# VOLUME 3 SUBJECT INDEX


A

*Ab initio* calculations
diphosphenes, 419, 432
Acetamide, oxidation by manganese(III), 977
Acetate complexes
gadolinium(III), holmium(III), 31
iron(III), 651
lanthanum(III), 31
molybdenum(II, III), 347
neodymium(III), 31
palladium(II), 1052
tungsten(II), 759
Acetic acid, effect on rhodium(III) substitution kinetics, 811
Acetone, reaction with rhodium(I) aldehyde complex, 1151
Acetonitrile, solvent for equilibrium studies, 251
Acetonitrile complexes
osmium(0), 1177, 1204, 1206, 1215, 1220
Acetophenone, 1181
Acetophenone–glycine Schiff base complexes, cobalt(II), copper(II), vanadium(IV), 575
Acetylene, *see* alkyne
4-Acetyl-2,4-dihydro-5-methyl-2-phenyl-5*H*-pyrazolonate, boron compound, 929
*N*-α-Acetylhistidine, induction of Pfeiffer effect, 1087
4-Acetyl-3-methyl-1-phenyl-2-pyrazolin-5-one, 929
Acidity, carbaborane amine complexes, 1351
Acrolein complexes
rhodium(I), 1151
Acrylamide, effect on
arsenic(III) oxidation by gold(III), 805
Acrylonitrile, reaction with
rhodium(II) aldehyde complex, 1151
Actinides, diketonate phosphine oxide complexes, distribution coefficients, formation constants, solvent extraction, separation factors, 1125
Activation energy, *see* free energy of activation
Activation enthalpy, *see* enthalpy of activation
Activation entropy, *see* entropy of activation
Acyl complexes
osmium, 1177, 1181, 1199, 1215
rhodium(III), 1047
1-Adamantylmethyl compounds
platinum(II), 87
Adenosine complexes
palladium(II), 9
Adenosine-5′-phosphate complexes
cadmium(II), 1105
Adipic acid, 607
Air, cyclohexanol oxidation, 607
Alanine complexes, cobalt(III), 49
Alcohol complexes
aluminium(II), 265
bismuth(III), 71
copper(II), 113
gallium(III), 265
Aldehydes
hydrogenation, oligomerisation, catalysis, 1151
reactions with osmium carbonyl cluster compounds, 1181, 1202
Aldehyde complexes, rhodium(I), 1151
Alizarin, *see* 1,2-dihydroxy-9,10-anthracenedione
Alkali metals
quinoline carboxylate complexes, synthesis, IR spectra, electric conductance, 240
Alkenes
addition to in cyclometallation, 1039
reactions with osmium carbonyl cluster compounds, 1183
Alkene complexes
platinum(II), 513
ruthenium(0), 1255
Alkoxide complexes
antimony(III), 661
boron, 589
copper(II), 641
molybdenum(II), 475
nickel(II), 641
osmium, 1178
tin(IV), 21
titanium(IV), 125
tungsten(VI), 1033
Alkyl compounds
cobalt(III), 79
gallium(III), 581
germanium, 757
indium(III), 581
iridium(III), 79
lead(IV), 297
nickel(II), 317
palladium(II), 117, 1042
platinum(II), 87, 373
rhodium(III), 79
ruthenium(II), 1255
silicon, 757
tin(IV), 297, 485, 681, 757
zirconium(IV), 79
Alkylamides
cadmium(II), 509
reactions with osmium carbonyl cluster compounds, 1177
titanium(IV), 1121
zirconium(IV), 1121
Alkylenedithiophosphates
antimony(III), arsenic(III), bismuth(III), 1337

Alkylidyne complexes
osmium, 1181
Alkynes, reactions with
disilenes, 392
methylborylene, 271
osmium carbonyl cluster compounds, 1187, 1219
Alkyne complexes
cobalt(0), iron(0), 175
Allene, 1185
Allyl compounds
cluster, 1279
osmium, 1181, 1186, 1205
Allylxanthate compounds
arsenic(III), 721
Aluminium(III)
alcohol water complexes, halide salts, NMR ($^{19}F$) spectra, second coordination sphere, 265
aminopolycarboxylate complex, reaction with indicator, kinetic study, free energy of activation, 917
carboxylate thiolate complexes, potentiometric titrations, formation constants, 871
heteropolytungstate, 1071
sialon ceramics, 1267
Americium(III), diketonate phosphine oxide complexes, distribution coefficients, formation constants, solvent extraction, 1125
Amides
oxidation by manganese(III), 977
reactions with osmium carbonyl cluster compounds, 1192
Amide complexes
cobalt(II), 99
copper(II), 99, 559
iron(III), 443
manganese(II), 99
nickel(II), 99, 551
osmium, 1196, 1217
tin(II), 627
Amidines, reactions with osmium carbonyl cluster compounds, 1192
Amidine complex, palladium(II), formation from aniline–nitrile complex reaction, 117
Amines
formation in amide oxidation by manganese(III), 977
reactions with osmium carbonyl cluster compounds, 1193
Amine complexes
boron, 589
cobalt(II), 357, 635
copper(II), 113, 137, 291, 357, 559
lithium, 307
manganese(I), 347
nickel(II), 551, 839, 1227
palladium(II), 969, 1227
platinum(II), 753
rhodium(III), 811
Aminoacid complexes
chromium(III), 17
cobalt(III), 49
nickel(II), 523, 1329
palladium(II), 9
Aminoalkoxide compounds
boron, 589
2-Aminobenzaldehyde, 257
2-Aminomethylpyridine complex, cobalt(II), 635
Aminopolycarboxylate complexes
aluminium(III), cobalt(II), 917
iron(II), 623
tin(IV), 1099
uranium(VI), 469
Aminopolyphosphonate complexes
cadmium(II), cobalt(II), copper(II), lead(II), manganese(II), nickel(II), zinc(II), 527
3-Aminopropanethiolate complex, nickel(II), 839
2-Aminopyridine, 1045, 1209
8-Aminoquinoline-2-carboxylic acid complexes
manganese(II), 491
Ammonia
reaction with cobalt(III) complex, 895
solvent, 133
Ammonia complexes
manganese(I), 347
platinum(II), 729
rhenium(I), 347
ruthenium(II), 1
Amylxanthate complexes
titanium(IV), 695
Aniline, 1193
Anilines, reaction with nitrile complexes, 117
Aniline complexes copper(II), 291
4-Anisaldehyde thiosemicarbazone complexes
cadmium(II), copper(II), mercury(II), zinc(II), 1237
4-Anisidine, 117
4-Anisyl(dimethyl)arsine complexes, osmium(0), 1219
Antifungal activity
thiosemicarbazone complexes, 1237
Antimicrobial activity
copper(II) pyridine Schiff base thione complexes, 1271
zinc(II) Schiff base thione complexes, 1271
Antimony
cluster compounds, 1307
double bonds, 403, 423
Antimony(III)
alkoxide phenolate semicarbazone thiosemicarbazone complexes, IR, Mössbauer, NMR ($^{1}H$) spectra, 661
alkylenedithiophosphate chloride compounds, synthesis, IR, NMR ($^{1}H$, $^{31}P$) spectra, 1337
germanium(IV), iron(−II) silicon complexes, synthesis, IR, NMR ($^{1}H$) spectra, 757
trichloro-, 1307
tris(trimethylstannyl)-, 757
Antimony(V)
alkyl aryl chloride compounds, preparation, reactions with tin(IV) compounds, NMR ($^{119}Sn$) spectra, 957
pentachloro-, 957
Apocytochrome-*c* complexes
vanadium(IV), zinc(II), 129
Arene complexes
rhodium(I), 497
Arsenic
cluster compounds, 1307
double bonds, 403, 408, 420

Arsenic(III)
alkylenedithiophosphate chloride compounds, synthesis, IR, NMR ($^1H$, $^{31}P$) spectra, 1337
aryl xanthate compounds, synthesis, IR, mass, NMR ($^1H$, $^{13}C$) spectra, 721
dichloro(phenyl)-, 721
oxidation by gold(III), kinetic study, enthalpy, entropy of reaction, 805
polymolybdates, 341
tribromo-, 297
Arsenic(V), polymolybdates, 341
Arsenious acid, 805
Arseno radicals, 631
Arsenoaminoxyl radical, formation, ESR spectrum, 631
Arsines, reactions with osmium carbonyl cluster compounds, 1217
Arsine complexes
platinum(II), 373
rhodium(III), 811
titanium(IV), 505
Arsine oxide complexes
iron(II), (III), 911
Aryl compounds
arsenic(III), 721
chromium(III), 1041
gold(I), 1040
iridium(III), 1048
osmium, 1039, 1179
palladium(II), 1039
platinum(II), 87, 1038
tin(IV), 485
titanium(III), 1041
Ascadians, absorption of niobium, 1033
ATP, *see* adenosine-5′-triphosphate
3-Azabicyclo[3.2.2]-nonane-3-thiocarboxylic acid-2-[1-(2-pyridinyl)ethylidene]hydrazide complexes, copper(II), 921
3-Azabicyclo[3.2.2]-nonane-3-thiocarboxylic acid-2-[1-(2-pyridinyl-*N*-oxide)ethylidene]-hydrazide complexes, copper(II), 921
Azides, reactions with osmium carbonyl cluster compounds, 1195
Azide complexes
cobalt(I), (III), 79
copper(II), 921
iridium(III), 79
rhodium(III), 79, 811
ruthenium(II), zirconium(IV), 79
Azidobenzene, 79, 1197
2-Azidobenzimidazole, 1197
2-Azido-6-chloropyridine, 1206
1-Azidophenylethene, 1196
2-Azidopyridine, 1208
Azidotrimethylsilane, 79
Azine complex, cobalt(III), 635
Azoles, induction of Pfeiffer effect, 1087
Azole complexes
cadmium(II), 509, 619
cobalt(II), 251
copper(II), 113, 261, 463, 787, 833, 1147
gold(I), 213, 497
iridium(I), 213
iron(−II), 1065
manganese(0), (I), (II), 707
mercury(II), 619
platinum(IV), 121
rhodium(I), 213
zinc(II), 619
Azomethines, *see* Schiff bases

## B

Barium phosphetanate, 325
Benzaldehyde, 393
Benzene complex, osmium, 1185
Benzil-*S*-benzyldithiocarbazate Schiff base complexes
cobalt(III), copper(II), nickel(II), rhodium(III), 517
Benzimidazole, 1207
Benzimidazole complexes
copper(II), 463
Benzoate complexes
iron(III), 651
Benzonitrile complex
thorium(IV), uranium(IV), 107
Benzophenone anion, reactions with osmium carbonyl cluster compounds, 1177, 1215
7,8-Benzoquinoline, 1038, 1040, 1042, 1046, 1051
2-Benzothiazolyl-3-tolyl compound
palladium(II), 1052
Benzoxazole, 1207
2-Benzoxazolyl-3-tolyl compound
palladium(II), 1052
Benzoyl chloride, reaction with carbaborane amine complex, 1351
4-Benzoyl-2,4-dihydro-5-methyl-2-phenyl-5*H*-pyrazolonate compound, boron, 929
4-Benzoyl-3-methyl-1-phenyl-2-pyrazolin-5-one, 929
complexes, actinides, 1125
2-Benzoylpyridine, 1052
Benzyl alcohol, *see* phenylmethanol
2-Benzylaminopyridine, 1045, 1052, 1209
*N*-Benzyldithiocarbamate complexes, palladium(II), platinum(II), 735
*S*-Benzyldithiocarbazate, 517
*S*-Benzyl-3(2′-hydroxyphenyl)methylendithiocarbazate complexes, copper(II), 595
2-Benzylmethylpyridine, 1052
2-Benzyloxypyridine, 1052
2-Benzylpyridine, 1052, 1208
2-(3-Benzyl)pyridyl compounds
osmium, 1045
Benzyne complexes
osmium, 1179, 1187
4-Benzylquinoline, 1044
*N*-Benzylsalicylaldimine, 1179
2-Benzylthioyridine, 1052
Berkelium(III), diketonate phosphine oxide complexes, distribution coefficients, formation constants, solvent extraction, separation factors, 1125
Beryllium, bromide chloride cyclopentadienyl compounds, synthesis, IR spectra, 1347

Biguanide, 983
Binuclear complexes
boron carboxylate oxo, 929
chromium(III) aminoacid hydroxide, 17
copper(II) planar, 157
gold(I), rhodium(I), (III), 497
iron(III) chloride oxo, 443
iron(III) chloride thione, 39
iron(III) magnesium chloride ether, 45
manganese(0), (I) azole carbonyl, 707
molydenum(III) chloride phosphine, 347
molydenum(IV) macrocyclic Schiff base, 257
nickel(II) carboxylate water, 689
palladium(II) acetate, 1052, 1053
palladium(II) alkyl nitrile phosphine, 117
palladium(II) aminoacid halide nucleoside, 9
palladium(II) chloride, 1052
palladium(II) chloride thiolate, 969
palladium(II) cyclometallated, 1048, 1051
platinum(II) diimine, 87
platinum(II) cyclometallated, 1051
rhodium(III) cyclometallated, 1046
silver(I) porphyrin, 1077
sodium crown ether hexafluorophosphate, 675
tungsten(II) carboxylates, 759
tungsten(V) dithiocarbamate oxo thio, 25
tungsten(V) dithiocarbamate thio, 1021
tungsten(VI) alkoxide, 1033
uranium(VI) dioxo hydroxide water, 143
vanadium(V) fluoride oxo peroxide, 287
Biorad AG50WX8 ion exchange resin, 667
Biphenyl complex, rhodium(I), 497
2,2′-Bipyridyl, reactions with
cyclometallated complex, 1046
osmium carbonyl cluster compounds, 1209
2,2′-Bipyridyl complexes
chromium(III), 1141
cobalt(III), 49
copper(II), 137, 595
cyclometallated, 1047
iridium(III), 1047
molybdenum(VI), 377
ruthenium(III), 639
titanium(IV), 125
6(2:2′-Bipyridyl)pyridyl compound, osmium, 1045
2,2′-Bipyrimidyl complexes
platinum(II), 87
Bis(3-acetyl-pentane, 2,4-dione)-ethylenediimine complex, copper(II), 157
Bis(2-aminoethyl)methoxide complex, copper(II), 157
*N*,*N*-Bis(2-benzimidazolylmethyl)-benzylamine complex, copper(II), 113
2-(Bis-*t*-butylphosphinomethyl)-8-methylquinoline, 1042
2-(Bis-*t*-butylphosphinomethyl)-quinoline, 1053
*N*,*N*′-Bis(2-carbamoylethyl)-1,2-diaminoethane complexes, copper(II), 559
*N*,*N*′-Bis(2-carbamoylethyl)-1,2-diaminopropane complexes, copper(II), 559
*N*,*N*′-Bis(2-carbamoylethyl)-1,3-diaminopropane complexes, copper(II), 559
*N*,*N*′-Bis(2-carbamoylethyl)-2-hydroxy-1,3-diaminopropane complexes, copper(II), 559
Bis(dimethylamino)tetrachlorophosphazene, 867
1,2-Bis(dimethylarsino)benzene complex, titanium(IV), 505
Bis(dimethyl{phenyl}silyl)amide, cadmium(II), 509
1,2-Bis(dimethylphosphino)ethane complexes
nickel(II), 317
palladium(II), 1025
ruthenium(0), (II), 1255
titanium(IV), 505
4,6-Bis(3,5-dimethylpyrazole-1-yl)pyrimidine complexes
gold(I), iridium(I), rhodium(I), 213
1,2-Bis(diphenylphosphino)ethane complex
titanium(IV), 505
Bis(diphenylphosphino)methane complex, ruthenium(0), 567
1,3-Bis(2-hydroxyphenyl)-1,3-propanedione complexes
cobalt(II), (III), copper(II), lithium, nickel(II), zinc(II), 1017
2-[1,1-Bis(methoxycarbonyl)propyl]pyridine, 1050
Bismuth(III)
alcohol mercaptide complexes, synthesis, electronic, IR spectra, formation constants, X-ray crystal structure, 71
alkylenedithiophosphates, synthesis, IR, NMR ($^{1}H$, $^{31}P$) spectra, 1337
*N*,*N*′-Bis-8-quinolinyl-1,2-diaminoethane complexes
cobalt(II), copper(II), 357
Bis(salicylaldehyde)ethylenediimine complex, copper(II), 157
Bis(salicylaldehyde)-*m*-phenylenediimine complex
copper(II), 157
Bis[2-(salicylideneamino)ethyl]amine, 939
Bis(trimethylsilyl)amide cadmium(II), 509
Biuret complexes, cobalt(II), copper(II), manganese(II), nickel(II), 99
Bonding schemes, *closo*-clusters, 199
Book reviews
inorganic coordination chemistry, 1169
lanthanides, 1169
molybdenum reactions, 515
technetium chemistry, 763
Boranes
dibromomethyl-, 271
oxobis(diacetato-), 929
polyhedral, bonding schemes, 199, 1321
trichloro-, 957
Borirene, 271
Borohydrides and borohydride complexes, uranium(III), (IV), 457
Boron
alkoxide amine phenolate compounds, synthesis, NMR ($^{1}H$, $^{11}B$, $^{13}C$) spectra, configurational isomerism, free energy of activation, 589
carboxylate diketonate oxo binuclear compounds, synthesis, IR, NMR ($^{1}H$, $^{11}B$) spectra, reactions with glycols, 929
chloride, reactions with tin(IV) compounds, NMR ($^{11}B$, $^{119}Sn$) spectra, 957
cluster compounds, 1299

organo compounds, synthesis, mass, NMR ($^1$H) spectra, 271
oxide, 151
subhalides, synthesis by radiofrequency discharge, intermediates, 369
trichloride, 957
Borosilicate glass, as nuclear waste immobilising agent, 151
Bromide, catalysis of iodide oxidation by tungstocobaltate(III), 191
Bromides and bromide complexes
aluminium(III), 265
arsenic(III), 297
beryllium, 1347
boron, 369
cadmium(II), 615
cluster, 1307
cobalt(II), 99, 357
copper(II), 99, 261, 357, 921, 1135, 1233
gallium(III), 265
iron(III), 911
manganese(II), 99
mercury(II), 297, 615
nickel(II), 99, 983
osmium(II), 385
palladium(II), 9, 1039
platinum(IV), 121
reactions with diimine complexes, kinetic study, 701
rhenium(I), 331
rhenium(III), 1059
ruthenium(II), 325
titanium(IV), 897
zinc(II), 615
Bromination
copper(II) diketonate complex, 1233
nickel(II) ketoimine complex, 239
Bromoethane, reaction with carbaborane amine complex, 1351
8-Bromoethylquinoline, 1052
8-Bromomethylquinoline, 1042
2-Bromo-1-phenylbutane-1,3-dione-1,2-diaminoethane-1-phenyl-2-succinimido-butane-1,3-dione Schiff base complex, nickel(II), 239
2-Bromopyridine, 1039
5-Bromosalicyl-2′-mercaptobenzaldimine complex molybdenum(VI), 55
5-Bromosalicyl-2′-mercaptoethaldimine complex molybdenum(VI), 55
Brucine sulphate, interaction with heteropolyanions, 1071
Buta-1,3-diene, 1187
*n*-Butane, 175
2,3-Butanedionebis(anisylimine) complexes, rhodium(I), 799
2,3-Butanedionebis(cyclohexyldiimine) complexes rhodium(I), 799
2,3-Butanedionebis(4-hydroxyphenylimine) complexes rhodium(I), 799
2,3-Butanedionebis(phenylimine) complexes, rhodium(I), 799
1-Butene, 175
2-Butene, 175
*n*-Butyl compounds
tin(IV), 485, 681
Butylamine, 1220
4-*t*-Butyl-1,2,6-cyclohexanetrione oxime complexes copper(II), nickel(II), 479
4-*t*-Butyl-1,2,6-cyclohexanetrione oxime furazan complexes, copper(II), nickel(II), 479
*t*-Butylcyclopentadienyl complexes
titanium(IV), 897
*N*-*t*-Butyldithiocarbamate complexes, palladium(II), platinum(II), 735
*O*-Butyldithiophosphate complexes
platinum(II), 231
2,3-Butylenedithiophosphate complexes, antimony(III), arsenic(III), bismuth(III), 1337
1-*n*-Butylimidazole, hexahaloplatinate(IV) salts, 121
*t*-Butylisocyanide complex
osmium(II), 385
4-*t*-Butylpyridine complex
cadmium(II), 509
*t*-Butylthiolate complexes
chromium(III), 775
copper(I), 535
platinum(II), 231
titanium(IV), 505
*t*-Butyl(trimethylsilyl)amide cadmium(II), 509
Butylxanthate complexes
titanium(IV), 695
But-1-yne, 1191
But-2-yne, 271
But-2-ynyl complex, cobalt(0), iron(0), 175
Butyronitrile complexes
manganese(I), rhenium(I), 353

## C

Cadmium(II)
alkylamide azole pyridine complexes, NMR ($^1$H, $^{29}$Si, $^{113}$Cd) spectra, 509
aminopolyphosphonate complexes, synthesis, 527
azole halide complexes, synthesis, IR, NMR ($^1$H, $^{13}$C) spectra, TGA study, 619
carboxylate *N*-oxide water complex, X-ray crystal structure, 303
chloride thiosemicarbazone complex, synthesis, IR spectrum, antifungal activity, 1237
hydrazone ketone pyridine complex, synthesis, IR, NMR ($^1$H, $^{13}$C) spectra, 281
nucleotide phosphate complexes, NMR ($^1$H, $^{31}$P) spectra, potentiometric titrations, formation constants, 1105
Caesium
fluoride complex, potentiometric titration, formation constant, 845
phosphetanate, 325
quinoline carboxylate complexes, synthesis, IR spectra, electric conductance, 240
Calcium, dicarboxylate complexes, calorimetry, formation constants, enthalpies, entropies, free energies of formation, effects of C=C bonds, 545

Californium(III), diketonate phosphine oxide complexes, distribution coefficients, formation constants, solvent extraction, separation factors, 1125
Calmagite, reactions with aminocarboxylate complexes, 917
Calorimetry, calcium dicarboxylate complexes, 545
Carbaboranes
  amine complex, reactions, IR, NMR ($^{1}H$, $^{11}B$) spectra, potentiometric titrations, 1351
  bonding schemes, electron counting, 199, 1321
1-Carbamoylindazolate complexes, copper(II), 1147
Carbanions, reactions with osmium carbonyl cluster compounds, 1177, 1199
Carbazole complexes
  gold(I), rhodium(I), (III), 497
Carbene complexes, osmium, 1202
Carbide cluster complexes, 1046, 1279, 1307, 1321
Carbocations, reactions with osmium carbonyl cluster compounds, 1199
Carbodiimides, reactions with osmium carbonyl cluster compounds, 1200
Carbomethoxymethylidyne complex
  iron(I) cluster, 1307
Carbon–carbon double bonds, effect on dicarboxylate complex formation, 545
Carbon–hydrogen bond activation cyclopentadienyl complex, 771
  insertion into, 1039
  thermal, 1038
Carbon dioxide, 1053
Carbon disulphide, 1200, 1307
Carbon monoxide, 79, 317, 1043, 1048, 1187
Carbon tetrachloride
  reaction with cluster complex, 1307
  reaction with rhenium(III) complex, 771
Carbonyl complexes
  cluster, 1175, 1279, 1307, 1321
  cobalt(0), 175
  cobalt(I), 79
  iridium(I), 213, 1093
  iron(−II), 757
  iron(0), 175, 365, 757, 889
  iron(II), 911
  manganese(−I), (0), 707
  manganese(I), 353, 707
  molybdenum(−I), 1131
  molybdenum(0), 235, 365, 1131
  molybdenum(II), 347
  osmium, 1175
  platinum(0), 1093
  rhenium(I), 331, 353
  rhenium(III), 1059
  rhodium(I), 213, 799, 1151
  ruthenium(0), 567
  tungsten(0), 365
Carboranes, *see* carbaboranes
Carboxylate complexes
  aluminium(III), 871
  boron, 929
  cadmium(II), 303
  chromium(III), 1141
  cobalt(II), 575
  copper(II), 575, 833
  gallium(III), indium(III), 871
  iron(III), 651
  molybdenum(II, III), 347
  neptunium(V), 667
  nickel(II), 689, 963
  niobium(V), 1029
  osmium, 1202
  terbium(III), 1087
  tungsten(II), 759
  vanadium(IV), 575
Carboxylic acids, reactions with osmium carbonyl cluster compounds, 1202
Catalysis
  aldehyde hydrogenation, oligomerisation by rhodium(I) complex, 1151
  hydrogen peroxide decomposition by copper(II) planar complexes, 157
  polycondensation by chiral heteropolyanion, 381
  tungstocobaltate(III) oxidations by halide ions, 191
Catechole, reactions with boron compounds, 589, 929
Catecholate complexes, boron, 589
Catecholborane, 589
CD spectra
  chromium(III) dicarboxylate diimine complexes, 1141
  cobalt(II) heteropolytungstate, 1071
  cobalt(III) aminoacid diimine complexes, 49
  heteropolymolybdates, 381, 1071
  heteropolytungstates, 1071
  phosphomolybdates, 1071
  polybenzyl, 381
  silicopolymolybdates, 1071
  vanadium(IV), zinc(II) apocytochrome-*c* phthalocyanine complexes, 129
Charcoal, effect on cyclohexanol oxidation, 607
Chelate effect, organometallic compounds, 1038
Chemical potential, relationship to electronegativity, 853
Chemisorption, nitric oxide, sulphur dioxide on iron(III) hydroxide, oxide, 223
Chirality, nickel(II) amide amine complexes, 551
Chlorides and chloride complexes
  aluminium(III), 265
  antimony(III), arsenic(III), 1337
  beryllium, 1347
  boron, 369
  cadmium(II), 619, 1237
  catalysis of iodide oxidation by tungstocobaltate(III), 191
  chromium(III), 775
  cluster, 1307
  cobalt(II), 99, 297, 357, 363
  copper(II), 99, 157, 261, 291, 297, 357, 921, 1135
  gallium(III), 265, 581
  germanium(IV), 297
  gold(0, I), 1289
  gold(III), 805, 1365
  iridium(I), 213
  iridium(III), (IV), 1013
  iron(III), 39, 45, 443, 911
  magnesium, 45

manganese(II), 99
mercury(II), 619, 1237
molybdenum(II), 347, 475
molybdenum(III), 347, 1131
molybdenum(IV), 257, 347, 1131
nickel(II), 21, 99, 317, 983
palladium(II), 9, 701, 969
platinum(II), 373, 701, 729
platinum(IV), 121
rhenium(I), 331
rhodium(I), 213, 799
rhodium(III), 811
ruthenium(II), 325
silicon, 603
thorium(IV), 107
tin(IV), 21
titanium(IV), 125, 505, 695, 897, 1121
uranium(IV), 107
zinc(II), 619, 1237
zirconium(IV), 611, 1121
Chlorination, nickel(II) ketoimine complexes, 239
Chloroacetic acid, 939
effect on rhodium(III) substitution kinetics, 811
4-Chloroaniline complexes
copper(II), 291
4-(4′-Chlorobenzoyl)-2,4-dihydro-5-methyl-2-phenyl-5*H*-pyrazolonate compound, boron, 929
4-(4′-Chlorobenzoyl)-3-methyl-1-phenyl-2-pyrazolin-5-one, 929
5-Chloro-2[3′-(4-chlorophenyl)]-pyridyl compound
palladium(II), 1052
Chloroform, solvent for equilibrium studies, 251
Chloromethyl methyl ether, 939
4-Chloro-3-methyl-5-phenylisoxazole complexes
copper(II), 261
2-Chloromethylpyridine, 1042
4-Chlorophenolate complexes, zirconium(IV), 611
2-Chlorophenoxyethanoate complex, nickel(II), 689
2-Chloro-1-phenylbutane-1,3-dione-1,2-diaminoethane-1-phenyl-2-succinimidobutane-1,3-dione Schiff base complex, nickel(II), 239
2-Chloropyridine, 1048, 1208
2(3-Chloro)pyridyl compound
osmium, 1045
2(6-Chloro)pyridyl compounds
nickel(II), palladium(II), platinum(II), 1048
2(6-Chloro)pyridylcarbonyl compounds, palladium(II), 1048
5-Chlorosalicylaldoximate complexes, nickel(II), 603
5-Chlorosalicyl-2′-mercaptobenzaldimine complex
molybdenum(IV), 61
molybdenum(VI), 55, 61
5-Chlorosalicyl-2′-mercaptoethaldimine complex
molybdenum(VI), 55
Chromium(0)
7,8-benzoquinoline(tricarbonyl)-, 1042
diarsene complexes, 415
diphosphene complex, 415, 428
Chromium(I)
cyanide nitrosyl water complexes, oxidation, photochemistry, electronic spectra, 247
Chromium(II)
diarsene complex, 417
Chromium(III)
aminoacid hydroxide complexes, synthesis, ESR spectra, magnetic moments, 17
*t*-butylthiolato(cyclopentadienyl)bis-thioether, 775
*t*-butylthiolato(methylcyclopentadienyl)bis-thioether, 775
chloride cyclopentadienyl thio thiolate palladium(II) polynuclear complexes, synthesis, IR spectra, magnetic moments, X-ray crystal structure, 775
cyanide water complex, magnetic moment, 183
cyclometallated complex, 1041
dicarboxylate diimine complexes, synthesis, CD, electronic, ORD spectra, 1141
diketonate complex, formation, electronic spectra, solvent extraction, kinetic study, 781
dithiocarbamate iodine complexes, synthesis, electronic, IR spectra, formation constants, enthalpy, entropy of formation, 1241
heteropolytungstate, electronic spectrum, 1161
2-phenylpyridyl, 1041
phosphetanate, synthesis, IR spectrum, magnetic moment, 1155
Chromium(VI)
tetroxo-, formation from chromium(I), 247
Circular dichroism, *see* CD
Circularly polarised luminescence spectra, terbium(III) carboxylate pyridine complex, 1087
Citrate complexes
iron(II), (III), 169
neptunium(V), 667
Cluster compounds
boron, 1299
carbonyl, 1321
*closo* bonding schemes, 199
gold, 1289
heteroatoms in, 1307
iridium(I), platinum(0) carbonyl, 1093
iron nitrosyl selenide sulphide, 1165
osmium, 1175, 1279
rhenium, 1279
ruthenium, 1279
structure and bonding, 1277 *et seq.*
*see also* polynuclear complexes
Cobalt
alkyl, 1046
cluster complexes, 1307
cyclometallated complex, 1046
Cobalt(0)
alkyne carbonyl iron(0) complex, hydrogenation, kinetic study, 175
octacarbonyldi-, 175
Cobalt(I)
azide carbonyl phosphine complex, synthesis, IR, NMR ($^{1}H$, $^{31}P$) spectra, X-ray crystal structure, 79
Cobalt(II)
amide halide complexes, synthesis, electronic, IR spectra, magnetic moments, X-ray diffraction, 99
amine halide nitrate quinoline thiocyanate complexes, synthesis, electronic, IR spectra, 357

amine pyridine complex, oxidation, 635
aminopolycarboxylate complex, reaction with indicator, kinetic study, free energy of activation, 917
aminopolyphosphonate complexes, electronic spectra, magnetic moments, 527
azole thiocyanate complexes, electronic spectra, equilibrium constants, electric conductance, solvent dependence, 251
carboxylate Schiff base complex, synthesis, electronic, IR spectra, electric conductance, magnetic moment, 575
chloride, 297
chloride complexes, diamine salts, electronic, IR spectra, magnetic moments, 363
cyanide water complexes, magnetic moments, 183
diketonate ketophenol complexes, synthesis, IR spectra, 1017
heteropolytungstate, 1071
phosphetanate, 325, 1155
pyridine Schiff base thione complex, synthesis, electronic, IR spectra, magnetic moment, 1271
separation from $Ni^{2+}$, 939
Cobalt(III)
alkyl azide phosphine complex, synthesis, IR, NMR ($^1H$, $^{31}P$) spectra, reaction with CO, X-ray crystal structure, 79
alkyl phosphine triazene complex, synthesis, IR, NMR ($^1H$, $^{31}P$) spectra, 79
aminoacid diimine, complexes, synthesis, CD, electronic spectra, optical rotation, 49
azine complex, synthesis, ligand synthesis, mass, NMR ($^1H$) spectra, 635
bis(2,2′-bipyridyl)dichloro-, chloride, 49
cyanide sulphite water complex, substitutions, kinetic studies, 895
dichlorobis(1,10-phenanthroline)-, chloride, 49
diimine complex, reactions with nucleophiles, electronic spectra, 701
diketonate ketophenol complexes, synthesis, IR spectra, 1017
heteropolytungstate, oxidation of iodide, thiocyanate, kinetic study, enthalpy, entropy of activation, catalysis by anions, 191
ketone Schiff base thiolate complexes, synthesis, ligand synthesis, electronic, IR, NMR ($^1H$) spectra, electric conductance, 517
pyrazolate thiosemicarbazone complex, synthesis, ligand synthesis, electronic, IR spectra, electric conductance, 1135
Schiff base thione complex, synthesis, electronic, IR, NMR ($^1H$), photoacoustic spectra, 1271
trimethyltris(trimethylphosphine)-, 79
12-tungsto-, 191
Coexistence index, plutonium oxidation states, 761
Compression pressure, effect on iron(III) hydroxide oxide chemisorption, 223
Conductivity, *see* electric conductance
Cone angles, carboranol ligand, 307
Configurational isomerism
copper(II) amide amine complexes, 559
gold(0, I), ruthenium(0) carbonyl hydride phosphine complexes, 567
spiroborates, 589
Conformational analysis, polysiloxanes, 1109
Conformational isomerism, thioether complexes, 331
Constitutional isomerism
copper(II) azole cyanate complexes, 1147
Controlled potential coulometry
copper(II) dipeptide complexes, 861
Controlled potential electrolysis, nickel(II) tetradentate complexes, 585
Copper, formation in copper(II) complex electrochemistry, 861
Copper(I)
chloride complex, formation from copper(II), magnetic moment, X-ray crystal structure, 771
cyclometallated complexes, 1055
dipeptide complexes, formation from copper(II) complex electrochemistry, 861
dithiocarbamate complexes, reaction with haloalkanes, 291
iodide rhenium(III) polynuclear complex, X-ray crystal structure, 749
Schiff base thione complex, synthesis, IR spectrum, 1271
thiolate polynuclear complexes, synthesis, IR, NMR ($^1H$) spectra, X-ray crystal structures, 535
Copper(II)
alcohol amine azole nitrate complex, synthesis, X-ray crystal structure, 113
alkoxide oxime sulphate polynuclear complexes, synthesis, electronic, IR spectra, magnetic moments, viscosity, DTA, TGA study, 641
amide amine complexes, ligand synthesis, electronic spectra, potentiometric titrations, formation constants, configurational isomerism, 559
amide halide complexes, synthesis, electronic, IR spectra, magnetic moments, X-ray diffraction, 99
amine diimine diketonate nitrate perchlorate complexes, synthesis, electronic, ESR, photoacoustic spectra, 137
amine halide nitrate quinoline thiocyanate complexes, synthesis, electronic, IR spectra, magnetic moments, 357
aminopolyphosphonate complexes, synthesis, electronic, IR spectra, magnetic moments, DTA, TGA study, 527
azide bromide chloride nitrate pyridine pyridine-*N*-oxide thiocyanate thiosemicarbazone complexes, synthesis, electronic, ESR, IR spectra, 921
azole bromide chloride nitrate perchlorate complexes, synthesis, electronic, ESR, IR spectra, 261
azole carboxylate peptide complexes, formation, electronic, ESR spectra, 833
azole cyanate complexes, electronic, IR spectra, constitutional isomerism, 1147
azole peptide complexes, synthesis, electronic, ESR, IR spectra, 463
azole peptide pyridine complexes, potentiometric titrations, formation constants
bis(3-nitro-2,4-pentanedionato)-, 1357

bromide diketonate complex,
synthesis, electronic, ESR spectra, 1233
carboxylate Schiff base complex, synthesis, electronic, IR spectra, electric conductance, magnetic moment, 575
cyanide water complex, magnetic moment, 183
diimine complex, reactions with nucleophiles, electronic spectra, 701
diimine phenolate pyridine Schiff base complexes, synthesis, electronic, IR spectra, magnetic moments, 595
diketonate ketophenol complexes, synthesis, IR spectra, 1017
diketone–diamine–salicylaldehyde Schiff base complexes, synthesis, electronic, IR spectra, magnetic moments, TLC, 713
dioxime complex, synthesis, ESR, IR spectra, solvent extraction, 821
dipeptide complexes, controlled potential voulometry, cyclic voltammetry, 861
diselenocarbamate dithiolate complex, ESR spectrum, EHMO calculations, 433
dithiocarbamate chloride diketonate complexes, formation, ESR spectra, 291
dithiocarbamate electrophile complexes, formation, ESR spectra, 297
ketone Schiff base thiolate complexes, synthesis, ligand synthesis, electronic, IR spectra, electric conductance, magnetic moments, 517
macrocyclic Schiff base complex, synthesis, ligand synthesis, electronic, IR spectra, polarography, solvent extraction, 1357
oxime complexes, synthesis, ligand synthesis, solvent extraction, 479
2,4-pentanedionato-, 1233
phosphetanate, synthesis, IR spectrum, magnetic moment, 1155
planar complexes, electronic spectra, cyclic voltammetry, reactions with hydrogen peroxide, 157
pyrazolate thiosemicarbazone complexes, synthesis, ligand synthesis, electronic, IR spectra, electric conductance, magnetic moments, 1135
pyridine Schiff base thione complex, synthesis, electronic, IR, photoacoustic spectra, magnetic moment, antimicrobial activity, 1271
quinone water complexes, synthesis, electronic, IR spectra, magnetic moments, 729
semicarbazone thiosemicarbazone complexes synthesis, electronic, ESR, IR spectra, magnetic moments, 991
separation from $Ni^{2+}$, $Zn^{2+}$, 939
sulphate thiosemicarbazone complex, synthesis, IR spectrum, magnetic moment, antifungal activity, 1237
Cotton effect, heteropolyanions, 1071
Creatinine complexes
cadmium(II), mercury(II), zinc(II), 619
Crotonaldehyde complex
rhodium(I), 1151
Crown ether complex, sodium, 675
Crystal structure, *see* X-ray crystal structure
Curium(III), diketonate phosphine oxide complexes, distribution coefficients, formation constants, solvent extraction, 1125
Cyanate complexes
copper(II), 1147
molybdenum(IV), 347
osmium, 1212
Cyanide, reaction with cobalt(III) complex, 895
Cyanide complexes
chromium(I), 247
chromium(III), 183
cobalt(III), 183, 895
copper(II), 183
iron(I), 1165
iron(II), (III), manganese(II), ruthenium(II), 183
tungsten(IV), 743
2-Cyanobenzyl complex
palladium(II), 117
2-Cyanopyridine, 1208
2(3-Cyano)pyridyl compound
osmium, 1045
Cyclic voltammetry
copper(II) dipeptide complexes, 861
copper(II) planar complexes, 157
molybdenum(V) oxo dithiocarbamate thiocyanate complex, 907
molydenum(VI) dioxo mercaptide phenolate Schiff base complexes, 55
nickel(II) tetradentate ketoimine complexes, 585
ruthenium(II) ammine thiocyanate complexes, 1
Cyclohexa-1,3-diene complexes
osmium, 1185
Cyclohexanediamine complexes, iron(II), 623
Cyclohexanol, oxidation, 607
Cyclohexanone, 607, 1182
2-Cyclohexenone, 1182
*N*-Cyclohexyl-*N*-methyldithiocarbamate complexes
tungsten(V), 1021
Cyclometallation
osmium carbonyl cluster compounds, 1178, 1185, 1190, 1206, 1217
review, 1037
Cyclonona-1,3-diene, 1186
1,5-Cyclooctadiene complexes
rhodium(I), 213, 497
Cyclooctene, 1185, 1192
Cyclopentadiene, 1185
Cyclopentadienyl complexes
beryllium, 1347
chromium(III), 775
cluster, 1307, 1321
iridium(I), 1093
iron(0), molybdenum(0), 365
molybdenum(IV), 765
nickel(II), 317
rhenium(III), 749, 771
titanium(IV), 695, 883, 897
tungsten(0), 365
zirconium(IV), 79, 611, 883
1,2,3-Cyclopentanetrione trioxime complexes
copper(II), nickel(II), 479

1,2,3-Cyclopentanetrione trioxime furazan complexes
copper(II), nickel(II), 479
Cyclopentanone, 1183
Cyclopentene, 1185
Cyclotetraphosphine, 400
Cyclotetrasilane, 395
Cyclotrigermane, 397
Cyclotrisilane, 397, 432
Cytidine complexes
palladium(II), 9

## D

Decahydrodecaborate(2), 199, 901
Decynes, 271
Demethylation, carbaborane amine complex, 1351
Density functional theory, application to electronegativity, 853
Deuteration, cyclometallated complex, 1041
Deuterium oxide, solvent for electronic spectra, 161
2,6-Diacetylpyridine-5-methyl-1,5,9-triazanonane Schiff base complex, copper(II), 157
*N,N'*-Dialanyl-1,2-diaminoethane complexes, nickel(II), 551
*N,N'*-Dialanyl-2,3-diaminopropane complexes
nickel(II), 551
Dialkylamides, *see* alkylamides
Diamine salts
tetrachlorocobaltate(II), 363
Diamine Schiff base complexes
copper(II), 713
1,2-Diaminodecane, 363
Diaminodiamide complexes
copper(II), 559
nickel(II), 551
1,2-Diaminoethane, 363
1,2-Diaminoheptane, 363
1,2-Diaminohexane, 363
1,2-Diaminononane, 363
1,2-Diaminooctane, 363
1,2-Diaminopentane, 363
1,2-Diaminopropane, 363
1,3-Diaminopropane complex
zinc(II), 1333
Diarsenes, 405, 408
Diarsene complexes, 413, 415
Diazo compounds, reactions with osmium carbonyl cluster compounds, 1202
Diazomethane, 1205
Diazonium salts, reactions with osmium carbonyl cluster compounds, 1206
2-Diazopropane, 1203
Dibenzo-36-crown-12 complex
sodium, 675
*N,N*-Dibenzyldithiocarbamate complexes
chromium(III), 1241
1,4-Diboracyclohexadienes, 271
Diboretene, 271
Diboron halides, 369
Di-*t*-butylacetylene, *see* tetramethylhex-3-yne
*N,N*-Di-*i*-butyldithiocarbamate complex, platinum(II), 231
*N,N*-Di-*n*-butyldithiocarbamate complex, platinum(II), 231
*O,O*-Dibutyldithiophosphate complexes, platinum(II), 231
Dicarba-*closo*-decaborane(10), 199
Dicarba-*closo*-dodecaborane(12), 199
Dicarba-*closo*-hexaborane(6), 199
Dicarba-*closo*-nonaborane(9), 199
Dicarba-*closo*-octaborane(7), 199
Dicarba-*closo*-pentaborane(7), 199
Dicarba-*closo*-undecaborane(11), 199
Dicarboxylate complexes
calcium, 545
chromium(III), 1141
terbium(III), 1087
2,6-Dicarboxylatopyridine complexes, terbium(III), 1087
Dichloroacetic acid, effect on rhodium(III) substitution kinetics, 811
6,6'-Dichloro-2,2'-bipyridyl, 1048
Dichloromethane, solvent for equilibrium studies, 251
Dicyclohexyl-18-crown-6 complexes uranium(VI), 143
Dicyclohexyl(phenyl)phosphine complexes, gold(0, I), 1289
Dielectric constant, iron(III) chloride thione complexes, 39
Dienes, reactions
disilenes, 392
osmium carbonyl cluster compounds, 1185
1,1-Di(ethoxycarbonyl)-2(2'-pyridyl)ethyl compounds
palladium(II), 1049
3-(2'-Diethylamino)ethylamino-*n*-propoxide complex
copper(II), 157
Diethylammonium phosphetanate, 325
*N,N*-Diethyldiselenocarbamate complexes, copper(II), nickel(II), 433
*N,N*-Diethyldithiocarbamate complexes
chromium(III), 1241
iron(I), 1065
molybdenum(IV), 347
platinum(II), 231
Diethylenetriamine, linked to polystyrene, metal ion separations, 939
Diethylenetriaminepentaacetate complexes, tin(IV), 1099
Di(2-ethylhexyl)phosphoric acid, iron(III) solvent extraction, 615
5,8-Diethyl-7-hydroxy-6-dodecanone oxime complexes
copper(II), nickel(II), 641
Diethyl(phenyl)phosphine complexes
molybdenum(II), 347
rhenium(III), 1059
Diethylphosphide complexes
gallium(III), indium(III), 581
2,2-Diethylpropylenedithiophosphate complexes
antimony(III), arsenic(III), bismuth(III), 1337
Difference absorption spectra, *see* electronic difference spectra
Digermenes, 395, 397, 418
*N,N'*-Diglycyl-1,2-diaminoethane complexes, nickel(II), 551

*N,N'*-Diglycyl-2,3-diaminopropane complexes
nickel(II), 551
*O,O*-Dihexyldithiophosphate complexes, platinum(II), 231
9,10-Dihydroanthracene complex
rhodium(I), 497
1,2-Dihydroxy-9,10-anthracenedione complexes
copper(II), manganese(II), nickel(II), palladium(II), 729
1,4-Dihydroxybut-2-yne, 1181
Diimine complexes
chromium(III), 1141
cobalt(II), 701
cobalt(III), 49
copper(II), 137, 595, 701
iron(III), 443
molybdenum(VI), 377
nickel(II), palladium(II), 701
platinum(II), 87, 701
reactions with nucleophiles, electronic spectra, kinetic studies, 701
rhodium(I), 799
ruthenium(III), 639
titanium(IV), 125
Diketonate complexes
americium(III), berkelium(III), 1125
boron, 929
californium(III), 1125
chromium(III), 781
cobalt(II), 1017
copper(II), 137, 291, 1017, 1233
curium(III), 1125
lithium, 1017
molybdenum(II), 347
zinc(II), 1017
Dimeric complexes, *see* binuclear complexes
Dimethylamides, titanium(IV), zirconium(IV), 1121
Dimethylamine, formation in amide oxidation by manganese(III), 977
Dimethylamine complex
carbaborane, 1351
1-Dimethylamine-1-carba-*closo*-dodecaborane, 1351
*N,N'*-Dimethyl-3-aminopropanethiol complex
nickel(II), 969
*N,N'*-Dimethyl-3-aminopropanethiolate complexes
nickel(II), palladium(II), 969
*N,N*-Dimethylaniline complexes
copper(II), 291
*N,N*-Dimethylbenzylamine, 1194
2,3-Dimethylbutane-2,3-diol reactions with boron compounds, 929
1,4-Dimethyl-2,3-butylenedithiophosphate complexes
antimony(III), arsenic(III), 1337
7,7-Dimethyl-4,7-diazaheptyloxamide complexes
copper(II), 157
Dimethyl(2-dimethylaminophenyl)arsine complexes
rhodium(III), 811
*N,N'*-Dimethylethylenediamine complex, zinc(II), 1333
*N,N*-Dimethylformamide
oxidation by manganese(III), 977
solvent for complex formation studies, 939
solvent for electronic spectra, 161
*N,N*-Dimethylformamide complexes
iron(III), 443
tin(II), 623
4,6-Dimethyl-2-guanidinopyrimidine complexes
nickel(II), 983
1,2-Dimethylimidazole complexes
platinum(IV), 121
*N,N*-Dimethyl-2-mercaptoethylamine complexes
nickel(II), palladium(II), 1227
*N,N*-Dimethyl-1,4-phenylenediamine complexes
copper(II), 291
4,6-Dimethyl-2-phenylguanidinopyrimidine complexes
nickel(II), 983
Dimethylphenylmethanamine, *see* dimethylbenzylamine
Dimethyl(phenyl)phosphine complexes
gold(0, I) 1289
iridium(III), 79
molybdenum(II), 347
osmium, 1201, 1216, 1220
rhenium(III), 1059
3,5-Dimethyl-1-phenylpyrazole, 1046
4,5-Dimethyl-2-phenylthiazole, 1051
Dimethylphosphinate complexes
platinum(II), 231
2,2-Dimethylpropylenedithiophosphate complexes
antimony(III), arsenic(III), bismuth(III), 1337
3-(3,5-Dimethylpyrazol)-6-chloropyradazine complexes
gold(I), iridium(I), rhodium(I), 213
3,5-Dimethylpyrazole complexes
cobalt(II), 251
4,6-Dimethylpyrimidine complexes
rhodium(I), 213
5,5-Dimethyl-1-pyrroline-1-oxide, 631
Dimethylsulphate, reaction with carbaborane amine complex, 1351
Dimethylsulphoxide, solvent for complex formation studies, 939
Dimethylsulphoxide complex
tin(II), 627
*N,N'*-Dimethylthiourea complexes
molybdenum(0), 235
Dimethyl(2-tolyl)arsine complexes, osmium(0), 1219
Dimethyl(vinyl)arsine, 1219
4-(3',5'-Dinitrobenzoyl)-3-methylpyrazolone-5 complexes, actinides, 1125
Dinitrogen complexes
iron(II), 623
6,13-Dinitro-5,7,12,14-tetramethyl-1,4,8,11-tetraazacyclotetradeca-1,5,7,12-tetraene, synthesis, IR, NMR ($^1$H) spectra, copper(II), nickel(II) complexes, 1357
Dioxime complexes
copper(II), nickel(II), 821
Dioxygen
cyclohexanol oxidation, 607
reaction with chromium(I) complexes, 247
reaction with platinum(0) complex, 513
Dipeptide complexes
copper(I), 861
copper(I), (II), 463, 861

1,5-Diphenyl-2,4-dithiobiuret complexes, iron(III), 39
*N,N*-Diphenyldithiocarbamate complexes, iron(I), 1065
1,2-Diphenylethene, 1189, 1205
Diphenylethyne, 1188
*N,N*-Diphenylmethamidine, 1193
Diphenyl(methyl)phosphine complexes
  osmium, 1204, 1214, 1216
  rhenium(III), 1059
2,5-Diphenyloxazole, 1042
Diphenylphosphinate complexes
  platinum(II), 231
Diphenylphosphinomethane complexes
  molybdenum(II), 347
1,4-Diphenylphthalazine, 1042
2,6-Diphenylpyridine, 1054
Diphenyl(pyridino)phosphine complexes, ruthenium(II), 325
2,3-Diphenylquinoxaline, 1042
Diphenyl(tetrachloro)cyclotriphosphazene, 867
*N,N'*-Diphenylthiourea complexes
  molybdenum(0), 235
Diphenyl(4-tolyl)phosphine complexes, rhenium(III), 1059
1,3-Diphenyltriazene complex
  zirconium(IV), 79
Diphenyl(vinyl)phosphine, 1219
Diphenyl(2-vinyl phenyl)phosphine, 1219
Diphosphenes, 390, 398, 408, 418, 432
Diphosphene complexes, 412
Diphosphene monosulphide, 410
Diphosphene monoxide, 409
Diphosphines, 390, 399
Diphosphooctadecamolybdate $(Mo_{18}P_2O_{62})^{6-}$, 381
Diphosphooctadecatungstate $(P_2W_{18}O_{62})^{6-}$, 381
Di-*i*-propylcarbodiimide, 1200
*N,N*-Di-*i*-propyldithiocarbamate complexes
  iron(I), 1065
  platinum(II), 231
Dipyridyl, *see* bipyridyl
Diselenocarbamate complexes
  copper(II), nickel(II), 433
Disilacycloalkenes, 392, 394
Disilanes, 390, 407
Disilenes, 390, 396, 406, 418, 420, 423, 429, 432
Distannenes, 398, 418
Distibene complexes, 417
Distribution coefficients, actinide diketonate phosphine oxide complexes, 1125
Disulphides, reactions with osmium carbonyl cluster compounds, 1220
Dithiocarbamate complexes
  chromium(III), 1241
  copper(II), 291, 297
  iron(I), 1065
  molybdenum(IV), 347
  molybdenum(V), 907
  palladium(II), 735, 1051
  platinum(II), 231, 735
  tungsten(V), 1021
Dithiolate complexes
  copper(II), 433
  iron(I), 1065
  nickel(II), 433
Dithiophosphate complexes
  iron(I), 1065
  tin(IV), 485
1,5-Di(2-tolyl)-2,4-dithiobiuret complexes, iron(III), 39
1,5-Di(4-tolyl)-2,4-dithiobiuret complexes, iron(III), 39
Dodecahydrododecaborate(2), 199
Dodecapolytungstate, 1071
Double bonding by main group elements, 389
Doyle and Wiedeman plots,
  lanthanum(III) sulphate complexes, 451
DTA studies
  copper(II) alkoxide oxime sulphate complexes, 641
  copper(II)aminopolyphosphonate complex, 527
  iron(II) aminocarboxylate dinitrogen complexes, 623
  iron(II) thiocyanate thiocyanogen complex, 997
  lanthanide ketone nitrate Schiff base complexes, 67
  lanthanum(III) sulphate complex, 451
  nickel(II) alkoxide oxime complexes, 641
  nickel(II) aminopolyphosphonate complex, 527
Dysprosium(III)
  electronic spectrum, solvent effects, oscillator strengths, Judd–Ofelt parameters, 161
  ketone nitrate Schiff base complexes, synthesis, electronic, IR spectra, DTA study, electric conductance, magnetic moments, 67

## E

EDTA, *see* ethylenediamine tetraacetate
EHMO calculations, copper(II) diselenocarbamate dithiolate complex, 433
Electric conductance
  alkali metal quinoline carboxylate complexes, 240
  cobalt(II) azole thiocyanate complexes, 251
  cobalt(II) carboxylate Schiff base complex, 575
  cobalt(III) pyrazole thiosemicarbazone complex, 1135
  cobalt(III) Schiff base thiolate complexes, 517
  copper(II) bromide diketone complex, 1233
  copper(II) carboxylate Schiff base complex, 575
  copper(II) pyrazole thiosemicarbazone complexes, 1135
  copper(II) Schiff base thiolate complexes, 517
  gold(I) azole rhodium(I), (III) complexes, 497
  iron(III) chloride thione complexes, 39
  iron(III) phosphetanate, 1155
  lanthanide ketone nitrate Schiff base complexes, 67
  magnesium chloride ether complex, 45
  manganese(II) phosphetanate, 115
  nickel(II) carboxylate phosphine complexes, 963
  nickel(II) imine pyridimidine complexes, 983
  nickel(II) oxime chlorosilane complexes, 603
  nickel(II) phosphetanate, 1155
  nickel(II) pyrazole thiosemicarbazone complexes, 1135
  nickel(II) Schiff base thiolate complexes, 517
  octylammonium salts, 313
  rhenium(V) oxo phosphine complexes, 1083
  rhenium(VII), tetraoxo salt, 1083

rhodium(I) aldehyde carbonyl phosphine complexes, 1151
rhodium(I) alkene arene gold(I) complexes, 497
rhodium(I) carbonyl chloride diimine complexes, 799
rhodium(III) arene gold(I) complexes, 497
rhodium(III) Schiff base thiolate complexes, 517
ruthenium(II) ammine thiocyanate complexes, 1
tin(II) amide sulphoxide complexes, 627
tin(IV) chloride complexes, 313
titanium(IV) cyclopentadienyl oxoquinolate complexes, 883
vanadium(IV) oxo carboxylate Schiff base complex, 575
zirconium(IV) cyclopentadienyl oxoquinolate complexes, 883
*see also* solid state electric conductance
Electron counting
boron cluster compounds, 1299
carbonyl cluster complexes, 1321
gold cluster compounds, 1289
iron triad cluster compounds, 1279
Electronegativity, density functional theory, relationship to chemical potential, 853
Electronic difference spectra
heteropolymolybdates, -tungstates, 1071
vanadium(IV) oxo apocytochrome-*c* phthalocyanine complex, 129
Electronic spectra
antipyrine Schiff base, 67
bismuth(III) alcohol mercaptide complexes, 71
chromium(I) cyanide nitrosyl complex, 247
chromium(III) dicarboxylate diimine complexes, 1141
chromium(III) diketonate complex formation, 781
chromium(III) dithiocarbamate iodine complexes, 1241
chromium(III) heteropolytungstate, 1161
cobalt(II) amide halide complexes, 99
cobalt(II) aminopolyphosphonate complexes, 527
cobalt(II) aminoquinoline complexes, 357
cobalt(II) azole thiocyanate complexes, 251
cobalt(II) carboxylate Schiff base complex, 575
cobalt(II) chloride complexes, 363
cobalt(II) diimine complex, 701
cobalt(II) heteropolytungstate, 1071
cobalt(II) phosphetanate complexes, 325
cobalt(II) pyridine Schiff base thione complex, 1271
cobalt(III) aminoacid diimine complexes, 49
cobalt(III) pyrazole thiosemicarbazone complex, 1135
cobalt(III) Schiff base thiolate complexes, 517
cobalt(III) Schiff base thione complex, 1271
copper(II) alkoxide oxime sulphate complexes, 641
copper(II) amide amine complexes, 559
copper(II) amine diketonate complexes, 137
copper(II) aminopolyphosphonate complexes, 527
copper(II) aminoquinoline complexes, 357
copper(II) azole complexes, 261
copper(II) azole cyanate complexes, 1147
copper(II) azole peptide complexes, 463
copper(II) bromide diketonate complex, 1233
copper(II) carboxylate Schiff base complex, 575
copper(II) diimine complex, 701
copper(II) insulin complexes, 833
copper(II) macrocyclic Schiff base complexes, 1357
copper(II) planar complexes, 157
copper(II) pyrazole thiosemicarbazone complexes, 1135
copper(II) pyridine Schiff base thione complex, 1271
copper(II) pyridyl thiosemicarbazone complexes, 921
copper(II) quinone complexes, 729
copper(II) Schiff base complexes, 595, 713
copper(II) Schiff base thiolate complexes, 517
copper(II) semicarbazone thiosemicarbazone complexes, 991
diarsenes, diphosphenes, disilenes, 420
dysprosium(III), solvent effects, 161
gadolinium(III) acetate complexes, 31
gold cluster compounds, 1289
gold(III) chloride complex, 805
gold(III) chloride thiolate, 1365
heteropolyanions, 381, 1071
holmium(III) acetate complexes, 31
holmium(III) antipyrine Schiff base complex, 67
hot ions, 1131
iron(II) aminocarboxylate dinitrogen complexes, 623
iron(II) arsine oxide complexes, 911
iron(II) pyridine Schiff base thione complex, 1271
iron(II) quinone complexes, 729
iron(II) thiocyanate thiocyanogen complex, 997
iron(III) arsine oxide complexes, 911
iron(III) carboxylate porphyrin complexes, 651
iron(III) chlorine thione complexes, 39
lanthanum(III) acetate complexes, 31
manganese(II) quinone complexes, 729
manganese(II) semicarbazone thiosemicarbazone complexes, 911
manganese(III) fluoride sulphate complexes, 599
manganese(IV) heteropolytungstate, 1161
molybdenum(−I) carbonyl complex, hot ion, 1131
molybdenum(0) carbonyl thione complexes, 235
molybdenum(III) chloride oxo phosphine complex, hot ion, 1131
molybdenum(V) oxo dithiocarbamate thiocyanate complex, 907
molybdenum(VI) dioxo mercaptide phenolate Schiff base complexes, 55
multiple bonds, 420
neodymium(III) acetate complexes, 31
neodymium(III) antipyrine Schiff base complex, 67
nickel(II) alkoxide oxime complexes, 641
nickel(II) amide amine complexes, 551
nickel(II) amide halide complexes, 99
nickel(II) amine thiolate complexes, 839, 1227
nickel(II) aminopolyphosphonate complexes, 527
nickel(II) carboxylate phosphine complexes, 963
nickel(II) chloride salicylhydrazone complexes, 21
nickel(II) diimine complex, 701
nickel(II) imine pyrimidine complexes, 983
nickel(II) ketoimine complexes, 239
nickel(II) macrocyclic Schiff base complex, 1357
nickel(II) oxime chlorosilane complexes, 603
nickel(II) pyrazole thiosemicarbazone complex, 1135
nickel(II) pyridine Schiff base thione complex, 1271

nickel(II) quinone complexes, 729
nickel(II) Schiff base thiolate complexes, 517
nickel(II) thiol thiolate complexes, 969
nickel(II) water complex, 963
palladium(II) diimine complexes, 701
palladium(II) dithiocarbamate phosphine complexes, 735
palladium(II) quinone complexes, 729
phospha-arsenes, 421
phosphopolymolybdates, 1071
platinum(II) diimine complexes, 87, 701
platinum(II) quinone complexes, 729
platinum(IV) azole halide complexes, 121
polybenzyl, 381
porphyrin complexes, 107, 889
rhodium(I) aldehyde carbonyl phosphine complexes, 1151
rhodium(I) carbonyl chloride diimine complexes, 799
rhodium(III) Schiff base thiolate complexes, 517
ruthenium(II) ammine thiocyanate complexes, 1
silicopolymolybdates, 1071
silver(I) porphyrin complexes, 1065
tungsten(IV) cyanide complex, 743
tungsten(V) carbamate oxo thio binuclear complexes, 25
tungsten(V) dithiocarbamate thio binuclear complexes, 1021
vanadium(IV) oxo carboxylate Schiff base complex, 575
vanadium(IV) oxo apocytochrome-*c* phthalocyanine complex, 129
zinc(II) quinone complexes, 729
zirconium(IV) phenolate complexes, 611
Electrophiles, reaction with dithiocarbamate complexes, 297
Endocyclic alkenes, reactions with osmium caronyl cluster compounds, 1185
Enthalpy of activation
anolines–coordinated nitrile reaction, 117
arsenic(III)–gold(III) reaction, 805
conformational isomerism, 331
iron(III) solvent extraction, 615
tungstocobaltate(III) oxidations, 191
Enthalpy of formation
alkali metal fluoride complexes, 845
calcium dicarboxylate complexes, 545
chromium(III) dithiocarbamate iodine complexes, 1241
iodine thiuram disulphide complexes, 1241
neptunium(V) dioxo carboxylate phosphate complexes, 667
Entropy of activation
amides–manganese(III) reaction, 977
anilines–coordinated nitrile reaction, 117
arsenic(III)–gold(III) reaction, 805
conformational isomerism, 331
tungstocobaltate(III) oxidations, 191
Entropy of formation
alkali metal fluoride complexes, 845
calcium dicarboxylate complexes, 545
chromium(III) dithiocarbamate iodine complexes, 1241
iodine thiuram disulphide complexes, 1241
neptunium(V) dioxo carboxylate phosphate complexes, 667
Ephedrine complexes, boron, 589
Equilibrium constants
cobalt(II) azole thiocyanate complexes, 251
*see also* formation constants
ESR spectra
arseno, arsenoaminoxyl radicals, 631
chromium(III) aminoacid complexes, 17
copper(II) amine diketonate complexes, 137
copper(II) azole complexes, 261
copper(II) azole peptide complexes, 463
copper(II) bromide diketonate complexes, 1233
copper(II) dioxime complex, 821
copper(II) diselenocarbamate dithiolate complex, 433
copper(II) dithiocarbamate chloride diketonate complexes, 291
copper(II) dithiocarbamate electrophile complexes, 297
copper(II) insulin complexes, 833
copper(II) pyridyl thiosemicarbazone complexes, 921
copper(II) semicarbazone thiosemicarbazone complexes, 991
hot ion, 1131
iron(−II) nitrosyl azole complexes, 1065
iron(0) nitrosyl thiolate complexes, 1065
iron(I) nitrosyl dithiolate complexes, 1065
iron(III) arsine oxide complexes, 911
iron(III) carboxylate porphyrin complexes, 651
manganese(II) semicarbazone thio semicarbazone complexes, 911
molybdenum(III) chloride oxo phosphine complex, hot ion, 1131
molybdenum(V) oxo dithiocarbamate thiocyanate complex, 907
nickel(I) ketoimine complexes, 585
nickel(II) ketoimine radical anion complexes, 585
Esters, unsaturated, reactions with osmium carbonyl cluster compounds, 1187
Ethanethiolate complexes cluster, 1307
Ethanol complexes
aluminium(III), 265
cobalt(III), 1017
gallium(III), 265
zinc(II), 1017
Ethanol, solvent for electronic spectra, 161
Ethene complexes
osmium, 1178, 1183
platinum(II), 513
ruthenium(0), 1255
Ether complexes
magnesium, 45
uranium(III), (IV), 457
Ethionine complexes
nickel(II), 523, 1329
Ethoxide compounds, 1179
4-Ethoxyaniline complexes, copper(II), 291

Ethyl compounds
gallium(III), indium(III), 581
lead(IV), 297
ruthenium(II), 1255
tin(IV), 297, 485
Ethylamine, formation in amide oxidation by manganese(III), 977
*N*-Ethylanilinedithiocarbamate complexes, tungsten(V), 1021
Ethylation, carbaborane amine complex, 1351
Ethyl bromide, *see* bromoethane
Ethyldiazoacetate, 1203
Ethyl(diphenyl)phosphine, 61
Ethyl(diphenyl)phosphine oxide complexes
molybdenum(IV), 61
Ethylene, *see* ethene
*N,N'*-Ethylene(acetylacetoneiminate)salicylideneiminate complex, nickel(II), 585
*N,N'*-Ethylenebis(acetylacetoneiminate) complex
nickel(II), 585
*N,N'*-Ethylenebis(salicylideneiminate) complex
nickel(II), 585
Ethylenediamine, 363
reaction with cyclometallated complex, 1046
Ethylenediamine complex
zinc(II), 1333
Ethylenediaminetetraacetate complexes, aluminium(III), cobalt(II), 917
iron(II), 623
Ethylenediamine-*N,N,N',N'*-tetramethylenephosphonate complexes, cadmium(II), cobalt(II), copper(II), lead(II), manganese(II), nickel(II), zinc(II), 527
Ethylenediphosphinetetraacetate acid complexes
nickel(II), 963
Ethylene glycol, reactions with boron compounds, 929
Ethylidyne complexes
osmium(I), 1184
2-Ethylimidazole complexes
platinum(IV), 121
Ethylmethylamine complex
carbaborane, 1351
*N*-Ethyl-*N*-phenyl dithiocarbamate complex, iron(I), 1065
Ethyl(tetramethyl)cyclopentadienyl complexes
titanium(IV), 897
Ethylxanthate complexes
arsenic(III), 721
titanium(IV), 695
Ethyne, 1190

## F

Ferromagnetism
chromium(III) aminoacid complexes, 17
chromium(III) thio complexes, 775
Five coordination, detection in copper(II) complexes, 137
Flexibility, polysiloxanes, 1109
Fluorene complex, rhodium(I), 497
Fluorides and fluoro complexes
alkali metals, 845
aluminium(III), gallium(III), 265
manganese(III), 599
vanadium(V), 287
Fluoroalkynes, reactions with osmium carbonyl cluster compounds, 1191
4-Fluorobenzisothiocyanate, 1214
Fluoronium ion ($H_2F^+$), non-formation in aqueous solution, ion-selective electrode potentiometry, 75
Fluxional processes
gold cluster compounds, 1289
thioether complexes, 331
Force constants, carbonyl complexes, 1333
Formaldehyde, 939, 1202, 1351
Formamide, oxidation by manganese(III), 977
Formate complex, osmium, 1202
Formation constants
actinide diketonate phosphine oxide complexes, 1125
alkali metal fluoride complexes, 845
aluminium(III) carboxylate thiolate complexes, 871
bismuth(III) alcohol mercaptide complexes, 71
cadmium(II) nucleotide phosphate complexes, 1105
calcium dicarboxylate complexes, 545
chromium(III) dithiocarbamate iodine complexes, 1241
copper(II) amide amine complexes, 559
copper(II) azole peptide pyridine complexes, 787
gallium(III), indium(III) carboxylate thiolate complexes, 871
iodine thiuram disulphide complexes, 1241
lanthanide acetate complexes, 31
neptunium(V) dioxo carboxylate phosphate complexes, 667
nickel(II) amide amine complexes, 551
nickel(II) aminoacid aminosulphonate thioether complexes, 1329
nickel(II) aminoacid thioether complexes, 523
silver(I) porphyrin complexes, 1077
terbium(III) carboxylate pyridine complex Pfeiffer effect, 1087
uranium(VI) dioxo aminopolycarboxylate complexes, 469
Formylation, carbaborane amine complex, 1351
Free energy of activation
amides–manganese(III) reaction, 977
aminopolycarboxylate complex substitutions, 917
B—N bond breaking, 589
chemisorption on iron(III) hydroxide oxide, 223
conformational isomerism, 331
Free energy of complexation
neptunium(V) dioxo carboxylate phosphate complexes, 667
Free energy of formation
calcium dicarboxylate complexes, 545
Fumarate complexes, calcium, 545
2-Furaldehyde-*S*-benzyldithiocarbazate Schiff base complexes, cobalt(II), copper(II), nickel(II), rhodium(III), 517
Furazan, nopinoquinone dioxime, 821

## G


Gadolinium(III)
  acetate complexes, electronic spectra, formation constants, 31
  ketone nitrate Schiff base complexes, synthesis, electronic, IR spectra, DTA study, electric conductance, magnetic moments, 67
Gallium(III)
  alcohol water complexes, halide salts, NMR ($^{19}F$) spectra, outer coordination sphere, 265
  alkyl chloride phosphide polynuclear compounds, synthesis, IR, mass, NMR ($^{1}H$, $^{31}P$) spectra, 581
  carboxylate thiolate complexes, potentiometric titrations, formation constants, 871
  chlorodimethyl-, 581
  triethyl-, 581
Gel permeation, chromatography, silicate trimethylsilylation, 503
Germanium
  double bonds, 395, 397, 418
  metal cluster compounds, 1307
Germanium(II), porphyrin iron(0) complexes, synthesis, electronic, IR, NMR ($^{1}H$) spectra, X-ray crystal structure, 889
Germanium(IV)
  alkyl stibine complexes, synthesis, IR, NMR ($^{1}H$) spectra, 757
  dichloro(octaethylporphyrin)-, 889
  dichloro(tetra-4-tolylporphyrin)-, 889
    tetrachloro-, 297
Glycinate complexes
  cobalt(II), 49
Glycine–acetophenone Schiff base complexes, cobalt(II), copper(II), vanadium(IV), 575
Glycollate complexes
  niobium(V), 1029
Glycols, reactions with boron compounds, 929
Glycylglycine complexes
  copper(I), 861
  copper(II), 463, 787, 861
Glycyl-*i*-leucine complexes
  copper(I), (II), 861
Glycylphenylalanine complexes
  copper(I), 861
  copper(II), 463, 861
Glycylserine complexes
  copper(I), (II), 861
Glycylthreonine complexes
  copper(I), (II), 861
Glycyltryptophan complexes
  copper(I), 861
  copper(II), 463, 861
Glycyltyrosine complexes
  copper(I), 861
  copper(II), 463, 861
Glyoxalbis(anisylimine) complexes, rhodium(I), 799
Glyoxalbis(cyclohexyldiimine) complexes, rhodium(I), 799
Glyoxalbis(4-hydroxyphenylimine) complexes
  rhodium(I), 799
Glyoxalbis(phenylimine) complexes, rhodium(I), 799
Glyoxalbis(4-tolylimine) complexes, rhodium(I), 799
Gold, cluster complexes, 567, 1289, 1307
Gold(0, I) hydride phosphine ruthenium(0) polynuclear complexes, synthesis, IR, NMR ($^{1}H$, $^{13}C$, $^{31}P$) spectra, X-ray crystal structure, configurational isomerism, 567
Gold(I)
  azole phosphine complexes, synthesis, IR spectra, 213
  carbazole(triphenylphosphine)-, 497
  cyclometallated complexes, 1040, 1055
  2-pyridyl compound, 1040
Gold(III)
  chloride complex, oxidation of arsenic(III), electronic spectra, kinetic study, enthalpy, entropy of reaction, 805
  chloride thiolate compound, synthesis, electronic, IR, Raman spectra, 1365
Graphite, potassium ($C_8K$), 271
Guanidinopyrimidines, synthesis, mass, NMR ($^{1}H$) spectra, 983
Guanosine complexes
  palladium(II), 9


## H


Hemimorphite, 151
Heptahydroheptaborate(2), 199
Heptasulphurmonoimide, 1365
Heteroatoms, in metal cluster compounds, 1307
Heterocyclic compounds, reactions with osmium carbonyl cluster compounds, 1206
Heterocyclic ligands, cyclometallation, 1037
Heteropolyanions
  chromium(III), 1161
  cyclohexanol oxidation catalysis, 607
  manganese(IV), 1161
  Pfeiffer effect, 381, 1071
  polymerisation catalysis, 381
  structure and stability, 341, 1171
Hexadecaphenyloctasiloxide complex, titanium(IV), 95
Hexa-2,4-diene, 1186
Hexafluorobut-2-yne, 1191
Hexafluorophosphate complex, sodium, 675
Hexahydrohexaborate(2), 199
Hexamethyldisiloxane, 503
Hexaphenylbenzene, 1188
*O*-Hexyldithiophosphate complexes
  platinum(II), 231
Histamine complexes
  iron(−II), 1065
Histidine, induction of Pfeiffer effect, 1087
Histidine complexes
  chromium(III), 17
Histidine methyl ester, induction of Pfeiffer effect, 1087
Histidinol, induction of Pfeiffer effect, 1087
Holmium(III)
  acetate complexes, electronic spectra, oscillator strengths, formation constants, 31
  ketone nitrate Schiff base complexes, synthesis, electronic, IR spectra, DTA study, electric conductance, magnetic moments, 67

Hot ions, molydenum(−I), (III), electronic ESR spectra, 1131
Hydrazine, 907
Hydrazone complexes
  cadmium(II), mercury(II), 281
  osmium, 1202
  zinc(II), 281
Hydride complexes
  cluster, 567, 1177, 1279, 1307, 1321
  gold(0, I), 567
  molybdenum(IV), 765
  osmium, 1039, 1044, 1177
  rhenium(I), 1043
  rhenium(III), 749
  ruthenium(0), 567
  ruthenium(II), 1255
Hydrofluoric acid, 75
Hydrogen chloride, 1201
Hydrogen peroxide
  cyclohexanol oxidation, 607
  decomposition, catalysis by copper(II) planar complexes, 157
Hydrogen sulphide, reaction with cluster compounds, 1307
Hydrogenation, alkyne complex, 175
Hydroxide, reactions with osmium carbonyl cluster compounds, 1177
Hydroxides and hydroxo complexes
  chromium(III), 17
  iron(III), 223
  niobium(V), 1029
  titanium(III), 639
  tungsten(IV), 743
  uranium(VI), 143
  vanadium(V), 287
Hydroxyalkynes, reactions with osmium carbonyl cluster compounds, 1179
Hydroxyallyl complexes
  osmium, 1190
4-*N*-(2′-Hydroxybenzylidene)aminoantipyrine complexes, lanthanides, 67
Hydroxybenzylidenemethylamine carbaborane complex, 1351
Hydroxycarboxylate complexes
  niobium(V), 1029
Hydroxymethylenemethylamine carbaborane complex, 1351
6-Hydroxymethylpyridine-2-carboxylic acid complexes
  manganese(II), 491
5-Hydroxy-1,4-naphthalenedione complexes, iron(II), nickel(II), palladium(II), platinum(II), 729
2-Hydroxypyridine, 1209
8-Hydroxyquinoline, 883
8-Hydroxyquinoline-2-carboxylic acid complexes
  manganese(II), 491

## I

Imidazole, 1206
Imidazole complexes
  copper(II), 463, 787
  iron(−II), 1065
  manganese(0), (II), 707
Imide complex, osmium, 1196
Imines, reactions with osmium carbonyl cluster compounds, 1210
Imine complexes
  nickel(II), 983
  osmium, 1216
Iminoacyl complex
  rhodium(III), 1047
Indene, 1185
Indenyl complexes
  rhodium(I), 497
  titanium(IV), 883
  zirconium(IV), 611, 883
Indium(III)
  alkyl phosphide polynuclear compounds, synthesis, IR, mass, NMR ($^{1}H$, $^{31}P$) spectra, 581
  carboxylate thiolate complexes, potentiometric titrations, formation constants, 871
  triethyl-, 581
Induced Cotton effect, *see* Pfeiffer effect
Inosine complexes, palladium(III), 9
Insulin complexes, copper(II), 833
Inverse solubilities
  phosphetanates, 1155
Iodides and iodide complexes
  boron, 369
  cadmium(II), 619
  cluster, 1307, 1321
  cobalt(II) 99
  copper(I), 749
  gold(0, I), 1289
  iron(II), (III), 911
  mercury(II), 297, 619
  nickel(II), 99, 983
  oxidation by cobalt(III), 191
  palladium(II), platinum(II), 735
  rhenium(I), 331
  titanium(IV), 897
  zinc(II), 619
Iodine, reaction with
  caraborane amine complex, 1351
  cyclometallated compounds, 1041
Iodine complexes, chromium(III), thiuram disulphides, 1241
Ion exchange behaviour
  neptunium(V) complexes, 667
Ionic strength, effect on copper(II) solvent extraction, 1357
Ion-selective electrode, fluoride, 845
Ion-selective electrode potentiometry, hydrofluoric acid, 75
IR spectra
  acetyl complexes, 1042, 1043, 1048
  acyl compounds, 317
  alcohol complexes, 71
  aldehyde complexes, 1151
  alkoxide complexes, 21, 641, 661
  alkyl compounds, 581, 681
  alkylammonium salt, 535

alkylenedithiophosphate complexes, 1337
amide complexes, 99, 627
amine complexes, 125, 353, 1227, 1351
aminoacid complexes, 9
aminopolycarboxylate complexes, 623
aminopolyphosphonate complexes, 527
aminoquinoline complexes, 357
ammine complexes, 353
ammonium salts, 313, 599
arsine oxide complexes, 911
azide complexes, 79, 921
azole complexes, 121, 213, 261, 619, 707, 1147
bromide complexes, 9, 121, 261, 357, 619, 911, 921, 963, 983, 1347
carbaborane amine complexes, 1351
carbonyl complexes, 79, 213, 235, 331, 347, 353, 567, 707, 757, 799, 889, 911, 1043, 1044, 1059, 1093, 1151, 1333
carboxylate complexes, 240, 575, 651, 929, 963, 1025, 1029, 1099
carboxylate on polystyrene, 939
carboxylic acid, 1099
chloride complexes, 9, 21, 107, 121, 125, 213, 261, 347, 357, 363, 619, 799, 883, 911, 921, 983, 1337, 1347, 1365
citrate complexes, 169
cyanate complexes, 347, 1147
cyclopentadienyl complexes, 695, 1347
diamine salts, 363
diimine complexes, 87, 125, 799
diketonate complexes, 347, 929, 1017
dinitrogen complexes, 623
dioxime complexes, 821
diphosphenes, disilenes, 429
dithiocarbamate complexes, 25, 749, 907, 1021, 1241
dithiophosphate complexes, 485
fluoride complexes, 287, 599
guanadinyl complexes, 983
heteropolyanions, 1071
hydrazone complexes, 21, 281
hydroxide complexes, 287
imine complexes, 983
iminoacyl complex, 1047
indenyl complexes, 611
iodide complexes, 619
isocyanide complex, 385
ketoimine complexes, 239
ketone complexes, 67, 281, 517
ketophenol complexes, 1017
macrocyclic complexes, 1357
metallacarborane, 307
nitrate complexes, 67, 357, 921, 983, 1135
nitrile complexes, 353
oxime complexes, 641
oxocomplexes, 25, 55, 287, 347, 575, 907, 1083
peptide complexes, 463, 883
perchlorate complexes, 911, 1135
perchlorate salts, 353, 627, 921, 1151
peroxide complexes, 287, 513
phenol complexes, 463
phenolate complexes, 125, 595, 611, 661
phenyl compounds, 721
phosphetanate complexes and salts, 325, 1155
phosphide complexes, 581
phosphine complexes, 347, 963
pyrazole complexes, 1135
pyridine complexes, 281
pyrimidine complexes, 983
quinoline complexes, 240
quinone complexes, 729
Schiff base complexes, 67, 257, 517, 575, 595, 713, 1357
semicarbazone complexes, 661, 681, 991
stibine complexes, 757
sulphate complexes, 451, 599, 641, 1135
sulphoxide complexes, 627
sulphur–nitrogen ligand complex, 1365
tetrafluoroborate complexes, 1135
thio complexes, 25, 1021
thiocarbonyl complexes, 21
thiocyanate complexes, 1, 347, 357, 911, 921, 983, 997
thiocyanogen complex, 997
thiol complexes, 969
thiolate complexes, 71, 517, 595, 969, 1227
thione complexes, 235
thiosemicarbazone complexes, 661, 681, 921, 991, 1135, 1237
water complexes, 911
xanthate compounds, 695, 721
Iridium, recovery from iridium(IV) by zinc reduction, 1013
Iridium(I)
alkene azole carbonyl chloride phosphine complexes, synthesis, IR spectra, 213
carbonyl cyclopentadienyl platinum(0) cluster complex, synthesis, IR, NMR ($^{1}H$, $^{13}C$, $^{195}Pt$) spectra, X-ray crystal structure, 1093
cyclopentadienyl(dicarbonyl)-, 1093
Iridium(II)
alkyl azide phosphine complex, synthesis, IR, NMR ($^{1}H$, $^{31}P$) spectra, 79
chloride water complexes, polarography, 1013
cyclometallated complexes, 104
trimethyltris[dimethyl(phenyl)phosphine]-, 79
Iridium(IV)
chloride water complexes, reduction by zinc, polarography, 1013
Iron
cluster compounds, 1307, 1321
nitrosyl selenide sulphide cluster complexes, NMR ($^{15}N$) spectra, 1165
Iron(−II)
carbonyl tin(IV) complex, synthesis, IR, mass, NMR ($^{1}H$) spectra, 757
nitrosyl azole complexes, ESR spectra, 1065
tetracarbonyl-, sodium, 889
Iron(−I), nitrosyl(tricarbonyl)-, potassium, 1043
Iron(0)
alkyne carbonyl cobalt(0) complex, hydrogenation, kinetic study, 175
carbonyl cyclopentadienyl mercury(II) complexes, Mössbauer spectra, 365

carbonyl germanium(II), tin(II) complexes, synthesis, electronic, IR, Mössbauer, NMR ($^1$H) spectra, X-ray crystal structure, 889
carbonyl stibine complexes, synthesis, IR, NMR ($^1$H) spectra, 757
carbonyl zinc complexes, synthesis, IR, Raman spectra, force constants, 1333
diphosphene complexes, 414, 428
hydrido(tetracarbonyl)-, 1333
nitrosyl thiolate complexes, ESR spectra, 1065
nonacarbonyldi-, 757
pentacarbonyl-, 175
Iron(I), nitrosyl dithiolate complexes, ESR spectra, 1065
Iron(II)
aminopolycarboxylate dinitrogen complexes, synthesis, electronic, IR spectra, DTA, TGA study, 623
aquo(cyclohexanediaminetetraacetato)-, 623
aquo(ethylenediaminetetraacetato)-, 623
arsine oxide carbonyl iodide complexes, synthesis, electronic, IR spectra, electric conductance, magnetic moments, X-ray diffraction, 911
cyanide water complexes, Mössbauer spectra, magnetic properties, 183
diphosphene complexes, 413, 417, 428
formation in iron(III) citrate complex photolysis, $\gamma$-radiolysis, 169
pyridine Schiff base thione complex, synthesis, electronic, IR, Mössbauer spectra, 1271
quinone complex, synthesis, electronic IR spectrum, magnetic moment, 729
thiocyanate thiocyanogen complex, synthesis, electronic, IR spectra, DTA, X-ray diffraction, 997
triiodo-, iron(II) arsine oxide complex salt, 911
Iron(III)
amide chloride diimine complex, magnetic moments, Mössbauer spectra, 443
arsine oxide halide perchlorate thiocyanate water complexes, synthesis, electronic, ESR, IR spectra, electric conductance, magnetic moments, TGA, X-ray diffraction, 911
carboxylate porphyrin complexes, syntheis, electronic, ESR, IR, mass, NMR ($^1$H) spectra, magnetic moments, X-ray crystal structure, 651
chloride magnesium complexes, synthesis, electric conductance, X-ray crystal structure, 45
chloride oxo binuclear complexes, formation, magnetic moments, 443
chloride thione binuclear complexes, synthesis, electronic, IR spectra, dielectric constant, magnetic moment, pyroelectricity, solid state electric conductance, 39
citrate complexes, photolysis, $\gamma$-radiolysis, IR, Mössbauer spectra, 169
cyanide water complexes, Mössbauer spectra, magnetic properties, 1983
heteropolymolybdates, heteropolytungstates, 1071
hydroxide oxide, chemisorption of NO, $SO_2$, solid state electric conductance, kinetic study, energy of activation, pressure effects, 223
phosphetanate, synthesis, IR spectrum, electric conductance, magnetic moment, 1155
solvent extraction, enthalpy, 615
tetrabromo-, tetrachloro-, iron(III) arsine oxide complex salt, 911
Irradiation, molybdenum(0) (IV) complexes, 1131
Isocyanides, reactions with cyclometallated compounds, 1048
osmium carbonyl cluster compounds, 1177, 1212
Isocyanide complexes
osmium(II), 385
Isonicotinate-*N*-oxide complex
cadmium(II), 303
Isonicotinate-*N*-oxide salt
zinc(II), 303
Isonicotinic acid hydrazide complexes, copper(II), 137
Isopolyanions
light, X-ray scattering, Raman spectra, 1001
structure and stability, 341
Isothiocyanates, reactions with osmium carbonyl cluster compounds, 1212
Itaconate complexes, calcium, 545

## J

Judd–Ofelt parameters, dysprosium(III), 161
Juglone, *see* 5-hydroxy-1,4-naphthalenedione

## K

Ketenes, reactions with osmium carbonyl cluster compounds, 1215
Ketene complex, osmium, 1204
Ketoimine complexes
nickel(II), 239, 585
Ketones, reactions with osmium carbonyl cluster compounds, 1181
Ketone complexes
cadmium(II), 281
cobalt(II), copper(II), 517
lanthanides, 67
mercury(II), 281
nickel(II), rhodium(III), 517
zinc(II), 281
Kinetic studies
chemisorption on iron(III) hydroxide oxide, 223
complex formation, chromium(III) diketonate, 781
complex formation, silver(I) porphyrins, 1077
conformational isomerism, thioether complexes, 331
coordinated nitrile, addition, 117
ligand substitution, diimine complexes, 701
ligand substitution, nickel(II) ketoimine complex, 239
redox reaction, gold(III) + arsenic(III), 805
redox reaction, manganese(III) + amides, 977
redox reaction, molybdenum(VI) complex + phosphine, 61
redox reaction, ruthenium(III) + titanium(III), 639
redox reaction, tungstocobaltate(III) + iodide thiocyanate, 191
substitution, aminopolycarboxylate complexes, 917
substitution, cobalt(III) complex, 895
substitution, rhodium(III) complexes, 811

## L


Lactate complexes
  niobium(V), 1029
Ladder polymers, siloxanes, 1109
Lanthanides, book review, 1169
Lanthanides(−I), improbability of existence in liquid ammonia, 133
Lanthanides(II)
  acetate complexes, electronic spectra, oscillator strength, formation constants, 31
  ketone nitrate Schiff base complexes, synthesis, electronic, IR spectra, DTA study, electric conductance, magnetic moments, 67
Lanthanum(III)
  acetate complexes, electronic spectra, oscillator strength, formation constants, 31
  ketone nitrate Schiff base complexes, synthesis, electronic, IR spectra, DTA study, electric conductance, 67
  sulphate complex, cobalt(III) ammine hydrated salts, synthesis, IR spectra, TGA, DTA, 451
Lead(II)
  aminopolyphosphonate complex, synthesis, 527
  thiolate complexes, synthesis, X-ray crystal structure, 1247
Lead(IV)
  tetraethyl-, 297
Leucinate complexes, cobalt(III), 49
Lewis acid, *see* electrophile
Librational frequencies, phosphazenes, 867
Ligand reaction
  ketoimine substitution, 239
  nitrile addition, 117
Ligand synthesis
  benzil-*S*-benzyldithiocarbazate Schiff base, 517
  diaminodiamides, 559
  fluorophenyldiamine, 753
  2-furaldehyde-*S*-benzyldithiocarbazate Schiff base, 517
  furazan oximes, 479
  macrocyclic Schiff base, 1357
  mercaptosalicylaldimines, 55
  pyrazole thiosemicarbazone, 1135
  quinaldic acid, 491
  tetrapyridylpyrazine, 635
  trioximes, 479
Light scattering
  isopolyanions, 1001
Linkage isomerism, thiocyanate complexes, 1
Lithium
  aluminium hydride, reaction with cyclometallated complexes, 1049, 1051
  *n*-butyl-, 307
  carborane amine complex, synthesis, IR, mass spectra, X-ray crystal structure, 307
  diketonate complexes, synthesis, IR spectra, 1017
  ethoxide, 1017
  fluoride complex, potentiometric titration, formation constant, enthalpy, entropy of formation, 845
  methyl-, 1199
  phosphetanate, 325
  2(2′-pyridyl), 1039
  2(2′-pyridyl)phenyl, 1041
Luminescence spectra
  terbium(III) carboxylate pyridine complex, 1087


## M


Macrocyclic complex
  copper(II), 1357
  molybdenum(IV), 257
  nickel(II), 1357
Magnesium
  chloride ether iron(III) complexes, synthesis, electric conductance, X-ray crystal structure, 45
  chloro(*neo*-pentyl)-, 317
Magnetic moments
  chromium(III) aminoacid complexes, 17
  chromium(III) chloride cyclopentadienyl thio thiolate palladium(II) complexes, 775
  chromium(III) phosphetanate, 1155
  cobalt(II) amide halide complexes, 99
  cobalt(II) aminopolyphosphonate complexes, 357
  cobalt(II) aminoquinoline complexes, 357
  cobalt(II) carboxylate Schiff base complex, 575
  cobalt(II) chloride complexes, 363
  cobalt(II) phosphetanate, 325
  cobalt(II) pyridine Schiff base thione complex, 1271
  copper(I) chloride complex, 771
  copper(II) alkoxide oxime sulphate complexes, 641
  copper(II) amide halide complexes, 99
  copper(II) aminopolyphosphonate complexes, 357
  copper(II) aminoquinoline complexes, 357
  copper(II) carboxylate Schiff base complex, 575
  copper(II) phosphetanate, 1155
  copper(II) pyrazole thiosemicarbazone complexes, 1135
  copper(II) pyridine Schiff base thione complex, 1271
  copper(II) quinone complexes, 729
  copper(II) Schiff base complexes, 595, 713
  copper(II) Schiff base thiolate complexes, 517
  copper(II) semicarbazone thiosemicarbazone complexes, 991
  copper(II) sulphate thiosemicarbazone complexes, 1237
  dysprosium(III) antipyrine Schiff base complex, 67
  gadolinium(III) antipyrine Schiff base complex, 67
  holmium(III) antipyrine Schiff base complexes, 67
  iron(II) arsine oxide complexes, 911
  iron(II) quinone complexes, 729
  iron(III) arsine oxide complexes, 911
  iron(III) carboxylate porphyrin complexes, 651
  iron(III) chloride thione complexes, 39
  iron(III) phosphetanate, 1155
  manganese(II) amide halide complexes, 99
  manganese(II) aminopolyphosphonate complexes, 527
  manganese(II) phosphetanate, 1155
  manganese(II) pyridine Schiff base thione complex, 1271

manganese(II) quinone complexes, 729
manganese(II) semicarbazone thiosemicarbazone complexes, 991
manganese(III) fluoride sulphate complexes, 599
molybdenum(III) chloride phosphine complex, 347
molybdenum(V) oxo dithiocarbamate thiocyanate complex, 907
neodymium(III) antipyrine Schiff base complex, 67
nickel(II) alkoxide oxime sulphate complexes, 641
nickel(II) amide halide complexes, 99
nickel(II) aminopolyphosphonate complexes, 357
nickel(II) carboxylate phosphine complexes, 963
nickel(II) chloride salicylidenehydrazone complexes, 21
nickel(II) imine pyrimidine complexes, 983
nickel(II) oxime complexes, 603
nickel(II) phosphetanate, 1155
nickel(II) pyrazole thiosemicarbazone complexes, 1135
nickel(II) pyridine Schiff base thione complex, 1271
nickel(II) quinone complexes, 729
nickel(II) Schiff base thiolate complexes, 517
praseodymium(III) antipyrine Schiff base complex, 67
Prussian blue analogues, 183
rhenium(III) cyclopentadienyl complex, 771
ruthenium(II) amine thiocyanate complexes, 1
samarium(III), terbium(III) antipyrine Schiff base complexes, 67
tungsten(V) binuclear dithiocarbamate complexes, 25
vanadium(III) phosphetanate, 1155
vanadium(IV) carboxylate oxo Schiff base complex, 575

Malate complexes
chromium(III), 1141
niobium(V), 1029

Maleate complexes, calcium, 545

Maleonitriledithiolate complexes, copper(II), nickel(II), 433

Manganese
cluster compounds, 1307

Manganese(−I)
azole carbonyl complexes, synthesis, IR, mass, NMR ($^1$H) spectra, 707

Manganese(0)
azole carbonyl binuclear complexes, synthesis, IR, mass, NMR ($^1$H) spectra, 707
decacarbonyldi-, 707

Manganese(I)
amine ammine carbonyl nitrile complexes, synthesis, IR, NMR ($^1$H) spectra, 347
azole carbonyl binuclear complexes, synthesis, IR, mass, NMR ($^1$H) spectra, 707
cyclometallated complexes, 1042

Manganese(II)
amide halide complexes, synthesis, IR spectra, magnetic moments, X-ray diffraction, 99
aminopolyphosphonate complexes, synthesis, magnetic moment, 527
cyanide water complex, Mössbauer spectrum, magnetic moment, 183
formation in manganese reduction by amides, 977
phosphetanate, 325, 115
pyridine Schiff base thione complex, synthesis, IR spectrum, magnetic moment, 1271
quinaldic acid complexes, ligand synthesis, NMR ($^1$H, $^{13}$C) spectra, relaxation studies, molecular structure, 491
quinone water complexes, synthesis, electronic, IR spectra, magnetic moments, 729
semicarbazone thiosemicarbazone complexes, synthesis, electronic, ESR, IR spectra, magnetic moments, 991
water complex, nickel(II) carboxylate phosphine complex anion, 963

Manganese(III)
fluoride sulphate complexes, synthesis, electronic, IR spectra, magnetic moments, pyrolysis, 599
reduction by amides, kinetic study entropy, free energy of activation, 977

Manganese(IV)
heteropolytungstate, electronic, MCD spectra, 1161

MASNMR, see NMR spectra, solid state, 1267

Mass spectra
copper(II) alkoxide oxime sulphate complexes, 641
gallium(III), indium(III) alkyl phosphide compounds, 581
iron(−II) carbonyl tin(IV) complex, 757
iron(III) carboxylate porphyrin complexes, 651
manganese azole carbonyl complexes, 707
metallacarborane, 307
nickel(II) alkoxide oxime complexes, 641
organoboron compounds, 271
platinum(II) dithiocarbamate complexes, 735
pyrazole thiosemicarbazone, 1135
pyrimidine derivatives, 983
tetrapyridylpyrazine, 635
tin(IV) alkyl phenolate semicarbazone thiosemicarbazone complexes, 681
titanium(IV) chloride phenoxide pyridine complex, 125
tripyridyloxazole, 635
xanthates, 721

MCD spectrum, manganese(IV) heteropolytungstate, 1161

Mercaptide, *see* thiolate

Mercaptoacetate complexes
aluminium(III), gallium(III), indium(III), 871

Mercaptobenzoate, *see* thiosalicylate

2-Mercaptoethanol complexes
bismuth(III), 71

2-Mercaptoethylamine complexes
nickel(II), palladium(II), 1227

6-Mercaptoguanine complex
iron(0), 1065

Mercaptopropionate complexes
indium(III), 871

3-Mercaptopropylamine complex
nickel(II), 839, 1227
palladium(II), 1227

6-Mercaptopurine complex
iron(0), 1965

2-Mercaptopyridine, 1209

2-Mercaptopyridine complex
iron(0), 1065
Mercury(II)
azole halide complexes, synthesis, IR, NMR ($^1H$, $^{13}C$) spectra, TGA study, 619
bromide, 297
chloride thiosemicarbazone complex, synthesis, IR spectrum, antifungal activity, 1237
hydrazone ketone pyridine complex, synthesis, IR, NMR ($^1H$, $^{13}C$) spectra, 281
iodide, 297
iron(0), molybdenum(0), tungsten(0), complexes, Mössbauer spectra, 365
thiolate complexes, synthesis, X-ray crystal structure, 1247
Metadithiophosphate, 432
Metal exchange, cyclometallation, 1039
Metallaazirane, 1041
Metallaborane, ruthenium, 901
Metallacarborane, lithium, 307
Metallation, *see* cyclometallation
Metal–metal bonds
cobalt(0)–iron(0), 175
copper(I)–copper(I), 749
copper(I)–rhenium(III), 749
germanium(II)–iron(0), 889
gold(0)–gold(I), 567
gold(0, I)–ruthenium(0), 567
iron(−II)–tin(IV), 757
iron(0)–mercury(II), 365
iron(0)–palladium(II), 1043
manganese(0)–manganese(0), 707
manganese(I)–manganese(I), 707
mercury(II)–molybdenum(0), 365
mercury(II)–tungsten(0), 365
molybdenum(0)–palladium(II), 1042
molybdenum(II)–molybdenum(III), 347
molybdenum(IV), 257
tungsten(II)–tungsten(II), 759
Metaphosphonate, 410
Methanal, *see* formaldehyde
Methane, 175
Methanol, solvent for electronic spectra, 161
Methanol complex
aluminium(III), 265
copper(II), 113
gallium(III), 265
zinc(II), 1017
Methionine complexes
nickel(II), 523, 1329
Methoxide complexes
molybdenum(II), 475
1-Methoxynaphthalene, 1051
2-Methoxy-2(2′-pyridyl)ethyl compounds, palladium(II), 1048
8-Methoxyquinoline-2-carboxylic acid complexes
manganese(II), 491
5-Methoxysalicyl-2′-mercaptobenzaldimine complex
molybdenum(IV), 61
molybdenum(VI), 55, 61
5-Methoxysalicyl-2′-mercaptoethaldimine complex
molybdenum(VI), 55
Methyl compounds
cobalt(III), 79
gallium(III), 581
germanium(IV), 757
iridium(III), 79
palladium(II), 1025
platinum(II), 87, 373
rhodium(III), 79
silicon, 757
tin(IV), 485, 757
zirconium(IV), 79
Methylamine
formation in amide oxidation by manganese(III), 977
reaction with cobalt(III) complex, 895
*N*-Methyl-4-anisidine, 117
Methylation, carbaborane amine complex, 1351
4-Methylbenzenediazonium compounds, 1206
Methylborylene, 271
*N*,*N*-Methylcyclohexyldithiocarbamate, *see* *N*-cyclohexyl-*N*-methyldithiocarbamate
Methylcyclopentadienyl complexes
chromium(III), 775
titanium(IV), 897
2-Methyl-1,2-dicarba-*closo*-dodecaborane compound
lithium, 307
*N*-Methylethylenediamine complex
zinc(0), 1333
*N*-Methylformamide
oxidation by manganese(III), 977
solvent for electronic spectra, 161
Methylidyne complexes
iron(I) cluster, 1307
osmium, 1199, 1203
1-Methylimidazole complexes
cadmium(II), 509
platinum(IV), 121
2-Methylimidazole complexes
copper(II), 457
platinum(IV), 121
4-Methylimidazole complexes
platinum(IV), 121
Methylisocyanate, 1213
2-Methyl-2-nitrosopropane, 631
1-Methylpentylenedithiophosphate complexes
antimony(III), arsenic(III), bismuth(III), 1337
(*N*-Methyl)phenylmethimine, 1211
4-Methylphenylpyruvic acid semicarbazone thiosemicarbazone complexes, copper(II), manganese(II), 991
1-Methyl-3-phenyltriazene complex, zirconium(IV), 79
5-Methylpyrazole-3-aldehydothiosemicarbazone complexes, cobalt(II), copper(II), nickel(II), 1135
2-Methylpyridine, 1039, 1041, 1045, 1208
2-Methylpyridine complexes
platinum(IV), 121
3-Methylpyridine complexes
titanium(IV), 125
4-Methylpyridine, reaction with cyclometallated complexes, 1044
4-Methylpyridine complexes
cadmium(II), 509
titanium(IV), 125

2(3-Methyl)pyridyl compound
osmium, 1045
7-Methylquinoline, 1044
1-Methyl(8′-quinolyl)ethyl compounds, palladium(II), 1052
Methylsalicylaldoximate complexes, nickel(II), 603
1-Methyl-3-(4-tolyl)triazene complex, cobalt(III), 79
Methyltrifluoromethanesulphonate, 1199
2-Methyl-1-vinylimidazole complexes, platinum(IV), 121
Methyl vinyl ketone, 1051
Methylxanthate compounds
arsenic(III), 721
titanium(IV), 695
Mica, trimethylsilylation, 503
Mobil 190/210, solvent extraction, 615
Molecular orbital calculations
cluster compounds, 1299
copper(II) diselenocarbamate dithiolate complexes, 433
multiple bonds, 418
Molecular structure determination (other than by diffraction), manganese(II) quinaldinic acid complexes, 491
Molybdate, 607
Molydenum
cluster compounds, 1307, 1321
reactions, book review, 515
Molybdenum(−I)
carbonyl complex, hot ion, electronic spectrum, 1131
Molybdenum(0)
carbonyl cyclopentadienyl mercury(II) complex, Mössbauer spectra, 365
carbonyl thione complexes, synthesis, electronic, IR, NMR ($^1$H) spectra, 235
hexacarbonyl-, 235, 1131
Molybdenum(II)
carbonyl carboxylate chloride diketonate phosphine complexes, synthesis, IR, NMR ($^1$H) spectra, 347
chloride methoxide polynuclear complexes, X-ray crystal structure, 475
cyclometallated complex, 1042
octachlorodi-, 257
Molybdenum(II, III)
carboxylate chloride binuclear complex, synthesis, IR spectrum, 347
Molybdenum(III)
chloride oxo phosphine complex, hot ion, electronic, ESR spectra, 1131
chloride phosphine binuclear complexes, synthesis, IR, NMR ($^{31}$P) spectra, magnetic moment, 347
tris(tetrahydrofuran)trichloro-, 347
Molybdenum(IV)
chloride cyanate dithiocarbamate oxo phosphine thiocyanate complexes, synthesis, IR, NMR ($^1$H) spectra, 347
chloride macrocyclic Schiff base water binuclear complex, synthesis, IR, NMR ($^1$H) spectra, 257
chlorobis(1,2-bis{diphenylphosphino}ethane)oxo-, irradiation product, 1131
chlorostannate(II), cyclopentadienyl hydride complex, X-ray crystal structure, 765
diphosphene complex, 412, 427
formation in molybdenum(V) electrochemistry, 907
mercaptide oxo phenolate Schiff base complexes, 61
Molybdenum(V)
oxo dithiocarbamate thiocyanate complex synthesis, electronic, ESR, IR spectra, cyclic voltammetry, magnetic moment, 907
Molybdenum(VI)
cyclohexanol oxidation catalysis, effects of air, charcoal, hydrogen peroxide, oxygen, 607
dichlorodioxo-, 55
diimine oxo peroxide complex, X-ray crystal structure, 377
dioxobis(pentane-2,4-dionato)-, 55
dioxo mercaptide phenolate Schiff base water complexes, synthesis, ligand synthesis, electronic, IR spectra, cyclic voltammetry, 55
dioxo mercaptide phenoxide Schiff base complexes, phosphine oxidation, kinetic study, 61
heteropolyanion, Pfeiffer effect, CD, electronic spectra, polymerisation catalysis, 381
heteropolyanions, Pfeiffer effect, CD, electronic, electronic difference, IR spectra, 1071
light, X-ray scattering, Raman spectra, 1001
oxide, 907
polyanions, 341, 1171
Morpholine complexes
chromium(III), 1241
copper(II), 137
Morpholine-*N*,*N*-dithiocarbamate complexes
tungsten(V), 25, 1021
Mössbauer spectra
antimony(III) alkoxide phenolate semicarbazone thiosemicarbazone complexes, 661
iron(0) carbonyl tin(II) complex, 889
iron(0)–mercury(II) compounds, 365
iron(II), (III) citrate complexes, 169
iron(II), (III) cyanide complexes, 183
iron(II) pyridine Schiff base thione complex, 1271
tin(IV) alkyl phenolate semicarbazone thiosemicarbazone complexes, 681
Mulliken, R. S., electronegativity scale, 853
Multiple bonds, heavy main group elements, 389

## N

Naphtholate complexes
zirconium(IV), 611
1-Naphthylamine complexes
copper(II), 291
2-Naphthyloxide complexes
titanium(IV), 125
Neodymium(III)
acetate complexes, electronic spectra, oscillator, strength, formation constants, 31
ketone nitrate Schiff base complexes, synthesis, electronic, IR spectra, DTA study, electric conductance, magnetic moments, 67

Neophyl complex
nickel(II), 317
palladium(II), 1025
Neptunium(V)
dioxo carboxylate phosphate complexes, ion exchange behaviour, formation constants, enthalpies, entropies, free energies of reaction, 667
Nickel
cluster compounds, 1279, 1321
Nickel(0)
diphosphene complex, 414
Nickel(I)
tetradentate complexes, formation, ESR spectra, 585
Nickel(II)
acyl alkyl chloride cyclopentadienyl phosphine thiocyanate complexes, synthesis, IR, NMR ($^1$H) spectra, X-ray crystal structure, 317
alkoxide oxime polynuclear complexes, synthesis, electronic, IR, mass, NMR ($^1$H) spectra, magnetic moments, viscosity, DTA, TGA study, 641
amide amine complexes, electronic, ORD spectra, potentiometric and spectrophotometric titrations, formation constants, 551
amine thiolate polynuclear complex, synthesis, electronic, IR spectra, X-ray crystal structure, 839, 1227
aminoacid aminosulphonate thioether complexes, potentiometric titrations, formation constants, 1329
aminoacid thioether complexes, potentiometric titrations, formation constants, 523
aminopolyphosphonate complexes, electronic spectra, magnetic moments, DTA, TGA study, 527
bis(neophyl)tetramethylethylenediamine-, 317
bis(pyridine)bis(trimethylsilylmethyl)-, 317
carboxylate phosphine complexes, synthesis, electronic, IR, NMR ($^1$H, $^{31}$P), XPE spectra, electric conductance, magnetic moments, 963
carboxylate pyridine water binuclear complex, synthesis, X-ray crystal structure, 689
chloride salicylidene hydrazone complexes, synthesis, electronic, IR spectra, magnetic moments, 21
chloro(cyclopentadienyl)triphenylphosphine-, 317
cyclometallated complexes, 1048
dichlorobis(trimethylphosphine)-, 317
diimine complex, reactions with nucleophiles, electronic spectra, 701
dioxime complex, synthesis, IR, NMR ($^1$H) spectra, solvent extraction, 821
diphosphene complexes, 413, 427
diselenocarbamate dithiolate complex, X-ray crystal structure, 433
halide imine nitrate pyrimidine thiocyanate complexes, synthesis, ligand synthesis, electronic, IR spectra, electric conductance, magnetic moments, 983
ketone Schiff base thiolate complexes, synthesis, ligand synthesis, electronic, IR, NMR ($^1$H) spectra, electric conductance, magnetic moments, 517
ketophenol complexes, synthesis, IR spectra, 1017
macrocyclic Schiff base complex, synthesis, ligand synthesis, electronic, IR spectra, polarography, 1357
oxime complexes, synthesis, ligand synthesis, solvent extraction, 479
oxime silicon complexes, synthesis, electronic, IR spectra, electric conductance, magnetic moments, 603
phosphetanate, synthesis, IR spectrum, electric conductance, magnetic moment, solubility, 1155
pyrazole thiosemicarbazone complexes, synthesis, ligand synthesis, electronic, IR spectra, electric conductance, 1135
pyridine Schiff base thione complexes, synthesis, electronic, IR, photoacoustic spectra, magnetic moments, 1271
quinone water complexes, synthesis, electronic, IR spectra, magnetic moments, 729
separation from Co(II), Cu(II), Zn(II), 939
tetradentate ketoimine complex, synthesis, electronic, IR, NMR ($^1$H) spectra, halogenation, kinetic study, 239
tetradentate ketoimine complexes, controlled potential electrolysis, coulometry, cyclic voltammetry, radical anion formation, reduction, ESR spectra, 585
thiol polynuclear complex, synthesis, electronic, IR spectra, X-ray crystal structure, 969
thiolate polynuclear complex, synthesis, electronic, IR spectra, 969
water complex, nickel(II) carboxylate phosphine complex anion, 963
Nickel(II, III), cluster complexes, 1307
Niobium, cluster compounds, 1307
Niobium(V)
hydroxycarboxylate hydroxide complexes, synthesis, IR spectra, absorption by ascadians, 1029
Nitrate complexes
cobalt(II), 357
copper(II), 113, 137, 261, 357, 929, 1135
Nitrene complexes, osmium, 1193, 1205, 1213
Nitric oxide
chemisorption on iron(III) hydroxide oxide, 223
cluster compounds, 1321
Nitride, sialon ceramics, 1267
Nitride complexes, cluster, 1279, 1307
Nitriles, reactions with osmium carbonyl cluster compounds, 1215
Nitrile complexes
manganese(I), 347
palladium(II), 117
rhenium(I), 347
Nitrite, reactions with osmium carbonyl cluster compounds, 1177
Nitrite complexes
copper(II), 297
palladium(II), 701
rhodium(III), 811
4-Nitroaniline complexes
copper(II), 291
Nitrobenzene, solvent for equilibrium studies, 251
Nitromethane, solvent for equilibrium studies, 251
5-Nitro-1,10-phenanthroline complexes, cobalt(II), copper(II), nickel(II), palladium(II), platinum(II), 701

4-Nitro-2(2'-pyridyl)phenyl compound, palladium(II), 1052
Nitrosyl complexes
chromium(I), 247
cluster, 1165, 1321
iron, 1065, 1165
osmium, 1177
Nitroxide, 631
NMR ($^{1}$H) spectra
aldehyde complexes, 1151
alkene complexes, 497, 1255
alkoxide complexes, 641
alkyl compounds, 79, 87, 317, 485, 581, 681, 757, 1025, 1043, 1255
alkylamide complexes, 509, 1121
alkylammonium salt, 535
alkylenedithiophosphate complexes, 1337
amide complex, 627
amine complexes, 1351
aminoalkoxide complexes, 589
arene complexes, 497
arsine complex, 505
aryl compounds, 87, 485
azole complexes, 121, 213, 619, 707
borohydride complexes, 457
carboxylate complexes, 929, 963
catecholate compounds, 589
cyclometallated complexes, 1042, 1048
cyclopentadienyl complexes, 79, 317, 695, 771, 1093
diimine complexes, 87, 799
diketonate complexes, 347, 929, 1017
dioxime complex, 821
dithiocarbamate complexes, 347, 735
dithiophosphate complexes, 485
hydrazone complexes, 281
hydride complexes, 567, 1047, 1307
indenyl complexes, 611
isocyanide complex, 385
ketoimine complexes, 239
ketone complexes, 281
manganese(II) complexes, 491
methyl complex, 373, 1025
nitrile complexes, 353
nucleotide complexes, 1105
organoboron compounds, 271
oxime complexes, 641
oxoquinolinate complexes, 883
phenolate complexes, 611, 661, 1121
phenyl compounds, 721
phosphetanate complexes, salts, 325
phosphide compounds, 581
phosphine complexes, 79, 317, 347, 505, 567, 735, 963, 1025, 1059, 1083, 1151, 1255
porphyrin complexes, 107, 651, 879, 889
pyrazole thiosemicarbazone, 1135
pyridine complexes, 281, 509
pyrimidine derivatives, 983
quinaldic acid complexes, 491
Schiff base complexes, 257, 517
semicarbazone complexes, 661, 681
tetrapyridylpyrazine, 635
thiolate complexes, 505, 535
thione complexes, 235
thiosemicarbazone complexes, 661, 681
tripyridyloxazole, 635
xanthate compounds, 695, 721
NMR ($^{11}$B) spectra
boron alkyls, aryls, chloro compounds, 957
boron carboxylate diketonate oxo complexes, 929
carbaborane amine complexes, 1351
spiroborates, 589
NMR ($^{13}$C) spectra
alkene complexes, 213
alkyl compounds, 485, 681
alkylamide complexes, 1121
aminoalkoxide compounds, 589
aryl compounds, 485, 721
azole complexes, 213, 619
carbonyl complexes, 567, 1059, 1093
catecholate compounds, 589
cyanide complex, 1165
cyclometallated complexes, 1042, 1044, 1046
cyclopentadienyl complexes, 79, 1093
dithiophosphate complexes, 485
hydrazone complexes, 281
ketone complexes, 281
manganese(II) complexes, 491
phenolate complexes, 681, 1121
phosphine complexes, 567, 1059
porphyrin complexes, 879
pyridine complexes, 281
quinaldic acid complexes, 491
semicarbazone thiosemicarbazone complexes, 681
triazene complexes, 79
xanthate compounds, 721
NMR ($^{15}$N) spectra
nitrosyl complex, 1165
NMR ($^{19}$F) spectra
fluoride complexes, 265
fluoroalkyl compounds, 87
NMR ($^{27}$Al) spectra
sialon ceramics, 1267
NMR ($^{29}$Si) spectra
disilenes, 423
sialon ceramics, 1267
silylamide complexes, 509
NMR ($^{31}$P) spectra
alkylenedithiophosphate complexes, 1337
diphosphenes, 423
dithiophosphate complexes, 485
organophosphate compounds, 1105
phospha-arsenes, 423
phosphastibines, 423
phosphetanate complexes and salts, 325, 1155
phosphide compounds, 581
phosphine complexes, 79, 347, 373, 567, 963, 1025, 1083, 1255
NMR ($^{113}$Cd) spectra
cadmium alkylamide complexes, 509
NMR ($^{119}$Sn) spectra
tin(IV) alkyl aryl chloro compounds, 957
tin(IV) alkyl aryl dithiophosphates, 485

NMR ($^{195}$Pt) spectra
platinum(0), carbonyl iridium(I) cluster complex, 1093
platinum(II) dithiocarbamate dithiophosphate dithiophosphinate phosphine complexes, 231
NMR spectra, relaxation studies, manganese(II) quinaldic acid complexes, 491
NMR spectra, solid state, ceramics, 1267
Nonachlorononaborane(9), 199
Nonahydrononaborate(2), 199
Nopinoquinonedioxime, configurational isomerism, copper(II), nickel(II) complexes, furazan formation, 821
2,5-Norbornadiene complexes
osmium(0), 1187
rhodium(I), 213
NQR spectra, phosphazenes, 867
Nucleophiles, reactions with
diimine complexes, kinetic study, 701
osmium carbonyl cluster compounds, 1176
Nucleoside complexes
palladium(II), 9
Nucleotide complexes
cadmium(II), 1105

O

Octachlorooctaborane(8), 199
Octaethylporphyrin complexes
germanium(II), 889
iron(III), 651
thorium(IV), 187
tin(II), 889
uranium(IV), 107
Octahydrooctaborate(2), 199
Octapolymolybdate, 607
Oligomerisation, osmium carbonyl cluster compounds, 1178
Optical rotation
cobalt(III) aminoacid diimine complexes, 49
ORD spectra
chromium(III) dicarboxylate diimine complexes, 1141
nickel(II) amide amine complexes, 551
Oscillator strengths
dysprosium(III), 161
iron(III) chloride thione complexes, 39
lanthanide acetate complexes, 31
Osmium
allyl complex, 1279
aryl compounds, 1044
carbonyl cluster compounds, review, 1175
cluster complexes, 1039, 1044, 1279, 1307, 1321
cyclometallated complexes, 1039, 1044
Osmium(0)
dodecacarbonyltri-, 1176
Osmium(II)
aryl compound, 1043
bromide isocyanide complex, synthesis, IR, NMR ($^{1}$H) spectra, X-ray crystal structure, 385
cyclometallated complexes, 1043
Osmium(IV)
hexabromo-, ammonium, 385
Oxides and oxo complexes
boron, 929
chromium(VI), 247
cluster, 1307
iron(III), 223, 443
molybdenum(III), 1131
molybdenum(IV), 61, 347, 1131
molybdenum(V), 907
molybdenum(VI), 55, 61, 377
neptunium(V), 667
rhenium(V), 1083
sialon ceramics, 1267
tungsten(IV), 743
tungsten(V), 25
uranium(VI), 143, 469
vanadium(IV), 129, 575
vanadium(V), 287
*N*-Oxide complexes
cadmium(II), 303
Oxime complexes
copper(II), 479, 641
nickel(II), 479, 603, 641
8-Oxoquinolinate complexes
titanium(IV), zirconium(IV), 883
Oxygen, *see* dioxygen

P

Palladium(II)
alkyls, 1042, 1043
alkyl nitrile phosphine binuclear complex, reaction with anilines, kinetic study, 117
alkyl phosphine complexes, synthesis, IR, NMR ($^{1}$H, $^{31}$P) spectra, 1025
amine chloride thiolate binuclear complex, synthesis, IR spectrum, 969
amine thiolate complex, synthesis, electronic, IR spectrum, 1227
aminoacid halide nucleoside binuclear complexes, synthesis, IR, NMR ($^{1}$H, $^{13}$C) spectra, electric conductance, 9
chloride, 9
cyclometallated complexes, 1039, 1042, 1048
diacetatobis(trimethylphosphine)-, 1025
dichlorobis(triphenylphosphine)-, 775
diimine complexes, reactions with nucleophiles, electronic spectra, kinetic studies, 701
diphosphene complex, 413
dithiocarbamate phosphine complexes, synthesis, electronic, IR, NMR ($^{1}$H) spectra, 735
octaacetatotetra-, 1025
phosphine thio thiolate chromium(III) polynuclear complexes, synthesis, IR spectra, magnetic moments, X-ray crystal structure, 775
porphyrin complexes, NMR ($^{1}$H, $^{13}$C) spectra, 879
quinone water complexes, synthesis, electronic, IR spectra, magnetic moments, 729
Pauling, L., electronegativity scale, 853
PE spectra, diphosphene, 432
Pentamethylcyclopentadienyl complexes
rhodium(I), (III), 497
titanium(IV), 897

Pentamethyldiethylenetriamine complex, lithium, 307
2,2,3,4,4-Pentamethylphosphetanates, 1155
2,2,3,4,4-Pentamethylphosphetanic acid, 325
2,4-Pentanedionate complexes
chromium(III), 781
copper(II), 137, 291, 1233
molybdenum(II), 347
2,4-Pentanedione, 983
2,4-Pentanedione Schiff base complexes, copper(II), 157, 713
2,4-Pentanedione(3-hydroxpropylimine) complex, copper(II), 157
*neo*-Pentoxide complexes
tungsten(VI), 1033
Peptide complexes
copper(I), 861
copper(II), 463, 787, 833, 861
Perchlorate complexes
copper(II), 137, 261, 1135
iron(III), 911
Peroxide complexes
molybdenum(VI), 377
platinum(II), 513
uranium(VI), 469
vanadium(V), 287
Peroxouranyl, *see* uranium(VI)
Pfeiffer effect
heteropolyanions, 381, 1071
terbium(III) carboxylate pyridine complex, 1087
Phenacylazide, 1197
1,10-Phenanthroline complexes
chromium(III), 1141
cobalt(III), 49
copper(II), 137, 595
iron(III), 443
titanium(IV), 125
Phenoxide complexes
antimony(III), 661
boron, 589
copper(II), 595
molybdenum(IV), 61
molybdenum(VI), 55, 61
tin(IV), 681
titanium(IV), 1121
zirconium(IV), 611, 1211
Phenyl compounds
arsenic(III), 721
platinum(II), 87
tin(IV), 485
Phenylacetonitrile complexes
manganese(I), rhenium(I), 353
Phenylalaninate complexes
cobalt(III), 49
Phenylamine, *see* aniline
Phenyl azide, *see* azidobenzene
2-Phenylbenzothiazole, 1051
2-Phenylbenzoxazole, 1051
Phenylbiguanidinium chloride, 983
1-Phenylbutane-1,3-dione-1,2-diaminoethane-1-phenyl-2-succinimidobutane-1,3-dione Schiff base complex
nickel(II), 239
Phenyl(*t*-butyl)nitrone, 631
Phenylenethiourea complex
tellurium(II), 921
1-Phenylethylamine, 1052
1-Phenylethylcyclopentadienyl complexes, titanium(IV), 897
2-Phenylimidazole, 1051
Phenylisocyanate, 1214
2-Phenylisoxazole, 1051
Phenylmethanol, 381
Phenylmethyl compound
palladium(II), 1025
1-Phenyl-3-methyl-4-benzoylpyrazolone-5, *see* 4-benzoyl-3-methyl-1-phenylpyrazolone-5
1-Phenyl-3-methyl-4-(3:5-dinitrobenzoyl)-pyrazolone-5, *see* 4-(3′,5′-dinitrobenzoyl)-3-methyl-1-phenylpyrazolone-5
*N*-Phenylnaphthylamine complexes
copper(II), 291
Phenylphosphide complexes
osmium, 1217
Phenylphosphine complexes
osmium(0), 1217
1-Phenylpyrazole, 1042, 1043, 1046, 1047, 1051
2-Phenylpyridine, 1040–1043, 1046, 1047, 1051, 1054
4-Phenylpyrimidine, 1042
Phenylpyruvic acid semicarbazone thiosemicarbazone complexes, copper(II), manganese(II), 991
2-Phenylquinoline, 1051
2-Phenylthiazole, 1051
1-Phenyl-2-(4-tolyl)-2,4-dithiobiuret complexes
iron(III), 39
1-Phenyl-5-(4-tolyl)-2,4-dithiobiuret complexes
iron(III), 39
Phospha-arsenes, 403, 408, 421
Phosphastibenes, 403, 423
Phosphate complexes
cadmium(II), 1105
neptunium(V), 667
Phosphazenes, NQR spectra, torsional frequencies, 867
Phosphetanate complexes, salts synthesis, electronic, IR, NMR ($^{1}H$, $^{31}P$) spectra, magnetic moment, 325
synthesis, IR, NMR ($^{31}P$) spectra, electric conductance, magnetic moment, solubility, 1155
Phosphide complexes
gallium(III), 581
indium(III), 581
osmium, 1217
Phosphine, reduction of molybdenum(VI), 61
Phosphines, reactions with osmium carbonyl cluster compounds, 1217
Phosphine complexes
cobalt(I), (III), 79
gold(0, I), 567, 1289
gold(I), iridium(I), 213
iridium(III), 79
molybdenum(II), 347
molybdenum(III), (IV), 347, 1131
nickel(II), 317, 963
osmium, 1177, 1214

palladium(II), 117, 735, 775, 1025
platinum(II), 231, 373, 735
rhenium(I), 353
rhenium(III), 1059
rhenium(V), 1083
rhodium(I), 213, 1151
rhodium(III), 79
ruthenium metallaborane, 901
ruthenium(0), 567, 1255
ruthenium(II), 325, 1255
ruthenium(III), 79
titanium(IV), 505
Phosphine oxide complexes
americium(III), berkelium(III), californium(III), curium(III), 1125
Phosphinyl radicals, 411
Phosphite, reaction with cluster compounds, 1307
Phosphododecamolybdate $(PMo_{12}O_{40})^{3-}$, 607
Phosphododecatungstate $(PW_{12}O_{40})^{3-}$, 607
Phosphoric acid, iron (III) solvent extraction, 615
Phosphorous acid, 939
Phosphorus
double bonds, 390, 395, 398, 408, 418, 432
metal cluster compounds, 1307, 1321
Phosphorus(III)
trichloro-, reaction with cluster compounds, 1307
Phosphorus(V)
decathiotetra-, 1021
heteropolyanion, 381, 1071
Photoacoustic spectra
cobalt(III) Schiff base thione complex, 1271
copper(II) amine diketonate complexes, 137
copper(II), nickel(II) pyridine Schiff base thione complexes, 1271
Photochemistry
chromium(I) complex, oxidation, 247
iron(III) citrate complexes, reduction, 169
molybdenum(0) carbonyl thione complexes, synthesis, 235
tungsten(IV) cyanide complex, 743
Phthalate complexes
neptunium(V), 667
Phthalocyanine complexes
vanadium(IV), zinc(II), 129
Picoline, *see* methylpyridine
Piperidine, reactions with diimine complexes, kinetic study, 701
Piperidine complexes
copper(II), 137
titanium(IV), 125
tungsten(V), 1021
Piperidine-*N*,*N*-dithiocarbamate complexes
tungsten(V), 25
Platinum(0)
bis(ethene)-, 513
carbonyl iridium(I) cluster compound, synthesis, IR, NMR ($^1H$, $^{13}C$, $^{195}Pt$) spectra, X-ray crystal structure, 1093
cluster compound, 1307
tris(ethene)-, 1093
Platinum(II)
alkene peroxide complex, formation, IR spectrum, reactivity, 513
alkyl arsine chloride phosphine complex, synthesis, NMR ($^1H$, $^{31}P$) spectra, X-ray crystal structure, 373
alkyl aryl diimine binuclear complexes, synthesis, electronic, IR, NMR ($^1H$) spectra, 87
amine pyridine complex, synthesis, ligand synthesis, X-ray crystal structure, 753
ammonia chloride quinone complexes, synthesis, electronic, IR spectra, 729
bis(dimethyl)triethylphosphine(triphenylarsine)-, 373
cyclometallated complexes, 1038
diaminoethane(dichloro)-, 753
diimine complex, reactions with nucleophiles, electronic spectra, kinetic studies, 701
diphosphine complex, 412
dithiocarbamate dithiophosphate dithiophosphinate phosphine complexes, NMR ($^{195}Pt$) spectra, 231
dithiocarbamate phosphine complexes, synthesis, electronic, IR, mass, NMR ($^1H$) spectra, 735
porphyrin complexes, NMR ($^1H$, $^{13}C$) spectra, 879
Platinum(IV)
azole halide complexes, synthesis, electronic, NMR ($^1H$) spectra, 121
chloride, 121
cyclometallated complexes, 1048
hexabromo-, potassium, 121
Plutonium, coexistence of oxidation states, 761
Polarography
copper(II) macrocyclic Schiff base complex, 1357
iridium(III), (IV) chloride water complexes, 1013
nickel(II) macrocyclic Schiff base complex, 1357
Polyaminopolycarboxylic acid, linked to polystyrene, IR spectra, metal ion separations, 939
Polyaminopolymethylphosphonate, linked to polystyrene, metal ion separations, 939
Polycondensation, phenylmethanol, 381
Polyhedral boranes, bonding schemes, 199
Polymerisation
benzyl, 381
siloxanes, 1109
Polymolybdates, polytungstates
cyclohexanol oxidation catalysis, 607
structure and stability, 341
Polynuclear complexes
chromium(III) palladium(II) thio thiolate, 775
copper(I) rhenium(III) iodide, 749
copper(I) thiolate, 535
copper(II) alkoxide oxime, 641
gallium(III) alkyl phosphide, 581
gold(0,I) ruthenium(0) carbonyl hydride phosphine, 567
gold(I) cyclometallated, 1055
gold(I) rhodium(I) alkene arene, 497
indium(III) alkyl phosphide, 581
molybdenum(II) chloride methoxide, 475
nickel(II) alkoxide oxime, 641
nickel(II) amine thiolate, 839
nickel(II) thiol, thiolate, 969
Polypyridine, *see* diimine
Polystyrene, support for polydentate ligands, 939

Pope, M. T., polyanion classification, 341
Porphyrin complexes
germanium(II), 889
iron(III), 651
palladium(II), platinum(II), 879
silver(I), 1077
thorium(IV), 107
tin(II), 889
uranium(IV), 107
Potassium
fluoride complex, potentiometric titration, formation constant, 845
graphite ($C_8K$), 271
phosphetanate, 325
quinoline carboxylate complexes, synthesis, IR spectra, electric conductance, 240
Potential function calculations
polysiloxanes, 1109
Potentiometric titrations
alkali metal fluoride complexes, 845
aluminium(III) carboxylate thiolate complexes, 871
cadmium(II) nucleotide phosphate complexes, 1105
carbaborane amine complexes, 1351
copper(II) amide amine complexes, 559
copper(II) azole peptide pyridine complexes, 787
gallium(III) carboxylate thiolate complexes, 871
hydrofluoric acid, 75
indium(III) carboxylate thiolate complexes, 871
nickel(II) amide amine complexes, 551
nickel(II) aminoacid aminosulphonate thioether complexes, 1329
nickel(II) aminoacid thioether complexes, 523
tin(IV) aminopolycarboxylate complexes, 1099
uranium(VI) dioxo aminopolycarboxylate peroxo complexes, 469
Praseodymium(III)
ketone nitrate Schiff base complexes, synthesis, electronic, IR spectra, DTA study, electric conductance, magnetic moments, 67
Prolinate complexes
cobalt(III), 49
palladium(II), 9
Propanediamine, *see* diaminopropane
*n*-Propanol, solvent for electronic spectra, 161
*n*-Propanol complexes
aluminium(III), gallium(III), 265
Propanone, 1183
Propene, 175
Propionate complexes
iron(III), 651
tungsten(II), 759
Propionitrile, reaction with rhodium(I) aldehyde complex, 1151
Propionitrile complexes
manganese(I), rhenium(I), 353
4-Propionyl-2,4-dihydro-5-methyl-2-phenyl-5*H*-pyrazolonate compound, boron, 929
4-Propionyl-3-methyl-1-phenyl-2-pyrazolin-5-one, 929
*i*-Propoxide complexes
antimony(III), 661
*n*-Propyl complex, ruthenium(II), 1255
*n*-Propylamine, reactions with diimine complexes kinetic study, 701
*i*-Propylcyclopentadenyl complexes, titanium(IV), 897
2-*i*-Propylimidazole complexes
platinum(IV), 121
Propylxanthate compounds
arsenic(III), 721
titanium(IV), 695
Propyne, 1190
Prussian blue analogues, 183
Purine complex, iron(−II), 1065
Pyramidal inversion thioether complexes, 331
Pyrazine complex
iron(II), 183
Pyrazole, 1206
Pyrazole complexes
cobalt(III), copper(II), 1135
iron(−II), 1065
manganese(0), (I), (II), 707
nickel(II), 1135
Pyrazole thiosemicarbazone, synthesis, IR, mass, NMR ($^1$H) spectra, 1135
5-(1-Pyrazolylmethyl)pyrazolyl compound, platinum(II), 1054
Pyridazine, 1210
Pyridazine complexes
rhodium(I), 213
Pyridine
reaction with cluster compounds, 1307
reaction with cyclometallated compounds, 1044
Pyridine complexes
cadmium(II), 281, 509
cluster, 1321
cobalt(II), 635, 1271
cobalt(III), copper(I), 1271
copper(II), 291, 595, 787, 921, 1271
iron(II), manganese(II), 1271
mercury(II), 281
nickel(II), 689, 1271
osmium(0), 1197
platinum(II), 753, 1038
ruthenium(II), 1044
terbium(III), 1087
thorium(IV), 107
titanium(IV), 125
uranium(IV), 107
zinc(II), 281, 1271
2-Pyridinecarbaldehyde, 1045
2-Pyridinecarbaldehyde salicylhydrazone complexes
cadmium(II), mercury(II), zinc(II), 281
Pyridine-2-carboxaldehyde-2-furanthiocarboxyhydrazone complexes, cobalt(II), (III), copper(I), (II), iron(II), manganese(II), nickel(II), zinc(II), 1271
Pyridine-4-carboxyaldehyde-2-furanthiocarboxyhydrazone complexes, cobalt(II), (III), copper(I), (II), iron(II), manganese(II), nickel(II), zinc(II), 1271
Pyridine-2-carboxylic acid–3-hydroxypropylamide complex, copper(II), 157

Pyridine-*N*-oxide complexes
copper(II), 921
2(1*H*)-Pyridinethione, 1045
2(1*H*)-Pyridone, 1045
Pyridoxamine complexes
copper(II), 787
2-Pyridyl compounds
copper(I), gold(I), 1055
nickel(II), 1048
osmium, 1039, 1044, 1046, 1181, 1208
palladium(II), 1039, 1048
rhenium(I), 1043
titanium(III), 1041
2-(2′-Pyridyl)acetyl compound
molybdenum(II), 1042
platinum(IV), 1048
2-(2′-Pyridyl)ethyl compounds
cobalt, 1046
ruthenium(II), 1044
2-Pyridylferrocene, 1051
2-Pyridylmethyl compound
iron(II), 1043
3-(2:2′-Pyridyl)thienyl compound
ruthenium(II), 1044
2-(2′-Pyridyl)vinyl compound
rhenium(I), 1042
Pyrimidines, synthesis, mass, NMR ($^1$H) spectra, 983
Pyrimidine complexes
nickel(II), 983
Pyroelectricity, iron(III) chloride thione complexes, 39
Pyrrole, 1206
Pyrrolidinyldithiocarbamate complex, molybdenum(V), 907

## Q

Quinaldic acid, *see* quinoline-2-carboxylic acid
Quinaldinic acid, *see* quinoline-2-carboxylic acid
Quinoline complexes
cobalt(II), copper(II), 357
Quinoline-8-aldehyde, 1047
Quinoline-8-*t*-butylketone, 1047
Quinoline-2-carboxylic acid complexes
alkali metals, 240
manganese(II), 491
Quinolyl compounds
gold(I), 1055
manganese(I), 1042
osmium, 1044
rhenium(I) 1042
8-Quinolylethyl compounds
palladium(II), 1052
8-Quinolylformyl compound
palladium(II), 1053
8-Quinolylmethyl compounds
molybdenum(II), 1042
palladium(II), 1042, 1043, 1052, 1053
platinum(II), 1051
Quinone complexes, copper(II), iron(II), manganese(II), nickel(II), palladium(II), platinum(II), zinc(II), 729

## R

Radical anions, formation in nickel(II) ketoimine complex electrochemical reduction, 585
Radiofrequency discharge, boron subhalide synthesis, 369
γ-Radiolysis, iron(III) citrate complexes, 169
Raft cluster complex, iridium(I) platinum(0) carbonyl, 1093
Raman spectra
carbonyl complexes, 1333
chloride complex, 1365
fluoride hydroxide complexes, 287
isopolyanions, 1001
oxo peroxide complexes, 287
sulphur–nitrogen ligand complex, 1365
Reviews
cyclometallation, 1037
double bonding by main group elements, 389
osmium carbonyl cluster compounds, 1175
Rhenium, cluster compounds, 1279, 1307
Rhenium(0)
nonacarbonyl(pyridine)di-, 1043
Rhenium(I)
alkyl, 1042
ammine carbonyl nitrile phosphine complexes, synthesis, IR, NMR ($^1$H) spectra, 347
aryl, 1042
bromide carbonyl phosphine complexes, oxidation with bromine, 1059
carbonyl halide thioether complexes, synthesis, IR, NMR ($^1$H) spectra, conformational isomerism, kinetic study, enthalpies, entropies, free energies of activation, 331
cyclometallated complexes, 1042
Rhenium(III)
bromide carbonyl phosphine complexes, synthesis, IR, NMR ($^1$H, $^{13}$C) spectra, X-ray crystal structure, 1059
copper(I) cyclopentadienyl hydride polynuclear complex, X-ray crystal structure, 749
cyclopentadienyl complex, magnetic moment, NMR ($^1$H) spectrum, X-ray crystal structure, reaction with $CCl_4$, 771
Rhenium(V)
oxo phosphine complex, synthesis, IR, NMR ($^1$H, $^{31}$P) spectra, electric conductance, X-ray crystal structure, 1083
Rhenium(VII)
heptaoxodi-, 1083
tetraoxo-, rhenium(V) complex salt, 1083
Rhodium, cluster compounds, 1279, 1307, 1321
Rhodium(I)
aldehyde carbonyl phosphine complexes, synthesis, electronic, IR, NMR ($^1$H) spectra, electric conductance, reactions, aldehyde hydrogenation catalysis, oligomerisation catalysis, 1151
alkene arene gold(I) complexes, synthesis, electric conductance, NMR ($^1$H) spectra, 497
alkene azole carbonyl chloride phosphine complexes, synthesis, IR, NMR ($^1$H, $^{13}$C) spectra, 213

carbonyl diimine complexes, synthesis, electronic, IR, NMR ($^1$H) spectra, electric conductance, 799
carbonyl(perchlorato)bis(triphenylphosphine)-, 1151
dicarbonyldichloro-, 799
dichloro(tetracarbonyl)di-, 799
Rhodium(III)
alkyl azide phosphine complex, synthesis, IR, NMR ($^1$H, $^{31}$P) spectra, reaction with carbon monoxide, 79
amine arsine azide chloride nitrite complexes, substitutions, kinetic study, 811
arene gold(I) complexes, synthesis, electric conductance, 497
cyclometallated complexes, 1046
ketone Schiff base thiolate complexes, synthesis, ligand synthesis, IR spectra, electric conductance, 517
trimethyltris(trimethylphosphine)-, 79
Rings, siloxanes, 1109
Roussin salts, 1165
Rubidium
fluoride complex, potentiometric titration, formation constant, 845
phosphetanate, 325
quinoline carboxylate complexes, synthesis, IR spectra, electric conductance, 240
Ruthenium
borane phosphine complex, synthesis, X-ray crystal structure, 901
cluster compounds, 1279, 1307, 1321
Ruthenium(0)
alkene phosphine complex, synthesis, NMR ($^1$H, $^{31}$P) spectra, X-ray crystal structure, 1255
carbonyl hydride phosphine gold(0, I) polynuclear complexes, synthesis, IR, NMR ($^1$H, $^{13}$C, $^{31}$P) spectra, X-ray crystal structure, configurational isomerism, 567
Ruthenium(II)
alkyl hydride phosphine complexes, synthesis, NMR ($^1$H, $^{31}$P) spectra, X-ray crystal structure, 1255
ammine thiocyanate complexes, synthesis, electronic, IR spectra, cyclic voltammetry, electric conductance, magnetic moments, configurational isomers, 1
aryl, 1043
azide phosphine complex, synthesis, IR, NMR ($^1$H, $^{31}$P) spectra, 79
cyanide water complex, magnetic moment, 183
cyclometallated complexes, 1043
dichlorotris(triphenylphosphine)-, 901
dimethyltetrakis(trimethylphosphine)-, 79
halide phosphetanate complexes, synthesis, IR spectra, 325
pentammine(dinitrogen)-, bromide, 1
Ruthenium(III)
diimine complex, reduction by titanium(III), kinetic study, 639

## S

Salicylaldehyde–diamine Schiff base complexes
copper(II), 713
Salicylaldehyde(3-hydroxypropylimine) complex
copper(II), 157
Salicylaldoximate complexes
nickel(II), 603
Salicylate complexes
neptunium(V), 667
Salicylidene hydrazone complexes
nickel(II), 21
Salicyl-2′-mercaptobenzaldimine complex
molybdenum(IV), 61
molybdenum(VI), 55, 61
Salicyl-2′-mercaptoethaldimine complex
molybdenum(VI), 55
Samarium(III)
ketone nitrate Schiff base complexes, synthesis, electronic, IR spectra, DTA study, electric conductance, magnetic moment, 67
Sauconite, 151
Scandium, book review, 1169
Scandium(III) phosphetanate, synthesis, IR spectrum, solubility, 1155
Schiff base complexes
cobalt(II), 575, 1271
cobalt(III), 517, 1271
copper(I), 1271
copper(II), 517, 575, 595, 713, 1271, 1357
dysprosium(III), 67
gadolinium(III), 67
holmium(III), 67
iron(II), 1271
lanthanum(III), 67
manganese(II), 1271
molybdenum(IV), 55, 257
molybdenum(VI), 55, 61
neodymium(III), 67
nickel(II), 239, 517, 1271, 1357
praseodymium(III), 67
rhodium(III), 517
samarium(III), terbium(III), 67
vanadium(IV), 575
yttrium(III), 67
zinc(II), 1271
Schubert plots, neptunium(V) complex formation, 667
Second coordination sphere
aluminium(III), gallium(III) alcohol water–halide complexes, 265
Selenide complexes, iron, 1165
Selenium, cluster compounds, 1307
Semicarbazone complexes
antimony(III), 661
copper(II), 991
manganese(II), 991
tin(IV), 681
Separation factors
berkelium(III)–californium(III), 1125
Sericite, 503
Sialon ceramics, NMR ($^{27}$Al, $^{29}$Si) spectra, 1267
Silica, 151
Silacycloalkenes, 394
Silanes, reactions with osmium carbonyl cluster compounds, 1220

Silaphosphene, 396
Silicates
  trimethylsilylation, 503
  zinc(II), 151
Silicon
  alkyl antimony complexes, synthesis, IR, NMR ($^1$H) spectra, 757
  chloride nickel(II) oxime complexes, 603
  cluster compounds, 1307
  double bonds, 390, 396, 406, 418, 420, 423, 429, 432
  heteropolyanions, 1071
  sialon ceramics, 1267
Siloxanes, 393
  polymers, conformational analysis, flexibility, potential function calculations, torsion angles, 1109
Siloxide complex,
  titanium(IV), 95
Silver(I)
  phosphetanate, 325
  porphyrin binuclear complexes, electronic spectra, spectrophotometric titrations, formation constants, kinetic study, 1077
Silylenes, 391
Sodium
  amalgam, 385
  crown ether hexafluorophosphate binuclear complex, synthesis, X-ray crystal structure, 675
  fluoride complex, potentiometric titration, formation constant, enthalpy, entropy of formation, 845
  oxide, 151
  phosphetanate, 325
  quinoline carboxylate complexes, synthesis, IR spectra, electric conductance, 240
  tungstate dihydrate, 25
Solid state electric conductance,
  iron(III) chloride thione complexes, 39
  iron(III) hydroxide oxide chemisorption, 223
Solubility, phosphetanates, 1155
Solvent effects, dysprosium(III) electronic spectra, 161
Solvent extraction
  actinide diketonate phosphine oxide complexes, 1125
  chromium(III) diketonate complex formation, 781
  copper(II) macrocyclic Schiff base complex, 1357
  copper(II) oxime complexes, 479, 821
  iron(III), 615
  nickel(II) oxime complexes, 479, 821
  tin(IV) chloride complexes, 313
Spectra, *see* CD, circularly polarised luminescence, electronic, electronic difference, ESR, IR, luminescence, mass, MCD, Mössbauer, NMR, NQR, ORD, PE, photoacoustic, Raman, XPE
Spectrophotometric titrations
  nickel(II) amide amine complexes, 551
  silver(I) porphyrin complexes, 1077
Spin traps, 631
Spiroborates, 589
Stability constants, *see* formation constants
Stannanes, reactions with osmium carbonyl cluster compounds, 1220
Stereochemical non-rigidity, gold cluster compounds, 1289
Stibine complexes
  iron(0), 757
Strontium
  phosphetanate, 325
Structural stability index, polyanions, 341
Styrene, 1051
Subhalides, boron, 369
Substitutions
  cobalt(III) complex, 895
  rhodium(III) amine arsine complexes, 811
Succinate complexes
  calcium, 545
Sulphate complexes
  copper(II), 641, 1135, 1237
  lanthanum(III), 451
  manganese(III), 599
2-Sulphatophenyl(*t*-butyl)nitrone, 631
Sulphido, *see* thio
Sulphite complex
  cobalt(III), 895
Sulphonate complexes
  nickel(II), 1329
Sulphoxide complexes
  tin(II), 627
Sulphur
  cluster complexes, 1279, 1307, 1321
  double bonds, 396
Sulphur dioxide
  chemisorption on iron(III) hydroxide oxide, 223
  reaction with cluster compounds, 1307
Sulphur–nitrogen ligand gold(III) complex, 1365
Surface vector harmonics, cluster compounds, 1299

## T

Tantalum, cluster compounds, 1307
Tartrate complexes
  niobium(V), 1029
Taurine complexes
  nickel(II), 1329
Technetium, book review, 763
Tellurium(II)
  thione complex, synthesis, X-ray crystal structure, 921
Tellurium(IV) oxide, 921
Template reaction
  molybdenum(II) binuclear complex, 257
Terbium(III)
  carboxylate pyridine complex, Pfeiffer effect of azoles, luminescence, circularly polarised luminescence spectra, formation constants, 1087
  ketone nitrate Schiff base complex, synthesis, electronic, IR spectra, DTA study, electric conductance, magnetic moment, 67
Tetrachlorotetraborane(4), 199
Tetraethylthiourea complexes
  molybdenum(0), 235
Tetrafluorobenzobarrelene complexes,
  rhodium(I), 213
Tetrafluoroborate complex
  copper(II), 1135
Tetrahydroborate, *see* borohydride

Tetrahydrofuran complexes
magnesium, 45
thorium(IV), uranium(IV), 107
Tetramethylene compound
platinum(II), 87
2,2,5,5-Tetramethylhex-3-yne, 271
*N,N,N',N'*-Tetramethyl-1,4-phenylenediamine complexes, copper(II), 291
Tetraethylthiourea complexes
molybdenum(0), 235
Tetralin complexes
rhodium(I), 497
Tetra(3-*N*-methylpyridinium)porphyrinate complexes
silver(I), 1077
Tetranitromethane, 297
2,2,6,6-Tetramethylpiperidine complex, cadmium(II), 509
Tetraphenylcyclopentadienone, 1183
Tetraphenylporphyrinate complexes
iron(II), 651
palladium(II), platinum(II), 879
2,3,5,6-Tetra-2-pyridylpyrazine, synthesis and cobalt(III) complex, 635
Tetrasulphophthalocyanine complexes, vanadium(IV), zinc(II), 129
*N,N,N',N'*-Tetra(2,3,5,6-tetrafluorophenyl)diaminoethane, synthesis, platinum(II) complex, 753
Tetra(3-tolyl)porphyrinate complexes, iron(III), 651
Tetra(4-tolyl)porphyrinate complexes
germanium(II), 889
iron(III), 651
tin(II), 889
Tetra(4-trimethylammoniumphenyl)porphyrinate complexes, silver(I), 1077
TGA studies
cadmium(II) azole halide complexes, 619
copper(II) alkoxide oxime sulphate complexes, 641
copper(II) aminopolyphosphonate complexes, 527
iron(II) aminopolycarboxylate dinitrogen complex, 623
iron(III) arsine oxide water complex, 911
lanthanum(III) sulphate complex, 451
mercury(II) azole halide complexes, 619
nickel(II) alkoxide oxime complexes, 641
nickel(II) aminopolyphosphonate complexes, 527
tin(IV) aminopolycarboxylate complexes, 1099
zinc(II) azole halide complexes, 619
Thallium(I)
2,4-pentanedionato-, reaction with cyclometallated compounds, 1044
pentafluorobenzoate, 753
2-Thienylpyrazole, 1046
2-Thienylpyridine, 1044, 1046, 1051
Thiiranes, 410
Thin layer chromatography, *see* TLC
Thio complexes
chromium(III), 775
iron, 1165
osmium, 1200, 1220
osmium(I), 1183, 1214
palladium(II), 775
tungsten(V), 25, 1021
Thiocarbonyl complexes
osmium, 1200
Thiocarbonylbis(salicylidenehydrazone) complexes, nickel(II), 21
Thiocyanate, oxidation by cobalt(III), 191
Thiocyanate complexes
cluster, 1307
cobalt(II), 251, 357
configurational isomers, 1
copper(II), 357, 921
gold(0, I), 1289
iron(II), 911, 997
molybdenum(IV), 347
molybdenum(V), 907
nickel(II), 317, 983
palladium(II), 701
platinum(II), 735
ruthenium(II), 1
Thiocyanogen, reaction with cyclometallated complexes, 1051
Thiocyanogen complex
iron(II), 997
Thioether complexes
conformational isomers, 331
nickel(II), 523, 1329
rhenium(I), 331
Thiols, reactions with osmium carbonyl cluster compounds, 1220
Thiol complexes
nickel(II), 969
Thiolate complexes
aluminium(III), 871
bismuth(III), 71
chromium(III), 775
cluster, 1307
cobalt(III), 517
copper(I), 535
copper(II), 517, 595
gallium(III), 871
gold(III), 1365
indium(III), 871
iron(0), 1065
lead(II), mercury(II), 1247
molybdenum(IV), 61
molybdenum(VI), 55, 61
nickel(II), 517, 839, 969, 1227
osmium, 1178, 1183, 1201, 1220
palladium(II), 775, 969, 1227
rhodium(III), 517
titanium(IV), 505
Thione complexes
cobalt(II), (III), 1271
copper(I), (II), iron(II), 1271
iron(III), 39
manganese(II), 1271
molybdenum(0), 235
nickel(II), 1271
tellurium(II), 921
zinc(II), 1271
Thiophenolate complexes
lead(II), mercury(II), 1247

Thiosalicylate complexes
gallium(III), indium(III), 871
Thiosemicarbazone complexes
antimony(III), 661
cadmium(II), 1237
cobalt(III), 1135
copper(II), 921, 991, 1135, 1237
manganese(II), 991
mercury(II), 1237
nickel(II), 1135
tin(IV), 681
zinc(II), 1237
Thiourea complexes
molybdenum(0), 235
Thioxanthate complexes
iron(I), 1065
Thiuram disulphides, iodine complexes, formation constants, enthalpy, entropy of formation, 1241
Thorium(IV)
chloride porphyrin complexes, synthesis, electronic, IR, NMR ($^1$H) spectra, 107
tetrachloride, 107
Three coordination, lead(II), mercury(II) thiophenolate complexes, 1247
Tin
cluster compounds, 1307, 1321
double bonds, 395, 398, 418
Tin(II)
amide complex, synthesis, IR, NMR ($^1$H) spectra, electric conductance, 627
dichloro(iodo)-, platinum(II) complexes, 735
porphyrin iron(0) complexes, synthesis, electronic, IR, Mössbauer, NMR ($^1$H) spectra, X-ray crystal structure, 889
sulphoxide complex, synthesis, IR spectrum, electric conductance, 627
trichloro-, molybdenum(IV) complex, 765
Tin(IV)
alkoxide chloride complexes, synthesis, IR spectra, 21
alkyl aryl chloride compounds, preparation, reactivity with antimony(V), boron compounds, NMR ($^{11}$B, $^{119}$Sn) spectra, 957
alkyl aryl dithiophosphates, synthesis, IR, NMR ($^1$H, $^{13}$C, $^{31}$P, $^{119}$Sn) spectra, 485
alkyl iron(−II) complex, synthesis, IR, mass, NMR ($^1$H) spectra, 757
alkyl phenolate semicarbazone thiosemicarbazone complexes, synthesis, IR, mass, Mössbauer, NMR ($^1$H, $^{13}$C) spectra, X-ray diffraction, 681
aminocarboxylate complexes, synthesis, IR spectra, potentiometric titrations, TGA, X-ray crystal structure, 1099
chloride complexes, octylammonium salts, synthesis, IR spectra, electric conductance, solvent extraction, 313
chlorotrimethyl-, 957
chlorotriphenyl-, 957
dichlorodimethyl-, 957
dichlorodiphenyl-, 957
dichloro(octaethylporphyrin)-, 889
dichloro(tetra-4-tolylporphyrin)-, 889
tetrachloro-, 939, 957
tetraethyl-, 297
tetramethyl-, 957
tetraphenyl-, 957
trichloro(methyl)-, 957
trichloro(phenyl)-, 957
Titanium, cluster compounds, 1307
Titanium(III)
hydroxide water complexes, oxidation by ruthenium(III), kinetic study, 639
2-pyridyl compounds, 1041
Titanium(IV)
alkylamide chloride phenolate complexes, synthesis, IR, NMR ($^1$H, $^{13}$C) spectra, X-ray crystal structure, 1121
arsine chloride phosphine thiolate complexes, synthesis, IR, NMR ($^1$H) spectra, X-ray crystal structure, 505
chloride cyclopentadienyl xanthate complexes, synthesis, IR, NMR ($^1$H) spectra, 695
cyclopentadienyl halide complexes, NMR ($^{47}$Ti, $^{49}$Ti) spectra, 897
cyclopentadienyl oxoquinolinate complexes, synthesis, IR, NMR ($^1$H) spectra, electric conductance, 883
cyclopentadienyl(trichloro)-, 695
dichlorobis(indenyl)-, 883
phenolate amine chloride diimine complexes, synthesis, IR, mass spectra, 125
phosphetanoate, synthesis, IR spectrum, 1155
siloxide complex, synthesis, X-ray crystal structure, 95
tetrachloro-, 505
tetrakis(dimethylamido)-, 1121
TLC, copper(II) Schiff base complexes, 713
4-Toluidine, 117
4-Toluidine complexes
copper(II), 291
2-(4′-Tolyl)-4,5-dimethyltriazole 1046, 1051
Torsion angles, polysiloxanes, 1109
Torsional frequencies, phosphazenes, 867
Tri-4-anisylphosphine complexes gold(0, I), 1289
rhenium(III), 1059
1,4,7-Triazaheptane complexes
manganese(I), 347
Triazene complexes
cobalt(III), 79
osmium(I), 1196
zirconium(IV), 79
Tribromide complex
copper(II), 1233
2,4,6-Tri-*t*-butylphenoxide complexes, titanium(IV), zirconium(IV), 1121
Tri-*n*-butylphosphine, reaction with cyclometallated complexes, 1044
Tributylphosphine complexes
platinum(II), 231
Trichloroacetic acid, effect on rhodium(III) substitution kinetics, 811
Trichlorostannate(II) complex
molybdenum(IV), 765

Tricyclohexylphosphine complexes
gold(0, I), 1289
palladium(II), platinum(II), 735
Triethylamine, 1194
Triethylphosphine complexes
molybdenum(II), 347
osmium(0), 1217
palladium(II), 1048
platinum(II), 373
Trifluoroacetonitrile, 1216
Trifluoromethyl compound
platinum(II), 87
Tri-4-fluorophosphine complexes
gold(0, I), 1289
Trimethylacetate complexes
tungsten(II), 759
Trimethylamine
formation in amide oxidation by manganese(III), 977
reaction with osmium carbonyl cluster compounds, 1194
Trimethylamine-*N*-oxide, 1043
reactions with osmium carbonyl cluster compounds, 1177
Trimethylphosphine complexes
cobalt(I), (III), 79
molybdenum(II), (III), (IV), 347
nickel(II), 317
osmium(0), 1216
palladium(II), 1025
rhenium(V), 1083
rhodium(III), 79
ruthenium(0), 1255
ruthenium(II), 79, 1255
Trimethylsilylation silicate mineral, 503
Trimethylsilylazide, 1196
Trimethylsilylmethyl compounds
nickel(II), 317
palladium(II), 1025
Trimethylstannane, 1220
Tri-*n*-octylamine complex
tin(IV), 313
Tri-*n*-octylammonium salts, 313
Trioctylphosphine oxide
americium(III), berkelium(III), californium(III), curium(III), 1125
iron(III) solvent extraction, 615
Triphenylarsine, reaction with cluster compounds, 1307
Triphenylarsine complexes
platinum(II), 373
ruthenium(II), 325
Triphenylmethyl cation, 1185
Triphenylphosphine complexes
gold(0, I), 567, 1289
gold(I), iridium(I), 213
nickel(II), 317
osmium, 1218
palladium(II), 117, 735
platinum(II), 231, 735
rhenium(III), 1059
rhodium(I), 213, 1151
ruthenium metallaborane, 901
ruthenium(0), 567
ruthenium(II), 325
Triphenylphosphine, reactions
cluster compounds, 1307
cyclometallated compounds, 1044
rhodium(I) aldehyde complex, 1151
Triphenylphosphite, 1048
*Triphenylsilane*, 1220
Triphenylsilyl, osmium, 1204
Triphenylstibine, reaction with cluster compounds, 1307
2,4,5-Tri-2-pyridyloxazole, 635
1,1,1-Tris(diphenylphosphinomethyl)ethane complexes
rhenium(I), 353
1,2,4-Trithia-3-azabut-2-ene compound, gold(III), 1365
2,4,6-Trithiaheptane complexes
rhenium(I), 331
Tri-4-tolylarsine oxide complexes
iron(II), (III), 911
Tri-4-tolylphosphine complexes
gold(0, I), 1289
Tungstate(VI), 607, 1001
sodium, dihydrate, 25
Tungsten, cluster compounds, 1307
Tungsten(0)
carbonyl cyclopentadienyl mercury(II) complexes, Mössbauer spectra, 365
distibene complex, 417
Tungsten(II)
carboxylate binuclear compounds, synthesis, X-ray crystal structure, 759
distibene complex, 417
Tungsten(III)
diethyltetrakis(dimethylamido)di-, 759
Tungsten(IV)
cyanide hydroxide oxo complexes, photochemical preparation, electronic spectra, 743
octacyano-, photochemical substitution, 743
Tungsten(V)
dithiocarbamate oxo thio binuclear complexes, synthesis, electronic, IR spectra, magnetic moments, 25
dithiocarbamate thio binuclear complexes, synthesis, electronic, IR spectra, 1021
Tungsten(VI)
alkoxide, binuclear complex, synthesis, X-ray crystal structure, 1033
polyanions, 191, 341, 381, 1161
cyclohexanol oxidation catalysis, effects of air, charcoal, dioxygen, hydrogen peroxide, 607
light, X-ray scattering, Raman spectra, 1001
Pfeiffer effect, CD, electronic, electronic difference, IR spectra, 1071

## U

Undecahydroundecaborate(2), 199
Uranium(III)
borohydride ether complexes, NMR ($^{1}H$, $^{11}B$) spectra, 457
Uranium(IV)
borohydride ether complexes, NMR ($^{1}H$, $^{11}B$) spectra, 457

chloride porphyrin complexes, synthesis, electronic, IR, NMR ($^1$H) spectra, 107
tetrachloride, 107
Uranium(VI)
dioxo aminopolycarboxylate peroxo complexes, potentiometric titrations, formation constants, 469
dioxo crown ether complex, X-ray crystal structure, 143
dioxo hydroxide water binuclear complex, X-ray crystal structure, 143
Uranyl, *see* uranium(VI), dioxo
UV spectra, *see* electronic spectra

V

Vanadium(III) phosphetanate, synthesis, IR, NMR ($^{31}$P) spectrum, magnetic moment, 1155
Vanadium(IV)
oxoapocytochrome-*c* phthalocyanine complex, formation, CD, electronic difference spectra, 129
oxo carboxylate Schiff base complex, synthesis, electronic, IR spectra, electric conductance, magnetic moment, 575
Vanadium(V)
fluoride hydroxide oxo peroxide complexes, synthesis, IR, Raman spectra, 287
Vinyl complexes, osmium(I), 1183, 1188, 1205, 1217
Vinylidene complexes, osmium(I), 1184, 1190, 1219
1-Vinylimidazole complexes
platinum(IV), 121
2-Vinylpyridine, 1039, 1041, 1044, 1047
Viscosity, copper(II), nickel(II) alkoxide oxime sulphate complexes, 641

W

Wang–Parr, electronegativity scale, 853
Water complexes
aluminium(III), 265
cadmium(II), 303
chromium(I), 247
chromium(III), 183
cobalt(II), 183, 1017
cobalt(III), 895, 1017
copper(II), 183
gallium(III), 265
iridium(III), (IV), 1013
iron(II), 183
iron(III), 183, 911
manganese(II), 183, 963
molybdenum(IV), 257
molybdenum(VI), 55
nickel(II), 689, 693, 1017
ruthenium(II), 183
titanium(III), 639
uranium(VI), 143
zinc(II), 303, 1017

X

Xanthate complexes
arsenic(III), 721
iron(I), 1065
titanium(IV), 695
XPE spectra, nickel(II) carboxylate phosphine and water complexes, 963
X-ray crystal structures
alkylammonium salts, 535
bismuth(III) alcohol mercaptide complex, 71
cadmium(II) carboxylate *N*-oxide water complex, 303
cobalt(I) azide carbonyl phosphine complex, 79
cobalt(III) alkyl azide phosphine complex, 79
copper(I) rhenium(III) cyclopentadienyl hydride iodide complex, 749
copper(II) alcohol amine azole nitrate complex, 113
copper(II) chloride complex, 771
copper(II) thiolate complexes, 535
gold(0, I) ruthenium(0) carbonyl hydride phosphine cluster complex, 567
iridium(I) platinum(0) carbonyl cyclopentadienyl cluster complex, 1093
iron(0) carbonyl tin(II) complex, 889
iron(III) carboxylate porphyrin complex, 651
iron(III) magnesium chloride ether complex, 45
lead(II) thiophenolate complex, 1247
lithium carborane amine complex, 307
mercury(II) thiophenolate complexes, 1247
molybdenum(IV) chloride methoxide polynuclear complexes, 475
molybdenum(IV) chlorostannate(II) cyclopentadienyl hydride complex, 765
molybdenum(VI) diimine oxo peroxide complex, 377
nickel(II) alkyl phosphine complex, 317
nickel(II) amine thiolate polynuclear complexes, 839, 1227
nickel(II) carboxylate pyridine water binuclear complex, 689
nickel(II) diselenocarbamate dithiolate complex, 433
nickel(II) thiol polynuclear complex, 969
osmium(II) bromide isocyanide complex, 385
platinum(II) alkyl arsine chloride phosphine complex, 373
platinum(II) amine pyridine complex, 753
rhenium(III) bromide carbonyl phosphine complex, 1059
rhenium(III) copper(I) cyclopentadienyl hydride iodide complex, 749
rhenium(III) cyclopentadienyl complex, 771
rhenium(V) oxo phosphine complex, rhenium(VII) tetraoxo salt, 1083
ruthenium borane phosphine complex, 901
ruthenium(0) alkene phosphine complex, 1255
ruthenium(II) alkyl hydride phosphine complex, 1255
sodium crown ether hexafluorophosphate binuclear complex, 675
tellurium(II) thione complex, 921
tin(II) porphyrin iron(0) complex, 889
tin(IV) aminopolycarboxylate complex, 1099
titanium(IV) alkylamide phenolate complex, 1121
titanium(IV) arsine chloride thiolate complex, 505
titanium(IV) soloxide complex, 95
tungsten(II) carboxylate binuclear complex, 759
tungsten(VI) alkoxide binuclear complex, 1033

uranium(VI) dioxo hydroxide water binuclear complex, 143
uranium(VI) dioxo crown ether complex, 143
zinc(II) water complex nicotinate, 303
X-ray diffraction
amide halide complexes, 99
iron(II) arsine oxide complexes, 911
iron(II) thiocyanate thiocyanogen complex, 997
iron(III) arsine oxide complexes, 911
tin(IV) alkyl phenolate semicarbazone thiosemicarbazone complexes, 681
zinc(II) silicates, 151
X-ray scattering, isopolyanions, 1001

## Y

Yttrium, book review, 1169
Yttrium(III)
ketone nitrate Schiff base complexes, synthesis, electronic, IR spectra, DTA study, electric conductance, 67

## Z

Zinc, 347
oxidation by iridium(IV), 1013
Zinc(0)
amine ammonia iron complexes, synthesis, IR, Raman spectra, force constants, 1333
Zinc(II)
aminopolyphosphonate complexes, synthesis, 527
apocytochrome-*c* phthalocyanine complex, formation, CD, electronic difference spectra, 129
azole halide complexes, synthesis, IR, NMR ($^1$H, $^{13}$C) spectra, TGA study, 619
chloride thiosemicarbazone complex, synthesis, IR spectrum, antifungal activity, 1237
diketonate ketophenol complexes, synthesis, IR, NMR ($^1$H) spectra, 1017
heteropolytungstate, 1071
hydrazone ketone pyridine complex, synthesis, IR, NMR ($^1$H, $^{13}$C) spectra, X-ray crystal structure, 281
oxide, 151
phosphetanate, synthesis, IR spectrum, 1155
pyridine Schiff base thione complex, synthesis, electronic, IR spectra, antimicrobial activity, 1271
quinone water complexes, synthesis, electronic, IR spectra, 729
separation from $Cu^{2+}$, $Ni^{2+}$, 939
silicates, synthesis, X-ray diffraction, 151
water complex, nicotinate salt, X-ray crystal structure, 303
Zirconium(IV)
alkyl azide cyclopentadienyl complex, synthesis, IR, NMR ($^1$H) spectra, 79
alkyl cyclopentadienyl triazene complex, synthesis, IR, NMR ($^1$H, $^{13}$C) spectra, 79
alkylamide phenolate complexes, synthesis, IR, NMR ($^1$H, $^{13}$C) spectra, 1121
aryl cyclopentadienyl triazene complex, synthesis, IR, NMR ($^1$H) spectra, 79
bis(cyclopentadienyl)diphenyl-, 79
chloride cyclopentadienyl phenolate complexes, synthesis, electronic, IR, NMR ($^1$H) spectra, 611
cyclopentadienyl oxoquinolinate complexes, synthesis, IR, NMR ($^1$H) spectra, electric conductance, 883
dichlorobis(indenyl)-, 883
tetrakis(dimethylamido)-, 1121

*Polyhedron* Vol. 4, No. 1, p. v, 1985
Pergamon Press Ltd. Printed in Great Britain

# ERRATUM

M. J. Freeman, A. D. Miles, M. Murray, A. G. Orpen and F. G. A. Stone, The synthesis and X-ray crystal structure of the hexanuclear metal cluster complex $[Ir_3Pt_3(\mu\text{-}CO)_3(CO)_3(\eta\text{-}C_5Me_5)_3]$. *Polyhedron* 1984, **3**, 1093–1097.

The publishers regret that one line was omitted from and another repeated in the introductory paragraph on p. 1093 of the published version of the above paper. Lines 15–17 of that paragraph should read: "... the dimetal salts $[IrPt(H)(R)(\mu\text{-}H)_2(PEt_3)_4][BPh_4]$(R = H or Ph).[4] Recently we have employed $[Rh(CO)_2(\eta\text{-}C_5Me_5)]$ as a reagent for obtaining..." The corrected p. 1093 is reprinted overleaf.

*Polyhedron* Vol. 3, No. 1, pp. 1–8, 1984
Printed in Great Britain.

0277–5387/84 $3.00 + .00
© 1984 Pergamon Press Ltd.

# STUDIES OF THE REACTIONS OF THIOCYANATE ION WITH PENTAMMINE DINITROGEN RUTHENIUM(II) DIBROMIDE AT DIFFERENT TEMPERATURES

**S. K. S. YADAV and U. C. AGARWALA***
Department of Chemistry, Indian Institute of Technology, Kanpur 208 016, India

(*Received* 13 *October* 1982; *accepted* 31 *May* 1983)

**Abstract**—The salts of the linkage isomers of thiocyanatopentammineruthenium(III) $[Ru(NH_3)_5(NCS)]^{2+}$, $[Ru(NH_3)_5(SCN)]^{2+}$ and dithiocyanatotetrammineruthenium(III) $[Ru(NH_3)_4(NCS)_2]^{+}$ along with those of tetrathiocyanatodiammineruthenate(III) $[Ru(NH_3)_2(SCN)_4]^{-}$ have been synthesized. The insoluble polymeric complex $[Ru(NH_3)_2(SCN)_2]_n$ has also been prepared. The compounds have been characterized by chemical analyses, spectral (IR, UV and visible), magnetic susceptibility, conductivity, cyclic voltammetry and chromatography studies.

Although the procedures for the syntheses of the species $[Ru(NCS)_6]^{3-}$ and $[Ru(NH_3)_5(NCS)]^{2+}$ have been reported in the literature,[1–3] those of the intermediate species and their isomers having two to five thiocyanate ions coordinated to ruthenium(III) are totally missing. Furthermore, since the modes of linkage of thiocyanate ion with ruthenium ammines are still the subject of investigation,[2,3] it was considered worthwhile to study the reactions of $SCN^-$ with ruthenium in its different oxidation states and under different experimental conditions. Recently[4,5] we have reported the reactions of $NH_4SCN$ with $[Ru(NH_3)_5X]X_2$ (X = Cl, Br, I) at different temperatures. This paper reports the results of the reactions of $[Ru(NH_3)_5N_2]Br_2$ with $NH_4SCN$ at different temperatures.

## EXPERIMENTAL

All the chemicals used were of chemically pure or Analar grade.

*Author to whom correspondence should be addressed.

(A) $[Ru(NH_3)_5N_2]Br_2$: was prepared by the literature method.[6]

(B) *Reactions of* $[Ru(NH_3)_5N_2]Br_2$ *with* $NH_4SCN$ *in the range* 60–70°C

(B1) *Preparations of* $[Ru(NH_3)_5NCS]Br_2$, $[Ru(NH_3)_5SCN]Br_2$ *and* $[Ru(NH_3)_4(NCS)_2][Ru(NH_3)_2(SCN)_4]$. Approximately 1.5 g of $NH_4SCN$ was added to 20 $cm^3$ of an aqueous solution of $[Ru(NH_3)_5N_2]Br_2$ (0.2 g). On stirring the mixture for about 3 hr at 65°C, the colour of the solution changed from yellow to reddish–violet. It was filtered to remove any insoluble impurities formed during the reaction. The slow addition of 3–4 $cm^3$ of conc. HBr to the filtrate changed its colour to violet. On keeping it for a few minutes either at room temperature or at 0°C, a black compound *B* precipitated out which was separated by centrifugation and washed several times with alcohol to remove unreacted $NH_4SCN$ and finally with ether. It was dried under vacuum. Similar reactions were repeated at a number of different temperatures between 60° and 70°C. The compound *B* was found to be a mixture of a number of complexes, which were separated as follows: 0.12 g of *B* was stirred in 100 $cm^3$ of water for some time and centrifuged. The centrifugate *B*1 was used for the

separation of other compounds. The insoluble residue which is paramagnetic, is under study.

(B2) *N-Thiocyanatopentammineruthenium(III) bromide*, $[Ru(NH_3)_5(NCS)]Br_2$. The centrifugate *B*1 was passed through an anion exchange resin (Dowex 1-X8) column in the chloride form at the rate of 0.5 $cm^3$/min. The column was washed with water until the eluate was colourless. The eluate was concentrated to about one third of its volume either at room temperature or in a lyophilizer. Two to three centimeters of conc. HBr was added to the resulting concentrate to precipitate the dark reddish bromide salts of the cation species. It was centrifuged and the residue (~100 mg) was redissolved in the minimum amount of distilled (*ca.* 25 $cm^3$) and passed through a column (100 × 1 cm) of Sephadex G-10. The column was eluted with a solution of HBr (*ca.* $10^{-3}$ M) at the rate of 3–4 $cm^3$/hr whereupon three bands appeared on the column. At higher elution rate, the bands did not separate because of the diffusion of the bands over the column. The eluates from the three bands were separately collected. (When $10^{-3}$ M HBr solution was used as eluant, the third band moved very slowly over the column. However, by using $10^{-2}$ M HBr solution the rate of the movement became quite fast. It is not possible to use $10^{-2}$ M HBr solution to eluate all the three bands because of the precipitation of $[Ru(NH_3)_5(NCS)]Br_2$ on the column itself.) Concentrated HBr (~2 $cm^3$) was added to the eluate of the first band whereby a reddish compound was precipitated out in near quantitative yield. It was centrifuged, washed with a little cold water, ethanol, ether and dried in vacuum. It was analysed for $[Ru(NH_3)_5(NCS)]Br_2$ (yield, ~60 mg).

(B3) *S-Thiocyanatopentammineruthenium(III) bromide*, $[Ru(NH_3)_5(SCN)]Br_2$. From the eluate of the second band the cationic species $[Ru(NH_3)_5(SCN)]^{2-}$ could not be precipitated out by adding concentrated acid, probably because of very high solubility or highly dilute solution of the complex dissolved therein. It (*ca.* 25 $cm^3$) was therefore concentrated nearly to dryness in a lyophilizer (*ca.* 2 $cm^3$) and approx. 1 $cm^3$ of conc. HBr was added to it whereby a reddish violet precipitate appeared. It was centrifuged, washed with a little cold (0°C) ethanol, ether and dried under vacuum. It was analysed for $[Ru(NH_3)_5(SCN)]Br_2$ (yield, ~8 mg).

(B4) *Dithiocyanatotetraammineruthenium(III) bromide*, $[Ru(NH_3)_4(NCS)_2]Br$. The compound in the third band could also not be precipitated by adding conc. HBr because of its high solubility in water. It (*ca.* 25 $cm^3$) was, therefore, concentrated in a lyophilizer nearly to dryness (*ca.* 2 $cm^3$) and 1 $cm^3$ of conc. HBr was added to it whereupon the complex was partially precipitated on keeping the solution at 0°C for about 2 hr. The precipitate was centrifuged, washed with a little (3–4 drops) cold (0°C) ethanol and finally with ether. Its washing should be carried out very carefully because of its high solubility in ethanol. It was dried under vacuum and analysed for $[Ru(NH_3)_4(NCS)_2]Br$ (yield, ~30–40 mg).

(B5) *Preparation of* $(H_3O)^+[Ru(NH_3)_2(SCN)_4]^-$. The centrifugate *B*1 was passed through a cation exchange resin (Dowex 50W × 10) column in the $H^+$ form at the rate of 0.5 $cm^3$/min. The column was washed with water until the eluate was colourless. The eluate was dried in a lyophilizer. The dried solid mass was partially dissolved in dry ethanol. The alcoholic solution was centrifuged and the centrifugate was dried in a lyophilizer. The residue was partially redissolved in dry ethanol and the mixture was centrifuged. The centrifugate was redried. The processes of drying, partial dissolving and centrifuging were repeated three to four times whereby it was possible to separate pure acid $(H_3O)^+[Ru(NH_3)_2(SCN)_4]^-$. It appears that the acid was quite stable in aqueous and alcoholic solution but on drying it slightly decomposes to give an insoluble species which could not be conclusively characterized.

(B6) *Tetraphenylarsonium tetrathiocyanatodiammineruthenate(III)* $[As(C_6H_5)_4][Ru(NH_3)_2(SCN)_4]$. The compound was precipitated by adding $[As(C_6H_5)_4]Cl$ to a concentrated aqueous solution of the acid, $(H_3O)^+[Ru(NH_3)_2(SCN)_4]^-$ obtained by the procedure B5. It was centrifuged and washed successively with a little water, alcohol and finally with ether. It was dried under vacuum and analysed.

(C) *Reactions of* $[Ru(NH_3)_5N_2]Br_2$ *with* $NH_4SCN$ *under refluxing conditions.* 1.5 g of $NH_4SCN$ was added to 20 $cm^3$ of an aqueous solution of $[Ru(NH_3)_5N_2Br_2$ (0.2 g). The mixture was refluxed for about 10 hr whereby a black compound, insoluble in almost all the solvents, was precipitated out. It was centrifuged, washed with an excess of water, alcohol and finally with ether. It was analysed for $[Ru(NH_3)_2(SCN)_2]_n$.

(D) *Reaction of* $[Ru(NH_3)_5N_2]Br_2$ *with* $NH_4SCN$ *at room temperature.* The procedure for the reaction was the same as that given in (B). The rate of reaction was so slow that even after running the reaction for three days, the colour of the reaction mixture was not deep violet and a small amount of $[Ru(NH_3)_5N_2]Br_2$ was left in the solution. The violet coloured solution on treating it by the

procedure given in (B), yielded the same series of compounds but in different yields as those obtained by the reactions carried out between 60–70°C (see Procedure (B)).

(E) *Preparation of the related compounds*

(E1) *Preparation of* $[Ru(NH_3)_5(NCS)]X_2$ (X = I, $ClO_4$, $NO_3$, $(C_6H_5)_4B$). These salts were obtained by the addition of HI, $HClO_4$, $NaNO_3$ or $Na[B(C_6H_5)_4]$ solutions to a conc. solution of $[Ru(NH_3)_5NCS]Br_2$ whereby the corresponding salts of the cation $[Ru(NH_3)_5(NCS)]^{2+}$ were precipitated out. These were centrifuged, washed with a little cold water, alcohol, ether and dried under vacuum. Precipitation of all these species was nearly quantitative.

(E2) *Preparation of* $[Ru(NH_3)_5(NCS)]Cl_2$, $[Ru(NH_3)_5(SCN)]Cl_2$ *and* $[Ru(NH_3)_4(NCS)_2]Cl$. The chloride salts of the cations $[Ru(NH_3)_5(NCS)]^{2+}$, $[Ru(NH_3)_5(SCN)]^{2+}$ and $[Ru(NH_3)_4(NCS)_2]^{+}$ could not be precipitated out by adding HCl or any other chlorosalts to the corresponding bromide salts. These salts were however prepared by the method that follows. The centrifugate *B*1 was passed through a column of an anion exchange resin (Dowex 1-X8) in the chloride form at the rate of 0.5 $cm^3$/min and the column was washed with water to a colourless eluate. It was concentrated in a lyophilizer to about one fourth of its volume and the concentrate was passed through a Sephadex G-10 column in the same way as described in (B2) except that $10^{-2}$ M HCl was used as an eluant. The order of the three bands which appeared on the column was the same as that when HBr was used as eluant. The eluates from the three bands were collected separately and dried in a lyophilizer. The complexes in the first, second and third bands were characterised as $[Ru(NH_3)NCS)]Cl_2$, $[Ru(NH_3)_5(SCN)]Cl_2$ and $[Ru(NH_3)_4(NCS)_2]Cl$, respectively.

(E3) *Alternate method for the syntheses of* $[Ru(NH_3)_5(NCS)]X_2$ $[Ru(NH_3)_5(SCN)]X_2$ *and* $[Ru(NH_3)_4(NCS)_2]X$ (X = I, $ClO_4$). These salts could also be synthesized by the same procedure as those given in (B2) except that the solutions of the cationic salts, obtained by passing the centrifugate (B1) through the anion exchange resin in the appropriate form, were concentrated and the corresponding cationic salts were precipitated from them. The solutions of these salts were passed through Sephadex G-10 column and the eluates from the bands were concentrated in lyophilizer and the corresponding salts were precipitated by the addition of HI or $HClO_4$.

(E4) *Precipitation of* $[Ru(NO_3)_5(NCS)]I_2$. Deuteriated complex was freshly prepared by dissolving a portion of $[Ru(NH_3)_5(NCS)]I_2$ in deaerated $D_2O$ and stirring the solution under argon for about an hour. A small amount of KI was added to the solution whereby a black compound precipitated out which was centrifuged, washed with 3–4 drops of ethanol and finally with ether. It was dried under vacuum and its IR spectrum was taken immediately. The process of separation, washing and drying was carried out very fast, otherwise there was a possibility of exchanging deuterium of $ND_3$ with hydrogen of atmospheric water.

Attempts to prepare $[Ru(ND_3)_5(SCN)]I_2$ and $[RU(ND_3)_4(NCS)_2]I$ failed because of their very high solubilities in water and ethanol.

(F) *Reactions in the absence of air*. The reactions of $NH_4SCN$ with $[Ru(NH_3)_5N_2]Br_2$ did not take place in the absence of air or oxygen at any temperature (below 80°C).

*Physical and chemical measurements*

Carbon, hydrogen and nitrogen in the complexes were analysed by the microanalytical laboratory of the Indian Institute of Technology, Kanpur, India. The sulphur, halides, $ClO_4^-$, $NO_3^-$ etc. were analysed by the methods given elsewhere.[4] The results are given in Table 1.

The procedures for the IR, the electronic spectra, the magnetic, the conductivity, the ion-exchange and the electrochemical studies were carried out by the methods given in the literature.[4]

*Chromatographic studies*

Sephadex G-10 and Sephadex LH-20 columns were used for the separation of the different species. Sephadex G-10 was allowed to swell overnight in water and a column (100 × 1 cm) was prepared by the swelled Sephadex G-10. Sephadex LH-20 column was prepared by the same procedure as that given for Sephadex G-10 column except that LH-20 was allowed to swell in ethanol.

## RESULTS AND DISCUSSION

All the complexes except the polymeric species $[Ru(NH_3)_2(SCN)_2]_n$ are highly soluble in water and relatively less soluble in alcohol. However, the complex $[As(C_6H_5)_4][Ru(NH_3)_2(SCN)_4]$ is highly soluble in alcohol but relatively less soluble in water. It is interesting to note that the reactions between $[Ru(NH_3)_5N_2]^{2+}$ and $NH_4SCN$ did not take place in the absence of air or oxygen suggesting that $NH_4SCN$ is incapable of reacting in +2 oxidation state. Possibly the ruthenium got

Table 1.

| Compound | Analytical Data, Found (Calc) (%) | | | | | | | $\mu_{eff}$ (BM) |
|---|---|---|---|---|---|---|---|---|
| | C | H | N | $S_{total}$ | $S_{cation}$ | $X^-_{total}$ | $X^-_{anion}$ | |
| 1 | 2 | 3 | 4 | 5 | 6 | 7 | 8 | 9 |
| $[Ru(NH_3)_5\underline{N}CS]I_2$ | 2.8 (2.4) | 3.4 (3.0) | 17.5 (16.8) | 6.8 (6.4) | 6.3 (6.4) | 51.8 (51.0) | 49.6 (51.0) | |
| $[Ru(NH_3)_5\underline{N}CS]Br_2$ | 3.1 (2.9) | 4.0 (3.7) | 21.4 (20.8) | 8.2 (7.9) | 7.6 (7.9) | 40.4 (39.6) | 39.2 (39.6) | |
| $[Ru(NH_3)_5\underline{N}CS](ClO_4)_2$ | 2.9 (2.8) | 3.5 (3.4) | 19.0 (18.9) | 7.0 (7.2) | 6.7 (7.2) | 16.5 (16.0) | 45.6 (44.9) | 2.0 |
| $[Ru(NH_3)_5\underline{N}CS](NO_3)_2$ | 3.5 (3.2) | 4.5 (4.1) | 31.3 (30.4) | 9.2 (8.7) | 8.4 (8.7) | - - | 34.5 (33.7) | |
| $[Ru(NH_3)_5\underline{N}CS]Cl_2$ | 4.1 (3.8) | 5.1 (4.7) | 25.8 (26.6) | 10.5 (10.1) | 9.7 (10.1) | 23.0 (22.5) | 22.6 (22.5) | |
| $[Ru(NH_3)_5\underline{N}CS][B(C_6H_5)_4]_2$ | 65.7 (66.6) | 6.6 (6.2) | 9.2 (9.5) | 3.9 (3.6) | 3.3 (3.6) | - - | 73.2 (72.3) | |
| $[Ru(NH_3)_5\underline{S}CN]Br_2$ | 3.2 (2.9) | 4.1 (3.7) | 21.5 (20.8) | 8.4 (7.9) | 8.0 (7.9) | 39.9 (39.6) | 39.5 (39.6) | |
| $[Ru(NH_3)_5\underline{S}CN]I_2$ | 2.7 (2.4) | 3.5 (3.0) | 17.6 (16.8) | 6.9 (6.4) | 6.5 (6.4) | 51.6 (51.0) | 50.5 (51.0) | |
| $[Ru(NH_3)_5\underline{S}CN]Cl_2$ | 3.5 (3.8) | 5.0 (4.7) | 26.0 (26.6) | 10.5 (10.1) | 9.7 (10.1) | 23.0 (22.5) | 22.1 (22.5) | |
| $[Ru(NH_3)_5\underline{S}CN](ClO_4)_2$ | 3.0 (2.8) | 3.5 (3.4) | 19.1 (18.9) | 7.7 (7.2) | 7.0 (7.2) | 15.6 (16.0) | 45.8 (44.9) | 2.0 |
| $[Ru(NH_3)_4(NCS)_2]ClO_4$ | 6.6 (6.2) | 3.4 (3.1) | 21.3 (21.8) | 16.0 (16.6) | 15.8 (16.6) | 9.6 (9.2) | 26.5 (25.8) | 2.0 |
| $[Ru(NH_3)_5(NCS)_2]I$ | 5.4 (5.8) | 3.4 (2.9) | 19.8 (20.4) | 15.9 (15.5) | 15.2 (15.5) | 31.5 (30.8) | 30.4 (30.8) | |
| $[Ru(NH_3)_5(NCS)_2]Cl$ | 7.8 (7.5) | 4.0 (3.7) | 25.7 (26.2) | 19.6 (20.0) | 19.5 (20.0) | 11.4 (11.1) | 11.0 (11.1) | |
| $[Ru(NH_3)_5(NCS)_2]Br$ | 5.3 (5.6) | 3.6 (3.3) | 23.4 (23.0) | 17.9 (17.5) | 17.3 (17.5) | 22.4 (21.9) | 21.4 (21.9) | |
| $H_3O[Ru(NH_3)_2(SCN)_4]$ | 12.6 (12.4) | 2.3 (2.3) | 22.3 (21.8) | 34.0 (33.2) | - - | - - | - - | 1.9 |
| $[(C_6H_5)_4As][Ru(NH_3)_2(SCN)_4]$ | 45.2 (44.7) | 3.8 (3.4) | 10.5 (11.2) | 16.0 (17.0) | - - | - - | - - | 1.9 |
| $[Ru(NH_3)_2(SCN)_2]_n$ | 8.3 (9.5) | 2.8 (2.4) | 21.4 (22.3) | 26.0 (25.5) | - - | - - | - - | Diamagnetic |

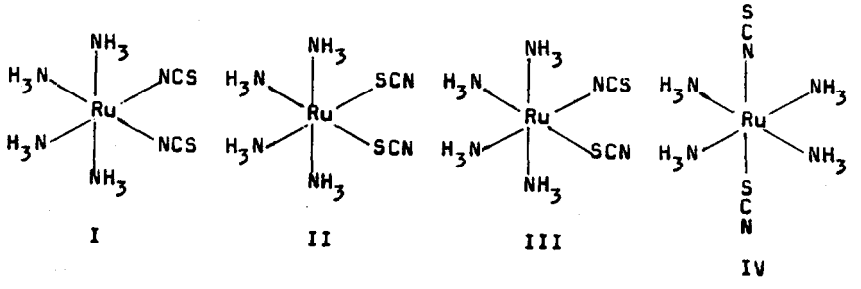
oxidized to +3 state by the oxygen which subsequently reacted to give thiocyanato complexes. Further, two complexes having the same composition $[Ru(NH_3)_5SCN]^{2+}$ have been obtained. The only possibility in such a situation is that they must be linkage isomers. Various physical methods have been employed to get some indication regarding the mode of linkage of SCN with ruthenium.

(a) *IR spectra*

The IR spectra of all the complexes showed characteristic bands of the coordinated thiocyanate ion[7-14] in the region 2000–2150 $cm^{-1}$ ($\nu_{CN}$); 650–800 $cm^{-1}$ ($\nu_{CS}$) and 450–480 $cm^{-1}$ ($\delta_{NCS}$ or $\nu_{M-NH_3}$) besides those of coordinated ammonia bands around 3400(w), 3200, 1600, 1300, 800 and 456 $cm^{-1}$. In general, the band due to $\nu_{CN}$ in the case of N-bonded SCN appears at lower wave numbers compared to that of S-bonded one.[15-17] The two isomers of $[Ru(NH_3)_5NCS]^{2+}$ showed strong bands due to $\nu_{CN}$ at 2057 $cm^{-1}$ (half width, 85 $cm^{-1}$) and 2073 $cm^{-1}$ (half width, 80 $cm^{-1}$). The positions of these bands[15-17] suggested that the one absorbing at 2057 $cm^{-1}$ should be the N-bonded while other, absorbing at 2073 $cm^{-1}$ S-bonded one. It is believed that the position of the band due to $\nu_{CN}$ alone is not a safe criterion to distinguish the NCS linkage isomers and it should be better judged along with those of $\nu_{CS}$ and $\delta_{NCS}$. Since the positions of these bands were masked by

the one due to $\tau_{NH}$ of $NH_3$ molecule, the IR-spectrum of the deuteriated species of the less soluble isomer $[Ru(ND_3)NCS]^{2+}$ (absorbing at 2057 $cm^{-1}$) was taken. As a result the positions of all the characteristic bands of $NH_3$ molecule shifted towards lower wave numbers and a weak band appeared around 800 $cm^{-1}$ suggesting[10] the bonding mode of NCS group through N atom in the complex. Unfortunately, all attempts to deuteriate the second isomer (more soluble one, $\nu_{CN}$ at 2073 $cm^{-1}$) failed. There have been reports[10,18] that in the 400 $cm^{-1}$ region the S-bond SCN group generally absorbs at relatively lower wave number than the N-bonded one. In the spectrum of the less soluble isomer ($\nu_{CN}$, 2057; $\nu_{CS}$, 800 $cm^{-1}$) a weak broad band appeared at 460 $cm^{-1}$ while the band position was around 420 $cm^{-1}$ in the second isomer. Since only two isomers are possible with the formulation $[Ru(NH_3)_5NCS]^{2+}$, it is concluded that the less soluble isomer ($\nu_{CN}$, 2057 $cm^{-1}$) is N-bonded while the more soluble one ($\nu_{CN}$, 2073 $cm^{-1}$) is S-bonded.

IR spectra of $[Ru(NH_3)_4(NCS)_2]^+$ showed two distinct bands at 2040 and 2100 $cm^{-1}$. Although there could be various possible isomers with this formulation (*cis*- and *trans*- with N, and/or S-bonded SCN groups) it is presumed that the splitting of the $\nu_{CN}$ band (2040 and 2100 $cm^{-1}$) is due to either coupling of the two *cis*-SCN groups or it could be the *trans*-form with one SCN group as N-bonded and other as S-bonded. However, the possibility of splitting in the *trans*-form with both SCN groups as N-bonded or as S-bonded is meagre. Further, it being a mixture of a number of isomers, was also ruled out by the fact that the band having this isomer was not separated on the Sephadex column under various experimental conditions and also on columns of different length. It is therefore concluded that the complex ion $[Ru(NH_3)_4(NCS)_2]^+$ is a single isomer having one of the following formulations:




The spectrum of $[As(C_6H_5)_4][Ru(NH_3)_2(SCN)_4]$ showed a broad and split band around 2100 $cm^{-1}$. The splitting and broadness of the band indicated the various modes of linkage of four SCN groups to the metal.

The black insoluble compound $[Ru(NH_3)_2(SCN)_2]_2$ assumed to be polymeric because of its insolubility in all the solvents exhibited a broad band around 2100 $cm^{-1}$ (half width, 140 $cm^{-1}$) and two bands around 1400 and 1250 $cm^{-1}$ instead of 1300 $cm^{-1}$. The splitting of $\delta_{NH}$ band could be due to the lowering of molecular symmetry.[19]

(b) *Electronic spectra*

The electronic spectra of all the complexes showed two intraligand bands around 210 nm ($\epsilon = 1.2$–$6.2 \times 10^4$) and 330(w) nm ($\epsilon = 2.0$–$5.0 \times 10^2$) assigned to $^1\Sigma^+ \rightarrow {}^1\Sigma^-$ and $^1\Sigma^+ \rightarrow {}^3\Sigma^-$, respectively.[20-22] The visible spectrum of one of the isomers of $[Ru(NH_3)_5NCS]^{2+}$ showed an intense broad band at 495 nm ($\epsilon = 3 \times 10^3$) in aqueous solution while the other at 515 nm ($\epsilon = 2.45 \times 10^3$). Although these bands could be assigned to the *d*–*d* transition, their higher intensities suggested them to be charge transfer bands,[23-26] possibly due to $t_{1u}(NCS) \rightarrow t_{2g}Ru(III)$. It is suggested that the isomer with the band at 495 nm ($\epsilon_{495} = 3000\ M^{-1}\ cm^{-1}$) is N-bonded thiocyanato complex while the second having a band at 515 nm ($\epsilon_{515} = 2450\ M^{-1}\ cm^{-1}$) is S-bonded isomer as suggested by Earley *et al.*[3,27] This conclusion is also in conformity with that derived by the IR spectral studies.

The spectra of $[Ru(NH_3)_4(NCS)_2]^+$ showed bands at 210, 270, 330, 470 and 530 nm. The assignments of the higher energy transitions are given in Table 1. It is preferred to assign broad bands at 470 nm and 530 nm to charge transfer transitions involving the NCS group and the metal. As described under the discussion section of IR spectral data, theoretically there are four possible isomers according to whether two SCN groups are in *cis* or *trans* positions. It is however difficult to decide one isomer over the other possible ones on the basis of these band positions but our choice is to assign *cis*-geometry to the complex. The reason for such a preference is that in the spectrum of

S-bonded monothiocyanato pentammine ruthenium(III) complex the same band appeared around 515 nm while in that of the N-bonded one, at 495 nm. The difference in the band positions of the two linkage isomers ($\Delta\lambda = 20$ nm) is appreciably low as compared to that found ($\Delta\lambda = 60$ nm) in $[Ru(NH_3)_4(NCS)_2]^+$. The large splitting indicated a strong coupling between the energy levels of the thiocyanato groups, which is possible, in case both SCN groups are *cis*-bonded. Another possibility which could not however be ruled out is that the two NCS groups may be in *trans*- or in *cis*-positions and bonded through N and S atom of the SCN groups as well.

The acid $H_3O[Ru(NH_3)_2(SCN)_4]$ showed bands at 535, 465, 340, 265 and 212 nm in aqueous solution while in alcoholic solution the position of the 535 nm band was shifted to lower energy (550 nm broad). The spectrum of $[As(C_6H_5)_4][Ru(NH_3)_2(SCN)_4]$ showed bands at 545, 440, 340, 250 and 215 nm along with the characteristic bands at 278, 270 and 215 nm of $[As(C_6H_5)_4]^+$. It has however been found that the anion was a mixture of four isomers which have been detected by passing an alcoholic solution of either the acid or that of $[As(C_6H_5)_4][Ru(NH_3)_2(SCN)_4]$ through Sephadex LH-20 column. Four separate bands appeared on the column when eluted with alcohol. The eluates of the four bands were separately collected and their solution spectra were taken and showed broad bands at 565, 560, 550 and 540 nm, respectively. Since the anionic

Table 2.

| Compound | Molar conductance and UV-visible band assignments of some of the complexes‡ | | |
|---|---|---|---|
| | $\lambda_m$ (25°C) ($ohm^{-1}cm^2mol^{-1}$) | $\lambda_{max}$ (log$\epsilon$) | Assignment |
| 1 | 2 | 3 | 4 |
| $[Ru(NH_3)_5\underline{N}CS](ClO_4)_2$ | 230 | 208 (4.12) | $^1\Sigma^+ \longrightarrow {}^1\Sigma^-$ |
| | | 265 (2.89) | $^2E_u \longrightarrow {}^2T_{2g}$, CT |
| | | 325 (2.20) | $^3\Sigma^+ \longrightarrow {}^3\Sigma^-$ |
| | | 495 (3.48) | $T_{1u}(NCS) \longrightarrow {}^2T_{2g}(Ru)$, CT |
| $[Ru(NH_3)_5\underline{S}CN](ClO_4)_2$ | 220 | 208 (4.30) | $^1\Sigma^+ \longrightarrow {}^1\Sigma^-$ |
| | | 265 (2.78) | $^2E_u \longrightarrow {}^2T_{2g}$, CT |
| | | 325 (2.32) | $^3\Sigma^+ \longrightarrow {}^3\Sigma^-$ |
| | | 515 (3.39) | $T_{1u}(NCS) \longrightarrow {}^2T_{2g}(Ru)$, CT |
| $[Ru(NH_3)_4(NCS)_2]ClO_4$ | 115 | 208 (4.33) | $^1\Sigma^+ \longrightarrow {}^1\Sigma^-$ |
| | | 270 (2.83) | $^2E_u \longrightarrow {}^2T_{2g}$, CT |
| | | 330 (2.59) | $^3\Sigma^+ \longrightarrow {}^3\Sigma^-$ |
| | | 530 (3.60) | $T_{1u}(NCS) \longrightarrow {}^2T_{2g}(Ru)$, CT |
| | | 470 (3.44) | $^2T_{2g} \longrightarrow {}^2A_g$ |
| $H_3O[Ru(NH_3)_2(SCN)_4]$ | 800 | 212 (4.11) | $^1\Sigma^+ \longrightarrow {}^1\Sigma^-$ |
| | | 265 (2.81) | $^2E_u \longrightarrow {}^2T_{2g}$, CT |
| | | 340 (2.57) | $^3\Sigma^+ \longrightarrow {}^3\Sigma^-$ |
| | | 535 (3.45) | $T_{1u}(NCS) \longrightarrow {}^2T_{2g}(Ru)$, CT |
| | | 465 (3.06) | $T_{2u}(NCS) \longrightarrow {}^2T_{2g}(Ru)$, CT |
| $[(C_6H_5)_4As][Ru(NH_3)_2(SCN)_4]$‡‡ | - | 215 (4.79) | $^1\Sigma^+ \longrightarrow {}^1\Sigma^-$ |
| | | 545 (3.91) | $T_{1u}(NCS) \longrightarrow {}^2T_{2g}(Ru)$, CT |
| | | 440 (3.04) | $T_{2u}(NCS) \longrightarrow {}^2T_{2g}(Ru)$, CT |

‡ Spectra recorded in aqueous solution.

‡‡Spectra recorded in ethanol.

complex was found to be a mixture of four isomers, the band assignments have not been made.

(c) *Magnetic properties*

The values of the room temperature magnetic moment per ruthenium atom of all the complexes ($\mu_{eff}$, 2.1 B.M.) except that of diamagnetic $[Ru(NH_3)_2(SCN)_2]_n$, indicate the presence of ruthenium in these complexes in +3 oxidation state. Magnetic moment values are given in Table 1.

(d) *Conductivity measurements*

The molar conductance values for all the water soluble complexes are shown in Table 2. The acid $H_3O[Ru(NH_3)_2(SCN)_4]$ showed quite high value of the molar conductance (800 $ohm^{-1}\,cm^2\,mole^{-1}$) which could be due to very high mobility of the $H_3O^+$ ions. The values for $[Ru(NH_3)_5NCS]^{2+}$ and $[Ru(NH_3)_4(NCS)_2]^+$ are comparable to those of known electrolytes having +2 and +1 charges, respectively.[28]

(e) *Electrochemical studies*

The cyclic voltammogrames of the complexes are shown in Fig. 1. The monothiocyanato complexes, $[Ru(NH_3)_5SCN]^{2+}$ showed $E_{1/2}$ value at 0.17 V and $\Delta E_p = 110$ mV, suggesting the system being quasi-reversible. After a second scan a new wave having broad cathodic peak at 0.65 V started appearing which indicated the formation of an unstable intermediate species A. $[Ru(NH_3)_4(NCS)_2]^+$ showed cathodic peak, $E_{pc}$ at 0.125 V, indicating the species to be easily reducible. After a few scans a new broad peak started appearing at 0.67 V indicating the formation of an unstable intermediate species B. The following electron transfer processes are tentatively surmized on the basis of these $E_{1/2}$ values. But these species could not be confirmed because of the lack of coulometric data.

$$\text{(I)}\ [Ru(NH_3)_5SCN]^{2+} \overset{+e^-}{\rightleftharpoons} [Ru(NH_3)_5SCN]^{1+}$$

$$\downarrow +e^- \qquad \mathbf{A}$$

$$[Ru(NH_3)_5SCN] \quad (1)$$

$$\text{(II)}\ [Ru(NH_3)_4(NCS)_2]^{+1} \underset{-e^-}{\overset{+e^-}{\rightleftharpoons}} [Ru(NH_3)_4(NCS)_2]$$

$$\mathbf{B}$$

$$\xrightarrow[-SCN]{+H_2O} [Ru(NH_3)_4(SCN)H_2O]^{1+} \xrightarrow{+e^-}$$

$$[Ru(NH_3)_4SCN(H_2O)]. \quad (2)$$

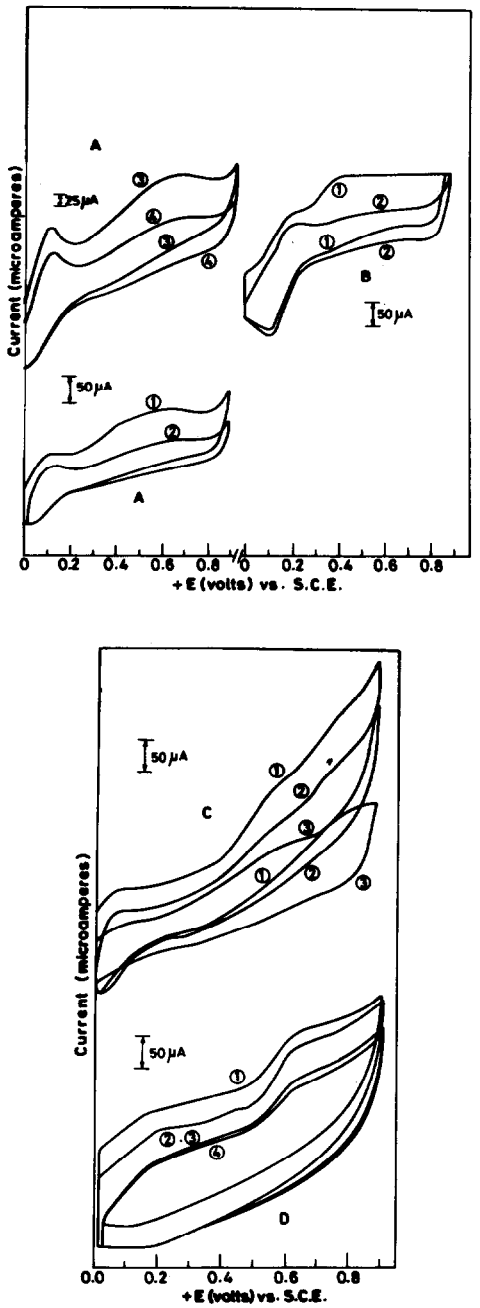



Fig. 1. Cyclic voltammogrames of A. $[Ru(NH_3)_4(SCN)_2]I$. B. $[Ru(NH_3)_5NCS]I_2$. C. $H_3O[Ru(NH_3)_2(SCN)_4]$. D. $[Ru(NH_3)_5SCN](ClO_4)_2$. Values given in parentheses represent the number of scans taken.

Acid $H_3O[Ru(NH_3)_2(SCN)_4]$ showed in the first scan a cathodic peak at 0.075 V and a weak anodic peak at 0.275 V. In the subsequent scans these peaks disappeared and a new peak appeared at 0.64 V.

## CONCLUSION

The following conclusions can be drawn from the reactions of $NH_4SCN$ with $[Ru(NH_3)_5N_2]Br_2$.

(a) The reaction did not occur in the absence of oxygen indicating that ruthenium in +2 oxidation state did not react with $NH_4SCN$. It appears that the metal ion during the reaction was first oxidized to +3 oxidation state by air and subsequently reacted with $NH_4SCN$ to give the products.

(b) The reactions at lower temperature (*ca.* 30°C) were very slow. It took a few days for the reaction to develop the red colour at room temperature.

(c) The formation of trinuclear species[4] which was obtained during the study of reaction of $NH_4SCN$ with $[Ru(NH_3)_5X]X_2$, could not be detected in this system. It may possibly be due to the instability of dinitrogen bridges in the ruthenium(III) complexes.

(d) Both the linkage isomers of $[Ru(NH_3)_5SCN]^{2+}$, one isomer of $[Ru(NH_3)_4(SCN)_2]$ and a mixture of four isomers of the anionic species, $[Ru(NH_3)_2(SCN)_4]^-$ have been formed.

(e) The aqueous solution of $H_3O[Ru(NH_3)_2(SCN)_4]$ on drying decomposed partially to some insoluble compound.

(f) The polymeric complex $[Ru(NH_3)_2(SCN)_2]_n$ was formed under refluxing conditions.

*Acknowledgements*—Authors wish to express their deep sense of gratitude to the referees who have suggested many points to help improve the manuscript.

## REFERENCES

1. H. H. Schmidke, *Ber. Bunsenges. Physik. Chem.* 1967, **71**, 1138.
2. S. W. Lin and A. F. Schreiner, *Inorg. Chim. Acta* 1971, **5**, 290.
3. H. S. Lim, D. J. Barclay and F. C. Anson, *Inorg. Chem.* 1972, **11**, 1460.
4. Rajinder Parashad, S. K. S. Yadav and U. Agarwala, *J. Inorg. Nucl. Chem.* 1981, **43**, 2359.
5. S. K. S. Yadav and U. C. Agarwala, *Ind. J. Chem.* 1982, **21A**, 175.
6. A. D. Allen, F. Bottomley, V. P. Remsolu and C. V. Senoff, *J. Am. Chem. Soc.* 1967, **89**, 5595.
7. J. Chatt and L. A. Duncanson, *Nature* 1956, **178**, 997.
8. K. R. Laing and W. R. Roper, *J. Chem. Soc.* (*A*) 1970, 2149.
9. A. Sabitini and I. Bertini, *Inorg. Chem.* 1965, **4**, 1665.
10. J. Lewish, R. S. Nyholm and P. W. Smith, *J. Chem. Soc.* 1971, 1950.
11. K. Nakamoto, *Infrared of Inorganic and Coordination Compounds*, 3rd Edn. Wiley, New York (1978).
12. F. Bottomley and J. R. Crawford, *J. Chem. Soc. Dalton* 1972, 2145.
13. H. A. Scherdegger, J. N. Armor and H. Taube, *J. Am. Chem. Soc.* 1968, **90**, 3263.
14. P. C. Ford and C. Sulton, *Inorg. Chem.* 1969, **8**, 1544.
15. Mitchell, P. C. H., *J. Chem. Soc.* 1960, 1912.
16. A. Tramer, *C.R. Acad. Soc.* 1960, **250**, 3150.
17. A. Tramer, *J. Chem. Phys.* 1962, **89**, 232.
18. A. Sabitini, *Inorg. Chem.* 1965, **4**, 954.
19. J. A. Stanko and T. W. Starnishak, *Inorg. Chem.* 1969, **8**, 2156.
20. J. R. McDonald, V. M. Scherr and S. P. McGlynn, *J. Chem. Phys.* 1969, **51**, 1723.
21. J. W. Rabalias, J. R. McDonald and S. P. McGlynn *J. Chem. Phys.* 1969, **51**, 5103.
22. J. W. Rabalias, J. R. McDonald, V. M. Scherr and S. P. McGlynn, *Chem. Rev.* 1971, **71**, 73.
23. M. D. Rowe, A. J. McCaffery, R. Gale and D. N. Copsey, *Inorg. Chem.* 1972, **11**, 3090.
24. G. N. Henning, A. J. McCaffery and P. N. Schatz, *J. Chem. Phys.* 1968, **48**, 565.
25. P. N. Schatz, A. J. McCaffery, W. Suetka, G. N. Henning and A. B. Ritchie, *J. Chem. Phys.* 1966, **45**, 722.
26. P. Day, *Inorg. Chem.* 1966, **5**, 1619.
27. R. A. Lee and Joseph E. Earley, *Inorg. Chem.* 1981, **20**, 1739.
28. R. D. Feltham and R. G. Hayter, *J. Chem. Soc.* 1964, 4587.

*Polyhedron* Vol. 3, No. 1, pp. 9–15, 1984
Printed in Great Britain.

0277–5387/84 $3.00 + .00
© 1984 Pergamon Press Ltd.

# COMPLEXES OF PALLADIUM (II) WITH L-PROLINE. MIXED L-PROLINATO NUCLEOSIDE COMPLEXES OF PALLADIUM (II)

**GEORGE PNEUMATIKAKIS**
University of Athens, Department of Chemistry, 13A Navarinou Street, Athens 144, Greece

(*Received* 25 *October* 1982; *accepted* 22 *June* 1983)

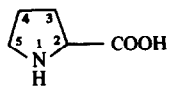
**Abstract**—The reaction of Palladium (II) chloride and L-proline (ProH) in aqueous solution gave the dimeric complex, $\{Pd(Pro)Cl\}_2$, which was characterized by elemental analysis, molecular weight, conductivity measurements and IR and NMR spectra. The complex, reacted further with the purine nucleosides inosine or guanosine (Nucl) and the complexes $\{Pd(Pro)(Nucl\text{-}H^+)\}$ were isolated from aqueous solution. The insolubility of these complexes suggested a rather polymeric structure in which the nucleoside bridges two adjacent palladium atoms through its N(7) and the exocyclic O(6) atoms. Reaction in dmso gave the complex $\{Pd(Pro)(Nucl)Cl\}$ in which the nucleoside act as monodentate ligands with their N(7) atom as ligation site. In aqueous solutions these complexes are quantitatively transformed to the polymeric analogues with the liberation of HCl. The nucleoside adenosine (Ado) reacted in a different way giving only the dimeric complex $\{Cl(Pro)PdAdoPd(Pro)Cl\}$ in which adenosine bridges two palladium atoms through its N(1) and N(7) atoms. Finally with the pyrimidine nucleoside cytidine (Cyd) the monomer Pd(Pro)(Cyd)Cl was isolated.

The Pd(II) complexes are interesting in biological chemistry. For example, Kirschner and collaborators noted that *cis*-dichloropiperidine palladium (II) can induce filamental growth in *E.Coli.*[1] The same effect was also noted by Charlon *et al.* with caesium *cis*-dichloro-L-serinato palladium (II).[2] Kirschner and collaborators also reported that some Pd(II) complexes with sulphur and nitrogen ligands, exhibit potential antitumour activity.[3]

It is clear from the active (against tumours) complexes discovered to date that *cis* displaceable ligands are necessary, and therefore the "carrier" ligand(s) should also occupy *cis* co-ordination sites in a four coordinate planar complex. When only monodentate "carrier" ligands are used one risks a *cis* complex isomerizing into the thermodynamically more stable *trans* configuration. Bidentate ligands remove this possibility of a drug deteriorating during storage. An L-amino-acid anion would seem to be an ideal choice of bidentate ligand for this task of conformation locking. Amino-acids may also be particularly useful "carrier" ligands because not only do cells have active transport processes for most of them but also, healthy cells tolerate them well and have means of using, or of disposing of, the amino-acids after therapy. In this respect it is very important to study the interaction of Pd(II) with α-amino-acids with the main purpose to prepare complexes with possible antitumour activity.

It is also very important to investigate the interaction of these complexes with the nucleic acid constituents in order to note any similarities in their behaviour, with that of the well established antitumour agent *cis*-$Pt(NH_3)_2Cl_2$ and the palladium analogue.

This paper describes the synthesis and some properties of some complexes of Pd(II) with L-proline, together with their interaction with nucleosides.




L-proline. a cyclic amino-acid widely distributed in nature, can form chelate and non-chelate complexes with various metals. Complexes are known for copper,[4–6] cobalt,[7–12] nickel,[13] palladium,[14–16] rare earth,[17] rhodium[18] and platinum.[18–26] In these complexes L-proline acts either as unidentate (as molecule or anion) or as bidentate (as anion) ligand,

and coordination is effected through the imino group, or both, respectively. Unlike other optically active α-amino-acids, the optically active proline anion is coordinated stereospecifically with the metal ion in the formation of rings: the asymmetric environment of the donor nitrogen atom takes the obligatory S-absolute configuration.

## RESULTS AND DISCUSSION

(1) *Interaction of palladium (II) chloride with L-proline*

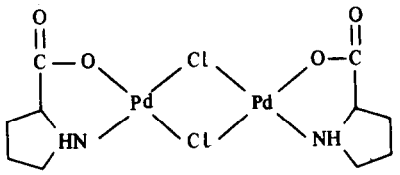
Anhydrous palladium (II) chloride is insoluble in water, but becomes soluble in presence of L-proline, in 1:1 stoichiometry, and gave the dimeric complex $\{Pd(Pro)Cl\}_2$, according to the eqn (1):

$$2PdCl_2 + 2ProH \xrightarrow{H_2O,\ R.T.} \{Pd(Pro)Cl\}_2 + 2HCl. \quad (1)$$

The complex was a non-electrolyte in water and the analytical results were in agreement with the proposed formulation (see Table 1). Its dimeric nature was established by a molecular weight determination in ethanol (Found 517; Calc. 511.8).

In the IR spectrum of the complex of palladium with L-proline there are three new bands, compared with the spectrum of L-proline alone. The first band at 485 $cm^{-1}$ is due to the metal–nitrogen vibrations. The second band at 305 $cm^{-1}$ may be assigned to the Pol-Cl-Pol vibrations, since it disappears in the bromide analogue. The third band at 295 $cm^{-1}$ may be assigned to the metal–oxygen vibrations. The $NH_2^+$ bands at 1475 and 1380 $cm^{-1}$ in the spectrum of L-proline do not appear in the spectrum of the complex, while the NH stretching vibrations shift from 3280 and 3190 $cm^{-1}$ to 3340 and 3210 $cm^{-1}$. In addition the antisymmetric, symmetric, and deformation vibrations of the carboxylate group shift from 1610, 1415 and 680 $cm^{-1}$ to 1587, 1435 and 750 $cm^{-1}$ respectively (see Table 2).

These results are consistent with L-proline acting as a bidentate ligand, through its carboxylate group and the amino nitrogen in a chelate form. On the other hand the position of the ν(Pd–Cl) band at (305-$cm^{-1}$), is consistent with the presence of chloride bridges in the complex, giving rise to the possible structure:




The mode of L-proline coordination to palladium in this complex has further been confirmed by comparing the $^1H$ and $^{13}C$ NMR spectra of the complexed and the free L-proline.

The $^1H$ NMR chemical shifts of L-proline and

Table 1. Analytical and conductivity data of the complexes*

| Compounds | %C | %H | %N | %Pd | $\Lambda_M$, $\Omega^{-1}$ $cm^2$ $Mol^{-1}$ | |
|---|---|---|---|---|---|---|
| | | | | | $10^{-3}$M in dmf | $10^{-3}$M in $H_2O$ |
| {Pd(Pro)Cl}$_2$ | 23.50 (23.44) | 3.19 (3.13) | 5.70 (5.47) | 41.85 (41.56) | 6 | 8 |
| {Pd(Pro)Br}$_2$ | 20.20 (19.98) | 2.80 (2.66) | 4.72 (4.66) | 35.14 (35.43) | 5 | 6 |
| {Pd(Pro)(Ino)Cl} | 34.51 (34.34) | 3.72 (3.82) | 13.50 (13.36) | 20.50 (20.30) | 8 | 120 |
| {Pd(Pro)(Ino-H$^+$)} | 36.58 (36.91) | 3.79 (3.90) | 14.61 (14.36) | 21.53 (21.82) | — | — |
| {Pd(Pro)(Guo)Cl} | 33.52 (33.38) | 3.96 (3.89) | 15.60 (15.29) | 19.48 (19.73) | 7 | 115 |
| {Pd(Pro)(Guo-H$^+$)} | 35.60 (35.80) | 3.90 (3.98) | 16.00 (16.38) | 21.42 (21.16) | — | — |
| {Pd(Pro)(Cyd)Cl} | 33.80 (33.66) | 4.35 (4.21) | 11.50 (11.22) | 21.50 (21.32) | 8 | 10 |
| {Pd(Pro)Cl}$_2$Ado | 31.04 (30.81) | 3.85 (3.72) | 12.69 (12.58) | 27.50 (27.32) | 6 | — |

* The numbers in parentheses represent the calculated figures

Table 2. Some characteristic IR bands of L-proline and $\{Pd(Pro)Cl\}_2$ ($cm^{-1}$)*

| Compound | ν(NH) | $\nu_a$(COO) | $\nu_s$(COO) | $\nu_{def}$(COO) | $\delta(NH_2^+)$ | ν(Pd–N) | ν(Pd–X) | ν(Pd–O) |
|---|---|---|---|---|---|---|---|---|
| L - Proline | 3190<br>3280 | 1610 | 1415 | 680 | 1475<br>1380 | — | — | — |
| $\{Pd(Pro)Cl\}_2$ | 3210<br>3340 | 1587 | 1435 | 750 | — | 485 | 305 | 295 |
| $\{Pd(Pro)Br\}_2$ | 3210<br>3340 | 1583 | 1432 | 745 | — | 487 | 252 | 297 |

* measured in KBr discs.

its complex are given in Table 3. There is a downfield shift for all four kinds of protons, in the complex relatively to free ligand, but the ones at positions (2), (3) and (5), which are adjacent to the ligation sites are shifted the most, 1.50, 1.02 and 0.54 ppm respectively. This confirms coordination of L-proline to palladium through both the carboxylate group and the imino nitrogen, in agreement with the IR data.

The $^{13}C$ NMR spectra also confirm the above postulations. In Table 4 are given the $^{13}C$ NMR chemical shifts of L-proline and the complex $\{Pd(Pro)Cl\}_2$.

The most pronounced change was observed for the carboxyl carbon of the complex, which was shifted by 15.0 ppm downfield with respect to the uncomplexed ligand. A large downfield shift was also observed for the carbons C(2) and C(5) (4.8 and 4.0 ppm respectively). This again confirms the participation of both the carboxylate group and the iminonitrogen in coordination, and is in agreement with the observation that the changes of chemical shift on chelation of α-amino-acids to Co(III) ($H_3N^+RCOOH \rightarrow$chelate) were about 15 and 5 ppm for the carboxy-carbon and α-carbon respectively.[27]

(2) *Mixed prolinato-nucleoside complexes of palladium (II)*

The dimeric complex, $\{Pd(Pro)Cl\}_2$, prepared and characterized above, reacted with purine and pyrimidine nucleosides (Nucl) with the cleavage of the chloride bridges between the two palladium atoms, and monomeric complexes were formed, according, to eqn (1):

$$\{Pd(Pro)Cl\}_2 + 2Nucl \xrightarrow{dmso} 2\{Pd(Pro)(Nucl)Cl\}. \quad (1)$$

The proposed formulae are in agreement with the

Table 3. $^1H$ NMR chemical shifts of L-proline and $\{Pd(Pro)Cl\}_2$ (ppm)

| Compound | H(2) | H(3) | H(4) | H(5) | Solvent |
|---|---|---|---|---|---|
| L - Proline | 4.10 | 2.18 | 2.18 | 3.36 | $D_2O$ |
| $\{Pd(Pro)Cl\}_2$ | 5.60 | 3.20 | 2.43 | 3.90 | $D_2O$ |

Table 4. $^{13}C$ NMR chemical shifts of L-proline and $\{Pd(Pro)Cl\}_2$ (ppm)

| Compound | C=O | C(2) | C(3) | C(4) | C(5) |
|---|---|---|---|---|---|
| L-Proline | 174.2 | 63.6 | 29.5 | 23.9 | 50.5 |
| $\{Pd(Pro)Cl\}_2$ | 189.2 | 68.4 | 31.7 | 25.0 | 54.5 |

analytical results (see Table 1). These mixed ligand complexes are non-electrolytes in dmf, as well as other organic solvents, e.g. ethanol, acetone, etc. However, those complexes with one ionizable N(1) H imino proton, e.g. inosine and guanosine, decompose in water giving insoluble yellow material and HCl, and consequently the mixtures develop high conductivities. These insoluble materials are free from chloride and correspond to the formulae; Pd(Pro)(Nucl-H). The decomposition reaction follows the equation:

$$\text{Pd(Pro)(Nucl)Cl} \xrightarrow{H_2O} \text{Pd(Pro)(Nucl-H)} + \text{HCl}. \quad (2)$$

In acidic solution the reaction (2) was reversed and the protonated complexes, Pd(Pro)(Nucl)Cl can be recovered. The deprotonated complexes, Pd(Pro)(Nucl-H) were also prepared by performing the reaction (1) in aqueous solutions:

$$\{\text{Pd(Pro)Cl}\}_2 + 2\text{Nucl} \xrightarrow{H_2O} 2\,\text{Pd(Pro)(Nucl-H)} + 2\text{HCl}. \quad (3)$$

Reaction (3) may proceed in two main steps. First the chloride bridges may be cleaved by the nucleosides, which then remain attached to palladium with their N(7) atom (as will be shown below) and this is seen by the formation of a transient clear yellow solution. In the second step, the compounds Pd(Pro)(Nucl-H) are precipitated, and this may involve: (i) the ionization of the N(1)-H iminoproton, due to the very large lowering of the $pK_a$ of this proton when the nucleosides are coordinated to metals and especially to Pd(II), through their N(7) atom;[28-30] (ii) the accumulation, due to resonance, of a negative charge on the exocyclic O(6) atom; and (iii) the nucleophilic substitution of the coordinated chloride by this negatively charged oxygen atom. This behaviour is similar to that observed in reacting the dimeric complex $\{\text{Pd(O-Mecys)Cl}\}_2$ with nucleosides.[31] However it is in contrast to the behaviour of analogous platinum complexes, where attempts to prepare complexes with the O(6) atom of the nucleosides, participating in coordination, resulted in the destruction of the parent compounds.[32]

The binding sites of the nucleosides in these mixed ligand complexes were deduced from their $^1$H NMR, $^{13}$C NMR and IR spectra.

The $^1$H NMR bands of the proline are not shown clearly because they coincide with some of the bands of the nucleosides. However, the bands in the aromatic proton region are very useful in assigning the coordination sites of the nucleosides, and they are given in Table 5.

The complex Pd(Pro)(Ino)Cl gave two resonances at 8.79 and 8.20 ppm assigned to H(8) and H(2) respectively. The downfield shift of the H(8) resonance by 0.57 ppm, is comparable to the one found in other similar cases[28,33,34] and may be taken as a good indication of the N(7) coordination of inosine to Pd(II). The complex Pd(Pro)(Guo)Cl shows one resonance at 8.46 ppm, assigned to H(8), and this again indicates N(7) coordination of guanosine to Pd(II). The complex $\{\text{Pd(Pro)Cl}\}_2$ Ado shows two resonances at 8.70 and 8.90 ppm assigned to H(2) and H(8) respectively. The downfield shift of both H(2) and H(8) resonances by about 0.75 ppm as compared with the uncomplexed adenosine is consistent with the participation of both N(1) and N(7) in coordination to Pd(II).[28,32,33] In the complex

Table 5. H$^1$ NMR chemical shifts of the mixed ligand complexes (ppm)

| Compounds | H(2) | H(5) | H(6) | H(8) | | Solvent |
|---|---|---|---|---|---|---|
| Inosine | 8.11 | — | — | 8.22 | 6.03, 5.93 | dmso-$d_6$ |
| {Pd(Pro)(Ino)Cl} | 82.0 | — | — | 8.79 | 5.85, 5.76 | dmso-$d_6$ |
| Guanosine | — | — | — | 7.80 | 5.74, 5.68 | dmso-$d_6$ |
| {Pd(Pro)(Guo)Cl} | — | — | — | 8.46 | 5.85, 5.78 | dmso-$d_6$ |
| Cytidine | — | 5.75, 5.66 | 7.78, 7.79 | — | 6.24, 6.17 | dmso-$d_6$ |
| {Pd(Pro)(Cyd)Cl} | — | 6.18, 6.19 | 8.11, 8.20 | — | 6.26, 6.24 | dmso-$d_6$ |
| Adenosine | 7.95 | — | — | 8.17 | 5.90, 5.80 | dmso-$d_6$ |
| $\{\text{Pd(Pro)Cl}\}_2$ Ado | 8.70 | — | — | 8.90 | 6.31, 6.23 | dmso-$d_6$ |

{Pd(Pro)(Cyd)Cl}, both H(5) and H(6) shifted downfield, with the larger shift for H(5). This indicates that H(5) is closer to the coordination site on the ligand, probably the N(3) atom.[33,34(b)]

The postulations on the binding sites of nucleosides made from $^1$H NMR spectra are further confirmed by the $^{13}$C NMR spectra of the complexes. The $^{13}$C NMR chemical shifts of the ligands and complexes are given in Table 6.

In the complex {Pd(Pro)(Ino)Cl}, the downfield shifts observed for the C(5) and C(8) resonances (2.3 and 3.8 ppm respectively) are consistent with N(7) coordination, since these carbons are adjacent to this nitrogen. The same sort of pattern was also observed in the $^{13}$C NMR spectra of the guanosine complex, suggesting again N(7) coordination. In the adenosine complex the resonances of all four carbon atoms, C(2), C(6), C(5) and C(8), adjacent to both N(1) and N(7) atoms are shifted downfield upon coordination, and this further supports the participation of both these nitrogens in coordination.[32-35] The resonances of the proline carbons in these mixed ligand complexes remain essentially at the same positions as in the parent dimeric complex.

The deprotonated complexes Pd(Pro)(Nucl-H) are insoluble in all common solvents and the information concerning their structure was deduced only from their chemical behaviour and IR spectra.

The preparation of these complexes from the complexes Pd(Pro)(Nucl)Cl and their reversible conversion to them suggested that the Pd–N(7) bonding, present in the latter complexes, exists also in the deprotonated complexes. These deprotonated complexes do not contain any chloride, and the $\nu$(Pd–Cl) vibration, which occurs at 305 cm$^{-1}$ in the starting dimeric complex, $\{Pd(Pro)Cl\}_2$ and is shifted at about 330 cm$^{-1}$ in the complexes {Pd(pro)(Nucl)Cl} (the normal position for the stretching vibration of the Pd–Cl terminal group) is absent from the spectra of these complexes.

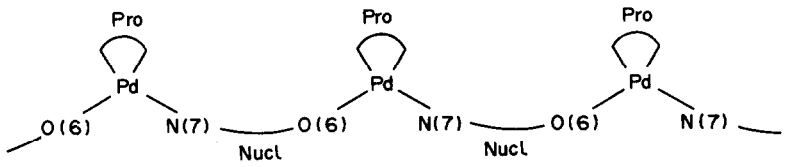
On the other hand, the IR spectra of these complexes in the carbonyl stretching region, may give an indication for the exocyclic O(6) atom participating in bonding with Pd(II), in these deprotonated complexes. The $\nu$(C = O) of the exocyclic carbonyl oxygen of the nucleosides inosine and guanosine appears at about 1700 cm$^{-1}$ and remains at the same frequency in the complexes Pd(Pro)(Nucl)Cl thus excluding its participation in bonding with palladium in these complexes.[28,33,34,36] However in the complexes Pd(Pro)(Nucl-H$^+$) this band is shifted to lower frequencies by about 75 cm$^{-1}$ and appears at 1625 cm$^{-1}$. This lowering of the $\nu$(C = O) frequency may be taken as a good indication of the O(6) keto oxygen involvement in bonding with the metals.[28,33,34(a),36-38] The shift to lower frequencies

Table 6. $^{13}$C NMR chemical shifts of the mixed ligand complexes (ppm)

| Compounds | L - Proline Carbons | | | | | Nucleoside Carbons | | | | | | | | | |
|---|---|---|---|---|---|---|---|---|---|---|---|---|---|---|---|
| | C=O | $C_2$ | $C_3$ | $C_4$ | $C_5$ | $C_2$ | $C_4$ | $C_5$ | $C_6$ | $C_8$ | $C_1'$ | $C_2'$ | $C_3'$ | $C_4'$ | $C_5'$ |
| Inosine | — | — | — | — | — | 146.0 | 148.2 | 124.4 | 156.5 | 138.7 | 87.4 | 74.0 | 70.2 | 85.6 | 61.2 |
| {Pd(Pro)(Ino)Cl} | 189.0 | 68.5 | 31.5 | 25.2 | 54.6 | 146.7 | 150.0 | 126.8 | 157.5 | 142.5 | 88.2 | 74.5 | 70.0 | 85.9 | 60.8 |
| Guanosine | — | — | — | — | — | 153.6 | 151.3 | 116.6 | 156.7 | 135.6 | 86.3 | 73.7 | 70.3 | 85.1 | 61.7 |
| {Pd(Pro)(Guo)Cl} | 189.1 | 68.4 | 31.7 | 25.0 | 54.5 | 154.6 | 152.6 | 118.7 | 158.2 | 139.0 | 87.1 | 74.0 | 69.7 | 85.6 | 61.1 |
| Cytidine | — | — | — | — | — | 152.9 | 163.7 | 99.6 | 148.6 | — | 90.8 | 74.6 | 69.8 | 83.8 | 61.3 |
| {Pd(Pro)(Cyd)Cl} | 188.8 | 68.3 | 31.5 | 25.3 | 54.8 | 156.5 | 166.0 | 98.0 | 147.2 | — | 90.7 | 74.9 | 69.7 | 84.0 | 61.0 |
| Adenosine | — | — | — | — | — | 148.5 | 147.0 | 114.5 | 152.0 | 135.8 | 88.4 | 71.0 | 73.9 | 86.3 | 61.0 |
| $\{Pd(Pro)Cl\}_2$ Ado | 189.0 | 68.7 | 31.4 | 25.1 | 54.7 | 156.0 | 147.6 | 116.9 | 157.0 | 143.5 | 88.6 | 71.3 | 74.3 | 86.8 | 61.3 |

of the $\nu$(C = O) band upon ionization of the N(1) H imino proton in inosine and guanosine, indicates the loss of the double bond character of the C = O group.[39,40] This is more pronounced in the ionic salt of guanosine (shift to 1595 $cm^{-1}$),[38] and less whenever the metal–oxygen bonding is more covalent, as in the case of Pd(II).[28,33] Certainly, the double bond character of the C = O is also lowered when the oxygen interacts with a metal, without ionization of the N(1)H imino proton.[34(a)] Oxygen involvement in bonding with metals, following deprotonation of the imino proton, has also been found in the crystal structure of *cis*-diamminoplatinum a-pyridone blue,[41] where both $O^-$ and N atoms bridge two platinum atoms. Kistenmacher *et al.*[42] have also found an O–Ag(I) interaction in the crystal structure of (nitrato) (1-methylcytosine) silver (1). Recently, Bau *et al.*[43] showed the participation of the exocyclic O(6) in coordination, in the crystal structure of a tetranuclear copper (II)—inosine monophosphate *o*-phenanthroline complex, where inosine acts as an O(6) N(7) bridging ligand with Cu–O(6) distance 1.956 Å. Very recently, Marzilli *et al.*,[44] have presented evidence for O(6) binding with metals mainly from $^{13}C$ NMR spectra.

In view of the above discussion, there must exist a strong O(6)–Pd interaction in the complexes Pd(Pro)(Nucl-H), which may be formulated as polymers with O(6) N(7) bridges:




The postulation that the bridging occurs with N(7) N(1) bridges, without participation of the carbonyl O(6) in bonding does not explain the large lowering of the $\nu$(C = O) frequency, and does not seem very likely to occur.

## EXPERIMENTAL

The experimental techniques have been described elsewhere.[33]

*Preparation of complexes*

(1) *L-Prolinato palladium (II)-μ-dichloro-L-prolinato palladium (II)*, $\{Pd(pro)Cl\}_2$

Palladium (II) chloride (0.356 g, 2 mmoles) and L-proline (0.230 g, 2 mmoles) were suspended in 25 $cm^3$ water and stirred at 60°C for 2 hr. The resulting clear red solution was roto-evaporated to dryness at 50°C. The residue was taken with 20 $cm^3$ absolute ethanol and filtered. The compound was then precipitated with excess ether. Yield, 90%.

(2) *Chloro-(L-prolinato)(nucleoside) palladium (II)*, Pd(pro)(Nucl)Cl, (Nucl = Ino, Guo, Cyd)

0.5 mmol $\{Pd(Pro)Cl\}_2$ and 1 mmol of the respective nucleoside were suspended in 3 $cm^3$ dmso-$d_6$ and stirred for 1 hr at room temperature. The $^1H$ NMR spectra of the solution showed the existence of only one species in the solution and the compound was precipitated with excess acetone. Yield, 85–90%.

(3) *L-prolinato (guanosinato) palladium (III)*, Pd(pro)(Guo-$H^+$) *and L-prolinato (insosinato) palladium (II)*, Pd(pro)(Ino-$H^+$)

(a) 0.5 mmol $\{Pd(Pro)Cl\}_2$ was dissolved in 10 $cm^3$ $H_2O$ and to that was added 1 mmol of the respective nucleoside dissolved in 25 $cm^3$ $H_2O$ (hot in the case of guanosine). The mixture was stirred at room temperature for 2 hr and the precipitate formed, was filtered, washed with hot water, ethanol, ether and dried at 80°C under vacuum. Yield, *ca.* 80%.

(b) 1 mmol of the respective complexes Pd(Pro)(Nucl)Cl (Nucl = Ino or Guo) was suspended in 25 $cm^3$ water and stirred for 2 hr at room temperature. The precipitate formed was filtered, washed with water, ethanol, ether and dried as above.

(4) *Chloro L-prolinato-palladium (II)-μ-Adenosine (N1 N7)-chloro L-prolinato palladium (II)*, Cl(Pro)Pd Ado Pd (Pro)Cl

1 mmol $\{Pd(Pro)Cl\}_2$ was dissolved in 10 $cm^3$ $H_2O$ and to that was added 1 mmol Adenosine dissolved in 20 $cm^3$ water and stirred for 2 hrs. The yellow precipitate formed, was filtered, washed with water, ethanol, ether and dried at 60°C under vacuum. Yield *ca.* 85%.

## REFERENCES

1. S. Kirschner, A. Maurer and D. Dragulesku, *J. Clin. Hematol. Oncol.* 1977, **7**, 293.
2. A. J. Charlson, N. T. McArdle and E. C. Watton, *Inorg. Chim. Acta* 1981, **56**, L35.
3. S. Kirschner, A. Maurer and C. Dragulescu, *J. Clin. Hematol. Oncol* 1977, **7**, 190.
4. T. Yasui, J. Hidaka and Y. Shimura, *J. Am. Chem. Soc.* 1965, **87**, 2762.

5. T. Yasui, *Bull. Chem. Soc. Japan* 1965, **38**, 1746.
6. A. M. Mathieson and K. H. Welsh, *Acta Cryst.* 1952, **5**, 599.
7. R. G. Denning and T. S. Piper, *Inorg. Chem.* 1966, **5**, 1056.
8. H. C. Freeman and J. E. Maxwell, *Inorg. Chem.* 1970, **9**, 649.
9. T. Yasui, J. Hidaka and Y. Shimure, *Bull. Chem. Soc. Japan* 1966, **39**, 2417.
10. T. Yasui, J. Fujita and Y. Shimure, *Bull. Chem. Soc. Japan* 1969, **42**, 2081.
11. T. Yasui, J. Hidaka and Y. Shimure, *Bull. Chem. Soc. Japan* 1965, **38**, 2025.
12. G. Brookes and L. D. Pettit, *J. Chem. Soc., Chem. Commun.* 1974, 813.
13. J. Hidaka and Y. Shimure, *Bull. Chem. Soc. Japan* 1970, **43**, 2999.
14. K. Freund and H. Frye, *Inorg. Nucl. Chem. Lett.* 1971, **7**, 107.
15. T. Ito, F. Marumo and J. Saito, *Acta Cryst.*, Sect. B. 1971 **27**, 1062.
16. J. Kollmar, C. Schroeter and E. Hoyer, *J. Prakt. Chem.* 1975, **317**, 515.
17. S. Zielinski, K. Lomozik and A. Wojciechowska, *Russ. J. Inorg. Chem.* 1980, **25**, 1573.
18. A. E. Bukanova, I. V. Prokoféva, Ya. V. Salyń and L. K. Shubochkin, *Russ. J. Inorg. Chem.* 1981, **26**, 82.
19. J. Fujita, K. Konya and K. Nakamoto, *Inorg. Chem.* 1970, **9**, 2794.
20. K. Konya, J. Fujita and K. Nakamoto, *Inorg. Chem.* 1971, **10**, 1699.
21. L. M. Volshtein and O. P. Slyudkin, *Russ. J. Inorg. Chem.* 1972, **17**, 236 and 1168.
22. L. M. Volshtein and O. P. Slyudkin, *Russ. J. Inorg. Chem.* 1974, **19**, 71.
23. R. D. Gillard and O. P. Slyudkin, *J. Chem. Soc. Dalton* 1978, 152.
24. L. M. Volshkein, O. P. Slyudkin and M. A. Kerzhentsev, *Russ. J. Inorg. Chem.* 1977, **22**, 1506.
25. R. D. Gillard, S. M. Laurie, D. C. Price, D. A. Phipps and C. F. Weick, *J. Chem. Soc. Dalton* 1974, 1385.
26. O. P. Slyudkin and M. A. Kerzhentser, *Russ. J. Inorg. Chem.* 1979 **24**, 1695.
27. A. Tomoharu and Y. Takaji, *Bull. Chem. Soc. Japan* 1976, **49**, 472.
28(a). G. Pneumatikakis, N. Hadjiliadis and T. Theophanides, *Inorg. Chim. Acta* 1977, **22**, L1. (b). G. Pneumatikakis, N. Hadjiliadis and T. Theophanides, *Inorg. Chem.* 1978, **17**, 915. (c) N. Hadjiliadis and G. Pneumatikakis, *J. Chem. Soc. Dalton* 1978, 1691.
29. G. Y. H. Chu and R. S. Tobias, *J. Am. Chem. Soc* 1976, **98**, 2641.
30. G. Y. H. Chu, S. Mansy, R. E. Duncan and R. S. Tobias, *J. Am. Chem. Soc.* 1978, **100**, 593.
31. G. Pneumatikakis, *Proc. XXII ICCC*, Vol. 2, p. 565, 23–27 August, Budapest, 1982.
32. N. Hadjiliadis and G. Pneumatikakis, *Inorg. Chim. Acta* 1980, **46**, 255.
33. (a) G. Pneumatikakis, *Inorg. Chim. Acta* 1980, **46**, 243. (b) *Ibid.* 1982, **66**, 131.
34. (a) J. Dehand and J. Jordanov, *J. Chem. Soc. Chem. Commun* 1976, 598. (b) J. Dehand and J. Jordanov, *J. Chem. Soc. Dalton* 1977, 1588.
35. D. J. Nelson, P. I. Yeagle, T. I. Miller and R. B. Martin, *Bioinorg. Chem.* 1976, **5**, 353.
36. M. Ogawa and T. Sakaguchi, *Chem. Pharm. Bull.* 1971, **19**, 1650.
37. A. T. Tu and M. J. Heller, In *Metal Ions in Biological Systems*, Vol. 1, p. 1 (1974).
38. A. J. Canty and R. S. Tobias, *Inorg. Chem.* 1979, **18**, 413.
39. R. M. Izatt, J. J. Christensen and J. H. Rytting, *Chem. Rev.* 1971, **71**, 439.
40. R. Shapiro, *Progr. Nucl. Acid Res.* 1968, **73**, 8.
41. J. K. Barton, H. N. Rabinowith, D. H. Szalda and R. S. Lippard, *J. Am. Chem. Soc.* 1977, **99**, 2827.
42. T. J. Kistenmacher, M. Rossi and L. G. Marzilli, *Inorg. Chem.* 1979, **18**, 240.
43. R. W. Gellert, B. E. Fischer and R. Bau, *J. Am. Chem. Soc.* 1980, **102**, 7812.
44. L. G. Marzilli, C. Baltazar and C. Solorzano, *J. Am. Chem. Soc.* 1982, **104**, 461.

*Polyhedron* Vol. 3, No. 1, pp. 17–20, 1984
Printed in Great Britain.

0277-5387/84 $3.00 + .00
Pergamon Press Ltd.

# MAGNETIC SUSCEPTIBILITY AND ESR STUDIES OF THREE COMPLEXES OF CHROMIUM(III) AND L-HISTIDINE. FERROMAGNETIC INTERACTIONS IN THE DIMERIC COMPLEX $[Cr(L\text{-}HISTIDINE)_2(OH)]_2$

**ETIM E. EDUOK, JOHN W. OWENS and CHARLES J. O'CONNOR***
Department of Chemistry, University of New Orleans, New Orleans, LA 70148, U.S.A.

(*Received* 4 *January* 1983; *accepted* 31 *May* 1983)

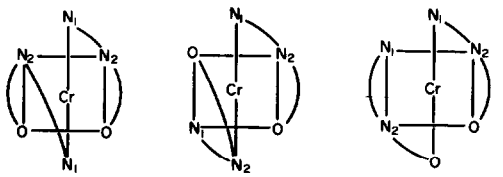
**Abstract**—Three complexes of chromium(III) and histidine were investigated by variable temperature magnetic susceptibility and ESR. Two monomeric stereosoimers of Cr(L-histidine)$_2$(NO$_3$) were studied; the *trans*(imidazole) and *trans*(carboxylate) isomers exhibited Curie–Weiss behaviour in the 6–300 K temperature region. The magnetic susceptibility of the related binuclear complex, $[Cr(L\text{-histidine})_2(OH)]_2$, showed ferromagnetic behaviour at low temperature ($J/k = +0.15$ K) lending strong support to the proposed hydroxo-bridged structure.

Transition metal complexes with amino acids are rudimentary steps in modelling the metal–protein interactions of many metallobiomolecules. Complexes of amino acids are often studied in solution to obtain information on the dynamic structural models of metal–peptide bonding.[1–5] However, the lability of amino acid ligands when coordinated to many metals renders the labile metal complex to be an unsuitable model of stable native metal–protein complexes. If the metal amino acid adduct is to be studied in solution, the chemistry of the metal dictates the use of substitutionally inert metals such as cobalt(III) or chromium(III). There are several reports in the literature which describe kinetic and spectral investigations of Co(III) and Cr(III) complexes of amino acids,[6–9] including several mixed ligand studies,[10–11] and crystal structure reports.[12–19]

An interesting outgrowth of the study of amino acid complexes concerns the tridentate amino acids, such as histidine and aspartine. These complexes are interesting because three stereoisomers are possible upon complex formation. Several authors have made structural assignments to species observed in solution from spectral measurements on the substitutionally inert complexes. In addition, complexes of the more labile metal(II) ions coordinated to tridentate amino acid have also been studied.[20,22]

*Author to whom correspondence should be addressed.

Hoggard recently reported the synthesis and spectral study of isomers **1** and **2** of Cr(L-histidine)$_2$NO$_3$ and a novel binuclear complex $[Cr(L\text{-histidine})(OH)]_2$.[6] The third isomer of Cr(L-histidine)$_2$(NO$_3$)(**3**, *trans*-amine) was not isolated.




**1** **2** **3**

Following Hoggard's report, we have investigated the ground state electronic properties of this series of chromium(III) histidine complexes using variable temperature magnetic susceptibility and ESR measurements. We report here on the magnetic susceptibility measured from 6–300 K and the ESR spectrum at 77 and 300 K for the *trans*(imidazole) and *trans*(carboxylate)isomers of Cr(L-histidine)$_2$NO$_3$, and the binuclear complex $[Cr(L\text{-histidine})_2(OH)]_2$. The mononuclear complexes exhibit Curie–Weiss behaviour over the entire temperature region as expected. The binuclear complex shows weak ferromagnetic coupling between the two hydroxide bridged chromium(III) centres.

## EXPERIMENTAL

*Synthesis of the complexes*

*Trans*(imidazole)[Cr(L-histidine)$_2$](NO$_3$). The procedures published by Hoggard were used for the preparation of this compound. Found: C, 33.87; H, 4.16; N, 23.09; Cr, 12.45; O, 26.0; Calc. for [Cr(C$_6$H$_8$H$_3$O$_2$)$_2$](NO$_3$): C, 34.1; H, 3.8; N, 23.2; Cr, 12.3; O, 26.5%.

*Trans*(carboxylate)[Cr(L-histidine)$_2$](NO$_3$). The mother liquor from *trans*-imidazole synthesis was left covered in a beaker for about 2 weeks, whereby large red cyrstalline products were collected. Found: C, 33.71: H, 3.82; N, 23.21; Cr, 12.20; O, 26.19%.

[(L-histidine)$_2$Cr(OH)$_2$Cr(L-histidine)$_2$]. Hoggard's method was modified to prepare this complex. Dowex 1-X8 in Cl-form was packed in a 30 mm × 25 cm column. This column was washed with 0.1 N NaOH (500 mls) for 2 days and tested with 0.1 N AgNO$_3$ to make sure there was no more Cl$^-$ ion in the column. The column was finally washed with distilled water to remove excess hydroxide. A 10 g sample of the trans-(imidazole)[Cr(L-histidine)$_2$](NO$_3$) dissolved in 60 cm$^3$ of water and heated to 56°C was passed through the column, while the solution was still warm. A pink precipitate began to form on collection. The precipitate was filtered and dried in air. Yield 70%. Found: C, 31.99; H, 5.56; N, 18.65; Cr. 11.81; O, 31.83; Calc. for [Cr$_2$(C$_6$H$_8$N$_3$O$_2$)$_4$-(OH)$_2$]. 6H$_2$O: C, 33.41; H, 5.33; N, 19.48; Cr, 12.06; O, 29.69%.

*Magnetic measurements*

Magnetic susceptibility measurements were carried out on an alternating force magnetometer (AFM).[23,24] The instrument was calibrated with HgCo(NCS)$_4$[25] and data was recorded over the temperature range 6–300 K. Measurement techniques are described elsewhere.[26] Tables of the variable temperature magnetic susceptibility data for the three complexes are available as supplementary material†. Electron spin resonance spectra were recorded on a Varian E-3 ESR spectrometer equipped with a nirtogen flow variable temperature unit. The spectra were recorded between 77 and 300 K.

## RESULTS AND DISCUSSION

The two monomeric complexes exhibit a linear dependence of the inverse magnetic susceptibility as a function of temperature. A plot of these data for *trans*(imidazole)Cr(L-histidine)$_2$NO$_3$ is shown in Fig. 1. The temperature dependent magnetic susceptibility data were fitted to the Curie–Weiss law (eqn 1) using the expression:

$$\chi = \frac{Ng^2\mu_B^2 S(S+1)}{3K(T-\theta)} \quad (1)$$

as shown in Fig. 1. The fitted parameters of each of the complexes to the Curie–Weiss law are listed in Table 1.

A plot of the magnetic data for [Cr(L-histidine)$_2$(OH)]$_2$ is shown in Fig. 2. An increase in the effective magnetic moment is seen as the temperature is lowered below 10 K. The inverse susceptibility was nearly linear and was also fitted to

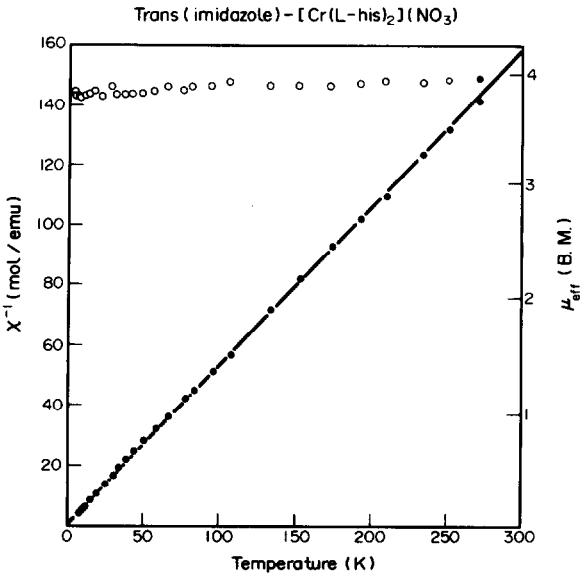



Fig. 1. Inverse magnetic susceptibility and effective magnetic moment plotted as a function of temperature for *trans*(imidazole)Cr(L-histidine)$_2$NO$_3$.

Table 1. Magnetic parameters for the chromium(III) histidine complexes

| | g | (K) | J(cm$^{-1}$) |
|---|---|---|---|
| (trans-carboxylate)Cr(histidine)$_2$NO$_3$ | 1.97 | -0.41 | - |
| (trans-imidazole)Cr(histidine)$_2$NO$_3$ | 2.00 | -0.31 | - |
| [Cr(histidine)$_2$(OH)]$_2$ | 1.99 | +0.43 | |
| | 1.99 | | +0.15 |

†Data has been deposited with the Editor and is available on request.

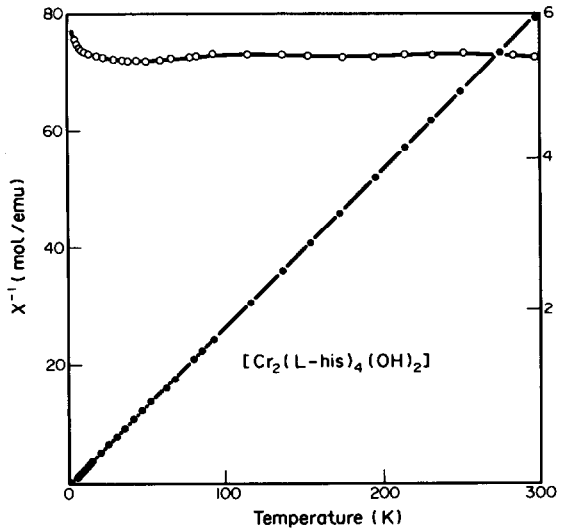



Fig. 2. Inverse magnetic susceptibility and effective magnetic moment plotted as a function of temperature for [Cr(L-histidine)$_2$OH]$_2$.

the Curie–Weiss law (eqn 1). The line through the inverse susceptibility points is the best fit of the magnetic data of [Cr(L-histidine)$_2$(OH)]$_2$ to eqn (1) with the parameters listed in Table 1. The positive value for $\theta$ and the increase in the effective magnetic moment at low temperature is consistent with ferromagnetic coupling between the two chromium(III) centres.

Ferromagnetic coupling between two neighbouring spins is usually described by the Heisenberg–Dirac–VanVleck spin Hamiltonian given in eqn (2).

$$\hat{\mathcal{H}} = 2J\hat{S}_1 \cdot \hat{S}_2. \quad (2)$$

For the case of binuclear chromium(III) where $S_1 = S_2 = 3/2$, the Hamiltonian in eqn (2) is incorporated into the Van Vleck equation to yield the closed form equation defining the temperature dependence of the magnetic susceptibility given in eqn (3).

$$\chi = \frac{Ng^2\mu_B^2[2e^{2x} + 10e^{6x} + 28e^{12x}]}{kT[1 + 3e^{2x} + 5e^{6x} + 7e^{12x}]} \quad (3)$$

where $x = J/kT$. The magnetic susceptibility data were fitted to eqn (3) and the curve drawn through the effective magnetic moment points ($\mu_{eff} = \sqrt{8\chi T}$) in Fig. 2 is the best fit of the data to eqn (3) with the parameters listed in Table 1.

ESR spectra for each of the complexes were recorded over the 77–300 K temperature range. Figure 3 shows the spectra recorded for polycrystalline samples of *trans*(imidazole)Cr(L-histidine)$_2$NO$_3$ and [Cr(L-histidine)$_2$(OH)]$_2$. The spectrum of the *trans*(carboxylate) isomer is very similar to the spectrum of the *trans*(imidazole)isomer.

We have attempted to isolate single crystals of the binuclear hydroxide-bridged complex but have been unsuccessful. Hodgson[27] and Hatfield[28] have described a linear relationship between the bridging angle and the size and magnitude of magnetic coupling for a series of hydroxo-bridged copper(II) complexes. It would be interesting to determine if the same correlation applied to chromium(III) hydroxo-bridged systems.

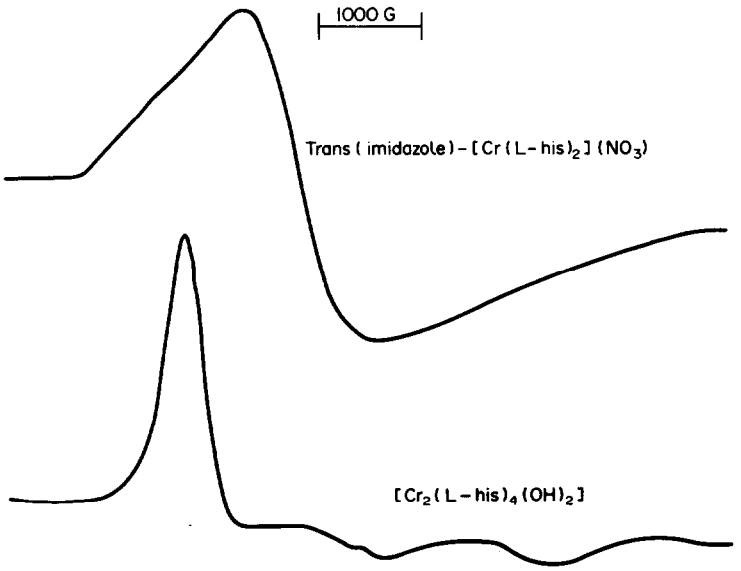



Fig. 3. The ESR spectra of *trans*(imidazole)Cr(L-histidine)$_2$NO$_3$ and [Cr(L-histidine)$_2$OH]$_2$ recorded at X-band at 77 K.

## REFERENCES


1. N. Nakamoto, V. Morinmoto and A. E. Martell, *J. Am. Chem. Soc.* 1961, **83**, 4528.
2. W. S. Eilbeck, F. Holmes and A. E. Underhill, *J. Chem. Soc.* (*A*) 1967, 757.
3. L. Cosella and M. Gullotti, *Inorg. Chem.* 1981, **20**, 1306.
4. P. Amico, G. Arena, P. G. Daniele, G. Ostacoli, E. Rizzarelli and S. Sammartano, *Inorg. Chem.* 1981, **20**, 772.
5. L. Antolini, L. P. Battaglio, A. B. Corradi, G. Marcotrigiano, L. Menabue, G. C. Pellacani and M. Saladini, *Inorg. Chem.* 1982, **21**, 1391.
6. P. E. Hoggard, *Inorg. Chem.* 1981, **20**, 415.
7. L. S. Zompa, *J. Chem. Soc. Chem. Coomun.* 1969, **9**, 783.
8. H. Oki, *Bull. Chem. Soc. Japan*, 1977, **50**, 680.
9. S. Yamada, J. Hidaka and B. E. Douglas, *Inorg. Chem.* 1971, **10**, 2187.
10. P. E. Hoggard and H.-H. Schmidtkey, *Inorg. Chim. Acta* 1979, **34**, 77.
11. L. A. Meiske and R. J. Angelici, *Inorg. Chem.* 1982, **21**, 731; 738.
12. M. Watabe, H. Yano, Y. Odaka, H. Kobayashi, *Inorg. Chem.* 1981, **20**, 3623.
13. R. Candlin and M. M. Harding, *J. Chem. Soc.* (*A*) 1967, 421.
14. K. A. Fraser and M. M. Harding, *J. Chem. Soc.* (*A*) 1967, 415.
15. M. M. Harding and S. J. Cole, *Acta Cryst.* 1963, **16**, 643.
16. R. H. Kretsinger, F. A. Cotton and R. F. Bryan, *Acta Cryst.* 1963, **16**, 651.
17. M. M. Harding and H. A. Long. *J. Chem. Soc.* (*A*) 1968, 2554.
18. K. A. Fraser, H. A. Long, R. Candlin and M. Harding, *J. Chem. Soc. Chem. Commun.* 1965, 344.
19. R. F. Bryan, P. T. Greene, P. F. Stokely and E. W. Wilson, Jr., *Inorg. Chem.* 1971, **10**, 1468.
20. A. Miyanaga, U. Sakaguchi, Y. Morimoto, Y. Kushi and H. Yoneda, *Inorg. Chem.* 1982, **21**, 1387.
21. M. S. Nair, K. Venkatachalapathi, M. Santappa and P. K. Murugan, *J. Chem. Soc., Dalton* 1982, 55.
22. J. J. Led and D. M. Grant, *J. Am. Chem. Soc.* 1975, **97**, 6962.
23. C. J. O'Connor, *Prog. Inorg. Chem.* 1982, **29**, 202.
24. R. T. Lewis, *Rev. Sci. Instrum.* 1971, **42**, 31.
25. C. J. O'Connor, E. J. Cucauskas, B. S. Deaver, Jr. and E. Sinn, *Inorg. Chim. Acta* 1979, **32**, 29.
26. C. J. O'Connor, C. L. Klein, R. J. Majeste and L. M. Trefonas, *Inorg. Chem.* 1982, **21**, 64.
27. D. J. Hodgson, *Prog. Inorg. Chem.* 1975, **19**, 173.
28. V. H. Crawford, W. H. Richardson, J. R. Wasson, D. J. Hodgson and W. E. Hatfield, *Inorg. Chem.* 1976, **15**, 2107.

*Polyhedron* Vol. 3, No. 1, pp. 21–24, 1984
Printed in Great Britain.

0277-5387/84 $3.00 + .00
Pergamon Press Ltd.

# SPECTRAL AND MAGNETIC STUDIES OF TIN(IV) COMPLEXES WITH NICKEL(II) THIOCARBOHYDRAZONES

SANGAMESH A. PATIL and VASANT H. KULKARNI*
Department of Chemistry, Gulbarga University, Gulbarga 585 106, India

(*Received* 18 *January* 1983; *accepted* 5 *April* 1983)

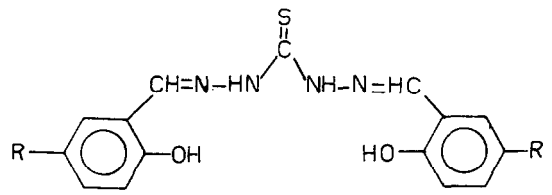
**Abstract**—Tin(IV) chloride derivatives of nickel(II) thiocarbohydrazones were obtained by reacting tin(IV) chloride with nickel(II) thiocarbohydrazones in chloroform medium. All the complexes are greenish coloured solids and appear to be non-electrolytes in DMF. Elemental analyses conform to the 1:1 stoichiometry. Magnetic, electronic and IR spectral information suggest that square planar nickel(II) thiocarbohydrazones have changed their configuration to octahedral as a result of reaction with tin (IV) chloride.

That metal complexes can behave as neutral ligands, and form complexes with both transition and non-transition metal ions, has marked the beginning of a new chapter in the coordination chemistry.[1-3] Sinn *et al.* have reported quite a large number of homonuclear bimetallic complexes for which the structural informations were accomplished with spectrochemical and magnetochemical means.

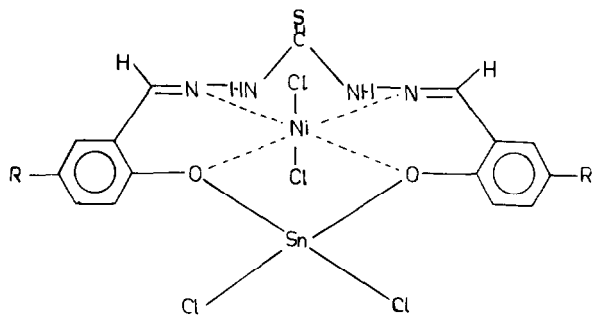
Hobday and Smith[4,5] have shown that N,N′-ethylene bis(salicylideneiminato)Co(II) having square-planar configuration reacts with $SnCl_4$ without undergoing any configurational changes, whereas, reaction with $AsCl_3$ and $PCl_3$ changes the configuration from square-planar to tetrahedral. Kogan *et al.*[6] have demonstrated that titanium(IV) chloride forms substitution complexes with transition metal complexes of bidentate Schiff bases. Biradar *et al.*,[7] have synthesized the bimetallic complexes of N,N′-ethylene bis(salicylideneiminato)Co(II) and N,N′-1,3-propane-bis-(salicylideneiminato)Co(II) with $SnCl_4$ and have deduced from magnetic and spectral data that the square-planar cobalt(II) complexes change their configuration to tetrahedral as a result of reaction with $SnCl_4$.

Voiculescu *et al.*,[8] have reported the reactions of organoaluminum compounds with Ni(II), Cu(II), Pd(II) dimethylglyoximates and salicylaldoximates. It is emphatically proven that organoaluminum compounds do not produce any configurational changes in nickel(II) glyoximates and aldoximates. However, Birader *et al.*[9] have indicated that tin(IV) chloride does produce such changes in nickel(II) aldoximates.

In this paper we report a new series of bimetallic complexes resulting from reaction of nickel(II) thiocarbohydrazones with tin(IV) chloride. The following thiocarbohydrazones were used for preparing nickel(II) complexes:




| | R |
|---|---|
| I | H |
| II | $CH_3$ |
| III | Cl |
| IV | $OCH_3$ |




## EXPERIMENTAL

Substituted salicylaldehydes, thiocarbohydrazide and their respective thiocarbohydra-

*Author to whom correspondence should be addressed.

zones were prepared as reported earlier.[10] Nickel(II) complexes of thiocarbohydrazones (**I–IV**) were prepared according to the method described earlier.[10]

*Preparation of tin(IV) complexes*

Nickel(II) thiocarbohydrazone (0.01 mol) was suspended in chloroform and treated with anhydrous tin(IV) chloride (0.01 mol) in the same solvent with vigorous shaking. The reaction mixture was left to stand at room temperature for several hours with occasional shaking. The precipitated binuclear complex was filtered, washed with chloroform and dried in vacuo over fused calcium chloride.

The complex was powdered and extracted with chloroform in a Soxhlet thimble for about 4–5 hr and then dried in vacuo over fused calcium chloride.

*Analysis*

Nickel(II) and tin(IV) in the complexes were determined gravimetrically as dimethylglyoximate and $SnO_2$ respectively. Nitrogen was determined by Dumas' method and sulphur gravimetrically as $BaSO_4$.[11]

The results of the elemental analyses are listed in Table 1.

*Physical measurements*

The IR spectra of the ligand and their complexes were recorded on a Perkin–Elmer 297 spectrophotometer in the region 4000–600 $cm^{-1}$ and the far IR spectra were obtained using a Perkin–Elmer 599 spectrophotometer.

The magnetic susceptibilities of the complexes at room temperature were obtained with a Gouy balance using $Hg[Co(SCN)_4]$ as a calibrant.

The electronic spectra of the complexes in nujol-mulls were recorded on a DMR-spectrophotometer in the 350–1500 nm region.

## RESULTS AND DISCUSSION

The complexes are brownish green in colour, soluble to a limited extent in common organic solvents, and to a considerable extent in pyridine, DMF and DMSO. The elemental analyses (Table 1) show that these complexes have 1:1 stoichiometry.

The molar conductance values in DMF at the concentration $10^{-3}$ M fall in the range of 5–10 $ohm^{-1}\,cm^2\,mole^{-1}$ indicating that all the complexes are non-electrolytes in DMF.

*IR spectra*

The important IR frequencies of the complexes along with their assignments are listed in Table 2.

The band due to the intramolecular hydrogen bonded OH,[12,13] appearing in the region 2675–2630 $cm^{-1}$ in the ligands disappears in the nickel(II) complexes, and the high intensity band of the ligands around 1280 $cm^{-1}$ due to the phenolic C–O vibration appears in the vicinity of 1320 $cm^{-1}$. These observations emphasize that the –OH groups of the ligands have reacted with nickel(II) via deprotonation.

The information regarding coordination of (C=N) groups[14] of the ligands to Ni(II) moiety is obtained by the low frequency shift of $\nu$(C=N) around 1630–1610 $cm^{-1}$ to 1620–1600 $cm^{-1}$.

The (C=S) group in thiamides[15,16] is expected to appear around 780 $cm^{-1}$. For these ligands this band is located in the region between 750 and 740 $cm^{-1}$. In the complexes this band does not show any shift suggesting that the C=S group is not involved in the coordination.

In view of the recent data on $\nu$(M–N) and $\nu$(M–O) vibrations of transition metal complexes of N- and O-donor ligands,[17] we have assigned the high intensity bands appearing in 415–405 and 370–350 $cm^{-1}$ regions to the $\nu$(Ni–N) modes. The bands appearing in the regions 345–335 $cm^{-1}$ and 255–240 $cm^{-1}$ have been assigned to the $\nu$(Ni–O) + $\nu$ ligand vibrations. Whereas, those found in the 310–305 $cm^{-1}$ and 285–270 $cm^{-1}$ regions to the $\nu$(Ni–O) vibrations.

In the bimetallic complexes, we do not observe significant changes in the NH, C=N and aromatic C=C vibrations. However, the phenolic C–O shows a low frequency shift and appears in the region 1280–1270 $cm^{-1}$ as a medium intensity band. This emphasizes the probable cleavage of the existing Ni–O bonds and formation of Sn–O bonds.

The $\nu$(Ni–N) bands of bimetallic complexes appear almost in the same region as those of parent complexes indicating that Ni–N linkages of the complexes have not undergone any changes in the bimetallic complexes. However, $\nu$(Ni–O) bands show considerable variation suggesting the involvement of Ni–O bonds of the complexes in the reaction with $SnCl_4$.

In addition to these bands we observe a few new bands in the spectra of those bimetallic complexes, and these have been assigned to the various $\nu$(Ni–Cl), $\nu$(Sn–O) and $\nu$(Sn–Cl) vibrations. A medium intensity band observed in the region 305–295 $cm^{-1}$ is attributed to the $\nu$(Ni–Cl) vibration in view of previous assignments.[18,19]

Nakamoto *et al.*[17] have assigned the region between 500 and 400 $cm^{-1}$ for $\nu$(M–O) in the case of transition metal acetylacetonates. Fay and Pinnavaia[20] also assign almost the same region for Zr and Hf acetylacetonates. In Sn(IV) acetylacetonates[21] the $\nu$(Sn–O) band has been lo-

Table 1. Elemental analysis, magnetic moments and electronic spectra of Sn(IV) bimetallic complexes

| Lig. No. | Comp. No. | Empirical Formula | % Sn | % Ni | % N | % S | % Cl | Mag. moments ($\mu_{eff}$ B.M.) | ($\bar{\nu}_1$) | ($\bar{\nu}_2$) | ($\bar{\nu}_3$) |
|---|---|---|---|---|---|---|---|---|---|---|---|
| I | V | $(C_{15}H_{12}N_4O_2SNi)SnCl_4$ | 18.25 (18.71) | 9.15 (9.30) | 8.76 (8.88) | 4.92 (5.06) | 22.25 (22.52) | 3.35 | 9980 | 12903 | 26666 |
| II | VI | $(C_{17}H_{16}N_4O_2SNi)SnCl_4$ | 17.42 (17.92) | 8.72 (8.91) | 8.49 (8.50) | 4.91 (4.85) | 21.32 (21.56) | 3.03 | 10260 | 12820 | 26316 |
| III | VII | $(C_{15}H_{10}N_4O_2SCl_2Ni)SnCl_4$ | 16.82 (16.87) | 8.28 (8.38) | 7.72 (8.00) | 4.51 (4.56) | 20.51 (20.30) | 2.96 | 10120 | 14290 | 25641 |
| IV | VIII | $(C_{17}H_{16}N_4O_4SNi)SnCl_4$ | 17.20 (17.09) | 8.35 (8.50) | 8.01 (8.11) | 4.52 (4.62) | 20.65 (20.56) | 3.12 | 10260 | 12900 | 26666 |

NOTE: 1. Values in the parenthesis are the calculated values.
2. Nickel(II) complexes of thiocarbohydrazones are diamagnetic and have square-planar configuration.
3. $\bar{\nu}_1$ is $^3A_{2g} \rightarrow {}^3T_{2g}$; $\bar{\nu}_2$ is $^3A_{2g} \rightarrow {}^3T_{1g}(F)$; $\bar{\nu}_3$ is $^4A_{2g} \rightarrow {}^3T_{1g}(P)$

Table 2. The important infrared frequencies (in $cm^{-1}$) of bimetallic complexes and their assignments

| Comp. | $\bar{\nu}$(NH) | $\bar{\nu}$(C=N) | $\bar{\nu}$(C=C) | $\bar{\nu}$(C-O) | $\bar{\nu}$(C=S) | $\bar{\nu}$(Ni-N) + $\bar{\nu}$Lig. | $\bar{\nu}$(Ni-N) | $\bar{\nu}$(Ni-O) | $\bar{\nu}$(Ni-O) + $\bar{\nu}$Lig | $\bar{\nu}$(Ni-Cl) | $\bar{\nu}$(Sn-O) | $\bar{\nu}$(Sn-Cl) |
|---|---|---|---|---|---|---|---|---|---|---|---|---|
| V | 3400brm<br>3150m | 1610s | 1560m<br>1540m<br>1500w | 1280s | 735s | 565m | 410w<br>360m | 365s<br>315s<br>290m | 330s | 340s<br>300m | 460m<br>400w<br>385m | 325s<br>310s<br>280m |
| VI | 3400brm<br>3200m | 1600s | 1550brm<br>1500w | 1280m | 740m | 560m | 410w<br>365m | 375m<br>325m<br>295sh | 345m | 360m<br>305m | 465w<br>400w<br>385m | 335m<br>315m<br>275sh |
| VII | 3410brm<br>3200m | 1600s | 1580w<br>1540m | 1275m | 740s | 560brm | 410w<br>365m | 380w<br>325s<br>280m | 330s | 375m<br>305m | 460m<br>400w<br>390m | 330s<br>315m<br>260w |
| VIII | 3400m<br>3200m | 1605s | 1560m<br>1540m | 1280m | 730s | 550m | 410m<br>370m | 350m<br>310m<br>280w | 335s | 340m<br>295w | 410m<br>390m | 330s<br>250m |

cated in the vicinity of 450 $cm^{-1}$. Taking into consideration these assignments we have located the $\nu$(Sn–O) modes in these complexes in the region 460–385 $cm^{-1}$.

*Magnetic data*

All the nickel(II) complexes of the ligands **I–IV** are diamagnetic suggesting that these complexes have square-planar configuration. The binuclear complexes formed by the action of tin(IV) chloride on nickel(II) thiocarbohydrazones are paramagnetic. The magnetic moments obtained at room temperature are in the range of 2.96–3.35 B.M. emphasizing that the nickel(II) has undergone a configurational change from square-planar to octahedral,[22] in these bimetallic complexes.

*Electronic spectra*

It is documented in the literature that square-planar complexes of nickel(II) are generally orange or red in colour.[22] However, examples of purple and green are also known. These complexes exhibit bands in the regions, 15,000–23,000 $cm^{-1}$ and 23,000–27,000 $cm^{-1}$ that can be ascribed respectively to $^1A_{1g} \rightarrow {}^1A_{2g}$ and $^1A_{1g} \rightarrow {}^1B_{1g}$ transitions. These nickel(II) thiocarbohydrazone complexes exhibit medium intensity broad bands in the regions, 14,710–15,500 $cm^{-1}$ and 22,730–21,740 $cm^{-1}$ that can be attributed to $^1A_{1g} \rightarrow {}^1A_{2g}$ and $^1A_{1g} \rightarrow {}^1B_{1g}$ transitions. These observations are suggestive of square-planar configuration prevailing in these complexes.

The electronic spectra of bimetallic complexes show three band maxima in the region 9980–26,666 $cm^{-1}$ (Table 1). It is obvious from the literature[22] that octahedral nickel(II) complexes display three bands attributable to the $^3A_{2g} \rightarrow {}^3T_{2g}$ ($\nu_1$), $^3A_{2g} \rightarrow {}^3T_{1g}(F)$ ($\nu_2$) and $^3A_{2g} \rightarrow {}^3T_{1g}(P)$ ($\nu_3$) transitions respectively in the following regions; 7000–13,000, 11,000–20,000 and 19,000–27,000 $cm^{-1}$. These bands shift to higher wave length in weaker fields. In these complexes we observe two broad bands in the regions 9980–10,260 $cm^{-1}$ and 12,820–12,900 $cm^{-1}$. The third band is observed as an inflection on the high intensity charge transfer band in the region 25,641–26,666 $cm^{-1}$. These observations suggest that square planar nickel(II) complexes have been transformed into the octahedral configuration as a result of reaction with tin(IV) chloride.

The analytical data, spectral and magnetic data taken together focus upon the conclusion that the square-planar nickel(II) complexes of thiocarbohydrazone have been transformed into octahedral configuration as a result of reaction with tin(IV) chloride.

*Acknowledgement*—Authors are grateful to Prof. S. P. Hiremath, Head of the Chemistry Department, Gulbarga University, for the facilities. One of the authors (SAP) acknowledges with thanks the financial assistance from the C.S.I.R., New Delhi.

## REFERENCES

1. E. Sinn and C. M. Harris, *Coord. Chem. Rev.* 1969, **4**, 391; E. N. Baker, D. Hall and T. N. Waters, *J. Chem. Soc.*, (A) 1970, 400; P. A. Yeats, J. R. Sams and F. Aubke, *Inorg. Chem.*, 1970, **6**, 1675.
2. H. S. Maslen and T. N. Waters, *Coord. Chem. Rev.* 1975, **17**, 137.
3. P. K. Bhattacharya, *J. Indian Chem. Soc.* 1982, **59**, 505.
4. M. D. Hobday and T. D. Smith, *J. Chem. Soc. (A)* 1970, 1085.
5. M. D. Hobday and T. D. Smith, *J. Chem. Soc. (A)* 1971, 1453.
6. V. A. Kogan, V. D. Sokolov, O. A. Osipov and V. N. Evreev, *Zh, Neorg. Khim.* 1970, 778.
7. N. S. Biradar, V. B. Mahale and V. H. Kulkarni, *Rev. Roum. Chim.* 1973, **19**, 809.
8. N. Voiculesen and I. Popesen, *Rev. Roum. Chim.* 1972, **17**, 719; N. Voiculesen, I. Popesen and L. Roman, *Rev. Roum. Chim.* 1973, **18**, 1595; N. Voiculesen, I. Popesen and N. Luchian, *Rev. Roum. Chim.* 1973, **18**, 1609; N. Voiculesen and I. Popesen, *Rev. Roum. Chim.* 1973, **18**, 1911.
9. N. S. Biradar, B. R. Patil and V. H. Kulkarni, *J. Inorg. Nucl. Chem.* 1975, **37**, 1901.
10. S. A. Patil, B. M. Badiger and V. H. Kulkarni, *Acta, Chim. (Hungeri)* in press.
11. A. I. Vogel, *Quantitative Inorganic Analysis.* Longmans Green, London (1962).
12. A. W. Baker and A. T. Shulgin, *J. Am. Chem. Soc.* 1959, **81**, 1523.
13. N. S. Biradar and V. H. Kulkarni, *J. Inorg. Nucl. Chem.* 1971, **33**, 3847.
14. N. S. Biradar and V. H. Kulkarni, *J. Inorg. Nucl. Chem.* 1971, **33**, 2451.
15. I. Suzuki, *Bull. Chem. Soc.* 1962, **35**, 1286, 1449.
16. B. L. Singh and U. Agarwala, *Inorg. Chem.* 1969, **8**, 2941.
17. K. Nakamoto, *IR and Raman Spectra of Inorganic and Coordination Compounds*, 3rd Edn. Wiley, New York (1978).
18. R. J. H. Clark, *Spectrochim. Acta.* 1965, **21**, 955.
19. D. M. Adams and P. J. Chandler, *Chem. Commun.* 1966, **3**, 69.
20. R. C. Fay and T. J. Pinnavaia, *Inorg. Chem.* 1968, **7**, 508.
21. Y. Kawasaki, T Tanaka and R. Okawara, *Spectrochim. Acta.* 1966, **22A**, 1571; R. W. Jones and R. C. Fay, *Inorg. Chem.* 1973, **12**, 2599; V. H. Kulkarni, B. R. Patil and B. K. Prabhakar, *J. Inorg. Nucl. Chem.* 1981, **43**, 17.
22. D. Nicholls, *Comprehensive Inorganic Chemistry* (Edited by J. C. Bailar Jr., H. I. Emeleus, R. S. Nyholm and A. F. T. Dickenson, Vol. 5. Pergamon Press, Oxford (1973).

*Polyhedron* Vol. 3, No. 1, pp. 25–29, 1984
Printed in Great Britain.

0277-5387/84 $3.00 + .00
Pergamon Press Ltd.

# TUNGSTEN(V) DIMERIC COMPLEXES WITH HETEROCYCLIC DITHIOCARBAMATES

**R. LOZANO*, E. ALARCON, A. L. DOADRIO and A. DOADRIO**
Departamento de Química Inorgánica, Facultad de Farmacia,
Universidad Complutense de Madrid, Madrid (3), Spain

(*Received* 8 *February* 1983; *accepted* 31 *May* 1983)

**Abstract**—In this paper we report the syntheses and study of a number of oxo- and sulphido-bridged tungsten(V) complexes with morpholine dithiocarbamate and piperidine dithiocarbamate as ligands. We assign the following formulae to the complexes: $W_2O_3(Rdtc)_4$, $W_2O_4(Rdtc)_2$, $W_2O_2S_2(Rdtc)_2$ and $W_2O_3S(Rdtc)_2$ (where R = morpholine and piperidine), based on the analytical data. We have studied the complexes by IR and electronic spectra, and magnetic susceptibility measurements. We assign in the IR spectra the following bands: W=O ($\nu_s$ = 939–948 $cm^{-1}$), W–$O_b$($\nu_a$ = 813–819 $cm^{-1}$, $\nu_s$ = 431–448 $cm^{-1}$), W–$S_b$ ($\nu_a$ = 470–476 $cm^{-1}$, $\nu_s$ = 368–370 $cm^{-1}$), C–N ($\nu$ = 1511–1519 $cm^{-1}$) and C–S ($\nu$ = 1090–1113 $cm^{-1}$). The low values of the magnetic moments (0.03–0.60 B.M.) are in accordance with a dimeric species of tungsten(V).

In previous communications, we have reported the isolation and study of monomeric and dimeric Mo(V) complexes with xanthates, oxines and dithiocarbamates as ligands.[1-3]

Although there is a great analogy between molybdenum and tungsten, no compounds of tungsten(V) with dimeric structure had been isolated. However, recently, we have reported the syntheses and study of several dimeric complexes of tungsten(V) with N,N-dialkyldithiocarbamates and N,N-alkylaryldithiocarbamates.[4,5]

In this paper, we describe the isolation of four complexes with different structures of W(V) with heterocyclic dithiocarbamates, as ligands. The four structures are due to dimeric complexes with monoxo bridge of formula $W_2O_3(Rdtc)_4$, dimeric complexes with dioxo bridge $W_2O_4(Rdtc)_2$, dimeric ones with disulphido bridge $W_2O_2S_2(Rdtc)_2$ and dimeric complexes with oxo-sulphido bridge $W_2O_3S(Rdtc)_2$, where R = morpholine and piperidine.

We have proved too that the four kinds of dimeric tungsten(V) complexes that have been obtained here, have the same structure and characteristics as the dimeric complexes of molybdenum(V) with dithiocarbamate as ligands, obtained by Schultz *et al.*,[6] showing the great similarity between molybdenum and tungsten.

The syntheses of the dimeric complexes of tungsten(V) present a great problem due to the polymerization and formation of polytungstates. We solved this question by treating the solution of $Na_2WO_4 \cdot 2H_2O$ in water with concentrated NaOH.

## EXPERIMENTAL

(a) *Materials.* $Na_2WO_4 \cdot 2H_2O$, morpholine, piperidine and potassium hydroxide were Merck commercial products. Potassium morpholine dithiocarbamate and potassium piperidine dithiocarbamate were prepared as reported previously.[7] The solvents used to prepare complexes were Carlo Erba or Merck. The solutions for absorption spectra were prepared using dimethylsulphoxide(DMSO) and $CH_2Cl_2$ spectral grade Merck–Uvasol.

(b) *Analytical procedures.* Elemental analyses were performed by the "Instituto de Química Or-

*Author to whom correspondence should be addressed.

gánica", Madrid, Spain. Tungsten was determined by Atomic Absorption with a Perkin–Elmer model 430 Atomic Absorption Spectrophotometer, after decomposing the complexes with a mixture of concentrated sulphuric acid and concentrated nitric acid (50%): Analytical data are collected in Table 1.

(c) *Methods.* Magnetic susceptibilities were measured by the Gouy method at room temperature in a Mettler H-51 A.R. balance and a type C Newport electromagnet. Molar susceptibilities have been corrected for the diamagnetism of the constituent atoms.[8] The magnetic moments were calculated according to the formula $\mu = 2.84(\chi_M \cdot T)^{0.5}$B.M., were $\chi_M$ is the corrected molar susceptibility.

The IR spectra have been registered on a Perkin–Elmer recording spectrophotometer model 283. The samples were run, in solid state as KBr pellets. Important IR absorption peaks for the compounds prepared in this study are listed in Table 2.

The visible and near ultraviolet spectra of the compounds were measured in the range 220–900 nm on a Perkin–Elmer recording spectrophotometer model 554 over dissolutions of the complexes in DMSO and $CH_2Cl_2$. The peaks obtained with both solvents are the same, however, we

Table 1. Elemental analyses (%) of tungsten(V) oxo-complexes

| Compound | % Calc | | | | | % Found | | | | |
|---|---|---|---|---|---|---|---|---|---|---|
| | C | H | N | S | W | C | H | N | S | W |
| $W_2O_3(S_2CNC_4H_8O)_4$ | 22.55 | 3.00 | 5.26 | 24.06 | 34.58 | 22.42 | 3.08 | 5.31 | 24.18 | 34.47 |
| $W_2O_3(S_2CNC_5H_{10})_4$ | 27.27 | 3.78 | 5.30 | 24.24 | 34.84 | 27.41 | 3.83 | 5.15 | 24.22 | 34.87 |
| $W_2O_4(S_2CNC_4H_8O)_2$ | 15.87 | 2.11 | 3.70 | 16.93 | 48.67 | 15.92 | 2.19 | 3.67 | 16.80 | 48.71 |
| $W_2O_4(S_2CNC_5H_{10})_2$ | 19.14 | 2.65 | 3.72 | 17.02 | 48.93 | 19.10 | 2.69 | 3.81 | 17.05 | 48.85 |
| $W_2O_2S_2(S_2CNC_4H_8O)_2$ | 15.22 | 2.03 | 3.55 | 24.36 | 46.70 | 15.31 | 2.05 | 3.50 | 24.22 | 46.66 |
| $W_2O_2S_2(S_2CNC_5H_{10})_2$ | 18.36 | 2.55 | 3.57 | 24.48 | 46.93 | 18.30 | 2.61 | 3.64 | 24.31 | 46.98 |
| $W_2O_3S(S_2CNC_4H_8O)_2$ | 15.54 | 2.07 | 3.62 | 20.72 | 47.66 | 15.46 | 2.01 | 3.73 | 20.91 | 47.62 |
| $W_2O_3S(S_2CNC_5H_{10})_2$ | 18.75 | 2.60 | 3.64 | 20.83 | 47.91 | 18.65 | 2.71 | 3.65 | 20.70 | 47.98 |

Table 2. IR absorption maxima, in $cm^{-1}$, of tungsten(V) oxo-complexes

| Compound | ν C-N | ν C-S | $\nu_s$ W=O | $\nu_a$ W-$O_b$ | $\nu_s$ W-$O_b$ | $\nu_a$ W-$S_b$ | $\nu_s$ W-$S_b$ |
|---|---|---|---|---|---|---|---|
| $W_2O_3(S_2CNC_4H_8O)_4$ | 1512 | 1109 | 940 | 819 | 448 | - | - |
| $W_2O_3(S_2CNC_5H_{10})_4$ | 1518 | 1090 | 939 | 818 | 446 | - | - |
| $W_2O_4(S_2CNC_4H_8O)_2$ | 1518 | 1108 | 944 | 814 | 442 | - | - |
| $W_2O_4(S_2CNC_5H_{10})_2$ | 1516 | 1109 | 943 | 815 | 440 | - | - |
| $W_2O_2S_2(S_2CNC_4H_8O)_2$ | 1513 | 1113 | 947 | - | - | 473 | 370 |
| $W_2O_2S_2(S_2CNC_5H_{10})_2$ | 1514 | 1099 | 948 | - | - | 470 | 369 |
| $W_2O_3S(S_2CNC_4H_8O)_2$ | 1511 | 1112 | 946 | 813 | 431 | 475 | 368 |
| $W_2O_3S(S_2CNC_5H_{10})_2$ | 1519 | 1108 | 945 | 816 | 437 | 476 | 368 |

Table 3. Electronic absorption spectra of tungsten(V) oxo-complexes with heterocyclic dithiocarbamates

| Compound | $\tilde{\nu}$ (kk) |
|---|---|
| $W_2O_3(S_2CNC_4H_8O)_4$ | 14.1(41), 17.0(203), 21.1(3141), 24.0(8253) 28.9(15417), 33.0(37297), 37.1(41046) |
| $W_2O_4(S_2CNC_4H_8O)_2$ | 15.5(103), 18.3(452), 21.3(4351), 23.6(6708) 28.7(9919), 33.0(17074), 36.9(32560) |
| $W_2O_2S_2(S_2CNC_4H_8O)_2$ | 15.4(57), 17.4(326), 20.9(4701), 22.5(4503) 23.2(8226), 29.0(17723), 33.0(28547), 37.0(51909) |
| $W_2O_3S(S_2CNC_4H_8O)_2$ | 15.4(98), 18.1(524), 21.2(4199), 22.2(4623) 23.5(8610), 29.1(12742), 32.8(43063), 36.7(61124) |
| $W_2O_3(S_2CNC_5H_{10})_4$ | 14.1(55), 16.8(213), 21.0(3640), 24.4(6228) 28.6(10453), 33.5(17604), 37.3(32912) |
| $W_2O_4(S_2CNC_5H_{10})_2$ | 15.3(154), 17.8(706), 21.0(5114), 23.5(8723) 28.6(14520), 33.4(22719), 36.7(48065) |
| $W_2O_2S_2(S_2CNC_5H_{10})_2$ | 15.4(131), 18.3(504), 20.8(6173), 22.3(5418) 23.8(7983), 29.0(11654), 33.3(27473) 36.7(35245) |
| $W_2O_3S(S_2CNC_5H_{10})_2$ | 15.4(95), 18.5(489), 21.0(4140), 22.6(5247) 25.0(9213), 28.9(13724), 33.0(22054) 36.6(39515) |

give in Table 3 the results in DMSO as solvents, as these complexes are not completely soluble in $CH_2Cl_2$.

(d) *Preparation of complexes.* All the complexes prepared in this study were susceptible to air oxidation, therefore all manipulations and reactions were carried out in a nitrogen atmosphere dry box or on a vacuum line.

$W_2O_3(S_2CNC_4H_8O)_4$

$Na_2WO_4 \cdot 2H_2O$ (1.65 g) was dissolved in water (30 $cm^3$) and was depolymerized. The solution was added to a solution of potassium morpholine dithiocarbamate (2.01 g) in water (30 $cm^3$), with vigorous stirring, and a solution (freshly prepared) of sodium dithionite (0.5 g) in water (10 $cm^3$) was added. Drop by drop, and with stirring, glacial acetic acid was added, till reaching pH = 5. The solution turns dark violet, and a solid of the same colour precipitates, which we separated by filtration *in vacuo*. It was washed repeatedly with a boiling water–ethanol mixture (75%), and dried over $P_2O_5$. Yield: 62%. $\mu = 0.60$ B.M.

$W_2O_4(S_2CNC_4H_8O)_2$

$Na_2WO_4 \cdot 2H_2O$ (3.30 g) was dissolved in water (40 $cm^3$) and it was depolymerized. Another solution of potassium morpholine dithiocarbamate (2.01 g) in water (35 $cm^3$) was prepared and added to the previous one and the resultant solution was treated with a solution of sodium dithionite (0.5 g) in water (10 $cm^3$). Drop by drop, dilute hydrochloric acid was added, till reaching pH = 2. The solution turns dark violet and a dark violet solid

precipitates, which was separated by filtration *in vacuo*, and washed repeatedly with a boiling water–ethanol mixture (50%).

The solid was filtered hot and *in vacuo*, in order to obtain a powder which was dried over $P_2O_5$. Yield: 59%. $\mu = 0.15$ B.M.

$W_2O_2S_2(S_2CNC_4H_8O)_2$

A solution of $NaWO_4 \cdot 2H_2O$ (3.30 g) in water (40 $cm^3$) previously depolymerized, was treated with potassium morpholine dithiocarbamate (2.01 g) in water (30 $cm^3$). Hydrogen sulphide was passed through the resultant solution with simultaneous cooling in freezing mixture, for about 30 min. The colour of the solution was gradually changed to brown. Lastly, dilute acetic acid was added dropwise till reaching pH = 5, and total precipitation. The solution was filtered and a brown residue was washed with hot water and dried *in vacuo* over $P_2O_5$. Yield: 83%. $\mu = 0.03$ B.M.

$W_2O_3S(S_2CNC_4H_8O)_2$

$Na_2WO_4 \cdot 2H_2O$ (3.30 g) was dissolved in water (40 $cm^3$), and was depolymerized. Dilute hydrochloric acid was added dropwise till reaching pH = 4, and afterwards, hydrogen sulphide was bubbled slowly through the resultant solution for *ca.* 1 hr. After this time, a solution of potassium morpholine dithiocarbamate (2.01 g) in water (30 $cm^3$) was added, and acetic acid was added dropwise till reaching pH = 5. A brown solid precipitated, and it was separated by filtration *in vacuo* and washed with hot water, and dried over $P_2O_5$. Yield: 69%. $\mu = 0.05$ B.M.

A similar preparation was realised for the corresponding complexes with piperidine dithiocarbamate as ligand.

## DISCUSSION

In this study, we have synthesized four different complexes of tungsten(V) with morpholine dithiocarbamate and piperidine dithiocarbamate as ligands. According to the results of the analytical and spectroscopic data, the four complexes present dimeric structures.

If we effect the precipitation at pH = 5, with acetic acid, the complexes obtained present a monoxo bridge, the stoichiometry is 2:1, and the tungsten is 6-coordinated. The formula which most closely fits the analyses is $[W_2O_3(Rdtc)_4]$. However, if we precipitate the complexes at pH = 2, with dilute hydrochloric acid, the stoichiometry of the compounds is 1:1, the tungsten is 5-coordinated, and these complexes present a dioxo bridge. The formula that we assign to these complexes is $[W_2O_4(Rdtc)_2]$. The complexes obtained by bubbling $H_2S$ into the $Na_2WO_4 \cdot 2H_2O$ solution and the corresponding heterocyclic dithiocarbamate, and the ones synthesized from $H_2S$ and $Na_2WO_4 \cdot 2H_2O$ solution in dilute hydrochloric acid, with subsequent addition of the heterocyclic dithiocarbamate gave a stoichiometry of 1:1, the tungsten being 5-coordinated. In the first case, we assign a formula $[W_2O_2S_2(Rdtc)_2]$ involving a disulphido bridge. In the second reaction, the formula assigned to the complexes is $[W_2O_3S(Rdtc)_2]$, involving an oxo-sulphido bridge.

The low values of the magnetic moments (0.03–0.60 B.M.) are concordant with a dimeric species of tungsten(V) due to W–W interaction (direct or indirect).

The IR spectra of the four different kinds of complexes studied here show a band at 939–948 $cm^{-1}$, which we attribute to the symmetric stretching mode of the terminal W=O bond, but the antisymmetric stretching mode has not been detected. However, the appearance of the symmetric mode, is sufficient to designate, in the dimeric complexes, a *cis* disposition of two terminal W=O.[9] Although the terminal oxygen metal bonds are quite sensitive to the variations of the metal–donor atoms, we have not seen any particular change for the frequency of the W=O terminal bond.

In the IR spectra of the complexes with monoxo bridge, dioxo bridge and oxo-sulphido bridge, we assign the bands corresponding to the W–O–W bridge at 813–819 and 431–448 $cm^{-1}$, which we attribute to the vibrations of the antisymmetric and symmetric mode, respectively, of the W–O bridge bond. The compounds with disulphido and oxo-sulphido bridge, show two bands over 470–476 and 368–370 $cm^{-1}$, which we attribute to the vibrations of antisymmetric and symmetric stretching mode of the W–S bridge bond.

The IR spectra of the W(V) dithiocarbamates complexes, show the vibrations bands of the C–N and C–S bonds at 1511–1519 and 1090–1113 $cm^{-1}$, respectively.

The electronic spectra of the dimeric complexes with monoxo bridge and formula $W_2O_3(Rdtc)_4$, exhibit two bands at 14,100 and 17,000 $cm^{-1}$ region, which we attribute to *d–d* transitions $^2B_2 \rightarrow {}^2E(I)$ and $^2B_2 \rightarrow {}^2B_1$ respectively, according to the Balhausen–Gray scheme[10] for a distorted octahedral structure. There are two other bands, in the 21,100 and 24,100 $cm^{-1}$ region, that we assign to charge-transfer (ligand-to-metal). These complexes show three bands over 28,700, 33,300 and

37,200 $cm^{-1}$, which are due to intra-ligand transitions. The potassium salts exhibit also three bands over 28,700, 34,000 and 38,500 $cm^{-1}$ region. The differences are not terribly significant. We attribute the first band to a $n \rightarrow \pi^*$ transition, the second to a $\pi \rightarrow \pi^*$ and the last to a $n \rightarrow \sigma^*$ transition.

The electronic spectra of the dimeric complexes with dioxo $[W_2O_4(Rdtc)_2]$, oxo-sulphido $[W_2O_3S(Rdtc)_2]$ and disulphido $[W_2O_2S_2(Rdtc)_2]$ bridges, are very similar and we propose the same structure for all these complexes. They exhibit two bands at 15,400 and 17,900 $cm^{-1}$, which we attribute to $^2B_2 \rightarrow {}^2E(I)$ and $^2B_2 \rightarrow {}^2B_1$ transitions, respectively, for a possible square-pyramidal structure.[11] In the visible region, two bands at 21,000 and 23,500 $cm^{-1}$, are attributed to charge-transfer transitions. The dimeric complexes with disulphido and oxo-sulphido bridges, present another transition around 22,400 $cm^{-1}$ which we assign to a charge-transfer transition as we have observed in similar complexes of molybdenum(V).[12] In UV region, three transitions are detected at 29,000, 33,000 and 37,000 $cm^{-1}$, which we attribute to intra-ligand transitions like $n \rightarrow \pi^*$, $\pi \rightarrow \pi^*$ and $n \rightarrow \sigma^*$, respectively.

## REFERENCES


1. A. Doadrio and A. Doadrio Villarejo, *An Quim.* 1977, **73**, 959.
2. A. Doadrio, R. Lozano and A. L. Doadrio, *An Quim.* 1980, **76B**, 193.
3. R. Lozano, A. Doadrio and A. L. Doadrio, *Polyhedron* 1982, **1**, 163.
4. R. Lozano, E. Alarcón, A. L. Doadrio and A. Doadrio, *Polyhedron*, 1983, **2**, 435.
5. R. Lozano, A. L. Doadrio, E. Alarcón, J. Roman and A. Doadrio, *Revue de Chimie Minérale* 1983, **20**, 109.
6. F. A. Schultz, V. R. Ott, D. S. Rolison, D. C. Braward, J. W. McDonald and W. E. Newton, *Inorg. Chem.* 1978, **17**, 7; 1758.
7. A. Doadrio and A. Doadrio Villarejo, *An Quim.* 1978, **74**, 1054.
8. P. W. Selwood, *Magnetochemistry*. Interscience, New York (1956).
9. F. A. Cotton, D. L. Hunter, L. Ricard and R. Weiss. *J. Coord. Chem.* 1974, **3**, 259.
10. C. J. Ballhausen and H. B. Gray, *Molecular Orbital Theory*, W. A. Benjamin, New York (1965).
11. G. Bunzey and J. H. Enemark, *Inorg. Chem.* 1978, **17**, 3; 682.
12. A. Kay and P. C. H. Mitchell, *J. Chem. Soc.(A)*, 1970, 2421.

*Polyhedron* Vol. 3, No. 1, pp. 31–38, 1984
Printed in Great Britain.

0277–5387/84 $3.00 + .00
Pergamon Press Ltd.

# SPECTROSCOPIC STUDIES ON THE MIXED $Nd^{3+}$–$La^{3+}$ AND $Ho^{3+}$–$Gd^{3+}$ ACETATE SYSTEMS AS AN EXAMPLE OF THE DETERMINATION OF STABILITY CONSTANTS FROM ELECTRONIC SPECTROSCOPIC DATA

**K. BUKIETYŃSKA* and A. MONDRY**
Institute of Chemistry, University of Wrocław 50383 Wrocław, Poland

(*Received* 22 *February* 1983; *accepted* 31 *May* 1983)

**Abstract**—The previously worked out spectroscopic method of determination of stability constants of lanthanide ions displaying hypersensitive transitions in absorption spectra [ions of $f^2$–$f^6$ and $f^8$–$f^{12}$ configurations] has been extended to all the lanthanide ions. The method is based upon measurements of the oscillator strength of hypersensitive transitions of mixed systems of equimolar concentrations containing two different lanthanide ions, in the spectrum one of which a hypersensitive transition is easily observed. The method was proved on the $La^{3+}$–acetate and $Gd^{3+}$–acetete systems, both the lanthanide ions having no hypersensitive transitions within the generally available UV and VIS measurement range.

Recent research[1–5] showed that the oscillator strength of "hypersensitive" $f$–$f$ transitions of the lanthanide ions can be applied to the evaluation of the stability constants and thermodynamic functions of lanthanide complexes. This method, however, is limited to lanthanide ions for which the oscillator strength of the "hypersensitive" transition can be measured in the available spectral region, namely $Nd^{3+}$, $Pm^{3+}$, $Eu^{3+}$, $Ho^{3+}$, $Er^{3+}$ and $Tm^{3+}$. "Hypersensitive" transitions of some lanthanide ions ($Pr^{3+}$, $Sm^{3+}$ and $Dy^{3+}$) are observed in the near IR spectral region, where it is difficult to measure the oscillator strength precisely because of the solvent and/or ligand (particularly $H_2O$) overtones. For the $Ce^{3+}$, $Gd^{3+}$, $Yb^{3+}$ and $Lu^{3+}$ ions no measurable $f$–$f$ transitions appear. This limitation is a very important one because any general conclusion concerning the physical properties of lanthanide complexes requires complete information for the whole lanthanide series to be available.

In the present paper the spectroscopic method was applied to the determination of stability constants for lanthanide ions having no "hypersensitive" transitions in the available spectral region. For this purpose, the method of mixtures of two lanthanide ions of molar ratio of solutions of 1:1 has been used. The measurements are based on the assumption that in the mixed solution to which some amount of ligand is added, the distribution of ligand molecules between two lanthanide ions is proportional to the stability constants of their complexes. Under those conditions, a lowering of the oscillator strength is observed for a given free ligand concentration, in comparison with that of a corresponding ligand solution containing only one ion, for which a "hypersensitive" transition is observed. In order to establish this method the systems: $Nd^{3+}$–$La^{3+}$–acetates and $Ho^{3+}$–$Gd^{3+}$–acetates have been chosen.

## EXPERIMENTAL

The stock solutions of the lanthanide perchlorates were prepared from 99.9% lanthanide oxides (Merck) by an already published method.[2] The concentrations of $Ln^{3+}$ ions were determined gravimetrically. The ligand solutions were prepared by the half-neutralization method. Preparation of solutions and measurements have been described earlier.[2] Mixed solutions of $Nd^{3+}$: $La^{3+}$ and $Ho^{3+}$: $Gd^{3+}$ with molar ratio 1:1 were prepared.

The series with the following concentrations of the equimolar mixtures of two lanthanide ions were prepared: **I**—0.02M, **II**—0.04M, **III**—0.06M, **IV**—0.08M. The total acetate concentrations varied within the range:

| | |
|---|---|
| **I** | 0.015–0.4M, |
| **II** | 0.015–0.8M, |
| **III** | 0.015–1.2M, |
| **IV** | 0.015–1.0M. |

The ionic strength equal to 2M was kept constant.

*Author to whom correspondence should be addressed.

## CALCULATIONS AND RESULTS

Stability constants for the $Nd^{3+}$–acetates and $Ho^{3+}$–acetates were determined by the spectral method described previously.[2,3,5] It was necessary however to measure also the oscillator strengths of "hypersensitive" transitions for the pure $Nd^{3+}$ and $Ho^{3+}$ systems because of the difficulties in achieving exactly the same concentrations of the solutions of the metal and ligand ions. The total ligand concentration in all the solutions was calculated from the relation:

$$c_A = c'_A + [H^+] - c_H \qquad (1)$$

where $c_A$ is the actual total concentration of the acetate, $c'_A$ is the stoichiometric concentration of $CH_3COONa$ calculated from the amount of buffer added to the complex solution, $[H^+]$ is the concentration of hydrogen ion of the complex solution and $c_H$ is the hydrogen ion concentration arising from the stock solution of the lanthanide perchlorate.

The oscillator strengths of "hypersensitive" transitions of the lanthanide ions in the investigated solutions were calculated using a graphical method of band integration and an appropriate computer program (ICH 31). The measured systems ($Nd^{3+}$ and $Ho^{3+}$ acetate and $Nd^{3+}$–$La^{3+}$ and $Ho^{3+}$–$Gd^{3+}$ acetate solutions) should obey the following general equation:[2]

$$P_{ij} = a_i c_{A_{ij}}^{1/2J+1} + b_i \qquad (2)$$

where $P_{ij}$ is the oscillator strength for the particular $c_M$ and $c_A$ value, $a_i$, $b_i$ are the coefficients for different $c_A$ and constant $c_M$ values, $c_{A_{ij}}$ is the total ligand concentration for the particular $c_M$ and $c_A$ value and $1/2J + 1$ equals $\frac{1}{10}$ and $\frac{1}{17}$ for the $Nd^{3+}$ and $Ho^{3+}$ ions, respectively. This analytical form of the $P = f(c_A)$ relation was checked numerically for all the investigated systems. For the $Nd^{3+}$–acetate, $Ho^{3+}$–acetate and mixed $Nd^{3+}$–$La^{3+}$ and $Ho^{3+}$–$Gd^{3+}$ acetates, the $a_i$, $b_i$ coefficients of the eqn (2) have been calculated from the experimental values of the oscillator strengths for different M:L ratios and different $c_M$ concentrations.

Typical results for $Ho^{3+}$–acetate and $Ho^{3+}$–$Gd^{3+}$–acetate are shown at a particular $c_M$ concentration (Table 1). These results were used for the evaluation of the formation curves of the investigated systems.

For the calculation of the average ligand number

Table 1. Total ligand concentrations ($c_A$), experimental ($P_{exp}$) and calculated ($P_{calc}$) oscillator strength values of the $^5G_6 \leftarrow {}^5I_8$ transition of $Ho^{3+}$ ion, the a and b values and the mean square error (s) for a given metal concentration for the $Ho^{3+}$–acetate and $Ho^{3+}$–$Gd^{3+}$–acetate systems

| | $c_{Ho}$ = 0.02000 M<br>a=9.7119·10$^{-5}$, b=−6.9062·10$^{-5}$<br>s = 6.35·10$^{-8}$ | | | $c_{Ho}$=0.02000M, $c_{Gd}$=0.02001M<br>a=1.0833·10$^{-4}$, b =−8.0429·10$^{-5}$<br>s = 2.37·10$^{-8}$ | | |
|---|---|---|---|---|---|---|
| N | $c_A \cdot 10^2$ [M] | $P_{exp} \cdot 10^6$ | $P_{calc} \cdot 10^6$ | $c_A \cdot 10^2$ [M] | $P_{exp} \cdot 10^6$ | $P_{calc} \cdot 10^6$ |
| 1 | 2.686 | 9.6175 | 9.4509 | 3.669 | 8.7000 | 8.7683 |
| 2 | 4.686 | 11.7662 | 12.0615 | 4.667 | 10.0617 | 10.0390 |
| 3 | 5.686 | 13.2507 | 12.9890 | 6.665 | 12.0334 | 11.8470 |
| 4 | 7.685 | 14.1752 | 14.4555 | 8.664 | 13.3837 | 13.3908 |
| 5 | 9.685 | 15.2983 | 15.5995 | 13.662 | 15.8047 | 15.9366 |
| 6 | 14.684 | 17.9767 | 17.6973 | 14.661 | 16.3648 | 16.3385 |
| 7 | 15.684 | 18.2206 | 18.0333 | 18.660 | 17.8915 | 17.7197 |
| 8 | 19.683 | 19.3512 | 19.2046 | 23.659 | 19.0545 | 19.0999 |
| 9 | 24.683 | 20.3789 | 20.3875 | 28.658 | 20.2160 | 20.2276 |
| 10 | 29.683 | 21.4622 | 21.3626 | 33.658 | 21.1548 | 21.1842 |
| 11 | 34.682 | 22.0388 | 22.1939 | 38.658 | 22.0097 | 22.0151 |
| 12 | 39.682 | 22.8183 | 22.9194 | | | |

($\bar{n}$) and free ligand concentration ($c_f$), the method of the corresponding solutions have been applied as previously.[2] It was assumed that at the same free ligand concentration, the same oscillator strength value is observed for different total ligand and metal concentrations:

$$P = a_1 c_{A_1}^{1/2J+1} + b_1 = a_2 c_{A_2}^{1/2J+1} + b_2 = a_3 c_{A_3}^{1/2J+1} + b_3 = a_4 c_{A_4}^{1/2J+1} + b_4. \quad (3)$$

Knowing the values of $a_i$ and $b_i$ the $Nd^{3+}$–acetate and $Ho^{3+}$–acetate systems, the $c_{A_i}$ values for different oscillator strength values can be evaluated. From the relation:

$$c_{A_i} = \bar{n} c_{M_i} + c_f \quad (4)$$

the free ligand concentration $c_f$ and the average ligand number $\bar{n}$ have been calculated.

As it is seen from the Table 1, the formation of $Gd^{3+}$–acetate distinctly influences the oscillator strength value at a given $c_M$ and $c_A$ concentration of $Ho^{3+}$–acetate. This is even more clearly seen in Fig. 1 where the hypersensitive transitions of the systems $Ho^{3+}$–acetate and $Ho^{3+}$–$Gd^{3+}$–acetate are shown.

The above results constitute strong evidence for the validity of the assumption of a distribution of the ligand between the two complexing ions. Knowing $a_i$, $b_i$ values for one of the lanthanide ions and the mixture ($Nd^{3+}$–$La^{3+}$, $Ho^{3+}$–$Gd^{3+}$) and applying the method of the corresponding solutions, the free ligand concentration in the $La^{3+}$ and $Gd^{3+}$ ion solutions can be calculated:

$$c_{A_f(M_I)} = \bar{n}_{M_I} c_{M_I} + c_f \quad (5)$$

$$c_{A_f(M_I, M_{II})} = \bar{n}_{M_I} c_{M_I} + \bar{n}_{M_{II}} c_{M_{II}} + c_f \quad (6)$$

$$c_{A_f(M_I, M_{II})} - c_{A_f M_I} = \bar{n}_{M_{II}} c_{M_{II}} \quad (7)$$

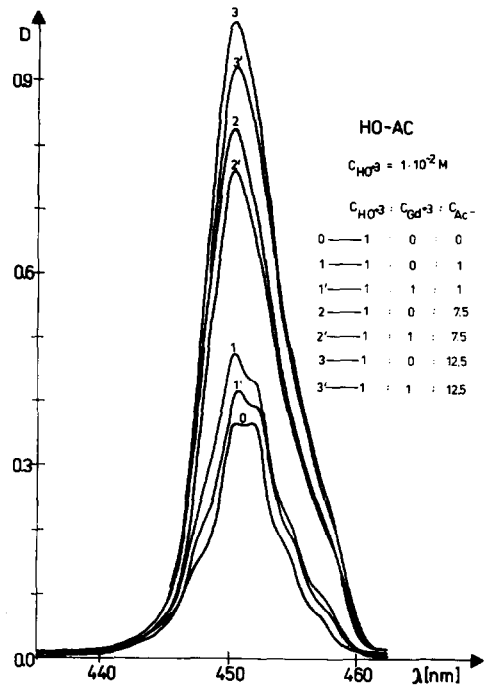



Fig. 1. The effect of the acetate ion concentration on the $^5G_6 \leftarrow {}^5I_8$ transition of $Ho^{3+}$ ion for the $Ho^{3+}$–acetate and $Ho^{3+}$–$Gd^{3+}$–acetate systems.

where $c_{A_f(M_I)} = c_{A_f(Nd^{3+})}$ or $c_{A_f(Ho^{3+})}$–total ligand concentration in the $Nd^{3+}$ or $Ho^{3+}$ acetate system

$$c_{A_f(M_I, M_{II})} = c_{A_f(Nd^{3+}, La^{3+})} \quad \text{or} \quad c_{A_f(Ho^{3+}, Gd^{3+})}$$

in $Nd^{3+}$–$La^{3+}$ or $Ho^{3+}$–$Gd^{3+}$–acetate system.

All data necessary for application of the discussed method are given in the Tables 2 and 3 for $Nd^{3+}$–$La^{3+}$ and $Ho^{3+}$–$Gd^{3+}$ acetates, respectively.

These data enabled us to evaluate the stability constant set values of the $La^{3+}$, $Nd^{3+}$, $Gd^{3+}$, $Ho^{3+}$ acetates which are collected in Table 4.

Table 4. Stability constants of $Ln^{3+}$–acetate systems ($\mu = 2$ M $NaClO_4$, $t = 21°C$) determined by (a) the spectroscopic method and (b) the potentiometric method (b) –Refs. [6, 7]

| System | | $\beta_1$ [$M^{-1}$] | $\beta_2$ [$M^{-2}$] | $\beta_3$ [$M^{-3}$] | $\beta_4$ [$M^{-4}$] |
|---|---|---|---|---|---|
| $La^{3+}$ – Ac | a | 46 ± 6 | 200 ± 50 | 1000 ± 800 | 1900 ± 900 |
| | b | 36 ± 1 | 300 ± 30 | 950 ± 200 | ~900 |
| $Nd^{3+}$ – Ac | a | 85 ± 1 | 870 ± 20 | 4300 ± 100 | 2600 ± 200 |
| | b | 80 ± 3 | 1020 ± 100 | 2900 ± 500 | ~3500 |
| $Gd^{3+}$ – Ac | a | 91 ± 10 | 1280 ± 110 | 6600 ± 3000 | 6100 ± 3600 |
| | b | 69 ± 2 | 1320 ± 150 | 5200 ± 1000 | ~5000 |
| $Ho^{3+}$ – Ac | a | 56 ± 1 | 870 ± 20 | 4500 ± 200 | 9800 ± 800 |
| | b | 43 ± 2 | 730 ± 70 | 5600 ± 800 | ~4000 |

Table 2. Results of the calculations all quantities necessary for the calculation of stability constants for $Nd^{3+}$-acetate and $Nd^{3+}$–$La^{3+}$-acetate systems

| $c_{Nd}$ [M] | 0.01005 | 0.01005 | | 0.02010 | 0.02010 | | 0.03024 | 0.03024 | | | | |
|---|---|---|---|---|---|---|---|---|---|---|---|---|
| $c_{La}$ [M] | | 0.01006 | | | 0.02011 | | | 0.03027 | | | | |
| $a \cdot 10^5$ | 3.4476 | 3.5371 | | 3.6749 | 3.8146 | | 3.8558 | 4.0305 | | | | |
| $b \cdot 10^5$ | -1.1442 | -1.2509 | | -1.3690 | -1.5424 | | -1.5567 | -1.7840 | | | | |
| $s \cdot 10^8$ | 2.32 | 3.06 | | 4.13 | 3.14 | | 4.94 | 4.92 | | | | |
| $P \cdot 10^5$ | $c_{A(Nd)} \cdot 10^2$ [M] | $c_{A(Nd,La)} \cdot 10^2$ [M] | $\bar{n}_{La_1}$ | $c_{A(Nd)} \cdot 10^2$ [M] | $c_{A(Nd,La)} \cdot 10^2$ [M] | $\bar{n}_{La_2}$ | $c_{A(Nd)} \cdot 10^2$ [M] | $c_{A(Nd,La)} \cdot 10^2$ [M] | $\bar{n}_{La_3}$ | $c_f \cdot 10^2$ [M] | $\bar{n}_{Nd}$ | $\bar{n}_{La}$ |
| 1.200 | 2.112 | 2.551 | 0.4364 | 2.787 | 3.688 | 0.4480 | | | | 1.437 | 0.6716 | 0.4420 |
| 1.215 | 2.252 | 2.712 | 0.4573 | 2.954 | 3.895 | 0.4679 | | | | 1.550 | 0.6985 | 0.4626 |
| 1.225 | 2.349 | 2.824 | 0.4722 | 3.071 | 4.039 | 0.4814 | | | | 1.627 | 0.7184 | 0.4768 |
| 1.250 | 2.609 | 3.122 | 0.5099 | 3.380 | 4.419 | 0.5167 | 4.177 | 5.842 | 0.5501 | 1.825 | 0.7766 | 0.5256 |
| 1.275 | 2.894 | 3.449 | 0.5517 | 3.717 | 4.831 | 0.5540 | 4.564 | 6.342 | 0.5874 | 2.060 | 0.8272 | 0.5644 |
| 1.300 | 3.208 | 3.806 | 0.5944 | 4.083 | 5.277 | 0.5937 | 4.983 | 6.879 | 0.6264 | 2.322 | 0.8792 | 0.6048 |
| 1.325 | 3.551 | 4.196 | 0.6412 | 4.483 | 5.760 | 0.6350 | 5.437 | 7.458 | 0.6677 | 2.610 | 0.9341 | 0.6480 |
| 1.350 | 3.928 | 4.621 | 0.6889 | 4.916 | 6.282 | 0.6793 | 5.927 | 8.080 | 0.7113 | 2.931 | 0.9901 | 0.6932 |
| 1.375 | 4.340 | 5.085 | 0.7406 | 5.387 | 6.847 | 0.7260 | 6.457 | 8.748 | 0.7569 | 3.281 | 1.0505 | 0.7412 |
| 1.400 | 4.790 | 5.591 | 0.7962 | 5.899 | 7.456 | 0.7742 | 7.030 | 9.465 | 0.8044 | 3.673 | 1.1095 | 0.7916 |

| | | | | | | | | | | | | |
|---|---|---|---|---|---|---|---|---|---|---|---|---|
| 1.450 | 5.819 | 6.739 | 0.9145 | 7.055 | 8.825 | 0.8802 | 8.313 | 11.061 | 0.9078 | 4.576 | 1.2353 | 0.9008 |
| 1.500 | 7.043 | 8.096 | 1.0467 | 8.411 | 10.415 | 0.9965 | 9.804 | 12.896 | 1.0215 | 5.667 | 1.3675 | 1.0216 |
| 1.550 | 8.494 | 9.694 | 1.1928 | 9.997 | 12.259 | 1.1248 | 11.531 | 14.999 | 1.1457 | 6.979 | 1.5042 | 1.1544 |
| 1.600 | 10.209 | 11.570 | 1.3529 | 11.848 | 14.392 | 1.2650 | 13.527 | 17.407 | 1.2818 | 8.553 | 1.6434 | 1.2999 |
| 1.650 | 12.229 | 13.767 | 1.5288 | 14.002 | 16.853 | 1.4177 | 15.828 | 20.156 | 1.4298 | 10.431 | 1.7826 | 1.4588 |
| 1.700 | 14.603 | 16.333 | 1.7197 | 16.501 | 19.687 | 1.5843 | 18.477 | 23.291 | 1.5904 | 12.664 | 1.9188 | 1.6315 |
| 1.750 | 17.383 | 19.322 | 1.9274 | 19.395 | 22.942 | 1.7638 | 21.518 | 26.858 | 1.7641 | 15.309 | 2.0481 | 1.8184 |
| 1.800 | 20.630 | 22.793 | 2.1501 | 22.739 | 26.674 | 1.9567 | 25.002 | 30.909 | 1.9514 | 18.431 | 2.1655 | 2.0194 |
| 1.850 | | | | 26.592 | 30.944 | 2.1641 | 28.986 | 35.503 | 2.1530 | 21.846 | 2.3610 | 2.1586 |
| 1.900 | | | | 31.024 | 35.820 | 2.3849 | 33.533 | 40.701 | 2.3680 | 26.051 | 2.4744 | 2.3765 |
| 1.950 | | | | 36.109 | 41.376 | 2.6191 | 38.712 | 46.575 | 2.5976 | 30.949 | 2.5671 | 2.6084 |
| 1.975 | | | | 38.923 | 44.435 | 2.7409 | 41.562 | 49.789 | 2.7179 | 33.692 | 2.6026 | 2.7294 |
| 2.000 | | | | 41.933 | 47.696 | 2.8657 | 44.599 | 53.201 | 2.8418 | 36.648 | 2.6292 | 2.8538 |

$c_{Nd}$ total $Nd^{3+}$ ion concentration
$c_{La}$ total $La^{3+}$ ion concentration
$a, b$ values of the coefficients in eqn (2) for the $Nd^{3+}$–acetate and $Nd^{3+}$–$La^{3+}$ acetate systems
$s$ mean square error
$c_{A(Nd)}$ total ligand concentration of $Nd^{3+}$–acetate system
$c_{A(Nd, La)}$ total ligand concentration of $Nd^{3+}$–$La^{3+}$-system
$P$ oscillator strength values of the $Nd^{3+}$ "hypersensitive" transition ${}^2G_{7/2}, {}^4G_{5/2} \leftarrow {}^4I_{9/2}$ for a given $c_{Nd}$ with different ligand concentrations ($c_{A(Nd)}$, $c_{A(Nd, La)}$)
$\bar{n}_{La_i}$ average ligand number of $La^{3+}$–acetates for a given $c_{La}$ and different $c_{A(Nd, La)}$ concentrations (eqn 7)
$c_f$ free ligand concentration
$\bar{n}_{Nd}$ average ligand number of $Nd^{3+}$–acetates
$\bar{n}_{La}$ mean value of the average ligand number of $La^{3+}$–acetates
This mean value is calculated from $\bar{n}_{La_i}$ values for a given $c_{A(Nd, La)}$ and different $c_{La}$ concentrations

Table 3. Results of the calculations all quantities necessary for the calculation of stability constants for $Ho^{3+}$-acetate and $Ho^{3+}$–$Gd^{3+}$-acetate systems

| $c_{Ho}$ [M] | 0.01000 | 0.01000 | | 0.02000 | 0.02000 | | 0.03000 | 0.03000 | | 0.04000 | 0.04000 | | | | |
|---|---|---|---|---|---|---|---|---|---|---|---|---|---|---|---|
| $c_{Gd}$ [M] | | 0.01000 | | | 0.02001 | | | 0.02997 | | | 0.04010 | | | | |
| $a \cdot 10^5$ | 9.2043 | 9.9580 | | 9.7119 | 10.833 | | 10.231 | 11.591 | | 10.682 | 12.166 | | | | |
| $b \cdot 10^5$ | -6.3805 | -7.1238 | | -6.9062 | -8.0429 | | -7.4388 | -8.8468 | | -7.9077 | -9.4770 | | | | |
| $s \cdot 10^8$ | 5.81 | 3.24 | | 6.35 | 2.37 | | 4.51 | 2.45 | | 4.41 | 4.40 | | | | |
| $P \cdot 10^5$ | $c_{A(Ho)} \cdot 10^2$ [M] | $c_{A(Ho,Gd)} \cdot 10^2$ [M] | $\bar{n}_{Gd_1}$ | $c_{A(Ho)} \cdot 10^2$ [M] | $c_{A(Ho,Gd)} \cdot 10^2$ [M] | $\bar{n}_{Gd_2}$ | $c_{A(Ho)} \cdot 10^2$ [M] | $c_{A(Ho,Gd)} \cdot 10^2$ [M] | $\bar{n}_{Gd_3}$ | $c_{A(Ho)} \cdot 10^2$ [M] | $c_{A(Ho,Gd)} \cdot 10^2$ [M] | $\bar{n}_{Gd_4}$ | $c_L \cdot 10^2$ [M] | $\bar{n}_{Ho}$ | $\bar{n}_{Gd}$ |
| 1.05 | 2.629 | 3.486 | 0.8570 | 3.372 | 5.096 | 0.8616 | | | | | | | 1.886 | 0.7430 | 0.8593 |
| 1.10 | 2.946 | 3.866 | 0.9200 | 3.750 | 5.594 | 0.9215 | | | | | | | 2.142 | 0.8040 | 0.9208 |
| 1.30 | 4.614 | 5.817 | 1.2030 | 5.705 | 8.081 | 1.1874 | 6.856 | 10.412 | 1.1865 | | | | 3.483 | 1.1210 | 1.1923 |
| 1.40 | 5.749 | 7.110 | 1.3610 | 7.009 | 9.684 | 1.3368 | 8.319 | 12.301 | 1.3287 | 9.621 | 14.898 | 1.3160 | 4.443 | 1.2926 | 1.3356 |
| 1.45 | 6.406 | 7.853 | 1.4470 | 7.762 | 10.594 | 1.4153 | 9.156 | 13.362 | 1.4034 | 10.539 | 16.107 | 1.3885 | 5.018 | 1.3793 | 1.4136 |
| 1.50 | 7.143 | 8.669 | 1.5260 | 8.591 | 11.583 | 1.4953 | 10.073 | 14.509 | 1.4802 | 11.538 | 17.406 | 1.4633 | 5.670 | 1.4667 | 1.4912 |
| 1.60 | 8.850 | 10.546 | 1.6960 | 10.503 | 13.829 | 1.6622 | 12.170 | 17.087 | 1.6406 | 13.810 | 20.308 | 1.6205 | 7.197 | 1.6547 | 1.6548 |

| | | | | | | | | | | | | | | | |
|---|---|---|---|---|---|---|---|---|---|---|---|---|---|---|---|
| 1.70 | 10.937 | 12.800 | 1.8630 | 12.812 | 16.481 | 1.8336 | 14.673 | 20.091 | 1.8078 | 16.498 | 23.660 | 1.7860 | 9.094 | 1.8544 | 1.8226 |
| 1.80 | 13.480 | 15.503 | 2.0230 | 15.592 | 19.605 | 2.0055 | 17.655 | 23.587 | 1.9793 | 19.674 | 27.528 | 1.9586 | 11.439 | 2.0645 | 1.9916 |
| 1.90 | 16.572 | 18.737 | 2.1650 | 18.934 | 23.281 | 2.1724 | 21.200 | 27.650 | 2.1522 | 23.418 | 31.986 | 2.1367 | 14.330 | 2.2804 | 2.1566 |
| 2.00 | 20.324 | 22.598 | 2.2740 | 22.940 | 27.598 | 2.3278 | 25.408 | 32.365 | 2.3213 | 27.826 | 37.117 | 2.3170 | 17.881 | 2.4974 | 2.3100 |
| 2.10 | | | | 27.735 | 32.661 | 2.4618 | 30.394 | 37.829 | 2.4808 | 33.006 | 43.015 | 2.4960 | 22.472 | 2.6355 | 2.4795 |
| 2.20 | | | | 33.463 | 38.589 | 2.5617 | 36.290 | 44.153 | 2.6236 | 39.084 | 49.787 | 2.6691 | 27.848 | 2.8105 | 2.6181 |
| 2.25 | | | | 36.727 | 41.919 | 2.5947 | 39.626 | 47.677 | 2.6864 | 42.504 | 53.538 | 2.7516 | 30.954 | 2.8885 | 2.6776 |
| 2.30 | | | | 40.290 | 45.519 | 2.6132 | 43.250 | 51.463 | 2.7404 | 46.204 | 57.554 | 2.8304 | 34.377 | 2.9570 | 2.7280 |
| 2.35 | | | | | | | 47.184 | 55.532 | 2.7855 | 50.206 | 61.852 | 2.9042 | 38.118 | 3.0220 | 2.8449 |

$c_{Ho}$ total $Ho^{3+}$ ion concentration

$c_{Gd}$ total $Gd^{3+}$ ion concentration

$a, b$ values of the coefficients in eqn (2) for the $Ho^{3+}$–acetate and $Ho^{3+}$–$Gd^{3+}$–acetate systems

$s$ mean square error

$c_{A(Ho)}$ total ligand concentration of $Ho^{3+}$–acetate system

$c_{A(Ho, Gd)}$ total ligand concentration of $Ho^{3+}$–$Gd^{3+}$–acetate system

$P$ oscillator strength values of the $Ho^{3+}$ "hypersensitive" transition $^5G_6 \leftarrow {}^5I_8$ for a given $c_{Ho}$ with different ligand concentrations $c_{A(Ho)}$, $c_{A(Ho, Gd)}$

$\bar{n}_{Gd_i}$ average ligand number of $Gd^{3+}$–acetates for a given $c_{Gd}$ and different $c_{A(Ho, Gd)}$ concentrations (eqn 7)

$c_f$ free ligand concentration

$\bar{n}_{Ho}$ average ligand number of $Ho^{3+}$–acetates

$\bar{n}_{Gd}$ mean value of the average ligand number of $Gd^{3+}$–acetates.

This mean value is calculated from $\bar{n}_{Gd_i}$ values for a given $c_{A(Ho, Gd)}$ and different $c_{Gd}$ concentrations

The comparison of the stability constants calculated by different methods[6,7] (Table 4) made us conclude, that better results can be reached when the stability constants of the two lanthanide ions investigated in the mixed system do not differ significantly. In each case, however, the results are quite reasonable.

The results presented confirmed our assumption that spectroscopic method based on the oscillator strength measurements can be applied to the investigation of complex equilibria of lanthanide complexes for the whole series.

## REFERENCES

1. K. Bukietyńska, A. Mondry and E. Osmęda, *J. Inorg. Nucl. Chem.* 1977, **39**, 483.
2. K. Bukietyńska, A. Mondry and E. Osmęda, *Ibid.* 1981, **43**, 1311.
3. K. Bukietyńska, A. Mondry and E. Osmęda, *Ibid.* 1981, **43**, 1321.
4. K. Bukietyńska, A. Mondry and E. Osmęda, *Bull. Acad. Pol. Chim.* 1980, **28**, 439.
5. K. Bukietyńska, A. Mondry and E. Osmęda, *Ibid.* 1980, **28**, 451.
6. A. Sonesson, *Acta Chem. Scand.* 1958, **12**, 165.
7. A. Sonesson, *Ibid.* 1958, **12**, 1937.

*Polyhedron* Vol. 3, No. 1, pp. 39–44, 1984
Printed in Great Britain.

0277-5387/84 $3.00 + .00
© 1984 Pergamon Press Ltd.

# SYNTHESIS AND ELECTRICAL PROPERTIES OF MONOMERIC AND DIMERIC IRON-1,5-DISUBSTITUTED 2,4-DITHIOBIURETS

**K. L. MADHOK**
School of Studies in Chemistry, Jiwaji University, Gwalior 474011(M.P.), India

(*Received* 14 *March* 1983; *accepted* 31 *May* 1983)

**Abstract**—The synthesis of monomeric and polymeric iron-1,5-disubstituted 2,4-dithiobiurets having the general empirical formula ($FeCl_3$·L) where L = 1,5-diphenyl-2,4-dithiobiuret (DPDTB); 1,5-diparatelyl 2,4-dithiobiuret (DpTDTB); 1,5-diorthotolyl 2,4-dithiobiuret (DoTDTB); 1-phenyl 5-paratolyl-2,4-dithiobiuret (PpTDTB); 1-phenyl 5-orthotolyl 2,4-dithiobiuret (PoTDTB) is described. The complexes were characterized by elemental analysis, molar conductance, magnetic susceptibility, IR and UV spectra. The dielectric constant and resistivity of characterized samples were studied as a function of temperature. The data indicate possible transitions at 90 and 185°C for monomeric iron-complexes whereas polymeric iron-1,5-disubstituted-2,4-dithiobiuret shows no breaks.

Metal complexes of sulphur donor ligands have received great attention during recent years because of their versatile use as antifungal and antibacterial agents.[1] Iron complexes have found a wide spectrum of applications[2–7] as catalyst,[2] in dehydrogenation,[3] dehalogenation,[4] decarboxylation,[5] isomerization[6] and electrolytic reduction.[7] Among biomedical applications are tumour localizing studies in the brain,[8] as blood coagulation inhibiter[9] and bactericide.[10] Applications as semiconductors[11] and for gas detection[12] have been reported. Earlier communications[13–20] have described the metal chelates of C=S, C=O and C=NH donor ligands. However, less work is available on the synthesis and physicochemical properties of polymeric iron-1,5-disubstituted 2,4-dithiobiurets. The present work describes simple methods of synthesis of both monomeric and polymeric iron-1,5-disubstituted-2,4-dithiobiurets and the results of the studies on their electrical properties.

## EXPERIMENTAL

All the chemicals used were either BDH "AnalaR" quality or E. Merck "G.R." quality.

The ligands used in the present study were 1,5-diphenyl 2,4-dithiobiurets (DPDTB); 1,5-diorthotolyl 2,4-dithiobiurets (DoTDTB); 1,5-diparatolyl 2,4-dithiobiuret (DpTDTB); 1-phenyl 5-orthotolyl 2,4-dithiobiuret (PoTDTB), 1-phenyl 5-paratolyl 2,4-dithiobiuret (PpTDTB) and were prepared by the method reported earlier.[19] Purity of these ligands was checked by melting point, elemental analysis and infrared studies.

## SYNTHESIS OF MONOMERIC IRON-COMPLEXES (FeL)

0.4 mol of the ligand, 0.0025 mol of ammonium molybdate in finally powdered state were taken in a 500 $cm^3$ round bottom flask fitted with reflux condenser and guard tube. 0.2 mol of anhydrous $FeCl_3$ was weighed into a closed dry bottle and the contents transferred to the flask, followed by addition of 200 $cm^3$ nitrobenzene (dried over fused $CaCl_2$ for 24 hr and redistilled). First the flask was heated at 150°C on a regulated heating mantle for half an hour. During this stage a brisk exothermic reaction takes place and the temperature rose sharply by 40°C. Next the flask was heated at 200°C for 4 hr. The reaction mixture was cooled, filtered and washed with distilled water. The crude product was treated with a solution of 30 g NaOH in 100 $cm^3$ water in a 1 L flask. The product was further purified by steam distillation until nitrobenzene was completely removed. The alkaline solution was then neutralized with 1% HCl and heated at 70°C for 1 hr. Contents of the flask were filtered off and washed with distilled water. The product was extracted with acetone using a Soxhlet apparatus. Final pufification was done by heating the sample at 170°C at low pressure ($10^{-3}$ mm Hg) by which any traces of impurities were sublimed.

## SYNTHESIS OF POLYMERIC IRON-COMPLEXES

A chloroform solution (0.1 M) of the ligand was added dropwise with constant stirring to an etherial solution of anhydrous $FeCl_3$ (0.08 M). During the course of the reaction temperature was maintained below 10°C. After the completion of the reaction, the reaction mixture was allowed to stand for 1 hr to attain equillibrium. The coloured complexes were separated by distilling out the excess solvent and purified by recrystallization.

## CHARACTERISATION OF THE SAMPLES

Monomeric and polymeric Fe-complexes were analysed for Fe, N, Cl and S. Iron[21] was estimated gravimetrically by heating at 400°C for 2 hr to convert it to $Fe_2O_3$. Nitrogen, sulphur and chlorine, were estimated by standard methods.[22, 17, 18]

The magnetic moments of the complexes were determined by Gouy's method. The molar conductance of these complexes in ethanol were determined with a conductivity meter (type LBR) using a dip type cell.

The infrared spectra of ligands and complexes were recorded in KBr on a Perkin–Elmer grating IR spectrophotometer model 237 B and in Nujol on c.r.-Beckman-20 instrument. The spectra are complicated due to the presence of many functional groups. However only those peaks which could be assigned with reasonable certainity are taken into consideration.

Absorption spectra of Fe (III) chloride complexes were measured by standard method using Perkin–Elmer UV-VIS spectrophotometer model 139. Transition energy ($E_T$ )was calculated from the relation

$$E_T = \frac{2.859 \times 10^5}{\lambda_{max} - (\text{in Å})}$$

and the oscillatory strength "$f$" was calculated from the equation

$$f = 4.32 \times 10^{-9} \int E dv$$

utilizing

$$E_{max}\, \Delta\bar{v} = \int E dv$$

where $\Delta\bar{v}$ is the wave number of the half band width. All the data are recorded in Table 2.

## ELECTRICAL MEASUREMENTS

Dielectric constant was defined as the ratio $\epsilon = C/C_0$, where $C$ is the capacitance of parallel plate condenser containing the material as a pellet and $C_0$ is the corresponding capacitance in air. The capacitance was measured with a standard LCR bridge at 1 and 10 kHz. The area $A$ of pellet was measured both geometrically and graphically and the thickness $d$ was measured by a micrometer screw up to 0.001 cm. The dielectric constant, $\epsilon$, was calculated from

$$\epsilon = C_0 d/(\epsilon_0 \times A)$$

Table 1. Analytical data of Fe (III) chloride complexes with 1,5-disubstituted 2,4-dithiobiurets

| Complex | M.P. (°C) | Analysis of Complexes | | | | | | Molecular Weight | |
|---|---|---|---|---|---|---|---|---|---|
| | | % Calculated | | | % Found | | | Calculated | Found |
| | | Fe | Cl | S | Fe | S | Cl | | |
| $FeCl_3$·DPDTB | 219 | 6.2 | 25.4 | 15.2 | 6.1 | 15.0 | 25.5 | 419.5 | 416.0 |
| $FeCl_3$·DoTDTB | 237 | 5.8 | 24.0 | 14.3 | 5.9 | 14.0 | 24.0 | 447.5 | 440.0 |
| $FeCl_3$·DpTDTB | 238 | 5.8 | 24.0 | 14.3 | 5.6 | 14.4 | 24.2 | 447.5 | 439.5 |
| $FeCl_3$·PoTDTB | 222 | 6.0 | 24.5 | 14.9 | 6.1 | 14.8 | 24.7 | 433.5 | 435.5 |
| $FeCl_3$·PpTDTB | 220 | 6.0 | 24.5 | 14.9 | 6.2 | 14.5 | 24.4 | 433.5 | 434.0 |
| $(FeCl_3$·DPDTB$)_2$ | 233 | 12.38 | 50.4 | 30.4 | 12.4 | 30.8 | 51.2 | 839.0 | 835.0 |
| $(FeCl_3$·DoTDTB$)_2$ | 235 | 11.5 | 11.5 | 28.5 | 12.0 | 29.0 | 11.0 | 895.0 | 870.5 |
| $(FeCl_3$·DpTDTB$)_2$ | 240 | 11.5 | 11.5 | 28.5 | 12.8 | 29.1 | 11.1 | 895.0 | 869.5 |
| $(FeCl_3$·PoTDTB$)_2$ | 241 | 12.0 | 49.0 | 29.8 | 11.9 | 29.2 | 49.4 | 867.0 | 852.2 |
| $(FeCl_3$·PpTDTB$)_2$ | 238 | 12.0 | 49.0 | 29.8 | 12.0 | 29.0 | 48.8 | 867.0 | 861.8 |

where

$$\epsilon_0 = 8.85 \times 10^{-14}\ \text{F/cm}$$

also, conductivity at different temperatures was determined using a stabilizing power supply and a d.c. microvoltmeter.

## RESULTS AND DISCUSSIONS

All the iron (III) complexes are dark-brown crystals, soluble in common organic solvents and insoluble in water. All these complexes decompose above 219°C. The analytical results (Table 1) correspond to general empirical formula $FeCl_3L$. Since there is almost no loss of chlorine (w%) in monomer or dimer, reduction of Fe (III) to Fe (II) may not be taking place. Cryoscopic determination of the molecular weights (Table 1) are in good agreement with $FeCl_3L$ and $Fe_2Cl_6L_2$ composition of the iron-complexes.

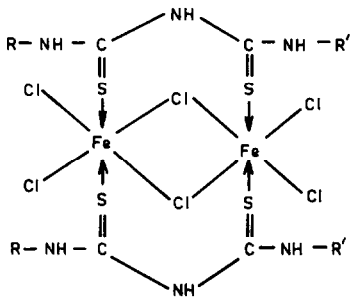
The electrolytic conductance measurements of these complexes (2.6–5.0 mhos) in freshly distilled ethanolic solution indicate non-electrolytic nature of these complexes (the molar conductance of uni-univalent electrolytes are 80–90 mhos).[24] The magnetic moments of these complexes at 25°C was observed to be very low (3.36–3.96 B.M.), which indicates the dimeric nature of these complexes.[26,27] On the basis of magnetic and conductance results, a dinuclear chlorobridged structure is proposed for these Fe (III) chloride complexes.

The molar absorptivity, the wave length corresponding to maximum absorption, transition energy and oscillatory strength of iron (III) chloride complexes are listed in Table 2. On the examination of UV spectra of the ligands and their complexes in ethanol, it is observed that the absorption bands of the ligands (285–295 nm) has been shifted to 300–310 nm (33300–32300 $cm^{-1}$) in complexes. This shift is attributed to the fact that during the complex formation the $\pi^*$ energy level is lowered due to stabilization of the excited state, so that the $n - \pi^*$ energy level is lowered in frequency and consequently lower energy. This also accounts for the fact that the thiocarbonyl group is acting as a donor in the complexes.

On examination of IR spectra of ligands and complexes it is observed that there is no remarkable change in N–H stretching and bending vibrations, but there is a considerable decrease in the intensity and frequency of C=S (10–35 $cm^{-1}$) stretching bands. This indicates that coordination is through thiocarbonyl sulphur in these complexes. Furthermore slight increase in the C–N stretching frequency on coordination also supports the view that the bonding is through sulphur in these complexes. The Fe (III) complexes show $\nu$Fe–Cl frequencies that seem too low for terminal Fe–Cl bands and correspond to bridging chlorine (245–200 $cm^{-1}$) groups. However bands in the region 355–380 $cm^{-1}$ may be attributed to terminal Fe–Cl groups, corresponding to which there are no ligand bands. These assignments are in good agreement with the assignment given by Woodward and Taylor.[28] On the basis of IR, magnetic, conductance measurements and electronic spectra, the following chlorobridged dimeric structure is proposed for $(FeCl_3L)_2$ complexes—

Table 2. Magnetic susceptibility, molar conductance and UV spectral data of Fe (III) chloride complexes

| Complex | Magnetic moment (B.M.) | Molar Conductance, $\lambda_m$, $cm^2$ mole $\Omega^{-1}$ | UV- Spectral Data in Ethanol | | | |
|---|---|---|---|---|---|---|
| | | | $\lambda_{max}$ (nm) | $E_{max} \times 10^4$ | $E_T$ (K cal/mole) | f |
| $FeCl_3$. DPDTB | 3.34 | 4.2 | 308 | 1.230 | 92.81 | 0.1990 |
| $FeCl_3$.DoTDTB | 3.35 | 3.8 | 320 | 1.329 | 89.35 | 0.2935 |
| $FeCl_3$.DpTDTB | 3.34 | 2.9 | 305 | 1.278 | 93.74 | 0.3639 |
| $FeCl_3$.PoTDTB | 3.35 | 3.0 | 320 | 1.4180 | 89.35 | 0.3378 |
| $FeCl_3$.PpTDTB | 3.36 | 2.6 | 308 | 2.9780 | 92.81 | 0.2000 |
| $(FeCl_3.DPDTB)_2$ | 3.36 | 4.8 | 300 | 4.616 | 95.30 | 1.615 |
| $(FeCl_3.DoTDTB)_2$ | 3.55 | 5.0 | 310 | 4.543 | 92.21 | 1.566 |
| $(FeCl_3.DpTDTB)_2$ | 3.58 | 5.0 | 310 | 4.543 | 92.21 | 1.566 |
| $(FeCl_3.PoTDTB)_2$ | 3.62 | 4.9 | 302 | 4.943 | 94.66 | 1.858 |
| $(FeCl_3.PpTDTB)_2$ | 3.96 | 4.5 | 305 | 4.754 | 93.74 | 1.746 |



Structure 1. Dinuclear CHloro bridged structure of $(FeCl_3l)_2$

Fe (III) chloride complexes with 1,5-disubstituted 2,4-dithiobiurets.

For

| | | |
|---|---|---|
| $FeCl_3$·DPDTB | $R = -C_6H_5$; | $R' = -C_6H_5$ |
| $FeCl_3$·DoTDTB5 | $R = -C_6H_4(CH_3)$; ortho | $R' = -C_6H_4(CH_3)$ ortho |
| $FeCl_3$·DpTDTB | $R = -C_6H_4(CH_3)$; para | $R' = -C_6H_4(CH_3)$ para |
| $FeCl_3$·PoTDTB | $R = -C_6H_5$; | $R' = -C_6H_4(CH_3)$ ortho |
| $FeCl_3$·PpTDTB | $R = -C_6H_5$; | $R' = -C_6H_4(CH_3)$ para |

## ELECTRICAL PROPERTIES

Eley[29] and Yartanyn[30] first observed the semiconducting properties of organic ligands. Eley[31] proposed that the conductivity arose through thermal or optical excitation of electrons from the highest filled to the lowest empty orbital. The mechanism of conductivity is associated with the mobile electrons of the ligand rings. Earlier Day *et al.*[33] reported the resistivity of iron–phthalocyanine as $4.10^9\ \Omega$ cm by single crystal method. The present data on specific resistance of monomeric complex is plotted as a function of temperature in Fig. 1. At room temperature $P$ is of the order of $10^{11}\ \Omega$ cm and decreases with increasing of $T$. The log $\rho$ vs $1/T$ plot is linear showing breaks at 90, 150 and 180°C. Below 90°C the activation energy as calculated from Arrhenius equation (Ea) is 0.47 eV. The Ea above 90°C (up to 150°C) is 0.35 eV. In the temperature ranges 150–180 and 180–240°C, Ea was found to be 0.26 and 0.69 eV respectively. This indicates the possibility of transitions at about 90, 150 and 180°C. In literature a transition from $\alpha$ to $\beta$ phase is reported at 180°C.

Table 3. IR spectral data of ligands and their Fe (III) chloride chelates (in $cm^{-1}$)[a]

| Complex | ν(N–H) | (N–H) | ν(C–N) | νN–H + ν(C–N) + (C=S) | $\nu_{cs}$(C=S) | ν(C=S) | νFe–Cl bridge | νFe–Cl terminal |
|---|---|---|---|---|---|---|---|---|
| DPDTB | 3200m | 1625m | 1535 | 1425 | 1255s | 750 | – | – |
| $FeCl_3$DPDTB | 3200m | 1622b | 1545 | 1425m | 1525m | 740m | 240 | 360 |
| $(FeCl_3DPDTB)_2$ | 3200m | 1620sb | 1542 | 1425 | 1222 | 749 | 245 | 355 |
| DoTDTB | 3210m | 1620m | 1549 | 1430 | 1260 | 750s | – | – |
| $FeCl_3$DoTDTB | 3215m | 1620m | 1550sb | – | 1225m | 740m | 205 | 370 |
| $(FeCl_3DoTDTB)_2$ | 3210m | 1618m | 1548 | 1428 | 1230m | 735m | 208 | 362 |
| DpTDTB | 3220m | 1618sb | 1535 | 1430m | 1235m | 750 | – | – |
| $FeCl_3$DpTDTB | 3218m | 1620m | 1542 | 1430m | 1230m | 730 | 212 | 375 |
| $(FeCl_3DpTDTB)_2$ | 3220m | 1615m | 1540 | 1425m | 1225 | 215 | 215 | 370 |
| PoTDTB | 3230b | 1620s | 1540 | 1415 | 1260s | 750s | – | – |
| $FeCl_3$PoTDTB | 3228m | 1615b | 1545 | 1420m | 1225m | 740m | 220 | 380 |
| $(FeCl_3PoTDTB)_2$ | 3225m | 1615b | 1550 | 1418m | 1230m | 738m | 220 | 365 |
| PpTDTB | 3225mb | 1600b | 1540 | 1425s | 1260s | 750s | – | – |
| $FeCl_3$PpTDTB | 3225m | 1608sb | 1560s | 1420m | 1228s | 740s | 215 | 378 |
| $(FeCl_3PpTDTB)_2$ | 3223m | 1605s | 1558s | 1425m | 1235m | 735m | 210 | 365 |

[a] s = strong, m = medium, b = bread, w = weak

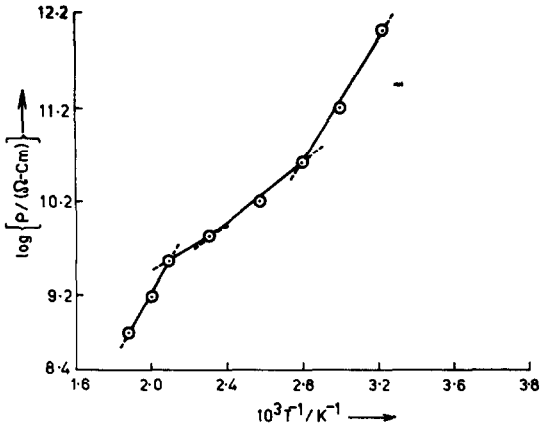



Fig. 1. Plot of log resistivity ($P$) vs $1/T$ for monomeric iron–DPDTB.

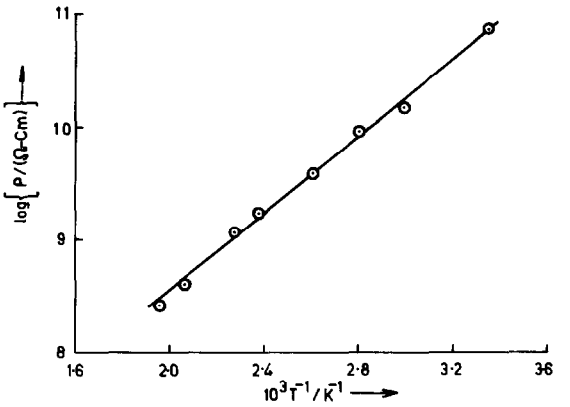



Fig. 2. Plot of log resistivity ($P$) vs $1/T$ for polymeric iron–DPDTB.

Table 4. Dielectric constant of monomeric and polymeric iron–DPDTB measured at 1 and 10 kHz as a function of temperature

| Temperature °C | Dielectric Constant | | | |
|---|---|---|---|---|
| | Monomeric $FeCl_3$.DPDTB | | Plymeric $FeCl_3$.DPDTB | |
| | 10 kHz | 1 kHz | 10 kHz | 1 KHz |
| 30 | 8.5 | 19 | 46 | 73 |
| 60 | 20.0 | 30 | 52 | 89 |
| 90 | 27.0 | 60 | 73 | 97 |
| 120 | 46.0 | 75 | 81 | 113 |
| 150 | 50.0 | 92 | 89 | 129 |
| 180 | 67.0 | 120 | 97 | 145 |
| 210 | 82.0 | 180 | 109 | 167 |
| 240 | 115.0 | 270 | 121 | 187 |

The specific resistance for the polymeric complex at room temperature is $10^{10}\,\Omega$ cm. This is lower than that of the monomeric complex by an order. The log $\rho$ vs $1/T$ plot (Fig. 2) is linear without any break, and the Ea is 0.20 eV. Both the monomeric and polymeric complexes show high dielectric constants. At room temperature these are in the range of 10–20 and 40–75 for monomeric and polymeric complexes respectively. On heating the dielectric constant increases rapidly at 180°C (Table 4) thus exihibiting a pyroelectric effect. Detailed studies on the changes in electrical properties in this region are underway.

## REFERENCES

1. J. G. Horsfall and S. Rich, *Contrib. Boyce Thompson Inst.* 1951, **16**, 361.
2. H. Meir, U. Tschirwitz, E. Zimmerchakt and W. Albercht, *Report BM Vg-FBWT* 1975, 756, 103.
3. S. A. Borisenkova, I. M. Ilina, A. P. Rudenko and A. P. Savilov, *Vestn. Mosk. Univ. Khim.* 1973, **14**, 494.
4. I. Hirco A. Ryuji and I. Eiji, *Chem. Lett.* 1974, **10**, 1157.
5. S. A. Borisenkova, I. M. Illina, E. V. Leonova and A. P. Radenko, *Zh. Org. Khim.* 1973, **9**, 1827.
6. S. A. Borisenkova, I. M. Ilina, A. P. Rudenko and A. P. Savilev, *Vestn. Mosk. Uiv. Khim.* 1973, **14**, 494.
7. A. J. Appleby and M. Savi, *Electrochim. Acta* 1979, **22**, 1315.
8. A. J. Cetosome, Ohio State University Microfilm Int. Order No. 7731919 (1979).
9. A. J. Cetosome, H. Brauner, M. Schaldach, R. Thull, R. Blaser and F. Johrestag, *Deutsch. Ges. Biomed. Tech.* 1973, 11.

10. P. Rudolf G. Reinert, H. Gerd, P. Andre and V. Rodolphe, Ger. Offen, 2812262 (1978).
11. W. Zygfryd and D. Brown, *Wiad. Chem* 1973, **27**, 38.
12. N. R. Byrd and M. B. Sheratte, *Sci. Tech. Aerosp. Rep.* 1976, 14(4).
13. K. L. Madhok and K. P. Srivastava, *Ind. J. Chem.* 1980, **A19**, 808.
14. K. L. Madhok, *Proc. Ind. Acad. Sci. (Chem. Sci.)* 1982, **91**, 165.
15. K. L. Madhok, *Inorg. Chim. Acta* 1982, **61**, 103.
16. K. P. Srivastava and K. L. Madhok, *Ind. J. Chem.* 1978, **16A**, 359.
17. K. P. Srivastava and K. L. Madhok, *J. Inorg. Nucl. Chem.* 1978, **40**, 1821.
18. K. P. Srivastava and K. L. Madhok, *J. Chem. Engng Data (ACS)* 1978, **23**, 256.
19. K. P. Srivastava, G. P. Srivastava, S. K. Arya and K. L. Madhok, *J. Chem. Engng Data (ACS)* 1980, **25**, 173.
20. K. P. Srivastava, I. K. Jain and K. L. Madhok, *Proc. Ind. Acad. Sci. (Chem. Sci.)* 1981, **90**, 309.
21. R. P. Linstead, *J. Chem. Soc.* 1934, 1017.
22. R. P. Linstead, *J. Chem. Soc.* 1934, 1016.
23. C. N. R. Rao, *Chemical Applications of Ultraviolet and Visible Spectroscopy*, p. 14. Butterworth, London (1967).
24. A. R. Nicholson and G. J. Sutton, *Austral. J. Chem.* 1969, **22**, 1543.
25. G. J. Sutton, *Austral. J. Chem.* 1971, **24**, 919.
26. R. R. Berrett, W. B. Fitzsimmon and A. A. Ownsu, *J. Chem. Soc. (A)* 1968, 1575.
27. W. M. Reiff, W. A. Baker and N. E. Ericksen, *J. Am. Chem. Soc.* 1968, **90**, 4794.
28. L. A. Woodward and M. J. Taylor, *J. Chem. Soc.* 1960, 4473.
29. D. D. Eley, *Nature* 1948, **162**, 819.
30. A. T. Yartanyan, *Zh. Fiz. Khim.* 1948, **22**, 769.
31. D. D. Eley, G. D. Perfitt, M. J. Perry and D. H. Taysum, *Trans Faraday Soc.* 1953, **49**, 79.
32. J. A. Elvidge and R. P. Linstead, *J. Chem. Soc.* 1955, 3536.
33. P. Day, G. Scregg and R. J. P. Williams, *Nature* 1963, **197**, 589.

*Polyhedron* Vol. 3, No. 1, pp. 45–47, 1984
Printed in Great Britain.

0277–5387/84 $3.00 + .00
© 1984 Pergamon Press Ltd.

# REACTION BETWEEN MAGNESIUM CHLORIDE AND IRON(III) CHLORIDE IN TETRAHYDROFURAN. THE CRYSTAL STRUCTURE OF DI-$\mu$-CHLORODICHLOROIRON(II) TETRAKIS(TETRAHYDROFURAN)MAGNESIUM(II)

**PIOTR SOBOTA*, TADEUSZ PŁUZIŃSKI and TADEUSZ LIS**
Institute of Chemistry, University of Wrocław, 14, Joliot-Curie, 50–383 Wrocław, Poland

(*Received* 21 *March* 1983; *accepted* 5 *July* 1983)

**Abstract**—The direct reaction between magnesium chloride and iron(III) chloride in tetrahydrofuran (THF) yields the $[MgCl(THF)_5][FeCl_4]$ complex (I). It is unstable and in reacting with THF undergoes reduction to produce the complex $FeCl_2(\mu\text{-}Cl)_2Mg(THF)_4$ (II). Crystals of (II) are orthorhombic, space group *Pbcn*, with $a = 9.18(1)$ $b = 16.30(2)$ $c = 15.85(1)$Å. The structure was solved by the heavy atom method and refined by least squares to $R = 0.053$ *for* 1194 observed diffractometer data. The molecule is heterobimetallic with an Fe ... Mg distance 3.455(3)Å and the Fe and Mg atoms are bridged by two Cl atoms.

Transition metal halogenide compounds ($MX$) in non-aqueous solutions ($D$), having the donor properties—undergo the heterolytic fission of a covalent bond when the solvent—solute interaction permits the complete transformation of an electron from the more electropositive to the more electronegative partner of the bond.[1]

$$D + 2MX \rightleftharpoons DM^+ + MX_2^-. \quad (1)$$

In many chemical reactions the I–III group elements ($A$) are used as reductors of the $MX$ in $D$. Such reactions yield the $AX$ which in solution could undergo ionization with formation of complex cation.

$$D + AX \rightleftharpoons DA^+ + X^-. \quad (2)$$

Such properties have been stated for $BeCl_2$,[2] $BCl_3$[3] and $AlCl_3$.[4]

In this paper the studies of magnesium chloride were undertaken to determine whether $MgCl_2$ would undergo ionization under the influence of a solvent, according to the eqn (2), and, whether this compound could have the influence upon the course of reaction (1). We have chosen $FeCl_3$, because it is known readily to form the $FeCl_4^-$ ion with $Cl^-$. Tetrahydrofuran was used as a solvent since both the magnesium chloride and iron (III) chloride are easily soluble in it.

*Author to whom correspondence should be addressed.

## RESULTS AND DISCUSSION

The addition of $MgCl_2(THF)_2$ to $FeCl_3$ in tetrahydrofuran gave a yellow precipitate, in which Fe:Mg:Cl = 1:1:5. This composition would suggest either $[MgCl(THF)_5][FeCl_4]$ or $[Mg(THF)_4][FeCl_5]$ as structures of the formed compound. To determine the composition of the anion, the magnesium cation was replaced by $Bu_4N^+$. The reaction produced a yellow homogeneous solution from which the previously synthesized compound $[Bu_4N][FeCl_4]$ was precipitated.[5] This is the evidence for the formation of $[MgCl(THF)_5][FeCl_4]$ (I) in the reaction (3)

$$FeCl_3 + MgCl_2(THF)_2 + 3THF \rightarrow [MgCl(THF)_5][FeCl_4]. \quad (3)$$

This result confirms the previous observation that the $[FeCl_5]^{2-}$anion does not exist in the aprotic medium. Thus, only the $[FeCl_4]^-$ anion is formed, which may form the double salts with the appropriate halogenide compounds.[6,7]

To determine, whether $MgCl_2(THF)_2$ actually undergoes ionization, its electrical conductivity in THF was measured as 0.5 $\mu$S. This value is very low and indicative of a low degree of dissociation.

In ether solution the $FeCl_3$ undergoes the autocomplex formation, according to the equation:[8]

$$2(THF)FeCl_3 + 2THF \rightleftharpoons [(THF)_4FeCl_2]^+ + [FeCl_4]^-. \quad (4)$$

The low value of the electrical conductivity of

$MgCl_2(THF)_2$ in THF prevents the unequivocal formation of the reaction (3) mechanism. The compound (I) could be formed either by coordination of the $MgCl_2(THF)_2$ molecule (where the magnesium—chlorine bonding could be broken) or in a reaction between the magnesium chloride dissociation products and the $FeCl_3$ autocomplexation products.

The compound (I) is sparingly soluble in tetrahydrofuran. Attempts to prepare it in a form suitable for X-ray investigations failed, because it is unstable in solution. After 2 days air—sensitive crystals of $[FeCl_2(\mu\text{–}Cl)_2Mg(THF)_4]$ (II) precipitated from solution. Its structure is shown in Fig. 1.

## SINGLE CRYSTAL X-RAY STUDIES

In the heterobimetallic compound (II) the Fe and Mg atoms are bridged by two $Cl^-$ atoms. Since both metal atoms lie on two-fold crystallographic axis, the molecule as a whole has also the $C_2$ point symmetry. The iron-magnesium distance of 3.455(3)Å suggests no direct metal–metal interaction. The geometry around the Fe atom is distorted tetrahedral. The terminal Fe–Cl(2) bond lengths of 2.228(2)Å are shorter than the bridging Fe–Cl(1) distances of 2.377(2)Å. The Cl–Fe–Cl angles also differ from the ideal tetrahedral values (Table 1). It is to be noted that the average Fe–Cl bond length of 2.30Å is almost the same as that found[9] for Fe(II) in $[N(CH_3)_4]_2[FeCl_4]$, 2.292(2)Å, but longer from that found for Fe(III) in $[PCl_4][FeCl_4]$[10], which is 2.185(4)Å. This difference is due to the cation radius increase and to the $Fe^{2+}$ ionic potential decrease on transition from $[FeCl_4]^-$ to $[FeCl_4]^{2-}$. That the Fe–Cl(2) bonding distance is shorter than the Fe–Cl(1) is undoubtedly caused by the presence of the de-$\mu$-chloro bridge. The chlorine atoms Cl(1) are coordinated by the $(THF)_4Mg^{2+}$ cation to form the bridge between the iron and the magnesium atoms. This results also in decrease of the Cl(1)FeCl(1)′ angle to 92.8(1)°, and, in consequence to increase of the Cl(2)FeCl(2)′ and Cl(1)FeCl(2) to 118.4(1)° and 115.5(1)° respectively.

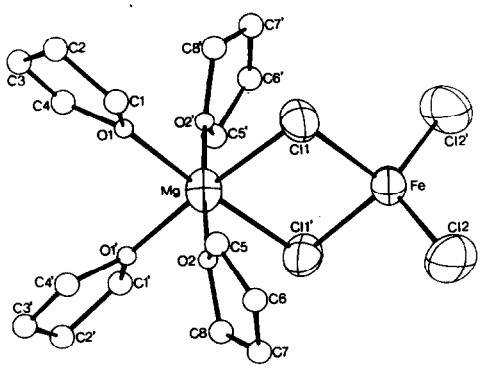



Fig. 1. The molecular structure of $[FeCl_2(\mu\text{-}Cl)_2Mg(THF)_4]$.

Table 1. Selected distances (Å) and angles (°) for $[FeCl_2(\mu\text{–}Cl)_2Mg(THF)_4]$

| | |
|---|---|
| (a) Bond lengths | |
| Fe–Cl(1) | 2.377(2) |
| Fe–Cl(2) | 2.228(2) |
| Mg–Cl(1) | 2.501(2) |
| Mg–O(1) | 2.073(5) |
| Mg–O(2) | 2.111(4) |
| O–C | 1.39–1.42(2) |
| C–C | 1.30–1.51(3) |
| (b) Interbond Angles | |
| (Atoms marked with a prime are related to those at $x, y, z$ by the two-fold axis at 0, $y$, $\frac{1}{4}$.) | |
| Cl(1)–Fe–Cl(1′) | 92.8(1) |
| Cl(2)–Fe–Cl(2′) | 118.4(1) |
| Cl(1)–Fe–Cl(2) | 115.5(1) |
| Cl(1)–Fe–Cl(2′) | 106.0(1) |
| Fe–Cl(1)–Mg | 90.2(1) |
| Cl(1)–Mg–Cl(1′) | 86.9(1) |
| Cl(1)–Mg–O(1) | 91.5(2) |
| Cl(1)–Mg–O(1′) | 174.8(2) |
| Cl(1)–Mg–O(2) | 87.2(2) |
| Cl(1)–Mg–O(2′) | 91.0(2) |
| O(1)–Mg–O(1′) | 90.5(2) |
| O(1)–Mg–O(2) | 93.9(2) |
| O(1)–Mg–O(2′) | 87.9(2) |
| O(2)–Mg–O(2′) | 177.5(2) |
| Mg–O–C | 124–131(1) |
| C–O–C | 101–105(1) |
| O–C–C | 107–121(2) |
| C–C–C | 104–108(2) |

The $Mg^{2+}$ cation has the coordination number 6 and besides the two Cl atoms, is also coordinated by four THF molecules, as shown in Fig. 1. The parameters (see Table 1) presented for the coordinated tetrahydrofuran molecules are close to those for $(THF)_4Mg^{2+}$ cation in the other compounds.[11]

## CONCLUSION

The composition of the compounds (I) and (II) is evidence for reaction of the magnesium chloride with the transition metal halogenides in a solvent like tetrahydrofuran. Complex (I) is unstable and in THF undergoes reduction to produce the heterobimetallic complex (II).

$$[MgCl(THF)_5][FeCl_4] \xrightarrow[-THF]{+e} [FeCl_2(\mu\text{–}Cl)_2Mg(THF)_4] + Cl^- . \quad (5)$$

The reduction is most likely caused by the THF, which reacts with $FeCl_3$, with ring—opening and polymerization.[12]

## EXPERIMENTAL

All manipulations were carried out under pure, dry dinitrogen, using Schlenk-tube and vacuum line techniques. Tetrahydrofuran was freshly distilled from sodium benzophenone ketyl. The $FeCl_3$ was obtained commercially from Fluka A. G and magnesium chloride was obtained by literature methode.[13]

*Preparation of* $[MgCl(THF)_5][FeCl_4]$ **(I)** Reaction of $FeCl_3$ with $MgCl_2(THF)_2$.

$FeCl_3$, 1g ($6.1 \times 10^{-3}$ mole) was dissolved under dinitrogen in 50 $cm^3$ tetrahydrofuran and mixed with $MgCl_2(THF)_2$, 2.9g ($1.2 \times 10^{-2}$ mole) dissolved in 20 $cm^3$ THF. Immediately, the yellow precipitate settled down, and was filtered off, washed with THF ($3 \times 10$ $cm^3$) and dried *in vacuo*. Yield: 3.4g; 90%. Found: C, 38.41; H, 6.34; Cl, 28.83; Mg, 3.79; Fe, 9.43%. Calc. for $C_{20}H_{40}O_5Cl_5MgFe$: C, 38.87; H, 6.47; Cl, 28.70; Mg, 3.93; Fe, 9.04%.

*Preparation of* $[Bu_4N][FeCl_4]$

To the suspension of the compound **(I)**, 0.5g in 20 $cm^3$ THF, $(Bu_4N)BF_4$ 0.7g was added with stirring. The reaction produced a homogeneous solution, which was next evaporated under vacuum to 50%; 10 $cm^3$ ethyl alcohol was then added. The yellow crystals precipitated slowly from the solution; after 24 h they were filtered off and washed with ethanol ($2 \times 5$ $cm^3$). Yield: 0.25g; 54%. Found: C, 43.31; H, 8.20; N, 3.45; Cl, 32.17; Fe, 12.62. Calc. for $C_{16}H_{38}NCl_4Fe$: C, 43.61; H, 8.18; N, 3.18; Cl, 32.25; Fe, 12.71%.

*Preparation of* $[FeCl_2(\mu\text{–}Cl)_2Mg(THF)_4]$ **(II)**

$[MgCl(THF)_5][FeCl_4]$, 0.5g, was dissolved in 40 $cm^3$ THF, filtered and distilled off under vacuum to 50%, and left upon standing for crystallization. The solution slowly changed its colour from yellow into brown–green; after 2–3 days the *colourless or yellow* air sensitive crystals were formed. Found: C, 37.51; H, 6.09; Cl, 27.69; Mg, 4.84; Fe, 11.07. Calc. for $C_{16}H_{32}O_4Cl_4MgFe$: C, 37.65; H, 6.27; Cl, 27.80; Mg, 4.76; Fe, 10.97%.

*X-Ray structure analysis of* $[FeCl_2(\mu\text{-}Cl)_2Mg(THF)_4]$

*Crystal data.* $C_{16}H_{32}O_4Cl_4FeMg$, $M = 510.4$, orthorhombic, $a = 9.18(1)$, $b = 16.30(2)$, $c = 15.85(1)$Å, $U = 2372$Å$^3$, $Z = 4$, $D_c = 1.43$g/cm$^3$, $D_0 = 1.43$g/cm$^3$, $F(000) = 1064$, space group *Pbcn*, Mo-$K_\alpha$ radiation $\lambda = 0.71069$Å, $\mu = 11.4$ cm$^{-1}$.

A specimen $0.60 \times 0.55 \times 0.50$ mm was cut from a large crystal and sealed in a capillary. 3580 intensities were recorded on a Synthex $P2_1$ diffractometer using graphite monochromated Mo-$K_\alpha$ radiation. The structure was solved by heavy atoms method using 1194 reflexions with $I > 3\sigma(I)$. All calculations were performed with the Synthex XTL/XTLE programs.[14] The hydrogen atoms were placed in geometrically calculation positions at a distance of 1.0Å and fixed. Full-matrix least-squares refinement, with anisotropic thermal parameters for Fe, Mg, Cl, O and C gave final $R = \Sigma||F_0| - |F_c||/\Sigma|F_0| = 0.053$ and $R_w = (\Sigma W \Delta F^2/\Sigma W F_0^2)^{1/2} = 0.045$.

Final thermal parameters for C(4) and C(8), were rather high. Furthermore the highest peaks on the final difference synthesis $\sim 0.3$ eÅ$^{-3}$ around them suggest small disordering of both atoms. Final atomic coordinates, thermal parameters and list of $F_0$ and $F_c$ values have been deposited with the Editor as supplementary data and may be obtained from him or the authors on request. Atomic coordinates have also been deposited with the Cambridge Crystallographic Centre.

## REFERENCES


1. V. Gutmann, *Coordination Chemistry in Non-Aqueous Solution*. Springer, Wien (1968).
2. B. M. Mikhaikov, T. A. Shchegoleva and V. D. Sheludyakov, *Izv. Acad. Nauk SSSR Ser Khim.* 1964, 2165.
3. T. H. Shchegoleva, V. D. Sheludyakov and B. M. Mikhailov, *Dokl. Akad. Nauk* 1963, **152**, 888.
4. R. E. Van Dyke and H. E. Crawford, *J. Am. Chem. Soc.* 1949, **71**, 2694.
5. J. S. Avery, C. D. Burbridge and D. M. L. Goodgame, *Spectrochim. Acta*, 1968, **24(A)**, 1721.
6. B. D. James, M. B. Millikan and M. F. MacKey, *Inorg. Chem. Acta Lett.* 1982, **64**, L 55.
7. M. B. Millikan and B. D. James, *J. Inorg. Nucl. Chem.* 1981, **43**, 1174.
8. V. Gutmann and K. H. Wegleitner *Monatsh. Chem.* 1970, **101**, 1532; R. S. Drago, *Progr. Inorg. Chem.* 1964, **6**, 371.
9. J. W. Lancher and J. A. Ibers, *Inorg. Chem.* 1975, **14**, 348.
10. T. J. Kistenmacher and G. D. Stucky, *Inorg. Chem.* 1968, **7**, 2150.
11. R. Hammer, H. F. Klein, U. Schubert, A. Frank and G. Huttner, *Angew. Chem. Int. Ed.* 1976, **15**, 612.
12. R. J. Kern, *J. Inorg. Nucl. Chem.* 1962, **24**, 1105.
13. E. C. Ashby and R. C. Arnott, *J. Organometall. Chem.* 1968, **14**, 1.
14. Syntex (1976). XTL/XTLE Structure Determination System. Syntex Analytical Instruments, Cupertino, California.

*Polyhedron* Vol. 3, No. 1, pp. 49–54, 1984
Printed in Great Britain.

0277–5387/84 $3.00 + .00
© 1984 Pergamon Press Ltd.

# SYNTHESIS AND CIRCULAR DICHROISM STUDIES OF SOME COBALT(III) COMPLEXES CONTAINING 2,2′ BIPYRIDINE, 1,10 PHENANTHROLINE, AND SOME OPTICALLY ACTIVE AMINO ACIDS

**MANUS B. MONROE*, DANIEL R. BOONE and ROGER N. KUST**
Chemistry Department, Indian Valley Colleges, Novato, CA 94947, U.S.A.

(*Received* 11 *April* 1983; *accepted* 31 *May* 1983)

**Abstract**—Two series of cobalt(III) complexes were synthesized and spectrally analyzed, [Co(2,2′-bipyridyl)$_2$(*aa*)]$I_2$ and [Co(1,10-phenanthroline)$_2$(*aa*)]$I_2$ (where the letters *aa* refer to an optically active, bidentate amino acid). The following amino acids were used: *l*-alanine, glycine, *l*-leucine, *l*-phenylalanine, and *l*-proline.

This research is an analogue to the chemical systems studied by Mason *et al.*[1,2] They investigated complexes such as $[Co(phen)_3]^{3+}$, $[Co(dipy)_3]^{3+}$, $[Co(phen)_2(dipy)]^{3+}$, $[Co(dipy)_2(phen)]^{3+}$, $[Co(phen)_2(ox)]^{2+}$, and $[Co(dipy)_2(ox)]^{2+}$. The series of $[Co(dipy)_2(na)]^{2+}$ and $[Co(phen)_2(na)]^{2+}$ complexes, where the letters *na* refer to a non-optically active, bidentate ligand, have exhibited exciton-splitting. We used optically active amino acids to ascertain whether or not the exciton-splitting phenomenon would occur when a non-optically active ligand was substituted by an optically active amino acid. In addition, a series of optically active amino acids was selected with the intention of determining whether small differences among the amino acid ligands would affect the circular dichroism (CD) spectra of the different complexes and if the formation of these complex ions would be steroselective.

## SYNTHESIS OF COMPLEX COMPOUNDS

The following is a list for the preparation of seven different cobalt(III) complex compounds.

*Compound* 1. $(-)_{589}$*l-prolinatobis*(2,2′-*bipyridyl*) *cobalt*(III) *iodide*

6.0 g of dichlorobis(2,2′-bipyridyl)cobalt(III) chloride[3] were dissolved in 100 cm$^3$ of absolute methanol and 1.5 g of *l*-proline was added with stirring and neutralized by adding lithium hydroxide, using universal pH paper, to "pH9".

After stirring for 30 min at room temperature in an open beaker concentrated hydrochloric acid was added to the vigorously stirred purple solution until the "pH" reached 7. Next, 6.0 g of potassium iodide was added and stirred for several minutes forming a precipitate of potassium chloride which was removed by vacuum filtering using a Gooch crucible with a medium porosity fritted disk.

The volume of the solution was reduced to approx. 20 cm$^3$ by passing air over the solution and the salmon-coloured product began to precipitate after approx. 30 min.

The product was filtered and dissolved in 20 cm$^3$ of warm (50°C) deionized water and the solution vacuum filtered to remove a water insoluble, yellow precipitate. Next, the solution, in a covered beaker, was placed in a 2°C refrigerator for at least 5 days so that red-coloured crystals formed. This technique gave a 28% (2.5 g) yield.

For analysis, the product was recrystallized three times from double distilled water and dried overnight in a 60°C oven. Found: C, 40.37; H, 3.29; N, 9.37. $CoN_5O_2I_2C_{25}H_{24}$ requires: C, 40.62; H, 3.27; N, 9.47%.

*Author to whom correspondence should be addressed.

*Compound* 2. *Glycinatobis(2,2′-bipyridyl)cobalt* (III) *iodide*

3.0 g of $[Co(dipy)_2Cl_2]Cl$[3] was dissolved in 50 cm$^3$ of absolute methanol and 0.45 g of glycine added with stirring and then LiOH until the solution attained a "pH of 8". The red-coloured solution was stirred for 3 hrs. at a temperature of 35°C. 4.0 g of KI added and the LiCl precipitate removed by vacuum filtration. The product was isolated as described above for compound 1. This technique gave a 25% (1.6 g) yield of red crystals.

For analysis, the crystals were recrystallized three times from double distilled water that contained two drops of 48% HI and were dried in a 60°C vacuum oven. Found: C, 38.13; H, 3.08; N, 9.71; $CoN_5O_2I_2C_{22}H_{20}$ requires: C, 37.79; H, 2.86; N, 10.02%.

*Compound* 3. $(-)_{589}$l-*leucinatobis(2,2′-bipyridyl) cobalt*(III) *iodide trihydrate*

3.0 g of the initial complex $[Co(dipy)_2Cl_2]Cl$ was dissolved in 50 cm$^3$ of absolute methanol and 0.9 g of l-leucine added with stirring followed by LiOH to produce a "pH of 7". The solution was stirred for 30 min at room temperature before increasing the volume to 80 cm$^3$ with deionized water.

To the aqueous red–orange solution was added 5.4 g of NaI and the solution placed in an ice bath for 4 hr. After vacuum filtering the water-insoluble yellow precipitate, the clear red–orange solution was kept undisturbed at room temperature for at least 2 days. Red–orange, hygroscopic needles[4] were formed in 60% (2.9 g) yield.

For analysis, the crystals were recrystallized three times from double distilled water and dried in an 80°C vacuum oven. Found: C, 38.48; H, 4.53; N, 8.10; $[CoN_5O_5I_2C_{26}H_{34}]$ requires: C, 38.59; H, 4.20; N, 8.66%.

*Compound* 4. $(-)_{589}$l-*alaninatobis(2,2′-bipyridyl) cobalt*(III) *iodide*

3.0 g of the parent compound $[Co(dipy)_2\ Cl_2]Cl$ was dissolved in 50 cm$^3$ of absolute methanol and 0.8 g of l-alanine added with stirring followed by LiOH to maintain the solution at a "pH of 7". Stirring was continued for 30 min at room temperature before increasing the volume to 80 cm$^3$ with deionized water. 5.4 g of NaI was then added to the aqueous red solution which was kept undisturbed in an ice bath for 4 hr and then vacuum filtered to remove the yellow precipitate. The red solution was kept in a 2°C refrigerator for at least 4 days. Dark red platelets (2.5 g, 60% yield) were formed.

For analysis, the platelets were recrystallized three times from double distilled water and dried in a 60°C vacuum oven. Found: C, 38.58; H, 3.36; N, 9.55. $CoN_5O_2I_2C_{23}H_{22}$ requires: C, 38.74; H, 3.09; N, 9.82%.

*Compound* 5. $(-)_{589}$l-*phenylalaninatobis(2,2′-bipyridyl)cobalt*(III) *iodide*

Into 50 cm$^3$ of absolute methanol, 3.0 g of $[Co(dipy)_2Cl_2]Cl$ were dissolved and 1.1 g of l-phenylalanine added with vigorous stirring followed by LiOH to maintain a "pH of 7". The solution was stirred for 30 min at room temperature and then its volume is increased to 80 cm$^3$ with deionized water. The red, crystalline product (2.35 g, 50% yield) was obtained using the previously described procedure.

For analysis, the needles were recrystallized once from 15 cm$^3$ of double distilled water, twice from absolute ethanol and, finally, twice from absolute propanol. The distilled water and both alcohols contained two drops of 48% HI. The needles were dried in an 80°C vacuum oven. Found: C, 44.41; H, 3.49; N, 8.70. $CoN_5O_2I_2C_{29}H_{26}$ requires: C, 44.13; H, 3.29; N, 8.88%.

*Compound* 6. *Glycinatobis(1,10-phenanthroline)-cobalt*(III) *iodide trihydrate.*

Into 100 cm$^3$ of absolute methanol, 3.0 g of dichlorobis (1,10-phenanthroline)cobalt(III) chloride[5] were dissolved and 0.45 g of glycine added with stirring followed by LiOH to maintain a "pH of 7". The red solution was stirred for 3 hr at a temperature of 45°C. Next, 4.0 g of KI were added and the solution's volume reduced to 20 cm$^3$ by passing air over the beaker. 15 cm$^3$ of deionized water was then added and allowed to sit undisturbed for 12 hr. After removing the yellow precipitate the clear, reddish solution was kept in a 20°C refrigerator for at least 3 days. Red–brown crystals were formed (2.8 g, 60% yield).

For analysis, the crystals were recrystallized three times from double distilled water and dried in a 60°C vacuum oven. Found: C, 35.85; H, 3.14; N, 9.09. $CoN_5O_5I_2C_{24}H_{26}$ requires: C, 35.93; H, 3.24; N, 8.73%.

*Compound* 7. $(-)_{589}$l-*alaninatobis(1,10-phenanthroline)cobalt*(III) *iodide monohydrate*

3.0 g of the parent compound $[Co(phen)_2Cl_2]Cl$[5] were dissolved in 100 cm$^3$ of absolute methanol and 0.8 g of l-alanine then added. Next, enough LiOH was added to the solution to maintain a "pH of 8". The red solution was first vigorously stirred for 1 hr at room temperature before 4.0 g of KI

were added followed by 20 $cm^3$ of deionized water. After stirring for 15 min the yellow precipitate was removed by vacuum filtration and the red–orange solution was kept undisturbed in a 2°C refrigreator for at least 3 days. Red crystals (2.3 g, 50% yield) were formed.

For analysis, the same procedure as for Compound 5 was followed. Found: C, 38.18; H, 3.51; N, 9.21. $CoN_5O_3I_2C_{25}H_{24}$ requires: C, 38.48; H, 3.08; N, 8.98%.

## SEPARATION OF THE MIXED DISSYMMETRIC COMPLEX COMPOUNDS

For separation of the mixed dissymmetric complex compounds **2**, **3** and **4** an ion exchange column was employed. The 10 cm × 3 cm column was packed with cellex P. 80 mg of a sample was placed on the column, and eluted with 0.05 molar NaI at a flow rate of 0.5 $cm^3$ per minute. Aqueous samples were collected, air dried, and recrystallized from absolute methanol.

For separation of the mixed dissymmetric complex compounds **5–7**, freshly precipitated silver antimonyl *d*-tartrate was used. Into 25 $cm^3$ of double distilled water, 6 mmoles of sample were dissolved. While stirring the solution, 3 mmoles of the tartrate precipitate were added. 30 min later, the AgI precipitate was filtered off and the clear solution placed in a 2°C refrigerator and vacuum filtered every 6 hr. Ultraviolet absorption spectra, using extinction coefficients, substantiated that the silver salt of antimonyl *d*-tartrate did not destroy the original complexes.

Table 1. Significant spectral data for the $[Co(dipy)_2(pro)]^{2+}$ complex

| | | | | |
|---|---|---|---|---|
| a) | polarimeter data: | | | |
| | resolved $[\alpha]_{589}^{25°C}$ | -255 | | |
| b) | absorption and CD data of the resolved complex. | | | |
| $\bar{\nu}$(kK) | | ε | $\bar{\nu}$(kK) | Δε |
| 20.6 | | 148 | 20.2 | - 3.07 |
| 23.8 | | 19.7 | 23.5 | 0.00 |
| 27.9 | (sh) | 341 | 27.8 | + 1.85 |
| 32.2 | | 15,800 | ---- | -- |
| 32.3 | (sh) | 15,500 | -- | -- |
| -- | | -- | 33.3 | +11.2 |
| -- | | -- | 37.0 | + 3.73 |
| 40.000 | (sh) | 29,500 | 40.0 | +36.6 |
| 44.3 | | 86,900 | -- | -- |

Table 2. Significant spectral data for the Co $(dipy)_2(gly)^{2+}$ complex

| | | | | |
|---|---|---|---|---|
| a) | Polarimeter data | | | |
| | racemic: | $\alpha_{589}^{25°C}$ | zero | |
| | resolved | λ | $\alpha_{\lambda}^{25°C}$ | |
| | | 589 | +114 | |
| | | 546 | +357 | |
| | | 436 | -826 | |
| b) | absorption and CD data | | | |
| $\bar{\nu}$(kK) | | ε | $\bar{\nu}$(kK) | Δε |
| 20.6 | | 178 | 20.2 | + 2.61 |
| 23.8 | | 46.1 | 23.8 | 0.00 |
| -- | | -- | 29.4 | - 0.545 |
| 28.9 | (sh) | 1,290 | -- | -- |
| 32.5 | | 20,900 | 32.8 | - 5.83 |
| 35.7 | | 9,520 | -- | -- |
| -- | | -- | 40.0 | -23.8 |
| -- | | -- | 42.4 | -24.7 |
| 44.3 | | 94,400 | 44.4 | -42.4 |

Table 3. Significant spectral data for the Co $(dipy)_2(leu)^{2+}$ complex

| | | | | |
|---|---|---|---|---|
| a) | Polarimeter data | | | |
| | racemic: | $\alpha_{589}$ | -150 | |
| | resolved | λ | $\alpha_{\lambda}^{25°}$ | |
| | | 589 | +260 | |
| | | 546 | -450 | |
| | | 436 | +1000 | |
| b) | absorption and CD data of the resolved complex | | | |
| $\bar{\nu}$(kK) | | ε | $\bar{\nu}$(kK) | Δε |
| 20.8 | | 132 | 20.6 | - 2.94 |
| 24.4 | | 27.9 | -- | -- |
| -- | | -- | 25.0 | 0.00 |
| 28.9 | (sh) | 923 | 28.2 | + 0.784 |
| 32.3 | | 14,600 | 32.3 | + 6.74 |
| -- | | -- | 37.8 | + 6.13 |
| 37.0 | | 5,940 | 37.1 | + 0.613 |
| 41.7 | (sh) | 34,300 | 41.7 (sh) | +29.3 |
| -- | | -- | 42.6 | +38.1 |
| 43.5 | | 102,000 | 43.9 | 0.00 |

Note: the first compound $[Co(dipy)_2(pro)]I_2$ is apparently stereoselective. The CD activity of this compound is quite large and has a $\Delta\epsilon$ in the visible region of 3.07. Douglas[6] has shown stereoselectivity for *l*-proline in the $[Co(en)_2(pro)]^{2+}$ complex ion, and it has a $\Delta\epsilon$ of 1.86 in the visible region.

## SPECTRAL MEASUREMENTS

Visible and UV absorption spectra were recorded on a Cary Model 14 Spectrophotometer. Circular dichroism spectra were recorded on a

Table 4. Significant spectral data for the $[Co(dipy)_2(alan)]^{2+}$ complex. All attempts to improve the resolution failed, and this complex may be considered partially resolved

a) polarimeter data

| | | |
|---|---|---|
| racemic: | $[\alpha]_{589}^{25°C}$ | -80 |
| partially resolved: | $\lambda$ | $[\alpha]_{\lambda}^{25°C}$ |
| | 589 | -127 |
| | 546 | -170 |
| | 436 | +436 |

b) absorption and CD data of the partially resolved complex.

| $\bar{\nu}$(kK) | | $\epsilon$ | $\bar{\nu}$(kK) | $\Delta\epsilon$ |
|---|---|---|---|---|
| 20.8 | | 138 | -- | -- |
| -- | | -- | 21.3 | - 1.27* |
| -- | | -- | 25.0 | 0 |
| -- | | -- | 27.8 | + 0.377 |
| 28.6 | (sh) | 517 | -- | -- |
| 32.3 | | 13,800 | 32.3 | + 2.77 |
| 32.5 | (sh) | 13,300 | 32.8 | + 2.22 |
| -- | | -- | 35.7 | 0 |
| 36.4 | | 4,470 | -- | -- |
| -- | | -- | 37.7 | - 0.554 |
| 39.4 | (sh) | 18,300 | -- | -- |
| 42.3 | | 34,900 | -- | -- |
| -- | | -- | 43.5 | +14. |

Table 5. Significant spectral data of the $[Co(dipy)_2(phenalan)]^{2+}$ complex

a) polarimeter data

| | | |
|---|---|---|
| racemic: | $[\alpha]_{589}^{25.8°C}$ | -216 |
| resolved: | $\lambda$ | $[\alpha]_{\lambda}^{25°C}$ |
| | 589 | 0 |
| | 546 | +120 |
| | 436 | +582 |

b) absorption and CD data

| $\bar{\nu}$(kK) | | $\epsilon$ | $\bar{\nu}$(kK) | | $\Delta\epsilon$ |
|---|---|---|---|---|---|
| 20.8 | | 119 | 20.0 | | + 3.23 |
| -- | | -- | 21.6 | | 0.00 |
| 24.4 | | 21.0 | -- | | -- |
| 28.7 | (sh) | 427 | -- | | -- |
| 32.3 | | 12,900 | -- | | -- |
| 32.9 | (sh) | 12,100 | -- | | -- |
| -- | | -- | 33.3 | (sh) | - 7.65 |
| 44.6 | | 47,800 | 40.0 | | -45.8 |

Table 6. Significant spectral data for the $[Co(phen)_2(gly)]^{2+}$ complex

| | | | | | |
|---|---|---|---|---|---|
| a) | polarimeter data | | | | |
| | racemic: | $[\alpha]^{25°C}_{589}$ | zero | | |
| | resolved: | $\lambda$ | $[\alpha]^{25°C}_{\lambda}$ | | |
| | | 589 | +140 | | |
| | | 546 | +280 | | |
| | | 550 | -550 | | |
| b) | absorption and CD data | | | | |
| $\bar{\nu}$(kK) | | $\epsilon$ | $\bar{\nu}$(kK) | | $\Delta\epsilon$ |
| 20.6 | | 150 | 20.0 | | + 3.15 |
| 23.8 | | 48.1 | 23.8 | | 0.00 |
| -- | | -- | 27.8 | | - 0.757 |
| 28.9 | | 740 | -- | | - -- |
| 31.3 | (sh) | 2,140 | 31.8 | (sh) | - 2.91 |
| 36.5 | | 41,100 | 36.4 | | -36.9 |
| -- | | -- | 42.6 | | -60.1 |
| 44.6 | (sh) | 55,100 | -- | | -- |

Table 7. Significant spectral data for the $[Co(phen)_2(alan)]^{2+}$ complex

| | | | | | |
|---|---|---|---|---|---|
| a) | polarimeter data | | | | |
| | racemic: | $[\alpha]^{25°C}_{589}$ | -77 | | |
| | resolved: | $\lambda$ | $[\alpha]^{25°C}_{\lambda}$ | | |
| | | 589 | zero | | |
| | | 546 | -300 | | |
| | | 436 | +1000 | | |
| b) | absorption and CD data | | | | |
| $\bar{\nu}$(kK) | | $\epsilon$ | $\bar{\nu}$(kK) | | $\Delta\epsilon$ |
| 20.8 | | 135 | 20.4 | | - 4.33 |
| 24.2 | | 20.8 | 24.3 | | 0.00 |
| -- | | -- | 27.8 | | + 1.37 |
| -- | | -- | 31.8 | | + 3.56 |
| -- | | -- | 32.3 | | + 2.85 |
| 33.3 | (sh) | 8,840 | -- | | -- |
| 36.5 | | 36,400 | 36.5 | | +51.6 |
| 44.6 | | 48,800 | -- | | -- |

Cary Model 60 Spectrophotometer. The concentration of the aqueous solutions for the visible region was approx. $10^{-3}$ molar while that for the UV region was approx. $10^{-5}$ molar.

Optical rotation measurements at the sodium-D line were made on a Perkin–Elmer 141 Polarimeter. The concentration of all aqueous solutions was approx. $10^{-3}$ molar.

## SPECTRAL RESULTS

The following tables list the significant spectral data obtained for the $[Co(dipy)_2(aa)]^{2+}$ and [Co

Table 8. Spectral data for the assignment of absolute configuration

| resolved complex | $\Delta\varepsilon$ of the assigned $^1E_a$ transition | $\tilde{\nu}$(kK) | assigned absolute configuration |
|---|---|---|---|
| $[Co(dipy)_2(pro)]^{2+}$ | -3.07 | 20.202 | Δ |
| $[Co(dipy)_2(gly)]^{2+}$ | +2.61 | 20.202 | Λ |
| $[Co(dipy)_2(leu)]^{2+}$ | -2.94 | 20.619 | Δ |
| $[Co(dipy)_2(alan)]^{2+}$ | -1.27 | 21.277 | Δ |
| $[Co(dipy)_2(phenalan)]^{2+}$ | +3.23 | 20.000 | Λ |
| $[Co(dipy)_2(gly)]^{2+}$ | +3.15 | 20.000 | Λ |
| $[Co(dipy)_2(alan)]^{2+}$ | -4.33 | 20.408 | Δ |

(phen)(*aa*)]$^{2+}$ ions. The letters sh refer to a shoulder on either the absorption or CD spectrograph. The energies associated with absorption and CD peaks are given in units of kilokaysers (1kK = $10^3$ cm$^{-1}$) rather than cm$^{-1}$ or nm.

## SUMMARY

All of the synthesized compounds were mixed dissymmetric complexes except for $[Co(dipy)_2(pro)]I_2$, which is stereoselective.

The visible and ultraviolet absorption spectra of the synthesized complexes were similar to those of $[Co(dipy)_2(na)]^{2+}$ and $[Co(phen)_2(na)]^{2+}$ chemical systems[6]. However, the circular dichroism spectra in the UV region for our synthesized complex ions suggested, but didn't show, exciton splitting. This apparent lack of splitting is due to the presence of the optically active amino acids. Further investigations, using optically active ligands, are needed to explain why the exciton phenomenon did not occur. In addition, we could neither discern nor correlate how the small differences in the optically active ligands affected the CD spectra of the different ions.

The empirical method of using CD visible spectra ($^1E_a$ band) was employed to assign tentatively the absolute configurations (see Table 8). Gillard[7] stated that for complexes in which the $^1E_a$ transition, where it can be assigned, has a positive rotational strength, they have an absolute configuration of Λ. Thus for those with a negative rotational strength, an absolute configuration of Δ can be assigned. Gillard also assumed that the $^1E_a$ component dominates over the $^1A$ transition and usually has a large rotational strength. By assuming $^1E_a$ transitions, we are also presuming $D_3$ symmetry for these complexes.

## REFERENCES

1. A. J. McCaffery and S.F. Mason, *Proc. Chem. Soc.* 1963, 211.
2. A. J. McCaffery, S.F. Mason, and B. J. Norman, *Proc. Chem. Soc.* 1964, 259.
3. A. A. Vlcek, *Inorg. Chem.* 1967, **6**, 1425.
4. M–H–W Laboratories, Garden City, Michigan, reported that these needles are extremely hygroscopic.
5. P. Pfeiffer and B. Werdelman, *Z. Anorg. u. Allgem. Chem.* 1936, **227**, 263.
6. J. Hidaka and B. E. Douglas, *Inorg. Chem.* 1964, **3**, 1180.
7. R. D. Gillard, R.E.E. Hill, and R. Maskill, *J. Chem. Soc. A*, 1970, 1447.

*Polyhedron* Vol. 3, No. 1, pp. 55–60, 1984
Printed in Great Britain.

0277–5387/84 $3.00 + .00
© 1984 Pergamon Press Ltd.

# SYNTHESIS AND ELECTROCHEMISTRY OF *cis*-DIOXOMOLYBDENUM(VI) COMPLEXES WITH TRIDENTATE SCHIFF BASE LIGANDS CONTAINING O, N AND S DONOR ATOMS

**JOSEPH TOPICH* and JAMES T. LYON, III**
Department of Chemistry, Virginia Commonwealth University, Richmond, VA 23284, U.S.A.

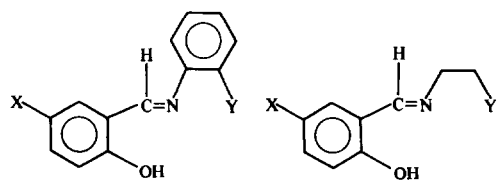
(*Received* 11 *April* 1983; *accepted* 23 *May* 1983)

**Abstract**—The synthesis and characterization of a number of *cis*-dioxomolybdenum(VI) coordination complexes involving tridentate (ONS) ligands is described. The Schiff base ligands were obtained by condensation of 5-substituted salicylaldehydes with *o*-aminobenzenethiol or 2-aminoethanethiol. The chemical properties of these molybdenum complexes are compared with those having tridentate ligands with the ONO donor atom set. Cyclic voltammetry was used to obtain cathodic reduction potentials ($E_{p_c}$) for the irreversible reduction of the Mo(VI) complexes. Although the reductions are irreversible, trends are observed in $E_{p_c}$ both within each series and when different series are compared. Cathodic reduction potentials for the four series examined span the range from $-1.53$ to $-1.05$ V versus NHE. There are three ligand features whose effect systematically alters the Mo(VI) cathodic reduction potentials. These include (1) the X-substituent on the salicylaldehyde portion of each ligand; (2) the degree of ligand delocalization; and (3) the substitution of a sulphur donor atom for an oxygen donor atom. Each of these effects is considered separately with regard to the Mo(VI) cathodic reduction potentials and then their cumulative effect is described.

Molybdenum is a versatile transition element because it possesses a large number of stable and accessible oxidation states as well as coordination numbers which can vary from four to eight.[1] A large number of important chemical reactions are catalyzed by molybdenum compounds. Industrial processes such as hydrodesulphurization[2] and olefin epoxidation[3] are carried out over molybdenum catalysts. Nature has also incorporated molybdenum into a number of important redox enzymes.[4] These include among others aldehyde, sulphite, and xanthine oxidase, nitrate reductase, and nitrogenase. Nitrate reductase and nitrogenase are important reducing enzymes involved in the nitrogen cycle of plants.

The higher oxidation states of molybdenum are dominated by complexes that contain the molybdenum-oxo group. Monooxo- or *cis*-dioxomolybdenum species are observed. Most simple Mo(VI) coordination complexes contain the *cis*-dioxo $MoO_2^{2+}$ cation. Recent EXAFS studies have shown the presence of this group as well as sulphur in the vicinity of the molybdenum in the oxidized forms of xanthine oxidase[5] and sulphite oxidase.[6]

It has been shown that stable *cis*-dioxomolybdenum(VI) coordination complexes can be prepared from the tridentate Schiff base ligands 5-X–SAP–$H_2$ and 5-X–SAE–$H_2$ (X = H, Br, Cl, $NO_2$, $CH_3O$; Y = OH).[7]




Y=OH: 5–X–SAP–$H_2$ 5–X–SAE–$H_2$
Y=SH: 5–X–SSP–$H_2$ 5–X–SSE–$H_2$

X=H, Br, Cl, $NO_2$, $CH_3O$

*Author to whom correspondence should be addressed.

The cathodic reduction potentials ($E_{p_c}$) for the Mo(VI) complexes in each series spanned a range of $\sim 200$ mV on going from $X = NO_2$ to $X = CH_3O$ with the entire series of $E_{p_c}$'s for the 5-X–SAP–$H_2$ series more anodic than the 5-X–SAE–$H_2$ series. A linear relationship was observed between $E_{p_c}$ and the Hammet $\sigma_p$ parameter for the X-substituent on the ligands in each series. Previous electrochemical data[8] has also shown that Mo(VI) complex reducibility is facilitated by the presence of a sulphur donor atom in the coordinating ligand. In an effort to further elucidate the role of ligand structure on Mo(VI) cathodic reduction potentials, we present in this paper electrochemical data on some new Mo(VI) coordination complexes with tridentate ligands incorporating the ONS donor atom set. The synthesis, characterization and cyclic voltammetry will be described for the Mo(VI) complexes of the ligands 5-X–SSP–$H_2$ and 5-X–SSE–$H_2$. Trends in the Mo(VI) cathodic reduction potentials will be discussed in terms of ligand donor atom set, ligand electron delocalization and ligand X-substituents.

## EXPERIMENTAL

*Materials*

All ligand components (5-X-salicylaldehyde (X = H, Cl, Br, $CH_3O$), *o*-aminobenzenethiol, and 2-aminoethanethiol hydrochloride) were obtained from commercial sources and used without further purification. Dimethyl sulphoxide ($Me_2SO$) and N,N-dimethylformamide (DMF) were reagent grade and DMF was dried over type 3A molecular sieves. $MoO_2Cl_2$ was obtained from Alfa and stored in a drybox to prevent hydrolysis. $MoO_2(acac)_2$ ($acac^-$ = acetylacetonate monoanion) was prepared according to a literature procedure[9] and characterized by its IR spectrum.

*Synthesis of ligands*

The hydrochloride salt of 2-aminoethanethiol was converted to the free amine by reaction with one equivalent of triethylamine. The ligands were prepared by reacting equi-molar amounts of the appropriate aldehyde and amine in absolute ethanol at 0°C under a $N_2$ atmosphere and after stirring for approx. 2 hr the ligands were isolated. All of the ligands except one were obtained as pale yellow solids. 5-H–SSE–$H_2$ was obtained as a yellow oil. The ligands were characterized by IR and NMR spectroscopy.

$MoO_2$(5-*X*–*SSP*)

A 1 mmol sample of the appropriate ligand was dissolved in 100 $cm^3$ of absolute ethanol. $MoO_2(acac)_2$ (1 mmol) was added as a solid to the ethanol ligand solution. The reaction mixture was refluxed for 8 hr during which time the product precipitates as a brown solid. The Mo(VI) complex was filtered, dried and recrystallized by dissolving in $Me_2SO$ followed by addition of $H_2O$ until the complex reprecipitated.

$MoO_2$(5-*X*–*SSE*)

A 1 mmol sample of the appropriate ligand was dissolved in 100 $cm^3$ of absolute ethanol. Triethylamine (2 mmol) was aded to this solution. $MoO_2Cl_2$ (1 mmol) was dissolved in a minimum amount of absolute ethanol. The two solutions were mixed and stirred at room temperature for approx. 2 hr. The Mo(VI) complex precipitated as an orange solid and was recrystallized as described above.

Elemental analyses were performed by Atlantic Microlab, Atlanta, GA.

*Physical measurements*

Cyclic voltammetry measurements were made with a home-made potentiostat of conventional design utilizing a three-electrode cell. The working electrode was a Bioanalytical Systems glassy carbon electrode and the auxiliary electrode was a Pt wire. A saturated calomel reference electrode was employed. All potentials were referenced to the ferrocenium/ferrocene couple (0.400 V vs NHE).[10] The ferrocene concentration was $\sim 3 \times 10^{-4}$ M. All cyclic voltammetry measurements were done in dry and deaerated DMF with tetrabutylammonium perchlorate (TBAP, $\sim 5 \times 10^{-2}$ M) as the supporting electrolyte and with a molybdenum complex concentration $\sim 10^{-3}$ M. IR spectra were obtained using a Perkin–Elmer Model 283 spectrophotometer. A Beckman Acta M VII spectrophotometer was used to obtain UV-visible data. $^1$H NMR data were obtained using a Varian T60 or JEOL FX-90Q spectrometer.

## RESULTS AND DISCUSSION

The ligands used in this study are tridentate Schiff base ligands with O, N and S donor atoms and two potential ionizable hydrogens. The Mo(VI) complex derived from 5-H–SSP–$H_2$ has been described previously in the literature.[8,11] Hill *et al.*[11] claim that 5-H–SSP–$H_2$ binds to Mo(VI) as a monoanionic bidentate ligand resulting in the $MoO_2$(5-H-SSP-H)$_2$ stoichiometry. Chakravorty and Rajan[8] state that the ligand, 5-H-SSP-$H_2$, coordinates to Mo(VI) as a dianionic tridentate Schiff base ligand with a solvent molecule, e.g. DMF, occupying the sixth coordination site. Our work supports the conclusions of Chakravorty *et al.* with regard to the stoichiometry of this complex.

Table 1. Spectroscopic and elemental analysis data for *cis*-dioxomolybdenum(VI) complexes

| Mo Complex | IR $\nu$(Mo = O) $cm^{-1}$ | Electronic Spectra $\lambda$, nm (log $\varepsilon$) | Analysis, % found (% calcd) C | H | N |
|---|---|---|---|---|---|
| $MoO_2$(5-H-SSP) | 925 | 374 (3.84), 460 sh | 44.03 (43.96) | 2.62 (2.56) | 3.95 (3.94) |
| $MoO_2$(5-Cl-SSP) | 934, 943 | 378 (3.75), 453 sh | 40.11 (40.07) | 2.12 (2.07) | 3.53 (3.59) |
| $MoO_2$(5-Br-SSP) | 926, 940 | 378 (3.81), 456 sh | 36.03 (35.97) | 1.91 (1.86) | 3.20 (3.23) |
| $MoO_2$(5-$CH_3O$-SSP) | 912 | 319 (4.18), 380 (3.72), 429 sh, 465 sh | 43.43 (43.65) | 2.91 (2.88) | 3.53 (3.64) |
| $MoO_2$(5-H-SSE) | 902, 947 | 346 (3.65) | 35.26 (35.19) | 2.99 (2.95) | 4.51 (4.56) |
| $MoO_2$(5-Cl-SSE) | 918 | 349 (3.63) | 31.68 (31.64) | 2.39 (2.36) | 4.09 (4.10) |
| $MoO_2$(5-Br-SSE)($H_2O$) | 914, 922 | 330 sh, 350 (3.53) | 26.66 (26.75) | 2.35 (2.49) | 3.54 (3.46) |
| $MoO_2$(5-$CH_3O$-SSE) | 887, 906, 920 | 346 (3.66) | 35.52 (35.62) | 3.36 (3.29) | 4.14 (4.15) |

The two series of Mo(VI) coordination complexes were prepared by reaction of either $MoO_2(acac)_2$ or $MoO_2Cl_2$ with the substituted dibasic Schiff base ligands in a 1:1 molar ratio in absolute ethanol. Elemental analyses and IR and UV-visible spectral data for $MoO_2$(5-X–SSP) and $MoO_2$(5-X–SSE) are presented in Table 1. The X = $NO_2$ derivatives could not be prepared for these two series. In the solid state, the IR spectra[12] indicate that some of these complexes may be oligomeric with an oxo-oxygen of one molybdenum complex acting as a donor atom coordinating to the sixth coordination site on an adjacent molybdenum complex. However, in donor solvents such as $Me_2SO$ or DMF the oligomeric chains are broken and monomeric *cis*-dioxomolybdenum(VI) complexes are obtained in solution. In one case, $MoO_2$(5-Br–SSE), we find $H_2O$ in the coordination sphere in the solid state. In solution, the tridentate Schiff base ligands may be assumed to occupy three meridional coordination sites about the $MoO_2^{2+}$ unit with a solvent molecule *trans* to an oxo oxygen.

Cyclic voltammetry was used to obtain cathodic reduction potentials. All cyclic voltammetry measurements were performed in anhydrous, deareated DMF with TBAP as the supporting electrolyte. Ferrocene was used as an internal electrochemical standard. All cyclic voltammetry potential measurements were directly compared to the potential of the ferrocenium/ferrocene couple[10] so that errors, particularly those arising from junction potentials are eliminated. A truly reversible one-electron transfer will have an $E_p$ value independent of scan rate, a $\Delta E$ value of 58 mV, and a ratio of 1.00 for cathodic to anodic peak current. For all the *cis*-dioxomolybdenum(VI) complexes described in this study, we observe irreversible redox behaviour. This is evidenced by no observable oxidation wave upon the reverse anodic scan in the cyclic voltammogram. Electrochemical studies on other *cis*-dioxomolybdenum(VI) complexes[13,14] have generally shown irreversible or quasi-reversible behaviour. Spence[13] has shown for a series of molybdenum complexes that Mo(V) monomers are not obtainable by electrochemical reduction of the corresponding Mo(VI) complexes. He also has shown that Mo(V) monomers cannot be oxidized to the corresponding dioxomolybdenum(VI) complexes, most likely due to the difficulty in adding a second oxo group to OMo(V) in non-aqueous solvents.

Since all the reductions that are observed are irreversible, the data that are presented are for the cathodic reduction potential, which is the potential measured where the cathodic peak current is at its maximum. It must be emphasized that the cyclic voltammetry data are for cathodic reduction potentials and not thermodynamic reduction potentials, which are obtained from reversible cyclic voltammograms. The ligands do not exhibit any redox activity in the potential range where the molybdenum reductions are observed. The cyclic voltammogram for $MoO_2$(5-H–SSP) is shown in Fig. 1 as a typical example of what is observed for these complexes. Table 2 contains cathodic reduction potentials for $MoO_2$(5-X–SSP) and $MoO_2$(5-X–SSE) obtained in this study and also $E_{p_c}$'s for $MoO_2$(5-X–SAP) and $MoO_2$(5-X–SAE) for comparison.

We have been interested in seeing how the cathodic reduction potentials of a number of

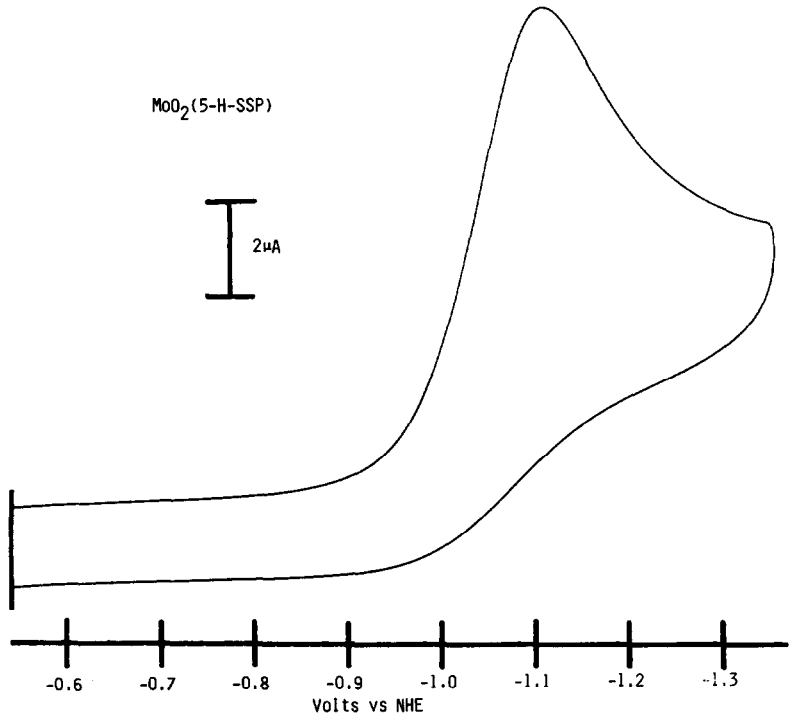



Fig. 1. Cyclic voltammogram for $MoO_2$(5-H-SSP). Scan rate was 100 mV/s.

Table 2. Cyclic voltammetry data for *cis*-dioxomolybdenum(VI) complexes

| Mo Complex | $E_{p_c}$,V[a] | Δ,mV[b] |
|---|---|---|
| $MoO_2$(5-Cl-SSP) | -1.06 | +180 |
| $MoO_2$(5-Br-SSP) | -1.05 | +190 |
| $MoO_2$(5-H-SSP) | -1.11 | +130 |
| $MoO_2$(5-$CH_3O$-SSP) | -1.13 | +110 |
| $MoO_2$(5-Cl-SSE) | -1.22 | + 20 |
| $MoO_2$(5-Br-SSE) | -1.22 | + 20 |
| $MoO_2$(5-H-SSE) | -1.25 | - 10 |
| $MoO_2$(5-$CH_3O$-SSE) | -1.27 | - 30 |
| $MoO_2$(5-$NO_2$-SAP) | -1.11 | +130 |
| $MoO_2$(5-Cl-SAP) | -1.17 | + 70 |
| $MoO_2$(5-Br-SAP) | -1.17 | + 70 |
| $MoO_2$(5-H-SAP) | -1.24 | 0 |
| $MoO_2$(5-$CH_3O$-SAP) | -1.25 | - 10 |
| $MoO_2$(5-$NO_2$-SAE) | -1.25 | - 10 |
| $MoO_2$(5-Cl-SAE) | -1.48 | -240 |
| $MoO_2$(5-Br-SAE) | -1.48 | -240 |
| $MoO_2$(5-H-SAE) | -1.49 | -250 |
| $MoO_2$(5-$CH_3O$-SAE) | -1.53 | -290 |

[a]Volts vs. NHE with reference to the $Fc^+/Fc$ redox couple. Scan rate = 100 mV/s.

[b]$\Delta = E_{p_c}$(Mo complex) - $E_{p_c}$($MoO_2$(5-H-SAP)).

Mo(VI) coordination complexes are affected through systematic changes in ligand structure. The $E_{p_c}$'s are plotted as a function of the Hammett $\sigma_p$ parameter for each series and the results are shown in Fig. 2. The Hammett *para* parameter was chosen because the X-substituent on the ligand is *para* to the salicylaldehyde oxygen donor atom. For all four series, the range of potentials spanned is $-1.53$ to $-1.05$ V ($MoO_2$(5-X–SAP), $-1.25$ to $-1.11$ V; $MoO_2$(5-X–SAE), $-1.25$ to $-1.53$ V; $MoO_2$(5-X–SSP), $-1.05$ to $-1.13$ V; $MoO_2$(5-X–SSE), $-1.22$ to $-1.27$ V). A linear relationship between $E_{p_c}$ and $\sigma_p$ for each of the four series of Mo complexes is satisfying and indicates that in fact the systematic changes in the ligands are bringing about systematic and predictable changes in cathodic reduction potentials. Recently, Chakravorty reported cyclic voltammetry data[8] on a number of Mo(VI) complexes similar to those described in this report. He defined a parameter $\Delta = (E_{p_c})_{complex} - (E_{p_c})_{standard}$ to indicate facile or non-facile reducibility of Mo complexes as compared to a standard complex ($MoO_2$(5-H–SAP)). These $\Delta$ values are compiled in Table 2 along with the $E_{p_c}$'s. A negative $\Delta$ value indicates that the molybdenum complex is reduced at a more cathodic potential (more difficult to reduce) than the standard. A positive $\Delta$ value means the Mo complex is reduced at a more anodic potential (easier to reduce) than the standard. $\Delta$ values in our table which differ from those listed by Rajan and Chakrovorty can be explained as resulting from more accurate measurements of $E_{p_c}$ when ferrocene is used as an internal standard.

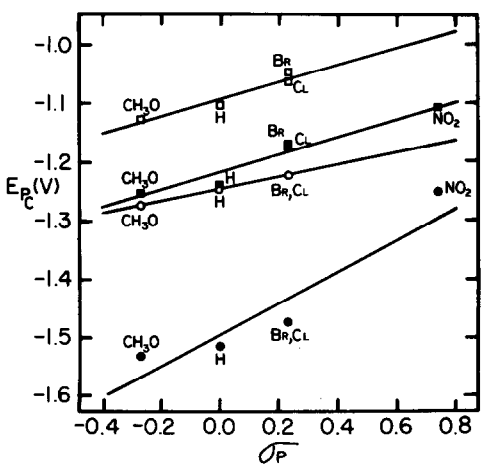



Fig. 2. Correlation of $E_{p_c}$(V) with the Hammett $\sigma_p$ parameter for the molybdenum(VI) complexes: □, $MoO_2$(5-X–SSP); ○, $MoO_2$(5-X–SSE); ■, $MoO_2$(5-X–SAP); ●, $MoO_2$(5-X–SAE); (X = $CH_3O$, H, Cl, Br, $NO_2$).

Even though the reductions observed for the *cis*-dioxomolybdenum(VI) complexes in this study are not reversible, there are trends seen in the cathodic reduction potentials both within each series and between series. There are three ligand features whose effect is to systematically alter the Mo(VI) cathodic reduction potential. These include (1) the X-substituent on the salicylaldehyde portion of each ligand; (2) the degree of ligand delocalization (5-X–$SAP^{2-}$ and 5-X–$SSP^{2-}$ vs 5-X–$SAE^{2-}$ and 5-X–$SSE^{2-}$); and (3) the substitution of a sulphur donor atom in 5-X–$SSP^{2-}$ and 5-X–$SSE^{2-}$ for an oxygen donor atom in 5-X–$SAP^{2-}$ and 5-X–$SAE^{2-}$. Each of these effects will be considered separately with regard to the Mo(VI) cathodic reduction potentials and then their cumulative effect will be discussed.

As the X-substituent becomes more electron withdrawing (X = $CH_3O$ < H < Cl, Br < $NO_2$) the Mo(VI) $E_{p_c}$'s are shifted in the anodic direction which means the Mo(VI) complexes become easier to reduce. The effect of electron withdrawing groups, although not bonded directly to the molybdenum, is to draw electron density away from the metal and hence allow the molybdenum to be more easily reduced. The opposite effect is observed when the substituent is the electron donating $CH_3O$ group. Some Mn(III) Schiff base complexes exhibit similar substituent effects on the metal reduction potential.[15,16]

The $MoO_2$(5-X–SSP) complexes are easier to reduce than the $MoO_2$(5-X–SSE) complexes and the $MoO_2$(5–SAP) complexes are easier to reduce than the $MoO_2$(5-X–SAE) complexes. Both $MoO_2$(5-X–SSP) and $MoO_2$(5-X–SAP) are complexes whose ligand systems are completely delocalized with extended $\pi$ systems. On the other hand, the ligand systems associated with $MoO_2$(5-X–SSE) and $MoO_2$(5-X–SAE) are not completely delocalized having limited $\pi$ systems because of the aliphatic amine portion of the ligand which was used in the synthesis of the Schiff base. This ease of molybdenum complex reducibility that is observed with delocalized ligand systems can be rationalized as follows. During the reduction process an additional electron is added to the metal. If this electron can be delocalized throughout the complex, the reduction will be easier to accomplish. An extended ligand $\pi$ system will facilitate this process. This is in fact what is observed when comparing $MoO_2$(5-X–SSP) and $MoO_2$(5-X–SAP) with $MoO_2$(5-X–SSE) and $MoO_2$(5-X–SAE).

The introduction of a sulphur donor atom in place of an oxygen donor atom on the ligand makes the molybdenum reduction more facile. $MoO_2$(5-X–SSP) is easier to reduce than

$MoO_2$(5-X–SAP) and $MoO_2$(5-X–SSE) is easier to reduce than $MoO_2$(5-X–SAE). Nakamura *et al.* recently studied the ESCA binding energies of some molybdenum complexes with sulphur containing chelates.[17] These workers found that sulphur donor atoms lower the binding energy and effective charge on the molybdenum. It appears that this effect may be attributed to increased covalency of the Mo–S bond as compared to the Mo–O or Mo–N bonds. The added covalency enhances $\pi$-interactions between metal $d$-orbitals and empty sulphur $d$-orbitals. Our cyclic voltammetry results indicate that the sulphur donor atom coordinated to the molybdenum in the two series $MoO_2$(5-X–SSP) and $MoO_2$(5-X–SSE) has effectively reduced the charge on the molybdenum through metal–ligand $\pi$-interactions. This results in $E_{p_c}$'s that are more anodic than those for the complexes with analogous oxygen containing ligands.

These three ligand variations by themselves can affect the molybdenum reduction and when they are found together their effects tend to be cumulative. The easiest Mo(VI) complex to reduce of the four series discussed here should be the one with a ligand having an extended $\pi$-system, a sulphur donor atom, and an effective electron withdrawing substituent. Two complexes fall into this category because Cl and Br have the same Hammett $\sigma_p$ value. They are $MoO_2$(5-Cl–SSP) and $MoO_2$(5-Br–SSP). These two molybdenum complexes have the most anodic $E_{p_c}$'s (for X = Cl, $E_{p_c} = -1.06$ V; for X = Br, $E_{p_c} = -1.05$ V) of the eighteen complexes discussed in this report. It is worthwhile to note that the $E_{p_c}$'s for $MoO_2$(5-X–SSE) and $MoO_2$(5-X–SAP) are very similar. This indicates for these types of molybdenum complexes that the effect of incorporating a sulphur donor into the ligand is about as effective as going to an extended $\pi$-system for the ligand in altering Mo(VI) cathodic reduction potentials.

This report has shown that cathodic reduction potentials for *cis*-dioxomolybdenum(VI) complexes can be systematically controlled through careful ligand design. Within each series, there is an X-substituent effect which causes predictable shifts in the Mo(VI) $E_{p_c}$'s as is evidenced by a linear relationship in each series between $E_{p_c}$ and $\sigma_p$ for the X-substituent. Even though the X-group is not bonded directly to the metal its effect is still transmitted to the molybdenum. We have also shown that ligands with extended $\pi$-systems also facilitate Mo complex reducibility. Finally, when a sulphur donor atom is substituted in the ligand for an oxygen, significant anodic shifts in $E_{p_c}$ are observed for these Mo(VI) complexes.

## REFERENCES


1. E. I. Stiefel, *Prog. Inorg. Chem.* 1977, **22**, 1 and references therein.
2. B. C. Gates, J. R. Katzer and G. C. A. Schuit, *Chemistry of Catalytic Processes*, p. 390. McGraw-Hill, New York (1979).
3. M. L. H. Green, *Proc. 3rd Int. Conf. on the Chemistry and Uses of Molybdenum* (Edited by H. F. Barry and P. C. H. Mitchell), p. 34. Climax Molybdenum Co., Ann Arbor, MI (1979).
4. R. C. Bray, *Enzymes* 1975, **12**, 299.
5. T. D. Tullius, D. M. Kurtz, Jr., S. D. Conradson and K. O. Hodgson, *J. Am. Chem. Soc.* 1979, **101**, 2776.
6. S. P. Cramer, H. B. Gray and K. V. Rajagopalan, *J. Am. Chem. Soc.* 1979, **101**, 2772.
7. J. Topich, *Inorg. Chem.* 1981, **20**, 3704.
8. O. A. Rajan and A. Chakravorty, *Inorg. Chim. Acta* 1979, **37**, L503.
9. G. J.-J. Chen, J. W. McDonald and W. E. Newton, *Inorg. Chem.* 1976, **15**, 2612.
10. R. R. Gagné, C. A. Koval and G. C. Lisensky, *Inorg. Chem.* 1980, **19**, 2854.
11. W. E. Hill, N. Atabay, C. A. McAuliffe, F. P. McCullough and S. M. Razzoki, *Inorg. Chim. Acta* 1979, **35**, 35.
12. O. A. Rajan and A. Chakravorty, *Inorg. Chem.* 1981, **20**, 660.
13. R. D. Taylor, J. P. Street, M. Minelli and J. T. Spence, *Inorg. Chem.* 1978, **17**, 3207.
14. C. A. Cliff, G. D. Fallon, B. M. Gatehouse, K. S. Murray and P. J. Newman, *Inorg. Chem.* 1980, **19**, 773.
15. W. M. Coleman, R. R. Goehring, L. T. Taylor, J. G. Mason and R. K. Boggess, *J. Am. Chem. Soc.* 1979, **101**, 2311.
16. R. K. Boggess, J. W. Hughes, W. M. Coleman and L. T. Taylor, *Inorg. Chim. Acta*, 1980, **38**, 183.
17. A. Nakamura, M. Nakayama, K. Sugihashi and S. Otsuka, *Inorg. Chem.* 1979, **18**, 394.

*Polyhedron* Vol. 3, No. 1, pp. 61–65, 1984
Printed in Great Britain.

0277–5387/84 $3.00 + .00
Pergamon Press Ltd.

# KINETIC STUDY ON THE REACTION OF *cis*-DIOXO-(N-(5-X-SALICYLIDENE)-2-AMINOBENZENETHIOLATO) MOLYBDENUM(VI) WITH ETHYLDIPHENYLPHOSPHINE

**JOSEPH TOPICH* and JAMES T. LYON, III**
Department of Chemistry, Virginia Commonwealth University, Richmond, VA 23284, U.S.A.

(*Received* 25 *April* 1983; *accepted* 23 *May* 1983)

**Abstract**—The reactions of ethyldiphenylphosphine with a number of *cis*-dioxomolybdenum(VI) Schiff base coordination complexes are described. These molybdenum complexes incorporate tridentate Schiff base ligands obtained from the condensation of 5-X-salicylaldehyde (X = Cl, Br, H, $CH_3O$) with *o*-aminobenzenethiol. Oxomolybdenum(IV) Schiff base complexes were observed as products of the reaction of these Mo(VI) complexes with $PEtPh_2$. The kinetics for these reactions were followed spectrophotometrically and the applicable rate law is $-d[MoO_2L]/dt = k_1[MoO_2L][PEtPh_2]$. The $k_1$'s were shown to vary systematically as the X-substituent on the ligand was changed. For $MoO_2$(5-X-SSP), the specific rate constants at 30°C span the range from $19.6 \times 10^{-4}\,M^{-1}\,sec^{-1}$ (X = Br) to $8.4 \times 10^{-4}\,M^{-1}\,sec^{-1}$ (X = $CH_3O$). It was also observed that a correlation exists between the cathodic reduction potentials ($E_{p_c}$) and the $k_1$'s within the series. The rate of reaction of $MoO_2$(5-X-SSP) with $PEtPh_2$ was altered and systematically controlled through ligand design.

Coordination complexes of molybdenum in the higher oxidation states are dominated by the molybdenum–oxo group. In particular, Mo(VI) complexes possess the *cis*-dioxomolybdenum moiety.[1] The molybdenum–oxo group is not restricted to only molybdenum coordination complexes. Recent EXAFS studies have also confirmed the presence of terminal molybdenum–oxo groups in the oxidized forms of the enzymes xanthine oxidase[2] and sulphite oxidase.[3] The current understanding of these enzymes indicates that the molybdenum cycles between the 6+ and 4+ oxidation states in their reaction with substrate and subsequent reactivation.[4] In examining the reactions carried out by xanthine, sulphite and aldehyde oxidase and also nitrate reductase one finds that the only difference between the substrate before and after the reaction is the addition or removal of an oxygen atom. The two-electron oxygen atom transfer reaction[5] may be relevant to the understanding of the reactions of molybdoenzymes, although other mechanisms are certainly possible.[6]

Attempts have been made to prepare molybdenum coordination complexes which can carry out oxygen atom transfer reactions. Mo(VI) complexes have been found to oxidize thiols,[7] hydrazine,[8] polyketones[9] and tertiary phosphines.[5] The *cis*-dioxomolybdenum(VI) dialkyldithiocarbamates $[MoO_2(S_2CNR_2)_2]$ have been extensively studied with regard to these reactions. Barral *et al.*[5] have reported on the oxidation of triphenylphosphine ($PPH_3$) by $MoO_2(S_2CNEt_2)_2$. McDonald and Shulman[10] have described an analytical procedure for the spectrophotometric determination of $PPh_3$ using $MoO_2(S_2CNEt_2)_2$. Newton *et al.*[11] have synthesized $Mo(V)_2O_3L_4$ (L = $S_2CNR_2$, $S_2PR_2$, cysteinato methyl ester, acetylacetonato and 8-hydroxyquinolinato) and $Mo(IV)OL_2$ (L = $S_2CNR_2$ and $S_2PR_2$) complexes starting with the Mo(VI) complexes and using ethyldiphenylphosphine ($PEtPh_2$) to carry out the oxo abstraction.

For Mo(VI) dialkyldithiocarbamates an equilibrium is established,[5,12]

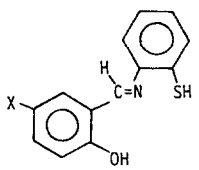
$$MoO_2(S_2CNR_2)_2 + MoO(S_2CNR_2)_2 \rightleftarrows Mo_2O_3(S_2CNR_2)_4 \quad (1)$$

from the oxo abstraction reaction when an excess of the Mo(VI) complex is present in solution. Durant *et al.*[13] have described the kinetics and mechanism of the oxygen atom transfer reaction between $MoO_2(S_2CNEt_2)_2$ and $PPh_3$. Deli and

*Author to whom correspondence should be addressed.

Speier[14] have described a similar study involving $MoO_2$(ethyl-L-cysteinate)$_2$ and $PPh_3$. Oxygen atom abstraction from $MoO_2(S_2CNR_2)_2$ can also be effected by acids[15,16] with the oxygen removed showing up as water.

In a recent report[17] from this laboratory, the electrochemistry of a series of *cis*-dioxomolybdenum(VI) Schiff base coordination complexes was described. Tridentate Schiff base ligands with the following structure were employed.




5-X-SSP-$H_2$

(X = Cl, Br, H, $CH_3O$)

The Mo(VI) complexes are soluble and stable in dimethylsulphoxide ($Me_2SO$) and N, N-dimethylformamide (DMF). In solution, a solvent molecule occupies the vacant coordination site *trans* to an oxo group. The electrochemistry of these Mo(VI) complexes in DMF showed them to undergo an irreversible reduction with the cathodic reduction potentials ($E_{p_c}$) shifted as the X-substituent on the ligand was changed. Electron-withdrawing substituents cause an anodic shift in $E_{p_c}$ while the opposite effect is observed for electron-donating ligand substituents. A linear relationship is observed between $E_{p_c}$ and the Hammett $\sigma_p$ parameter for the ligand substituent. It is satisfying to see the correlation between $E_{p_c}$ and the changes in the ligand substituents for the Mo(VI) complexes. Keeping in mind the fact that the molybdo-enzymes are redox enzymes, it would be interesting to see if the ligand modifications that caused changes in $E_{p_c}$ would also alter the relative reactivities of the Mo(VI) complexes toward suitable substrates. To this end, the Mo(VI) complexes were reacted with $PEtPh_2$. This paper reports on the kinetic data obtained and its relationship to the cathodic reduction potentials obtained previously.

## EXPERIMENTAL

### *Materials*

Ethyldiphenylphosphine was obtained from Strem Chemicals and used without further purification. DMF was reagent grade and was dried over type 3A molecular sieves. The synthesis and characterization of the complexes $MoO_2$(5-X-SSP) (X = Cl, Br, H, $CH_3O$) has been described in a previous publication.[17]

### *Kinetic measurements*

All manipulations associated with the kinetic measurements were performed under a nitrogen atmosphere. Mo(VI) complex solutions of approx. $10^{-3}$ M in DMF were employed. Pseudo-first order conditions were used throughout the study of these reactions by maintaining the concentration of $PEtPh_2$ between 25-fold and 100-fold molar excess over the molybdenum concentration. The solutions were maintained at $30.0 \pm 0.5$°C with a thermostated bath. Spectra were recorded for several hours at 30–60 min intervals, between 650 and 300 nm, using a Beckman Acta M VII spectrophotometer. The pseudo-first order rate constants, $k_{obs}$($k_{obs} = k_1[PEtPh_2]$), were determined for each reaction from plots of $\ln(A_\infty - A_t)$ vs time. $A_t$ is the optical density at time $t$. $A_\infty$ was determined as the optical density when the final two spectral traces overlapped. Kinetic experiments were performed at least three times for each molybdenum complex studied, with the plots in each case being linear over at least three half lives.

## RESULTS AND DISCUSSION

The reactions of $MoO_2(S_2CNR_2)_2$ with $PPh_3$ are well documented in the literature.[5,10–14] This substrate, however, did not react at any reasonable rate with the Mo(VI) Schiff base complexes described in this report. A more suitable phosphine substrate, ethyldiphenylphosphine, was finally chosen because it reacted with the Mo(VI) complexes at room temperature. The reaction followed in this study was

$$MoO_2(5\text{-X–SSP}) + PEtPh_2 \xrightarrow{k_1} MoO(5\text{-X–SSP}) + OPEtPh_2. \quad (2)$$

A qualitative examination of this reaction showed that it was a slow reaction that could be followed spectrophotometrically by observing changes in the optical spectra. Both $Me_2SO$ and DMF are excellent solvents for the Mo(VI) complexes described here. However, there is the possibility of oxidizing the $PEtPh_2$ by $Me_2SO$[18] itself. Therefore, $Me_2SO$ was not used and instead dry DMF was employed as the solvent for these reactions.

The $MoO_2$(5-X–SSP) complexes exhibit charge transfer electronic transitions in the 470–300 nm region of the spectrum. For all the $MoO_2$(5-X–SSP) complexes, the intensities of the electronic transitions associated with the Mo(VI) species decreased as a function of time on reaction with $PEtPh_2$. A new absorbance appeared around 465 nm and increased in intensity as a function of

time. Absorbance changes in this region of the spectrum were monitored as a function of time to obtain the kinetic parameters presented here.

Figure 1 shows a series of spectra recorded for the reaction of $MoO_2$(5-H–SSP) with $PEtPh_2$. This result is typical of the type of spectral changes observed for these complexes. The appearance of an isosbestic point strongly suggests[19] that the molybdenum complex reactant is being converted to product without going through some type of reaction intermediate. Boyd and Spence[20] have described the electronic spectrum of the Mo(IV) complex, MoO(5-H–SSP). They report a $\lambda_{max}$ at 465 nm which is identical to what is observed for the product in the reaction of $MoO_2$(5-H–SSP) with $PEtPh_2$. It is interesting to note that we observe the production of oxomolybdenum(IV) complexes and not the $\mu$-oxo-Mo(V) dimers ($Mo_2O_3L_2$). The absorption spectra were recorded beginning at 650 nm and as the reactions proceeded no absorption bands were observed above 465 nm for any complex in the series.

In the introduction it was mentioned that $MoO_2(S_2CNR_2)_2$ complexes are reduced by phosphines to produce the corresponding Mo(IV) complexes. If, during the reduction, excess Mo(VI) complex is present in solution an equilibrium is established (see reaction 1). The Mo(V) dimer produced in this equilibrium has a unique absorption spectrum. The $\mu$-oxo-Mo(V) dimers ($Mo_2O_3L_n$) have a characteristic absorption at $\sim 525$ nm[1] which is essentially unchanged as the ligands L are varied. The absorption is believed to be associated with a charge transfer transition that is localized in the Mo–O–Mo bridge. The spectral data that are obtained here are not characteristic of Mo(V) $\mu$-oxo-dimers. Thus, the spectral changes that are observed are most likely due to the conversion of the Mo(VI) complex into its Mo(IV) analogue by way of the oxygen atom abstraction reaction producing $OPEtPh_2$. There does not appear to be an equilibrium between the Mo(VI) and Mo(IV) complexes to produce the $\mu$-oxo-Mo(V) dimer.

The kinetic study of the reaction of $MoO_2(S_2CNEt_2)_2$ with $PPh_3$[13] was found to be first order in both reactants. In order to see if the reactions described here were also first order in phosphine, experiments were run to determine the dependence of $k_{obs}$ on $PEtPh_2$ concentration. Since these reactions are slow, only one complex [$MoO_2$(5-Cl–SSP)] was examined under conditions of varying $PEtPh_2$ concentration. Figure 2 shows a plot of $k_{obs}$ vs [$PEtPh_2$]. The linear dependence of $k_{obs}$ on [$PEtPh_2$] shows that these reactions are also first order in $PEtPh_2$.

The kinetic data obtained in this study is interpreted as resulting from a simple second order reaction involving a Mo(VI) Schiff base complex interacting with $PEtPh_2$. The applicable rate law is $-d[MoO_2L]/dt = k_1[MoO_2L][PEtPh_2]$. The second order rate constants ($k_1$) are listed in Table 1 along with cathodic reduction potentials ($E_{p_c}$) reported previously.[17] Newton *et al.*[21] have discussed the reaction of $MoO_2(S_2CNR_2)_2$ with $PR_3$ as an electrophilic attack of the oxo ligand on the electron rich $PR_3$ base. This mechanism is consistent with the kinetic data obtained here. The Mo(VI) complexes described here contain ligand substituents that span the range from electron-withdrawing (Cl, Br) to electron-donating ($CH_3O$). Even though the substituents are not directly bonded to the molybdenum, their effect is trans-

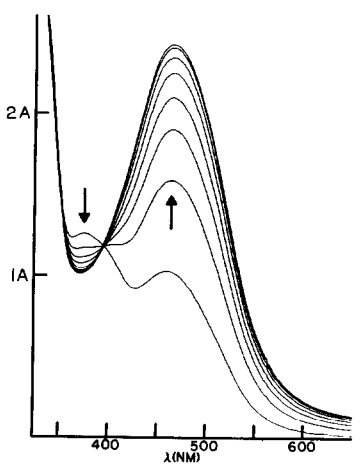



Fig. 1. Spectral changes observed during the reaction of $MoO_2$(5-H–SSP) with $PEtPh_2$. (The initial $MoO_2$(5-H–SSP) and $PEtPh_2$ concentrations were $3.12 \times 10^{-3}$ M and $3.12 \times 10^{-1}$ M respectively. Spectra were recorded at 30 min intervals.)

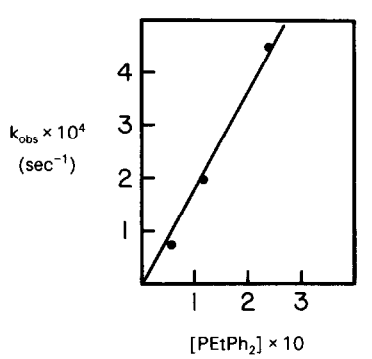



Fig. 2. Variation of $k_{obs}$ vs [$PEtPh_2$] for the reaction of $MoO_2$(5-Cl–SSP) with $PEtPh_2$.

Table 1. Kinetic and electrochemical data for the molybdenum(VI) complexes

| Mo Complex | $k_1$($M^{-1}$ $sec^{-1}$) at 30°C | $E_{p_c}$(V vs NHE) |
|---|---|---|
| $MoO_2$(5-Br-SSP) | 19.6(±0.6) x $10^{-4}$ | -1.05 |
| $MoO_2$(5-Cl-SSP) | 18.7(±0.2) x $10^{-4}$ | -1.06 |
| $MoO_2$(5-H-SSP) | 10.2(±0.9) x $10^{-4}$ | -1.11 |
| $MoO_2$(5-$CH_3O$-SSP) | 8.4(±0.4) x $10^{-4}$ | -1.13 |

mitted through the ligand to the Mo-oxo core. This transmitted electronic effect shows up in the changes that are observed for the $k_1$'s. For the complexes $MoO_2$(5-X–SSP)(X = Cl, Br), the substituents make the ligands the most electronegative of the series because of their electron-withdrawing capacity. Some electron density is also removed from the Mo-oxo core making the oxo ligands the most electrophilic of the series. In contrast, the complex $MoO_2$(5-$CH_3O$–SSP) contains the methoxy group which makes this particular ligand the least electronegative of the series. The electron-donating ability of the methoxy group is also transmitted to the Mo-oxo core making the oxo ligands in this complex the least electrophilic of the series. This difference in electrophilic character is manifested in the variation of the specific rate constants that are obtained for the reaction with $PEtPh_2$.

Since the reaction of phosphines with Mo(VI) coordination complexes is a redox reaction, it is worth considering the relationship between $k_1$ and $E_{p_c}$. Figure 3 shows a plot of $k_1$ vs $E_{p_c}$ for the series

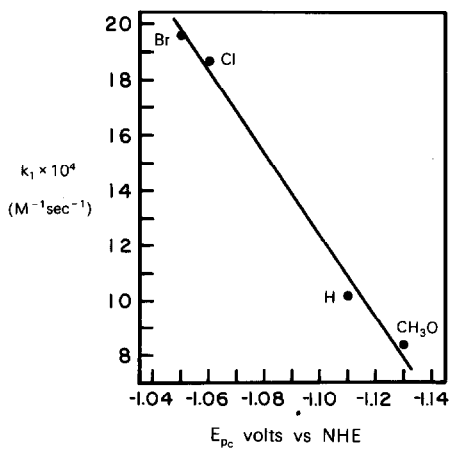



Fig. 3. Plot of $k_1$ vs $E_{p_c}$ for $MoO_2$(5-X–SSP)(X = Cl, Br, H, $CH_3O$).

$MoO_2$(5-X–SSP). It is interesting to note the correlation that exists within the series. It was not unexpected that a correlation of this type might exist since $k_1$ does represent the specific rate constant for a redox reaction. The same electronic effects which alter the electrophilic nature of the Mo(VI) oxo-group also cause changes in the cathodic reduction potentials for these complexes.

## CONCLUSIONS

The molybdenum complexes $MoO_2$(5-X–SSP) react with $PEtPh_2$ in DMF at room temperature. The reactions were shown to be first order in both molybdenum complex and $PEtPh_2$. The second order specific rate constants show a correlation with cathodic reduction potentials reported earlier. The data presented here are consistent with a mechanism involving electrophilic attack of the oxo ligand on the basic $PEtPh_2$ leading to a Mo(IV) complex and $OPEtPh_2$. To the best of our knowledge, this is the first report of a detailed study on Mo(VI) complexes whereby changes in rates of reaction were correlated with cathodic reduction potentials. This work has shown that for a series of structurally similar *cis*-dioxomolybdenum(VI) coordination complexes the rate of reactivity toward a particular substrate can be altered systematically through careful ligand design. The change in reactivity is also paralleled by a change in cathodic reduction potential. For the series, the rate of $PEtPh_2$ oxidation is increased as the Mo(VI) complex is more easily electrochemically reduced.

*Acknowledgment*—We gratefully acknowledge support of this work by the National Institutes of Health, Grant No. GM28659.

## REFERENCES

1. E. I. Stiefel, *Prog. Inorg. Chem.* 1977, **22**, 1 and references therein.
2. T. D. Tullius, D. M. Kurtz, Jr., S. D. Conradson and K. O. Hodgson, *J. Am. Chem. Soc.* 1979, **101**, 2776.

3. S. P. Cramer, H. B. Gray and K. V. Rajagopalan, *J. Am. Chem. Soc.* 1979, **101**, 2772.
4. S. Gutteridge and R. C. Bray, *Proc. 3rd Int. Conf. on the Chemistry and Uses of Molybdenum* (Edited by H. F. Barry and P.C.H. Mitchell), p. 275. Climax Molybdenum Co., Ann Arbor, MI (1979).
5. R. Barral, C. Bocard, I. Seree de Roch and L. Sajus, *Tetrahedron Lett.* 1972, 1693.
6. E. I. Stiefel, *Proc. Nat. Acad. Sci. USA* 1973, **70**, 988.
7. L. S. Meriwether, W. F. Marzluff and W. G. Hodgson, *Nature* (*London*) 1966, **212**, 465.
8. T. Huang and J. T. Spence, *J. Phys. Chem.* 1968, **72**, 4198 4573.
9. J. -F. Verchere and M. -B. Fleury, *Bull. Soc. Chim. France* 1972, 2611.
10. D. B. McDonald and J. I. Schulman, *Anal. Chem.* 1975, **47**, 2023.
11. G. J. -J. Chen, J. W. McDonald and W. E. Newton, *Inorg. Chem.* 1976, **15**, 2612.
12. W. E. Newton, J. L. Corbin, D. C. Bravard, J. E. Searles and J. W. McDonald, *Inorg. Chem.* 1974, **13**, 1100.
13. R. Durant, C. D. Garner, M. R. Hyde and F. E. Mabbs, *J. Chem. Soc., Dalton Trans.* 1977, 955.
14. J. Deli and G. Speier, *Transition Met. Chem.* 1981, **6**, 227.
15. J. Dirand, L. Ricard and R. Weiss, *J. Chem. Soc., Dalton Trans.* 1976, 278.
16. G. J. -J. Chen, J. W. McDonald and W. E. Newton, *Inorg. Chim. Acta* 1980, **41**, 49.
17. J. Topich and J. T. Lyon, III, *Polyhedron* 1984, **3**, 55.
18. E. G. Amonoo, S. K. Ray, R. A. Shaw and B. C. Smith, *J. Chem. Soc.* 1965, 4296.
19. M. D. Cohen and E. Fischer, *J. Chem. Soc.* 1962, 3044.
20. I. W. Boyd and J. T. Spence, *Inorg. Chem.* 1982, **21**, 1602.
21. W. E. Newton, G. D. Watt and J. W. McDonald, *Proc. 3rd Int. Conf. on the Chemistry and Uses of Molybdenum* (Edited by H. F. Barry and P. C. H. Mitchell), p. 259. Climax Molybdenum Co., Ann Arbor, MI (1979).

*Polyhedron* Vol. 3, No. 1, pp. 67–70, 1984
Printed in Great Britain.

0277-5387/84 $3.00 + .00
© 1984 Pergamon Press Ltd.

# COMPLEXES OF LANTHANIDE NITRATES WITH 4N-(2′-HYDROXY BENZYLIDENE)-AMINOANTIPYRINE

**P. K. RADHAKRISHNAN, P. INDRASENAN* and C. G. R. NAIR***
Department of Chemistry, University of Kerala, Trivandrum 695034, India

(*Received* 26 *April* 1983; *accepted* 31 *May* 1983)

**Abstract**—New complexes of lanthanide nitrates with 4N-(2′-hydroxy benzylidene)-aminoantipyrine (HBAAP) having the general formula $[Ln(HBAAP)_2(NO_3)_3]$ (where Ln = La, Pr, Nd, Sm, Gd, Tb, Dy, Ho and Y) have been prepared and characterized. Conductance studies indicate non-electrolytic behaviour for these complexes. Their infrared spectra show that both the ligand and the nitrate group are bound to the metal ion in a bidentate fashion. Electronic spectra indicate weak covalent character in the metal–ligand bond. Thermogravimetric studies indicate that these complexes are stable up to ~200°C and undergo complete decomposition in the range 200–550° resulting in the formation of the stable lanthanide oxides.

Earlier reports on the syntheses of lanthanide complexes of pyrazol-5-one derivatives, such as antipyrine,[1-4] 4-dimethylaminoantipyrine,[1,5] 4-aminoantipyrine,[6-8] and 3-methyl-1-phenylpyrazol-5-one[9] are of particular interest in that in all of them the carbonyl oxygen is the strong donor site. In the complexes of 4-dimethylamino antipyrine the amino nitrogen is also coordinated to the metal ion forming a 5-membered ring. In this paper we are reporting on the synthesis and characterization of some lanthanide nitrate complexes of the Schiff base derived from 4-amino antipyrine and 2-hydroxybenzaldehyde, viz. 4N-(2′-hydroxy benzylidene)-aminoantipyrine (HBAAP). This ligand is expected to behave as monovalent terdentate since this will result in the formation of two ring systems and is likely to impact considerable stability to the complexes. In addition to the carbonyl oxygen, the nitrogen of the azomethine group and the phenolic oxygen may be the donor sites in HBAAP.

## EXPERIMENTAL

### *Reagents*

The lanthanide nitrates of La, Pr, Nd, Sm, Gd, Tb, Dy, Ho and Y were prepared from the respective oxides (99.9% pure) as reported earlier.[7] The ligand was prepared from 4-aminoantipyrine and 2-hydroxybenzaldehyde by the method reported earlier.[10]

### *Preparation and analyses of the complexes*

Solutions of lanthanide nitrate (0.2 mole) and HBAAP (0.6 mole) in hot acetone were mixed and the resulting solution was kept under reflux for 1 hr. It was then concentrated to get a viscous black mass which was washed several times with hot benzene to remove excess of the ligand. The solid mass obtained was dissolved in minimum quantity of acetone and was stirred vigorously with the addition of diethyl ether. The complex separated was dried in vacuum over $P_4O_{10}$. These complexes were analysed for metal, carbon, hydrogen and nitrogen by the conventional methods.[7,11]

### *Physical methods*

Conductivities of the complexes in nitrobenzene ($\sim 10^{-3}$ M solution) were taken at room temperature ($28 \pm 2$°C) using an ELICO type M82T conductivity bridge with dip type cell (type CC-03) and platinum electrodes (cell constant = 1.4 $cm^{-1}$). Magnetic susceptibilities were measured at room temperature by the Gouy method using mercury(II) tetrathiocyanato cobaltate(II) as the calibrant. The IR spectra of the ligand and the complexes were recorded in the 400–4000 $cm^{-1}$ range on a Perkin–Elmer 397 IR Spectrophotometer using KBr disc technique. Electronic spectra of the ligand and the complexes in acetonitrite ($\sim 10^{-3}$ M) were recorded in the range 200–850 nm on a Shimadzu UV-200S spectrophotometer. Ther-

*Authors to whom correspondence should be addressed.

mal decomposition studies of the complexes were carried out on a Perkin–Elmer TGS-1 thermobalance (sample mass: 1.5–2.5 mg; heating rate; 10° $min^{-1}$; atmosphere: static air).

## RESULTS AND DISCUSSION

Analytical data of the complexes (Table 1) show that all the nine complexes have the general formula $Ln(HBAAP)_2(NO_3)_3$ (where Ln = La, Pr, Nd, Sm, Gd, Tb, Dy, Ho and Y). All are mushroom coloured non-hygroscopic solids. They are soluble in polar solvents such as acetone, acetonitrile, methanol and ethanol and insoluble in solvents of low polarity such as benzene, carbon tetrachloride and chloroform.

*Electrical conductance*

The conductance data of the complexes are presented in Table 1. From these data it is clear that all the complexes show non-electrolytic behaviour in nitrobenzene.[10,12] Hence the present complexes may be formulated as $[Ln(HBAAP)_2(NO_3)_3]$.

*Magnetic behaviour*

The magnetic data of the complexes are presented in Table 1. La and Y complexes were diamagnetic, as expected. The measured magnetic moments of the complexes agreed well with the theoretical values calculated from the Van Vleck formula.[13]

*IR spectra*

The important IR frequencies of the free ligand and those of the complexes are presented in Table 2. The IR spectrum of the free ligand shows a broad medium intensity band around 3440 $cm^{-1}$ attributed to the stretching vibration of the phenolic OH group. This band occurs at the same region in the spectra of the complexes showing that the phenolic OH group is not participating in coordination. The spectrum of HBAAP shows a very strong band at 1655 $cm^{-1}$ which is assigned to the carbonyl stretching virbation. On complexation this band is shifted to the region 1600–1605 $cm^{-1}$ showing that the carbonyl oxygen is coordinated to the metal ion. A very strong band at 1590 $cm^{-1}$ in the spectrum of BHAAP is attributed to the hydrogen-bonded C=N stretching vibration.[14] This band is shifted to the region 1560–1575 $cm^{-1}$ in the spectra of the complexes indicating that the nitrogen of the azomethine group is also coordinated to the lanthanide ions. Thus HBAAP acts as a bidentate neutral ligand coordinating through the carbonyl oxygen and nitrogen of the azomethine group forming a 5-membered ring.

The IR spectra of the complexes show two strong absorptions at ~1475 and ~1290 $cm^{-1}$ which are assigned respectively to the $\nu_4$ and $\nu_1$ vibrations of the coordinated $C_{2v}$ nitrate group.[15] The magnitudes of $\nu_4$–$\nu_1$ are in the range 180–190 $cm^{-1}$ in all the cases indicating that the nitrate group is coordinated in a bidentate fashion.

*Electronic spectra*

The electronic spectrum of the ligand shows the following absorption maxima: $n \rightarrow \pi^*$ transition at 28,750 $cm^{-1}$ and two $\pi \rightarrow \pi^*$ transitions at 37,040 and 42,010 $cm^{-1}$, the latter being the more intense band. In the spectra of the complexes, the $n \rightarrow \pi^*$ band is slightly red-shifted to 28,330 $cm^{-1}$ and the low energy and high energy $\pi \rightarrow \pi^*$ bands are also red shifted to 35,450 and 39,210 $cm^{-1}$, respectively. The very broad band observed in the visible region with absorption maximum around 17,500 $cm^{-1}$ in all the complexes may be assigned to the very strong ligand to metal charge-transfer transition. Most of the absorption bands due to *f–f* transitions of the lanthanide ions in the visible region are obscured in the present complexes by the very broad charge transfer band that spreads over the whole visible region. However, in the Nd and Ho complexes the following *f–f* bands are observed, the tentative assignments of which are given in brackets: Nd complex:

19,380 $cm^{-1}$ ($^4I_{9/2} \rightarrow {}^4G_{9/2}$); 19,010 $cm^{-1}$ ($^4I_{19/2} \rightarrow {}^4G_{7/2}$); 17,150 $cm^{-1}$ ($^4I_{9/2} \rightarrow {}^4G_{5/2}, {}^2G_{7/2}$); 13,590 $cm^{-1}$ ($^4I_{9/2} \rightarrow {}^4F_{7/2}$); 13,400 $cm^{-1}$ ($^4I_{9/2} \rightarrow {}^4S_{3/2}$) and 12,523 $cm^{-1}$ ($^4I_{9/2}{}^4H_{9/2}$).

Ho complex:

22,075 $cm^{-1}$ ($^5I_8 \rightarrow {}^5G_6, {}^5F_1$); 18,590 $cm^{-1}$ ($^5I_8 \rightarrow {}^5S_2, {}^5F_4$) and 15,550 $cm^{-1}$ ($^5I_8 \rightarrow {}^5F_5$).

A small red-shift is observed in these *f–f* bands compared to the aquo ions.[16,17] Sinha's covalency parameters[17] calculated for these two complexes ($\delta = 0.9082$ for Nd complex and $\delta = 0.3311$ for Ho complex) suggest a weak covalent character in the metal–ligand bond.

*Thermal behaviour*

The thermal decomposition data of the complexes (Table 2) show that all the complexes are stable up to ~200°C. The lighter lanthanide complexes (La, Pr, Nd, Sm and Gd) undergo decomposition in three stages as denoted by the DTG peaks in the ranges 275–310, 330–405 and 430–450°C. The heavier lanthanide complexes (Tb, Dy, Ho and Y) undergo decomposition in two

Table 1. Analytical,* magnetic and conductance data of lanthanide nitrate complexes of HBAAP

| No | Complex | % Metal | % Carbon | % Hydrogen | % Nitrogen | $\mu_{eff}$ in B.M. | Molar conductance** in nitrobenzene |
|---|---|---|---|---|---|---|---|
| 1 | $[LaL_2(NO_3)_3]$ | 14.69 (14.80) | 46.27 (46.01) | 3.63 (3.62) | 13.58 (13.42) | .. | 4.81 |
| 2 | $[PrL_2(NO_3)_3]$ | 14.78 (14.98) | 46.23 (45.91) | 3.65 (3.61) | 13.12 (13.39) | 3.49 | 6.56 |
| | $[NdL_2(NO_3)_3]$ | 15.19 (15.28) | 44.97 (45.75) | 3.57 (3.60) | 13.47 (13.34) | 3.51 | 6.97 |
| 4 | $[SmL_2(NO_3)_3]$ | 15.86 (15.82) | 44.85 (45.46) | 3.59 (3.58) | 13.43 (13.26) | 1.64 | 7.17 |
| 5 | $[GdL_2(NO_3)_3]$ | 16.14 (16.43) | 45.22 (45.13) | 3.56 (3.55) | 13.13 (13.16) | 7.83 | 6.23 |
| 6 | $[TbL_2(NO_3)_3]$ | 16.54 (16.57) | 44.69 (45.05) | 3.55 (3.55) | 12.92 (13.14) | 9.61 | 7.33 |
| 7 | $[DyL_2(NO_3)_3]$ | 16.82 (16.88) | 44.76 (44.88) | 3.50 (3.53) | 13.14 (13.09) | 10.52 | 5.57 |
| 8 | $[HoL_2(NO_3)_3]$ | 17.15 (17.09) | 44.63 (44.77) | 3.54 (3.52) | 12.85 (13.06) | 10.34 | 6.18 |
| 9 | $[YL_2(NO_3)_3]$ | 9.71 (10.00) | 48.80 (48.60) | 3.95 (3.82) | 14.11 (14.17) | .. | 5.46 |

L = HBAAP

*Calculated values in parenthesis; **$Ohm^{-1}$ $cm^2$ $mole^{-1}$; $\sim 10^{-3}$M solution used

Table 2. Important IR bands (in $cm^{-1}$) and thermal data of lanthanide nitrate complexes of HBAAP

| No. | Compound | $\nu_{C=O}$ | $\nu_{C=N}$ | $\nu_4(NO_3)$ | $\nu_1(NO_3)$ | $\nu_2(NO_3)$ | Stability range in TG(°C) | Peaks in DTG (°C) |
|---|---|---|---|---|---|---|---|---|
| 1 | L | 1655 vs | 1590 s | | | | | |
| 2 | $[LaL_2(NO_3)_3]$ | 1605 " | 1560 " | 1480 vs | 1295 vs | 1025 s | upto 200 | 275m· 330m; 452s |
| 3 | $[PrL_2(NO_3)_3]$ | 1605 " | 1570 " | 1480 " | 1290 " | 1025 " | upto 200 | 285m· 383w; 430s |
| 4 | $[NdL_2(NO_3)_3]$ | 1600 " | 1570 " | 1480 " | 1290 " | 1025 " | upto 200 | 305m; 370w; 430s |
| 5 | $[SmL_2(NO_3)_3]$ | 1605 " | 1570 " | 1475 " | 1295 " | 1025 " | upto 200 | 310m· 390m; 430s |
| 6 | $[GdL_2(NO_3)_3]$ | 1605 " | 1570 " | 1475 " | 1295 " | 1025 " | upto 240 | 310m· 405m 450s |
| 7 | $[TbL_2(NO_3)_3]$ | 1605 " | 1575 " | 1475 " | 1295 " | 1025 " | upto 220 | 300m; 410s |
| 8 | $[DyL_2(NO_3)_3]$ | 1605 " | 1575 " | 1475 " | 1295 " | 1025 " | upto 220 | 290m; 410s |
| 9 | $[HoL_2(NO_3)_3]$ | 1605 " | 1575 " | 1475 " | 1295 " | 1025 " | upto 220 | 300m; 417s |
| 10 | $[YL_2(NO_3)_3]$ | 1605 " | 1575 " | 1475 " | 1295 " | 1025 " | upto 220 | 320m; 445s |

L = HBAAP;

vs = very strong; s = strong; m = medium; w = weak

stages which are represented by DTG peaks in the ranges 290–300 and 410–445°C. All the complexes undergo complete decomposition at ~550°C after which they yield the respective stable oxides.

## REFERENCES


1. D. I. Ryabchikov and E. A. Terent'eva, *Izv. Akad. Nauk SSSR, Otdel Khim. Nauk.* 1949, **44**; *Chem. Abstr.* 1949, **43**, 4969i.
2. V. N. Krishnakurthy and S. Soundararajan, *Proc. Ind. Acad. Sci.* 1967, **65A**, 148.
3. S. S. Krishnamurthy and S. Soundararajan, *J. Less Common Metals* 1967, **13**, 619.
4. R. W. Bashioum, R. L. Dieck and T. Moeller, *Inorg. Nucl. Chem. Lett.* 1973, **9**, 773.
5. L. J. Sauro and T. Moeller, *J. Inorg. Nucl. Chem.* 1968, **30**, 953.
6. Jacob Chacko, C. P. Prabhakaran and C. G. R. Nair, *Ind. J. Chem.* 1975, **13**, 411.
7. Jacob Chacko, C. P. Prabhakaran and C. G. R. Nair, *J. Inorg. Nucl. Chem.* 1976, **38**, 1555.
8. C. G. R. Nair and Jacob Chacko, *Curr. Sic. (Ind.).* 1976, **45**, 452.
9. C. G. R. Nair and P. K. Radhakrishnan, *Proc. Ind. Acad. Sci. (Chem. Sci.)* 1981, **90**, 541.
10. T. Radhakrishnan, P. T. Joseph and C. P. Prabhakaran, *J. Inorg. Nucl. Chem.* 1976, **38**, 2217.
11. I. M. Kolthoff and P. J. Elving (Editors), *Treatise on Analytidal Chemistry*, Vol. 8, Part II. Interscience, New York (1963).
12. W. J. Geary, *Coordination Chem. Rev.* 1971, **7**, 81.
13. J. H. Van Vleck and N. Frank, *Phy. Rev.* 1929, **34**, 1494.
14. K. Ueno and A. E. Martell, *J. Phys. Chem.* 1956, **60**, 1270.
15. N. F. Curtis and Y. M. Curtis, *Inorg. Chem.* 1965, **4**, 804.
16. S. P. Sinha, *J. Inorg. Nucl. Chem.* 1965, **27**, 115.
17. S. P. Sinha, *Spectrochim Acta* 1966, **22**, 57.

*Polyhedron* Vol. 3, No. 1, pp. 71–73, 1984
Printed in Great Britain.

0277-5387/84 $3.00 + .00
© 1984 Pergamon Press Ltd.

# A SPECTROPHOTOMETRIC INVESTIGATION INTO THE COMPLEX FORMATION BETWEEN BISMUTH(III) AND 2-MERCAPTOETHANOL IN AQUEOUS SOLUTION

**GRAHAM E. JACKSON***
Department of Inorganic Chemistry, University of Cape Town, Rondebosch 7700, South Africa

and

**ROBERT D. HANCOCK**
Department of Chemistry, University of Witwatersrand, Johannesburg, South Africa

(*Received* 18 *May* 1983; *accepted* 21 *June* 1983)

**Abstract**—Complex formation between bismuth(III) and 2-mercaptoethanol was studied at 25°C and I = 1.0 mol dm$^{-3}$ $HClO_4$. The results were used to test the validity of an empirical equation for the calculation of formation constants.

Recently[1,2] an empirical equation was used to correlate formation constants of monodentate ligands with Lewis acids in aqueous solution.

$$\log K_1 = E_A^{aq} \cdot E_B^{aq} + C_A^{aq} \cdot C_B^{aq} - D_A \cdot D_B. \quad (1)$$

The equation relates the ionic ($E$), covalent ($C$) and steric ($D$) contributions to bond formation to the equilibrium constant $K$. The values of $E$, $C$ and $D$ have been adjusted to give a best fit using all the formation constant data available on some thirty Lewis acids (e.g. $H^+$, $Ag^+$, $Pb^{2+}$, $Fe^{3+}$ and $La^{3+}$) with some twenty different ligands. To date, however, no empirical correlation has been attempted for the sulphur donor ligands for which there is a large number of gaps in the matrix of experimental $\log K_1$ values. In this paper we report such a correlation and attempt to fill one of the gaps with the study of bismuth(III) and mercaptoethanol. Bismuth(III) itself is interesting in that very few studies on this metal-ion have been reported.

## EXPERIMENTAL

Stock solutions of redistilled, 2-mercaptoethanol (Merck) were prepared and standardised by potentiometric titration using a Gran plot.[3] Bismuth(III) perchlorate stock solutions were prepared from $Bi_2O_3$ by the action of concentrated perchloric acid. Because of the high stability of the bismuth(III)-2-mercaptoethanol complexes and the facility with which bismuth(III) hydrolyses, all reactions were carried out in 1 M $HClO_4$. Complexation was followed spectrophotometrically on a Beckman Acta Mm spectrophotometer at 25.00 ± 0.05°C. The protonation constant of 2-mercaptoethanol has been determined previously[4] to be $2.5 \times 10^9$.

IR spectra were recorded as a Nujol mull between polyethylene plates (500–80 cm$^{-1}$) on a Digilab FTS 16B/D interferometer.

## RESULTS AND DISCUSSION

A typical set of absorption spectra of solutions containing 0.4 mM bismuth(III) (M) and varying amounts of 2-mercaptoethanol (LH) is given in Fig. 1. The absorption peak at 190 nm is due to the metal-ion and the ligand, while the peak at 220 nm is due entirely to the metal-ion. Clearly as the ligand concentration is increased so the amount of free metal decreases resulting in a decreased absorption at $\lambda = 220$ nm. At the same time the peak centred at 261 nm, ascribed to the species ML, increases. The isosbestic point between these two absorption peaks is indicative of two species in equilibrium. At higher ligand concentrations two new peaks centred at 330 and 550 nm appeared and were assigned to the species $ML_2$ and $ML_3$ respectively. Since there was a ten-fold difference in concentration of the ligand between the appearance of these absorption bands a graphic interpretation of the data was possible.

Figure 2 shows a plot of Absorbance ($\lambda = 261$ nm) against total metal concentration at

*Author to whom correspondence should be addressed.

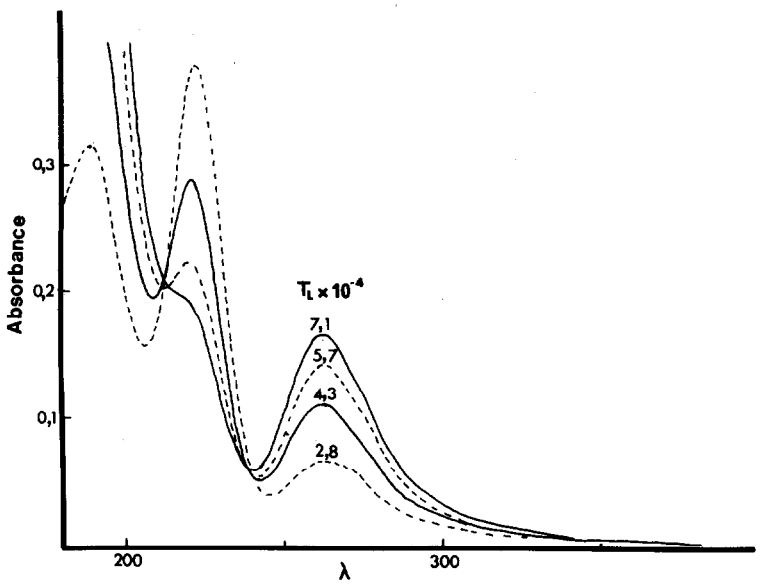



Fig. 1. Absorption spectra of bismuth(III) in the presence of 2-mercaptoethanol. 0.101 cm cells, $T_M = 4 \times 10^{-4}$ mol dm$^{-3}$, $T_H = 1.0$ mol dm$^{-3}$.

constant total ligand and proton concentrations. From the slopes of these curves the extinction coefficient $\epsilon_1$, and the formation constant $\beta_1$ of the ML species were obtained. Similarly using $\lambda = 330$ nm and 550 nm $\epsilon_2$, $\beta_2$ and $\epsilon_3$, $\beta_3$ were obtained. The results of this graphic analysis are collated in Table 1.

Since the modern trend in spectrophotometric determination of stability constants is away from the more traditional graphical analysis to numerical, computer analysis, this approach was also used. Several published programs exist for this, LETAGROP[5] being the most widely used. The very low free ligand concentrations existing in 1 M $HClO_4$ was problematic but could be overcome by using double precision. The results of the computer

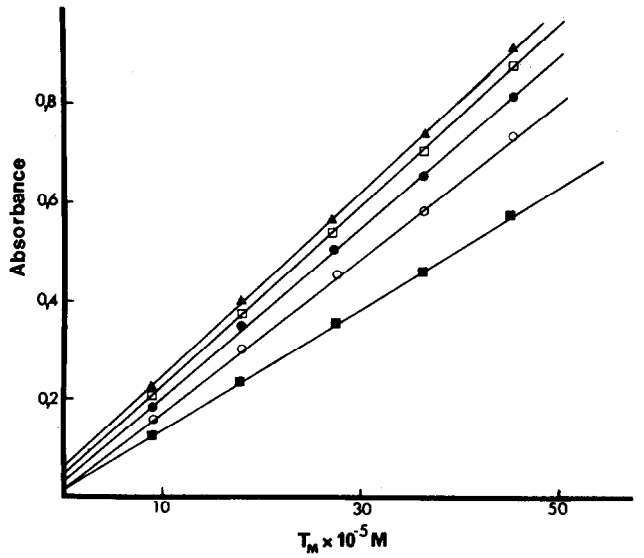



Fig. 2. Plot of absorbance at 261 nm against total bismuth(III) concentration at constant total 2-mercaptoethanol and $[H]^+$ concentration. $T_L =$ ■ 1.42; ○ 2.84; ● 4.26; □ 5.68; ▲ 7.11 mmol dm$^{-3}$.

Table 1. Formation constant for the Bi(III) mercaptoethanol system from graphic and computer analysis

| Species | log β | Extinction Coefficients λ = 220 | 261 | 330 | 550 |
|---|---|---|---|---|---|
| M | - | 11650.0 | 32.9 | 0.0 | 0.0 |
| L | - | 232.2 | 2.0 | 0.0 | 0.0 |
| | | Computer | | | |
| ML | 13.77 | 65.0 | 4389.0 | 0.0 | 0.0 |
| $ML_2$ | 25.10 | 0.0 | 0.0 | 2343.5 | 0.0 |
| $ML_3$ | 35.58 | 0.0 | 0.0 | 0.0 | 40.9 |
| | | Graphic | | | |
| ML | 13.63 | - | 4670.0 | - | - |
| $ML_2$ | 25.03 | - | - | 2127.6 | - |
| $ML_3$ | 35.48 | - | - | - | 40.87 |

analysis of the experimental data are given in Table 1. The agreement between the two methods is gratifying.

When the two reactants were mixed in a 1 : 1 ratio, at a high concentration, in aqueous solution, a yellow crystalline solid was isolated. This analysed for $Bi\text{-}(SCH_2CH_2OH)_2 \cdot ClO_4$ (Found: C 10.2; H 2.2; Calc.: C 10.4; H 2.2%). X-Ray crystal structure analysis[6] showed the ligand to be bidentate coordinating through both the oxygen and the sulphur atoms. A distorted, *cis*-octahedral arrangement about a central bismuth ion was obtained by coordination to the mercapto groups of two neighbouring molecules. In this way the mercapto groups are bridging, having one long (2.97 Å) and one short (2.61 Å) Bi–S bond. The far-IR spectrum of the solid showed three bands which we have tentatively assigned to $\nu_{Bi\text{-}O}$ (265 $cm^{-1}$) $\nu_{Bi\text{-}S}$ (222 $cm^{-1}$) and $\nu_{Bi\text{-}S}$ (197 $cm^{-1}$). On symmetry grounds two Bi–O stretches would be expected but, possibly due to the very weak Bi–O bond, are not resolved.

The agreement between the predicted value of $\log K_1$ for mercaptoethanol and Bi(III) must be regarded as most encouraging, with $\log K_1$ predicted as 13.8, and measured as 13.6. However, if one examines the available $\log K_1$ values for mercaptoethanol with those predicted by the model, the level of agreement is not as good as generally achieved by the model for other ligands where the standard deviation between calculated and observed is about 0.2 log units.[1] It is a general feature of the model that the accuracy of prediction falls off as the absolute covalent bond strength of the metal to ligand bond increases. This is to be expected from the work of Drago,[7] where he has found the same limitation wth the "*E* and *C*" type of equation applied to reactions in the gas-phase. In spite of this, the level of accuracy in predicting $\log K_1$ for mercaptoethanol is still reasonable, and we would only suggest altering eqn (1) if very considerable improvements in the accuracy of prediction could be achieved without losing the simplicity of the relation.

*Acknowledgements*—We wish to acknowledge the C.S.I.R., the University of Cape Town and MINTEK for financial assistance.

## REFERENCES

1. R. D. Hancock and F. Marsicano, *Inorg. Chem.* 1978, **17**, 560.
2. R. D. Hancock and F. Marsicano, *Inorg. Chem.* 1980, **19**, 2709.
3. C. Gran, *Analyst.* 1952, **77**, 661.
4. G. E. Jackson, *S. Afr. J. Chem.* 1982, **35**, 1.
5. L. G. Sillén, *Acta Chem. Scand.* 1962, **16**, 159.
6. M. Niven, L. R. Nassimbeni and G. E. Jackson, Structure in progress. Space group *C*2/*c*, *a*/Å 24.56(1), *b*/Å 11.127(5), *c*/Å 20.16(1), β/° 123.74(2).
7. R. S. Drago, G. C. Vogel and T. E. Needham, *J. Am. Chem. Soc.*, 1971, **93**, 6014.
8. *Stability Constants of Metal-ion Complexes* (Edited by L. G. Sillén and A. E. Martell). Chemical Society Special Publication No. 17 (1964); No. 25 (1971).
9. G. E. Jackson and R. D. Hancock, *Polyhedron* 1982, **1**, 836.

| Lewis acid: | $Ag^+$ | $CH_3Hg^+$ | $In^{3+}$ | $Cd^{2+}$ | $H^+$ | $Pb^{2+}$ | $Bi^{3+}$ |
|---|---|---|---|---|---|---|---|
| Log $K_1$ predicted: | 11.3 | 18.8 | 10.3 | 8.3 | 9.7 | 5.7 | 13.8 |
| observed[8]: | 13.2 | 16.3 | 9.8 | 8.0 | 9.8 | 6.7[9] | 13.6 |

*Polyhedron* Vol. 3, No. 1, pp. 75–78, 1984
Printed in Great Britain.

0277–5387/84 $3.00 + .00
© 1984 Pergamon Press Ltd.

# ON THE EXISTENCE OF $H_2F^+$ IN DILUTE HYDROFLUORIC ACID SOLUTIONS

**G. T. HEFTER**
School of Mathematical and Physical Sciences, Murdoch University, Murdoch, W.A. 6150 Australia

(*Received* 24 *May* 1983; *accepted* 21 *June* 1983)

**Abstract**—The existence of $H_2F^+$, which has been long postulated in dilute aqueous HF solutions, was investigated by fluoride ion-selective electrode potentiometry. Even under conditions conducive to its formation precise measurements yielded only equivocal evidence for its occurrence. It is thought that $H_2F^+$ will exist only in very concentrated HF solutions with low water activities.

A variety of polymeric ions and molecules, including the fluoronium ion $H_2F^+$, have been well characterized in liquid (anhydrous) HF by physical and spectroscopic measurements.[1–3] Similar species have also long been postulated, usually by analogy, to exist in dilute aqueous HF solutions.[4] For example, Forero *et al.*[4] have presented a detailed quantum mechanical description of the structure of $H_2F^+$ in aqueous HF, although the evidence they cite for its existence refers exclusively to anhydrous HF. Since, apart from the well documented[5] $HF_2^-$ and one claim[6] for $H_2F_2$, no polymeric species have ever been reported in any of the numerous equilibrium studies of the $H^+/F^-$system,[3,5] it seems worthwhile to investigate the existence of $H_2F^+$ under conditions conducive to its formation and detection.

## EXPERIMENTAL

The preparation, purification and standardization of all reagents were as described elsewhere.[7,8] Equilibria were investigated at $25.00 \pm 0.02$°C by potentiometric titrations (at least five per medium) using a fluoride ion-selective electrode (Orion, Model 94–09) and procedures and apparatus described previously.[7,9]

In solutions where $[H^+] \gg [F^-]$ the formation of $HF_2^-$ will be suppressed[7] and only the equilibria

$$H^+(aq) + F^-(aq) \overset{\beta_1}{\rightleftharpoons} HF(aq) \qquad (1)$$

$$2H^+(aq) + F^-(aq) \overset{\beta_{21}}{\rightleftharpoons} H_2F^+(aq) \qquad (2)$$

need be considered.[3,5] These conditions are also the most favourable for detection of "polyprotic" $H_nF^{(n-1)+}$ species with a fluoride-responsive electrode.[7]

Using the usual mass balance for fluoride and the stability constant expressions for equilibria (1) and (2), and assuming activity coefficients are constant at constant ionic strength, it is readily shown that

$$\frac{1}{[H^+]}\left[\frac{[F^-]_T}{[F^-]} - 1\right] = F_0(X) = \beta_1 + \beta_{21}[H^+] \qquad (3)$$

where $F_0(X)$ is introduced for convenience to represent the experimentally determinable left hand side of eqn (3). Clearly, if $H_2F^+$ exists, a plot of $F_0(X)$ vs $[H^+]$ will be a straight line of slope $\beta_{21}$ and intercept $\beta_1$. The existence of higher order polyprotic species would be indicated by curvature of a plot of $F_0(X)$ vs $[H^+]$.

As most work on the $H^+/F^-$ system has been reported[5] at an ionic strength of 1 *M* this was also chosen for the present study. The cells used may be represented

| Reference half-cell | Salt bridge | Indicating half-cell | |
|---|---|---|---|
| 0.1 *M* MCl | | *x M* $HClO_4$ | |
| Ag AgCl | I ($MClO_4$) | *y M* MF | FE |
| I ($MClO_4$) | | I ($MClO_4$) | |
| $E_{j1}$ | | $E_{j2}$ | |

(4)

where FE represents the fluoride electrode, I ($MClO_4$) represents a solution maintained at constant total ionic strength ($=\frac{1}{2}\Sigma[i]Z_i^2 = I$) by addition of $MClO_4$, and $E_{j1\&2}$ are liquid junction potentials (LJPs).

The procedures for obtaining stability constants from the raw data have been described in detail elswhere.[7] It should be noted, however, that because of the necessarily high concentrations of $H^+$, attention must be given to LJPs despite the high ionic strength.[10] In fact only $E_{j2}$ must be considered as $E_{j1}$ is essentially constant and may be incorporated into the "standard" cell potential.[10] As shown elsewhere $E_{j2}$ can be accurately calculated from the Henderson equation for the type of junction shown in cell (4).[10]

## RESULTS AND DISCUSSION

Table 1 shows an abbreviated summary (20 data points were actually obtained over the concentration range indicated) of a typical titration in $I = 1\ M$ ($NaClO_4$) media. Similar results were obtained over widely varying $[H^+]$ and $[F^-]$, and the average $\beta_1$ (HF) value is in excellent agreement with literature values.[5] Considering the first four data points (ten in the actual experiment) covering $[H^+]/[F^-]$ ratios up to 4000, clearly only HF (aq) is being detected. At even higher $[H^+]/[F^-]$ ratios, $F_0(X)$ actually *decreases* slightly (see eqn 3).

There are three likely causes for this decrease: LJP errors, deterioration in the fluoride electrode response at the necessarily low $[F^-]$, or activity coefficient effects. The first two of these are unlikely to be significant. Although errors in the calculation of $E_{j2}$ are difficult to quantify, on the basis of previous experience with similar junctions they are probably small ($\simeq 0.1$ mV, corresponding to an error of 3 $M^{-1}$ in $F_0(X)$).[8,10] The performance of the fluoride electrode in fluoride-buffered $NaClO_4/HClO_4$ solutions has been shown[11] to be Nernstian to $\sim 10^{-7}\ M$ well below that employed here (see Table 1, column 4).

On the other hand, activity coefficient variation in constant ionic strength mixtures of $NaClO_4$ and $HClO_4$, although small, is well known.[12,13] This variation, which is due to "specific ionic interactions",[12-14] may be appreciable ($\sim 10\%$) when a substantial fraction of $NaClO_4$ is replaced by $HClO_4$ at constant I. Thus, it may be that the anticipated increase in $F_0(X)$ due to $H_2F^+$ formation (eqn 3) is being swamped by activity coefficient variation.

This suggested that it might be worthwhile repeating these measurements in $LiClO_4$ media since activity coefficient variation in $LiClO_4/HClO_4$ mixtures is known to be almost negligible ($< 1\%$) even at high levels of replacement.[12,13] Typical results of measurements in $I = 1\ M$ ($LiClO_4$) media, analogous to those of Table 1 but at much higher $[H^+]/[F^-]$ ratios, are shown in Fig. 1. In this case $F_0(X)$ does appear to increase with $[H^+]$. Application of eqn (3) yielded a value of $\beta_{21}$ ($H_2F^+$) $= 73 \pm 6\ M^{-2}$ indicating a very feeble complex (stepwise equilibrium constant $K_{21} = \beta_{21}/\beta_1 = 0.16\ M^{-1}$).

Unfortunately, the interpretation of these data is ambiguous. Even assuming activity coefficient variation is negligible, the magnitude of the LJP correction at high proton concentrations is very large ($E_{j2} = 21.6$ mV at $[H^+] = 0.4\ M$). More importantly, an increase in the *apparent* value of $\beta_1$(HF) and hence $F_0(X)$ in eqn (3) might be anticipated when a substantial fraction of the $LiClO_4$ medium is replaced by $HClO_4$ because of the small but significant complexation of $F^-$ by $Li^+$.[15] The competition between $H^+$ and $Li^+$ for $F^-$ lowers the apparent value of $\beta_1$(HF) in $LiClO_4$ media below that observed in a truly "indifferent"

Table 1. Determination of $\beta_1$(HF) at $I = 1\ M$ ($NaClO_4$), $T = 25.00°C$

| $E_{corr}$ mV [a] | $-E_{j2}$ mV [b] | $[F^-]_T$ $\times 10^4 M$ | $[F^-]$ $M$ | $[H^+]_T$ $M$ | $[H^+]$ $M$ | $F_o(X)$ $M^{-1}$ [c] |
|---|---|---|---|---|---|---|
| -64.1 | 0.1 | 5.333 | $1.720 \times 10^{-4}$ | $2.689 \times 10^{-3}$ | $2.328 \times 10^{-3}$ | 902 |
| -40.1 | 0.5 | 5.179 | $6.760 \times 10^{-5}$ | $7.835 \times 10^{-3}$ | $7.385 \times 10^{-3}$ | 902 |
| -17.7 | 1.2 | 4.864 | $2.827 \times 10^{-5}$ | $1.840 \times 10^{-2}$ | $1.794 \times 10^{-2}$ | 903 |
| 7.0 | 2.7 | 4.161 | $1.081 \times 10^{-5}$ | $4.197 \times 10^{-2}$ | $4.156 \times 10^{-2}$ | 902 |
| 22.9 | 4.2 | 3.461 | $5.822 \times 10^{-6}$ | $6.544 \times 10^{-2}$ | $6.510 \times 10^{-2}$ | 898 |
| 40.5 | 6.2 | 2.544 | $2.935 \times 10^{-6}$ | $9.620 \times 10^{-2}$ | $9.595 \times 10^{-2}$ | 893 |

[a] Corrected cell potential ($= E_{observed} - E_{j2}$).

[b] Calculated from Henderson equation

[c] See eqn. (3); average (20 points) $\beta_1$(HF) = 901 ± 3 $M^{-1}$

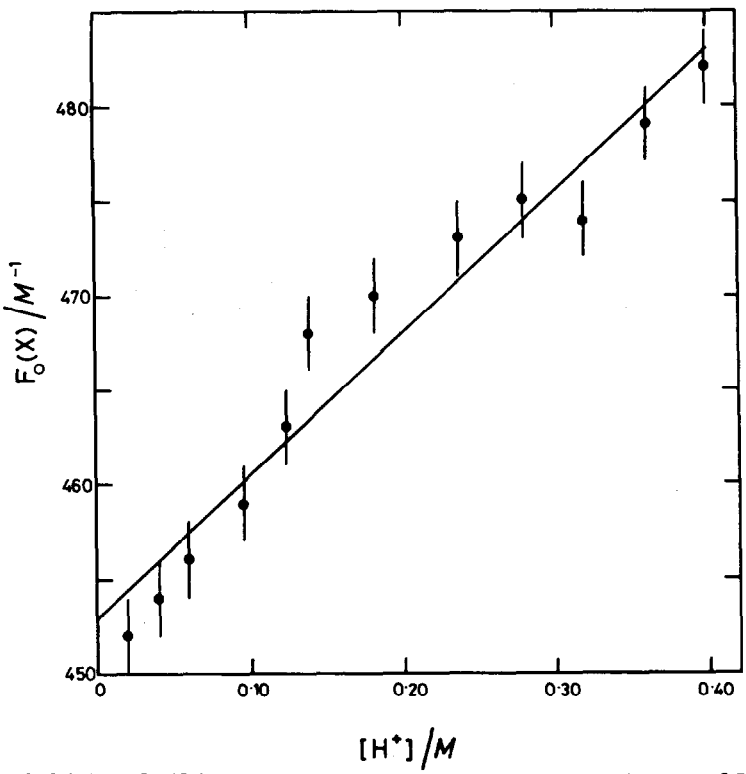



Fig. 1. Plot of $F_0(X)$ vs $[H^+]$ in $I = 1\ M$ ($LiClO_4$) showing possible existence of $H_2F^+$ (see text however). Error bars correspond to $\pm 0.1$ mV uncertainty.

electrolyte. For example, at $I = 1\ M$, log $\beta_1$ (HF) has been reported as 2.95, 2.90 and 2.95 in NaCl, $NaNO_3$ and $NaClO_4$ respectively, but has a value of only 2.66 in $LiClO_4$ (see Fig. 1). The expected increase in the apparent value of $\beta_1$ (HF) may well account for the variation of $F_0(X)$ in Fig 1. Added credence for this interpretation is provided by measurements in $I = 1\ M$ ($NaNO_3$) solution analogous to those of Table 1. As with $NaClO_4$ no evidence was obtained for $H_2F^+$ up to $[H^+]/[F^-]$ ratios of $5 \times 10^4$.

Thus, on balance, the evidence for $H_2F^+$ in dilute aqueous HF solutions is extremely tenuous even under conditions favourable to its formation. This conclusion is consistent with the apparent failure of physical and spectroscopic studies to detect $H_2F^+$.[1,2,16–18] Detailed quantum mechanical studies of its shape and properties in such solutions[4] might therefore be regarded as somewhat premature.

Since $H_2F^+$ *is* firmly established in anhydrous HF solutions it remains to reconcile this with the present results. Giguere and others[16,17] have shown from spectroscopic studies that associated HF (aq) is probably best represented as an ion-pair "$H_3O^+F^-$" (thermodynamics does not provide direct information about structures of species in equilibrium).[3] Thus, the formation of $H_2F^+$ (aq) may be considered as a competitive equilibrium

$$\text{"}H_3O^+F^-\text{"}\ (aq) + H^+(aq) \rightleftharpoons H_2F^+\ (aq) + H_2O.$$

In dilute aqueous solution this reaction will not be favoured because of the high activity of $H_2O$ and the inherent stability of associated HF ("$H_3O^+F^-$") regardless of the proton activity. Appreciable formation of $H_2F^+$ will only be expected in very concentrated HF solutions where the activity of water is considerably lowered.

*Acknowledgement*—Much of the experimental work was performed by the author at the University of Malaya and was funded by that institution.

## REFERENCES

1. T. C. Waddington, in *MPT International Review of Science. Inorganic Chemistry. Series* 1 (Edited by V. Gutmann), Vol. 3. Butterworths, London (1972).
2. T. A. O'Donnell, in *Comprehensive Inorganic Chemistry* (Edited by J. C. Bailar *et al.*), Chap. 25. Pergamon Press, Oxford (1973).
3. L. G. Hepler and H. P. Hopkins, *Rev. Inorg. Chem.* 1979, **1** 303.
4. O. Forero, J. I. Fernandez-Alonso and J. Bertran, *J. Chem. Soc. Dalton Trans.* 1979, 254, and references cited therein.

5. A. M. Bond and G. T. Hefter. *Critical Survey of Stability Constants and Related Thermodynamic Data of Fluoride Complexes in Aqueous Solution*, IUPAC Chemical Data Series No. 27. Pergamon Press, Oxford (1980).
6. L. J. Warren, *Anal. Chim. Acta*, 1971, **53** 199.
7. G. T. Hefter, *J. Solution Chem.*, 1982, **11** 45.
8. G. T. Hefter, Unpublished observations.
9. G. T. Hefter, *J. Electroanal. Chem.* 1972, **39** 345.
10. G. T. Hefter, *Anal. Chem.* 1982, **54** 2518.
11. E. W. Baumann, *Anal. Chim. Acta*, 1971, **54** 189.
12. J. E. Prue and A. J. Read, *J. Chem. Soc. A.*, 1966, 1812.
13. J. B. Macaskill, A. D. Pethybridge and J. E. Prue, *J. Chem. Thermodyn.* 1975, **7** 131.
14. R. A. Robinson and R. H. Stokes, *Electrolyte Solutions*, 2nd Edn. Butterworths, London (1970).
15. A. D. Pethybridge and D. J. Spiers, *J. Chem. Soc. Faraday Trans. I* 1977, **73** 768.
16. P. A. Giguere and S. Turrell, *J. Am. Chem. Soc.* 1980, **102** 5473.
17. O. D. Bonner and N. M. Nunn, *J. Solution Chem.* 1981, **10** 189.
18. K. Schaumburg and C. Deverell, *J. Am. Chem. Soc.* 1968, **90** 2495.

*Polyhedron* Vol. 3, No. 1, pp. 79–85, 1984
Printed in Great Britain.

0277–5387/84 $3.00 + .00
© 1984 Pergamon Press Ltd.

# INTERACTION OF ORGANIC AZIDES WITH METHYL COMPOUNDS OF COBALT, RHODIUM, IRIDIUM, RUTHENIUM AND ZIRCONIUM TO GIVE AZIDO OR 1,3-TRIAZENIDO COMPLEXES. THE CRYSTAL STRUCTURES OF TRIS-TRIMETHYLPHOSPHINEAZIDO-DIMETHYLCOBALT(III) AND BIS(CARBONYL)TRI-METHYLPHOSPHINEAZIDOCOBALT(I)

**KWOK W. CHIU and GEOFFREY WILKINSON***
Chemistry Department, Imperial College, London, SW7 2AY, England

**and**

**MARK THORNTON-PETT and MICHAEL B. HURSTHOUSE***
Chemistry Department, Queen Mary College, Mile End Road, London, E1 4NS, England

(*Received* 9 *June* 1983; *accepted* 21 *June* 1983)

**Abstract**—The interaction of azidotrimethylsilane with *mer*-$CoMe_3(PMe_3)_3$, *fac*-$RhMe_3(PMe_3)_3$, *fac*-$IrMe_3(PMe_2Ph)_3$, *cis*-$RuMe_2(PMe_3)_4$ and $(\eta^5\text{-}C_5H_5)_2ZrMe_2$ gives tetramethylsilane and, respectively, the azido compounds $MMe_2(N_3)(PMe_3)_3$, M = Co, Rh, $IrMe_2(N_3)(PMe_2Ph)_3$, *cis*-$Ru(N_3)_2(PMe_3)_4$ and $(\eta^5\text{-}C_5H_5)_2ZrMe(N_3)$. The crystal structures of $CoMe_2(N_3)(PMe_3)_3$ and of the derived complex $Co(N_3)(CO)_2(PMe_3)_2$ have been determined by X-ray diffraction.

The dimethyl cobalt(III) compound has an octahedral structure with a *mer* arrangement of the three $PMe_3$ groups. The $Co^{III}$–N distance is rather long, at 2.071(4) Å. The cobalt(I) carbonyl compound has a trigonal bipyramidal structure with the two phosphines occupying the axial sites. The $Co^{I}$–N distance is 2.03(1) Å.

The interaction of $PhN_3$ with $(\eta^5\text{-}C_5H_5)_2ZrR_2$, R = Me, Ph, gives the 1,3-triazenido complexes $(\eta^5\text{-}C_5H_5)_2ZrR(RNNNPh)$ while *mer*-$CoMe_3(PMe_3)_3$ and *p*-$MeC_6H_4N_3$ react to give $CoMe_2(MeNNNp\text{-tol})(PMe_3)_2$. In all three cases the triazenido group appears to be bidentate.

Organic azides are well known sources of nitrene species in organometallic chemistry;[1] their reactivity towards metal–carbonyl,[2] metal–hydride,[3] metal–phosphine,[4] and metal–alkene[5] complexes have been extensively studied.

The interaction of organic azides with transition metal alkyl compounds appears not to have been investigated although the alkyl azide compounds, $MeZn(N_3)$,[6] $MeHg(N_3)$[7] and $[Me_2Au(N_3)]_2$,[8] have been made from the corresponding halides by action of $NaN_3$.

The interaction of the tertiary phosphine and $\eta^5$-cyclopentadienyl methyl compounds studied here with azidotrimethylsilane always leads to elimination of tetramethylsilane and formation of the azide according to the general reaction:

$$L_nMMe + Me_3Si(N_3) = L_nM(N_3) + SiMe_4.$$

Phenyl azide also reacts with the phosphine complexes, but the products are always contaminated with the petroleum soluble $PhN{=}PMe_3$,[9] and consequently the products which are all air-sensitive are difficult to isolate pure.

Azido complexes have been extensively reviewed.[10]

The reactions of phenyl azide with

*Authors to whom correspondence should be addressed.

$(\eta^5\text{-}C_5H_5)_2ZrR_2$ R = Me, Ph, and of p-tolylazide with *mer*-$CoMe_3(PMe_3)_3$ by contrast give 1,3-triazenido complexes where the R group of the metal is transferred to nitrogen.

1. *Reactions giving azido complexes*

*Cobalt.* The interaction of $CoMe_3(PMe_3)_3$ with $Me_3Si(N_3)$ occurs readily in petroleum–ether at 0°C. The orange crystalline $CoMe_2(N_3)(PMe_3)_3$, is moderately air-sensitive and crystals suitable for X-ray study were obtained from tetrahydrofuran.[11]

The structure found is shown in Fig. 1, whilst selected bond lengths and angles are given in Table 1. The molecule has an octahedral configuration, with retention of the meridional arrangement of phosphines present in the starting material. The coordination of the azido group is as expected, with a Co–N–N angle of *ca.* 126°, although the Co–N bond length is considerably longer than distances of *ca.* 1.95 Å found in other azides.[11] This apparent lengthening may well be due to increased crowding in the molecule due to the presence of the three phosphines. The Co–P distances are normal, however.

The spectroscopic data are consistent with the structure. The IR spectrum shows asymmetric and symmetric stretches of $N_3$ at 2015 and 1278 $cm^{-1}$ respectively. The $^{31}P\{^1H\}$ NMR spectrum shows a very broad peak at 7.2 ppm at room temperature and two broad singlets at 16.9 and 1.9 ppm with relative intensity 2:1 at −60°C.

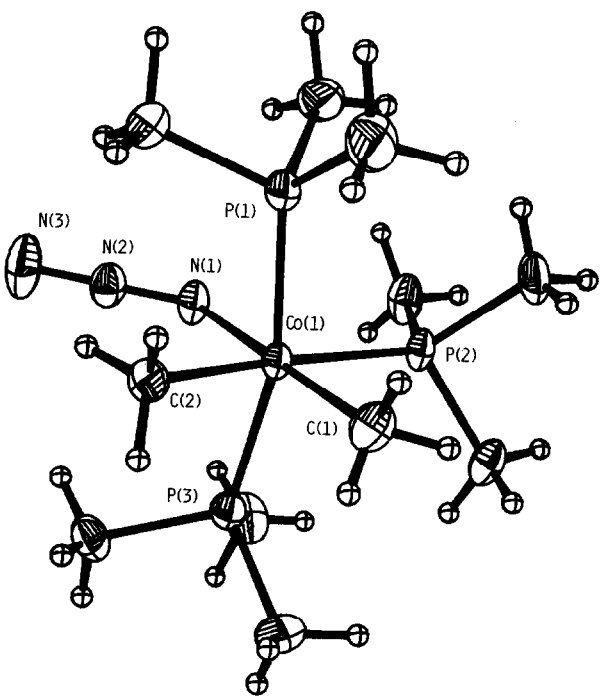



Fig. 1.

The compound reacts with CO (2 atm) to give a mixture of compounds, one of which has been identified as $Co^I(CO)_2(PMe_3)_2(N_3)$. This orange crystalline, air sensitive complex is soluble in diethylether or aromatic hydrocarbons. Crystals suitable for X-ray study were obtained from diethylether. The structure of this molecule, which has a trigonal bipyramidal configuration with axial phosphines, is shown in Fig. 2; selected bond lengths and angles are given in Table 2. As far as we can ascertain this appears to be the first azide complex of $Co^I$ to be characterised, although many other $Co^I$ carbonyl phosphines are known. The $Co–N_3$ geometry is similar to that in the $Co^{III}$ complex, above, with a Co–N–N angle of 128°C and a Co–N distance of 2.03 A. The Co–P and Co–C (carbonyl) distances are all short, and consistent with significant backbonding from the 18-electron Co atom to the $\pi$-acceptor ligands.

The spectroscopic data are consistent with the structure determined; thus the IR spectrum shows asymmetric and symmetric stretches of $N_3$ at 2050 and 1290 $cm^{-1}$ and CO stretches are 1970 and 1920 $cm^{-1}$, while the $^{31}P\{^1H\}$NMR spectrum shows broad singlets at 27.3 and 28.8 ppm at −60°C.

The compound $CoMe_2(N_3)(PMe_3)_3$ reacts with $HBF_4$, acetylene, olefins and $^t$BuNC, but no pure compounds have been isolated.

*Rhodium.* Azidotrimethylsilane reacts with $RhMe_3(PMe_3)_3$ in the same way as the cobalt methyl to give the orange crystalline complex, $RhMe_2(N_3)(PMe_3)_3$ which is air sensitive and soluble in aromatic hydrocarbons and ether. The $^{31}P\{^1H\}$ NMR spectrum shows a doublet of doublets at $\delta$ − 5.7 ppm ($^2J_{P\text{-}P}$ = 35 Hz, $^1J_{Rh\text{-}P}$ = 97 Hz) and a doublet at 14.7 d ppm ($^1J_{Rh\text{-}P}$ = 144 Hz); the IR spectrum shows asymmetric and symmetric stretches of $N_3$ at 2030 and 1280 $cm^{-1}$.

*Iridium.* The reaction of $Me_3Si(N_3)$ with *fac*-$IrMe_3(PMe_2Ph)_3$ gives the white crystalline complex, $IrMe_2(N_3)(PMe_2Ph)_3$, which is air sensitive and soluble in aromatic hydrocarbons and ether. The IR spectrum shows asymmetric and symmetric stretches of $N_3$ at 2040 and 1270 $cm^{-1}$, while the $^{31}P\{^1H\}$ NMR spectrum shows a doublet and a triplet at $\delta$ − 30.1 ppm ($^2J_{P\text{-}P}$ = 20 Hz) and −43.0 ppm ($^2J_{P\text{-}P}$ = 20 Hz) with relative intensity 2:1 respectively. Both the Rh and Ir complexes appear to have the same structure as the cobalt compound.

*Ruthenium.* Reaction of azidotrimethylsilane with *cis*-$RuMe_2(PMe_3)_4$ under reflux in toluene to

Table 1. Selected molecular geometry parameters for $CoMe_2(N_3)(PMe_3)_3$

(a) Bond Lengths A.

| | | | |
|---|---|---|---|
| Co-P(1) | 2.222(3) | Co-P(1) | 2.071(4) |
| Co-P(2) | 2.266(3) | Co-C(1) | 2.031(5) |
| Co-P(3) | 2.232(3) | Co-C(2) | 2.027(5) |
| N(1)-N(2) | 1.175(4) | N(2)-N(3) | 1.168(4) |
| P-C(Me) | 1.817(5) - 1.833(5) | | |

(b) Bond Angles (deg.)

| | | | |
|---|---|---|---|
| P(1)-Co-P(2) | 95.4(1) | N(1)-Co-P(1) | 84.9(2) |
| P(1)-Co-P(3) | 165.2(1) | N(1)-Co-P(2) | 92.7(2) |
| P(2)-Co-P(3) | 96.0(1) | N(1)-Co-P(3) | 85.2(2) |
| P(1)-Co-C(1) | 95.8(2) | N(1)-Co-C(1) | 178.6(1) |
| P(1)-Co-C(2) | 84.4(2) | N(1)-Co-C(2) | 97.0(2) |
| P(2)-Co-C(1) | 86.0(2) | C(1)-Co-C(2) | 84.3(3) |
| P(2)-Co-C(2) | 170.2(1) | | |
| P(3)-Co-C(1) | 94.4(2) | Co-N(1)-N(2) | 125.6(3) |
| P(3)-Co-C(2) | 85.9(2) | N(1)-N(2)-N(3) | 177.8(3) |

give *cis*-$Ru(N_3)_2(PMe_3)_4$ which is soluble in $CH_2Cl_2$ and is fairly stable in air. The IR spectrum shows asymmetric and symmetric stretches of $N_3$ at 2030 and 1280 $cm^{-1}$. The $^{31}P\{^1H\}$ NMR spectrum shows two triplets at 8.4 and −4.9 ppm both with $^2J_{P-P} = 31.5$ Hz consistent with a structure having *cis*-azido groups.

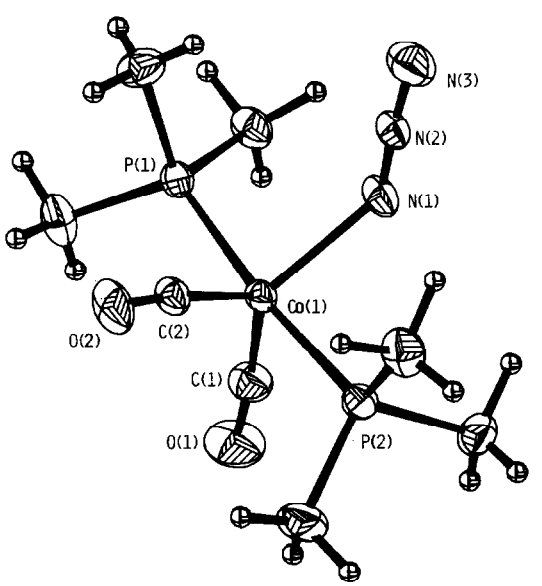



Fig. 2.

*Zirconium.* The reaction of $(\eta^5\text{-}C_5H_5)_2ZrMe_2$ with $Me_3Si(N_3)$ gives white crystalline $(\eta^5\text{-}C_5H_5)_2ZrMe(N_3)$, which is air sensitive, soluble in aromatic hydrocarbons and in thf. The IR spectrum shows asymmetric and symmetric stretches of $N_3$ at 2080 and 1270 $cm^{-1}$. The *bis*-azide, $(\eta^5\text{-}C_5H_5)_2Zr(N_3)_2$[12] has been long known.

2. *Reactions giving* 1,3-*diazenido complexes*

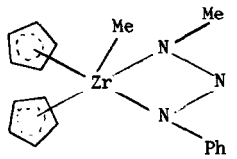
In the above reactions, part of the driving force would appear to be the ease of elimination of tetramethylsilane leading to only the azido complex. By contrast for aryl azides where C–Si bond formation is less likely we find that there is a formal insertion reaction in which a methyl or phenyl group on the metal is transferred to nitrogen giving a 1,3-diazenido ligand. Such an insertion has not previously been observed although hydride transfer in the reaction of $(\eta^5\text{-}C_5Me_5)_2HfH_2$ with $PhN_3$ has been recently observed and a bidentate 1,3-triazenido group proposed.[3a] The distinction betwen unidentate and bidentate binding of triazenido ligands on the basis of IR spectra appears uncertain.[3a,13] The spectra we observe (see Experimental) are consistent with a chelate group which would give the species the 18-electron configuration.

Interaction of $(\eta^5\text{-}C_5H_5)_2ZrR_2$, R = Me, Ph with phenylazide gives very air sensitive yellow (Me) or

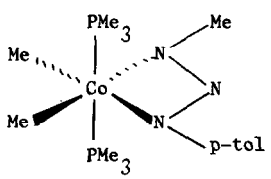
Table 2. Selected molecular geometry parameters for $Co(N_3)(CO)_2(PMe_3)_2$

| | | | |
|---|---|---|---|
| (a) Bond Lengths (Å) | | | |
| Co(1)-P(1) | 2.192(3) | Co(1)-C(1) | 1.749(5) |
| Co(1)-P(2) | 2.184(3) | Co(1)-C(2) | 1.739(6) |
| Co(1)-N(1) | 2.029(5) | | |
| N(1)-N(2) | 1.185(5) | C(1)-O(1) | 1.134(5) |
| N(2)-N(3) | 1.163(6) | C(2)-O(2) | 1.145(6) |
| P-C(Me) | 1.803(6) - 1.812(6) | | |
| (b) Bond Angles (deg.) | | | |
| N(1)-Co(1)-C(1) | 117.4(2) | P(1)-Co(1)-P(2) | 173.5(1) |
| N(1)-Co(1)-C(2) | 121.4(3) | Co(1)-N(1)-N(2) | 127.9(3) |
| C(1)-Co(1)-C(2) | 121.1(3) | N(1)-N(2)-N(3) | 175.9(4) |
| P(1)-Co(1)-N(1) | 87.5(2) | P(2)-Co(1)-N(1) | 86.2(2) |
| P(1)-Co(1)-C(1) | 94.2(2) | P(2)-Co(1)-C(1) | 90.2(2) |
| P(1)-Co(1)-C(2) | 90.7(2) | P(2)-Co(1)-C(2) | 91.2(2) |
| Co(1)-C(1)-O(1) | 172.6(3) | Co(1)-C(2)-O(2) | 172.5(5) |

orange (Ph) needles but crystals of X-ray quality have not yet been obtained. For the methyl compound the $^{13}C\{^1H\}$ NMR spectrum shows singlets at $\delta$ 28.5 (Zr–Me), 42.2 (N–Me), 109.2 ($\eta^5$-$C_5H_5$) and 100.2, 111.6, 116.1 and 122.5 (Ph) ppm. This spectrum, the spectra of the phenyl compound, as well as the $^1H$ and $^{31}P\{^1H\}$ spectra of the air sensitive green crystalline $CoMe_2(MeNNN\,p\text{-tol})(PMe_3)_2$, obtained from reaction of $CoMe_3(PMe_3)_3$ are consistent with the structures 1 and 2 for the Zr and Co compounds respectively.




1




2

Structures 1 and 2.

## EXPERIMENTAL

Microanalyses were by Pascher (Bonn) and Imperial College microanalytical laboratories.

*Spectrometers.* NMR: Perkin–Elmer R32 ($^1H$); Bruker WM 250 ($^1H$ 250 MHz, $^{31}P$ 101.2 MHz, $^{13}C$ 62.9 MHz, 28°C). $^1H$ data referenced to $Me_4Si$, and $^{31}P\{^1H\}$ to external 85% $H_3PO_4$; data in ppm. IR: Perkin–Elmer 627; data in $cm^{-1}$, for spectra in Nujol mulls.

All operations were performed under oxygen-free nitrogen or argon or *in vacuo*, and all solvents except $CH_2Cl_2$ were dried over sodium and distilled from sodium benzophenone under nitrogen immediately before use. $CH_2Cl_2$ was dried over calcium hydride and distilled under nitrogen. Petroleum had b.p. 40–60°C. Melting points were determined in sealed tubes under nitrogen (uncorrected).

*mer*-$CoMe_3(PMe_3)_3$,[15] *fac*-$IrMe_3(PMe_2Ph)_3$,[16] *fac*-$RhMe_3(PMe_3)_3$,[17] *cis*-$RuMe_2(PMe_3)_4$,[17] $(\eta^5\text{-}C_5H_5)_2ZrMe_2$,[18] $PhN_3$,[18] and *p*-tolyl$(N_3)$[19] were prepared according to the literature, $Me_3SiN_3$ was purchased from Aldrich.

1. *Azidobis(methyl)tris(trimethylphosphine) cobalt(III)*

Excess $Me_3SiN_3$ (1 $cm^3$, 7.5 mmol) was added to a solution of *mer*-$CoMe_3(PMe_3)_3$ (0.8 g, 2.4 mmol) in 90 $cm^3$ petroleum–$Et_2O$ (1:2) at 0°C. The mix-

ture was stirred for 12 hr at room temperature. The orange solid was collected and washed with cold petrol (2 × 30 $cm^3$) and extracted with thf (30 $cm^3$); the solution was filtered, concentrated to *ca.* 10 $cm^3$ and cooled to −20°C to give orange crystals. Yield, 0.5 g, 60%; m.p., 110°C. [*Found*: C, 36.7 (36.4); H, 9.0 (9.2); N, 11.1 (11.7); P, 25.6 (25.9)%. *M*, 330 (359).]

IR 2015 vs, 1435 m, 1420 m, 1405 m, 1320 m, 1300 m, 1278 s, 1195 m, 1160 m, 945 vs, 850 s, 790 w, 760 w, 725 s, 715 s, 705 s, 660 s.

NMR $^1H$ ($C_6D_6$): −1.27 *q* (b) ($^3J_{P-H}$ = 9 Hz), Co–*Me*; 0.88 *d* (9) ($^2J_{P-H}$ = 6.2 Hz), 1.0 *br.s* (18), P*Me*$_3$.

$^{31}P\{^1H\}$ ($C_6H_6$ + 10% $C_6D_6$): see text.

2. *Azidobis(carbonyl)bis(trimethylphosphine) cobalt(I)*

A solution of $Co(N_3)Me_2(PMe_3)_3$ (0.3 g, 0.84 mmol) in thf (50 $cm^3$) was treated with CO(2 atm) in a pressure bottle at room temperature and the solution stirred for 5 hr when the pale orange solution was evaporated under vacuum. The solid was extracted into $Et_2O$ (30 $cm^3$), the orange solution filtered, concentrated to *ca.* 10 $cm^3$ and cooled to −20°C to give mixtures of white and orange crystals. Careful recrystallisation from $Et_2O$ allows separation of the orange crystals. Yield, 0.1 g, 40%; m.p., 99°C. [*Found*: C, 31.0 (31.0); H, 5.9 (5.8); N, 13.4 (13.6); O, 10.5 (10.4); P, 19.5 (20.0)%. *M*, 300 (309).]

IR 2218 w, 2050 vs, 1970 s, 1920 s, 1435 w, 1420 m, 1330 w, 1310 w, 1290 m, 950 vs, 860 m, 725 m, 680 s, 640 w.

NMR $^1H$ ($C_6D_6$): 1.1 *t* ($^2J_{P-H}$ = 4.2 Hz), P*Me*$_3$. $^{31}P\{^1H\}$: see text.

3. *Azidobismethyltris(trimethylphosphine) rhodium(III)*

Excess $Me_3SiN_3$ (1 $cm^3$, 7.5 mmol) was added to a solution of *fac*-$RhMe_3(PMe_3)_3$ (0.5 g, 1.33 mmol) in toluene and the mixture stirred for 12 hr. The solvent was recovered under reduced pressure, the solid washed with petroleum (20 $cm^3$) and extracted with toluene (30 $cm^3$). The orange solution was filtered, concentrated to *ca.* 50 $cm^3$ and cooled to −20°C to give a solid, which was recrystallised from $Et_2O$ to give orange crystals. Yield, 0.3 g, 60%; m.p., 121–122°C. [*Found*: C, 31.8 (32.3); H, 8.0 (8.18); N, 10.2 (10.4); P, 22.5 (23.1)%. *M*, 390 (403)].

IR 2030 vs, 1435 s, 1420 s, 1325 w, 1300 m, 1284 s, 1280 s, 1260 msh, 1215 w, 1181 w, 972 s, 940 vs, 860 m, 855 m, 800 w, 721 s, 665 s.

NMR $^1H$ ($C_6D_6$): −0.25 (6) Rh–Me, 1.55 *m* (27) P*Me*$_3$.

$^{31}P\{^1H\}$ ($C_6H_6$ + 10% $C_6D_6$): see text.

4. *Azidobis(methyl)tris(dimethylphenylphosphine) iridium(III)*

Excess $Me_3SiN_3$ (1.0 $cm^3$, 7.5 mmol) was added to a solution of *fac*-$IrMe_3(PMe_2Ph)_3$ (7.0 g, 1.07 mmol) in toluene (50 $cm^3$) and the mixture stirred for 12 hr, then evaporated to dryness under vacuum. The solid was washed with petroleum (2 × 30 $cm^3$), then extracted into toluene (2 × 30 $cm^3$), the solution filtered, concentrated to *ca.* 25 $cm^3$ and cooled to −20°C to give a white microcrystalline solid, which was filtered and recrystallised from thf to give white crystals. Yield, 0.5 g, 70%; m.p., 158–159°C. [*Found*: C, 45.3 (46.0); H, 5.5 (5.8); N, 6.0 (6.2); P, 13.0 (13.7)%. *M*, 640 (678).]

IR 3060 w, 3050 w, 2040 vs, 1490 w, 1435 m, 1420 m, 1410 m, 1320 w, 1300 w, 1295 m, 1270 s, 1100 m, 960 s, 920 s, 910 s, 840 w, 750 s, 725 s, 709 s, 700 s, 685 s, 515 s, 500 s.

NMR $^1H$ ($CD_2Cl_2$): 7.3 *m* (15) *Ph*$Me_2P$; 1.48 *d* ($^2J_{P-H}$ = 7.5 Hz), 1.41 t ($^2J_{P-H}$ = 7.5 Hz), P*Me*$_2$Ph. $^{31}P\{^1H\}$ ($CH_2Cl_2$ + 10% $CD_2Cl_2$): see text.

5. *cis-Bisazidotetrakis(trimethylphosphine)ruthenium(II)*

Excess $Me_3SiN_3$ (1.0 $cm^3$, 7.5 mmol) was added to a solution of *cis*-$RuMe_2(PMe_3)_4$ (0.6 g, 1.38 mmol) in toluene (50 $cm^3$) and the mixture stirred under reflux for 12 hr. After cooling, the white solid was collected, washed with $Et_2O$ (2 × 30 $mc^3$) and then extracted into $CH_2Cl_2$ (40 $cm^3$); the solution was filtered, concentrated to *ca.* 30 $cm^3$ and cooled to −20°C to give a white crystalline solid. Yield, 0.5 g, 75%; m.p., 258–260°C (dec.). [*Found*: C, 29.6 (29.5); H, 7.3 (7.4); N, 16.5 (17.1); P, 24.9 (25.3)%. *M*, 450 (489).]

IR 2030 vs, 1440 m, 1420 m, 1410 w, 1335 w, 1305 m, 1290 m, 1280 s, 975 m, 948 vs, 860 m, 720 s, 710 m, 670 s.

NMR $^1H$ ($CD_2Cl_2$): 1.49 *t* (18), 1.37 *t* (18) ($^2J_{P-H}$ = 3.5 Hz), P*Me*$_3$. $^{31}P\{^1H\}$ ($CH_2Cl_2$ + 10% $CD_2Cl_2$): see text.

6. *Azidobis(η⁵-cyclopentadienyl)methyl zirconium(IV)*

$Me_3SiN_3$ (0.5 $cm^3$, 3.8 mmol) was added to a solution of $Cp_2ZrMe_2$ (0.75 g, 3.0 mmol) in $Et_2O$ (50 $cm^3$) and the mixture was stirred at room temperature for 12 hr. After removal of solvent, the solid was washed with petroleum (2 × 20 $cm^3$) and extracted into toluene (30 $cm^3$); the solution

was filtered, concentrated to *ca.* 15 $cm^3$ and cooled to −20°C to give a microcrystalline solid. Yield, 0.5 g, 60%; m.p., 120°C. [*Found*: C, 47.0 (47.4); H, 4.62 (4.67); N, 14.7 (15.1)%. *M*, 260 (278.2).]

IR 3090 w, 3080 w, 2800 w, 2080 vs, 1610 w br, 1420 m, 1370 m, 1350 m, 1270 s, 1250 w, 1155 w, 1130 m, 1115 m, 1070 m, 1015 s, 960 m, 792 vs, 780 s, 770 s, 740 s, 680 m, 650 m, 600 m.

NMR $^1H$ ($C_6D_6$): 5.7 *s* (10) *Cp*, 0.27 *s* (3) Zr–*Me*.

7. *Bis*($\eta^5$-*cyclopentadienyl*)*methyl*($\eta^2$-1-*phenyl*-3-*methyltriazenido*)*zirconium*(*IV*)

One equivalent of $PhN_3$ (0.67 $cm^3$, 2 M in $Et_2O$) was added to a solution of $Cp_2ZrMe_2$ (0.34 g, 1.35 mmol) in toluene (30 $cm^3$) and the solution stirred for 18 hr at room temperature. After removal of solvent, the solid was extracted into petroleum (2 × 35 $cm^3$); the pale orange solution was filtered, concentrated to *ca.* 40 $cm^3$ and cooled to −20°C to give pale yellow needles. Yield, 0.4 g, 80%; m.p., 127–128°C. [*Found*: C, 58.5 (58.3); H, 5.7 (5.8); N, 10.8 (11.3)%. *M*, 350 (370).]

IR 3090 w, 3080 w, 2810 w, 1970 w, 1945 w, 1880 w, 1828 w, 1598 s, 1580 m, 1506 w, 1488 m, 1415 m, 1370 m, 1360 m, 1325 m, 1300 s, 1285 vs, 1260 s, 1170 m, 1160 w, 1130 w, 1125 w, 1115 w, 1080 m, 1070 w, 1065 w, 1025 m, 1015 m, 1010 m, 995 w, 910 w, 898 w, 820 w, 805 s, 760 m, 755 m, 695 m, 655 w, 631 w, 608 w.

NMR $^1H$ ($C_6D_6$): 7.3 *m* (5) *Ph*; 5.63 *s* (10) *Cp*, 3.13 *s* (3) *Me*–N, 0.02 *s* (3) *Me*–Zr.

$^{13}C\{^1H\}$: see text.

8. *Bis*($\eta^5$-*cyclopentadienyl*)*phenyl*($\eta^2$-1,3-*diphenyltriazenido*)*zirconium*(*IV*)

One equivalent of $PhN_3$ (1.3 $cm^3$, 2 M in diethyl ether) was added to a solution of $(\eta^5\text{-}C_5H_5)_2ZrPh_2$ (1.03 g, 2.66 mmol) in toluene (40 $cm^3$) and the solution stirred for 16 hr at room temperature. After removal of solvent, the solid was washed with petroleum (2 × 30 $cm^3$), then extracted into diethylether (2 × 30 $cm^3$), the orange solution filtered, concentrated to *ca.* 20 $cm^3$ and cooled to −20°C to give an orange solid, which was collected and recrystallised from diethylether to give orange crystals. Yield: 0.78 g, 60%; m.p., 129–130°C. [*Found*: C, 67.1 (68.0); H, 4.7 (5.1); N, 8.1 (8.5)%. *M*, 478 (490).]

IR 3080 w, 3040 w, 1592 m, 1480 s, 1410 w, 1350 w, 1325 w, 1300 s, 1275 vs, 1235 m, 1190 w, 1165 w, 1100 w, 1050 m, 1015 s, 980 w, 955 w, 900 w, 805 vs, 760 m, 730 s, 700 s, 695 m sh, 660 w, 640 w, 610 w, 520 w, 455 w.

NMR $^1H$ ($C_6D_6$): 7.3 *m*, 7.1 *m*, (15) *Ph*; 5.7 s (10) *Cp*.

9. 1,6-*Bis*(*trimethylphosphine*)-2,3-*dimethyl*($\eta^2$-1-*p-tolyl*-3-*methyltriazenido*)*cobalt*(*III*)

One equivalent of *p*-tolylazide (4.0 $cm^3$, 0.15 M in benzene) was added to a solution of *mer*-$CoMe_3(PMe_3)_3$ in diethylether (50 $cm^3$) and the solution stirred for 16 hr at room temperature. After removal of solvent, the solid was extracted with petroleum (2 × 30 $cm^3$), the green solution filtered, concentrated to *ca.* 10 $cm^3$ and cooled to −20°C to give a solid, which was collected and recrystallised from petroleum to give green crystals. Yield: 0.12 g, 55%; m.p., 210°C (dec.). [*Found*: C, 48.9 (49.4); H, 8.5 (8.7); N, 10.0 (10.8); P, 15.1 (15.9)%. *M*, 360 (389).]

IR 3060 w, 1575 w, 1445 m, 1430 m, 1420 m, 1400 w, 1375 m, 1305 s, 1298 vs, 1280 s, 1250 w, 1235 m, 1170 w, 1155 m, 1008 m, 945 vs, 910 w, 850 w, 810 m, 730 m, 710 w, 670 w, 590 m, 580 w, 520 w, 470 w.

NMR $^1H$ ($C_6D_6$): 6.8–7.6 *m* (4) $C_6H_4$; 2.2 *s* (3) $C_6H_4Me$; 2.8 *br s* (3) N–*Me*; 0.75 *t* (18), ($^2J_{P\text{-}H}$ = 3.6 Hz), P$Me_3$; 0.46 *d* (6), ($^3J_{P\text{-}H}$ = 2.5 Hz), Co–*Me*.

$^{31}P\{^1H\}$ ($C_6H_6$ + 10% $C_6D_6$): 0.51 s.

*Crystallographic studies*

Crystals of both compounds were sealed under argon in Lindemann capillaries for X-ray work. Intensity data were collected using a CAD4 diffractometer and graphite monochromated Mo–$K_\alpha$ radiation ($\theta$ = 0.71069 Å), in a manner described in detail previously.[20] The structures were solved and refined via standard heavy atom procedures and full-matrix least squares methods, using programs listed previously.[20]

*Crystal data*; *Compound* 1. $C_{11}H_{33}N_3P_3Co$, M = 360.3, monoclinic, $a$ = 9.056(1), $b$ = 15.815(1), $c$ = 13.156(1) Å, $\alpha$ = 91.0(1)°, U = 1884 $Å^3$, space group $P_{2_1}/c$ Z = 4, $D_c$ = 1.27 g $cm^{-3}$, (Mo–$K_\alpha$) = 10.90 $cm^{-1}$. 5984 intensity data measured $2.0 \leq \theta \leq 30°$, $h$, $k$, $\pm 1$); 5484 were unique and 3524 observed ($I > 1.56\sigma(I)$). Final R, R$\omega$ values were 0.0399 and 0.0368 (with $\omega = 1/[\sigma^2(F_0) + 0.0005\ (F_0)^2]$, with all non-hydrogen atoms aniso tropic and hydrogen atoms isotropic (number of parameters = 295).

*Compound* 2. $C_8H_{18}O_2N_3P_2Co$, M = 302.2, monoclinic, $a$ = 6.656(3), $b$ = 12.038(3), $c$ = 9.421(4) Å, $\beta$ = 103.59(4)°, U = 733.7 $Å^3$, space group $P2_1$, Z = 2, $D_c$ = 1.37 g $cm^{-3}$. 1809 intensity data measured ($2.0 \leq \theta \leq 27.0°$, $h$, $k$, $\pm 1$), 1675 were unique and 1522 observed ($I > 1.5\sigma(I)$). Final R, $R_\omega$ scan values were 0.0256, 0.0257 (with $\omega = 1/[\sigma^2(F_0) + 0.00025(F_0)^2]$) with isotropic and anisotropic thermal parameters for hydrogen and

nonhydrogan atoms respectively. Tables of atomic coordinates, thermal parameters, bond lengths and angles and $F_0/F_c$ values have been deposited as supplementary material with the Editor, from whom copies are available on request. Atomic coordinates have also been deposited with the Cambridge Crystallographic Data Centre.

*Acknowledgement*—We thank the S.E.R.C. for post-doctoral support (K.W.C.) and for provision of the diffractometer and Johnson Matthey PLC for loan of platinum metal salts.

## REFERENCES

1. S. Cenini and G. La Monica, *Inorg. Chim. Acta* 1976, **18**, 279.
2. S. Cenini, M. Pizzotti, F. Porta and G. La Monica, *J. Organomet. Chem.* 1975, **88**, 237.
3. (a) G. L. Hillhouse and J. E. Bercaw, *Organometallics* 1982, **1**, 1025. (b) W. Beck, W. Rieber, S. Cenini, F. Porta and G. La Monica, *J. Chem. Soc., Dalton Trans.* 1974, 298. (c) B. Bell, J. Chatt and G. J. Leigh, *J. Chem. Soc., Dalton Trans.* 1973, 997. (d) W. Beck and M. Bauder, *Chem. Ber.* 1970, **103**, 583.
4. W. Beck, M. Bauder, G. La Monica, S. Cenini and R. Ugo, *J. Chem. Soc.* (*A*) 1971, 113.
5. P. Overbosch, G. van Koten, D. M. Grove, A. L. Spek and A. J. M. Duisenberg, *Inorg. Chem.* 1982, **11**, 3253.
6. J. Muller and K. Dehnicke, *J. Organomet. Chem.* 1967, **10**, 1.
7. K. Dehnicke and D. Seybold, *J. Organomet. Chem.* 1968, **11**, 227.
8. W. Beck, W. P. Fehlhammer, P. Pollmann and R. S. Tobias, *Inorg. Chim. Acta* 1968, **2**, 467.
9. This compound is new. It is very air and moisture sensitive [Found: C, 64.6 (64.7); H, 8.5 (8.4); N, 8.3 (8.4); P, 18.5 (18.5)%]. NMR $^1$H, 0.9 s ($PMe_3$), 6.8–7.3 m (Ph). $^{31}P\{^1H\}$ 1.7 s. Compounds of the type $R_3^1P{=}NR^2$ are well known see *Comprehensive Organic Chemistry* (Edited by D. H. R. Barton and W. D. Ollis), Vol. 2, p. 1301. Pergamon Press, Oxford (1979).
10. Z. Dori and R. F. Ziolo, *Chem. Rev.* 1973, 73, 247.
11. R. J. Restivo, G. Ferguson, R. W. Hay and D. P. Piplani, *J. Chem. Soc., Dalton Trans.* 1978, 1131; A. Clearfield, R. Gopal, R. J. Kline, M. L. Sipski and L. O. Urban, *J. Coord. Chem.* 1978, **8**, 5; L. F. Druding and F. Sancilio, *Acta. Cryst* 1974, **30B**, 2386.
12. R. S. P. Coutts and P. C. Wailes, *Aust. J. Chem.* 1971, **24**, 1075.
13. K. R. Laing, S. D. Robinson and M. F. Uttley, *J. Chem. Soc., Dalton Trans.* 1976, 1205.
14. F. A. Cotton and G. Wilkinson, *Advanced Inorganic Chemistry*, 4th Edn, p. 131. Wiley, New York (1980).
15. H-F. Klein and H. H. Karsch, *Chem. Ber.* 1975, **108**, 956.
16. B. L. Shaw and A. C. Smithles, *J. Chem. Soc.* (*A*) 1967, 604.
17. R. A. Andersen, R. A. Jones and G. Wilkinson, *J. Chem. Soc., Dalton Trans.* 1978, 446.
18. E. Samuel and M. D. Rausch, *J. Am. Chem. Soc.* 1973, **95**, 6263.
19. E. Noelting and O. Michel, *Ber. Dtsch. Chem. Ges.* 1893, **26**, 86.
20. R. A. Jones, K. M. A. Malik, M. B. Hursthouse and G. Wilkinson, *J. Am. Chem. Soc.* 1979, **101**, 4128.

*Polyhedron* Vol. 3, No. 1, pp. 87–94, 1984
Printed in Great Britain.

0277–5387/84 $3.00 + .00
© 1984 Pergamon Press Ltd.

# ORGANOMETALLIC AND ORGANOBIMETALLIC COMPLEXES OF PLATINUM(II) CONTAINING 2,2′-BIPYRIMIDYL: SYNTHESES AND SPECTROSCOPIC CHARACTERISTICS

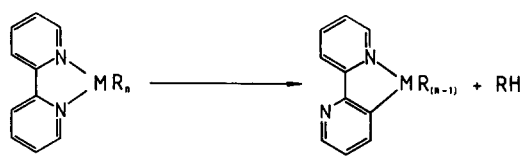
VIVIENNE F. SUTCLIFFE and G. BRENT YOUNG*
Chemistry Department, Imperial College, London, SW7 2AY, England

(*Received* 13 *June* 1983; *accepted* 21 *June* 1983)

**Abstract**—Preparations are described of several monometallic complexes (bipym)$PtR_2$ [bipym = 2,2′-bipyrimidyl; R = Me, $CF_3$, Ph, 1-adamantylmethyl (adme); $R_2 = (CH_2)_4$] and bimetallic analogues $R_2Pt(\mu\text{-bipym})PtR'_2$ [R = R′ = $CH_3$, $C_6H_5$, adme; R = $CH_3$, R′ = Ph, adme, $CF_3$]. IR, $^1H$ NMR and UV/visible spectroscopic characteristics of the two modes of bipyrimidyl coordination are discussed.

Numerous organometallic derivatives of the nickel group have featured 2,2′-bipyridyl (bipy) as ancillary ligand.[1] As part of our study of organotransition metal mechanistics, we are investigating the reactivity of a series of organoplatinum compounds which contain the related ligand 2,2′-bipyrimidyl (bipym). Although bipyrimidyl is increasingly popular as a coordinating ligand,[2] its appearance in organometallic complexes to date is rare.[1d,3]

Our study has been prompted by several considerations. Bipyrimidyl has the capacity to function as a bidentate ligand on a single metal (monobidentate) or as a bridging ligand between two metal centres (bis-bidentate). Both types of coordination raise interesting mechanistic possibilities. One aim of our current work is to restrict intramolecular hydrogen abstraction (of any type) from ligand sites. In its mono-bidentate mode, 2,2′-bipyrimidyl is denied the "flip-over" 3-metallation, available to 2,2′-bipyridyl[4] (Scheme 1). In addition, evidence has recently been presented[2,3] for electronic communication between metals bridged by bis-bidentate bipyrimidyl. These interactions should be manifest in modified organometallic reactivity, as well as in ground state effects. Here, we report the synthesis and spectroscopic characteristics which preface our mechanistic studies[4,5] on these compounds.




Scheme 1. R = alkyl, aryl.

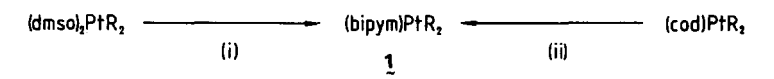
## EXPERIMENTAL

### *General and instrumental*

Elemental analyses were by Imperial College microanalytical laboratories. Measurement of NMR spectra was performed on Bruker ($^1H$, 250 MHz) and Perkin–Elmer R32 ($^{19}F$, 84 MHz) spectrometers. IR data were collected on a Perkin–Elmer 683 instrument and electronic spectra were recorded on a Perkin–Elmer 55 spectrometer.

Reactions involving alkyl transfer reagents were executed under an inert atmosphere of nitrogen or argon. Diethyl ether used in these anaerobic manipulations was distilled under nitrogen from sodium benzophenone dianion. Melting/decomposition points were determined in open capillaries and are uncorrected. Chlorotrimethyltin, tetramethyltin and methyllithium were supplied by Aldrich Chemical Co., 2,2′-bipyrimidyl was obtained from Lancaster Synthesis and trifluoroiodomethane was provided by Rose Chemicals. All were used as supplied. Phenyllithium was prepared from bromobenzene and lithium foil. 1,4-Bis(bromomagnesio)butane[6]

*Author to whom correspondence should be addressed.




Scheme 2. (i) R = Me (a), Ph (b). (ii) R = $CF_3$ (c), adme (d), $R_2 = C_4H_8$(e).

and trimethylphenyltin[7] were synthesised according to published methods. Further, (1,4-tetramethylene)(1,5 - cyclooctadiene)platinum(II),[1i] dimethyl(1,5 - cyclooctadiene)platinum(II),[8] bis(trifluoromethyl(1,5-cyclooctadiene)platinum(II)[8] and bis(adamantylmethyl)(1,5-cyclooctadiene) platinum(II)[1d] were prepared by established routes. Dimethylbis(dimethylsulphoxide)platinum(II) and diphenylbis(dimethylsulphoxide)platinum(II) were prepared by the interaction, respectively, of tetramethyltin(IV) or trimethylphenyltin(IV) with dichlorobis(dimethylsulphoxide)platinum(II) under the conditions described by Pidcock *et al.*[9]

*Monometallic derivatives of 2,2′-bipyrimidyl* (Scheme 2)

Unless stated otherwise, the following reactions were carried out at ambient temperature in air.

*Dimethyl(2,2′-bipyrimidyl)platinum(II)*

A solution of (dmso)$_2$PtMe$_2$ (0.50 g, 1.31 mmoles) in dichloromethane (40 cm$^3$) was slowly added to a rapidly stirred solution of bipyrimidyl (0.41 g, 2.62 mmoles) in the same solvent (40 cm$^3$). The colourless solution began to turn red immediately; reaction was complete after stirring for 2 hr at room temperature.

The reaction mixture was filtered to remove the small quantity of binuclear product produced (0.08 g, 20% based on Pt) and the solvent removed under reduced pressure.

Crystallisation of the brown–red residue from warm (35°C) acetone afforded deep red needles of (bipym)PtMe$_2$ (1a) in 63% overall yield which decomposed above 120°C. Found: C, 30.96; H, 3.01; N, 14.45. Calc. for $C_{10}H_{12}N_4Pt$: C, 31.33; H, 3.16; N, 14.62%.

*Diphenyl(2,2′-bipyrimidyl)platinum(II)*

Following a procedure essentially similar to that outlined for 1a, (bipym)PtPh$_2$ (1b) was prepared by the reaction of (dmso)$_2$PtPh$_2$ (0.3 g, 0.59 mmoles) with bipyrimidyl (0.14 g, 0.89 mmoles) in dichloromethane.

Golden plates of (bipym)PtPh$_2$ were recovered from warm (35°) acetone in 71% yield which decomposed above 175°. $^1$H NMR spectroscopy indicated that both acetone (1/6 equivalent) and uncoordinated bipyrimidyl (1/7 equivalent) were included in the crystal lattice. Found: C, 48.15; H, 3.28; N, 11.80. Calc. for $C_{20}H_{16}N_4Pt.1/6C_3H_60.1/7C_8H_6N_4$: C, 48.34; H, 3.33; N, 11.86%.

*1,4-Tetramethylene(2,2′-bipyrimidyl)platinum(II)*

Equimolar amounts of (cod)Pt(CH$_2$)$_4$ (0.4 g, 1.12 mmoles) and bipyrimidyl (0.18 g, 1.12 mmoles) were dissolved in toluene (*ca.* 20 cm$^3$) and left to react in the dark. After 2 hr, the initially colourless solution had acquired a pink tinge; after 7 days the solution was deep red in colour, and a small amount of uncharacterised orange powder had appeared. This was removed by filtration and the reaction mixture set aside for *ca.* 90 days during which time dark red (bipym)Pt(CH$_2$)$_4$ (1c) deposited from the solution in 30% yield. This was collected, recrystallised carefully from acetone/ethanol and found to decompose above 197°C. Found: C, 35.0; H, 3.54; N, 13.69. Calc. for $C_{12}H_{14}N_4Pt$: C, 35.21; H, 3.45; N, 13.69%.

*Bis(trifluoromethyl)(2,2′-bipyrimidyl)platinum(II)*

An initially colourless solution of (cod)Pt(CF$_3$)$_2$ (0.29 g, 0.68 mmoles) and bipyrimidyl (0.14 g, 0.90 mmoles) in acetone (*ca.* 100 cm$^3$) was kept at 50°C for 2 days. During this time the reaction mixture became increasingly orange in colour.

Removal of the solvent and washing the residue with ether (20 cm$^3$) afforded a fine orange powder. Orange prisms of (bipym)Pt(CF$_3$)$_2$ (1e) were obtained in 82% yield by slow evaporation of an acetone solution at room temperature. The crystals decomposed without melting above 250°C. Found: C, 24.47; H, 1.30; N, 11.79. Calc. for $C_{10}H_6F_6N_4Pt$: C, 24.45; H, 1.23; N, 11.40%.

*Bimetallic derivatives of bipyrimidyl*

*Tetramethyl(μ-2,2′-bipyrimidyl)diplatinum(II).* A solution of bipyrimidyl (0.053 g, 0.33 mmoles) in dichloromethane (30 cm$^3$) was added over a period of 1 hr to a stirred solution of (dmso)$_2$PtMe$_2$ (0.25 g, 0.66 mmoles) in the same solvent (30 cm$^3$). The colourless solution attained a dull red colour and a brown–black solid precipitated. The mixture was allowed to stand overnight and further, microcrystalline, product was deposited. Microcrystalline (μ-bipym)[PtMe$_2$]$_2$ (2a) was collected by filtration, washed with dichloromethane (2 × 30 cm$^3$) then dried *in vacuo* (Yield = 84%).

Found: C, 23.14; H, 2.73; N, 9.05. Calc. for $C_{12}H_{18}N_4Pt_2$: C, 23.69; H, 2.98; N, 9.21%.

*Tetraphenyl(μ-2,2′-bipyrimidyl)diplatinum(II)*

Conditions analogous to those for (μ-bipym)[$PtMe_2$]$_2$ were used to prepare (μ-bipym)[$PtPh_2$]$_2$ (2b). A solution of $(dmso)_2PtPh_2$ and bipym in 2:1 ratio was allowed to stand overnight. The dark red microcrystals of (μ-bipym)[$PtPh_2$]$_2$ were filtered off, washed with dichloromethane and dried *in vacuo*. The complex was found to decompose above 170°C (Yield = 88%). (Found: C, 44.46; H, 3.03; N, 6.51. Calc. for $C_{32}H_{26}N_4Pt_2$: C, 44.86; H, 3.06; N, 6.54%.

Pt-*dimethyl*-Pt′-*diphenyl*(μ-2,2′-*bipyrimidyl*) *diplatinum(II)*

A colourless solution of $(dmso)_2PtPh_2$ (0.109 g, 0.215 mmoles) in dichloromethane (30 cm$^3$) was added to a red solution of (bipym)$PtMe_2$ (0.082 g, 0.215 mmoles) in the same solvent (30 cm$^3$). The intensity of the colour deepened at once; the reaction mixture was left overnight to complete decomposition of (μ-bipym)[$PtMe_2$][$PtPh_2$] (2c) as dark brown microcrystals in 93% yield.

Pt-*dimethyl*-Pt′-*bis(trifluoromethyl)*(μ-2,2′-*bipyrimidyl)diplatinum(II)*

$(dmso)_2PtMe_2$ (0.11 g, 0.29 mmoles) was added to a stirred solution of (bipym)$Pt(CF_3)_2$ (0.14 g, 0.29 mmoles) in acetone (250 cm$^3$). When the $(dmso)_2PtMe_2$ had completely dissolved, the rapidly darkening solution was allowed to stand overnight. The resultant brown–black microcrystalline precipitate of (μ-bipym)[$PtMe_2$][$Pt(CF_3)_2$] (2e) was isolated by filtration, washed with acetone and dried *in vacuo*. Yield = 81%. Found: C, 19.73; H, 1.87; N, 7.94. Calc. for $C_{12}H_{12}N_4F_6Pt_2$: C, 20.12; H, 1.69; N, 7.82%.

Pt-*dimethyl*-Pt′-*bis(adamantylmethyl)*(μ-2,2′-*bipyrimidyl)diplatinum(II)*

A solution of $(dmso)_2PtMe_2$ (0.06 g, 0.15 mmol) in acetone (8 cm$^3$) was added to (bipym)$Pt(adme)_2$ (0.10 g, 0.15 mmol) in the same solvent (60 cm$^3$). The dark red mixture was allowed to stand for 15 hr at ambient temperature, during which green–brown filamentous crystals of (μ-bipym)[$PtMe_2$][Pt adme$_2$].$(Me)_2CO$ were deposited. These were filtered off, washed with acetone (2 × 10 cm$^3$) and dried *in vacuo* (Yield = 93%). Found: C, 44.41; H, 5.45; N, 6.18. Calc. for $C_{34}H_{52}N_4OPt_2 \cdot \frac{1}{2}C_3H_6O$: C, 43.78; H, 5.12; N, 5.96%.

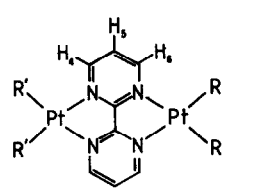
## RESULTS AND DISCUSSION

Dialkyl- and diaryl(2,2′-bipyrimidyl)diplatinum(II) species **1** were prepared by interaction of 2,2′-bipyrimidyl with an equivalent amount of an organoplatinum precursor containing a labile ligand, either 1,5-cyclooctadiene (cod) or dimethylsulphoxide, (dmso). The conversions proceed at ambient temperatures to give air-stable orange or red crystalline products in moderate to high yields. For the dimethyl, (**1a**) and diphenyl (**1b**) complexes, the dmso route 2(i) was the favoured path, principally because of its speed; conversion was complete in *ca.* 2 hr. The utility of this approach was only limited by the range of $(dmso)_2PtR_2$ accessible via organotin precursors.[9] Formation of **1a** and **1b** from (cod)$PtR_2$ [Route 2(ii)] took several weeks.[10] This was also true of the platinacyclopentane (bipym)Pt$(CH_2)_4$ (**1c**), in parallel with its bipyridyl analogue.[11] Useful yields were recovered only after *ca.* 90 days (alternative syntheses are being explored). As previously reported, however, metathesis of the diene in (cod)Pt(adme)$_2$, to give **1d**, is less sluggish.[1d] This labilisation is probably steric in origin; we have found similar effects on the displacement rate of cyclooctadiene from complexes with other bulky alkyl ligands.[5] The rapid formation of **1e** is, in contrast, ascribable to an electronically controlled, high kinetic *trans*-effect for the perfluoroalkyl ligands in (cod)$Pt(CF_3)_2$.[8] Synthesis of **1e** required 2 days at 50°C.

Bimetallic derivatives **2** (Fig. 1) were isolated as extremely dark, microcrystalline solids[10] by reaction of **1** with $(dmso)_2PtR_2$ in dichloromethane solution. With the exception of (cod)Pt(adme)$_2$,[1d] (cod)$PtR_2$ reacts too slowly to be a useful precursor. Consequently, (μ-bipym)[$Pt(CH_2)_4$]$_2$ and (μ-bipym)[$Pt(CF_3)_2$]$_2$ have not yet been isolated in sufficient quantity for rigorous analysis. Satisfactory microanalytical results have been obtained for all other compounds (see Experimental).

## $^1$H NMR SPECTROSCOPY

$^1$H NMR emerged as an especially useful technique for analysis of monometallic complexes. The




**2**

Fig. 1. (a) R = R′ = Me. (b) R = R′ = Ph. (c) R = Me, R′ = Ph. (d) R = R′ = adme. (e) R = Me, R′ = $CF_3$. (f) R = Me, R′ = adme.

results are summarised in Table 1. Resonances assigned to the coordinated bipyrimidyl ligand show characteristic downfield shifts relative to those for the free ligand,[11] consistent with a net loss of electron density from the bipyrimidyl skeleton via $\sigma$-donation. All three hydrogens generate doubled doublets due to coupling with their two neighbours. Additionally, $H_6$ displays substantial spin–spin interaction with 34% abundant $^{195}Pt$. There is no evidence for $H_6$–$H_4$ scrambling via 1–3 exchange of the ligating nitrogen at ambient temperature.

Although the magnitudes of the coordination shifts $\Delta\delta$[12] are not large (generally $< 1$ ppm) several trends are immediately apparent (Fig. 2). The general pattern for any (bipym)$PtR_2$ is an increase in $\Delta\delta$ in the order $\Delta\delta H_5 < \Delta\delta H_4 < \Delta\delta H_6$. From complex to complex, $\Delta\delta H_4$ varies least, whilst $\Delta\delta H_6$ has the widest range. $\Delta\delta H_5$ increases in the same order as $\Delta\delta H_4$ as R is varied. The chemical shift of the ring hydrogens must reflect the skeletal $\sigma$-electron density in the ring. The trends in $\Delta\delta H_5$ and $\Delta\delta H_4$ are ascribed to the

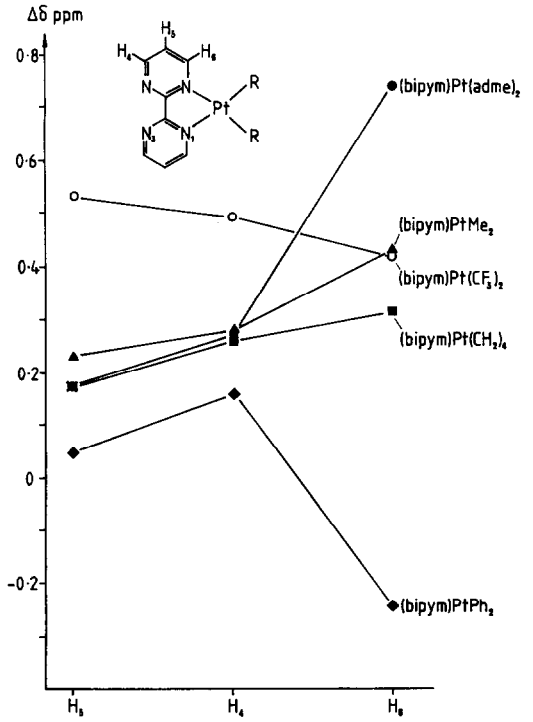



Fig. 2. $^1H$ NMR coordination shifts ($\Delta\delta$) for monobidentate 2,2′-bipyrimidyl.†

relative electron withdrawing capacities of the $PtR_2$ moiety. These decrease in order R = $CF_3 > CH_3 \simeq$ adme $\simeq CH_2$(cyclic) $> C_6H_5$.[13] This appears to be largely an inductive ($\sigma$) effect, since it is the $H_4$ position which should be the more sensitive to hyperconjugative and mesomeric ($\pi$) electron withdrawal, in contrast to our observations. The anomalous reversal of the general trend in (bipym)$Pt(CF_3)_2$, where $\Delta\delta H_6 < \Delta\delta H_4 < \Delta\delta H_5$, is further indication that $H_5$ is the most affected by increasing electronegativity of $PtR_2$.

The relatively larger variations in $\Delta\delta H_6$ in (bipym)$PtR_2$ are less easily explained in similarly broad terms and are, we suspect, locally dictated by the nature of the adjacent R. For instance, $H_6$ in (bipym)$Pt(C_6H_5)_2$ displays a significant *upfield* shift relative to bipyrimidyl itself. This shielding may be attributed to proximity to the phenyl ligand; if the favoured conformation for the arylplatinum segment places the ring perpendicular to the coordination plane, then $H_6$ is suitably placed to experience shielding by the induced anisotropic magnetic field of the aromatic group.

We are unable to provide a convincing argument for the contrasting deshielding of $H_6$ in the adamantylmethyl analogue, unless the bulky alkyl ligand induces substantial distortion in the molecular geometry. It may be significant, from this point of view, that $\Delta\delta H_6$ for the sterically similar methyl and trifluoromethyl derivatives are almost identical to each other. That $\Delta\delta H_6$ is to an extent controlled by an electronic *trans*-influence of R cannot be entirely excluded, of course, but we feel that such variation in *trans*-influence—which should, *inter alia*, alter the relative contribution of the platinum 6s orbital to metal–ligand bonds—would produce a wider range in $J(^1H_6$–$^{195}Pt)$ than is observed here.

Only the bimetallic species which contain adamantylmethyl groups are sufficiently soluble to allow measurement of $^1H$ NMR spectra. This is unfortunate, since the data provide excellent characterisation of the bis-bidentate mode of coordination. In both **2d** and **2e**, $\Delta\delta H_5$ is greater than that in the mononuclear complexes, indicating further electron withdrawal from bipyrimidyl. $H_4$ and $H_6$ are now *both* adjacent to coordinated organoplatinum, and this is reflected in increased downfield shifts. This is most dramatic in **2d** and underlines the strongly deshielding influence of the bis(adamantylmethyl)platinum moiety observed for $H_6$ in **1d**. The effect is also noted in the asymmetric **2e**; here $H_6$, which is *syn* to the dimethylplatinum fragment, is also less shielded than in the mononuclear analogue.

†$\Delta\delta$(ppm) for dimers: ($\mu$-bipym)[Pt(adme)$_2$]$_2$; $H_4 = H_6 = 1.08$, $H_5 = 0.44$; ($\mu$-bipym)[PtMe$_2$][Pt(adme)$_2$]; $H_4$ (adjacent to adme) = 1.03, $H_5 = 0.42$, ($H_6$ adjacent to Me) = 0.74.

Table 1. $^1$H NMR characteristics of 2,2′-bipyrimidyl (L) in organoplatinum(II) complexes

| Complex | $H_4$[a] | $H_5$[a] | $H_6$[a] | Coupling Constants (Hz) $H_4$–$H_6$ | $H_4$–$H_5$ | $H_5$–$H_6$ | Pt–$H_6$ | Other $^1$H and $^{19}$F Parameters |
|---|---|---|---|---|---|---|---|---|
| 1a $LPtMe_2$[c] | 9.31 | 7.68 | 9.46 | 2.2 | 4.8 | 5.4 | 20 | Methyl: $\delta$ = 1.18, J(Pt–H) = 87 Hz |
| 1b $LPtPh_2$[c] | 9.19 | [b] | 8.79 | 2.2 | 4.8 | 5.5 | 22 | Phenyl: $\delta$ = 7.54, $H_2'$, $H_6'$, J(Pt–$H_6'$) = 72 Hz; $\delta$ = 7.04, $H_3'$,$H_5'$; $\delta$ = 6.90, $H_4'$ |
| 1c $LPt(CH_2)_4$[c] | 9.29 | 7.62 | 9.35 | 2.2 | 4.3 | 5.2 | 20 | Methylene: $\delta$ = 1.30, $\alpha$-$CH_2$, J(Pt–H) = 93 Hz; $\delta$ = 2.65, $\beta$-$CH_2$, J(Pt–H) = 101 Hz |
| 1d $LPt(adme)_2$[c,f] | 9.33 | 7.64 | 9.79 | 2.2 | 4.6 | 5.6 | 22 | Methylene: $\delta$ = 2.11, J(Pt–H) = 90 Hz<br>Adamantyl: $\delta$ = 1.58(6H), $\delta$ = 1.69(6H)<br>$\delta$ = 1.81(3H) |
| 1e $LPt(CF_3)$[d] | 9.45 | 8.11 | 9.38 | 2.1 | 4.8 | 5.8 | 22 | Trifluoromethyl[g]: $\delta$ = 36.37, J(Pt–F) = 758 Hz |
| 2d ($\mu$-L)$[Pt(adme)_2]_2$[e,f] | 10.11 | 7.89 | 10.11 | 0 | 5.5 | 5.5 | 26 | Methylene: $\delta$ = 2.12, J(Pt–H) = 92 Hz<br>Adamantyl: $\delta$ = 1.58(6H), $\delta$ = 1.69(6H)<br>$\delta$ = 1.81(3H) |
| 2e ($\mu$-L)$(PtMe_2)[Pt(adme)_2]$[e] | 10.06 | 7.87 | 9.78[h] | 1.7 | 5.4 | 5.4 | 28[i]<br>30 | Methyl: $\delta$ = 1.21, J(Pt–H) = 89 Hz<br>Methylene: $\delta$ = 2.11, J(Pt–H) = 91 Hz<br>Adamantyl: $\delta$ = 1.58(6H), $\delta$ = 1.69(6H), $\delta$ = 1.81(3H) |

a: ppm relative to tetramethylsilane; b: obscured by phenyl resonances; c: d-chloroform solution; d: $d_6$-acetone solution; e: $d_2$-dichloromethane solution; f: re-examined at 250 MHz (see Ref. 3a); g: $^{19}$F NMR in ppm relative to $CFCl_3$ external standard, upfield shifts negative; h: $H_6$ adjacent to Me group; i: J(Pt–$H_4$), $H_4$ adjacent to adme group.

The NMR characteristics for the $PtR_2$ skeleton in both mono- and binuclear complexes are typical of such compounds.

## IR SPECTROSCOPY

The IR spectra of monometallic species (bipym)$PtR_2$ contain a number of absorptions that appear to be especially characteristic of the skeleton. These are assigned in Table 2.[14] Vibrational characteristics are most useful in distinguishing bimetallic derivatives from their monometallic precursors. The latter invariably have two prominent bands near 1570 and 1550 $cm^{-1}$, assigned to ring-stretching modes of the coordinated ligand. In the bis-bidentate mode of coordination, the lower energy absorption, in particular, is nearly or wholly absent. In the dinuclear complexes which feature adamantylmethyl, both bands have dissappeared. Perhaps less dramatic is an invariable decrease in energy, by *ca.* 20 $cm^{-1}$, of the C–H bending mode initially at 745–750 $cm^{-1}$. Finally, addition of the second metal leads generally to loss of the band near 660 $cm^{-1}$. The persistance of this feature to some degree in **2b** and **2c** may be ascribed to a similar ring bending mode of the phenyl ligands. Absorptions near 580 $cm^{-1}$ attributable to Pt–C stretching modes, are evident for both mono- and binuclear methyl–platinum complexes, but not for those with trifluoromethyl or more heavily substituted organic ligands.

## ELECTRONIC SPECTROSCOPY

Characteristics of UV and visible spectra have been used as a sensitive indication of electron energetics of the related bipyridyl complexes.[1g] We exploit our data in two such ways. First of all, we wish to compare the relative electronic effects of 2,2′-bipyridyl and monobidentate 2,2′-bipyrimidyl as (isosteric) ligands. Second, electronic spectroscopy identifies the electronic adjustments which accompany the bis-bidentate mode of binding and which we expect also to produce modified reactivity. The main features of the electronic spectra appear in Table 3. Dichloromethane and 1,1,2,2-tetrachloroethane were employed as solvents, the former to allow comparison with previous results for (bipy)$PtR_2$, the latter in order to compare the mononuclear complexes with their dinuclear analogues, for which it is the only generally satisfactory solvent.

The spectra of (bipym)$PtR_2$ are characterised by two absorptions which we attribute to MLCT ($d\pi$–$\pi^*$) transitions. The energies of these bands are sensitive both to the nature of R and of the solvent. The higher of the two in energy, $\lambda_2$, is often obscured by the more intense ligand $\pi$–$\pi^*$ transitions in the near UV. The lower energy absorption $\lambda_1$ can always be observed at 130–160 nm to longer wavelength. This feature is therefore the more reliable gauge of electronic variations.

The energy of this transition is invariably lower for (bipym)$PtR_2$ than for the corresponding (bipy)$PtR_2$. This is consistent with the general observation that energies of MLTC absorptions in complexes of N-bonded heterocyclic ligands are lowered by introduction of electronegative ring atoms or substituents.[2] Molecular orbital calculations which place the LUMO ($\pi^*$) for 2,2′-bipyrimidyl lower than that for 2,2′-bipyridyl are in accord with a smaller separation from the $d\pi$ orbitals of platinum.[2g] As with the bipyridyl analogues,[1g] increasing the electronegativity of R in (bipym)$PtR_2$ shifts $\lambda_1$ to shorter wavelength, pre-

Table 2. IR characteristics of mono-bidentate and bis-bidentate bipyrimidyl complexes

| Complex | Ring Stretch (C–N,C–C) | | | Ring Breathing | H In Plane Bend | H Out of Plane Bend | Ring Bend | M–C Stretch |
|---|---|---|---|---|---|---|---|---|
| 1a (bipym)$PtMe_2$ | 1570s | 1549s | 1400vs | 1020mw | 830mw | 745s | 664ms | 577br,m |
| 1b (bipym)$PtPh_2$ | 1572vs | 1548ms | 1404vs | 1025vs | 820ms | 750vs | 662mw | |
| 1c (bipym)$Pt(CH_2)_4$ | 1570s | 1551ms | 1402vs | 1020m | 819m | 746s | 664m | |
| 1d (bipym)Pt(adme)$_2$ | 1572ms | 1547m | 1403vs | 1013m | 808s | 750vs | 662w | |
| 1e (bipym)$Pt(CF_3)_2$ | 1583s | 1559m | 1418s | a | 820mw | 750s | 664ms | |
| 2a (μ-bipym)$(PtMe_2)_2$ | 1568s | | 1401vs | 1025s | 810m | 723vs | | 582,578m |
| 2b (μ-bipym)$(PtPh_2)_2$ | 1570s | | 1410vs | 1025ms | 819m | 730vs | 665m | |
| 2c (μ-bipym)$(PtMe_2)(PtPh_2)$ | 1569vs | | 1406vs | 1023ms | 818ms | 724s | 661vw | 580br,w |
| 2d (μ-bipym)$[Pt(adme)_2]_2$ | | | 1400s | 1030w | 803s | 736s | | |
| 2e (μ-bipym)$(PtMe_2)[Pt(CF_3)_2]$ | 1580vs | | 1415vs | a | 820m | 728ms | | 580br,w |
| 2f (μ-bipym)$(PtMe_2)[Pt(adme)_2]$ | | | 1400vs | 1030w | 806s | 729s | | 582w |

a: obscured by ν(C–F).

Table 3. UV and visible characteristics of (i) $L_2PtR_2$ (ii) $R_2Pt(bipym)PtR'_2$

(i)

| $L_2$/Solvent / $R_2$ | bipy/ $CH_2Cl_2$ | | bipym/ $CH_2Cl_2$ | | bipym/ $Cl_2CHCHCl_2$ | |
|---|---|---|---|---|---|---|
| | $\lambda_1$ | $\lambda_2$ | $\lambda_1$ | $\lambda_2$ | $\lambda_1$ | $\lambda_2$ |
| $Me_2$ | 448[a] | | 478 | 347 | 464 | c |
| $Ph_2$ | 441[a] | | 458 | c | 465 | c |
| $(CH_2)_4$ | 476 | | 496 | 356 | d | d |
| $(adme)_2$ | 498 | 342 | 525 | 368 | 527 | 375 |
| $(CF_3)_2$ | 423 | c | 432 | c | 440 | c |

(ii)

| R | R' | $\lambda_1$[e] | $\lambda_2$[e] |
|---|---|---|---|
| Me | Me | 610<br>560 | 383 |
| Ph | Ph | f | f |
| Me | Ph | 600<br>560 | 379 |
| adme | adme | 655<br>600 | 410 |
| Me | $CF_3$ | f | f |
| Me | adme | 623[g]<br>568 | c |

a: from reference 7; b: unavailable;
c: obscured; d: decomposed; e: in sym-tetrachloroethane;
f: insufficiently soluble; g: in dichloromethane.

sumably since increased electron withdrawal from the metal contracts the $d\pi$ orbitals, thus increasing the $d\pi-\pi^*$ energy gap.

For the dinuclear complexes, the first MLCT absorption occurs at longer wavelength than in corresponding mononuclear species. The $\lambda_1$ band comprises two peaks of about equal intensity with 40–60 nm separation between the maxima. The bathochromic shift is most marked for adamantylmethyl derivatives, which give green solutions. The lowered energy of this transition could be due to further stabilisation of the LUMO on the ligand by the electron withdrawing influence of the second metal centre and/or to the presence of a relatively high energy, less stable, largely nonbonding HOMO spanning both metals in the dinuclear complex.[2g] The absorption pattern for the asymmetric bimetallic species, **2e**, lies intermediate between those for **2a** and **2d**. We note that distinct MLCT bands assignable to the different metal centres in mixed bimetallic complexes were not observed previously.[3a] Reasons for the splitting of this band are not immediately clear, especially in the highly symmetrical ($D_{2h}$) **2a** and **2d**.

Reactivity studies of these complexes are currently under way and we are examining the chemistry of the analogous palladium and nickel systems. We are also investigating substituted 2,2′-bipyrimidyl in an effort to improve the solubilities of those complexes.

*Acknowledgements*—The award of a studentship by the S.E.R.C. (to V.F.S.) and the generous loan of platinum by Johnson Matthey Ltd., are gratefully acknowledged. We are additionally grateful to the Royal Society and the Central Research Fund of the University of London for equipment grants in support of this work. We also thank Sue Johnson and Dick Sheppard for F.T. NMR measurements and Niall Watkins for preparing (cod)Pt(adme)$_2$.

## REFERENCES

1. (a) G. Wilke and G. Hermann, *Angew. Chem. Int. Edn.* 1966, **51**, 581. (b) T. Saito, Y. Uchida, A. Misono, A. Yamamoto, K. Morifuji and S. Ikeda, *J. Am. Chem. Soc.* 1966, **88**, 5198. (c) M. J. Doyle, J. McMeeking and P. Binger, *J. Chem. Soc., Chem. Commun.* 1976, 376; S. Takahashi, Y. Suzuki, K. Sonogashira and N. Hagihara, *Ibid.* 1976, 839. (d) M. Bochmann, G. Wilkinson and G. B. Young, *J. Chem. Soc., Dalton* 1980, 1879. (e) G. Calvin and G. E. Coates, *J. Chem. Soc.* 1960, 2008. (f) P. Diversi, G. Ingrosso, A. Lucherin and S. Murtas, *J. Chem. Soc., Dalton* 1980, 1633. (g) N. Chaudhury and R. J. Puddephatt, *J. Organomet. Chem.* 1975, **84**, 105. (h) J. Kuyper, *Inorg. Chem.* 1978, **16**, 2171. (i) G. B. Young and G. M. Whitesides, *J. Am. Chem. Soc.* 1978, **100**, 5808.
2. (a) A. Teurstein, B. A. Fert and G. Navon, *J. Inorg. Nucl. Chem.* 1974, **36**, 1055. (b) J. C. Bailar Jr., D. J. Baker, R. A. Bauer, Gov. Rep. Announce. Index (U.S.) 1975, **75**, 50 (Chem. Abs. 1976, **84**, 115243h). (c) M. Hunziker and A. Ludi, *J. Am. Chem. Soc.* 1977, **99**, 7370. (d) F. V. Dose and L. J. Wilson, *Inorg. Chem.* (1978), **17**, 2660. (e) P. M. Kiernan and A. Ludi, *J. Chem. Soc., Dalton* 1978, 1127. (f) R. H. Petty and L. J. Wilson, *J. Chem. Soc., Chem. Commun.* 1978, 483. R. H. Petty, B. R. Welch, L. J. Wilson, L. A. Bottomley and K. M. Kadish, *J. Am. Chem. Soc.* 1960, **102**, 611. (g) R. R. Ruminski and J. D. Petersen, *Inorg. Chem.* 1982, **21**, 3706. (h) N. Kuhn, A. Voss and P. Sartori, *Chem. Zeit.* 1982, **106**, 298.

3. (a) C. Overton and J. A. Connor, *Polyhedron* 1982, **1**, 53. (b) K. J. Moore and J. D. Petersen, *Ibid.* 1983, **2**, 279.
4. These aspects are currently under independent investigation; V. F. Sutcliffe and G. B. Young, unpublished work.
5. D. C. Griffiths and G. B. Young, *Polyhedron*, 1983, **2**, 1095. in press.
6. J. X. McDermott, J. F. White and G. M. Whitesides, *J. Am. Chem. Soc.* 1976, **98**, 6521, and references cited therein.
7. C. Eaborn, K. Kunden and A. Pidcock, *J. Organomet. Chem.* 1967, **10**, 529.
8. H. C. Clark and L. E. Manzer, *J. Organomet. Chem.* 1873, **59**, 411.
9. C. Eaborn, K. Kunden and A. Pidcock, *J. Chem. Soc., Dalton* 1981, 933.
10. The extremely dark colour of many of these compounds meant that decomposition points were not visible.
11. $^1$H NMR data for 2,2′-bipyrimidyl (i) chloroform-*d*: $H_{4,6} = 9.04$ ppm, $H_5 = 7.45$ ppm, $^3J(H–H)) = 6$ Hz; (ii) acetone-$d_6$: $H_{4,6} = 8.96$ ppm, $H_5 = 7.58$ ppm, $^3J(H–H) = 5$ Hz; (iii) dichloromethane-$d_2$; $H_{4,6} = 9.03$ ppm, $H_5 = 7.45$ ppm, $^3J(H–H) = 1$ Hz.
12. Coordination shift $\Delta\delta = \delta$ ($H_n$ in coordinated bipym)—$\delta$($H_n$ in free bipym); thus, downfield shifts are positive.
13. In order that $H_5$ be obscured in (bipym)$PtPh_2$ the magnitude of $\Delta\delta H_5$ must be 0–0.5 ppm.
14. Assignments by analogy with related (bipy)$PtX_2$. J. S. Strukl and J. L. Walter, *Spectrochim Acta* 1971, **27A**, 22.

*Polyhedron* Vol. 3, No. 1, pp. 95–97, 1984
Printed in Great Britain.

0277–5387/84 $3.00 + .00
Pergamon Press Ltd.

# THE CRYSTAL AND MOLECULAR STRUCTURE OF HEXADECAPHENYLOCTASILOXYSPIRO(9,9)TITANATE(IV)

MICHAEL B. HURSTHOUSE* and Md. ALTAF HOSSAIN

Department of Chemistry, Queen Mary College, London E1 4NS, England

(*Received* 27 *June* 1983; *accepted* 5 *July* 1983)

**Abstract**—The crystal and molecular structures of the title compound have been determined by single crystal X-ray diffraction methods. In the spiro molecule, the metal atom has a geometry very close to tetrahedral, with O–Ti–O angles of 107.9–111.0(2)° and very short Ti–O bonds of length 1.777–1.791(5)Å. The two $TiO_5Si_4$ rings have different, ill-defined conformations; the Si–O bond lengths and Si–O–Si angles are similar to those in $(SiO)_n$ rings.

Although metallosiloxanes containing titanium have been extensively studied,[1] many of them are intractable polymers. Of the molecular species which have been described, the large majority are derivatives of the monodentate triorganosiloxy ligands [–$OSiR_3$]. Exceptions to this group are two spiro-titanium species $Ti[OSiPh_2OSiPh_2OSiPh_2O]_2$ and $Ti[OSiPh_2OSiPh_2O]_2$, the syntheses and properties of which were reported by Brown[2] and Andrianov[3] respectively, although in neither case were the molecules structurally characterised. As part of a study of the bonding characteristics of metallosiloxane systems, we have determined the structure of the title compound by single-crystal X-ray techniques.

## RESULTS AND DISCUSSIONS

A molecule of the compound, confirmed as the spiro (9,9)titanate is shown in the Fig. 1. Some of the more important bond lengths and angles are given in the Table and in Fig. 2; full lists have been deposited in the Supplementary Publication.

The titanium atom has an almost regular tetrahedral geometry as can be seen from the O–Ti–O angles of 108–111(1)° and the dihedral angle of 90.5(5)° between the two intersecting $O_2Ti$ chelate planes. Four coordination (and tetrahedral geometry) is in fact quite rare for Ti(IV) if we discount the $\psi$-tetrahedral structures adopted by the many dicyclopentadienyl titanium(IV) derivatives. Occasionally the "$Ti^{4+}$ ions" in titanates have been found to occupy tetrahedral sites,[6] and examples from the area of metallo-organic complexes are the $TiN_4$ species $Ti[N(Me)–Si(Me)_2–Si(Me)_2–(Me)N]_2$ [7] and $Ti[N(Bu^t)Si(Me)_2(Bu^t)N]_2$,[8] also *spiro* molecules), $TiCl[N(SiMe_3)_2]_3$,[9] tetrabenzyl titanium,[10] $\mu$-oxobis(tribenzyl titanium)[11] and dibenzylbis(octamethyl-2,4,6-trisila-1,3,5-triazacyclohex-1-yl)titanium.[12]

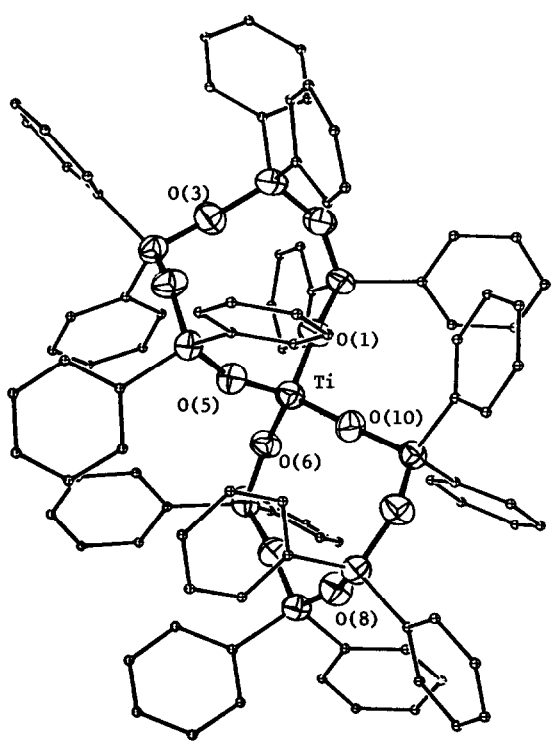



Fig. 1. Ortep drawing of a molecule of $Ti(OSiPh_2.OSiPh_2.OSiPh_2.OSiPh_2.O–)_2$.

*Author to whom correspondence should be addressed.

Table 1. Selected bond lengths and angles

a) Bond Angles (Å)

| | | | |
|---|---|---|---|
| Ti -O(1) | 1.777(5) | Ti -O(6) | 1.780(3) |
| Ti -O(5) | 1.791(5) | Ti -O(10) | 1.779(3) |
| Si(1)-O(1) | 1.635(5) | Si(5)-O(6) | 1.637(5) |
| Si(1)-O(2) | 1.610(5) | Si(5)-O(7) | 1.611(5) |
| Si(2)-O(2) | 1.608(5) | Si(6)-O(7) | 1.616(5) |
| Si(2)-O(3) | 1.621(5) | Si(6)-O(8) | 1.618(5) |
| Si(3)-O(3) | 1.612(5) | Si(7)-O(8) | 1.609(5) |
| Si(3)-O(4) | 1.617(5) | Si(7)-O(9) | 1.622(5) |
| Si(4)-O(4) | 1.630(5) | Si(8)-O(9) | 1.629(5) |
| Si(4)-O(5) | 1.629(5) | Si(8)-O(10) | 1.621(5) |

Si-C(phenyl) 1.850(6) - 1.868(6), Av. 1.8

b) Angles ( deg)

| | | | |
|---|---|---|---|
| O(1)-Ti-O(5) | 110.0(2) | O(5)-Ti-O(6) | 111.0(2) |
| O(1)-Ti-O(6) | 109.6(2) | O(5)-Ti-O(10) | 109.1(2) |
| O(1)-Ti-O(10) | 109.2(2) | O(6)-Ti-O(10) | 107.9(2) |

O-Si-O 107.3(2) - 110.6(2) Av. 109.2

C-Si-C 110.3(3) - 114.6(3) Av. 112.0

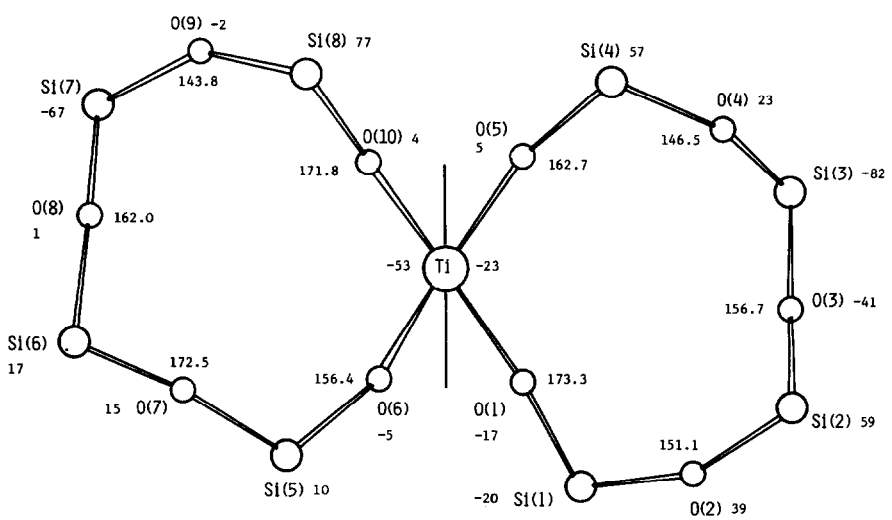



Fig. 2. Schematic representation of the $[TiO_5Si_4]$ ring conformation. Each ring is drawn as seen in projection perpendicular to the least squares plane. Atomic deviations from this plane (Å × $10^2$) are given by each atom symbol; the numbers inside the rings are the Si–O–Si angles.

The Ti–O bonds in the title compound are short in comparison with the Ti–L bonds in the organometallic complexes mentioned above (e.g. Ti–N 1.89–1.94 A, Ti–C 2.07–2.09) although they are close to the Ti–O bond lengths in the oxo bridged complex (1.804(7)Å)[11] and in the titanates, $\beta Ba_2TiO_4$[6a] (1.808(7)Å) and $Rb_2TiO_3$[6b] (1.73–1.87 Å). We consider these distances to indicate very strong bonds, presumably reinforced by O→Ti $\pi$-bonding. This would explain the high thermal stability of the compound and, perhaps, the large (i.e.→180°) Ti–O–Si angles in the rings.

The titanosiloxane rings have different and ill-defined conformations, as can be seen from the

atom deviations from the ligand best planes, included in Fig. 2. These, and the wide variation in Si–O–Si angles point to a flexible ring system and it is therefore unlikely that the ring structure and conformation will have had much effect on the $TiO_4$ stereochemistry. The Si–O distances in the rings are similar to those found in the parent siloxane rings,[13] although there is a slight tendency for those next to the Ti–O bonds to be lengthened.

## EXPERIMENTAL

Hexadecaphenyloctasiloxyspiro(9,9)titanate(IV) was prepared according to Brown *et al.*[2] except that tetraisopropoxytitanium[4] was used instead of the butoxide. Colourless plates were obtained directly from the preparation, in which the solvent was THF.

*Crystal data*

$C_{96}H_{80}O_{10}Si_8Ti$, M = 1664.59, Monoclinic, $a = 13.829(1)$, $b = 27.594(2)$, $c = 23.514(2)$Å, $\beta = 94.39(1)$, $U = 8946.3$ Å$^3$, space group $P2_1/n$, $Z = 4$, $D_c = 1.24$ g cm$^{-3}$, $F_{(000)} = 3480$, $\mu$(Cu–$K\alpha$) = 21.9 cm$^{-1}$.

*Data collection*

CADA4 Diffractometer, $\omega/2\theta$ scan, $\omega$ scan width = $0.80 + 0.15 \tan\theta$, Cu–$K\alpha$ radiation, $3 < \theta < 60°$, $\pm h,k,l$; $T_{max} = 60$ s, crystal size 0.45 × 0.13 × 0.10 mm, total data measured = 14440, unique = 13269, observed = 10652 [$Fo > 3\sigma(Fo)$].

*Structure solution and refinement*

Automatic direct methods (SHELX) + difference syntheses; blocked-cascade least square; all non-H atoms anisotropic, H-atoms not included, weighting scheme $\omega = 1/[\sigma^2(Fo) + 0.002Fo^2]$, $R = 0.066$, $R\omega = 0.075$. Programs, computers and scattering factor data as in Ref. 5.

Lists of atomic coordinates, thermal parameters, bond lengths and angles and Fo/Fc values have been deposited as Supplementary Material with the Editor, from whom copies are available on request. Atomic coordinates have also been deposited with the Cambridge Crystallographic Data Centre.

*Acknowledgments*—We thank the University of Dacca, Bangladesh, for a research studentship (MAH) and the SRC and Royal Society for assistance in the purchase and enhancement of the diffractometer.

## REFERENCES

1. K. A. Andrianov, *Inorg. Macromol. Rev.* 1970, **1**, 33, F. Schindler and H. Schmidbauer, *Angew. Chemie Int. Edn* 1967, **6**, 683.
2. V. A. Zeitler and C. A. Brown, *J. Am. Chem. Soc.* 1957, **79**, 4618.
3. K. A. Andrianov, N. A. Kurasheva and L. I. Kuteinikova, *Zh. Obshchei khim* 1976, **46**, 1533.
4. D. C. Bradley, *Prog. Inorg. Chem.* 1960, **2**, 303.
5. Md. A. Hossian, Ph.D. Thesis. University of London (1980).
6. a) K. I. Wu and I. D. Brown, *Acta Cryst.* 1973, **B29**, 2009;
   b) W. Schartan and R. Hoppe, *Z. Anorg. Chem.* 1974, **408**, 60.
7. H. Bürger, K. Wiegel, U. Thewalt and D. Schomburg, *J. Organometallic Chem.* 1975, **87**, 301.
8. D. J. Brauer, H. Bürger, E. Essig and W. Geschwandtner, *J. Organometallic Chem.* 1980, **190**, 343.
9. C. Airoldi, D. C. Bradley, H. Chudzynska, M. B. Hursthouse, K. M. A. Malik, *J. Chem. Soc. Dalton* 1980, 2010.
10. G. R. Davies, J. A. J. Jarvis, B. T. Kilbourn, *J. Chem. Soc.(D)*, 1971, 1511; I. W. Bassi, G. A. Negra, R. Scordamaglia, G. Chioccola, *J. Am. Chem. Soc.* 1971, **93**, 3787.
11. H. Stoeckli-Evans, *Helv. Chim. Acta* 1974, **57**, 684.
12. D. J. Brauer, H. Bürger, K. Wiegel, *J. Organometallic Chem.* 1978, **150**, 215.
13. M. A. Hossain, M. B. Hursthouse and K. M. A. Malik, *Acta Cryst.* 1979, **B35**, 522.

*Polyhedron* Vol. 3, No. 1, pp. 99–106, 1984
Printed in Great Britain.

0277-5387/84 $3.00 + .00
Pergamon Press Ltd.

# BIURET COMPLEXES OF DIVALENT TRANSITION METALS.

N'DONGUI MABIALA, J.P. BARBIER and R.P. HUGEL*

Laboratoire de Chimie Minérale, Université de REIMS, B.P. 347
51062 REIMS - Cédex - FRANCE.

**(Received 25 July 1983; accepted 10 October 1983)**

## ABSTRACT

The complexes M $bi_2$ $X_2$ with M = Mn, Co, Ni and Cu, X = Cl, Br and I have been prepared. IR spectra and magnetic properties are given. The analysis of the ligand field parameters obtained from the electronic spectra for the cobalt and nickel compounds are in agreement with a *trans* octahedral structure.

## INTRODUCTION

The biuret reaction first reported by Wiedemann (1) is used to show the presence of peptide groups : the addition of a cupric salt to an alkaline biuret solution gives a characteristic red violet colour. This reaction has been extensively studied (2) but the complexes obtained from neutral solution have not been detailed except for the bis(biuret) copper(II) chloride (3-6) and a far-infrared study (7). Some other bis(biuret) metal(II) chloride compounds were also reported by Mac Lellan and Melson (4) mainly an infrared study : bands shifts indicate that biuret is bonded through oxygen atoms.

* Author for correspondence

In the present work, neutral biuret complexes with divalent metal halides (M = Cu, Ni, Co and Mn ; X = Cl, Br, I) are prepared and characterized. Electronic and infrared spectra, magnetic properties are discussed, ligand field parameters are determined in the case of Ni(II) and Co(II) compounds.

## EXPERIMENTAL

The ligand biuret (FLUKA puriss.) was used without further purification. All chemicals (PROLABO R.P.) were of reagent grade. Ni(II) and Co(II) iodide were obtained from reaction of $BaI_2$ with $NiSO_4$ an $CoSO_4$. All halides were dehydrated under vacuum for the iodides or by heating for the others.

### Preparation of compounds and analyses.

All complexes were prepared as previously reported (4). Metals were determined by EDTA titration or by atomic absorption spectrometry and halides by potentiometry with silver nitrate. (Table I).

### Measurements.

Solid state electronic spectra were recorded with a Beckman 5240 spectrophotometer. Infrared spectra were recorded on a Perkin-Elmer 521 in KBr discs or Nujol mulls (4000-400 $cm^{-1}$). Magnetic data were measured, at room temperature, with a Curie-Cheneveau balance using $HgCo(SCN)_4$ as calibrant. X-ray powder patterns were obtained with a Debye-Scherrer camera, using Cu-$K_\alpha$ radiation.

TABLE I : Analytical results for biuret complexes.

| Compound | Color | Melting Point °C | % Carbon | | % Hydrogen | | % Nitrogen | | % Metal | | % Halogen | |
|---|---|---|---|---|---|---|---|---|---|---|---|---|
| | | | Calcd | Found | Calcd | Found | Calcd | Found | Calcd | Found | Calcd | Found |
| Mn $bi_2$ $Cl_2$ | White | 260 | 14.47 | 14.77 | 3.04 | 3.18 | 25.31 | 25.20 | 16.5 | 16.2 | 21.4 | 21.2 |
| Co $bi_2$ $Cl_2$ | Pink | 265 | 14.30 | 14.60 | 3.00 | 3.21 | 25.01 | 25.08 | 17.5 | 16.8 | 21.1 | 21.1 |
| Ni $bi_2$ $Cl_2$ | Pale green | 302 dec | 14.31 | 14.52 | 3.00 | 3.20 | 25.03 | 25.04 | 17.5 | 17.0 | 21.1 | 21.2 |
| Cu $bi_2$ $Cl_2$ | Blue green | 240 | 14.11 | 14.39 | 2.96 | 3.10 | 24.67 | 24.80 | 18.6 | 18.3 | 20.8 | 21.0 |
| Mn $bi_2$ $Br_2$ | White | 270 | 11.41 | 11.71 | 2.39 | 2.38 | 19.97 | 20.04 | 13.0 | 12.9 | 38.0 | 38.0 |
| Co $bi_2$ $Br_2$ | Pink | 265 | 11.31 | 11.82 | 2.37 | 2.40 | 19.78 | 19.76 | 13.9 | 13.5 | 37.6 | 37.5 |
| Ni $bi_2$ $Br_2$ | Pale green | 250 dec | 11.31 | 11.73 | 2.37 | 2.44 | 19.79 | 19.87 | 13.8 | 13.5 | 37.6 | 37.5 |
| Cu $bi_2$ $Br_2$ | Blue green | 240 dec | 11.13 | 11.31 | 2.35 | 2.37 | 19.57 | 19.49 | 19.6 | 19.5 | 37.2 | 37.2 |
| Co $bi_2$ $I_2$ | Pink | 255 | 9.26 | 9.57 | 1.94 | 2.31 | 16.20 | 17.02 | 11.3 | 11.1 | 48.9 | 48.5 |
| Ni $bi_2$ $I_2$ | Pale green | 290 | 9.26 | 9.76 | 1.94 | 2.29 | 16.20 | 15.74 | 11.3 | 10.8 | 48.9 | 48.0 |

## RESULTS AND DISCUSSION

### Electronic spectra.

Electronic spectra of Co(II) compounds are discussed on octahedral ligand field basis. They show one band at 8000 $cm^{-1}$ ($\nu_1$ : $^4T_{1g}$ (F) → $^4T_{2g}$ (F) transition) and a band system around 18000 $cm^{-1}$ ($\nu_3$ : $^4T_{1g}$ (F) → $^4T_{1g}$ (P) transition) ; the $\nu_2$ band is not observed being a two-electron jump process.
The fine structure of the $\nu_3$ band can be explained by spin-orbit coupling, vibrational interactions, forbidden doublet states transitions and mainly great distortions (irregularity of the ligand field).

The ligand field parameters are listed on Table II. $D_q$ and B values are obtained from the transition energy ratios given by Lever (8).

TABLE II : Electronic Spectra of Co(II) complexes.

| Compound | $\nu_1(cm^{-1})$ | $\nu_3(cm^{-1})$ | $D_q(cm^{-1})$ | $B(cm^{-1})$ | $\beta = \frac{B}{B_o}$ |
|---|---|---|---|---|---|
| Co $bi_2$ $Cl_2$ | 8200 | 19050 | 935 | 800 | 0.82 |
| Co $bi_2$ $Br_2$ | 8050 | 18400 | 925 | 755 | 0.78 |
| Co $bi_2$ $I_2$ | 8000 | 17540 | 900 | 705 | 0.73 |

($B_o$ value for free Co(II) ion : 971 $cm^{-1}$).

$D_q$ and B decrease from chloride to iodide compounds.

These results, indicative of a Co $O_4$ $X_2$ chromophore, are in agreement with the spectrochemical and nephelauxetic series.

In the case of Ni(II) compounds the $\nu_2$ around 14500 $cm^{-1}$ and $\nu_3$ (25000 $cm^{-1}$) agree with an octahedral metal ion surrounding but the calculated ligand field parameters are too high for this type of compounds. The splitting of the first band is characteristic of a lower symmetry. The Ni(II) electronic spectra have then been assigned in the basis of the tetragonal ligand field model with $D_{4h}$ symmetry. The bands in the 7000-10000 $cm^{-1}$ region can be assigned to the electronic transition, $^3A_{2g} \rightarrow {}^3T_{2g}$, in $O_h$ symmetry which splits in $D_{4h}$ symmetry into the lower $^3E_g$ and the higher $^3B_{2g}$. According to the tetragonal ligand field model the transition energy of the second lowest band $^3B_{1g}(F) \rightarrow {}^3B_{2g}(F)$ corresponds in a first approximation to the inplane ligand field strength $D_q^{xy}$

The two first bands energies are given by the relations

$$10\, D_q^{xy} - \frac{35}{4} D_t \quad \text{for} \quad {}^3B_{1g}(F) \rightarrow {}^3E_g(F)$$

$$10\, D_q^{xy} \quad \text{for} \quad {}^3B_{1g}(F) \rightarrow {}^3B_{2g}(F)$$

and the ligand field strength on the z axis by $D_q^z = D_q^{xy} - \frac{7}{4} D_t$ (8b).

All these results are listed in Table III.

TABLE III : Electronic spectra of Ni(II) complexes.

| Compound | $^3B_{1g} \rightarrow {}^3E_g$ ($cm^{-1}$) | $^3B_{1g} \rightarrow {}^3B_{2g}$ ($cm^{-1}$) | $D_t$($cm^{-1}$) | $D_q^{xy}$($cm^{-1}$) | $D_q^z$ ($cm^{-1}$) |
|---|---|---|---|---|---|
| Ni $bi_2$ $Cl_2$ | 7450 | 9750 | 265 | 975 | 515 |
| Ni $bi_2$ $Br_2$ | 7150 | 9800 | 305 | 980 | 450 |
| Ni $bi_2$ $I_2$ | 6900 | 10100 | 365 | 1010 | 370 |

The larger $D_t$ value for the iodide shows that the tetragonal distortion increases with the halide anion size. The fact that practically the same $D_q^{xy}$ value is obtained for the three Ni(II) compounds indicates that the two biuret ligands are in a plane. The $D_z$ ligand field strength decrease from chloride to iodide in agreement with the spectrochemical series.

The Cu(II) compounds show a broad band (around 13300 $cm^{-1}$) as usually observed with copper (II) in $D_{4h}$ symmetry.

Infrared spectra.

In agreement with Nakamoto *et al* (6), band shifts given in Table IV ($\nu_{C=O}$ decreases, $S_{N-H}$ and $\nu_{C-N}$ increase) indicate a coordination through the oxygen atoms. Band shifts of N-H stretching vibration are not significant because of hydrogen bonds.

TABLE IV : Significant Bands in the Infrared Spectra.

| Compound | $\nu_{C=O}$ Stretching | $\nu_{C-N}$ Stretching | $S_{N-H}$ Bending |
|---|---|---|---|
| Biuret | 1725,1680 s | 1420 m | 1325 s |
| Mn $bi_2$ $Cl_2$ | 1690 vs | 1490 s | 1330 s |
| Co $bi_2$ $Cl_2$ | 1690 vs | 1490 s | 1335 s |
| Ni $bi_2$ $Cl_2$ | 1690 vs | 1495 s | 1335 s |
| Cu $bi_2$ $Cl_2$ | 1680 s | 1490 s | 1350 s |
| Mn $bi_2$ $Br_2$ | 1690 s | 1490 s | 1330 s |
| Co $bi_2$ $Br_2$ | 1690 s | 1490 s | 1335 s |
| Ni $bi_2$ $Br_2$ | 1690 s | 1495 s | 1335 s |
| Cu $bi_2$ $Br_2$ | 1675 s | 1490 s | 1350 s |
| Co $bi_2$ $I_2$ | 1695 s | 1490 s | 1335 s |
| Ni $bi_2$ $I_2$ | 1700 s | 1500 s | 1340 s |

Magnetic data.

The magnetic data at room temperature (20°C) are listed in Table V.

TABLE V : Magnetic Data for the Biuret Compounds

| Compounds | Diamagnetic correction ($\times 10^6$) | $\chi_M^{corr}$ ($\times 10^6$) | $\mu_{eff}$ (B.M.) |
|---|---|---|---|
| Mn $bi_2$ $Cl_2$ | - 121 | 14500 | 5.83 |
| Co $bi_2$ $Cl_2$ | - 119 | 11400 | 5.18 |
| Ni $bi_2$ $Cl_2$ | - 119 | 4250 | 3.16 |
| Cu $bi_2$ $Cl_2$ | - 118 | 1540 | 1.90 |
| Mn $bi_2$ $Br_2$ | - 143 | 14700 | 5.87 |
| Co $bi_2$ $Br_2$ | - 141 | 11400 | 5.17 |
| Ni $bi_2$ $Br_2$ | - 141 | 4150 | 3.11 |
| Cu $bi_2$ $Br_2$ | - 140 | 1440 | 1.83 |
| Ni $bi_2$ $I_2$ | - 173 | 5200 | 3.49 |
| Co $bi_2$ $I_2$ | - 173 | 10900 | 5.05 |

Diamagnetic corrections are obtained from reference (9).

All these values are in agreement with a six coordinate octahedral configuration. We can notethe abnormally high magnetic susceptibility for the biuret nickel iodide as previously reported for strongly tetragonally distorted nickel (II) compound (10).

X-ray powder diffraction patterns.

The X-ray powder diagrams are compared in Table VI.

For the same anions, powder diagrams are identical except for copper (II). The interplanar spacings are slightly larger for Mn(II) complexes in agreement with the metal ion size. The different behaviour of copper can be explained by the Jahn-Teller effect.

TABLE VI : X-Ray Powder Types for M $bi_2$ $X_2$ Compounds.

| M $bi_2$ $X_2$ | Cl | Br | I |
|---|---|---|---|
| Mn | A | C | |
| Co | A | C | E |
| Ni | A | C | E |
| Cu | B | D | |

## CONCLUSION

The results indicate clearly an octahedral *trans* structure for the M $bi_2$ $X_2$ compounds, with the two biuret molecules coordinated through the oxygen atoms in the equatorial plane and the halides in axial positions. Racah parameters B decrease from chloride to iodide in agreement with a more covalent bonding in the case of iodide. The large value of $D_t$ and the abnormally high magnetic susceptibility indicate a strongly tetragonally distorted geometry for Ni $bi_2$ $I_2$.

## REFERENCES

1. G. WIEDEMANN, Ann. 1848, 68, 324
2. F. KURZER, Chem. Rev. 1956, 56, 95
3. H.C. FREEMAN and J.E.W.L. SMITH,Acta Crystallogr. 1966, 20, 153
4. A.W. Mc LELLAN and G.A. MELSON, J.Chem.Soc (A), 1967, 137
5. G.A. MELSON, J. Chem. Soc. (A) 1967, 669
6. B.B. KEDZIA, P.X. ARMENDAREZ and K. NAKAMOTO, J. Inorg. Nucl. Chem. 1968, 30, 669
7. R.H. NUTTALL and G.A. MELSON, J.Inorg.Nucl.Chem. 1969,31,2979
8. A.B.P. LEVER a) J. Chem. Educ. 1968, 45, 711
   b) "Inorganic Electronic Spectroscopy" Elsevier,Amsterdam (1968)
9. A. EARNSHAW "Introduction to Magnetochemistry" Academic Press, London (1968)
10. A.B.P. LEVER, Inorg. Chem. 1965, 4, 763

*Polyhedron* Vol. 3, No. 1, pp. 107–112, 1984
Printed in Great Britain.

0277–5387/84 $3.00 + .00
Pergamon Press Ltd.

# UNUSUAL METALLOPORPHYRINS : THORIUM AND URANIUM COMPLEXES OF OCTAETHYLPORPHYRIN.

ALAIN DORMOND, BOUSSAD BELKALEM and ROGER GUILARD*
Laboratoire de Synthèse et d'Electrosynthèse Organométallique associé au C.N.R.S. (LA 33), Faculté des Sciences "Gabriel", 6, Bd Gabriel, 21100 Dijon, France.

(Received 15 June 1983 ; accepted 10 October 1983)

Abstract The action of thorium or uranium tetrachloride with octaethylporphyrin [$(oep)H_2$] affords the dichlorometal (IV) complexes [$M(IV)(oep)Cl_2$, $L_n$] (M(IV) = Th or U, L = benzonitrile, tetrahydrofuran or pyridine). Spectral properties of these complexes are in good agreement with a *cis* octa-coordination.

During the last decade, almost all metals and some semimetals have been coordinated with a porphyrin ligand[1]. Although the "periodic table of metalloporphyrin is very large", complexes of uranium have never been reported and very few studies of thorium porphyrins have been reported[2,3]. Interest in these classes of porphyrins stems from the existence of various possible oxidation states and coordination schemes for the central metal. Such model compounds provide a structural framework for understanding the central metal influence on the chemical reactivity of the porphyrins.

In this paper we report the synthesis and structural characterization of thorium(IV) and uranium(IV) porphyrins [$M(IV)(oep)Cl_2$, $L_n$] [M(IV) = Th or U ; L = pyridine (Py), tetrahydrofuran (THF) or benzonitrile (Bzn) ; oep = octaethylporphinato]. The complexes 1a and 2a (L = Bzn ; n = 2) were prepared ac-

*Author for correspondence.

cording to the following general method. All operations were carried out in Schlenk tubes under purified argon using freshly distilled over sodium and oxygen free solvents. A mixture of $MCl_4$ (0.03 mol) and porphyrin $(oep)H_2$ (0.01 mol) in benzonitrile (30 $cm^3$) was introduced under argon in a reactor provided with magnetic stirring and pyridine (10 $cm^3$) was then added. The mixture was then heated under reflux for 4 h. The reaction was monitored by UV-visible spectroscopy. After completion of the transformation, the solution was cooled and the excess of pyridinium metal tetrachloride was filtered. The solution was evaporated under reduced pressure and the crude material was recrystallised from toluene to give 25 % yield of $[Th(oep)Cl_2, (Bzn)_2]$, 2a, (20 % for $[U(oep)Cl_2, (Bzn)_2]$, 1a .

Analysis. 1a : Found. C, 57.0 ; H, 5.3 ; N, 7.9 ; Cl, 6.6 ; U, 21.9. Calculated for $C_{50}H_{54}N_6Cl_2U$ : C, 57.3 ; H, 5.15 ; N, 8.0 ; Cl, 6.8 ; U, 22.7. 2a : Found. C, 56.1 ; H, 5.5 ; N, 8.2 ; Cl, 5.5 ; Th, 22.0. Calculated for $C_{50}H_{54}N_6Cl_2Th$ : C, 57.65 ; H, 5.2 ; N, 8.1 ; Cl, 6.8 ; Th, 22.3.

Recrystallisation of $[U(oep)Cl_2, (Bzn)_2]$, 1a, in a mixture of methylene chloride-THF (1/1) yielded $[U(oep)Cl_2, (THF)_2]$, 1b. The complexes $[U(oep)Cl_2, (Py)_2]$, 1c and $[Th(oep)Cl_2, (Py)_2]$, 2c were prepared according to the same method. The derivative $[U(oep)Cl_2]$, 1d was obtained by heating the complex 1a at 200°C under vacuum for 2 h.

Analysis. $[U(oep)Cl_2]$, 1d : Found. C, 51.1 ; Cl, 8.7 ; U, 27.0. Calculated for $C_{36}H_{44}N_4Cl_2U$ : C, 51.45 ; Cl, 8.45 ; U, 28.3.

The analytical results and the mass spectral data of the isolated compounds agree with the general formula $[M(oep)Cl_2, L_n]$. The parent peak corresponds either to the ion $[M(oep)Cl, L]^+$ (uranium series) resulting from the elimination of a chlorine

atom and a ligand or to the molecular ion $[M(oep)Cl_2]^{+\cdot}$ (thorium series).

Nuclear magnetic resonance spectra were recorded in the pulse Fourier transform mode with use of a Jeol FX 100 instrument. Complexes 2a and 2c exhibit typical $^1H$ n.m.r. features of diamagnetic metalloporphyrins[4] (Table 1) : *meso* protons resonance signals appear at 10.25 - 10.50 ppm as already shown for seven-coordinated niobioporphyrins[5], methylene and methyl protons are normally located around 4.20 and 1.90 ppm. The observed non-equivalence of the methylene protons results from the specific asymmetry of the complex, not from a hindered rotation of the lateral ethyl chains[6]. Uranium(IV) octaethylporphyrins exhibit characteristic spectra of paramagnetic species[7]. Very broad signals appear around 2.5 ppm (line width $\sim$ 30 Hz) for the *meso* protons ; β protons show a triplet around 0.2 ppm whereas the α-$CH_2$ protons present two well resolved signals at 1.5 and 1.0 ppm. The multiplet observed for the methylene protons can be explained by an $ABX_3$ system[6]. Thus from this study it appears that the $^1H$ n.m.r. data are those of *cis* coordinated metalloporphyrins.

Electronic spectra of complexes 1 and 2 are similar to those of the metalloporphyrins belonging to the normal class[8]. They show a Soret band near to 405 nm and two extra bands between 534-572 nm.

Infrared spectroscopy is a poor tool in the structural determination of uranium and thorium porphyrins. An absorption of medium intensity located at 250 $cm^{-1}$ is attributable to the M - Cl stretching. Such absorptions have already been reported for several actinide organochlorides (near to 230-250 $cm^{-1}$) for uranium[9-10] and thorium compounds[10].

Table : $^1$H n.m.r. data ($CDCl_3$, TMS).

| Complex | meso H m/i[a] | δ | $CH'_2$ m/i | δ | $CH_3$ m/i | δ | L δ |
|---|---|---|---|---|---|---|---|
| $[U(oep)Cl_2, (Bzn)_2]$ 1a | s[b]/4 | 2.80 | M/8[c]<br>M/8[c] | 1.49<br>1.17 | t/24 | 0.00 | 7.3 , 6.8 |
| $[U(oep)Cl_2, (THF)_2]$ 1b | s[b]/4 | 2.67 | m/8<br>m/8 | 1.61<br>1.09 | t/24 | 0.43 | - 3.5 , - 8.9 |
| $[U(oep)Cl_2, (Py)_2]$ 1c | s[b]/4 | 2.32 | m/8<br>m/8 | 1.43<br>0.92 | t/24 | 0.28 | 7.3 , 8.4[d] |
| $[Th(oep)Cl_2, (Bzn)_2]$ 2a | s/4 | 10.49 | m/8<br>m/8 | 4.28<br>4.21 | t/24 | 1.89 | 7.5 , 7.0 |
| $[Th(oep)Cl_2, (Py)_2]$ 2c | s/4 | 10.26 | q/8<br>q/8 | 4.14<br>4.07 | t/24 | 1.85 | 7.3 ; 8.4 |

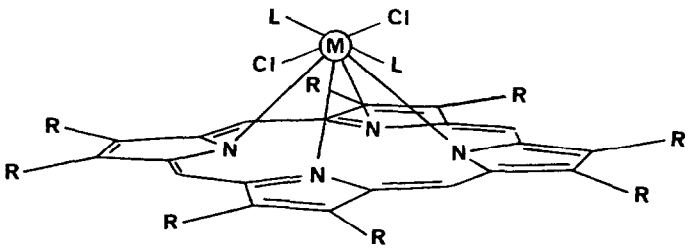
(a) m : multiplicity ; i : intensity ; s : singlet ; q : quadruplet ; t : triplet ; m : multiplet ; M : massive.

(b) Very broad signals.

(c) At 60°C the two signals of methylene protons coalesce into a multiplet centered at 2.03 ppm.

(d) Pyridine protons signals (spectrum recorded with free pyridine).

On the basis or our physicochemical measurements we propose the structure of the thorium and uranium prepared complexes to involve eight coordination as shown in figure.




R : $C_2H_5$ ; M = Th or U ; L = Bzn, THF or Py.

It thus appears that big ions can attain higher coordination number than 6 and a similar eight coordination was observed by Hoard[11] for $[Zr(oep)(OAc)_2]$. The proposed structure of thorium and uranium porphyrins is not surprising if we refer to the ionic radii of these metals ( .99 and .93 respectively for Th(IV) and U(IV) compared to .77 for Zr(IV)) and structural data of organoactinide compounds.

REFERENCES

[1] J. W. Buchler, *The Porphyrins* (Edited by D. Dolphin), Vol. I, Chap. 10, Academic Press, New York, 1978.

[2] L. P. Wong and W. D. Horrocks, Jr., *Tetrahedron Lett.*, 1975, 31, 2637.

[3]M. Gouterman, private communication.

[4]T. R. Janson and J. J. Katz, *The Porphyrins* (Edited by D. Dolphin), Vol. IV, Chap. 1, Academic Press, New York, 1979.

[5]C. Lecomte, J. Protas, R. Guilard, B. Fliniaux and P. Fournari, *J. Chem. Soc., Dalton Trans.*, 1979, 1306.

[6]C. A. Busby and D. Dolphin, *J. Magnetic Resonance*, 1976, 23, 211.

[7]G. N. La Mar and F. A. Walker (Jensen), *The Porphyrins* (Edited by D. Dolphin), Vol. IV, Chap. 2, Academic Press, New York, 1979.

[8]M. Gouterman, *The Porphyrins* (Edited by D. Dolphin), Vol. III, Chap. 1, Academic Press, New York, 1979.

[9]K. W. Bagnall, J. Edwards, A. G. Tempest, *J. Chem. Soc., Dalton Trans.*, 1978, 295.

[10]T. J. Marks and R. D. Fischer, *Organometallics of the f elements*, p. 493, D. Reidel Publishing Company, Dordrecht, Holland, 1979.

[11]J. L. Hoard, *"Porphyrins and Metalloporphyrins"* (Edited by K. M. Smith), Elsevier, Amsterdam, 1975.

*Polyhedron* Vol. 3, No. 1, pp. 113-116, 1984
Printed in Great Britain.

0277-5387/84 $3.00 + .00
Pergamon Press Ltd.

# NOTE

## CRYSTAL STRUCTURE OF COPPER(II) COMPLEX WITH N,N-BIS(2-BENZIMIDAZOLYLMETHYL)BENZYLAMINE

Kazuhiro Takahashi*, Yuzo Nishida and Sigeo Kida

Department of Chemistry, Faculty of Science, Kyushu University, Fukuoka 812, Japan

(Received 16 May 1983; accepted 11 October 1983)

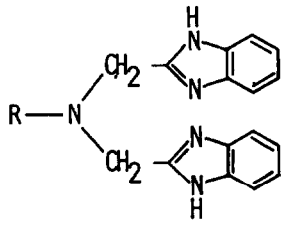
Abstract— The copper(II) complex with N,N-bis(2-benzimidazolylmethyl)-benzylamine has been synthesized and its crystal structure was determined by X-ray diffraction methods.

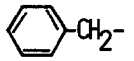
In preceding papers, we have reported the syntheses, magnetic and optical properties, and crystal structures of several Cu(II) complexes with multidentate ligands containing benzimidazolyl groups[1-6]. The crystal structure determinations of the complexes ([Cu(eta-dbz)X]$ClO_4 \cdot CH_3OH$, X = $Cl^-$ and $Br^-$ [1], and $[Cu(ibz)Cl_2] \cdot CH_3OH$ [2]: for the abbreviations of the ligands, see Fig. 1) revealed that two molecules of Cu(II) complex are stacked, forming a "face-to-face" like binuclear structure. The stacking between two Cu(II) complexes observed was attributed to an intermolecular interaction between benzimidazolyl groups. In this study, we have synthesized the Cu(II) complex with N,N-bis-(2-benzimidazolylmethyl)benzylamine (babz; cf. Fig. 1), and determined its crystal structure by X-ray diffraction methods in order to gain further insight into the stacking mode of the benzimidazolyl moiety.

The ligand, babz, was prepared by the conventional method[7] from benzylamine diacetic acid and 1,2-diaminobenzene. Its complex with Cu(II) was obtained by mixing equivalent stoichiometric amount of methanolic solutions of babz and $Cu(NO_3)_2 \cdot 3H_2O$, and recrystallized from an absolute methanol. The blue prismatic crystals thus obtained were suitable for X-ray study. Found, C, 49.11; H, 4.40; N, 16.65; Calc. for $C_{24}H_{25}N_7O_7Cu$, C, 49.10; H, 4.29; N, 16.70 %.

Crystal data[8]; Space group $P2_1/n$(monoclinic), a = 10.409(4) Å, b = 16.237(5) Å, c = 15.828(5) Å, β = 103.82(3)°, V = 2598(2) Å$^3$, Z = 4, Dm = 1.50g/cm$^3$, Dc = 1.51g/cm$^3$, T = 296K

Fig. 1. Illustration and abbreviation of the ligands



| R | Abbreviation |
|---|---|
| H | ibz |
| $-CH_2CH_2OH$ | eta-dbz |
|  | babz |

An ORTEP drawing and the atomic numbering system of the complex are shown in Fig. 2. Selected interatomic bond distances and angles are listed in Table 1.

The coordination number of Cu(II) is six, consisting of three nitrogen atoms (imidazole N1, N3 and tertiary amine N5) and three oxygen atoms (methanol O1A and nitrate O1B, O2B). The bond length of Cu-O2B is 2.637(5) Å showing very weak bonding, yet the

* Author for correspondence

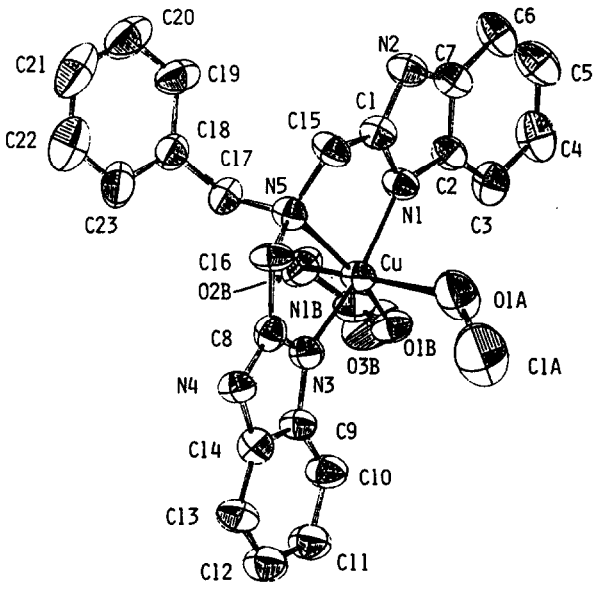



Fig. 2. ORTEP drawing of $[Cu(babz)(NO_3)(CH_3OH)]^+$.

Table 1. Interatomic distances(Å) and angles(°) in the coordination sphere with their standard deviations in parenthesis.

| | | | | | |
|---|---|---|---|---|---|
| Cu - N1 | 1.943(5) | Cu - N3 | 1.940(6) | Cu - N5 | 2.109(6) |
| Cu - O1A | 2.266(6) | Cu - O1B | 1.998(4) | Cu - O2B | 2.637(5) |
| N1-Cu-N3 | 163.4(2) | N1-Cu-N5 | 82.7(2) | N1-Cu-O1A | 84.8(2) |
| N1-Cu-O1B | 97.4(2) | N1-Cu-O2B | 85.8(2) | N3-Cu-N5 | 82.0(2) |
| N3-Cu-O1A | 93.2(2) | N3-Cu-O1B | 99.2(2) | N3-Cu-O2B | 104.1(2) |
| N5-Cu-O1A | 105.4(2) | N5-Cu-O1B | 157.2(2) | N5-Cu-O2B | 104.2(2) |
| O1A-Cu-O1B | 97.2(2) | O1A-Cu-O2B | 147.5(2) | O1B-Cu-O2B | 53.3(2) |

Table 2. Best-plane equation of the N1-N3-N5-O1B plane and the deviations of the atoms of the coordination sphere from the plane.

| | | | | | | | | |
|---|---|---|---|---|---|---|---|---|
| Equation ; | 0.9260 x | - | 0.1876 y | + | 0.0969 | = | 7.0251 | |
| Deviation(Å); | Cu | 0.177, | N1 | 0.228, | N3 | 0.229, | N5 | -0.254, |
| | O1B | -0.203, | O1A | 2.432, | O2B | -2.162 | | |

arrangement of the nitrate ion definitely shows its bidentate coordination (cf. Fig. 2 ). Judging from the above facts, the coordination geometry is roughly an octahedron elongated along the O1A-Cu-O2B axis.

As seen in Fig. 3-a, two molecules form a loosely bound dimeric unit across the inversion center. Fig. 3-a shows the stacking between the benzimidazolyl and phenyl groups in the dimeric unit. The projection of the phenyl ring of one complex (C18'~ C23') on the benzimidazolyl plane of the other complex is illustrated in Fig. 3-b.
The deviations of the atoms of the benzimidazolyl group from the plane, and distances of the phenyl atoms to the plane are summarized in Table 3. The average distance and

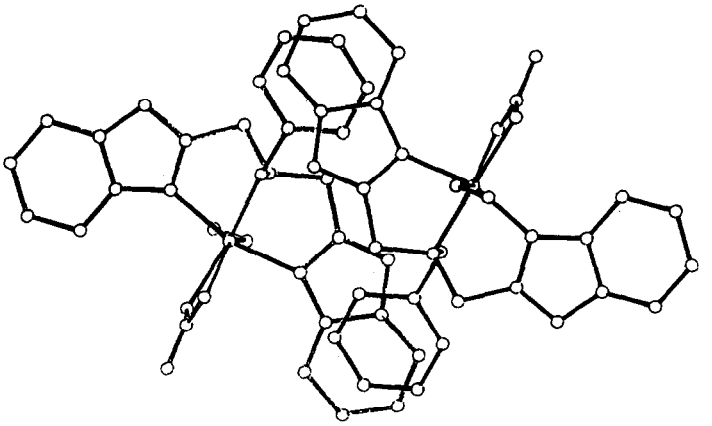


Fig. 3-a. Perspective view of the dimeric unit.

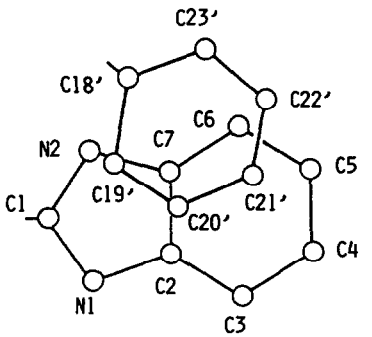



Fig. 3-b. Projection of the phenyl ring on the benzimidazolyl plane.

Table 3. Best-plane equation of the benzimidazolyl group and the deviations of the atoms from the plane, and the distances of the phenyl atoms (cf. Fig. 3-b) to the plane.

Equation : $0.9138\,x - 0.1893\,y + 0.1307\,z = 7.3982$

| Ring | benzimidazolyl | | | | phenyl | |
|---|---|---|---|---|---|---|
| Equivalent position | x,y,z | | | | 1-x,1-y,1-z | |
| | Deviation (Å) | | | | Distance (Å) | |
| | N1 | 0.014 | C3 | 0.004 | C18' | 3.947 |
| | N2 | -0.016 | C4 | -0.030 | C19' | 3.754 |
| | C1 | -0.019 | C5 | 0.001 | C20' | 3.417 |
| | C2 | 0.019 | C6 | 0.017 | C21' | 3.289 |
| | | | C7 | 0.009 | C22' | 3.444 |
| | | | | | C23' | 3.776 |

dihedral angle between the benzimidazolyl and phenyl planes are ca. 3.6 Å and 13.7°, respectively.

As for the stacking between heterocyclic and aromatic rings in transition metal complexes[10], the present result is a rare example revealed by the X-ray analysis. Such a stacking may play some role in the biological reaction involving nucleoside bases.

## References


1. Y. Nishida, K. Takahashi and S. Kida, Mem. Fac. Sci., Kyushu Univ., ser C, 13(1), 27 (1981).
2. ibid., 13(2), 343 (1982).
3. K. Takahashi, E. Ogawa, N. Oishi, Y. Nishida and S. Kida, Inorg. Chim. Acta, 66, 97 (1982).
4. Y. Nishida, K. Takahashi, H. Kuramoto and S. Kida, ibid., 54, L103 (1981).
5. Y. Nishida, N. Oishi and S. Kida, ibid., 44, L257 (1980).
6. K. Takahashi, Y. Nishida and S. Kida, Bull. Chem. Soc. Jpn., 56, 339 (1983).
7. L. K. Thompson, B. S. Ramaswamy and E. A. Seymour, Can. J. Chem., 55, 878 (1977).
8. The unit cell parameters were determined from 20 reflections($20°<2\theta<30°$) on a Rigaku Automatic Four Circle Diffractometer AFC-5. Intensity data were recorded by the $\theta$-$2\theta$ scan technique($2.5°<2\theta<50°$), using graphite monochromated Mo K$\alpha$ radiation and monitoring 3 reflections after each 97 measurements. The structure was solved by Patterson and Fourier methods using the UNICS II program system[9] and 2760 unique refrections($Fo>3\sigma(Fo)$). The structure was refined to $R(=\Sigma(Fo-Fc)/\Sigma Fo)=0.057$ by the block-diagonal least-squares method of UNICS II using anisotropic thermal parameters for non-hydrogen atoms. Atomic coordinates, thermal parameters and lists of Fo/Fc values have been deposited on Supplementary Material with the Editor, from whom copies are available on request. Atomic coordinates have also been deposited with the Cambridge Crystallographic Data Center.
9. "Universal Crystallographic Computer Program System" ed. by T. Sakurai, The Crystallographic Society of Japan, Tokyo (1967).
10. K. Aoki, J. Am. Chem. Soc., 100, 7106 (1978).

*Polyhedron* Vol. 3, No. 1, pp. 117–120, 1984
Printed in Great Britain.

0277–5387/84 $3.00 + .00
© 1984 Pergamon Press Ltd.

# NOTE

## KINETICS OF NUCLEOPHILIC ATTACK BY ANILINES ON THE NITRILE GROUP IN PALLADIUM(II) ORTHO-CYANOBENZYL COMPLEXES

LEO CALLIGARO

Istituto di Chimica Industriale, Facoltà di Ingegneria, Università di Padova, Via Marzolo 9, 35100 Padua, Italy

(Received 17 June 1983; accepted 25 July 1983)

**Abstract**

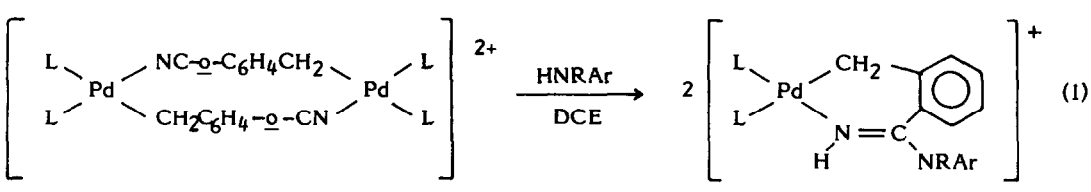
A kinetic study of the reactions of anilines with the dimeric cationic complex of palladium(II) $[Pd(o\text{-}CH_2C_6H_4CN)(PPh_3)_2]_2(BF_4)_2$ emphasized the production of amidino mononuclear complexes through the breaking of the Pd-CN bonds, and the formation of an intermediate with the activated nitrile group where the amine reacts through an analogous two-step mechanism for both primary and secondary anilines.

---

There has been considerable interest in the mechanisms of reactions of the metal bound CN group and its activation upon coordination towards addition of nucleophiles,such as alcohols,thiols, water, or amines, yielding stable N-bonded iminoether, iminothioether, amide, and amidine complexes, respectively.[1] Several cationic cyanobenzyl palladium(II) complexes were prepared, and the reactivity of the CN group towards nucleophiles was investigated,[2,3] whereas few kinetic studies on the hydrolysis of coordinated nitriles have appeared,[4] and the mechanism of reaction of anilines has been examined only for platinum(II) analogues.[5]

### Results and discussion

Similarly with the behaviour of primary and secondary anilines with analogous dimeric Pt(II) compounds,[5] the cationic dimeric complex I forms chelate amidino complexes II by reaction with both primary and secondary anilines (1):[6]

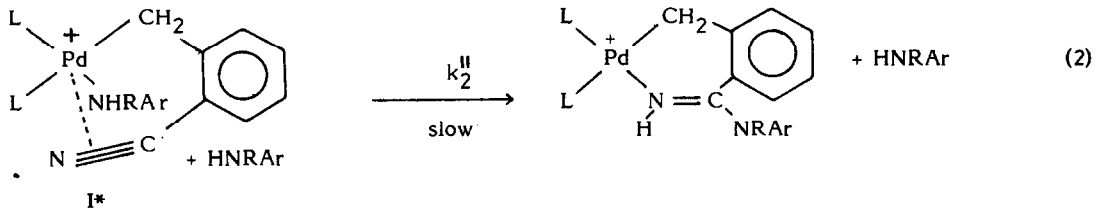



I II (1)

( L = $PPh_3$; Ar = p-$CH_3OC_6H_4$, p-$CH_3C_6H_4$; R = H, Me; DCE = 1,2-dichloroethane )

where a first stage of the mechanism of reaction is thought to involve fast breaking of the Pd-CN bridges in I by the aniline, | which produces a nucleophilic substitution at the palladium center, bearing the uncoordinated nitrile group I* (2). The observed high rate of opening of the o-cyanobenzyl bridges seems due to the role of the trans effect of triphenylphosphine in I, accompanied by the steric strain of the o-cyanobenzyl bridges in the dimeric I Pt-analogous compounds.[6]

Dreiding molecular models show that the nitrile group may occupy an axial position at sufficient distance from the central palladium ion to allow a possible "side-on" interaction with the latter.[7] Such electronic interaction activates the CN group towards nucleophilic attack which takes place in the second slower step of the reaction (2) :

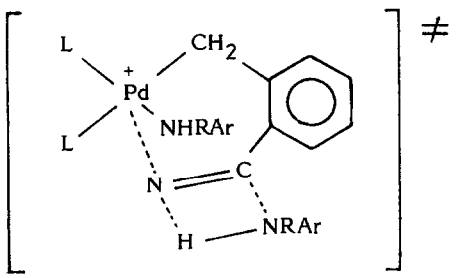



(2)

This has been followed kinetically by spectrophotometry under pseudo-first-order conditions with an excess of amine. The pseudo-first-order constant for the second step (2) is first-order in amine concentration:

$$k^{II}_{obs} = k^{II}_2 [A] \qquad (3)$$

this supporting a direct nucleophilic attack of the amine on the CN group and an intramolecular proton exchange between the amine and the nitrile nitrogens, involving a cyclic 4-center transition state:




at the same time the new Pd-amidino bond is formed and the existing Pd-amine bond breaks. In Table I are listed rate data for the reactions of I with N-methyl-p-anisidine at some temperatures, as computed by linear regression; in Table II analogous data are reported for the reactions of I with p-anisidine and p-toluidine. In Fig.1 the Eyring plot is reported for N-methyl-p-anisidine.

Table I. Rate Data for the Second Stage of Reaction of $[Pd(o\text{-}CH_2C_6H_4CN)(PPh_3)_2]_2(BF_4)_2$ with N-methyl-p-anisidine in 1,2-dichloroethane.

| Temperature (°C) | $10^2$ [A] (M) | $10^2 k^{II}_{obs}$ ($min^{-1}$) | $10^2 k^{II}_2$ ($M^{-1} min^{-1}$) |
|---|---|---|---|
| 20 | 1.99 | 0.20 | 10.62 ± 0.32 |
| | 3.44 | 0.36 | |
| | 6.36 | 0.64 | |
| | 9.44 | 1.00 | |
| 25 | 3.06 | 0.50 | 19.36 ± 0.98 |
| | 4.45 | 0.73 | |
| | 5.05 | 0.84 | |
| | 6.85 | 1.31 | |
| | 8.30 | 1.53 | |
| | 9.86 | 1.76 | |
| 35 | 1.24 | 0.51 | 53.13 ± 1.56 |
| | 1.85 | 0.94 | |
| | 3.49 | 1.77 | |
| | 5.74 | 2.94 | |
| 45 | 1.44 | 1.88 | 139.10 ± 0.84 |
| | 2.14 | 2.81 | |
| | 3.41 | 4.60 | |
| | 4.93 | 6.72 | |

Table II. Rate Data for the Second Stage of Reaction of $[Pd(o\text{-}CH_2C_6H_4CN)(PPh_3)_2]_2(BF_4)_2$ with p-anisidine and p-toluidine in 1,2-dichloroethane at 40 °C.

| | $10^2$ [ A ] (M) | $10^3 k^{II}_{obs}$ ($min^{-1}$) | $10^2 k^{II}_2$ ($M^{-1} min^{-1}$) |
|---|---|---|---|
| p-anisidine | 5.03 | 1.29 | 2.62 ± 0.03 |
| | 6.85 | 1.74 | |
| | 9.01 | 2.34 | |
| | 12.10 | 3.13 | |
| p-toluidine | 3.51 | 0.87 | 2.47 ± 0.02 |
| | 5.81 | 1.43 | |
| | 7.74 | 1.92 | |
| | 9.02 | 2.23 | |

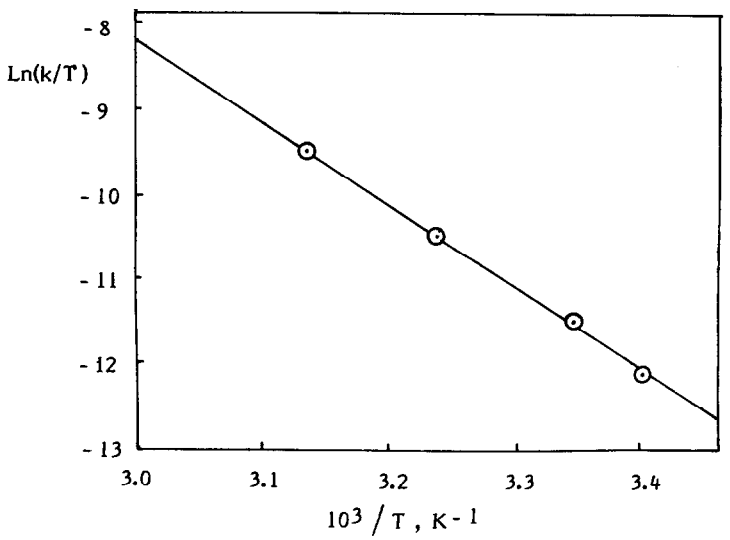



Fig. 1. Eyring Plot of $k^{II}_2$ for the Reaction of I with N-methyl-p-anisidine.

The amine reactivity order is N-methyl-p-anisidine ≫ p-anisidine ≈ p-toluidine. The activation parameters for N-methyl-p-anisidine ($\Delta H_2^{\neq}$ = 18.13 ± 0.12 kcal/mol, $\Delta S_2^{\neq}$ = - 9.16 ± 0.38 e.u. ) indicate that the negative activation entropy is in agreement with the bimolecular nature of the activation process. The nucleophilic ability of the amine greatly influences the rate of the second stage; N-methyl-p-anisidine has higher nucleophilicity and relatively few steric hindrance around the reacting center than p-anisidine and p-toluidine; for N-ethyl-p-toluidine whose kinetics are too slow to be studied, steric hindrance decreases markedly the possibility of formation of a constrained oriented cyclic transition state. In the case of p-anisidine and p-toluidine we kinetically observed the later part of the first stage, but the treatment of absorbance data for the two consecutive step model gave not so consistent results. Unlike with the analogous Pt-containing system[5] here both primary and secondary anilines appear to follow the same mechanistic pattern.

## Experimental

Kinetics The reactions were followed spectrophotometrically by measuring changes in optical density in the range 330-370 nm with time by means of a Cary-219 Varian double-beam recording instrument. Freshly prepared solutions of the complex, stored under nitrogen, were used for each kinetic run. All reactions were started by mixing known volumes of pre-thermostatted standard solutions of the reagents in the thermostatted ( ± 0.1 °C ) cell compartment of the spectrophotometer.

A solution containing the same concentration of the entering amine was used as a reference. The entering amine was present in sufficient excess to provide pseudo-first-order conditions and to force the reactions to completion. The final spectra were generally in good agreement with those of the products prepared and characterized independently. The values of pseudo-first-order rate constants, $k_{obs}$, and activation parameters were obtained as described elsewhere.[8]

Statistical Data Treatment All statistical and graphical analyses of kinetic data were performed with a comprehensive software package implemented on a Tektronix 4052 Graphic System. The package was in part derived from the Tektronix Plot 50 Statistical Software and locally tailored to suit the needs of the system under study.

## References

[1] B.N.Storhoff and H.Lewis, Coord. Chem. Rev., 1977,**23**,1.

[2] R.Ros, M.Lenarda, T.Boschi and R.Roulet, Inorg. Chim. Acta, 1977,**25**, 61.

[3] R.Ros, R.A.Michelin, T.Boschi, and R.Roulet, Inorg. Chim. Acta, 1979, **35**, 43.

[4] R.J.Balahura and W.L.Purcell, Inorg. Chem., 1981,**20**, 4159; R.J.Balahura, P.Cock, and W.L. Purcell,J.Am.Chem.Soc., 1976,**96**, 393.

[5] L.Calligaro, R.A.Michelin, and P.Uguagliati, Inorg. Chim. Acta, 1983, **76**, L83.

[6] R.Ros,J.Renaud, and R.Roulet, J. Organomet. Chem., 1976, **104**, 393.

[7] H.C.Clark and L.Manzer, Inorg. Chem., 1971,**10**, 2699.

[8] P.Uguagliati, R.A.Michelin, U.Belluco, and R.Ros, J.Organomet.Chem., 1979, **169**, 115.

*Polyhedron* Vol. 3, No. 1, pp. 121–124, 1984
Printed in Great Britain.

0277-5387/84 $3.00 + .00
© 1984 Pergamon Press Ltd.

# NOTE

## SUBSTITUTED IMIDAZOLE COMPLEXES OF PLATINUM(IV) HALIDES

Tulendra Nath Hazarika and Tankeswar Bora*

Department of Chemistry, Dibrugarh University,
Dibrugarh - 786 004 (Assam), India.

(Received 21 June 1983, accepted 11 October, 1983)

Abstract - Platinum(IV) halides formed complexes of the type $PtL_2X_4$ [L=1-vinyl imidazole (1-VIm), 1-methylimidazole (1-MeIm), 1,2-dimethylimidazole (1,2-$Me_2$Im), 1-vinyl-2-methylimidazole (1-V-2-MeIm), 2-methylimidazole (2-MeIm), 2-ethylimidazole (2-EtIm), 2-isopropylimidazole (2-i-PrIm), and 4-methylimidazole (4-MeIm); X=Cl,Br] in neutral aqueous solution. The 1-n-butylimidazole (1-n-BuIm) ligand yielded only $(LH)_2PtX_6$ compound in the same medium. The compounds were characterised by elemental analyses, IR, UV-VIS and $^1$HNMR spectra.

The coordination compounds of imidazole and substituted imidazoles with platinum metals have been studied by a number of authors[1-8]. Recently, complexes of these ligands with palladium(II)/platinum(II) have been reported from this laboratory[9,10]. We now report here some more compounds of substituted imidazoles with platinum(IV) halides.

## EXPERIMENTAL

The ligand samples were supplied by M/S BASF (W. Germany) and were used as such. Chloroplatinic acid ($H_2PtCl_6.xH_2O$) and potassium chloroplatinate ($K_2PtCl_6$) were obtained from M/S Arora Matthey Ltd. The chloroplatinic acid was evaporated with conc. HCl several times and the resulting dried mass was heated at 300°C to convert it into $PtCl_4$[11]. $K_2PtCl_6$ was refluxed with $Br_2$/HBr mixture for ~2hrs. and the resulting mass was evaporated on a water bath to dryness to get $K_2PtBr_6$.

The IR and UV-VIS spectra were recorded as reported earlier[9]. $^1$HNMR spectra were recorded at RSIC, IIT Bombay. C, H and N were determined by microanalytical technique at CDRI, Lucknow. Platinum was determined as metal[12] and the halides were determined as silver halides.

Preparation of complexes: (i) $PtL_2Cl_4$ (L=1-VIm, 1-MeIm, 1-V-2-MeIm and 1,2-$Me_2$Im) and $(1\text{-n-BuImH})_2PtCl_6$ — An aqueous solution of $PtCl_4$(1mmol in 10$cm^3$) and the ligand(2mmol in 5$cm^3$) was warmed on a water bath when the pale yellow precipitate of the complexes occured on concentration. It was then cooled, filtered and the precipitate was washed with water several times and kept in a desiccator overnight (yield ~70%). (ii) $PtL_2Cl_4$(L= 2-MeIm, 2-EtIm and 4-MeIm) — An ethanolic solution of $PtCl_4$(1mmol in 10$cm^3$) and the ligand (2mmol in 5 $cm^3$) was prepared. Any precipitate that occured initially was ignored and the whole solution evaporated almost to dryness on a water bath. The dried mass was kept overnight in a desiccator. It was

*Author for correspondence

Table-1. Melting points, analytical data and $\nu$(Pt-X) of some platinum(IV) imidazole complexes.

| Compound | m.pt. °C | Found (Calc),% Pt | X | C | H | $\nu$(Pt-X) ($cm^{-1}$) |
|---|---|---|---|---|---|---|
| $Pt(1\text{-VIm})_2Cl_4$ | 220 | 37.1(37.1) | 26.2(27.0) | 22.9(22.8) | 2.4(2.3) | 350vs,320sh |
| $Pt(1\text{-VIm})_2Br_4$ | 165 | 29.2(27.8) | 43.7(45.5) | 16.9(17.1) | 1.8(1.7) | 238s,222sh |
| $Pt(1\text{-MeIm})_2Cl_4$ | 258 | 38.1(38.9) | 28.4(28.3) | 19.3(19.1) | 2.5(2.4) | 348vs |
| $Pt(1\text{-MeIm})_2Br_4$ | 248 | 28.2(28.7) | 47.0(47.1) | 13.9(14.1) | 2.0(1.8) | 257vs,222m |
| $(1\text{-n-BuImH})_2PtCl_6$ | 185 | 30.0(29.6) | 32.6(32.3) | 26.9(27.0) | 4.1(4.2) | |
| $(1\text{-n-BuImH})_2PtBr_6$ | 152 | 22.2(21.1) | 50.0(51.8) | 18.4(18.2) | 2.8(2.6) | |
| $Pt(1\text{-V-2-MeIm})_2Cl_4$ | 190 | 36.0(35.3) | 24.9(25.7) | 26.1(26.0) | 3.0(2.9) | 332vs |
| $Pt(1\text{-V-2-MeIm})_2Br_4$ | 170 | 26.6(26.7) | 42.1(43.7) | 19.9(19.7) | 2.3(2.2) | 233vs,212sh |
| $Pt(1,2\text{-Me}_2\text{Im})_2Cl_4$ | 183 | 38.0(39.5) | 22.5(21.6) | 24.5(24.3) | 3.2(3.3) | 332vs bd |
| $Pt(1,2\text{-Me}_2\text{Im})_2Br_4$ | 160 | 26.9(27.6) | 44.1(45.2) | 17.1(16.9) | 2.3(2.3) | 240vs,220sh |
| $Pt(2\text{-MeIm})_2Cl_4$ | 218 | 38.2(38.9) | 29.5(28.3) | 19.0(19.1) | 2.4(2.4) | 350s bd, 328sh |
| $Pt(2\text{-MeIm})_2Br_4$ | 270[d] | 27.9(28.7) | 46.2(47.1) | 14.3(14.1) | 1.9(1.8) | 242m,235m |
| $Pt(2\text{-EtIm})_2Cl_4$ | 208 | 36.9(36.4) | 25.0(26.8) | 22.5(22.7) | 3.1(3.0) | 350vs,325sh |
| $Pt(2\text{-EtIm})_2Br_4$ | 194 | 27.9(27.6) | 44.1(45.2) | 16.8(16.9) | 2.3(2.3) | 235s,225w |
| $Pt(2\text{-i-PrIm})_2Cl_4$ | 180 | 34.7(35.0) | 25.1(25.5) | 26.0(25.8) | 3.5(3.6) | |
| $Pt(2\text{-i-PrIm})_2Br_4$ | 183 | 26.1(26.5) | 42.3(43.5) | 19.7(19.6) | 2.8(2.7) | |
| $Pt(4\text{-MeIm})_2Cl_4$ | 221 | 38.4(38.9) | 28.5(28.3) | 19.1(19.1) | 2.3(2.4) | 345vs,310sh |
| $Pt(4\text{-MeIm})_2Br_4$ | 245[d] | 29.1(28.7) | 47.9(47.1) | 14.3(14.1) | 1.8(1.8) | 257m,240w |

d=decomposes, vs=very strong, s=strong, m=medium, w=weak, sh=shoulder, bd=broad.

Table-2. $^1$HNMR parameters of some imidazoles and their complexes with platinum(IV) halides.

| Compound | H-2 | H-4 | H-5 | $C_1$-Me | $C_2$-Me | $H_\alpha$ | $H_\beta$ | $H_\gamma$ |
|---|---|---|---|---|---|---|---|---|
| 1-VIm | 8.2 | 7.6 | 7.06 | | | 7.24[q] | 4.90[q] | 5.54[q] |
| $Pt(1\text{-VIm})_2Cl_4$ | 8.77(16) | 8.0(8) | 7.18(10) | | | 7.45[m] | 5.24[m] | 5.87[m] |
| 1-MeIm | 7.58 | 7.10 | 6.92 | 3.67 | | | | |
| $Pt(1\text{-MeIm})_2Cl_4$ | 8.42(7) | 7.44(11) | 7.12(8) | 3.90 | | | | |
| $Pt(1\text{-MeIm})_2Br_4$ | 8.46(7) | 7.40(6) | 7.20(10) | 3.88 | | | | |
| 1-V-2-MeIm | | 7.6 | 7.06 | | 2.30 | 7.24[q] | 4.93[q] | 5.54[q] |
| $Pt(1\text{-V-2-MeIm})_2Cl_4$ | | 7.84(8) | 7.16(10) | | 2.84[m] | 7.40[m] | 5.28[m] | 5.77[m] |

q=quartet, m=multiplet, coupling constants of $^{195}Pt$-$^1H$ are in parentheses, $H_\alpha$, $H_\beta$, $H_\gamma$, denote vinyl protons.

then stirred vigorously with hot water when the yellow precipitate of the compound was obtained (yield~75%). (iii) $Pt(2\text{-}i\text{-}PrIm)_2Cl_4$ — To an ethanolic solution of $PtCl_4$(1mmol in $5cm^3$) with the ligand (2mmol in $5cm^3$) was added $5cm^3$ of triethylorothoformate(TEOF). The solution was then refluxed for 2 hrs. and allowed to cool. The yellow precipitate occured on slight evaporation (yield~65%). (iv) $Pt(1\text{-}VIm)_2Br_4$ and $(1\text{-}n\text{-}BuImH)_2PtBr_6$ — A solution of $Pt(1\text{-}VIm)_2Cl_4$ or $(1\text{-}n\text{-}BuImH)_2PtCl_6$ in acetone (3gm in $10cm^3$) was refluxed for 1 hr. with 20 fold excess of LiBr. The resulting deep-red solution was then evaporated to dryness on a water bath. The dried mass was stirred with water and warmed slowly. The brownish yellow precipitate of the complex was obtained (yield~55%). (v) $Pt(1\text{-}MeIm)_2Br_4$ — This compound was prepared by a similar method applied to imidazole compounds of Pt(II) by Reedijk et al.[4] (vi) $PtL_2Br_4$(L=1-V-2-MeIm, 1,2-$Me_2$Im , 2-MeIm, 2-EtIm, 2-i-PrIm and 4-MeIm) — An aqueous solution of $K_2PtBr_6$(1mmol in $10cm^3$) and the ligand (2mmol in $5cm^3$) was warmed slightly when a deep-yellow precipitate was obtained. In case of 2-MeIm, evaporation of the solution to almost 50% of the original volume was necessary. For the preparation of 2-EtIm and 2-i-PrIm complexes, the mixture was evaporated very carefully to dryness at low temperature. The compound was obtained by leaching the dried mass with water and warming (yield~50%).

All the chloro complexes are light-yellow while the bromo derivatives are deep-yellow in colour. They are soluble in DMF and DMSO.

## RESULTS AND DISCUSSION

Conductivity data in DMF (7 to 27 $ohm^{-1}cm^2mol^{-1}$) indicate that they are non-electrolytes. The compound $(1\text{-}n\text{-}BuImH)_2PtX_6$, however, shows a conductance value of 136 $ohm^{-1}$ in DMF. Their melting points lie in the range 152°C-258°C (Table-1). The elemental analyses agree with 1:2 metal-ligand ratio.

In all the complexes, the ligand vibrations with decreased intensity or with slight shift in position are present. The broad intermolecular H-bonding mode at ~3100-2500$cm^{-1}$ region in the 2- and 4-substituted imidazoles is replaced by one or two medium intensity bands. The ring vibration $R_6$, at ~925-888$cm^{-1}$ however, shows considerable shift ($\Delta\nu$ ~ 50$cm^{-1}$) in 1-substituted imidazole complexes. $\nu$ Pt-X bands for $PtL_2X_4$ complexes are observed at ~350-332$cm^{-1}$ and ~257-235$cm^{-1}$ respectively (Table-1) for the chloro and bromo complexes. This is in agreement with $D_{4h}$ symmetry of the complexes. The electronic spectra of $PtCl_6^{2-}$ and $PtBr_6^{2-}$ reveal spin-forbidden $^1A_{1g} \rightarrow {}^3T_{1g}$ transition at ~22,000$cm^{-1}$ and~19,000$cm^{-1}$ respectively while spin-allowed $^1A_{1g} \rightarrow {}^1T_{1g}$ transition at ~ 28,400$cm^{-1}$ and ~ 23,000$cm^{-1}$ regions[13]. The weak transition $^1A_{1g} \rightarrow {}^3T_{1g}$, is observed in $PtL_2Br_4$ (L= 1,2-$Me_2$Im and 2-i-PrIm) at ~ 19,500$cm^{-1}$. The $PtL_2Cl_4$ species (except 1-VIm complex) exhibit only the $^1A_{1g} \rightarrow {}^1T_{1g}$ transition at ~ 26,000$cm^{-1}$ region. This is absent in the bromo complexes, probably due to the strong and broad C.T. bands in the low energy region. The $^1$HNMR signals (in ppm, with respect to internal TMS) of 1-MeIm, 1-VIm and 1-V-2-MeIm and their complexes with Pt(IV) halides in DMSO-$d_6$ at 100MHz are recorded in Table-2. All the complexes, in general, exhibit a downfield shift of $^1$HNMR signals compared

to the free ligands. Also, in comparison to the signals of H-4 and H-5 protons, the H-2 proton exhibits larger chemical shifts due to its proximity to the coordinating N-3 atom. The $^{195}Pt-^{1}H$ coupling constant ranges from 6-16 Hz in all the complexes. The $C_2$-methyl protons as well as the vinyl protons show multiplet splittings. As a result, the $^{195}Pt-^{1}H$ coupling constant for these protons could not be ascertained.

Acknowledgement - The authors are grateful to Dr. S.K. Barooah for recording the IR and UV-VIS spectra. They also acknowledge the services of CDRI, Lucknow for elemental analyses; RSIC, IIT Madras for far IR spectra and RSIC, IIT Bombay for $^{1}H$NMR spectra. The work has been supported by a UGC grant (T.B.) and a fellowship award (T.N.H.).

## REFERENCES

[1] S.P. Ghosh, P. Bhattacharjee, L. Dubey and L.K. Mishra, J. Indian Chem. Soc. 1977, 54, 230.

[2] C.G. van Kralingen and J. Reedijk, Inorg. Chim. Acta. 1978, 30, 171.

[3] M.C. Navarro Ranninger and M. Gayoso, An Quim. 1978, 74, 717 & 722.

[4] C.G. van Kralingen, J. K. deRidder and J. Reedijk, Inorg. Chim. Acta. 1979, 36, 69.

[5] A.T.M. Marcelis, C.G. van Kralingen, J. Opschoor and J. Reedijk Rec. Trav. Chim. Pays-Bas. 1980, 99, 198.

[6] M.B. Cingi, A.M. Manotti Lanfredi and A. Tiripicchio, Inorg. Chim. Acta. 1980, 39, 265.

[7] K.H. Juergen, K. Bernt, C.G. van Kralingen, A.T.M. Marcelis and J. Reedijk, Inorg. Chim. Acta. 1981, 52, 61.

[8] R.N. Shchelokov, G.S. Muraveiskaya, V.N. Voropaev, G.G. Skvortsova and E.S. Dominina, Koord Khim. 1982, 8, 513.

[9] T.N. Hazarika and T. Bora, Transition Met. Chem. 1982, 7, 210.

[10] T.N. Hazarika and T. Bora, Indian J. Chem. A. (in press).

[11] S.E. Livingstone, The chemistry of ruthenium, rhodium, palladium, osmium iridium and platinum, Monograph Vol 25, Pergamon Press, (1975) 1332.

[12] A.I. Vogel, A text book of quantitative inorganic analysis, 4th edn., The English Language Book Society, (1978) 474.

[13] C.J. Ballhausen, Introduction to Ligand Field Theory, McGraw-Hill Book Company, London, (1962) 283.

*Polyhedron* Vol. 3, No. 1, pp. 125–128, 1984
Printed in Great Britain.

0277-5387/84 $3.00 + .00
Pergamon Press Ltd.

# NOTE

## ACCEPTOR PROPERTIES OF TITANIUM 2-NAPHTHYLOXIDES

**K. C. MALHOTRA,* K. C. MAHAJAN and S. C. CHAUDHRY**
Department of Chemistry, Himachal Pradesh University, Simla 171005, India

(*Received* 7 *December* 1982; *Accepted* 21 *March* 1983)

**Abstract**—The behaviour of 2-naphthyloxy titanium compounds towards several aromatic tertiary bases has been studied and a number of complexes $TiCl_x(OC_{10}H_7)_{4-x}$, $L_y$($x = 0 - 4$; $L$ = tertiary base) have been isolated and their properties studied by spectroscopic and thermogravimetric techniques.

Acceptor properties of metal phenoxides[1,2] like metal alkoxides[3] are low in contrast to the corresponding metal halides. It has been reported by Yoshino *et al.*[4] that addition compounds of titanium tetraphenoxides are more stable than those of titanium tetraalkoxides. Nitrogen[5] and oxygen[2,6] donors are known to form addition compounds with titanium tetraphenoxides but the acceptor properties of titanium naphthyloxides on the other hand are not established although metal naphthyloxides also find applications as homogeneous catalysts in synthetic organic reactions.[7,8] Establishment of the acceptor properties of metal naphthyloxides may help to elucidate some reaction mechanism. Presently, therefore, acceptor properties of titanium naphthyloxides with tertiary bases have been explored.

### EXPERIMENTAL

Titanium naphthyloxides of composition $Ti(OC_{10}H_7)_4.C_{10}H_7OH$, $Ti(OC_{10}H_7)_4$, $TiCl(OC_{10}H_7)_3$, $TiCl_2(OC_{10}H_7)_2$ and $TiCl_3(OC_{10}H_7)$ (where $C_{10}H_7O^-$ is the anion of 2-naphthol) were prepared by the methods reported earlier.[9,10] Nitrogenous bases were purified by the usual methods. Adducts of these titanium naphthyloxides were prepared by reacting benzene solution or suspension of a known weight (0.1 mole) of the parent titanium naphthyloxide with a benzene solution of the base (0.2 mole) when an exothermic reaction took place. The resulting solution was stirred for 6 hr. and allowed to stand overnight when solid crystalline compound separated out. In some cases, the products remained in solution and the compounds were isolated by the addition of petroleum spirit. They were filtered and then dried under vacuum. Molecular weights of some of these compounds were determined cryoscopically in nitrobenzene or benzene. IR spectra were recorded on a Perkin–Elmer 337 (4000–400 $cm^{-1}$) and 521 (600–250 $cm^{-1}$) spectrophotometer in KBr pellets. Thermogravimetric analysis of adducts was carried out on a thermogravimetric balance, Stanton model No. AD-2. Mass spectrum was recorded using E–MS Mass Spectrometer, the activation energy being 70 eV.

### RESULTS AND DISCUSSION

All the compounds isolated in the present studies are given in Table 1. Stoichiometric composition of these adducts has been established by elemental analysis. Evidently $Ti(OC_{10}H_7)_4$ forms compounds of 1:1 composition while $TiCl_3(OC_{10}H_7)$ and $TiCl_2(OC_{10}H_7)_2$ form compounds of 1:2 stoichiometry with monodentate ligands (L). However, with bidentate ligands (B), viz. 2, 2′-bipyridyl and 1, 10-phenanthroline, while $TiCl_3(OC_{10}H_7)$ and $TiCl_2(OC_{10}H_{10})_2$ form 1:1 adducts, $Ti(OC_{10}H_7)_4.C_{10}H_7OH$ does not react at all. Attempts to isolate adducts of $Ti(OC_{10}H_7)_4$ and $TiCl(OC_{10}H_7)_3$ with these bases of either stoichiometry have failed which may be due to steric effects. The fact that $Ti(OC_{10}H_7)_4.C_{10}H_7OH$ readily forms addition compounds with monodentate bases shows the ease of replacement of the coordinated naphthol molecule. Molar conductance values of millimolar solutions of these adducts in nitrobenzene are low (Table 1) suggesting their non-ionic character. Molecular weight determination of some of these adducts in very dilute solutions, where solubility permitted, suggests that they are monomeric.

Except in the case of titanium naphthyloxide naphtholate wherein a dimeric structure seems to

*Author to whom correspondence should be addressed.

Table 1. Analytical data of the adducts of naphthoxides of titanium(IV) with nitrogenous bases

| Compound | Colour | M.pt. (°C) | Elemental analysis | | | | Molar conductance in nitrobenzene ($ohm^{-1}cm^2mole^{-1}$) | Molecular weight in nitrobenzene | |
|---|---|---|---|---|---|---|---|---|---|
| | | | % Titanium | | % Chlorine | | | Found* | Calcd. |
| | | | Found | Calcd | Found | Calcd | | | |
| $TiCl_3(OC_{10}H_7).2py$ | Brown | 135 | 10.47 | 10.53 | 23.26 | 23.38 | 3.1 | 403 | 455.5 |
| $TiCl_3(OC_{10}H_7).2pip$ | Light brown | 180 | 10.02 | 10.26 | 22.57 | 22.78 | 3.2 | 440 | 467.5 |
| $TiCl_3(OC_{10}H_7).2\alpha$-pic | Brown | 129 | 9.82 | 9.93 | 21.89 | 22.03 | 2.9 | - | - |
| $TiCl_3(OC_{10}H_7).2\beta$-pic | Brown | 130 | 9.78 | 9.93 | 21.90 | 22.03 | 3.0 | 458 | 483.5 |
| $TiCl_3(OC_{10}H_7).2\gamma$-pic | Brown | 85 | 9.73 | 9.93 | 21.81 | 22.03 | 2.7 | 455.5 | 483.5 |
| $TiCl_3(OC_{10}H_7).bipy$ | Brown | 178 | 10.46 | 10.58 | 23.37 | 23.48 | 2.5 | - | - |
| $TiCl_3(OC_{10}H_7).phen$ | Brown | 160 | 9.91 | 10.05 | 22.19 | 22.30 | 3.0 | 438 | 477.5 |
| $TiCl_2(OC_{10}H_7)_2.2py$ | Light brown | 58 | 8.40 | 8.53 | 12.51 | 12.61 | 2.6 | - | - |
| $TiCl_2(OC_{10}H_7)_2.2pip$ | Brown | 65 | 8.29 | 8.34 | 12.25 | 12.34 | 2.1 | 546 | 575 |
| $TiCl_2(OC_{10}H_7)_2.2\alpha$-pic | Brown | 112 | 8.00 | 8.12 | 11.85 | 12.01 | 1.9 | - | - |
| $TiCl_2(OC_{10}H_7)_2.2\beta$-pic | Brown | 79 | 7.99 | 8.12 | 11.89 | 12.01 | 2.3 | 560 | 591 |
| $TiCl_2(OC_{10}H_7)_2.2\gamma$-pic | Brown | 87 | 8.05 | 8.12 | 11.93 | 12.01 | 2.7 | 558 | 591 |
| $TiCl_2(OC_{10}H_7)_2.bipy$ | Light brown | 215-216 | 8.43 | 8.56 | 12.53 | 12.66 | 2.0 | 532 | 561 |
| $TiCl_2(OC_{10}H_7)_2.phen$ | Brown | 118 | 8.09 | 8.21 | 12.00 | 12.14 | 2.9 | 548 | 585 |
| $Ti(OC_{10}H_7)_4.py$ | Light brown | 178 | 6.61 | 6.87 | - | - | 1.1 | 1358 | 1398 |
| $Ti(OC_{10}H_7)_4.pip$ | Light brown | 182 | 6.75 | 6.80 | - | - | 1.0 | - | - |
| $Ti(OC_{10}H_7)_4.\alpha$-pic | Light brown | 180 | 6.61 | 6.73 | - | - | 1.4 | 1392 | 1426 |
| $Ti(OC_{10}H_7)_4.\beta$-pic | Light brown | 172 | 6.67 | 6.73 | - | - | 1.3 | - | - |
| $Ti(OC_{10}H_7)_4.\gamma$-pic | Light brown | 185 | 6.65 | 6.73 | - | - | 1.6 | - | - |

* The value reported is the mean of three determinations.

be retained even on adduct formation, a breakdown of dimeric structures of titanium naphthyloxides viz. $TiCl_2(OC_{10}H_7)_2$ and $TiCl_3(OC_{10}H_7)$ on adduct formation with bases has been observed. This has been ascertained from the fact that bands due to bridging $Ti{<}O{>}Ti$ modes of the parent titanium naphthyloxides observed in the lower frequency region have been found to shift to higher spectral regions which correspond to terminal $\nu$(Ti–O) stretching modes on adduct formation. Similar observations have been made earlier also in case of addition compounds of naphthyloxides.[2] In case of addition compounds $Ti(OC_{10}H_7)_4.L$, however, bands due to both bridging $Ti{<}O{>}Ti$ as well as terminal $\nu$(Ti–Cl) modes have been observed, suggesting the retention of dimeric structure even on complex formation which is also supported by molecular weight determinations (Table 1). Bands due to (Ti–Cl) in the IR spectra of compounds $TiCl_3(OC_{10}H_7).2L$, $TiCl_3(OC_{10}H_7).L$, $TiCl_2(OC_{10}H_7)_2.2L$ and $TiCl_2(OC_{10}H_7)_2.B$ have been observed in the region 340–350 $cm^{-1}$ which are in the same range as reported earlier in the adducts of chloroalkoxides and chlorophenoxides of titanium in an octahedral environment.[2,11] Apart from the bands due to $\nu$(Ti–O) and $\nu$(Ti–Cl), new bands in the region 280–290 $cm^{-1}$ (not present in parent titanium naphthyloxides) have been observed and may be assigned to $\nu$(Ti–N) stretching modes.[12] thus suggesting the coordination of bases through nitrogen.

The coordination of pyridine, $\alpha$-, $\beta$- and $\gamma$-picolines has been further confirmed by the fact that four principal bands in the region 1400–1600 $cm^{-1}$ assigned to C = C and C = N in plane ring deformation vibrations shift to higher frequencies in agreement with the earlier reports.[13,14] All important bands which are characteristic of coordinated tertiary bases are present in these adducts.[13–15] In the case of addition compounds of titanium naphthyloxides with piperidine, however, in addition to these bands a band present at 3291 $cm^{-1}$ assigned to hydrogen bonded $\nu$(N–H) stretching mode[14] gets lowered by 50–60 $cm^{-1}$. All these observations support the coordination of piperidine through nitrogen and is quite in agreement with the earlier reports of its adducts with metal halides.[14] Similarly adduct formation of these titanates with bidentate ligands has been ascertained from the shifts in C = C and C = N stretching frequencies and C–H out of plane deformation bands to the higher spectral frequencies.[16–18]

Thermogravimetric analysis of some of these adducts has been studied to determine their stability and mode of decomposition. From the weight changes noted from thermograms of different compounds, it is inferred that the first step of decomposition involves the loss of base molecule followed by a similar trend of decomposition as observed for the parent titanium naphthyloxides[9,10], e.g.

$$TiCl_2(OC_{10}H_7)_2.2L \xrightarrow{150\text{–}200^\circ C} TiCl_2(OC_{10}H_7)_2 + 2L$$

$$TiCl_2(OC_{10}H_7)_2 \xrightarrow{350^\circ C} TiOCl_2 + C_{10}H_7C_{10}H_7$$

$$2TiOCl_2 \xrightarrow{\text{above } 600^\circ C} TiO_2 + TiCl_4.$$

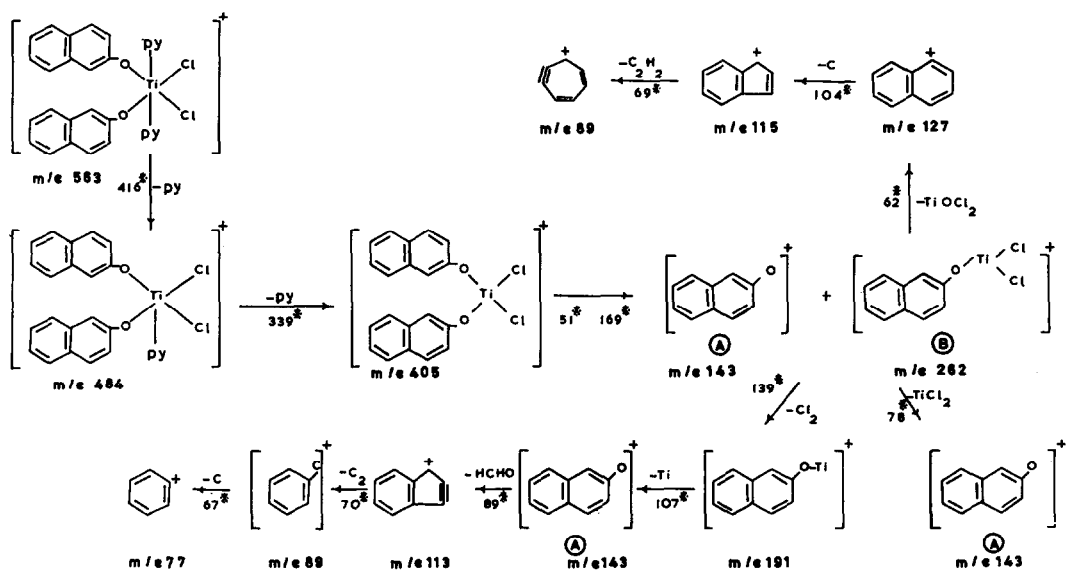



Fig. 1. Fragmentation pattern of dipyridine dichlorodinaphtoxy titanium(IV).

Apparently the base dissociation shows their weak acceptor character. The *m/e* ions peaks observed in the mass spectral study of the compound of composition $TiCl_2(OC_{10}H_7)_2.2Py$ also indicates that there is successive loss of base molecules. Based upon different peaks observed in its mass spectra, it is possible to assign molecular weights to various species. The fragmentation scheme shown in Fig. 1 is supported by the appropriate metastable peaks. Similar type of patterns can be suggested for other adducts as well.

It can thus be concluded that titanium naphthyloxides behave as Lewis acids and are able to form fairly stable adducts with bases.

## REFERENCES


1. R. J. H. Clark, *The Chemistry of Titanium and Vanadium*, p. 289. Elsevier, New York (1968).
2. K. C. Malhotra, N. Sharma and S. C. Chaudhry, *Trans. Metal Chem.* 1981, **6**, 238.
3. D. C. Bradley, *Prog. in Inorg. Chem.* 1960, **2**, 303.
4. T. Yoshino, I. Kijima and M. Ochi, *Bull. Chem. Soc. Japan* 1961, **34**, 459.
5. V. R. Masthoff, H. Kohler, H. Bohland and F. Schmeil, *Z. Chem.* 1965, **5**, 122.
6. K. C. Malhotra, U. K. Banerjee and S. C. Chaudhry, *Trans. Metal Chem.* 1982, **7**, 14.
7. S. M. Oblberg and P. A. Vander Maulen, *J. A. Chem. Soc.* 1953, **75**, 997.
8. C. Koneeny, *Collection Czech. Chem. Commun.* 1962, **27**, 2596.
9. K. C. Mahajan, Ph.D. Thesis, H. P. University, Simla (India), 1982.
10. K. C. Malhotra, K. C. Mahajan and S. C. Chaudhry, *J. Ind. Chem. Soc.* in press.
11. R. C. Paul, P. K. Gupta, M. Gulati and S. L. Chadha, *Inorg. Nucl. Chem. Letters* **1977, 13**, 665.
12. D. Horley and E. G. Torrible, *Can. J. Chem.* 1965, **43**, 3201.
13. N. Vuletic and C. Djordjevic, *J. Chem. Soc. Dalton* 1972, 2322.
14. N. N. Greenwood and K. Wade, *J. Chem. Soc.* 1960, 1130.
15. N. S. Gill, R. H. Nuttall, D. E. Scaife and D. W. A. Sharp, *J. Inorg. Nucl. Chem.* 1961, **18**, 79.
16. R. G. Inskeep, *J. Inorg. Nucl. Chem.* 1962, **24**, 763.
17. A. S. Schilt and R. C. Taylor, *J. Inorg. Nucl. Chem.* 1959, **9**, 211.
18. K. C. Malhotra and Bal Krishan, *Ind. J. Chem.* 1976, **14A**, 869.

*Polyhedron* Vol. 3, No. 1, pp. 129–131, 1984
Printed in Great Britain.

0277–5387/84 $3.00 + .00
© 1984 Pergamon Press Ltd.

# NOTE

## Interaction between some metal tetrasulphonated phthalocyanines and apocytochrome-*c*

HELENA PRZYWARSKA-BONIECKA*, ŁUCJA OSTROPOLSKA and HANNA SWIRSKA
Institute of Chemistry, University of Wrocław, Poland

(*Received* 11 *April* 1983: *Accepted* 31 *May* 1983)

**Abstract**—Artificial cytochromes-*c* have been prepared with zinc and vanadyl tetrasulphonated phthalocyanines in place of heme. Their structure and properties have been investigated by CD and difference spectroscopy, molecular weight determination and peptide fragments examination.

It has been shown that metalloporphyrins other than heme may be incorporated into the heme crevice of apohemoglobin,[1–5] apomyoglobin and apocytochrome-*c*.[6–9]

Earlier we have shown that substitution of heme in hemoglobin and cytochrome-*c* by iron and cobalt tetrasulphonated phthalocyanines gave complexes which can be regarded as models of these hemoproteins.[10–14] Phthalocyanine substituted hemoglobins are able to combine reversibly with oxygen. Modification of cytochrome *c* by phthalocyanine derivatives causes significant conformational changes of the protein but does not produce the major alteration in activity of the enzyme with succinate-cytochrome-*c*-reductase.[13]

In this paper we report the results of our studies of Zn, Cu, V, Cr and Mo tetrasulphonated phthalocyanines with apocytochrome-*c*.

## EXPERIMENTAL

Pig heart cytochrome-*c* was purchased from Biomed [Kraków] and purified chromatographically.[15] Apocytochrome-*c* was prepared by modification of the silver sulphate method.[13] The preparation and purification of metal tetrasulphonated phthalocyanines was performed according to the method described earlier for the manganese tetrasulphonated phthalocyanine.[12] Stock solutions were obtained by weighing appropriate amounts of the solid and dissolving the latter in 100 $cm^3$ of 0.2 M acetic acid. Protein concentrations were determined spectrophotometrically with Specord Spectrophotometer. Molar absorptivities used for ferric cytochrome-*c* and apocytochrome-*c* were: $\epsilon_{408} = 1.1 \times 10^5$ and $\epsilon_{276} = 1.15 \times 10^4\ M^{-1}cm^{-1}$, respectively.

The synthesis of the phthalocyanine substituted cytochromes-*c* involved incubation of apocytochrome-*c* with twice excess of the metal tetrasulphonated phthalocyanine in 0.2 M acetic acid for 3 days at 4°C. The reaction mixture was separated by gel filtration on Sephadex G50. Preparation of the carboxymethylated derivatives was performed according to the method described earlier.[16] The cleavage of the methionyl residue bonds with cyanogen bromide was carried out according to Corradin and Harbury.[17]

Most of the experiments were performed with the model complexes in unlyophilizated form. The concentrations of the complexes in the solutions were determined spectrophotometrically, from the protein content.

Absorption spectra and difference spectra were obtained with Cary 15 recording spectrophotometer with a cell compartment thermostatically controlled at 4°C. The measurements were made under equilibrium conditions.

Polyacrylamide gel electrophoresis was carried out as described earlier.[11]

Circular dichroism measurements were performed using a model ORD/UV-5 Japan Spectropolarimeter with CD attachment. The solutions for electrophoretic and CD experiments were prepared as follows: The mixture of the reactants containing excess of metal tetrasulphonated phthalocyanine was incubated in acetate buffer, pH 5.8 for three days at 4°C and then examinatd without isolation of the reaction products.

## RESULTS AND DISCUSSION

Incubation of apocytochrome-*c* with copper, chromium and molybdenum tetrasulphonated phthalocyanines in acetate buffer pH 5.8 gave highly unstable complexes which undergo irreversible denaturation after the 2 days' reaction. Formation of the complexes was suggested on the basis of difference spectra of reaction systems in carbonate buffer (pH 9.16). However, low stability of these compounds does not allow their thorough examination.

*Author to whom correspondence should be addressed.

Interaction of apocytochrome-*c* with vanadyl and zinc tetrasulphonated phthalocyanines in acetate buffer led to the formation of more stable complexes. Visible difference spectra of the mixtures of vanadyl and zinc tetrasulphonated phthalocyanines with apocytochrome-*c* showed characteristic positive peaks at 655 and 715 nm, respectively, which were indicative of complex formation. Negative bands of these spectra correspond to the main absorptivities of unbonded vanadyl and zinc tetrasulphonated phthalocyanines (Figs 1A and B).

Electrophoresis and molecular weight estimations point to the monomeric character of the complexes. The approximate molecular weights of the vanadyl and zinc model compounds are 12,800 and 12,600, respectively.

Spectroscopic studies of the vanadyl and zinc phthalocyanine interactions with the cytochrome-*c* peptide fragments demonstrated the complex formation entirely with the heme fragment apopeptides. However, no interactions were observed with non-heme peptides of cytochrome-*c*. Visible difference spectrum of the mixtures of Zn(II)L with apopeptide (1–65) heme peptide in acetate buffer are presented in Fig. 1(C). It shows a positive peak at 715 nm and two negative peaks at 645 and 680 nm, belonging to Zn(II)L. This spectrum is identical with that of the Zn(II)L-apocytochrome-*c* system.

L = tetrasulphonated phthalocyanine ligand $C_{32}H_{12}N_8(SO_3Na)_4$.

The results of the spectroscopic investigations support the statement that the binding site of zinc phthalocyanine and heme in apoprotein is the same.

The conformational properties of the zinc and vanadyl phthalocyanine cytochrome-*c* were examined by a CD technique. In Fig. 2 UV CD spectra of the model complexes are presented in comparison with that of

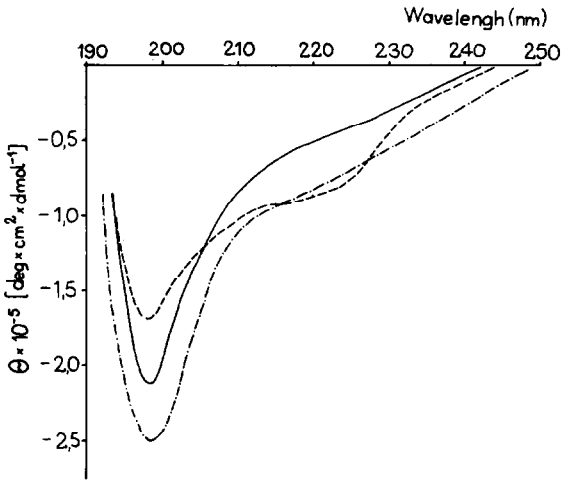



Fig. 2. UV CD spectra of (VO)L-apocyt. (----), Zn(II)L-apocyt. (-·-·-) and apocytochrome-*c* (———) in acetate buffer pH = 5.8.

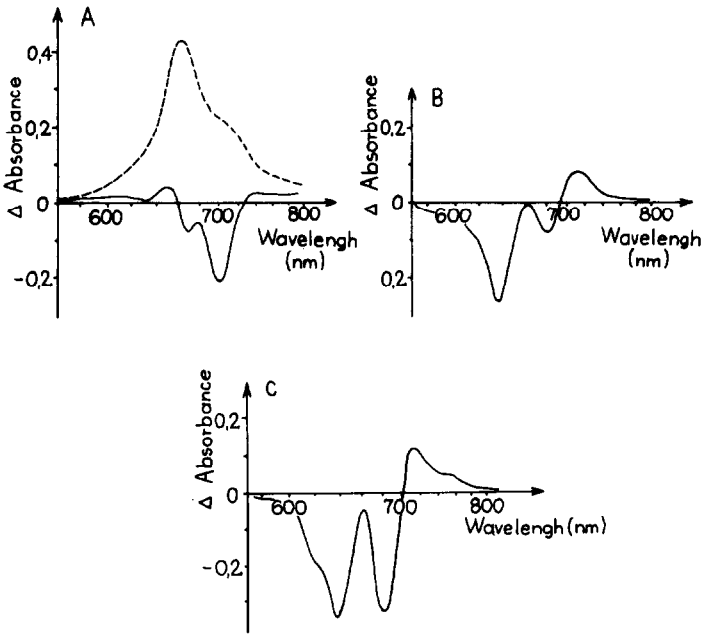



Fig. 1. Difference spectra of (A) (VO)L + apocytochrome-*c*, (B) Zn(II)L + apocytochrome-*c*, (C) Zn(II)L + (1–65) fragment apopeptide (———) and absorption spectrum of (VO)L-apocyt. (---) in acetate buffer pH = 5.8 Concentrations: (A) (VO)L = $6 \times 10^{-5}$M, apocytochrome-*c* = $1 \times 10^{-4}$M. (B) Zn(II)L = $6.2 \times 10^{-5}$M, apocytochrome-*c* = $5.8 \times 10^{-5}$M. (C) Zn(II)L = $1 \times 10^{-5}$M, (1–65) apopeptide = $2.15 \times 10^{-5}$M.

apocytochrome-*c*. In acetate buffer, apocytochrome-*c* exhibits an intense negative band at about 198 nm with ellipticity $-2.1$ deg cm$^2$ dmole$^{-1}$. This is indicative of a predominantly unordered conformation. Coordination of the apocytochrome-*c* with the vanadyl or zinc phthalocyanine derivative resulted in the appearance of the negative Cotton effects at 223 nm of ellipticity $-0.85$ and 0.75 deg cm$^2$ dmole$^{-1}$, respectively. In the case of the vanadyl complex the negative ellipticity at 198 nm is lowered at the same time to $-1.7$ deg cm$^2$ dmole$^{-1}$. These results point to the slight increase of the helix content in the model complex, although the protein conformation remains virtually unordered. The zinc phthalocyanine modified cytochrome-*c* exhibited higher negative ellipticity at 198 nm ($-2.5$ deg cm$^2$ dmole$^{-1}$) compared with that of apocytochrome-*c*. This indicated an increase of a random coil conformation upon coordination. It is probably due to the change of the electronic configuration of the Zn(II) ion on coordination with protein. A completely filled electronic system like Zn(II), tends to favour a tetrahedral configuration. Coordination with square-planar phthalocyanine ligand must lead to deformation of the zinc phthalocyanine complex that bring about conformational changes of the protein.[12]

Both phthalocyanine cytochromes-*c* as well as complexes of vanadyl and zinc phthalocyanines with apopeptides of the cytochrome heme fragments have no affinity for additional ligands characteristic for iron. This suggests that the phthalocyanine prosthetic group in the model complexes is axially coordinated with protein by strong field ligands. On the contrary to the native cytochrome-*c*, carboxymethylation of the model complexes at methionines 65 and 80 does not change the properties of these complexes. This fact excludes the possibility of coordination with protein by methionine 80 as it is in the native cytochrome-*c*.

The examined model complexes are not reduced with ascorbic acid. With dithionite they undergo irreversible reduction with degradation of the phthalocyanine ring. This fact may suggest that model complexes have the open crevice structure with the altered environment of the phthalocyanine moiety. It is possible that in such conditions one of the axially coordinated groups is histidine-33 or lysine-79, neighbouring methionine-80.

Zn(II)L-apocyt and (VO) L-apocyt = complexes of zinc and vanadyl tetrasulphonated phthalocyanines with apocytochrome-*c*.

## REFERENCES


1. B. M. Hoffmann and D. H. Petering, *Proc. Natl Acad. Sci. U.S.A.* 1970, **67**, 637.
2. T. L. Fabry, C. Simo and K. Javaherian, *Biochim. Biophys. Acta* 1968, **160**, 118.
3. T. Yonetani, H. R. Drott, J. S. Leigh, G. Reed, M. R. Waterman and T. Asacura, *J. Biol. Chem.* 1970, **245**, 2998.
4. S. F. Andres and M. Z. Atassi, *Biochem.* 1970, **9**, 2268.
5. J. L. Leonard, T. Yonetani and J. B. Callis, *Biochem.* 1974, **13**, 1460.
6. L. C. Dickinson and J. C. W. Chien, *Biochem.* 1975, **14**, 3526.
7. L. C. Dickinson and J. C. W. Chien, *J. Biol. Chem.* 1977, **252**, 6156.
8. M. C. Findlay and J. C. W. Chien, *Eur. J. Biochem.* 1977, **76**, 79.
9. M. C. Findlay, L. C. Dickinson and J. C. W. Chien, *J. Am. Chem. Soc.* 1977, **99**, 5168.
10. H. Przywarska-Boniecka, L. Trynda and E. Antonini, *Eur. J. Biochem.* 1975, **52**, 567.
11. H. Przywarska-Boniecka and L. Trynda, *Eur. J. Biochem.* 1978, **87**, 569.
12. H. Przywarska-Boniecka and H. Swirska, *J. Inorg. Chem.* 1980, **13**, 283.
13. H. Przywarska-Boniecka and Ł. Ostropolska, *J. Inorg. Biochem.* 1982, **16**, 183.
14. H. Przywarska-Boniecka and Ł. Ostropolska, *J. Inorg. Biochem.* (in press).
15. W. R. Fischer, H. Taniuchi and C. B. Anfinsen, *J. Biol. Chem.* 1973, **248**, 3188.
16. K. Ando, H. Matsubara and K. Okunuki, *Biochim. Biophys. Acta* 1966, **118**, 240.
17. G. Corradin and H. A. Harbury, *Biochim. Biophys. Acta* 1970, **221**, 489.

*Polyhedron* Vol. 3, No. 1, pp. 133–135, 1984
Printed in Great Britain.

0277–5387/84 $3.00 + .00
Pergamon Press Ltd.

# NOTE

## LANTHANIDE THERMODYNAMIC PREDICTIONS—V. STABILITIES OF LANTHANIDE ANIONS IN LIQUID AMMONIA

**STEVEN G. BRATSCH* and J. J. LAGOWSKI**
Department of Chemistry, The University of Texas, Austin, TX 78712, U.S.A.

(*Received* 6 *June* 1983; *accepted* 28 *June* 1983)

**Abstract**—The stabilities (as $\Delta G_f^0$) of monatomic lanthanide anions in liquid ammonia are estimated from a simple electrostatic model. It is shown that the existence of lanthanide anions in this solvent is highly improbable.

This paper is the latest of a series concerning the thermodynamic properties of compounds and ions of the lanthanides.[1-4] It is possible in many cases to correlate and predict these properties with surprising accuracy. The ability of some metals to form anions[5-9] represents a new and unusual area of inorganic chemistry, and it is natural to enquire whether the lanthanides may also form anionic species. Monatomic metal anions known in non-aqueous solvents and/or solids include $Na^-$, $K^-$, $Rb^-$, $Cs^-$ and $Au^-$.[5-9] The stabilities of metal anions in various environments can often be predicted from simple electrostatic models.[5-7,9a,10] We present here an analysis of the thermodynamic stability of monatomic lanthanide anions in liquid ammonia solution.

The standard Gibbs free energy of formation of a metal anion $M^-$ in liquid ammonia may be derived from the following thermochemical cycle:

| | | |
|---|---|---|
| Step 1 | $0.5\,H_2(g) \rightarrow H^+(g) + e^-$ | $\Delta G_f^\circ(H^+, g)$ |
| Step 2 | $M(c) + e^- \rightarrow M^-(g)$ | $\Delta G_f^\circ(M^-, g)$ |
| Step 3 | $H^+(g) \rightarrow H^+(am)$ | $\Delta G_{am}^\circ(H^+)$ |
| Step 4 | $M^-(g) \rightarrow M^-(am)$ | $\Delta G_{am}^\circ(M^-)$ |
| SUM | $M(c) + 0.5\,H_2(g) \rightarrow M^-(am) + H^+(am)$ | $\Delta G_f^\circ(M^-, am)$ |

The value for Step 1 is 1517.0 kJ mol$^{-1}$ at 298 K.[10] Values for Step 2 can be derived from $\Delta H_f^\circ(M, g)$, the electron affinities EA(M) and the appropriate entropy terms; these are given in Table 1 for the elements Cs–Lu at 298 K. The value for Step 3 has been estimated as $-1163$ kJ mol$^{-1}$ at 298 K.[11] (Note that $H^+(am)$ is a shorthand for $NH_4^+(am)$ just as $H^+(aq)$ is a shorthand for $H_3O^+(aq)$, $H_9O_4^+(aq)$, etc.[12] The sum of thermochemical steps may be rewritten as

$$\Delta G_f^\circ(M^-, am) = \Delta G_f^\circ(M^-, g) + \Delta G_{am}^\circ(M^-) + 354\ \text{kJ mol}^{-1}. \quad (1)$$

The value for Step 4 at 298 K may be estimated by[10]

$$\Delta G_{am}^\circ(M^-) = -\frac{50.3}{r - 0.017} \pm 8.7\ \text{kJ mol}^{-1} \quad (2)$$

where $r$ is the crystal anionic radius expressed in nanometers. An extension of a method developed previously for cations[1-3] leads to

$$r_M = \frac{2.41}{q + 14} + 0.18\ \text{nm} \quad (3)$$

where $q$ is the sum of the $4f$ and $5d$ electrons in the anion and ranges from 0 ($Cs^-$) to 16 ($Lu^-$). Equation (3) gives $r_{Cs^-} = 0.352$ nm which agrees with a spectroscopically derived estimate[9b] and $r_{Lu^-} = 0.26$ nm which reflects our estimate of the contraction in anionic radii across the lanthanide

*Author to whom correspondence should be addressed.

Table 1. Thermodynamics of gas-phase ions

| M | $\Delta H_f^\circ(M, g)$ (a) | $\Delta H_f^\circ(M^-, g)$ (b) | $S^\circ(M, c)$ (c) | $S^\circ(M^-, g)$ (d) | $\Delta G_f^\circ(M^-, g)$ (e) |
|---|---|---|---|---|---|
| Cs | 76.1 | 24.4 | 85.2 | 169.73 | 5.4 |
| Ba | 180 | 203 | 62.8 | 181.66 | 174 |
| La | 431.0 | 377 | 57.0 | 183.66 | 345 |
| Ce | 420.1 | 366 | 72.0 | 189.5 | 337 |
| Pr | 356.9 | 351 | 73.2 | 191.8 | 322 |
| Nd | 326.9 | 350 | 71.5 | 192.7 | 320 |
| Pm | 318 | 341 | 71 | 189 | 312 |
| Sm | 206.7 | 172 | 69.6 | 188.56 | 143 |
| Eu | 177.4 | 200 | 77.8 | 191.3 | 172 |
| Gd | 397.5 | 343 | 68.1 | 192.5 | 312 |
| Tb | 388.7 | 334 | 73.2 | 195.5 | 304 |
| Dy | 290.4 | 313 | 74.8 | 197.1 | 283 |
| Ho | 300.6 | 323 | 75.3 | 196.9 | 293 |
| Er | 316.4 | 339 | 73.2 | 195.6 | 309 |
| Tm | 232.2 | 197 | 74.0 | 172.72 | 174 |
| Yb | 155.6 | 178 | 59.9 | 184.54 | 147 |
| Lu | 427.6 | 373 | 51.0 | 186.54 | 339 |

Notes to Table 1:

(a) kJ $mol^{-1}$: $\Delta H_f^\circ(Cs, g)$ from 13.
$\Delta H_f^\circ(Ba, g)$ from 14.
All others from 15.
(b) kJ $mol^{-1}$; calculated by (16a)
$\Delta H_f^\circ(M^-, g) = \Delta H_f^\circ(M, g) - EA(M) - 2.5\ RT$.
EA(Cs) from 17.
All other EA from 4 (estimated uncertainty = ±0.3 eV).
(c) J $K^{-1}mol^{-1}$: $S^\circ(Cs, c)$ from 13.
$S^\circ(Ba, c)$ from 14.
All others from 15.
(d) J $K^{-1}mol^{-1}$; calculated by (16b)
$S^\circ = 1.5\ R\ \ln(\text{at wt}) + R\ \ln(2J + 1) + 108.745$
where J is the total angular momentum quantum number (L-S coupling) ignoring 4f/5d electronic interaction.
(e) kJ $mol^{-1}$ from $\Delta G_f^\circ = \Delta H_f^\circ - T\ \Delta S_f^\circ$. $S^\circ(e^-) = 20.87$ J $K^{-1}mol^{-1}$ included in the calculation (16c).
Estimated uncertainty (other than $Cs^-$) = ±30 kJ $mol^{-1}$.

Table 2. Predicted Gibbs free energies in liquid ammonia

| M | $r_{M^-}$ (a) | $\Delta G_{am}^\circ(M^-)$ (b) | $\Delta G_f^\circ(M^-, am)$ (c) | $E^\circ(M/M^-)$ (d) |
|---|---|---|---|---|
| Cs | 0.352 | -150.1 | 209.3 | -2.17 |
| Ba | 0.341 | -155.4 | 373 | -3.9 |
| La | 0.331 | -160.4 | 539 | -5.6 |
| Ce | 0.322 | -165.0 | 526 | -5.5 |
| Pr | 0.314 | -169.4 | 507 | -5.3 |
| Nd | 0.307 | -173.5 | 500 | -5.2 |
| Pm | 0.300 | -177.4 | 489 | -5.1 |
| Sm | 0.295 | -181.1 | 316 | -3.3 |
| Eu | 0.290 | -184.6 | 341 | -3.5 |
| Gd | 0.285 | -187.8 | 478 | -5.0 |
| Tb | 0.280 | -191.0 | 467 | -4.8 |
| Dy | 0.276 | -193.9 | 443 | -4.6 |
| Ho | 0.272 | -196.7 | 450 | -4.7 |
| Er | 0.269 | -199.4 | 464 | -4.8 |
| Tm | 0.266 | -202.0 | 326 | -3.4 |
| Yb | 0.263 | -204.4 | 297 | -3.1 |
| Lu | 0.260 | -206.7 | 486 | -5.0 |

Notes to Table 2:

(a) nm: Equation 3.
(b) kJ $mol^{-1}$: Equation 2.
(c) kJ $mol^{-1}$: Equation 1.
Estimated uncertainty: $Cs^-$ = ±20 kJ $mol^{-1}$; all others = ±40 kJ $mol^{-1}$.
(d) V. Estimated uncertainty: Cs = ±0.2 V; all others = ±0.4 V.

series. Equation (3) is not sufficiently accurate to account for irregularities in the electron configurations of $M^-$,[4] nor for a slight discontinuity which may occur near the middle of the lanthanide series. Taken together, eqns (1)–(3) are expected to produce a maximum error of about 20 kJ $mol^{-1}$.

Calculated values of $r_{M^-}$, $\Delta G_{am}^\circ(M^-)$, $\Delta G_f^\circ(M^-, am)$ and $E^\circ(M/M^-)$ are given in Table 2. The $E^\circ$ values are illustrated in Fig. 1. The most stable metal anion of those considered is predicted to be $Cs^-$. This species has been detected spectroscopically in cyclic ethers and organic amines, but not in liquid ammonia.[5-7] The next most stable metal anion of those considered is predicted to be $Yb^-$, which is calculated to be even less stable than $Cs^-$, by 88 kJ $mol^{-1}$ (0.9 V). All the lanthanide anions are predicted to be considerably less stable than the ammoniated electron, for which $E^\circ(e^-/e^-, am) = -1.93$ V at 298 K.[9c] It is doubtful whether the order of stability will change

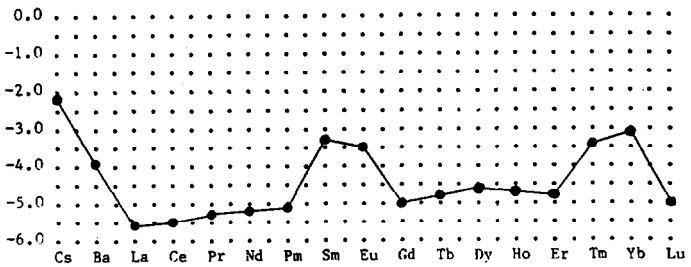



Fig. 1. Predicted $E^{\circ}(M/M^{-})$ in liquid ammonia (volts).

appreciably in moving from one solvent to another. Therefore, it appears that the preparation of monatomic lanthanide anions, at least in solution, is highly unlikely.

*Acknowledgements*—We wish to acknowledge the generous financial support of the Robert A. Welch Foundation (Grant Number FO81).

## REFERENCES

1. S. G. Bratsch and H. B. Silber, *Polyhedron* 1982, **1** 219.
2. S. G. Bratsch and H. B. Silber, In *The Rare Earths in Modern Science and Technology* (Edited by G. J. McCarthy, H. B. Silber and J. J. Rhyne), Vol. 3, pp. 291–292. Plenum Press, New York (1982).
3. S. G. Bratsch and H. B. Silber, *Inorganica Chim. Acta* 1982, **65** L53.
4. S. G. Bratsch, *Chem. Phys. Lett.* 1983, **98** 113.
5. J. L. Dye, C. W. Andrews and S. E. Mathews, *J. Phys. Chem.* 1975, **79** 3065.
6. J. L. Dye, *J. Chem. Educ.* 1977, **54** 332.
7. J. L. Dye, *Angew. Chem. Int. Ed. Engl.* 1979, **18** 587.
8. W. J. Peer and J. J. Lagowski, *J. Am. Chem. Soc.* 1978, **100** 6260.
9. W. J. Peer, Ph.D. Dissertation (a) pp. 261–263, (b) p. 313, (c) p. 260. The University of Texas, Texas (1979).
10. S. G. Bratsch and J. J. Lagowski *J. Phys. Chem.* (submitted).
11. N. A. Izmailov, *Dokl. Akad. Nauk. SSSR* (*English Translation*) 1963, **149** 288.
12. W. L. Jolly, *J. Chem. Educ.* 1956, **33** 512.
13. NBS Technical Note 270-8 (National Bureau of Standards, Washington, DC, 1981).
14. NBS Technical Note 270-6 (National Bureau of Standards, Washington, DC, 1971).
15. L. R. Morss, *Chem. Rev.* 1976, **76** 827.
16. D. A. Johnson, *Some Thermodynamic Aspects of Inorganic Chemistry* 2nd Edn. (a) p. 251, (b) p. 8, (c) p. 25. Cambridge University Press, New York (1982).
17. H. Hotop and W. C. Lineberger, *J. Phys. Chem. Ref. Data* 1975, **4** 539.

*Polyhedron* Vol. 3, No. 2, pp. 137–142, 1984
Printed in Great Britain.

0277-5387/84 $3.00 + .00
Pergamon Press Ltd.

# DISTORTION OF THE COORDINATION POLYHEDRON IN MONONUCLEAR COPPER(II) COMPLEXES. OPTICAL ABSORPTION AND ELECTRON SPIN RESONANCE STUDIES ON SOME FIVE-COORDINATE COPPER(II) COMPLEXES

RAGHUVIR SINGH* and L. V. K. N. RAMLINGESWARA RAO
School of Chemistry, University of Hyderabad, Hyderabad 500 134, India

(*Received* 18 *August* 1981; *accepted* 23 *December* 1982)

**Abstract**—The preparation and spectral properties are reported for a series of ten mixed-ligand copper(II) complexes of the form $[Cu(A)(B)_n](X)$, where $A$ is acetylacetonate anion, $B$ represents a mono- or bidentate ligand such as morpholine, piperidine, isonicotinic acid hydrazide, 2,2′-bipyridine, 1,10-phenanthroline and $X$ is variously $NO_3^-$ or $ClO_4^-$ anion and $n = 1$ or 2. The coordination of the anions and ligands has been demonstrated by infrared and electronic spectral methods. Electron spin resonance spectral data show the square-pyramidal five-coordinated arrangement around copper(II) in these complexes. Parameters such as $g_\parallel$, $g_\perp$, $A_\parallel$, $A_\perp$, $\langle g \rangle$ and $\langle A \rangle$ calculated from electron spin resonance data in solid and solution state at room temperature as well as frozen solution indicate the presence of the unpaired electron in the $d_{x^2-y^2}$ or $d_{z^2}$ orbital. These results are in good agreement with electronic and photoacoustic spectral studies.

Although the coordination compounds of copper(II) with various mono- or bidentate ligands have been studied extensively in the light of different stereochemistries, the structural aspects of five-coordinate copper(II) complexes are still under extensive investigation in various laboratories. Generally the copper forms octahedral complexes with the weakening of two axial bonds or square planar complexes. There is another possibility of a five-coordinated environment around the copper(II) giving square-pyramidal or trigonal bipyramidal structures in which one ligand is weaker at the axial position. Electron spin resonance is one of the most suitable techniques for studying the changes in molecular structure of paramagnetic complexes in solution. These changes in structure may be brought about by the solvent molecules in various ways. The solvent may enter into the coordination sphere of the metal ion, detach some of the coordinated atoms from the metal ions, or completely change the structure due to the formation of new complexes. When square planar complexes (with small $g$ and large $A$) are dissolved in a solvent, the solvent molecules will, in general, be attached at the apical positions.[2] This type of axial bonding has two effects. One is that the copper ions in a four-coordinate complex will in general be pulled out of the equatorial plane, thus weakening the equatorial bonds; this will increase $g_\parallel$ and $g_\perp$ and decrease $\Delta E_{xy}$ and $\Delta E_{xz}$. The second effect is that the value of K would be dependent on the 4$s$ and 4$p$ contribution of the ground state which reduces the value of K. Therefore, the value of K in the presence of 4$s$ contribution can be deduced as $K = K_0\alpha^2 - 4s$. On the other hand the weakening of the equatorial bond will tend to increase the value of $\alpha^2 K_0$. Therefore, it may not be possible to predict whether $K$ will increase or decrease due to axial bond formation. It is also difficult to predict the changes in the hyperfine line separation in a five-coordinate complex, because the separation is determined by the sum of $K$, the direct dipolar term, and the indirect dipolar terms which depend on $\alpha^2$ and on the principal $g$ values ($g_\parallel$ and $g_\perp$). If the equatorial bonds are not weakened much by the axial field, the resultant change will be a reduction in the hyperfine line separation constants ($A_\parallel$ and $A_\perp$) which is commonly observed in five-coordinate complexes.[3] If the solvent molecule occupies the sixth position in the coordination sphere the metal ions may once again be brought back into the equatorial plane and the changes in $g$ and $A$ values will be difficult to predict. Therefore, it was of interest to study the five-coordinate complexes of copper(II) by electron spin resonance studies in formamide/dimethylformamide solution to examine the changes produced in the coordination sphere of these complexes due to solute–solvent interactions. Further, these results on ESR were compared with our findings on electronic and photoacoustic spectral data.

## EXPERIMENTAL

All commercial reagents were of high grade and were distilled or recrystallized, where necessary, before use.

To a copper(II) acetate solution (0.005 M) in ethanol/methanol (50 ml) was added a mixture of equimolar quantities of acetylacetonate and amine ligand solutions. The resulting solution was refluxed on a water bath for 1 hr and then a solution of sodium perchlorate or nitrate was added slowly till the precipitation of the complex was complete. In some cases the addition of nitrate/perchlorate did not precipitate the material and in such cases the

*Author to whom correspondence should be addressed. Present address: Department of Chemistry, Harvard University, Cambridge, MA 02138, U.S.A.

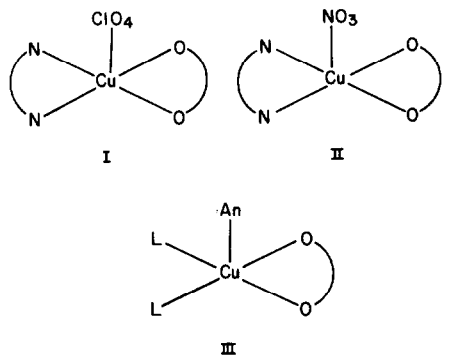
solution was kept at 0°C for few days. The solid was filtered, washed with ether and dried in an inert atmosphere and analyzed by standard methods. The copper was estimated as oxinate/iodometrically and C, H and N by micro analysis.

The IR spectra were recorded as CsI pellets in the range 4000–200 $cm^{-1}$ with a Perkin–Elmer-283 spectrophotometer. The electronic spectra of the complexes were recorded in the solid state as Nujol mulls in the range 1500–350 nm on a Cary-17D recording spectrophotometer. The photoacoustic spectra (PAS) were measured in the solid state with a Princeton Applied Research Model 6001 instrument with a 1000 W xenon lamp modulated electronically: the modulated frequency used in the present study was 40 Hz with a monochromator slit width of 2 mm that corresponds to a spectral band width of 2–5 nm in the range 1500–200 nm. The scan rate in this experiment was set at 200 nm $min^{-1}$.

The electron spin resonance spectra of the copper(II) complexes under study were recorded at room temperature and at −150°C with a JEOL PE–3X spectrometer operating at about 9.45 and 9.28 GHz using 100 KHz field modulated on a 12 in. electromagnet. The frequency was monitored with a calibrated absorption wavemeter incorporated in a microwave unit. Spectra of powder samples and formamide solutions of each complex were recorded. The magnetic field calibration was checked using diphenylpicrylhydrazyl (DPPH) free radical for which $g = 2.0023$. The magnetic field homogeneity around the sample was approx. ±25 mG and the maximum errors in $g$ and hyperfine line separation are ±0.001 and ±2 Gauss, respectively. Quartz sample tubes were employed in measurements of the electron spin resonance spectra of powdered solids.

## RESULTS AND DISCUSSION

Table 1 summarizes the copper(II) complexes together with their analytical data. The analytical data correspond with the assigned molecular formulae. Weight loss experiments show the absence of coordinated water. Conductivity measurements[4] show these complexes in dimethylformamide solution behave as uni-univalent electrolytes indicating the dissociation of bonds between metal and anions and support the presence of nitrate and perchlorate anions inside the coordination sphere. This could be explained on the basis of strong π-interaction in the complexes containing acetylacetonate/bipyridine ligands which leave the metal ion with a high positive charge to accommodate negatively charged ligands. The structures of complexes can be represented as follows.




### *IR spectra*

Ir spectra of ligands and diketone anions contained in complexes are quite characteristic of the modes of

Table 1.

| Compound# | Copper % | Carbon % | Hydrogen % | Nitrogen % |
|---|---|---|---|---|
| Cu(acac)(bipy)$ClO_4$ | 15.7 (15.0) | 43.5 (42.9) | 3.9 (3.8) | 6.9 (6.7) |
| Cu(acac)(bipy)$NO_3$ | 16.3 (16.0) | 47.3 (47.0) | 4.3 (4.2) | 10.9 (10.9) |
| Cu(acac)(phen)$ClO_4$ | 14.5 (14.5) | 46.5 (46.3) | 3.7 (3.6) | 6.9 (6.4) |
| Cu(acac)(phen)$NO_3$ | 15.9 (15.7) | 50.9 (50.5) | 4.1 (3.9) | 10.9 (10.4) |
| Cu(acac)(inh)$ClO_4$ | 16.3 (15.9) | 35.8 (35.5) | 3.9 (3.8) | 10.5 (10.5) |
| Cu(acac)(inh)$NO_3$ | 17.2 (17.5) | 39.3 (39.0) | 4.3 (4.0) | 15.8 (15.4) |
| Cu(acac)(morph)$_2ClO_4$ | 14.7 (14.5) | 36.0 (35.7) | 6.2 (5.9) | 6.9 (6.4) |
| Cu(acac)(morph)$_2NO_3$ | 16.6 (15.9) | 39.5 (39.0) | 6.7 (6.5) | 10.3 (10.5) |
| Cu(acac)(pip)$_2ClO_4$ | 14.6 (14.7) | 41.9 (41.5) | 7.0 (6.9) | 6.7 (6.5) |
| Cu(acac)(pip)$_2NO_3$. | 16.3 (16.0) | 45.5 (45.5) | 7.6 (7.5) | 10.6 (10.6) |

*Calculated values are given in parentheses.

#acac = acetylacetonate
bipy = 2,2'-bipyridine
phen = 1,10-phenanthroline
inh = isonicotinic acid hydrazide
morph = morpholine
pip = piperidine

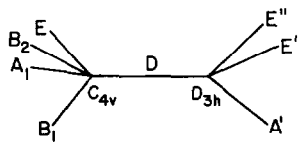
coordination.[5] These frequencies are in good accord with the modes obtained for other metal complexes with various ligands reported earlier and by other workers. The absence of bands in the region $\sim 3400\,cm^{-1}$ indicates the absence of water in these complexes.[6] However, bands in the region $\sim 3300\,cm^{-1}$ are found in the case of amine-bonded complexes due to N–H stretching frequencies. Bands in the range 1580 and 1530 $cm^{-1}$ correspond to C=O stretching of the acetylacetonate anion.[5,6] The ligands such as morpholine, piperidine, 2,2′-bipyridine, 1,10-phenanthroline and isonicotinic acid hydrazide are coordinated and act as mono/bidentate molecules by coordination through the ring nitrogen atoms. To investigate the coordination of ligands we compared the spectra of the uncoordinated ligands with that of the complexes. Positive shifts are observed in the bands of ring vibration which clearly indicate the involvement of ring nitrogen.[7] In the case of inh, shifts were observed in the carbonyl stretching frequencies which indicate that the carbonyl groups are participating in coordination.[8] However, N–H stretching frequencies are undisturbed in the case of this ligand.

The free perchlorate ion gives rise to two IR bands. A weak band at $\sim 920\,cm^{-1}$ is due to symmetric stretching mode $\nu_1$, which is strictly IR forbidden; $\nu_3$ the asymmetric stretching mode at $\sim 1100\,cm^{-1}$ and $\nu_2$ the asymmetric stretching at $625\,cm^{-1}$ are IR active when perchlorate is coordinated to a metal ion.[9] Its symmetry is lowered from $T_d$ to $C_{3v}$ and then the symmetric stretch becomes IR allowed as the triple degeneracy of $\nu_3$ is partly lifted. Consequently the IR spectral band at $\sim 920\,cm^{-1}$ becomes more intense and 1100 and $625\,cm^{-1}$ bands are resolved into two. In the present complexes containing the $ClO_4^-$ group, bands in the regions at 628, 960 and $1100\,cm^{-1}$ are observed. This shows that perchlorate ion is coordinated through one oxygen atom and inside the coordination sphere of the complex.[10] As a result these complexes contain two nitrogen atoms and three oxygen atoms (two from acetylacetonate) and in others contain four nitrogen atoms and one oxygen atom in a five coordinate square pyramidal structure around copper(II) ion. IR spectra of the nitrate-containing complexes indicate the presence of coordinated nitrate groups.[11] In addition to the ligand bands, modified slightly on account of coordination, IR spectra of the nitrate-containing complexes show absorption bands at $\sim 1310$, 1025, 710, 1410, 740 and $800\,cm^{-1}$ due to coordinated nitrate groups. These bands are assigned as $\nu_1$, $\nu_2$, $\nu_3$, $\nu_4$, $\nu_5$ and $\nu_6$, respectively[12] and their frequencies correspond with those associated with terminally bonded monodentate nitrate groups. In addition to these, two weak bands with a separation of $\sim 15\,cm^{-1}$ appear in the $1800–1700\,cm^{-1}$ combination band region indicating[13] clearly the exclusive presence of terminal monodentate nitrate groups.

*Electronic and photoacoustic spectra*

Table 2 summarizes the electronic and photoacoustic spectral data in the visible range for complexes of copper with nitrate/perchlorate anions in the coordination sphere. All the compounds have at room temperature magnetic moments in the range 1.7–2.2 BM which suggests that negligible magnetic interactions are present in the complexes.[14]

The two stereochemistries of highest symmetry among five-coordinate complexes are the trigonal bipyramidal ($D_{3h}$) and the square-pyramid ($C_{4v}$).[15] In the case of $D_{3h}$ symmetry the chromophore has $C_{3v}$ symmetry if the axial ligands are not the same and/or if the metal does not lie in the plane of the equatorial ligands. In the second case the chromophores have $C_{4v}$ symmetry even if the metal lies out of the plane of the ligands. The only term which can be derived from the copper $d^9$ is $^2D$. Application of the Van Vleck[16] or Paul[16] operators show that the energy level diagram in the case of $d^9$ would look like the following. Using this diagram, assignment of the observed bands in the electronic spectra of square pyramidal complexes can be easily made.




IV

Table 2. Photoacoustic and electronic spectral data

| Compound | PAS bands $cm^{-1}$ | eV | Electronic bands $cm^{-1}$ | nm |
|---|---|---|---|---|
| Cu(acac)(bipy)$ClO_4$ | 17241 | 2.1 | 17241 | 580 |
| Cu(acac)(bipy)$NO_3$ | 17094 | 2.1 | 17094 | 585 |
| Cu(acac)(phen)$ClO_4$ | 17094 | 2.1 | 16666 | 600 |
| Cu(acac)(phen)$NO_3$ | 17850 | 2.2 | 18018 | 555 |
| Cu(acac)(inh)$ClO_4$ | 17241 | 2.1 | --- | --- |
| Cu(acac)(inh)$NO_3$ | 16666 | 2.0 | — | — |
| Cu(acac)(morph)$_2ClO_4$ | 17850 | 2.2 | 18180 | 550 |
| Cu(acac)(morph)$_2NO_3$ | 17850 | 2.2 | 18020 | 555 |
| Cu(acac)(pip)$_2ClO_4$ | 17820 | 2.2 | 15160 | 660 |
| Cu(acac)(pip)$_2NO_3$ | 17241 | 2.1 | 15380 | 650 |

Based on the following arguments concerning electronic spectra, a square-pyramidal structure is assigned to the complexes rather than a trigonal-bipyramidal structure. The reflectance spectrum of a square-pyramidal complex [Cu(trien)SCN]NCS whose structure was determined by X-ray diffraction[17] has a broad asymmetric band at 17 400 $cm^{-1}$. Also the members of a series of bis(en)copper(II)–monoamine complexes are assigned square pyramidal structures[18] from the electronic spectra, each of which has an intense band at 17 000 $cm^{-1}$ with a very weak shoulder near 11 000 $cm^{-1}$. In contrast the reflectance spectra of $Cu(NH_3)_2Ag(SCN)_3$ which has been assigned a regular trigonal-bipyramidal structure from X-ray analysis[19] has two strong broad bands of high intensity at 12 800 and 14 500 $cm^{-1}$ (which appear almost a single band). Other complexes of the type $[Cu(NH_3)_6][CuCl_5]$ and [Cu(NCS)tren]SCN, with electronic spectra similar to $Cu(NH_3)_2Ag(SCN)_3$ were assigned[20] trigonal-bipyramidal structures. Using these results and based upon the position of electronic bands (Table 2) (Fig. 1), a similar square-pyramidal structure can be assigned to these complexes under study. These results are consistent with the ESR spectra (*vide infra*).

The photoacoustic spectra of the solid copper(II) complexes are collected in Table 2. In this spectroscopy[21] the solid samples absorb the light which is detected as an acoustic signal. With this technique it is possible to obtain optical absorption spectra in UV, visible and IR regions of all kinds of material, irrespective of whether the sample is crystalline, microcrystalline, amorphous, a powder or a gel. Scattered light poses no problem when dealing with solid samples in PAS because only the absorbed light is converted into sound. The photoacoustic spectra of our complexes show strong bands (Fig. 2) in the range 1.5–3.0 eV (~17 000 $cm^{-1}$) which are due to *d–d* transitions and are quite comparable to bands obtained in the electronic spectra. These bands near ~17 000 $cm^{-1}$ further confirm the proposed square-pyramidal stereochemistry around copper(II) ions.

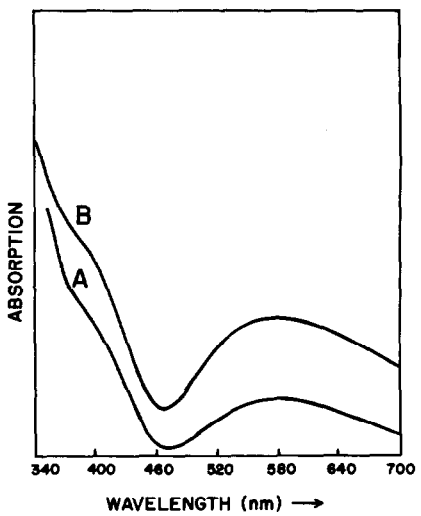



Fig. 1. Electronic spectra of (A) Cu(acac)(bipy)$ClO_4$ and (B) Cu(acac)(phen)$ClO_4$.

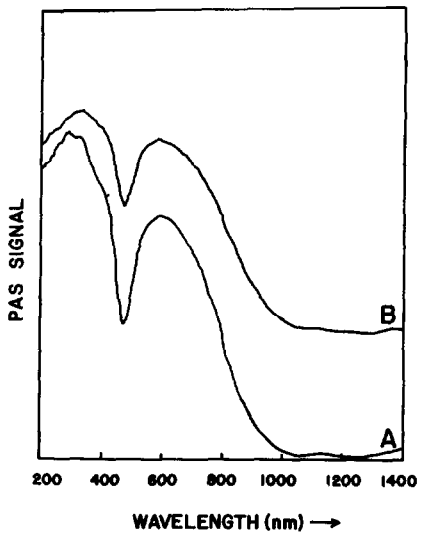



Fig. 2. Photoacoustic spectra of (A) Cu(acac)(bipy)$ClO_4$ and (B) Cu(acac)(bipy)$NO_3$ in the solid state.

*Electron spin resonance spectra*

To obtain further information about the stereochemistry and the site of metal ligand bonding and to determine the magnetic interactions in copper complexes we recorded the paramagnetic resonance spectra of the complexes in solid and solution state at room and low temperature.

The solid state ESR spectra of these complexes at room temperature as well as at low temperature consisted of a single line (Figs. 3 and 4). The corresponding spectra in formamide solution show four lines (Fig. 5), indicating the formation of a *single* complex in the above solution. The $\langle g \rangle$, $\langle A \rangle$ values are given in Table 3. The above values in formamide/dimethylformamide are found to be the same, indicating that the solvation of these complexes in the above solvents is the same. One cannot rule out the possibility of solvent interaction in solution. But the present studies on ESR as well as electronic spectral data indicate clearly the presence of one type of stereochemistry (five-coordinate) in solution. This means probably the solvent molecule displaces an atom of ligand or anion from the coordination sphere retaining the square-pyramidal five-coordinate geometry. In some of these spectra, the fourth hyperfine line of the parallel component is superimposed in the perpendicular component.[22] Recently similar spectra were observed in frozen solutions of bis(8-quinolinethiolato)-copper(II) and bis(8-quinolinolato)copper(II)[23] in chloroform, pyridine, water and dioxan. The $g_\parallel$ and $A_\parallel$ values are accurately measured from the ESR spectra of the frozen solution. Assuming that the symmetry is axial, the $\langle g \rangle$ and $\langle A \rangle$ values are calculated from the expressions:

$$\langle g \rangle = \left[\frac{g_\parallel + 2g_\perp}{3}\right]$$

$$\langle A \rangle = \left[\frac{A_\parallel + 2A_\perp}{3}\right].$$

The methods described by Sand[24] and Kneubuhl[25] were used to calculate the values of $g_\parallel$, $g_\perp$, $A_\parallel$ and $A_\perp$.

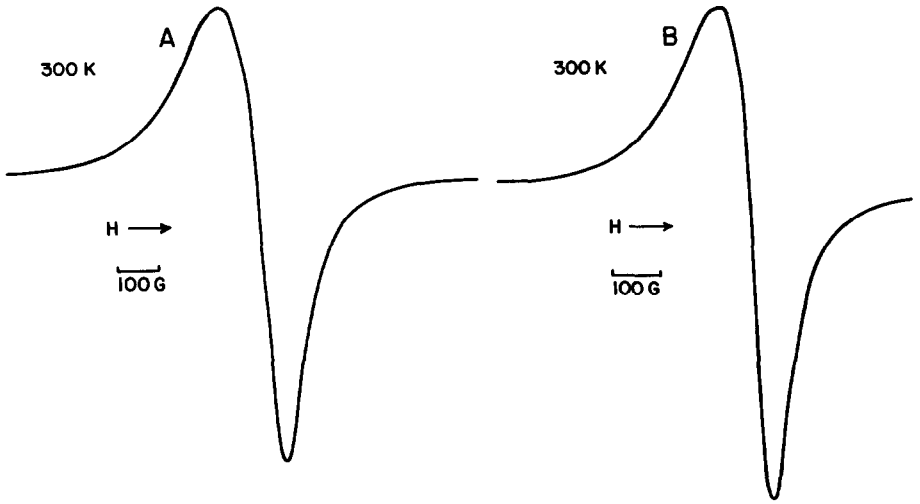



Fig. 3. Electron spin resonance spectra of (A) Cu(acac)(phen)$NO_3$ and (B) Cu(acac)(morph)$_2ClO_4$ in the solid state.

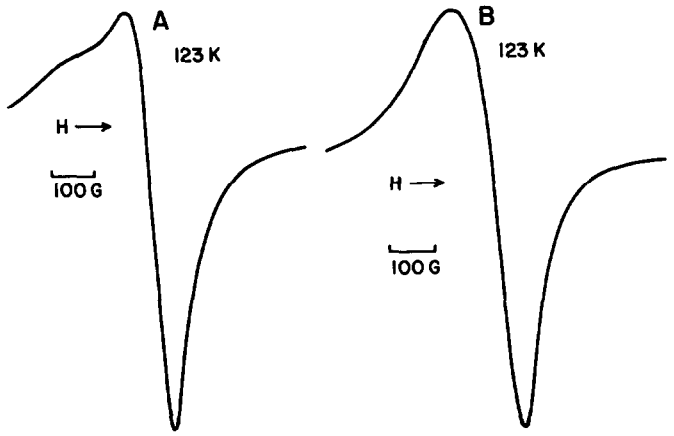



Fig. 4. Electron spin resonance spectra of (A) Cu(acac)(phen)$ClO_4$ and (B) Cu(acac)(phen)$NO_3$ in the solid state.

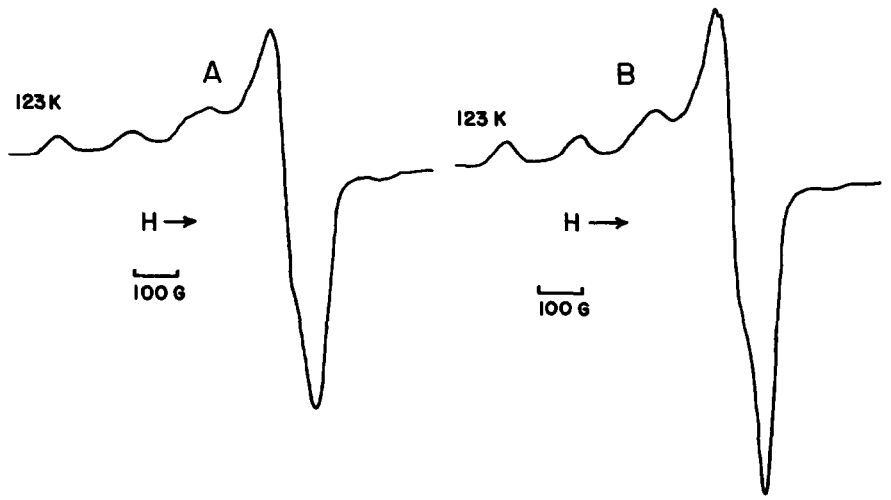



Fig. 5. Electron spin resonance spectra of (A) Cu(acac)(bipy)$ClO_4$ and (B) Cu(acac)(bipy)$NO_3$ in formamide solution.

Table 3. Spin-Hamiltonian parameters for copper(II) complexes in formamide solution

| Compound | <g> r.t. | $g_{\parallel}$ | $g_{\perp}$ | <g> | $A^*_{\parallel}$ | $A^*_{\perp}$ | <A>* |
|---|---|---|---|---|---|---|---|
| Cu(acac)(bipy)$ClO_4$ | 2.0991 | 2.2675 | 2.0536 | 2.1582 | 165.0 | 38.3 | 80.5 |
| Cu(acac)(bipy)$NO_3$ | 2.0696 | 2.2678 | 2.0520 | 2.1239 | 165.0 | 40.0 | 81.6 |
| Cu(acac)(phen)$ClO_4$ | 2.0659 | 2.2313 | 2.0488 | 2.1096 | 196.6 | 46.6 | 96.6 |
| Cu(acac)(phen)$NO_2$ | 2.1120 | 2.2836 | 2.0620 | 2.1358 | 181.6 | 30.0 | 80.5 |
| Cu(acac)$(inh)_2ClO_4$ | 2.0664 | 2.2625 | 2.0511 | 2.1215 | 166.6 | 35.0 | 78.8 |
| Cu(acac)(inh)$NO_3$ | 2.0659 | 2.1900 | 2.0482 | 2.0954 | 165.0 | 41.6 | 82.7 |
| Cu(acac)(morph)$ClO_4$ | 2.1084 | 2.2753 | 2.0584 | 2.1307 | 171.6 | 33.3 | 79.4 |
| Cu(acac)$(morph)_2NO_3$ | 2.1055 | 2.2741 | 2.0574 | 2.1296 | 173.3 | 31.6 | 78.8 |
| Cu(acac)$(pip)_2ClO_4$ | 2.1053 | 2.2760 | 2.0606 | 2.1324 | 171.6 | 31.6 | 78.3 |
| Cu(acac)$(pip)_2NO_3$ | 2.1088 | 2.2839 | 2.0654 | 2.1382 | 171.6 | 33.3 | 79.4 |

*All values in Gauss units.

r.t. = room temperature. All others at 123 K temperature.

The shape of ESR lines indicate that the geometry around copper(II) ions is not trigonal bipyramidal in any of the complexes because this symmetry would require the low field side of the ESR spectra to be more intense than the high field side and the order of $g$ values would be $2.00 \geqslant g_{\parallel} < g_{\perp}$.[26] This is in agreement with our results on electronic and photoacoustic spectral data.

*Acknowledgement*—The authors wish to express their thanks to the referee for useful suggestions.

## REFERENCES

[1]J. R. Wasson and P. Zacharopoulos, *J. Inorg. Nucl. Chem.* 1969, **31**, 3881; J. M. Assour, *J. Chem. Phys.* 1965, **43**, 2477.
[2]B. R. McGarvey, *J. Phys. Chem.* 1956, **60**, 71; D. Hall, S. V. Sheat-Rumball and T. N. Waters, *J. Chem. Soc.* 1968, A, 2761.
[3]S. Misumi, T. Isobe and K. Sugiyama, *Bull. Chem. Soc. Jap.* 1974, **47**, 1; D. K. Johnson, H. J. Stokloss, J. R. Wasson wnd G. L. Seebach, *J. Inorg. Nucl. Chem.* 1975, **37**, 1397.
[4]W. J. Geary, *Coord. Chem. Rev.* 1971, **7**, 81.
[5]Raghuvir Singh and R. S. Srinivas Rao, *J. Mol. Struc.* 1981, **71**, 23.
[6]K. Nakamoto, *Infrared and Raman Spectra of Inorganic Coordination Compounds*, 3rd Edn. Wiley, New York (1977).
[7]N. S. Gill, R. H. Nuttall, D. E. Scaife and D. W. A. Sharp, *J. Inorg. Nucl. Chem.* 1961, **18**, 79; I. S. Ahuja and Raghuvir Singh, *J. Inorg. Nucl. Chem.* 1974, **36**, 1505; R. J. H. Clark and C. S. Williams, *Inorg. Chem.* 1965, **4**, 350.
[8]I. S. Ahuja and Indra Prasad, *Inorg. Nucl. Chem. Lett.* 1976, **12**, 777.
[9]B. J. Hathaway and A. E. Underhill, *J. Chem. Soc.* 1961, 3091.
[10]S. F. Pavkovic and D. W. Meek, *Inorg. Chem.* 1965, **4**, 1091.
[11]I. S. Ahuja, Raghuvir Singh and C. L. Yadava, *J. Mol. Struc.* 1980, **68**, 333; M. Choca and J. R. Ferraro and K. Nakamoto, *J. Chem. Soc. Dalton Trans.* 1972, 2297.
[12]N. F. Curtis and Y. M. Curtis, *Inorg. Chem.* 1965, **4**, 804.
[13]A. B. P. Lever, E. Mantovani and B. S. Ramaswamy, *Can. J. Chem.* 1971, **49**, 1957.
[14]B. N. Figgis and J. Lewis, *Prog. Inorg. Chem.* 1964, **6**, 37.
[15]M. Cinampolini, *Structure and Bonding* 1969, **6**, 57.
[16]C. E. Schaffer and C. K. Jorgensen, *Mat. Fys. Medd. Dan. Vid. Selskab.* 1965, **34**(13).
[17]R. Barbucci, G. Cialdi, G. Ponticelli and P. Paoletti, *J. Chem. Soc.* (A) 1969, 1775.
[18]A. A. G. Tomilson and B. J. Hathaway, *J. Chem. Soc.* (A) 1968, 1685.
[19]R. C. Slade, A. A. G. Tomilson, B. J. Hathaway and D. E. Billing, *J. Chem. Soc.* (A), 1968, 61.
[20]M. Ciampolini and G. P. Speroni, *Inorg. Chem.* 1966, **5**, 45; B. J. Hathaway, I. M. Procter, R. C. Slade and A. A. G. Tomilson, *J. Chem. Soc.* (A) 1969, 2219.
[21]A. Rosencwaig, *Anal. Chem.* 1975, **47**, 592A.
[22]M. N. Chary, B. A. Sastry, G. Ponticelli and M. Massacesi, *Ind. J. Pure and Appl. Phys.* 1977, **15**, 167.
[23]N. D. Yordanov, M. Stankova and D. Shopov, *Chem. Phys. Lett.* 1976, **39**, 174.
[24]R. H. Sands, *Phys. Rev.* 1955, **99**, 1222.
[25]F. K. Kneubuhl, *J. Chem. Phys.* 1960, **33**, 1074.
[26]R. Barbucci and M. J. M. Campbell, *Inorg. Chim. Acta* 1975, **15**, L15; M. N. Chary, B. A. Sastry, G. Ponticelli and G. Devote, *J. Inorg. Nucl. Chem.* 1978, **40**, 1442.

*Polyhedron* Vol. 3, No. 2, pp. 143–149, 1984
Printed in Great Britain.

0277-5387/84 $3.00 + .00
© 1984 Pergamon Press Ltd.

# CRYSTAL STRUCTURES OF THE DICYCLOHEXYL-(18-CROWN-6) URANYL PERCHLORATE COMPLEX AND OF ITS HYDROLYSIS PRODUCT

A. NAVAZA* and F. VILLAIN
Faculté de Pharmacie, 92290 Chatenay Malabry, France

and

P. CHARPIN
Commissariat à l'Energie Atomique, Département de Physico-Chimie, 91 Saclay, France

(*Received* 21 *October* 1982; *accepted* 25 *July* 1983)

**Abstract**—The structures of dicyclohexyl-(18-crown-6) uranyl perchlorate, $[(C_{20}H_{36}O_6)UO_2]$ $(ClO_4)_2$ (complex **I**) and of dicyclohexyl-(18-crown-6) uranyl hydroxyperchlorate $[C_{20}H_{36}O_6]_3$ $[(UO_2)_2(H_2O)_6] \cdot (ClO_4)_2$, $CH_3CN$, (complex **II**) have been determined from three dimension X-ray diffraction data.

The uranyl group is directly coordinated to the oxygen atoms of the polyether ring in complex **I**; its hydrolysis (complex **II**) leads to a dimerization of the uranyl ions by sharing two OH groups with an U-U distance of only 3.827(8) Å. The polyether molecules are connected by hydrogen bonds with the dimeric ion $[(UO_2)_2$ $(OH)_2$ $(H_2O)_6]^{2+}$.

The insertion of uranium in a macrocyclic ligand has proved to be more difficult to achieve than the insertion of elements of the first two rows. The crystal structures of the hydrates of (18-crown-6) uranyl nitrate complex have shown that the uranyl cation is only bonded to the nitrate and water oxygens.[1-3] In a (18-crown-6) uranium (IV) thiocyanate complex,[4] the cation was shown to be surrounded by four nitrogen atoms of thiocyanate groups and four oxygen atoms of water molecules but not to the polyether ligand. Insertion complexes of uranium can be obtained in anhydrous solvents such as acetonitrile, nitromethane or nitrobenzene, the first of such compounds was the $[UCl_6]^{2-}$ $[UCl_3(syn\text{-}dcc)]_2^+$,[5] (syn-dcc: *cis-syn-cis*-dicyclohexyl-(18-crown-6)), obtained in acetonitrile. A similar (18-crown-6) uranium (IV) complex has been reported by Bombieri *et al.*[6] while Moody *et al.* claimed the isolation of uranium(III) crown ether complexes.[7] The synthesis of uranyl and uranium(IV) crown–ether complexes requires precautions to avoid hydrolysis. In the case of uranyl a suitable anion weakly bonded to it has to be used.

The complexes of the uranyl perchlorate with (18-crown-6) and dicyclohexyl-(18-crown-6) (dcc) have been synthesized and preliminary crystal data reported.[8] The crystal structure of the latter together with the crystal structure of its hydrolysis product are presented in this paper. Both structural determinations suffer from a lack of accuracy in the positions of light atoms, but their interest is to prove the insertion of uranyl in complex **I** and show the effect of the presence of water which eliminates crown–ether molecules of the uranium environment in complex **II**.

## EXPERIMENTAL SECTION

*Dicyclohexyl-(18-crown-6) uranyl perchlorate* $[(C_{20}H_{36}O_6)UO_2](ClO_4)_2$

*Crystal data.* M = 841, monoclinic, space group $P2_1/c$, $a = 12.947(5)$, $b = 12.850(8)$, $c = 17.539(12)$ Å, $\beta = 91.4(1)$ °, $V = 2916$ Å$^3$, $Z = 4$, $\rho_{calc.} = 1.916$ Mg · m$^{-3}$, $\mu(MoK\alpha) = 5.53$ mm$^{-1}$.

*X-Ray data collection and refinement.* A single crystal of approximate dimensions $0.1 \times 0.1 \times 0.2$ mm was mounted in a capillary. The unit cell dimensions and their estimated standard deviations were obtained from a least-squares fit of the optimized diffractometer setting angles of 15

*Author to whom correspondence should be addressed.

selected reflections. 2082 intensities were recorded ($1.5° < \theta < 20°$) on a CAD-4 Enraf–Nonius diffractometer using graphite monochromated Mo$K\alpha$ radiation with the $\omega$ scan technique. Only 1195 reflections ($I > 2\sigma(I)$) were observed due to pseudo A face centering in the uranium atom positions. The intensities of three standard reflections monitored every 100 measures, showed no significant fluctuation during the data collection. The large width and the high background of most of the reflections evidenced the imperfection of the crystals. The data were corrected for Lorentz-polarization effects but not for absorption or extinction. The structure was solved by a combination of direct methods and Fourier difference techniques. The uranium atom position was determined by Multan[11] and the other atoms were located by difference Fourier maps. The structure was refined by blocked full matrix least squares to $R = 0.079$. Only thermal parameters of uranium and chlorine atoms were refined anisotropically. The hydrogen atoms were placed respecting stereochemistry. The final difference Fourier map revealed residual peaks (height 0.7–1 e/Å$^3$) in the vicinity of one side of the crown–ether and of the perchlorate ion. This fact together with high thermal parameters and abnormal distances found for the dcc confirmed the existence of disorder in the structure, the poor quality of data did not permit us to proceed further its interpretation. The disordered positions of oxygen around chlorine atoms are frequently observed and, as will be seen in the discussion, the presence of two isomers of dcc provides a possible explanation of crown disorder. Data collection with Cu$K\alpha$ radiation corresponding to a different crystal was used after resolution of the structure, but no improvement in accuracy was obtained.

*Dicyclohexyl (18-crown-6) uranyl hydroxyperchlorate acetonitrile* $[C_{20}H_{36}O_6]_3$, $[(UO_2)_2(OH)_2(H_2O)_6] \cdot (ClO_4)_2$, $CH_3CN$ (*complex* **II**)

In the course of attempts to improve the quality of crystals of complex **I** by means of recrystallization in acetonitrile, a second complex was found in the preparation, its formation being probably due to a slow hydration of the solvent.

*Crystal data.* M = 2038, triclinic, space group $P\bar{1}$, $a = 9.693(4)$, $b = 13.836(3)$, $c = 17.888(2)$ Å, $\alpha = 70.90(8)$, $\beta = 75.83(8)$, $\gamma = 74.02(3)$°, $V = 2147$ Å$^3$, $Z = 1$, $\rho_{calc.} = 1.577$ Mg · m$^{-3}$, $\mu$(Cu$K\alpha$) = 12.63 mm$^{-1}$.

*X-Ray data collection and refinement.* A crystal of approximate dimensions 0.075 × 0.10 × 0.20 mm was selected and sealed in a Lindeman capillary. Unit cell dimensions were obtained in the same conditions as complex **I**. 3584 unique reflections ($1.5 < \theta < 55°$) were measured with the $\omega/2\theta$ scan technique using graphite monochromatized Cu$K\alpha$ radiation. Of these, 422 were considered as unobserved ($I < 2\sigma(I)$). The intensities of three standard reflections monitored every 100 measures, showed a linear decrease of about 20%. The data were appropriately scaled and corrected for Lorentz-polarization effects. During the decomposition of the crystal a variation of its shape was observed and a broadening of the reflections appeared. As a consequence no absorption correction was applied although the absorption is not negligible for this crystal.

Uranium atom was located from the three-dimensional Patterson synthesis. After two difference Fourier syntheses all atoms of the chemical formula, including one molecule of solvent (acetonitrile) were located. Two cycles of isotropic refinement and two cycles where anisotropic thermal parameters were given to uranium and chlorine atoms, using all the data, reduced the *R* factor to a final value of 0.09. Hydrogen atoms were not included.

In both structures values for the atomic scattering factors and anomalous terms for U(VI) were taken from International Tables for X-Ray Crystallography.[9]

All calculations were performed by means of the X-ray system[10] and Multan program.[11] Atomic positional and thermal parameters and lists of $F_0F_c$ have been deposited as supplementary material with the Editor, from whom copies are available on request. Atomic co-ordinates have also been deposited with the Cambridge Crystallographic Data Centre.

## DISCUSSION

Table 1 and Fig. 1 show the uranium coordination in the complex **I**. The uranyl is coordinated to six heteroatoms of dcc giving a puckered hexagonal bipyramid. The uranium atom is contained in the least-squares equatorial plane (Table 2) and the quasi-linear uranyl bond (176.7(1.7)°) is perpendicular to it. The adjacent O–O distances in the equatorial plane are shorter than the sum of their van der Waals radii. Figures 2(a) and (b) show the projections of the molecular unit perpendicular and parallel to the uranyl bond respectively. The distances and angles of dcc are affected by the disorder. The mean aliphatic C–C distances are 1.53 Å in the macrocycle and 1.51 Å in the cyclohexyl rings, the mean C–O bond lengths is 1.42 Å; the dcc angles range from 103 to 124°. All these figures have a high standard deviations which corresponds to an error ranging from 5 to 10%.

Table 1. Uranium–Oxygen bond distances (Å) in complex I

| | | | |
|---|---|---|---|
| U - O(11) | 1.77(4) | | |
| U - O(12) | 1.77(4) | | |
| U - O(1) | 2.44(4) | U - O(4) | 2.68(4) |
| U - O(2) | 2.48(4) | U - O(5) | 2.46(4) |
| U - O(3) | 2.43(4) | U - O(6) | 2.56(4) |
| O(1) - O(2) | 2.39(6) | O(4) - O(5) | 2.64(6) |
| O(2) - O(3) | 2.53(6) | O(5) - O(6) | 2.60(6) |
| O(3) - O(4) | 2.57(6) | O(6) - O(1) | 2.54(6) |
| O(11) - O(1) | 3.17(6) | O(12) - O(1) | 2.90(5) |
| O(11) - O(2) | 3.06(6) | O(12) - O(2) | 3.00(5) |
| O(11) - O(3) | 2.68(6) | O(12) - O(3) | 3.23(6) |
| O(11) - O(4) | 3.39(6) | O(12) - O(4) | 2.97(5) |
| O(11) - O(5) | 3.04(6) | O(12) - O(5) | 3.06(6) |
| O(11) - O(6) | 2.97(6) | O(12) - O(6) | 3.32(5) |

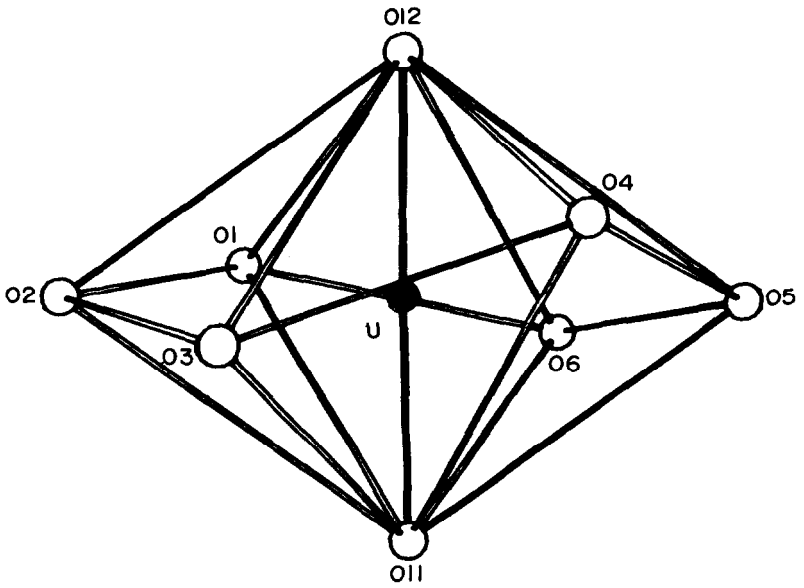



Fig. 1.

Table 2. Deviations (Å) from the least-squares planes through the polyether–oxygen atoms

| a) In the complex I | | | |
|---|---|---|---|
| U | 0.02 | | |
| O(1) | 0.28 | | |
| O(2) | 0.10 | | |
| O(3) | -0.44 | | |
| O(4) | 0.37 | | |
| O(5) | -0.02 | | |
| O(6) | -0.29 | | |
| b) In the complex II | | | |
| non centrosymmetric | | centrosymmetric crown | |
| O(1) | 0.71 | O(7) | -0.12 |
| O(2) | 0.05 | O(8) | 0.15 |
| O(3) | -0.68 | O(9) | -0.12 |
| O(4) | 0.51 | O(7') | 0.12 |
| O(5) | 0.23 | O(8') | -0.15 |
| O(6) | -0.82 | O(9') | 0.12 |

Torsion angles are given in Table 3; in spite of the inaccurate data they are close to those found in other cyclic polyether complexes where all six heteroatoms coordinate in a planar configuration about the cation. A non-crystallographic two-fold axis lies along the O(2)UO(5) line. Its standard deviation ($\sigma$) is 0.14 Å excluding the oxygen atoms of the perchlorate groups, with a maximum dispersion 0.36 Å corresponding to Cl(1)–Cl(2); omitting the chlorine atoms $\sigma$ is 0.10 Å with a maximum dispersion of 0.15 Å corresponding to C(1)–C(4). This local symmetry is characteristic of the *cis-anti-cis* (or B) isomer, $(^{ax\,ax}_{eq\,eq})$ conformer of dcc. The perchlorate anions have the usual tetrahedral configuration with the mean O–Cl distances 1.31(9) Å for Cl(1) and 1.33(10) Å for Cl(2).

The structure of the Complex I consists of infinite chains, related by $2_1$ axis, of $[UO_2\ dcc]^{2+}$

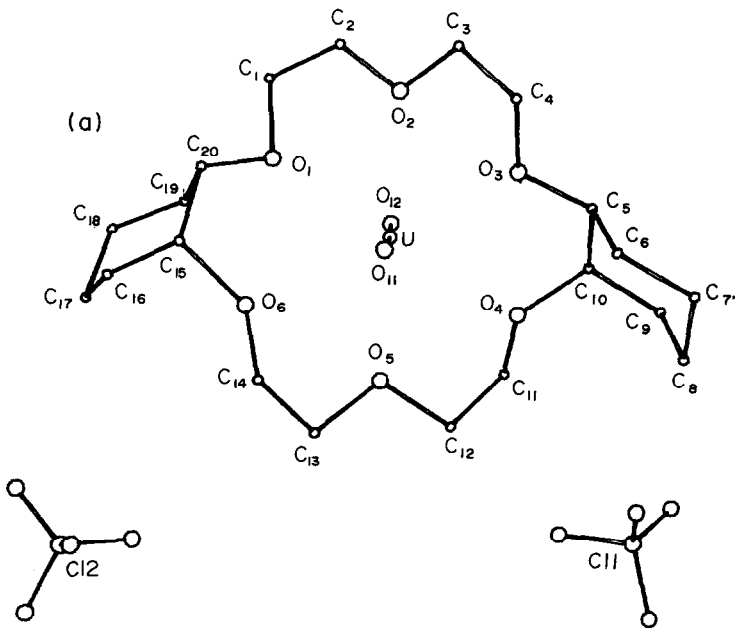



Fig. 2(a)

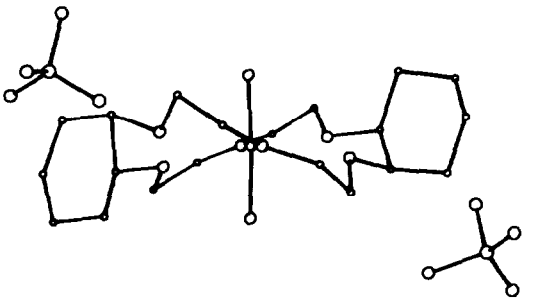


Fig. 2(b).

Table 3. Torsion angles (°) of the polyether in complex **I** ($\sigma$ range from 5° to 9°)

a) In the cyclic ether ring

| | | | |
|---|---|---|---|
| O(1)-C(1)-C(2)-O(2) | 42 | O(4)-C(11)-C(12)-O(5) | 51 |
| C(1)-C(2)-O(2)-C(3) | 169 | C(11)-C(12)-O(5)-C(13) | 165 |
| C(2)-O(2)-C(3)-C(4) | 169 | C(12)-O(5)-C(13)-C(14) | 170 |
| O(2)-C(3)-C(4)-O(3) | 27 | O(5)-C(13)-C(14)-O(6) | 49 |
| C(3)-C(4)-O(3)-C(5) | 152 | C(13)-C(14)-O(6)-C(15) | 162 |
| C(4)-O(3)-C(5)-C(10) | -151 | C(14)-O(6)-C(15)-C(20) | -180 |
| O(3)-C(5)-C(10)-O(4) | -56 | O(6)-C(15)-C(20)-O(1) | -64 |
| C(5)-C(10)-O(4)-C(11) | 176 | C(15)-C(20)-O(1)-C(1) | -172 |
| C(10)-O(4)-C(11)-C(12) | 173 | C(20)-O(1)-C(1)-C(2) | 153 |

b) In the cyclohexyl ether rings

| | | | |
|---|---|---|---|
| C(5)-C(6)-C(7)-C(8) | -61 | C(15)-C(16)-C(17)-C(18) | -58 |
| C(6)-C(7)-C(8)-C(9) | 43 | C(16)-C(17)-C(18)-C(19) | 65 |
| C(7)-C(8)-C(9)-C(10) | -45 | C(17)-C(18)-C(19)-C(20) | -62 |
| C(8)-C(9)-C(10)-C(5) | 46 | C(18)-C(19)-C(20)-C(15) | 55 |
| C(9)-C(10)-C(5)-C(6) | -47 | C(19)-C(20)-C(15)-C(16) | -59 |
| C(10)-C(5)-C(6)-C(7) | 59 | C(20)-C(15)-C(16)-C(17) | 62 |

units packed along the [100] axis with the distances: U–U: 6.47 Å; O(11)–O(11′): 3.60 Å; O(12)–O(12′): 3.51 Å (successive units are obtained by the inversion center). Each uranium unit has four neighbouring perchlorate ions (U–Cl distances: 5.42, 5.56, 6.14 and 6.23 Å), which give the negative charge between the chains.

As we have seen, the formation of complex **II** may be regarded as due to hydrolysis of complex **I** by some water molecules accidentally present in the acetonitrile solvent. This results in a complete modification of the environment of the uranyl ion, which is no more inserted in the crown ether but surrounded by water molecules, forming a dimeric ion $[(UO_2)_2(OH)_2(H_2O)_6]^{2-}$ as shown in Fig. 3. Two pentagonal bipyramids sharing an edge (O(21)–O(21′)) are related by the inversion center (0 1/2 0) located on this edge, which should be a double hydroxy-bridge between the two uranium atoms according to the hydrogen arrangement proposed below. Hydroxyl-bridged dimers have been reported for $Th_2(OH)_2(NO_3)_6(H_2O)_8$ and $^{12}U_2(OH)_2(ClO_4)_6(H_2O)_x$ ($x \sim 13$)[13] with Th–Th and U–U distances 3.99 and 4.03 Å respectively; in the structure of complex **II** the U–U distance is only 3.827(8) Å. Bond distances in the dimeric ion are given in Table 4. The shortest U–O distance observed in the equatorial plane is that involving the bridging oxygen O(21); the other U–O distances are in the standard range of a water molecule. The distances of these oxygen and uranium atoms to the least-squares equatorial plane are the following (Å): −0.008(U), −0.04(0(21)), +0.00(0(21′)), −0.06(0(22)), +0.06(0(23)) and +0.04(0(24)). The uranyl bond deviates slightly from linearity (174.6(0.07)°).

There are two different uncomplexed dcc molecules in the complex. One of these is a *cis-anti-cis* (or B) isomer ($(^{eq\ ax}_{ax\ eq})$ conformer) (Fig. 4a) and is located on the (1/2 1/2 0) symmetry center (centric - crown); the other is *cis-syn-cis* (or A) isomer ($(^{eq\ ax}_{ax\ eq}$) conformer) (Fig. 4b), (non-centric crown). The presence in this structure of the two isomers of dcc seems an indication of their coexistence in complex **I** and, as a consequence, provides a possible explanation of the disorder found in its crystal structure. As in the structure of $[U(NCS)_4(H_2O)_4]$ (18-crown-6), $3H_2O$, $CH_3CN$,[4]

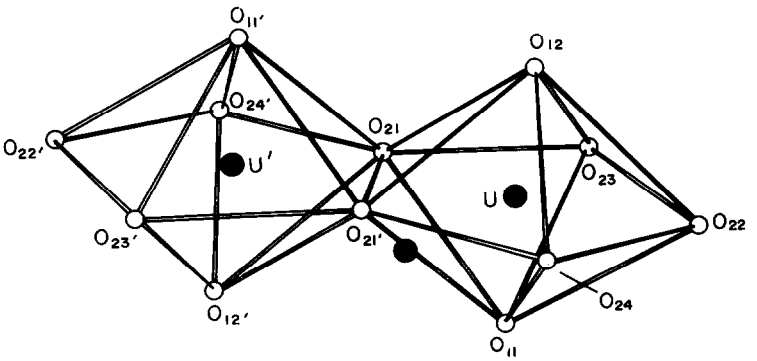



Fig. 3.

Table 4. Uranium–oxygen bond distances (Å) in complex **II**

| | | | |
|---|---|---|---|
| U - U | 3.83(1) | | |
| U - O(11) | 1.73(2) | | |
| U - O(12) | 1.70(2) | | |
| U - O(21′) | 2.27(1) | O(21′) - O(21) | 2.51(2) |
| U - O(21) | 2.31(1) | O(21′) - O(24) | 2.78(2) |
| U - O(22) | 2.44(2) | O(24) - O(22) | 2.95(2) |
| U - O(23) | 2.44(1) | O(22) - O(23) | 2.86(2) |
| U - O(24) | 2.47(2) | O(23) - O(21) | 2.93(2) |
| O(11) - O(21) | 2.89(3) | O(12) - O(21) | 2.91(2) |
| O(11) - O(21′) | 2.99(3) | O(12) - O(21′) | 2.82(2) |
| O(11) - O(22) | 2.94(2) | O(12) - O(22) | 2.92(3) |
| O(11) - O(23) | 2.78(2) | O(12) - O(23) | 3.06(2) |
| O(11) - O(24) | 3.10(2) | O(12) - O(24) | 2.96(3) |

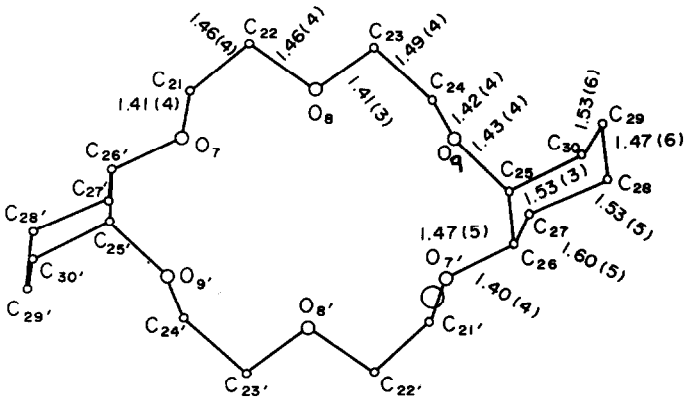



Fig. 4(a).

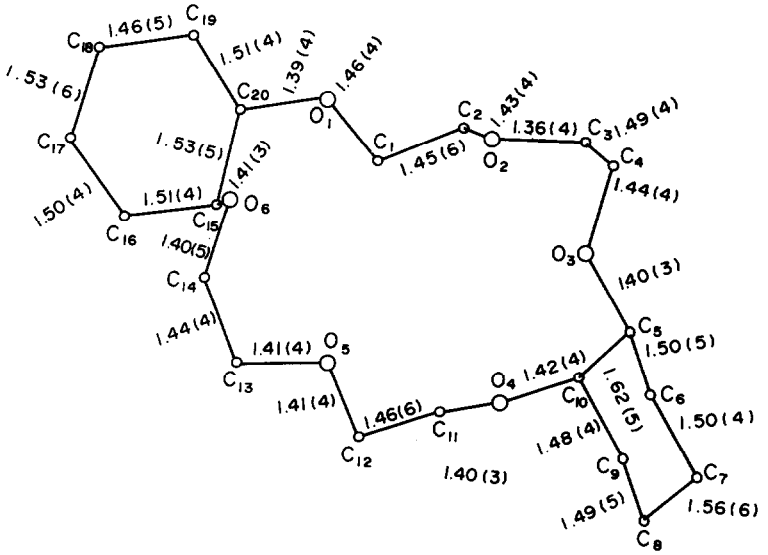



Fig. 4(b).

the oxygen atoms of two crown molecules are engaged in hydrogen bonds with water molecules. Several O–H . . . O connections are possible: the oxygen atoms of the centric crown: O(7), O(8′) and O(9) may be bonded to O(24) with distances 2.79(3), 2.77(3) and 2.81(2) Å respectively; those belonging to the non centric crown O(6), O(1) and O(2) may be connected to O(22), and O(3), O(4), O(5) to O(23) with the following distances 2.51(3), 2.98(2), 2.83(3) and 2.71(3), 2.83(2), 2.60(2) Å.

Table 5 gives torsion angles and Table 2 shows the atomic deviations from least-squares planes through the oxygen atoms, in both dcc molecules. The figures indicate that the six O centric-crown atoms, alternately above and below their mean plane, are fairly planar, while the hexagon formed by the six heteroatoms in the non-centric crown takes on a boat conformation. The origin of the conformational strain in the non-centric crown is evidently the asymmetric hydrogen bonding.

A stereoscopic ORTEP packing diagram is shown in Fig. 5. The structure is built of dimeric units which alternate along the [100] direction with the centric-crown molecules and along the [001] direction with two non-centric crown related by an inversion center. The perchlorate anion is contained in the [001] stacking and does not form closed contracts, as well as the solvate molecules, with the binuclear unit.

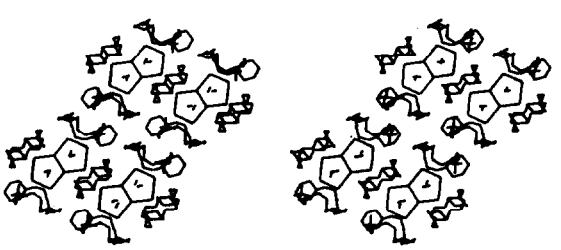


Fig. 5.

Table 5. Torsion angles (°) of the polyethers in complex **II** ($\sigma$ range from 3° to 4°)

| | | | |
|---|---|---|---|
| a) In the centric-crown | | | |
| In the cyclic ether ring | | In the cyclohexyl ring | |
| O(7)-C(21)-C(22)-O(8) | 65 | C(25)-C(30)-C(29)-C(28) | -59 |
| C(21)-C(22)-O(8)-C(23) | 177 | C(30)-C(29)-C(28)-C(27) | 65 |
| C(22)-O(8)-C(23)-C(24) | 176 | C(29)-C(28)-C(27)-C(26) | -60 |
| O(8)-C(23)-C(24)-O(9) | 63 | C(28)-C(27)-C(26)-C(25) | 62 |
| C(23)-C(24)-O(9)-C(25) | -178 | C(27)-C(26)-C(25)-C(30) | -60 |
| C(24)-O(9)-C(25)-C(26) | -163 | C(26)-C(25)-C(30)-C(29) | 54 |
| O(9)-C(25)-C(26)-O(7') | -57 | | |
| C(25)-C(26)-O(7')-C(21') | -69 | | |
| C(26)-O(7')-C(21')-C(22') | -162 | | |
| b) In the non-centric-crown | | | |
| In the cyclic ether ring | | | |
| O(1)-C(1)-C(2)-O(2) | 69 | O(4)-C(11)-C(12)-O(5) | 70 |
| C(1)-C(2)-O(2)-C(3) | 149 | C(11)-C(12)-O(5)-C(13) | 157 |
| C(2)-O(2)-C(3)-C(4) | -176 | C(12)-O(5)-C(13)-C(14) | -174 |
| O(2)-C(3)-C(4)-O(3) | 62 | O(5)-C(13)-C(14)-O(6) | 63 |
| C(3)-C(4)-O(3)-C(5) | 50 | C(13)-C(14)-O(6)-C(15) | 79 |
| C(4)-O(3)-C(5)-C(10) | 174 | C(14)-O(6)-C(15)-C(20) | -104 |
| O(3)-C(5)-C(10)-O(4) | 59 | O(6)-C(15)-C(20)-O(1) | -58 |
| C(5)-C(10)-O(4)-C(11) | 69 | C(15)-C(20)-O(1)-C(1) | 158 |
| C(10)-O(4)-C(11)-C(12) | 168 | C(20)-O(1)-C(1)-C(2) | 180 |
| In the cyclohexyl ring | | | |
| C(5)-C(6)-C(7)-C(8) | 59 | C(15)-C(16)-C(17)-C(18) | -54 |
| C(6)-C(7)-C(8)-C(9) | -55 | C(16)-C(17)-C(18)-C(19) | 56 |
| C(7)-C(8)-C(9)-C(10) | 55 | C(17)-C(18)-C(19)-C(20) | -54 |
| C(8)-C(9)-C(10)-C(5) | -61 | C(18)-C(19)-C(20)-C(15) | 54 |
| C(9)-C(10)-C(5)-C(6) | 61 | C(19)-C(20)-C(15)-C(16) | -56 |
| C(10)-C(5)-C(6)-C(7) | -58 | C(20)-C(15)-C(16)-C(17) | 55 |

*Acknowledgements*—The authors wish to thank G. Folcher, G. de Villardi and N. Keller for supplying the crystals. We also thank C. de Rango for helpful discussions.

## REFERENCES

1. P. G. Eller and R. A. Penneman, *Inorg. Chem.* 1976, **15**, 2439.
2. G. Bombieri, G. de Paoli, A. Cassol and A. Immirzy, *Inorg. Chim. Acta* 1976, **18**, L24.
3. G. Bombieri and G. de Paoli, *J. Inorg. Nucl. Chem.* 1978, **40**, 799.
4. P. Charpin, R. M. Costes, G. Folcher, P. Plurien, A. Navaza and C. de Rango, *Inorg. Nucl. Chem. Lett.* 1977, **13**, 341.
5. G. C. de Villardi, P. Charpin, R. M. Costes, G. Folcher, P. Plurien, P. Rigny and C. de Rango, *J.C.S. Chem. Comm.* 1978, 90.
6. G. Bombieri and G. de Paoli, *J. Inorg. Nucl. Chem.* 1978, **40**, 1889.
7. D. C. Moody, R. A. Penneman and K. V. Salazar, *Inorg. Chem.* 1979, **18**, 208.
8. G. Folcher, P. Charpin, R. M. Costes, N. Keller and G. C. de Villardi *Inorg. Chim. Acta*, 1979, **34**, 81.
9. *International Tables for X-Ray Crystallography*. Vol. IV. Kynoch Press, Birmingham (1974).
10. J. M. Stewart, F. A. Kundell and J. C. Baldwin, The X-Ray System Computer Science Center. University of Maryland, College Park, Maryland (1972).
11. P. Main, M. M. Woolfson, L. Lessinger, G. Germain and J. P. Declerq, Multan, A system of Computer Programs for the Automatic Solution of Crystal Structures from X-Ray Diffraction Data. University of York, England and Louvain-la-Neuve, Belgium (1978).
12. G. Johansson, *Acta Chem. Scand.* 1968, **22**, 389.
13. S. Pocev, *Acta Chem. Scand.* 1974, **28A**, 932.
14. C. K. Johnson, ORTEP II, Report ORNL-3794, Oak Ridge Nat. Lab.

*Polyhedron* Vol. 3, No. 2, pp. 151–155, 1984
Printed in Great Britain.

0277–5387/84 $3.00 + .00
Pergamon Press Ltd.

# HYDROTHERMAL SYNTHESIS OF ZINC SILICATES FROM BOROSILICATE GLASSES AND FROM MIXTURES OF ZINC OXIDE AND SILICA†

**PETER TAYLOR* and DERREK G. OWEN**
Research Chemistry Branch, Atomic Energy of Canada Limited, Whiteshell Nuclear Research Establishment, Pinawa, Manitoba, Canada R0E 1L0

(*Received* 22 *November* 1982; *accepted* 25 *July* 1983)

**Abstract**—The formation of sauconite and hemimorphite from glasses and oxide precursors in aqueous solution at 150–200°C is described. A tentative schematic stability diagram for a portion of the system $Na_2O$–$ZnO$–$SiO_2$–$H_2O$ at 150°C is presented. The relevance of this work to the use of a sodium zinc borosilicate glass as a matrix for the immobilization of nuclear fuel reprocessing wastes is discussed briefly.

The system $ZnO$–$SiO_2$–$H_2O$ includes two well-characterized zinc silicates: willemite, $Zn_2SiO_4$ and hemimorphite, $Zn_4Si_2O_7(OH)_2 \cdot H_2O$ (empirically, $Zn_2SiO_4 \cdot H_2O$). The univariant pressure-temperature curve for equilibrium (1) at pressures from 70 MPa to 10 GPa has been determined by Roy and Mumpton,[1] and by Pistorius.[2] Several zinc-containing phyllosilicates have

$$Zn_4Si_2O_7(OH)_2 \cdot H_2O \rightleftharpoons 2Zn_2SiO_4 + 2H_2O \quad (1)$$

been reported, both in nature[3–6] and in preparative studies;[7–9] little is known about their stability. Roy and Mumpton[1] concluded that a zinc end-member sauconite, namely $Zn_{x+y}[Zn_{3-x}(Si_{4-y}Zn_y)O_{10}(OH)_2]$ can occur stably below about 210°C at pressure near 100 MPa, and indicated that its stability is enhanced by partial substitution of Al for Zn. An Al-free natural sauconite was formulated by Smol'yaninova *et al.* as $Zn_3Si_4O_{10}(OH)_2 \cdot nH_2O$, and named zincsilite (see Ref. 4).

We have observed hemimorphite and a sauconite-like phase as products of hydrothermal devitrification of sodium zinc borosilicate glasses. This work formed part of an assessment of such glasses as host materials for nuclear fuel reprocessing wastes.[10] In an attempt to clarify the occurrence of hemimorphite and sauconite, we have also examined their formation from the parent oxides.

## EXPERIMENTAL

Experiments were performed in 0.3 $dm^3$-capacity titanium autoclaves using a heater and temperature control assembly described previously.[11] The preparation of sodium zinc borosilicate glasses has been described elsewhere;[12] experiments were run on both glass coupons and powders. The twelve glasses examined covered the composition range (mol per cent) 5–10 $Na_2O$, 5–30 $ZnO$, 10–40 $B_2O_3$, 40–70 $SiO_2$. Reagent grade powders of $ZnO$ (surface area, estimated by BET method, $4\ m^2 \cdot g^{-1}$), quartz ($1\ m^2 \cdot g^{-1}$) and fused silica ($1\ m^2 \cdot g^{-1}$) were used. Crystalline products were isolated by filtration, air-dried and identified by X-ray powder diffractometry, using Cu$K_\alpha$ radiation and a Philips PW–1150 diffractometer with a diffracted-beam monochromator.

## RESULTS AND DISCUSSION

### (a) *Hydrothermal reactions of glasses*

All the glasses examined underwent detectable surface crystallization during exposure to water for one day at 150°C. As expected, the quantity of crystalline products decreased, i.e. glass durability increased, with increasing silica content of the glass. These products were usually only loosely adherent on the surfaces of glass coupons. The solution pH, measured after cooling to room temperature, was usually 9–10.

The only observed crystalline products were hemimorphite and a sauconite-like clay. Most fea-

*Author to whom correspondence should be addressed.

†Issued as Atomic Energy of Canada Limited Report No. AECL–7356.

tures in the diffraction pattern of the latter phase (see Table 1), were broad and ill-defined, which is typical of synthetic clays of this type.[1] The basal spacing of acetone-washed, air-dried material was near 12 Å, expanding to about 18 Å on saturation with glycerol or ethylene glycol. This clay was not chemically analyzed, since it was never obtained free of hemimorphite and/or amorphous material; we refer to it hereafter as sauconite.

In the reactions with glass coupons, sauconite occurred only on the most severely corroded glasses, which had low silica content; hemimorphite occurred on all other glasses. In the reactions with glass powders, sauconite was formed on most of the silica-rich glasses as well. Sauconite formation is thus favoured by a high ratio of glass surface area to solution volume, presumably due to more rapid glass dissolution. This suggests that sauconite occurred metastably in at least some experiments.

Sauconite persisted as the major solid product for up to 33 days at 200°C in some runs. However, when the solution was then replaced daily with distilled water, sauconite was converted to hemimorphite within three days. This shows that sauconite is not a congruently saturating phase (see Ref. 12), but it still could be stable at high silica and/or alkali activities.

(b) *Hydrothermal reactions between ZnO and $SiO_2$*

These experiments were intended to clarify the occurrence of sauconite; results are summarized in Table 2.

(i) *Occurrence of willemite.* Willemite was the sole product of reaction of a 2:1 mole ratio of ZnO and quartz in water at 225°C for 1 week. A similar reaction at 175°C yielded hemimorphite, with traces of willemite and residual starting materials. These results indicate that the equilibrium water partial pressure curve for reaction (1) intersects the water vapor pressure curve near 200°C, which is consistent with reported data at higher pressures.[1,2]

(ii) *Occurrence of hemimorphite.* This phase occurred in 29 of 30 experimental runs with ZnO and quartz or fused silica in aqueous solutions at 150°C. It was the only zinc silicate formed in all runs with quartz, and in reactions between ZnO, fused $SiO_2$ and distilled water. It was also formed in about 20

Table 1. X-ray diffraction data for synthetic sauconite and related solids

| | Synthetic Sauconite[a] | | Natural Sauconite[b] | | Montmorillonite[c] | |
|---|---|---|---|---|---|---|
| *hkl* | *d*,Å | *I*[e] | *d*,Å | *I*[e] | *d*,Å | *I*[e] |
| 001 | 18.0 | vs | 16.6 | 100 | 17.6 | 100 |
| 002 | 9.0 | s | 8.33 | 100 | 9.00 | 50 |
| 003 | 6.1 | vw? | (5.41?) | 50b[j] | 5.99 | 10 |
| 110 etc. | 4.6 | m,vb[f] | 4.60 | 100 | 4.49 | 80 |
| 005 | 3.62 | m | 3.34 | 75 | 3.58 | 40 |
| 006 | 3.0 | w,b?[g] | — | | 2.99 | 30 |
| 130 etc. | 2.6 | m,vb[i] | 2.62 | 75d | 2.57 | 40b |
| 220 etc. | | | 2.473 | | 2.242 | 10 |
| 009 | — | | — | | 1.989 | 5 |
| 240 etc. | 1.7 | w,vb | 1.753 | 10 | 1.699 | 20 |
| 060 etc. | 1.526 | m | 1.550 | 100 | 1.504 | 60 |

*a* Glycerol saturated, this work.
*b* Ethylene glycol saturated, JCPDS file card No. 8–444.
*c* Glycerol saturated sodium montmorillonite, JCPDS file card No. 12–219.
*e* b = broad, d = diffuse, m = medium, s = strong, v = very, w = weak.
*f* Peak at 4.6 Å with very broad asymmetric tail toward lower *d*.
*g* Obscured by hemimorphite peaks.
*i* Peak at 2.6 Å with very broad asymmetric tail toward lower *d*.
*j* Obscured by "Duco" band.

per cent yield from ZnO and quartz at 100°C for 1 week. In some reactions between ZnO and fused silica in alkaline solutions it occurred in association with sauconite.

(iii) *Occurrence of sauconite.* This phase was formed in several reactions between ZnO and fused silica in alkaline solutions (0.01 mol · dm$^{-3}$ $Na_2B_4O_7$ or NaOH; 0.1 mol · dm$^{-3}$ NaOH) at 150°C. It did not occur in corresponding reactions with quartz replacing fused silica. It usually occurred in association with hemimorphite, but was the sole zinc silicate formed in one reaction between 1.0 g of ZnO and 2.4 g of fused silica in 150 cm$^3$ of 0.1 mol · dm$^{-3}$ NaOH, unstirred, at

Table 2. Products of reactions among ZnO, $SiO_2$ and various aqueous solutions[a]

| $ZnO:SiO_2$ mole ratio | Solution (M = mol·dm$^{-3}$) | Temperature (°C) | Time (d) | Crystalline Products[b] |
|---|---|---|---|---|
| | | (A) *Reactions using quartz* | | |
| 2.0 | $H_2O$ | 225 | 7 | W |
| 2.0 | $H_2O$ | 175 | 7 | H (major)<br>Q,Z,W (minor) |
| 0.75 | $H_2O$ | 175 | 7 | H,Q (major)<br>Z (minor) |
| 0.75 | $H_2O$ | 150 | 7 | H,Q (major)<br>Z (minor) |
| 0.75 | $H_2O$ | 100 | 7 | Z,Q (major)<br>H (minor) |
| 0.62 | 0.01 M NaOH | 137 | 4 | H,Q (major)<br>Z (trace) |
| | | (B) *Reactions using fused* $SiO_2$ | | |
| 0.62 | $H_2O$ | 150 | 4 | H (major)<br>Z (trace) |
| 0.62 | $H_2O$ | 150 | 4 | H |
| 0.30 | $H_2O$ | 150 | 1 | Z,H (major) |
| | | | 7 | H |
| | | | 28 | H |
| 0.62 | 0.001 M NaOH | 150 | 4 | H |
| 0.62 | 0.01 M NaOH | 150 | 4 | H (major)<br>S (minor) |
| 0.62 | 0.01 M NaOH | 150 | 5,14 | S (major)<br>H (minor) |
| 0.62[c] | 0.01 M NaOH | 150 | 5 | S (major)<br>H (minor) |
| 0.62[d] | 0.01 M NaOH | 150 | 4 | H |
| 0.62 | 0.1 M NaOH | 150 | 5 | H (major)<br>S (minor) |
| 0.30 | 0.1 M NaOH | 150 | 1 | S (major)<br>Z (minor) |
| | | | 7,21 | S |
| 0.62 | 0.01 M LiOH | 150 | 4 | S (major)<br>H (minor) |
| 0.62[e] | 0.01 M $Na_2B_4O_7$ | 150 | 4 | S (major)<br>H (minor) |
| 0.62 | 0.005 M $Na_2SO_4$ | 150 | 4 | Z |

*a* Unless otherwise stated, reactions used 1.0 g ZnO and 175 cm$^3$ of unstirred solution

*b* H = hemimorphite, Q = quartz, S = sauconite, W = willemite, Z = ZnO

*c* 4.0 g ZnO, 4.8 g $SiO_2$, 700 cm$^3$ solution, stirred

*d* 0.5 g ZnO, 0.6 g $SiO_2$, 700 cm$^3$ solution, stirred

*e* Duplicated run.

150°C for seven days. Analysis of this material, which was contaminated with unreacted ZnO and $SiO_2$, indicated a sodium content of about 1 wt.%, compared with 1.5% expected for the ideal montmorillonoid composition $Na_{0.333}Zn_{2.833}Si_4O_{10}(OH)_2$. We conclude that sodium is probably an essential constituent of the sauconite prepared in these reactions.

(iv) *Interconversion of sauconite and hemimorphite.* Several experiments were run to try to determine the conditions of equilibrium (2) at 150°C.

$$\underset{\text{hemimorphite}}{17Zn_4Si_2O_7(OH)_2 \cdot H_2O} + 8Na^+ + 8OH^- + 62SiO_2 \rightleftharpoons \underset{\text{sauconite}}{24Na_{0.333}Zn_{2.833}Si_4O_{10}(OH)_2} + 14H_2O \qquad (2)$$

In the presence of fused silica at 150°C, hemimorphite persisted unchanged for 28 days in water, and for 7 days in 0.1 mol · $dm^{-3}$ NaOH. Sauconite also persisted in the presence of fused silica in 0.1 mol · $dm^{-3}$ NaOH for 21 days. Under somewhat more aggressive conditions—0.5 mol · $dm^{-3}$ NaOH at 175°C—both sauconite and hemimorphite reacted in the presence of fused silica to produce quartz and at least one unidentified phase. The latter did not correspond to any of the numerous sodium zinc silicates reported in Refs. 14–17. Kinetic limitations would thus not permit direct determination of the conditions of equilibrium (2). However, when a mixture of sauconite and hemimorphite (0.5 g total) was allowed to react with 0.1 mol · $dm^{-3}$ NaOH (700 $cm^3$) at 150°C for seven days, the solid product was pure hemimorphite. This supports our earlier deduction that sauconite is not a congruently saturating phase.

(c) *Deduction of stability relationships*

Although equilibrium relationships could not be determined, we can deduce certain limitations on the stability of sauconite, as shown in Fig. 1. This figure shows schematically the solubilities of the various solids, expressed as activities of aqueous $Si(OH)_4^\circ$ and $Zn(OH)_2^\circ$. Since the formation of ZnO, $SiO_2$ and hemimorphite from these two species does not involve net reaction of protons, these solubility lines are pH-independent. (The solubilities expressed as total Zn and/or Si concentrations are pH-dependent.) However, sauconite formation probably involves NaOH (e.g. reaction (2)), so the sauconite solubility line will move to the left with increasing $Na^+$ and $OH^-$ activities.

The horizontal and two vertical lines in Fig. 1 represent the solubilities of ZnO (Z), quartz (Q) and fused silica (F), respectively. The solubility limit of hemimorphite (H) is a line of slope −0.5. A parallel line at slightly higher solute activities represents the solubility of willemite (W). Lines H and W will approach one another with increasing temperature, and cross over at the hemimorphite + willemite + solution + vapour quadruple point near 200°C. The solubility of sauconite (S) is a line of approximate slope −1.4, the precise value depending on the exact stoichiometry.

Sauconite was formed from ZnO and fused silica in 0.01 mol · $dm^{-3}$ NaOH, so line S lies to the left of point *a* (Fig. 1) under these conditions. Since sauconite is not a stable saturating phase in 0.1 mol · $dm^{-3}$ NaOH, line S must lie to the right of point *b*. Our inability to produce sauconite from ZnO and quartz, even in alkaline solution, implies that conditions for sauconite nucleation are hard to achieve to the left of line *Q*, but does not impose definite limits on sauconite stability.

## CONCLUSIONS

Hemimorphite appears to be the only stable solid zinc silicate in the system ZnO–$SiO_2$–$H_2O$ at 150°C. Sauconite is stable with respect to ZnO and fused silica in 0.01 mol · $dm^{-3}$ NaOH at 150°C, but is probably metastable with respect to hemimorphite and quartz, even in NaOH solution. However, sauconite can be persistent, and its conversion to hemimorphite, even at 200°C, can be very slow.

The reaction of stoichiometric quantities of ZnO and $SiO_2$ in water provides convenient small-scale synthetic routes to hemimorphite (at 150–175°C) and willemite (at 225°C). It is very difficult to

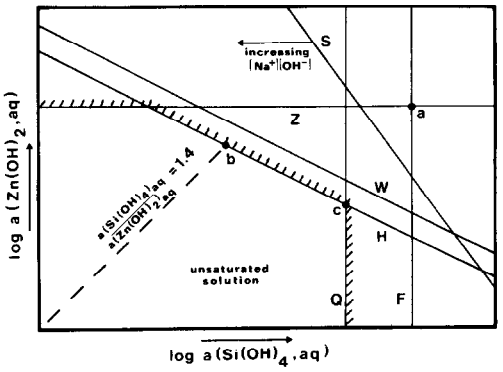



Fig. 1. Schematic representation of solubility relationships among solids in the system ZnO–$SiO_2$–$H_2O$ at 150°C, expressed as activities of $Zn(OH)_2^\circ$(aq) and $Si(OH)_4^\circ$(aq). F = fused $SiO_2$, H = hemimorphite, Q = quartz, S = Na-containing sauconite, S′ = Na-free sauconite, W = willemite, Z = zinc oxide. The hatched lines indicate equilibrium saturating solids.

prepare pure sauconite from ZnO and fused silica, but the best conditions are near 150°C, unstirred, in 0.1 mol · $dm^{-3}$ NaOH.

We reach the following tentative conclusions about hydrothermal alteration of a high-level radioactive waste product comprising a dilute solution of radionuclides in a zinc-containing sodium borosilicate glass:

(i) Crystallization of hydrated zinc silicates is likely to occur readily on exposure to water at 150–200°C, and probably also at lower temperatures.

(ii) Since these products are only loosely adherent on corroding glass surfaces, they are unlikely to aid passivation of the glass. Indeed, they could promote corrosion by providing a sink for dissolved Zn and Si close to the corroding surface.

(iii) The formation of sauconite is probably preferable to that of hemimorphite, since a montmorillonoid product is likely to have more desirable ion-exchange and solid-solution properties for the retention of some radionuclides. However, being metastable, sauconite is unlikely to persist indefinitely. In general, it may be possible to tailor radioactive waste glass compositions to promote their alteration to stable clay products, perhaps by addition of $Al_2O_3$.

## REFERENCES


1. D. M. Roy and F. A. Mumpton, *Econ. Geol.* 1956. **51**, 432.
2. C. W. F. T. Pistorius, *Neues Jahrb. Mineral. Monatsh.* 1963. 30.
3. C. S. Ross, *Am. Min.* 1946. **31**, 411.
4. M. Fleischer, *Am. Min.* 1961. **46**, 241.
5. B. W. Evans and R. G. J. Strens, *Nature* 1966. **211**, 619.
6. C. Frondel and J. Ito, *Am. Min.* 1966. **51**, 1107.
7. J. Esquevin, *Ann. Agron.* 1960. **11**, 497.
8. A. G. Merkulov and B. S. Khristoforov, *Tr. Soveshch. Eksp. Tekh. Mineral. Petrogr.*, 8th 1968, 322.
9. R. M. Barrer and W. Sieber, *J. Chem. Soc. Chem. Comm.* 1977, 905.
10. G. G. Strathdee, N. S. McIntyre and P. Taylor. *Proc. Int. Symp. on Ceramics in Nuclear Waste Management*, Cincinnati, Ohio, 1979 (CONF-790420), 243.
11. P. Taylor, T. E. Rummery and D. G. Owen, *J. Inorg. Nucl. Chem.* 1979. **41**, 1683.
12. P. Taylor and D. G. Owen, *J. Am. Ceram. Soc.* 1981. **64**, 360.
13. A. Findlay, A. N. Campbell and N. O. Smith, *The Phase Rule and its Applications*, pp. 346–349. Dover, New York (1951).
14. A. E. Holland and E. R. Segnit, *Aust. J. Chem.* 1966. **19**, 905.
15. B. N. Litvin, O. S. Tarasenkova and N. V. Belov, *Ocherki Fiz.-Khim. Petrol.* 1974. **4**, 89.
16. M. A. Simonov and N. V. Belov, *Vestn. Mosk. Univ. Ser. 4 Geol.* 1978. **3**, 56.
17. Powder Diffraction File, Joint Committee on Powder Diffraction Standards, Swarthmore, PA 19081, U.S.A.

*Polyhedron* Vol. 3, No. 2, pp. 157–160, 1984
Printed in Great Britain.

0277-5387/84 $3.00 + .00
© 1984 Pergamon Press Ltd.

# CATALYTIC ACTIVITY OF BINUCLEAR PLANAR COPPER(II) COMPLEXES FOR THE DECOMPOSITION OF HYDROGEN PEROXIDE

**NAOYASU OISHI, MASATAKA TAKEUCHI, YUZO NISHIDA* and SIGEO KIDA**

Department of Chemistry, Faculty of Science, Kyushu University 33, Fukuoka 812, Japan

(*Received* 2 *February* 1983; *accepted* 25 *July* 1983)

**Abstract**—Planar binuclear copper(II) complexes generally showed high catalytic activities for the decomposition of hydrogen peroxide compared with the relevant planar mononuclear copper(II) complexes. This result was explained on the assumption that the two-electron transfer occurs between $H_2O_2$ molecules via an intervening binuclear copper(II) complex.

We have been investigating the reactivities and the catalytic activities of the synthetic binuclear copper(II) complexes in the redox systems in order to elucidate the relationship between the functions and the structures of the Type-III copper ion in enzymes such as tyrosinase and laccase, etc. We already reported that planar binuclear copper(II) complexes generally show high reactivities in the redox reactions with ascorbic acid, catechol and N,N,N′,N′-tetramethyl-*p*-phenylenediamine, etc. compared with the relevant planar mononuclear copper(II) complexes, and pointed out the importance of the structural factors of the complexes participated in the reactions.[1-6]

It has been well known that the decomposition of hydrogen peroxide is catalyzed by various metal complexes, and catalytic activity of copper(II) complexes has been extensively studied.[7] Sigel *et al.* studied the catalytic action of copper(II)-ethylenediamine complex on the decomposition of hydrogen peroxide, and proposed a binuclear model as an intermediate complex.[8] In the biological systems hydrogen peroxide is most effectively decomposed by catalase, but some methemocyanins are also known to decompose hydrogen peroxide.[9,10] According to the recent work by Solomon *et al.*, methemocyanins of Molluscs can decompose hydrogen peroxide via the formation of an oxyhemocyanin.[11] Thus, we have assumed that in the methemocyanin-catalyzed decomposition of hydrogen peroxide a peroxide adduct with copper (II) ions of methemocyanin as depicted in Fig. 1(2) is formed as an intermediate which plays an important role in the catalytic reaction. In order to confirm our assumption, we have undertaken a model study of this reaction, using various types of synthetic copper(II) complexes as catalysts.

## EXPERIMENTAL

*Materials.* Copper(II) complexes used in this study, (D),[12] (E),[13] (F),[14] (G),[15] (H),[16] (I),[2] and (J)[17] (Fig. 2) were prepared according to the literature methods. Hydrogen peroxide (Nakarai Chemicals, Guaranteed Grade 30% in water) was obtained commercially.

Decomposition of $H_2O_2$ in the presence of a copper(II) complex. The solution (5 $cm^3$) of a copper(II) complex ($[Cu^{2+}] = 2 \times 10^{-4}$ mol $dm^{-3}$) was mixed with a $H_2O_2$ solution (5 $cm^3$, $[H_2O_2] = 1 \times 10^{-3}$ mol $dm^{-3}$) at 25°C, and the content of $H_2O_2$ was determined by the $Fe^{2+}$-$NH_4NCS$ method.[18]

*Measurements.* The absorption spectra were measured with a Shimazdu spectrophotometer model MPS-5000. The cyclicvoltammograms (in

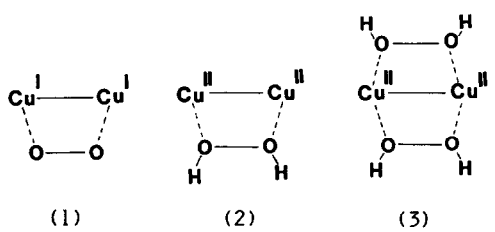



Fig. 1. Binuclear copper complexes with dioxygen molecule and/or hydrogen peroxide.

*Author to whom correspondence should be addressed.

dmf) of [Cu(m–cr)] $(ClO_4)_2$ and $[Cu_2(pc–1, 3)_2]$ were measured by the procedure as described in the literature.[19] The potentials were referenced to SCE, $E_{1/2}$ in Table 1 being calculated by the equation, $E_{1/2} = (E_{pc} + E_{pa})/2$.

## RESULTS AND DISCUSSION

Among the copper(II) complexes in Fig. 2, [Cu(m–cr)] $(ClO_4)_2$, $[Cu_2(dpl)_2]Cl_2$ and [Cu(me–ox)] $(PF_6)_2$ are soluble in water. Hence, the decomposition of hydrogen peroxide in the presence of these copper(II) complexes was investigated in an aqueous solution. Organic solvents were used in the cases of the other copper(II) complexes (see Table 1).

In Fig. 3, the spectral change (in water) of $(Cu_2(dpl)_2]^{2+}$ by the addition of hydrogen peroxide is shown. According to Murase *et al.*[15], $[Cu_2(dpl)_2]^{2+}$ shows two distinct absorption bands at 17,700 and 28,400 $cm^{-1}$, which were assigned to the *d–d* and charge-transfer bands, respectively. The charge-transfer band at 28400 $cm^{-1}$ is characteristic of the alkoxo-bridged binuclear copper(II) complexes,[14,20] thus it is clear that $[Cu_2(dpl)_2]^{2+}$ keeps the binuclear structure[21] in water. As shown in Fig. 3, little change was observed for the *d–d* and the charge-transfer bands, but a broad absorption centered at $22 \times 10^3$ $cm^{-1}$ appeared. Similar spectral changes were also observed for $[Cu_2(pia)_2]$ and $[Cu_2(et\text{-}2\text{-}3)_2]^{2+}$, etc. This fact implies that there exists some interaction between $H_2O_2$ and the binuclear copper(II) complexes. However, no spectral change was observed for [Cu(salen)], $[Cu(m–cr)]^{2+}$, [Cu(J–en)], $[Cu_2(me–ox)]^{2+}$ and $[Cu_2(sal\text{-}m\text{-}phen)_2]$ in the 10–27 $\times$ $10^3$ $cm^{-1}$ region.

The time course of the decomposition of $H_2O_2$ in the presence of $[Cu_2(dpl)_2]^{2+}$ is shown in Fig. 4, where the rate appears to be first-order with respect to $H_2O_2$. Similar experiments have been carried out by using various binuclear copper(II)

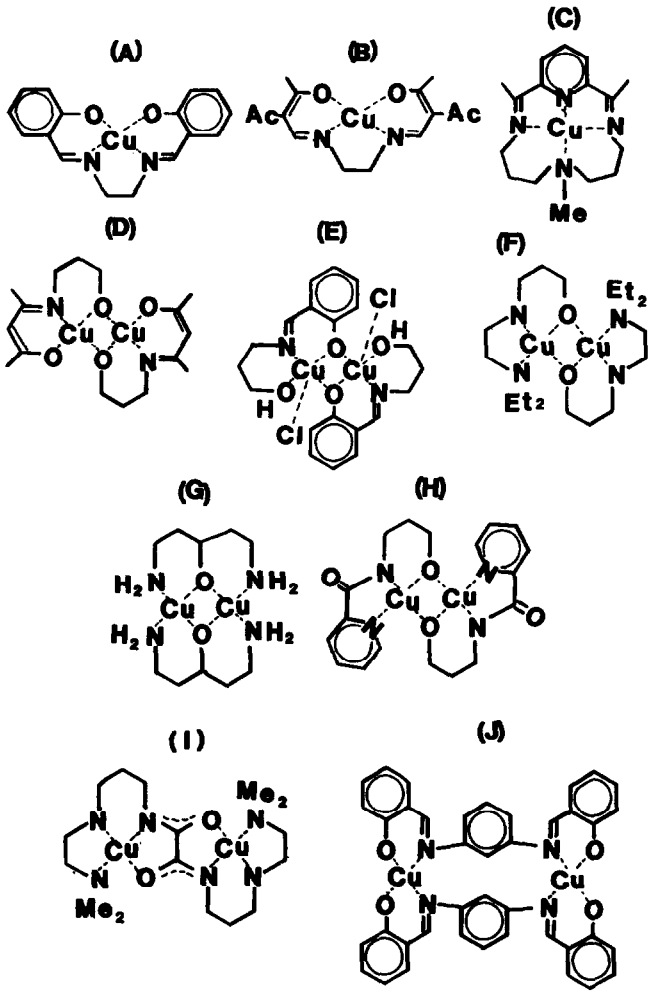



Fig. 2. Copper(II) complexes cited in this study and their abbreviations. (A) [Cu(salen)], (B) [Cu(J–en)], (C) $[Cu(m–cr)](ClO_4)_2$, (D) $[Cu_2(pia)_2]$, (E) $[Cu_2(salpa)_2]Cl_2$, (F) $[Cu_2(et–2–3)_2](ClO_4)_2$, (G) $[Cu_2(dpl)_2]Cl_2$, (H) $[Cu_2(pc–1, 3)_2]$, (I) $[Cu_2(me–ox)](PF_6)_2$, (J) $[Cu_2(sal–m–phen)_2]$.

Table 1. Catalytic activities for the decomposition of $H_2O_2$ and polarographic reduction potentials of the copper(II) complexes

| complex | catalytic activity for $H_2O_2$ decomposition (solvent) | $E_{1/2}$ (V vs SCE) |
|---|---|---|
| [Cu(salen)] | X (dmf) | -1.12[17] |
| [Cu(J-en)] | X ($CH_3OH$,dmf) | -1.09[4] |
| $[Cu(m\text{-}cr)]^{2+}$ | X ($H_2O$,$CH_3OH$,dmf) | -0.40[a] |
| $[Cu_2(pc\text{-}1,3)_2]$ | $t_{1/2}$ < 0.2 min.($CH_3OH$) | -0.96[a] |
| $[Cu_2(pia)_2]$ | $t_{1/2}$ ~ 1 min.($CH_3OH$) | -1.41[4] |
| $[Cu_2(dpl)_2]^{2+}$ | $t_{1/2}$ ~ 10 min.($H_2O$) | -0.79[25] |
| $[Cu_2(et\text{-}2\text{-}3)_2]^{2+}$ | $t_{1/2}$ < 0.5 min.($CH_3OH$) | -0.39[4] |
| $[Cu_2(salpa)_2]^{2+}$ | $t_{1/2}$ ~ 3 min.($CH_3OH$) | —— |
| $[Cu_2(me\text{-}ox)]^{2+}$ | X ($H_2O$,$CH_3OH$,dmf) | -0.69,-1.06[4] |
| $[Cu_2(sal\text{-}m\text{-}phen)_2]$ | X (dmf) | -0.70[17] |

X : practically inactive. $t_{1/2}$: half-life time of $H_2O_2$ in the presence of a copper(II) complex(1/10 of $H_2O_2$ in mole ratio) at 25°C.
a : this work.

complexes as well as mononuclear ones, and the results are summarized in Table 1. As seen in the table, the catalytic activities of the binuclear copper(II) complexes, except for $[Cu_2(me\text{-}cr)]^{2+}$ and $[Cu_2(sal\text{-}m\text{-}phen)_2]$, are much higher than those of the relevant mononuclear complexes.

The velocity of $H_2O_2$ decomposition in dmf solution is slower than that in methanol solution, however the trend observed for methanol solutions was similar to that observed in dmf solutions, i.e. $[Cu(m\text{-}cr)]^{2+}$ showed no catalytic function, whereas $[Cu_2(pia)_2]$ showed activity. In Table 1, the reduction potentials (in dmf) of the copper(II) complexes used in this study are summarized. These data indicated that there is no discrete correlation between the catalytic activity and the reduction potentials of the complexes. Similar results were obtained in the previous studies on the

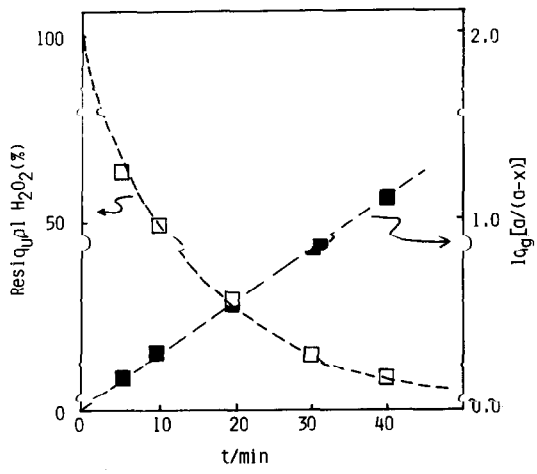



Fig. 4. Time course of the decomposition of $H_2O_2$ in the presence of $[Cu_2(dpl)_2]Cl_2$, and their $\log[a/(a-x)]$ plots, where $a$ and $x$ represent the initial and the decomposed quantities of $H_2O_2$, respectively.

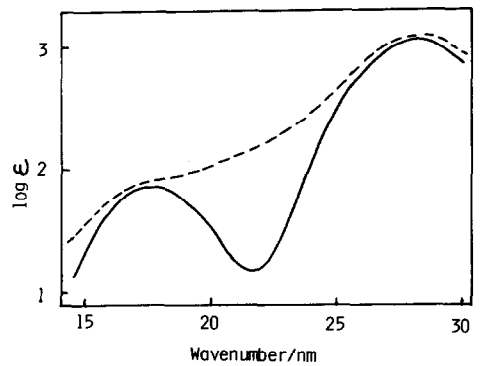



Fig. 3. Absorption spectra (in water) of $[Cu_2(dpl)_2]Cl_2$ (———). and $[Cu_2(dpl)_2]Cl_2 + H_2O_2$ (·--------·). ($[Cu^{2+}]/[H_2O_2] = 1/100$). Each spectrum was measured immediately after $H_2O_2$ was added to the copper(II) solution.

oxidation of ascorbic acid, 3,5-di-tert-butyl-catechol and N,N,N′,N′-tetramethyl-*p*-phenylenediamine.[2,4] All these results suggest that the structural factor is most important in the catalytic function of copper(II) complexes.

The decomposition of hydrogen peroxide is a redox-disproportionation. In Fig. 5, the reduction potentials concerning this reaction are illustrated. Based on the discussion by Fee[22] and our experimental results, we assume that the decompositon of hydrogen peroxide catalyzed by binuclear copper(II) complexes proceeds in the following steps: (1) the formation of a $H_2O_2$-adduct as depicted in Fig. 1(2), (2) approaching of another $H_2O_2$ molecule to the vacant site of the coordination plane

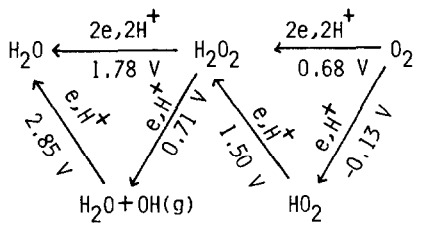



Fig. 5. Reduction potentials (V vs NHE)[24] concerning the reduction products of dioxygen molecule.

(see Fig. 1(3)), and (3) two-electron transfer between the $H_2O_2$ molecules through the copper atoms, where the electron-transfer between $H_2O_2$ and copper atoms is assumed to proceed in the inner-sphere mechanism.[23] The last step would be the rate-determinating step. This mechanism well explains the experimental results that planar binuclear copper(II) complexes with an appropriate Cu–Cu distance catalyze the reaction much better than the relevant mononuclear complexes. Thus, the very low catalytic activity of binuclear copper(II) complexes with a long Cu–Cu distance such as $[Cu_2(me\text{–}ox)]^{2+}$ and $[Cu_2(sal\text{-}m\text{-}phen)_2]$ can readily be understood.

## REFERENCES


1. Y. Nishida, N. Oishi and S. Kida, *Inorg. Chim. Acta* 1980, **46**, L69.
2. N. Oishi, Y. Nishida, K. Ida and S. Kida, *Bull. Chem. Soc. Jpn.* 1980, **53**, 2847.
3. N. Oishi, Y. Nishida and S. Kida, *Chem. Lett.* 1981, 1031.
4. Y. Nishida, N. Oishi, H. Kuramoto and S. Kida, *Inorg. Chim. Acta* 1982, **57**, 253.
5. M. Okamoto, N. Oishi, Y. Nishida and S. Kida, *Inorg. Chim. Acta* 1982, **64**, L217.
6. N. Oishi, M. Takeuchi, Y. Nishida and S. Kida, *Bull. Chem. Soc. Jpn.* 1982, **55**, 3747.
7. H. Sigel, *Angew. Chem. Internat. Edit.* 1969, **8**, 167.
8. T. Kadan and H. Sigel, *Helv. Chim. Acta* 1968, **51**, 947.
9. F. Ghiretti, *Arch. Biochem. Biophys.* 1956, **63**, 165.
10. G. Felsenfeld and M. P. Printz, *J. Am. Chem. Soc.* 1959, **81**, 6259.
11. R. S. Himmelwright, N. C. Eickman, C. D. LuBien and E. I. Solomon, *J. Am. Chem. Soc.* 1980, **102**, 5378.
12. J. A. Bertrand and J. A. Kelley, *Inorg. Chim. Acta* 1970, **4**, 203.
13. J. A. Bertrand, J. A. Kelley and J. L. Breese, *Inorg. Chim. Acta* 1970, **4**, 247.
14. Y. Nishida, F. Numata and S. Kida, *Inorg. Chim. Acta* 1974, **11**, 189.
15. I. Murase, M. Hatano, S. Ueno, M. Tanaka, H. Okawa and S. Kida, *Bull. Chem. Soc. Jpn.* 1982, **55**, 2402.
16. H. Ojima, *Nippon Kagaku Zasshi* 1967, **88**, 1056.
17. G. S. Patterson and R. H. Holm, *Bioinorg. Chem.* 1975, **4**, 257.
18. R. G. Thurman, H. G. Ley and R. Sholz, *Eur. J. Biochem.* 1972, **25**, 420.
19. M. Nakamura, H. Okawa and S. Kida, *Inorg. Chim. Acta* 1982, **62**, 201.
20. Y. Nishida and S. Kida, *J. Inorg. Nucl. Chem.* 1976, **38**, 451.
21. The crystal structural determination of $Cu_2(dpl)_2Cl_2$ was already reported. Y. Nishida and S. Kida, *Mem. Fac. Sci. Kyushu Univ. Ser. C*, 1981, **13(1)**, 35.
22. J. A. Fee, *Structure and Bonding*, Vol. 23, pp. 22–23. Springer-Verlag, Berlin (1975).
23. R. A. Holwerda, S. Wherland and H. B. Gray, *Ann. Rev. Biophys. Bioeng.* 1976, **5**, 363. It should be noted that in the cyclic voltammetry the electron-transfer between a metal ion and the electrode must involve an "outer-sphere mechanism", see *Mechanisms in Inorganic Reactions* (Edited by F. Basolo and R. G. Pearson), 2nd Edn, Chap 6. Wiley New York (1967).
24. *Kagakubinran*, (Edited by Chem. Society Japan, 2nd Edn, pp. 1204–1206. Maruzen, Tokyo (1975).
25. M. Mikuriya, M. Nakamura, H. Okawa and S. Kida, *Chem. Lett.* 1982, 839.

*Polyhedron* Vol. 3, No. 2, pp. 161–168, 1984
Printed in Great Britain.

0277-5387/84 $3.00 + .00
© 1984 Pergamon Press Ltd.

# ABSORPTION SPECTRA OF DYSPROSIUM COMPOUNDS IN NONAQUEOUS SOLUTIONS. SPECTRAL INTENSITY ANALYSIS

JANINA LEGENDZIEWICZ,* GRAŻYNA OCZKO and BARBARA KELLER
Institute of Chemistry, University of Wrocław, Wrocław, Poland

(*Received* 11 *April* 1983; *accepted* 25 *July* 1983)

**Abstract**—Absorption spectra of dysprosium compounds were measured in amides and $D_2O$ within the 5500–35000 $cm^{-1}$ region and in alcohols within the 7000–34300 $cm^{-1}$ region. The oscillator strengths of $f$–$f$ absorptions bands below 35000 $cm^{-1}$ were determined. The intensities of the $Dy^{3+}$ ground state absorption were analyzed according to the Judd–Ofelt theory of forced electric dipole transitions.

A good fit to the measurements was obtained with the intensity parameter given in Tables 4–6. The polarizability effect on the intensity of the $f$–$f$ transition with high value matrix elements $U^{(4)}$ and $U^{(6)}$ were considered.

Our hitherto spectroscopic investigations of lanthanide ions in nonaqueous solutions have proved not only the applicability of the Judd theory to those systems, but have provided also some insight into the nature of the so-called hypersensitive transitions that are extremely sensitive to the variations occurring in the immediate neighbourhood of the lanthanide ion.[1-9] From the intensity analysis, it was possible to determine the Judd parameters and fit the calculated values to the experimental ones. Up to the present, one has been faced with difficulties in the analysis of the $Pr^{3+}$, $Eu^{3+}$ and $Dy^{3+}$ spectra.[1,2,10-13] Since only for $Dy(NO_3)_3$ in the $LiNO_3$–$KNO_3$ eutectic was it possible so far to get a set of acceptable parameters,[10] we have started a study of dysprosium compounds in nonaqueous solvents in which the measurement range is as broad as that in $H_2O$ (alcohols) or even somewhat broader, particularly in the infrared spectral part. This was particularly important since an unsatisfactory approximation of the parameters may be due either to a low lying of the disturbing configurations of a different parity (e.g. $4f5d$) or to an erroneous experimental determination of the intensities of $f$–$f$ transitions, particularly of those of the hypersensitive transitions. On the other hand, however, the effect of the disturbing configurations of the $Dy^{3+}$ ion should not exceed that of the $Nd^{3+}$ ion.[14]

*Author to whom correspondence should be addressed.

*Analysis of the transition probabilities in the absorption spectrum*

Considerable progress has been made in the analysis of the energy level structure within the $4f^N$ configuration of trivalent lanthanide ions. Particularly, the assignment of transitions of the lanthanide aquoions in a broad range is helpful in the identification of the transitions and warrants the discussion of the intensities of transitions from the $J$ ground state to the excited $J'$ states.[11,14-16] The observed absorption bands are complex resulting from transitions to the levels of more than one excited state.

In the analysis of intensities it was assumed that the populations of all the crystal field components of the ground state are equalized.[15]

For the measurements, hydrated salts were used since, as proved previously by the results of studies on the anhydrous and hydrated lanthanide chlorides, the amide solvents eliminate water molecules from the first coordination sphere, so that in any case the lanthanide ion is solvated exclusively by the amide molecules (e.g. $LnCl_3$ and $LnCl_3 \cdot xH_2O$).[1,2] In alcoholic solutions, the methanol and ethanol molecules also remove water molecules from the coordination sphere, while in hydrated salts dissolved in propanol, the hydration waters may be partly maintained.[7,17]

The analysis of energy levels in spectra of the $Dy^{3+}$ ion in non-aqueous solutions was based both on data of the structure of levels $Ln^{3+}:LaF_3$[18] and on Carnall's data for spectra of the $Dy^{3+}$ aquoion.[11]

The analysis of intensities was carried on similarly as for previous investigations.[15]

From the experimentally measured oscillator strengths the values $\Omega_\lambda$ were calculated.

In accordance with the mechanism of energy absorption:

$$P_{exp} = \frac{8\pi^2 mc\sigma}{3he^2(2J+1)}(xS_{ED} + nS_{MD})$$

where

$$S_{ED} = e^2 \sum_{\lambda=2,4,6} \Omega_\lambda (\psi' J \| U^{(\lambda)} \| \psi' J')^2.$$

The $\Omega_\lambda$ are three quantities which are treated as parameters to be evaluated by an optimised fit to experimental data. The matrix elements of $U^{(\lambda)}$ employed here were the same as those for aquoion.[11]

## EXPERIMENTAL

The dysprosium compounds were obtained from $Dy_2O_3$ (Merck, 99.99%) by dissolving this oxide in the required acids and recrystallizing the salts from $H_2O$. Repeated crystallization of $Dy(ClO_4)_3 \cdot H_2O$ from heavy water led to the formation of $Dy(ClO_4)_3 \cdot D_2O$. The concentration of $Dy^{3+}$ was determined gravimetrically[19] and by titration with EDTA using xylenol orange as the end-point indicator.[20]

The solvents were purified as described previously.[1,2,5,7] The IR spectra of the purified DMF evidenced the absence of water, at least of considerable amounts of the latter. The refractive indexes of DMF, MFA, $CH_3OH$, $C_2H_5OH$ and $C_3H_7OH$ were $n_D^{25} = 1.4294$, $n_D^{25} = 1.4319$, $n_D^{25} = 1.329$, $n_D^{25} = 1.362$ and $n_D^{25} = 1.385$, respectively. The water contents in the alcohols did not exceed $10^{-4}$%.

The spectra were recorded with a "Cary 14" spectrophotometer within the 5500–35000 $cm^{-1}$ region. Appropriate solvents were used as standard liquids. Several different concentrations were studied for each dysprosium salts in each solvent. The refractive index at 25°C of the respective solutions are given in Table 1.

The reported oscillator strengths did not differ from those obtained for the other concentrations measured.

## RESULTS AND DISCUSSION

The absorption spectra of dysprosium perchlorate and nitrate in amide solvents are shown in Fig. 1.

In the figure, the absorption band centres of gravity as well as the energies used in the calculation of the $\Omega_\lambda$ parameters are marked.

The oscillator strength values of the bands attributed to $f$–$f$ transitions of the $Dy^{3+}$ ion, calculated by graphical integration, are given in Tables 2 and 3. In these tables, also the oscillator strength values, calculated from the Judd's equation by applying the estimated $\Omega_\lambda$ parameter values, are given.

There is a distinct intensity increase of the $f$–$f$ transitions for all the nonaqueous solutions compared with those obtained for $Dy(ClO_4)_3 \cdot xD_2O$ in $D_2O$. A considerable increase is observed in the intensity of the so-called hypersensitive band for which the matrix element $U^{(2)}$ assumes a high value, i.e. $^6H_{15/2} \rightarrow {}^6F_{11/2}$, $^6H_{9/2}$. Nevertheless, unlike the hitherto results obtained for the $Nd^{3+}$, $Ho^{3+}$ and $Er^{3+}$ ions, a considerable increase in intensity is observed also for the transitions for which the $U^{(2)}$ matrix element is different from zero and achieves a small value. Moreover, a significant intensity increase is observed also for the transitions for which the $U^{(4)}$ and $U^{(6)}$ elements have large values and $U^{(2)} = 0$ ($^6H_{15/2} \rightarrow {}^6F_{9/2}$, $^6H_{7/2}$; $^6H_{15/2} \rightarrow {}^6P_{7/2}$). The same applies to the bands in which those transitions overlap transitions with

Table 1. Refraction indices of the dysprosium salt solutions

| | DMF | | MFA | |
|---|---|---|---|---|
| $Dy(NO_3)_3 \cdot xH_2O$ | c=0.1129M | 1.4340 | c=0.1129M | 1.4358 |
| $DyCl_3 \cdot xH_2O$ | c=0.0925M | 1.4340 | c=0.0968M | 1.4352 |
| $Dy(ClO_4)_3 \cdot xH_2O$ | c=0.1139M | 1.4342 | c=0.1036M | 1.4328 |
| | $CH_3OH$ | $C_2H_5OH$ | n- $C_3H_7OH$ | |
| $DyCl_3 \cdot xH_2O$ | c=0.0502M | c=0.0498M | c=0.0496M | |
| | 1.3267 | 1.3596 | 1.3754 | |

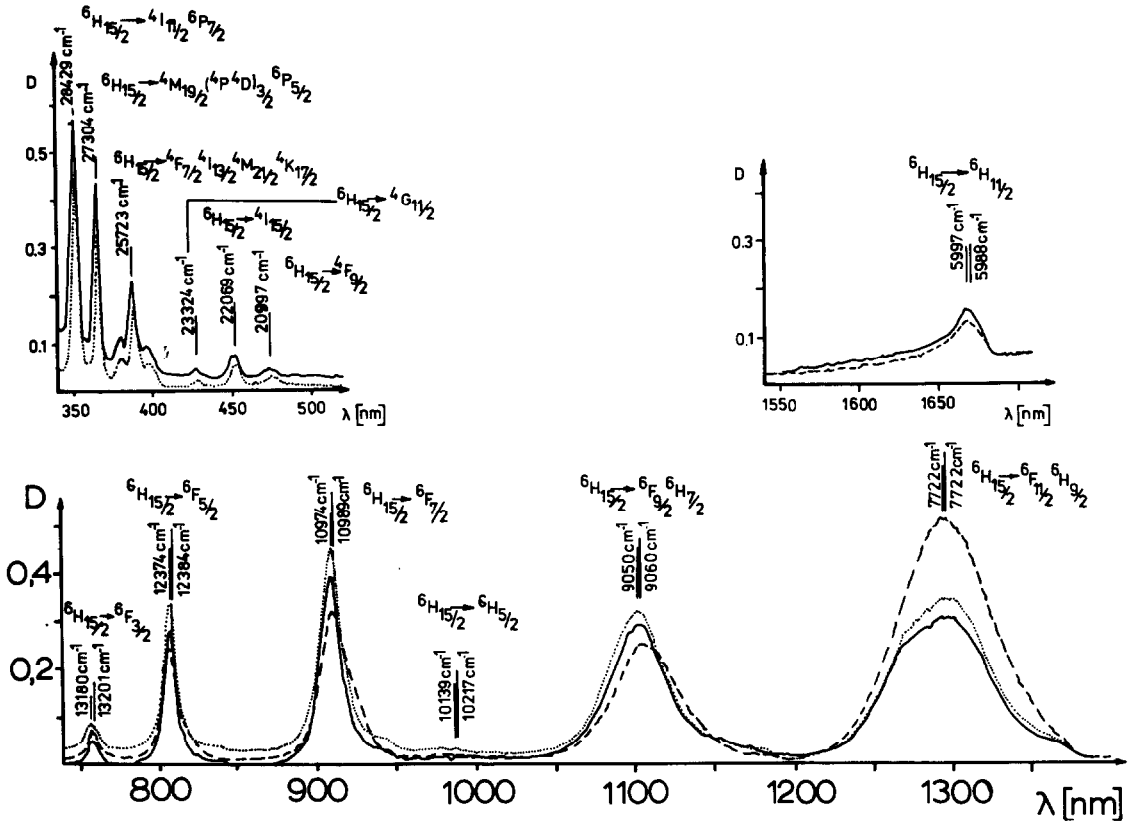



Fig. 1. Absorption spectrumof $Dy(ClO_4)_3 \cdot H_2O$ in MFA $c = 0.0541$ M $d = 2$ cm—; $Dy(ClO_4)_3 \cdot H_2O$ in DMF $c = 0.0543$ M $d = 2$ cm . . . ; $Dy(NO_3)_3 \cdot H_2O$ in DMF $c = 0.0543$ M $d = 2$ cm——; with identification of $4f$–$4f$ transitions.

$U^{(2)} \neq 0$. ($^6H_{15/2} \rightarrow {}^4F_{7/2}$, $^4I_{13/2}$ $^4M_{21/2}$ $^4K_{17/2}$). For the latters, the contributions from the individual transitions are difficult to estimate.

The values of the particular $\tau_\lambda$ parameters of the Judd's equation related to the $\Omega_\lambda$ parameters in the following way $\Omega_\lambda = (8\pi^2 mc\chi/3h)^{-1}\tau_\lambda = (1.085 \times 10^{11}\chi)^{-1}\tau_\lambda$ where $\chi = (n^2+2)^2/9n$ are collected in Tables 4–6.

Since the measurable range of the spectra of dysprosium nitrate in mono- and di-substituted amides ($28000\ cm^{-1}$) is narrower than those for the chlorides and perchlorates in amide and alcoholic solutions ($\sim 35000\ cm^{-1}$), the $\Omega_\lambda$ parameters for dysprosium chloride in alcohols were approximated taking into account all the transitions up to $32200\ cm^{-1}$ ($^4L_{19/2}$), while for the dysprosium salts in amide solvents, the transitions up to $28500\ cm^{-1}$ ($^6P_{7/2}$) were used (Tables 5 and 6, variant I). For the chloride and perchlorate, the transitions taken into account extend to the limit assumed for the alcoholic solutions (Tables 5 and 6, variant II).

It would be worthwhile noting that for $Dy^{3+}$ ion the first time the $\Omega_\lambda$ parameter values for alcoholic solutions were determined from experimental data with so high accuracy. In the spectra of the alcoholic solutions, the contribution of OH vibrations to the intensity in the IR range was successfully separated from that due to the $^6H_{15/2} \rightarrow {}^6F_{11/2}$, $^6H_{9/2}$ transition. Because of the intensity distribution of the $^4M_{19/2}$, $(^4P,^4D)_{3/2}$, $^6P_{5/2}$, $^4I_{11/2}$, $^6P_{7/2}$ bands, it seemed to be reasonable to attribute the intensity of the $^6H_{15/2} \rightarrow {}^4I_{11/2}$ transition to the band corresponding to $^6H_{15/2} \rightarrow {}^6P_{7/2}$. It improved considerably the fit of the calculated oscillator strength values, $P_{calc}$, to those obtained from experiment, $P_{exp}$ (Table 4–6, Variant III). The uncertainty in the parameter values is extremely small (Table 4). The calculations of the $\Omega_\lambda$ parameters repeated for the same spectral region of $Dy(ClO_4)_3 \cdot xD_2O$ in $D_2O$ resulted at the same identification in positive values with low errors (Table 6, variant IV). The $\tau_2$ parameter increases in the sequence $1.63 \pm 0.55$ in $D_2O$, $2.60 \pm 0.69$ in $CH_3OH$, $5.62 \pm 0.58$ in $C_2H_5OH$ and $10.54 \pm 0.49$ in $C_3H_7OH$. Of importance is the much higher increase in the $\tau_2$ parameter value and thereby in the $\Omega_2$ for heavy lanthanides[17] if compared with those for the light

Table 2. Oscillator strength values of $DyCl_3$ and $Dy(NO_3)_3$ in amide and alcohol solutions

| P x $10^8$ | $Dy(NO_3)_3 \cdot xH_2O$ | | | | $DyCl_3 \cdot xH_2O$ | | | | | | | | | |
|---|---|---|---|---|---|---|---|---|---|---|---|---|---|---|
| | MFA | | DMF | | MFA | | DMF | | $CH_3OH$ | | $C_2H_5OH$ | | n-$C_3H_7OH$ | |
| | c=0.1129M | | c=0.1129M | | c=0.0968M | | c=0.0925M | | c=0.0502M | | c=0.0498M | | c=0.0496M | |
| | $P_{exp}$ | $P_{cal}$ | $P_{exp}$ | $P_{cal}$ | $P_{exp}$ | $P_{cal}$ | $P_{exp}$ | $P_{cal}$ | $P_{exp}$ | $P_{cal}$ | $P_{exp}$ | $P_{cal}$ | $P_{exp}$ | $P_{cal}$ |
| $^6H_{11/2}$ | - | - | 54.9 | - | - | - | - | - | - | - | - | - | - | - |
| $^6F_{11/2}\,^6H_{9/2}$ | 497.3 | 500.4 | 814.2 | 816.6 | 490.7 | 497.9 | 681.1 | 686.7 | 324.2 | 326.4 | 416.1 | 415.3 | 663.2 | 664.5 |
| $^6F_{9/2}\,^6H_{7/2}$ | 434.6 | 549.7 | 409.4 | 469.4 | 456.6 | 604.0 | 259.3 | 357.1 | 225.1 | 261.3 | 155.4 | 192.0 | 181.2 | 220.1 |
| $^6H_{5/2}$ | 14.1 | 1.2 | 19.5 | 1.3 | 16.5 | 1.4 | 10.3 | 0.8 | - | - | - | - | - | - |
| $^6F_{7/2}$ | 390.1 | 432.1 | 363.9 | 413.5 | 403.2 | 482.9 | 220.9 | 273.9 | 174.4 | 201.0 | 145.3 | 140.3 | 154.2 | 162.0 |
| $^6F_{5/2}$ | 221.9 | 199.6 | 208.8 | 202.7 | 224.5 | 225.1 | 126.5 | 123.8 | 106.9 | 92.1 | 82.0 | 61.4 | 89.8 | 71.2 |
| $^6F_{3/2}$ | 47.1 | 37.6 | 42.2 | 38.2 | 45.8 | 42.4 | 25.9 | 23.3 | 19.0 | 17.5 | 13.2 | 12.4 | 14.9 | 13.0 |
| $^4F_{9/2}$ | 34.0 | 33.3 | 33.2 | 32.2 | 30.4 | 37.3 | 20.9 | 21.0 | | | | | | |
| $^4I_{15/2}$ | 70.0 | 69.3 | 83.5 | 80.0 | 64.5 | 77.2 | 62.1 | 51.0 | 56.3 | 57.0 | 45.9 | 44.4 | 63.0 | 55.3 |
| $^4G_{11/2}$ | 21.3 | 15.3 | 21.6 | 10.3 | 21.9 | 16.1 | 15.9 | 11.0 | | | | | | |
| $^4F_{7/2}\,^4I_{13/2}\,^4M_{21/2}\,^4K_{17/2}$ | 442.1 | 387.3 | 412.7 | 372.9 | 452.8 | 425.5 | 295.4 | 266.6 | 199.0 | 186.4 | 114.1 | 142.9 | 169.0 | 157.4 |
| $^4M_{19/2}\,(^4P,\,^4D)_{3/2}\,^6P_{5/2}$ | 412.4 | 297.4 | 382.8 | 293.4 | 447.6 | 332.6 | 246.7 | 185.5 | 153.0 | 137.4 | 118.9 | 93.4 | 140.0 | 109.1 |
| $^4I_{11/2}\,^6P_{7/2}$ | 712.7 | 679.4 | 452.1 | 434.4 | 760.6 | 717.8 | 495.2 | 467.7 | 344.1 | 344.4 | 291.0 | 276.9. | 322.0 | 311.3 |
| $(^4M,\,^4I)_{15/2}\,(^4F,\,^4D)_{5/2}\,^4I_{9/2}$ | | | | | 73.6 | 41.9 | 43.2 | 26.7 | 18.2 | 18.4 | 11.3 | 14.1 | 14.1 | 18.4 |
| $^4G_{9/2}\,^6P_{3/2}\,^4M_{17/2}\,(^4G,\,^4F)_{7/2}$ | | | | | 450.6 | 245.2 | 282.7 | 149.2 | 164.3 | 105.2 | 113.4 | 78.2 | 92.3 | 95.4 |
| $^4K_{15/2}\,^4L_{19/2}$ | | | | | | | | | | | | | | |
| Sx$10^7$ | 6.1 | | 4.5 | | 8.9 | | 5.7 | | 2.8 | | 2.4 | | 2.1 | |

Table 3. Oscillator strength values of $Dy(ClO_4)_3$ in $D_2O$ and amide solutions

| $P \times 10^8$ | $Dy(ClO_4)_3 \cdot xH_2O$ | | $Dy(ClO_4)_3 \cdot xH_2O$ | | | |
|---|---|---|---|---|---|---|
| | MFA | | DMF | | $D_2O$ | |
| | $c = 0.1036$ M | | $c = 0.1139$ M | | $c = 0.1033$ M | |
| | $P_{exp}$ | $P_{cal}$ | $P_{exp}$ | $P_{cal}$ | $P_{exp}$ | $P_{cal}$ |
| $^6H_{11/2}$ | — | — | 76.84 | — | 127.20 | — |
| $^6F_{11/2}{}^6H_{9/2}$ | 506.47 | 513.37 | 549.13 | 555.04 | 210.37 | 213.84 |
| $^6F_{9/2}{}^6H_{7/2}$ | 432.90 | 576.65 | 528.65 | 654.69 | 267.68 | 285.08 |
| $^6H_{5/2}$ | 3.19 | 1.30 | 24.62 | 1.51 | 14.27 | 1.04 |
| $^6F_{7/2}$ | 372.07 | 454.15 | 446.93 | 522.18 | 270.38 | 313.31 |
| $^6F_{5/2}$ | 217.03 | 210.12 | 245.56 | 242.99 | 151.77 | 168.45 |
| $^6F_{3/2}$ | 46.16 | 39.58 | 49.23 | 45.74 | 32.18 | 31.73 |
| $^4F_{9/2}$ | 36.40 | 35.00 | 37.25 | 40.22 | 17.89 | 24.74 |
| $^4I_{15/2}$ | 72.18 | 72.72 | 76.64 | 83.50 | 39.53 | 58.72 |
| $^4G_{11/2}$ | 20.40 | 15.86 | 20.26 | 17.54 | 13.20 | 1.26 |
| $^4F_{7/2}{}^4I_{13/2}$ | 413.04 | 404.60 | 459.34 | 461.01 | 235.26 | 244.09 |
| $^4M_{21/2}{}^4K_{17/2}$ $^4M_{19/2}(^4P, ^4D)_{3/2}$ $^6P_{5/2}$ | 424.68 | 311.55 | 463.12 | 358.74 | 235.41 | 234.67 |
| $^4I_{11/2}{}^6P_{7/2}$ | 748.50 | 704.71 | 819.26 | 780.49 | 413.95 | 413.56 |
| $(^4M, ^4I)_{15/2}$ $(^4F, ^4D)_{5/2}$ $^4I_{9/2}$ | 70.72 | 39.52 | 59.63 | 45.37 | 40.43 | 31.12 |
| $^4G_{9/2}{}^6P_{3/2}{}^4M_{17/2}$ $(^4G, ^2F)_{7/2}{}^4K_{15/2}$ $(^4D, ^4G)_{5/2}{}^4D_{1/2}$ $^4L_{19/2}$ | 452.49 | 231.79 | 481.38 | 265.26 | 314.62 | 157.15 |
| $S = 10^6$ | 0.91 | | 0.86 | | 0.51 | |

Table 4. The $\Omega_\lambda$ parameters for $DyCl_3$ in alcohols

| $\Omega_\lambda \cdot 10^{20}$ | $DyCl_3 \cdot xH_2O$ | | |
|---|---|---|---|
| | $CH_3OH$ | $C_2H_5OH$ | $n\text{-}C_3H_7OH$ |
| | c = 0.0502 M | c = 0.0498 M | c = 0.0496 M |
| $\Omega_2$ | 2.02 ± 0.54 | 4.27 ± 0.44 | 7.39 ± 0.37 |
| $\Omega_4$ | 2.69 ± 0.19 | 2.20 ± 0.20 | 2.42 ± 0.16 |
| $\Omega_6$ | 2.67 ± 0.25 | 1.74 ± 0.21 | 2.00 ± 0.18 |

lanthanides. The parameters for the heavy lanthanides decrease in the sequence *n*-$C_3H_7OH > C_2H_5OH > CH_3OH$ while for the light lanthanides they decrease in the sequence $C_2H_5OH > nC_3H_7OH > CH_3OH$. It is worthy of notice that the sequences do not change on going from $LnCl_3$ anhydrate to the corresponding hydrates and that the $\tau_2$ values almost do not change as well. Since the character of the alcohols remains constant, the variations observed must be caused by structural changes in the solvates formed possibilities of change of coordination number.

Table 5. The $\Omega_\lambda$ parameters for $DyCl_3$ and $Dy(NO_3)_3$ in amide solutions

| $\Omega_\lambda \cdot 10^{20}$ | | $Dy(NO_3)_3 \cdot xH_2O$ | | | | $DyCl_3 \cdot xH_2O$ | | | |
|---|---|---|---|---|---|---|---|---|---|
| | | MFA | | DMF | | MFA | | DMF | |
| | | c=0.1129 M | c=0.0565 M | c=0.1129 M | c=0.0564 M | c=0.0968 M | c=0.0520 M | c=0.0925 M | c=0.0522 M |
| I | $\Omega_2$ | 1.02±1.03 | 0.72±0.82 | 7.76±0.72 | 8.43±0.67 | 0.51±1.15 | 0.29±1.18 | 6.34±0.73 | 6.75±0.87 |
| | $\Omega_4$ | 5.15±0.45 | 4.92±0.35 | 3.26±0.31 | 3.30±0.30 | 5.51±0.50 | 5.55±0.51 | 3.62±0.32 | 3.58±0.38 |
| | $\Omega_6$ | 5.35±0.51 | 5.31±0.40 | 5.44±0.35 | 5.47±0.33 | 5.56±0.56 | 5.71±0.58 | 3.01±0.36 | 2.99±0.43 |
| II | $\Omega_2$ | | | | | 0.43±1.54 | 0.20±1.68 | 6.27±0.99 | 6.70±1.04 |
| | $\Omega_4$ | | | | | 5.45±0.67 | 5.47±0.73 | 3.57±0.43 | 3.55±0.46 |
| | $\Omega_6$ | | | | | 6.04±0.73 | 6.26±0.80 | 3.33±0.47 | 3.28±0.49 |
| III | $\Omega_2$ | 1.06±1.05 | 0.77±0.84 | 7.80±0.75 | 8.47±0.71 | 0.56±1.17 | 0.34±1.20 | 6.37±0.75 | 6.78±0.88 |
| | $\Omega_4$ | 5.07±0.46 | 4.84±0.37 | 3.18±0.33 | 3.22±0.31 | 5.43±0.52 | 5.47±0.53 | 3.57±0.33 | 3.54±0.39 |
| | $\Omega_6$ | 5.39±0.52 | 5.36±0.42 | 5.48±0.37 | 5.52±0.36 | 5.60±0.58 | 5.76±0.60 | 3.04±0.44 | 3.01±0.43 |
| IV | $\Omega_2$ | 4.00±1.19 | 3.17±0.90 | 9.33±1.02 | 10.03±0.93 | 3.73±1.37 | 3.39±1.49 | 8.43±0.87 | 9.08±1.10 |
| | $\Omega_4$ | 1.28±1.26 | 1.74±0.95 | 1.21±1.08 | 1.22±0.99 | 1.34±1.45 | 1.52±1.58 | 0.91±0.93 | 0.57±1.17 |
| | $\Omega_6$ | 6.53±0.52 | 6.28±0.39 | 6.06±0.44 | 6.11±0.41 | 6.83±0.60 | 6.94±0.65 | 3.84±0.38 | 3.91±0.48 |

The parameters $\Omega_\lambda$ determined from the dysprosium salt for spectra in amide solutions are given in Tables 5 and 6.

Since the IR measurement range for the amide solutions is broader than that for the alcoholic solutions, the DMF solutions were expected to be most suitable for the estimation of the oscillator strength of the hypersensitive $^6H_{15/2} \rightarrow {}^6F_{11/2}$, $^6H_{9/2}$ transition. In the latter solutions also the $^6H_{15/2} \rightarrow {}^6H_{11/2}$ transition may be observed. If the errors in determination of the $\Omega_\lambda$ parameters were caused only by the inaccuracy in determination of $P_{exp}$ for the hypersensitive transition, the deviations resulting from the spectra in DMF should be considerably smaller than those obtained from the spectra in alcoholic or MFA solutions. However, the measurement results contradict this expectation. The error in the $\Omega_\lambda$ parameters, calculated by assuming an identification identical with that used for alcoholic solutions, decreases only for $DyCl_3$ and $Dy(NO_3)_3$ in DMF (see Table 5, variant III). For the other solutions, the error varies insignificantly (see Tables 5 and 6, variant III).

Similarly to the $Nd^{3+}$, $Ho^{3+}$ and $Er^{3+}$ salts in the amide solvents studied previously, the variations in the $\Omega_2$ parameter values seem to be unaccountable. There is an odd change in the intensity of the $^6H_{15/2} \rightarrow {}^6P_{7/2}$ transition: for $DyCl_3$ and $Dy(NO_3)_3$ in DMF the intensity decreases twice in relation to $Dy(ClO_4)_3$ in the same solvent, although the intensity of the $^6H_{15/2} \rightarrow {}^4M_{19/2}$, $(^4P, {}^4D)_{3/2}$, $^6P_{5/2}$, $^4I_{11/2}$ band is reduced significantly only for the chloride. It may be presumed that the formation of innersphere complexes is accompanied by a change in symmetry resulting in a different intensity distribution of those two adjoining bands. The contribution to those bands of the $^6H_{15/2} \rightarrow {}^4I_{11/2}$ transition with a nonzero matrix element $U^{(2)}$ are difficult to estimate. If the $^6H_{15/2} \rightarrow {}^6P_{7/2}$ transition is not taken into account, all the $\Omega_\lambda$ parameters can be determined with the error which is not so satisfactory as it is in the case of the variant III but still is a satisfactory uncertainty (see Tables 5 and 6, variant IV). In accordance with the Mason's[21] dynamic coupling mechanism, and assuming as stated by Malta[22], that the contribution of transitions with large $U^{(4)}$ and $U^{(6)}$ values in the intensity of hypersensitive transitions is significant, this contribution being due only to the change in the polarizability but being independent of structural factors, the intensity variations become explicable since a replacement of solvent molecules by $Cl^-$ and $NO_3^-$ should result in a change in polarizability, (see Tables 2 and 3), since it is well-known that in DMF solvent are formed the inner-sphere complexes $[LnX\ Amid]^{2+}$ (where $X = Cl^-$, $NO_3^-$).

However the significant effect of those transitions on the $\Omega_2$ parameter value of dysprosium (see Tables 5 and 6) remains still obscure.

The attribution of the negative $\Omega_2$ values to the noticeable influence of the disturbing configurations of dysprosium, (e.g. $4f5d$), and assumption that the parameters of the low energy

POLY Vol. 3, No. 2—C

Table 6. The $\Omega_\lambda$ parameters for $Dy(ClO_4)_3$ in amide solutions and $D_2O$

| $\Omega_\lambda \cdot 10^{20}$ | | $Dy(ClO_4)_3 \cdot xH_2O$ | | | | |
|---|---|---|---|---|---|---|
| | | MFA | | DMF | | $D_2O$ |
| | | c = 0.1036 M | c = 0.0541 M | c = 0.1139 M | c = 0.0543 M | c = 0.1033 M |
| I | $\Omega_2$ | 1.07 ± 1.18 | 1.35 ± 1.21 | 1.11 ± 1.08 | 0.98 ± 1.51 | -0.77 ± 0.58 |
| | $\Omega_4$ | 5.23 ± 0.52 | 5.25 ± 0.54 | 5.46 ± 0.47 | 6.08 ± 0.65 | 3.08 ± 0.25 |
| | $\Omega_6$ | 5.28 ± 0.59 | 5.41 ± 0.60 | 6.06 ± 0.53 | 6.12 ± 0.75 | 3.65 ± 0.29 |
| II | $\Omega_2$ | 0.98 ± 1.60 | 1.27 ± 1.55 | 1.02 ± 1.53 | 0.80 ± 1.50 | -0.83 ± 1.10 |
| | $\Omega_4$ | 5.17 ± 0.70 | 5.18 ± 0.69 | 5.39 ± 0.67 | 5.77 ± 0.66 | 3.02 ± 0.48 |
| | $\Omega_6$ | 5.79 ± 0.77 | 5.88 ± 0.75 | 6.56 ± 0.73 | 6.64 ± 0.72 | 4.07 ± 0.53 |
| III | $\Omega_2$ | 1.06 ± 1.14 | 1.35 ± 1.16 | 1.05 ± 1.04 | 0.89 ± 1.02 | -0.80 ± 0.57 |
| | $\Omega_4$ | 5.36 ± 0.50 | 5.38 ± 0.51 | 5.57 ± 0.46 | 5.91 ± 0.45 | 3.12 ± 0.26 |
| | $\Omega_6$ | 5.17 ± 0.56 | 5.30 ± 0.58 | 5.96 ± 0.51 | 6.07 ± 0.51 | 3.62 ± 0.21 |
| IV | $\Omega_2$ | 4.41 ± 1.41 | 4.69 ± 1.50 | 3.59 ± 1.53 | 3.79 ± 1.28 | 1.26 ± 0.42 |
| | $\Omega_4$ | 0.90 ± 1.51 | 0.92 ± 1.59 | 2.25 ± 1.62 | 2.07 ± 1.36 | 0.45 ± 0.45 |
| | $\Omega_6$ | 6.61 ± 0.62 | 6.74 ± 0.65 | 7.04 ± 0.66 | 7.30 ± 0.56 | 4.46 ± 0.19 |

I to $^6H_{15/2} \rightarrow {}^6P_{7/2}$

II to $^6H_{15/2} \rightarrow {}^4L_{19/2}$

III to $^6H_{15/2} \rightarrow {}^4I_{11/2}$ $^6P_{7/2}$

IV to $^6H_{15/2} \rightarrow {}^4I_{11/2}$

levels of dysprosium can be determined most reliably,[13] is contradicted by the calculations for alcoholic solutions and seems therefore to be unacceptable.

## REFERENCES


1. K. Bukietyńska and J. Legendziewicz, *Rocz. Chemii* 1973, **47**, 1809.
2. J. Legendziewicz, K. Bukietyńska and B. Jeżowska-Trzebiatowska, *Acta Phys. Hung.* 1974, **35**, 167.
3. J. Legendziewicz, K. Bukietyńska, Z. Bajsarowicz and B. Jeżowska-Trzebiatowska, *Ibid.* 1975, **39**, 149.
4. B. Keller, K. Bukietyńska and B. Jeżowska-Trzebiatowska, *Bull. Acad. Polon. Sci.* 1976, **24**, 763.
5. J. Legendziewicz, K. Bukietyńska, Z. Kopaczyńska and B. Jeżowska-Trzebiatowska, *Optika i Spektroskopia* 1978, **45**, 288.
6. J. Legendziewicz, K. Bukietyńska, G. Oczko, S. Ernst and B. Jeżowska-Trzebiatowska, *Chem. Phys. Lett.* 1980, **73**, 576.
7. K. Bukietyńska, B. Jeżowska-Trzebiatowska and B. Keller, *Ibid.* 1981, **43**, 1065.
8. J. Legendziewicz, G. Oczko and W. Stręk, *Z. Naturforsch.* 1983, **38a**, 47.
9. J. Legendziewicz, B. Keller and W. Stręk, *Chem. Phys. Lett.* 1982, **92**, 205.
10. W. T. Carnall, J. P. Hessler and F. Wagner, Jr., *J. Phys. Chem.* 1978, **82**, 2152.
11. W. T. Carnall, D. R. Fields and K. Rajnak, *J. Phys. Chem.* 1968, **49**, 4412.
12. K. Bukietyńska and G. R. Choppin, *J. Phys. Chem.* 1970, **52**, 2875.
13. K. Bukietyńska and B. Radomska, *Chem. Phys. Lett.* 1981, **79**, 162.
14. W. T. Carnall, *Handbook on the Physics and Chemistry of Rare Earths.* North-Holland, Amsterdam (1976).
15. B. R. Judd, *Phys. Rev.* 1962, **127**, 750.
16. W. T. Carnall, P. R. Fields and K. Rajnak,, *J. Chem. Phys.* 1968, **49**, 4424.
17. B. Keller, Dissertation.
18. W. T. Carnall, H. Crosswhite and H. M. Crosswhite, *Energy Level Structure and Transition Probabilities of the Trivalent Lanthanides in* $LaF_3$. Chemistry Division Report Argonne National Laboratory, Argonne III (1977).
19. W. T. Hillebrandt and G. E. Lundell, *Applied Inorganic Analysis.* Wiley, New York (1953).
20. S. J. Lyle and M. Rahman, *Talanta*, 1963, **10**, 1177.
21. S. F. Mason, R. D. Peacock and B. Stewart, *Mol. Phys.* 1975, **30**, 1820.
22. O. L. Malta and G. F. de Sá, *Chem. Phys. Lett.* 1980, **74**, 101; *Phys. Rev. Lett.* 1980, **45**, 890.

*Polyhedron* Vol. 3, No. 2, pp. 169–173, 1984
Printed in Great Britain.

0277–5387/84 $3.00 + .00
© 1984 Pergamon Press Ltd.

# MÖSSBAUER STUDY OF PHOTOLYSIS AND γ-RADIOLYSIS OF ALKALI BIS(CITRATO) FERRATES(III)

**A. S. BRAR* and B. S. RANDHAWA**
Chemistry Department, Guru Nanak Dev University, Amritsar 143005, India

(*Received* 18 *April* 1983; *accepted* 16 *June* 1983)

**Abstract**—The photolysis of alkali bis(citrato) ferrates(III) $M_3Fe(cit)_2 \cdot xH_2O$ (M = Li, Na, K, Cs, $NH_4$) in solid and solution phases and γ-radiolysis in solid state has been investigated using Mössbauer and IR spectroscopic techniques. The formation of iron(II) species as the ultimate product in all these complexes has been observed except the solid state photolysis of potassium bis(citrato) ferrate(III) in which the intermediate iron(II) moiety is oxidized to an octahedral iron(III) species.

Recently Mössbauer spectroscopy has been extensively used to detect the change in oxidation state, bonding and local environment of the iron complexes, especially iron(III) carboxylates, during photolysis and radiolysis.[1–7] Buchanan[1] studied the solid state photolysis and γ-radiolysis of iron(III) citrate using Mössbauer spectroscopy and reported the formation of iron(II) citrate as the final product. The reduction of iron(III) to iron(II) species has also been observed during solid state radiolysis of iron(III) citrate, iron(III) lactate and iron(III) maleate using Mössbauer spectroscopy.[2] Frahn[8] studied the photolysis of iron(III) citrate in the liquid state using bright sunlight and reported the formation of iron(II) moiety as the end product. In the present investigation, our aim was to observe the effect of outer monovalent cations ($Li^+$, $Na^+$, $K^+$, $Cs^+$, $NH_4^+$) on the intermediates and products formed during photolysis (in solid and solution phases) and solid state γ-radiolysis using Mössbauer and IR spectroscopic techniques.

## EXPERIMENTAL

The methods of preparation and chemical analysis of alkali bis(citrato) ferrates(III) (Li, Na, K, Cs, $NH_4$) have already been reported.[9] For photoirradiation in the solid state, the finely powdered samples were exposed to medium pressure mercury lamp radiations in the UV and visible regions. For solution phase photolysis,[10] an acidic aqueous solution containing 90% of 0.15 mol $dm^{-3}$ complex solution and 10% of 1.0 N sulphuric acid was taken in a Pyrex glass reactor. The reaction solution was exposed to radiations from a 125 W medium pressure mercury lamp having intensity $7.07 \times 10^{17}$ quanta/sec. After a certain interval of time, 10 $cm^3$ of the irradiated solution was injected out of the reactor into a black painted beaker containing excess methanol to precipitate the irradiated product for Mössbauer study. For γ-radiolysis, the well powdered samples were irradiated at room temperature (25 ± 2°C) in the Frickle 2 KCi $^{60}Co$ irradiation chamber at the Chemistry Department, University of Poona, Pune (India). The samples were sealed in glass tubes in the presence of air and then subjected to a total dose of $10^8$ rads.

The experimental details of Mössbauer investigation have been reported in our earlier publications.[11,12] The values of isomer shift have been reported with respect to natural iron. All the spectra have been fitted to Lorentzian line shape using programme IBM 370/155, Fortran IV, University of Akron, U.S.A. and fitting procedures on ICL-2960 computer at I.I.T., New Delhi. The infrared spectra were recorded on MOM-2000 spectrophotometer (Hungarian Optical Works, Hungary) in the range 4000–700 $cm^{-1}$ using KBr pellet technique.

## RESULTS AND DISCUSSION

The Mössbauer spectra of alkali bis(citrato) ferrates(III) (Li, Na, Cs, $NH_4$) at room tem-

*Author to whom correspondence should be addressed. Present address: Chemistry Department, I.I.T. New Delhi 110016, India.

perature consist of a doublet. The isomer shift values (0.39–0.56 $mms^{-1}$) indicate these complexes be high spin (+ 3) oxidation state of iron while the quadrupole splitting values (0.59–0.65 $mms^{-1}$) show their distortion from the cubic symmetry. However, in case of potassium bis(citrato) ferrate(III) a single broad absorption band has been observed which is due to electronic-spin relaxation effect.[13] The Mössbauer parameters of these complexes are listed in Table 1.

(i) *Solid state photolysis*

In the cases of lithium bis(citrato) ferrate(III) hexahydrate, no significant change in the Mössbauer parameters has been observed up to 100 hr of irradiation. The Mössbauer spectrum of the lithium bis(citrato) ferrate(III) irradiated for a period of 150 hr (Fig. 1b) exhibits two quadrupole doublets, one with isomer shift and quadrupole splitting values of 1.21 and 2.60 $mms^{-1}$ respectively, indicating the formation of iron(II) citrate and the other doublet is due to the parent complex. The computer analysis of the spectrum has shown the percentage of iron(II) species to be 37.0. The reported values of isomer shift and quadrupole splitting for ferrous citrate obtained by the solid state photolysis of ferric citrate are 1.20 and 2.60 $mms^{-1}$ respectively.[2] For the sample irradiated for 200 hr, the Mössbauer spectrum shows significant increase in the value of quadrupole doublet due to iron(II) species (Fig. 1c) with isomer shift and quadrupole splitting values of 1.16 and 3.13 $mms^{-1}$ respectively. The higher value of quadrupole splitting compared to that of ferrous citrate indicates the formation of another iron(II) containing species due to some solid state reaction and which may be $LiFe^{II}$(cit). On further irradiation of the sample, the Mössbauer spectrum shows a significant increase and decrease in the intensities of the doublets due to iron(II) and iron(III) species respectively. The Mössbauer spectrum of the final photolysis product obtained by irradicating the sample for 600 hr, represents a quadrupole splitting values of 1.15 and 3.09 $mms^{-1}$ respectively indicating the complete reduction to iron(II) citrate, i.e. $LiFe^{II}$(cit). The IR spectrum does not show any significant change in the carboxyl stretching frequencies due to the presence of both citrate and acetone–dicarboxylate groups. The pattern of solid state photodecomposition of sodium bis(citrato) ferrate(III) pentahydrate is very similar to that of lithium derivative in which the reduction to iron(II) state also occurs after 150 hr of irradiation.

Thus the mechanism of photodecomposition of lithium and sodium bis(citrato) ferrates(III) in the solid state might be postulated as follows:

$$2M_3Fe^{III}(cit)_2 \xrightarrow[air]{h\nu} Fe^{II}_3(cit)_2 \rightarrow 2MFe^{II}(cit) + 2M_2(C_5H_4O_5) + 2CO_2 + H_2O \quad (M = Li, Na)$$

The decomposition of citrate ion into acetone-dicarboxylate ion, $(C_5H_4O_5)^{2-}$ during photolysis has been reported.[14]

In case of potassium bis(citrato) ferrate(III) tetrahydrate, the photoreduction starts after 200 hr of irradiation as indicated by the presence of a quadrupole doublet in the Mössbauer spectrum with isomer shift and quadrupole splitting values of 1.12 and 2.72 $mms^{-1}$ respectively, suggesting the formation of ferrous citrate. The presence of a broad absorption band in the spectrum is due to the parent complex. The Mössbauer spectrum of the sample irradiated for 300 hr exhibits two quadrupole doublets, one with isomer shift and quadrupole splitting values of 1.14 and 2.73 $mms^{-1}$ respectively, indicating the formation of ferrous citrate and the other doublet with isomer shift and quadrupole splitting values of 0.43 and 0.68 $mms^{-1}$ respectively due to a high spin octahedral iron(III) species. Similar obser-

Table 1. Mössbauer parameters of alkali bis(citrato) ferrate(III)

| Name of complex | Isomer Shift* ( $mm.s^{-1}$) | Quadrupole splitting ( $mm.s^{-1}$) |
|---|---|---|
| $Li_3Fe(C_6H_5O_7)_2.6H_2O$ | 0.41±0. 03 | 0.61±0.03 |
| $Na_3Fe(C_6H_5O_7)_2.5H_2O$ | 0.47±0.03 | 0.65±0.03 |
| $K_3Fe(C_6H_5O_7)_2.4H_2O$ | 0.35±0.03 | - |
| $Cs_3Fe(C_6H_5O_7)_23H_2O$ | 0.56±0.03 | 0.64±0.03 |
| $(NH_4)_3\ Fe(C_6H_5O_7)_2.\ 2H_2O$ | 0.39±0.03 | 0.59±0.03 |

* With respect to natural iron.

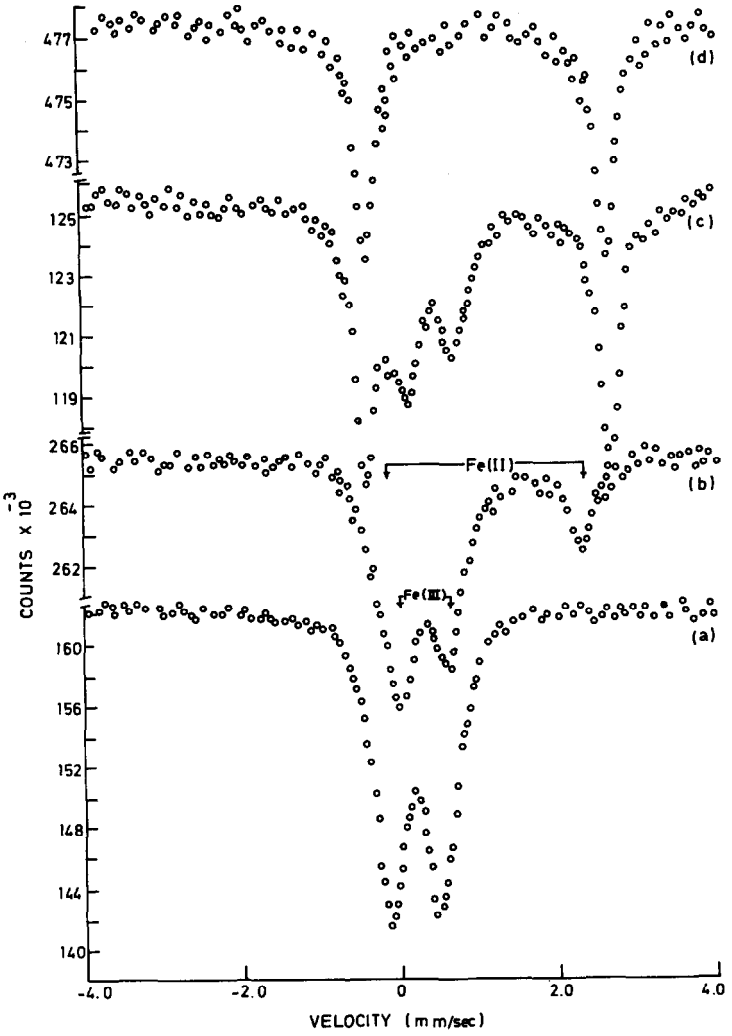



Fig. 1. Mössbauer spectra of lithium bis(citrato) ferrate(III) hexahydrate (a) unirradiated (b) irradiated for 150 hr (c) irradiated for 200 hr (d) irradiated for 600 hr.

vation has also been observed during solid state photolysis of potassium tris(oxalato) ferrate(III) trihydrate.[3] The computer analysis of the spectrum has shown the percentage of iron(II) and iron(III) species to be 47.0 and 53.0 respectively. On further irradiation the intensity of the doublet due to iron(II) citrate goes on decreasing while that of iron(III) species increase. The Mössbauer spectrum of the sample irradiated for 600 hr shows only an intense doublet indicating the complete oxidation of iron(II) citrate. The values of isomer shift (0.44 $mms^{-1}$) and quadrupole splitting (0.68 $mms^{-1}$) for the iron(III) species are in close agreement with the reported values for ferric citrate.[15] The IR spectrum of this sample shows a broad band at 1605 $cm^{-1}$ to asy(C=O) and bands at 1420 and 1380 $cm^{-1}$ due to sym(C=O) of the coordinated carboxylate groups of the citrate ligand.

On the basis of the above observations, the following mechanism for the solid state photolysis os potassium bis(citrato) ferrate(III) may be suggested:

$$K_3Fe^{III}(cit)_2 \xrightarrow[air]{h\nu} \text{ferrous citrate} \xrightarrow[air]{h\nu} \text{ferric citrate.}$$

The photoreduction of caesium bis(citrato) ferrate(III) trihydrate takes place after 300 hr of irradiation as indicated by the presence of two quadrupole doublets in the Mössbauer spectrum one with isomer shift and quadrupole splitting values of 1.15 and 2.52 $mms^{-1}$ respectively, indicating the formation of ferrous citrate and the other doublet is due to parent complex. No significant change in Mössbauer and IR parameters has been observed on further irradiation up to 600 hr. The trend of solid

state photolysis of ammonium bis(citrato) ferrate(III) dihydrate is similar to that of caesium derivative, but the reduction occurs after 200 hr of irradiation. The IR spectra of the irradiated products of these complexes does not show a considerable change compared to that taken for the unirradiated complexes due to the presence of both ferrous citrate and the parent complex.

The comparison shows that alkali bis(citrato) ferrates(III) are much less photosensitive compared to the alkali tris(oxalato) ferrates(III). The photo-decomposition for the latter is complete up to 200 hr of irradiation[12] while it starts after 150 hr of irradiation in the former. This may be due to the bulky and tridentate nature of citrate ligands relative to the bidentate oxalate ligands.

(ii) *Solution phase photolysis*

In case of lithium bis(citrato) ferrate(III) hexahydrate, the photoreduction starts after 45 min of irradiation as indicated by the presence of two quadrupole doublets in the Mössbauer spectrum, one with isomer shift and quadrupole splitting values of 1.12 and 2.63 $mms^{-1}$ respectively, indicating the formation of ferrous citrate and the other doublet is due to parent complex. No significant change in Mössbauer parameters has been observed on further irradiation of the sample. Thus only a partial reduction to iron(II) citrate takes place and the parent complex remains present in considerable amount during the course of photolysis and hence the IR spectrum does not show much difference from the parent complex. Similar observations have been observed in case of sodium bis(citrato) ferrate(III) pentahydrate, but it undergoes photo-reduction after 1 hr of irradiation.

The Mössbauer spectrum of unirradiated potassium bis(citrato) ferrate(III) tetrahydrate consists of a single broad absorption band but, however, the unirradiated sample obtained by the precipitation from the acidic solution by the addition of excess methanol, shows a doublet with isomer shift and quadrupole splitting values of 0.37 and 0.63 mm $s^{-1}$ respectively indicating the acidic sample to be high spin with distorted octahedral symmetry. Similar observations have been reported by Sato and Tominaga[3] during the course of photolysis of potassium tris(oxalato) ferrate(III) trihydrate in acidic solutions. The acidic complex undergoes photoreduction in the same way as has been observed in case of lithium and sodium bis(citrato) ferrates(III). The reduction to iron(II) state starts after 1 hr of irradiation as indicated by the Mössbauer spectrum.

The pattern of photodecomposition in case of caesium and ammonium bis(citrato) ferrates(III) is also similar to that of other alkali bis(citrato) ferrates(III). The reduction to iron(II) state starts after 60 and 45 min of irradiation in case of caesium and ammonium bis(citrato) ferrates(III) respectively.

The above observations reveal that the rate of photodecomposition is influenced by the outer alkali metal cations ($Li^+$, $Na^+$, $K^+$, $Cs^+$, $NH_4^+$) and is in the following order:

Lithium- $\approx$ ammonium- > Sodium-, Potassium- $\approx$ Caesium bis(citrato ferrates(III).

The comparison with alkali tris (oxalato)-ferrates(III) shows that the rate of photoreduction for alkali bis(citrato) ferrates(III) is much slower than that of the former in which the reduction to iron(II) state starts after 8–16 min of irradiation.[11] This may be due to greater ease of the removal of carbon dioxide from the bidentate oxalate group than that of the bulky tridentate citrate group.

(iii) *Solid state radiolysis*

The Mössbauer spectrum of radiolysed sample of lithium bis(citrato) ferrate(III) hexahydrate consists of two quadrupole doublets one with isomer shift and quadrupole splitting values of 1.18 and 2.63 mm $s^{-1}$ respectively, indicating the formation of ferrous citrate[2] and the other doublet is due the parent complex. Since the parent complex is present in significant amount, the IR spectrum of the radiolysed sample is similar to that taken for the unirradiated sample. The similar trend has been observed in other alkali bis(citrato) ferrates(III). The Mössbauer spectrum of radiolysed sample of potassium bis(citrato) ferrate(III) exhibits a single broad absorption band due to the parent complex and a quadrupole doublet with isomer shift and quadrupole splitting values of 1.15 and 2.75 mm $s^{-1}$ due to ferrous citrate.

Thus the end product of $\gamma$-radiolysis, i.e. ferrous citrate for all the alkali bis(citrato) ferrates(III) is the same. These results are similar to that of alkali tris(oxalato)ferrates(III) in which ferrous oxalate is formed as the ultimate radiolysis product except in case of potassium tris(oxalato) ferrate(III) where iron(III) species is formed via the oxidation of iron(II) intermediates.[16]

*Acknowledgement*—One of the authors (B.S.R.) wishes to express his sincere thanks to the Council of Scientific and Industrial Research, New Delhi for the financial assistance.

## REFERENCES

1. D. N. E. Buchanan, *J. Inorg. Nucl. Chem.* 1970, **32**, 3531.

2. N. Saito, T. Tominaga and T. Morimoto, *J. Inorg. Nucl. Chem.* 1970, **32**, 2811.
3. H. Sato and T. Tominaga, *Bull. Chem. Soc. Japan* 1979, 52, 1402.
4. N. Saito, H. Sano, T. Tominaga and F. Ambe, *Bull. Chem. Soc. Japan* 1965, **38**, 681.
5. A. Sugimori, *Bull. Chem. Soc. Japan* 1966, **39**, 2583.
6. A. A. Temperley and D. W. Pumplin, *J. Inorg. Nucl. Chem.* 1969, **31**, 2711.
7. G. M. Bancroft, K. G. Dharmawardena and A. G. Maddock, *J. Chem. Soc.* (*A*), 1969, 2941.
8. J. L. Frahn, *Australian J. Chem.* 1958, **11**, 399.
9. A. S. Brar and B. S. Randhawa, *J. De Physique* (Communicated).
10. J. G. Calvert and J. N. Pitts, *Photochemistry*, p. 784. Academic Press, New York (1967).
11. A. S. Brar and B. S. Randhawa, *Radiochem. Radioanal. Lett.* 1981, **47**, 219.
12. A. S. Brar and B. S. Randhawa, *Bull Chem. Soc. Japan* 1981, **54**, 3166.
13. M. Blume, *Phys. Rev. Lett.* 1965, **14**, 96.
14. H. S. Fry and E. G. Gerwe, *Ind. Eng. Chem.* 1928, **20**, 1392; *Chem. Abs.* 1929, **23**, 1058.
15. J. J. Bara, K. Krolas and T. Matlak, *Applications of Mössbauer 'Effect'*, p. 769. Academia Kiado, Budapest (1971).
16. B. S. Randhawa, A. S. Brar and T. K. Bansal, *Radiochem. Radioanal. Lett.* 1982, **53**, 359.

*Polyhedron* Vol. 3, No. 2, pp. 175–181, 1984
Printed in Great Britain.

0277–5387/84 $3.00 + .00
© 1984 Pergamon Press Ltd.

# STOICHIOMETRIC HYDROGENATION OF THE HETEROBIMETALLIC (α-ALKYNYL) COMPLEX $[\mu(1\text{–}\sigma, 2\text{–}3\eta^2\text{–}H_2C\text{–}C\equiv C\text{–}CH_3)][(CO)_3Fe\text{–}Co(CO)_3]$

SILVIO AIME, MARIO CASTIGLIONI, ROBERTO GOBETTO and DOMENICO OSELLA*
Istituto di Chimica Generale ed Inorganica dell'Università, Corso Massimo d'Azeglio 48, 10125 Torino, Italy

(*Received* 4 *May* 1983; *accepted* 21 *June* 1983)

**Abstract**—The title compound reacts with molecular hydrogen at 60°C giving rise to the homometallic complexes $Fe(CO)_5$ and $Co_2(CO)_8$, and a very rich mixture of gaseous hydrocarbons (e.g. butenes from partial hydrogenation, butane from total hydrogenation and methane and propene from selective hydrogenolysis of the organic chain).

The influence of concentration of the title complex, and partial pressure of hydrogen or carbon monoxide on the hydrogenation rate have been investigated. Although an unequivocal mechanism cannot be ascertained from the kinetic data owing to the complexity of the reaction, the pattern of products strongly indicates that the σ-interaction between the iron atom and the organic chain is preserved in the transition state.

Muetterties[1] has investigated the hydrogenation of alkynes coordinated to transition metal compounds. For alkyne-dimetal complexes, the most common structural feature is the acetylene moiety bridging the two metal atoms in a crosswise manner, so that the $M_2C_2$ framework describes a tetrahedron (Fig. 1). This kind of bonding scheme (namely $\mu_2\text{–}\eta^2$) has been established for $[Mo_2Cp_2(CO)_4(RC\equiv CR)]$[2], $[Fe_2(CO)_6(RC\equiv CR)]$[3], $[Co_2(CO)_6(RC\equiv CR)]$[4], $[Ni_2Cp_2(RC\equiv CR)]$[5], $[Ni_2(COD)_2(RC\equiv CR)]$[6] and $[CoNiCp(CO)_3(RC\equiv CR)]$[7] complexes. In all these binuclear complexes the triple bond has been reduced upon coordination as confirmed by the C–C bond lengthening (beyond 1.30Å). Muetterties[1] pointed out that this bond order reduction should be sufficient to activate the acetylene for hydrogenation. The reactivity towards hydrogen should depend on the energy barrier required to reach an "unsaturated" transition state. Indeed, among the isostructural $\mu_2\text{–}\eta^2$ alkyne complexes, only the class of coordinatively unsaturated species, i.e. $Fe_2(CO)_6(RC\equiv CR)$ and $Ni_2(COD)_2(RC\equiv CR)$, reacts with hydrogen under mild conditions of temperature and pressure.[8]

Within the class of coordinatively saturated complexes, the $Mo_2Cp_2(CO)_4(RC\equiv CR)$ compound has been shown to undergo hydrogenation under more forcing conditions and the first step has been suggested to involve CO ligand dissociation.[9] Available data are briefly reported in Table 1.




Fig. 1. $M_2C_2$ tetrahedral framework.

Apart from the case of $Fe_2(CO)_6(Bu^t\text{–}C\equiv C\text{–}Bu^t)$, for which an explanation in terms of the character of the L.U.M.O. has been sought,[8] *cis*-olefin is the invariable product of these hydrogenation. Muetterties[11] again rationalized this selectivity suggesting that the intermediate (not always precisely defined) stereochemically requires *cis*-addition of hydrogen and then the *cis*-olefin is expelled as it is formed, so no isomerization to *trans*-olefin, no further hydrogenation to alkane can take place in spite of these products being thermodynamically favoured.

We have recently synthesized and characterized the heterobimetallic iron-cobalt *a*-alkynyl complexes $[FeCo(CO)_6(R_2C\text{–}C\equiv CR')]$.[12] Their bonding scheme is strictly related to the $\mu_2\text{–}\eta^2$ one: the triple bond $C^2\equiv C^3$ lies over and perpendicular to the

*Author to whom correspondence should be addressed.

Table 1. Reported results of stoichiometric hydrogenation of $\mu_2$–$\eta^2$ alkyne-dimetal complexes (Cp = cyclopentadienyl; COD = 1,5 cyclooctadiene)

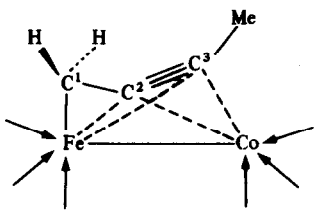
| Complex | Temperature (°C) | Reaction time (h) | $P_{H_2}$ (torr) | hydrogenation products | Ref. |
|---|---|---|---|---|---|
| $Fe_2(CO)_6(^tBuC_2Bu^t)$ | 20 | 2 | 1200 | trans-olefin (90%) cis-olefin (10%) | 8 |
| $Ni_2(COD)_2(PhC_2Ph)$ | 20 | 1 | 400 | cis-olefin | 8 |
| $Mo_2Cp_2(CO)_4(EtC_2Et)$ | 150 | 2 | 760 | cis-olefin | 9 |
| $Co_2(CO)_6(PhC_2Ph)$ | 60 | 168 | 500 | none | 8 |
| $CoNiCp(CO)_3(PhC_2Ph)$ | 80 | - | 1200 | none | 8 |
| $Ni_2Cp_2(PhC_2Ph)$ | 80 | - | 1200 | none | 8 |
| $Ni_2Cp_2(PhC_2Ph)$ | 150 | 12 | 760 | none | 10 |

Fe–Co bond while the $C^1$ atom $\sigma$-interacts with the iron (Fig. 2). The presence of this $\sigma$-interaction has been further corroborated by obtaining a racemate when a prochiral acetylene is employed, i.e. $[FeCo(CO)_6(RR'C^*–C{\equiv}CR'')]$.[13] These complexes are coordinately saturated because the organic chain acts as an overall 5-electron donor. This unique bonding feature prompted us to study the reactivity of the simplest of these compounds, namely $[FeCo(CO)_6(H_2C–C{\equiv}C–CH_3)]$ **1** towards molecular hydrogen under mild conditions. The results of the stoichiometric hydrogenation of complex **1** are reported herein.

## EXPERIMENTAL

### *Material*

Toluene was distilled from sodium, stored on 4 A molecular sieve and saturated with dry nitrogen prior to use. Hydrogen, carbon monoxide, 1-butene, *cis*-2-butene, *trans*-2-butene and *n*-hexane were C. Erba pure grade, $Fe(CO)_5$ and $Co(CO)_8$ were purchased from Strem Chemical Co. and used without further purification. $[FeCo(CO)_6(H_2C–C{\equiv}C–CH_3)]$ **1** was synthesized according to previously reported procedures[12], its purity was checked by IR and MS spectroscopy.




(1)

Fig. 2. Structure of bimetallic complex **1**.

### *Analyses*

Separation of reaction solutions was performed by tlc (absorbent Kieselgel PF Merck, eluent light petroleum and 5% diethyl ether). Elemental analysis of the metallic residue was carried out with a Perkin–Elmer 303 Atomic Absorption Spectrophotometer. Infrared spectra were recorded on a Perkin–Elmer 580 B instrument, using matched 0.5 mm NaCl cells, and mass spectra on a Hitachi Perkin–Elmer RMU–6H.

### *General procedure*

Complex **1** was chosen among the several heterobimetallic iron–cobalt $\alpha$-alkynyl compounds because it gives the simplest mixture of hydrocarbons. An unique toluene standard solution was prepared (150 $cm^3$, 0.05 M) from which all the others were obtained by dilution. All the solutions were saturated with nitrogen and added with an appropriate amount of *n*-hexane as internal standard for gc measurements.

Required volumes (2 $cm^3$) of toluene solutions of complex **1** were introduced into glass vials (estimated volume of 75 $cm^3$) equipped with a gc septum. The vials were connected to a vacuum line, degassed by three freeze–pump–thaw cycles, filled with the desired gas mixture and finally sealed hermetically. The ampoules were placed in a thermostatic bath at $+60.0 \pm 0.2$°C. Sample of the gases above the reaction solution were withdrawn at regular intervals by a syringe and analyzed quantitatively on a C. Erba 4200 FID gas chromatograph with a 2m × 4mm column filled with *n*-octane (porosil C 100/120 mesh) using $N_2$ as carrier gas, 25 $cm^3$/min.

The reactant solutions were checked by tlc and IR spectroscopy.

*Blank tests*

A large ampoule equipped with a gc septum was connected to a vacuum line and filled with 1-butene, *cis*-2-butene and *trans*-2-butene in molecular ratio *ca.* 1 : 1 : 1 (checked by gc analysis) up to a total pressure of 760 Torr. Required volumes of this $C_4H_8$ gaseous mixture were transferred to the vials by a syringe through the gc septa.

*Complex* **1** *as isomerization catalyst.* A toluene solution of complex (1) (0.025 M, 2 $cm^3$) was sealed in a vial under 760 torr of nitrogen and added with 1 $cm^3$ (0.04 mmol) of the $C_4H_8$ gaseous mixture. The vial was kept at 60°C for 1 day, gc analysis showed no change in hydrocarbon composition within the experimental error.

*$FeCO)_5$ as catalyst.* A toluene solution of $Fe(CO)_5$ (0.017 M, 2 $cm^3$) was sealed in a vial under 760 torr of hydrogen and added with 1 $cm^3$ of $C_4H_8$ mixture. The vial was kept at 60°C for 1 day, very little isomerization and no hydrogenation were detected by gc analysis.

$Co_2(CO)_8$ *as catalyst.* A toluene solution of $Co_2(CO)_8$(0.008 M, 2 $cm^3$) was prepared as above. After one day at 60°C moderate isomerization (1-butene = 9% *trans*-2-butene = 60% and *cis*-2-butene = 27%) and little hydrogenation (*n*-butane = 4%) had taken place. Tlc and IR analyses of the final solution showed the presence of $Co_4(CO)_{12}$ only.

*Metallic residue as catalyst.* The vials in which complex **1** underwent stoichiometric hydrogenation had a black metallic residue. One of these vials was opened under nitrogen atmosphere, the residue washed three times with fresh toluene and the vial sealed again under 760 Torr of hydrogen. 1 $cm^3$ of the $C_4H_8$ mixture was added and the ampoule kept for 1 day at 60°C. Very little isomerization and hydrogenation were detected.

## RESULTS AND DISCUSSION

The $[FeCo(CO)_6(H_2C–C{\equiv}CCH_3)]$ compound slowly reacted at 60°C with molecular hydrogen in a pressure range (190–760 Torr) giving rise to a very complex mixture of gaseous hydrocarbons. The most abundant components were butenes (up to 90%) deriving from partial hydrogenation of the organic moiety. A small amount of *n*-butane from total hydrogenation and hydrogenolysis products (mainly methane and propene in a rough molecular ratio 1 : 1 with traces of propane, ethane and ethylene) were found even at low conversion of the complex. Concomitant to the hydrogenation of the organic chain, complex **1** disproportionated to $Fe(CO)_5$ (established by MS spectrometry in gas phase) and $Co_2(CO)_8$. The latter promptly changed into $Co_4(CO)_{12}$ (checked by IR spectroscopy) especially in the absence of added CO.[14] A dark precipitate was always present at the end of all stoichiometric hydrogenations; elemental analyses established a mixture of iron and cobalt in an atomic ratio *ca.* 1:1. All the analytical data were in fair agreement with the following equations:

$$3FeCo(CO)_6(H_2C–C_2–CH_3) + 9/2H_2 \rightarrow 3C_4H_8 + 2Fe(CO)_5 + Co_2(CO)_8 + \downarrow[Fe,Co] \quad (1)$$

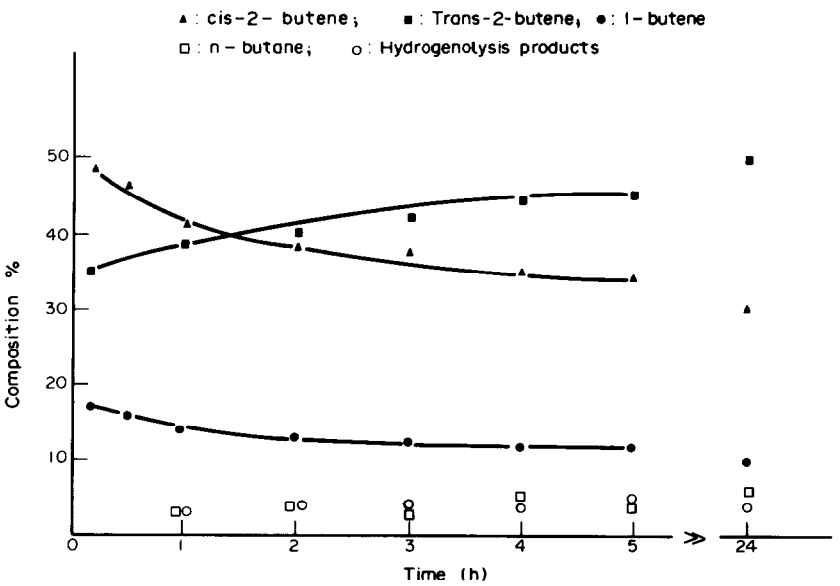



Fig. 3. Composition of hydrocarbon mixture during the stoichiometric hydrogenation of complex **1** (60°C; [**1**] = 25.0 mM; $P_{H_2}$ = 360 Torr).

$$2Co_2(CO)_8 \rightleftarrows Co_4(CO)_{12} + 4CO. \quad (2)$$

Figure 3 shows the composition of the hydrocarbon mixture as a function of the reaction time at 60°C under 360 Torr of hydrogen. At very low conversion of complex **1**, *cis*-2-butene was the most abundant $C_4H_8$ isomer (48%), but interestingly this reaction was not so stereoselective as generally found for $\mu_2$-$\eta^2$ alkyne–dimetal complexes.[8,9] Furthermore during the course of hydrogenation, the butene isomers smoothly changed their ratio, but the thermodynamic equilibrium value, calculated from free energies of formation[15] was not achieved even after 24 hr.

The amount of hydrogenolysis products (mainly $CH_4$ and $CH_2$=CH–$CH_3$) was constant within experimental error, while that of *n*-butane slowly increased up to 10%. Blank runs gave some insight into this puzzle of concomitant reactions. Complex **1** was not able to catalyze the isomerization process, on the contrary the reaction products, mainly $Co_2(CO)_8$,[16] in the concentration suggested by eqn (1), act as catalysts for isomerization and, less effectively, for hydrogenation of the gaseous hydrocarbon mixture. This behaviour accounts for the change in olefinic distribution and the increase of alkane yield during the course of the reaction. The variation of complex **1** concentration (12.5–50.0 mM) does not change the composition of hydrocarbon mixture, the increase in hydrogen pressure (190–760 Torr) enhanced the *n*-butane yield but did not substantially alter the $C_4H_8$ ratio. The presence of CO added or the use of deuterium in place of hydrogen quenched the $C_4H_8$ isomerization process.

The absolute yield of hydrocarbon products was obtained by their peak area integration with respect to that of the internal standard, *n*-hexane. For the hydrogenolysis products the sum of the amounts of $CH_4$ and $CH_2$=CH–$CH_3$ was divided by two, according to the fact that just one molecule of complex **1** produces both; the amounts of the other hydrogenolysis products were always negligible. The hydrocarbon yield was proportional to the reaction time for at least 50 min. The slope of the best straight line, obtained by means of the least-squares treatment of the data at low conversion, gave the initial hydrogenation rate R. The error, calculated as standard deviation, was less then 10%. Figure 4 shows a typical plot of the stoichiometric hydrogenation of complex **1**, an alternative scale (on the right) shows the percent of conversion of complex **1** as function of the reaction time.

The initial rate values at 60°C under different experimental conditions are collected in Table 2.

The hydrogenation rate is first order with respect

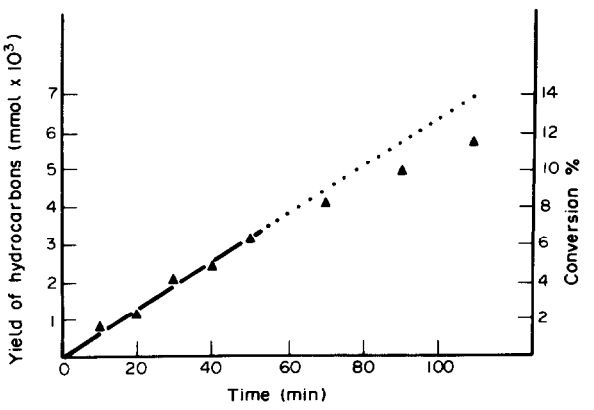



Fig. 4. Representative hydrocarbon yield plot for stoichiometric hydrogenation (60°C; [**1**] = 25.0 mM; $P_{H_2}$ = 360 Torr). Initial rate, R = 3.75 $10^{-3}$ mmol $h^{-1}$; conversion 7.5% $hr^{-1}$.

to the concentration of complex **1** (Fig. 5) and with respect to the hydrogen partial pressure, at least in the range 190–760 Torr (Fig. 6).

The addition of CO into the vials causes remarkable suppression in the hydrogenation process, Fig. 7 shows the inverse relation between the hydrogenation rate and the pressure (or molecular ratio) of CO added. When $D_2$ was used in lieu of $H_2$, the rate of stoichiometric hydrogenation quenches and the kinetic isotope effect is 3.3 in the following experimental conditions: 60°C, [complex] = 25.0 mM, $P_{H_2}$ or $P_{D_2}$ = 360 Torr. No attempt to examine the deuterium distribution in the products was made. Kinetic data are consistent with eqn (3), which summarizes the experimental relationship between the initial rate and the reactants:

$$\frac{d[\text{hydrocarbons}]}{dt} = R = K\frac{[\text{complex}]P_{H_2}}{P_{CO}} \quad (3)$$

Since complex **1** is coordinatively saturated, the first step should involve the creation of a vacant coordination site. This can be achieved by dissociation of a ligand like CO or by intramolecular rearrangement of the organic chain, i.e. conversion from $\mu_2$ to $\mu_1$ coordination mode, or by cleavage of the metal-metal bond. The suppression of hydrogenation rate by added CO suggests an initial step involving CO dissociation, as pointed out for stoichiometric and catalytic hydrogenation of $[Mo_2Cp_2(CO)_4(RC_2R)]$.[9] On the contrary the quite large value obtained for the deuterium isotope effect suggests that the H–H bond cleavage should be relevant in the rate-determining step.[18] A number of mechanisms could account for eqn (3),

Table 2. Values of the observed initial rate R of the stoichiometric hydrogenation of complex **1** in toluene at 60°C

| R (mmol $h^{-1}$ x $10^3$) | [complex 1] (mM) | $P_{H_2}$ (torr) | $P_{CO}$ (torr) |
|---|---|---|---|
| 1.97 | 12.5 | 360 | - |
| 3.75 | 25.0 | 360 | - |
| 6.19 | 37.5 | 360 | - |
| 8.33 | 50.0 | 360 | - |
| 2.10 | 25.0 | 190 | - |
| 5.92 | 25.0 | 570 | - |
| 7.03 | 25.0 | 760 | - |
| 2.86 | 25.0 | 360 | 10 |
| 2.04 | 25.0 | 360 | 20 |
| 1.74 | 25.0 | 360 | 30 |
| 1.36 | 25.0 | 360 | 40 |
| 1.12 | 25.0 | 360($D_2$) | - |

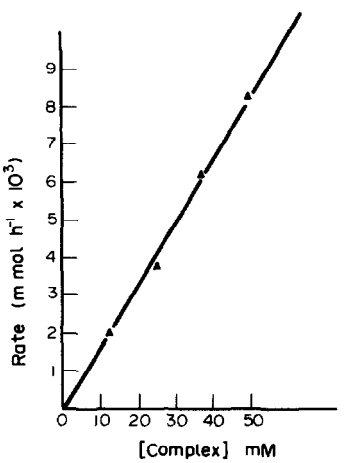



Fig. 5. Rate of hydrogenation as a function of complex **1** concentration (60°C; $P_{H_2}$ = 360 Torr).

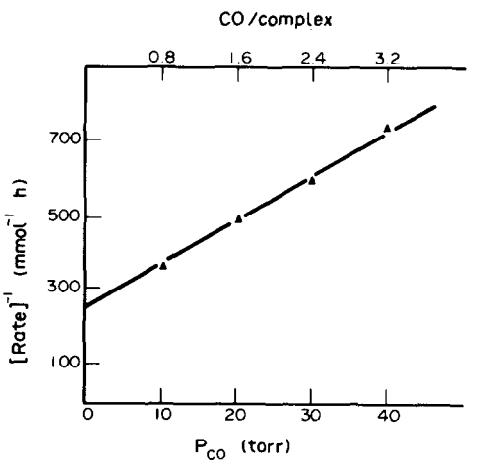



Fig. 7. Plot of 1/Rate vs $P_{CO}$(60°C; [1] = 25.0 mM, $P_2$ = 360 Torr).

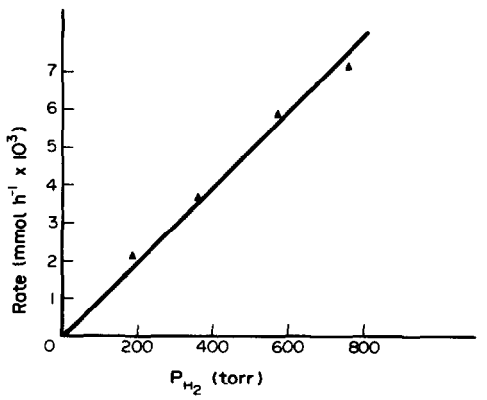



Fig. 6. Rate of hydrogenation as a function of hydrogen pressure (60°C, [1] = 25.0 mM).

depending on the value attributed to the rate constants of the single step. Thus we prefer to propose only a qualitative description of the phenomenon. The striking feature of this hydrogenation is the unusual hydrocarbon distribution, i.e.

(a) no total selectivity toward *cis*-olefin

(b) occurrence of hydrogenation to alkane

(c) occurrence of hydrogenolysis specifically on the terminal C–C bond.

All these data suggest that the $\sigma$-interaction between the organic chain and the iron atom is preserved in the transition state (Fig. 8). The organic chain, even if selective *cis*-addition of dihydrogen occurs, remains linked to the bimetallic

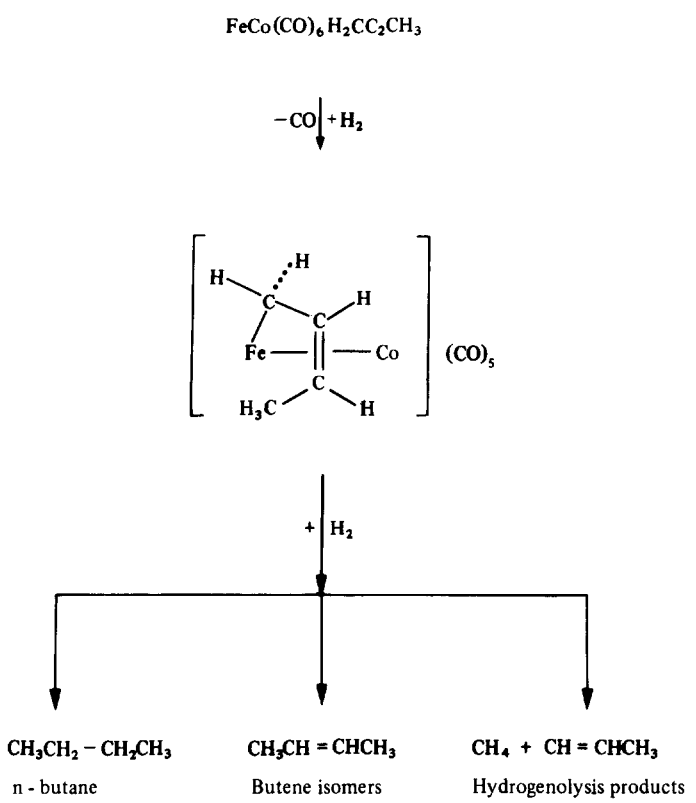



Fig. 8. Scheme of the hydrogenation of complex **1**.

fragment long enough to transpose the double bond and further hydrogenation takes place. The occurrence of hydrogenolysis is in tune with this description. The first step of hydrogenolysis on metal catalyst is the formation of a carbon–metal bond, then carbon–carbon scission follows.[19] The proposed transition state fulfils this bonding model and selective formation of propene is expected.

The $\mu_2$-$\eta^2$ diphenylacetylene complexes reported in Table 1 did not give any detectable yield of hydrocarbons in experimental condition even more forced than those employed for hydrogenation of **1**. The enhanced reactivity of **1** towards hydrogen is probably due to the unique coordination mode of the organic chain, although polarity of the hetero-bimetallic bond may play a role.

*Acknowledgements*—This research was supported by the Italian C.N.R. (Progetto Finalizzato Chimica Fine e Secondaria, Contratto No. 8100727.95). We are indebted to Dr. P. L. Stanghellini for helpful discussions.

## REFERENCES

1. (a) E. L. Muetterties, *Bull. Soc. Chim. Belg.* 1976, **85**, 451. (b) E. L. Muetterties, *Pure Appl. Chem.* 1978, **50**, 941.
2. (a) W. I. Bailey, F. A. Cotton, J. D. Jamerson and J. R. Kolb, *J. Organomet. Chem.* 1976, **121**, C23. (b) W. I. Bailey, D. M. Collins and F. A. Cotton, *J. Organometal. Chem.* 1978, **135**, C53.
3. F. A. Cotton, J. D. Jamerson and B. R. Stults, *J. Am. Chem. Soc.* 1976, **98**, 1774.
4. W. G. Sly, *J. Am. Chem. Soc.* 1959, **81**, 18.
5. Y. Wong and P. Coppens, *Inorg. Chem.* 1976, **15**, 1123.
6. V. W. Day, S. S. Abdel-Meguid, S. Dahestani, M. G. Thomas, W. R. Pretzer and E. L. Muetterties, *J. Am. Chem. Soc.* 1976, **98**, 8289.
7. B. H. Freeland, T. E. Hux, N. C. Payne and K. G. Kyers, *Inorg. Chem.* 1980, **19**, 693.
8. E. L. Muetterties, W. R. Pretzer, M. G. Thomas, B. F. Beier, D. L. Thorn, V. W. Day and A. B. Anderson, *J. Am. Chem. Soc.* 1978, **100**, 2090.
9. S. Slater and E. L. Muetterties, *Inorg. Chem.* 1980, **19**, 3337.
10. S. Slater and E. L. Muetterties, *Inorg. Chem.* 1981, **20**, 1604.
11. E. L. Muetterties, *Inorg. Chim. Acta* 1981, **50**, 1.
12. S. Aime, D. Osella, L. Milone and A. Tiripicchio, *Polyhedron* 1983, **2**, 77.
13. S. Aime, L. Milone, D. Osella, A. Tiripicchio and A. M. Manotti-Lanfredi, *Inorg. Chem.* 1982, **21**, 501.
14. (a) G. Bor and U. K. Dietler, *J. Organometal. Chem.* 1980, **191**, 295. (b) F. Ungvary and I. Marko, *J. Organomet. Chem.* 1974, **71**, 283.

15. F. D. Rossini, *Chemical Thermodynamics*. Wiley, New York (1950).
16. In these experimental conditions the active species is likely $HCo(CO)_4$.[17]
17. M. Orchin, *Acc. Chem. Res.* 1981, **14**, 259.
18. (a) K. B. Wiberg, *Chem. Rev.* 1955, **55**, 713. (b) B. R. James, *Homogeneous Hydrogenation*. Wiley, New York (1973).
19. J. H. Sinfelt, *Adv. Catal.* 1973, **23**, 91.

*Polyhedron* Vol. 3, No. 2, pp. 183–190, 1984
Printed in Great Britain.

0277–5387/84 $3.00 + .00
© 1984 Pergamon Press Ltd.

# AN INVESTIGATION OF PRUSSIAN BLUE ANALOGUES BY MÖSSBAUER SPECTROSCOPY AND MAGNETIC SUSCEPTIBILITY

**PAUL G. RASMUSSEN* and E. A. MEYERS**
The University of Michigan, Department of Chemistry, Ann Arbor, MI 48109, U.S.A.

(*Received* 17 *May* 1983; *accepted* 25 *July* 1983)

**Abstract**—The Mössbauer spectra and magnetic susceptibilities have been obtained for a series of Prussian Blue analogues of general formula $M_j^A[M^B(CN)_6]_k \cdot mH_2O$ where $M^A$ and $M^B$ are transition metal ions, $j$ and $k$ vary with the oxidation states of $M^A$ and $M^B$ and $m$ typically has values from 8 to 14. The compounds were prepared from the hexacyano acids or with large quaternary ammonium counterions and are therefore not contaminated with alkali cations. In each analogue, A or B is iron and the second metal is Mn, Cu, Co, Cr or Ru. In each case it was possible to assign the site (A or B), oxidation state and spin state to each transition metal ion. This group of compounds are all class II mixed valence species from their colours, but do not show evidence of linkage isomerism or redox changes compared to the starting materials. The Mössbauer linewidths are consistent with the Ludi model of Prussian Blue.

The structure of Prussian Blue, $Fe_4[Fe(CN)_6]_3 \times H_2O$, prototype of a series of polymeric cyanides, has been the object of intensive investigations.[1] Historically, it was the first documented synthetic coordination complex and its unexpected deep blue colour has triggered many investigations. Many of these studies have attempted to discern whether there were discrete oxidation states or valence equivalency for the structurally different iron atoms. The bulk of information accumulated by X-ray diffraction,[2–4] infrared spectroscopy,[5,6] magnetic susceptibility,[5,7,8] electronic structure,[9] Mössbauer studies,[10–16] photoelectron spectroscopy,[17,18] and neutron diffraction studies[19] support the assignment of discrete oxidation states as

$$Fe(II)–C{\equiv}N–Fe^{3+}$$[20]

an $Fe^{3+}$ salt of the hexacyanoferrate(II) ion.

Prussian Blue and its many analogues are generally obtained as fine powders. A wide variety of colours, stoichiometries, oxidation states and electronic properties are obtained by substituting different transition metals for the iron atoms in Prussian Blue. This series of polymeric cyanides has the general formula

$$M_j^A[M^B(CN)_6]_k \cdot mH_2O$$

where $M^A$ and $M^B$ represent transition metal ions, $j$ and $k$ are the stoichiometric numbers of the compound and vary with the oxidation states of the metals, A and B. These compounds are heavily hydrated; so that $m$ typically has a value of 8–14.

The basic features of the crystal structure for Prussian Blue and the analogues were described in the pioneering work by Keggin and Miles[2] who defined the unit cell as f.c.c. with a cell edge of about 10 Å. In their model, position 4*a* (0, 0, 0) and 4*b* (1/2, 1/2, 1/2) are occupied by $M^A$ and $M^B$, respectively. The carbon and the nitrogen of the cyanide ligand are located on the two sets of the 24-fold position ($x$, 0, 0). The eight fold positions (1/4, 1/4, 1/4) and (3/4, 3/4, 3/4) are randomly occupied by $M^A$ or alkali metals as required for electroneutrality. All $M^B$ atoms are octahedrally coordinated to the carbon end of the cyanide (i.e. $M^BC_6$), and the $M^A$ atoms are either present as octahedrally coordinated to the nitrogen (i.e. $M^AN_6$) or as uncoordinated interstitial ions. In this model, water molecules do not occupy crystalline sites, but rather are present only as zeolitic or surface water.

*Author to whom correspondence should be addressed.

The model proposed by Ludi *et al.*[21] retains some of the features of that of Keggin and Miles. Much of the new model is described in the context of the space group ($Fm3m$), with a cell edge ranging between 9.9 and 10.9 Å. The exact cell edge is a function of the specific compound and the differences reflect the $M^B$–C and the $M^A$–N bond distances. Their discovery of primitive reflections from single crystals of Prussian Blue changes the space group to $Pm3m$. The $M^A$ and the $M^B$ atoms occupy the four-fold positions exclusively, and are, therefore, octahedrally coordinated to the nitrogen and the carbon atoms, respectively. The assumption of randomly distributed $M^A$ atoms in uncoordinated interstitial sites (8c) is discarded. The occupancy rate of the sites 4*a* and 4*b* is a function of the stoichiometry of the analogue. For example, when $j = 1$ and $k = 1$, then there will be a 100% occupancy of both sites 4*a* and 4*b*. However, when the $j:k$ ratio is greater than 1, the occupancy of site 4*a* remains at 100%, while that for site 4*b* becomes less than 100%. Specifically, when the $j:k$ ratio is 4:3, as is the case for Prussian Blue, the average composition is postulated to be $M^BC_6$ and $M^AN_{4.5}O_{1.5}$. The absence of whole $M^B(CN)_6$ octahedra leads to interruptions in the very tight three dimensional $M^A$–NC–$M^B$–CN–$M^A$ lattice postulated by Keggin and Miles. Coordinated water in sites normally occupied by the nitrogens has been suggested to explain the infrared spectra of the analogues.[22,23] As the ratio of $j:k$ increases, the differences between the two models becomes more pronounced because as $j:k$ increases the density should decrease for the Ludi model and increase for that by Keggin and Miles.

The problem in differentiating between the two models on the basis of density measurements is, that such measurements are also a reflection of the chemical composition. If there are any unspecified alkali metals or water molecules in the compound under study, then the density measurements can be misleading. In the past, very little specific analytical data was ever included with the results, and it is likely that a variety of analytically different compounds were synthesized and studied as Prussian Blue. The structural implications of the two models and the relationship of the non-cubic analogues is reviewed elsewhere.[24]

We have carried out a systematic study of a series of Prussian Blue analogues. In each, at least one of the metal atoms (and in the case of Prussian Blue–both) is iron. One objective of this investigation was to determine whether or not linkage isomerism and/or oxidation-reduction occurs for the analogs by determining the site configuration and spin state for metal ions.

In the preparation of the compound which has been called "Turnbull's blue" but which is actually Prussian Blue, it is clear that linkage isomerism or oxidation-reduction has occurred.[25] Underlying the study of the analogs is the question of whether this linkage isomerism is typical or even common. Note that while linkage isomerism is indistinguishable from oxidation-reduction in Prussian Blue, this is not the case when $M^A$ is a different atom from $M^B$.

## EXPERIMENTAL SECTION

Prussian Blue analogues were kindly supplied from the laboratory of Dr. A. Ludi, Universität Bern, Bern, Switzerland. These compounds were prepared with careful attention to analytical composition as described by Buser.[26] The preparations avoid contamination by alkali cations by using the acid form of the hexacyano species, or by using large quaternary ammonium counterions.

*Magnetic susceptibilities*

Magnetic susceptibilities were measured by the Faraday method. Samples (about 15 mg) in an open quartz bucket were suspended from a R-100 Cahn Electrobalance into a V-3400 Varian electromagnet fitted with Heyding pole pieces. A Varian Fieldial Mark I was used to regulate the field strength. Susceptibilities were corrected for diamagnetic contributions using values listed by Figgis and Lewis.[27] The system was checked by calibration with $Ni(NH_4)_2(SO_4)_2 \cdot 6H_2O$ against $HgCo(SCN)_4$. Results corresponded closely to those reported by Simmons.[28] The magnetic data is summarized in Table 2.

The Mössbauer spectra were obtained using a constant accceleration drive unit coupled with a multichannel analyzer operated in the time mode. In the temperature range $84° < T < 298K$, the spectrometer employed was built by T. M. Gould and has been described in detail in his thesis.[29] For this temperature range, a styrofoam insulated dewar was used; the temperature was monitored with a Cu constantin thermocouple. All reported Mössbauer spectra were gathered with temperature variations of less than $\pm 2\%$°C. A very thin piece of circular carboard was cut to a diameter of 3.5 cm with an inner hole of diameter 2.7 cm. One side was covered with mylar film attached with double sided tape. A finely ground powder (40–90 mg) as then pressed into the hole and covered with a second piece of mylar. These samples were fitted into the aluminum block of the cryostat.

An enriched $^{57}Fe$ sample was used to calibrate the velocity. All chemical shifts (cs) are relative to

sodium nitroprusside ($T$ = ambient). The source temperature remained at room temperature for all spectra obtained with this system.

A second system was used to obtain the spectra in the temperature range 4.2 K < $T$ < 77 K.[30] Samples (30–50 mg) were pressed in small plastic vials (1 cm dia.) and stoppered with styrofoam. Velocities were internally calibrated. The CS are relative to sodium nitroprusside. Since the source is immersed in the dewar, the source temperature was monitored and maintained at 18 K. No corrections were made for the variance in source temperature between the two systems.

The Mössbauer data points were fitted to a series of Lorentzian or Gaussian-distribution of Lorentzian shaped peaks by a nonlinear least squares analysis. The non-resonant background is fit to a parabola. The method used to fine the parameters which minimize the chi-squared value is the Gauss–Newton iteration method. Specific details (including a listing of the main program and the subroutines) are given in Gould's thesis.[29]

The print-out for this program includes the normalized chi-squared ($\chi^2$) value after each iteration and after the final calculation, a list of the best fitting parameters, with a measured fitting error, experimental vs the fitted area, individual line and/or pair areas and estimated diagonalized areas. The goodness of fit parameter $\chi^2$ was compared for various initial conditions, e.g. one line 2 independent lines, QS pair, etc. An acceptable value of $\chi^2$ was $0.95 \leq \chi^2 \leq 1.25$. Two independent lines were considered a QS pair if the areas were within 5% of each other and if the $\chi^2$ did not radically change constraining the data to fit a QS pair. A typical spectrum is shown in Fig. 1. In all spectra, over one million counts per channel were accumulated.

Guinier X-ray photographs were obtained for samples where the number of phases was in doubt.

## RESULTS AND DISCUSSION

The results are divided into two parts: the first deals with iron atoms expected to be in $M^BC_6$ sites; the second deals with iron atoms expected to be bonded to the nitrogen end of the cyanide ($M^A$). The discussion will be directed towards confirming the oxidation and spin state, and elucidating insofar as possible the site symmetry.

Room temperature Mössbauer spectra obtained for $K_3[Fe(CN)_6]$ and $K_4[Fe(CN)_6]$ are used as references for line width (FWHM), position (CS) relative to sodium nitroprusside, and quadrupole splitting (QS) for this series of compounds. For $K_3[Fe(CN)_6]\cdot 3H_2O$ the values are CS = 0.136 ± 0.007 mm/sec; QS = 0.269 ± 0.008 mm/sec; FWHM = 0.365 ± 0.008 mm/sec, in close agreement with the results published by Garg and Goel.[31] $K_4[Fe(CN)_6]\cdot 2H_2O$, our experimental parameters are: CS = 0.234 ± 0.005 mm/sec; QS = 0.0 mm/sec; FWHM = 0.324 ± 0.06 mm/sec. in good agreement with Hall *et al.*[32] Note that there is little difference in CS between the Fe(II) and Fe(III) cyanide complexes. Differentiation between Fe(II) and Fe(III) cyanide complexes is based on the presence/absence of temperature-dependent QS.

*Compound*: $Co_3[Fe(CN)_6]_2\cdot 14H_2O$

The compound $Co_3[Fe(CN)_6]_2\cdot 14H_2O$ is a deep

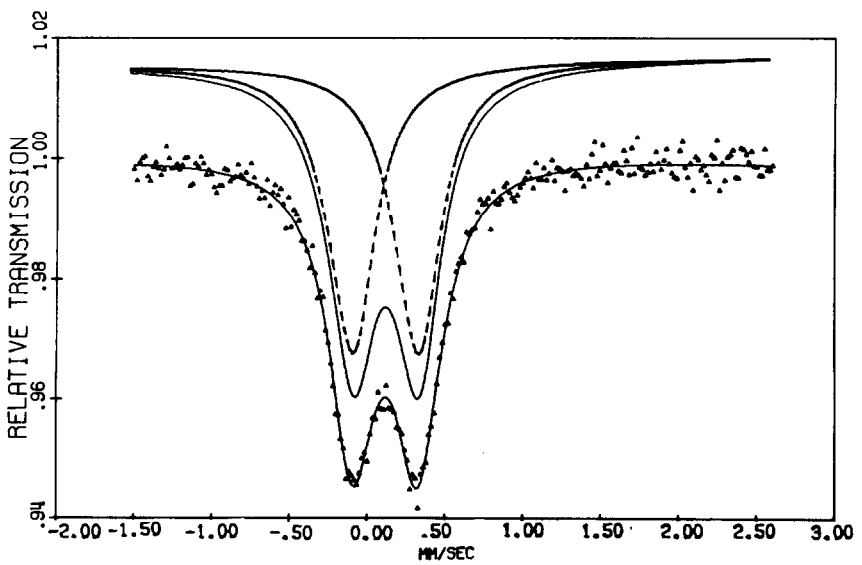



Fig. 1. Mössbauer spectrum of $Co_3[Fe(CN)_6]_2\cdot 14H_2O$ at 298 K.

red–brown with a well defined crystaline phase.[24] The magnitude of the CS is that expected for low spin iron. The QS is temperature dependent (Table 1). The temperature dependent spectra were fitted by the usual techniques described elsewhere.[29] The size of the QS and the extent of variation with temperature clearly indicate low spin Fe(III) behaviour and suggest a splitting with the $t_{2g}$ octahedral orbitals of the order of $kT$ ($\sim 170\,cm^{-1}$).

The magnetic susceptibility is given in Table 2. Since both Co(II) and Fe(III) are contributing to the paramagnetism of the compound, attribution of the magnetism to the two species can only be approximate. Assuming no interaction, the form for the magnetic moment of an $A_nB_m$ salt is[33]

$$\mu_{AB} = [n\mu_A^2 + m\mu_B^2]^{1/2}. \quad (1)$$

Using spin only values for Co(II), Fe(III), one calculates a room temperature moment of $\mu_{AB} = 6.7$. However, substantial contribution to the observed or orbital contribution from both species is likely. If one takes accepted values[27] of $\mu = 2.4$ for $K_3Fe(CN)_6$ and $\mu = 5.1$ for $(NH_4)_2Co((SO_4)_2 \cdot 6H_2O$ and uses the formula above, one calculates $\mu = 9.46$. The observed value of $\mu = 7.8$ falls reasonably between these values. Thus the Mössbauer and magnetic susceptibility data confirm the assignment Co(II)–N≡C–Fe(III). Interestingly, this compound does not undergo transformation at room temperature to $Fe_3[Co(CN)_6]\cdot 14H_2O$ whose parameters are given below.

*Compound*: $Na_3[Fe(CN)_5pyrazine]\cdot 3H_2O$

The compound $Na_3[Fe(CN)_5pyrazine]\cdot 3H_2O$ is bright red. The Mössbauer data, in the temperature range $83 \leq T \leq 294$ K, give a well-resolved doublet.

The QS is independent of temperature and is apparently due to the difference in covalency between the pyrazine and cyanide ligands. The data agree closely with that reported by Weihofen[34] for the pyrrolidine-substituted complex.

The compound is diamagnetic which, coupled with the Mössbauer data prescribes a $Fe(II)C_5N_1$ site configuration. Although this compound is not a Prussian Blue analogue, the data are useful for comparison purposes to other low spin iron(II) cyanides. In particular, they show the sensitivity of the quadrupole splitting of low spin iron(II) to lowered symmetry.

Table 1. Mössbauer data

| | Temp K±2% | CS, mm/sec | QS, mm/sec | FWHM, mm/sec |
|---|---|---|---|---|
| $Co_3[Fe(CN)_6]_2\cdot 14H_2O$ | 298.0 | 0.115 ± 0.004 | 0.422 ± 0.004 | 0.361 ± 0.004 |
| | 294.2 | 0.116 ± 0.002 | 0.426 ± 0.010 | 0.487 ± 0.010 |
| | 153.8 | 0.142 ± 0.003 | 0.738 ± 0.006 | 0.527 ± 0.006 |
| | 113.6 | 0.153 ± 0.006 | 0.828 ± 0.010 | 0.511 ± 0.007 |
| | 88.4 | 0.182 ± 0.007 | 0.877 ± 0.009 | 0.583 ± 0.009 |
| | 84.7 | 0.184 ± 0.005 | 0.884 ± 0.011 | 0.569 ± 0.001 |
| | *77.0 | 0.049 ± 0.009 | 0.894 ± 0.010 | 0.511 ± 0.006 |
| | *60.0 | 0.056 ± 0.003 | 0.910 ± 0.009 | 0.524 ± 0.005 |
| | *40.0 | 0.056 ± 0.005 | 0.917 ± 0.004 | 0.518 ± 0.006 |
| | *18.0 | 0.056 ± 0.005 | 0.950 ± 0.006 | 0.523 ± 0.005 |
| *Source temperature: 5-10 K. | | | | |
| $Na_3[Fe(CN)_6pyz\cdot 3H_2O$ | 294.0 | 0.283 ± 0.002 | 0.749 ± 0.008 | 0.484 ± 0.007 |
| | 84.0 | 0.362 ± 0.003 | 0.758 ± 0.006 | 0.427 ± 0.005 |
| $Mn_2[Fe(CN)_6]\cdot 8H_2O$ | 294.0 | 0.164 ± 0.002 | -- | 0.498 ± 0.007 |
| | 84.2 | 0.252 ± 0.003 | -- | 0.536 ± 0.006 |
| $Cu_2[Fe(CN)_6]\cdot 14H_2O$ | 297.0 | 0.168 ± 0.002 | -- | 0.401 ± 0.006 |
| | 87.0 | 0.219 ± 0.003 | -- | 0.420 ± 0.005 |
| $Co_2[Fe(CN)_6]\cdot 8H_2O$ | 298.0 K | 0.150 ± 0.006 | -- | 0.426 ± 0.006 |
| | 87.4 K | 0.240 ± 0.009 | -- | 0.498 ± 0.009 |
| $Co_2[Fe(CN)_6]\cdot 9H_2O$ | 298.0 K | 0.148 ± 0.009 | -- | 0.487 ± 0.004 |
| | 87.2 K | 0.228 ± 0.006 | -- | 0.568 ± 0.003 |

Table 1 (*Contd*)

| | Temp K±2% | CS, mm/sec | QS, mm/sec | FWHM, mm/sec |
|---|---|---|---|---|
| $Cr_4[Fe(CN)_6]_3 \cdot 14H_2O$ | 298.0 | 0.155 ± 0.005 | -- | 0.578 ± 0.004 |
| | 87.4 | 0.229 ± 0.004 | -- | 0.580 ± 0.007 |
| | 4.3 | 0.261 ± 0.006 | -- | 0.598 ± 0.007 |
| $Fe_3[Co(CN)_6]_2 \cdot 14H_2O$ | 298.0 | 1.48 ± .03 | 1.667 ±0.004 | 0.823 ±0.018 |
| | 282.1 | 1.49 ± .02 | 1.723 ±0.004 | 0.831 ±0.014 |
| | 187.2 | 1.51 ± .03 | 2.294 ±0.003 | 0.877 ±0.021 |
| | 134.2 | 1.54 ± .01 | 2.506 ±0.001 | 0.926 ±0.031 |
| | 99.5 | 1.55 ± .04 | 2.588 ±0.004 | 0.941 ±0.011 |
| | 87.8 | 1.54 ± .06 | 2.603 ±0.005 | 0.989 ±0.034 |
| | 84.2 | 1.55 ± .06 | 2.619 ±0.003 | 0.996 ±0.007 |
| | 40.0 | 1.72 ± .05 | 2.620 ±0.005 | 0.904 ±0.021 |
| | 4.2 | 1.77 ± .06 | 2.620 ±0.006 | 0.904 ±0.008 |
| $Fe_4[Ru(CN)_6]_3 \cdot 14H_2O$ | 298.0 | 0.617 ± 0.002 | 0.628 ± 0.004 | 0.646 ± 0.004 |
| | 273.0 | 0.643 ± 0.002 | 0.617 ± 0.006 | 0.543 ± 0.006 |
| | 87.0 | 0.751 ± 0.003 | 0.676 ± 0.004 | 0.638 ± 0.008 |
| | 84.0 | 0.801 ± 0.004 | 0.715 ± 0.006 | 0.672 ± 0.011 |
| | 5.0 | 0.807 ± 0.004 | 0.692 ± 0.005 | 0.549 ± 0.008 |
| Prussian Blue | 298.0 | 0.669 ± 0.005 | 0.868 ± 0.009 | 0.606 ± 0.014 |
| | | 0.109 ± 0.006 | -- | 0.378 ± 0.007 |
| | 281.2 | 0.671 ± 0.006 | 0.613 ± 0.009 | 0.577 ± 0.008 |
| | | 0.113 ± 0.002 | -- | 0.403 ± 0.004 |
| | 87.4 | 0.775 ± 0.004 | 0.696 ± 0.006 | 0.647 ± 0.006 |
| | | 0.183 ± 0.002 | -- | 0.462 ± 0.005 |
| | 82.4 | 0.764 ± 0.004 | 0.707 ± 0.019 | 0.682 ± 0.006 |
| | | 0.159 ± 0.002 | -- | 0.491 ± 0.008 |

Table 2. Magnetic susceptibility data

| | (X $10^{-3}$) $\chi'_M$(293 K) | $\mu_{BM}$(Curie Law) |
|---|---|---|
| $Co_3[Fe(CN)_6]_2 \cdot 14H_2O$ | 23.5/mole | 7.4 |
| $Mn_2[Fe(CN)_6] \cdot 8H_2O$ | 15.4/Mn | 6.0 |
| $Cu_2[Fe(CN)_6] \cdot 14H_2O$ | 1.9/Cu | 2.1 |
| $Co_2[Fe(CN)_6] \cdot 8H_2O$ | 11.2/Co | 5.2 |
| $Co_2[Fe(CN)_6] \cdot 9H_2O$ | 9.2/Co | 4.6 |
| $Cr_4[Fe(CN)_6]_3 \cdot 14H_2O$ | 6.73/Cr | 3.9 |
| $Fe_3[Co(CN)_6]_2 \cdot 14H_2O$ | 14.0/Fe | 5.7 |
| $Fe_4[Ru(CN)_6]_3 \cdot 14H_2O$ | 15.3/Fe | 6.0 |
| $Fe_4[Fe(CN)_6]_3 \cdot 14H_2O$ | 13.9/Fe | 5.7 |

*Compound*: $Mn_2[Fe(CN)_6] \cdot 8H_2O$

The compound $Mn_2[Fe(CN)_6] \cdot 8H_2O$ is pale blue. The Mössbauer spectra obtained in the temperature range $294 \geq T \geq 84$ K show a single resonance peak. The magnitude of the CS and the lack of a QS is consistent with a low spin iron(II) and the magnetic susceptibility substantiates a Mn(II) assignment as the only paramagnetic ion and confirms the configuration, Fe(II)–C≡N–Mn(II). This compound is isostructural to $Mn_2[Ru(CN)_6] \cdot 8H_2O$[35] which has non-cubic structure and bridged pairs of manganese ions. Although the iron is not at a cubic site, the Mössbauer parameters indicate an octahedral cyanide site (no discernible quadruple splitting and typical linewidth).

*Compound*: $Cu_2[Fe(CN)_6] \cdot 14H_2O$

$Cu_2[Fe(CN)_6] \cdot 14H_2O$ is a brown compound; this colour is caused by strong ultraviolet charge transfer bands tailing off into the blue end of the visible spectrum.[36] The Mössbauer parameters indicate

that the iron atom is in an octahedral environment as low spin iron(II). The configuration of Fe(II)–C≡N–Cu(II) is consistent with both the Mössbauer and magnetic susceptibility data.

*Compounds*: $Co_2[Fe(CN)_6]\cdot 8H_2O$ *and* $Co_2[Fe(CN)_6]\cdot 9H_2O$

The compound $Co_2[Fe(CN)_6]\cdot 8H_2O$ is a deep blue–green. The compound $Co_2[Fe(CN)_6]\cdot 9H_2O$ is black. The Mössbauer spectra obtained for both show a single resonance peak, indicating iron atoms in similar sites, defined by: $Fe(II)C_6$.

The magnetic moments indicate that in both cases the $Co^{2+}$ are weak but slightly different fields. Given the importance in the Ludi model of water in the crystal field around the $M_A$ site,[24] the addition of one water per mole of compound might strengthen the crystal field enough to result in observable orbital quenching. More definite descriptions of the ligand fields surrounding the $Co^{2+}$ ions can not be made.

*Compound*: $Cr_4[Fe(CN)_6]_3\cdot 14H_2O$

The compound $Cr_4[Fe(CN)_6]_3\cdot 14H_2O$ is dark green. The Mössbauer spectra obtained in the temperature range $298 \geq T \geq 4.3$ K have a single resonance peak.

The lack of QS and the magnitude of the CS indicate that the site assignment for the iron atom is $Fe(II)C_6$. Any observed paramagnetism should be a function of only the chromium atom. The experimentally observed magnetic moment is close to the spin-only value for Cr(III). The configuration Fe(II)–C≡N–Cr(III) is substantiated by both the experimental measurements.

*Iron atoms in* $M^A$ *sites*

There remains controversy concerning the positions of the $M^A$ metal atoms. The two models assign different locations for these atoms. That the stoichiometry will influence the kinds of sites occupied by the $M^A$ atoms is agreed to by both. In the Keggin model, $M^A$ atoms are in well-defined nitrogen octahedra and interstitial sites. The number of interstitial sites occupied is a function of the stoichiometry. In the Ludi model, the $M^A$ atoms are all in six-coordinate sites. No interstitial sites are postulated to be occupied by $M^A$ atoms. In order to define the $M^A$ site more exactly, Mössbauer and magnetic susceptibilities were obtained.

We have redone the magnetic susceptibility and Mössbauer spectra for Prussian Blue and include it for comparison. The primary motive for repeating earlier work was the paucity of analytical data for compounds labeled as Prussian Blue. The water content has been analytically well-defined in our preparations, whereas in the past, water has been assumed to be zeolitic in nature. The single-crystal work done on Prussian Blue[21,37] substantiates water occupying crystalline sites.

*Compound*: $Fe_3[Co(CN)_6]_2\cdot 14H_2O$

The compound $Fe_3[Co(CN)_6]_2\cdot 14H_2O$, is green–yellow. From the CS values, it is obvious that this is a high spin ferrous complex. The temperature dependence of the QS suggests a splitting in levels on the order of 340 $cm^{-1}$ or about double that found for the $Fe(II)C_6$ site.

In addition to the QS, the magnitude of the FWHM for this compound is almost twice that obtained for similary prepared samples where the iron atoms is in the $M^B$ site. If two or more similar iron sites are present, broadened lines would be expected. Two lattice effects can explain this situation: (1) impurities in the sample, that is, the iron atoms are not in the well-defined $M^A$ sites for a face center cubic crystal, as expected. Or, (2) two nearly equivalent sites exist (i.e. *cis/trans* orientation of water ligands about the iron atoms). The magnetic data are consistent with a high spin ferrous complex with orbital contribution to the moment. The Guiniér photographs indicate only one phase is present. In this case the evidence parallels the Ludi model quite closely.

*Compound*: $Fe_4[Ru(CN)_6]_3\cdot 14H_2O$

The compound $Fe_4[Ru(CN)_6]_3\cdot 14H_2O$ is dark blue, quite similar to Prussian Blue.

The Mössbauer spectra obtained are rather diffuse at temperatures higher than 87.2 K and of relatively low intensity. The values obtained for the CS vary strongly with temperature; quite similar to that postulated for other Fe(III) complexes.[38] The QS varies with temperature in a manner that may be a function of fitting the rather diffuse spectra.

The FWHM is again larger than what is obtained for similarly prepared samples where the iron atoms is in well-defined $M^B$ site. The FWHM is indicative of two or more lattice sites being occupied by the Fe(III) ($M^A$). If the sites were extremely different (i.e. interstitial site vs $M^A$ site) the two sets of doublets would probably be resolvable.

The magnetic data are consistent with the site assignments

Fe(III)–N≡C–Ru(II).

There is no evidence for linkage isomerism in this species.

*Compound: Prussian Blue* $Fe_4[Fe(CN)_6]_3 \cdot 14H_2O$

A wide variety of methods have been used to elucidate the structure of Prussian Blue and consequently there exists a large volume of published data. *Vide supra.*

The Mössbauer spectra obtained in the temperature range: $84 < T < 298$ K vary rather little. The variation in the CS and QS with temperature is probably a function of the curve fitting process, the overlaps making resolution difficult. The asymmetry on the r.h.s. of the more intense peak indicates that the observed envelope is the sum of two unresolved peaks. An investigation using an $^{56}Fe$ labeled Prussian Blue[39] substantiates this type of fitting, where both an Fe(III) (non-octahedral symmetry) and Fe(II) (octahedral symmetry) are present, as do our data for the analogues.

Our magnetic moment value is in general agreement with those previously obtained[7,8] although some of the discrepancies may be due to differences in formulation especially regarding potassium ion or water.

## CONCLUSIONS

In all the cases examined here, the ions bonded to the carbon end of the cyanide ($M^B$) are in low spin configurations, and all ions in $M^A$ sites are high spin. None of this group is involved in linkage isomerism and the location of the ions has been determined to be that predicted based on the starting materials. All compounds in the group (with the exception of course of $Na_3[Fe(CN)_5pyz]\cdot 3H_2O$) appear to be Prussian Blue analogues in the sense of having well defined octahedral cyanide sites, extensive water of hydration, and variations in the $M^A$ sites. This latter property is particularly evident in the Mössbauer linewidths which are substantially greater for ions in $M^A$ sites, in accord with the Ludi model. In Prussian Blue itself the linewidths are uncertain because of overlapping peaks whereas in the analogs the effect is clear. Conversely, the $M^B$ linewidths are relatively narrow and no quadrupole splitting is observed for the low spin iron(II) cases. All of these compounds fit the class II description of mixed valency, having colors which are not composites of the constituents. The determination of magnetic ordering at low temperature awaits further investigation.

## REFERENCES


1. B. M. Chadwick and A. G. Sharpe, *Adv. Inorg. Chem. Radiochem.* 1966, **8**, 83.
2. J. F. Keggin and F. D. Miles, *Nature*, 1936, **137**, 577.
3. H. B. Weiser, W. O. Milligan and J. Bates, *J. Phys. Chem.* 1942, **46**, 99.
4. A. Ludi, H. U. Güdel and R. Hugi, *Chimia* 1969, **23**, 194.
5. G. Emschwiller, *Compt. Rend.* 1954, **238**, 1414.
6. R. E. Wilde, S. N. Ghosh and B. J. Marshall, *Inorg. Chem.*, 1970, **9**, 2512.
7. D. Davidson and L. A. Welo, *J. Phys. Chem.* 1928, **32**, 1191.
8. K. Chandra, D. Raj and S. P. Puri, *J. Chem. Phys.* 1967, **46**, 1466.
9. M. B. Robin, *Inorg. Chem.* 1962, **1**, 337.
10. E. Fluck, W. Kerler and W. Neuwirth, *Angew Chem.* 1963, **75**, 461.
11. J. F. Duncan and P. W. R. Wigley, *J. Chem. Soc.* 1963, 1020.
12. S. C. Fung and H. G. Drickamer, *J. Chem. Phys.* 1969, **51**, 4353.
13. A. Ito, M. Suenaga and K. Ono, *J. Chem. Phys.* 1968, **48**, 3597.
14. N. Erickson and N. Elliot, *J. Phys. Chem. Solids* 1970, **31**, 1195.
15. J. F. Allen and B. R. Edwards, *J. Inorg. Nucl. Chem.* 1973, **35**, 3547.
16. K. Maer, Jr., M. L. Beasley, R. L. Collins and W. O. Milligan, *J. Am. Chem. Soc.* 1968, **90**, 3201.
17. D. Liebfritz and W. Bremser, *Chemiker-Zeitung* 1970, **94**, 982.
18. G. K. Wertheim and A. Rosenwaig, *J. Chem. Phys.* 1971, **54**, 3235.
19. H. J. Buser, A. Ludi, P. Fischer, T. Studach and B. W. Dale, *Z. Phys. Chem.* 1974, **92**, 354.
20. We will use Arabic numerals to indicate the charges on high spin ions and Roman numerals to indicate the charges on low spin ions throughout this paper.
21. H. J. Buser, D. Schwarzenbach, W. Petter and A. Ludi, *Inorg. Chem.* 1977, **16**, 2704.
22. D. B. Brown, D. F. Shriver and L. H. Schwartz, *Inorg. Chem.* 1968, **7**, 77.
    D. B. Brown and D. F. Shriver, *Inorg. Chem.* 1969, **8**, 37.
23. A. Ludi and H. U. Güdel, *Helv. Chim. Acta.* 1968, **51**, 2006.
24. A. Ludi and H. U. Güdel *Structure and Bonding*, Vol. 14, Chap. 1. Springer-Verlag, Berlin (1973).
25. A. K. Bonnette and J. F. Allen, *Inorg. Chem.* 1971, **10**, 1613.
26. H. J. Buser, Ph.D. Thesis. Universität Bern (1974).
27. B. N. Figgis and J. Lewis, *Progress in Inorganic Chemistry*, Vol. 6, Chap. 2. Interscience, New York (1964).
    B. N. Figgis and J. Lewis, *Techniques of Inorganic Chemistry*, Vol. IV, Chap. 4. Interscience, New York (1965).
28. V. E. Simmons, Ph.D. Thesis. Boston University (1963).
29. T. H. Gould, Ph.D. Thesis. The University of Michigan (1974).
    P. W. Merrithew, Ph.D. Thesis. The University of Michigan (1969).
30. W. R. Dunham, C. T. Wu, R. M. Polichar, R. H.

Sands and L. J. Harding, *Nucl. Inst. and Methods* 1977, **145**, 537.
31. A. N. Garg and P. S. Geol, *J. Inorg. Nucl. Chem.* 1970, **32**, 1547.
32. D. Hall, J. H. Slater, B. W. Fitzsimmons and K. Wade, *J. Chem. Soc. A* 1971, 800.
33. A. W. Chester and A. E. Schweizer, *Inorg. Nucl. Chem. Lett.* 1977, **7**, 451.
34. U. Weihofen, *Z. Naturforsch* 1972, **274**, 565.
35. M. Ruegg, A. Ludi and K. Ruder, *Inorg. Chem.* 1971, **10**, 1773.
36. D. W. Smith, *Inorg. Chem.* 1966, **5**, 2336.
37. F. Herren, P. Fischer, A. Ludi and W. Halg, *Inorg. Chem.* 1980, **19**, 956.
38. W. Perkins and Y. Hazony, *Phys. Rev. B* 1972, **5**, 7. G. K. Wertheim, D. N. E. Buchanen and H. J. Guggenheim, *Phys. Rev. B* 1970, **2**, 1392.
39. J. F. Allen and B. R. Edwards, *J. Inorg. Nucl. Chem.* 1973, **35**, 3547.
40. M. B. Robin and P. Day, *Adv. Inorg. Chem. Radiochem.* 1967, **10**, 248.

*Polyhedron* Vol. 3, No. 2, pp. 191–197, 1984
Printed in Great Britain.

0277–5387/84 $3.00 + .00
© 1984 Pergamon Press Ltd.

# THE KINETICS OF THE OXIDATION OF IODIDE AND THIOCYANATE IONS BY 12-TUNGSTOCOBALTATE(III)

**M. ADEGBOYEGA OLATUNJI* and G. ADEFIKAYO AYOKO**
Department of Chemistry, Ahmadu Bello University, Zaria, Nigeria

(*Received* 25 *May* 1983; *accepted* 21 *June* 1983)

**Abstract**—The rates and mechanism of the reaction of 12-tungstocobaltate(III) anion with thiocyanate and iodide ions have been examined in aqueous acidic solution and constant ionic strength I = 1.00M ($LiClO_4$). The reactions follow second-order kinetics, i.e. first-order in both the oxidant and the reductant and the rate constants are found to be independent of hydrogen ions in the range $[H^+] = 0.10$–1.00M. Outer-sphere mechanism is postulated for the systems based on the relative inertness of the oxidant and linear free energy relations are employed in demonstrating that in the reaction involving thiocyanate ion, the rate determining step is the diffusion apart of the product while the corresponding step in the iodide reaction is the electron transfer. The latter reaction is also catalysed by both bromide and chloride ions and this is rationalised in terms of possible stabilization of atomic iodine as product by these halide ions.

The oxidation of iodide by transition metal ions very often occurs through the formation of a metal–iodide complex. This has led in many instances to complex rate expressions such as those encountered in the reactions of aquoiron(III)[1] and ferricyanide complexes[2] with iodide ion. Similarly, the reduction of neptunium(V) by iodide ion was rationalized in terms of a fifth-order rate law[3] while second-order rate was observed by Ford-Smith and Rawsthorne[4] in the reaction of $Mo(CN)_8^{3-}$ with the same reductant. However, in a similar investigation of the latter reaction by Ferranti[5] the orders with respect to $Mo(CN)_8^{3-}$ and $I^-$ were found to be slightly greater than unity. Various workers[6–8] have also studied the reaction of $Fe(phen)_3^{3+}$ with $I^-$ and concluded that the reaction obeys a second-order rate-law. In their own contribution Ojo *et al.*[6] postulated an outer-sphere mechanism based on the relative inertness of the oxidant and supported by the observed catalysis of the reaction by added chloride and bromide ions while Kimura and Wada[8] discussed the mechanisms of the same reaction in aqueous mixtures of methanol and ethanol in terms of the effect of ionic strength and dielectric constant on the rate of reaction. More recently, in the oxidation of thiocyanate and/or iodide ions by iridium(IV), $Ir(bpy)_3^{3+/4+}$, $Ir(phen)_3^{3+/4+}$ and substituted poly-pyridine) iron(III) complexes[7] a two term rate-law, one first-and the other second-order in the ligands was observed in each case. As part of the continuing interest in the kinetics of the redox reactions involving iodide ion, its oxidation by 12-tungstocobaltate(III) anion was studied using the stopped-flow apparatus. The investigation was extended to the thiocyanate ion.

There are very few reports in the literature of redox reactions involving 12-tungstocobaltate(III) anion. The studies of the electron exchange between 12-tungstocobaltate(III) $[Co(III)O_4W_{12}O_{36}]^{5-}$ and 12-tungstocobaltate(II) $[Co(II)O_4W_{12}O_{36}]^{6-}$ anions (referred to in the text as [Co(III)] and [Co(II)] respectively) by Brubaker and Rasmussen[11] could be described as the pioneering work probably followed by those involving

*Author to whom correspondence should be addressed.

the thioureas as the reductants.[12] Recently, McAuley *et al.*[13] investigated the reactions of [Co(III)] with ascorbic acid, hydroquinone and catechol while the authors of this paper have just concluded the studies of the oxidation of some thiols[14] and aliphatic diols[15] by the same oxidant.

The present investigation was undertaken to accumulate more data on the reaction of 12-tungstocobaltate(III) anion and to investigate the effect, if any, of the symmetry of the central cobalt atom on the rate of redox reactions involving this oxidant and $Co_{aq}^{3+}$. Cobalt atom is in a tetrahedral environment in 12-tungstocobaltate(III) anion[16,17] while it is octahedrally surrounded by water molecules in aquocobaltic ion[18] whose reactions with iodide and thiocyanate ions have been reported by Davies and Watkins.[19]

## EXPERIMENTAL

### *Materials*

Potassium 12-tungstocobaltate(III) was prepared by the method given in the literature.[20,14] The molar extinction coefficient $\epsilon$ obtained at 390 nm is $1180 \pm 20\ M^{-1}\,cm^{-1}$ which is in good agreement with values of $1185\ M^{-1}\,cm^{-1}$ at $\lambda = 390$ nm,[12] and $1150 \pm 5\ M^{-1}\,cm^{-1}$ at $\lambda = 388$ nm.[13]

Analar grade sodium thiocyanate and sodium iodide were used without further purification. Stock solution of sodium iodide was standardised gravimetrically as AgI while the concentration of the corresponding solution of sodium thiocyanate was determined by titration with $AgNO_3$, using ferric ammonium sulphate as the indicator. Perchloric acid was used to investigate the effect of hydrogen ions on the reactions while the ionic strength was kept constant at 1.00 M using lithium perchlorate. All other reagents were used without further purification.

### *Stoichiometry*

The stoichiometries of the reactions were determined by spectrophotometric titration at $\lambda = 390$ nm using constant initial concentrations of $[Co(III)] = 2.00 \times 10^{-4}$ M and $[H^+] = 0.05$ M but varying concentrations of the two ligands in the range $(0.80 - 9.60) \times 10^{-4}$ M. The ionic strength was kept constant at 1.00 M using $LiClO_4$ solution.

### *Kinetics*

The oxidation of $SCN^-$ by [Co(III)] was slow under the conditions employed in the kinetic investigation, its rate was therefore measured at 390 nm using Pye Unicam SP 8000 spectrophotometer. The rate of the faster reaction involving $I^-$ with [Co(III)] was monitored using a Durrum–Gibson stopped-flow spectrophotometer. Unlike the former reaction where the decrease in the concentration of [Co(III)] with time was measured, in the reaction of $I^-$ with [Co(III)] the rate of formation of the product was monitored at 370 nm where triiodide is the only absorbing species at the concentrations used. All measurements were made under pseudo-first-order conditions using the following reactant concentrations: $[Co(III)] = 2.00 \times 10^{-4}$ M; [Ligand] = $(2.00 - 12.00) \times 10^{-3}$ M; $[H^+] = 0.10$–$1.00$ M and $I = 1.00$ M ($LiClO_4$).

## RESULTS AND DISCUSSION

Stoichiometric studies indicated that for each mole of [Co(III)], $1.04 \pm 0.01$ mole of iodide and $1.03 \pm 0.03$ mole of thiocyanate ions were oxidized. The equations for the overall reactions are as follows:

$$2[Co(III)] + 3\,I^- \rightarrow 2[Co(II)] + I_3^- \quad (1)$$

$$2[Co(III)] + 2\,SCN^- \rightarrow 2[Co(II)] + (SCN)_2. \quad (2)$$

In reaction (I), the products were confirmed by spectral measurement of reaction mixtures which exhibited absorption peaks at 350 nm and 625 nm characteristic of $I_3^-$[1,4] and [Co(II)][13] respectively. Although thiocyanogen is indicated as one of the reaction products of the oxidation of thiocyanate by the same oxidant, it is known[21,22] to undergo hydrolysis quite readily in aqueous solution according to eqn (3).

$$4H_2O + 3(SCN)_2 \rightarrow 7H^+ + 5SCN^- + HCN + SO_4^{2-}. \quad (3)$$

Using the method employed by Ng and Henry[23] cyanide was identified as one of the reaction products by the precipitation of AgCN using $AgNO_3$ and comparing its IR spectrum with a known sample. Similarly $SO_4^{2-}$ was shown to be present by the production of a white precipitate on addition of $BaCl_2$ to a reaction mixture in which [Co(III)] had been completely reduced to [Co(II)]. $SO_4^{2-}$ and $CN^-$ ions have also been indicated or confirmed as reaction products of thiocyanate oxidations by $Fe(phen)_3^{3+}$ and its derivatives,[23] $Fe_{aq}^{3+}$,[24] $H_2O_2$,[25] Cr(VI)[26] and Ir(IV)[9] in acidic media. However, in the reduction of $Co_{aq}^{3+}$ in aqueous solution[19] and $Fe_{aq}^{3+}$ in acetonitrile[27] by $SCN^-$ ions, thiocyanogen was confirmed as the reaction products.

Under the conditions employed for the kinetic investigations, pseudo-first-order plots were linear

to more than 90% of the reaction, suggesting that the reactions were all first-order in [Co(III)]. From the slopes of such linear plots, the pseudo-first-order rate constants $k_{obs}$ were determined at different initial concentrations of the ligands and hydrogen ions. The values of the $k_{obs}$ thus evaluated are presented in Table 1. These were found to be independent of $[H^+]$ varied between 0.10 and 1.00 M. Plots of $k_{obs}$ vs ligand concentrations were linear suggesting that the reactions were first-order in each of the ligands. Values of the second-order rate constants $k'$ obtained from these plots are also shown in Table 1. Added bromide and chloride ions catalysed the rate of oxidation of iodide ions by [Co(III)] with the bromide ions having a much greater catalytic effect (Table 1 and Fig. 1).

From the results obtained above, the general rate law for the oxidation of iodide and thiocyanate ions by [Co(III)] can be written as

$$\frac{-\frac{1}{2}\mathrm{d[Co(III)]}}{\mathrm{d}t} = \frac{\mathrm{d}(X_2)}{\mathrm{d}t} = k'[\mathrm{Co(III)}][X^-] \quad (4)$$

where $X$ is either I or SCN.

A general mechanism consistent with the rate law is suggested below for the two reactions where $X^-$ represents either iodide or thiocyanate ion.

$$[\mathrm{Co(III)}] + X^- \underset{k_{-1}}{\overset{k_1}{\rightleftharpoons}} [\mathrm{Co(II)}] + X^{\cdot} \quad (5)$$

$$X^{\cdot} + X^- \underset{k_{-2}}{\overset{k_2}{\rightleftharpoons}} X_2^{\cdot-} \quad (6)$$

$$[\mathrm{Co(III)}] + X_2^{\cdot-} \xrightarrow{k_3} [\mathrm{Co(II)}] + X_2. \quad (7)$$

If the steady state approximation is applied to reactions 5–7 above, assuming eqns (3) and (7) are rapid, a rate-law given by eqn (8) is obtained.

$$\frac{-\mathrm{d[Co(III)]}}{\mathrm{d}t} = \frac{2k_1k_2k_3[\mathrm{Co(III)}]^2[X^-]^2}{k_{-1}k_{-2}[\mathrm{Co(II)}] + k_{-1}k_3[\mathrm{Co(II)}][\mathrm{Co(III)}] + k_2k_3[\mathrm{Co(III)}][X^-]}. \quad (8)$$

Table 1. Second-order rate constants at various $[H^+]$ and $[X^-]$ concentrations. $[\mathrm{Co(III)}] = 2.00 \times 10^{-4}$ M; I = 1.00 M; $[X^-]$ = iodide or thiocyanate ion

a. $[X^-]$ = Iodide ion, T = 25.0°C λ = 370nm.

| $[H^+]$/M | $10^3[X^-]$/M | $[Cl^-]$/M | $[Br^-]$/M | $k_{obs}/s^{-1}$ | $[H^+]$/M | $10^3[X^-]$/M | $k_{obs}/s^{-1}$ |
|---|---|---|---|---|---|---|---|
| 0.50 | 1.00 | | | 0.34 | 0.10 | 4.00 | 1.38 |
| 0.50 | 2.00 | | | 0.68 | 0.20 | 4.00 | 1.41 |
| 0.50 | 4.00 | | | 1.33 | 0.30 | 4.00 | 1.38 |
| 0.50 | 4.00 | 0.01 | | 1.41 | 0.50 | 4.00 | 1.33 |
| 0.50 | 4.00 | 0.10 | | 1.44 | 0.80 | 4.00 | 1.36 |
| 0.50 | 4.00 | 0.50 | | 1.56 | 1.00 | 4.00 | 1.41 |
| 0.50 | 4.00 | | 0.01 | 2.69 | | | |
| 0.50 | 4.00 | | 0.05 | 4.50 | | | |
| 0.50 | 4.00 | | 0.10 | 7.28 | | | |
| 0.50 | 6.00 | | | 1.82 | | | |
| 0.50 | 8.00 | | | 2.75 | | | |
| 0.50 | 10.00 | | | 3.54 | | | |
| 0.50 | 12.00 | | | 4.15 | | | |

[a] $k' = 341 \pm 42\ M^{-1}s^{-1}$

b. $[X^-]$ = Thiocyanate ion T = 25.3°C λ = 390nm.

| $[H^+]$/M | $10^3[X^-]$/M | $k_{obs}/s^{-1}$ | $[H^+]$/M | $10^3[X^-]$/M | $k_{obs}/s^{-1}$ |
|---|---|---|---|---|---|
| 0.10 | 2.00 | 0.59 | 0.50 | 2.00 | 0.56 |
| 0.10 | 4.00 | 1.16 | 0.50 | 4.00 | 1.20 |
| 0.10 | 6.00 | 1.75 | 0.50 | 6.00 | 1.73 |
| 0.10 | 8.00 | 2.25 | 0.50 | 8.00 | 2.32 |
| 0.10 | 10.00 | 2.88 | 0.50 | 10.00 | 3.06 |
| 0.10 | 12.00 | 3.47 | 0.50 | 12.00 | 3.67 |

[a] $k' = 0.292 \pm 0.006\ M^{-1}s^{-1}$

[a] Error expressed as standard deviation

Provided $k_{-1}[Co(II)] \{k_{-2} + k_3[Co(III)]\} \ll k_2k_3[Co(III)](X^-)$ eqn (8) reduces to the observed rate law where $k^1 = 2k_1$. In the mechanism above, the final fast step of the reaction involving the iodide ion (i.e. when $X^- = I^-$) is the reaction of iodine generated from the redox steps with excess $I^-$ to give the identified triiodide product.

$$I_2 + I^- \overset{K_{I_3^-}}{\rightleftharpoons} I_3^- \qquad (9)$$

where $K_{I_3^-}$ is 768 $M^{-1}$.[28]

The standard redox potential for $I^{\cdot}/I^-$ and $I_2^{\cdot-}/I^-$ couples are in the ranges 1.33–1.42 and 1.04–1.18 V respectively,[9,10,29] while for the $SCN^{\cdot}/SCN^-$ couple, $E^{\ominus}$ is 1.62–1.66[9,10] V although a value of 1.80 V has been reported by Malone and Endicott.[30] On the other hand, the standard reduction potential of the oxidant is 1.00 V.[16] These values imply that the free energy of reaction $\Delta G^{\ominus}$ for the step involving the transfer of an electron has a value greater than zero. However, although the equilibrium in reaction 5 may lie heavily to the left, a substantial amount of the intermediate species $X^{\cdot}$ may still be produced to allow the overall reaction to occur. It is suggested that the depletion of the $X^{\cdot}$ radical formed may provide a force for driving the equilibria in reaction 5 to the right against unfavourable thermodynamic factors. The existence of the ion-radical $X_2^{\cdot-}$ as an intermediate in reactions of $SCN^-$ and $I^-$ ions is well documented.[7,9,10,23] In reactions of the iodide ion, the free energy change accompanying the formation of $I_2^{\cdot-}$ from iodide radical (eqn 10) is highly favourable

$$I^{\cdot} + I^- \overset{K_{I_2^{\cdot-}}}{\rightleftharpoons} I_2^{\cdot-}$$

$$K_{I_2^{\cdot-}} \text{ is } 1.30 \times 10^5\ M^{-1}[31]. \qquad (10)$$

Under the conditions used for the kinetic investigations (i.e. pseudo first-order) the formation of this reactive intermediate is proposed to be an important step in the reaction involving these reductants. Based on the established substitution inertness of the oxidant[13] and the fact that it has no empty and low-lying $\pi$ or $\pi^*$ orbitals to overlap with $\pi$ orbitals of the reductants, outer-sphere ion pairs are also assumed to be the precursor complexes in these reactions.

*Intimate mechanism*

Stanbury *et al.*[9] interpreted the observed data in the outersphere oxidations of $I^-$ and $SCN^-$ ions by Ir(IV) using a combination of intimate mechanism and linear free energy relationship (LFER). Their proposed scheme for such reactions having a bimolecular rate law was

$$Ox + X^- \overset{K_{lip}}{\rightleftharpoons} Ox,\ X^- \qquad (11)$$

$$Ox,\ X^- \underset{k_{-let}}{\overset{k_{let}}{\rightleftharpoons}} Red,\ X^{\cdot} \qquad (12)$$

$$Red,\ X^{\cdot} \underset{k_{-1d}}{\overset{k_{1d}}{\rightleftharpoons}} Red + X^{\cdot} \qquad (13)$$

which on application of steady-state approximation gave

$$k_1 = \frac{k_{lip}k_{let}k_{1d}}{k_{-let} + k_1 d}. \qquad (14)$$

In the application of the LFER to the systems, Stanbury *et al.*[9] plotted log $k_1$ (as defined in this text) as a function of log $K_{eq}$($K_{eq}$ is the equilibrium constant for reaction 5 and was calculated from the relationship $23.06\Delta E^{\ominus} = -RT \ln K_{eq}$) for a series of outer-sphere reactions involving one electron oxidants with $SCN^-$ and $I^-$ ions and obtained a straight line with a slope of unity. This they interpreted to mean the insensitivity of the rates to the nature of the oxidant and by implication that the rate-determining step was not electron-transfer but diffusion apart of the products.

Using the data provided by them and other references contained there in, together with those obtained from this work, Table 2 was constructed from which Fig. 2 was also obtained. Using the method of least squares, a slope of 0.88 was arrived at which is in good agreement with the value of 1.00 obtained by them. Considering the title reactions, only the point corresponding to the reaction of [Co(III)] with $SCN^-$ was found to fall in line (Fig. 2, Point 9). However, when the other known value of $E^{\ominus}$ (1.80 V)[30] for the $SCN^{\cdot}/SCN^-$ couple was used in calculating $K_{eq}$ for the cross-reaction that point too was found to be off the line (Fig. 2, point 12). We therefore conclude that while the rate-determining step in the oxidation of $SCN^-$ ion by [Co(III)] may be the diffusion apart of the products, the corresponding step in the oxidation of the iodide is the electron-transfer process. This latter conclusion is in good agreement with similar observations made by other workers[4,7,10] while the former could also be assumed to be in line with an argument put forward by Ng and Henry[23] that the thiocyanate radical being a high energy species

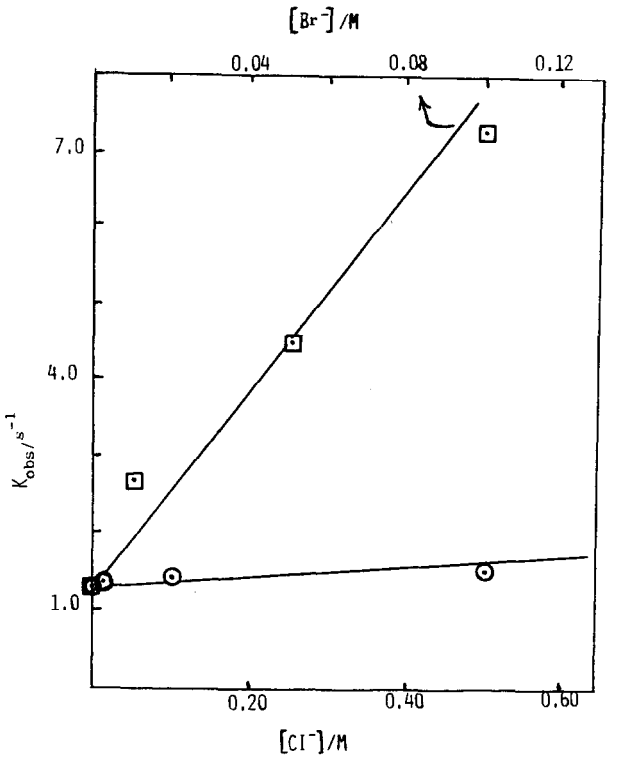



Fig. 1. Effect of added bromide and chloride ions on observed second-order rate constants for [Co(III)] + $I^-$ reaction at $T = 25°C$. ⊡, Bromide ion; ⊙, chloride ion $[H^+] = 0.50$ M, I = 1.00 M ($LiClO_4$).

Table 2. Kinetic and thermodynamic parameters for the oxidation of iodide[a] and thiocyanate[b] ions by one electron oxidants

| No. | Oxidant | Reductant | $k_1/M^{-1}s^{-1}$ | $E^{\circ}/V$ |
|---|---|---|---|---|
| 1. | $IrBr_6^{2-}$ | $I^-$ | 28 | 0.843[c] |
| 2. | $IrCl_6^{2-}$ | $I^-$ | 409[d] | 0.892[e] |
| 3. | $Mo(CN)_8^{3-}$ | $I^-$ | 1.5[f] | 0.75[g] |
| 4. | $Fe(bpy)_3^{3+}$ | $I^-$ | $1.0 \times 10^5$[h] | 1.06[i] |
| 5. | $Os(bpy)_3^{3+}$ | $I^-$ | 16.5[j] | 0.837[j] |
| 6. | $Os(phen)_3^{3+}$ | $I^-$ | 26[j] | 0.84[j] |
| 7. | $Fe(phen)_3^{3+}$ | $I^-$ | $3.24 \times 10^5$[k] | 1.06[i] |
| 8. | {Co(III)} | $I^-$ | 341[m] | 1.00[n] |
| 9. | {Co(III)} | $SCN^-$ | 0.146[m] | 1.00[n] |
| 10. | $Fe(bpy)_3^{3+}$ | $SCN^-$ | 5.495[h] | 1.06[i] |
| 11. | $IrCl_6^{2-}$ | $SCN^-$ | $4.6 \times 10^{-3}$[d] | 0.892[e] |

[a] $I^{\cdot} + e \rightarrow I^-$, $E^{\circ} = 1.33V$[g]. [b] $SCN^{\cdot} + e \rightarrow SCN^-$, $E^{\circ} = 1.66V$[g]. [c] Reference 33. [d] Reference 9. [e] Reference 34. [f] Reference 5. [g] Reference 35. [h] Reference 36. [i] Reference 37. [j] Reference 10. [k] Reference 8. [l] Reference 23. [m] This work. [n] Reference 16.

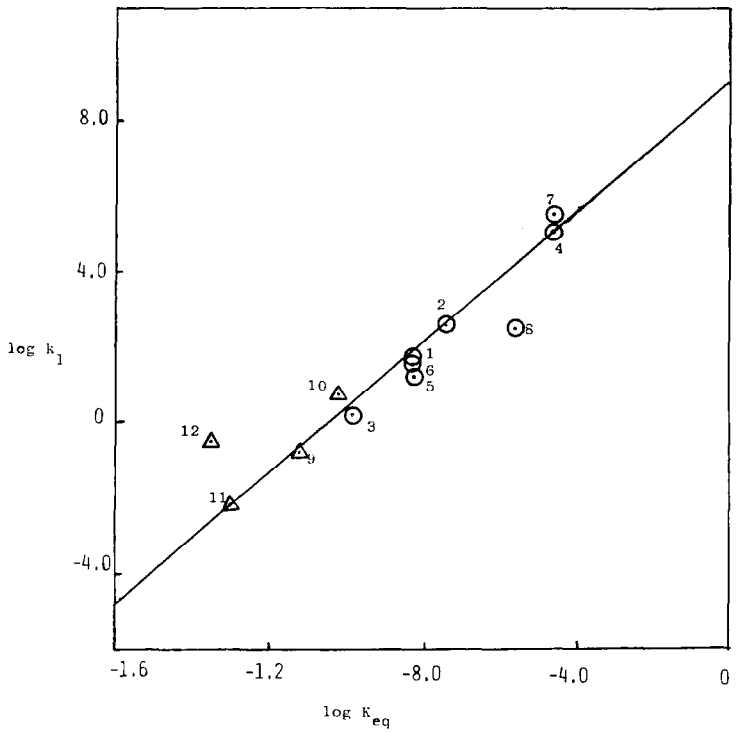



Fig. 2. LFER for oxidations of $I^-$ and $SCN^-$ ions. Points are numbered as in Table 2. △, $SCN^-$ reactions; ⊙, $I^-$ reactions.

dissociates with reluctance from a formed intermediate or ion-pair complex after the electron-transfer. However such conclusion must be made with some reservations in view of the inherent errors in the estimation of the $E^\ominus$ for the various couples.

The observed increase in rate on addition of halide ions in the reduction of [Co(III)] by $I^-$ ion could be due to the association of the halide ion with atomic iodine when it is in the process of being formed. This association stabilizes the atomic iodine and lowers the potential energy barrier for the redox process. Since 5*p* orbitals of iodide ion are more comparable with the 4*p* orbitals of $Br^-$ ion in size than the 3*p* of $Cl^-$, the former would produce greater stabilization and therefore higher catalysing effect, as was found in this study (Table 1 and Fig. 1). Similar observations have been made in the oxidation of $Fe(phen)_3^{3+}$ with $I^-$[6] and also by Wilmarth and Haim[32] in the oxidation of halides and pseudo-halides. However, it is difficult to see why $I^-$ should not be self-catalyzing, i.e. the order in $[I^-]$ to be greater than one in view of the fact that the greater stabilization would be the formation of $I_2^-$. The only explanation the authors could offer is the low concentration of the reductants employed in the kinetic studies. At higher iodide concentrations the rate law may contain the $[I^-]^2$ term. This is not unreasonable in view of the higher concentrations of the $Cl^-$ and $Br^-$ ions employed to bring about the observed catalysis.

The energies of activation for the reactions of various ligands with [Co(III)] are lower than those of the corresponding reactions of the ligands with $Co_{aq}^{3+}$ (Table 3). This is attributed to the symmetries of the central cobalt atom in $Co_{aq}^{3+}$ (octahedral)[18] and [Co(III)] (tetrahedral)[16,17] and the attendant difference in electronic configurations of the cobalt atom in these complexes. In going from $Co_{aq}^{3+}$ ($t_{2g}^6$) to $Co_{aq}^{2+}$ ($t_{2g}^5 e_g^2$) an electron is transferred from a $t_{2g}$ to an $e_g$ level. This process would be expected to be accompanied by a drastic internal rearrangement and hence high energy requirement while in the reduction of [Co(III)] ($e^3 t_2^3$) to [Co(II)] ($e^4 t_2^3$) where spin inversion is not expected, lower energies of activation should be observed as Table 3 shows.

In conclusion, the first electron-transfer step in the reduction of [Co(III)] by iodide ion is the intramolecular electron transfer within an ion pair complex. This step for which the quoted values of

Table 3. Activation parameters for some reactions involving $Co^{3+}_{aq}$ and [Co(III)] in aqueous perchloric acid at 25°C

| Reductant | Oxidant | $\Delta H^{\ddagger}$/KJ $mol^{-1}$ | $\Delta S^{\ddagger}/JK^{-1}mol^{-1}$ | Ref. |
|---|---|---|---|---|
| $SCN^-$ | $Co^{3+}_{aq}$ | 86.19 | 83.68 | 19 |
| $SCN^-$ | [Co(III)] | 27.45 | -163.22 | a |
| $HNO_2$ | $Co^{3+}_{aq}$ | 76.57 | 37.66 | 19 |
| $H_2Q^b$ | $Co^{3+}_{aq}$ | 76.15 | 75.31 | 19 |
| $H_2Q^b$ | [Co(III)] | 15.06 | -142.26 | 13 |
| $I^-$ | $Co^{3+}_{aq}$ | 81.17 | 104.60 | 19 |

[a] This work

$H_2Q^b$ = Hydroquinone

the redox potentials show that $\Delta G^{\ddagger} > 0$, is proposed as the rate-determining step while in the reaction involving thiocyanate ion the corresponding step is the diffusion apart of the products.

*Acknowledgement*—We thank Ahmadu Bello University for the award of Graduate-Assistantship to G.A.A.

## REFERENCES


1. (a) A. J. Fudge and K. W. Sykes, *J. Chem. Soc.* 1952, 119. (b) K. W. Sykes, *Ibid.* 1952, 124.
2. Y. A. Majid and K. E. Howlett, *J. Chem. Soc. (A)* 1968, 679.
3. N. K. Shastri, T. O. Wear and E. S. Amis, *J. Inorg. Nucl. Chem.* 1962, **24**, 535.
4. M. H. Ford-Smith and J. H. Rawsthorne, *J. Chem. Soc.(A)* 1969, 160.
5. F. Ferranti, *J. Chem. Soc. (A)* 1970, 134.
6. J. Ige, J. F. Ojo and O. Olubuyide, *Can. J. Chem.* 1979, **57**, 2065.
7. C. O. Adedinsewo and A. Adegite, *Inorg. Chem.* 1979, **18**, 3597.
8. M. Kimura and G. Wada, *Inorg. Chem.* 1978, **17**, 2239.
9. D. M. Stanbury, W. K. Wilmarth, S. Khalaf, H. N. Po and J. E. Byrd, *Inorg. Chem.* 1980, **19**, 2715.
10. G. Nord, B. Pedersen and O. Farver, *Inorg. Chem.* 1978, **17**, 2233.
11. C. H. Brubakar and P. G. Rasmussen, *Inorg. Chem.* 1964, **3**, 977.
12. M. A. Olatunji, Ph.D. Thesis. University of Glasgow, Glasgow (1975).
13. Z. Amjad, J. C. Brodovitch and A. McAuley, *Can. J. Chem.* 1977, **55**, 3581.
14. G. A. Ayoko and M. A. Olatunji, *Polyhedron*, 1983, **2**, 577.
15. G. A. Ayoko and M. A. Olatunji, to be submitted.
16. L. C. W. Baker and V. E. Simons, *J. A.m. Chem. Soc.* 1959, **81**, 4744.
17. F. A. Cotton and G. Wilkinson, *Advanced Inorganic Chemistry*, 3rd Edn, p. 954. Wiley, New Delhi (1979).
18. *Ibid.* p. 884.
19. G. Davies and K. O. Watkins, *J. Phys. Chem.* 1970, **74**, 3388.
20. L. C. W. Baker and T. P. McCutcheon, *J. Am. Chem. Soc.* 1956, **78**, 4503.
21. H. Lecher, M. Wittwer and W. Speer, *Ber.* 1923, **56**, 1104.
22. R. Gauguin, *J. Chim. Phys.* 1945, **42**, 138.
23. F. T. T. Ng and P. M. Henry, *Can. J. Chem.* 1975, **53**, 3319.
24. R. H. Betts and F. S. Dainton, *J. Am. Chem. Soc.* 1953, **75**, 5721.
25. I. R. Wilson and G. M. Harris, *J. Am. Chem. Soc.* 1961, **83**, 286.
26. K. A. Muirhead and G. P. Haight Jr., *Inorg. Chem.* 1973, **12**, 1116.
27. B. Kratochvil and R. Long, *Anal. Chem.* 1970, **42**, 43.
28. M. Davies and E. Gwynne, *J. Am. Chem. Soc.* 1952, **74**, 2748.
29. W. H. Woodruff and D. W. Margerum, *Inorg. Chem.* 1973, **12**, 962.
30. S. D. Malone and J. F. Endicott, *J. Phys. Chem.* 1972, **76**, 2223.
31. J. H. Baxendale, P. L. T. Beyan and D. A. Stott, *Trans. Faraday Soc.* 1964, **64**, 2389.
32. W. K. Wilmarth and H. Haim, *Peroxide Reaction Mechanisms* (Edited by J. O. Edwards), p. 175. Wiley-Interscience, New York (1962).
33. P. Hurwitz and K. Kustin, *Trans Faraday Soc.* 1966, **62**, 427.
34. D. W. Margerum, K. L. Chellapa, F. P. Bossu and G. L. Burce, *J. Am. Chem. Soc.* 1975, **97**, 6894.
35. W. U. Malik and S. I. Ali, *Indian J. Chem.* 1963, **1**, 347.
36. J. E. Byrd, J. Y. Chen, H. N. Po, C. P. Chua and W. K. Wilmarth, *Abstracts, 167th National Meeting of the American Chemical Society Los Angeles*, CA, 31 March–5 April, 1974, Abstract No. INOR 102.
37. A. A. Schilt, *Analytical Applications of 1,10-Orthophenanthroline and Related Compounds*, p. 118. Pergamon Press, New York (1969).

*Polyhedron* Vol. 3, No. 2, pp. 199–212, 1984
Printed in Great Britain.

0277–5387/84 $3.00 + .00
© 1984 Pergamon Press Ltd.

# CLOSO CLUSTERS WITH UNUSUAL ELECTRON NUMBERS: LOCALIZED BOND SCHEMES FOR *n*-ATOM CLUSTERS WITH *n*, (*n* + 1) OR (*n* + 2) SKELETAL ELECTRON PAIRS

**MARION E. O'NEILL and KENNETH WADE***
Chemistry Department, Durham University, South Road, Durham DH1 3LE, England

(*Received* 1 *June* 1983; *accepted* 25 *July* 1983)

**Abstract**—This paper considers whether satisfactory localized 2- and 3-centre bond schemes may be devized for real or hypothetical clusters $B_nH_n^{c-}$ ($c = 0$, 2 or 4; $n = 4 \rightarrow 12$) or isoelectronic analogues thereof, with *closo* deltahedral shapes. As expected, localized bond schemes can be devized for all the species that would be predicted, using MO approaches, to have closed shell electronic configurations: these include species $B_nH_n^{2-}$ ($n = 5 \rightarrow 12$) and $B_nH_n^{c-}$ ($c = 0$ or 4; $n = 4$, 8, 9 or 11). There is also generally good agreement with MO treatments as to which systems are *not* expected to be stable: these include $B_4H_4^{2-}$ and $B_nH_n^{c-}$ ($c = 0$ or 4; $n = 5$, 7 or 10). Localized bond treatments have value for estimating the bond orders of cluster bonds in species $B_nH_n$ and $B_nH_n^{2-}$, though they overestimate the bond orders in species $B_nH_n^{4-}$ (except when $n = 4$). They are misleading, when applied to octahedral and icosahedral systems, in indicating the former shape to be feasible for hypothetical species $B_6H_6$ and $B_6H_6^{4-}$, and the latter shape to be feasible for hypothetical species $B_{12}H_{12}$ and $B_{12}H_{12}^{4-}$.

A striking feature of the structural chemistry of the higher boranes and related clusters is the link that exists between skeletal shapes and electron numbers.[1–8] Closed cage (*closo*) deltahedral shapes are normally adopted when the number of skeletal electron pairs exceeds the number of skeletal atoms by one, as in the case of anions $B_nH_n^{2-}$ and related neutral molecules $C_2B_{n-2}H_n$ ($n = 5 \rightarrow 12$). More open structures are adopted by species with more skeletal electrons, though even for these the normal pattern is for the structure to be based on a polyhedron with one vertex fewer than the number of skeletal electron pairs. There are, however, a few important systems that are our concern here, in which a *closo* *n*-vertex deltahedral structure is found to be associated with *n* or (*n* + 2) skeletal electron pairs instead of the more usual (*n* + 1) pairs. Examples include the neutral chlorides $B_8Cl_8$[9] and $B_9Cl_9$[10] which, like the metallaborane $(C_5H_5)_4Co_4B_4H_4$[11], are *n*-atom *n*-electron pair systems. Examples of *n*-atom (*n* + 2)-electron pair systems with *closo* deltahedral structures include the metallaborane $(C_5H_5)_4Ni_4B_4H_4$[12] and the cationic bismuth cluster $Bi_9^{5+}$.[13] It has been suggested[14] that an explanation for the unusual numbers of electrons these clusters contain lies in the fact that localized 2- and 3-centre bond schemes using *n*, (*n* + 1) or (*n* + 2) bond pairs can be devized for the deltahedra in question ($D_{2d}$ dodecahedron for the 8-atom clusters, $D_{3h}$ tricapped trigonal prism for the 9-atom clusters). We have elsewhere pointed out that a consideration of the degeneracies of the frontier orbitals of such clusters provides a better guide as to which shapes can tolerate other than the usual (*n* + 1) skeletal bond pairs, and that localized 2- and 3-centre bond schemes can be devized for such unlikely species as $B_6H_6$ and $B_6H_6^{4-}$.[15] Here we elaborate and extend our earlier discussion of localized bonds and explore further merits and defects of 2- and 3-centre bond treatments of *closo* borane-type clusters.

## LOCALIZED BOND SCHEMES. ASSUMPTIONS AND GENERALISATIONS

Our approach has been to explore whether the *closo* deltahedral structures of anions $B_nH_n^{2-}$ and carboranes $C_2B_{n-2}H_n$ might be compatible with the presence of *n* or (*n* + 2) skeletal electron pairs, as

*Author to whom correspondence should be addressed.

well as the more usual $(n + 1)$ bond pairs, by assigning these electrons to localized 2-centre B–B bonds along edges of the $B_n$ polyhedra, or to localized 3-centre BBB bonds in the polyhedral faces. To deduce how many of each bond type should be used, and how they should be distributed about the surfaces of the $B_n$ polyhedra, we have used Lipscomb's topological treatment of borane bonding[16,17] which has for long provided the standard treatment of the bonding in neutral *nido* or *arachno* boranes $B_nH_{n+4}$ or $B_nH_{n+6}$, although it has found only occasional application to *closo* species because these generally require large numbers of canonical forms to be considered. Computer programmes to search exhaustively for these canonical forms have been developed, and Epstein and Lipscomb[17] have listed the results of such searches for most known neutral *nido* and *arachno* boranes and for many *closo* borane anions $B_nH_n^{2-}$. Our intention here is to supplement their work by considering some systems they ignored, and by drawing attention to some general characteristics of localized bond schemes that have hitherto gone unremarked.

To start with, it is necessary to consider the salient features of the topological approach to borane bonding, and to note the assumptions on which it is based. Neutral boranes $B_nH_{n+m}$ are treated as aggregates of $n$ BH units, held together by $(2n + m)$ electrons—two provided by each BH unit, one by each of the extra $m$ hydrogen atoms. These framework or skeletal electrons are allocated to $s$ BHB bonds, $t$ BBB bonds, $y$ BB bonds and $x$ extra terminal BH bonds. For ionic species $B_nH_n^{c-}$, with no additional hydrogen atoms to be accommodated in BHB bonds or in extra terminal BH bonds, the equations relating $s$, $t$, $y$ and $x$ to each other reduce to the unique solutions $s = x = 0$, $t = n - c$ and $y = 3c/2$.[17,18] Values of $t$ and $y$ that concern us here, i.e. for values of $n$ ranging from 4 to 12 and values of $c$ of 0, 2 or 4, are listed in Table 1.

To allocate these bonds satisfactorily to polyhedral clusters like the *closo* anions $B_nH_n^{2-}$, one must take account of further basic assumptions of the topological approach. These are as follows.

(1) Each skeletal atom is assumed to participate in three skeletal bonds (the other bond it can form, by use of the fourth of its valence shell orbitals, links it to the *exo* hydrogen atom).

(2) Each point of contact between bonded atoms—each edge of the skeletal $B_n$ polyhedron—must be accounted for, either by a 2-centre bond along that edge, by two 3-centre bonds adjacent to that edge, or by one 3-centre bond adjacent to it (Fig. 1a).

(3) Two boron atoms cannot simultaneously be bonded to each other by both a 2-centre BB bond and one or two 3-centre BBB bonds, as shown in Fig. 1(b), as these arrangements would require too close an alignment of the atomic orbitals involved, and would imply a greater concentration of electronic charge near to one polyhedron edge than is reasonable in these systems, which generally contain far fewer skeletal electron pairs [$(n + 1)$ pairs for systems $B_nH_n^{2-}$] than polyhedral edges [$3(n - 2)$ for $n$-vertex deltahedra].

(4) Cross-polyhedral interactions, which are generally significantly longer than polyhedral edge interactions, are considered to be nonbonded.

(5) Where individual bond networks do not match the symmetry of the polyhedron in question (as is generally the case), resonance between all plausible canonical forms needs to be invoked.

Bearing in mind these assumptions, we can deduce what bond arrangements are possible for specific cluster systems. In doing so, it is helpful to take account of the skeletal coordination numbers

Table 1. Values of $t$ (the number of 3-centre BBB bonds) and $y$ (the number of 2-centre BB bonds) for clusters $B_nH_n^{c-}$ ($c = 0$, 2 or 4)

| | | n | 4 | 5 | 6 | 7 | 8 | 9 | 10 | 11 | 12 |
|---|---|---|---|---|---|---|---|---|---|---|---|
| c = 0 | y = 0 | t | 4 | 5 | 6 | 7 | 8 | 9 | 10 | 11 | 12 |
| c = 2 | y = 3 | t | 2 | 3 | 4 | 5 | 6 | 7 | 8 | 9 | 10 |
| c = 4 | y = 6 | t | 0 | 1 | 2 | 3 | 4 | 5 | 6 | 7 | 8 |

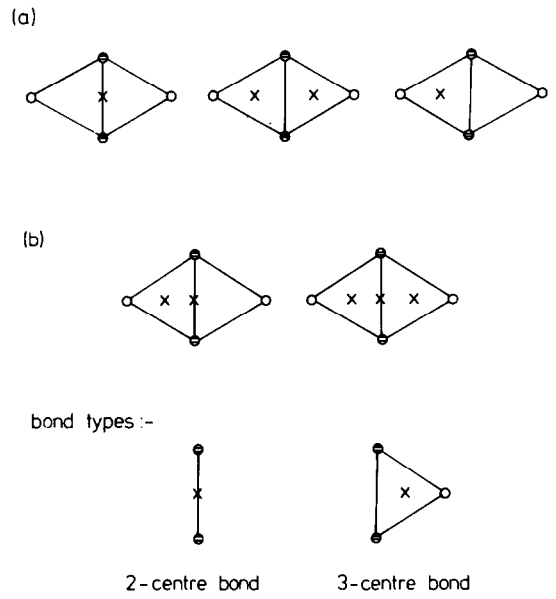



Fig. 1. Localized bond arrangements by which points of contact (the point of contact under consideration is that between the shaded atoms) between skeletal atoms (polyhedral edges) can be accounted for: (a) plausible arrangements (b) arrangements excluded.

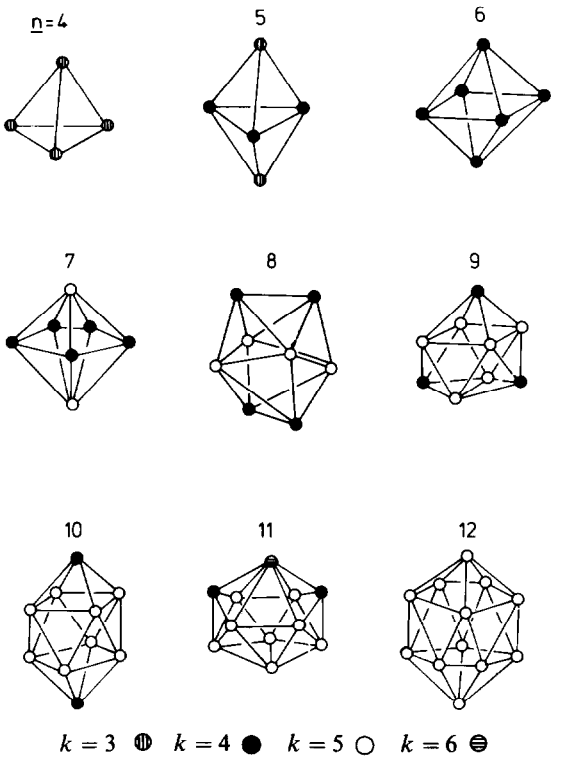



Fig. 2. The polyhedral skeletons of boron halide clusters $B_nX_n$ ($n = 4$, 8 or 9), borane anions $B_nH_n^{2-}$ ($n = 6 \rightarrow 12$) or carboranes $C_2B_{n-2}H_n$ ($n = 5 \rightarrow 12$) showing skeletal connectivities $k$.

or skeletal connectivities, $k$, of individual skeletal atoms—the numbers of neighbouring skeletal atoms to which particular atoms are directly linked by polyhedral edges. Figure 2 shows the series of polyhedra known for boron halide clusters $B_nX_n$ ($n = 4$, 8 or 9) or for borane anions $B_nH_n^{2-}$ ($n = 6 \rightarrow 12$) or carboranes $C_2B_{n-2}H_n$ ($n = 5 \rightarrow 12$). In these, $k$ ranges from 3 to 6. The localized bonding arrangements that are compatible with these connectivities, and with the assumptions listed above, are shown in Fig. 3. From this, we see that a skeletal atom with only three skeletal neighbours can bond to these either by using three 2-centre bonds along the polyhedral edges or by using three 3-centre bonds in the polyhedral faces that meet at that atom. Combinations of two 2-centre bonds and one 3-centre bond, or of one 2-centre bond and two 3-centre bonds, are excluded by assumption 3 above. An atom with four skeletal neighbours cannot bond exclusively to them by means of 2-centre bonds, since that would require it to participate in four skeletal bonds, contravening assumption 1 above. It can, however, use exclusively 3-centre bonds, or combinations of one 2-centre bond and two 3-centre bonds, or one 3-centre bond and two 2-centre bonds. An atom with five skeletal neighbours can use three 3-centre bonds, or two 3-centre bonds and one 2-centre bond, while an atom with six skeletal neighbours

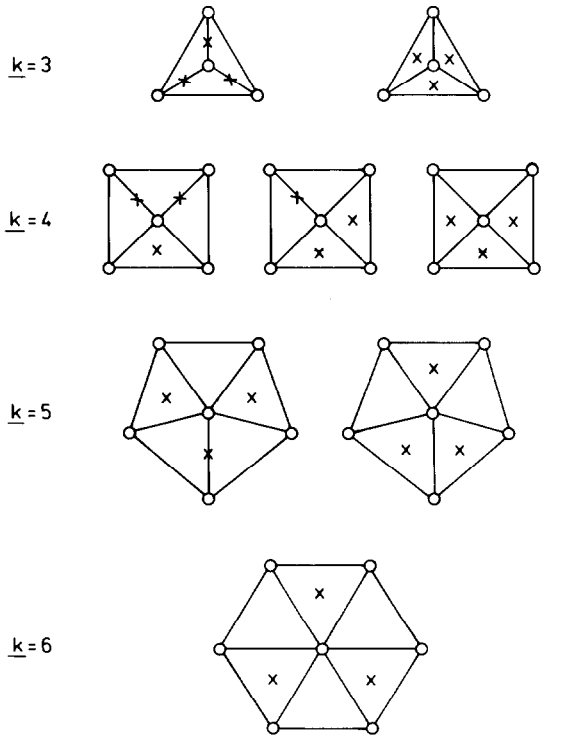



Fig. 3. The bonding networks by which atoms of particular connectivities $k$ can bond to their skeletal neighbours.

has only one bonding option open to it, which is to use three 3-centre bonds.

Before exploring the compatibility of these localized bond arrangements with the connectivity requirements of all the atoms of complete polyhedra, it is worth noting how strongly the bond arrangements shown in Fig. 3 connect the central atoms to their neighbours. As we shall be trying to rationalise the lengths of the edges in specific polyedra, it is convenient to regard the bonding power of the skeletal bond pairs as channelled along the polyhedral edges, whether the bond pairs occupy 2-centre edge bonds or 3-centre face bonds, and to estimate the *edge bond order*, $e$, of each polyhedral edge (which will generally prove to be $< 1$). An edge to which a 2-centre edge bond is assigned is assumed to have $e = 1.0$. Each of the three edges surrounding a 3-centre face bond is assumed to have a bond order of 1/3 (0.33′). Edges between two 3-centre face bonds are assumed to have a bond order of 2/3 (0.66′). Intermediate values of the edge bond order, $e$, are possible for edges to which two or more different bond arrangements contribute as resonance canonical forms.

The two bonding possibilities (Fig. 3) open to an atom of skeletal connectivity $k = 3$, for example, generate edge bond orders $e$ of 1.0 and 2/3 (0.66′) respectively. If both bond arrangements are equally possible, resonance between the two will lead to an average edge bond order $e$, of 5/6 (0.83′), and a *total* bond order, $ke$, of 2.5 for the three skeletal bonds formed by such an atom. The edge bond orders corresponding to the other possible values of $k$ illustrated in Fig. 3 are given in Table 2, which reveals some interesting trends. Not surprisingly, the mean bond order of the edge bonds formed by a particular atom decreases as the skeletal connectivity, $k$, of that atom increases, since a higher proportion of 3-centre bonds needs to be used as $k$ increases. Perhaps less obviously expected is the trend in $ke$, the total order of the $k$ skeletal bonds formed by a particular atom, which also decreases as $k$ increases, provided that all the bonding options shown in Fig. 3 can be utilised, and are given equal weight. The implication of this trend is that atoms of low coordination number in clusters require a greater share of the skeletal bonding electrons than their more highly coordinated neighbours, and so are expected to be the more negatively charged, a conclusion consistent with the results of MO calculations and also with studies of the spectra and reactions of specific clusters.[16-21]

In the following section, we illustrate the localized bond networks with which the skeletal bonding in some specific systems can be described, and draw attention to respects in which these networks appear either particularly apt or particularly misleading.

## APPLICATIONS TO SPECIFIC POLYHEDRAL SYSTEMS $B_nH_n^{c-}$ ($c = 0$, 2 OR 4)

### *Tetrahedral* $B_4H_4$ *systems*

It has long been recognized that tetrahedral clusters in which each skeletal atom is capable of forming 3 skeletal bonds can be held together either by six 2-centre edge bonds (as exemplified by tetrahedrane, $C_4H_4$, the carbon counterpart of $B_4H_4^{4-}$) or by four 3-centre face bonds (as exemplified by $B_4Cl_4$). In MO terms, these correspond to occupancy of the A, T and E-symmetry bonding MO's, or of only the A and T-symmetry bonding MO's, respectively. What is less generally recognized is that a localized bond treatment of a hypothetical species $B_4H_4^{2-}$, which on the arguments outlined above would require the use of three 2-centre BB bonds and two 3-centre BBB bonds, cannot be devized without recourse to

Table 2. Dependence of edge bond orders, $e$, on skeletal atom connectivities, $k$

| Connectivity, k | 3 | 3 | 4 | 4 | 4 | 5 | 5 | 6 |
|---|---|---|---|---|---|---|---|---|
| Number of 2-centre bonds | 3 | 0 | 2 | 1 | 0 | 1 | 0 | 0 |
| Number of 3-centre bonds | 0 | 3 | 1 | 2 | 3 | 2 | 3 | 3 |
| Mean edge bond order, e | 1 | 2/3 | 2/3 | 7/12 | 1/2 | 7/15 | 2/5 | 1/3 |
| ke | 3.0 | 2.0 | 2.6′ | 2.3′ | 2.0 | 2.3′ | 2.0 | 2.0 |
| Average ke* | 2.5 | | | 2.3′ | | 2.16′ | | 2.0 |

*Assuming all of the bond arrangements listed for a particular value of k are equally possible.

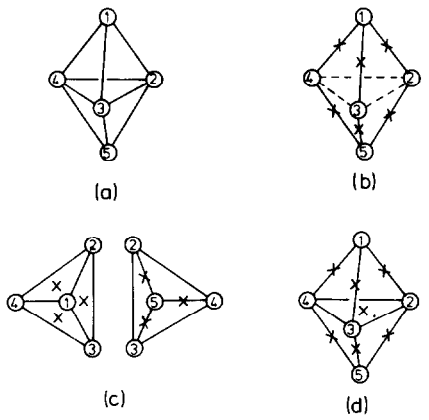



Fig. 4. (a) Skeletal structure of 1,5-$C_2B_3H_5$; (b) Classically bonded network of six 2-centre B–C bonds; (c) Alternative bond network, using three 2-centre and three 3-centre bonds; (d) Inappropriate network of one 3-centre and six 2-centre bonds for a hypothetical $D_{3h}$ species $B_5H_5^{4-}$.

unsatisfactory bond arrangements of the type shown in Fig. 1(b). Molecular orbital considerations would lead to the conclusion that a tetrahedral species $B_4H_4^{2-}$ would be paramagnetic and susceptible to Jahn–Teller distortion.[27] For the series $B_4Cl_4$, $B_4H_4^{2-}$ and $C_4H_4$, localized bond and MO treatments are thus in accord, in showing the tetrahedral arrangement of four BH or similar isolobal units to be compatible with four or six bond pairs, but not five pairs.

$D_{3h}$ $B_5H_5$ *systems*

Although $B_5H_5^{2-}$ is unknown, it would be expected to have a structure like that of its carborane counterpart, 1,5-$C_2B_3H_5$, which is familiar as the smallest *closo* carborane known. This has a trigonal bipyramidal structure[23] (Fig. 4a) with axial carbon and equatorial boron atoms. The equatorial bonds are relatively long (1.85 Å) for a carborane. Their length is usually dismissed as implying a nonbonding interaction between the equatorial boron atoms, as might be expected for a classically bonded structure (Fig. 4b) in which the six skeletal bond pairs are assigned to the six polyhedral edges linking axial atoms to equatorial atoms, i.e. to the six C–B links. This description involves each boron atom in only *two* skeletal bonds.

A much better description, that is fully compatible with all the requirements of the topological treatment of borane bonding, including the assumption that each atom forms *three* skeletal bonds, involves use of the required three 2-centre skeletal bonds and three 3-centre skeletal bonds (Table 1 and Fig. 4c). The low coordination numbers of the axial atoms require these sets of bonds to occupy opposite hemispheres of the pseudospherical structure, though resonance between the two possible canonical forms leads to edge bond orders $e$ of 5/6 (0.83′) and 1/3 (0.33′) for the axial and equatorial bonds respectively. Although the disparity between these bond orders is likely to be even greater in $C_2B_3H_5$ than in $B_5H_5^{2-}$, since the more electro-negative axial carbon atoms in the carborane will drain electron density away from the equatorial boron atoms, these bond orders are more in line with the observed bond lengths[23] (B–C 1.56 Å, B–B 1.85 Å) and with the results of MO calculations[24] than the description in terms of six 2-centre B–C bonds.

The equations of balance, applied to a hypothetical neutral species $B_5H_5$, require its skeletal bonding to be described in terms of five 3-centre bonds. The connectivities required for a trigonal bipyramid, however, are incompatible with the use of five 3-centre bonds, so this species appears unlikely on the basis of localized bond arguments. It appears equally unlikely on the basis of MO treatments, which in view of the degeneracy of the HOMO of $B_5H_5^{2-}$ require $D_{3h}$ $B_5H_5$ to be a paramagnetic species susceptible to Jahn–Teller distortion.[15,22]

A trigonal bipyramidal structure is also incompatible with a bonding rationale involving seven skeletal bond pairs in six 2-centre bonds and one 3-centre bond as would be required for a species $B_5H_5^{4-}$. Allocation of six 2-centre bonds to the axial edges and one cross-polyhedral 3-centre bond to the equatorial triangle as in Fig. 4(d) would conflict with assumption 4 above, and can be eliminated on the grounds that the four bonds formed by each of the equatorial atoms, including the *exo* B–H bond, would then all be coplanar. MO arguments[16] also lead to the conclusion that a $D_{3h}$ structure for a hypothetical species $B_5H_5^{4-}$ would be unsatisfactory since the doubly degenerate HOMO would then be only half full.

Thus, both localized bond and MO treatments lead to the same conclusion: that the *closo* trigonal bipyramidal structure adopted by $C_2B_3H_5$, and expected for $B_5H_5^{2-}$, is *not* expected to be retained by species with two electrons more or fewer.

*Octahedral* $B_6H_6$ *systems*

MO treatments of octahedral arrangements of six BH units indicate a closed shell electronic configuration for the species $B_6H_6^{2-}$ which contains the seven skeletal bond pairs needed to fill all seven of the $A$, $T_{1u}$ and $T_{2g}$ bonding MO's.[16,25]

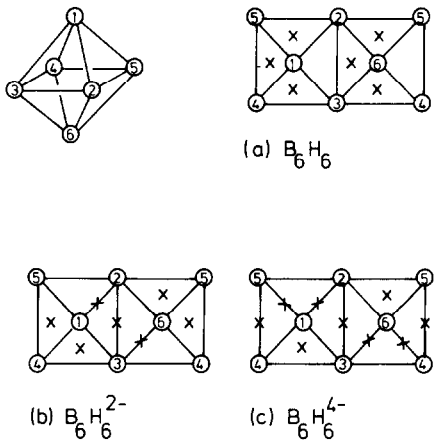



Fig. 5. Apparently satisfactory bond networks for octahedral species $B_6H_6$ (six 3-centre bonds), $B_6H_6^{2-}$ (three 2-centre and four 3-centre bonds) and $B_6H_6^{4-}$ (six 2-centre and two 3-centre bonds).

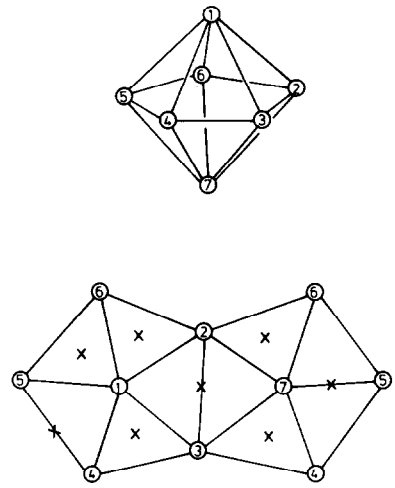


Fig. 6. The localised bond network of three 2-centre and five 3-centre bonds compatible with the $D_{5h}$ pentagonal bipyramidal structure of $B_7H_7^{2-}$.

However, localized bond treatments (Fig. 5), whether using six 3-centre bonds for a hypothetical species $B_6H_6$, or three 2-centre and four 3-centre bonds for $B_6H_6^{2-}$, or six 2-centre and two 3-centre bonds for a hypothetical octahedral species $B_6H_6^{4-}$, appear to indicate that an octahedral structure is compatible with six, seven or eight skeletal bond pairs, and that the bond orders of the octahedral edges would be expected to increase with the number of electrons available for skeletal bonding. The localized bond treatment thus has no predictive value for these systems' likely existence, and gives no clear indication of why seven skeletal bond pairs are needed.

### $D_{5h}$ *pentagonal bipyramidal* $B_7H_7$ *systems*

Although the structure of $B_7H_7^{2-}$ has not been confirmed by X-ray crystallographic studies, a $D_{5h}$ pentagonal bipyramidal structure like that established for the carborane 2,4-$C_2B_5H_7$[26] is indicated by NMR studies[27] and by MO treatments[16] which, moreover, show both HOMO and LUMO to be doubly degenerate. Hypothetical pentagonal bipyramidal species $B_7H_7$ or $B_7H_7^{4-}$ would therefore be expected to be paramagnetic and so highly reactive species, susceptible to distortion to relieve the degeneracy of their highest occupied molecular orbitals.

Interestingly, localized bond treatments also indicate that eight skeletal bond pairs, but *not* seven or nine pairs, are appropriate for a pentagonal bipyramidal arrangement of seven BH units. The three 2-centre bonds and five 3-centre bonds required by the equations of balance for $B_7H_7^{2-}$ can be allocated as shown in Fig. 6, using the two bonding networks possible for an atom of skeletal connectivity $k = 5$ (Fig. 3). Two 3-centre bonds must be allocated to one pentagonal pyramid, three 3-centre bonds to the other, and so only one of the 2-centre bonds can be used for edges connecting axial to equatorial atoms. All three of the bonding schemes shown in Fig. 3 as possible for an atom of connectivity $k = 4$ must therefore be used. Allowing for resonance, this bond scheme corresponds to edge bond orders $e$ of 0.43′ for the edges linking axial atoms to equatorial atoms, and 0.583′ for the equatorial edges. These values in turn correspond to total bond orders $ke$ of 2.16′ for the axial atoms, and 2.3′ for the equatorial atoms, implying that the latter, which have the lower coordination number, are the more negatively charged, as indicated also by MO treatments.[16]

Hypothetical $D_{5h}$ species $B_7H_7$ and $B_7H_7^{4-}$ would need the following localized bond networks. For $B_7H_7$, seven 3-centre BBB bonds would need to be allocated to seven of the ten pentagonal bipyramidal faces, while for $B_7H_7^{4-}$, six 2-centre BB bonds and three 3-centre BBB bonds would have to be used. From Fig. 3 it is apparent that neither bond arrangement is compatible with the presence of two non-adjacent atoms with $k = 5$, which between them would require a minimum of four and a maximum of six 3-centre bonds to be used.

### $D_{2d}$ *dodecahedral* $B_8H_8$*-systems*

Molecular orbital treatments of $B_8H_8^{2-}$ have identified the HOMO and LUMO as having $b_2$ and $a_2$ symmetry respectively.[16,28] Neither is degenerate—degeneracies could of course only be

accidental in a system with 2-fold symmetry. In contrast to the situation that obtains for the deltahedra of $B_5H_5^{2-}$, $B_6H_6^{2-}$ and $B_7H_7^{2-}$ (which are $n$-vertex shapes compatible only with $(n+1)$ skeletal bond pairs), the $D_{2d}$ dodecahedral cluster shape of $B_8H_8^{2-}$ is therefore compatible with $n$, $(n+1)$ or $(n+2)$ (i.e. 8, 9 or 10) skeletal bond pairs, as illustrated by the chloride $B_8Cl_8$[9] (8 pairs), the cobaltaborane $(C_5H_5)_4Co_4B_4H_4$[11] (8 pairs), the anion $B_8H_8^{2-}$[29] (9 pairs), the carborane $C_2B_6H_8$[30] (9 pairs) and many other 9-pair systems, and the nickelaborane $(C_5H_5)_4Ni_4B_4H_4$[12] (ten pairs).

The localized bond networks that can be drawn for these three different numbers of skeletal electron pairs are illustrated in Fig. 7. The average edge bond orders that they imply are given in Table 3, which also gives the interatomic distances in $B_8Cl_8$[9] and $B_8H_8^{2-}$.[29] Qualitatively, the localized bond schemes provide a satisfactory explanation of the differences in edge lengths between these two octaborane clusters—bond orders increase where B–B distances decrease. Moreover, the two types of edge that link 4-coordinate to 5-coordinate atoms (types $x$ and $y$ in Fig. 7) suffer a reversal of their relative bond orders on going from $B_8Cl_8$ to $B_8H_8^{2-}$, a reversal matched by their relative lengths. These features correlate precisely with the character of the HOMO of $B_8H_8^{2-}$,[28] which is

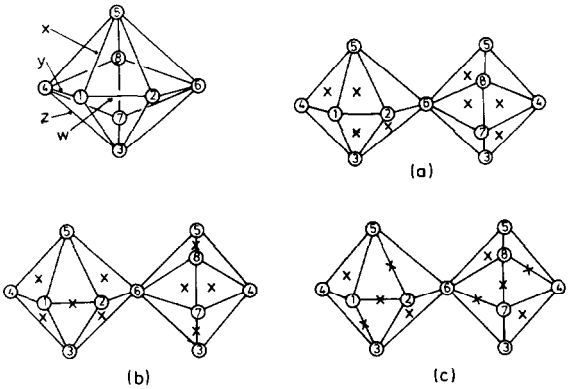



Fig. 7. Localized bond networks appropriate for $D_{2d}$ 8-atom clusters with (a) eight skeletal electron pairs (e.g. $B_8Cl_8$; eight 3-centre bonds), (b) nine skeletal electron pairs (e.g. $B_8H_8^{2-}$; three 2-centre and six 3-centre bonds), or (c) ten skeletal electron pairs (e.g. $(C_5H_5)_4Co_4B_4H_4$; six 2-centre and four 3-centre bonds).

bonding for edges of types $w$, $y$ and $z$, but antibonding for edges of type $x$.

No homonuclear 8-atom 10-electron pair $D_{2d}$ dodecahedral cluster is known at present with which to test the capacity of localized bond schemes to explain or predict the interatomic distances in such a system. From the character of the LUMO of $B_8H_8^{2-}$ (the orbital that must accommo-

Table 3. Average edge bond orders, $e$, predicted for $D_{2d}$ $B_8Cl_8$, $B_8H_8^{2-}$ and $B_8H_8^{4-}$ from the localized bond networks shown in Fig. 7, compared with interatomic distances $d$ (pm)

| | | Edge type (Fig. 7) | | | | Ref. |
|---|---|---|---|---|---|---|
| | | w | x | y | z | |
| $B_8Cl_8$ | e | 0.66' | 0.50 | 0.33' | 0.33' | |
| | d | 168 | 175 | 178 | 200 | 9 |
| $B_8H_8^{2-}$ | e | 0.83' | 0.33' | 0.83' | 0.33' | |
| | d | 158 | 178 | 174 | 193 | 29 |
| $B_8H_8^{4-}$ | e | 1.0 | 0.83' | 0.33' | 0.33' | |
| $B_8H_8^{2-}$ | HOMO* | b | ab | b | b | 16,28 |
| $B_8H_8^{2-}$ | LUMO* | ab | ab | ab | b | 16,28 |

*Entries in these rows indicate the bonding (b) or antibonding (ab) character of the HOMO and LUMO of $B_8H_8^{2-}$.

date the tenth pair of electrons), which is antibonding for polyhedron edges of types *w*, *x* and *y*, and bonding for edges of type *z*, one would expect the former to be longer and latter shorter in a $D_{2d}$ species $B_8H_8^{4-}$ than in $B_8H_8^{2-}$. The related nickelaborane $(C_5H_5)_4Ni_4B_4H_4$[12] contains four B——B polyhedral edge bonds, all of type *z* (Fig. 7), for which all three localized bond schemes, whether using eight, nine or ten skeletal electron pairs, predict a bond order of 0.33′. Type *z* bond lengths are 200 pm in $B_8Cl_8$,[9] 193 pm in $B_8H_8^{2-}$,[29] and 192 pm in $(C_5H_5)_4Ni_4B_4H_4$.[12] The consistency of these last two figures with the expectations of a localized bond treatment must be regarded as fortuitous, since the effect of replacing boron atoms by nickel atoms on going from $B_8H_8^{4-}$ to the nickelaborane is ignored. Anyway, the localized bond treatment using ten skeletal bond pairs can be faulted because it assigns a bonding role to the tenth pair of electrons which MO treatments,[28] as mentioned above, show to be essentially *anti*-bonding (antibonding for *w*, *x* and *y*, bonding for *z*). However, Table 3 shows that the localized bond treatment requires the tenth pair of electrons to make edges of types *w* and *x* more strongly bonded, edges of type *y* to be less strongly bonded, and edges of type *z* to remain the same compared with the 9-skeletal pair system $B_8H_8^{2-}$.

Localized bond and MO treatments are thus in agreement in indicating that the 8-atom $D_{2d}$ dodecahedral skeleton is compatible with the presence of eight, nine or ten skeletal electron pairs, and in their assessment of how the eight or nine pairs are distributed about the skeleton. However, the localized bond treatment overestimates the bonding role of the tenth pair of electrons, which it distributes misleadingly.

### $D_{3h}$ *tricapped trigonal prismatic* $B_9H_9$ *systems*

Like the $D_{2d}$ dodecahedral $B_8H_8^{2-}$, the $D_{3h}$ tricapped trigonal prismatic $B_9H_9^{2-}$ has non-degenerate frontier oribitals.[13] The HOMO has symmetry $a_2'$, and is antibonding for edges of type *f* (Fig. 8), bonding for edges of types *g* and *h*. The LUMO has symmetry $a_2''$, with precisely the reverse edge-bonding or -antibonding characteristics: it is bonding for edges of type *f*, antibonding for edges of types *g* and *h*. Closed shell electronic configurations are therefore possible for $D_{3h}$ tricapped trigonal prismatic nine-atom clusters with nine, ten or eleven skeletal electron pairs, exemplified by the homonuclear clusters $B_9Cl_9$[10], $B_9H_9^{2-}$,[31] and $Bi_9^{5+}$[13] respectively. Bonding is expected to be strongest when there are ten skeletal bond pairs available. Adding or removing one or two electrons to or from the 10-pair system is expected to give rise to precisely the same type of distortion. As one moves away from the ideal number of ten skeletal bond pairs, the trigonal prism is expected to get longer and narrower as *g* increases and *f* decreases in length, while the bonds (type *h*) to the capping atoms are also expected to lengthen.

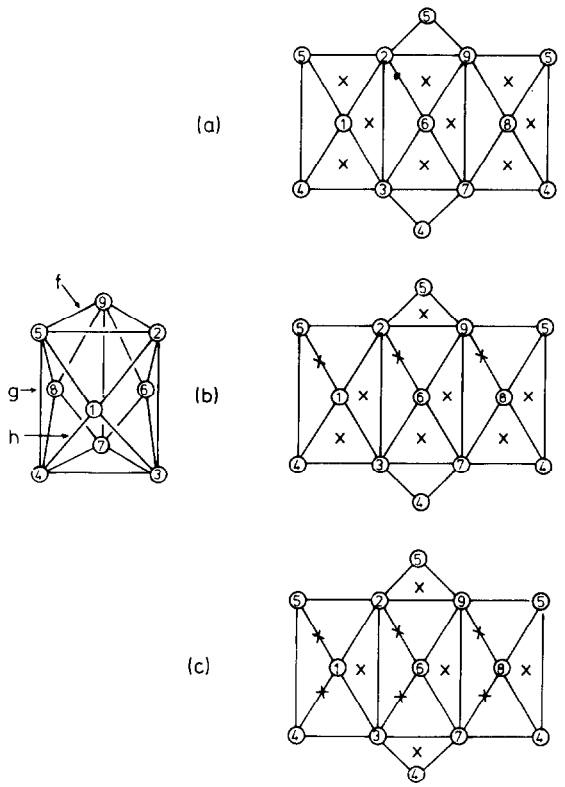



Fig. 8. Localized bond networks appropriate for $D_{3h}$ 9-atom tricapped trigonal prismatic clusters with (a) nine skeletal electron pairs (e.g. $B_9Cl_9$; nine 3-centre bonds), (b) ten skeletal electron pairs (e.g. $B_9H_9^{2-}$; three 2-centre and seven 3-centre bonds) or (c) eleven skeletal electron pairs (e.g. $Bi_9^{5+}$; six 2-centre and five 3-centre bonds).

Localized bond networks for such systems are illustrated in Fig. 8. The mean bond orders that they imply for the three types of edge are given in Table 4, which also lists the edge lengths in $B_9Cl_9$[10], $B_9H_9^{2-}$ and $Bi_9^{5+}$.[13] Interestingly, a bond order of 0.33′ is indicated for *both* types of prism edge (*f* and *g*), irrespective of the number of electrons available, though the edges of type *h* connecting the capping atoms to the rectangular prism faces are expected to increase in bond order from 0.50 through 0.58–0.66′ as the number of skeletal electron pairs increases from nine to eleven. The lengths of these edges should therefore decrease relative to the lengths of the other edges going from $B_9Cl_9$ through $B_9H_9^{2-}$ to $Bi_9^{5+}$. The inter-

Table 4. Average edge bond orders, $e$, predicted for $D_{3h}$ 9-atom clusters with 9, 10 or 11 skeletal electron pairs from the localized bond networks shown in Fig. 8, with interatomic distances $d$ (pm) in some representative systems

| | | Edge type (Fig. 8) | | | Ref. |
|---|---|---|---|---|---|
| | | f | g | h | |
| $B_9Cl_9$ | e | 0.33' | 0.33' | 0.50 | |
| | d | 180 | 208 | 175 | 10 |
| $B_9H_9^{2-}$ | e | 0.33' | 0.33' | 0.583' | |
| | d | 188 | 181 | 171 | 31 |
| $Bi_9^{5+}$ | e | 0.33' | 0.33' | 0.66' | |
| | d | 324 | 374 | 309 | 13 |
| $B_9H_9^{2-}$ | HOMO* | ab | b | b | 31 |
| $B_9H_9^{2-}$ | LUMO* | b | ab | ab | 31 |

* Entries in these rows indicate the bonding (b) or antibonding (ab) character of the HOMO and LUMO of $B_9H_9^{2-}$.

atomic distances listed in Table 4, however, show poor correlation with these predictions. For $B_9Cl_9$, for example, the edges of types $f$ and $g$, both formally of bond order 0.33', and both linking atoms of connectivity $k = 5$, actually differ in length by as much as 28 pm. The edges of type $h$ are admittedly the shortest in this compound, as required of those of highest bond order, but this feature might otherwise be attributed to the lower connectivity ($k = 4$) of the capping atoms.

The anion $B_9H_9^{2-}$, with ten skeletal bond pairs assigned to three 2-centre and seven 3-centre skeletal bonds, presents a slightly less unsatisfactory picture, with the links formally of bond order 0.33' (types $f$ and $g$) differing in length by only 7 pm, both being significantly longer than those of formal order 0.58 (type $h$). The bismuth cluster $Bi_9^{5+}$, with eleven skeletal electron pairs, cannot be compared directly with the other two 9-atom clusters because of the different covalent radii of bismuth and boron atoms. The edges predicted to be of highest bond order (type $h$) are indeed the shortest (310 pm), but the other edges, each formally of bond order 0.33, differ by *ca.* 50 pm in length.

For these nine-vertex systems it can be seen, therefore, that although localized bond networks can be drawn for all three possible electron numbers, the electron distributions they imply appear to be quite misleading, particularly in the case of the systems containing nine or eleven skeletal electron pairs.

### $D_{4d}$ *bicapped square antiprismatic* $B_{10}H_{10}$ *systems*

Molecular orbital treatments of the bicapped square antiprismatic anion $B_{10}H_{10}^{2-}$ have shown both HOMO and LUMO to be doubly degenerate.[16] Adding or removing two electrons to or from the twenty-two involved in skeletal bonding would generate paramagnetic reactive species if there were no change in symmetry. The *closo* shape is therefore compatible with eleven skeletal bond pairs, but *not* with ten or twelve skeletal pairs.

The eleven skeletal pair system $B_{10}H_{10}^{2-}$ can be treated in terms of three 2-centre and eight 3-centre localized bonds in a variety of ways[17] (Fig. 9). The average bond orders of the three types of edge, giving equal weight to each of the six possible types of bond arrangement, are 0.583' for edges of type $a$, 0.375 for edges of type $b$, and 0.416' for type $c$. The actual edge lengths are $a = 173$ pm, $b = 186$ pm, $c = 181$ pm.[3] The sequence $a < c < b$ is thus entirely consistent with the sequence of decreasing bond order. Moreover, the total bond order, $ke$, for the two types of skeletal atom is 2.33' for the capping (polar) atoms of connectivity $k = 4$, and 2.16' for the other (tropical) atoms of connectivity $k = 5$, indicating that the atoms of lower connectivity, by forming a set of bonds of higher total bond order than their more highly coordinated neighbours, are evidently the more negatively charged atoms. These localized bond networks thus provide a satisfactory rationale for the interatomic distances and charge distribution

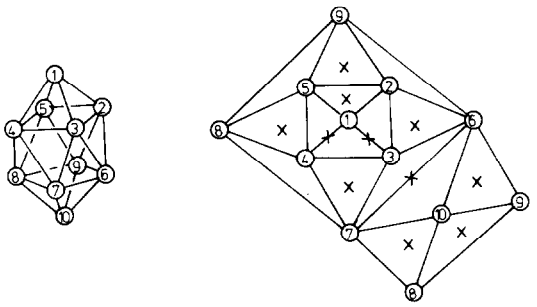


Fig. 9. Localized bond networks (only one of the six possible networks shown; the other networks have the 2-centre bonds linking the following pairs of atoms; (i) 1–3, 1–4, 5–9, (ii) 1–3, 1–4, 6–9, (iii) 1–3, 1–4, 9–10, (iv) 1–3, 4-8, 2–9, (v) 1–3, 4-8, 9–10.) of the three 2-centre and eight 3-centre bonds compatible with the $D_{4d}$ bicapped square antiprismatic structure of $B_{10}H_{10}^{2-}$.

in the anion $B_{10}H_{10}^{2-}$, and the large number of alternative networks consistent with the connectivity requirements of this anion suggests that it is likely to benefit from considerable resonance stabilisation, as indeed is indicated by its chemistry.[20]

If one attempts to describe the skeletal bonding in hypothetical species $B_{10}H_{10}$ and $B_{10}H_{10}^{4-}$, assuming $D_{4d}$ structures like that of $B_{10}H_{10}^{2-}$, and using localized 2- and 3-centre bonds, a different picture emerges. A species $B_{10}H_{10}$, having ten skeletal electron pairs, would require these to be allocated to ten 3-centre bonds if each boron atom is to participate in three skeletal bonds. Considering firstly the requirements of the capping atoms of connectivity, $k = 4$, one would need to allocate six of the ten 3-centre bonds to these atoms, three to each of the square pyramids, leaving four 3-centre bonds to be allocated to faces linking the tropical atoms of one hemisphere to those of the other, an allocation that is not compatible with the bonding requirements of these tropical atoms once the polar bonds have been assigned as described. A ten-atom ten-electron pair cluster with a $D_{4d}$ bicapped square antiprismatic structure is therefore *not* expected either on MO or on localized bond considerations.

The hypothetical 10-atom 12-electron pair species $B_{10}H_{10}^{4-}$ poses similar problems if one attempts to allocate the required six 2-centre and six 3-centre bonds to a $D_{4d}$ bicapped square antiprismatic structure, such bonds being incompatible with the connectivities of this polyhedron. Thus both MO and localized bond treatments are in agreement that eleven skeletal bond pairs, but not ten or twelve pairs, are appropriate for the $D_{4d}$ bicapped square antiprism.

### $C_{2v}$ *octadecahedral* $B_{11}H_{11}$ *systems*

Although the structure of the anion $B_{11}H_{11}^{2-}$ has not been confirmed by an X-ray crystallographic study, its spectra[32] are consistent with a $C_{2v}$ structure related to that of decaborane, $B_{10}H_{14}$, with the extra atom completing the 11-vertex polyhedron by occupying the highly coordinated ($k = 6$) site on the 2-fold axis. This structure is analogous to that established for the isoelectronic carborane $C_2B_9H_{11}$,[33] and is supported by MO calculations.[34] Although these latter gave no details of the frontier orbitals, the $C_{2v}$ symmetry requires both HOMO and LUMO to be nondegenerate. Removal or addition of an electron pair need not therefore distort the cage substantially, and so species $B_{11}H_{11}$ or $B_{11}H_{11}^{4-}$, like $B_{11}H_{11}^{2-}$, might in principle have *closo* $C_{2v}$ structures. No such species are as yet known, though a *nido* type geometry based on an icosahedron is indicated for derivatives of $B_{11}H_{11}^{4-}$ and the isoelectronic carborane anions $CB_{10}H_{11}^{3-}$ and $C_2B_9H_{11}^{2-}$.[20]

Localized bond networks compatible with a $C_{2v}$ octadecahedral *closo* shape can be devised for all three species $B_{11}H_{11}$, $B_{11}H_{11}^{2-}$ and $B_{11}H_{11}^{4-}$ (Fig. 10). The distribution of the bonds is effectively governed by the presence of the unique atom with $k = 6$, which must participate in three 3-centre bonds (Fig. 3). Each edge radiating from that atom therefore acquires a formal bond order of 0.33′. The problem of allocating the remaining bonds to the decaborane-like residue thus reduces to allocating eight 3-centre bonds ($B_{11}H_{11}$), three 2-centre and six 3-centre bonds ($B_{11}H_{11}^{2-}$), or six 2-centre and four 3-centre bonds ($B_{11}H_{11}^{4-}$) to meet the connectivity requirements of the two atoms with $k = 4$ and eight with $k = 5$. The ways in which this can be achieved are illustrated in Fig. 10. The "normal" species $B_{11}H_{11}^{2-}$ offers the greatest scope for alternative bonding networks, and so may be regarded as that most likely to benefit from resonance stabilization, though plausible bond networks for $B_{11}H_{11}$ and $B_{11}H_{11}^{4-}$ can be devised. The bond orders they imply for the nine distinct types of bond in the $C_{2v}$ octadecahedron are listed in Table 5, which also shows how the total order of the bonds to particular atoms varies with their connectivity and with the number of skeletal electron pairs.

The $C_{2v}$ octadecahedron of $B_{11}H_{11}^{2-}$ or $C_2B_9H_{11}$ thus resembles the $D_{2d}$ dodecahedron of $B_8H_8^{2-}$ and the $D_{3h}$ tricapped trigonal prism of $B_9H_9^{2-}$ in being an $n$-vertex deltahedron which, on both MO and localized bond grounds, is compatible with the presence of $(n + 1)$ skeletal electron pairs. Both MO and localized bond arguments are in agree-

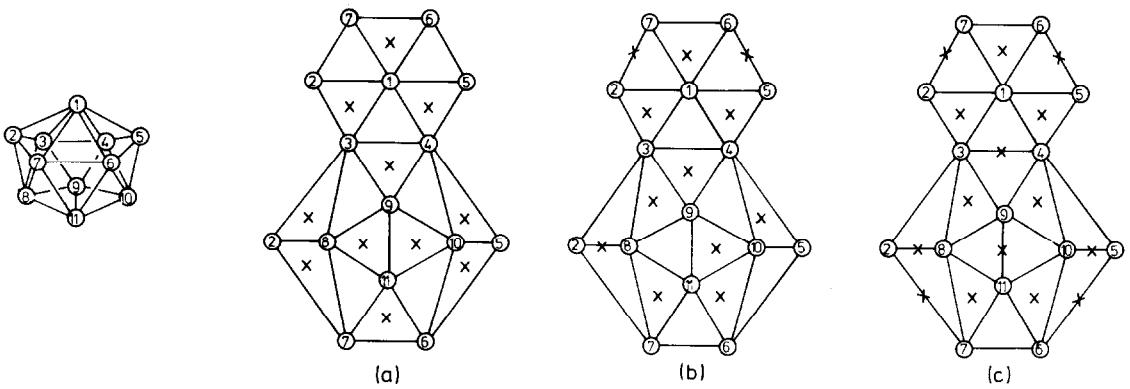



Fig. 10. Localized bond networks appropriate for $C_{2v}$ 11-atom octadecahedral clusters with (a) eleven skeletal pairs (e.g. a hypothetical $B_{11}H_{11}$; eleven 3-centre bonds), (b) twelve skeletal electron pairs (only one of the four possible bond networks shown; the other networks have the 2-centre bonds linking the following pairs of atoms (i) 2–3, 4-5, 8–11, (ii) 2–3, 4-9, 2–8, (iii) 2–3, 4-9, 8–11.) (e.g. $B_{11}H_{11}^{2-}$: three 2-centre and nine 3-centre bonds) or (c) thirteen skeletal electron pairs (e.g. a hypothetical $B_{11}H_{11}^{4-}$; six 2-centre and seven 3-centre bonds).

ment in predicting weaker bonding when there are only $n$ skeletal electron pairs, but the localized bond treatment in all cases is misleading in implying stronger bonding when there are $(n + 2)$ skeletal bond pairs.

### $I_h$ *icosahedral* $B_{12}H_{12}$ *systems*

The icosahedral arrangement of twelve BH units is of interest in the development of cluster bonding in that it was predicted by Longuet-Higgins and Roberts,[35] from MO considerations, that this would require thirteen skeletal electron pairs for a closed shell electronic configuration, with quadruply degenerate HOMO and LUMO (of symmetries $U_u$ and $U_g$ respectively). This prediction was later confirmed by the isolation and structural characterization of the anion $B_{12}H_{12}^{2-}$.[16,19,20] Adding two electrons to or removing two electrons from this

Table 5(a). Average edge bond orders, $e$, predicted for $C_{2v}$ octadecahedral $B_{11}H_{11}$, $B_{11}H_{11}^{2-}$ and $B_{11}H_{11}^{4-}$ species from the localized bond networks shown in Fig. 10

| | Edge type (Fig. 10) | | | | | | | | |
|---|---|---|---|---|---|---|---|---|---|
| | a | b | c | d | e | f | g | h | i |
| $B_{11}H_{11}$ | 0.33' | 0.33' | 0.50 | 0.50 | 0.66' | 0.33' | 0.33' | 0.33' | 0.66' |
| $B_{11}H_{11}^{2-}$ | 0.33' | 0.33' | 0.75 | 0.33' | 0.50 | 0.38 | 0.38 | 0.50 | 0.33' |
| $B_{11}H_{11}^{4-}$ | 0.33' | 0.33' | 0.66' | 0.66' | 1.00 | 0.33' | 0.33' | 0.33' | 1.00 |

Table 5(b). Total bond order, $ke$, of the bonds radiating from atoms in $C_{2v}$ octadecahedral species $B_{11}H_{11}$, $B_{11}H_{11}^{2-}$ and $B_{11}H_{11}^{4-}$ as a function of their connectivities $k$

| Atom Number (Fig. 10) | Connectivity $k$ | Total bond order, $ke$ | | |
|---|---|---|---|---|
| | | $B_{11}H_{11}$ | $B_{11}H_{11}^{2-}$ | $B_{11}H_{11}^{4-}$ |
| 1 | 6 | 2.0 | 2.0 | 2.0 |
| 2,5 | 4 | 2.0 | 2.33' | 2.66' |
| 3,4,6,7 | 5 | 2.0 | 2.33' | 2.33' |
| 8,10 | 5 | 2.0 | 2.25 | 2.33' |
| 9,11 | 5 | 2.0 | 2.08 | 2.33' |

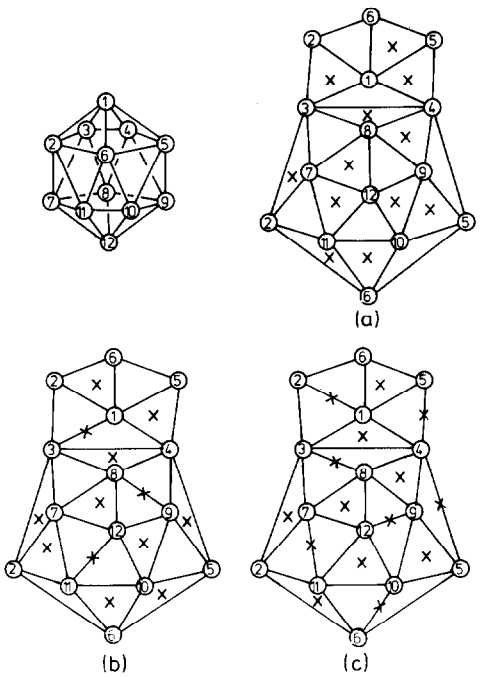



Fig. 11. Apparently satisfactory bond networks for icosahedral species (a) $B_{12}H_{12}$ (twelve 3-centre bonds) (b) $B_{12}H_{12}^{2-}$ (three 2-centre and ten 3-centre bonds) (c) $B_{12}H_{12}^{4-}$ (six 2-centre and eight 3-centre bonds).

species would generate products $B_{12}H_{12}^{4-}$ or $B_{12}H_{12}$ with incomplete electron configurations, prone to Jahn–Teller type distortions.

Localized bond treatments of icosahedral species $B_{12}H_{12}$ with twelve, thirteen or fourteen skeletal electron pairs give no indication that the systems with twelve or fourteen pairs are in any way unsatisfactory. Indeed, as illustrated in Fig. 11, the allocation of six 2-centre bonds to an octahedrally-related set of edges, with eight 3-centre bonds symmetrically disposed in relation to these, appears to provide a particularly apt bonding network for a hypothetical icosahedral species $B_{12}H_{12}^{4-}$. Likewise, twelve 3-centre bonds can be allocated in a symmetrical manner (Fig. 11) to all but eight of the icosahedral faces to provide an apparently satisfactory bonding description for a hypothetical species $B_{12}H_{12}$. Allowing for resonance, these localized bond networks correspond to average edge bond orders $e$ of 12/30, 13/30 and 14/30 for $B_{12}H_{12}$, $B_{12}H_{12}^{2-}$ and $B_{12}H_{12}^{4-}$ respectively.

The icosahedron of $B_{12}H_{12}^{2-}$, like the octahedron of $B_6H_6^{2-}$, is thus another shape for which MO treatments suggest a compatibility with only $(n+1)$ skeletal bond pairs, whereas localized bond treatments suggest that $n$, $(n+1)$ or $(n+2)$ skeletal pairs are all possible.

## CONCLUSIONS

In this paper, we have attempted to describe the bonding in a series of real and hypothetical deltahedral *closo* boranes $B_nH_n^{2-}$, where $c = 0$, 2 or 4, by using 2- and 3-centre bond networks that ensure that each boron atom participates in three bonds and that each polyhedron edge is always accounted for, either by a 2-centre bond along that edge, by one or two 3-centre bonds adjacent to that edge, or by a combination of these in resonance. For all species shown by MO calculations to have closed shell electronic configurations, i.e. for $B_nH_n$ ($n = 4$, 8, 9 or 11), for $B_nH_n^{2-}$ ($n = 5 \rightarrow 12$), and for $B_nH_n^{4-}$ ($n = 4$, 8, 9 or 11), it was found possible to devise localized bond networks compatible with the atom connectivities involved. This is not unexpected, since the localized bonds used represent acceptable though rather crude alternative ways of describing how the electron density is distributed about the surfaces of these clusters. What is perhaps less expected is the way that topological factors—local connectivity requirements—prevent satisfactory bond networks from being devised for systems that, on MO grounds, would contain unpaired electrons. The systems $B_4H_4^{2-}$, and $B_nH_n^{4-}$ ($n = 5$, 7 or 10) fall into this category (Table 6). Such species are thus predicted to be unstable on both MO and localized bond arguments. It is only for the octahedron and icosahedron that discrepancies arise between the two approaches as to what electron numbers are expected. Apparently satisfactory localized bond networks can be devised for such species using $n$, $(n+1)$ or $(n+2)$ bond pairs, whereas MO treatments indicate that only the dianions $B_6H_6^{2-}$ and $B_{12}H_{12}^{2-}$, i.e. the systems with $(n+1)$ skeletal bond pairs, are expected to be stable for these particular polyhedra. The disagreement between localized bond and MO arguments in these cases may be associated with their high symmetry.

A more serious discrepancy between the localized bond approach and MO theory is in the assignment of a bonding role to the $(n+2)$'th electron pair in the former, whereas these electrons are antibonding according to the latter. The electrons are, moreover, distributed misleadingly about the polyhedra. For the systems with $n$ or $(n+1)$ bonding electron pairs, however, the localized bond treatment provides at worst a rough but realistic indication of how they are distributed, and at best, provided the various canonical forms are considered, a very helpful indication of the electron distribution, allowing edge bond orders to be estimated.

Table 6. The numbers of skeletal electron pairs predicted by molecular orbital and localized bond treatments to be compatible with $n$-vertex *closo* deltahedral shapes for clusters $B_nH_n^{c-}$ ($c = 0$, 2 or 4) and related clusters

| Number of skeletal pairs | Number of polyhedron vertices, n | | | | | | | | |
|---|---|---|---|---|---|---|---|---|---|
| | 4 | 5 | 6 | 7 | 8 | 9 | 10 | 11 | 12 |
| n | + | - | 0 | - | + | + | - | + | 0 |
| n + 1 | - | + | + | + | + | + | + | + | + |
| n + 2 | + | - | 0 | - | + | + | - | + | 0 |

\+ Systems shown by MO treatments to have closed shell electronic configurations for which localized bond networks can be devised.

\- Systems shown by MO treatments to have incompletely filled MO's, for which localized bond networks cannot be devised.

0 Systems shown by MO treatments to have incompletely filled MO's, for which localized bond networks can be devised.

*Acknowledgements*—We thank SERC for support, and the University of Notre Dame (where this paper was written) for the generous hospitality shown to KW as a visiting professor.

## REFERENCES

1. R. E. Williams, *Inorg. Chem.* 1971 **10**, 210.
2. K. Wade, *J. Chem. Soc. D* 1971, 792.
3. R. W. Rudolph and W. R. Pretzer, *Inorg. Chem.* 1972, **11**, 1974.
4. D. M. P. Mingos, *Nature Phys. Sci.* 1972, **236**, 99.
5. R. N. Grimes, *Ann. N. Y. Acad. Sci.* 1974, **239**, 180.
6. R. W. Rudolph, *Acc. Chem. Res.* 1976, **9**, 466.
7. K. Wade, *Advan. Inorg. Chem. Radiochem.* 1976, **18**, 1.
8. R. N. Grimes (Editor), *Metal Interactions with Boron Clusters*. Plenum Press, New York (1982).
9. G. S. Pawley, *Acta Cryst.* 1966, **20**, 631.
10. M. B. Hursthouse, J. Kane and A. G. Massey, *Nature* 1970, **228**, 659; M. B. Hursthouse, personal communication.
11. J. R. Pipal and R. N. Grimes, *Inorg. Chem.* 1979, **18**, 257.
12. J. R. Bowser, A. Bonny, J. R. Pipal and R. N. Grimes, *J. Am. Chem. Soc.* 1979, **101**, 6229.
13. J. D. Corbett, *Prog. Inorg. Chem.* 1976, **21**, 140.
14. R. B. King, *Polyhedron* 1982, **1**, 133.
15. M. E. O'Neill and K. Wade, *Inorg. Chem.* 1982, **21**, 461; *Polyhedron* 1983, **2**, 963.
16. W. N. Lipscomb, *Boron Hydrides*. W. A. Benjamin, New York(1963).
17. I. R. Epstein and W. N. Lipscomb, *Inorg. Chem.* 1971, **10**, 1921.
18. K. Wade, *Electron Deficient Compounds*. Nelson, London (1971).
19. E. L. Muetterties and W. H. Knoth, *Polyhedral Boranes*. Marcel Dekker, New York (1968).
20. E. L. Muetterties, *Boron Hydride Chemistry*. Academic Press, New York (1975).
21. M. J. S. Dewar and M. L. McKee, *Inorg. Chem.* 1978, **17**, 1569.
22. C. Glidewell, *J. Organometal Chem.* 1977, **128**, 13.
23. I. A. McNeill, K. L. Gallaher, F. R. Scholer and S. H. Bauer, *Inorg. Chem.* 1973, **12**, 2108.
24. R. N. Camp, D. S. Marynick, G. D. Graham and W. N. Lipscomb, *J. Am. Chem. Soc.* 1978, **100**, 6781.
25. H. C. Longuet-Higgins, *Quart. Rev. Chem. Soc.* 1957, **11**, 121.
26. T. Onak, G. B. Dunks, R. A. Beaudet and R. L. Poynter, *J. Am. Chem. Soc.* 1966, **88**, 4622.
27. F. Klanberg, D. R. Eaton, L. J. Guggenberger and E. L. Muetterties, *Inorg. Chem.* 1967, **6**, 1271.
28. D. A. Kleir and W. N. Lipscomb, *Inorg. Chem.* 1979, **18**, 1312.
29. L. J. Guggenberger, *Inorg. Chem.* 1969, **8**, 2771.
30. H. V. Hart and W. N. Lipscomb, *J. Am. Chem. Soc.* 1967, **89**, 4220.

31. L. J. Guggenberger, *Inorg. Chem.* 1968, **7**, 2260.
32. F. Klanberg and E. L. Muetterties, *Inorg. Chem.* 1966, **5**, 1955.
33. C. Tsai and W. E. Streib, *J. Am. Chem. Soc.* 1966, **88**, 4513.
34. M. J. S. Dewar and M. L. McKee, *Inorg. Chem.* 1978, **17**, 1569. See also E. H. Wong, L. Prasad, E. J. Gabe and M. G. Gatter, *Inorg. Chem.* 1983, **22**, 1143 for the structure of $Et_4N^+B_{11}H_{10}SMe_2^-$.
35. H. C. Longuet-Higgins and M. de V. Roberts, *Proc. Roy. Soc.* (*London*) 1955, **A230**, 110.

*Polyhedron* Vol. 3, No. 2, pp. 213–221, 1984
Printed in Great Britain.

0277-5387/84 $3.00 + .00
© 1984 Pergamon Press Ltd.

# RHODIUM(I) COMPLEXES WITH PYRIDAZINE, 4,6-DIMETHYL-PYRIMIDINE, 4,6-BIS(3,5-DIMETHYLPYRAZOL-1-YL)PYRIMIDINE, 3,6-BIS(3,5-DIMETHYLPYRAZOL-1-YL)PYRIDAZINE AND 3-(3,5-DIMETHYLPYRAZOL-1-YL)-6-CHLOROPYRIDAZINE

**R. USON, L. A. ORO,* M. ESTEBAN and D. CARMONA**
Departamento de Química Inorgánica, Universidad de Zaragoza, Zaragoza, Spain

**and**

**R. M. CLARAMUNT and J. ELGUERO***
Instituto de Química Médica, Juan de la Cierva 3, Madrid-6, Spain

(*Received* 13 *June* 1983; *accepted* 25 *July* 1983)

**Abstract**—The synthesis and properties of rhodium(I) complexes of formulae $[\{RhCl(diolefin)\}_2(L)]$ (or $[RhCl(diolefin)(L)]$), and $[Rh(diolefin)(L)]_n(ClO_4)_n$ are reported. These complexes react with carbon monoxide to yield the related carbonyl derivatives. Ligands used were pyridazine, 4,6-dimethyl-pyrimidine, 4,6-bis(3,5-dimethylpyrazol-1-yl)pyrimidine, 3,6-bis(3,5-dimethylpyrazol-1-yl)pyridazine and 3-(3,5-dimethyl-pyrazol-1-yl)-6-chloropyridazine. Related iridium(I) and gold(I) compounds are also reported.

In recent years we have reported several types of polynuclear rhodium(I) complexes using ligands containing two or more nitrogen atoms, which are potentially capable of coordination to the metal ion.[1-4] In this paper we report some mono- or polynuclear rhodium(I) complexes with pyridazine ($L^1$), 4,6-dimethyl-pyrimidine ($L^2$), 4-6-bis(3,5-dimethylpyrazol-1-yl)pyrimidine ($L^3$), 3,6-bis(3,5-dimethylpyrazol-1-yl)pyridazine ($L^4$), 3-(3,5-dimethylpyrazol-1-yl)-6-chloro-pyridazine ($L^5$) and 3-(3,5-dimethylpyrazol-1-yl)pyridazine ($L^6$), as well as some iridium(I) or gold(I) related complexes.

## RESULTS AND DISCUSSION

### *Complexes with pyridazine* ($L^1$) *and* 4,6-*dimethyl-pyrimidine* ($L^2$)

The reaction of the pyridazine ligand ($L^1$) with binuclear rhodium(I) complexes of the type $[RhCl(diolefin)]_2$ (diolefin = tetrafluorobenzobarrelene, TFB,[5] 2,5-norbornadiene, NBD[6] or 1,5-cyclooctadine, COD[7]) ($Rh/L^1 = 2$ or 1) yielded mononuclear $[RhCl(diolefin)(L^1)]$ complexes.[8] In these reactions the pyridazine ligand behaved like pyridine.[9] However, the 4,6-dimethyl-pyrimidine ligand ($L^2$) reacted with $[RhCl(diolefin)]_2$ complexes ($Rh/L^2 = 2$ or 1) with formation of binuclear complexes of formula $[\{RhCl(diolefin)\}_2(L^2)]$ (diolefin = TFB or NBD), although molecular weight measurements (see Table 1) suggested a significant dissociation of the $[\{RhCl(diolefin)\}_2(L^2)]$ complexes in chloroform solution.

Cationic complexes of formulae $[Rh(diolefin)(L)]_n(ClO_4)_n$ ($L = L^1$ or $L^2$) were formed by reaction of $[Rh(diolefin)(Me_2CO)_x]ClO_4$[10,11] with the corresponding $L^1$ or $L^2$ ligand. In these compounds the two nitrogen atoms should be involved in bonding, but the products were generally too insoluble to establish the nuclearity.[12] The derived $[Rh(CO)_2(L^2)]_n(ClO_4)_n$ complex was obtained by bubbling carbon monoxide through a dichloromethane solution of $[Rh(TFB)(L^2)]_n(ClO_4)_n$ (Table 2).

### *Complexes with* 4,6-*bis*(3,5-*dimethylpyrazol*-1-*yl*)*pyrimidine*($L^3$), 3,5-*bis*(3,5-*dimethylpyrazol*-1-*yl*)*pyridazine*($L^4$) *and* 3-(3,5-*dimethylpyrazol*-1-*yl*)-6-*chloropyridazine*($L^5$)

While the binuclear cationic complex $[\{Rh(COD)\}_2(L^3)](ClO_4)_2$ was obtained by reaction of $[Rh(COD)(Me_2CO)_x]ClO_4$ with 4,6-bis(3,5-

*Authors to whom correspondence should be addressed.

Table 1. Analytical results and properties for neutral complexes with $L^1$ and $L^2$ ligands

| Complex | Analysis(found(calcd)(%)) C | H | N | Mol.wt.($CHCl_3$) (found(calcd.)) | Yield (%) | I.R. bands ($cm^{-1}$) |
|---|---|---|---|---|---|---|
| [RhCl(TFB)($L^1$)] (I) | 42.91 (43.22) | 2.26 (2.27) | 6.17 (6.30) | 462 (445) | 83 | 1570 ν(CN) 285 ν(RhCl) |
| [RhCl(NBD)($L^1$)] (II) | 42.99 (42.54) | 3.78 (3.89) | 8.72 (9.02) | 329 (311) | 66 | 1570,1575sh ν(CN) 270 ν(RhCl) |
| [RhCl(COD)($L^1$)] (III) | 44.08 (44.13) | 4.88 (4.94) | 8.48 (8.58) | 312 (327) | 73 | 1570 ν(CN) 280 ν(RhCl) |
| [IrCl(COD)($L^1$)] (IV) | 34.26 (34.65) | 3.82 (3.88) | 6.40 (6.73) | | 60 | 1565 ν(CN) 300 ν(IrCl) |
| [{RhCl(TFB)}$_2$($L^2$)] (V) | 43.26 (43.03) | 2.44 (2.40) | 3.51 (3.34) | 519 (837) | 71 | 1610 ν(CN) 270 ν(RhCl) |
| [{RhCl(NBD)}$_2$($L^2$)] (VI) | 42.84 (42.21) | 4.42 (4.25) | 4.68 (4.92) | 373 (569) | 76 | 1610 ν(CN) 270 ν(RhCl) |

Table 2. Analytical results and properties for cationic complexes with $L^1$ and $L^2$ ligands

| Complex | Analysis(found(calcd)(%)) C | H | N | Colour | Yield (%) | I.R. bands ($cm^{-1}$) |
|---|---|---|---|---|---|---|
| [Rh(TFB)($L^1$)]$_n$($ClO_4$)$_n$ (VII) | 37.06 (37.78) | 1.95 (1.98) | 5.40 (5.51) | orange | 67 | 1580 ν(CN) |
| [Rh(NBD)($L^1$)]$_n$($ClO_4$)$_n$ (VIII) | 34.65 (35.27) | 2.88 (3.23) | 7.12 (7.48) | red | 65 | 1575 ν(CN) |
| [Rh(COD)($L^1$)]$_n$($ClO_4$)$_n$·$Me_2CO$ (IX) | 37.87 (38.64) | 4.78 (4.56) | 6.43 (6.67) | red | 83 | 1580 ν(CN) 1710 ν(CO) |
| [Rh(TFB)($L^2$)]$_n$($ClO_4$)$_n$ (X) | 38.96 (40.28) | 2.70 (2.63) | 5.11 (5.22) | yellow | 76 | 1625 ν(CN) |
| [Rh(CO)$_2$($L^2$)]$_n$($ClO_4$)$_n$ (XI) | 26.19 (26.22) | 2.20 (2.20) | 6.70 (7.64) | pale yellow | 70 | 2110,2050 ν(CO) |

dimethylpyrazol-1-yl)pyrimidine ($L^3$) ($Rh/L^3$ = 2/1) (see Fig. 1a), mononuclear [Rh(diolefin)($L^4$)]$ClO_4$ complexes (see Fig. 1b) were obtained by reaction of [Rh(diolefin)($Me_2CO$)$_x$]$ClO_4$ with 3,6-bis(3,5-dimethylpyrazol-1-yl)pyridazine ($L^4$) ($Rh/L^4 = 2$ or 1/1). The related [Rh(diolefin)($L^5$)]$ClO_4$ complexes (see Fig. 1c) were similarly prepared. Furthermore, the tetrafluorobenzobarrelene mononuclear complexes [Rh(TFB)(L)]$ClO_4$ (L = $L^4$ or $L^5$) react with triphenylphosphine ($Rh/PPh_3$ = 1/1) with formation of the presumed five-coordinated [Rh(TFB)(L)($PPh_3$)]$ClO_4$ complexes.[14]

On the other hand, the reaction of [Au($PPh_3$)($Me_2CO$)$_x$]$ClO_4$ with $L^4$ ($Au/L^4$ = 4/1) or $L^5$ ($Au/L^5$ = 3/1) gave the trinuclear gold(I) complexes of formula [{Au($PPh_3$)}$_3$(L)]($ClO_4$)$_3$, where all the nitrogen was involved in coordination with gold for L = L,[5] but only three nitrogen atoms of the four potentially capable of coordination, were used for L = L.[4]

Attempts to prepare an heterobinuclear rhodium(I)–gold(I) complex, by reaction of [Rh(TFB)($L^4$)]$ClO_4$ with [Au($PPh_3$)($Me_2CO$)$_x$]$ClO_4$ in acetone as solvent were unsuccessful. The only isolated rhodium complex was [Rh(TFB)($L^6$)]$ClO_4$ (see Fig. 1d) ($L^6$ = 3-(3,5-dimethylpyrazol-1-yl)-pyridazine). The formulation of the complex was confirmed by preparing the $L^6$ ligand and subsequent reaction with [Rh(TFB)($Me_2CO$)$_x$]$ClO_4$. The formation of [Rh(TFB)($L^6$)]$ClO_4$ from [Rh(TFB)($L^4$)]$ClO_4$ corresponded to the hydrogenolysis of the $C_6$–$N_{1'}$ bond between the pyridazine and the pyrazole. The *N*-unsubstituted 3,5-dimethylpyrazole has not been isolated; probably it forms gold complexes. A potential source of hydrogen could be the acetone used as solvent.

Bubbling carbon monoxide at atmospheric pres-

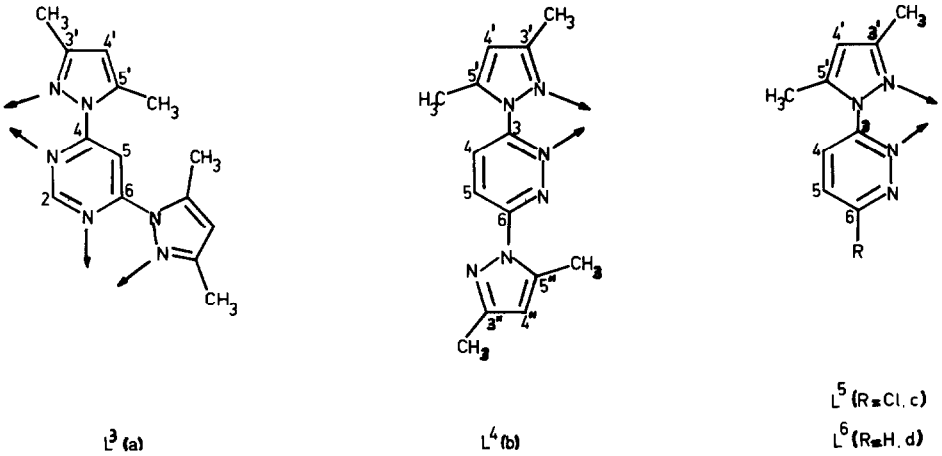



Fig. 1.

sure through dichloromethane solutions of the $[Rh(diolefin)(L)]ClO_4$ complexes (L = $L^4$ or $L^5$) gave rise to the formation of $[Rh(CO)_2(L)]ClO_4$ derivatives. In particular the $[Rh(CO)_2(L^5)]ClO_4$ was also obtained by reacting $[Rh(CO)_2(Me_2CO)_x]ClO_4$[10] with $L^5$. Furthermore, these dicarbonyl $[Rh(CO)_2(L)]ClO_4$ complexes reacted with triphenylphosphine with formation of the corresponding mononuclear $[Rh(CO)(L)(PPh_3)]ClO_4$ derivatives (see Scheme 1 and Table 3).

Binuclear neutral rhodium complexes of formula $[\{RhCl(diolefin)\}_2(L)]$ (L = $L^4$, $L^5$ or $L^6$) were obtained by reacting $[RhCl(diolefin)]_2$ with L(Rh/L = 2/1). The rhodium atoms should be in a square planar arrangement where the $L^4$, $L^5$ or $L^6$ ligands act as bridge between two "RhCl(diolefin)" units. Molecular weight measurements for $L^4$ complexes suggest the existence, in some cases, of dissociation in chloroform solutions (Table 4).

The $^1H$ NMR measurements on these neutral complexes showed that only the 4-H and 5-H protons (see Fig. 1 for numbering scheme) were significantly broadened and shifted to lower field (*ca.* 0.6 ppm) by the coordination to the rhodium atom. The $^{13}C$ NMR spectra of neutral complexes $[\{RhCl(COD)\}_2(L)]$, (L = $L^4$, $L^5$ or $L^6$) were also recorded. Some of the quaternary carbons were not observed (marked with an asterisk in Fig. 2). The values in parentheses correspond to the $\Delta\delta$ differences in ppm between the chemical shifts of the free ligands (Table 6) and those of the complexes. The olefinic carbons of 1,5-cyclooctadiene appear at 80.1–80.5 ppm and are coupled with rhodium ($^1J$ = 13 Hz); the saturated carbons appear at 30.8 ppm. No conclusion concerning the type of nitrogen atom involved in coordination, could be reached from these measurements.

The related $[\{RhCl(CO)_2\}_2(L)]$ complexes were

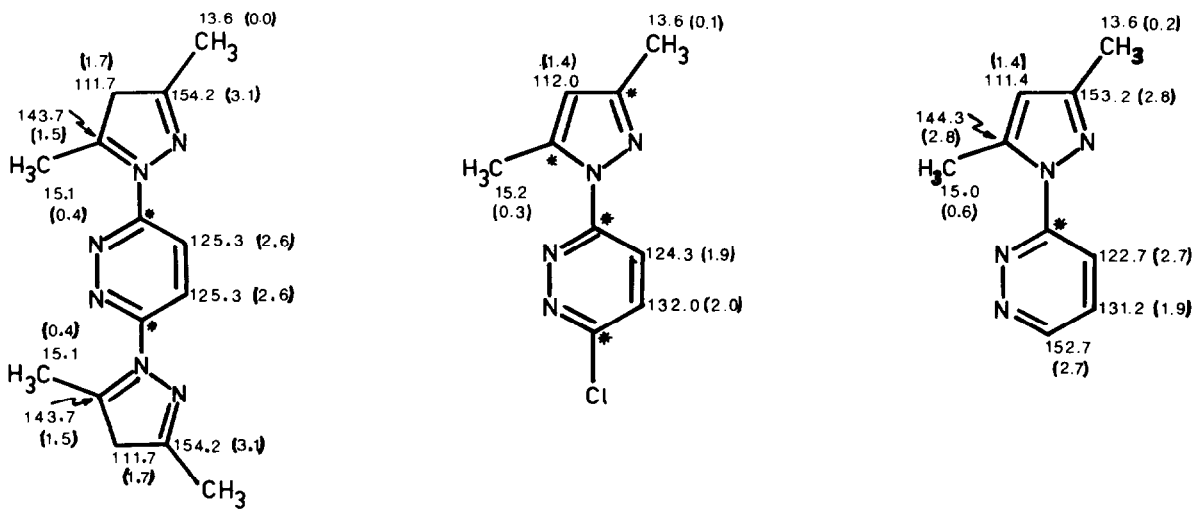



Fig. 2.

Table 3. Analytical results and properties for cationic complexes with $L^3$, $L^4$, $L^5$ and $L^6$ ligands

| Complex | Analysis (found (calcd) (%)) C | H | N | Colour | $\Lambda_M$ (ohm$^{-1}$ cm$^2$ mol$^{-1}$) | Yield (%) | I.R. bands (cm$^{-1}$) |
|---|---|---|---|---|---|---|---|
| $[\{Rh(COD)\}_2(L^3)](ClO_4)_2$ (XII) | 40.84 (40.51) | 4.53 (4.53) | 9.30 (9.45) | orange | 180 | 89 | 1615,1580ν(CN) |
| $[Rh(TFB)(L^4)]ClO_4$ (XIII) | 44.88 (44.81) | 3.30 (3.18) | 11.99 (12.06) | orange | 128 | 86 | 1586,1560ν(CN) |
| $[Rh(NBD)(L^4)]ClO_4$ (XIV) | 44.16 (44.82) | 4.16 (4.30) | 14.90 (14.93) | orange | 138 | 81 | 1565,1540ν(CN) |
| $[Rh(COD)(L^4)]ClO_4$ (XV) | 44.82 (45.64) | 5.16 (4.87) | 13.89 (14.51) | pink | 131 | 79 | 1580,1550ν(CN) |
| $[Rh(TFB)(L^5)]ClO_4$ (XVI) | 38.76 (39.58) | 2.81 (2.37) | 8.21 (8.79) | orange | | 88 | 1575,1540ν(CN) |
| $[Rh(NBD)(L^5)]ClO_4$ (XVII) | 37.29 (38.19) | 3.38 (3.40) | 10.78 (11.13) | orange | 146 | 80 | |
| $[Rh(COD)(L^5)]ClO_4$ (XVIII) | 38.46 (39.33) | 3.96 (4.07) | 11.02 (10.79) | pink | 147 | 88.5 | 1575 ν(CN) |
| $[Rh(TFB)(L^4)(PPh_3)]ClO_4$ (XIX) | 54.60 (55.10) | 4.20 (3.89) | 8.43 (8.76) | pale yellow | | 91 | 1585,1575, 1550 ν(CN) |
| $[Rh(TFB)(L^5)(PPh_3)]ClO_4$ (XX) | 51.44 (52.08) | 3.35 (3.36) | 5.80 (6.23) | yellow | 140 | 92 | 1580,1540ν(CN) |
| $[Ir(CO)(L^4)(PPh_3)_2]ClO_4$ (XXI) | 54.23 (55.06) | 4.74 (4.17) | 7.33 (7.55) | red brown | | 77 | 1935 ν(CO) 1580,1550ν(CN) |
| $[Ir(CO)(L^5)(PPh_3)_2]ClO_4$ (XXII) | 50.68 (52.47) | 3.73 (4.85) | 5.32 (5.84) | pale orange | | 69 | 1910 ν(CO) |
| $[\{Au(PPh_3)\}_3(L^4)](ClO_4)_3$ (XXIII) | 41.53 (42.00) | 3.73 (3.16) | 4.81 (4.32) | white | 298 | 46 | 1575,1560ν(CN) |
| $[\{Au(PPh_3)\}_3(L^5)](ClO_4)_3$ (XXIV) | 40.07 (40.15) | 2.95 (2.88) | 3.48 (2.97) | white | 267 | 70 | 1560 ν(CN) |
| $[Rh(TFB)(L^6)]ClO_4$ (XXV) | 42.55 (41.85) | 2.93 (2.67) | 8.82 (9.29) | orange | 113 | 73 | 1595 ν(CN) |
| $[Rh(CO)_2(L^4)]ClO_4$ (XXVI) | 36.90 (36.49) | 3.36 (3.06) | 15.63 (15.95) | orange | | 92 | 2105,2050ν(C |
| $[Rh(CO)_2(L^5)]ClO_4$ (XXVII) | 27.75 (28.29) | 1.80 (1.94) | 11.57 (11.99) | violet | --- | 75 | 2100,2060ν(C |
| $[Rh(CO)(L^4)(PPh_3)]ClO_4$ (XXVIII) | 50.68 (52.09) | 4.35 (4.11) | 10.85 (11.04) | pale orange | | 89 | 1945 ν(CO) |
| $[Rh(CO)(L^5)(PPh_3)]ClO_4$ (XXIX) | 48.20 (47.95) | 3.68 (3.45) | 7.87 (7.99) | orange | 144 | 76 | 1995 ν(CO) |

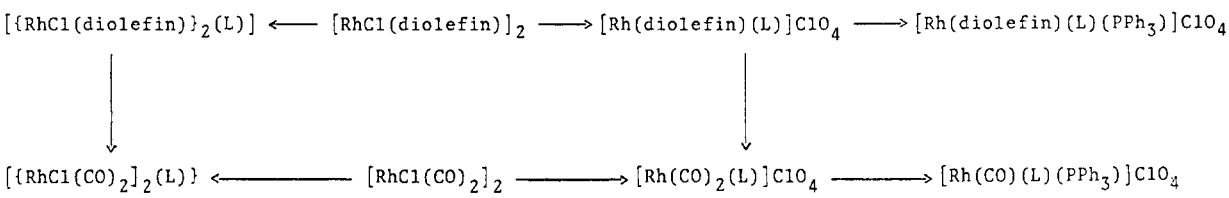
prepared by carbonylation of the corresponding diolefinic parent complexes, or by reaction of $[RhCl(CO)_2]_2$[15] with L (see Scheme 1). However, an alternative formulation for these complexes is $[Rh(CO)_2(L)][RhCl_2(CO)_2]$, supported by the presence of four $\nu$(CO) bands in the range 1985–2110 cm$^{-1}$, but the insolubility of these materials prevents us from conductivity measurements.

## EXPERIMENTAL

Melting points are uncorrected and were measured on a Büchi–Tottoli instrument. The C, H and N analyses were carried out with a Perkin–Elmer 240B microanalyzer. IR spectra were recorded on a Perkin–Elmer 577 spectrophotometer. $^1$H NMR and $^{13}$C NMR were obtained with a Bruker WP 80SY spectrometer using $CDCl_3$ solvent. Chemical shifts are given in ppm ($\delta$ scale) relative to internal TMS. Molecular weights were determined osmometrically with a Perkin–Elmer 115 instrument. Conductivities were measured in $5 \times 10^{-4}$ M acetone solution with a

Table 4. Analytical results and properties for neutral complexes with $L^4$, $L^5$ and $L^6$ ligands

| Complex | Analysis (found(calcd.)(%)) C | H | N | Mol.wt.($CHCl_3$) (found(calcd)) | Colour | Yield (%) | I.R. bands ($cm^{-1}$) |
|---|---|---|---|---|---|---|---|
| $[\{RhCl(TFB)\}_2(L^4)]$ (XXX) | 45.84 (45.76) | 2.89 (2.83) | 8.33 (8.43) | 1168 (998) | orange | 85 | 1575,1545 ν(CN) 298 ν(RhCl) |
| $[\{RhCl(NBD)\}_2(L^4)]$ (XXXI) | 45.42 (46.11) | 4.43 (4.42) | 11.62 (11.52) | 623 (729) | orange | 78 | 1587,1571,1550 ν(CN) 259 ν(RhCl) |
| $[\{RhCl(COD)\}_2(L^4)]$ (XXXII) | 46.95 (47.32) | 5.25 (5.29) | 11.24 (11.04) | 419 (761) | yellow | 88 | 1575,1550 ν(CN) 250 ν(RhCl) |
| $[\{RhCl(TFB)\}_2(L^5)]$ (XXXIII) | 41.64 (42.27) | 2.35 (2.26) | 5.44 (5.97) | | red-brown | 63 | 1580,1565 ν(CN) 290 ν(RhCl) |
| $[\{RhCl(NBD)\}_2(L^5)]$ (XXXIV) | 40.45 (41.25) | 3.76 (3.85) | 8.37 (7.76) | | red-brown | 73 | 1580,1540 ν(CN) 265 ν(RhCl) |
| $[\{RhCl(COD)\}_2(L^5)]$ (XXXV) | 41.66 (42.79) | 4.33 (4.74) | 8.24 (7.98) | | pink | 85 | 1580,1540 ν(CN) 270 ν(RhCl) |
| $[\{RhCl(CO)_2\}_2(L^4)]$ (XXXVI) | 32.65 (32.90) | 2.36 (2.45) | 12.65 (12.79) | | dark-blue | 85 | 2110,2070,2045,1985 ν(CO) 320,290 ν(RhCl) |
| $[\{RhCl(CO)_2\}_2(L^5)]$ (XXXVII) | 25.95 (26.13) | 1.54 (1.52) | 9.83 (9.38) | | blue | 78 | 2100,2060,2030,1990 ν(CO) 320,290 ν(RhCl) |
| $[\{RhCl(COD)\}_2(L^6)]$ (XXXVIII) | 44.78 (45.00) | 4.98 (5.13) | 8.30 (8.40) | | orange | 81 | 1580,1540 ν(CN) 250 ν(RhCl) |




Scheme 1. L = $L^4$ or $L^5$.

Table 5. $^1$H NMR data for $L^3$, $L^4$, $L^5$ and $L^6$ ligands

| Ligand[a,e] | 2-H | 4-H | 5-H | 6-H | 4'-H | 3'-$CH_3$ | 5'-$CH_3$ |
|---|---|---|---|---|---|---|---|
| $L^3$ [b] | 8.72 | - | 8.37 | - | 6.00 | 2.28 | 2.70 |
| $L^4$ | - | 8.19 | 8.19 | - | 6.02 | 2.27 | 2.72 |
| $L^5$ [c] | - | 8.23 | 7.66 | - | 6.13 | 2.32 | 2.77 |
| $L^6$ [d] | - | 8.09 | 7.45 | 9.00 | 6.00 | 2.27 | 2.73 |

[a]For numbering scheme. see Fig 1. [b]J(1-H,$CH_3$)= 0.83 Hz, J(2-H,5-H)= 1.04 Hz. [c]J(4-H,5-H)= 9.4 Hz. [d]J(4-H,5-H)= 8.9 Hz, J(4-H,6-H)= 1.54 Hz, J(5-H,6-H)= 4.8 Hz. [e]Solvent was $CDCl_3$.

Table 6. $^{13}$C NMR data for $L^3$, $L^4$, $L^5$ and $L^6$ ligands

| Ligand[a,b] | 2-C | 3-C | 4-C | 5-C | 6-C | 3'-C | 4'-C | 5'-C | 3'-$CH_3$ | 5'-$CH_3$ |
|---|---|---|---|---|---|---|---|---|---|---|
| $L^3$ | 156.8 | -- | 160.3 | 98.6 | -- | 151.2 | 110.7 | 142.7 | 13.6 | 15.2 |
| $L^4$ | -- | 155.0 | 122.7 | - | -- | 151.1 | 110.0 | 142.2 | 13.6 | 14.7 |
| $L^5$ | -- | 156.0 | 122.4 | 130.0 | 153.4 | 151.6 | 110.6 | 142.5 | 13.5 | 14.9 |
| $L^6$ | -- | 156.6 | 120.0 | 129.3 | 150.0 | 150.4 | 110.0 | 141.5 | 13.4 | 14.4 |

[a]For numbering scheme see Fig 1. [b]Solvent were: $CDCl_3$ (for $L^4$ and $L^5$), DMSO-$d_6$ (for $L^6$) and $CDCl_3$ + DMSO-$d_6$ (for $L^3$).

Philips 9501/01 conductimeter. Direct inlet MS were registered on a Hitachi Perkin–Elmer RMU-6M spectrometer.

*Synthesis of ligands*

The synthesis of 3,6-bis(3,5-dimethylpyrazol-1-yl)pyridazine ($L^4$) and 3-(3,5-dimethylpyrazol-1-yl)-6-chloro-pyridazine ($L^5$) have been previously reported.[16]

*Synthesis of* 4,6-*bis*(3,5-*dimethylpyrazol*-1-*yl*)-*pyrimidine* ($L^3$)

To a solution of 4,8 g (0.05 mol) of 3,5-dimethylpyrazole in 250 cm$^3$ of anhydrous xylene, 1.2 g (0.052 mol) of finely divided sodium metal were added. The reaction mixture was stirred overnight at room temperature. Then 3.72 g (0.025 mol) of 4,6-dichloropyrimidine in anhydrous xylene were added with a dropping funnel to the suspension of 3,5-dimethylpyrazole sodium salt. After heating under reflux for 12 hr, the solution was filtered and the filtrate evaporated under vacuum. The resulting solid was crude 4,6-bis(3,5-dimethylpyrazol-1-yl)pyrimidine (Yield: 93%), which was purified by column chromatography on silica-gel (60 Merck) using chloroform as eluent. M.p., 148°C. Mass spectrum: *m/e* 268 ($M^+$).

*Synthesis of* 3-(3,5-*dimethylpyrazol*-1-*yl*)*pyridazine* ($L^6$)

A mixture of 0.6 g (0.003 mol) of 3-(3,5-dimethylpyrazol-1-yl)-6-chloropyridazine, 5 cm$^3$ of aqueous $NH_4OH$ (25%) 70 cm$^3$ of methanol and

0.5 g of Pd/C (10%) was catalytically hydrogenated at an initial pressure of 35 psi. After 20 min, the reaction was ceased and worked up, filtered, washed with chloroform (100 $cm^3$) and evaporated *in vacuo*. The low melting solid (m.p., 40°C) obtained was 3-(3,5-dimethylpyrazol-1-yl)pyridazine. Mass spectrum: *m/e* 174 ($M^+$).

When the reaction time was longer the pyridazine ring was hydrogenated too. Thus after 6 hr the tetrahydropyridazine was formed (m.p.: 88–90°C); mass spectrum (*m/e* 178($M^+$)) and proton magnetic resonance confirming the assigned structure: $^1H$ NMR ($CDCl_3$) $\delta$: 1.8–3.3(*m*, 6H), 2.27(*s*,3H), 2.44(*s*,3H), 5.47(*br*,NH) and 5.94(*s*, pyrazolic proton).

$^1H$ NMR and $^{13}C$ NMR for $L^3$, $L^4$, $L^5$ and $L^6$ ligands are listed in Tables 5 and 6.

*Preparation of complexes of the type* [RhCl(*diolefin*)($L^1$)]

The preparation of [RhCl(TFB)($L^1$)] is described as an example.

Addition of 13 $\mu$l (0.179 mmol) of $L^1$ to a suspension of 58.9 mg (0.08 mmol) of $[RhCl(TFB)]_2$[5] in 5 $cm^3$ of acetone caused immediate dissolution of the solid. The resulting yellow solution was stirred for 20 min and *vacuum*-concentrated to *ca.* 2 $cm^3$. Slow addition of hexane caused precipitation of a yellow solid, which was filtered off, washed with hexane and air-dried.

*Preparation of complexes of the type* [{RhCl(*diolefin*)}$_2$($L^2$)]

The preparation of [{RhCl(NBD)}$_2$($L^2$)] is described as an example.

To a suspension of 101.8 mg (0.220 mmol) of $[RhCl(NBD)]_2$[6] in 5 $cm^3$ of acetone were added 27 $\mu$l (0.245 mmol) of $L^2$, which caused immediate dissolution of the initial complex and formation of a yellow solid. After 20 min stirring, the suspension was *vacuum*-concentrated to half its volume and the precipitation was completed by addition of hexane. The yellow solid was filtered off, washed with hexane and air-dried.

*Preparation of* [IrCl(COD)($L^1$)]

Addition of 11 $\mu$l (0.151 mmol) of the ligand to a suspension of 40.4 mg (0.061 mmol) of $[IrCl(COD)]_2$[17] in 5 $cm^3$ of acetone gives an orange solution. After stirring, under nitrogen, this solution for 15 min, was *vacuum*-concentrated to *ca.* 1 $cm^3$ and a lemon–yellow solid appeared, which was filtered off and air-dried.

*Preparation of complexes of the type* [Rh(*diolefin*)(L)]$_n$($ClO_4$)$_n$ (L = $L^1$, $L^2$)

The preparation of [Rh(TFB)($L^1$)]$_n$($ClO_4$)$_n$ is described as an example.

To a suspension of 50.8 mg (0.070 mmol) of $[RhCl(TFB)]_2$ in 5 $cm^3$ of acetone was added silver perchlorate (31.5 mg, 0.152 mmol) in 2 $cm^3$ of the same solvent. Silver chloride was immediately precipitated. After 30 min stirring the silver chloride was filtered off and 11 $\mu$l (0.151 mmol) of $L^1$ were added to the filtrate. The colour changes from yellow to orange and an orange solid appeared. After 20 min stirring, the suspension was concentrated to half its volume and addition of hexane completed the precipitation of the complex, which was filtered off, washed with hexane and air-dried.

*Preparation of* [Rh(CO)$_2$($L^2$)]$_n$($ClO_4$)$_n$

Carbon monoxide at normal pressure was bubbled through a suspension of [Rh(TFB)($L^2$)]$_n$($ClO_4$)$_n$ in dichloromethane, for 45 min, during which a pale yellow solid precipitated. This solid was filtered off, washed with ether and air-dried.

*Preparation of* [{Rh(COD)}$_2$($L^3$)]($ClO_4$)$_2$

Addition of 69.1 mg (0.333 mmol) of silver perchlorate in 2 $cm^3$ of acetone to a suspension of 76.2 mg (0.154 mmol) of $[RhCl(COD)]_2$[7] in 10 $cm^3$ of the same solvent gave an immediate precipitation of silver chloride. The suspension was stirred for 30 min, the precipitate was filtered off, and the filtrate was added to a solution of 42.5 mg (0.158 mmol) of the ligand in 10 $cm^3$ of acetone. The resulting orange solution was stirred for 15 min and *vacuum*-concentrated to *ca.* 2 $cm^3$, whereupon an orange solid separated. The precipitation was completed by adding ether, and the solid was filtered off, washed with ether and air-dried.

*Preparation of complexes of the type* [Rh(*diolefin*)(L)]$ClO_4$ (L = $L^4$, $L^5$)

The preparation of [Rh(COD)($L^5$)]$ClO_4$ was described as an example.[18]

To a suspension of 50.9 mg (0.103 mmol) of $[RhCl(COD)]_2$ in 10 $cm^3$ of acetone was added silver perchlorate (43.9 mg; 0.212 mmol) in 2 $cm^3$ of the same solvent. After 45 min stirring the formed silver chloride was filtered off and the filtrate was added to 43.1 mg (0.206 mmol) of the ligand in 10 $cm^3$ of acetone. The colour changed from yellow to red. This solution was stirred for 20 min and *vacuum*-concentrated to *ca.* 1 $cm^3$ and slow addition of ether gave a precipitate of a pink solid, which was filtered off, washed with ether and air-dried.

*Preparation of complexes of the type* $[Rh(TFB)(L)(PPh_3)]ClO_4$ ($L = L^4$, $L^5$)

The preparation of $[Rh(TFB)(L^4)(PPh_3)]ClO_4$ is described as an example.

A stoichiometric amount of triphenylphosphine in dichloromethane was added to a solution of $[Rh(TFB)(L^4)]ClO_4$ in 10 $cm^3$ of the same solvent. The colour changed from orange to orange–yellow. After 25 min stirring, the solution was *vacuum*-concentrated to *ca.* 1 $cm^3$ and slow addition of ether gave a yellow solid, which was filtered off, washed with ether and air-dried.

*Reaction between* $[Rh(TFB)(L^4)]ClO_4$ *and* $[Au(PPh_3)(Me_2CO)_x]ClO_4$

To a solution of 21.8 mg (0.044 mmol) of $AuCl(PPh_3)$ in 10 $cm^3$ of acetone were added 9.7 mg (0.047 mmol) of silver perchlorate in 2 $cm^3$ of the same solvent. The silver chloride formed was filtered off after 25 min stirring and the filtrate was added to a suspension of 30.6 mg (0.044 mmol) of $[Rh(TFB)(L^4)]ClO_4$ in 5 $cm^3$ of acetone. The resulting orange solution was stirred for 20 min and *vacuum*-concentrated to *ca.* 2 $cm^3$; the precipitation of the orange complex was completed by slow addition of ether. The solid was filtered off, washed with ether, air-dried and identified as $[Rh(TFB)(L^4)]ClO_4$ .

*Preparation of complexes of the type* $[Rh(CO)_2(L)]ClO_4$ ($L = L^4$, $L^5$)

These complexes were made by the two routes described below.

(i) Preparation of $[Rh(CO)_2(L^4)]ClO_4$. Carbon monoxide at normal pressure was bubbled for 30 min through a dichloromethane solution of 39.8 mg (0.07 mmol) of $[Rh(NBD)(L^4)]ClO_4$. The colour changed from orange to yellow. This solution was *vacuum*-concentrated and slow addition of ether completed the precipitation of a yellow solid, which was filtered off, washed with ether and air-dried.

(ii) Preparation of $[Rh(CO)_2(L^5)]ClO_4$. Addition of 36.9 mg (0.178 mmol) of silver perchlorate in 2 $cm^3$ of acetone to a solution of 33.4 mg (0.086 mmol) of $[RhCl(CO)_2]_2$[15] in 10 $cm^3$ of acetone gave an immediate precipitate of silver chloride. After 30 min stirring, the silver chloride was filtered off and the filtrate was added to 36.3 mg (0.173 mmol) of $L^5$ in 5 $cm^3$ of acetone. The resulting green suspension was stirred for 20 min and *vacuum*-concentrated to half its volume. The precipitation was completed by adding ether and the resulting violet solid was filtered off, washed with ether and air-dried.

*Preparation of complexes of the type* $[Rh(CO)(L)(PPh_3)]ClO_4$ ($L = L^4$, $L^5$)

These two complexes were prepared by the method described below.

Carbon monoxide was bubbled for 60 min through a solution of $[Rh(TFB)(L)]ClO_4$ ($L = L^4$, $L^5$) and a stoichiometric amount of triphenylphosphine in dichloromethane was added. The resulting orange solution was *vacuum*-concentrated to *ca.* 1 $cm^3$ and slow addition of ether completed the precipitation of an orange solid, which was filtered off, washed with ether and air-dried.

*Preparation of complexes of the type* $[\{Au(PPh_3)\}_3(L)](ClO_4)_3$ ($L = L^4$, $L^5$)

The preparation of $[\{Au(PPh_3)\}_3(L^4)](ClO_4)_3$ is described as an example.

To a suspension of 99.7 mg (0.201 mmol) of $AuCl(PPh_3)$[19] in 10 $cm^3$ of acetone were added 43.8 mg (0.211 mmol) of silver perchlorate in 2 $cm^3$ of the same solvent. After 20 min stirring, under nitrogen, the silver chloride was filtered off and the filtrate was added to a solution of 13.5 mg (0.05 mmol) of $L^4$. The resulting colorless solution was stirred for 20 min. Slow addition of ether to a *vacuum*-concentrated solution gave a white solid, which was filtered off, washed with ether and air-dried. The complex was recrystallised from dichloromethane/ether.

*Preparation of complexes of the type* $[Ir(CO)(L)(PPh_3)_2]ClO_4$ ($L = L^4$, $L^5$)

The synthesis of $[Ir(CO)(L^4)(PPh_3)_2]ClO_4$ is described as an example.

A suspension of 59.5 mg (0.076 mmol) of *trans*-$IrCl(CO)(PPh_3)_2$[20] in 10 $cm^3$ of acetone was stirred, under nitrogen, for 30 min together with 17.4 mg (0.084 mmol) of silver perchlorate. The resulting silver chloride was filtered off and the filtrate was added to a solution of 20.6 mg (0.077 mmol) of $L^4$ in 10 $cm^3$ of acetone. The colour changed from yellow to orange. After 15 min stirring, the orange solution was *vacuum*-concentrated to *ca.* 2 $cm^3$. Addition of ether completed the precipitation of a red–brown solid which was filtered off, washed with ether and air-dried.

*Preparation of complexes of the type* $[\{RhCl(diolefin)\}_2(L)]$ ($L = L^4$, $L^5$, $L^6$)

These complexes were prepared as is described below for $[\{RhCl(COD)\}_2(L^4)]$.

To a suspension of 50.3 mg (0.102 mmol) of $[RhCl(COD)]_2$ in 10 $cm^3$ of acetone were added 27.7 mg (0.103 mmol) of $L^4$. The colour changed from yellow to orange. The suspension was stirred

for 20 min and *vacuum*-concentrated to *ca.* 2 $cm^3$. Addition of ether completed the precipitation of the complex, which was filtered off, washed with ether and air-dried.

*Preparation of complexes of the type* $[\{RhCl(CO)_2\}_2(L)]$ ($L = L^4$, $L^5$)

These complexes were prepared by the two routes described below.

(i) Carbon monoxide at normal pressure was bubbled through a solution of $[\{RhCl(COD)\}_2(L)]$ ($L = L^4$ or $L^5$) in dichloromethane for 30 min, which caused the precipitation of the carbonylated complex which was filtered off, washed with ether and air-dried.

(ii) 17.6 mg (0.084 mmol) of $L^5$ were added to a solution of $[RhCl(CO)_2]_2$ (32 mg, 0.082mmol) in dichloromethane. A green solid precipitated immediately. The suspension was stirred for 30 min and concentrated to *ca.* 2 $cm^3$. Slow addition of ether completed the precipitation of the solid, which was filtered off, washed with ether and air-dried.

*Acknowledgements*—We are indebted to Dr. Géza Szilagyi (Institute for Drug Research, Budapest, Hungary) for helpful advice about cloropyridazine reduction. We would like to thank Mrs. M. D. Casado and M. Plaza, who obtained the NMR spectra.

## REFERENCES

1. R. Usón, L. A. Oro, D. Carmona and M. Esteban, *J. Organometal. Chem.* 1981, **220**, 103.
2. R. Usón, L. A. Oro, M. Esteban, A. M. Cuadro, P. Navarro and J. Elguero, *Transition Met. Chem.* 1982, **7**, 234.
3. L. A. Oro, D. Carmona and J. Reedijk, *Inorg. Chim. Acta* 1983, **71**, 115 and references therein.
4. R. Usón, L. A. Oro and J. A. Cabeza, *J. Organometal. Chem.* 1983, **247**, 105 and references therein.
5. D. M. Roe and A. G. Massey, *J. Organometal. Chem.* 1971, **28**, 273.
6. E. W. Abel, M. A. Bennett and G. Wilkinson, *J. Chem. Soe.* 1959, 3178.
7. G. Giordano and R. H. Crabtree, *Inorg. Synth.* 1979, **19**, 218.
8. The related $[IrCl(COD)(L^1)]$ was similarly obtained.
9. P. Fougeroux, B. Denise, R. Bonnaire and G. Pannetier, *J. Organometal. Chem.* 1973, **60**, 375.
10. R. R. Schrock and J. A. Osborn, *J. Am. Chem. Soc.* 1971, **93**, 3081.
11. R. Usón, L. A. Oro, R. Sariego, M. Valderrama and C. Rebullida, *J. Organometal. Chem.* 1980, **197**, 87.
12. Conductivity measurements in acetone at different concentrations ($10^{-3}$ N – $10^{-4}$N) on the complex $[Rh(TFB)(L^1)]_n(ClO_4)_n$ give a value of A in Onsagers equation ($\Lambda_e = \Lambda_0 - A\sqrt{c}$) that suggested a value of $n = 2$. A similar coordination of $L^1$ was recently reported.[13]
13. M. G. B. Drew, P. J. Baricelli, P. C. H. Mitchell and A. R. Read, *J. Chem. Soc., Dalton Trans* 1983, 649.
14. Five-coordinated iridium(I) complexes of formula $[Ir(CO)(L)(PPh_3)_2](ClO_4)$ can be prepared by reacting trans-$IrCl(CO)(PPh_3)_2$ with $AgClO_4$ in the presence of the corresponding ligand ($L = L^4$ or $L^5$).
15. J. A. McCleverty and G. Wilkinson, *Inorg. Synth.* 1966, **8**, 211.
16. J. Elguero, R. Jacquier and S. Mondon, *Bull. Soc. Chim. Fr.* 1970, 1346.
17. J. L. Herde, J. C. Lambert and C. V. Senoff, *Inorg. Synth.* 1974, **15**, 19.
18. The related complex $[Rh(TFB)(L^6)]ClO_4$ was prepared by the same method.
19. E. A. Allen and W. Wilkinson, *Spectrochim. Acta* 1972, **28A**, 2257.
20. J. P. Collman, C. T. Sears, Jr., and M. Kubota, *Inorg. Synth.* 1978, **11**, 101.

*Polyhedron* Vol. 3, No. 2, pp. 223–230, 1984
Printed in Great Britain.

0277–5387/84 $3.00 + .00
© 1984 Pergamon Press Ltd.

# FAST CHEMISORPTION OF NO AND $SO_2$ ON FeOOH CRYSTALS

**KATSUMI KANEKO and KATSUYA INOUYE***
Department of Chemistry, Faculty of Science, Chiba University, Chiba 260, Japan

(*Received* 27 *June* 1983; *accepted* 8 *August* 1983)

**Abstract**—The electrical conductivity changes of α-, β- and γ-FeOOH by adsorption of NO and $SO_2$ during 1 ms–1 min were determined. The conductivity change consists of fast and slow processes which are presumably caused by fast chemisorption on the oxygen vacancies and by slow one on the surface anions. The rate constants of fast and slow chemisorption were determined from the conductivity changes. The correlations of the rate constants with the compression pressure of specimen, adsorption temperature and original electrical conductivity are given. The order of magnitude of the fast chemisorption rate constants of the three polymorphs is related to the difference in the surface structure.

The presence of fast chemisorption of gas molecules on oxide surface, taking less than 1 min, can be anticipated for several reasons. First, the electrical conductivity of transition metal oxides changes by 50% of the original conductivity on $O_2$ or CO admission within 1 min.[1–3] Second, the chemisorption rate of CO on $Sc_2O_3$ shows the maximum at 3 s after the gas admission.[4] Third, the parameter $t_0$ in the widely applicable Elovich equation has often smaller values than several minutes.[5–7] It has been known that the non-activated chemisorption on a clean metal surface is complete within a few seconds at room temperature.[8,9] Nevertheless, insufficient studies have been done on the fast chemisorption with regard to metal oxides. Even the Hayward-Trapnell's so-called rapid chemisorption,[8] as in the case of $O_2$ and CO adsorption on transition metal oxides, lasts several minutes.

One must find a suitable experimental method which is able to follow the change in seconds in order to study the fast chemisorption process. The chemisorption with an electron transfer gives rise to an electrical conductivity change of adsorbent.[10,11] The electrical conductivity measurement of oxides on introducing gas molecules can be followed sensitively and swiftly and chemisorption separated from physisorption. The present study employed the electrical conductivity measurement for examining the chemisorption of NO and $SO_2$ on iron(III) hydroxide oxide (FeOOH) in a duration between ms and min.

α-FeOOH, β-FeOOH and γ-FeOOH occur naturally as minerals and the main components in the corrosion products of iron-base alloys. As explained more comprehensively in the Discussion, FeOOH crystals have advantages as the adsorbents for three reasons: high chemisorptive activity for NO and $SO_2$,[12–14] characteristic surface structures consisting $O^{2-}$ and $OH^-$ ions[15] and the electrical conductivity increase with rise in preheating temperature.[16]

The existence of fast ( < 10 s) and slow (10–60 s) changes in electrical conductivity of FeOOH crystals with the NO and $SO_2$ chemisorption are here reported. Both the geometrical and electronic factors controlling the fast conductivity-change are discussed.

## EXPERIMENTAL

*Samples*

Synthetic α-, β- and γ-FeOOH crystals with specific surface areas of 75, 36 and 71 $m^2/g$, respectively, were used. α-FeOOH was obtained by hydrolyzing 0.6 M ferric sulfate solution with 1 M NaOH at pH 13 and 50°C,[17] and β-FeOOH from 0.1 M ferric chloride solution with addition of urea at 95–99°C.[18] γ-FeOOH was prepared by the oxidation of 0.2 M ferrous chloride solution with sodium nitrite at 60°C in the presence of urotropin.[17] $Fe^{2+}$ content in crystals was determined

*Author to whom correspondence should be addressed.

by titrating the dissolved $Fe^{2+}$ ions in HCl solution under an $N_2$ atmosphere with 0.005 N cerium sulfate solution. The total Fe content was obtained by the Zimmerman–Reinhardt method using 0.1 N $K_2Cr_2O_7$ solution.

*Effect of compression on electrical conductivity change*

The sample disk of both good electrical contact among crystals and intergranular gaps through which molecules can be adsorbed on most crystal surfaces must be prepared in order to determine the chemisorption rate from the electrical conductivity measurement. If possible, it is preferable to get an absolute chemisorption rate constant from the electrical conductivity change under the ideal conditions that molecules can be adsorbed on all interfaces in the disk with no intergranular gaps. Thus the effect of the compression against samples (60 mg) on the electrical conductivity change was examined in the compression pressure range of $4.0 \times 10^6$ to $1.0 \times 10^8$ N m$^{-2}$. The conductivity change with admission of NO was measured at room temperature (20–24°C) by means of the cell in Fig. 1 and a d.c.-meter (Kawaguchi Denki NA-14E) connected with amplifier (Ohkura Denki AM-1001), transient time convertor (Riken Denshi TC-1000) and recorder. The cell has a sample-compression cell (0.154 dm$^3$) and gas container (0.36 dm$^3$). NO was introduced into the sample cell by opening a valve at room temperature, after the sample was pretreated at 110°C and $10^{-3}$ Pa for 15 hr.

*Electrical conductivity changes under the compression of* $1.5 \times 10^7$ *N m*$^{-2}$

The electrical conductivity change of the sample compressed at $1.5 \times 10^7$ N m$^{-2}$ was examined to obtain a practical chemisorption rate constant. The correlations of the electrical conductivity change with temperature, gas pressure and original electrical conductivity were examined for the sample compressed under $1.5 \times 10^7$ N m$^{-2}$. The conductivity change with admission of NO or $SO_2$ was measured by use of a glass cell and the electrical meters in Fig. 2. The glass cell consists of a sample room (0.033 dm$^3$), in which the sample disk is mounted, and a gas container (0.196 dm$^3$). The disk of 60 mg sample was formed between Au–plated brass electrodes. Both the sample room and gas container were kept at measuring temperatures between 30.0 and 50.0°C. By breaking the glass seal, a gas was admitted into the sample room. Most preheating conditions were the same as those in the compression effect experiment. In order to examine the relationship between the NO chemisorption rate constant and original electrical conductivity $\sigma_0$ at 30°C, samples were preheated at various temperatures (80–150°C) for obtaining the different $\sigma_0$ values.

*Gases*

High purity NO (Takachiho Kagaku) was purified by repeated bulb-to-bulb distillations. $SO_2$ (Showa Denko) of 99.9% purity was dried over $P_2O_5$. The pressures of gases to be adsorbed were $270 \pm 40$ Pa for NO and $130 \pm 20$ Pa for $SO_2$. Gases of different pressures between 70 and

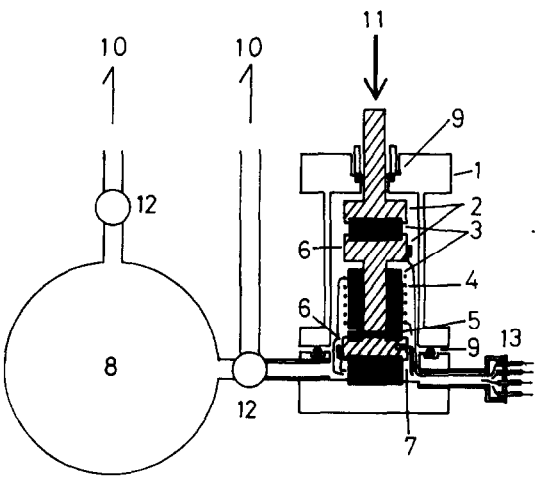



Fig. 1. Sample-compression apparatus. 1 Brass, 2 phosphor bronze, 3 steatite, 4 heater, 5 sample, 6 electrodes, 7 C · A thermocouple, 8 gas container, 9 *o*-ring, 10 to vacuum, 11 compression pressure, 12 vacuum glass tap, 13 lead wires.

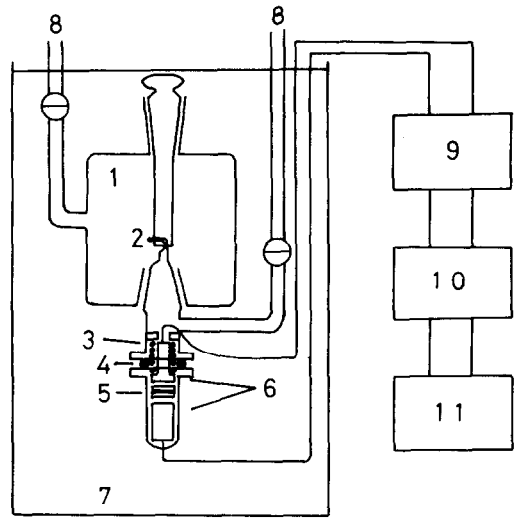



Fig. 2. Apparatus for the electrical conductivity measurement. 1 Absorbed gas, 2 breakable seal, 3 spring, 4 *o*-ring, 5 sample, 6 electrodes, 7 thermostat, 8 vacuum line, 9 dc-meter, 10 transient convertor, 11 recorder.

$2.0 \times 10^3$ Pa and NO and 70 to 330 Pa for $SO_2$ were used to examine the dependence of the conductivity change on the gas pressure. The equilibrium gas pressure of 100–300 Pa corresponds to the adsorption coverage of 0.01–0.05 with reference to the adsorption isotherms reported by Inouye *et al.*[12,13]

*Temperature dependence of the electrical conductivity*

After adsorption of NO at $500 \pm 30$ Pa, the specimen was evacuated at $10^{-3}$ Pa and 30°C for 15 hr to desorb the physisorbed NO molecules. The electrical conductivity was measured at various temperatures from 30 to 100°C. The slope of the linear log $\sigma$ vs 1/T plot gave the activation energy for conduction, where $\sigma$ and T are the electrical conductivity and measuring temperature in Kelvin, respectively.

## RESULTS

*Conductivity change and compression effect*

The $\sigma_0$ increases steeply with the compression pressure up to $1.5 \times 10^7$ N m$^{-2}$ and slightly beyond the pressure as shown in Fig. 5(A). Most of the contact resistance can be eliminated by the compression at $1.5 \times 10^7$ N m$^{-2}$. Figure 3 shows the electrical conductivity change of $\alpha$-FeOOH compressed at various pressures with admission of NO. A fast drop of the electrical conductivity within 2 s is followed by a much slower decrease. Under a lower compression pressure, the initial change is more remarkable. Application of the first order reaction plot to the conductivity change is shown in Fig. 4(A). The plot of $\ln \sigma/\sigma_0$ vs $t$ consists of two lines: one line with larger inclination ($k_f$) for the initial change and another line having smaller inclination ($k_s$) and an intercept ($C$). The slope of the initial change becomes smaller with the compression pressure as shown in Fig. 4(B). Two kinds of lines in Fig. 4(A) are expressed by the first order equations,

$$-\ln \sigma/\sigma_0 = k_f t \qquad (t \leq t_c) \tag{1}$$

$$-\ln \sigma/\sigma_0 = k_s t + C, \quad (t > t_c) \tag{2}$$

where $t_c$ is a time at the crossing of two lines. Let us call $k_f$ and $k_s$ the rate constants of the fast and slow conductivity changes, respectively. Changes of $k_f$ for NO on $\alpha$-, $\beta$- and $\gamma$-FeOOH with the rise of the compression pressure are exhibited in Fig. 5(B). The $k_f$ drops up to $1.5 \times 10^7$ N m$^{-2}$, followed by a gradual decrease beyond the pressure. The $k_f$ for $\gamma$-FeOOH decreases remarkably with the compression pressure, whereas that for $\beta$-FeOOH shows a slight decrease.

The specific surface area (determined from $N_2$ adsorption, $S_{N_2}$) of $\alpha$-FeOOH disk varied with the compression; 75 m$^2$/g of $\alpha$-FeOOH powder became 62 m$^2$/g at $1.5 \times 10^7$ N m$^{-2}$ and constant ($61 \pm 2$ m$^2$/g) over the pressure.

The compression under $1.5 \times 10^7$ N m$^{-2}$ seems to be sufficient for guaranteeing gaps for chemisorption and at the same time electrical contact among crystal particles. The $k_f$ and $k_s$ under the $1.5 \times 10^7$ N m$^{-2}$ compression pressure are denoted $k_f^*$ and $k_s^*$.

*Dependence of the rate constant on temperature and gas pressure*

The Arrhenius plot of $k_f^*$ with regard to NO adsorption is shown in Fig. 6. The activation energy for the fast conductivity changes for $\beta$- and $\gamma$-FeOOH is 0.5 and 0.6 eV, respectively. The Arrhenius plot for $\alpha$-FeOOH is a convex curve. Figure 7 illustrates the Arrhenius plot of $k_f^*$ for $SO_2$ adsorption. The $k_f^*$ for $\alpha$-FeOOH deviates from the linear relationship in the temperature range 40–47°C, showing a peak at 47°C. Table 1 gives the two rate constants ($k_f^*$,$k_s^*$) and the corresponding activation energy ($E_f^*$, $E_s^*$) for the fast and slow processes. The $k_f^*$ for NO is in the order of 1 s$^{-1}$, whereas that for $SO_2$ is 0.1 s$^{-1}$ or less. For both the adsorption results of NO and $SO_2$, $k_f^*$ and $E_f^*$ are much larger than $k_s^*$ and $E_s^*$.

The variation of $k_f^*$ for NO adsorption on $\gamma$-FeOOH with the initial gas pressure $P$ in the range of 70 to $2.0 \times 10^3$ Pa is expressed by,

$$k_f^* \propto P^{0.6}, \tag{3}$$

while the $k_f^*$ for $SO_2$ is almost constant at $0.065 \pm 0.008$ s$^{-1}$ in the pressure range 70–330 Pa.

*Dependence of $k_f^*$ on the original electrical conductivity*

A remarkable dependence of $k_f^*$ for NO adsorption of $\alpha$- and $\gamma$-FeOOH at 30°C on the original electrical conductivity $\sigma_0$ is illustrated in Fig. 8. There are sharp peaks around $3 \times 10^{-10}\ \Omega^{-1}$m$^{-1}$ for both $\alpha$- and $\gamma$-FeOOH.

*Activation energy change with chemisorption*

The linear plots of log $\sigma$ vs 1/T for both pure and NO-chemisorbed FeOOH gave the activation energy values for conduction before and after the chemisorption which are agreed with each other, as shown in Table 2.

## DISCUSSION

*True and apparent fast chemisorption rate constants*

The chemisorption of NO and $SO_2$, electron-attractive molecules, on $n$-type FeOOH surfaces

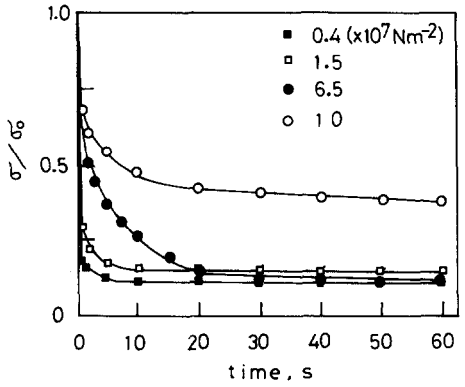



Fig. 3. Electrical conductivity change with admission of NO for α-FeOOH compressed at various pressures.

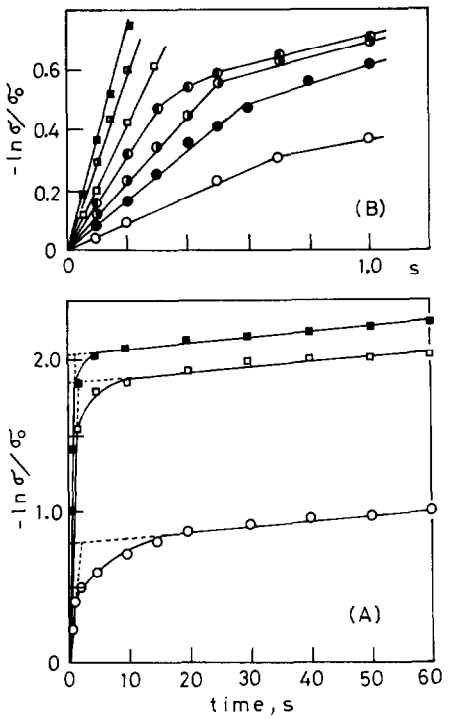



Fig. 4. The first order plot for the electrical conductivity change of α-FeOOH compressed at various pressures during 60 s (A) and 1 s (B). ■, 0.4; ◨, 0.8; □, 1.5; ◐, 2.8; ◑, 4.0; ●, 6.5 and ○, 10 ($\times 10^7$ N m$^{-2}$).

should bring about electron transfer from FeOOH to the molecule, lowering the electrical conductivity of FeOOH crystals. The conductivity decrease described by eqns (1) and (2) must arise from the chemisorption. The activation energy for electrical conduction does not vary with the NO chemisorption (Table 2). As the activation energy is nearly equal to hopping energy of the mobility term in a hopping conduction system, the electron mobility is same during the chemisorption. Ac-

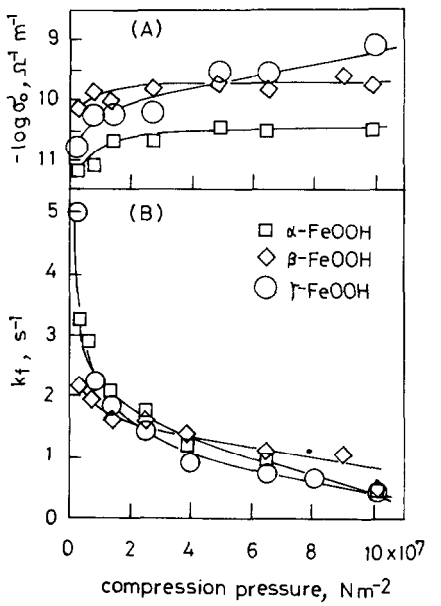



Fig. 5. Changes of the original electrical conductivity (A) and $k_f$ for NO (B) with the compression pressure.

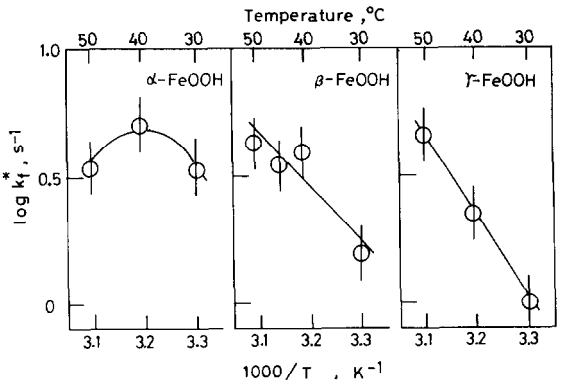



Fig. 6. The Arrhenius plots for $k_f^*$ in the case of NO adsorption on α-FeOOH, β-FeOOH and γ-FeOOH.

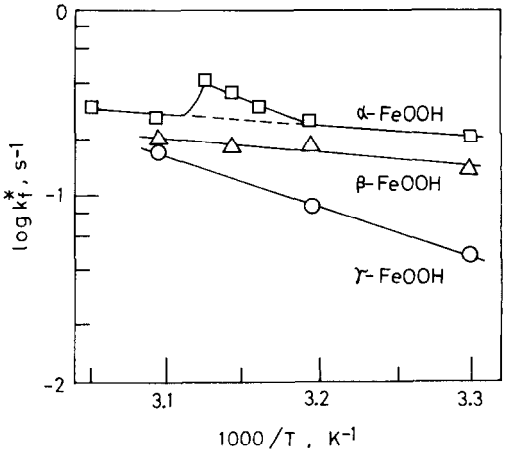



Fig. 7. The Arrhenius plots for $SO_2$ fast chemisorption on α-FeOOH, β-FeOOH and γ-FeOOH.

Table 1. Chemisorption rate constants ($k_f^*$, $k_s^*$) at 30°C and activation energy values ($E_f^*$, $E_s^*$)

| | | α-FeOOH | β-FeOOH | γ-FeOOH |
|---|---|---|---|---|
| NO | $k_f^*$, $s^{-1}$ | 3 ± 1 | 1.3 ± 0.3 | 1 ± 0.3 |
| | $E_f^*$, eV | — | 0.5 ± 0.3 | 0.6 ± 0.1 |
| | $k_s^*$, $s^{-1}$ | 0.008 | 0.02 | 0.009 |
| | $E_s^*$, eV | 0.2 ± 0.3 | 0.0–0.3 | 0.0–0.3 |
| $SO_2$ | $k_f^*$, $s^{-1}$ | 0.22 | 0.17 | 0.052 |
| | $E_f^*$, eV | 0.11 | 0.18 | 0.53 |
| | $k_s^*$, $s^{-1}$ | 0.005 | 0.006 | 0.002 |
| | $E_s^*$, eV | 0.03 | 0.03 | 0.35 |

cordingly $\sigma/\sigma_0$ in eqns (1) and (2) can be replaced by $n/n_0$ as

$$-\ln n/n_0 = k_f t \tag{4}$$

$$-\ln n/n_0 = k_s t + C, \tag{5}$$

where $n$ and $n_0$ are the carrier concentration at time $t$ and the original concentration, respectively. Equation (4) and (5) express two chemisorption rate equations of the first order; the $k_f$ and $k_s$ mean the fast and slow chemisorption rate constants.

The compressed specimen of FeOOH crystals has intergranular gaps. The concentration of effective carriers migrating through the intergranular conducting paths is smaller than the bulk concentration; $n_0$ in eqns (4) and (5) for the compressed specimen is less than the true concentration in the bulk. The $k_f$ and $k_s$ for the compressed specimen are the apparent chemisorption rate constants. The $k_f$-decrease with the compression in Fig. 5(B) characterizes the apparent rate constant, because the concentration of effective carriers approaches to the true one with the compression. The $k_f$ values determined under $1.5–10 \times 10^7$ N m$^{-2}$ compression seem to express still apparent magnitude, although the compression over $1.5 \times 10^7$ N m$^{-2}$ guarantees the conducting paths in the specimen as mentioned in Results.

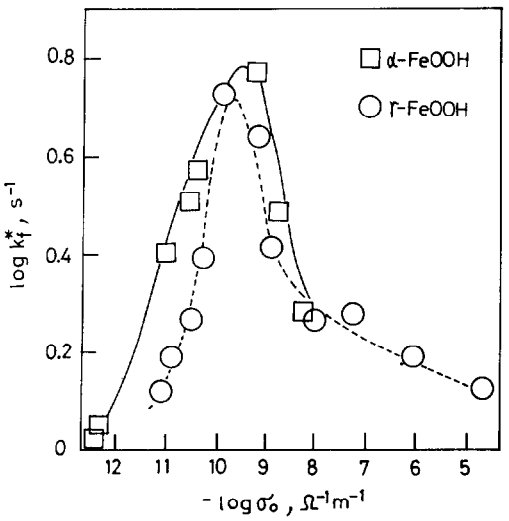



Fig. 8. The relationship between $k_f^*$ and the original electrical conductivity for NO chemisorption on α-FeOOH and γ-FeOOH at 30°C.

A true rate constant of chemisorption must be determined from the specimen compressed under such a high pressure that all intergranular gaps collapse and $n_0$ agrees with the bulk concentration. Figure 9 shows log $k_f$ vs $d^{true}/d^{app}$ plots for NO chemisorption, where $d^{true}$ and $d^{app}$ are true density of crystals and the apparent density of the specimen, respectively. The density values in the literature were used as true density: α-FeOOH, 4.28[19]; β-FeOOH, 3.0[20]; γ-FeOOH, 4.07.[21] It is noted that each line has the same slope but different intercepts at $d^{true}/d^{app} = 1$. The same inclination leads to the conclusion that $k_f$ does not depend on the size and state of the gaps, but does on the volume. The intercept gives the true rate constant, $k_f^0$, for the specimen without intergranular gaps. $k_f^0$ and slope are given in Table 3. The order of magnitude of $k_f^0$ is β-FeOOH > α-FeOOH > γ-FeOOH. It appears that the NO chemisorption for gap-free FeOOH specimen finishes within 3–20 s as shown by the reciprocal of $k_f^0$. It can be concluded that the fast chemisorption is an inherent characteristic of the FeOOH surfaces.

The $d^{true}/d^{app}$ values for α- and γ-FeOOH specimens under $1.5 \times 10^7$ N m$^{-2}$ are similar, while

Table 2. Activation energy for electrical conduction of pure and NO-chemisorbed FeOOH crystals

| | pure FeOOH, eV | FeOOH with NO, eV |
|---|---|---|
| α-FeOOH | 0.80 ± 0.03 | 0.87 ± 0.04 |
| β-FeOOH | 0.91 ± 0.03 | 0.91 ± 0.04 |
| γ-FeOOH | 0.64 ± 0.03 | 0.69 ± 0.04 |

β-FeOOH shows a smaller value. Therefore, the $k_f^*$ seems to be unsuitable for comparing three FeOOH polymorphs with regard to the chemisorption rate. The $k_f^*$, however, is useful for examining the characteristics of the fast chemisorption on an FeOOH; the correlation of $k_f$ and $k_s$ with adsorption temperature and $\sigma_0$ can be discussed on basis of $k_f^*$.

*Surface structure and fast and slow chemisorption*

Regardless of the difference in crystal shape of α-, β- and γ-FeOOH, each crystal has characteristic predominant face: (100) for α-FeOOH,[22] (100) for β-FeOOH[20] and (010) for γ-FeOOH.[21,22] These predominant faces cover more than 95% of the total surface area.[15] It may well be that the surface properties of such substances are governed almost by those of predominant crystal faces.

The predominant face of each FeOOH homologue has typical arrays of oxygen and hydroxyl ions in parallel with the *c*-axis. The surface of α-FeOOH shown in Fig. 10(A) has grooves along the *c*-axis. There are two kinds of hydroxyl ions inside and outside of the groove. β-FeOOH surface has two kinds of concaves, narrow and wide ones as shown in Fig. 10(B). In β-FeOOH crystals, there are tunnels parallel to *c*-axis, containing chloride ions and water molecules. The water adsorption

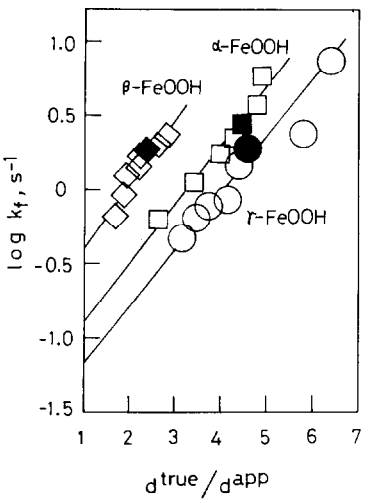



Fig. 9. The log $k_f$ vs $d^{true}/d^{app}$ plots for NO chemisorption.

experiment by the present authors[15] indicates that β-FeOOH crystals have the inner surface due to the vacant tunnels, amounting to 70% of the outer specific surface area. Conzalez–Calbet *et al.*[23] reported that the tunnels can adsorb nitrogen molecules. Surface hydroxyl ions of γ-FeOOH are situated at ridges that are parallel to *c*-axis, whereas oxygen ions are placed beneath shallow valleys (Fig. 10(C)).

It was proposed by the present authors[13,24] that NO and $SO_2$ are chemisorbed on the oxygen ions for α- and β-FeOOH and on the hydroxyl ions for γ-FeOOH. The large shaded circles in Fig. 10 indicate the active oxygen and hydroxyl ions regarded as chemisorptive sites.

α-, β- and γ-FeOOH evacuated at 110°C and $10^{-3}$ Pa have 0.5, 1.0 and 1.7 atomic % $Fe^{2+}$/total Fe. The presence of $Fe^{2+}$ ions is caused by the formation of oxygen vacancy $V_0$ at the removal of hydroxyls ($Fe^{3+} + 2\,OH^- \rightarrow Fe^{2+} + H_2O + O^- + V_0$).[16] The oxygen vacancies produced in arrrays of hydroxyl ions can attract both NO and $SO_2$ molecules by stronger force than that of the surface anions. If the surface structure around the vacancies is suitable to the adsorbate molecule, the adsorption will be stronger.

We presume two kinds of chemisorption site; one is the oxygen vacancy which is in low concentration but is a strong site and another is the surface anion which is numerous but a weak site. If the chemisorption of molecules occurs on the two kinds of sites simultaneously, the presence of fast and slow chemisorption described by eqns (4) and (5) can be explained as the chemisorption processes on the oxygen vacancies and on the surface anions, respectively.

*Geometrical factor in fast chemisorption*

Fast chemisorption sites on the predominant surfaces are shown in Fig. 10. Oxygen vacancies on α- and β-FeOOH surfaces exist in the spaces that fit with adsorbate molecules. On the other hand, γ-FeOOH does not have any surface structure suitable to embrace the molecules. The fact that $k_f^0$ for α- and β-FeOOH is larger than that of γ-FeOOH will be due to the difference in the structure around the vacancy. The site structure of α-FeOOH appears more adaptable to an NO

Table 3. $k_f^0$ and slopes of relationship between log $k_f$ and $d^{true}/d^{app}$

| | $k_f^0$, $s^{-1}$ | slopes |
|---|---|---|
| α-FeOOH | 0.13 | 0.4 |
| β-FeOOH | 0.3 | 0.5 |
| γ-FeOOH | 0.06 | 0.4 |

molecule than β-FeOOH, but $k_f^0$ of α-FeOOH is less than $k_f^0$ of β-FeOOH. The β-FeOOH surface has the open tunnels where NO molecules can be adsorbed. The tunnel will bind NO molecules more firmly than the vacancy. It is assumed that the fast chemisorption sites of β-FeOOH exist mainly in the open tunnels.

Also the fact that $k_f^*$ for NO is much larger than that for $SO_2$ seems to be pertinent to the geometrical factor; small and linear NO molecule can approach closer to the iron ion than larger $SO_2$ molecule.

*Electronic factor in fast chemisorption*

The electron migration to the site is possibly a rate-determining step in the fast chemisorption of NO on β- and γ-FeOOH (0.5–0.6 eV) is close to that for the electrical conduction (0.6–0.9 eV). If this is the case, higher electrical conductivity will result in a larger $k_f$.

The facts that the $k_f^*$ for $SO_2$ α-FeOOH drops in the temperature range above 47°C and that the $k_f^*$ for NO is larger than $k_f^*$ at 50°C, are relevant to the particular change of electrical conductivity of α-FeOOH near 47°C. It was reported in the previous paper[25] that synthetic α-FeOOH is an antiferromagnetic substance having the Néel point at 47°C and the linear plot of log σ vs 1/T bends upward at the temperature. As the activation energy for conduction increases above the Néel point, the fast chemisorption rate drops above the Néel point according to the correlation between σ and $k_f$.

Also the fact that the $k_f^*$ values for NO on α- and γ-FeOOH increase with $\sigma_0$ (Fig. 8) supports the importance of electron migration to the site. However, the decrease of $k_f^*$ for a conductive specimen is inconsistent with the assumption mentioned above. There is a possibility that excess carriers near the surface may suppress the electron migration to the site. Further investigation needs to be done before the electronic mechanism of fast chemisorption is fully understood.

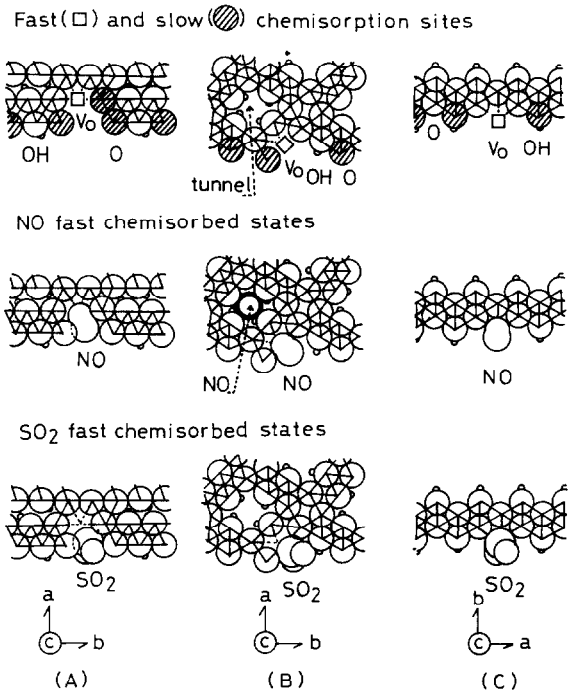



Fig. 10. Surface structures and chemisorption sites viewed from the direction of c-axis for α-FeOOH (A), β-FeOOH (B) and γ-FeOOH (C).

## SUMMARY

The electrical conductivity of FeOOH crystals due to the adsorption of NO and $SO_2$ changes in fast and slow processes of the first order. The fast change finishes within several seconds. The fast and slow conductivity changes are assumed to be caused by fast and slow chemisorption on surface oxygen vacancies and active surface anions, respectively. The fast and slow chemisorption rate constants, $k_f$ and $k_s$, were obtained for α-, β- and γ-FeOOH. The $k_f$ was examined with respect to the adsorption temperature, original electrical conductivity and compression-pressure of the specimen. The activation energy for fast chemisorption was close to that for electrical conduction; the importance of electron-migration to site being suggested. The true rate constant $k_f^0$ of fast chemisorption for the specimen without intergranular gaps, we obtained under higher pressure. The order of magnitude of $k_f^0$ was β-FeOOH > α-FeOOH > γ-FeOOH. The difference in $k_f^0$ was correlated with the difference in the surface structure of each FeOOH.

*Acknowledgement*—This work was supported in part by the Science Research Grant from the Ministry of Education, Japanese Government.

## REFERENCES

1. W. E. Garner and F. S. Stone, *Proc. Roy. Soc.* 1949, **A197**, 294.

2. J. Cunningham, J. J. Kelly and A. L. Penny, *J. Phys. Chem.* 1970, **74**, 1992.
3. M. Komuro, *Bull. Chem. Soc. Japan* 1975, **48**, 756.
4. J. A. Pajares, J. L. Garia Fierro and S. W. Weller, *J. Catal.* 1978, **52**, 521.
5. H. A. Taylor and N. Thon, *J. Am. Chem. Soc.* 1952, **74**, 4169.
6. C. Aharoni and F. C. Tompkins, *Adv. Catal.* 1970, **21**, 1.
7. C. Aharoni and M. Ungarish, *J. Chem. Soc. Faraday Trans. I*, 1976, **72**, 4000.
8. D. O. Hayward and B. M. W. Trapnell, *Chemisorption.* Butterworths, London (1964).
9. D. O. Hayward, *Chemisorption and Reaction on Metallic Films* (Edited by J. R. Anderson), p. 258. Academic Press, New York (1971).
10. G. Wedler, *Chemisorption*, Chap. 5. Butterworths, London (1970).
11. A. Clark, *The Chemisorptive Bond*, Chap. 5. Academic Press, New York (1974).
12. T. Ishikawa and K. Inouye, *Bull. Chem. Soc. Japan* 1972, **45**, 2350.
13. T. Hattori, K. Kaneko, T. Ishikawa and K. Inouye, *Nippon Kagaku Kaishi* 1979, 423.
14. K. Kaneko and K. Inouye, *Nippon Kagaku Kaishi* 1980, 1653.
15. K. Kaneko, M. Serizawa, T. Ishikawa and K. Inouye, *Bull. Chem. Soc. Japan* 1975, **48**, 1764.
16. K. Kaneko and K. Inouye, *J. Chem. Soc. Faraday Trans. I*, 1976, **72**, 1258.
17. K. Kaneko and K. Inouye, *Bull. Chem. Soc. Japan* 1974, **47**, 1139.
18. K. Inouye, H. Imamura, K. Kaneko and T. Ishikawa, *Bull. Chem. Soc. Japan*, 1974, **47**, 743.
19. R. F. Conley, *J. Am. Ceram. Soc.* 1967, **50**, 124.
20. A. L. Mackay, *Miner. Mag.* 1960, **32**, 545.
21. F. J. Ewing, *J. Chem. Phys.* 1935, **3**, 420.
22. G. W. Van Oosterhout, *Acta Cryst.* 1960, **13**, 932.
23. J. M. Gonzalez-Calbet, M. A. Alario-Franco and M. Gayoso-Andrade, *J. Inorg. Nucl. Chem.* 1981, **43**, 257.
24. K. Kaneko, T. Ishikawa and K. Inouye, *Nippon Kagaku Kaishi* 1977, 162.
25. K. Inouye and K. Kaneko, *Proc. 5th Int. Conf. on Thermal Analysis* (Edited by H. Chihara), p. 251. Kagaku Gijutsu-sha, Japan (1977).

*Polyhedron* Vol. 3, No. 2, pp. 231–234, 1984
Printed in Great Britain.

0277-5387/84 $3.00 + .00
© 1984 Pergamon Press Ltd.

# PLATINUM-195 NMR STUDIES OF $Pt(L–L)_2$ (L–L = $^-S_2PR_2$, $^-S_2P(OR)_2$, $^-S_2CNR_2$) AND THEIR DERIVATIVES WITH PHOSPHORUS CONTAINING LIGANDS

RAY COLTON
Department of Inorganic Chemistry, University of Melbourne, Parkville 3052, Australia

**and**

T. ANTHONY STEPHENSON*
Department of Chemistry, University of Edinburgh, Edinburgh, EH9 3JJ, Scotland

(*Received* 4 *July* 1983; *accepted* 2 *August* 1983)

**Abstract**—Platinum-195 NMR spectra have been recorded for $CH_2Cl_2$ solutions of a range of $Pt(L–L)_2$ (L–L = $^-S_2PR_2$, $^-S_2P(OR)_2$, $^-S_2CNR_2$) and their derivatives with phosphorus containing ligands. Platinum chemical shifts cover a range of almost 2000 ppm.

Over the last 15 years a substantial number of papers have been published on the reactions of various tertiary phosphines and phosphinites with square planar $M(L–L)_2$ complexes (M = Pd or Pt, L–L = $^-S_2PR_2$, $^-S_2P(OR)_2$, $^-S_2CNR_2$, $^-Se_2CNR_2$, etc.).[1] The main types of reaction which occur are shown in the Scheme and the authenticity of the products has been verified by several X-ray structural analyses,[1] together with detailed variable temperature $^1H$, $^{31}P–\{^1H\}$ and $^{13}C–\{^1H\}$NMR spectral studies. In this paper we report $^{195}Pt–\{^1H\}$ NMR spectral studies on these compounds which helps to confirm their structures in solution and also the previously proposed rearrangement steps.

## RESULTS AND DISCUSSION

The $^{195}Pt–\{^1H\}$ NMR spectra of these $Pt(L–L)_2$ complexes are readily observed and the data are given in Table 1. Interestingly, a substantial range of $\delta^{195}Pt$ values are observed with $Pt(S_2PPh_2)_2$ at highest frequency, followed by $Pt(S_2CNR_2)_2$, then $[Pt(S_2PMe_2)(PPh_3)_2]^+$ cation with $PBu_3$ in $CH_2Cl_2$ est frequency. Note that the resonance frequencies for the complexes $[Pt(S_2CNR_2)(S^tBu)]_2$ are some 300 ppm above those for the corresponding $Pt(S_2CNR_2)_2$ compounds.

The most interesting systems are those in which a tertiary phosphine, ($PPh_3$ or $PBu_3$ in this case), is added to these $Pt(L–L)_2$ compounds. The reactions are as shown in Scheme 1 and for the monophosphine derivatives, $Pt(L–L)_2PR_3$, (**I**), extensive $^1H$[2], $^{13}C–\{^1H\}$[1,2d] and $^{31}P–\{^1H\}$[1,2d,3] NMR studies have established that at ambient temperature there is a rapid exchange between the mono- and bi-dentate L–L ligands. Figure 1 shows the $^{195}Pt–\{^1H\}$ NMR spectrum of *in situ* generated $Pt(S_2P\{OBu\}_2)_2PPh_3$ at various temperatures. Thus, at 25°C, rapid dithiophosphate exchange produces a doublet of triplets whereas at −40°C, the exchange is slow on the NMR time scale giving rise to separate couplings to the two, now non-equivalent, $^-S_2P(OBu)_2$ ligands. The coupling constant between platinum and the $^{31}P$ in the $^-S_2P(OBu)_2$ groups at room temperature (225 Hz) is the average of the two coupling constants (337 and 117 Hz) observed at lower temperatures for bidentate and unidentate $^-S_2P(OBu)_2$ coordination respectively. Similar spectra are observed for the other $Pt(L–L)_2PR_3$ complexes (Table 1) (L–L = $^-S_2PR_2$, $^-S_2P(OR)_2$), except that for the $PBu_3$ derivatives, there is an intermediate exchange pattern observed at 25°C, indicating that intramolecular exchange of dithioacid groups is slightly slower in complexes of this phosphine.

Further addition of $PR_3$ generates the ionic $[Pt(L–L)(PR_3)_2](L–L)$ complexes (**II**) and for L–L = $^-S_2PPh_2$ and $^-S_2PMe_2$, the $^{195}Pt–\{^1H\}$ NMR spectra consist of the expected triplet of doublets pattern (Table 1). Furthermore, $^{195}Pt$ NMR studies show that treatment of the $[Pt(S_2PMe_2)(PPh_3)_2]^+$ cation with $PBu_3$ in $CH_2Cl_2$

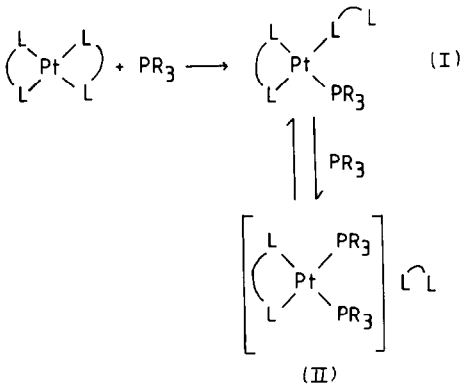
*Author to whom correspondence should be addressed.

Table 1. $^{195}Pt\{^1H\}$ NMR data in $CH_2Cl_2$

| Compound | °C | δ(Pt) | $^1J_{Pt,P}$ | $^2J_{Pt,P}$ |
|---|---|---|---|---|
| $[Pt(S_2CN^iBu_2)S^tBu]_2$ | 25 | -3357 s | | |
| $[Pt(S_2CNEt_2)S^tBu]_2$ | 25 | -3419 s | | |
| $Pt(S_2CN^iPr_2)_2$ | 25 | -3779 s | | |
| $Pt(S_2CNEt_2)_2$ | 25 | -3835 s | | |
| $Pt(S_2CN^nBu_2)_2$ | 25 | -3843 s | | |
| $Pt(S_2P\{Ohexyl\}_2)_2$ | 25 | -3995 t | | 445 |
| $Pt(S_2P\{OBu\}_2)_2$ | 25 | -4015 t | | 445 |
| $[Pt(S_2P\{Ohexyl\}_2)_2PPh_3]$ | 25 | -4501 d of t | 3848 | 220 |
| | -40 | -4525 br. d | 3805 | |
| | -65 | -4534 d of d of d | 3770 | 320, 112 |
| $[Pt(S_2P\{OBu\}_2)_2PPh_3]$ | 25 | -4494 d of t | 3850 | 225 |
| | -10 | -4560 d (exchange) | 3812 | |
| | -40 | -4568 d of d of d | 3780 | 337, 117 |
| $[Pt(S_2P\{OBu\}_2)_2PBu_3]$ | 25 | -4494 d of t | 3585 | |
| | -10 | -4507 d of d of d | 3550 | 315, 135 |
| $[Pt(S_2PPh_2)_2PPh_3]$ | -50 | -4186 d of d of d | 3695 | 290, 100 |
| $[Pt(S_2PPh_2)_2PBu_3]$ | -50 | -4108 d of d of d | 3480 | 280, 124 |
| $[Pt(S_2PMe_2)_2PPh_3]$ | -30 | -4135 d of d of d | 3710 | 270, 110 |
| $[Pt(S_2PMe_2)_2PBu_3]$ | -30 | -4146 d of d of d | 3512 | 255, 115 |
| $[Pt(S_2P\{Ohexyl\}_2)(PBu_3)_2]^+$ | 25 | -4832 t of d | 3275 | 265 |
| $[Pt(S_2P\{Ohexyl\}_2)(PPh_3)_2]^+$ | 25 | -4827 t of d | 3305 | 300 |
| $[Pt(S_2P\{O\}Ohexyl)(PPh_3)_2]$ | 25 | -4856 t of d | 3455 | 264 |
| $[Pt(S_2P\{OBu\}_2)(PBu_3)_2]^+$ | 25 | -4841 t of d | 3295 | 268 |
| $[Pt(S_2P\{O\}OBu)(PBu_3)_2]$ | 25 | -4859 t of d | 3170 | 244 |
| $[Pt(S_2P\{OBu\}_2)(PPh_3)_2]^+$ | 25 | -4876 t of d | 3450 | 220 |
| $[Pt(S_2P\{O\}OBu)(PPh_3)_2]$ | 25 | -4903 t of d | 3310 | 270 |
| $[Pt(S_2PMe_2)(PPh_3)_2]^+$ | 25 | -4426 t of d | 3385 | 254 |
| $[Pt(S_2PPh_2)(PPh_3)_2]^+$ | -50 | -4559 t of d | 3375 | 260 |
| $[Pt(S_2PPh_2)(PBu_3)_2]^+$ | -50 | -4538 t of d | 3235 | 225 |
| $[Pt(S_2PMe_2)(PPh_3)_2]^+$ | -30 | -4530 t of d | 3370 | 250 |
| $[Pt(S_2PMe_2)(PBu_3)_2]^+$ | -30 | -4503 t of d | 3215 | 220 |
| $Pt(S_2CN^iPr_2)$-$(Ph_2P\{S\}HP\{O\}Ph_2)$ | 25 | -4482 d of d | 3715 (P-O)<br>3130 (P-S) | |
| $Pt(S_2CNEt_2)(Ph_2PO)_2H$ | 25 | -4587 t | 3495 | |
| $[Pt(S_2CNMe_2)(PPh_3)_2]^+$ | 25 | -4647 t | 3280 | |

produces a clean sample of $[Pt(S_2PMe_2)(PBu_3)_2]^+$.

However, for the dithiophosphate complexes, addition of an excess of $PR_3$ to $Pt[S_2P(OR)_2]_2$ in $CH_2Cl_2$ gives rise to *two* triplets of doublets in their $^{195}Pt$–$\{^1H\}$ NMR spectra, (see Fig. 2(a) for $Pt(S_2P\{Ohexyl\}_2)_2/PPh_3$ and Table 1 for others). This is because in addition to the formation of $[Pt\{S_2P(OR)_2\}(PR_3)_2]S_2P(OR)_2$ (**II**) by stepwise cleavage of the Pt–S bonds, further irreversible rearrangement occurs to give the neutral $Pt\{S_2P(O)OR\}(PR_3)_2$ (**III**) and $RS_2P(OR)_2$ (equation)[1,2a,2b].




Scheme 1.

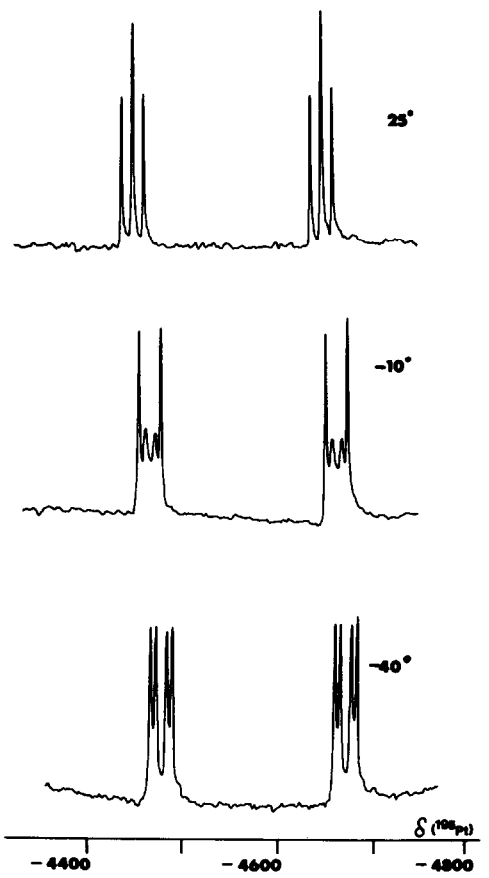
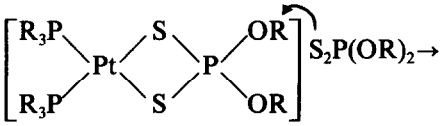
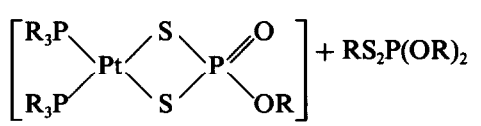



Fig. 1. $^{195}Pt$–$\{^1H\}$ NMR spectra of $Pt(S_2P\{OBu\}_2)_2PPh_3$ in $CH_2Cl_2$ at (a) 25°, (b) −10°, (c) −40°C.



(II)



(III)

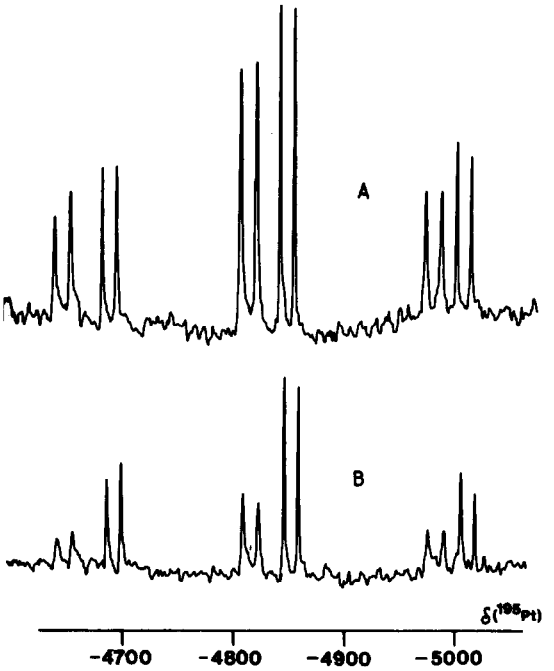



Fig. 2. $^{195}Pt$–$\{^1H\}$ NMR spectra of $Pt(S_2P\{Ohexyl\}_2)_2$ and an excess of $PPh_3$ in $CH_2Cl_2$: (a) at 25°C shortly after mixing, (b) at 25°C after addition of $K[S_2P\{Ohexyl\}_2]$.

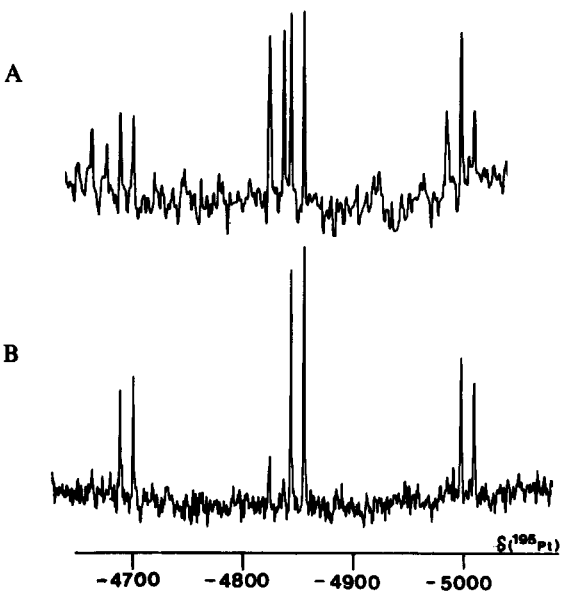



Fig. 3. $^{195}Pt$–$\{^1H\}$ NMR spectra of $[Pt(S_2P\{OBu\}_2)_2]$ and an excess of $PBu_3$ in $CH_2Cl_2$ (a) at 25°C about 30 min after mixing, (b) at 25°C, 12 hr after mixing.

In order to determine which of these $^{195}Pt$ NMR signals correspond to (II) and (III), some excess $K[S_2P(Ohexyl)_2]$ was added to the $[Pt(S_2P\{Ohexyl\}_2)]/PPh_3$ system. As shown in Fig. 2(b), one signal is unaffected while the other is reduced in intensity and broadened, which strongly

suggests that the triplet of doublets at higher frequency is due to compound (II). The broadening is due to slow exchange between free and coordinated $^{-}S_2P(Ohexyl)_2$ and the reduction in intensity is due to attack by the excess $^{-}S_2P(Ohexyl)_2$ to give more of compound (III).

Further proof that this assignment is correct comes from an *in situ* NMR study of the reaction between $[Pt(S_2P\{OBu\}_2)_2]$ and an excess of $PBu_3$ in $CH_2Cl_2$. Figure 3(a) shows the $^{195}Pt$ NMR spectrum of this solution recorded 30 min after mixing the reagents. This is similar to Fig. 2(b) except that accidental coincidence converts the two doublets at lower frequency to an apparent triplet. However, on recording the $^{195}Pt$ NMR spectrum of the same solution, 12 hr later (Fig. 3b), the triplet of doublets at higher frequency has now almost disappeared due to completion of the irreversible reaction to form compound (III).

Finally, Table 1 also lists data for a number of related compounds such as $[Pt(S_2CNEt_2)(Ph_2PO)_2H]$ and $[Pt(S_2CN^iPr_2)(Ph_2P(S)HP(O)Ph_2]$.

## EXPERIMENTAL

The $Pt(L–L)_2$ complexes were prepared according to the literature methods: $Pt(S_2CNR_2)_2$ (R = Et, $^i$Pr),[2b] $Pt(S_2PMe_2)_2$,[2c] $Pt(S_2PPh_2)_2$,[4] $[Pt(S_2CNR_2)S^tBu]_2$,[5] $Pt\{S_2P(OR)_2\}_2$ (R = Bu, hexyl),[6] $Pt(S_2CNEt_2)(Ph_2PO)_2H$[7] and $Pt(S_2CN^iPr_2)\{Ph_2P(S)HP(O)Ph_2\}$.[7] The $[Pt(L–L)_2PR_3]$ and $[Pt(L–L)(PR_3)_2]L–L$ complexes were generated *in situ* in the NMR tube by addition of the appropriate quantity of $PR_3$ to $Pt(L–L)_2$.

NMR spectra were recorded using a JEOL FX 100 spectrometer operating at 21.31–21.33 MHz using 1 M $H_2PtCl_6$ in conc. HCl as an external reference. High frequency positive convention is used. Temperatures were maintained using a JEOL NM 5471 controller calibrated against a platinum resistance thermometer.

*Acknowledgement*—We thank Johnson Matthey PLC for the loan of $K_2PtCl_4$.

## REFERENCES

1. J. P. Fackler Jr., L. D. Thompson, I. J. B. Lin, T. A. Stephenson, R. O. Gould, J. M. C. Alison and A. J. F. Fraser, *Inorg. Chem.* 1982, **21**, 2397 and references therein.
2. [a]J. P. Fackler Jr., J. A. Fetchin and W. C. Seidel, *J. Am. Chem. Soc.* 1969, **91**, 1217. [b]J. M. C. Alison and T. A. Stephenson, *J. Chem. Soc. Dalton Trans.* 1973, 254. [c]D. F. Steele and T. A. Stephenson, *J. Chem. Soc. Dalton Trans.* 1973, 2124. [d]I. J. B. Lin, H. W. Chen and J. P. Fackler Jr., *Inorg. Chem.* 1978, **17**, 394.
3. [a]M. C. Cornock and T. A. Stephenson, *J. Chem. Soc. Dalton Trans.* 1977, 501. [b]J. P. Fackler Jr. and W.-H. Pan, *J. Am. Chem. Soc.* 1979, **101**, 1607.
4. J. M. C. Alison, T. A. Stephenson and R. O. Gould, *J. Chem. Soc.* (*A*) 1971, 3690.
5. J. A. M. Andrews, J. P. Fackler Jr. and D. Coucouvanis, *Inorg. Chem.* 1972, **11**, 494.
6. C. K. Jorgensen, *J. Inorg. Nucl. Chem.* 1962, **24**, 1571.
7. D. M. Anderson, E. A. V. Ebsworth, T. A. Stephenson and M. D. Walkinshaw, *J. Chem. Soc. Dalton Trans.* 1982, 2343.

*Polyhedron* Vol. 3, No. 2, pp. 235–238, 1984
Printed in Great Britain.

0277–5387/84 $3.00 + .00
© 1984 Pergamon Press Ltd.

# NOTE

## SOME SUBSTITUTED THIOUREA COMPLEXES OF MOLYBDENUM CARBONYL

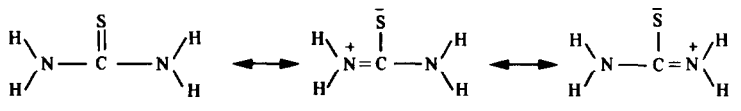
**A. O. BAGHLAF*, M. ISHAQ and A. S. DAIFULIAH**

King Abdul Aziz University College of Science, Department of Chemistry P.O. Box 9028, Jeddah, Kingdom of Saudi Arabia

(*Received* 15 *March* 1983; *accepted* 25 *July* 1983)

**Abstract**—Preparation of monosubstituted thiourea complexes of molybdenum carbonyl $[Mo(CO)_5L]$ both by thermal and UV irradiation methods have been described. The ligands (L) used were N,N′-dimethylthiourea (DMTU), N,N′-diphenylthiourea (DPTU), tetramethylthiourea (TMTU) and tetraethylthiourea (TETU). The complexes $[Mo(CO)_5(L)]$ were characterised by NMR, IR, UV-visible and elemental analyses.

Transition metal carbonyls are known to form complexes with ligands containing sulphur,[1] but it is only in the recent past that thiourea and substituted thioureas have been reported as ligands with transition metal carbonyls.[2–5] The canonical structure of thiourea can be represented as structure 1–3. The ambidentate nature of thiourea has been shown and reported by various workers. For example in thiourea complexes of Zn(II) and Cd(II) the coordination through S has been reported,[7] while in case of Pd(II), Pt(II) and Cu(I) the coordination through N has been suggested.[8] In order to investigate the nature of chemical bonding in this system the studies of molybdenum hexacarbonyl and substituted thiourea derivatives were undertaken.



1 2 3

The compounds were prepared either thermally or on irradiation with UV light. Both the methods gave only monosubstituted thiourea derivatives of the type $[Mo(CO)_5L]$. While this work was in progress Granifo *et al.* reported some substituted thiourea complexes of Cr and W carbonyls.[9]

## RESULTS AND DISCUSSION

### *IR spectra*

All the complexes (I–IV) were monosubstituted $[Mo(CO)_5L]$ and behaved as distorted $C_{4v}$ symmetry showing four bands due to M–CO stretching vibrations, see Table 1.

The low M–CO stretching frequencies in this system may be attributed to the metal-ligand complexation. If the coordination of the ligands to metal was through S it would enhance the canonical forms **2** and **3** thus decrease the bond order of C=S towards the value of a single bond while the value of C–N bond would have more double bond character. This means that the C–S stretching frequency should decrease and whilst the C–N stretching frequency should increase. On the other hand if nitrogen–metal bond is formed just the opposite effect would be expected.

Gosavi and Rao have studied the IR spectra of N,N′-dimethylthiourea complexes of Cu(I) and

*To whom all the correspondence should be addressed.

Table 1.

| Compound | IR spectra in KBr (pellets ($cm^{-1}$) | IR spectra in $CHCl_3$ soln. ($cm^{-1}$) |
|---|---|---|
| DMTU | 1565, 1525, 1450, 1287, 1030 | |
| DPTU | 1547, 1450, 1290, 1067, 1020, 1000, 750, 690. | |
| TMTU | 1505, 1430, 1119, 1092, 1054, 1003, 700, 660. | |
| TETU | 1485, 1373, 1413, 1252, 1080, 890 , 780. | |
| $[Mo(CO)_5DMTU]$ (I) | 1575, 1500, 1455, 1415, 1260, 1085, 1025 | 2070, 1985, 1935, 1905. 1575, 1500, 1025 |
| $[Mo(CO)_5DPTU]$ (II) | 1520, 1460, 1280, 1100, 1066, 1018, 998, 750, 720 682, 260 | 2070, 1992, 1943, 1905 1420, 1100, 1018, 750, 250. |
| $[Mo(CO)_5TMTU]$ (III) | 1538, 1432, 1104, 1051, 1000, 695, 633, 260 | 2070, 1984, 1935, 1888, 1104, 1051, 695, 260. |
| $[Mo(CO)_5TETU]$ (IV) | 1488, 1380, 1434, 1405, 1276, 1255, 995, 1070, 876, 790, 775, 700, 660, 260 | 2080, 1982, 1932, 1890, 1070, 995, 775, 260. |

Pd(II) belonging to the first group and the Cd(II), Zn(II) and Hg(II) complexes belonging to the second group.[7,10] They have shown that in the former group there is a small increase 10–15 $cm^{-1}$ for a composite band around 1500 $cm^{-1}$ (NH bend + C=S + N–C–N bend) compared to the later group, i.e. Zn(II) which show higher value 25–37 $cm^{-1}$. Similarly the bands around 760 $cm^{-1}$ (which is C=S region) are shifted towards the higher frequencies in the complexes of the first group and to lower frequencies in the second group. Recently Khan *et al.*[11] have shown that in complexes $Co[Cu(SCN)_2]$. 2L (L = dimethyl or diphenylthiourea) $\nu$ C=S is shifted to lower frequency ~20–35 $cm^{-1}$ while there is a very small or no shift in the $\nu$ N–H band which clearly shows that sulphur is a donor site in open chain substituted thiourea complexes. The C=S stretching in the infrared spectra of $MX_5$. TMTU (where M=Nb, Ta; X=Cl, Br) has been reported at 1120 $cm^{-1}$.[14] A similar trend has been observed in all complexes **I–IV**. Further consideration of the spectra of complexes leads us to assign the bands at 1025, 1066, 1104 and 1070 $cm^{-1}$, tentatively, to the $\nu$ C=S stretching vibration in complexes **I–IV** respectively, suggesting that coordination is through S see Table 1. The far infrared spectra of complexes **II–IV** show a band of medium intensity at 260 $cm^{-1}$ which may be assigned to Mo–S bond.[8,12,13]

*Proton magnetic resonance spectra*

The spectrum of the complex $[Mo(CO)_5(TMTU)]$ shows a band at 6.8$\tau$ corresponding to the co-ordinated (TMTU) protons and another weak band at 6.9$\tau$ which corresponds to the free ligand. After an interval of 3 hr the latter band shows an increase in its intensity while the former band shows a decrease, which indicates the dissociation of the complex in solution.

The sharpness of the signals is an indication that the compounds are all diamagnetic. All the spectra of the complexes **I–IV** are consistent with the proposed structures and are shown in Table 2.

*Visible and UV-spectra*

The complexes **I–IV** and their solution in common organic solvents were yellow in colour. The visible UV spectra were taken in chloroform and ethanol and show a band around 400 nm while the UV spectra were observed around 272–281 nm. See Table 2.

## EXPERIMENTAL

*Materials*

All the reactions were carried out in an atmosphere of dry nitrogen or in vacuum. The ligands DMTU, DPTU, TMTU and TETU were commercially available and were purchased from Aldrich Chem. Company. They were used without further purifications. $Mo(CO)_6$ was obtained from Koch-Light Chem. Co. and was used as such. Solvents were dried before use and THF was dried over $LiAlH_4$ and distilled under nitrogen.

*Physical measurements*

Infrared spectra were measured in chloroform solution or in KBr pellets on Pye Unicam Model 110 spectrophotometer.

Proton magnetic resonance spectra were measured in deuteriochloroform on a 200 MHz Varian Instrument using TMS as internal reference.

Table 2.

| COMPOUND | Proton magnetic resonance spectra Chem. Shift in ( $\tau$ ) | Multiplicity | Assignment | Visible in ethanol. $\lambda$ max. $\epsilon$ mol$^{-1}$ nm. | cm$^{-1}$ | UV. in chloroform $\lambda$ max. $\epsilon$ mol nm. | cm$^{-1}$ |
|---|---|---|---|---|---|---|---|
| [Mo(CO)$_5$(DMTU)] (I) | 6.9 | doublet | $CH_3$ | 385 | 1920 | 272 | (5048) |
| | 4.2 | broad | N-H | | | | |
| [Mo(CO)$_5$(DPTU)] (II) | 2.66 | doublet | $C_6H_5$ protons | 405 | 1235 | 281 | (7331) |
| | 2.1 | broad | NH | | | | |
| [MO(CO)$_5$(TMTU)] (III) | 6.9 | singlet | $CH_3$(free ligand) | 405 | - | 272 | (4811) |
| | 6.8 | singlet | $CH_3$ | | | | |
| [MO(CO)$_5$(TETU)] (IV) | 8.8 | triplet | $CH_3$ | - | - | 281 | (3281) |
| | 6.5 | quartet | $CH_2$ | | | | |

Visible-UV absorption spectra were obtained on a Beckman spectrophotometer using aboslute ethanol and quartz cuvettes. The electronic spectra in the UV region were obtained on a Zeiss spectrometer Model PMQ using chloroform as solvent.

Elemental analysis were carried out by Microanalysis Laboratory of the King Saud University at Riyadh. Molybdenum analysis was determined by the thiocyanate method.[6]

*Preparation of the compounds*

The compounds (I–IV) were prepared by both (a) Thermal method and (b) UV-Irradiation method (a) gave better yields than the method (b).

(a) *Thermal method.* A typical example is described. *Preparation of dimethylthiourea pentacarbonyl molybdenum*: $Mo(CO)_6$ (528 mg, 2 mmol) was dissolved in 40 cm$^3$ THF and (20 mg, 2 mmol) of the ligand DMTU was added. The solution was refluxed for 2 hr. under constant stirring. The solvent was removed under reduced pressure. The residue was extracted with benzene and the volume was reduced to half. This was poured on an alumina column made in petroleum ether and elution with the benzene separated a yellow band. This was collected and the solvent was evaporated under reduced pressure. A pale yellow solid was obtained. This was recrystallised from benzene/petroleum ether (40–60°C) yield ~20% m.p. 82°C. Calc. for $[Mo(CO)_5DMTU]$: C, 29.3; H, 2.4– N, 8.5; S, 6.4; Mo, 28.2. Found: C, 29.5; J. 3.0; N, 9.3; S, 6.3; Mo, 27.4%.

*Preparation of diphenylthiourea pentacarbonyl molybdenum*

$Mo(CO_6)$ (528 mg, 2 mmol) was dissolved in 40 cm$^3$ THF. To this was added (456 mg, 2 mmol) of the ligand (DPTU) and the mixture was refluxed for 1 hr. The product was obtained as described above. A yellow solid was obtained, yield ~16% and m.p. 103°C. Calc. for $[Mo(CO)_5DPTU]$; C, 46.6; H, 2.6; N, 6.0; S, 6.9; Mo, 20.7. Found: C, 47.0; H, 3.9; N, 4.3; S, 6.7; Mo, 21.1%.

*Preparation of tetramethylthiourea pentacarbonyl molybdenum*

$Mo(CO)_6$ (628 mg, 2 mmol) was dissolved in 50 cm$^3$ *n*-hexane. To this was added (250 mg, 2 mmol) of the ligand (TMTU). The mixture was refluxed for 1 hr. The method (a) was followed for the purification of the product which gave yellow solid, yield ~20% and m.p. 85°C. Calc for $[Mo(CO)_5TMTU]$; C, 32.6; H, 3.3; N, 7.6; S, 8.6; Mo, 26.0. Found: C, 30.7; H, 3.3; N, 7.6; S, 8.5; Mo, 18.3%.

*Tetraethylthiourea pentacarbonyl molybdenum*

$Mo(CO)_6$ 792 mg (3 mmol) was mixed with the ligand (TETU) 564 mg (3 mmol) in 40 cm$^3$ *n*-hexane. The mixture was refluxed for 1 hr. The product was purified as described above in procedure (a). A yellow waxy solid was obtained yield 20%. The elemental analysis of this compound was not obtained due to the difficulty in handling the product.

(b) *UV irradiation method.* All the compounds **I–IV** were obtained on irradiation (1–2 hr) with the UV lamp. The products were purified by using the method (a) as described above.

*Acknowledgement*—A. S. D. thanks the King AbdulAziz University for the Scholarship.

## REFERENCES

1. E. W. Abel and B. C. Crosse, *Organometal. Chem. Rev.* 1967, **2**, 443.
2. F. A. Cotton and F. Zingales. *Inorg. Chem.* 1962, **1**, 145.
3. L. M. Houk and G. R. Dobson, *Inorg. Chem.* 1966, **5**, 2119.
4. H. C. E. Mannenkantz and G. Wilkinson, *J. Chem. Soc.* 1962, 4454.
5. W. Hieber and W. Rhom, *Ber.* 1969, **102**, 2787; 1969, *Ibid.* 1966, **99**, 2312.
6. A. I. Vogel, *A Text-book of Quantitative Inorganic Analysis*, 3rd Edn, p. 903 (1961).
7. T. J. Lane, C. S. C. A. Yamaguchi, J. V. Qugliano, J. A. Ryan and S. Mizushima, *J. Am. Chem. Soc.* 1959, **81**, 3824.
8. R. K. Gosavi and C. R. R. Rao, *J. Inorg. Nucl. Chem.* 1967, **29**, 1937.
9. J. Granifo, J. Costamagna, A. Garro and M. Pieber, *J. Inorg. Nucl. Chem.* 1980, **42**, 1587.
10. R. K. Gossavi, U. Agarwala and C. N. R. Rao, *J. Am. Chem. Soc.* 1967, **89**, 235.
11. S. A. Khan. *J. Inorg. Nucl. Chem.* 1980, **42**, 919.
12. D. M. Adams and J. B. Cornell, *J. Chem. Soc.* 1967, 884.
13. M. B. Adi and A. S. R. Murty, *J. Inorg. Nucl. Chem.* 1977, **39**, 692.
14. A. O. Baghlaf, K. Behzadi and A. Thompson, *J. Less-Common Met.* 1978, **61**, 31.

*Polyhedron* Vol. 3, No. 2, pp. 239–242, 1984
Printed in Great Britain.

0277–5387/84 $3.00 + .00
© 1984 Pergamon Press Ltd.

# NOTE

# KINETICS FOR THE REACTION OF METHINE PROTON OF AN UNSYMMETRICAL TETRADENTATE SCHIFF BASE COMPLEX OF NICKEL(II) WITH N-CHLOROSUCCINIMIDE

**KUNINOBU KASUGA,* TAKEO NAGAHARA, SHUNJI KIYOTA and YASUO YAMAMOTO**
Department of Chemistry, Faculty of Science, Shimane University, Matsue 690, Japan

(*Received* 4 *May* 1983; *accepted* 25 *July* 1983)

**Abstract**—The substitution reaction of the methine proton of an unsymmetrical tetradentate Schiff base complex of nickel(II) with *N*-chlorosuccinimide was kinetically studied in a dichloromethane solution. While the rate of chlorination was decreased by the addition of acetone or ether, the rate was significantly increased by the addition of ethanol. The rate of bromination was faster than that of chlorination. A four-centred intermediate was proposed for the halogenation reaction of the Schiff base nickel(II) complex.

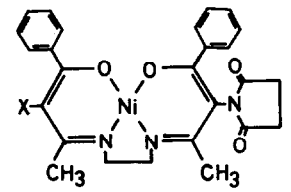
Reactions of coordinated ligands have received considerable attention to elucidate the mechanism of organic syntheses catalyzed by metal ions and the role of metallo-coenzyme.[1] For instance, the numerous substitution reactions of metallo $\beta$-diketone complexes have been reported.[2] Recently, a few studies on the reactions of the methine proton of Schiff base complexes have also been reported.[3–5] While synthetic aspects of the reactions of coordinated ligands are extensively studied, only a few studies on the reaction mechanism are reported.[5–7] In this paper, we report the kinetics for the substitution reactions of [N,N′ - (1 - methyl - 3 - oxo - 3 - phenylpropylidene)(1 - methyl - 2 - succinimido - 3 - oxo - 3 - phenylpropylidene) - ethylenediaminato]nickel(II) (abbr. Ni(L–H) having only one reactive site) with *N*-chlorosuccinimide (NCS).

## EXPERIMENTAL

### *Syntheses*

*Preparation of* Ni(L–H). Benzenethiol (0.33 g, 3 mmol) was added to a dichloromethane solution (80 $cm^3$) of Ni(L–Br) (1.16 g, 2 mmol) which was prepared by the method described before.[4] Then, the solution was left standing with stirring for 1 hr at room temperature. Ni(L–H) was precipitated by the addition of an adequate amount of methanol to the solution. Yields. 0.40 g, 40%. Found: C, 62.06; H, 5.04; N, 8.32. Calc. for $C_{26}H_{25}N_3O_4Ni$; C, 62.18; H, 5.02; N, 8.39%. IR: $\nu$CO (1705 $cm^{-1}$). $^1$H–NMR: $\delta = 1.98$ (s, 3H, $CH_3$), 2.31–2.95 (m, 4H, $CH_2$ of succinimide), 3.53 (s, 4H, $CH_2$ of chelate ring,), 6.24 (s, H, CH) and 7.99–8.42 ppm (m, 10H, $C_6H_5$).

*Preparation of* Ni(L–Cl). NCS (0.40 g, 3 mmol) was added to a dichloromethane solution (50 $cm^3$) of Ni(L–H) (1.00 g, 2 mmol), after which the solution was left standing with stirring for 20 min at room temperature. After the small amounts of




| substituent | X |
|---|---|
| hydrogen | H |
| chloro | Cl |
| bromo | Br |

NI(L-X)

Fig. 1. Abbreviation of the Schiff base nickel(II) complexes.

*Author to whom correspondence should be addressed.

precipitates were filtered off, the filtrate was concentrated under reduced pressure. Then, Ni(L–Cl) was precipitated by the addition of an adequate amount of methanol. Subsequently, the complex was recrystallized from dichloromethane and a small amount of methanol. Yields. 0.57 g, 53%. Found: C, 58.42; H, 4.58; N, 7.85. Calc. for $C_{26}H_{24}N_3O_4ClNi$, C, 58.19; H, 4.51; N, 7.83%. IR: $\nu$CO (1703 $cm^{-1}$). $^1$H-NMR: $\delta = 1.95$ (s, 3H, $CH_3$), 2.33–2.93 (m, 4H, $CH_2$ of succinimide), 3.50 (s, 4H, $CH_2$ of the chelate ring) and 7.72–7.95 ppm (m, 10H, $C_6H_5$).

*Measurements*

NCS was recrystallized from ethanol and dried under reduced pressure. The other reagents were reagent grade, and used without further purification. The change in the absorbance with the time was followed with a Hitachi 215 spectrophotometer. The temperature was controlled at 20.0 ± 0.1°C. The $^1$H-NMR spectra were recorded with a JEOL-MH 100 spectrophotometer at a frequency of 100 MHz. The chemical shifts were determined in ppm, using TMS as the internal standard. The electronic spectra in solution and the infrared spectra using Nujol-mull methods were measured on a Hitachi 215 spectrophotometer and a Hitachi 124 spectrophotometer respectively.

## RESULTS AND DISCUSSION

Ni(L–H) was prepared from Ni(L–Br) by reducing with benzenethiol, where the preparation of Ni(L–Br) was previously reported from our laboratory.[4] The $^1$H-NMR spectrum of Ni(L–H) shows the signal arising from the methine proton at 6.24 ppm, which indicates the displacement of bromine by hydrogen on the methine carbon. By the addition of NCS to the Ni(L–H) solution, Ni(L–Cl) was prepared, which was also confirmed by the disappearance of the $^1$H-NMR signal arising from the methine proton.

Ni(L–H) shows the absorption maxima at 248 (log $\epsilon = 4.56$), 283 (4.32), 397(3.87), 440$^{sh}$ (3.39) and 570 nm (2.11) in the dichloromethane solution. Ni(L–Cl) also shows the maxima at 252 (4.49), 283$^{sh}$ (4.32), 391 (3.73), 430$^{sh}$ (3.25) and 562 nm (2.18). The spectrum changed with the time by the addition of NCS to that of Ni(L–Cl) with isosbestic points at 257 and 275 nm (Fig. 2).

The rate of the chlorination was determined by an absorbance change at 410 nm. The plot of $(a-b)^{-1}$ ln $[b(A_t - A_\infty)/\{(b(A_0 - A_\infty) - a(A_0 - A_t)\}]$ vs the time was linear for at least 90% completion; $a$ and $b$ are initial concentrations of Ni(L–H) and NCS. $A_0$, $A_t$ and $A_\infty$ represent the absorbances at initial, time $t$ and infinity, respectively. From the slope, the second-order rate constant was estimated at $(3.26 \pm 0.15) \times 10/mol^{-1}$ $dm^3$ $s^{-1}$. The rate was also measured at 400 nm. The rate constant ($(3.25 \pm 0.18) \times 10/mol^{-1}$ $dm^3$ $s^{-1}$) obtained was almost the same with that measured at 410 nm, showing no wavelength dependence of the rate.

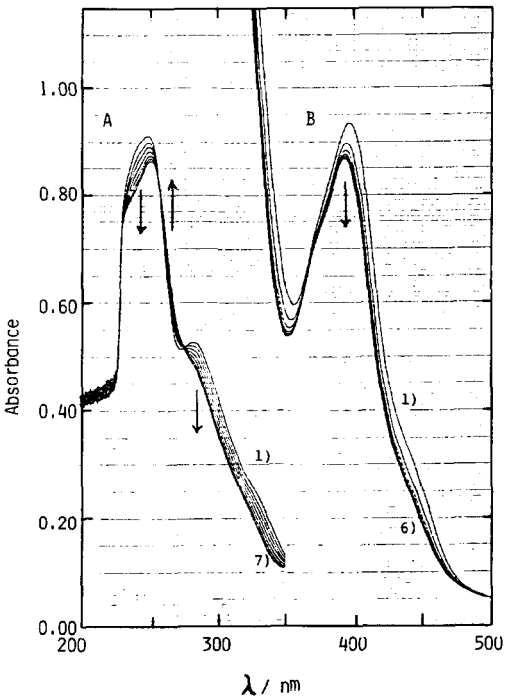



Fig. 2. Spectra changes during the reaction of Ni(L–H) with NCS in the dichloromethane solution at 20°C. (A) [Ni(L–H)] = $2.50 \times 10^{-5}$ mol $dm^{-3}$, [NCS] = $5.00 \times 10^{-5}$ mol $dm^{-3}$: (1) 0.5, (2) 2.5, (3) 4.5, (5) 11.5, (6) 16.5 and (7) 22.5 min after the reaction. (B) [Ni(L–H)] = $1.50 \times 10^{-4}$ mol $dm^{-3}$dm, [NCS] = $3.00 \times 10^{-4}$ mol $dm^{-3}$: (1) 0.5, (2) 2.5, (3) 4.5, (4) 6.5, (5) 8.5 and (6) 12.5 min after the reaction.

A few further experiments were performed to elucidate the reaction mechanism. (1) 2,6-di-tert-butylphenol was added to the reaction solution of Ni(L–H) and NCS. However, the rate was not affected by the radical scavenger so that the radical mechanism might be excluded, as reported in the case of the chlorination of [N,N′ - bis(1 - methyl - 3 - oxo - 4 - trifluorobutylidene) - ethylenediaminato] nickel(II) with NCS.[5] It is reported that the reaction of *N*-halogenosuccinimide (NXS) involves the radical mechanism in nonpolar solvents such as carbon tetrachloride and cyclohexane in which NXS is insoluble or hardly soluble; the radical mechanism occurs at the surface of the NXS crystal lattice.[8] On the other hand, in polar solvents such as tetrachloroethane and nitrobenzene, NXS is soluble and reacts like a halogen molecule via an ionic mechanism.[8] In the

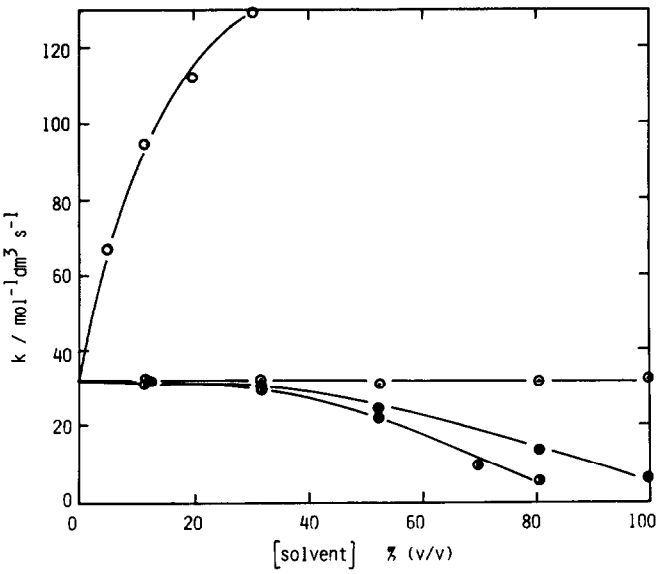



Fig. 3. The effect of solvents on the rate constant of the chlorination: ○, ethanol; ⊙, acetonitrile; ●, acetone; ◑, ethyl ether (the complex was undissolved in 100% ethyl ether).

kinetic measurements, NCS was completely dissolved in the dichloromethane solution ($5.00 \times 10^{-5}$ mol dm$^{-3}$), and thus the reaction may proceed via the ionic mechanism. (2) The rate of bromination with *N*-bromosuccinimide was faster than that of chlorination (the rate of the bromination was so fast that the rate constant could not be obtained). The polarizability of the halogen atom in the electrophile seems to be more important than its electronegativity. (3) The effects of solvents on the chlorination are shown in Fig. 3. The rate constant was little affected by the addition of acetonitrile. While the rate constant was decreased by the addition of acetone or diethyl ether, it was significantly increased by the addition of ethanol.

For an intermediate of the chlorination, the following two types can be proposed. In the intermediate (**I**), breakage of a C–H bond might be a rate-determining step, as was reported for iodination of phenol.[9] Thus, the rate constant may be little affected by the kinds of the halogen atoms of electrophiles, in contrast to the experimental results. The polar solvents such as acetonitrile and acetone must promote the heterolytic fission of NCS, and hence accelerate the rate of the chlorination. However, the rate constant was not affected or decreased by the addition of the solvents. These results exclude the intermediate (**I**) for the chlorination. In the intermediate (**II**), the bromine atom must stabilize the four-centred system more than the chlorine atom because of the larger polarizability of bromine. Furthermore, the strong

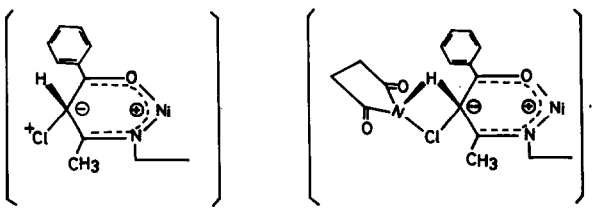



Fig. 4. The proposed intermediates.

proton-acceptor solvents such as acetone and ethyl ether might make a hydrogen bonding with hydrogen in the four-centred system, resulting in the destabilization of the intermediate (**II**) which decreases the rate constant. These results support the intermediate (**II**) for the chlorination on the methine carbon by *N*-chlorosuccinimide.

It is reported that chlorine is liberated from NCS by the addition of alcohols.[10] That is, the chlorine thus liberated by ethanol may accelerate the rate of the chlorination presumably *via* the intermediate (**I**). Further studies will be performed to elucidate the detailed reaction mechanism.

## REFERENCES

1. M. M. Jones, *Ligand Reactivity and Catalysis*. Academic Press, New York (1968); R. H. Holm, *Inorganic Chemistry* (Edited by G. L. Eichorn), Vol. 2, p. 1137. Elsevier, Amsterdam (1973); A. Nakahara, O. Yamanouchi and Y. Nakao, *Bioorganic Chemistry* (Edited by E. E. van Tamelen), Vol. 4, p. 349. Academic Press (1978).

2. J. P. Collman, *Angew. Chem.* 1965, **77**, 154; K. C. Joshi and V. N. Pathak, *Coord. Chem. Rev.* 1977, **22**, 37; T. J. Cardwell and T. H. Lorman, *Inorg. Chim. Acta* 1981, **53**, L104.
3. T. Nagahara, K. Kasuga and Y. Yamamoto, *Inorg. Chim. Acta* 1981, **47**, 37.
4. T. Nagahara, K. Kasuga and Y. Yamamoto, *Inorg. Nucl. Chem. Lett.* 1981, **17**, 235.
5. Y. Fujii, M. Ito and K. Akiyama, *Bull. Chem. Soc. Jpn.* 1981, **54**, 2527.
6. R. W. Kluiber, *J. Am. Chem. Soc.* 1961, **83**, 3030.
7. K. Kuroda, K. Yoshitani, K. Kunigita, Y. Kamiiba and K. Watanabe, *Bull. Chem. Soc. Jpn.* 1976, **49**, 2445.
8. S. D. Ross, M. Finkelstein and R. C. Petersen, *J. Am. Chem. Soc.* 1958, **80**, 4327; F. Dewhurst and P. K. J. Shah, *J. Chem. Soc. (C)*, 1970, 1737; L. Horner and E. H. Winkelmann, *N*-bromosuccinimide, its properties and reactions. In *Newer Methods of Preparative Organic Chemistry* (Edited by W. Forerst), Vol. 3, pp. 151–198. Academic Press, New York (1964) and the articles cited therein.
9. E. Grovenstein and D. C. Kilby, *J. Am. Chem. Soc.* 1957, **79**, 2972.
10. L. Zechmeister and L. Walleave, *J. Am. Chem. Soc.* 1953, **75**, 4493; F. J. Petracek and L. Zechmeister, *J. Am. Chem. Soc.* 1956, **78**, 1427.

*Polyhedron* Vol. 3, No. 2, pp. 243–246, 1984
Printed in Great Britain.

0277–5387/84 $3.00 + .00
© 1984 Pergamon Press Ltd.

# NOTE

# ALKALI METAL COMPLEXES: COMPLEXES OF ALKALI METALS WITH QUINALDINIC ACID

**DHARM PRAKASH***
Department of Chemistry, Patna University, Patna 800005, India

and

**SHANKAR PRASAD SINGH**
Department of Chemistry, A. N. College, Patna 800013, India

(*Received* 17 *May* 1983; *accepted* 28 *June* 1983)

**Abstract**—Complexes having the general formula ML.HL, where M = Na, K, Rb or Cs and HL = quinaldinic acid, have been obtained. The isolation of adducts in the solid state appeared to be favoured by increase in atomic radius, and hence decrease in ionisation potential of the metal. Attempts to synthesise similar adducts of picolinic acid N-oxide and quinaldinic acid N-oxide did not succeed. Complexes have been characterised by elemental analyses, thermal, IR spectral and solution studies. Our findings suggest that pK value of the ligands cannot be regarded a dominant factor in the synthesis and isolation of alkali metal complexes.

Extending our investigations, and those of others,[1–6] to the syntheses of pure neutral complexes of alkali metals, with a view to exploring the mechanism of selective absorption of alkali metal ions by plants, our attention has been drawn to the ligand quinaldinic acid.

Quinaldinic acid has been extensively investigated for its possible use in analytical determination of metal ions.[8–15] Its complexes with transition metals as well as rare earths are well investigated.[16–24] However, a survey of the literature revealed that no alkali metal complex with this ligand had previously been reported.

In the present communication, the syntheses and characterisation of a number of complexes of alkali metals with quinaldinic acid are described. They have the general formula ML.HL where M = Na, K, Rb or Cs and HL = quinaldinic acid, hereafter designated as HQuinA. The isolation of adducts in the solid state appeared to be favoured by increase in atomic radius, and hence decrease in ionisation potential of the metal.

*Author to whom correspondence should be addressed.

## EXPERIMENTAL

*Preparation of alkali metal salts of quinaldinic acid*

Equimolar proportions of metal hydroxide and the quinaldinic acid were refluxed in 95% ethanol in a water bath for about 15 min. The solution was filtered, concentrated and then cooled, when the alkali metal salts precipitated out. It was filtered, washed with the solvent and then dried in an electric oven at 80°C.

*Preparation of the complexes*

To the suspension of alkali metal salt of quinaldinic acid in absolute ethanol, quinaldinic acid was added in 1:1 mole ratio. The contents went into solution and almost instantaneously a white adduct precipitated. On refluxing with continuous stirring on a hot plate, the contents went into solution again. The clear solution so obtained was cooled, when the white adduct reappeared. It was filtered, washed with absolute ethanol and dried in an electric oven at 80°C. No adduct separated in the case of lithium.

We also attempted to synthesise similar adducts of picolinic acid N-oxide and quinaldinic acid N-oxide with alkali metals, but our attempts did not succeed. This leads us to suggest that the

conversion of picolinic acid and quinaldinic acid into their corresponding N-oxides has caused a decrease in their chelating ability.

## RESULTS AND DISCUSSION

Some physical properties and analytical data of the ligand, its alkali metal salts and the hitherto unknown alkali metal complexes are listed in Table 1.

All the complexes are white in colour. They are stable under dry conditions, e.g. over anhydrous $CaCl_2$ in a desiccator.

The complexes showed no change in stoichiometry or in physical properties even after 1 yr. On exposure to moisture, the complexes appeared to hydrolyse. This was confirmed by the analysis as well as by studying the IR spectra, which were not identical with that of the original complex.

All the complexes are soluble in polar solvents such as methanol. However, a few complexes have also been found to be sparingly soluble in non-polar solvents such as chloroform and toluene too.

Quinaldinic acid, although it has a low pK value (4.92), has been found to form neutral complexes with all the alkali metals except lithium (Table 2). This is in conformity with the observations of Banerjee *et al.*[25] in the case of 2-nitroso-1-naphthol, but appears inconsistent with their findings, reported in the same communication that ligands with higher pK values formed complexes with most of the alkali metals; whereas the ligands with low pK values gave complexes only with rubidium and caesium. Our findings suggest that pK value of the ligands cannot be regarded as a dominant factor in the synthesis and isolation of alkali metal complexes.

From the results (Table 1), it is evident that all these complexes undergo a transformation at temperatures which are considerably higher than the melting point of the ligand, indicating thereby their greater thermal stability.

### *IR Spectra*

IR spectra of the ligand, the salts and the complexes have been recorded in the region 4000–650 $cm^{-1}$ in Nujol mulls using a Perkin–Elmer Spectrophotometer. The pertinent IR data are listed in Table 3.

The multiple bands in the region 2700–1800 $cm^{-1}$ in the spectrum of the ligand HQuinA point to the presence of strong intramolecular hydrogen bonding involving the carboxyl hydrogen atom and the N-atom of the quinoline ring. In the spectra of the complexes, these bands have disappeared. However, the spectra of all the complexes exhibit a new broad band of weak to medium intensity at 2350 $cm^{-1}$ which may be attributed to O–H...O/N...H–O absorption. This suggests hydrogen bonding to be a dominant factor in stabilising these complexes.

Koramantzon and Pneumaticakis[26] have reported the antisymmetric stretching frequency of the –COOH group in the quinaldinic acid at 1670 $cm^{-1}$. However, we did not find any peak in the spectrum of the ligand at this wave number. The medium intensity band at 1680 $cm^{-1}$ in the spectrum of the ligand may, in all probability, be assigned to the antisymmetric stretching frequency of the –COOH group. Shifting of this band to lower frequency by 20 $cm^{-1}$ in the sodium complex and to higher frequencies in other complexes appears to suggest coordination of the ligand through carboxylic group. Besides, the shifting of the 1620 $cm^{-1}$ band to lower frequencies by about

Table 1.

| Compound | Colour | m.p./decomp./transition temp. (°C) | Conductivity ($Ohm^{-1}cm^2mole^{-1}$) | (%) Found | | | | (%) Calculated | | | |
|---|---|---|---|---|---|---|---|---|---|---|---|
| | | | | C | H | N | M | C | H | N | M |
| HQuinA | White | 156–158 m | – | | | | | | | | |
| LiQuinA | White | >300 d | 3.3 | 67.45 | 3.56 | 7.78 | – | 67.04 | 3.35 | 7.82 | – |
| NaQuinA | White | >300 d | 3.3 | 61.99 | 3.37 | 7.00 | 11.50 | 61.54 | 3.08 | 7.18 | 11.79 |
| NaQuinA.HQuinA | White | 220 t | 3.6 | 65.80 | 3.88 | 7.60 | 6.25 | 65.22 | 3.53 | 7.61 | 6.25 |
| KQuinA | White | >300 d | 4.4 | 56.96 | 2.89 | 6.65 | 18.00 | 56.87 | 2.84 | 6.53 | 18.48 |
| KQuinA.HQuinA | White | 235 t | 4.5 | 62.80 | 3.88 | 7.30 | 10.00 | 62.50 | 3.38 | 7.29 | 10.16 |
| RbQuinA | White | >300 d | 2.5 | 46.83 | 2.88 | 5.78 | 33.50 | 46.60 | 2.33 | 5.43 | 33.25 |
| RbQuinA.HQuinA | White | 205 t | 3.3 | 55.95 | 3.50 | 6.50 | 19.50 | 55.75 | 3.02 | 6.50 | 19.86 |
| CsQuinA | White | >300 d | 4.7 | 40.06 | 2.40 | 4.62 | 43.85 | 39.34 | 1.96 | 4.59 | 43.60 |
| CsQuinA.HQuinA | White | 190 t | 4.4 | 50.80 | 2.95 | 5.85 | 27.80 | 50.21 | 2.72 | 5.86 | 27.82 |

5 $cm^{-1}$ and that of 1535 $cm^{-1}$ band to higher frequencies by 7 $cm^{-1}$ in the complexes indicate the coordination of the ligand through carboxylic group.

The 1580 $cm^{-1}$ band of the ligand has split into two in all the complexes. While one of the split bands has appeared in the higher frequency side (*ca.* positive shift of 15–20 $cm^{-1}$), the other is in the lower frequency side (*ca.* negative shift of 2–5 $cm^{-1}$). A probable explanation for this splitting seems to be the simultaneous presence of the two quinoline ring –C=N– moiety, one of which is in the salt and the other belongs to the quinaldinic acid molecule, acting as the secondary

Table 2.

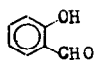
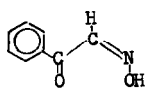
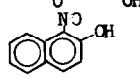
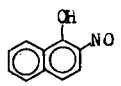
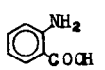
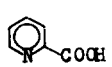
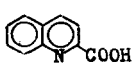
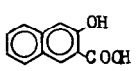
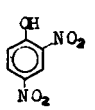
| | pK value | Neutral complexes | | | | |
|---|---|---|---|---|---|---|
| | | Li | Na | K | Rb | Cs |
|  | 9.58 | 1:2 | 1:2 | 1:2<br>1:3 | 1:2<br>1:3 | 1:2<br>1:3 |
|  | 9.51 | 1:2 | 1:2 | 1:2 | 1:3 | 1:3 |
|  | 8.50 | – | 1:2 | 1:2 | 1:2 | 1:2 |
|  | 7.70 | – | – | 1:2 | 1:2 | 1:2 |
|  | 7.48 | 1:2 | 1:2 | 1:2 | 1:2 | 1:2<br>1:3 |
|  | 7.17 | – | – | 1:3 | 1:3 | 1:2 |
|  | 6.97 | – | – | 1:2 | 1:2 | 1:2 |
|  | 5.86 | – | – | 1:2 | 1:2 | 1:2 |
|  | 4.92 | – | 1:2 | 1:2 | 1:2 | 1:2 |
|  | 4.50 | – | – | – | 1:2 | 1:2 |
|  | 3.86 | – | – | – | – | 1:3 |

Table 3.

| Compound | Selected i.r. absorption bands ($cm^{-1}$) | | | | | |
|---|---|---|---|---|---|---|
| HQuinA | 2700–1800v | 1680m | 1620s | 1580sh | | 1535s |
| NaQuinA.HQuinA | 2350br | 1660s | 1615m | 1595s | 1575w | 1542m |
| KQuinA.HQuinA | 2350br | 1685s | 1615m | 1600s | 1578m | 1542m |
| RbQuinA.HQuinA | 2350br | 1680s | 1615m | 1600s | 1575m | 1542m |
| CsQuinA.HQuinA | 2350br | 1730s | 1615m | 1600s | 1575w | 1542m |

ligand. These features are suggestive of the coordination of the ligand with alkali metals through nitrogen atom of its quinoline ring.

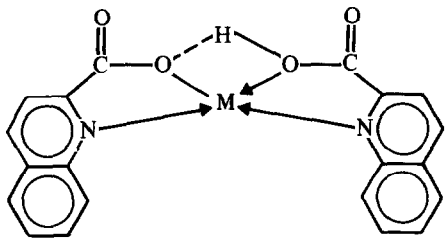
*Conductivities*

Molar conductivities were measured in methanol at 23°C at a concentration of $10^{-3}$ M.

From Table 1, it is evident that the molar conductivities of the neutral complexes are almost equal to those of corresponding alkali metal salts of quinaldinic acid. It appears that in the methanolic solutions, all these neutral complexes are completely dissociated.

*Probable structure*

The above discussion suggests that in all the complexes, the ligand HQuinA behaves as a bidentate ligand, coordination sites being the nitrogen atom of its quinoline ring as well as the oxygen atom of the –COOH group. IR spectra of the complexes point to the presence of hydrogen-bonding in them. These facts suggest the following possible structure for these complexes:




## REFERENCES

1. N. V. Sidgwick and S. G. P. Plant, *J. Chem. Soc.* 1925, **127**, 209.
2. N. V. Sidgwick and F. M. Brewer, *J. Chem. Soc.* 1925, **127**, 2379.
3. F. M. Brewer, *J. Chem. Soc.* 1931, 361.
4. A. K. Banerjee, A. J. Layton, R. S. Nyholm and M. R. Truter, *Nature* 1968, **5134**, 1147.
5. A. K. Banerjee, A. J. Layton, R. S. Nyholm and M. R. Truter, *J. Chem. Soc.* (*A*), 1969, 2536.
6. A. J. Kolombos, Ph.D. Thesis. University of London, 1970.
7. A. K. Banerjee, Dharm Prakash and S. K. Roy, *J. Ind. Chem. Soc.* 1976, **53**, 458.
8. P. Ray and M. K. Bose, *Mikrochemie* 1935, **17**, 11.
9. P. Ray and J. Gupta, *Mikrochemie* 1935, **17**, 14.
10. P. Ray and A. K. Majumdar, *Z. Anal. Chem.* 1935, **100**, 324.
11. P. Ray and M. K. Bose, *Mikrochemie* 1935, **18**, 89.
12. P. Ray and N. K. Durra, *Z. Anal. Chem.* 1939, **115**, 265.
13. P. Ray and T. C. Sarkar, *Mikrochemie* 1939, **27**, 64.
14. John F. Flogg and D. W. Vanas, *Ind. Eng. Chem. Anal. Ed.* 1946, **18**, 436.
15. O. Erametsa, *Suom. Kemi* 1944, **178**, 30.
16. M. Singh, R. Singh and S. S. Sandhu, *Ind. J. Chem.* 1976, **14A**, 361.
17. R. L. Dutta and S. Lahiry, *J. Ind. Chem. Soc.* 1961, **38**, 1001.
18. R. L. Dutta and S. Lahiry, *J. Ind. Chem. Soc.* 1962, **39**, 871.
19. R. L. Dutta and B. Chatterjee, *J. Ind. Chem. Soc.* 1967, **44**, 758.
20. N. K. Dutt and S. Upadhyay, *J. Inorg. Nucl. Chem.* 1967, **29**, 1368.
21. N. K. Dutt and K. Nag, *J. Inorg. Nucl. Chem.* 1969, **31**, 1867.
22. N. K. Dutt and S. Sur, *J. Inorg. Nucl. Chem.*, 1969, **31**, 3171.
23. S. P. Ghosh and A. Mishra, *J. Ind. Chem. Soc.* 1970, **47**, 79.
24. B. Chatterjee, *J. Ind. Chem. Soc.* 1976, **53**, 1212.
25. A. K. Banerjee, Dharm Peakash and S. K. Roy, *J. Ind. Chem. Soc.* 1976, **53**, 773.
26. M. B. Koromantzon and G. A. Pneumaticakis, *Chem. Ind.* 1967, **25**, 1089.

*Polyhedron* Vol. 3, No. 2, pp. 247–250, 1984
Printed in Great Britain.

0277–5387/84 $3.00 + .00
© 1984 Pergamon Press Ltd.

# NOTE

# THERMAL AND PHOTOCHEMICAL PRODUCTION OF CHROMATE(VI) IONS FROM SOME COMPLEXES CONTAINING THE $\{CrNO\}^{2+}$ GROUP

**GRZEGORZ STOPA and ZOFIA STASICKA***

Department of Inorganic Chemistry, Jagiellonian University, 30-060 Kraków, Poland

(*Received* 7 *June* 1983; *accepted* 28 *June* 1983)

**Abstract**—Results are reported for the oxidation of complexes of the type $[Cr(CN)_{5-x}(H_2O)_xNO]^{x-3}$ by molecular oxygen in alkaline medium. In the case of the $[Cr(CN)_5NO]^{3-}$ complex the reaction proceeded photochemically, whereas in other cases the thermal oxidation was also observed. The influence of pH, $CN^-$ concentration and energy of radiation was investigated.

Recently, production of chromate(VI) in photoredox reactions of the $[Cr(CN)_{6-x}(OH)_x]^{3-}$ complexes was reported.[1] We have found[2] that other chromium complexes are also susceptible to oxidation by oxygen yielding $CrO_4^{2-}$ in alkaline medium upon exposure or even thermally. Such behaviour has been demonstrated by complexes of the type $[Cr(CN)_{5-x}(H_2O)_xNO]^{x-3}$, where $x = 0$, 3 or 5.

We now report details of the study.

## RESULTS AND DISCUSSION

So far, complexes of the type $[Cr(CN)_{5-x}(H_2O)_xNO]^{x-3}$ have been studied in acidic or neutral medium.[3–13] In this work, their behaviour in alkaline solutions was followed. More stable members of the series, i.e. the $[Cr(CN)_5NO]^{3-}$, $[Cr(CN)_2(H_2O)_3NO]$ and $[Cr(H_2O)_5NO]^{2+}$ complexes, were chosen for this study. The fate of the complexes was found to depend strongly on the presence of light and oxygen as well as on the concentrations of the $OH^-$ and $CN^-$ ions.

Nitrosylpentacyanochromate, $[Cr(CN)_5NO]^{3-}$, appeared to be thermally stable at pH $\geqslant$ 7, whereas its aquo derivatives underwent relatively fast thermal reactions in alkaline medium.

In the presence of an excess of KCN, the $[Cr(CN)_2(H_2O)_3NO]$ complex and, in part, also the $[Cr(H_2O)_5NO]^{2+}$ one, were transformed rapidly into a thermally stable species characterized by bands at $16.4 \times 10^3\ cm^{-1}$ ($\epsilon = 20\ dm^3\ mole^{-1}\ cm^{-1}$) and $21.3 \times 10^3\ cm^{-1}$ ($\epsilon = 140\ dm^3\ mole^{-1}\ cm^{-1}$) and increasing absorption towards higher wave numbers (Fig. 1).

In the absence of added KCN, a decay of the band near $22 \times 10^3\ cm^{-1}$ was observed indicating the cleavage of the metal–ligand bond in the $\{CrNO\}^{2+}$ group.[4,14] In the oxygenated system the product spectra (Fig. 1) were characteristic of a mixture of the $[CrO_2(H_2O)_n]_2^-$ complex[1] ($\tilde{\nu}_1 = 16.8 \times 10^3\ cm^{-1}$ and $\tilde{\nu}_2 = 23.3 \times 10^3\ cm^{-1}$) and the $CrO_4^{2-}$ ions ($\tilde{\nu}_1 = 26.8 \times 10^3\ cm^{-1}$ and $\tilde{\nu}_2 = 36.6 \times 10^3\ cm^{-1}$). This conclusion was

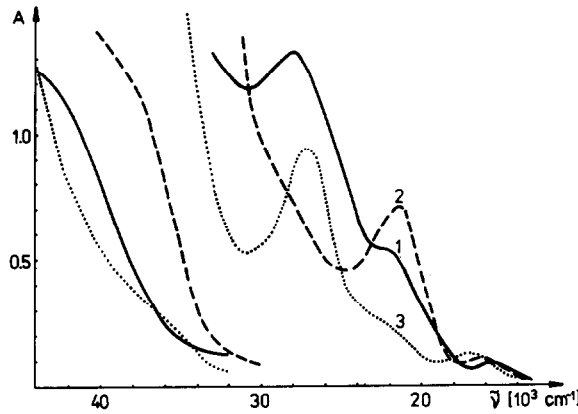



Fig. 1. Spectra of $5 \times 10^{-3}$ M $[Cr(CN)_2(H_2O)_3NO]$ at pH = 3 (curve 1) and products of its thermal equilibration at 295 K in 1 M KOH: in the presence of 0.1 M KCN (curve 2) and in oxygen saturated solution (curve 3).

*Author to whom correspondence should be addressed.

confirmed by chemical analysis. Moreover, the reaction was accompanied by production of the $NO_2^-$ ions, and, in case of the $[Cr(CN)_2(H_2O)_3NO]$ complex, by release of the $CN^-$ ions.

The results suggested generation of a deprotonated form of nitrosylaquocyanochromate in the presence of an excess of KCN, whereas complete decomposition of the $[Cr(CN)_2(H_2O)_3NO]$ and $[Cr(H_2O)_5NO]^{2+}$ complexes in the other case. Products of the decomposition were oxidized by molecular oxygen to Cr(III) and Cr(VI) species according to overall reaction

$$[Cr(CN)_{5-x}(H_2O)_xNO]^{x-3} \xrightarrow[O_2,\,OH^-]{kT(h\nu)} \begin{cases} [CrO_2(H_2O)_n]^- + NO_2^- + (5-x)CN^- & (1a) \\ CrO_4^{2-} + NO_2^- + (5-x)CN^- & (1b) \end{cases}$$

where $x = 3$ or 5.

Yield of the second path (1b) was found to be relatively low (not higher than 20%) and considerably dependent on the concentrations of the $OH^-$ and $CN^-$ ions and molecular oxygen in the system. This is illustrated in Figs. 2(a) and (b) for the $OH^-$ and $CN^-$ ions, respectively. Moreover, the yield of chromate(VI) ions appeared to be significantly increased by irradiation of the system (Fig. 2c).

The $CrO_4^{2-}$ ions were found to be produced also in oxygenated alkaline solutions of the $[Cr(CN)_5NO]^{3-}$ complex but only upon exposure to radiation of $\tilde{\nu} \gtrsim 23 \times 10^3\ cm^{-1}$ (Fig. 3). This was accompanied by release of the $CN^-$ and $NO_2^-$ ions. In more concentrated solutions generation of the $[CrO_2(H_2O)_n]^-$ complex could be also observed.

*It should be, however, mentioned that Nikolskii and Popov[17] postulated another mechanism for the photochemical reaction in non-alkaline medium.

The same reaction products as in eqn (1) and relatively low energy of the radiation inducing the photooxidation of the $[Cr(CN)_5NO]^{3-}$ complex have led us to believe that the oxidation was preceded by photosubstitution of the $CN^-$ ligands by the $H_2O$ molecules or $OH^-$ ions*.

$$[Cr(CN)_5NO]^{3-} \xrightarrow[H_2O]{h\nu} [Cr(CN)_{5-x}(H_2O)_xNO]^{x-3} + xCN^- \quad (2)$$

Secondary thermal and photochemical reactions of

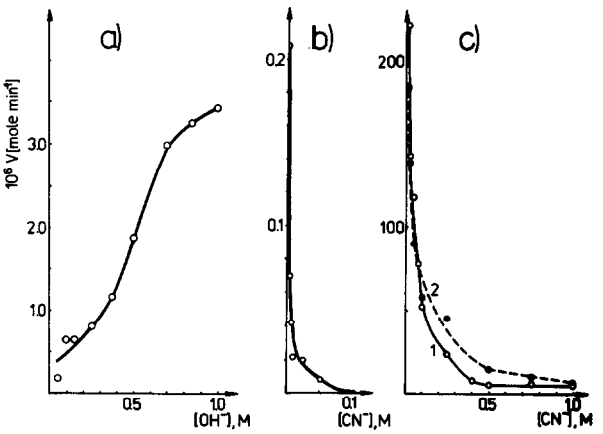



Fig. 2. Concentration dependence of chromate (VI) production rate at 295 K: (a) in thermal reaction of $2.5 \times 10^{-3}$ M $[Cr(CN)_2(H_2O)_3NO]$; (b) in thermal reaction of $2.5 \times 10^{-3}$ M $[Cr(CN)_2(H_2O)_3NO]$ in 0.1 M NaOH; (c) in photochemical reaction (polichromatic light) of $2.5 \times 10^{-3}$ M $[Cr(CN)_2(H_2O)_3NO]$ in 0.1 M NaOH (curve 1) and of $2.5 \times 10^{-3}$ M $[Cr(CN)_5NO]^{3-}$ in 0.1 M NaOH (curve 2).

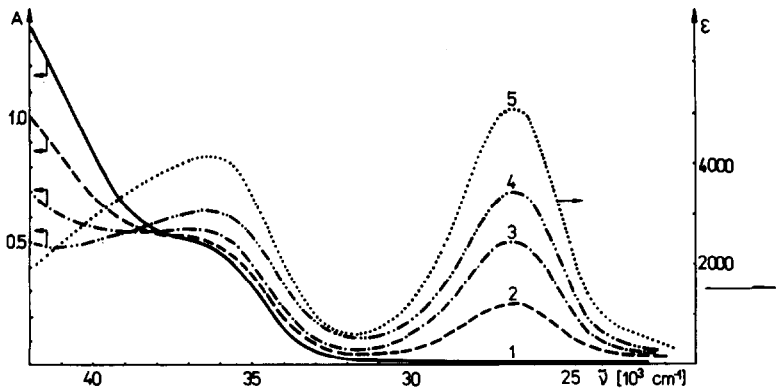



Fig. 3. Spectral changes recorded for oxygenated $2.5 \times 10^{-4}$ M solution of $K_3[Cr(CN)_5NO]$ in 0.01 M KOH (curve 1) upon irradiation with polichromatic light within 1, 2.5 and 11 min (curves 2–4 respectively); for a comparison, the spectrum of $K_2CrO_4$ in 0.01 M KOH is presented as curve 5.

Table 1. Quantum yields of chromate(VI) production from the $[Cr(CN)_5NO]^{3-}$ complex ($\Phi \times 10^2$; $T = 293 \pm 0.5$ K)

| pH | λ [nm] | | |
|---|---|---|---|
| | 436 | 366 | 313 |
| 7[a] | 0.02 ± 0.007[c] | 0.12 ± 0.002 | 0.16 ± 0.01 |
| 9[a] | 0.17 ± 0.07 | 0.68 ± 0.07 | 1.23 ± 0.08 |
| 11[a] | 0.17 ± 0.07 | 1.00 ± 0.13 | 1.58 ± 0.10 |
| 13[b] | 0.21 ± 0.08 | 1.19 ± 0.12 | 1.96 ± 0.24 |

[a]Britton-Robinson buffer; [b]0.1 M KOH; [c]standard deviation

the nitrosylaquochromates in alkaline oxygenated solutions (eqn 1) would be thus responsible for generation of the Cr(VI) and Cr(III) species.

The conclusion was supported by the results of flash photolysis experiments which revealed that chromate(VI) appeared not earlier than within milliseconds upon flashing and increased up to delay times of the order of seconds.

The postulated mechanism is consistent as well with the influence of concentration of the $OH^-$ and $CN^-$ ions on the yield of Cr(VI) production from the $[Cr(CN)_5NO]^{3-}$ complex. This is illustrated in Fig. 2(c) for the $CN^-$ ions, whereas data presented in Table 1 show that quantum yields of $CrO_4^{2-}$ production depend considerably on concentration of the $OH^-$ ions. Moreover, the photochemical reaction was found to proceed both in *d–d* and CT bands (see, e.g.[14–16]) although the yield was the higher with the more energetic radiation (Table 1).

## EXPERIMENTAL

*Materials.* Potassium nitrosylpentacyanochromate, $K_3[Cr(CN)_5NO]$ was prepared and purified according to procedure of Griffith *et al.*[18] Its purity was checked by chemical analysis and IR and UV spectroscopy. The nitrosylaquochromates, $[Cr(CN)_2(H_2O)_3NO]$ and $[Cr(H_2O)_5NO]^{2+}$, were obtained in aqueous solution following the literature method.[4,6] Their purity was tested spectrally.[5] Other chemicals were best available commercial reagents used without further purification.

Apparatus and procedure. A high pressure mercury lamp (HBO 200, Narva, DDR) was used to irradiate samples set in a thermostated rectangular quartz cell ($d = 1$ cm). For quantum yield measurements, glass filters (Schott, Jena, DDR) were used to isolate 436, 366 and 313 nm wavelengths. Irradiations were performed at $293 \pm 0.5$ K with a continuous flow of oxygen. The reaction progress was followed spectrally (Specord UV-Vis, Zeiss, DDR). Irradiations were limited to less than 10% conversion. Quantum yield values were corrected for inner filter effect.[19,20] Actinometry was carried out with trisoxalatoferrate(III).[21,22] Flash photolysis apparatus was that described elsewhere.[23]

*Acknowledgement*—We thank the Polish Academy of Sciences for support.

## REFERENCES

1. A. Marchaj and Z. Stasicka, *Polyhedron* 1983, **2**, 1287.
2. Preliminary results were presented at the 3rd Symposium on Coordination Compounds, Mogilany-Kraków, Poland, May 1980 and at the 22nd International Conference on Coordination Chemistry, Budapest, Hungary, August 1982.
3. J. Burgess, B. A. Goodman and J. B. Raynor, *J. Chem. Soc. A* 1968, 501.
4. D. I. Bustin, J. E. Earley and A. A. Vlček, *Inorg. Chem.* 1969, **8**, 2062.
5. J. Mocák, D. I. Bustin and M. Žiaková, *Inorg. Chim. Acta* 1977, **22**, 185.
6. J. Mocák, D. I. Bustin and M. Žiaková, *Inorg. Chim. Acta* 1977, **23**, 111.
7. D. I. Bustin, M. Rievaj and J. Mocák, *Inorg. Chim. Acta* 1978, **26**, 5.
8. D. I. Bustin, M. Rievaj and J. Mocák, *Inorg. Chim. Acta* 1978, **26**, 11.
9. D. I. Bustin, M. Rievaj and J. Mocák, *Inorg. Chim. Acta* 1978, **27**, 53.
10. D. I. Bustin, M. Rievaj and J. Mocák, *Inorg. Chim. Acta* 1978, **27**, 59.
11. J. Labuda, D. I. Bustin and J. Mocák, *J. Inorg. Nucl. Chem.* 1980, **42**, 1739.
12. J. Labuda, D. I. Bustin and J. Mocák, *Chem. Zvesti* 1981, **35**, 459.
13. D. I. Bustin, M. Rievaj and J. Mocák, *Proc. 8th Conf. Coord. Chem.*, p. 55. Smolenice-Bratislava (1980).

14. P. T. Manoharan and H. B. Gray, *Inorg. Chem.* 1966, **5**, 823.
15. Y. J. Israeli, *Bull. Soc. Chim. France* 1964, 1145.
16. R. F. Fenske and R. L. DeKock, *Inorg. Chem.* 1972, **11**, 437.
17. A. B. Nikolskii and A. M. Popov, *Dokl. Akad. Nauk SSSR* 1980, **250**, 902.
18. W. P. Griffith, J. Lewis and G. Wilkinson, *J. Chem. Soc.* 1959, 872.
19. H. F. Wasgestian and H. L. Schläfer, *Ber. Bunsenges. Phys. Chem.* 1967, **71**, 489.
20. H. F. Wasgestian, *Z. Phys. Chem.* (*Frankfurt am Main*) 1969, **67**, 39.
21. C. A. Parker, *Proc. Roy. Soc. A* 1953, **220**, 104.
22. C. G. Hatchard and C. A. Parker, *Proc. Roy. Soc. A* 1956, **235**, 518.
23. T. Jarzynowski, T. Senkowski and Z. Stasicka, *Polish J. Chem.* 1981, **55**, 3.

*Polyhedron* Vol. 3, No. 2, pp. 251–255, 1984
Printed in Great Britain.

0277-5387/84 $3.00 + .00
© 1984 Pergamon Press Ltd.

# NOTE

# THE INFLUENCE OF SOLVENT POLARITY ON THE TETRAHEDRAL–OCTAHEDRAL EQUILIBRIUM OF Co(II)COMPLEXES WITH 3,5-DIMETHYLPYRAZOLE

**A. ANAGNOSTOPOULOS* and S. HADJISPYROU**
Chemical Engineering Department, Polytechnic School, University of Thessaloniki, Thessaloniki, Greece

(*Received* 27 *June* 1983; *accepted* 5 *July* 1983)

**Abstract**—The configuration equilibrium: $[Co(SCN)_2(DMPz)_4] \overset{K}{\rightleftharpoons} Co(SCN)_2(DMPz)_2 + 2DMPz$; (where DMPz = 3,5-dimethylpyrazole), has been studied spectrophotometrically in various non-aqueous polar solvents. The influence of solvent polarity on the K value has been investigated. Solvation studies have also been carried out on the tetrahedral species $Co(SCN)_2(DMPz)_2$, and the results are interpreted in terms of the polarity of the various solvents.

The configuration equilibria in solutions of the type:

$$CoB_4X_2 \rightleftharpoons CoB_2X_2 + 2B \qquad (1)$$

(octahedral) (tetrahedral)

where B = organic base and X = halide or pseudohalide, have been studied and the relative stabilities of the tetrahedral and the octahedral configurations were found to be affected by the ligand properties, such as size, shape, polarisability and $\pi$-acceptor capacity.[4–6] Nelson *et al.* gave significance to the existence of Co–B $\pi$-bonding which depends mainly on $X^-$ and to a lesser extent on B and its pKa value.[7(a–d)] However, although the influence of B and X on the relative stabilities of the tetrahedral and the octahedral forms has been intensively studied, the effect of the solvent used has received only little attention.[6]

In this paper, we are investigating the effect of the solvent polarity on the K value of equilibrium (1) and the solvation behaviour of the tetrahedral form in non-aqueous solvents of different polarity. The aim of this work is to elucidate the kind of solvation mechanism and how this mechanism is affected by the solvent polarity.

*Author to whom correspondence should be addressed.



## EXPERIMENTAL

*Substances*

The Co(II) complexes were prepared as described earlier.[1] The 3,5-dimethylpyrazole has been prepared according to the literature.[2] The solvents have been purified according to published procedures.[3] Throughout the text, the substances will be referred to as:

$Co(SCN)_2(DMPz)_4$ = P (pink, octahedral)

$Co(SCN)_2(DMPz)_2$ = B (blue, tetrahedral)

DMPz = 3,5-dimethylpyrazole = L, ligand.

*Physical measurements*

Electronic spectra were run on a Shimadzu-200S spectrophotometer. Electrical conductances were measured with a Metrohm E 527 conductivity bridge.

*Part A. (Procedure)*

The equilibrium (1) has been confirmed and the influence of the solvent's polarity on its K value assessed. This has been done as follows: The visible spectra of $10^{-3}$ M solutions of B and P were obtained in each solvent, in order to estimate the $\lambda_{max}$ of each complex (Table 1). The absorbance of different solutions of B were measured at $\lambda_{max}$ and the $\epsilon_B$ value was estimated for each solvent.

Table 1. Spectroscopic data of $Co(DMPz)_2(NCS)_2$ and K values in various solvents, at 20°C

| Solvent | B $\lambda$max (nm) | B emax | $K_1$ | $K_2$ |
|---|---|---|---|---|
| $CHCl_3$ | 590 | 1100 | $8,18X10^{-7}$ | $8,4X10^{-7}$ |
| $CH_3NO_2$ | 598 | 1200 | $5,89X10^{-6}$ | $5,98X10^{-6}$ |
| $CH_3CN$ | 600 | 1220 | $8,27X10^{-6}$ | $8,38X10^{-6}$ |
| $C_6H_5NO_2$ | 605 | 1225 | $2,57X10^{-5}$ | $2,32X10^{-5}$ |
| $CH_2Cl_2$ | 613 | 1250 | $5,89X10^{-5}$ | $5,99X10^{-5}$ |

(Table 1). Further, the K of the equilibrium $P \rightleftharpoons B + 2L$ has been estimated:

$$K = \frac{[B][L]^2}{[P]} \quad (1)$$

Replacing in (1) the concentration values in equilibrium and considering Beer's law,the following equation results:

$$4\left(\frac{A - \epsilon_p P_0}{\epsilon_B - \epsilon_p}\right)^3 + K\left(\frac{A - \epsilon_p P_0}{\epsilon_B - \epsilon_p}\right) - KP_0 = 0 \quad (2)$$

where: A = absorbance at $\lambda_{max}$, $\epsilon_B$, $\epsilon_p$ = molar extinction coefficients of the corresponding complexes and $P_0$ = initial concentration of P(moles/lit). This method is necessary, because from the spectra it is shown that the two forms, the octahedral P and the tetrahedral B exist in the solution simultaneously. The $A_{\lambda max}$ in different $P_0$ concentrations was measured and the $\epsilon_p$ and K values were obtained (Table 1, $K_1$). Finally, the equilibrium:

$$P \rightleftharpoons B + 2L$$

has been confirmed, by adding increasing amounts of L in decreasing amounts of B, in order to move the above equilibrium to the left. The K value remains constant, ($K_2$) at the same temperature. The mathematical transformation of the equilibrium (1) at this point, gives the eqn (3):

$$4\left(\frac{A - \epsilon_B B_0}{\epsilon_p - \epsilon_B}\right)^3 - 4(B_0 + L_0)\left(\frac{A - \epsilon_B B_0}{\epsilon_p - \epsilon_B}\right)^2$$

$$+ (L_0^2 + 4B_0L_0 + K)\left(\frac{A - \epsilon_B B_0}{\epsilon_p - \epsilon_B}\right) - B_0L_0^2 = 0 \quad (3)$$

where $B_0$, $L_0$ = initial concentrations of B and L (moles/lit).

Measuring the $A_{\lambda max}$ for different $B_0$ and $L_0$, with known values of $\epsilon_p$ and $\epsilon_B$, the K was estimated (Table 1).

*Part B (Solvation studies)*

The study of the solvation mechanism has been carried out by spectroscopic and conductometric measurements, according to previous work.[4]

In this work, the solvation mechanism of $Co(SCN)_2(DMPz)_2 = B$ has been determined in different polar solvents and estimated the % solvation in each solvent.

*Procedure*

A 100 $cm^3$ solution of B, has been prepared, conc. $5.0 \times 10^{-4}$ M, in each solvent. The conductivity and the absorbance value are obtained at the corresponding $\lambda_{max}$. Afterwards, to the above solution, 0.02 mmole of base (DMPz) has been added (equal amount each time). Then, the conductivity and the absorbance were measured again, until two consecutive measurements were equal (equilibrium situation) (Tables 2 and 3).

## RESULTS AND DISCUSSION

In the first part of this work, the existence of the equilibrium:

$$Co(SCN)_2(DMPz)_4 \overset{K}{\rightleftharpoons} Co(SCN)_2(DMPz)_2 + 2DMPz \quad (1)$$

has been confirmed and its K value was measured in different polar non-aqueous solvents. The more polar the solvent, the greater the K value (Table 1). This means that with more polar solvent, we have greater proportion of the tetrahedral form in the solution. The octahedral P complex exhibits the above disproportionation (1) in each solvent, whereas the tetrahedral form B is stable in the solvents used. The relatively small difference in CFSE between octahedral and tetrahedral Co(II) complexes is responsible, in part, for the formation of more tetrahedral complexes than any other

Table 2. Solvation studies in a $Co(DMPz)_2(NCS)_2$ solution in chloroform. $C = 5 \times 10^{-4}M$. $\Theta = 20°C$

| mmoles of added $DMP_z$ | $A^{590}$ | Conductivity $\Lambda$(mS) | Specific Conductivity, $K(mS.cm^{-1})$ |
|---|---|---|---|
| 0 | 0,550 | 56,5 | 0,05053 |
| 0,02 | 0,558 | 54 | 0,04830 |
| 0,04 | 0,565 | 50,8 | 0,04544 |
| 0,06 | 0,570 | 47,2 | 0,04222 |
| 0,08 | 0,579 | 44,5 | 0,03980 |
| 0,10 | 0,585 | 41,3 | 0,03698 |
| 0,12 | 0,594 | 39 | 0,03488 |
| 0,14 | 0,594 | 39 | 0,03488 |

Table 3. Solvation studies in a $Co(DMPz)_2(NCS)_2$ solution in nitromethane. $c = 5 \times 10^{-4}M$. $\Theta = 20°C$

| mmoles of added $DMP_z$ | $A^{598}$ | Conductivity $\Lambda(\mu S)$ | Specific Conductivity, $K(\mu S.cm^{-1})$ |
|---|---|---|---|
| 0 | 0,600 | 20 | 17,888 |
| 0,02 | 0,585 | 22,5 | 20,124 |
| 0,04 | 0,570 | 23,8 | 21,287 |
| 0,06 | 0,560 | 24,2 | 21,644 |
| 0,08 | 0,5425 | 24,9 | 22,270 |
| 0,10 | 0,528 | 25,3 | 22,628 |
| 0,12 | 0,515 | 25,8 | 23,075 |
| 0,14 | 0,500 | 26,1 | 23,344 |
| 0,16 | 0,495 | 26,6 | 23,791 |
| 0,18 | 0,490 | 27,2 | 24,328 |
| 0,20 | 0,4875 | 27,6 | 24,685 |
| 0,22 | 0,4875 | 27,6 | 24,685 |

transition metal ion.[8] This difference becomes greater with the polarity of the solvent. With more polar solvent, we have greater stabilization of the tetrahedral form.

As pointed out, for solvents with low dipole moment value (e.g. $CHCl_3$ and $CH_2Cl_2$), there is simple solvation, which is concluded from the increase in intensity of absorption, paralleled with a decrease in conductivity value (Fig. 1). That is mechanism of type SS (simple solvation, eqn 2).

$$\underset{\text{tet}-}{Co(SCN)_2(DMPz)_2} + zS \rightleftharpoons \underset{\text{oct}-}{[Co(DMPz)_{2-x}(SCN)_{2-y}S_z]^{y+}} + xDMPz + ySCN^- \quad (2)$$

where $S$ = solvent and $X + y + 2 = Z$.

For more polar solvents (e.g. $CH_3NO_2$, $CH_3CN$ and $C_6H_5NO_2$) there is different solvation type. This is ionic side reaction (IS), where the solvent S enters the coordination sphere of the complex and the equilibrium (1) moves to a charged, octahedral ion, with a decrease of absorbance paralleled with an increase of conductivity value (Fig. 2 and eqn 3).

$$\underset{\text{tet}-}{Co(SCN)_2(DMPz)_2} + zS + (x-2)DMPz \rightleftharpoons \underset{\text{oct}-}{[Co(DMPz)_x(SCN)_yS_z]^{(2-y)+}} + (2-y)SCN^- \quad (3)$$

where $x + y + z = 6$.

The degree of solvation or percentage of solvation, increases with the solvent's polarity (Table 4). For solvents which exhibit simple solvation (type SS), low percentages of solvation are ob-

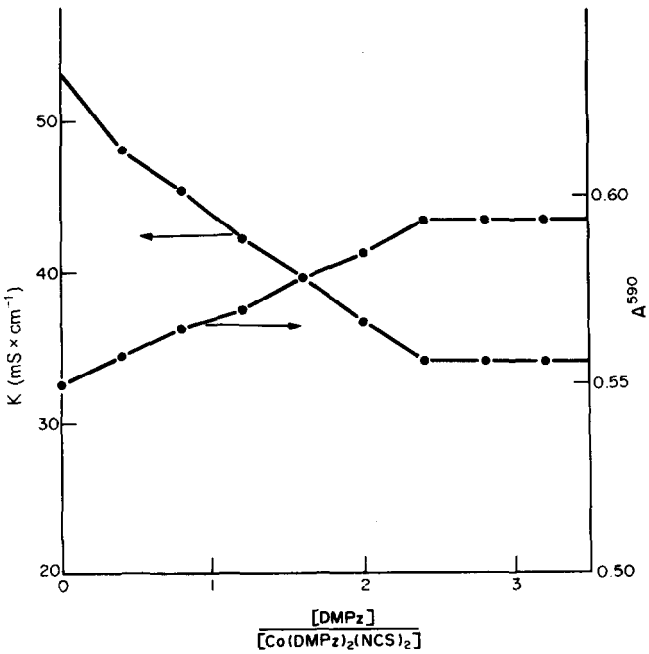



Fig. 1. Specific conductivity (k) and absorbance (590 nm) of $Co(DMPz)_2(NCS)_2$ vs molar ratio $[DMPz]/[Co(DMPz)_2(NSC)_2]$ at 20°C in chloroform. $[Co(DMPz)_2(NCS)_2] = 5 \times 10^{-4}M$.

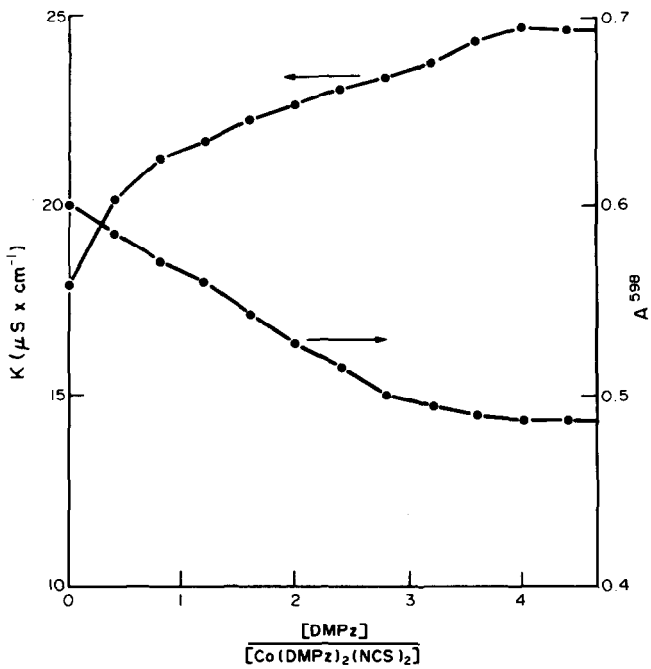



Fig. 2. Specific conductivity (k) and absorbance (598 nm) of $Co(DMPz)_2(NCS)_2$ vs molar ratio $[DMPz]/[Co(DMPz)_2(NCS)_2]$ at 20°C in nitromethane: $[Co(DMPz)_2(NCS)_2] = 5 \times 10^{-4}M$.

served, whereas for the type IS solvents, high solvation percentages are obtained. That is in agreement with the solvent polar properties. The solvents of the SS type, possess low values of dipole moment ($\mu$) and dielectric constant, ($\epsilon$). Low value of $\epsilon$, means low ability of stabilizing the ions formed, leading to ion-pairs and also the dipole-ion interaction is very confined in this case, due to the low value of $\mu$. Inversely, the high $\mu$ and $\epsilon$ values of the IS type solvents are responsible, in

Table 4. Polar and donor characteristics and % solvation of various solvents

| Solvent | Dipole (Debye) moment (μ) | Dielectric constant, ε | Donor number D.N. | % Solvation |
|---|---|---|---|---|
| $CHCl_3$ | 1,01 | 5,04 | 0,01 | 8 |
| $CH_2Cl_2$ | 1,60 | 9,20 | 0,02 | 10,72 |
| $CH_3NO_2$ | 3,46 | 38,93 | 2,7 | 18,75 |
| $CH_3CN$ | 3,92 | 37,76 | 14,1 | 15,24 |
| $C_6H_5NO_2$ | 4,22 | 37 | 4,4 | 15,03 |
| DMSO | 3,96 | 49 | 29,8 | ——— a |
| DMF | 3,82 | 39 | 26,6 | ——— a |

a= Equilibrium (1) not existed.

part, for the reversible to the above phenomena, which are the IS type features.

However, although $CH_3CN$ has higher dipole moment than $CH_3NO_2$ (Table 4) the percentage of solvation is lower for $CH_3CN$. For $C_6H_5NO_2$, with even higher dipole moment (4.22 D) the percentage of solvation is even lower. This is attributed to the factor donor number (DN) which, for a coordinating solvent, is of fundamental importance in determining the donor strength of the solvent molecule.[10] From this point of view, the $DN_{CH_3CN}(=14.1)$ is much greater than that of $CH_3NO_2(=2.7)$ and $C_6H_5NO_2(=4.4)$. The DN values for chlorinated hydrocarbons are less than unity (Table 4). The spectral data for the solvents DMF and DMSO do not include the characteristic absorptions of the two forms, as in the other solvents used. Thus, we were unable to obtain any comparable results. This is attributed to the high donor strength (Table 4) which exhibit these solvents. They enter the inner coordination sphere of the complex. They form octahedral species, replacing totally the ligand L, destroying in this way the equilibrium (1), as it is shown in eqns (4) and (5). This case has been established in other systems.[9,10]

$$Co(SCN)_2(DMPz)_2 + 5DMSO \rightleftharpoons [Co(SCN)(DMSO)_5]^+ + SCN^- + 2DMPz \quad (4)$$

$$Co(SCN)_2(DMPz)_2 + 5DMF \rightleftharpoons [Co(SCN)(DMF)_5]^+ + SCN^- + 2DMPz. \quad (5)$$

*Supplementary material available*

Tables, graphs and spectral data are available on request from the authors.

## REFERENCES


1. A. Anagnostopoulos, *J. Inorg. Nucl. Chem.* 1976, **58**, 435.
2. *Org. Synthesis* 1951, **31**, 43.
3. D. D. Perrin and W. L. F. Armarego, *Purification of Laboratory Chemicals*. Pergamon Press (1966).
4. C. F. Tshabalala, E. W. Giesekke, N. H. Agnew, *J. Inorg. Nucl. Chem.* 1978, **40**, 225.
5. C. L. Sharma and P. K. Jain, *Ibid.* 1979, **41**, 805.
6. W. Libus, K. Chachulska, M. Mecik, *Inorg. Chem. 1980, 19, 2259.*
7. S. M. Nelson, H. C. A. King and E. Körös, (a) *J. Chem. Soc.* 1963, 5449. (b) *Ibid*, 1965, 3276. (c) *Ibid*, 1965, 3284. (d) *Ibid*, 1966, 1348.
8. Nyholm, Pauling and Gill, *Nature* 1958, **182**, 168.
9. V. Gutmann, O. Bohunovsky, *Monatsh. Chem.* 1968, **99**, 751.
10. V. Gutmann, In *New Pathways in Inorganic Chemistry* (Edited by E. A. V. Ebsworth, A. G. Maddock and A. G. Sharpe), p. 69. Cambridge University Press, Cambridge (1968).

*Polyhedron* Vol. 3, No. 2, pp. 257–260, 1984
Printed in Great Britain.

0277-5387/84 $3.00 + .00
Pergamon Press Ltd

# NOTE

## TEMPLATE REACTIONS WITH POLYNUCLEAR COMPLEXES. THE REACTION OF OCTACHLORODIMOLYBDATE(II) WITH 2-AMINOBENZALDEHYDE

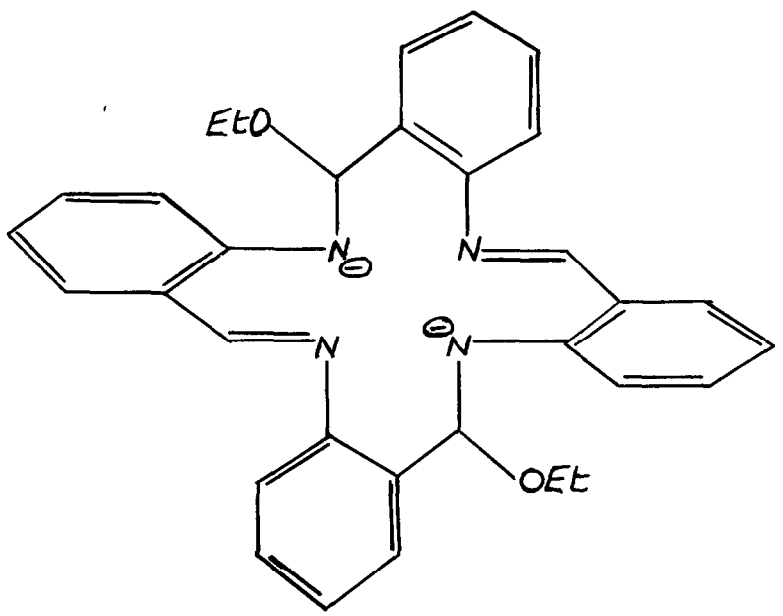
Arvind Sahajpal and Peter Thornton*

Department of Chemistry, Queen Mary College,
Mile End Road, London E1 4NS.

(Received 18 August 1983; accepted 3 November 1983)

The binuclear molybdenum(II) anion $[Mo_2Cl_8]^{4-}$ acts as a template for the self-condensation of 2-aminobenzaldehyde. The dimolybdenum unit is retained in the molybdenum(IV) product, $[Mo_2(A)_2(H_2O)]^{4+}.4Cl^-$, where A is a macrocyclic tetradentate ligand containing two Schiff base nitrogen donors. The product forms as two isomers, whose $^1H$ nmr spectra are discussed.

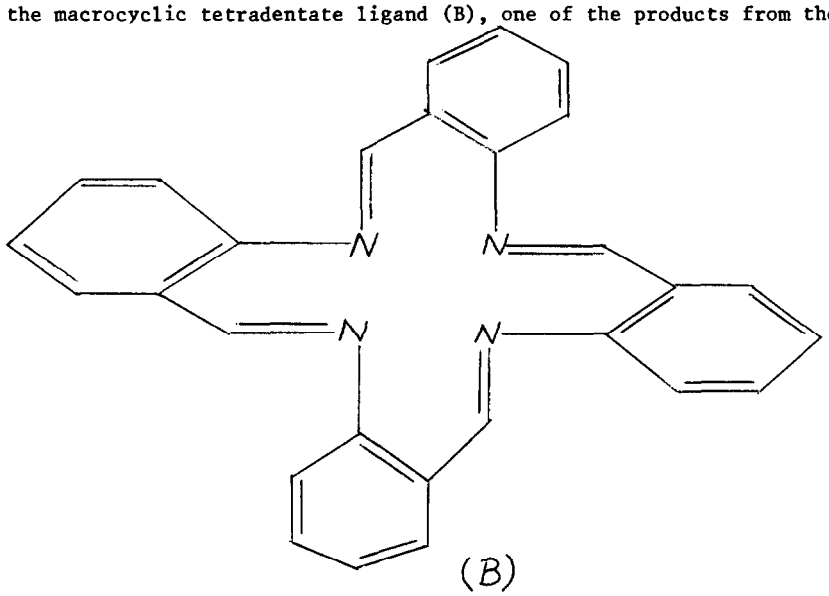
All previously reported template reactions, in which metal ions control the course of an organic reaction, involve just a single metal ion.[1] This paper describes our first attempts at performing template reactions round a binuclear centre, the quadruply bonded $[Mo_2Cl_8]^{4-}$. We selected for study the self-condensation of 2-aminobenzaldehyde as this reaction is particularly sensitive to the choice of metal ion used as template, giving complexes of a tetradentate ligand with $Cu^{2+}$, of a tridentate ligand with $Co^{2+}$, and of both with $Ni^{2+}$. The fairly soluble salt $(NH_4)_5[Mo_2Cl_8]Cl.H_2O$ reacts with 2-aminobenzaldehyde in ethanol to give a mixture of products from which $[Mo_2(A)_2(H_2O)Cl_2]^{2+}.2Cl^-$ has been




(A)

*Author for correspondence

isolated. Ligand (A) was first prepared[2] by the partial base hydrolysis of a nickel(II) complex of the macrocyclic tetradentate ligand (B), one of the products from the



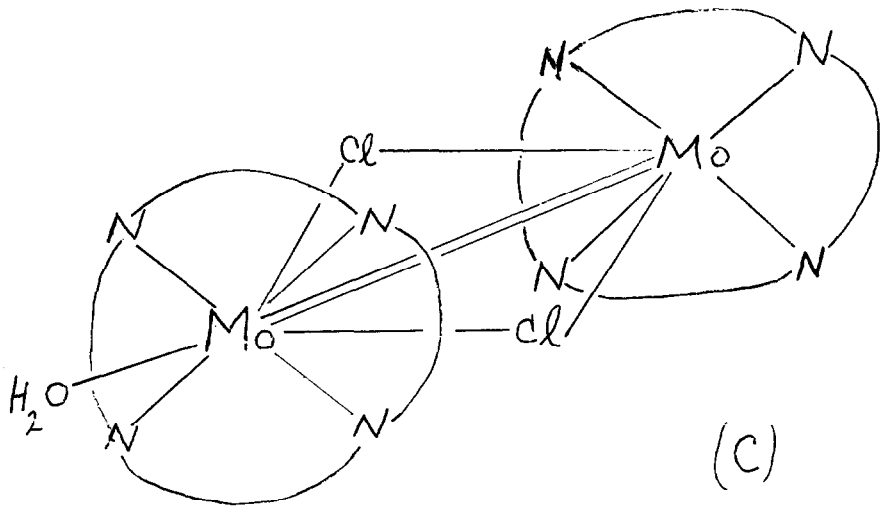
(B)

nickel(II)-controlled 2-aminobenzaldehyde self-condensation. In that work the complex of (B) was isolated and then subjected to base hydrolysis, but in our reaction the presence of ethanol, perhaps with intervention by $NH_4^+$ or ammonia formed from it, gives a complex of (A) directly.

The formulation of our product as binuclear $[Mo_2(A)_2(H_2O)Cl_2]^{2+}.2Cl^-$ and not as a mononuclear complex is based on its diamagnetism, which shows that the two d-electrons on each Mo(IV) atom are fully paired. There is a shortage of magnetochemical information on molybdenum(IV) complexes, and it is conceivable that a monomeric structure for our complex would give diamagnetism, but we think this unlikely in view of the contrast[3] between the diamagnetism of oligomeric molybdenum(IV) alkoxides and the paramagnetism of monomeric $[Mo(OSiMe_3)_4(NHMe_2)_2]$. Thus the quadruple molybdenum-molybdenum bond of the Mo(II) starting material has been converted to the double bond of the Mo(IV) dimer. We consider that at least some of the chlorine is present as uncoordinated chloride ions because the compound is soluble in polar solvents but insoluble in hydrocarbons, and because it reacts immediately with aqueous silver nitrate. The formulation as monohydrate, indicated by the elemental analysis, is confirmed by integration of the $^1H$ nmr signal at $\delta 1.22$. We have not accumulated sufficient material to obtain reproducible conductance data, nor have we succeeded in crystallising the compound, so our suggestions as to its structure must be tentative, but we propose a double chlorine bridged structure (C) as the most likely formulation on the present evidence. Work is continuing on related compounds.

Busch et al. have already noted[2] that ligand (A) can exist in a number of isomeric forms, depending on the cis- or trans-disposition of the two C=N bonds and whether the ethoxy groups are located on the same side of the macrocyclic ring. In our complex there is the additional complication that the two macrocyclic ligands may not have the same configuration. Our product is a mixture of two of these isomers, the major one having C=N stretching frequencies at 1630 and 1562 $cm^{-1}$, the minor fraction showing these at 1604 and 1562 $cm^{-1}$ in the ir spectrum. The 80 MHz $^1H$ nmr spectrum shows two overlapping triplets ($\delta 1.0$-$1.4$) for the methyl protons and a complex pattern ($\delta 3.2$-$4.5$) for the methylene protons. These regions are strikingly clarified by the 400 MHz spectrum, which shows two separate triplets at $\delta 1.12$ (weaker) and $\delta 1.46$ (stronger) for methyl protons. For the methylene protons one quartet is seen at $\delta 3.4$ superimposed on a weaker complex virtual coupling

pattern for the methylene protons of the minor isomer. This virtual coupling probably arises from interactions with CH protons, whose own spectrum is very complex, because both isomers have at least two different kinds of these hydrogens.




(C)

Assignment of a particular configuration to a particular nmr signal can only be tentative because we have not been able to separate or interconvert the isomers or crystallise the material. However, we suggest the major isomer has its C=N bonds trans at each molybdenum atom and the minor isomer to have its C=N bonds cis.

We believe this is the first report of the use of a metal–metal bond in a template reaction. Dimeric complexes with two macrocyclic ligands and a Rh-Rh bond have been prepared,[4] but not by a template reaction.

## Experimental

Synthesis. - A solution of 2-aminobenzaldehyde[5] (1.2g) in ethanol (250 $cm^3$) was refluxed under nitrogen and then cooled to room temperature. $(NH_4)_5.Mo_2Cl_9.H_2O$ (ref.6) (1.8g) was added to the resulting dark brown solution, was refluxed for 2 hr, cooled, filtered and evaporated to dryness to give a dark brown solid. This was washed with diethyl ether and extracted with acetone. This solution was evaporated to dryness and the residue was again washed with diethyl ether. The final purification was by extracting with ethanol, evaporating again and washing with diethyl ether to give a light brown microcrystalline product. Yield 0.8g (20%). Found: C, 56.02; H, 4.64; Cl, 10.52; N, 9.67. Calculated for $C_{64}H_{62}Cl_4Mo_2N_8O_5$: C, 56.50; H, 4.61; Cl, 10.46; N, 8.30.

Instrumentation. - NMR spectra were recorded at 80 and 400 MHz using Bruker HFX80 and 400 spectrometers; ir spectra were obtained on Nujol mulls with a Perking Elmer 577 grating spectrophotometer; microanalyses were obtained by the microanalyses laboratory, University College, London.

Acknowledgements

We are grateful to S.E.R.C. for financial support and U.L.I.R.S. for the 400 MHz spectra.

References

1. M. de S. Healy and A.J. Rest, Adv.Inorg.Chem.Radiochem., 1978, 21, 1.
2. L.T. Taylor, F.L. Urbach and D.H. Busch, J.Am.Chem.Soc., 1969, 91, 1072.
3. M.H. Chisholm, W.W. Reichert and P. Thornton, J.Am.Chem.Soc., 1978, 100, 2744.
4. L.F. Warren and V.L. Goedken, J.C.S.Chem.Comm., 1978, 909.
5. L.I. Smith and J.W. Opie, Organic Syntheses, 1948, 28, 11.
6. J.V. Brencic and F.A. Cotton, Inorg.Chem., 1970, 9, 346.

*Polyhedron* Vol. 3, No. 2, pp. 261–263, 1984
Printed in Great Britain.

0277–5387/84 $3.00 + .00
© 1984 Pergamon Press Ltd.

# COMMUNICATION

## COPPER(II) COMPLEXES OF 4-CHLORO,3-METHYL,5-PHENYLISOXAZOLE

**M. MASSACESI and G. PONTICELLI***
Institute of General, Inorganic and Analytical Chemistry, University of Cagliari, 09100 Cagliari, Italy

**S. CABIDDU**
Institute of Organic Chemistry, University of Cagliari, 09100 Cagliari, Italy

**B. A. SASTRY and B. BALAIAH**
Physics Department, Osmania University, Hyderabad 500007, India

(*Received* 8 *February* 1983, *accepted* 25 *July* 1983)

**Abstract**—4-chloro,3-methyl,5-phenylisoxazole copper(II) complexes of the type $Cu(L)X_2$(X = Cl, Br, $NO_3$) and $Cu(L)_2(ClO_4)_2$ have been prepared and studied by the IR, electronic, paramagnetic resonance spectroscopy and molar conductivity values. The ligand acts as monodentate N-bonded except to the nitrate derivative where this behaves as bridging bidentate. The halide complexes are tetrahedral, while the nitrate and perchlorate derivatives are square planar.

### RESULTS AND DISCUSSION

Previously we have reported the preparation and the characterization of cobalt(II), nickel(II) and copper(II) complexes of 3-methyl,5-phenylisoxazole (3-Me,5-Phisox). This ligand behaves as monodentate N-bonded and as bridging N- and O-bonded. These complexes have different stereochemistries.[1]

This paper presents the results with 4-chloro,3-methyl,5-phenylisoxazole (4-Cl, 3-Me, 5-Phisox) and copper(II) salts and the study of the mesomeric effects of the chloro in four position respect to the 3-Me, 5-Phisox.

The isolated complexes with the analytical data, the far IR, the reflectance electronic and the EPR spectra are shown in Table 1.

The compounds are powder-like, magnetically dilute and soluble in MeOH, MeCN and DMF.

On the basis of the reflectance electronic and near and far IR spectra the monomeric $Cu(4\text{-Cl,3-Me,5-Phisox})_2Cl_2$ and the dimeric $Cu(4\text{-Cl,3-Me,5-Phisox})Br_2$ are tetrahedral,[2] while the monomeric $Cu(4\text{-Cl,3-Me,5-Phisox})_2(ClO_4)_2$ and the dimeric $Cu(4\text{-Cl,3-Me,5-Phisox})(NO_3)_2 \cdot H_2O$ are square planar.[3–9]

The ligand behaves as monodentate N-bonded with the exception of the nitrate derivative where it behaves as bidentate O- and N-bonded [$\nu$(Cu-N) = 236–211 $cm^{-1}$, $\nu$(Cu–O) = 358 $cm^{-1}$].[5]

In order to gain information regarding the stereochemistry and disposition of the molecules in the unit cell, ESR spectra of these complexes in polycrystalline form have been recorded at room temperature and Q-band microwave frequency (35 GHz). The $g$ values are given in Table 1. From the table it is found that the values obtained in the case of $Cu(4\text{-Cl,3-Me,5-Phisox})Cl_2$ corresponds to molecular $g$ values since the value of $G(G = g_3 - 2/(g_1 + g_2/g) - 2)$ falls generally between 3.5 and 5.[10–13] These $g$ values are also supporting the tetrahedral stereochemistry,[14,15] predicted by IR and electronic spectra. Since only a single line is obtained in the case of $Cu(4\text{-Cl,3-Me,5-Phisox})Br_2$, it is not possible to predict the stereochemistry of the molecule, except to say that the unit cell contains more than one

*Author to whom correspondence should be addressed.

Table 1. Analytical data, far, reflectance electronic and ESR spectra

| Compound | Found(calcd.)% | | | $\nu$(Cu–X) | $\nu$(Cu–L) | $d$–$d$ bands ($cm^{-1}$) | $g_1$ | $g_2$ | $g_3$ | $G$ |
|---|---|---|---|---|---|---|---|---|---|---|
| | C | H | N | | | | | | | |
| Cu(4-Cl,3-Me,5-Phisox)$_2$Cl$_2$ | 46.2 (46.0) | 3.1 (3.1) | 5.6 (5.4) | 317 vsbr | 221s, 211 vsbr | 12660 | 2.062 | 2.062 | 2.290 | 4.7 |
| Cu(4-Cl,3-Me,5-Phisox)Br$_2$ | 28.6 (28.8) | 1.8 (1.9) | 3.5 (3.4) | 250 msbr, 227 vsbr$_b^*$ | 227 vsbr* | 12130 | 2.168 | 2.168 | 2.168 | 0 |
| Cu(4-Cl,3-Me,5-Phisox)$_2$(ClO$_4$)$_2$ | 37.1 (36.9) | 2.7 (2.5) | 4.4 (4.3) | | 236 vs | 12420 sh, 15040 | 2.065 | 2.071 | 2.213 | 3.1 |
| Cu(4-Cl,3-Me,5-Phisox)(NO$_3$)$_2$ · H$_2$O | 30.9 (30.1) | 2.7 (2.5) | 10.7 (10.5) | | 358 s, 231 wbr | 12950 sh, 16950 | | | | |

b = bridging

magnetically inequivalent molecules and the "overall" symmetry of the unit cell is cubic. Whereas in the case of $Cu(4\text{-}Cl,3\text{-}Me,5\text{-}Phisox)_2(ClO_4)_2$, the $G$ values is found to be less than 3.5 and hence the three $g$ values (Table 1) obtained do not correspond to molecular $g$ values. However one can say that the "overall" symmetry of the unit cell is rhombic[16] and the $g$ values are characteristic of $CuN_2O_2$ stereochemistry[17] arranged in a square planar fashion as predicted by IR and electronic studies.

## EXPERIMENTAL

The 4-Cl,3-Me,5-Phisox was obtained by reaction of hydroxylamine on the 2-chloro,1-phenyl,1,3-butanedione ($C_{10}H_8NOCl$ Yield 81%; Found b.p. 140–41°C at 10 mmHg; lit. b.p. 137°C at 9 mmHg).[18]

The complexes were prepared and other physical measurements were made as previously described[1] with exception of the ESR measurements.

The ESR spectra are recorded with a Varian E-112 Q-band spectrometer having 70 KHz magnetic field modulation arrangement. DPPH is used as a $g$-marker. The error in $g$ is about $\pm 0.001$.

## REFERENCES


1. M. Massacesi, G. Ponticelli and C. Preti, *J. Inorg. Nucl. Chem.* 1975, **37**, 1641.
2. D. M. L. Goodgame, M. Goodgame and G. W. Rayner Canham, *Inorg. Chim. Acta* 1969, **3**, 406.
3. D. M. L. Goodgame, M. Goodgame and G. W. Rayner Canham, *Inorg. Chim. Acta* 1969, **3**, 399.
4. M. Choca, J. R. Ferraro and K. Nakamoto, *J. Chem. Soc.* (*Dalton*) 1972, 2297.
5. E. J. Duff and M. N. Hughes, *J. Chem. Soc.* (*A*) 1968, 2144.
6. E. J. Duff and M. N. Hughes, *J. Chem. Soc.* (*A*) 1969, 477. M. N. Hughes and K. J. Rutt, *J. Chem. Soc.* (*A*), 1970, 3015.
7. M. E. Farago, I. M. James and V. G. C. Trew, *J. Chem. Soc.* (*A*) 1967, 820; 1968, 48 and references therein.
8. G. Devoto, M. Massacesi, R. Pinna and G. Ponticelli, *Transition Met. Chem.* 1977, **2**, 236.
9. J. R. Ferraro, *Low Frequency Vibrations of Inorganic and Coordination Compounds*. Plenum Press, New York (1971).
10. J. M. Procter, B. J. Hathaway and P. Nichols, *J. Chem. Soc.* (*A*), 1968, 1678.
11. A. A. G. Tomlinson and B. J. Hathaway, *J. Chem. Soc.* (*A*), 1968, 1685.
12. M. J. Bew, B. J. Hathaway and R. J. Fereday, *J. Chem. Soc.* (*A*), 1972, 1229.
13. A. A. G. Tomlinson and B. J. Hathaway, *J. Chem. Soc.* (*A*), 1968, 1905.
14. C. A. Bates, W. S. Moore, K. J. Standley and K. W. H. Stevens, *Proc. Phys. Soc.* (*London*), 1962, **79**, 75.
15. G. F. Kokoszka, C. W. Reissen and H. C. Hallen, *J. Phys. Chem*, 1967, **71**, 121.
16. B. A. Sastry and G. S. Sastry, *Physica* 1971, **54**, 20.
17. N. D. Yordanov, M. Stankova and D. Shapov, *Chem. Phys. Lett.* 1976, **39**, 174.
18. A. Quilico, G. Speroni, L. C. Behr and R. L. McKee, *The Chemistry of Heterocyclic Compounds. Five- and Six-Membered Compounds with Nitrogen and Oxygen*. Wiley, New York (1962). S. D. Sokolov and N. K. Kochetkov, *Zn. Obshch. Khim.*, 1963, **33**, 1192; *Chem. Abstr.* 1963, **59**, 11464f.

*Polyhedron* Vol. 3, No. 3, pp. 265–270, 1984
Printed in Great Britain.

0277–5387/84 $3.00 + .00
© 1984 Pergamon Press Ltd.

# SECOND COORDINATION SPHERE OF ALUMINIUM AND GALLIUM HEXACOORDINATION COMPLEXES

YU. A. BUSLAEV* and S. P. PETROSYANTS
N. S. Kurnakov Institute of General and Inorganic Chemistry, Academy of Sciences of the USSR, Moscow 117071, U.S.S.R.

(*Received* 14 *September*, 1981; *accepted* 9 *May* 1983)

**Abstract**—It is shown by means of $^{19}F$ NMR that the hexacoordinated solvates of aluminium and gallium in solutions of methyl, ethyl and *n*-propyl alcohols form outer-sphere complexes with the halide ions, $F^-$, $Cl^-$ and $Br^-$, in which the acidoligands are situated in the second coordination sphere. The outer-sphere complexes are formed on the basis of purely alcoholic solvates, $M(ROH)_6^{3+}$, as well as the complexes containing the mixed coordination sphere, $M(ROH)_{6-n}(H_2O)_n^{3+}$, and $Al(CH_3OH)_{6-n}(C_2H_5OH)_n^{3+}$.

Octahedral coordination of the $Al^{3+}$ ion in aqueous solutions of salts has been reliably confirmed by means of X-ray diffraction,[1] $^{17}O$ NMR[2] and $^1H$ NMR.[3,4] No evidence was found to prove the participation of acido-ligands ($ClO_4^-$, $NO_3^-$, $Cl^-$, $Br^-$, $I^-$) in the formation of the first coordination sphere. The composition of the compounds resulting from the dissolving of aluminium and gallium halides in non-aqueous solvents is in many ways dependent on the solvation power of the solvent. As a rule, aluminium and gallium have the coordination number of six in complexes with neutral donor molecules, for example, acetonitrile,[5] dimethylformamide and dimethylsulphoxide,[6] trialkylphosphates.[7] Much attention has been given to the state of aluminium halides in aliphatic alcohols. The mean solvation number (MSN) for the solution of $AlCl_3$ in methanol was six.[8] The $^{27}Al$ NMR data on $AlCl_3$ solutions in ethyl and n-propyl alcohols have led to a conclusion of the predominant formation of the cation of $Al(ROH)_6^{3+}$ in the solution.[9]

Analysis of aluminium and gallium of $^1H$ NMR, $^{27}Al$ NMR and $^{69,71}Ga$ NMR[10] have shown that the MSN for aluminium in ethanol solutions of $AlCl_3$ is close to six at $-40°$. The molecules of the alcohol in the inner sphere of the hexacoordination solvate form fairly stable (on the NMR time scale) hydrogen bonds with the chloride ion. The ratio of intensities of PMR signals from OH groups in the solvate $Al(C_2H_5OH)_6^{3+}$ as well as in the ion $Al(C_2H_5OH)_6^{3+}\ldots X^-$ indicate that the second sphere contains one or two acidoligands.[10] The solvation number of $Al^{3+}$ in the methanolic solution was found according to the ratio of intensities of the signals of free and coordinated groups $CH_3$ or OH. In the first case, the MSN = 5.6 at $-20°$; the MSN calculated according to hydroxyl groups depends on the temperature and is equal to 5.6 at $-60°$. The MSN thus obtained are close to six. Therefore, in methanol solution of $AlCl_3$, the aluminium ion is surrounded by six alcohol molecules which also participate in the formation of hydrogen bonds with the halide ions in the second coordination sphere.

Unlike aluminium, gallium retains the Ga–Cl bond. According to our data,[11] not less than 50 per cent of gallium in the form of $GaCl_4^-$ appear to be present in the methanol solution of $GaCl_3$. In addition, some forms of $Ga(CH_3OH)_{4-n}Cl_n$ type containing the Ga–Cl bond are also present in the solution along with the solvate $Ga(CH_3OH)_6^{3+}$ which forms the associate $Ga(CH_3OH)_6Cl_x$. In ethanol solutions, $GaCl_3$ poorly dissociates and forms the adduct $GaCl_3 \cdot C_2H_5OH$.[10]

It seems likely, that the solvates of aluminium and gallium containing six molecules of alcohol in the first coordination sphere are characterized by the formation of the outer-sphere associates with acido-ligands. This formation is due to the system of hydrogen bonds between the hydroxy-group protons of the coordinated alcohol molecules with the $Cl^-$ and $Br^-$ anions as well as to the ion–ion interaction, with the acido-ligands being possibly situated on the two opposite faces of the solvated complex octahedron.[10,11]

Spectroscopic and thermodynamic data indicate that fluoride ions form stronger hydrogen bonds than other halide ions.[12,13] Therefore, the fluoride ion is likely to give rise to rather stable ion pairs with $M(ROH)_6^{3+}$.

The present paper concerns the participation of the fluoride ion, along with the chloride and bromide ions, in the formation of the outer-sphere

*Author to whom correspondence should be addressed.

associates of Al(III) and Ga(III) solvated complexes. A $^{19}F$ NMR study of the associates formed from the side of the outer-sphere ligand has suggested a consideration of the stereochemistry of the second coordination sphere of the solvated complexes.

## EXPERIMENTAL

Aluminium chloride and bromide, as well as gallium chloride (pure for analysis) were not purified further. Methanol, ethanol and propanol were dehydrated by standard methods and stored over 3 Å molecular sieves in sealed ampoules. All the operations on sample preparations were performed in a glove-box under dry nitrogen. The fluoride ion was introduced into alcoholic solution of halides in the form of $(C_4H_9)_4NF$ solutions in methanol or ethanol; in some instances $(CH_3)_4NF\cdot(H_2O)_x$ or KF in $CH_3OH$ were used. The $^{19}F$ NMR spectra were recorded on a Varian XL–100 spectrometer at 94.1 MHz in the temperature range from room temperature to $-60°C$. The chemical shifts were calculated using $CFCl_3$ as an external reference.

## RESULTS AND INTERPRETATION

The $^{19}F$ spectra of $(C_4H_9)_4NF$ solutions in methanol and ethanol contained one signal with the chemical shift 148.5 and 137.6 ppm, respectively, this being close to the chemical shifts of KF solutions in the same alcohol.[14] The addition of fluoride to alcoholic solutions of the chloride or bromide of aluminium at a rather small ratio F:Al ($\sim 0.5$) produced several signals (A, B, C, etc.) in the high field up to 180 ppm (Fig. 1). The spectra of the $AlCl_3$ and $AlBr_3$ solutions largely coincide in terms of the number of signals, chemical shifts and the dependence on the amount of the fluoride added. This fact is consistent with the absence of interaction between the ions of fluorine and chlorine (or bromine) via the aluminium atom. If the fluoride ions were present in the first coordination sphere along with the chloride (or bromide) ion, the chemical shifts of these fluorine nuclei would have certainly been situated in a lower field, as is well known from the previous publications.[15] The signals A, B, C, etc. differ from those of the fluoride ion, bound to aluminium in aqueous solutions of aluminium chloride and nitrate,[16] in their greater number, their chemical shifts, distribution of intensities and the line widths (Fig. 2). It should be also mentioned that addition of up to 60% of alcohol to aqueous solutions of fluoroaluminates did not lead to any shift of the equilibrium towards the formation of any new forms (Fig. 2). Among the above-mentioned distinctions the most prominent one is the presence of the signal of the "free", i.e. solvated, fluoride ion (137 ppm) in the spectra of $AlCl_3$ solutions in ethyl and *n*-propyl alcohols when the first portions of fluoride are added (Fig. 3) and the absence of such a signal in methyl alcohol solutions. Upon further addition of $F^-$ the signal of the solvated fluoride ion disappeared. These peculiarities are sharply different from those observed in aqueous solutions of aluminium and gallium fluorides where the signals of hydrated fluoride ion are recorded only at F:Al $\sim 5$ and F:Ga $\sim 4$[17] molar ratios, i.e. when the coordination sphere of the cation is saturated with the fluoride ion.

Another peculiarity of alcoholic solutions shows that at molar ratios F:Al $\sim 3$ and 1.5, respectively, for methyl, ethyl and propyl alcohols and upon

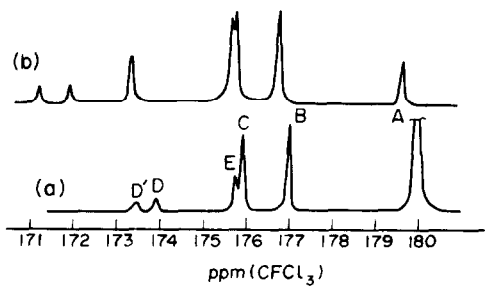



Fig. 1. $^{19}F$ NMR spectra of solutions in methyl alcohol (the concentration of the salt is given in moles per 1000 g of the solution). (a) 0.5 M $AlCl_3$, F:Al = 0.5, $-30°$. (b) 0.6 M $AlBr_3$, F:Al = 0.7, $-30°$.

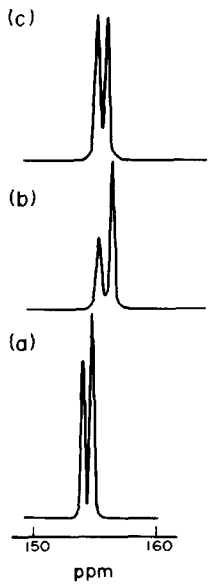



Fig. 2. $^{19}F$ NMR spectra at $-10°$. (a) 0.46 M $Al(NO_3)_3$ in water, F:Al = 1.3. (b) 0.7 M $Al(NO_3)_3$, 60% of ethyl alcohol, F:Al = 1.0. (c) 0.6 M $AlCl_3$, 60% of ethyl alcohol, F:Al = 1.6.

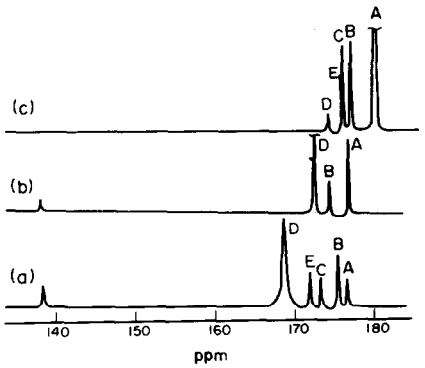
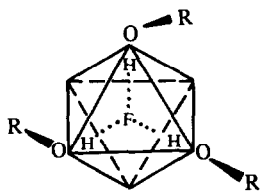



Fig. 3. $^{19}F$ NMR spectra of $AlCl_3$ solutions. (a) 0.5 M in *n*-propyl alcohol, F:Al = 0.8, 0°. (b) 0.7 M in ethyl alcohol, F:Al = 0.6, −30°. (c) 0.7 M in methyl alcohol, F:Al = 0.5, −25°.

hydration of these solutions, the spectra of such solutions contain wide unresolved signals at 155–165 ppm due to the formation of compounds with $(ROH)(H_2O)Al–F$ bonds.

The above observations have suggested a conclusion that the narrow signals A, B, C, etc. observed in the spectra would belong to the fluoride ions situated in the outer-sphere of aluminium. It may be assumed that in hexasolvate $Al(ROH)_6^{3+}$, the fluoride ions are attached to the face of the octahedron due to the formation of a system of hydrogen bonds between the fluoride ion and the hydroxyl protons as well as to the ion–ion interaction between $Al^{3+}$ and $F^-$. (Dotted lines in the schematic show the system of hydrogen bonds of the fluoride ion.) Such interactions were assumed for the chloride ion in alcoholic solutions of aluminium chloride.[10]




Since only the three molecules of the alcohol situated on one face form a bond with the halide ion, the above-considered interaction can involve only the opposite face because the alkyl groups would screen the other faces of the octahedron. Thus, it becomes possible to place one or two halide ions on the two opposite faces of the octahedron.

Comparison of the spectra in methyl and ethyl alcohols (Fig. 3) reveals a difference in the distribution of fluorine. In methyl alcohol at the ratios F:Al ≤ 1 the associate A prevails, with the intensity of its signal being three times as high as the overall intensity of all the other signals. In ethyl alcohol, on the other hand, the complex A accounts for only one fourth of all the fluorine-containing species. This most likely results from a higher concentration of complexes (in which the chloride ions occupy opposite faces) in ethanol than in methanol,[10] i.e. the ethanol solvate of aluminium preferably reacts with the chloride ion while the methanol solvate does so with the fluoride ion. Since the concentration of the chloride ion in the solutions under investigation was higher than that of the fluoride ion (the ratio Cl:Al = 3), it appears that the complex A contains both the fluoride ion and the chloride ion in the second coordination sphere. This tendency is also accounted for by a decreasing intensity of the signal A in the spectra of the aluminium bromide solutions as compared with aluminium chloride, for the tendency towards the formation of hydrogen bonds becomes weaker along the range $F^- > Cl^- > Br^-$. The assumption concerning the participation of chloride- and bromide ions along with fluoride in the formation of the outer-sphere associates was confirmed in the following experiment. A solution of $NaBPh_4$ in methanol was added to the initial $AlCl_3$ in $CH_3OH$ to the mole ratios Na:Al ≤ 3, the NaCl precipitate was separated and KF in $CH_3OH$ was added to the filtrate obtained. In the spectrum of the resulting solution (Fig. 4), the intensity of A decreased sharply, which definitely indicates that the chloride ion is present in this form and suggests $\{Al(ROH)_6^{3+}F^-Cl^-\}$ as the formula of A.

Two coordination places in the second sphere of hexa-alcohol solvates of aluminium and the participation of one or two fluoride ions as well as the fluoride and chloride ions in coordination did not

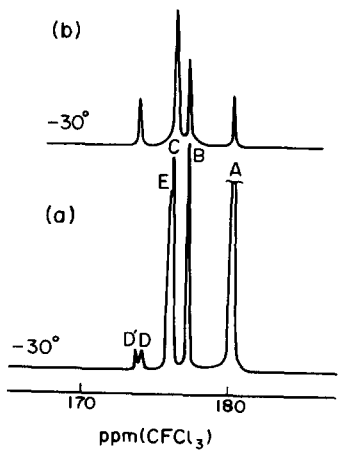



Fig. 4. $^{19}F$ NMR spectra of $AlCl_3$ solutions in methyl alcohol with the ratio F:Al = 1. (a) The initial solution. (b) After treating with $NaBPh_4$.

account for the existence of all the signals observed, whose number in the lower field increases upon addition of the fluoride ion and water to the system (Fig. 5). Water molecules seem to substitute one or more molecules of alcohol and thus the number of non-equivalent states of the fluorine ion on the faces of the octahedron increases considerably. The resulting outer-sphere complexes A, B, C, etc. are fairly stable. The temperature dependences show that the fluoride ion in A does not participate in the intermolecular exchange even at room temperature. The signal width of A is the smallest (5–6 Hz at $-30 \div -40°$) in $CH_3OH$, which corresponds to the lifetime of the fluoride ion $\sim 0.05$ sec. The maximum line width of all the signals in $CH_3OH$ in slow-exchange region ($-30 \div 40°$) was one and the same order of magnitude and did not exceed 10 Hz. At room temperature the intermolecular exchange involves complexes which correspond to the signals B, C, E. The presence of water in the coordination sphere of a cation is known to increase the rate of exchange of coordinated ligands;[18] this may be regarded as further evidence supporting the attribution of B, C and E signals to aqua-alcohol solvates.

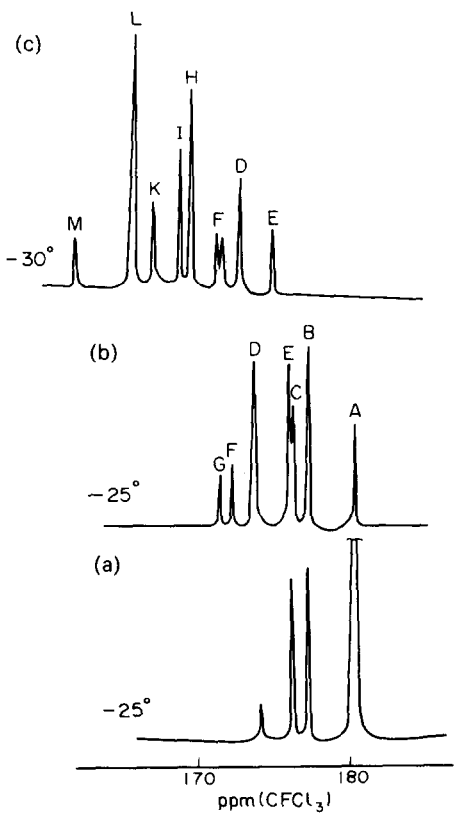



Fig. 5. $^{19}F$ NMR spectra of $AlCl_3$ solutions in methyl alcohol with the ratio $F:Al = 0.5$ and $H_2O:Al = 0$(a), 1.45(b) and 3.4(c).

Comparison of the spectra in Fig. 4 shows that the removal of the chloride ion from the solution exerts virtually no effect on the signals of B and E, which means that they are due to the solvates containing the fluoride ion. These limitations, as well as the redistribution of intensities of signals B and E depending on $F^-$ concentration in the solution suggest that the signal B refers to an outer-sphere complex $\{Al(ROH)_5(H_2O)^{3+}F^-\}$, and the signal E belongs to $\{Al(ROH_5)(H_2O)^{3+}F^-,F^-\}$.

The signal C proved to feature the highest sensitivity to such factors as addition of water and the fluoride ion, and removal of the chloride ion from the system. Therefore, it is likely that this complex appears as a monoaquo solvate containing one fluoride ion and one chloride ion in the outer sphere $\{Al(ROH)_5(H_2O)^{3+}F^-, Cl^-\}$.

The effect of another acido-ligand in the second coordination sphere of aluminium solvates on the chemical shifts of fluorine is less pronounced than that of the neutral ligand ($H_2O$) in the first coordination sphere of aluminium. For instance, the difference in chemical shifts between the signals B and C, E is equal to 100 Hz and characterizes the influence of the second acido-ligand on the chemical shift of $^{19}F^-$. The change in the shielding of fluorine when passing from $A = \{Al(ROH)_6^{3+}F^-, Cl^-\}$, $E = \{Al(ROH)_5(H_2O)^{3+}F^-, F^-\}$ and $C = \{Al(ROH)_5(H_2O)^{3+}F^-, Cl^-\}$ is determined primarily by the presence of water in the coordination sphere of aluminium and may be regarded as the measure of the effect of one water molecule on the deshielding of $^{19}F$. In methanol solution, this value is equal to $\Delta = \delta_{C,E} - \delta_A = 390$ Hz. These semi-quantitative estimations along with other factors were used for the identification of the remaining signals in the spectra of $^{19}F$ which were due to the formation of the outer-sphere associates on the basis of the aqua-alcoholic solvates of aluminium.

According to the literature, the state of aluminium chloride in ethyl alcohol and in propyl alcohol is similar.[3,6] Hence, the presence of the fluoride ion in the solution of propyl alcohol would affect aluminium solvates in the same manner as in ethanol solution. Indeed, a similar distribution of fluoride in complexes producing signals A, B, C, E and D are observed (Fig. 3). The ratio between the concentrations of these complexes is similar to that in ethyl alcohol solutions when judged by the intensities of the $^{19}F$ signals. In ethanol and propanol, unlike in methanol, at low F:Al molar ratios the fluorine-containing complexes are predominant and are based on solvates with one or two water molecules in the first coordination sphere of aluminium (B, E and D).

The spectra of solutions in propanol, like those in ethanol, at F:Al ~ 0.5 contain the signals of the free fluoride ion in addition to narrow lines of outer-sphere complexes (Fig. 3). The broadened lines which reveal the formation of fluoroaluminates appear at F:Al ~ 1.5 which indicates that propyl alcohol has a lower solvating power than ethanol and methanol.

Now, the dependence of the spectra on the addition of water (Fig. 5) to methanol solution has the following aspects. The signals due to the complexes with one and, to a lesser extent, with two molecules of water disappear, the associates containing the chloride ion in the outer sphere being less stable. New lines H, I, K and L appear. The resonance lines H and I were attributed to the complexes with three water molecules in the inner sphere of aluminium $\{Al(ROH)_3(H_2O)_3^{3+}F^-\}$. The signal K, like G, exists in a narrow range of concentrations and most likely is due to the complex $\{Al(ROH)_3(H_2O)_3F^-, Cl^-\}$. The line L arises from $\{Al(ROH)_3(H_2O)_3^{3+}F^-, F^-\}$.

Addition of water to solutions in ethanol and propanol led to a less sharp shift of the equilibrium towards the formation of fluorine-containing outerspheric associates based on aqua-alcohol solvates. At the same molar ratio F:Al as in methyl alcohol ethanol and propanol contained virtually no complexes with three water molecules.

It was mentioned above that in contrast to aluminium, gallium features a tendency to retain the Ga–Cl bond. It would be of interest to find out whether this affects the formation of the outer-sphere complexes. On addition of $F^-$ to solutions of $GaCl_3$ in methanol, ethanol and propanol the formation of the precipitates of composition $[(C_4H_9)_4N]GaCl_4$ was observed. The spectra of $^{19}F$ were recorded after the solid phase was separated. In all alcohols the spectra had the same number of resonance lines and the same dependence on the molar ratio F:Ga or $H_2O$:Ga and temperature (Fig. 6). This indicates that the fluorine-containing forms of gallium chloride in alcohol solutions are similar. As in the case of $AlCl_3$ solutions in alcohols, the resonance signals of $^{19}F$ in alcoholic gallium chloride solutions are shifted upfield with respect to the free fluoride ion. Hexacoordination solvates of $Ga(ROH)_6^{3+}$, similar to the corresponding solvates of aluminium, seem to form outer-sphere ion pairs of $Ga(ROH)_6^{3+}X$ both with chloride and fluoride ions.

The resonance signals in the spectra of gallium solutions were attributed to the outer-sphere complexes on the basis of a purely alcoholic solvate of $Ga(ROH)_6^{3+}F^-, Cl^-$ (signal A) and aqua-alcoholic forms (signals C, E, D). Gallium fluorine-containing forms have shorter lifetimes of the ligands as compared to the aluminium forms; this feature is manifested in the temperature range of the slow exchange state and in the line widths. The narrowest signals in gallium solution spectra were 20–30 Hz wide, i.e. 2–3 times as broad as those in aluminium solutions which corresponds to shorter lifetime of the ligands due to higher exchange rates in gallium solvatocomplexes.[18]

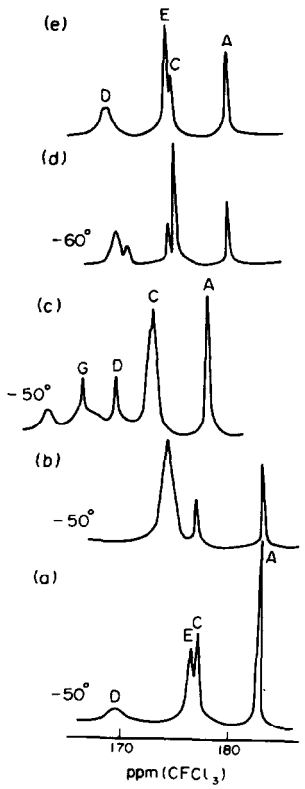



Fig. 6. $^{19}F$ NMR spectra of $GaCl_3$ solutions: in methyl alcohol (a,b), in ethyl alcohol (c), in *n*-propyl alcohol (d,e) with the ratio F:Al = 0.5(a), 1.8(b), 0.3(c, d) and 0.6(e).

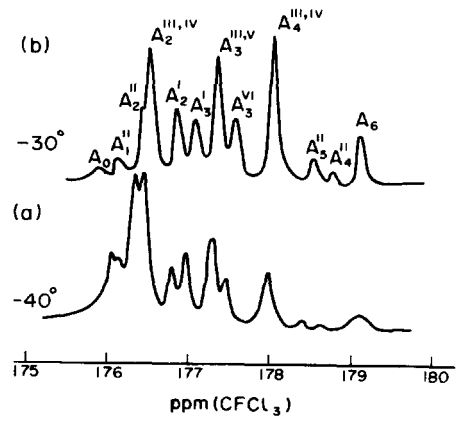



Fig. 7. $^{19}F$ NMR spectra. (a) F:Al:$C_2H_5OH$:$CH_3OH$ = 0.6:1:29:8. (b) F:Al:$C_2H_5OH$:$CH_3OH$ = 1:1:29:13.

The data obtained suggest the possibility of the formation of outer-sphere complexes which have a mixed inner sphere containing the molecules of methanol as well as those of ethanol. Indeed, in the system $AlCl_3$–$CH_3OH$–$C_2H_5OH$, the redistribution of molecular ligands took place in the first solvate shell of aluminium to produce a number of complexes $Al(CH_3OH)_{6-n}(C_2H_5OH)_n^{3+}F^-$, $Cl^-$ corresponding to signals $A_n$ situated in the 300 Hz range from $A_0$ (ethanol solvate) with the chemical shift 176.1 ppm to $A_6$ (methanol solvate) with the chemical shift 179.1 ppm (Fig. 7). To assign the 12 lines observed in Fig. 7 it is necessary to consider the geometric isomerism of the octahedral solvates $Al(CH_3OH)_{6-n}(C_2H_5OH)_n^{3+}$ which would explain the difference in the surrounding of the acidoligand, the fluoride ion, in the outer sphere. This would make it necessary to consider the stereochemistry of the outer-spheric associates.

The authors acknowledge for useful suggestions from the referee.

## REFERENCES

1. R. Caminiti, G. Licheri, G. Piccaluge, G. Pinna and T. Radnari, *J. Chem. Phys.* 1979, **71**, 2473.
2. R. E. Connick and D. N. Fiat, *J. Chem. Phys.* 1963, **39**, 1349.
3. G. K. Schweitzer and J. F. Stephens, *Spectrosc. Lett.* 1970, **3**, 11.
4. J. W. Akitt, *J. Chem. Soc.* 1973, 43.
5. Yu. A. Buslaev, V. P. Tarasov, S. P. Petrosyants and N. N. Mel'nikov, *Zh. Strukt. Chimii* 1974, **15**, 617.
6. S. F. Lincoln, *Coord. Chem. Rev.* 1971, **6**, 309.
7. J. J. Delpuech, M. R. Khaddar, A. Peguy and P. Rubini, *J. Chem. Soc.* Chem. Commun. 1974, 154.
8. S. Nakamura and S. Meiboom, *10th Int. Conf. Coord. Chem.*, p. 2. Nikko, Japan (1967). 2.
9. H. Haraguchi and S. Fujiware, *J. Phys. Chem.* 1967, **73**, 3467.
10. Yu. A. Buslaev, V. P. Tarasov, S. P. Petrosyants and G. A. Kirokosyan, *Koord. Kchimiya* 1978, **4**, 1346.
11. Yu. A. Buslaev, V. P. Tarasov, S. P. Petrosyants and G. A. Kirokosyan, *Dokl. Akademii Nauk SSSR* 1978, **241**, 838.
12. J. Sadley, *Adv. in Molec. Relax. and Interact. Proc.* 1979, **15**, 163.
13. M. C. R. Symons, *Pure and Appl. Chem.* 1979, **51**, 1671.
14. C. Deverell, K. Schaumburg and H. J. Bernstein, *J. Chem. Phys.* 1968, **49**, 1276.
15. M. J. Bula, D. F. Hamilton and J. S. Hartman, *J. Chem. Soc.* 1972, 1405.
16. Yu. A. Buslaev and S. P. Petrosyants, *Koord. Kchimiya* 1979, **5**, 163.
17. D. Hass, S. P. Petrosyants, Yu. A. Buslaev and I. Hartleb, *Dokl. Akademii Nauk SSSR* 1983, **269**, 380.
18. Yu. A. Buslaev, *Thermodynamics and Structure of Solutions*, p. 36. Ivanovo (1977).

*Polyhedron* Vol. 3, No. 3, pp. 271–280, 1984
Printed in Great Britain.

0277–5387/84 $3.00 + .00
© 1984 Pergamon Press Ltd.

# THE ADDITION OF METHYLBORYLENE TO ACETYLENES

## SYNTHESIS OF 1,4-DIBORACYCLOHEXA-2,5-DIENES, AND OF A BORIRENE AND A DIBORETENE DERIVATIVE

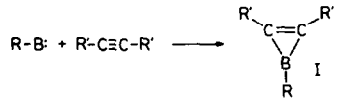
S. M. VAN DER KERK,*† P. H. M. BUDZELAAR, A. L. M. VAN EEKEREN and G. J. M. VAN DER KERK
Laboratory for Organic Chemistry, State University of Utrecht, Croesestraat 79, 3522 AD Utrecht, The Netherlands

(*Received* 4 *March* 1983; *accepted* 16 *June* 1983)

**Abstract**—The synthesis of 1,4-dimethyl-2,3,5,6-tetra-*n*-alkyl-1,4-diboracyclohexa-2,5-dienes from the reaction of di-*n*-alkylacetylenes with the methylborylene-generating system $2C_8K/MeBBr_2$ is described. A mechanism for these reactions is proposed. The addition of methylborylene to di-*t*-butylacetylene results in the formation of 1-methyl-2,3-di-*t*-butylborirene and of 1,3-dimethyl-2,4-di-*t*-butyl-1,3-diboretene.

The concept of three-membered heteroaromatic compounds was broached in 1962 by Volpin *et al.*;[1] in their pioneering paper they suggested as a route, possibly leading to these compounds, the addition of carbene analogues to acetylenes. Further, they made an outline of species that might qualify as carbene analogues and suggested a number of their possible reactions. In their publication the potential aromaticity of borirene (I) is first mentioned.

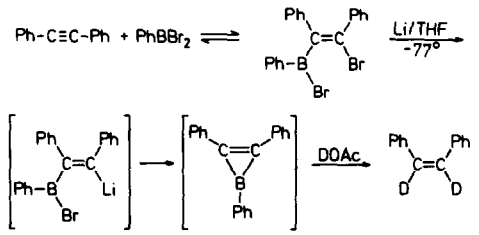
Thus, according to Volpin *et al.*,[1] addition of a borylene to an acetylene might yield a borirene (I):



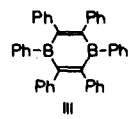
Both possibilities, generating a borylene and synthesizing a borirene derivative have intrigued chemists in the years following.

Kuchen and Brinkmann[2,3] treated phenylboron dichloride with sodium in toluene, to obtain polymeric $[PhB]_n$. The suggestion that in this way, by abstraction of the halogen atoms from $PhBCl_2$, phenylborylene might have been generated was made in 1966 by Nefedow and Manakow.[4] Köster and Grassberger[7] treated ethylboron difluoride with lithium in THF, to obtain carboranes.

In 1967 Eisch and Gonsior[8] presented indirect chemical evidence for the initial formation of the borirene ring in solution. They did not generate a borylene, but chose a route involving reductive ring closure of the haloboration product of diphenylacetylene (Fig. 2). The compounds in square



brackets were not isolated. The occurrence of triphenylborirene (II) was inferred from the product obtained upon deuteroacetolysis. It should be noted that the formal dimer of triphenylborirene, hexaphenyl-1,4-diboracyclohexa-2,5-diene (III, hexaphenyl-DBCH) would yield the same acetolysis product (Fig. 3). The DBCH structure (III)

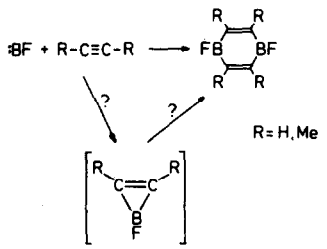


*Author to whom correspondence should be addressed.

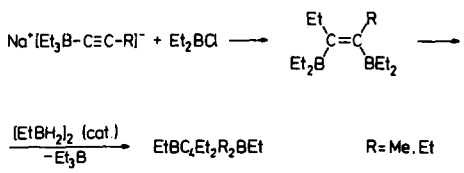
†Present address: Laboratory for Organic Chemistry, University of Amsterdam, Nieuwe Achtergracht 129, 1018 WS Amsterdam, The Netherlands.

was postulated by Lappert *et al.*[5] in analogy to the products of similar reactions with silylenes and germylenes.[4]

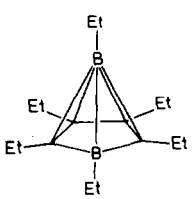
Timms[9-11] obtained high yields of boron monofluoride, or fluoroborylene, by passing boron trifluoride over crystalline boron at 2000° under low pressure. The short-lived BF was made to react with acetylenes by co-condensation. In this way 1,4-diboracyclohexa-2,5-diene (DBCH) derivatives were formed; no trace of the expected borirenes was found. Timms supposed that the borirene formed immediately dimerized to the corresponding DBCH derivative. By cracking $B_2Cl_4$ at 1100°




Timms was able to produce BCl, chloroborylene,[11] which reacts with acetylenes in the same fashion as BF.[9-11] Timms found the $[FBC_4R_4BF]$ and $[ClBC_4R_4BCl]$ species isolated to be planar. Contrary to this, the compounds $[EtBC_4Et_2R_2BEt]$ reported in 1966 by Binger[12] were concluded to have a non-planar carborane structure. These compounds, however, were synthesized along a totally

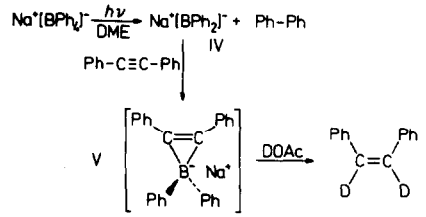



different route (Fig. 5). For R=Et the following *nido*-carborane structure was proposed:

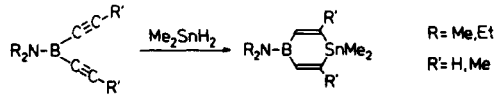


Lipscomb *et al.*[13] compared the geometries of the possible isomers of $[HBC_4H_4BH]$ and $[FBC_4H_4BF]$ by means of PRDDO calculations. For $[HBC_4H_4BH]$ the carborane structure appeared to be more stable (by 9 kcal/mole) than the planar isomer. Placing electron-rich substituents on the boron atoms proved to stabilize the planar structure: planar $[FBC_4H_4BF]$ was found to be 43 kcal/mole more stable than the carborane isomer, thus confirming the conclusions drawn by Timms.[10]

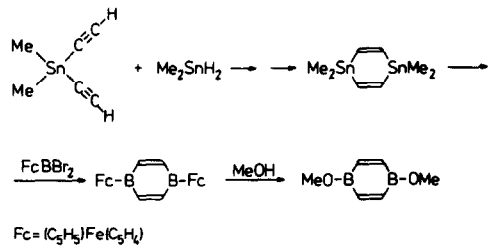
In 1975 Eisch *et al.* reported[14] borylene character for the diphenylborate(I) anion (**IV**). When sodium tetraphenylborate was irradiated in DME in the presence of diphenylacetylene, subsequent acetolysis yielded (among other products) *cis*-stilbene, the formation of which was ascribed to the intermediate occurrence of the diphenyl(diphenylvinylene)borate(III) anion (**IV**), a species possessing a borirene nucleus (Fig. 7).




Nöth *et al.*[15,16] synthesized 1-bora-4-stannacyclohexa-2,5-diene derivatives via hydrostannation of dialkinylboranes (Fig. 8). However,




exchange of tin by boron, to yield a DBCH derivative, failed. A slightly different route was followed by Herberich and Hessner,[17,18] leading to DBCH derivatives (Fig. 9).




In 1979 Eisch and Becker[6] reported on another attempt to generate borylenes by abstracting the halogen atoms from organoboron dihalides by suitable reducing agents and, subsequently, to trap the borylenes with diphenylacetylene to produce a borirene. No positive results were obtained.

Bock *et al.* published a study[19] of the He(I) photoelectron spectrum, the one electron-reduction behaviour and the electronic structure of 1,4-difluoro-2,3,5,6-tetramethyl-1,4-diboracyclohexa-2,5-diene, in comparison to the isoelectronic duroquinone.

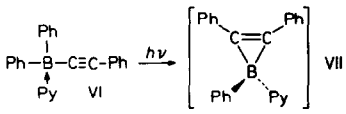
A theoretical study of (amongst others) the

borirene system was published by von Schleyer *et al.*[20] (*vide infra*).

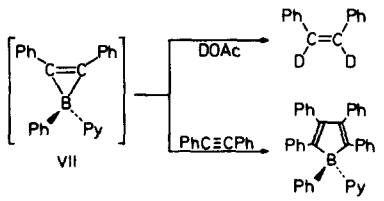
With DBCH derivatives a number of transition metal sandwich complexes have been synthesized; those marked with an asterisk have been characterized by X-ray analysis: $(FBC_4Me_4BF)Ni(CO)_2^*$, $(FBC_4Me_4BF)_2Ni^*$, $(FBC_4Me_4BF)Co(C_5H_5)$, $(FBC_4Me_4BF)Fe(CO)_3$, $(FBC_4Me_4BF)Ni(cyclo\text{-}octa\text{-}1,5\text{-}diene)$,[21,22] $(MeOBC_4H_4BOMe)_2Ni$,[18] and $(MeBC_4H_4BMe)Co(C_5H_5)^*$.[23] Due to the fact that in the crystals of $(FBC_4Me_4BF)Ni(CO)_2$ molecules of free $[FBC_4Me_4BF]$ were present, the structure of the latter was determined as well.[22]

Herberich *et al.* reported the synthesis and structure determination of a triple-decker sandwich complex with DBCH as a bridging ligand: $(C_5H_5)Rh(MeBC_4H_4BMe)Rh(C_5H_5)$,[24] and the He(I) photoelectron spectrum and the electronic structure of the sandwich complex $(MeBC_4H_4BMe)Co(C_5H_5)$.[25]

Recently, Eisch *et al.* stated[26] that irradiation of diphenyl(phenylethynyl)borane-pyridine (**VI**) in THF or benzene leads to the formation of the pyridine complex of triphenylborirene (**VII**) (Fig. 10). Eisch *et al.* did not isolate (**VII**) but its




occurrence was inferred from the products obtained upon treatment of the reaction mixture (in benzene) with deuteroacetic acid and upon irradiation of a mixture of (**VI**) and diphenylacetylene in benzene. In the latter reaction the pyridine complex of pentaphenylborole was produced (Fig. 11). The borirene complex (**VII**) was reported to be extremely labile towards oxygen and protic agents.




This was ascribed to a lack of aromatic stabilization. It is evident that hardly any degree of aromaticity is to be expected in a Lewis base adduct of a borirene, as in such a complex the boron atom is 4-coordinated and thus cannot provide an empty *p* orbital to partake in the $\pi$ electronic system.

In a recent publication[27] Herberich and Hessner described the synthesis of the $6\pi$-electron system $[FcBC_4H_4BFc]^{2-}$ $(Fc=(C_5H_5)Fe(C_5H_4))$, obtained by reduction of $[FcBC_4H_4BFc]$ by sodium amalgam. Further, a number of transition metal sandwich complexes of this DBCH, and nucleophilic substitution reactions on these complexes were reported.[27,27a]

It occurred to us that most attempts to synthesize a borirene by addition of a borylene to an acetylene had been undertaken using diphenylacetylene as a substrate. As it is to be expected that borylenes have an even more electrophilic character than carbenes, acetylenes with electron-donating groups, in our opinion, should offer better chances of trapping a borylene than diphenylacetylene. In view of our earlier finding that the system $2C_8K/MeBBr_2$ is a suitable methylborylene generator,[28] it was decided to study the reactions of methylborylene with dialkylacetylenes.†

## RESULTS

In Table 1 the results of the reactions of the system $2C_8K/MeBBr_2$ with various acetylenes are summarized.

When diphenylacetylene was subjected to the system $2C_8K/MeBBr_2$ in boiling cyclohexane, inspection by $^1H$ NMR showed that no reaction had

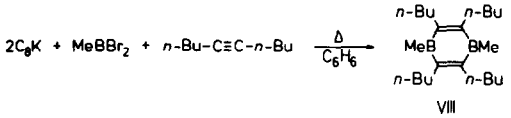
†Parts of this work were published in preliminary publications.[29,30]

Table 1. Identified products of the reaction of the system $2C_8K/MeBBr_2$ with various acetylenes

| acetylene | major product | benzene derivative | other products |
|---|---|---|---|
| Ph–C≡C–Ph | no reaction | | |
| *n*-Bu–C≡C–*n*-Bu | DBCH (1 isomer) | *n*-$Bu_6$-benzene | |
| *n*-Pr–C≡C–*n*-Pent | DBCH (2 isomers) | *n*-$Pr_3$-*n*-$Pent_3$-benzene | |
| Et–C≡C–*n*-Hex | DBCH (2 isomers) | $Et_3$-*n*-$Hex_3$-benzene | |
| *t*-Bu–C≡C–*t*-Bu | borirene + 1,3-diboretene | | |
| Me–C≡C–Me | carborane (1 isomer) | | $[C_2Me_2]_2[MeB]_4$ + $[C_2Me_2]_3[MeB]_4$ |
| Et–C≡C–Et | DBCH + carborane (both 1 isomer) | | |

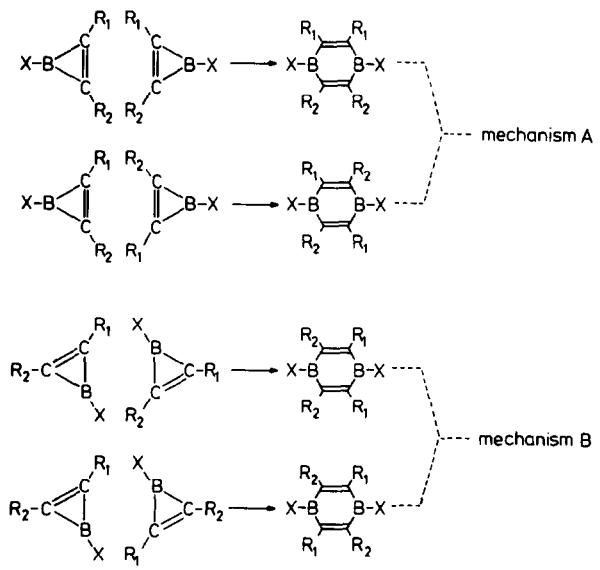
taken place. After filtering off all solid material and removal of all volatile components, the residue was subjected to GC/MS. Only diphenylacetylene could be detected. No 1-methyl-2,3-diphenylborirene or 1,4-dimethyl-2,3,5,6-tetraphenyl-1,4-diboracyclohexa-2,5-diene had been formed (thus confirming the results of Eisch and Becker[6]), but no haloboration products[6,8] either.

Next, di-*n*-butylacetylene (5-decyne) was chosen as a substrate. The reaction with the system $2C_8K/MeBBr_2$ was carried out in boiling benzene. In the course of hours, inspection by $^1H$ NMR showed that reaction had taken place and the potassium–graphite turned black. When no further change in the $^1H$ NMR spectra was observable, the solid material was filtered off, the volatile components were removed *in vacuo* and the residue was subjected to vacuum fractionation. The fractions collected were investigated by GC/MS. It appeared that a DBCH derivative, 1,4-dimethyl-2,3,5,6-tetra-*n*-butyl-1,4-diboracyclohexa-2,5-diene (**VIII**), had been obtained in a pure state. No trace of the expected borirene was present; neither were haloboration products found (Fig. 12). Compound



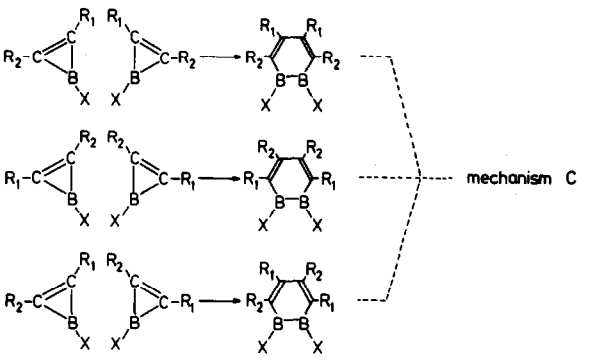

(**VIII**) is a viscous yellow liquid, boiling at 60–65°/$10^{-6}$ Torr, highly reactive towards air and water. The reaction was carried out in cyclohexane as well, to yield the same results.

If DBCH's are formed via the direct dimerization of borirenes, this reaction can be described by either or both of the following two mechanisms. Starting from an asymmetric acetylene, different

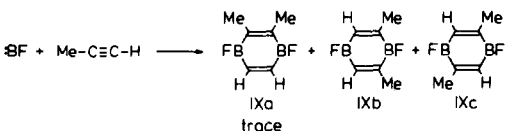



products will be obtained by either mechanism (Fig. 13).

It should be noted that the second and the fourth product are identical. A variation of mechanism *B* is a reaction course in which 1,2-diboracyclohexa-3,5-dienes are formed (mechanism *C*, Fig. 14). It is seen that, using an asymmetric




acetylene, both mechanism *A* and *B* yield two distinct products. Mechanism *C* yields three isomers. In one of his experiments with BF, Timms used propyne as a substrate.[10] He obtained three 1,4-DBCH's (one of them in a trace quantity), but no 1,2-DBCH's (Fig. 15). Compound (**IXa**) can




only stem from mechanism *A*, (**IXb**) only from mechanism *B*, and (**IXc**) from both *A* and *B*.

In order to get insight into the matter, the system $2C_8K/MeBBr_2$ was reacted with *n*-propyl-*n*-pentylacetylene (4-decyne). GC/MS investigation of the reaction mixture showed that two DBCH isomers had formed, with almost identical mass spectra, in a relative ratio of 1:2.6. No borirene was detected. The same experiment, carried out with ethyl-*n*-hexylacetylene (3-decyne) showed, upon GC/MS investigation, that two DBCH derivatives had formed, again with very similar mass spectra, in a relative ratio of 1:3.0. Again, no borirene was found.

In our opinion, acetolysis of the products of the reaction of methylborylene with an asymmetric acetylene should offer a possibility of deciding between mechanisms *A*, *B* and *C*. Timms did not observe a general pattern in the hydrolysis products of his DBCH's,[10] viz:

$$BF + CH{\equiv}CH \xrightarrow{H_2O} \text{90\% ethene + 10\% 1-butene}$$

$$BF + MeC{\equiv}CH \xrightarrow{H_2O}$$

complex mixture of hexenes with *ca.* 10% propene

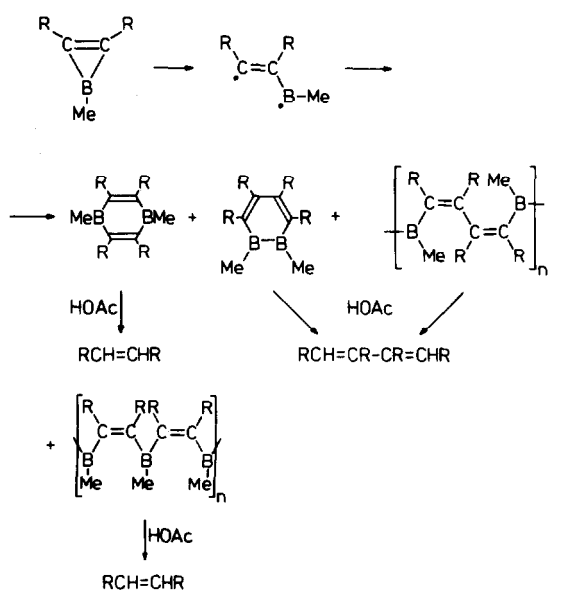
$$BF + MeC{\equiv}CMe \xrightarrow{H_2O}$$

3,4-dimethyl-2-hexene with a little cis-2-butene.

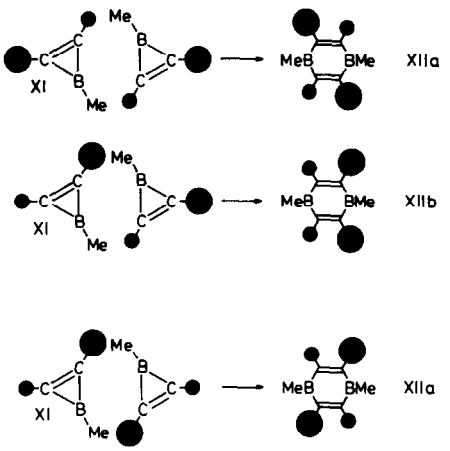
Timms supposed that hydrolysis was accompanied by polymerization. Acetolysis (with glacial acetic acid) of the crude mixture obtained upon reaction of $2C_8K/MeBBr_2$ with ethyl-*n*-hexylacetylene (3-decyne) yielded only 3-decene (according to GC/MS), thus accounting for mechanism *B*. Neither 3-hexene nor 7-tetradecene could be detected, so mechanism *A* could be ruled out. A $C_{20}$-olefin was not found either, so mechanism C could be excluded as well.

Of course, formation of a DBCH molecule by two borirene molecules might be preceded by ring opening of the borirenes, leading to biradicals. However, combination of the biradicals would, in our opinion, result in the formation of a large amount of polymeric material (apart from the formation of 1,4-DBCH and, possibly, 1,2-DBCH) which, in turn, would yield dienes upon acetolysis (Fig. 17). Dienes were never found upon acetolysis of crude reaction mixtures. Further, it is to be expected that a biradical would react with a molecule of acetylene to yield a borole. Boroles were never encountered in the reaction mixtures.

In the case of the formation of DBCH's from asymmetric acetylenes, the preponderance of one




isomer over the other (especially as the substituents show a larger difference in size) can be explained in terms of steric hindrance. In the dimerization of the asymmetric borirene (**XI**), DBCH (**XIIa**) is expected to be favoured over DBCH (**XIIb**), both on grounds of easier approach of the reactants and less steric hindrance in the product (Fig. 18). Compound (**XIIa**) can be formed in a second way; here, however, the approach is even more unfavourable (Fig. 19). These effects are expected to be more evident in the ratio of the products of the



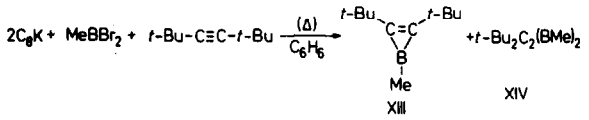

reaction of methylborylene with ethyl-*n*-hexylacetylene than with *n*-propyl-*n*-pentylacetylene, and, in fact, this was observed experimentally.

In personal discussions Prof. von Schleyer[31] suggested the use of an acetylene with very bulky substituents, since this might render the formation of a DBCH derivative impossible on two counts. First, in the DBCH molecule itself the steric hindrance might be so extensive, as to make the formation of the species thermodynamically unfavourable. Second, if DBCH is formed from the direct reaction of two molecules of borirene, a close approach of the two molecules could be impeded by the bulky substituents. Thus the reaction might halt at the stage of the borirene derivative.

It was decided to use di-*t*-butylacetylene (2,2,5,5-tetramethyl-3-hexyne) as a substrate, especially as the electron-donating properties of the tertiary butyl groups might impart an extra stability to the borirene molecule. Reactions were carried out between $C_8K$, $MeBBr_2$, and di-*t*-butylacetylene in benzene, both at reflux and at ambient temperature. The reactions were followed with $^1H$ NMR; it was necessary to use sweep widths down to 0.2 ppm in order to be able to distinguish between the various *t*-Bu signals, as the differences in chemical shifts between reactant and product(s) were very small. After work-up (see Experimental Part) the results of the reactions were

studied by GC/MS. No 1,4-dimethyl-2,3,5,6-tetra-*t*-butyl-1,4-diboracyclohexa-2,5-diene was found at all; instead, in both reactions a product had formed, the mass spectrum of which pointed to 1-methyl-2,3-di-*t*-butylborirene (**XIII**).

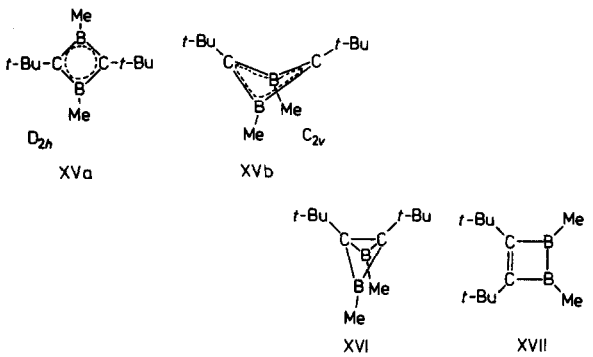
In both reactions, but especially in the one that had been carried out at room temperature, a second compound was present the fragmentation and isotope pattern of which pointed to the compound *t*-$Bu_2C_2(BMe)_2$ (**XIV**), the product of the reaction of two methylborylene units with one molecule of di-*t*-butylacetylene, a diboretene (Fig. 20). For the diboretene (**XIV**) several structural




XIII XIV

formulae can be envisaged: two 1,3-diboretenes (**XVa** and **XVb**, of symmetries $D_{2h}$ and $C_{2v}$ respectively), one diborabicyclo[1.1.0]butane (**XVI**) and one 1,2-diboretene (**XVII**):

Extensive calculations on the aromaticity in hypothetical small rings containing boron and




XVa XVb XVI XVII

carbon ($[CH]_2[BH]_n$, n = 1,2) have been carried out by von Schleyer *et al.*[20] It was predicted that the 1,3-diboretene $[CH]_2[BH]_2$ with the structure of compound (**XVb**) would be the most stable. In this puckered molecule (symmetry $C_{2v}$) the C–C distance is calculated to be extremely large (1.858 Å); the two extra valence electrons are found to remain delocalized over the entire ring. The angle between the planes defined by $B_1C_1C_2$ and $C_1C_2B_2$ is predicted to be 125.1°. The structures corresponding to (**XVa**) (symmetry $D_{2h}$) and (**XVI**) are not even local minima. The 1,2-diboretene (**XVII**) is calculated to be 7–17 kcal/mole higher in energy than the puckered 1,3-diboretene (**XVb**).

In the mass spectrum of (**XIV**) (*vide infra*) a fragment is found with half the molecular mass, with an intensity of 34%. In our opinion, this mass represents the fragment *t*-$BuCBMe^+$, originating from cleavage of the four-membered ring in a 1,3-diboretene (**XVa** or **XVb**). Fragmentation of the four-membered ring of the 1,2-diboretene (**XVII**) is not expected to proceed via C=C bond cleavage. Rather, cleavage of the B–C bonds should occur, to produce fragments *t*-$Bu_2C_2^+$ and/or $Me_2B_2^+$ (or $MeB^+$). These fragments were not found.

Our assignment of the 1,3-diboretene structure to (**XIV**) in preference to the 1,2-diboretene structure (**XVII**) is in accord with the results of the calculations by von Schleyer *et al.*[20]

The quantity of diboretene formed in the reaction carried out at reflux temperature was quite small as compared to the quantity of borirene (GC/MS, NMR). 1-Methyl-2,3-di-*t*-butylborirene (**XIII**) appears to be thermally quite stable, taking into account that in the course of one of its syntheses a reflux period (in benzene) of 24 hr was included, and that benzene could be removed from it by distillation under atmospheric pressure without noticeable decomposition. This is borne out by its calculated[20] resonance energy of 70–75% of that of its carbocation analogue (*cf.* the resonance energy of 1-methylborepin, which was calculated by us to be 75–85% of that of its analogue, the tropylium cation[36]).

*Mass spectra*

The mass spectra (electron impact) of the DBCH derivatives, synthesized starting from 3-decyne, 4-decyne, and 5-decyne are fairly complex. The base peak is always found at *m/e* 41 ($[Me_2B]^+$). The parent peaks (with intensity ratios 1:8:16, as expected for a molecule containing two boron atoms ($^{10}B:^{11}B = 1:4$)) are always found at *m/e* 326, 327, and 328 respectively, with intensities lying between 27 and 88%. The spectra further show a gradual breakdown of the molecules. As the starting acetylene becomes more asymmetrical, the differences in intensities of the parent peaks of the two DBCH isomers grow larger. The intensity of the parent peak of [$MeBC_4n$-$Bu_4BMe$] is 28%; the intensities of the parent peaks of the two isomers of [$MeBC_4n$-$Pr_2n$-$Pent_2BMe$] are 52% and 60%, respectively, those of [$MeBC_4Et_2n$-$Hex_2BMe$] 42 and 88%, respectively. In our opinion, the parent peak with the highest intensity originates from the least sterically hindered isomer.

There is a characteristic difference between the mass spectra of the 1,4-DBCH's on the one hand and the mass spectra of 1,4-disilacyclohexa-2,5-dienes and 1,4-digermacyclohexa-2,5-dienes[32] (synthesized by reaction of silylenes and germylenes, respectively, with diphenylacetylene) on the other. In the latter a main fragmentation pattern involves

formation of the starting acetylene. In none of the DBCH mass spectra any indication for this mechanism was found. This is probably due to the considerable $\pi$-interaction over the hetero atom in the DBCH's, which is absent in the corresponding silicon and germanium compounds.

The mass spectrum of 1-methyl-2,3-di-*t*-butylborirene (**XIII**) is characterized by the following fragmentation scheme, in which isotope peaks are omitted. $164 = M^+$ (64%), $149 = [M-CH_3]^+$ (63%), $107 = [M-C_4H_9]^+$ (100%), $93 = [149-C_4H_8]^+$ (22%), $77 = [93-CH_4]^+$ (7%), $65 = [107-C_3H_6]^+$ (75%), $51 = [93-C_3H_6]^+$ (17%), $41 = [(CH_3)_2B]^+$ (52%) (fragmentation of the ring). It is suggestive for the stability of (**XIII**) that throughout the fragmentation of the molecule the borirene-ring stays intact.

The main fragmentation scheme of 1,3-dimethyl-2,4-di-*t*-butyl-1,3-diboretene (**XVb**) is as follows (isotope peaks omitted): $190 = M^+$ (4%), $175 = [M-CH_3]^+$ (77%), $148 = [M-C_3H_6]^+$ (11%), $133 = [M-C_4H_9]^+$ and/or $[148-CH_3]^+$ (84%), $119 = [175-C_4H_8]^+$ (39%), $117 = [133-CH_4]^+$ (47%), $105 = [133-C_2H_4]^+$ (13%), $95 = [t\text{-BuCBMe}]^+$ (34%), $91 = [117-BCH_3]^+$ (23%), $77 = [119-C_3H_6]^+$ (12%), $65 = [91-C_2H_2]^+$ (51%), $41 = [(CH_3)_2B]^+$ (100%).

Preliminary NMR data for borirene (**XIII**) and diboretene (**XVb**) are given in Ref. 30 The $^1H$ NMR data of the DBCH derivatives described in this publication proved these compounds to be planar.

In the reactions of almost all dialkylacetylenes with the system $2C_8K/MeBBr_2$ hexaalkylbenzenes were formed: with di-*n*-butylacetylene hexa-*n*-butylbenzene, with *n*-propyl-*n*-pentylacetylene tri-*n*-propyl-tri-*n*-pentylbenzene, and with ethyl-*n*-hexylacetylene triethyl-tri-*n*-hexylbenzene. However, in each of the latter two cases, only one isomer could be detected by GC/MS.

The formation of hexaalkylbenzenes might be explained by the reaction of a molecule of borirene (**XVIII**) with one molecule of acetylene, leading to the formation of a borole (**XIX**). Another molecule of acetylene might undergo a Diels–Alder reaction with the borole, leading to the formation of a 7-borabicyclo[2.2.1]heptadiene (**XX**) which, via a [1,3] suprafacial sigmatropic rearrangement, would give a 7-borabicyclo[4.1.0]heptadiene (**XXI**). This compound, on the one hand might yield a borepin (**XXII**) via a disrotatory ring opening, or, on the other hand, might eliminate a borylene to form a benzene derivative (**XXIII**); see Fig. 2.

Recently, Eisch *et al.* reported[26] the photochemical reaction of diphenylacetylene with a solution assumed to contain the pyridine complex of

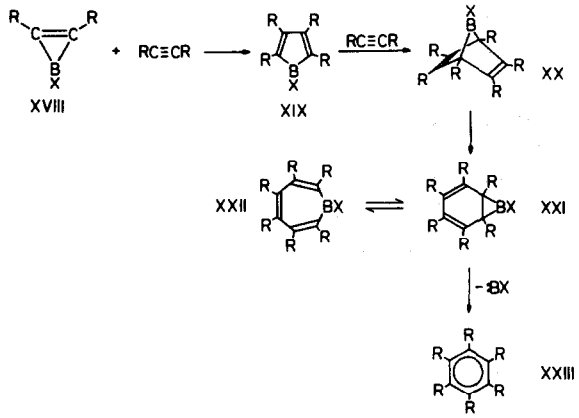



Fig. 2.

triphenylborirene, to produce the pyridine complex of pentaphenylborole. The formation of a benzene derivative from a borole via the Diels–Alder addition of an acetylene has been suggested by Grisdale and Williams.[33] The synthesis of heptaphenylborepin from pentaphenylborole and diphenylacetylene has been described by Eisch and Galle.[34] Our own researches have shown[35,36] that 1-methylborepin eliminates methylborylene in a symmetry-allowed reaction to yield benzene, probably via a 7-borabicyclo[4.1.0]heptadiene.

The apparent occurrence of only one "benzene isomer" in the case of asymmetrical acetylenes might be explained on grounds of steric hindrance. The same argument applies to the fact that in the reactions of di-*t*-butylacetylene absolutely no hexa-*t*-butylbenzene was found.

It should be noted that we never found any trace of boroles. This can be explained by assuming that the Diels–Alder reaction of an acetylene with a borole is much faster than the cycloaddition reaction of an acetylene with a borirene, an assumption that is borne out by orbital-symmetry arguments:[37] the latter reaction is forbidden in the ground state.

## DISCUSSION

In the foregoing it has been shown that $C_{10}$ dialkylacetylenes are suitable substrates for the synthesis of 1,4-diboracyclohexa-2,5-diene (DBCH) derivatives, upon reaction with the system $2C_8K/MeBBr_2$. When the extremely sterically crowded di-*t*-butylacetylene was used as a substrate, it proved possible to obtain the corresponding borirene and diboretene derivative. Therefore it is assumed that the formation of DBCH's proceeds *via* dimerization of initially formed borirenes.

When dimethylacetylene (2-butyne) is reacted with $C_8K$ and $MeBBr_2$ in benzene, the first reaction to take place is fast haloboration (as was estab-

lished by $^1$H NMR). Gradually, the haloboration product is converted by the $C_8K$, however, not in hexamethyl-DBCH, but in a compound the $^1$H NMR spectrum of which showed two MeB signals (of equal intensity) and two MeC resonances (of equal intensity). The intensity ratio of the MeB and the MeC peaks was 1:2. This provided strong evidence for a nido-carborane structure in which the boron atoms are inequivalent. The $^1$H NMR data of this compound matched those given in the literature for hexa- methyl-2,3,4,5-tetracarbahexaborane(6).[41]

In the same reaction, GC/MS investigation showed that, in small amounts, two species were present the fragmentation and isotope pattern of which suggested the compositions $[C_2Me_2]_2[MeB]_4$ and $[C_2Me_2]_3[MeB]_4$. These probably carborane-like structures proved to be resistant to acetolysis with glacial acetic acid.

Further, recent experiments have shown that, when diethylacetylene (3-hexyne) is reacted with the system $2C_8K/MeBBr_2$ at room temperature, the molecule $[MeBC_4Et_4BMe]$ with nido-carborane structure is formed. When the same reaction is carried out at reflux temperature, both the carborane and the DBCH structure are formed.

In our opinion the formation of the 2,3,4,5-tetracarbahexaboranes(6) takes place via reaction of $C_8K$ with the haloboration product.

Concerning the formation of the planar DBCH's, it should be noted that, in the reactions of the system $2C_8K/MeBBr_2$ with decynes, upon longer reaction times, when the potassium content of the surface of the graphite–potassium has become low, small amounts of the corresponding carboranes are formed.

At the moment, we are unable to discern between the following two possibilities.

(a) The formation of DBCH and carborane takes place via two independent reactions, the former involving the boron analogue of a carbenoid reaction with the acetylene, leading to the formation of a borirene which dimerizes, the latter involving an attack of the graphite–potassium on the haloboration product.

(b) Both borirene (and thus DBCH) and carborane are formed via the haloboration product. Whether DBCH or carborane is formed is determined by the bulkiness of the acetylene and the potassium content of the surface of the graphite–potassium.

## EXPERIMENTAL

All experiments were carried out in an atmosphere of dry, oxygen-free nitrogen. Solvents were purified and stored under nitrogen. Liquids were handled with syringes.

$^1$H NMR spectra were recorded using Varian EM 390 and HA-100 spectrometers. $^{13}$C NMR spectra were recorded on a Bruker WM 250 spectrometer by Dr. F. J. J. de Kanter at the Chemical Laboratory of the Free University at Amsterdam. GC/MS investigations were carried out on a Finnigan 3100 D Mass Spectrometer with 6110 Data System and Finnigan 9500 Gas Chromatograph by Miss E. Ch. Th. Gevers, Mrs. G. G. Versluis-de Haan, and Mrs. C. M. Bijlsma-Kreuger at the Institute for Organic Chemistry TNO at Utrecht, and on a Kratos MS 80 Mass Spectrometer with Data General Nova 3 Data System and Carlo Elba/Kratos Gas Chromatograph by Mrs. A. van der Kerk-van Hoof at the Laboratory for Analytical Chemistry of the State University at Utrecht.

Tetramethyltin was kindly provided by the Institute for Organic Chemistry TNO at Utrecht.

$MeBBr_2$ was synthesized from $Me_4Sn$ and $BBr_3$.[38,39] $C_8K$ was synthesized according to a literature procedure.[40] Concerning the latter, it should be noted that the graphite should be very thoroughly dried prior to the synthesis of $C_8K$, to prevent the formation of oxygen-containing products in the subsequent syntheses.

*Reactions of 5-decyne, 4-decyne and 3-decyne with the system* $2C_8K/MeBBr_2$

These reactions were all carried out in the same fashion. In a typical run, 24.74 g (183 mmole) of $C_8K$ were suspended in 100 cm$^3$ of benzene and 10.78 g (78 mmole) of 5-decyne were added. The mixture was heated to reflux and 14.67 g (79 mmole) of $MeBBr_2$, diluted with 20 cm$^3$ of benzene, were added dropwise over a period of *ca.* 1 hr. The reaction was followed with $^1$H NMR and the suspension turned black. The reaction mixture was refluxed for 20 hr and next stirred at room temperature for 3 more days. After that period all solid material was removed by filtration (or centrifugation). A dark-brown liquid was obtained from which all volatile components were removed *in vacuo*. The residue was subjected to fractional vacuum distillation. The fraction boiling at 60–65°/$10^{-6}$ Torr was, according to GC/MS, pure 1,4-dimethyl-2,3,5,6-tetra-*n*-butyl-1,4-diboracyclohexa-2,5-diene. This compound is a viscous yellow liquid, very air- and moisture sensitive, and thermally somewhat unstable. The same reaction, carried out in cyclohexane, yielded the same results.

*Reaction of 2-butyne with the system* $2C_8K/MeBBr_2$

In 100 cm$^3$ of benzene were suspended 20.56 g (152 mmole) of $C_8K$; 4.11 g (76 mmole) of 2-butyne

were added to this mixture. Next, 14.12 g (76 mmole) of $MeBBr_2$ diluted with 20 $cm^3$ of benzene were added dropwise. The ensuing reaction was slightly exothermic; the graphite-potassium slowly turned black. The mixture was stirred at room temperature for 6 days. After this period, all solid material was removed by centrifugation. The supernatant was investigated by GC/MS. The carborane was obtained in a pure state by fractionated vacuum distillation (b.p. 55–56°/4.5 Torr). It is a pale yellow liquid, extremely sensitive towards air and water.

The same product is obtained when 2-butyne is reacted first with one equivalent of $MeBBr_2$ (in benzene), and the reaction product is treated subsequently with two equivalents of $C_8K$.

In the mass spectrum of $[MeBC_4Me_4BMe]$ the base peak is the parent peak (*m/e* 160). The ratio of the peaks at *m/e* 158, 159 and 160 is 1:8:16. Further prominent peaks occur at *m/e* 145 ($[M-CH_3]^+$, 69%), *m/e* 65 ($[C_2BMe_2]^+$, 43%), and at *m/e* ($[Me_2B]^+$, 50%).

*Reaction of di-t-butylacetylene with the system* $2C_8K/MeBBr_2$; *formation of* 1-*methyl*-2,3-*di*-t-*butylborirene* (**XIII**) *and of* 1,3-*dimethyl*-2,4-*di*-t-*butyl*-1,3-*diboretene* (**XVb**)

Two portions of *ca.* 150 mmole of $C_8K$ were each suspended in 100 $cm^3$ of benzene. To each half an equivalent (75 mmole) of di-*t*-butylacetylene were added. One of the mixtures was heated to reflux, and to both half an equivalent of $MeBBr_2$, diluted with 20 $cm^3$ of benzene, were added dropwise. Next, both mixtures were stirred for 3 days, one at reflux temperature, one at ambient temperature. The reactions were followed by $^1H$ NMR. When the reactions would not proceed any further, all solid material was removed by centrifugation. From the supernatants all volatile components were removed by freezing them *in vacuo* ($10^{-1}$ Torr) into a trap cooled with liquid nitrogen. The liquids thus obtained appeared to contain air- and moisture-sensitive component(s). Most benzene was removed by careful distillation under atmospheric pressure over a Widmer column. The residues, colourless, extremely air- and moisture-sensitive liquids, contained, according to $^1H$ NMR, two *t*-butyl components, apart from di-*t*-butylacetylene. The residues of both distillations and the residues obtained after removal of all volatile components were investigated by GC/MS. The latter contained no identifiable compounds.

*Acetolysis of reaction mixtures*

Prior to acetolysis all solid material was removed by filtration or centrifugation. Next, an excess of glacial acetic acid was added and the mixture was refluxed for 1 hr.

Residues were diluted with benzene before the acetic acid was added.

*Acknowledgements*—We wish to thank Prof. Dr. L. Brandsma for kindly supplying samples of 3-decyne, 4-decyne, 5-decyne, and di-*t*-butylacetylene, and Dr. P. E. van Rijn for providing us with a sample of 2-butyne.

The authors are indebted to Prof. Dr. P. von R. Schleyer (University of Erlangen–Nürnberg, in 1982 Guest Professor in Utrecht) for stimulating discussions.

We are grateful to Mr. M. Hasselaar for helpful assistance in part of this work.

## REFERENCES

1. M. E. Volpin, Yu. D. Koreshkov, V. G. Dulova and D. N. Kursanov, *Tetrahedron* 1962, **18**, 107.
2. W. Kuchen and R. D. Brinkmann, *Angew. Chem.* 1960, **72**, 564.
3. W. Kuchen and R. D. Brinkmann, *Z. Anorg. Allgem. Chem.* 1963, **325**, 225.
4. O. M. Nefedow and M. N. Manakow, *Angew. Chem.* 1966, **78**, 1039.
5. F. Joy, M. F. Lappert and B. Prokai, *J. Organometal. Chem.* 1966, **5**, 506.
6. J. J. Eisch and H. P. Becker, *J. Organometal. Chem.* 1979, **171**, 141.
7. R. Köster and M. A. Grassberger, *Angew. Chem.* 1966, **78**, 590.
8. J. J. Eisch and L. J. Gonsior, *J. Organometal. Chem.* 1967, **8**, 53.
9. P. L. Timms, *J. Amer. Chem. Soc.* 1967, **89**, 1629.
10. P. L. Timms, *J. Amer. Chem. Soc.* 1968, **90**, 4585.
11. P. L. Timms, *Acc. Chem. Res.* 1973, **6**, 118.
12. P. Binger, *Tetrahedron Letters* 1966, 2675.
13. R. N. Camp, D. S. Marynick, G. D. Graham and W. N. Lipscomb, *J. Amer. Chem. Soc.* 1978, **100**, 6781.
14. J. J. Eisch, K. Tamao and R. J. Wilcsek, *J. Amer. Chem. Soc.* 1975, **97**, 895.
15. B. Wrackmeyer and H. Nöth, *Z. Naturforsch. B.* 1974, **29**, 564.
16. H.-O. Berger, H. Nöth, G. Rub and B. Wrackmeyer, *Chem. Ber.* 1980, **113**, 1235.
17. G. E. Herberich and B. Hessner, *Z. Naturforsch. B.* 1978, **33**, 180.
18. G. E. Herberich and B. Hessner, *J. Organometal. Chem.* 1978, **161**, C36.
19. H. Bock, W. Kaim, P. L. Timms and P. Hawker, *Chem. Ber.* 1980, **113**, 3196.
20. K. Krogh-Jespersen, D. Cremer, J. D. Dill, J. A. Pople and P. von R. Schleyer, *J. Amer. Chem. Soc.* 1981, **103**, 2589.
21. P. S. Maddren, A. Modinos, P. L. Timms and P. Woodward, *J. Chem. Soc., Dalton Trans.* 1975, 1272.
22. J. A. K. Howard, I. W. Kerr and P. Woodward, *J. Chem. Soc., Dalton Trans.* 1975, 2466.

23. G. E. Herberich, B. Hessner, S. Beswetherick, J. A. K. Howard and P. Woodward, *J. Organometal. Chem.* 1980, **192**, 421.
24. G. E. Herberich, B. Hessner, G. Huttner and L. Zsolnai, *Angew. Chem.* 1981, **93**, 471.
25. M. C. Böhm, M. Eckert-Maksić, R. Gleiter, G. E. Herberich and B. Hessner, *Chem. Ber.* 1982, **115**, 754.
26. J. J. Eisch, F. Shen and K. Tamao, *Heterocycles* 1982, **18**, 245.
27. G. E. Herberich and B. Hessner, *Chem. Ber.* 1982, **115**, 3115.
27a. G. E. Herberich and M. M. Kucharska-Jansen, *J. Organometal. Chem.* 1983, **243**, 45.
28. S. M. van der Kerk and G. J. M. van der Kerk, *J. Organometal. Chem.* 1980, **190**, C11.
29. S. M. van der Kerk, A. L. M. van Eekeren and G. J. M. van der Kerk, *J. Organometal. Chem.* 1980, **190**, C8.
30. S. M. van der Kerk, P. H. M. Budzelaar, A. van der Kerk-van Hoof, G. J. M. van der Kerk and P. von R. Schleyer, *Angew. Chem.* 1983, **95**, 61.
31. P. von R. Schleyer, private communication.
32. F. Johnson, R. S. Gohlke and W. A. Nasutavicus, *J. Organometal. Chem.* 1965, **3**, 233.
33. P. J. Grisdale and J. L. R. Williams, *J. Organometal. Chem.* 1970, **22**, C19.
34. J. J. Eisch and J. E. Galle, *J. Amer. Chem. Soc.* 1975, **97**, 4436.
35. S. M. van der Kerk, J. Boersma and G. J. M. van der Kerk, *J. Organometal. Chem.* 1981, **215**, 303.
36. S. M. van der Kerk, *J. Organometal. Chem.* 1981, **215**, 315.
37. S. M. van der Kerk and P. H. M. Budzelaar, to be published.
38. K. Niedenzu, *Organometal. Chem. Rev. A.* 1966, **1**, 305.
39. H. Nöth and H. Vahrenkamp, *J. Organometal. Chem.* 1968, **11**, 399.
40. H. Podall, W. E. Foster and A. P. Giraitis, *J. Org. Chem.* 1958, **23**, 82.
41. R. Köster and M. A. Grassberger, *Angew. Chem.* 1967, **79**, 197.

*Polyhedron* Vol. 3, No. 3, pp. 281–286, 1984
Printed in Great Britain.

0277–5387/84 $3.00 + .00
© 1984 Pergamon Press Ltd.

# AROYLHYDRAZONES AS CHELATING AGENTS: $d^{10}$-METAL COMPLEXES OF PYRIDINE-2-CARBALDEHYDE SALICYLOYLHYDRAZONE AND X-RAY STRUCTURE OF THE ZINC DERIVATIVE†

**PAOLO DOMIANO, CORRADO PELIZZI and GIOVANNI PREDIERI***
Centro di Studio per la Strutturistica Diffrattometrica del CNR, Istituti di Strutturistica Chimica e di Chimica Generale dell'Università, Via M. D'Azeglio 85, 43100 Parma, Italy

**CARLO VIGNALI**
Centro Interfacoltà di Misure dell'Università, Via Spezia 73, 43100 Parma, Italy

**and**

**GERARDO PALLA**
Istituto di Chimica Organica dell'Università, Via M. D'Azeglio 85, 43100 Parma, Italy

(*Received* 11 *April* 1983; *accepted* 25 *July* 1983)

**Abstract**—The title organic ligand (Hsip) gave, by reaction with $d^{10}$-metal acetates, complexes of the type $M(sip)_2$ (M = Zn, Cd, Hg), in which the ligand behaved as terdentate, producing a distorted octahedral environment around the metal. The $^1H$ and $^{13}C$ chemical shifts found for these complexes in DMSO are compared with the corresponding ones of the free ligand. The crystal structure of the zinc derivative has been determined from diffractometer data to $R = 0.072$ for 1086 independent reflections. Crystals are monoclinic, space group $C2/c$, with unit-cell dimensions $a = 18.193(2)$, $b = 24.532(6)$, $c = 11.535(2)$ Å, $\beta = 103.71(1)°$ and $Z = 8$. Coordination occurs through the carbonyl oxygens (Zn–O = 2.10, 2.16(1) Å), the azomethine nitrogens (Zn–N = 2.04, 2.07(1) Å) and the pyridine nitrogens (Zn–N = 2.24, 2.26(1) Å).

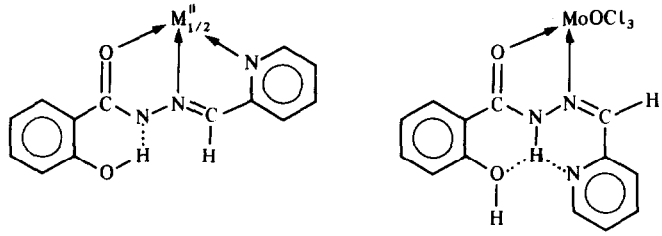
The chemical properties of hydrazones have been intensively investigated in recent years, owing to their coordinative capability,[1] their pharmacological activity[2] and their use in analytical chemistry as metal extracting agents.[3] In particular the chelating behaviour of aroylhydrazones of heteroaromatic aldehydes or ketones is currently being studied in our laboratories, with the aim of investigating the influence coordination exerts on their conformation and/or configuration, in connection with the nature of the metal and of the counter ion.[4]

We have recently shown[5] that the terdentate ligand *N*-pyridylmethylene-*N'*-salicylhydrazine (Hisp), having the **E** configuration, when free and when coordinated to transition metals of the first row, assumes the **Z** configuration in $[MoOCl_3(Hisp)]$ and behaves as bidentate (Scheme 1) Bond distances and angles in (**Z**)-Hsip (**1b**) indicates that some strain is present in the structure and this strain could be responsible for the *non*-existence of (**Z**)-Hsip in the free state.

Another interesting feature of these molecules is the possibility of coordinating either in the neutral (keto) or in the anionic (iminol) form via the loss of the "amide" hydrogen. For Hsip these forms exhibit small, but significant differences in the structural parameters of the central hydrazine chain, the anionic form ($sip^-$) showing more $\pi$ delocalization, probably involving also the pyridine ring.[6] Therefore, in order to gain more information on the nature of the changes, de-

*Author to whom correspondence should be addressed.

†Bis[*N'*-(2-pyridylmethylene)-*N''*-salicyloylhydrazido (1−)-*NN'O*]zinc(II)-methanol (1/0.5).




**1a** **1b**

Scheme 1.

protonation and coordination induce on these molecular systems, we have synthesized three $d^{10}$ metal complexes of the type [M(sip)$_2$], (M = Zn, Cd, Hg), suitable for $^1$H and $^{13}$C NMR investigations. We have determined the crystal structure of the zinc derivative and here we report together the results of these studies.

## EXPERIMENTAL

*Reagents.* Reagent grade metal acetates, methyl salicylate, hydrazine hydrate (C.Erba) and pyridine-2-carbaldehyde (Merck) were used without further purification. Solvents were distilled before use.

*Physical measurements.* IR spectra (KBr discs; 4000–250 cm$^{-1}$) were recorded on a Perkin–Elmer 283B spectrophotometer; $^1$H (100 MHz) and $^{13}$C(25 MHz) NMR spectra for saturated solutions in deuterated dimethyl sulphoxide, with TMS as internal reference, were recorded at 60°C on a Varian XL100 instrument equipped with Fourier-Transform facility. Elemental C, H, N analyses were made on a Perkin–Elmer 240 automatic equipment.

*Preparations.* The ligand Hsip was prepared as described in Ref. 7. Its main vibrational bands, were already reported.[8] $^1$H NMR: $\delta$ ppm 12.05 (NH), 11.67(OH), 8.50 (N = CH), 7.90 (H3 and H4), 7.48 (H5), 8.63 (H6), 7.00 (H3′ and H5′), 7.42 (H4′), 7.96 (H6′); $^{13}$C NMR data are quoted in Table 1.

The metal complexes [M(sip)$_2$), M = Zn, Cd, Hg, were prepared by heating under reflux ethanol solutions containing Hsip and the metal acetate (2:1). The pale yellow microcrystalline precipitates obtained on cooling were collected by filtration, washed several times and dried *in vacuo* giving satisfactory C, H, N elemental analyses. IR bands [Zn(sip)$_2$]: 3000–2500 w, br, 1600 vs, 1560 ms, 1515 s, 1490 s, 1470 s; 1360 vs, 1340 vs, 1250 s, 1155 s, 925 m, 830 m, 755 ms. [Cd(sip)$_2$] and (Hg (sip)$_2$] show practically the same vibrational bands. $^1$H NMR [Zn(sip)$_2$]: $\delta$ 13.20 (OH), 8.82 (N = CH), 6.75 ÷ 8.08 (arom.); [Cd(sip)$_2$]: $\delta$ 13.24 (OH), 8.74 (N = CH), 6.75 ÷ 8.15 (arom.); [Hg(sip)$_2$]: $\delta$ 13.15 (OH), 8.98 (N = CH), 6.80 ÷ 8.15 (arom); $^{13}$C data are quoted in Table 1.

*Crystallographic measurements.* Crystals of [Zn (sip)$_2$].$\frac{1}{2}$MeOH, suitable for *X*-ray analysis were obtained accidentally by slow evaporation of methanol solutions of [Zn(Hsip)Br$_2$][8] heated under reflux. The selected crystal was a pale yellow elongated prism of dimensions 0.14 × 0.09 × 0.38 mm$^3$. The unit cell parameters were obtained by a least-squares treatment of the 2$\theta$ values of 16 reflections, accurately centered on the four-circle diffractometer (on-line Siemens AED equipment), and are given in the Table 2 together with other crystal data.

The intensity data of 3158 independent reflections were collected at room temperature with the $\omega - 2\theta$ scan technique; 1086 of these, having

Table 1. $^{13}$C assignments for Hsip and its complexes

| Compound | CO | N=CH | C2 | C3 | C4 | C5 | C6 | C1' | C2' | C3' | C4' | C5' | C6' |
|---|---|---|---|---|---|---|---|---|---|---|---|---|---|
| Hsip | 165.0 | 148.5 | 152.7 | 119.9 | 136.5 | 124.2 | 149.2 | 119.2 | 158.8 | 117.1[b] | 133.6 | 118.7[b] | 128.4 |
| [Zn(sip)$_2$] | 174.9 | 140.8 | 148.4 | 125.2 | 139.9 | 126.0 | 147.2 | 117.5 | 160.0 | 116.6[b] | 132.6 | 117.9[b] | 129.3 |
| [Cd(sip)$_2$] | 174.0 | 141.5 | 148.8 | 125.5 | 139.5 | 125.5 | 148.5 | 118.5 | 160.1 | 116.5[b] | 132.2 | 117.6[b] | 129.2 |
| [Hg(sip)$_2$] | 172.1 | 141.7 | 148.8 | 126.5 | 139.5 | 126.5 | 148.7 | 118.5 | 159.9 | 116.6[b] | 132.3 | 117.9[b] | 129.1 |

(a) carbon labels are those of Figure 2

(b) assignments could be reversed

Table 2. Crystal data for the zinc complex

| | |
|---|---|
| $Zn(C_{13}H_{10}N_3O_2)_2 \cdot \frac{1}{2}CH_3OH$ | M = 561.87 |
| Monoclinic, space group C2/c | |
| a = 18.193(2), b = 24.532(6), c = 11.535(2) Å; β = 103.71(1)° | |
| V = 5002 (2) Å$^3$; Z = 8; $D_c$ = 1.49 g.cm$^{-3}$; | |
| F(000) = 2312; λ(CuKα) = 1.54178 Å; | |
| μ(CuKα) = 18.3 cm$^{-1}$ | |

$I > 2\sigma(I)$, were considered observed, were corrected for Lorentz and polarization, but not for absorption effects, and were used in the analysis. The structure was solved by direct methods, using the SHELX–76 system of programs,[9] in which the atomic scattering factors take into account the anomalous scattering effects, following the International Tables.[10]

The refinement was carried out by full-matrix least-squares anisotropically for the Zn atom and isotropically for the other ones, owing to the paucity of the observed data; in this way the observation-to-parameters ratio was 7.2/1 (1086/151).

No attempt was made in order to localize the hydrogen atoms.

During the last cycles of refinement a residual electron density on a twofold axis was attributed to the oxygen of a molecule of methanol, exhibiting orientational disorder; the final cycles led to the values of 0.072 for $R$ and 0.076 for $R_w$ ($w = 1/(\sigma^2(F) + 0.005\,F^2)$).

All calculations were performed on the computer of Consorzio per la Gestione del Centro di Calcolo Interuniversitario dell'Italia Nord Orientale with the financial support of the University of Parma.

Final positional and thermal parameters together with observed and calculated structure factors have been deposited with the Editor as supplementary material. Atomic coordinates have also been deposited with the Cambridge Crystallographic Data Centre.

## RESULTS AND DISCUSSION

The reaction of Hsip with metal(II) acetates in alcoholic medium produces metal complexes of the type $[M(sip)_2]$ in which the deprotonated ligand behaves as terdentate as depicted in the previous scheme (**1a**). They are pale yellow solids poorly soluble at room temperature in all common solvents, with the exception of DMSO. Their IR spectra present the same bands of the Ni(II) derivative,[7] a major feature being the lowering ($30\ cm^{-1}$) of the $\nu$(CO) value with respect to the free ligand.

*$^1H$ and $^{13}C$ NMR spectra.* As quoted in the experimental section, the amide proton in the free ligand exhibits a large downfield shift, probably as a consequence of the intramolecular hydrogen bond with the OH group, whose line is rather broad ($\Delta = 50$ Hz). At room temperature the NMR linewidth of NH is as sharp ($\Delta = 7$ Hz) as those of other *N*-aroylhydrazones,[11] and the line broadens, with increasing temperature, at the same rate observed for the same proton in methyl pyruvate benzoylhydrazone.[12] Assignments of the pyridine protons are based on previously reported spectra,[13] having also used selective decouplings for the purpose of confirmation. The shifts of the phenyl protons were assigned with the aid of less complicated spectra of simpler *N*-salicyloylhydrazones.[12]

The $^{13}C$ assignments for Hsip have been deduced taking into account the shifts and the J(CH) values of pyridine substituted compounds[14] and of salicylaldehyde.[15] The comparison with $^{13}C$ NMR data of picolinaldehyde acetylhydrazone[11] has been a successful aid. Two lines are present near 149 ppm: the N = CH carbon, assigned at 148.5 ppm gives, rise to a clear doublet with J(CH) = 167.0 Hz, when observed in non-decoupled conditions; the pyridine carbon C6, at 149.2 ppm, reveals, on the contrary, a more complex eight-line structure.

The $[M(sip)_2]$ complexes required, in the case of $^{13}C$, the use of $Cr(acac)_3$ as relaxation reagent, in order to reveal the carbonyl resonances. Some peak broadening occurs in their spectra, both for the azomethine proton and carbon, mainly in $[Hg(sip)_2]$. The spectrum of $[Hg(sip)_2]$ was recorded also in non-decoupled conditions in order to confirm the correctness of the assignments. In the $^1H$ spectra of the complexes, the hydroxyl protons show a significant downfield shift, owing to the strong intramolecular hydrogen bond with the deprotonated amide nitrogen (O...N = 2.53(2) A in the solid state). The same happens for the formyl proton, its shift being less remarkable ($8.74 \div 8.98\ \delta$).

As shown in the Table 1, the simultaneous effects of deprotonation and coordination strongly influence the carbon shifts in the metal complexes, particularly those of the hydrazide chain and of the pyridine ring, which directly interact with the metals. The carbonyl carbon undergoes a significant downfield shift, which is slightly dependent on the nature of the metal. The same

behaviour was already observed in an uranyl complex of a diacetylpyridine bis-aroylhydrazone[16] and seems to be a consequence of the lowering of electron density from the carbonyl carbon on coordination. More complex is the situation in the pyridine ring where the C3, C4 and C5 resonances shift downfield, whereas the C2 and C6 carbon exhibit upfield shifts, compared to the ligand. Such a tendency seems to be characteristic of coordinated pyridine rings, having been already reported.[17,18] It is interesting to note the behaviour of C2 and C6 and of C3 and C5, the lines of which, as the metal is changed in the series Zn, Cd, Hg, approach each other, as far as they collapse in $[Hg(sip)_2]$, giving rise to only two lines. Surprisingly the azomethine carbon exhibits an upfield shift, compared to the ligand, contrary to the behaviour of the similar carbon in the double hydrazone of Ref. 16 and in opposition to the downfield shift of the corresponding proton. The differences in the nature of the shifts in the $^{13}C$ and $^{1}H$, due to the different factors governing the shifts, could justify this effect. Furthermore the azomethine carbon could be shielded by the release of negative charge on deprotonation, which becomes delocalized throughout the ligand, probably to a greater extent than in the case of the double hydrazone,[16] whereas the formyl proton could be affected by the ring-current of the nearby pyridine ring.

*X-Ray structure.* The structure consists of discrete $[Zn(sip)_2]$ and methanol molecules, packing being determined by van der Waals interactions. As shown in the Fig. 1, the two terdentate anionic ligands coordinate to zinc through the oxygen and a nitrogen from the hydrazide groups and through the pyridine nitrogen, in a distorted octahedral environment. The molecular ensemble is practically the same as found in $[Ni(sip)_2]$,[7] where, however, the two ligand ions were related by a twofold axis through the metal.

Bond angles at Zn (Table 3) range from 74.5(5) to 115.1(5)°, thus showing relevant departures from the ideal octahedral values. A better view of the metal environment can be achieved considering the deviations from the three least-squares coordination planes quoted in Table 4. N(1), N(2), N(5), O(1) were very close to coplanarity, the largest deviation from the mean least-squares plane through them being 0.05 Å and Zn being displaced by only 0.03 Å.

Coordination distances, reported in Table 3, are significantly longer than those observed in $[Ni(sip)_2]$[7] in agreement with the different values of the effective ionic radii reported for six-coordinated $Zn^{2+}$ (0.75 Å) and $Ni^{2+}$ (0.70 Å).[19]

The two anionic ligands consist of three planar parts: the phenyl and pyridine rings and the central chain (Table 4). These latter are roughly coplanar, supporting the existence of $\pi$ interaction between

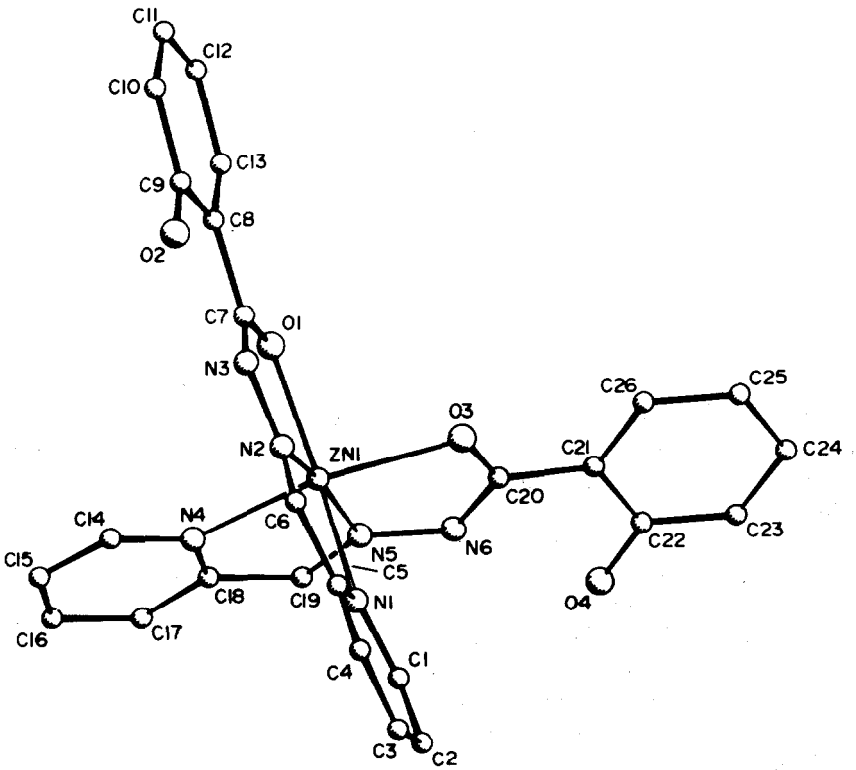



Fig. 1. Perspective view of the complex along [010].

Table 3. Bond distances and angles in the coordination polyhedron

| | | | |
|---|---|---|---|
| Zn-O(1) | 2.10(1) | O(3)-Zn-N(1) | 92.2(4) |
| Zn-O(3) | 2.16(1) | O(3)-Zn-N(2) | 105.8(5) |
| Zn-N(1) | 2.27(1) | O(3)-Zn-N(4) | 149.2(4) |
| Zn-N(2) | 2.04(1) | O(3)-Zn-N(5) | 75.1(5) |
| Zn-N(4) | 2.24(1) | N(1)-Zn-N(2) | 75.0(5) |
| Zn-N(5) | 2.07(1) | N(1)-Zn-N(4) | 95.0(5) |
| O(1)-Zn-O(3) | 92.4(4) | N(1)-Zn-N(5) | 94.4(4) |
| O(1)-Zn-N(1) | 150.4(4) | N(2)-Zn-N(4) | 105.0(5) |
| O(1)-Zn-N(2) | 75.6(5) | N(2)-Zn-N(5) | 169.4(5) |
| O(1)-Zn-N(4) | 95.9(4) | N(4)-Zn-N(5) | 74.5(5) |
| O(1)-Zn-N(5) | 115.1(5) | | |

Table 4. Deviations of atoms from least-squares planes

In the coordination polyhedron

(1) N(1), O(1), N(4), O(3). N(1), -0.50(1); O(1), -0.51(1); N(4), 0.76(1); O(3), 0.51(1); Zn, 0.051(3)

(2) N(1), N(2), N(5), O(1). N(1), -0.04(1); N(2), 0.05(1); N(5), 0.03(1); O(1), -0.02(1); Zn, 0.029(2).

(3) N(2), N(4), N(5), O(3). N(2), 0.09(1); N(4), -0.13(1); N(5), 0.14(1); O(3), -0.09(1); Zn, -0.073(2).

(1)-(2) = 87.0(4); (1)-(3) = 93.7(3); (2)-(3) = 90.9(3)

In the ligands

| | |
|---|---|
| (1) N(1), C(1), C(2), C(3), C(4), C(5) | max dev. 0.03 for C(2) |
| (2) C(8), C(9),C(10), C(11), C(12), C(13) | max dev. 0.02 for C(8) |
| (3) C(6), N(2), N(3), C(7), O(1) | max dev. 0.04 for N(2) |
| (4) N(4), C(14), C(15), C(16), C(17), C(18) | max dev. 0.04 for C(14) |
| (5) C(21), C(22), C(23), C(24), C(25), C(26) | max dev. 0.04 for C(24) |
| (6) C(19), N(5), N(6), C(20), O(3) | max dev. 0.03 for C(19) |

(1)-(2) = 12.3(5); (1)-(3) = 4.7(5); (2)-(3) = 7.9(6)

(4)-(5) = 18.0(5); (4)-(6) = 6.9(5); (5)-(6) = 11.1(4)

these moieties, in order to allow some delocalization of the negative charge also on the pyridine nitrogen. The structural parameters in the ligands (Fig. 2) are in substantial agreement with the corresponding ones found in other complexes of sip,[6,7,20] indicating that also the iminol form –(O)C = N–N = CH– contributes, to some extent, in describing the resulting structure. Nevertheless we suspect that these iminol forms, found in metal complexes and often postulated to form because of tautomeric equilibria involving aroylhydrazones, do not really exist, when they are free in solution. Our $^1H$ and $^{13}C$ NMR data, collected for a variety of aroylhydrazones in DMSO-$d_6$ and sometime in $CHCl_3$-$d$[11,12] revealed conformational and/or configurational equilibria but provided no evidence of keto-iminol tautomerism.

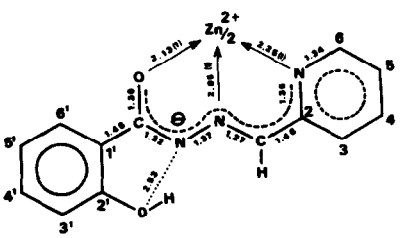


Fig. 2. Scheme of the molecular complex with averaged bond distances.

## REFERENCES


1. M. B. Hursthouse, S. A. A. Jayaweera and A. Quick, *J. Chem. Soc. (Dalton)* 1979, 279. M. F. Iskander, L. El-Sayed, S. Saddeck and M. A. Abno-Taleb, *Transition Met. Chem.* 1980, **5**, 168.
2. R. Haran, J. Gairin and G. Commenges, *Inorg. Chim. Acta* 1980, **46**, 63.
3. M. Gallego, M. Garcia–Vargas and M. Valcarcel, *Analyst* 1979, **104**, 613.
4. C. Pelizzi, G. Pelizzi, G. Predieri and S. Resola, *J. Chem. Soc. (Dalton)* 1982, 1349 and references therein.
5. P. Domiano, A. Musatti, M. Nardelli, C. Pelizzi and G. Predieri, *Transition Met. Chem.* 1980, **5**, 172.
6. P. Domiano, A. Musatti, M. Nardelli, C. Pelizzi and G. Predieri, *J. Chem. Soc. (Dalton)* 1979, 1266.
7. P. Domiano, A. Musatti, M. Nardelli and C. Pelizzi, *J. Chem. Soc. (Dalton)* 1975, 295.
8. C. Pelizzi and G. Predieri, *Gazz. Chim. Ital.* 1975, **105**, 413.
9. G. Sheldrick, *SHELX-76 system of computer programs.* University of Cambridge (1976).
10. *International Tables for X-ray Crystallography*, Vol. IV. Kynoch Press, Birmingham (1974).
11. G. Palla, C. Pelizzi, G. Predieri and C. Vignali, *Gazz. Chim. Ital.* 1982, **112**, 339.
12. C. Vignali, unpublished results
13. C. F. Bell, G. R. Mortimore and G. L. Reed, *Org. Magn. Reson* 1975, **7**, 512.
14. M. Hansen and H. J. Jakobsen, *J. Magn. Reson.* 1973, **10**, 74.
15. P. Äyräs, R. Laatikainen, S. Lötjönen, *Org. Magn. Reson.* 1980, **13**, 387.
16. G. Paolucci, G. Marangoni, C. Bandoli and D. A. Clemente, *J. Chem. Soc. (Dalton)* 1980, 1304.
17. M. Hughes, R. H. Prince and P. Wyeth, *J. Inorg. Nucl. Chem.* 1978, **40**, 713.
18. R. Jagannathan and S. Soundararajan, *J. Inorg. Nucl. Chem.* 1980, **42**, 145.
19. R. D. Shannon and C. T. Prewitt, *Acta Cryst.* 1970, **B26**, 1046.
20. P. Domiano, A. Musatti, M. Nardelli, C. Pelizzi and G. Predieri, *J. Chem. Soc. (Dalton)* 1975, 2357.

*Polyhedron* Vol. 3, No. 3, pp. 287–290, 1984
Printed in Great Britain.

0277-5387/84 $3.00 + .00
© 1984 Pergamon Press Ltd.

# FLUOROOXOPEROXO COMPLEXES OF VANADIUM(V)

**PETER SCHWENDT* and DANIELA JONIAKOVÁ**
Department of Inorganic Chemistry, Comenius University, Mlynská dol., 842 15 Bratislava, Czechoslovakia

(*Received* 11 *April* 1983, *accepted* 25 *July* 1983)

**Abstract**—Substances crystallizing under various conditions from the $MVO_3$–(MF, HF)–$H_2O_2$–$H_2O$ (M = $NH_4$, K) systems have been characterized by elemental analysis, infrared and Raman spectra and X-ray powder patterns. Besides the known $M_2[VO(O_2)_2F]$ complexes, complexes of two new types have been obtained: $M_3[HV_2O_2(O_2)_3F_4] \cdot 2H_2O$ and $(NH_4)_3[V_2O_2(O_2)_4F] \cdot nH_2O$ ($n \approx 2$). Vibrational spectra of new complexes are consistent with the presence of dimeric anions containing $V(\mu_2\text{–}O_2)V$ and V–F–V bridges, respectively.

The synthesis of several fluoroperoxovanadates (V) has been reported recently. $(NH_4)_2[VO(O_2)OHF_2]$,[1] $K_4[V_2O_3(O_2)_2F_4]$,[1] $K_2[VO(O_2)_2F]$,[2] $K_2[V_2O_3(O_2)_2F_2]$[3] have been prepared from acidic media, $M_2[VO(O_2)_2F]$[4] and $M_2[V(O_2)_3F]$ (M = Na, K, $NH_4$)[5] from alkaline media. Although information on the composition of fluorooxoperoxovanadate (V) ions in aqueous solution is entirely lacking, a greater variety of species in the solution can be expected, especially when the ability of all ligands to form bridges between two vanadium atoms is taken into account. With regard to this assumption a systematic study of products crystallizing from the $MVO_3$–(MF, HF)–$H_2O_2$–$H_2O$ systems under various conditions has been undertaken.

## EXPERIMENTAL

*Physical–chemical studies.* IR spectra were recorded in the 200–4000 $cm^{-1}$ region with Perkin Elmer 180 and Specord 75 IR spectrophotometers. The substances were prepared as Nujol and hexachlorobutadiene mulls between KBr and polyethylene plates. Raman spectrum for $K_3[HV_2O_2(O_2)_3F_4] \cdot 2H_2O$ was obtained using Jeol JRS 1 spectrophotometer and He–Ne laser. Decomposition occurred when the $Ar^+$ ion laser was used.

X-Ray powder patterns were obtained with a Phillips diffractometer (PW 1058) employing Cu $K_\alpha$ radiation.

*Author to whom correspondence should be addressed.

*Elemental analyses.* Vanadium (V) was reduced to vanadium (IV) using ascorbic acid. An excess of standard EDTA solution was added to the obtained solution and the vanadium content was estimated by a back titration with zinc chloride.[6] The peroxide content was determined by potentiometric titration with potassium permanganate. Fluorine was estimated using an ion-selective electrode (Crytur 09–17). Nitrogen ($NH_4^+$) was determined by Kjeldahls' method. Potassium was estimated by flame photometry.

*Preparation of complexes.* Almost 200 products were isolated from the $MVO_3$–(MF, HF)–$H_2O_2$–$H_2O$ (M = $NH_4$, K) systems. The following conditions were systematically changed: (i) Molar ratio $n(MF + HF)/n(MVO_3)$ (from 2 to 12); (ii) the concentration of $MVO_3$ (from 0.2 to 1.5 mol/$dm^3$); (iii) the acidity of solutions ($n(HF)/n(MVO_3)$ was between 0 and 12). Solid products were obtained by crystallization at lower temperatures (−25° to +5°C). In some cases, the crystallization was initiated by ethanol. The pH values of solutions before crystallization (estimated by a narrow range pH paper) were between 2 and 5. Preparative conditions and analyses of pure compounds are given in Table 1. Complex $(NH_4)_3[V_2O_2(O_2)_4F] \cdot nH_2O$ was obtained only in the following way: solutions A and B (Table 1) were cooled to 0°C, then mixed and 150 $cm^3$ of cold ethanol (−25°C) was immediately added. The complex obtained was quickly isolated from the solution.

Table 1. Preparative conditions and analyses of complexes

| Compound | Preparative conditions | | Analyses | | | | |
|---|---|---|---|---|---|---|---|
| | Solutions for crystallization | Temp.* | $K^+/NH_4^+$ | V | $(O_2^{2-})$ | F | H |
| $K_3[HV_2O_2(O_2)_3F_4].2H_2O$ orange | $KVO_3$ (10 mmol), 5% $H_2O_2$ (24 $cm^3$), $KHF_2$ (20 mmol) | 5°C | Found. 26.20<br>Calc. 25.49 | 22.52<br>22.13 | 20.50<br>20.86 | 16.97<br>16.51 | |
| $(NH_4)_3[HV_2O_2(O_2)_3F_4].2H_2O$ dark orange | $NH_4VO_3$ (10 mmol), 30% $H_2O_2$ (3 $cm^3$), 40% HF (5 $cm^3$), ethanol (12 $cm^3$) | -25°C | Found. 13.65<br>Calc. 13.61 | 25.90<br>25.67 | 24.90<br>24.19 | 18.68<br>19.14 | 4.23<br>4.32 |
| $(NH_4)_2[VO(O_2)_2F]$ orange-yellow | $NH_4VO_3$ (10 mmol), 15% $H_2O_2$ (14 $cm^3$), $NH_4F$ (120 mmol) | 0°C | Found. 19.32<br>Calc. 19.36 | 27.36<br>27.39 | 34.23<br>34.42 | 10.49<br>10.22 | 4.41<br>4.33 |
| $(NH_4)_3[V_2O_2(O_2)_4F].nH_2O$ yellow | A: $NH_4VO_3$ (10 mmol), 15% $H_2O_2$ (20 $cm^3$)<br>B: $NH_4F$ (30 mmol), $H_2O$ (20 $cm^3$), 40% HF (1.5 $cm^3$) | see text | Found.<br>Calc.** | | 28.04<br>27.46 | 34.40<br>34.50 | 4.92<br>5.12 |

*Temperature of the solution during crystallization

**For n=2

## RESULTS AND DISCUSSION

The main solid products crystallizing under given conditions from the $MVO_3$–(MF, HF)–$H_2O_2$–$H_2O$ (M = $NH_4$, K) systems are the complexes $M_2[VO(O_2)_2F]$, which crystallize from weakly acidic solutions (without hydrofluoric acid, the pH value about 5) and the complexes $M_3[HV_2O_2(O_2)_3F_4] \cdot 2H_2O$ which can be obtained from more acidic solutions (the pH about 3). By rapid precipitation of diluted, weakly acidic solutions, an unstable complex $(NH_4)_3[V_2O_2(O_2)_4F] \cdot nH_2O$ can be prepared. Formation of monoperoxo complexes was not observed. However, the products obtained from strongly acidified solutions often contained admixtures of decomposition products: $MVO_3$, $M_3[V_2O_4F_5]$, $M_2[VO_2F_3]$ and $M_6[V_4O_4(O_2)_6F_6]$ which were identified by means of the IR spectra and the X-ray powder patterns.[7] The prepared complexes with the exception of $(NH_4)_3[V_2O_2(O_2)_4F] \cdot nH_2O$ are stable if kept in a desiccator over silica gel at 0°C.

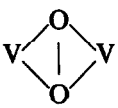
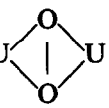
The structure of the vanadium (V) peroxo complexes can to a certain extent be determined from the vibrational spectra.[8–10] The $\nu(V–O_p)$ bands ($O_p$ stands for the peroxo oxygen) can be used for differentiation of diperoxo complexes, since the coupling of the stretching vibrations of two $V(O_2)$ groups depends on the coordination number of the central atom.[9] For pentagonal pyramidal complexes two absorption regions are characteristic: the first at about 630 $cm^{-1}$ (strong or very strong bands) and the second at about 520 $cm^{-1}$ (weak or medium bands). The difference between average wavenumbers of the bands from the first and from the second absorption region, $\Delta\tilde{\nu} = \tilde{\nu}_2 - \tilde{\nu}_3$, is approx. 110 $cm^{-1}$. The bands of almost equal, mostly medium intensity at about 625 and 585 $cm^{-1}$ are typical for pentagonal bipyramidal complexes while $\Delta\tilde{\nu}$ is about 40 $cm^{-1}$ in this case.

The IR spectra of $(NH_4)_2[VO(O_2)_2F]$ [$\Delta\tilde{\nu} = 108$ $cm^{-1}$ m Table 2), $K_2[VO(O_2)_2F]$ ($\Delta\tilde{\nu} = 101$ $cm^{-1}$) and $(NH_4)_3[V_2O_2(O_2)_4F] \cdot nH_2O$ ($\Delta\tilde{\nu} = 101$ $cm^{-1}$) are consistent with a pentagonal pyramidal structure of the complex anions. The IR spectrum of $(NH_4)_2[VO(O_2)_2F]$ is different from the reported one.[4] The $[V_2O_2(O_2)_4F]^{3-}$ ion probably consists of two pentagonal pyramidal groups $VO(O_2)_2F$ which are connected through the shared fluorine atom.

The presence of a bridging peroxo group can be expected in the complexes $M_3[HV_2O_2(O_2)_3F_4] \cdot 2H_2O$ on the basis of their unusual stoichiometry. In the case of the symmetrical V–O–O–V bridge the O–O stretching vibration is active only in the Raman spectrum. As it can be seen from Table 2 the $\nu$(O–O) bands in the Raman spectrum of $K_3[HV_2O_2(O_2)_3F_4] \cdot 2H_2O$ have corre-

Table 2. Structurally significant bands in the vibrational spectra of fluorooxoperoxo complexes of vanadium(V)

| $K_2[VO(O_2)_2F]$ | $(NH_4)_2[VO(O_2)_2F]$ | $(NH_4)_3[V_2O_2(O_2)_4F].nH_2O$ | $M_3[HV_2O_2(O_2)_3F_4].2H_2O$ M=$NH_4$ | | M=K | Assign. |
|---|---|---|---|---|---|---|
| IR | IR | IR | IR | IR | R | |
| | | | | 3180m | | ν(OH) |
| 955s | 915vs | 985vs<br>973vs | 970vs | 975vs | 982vs | ν(V=O) |
| | | | ? | 951m | 956w | δ(V-O-H) |
| 897s<br>876vs | 881vs | 897s<br>891s<br>876vs<br>856s | 890s<br>865m | 900s<br>867m | 900m<br>866s | ν(O-O) |
| 643vs | 641s<br>611s | 647sh<br>635s<br>600s | 615s | 611s | 620sh | $\nu_2(V\text{-}O_p)$ |
| 535m<br>531m | 518m | 536w<br>517w | 580s | 580s | 584s | $\nu_3(V\text{-}O_p)$ |
| 466m | 470m | 450w ? | 495m<br>465m<br>430m | 502m<br>430m | 510sh<br>447vs | ν(V-F) |

sponding bands in the IR spectrum. If we assume the existence of an approximately symmetrical bridge V  V analogous to U  U bridge in the structure of benzyltrimethylammonium - $\mu_2$ - peroxo - bis[trichlorouranate (VI)],[11] it is possible to propose a model for the $[HV_2O_2(O_2)_3F_4]^{3-}$ anion with three coplanar peroxo groups (Fig. 1). In such a structure, both coordination polyhedrons can be considered as diperoxo complexes with the coordination number 7. Evidence supporting the proposed structure can be summarized as follows:

(a) The IR spectra are in the region of $V\text{–}O_p$ stretching vibrations very similar to the IR spectra of diperoxo complexes with the coordination number 7. The $\nu(V\text{–}O_p)$ bands are of almost equal intensity and $\Delta\tilde{\nu}$ is 35 $cm^{-1}$ for ammonium complex and 31 $cm^{-1}$ for potassium complex (Table 2).

(b) The absence of the $\delta(OOH)$ and $\delta(HF_2)$ bands and the presence of bands which can be assigned to the O–H stretching and V–O–H bending vibrations, are in agreement with the proposed protonation place. The assignment of the band at 3180 $cm^{-1}$ to stretching vibration of OH group coordinated to vanadium atom is based on the fact that the intensity of this band does not change in the course of dehydration.†

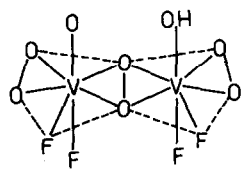


Fig. 1. The proposed structure of the $HV_2O_2(O_2)_3F_4^{3-}$ ion.

(c) There is no difference between the IR spectra of hydrated and anhydrous complexes in the range where the bands of coordinated water molecules should occur (200–800 $cm^{-1}$) therefore the water molecules are probably not coordinated.

It is noteworthy that the thermal decomposition of $K_3[HV_2O_2(O_2)_3F_4] \cdot 2H_2O$ begins with the release of water and hydrogen fluoride and complex $K_6[V_4O_4(O_2)_6F_6]$ with a more symmetrical anion, is thus formed.[12]

†Above $P_4O_{10}$ at room temperature.

## REFERENCES

1. M. C. Chakravorti and A. R. Sarka, *J. Fluorine Chem.* 1976, **8**, 255.
2. G. V. Jere and S. M. Kaushik, *Synth. React. Inorg. Met.-Org. Chem.* 1980, **10**, 255.

3. L. Surendra, S. M. Kaushik and G. V. Jere, *Synth. React. Inorg. Met.-Org. Chem.* 1982, **12**, 455.
4. M. K. Chaudhuri and S. K. Gosh, *Polyhedron* 1982, **1**, 553.
5. M. K. Chaudhuri and S. K. Ghosh, *Inorg. Chem.* 1982, **21**, 4020.
6. R. Přibil, Komplexometrie, p. 246, SNTL, Prague 1977.
7. P. Schwendt, D. Joniaková and V. Ezr, *Chem. Zvesti*, in press.
8. P. Schwendt, P. Petrovič and D. Úškert, *Z. Anorg. Allg. Chem.* 1980, **466**, 232.
9. P. Schwendt, *Collect. Czechoslov. Chem. Common.* 1983, **48**,248.
10. P. Schwendt and M. Pisárčik, *Collect. Czechoslov. Chem. Commun.* 1982, **47**, 1549.
11. R. Haegele and J. C. A. Boeyens, *J. Chem. Soc.*, (Dalton) 1977, 648.
12. P. Schwendt and D. Joniaková, *Thermochim. Acta*, 1983, **68**, 297.

*Polyhedron* Vol. 3, No. 3, pp. 291–296, 1984
Printed in Great Britain.

0277–5387/84 $3.00 + .00
© 1984 Pergamon Press Ltd.

# STUDIES ON THE INTERMOLECULAR INTERACTIONS OF METAL CHELATE COMPLEXES—VIII

## ON THE INTERACTIONS OF DITHIOCARBAMATO–COPPER(II) AND –COPPER(I) COMPLEXES WITH HALOALKANES[1]

**V. I. ILIEV, N. D. YORDANOV* and D. SHOPOV**
Institute of Organic Chemistry, Bulgarian Academy of Sciences, 1113 Sofia, Bulgaria

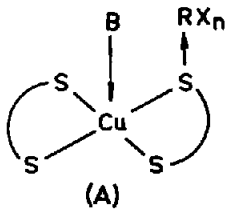
(*Received* 29 *April* 1983; *accepted* 25 *July* 1983)

**Abstract**—The interaction of Cu(II)(dtc)$_2$ and Cu(I)(dtc) complexes with haloalkanes were studied by the EPR method. It was found that the Cu(II)(dtc)$_2$ complex reacted with haloalkanes only in the presence of weak Lewis bases which formed adducts with it. The intermediate reaction product is the mixed-ligand complex Cu(II)(dtc)$X_n$ (X = Cl, Br, $n$ = 1 or 2); the final products being $CuX_2B_n$ (B = Lewis bases, $n$ = 1 or 2) and unstable resin-like residue. Cu(I)(dtc) reacted with haloalkanes without any promoters giving the mixed-ligand complex Cu(II)(dtc)$X_n$ as product. Free radicals were detected in the reaction of Cu(I)(dtc) using the method of "radical scavenger" and were not found in the reaction of Cu(II)(dtc)$_2$. The reported results confirmed one of the two reaction mechanisms proposed in the previous studies. The role of the solvent on the EPR parameters of the mixed-ligand Cu(II)(dtc)X complex is also discussed.

It was reported in Part IV of this series,[2] that haloalkanes interacted with copper(II) dithiocarbamate [Cu(II)(dtc)$_2$], dithiophosphate and thiooxine complexes only in the presence of weak Lewis bases. The complexes $CuX_2B_n$ (X = Cl, Br, B = Lewis bases, $n$ = 1 or 2) were found to be the final reaction products of all studied complexes. The formation of mixed-ligand complex Cu(II)(dtc)$X_n$ ($n$ = 1 or 2) has been observed by EPR[2], and electronic spectra[3] in the reaction of Cu(II)(dtc)$_2$. Free radical formation was not observed in the reaction. Two possible mechanisms have been discussed[2] explaining the interaction:

(a) As a result of axial adduct formation between the base and the metal chelate complex the latter is expanded in the plane $xy$ and some rhombic distortion in it takes place, the donor properties of sulphur atoms being increased.[4] This effect facilitates the formation of donor–acceptor (D–A) complex between the metal complex and the haloalkanes, which are known as weak acceptors. Furthermore electron transfer from the sulphur atom to the acceptor molecule is realized within the complex (A) (Scheme 1). The intermediate product—the mixed-ligand complex Cu(II)(dtc)X and the ester of the corresponding ligand are formed. The interaction of the mixed-ligand complex with a second molecule $RX_n$ is connected with the formation of the final product—$CuX_2B_n$.

(b) As a result of weak charge-transfer complex (CTC) formation between $RX_n$ and base (B) of the




a.

b.

Scheme 1.

*Author to whom correspondence should be addressed.

type (b)—Scheme 1, the reactivity of $RX_n$ is increased. This assumption is based on the available literature data about formation of such CTC.[4-7]

It is interesting to note that complexes with $CuO_4$ and $CuO_2N_2$ chromophores do not interact under the conditions described above.[2] However, Sacconi and Bertini[8] showed that Cu(II) complexes with tridentate Schiff bases form Cu(II)(sch.b.)X mixed-ligand complexes under synthesis or when heated in haloalkanes.

The purpose of the present paper was to study the role of the bases in the described interactions in order to test the proposed reaction mechanisms. Also, the results on the interaction of Cu(I)(dtc) complex with haloalkanes were investigated in order to find some differences in the interaction of $RX_n$ with Cu(II) and Cu(I) chelate complexes.

## EXPERIMENTAL

The $Cu(II)(dtc)_2$ complex was obtained by extraction from water solution of $CuCl_2$ and Na(dtc). The complex was purified by recrystallization from $CHCl_3$.

The Cu(I)(dtc) complex was synthesized by the method described in the literature,[10] using tetramethylthiuramdisulphide and elemental copper. The complex was obtained, kept and used in dry argon atmosphere.

Haloalkanes ($CCl_4$, $CHCl_3$, $C_2H_2Cl_4$, $CHBr_3$, $C_2H_2Br_4$) as well as the bases used (pyridine, 2-methylpyridine, 2,4,6-trimethylpyridine, aniline, N-methylaniline, N,N-dimethylaniline, N,N-dimethyl-1,4-phenylenediamine, N,N,N′,N′-tetramethyl-1,4-phenylenediamine) were purified by standard methods or were obtained from the corresponding hydrochlorides under argon atmosphere to prevent oxidation. $C_2Cl_6$ was purchased from Merck, and 1,1-diphenylpicrylhidrazine (DPPH–H) from Pluka.

The EPR spectra were recorded at 300 and 77 K on a 3BS–X spectrometer using 100 kHz modulation of the magnetic field. The magnetic field was calibrated with $Mn^{2+}$ doped in MgO. The $g$-values were calculated relatively to DPPH.

## RESULTS

(a) *Interactions of* $Cu(II)(dtc)_2$ *complex with haloalkanes in the presence of different weak Lewis bases.*

The interaction of $Cu(II)(dtc)_2$ ($\sim 10^{-3}$ M/l) dissolved in $CCl_4$, $CHCl_3$, $C_2H_2Cl_4$, $CHBr_3$, $C_2H_2Br_4$ and in presence of organic bases ($\sim 10^{-2}$ M/l) pyridine, 2-methylpyridine, 2,4,6-trimethylpyridine, aniline, N-methylaniline, N,N-dimethyl-1,4-phenylenediamine, N,N-dimethylaniline, and N,N,N′,N′-tetramethyl-1,4-phenylenediamine was studied. It was found that interaction of $Cu(II)(dtc)_2$ does not proceed only in the presence of the last two bases. The intermediate reaction product detected by EPR method was the mixed-ligand complex $Cu(II)(dtc)X_n$ containing one or two halogen atoms. Typical EPR spectra are shown on Fig. 1 and the data for all studied mixed-ligand complexes are listed in Table 1. Attempts to record frozen solution EPR spectra at 77 K were unsuccessful—only unresolved broad singlet EPR spectra were obtained. In all cases the final reaction products were the complex $CuX_2B_n$ and an unstable resin-like residue. In the case of N,N - dimethyl - 1,4 - phenylenediamine the EPR spectrum of the cation-radical of the base was recorded simultaneously with the appearance of the mixed-ligand complex.

As has been pointed out, in the presence of N,N-dimethylaniline and N,N,N′,N′ - tetramethyl-1,4 - phenylenediamine such interaction has not been observed. However, in sample containing N,N,N′,N′ - tetramethyl - 1,4 - phenylenediamine the EPR spectrum of the cation–radical of the base was recorded under illumination (diffuse day light),

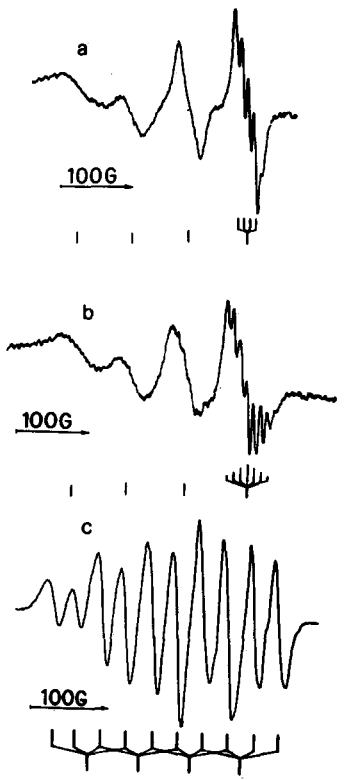



Fig. 1. Room temperature EPR spectra of the intermediate mixed–ligand complexes $Cu(II)(dtc)X_n$ obtained in the reactions of $Cu(II)(dtc)_2$ with: (a) $CCl_4$ + pyridine, $n = 1$. (b) $CCl_4$ + 2,4,6-trimethylpyridine, $n = 2$. (c) $C_2H_2Br_4$ + pyridine, $n = 1$.

Table 1. EPR parameters of the mixed-ligand complexes obtained in the reactions of adducts of $Cu(II)(dtc)_2$ and Cu(I)(dtc) with haloalkanes ($T = 300$ K)

| Complex | Base | Halo-alkane | Mixed-ligand complex | $g_o \pm 0.001$ | $Cu A_o$ ±1G | $X A_o$ ±0.5G |
|---|---|---|---|---|---|---|
| $Cu(II)(dtc)_2$ | - | $CCl_4$ | - | 2.046 | 79 | - |
| Cu(I)(dtc) | - | $CCl_4$ | Cu(II)(dtc)Cl | 2.063 | 73 | 8.0 |
| Cu(I)(dtc) | ethanol | $CCl_4$ | Cu(II)(dtc)Cl | 2.072 | 72 | 9.6 |
| $Cu(II)(dtc)_2$ | pyridine | $CCl_4$ | Cu(II)(dtc)Cl | 2.081 | 70 | 9.1 |
| Cu(I)(dtc) | pyridine | $CCl_4$ | Cu(II)(dtc)Cl | 2.081 | 70 | 9.1 |
| $Cu(II)(dtc)_2$ | 2,4,6-trimethylpyridine | $CCl_4$ | $Cu(II)(dtc)Cl_2$ | 2.072 | 75 | 10.2 |
| Cu(I)(dtc) | ethanol | $CCl_4$ | $Cu(II)(dtc)Cl_2$ | 2.071 | 75 | 10.2 |
| $Cu(II)(dtc)_2$ | aniline | $CCl_4$ | Cu(II)(dtc)Cl | 2.069 | 76 | 8.4 |
| $Cu(II)(dtc)_2$ | DMPDA[x] | $CCl_4$ | Cu(II)(dtc)Cl(?) | 2.072 | 77 | xx |
| $Cu(II)(dtc)_2$ | pyridine | $C_2Cl_6$ | Cu(II)(dtc)Cl | 2.080 | 72 | 9.3 |
| Cu(I)(dtc) | ethanol | $C_2Cl_6$ | Cu(II)(dtc)Cl | 2.072 | 72 | 9.4 |
| $Cu(II)(dtc)_2$ | pyridine | $C_2H_2Br_4$ | Cu(II)(dtc)Br | 2.081 | 64 | 33.0 |
| Cu(I)(dtc) | ethanol | $C_2H_2Br_4$ | Cu(II)(dtc)Br | 2.069 | 78 | 38.0 |
| $Cu(II)(dtc)_2$ | aniline | $C_2H_2Br_4$ | Cu(II)(dtc)Br | 2.065 | 77 | 37.0 |
| $Cu(II)(dtc)_2$ | DMPDA[x] | $C_2H_2Br_4$ | Cu(II)(dtc)Br | 2.077 | 68 | 36.0 |

[x] N,N-dimethyl-1,4-phenylenediamine

[xx] Not estimated due to the overlapping with the spectrum of the cation-radical of N,N-dimethyl-1,4-phenylenediamine

without any visible changes in the EPR spectrum of $Cu(II)(dtc)_2$ complex.

In order to explain the above results the adduct formation between $Cu(II)(dtc)_2$ and some of the bases used has been studied. The investigations were carried out in toluene solution at 300 and 77 K and the data obtained are listed in Table 2. The adduct formation between some of the bases and copper(II) acetylacetonate complex, which is known[11] to be a stronger Lewis acid than $Cu(II)(dtc)_2$ has also been studied (Table 2).

(b) *Interactions of* Cu(I)(dtc) *complex with haloalkanes.*

It was found that the Cu(I)(dtc) complex in haloalkanes/ethanol solution slowly reacted with the solvent with the formation of mixed-ligand $Cu(II)(dtc)X_n$ complex detected by EPR. Well resolved superhyperfine splitting (shfs) from one or two halogen nuclei (Fig. 2) was found in the EPR spectra at 300 K depending on the ratio $RX_n$/EtOH (from 1:4 to 4:1 v/v), whereas at low temperature (77 K) the spectrum was not resolved and only hf lines from $^{63,65}Cu$ were observed.

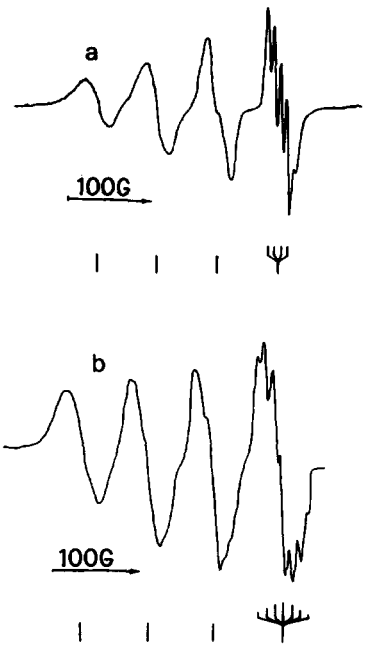



Fig. 2. Room temperature EPR spectra of the mixed-ligand complexes $Cu(II)(dtc)Cl_n$ obtained in the reactions of Cu(I)(dtc) with: (a) $CCl_4$, $n = 1$. (b) $CCl_4$ + ethanol, $n = 2$.

Table 2. EPR parameters of $Cu(dtc)_2$ and $Cu(acac)_2$ adducts with different Lewis bases

| Base | $Cu(acac)_2$ | | | | $Cu(dtc)_2$ | |
|---|---|---|---|---|---|---|
| | $g_{\parallel} \pm 0.003$ | $g_{\perp} \pm 0.002$ | $A_{\parallel}$ ±3 G | $A_{\perp}$ ±2 G | $g_{\parallel} \pm 0.003$ | $A_{\parallel}$ ±3 G |
| - | 2.250 | 2.052 | 180 | 25 | 2.087 | 164 |
| 4-nitroaniline | 2.277 | 2.065 | 162 | 19 | 2.087 | 164 |
| 4-chloraniline | 2.283 | 2.064 | 159 | 17 | 2.108 | 160 |
| N-phenyl-1-naphtylamine | 2.276 | - | 166 | - | 2.087 | 164 |
| 1-naphtylamine | 2.276 | 2.066 | 160 | 17 | 2.087 | 164 |
| aniline | 2.281 | 2.064 | 161 | 17 | 2.109 | 159 |
| p-toluidine | 2.277 | 2.064 | 160 | 16 | 2.109 | 159 |
| 4-ethoxyaniline | 2.283 | 2.064 | 158 | 16 | 2.109 | 157 |
| DMPDA[x] | 2.281 | 2.065 | 156 | 15 | 2.109 | 154 |
| pyridine | 2.290 | 2.067 | 152 | 13 | 2.110 | 147 |
| N,N-dimethyl-aniline | 2.250 | 2.052 | 180 | 25 | 2.087 | 164 |
| TMPDA[xx] | 2.250 | 2.052 | 180 | 25 | 2.087 | 164 |

[x] N,N-dimethyl-1,4-phenylenediamine

[xx] N,N,N',N'-tetramethyl-1,4-phenylenediamine

Cu(II)(dtc)X was found to be the final reaction product.

When 1,1-diphenyl-2-picrylhydrazine (DPPH–H) was added to the reaction mixture the EPR spectrum of DPPH free radical was recorded simultaneously with that of the mixed-ligand complex Cu(II)(dtc)X. However, the increase in concentration of the free radical was not proportional to that of Cu(II)(dtc)X complex.

When Lewis bases were added to the solution of Cu(II)(dtc)X complex in haloalkanes or in toluene the EPR parameters were shifted to higher $g$-values and lower $A$-values and the shfs from the halogen nuclei was not well resolved (see Table 3). These changes appeared very well at low temperature (77 K) too. The EPR spectrum obtained in ratio Cu(II)(dtc)X/py = 1:4 (v/v) at 77 K is given in Fig. 3.

In solution not containing halogen atoms (benzene, toluene, heptane, etc.) and in the absence of oxygen and moisture the Cu(I)(dtc) complex is stable and oxidation of copper(I) was not detected.

## DISCUSSION

It is well known[5–8] that the bases used form weak donor-acceptor complexes with haloalkanes. Based on the increase in the ionization potentials of the donors,[12] the stability of the D–A complexes should increase in the following order: aniline < N,N - dimethylaniline < N,N - dimethyl-

Table 3. EPR parameters of the mixed-ligand complexes depending on the bases (solvent–toluene) $T = 77$ K

| Mixed-ligand | Base | $g_{\parallel} \pm 0.003$ | $g_{\perp} \pm 0.002$ | $Cu_{A_{\parallel}}$ ±2G | $Cu_{A_{\perp}}$ ±2G | $shf_{A_{\perp}}$ ±1G |
|---|---|---|---|---|---|---|
| $Cu(dtc)_2$ | - | 2.087 | 2.025 | 164 | 41 | - |
| Cu(dtc)Cl | - | 2.110 | 2.040 | 159 | 30 | - |
| Cu(dtc)Cl | ethanol | 2.171 | 2,046 | 156 | 25 | - |
| Cu(dtc)Cl | pyridine | 2.240 | - | 152 | - | 11.5 |

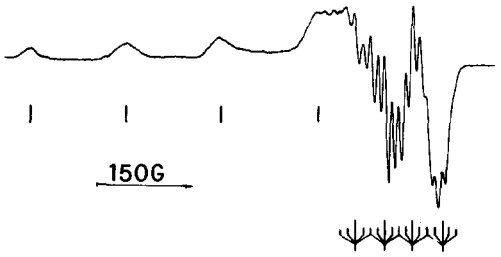
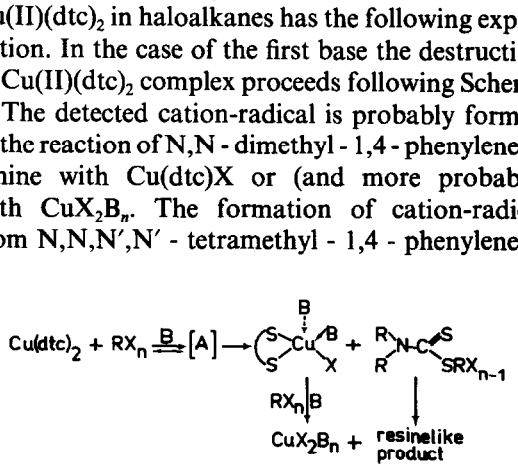



Fig. 3. EPR spectrum of Cu(II)(dtc)Cl complex dissolved in toluene–pyridine mixture (9:1 v/v) $T = 77$ K.

1,4 - phenylenediamine < N,N,N′,N′ - tetramethyl - 1,4 - phenylenediamine. Therefore, haloalkanes should follow the same order of activation provided CTC with the base is an intermediate product, necessary for the reaction to take place. However, the present studies have shown that $Cu(II)(dtc)_2$ does not react with haloalkanes in the presence of N,N-dimethylaniline and N,N,N′,N′ - tetramethyl - 1,4 - phenylenediamine independently of the strong CTC which they form with the solvent. On the other hand, it is evident from the data of Table 2 that the adduct formation is a necessary step for the reaction to take place. Therefore, it must be concluded that the complex (A) is the intermediate product of the reaction.

Having in mind the above results as well as the fact that the reaction proceeds without free radical formation,[2] the following alternative reaction mechanism (Scheme 2) is suggested. Electron transfer from S atom of the ligand to $RX_n$ is realized within the complex (A). Further the mixed-ligand complex Cu(II)(dtc)X and the ester dtc-$RX_{n-1}$ are formed without free radical formation.

The formation of cation-radical of N,N-dimethyl-1,4-phenylenediamine and N,N,N′,N′ - tetramethyl-1,4-phenylenediamine in solution of $Cu(II)(dtc)_2$ in haloalkanes has the following explanation. In the case of the first base the destruction of $Cu(II)(dtc)_2$ complex proceeds following Scheme 2. The detected cation-radical is probably formed in the reaction of N,N - dimethyl - 1,4 - phenylenediamine with Cu(dtc)X or (and more probably) with $CuX_2B_n$. The formation of cation-radical from N,N,N′,N′ - tetramethyl - 1,4 - phenylenediamine should be considered as a result of the formation of CTC with haloalkanes yielding free radicals under illumination.[5] The cation-radical does not react with $Cu(II)(dtc)_2$ independently of the fact that the latter reacts effectively with free radicals of the type $R^{\cdot}$, $RO^{\cdot}$, $RO_2^{\cdot}$.[11]




Scheme 2.

The interaction of Cu(I)(dtc) complex with haloalkanes without reaction promoters (Lewis bases) could be explained with the relatively higher donor properties of the complex. The interaction is connected with the oxidation of Cu(I)(dtc) to Cu(II)(dtc)X. This result is not surprizing since many reactions of Cu(I) salts with haloalkanes are known,[14–16] which are connected with a free radical formation ($\dot{C}Cl_3$ for example) and oxidation of copper(I). The appearance of DPPH free radical in our reaction system has shown the presence of free radicals in the reaction mixture.[15] The results obtained suggest the following reaction scheme:

$$Cu(I)(dtc) + RX_n \rightarrow Cu(I)(dtc) \ldots RX_n \rightarrow$$

$$Cu(II)(dtc)_X + \dot{R}X_{n-1}$$

The free radicals obtained may recombine with the formation of $X_{n-1}R\text{–}RX_{n-1}$ which could be involved again in the reaction with Cu(I)(dtc).

The difference in the EPR parameters of Cu(II)(dtc)X mixed–ligand complex obtained under different experimental conditions (in the presence or absence of the bases—Tables 1 and 3), suggested the coordination of base molecules to the complex. The Cu(II)(dtc)X complex has one free coordination place in the *xy* plane and additionally axial coordination is also possible. The dependence of the EPR parameters on the solvent properties is detectable even at 300 K. Whereas Cu(II)(dtc)X complex obtained in the interaction of Cu(I)(dtc) with $CCl_4$ in the presence of toluene shows the lowest $g$-value, the one recorded in the presence of pyridine shows highest $g$-values. The changes in the EPR parameters due to the coordination properties of the solvent are readily detectable at 77 K (Table 3). The fact that at 77 K in the presence of pyridine shfs from $^{14}N$ nuclei was observed in Cu(dtc)X mixed–ligand complex unambiguously shows that the base molecule is coordinated in the *xy* plane of copper(II).

## REFERENCES

1. Part VII of this series, N. D. Yordanov and V. Alexiev, *Commun. Dept. Chem. Bulg. Acad. Sci.* 1983, in press.
2. N. D. Yordanov, V. Iliev, V. Terziev and D. Shopov, *Inorg. Chim. Acta* 1982, **60**, 21.

3. N. D. Yordanov, V. Iliev and D. Shopov, *Compt. rend. Acad. Sci. Bulg.* 1976, **29**, 1653.
4. N. D. Yordanov, *J. Mol. Structure* 1978, **47**, 107.
5. S. Leach and R. Lopez-Delgado, *Compt. Rend.* 1963, **256**, 1299.
6. D. P. Stevenson and G. M. Coppinger, *J. Am. Chem. Soc.* 1962, **84**, 149.
7. V. Iliev and S. Dyankov, *Commun. Dept. Chem. Bulg. Acad. Sci.* 1976, **9**, 506.
8. J. M. Dumas, C. Geron, H. Paurichard and M. Gomel, *Bull. Soc. Chim. France* 1976, 720.
9. L. Sacconi and I. Bertini, *Inorg. Chem.* 1976, **5**, 1520.
10. S. Akerstrom, *Arkiv Kemi* 1959, **14**, 387; 403.
11. N. D. Yordanov and D. Shopov, In *Theory, Structure, Properties of Complex Compounds* (Edited by B. Jezowska-Trzebiatowska, J. Legendziewicz and M. F. Rudolf), p. 313. Polish Scientific Publishers (1979).
12. H. McConnell, J. S. Ham and J. R. Platt, *J. Chem. Phys.* 1953, **21**, 66.
13. M. Asscher and D. Vofsi, *J. Chem. Soc.* (*B*) 1968, 947; 1964, 962.
14. S. Uemura, A. Onoe and M. Okano, *J. Chem. Soc. Chem. Comm.* 1975, 925.
15. E. S. Huyser and R. H. S. Wang, *J. Org. Chem.* 1968, **33**, 3901.
16. J. K. Kochi (Editor) *Free Radicals*, Chap. 11. Wiley Interscience, New York (1973).

*Polyhedron* Vol. 3, No. 3, pp. 297–301, 1984
Printed in Great Britain.

0277–5387/84 $3.00 + .00
© 1984 Pergamon Press Ltd.

# STUDIES ON THE INTERMOLECULAR INTERACTIONS OF METAL CHELATE COMPLEXES—IX

## ON THE INTERACTION OF COPPER(II) DITHIOCARBAMATE WITH SOME LEWIS ACIDS

**V. ILIEV, N. D. YORDANOV* and D. SHOPOV**
Institute of Organic Chemistry, Bulgarian Academy of Sciences, 1113 Sofia, Bulgaria

(*Received* 29 *April* 1983; *accepted* 25 *July* 1983)

**Abstract**—The intermediate products of the reaction between copper(II) dithiocarbamate complex and some Lewis acids ($HgI_2$, $HgBr_2$, $GeCl_4$, $AsBr_3$, $CoCl_2$, $C(NO_2)_4$) as well as some organometallic compounds ($SnEt_4$ and $PbEt_4$) were studied using EPR spectroscopy. In non-polar and non-coordinating solvents $HgI_2$, $HgBr_2$ and $GeCl_4$ formed adducts with $Cu(dtc)_2$, whereas in polar and coordinating solvents the mixed-ligand complexes of the type $Cu(dtc)^+ \ldots A^-$ ($A = HgX_3$) were obtained with a complex counterion in the second coordination sphere of copper(II). With $C(NO_2)_4$ the intermediate reaction product in non-polar solvents was assumed to be $Cu(dtc)\cdot NO_2$ which dissociates to $Cu(dtc)^+ \ldots NO_2^-$ in polar solvents. Similar EPR spectra were obtained with $SnEt_4$ and $PbEt_4$. The reaction of $Cu(dtc)_2$ with $CoCl_2$, $AsBr_3$ and $SbCl_3$ yielded the mixed-ligand complexes of the type $Cu(dtc)X_n$ ($n = 1$ or 2) exhibiting well resolved superhyperfine splitting from one or two halogen nuclei. The influence of the medium on the above interaction is also discussed.

Previous papers from this laboratory[1–6] dealt with the interactions of copper(II) dithiocarbamates [$Cu(dtc)_2$], dithiophosphates and acetylacetonate with Lewis acids of the type $CuX_2$ (X = Cl, Br), $CuY_2$ (Y = $NO_3$, $ClO_4$), $SnCl_4$, $SbBr_3$. The formation of the mixed-ligand complex $CuLX_n$, $CuL^+ \ldots Y^-$ where L = dtc, dtp, acac and $n = 1$ or 2 was found. Evidence for the mixed-ligand complexation was found in the appearance of new EPR spectra with additional superhyperfine splitting (shfs) from one[1–6] or two[3,6] halogen nuclei in the case of $CuLX_n$. The observed shfs suggested the location of the halogen atom in the first coordination sphere of the metal ion. These conclusions have been recently confirmed by other authors with EPR[7] and X-ray diffraction data on Cu(dtc)X species.[8–10]

Metal complexes of the type $M(dtc)_n$ and $M(dtp)_n$ are widely applied as antioxidants in lubricating oils, motor fuel, plastics, resins, etc. On the other hand the hydrocarbons kept in stock or when used become often in contact with metal salts, organometallic compounds or contain them as ingredients or pollutants. The influence of these additives or ingredients on $M(dtc)_n$ and $M(dtp)_n$ have not been studied till now. The purpose of the present study is to find the changes appearing as a result of the interaction of different Lewis acids like $HgI_2$, $HgBr_2$, $GeCl_4$, $SbCl_3$, $AsBr_3$, $CoCl_2$, $C(NO_2)_4$ as well as the organometallic compounds $SnEt_4$ and $PbEt_4$ on a model complex—$Cu(dtc)_2$. The previous studies[1–6,11–13] have shown that EPR method is very sensitive and powerful in following such interactions and making definite conclusions on the reaction products.

## EXPERIMENTAL

$Cu(dtc)_2$ complex was obtained by $CHCl_3$ extraction from water solution of Na(dtc) and $CuCl_2$. The complex was purified by recrystallization from $CHCl_3$ and ethanol (1:1 v/v).

Reagent grade $HgI_2$, $HgBr_2$, $AsBr_3$, $SbCl_3$, $C(NO_2)_4$, $CoCl_2\cdot 6H_2O$ obtained from Fluka, $GeCl_4$ from Merck and $PbEt_4$ from Alfa were used without further purification.

$CoCl_2\cdot 6H_2O$ was dehydrated by heating under vacuum before use.

*Author to whom correspondence should be addressed.

All solvents—toluene, ethanol, $CCl_4$, diethylformamide (DEFA) were purified and dried by standard methods.

The EPR spectra were recorded at 300 and 77 K on a 3BS-X spectrometer using 100 kHz modulation of the magnetic field. The magnetic field was calibrated with $Mn^{2+}$ doped in MgO, and the $g$-values were calculated relative to DPPH.

## RESULTS

Depending on the solubility of the Lewis acids and the products of their interaction with $Cu(dtc)_2$ complex the studies have been carried out in non-polar and non-coordinating (toluene, $CCl_4$) as well as in more polar and coordinating (toluene–ethanol 1:1 v/v, toluene–DEFA 1:1 v/v) solvents. The EPR parameters of all studied complexes are listed in Table 1.

(1) *Interaction of* $Cu(dtc)_2$ *complex with Lewis acids in toluene*

The interaction of $Cu(dtc)_2$ ($\sim 10^{-3}$ M/l) with $HgI_2$, $C(NO_2)_4$ ($\sim 10^{-2}$ M/l) and $GeCl_4$, $SnEt_4$, $PbEt_4$ ($\sim 10^{-3}$ M/l) has been studied in toluene. Turbidity was observed at higher concentrations because of the low solubility of the Lewis acids and mainly that of the products of their interaction with $Cu(dtc)_2$.

The EPR spectra of $Cu(dtc)_2$ detected at 300 K remained unchanged in the presence of $HgI_2$ or $GeCl_4$. EPR spectrum with higher $g$-values and lower hyperfine splitting of $^{63,65}Cu$ compared with the initial $Cu(dtc)_2$ complex (Fig. 1a) was obtained in the case of $HgI_2$ at 77 K. In the presence of $GeCl_4$ two EPR spectra were obtained at 77 K—one of the initial $Cu(dtc)_2$ complex and a second one whose parameters were slightly different from those of $Cu(dtc)_2$—Fig. 1(b).

Two EPR spectra have been recorded at both 300 and 77 K in the reaction of $Cu(dtc)_2$ with $SnEt_4$, $PbEt_4$ and $C(NO_2)_4$—one of the initial $Cu(dtc)_2$ complex and a second one whose parameters were equal for all Lewis acids used (Fig. 2).

(2) *Interaction of* $Cu(dtc)_2$ *complex with Lewis acids in toluene–ethanol or toluene–DEFA*

The interaction of $Cu(dtc)_2$ complex ($\sim 10^{-3}$ M/l) with $HgBr_2$, $SbCl_3$, $AsBr_3$ and $CoCl_2$ ($\sim 10^{-2} \div 10^{-1}$ M/l) was studied. At higher concentrations $Cu(dtc)_2$ was completely destroyed and only a singlet EPR spectrum with $g \approx 2.15$ was recorded.

The interaction of $Cu(dtc)_2$ with $AsBr_3$, $SbCl_3$ or $CoCl_2$ yielded new EPR spectra with shfs from halogen nuclei additional to the $^{63,65}Cu$ hfs. EPR spectra with equal parameters and shfs from one

Table 1. EPR parameters of the products obtained in the reaction of $Cu(dtc)_2$ with the studied Lewis acids

| Lewis acid | Solvent | Associate or mixed-ligand complex | $g_o$ | $A_o$ | $A_o^X$ | $g_\parallel$ | $g_\perp$ | $A_\parallel$ | $A_\perp$ | $A^X$ |
|---|---|---|---|---|---|---|---|---|---|---|
| - | toluene | - | 2.046 | 79 | - | 2.087 | 2.025 | 164 | 41 | - |
| | toluene-ethanol | - | 2.046 | 79 | - | 2.087 | 2.025 | 164 | 41 | - |
| $HgI_2$ | toluene | $Cu(dtc)_2.HgI_2$ | 2.046 | 79 | - | 2.093 | 2.030 | 158 | 38 | - |
| $GeCl_4$ | toluene | $Cu(dtc)_2.GeCl_4$ | 2.046 | 79 | - | 2.093 | 2.026 | 159 | 41 | |
| $HgI_2$ | toluene-ethanol | $Cu(dtc)^+..HgI_3^-$ | 2.089 | 68 | - | 2.180 | 2.049 | 154 | 22 | - |
| $HgBr_2$ | toluene-ethanol | $Cu(dtc)^+...HgBr_3^-$ | 2.087 | 68 | - | 2.180 | 2.049 | 156 | 22 | - |
| $SnEt_4$ | toluene | (?) | 2.066 | 77 | - | 2.123 | 2.034 | 168 | 43 | - |
| $SnEt_4$ | toluene-ethanol | (?) | 2.066 | 77 | - | 2.123 | 2.034 | 168 | 44 | - |
| $PbEt_4$ | toluene | (?) | 2.066 | 77 | - | 2.120 | 2.038 | 168 | 43 | - |
| $PbEt_4$ | toluene-ethanol | (?) | 2.066 | 77 | - | 2.122 | 2.035 | 168 | 43 | - |
| $C(NO_2)_4$ | toluene | $Cu(dtc).NO_2$ | 2.066 | 78 | - | 2.122 | 2.032 | 165 | 42 | - |
| $C(NO_2)_4$ | toluene-ethanol | $Cu(dtc)^+...NO_2^-$ | 2.090 | 67 | - | 2.180 | 2.049 | 155 | 23 | - |
| $CoCl_2$ | toluene-ethanol | Cu(dtc).Cl | 2.073 | 74 | 8 | - | - | - | - | - |
| $SbCl_3$ | toluene-ethanol | Cu(dtc).Cl | 2.070 | 73 | 8 | - | - | - | - | - |
| $AsBr_3$ | toluene-ethanol | Cu(dtc).Br | 2.052 | 78 | 43 | - | - | - | - | - |
| $AsBr_3$ | toluene-DEFA | Cu(dtc).2Br | 2.050 | 77 | 43 | 2.060 | 2.030 | 142 | 42 | 52 |

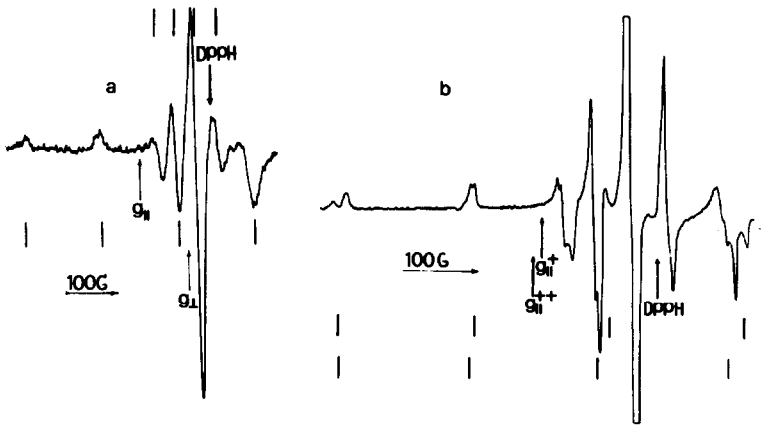



Fig. 1. Frozen solution EPR spectra recorded during the reaction of $Cu(dtc)_2$ with (a) $HgI_2$, (b) $GeCl_4$ ((+) $Cu(dtc)_2$ lines, and (+ +) $Cu(dtc)_2 \cdot GeCl_4$ in toluene).

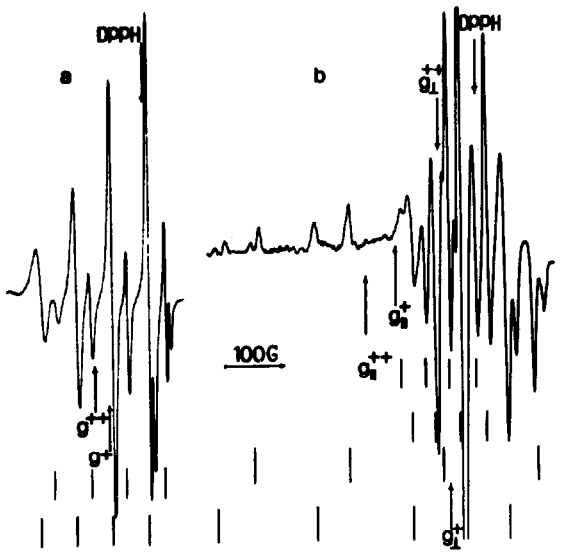



Fig. 2. EPR spectra recorded in the reaction of $Cu(dtc)_2$ with $SnEt_4$ in toluene: (a) room temperature spectrum; (b) frozen solution spectrum, (+) $Cu(dtc)_2$ lines and (+ +) mixed-ligand complex spectrum.

Cl nucleus not recorded at 77 K were recorded at 300 K in the presence of $CoCl_2$ or $SbCl_3$. In the presence of $AsBr_3$ in toluene–ethanol and toluene–DEFA solvents the 300 and 77 K EPR spectra revealed the appearance of a new mixed-ligand complex with two Br nuclei (Fig. 3).

The interactions of $Cu(dtc)_2$ with $HgI_2$, $HgBr_2$, $SnEt_4$, $PbEt_4$ or $C(NO_2)_4$ were studied in order to follow the influence of the polarity and the coordinating properties of the medium in toluene–ethanol mixture. New EPR spectra were recorded in the presence of $HgI_2$ or $HgBr_2$ at 300 K with equal parameters (compare with the parameters obtained in pure toluene—Table 1). The parameters of the EPR spectra at 77 K of the new complexes were also different from those recorded in toluene and in presence of $HgI_2$ (Fig. 4).

The EPR parameters of the complexes obtained in the reaction of $Cu(dtc)_2$ with $SnEt_4$, $PbEt_4$ in toluene–ethanol solution were equal to those recorded in pure toluene. Only in the presence of

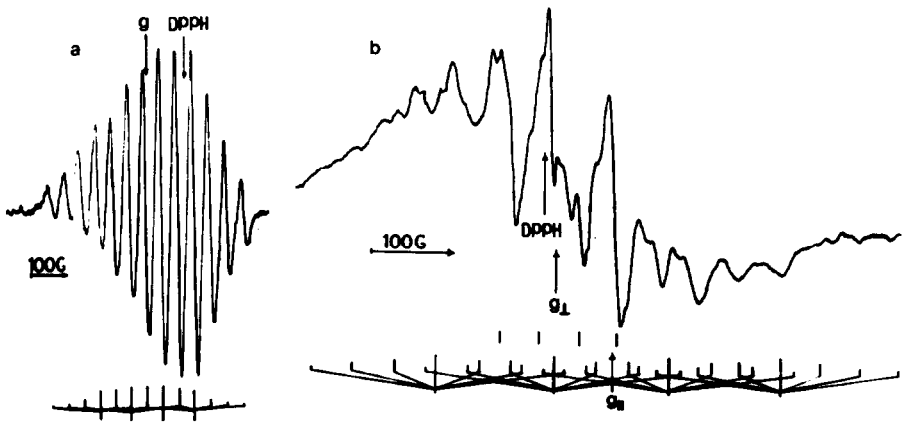



Fig. 3. EPR spectra recorded in the reaction of $Cu(dtc)_2$ with $AsBr_3$ in toluene–DEFA mixture: (a) 300 K, (b) 77 K.

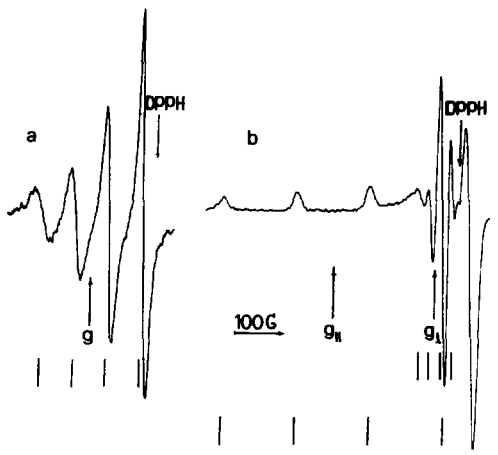
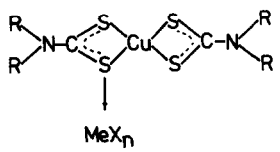



Fig. 4. EPR spectra recorded in the reaction of $Cu(dtc)_2$ with $HgI_2$ in toluene–ethanol mixture: (a) 300 K, (b) 77 K.

$C(NO_2)_4$ new EPR spectrum with higher $g$- and A-values has been recorded.

## DISCUSSION

In order to explain the above results it is reasonable to assume that the first stage of the reaction is the formation of donor–acceptor complex between $Cu(dtc)_2$ complex and the Lewis acids of the type (**I**) (Scheme 1). This assumption is based on




the data about the interaction of organic sulphur-containing hydrocarbons with the studied Lewis acids.[14] On the other hand, depending on the electron ability ($E_a$) as well as both the frequency shifts in the IR spectra of carbonyl compounds coordinated to the used acceptors,[15] and thermodynamic parameters of the D–A complexes,[14] the Lewis acids could form the following order of increasing acceptor properties:

$$CCl_4 < GeCl_4 < CoCl_2 < HgX_2 < AsBr_3 < SbCl_3 < C(NO_2)_4.$$

The formation of mixed-ligand complex within the D–A complex depends on the possibility of atomic rearrangement in it. This factor, as pointed out[12] depends to a great extent on the polarity and coordinating properties of the medium.

The EPR parameters of the complexes obtained during the interaction of $Cu(dtc)_2$ with the weak Lewis acids ($CCl_4$, $GeCl_4$, $HgI_2$) dissolved in toluene or toluene–ethanol could be interpreted in the following manner:

(i) In non-polar, non-coordinating solvents (toluene, $CCl_4$) the appearance of new EPR spectra suggested the formation of D–A complex of the type (**I**), according to $Cu(dtc)_2 + A \rightleftharpoons Cu(dtc)_2 \cdot A$, where $A = HgI_2$ or $GeCl_4$.

If this happens the changes in the EPR parameters at 77 K compared to the data obtained at 300 K could be attributed to the above equilibrium shifted to the right at lower temperature. Since the $g$-values are increased while A decreases comparing to the initial $Cu(dtc)_2$ complex decreasing of the electron density (or deformation) in the chelate ring might have happened. X-Ray diffraction data about the associates of $Cu(dtc)_2$ complex with $ZnCl_2$, $CdX_2$, or $HgX_2$,[10] have confirmed the above assumption. The EPR parameters obtained could be considered as characteristic for D–A complexes of $Cu(dtc)_2$ (structure (**I**)) with Lewis acids coordinated around the sulphur atom of the chelate ring. With $CCl_4$ such changes in the EPR parameters both at 300 and 77 K have not been detected probably due to its significantly low electron acceptor properties (for $CCl_4$ $E_a = 0.15$ eV, whereas for $GeCl_4$ $E_a = 0.87$ eV[16]).

(ii) In more polar medium (toluene–ethanol) the significant changes in the EPR parameters of the new complexes obtained in the reaction of $Cu(dtc)_2$ with $HgI_2$ or $HgBr_2$ at 300 and 77 K are probably due to mixed-ligand complexes of the type $Cu(dtc)^+ \ldots X^-$. The absence of shfs from halogen atoms and the equality of the EPR parameters suggest that $X^-$ are not coordinated in the first coordination sphere of copper(II). Similar EPR parameters have been obtained in the reaction of $Cu(dtc)_2$ complex with $Cu(NO_3)_2$ and $Cu(ClO_4)_2$.[2,6] The X-ray diffraction data on the product of the reaction of $Cu(dtc)_2$ with $CdX_2$,[10] suggest that the EPR parameters could be considered as characteristic for mixed-ligand complexes with the structure $Cu(dtc)^+ \ldots A^-$, where $A = HgX_3$, i.e. with complex counterion in the second coordination sphere.

The failure to obtain the EPR parameters corresponding to the D–A complex (**I**) with stronger Lewis acids $AsBr_3$, $C(NO_2)_4$, $SbCl_3$, $CoCl_2$, as well as with organometallic compounds $SnEt_4$ and $PbEt_4$ is probably due to the stronger D–A interaction yielding mixed-ligand complexes. (i) The higher $g$-values of the complexes obtained in the reaction of $Cu(dtc)_2$ with $SnEt_4$, $PbEt_4$ or $C(NO_2)_4$ in toluene suggest more ionic copper-ligand bonds compared to the initial complex. The EPR parameters of the product obtained in the reaction of $Cu(dtc)_2$ with $C(NO_2)_4$ and $Cu(dtc) \cdot NO_2$ are equal to the parameters of the mixed-ligand complexes obtained in the reaction of $Cu(dtc)_2$ with $NO_2$.[11] The EPR parameters obtained during the inter-

action of the same reagents in toluene–ethanol solution must be considered as mixed-ligand complex of the type $Cu(dtc)^+ \ldots NO_2^-$ in which $NO_2^-$ is located in the second coordination sphere of copper(II). This conclusion is supported by the previous EPR studies[2,6] on the interaction of $Cu(dtc)_2$ with $Cu(NO_3)_2$ and $Cu(ClO_4)_2$ as well as with the approximate equality of the parameters obtained in the interaction of $Cu(dtc)_2$ with $HgI_2$ or $HgBr_2$ in toluene–ethanol.

It is difficult to find a reasonable explanation of the new complexes obtained in the reaction of $Cu(dtc)_2$ with $SnEt_4$ and $PbEt_4$, however the interaction between them is experimentally established.

(ii) The interaction of $Cu(dtc)_2$ with $CoCl_2$, $AsBr_3$ or $SbCl_3$ in polar medium is connected with the formation of mixed-ligand complexes in which shfs from one Cl or two Br nuclei is an evidence of their coordination to copper(II). Having in mind our previous studies,[1–6] as well as X-ray diffraction data about similar complexes,[8–10] it is reasonable to consider these complexes as Cu(dtc)Cl and $[Cu(dtc)2Br]^-$ respectively.

## REFERENCES


1. N. D. Yordanov, *Teoret. Eksp. Khim.* 1973, **9**, 709.
2. N. D. Yordanov and D. Shopov, *J. Inorg. Nucl. Chem.* 1976, **38**, 137.
3. N. D. Yordanov, V. Terziev and D. Shopov, *Compt. rend. Acad. Sci. Bulg.* 1974, **27**, 1529.
4. N. D. Yordanov, N. Nicolov, A. Shishkov and D. Shopov, *Inorg. Nucl. Chem. Lett.* 1976, **12**, 527.
5. N. D. Yordanov, V. Terziev, V. Iliev and D. Shopov, *Compt. rend Acad. Sci. Bulg.* 1977, **30**, 675.
6. N. D. Yordanov, *J. Mol. Structure* 1978, **47**, 107.
7. W. J. Newton and B. J. Tabner, *J. Chem. Soc. Dalton* 1981, 466.
8. A. R. Hendrickson, R. L. Martin and D. Taylor, *J. Chem. Soc. Chem. Commun.* 1975, 843.
9. R. N. Furneaux and E. Sinn, *Inorg. Nucl. Chem. Lett.* 1976, **12**, 501.
10. J. Willemse, J. A. Cras, J. J. Steggerda and C. P. Keijzers, *Structure and Bonding* 1976, **28**, 83.
11. N. D. Yordanov, B. G. Zheliazkowa and V. Terziev, *Inorg. Chim. Acta* 1982, **58**, 213.
12. V. Iliev, N. D. Yordanov and D. Shopov, *Polyhedron* 1984, **3**, 291.
13. N. D. Yordanov and Yu. Karadzhov, *Polyhedron*, submitted for publication.
14. E. N. Gurijanova, I. P. Goldstein and I. P. Romm, Donorno-akzeptornaja svjaz, Khimia, Moscow (1973).
15. J. Yarwood (Editor), *Spectroscopy of Molecular Complexes*, Chap. 6. Plenum Press, New York (1973).
16. M. Hatano, Osh. Ito, *Bull. Chem. Soc. Japan* 1970, **43**, 3344.

*Polyhedron* Vol. 3, No. 3, pp. 303–305, 1984
Printed in Great Britain.

0277–5387/84 $3.00 + .00
© 1984 Pergamon Press Ltd.

# CRYSTAL AND MOLECULAR STRUCTURES OF HEXAAQUAZINC(II)ISONICOTINATE N-OXIDE AND CATENA-DIAQUABIS-$\mu$-(ISONICOTINATO N-OXIDE)CADMIUM(II)

PEKKA KNUUTTILA
Department of Chemistry, University of Jyväskylä, SF-40100 Jyväskylä 10, Finland

(*Received* 20 *May* 1983; *accepted* 2 *August* 1983)

**Abstract**—$[Zn(H_2O)_6](N\text{-inicO})_2$ is an ionic compound made up of hexaaqua metal cations and isonicotinate N-oxide anions. It forms an isomorphic series with the corresponding $Mg^{2+}$, $Fe^{2+}$, $Co^{2+}$ and $Ni^{2+}$ compounds.

In $[Cd(N\text{-inicO})_2(H_2O)_2]_n$ complex, coordination takes place through the N–O oxygen and one of the (COO) oxygens with ligand forming thus a double bridge between $Cd^{2+}$ ions. The structure is an endless chain stretching diagonally through the unit cell.

The coordination polyhedron in both compounds is almost undistorted octahedron.

The present work is a continuation of the X-ray structure determinations of metal complexes with monocarboxylic acid N-oxide carried out in this laboratory during recent years. The coordination with bivalent metal ions shows a wide variation. Picolinic acid N-oxide coordinates with 3*d* metals through the N–O oxygen and one of the (COO) oxygens, forming a stable six membered chelate ring.[1] Nicotinic acid N-oxides on the other hand, have been found to coordinate through the N–O oxygen only in three cases: *catena*-diaqua-di-$\mu$-hydroxo-bis-$\mu$-(nicotinato N-oxide)-bis-$\mu$-(nicotinato N-oxido)tricopper,[2] *catena*-diaquabis-$\mu$-(nicotinato N-oxido)copper(II)tetrahydrate[3] and dichlorobis(nicotinic acid N-oxide)copper(II).[4] In isonicotinic acid N-oxide 3*d* metal complexes the coordination occurs in different ways through the (COO) oxygens.[5–8]

The study on the coordination of monocarboxylic acid N-oxides is to be continued with bivalent non-transition elements. The structures of lead and calcium complexes have already been solved.

## RESULTS AND DISCUSSION

The coordination geometry around the central metal atom in $[Zn(H_2O)_6](N\text{-inicO})_2$ is almost undistorted octahedral, with bonding distances varying from 2.056(2) Å to 2.104(2) Å. The most important bond distances and angles are listed in Table 1. The Zn ion is situated at the special positions (0, 0, 0) and $(0, \frac{1}{2}, \frac{1}{2})$ of the space group $P2_1/c$. The compound forms an isomorphic series with $[Mg(H_2O)_6](N\text{-inicO})_2$,[9] $[Fe(H_2O)_6](N\text{-inicO})_2$,[5] $[Co(H_2O)_6](N\text{-inicO})_2$[6] and $[Ni(H_2O)_6](N\text{-inicO})_2$.[6] The bond lengths in aqua-octahedron lie between those of $Ni^{2+}$ and $Co^{2+}$ compounds, as would be expected on the basis of increasing ionic radius. The bonding distances in the isonicotinate N-oxide ions are comparable to those in the other members of the isomorphic series and are unexceptional. The angle and C–O distances in the carboxylate groups indicate complete ionization. The strong hydrogen bonds between aquo ligands and the oxygens of carboxylate and N-oxide groups stabilize the structure. The hydrogen bonds are listed in Table 1. All distances between the metal ion and the three oxygens of the isonicotinate N-oxide ion are greater than the contact distance 3.8 Å.

The coordination of isonicotinate N-oxide through N-oxide and carboxylic oxygens leads for steric reasons to a polymeric structure. However, the N-oxide group is a weaker coordinating group in aqueous solutions than the carboxylic group.[5–9] The distance between the N–O oxygen and the central metal Cd in $[Cd(N\text{–inicO})_2(H_2O)_2]_n$ is 2.332(1) Å, which is only slightly longer than Cd–O bond distances in the Cd coordination polyhedron, but the angle Cd–O1–N1 is 113.65(4)° and deviates considerably from the theoretical M–O–N angle of 120°. In polymeric copper complexes[2,3] the distances between copper and the N–O oxygen are about 0.5 Å longer than the other Cu–O distances,

Table 1. The most important bond distances and angles

| $\|Zn(H_2O)_6\|(N\text{-inicO})_2$ | | $\|Cd(N\text{-inicO})_2(H_2O)_2\|_n$ | |
|---|---|---|---|
| **In the coordination sphere** | | | |
| Zn-O4 | 2.056(2) Å | Cd-O1 | 2.332(1) Å |
| Zn-O5 | 2.059(2) | Cd-O2 | 2.253(1) |
| Zn-O6 | 2.104(2) | Cd-O4 | 2.299(1) |
| O4-Zn-O5 | 91.88(7)° | O1-Cd-O2 | 89.68(2)° |
| O4-Zn-O5 | 90.23(8) | O1-Cd-O4 | 92.56(2) |
| O5-Zn-O6 | 90.32(7) | O2-Cd-O4 | 91.10(2) |
| **In the isonicotinate N-oxide ions** | | | |
| N1-O1 | 1.327(3) Å | N1-O1 | 1.330(1) Å |
| C6-O2 | 1.248(4) | C6-O2 | 1.270(1) |
| C6-O3 | 1.250(3) | C6-O3 | 1.236(1) |
| C6-C5 | 1.509(3) | C6-C3 | 1.494(1) |
| O3-C6-O2 | 125.3(2)° | Cd-O2-C6 | 125.7(1)° |
| C6-C5-C3 | 120.5(3) | Cd-O1-N1 | 113.7(1) |
| | | O2-C6-O3 | 126.0(1) |
| | | C6-C3-C2 | 121.0(1) |
| **Hydrogen bonds** | | | |
| O6-H6...O1 | | O4-H5...O3 | |
| O6...O1 | 2.656(3) Å | O4...O3 | 2.622(1) Å |
| O6-H6 | 0.84(3) | O4-H5 | 1.21(1) |
| H6...O1 | 1.98(3) | H5...O3 | 1.41(1) |
| >O6-H6...O1 | 152(3)° | >O4-H5...O3 | 178(1)° |
| O5-H9...O2 | | O4-H6...O1 | |
| O5...O2 | 2.674(3) Å | O4...O1 | 2.734(1)·Å |
| O5-H9 | 0.76(4) | O4-H6 | 1.37(2) |
| H9...O2 | 1.97(4) | H6...O1 | 1.45(2) |
| >O5-H9...O2 | 162(4)° | >O4-H6...O1 | 152(1)° |
| O4-H8...O3 | | | |
| O4...O3 | 2.660(2) Å | | |
| O4-H8 | 0.69(4) | | |
| H8...O3 | 2.03(4) | | |
| >O4-H8...O3 | 152(5)° | | |

and the Cu–O–N angles are between 108.8(4)° and 125.8(1)°. In the $[CuCl_2(N\text{–nicOH})_2]$ complex coordination occurs only through the N–O oxygen, the bonding distance being 1.962(3) Å, and the angle, 120.1(2)°, is close to the theoretical value.[4]

The coordination to Cd does not change the angle O2–C6–O3. The bonding distances C6–O2 and C6–O3 are 1.270(1) Å and 1.236(1) Å, respectively, with the coordinated oxygen–carbon distance just slightly longer. The uncoordinated carboxylic oxygen atom O3 has a wider thermal motion than the coordinated atom O2.

## EXPERIMENTAL

The metal complexes of $[Zn(H_2O)_6](N\text{–inicO})_2$ and $[Cd(N\text{–inicO})_2(H_2O)_2]_n$ were prepared according to instructions given in the literature[6, 10, 11] except that solutions were more dilute. Gelfand *et al.*[11] have synthesized a compound formulated as $Zn(N\text{–inicO})_2(H_2O)_6$ and supposed that the N–inicO anion is coordinated to Zn–ion through the N–O oxygen and one of the (COO) oxygens, forming single bridges between adjacent metal ions. Palepu *et al.*[10] supposed $Cd(N\text{–inicO})_2(H_2O)_2$ to be coordinated in the same manner.

Crystal data $[Zn(H_2O)_6](N\text{–inicO})_2$, M = 449.68 monoclinic, $a = 7.775(3)$ Å, $b = 9.753(4)$ Å, $c = 11.405(5)$ Å, $\beta = 91.16°$, U = 864.6 Å$^3$; space group $P2_1/c$ $Z = 2$, $D_0 = 1.71$ gcm$^{-3}$, $D_c = 1.72$ F (000) = 464, $\mu$(Mo–K$\alpha$) = 15.37 cm$^{-1}$ $[Cd(H_2O)_2(N\text{–inicO}_2]_n$, M = 424.6 triclinic, $a = 5.696(2)$ Å, $b = 7.898(2)$ Å, $c = 11.900(4)$ Å, $\alpha = 90.86(3)°$, $\beta = 124.48(2)°$, $\gamma = 121.00(2)°$ and U = 340.8 Å$^3$; space group $P\bar{1}$ $Z = 1$, $D_0 = 2.06$ gcm$^{-3}$, $D_c = 2.07$, F (000) = 210, $\mu$(Mo–$K_\alpha$) = 16.46 cm$^{-1}$.

Data collection; for Zn compound, Syntex $P2_1$ diffractometer, Mo-$K_\alpha$ radiation ($\lambda = 0.71069$ Å graphite monochromator), $\omega$-scan technique $4° < 2\theta < 55°$, 2367 reflections measured, 1315 observed $|I > 3.0\delta(I)|$, no absorption correction. Cd compound, same as for Zn compound except $\theta/2\theta$ scan mode 1802 reflections measured, 1717 observed.

*Structure solution and refinement.* The structure of the Zn compound was refined by using the

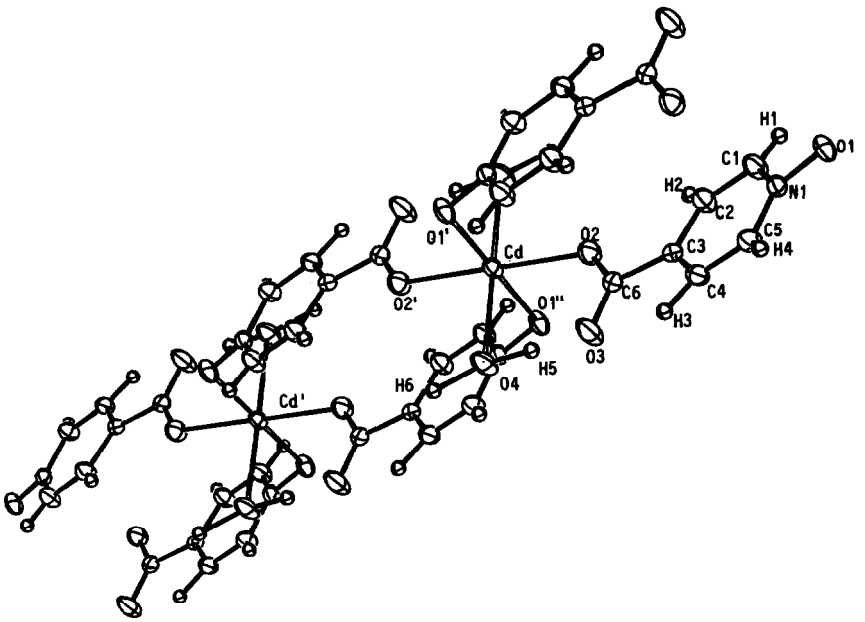



Fig. 1. An ORTEP drawing of $[Cd(N\text{–}inicO)_2(H_2O)_2]_n$ including the atomic labeling scheme. Thermal ellipsoids for nonhydrogen atoms are on 50% probability level.

coordinates of the other compounds in the isomorphic series.[6] Non-hydrogen atoms were assigned anisotropic and hydrogen atoms isotropic thermal parameters. Block-diagonal matrix least squares were used. The final R-value was 0.038

$$\left(R = \frac{\Sigma\|\Delta F_0| - |F_c\|}{\Sigma|F_0|}\right)$$

MULTAN 80[12] gave all coordinates for nonhydrogen atoms of $[Cd(H_2O)_2(N\text{–}inicO)_2]_n$. Refinement with those isotropic parameters gave an R-value of 0.08. After a final cycle in which hydrogen atoms located from a Fourier map were refined isotropically and all nonhydrogen atoms anisotropically, the final R-value was 0.035. More detailed information concerning the data collection, programs and other methods are given in Refs. 1–4, 6 and 7. Final atomic coordinates for both compounds with anisotropic thermal parameters and lists of $F_c/F_0$ factors have been deposited with the Editor as supplementary material and are available on request. Atomic coordinates have also been deposited with the Cambridge Crystallographic Data Centre.

*Acknowledgement*—The author wishes to express his gratitude to the Emil Aaltonen Foundation for financial support of this study.

## REFERENCES

1. P. Knuuttila, *Acta Chem. Scand.* 1982, **A36**, 767.
2. H. Knuuttila, *Inorg. Chim. Acta* 1981, **50**, 221.
3. H. Knuuttila, *Inorg. Chim. Acta* 1983, **69**, 173.
4. H. Knuuttila, *Acta Chem. Scand.* 1983, **A37**.
5. P. Knuuttila, *7th European Crystallographic Meeting*. Jerusalem (1982).
6. P. Knuuttila, *Inorg. Chim. Acta* 1981, **52**, 141.
7. P. Knuuttila, *Inorg. Chim. Acta* 1982, **58**, 201.
8. H. Knuuttila and P. Knuuttila, *Acta Chem. Scand.* 1983, **A37**, 227.
9. P. Knuuttila, unpublished result.
10. R. Palepu and M. M. Morrison, *Inorg. Chim. Acta* 1979, **36**, L437–L439.
11. L. S. Gelfand, L. L. Pytlewski, D. L. Cosgrove, C. M. Mikulski, A. N. Speca and N. M. Karayannis, *Inorg. Chim. Acta* 1979, **32**, 59.
12. P. Main, S. J. Fiske, S. E. Hull, L. Lessinger, G. Germain, J. P. Declerq and M. M. Woolfson *MULTAN* 80, Universities of York, England and Lonvain-la-Neuve, Belgium (1980).

*Polyhedron* Vol. 3, No. 3, pp. 307–311, 1984
Printed in Great Britain.

0277-5387/84 $3.00 + .00
© 1984 Pergamon Press Ltd.

# CRYSTAL STRUCTURE OF THE PENTAMETHYLDIETHYLENETRIAMINE ADDUCT OF 1-LITHIO-2-METHYL-1,2-DICARBA-*CLOSO*-DODECABORANE, $Li[C_2B_{10}H_{10}Me][MeN(CH_2CH_2NMe_2)_2]$, A COMPOUND CONTAINING A LITHIUM ATOM TERMINALLY BONDED TO A SIX-COORDINATE CARBON ATOM

WILLIAM CLEGG
Institut für Anorganische Chemie der Universität, Tammannstrasse 4, D-3400 Göttingen, Federal Republic of Germany

**and**

DAVID A. BROWN, STEPHEN J. BRYAN and KENNETH WADE*
Chemistry Department, Durham University Science Laboratories, South Road, Durham DH1 3LE, England

(*Received* 23 *May* 1983; *accepted* 25 *July* 1983)

**Abstract**—$Li[C_2B_{10}H_{10}Me][MeN(CH_2CH_2NMe_2)_2]$, prepared by successive reaction of equimolar amounts of *n*-butyl-lithium and pentamethyldiethylenetriamine with 1-methyl-1,2-dicarba-*closo*-dodecaborane, $C_2B_{10}H_{11}Me$, crystallises in the monoclinic space group $P2_1/m$, with $a = 8.242(1)$, $b = 13.522(1)$, $c = 10.799(1)$ Å, $\beta = 108.75(1)°$, $Z = 2$. The crystal structure has been refined to $R = 0.088$ from 1128 unique diffractometer data with $F > 6\sigma(F)$. The compound is unusual in that it contains a lithium atom terminally attached by a formally single Li–C bond to the six-coordinate carbon atom of a carborane. Features of the structure are compared with related features of other organolithium compounds, and used to calculate the cone angles and steric requirements of icosahedral carboranyl and methylcarboranyl ligands attached to metal atoms of various sizes.

A familiar feature of organolithium chemistry is the multicentre bonding which normally occurs between the metal atoms and ligand carbon atoms.[1–3] Lithio derivatives of unsaturated hydrocarbons have structures in which the metal atoms are within bonding distance of at least two (and usually three or four) ligand carbon atoms.[4] Lithium alkyls normally have strongly associated structures which persist even in solution in donor solvents, held together by four-centre two-electron bonds, as in tetrahedral tetrameric molecules like $(LiMe)_4$[5] or chair-shaped hexameric molecules like $(Li.cyclohexyl)_6$.[6] The number of ligand carbon atoms to which each lithium atom bonds (and the number of lithium atoms to which each ligand carbon atom bonds) can be reduced by the presence of chelating bases: phenyl-lithium, for example, crystallises in the presence of tetramethylethylenediamine (TMEDA) as the dimer $(LiPh.TMEDA)_2$, held together by three-centre Li . . . C . . . Li bonds.[7] The steric bulk of certain organic ligands can also be sufficient to prevent association, and it is significant that one of the only two organolithium compounds known prior to the present work to have unassociated structures, with their metal atoms terminally bonded to specific

*Author to whom correspondence should be addressed.

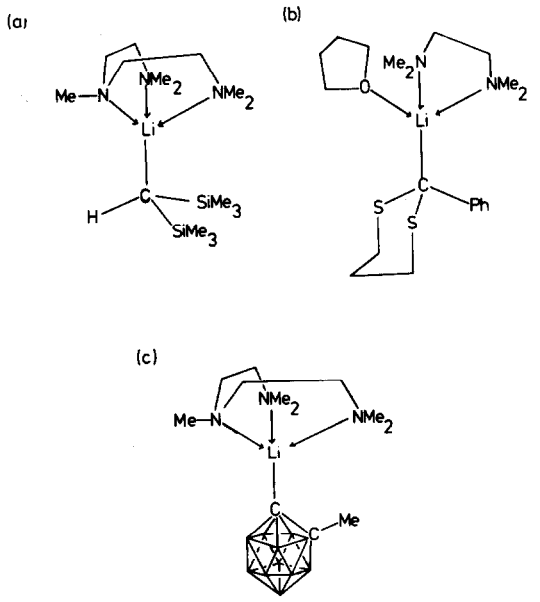



Fig. 1. Compounds known to contain a lithium atom terminally attached to one carbon of an organic residue. (a) Compound (1), $LiCH(SiMe_3)_2(PMDETA)$.[8] (b) Compound (2), $\overline{LiCPhSC_3H_6S}(TMEDA)(THF)$.[9] (c) Compound (3), $LiC_2B_{10}H_{10}Me(PMDETA)$.

carbon atoms, contains the very bulky ligand $CH(SiMe_3)_2$ (Compound (1), Fig. 1a).[8] The other compound already known to contain a two-centre two-electron Li–C bond (Compound (2), Fig. 1b)[9] also contains a relatively bulky ligand, though the electron-withdrawing effect of the two sulphur atoms attached to the lithiated carbon atom in this compound should not be ignored.

Here we describe the structure of a third compound containing a two-centre two-electron Li–C bond. This is the pentamethyldiethylenetriamine (PMDETA) adduct of 1-lithio-2-methyl-1,2-dicarba-*closo*-dodecaborane, $Li[C_2B_{10}H_{10}Me][MeN(CH_2CH_2NMe_2)_2]$ (Compound (3), Fig. 1c). It was studied in the expectation (now realised) that for a combination of electronic and steric reasons it would prove to be monomeric, so providing an unprecedented example of lithium terminally attached to hypercoordinate carbon. Despite the wealth of structural information now available on polyhedral boranes and carboranes and their metalla derivatives,[2,10–12] no carborane with an alkali metal atom covalently bonded in an *exo* position appears to have been structurally characterised, although such derivatives have found wide application as intermediates for the synthesis of *exo* functionally substituted carboranes.[10,11,13,14]

We also attempted to obtain crystals of the lithiocarborane 1-Li-1,2-$C_2B_{10}H_{11}$ or its adduct with TMEDA or PMDETA, but without success. A dimeric structure for the TMEDA adduct $[LiC_2B_{10}H_{11}.TMEDA]_2$, like that of the analogous phenyl-lithium adduct $[LiPh.TMEDA]_2$,[7] appeared sterically possible, even if unlikely on electronic grounds—the electron-withdrawing properties of the carboranyl ligand are expected to reduce the capacity of the carbon atoms to participate in multicentre bonding *outside* the polyhedron. The lithio-carborane 1-Li-1,2-$C_2B_{10}H_{11}$ is in any case unstable with respect to disproportionation into the parent carborane and the dilithio derivative 1,2-$Li_2$-1,2-$C_2B_{10}H_{10}$ in the presence of certain bases.[15] Use of the methylcarborane 1-Me-1,2-$C_2B_{10}H_{11}$ avoided this problem, and provided a bulkier organic residue less likely to allow association, even if that were electronically favoured. The tridentate base PMDETA was used to block the expected three spare lithium valences.

## EXPERIMENTAL

### *Preparation of* $Li(C_2B_{10}H_{10}Me)(PMDETA)$

1-Methyl-1,2-dicarba-*closo*-dodecaborane (1-methyl-*ortho*-carborane) was prepared via the bromomethyl derivative 1-$BrCH_2C_2B_{10}H_{11}$ from $B_{10}H_{12}(NCMe)_2$ and $BrCH_2C{\equiv}CH$.[16] The tridentate base PMDETA was dried by distillation from $CaH_2$ and then $P_2O_5$ (twice) under reduced pressure. Hydrocarbon solvents were dried over sodium wire. Manipulations were carried out using standard inert atmosphere (dry nitrogen) techniques.

A solution of *n*-BuLi (10 mmol) in hexane was added to a solution of 1-$MeC_2B_{10}H_{11}$ (1.58 g, 10 mmol) in toluene (30 $cm^3$). The mixture was stirred at 15°C for 3 hr, during which time the lithio-carborane 1-Li-2-$MeC_2B_{10}H_{10}$ precipitated. PMDETA (1.73 g, 10 mmol) was then added, and the mixture was warmed until all the precipitate dissolved. The product crystallised when the solution was cooled to −35°C. After recrystallisation from toluene in the form of colourless transparent blocks, it was identified as $Li[C_2B_{10}H_{10}Me][MeN(CH_2CH_2NMe_2)_2]$, m.p. 195–197°C (decomp.). Found: C, 42.5; H, 10.2; Li, 2.0; N, 12.1. Calc. for $C_{12}H_{36}B_{10}LiN_3$: C, 42.7; H, 10.8; Li, 2.1; N, 12.5%.

IR (Nujol mull), $cm^{-1}$: 2595 sh, 2580 s, 2550 sh, 2512 sh, 1358 m, 1318 w, 1308 m, 1297 sh, 1289 m, 1252 w, 1172 w, 1158 w, 1119 m, 1102 w, 1060 m, 1041 s, 1024 m, 992 w, 947 sh, 943 s, 937 sh, 905 w, 799 m, 783 m, 770 w, 758 w, 738 m, 730 sh, 694 w, 671 w, 660 w, 603 m, 577 w, 548 w, 508 w.

The compound was exceedingly air- and moisture-sensitive, decomposing immediately on exposure to air. Attempts to record its mass spectrum afforded evidence of the ligand PMDETA

($m/e$ 173) and fragments thereof, and of the carboranyl residue $C_2B_{10}H_{10}Me$ (a characteristic group of peaks, showing the appropriate isotope pattern, with that at $m/e$ 159 of highest mass) and its breakdown fragments.

## CRYSTALLOGRAPHIC STUDY

A crystal was sealed in a Lindemann glass capillary and examined at room temperature on a Stoe–Siemens AED diffractometer with Mo-$K\alpha$ radiation.[17]

*Crystal data*

$C_{12}H_{36}B_{10}LiN_3$, F.wt. = 337.5, monoclinic, $P2_1/m$; $a = 8.242(1)$, $b = 13.522(1)$, $c = 10.799(1)$ Å, $\beta = 108.75(1)°$, $U = 1139.7$ Å$^3$, $Z = 2$, $D_c = 0.983$ g cm$^{-3}$, $\mu = 0.47$ cm$^{-1}$, $F(000) = 364$.

*Data collection*

$\theta/\omega$ scan, real-time profile fitting[18]. 4524 reflections measured with $2\theta < 50°$, 2093 unique, 1128 with $F > 6\sigma(F)$.

*Structure solution and refinement*

Automatic direct metbods,[19] anisotropic thermal parameters for non-hydrogen atoms, B–H atoms refined freely (isotropic), other H atoms constrained to give C–H = 0.96 A°, H–C–H = 109.5° and $U(H) = 1.2U_{eq}(C)$. Final $R = 0.088$, $R_w = (\Sigma w\Delta^2/\Sigma wF_0^2)^{1/2} = 0.107$, with $w^{-1} = \sigma^2(F) + 0.0002F^2$. An isotropic extinction parameter $x$ refined to $3.2(8) \times 10^{-5}$, where $F_c$ is divided by $(1 + xF_c^2/\sin(2\theta))^{1/4}$. A final difference synthesis contained no significant features; the analysis of variance showed no unusual trends with indices, $F$ or $\sin\theta$.

Final atomic coordinates, thermal parameters, detailed geometry and structure factor lists have been deposited with the Editor as supplementary data. The molecular structure is shown in Fig. 2, which also gives the atom numbering scheme. Selected bond lengths and angles are given in Table 1. The molecule lies on a crystallographic mirror plane, passing through Li, the central nitrogen atom and the carborane icosahedron.

## RESULTS AND DISCUSSION

The four-coordinate lithium atom of compound (3) is terminally attached to the six-coordinate carbon atom of the carborane icosahedron by a bond of length 2.18(1) Å, which

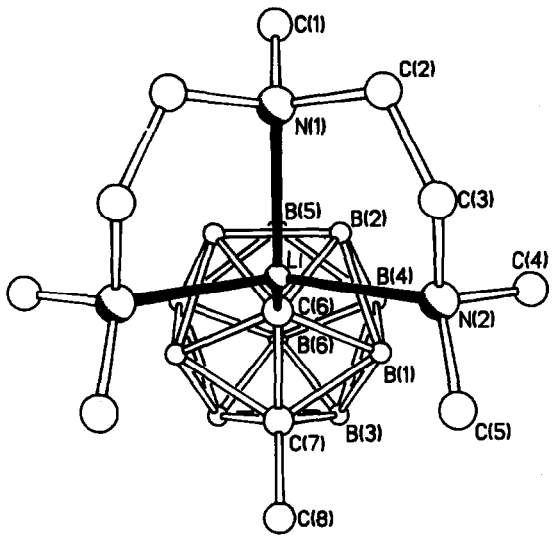



Fig. 2. Molecular structure of compound (3), $LiC_2B_{10}H_{10}Me$(PMDETA) showing atom numbering.

Table 1. Selected bond lengths (Å) and angles (°)

| | | | |
|---|---|---|---|
| Li-N(1) | 2.134(9) | Li-N(2) | 2.169(5) |
| Li-C(6) | 2.176(8) | C(6)-C(7) | 1.681(7) |
| C(6)-B(1) | 1.707(6) | C(6)-B(2) | 1.709(8) |
| C(7)-C(8) | 1.516(11) | C(7)-B(1) | 1.653(7) |
| C(7)-B(3) | 1.686(6) | C(2)-C(3) | 1.434(11) |
| N(1)-C(2) | 1.435(7) | N(2)-C(3) | 1.452(7) |
| N(1)-Li-N(2) | 85.6(2) | N(1)-Li-C(6) | 124.1(5) |
| N(2)-Li-C(6) | 119.1(2) | N(2)-Li-N(2)' | 114.4(4) |
| Li-C(6)-C(7) | 129.3(5) | Li-C(6)-B(1) | 122.4(2) |
| Li-C(6)-B(2) | 118.0(3) | C(8)-C(7)-C(6) | 115.7(4) |
| C(8)-C(7)-B(1) | 116.8(3) | C(8)-C(7)-B(3) | 120.1(4) |

may be compared with the lengths of 2.13(5) and 2.28 Å previously reported[8,9] for the two-centre Li–C bonds in compounds (1) and (2) respectively. The metal–carbon bond in compound (3) might have been expected to be rather longer, in view of the high coordination number of the carbon atom involved—compounds (1) and (2) contain four-coordinate carbon—though the *sp* hybridisation commonly assumed for the skeletal atoms of icosahedral carboranes would require a relatively short *exo* bond. Our terminal Li–C bonds are shorter than the fractional order Li–C bonds in unsolvated methyl-lithium (2.36 Å)[5] or its TMEDA adduct (2.23–2.27 Å),[20] though they are actually longer than some of the bonds formally of order $<1.0$ found in other associated lithium alkyls or aryls, for which bond lengths in the range 2.11–2.47 Å have been reported.[3] In organoaluminium chemistry, the fractional order Al–C bonds in associated aluminium alkyls or aryls are invariably some 0.20 Å longer than related terminal single Al–C bonds, as would be expected.[2,21] The correlation of bond length with formal bond order in organolithium chemistry is thus far less clear-cut, and indeed these bonds must be regarded as being at (or beyond) the limit of what can realistically be regarded as covalent,[1,22–24] so that other factors, such as the degree of ionic character, are as important as the formal bond order.

Those features of the lithium coordination related to the PMDETA ligand are unexceptional: the lithium–nitrogen bonds are of normal length (*ca.* 2.15 Å) and the N–Li–N bond angles reflect the characteristic "bite" of the tridentate PMDETA ligand. The orientation of the ligand is such that its plane of symmetry coincides with the plane of symmetry of the carborane residue, an orientation which minimises repulsive non-bonding interactions with the methyl group attached to the *ortho* carbon atom of the carborane residue. Surprisingly, the orientations of the *exo* bonds, from C(6) to Li, and from C(7) to its methyl group (C(8)) both show slight deviations from the expected direction as if both *exo* substituents were shifted parallel to the C(6)–C(7) axis in the *same direction* (bringing the methyl group attached to C(7) slightly nearer to C(6) than expected), rather than in opposite directions as might have been expected of two adjacent mutually repellent groups.

From the structure of compound (3), it is possible to calculate the effective cone angle subtended by the 2-methyl-*ortho*-carboranyl ligand at a metal atom such as lithium. The concept of cone angles, originally introduced by Tolmann[25] to facilitate the discussion of steric effects in crowded transition metal coordination complexes, can be particularly helpful in assessing how many bulky pseudo-spherical ligands like icosahedral carboranyl groups can be attached to a single metal atom. Table 2 gives the cone angles calculated for (a) unsubstituted icosahedral carboranyl ligands $C_2B_{10}H_{11}$ and (c) 2-methyl-*ortho*-carboranyl ligands $MeC_2B_{10}H_{10}$ for a representative range of metal–carbon bond distances. The cone angles were determined (Fig. 3) by calculating the angles between the *exo* C–M bond and the surface of the

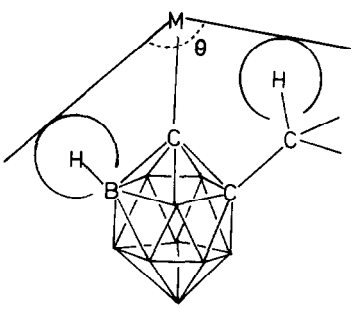



Fig. 3. Cone angles of carboranyl groups.

Table 2. Cone angles ($\theta°$) for aryl and carboranyl ligands as a function of the metal–carbon distance d(M–C)

| d(M–C) (Å) | 1.60 | 1.95 | 2.18 | 2.45 |
|---|---|---|---|---|
| (a) $\theta(C_2B_{10}H_{11}-)$ | 154 | 140 | 132 | 120 |
| (b) $\theta(C_6H_5-)$ | 153 | 138 | 130 | 120 |
| (c) $\theta$(2-Me-1,2-$C_2B_{10}H_{10}-$) | 169 | 158 | 149 | 138 |
| (d) $\theta(2\text{-}MeC_6H_4-)$ | 183 | 169 | 159 | 148 |

nearest hydrogen atoms. These are either of a B–H or C–H group or of a C–Me group in the *ortho* position relative to the metallated carbon atom. A van der Waals radius for hydrogen of 1.2 Å was assumed. Also included in Table 2 for comparison are the cone angles for (b) phenyl and (d) *ortho*-tolyl ligands. The latter, in the plane of the ring, are seen to be slightly more sterically demanding.

The cone angles in Table 2 indicate that there is room for uncoordinated 1-lithio-2-methyl-*ortho*-carborane to adopt a dimeric structure $[LiC_2B_{10}H_{10}Me]_2$, in which the carboranyl groups, like the phenyl groups of $[LiPh.TMEDA]_2$,[7] perform a bridging role between the metal atoms, even though association of this type is unlikely on electronic grounds. Further solution studies and attempts to grow crystals of the compound are planned.

A further implication of the data in Table 2 is that it is not realistic to expect more than two $C_2B_{10}H_{11}$ carboranyl units, let alone ortho-methylated carboranyl units, to be linked to a single boron, carbon or nitrogen atom, for which an *exo* bond of length *ca.* 1.52–1.62 Å can be assumed. A larger second-row element such as aluminium, silicon or phosphorus might just be big enough to accommodate three $C_2B_{10}H_{11}$ carboranyl icosahedra, though not when they are ortho-methylated.

*Acknowledgements*—We thank PEMOD (DAB), SERC (SJB) and the Verband der Chemischen Industrie (WC) for financial support.

## REFERENCES

1. B. J. Wakefield, *The Chemistry of Organolithium Compounds*. Pergamon Press, Oxford (1974).
2. M. E. O'Neill and K. Wade, In *Comprehensive Organometallic Chemistry* (Edited by G. Wilkinson, F. G. A. Stone and E. W. Abel), Vol. 1, p. 1. Pergamon Press, Oxford (1982).
3. J. L. Wardell, In *Comprehensive Organometallic Chemistry* (Edited by G. Wilkinson, F. G. A. Stone and E. W. Abel), Vol. 1, p. 43. Pergamon Press, Oxford (1982).
4. G. D. Stucky, *Adv. Chem. Ser.* 1974, **130**, 56.
5. E. Weiss and G. Hencken, *J. Organometal. Chem.* 1970, **21**, 265.
6. R. Zerger, W. Rhine and G. D. Stucky, *J. Am. Chem. Soc.* 1974, **96**, 6048.
7. D. Thoennes and E. Weiss, *Chem. Ber.* 1978, **111**, 3157.
8. M. F. Lappert, L. M. Engelhardt, C. L. Raston and A. H. White, *J. Chem. Soc. Chem. Commun.* 1982, 1323.
9. R. Amstutz, D. Seebach, P. Seiler, B. Schweizer and J. D. Dunitz, *Angew. Chem. Internat. Ed. Engl.* 1980, **19**, 53.
10. T. Onak in *Comprehensive Organometallic Chemistry* (Edited by G. Wilkinson, F. G. A. Stone and E. W. Abel), Vol. 1, pp. 411, 459, 543. Pergamon Press, Oxford (1982).
11. R. Thompson, D. E. Buck, N. N. Greenwood, R. W. Jotham, L. H. Long and J. H. Morris, *Supplement to Mellor's Comprehensive Treatise on Inorganic and Theoretical Chemistry*, Vol. 5BI: *Boron–Hydrogen Compounds*. Longman, London (1981).
12. R. N. Grimes, *Metal Interactions with Boron Clusters*. Plenum Press, New York (1982).
13. R. N. Grimes, *Carboranes*. Academic Press, New York (1970).
14. E. L. Muetterties, *Boron Hydride Chemistry*. Academic Press, New York (1975).
15. L. I. Zakharkin, A. V. Grebennikov and A. V. Kazantsev, *Izvest. Akad. Nauk. S.S.S.R., Ser. Khim.* 1967, 2077.
16. J. R. Reiner, R. P. Alexander and H. Schroeder, *Inorg. Chem.* 1966, **5**, 1460.
17. W. Clegg, *Acta Crystallogr.* 1981, **A37**, C313.
18. W. Clegg, *Acta Crystallogr.* 1981, **A37**, 22.
19. G. M. Sheldrick, SHELXTL program system. University of Göttingen (1978).
20. H. Köster, D. Thoennes and E. Weiss, *J. Organometal. Chem.* 1978, **160**, 1.
21. J. J. Eisch, In *Comprehensive Organometallic Chemistry* (Edited by G. Wilkinson, F. G. A. Stone and E. W. Abel), p. 555. Pergamon Press, Oxford (1982).
22. A. Streitwieser Jr., *J. Organometal. Chem.* 1978, **156**, 1.
23. G. Graham, S. Richtsmeier and D. A. Dixon, *J. Am. Chem. Soc.* 1980, **102**, 5759.
24. T. Clark, J. Chandrasekhar and P. von R. Schleyer, *J. Chem. Soc. Chem. Commun.* 1980, 672.
25. C. A. Tolman, *J. Am. Chem. Soc.* 1970, **92**, 2956.

*Polyhedron* Vol. 3, No. 3, pp. 313–316, 1984
Printed in Great Britain.

0277–5387/84 $3.00 + .00
© 1984 Pergamon Press Ltd.

# ON THE TRI-*n*-OCTYLAMMONIUM CHLOROCOMPLEXES OF Sn(IV) IN BENZENE SOLUTION

**CLAUS FISCHER* and HARALD WAGNER**
Central Institute of Solid State Physics and Material Research, Academy of Sciences of the GDR, 8027 Dresden, Helmholtzstraße 20, GDR

**and**

**VLADIMIR V. BAGREEV**
V. I. Vernadsky Institute of Geochemistry and Analytical Chemistry, USSR Academy of Sciences, Moscow, U.S.S.R.

(*Received* 15 *June* 1983; *accepted* 25 *July* 1983)

**Abstract**—Extracts with tri-*n*-octylammonium chlorocomplexes of Sn(IV) of various compositions, included the N-deuterated compounds, were prepared and investigated by IR spectroscopy and conductivity measurements. Three Sn(IV) complexes were found: $(TOAH^+)_2SnCl_6^{2-}$ (2:1-complex), $TOAH^+SnCl_5^-$ (1:1-complex) and a complex with the stoichiometric ratio TOA:Sn(IV) > 2. The cation of the latter contains the groups $(TOAH \ldots Cl \ldots HTOA)^+$ and $TOAH^+$ and that species is supposed to be a 3:1-complex $(TOAH \ldots Cl \ldots HTOA)^+TOAH^+SnCl_6^{2-}$.

In the series of studies on various halocomplexes in the system tri-*n*-octylammonium halide/$C_6H_6$ or $C_6D_6$–$MX_n$–HX (M = In(III), Fe(III), Ga(III), Cu(II), Zn(II), Co(II) or Sn(II); X = Cl, Br or I)[1–4] work was extended to the chlorocomplexes of Sn(IV).

Laskorin *et al.*[5] have dealt with the extraction of Sn(IV) from HCl solutions by technical grade trialkylamine ("TAA", $C_7$–$C_9$) in benzene. The molar ratio amine:$Sn(IV)_{(org)}$ in the extract, determined by loading experiments and slope analysis, amounted to 2:1. The extractable Sn(IV) containing species supposed was given in the form of the general gross formula $H_2SnCl_6 \cdot 2TAA$.

The present work comprises the preparation of Sn(IV) containing extracts and solutions of the above-mentioned system and their investigation by IR spectroscopy and conductivity measurements.

## EXPERIMENTAL AND PREPARATION OF THE EXTRACTS

$SnCl_4$ ("pure") was distilled before use. The reagents HCl and $C_6H_6$ were of analytical grade. Tri-*n*-octylamine (pract., $d_4^{20}$ 0.82; $n_D^{20}$ 1.4476) was supplied by Fluka AG (Switzerland), deuterobenzene (Benzol-$D_6$, b.p.$_{760}$; 99 ± 0.1 at% D) by the Zentralinstitut für Isotopen- und Strahlenforschung Leipzig, deuterium chloride (20% DCl in $D_2O$; 99.9%) by VEB Berlin–Chemie, Berlin–Adlershof. In general, the preparation of the extracts and the measurements of the IR spectra and specific conductivities were carried out as described earlier.[1,2]

The extracts prepared and their preparation conditions are compiled in Table 1. Extracts No. 1, 2, 5 and 6 were duplicated using benzene and deuterobenzene, respectively, as diluents. Extracts No. 1 and 2 were prepared according to Ref. 5; the extraction time was 30 min, the phase ratio $V_w/V_{org} = 1$. Though an excess of Sn(IV) in relation to TOA had been used, only the 2:1-complex with the anion $SnCl_6^{2-}$ was formed. This was to be expected, because the formation of four- or five-coordinate species is unlikely under solvent extraction conditions due to the ease of formation of six-coordinate Sn(IV).[6] Thus by analogy with the approach of Beattie *et al.*[7] mixtures of 2:1-complex and $SnCl_4$ were prepared to prove the existence of the 1:1-complex $TOAH^+SnCl_5^-$†.

The concentrations of Sn(IV) and $Cl^-$ of all extracts investigated were determined in the following way: back extraction by shaking 5 cm³ of the organic phase with 20 cm³ 6 M NaOH for 30 min,

*Author to whom correspondence should be addressed.

†Complexes are here and subsequently written in monomeric form.

Table 1. Preparation of the extracts

| No. | Sn(IV) bearing complex +) | Extract composition, M TOA | Sn(IV) | Cl | Diluent | Initial organic phase, M TOA | Initial aqueous phase, M ($H_2O$ or $D_2O$) | $D_{Sn(IV)}$, detd. |
|---|---|---|---|---|---|---|---|---|
| 1 | 2:1-H | 0.25 | 0.129 | 0.77 | $C_6H_6/C_6D_6$ | 0.25 | 1.5 $SnCl_4$ 6 HCl | 0.094 |
| 2 | 2:1-D | 0.25 | 0.129 | 0.77 | $C_6H_6/C_6D_6$ | 0.25 | 1.5 $SnCl_4$ 6 HCl | |
| 3 | 1:1-H | 0.25 | 0.27 | 1.26 | $C_6D_6$ | 10 $cm^3$ extract No. 1 + 0.15 $cm^3$ $SnCl_4$ (20 °C, 24 h) | | |
| 4 | 1:1-D | 0.25 | 0.27 | 1.26 | $C_6H_6$ | 10 $cm^3$ extract No. 2 + 0.15 $cm^3$ $SnCl_4$ (20 °C, 24 h) | | |
| 5 | 3:1-H++) | 0.25 | 0.0833 | | $C_6H_6/C_6D_6$ | 2 $cm^3$ extract No. 1 + 1 $cm^3$ 0.25 M $TOAH^+Cl^-$ | | |
| 6 | 3:1-H++) | 0.25 | 0.0625 | | $C_6H_6/C_6D_6$ | 2 $cm^3$ extract No. 1 + 2 $cm^3$ 0.25 M $TOAH^+Cl^-$ | | |

+) H: non-deuterated; D: N-deuterated
++) 3:1-complex supposed

precipitation of the Sn(IV) with diluted $HNO_3$ and gravimetric determination as $SnO_2$; argentometric titration of the $Cl^-$ in the filtrate (Volhard's method).

The molar ratios TOA:Sn(IV):Cl found were in good agreement with those to be expected: 2:1-complex $(TOAH^+)_2SnCl_6^{2-}$ 2:1.03:6.16; 1:1-complex $TOAH^+SnCl_5^-$ 1:1.08:5.04.

The extracts for the conductivity measurements were prepared in the same way but with benzene as diluent only. The extract with the molar ratio TOA:Sn(IV) = 3:1 was prepared according to extract No. 5, but starting from 0.3 M solutions of TOA and $TOAH^+Cl^-$, respectively.

## IR SPECTRA, CONDUCTIVITY MEASUREMENTS AND DISCUSSION

The IR spectra of the extracts and solutions were taken in the range 1800–3800 $cm^{-1}$. They are given in Fig. 1. The wave numbers of the $\nu$NH and $\nu$ND absorptions are summarized in Table 2.

The IR spectrum of the undeuterated 2:1-complex $(TOAH^+)_2SnCl_6^{2-}$ (extract No. 1) exhibits, in comparison with other complexes in-

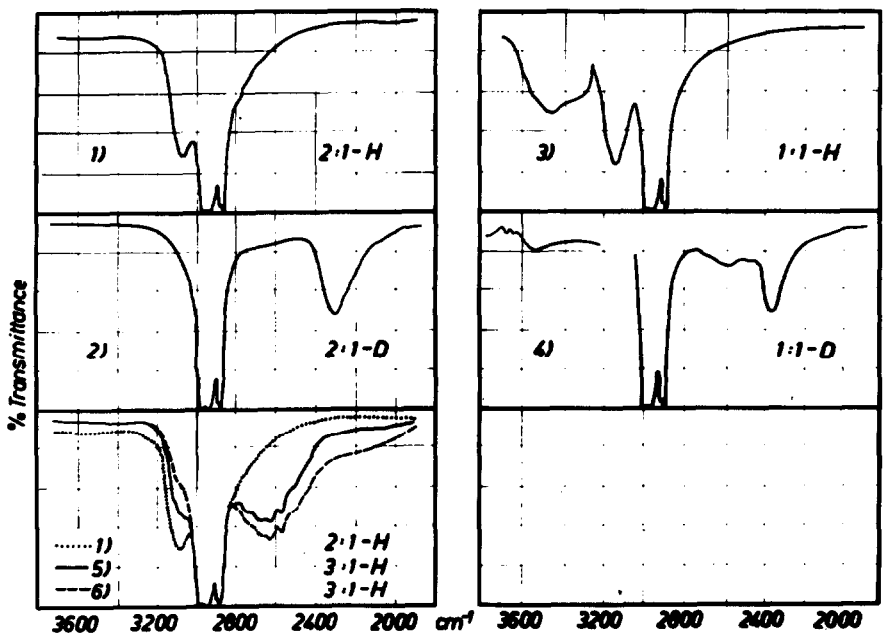



Fig. 1. IR spectra of the extracts (the numbers refer to Table 1).

Table 2. Wave numbers (in $cm^{-1}$) of the $\nu$NH and $\nu$ND absorptions

| No. (acc. to Table 1) | Complex | | $\nu$NH | $\nu$ND | $\nu$NH/$\nu$ND |
|---|---|---|---|---|---|
| 1 | $(TOAH^+)_2SnCl_6^{2-}$ | 2:1 | 3069 s | | 1.34 |
| 2 | $(TOAD^+)_2SnCl_6^{2-}$ | 2:1 | | 2293 s | |
| 3 | $TOAH^+SnCl_5^-$ | 1:1 | 3120 s | | 1.34 |
| 4 | $TOAD^+SnCl_5^-$ | 1:1 | | 2330 s | |
| 5 | $(TOAH...Cl...HTOA)^+TOAH^+SnCl_6^{2-}$ | 3:1[+)] | 2500 w, sh<br>2560 m<br>2615 m<br>2790 w<br>3060 m, sh[++)] | | |
| 6 | $(TOAH...Cl...HTOA)^+TOAH^+SnCl_6^{2-}$ | 3:1[+)] | 2500 w, sh<br>2560 m<br>2615 m<br>2790 w<br>3070 w, sh[++)] | | |

[+)] 3:1-complex supposed [++)] Some 2:1-complex present

volving anions of charge $-2$ which had previously been investigated, a striking high frequency of the $\nu$NH vibration at 3069 $cm^{-1}$. However, this value is evident, because the anion $SnCl_6^{2-}$ is a regular octahedron (point group $O_h$[8]) without any local concentrations of electrons. Thus the tendency to form H-bonds between cation and anion is weakly pronounced in spite of the anion charge $-2$. The degree of the shift of the $\nu$NH frequency with N-deuteration (extract No. 2), expressed by the ratio $\nu NH/\nu ND = 1.34$, coincides exactly with the ratios found for complexes, which exhibit $\nu$NH vibrations in the same frequency range (1:1-complexes of Fe(III), Cu(II) and Sn(II).[3,4]

These statements are valid for the 1:1-complex $TOAH^+SnCl_5^-$ (extract No. 3), too. Its $\nu$NH frequency at 3120 $cm^{-1}$ indicating an even weaker cation-anion-interaction coincides practically with those of the analogous 1:1-complexes of Fe(III), Ga(III) and In(III).[1] N-deuteration of the complex (extract No. 4) yields the ratio $\nu NH/\nu ND = 1.34$, too. The strong and medium absorptions near 3450 $cm^{-1}$ (undeuterated 1:1-complex) and near 2550 $cm^{-1}$ (N-deuterated 1:1-complex) must be considered as $\nu$OH and $\nu$OD vibrations respectively, which arise by reaction of the $SnCl_4$ added with traces of moisture. The decrease of the frequency in relation to the "pure" $\nu$OH vibration indicates a strong H-bond.[9]

The three peaks at 2500, 2560 and 2615 $cm^{-1}$ in the IR spectra of the extracts with the molar ratios TOA:Sn(IV) = 3:1 and 4:1 (extracts No. 5 and 6), which represent $\nu$NH vibrations (like the absorption at 2790 $cm^{-1}$), indicate the existence of at least one species containing the cationic group $(TOAH...Cl...HTOA)^+$. This assignment is evident according to the preceding work.[1-4] Therefore by analogy with[3] it may be suggested in the present case, too, that a 3:1-complex $(TOAH...Cl...HTOA)^+TOAH^+SnCl_6^{2-}$ can occur, though there is no complete evidence for it in the case of Sn(IV), too, and a possible formation of a 4:1-complex cannot fully be excluded. The shoulder at $\nu$3060 $cm^{-1}$ (molar ratio TOA/Sn(IV) = 3:1; extract No. 5) refers to the presence of quantities of 2:1-complex (due to the equilibrium $(TOAH...Cl...HTOA)^+ TOAH^+SnCl_6^{2-} \rightleftharpoons (TOAH^+)_2SnCl_6^{2-} + TOAH^+ Cl^-$), which decreases when going to the molar ratio TOA/Sn(IV) = 4:1 (extract No. 6).

The specific conductivity data $\kappa$ of the Sn(IV) containing extracts are given in Table 3 together with the data of corresponding complexes of Fe(III), Sn(II), Cu(II), Zn(II) and Co(II) previously determined.[1,3,4]

The $\kappa$ values of the supposed 3:1-complex and of the 2:1-complex are of the same order like those of the corresponding complexes of Zn(II) and Co(II), but differ clearly from each other by one order thus indicating two different species. The strikingly low value of the 1:1-complex (in comparison with the other 1:1-complexes mentioned) can possibly be caused by a partial decomposition of that species according to the equilibrium

Table 3. Specific conductivity data $\kappa$. (Metal concentration: 0.1 M; diluent: benzene)

| Complexes | $\kappa$ [$\Omega^{-1}cm^{-1}$] at 25 ± 0.02 °C |
|---|---|
| **1:1-Complexes** | |
| $TOAH^+FeCl_4^-$ | $2.75 \times 10^{-5}$ [1] |
| $TOAH^+SnCl_3^-$ | $2.18 \times 10^{-5}$ [4] |
| $TOAH^+CuCl_3^-$ | $1.84 \times 10^{-5}$ [3] |
| $TOAH^+SnCl_5^-$ | $1.23 \times 10^{-5}$ |
| **3:1-Complexes**[+)] | |
| $(TOAH...Cl...HTOA)^+TOAH^+CuCl_4^{2-}$ | $2.14 \times 10^{-5}$ [3] |
| $(TOAH...Cl...HTOA)^+TOAH^+ZnCl_4^{2-}$ | $1.85 \times 10^{-5}$ [3] |
| $(TOAH...Cl...HTOA)^+TOAH^+CoCl_4^{2-}$ | $1.72 \times 10^{-5}$ [3] |
| $(TOAH...Cl...HTOA)^+TOAH^+SnCl_6^{2-}$ | $1.36 \times 10^{-5}$ |
| **2:1-Complexes** | |
| $(TOAH^+)_2CuCl_4^{2-}$ | $1.54 \times 10^{-5}$ [3] |
| $(TOAH^+)_2SnCl_6^{2-}$ | $1.28 \times 10^{-6}$ |
| $(TOAH^+)_2ZnCl_4^{2-}$ | $8.89 \times 10^{-7}$ [3] |
| $(TOAH^+)_2CoCl_4^{2-}$ | $6.21 \times 10^{-7}$ [3] |

[+)] Complexes supposed

2 $TOAH^+SnCl_5^- \rightleftharpoons (TOAH^+)_2SnCl_6^{2-} + SnCl_4$. However, no IR spectroscopic evidence for this reaction could be found.

## REFERENCES


1. C. Fischer, H. Wagner, V. V. Bagreev and E. S. Stojanov, *J. Inorg. Nucl. Chem.* 1977, **39**, 513.
2. C. Fischer, H. Wagner and V. V. Bagreev, *J. Inorg. Nucl. Chem.* 1980, **42**, 891.
3. C. Fischer, H. Wagner and V. V. Bagreev, *Polyhedron* 1983, **2**, 1141.
4. C. Fischer, H. Wagner and V. V. Bagreev, *Polyhedron* 1983, **2**, 917.
5. B. N. Laskorin, V. S. Ulyanov, R. A. Sviridova, G. N. Melikhova and I. D. Akimova, *Zh. Prikl. Chim.* 1975, **48**, 1221.
6. M. J. Taylor, J. R. Milligan and D. L. Parnell, *J. Inorg. Nucl. Chem.* 1972, **34**, 2133.
7. I. R. Beattie, T. Gilson, K. Livingston, V. Fawcett and G. A. Ozin, *J. Chem. Soc.* (*A*) 1967, 712.
8. L. A. Woodward and L. E. Anderson, *J. Chem. Soc.* 1957, 1284.
9. H. Kriegsmann and G. Kessler, *Z. Anorg. Allg. Chem.* 1962, **318**, 277.

*Polyhedron* Vol. 3, No. 3, pp. 317–323, 1984
Printed in Great Britain.

0277–5387/84 $3.00 + .00
© 1984 Pergamon Press Ltd.

# FURTHER STUDIES ON ORGANONICKEL COMPOUNDS: THE SYNTHESIS OF SOME NEW ALKYL-, ACYL- AND CYCLOPENTADIENYL-DERIVATIVES AND THE CRYSTAL STRUCTURE OF *TRANS*- $[Ni(CH_2SiMe_3)_2(PMe_3)_2]$

**ERNESTO CARMONA,* MARGARITA PANEQUE and MANUEL L. POVEDA**
Departamento de Química Inorgánica, Facultad de Quimica, Universidad de Sevilla, Sevilla, Spain

**ROBIN D. ROGERS***
Department of Chemistry, Northern Illinois University, Dekalb, IL 60115, U.S.A.

**and**

**JERRY L. ATWOOD***
Department of Chemistry, University of Alabama, University, AL 35486, U.S.A.

(*Received* 28 *June* 1983; *accepted* 25 *July* 1983)

**Abstract**—The complex $[NiCl_2(PMe_3)_2]$ reacts with one equivalent of $Mg(CH_2CMe_3)Cl$ to yield the monoalkyl derivative *trans*-$[Ni(CH_2CMe_3)Cl(PMe_3)_2]$, which can be carbonylated at room temperature and pressure to afford the acyl $[Ni(COCH_2CMe_3)Cl(PMe_3)_2]$. Other related alkyl and acyl complexes of composition $[Ni(R)(NCS)(PMe_3)_2]$ ($R = CH_2CMe_3$, $COCH_2CMe_3$) and $[Ni(R)(\eta\text{-}C_5H_5)L]$ ($L = PMe_3$, $R = CH_2CMe_3$, $COCH_2CMe_3$; $L = PPh_3$, $R = CH_2CMe_2Ph$) have been similarly prepared. Dialkyl derivatives $[NiR_2(dmpe)]$ ($R = CH_2SiMe_3$, $CH_2CMe_2Ph$; dmpe = 1,2-bis(dimethylphosphine)ethane, $Me_2PCH_2$ $CH_2PMe_2$) have been obtained by phosphine replacement of the labile pyridine and NNN′N′-tetramethylethylenediamine ligands in the corresponding $[Ni(CH_2SiMe_3)_2(py)_2]$ and $[Ni(CH_2CMe_2Ph)_2(tmen)]$ complexes. A single-crystal X-ray determination carried out on the previously reported trimetylphosphine derivative $[Ni(CH_2SiMe_3)_2(PMe_3)_2]$ shows the complex belongs to the orthorhombic space group *Pbcn*, with $a = 14.345(4)$, $b = 12.656(3)$, $c = 12.815(3)$ Å, $Z = 4$ and $R$ 0.077 for 535 independent observed reflections. The phosphine ligands occupy mutually *trans* positions P–Ni–P 146.9(3)° in a distorted square-planar arrangement.

In spite of the high reactivity and instability often associated with $\sigma$-bonded organonickel(II) compounds, a large number of alkyl and acyl derivatives of composition $[NiX(R)L_2]$ and $[NiR_2L_2]$ is already known.[1] As a continuation of our own work in this area,[2] we have carried out the synthesis and characterization of several new alkyl- and acyl-complexes of Ni(II) stabilized by phosphine ligands. This paper deals with (i) neopentyl- and neopentylcarbonyl-complexes of composition $[Ni(R)X(PMe_3)_2]$ and $[Ni(COR)X(PMe_3)_2]$ (X = Cl,NCS), (ii) cyclopentadienyl derivatives $[Ni(R)(\eta\text{-}C_5H_5)L]$ ($L = PMe_3$, $R = CH_2CMe_3$; $L = PPh_3$, $R = CH_2CMe_2Ph$) and $[(C_5H_5)Ni(COCH_2CMe_3)(PMe_3)]$ and (iii) dialkyl complexes $[NiR_2(dmpe)]$ ($R = CH_2SiMe_3$, $CH_2CMe_2Ph$; dmpe = $Me_2PCH_2C$ $H_2PMe_2$). In addition, the crystal structure of the previously prepared[2b] $PMe_3$ derivative $[Ni(CH_2SiMe_3)_2(PMe_3)_2]$ is also reported. Analytical and spectral data for the new compounds are collected in Table 1.

*Authors to whom correspondence should be addressed.

## RESULTS AND DISCUSSION

### $[Ni(CH_2CMe_3)X(PMe_3)_2]$ *and* $[Ni(COCH_2CMe_3)X(PMe_3)_2]$ *complexes*

The addition of 1 equiv of the Grignard reagent

Table 1. Analytical and spectroscopic data for the new alkyl- and acyl-derivatives of nickel(II)

| | Compound | Colour | Analysis[a] C | Analysis[a] H | $^1$H NMR data[e] Me–P | C–Me or Si–Me | $NiCH_2$ or $NiCOCH_2$ | Others |
|---|---|---|---|---|---|---|---|---|
| (1) | $[Ni(CH_2CMe_3)Cl(PMe_3)_2]$ | Yellow | 41.6 (41.3) | 9.0 (9.2) | 1.24bt[g] | 1.42s | 0.72bt[h] | |
| (2) | $[Ni(COCH_2CMe_3)Cl(PMe_3)_2]$ | Yellow[c] | 41.2 (41.7) | 8.3 (8.4) | f 1.31bs | 0.94s | 2.98s | |
| (3) | $[Ni(CH_2CMe_3)(NCS)(PMe_3)_2]$ | Orange[d] | 41.9 (42.4) | 8.5 (8.5)[b] | 1.10bs | 1.29s | 0.47bs | |
| (4) | $[Ni(COCH_2CMe_3)(NCS)(PMe_3)_2]$ | Yellow[c,d] | 42.0 (42.4) | 7.9 (7.9) | f 1.23bs | 0.86s | 2.81s | |
| (5) | $[(\eta\text{-}C_5H_5)Ni(CH_2CMe_3)(PMe_3)]$ | Green | 57.9 (57.6) | 9.3 (9.2) | 0.97d[i] | 1.27s | 0.95d[i] | 5.35s (Cp) |
| (6) | $[(\eta\text{-}C_5H_5)Ni(COCH_2CMe_3)(PMe_3)]$ | Red[c] | 56.0 (56.2) | 8.4 (8.4) | 1.01d[i] | 1.19s | 3.01s | 5.34s (Cp) |
| (7) | $[(\eta\text{-}C_5H_5)Ni(CH_2CMe_2Ph)(PPh_3)]$ | Green | 75.6 (76.3) | 6.4 (6.4) | | 1.34s | 1.30d[i] | 5.10s (Cp) |
| (8) | $[Ni(CH_2SiMe_3)_2(dmpe)]$ | Yellow | 43.8 (43.9) | 9.9 (9.9) | 1.04d[j] | 0.45s | 0.23m[k] | 0.93m[k] ($CH_2P$) |
| (9) | $[Ni(CH_2CMe_2Ph)_2(dmpe)]$ | Yellow | 65.0 (65.7) | 8.7 (8.8) | 0.70d[j] | 1.86s | 1.86m[k] | 0.82m[k] ($CH_2P$) |

[a] Calculated values are in parentheses. [b] N: 4.1 (4.1). [c] $\nu$(CO) 1650 $cm^{-1}$. [d] $\nu$(NCS) 2085 $cm^{-1}$. [e] In $C_6H_6$ solution. [f] In $CH_2Cl_2$. [g] $J(HP)_{app}$ = 3Hz. [h] J(HP) 14Hz. [i] J(HP) 9Hz. [j] J(HP) 8Hz. [k] Complex multiplet.

$Mg(CH_2CMe_3)Cl$ to a suspension of $[NiCl_2(PMe_3)_2]$ in $Et_2O$ produces $[Ni(CH_2CMe_3)Cl(PMe_3)_2]$, (1), as yellow–brown crystals, in 60% yield. Formation of the dialkyl derivative is not detected, and the use of an excess of the alkylating reagent produces instead extensive decomposition and hence lower yields in complex 1.

IR and $^1$H NMR spectroscopic studies suggest 1 has a *trans* stereochemistry similar to that found for other $[Ni(R)X(PMe_3)_2]$ complexes.[2a] Thus, the $^1$H NMR spectrum shows, in the methylphosphine region, a triplet at $\delta$ 1.24 ppm characteristic of bis-phosphine complexes with strong coupling between the phosphorus nuclei; a slightly broad triplet, at 0.72 ppm, is due to coupling of the $NiCH_2R$ protons to two equivalent phosphorus nuclei. In the presence of traces of free $PMe_3$, these signals collapse to singlets, clearly indicating fast exchange of free and complexed $PMe_3$, possibly through a 5-coordinate intermediate species.[3] Formation of 5-coordinate derivatives is well documented[1,3,4] for complexes of this type and species of this sort have been postulated as intermediates in a number of their reactions, e.g. CO or alkyne insertions into the Ni–C bonds.

On bubbling CO through a solution of 1, at room temperature and pressure, a smooth, essentially quantitative reaction takes place, with formation of the corresponding acyl, $[Ni(COCH_2CMe_3)Cl(PMe_3)_2]$, (2), eqn (1),

$$[Ni(CH_2CMe_3)Cl(PMe_3)_2] + CO \rightarrow [Ni(COCH_2CMe_3)Cl(PMe_3)_2]. \quad (1)$$

Complex 2 is a yellow crystalline very thermally stable solid, which can be indefinitely stored at room temperature under $N_2$, without noticeable loss of carbon monoxide. Although sparingly soluble in petroleum it is very soluble in $Et_2O$, THF and aromatic hydrocarbons. While the presence of a strong IR band at *ca.* 1650 $cm^{-1}$ clearly indicates the existence of an acyl group coordinated to the nickel atom in the normal or monohapto fashion, the similarity of its $^1$H NMR spectrum with that of 1, is again indicative of *trans* geometry. Both 1 and 2 react with KNCS in acetone or tetrahydrofuran (THF) to yield the corresponding thiocyanate derivatives $[Ni(CH_2CMe_3)(NCS)(PMe_3)_2]$, (3) and $[Ni(COCH_2CMe_3)(NCS)(PMe_3)_2]$, (4) in high yield. Pertinent IR and $^1$H NMR data for these complexes are included in Table 1 and require no further comment.

*Cyclopentadienyl derivatives* $[Ni(R)(\eta\text{-}C_5H_5)L]$ *and* $[Ni(COR)(\eta\text{-}C_5H_5)L]$

Although complexes of composition $[NiR(\eta\text{-}C_5H_5)]$ are still unknown, closed-shell derivatives of the type $[NiR(\eta\text{-}C_5H_5)L]$, in which the

Ni(R)Cp unit is stabilized by a donor ligand have been known for many years.[1] More recently we have shown[2a] that the neophyl derivative $[Ni(CH_2CMe_2Ph)Cl(PMe_3)_2]$ reacts almost instantly with TlCp, in acetone, to afford $[NiR(\eta\text{-}C_5H_5)(PMe_3)]$, eqn (2),

$$[Ni(CH_2CMe_2Ph)Cl(PMe_3)_2] + TlCp \rightarrow$$
$$[Ni(CH_2CMe_2Ph)(\eta\text{-}C_5H_5)(PMe_3)] + PMe_3 + TlCl. \quad (2)$$

Surprisingly, no reaction is observed when complex **1** and TlCp are stirred in acetone, at room temperature, for a period of *ca.* 2–3 hr. The neopentyl derivative, $[Ni(CH_2CMe_3)(\eta\text{-}C_5H_5)(PMe_3)]$, (**5**), can however be obtained in high yield by using the more nucleophilic NaCp in diethyl ether solution. By an analogous procedure, the corresponding acyl derivative $[Ni(COCH_2CMe_3)(\eta\text{-}C_5H_5)(PMe_3)]$, (**6**) can be obtained from **2** and NaCp. It is important to note that complex **6** is not formed when **5** is reacted with carbon monoxide. The lack of reactivity towards CO can be explained by the inability of the complex to dissociate $PMe_3$ to form a reactive, sixteen-electron intermediate. This is in accord with the results of $^1H$ NMR studies carried out for this and other related compounds.[2a]

Infrared and $^1H$ NMR studies for complexes **5** and **6** are in agreement with the proposed formulations (see Table 1). Thus a singlet is observed for the Cp protons, indicating pentahapto coordination to the nickel atom, while the neopentylmethylene protons in **5** give rise to a doublet, with J(H–P) 9 Hz. On the other hand the addition of free $PMe_3$ to solutions of either **5** or **6** produces no changes in the spectrum, separate responses being observed for the free and the coordinated ligand. Thus, phosphine dissociation, if any, must be slow on the NMR time scale.

Finally, interaction of the complex $[NiCl(\eta\text{-}C_5H_5)(PPh_3)]$ with the neophyl Grignard reagent takes place as in eqn (3), affording the corresponding alkyl derivative **7**

$$[NiCl(\eta\text{-}C_5H_5)(PPh_3)] + Mg(R)Cl \rightarrow$$
$$[Ni(R)(\eta\text{-}C_5H_5)(PPh_3)] + MgCl_2 \quad R = CH_2CMe_2Ph. \quad (3)$$

The neophyl derivative **7** is a green crystalline solid, moderately air stable, which shows physical and spectral properties similar to those of the previously reported trimethylsilylmethyl and neopentyl analogues.[1,5]

*Dialkyl complexes* $[NiR_2(dmpe)]$. *The X-ray structure of* $[Ni(CH_2SiMe_3)_2(PMe_3)_2]$.

Although dialkyl derivatives of Ni(II) of composition $[NiR_2L_2]$ cannot be prepared[2b] by reacting $[NiCl_2L_2]$ complexes with an excess of the Grignard reagent, a number of complexes of this type can be obtained in good yields by taking advantage of the facility with which the unstable complexes $[Ni(CH_2SiMe_3)_2(py)_2]$ and $[Ni(CH_2CMe_2Ph)_2(tmen)]$ lose the nitrogen-containing ligands in solution. Using this we have now carried out the synthesis of the dmpe analogues $[NiR_2(dmpe)]$, eqn (4),

$$[Ni(CH_2SiMe_3)_2(py)_2] + dmpe \rightarrow$$
$$[Ni(CH_2SiMe_3)_2(dmpe)], \mathbf{8} + 2py$$
$$[Ni(CH_2CMe_2Ph)_2(tmen)] + dmpe \rightarrow$$
$$[Ni(CH_2CMe_2Ph)_2(dmpe)], \mathbf{9} + tmen. \quad (4)$$

Compounds **8** and **9** can be isolated as yellow, air-sensitive crystals, which are soluble in petroleum, benzene and non-hydrocarbon solvents.

Table 2. Crystal data and summary of intensity data collection and structure refinement

| | |
|---|---|
| Cmpd | $Ni(CH_2SiMe_3)_2(PMe_3)_2$ |
| Mol wt | 385.3 |
| Space group | Pbcn |
| Cell constants | |
| a, Å | 14.345(4) |
| b, Å | 12.656(3) |
| c, Å | 12.815(3) |
| Cell vol, $Å^3$ | 2326.6 |
| Molecules/unit cell | 4 |
| $\rho$(calc), g $cm^{-3}$ | 1.10 |
| $\mu$(calc), $cm^{-1}$ | 10.58 |
| Radiation | MoKα |
| Max crystal dimension, mm | 0.25 x 0.40 x 0.55 |
| Scan width | 0.80 + 0.20 tanθ |
| Standard reflections | 600, 040, 004 |
| Decay of standards | 39% |
| Reflections measured | 1012 |
| 2θ range | 36° |
| Reflections collected | 535 |
| No. of parameters varied | 87 |
| GOF | 1.93 |
| R | 0.077 |
| Rw | 0.076 |

For $R = CH_2CMe_3$, the instability of the pyridine or tmen intermediates has precluded isolation of analytically pure samples of $[Ni(CH_2CMe_3)_2(dmpe)]$.

While the IR spectra of **8** and **9** show absorptions characteristic of the alkyl and phosphine ligands, the $^1H$ NMR spectra are complex, due not only to the complexity of the spin system involved but also because of fortuitous similarities in the chemical shifts of some of the phosphine and alkyl groups protons. This makes the assignment of the resonances difficult and therefore, in some cases (see Table 1), we merely point out the position of the bands. The chemical shifts observed for the P–Me protons have similar values to those found in other dmpe complexes.[6]

We have shown recently that addition of a slight excess of $PMe_3$ to a petroleum solution of *cis*-$[Ni(CH_2SiMe_3)_2(py)_2]$ yields $[Ni(CH_2SiMe_3)_2(PMe_3)_2]$ in almost quantitative yield.[2b] $^1H$ and $^{31}P$ NMR studies for this complex suggest the presence in solution of *cis* and *trans* isomers in a *ca.* 4:1 ratio, the isomerization being slow on the NMR time scale, even in the presence of free base. An X-ray crystal structure determination shows the *trans* geometry to be the preferred in the solid state. The molecular structure and atom-labeling scheme for $[Ni(CH_2SiMe_3)_2(PMe_3)_2]$ are presented in Fig. 1. The molecule resides on a crystallographic two-fold axis containing the Ni atom. The overall geometry is that of a distorted square-planar arrangement with *trans*-phosphines (P–Ni–P′ = 146.9(3)°—Table 3).

Although high standard deviations in the bond distances and angles, a result of crystal decomposition (see experimental section), rule out a detailed study of the bonding in the title compound, some comparisons can be made. The Ni–P bond length, 2.158(4)Å, is somewhat shorter than the 2.206 and 2.201 Å averages found for $[Ni(CH_2SiMe_3)Cl(PMe_3)_2]$[2a] and $Ni(COCH_2SiMe_3)Cl(PMe_3)_2$,[2a] respectively. The title compound also exhibits a smaller P–Ni–P bond angle (146.9(3)° vs 164.0 and 167.6°). Correspondingly, a slightly longer Ni–C bond length of 2.08(2)Å is found in $[Ni(CH_2SiMe_3)_2(PMe_3)_2]$ than in $[Ni(CH_2SiMe_3)Cl(PMe_3)_2]$ (1.95Å), $[Ni(COCH_2SiMe_3)Cl(PMe_3)_2]$ (1.84Å) and $[Ni(CH_2SiMe_3)_2(NC_5H_5)_2]$ (1.89(1)Å).[2b] The C–Ni–C angle in the title compound is 170(1)°.

## EXPERIMENTAL

Microanalyses were by Pascher Microanalytical Laboratory, Bonn. The spectroscopic instruments

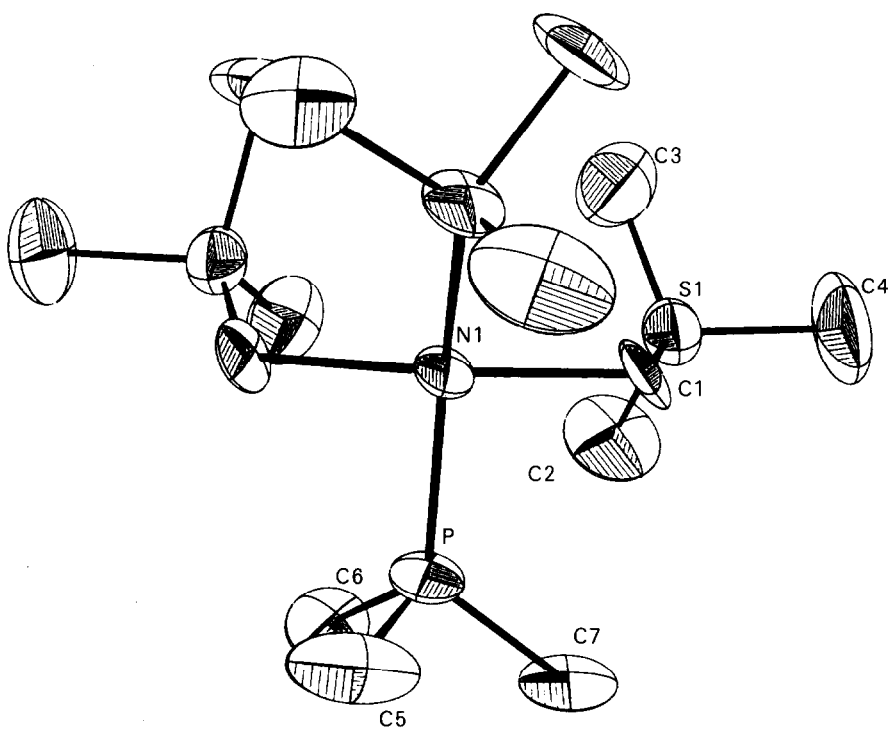



Fig. 1. Molecular structure and atom-labeling scheme for $Ni(CH_2SiMe_3)_2(PMe_3)_2$. The atoms are represented by their 50% probability ellipsoids for thermal motion. The molecule resides on a crystallographic two-fold axis.

Table 3. Bond lengths (Å) and bond angles (°) for $Ni(CH_2SiMe_3)_2(PMe_3)_2$

| Atom | x/a | y/b | z/c |
|---|---|---|---|
| Ni | 0.0000 | 0.1291(3) | 0.2500 |
| P | 0.1432(3) | 0.0805(4) | 0.2690(4) |
| Si | -0.0080(4) | 0.2789(5) | 0.4499(4) |
| C(1) | -0.023(1) | 0.143(2) | 0.409(1) |
| C(2) | 0.118(1) | 0.336(2) | 0.435(2) |
| C(3) | -0.086(2) | 0.376(2) | 0.385(2) |
| C(4) | -0.034(2) | 0.293(2) | 0.597(1) |
| C(5) | 0.150(1) | -0.051(2) | 0.217(2) |
| C(6) | 0.239(1) | 0.150(2) | 0.202(1) |
| C(7) | 0.195(1) | 0.055(2) | 0.398(2) |

used were a Perkin–Elmer model 577 for IR spectra and a Perkin–Elmer R12A for $^1H$ NMR spectra. All preparations and other operations were carried out under oxygen-free nitrogen, following conventional Schlenk techniques. Solvents were dried and degassed before use. The light petroleum used had b.p. 40–60°C. $PMe_3$,[7] $NiCl_2(PMe_3)_2$[8] and $[NiR_2L_2]$(L = py, tmen)[2b] were prepared according to literature methods.

*Chloro(neopentyl)bis(trimethylphosphine)nickel(II)* (1)

To a stirred suspension of $[NiCl_2(PMe_3)_2]$ (1.5 g, *ca.* 5.3 mmol) in diethyl ether (80 $cm^3$) cooled at −60°C was added $Mg(CH_2CMe_3)Cl$ (11.5 $cm^3$ of a *ca.* 0.6 mol $dm^{-3}$ diethyl ether solution, a slight excess). The mixture was stirred at this temperature for 30 min, then at 0°C for 2–3 hr, and finally at room temperature for 1 hr. The solvent was removed *in vacuo* and the residue extracted with 60 $cm^3$ of light petroleum. The solution was centrifuged and the product crystalized as light brown needles by removing part of the solvent and cooling at −30°C. Yield 60%.

*Chloro(neopentylcarbonyl)bis(trimethylphosphine)nickel(II)*, (2)

Carbon monoxide was bubbled, at room temperature and pressure, through a solution of the alkyl-complex **1** (0.31 g, *ca.* 1 mmol) in diethyl ether (30 $cm^3$) for about 10 min. The resulting solution, which had considerably faded was evaporated to dryness, the residue dissolved in 20 $cm^3$ of $Et_2O$ and the mixture centrifuged to remove a small amount of an insoluble material. Cooling overnight at −30°C afforded the title compound as yellow microcrystals. They were filtered off and dried *in vacuo*. Yield 90%. Crystals of analytical purity can be obtained by recrystallisation from $Et_2O$ at 5°C.

*Thiocyanate(neopentyl)bis(trimethylphosphine)nickel(II)*, (3)

Complex **1** (0.3 g, *ca.* 1 mmol) and an excess of KNCS, previously dried by heating at 110°C for *ca.* 24 hr, were stirred in THF or acetone (20 $cm^3$) for 1 hr at room temperature. The solvent was stripped off under reduced pressure and the residue extracted with an $Et_2O$-petroleum mixture. After centrifugation and cooling at −30°C the product was obtained as golden plates in *ca.* 70% yield. The neopentylcarbonyl derivative, $[Ni(COCH_2CMe_3)(NCS)(PMe_3)_2]$ (**4**), can be obtained similarly from $[Ni(COCH_2CMe_3)(PMe_3)_2]$ and KNCS. The compound crystallised as yellow microcrystals from $Et_2O$-acetone.

*(η-cyclopentadienyl)neopentyl(trimethylphosphine)nickel(II)*, (5)

A stirred solution of $[Ni(CH_2CMe_3)Cl(PMe_3)_2]$, **1**, (0.23 g, *ca.* 0.7 mmol) in $Et_2O$ (20 $cm^3$) was reacted at room temperature with an equimolecular amount of NaCp (0.7 $cm^3$ of a *ca.* 1.0 mol $dm^{-3}$ diethyl ether solution). A fine precipitate of NaCl immediately appeared and the colour of the solution changed to green-yellow. The mixture was stirred for 30 min and then evaporated to dryness. Petroleum ether was added (30 $cm^3$) and the suspension centrifuged. Green–yellow crystals were obtained in *ca.* 75% yield after removing part of the solvent and cooling at −80°C.

The reaction of the acyl complex $[Ni(COCH_2CMe_3)Cl(PMe_3)_2]$ with NaCp was carried out in a similar way to give $[Ni(\eta\text{-}C_5H_5)(COCH_2CMe_3)(PMe_3)]$, (**6**), as red crystals from light petroleum.

*(η-cyclopentadienyl)neophyl(triphenylphosphine) nickel (II), (7)*

To a stirred and cold (−80°C) suspension of $[(\eta\text{-}C_5H_5)NiCl(PPh_3)]$ (0.84 g, *ca.* 2 mmol) in $Et_2O$ (40 $cm^3$) 2 equiv of neophyl Grignard reagent (in $Et_2O$ solution) were added via syringe. The cold bath was then removed and the mixture stirred at room temperature for 1–2 hr until complete disappearance of the red starting material. The solvent was removed *in vacuo* and the residue extracted with light petroleum (30 $cm^3$). The green suspension was centrifuged and the volume of the solution partially reduced *in vacuo*. Cooling at −30°C afforded the product as green crystals in *ca.* 40% yield Analytically pure samples were obtained by recrystallisation of the crude product from petroleum at −30°C.

*Bis(trimethylsilylmethyl)- and bis(neophyl)-(1,2-bis(dimethylphosphine)ethane)nickel(II), (8) and (9)*

To a solid sample of $[Ni(CH_2SiMe_3)_2(py)_2]$ (0.64 g, *ca.* 1.6 mmol) a cold (−60°C) solution of dmpe (0.32 $cm^3$, *ca.* 1.6 mmol) in light petroleum (20 $cm^3$) was added. The mixture was allowed to reach room temperature with stirring, when the brown crystals of the pyridine complex dissolved to give a yellow solution. The stirring was continued for 30 min and the solvent evaporated to dryness. Extraction with petroleum (20 $cm^3$) and cooling at −30°C gave the title compound as yellow crystals in almost quantitative yield. The complex was recrystallised from petroleum at 5°C.

A similar procedure starting from $[Ni(CH_2CMe_2Ph)_2(tmen)]$ afforded $[Ni(CH_2CMe_2Ph)_2(dmpe)]$ as yellow crystals from petroleum in *ca.* 15% yield.

*X-Ray data collection, structure determination and refinement for* $[Ni(CH_2SiMe_3)_2(PMe_3)_2]$

Single crystals of the air-sensitive compound were sealed under $N_2$ in thin-walled glass capillaries. Final lattice parameters as determined from a least-squares refinement of $((\sin\theta)/\lambda)^2$ values for 15 reflections ($\theta > 20°$) accurately centered in the diffractometer are given in Table 2. The space group was uniquely determined as *Pbcn* from the systematic absences.

Data were collected on an Enraf–Nonius CAD–4 diffractometer by the $\theta$–$2\theta$ scan technique. The method has been previously described.[9] A summary of data collection parameters is given in Table 2. During data collection the crystal slowly decomposed in the X-ray beam. The intensities were corrected for Lorentz, polarization, and, decomposition effects, but not for absorption.

Calculations were carried out with the SHELX system of computer programs.[10] Neutral atom scattering factors for Ni, P, Si and C were taken from Cromer and Waber,[11] and the scattering for nickel was corrected for the real and imaginary components of anomalous dispersion using the table of Cromer and Liberman.[12] Scattering factors for H were from Ref. 13.

The position of the nickel atom was revealed by the inspection of a Patterson map. A difference Fourier map phased on the nickel atom readily revealed the positions of the nonhydrogen atoms. Least-squares refinement with isotropic thermal parameters led to $R = \Sigma\|F_o| - |F_c\|/\Sigma|f_o| = 0.099$. As a result of the problems associated with crystal decomposition, the hydrogen atoms could not be located and were not included in any refinement. Refinement with anisotropic temperature factors led to final values of $R = 0.077$ and $R_w = 0.076$. A final difference Fourier showed no feature greater than 0.5 $e^-/Å^3$. The weighting scheme was based on unit weights; no systematic variation of $w(|F_o| - |F_c|)$ vs $|F_o|$ or $(\sin\theta)/\lambda$ was noted. The final values of the positional and thermal parameters have been deposited as supplementary material with the Editor, from whom copies are available on request.†

*Acknowledgements*—We thank the Spanish C.A.I.C.Y.T. (E.C.) and the U.S.A. National Science Foundation (R.D.R. and J.L.A.)

## REFERENCES

1. P. W. Jolly, In *Comprehensive Organometallic Chemistry*, Vol. 6, Chap. 37.4. Pergamon Press, Oxford (1982).
2. (a) E. Carmona, F. González, M. L. Poveda, J. L. Atwood and R. D. Rogers, *J. Chem. Soc., Dalton* 1980, 2108. (b) E. Carmona, F. González, M. L., Poveda, J. L. Atwood and R. D. Rogers, *J. Chem. Soc. Dalton* 1981, 777. (c) E. Carmona, F. González, M. L. Poveda, J. M. Marín and A. Martínez, *An. Quím.* 1982, **78B**, 51; E. Carmona, F. González, M. L. Poveda and J. M. Marín, *Synth. React. Inorg. Met.-Org. Chem.* 1982, **12**, 185.
3. H. F. Klein and H. H. Karsch, *Chem. Ber.* 1972, **105**, 2628.
4. D. W. Firsich and R. J. Lagow, *J. Chem. Soc., Chem. Comm.* 1981, 1283; P. F. Meier, A. E. Merbach, M. Dartiguenave and Y. Dartiguenave, *Inorg. Chem.* 1979, **18**, 610.
5. P. W. Jolly and G. Wilke, In *The Organic Chemistry of Nickel*, Vol. 1. Academic Press, London (1974).

†Atomic coordinates have also been deposited with the Cambridge Crystallographic Data Centre.

6. See for instance S. J. Holmes, D. N. Clark, H. W. Turner and R. R. Schrock, *J. Am. Chem. Soc.* 1982, **104**, 6322.
7. W. Wolfsberger and H. Schmidbaur, *Synth. React. Inorg. Met.-Org. Chem.* 1974, **4**, 149.
8. O. Dahl, *Acta Chem. Scand.* 1969, **23**, 2342.
9. J. Holton, M. F. Lappert, D. G. H. Ballard, R. Pearce, J. L. Atwood and W. E. Hunter, *J. Chem. Soc., Dalton* 1979, 45.
10. SHELX, a system of computer programs for X-ray structures determination by G. M. Sheldrick, 1976.
11. D. T. Cromer and J. T. Waber, *Acta Cryst.* 1965, **18**, 104.
12. D. T. Cromer and D. Liberman, *J. Chem. Phys.* 1970, **53**, 1891.
13. *International Tables for X-ray Crystallography*, Vol. 4, p. 72. Kynoch Press, Birmingham (1974).

*Polyhedron* Vol. 3, No. 3, pp. 325–329, 1984
Printed in Great Britain.

0277–5387/84 $3.00 + .00
Pergamon Press Ltd.

# 2,2,3,4,4-PENTAMETHYLPHOSPHETANIC ACID, $C_8H_{16}PO_2H$: SALTS, COMPLEXES AND A HYDROGEN BONDED AMINE ADDUCT

**JOHN EMSLEY,* AMANDA P. DUNNING, ROBERT J. PARKER and JOHN K. WILLIAMS**

Department of Chemistry, King's College, Strand, London WC2R 2LS, England

**SHIRLEY BROWN, STELLA EARNSHAW and DAVID S. MOORE†**

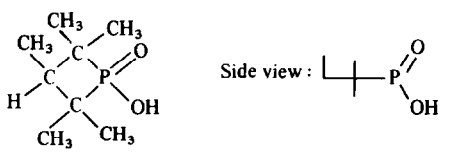
Department of Chemistry, Imperial College of Science and Technology, South Kensington, London SW7 2AY, England

(*Received* 1 *July* 1983; *accepted* 25 *July* 1983)

**Abstract**—The conjugate base of the title acid, i.e. $C_8H_{16}PO_2^-$, has been investigated as its simple salts, as a ligand in transition metal complexes of cobalt and ruthenium, and as a secondary amonium salt in which hydrogen bonding between anion and cation occurs.

1-Chloro-2,2,3,4,4-pentamethylphosphetan 1-oxide, $C_8H_{16}POCl$, can be easily synthesized from 2,4,4-trimethylpent-2-ene and $PCl_3$ in the presence of $Al_2Cl_6$.[1,2] This chloride is slowly hydrolysed in air. The products of hydrolysis may be the acid, a phosphetanic acid, $C_8H_{16}PO_2H$, or the anhydride, $C_8H_{16}P(O)OP(O)C_8H_{16}$, depending on conditions.[3] The latter is rapidly formed[4] and is remarkably stable to further hydrolysis.[3]

Little has been written about $C_8H_{16}PO_2H$ beyond reporting a few basic physical properties and spectra.[5] It is a fairly strong acid, $pK_a$ 2.85.[1] Its structure is assumed to be (I), based on that of other phosphetans.[6]




(I)

Whereas for the chloride there are two non-interconverting isomers, *cis* and *trans*, defined for the ring H and PO groups with respect to the plane of the ring, there can be only one form of the acid. The conjugate base, $C_8H_{16}PO_2^-$, has a plane of symmetry bisecting the phosphetan ring. Because of the similarity of $R_2PO_2H$ and $R_2PO_2^-$ to $RCO_2H$ and $RCO_2^-$, it was thought likely that this phosphinic acid might also display some of the properties of a typical carboxylic acid in its ability (i) to act as a ligand, and (ii) to involve itself in hydrogen bonding including possibly very strong hydrogen bonding.[7] These hopes have been realized and in this communication we present evidence of $C_8H_{16}PO_2^-$ acting as a ligand towards certain transition metals and of $C_8H_{16}PO_2H$ forming an adduct with secondary amines in which a cyclic hydrogen bonding system is suspected.

## EXPERIMENTAL

*Instruments.* IR spectra as KBr discs were run on PE457 and PE580 machines. Nuclear magnetic spectra were taken on JEOL PMX60 SI, Bruker HFX90 and Bruker WM250 spectrometers. $^{31}P$ NMR spectra at 36.4 MHz are referenced to external $H_3PO_4$. UV spectra were taken on a UNICAM SP800 spectrometer

*Preparation of* 2,2,3,4,4-*pentamethylphosphetanic acid,* $C_8H_{16}PO_2H$

$C_8H_{16}POCl$, made by the reported methods,[1,2] is hygroscopic. On exposure it the atmosphere for *ca.*

*Author to whom correspondence should be addressed.

†Present address: Priory House, Dover College, 6 Waterloo Crescent, Dover, Kent CT16 1LA, England.

1 week it is converted to the acid. Refluxing a mixture of $C_8H_{16}POCl$ and water for 3 hr produces a mixture of the acid and the anhydride $C_8H_{16}P(O)OP(O)C_8H_{16}$. Aqueous 2M NaOH solution and $C_8H_{16}POCl$ react to give the same mixture, although with less anhydride, from which the acid can be recovered by treatment with 2M HCl. The acid is only slightly soluble in water (1.33 g/100 $cm^3$ $H_2O$ at 20°C).

The $^{31}P$ NMR spectrum of $C_8H_{16}PO_2H$ in $CDCl_3$ consists of a multiplet of 13 peaks (3747 scans), with $^3J_{PCCH_3}$ 18.55 Hz, split into doublets due to $^3J_{PCCH}$, 5.86 Hz. Further fine structure from $^4J_{PCCH_3}$ was evident but not resolvable. No evidence of $J_{POH}$ coupling shows that rapid exchange in this solvent is occurring probably via hydrogen bonding. The proton decoupled spectrum has $\delta$ 59.04 ppm. In $D_2O$ the decoupled signal is at $\delta$ 59.18 ppm.

## SALTS

*Preparation of lithium 2,2,3,4,4-pentamethylphosphetanate.* To a solution of lithium hydroxide monohydrate (0.42 g, 10 mmol) in water (10 $cm^3$) was added $C_8H_{16}PO_2H$ (1.76 g, 10 mmol). The solution was evaporated to yield $C_8H_{16}PO_2Li$ which was dried at 130°C. The $^1H$ NMR spectrum of a solution in $D_2O$ gave signals at 1.50 (1H, CH, dq, $J_{HCCH_3} = 4.5$ Hz), 1.03 (12H, $CH_3$, dd, $J_{PCCH_3} = 17.5$ Hz) 0.78 ppm (3H, $CH_3$, dd, $J_{PCCH_3}$ 1.5 Hz). The calcium salt was made likewise.

In a similar reaction, but using metal carbonate, the following salts were made: Na, K, Rb, Cs, Sr, Ba and Ag. The silver salt darkened on exposure to light. The ammonium salt was made from $C_8H_{16}PO_2H$ and liquid $NH_3$ in toluene. All the salts gave similar IR spectra showing the characteristic phosphetan vibration absorptions. The $\nu_{as}(PO_2^-)$ and $\nu_s(PO_2^-)$ modes were recognizable as a pair of strong bands at 1160–1130 $cm^{-1}$ and 1050–1030 $cm^{-1}$ respectively. The $^{31}P$ NMR signal of $C_8H_{16}PO_2K$ in $D_2O$ gave a spectrum like that of the acid (2521 scans) from which $^3J_{PCCH_3} = 17.63$ Hz and $^3J_{PCCH_3} = 3.42$ Hz. The proton decoupled signal appeared at $\delta$ 49.1 ppm.

$C_{18}H_{16}PO_2K$ *and* $C_8H_{16}PO_2H$. An aqueous solution of $C_8H_{16}PO_2K$ is capable of dissolving more acid than the same volume of water. Thus a 0.187 M solution of $C_8H_{16}PO_2K$ was stirred for several hours with excess $C_8H_{16}PO_2H$ and the latter dissolved to give a solution of 0.204 M in acid; the mole ratio of salt: acid is 1:1.09. The $^{31}P$ NMR spectrum of the resulting solution showed only a 13 peak multiplet with $^3J_{PCCH_3} = 16.85$ Hz (5343 scans). The fine structure due to $^3J_{PCCH}$ was not evident but unresolved substructure was present. The proton decoupled signal was at $\delta$ 48.97 ppm.

## COMPLEXES

*Reaction of* $C_8H_{16}PO_2H$ *and cobalt(II) carbonate.* Cobalt(II) carbonate (2.0 g, 16 mmol) was added to a solution of $C_8H_{16}PO_2H$ (7.0 g, 40 mmol) dissolved in hot water; $CO_2$ was evolved. When all the $CoCO_3$ had reacted the pink solution was heated to boiling and a blue precipitate formed which was filtered hot. This was *bis*(2,2,3,4,4-pentamethylphosphetanato) cobalt(II), $Co(C_8H_{16}PO_2)_2$ (6.2 g, 12 mmol, 60%), m.p. > 360°C. The complex was stable in air. Found: C, 46.93; H, 7.82; P, 15.13. $C_{16}H_{32}CoO_4P_2$ requires: C, 46.94; H, 7.82; P, 15.16%.

$Co(C_8H_{16}PO_2)_2$ gave an IR spectrum with absorptions at 2975–2861 s ($CH_3$), 1460 m ($CH_3$, 1393–1370 w ($CH_3$), 1240 w (P), 1208 w, 1143 s (P), 1092 s ($PO_2$), 1062 s ($PO_2$), 1020 m ($CH_3$), 940 w (P), 760 w (P), 730 sh (P), 657 m (P), 545 m (CoOP), 534 sh (P), 418 w, 410 w (P), 312 m $cm^{-1}$, where P refers to the mode being a recognized phosphetan ring absorption.[5]

The UV spectrum of a $CHCl_3$ solution (blue) has $\lambda_{max}$ 500 nm (118,000 $mol^{-1}$ $cm^2$), 580 nm (138,000 $mol^{-1}$ $cm^2$), 626 nm (147,000 $mol^{-1}$ $cm^2$).

An aqueous solution (pink) has $\lambda_{max}$ 500 nm (1680 $mol^{-1}$ $cm^2$).

The blue crystals of $Co(C_8H_{16}PO_2)_2$ are soluble in cold water to form a pink solution which on heating to 79°C precipitates the blue complex. This in turn redissolves as the solution is allowed to cool. The blue complex is also soluble in $CHCl_3$ but can be extracted from this solvent into water as a pink solution. This technique can be used to remove unreacted $C_8H_{16}PO_2H$.

The blue complex can also be prepared by heating $Co(NO_3)_2$ and an excess of $C_8H_{16}PO_2H$ in an acetone solution for 2 hr.

From a cold aqueous solution of $Co(C_8H_{16}PO_2)_2$ pink crystals grow on evaporation of the solvent. On standing these slowly revert to the blue form, rapidly at 40°C or on being left in a desiccator.

The magnetic susceptibility of the blue complex was measured by the Gouy method at $19960 \times 10^{-12}$ $m^3$ $mol^{-1}$ from which a magnetic moment of 6.1 Bohr magnetons was calculated. The diamagnetic correction factor for $C_8H_{16}PO_2H$ was calculated as $-2561 \times 10^{-12}$ $m^3$ $mol^{-1}$.

*Reaction of* $C_8H_{16}PO_2H$ *and maganese(II) nitrate.* Manganese(II) nitrate (1.78 g, 10 mmol) and $C_8H_{16}PO_2H$ (5.0 g, 28 mmol) were refluxed together in acetone (20 $cm^3$) for 2 hr. On cooling, white microcrystalline needles of the complex *bis*(2,2,3,4,4-pentamethylphosphetanato) manganese(II) formed (2.9 g, 7.1 mol, 71%), m.p. > 360°C. Found: C, 46.81; H, 7.84; P, 14.75. Calculated for $C_{16}H_{32}MnO_4P_2$: C, 47.41; H, 7.90; P,

15.31%. The IR spectrum (Nujol mull) showed absorptions: 1239 m (P), 1147 s (P), 1089 m ($PO_2$), 1056 m ($PO_2$), 1019 m ($CH_3$), 989 w, 934 m (P), 758 m (P), 672 s (P), 641 m (P), 560 w (P), 540 s (P), 521 sh (MnOP) $cm^{-1}$.

*Preparation of* $RuX_2Y_2$ *(phosphetanato) complexes* [X = Cl, Br; Y = $PPh_3$, $AsPh_3$, $PpyPh_2$]

The $RuX_2Y_3$ complex, made by published methods,[8,9] was dissolved in benzene under aerobic conditions in the presence of $C_8H_{16}PO_2H$. The mixture was stirred for 3 hr, the solvent removed and the oily product crystallized from petroleum spirit (60/80°). The following compounds were prepared by this method: *dichloro*(2,2,3,4,4 - *pentamethylphosphetanato*) - *bis*(*triphenylphosphine*)*ruthenium*, dark green crystals m.p. 130°C, yield 31%, [Found: C, 59.40; H, 5.22; P, 10.29; $C_{44}H_{46}Cl_2O_2P_3Ru$ requires: C, 60.62; H, 5.28; P, 10.68%]; *dibromo*(2,2,3,4,4-*pentamethylphosphetanato*)*bis*(*triphenylphos* - *phine*)*ruthenium*, brown crystals, m.p. 142°C, yield 46% [Found: C, 54.86; H, 4.60; P, 9.62, $C_{44}H_{46}Br_2O_2P_3Ru$ requires: C, 55.00; H, 4.79; P, 9.69%]; *dichloro*(2,2,3,4,4-*pentamethylphos* - *phetanato*)*bis*(*tripyrridinodiphenylphosphine*)*ruth* - *enium*, orange–brown crystals, m.p. 118°C, yield 11%; [Found: C, 56.90; H, 5.02; P, 10.47; N, 3.15; $C_{42}H_{46}Cl_2N_2O_2P_3Ru$ requires: C, 57.60; H, 5.26; P, 10.63; N, 3.20%]; *dibromo*(2,2,3,4,4-*pentame* - *thylphosphetanato*)*bis*(*pyridinodiphenylphosphine*) - *ruthenium*, pale yellow crystals, m.p. 102°C, yield 11%; [Found: C, 52.17; H, 4.67; P, 9.58; N, 2.85; $C_{42}H_{46}Br_2N_2O_2P_3Ru$ requires: C, 52.28; H, 4.77; P, 9.65; N, 2.90%]; and *dichloro*(2,2,3,4,4-*penta* - *methylphosphetanato*)*bis*(*triphenylarsine*)*ruthenium*, *ruthenium*, brown crystals, m.p. > 230°C, yield 20%; [Found: C, 55.00; H, 4.73; P, 2.98; $C_{44}H_{46}As_2Cl_2O_2PRu$ requires: C, 55.05; H, 4.79; P, 3.23%].

## ADDUCTS

*Reaction of* $C_8H_{16}PO_2H$ *and diethylamine.* Diethylamine (0.73 g, 10 mmol) was mixed with water (5 $cm^3$) and $C_8H_{16}PO_2H$ (1.76 g, 10 mmol) added. This slowly dissolved and the solution was evaporated to dryness on a steam bath to yield 2.49 g of a solid that was recrystallized from benzene to yield the adduct $C_8H_{16}PO_2H.NEt_2H$, m.p. 153–156°. Found: C, 55.7; H, 11.25; N, 5.43. $C_{12}H_{28}NO_2P$ requires: C, 57.8; H, 11.24; N, 5.62%. The IR spectrum has absorbances at 3450 vw br (trace of free amine), 3000–2860 s ($CH_3$), 2700 sbr ($NH_2$), 2520 sbr ($NH_2$), 2410 sbr ($NH_2$), 2345 s ($NH_2$), 1942 wbr, 1717 wbr, 1627 m, 1514 m, 1465 s ($CH_3$), 1453 s ($CH_3$), 1333 w ($CH_3$), 1231 w (P) 1217 w (P), 1143 s (P), 1079 s ($PO_2$), 1037 s ($PO_2$), 1010 s, 982 w ($CH_3$), 932 w (P), 870 w, 813 s (P), 764 w, 756 w (P), 722 vw, 660 s (P), 634 m (P), 532 s (P), 503 w, 450 vw (P), 418 m (P), 384 m (P), 330 m $cm^{-1}$.

The $^1H$ NMR spectrum run in $CDCl_3$ has resonances at 0.83 (3H, ring $CH_3$, dd, $^4J_{PCCCH_3} = 1.61$, $^3J_{HCCCH_3} = 7.11$ Hz), 1.10 (6H, ring $CH_3$, d, $^3J_{PCCH_3} = 17.0$ Hz), 1.13 (6H, ring $CH_3$, d, $^3J_{PCCH_3} = 17.0$ Hz), 1.36 (6H, amine $CH_3$, t, $^3J_{H_2CCH_3} = 7.34$ Hz), 1.50 (1H, CH, dq, $^3J_{PCCH} = 5.28$ Hz, $^3J_{HCCH_3} = 7.11$ Hz); 2.90 (4H, $CH_2$, q, $^3J_{H_2CCH_3} = 7.34$ Hz), 10.5 (2H, $NH_2$, very broad) ppm. The $\delta$(NH) was sensitive to concentration. At infinite dilution this was projected to have a chemical shift of 9.75 ppm.

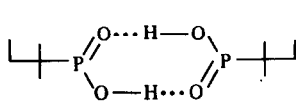
The $^{13}P$ NMR spectrum, proton decoupled, had $\delta = 49.05$ ppm in $D_2O$ and 37.38 ppm in $CDCl_3$. In an undecoupled spectrum (30307 scans) the 13 multiplet clearly showed $^3J_{PCCH_3}$ coupling (16.18 Hz) but the finer coupling could not be resolved.

## DISCUSSION

The physical and spectral features of 2,2,3,4,4-pentamethylphosphetanic acid, $C_8H_{16}PO_2H$, are given in Refs. 1 and 5 respectively. This acid is a phosphinic acid that, unlike most of this type, is easily made and is stable to hydrolysis. Moreover the phosphetan ring itself is very stable towards chemical attack. To date little has been said of its chemical behaviour as an acid and in this paper we report on the formation of some salts, complexes and an amine adduct.

$C_8H_{16}PO_2H$ is not very soluble in water. The hydrophobic tendency of the five methyl groups is enough to cancel the hydrophilicity of the acid centre. It is soluble in organic solvents. The metal salts of the acid are water soluble.

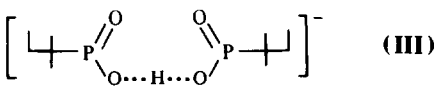
In some respects the behaviour of $C_8H_{16}PO_2H$ is expected to parallel that of carboxylic acids so that mutual hydrogen bond formation to give cyclic dimers would be anticipated, i.e. (II).[10] The $\nu_{OH}$ signal at *ca.*


(II)

3500 $cm^{-1}$ is not observed but two very broad and strong peaks at 2250 and 2600 $cm^{-1}$ can be attributed to $\nu$(OH · · O) of (II) by analogy with carboxylic acid dimers. Other broad bands at 955 and

500 $cm^{-1}$ are the corresponding in-plane and out-of-plane OH · · O bending modes. Dilution of $C_8H_{16}PO_2H$ in $CCl_4$ down to 0.001 M concentration failed to produce a signal in the spectrum at *ca.* 3500 $cm^{-1}$ that could arise from the monomeric acid species. This seems to be evidence that the hydrogen bonding of **(II)** is stronger than that of $(RCO_2H)_2$ where dilution disturbs the equilibrium towards the monomer sufficiently for the latter's OH bond vibration to be observed.

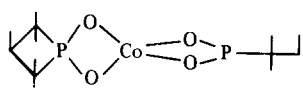
If the hydrogen bonding of acids is strong then that between an acid and its conjugate base is generally very strong.[7] Examples of this are the hydrogen bonds between the following combinations: $CH_3CO_2H + CH_3CO_2^-$;[11,12] $HNO_3 + NO_3^-$;[13] and even between $HSO_4^- + SO_4^{2-}$.[14] Indeed the first of these combinations, carboxylic acid and carboxylate, has yielded a large number of very strongly hydrogen bonded adducts.[15] Few examples of phosphorus acids interacting in this way are known but in $Ca_2(NH_4)H_7(PO_4)_4 \cdot 2H_2O$ there is a polymeric arrangement of $H_2PO_4^- + HPO_4^{2-}$.[16] There is thus high expectation that $C_8H_{16}PO_2H + C_8H_{16}PO_2^-$ would interact in this manner to form an adduct (III).




**(III)**

That this may occur is supported by the salting-in effect which occurs when $C_8H_{16}PO_2K$ is dissolved in water and the fact that this produces a solution that is approximately of the right composition for **(III)**. Unfortunately crystals which grew from slow evaporation of such solutions were unsuitable for X-ray investigation. However the IR spectrum showed a high water content and a continuum in the region 850–450 $cm^{-1}$ which may arise from a very strong hydrogen bond of the OHO type. Moreover the chemical shift of the phosphorus is not a weighted average of the acid and the anion, being almost the same as that of the anion. This suggests that both phosphetan parts have a deprotonated environment such as would be expected for **(III)** with the proton centred in the strong hydrogen bond.

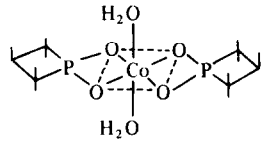
The ability of the conjugate base $C_8H_{16}PO_2^-$ to act as a ligand was demonstrated by the formation of several complexes and in particular the cobalt (II) complex. This occurs in two forms which interconvert at 79° in solution. Above this temperature the tetrahedra complex is favoured and the structure **(IV)** is proposed as the most likely form based on the




**(IV)**

IR and UV evidence.[17] This form is stable at room temperature in the solid state but in aqueous solution it dissolves to form a pink solution, although in $CHCl_3$ it retains the tetrahedral configuration as shown by its colour and UV spectrum. Changes in the vibrational frequencies for the $\nu_s$ and $\nu_{as}(PO_2)$ modes are not dramatically different as compared to those of the salts except the $\nu_{as}(PO_2)$ is at a lower and $\nu_{as}(PO_2)$ at a slightly higher frequency than expected. A band in the IR spectrum at 545 $cm^{-1}$ is not a phosphetan vibration and is tentatively assigned to a Co–O vibration.

The pink crystals which can be grown from aqueous solution at room temperature are presumably octahedral and structure (V) is a reasonable assumption which would explain their colour and spectra. These crystals readily lose water and turn blue which suggest that it is the coordinated water molecules that are lost.




**(V)**

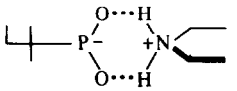
Whether this complex holds together in solution as V or exists in equilibrium with $Co(H_2O)_6^{2+}$ could not be determined conclusively from the UV spectrum; the $\lambda_{max}$ of 500 nm may overlap the $\lambda_{max}$ of $Co(H_2O)_6^{2+}$ at 530 nm, but the band was a single maximum with no suggestion of a second species so that V would appear to persist in aqueous solution.

The manganese complex of composition $Mn(C_8H_{16}PO_2)_2$ is insoluble in all solvents and may well be polymeric.

A selection of complexes were made of ruthenium showing that this ligand is capable of behaving in a manner analogous to carboxylic acids with $RuX_2(PPh_3)_3$.[18] The complexes $RuX_2(C_8H_{16}PO_2)(PPh_3)_2$, where X = Cl or Br, showed the expected IR bands associated with the phosphetan ligand. Yields of these and similar complexes were low due to higher solubility in the acetone used as solvent.

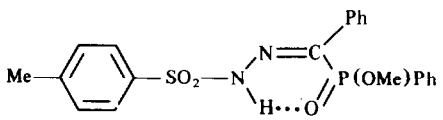
The combination of $C_8H_{16}PO_2H$ and diethylamine gave a material that analysed as the diethylammonium phosphetanate and in $D_2O$ the $^{31}P$ NMR spectrum showed the anion to be $C_8H_{16}PO_2^-$ by comparison with the potassium salt's spectrum.

In $CDCl_3$ the signal shifts to 37.4 ppm. This, and especially the IR spectrum of this material, suggests that there is close association between the cation and the anion, maybe in the formation of a cyclic hydrogen bonded structure (**VI**).[19] Because of the dimensions



**(VI)**

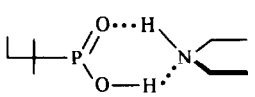
of the $PO_2^-$ moiety and the tetrahedral angle at nitrogen, it would not be feasible for linear OHN bonds to form. An intramolecular NHOP hydrogen bond that is non-linear ($\angle$ 143°) has been reported in **VII**.[20]



**(VII)**

The $\delta$(NH) chemical shift of the amine adduct is very downfield, again suggesting strong hydrogen bonding. In the system $CF_3CO_2H + Et_3N$ $\delta$(NH) varies from 7.5 to 10.5 ppm and separate signals can be distinguished for the two forms $CF_3CO_2H \cdots NEt_3$ and $CF_3CO_2^- \cdots HNEt_3^+$, even at 40°C.[21]

The combination $RCO_2H$ + imidazole[22] also has an IR spectrum in the region 3000–2000 $cm^{-1}$ like that reported here for $C_8H_{16}CO_2H + Et_2NH$, i.e. a hydrogen bonding continuum with several submaxima. Whether this is solely due to **VII** or involves contributions from (**VIII**) cannot be decided



**(VIII)**

at this stage. The $^{31}P$ chemical shift of **VIII** would resemble that of $C_8H_{16}PO_2H$ in $CDCl_3$ ($\delta$ = 59.0 ppm) but is much further upfield suggesting that contributions from **VIII** are small. In aqueous solution there is no evidence for **VIII** but a polar solvent would in any case favour the **VI** form. Yet type **VIII** structures have been postulated for adducts of $RCO_2H$ + amines.[19]

It has also been shown by matrix IR spectroscopy that whereas $CF_3CO_2H + Me_3N$ is of the proton-transfer/hydrogen bond type, as is **VI**, the combination $CH_3CO_2H + Me_3N$ is a molecular adduct, as is **VIII**.[23] Further investigation into the amine adducts of $C_8H_{16}PO_2H$ is being carried out.

*Acknowledgement*—The authors thank the SERC for a research grant for R. J. P.

## REFERENCES


1. E. Jugermann, J. McBride, R. Clutter and A. Mais, *J. Org. Chem.* 1962, **27**, 606 and 1833.
2. J. Emsley, T. B. Middleton and J. K. Williams, *J. Chem. Soc. Dalton* 1976, 979.
3. M. F. Crook, J. Emsley, T. B. Middleton and J. K. Williams, *Phosphorus* 1973, **3**, 45.
4. J. Emsley and J. K. Williams, *J. Chem. Soc. Dalton* 1973, 1756.
5. J. Emsley, T. B. Middleton and J. K. Williams, *J. Chem. Soc. Dalton* 1973, 2701.
6. D. D. Swank and C. N. Caughlan, *J. Chem. Soc. Chem. Commun* 1968, 1051; Mazhar-ul-Haque and C. N. Caughlan, *ibid*, 1968, 1228; Mazhar-ul-Haque, *J. Chem. Soc. B* 1970, 934; 1971, 117.
7. J. Emsley, *Chem. Soc. Revs.* 1980, **9**, 91.
8. T. A. Stephenson and G. Wilkinson, *J. Inorg. Nucl. Chem.* 1966, **28**, 945.
9. L. Vaska, *Chem. Ind. (London)* 1961, 1402.
10. D. F. Peppard, J. R. Ferraro and B. W. Mason, *J. Inorg. Nucl. Chem.* 1960, **16**, 246.
11. J. Emsley, O. P. A. Hoyte and R. E. Overill, *J. Am. Chem. Soc.* 1978, **100**, 3303.
12. M. Currie, *J. Chem. Soc. Perkin II* 1972, 832.
13. J. M. Williams, J. Rozière and M. T. Rozière-Bories, *Inorg. Chem.* 1976, **15**, 2490.
14. M. Calti, G. Ferraris and G. Ivaldi, *Acta Cryst.* 1979, **B35**, 525.
15. J. C. Speakman, *Structure and Bonding* 1972, **12**, 141.
16. S. Tagaki, M. Mathew and W. E. Brown, *Acta Cryst.* 1980, **B36**, 766.
17. F. A. Cotton and G. Wilkinson, *Advanced Inorganic Chemistry* 4th Edn, p. 769. (1980).
18. D. S. Moore and S. D. Robinson, *Inorg. Chem.* 1979, **18**, 2307.
19. G. S. Denisov and N. S. Golubev, *J. Mol. Struct.* 1981, **75**, 311.
20. G. Mass and R. Hodge, *Acta Cryst.* 1980, **B36**, 499.
21. F. Kohler, R. Gopal, G. Götze, H. Atrops, M. A. Demiriz, E. Libermann, E. Wilhelm, F. Ratkovics and B. Palagyl, *J. Phys. Chem.* 1981, **85**, 2524.
22. R. Lindemann and G. Zundel, *J. Chem. Soc. Faraday II* 1977, **73**, 788.
23. M. Wierzejewska-Hnat, Z. Mielke and H. Ratajczak, *J. Chem. Soc. Faraday II* 1980, **76**, 834.

*Polyhedron* Vol. 3, No. 3, pp. 331–339, 1984
Printed in Great Britain.

0277–5387/84 $3.00 + .00
© 1984 Pergamon Press Ltd.

# NMR STUDIES OF STEREOCHEMICAL NON-RIGIDITY IN THE COMPLEXES OF TRICARBONYLRHENIUM HALIDES WITH 2,4,6-TRITHIAHEPTANE

EDWARD W. ABEL, MOHAMED Z. A. CHOWDHURY, KEITH G. ORRELL* and VLADIMIR ŠIK
Department of Chemistry, University of Exeter, Exeter EX4 4QD, England

(*Received* 4 *July* 1983; *accepted* 25 *July* 1983)

**Abstract**—Mononuclear chelate complexes *fac*-[{$ReX(CO)_3$}($MeSCH_2SCH_2SMe$)] X = Cl, Br and I, have been isolated and examined by dynamic NMR methods. Energy data associated with the pyramidal inversion of the sulphur atoms and rotation of the chelated ligands have been obtained.

Metal complexes of sulphur and selenium ligands are known to undergo a wide variety of stereodynamic changes.[1] We have shown that sulphur coordinated complexes of [$(PtXMe_3)_4$] are particularly rich in fluxional motions.[2–5] These include pyramidal sulphur inversions, ligand rotations or switchings, and Pt-methyl scramblings. Recently, complexes with the chelate ligand 2,4,6-trithiaheptane have been shown to produce highly tractable NMR spectra from which the energies of each of these internal rate processes can be evaluated.[6] The isoelectronic nature of Re(I) and Pt(IV) is responsible for the moieties $PtXMe_3$ and $ReX(CO)_3$ yielding isostructural series of complexes with S or Se ligands. We have previously studied the fluxional properties of rhenium(I) complexes with aliphatic, aromatic and olefinic thio-, seleno-, and mixed thio/seleno-ethers, but have identified only pyramidal inversions of the S and/or Se atoms[7,8] in these complexes. In order to establish whether any ligand rotations occur in Re(I) complexes as they do in the Pt(IV) complexes, we have prepared the Re(I) complexes of 2,4,6-trithiaheptane [{$ReX(CO)_3$}($MeSCH_2SCH_2SMe$)], X = Cl, Br, I and report herein on their variable temperature NMR properties.

## EXPERIMENTAL

*Materials.* The pentacarbonylrhenium(I) halides were prepared by previously reported methods.[9] The ligand 2,4,6-trithiaheptane, prepared by literature methods,[10,11] was a pale-yellow oil (Yield 7.5 g, 49%), B.p 104–108°C/15 mmHg (Lit. B.p 106°C/5 mmHg,[12] 100–103°/3.5 mmHg[13]). $^1H$ NMR data: $\delta$ 2.15 (S–Me), $\delta$ 3.77 ($CH_2$).

The rhenium complexes were prepared as outlined below.

An excess of 2,4,6-trithiaheptane (250 mg, 1.62 mmol) was added to a solution of pentacarbonylrhenium(I) halide (1.11 mmol) in chloroform (15 $cm^3$) in a Schlenk tube equipped with a cold finger. The stirred solution was refluxed under dry nitrogen for an expedient length of time (viz. 3 days-chloride, 5 days-bromide, 13 days-iodide). The reaction was judged complete by the appearance of three new CO stretching bands in the IR spectrum and the disappearance of the CO bands due to the starting material. The near-equal intensities of the new bands were attributed to the *facial* isomers[14] of these complexes. The volume of the solution was reduced to 2 $cm^3$ under vacuum and an equal volume of heptane added. Slow cooling of the solution to −20°C yielded crystals of *fac*-[chloro-(2,4,6-trithiaheptane)-tricarbonylrhenium(I)] (0.489 g, 96%), *fac*-[bromo-(2,4,6-trithiaheptane)-tricarbonylrhenium(I)] (0.509 g, 91%), or *fac*-[iodo-(2,4,6-trithiaheptane)-tricarbonylrhenium(I)] (0.517 g, 85%). The crystals were washed with petroleum spirit (40–60°C) and dried under vacuum. Analytical and IR data of the complexes are collected in Table 1.

*Spectra.* IR spectra were recorded on either a Perkin–Elmer Model 299B or 398 spectrometer using chloroform solutions of the complexes.

NMR spectra were recorded on a JEOL PS/PFT-100 spectrometer operating in the Fourier transform mode at 100 MHz for $^1H$ studies. Variable temperature measurements were carried out as

*Author to whom correspondence should be addressed.

Table 1. Characterisation of the complexes

| Compound | Colour | M.P./°C | Analysis[a] | | $\nu$(CO)/cm$^{-1}$[b] |
|---|---|---|---|---|---|
| | | | %C | %H | |
| $[ReCl(CO)_3\{MeS(CH_2S)_2Me\}]$ | White | 117 | 18.21 (18.28) | 2.18 (2.19) | 2043, 1952, 1918 |
| $[ReBr(CO)_3\{MeS(CH_2S)_2Me\}]$ | Greyish-White | 153 | 16.58 (16.66) | 1.91 (1.99) | 2045, 1955, 1920 |
| $[ReI(CO)_3\{MeS(CH_2S)_2Me\}]$ | Grey | 167-168 | 15.21 (15.24) | 1.80 (1.82) | 2047, 1954, 1921 |

[a] Calculated values are given in parentheses

[b] Infrared spectra were recorded in $CHCl_3$ solution; all carbonyl stretching frequencies were very strong.

previously described.[5] For the temperature range $-75$°C to 50°C, complexes were examined in the mixed solvent $CD_2Cl_2/CS_2$. For higher temperatures the mixed solvent $C_6D_5NO_2/C_6D_6$ was employed.

## RESULTS

The NMR spectra of the ring protons of these Re(I) complexes are very closely related to those of the analogous Pt(IV) complexes which we have recently discussed in detail.[6] We will therefore only summarise the pertinent features of the spectra of the present Re(I) complexes.

In the absence of any internal exchange process, four diastereoisomers may exist, namely *meso*-1, *meso*-2 and a degenerate pair of *dl* isomers (Fig. 1). These were clearly distinguished at low temperatures (*ca.* $-60$°C to $-70$°C) by four sharp signals in the methyl region (Fig. 2) and four AB quartets in the ring methylene region. The chemical shifts of all these signals have been collected in Table 2. On warming the complexes to above-ambient temperatures (*ca.* 40°C), the methyl signals coalesced to a singlet and the methylene signals to a single AB quartet. The case of $[\{ReCl(CO)_3\}(MeSCH_2SCH_2SMe)]$ is illustrated in Fig. 3, and the high temperature data of all three complexes are included in Table 2. The changes are

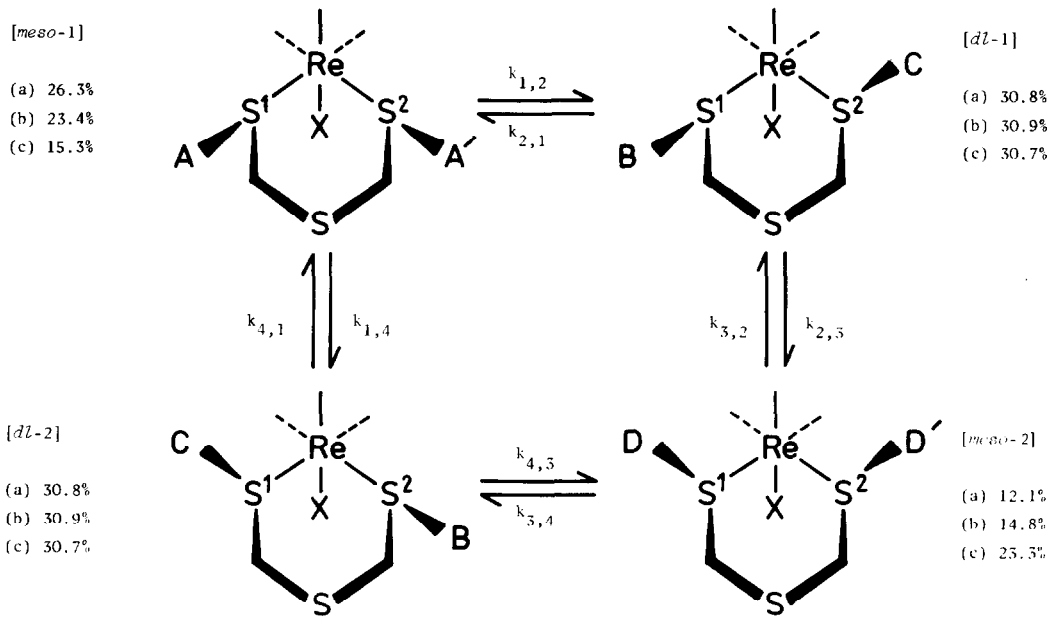



Fig. 1. Interconversion of the diastereoisomers of $[ReX(CO)_3\{MeS(CH_2S)_2Me\}]$. Percentage populations refer to the complexes (a) X = Cl, (b) X = Br and (c) X = I.

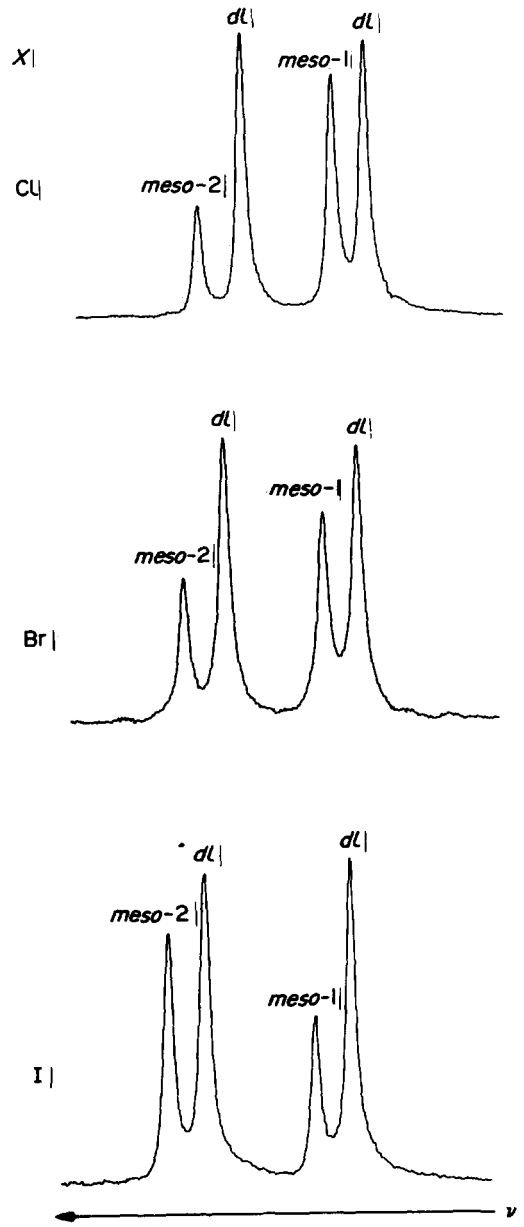



Fig. 2. Methyl proton spectra of $[ReX(CO)_3\{MeS(CH_2S)_2SMe\}]$ showing the halogen dependence of invertomer populations.

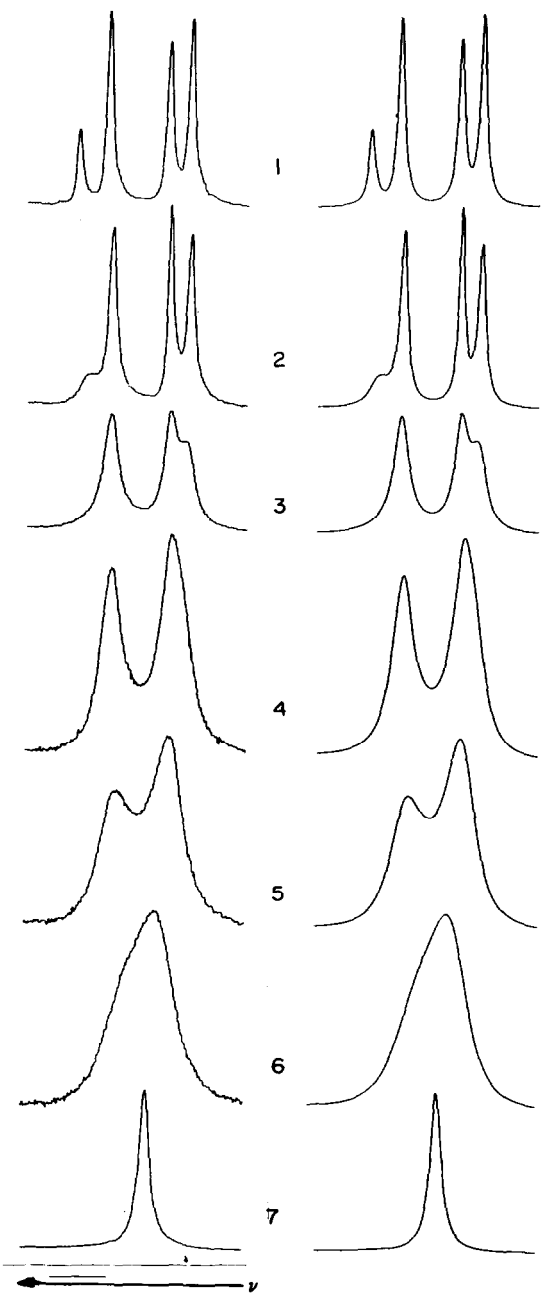



Fig. 3. Experimental and computer synthesised spectra of the methyl proton spectra of $[ReCl(CO)_3\{MeS(CH_2S)_2SMe\}]$ showing the effects of sulphur pyramidal inversion.

undoubtedly due to the increasing rate of sulphur pyramidal inversion with temperature,[6] and the energy of the process was computed from the line shape changes of the methyl region using standard fitting procedures.[1] The methylene region was not used for this purpose because of the added complexities in this region of the spectrum.

An essential preliminary to any band shape analysis is the correct assignment of the low temperature spectra. The assignments given in Fig. 2 are based on the fact that the two equal intensity signals must be due to the *dl* invertomer, while the remaining two signals are assigned on the basis that the halogen dependence will be such as to favour *meso*-2 at the expense of *meso*-1 as the halogen size increases.[3,7] It should be noted that in $ReX(CO)_3L$ complexes the halogen dependence of invertomer populations is very pronounced.[7] With bulky halogens, the E-methyls are forced *trans* to the halogen atom, methyl–carbonyl interactions being quite weak. In $PtXMe_3L$ complexes, the halogen dependence is smaller and the preferred

Table 2. Chemical shifts of $^1H$ NMR signals of [{$ReX(CO)_3$}{$MeS(CH_2S)_2Me$}] in the slow and fast inversion limits

| X | Temp./°C | δ(-$CH_2$-)/p.p.m. [a] | δ($CH_3$-)/p.p.m. |
|---|---|---|---|
| Cl | -72.1 | 5.19, 5.13, 5.03, 5.00 4.95, 4.91, 4.88, 4.81, | 3.80, 3.77, 3.73, 3.68, 3.64, 3.58, 3.56, 3.52, | 2.99, 2.91, 2.73, 2.67, |
| | 40.0 | 5.10, 4.97 | 3.65, 3.57 | 2.76 |
| Br | -59.0 | 5.27, 5.18, 5.15, 5.12, 5.05, 5.03, 5.00, 4.91, | 3.85, 3.80, 3.77, 3.72, 3.70, 3.64, 3.60, 3.56, | 3.03, 2.94, 2.75, 2.68, |
| | 43.0 | 5.20, 5.06 | 3.71, 3.64 | 2.79 |
| I | -62.1 | 5.33, 5.27, 5.21, 5.18, 5.13, 5.11, 5.05, 4.98, | 3.98, 3.94, 3.90, 3.85, 3.81, 3.79, 3.73, 3.67, | 3.05, 2.98, 2.77, 2.70 |
| | 36.5 | 5.28, 5.14 | 3.83, 3.69 | 2.84 |

a. Chemical shifts measured relative to $SiMe_4$.

orientations of E-methyls are governed by a balance between halogen-E-methyl and Pt-methyl-E-methyl repulsions.[3] In the trithiaheptane complexes of $PtXMe_3$ there is the added factor of the 6-membered ring conformation(s) to be considered, and in this case[6] the halogen dependence of invertomer populations shows a small, opposite trend to the present $ReX(CO)_3$ complexes.

The conformational nature of the trithiaheptane ring in these Re(I) complexes is not known since cooling the complexes to *ca.* −90°C did not reveal any significant changes in the spectra. This implies that either chair–chair interconversion is very fast on the NMR time scale or that one of the conformers is present in overwhelming abundance.

The effects of varying rates of pyramidal sulphur inversion on the methyl signals were computed in the usual way. The NMR spin problem for the interconversion of the invertomers may be represented by

$$\begin{array}{ccc} AA' & \overset{k}{\rightleftharpoons} & BC \\ \downdownarrows k & & \downdownarrows k' \\ CB & \overset{k'}{\rightleftharpoons} & DD' \end{array}$$

where the labelling of the methyls refers to Fig. 1. Since no methyl–methyl spin couplings were detected the spin system reduces to

$$\begin{array}{ccc} A & \overset{k}{\rightleftharpoons} & B \\ \downdownarrows k & & \downdownarrows k' \\ C & \overset{k'}{\rightleftharpoons} & D \end{array}$$

where $k$ is the rate constant for [*meso*-1]→[dl-1/2] and $k'$ is the rate constant for [*dl*-1/2]→[*meso*-2]. Band shapes were computed based on the static parameters (chemical shifts, invertomer populations and effective spin–spin relaxation times) listed in Table 3. The "best fit" spectra for [{$ReCl(CO)_3$}($MeSCH_2SCH_2SMe$)] are shown in Fig. 3 and the associated rate constants $k$ and $k'$ in Table 4. The close agreement in band shapes fully justified the assumption of independent inversion of the sulphur atom pairs. Activation parameters based on the Arrhenius and Eyring equations are given in Table 5.

The possibility that the signal coalescence was due to some type of dissociation–recombination process was excluded on the basis of the detection of a separate free ligand signal on adding some trithiaheptane to the chloride complex at a temperature considerably higher than its coalescence temperature.

When trithiaheptane is chelated to the $PtXMe_3$ moiety high temperature fluxions occur causing an effective rotation of the 6-membered ligand ring with respect to the equatorial Pt–Me plane. Such a fluxional movement was therefore sought in these Re(I) complexes. Heating the complexes did indeed cause a significant broadening of the methylene proton AB quartet but coalescence of the signals was not achieved at the highest temperature possible (165°C). The changes, however, were perfectly temperature reversible and it was possible to simulate the spectra quite accurately (Fig. 4). The static parameters on which these theoretical spectra are based are given in Table 6 and the activation energy parameters subsequently deduced are presented in Table 7. We are stongly of the opinion that these spectral changes indicate a 180° "pancake" rotation of the ligand, a process which may precede or may initiate or be simply a consequence

Table 3. Static parameters used in the computation of sulphur–methyl spectra of $[ReX(CO)_3\{MeS(CH_2S)_2Me\}]$ for pyramidal inversion studies

| X | Temp./°C | *meso*-1 isomer | | *dl*-isomers | | | *meso*-2 isomer | | $T_2^*$/s |
|---|---|---|---|---|---|---|---|---|---|
| | | $\nu_A$/Hz[a] | $p_A$ [b] | $\nu_B$/Hz | $\nu_C$/Hz | $p_B + p_C$ | $\nu_D$/Hz | $p_D$ | |
| Cl | -72.1 | 273.3 | 26.3 | 266.9 | 290.8 | 61.6 | 299.3 | 12.1 | 0.240 |
| Br | -69.2 | 274.9 | 23.4 | 268.3 | 293.6 | 61.8 | 301.5 | 14.8 | 0.205 |
| I | -72.5 | 277.5 | 15.3 | 270.7 | 298.6 | 61.4 | 305.4 | 23.3 | 0.275 |

[a]Solvent was $CD_2Cl_2/CS_2$ mixture, chemical shifts ($\nu_i$) measured relative to $SiMe_4$.

[b]% Populations of isomers (±0.5).

Table 4. The "best fit" rate constants used for the synthesis of the spectra shown in Fig. 3

| Spectrum[a] Number | Temp./°C | $k/s^{-1}$ | $k'/s^{-1}$ |
|---|---|---|---|
| 1 | -72.1 | 0.001 | 0.001 |
| * | -41.1 | 0.001 | 0.60 |
| * | -30.2 | 0.001 | 1.40 |
| 2 | -24.7 | 1.0 | 3.5 |
| * | -21.0 | 2.5 | 6.0 |
| 3 | -16.2 | 5.0 | 11.0 |
| 4 | -8.7 | 9.5 | 21.0 |
| 5 | -2.4 | 18.0 | 39.0 |
| 6 | 3.0 | 33.0 | 65.0 |
| * | 9.5 | 62.0 | 125.0 |
| * | 15.6 | 100.0 | 200.0 |
| 7 | 21.3 | 185.0 | 370.0 |
| * | 40.0 | 785.0 | 1590.0 |

[a]See Figure 3.

*Spectra not shown in Figure 3.

of scrambling of the groups (CO and X) attached to rhenium. Such a ligand rotation process was clearly identified in the trimethylplatinum(IV) complexes with trithiaheptane,[6] where in this case the scrambling of the Pt-methyl environments was also detected by $^1H$ NMR. In the present Re(I) complexes the carbonyl scrambling fluxion was not identified because of the considerable experimental difficulties in detecting $^{13}C$ carbonyl signals of nuclei attached to the highly quadrupolar rhenium nucleus ($I = 5/2$). Chemical intuition, however, strongly suggests that carbonyl/halogen scrambling will be occuring at an NMR detectable rate.

## DISCUSSION

*Pyramidal inversion.* The Arrhenius and Eyring activation parameters in Table 5 are reported for the interconversions [*meso*-1]→[*dl*-1/2] and [*dl*-1/2]→[*meso*-2]. In all cases the $\log_{10} A$ and $\Delta S^{\ddagger}$ values are in the region of 13 and 0 respectively, indicating purely intramolecular changes with non-dissociative transition states. $\Delta G^{\ddagger}$ values are of a magnitude expected for sulphur atoms coordinated to transition metals,[1] and are *ca.* 2 kJ $mol^{-1}$ higher

Table 5. Arrhenius and Eyring activation parameters for pyramidal inversion in the complexes $[ReX(CO)_3\{MeS(CH_2S)_2Me\}]$(X = Cl, Br and I)

| X | Interconversions | $E_a$/kJ $mol^{-1}$ | $\log_{10} A$ | $\Delta H^{\ddagger}$/kJ $mol^{-1}$ | $\Delta S^{\ddagger}$/J $K^{-1}$ $mol^{-1}$ | [a] $\Delta G^{\ddagger}$/kJ $mol^{-1}$ |
|---|---|---|---|---|---|---|
| Cl | *meso*-1 → *dl*-1/2 | 61.43 ± 1.09 | 13.13 ± 0.21 | 59.16 ± 1.09 | -1.0 ± 4.0 | 59.46 ± 0.10 |
| | *dl*-1/2 → *meso*-2 | 58.87 ± 1.03 | 12.97 ± 0.19 | 56.61 ± 1.01 | -4.15 ± 3.73 | 57.85 ± 0.09 |
| Br | *meso*-1 → *dl*-1/2 | 62.41 ± 1.34 | 13.29 ± 0.25 | 60.10 ± 1.34 | 1.81 ± 4.81 | 59.56 ± 0.09 |
| | *dl*-1/2 → *meso*-2 | 60.40 ± 1.47 | 13.30 ± 0.27 | 58.09 ± 1.45 | 2.01 ± 5.19 | 57.49 ± 0.10 |
| I | *meso*-1 → *dl*-1/2 | 62.54 ± 1.49 | 13.28 ± 0.29 | 60.31 ± 1.49 | 1.90 ± 5.58 | 59.74 ± 0.16 |
| | *dl*-1/2 → *meso*-2 | 61.11 ± 1.54 | 13.59 ± 0.30 | 58.88 ± 1.55 | 7.95 ± 5.77 | 56.50 ± 0.17 |

[a]At 298.15 K.

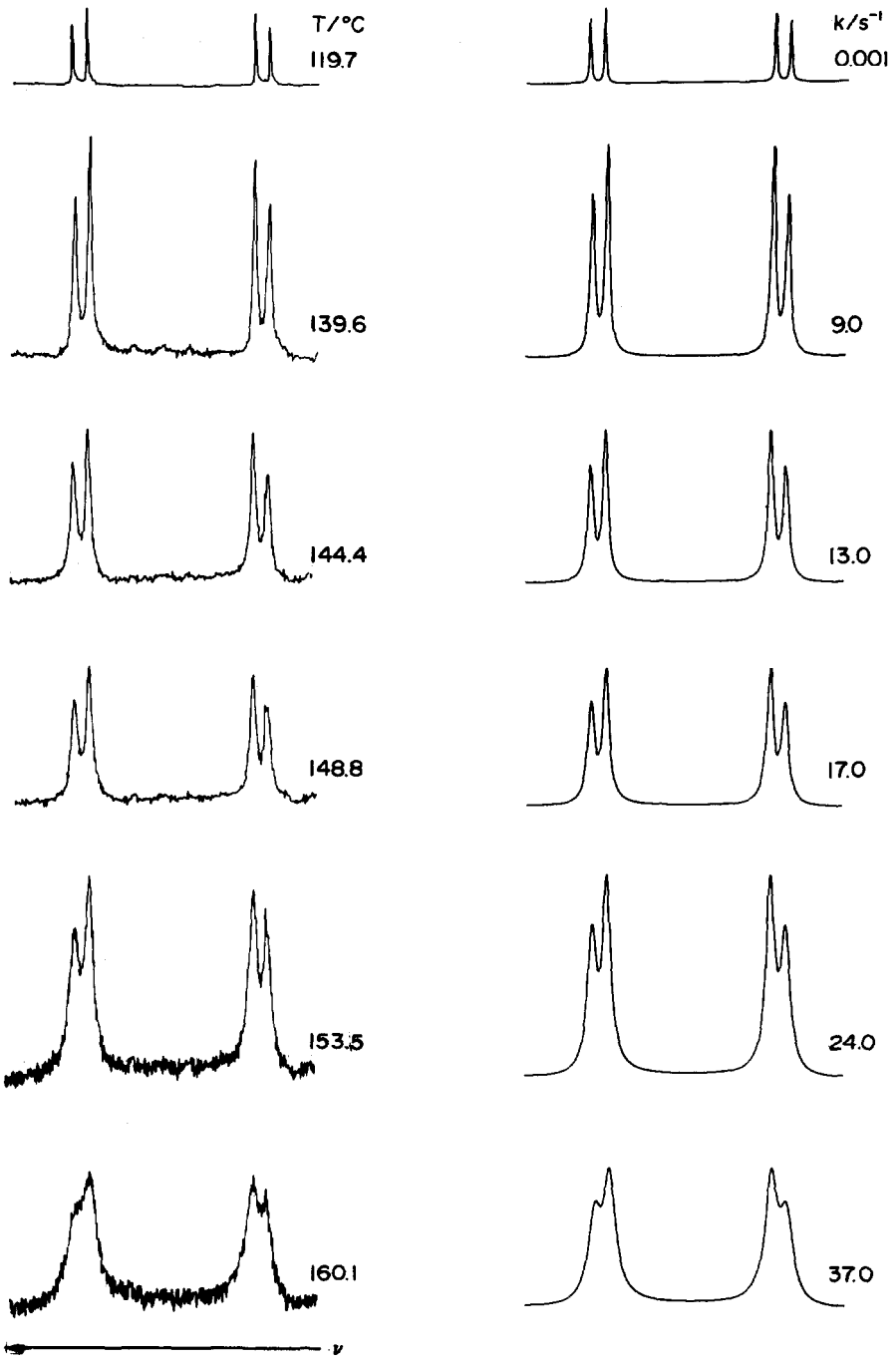



Fig. 4. Experimental and computer synthesised spectra of the methylene proton spectra of $[ReCl(CO)_3\{MeS(CH_2S)_2SMe\}]$ showing the effects of ligand rotation.

than in the corresponding trimethylplatinum(IV) complexes. This implies the somewhat greater strength of the Re(I)←S bond compared to Pt(IV)←S bond. No significant halogen dependence of the inversion energies was found in accord with the usually negligible *cis* influence of halogen.

The difference in barrier energies for the interconversions [*meso*-1]→[*dl*-1/2] and [*dl*-1/2]→[*meso*-2] can be mainly attributed to the difference in ground state energies of the invertomers. These differences have been calculated (Table 8) and expressed graphically in Fig. 5 where the $\Delta G^{\ominus}$ values have been evaluated from the equation $\Delta G^{\ominus} = -RT \ln K^{\ominus}$ where $K^{\ominus}$ is a standard equilibrium constant and represents the ratio

Table 6. Static parameters used in simulating the methylene region of $^1H$ NMR spectra of $[\{ReX(CO)_3\}\{MeS(CH_2S)_2Me\}]$ for ligand rotation studies

| Complex[a] | Temp./°C | $\nu_A$/Hz[b] | $\nu_B$/Hz | $^2J$/Hz[c] | $T_2^*$/s |
|---|---|---|---|---|---|
| $[ReCl(CO)_3\{MeS(CH_2S)_2Me\}]$ | 99.9 | 473.5 | 307.3 | 13.37 | 0.175 |
| $[ReBr(CO)_3\{MeS(CH_2S)_2Me\}]$ | 102.5 | 487.9 | 328.3 | 13.43 | 0.250 |
| $[ReI(CO)_3\{MeS(CH_2S)_2Me\}]$ | 94.0 | 497.9 | 338.7 | 13.67 | 0.320 |

[a]Solvent was $C_6D_5NO_2/C_6D_6$ mixture. [b]Chemical shifts measured relative to $Me_3SiOSiMe_3$.

[c]$^2J(^1H\text{-}C\text{-}^1H)$.

Table 7. Barrier energies calculated for the ligand rotation in $[\{ReX(CO)_3\}\{MeS(CH_2S)_2Me\}]$ (X = Cl, Br and I)

| X | $E_a$/kJ mol$^{-1}$ | $\log_{10}A$ | $\Delta H^{\ddagger}$/kJ mol$^{-1}$ | $\Delta S^{\ddagger}$/J K$^{-1}$ mol$^{-1}$ | [a]$\Delta G^{\ddagger}$/kJ mol$^{-1}$ |
|---|---|---|---|---|---|
| Cl | 101.69 ± 1.65 | 13.83 ± 0.20 | 98.23 ± 1.55 | 8.72 ± 3.67 | 95.63 ± 0.45 |
| Br | 98.53 ± 4.17 | 13.37 ± 0.50 | 94.98 ± 4.06 | -0.25 ± 9.37 | 95.05 ± 1.27 |
| I | 97.11 ± 4.95 | 12.90 ± 0.61 | 93.59 ± 4.95 | -9.19 ±11.68 | 96.33 ± 1.47 |

[a]Calculated at 298.15 K.

of the population of the appropriate *meso* invertomer to either *dl* invertomer. Figure 5 strikingly indicates the cross-over in relative *meso* populations as the halogen changes from bromine to iodine.

*Fluxional processes.* The activation parameters for the ligand rotation process are listed in Table 7. The values are *ca.* 35 kJ mol$^{-1}$ higher than those for pyramidal inversion and are essentially halogen independent. A comparison of the $\Delta G^{\ddagger}$ values with those for the corresponding process in the isoelectronic and isostructural trimethylplatinum(IV) complexes of the same ligand[6] shows that the barrier is *ca.* 15 kJ mol$^{-1}$ higher in the rhenium(I) complexes. Indeed, these high $\Delta G^{\ddagger}$ values (*ca.* 95–96 kJ mol$^{-1}$) represent some of the largest energies barriers which can be reliably measured by the $^1H$ NMR band coalescence method.

The above-ambient temperature spectral changes may be examined in terms of a number of dissociative or non-dissociative mechanisms. One such mechanism involves halogen dissociation–recombination via a highly fluxional

Table 8. The halogen dependence of the relative invertomer populations as expressed by the $\Delta G^{\theta}$ parameter (see text)

| X | $\Delta G^{\theta}$ (298.15 K)/kJ mol$^{-1}$ | |
|---|---|---|
| | *meso*-1 | *meso*-2 |
| Cl | 0.39 | 2.32 |
| Br | 0.69 | 1.83 |
| I | 1.73 | 0.68 |

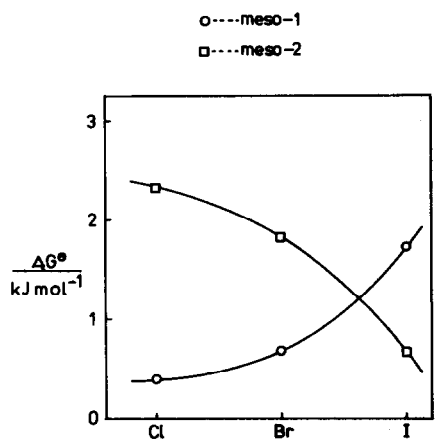



Fig. 5. The effects of halogen type on the populations of the *meso*-isomers relative to the *dl*-isomers as expressed by the $\Delta G^{\ddagger}$ parameter (see text).

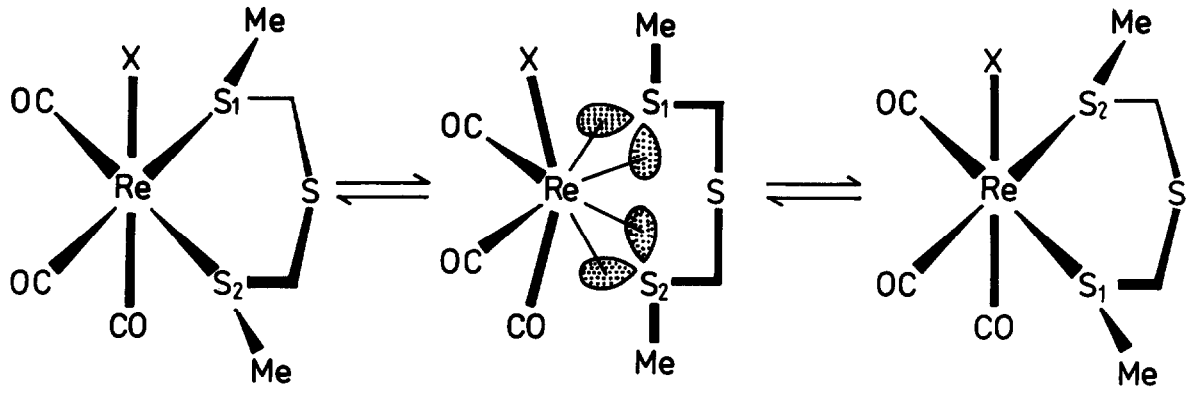



Fig. 6. Proposed mechanism for the ligand rotation process via an eight-coordinate intermediate.

five-coordinate intermediate which would allow the ligand to rotate. In order to test this explanation a halogen exchange experiment was performed. A molar equivalent of potassium iodide was added to a solution of [$ReCl(CO)_3\{MeS(CH_2S)_2Me\}$] in $C_6D_5NO_2/C_6D_6$ solvent mixture at 165°C, a temperature where ligand rotation was rapid. Spectra recorded before and after addition and again at room temperature, showed very little evidence of halogen exchange. Moreover, the existence of such a mechanism would have been reflected in a halogen dependence of the energy barrier.

An alternative dissociative mechanism may occur by the breaking and reforming of individual Re←S bonds. This possibility was checked by adding some free ligand to a solution of the chloro complex and re-recording the spectra. Separate, sharp signals for the added free ligand observed at 160°C eliminated ligand exchange as a possible explanation of the high temperature spectral changes.

Any non-dissociative mechanism for effective ligand rotation requires a twist of the ligand backbone. Such a movement may be a trigonal (Bailar) or a rhombic (Ray–Dutt) twist. When the distance between the two donor atoms in a chelate complex is small and the ring is slightly twisted in the ground state, a direct interaction between the donor atoms may cause the ligand to rotate about the metal atom.[15] A trigonal twist would not bring about averaging of the different carbonyl environments (i.e. *trans* S and *trans* X), whereas a rhombic twist would. Since ligand rotation and platinum-methyl scrambling are strongly correlated in the trimethylplatinum(IV) complexes of trithiaheptane, it would appear very likely that carbonyl/halogen scrambling will be accompanying ligand rotation in these rhenium(I) complexes although no direct evidence for it is available (*vide supra*). Thus, the most probable mechanism would seem to be a twist similar to a rhombic twist in which ligand rotation occurs via a highly fluxional eight-coordinate intermediate analogous to those proposed previously for trimethylplatinum(IV) complexes with thio- and seleno- ethers,[4] and trithiaheptane.[6] During the twist process, the two lone pairs of electrons on the chalcogens are considered to take part in the rehybridisation of the bonding orbitals of the metal (Fig. 6) such that the electronic environments of the three carbonyls as well as the methylene protons become averaged. The energy of this rehybridisation process is clearly considerable (*ca.* 96 kJ $mol^{-1}$).

We have shown previously[4] how a graph diagram in the form of a regular cube can neatly describe the effects of pyramidal inversions and ligand rotations in metal complexes. With mixed chalcogen complexes the eight corners of the cube represent the eight non-superimposable diastereoisomers of the complexes. Interconversion of any isomer to its mirror image form involves pyramidal inversion of both chalcogens and a 180° rotation. In the present rhenium complexes a cube diagram can again be used, but with the difference that there are now only four diastereoisomers, the isomers occupying the back corners of the cube being simply permutation (i.e. superimposable) isomers of the adjoining isomers on the front face. Bearing this difference in mind the cube diagram again presents a unified description of the stereodynamics of these rhenium(I) complexes.

## REFERENCES

1. E. W. Abel, S. K. Bhargava and K. G. Orrell, *Prog. Inorg. Chem.* 1983.
2. E. W. Abel, A. R. Khan, K. Kite, K. G. Orrell and V. Šik, *J. Chem. Soc., Dalton Trans.* 1980, 1169.

3. E. W. Abel, A. R. Khan, K. Kite, K. G. Orrell and V. Šik, *J. Chem. Soc., Dalton Trans.* 1980, 1169.
4. E. W. Abel, S. K. Bhargava, K. Kite, K. G. Orrell and V. Šik, *J. Chem. Soc., Dalton Trans.* 1982, 583.
5. E. W. Abel, K. Kite, K. G. Orrell, V. Šik and B. L. Williams, *J. Chem. Soc., Dalton Trans.* 1981, 2439, and references therein.
6. E. W. Abel, M. Z. A. Chowdhury, K. G. Orrell and V. Šik, *J. Organomet. Chem.* accepted for publication.
7. E. W. Abel, S. K. Bhargava, M. M. Bhatti, K. Kite, M. A. Mazid, K. G. Orrell, V. Šik, B. L. Williams, M. B. Hursthouse and K. M. A. Malik, *J. Chem. Soc., Dalton Trans.* 1982, 2065.
8. E. W. Abel, S. K. Bhargava, K. Kite, K. G. Orrell, V. Šik and B. L. Williams, *J. Chem. Soc., Dalton Trans.* accepted for publication.
9. W. Hieber, R. Schuh and H. Fuchs, *Z. Anorg. Allg. Chem.* 1941, **248**, 243.
10. F. G. Bordwell and B. M. Pitt, *J. Am. Chem. Soc.* 1955, **77**, 572.
11. F. Feher and K. Vogelbruch, *Chem. Ber.* 1958, **91**, 1003.
12. M. Ohsaku, Y. Shiro and H. Murata, *Bull. Chem. Soc. Japan* 1972, **45**, 113.
13. D. Welti and D. Whittaker, *J. Chem. Soc.* 1962, 4372.
14. E. W. Abel and S. P. Tyfield, *Canad. J. Chem.* 1969, **47**, 4627.
15. F. A. Cotton and G. Wilkinson, *Advanced Inorganic Chemistry*, 4th Edn, p. 1223. Wiley, New York (1980).

*Polyhedron* Vol. 3, No. 3, pp. 341–346, 1984
Printed in Great Britain.

0277–5387/84 $3.00 + .00
© 1984 Pergamon Press Ltd.

# STRUCTURAL STABILITY INDEX OF HETEROPOLY- AND ISOPOLY-ANIONS

**KENJI NOMIYA and MAKOTO MIWA***
Department of Industrial Chemistry, Faculty of Engineering, Seikei University, Musashino, Tokyo 180, Japan

(*Received* 4 *July* 1983; *accepted* 23 *September* 1983)

**Abstract**—On various types of heteropolyanion (HPA) and isopolyanion (IPA), there are some closed loops, each of which is formed by a junction of M ion and bridging oxygens (edge-sharing and/or corner-sharing). By using the structural stability index defined as the number of loops per $MO_6$ octahedral unit, the relative stability, the degree of condensation, the interconversion, and the formation of heteropoly blue anions of HPA and IPA can be clarified.

Heteropolyanions (HPA) and Isopolyanions (IPA) have been customarily represented as assemblages of metal-oxygen polyhedra, or as fragments of metal-oxide lattices and close-packed arrays.[1] We have introduced a new parameter, a structural stability index, which determines the structural feature and the degree of condensation of HPA and IPA, discussed the structural stability of their skeletons, classified the structural types and clarified the formation of heteropoly blue anion.

Concerning a general principle of HPA and IPA structures, Lipscomb has suggested that their structures might be limited to those in which each M atom is coordinated to no more than two unshared oxygens. His proposal leads to only a very limited number of predictions for the topology of HPA and IPA.[2] On the basis of this proposal, Pope has classified the known HPA and IPA structures into three types according to the number of unshared oxygen atoms attached to each M atom.[3] Type **I** structure has each M atom with a single unshared oxygen atom. The HPA such as Keggin-type $XM_{12}O_{40}^{n-}$ ($n = 3$–7) anion,[4–19] Dawson-type $X_2M_{18}O_{62}^{6-}$ anion,[20–22] and the IPA such as $M_6O_{19}^{n-}$ (n = 2–8) anion,[23–28] $W_{10}O_{32}^{4-}$ anion[29] belong to this type. Type **II** structure has each M atom with two mutually *cis* unshared oxygens. The HPA such as Anderson-type $XM_6O_{24}^{n-}$ ($n = 5$–8) and $XM_6O_{24}H_6^{n-}$ ($n = 3$–4) anions,[14,30–33] Waugh-type $XMo_9O_{32}^{6-}$ anion,[34] Silverton-type $XMo_{12}O_{42}^{8-}$ anion,[35] Evans–Showell-type $Co_2Mo_{10}O_{38}H_4^{6-}$ anion[36] and the IPA such as $Mo_7O_{24}^{6-}$ anion[31,37,38] and $\alpha$-$Mo_8O_{26}^{4-}$ anion[39] belong to this class. Type **III** anions have both sorts of M atom sites. Pope also pointed out that the formation of heteropoly blue anions appears to be restricted to complexes with type **I** or type **III** structure. Indeed, all of type **I** anions are known to be reducible,[40] but in the type **III** anions, only some examples of defect-structure anions[41–43] such as $PW_{11}O_{39}^{7-}$, $SiW_{11}O_{39}^{8-}$, $P_2W_{17}O_{61}^{10-}$, are known[40] and a reduced form of paratungstate $H_2W_{12}O_{42}^{10-}$ anion[44,45] and $\beta$-$Mo_8O_{26}^{4-}$ anion[46] has not been reported. According to the molecular orbital theory of oxo-type octahedral complexes,[47–49] a $MOL_5$ complex corresponding to the type **I** anion has one non-bonding $t_{2g}$ orbital ($b_2$ orbital), which can accommodate one or two electrons by reduction, however, a *cis*-$MO_2L_4$ complex corresponding to the type **II** has no such orbital, because of the participation of all $t_{2g}$ orbitals in the $\pi$-bonding with oxo-oxygens. However, taking consideration of the fact that only some of type **III** anions can be reduced, not only the reducibility of each $MO_6$ octahedron, but also the structural stability of overall inter-$MO_6$ octahedra should be considered.

## RESULTS AND DISCUSSION

Each $MO_6$ octahedron in the Keggin-type $XM_{12}O_{40}^{n-}$ anion, for example, is constituted with a central M atom, an unshared oxygen, i.e. terminal oxygen ($O_d$), bridging oxygens (corner-sharing, $O_b$ and edge-sharing, $O_c$) and a coordinating oxygen ($O_a$) to the heteroatom X, which occupies a *trans* position to the $O_d$ in the $MO_6$. These oxygens have a different $\pi$-bond order, that is, the $\pi$-bonding character of M–$O_d$ is the largest,

*Author to whom correspondence should be addressed.

whereas that of M–$O_a$ is the smallest, and those of M–$O_b$ and M–$O_c$ are in the middle order, and as a matter of fact, they are distinguished by the $^{17}O$–NMR technique.[50–52] These are consistent with their mean bond length established by X-ray analyses.[53] The M atom in HPA is always strongly displaced toward the unshared oxygens of their respective octahedra. Such a displacement can be also regarded as facilitating the $\pi$-bonding between M and terminal oxygen. Since the great $\pi$-bonding character of M–$O_d$ leads to the weak bond of M–$O_a$, the central $XO_4$ moiety of the Keggin-type anion appears to be isolated from surrounding $M_{12}O_{36}$ cage. Thus, the stability of the HPA will be governed by the stability of the cage. Terminal oxygens strongly connect with their respective $MO_6$ and therefore, bridging oxygens, $O_b$ and $O_c$, which link each $MO_6$ octahedron, will mainly contribute to the stability of cage-skeleton. Similar consideration can be applied for other types of HPA.

Here, as a means representing the contribution of $O_b$ and $O_c$, we propose an interpenetrating loop, $-O_c-M_1-O_b-M_2-O_c-$, around the HPA cage, which passes through the linkage of inter-$MO_6$ octahedra. If the loop is closed, it is regarded as a kind of macrocyclic $\pi$-bonding system. The $\sigma$- and $\pi$-bonding chains along the closed loop should significantly contribute to the structural stability of the cage. Thus, the larger is the number of closed loops, the more the cage will be stabilized. Alternately, the number of closed loops suggests to us the number of ways to fasten the HPA cage with a rope through $O_b$, M, $O_c$ as a hook. As a cage, the idealized model formed by removal of heteratom X from the HPA formed from perfect octahedral $MO_6$ units is used here for convenience.

In the Keggin-type anion, there exist four closed loops; all of which involve the linkage of six $MO_6$ octahedra. This is illustrated in Fig. 1. In the Dawson-type anion, there are two loops involving the linkage of six $MO_6$ octahedra and three loops involving the linkage of eight $MO_6$ octahedra, where the former are simultaneously orthogonal to the latter. As an index, we evaluated the mean value of the number of loops passing through each

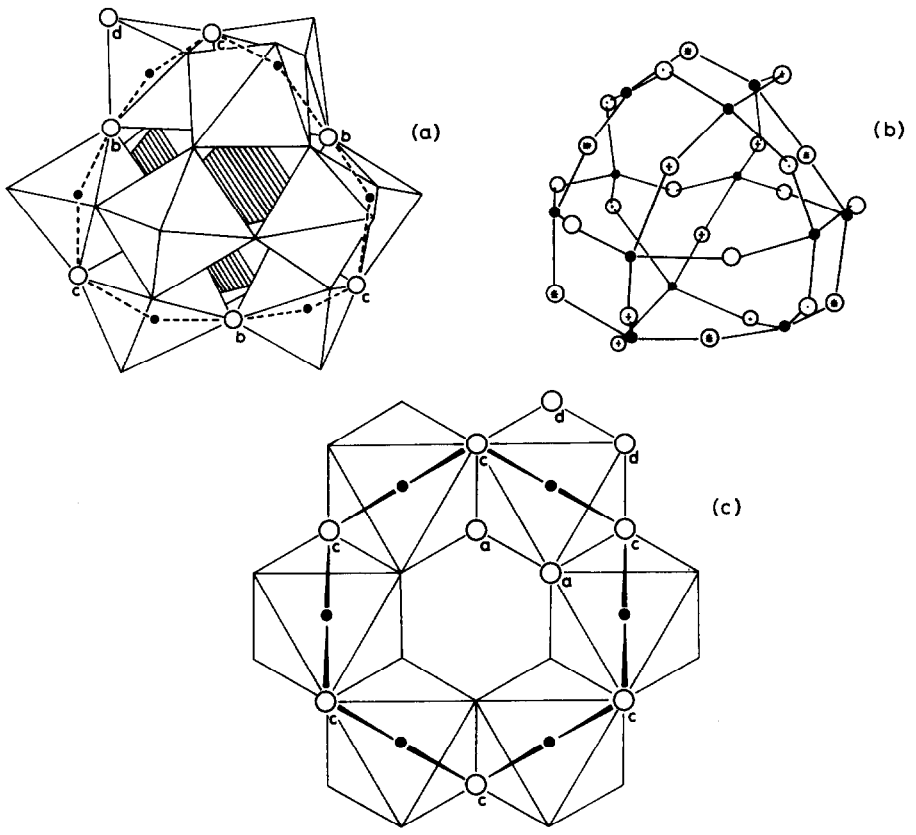



Fig. 1. Representation of the closed loop in the HPA cage. (a) One of the four interpenetrating loops of $-O_c-M-O_b-$ bonds in the Keggin-structure polyanion. (b) Four closed loops in the Keggin-structure polyanion. Small dark circles are molybdenum or tungsten atoms and open circles are oxygens. The uniformly marked oxygens identify one closed loop. (c) Only one interpenetrating loop of $-O_c-Mo-O_c-$ bond in the Anderson-structure polyanion.

$MO_6$ octahedron, or the divided value ($\eta$) of a sum of BC ($\Sigma$BC) with A, where A is the number of $MO_6$ octahedron constituting the cage, B the number of $MO_6$ constituting the loop and C the number of loops. The value represents a measure of the structural stability of the cage and frequently relates complementarily to the number of unshared oxygen attached to each M atom. For the Keggin-type anion, $\eta = 6 \times 4/12 = 2$ and for the Dawson-type anion, $\eta = (6 \times 2 + 8 \times 3)/18 = 2$, indicating that their structural stabilities are of the same degree. The index of $\eta = 2$ for these anions becomes complementary to that each octahedron constituting the cage has only one unshared oxygen, i.e. they belong to the type **I**.

In the case of Anderson-type $XM_6O_{24}^{n-}$ and $XM_6O_{24}H_6^{n-}$ anions (type **II**), there is one closed loop, $-O_c-M_1-O_c-M_2-O_c-$, around a crown of six octahedra formed only by edge-sharing, leading to $\eta = 1$. This index is also complementary to two *cis*-unshared oxygens attached to each $MO_6$ octahedron. The cage of Waugh-type $XMo_9O_{32}^{6-}$ anions belonging to the same type, has two partially penetrating boats of six octahedra formed by edge-sharing; there are two closed loops over them and the index $\eta = 4/3 = 1.33$. Silverton-type $XMo_{12}O_{42}^{8-}$ anion cage is constructed by corner-sharing of the $Mo_2O_9$-unit, which is formed by face-sharing of two octahedra. If the $-M_1-O_b-M_2-O_c-$ linkage is followed, it leads to the terminal oxygen. Thus, there is no closed loop as observed in other HPA and $\eta = 0$. The cage of Evans–Showell-type $Co_2Mo_{10}O_{38}H_4^{6-}$ anion also has no closed loop. These indicate that the different structural types of HPA have different structral stabilities. In Table 1, these are summarized together with Pope's classification. Various structures in the series of HPA having As or P atom as heteroatom are also known. The calculated index and type-classification are listed in Table 2. General rules are derived from Tables 1 and 2; (1) the HPA with the larger structural index are the more stabilized, (2) the HPA with an identical index within the same series can be interconverted or converted from one HPA to another, and (3) the index reveals the degree of condensation of the HPA. These can explain the following facts; the "reverse Keggin"-type $H_4As_4Mo_{12}O_{50}^{4-}$ anion[54] is more stable than the Keggin-type $AsMo_{12}O_{40}^{3-}$ anion,[55] and $(PhAs)_2Mo_6O_{25}H_2^{5-}$ anion is converted to $(PhAs)_2Mo_6O_{24}^{4-}$ anion by removal of water from an acetonitrile solution and the reverse process in the presence of water occurs upon heating.[56] Furthermore, we know that the Dawson-type $H_6P_2Mo_{18}O_{62}$ can be converted to the Keggin-type $H_3PMo_{12}O_{40}$ in the solid state on standing for a long time at room temperature. This can also be understood by the second rule. The conversion of the HPAs containing less molybdenum[57-61] might be possible between the

Table 1. Structural stability index of various types of HPA

| General formula of HPA | | A | B | C | Structural stability index; $\eta$ | Pope's classification |
|---|---|---|---|---|---|---|
| Keggin-structure; | $XM_{12}O_{40}^{n-}$ | 12 | 6 | 4 | 2 | I |
| Dawson-structure; | $X_2M_{18}O_{62}^{6-}$ | 18 | {6<br>8 | {2<br>3 | 2 | I |
| Anderson-structure; | | | | | | |
| | $XMo_6O_{24}^{n-}$<br>$XMo_6O_{24}H_6^{n-}$ | 6 | 6 | 1 | 1 | II |
| Waugh-structure; | $XMo_9O_{32}^{6-}$ | 9 | 6 | 2 | 1.33 | II |
| Silverton-structure; | | | | | | |
| | $XMo_{12}O_{42}^{8-}$ | 12 | 0 | 0 | 0 | II |
| Evans-Showell-structure; | | | | | | |
| | $Co_2Mo_{10}O_{38}H_4^{6-}$ | 10 | 0 | 0 | 0 | II |
| defect-structure; | $XM_{11}O_{39}^{n-}$ | 11 | 6 | 2 | 1.09 | III |
| | $X_2M_{17}O_{61}^{n-}$ | 17 | {6<br>8 | {2<br>1 or {1<br>2 | {1.18 or [a]<br>1.29 | III |
| half-Dawson structure; | | | | | | |
| | $XM_9O_{34}^{n-}$ | 9 | 6 | 1 | 0.67 | III |

a There are two indexes according to the removed positions of one $MO^{4+}$ group from the Dawson-structure anion.

Table 2. Structural stability index of various molybdoheteropolyanions containing As or P as heteroatom

| Formula | A | B | C | Structural stability index; η | Pope's classification |
|---|---|---|---|---|---|
| $AsMo_{12}O_{40}^{3-}$ (Keggin-type) | 12 | 6 | 4 | 2 | I |
| $As_2Mo_{18}O_{62}^{6-}$ (Dawson-type) | 18 | { 6 8 | { 2 3 | 2 | I |
| $H_4As_4Mo_{12}O_{50}^{4-}$ ; $(C_6H_5As)_4Mo_{12}O_{46}^{4-}$ | 12 | { 6 8 | { 4 3 | 4 | II |
| $AsMo_9O_{34}^{9-}$ (half-Dawson type) | 9 | 6 | 1 | 0.67 | III |
| $As_2Mo_6O_{26}^{6-}$ ; $(MeAs)_2Mo_6O_{24}^{6-}$ | 6 | 6 | 1 | 1 | II |
| $(PhAs)_2Mo_6O_{25}H_2^{4-}$ | 6 | 6 | 1 | 1 | II |
| $As_2Mo_5O_{23}^{6-}$ ; $(MeP)_2Mo_5O_{21}^{4-}$ | 5 | 5 | 1 | 1 | II |
| $(Me_2As)Mo_4O_{15}H^{2-}$ | 4 | 4 | 1 | 1 | II |

HPAs with an identical index in Table 2, because they are the metastable intermediates. Although the number (A) of octahedra constituting the cage of the Waugh-type and half-Dawson type anions is equal, their degrees of condensation are remarkably different. This is reflected in the index.

The rules are also compatible with the observation of IPA. The index and Pope's classification are represented in Table 3. One molybdenum atom with no oxo-type oxygen in the centre of a boat of six octahedra in $Mo_7O_{24}^{6-}$ anion and two tetrahedral molybdenum parts above and below a crown of six octahedra formed by edge-sharing in $\alpha$-$Mo_8O_{26}^{4-}$ anion could be treated as a kind of "heteroatom" on counting the loop and evaluating the index. Within the compounds of A = 6, the $M_6O_{19}^{n-}$ anion has the most close-packed structure; hence, its degree of condensation is larger than those of $Mo_7O_{24}^{6-}$ and $\alpha$-$Mo_8O_{26}^{4-}$ anions. The complementary relation between the index and the number of unshared oxygen in each octahedron appears, except the paratungstate $H_2W_{12}O_{42}^{10-}$ anion and the $\beta$-$Mo_8O_{26}^{4-}$ anion. Within the compounds of $\eta = 1$, the interconversion between Anderson-type $XM_6O_{24}^{n-}$ anion and $Mo_7O_{24}^{6-}$ anion, and between $\alpha$- and $\beta$-$Mo_8O_{26}^{4-}$ isomers have been fully discussed by using a cubic close-packed sphere model.[62] The index of $\eta = 2$ of the metatungstate anion, $H_2W_{12}O_{40}^{6-}$, implies just the structural stability of the Keggin-type cage itself. No closed loop could be found on both paratungstate anion (type III)

Table 3. Structural stability index of various types of IPA

| Formula | A | B | C | Structural stability index; η | Pope's classification |
|---|---|---|---|---|---|
| $M_6O_{19}^{n-}$ | 6 | 4 | 3 | 2 | I |
| $W_{10}O_{32}^{4-}$ | 10 | { 4 6 | { 2 2 | 2 | I |
| $H_2W_{12}O_{40}^{6-}$ (metatungstate) | 12 | 6 | 4 | 2 | I |
| $Mo_7O_{24}^{6-}$ (paramolybdate) | 6 [a] | 6 | 1 | 1 | II |
| $\alpha$-$Mo_8O_{26}^{4-}$ | 6 [b] | 6 | 1 | 1 | II |
| $\beta$-$Mo_8O_{26}^{4-}$ | 8 | 4 | 2 | 1 | III |
| $H_2W_{12}O_{42}^{10-}$ | 12 | 0 | 0 | 0 | III |
| $W_4O_{16}^{8-}$ ; $H_4W_4O_{16}^{4-}$ | 4 | 0 | 0 | 0 | — |

a Central Mo atom with no oxo-oxygen in the anion is treated as a heteroatom.

b Two Mo atoms in the tetrahedra above and below a crown of six octahedra in this anion are treated as heteroatoms.

and metastable $W_4O_{16}^{8-}$ or $H_4W_4O_{16}^{4-}$ anion. The degree of condensation of paratungstate anion is much less than that of metatungstate anion, as predicted by the index. These anions have marked difference on actual stability, which can be also understood by using their molecular models. The tetratungstate anion has a unique structure formed by each octahedron with three unshared oxygens[63] and is detectable only by a fast-reaction technique.[64]

Reducibility of HPA and IPA, or whether the reduced species of those anions are formed or not, appears to be dependent upon the magnitude of structural stability. As a matter of fact, all of type I anions, the reducibility of which is demonstrated, show large $\eta$ values. This is consistent with the first rule. In the type **III** anion, the reducibility of defect-structure $XM_{11}O_{39}^{n-}$ ($\eta = 1.09$) and $X_2M_{17}O_{61}^{n-}$ ($\eta = 1.18$ or 1.29 according to the lost position of $MO^{4+}$ group) anions is demonstrated, whereas that of $\beta$-$Mo_8O_{26}^{4-}$ anion ($\eta = 1$) and the paratungstate anion ($\eta = 0$) has not been reported yet. A heteropoly blue of half-Dawson type $XM_9O_{34}^{n-}$ ($\eta = 0.67$) will not be formed, because of its low structural stability.

The structural stability discussed here may not necessarily agree with the actual stability, because a contribution from the heteroatom has been ignored. In fact, although the metatungstate and Keggin-type anions have an identical index, the thermal stability of the latter is much larger than that of the former. This may be mainly caused by the effect of the heteroatom. Besides, in spite of low structural stability, Silverton-type $XMo_{12}O_{42}^{8-}$ anions ($X = Ce^{IV}$, $Th^{IV}$, $U^{IV}$) and Evans–Showell-type anion are actually isolated as stable compounds. These may be attributed to not only the degree of condensation, but also the strong interaction of high valence heteroatoms with the cage.

In this work, the respective stability of the mixed-HPA's, $XMo_{12-n}W_nO_{40}$ ($n = 0$–12), cannot be discussed, because the differences of poly-ion effect such as molybdenum and tungsten were not taken into account in the index. Moreover, subtle differences of stabilities in $\alpha$-, $\beta$- and another three isomers of Keggin-type anion, which are given as a consequence of gradual 60° rotations of $M_3O_{13}$ groups,[65] are also difficult to explain. However, we emphasize that many of structural points are best appreciated by the aspects of the closed loop over the linkage of many octahedra. Furthermore, since the –M–O–M– loop has a $\pi$-bonding character, it can be distingiushed as a chromophore from a great or $\pi$-bonding $M–O_d$. This may be shown in the charge transfer absorption and corresponding MCD spectra in the uv region of HPA and IPA.

## REFERENCES


1. F. A. Cotton and G. Wilkinson, *Advanced Inorganic Chemistry*, 4th Edn, p. 852. Wiley, New York (1980).
2. W. N. Lipscomb, *Inorg. Chem.* 1965, **4**, 132.
3. M. T. Pope, *Inorg. Chem.* 1972, **11**, 1973.
4. J. F. Keggin, *Proc. Roy. Soc. Ser. A* 1934, **144**, 75.
5. J. L. Hoard, *Z. Krist.* 1933, **84**, 217.
6. A. Ferrari, L. Cavalca, M. Nardelli, O. Scagnioli and E. Tognoni, *Gazz. Chim. Ital.* 1950, **80**, 352.
7. A. Kobayashi and Y. Sasaki, *Bull. Chem. Soc. Jpn.* 1975, **48**, 885.
8. R. Strandberg, *Acta Chem. Scand. Ser. A*, 1975, **29**, 359.
9. J. M. Fruchart, G. Herve, J. P. Launary and R. Massart, *J. Inorg. Nucl. Chem.* 1976, **38**, 1627.
10. R. Allmann, *Acta Chem. Scand. Ser. A* 1976, **30**, 152.
11. H. D'Amour and R. Allmann, *Z. Krist.* 1976, **143**, 1.
12. G. M. Brown, M. R. Noe-Spirlet, W. R. Busing and H. A. Levy, *Acta Cryst. Ser. B* 1977, **33**, 1038.
13. L. C. W. Baker and V. E. Simmons, *J. Am. Chem. Soc.* 1959, **81**, 4744.
14. K. Eriks, N. F. Yannoni, U. C. Agarwala, V. E. Simmons and L. C. W. Baker, *Acta Cryst.* 1960, **13**, 1139.
15. D. H. Brown, *J. Chem. Soc.* 1962, 3281.
16. D. H. Brown and J. A. Mair, *J. Chem. Soc.* 1962, 1512.
17. D. H. Brown, *J. Chem. Soc.* 1962, 3322.
18. D. H. Brown and J. A. Mair, *J. Chem. Soc.* 1962, 3946.
19. D. H. Brown, *J. Chem. Soc.* 1962, 4408.
20. B. Dawson, *Acta Cryst.* 1953, **6**, 113.
21. R. Strandberg, *Acta Chem. Scand. Ser. A* 1975, **29**, 350.
22. H. D'Amour, *Acta Cryst. Sect. B* 1976, **32**, 729.
23. I. Lindqvist, *Ark. Kemi* 1953, **5**, 247.
24. I. Lindqvist and B. Aronsson, *Ark. Kemi* 1954, **7**, 49.
25. H. R. Allcock, E. C. Bissel and E. T. Shawl, *Inorg. Chem.* 1973, **12**, 2963.
26. J. Fuchs, W. Freiwald and H. Hartl, *Acta Cryst. Sect. B* 1978, **34**, 1764.
27. C. D. Garner, N. C. Howlader, F. E. Mabbs, A. T. McPhail, R. W. Miller and K. D. Onan, *J. Chem. Soc. Dalton* 1978, 1582.
28. O. Nagao and Y. Sasaki, *Acta Cryst. Sect. B* 1979, **35**, 2387
29. J. Fuchs, H. Hartl, W. Schiller and U. Gerlach, *Acta Cryst. Sect. B* 1976, **32**, 740.
30. H. T. Evans, *J. Am. Chem. Soc.* 1948, **70**, 1291.
31. H. T. Evans, *J. Am. Chem. Soc.* 1968, **90**, 3275.
32. A. Perloff, *Inorg. Chem.* 1970, **9**, 2228.
33. H. T. Evans, *Acta Cryst. Sect. B* 1974, **30**, 2095.
34. J. L. T. Waugh, D. P. Shoemaker and L. Pauling, *Acta Cryst.* 1954, **7**, 438.
35. D. D. Dexter and J. V. Silverton, *J. Am. Chem. Soc.* 1968, **90**, 3589.

36. H. T. Evans and J. S. Showell, *J. Am. Chem. Soc.* 1969, **91**, 6881.
37. K. Sjobom and B. Hedman, *Acta Chem. Scand.* 1973, **27**, 3673.
38. H. T. Evans, B. M. Gatehouse and P. Leverett, *J. Chem. Soc. Dalton.* 1975, 505.
39. J. Fuchs and H. Hartl, *Angew. Chem.* 1976, **88**, 385.
40. See Ref. 3.
41. G. Schwarzenbach, G. Geier and J. Littler, *Helv. Chim. Acta* 1962, **45**, 2601.
42. P. T. Meiklejohn, M. T. Pope and R. A. Prados, *J. Am. Chem. Soc.* 1974, **96**, 6779.
43. A. Teze and G. Herve, *J. Inorg. Nucl. Chem.* 1977, **39**, 999.
44. R. Allmann and G. Weiss, *Acta Cryst. Sect. A* 1969, **25**, S106.
45. R. Allmann, *Acta Cryst. Sect. B* 1971, **27**, 1393.
46. T. J. R. Weakley, *Polyhedron* 1982, **1**, 17.
47. C. J. Ballhausen and H. B. Gray, *Inorg. Chem.* 1962, **1**, 111.
48. H. B. Gray and C. R. Hare, *Inorg. Chem.* 1962, **1**, 363.
49. W. P. Griffith, *Coord. Chem. Rev.* 1970, **5**, 459.
50. W. G. Klemperer, *Angew. Chem.* 1978, **90**, 258.
51. M. Filowitz, W. G. Klemperer, L. Messerle and W. Shum, *J. Am. Chem. Soc.* 1976, **98**, 2345.
52. M. Filowitz, R. K. C. Ho, W. G. Klemperer and W. Shum, *Inorg. Chem.* 1979, **18**, 93.
53. See Refs. 7–12.
54. T. Nishikawa and Y. Sasaki, *Chem. Lett.* 1975, 1185.
55. Y. Sasaki and K. Matsumoto, *Kagaku no Ryoiki* 1975, **29**, 853.
56. W. Kwak, L. M. Rajkovic, M. T. Pope, C. O. Quicksall, K. Y. Matsumoto and Y. Sasaki, *J. Am. Chem. Soc.* 1977, **99**, 6463.
57. W. Kwak, L. M. Rajkovic, J. K. Stalik, M. T. Pope and C. O. Quicksall, *Inorg. Chem.* 1976, **15**, 2778.
58. R. Strandberg, *Acta Chem. Scand. Sect. A* 1974, **28**, 217.
59. R. Strandberg, *Acta Chem. Scand.* 1973, **27**, 1004.
60. B. Hedman, *Acta Chem. Scand.* 1973, **27**, 3335.
61. K. M. Barkigia, L. M. Rajkovic, M. T. Pope and C. O. Quicksall, *J. Am. Chem. Soc.* 1975, **97**, 4146.
62. A. F. Masters, S. F. Gheller, R. T. C. Brownlee, M. J. O'Connor and A. G. Wedd, *Inorg. Chem.* 1980, **19**, 3866.
63. K.-H. Tytko and O. Glemser, *Adv. Inorg. Chem. Radiochem.* 1976, **19**, 239.
64. O. Glemser and K.-H. Tytko, *Z. Naturforsch. B* 1969, **24**, 648.
65. M. T. Pope, *Inorg. Chem.* 1976, **15**, 2008.

*Polyhedron* Vol. 3, No. 3, pp. 347–352, 1984
Printed in Great Britain.

0277–5387/84 $3.00 + .00
Pergamon Press Ltd.

# MONONUCLEAR AND DINUCLEAR TERTIARY PHOSPHINE MOLYBDENUM COMPLEXES. OXO-MOLYBDENUM(IV), DINUCLEAR $Mo_2Cl_4L_4$ AND RELATED DERIVATIVES

**ERNESTO CARMONA,* AGUSTIN GALINDO and LUIS SANCHEZ**
Departamento de Quimica Inorganica, Facultad de Quimica, Universidad de Sevilla, Sevilla, Spain

**and**

**ALASTAIR J. NIELSON† and GEOFFREY WILKINSON***
Chemistry Department, Imperial College, London SW7 2AY, England

(*Received* 27 *July* 1983; *accepted* 10 *August* 1983)

**Abstract**—Green and blue isomers of the oxo derivative $MoOCl_2(PMe_3)_3$ have been obtained by an oxygen-atom abstraction reaction between $MoCl_4(thf)_2$ and equimolar amounts of water in the presence of $PMe_3$. Methathesis with KX(X = NCO, NCS) yields $MoOX_2(PMe_3)_3$ and with $NaS_2CNEt_2$, $MoO(S_2CNEt_2)_2(PMe_3)$. The latter complex readily loses $PMe_3$ to give $MoO(S_2CNEt_2)_2$ from which it can be prepared by addition of the phosphine ligand.

Reaction of the blue purple complex, $MoCl_3(thf)_3$ (**I**), with excess $PMe_3$ gives *mer*-$MoCl_3(PMe_3)_3$ which loses $PMe_3$ on heating in toluene to afford $[MoCl_3(PMe_3)_2]_2$. Reduction of (**I**) with phosphines and zinc in tetrahydrofuran gives the dinuclear molybdenum(II) halide complexes $Mo_2Cl_4L_4$ (L = $PMe_3$, $PEt_3$, $PhMe_2Ph$, $PEt_2Ph$; $L_2$ = dppm), while Zn-acetic acid reduction yields $Mo_2(CO_2Me)_4$. Interaction of the chlorocarbonyl species $MoCl_2(CO)_2(PMe_3)_3$ with Tl(acac) affords Mo(acac)Cl(CO)$(PMe_3)_3$ which has an unusually low C–O stretching frequency for a terminal carbonyl group (1755 $cm^{-1}$).

Previous work from our laboratories has resulted[1] in the preparation of a variety of tertiary phosphine derivatives of group VI metals. More recently[2] we have reported the isolation and structural characterisation of the oxotungsten species $WOCl_2(PMe_3)_3$ and related complexes. As an extension of this work we report the facile conversion of the molybdenum(IV) adduct $MoCl_4(thf)_2$ to the oxo complex $MoOCl_2(PMe_3)_3$ by oxygen abstraction from water in wet acetone or tetrahydrofuran in the presence of trimethylphosphine. We also report additional chemistry of $MoCl_3(thf)_3$ (**I**), which relates to its reduction to dinuclear complexes containing the $Mo_2^{4+}$ core. Although this unit may be generated by different procedures[3–6] and several methods are now available for preparing the molybdenum(II) halide complexes,[7] $Mo_2X_4L_4$ (L = phosphine), no simple high yield route has however been devised for reduction in non-aqueous media of higher oxidation state molybdenum halides without metal–metal bonds. The reactions leading to the complexes studied in this work are shown in the Scheme.

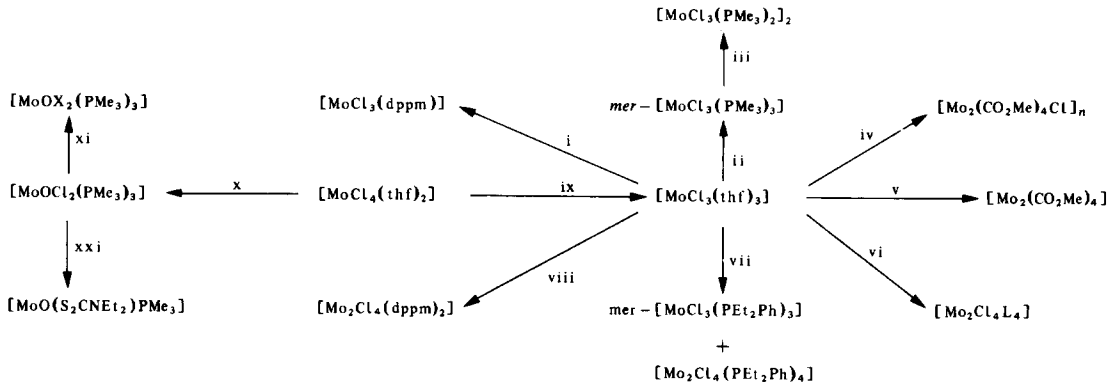
## RESULTS AND DISCUSSION

### (a) *Oxomolybdenum(IV) complexes*

Several synthetic methods have been devised for the preparation of oxomolybdenum(IV) complexes. These include oxygen abstraction by phosphine from dioxomolybdenum(VI) complexes,[8] reaction of a high oxidation state molybdenum halide with alcohol in the presence of the appropriate ligand[8,9] and ligand addition or displacement reaction of oxomolybdenum(IV) complexes.[8–11] As an extension of our earlier work on oxotungsten(IV) complexes, we have now prepared the trimethylphosphine derivative $MoOCl_2(PMe_3)_3$ by the reaction of $MoCl_4(thf)_2$ with equimolar amounts of water in the presence of an excess of

*Authors to whom correspondence should be addressed.

†Present address: Department of Chemistry, University of Auckland, Private Bag, Auckland, New Zealand.




(i) dppm; (ii) excess $PMe_3$ in thf; (iii) reflux toluene; (iv) $NaCO_2Me$ in thf; (v) Zn and $MeCO_2H$; (vi) phosphine and Zn in thf; (vii) $PEt_2Ph$ and Zn in thf; (viii) dppm and Zn in thf, 12 hr, in $CH_2Cl_2$, 4 hr; (ix) see references 6 and 7; (x) $H_2O$, $PMe_3$ in thf; (xi) KX (X = OCN, SCN) in thf; (xii) $NaS_2CNEt_2$, excess $PMe_3$.

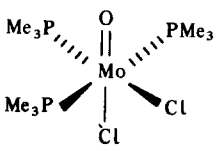
Scheme. Some reactions of *mer*-$[MoCl_3(thf)_3]$ and $[MoCl_4(thf)_2]$.

$PMe_3$ according to the equation.

$$MoCl_4(thf)_2 + H_2O + 5\,PMe_3 \xrightarrow{thf} MoOCl_2(PMe_3)_3 + 2[Me_3PH]Cl.$$

Interaction of $MoCl_4(thf)_2$ with trimethylphosphine in slightly wet acetone or thf at 50°C for 5–6 hr yielded a green solution from which green crystals of the diamagnetic $MoOCl_2(PMe_3)_3$ were isolated. In some instances the reaction carried out under apparently identical conditions, gave a blue solution from which blue crystals of the same stoichiometry and spectral properties as the green complex were obtained. Although for other related $MoOCl_2L_3$ complexes[9] the green isomers irreversibly convert to the blue complexes in warm organic solvents, green $MoOCl_2(PMe_3)_3$ seems to be the more stable of the two forms and we have been unable to ascertain the conditions under which the blue complex is generated. The IR spectrum of both isomers shows a strong absorption at 940 $cm^{-1}$ due to coordinated $PMe_3$ with a shoulder at *ca.* 960 $cm^{-1}$ possibly due to $\nu$(Mo=O). While for other $MoOCl_2L_3$ complexes[9] the green isomers show $\nu$(Mo=O) at slightly lower values than the blue ones, the overlapping of the $PMe_3$ and M=O bands in $MoOCl_3(PMe_3)_3$ makes difficult the precise determination of the Mo–O stretching frequency in the two isomers.

The $^1H$ NMR spectrum shows a pattern of five lines due to the P*Me*$_3$ protons, from which the components of a virtually-coupled triplet centred at $\delta$ 1.55 and of a doublet at 1.45 ppm can be clearly distinguished. This is consistent with *mer*-$PMe_3$ groups and by analogy with other similar




(1)

complexes *cis* chloride ligands; the structure is probably as in (**1**).

Interaction of the complex with KNCO and KNCS yielded the corresponding blue crystalline metathesis products $MoOX_2(PMe_3)_3$, (X = NCO, NCS); green isomers were not observed. Although the NCS derivative gives a distinct IR absorption at *ca.* 955 $cm^{-1}$ due to $\nu$(Mo = O), for the cyanate derivative the presence of an oxo group could only be inferred from the asymmetry of the strong band at 940 $cm^{-1}$ and the presence of a small shoulder at 960 $cm^{-1}$. Both complexes have two strong bands at 2210 and 2170 $cm^{-1}$ (NCO) and 2050 and 2020 $cm^{-1}$ (NCS) due to $\nu$(C–N) of the NCX ligands, thus confirming the structure type **1**.

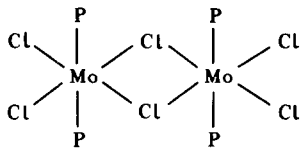
In contrast to the stability of the oxotungsten complexes $WO(S_2CNR_2)_2(PMe_3)$ towards dissociation of the phosphine ligand, the molybdenum analogues readily lose $PMe_3$ in solution to give $MoO(S_2CNR_2)_2$. Thus the interaction of $MoOCl_2(PMe_3)$ with anhydrous $NaS_2CNEt_2$ yielded mainly the 5-coordinate oxo complex $MoO(S_2CNEt_2)_2$. Synthesis of the phosphine adduct $MoO(S_2CNEt_2)_2PMe_3$ requires the presence of an excess of $PMe_3$ to solutions of $MoO(S_2CNEt_2)_2$; it forms green crystals moderately stable to air that can be kept at room temperature for several days under nitrogen without apparent conversion to $MoO(S_2CNEt_2)_2$. The room temperature $^1H$ NMR

spectrum shows broad resonances for the methylene (3.6 ppm, *q*) and methyl (1.0 ppm, *t*, $^3J_{H-H} = ca.$ 7 Hz) dithiocarbamate protons, and a broad doublet at 1.3 ppm ($^2J_{P-H} = ca.$ 9 Hz) for the phosphine ligand.

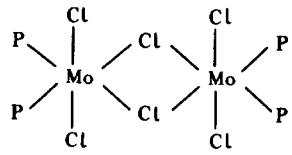
(b) *Reactions of $MoCl_3(thf)_3$ and its reduction to the $Mo_2^{4+}$ core*

In earlier work,[1a] we obtained the complex $MoCl_3(PMe_3)(thf)_2$ by reaction of $MoCl_3(thf)_3$ with one equivalent of $PMe_3$ while an excess gave $MoCl_3(PMe_3)_3$.[1b] The *tris*(phosphine) complex, prepared from blue–purple[12,13] $MoCl_3(thf)_3$ is a yellow solid which slowly decomposes above 55°C' under $N_2$, finally melting at 160°C. The IR spectrum shows bands at 340 and 290 $cm^{-1}$ while the $^{31}P\{^1H\}$ NMR spectrum consists of a doublet and a triplet (ratio 2:1) characteristic of a *mer* configuration of phosphines. It may be noted that two forms of $MoCl_3(PMe_2Ph)_3$ are obtained on reaction of orange $MoCl_3(thf)_3$ with $PMe_2Ph$.[12]

On refluxing in toluene *mer*-$MoCl_3(PMe_3)_3$ loses $PMe_3$ to form a diamagnetic red solid of stoichiometry $[MoCl_3(PMe_3)_2]_n$. This appears to be the chloro bridged dimeric species (**2a**, **b**) based on the molecular weight. By contrast, $MoCl_3(thf)_3$ on refluxing with $PEt_3$ has been shown to give an uncharacterised species, $MoCl_3(PEt_3)_2$, while




**(2a)**




**(2b)**

$PEt_2Ph$ formed $Mo_2Cl_6(PEt_2Ph)_3$ thought to be derived from the $Mo_2Cl_9^{3-}$ core.[12]

The reaction of 1,2-diphenylphosphinomethane (dppm) with (I) gave a red purple solid which analysed as $MoCl_3$(dppm) and showed a magnetic moment of 1.79 BM consistent with magnetically dilute $Mo^{III}$ centres suggesting the existence of weak Mo–Mo bonds. The complex has not been characterised further on account of its insolubility and inability to replace dppm with other phosphines. However, the IR spectrum is similar to that of $Mo_2Cl_6(dppe)_2$[14] prepared from $Mo_2Cl_6(MeCN)_3$ of which analogous complexes exhibit intermetallic bonding.[15]

During attempts to prepare $MoCl_2(PMe_3)_4$ we found that the reaction of (I) in thf with excess $PMe_3$ in the presence of granular zinc over long periods gave, after extraction of *mer*-$MoCl_3(PMe_3)_3$ small amounts of a blue complex. Repetition with zinc powder gave a green solution from which $Mo_2Cl_4(PMe_3)_4$ identical to a sample prepared from $(NH_4)_5Mo_2Cl_9 \cdot H_2O$ was obtained. The dinuclear molybdenum(II) complex could similarly be prepared from *mer*-$MoCl_3(PMe_3)_3$. Subsequent reactions with $PEt_3$, $PMe_2Ph$, $PEt_2Ph$ gave the respective $Mo_2Cl_4L_4$ complexes, while dppm yielded $Mo_2Cl_4$(dppm)$_2$ (see Table 1). $PPh_3$ gave a yellow gum which failed to solidify.

Table 1. Analytical data for $Mo_2Cl_4P_4$ complexes prepared from mer-$MoCl_3(thf)_3$

| Complex | Yield (%) | C | H | Cl | P |
|---|---|---|---|---|---|
| $Mo_2Cl_4(PMe_3)_4$ | 63 | 22.8 | 5.8 | 22.3 | 20.2 |
| | | (22.4) | (5.7) | (22.1) | (19.9) |
| $Mo_2Cl_4(PEt_3)_4$ | 68 | 36.1 | 7.6 | 17.5 | 15.9 |
| | | (35.8) | (7.5) | (17.6) | (15.4) |
| $Mo_2Cl_4(PMe_2Ph)_4$ | 69 | 43.7 | 5.3 | 16.5 | 14.1 |
| | | (43.4) | (5.0) | (16.0) | (14.0) |
| $Mo_2Cl_4(PEt_2Ph)_4$ | 64 | 47.8 | 6.1 | 13.9 | 12.1 |
| | | (48.1) | (6.1) | (14.2) | (12.4) |
| $Mo_2Cl_4(dppm)_2 \cdot 3CH_2Cl_2$ | 82 | 46.5 | 3.8 | 26.3 | 9.3 |
| | | (46.9) | (3.7) | (26.1) | (9.1) |

In light of these reactions it seemed possible that molybdenum(II) acetate could be prepared by the reductive procedure. Stirring a solution of (I) in acetic acid with zinc powder gave a green solution which darkened to yellow brown under reflux and after cooling deposited $Mo_2(CO_2Me)_4$. As yet the nature of the green intermediate formed during the reaction, or, alternatively, by reacting (I) with NaOAc in thf, has not been fully established. The poorly soluble material obtained from the latter reaction analysed closely to $Mo_2(CO_2Me)_4Cl$ and showed an identical IR spectrum to $Mo_2(OAc)_4$. While an $Mo^{II}$–$Mo^{III}$ core could be proposed, the diamagnetism suggests a higher polymeric species.

The above reactions indicate that molybdenum(III) may be readily reduced to dinuclear molybdenum(II) under the appropriate conditions. Although large scale preparations have not been carried out the method would seem to offer a viable alternative route to the $Mo_2^{4+}$ core considering the ease of preparing the starting material $MoCl_3(thf)_3$.[13]

As noted earlier[16] the complex *trans*-$MoCl_2(PMe_3)_4$ can be easily carbonylated to the seven-coordinate derivative $MoCl_2(CO)_2(PMe_3)_3$. While the reaction of the latter complex with sulphur chelating ligands is always accompanied by the loss of one or two of the coordinated phosphines to afford $Mo(S_2CNR_2)_2(CO)_n(PMe_3)_{3-n}$[16] ($n = 1, 2$), the interaction with Tl(acac) yields a complex of composition $Mo(acac)Cl(CO)(PMe_3)_3$. The IR spectrum shows two sharp bands at 1570 and 1515 $cm^{-1}$ due to vibrations derived from the acac group and a strong absorption at 1755 $cm^{-1}$ that indicates the presence of a carbonyl ligand. The unusually low frequency of this band suggests strong $\pi$-back donation from the metal to the CO $\pi^*$ orbitals. Although the band position lies in the bridging CO region the complex is monomeric by cryoscopic molecular weight determinations thus eliminating a dinuclear formulation; other related complexes[16] having terminal CO groups have $\nu$(C–O) in the range 1760–1735 $cm^{-1}$. In accord with the above formulation, the $^1H$ NMR shows a sharp singlet at $\delta$ 2.1 ppm and a slightly broad singlet at $\delta$ 5.7 ppm for the acac methyl and methyne protons (6:1). The phosphine ligands give rise to a filled-in doublet almost a pseudo triplet and a doublet at 1.6 and 1.2 ppm, (18:9 respectively). The first arises from two equivalent $PMe_3$ molecules with intermediate coupling between the phosphorus nuclei and the second to a unique phosphine *cis* with respect to the others. Due to the structural complexity inherent to seven-coordination chemistry[17] an unique stereochemical assignment cannot be made with the present data.

## EXPERIMENTAL

Microanalyses were by Pascher (Bonn) and Imperial College microanalytical laboratories.

*Spectrometers.* IR Perkin–Elmer 577 and 597. Spectra ($cm^{-1}$) in Nujol mulls. NMR Perkin–Elmer R-12A and R32 ($^1H$ 60 and 90 MHz), Varian XL100-12 ($^{31}P$ 40.5 MHz). $^1H$ NMR data in $C_5H_6$ at 35°C unless otherwise specified. $^{31}P$ data references to external 85% $H_3PO_4$.

All operations were performed under oxygen-free nitrogen; solvents were dried over sodium or calcium hydride and distilled prior to use. Melting points were determined in sealed tubes under nitrogen and are uncorrected. $MoCl_3(thf)_3$ was prepared according to the literature method[13] except that the reaction was prolonged to give the blue-purple isomer. $MoCl_4(thf)_2$ and $MoO(S_2CNEt_2)_2$ were also obtained as already reported.[13,18] For comparison the $Mo_2Cl_4L_4$ complexes ($L = PMe_3$, $PEt_3$, $PMe_2Ph$, $PEt_2Ph$) were prepared from $(NH_4)_5Mo_2Cl_9.H_2O$.[7b,c] Petroleum used had b.p. 40–60°C.

Magnetic susceptibility measurements were made at ambient temperature on a Gouy balance constructed by Prof. D. F. Evans, F.R.S.

*Oxodichlorotris(trimethylphosphine)molybdenum (IV) (Green isomer).* Trimethylphosphine (1.3 $cm^3$, *ca.* 13 mmol) and a few drops of oxygen-free water were added to a suspension of $MoCl_4(thf)_2$ (1 g, *ca.* 2.6 mmol) in thf (40 $cm^3$), and the mixture stirred at 50°C for 5–6 hr. (A large excess of water should be avoided otherwise considerable decomposition takes place.) The solution was filtered, evaporated and the residue extracted with EtOH (15 $cm^3$). Centrifugation, partial removal of the solvent *in vacuo* and cooling at −25°C afford the complex as green crystals in *ca.* 60% yield. [Found: C, 26.0; H, 6.6. $C_9H_{27}OCl_2P_3Mo$ requires C, 26.3; H, 6.6%].

IR 1410s, 1295m, 1275s, 960sh, 940s, 850m, 840sh, 730s, 665m.

NMR $^1H$: $\delta$ 1.45 (1) *d* ($^2J_{P-H} = 8$ Hz); 1.55 (2) *t* ($^2J_{P-H} = ca.$ 4 Hz).

In some instances the above reaction carried out under apparently the same conditions, yielded a blue solution from which blue crystals of a complex analysing for $MoOCl_2(PMe_3)_3$ and having IR and $^1H$ NMR spectra identical to those of the green isomer were isolated. [Found: C, 26.2; H, 6.7. $C_9H_{27}OCl_2P_3Mo$ requires C, 26.3; H, 6.6%].

*Oxobis(cyanato)tris(trimethylphosphine)molybdenum(IV).* $MoOCl_2(PMe_3)_3$ (0.41 g, *ca.* 1 mmol) and dry (100°C, 24 hr) KNCO (0.32 g, excess) were stirred at room temperature in thf (30 $cm^3$) for 9–10 hr. The suspension was centrifuged and the solution evaporated. Crystallisation of the residue from EtOH (10 $cm^3$) at −20°C overnight afforded

blue crystals. Yield *ca.* 70%. [Found: C, 30.3; H, 6.4. $C_{11}H_{27}O_3O_3N_2P_3Mo$ requires C, 31.3; H, 6.4%].

IR 2210s, 2170s, 1415m, 1330m, 1300m, 1280m, 960sh, 940s, 850m, 725s; 665m, 615s, 580w.

NMR $^1H$: $\delta$ 1.27 (1) *d* ($^2J_{P-H} = 8$ Hz); 1.31 (2) *t* ($^2J_{P-H} = ca.$ 4 Hz).

A similar metathesis with KSCN gave small blue crystals of $MoO(NCS)_2(PMe_3)_3$ from EtOH at $-25°C$ in *ca.* 60% yield. [Found: C, 28.5; H, 5.8. $C_{11}H_{27}OS_2N_2P_3Mo$ requires C, 28.9; H, 5.9%].

IR 2050s, 2020s, 1405m, 1300m, 1280m, 1255w, 995s, 940s, 845m, 835m, 725s, 665w.

NMR: $^1H(CH_2Cl_2, 35°C)$: $\delta$ 1.65 (2) *t* ($^2J_{P-H} = ca.$ 4 Hz); 1.68 (1) *d* ($^2J_{P-H} = 8$ Hz).

*Oxobis(N, N-diethyldithiocarbamato)trimethylphosphine molybdenum(IV).* To a stirred suspension of $MoO(S_2CNEt_2)_2$ (0.4 g, *ca.* 1 mmol) in $Et_2O$ (15 cm$^3$) an excess of $PMe_3$ (0.3 cm$^3$, *ca.* 3 mmol) was added dropwise. The mixture was stirred for 10 min at room temperature then centrifuged and the resulting solution concentrated *in vacuo*; cooling at $-25°C$ overnight afforded green needles. Yield: *ca.* 50% [Found: C, 32.3; H, 5.9. $C_{13}H_{29}OS_4N_2PMe$ requires C, 32.3, H, 5.9%].

IR 1480s, 1350s, 1295m, 1270s, 1205s, 1140s, 1090mm, 1070m, 1065sh, 1000m, 985sh, 945sh, 930s, 910sh, 840m, 775m, 665w.

NMR. $^1H$: $\delta$ 1.0 (12) *bt* ($^3J_{H-H}$ 7 Hz); 1.6 (9) *bd* ($^2J_{P-H} = 9$ Hz); 3.6 (8) *bq*.

*Chloro(2, 4-pentanedionato)carbonyltris(trimethylphosphine)molybdenum(II).* A solution of $MoCl_2(CO)_2(PMe_3)_3$ (0.5 g, *ca.* 1 mmol) in acetone or tetrahydrofuran (40 cm$^3$) was treated with Tl (acac) (0.6 g, *ca.* 2 mmol) at 50–60°C overnight. The colour of the solution changed from yellow to red. The solvent was stripped under vacuum and the residue crystallised from petroleum at $-25°C$ to give red crystals which were collected and dried *in vacuo*. Yield, 0.2 g, 40%. This preparation is not reproducible and in four more attempts only one further crop of crystals could be obtained. [Found: C, 37.2; H, 6.9; Cl 7.0. $C_{15}H_{34}O_3ClP_3Mo$ requires C, 37.0; H, 7.0; Cl 7.2%].

IR 1755s, 1570s, 1515s, 1420m, 1300m, 1280m, 1265m, 1200w, 1020w, 950s, 855w, 780w, 725m, 720m, 715m, 665m, 560m.

NMR. $^1H$: $\delta$ 1.20 d ($^2J_{P-H} = 8$ Hz); 1.6 "filled-in" doublet ($^2J_{P-H} = 10$ Hz); 2.10 s; 5.7 s.

*Trichloro(1,2 - diphenylphosphinomethane)dimolybdenum(III).* Trichlorotris(tetrahydrofuran)molybdenum(III) and excess diphenylphosphinomethane were heated to the melting point of the diphosphine for 10 mins giving a purple solution. On cooling the solid was washed repeatedly with hot toluene leaving the complex as a purple solid. Yield *ca.* 100%. [Found: C, 50.9; H, 3.7; Cl, 18.7; P, 10.5. $C_{50}H_{44}Cl_6P_4Mo_2$ requires C, 51.2; H, 3.8; Cl 18.1; P, 10.6%]. $\mu_{eff} = 1.79$ BM.

IR. 340m, 328s, 314s, 260w.

The complex dissolved very slighly in $CH_2Cl_2$ but is insoluble in other solvents. Phosphine exchange does not occur on refluxing with $PMe_2Ph$ or $PEt_3$ in thf or $CH_2Cl_2$.

*mer - Trichlorotris(trimethylphosphine)molybdenum(III).* This complex was prepared by a slight modification of the procedure already described.[7b] Details were as follows: trimethylphosphine (8 cm$^3$, 72.7 mmol) was added to a suspension of $MoCl_3(thf)_3$ (10 g, 23.9 mmol) in $Et_2O$ (450 cm$^3$) and the mixture stirred for 24 hr. A grey solid was removed by filtration and the yellow–brown solution evaporated until crystallisation began. On cooling to $-78°C$ the complex was deposited as yellow crystals. Yield: 9.2 g, 89%; m.p. decomp. 55°C finally melting *ca.* 160°C. [Found: C, 25.3; H, 6.4; Cl 24.5; P, 21.2. $C_9H_{27}Cl_3P_3Mo$ requires C, 25.1; H, 6.32; Cl, 24.7; P, 21.6%].

IR 330s, 280w.

NMR $^{31}P\{^1H\}$: $\delta$ $-63.25$ (2), *d*, $^2J_{P-P} = 24.5$ Hz; $-69.3$ (1) *t*, $^2J_{P-P}$ 24.5 Hz.

*Di - μ - chlorotetrachlorotetrakis(trimethylphosphine)dimolybdenum(III).* *mer*-Trichlorotris(trimethylphosphine)molybdenum(III) (1.0 g) was refluxed in toluene (50 cm$^3$) for 12 hr, the cooled solution filtered and the volume reduced to give a dark red solid which was collected and washed with cold $Et_2O$. Yield: 0.68 g, 83%; m.p., decomp. > 85°C. [Found: C, 21.3; H, 5.2; Cl 29.3; P, 17.3. $C_{12}H_{36}Cl_6P_4Mo_2$ requires C, 20.4; H, 5.1; Cl 3.1; P, 17.5%. *M*, 652 (708)].

IR 324m, 268w.

*Tetrachlorotetrakis(trimethylphosphine)dimolybdenum(II).* Trimethylphosphine (1.0 cm$^3$, 9 mmole) in thf (60 cm$^3$ was added to $MoCl_3(thf)_3$ (1 g, 2.3 mmol) and zinc powder (0.6 g, 9.2 mmol; prewashed with thf) and the mixture stirred overnight. The solution was filtered, the solvent removed and the green gum washed with cold petroleum. After dissolving in benzene (50 cm$^3$) and removing of a white solid, the solvent was stripped and the residue washed with cold methanol (2 × 20 cm$^3$). The residual blue solid was dissolved in toluene (30 cm$^3$), the volume reduced and the solution cooled at $-30°C$ to give the blue complex. Yield: 0.48 g, 63%, m.p., decomp. > 245°C. [Found: C, 22.8; H, 5.8; Cl 22.3; P, 20.2. $C_{12}H_{36}Cl_4P_4Mo_2$ requires C, 22.4; H, 5.7; Cl 22.1; P, 19.9%. *M*, 625 (638)].

*Trichlorotris(diethylphenylphosphine)molybdenum(III) and tetrachlorotetrakis(diethylphenylphosphine)dimolybdenum(II).* Diethylphenylphosphine (2 cm$^3$) in thf (60 cm$^3$) was added to $MoCl_3(thf)_3$

(1 g, 2.3 mmol) and zinc powder (0.6 g, 9.2 mmol). After stirring for 4 hr the mixture was filtered and the solution evaporated. The green gum was washed with petroleum ($4 \times 10\,cm^3$) to remove excess phosphine, then with methanol ($2 \times 10\,cm^3$) and the residue recrystallised from toluene/MeOH (1:1) to give $MoCl_3(PEt_2Ph)_3$ as a yellow crystalline solid. Yield: 0.72 g, 43%, m.p., 116°C. [Found: C, 51.4; H, 6.5; Cl 15.1; P, 13.3. $C_{30}H_{45}Cl_3P_3Mo$ requires C, 51.4; H, 6.5; Cl 15.2; P, 13.3% *M*, 480 (700)].

The methanol extracts from above were reduced in volume and cooled at −30°C to give tetrachlorotetrakis(diethylphenylphosphine)dimolybdenum(II) as a blue powder which was washed with cold methanol ($2 \times 5\,cm^3$) and dried *in vacuo*. Yield: 0.44 g, 37%. [Found: C, 47.8; H, 6.1; Cl, 13.9; P, 12.1. $C_{40}H_{60}Cl_4P_4Mo_2$ requires C, 47.9; H, 6.0; Cl, 14.2; P, 12.7%].

Repetition of the reaction with stirring for 24 hr gave a blue solution which was filtered from the solid and the solvent removed. The gum remaining was washed with petroleum ($2 \times 20\,cm^2$) and cold methanol ($2 \times 10\,cm^3$) to give the dimolybdenum complex (0.68 g, 5.7%) as a blue solid, identical in properties with a sample prepared from $(NH_4)_5Mo_2Cl_9.H_2O$.

*Tetra-acetato)dimolybdenum(II)*. Degassed glacial acetic acid ($50\,cm^3$) was added to $MoCl_3(thf)_3$ (1 g, 2.4 mmole) and zinc powder (0.8 g, 12.2 mmol) and the mixture stirred under reflux until a homogeneous solution was obtained. On cooling tetra(acetato)dimolybdenum(II) precipitated as yellow crystals which were collected and dried. Yield: 0.42 g, 41%.

The solvent was removed from the filtrate and the residue washed with cold thf ($5\,cm^3$) and diethyl ether ($2 \times 10\,cm^3$) to give a green solid which could not be obtained pure.

A similar product analysing as $Mo_2(O_2CMe)_4Cl$ was obtained as follows: Tetrahydrofuran ($50\,cm^3$) was added to $MoCl_3(thf)_3$ (0.92 g, 2.2 mmol) and sodium acetate (0.54 g, 6.6 mmol) and the solution refluxed for 4 hr and allowed to stand overnight. After filtering the solution and reducing the solvent volume, the complex precipitated as a green solid which was collected, washed with cold thf ($5\,cm^3$) followed by $Et_2O$ ($2 \times 10\,cm^3$) and dried *in vacuo*. Yield: 0.36 g, decomp. > 110°C. [Found: C, 20.1; H, 2.9; Cl, 8.3; O, 27.4. $C_8H_{12}O_8ClMo_2$ requires C, 20.7; H, 2.6; Cl, 7.7; O, 27.6%]. The diamagnetic complex is slightly soluble in thf; the IR spectrum is identical with that of $Mo_2(CO_2Me)_4$.

*Acknowledgement*—We thank the Spanish C.A.I.C.Y.T. (E.C.) and the S.E.R.C. (A.J.N.) for support.

## REFERENCES

1. See, e.g. (a) E. Carmona-Guzman and G. Wilkinson, *J. Chem. Soc., Dalton Trans.* 1978, 1139; (b) J. L. Atwood, W. E. Hunter, E. Carmona-Guzman and G. Wilkinson, *J. Chem. Soc., Dalton Trans.* 1980, 467.
2. (a) K. W. Chiu, D. Lyons, G. Wilkinson, M. Thornton-Pett and M. B. Hursthouse, *Polyhedron* 1983, **2**, 803. (b) E. Carmona, L. Sanchez, M. L. Poveda, R. A. Jones and J. G. Hefner, *Polyhedron* 1983, **2**, 797.
3. P. R. Brown, F. G. N. Cloke, M. L. H. Green and R. C. Tovey, *J. Chem. Soc. Chem. Commun.* 1982, 519.
4. D. A. Edwards and J. J. Maguire, *Inorg. Chim. Acta* 1977, **25**, L47; J. E. Armstrong, D. A. Edwards, J. J. Maguire and R. A. Walton, *Inorg. Chem.* 1979, **18**, 1172.
5. P. R. Sharp and R. R. Schrock, *J. Am. Chem. Soc.* 1980, **102**, 1430.
6. H. Bino and D. Gibson, *J. Am. Chem. Soc.* 1980, **102**, 4277.
7. See for example: (a) H. D. Glicksman, A. D. Hamer, T. J. Smith and R. A. Walton, *Inorg. Chem.* 1976, **15**, 2205; (b) J. San Filippo, H. J. Sniadoch and R. L. Grayson, *Inorg. Chem.* 1974, **13**, 2121; (c) J. V. Brencic and P. Segedin, *Z. Anorg. Allg. Chem.* 1976, **423**, 266; (d) J. San Filippo, *Inorg. Chem.* 1972, **11**, 3140.
8. I. W. Boyd and J. T. Spence, *Inorg. Chem.* 1982, **21**, 1602.
9. A. V. Butcher and J. Chatt, *J. Chem. Soc.* (*A*) 1970, 2652.
10. W. E. Newton, J. W. McDonald, J. L. Corbin, L. Ricard and R. Weiss, *Inorg. Chem.* 1980, **19**, 1997.
11. C. A. Rice and J. T. Spence, *Inorg. Chem.* 1980, **19**, 2845.
12. M. W. Anker, J. Chatt, G. J. Leigh and A. G. Wedd, *J. Chem. Soc., Dalton Trans.* 1975, 2639.
13. J. R. Dilworth and R. L. Richards, *Inorg. Synth.* 1980, **20**, 119.
14. C. Miniscloux, G. Martino and L. Sajus, *Bull. Soc. Chim. France* 1973, 2179.
15. J. E. Grey and P. W. Smith, *Austr. J. Chem.* 1969, **22**, 1627; I. W. Boyd and A. G. Wedd, *Austr. J. Chem.* 1976, **29**, 1829.
16. E. Carmona, K. Doppert, J. M. Marin, M. L. Poveda, L. Sánchez and R. Sánchez-Delgado, unpublished results.
17. M. G. B. Drew, *Prog. Inorg. Chem.* 1977, **23**, 68.
18. R. N. Jowitt and P. C. H. Mitchell, *J. Chem. Soc.* (*A*) 1969, 2632.

*Polyhedron* Vol. 3, No. 3, pp. 353–355, 1984
Printed in Great Britain.

0277–5387/84 $3.00 + .00
© 1984 Pergamon Press Ltd.

# THE PREPARATION AND SYNTHETIC VALUE OF *fac*-$[M(CO)_3(NCR)_3]^+$ CATIONS (M = Mn or Re; R = Et, Pr OR $PhCH_2$)

**D. A. EDWARDS and J. MARSHALSEA**
School of Chemistry, University of Bath, Bath, BA2 7AY, England

(*Received* 28 *July* 1983; *accepted* 10 *August* 1983)

**Abstract**—Treatment of $MBr(CO)_5$ (M = Mn or Re) with $AgClO_4$ and an organonitrile in a suitable solvent affords the complexes *fac*-$[M(CO)_3(NCR)_3][ClO_4]$, (R = Et, Pr or $PhCH_2$). The use of these complexes as synthetic precursors has been illustrated by the preparation of *fac*-$[M(CO)_3L_3][ClO_4]$, (M = Mn, L = $NH_3$ or $L_3$ = dien; M = Re, $L_3$ = triphos). Pure *fac*-$[Re(CO)_3(NH_3)_3][ClO_4]$ could not be prepared using this nitrile displacement route, but may be isolated, as the $PF_6^-$ salt, from the reaction of $[Re(CO)_3(toluene)][PF_6]$ and ammonia in chloroform.

In a recent publication[1] Kubas illustrated the use of the complexes *fac*-$W(CO)_3(NCR)_3$, (R = Et or Pr), as starting materials for the synthesis of several polyolefin- and phosphine-substituted tungsten carbonyls. These nitrile complexes were preferred to the commonly employed *fac*-$W(CO)_3(NCMe)_3$ because not only were they formed more rapidly than the acetonitrile complex from $W(CO)_6$ but they also possessed higher solubilities in solvents of synthetic utility. Subsequent nitrile substitution reactions could therefore be achieved more effectively. Kubas also suggested that the use of higher nitriles as ligands should be encouraged, rather few complexes containing these ligands having been explored.

We are therefore prompted to report the preparation, characterization and use of the complexes *fac*-$[M(CO)_3(NCR)_3][ClO_4]$ (M = Mn or Re; R = Et, Pr or $PhCH_2$), the rhenium cations with R = Et or Pr being isoelectronic and isostructural with *fac*-$W(CO)_3(NCR)_3$ reported by Kubas.[1]

## EXPERIMENTAL

All reactions were performed under dry nitrogen using anhydrous, deoxygenated solvents. IR spectra were recorded using Perkin–Elmer 597 and 599B spectrometers. The $^1H$ NMR spectra were recorded as $CDCl_3$ solutions using a Jeol PS 100 spectrometer with tetramethylsilane as internal standard.

*Preparation of* *fac*-$[Mn(CO)_3(NCR)_3][ClO_4]$, (R = Et, Pr or $PhCH_2$)

A solution of $MnBr(CO)_5$ (0.55 g, 2.00 mmol), $AgClO_4$ (0.42 g, 2.03 mmol) and EtCN (0.36 g, 6.50 mmol) in 30 $cm^3$ of chloroform was refluxed for 5 hr. The AgBr formed was filtered off and the filtrate evaporated to low bulk. Addition of diethyl ether afforded an orange precipitate of $[Mn(CO)_3(NCEt)_3][ClO_4]$, (0.71 g, 88%; $^1H$ NMR in $CDCl_3$: $\delta$, 1.43 (3), 2.86 (2)). Found: C, 35.1; H, 4.1; N, 10.6. $C_{12}H_{15}ClMnN_3O_7$ calc.: C, 35.7; H, 3.8; N, 10.4.

The PrCN complex was prepared in a similar fashion, except that PrCN (0.45 g, 6.50 mmol) was used with a reflux time of 16 hr. The product, isolated as a yellow oil which could not be induced to crystallize, was freed from excess PrCN by high vacuum pumping. Yield, 0.79 g (89%). $^1H$ NMR in $CDCl_3$: $\delta$, 1.10 (3), 1.82 (2), 2.83 (2). Found: C, 39.2; H, 4.8; N, 9.2. $C_{15}H_{21}ClMnN_3O_7$ calc.: C, 40.4; H, 4.8; N, 9.4.

The $PhCH_2CN$ analogue was also prepared in the above manner as an orange oil using $PhCH_2CN$ (0.70 g, 6.00 mmol) and a reflux time of 4 hr. Yield, 0.91 g (77%). $^1H$ NMR in $CDCl_3$: $\delta$, 4.23 (2), 7.33 (5). Found: C, 54.8; H, 3.5; N, 6.9. $C_{27}H_{21}ClMnN_3O_7$ calc.: C, 55.0; H, 3.6; N, 7.1.

*Preparation of* *fac*-$[Re(CO)_3(NCEt)_3][ClO_4]$. A mixture of $ReBr(CO)_5$ (1.00 g, 2.50 mmol), $AgClO_4$ (0.52 g, 2.51 mmol) and EtCN (25 $cm^3$) was refluxed for 16 hr. After removal of the AgBr, diethyl ether (70 $cm^3$) was added to the filtrate to give colourless crystals on standing. These were washed with diethyl ether and dried *in vacuo*. Yield, 0.86 g (65%). $^1H$ NMR in $CDCl_3$: $\delta$, 1.44 (3),

*Author to whom correspondence should be addressed.

2.96 (2). Found: C, 26.8; H, 2.8; N, 7.9. $C_{12}H_{15}ClN_3O_7Re$ calc.: C, 26.9; H, 2.8; N, 7.9.

*Preparation of fac*-$[Re(CO)_3(NCCH_2Ph)_3][ClO_4]$. A mixture of $ReBr(CO)_5$ (0.50 g, 1.25 mmol), $AgClO_4$ (0.25 g, 1.21 mmol), $PhCH_2CN$ (0.43 g, 3.69 mmol) and di-isopropyl ether (20 $cm^3$) was refluxed for 20 hr. Decantation of the solvent left a brown solid which was partly soluble in 20 $cm^3$ of chloroform leaving a residue of AgBr. Removal of the chloroform left a viscous liquid which crystallized after standing for a few days at room temperature. Yield, 0.73 g (82%). $^1H$ NMR in $CDCl_3$: $\delta$, 4.30 (2), 7.33 (5). Found: C, 44.6; H, 3.1; N, 5.6. $C_{27}H_{21}ClN_3O_7Re$ calc.: C, 45.0; H, 2.9; N, 5.8.

*Preparation of fac*-$[Mn(CO)_3(NH_3)_3][ClO_4]$. Ammonia gas was passed for 1 hr into solutions of *fac*-$[Mn(CO)_3(NCR)_3][ClO_4]$, (0.25 g; R = Et, Pr or $PhCH_2$) in 10 $cm^3$ of chloroform. The cream–yellow products were filtered, washed with chloroform and dried *in vacuo*. Yields at least 80%. Found: C, 12.5; H, 3.3; N, 14.5. $C_3H_9ClMnN_3O_7$ calc.: C, 12.5; H, 3.1; N, 14.5.

*Preparation of fac*-$[Mn(CO)_3(dien)][ClO_4]$. A mixture of *fac*-$[Mn(CO)_3(NCR)_3][ClO_4]$, (1.00 mmol; R = Et, Pr or $PhCH_2$), diethylenetriamine (0.11 g, 1.10 mmol) and chloroform (10 $cm^3$) was refluxed for 0.5 hr. The pale yellow products were filtered, washed with chloroform and dried *in vacuo*. Yields at least 90%. Found: C, 25.1; H, 3.9; N, 12.5. $C_7H_{13}ClMnN_3O_7$ calc.: C, 24.6; H, 3.8; N, 12.3.

*Preparation of fac*-$[Re(CO)_3(triphos)][ClO_4]$. A mixture of *fac*-$[Re(CO)_3(NCEt_3)][ClO_4]$, (0.26 g, 0.50 mmol), 1,1,1-tris(diphenylphosphinomethyl) ethane (0.34 g, 0.55 mmol) and acetone (20 $cm^3$) was refluxed for 2 hr. Removal of the acetone left a creamy–white residue which was redissolved in acetone, the solution filtered and the product precipitated by addition of light petroleum. Yield 0.32 g (65%). Found: C, 52.8; H, 3.9. $C_{44}H_{39}ClO_7P_3Re$ calc.: C, 53.1; H, 4.0.

*Preparation of fac*-$[Re(CO)_3(NH_3)_3][PF_6]$ *from* $[Re(CO)_3(\eta\text{-}C_6H_5Me)][PF_6]$. Ammonia gas was slowly passed for 6 hr through a suspension of $[Re(CO)_3(\eta\text{-}C_6H_5Me)][PF_6]$[2] (0.05 g) in chloroform (15 $cm^3$). The white solid produced was filtered, washed with diethyl ether and dried *in vacuo*. Yield, 0.038 g (82%). Found: C, 7.8; H, 2.0; N, 9.1. $C_3H_9F_6N_3O_3PRe$ calc.: C, 7.8; H, 1.9; N, 9.0.

## RESULTS AND DISCUSSION

High yields of the complexes *fac*-$[M(CO)_3(NCR)_3][ClO_4]$, (M = Mn, R = Et, Pr or $PhCH_2$; M = Re, R = Et or $PhCH_2$) have been isolated from the reactions of $MBr(CO)_5$ with RCN in the presence of $AgClO_4$. This method has previously been employed for the syntheses of the acetonitrile analogues.[3,4] The *fac*-$[Mn(CO)_3(NCR)_3][ClO_4]$ (R = Pr or $PhCH_2$) complexes were isolated as non-crystallizable viscous oils. The related *fac*-$[Mn(CO)_3L_3][ClO_4]$ (L = acetone or tetrahydrofuran) complexes are also known as oils.[5] IR data for the nitrile complexes are presented in Table 1 and are, not unexpectedly, similar to those of the acetonitrile analogues.[4] Two $\nu$(CO) bands ($A_1 + E$) are observed in the solution spectra, the lower frequency band being of greater half width. The presence of the $T_2$ $\nu$(ClO) and $\delta$(OClO) bands at *ca.* 1095 and *ca.* 625 $cm^{-1}$ coupled with the absence of $A_1$ $\nu$(ClO) bands at *ca.* 935 $cm^{-1}$ are indicative of ionic perchlorate and an increase in $\nu$(CN) from that of the free nitrile is typical of *N*-bonded nitrile. The $^1H$ NMR spectra are given in the Experimental section, the observation of a single set of resonances for each cation being further support for facial configurations.

As illustrations of the synthetic value of these nitrile complexes, we have prepared the complexes *fac*-$[M(CO)_3L_3][ClO_4]$ (M = Mn, $L = NH_3$ or $L_3$ = dien; M = Re, $L_3$ = triphos) in excellent yields by simple nitrile displacement reactions. Significant IR bands are listed in Table 1, *fac*-$[Re(CO)_3(triphos)][ClO_4]$ showing three $\nu$(CO) bands rather than the expected two due to solid state E mode splitting. Although *fac*-$[Mn(CO)_3(NH_3)_3][ClO_4]$ has not been reported previously, the corresponding chloride has been prepared[6] by a high pressure reaction of $MnCl(CO)_5$ with anhydrous liquid ammonia, and the $[Mn(CO)_5]^-$ salt by photolysis of a solution of $Mn_2(CO)_{10}$ in the presence of ammonia.[7] Clearly the present route offers a simple alternative. The complex *fac*-$[Mn(CO)_3(triphos)][Mn(CO)_5]$ has been prepared[8] by a similar disproportionation of $Mn_2(CO)_{10}$ using triphos, but the analogous cation *fac*-$[Re(CO)_3(triphos)]^+$, isolated here as its perchlorate salt, appears not to have been reported before.

Surprisingly, in view of the simplicity of the above reactions, we were unable to obtain pure samples of *fac*-$[Re(CO)_3(NH_3)_3][ClO_4]$ from reactions of solutions of *fac*-$[Re(CO)_3(NCR)_3][ClO_4]$ with ammonia gas. However, *fac*-$[Re(CO)_3(NH_3)_3][PF_6]$ was successfully isolated by displacement of arene from $[Re(CO)_3(\eta\text{-}C_6H_5Me)][PF_6]$. The tris-ammine cation has previously been prepared as its chloride by high pressure reactions of either $Re_2(CO)_{10}$ or $Re(CO)_5H$ with a solution of ammonium chloride in liquid ammonia,[9] and as the phosphinate $R_2PO_2^-$ (R = Me or Ph) salts from

Table 1. IR frequencies ($cm^{-1}$)[a]

| Compound | ν(CO) | ν(CN)[d] | ν(ClO)[d] | δ(OClO)[d,f] | ν(NH)[d] |
|---|---|---|---|---|---|
| $[Mn(CO)_3(NCEt)_3][ClO_4]$ | 2050, 1972[b] | 2293 w | 1099 br | 623 | |
| $[Mn(CO)_3(NCPr)_3][ClO_4]$ | 2048, 1966[b] | 2290 w | 1097 br | 627 | |
| $[Mn(CO)_3(NCCH_2Ph)_3][ClO_4]$ | 2045, 1965[b] | 2285 w | 1092 br | 625 | |
| $[Re(CO)_3(NCEt)_3][ClO_4]$ | 2045, 1935[b] | 2297 w | 1093 br | 625 | |
| $[Re(CO)_3(NCCH_2Ph)_3][ClO_4]$ | 2052, 1950[b] | 2300 w | 1096 br | 626 | |
| $[Mn(CO)_3(NH_3)_3][ClO_4]$ | 2043, 1919[c] | | 1096 br | 627 | 3358 m, 3296 w |
| $[Mn(CO)_3(dien)][ClO_4]$ | 2035, 1923[c] | | 1090 br | 626 | 3340 m, 3298 m |
| $[Re(CO)_3(triphos)][ClO_4]$ | 2035, 1967, 1948[d] | | 1098 br | 626 | |
| $[Re(CO)_3(NH_3)_3][PF_6]$ | 2028, 1902[b] | | 840 br[e] | 560[g] | 3370 m, 3300 m |

[a] All bands strong unless otherwise indicated. [b] $CHCl_3$ solution. [c] MeCN solution.
[d] Nujol mull. [e] $\nu_3$, $PF_6^-$. [f] Strong δ(MCO) bands also found between 700-600 $cm^{-1}$.
[g] $\nu_4$, $PF_6^-$.

$[Re(CO)_3(\mu\text{-}O_2PR_2)(THF)]_n$ and liquid ammonia.[10] Again the route suggested here represents an attractive alternative. The complex *fac*-$[Re(CO)_3(triphos)][PF_6]$ may also be prepared by a similar displacement reaction from $[Re(CO)_3(\eta\text{-}C_6H_5Me)][PF_6]$.

*Acknowledgement*—We thank the University of Bath Research Fund for partial support of this work.

## REFERENCES

1. G. J. Kubas, *Inorg. Chem.* 1983, **22**, 692.
2. L. A. P. Kane-Maguire and D. A. Sweigart, *Inorg. Chem.* 1979, **18**, 700.
3. R. H. Reimann and E. Singleton, *J. Organomet. Chem.* 1973, **59**, C 24; *J. Chem. Soc., Dalton Trans.* 1974, 808.
4. D. A. Edwards and J. Marshalsea, *J. Organomet. Chem.* 1977, **131**, 73.
5. D. Drew, D. J. Darensbourg and M. Y. Darensbourg, *Inorg. Chem.* 1975, **14**, 1579; R. Uson, V. Riera, J. Gimeno, M. Laguna and M. P. Gamasa, *J. Chem. Soc., Dalton Trans.* 1979, 996.
6. H. Behrens, E. Ruyter and H. Wakamatsu, *Z. Anorg. Allg. Chem.* 1967, **349**, 241.
7. M. Herberhold, F. Wehrmann, D. Neugebauer and G. Huttner, *J. Orgamomet. Chem.* 1978, **152**, 329.
8. J. Ellermann and H. A. Lindner, *Z. Naturforsch., B*; *Anorg. Chem., Org. Chem.* 1976, **31B**, 1350.
9. H. Behrens and P. Pässler, *Z. Anorg. Allg. Chem.* 1969, **365**, 128.
10. E. Lindner, S. Trad, S. Hoehne and H.-H. Oetjen, *Z. Naturforsch., B*; *Anorg. Chem., Org. Chem.*, 1979, **34B**, 1203.

*Polyhedron* Vol. 3, No. 3, pp. 357-362, 1984
Printed in Great Britain.

0277-5387/84 $3.00 + .00
Pergamon Press Ltd.

# COMPLEXES OF Cu(II) AND Co(II) WITH NN'-BIS-8-QUINOLYLETHYLENEDIAMINE

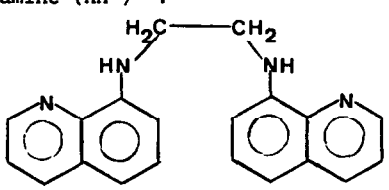
J.Ribas*, C.Diaz
Departament de Química Inorgànica.Facultat de Química.-Universitat de Barcelona. Diagonal,647 BARCELONA. SPAIN

J.Casabó
Departament de Química Inorgànica. Facultat de Ciències.Universitat Autònoma de Barcelona. Bellaterra.BARCELONA. SPAIN

Received, 4 July 1983 : accepted 25 November 1983)

ABSTRACT.- This article describes some complexes of Cu(II) and Co(II) with NN'-bis-8-quinolylethylenediamine ligand (nn'). All the compounds are of stoichiometry $[MX_2(nn')]$ (M = Cu or Co; X = $Cl^-$,$Br^-$,$I^-$,$NO_3^-$ or $SCN^-$). The electronic spectra are consistent with distorted octahedral geometry around the ions, indicating the four coordination of the nn' ligand. Magnetic susceptibility measurements down to 100 K show antiferromagnetic interactions in all the Cu(II) compounds demonstrating the existence of the ionic and bridging X group. Infrared spectra show the presence of ionic and bridging nitrate in the $[M(NO_3)_2(nn')]$ (M = Co or Cu) compounds and ionic and bridging NCS group in the $[Cu(NCS)_2(nn')]$ compound.

The chelating properties of 8-aminoquinoline and its derivatives have been neglected. Earlier, some of us have reported complexes with 8-aminoquinoline [1] and some derivatives , namely 5,7-dichloro-8-aminoquinoline ; 5,7-dibromo-8-aminoquinoline and 5,7-diiodo-8-aminoquinoline with Cu(II) [2], Ni(II)[3] and Co(II) [4] ions. A few compounds are known with the NN'-bis-8-quinolylethylenediamine (nn') [5].




(nn' ligand)

In aqueous solution, complexes of the $[M(H_2O)_2(nn')]$ type have been reported [6] and complexes of stoichiometry $[M(nn')_2]$ [7] were formed in strongly alkaline solution similarly to the analogous quinolinates. In this paper we describe some complexes of Cu(II) and Co(II) with the NN'-bis-8-quinolylethylenediamine ligand. The stoichiometry of these compounds is $[M(X)_2(nn')]$. The visible, i.r. and magnetic measurements down to 100 K (for Cu complexes) indicate hexacoordination with possible formation of polynuclear species with $\mu$-X ligand.

## EXPERIMENTAL

Preparation of the new compounds.-

The nn' ligand was prepared by a literature method [7]. For the synthesis of the new complexes we used anhydrous solvents distilled twice over $CaCl_2$. All the complexes are very inso-

* Author to whom all the correspondence should be adressed

luble in the most common solvents. In all cases the yield is nearly quantitative.

Complexes $[Cu(X)_2(nn')]$.

$[Cu(Cl)_2(nn')]$.- nn' (0.3 g) was dissolved in $Me_2CO$ (20 $cm^3$) ; an ethanolic solution of $CuCl_2aq$ (0.13 g) was added. The green powder which precipitates was filtered and washed with EtOH and $Et_2O$. Found: C, 52.7 ; N, 12.5 ; H, 4.0 ; Cl, 15.8%. Calc.: C, 53.49 ; N, 12.47; H, 4.04 ; Cl, 15.78%.

$[Cu(Br)_2(nn')]$.- The procedure was the same as in the corresponding chloro-compound, using 0.20 g of $CuBr_2aq$. The solid is green. Found: C, 45.3 ; N, 10.4 ; H, 3.4 ; Br, 12.5 %. Calc.: C, 44.65 ; N, 10.41 ; H, 3.37 ; Br, 13.18 %.

$[Cu(NO_3)_2(nn')]$.- A solution of nn' (0.3 g) in $Me_2CO$ (25 $cm^3$) was mixed with a solution of $Cu(NO_3)_2aq$ (0.18 g) in EtOH (30 $cm^3$). A powdery blue solid precipitated which was separated as above. Found : C, 48.7 ; N, 16.8 ; H, 3.6%. Calc.: C, 47.87 ; N, 16.73 ; H, 3.61 %.

$[Cu(NCS)_2(nn')]$.- To a solution of nn' (0.3 g) in $Me_2CO$ an ethanolic solution of $Cu(NO_3)_2aq$ (0.18 g) and a large excess of $NH_4SCN$ (2.5 g) were added. Green powder was precipitated immediately, which was treated as above. Found: C, 53.5 ; N, 16.9 ; H, 3.8 %. Calc.: C, 53.45 ; N, 17.00; H, 3.67%.

Complexes $[Co(X)_2(nn')]$.

Because of the facility of oxidation of the Co(II) to Co(III) with the ligands containing the $NH_2$ group, we have employed a nitrogen atmosphere in the preparation of these complexes.

$[Co(Cl)_2(nn')]$.- $CoCl_2aq$ (0.32 g) was dissolved in EtOH (40 $cm^3$). Acetone solution of nn' (0.3 g) was added. The mixture was refluxed for a few minutes. The brown solid which precipitated was filtered, washed with EtOH and $Me_2CO$ and left to dry in the air. Found : C, 51.8 ; N, 11.6 ; H, 4.3 ; Cl, 14.7 %. Calc.: C, 51.96 ; N, 12.12 ; H, 4.36 ; Cl, 15.34 %.

$[Co(Br)_2(nn')]$.- This complex was prepared as for $[Co(Cl)_2(nn')]$ using 0.31 g of $CoBr_2aq$. A brown solid precipitated, which was separated as above. Found : C, 45.3 ; N, 10.2 ; H, 3.4; Br, 12.3 % Calc .: C, 44.65 ; N, 10.41 ; H, 3.37 ; Br, 13.28 %.

$[Co(NO_3)_2(nn')]$.- This complex was prepared as for $[Co(Cl)_2(nn')]$ using 0.17 g of $Co(NO_3)_2aq$. A brown powder precipitated, which was separated as above. Found : C, 48.2 ; N, 16.8 ; H, 3.6 %. Calc.: C, 48.28 ; N, 16.89 ; H, 3.64 %.

$[Co(SCN)_2(nn')]$.- To a solution of nn' (0.3 g) in $Me_2CO$ (40 $cm^3$), an ethanolic solution of $Co(NO_3)_2aq$ (0.17 g) and a large excess of $NH_4SCN$ (2.5 g) was added. After the mixture was refluxed for a few minutes, a brown powder precipitated which was separated as above. Found : C, 53.6 ; N, 17.0 ; H, 3.7 %. Calc.: C, 53.95 ; N, 17.16 ; H, 3.70 %.

Techniques

The infrared spectra have been recorded on a Beckman IR-20 A spectrophotometer using the KBr pellet technique, at different concentrations. For the 600-250 $cm^{-1}$ zone it has been made in an approximate relation 1:1 to be able to assign metal-ligand bands of low intensity. The electronic spectra have been made in solid state because the low solubility of the complexes or the possibility of exchange of the ligand with the solvent. They have been made using Beckman DU-2 (visible, UV and near i.r.) and Beckman 5230 UV (visible and UV)spectrophotometers. We have as well used diffuse reflectance measurements with a Cary 17 spectrophotometer with MgO as reference.

For the magnetic measurements we have used a Cahn 2000 electrobalance sensitive to 0.001 mg; a Brucker N-177 electromagnet and a cryostat CF-100 of Oxford Instruments. Measurements were made for different values of magnetic field.

## RESULTS AND DISCUSSION

### Infrared spectra: general.-

Table 1 shows the frequencies of the bands assigned to vibrational modes of the NH group of the ligand and their complexes. In the 2800-3400 $cm^{-1}$ zone the stretching modes of the NH group of R-NH-R' appear. In all the complexes these bands appear at lower frequencies than for the free ligand and are split into two components in the Cu(II) complexes. This effect is a convincing proof of the coordination of the amine group in all the compounds [7-9]. In the 1650-1550 $cm^{-1}$ region the free ligand exhibits two resolved bands at 1600 and 1570 $cm^{-1}$ of relative intensity 1:3, due to partially coupled stretching vibrations $\nu$(C=C), $\nu$(C=N) of the aromatic rings and the deformation mode of the NH group. This was shown in the case of 8-aminoquinoline by deuteration studies [7]. Coordination changes the coupling of these modes. These two bands appear at higher frequencies than in the free ligand and the intensity is smaller. In all the Co(II) complexes the second of these bands is also split into two components (see Table 1). This splitting can be attibuted to the partial loss of coupling between $\delta$(NH) and aromatic ring vibrations.

In the 945-970 $cm^{-1}$ region there is a band corresponding to the deformation mode of the coordinated NH group. The behaviour of this band is analogous to that of the previously described wagging mode of the $NH_2$ group in 8-aminoquinoline [1].

### Complexes with halogen ligand.-

The compounds of Cu(II) with chlorine show two bands at 300 $cm^{-1}$ and 270 $cm^{-1}$, which can be assigned to $\nu$(Cu-Cl) terminal and bridging respectively, analogously to the complexes of ethylenediamine [10], bipyridyl [11] and 5,7-dibromo-8-aminoquinoline [2]. In the bromine complex we were limited by the range of the spectrophotometer used. For this reason only one band at 260 $cm^{-1}$ is shown, which can be attributed to Cu-Br vibration. In this region, the two Co(II) complexes do not show bands attributable to the Co-X vibrations which should appear at lower frequencies. This difference between Cu-X and Co-X was also found in the 8-aminoquinoline complexes [2,4].

### Complexes with nitrato ligand.-

Table 2 shows the wavenumbers assigned to the $NO_3^-$ group in the two prepared complexes with this ligand. In it we note the presence of some bands that may be assigned to the ionic nitrate group together with other bands corresponding to the coordinate nitrate group[12]. In the 1290-1450 $cm^{-1}$ region we can see the $\nu_3(E')$ mode split by the coordination into two components at 1440-1450 $cm^{-1}$ and 1300-1310 $cm^{-1}$. At the same time , there is a very intense band at 1390 $cm^{-1}$ attributed to the free ligand [12]. In this zone, the ligand nn' presents several bands which do not overlap the others, except one that coincides with the band assigned to the ionic nitrate group. However, making the infrared spectra with very dilute pellets of KBr it is possible to show the very intense and characteristic band corresponding to the $\nu_3(E')$ mode of the free nitrate ion. Under these conditions the nn' bands disappear almost completely.

In the 1020-1065 $cm^{-1}$ region, the Cu(II) complex presents two intense bands due to the $\nu_1(A_1')$ mode of the ionic and coordinate nitrate group. In the same region the Co(II) complex show only one band due to the same mode of the coordinated nitrate group because the other is overlapped by the ligand bands.

The $\nu_2(A_2'')$ mode due to coordinated nitrate group is observed with medium intensity in the 815-820 $cm^{-1}$ region. The $\nu_4(E')$ mode appears between 725-730 $cm^{-1}$ as a weak band and without splitting, because in this region there are several bands due to the amine ligand.

The coordination mode of the nitrate group cannot be unequivocally deduced from these data [12], but all the physicochemical characteristics of these complexes are compatible with

a polymeric structure with nitrato groups bridging Cu(II) and Co(II) ions and nitrate ionic group in the lattice, as in the corresponding complexes with 8-aminoquinoline derivatives[2,3].

Complexes with thiocyanate.-

Table 3 shows the wavenumbers assigned to the SCN group in the two complexes prepared with nn' ligand. The most interesting features are found in the Cu(II) complex. Effectively, in the 2080-2100 $cm^{-1}$ zone we find two intense bands which can be assigned to $\nu$(CN) stretching mode. Two other bands corresponding to the $\nu$(CS) stretching mode can be seen at 710 $cm^{-1}$ and 860 $cm^{-1}$. Only one band corresponding to the $\delta$(SCN) mode can be found at 460 $cm^{-1}$ [12]. These spectral characteristics may indicate two different thiocyanate groups in the complex. The previously reported compounds $[Cu(SCN)_2(en)]$ [13], $[Cu(SCN)_2(8aq)]$ [1] and $[Cu(SCN)_2(dbaq)]$ [2] have similar i.r. spectra, with two bands in the $\nu$(CN) stretching region.

The complex $[Cu(SCN)_2(en)]$ (en = ethylenediamine) presents an i.r. spectrum with bands corresponding to the SCN group at 2114, 2080 and 790 $cm^{-1}$ [13]. This compound has been analysed by X-ray diffraction [11] which showed that $[Cu(SCN)_2(en)]$ is a sulphur-bridged Cu(II) polymer. The thiocyanate compound contains tricoordinate bridging sulphur. There are two inequivalents Cu atoms associated with two types of chains, one containing only terminal N-thicyanate and the other all bridging [11]. In spite of the low wavenumbers for the stretching modes $\nu$(CN) of the thiocyanate group, this exists partially as a bridging group. In our case we can interpret the two bands corresponding to the SCN group, which appear at 2100 $cm^{-1}$ and 2080 $cm^{-1}$, as being due to the thiocyanate bridging (2100 $cm^{-1}$) and ionic (2080 $cm^{-1}$) groups. The physicochemical and stoichiometric particularities of this compound are compatible with this polymeric structure with bridging and ionic thiocyanate group.

The $[Co(SCN)_2(nn')]$ complex shows an intense band at 2180 $cm^{-1}$ which can be assigned to the $\nu$(CN) stretching mode and another band at 465 $cm^{-1}$ due to the $\delta$(SCN) bending mode. These spectral characteristics are compatible with a coordination via the sulphur atom of the thiocyanate group in the complex.In this case we cannot affirm the existence of a polynuclear compound rather than an octahedral discrete form.

Electronic spectra.-

Table 4 summarises the electronic spectra of all the compounds. The electronic spectra of the $[Cu(X)_2(nn')]$ compounds consist of a high frequency broad band (650-725 nm) with a low frequency shoulder (850-1250 nm). These spectra are consistent with approximately square-planar, elongated tetragonal-octahedral or square-pyramidal but not tetrahedral stereochemistry [5,13,14]. In the case of $[Cu(SCN)_2(nn')]$ the shoulder appears at higher frequency, comparable to that of the similar compounds of ethylenediamine and 8-aminoquinoline derivatives [2].

The electronic spectra of the compounds $[Co(X)_2(nn')]$ are consistent with octahedral geometry around the Co(II) ion. A very large number of six coordinate cobalt(II) complexes are known, but their spectra are difficult to interpret due to spin-orbit coupling, vibronic interactions and symmetry distortions [15-17].

Magnetic susceptibility measurements.-

We have measured the magnetic susceptibility of all the Cu(II) compounds down to 100 K (Table 5). At room temperature the magnetic moment is that expected for a $d^9$ ion in an octahedral environment and with little orbital contributions to the magnetic moment of spin only. All the compounds follow the Curie-Weiss law with good approximation down to the investigated temperature. All the g-values calculated from the Curie-Weiss law are also typical for Cu(II) complexes. All the complexes have small negative Curie-Weiss temperatures ($\theta$) showing the possibility of the existence of antiferromagnetic interactions among the Cu(II)

ions (Table 5). These interactions are explicable in terms of the polymeric structure with bridging X group. We conclude from our results that de nn' complexes closely resemble their 8-aminoquinoline and ethylenediamine analogues.

REFERENCES


1.- J.Casabó, J.Ribas and J.Bartrolí ; Rev.Chim.Min., 1976, 13, 149

2.- J.Casabó, M.Izquierdo, J.Ribas and C.Diaz; Trans.Metal Chem., 1983, 8, 110

3.- M.Izquierdo, J.Casabó, C.Diaz and J.Ribas; Polyhedron, 1983, 2, 529

4.- M.Izquierdo, J.Casabó, C.Diaz and J.Ribas; Synt.React.Inorg.Met.Chem., In press

5.- T.M.Suzuki, S.S.Kamiyana and T.Kinura; Bull.Chem.Soc.Jpn., 1978, 91, 1094

6.- H.Nielsen and O.Dahl; Acta Chem.Scand., 1966, 20, 1113

7.- K.A.Jansen and H.Nielsen; Acta Chem.Scand., 1964, 18, 1

8.- K.J.Badile, D.L.Koracic and J.R.Ferraro; Inorg.Chem., 1967, 6, 406

9.- L.J.Bellamy; The Infrared Spectra of Complex Molecules, Methuen.Co., London ,1962

10.- J.R.Ferraro; Low Frequency Vibrations of Inorganic and Coordination Compounds, Plenum Press, New York, 1971

11.- W.M.Reiff, H.Woing, B.Dockum, T.Brennan and C.Cheng; Inorg.Chim.Acta, 1978, 30, 69

12.- K.Nakamoto; Infrared Spectra of Inorganic and Coordination Compounds, John Wiley, New-York, 1978

13.- I.M.Procter, B.J.Hathaway and P.D.Hodgson; J.Inorg.Nucl.Chem., 1972, 34, 3689

14.- C.K.Jorgensen; Absorption Spectra and Chemical Bonding, Pergamon Press, Oxford, 1962

15.- A.B.P.Lever; Inorganic Electronic Spectroscopy, Elsevier, Amsterdam, 1968

16.- J.Ferguson; J.Cryst.Chem., 1963, 67, 1314

17.- J.Ferguson, D.L.Wool and J.Knox; J.Chem.Phys., 1963, 39, 881


**********

Table 1.- Selected i.r. band wavenumbers (4000-900 $cm^{-1}$) assigned to the ligand

| nn' | Cu/Cl | Cu/Br | Cu/SCN | $Cu/NO_3$ | Co/Cl | Co/Br | Co/SCN | $Co/NO_3$ |
|---|---|---|---|---|---|---|---|---|
| 3380(s) | 3180(s) | 3000(s) | 3200(s) | 3100(s) | 3160(s) | 3200(s) | 3200(s) | 3260(s) |
| | 3060(s) | 2800(s) | | 2870(s) | | | | |
| 1600(m) | 1620(m) | 1630(m) | 1620(m) | 1630(m) | 1620(m) | 1620(m) | 1620(m) | 1620(m) |
| 1570(vs) | 1595(m) | 1605(m) | 1590(m) | 1600(m) | 1600(m) | 1600(m) | 1610(m) | 1600(m) |
| | | | | | 1590(m) | 1590(m) | 1600(m) | 1590(m) |
| | 920(s) | 980(s) | 925(s) | 985(s) | 950(s) | 945(s) | 960(s) | 950(s) |

Table 2. I.r. band wavenumbers attributed to the $NO_3$ group

| $[Co(NO_3)(nn')]NO_3$ | $[Cu(NO_3)(nn')]NO_3$ | |
|---|---|---|
| 1440(s) | 1450(s) | $\nu_3(E')$,ligand |
| 1390(vs) | 1390(vs) | $\nu_3(E')$,ionic |
| 1310(s) | 1300(s) | $\nu_3(E')$,ligand |
| (a) | 1065(m) | $\nu_1(A_1')$ |
| 1030(m) | 1020(s) | |
| 820(m) | 815(m) | $\nu_2(A_2'')$ |
| 730(w) | 725(w) | $\nu_4(E')$ |

(a) overlapped with ligand bands

Table 3. I.r. band wavenumbers attributed to the NCS group.

| $[Co(SCN)_2(nn')]$ | $[Cu(SCN)(nn')]SCN$ | |
|---|---|---|
| 2180(vs) | 2100(vs) | |
| | 2080(vs) | $\nu$(CN) |
| | 860(m) | |
| (a) | 710(m) | $\nu$(CS) |
| 465(w) | 460(w) | $\delta$(SCN) |

(a) overlapped with ligand bands

Table 4. Electronic Spectra(nm) in the solid state

| $[CuCl_2(nn')]$ | $[CuBr_2(nn')]$ | $[Cu(SCN)(nn')]SCN$ | $[CuNO_3(nn')]NO_3$ |
|---|---|---|---|
| 1100(sh) | 960(sh) | 1450-1400(sh) | 1000(sh) |
| 660-650 | 720-705 | 720-700 | 680-665 |
| 665* | -- | -- | 680* |
| 400(sh) | 370(sh) | 350(sh) | -- |

| $[CoCl_2(nn')]$ | $[CoBr_2(nn')]$ | $[CoNO_3(nn')]NO_3$ | $[Co(SCN)_2(nn')]$ | |
|---|---|---|---|---|
| 1100-1000 | 1200-1210 | 1140-1100 | 1420(sh) | $^4T_{1g}(F) \rightarrow {}^4T_{2g}(F)$ |
| | | | 1150 | |
| 690 | 750(sh) | 725 | 750(sh) | |
| 670 | 725 | 705 | 715-710 | |
| 630 | - | 660 | 625 | $^4T_{1g}(F) \rightarrow {}^4A_{2g}(F)$ |
| 610 | 510-505 | 470 | 505(sh) | $^4T_{1g}(F) \rightarrow {}^4T_{1g}(P)$ |

(*) diffuse reflectance

Table 5. Magnetic measurements

| Compounds | B.M.(*) | θ(K) | g |
|---|---|---|---|
| $[CuCl_2(nn')]$ | 2.08 | -4.5 | 2.4 |
| $[CuBr_2(nn')]$ | 1.92 | -7.0 | 2.2 |
| $[Cu(NO_3)_2(nn')]$ | 1.91 | -3.8 | 2.2 |
| $[Cu(SCN)_2(nn')]$ | 1.92 | -7.5 | 2.2 |

* at room temperature

*Polyhedron* Vol. 3, No. 3, pp. 363-364, 1984
Printed in Great Britain.

0277-5387/84 $3.00 + .00
© 1984 Pergamon Press Ltd.

# NOTE

## PREPARATION AND CHARACTERIZATION OF TETRACHLOROCOBALTATES OF $\alpha,\omega$-ALKANEDIAMMONIUM

M. A. Bañares* A. Angoso and E. Rodriguez
Departamento de Química Inorgánica, Facultad de Química, Universidad de Salamanca
Salamanca, España

(Received 20 July 1983 ; accepted 25 November 1983)

ABSTRACT. Several tetrachlorocobaltates(II) of diprotonated $\alpha,\omega$-alkanediamines have been prepared using the following aliphatic diamines: $NH_2(CH_2)_nNH_2$, where n=2,3, 5,6,7,8,9 and 10. Analytical results show that the compounds prepared correspond to the empirical formula $(AAH_2)\left[CoCl_4\right]$, where $AAH_2^{2+}$ is the diprotonated diamine. The formula for the compound with ethylenediamine is, however, $(enH_2)_2CoCl_6$ . Magnetic moments and electronic spectra confirm the existence of $CoCl_4^{2-}$ in all compounds.

The existence of the $CoCl_4^{2-}$ anion in compounds such as $Cs_2CoCl_4$ and $Cs_3CoCl_5$ [1] is well known, as is the corresponding ammonium tetrachlorocobaltate [2] and numerous alkylammonium tetrachlorocobaltates [3]. In the dicationic species of quaternary ammonium ions, of special interest are the compounds with N,N' dimethyltriethylenediammonium [4] and the compounds described by Smith and Stratton [5] with ethylenediammonium.

The present work deals with the preparation and characterization of the tetrachlorocobaltates corresponding to the diprotonated species of the following aliphatic diamines: 1,2 ethylenediamine (en), 1,3 propylenediamine (tn), 1,5 pentamethylenediamine (pn), 1,6 hexamethylene diamine (hn), 1,7 heptamethylenediamine (hpn), 1,8 octamethylenediamine (on), 1,9 nonemathylenediamine (nn) and 1,10 decamethylenediamine (dn).

The compounds obtained all follow the general formula of $(AAH_2)\left[CoCl_4\right]$, where $AAH_2^{2+}$ is the corresponding diprotonated diamine except for the compound formed by ethylenediamine, which has a stoichometry of $(enH_2)_2CoCl_6$, in agreement with what was reported by Smith and Stratton [5].

EXPERIMENTAL. The compounds were prepared after the following method: A mixture is made of equimolecular solutions of the corresponding diamine and of $CoCl_2 \cdot 6H_2O$, both in water, inmediately yielding a blue-green precipitate. Following this, a burette is used to add with stirring, the necessary amount of 1N HCl dropwise to dissolve the precipitate in question. The resulting pink solution is subsequently subjected to evaporation at 60°C until it acquires an intense blue colour, after which it is placed in a desiccator with calcium chloride under reduced pressure. After several days blue acicular crystals begin to appear and these are collected by filtration and dried in an oven at 50°C. Yields ranged between 60 and 70% in all preparations.

All the compounds are stable in air, although the one corresponding to 1,6 hexamethylenediamine is slightly hygroscopic.

Table I shows the elementary analysis of the compounds obtained and compares the percentages observed with those calculated for the proposed formula. The cobalt content of the compounds was determined complexometrically with EDTA using murexide as an indicator, the chloride and nitrogen contents were determined by Mohr and micro-Kjeldahl methods respectively. The amounts of carbon and hydrogen present were determined in the Department of Instrumental Techniques at the C.S.I.C. (Madrid).

Magnetic moments were determined according to the Gouy method using a Stanton MC-5 microbalance equipped with a Newport electromagnet and an Ernest-Turner(0-3A) amperometer, previously calibrating the sample tube with $Hg\left[Co(SCN)_4\right]$, according to the method of Curtis.

* Author to whom correspondence should be addressed.

The electronic spectra were obtained in a Varian-Techtron model 635 spectrophotometer. The diffuse reflectante technique was employed, using magnesium carbonate as the reference blank, since the tetrahedral geometry adopted by the Co(II) in these compounds is easily altered by interaction with the solvent.

The I.R. spectra were recorded in the range 4000-600 $cm^{-1}$ with a Beckman Acculab 10 apparatus, suspending the sample in nujol mull and using sodium chloride plates as the support. In the range of 600-200 $cm^{-1}$, a Perkin-Elmer model 325 apparatus was used with the same technique as before except that caesium iodide plates were used.

RESULTS AND DISCUSSION. The magnetic moments of the compounds agree well with those expected for the Co(II) ion in a tetrahedral environment and are similar to those described for other tetrachlorocobaltates [6]. The diffuse reflectance spectra show a wide band of strong absorption which is responsible for the intense blue shown by these compounds. This band, accompanied by other weaker ones, corresponds to the transition $\nu_3\ ^4A_2 \rightarrow {}^4T_1(P)$ in the tetrahedral conformation adopted by Co(II) in these compounds and is present in other tetrachlorocobaltates [5,6]. In the I.R. spectra, of interest is the shift towards lower frequencies of the stretching and the deformation of the N-H bond due to the protonation of the amine groups and the formation of hydrogen bonds between these and the halocomplex [5,7]. The stretching frequency of the Co-Cl bond appears in all the compounds with a strong band around 300 $cm^{-1}$, in agreement with other tetrachlorocobaltates described in the literature [8].

TABLE I. DIFFUSE REFLECTANCE, MAGNETIC MOMENTS AND ELEMENTARY ANALYSIS

| COMPOUND | | N% | C% | H% | Cl% | Co% | $\mu$(MB) | $\nu_3\ cm^{-1}$ |
|---|---|---|---|---|---|---|---|---|
| $(enH_2)_2CoCl_6$ | cal. | 14.15 | 12.12 | 5.05 | 53.70 | 14.89 | | |
| | obs. | 14.16 | 11.98 | 4.97 | 53.62 | 15.33 | 4.64 | 15150 |
| $(tnH_2)[CoCl_4]$ | cal. | 10.11 | 13.00 | 4.33 | 51.22 | 21.18 | | |
| | obs. | 10.17 | 12.98 | 4.36 | 52.03 | 21.11 | 4.63 | 15130 |
| $(pnH_2)[CoCl_4]$ | cal. | 9.18 | 19.68 | 5.25 | 46.53 | 19.34 | | |
| | obs. | 9.32 | 19.62 | 5.31 | 46.25 | 19.23 | 4.66 | 15314 |
| $(hnH_2)[CoCl_4]$ | cal. | 8.78 | 22.58 | 5.64 | 44.49 | 18.48 | | |
| | obs. | 9.01 | 22.97 | 5.60 | 45.04 | 17.61 | 4.48 | 15197 |
| $(hpnH_2)[CoCl_4]$ | cal. | 8.41 | 25.24 | 6.01 | 42.60 | 17.60 | | |
| | obs. | 8.33 | 24.60 | 5.65 | 44.30 | 17.51 | 4.58 | 15150 |
| $(onH_2)[CoCl_4]$ | cal. | 8.07 | 27.67 | 6.34 | 40.89 | 16.99 | | |
| | obs. | 8.18 | 27.65 | 6.23 | 41.51 | 17.54 | 4.49 | 15150 |
| $(nnH_2)[CoCl_4]$ | cal. | 7.76 | 29.93 | 6.65 | 39.31 | 16.33 | | |
| | obs. | 7.40 | 28.39 | 6.36 | 37.78 | 18.32 | 4.63 | 14990 |
| $(dnH_2)[CoCl_4]$ | cal. | 7.47 | 32.01 | 6.93 | 37.83 | 15.72 | | |
| | obs. | 6.64 | 28.01 | 6.42 | 36.09 | 14.32 | 4.59 | 15150 |

REFERENCES

1-H.M. Powell, A.F. Wells; J.Chem.Soc. 1935, 359.

2-N. Fogel, C.C. Lin, C. Ford, W. Grindstaff; Inorg.Chem. 1964, 3, 720.

3-N.S. Gill, R.S. Nyholm; J.Chem.Soc. 1959, 3997.

4-A.K. Banerjee, L.M. Vallarino, J.V. Quagliano; Coord.Chem.Rev. 1966, 1, 239.

5-H.W. Smith, W.J. Stratton; Inorg.Chem. 1977, 16, 1640.

6-F.A. Cotton, D.L. Goodgame, M. Goodgame; J.Amer.Chem.Soc. 1961, 83, 4690.

7-L.J. Bellamy, "The Infrared Spectra of Complex Molecules", Chapman & Hall, London 1978.

8-A. Sabatini, L. Sacconi; J.Amer.Chem.Soc. 1964, 86, 17.

*Polyhedron* Vol. 3, No. 3, pp. 365–368, 1984
Printed in Great Britain.

0277–5387/84 $3.00 + .00
© 1984 Pergamon Press Ltd.

# NOTE

## TRANSITION METAL-MAIN GROUP METAL BOND. VI.[1] $^{199}Hg$ NMR AND $^{57}Fe$ MÖSSBAUER STUDY OF $(\eta^5\text{-}C_5H_5)(CO)_2FeHgX$ [X = Cl,Br,I,$S_2COC_2H_5$, $S_2CN(C_2H_5)_2$, $S_2P(OC_2H_5)_2$ AND $Fe(CO)_2(\eta^5\text{-}C_5H_5)$]COMPLEXES.

MAREK M. KUBICKI, RENE KERGOAT, JEAN-Y. DE VANSSAY, JEAN-Y. LE GALL and JACQUES E. GUERCHAIS*
Laboratoire Associé au C.N.R.S. N°322, Equipe de Chimie Inorganique Moléculaire, Université de Bretagne Occidentale, 29283 BREST-CEDEX - FRANCE

(Received 12 july 1983; accepted 25 november 1983)

Abstract : The $^{199}Hg$ NMR and $^{57}Fe$ Mössbauer spectra of iron-mercury bounded complexes are reported, compared with the $^{199}Hg$ NMR data for analogous molybdenum and tungsten compounds and discussed in terms of the polarization of the metal-metal bonds.

One of the more debated problems of compounds containing bonds between transition and non-transition metal atoms concerns the description of this bond. Although its covalency has been established, there is still some controversy over the exact nature of metal-metal bond, i.e. over its representation either as a simple polarized σ-bond or as a σ-bond with an additional π-back donation from the filled transition metal d orbitals to the vacant orbitals of the other metal [2].

Our recent $^{95}Mo$ and $^{199}Hg$ NMR study of $(\eta^5\text{-}C_5H_5)(CO)_2LMoHgX$ complexes indicated the existence of polarized Mo-Hg bonds, degree of which depends on the nature of ligand X [1]. Comparison of the $^{199}Hg$ chemical shifts in the molybdenum derivatives with those reported for the $(\eta^5\text{-}C_5H_5)(CO)_3WHgX$ ones [3] shows a good linear correlation $\delta(^{199}Hg)$ in Mo-Hg bonded complexes v.s. $\delta(^{199}Hg)$ in W-Hg bonded complexes for X = Cl,Br and I (figure 1). If the validity of this correlation could be extended on $[(\eta^5\text{-}C_5H_5)(CO)_3M]_2Hg$ compounds, the $^{199}Hg$ resonance in the molybdenum derivative should be observed at about + 70 ppm (in $CH_2Cl_2$). A value of + 236 ppm was found. Looking for the reasons of such a divergence one can suppose that different electronic properties (i.e. basicity, nucleophilicity etc..) induce a different degree of polarization over the transition metal-mercury bonds in the symmetrical organometalmercurials M-Hg-M. In this light we have undertaken a study of $^{199}Hg$ NMR resonances [4] in $(\eta^5\text{-}C_5H_5)(CO)_2FeHgX$ complexes [5]. The results, together with some $^{57}Fe$ Mössbauer [6], $^1H$ $(C_5H_5)$ NMR and carbonyl infrared data are given in Table 1.

The $^{199}Hg$ resonances exhibit a "normal" halogen dependence consistent with the electronegativity of halides (deshielding of mercury nucleus by more electronegative Cl as compared with Br and I). These resonances are shifted to higher frequencies with "dithio" ligands than with the halogenide ones (Cl, Br, I; figure 2). The most important result is supplied by the position of $^{199}Hg$ resonance in $(\eta^5\text{-}C_5H_5)(CO)_2Fe_2Hg$. It is only slightly shifted to lower field than in the "dithio" compounds. The significative information can be drawn from the comparison of differences between the $^{199}Hg$ chemical shifts in the series of M-Hg-M and

* Author to whom correspondence should be addressed.

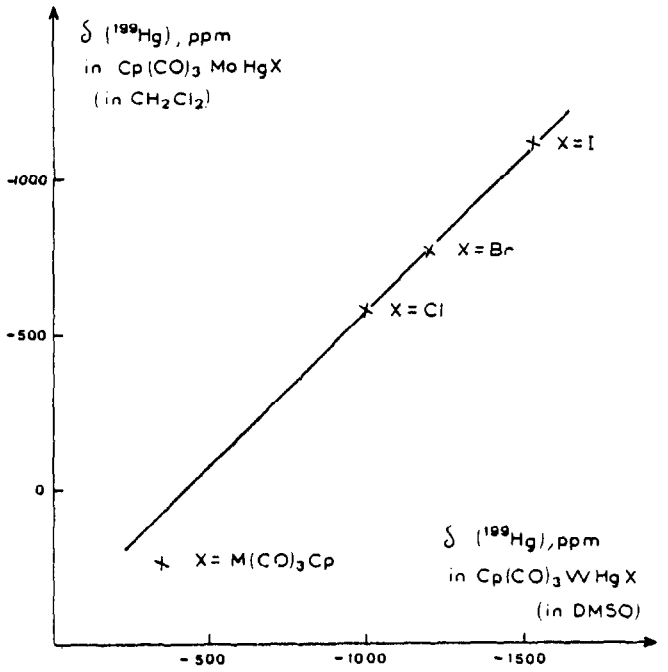



Figure 1 - Correlation of the $^{199}Hg$ chemical shifts in $(\eta^5\text{-}C_5H_5)(CO)_3MHgX$ complexes (M = Mo vs M = W)

Table 1 - Spectroscopic data for $(\eta^5\text{-}C_5H_5)(CO)_2FeHgX$ complexes

| X | $\delta(^1H)Cp$ [a] | $\delta(^{199}Hg)$ [b] | $\delta(^{57}Fe)$ [c] | $\Delta(^{57}Fe)$ [d] | $\nu(CO)$ [e] |
|---|---|---|---|---|---|
| Cl | 4.98 | - 1176(2) | 0.121 | 1.723 | 2020,1980 |
| Br | 4.97 | - 1370(2) | f | f | 2020,1977 |
| I | 4.96 | - 1704(3) | 0.136 | 1.731 | 2012,1968 |
| dtc | 4.87 | - 964(2) | 0.128 | 1.690 | 2000,1952 |
| dtp | 4.92 | - 1025(3) | 0.155 | 1.686 | 2011,1968 |
| xant | 4.94 | - 1032(3) | f | f | 2010,1965 |
| $Fe(CO)_2Cp$ | 4.72 | - 911(2) | 0.13 [g] | 1.60 [g] | 1993,1963, 1927 |

a. in $CDCl_3$ relative to internal TMS,ppm.
b. in $CH_2Cl_2/C_6D_6$ relative no neat $HgMe_2$,ppm.
c. isomer shift relative to Fe, mm/sec; δ values are ± 0.005.
d. quadruple splittings in mm/sec, δ values are ± 0.005.
e. in $CH_2Cl_2$,$cm^{-1}$.
f. not recorded.
g. N.N. GREENWOOD and T.C. GIBB, "Mössbauer Spectroscopy". Chapman and Hall Ltd, London,1971,p.234.

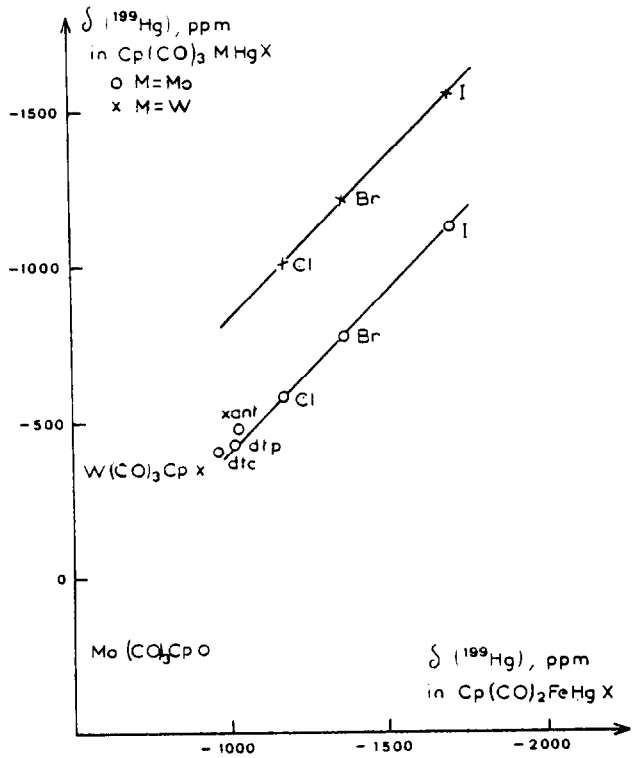



Figure 2 - $^{199}Hg$ chemical shifts in $(\eta^5\text{-}C_5H_5)(CO)_3MHgX$ complexes as a function of the corresponding (X) resonances in the $(\eta^5\text{-}C_5H_5)(CO)_2FeHgX$ compounds.

M-Hg-Cl complexes. They increase in the order M = Fe (265 ppm, Table 1) < M = W (649 ppm [7]) < M = Mo (810 ppm [8]) which is a decreasing order of nucleophilicities M = Fe > M = W > M = Mo[9]. A highest deshielding of mercury nucleus in the molybdenum symmetrical compound supports that the M-Hg-M linkage is more polarized in the case of molybdenum than in the case of tungsten and iron.

The inspection of the infrared and $^1H$ ($C_5H_5$) NMR together with the $^{199}Hg$ NMR data (Table 1) shows that there are three distinct groups of iron compounds corresponding to

i) X = Cl, Br and I

ii) X = dtc, dtp and xant

iii) X = $Fe(CO)_2(\eta^5\text{-}C_5H_5)$ in $[(\eta^5\text{-}C_5H_5)(CO)_2Fe]_2Hg$.

All these data indicate that the electron density retained at $(\eta^5\text{-}C_5H_5)(CO)_2Fe$ moiety increase in the order i < ii < iii showing once more a highest polarization of the Fe-Hg, or generally M-Hg, bond in symmetrical organometalmercurials.

The isomer shift values observed on $^{57}Fe$ Mössbauer spectra of the Fe-Hg bonded compounds are lower than in $(\eta^5\text{-}C_5H_5)(CO)_2FeX$ (X = Cl,Br,I) complexes [10] demonstrating, as expected, that the "HgX" ligands are better donors to iron than the X ligands. These δ values remain practically constant for whole compounds listed in Table 1. They are close to the I.S. values recorded for the complexes with iron-tin bonds [10] but are greater than that reported for $(\eta^5\text{-}C_5H_5)(CO)_2FeSC(S)NR_2$ complexe containing a monodente dithiocarbamate ligand [11].

There is a significant increase in quadrupole splittings Δ going from iii to i, suggesting that increased donation from mercury to iron atom decreases the electric field gradient at the latter. Otherwise, a low e.f.g. corresponds to a high polarization of the iron-mercury bond with the electron density (mostly s in character) displaced towards the iron atom.

The $^{199}Hg$ NMR and $^{57}Fe$ Mössbauer data presented above argue for the existance of polarization phenomena over the metal-metal σ-bonds.

*Acknowledgment* - We are grateful to Prof. F. Varret for helpfull discussion.

REFERENCES


1 Part V of this series : M.M. Kubicki, R. Kergoat, J.-Y. Le Gall, J.E. Guerchais, J. Douglade and R. Mercier, Aust.J.Chem.,(1982),38,1543.

2 P. Chini, "The Organic Chemistry of Iron", Vol.2,(1981),p.189. Edited by E.A. Koerner Von Gustorf, F.-W. Grevels and I. Fischer, Academic : New-York,N.Y.
D.J. Patmore and W.A.G. Graham, Inorg.Chem.,(1967),6,981; J.Dalton, I. Paul and F.G.A. Stone, J.Chem.Soc.(A),(1969),2744; N.A.D. Carey and H.C. Clark, Inorg.Chem., (1968),7,94; R. Ugo, S. Cenini and F. Bonati, Inorg.Chim.Acta,(1967),1,451; W.C. Cullen, J.R. Sams and J.A.J. Thompson, Inorg.Chem.,(1971),10,843.

3 M.J. Albright and J.P. Oliver, J.Organometal.Chem.,(1979),172,99.

4 NMR spectra were recorded on a JEOL JNM-FX 100 spectrometer operating at 99,60 MHz for $^{1}H$ and 17,78 MHz for $^{199}Hg$. $^{199}Hg$ chemical shifts were measured relative to neat $Hg(CH_3)_2$. Negative values indicate the highfield shifts.

5 $[(\eta^5\text{-}C_5H_5)(CO)_2Fe]_2Hg$ and $(\eta^5\text{-}C_5H_5)(CO)_2FeHgX$ (X = Cl, Br, I) complexes were prepared by literature methods : M.J. Mays and J.D. Robb, J.Chem.Soc.(A),(1968),329. New compounds with sulphur ligands were prepared in the same way as halogenide derivatives by stirring an equimolecular mixture of $[(\eta^5\text{-}C_5H_5)(CO)_2Fe]_2Hg$ with $HgX_2$ (X = dtc-diethyldithiocarbamate, dtp- diethyldithiophosphate, xant- ethylxanthate) in toluene at 30°C for 16h. The products were precipitated with *n*-heptane giving 50-80% yields. Correct elemental analyses were obtained for new complexes.

6 Mössbauer spectra were recorded with a 25-mCi $^{57}Co$ source on Rh using a symmetric triangular sweep mode.

7 $\delta(^{199}Hg)$ in $(\eta^5\text{-}C_5H_5)(CO)_3WHgCl$ = - 997 ppm and in $[(\eta^5\text{-}C_5H_5)(CO)_3W]_2Hg$ = - 348 ppm (DMSO solutions); data taken from ref.3.

8 $\delta(^{199}Hg)$ in $(\eta^5\text{-}C_5H_5)(CO)_3MoHgCl$ = - 574 ppm and in $[(\eta^5\text{-}C_5H_5)(CO)_3Mo]_2Hg$ = + 236 ppm ($CH_2Cl_2$ solutions); data taken from ref.1.

9 R.E. Dessy, R.L. Pohl and R.B. King, J.Amer.Chem.Soc.,(1966),88,5121.

10 R.J. Dickinson, R.V. (Dick) Parish, P.J. Rowbothom, A.R. Manning and P. Hackett, J.Chem.Soc.Dalton Trans.,(1975),424.

11 E. Roman, D. Catheline, D. Astruc, P. Batail, L. Ouahab and F. Varret, J.Chem.Soc., Chem.Comm.,(1982),129.

*Polyhedron* Vol. 3, No. 3, pp. 369-371, 1984
Printed in Great Britain.

0277-5387/84 $3.00 + .00
© 1984 Pergamon Press Ltd.

# NOTE

## POSSIBLE INTERMEDIATES IN THE DISCHARGE SYNTHESIS OF DIBORON TETRAHALIDES

**A. G. BRIGGS, A. G. MASSEY*, M. S. REASON and P. J. PORTAL**
Department of Chemistry, University of Technology, Loughborough, Leicestershire LE11 3TU, England

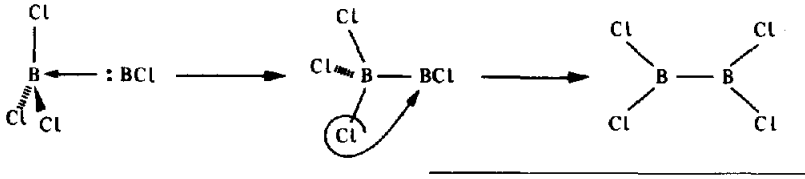
(*Received* 21 *March* 1983; *accepted* 25 *July* 1983)

**Abstract**—When boron trichloride and tribromide are passed through a radiofrequency discharge to prepare the corresponding sub-halides, BCl and BBr can be detected spectroscopically. It is suggested that they are intermediates in the formation of $B_2Cl_4$, $B_4Cl_4$ and $B_2Br_4$. By the same technique, good yields of $B_2I_4$ are obtained from $BI_3$, although no BI could be detected because of the presence of much free $I_2$. Using a microwave discharge, although no known BI bands were observed, four new bands assigned to BI were found in an emission spectrum once again largely dominated by $I_2$.

Schlesinger first prepared $B_2Cl_4$ by passing $BCl_3$ vapour through a mercury discharge and assumed the product arose by dimerization of $BCl_2$ radicals formed by chlorine atom abstraction from $BCl_3$ by excited mercury atoms.[1] It was shown much later[2] that the spectrum of such discharges contains no bands of $BCl_2$ whereas strong emission from BCl was present. Similarly, the spectrum of BCl was observed during the microwave excitation of $BCl_3$ vapour a system which also produced $B_2Cl_4$ (and chlorine[3]). These results suggest that BCl is a precursor in the formation of $B_2Cl_4$. Thermodynamically, the reaction:

$$\begin{array}{lrrl} & BCl_3 + & BCl \rightarrow & B_2Cl_4 \\ \Delta G_f^\circ & -388.7 & 120.9 & -460.7\,kJ\,mol^{-1}\ \text{(Ref. 4)} \end{array}$$

is favoured ($\Delta G^\circ = -192.9\,kJ\,mol^{-1}$) and presumably proceeds via the donation of a lone pair of electrons on BCl into the empty 2p orbital of $BCl_3$:




Urry[5] has objected to this mechanism for the mercury discharge system, mainly because mercury(I) chloride is a by-product (he presumably thought mercury(II) chloride would be a more obvious product of stripping two chlorine atoms from a $BCl_3$ molecule) but also because he observed no mixed chlorides when $BCl_3$ and $SiCl_4$ were passed through the discharge (BCl might be expected to insert into $SiCl_4$; viz. $BCl + SiCl_4 \rightarrow Cl_2BSiCl_3$).

However, it is known[6] that mercury(II) chloride reacts with mercury to form $Hg_2Cl_2$. Furthermore, $Cl_2BSiCl_3$ has indeed been isolated as a by-product in the discharge-preparation of $B_2Cl_4$, probably arising from $SiCl_4$ impurity[7] in the $BCl_3$. Thus, two of Urry's initially plausible objections can now be discounted. His other cognate objection was that no $Cl_2BPCl_2$ was detected when a mixture of boron and phosphorus trichlorides was passed through the mercury discharge;[8] perhaps this experiment ought to be repeated.

Whether or not BCl reacts with $BCl_3$ will depend of course on the prevailing conditions. For example, Timms and Maddren[9] have shown that BCl and $BCl_3$ do not form $B_2Cl_4$ when they are co-

*Author to whom correspondence should be addressed.

condensed at −196°C (under similar extreme conditions BF does insert into $BF_3$ to give diboron tetrafluoride[10], $\Delta G_f^\ominus = -140.2\,kJ\,mol^{-1}$). More recently,[11] it was found that $BCl_3$, when passed at low pressure through a radiofrequency discharge in the presence of mercury, produces $B_2Cl_4$ and $B_4Cl_4$.

Diener and Pflugmacher[12] prepared $B_2Br_4$ by passing $BBr_3$ through an electrical discharge maintained between nickel electrodes. Previously, an almost identical system had been used to study the emission spectrum of BBr in the discharge zone.[13] Again, when $BBr_3$ is passed at low pressure through a radiofrequency glow discharge, $B_2Br_4$ is formed.[14] Now for the reaction:

$$BBr_3 + BBr \rightarrow B_2Br_4$$
$$\Delta G_f^\ominus: \quad -232.5 + 195.4 \quad -kJ\,mol^{-1}$$

the value of $\Delta G_f^\ominus(B_2Br_4)$ is unknown, but the high positive value of $\Delta G_f^\ominus(BBr)$ ensures that $\Delta G^\ominus$ (reaction), given by $\Delta G_f^\ominus(B_2Br_4) - (-232.5 + 195.4)$, will be highly negative for any plausible value assigned to $\Delta G_f^\ominus(B_2Br_4)$. It is therefore, reasonable to suggest BBr as a possible intermediate in the formation of $B_2Br_4$ from $BBr_3$.

In this paper, we report the result of radio frequency and microwave discharges in $BI_3$ vapour, and of additional studies on $BCl_3$ and $BBr_3$.

## EXPERIMENTAL

The radiofrequency generator (30 MHz) was similar to that of Schumb[16]. The pyrex discharge cell was about 30 cm long by 7.5 cm dia. and had a silica window fused onto one end, using a graded seal. R. F. power was applied to seven turns of 1 mm dia. copper wire wrapped round one end of the tube. A boron halide under study (mixed with carrier gas when necessary) was evaporated in a high vacuum system, from a U-tube on one side of the cell into a U-tube at −196°C on the other side. The discharge produced in the vapour was photographed through the silica window using a Hilger medium quartz spectrograph, type E498. The R. F. generator was replaced by an Evans Electro-medical Supplies Microtron 200 microwave generator, operating at 2.450 GHz, for the microwave excitation studies. Boron trihalide vapour was flowed through a quartz tube which passed through a tuned cavity. Argon and helium gases (B.O.C.) were taken direct from the cylinders without further treatment.

## RESULTS AND DISCUSSION

It was found that the emission spectrum resulting from the radiofrequency discharge through $BCl_3$, in the presence of liquid mercury, contained not only the expected mercury atomic lines but also the (0,0), (1,0), (0,1), (1,1), (2,0), (2,1), (2,2), (0,3), (4,4), and (5,5) bands of the $A\,^1\Pi \rightarrow X\,^1\Sigma^+$ system of BCl[18]. This species has therefore been shown to be present with up to five quanta of vibrational energy (53.4 kJ $mol^{-1}$), and once again one is led to the conclusion that the production of the two subchlorides, $B_2Cl_4$ and $B_4Cl_4$, occurs via the BCl intermediate. The well-known doublet of atomic boron (249.7, 249.8 nm) was also detected, the longer wavelength line being relatively less intense than its calculated Boltzmann value. Analogous results were obtained for the effect of the radiofrequency discharge on pure $BBr_3$ vapour. An intense $A \rightarrow X$ band system[18] of BBr was observed in which the longest wavelength band was the (3,5), corresponding to a vibrational excitation energy of 43.7 kJ $mol^{-1}$. On the addition of liquid mercury to the system, the only observed change was the appearance of mercury lines in the spectrum.

Only in the case of $BI_3$ were any problems experienced due to the spectrum of free halogen. It was found that molecular iodine dominated the spectrum emitted by the radiofrequency discharge through pure $BI_3$ vapour, and no bands were observed which could be assigned to BI or any other molecule containing boron. Once more, atomic boron in a non-equilibrium state was detected. About 25 $cm^3$ of mercury were added to the discharge cell to diminish the intensity of the iodine spectrum, but it still proved impossible to detect any bands of the BI spectrum corresponding to those reported by either Briggs and Piercy[17] or Lebreton.[15] The only other molecule to be detected was HgI, for which bands of the $B\,^2\Sigma^+ \rightarrow X\,^2\Sigma$ and $C\,^2\Pi_{\frac{1}{2}} \rightarrow X\,^2\Sigma^+$ systems were present. Following Lebreton[15] who used the gas to suppress the iodine spectrum in his studies on BI (produced using a Schüler type discharge), argon was flowed through the discharge cell. The pressure was such as just to sustain the glow, but in spite of this iodine emission was still relatively intense.

In a further series of experiments, $BI_3$ vapour, mixed with argon or helium, was subjected to microwave discharge. Four bands, degrading to the red, were observed at 349.8, 350.8, 351.2 and 352.5 nm. None of these corresponds to bands reported for $I_2$ or $B_2$, and they are not present in the spectra of discharges in He, Ar or $I_2$, in the absence of $BI_3$. It seems reasonable to conclude that the new bands relate to BI, although once more neither the BI bands[17] at 349.1 and 349.3 nm, nor the system belonging to the semi-forbidden transition[15] $a^3\Pi_{o+} \rightarrow X^1\Sigma^+$ near 600 nm, was observed. This result is perhaps not unexpected, since

the former bands were obtained following the flash photolysis of $BI_3$, and the latter constitute a weak system overlaid in the present instance by iodine emission. Other spectral features in the $BI_3$ discharge were an intense atomic iodine line at 206.2 nm and two intense atomic boron doublets at 208.9 and 209.0, and at 249.7 and 249.8 nm.

It may be concluded reasonably that the available data are consistent with the hypothesis that the formation of boron subhalides in radio-frequency or microwave discharge systems does occur via the donation of BX lone pair electrons into the empty $2p$ orbital of $BX_3$ (X = Cl, Br or I).

## REFERENCES


1. G. Urry, T. Wartik, R. E. Moore and H. I. Schlesinger, *J. Am. Chem. Soc.* 1954, **76**, 5293.
2. A. G. Briggs, M. S. Reason and A. G. Massey, *J. Inorg. Nucl. Chem.* 1975, **37**, 313.
3. R. T. Holzmann and W. F. Morris, *J. Chem. Phys.* 1958, **29**, 677.
4. D. D. Wagman, W. H. Evans, V. B. Parker, I. Halow, S. M. Bailey and R. H. Schumb, *N. B. S. Technical Note* 270–3 (1968).
5. G. Urry, In *The Chemistry of Boron and its Compounds* (Edited by E. L. Muetterties), p. 325. Wiley, New York (1967).
6. A. G. Sharpe, *Inorganic Chemistry*, p. 641. Longman, London (1981).
7. A. G. Massey and D. S. Urch, *Proc. Chem. Soc.* 1964, 284.
8. A. G. Garrett and G. Urry, *Inorg. Chem.*, 1963, **2**, 400.
9. P. L. Timms, In *Cryochemistry* (Edited by M. Moskovits and G. A. Ozin), p. 61. Wiley–Interscience, New York (1976).
10. P. L. Timms, *J. Am. Chem. Soc.* 1967, **89**, 1629.
11. T. Davan and J. A. Morrison, *Inorg. Chem.* 1979, **18**, 3194.
12. W. Diener and A. Pflugmacher, *Angew. Chem.* 1957, **69**, 777.
13. E. Rosenthaler, *Helv. Phys. Acta* 1940, **13**, 355.
14. N. A. Kutz and J. A. Morrison, *Inorg. Chem.* 1980, **19**, 3295.
15. J. Lebreton, J. Ferran, A. Chatalic, D. Iacocca and L. Marsigny, *J. Chim. Phys. Physicochim. Biol.* 1974, **71**, 587.
16. W. C. Schumb, E. L. Gamble and M. D. Banus, *J. Am. Chem. Soc.* 1949, **71**, 3225.
17. A. G. Briggs and R. Piercy. *Spectrochim. Acta* 1973, **A29**, 851.
18. K. P. Huber and G. Herzberg, *Molecular Spectra and Molecular Structure—IV. Constants of Diatomic Molecules*, p. 74. Van Nostrand, New York (1979).

*Polyhedron* Vol. 3, No. 3, pp. 373–375, 1984
Printed in Great Britain.

0277–5387/84 $3.00 + .00
© 1984 Pergamon Press Ltd.

# NOTE

## CHEMISTRY OF MIXED LIGAND COMPLEXES OF PLATINUM: CRYSTAL AND MOLECULAR STRUCTURE OF *trans*-[PtCl(CH$_3$)(PEt$_3$)(AsPh$_3$)]

**ANIL B. GOEL*, SARLA GOEL and DON VANDERVEER**
School of Chemistry, Georgia Institute of Technology, Atlanta, GA 30332, U.S.A.

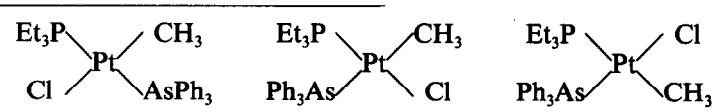
(*Received* 21 *March* 1983; *accepted* 25 *July* 1983)

**Abstract**—The dimethyl platinum(II) complex containing mixed ligands, *cis*-[Pt(CH$_3$)$_2$(PEt$_3$)(AsPh$_3$)] reacted with one equivalent of hydrogen chloride yielding *trans*-[PtCl(CH$_3$)(PEt$_3$)(AsPh$_3$)]. The X-ray crystal structure of the molecule shows the *trans* orientation of the PEt$_3$ and AsPh$_3$ ligands.

Metal complexes of low symmetry containing mixed ligands can be useful in studies such as (i) *trans*-effects of ligands having variable electronic and steric parameters,[1,2] (ii) asymmetric synthesis catalyzed by metal complexes and (iii) homogeneous hydrogenation and polymerization catalysis.[3,4] In the course of our recent investigations on mixed ligand complexes of platinum,[2–8] we have isolated a series of stable complexes, [PtCl(R)LL′][3] containing four different ligands on platinum. The fact that their five coordinate olefin complexes, [PtCl(R)(L)(L′)(olefin)], either isolable or occurring only as a reaction intermediate, would totally lack symmetry, offers many interesting possibilities. In view of this, the chemistry of mixed ligand complexes is of interest and we felt that the structural study of such low symmetry four coordinate complexes would be worthwhile. The complex, [PtCl(CH$_3$)(PEt$_3$)(AsPh$_3$)], **1**, was selected for the structural studies due to its much higher stability toward disproportionation.

The reaction of *cis*-[PtCl$_2$(PEt$_3$)(AsPh$_3$)] with excess methyllithium in anhydrous diethyl ether gave the corresponding dimethyl platinum(II) complex, *cis*-[Pt(CH$_3$)$_2$(PEt$_3$)(AsPh$_3$)]. Treatment of this with one mole equivalent of HCl afforded the desired mixed ligand complex, [PtCl(CH$_3$)(PEt$_3$)(AsPh$_3$)], **1**. Recrystallization of complex **1** from a mixture of CH$_2$Cl$_2$/hexane provided the suitable crystals for X-ray analysis ($^1$H NMR in CD$_2$Cl$_2$: $\delta$(CH$_3$) 0.35 ppm, $^2$J(PtH) = 80 Hz, $^3$J(PH) = 4.5 Hz.). The $^{31}$P NMR spectrum in CH$_2$Cl$_2$/C$_6$D$_6$ shows a sharp singlet at $\delta$(PEt$_3$) 13.07 ppm (w.r. to H$_3$PO$_4$) associated with platinum satellite, $^1$J(Pt–P) = 3738 Hz.

Out of three possible structural configurations (**1A–1C**), structure **1C** can be ruled out on the basis of the large platinum-phosphorus coupling constant observed in the $^{31}$P NMR spectrum (a much lower value of J(Pt–P) of the order of >2000 Hz is expected for such a system due to the high *trans*-effect of methyl group[9]).




**1A** **1B** **1C**

In order to differentiate between structures **1A** and **1B**, an X-ray crystal structure determination has been carried out.

*Author to whom correspondence should be directed at the present address: Ashland Chemical Company, P.O. Box 2211, Columbus, OH 43216, U.S.A.

The complex crystallizes in the orthorhombic system, space group $P2_12_12_1$ with 4 molecules in the unit cell (density: calc. 1.71, exp. 1.72 g cm$^{-3}$); the lattice constants are $a = 9.898$ (3), $b$, $= 10.719$ (3), $c = 24.342$ (3) Å. Intensity data were collected on a $P2_1$ four circle automated diffractometer with Mo$K_\alpha$-radiation. A total of 2635 independent reflections were measured. Intensities were corrected for Lorentz, polarization and absorption effects. The structure was determined by heavy-atom techniques and refined by full-matrix least squares procedures. The final conventional $R$ value is 0.0521.†

A perspective view of the molecule is presented in Fig. 1, where most of the relevant atoms are labeled. In the compound the Pt atom is four-coordinated and is surrounded in an approximately planar fashion by $PEt_3$ and $AsPh_3$ ligands (at mutually *trans* positions), a chlorine and a methyl group. Thus the orientations of $PEt_3$ and $AsPh_3$ is changed from *cis*- in the starting dimethyl platinum(II) complex to *trans*- in the final product (**1**). The deviations of the angles in the coordination sphere from those of the ideal square planar geometry are small and unimportant.

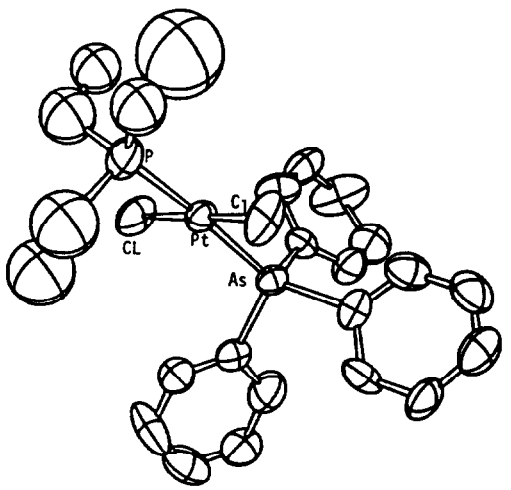



Fig. 1. ORTEP drawing of the complex [PtCl($CH_3$)($PEt_3$)($AsPh_3$)]. Most relevant atoms are labeled. Principal bond lengths (Å) are: Pt–P = 2.271 (6), Pt–As = 2.423 (2), Pt–Cl = 2.397 (5), Pt–$C_1$ = 2.076 (16) and angles (°): P–Pt–As = 175.5 (2), Cl–Pt–As = 87.1 (1), Cl–Pt–P = 92.2 (2), $C_1$–Pt–P = 89.6 (6), $C_1$–Pt–Cl = 177.8 (6).

†Atomic parameters, bond lengths and angles and Fo/Fc values have been deposited with the Editor as supplementary data. Copies are available on request. Atomic coordinates have also been deposited at the Cambridge Crystallographic Data Centre.

The much higher J(Pt–P) value (3738 Hz) compared to values of 2400-2600 Hz often found in the complexes *trans*-[$PtCl_2(PR_3)_2$][10] suggests a relatively strong Pt–P bond. Indeed, the Pt–P bond length found in complex **1**, 2.271 (6) Å, is shorter than in various other triethylphosphine platinum complexes,[11] e.g. 2.320 (3) in [PtCl(P–$HNNC_6H_4F$)($PEt_3$)$_2$]; however, is in good agreement with the value of 2.272 (4) Å found for *trans*-[$PtH(CH_2CN)(PPh_3)_2$][12]. This relatively shorter Pt–P bond length in complex **1** compared to other triethyl phosphine platinum(II) complexes, not only explains the higher value of the platinum–phosphorus coupling constant, but also indicates a lower *trans*-effect of $Ph_3As$ compared to tertiary phosphines. The Pt–As distance in **1** is quite long, 2.423 (2) Å, when compared to the complexes *symdl-trans*-[$Pt_2Cl_2(AsMe_3)_2$] (2.308 Å)[13] and *trans*-[$PtCl_2CN(CH_3) = CH$–(P–$CH_3C_6H_4$)($AsEt_3$)](2.346 Å)[14].

The Pt–C distance of 2.076 (16) Å is typical of Pt(II)–C($sp^3$) bonds (e.g. 2.081 (6) Å in *trans*-[$PtCl(CH_3)(PMePh_2)_2$][15], 2.079 (14) Å in *trans*-[$PtCl(CH_2SiMe_3)(PMe_2Ph)_2$][16] and 2.08 (1) in *trans*-[$PtCl(CH_2CN)(PPh_3)_2$][17]) and approximately the value expected from the sum of covalent radii (2.08 Å). The Pt–Cl distance of 2.397 (5), which is longer than predicted from radii-sum rules (2.30 Å) is probably due to the high *trans*-effect of methyl group. However this Pt-Cl bond distance is shorter than the values found in *trans*-[$PtCl(\eta'$-$C_3H_5(PPh_3)_2$][11]; 2.425 (2) Å and in *trans*-[$PtCl(CH_2SiMe_3)(PMe_2Ph)_2$],[16] 2.415 (5) Å.

## REFERENCES

1. C. A. Tolman, *Chem. Rev.* 1977, **77**, 313.
2. H. C. Clark, A. B. Goel, R. G. Goel and S. Goel, *Inorg. Chem.* 1980 **19**, 3220.
3. H. C. Clark, A. B. Goel and C. S. Wong *J. Organometal. Chem.* 1980 **190**, C101; H. C. Clark, C. S. Wong and C. Billard, *J. Organometal. Chem.* 1980 **190**, C105.
4. A. B. Goel, S. Goel and D. VanDeerVeer, *Inorg. Chim. Acta* 1981 **54**, L5.
5. A. B. Goel, S. Goel and D. VanDeerVeer, *Inorg. Chim. Acta* 1982, **64**, L173.
6. A. B. Goel, S. Goel, D. VanDerVeer and H. C. Clark, *Inorg. Chim. Acta* 1981, **53**, L117.
7. A. B. Goel, S. Goel and H. C. Clark, *Synth. React. Inorg. Metal Org. Chem* 1981, **11**, 289.
8. A. B. Goel and S. Goel, *Inorg. Chem. Acta* 1982, **59**, 237.
9. T. G. Appelton, H. C. Clark and L. E. Manzer, *Coord. Chem. Rev.* 1973, **10**, 335.
10. P. S. Pregosin and R. W. Kunz, *NMR Basic Principles and Progress*, Vol. 16 and references therein. Springer-Verlag Berlin (1979).

11. J. A. Kaduk and J. A. Ibers, *J. Organometal. Chem.* 1977, **139**, 199, and references therein.
12. R. Ros, R. A. Michelin, R. Bataillard and R. Roulet, *J. Organometal. Chem.* 1977, **139**, 355.
13. S. F. Watkins, *J. Chem. Soc. A* 1970, 168.
14. D. Hottentot and C. H. Stan, *Cryst. Struct. Comm.* 1975, **4**, 421.
15. G. B. Robertson and P. O. Whimp, *Inorg. Chem.* 1974, **13**, 2082.
16. B. Jovanovic, L. Manojlovic-Muir and K. W. Muir, *J. Chem. Soc. Dalton* 1974, 195.
17. A. Delpra, G. Zanotti, G. Bombieri and R. Ros, *Inorg. Chim. Acta* 1979, **36**, 121.

*Polyhedron* Vol. 3, No. 3, pp. 377–380, 1984
Printed in Great Britain.

0277-5387/84 $3.00 + .00
© 1984 Pergamon Press Ltd.

# NOTE

## CRYSTAL STRUCTURE OF OXO(DIPEROXO)BIPYRIDYLMOLYBDENUM(VI)

**E. O. SCHLEMPER***
Department of Chemistry, University of Missouri, Columbia, MI 65211, U.S.A.

**and**

**G. N. SCHRAUZER and L. A. HUGHES**
Department of Chemistry, University of California, San Diego, La Jolla, CA 92093, U.S.A.

(*Received* 11 *April* 1983; *accepted* 4 *August* 1983)

**Abstract**—Yellow oxo(diperoxo)bipyridylmolybdenum(VI), $C_{10}H_8MoN_2O_5$, $M_r = 332.1$ crystallizes in the monoclinic space group $P2_1/n$, $a = 6.261(3)$, $b = 12.726(1)$ $c = 13.752(3)$A, $\beta = 91.84(2)°$, $V = 1095.2(5)$A$^3$, $Z = 4$, $D_c = 2.014(1)$ g/cm$^3$, Mo$K\alpha$($\lambda = 0.7107$A), $\mu = 11.8$ cm$^{-1}$, $T = 22(1)°$C, $R = 0.034$, $\omega R = 0.040$, number of reflections in least squares ($F_0 > 2\sigma(F_0)$) = 1125. The molybdenum coordination (distorted trigonal bipyramidal) is as in the corresponding chromium complex, $C_{10}H_8CrN_2O_5$ which has closely similar bond angles but is not isomorphous. The difference in Mo–$N_{apex}$ and Mo–$N_{eq}$ bond distances (2.312(5) and 2.199(5)A) is similar to that in the Cr–$N_{apex}$ and Cr–$N_{eq}$ distances (2.23(2) and 2.11(2)A). The M–O distances for each peroxo ligand (ave. 1.910(2) and 1.950(2)A) are significantly different and slightly longer than those in the chromium complex as is the O–O distance of 1.459(6)A. The latter is indicative of greater negative charge on the $O_2$ ligands, approaching that of $O_2^{2-}$ in the molybdenum complex.

Although several peroxochromium and peroxo molybdenum complexes are known and have been structurally characterized,[1] direct comparisons between homologous complexes of chromium and molybdenum have thus far been impossible. Our current interest in molybdenum(VI) complexes carrying the 2,2′-bipyridyl (bpy) ligand.[2,3] prompted us to prepare the diperoxo derivative [Mo(O)$(O_2)_2$(bpy)][4] and to determine its structure by means of a single crystal X-ray crystallographic analysis for comparison with the corresponding chromium complex,[5] [Cr(O)$(O_2)_2$(bpy)] described by Stromberg and Ainalem.[6]

## EXPERIMENTAL

The complex was prepared by the method of Mimoun, Seree de Roch, and Sajus[4] and recrystallized from dimethylformamide.

Details of the crystal data, data collection, and structure refinement are included in Table 1. Data analysis and structure solution were done on a PDP11/34 computer using the Nonius SDP package. Atomic scattering factors, including anomalous contributions, were taken[7] from the International Tables for X-ray Crystallography, Vol. 4. The structure was solved by conventional Patterson and Fourier methods. All atom parameters (H's with fixed B = 5.0A$^2$, other atoms anisotropic) were obtained by full-matrix least squares methods minimizing $\Sigma w(F_c - F_o)^2$. The large decay in intensities occurred during the last third of data collection, and these reflections, after correction, agreed with their symmetry equivalent forms (see Table 1).

## DISCUSSION

The final atomic parameters and $F_o/F_c$ values have been deposited as supplementary material with the Editor, from whom copies are available on request†, and the pertinent bond distances and angles are in Table 2. The structure of the molecule with the atom numbering system is in Fig. 1.

The coordination number of the molybdenum atom may be viewed as five or seven, depending on interpretation of the peroxide bonding as monodentate or bidentate. The molybdenum is coordi-

*Author to whom correspondence should be addressed.

†Atomic coordinates have also been deposited with the Cambridge Crystallographic Data Centre.

Table 1. Crystal data, data collection parameters, refinment

| | | | |
|---|---|---|---|
| Crystal Dimensions | 0.05x0.10x0.40 mm | # of refl. measured | 2804 |
| Diffractometer | Enraf-Nonius CAD4 | # of unique refl. | 1529 |
| | | # above $2\sigma(F_o)$ | 1125 |
| X-ray Source | MoKα(λ0.7107Å) | $R_{int}$ | 0.045 |
| Crystal Centering | 25 reflections | # of variables | 187 |
| | | R | 0.034 |
| Systematic Absences | 0k0,k=2n+1 | | |
| | h0l,h+l=2n+1 | wR | 0.040 |
| Space Group | $P2_1/n$ | w | $1/\sigma^2(F_o)$ |
| Absorption correction method empirical ψ scan | T=0.91-0.99 | $\sigma^2(F_o)$ | $\sigma^2(F_o^2)/4F_o^2$ |
| $\mu(cm^{-1})$ | 11.8 | $\sigma^2(F_o^2)$ | $\sigma^2_{counting}+0.050F_o^2$ |
| 2θ range (deg) | 4-45 | max shift/error | 0.01 |
| | | max dif.density | $0.8e/Å^3$ |
| hkl range | h,±k,±l | extinction correction | none |
| intensity standards | 3(every 6000 sec) | | |
| orientation standards | 3(every 150 refl) | | |
| decay of standards | ∿50% | | |

Table 2. Bond distances in angstroms

TABLE OF BOND ANGLES IN DEGREES

| ATOM1 | ATOM2 | ATOM3 | ANGLE | ATOM1 | ATOM2 | ATOM3 | ANGLE | ATOM1 | ATOM2 | ATOM3 | ANGLE |
|---|---|---|---|---|---|---|---|---|---|---|---|
| O(1) | MO | O(2) | 165.4(2) | O(4) | MO | O(5) | 44.6(2) | C(6) | N(2) | C(10) | 118.5(6) |
| O(1) | MO | O(3) | 101.1(2) | O(4) | MO | N(1) | 86.5(2) | N(1) | C(1) | C(2) | 121.5(7) |
| O(1) | MO | O(4) | 101.7(2) | O(4) | MO | N(2) | 78.2(2) | C(1) | C(2) | C(3) | 119.9(7) |
| O(1) | MO | O(5) | 165.6(2) | O(5) | MO | N(1) | 129.9(2) | C(2) | C(3) | C(4) | 119.3(7) |
| O(1) | MO | N(1) | 92.4(2) | O(5) | MO | N(2) | 86.2(2) | C(3) | C(4) | C(5) | 118.7(7) |
| O(1) | MO | N(2) | 163.4(2) | N(1) | MO | N(2) | 70.9(2) | N(1) | C(5) | C(4) | 121.7(6) |
| O(2) | MO | O(3) | 44.4(2) | MO | O(2) | O(3) | 69.3(3) | N(1) | C(5) | C(6) | 115.6(5) |
| O(2) | MO | O(4) | 132.3(2) | MO | O(3) | O(2) | 66.4(2) | C(4) | C(5) | C(6) | 122.7(6) |
| O(2) | MO | O(5) | 98.1(2) | MO | O(4) | O(5) | 66.2(2) | N(2) | C(6) | C(5) | 114.5(5) |
| O(2) | MO | N(1) | 138.0(2) | MO | O(5) | O(4) | 69.1(3) | N(2) | C(6) | C(7) | 121.9(6) |
| O(2) | MO | N(2) | 86.0(2) | MO | N(1) | C(1) | 128.4(4) | C(5) | C(6) | C(7) | 123.6(6) |
| O(3) | MO | O(4) | 156.5(2) | MO | N(1) | C(5) | 128.7(4) | C(6) | C(7) | C(8) | 118.5(7) |
| O(3) | MO | O(5) | 132.2(2) | C(1) | N(1) | C(5) | 118.9(5) | C(7) | C(8) | C(9) | 119.7(7) |
| O(3) | MO | N(1) | 86.9(2) | MO | N(2) | C(6) | 118.2(4) | C(8) | C(9) | C(10) | 118.7(7) |
| O(3) | MO | N(2) | 78.3(2) | MO | N(2) | C(10) | 123.2(4) | N(2) | C(10) | C(9) | 122.6(7) |

TABLE OF BOND DISTANCES IN ANGSTROMS

| ATOM1 | ATOM2 | DISTANCE | ATOM1 | ATOM2 | DISTANCE | ATOM1 | ATOM2 | DISTANCE |
|---|---|---|---|---|---|---|---|---|
| MO | O(1) | 1.682(4) | O(4) | O(5) | 1.465(6) | C(4) | C(5) | 1.382(9) |
| MO | O(2) | 1.912(5) | N(1) | C(1) | 1.350(8) | C(5) | C(6) | 1.432(8) |
| MO | O(3) | 1.953(4) | N(1) | C(5) | 1.355(8) | C(6) | C(7) | 1.398(9) |
| MO | O(4) | 1.948(4) | N(2) | C(6) | 1.331(7) | C(7) | C(8) | 1.373(10) |
| MO | O(5) | 1.908(4) | N(2) | C(10) | 1.336(8) | C(8) | C(9) | 1.363(11) |
| MO | N(1) | 2.199(5) | C(1) | C(2) | 1.378(10) | C(9) | C(10) | 1.376(10) |
| MO | N(2) | 2.312(5) | C(2) | C(3) | 1.365(11) | | | |
| O(2) | O(3) | 1.459(6) | C(3) | C(4) | 1.392(10) | | | |

NUMBERS IN PARENTHESES ARE ESTIMATED STANDARD DEVIATIONS IN THE LEAST SIGNIFICANT DIGITS.

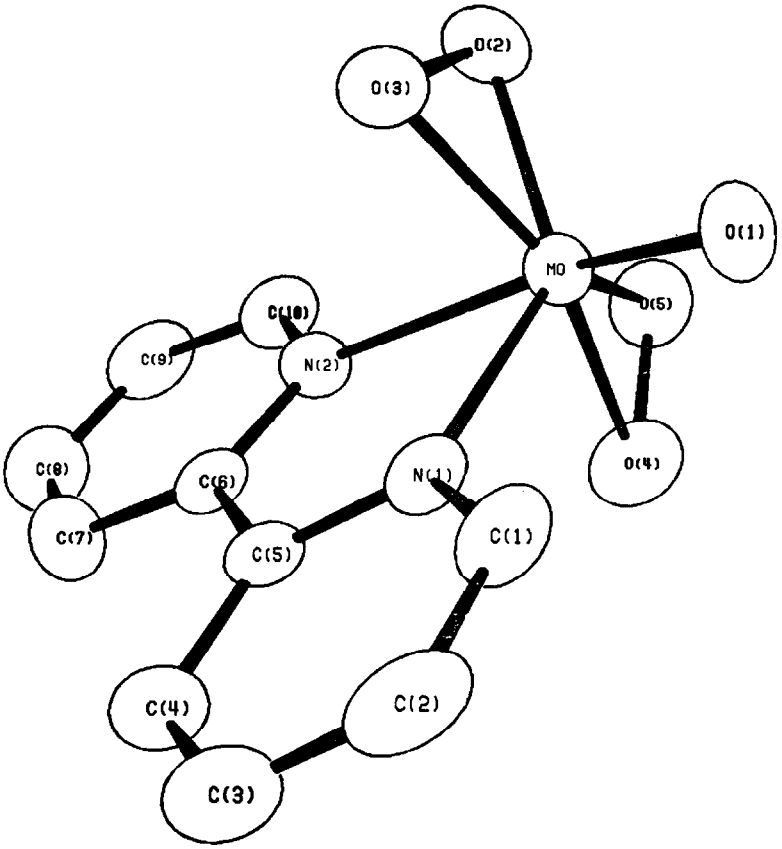



Fig. 1. Perspective view of the structure showing atom numbering and thermal ellipsoids.

nated to four oxygen atoms from two peroxide ligands, an oxo ligand, and two nitrogens from the bipyridyl ligand. If the peroxo ligands are considered to be monodentate, the coordination geometry is distorted trigonal bipyramidal with the peroxo ligands and one bipyridyl nitrogen N(1) occupying the equatorial positions and with the oxo ligand O(1) and the other bipyridyl nitrogen N(2) axial. The N(2)–Mo–O(1) angle of 163.4(2)° is significantly distorted from linear, presumably because of the limited bite of the bipyridyl ligand. Alternatively the structure may be considered to involve pentagonal bipyramidal, seven coordination of the molybdenum as suggested by Winter, *et al.*[8] and references therein for other oxodiperoxomolybdenum(VI) complexes. The molybdenum atom is 0.382(1)Å out of the least squares plane through the peroxo ligands and N(1) while those five atoms are all within 0.02 Å of that plane. As might be expected, the molybdenum displacement is in the direction of the strongly bonded oxo ligand.

The two Mo–N bond distances (2.199(5) and 2.312(5) Å) are quite different. The shorter distance involves the nitrogen (N(1)) in the equatorial position. These distances can be compared with those in $[Mo(O)_2(CH_3)_2$ bipyridyl] (Schrauzer, *et al.*[2]) where both nitrogens are *trans* to oxo groups, and the Mo–N distances are 2.314(2) and 2.346(2) Å. Apparently the oxo ligand has a strong *trans* effect on the Mo–N bond.

Another feature of significant interest is the asymmetric bonding of the peroxo ligands. The two oxygens (O(3) and O(4)) nearest to the equatorial nitrogen have longer Mo–O bonds (1.948(4) and 1.953(4) Å) than the two oxygens (0(2) and 0(5)) adjacent to each other (1.912(5) and 1.908(4) Å). A similar effect was observed by Winter, *et al.*[8] for $[MoO(O_2)_2 \cdot (S)$–$MeCH(OH)CONMe_2]$ as well as in earlier studies referenced therein of oxodiperoxomolybdenum (VI) complexes.

The structure compares favourably with that of the corresponding chromium complex.[6] However, detailed comparison of molecular parameters is hampered by the low accuracy of the structural parameters in the chromium study. Pertinent comparisons include (1) the nearly identical difference (0.12A) in $M–N_{apex}$ and $M–N_{eq}$ distances; (2) the unequal values of $M–O_{peroxo}$ distances for a given peroxide ligand (differing by 0.040(2) Å in the Mo case); and (3) the increase in the peroxo O–O

distances from Cr to Mo (1.40(2)→1.459(6) Å). The latter effect indicates a greater negative charge on the $O_2$ group in the Mo complex, approaching that observed[9] for an ionic peroxide (1.49 Å). The increase in negative charge on the $O_2$ group and concominant increase in positive charge on the metal is expected in going from Cr to Mo and has been observed[9] for other peroxo Mo and Cr complexes.

## REFERENCES

1. F. A. Cotton and G. Wilkinson, *Advanced Inorganic Chemistry* 4th Edn. Wiley–Interscience, New York, (1980) and references cited therein.
2. G. N. Schrauzer, L. A. Hughes, N. Strampach, P. R. Robinson and E. O. Schlemper, *Organometallics* 1982, **1**, 44.
3. G. N. Schrauzer, L. A. Hughes, N. Strampach, F. Ross, D. Ross and E. O. Schlemper, *Organometallics* 1983 **2**, 481.
4. H. Mimoun, I. Seree de Roch and L. Sajus, *Bull. Soc. Chim. Fr.* 1969, **5**, 1481.
5. O. F. Wiede, *Ber.* 1897, **30**, 2178.
6. R. Stomberg and B. Ainalem, *Acta Chem. Scand.* 1968, **22**, 1439.
7. *International Tables for X-ray Crystallography*, Vol. IV. Table 2.2B. Kynoch Press, Birmingham (1974).
8. W. Winter, C. Mark and V. Schurig, *Inorg. Chem.* 1980, **19**, 2045.
9. L. Vaska, *Acta Chem. Res.* 1976, **9**, 175.

*Polyhedron* Vol. 3, No. 3, pp. 381–383, 1984
Printed in Great Britain.

0277–5387/84 $3.00 + .00
Pergamon Press Ltd.

# NOTES

## CATALYSIS BY HETEROPOLYACID—VI. ASYMMETRIC POLYCONDENSATION OF BENZYL ALCOHOL TO OPTICALLY ACTIVE POLYBENZYL INITIATED BY BRUCINE-INDUCED CHIRAL DIPHOSPHOOCTADECAMOLYBDIC ACID

KENJI NOMIYA, MAKOTO MIWA* and YOSHIO SUGAYA
Department of Industrial Chemistry, Faculty of Engineering, Seikei University, Musashino, Tokyo 180, Japan

(*Received* 17 *June* 1983; *accepted* 25 *July* 1983)

**Abstract**—Diphosphooctadecamolybdic acid, the so-called Dawson-type heteropolyacid with a formula of $H_6[P_2Mo_{18}O_{62}]$, shows a Pfeiffer effect due to the equilibrium shift to one enantiomer in the presence of *l*-brucine sulphate in benzyl alcohol solution. Heating the homogeneous system caused polymerization of non-chiral benzyl alcohol to chiral polybenzyl. This reveals that the structure of the heteropolyanion-moiety plays an important role in the polymerization of benzyl alcohol.

A few years ago, it was demonstrated that oxidized and even-electron reduced forms of diphosphooctadecamolybdate anion, $[P_2Mo_{18}O_{62}]^{6-}$, showed the positive Cotton effect centred at 350 nm in acetonitrile or in DMF in the presence of *l*-brucine sulphate.[1] This is attributed to a Pfeiffer effect. On the other hand, it has been reported that Keggin-type heteropolyacids such as $H_4[SiM_{12}O_{40}]$ and $H_3[PM_{12}O_{40}]$ (M = Mo, W) promote catalytic polycondensation of benzyl alcohol to polybenzyl via carbonium ion mechanism generated by their Brønsted acidity.[2] The diphosphooctadecametallic acids, $H_6[P_2M_{18}O_{62}]$ (M = Mo, W), also promote effectively the polymerization, although their initial structure is not retained after the reaction. In this work, using benzyl alcohol as a solvent, the chirality of $H_6[P_2Mo_{18}O_{62}]$ in homogeneous system in the presence of *l*-brucine sulphate has been ensured and the polymerization of benzyl alcohol under the chiral environment has been examined.

### EXPERIMENTAL

The chiral environment substance, *l*-brucine sulphate, was obtained from a commercial source (Tokyo Kasei). The electronic and CD spectra were recorded by Hitachi Model-340 spectrophotometer and JASCO J40A-ORD spectropolarimeter, respectively.

*Author to whom correspondence should be addressed.

Free-acid forms $H_6[P_2M_{18}O_{62}]$ (M = Mo, W) were prepared by the established method.[3] The tetrabutylammonium salts were obtained by precipitation from the aqueous acid solution and recrystallized several times from acetonitrile. Found: C, 24.00; H, 4.49; N, 1.81. Calc. for $[(C_4H_9)_4N]_5H[P_2Mo_{18}O_{62}]$: C, 24.05; H, 4.53; N, 1.75%. Found: C, 19.93; H, 3.63; N, 1.46. Calc. for $[(C_4H_9)_4N]_6[P_2W_{18}O_{62}]$: C, 19.81; H, 3.72; N, 1.44%. Two-electron type of blue acid, $H_6[H_2P_2Mo_{18}O_{62}]$, was prepared by refluxing for about 24 hr the parent acid in isopropyl alcohol. The tetrabutylammonium salt was isolated as above. Found: C, 23.89; H, 4.44; N, 1.75. Calc. for $[(C_4H_9)_4N]_5H[H_2P_2Mo_{18}O_{62}]$: C, 24.04; H, 4.62; N, 1.75%. The brucinium ($bru^+$) salt of the parent anion was also obtained from acidic aqueous solution and purified by reprecipitation from the DMF solution with ethanol. Found: C, 31.12; H, 3.68; N, 4.63. Calc. for $(C_{23}H_{27}N_2O_4)_5H[P_2Mo_{18}O_{62}]\cdot 8DMF$: C, 31.24; H, 3.60; N, 4.72%. IR spectra of the isolated compounds were identified with the literature.[1]

The work-ups of the polymerization of benzyl alcohol and of the isolation of polybenzyl were previously reported.[2] The asymmetric polymerization occurs in the homogeneous solution of benzyl alcohol containing an appropriate molar ratio of the free acid of polyanion to the *l*-brucine sulphate as environment substance. The heating the solution on a hot-plate is preferable to the refluxing it.

## RESULTS AND DISCUSSION

The CD spectra of DMF solutions containing molar ratios of $H_6[P_2Mo_{18}O_{62}]$: *l*-brucine, 1:1, 1:2, 1:3, 1:4 and 1:5, showed the positive Cotton effect centred at 345 nm, whereas the spectrum of the solution of *l*-brucine alone had a negative Cotton effect centred at ca. 300 nm. This is in good agreement with the previously reported results.[1] The chirality of this polyanion is due to the loops of Mo–O–Mo bonding alternately "short" (~1.80 Å) and "long" (~2.05 Å), lowering the apparent symmetry $D_{3h}$ to $D_3$. In benzyl alcohol solution, the CD spectra show the positive CD band at 340 nm, as represented in Fig. 1 together with the electronic spectra. There is a noticeable change of CD and no noticeable change of absorption spectrum in the relatively low concentration ($\sim 10^{-5}$ mol dm$^{-3}$) of the environment substance. Thus, this is attributed to the Pfeiffer effect, as observed in the DMF solution. In the presence of *l*-brucine sulphate, the equilibrium shift of the racemic polyanion to the (+)-enantiomer occurs in the benzyl alcohol solution, the system of which may form a "chiral" catalyst for the polymerization of benzyl alcohol. The brucinium salt, $(bru^+)_5H[P_2Mo_{18}O_{62}]$, shows also the positive Cotton effect at *ca.* 340 nm both in DMF and in benzyl alcohol, where the brucinium ion as a counter cation will play a role of chiral environment substance leading to the Pfeiffer effect. Homogeneous DMF and benzyl alcohol solutions containing two-electron reduced acid, $H_6[H_2P_2Mo_{18}O_{62}]$, also showed the Pfeiffer effect in the prescence of *l*-brucine sulphate. However, analogous measurements with free acid and tetrabutylammonium salt of achiral $[P_2W_{18}O_{62}]^{6-}$ did not show such an effect in either solvent.

By heating the benzyl alcohol solutions containing the molar ratio of $H_6[P_2Mo_{18}O_{62}]$:*l*-brucine; 1:1, 1:2, 1:3 and 1:4, the polybenzyl was obtained, while from the solutions of more than the ratio of 1:5 the polybenzyl was not obtained. This may suggest that the number of protons as counter ions relates to the acidity necessary for the Brønsted-acid catalyzed reaction.[4] In fact, the polybenzyl was not obtained from the benzyl alcohol solution of $(bru^+)_5H[P_2Mo_{18}O_{62}]$. The polybenzyl isolated from the system of the ratios of 1:2, 1:3 and 1:4 showed the positive Cotton effect centred at 305 nm in $CH_2Cl_2$ solution (Fig. 2). The intensity of observed CD band is comparatively small. The uv spectrum of the chiral polybenzyl is identical with that of achiral polybenzyl obtained by catalysis of usual Keggin-type heteropolyacid. Analytical data of the chiral polybenzyl (Found: C, 93.61; H, 6.67. Calc. for $C_7H_6$: C, 93.33; H, 6.67%) suggest that the chirality does not come from the impurities or the contaminants of *l*-brucine and heteropolyacid, but from the intrinsic structure. In the solid state of the polymer, the chirality

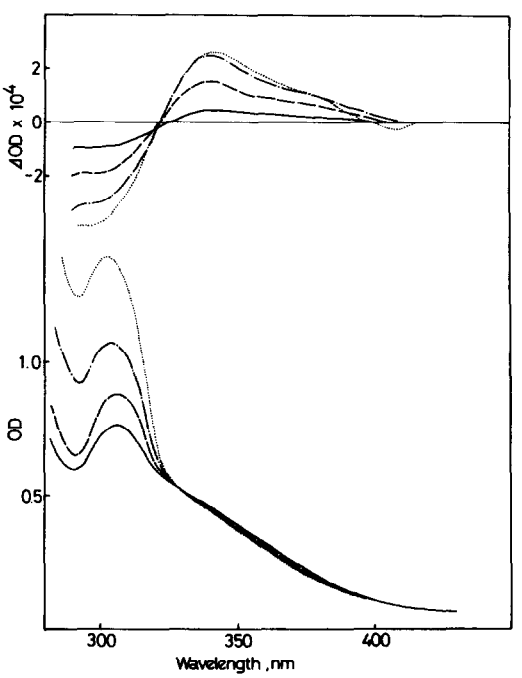



Fig. 1. Absorption and CD spectra of the diphosphooctadecamolybdic acid ($2.12 \times 10^{-5}$ mol dm$^{-3}$) in the benzyl alcohol solution containing various moles of *l*-brucine sulphate. Molar ratios of polyanion: brucine are 1:1 (——), 1:2 (– – – –), 1:3 (– – – – –) and 1:5 (- - - -).

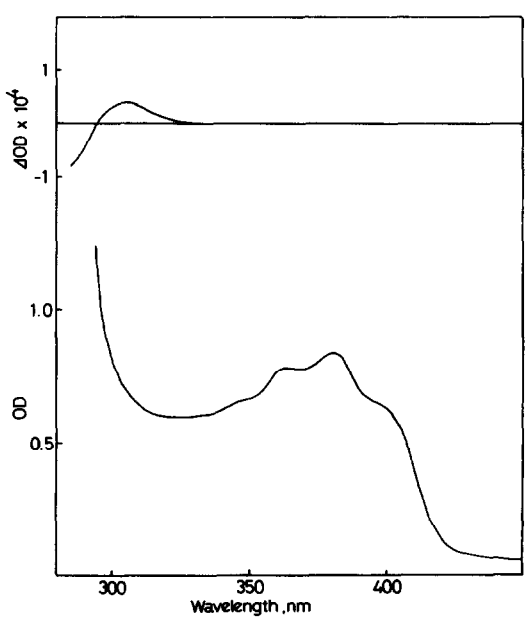



Fig. 2. Absorption and CD spectra of the obtained chiral polybenzyl (0.536 g dm$^{-3}$) in $CH_2Cl_2$ solution.

is maintained for relatively a long time. In solution, however, it is subject to mutarotation with an elapse of time. This fact may be interpreted as that the polybenzyl has a flexible structure leading to mutarotation in solution.

This polymer was colourless and amorphous. The viscosity $[\eta]$ was $0.07\,\mathrm{dl\,g^{-1}}$ (in N, N′-dimethylacetamide containing 1% LiCl, $c = 0.25\,\mathrm{g\,dl^{-1}}$ and at 25°C) and the decomposition temperature was 408°C. The $^1$H-NMR spectrum in *d*-chloroform showed the comparatively broad signals of methylene protons at 3.80 ppm and phenyl protons at 7.00 ppm, but showed no methyne proton of asymmetric carbon as a cause of the chirality. This implies that the chirality may be due to the helical part existing in the polymer structure.

The chiral two-electron reduced polyacid in the presence of brucine also gave polybenzyl with a positive CD at 305 nm. On the contrary, analogous experiments with the achiral heteropolyacid, $H_6[P_2W_{18}O_{62}]$, produced only achiral polybenzyl.

Under chiral environment substances other than *l*-brucine, such as *d*-cinchonine, strychnine, $\Delta$- and $\Lambda$-$[Co(en)_3]^{3+}$, the Pfeiffer effect was not observed because of their low solubility in benzyl alcohol, or of the formation of insoluble salts with the heteropolyacid.

In this asymmetric polymerization, the chiral heteropolyacid may catalyze only in the initial stage of reaction, because of its relatively low stability. However, the chiral structure of heteropolyanion has been found to participate significantly in the polymerization. Recently Knoth and Harlow have reported that a trimethyloxonium ion is alkylated to a surface bridged, rather than a terminal, oxygen atom of dodecamolybdo heteropolyanion.[5] If a benzyl cation, generated by the strong Brønsted acidity of the octadecamolybdic acid, is polymerized on the surface bridged oxygens of the chiral polyanion, the chiral structure of polybenzyl may be plausibly conformed. The measurement of the CD spectrum in the range less than 290 nm, which should be expected, was unsuccessful because of the influence of solvent.

## REFERENCES

1. J. F. Garvey and M. T. Pope, *Inorg. Chem.* 1978, **17**, 1115.
2. K. Nomiya, T. Ueno and M. Miwa, *Bull. Chem. Soc. Jpn.* 1980, **53**, 827.
3. H. Wu, *J. Biol. Chem.* 1920, **43**, 189.
4. K. Nomiya, S. Sasa and M. Miwa, *Chem. Lett.* 1980, 1075.
5. W. H. Knoth and R. L. Harlow, *J. Am. Chem. Soc.* 1981, **103**, 4265.

*Polyhedron* Vol. 3, No. 3, pp. 385–387, 1984
Printed in Great Britain.

0277–5387/84 $3.00 + .00
Pergamon Press Ltd.

# NOTE

## SYNTHESIS AND X-RAY CRYSTAL STRUCTURE OF $OsBr_2(CNBu^t)_4 \cdot 2CH_2Cl_2$

**RICHARD A. JONES* and BRUCE R. WHITTLESEY**
Department of Chemistry, University of Texas at Austin, Austin, TX 78712, U.S.A.

**and**

**JERRY L. ATWOOD* and WILLIAM E. HUNTER**
Department of Chemistry, University of Alabama, University, AL 35486, U.S.A.

(*Received* 4 *July* 1983; *accepted* 25 *July* 1983)

**Abstract**—Reaction of $(NH_4)_2OsBr_6$ with excess Na/Hg in THF in the presence of excess $^t$BuNC yields *trans*-$OsBr_2(CNBu^t)_4$ in high yield. The bis-dichloromethane solvate crystallises from $CH_2Cl_2$ solutions and its X-ray crystal structure has been determined. Crystal data: $C_{22}H_{40}Br_2Cl_4N_4Os$, M = 852.40, monoclinic, space group $P2_1/c$, $a = 9.702(3)$ Å, $b = 10.143(5)$ Å, $c = 18.497(5)$ Å, $\beta = 104.28(3)°$, $U = 1764(1)$ Å$^3$, $Z = 2$ for $D_c = 1.60$ gcm$^{-3}$. $\lambda(MoK_\alpha) = 0.71069$ Å (graphite monochromator), $\mu(MoK_\alpha) = 65.44$ cm$^{-1}$, final $R = 0.044$, $R_w = 0.056$ from 1105 observed reflections (1777 measured).

Isocyanide complexes of the transition metals have received increasing attention in the past few years. For the iron triad a variety of binary and mixed ligand isocyanide systems are known.[1–3] Binary (homoleptic) isocyanides such as $Fe(RNC)_5$ (R = $^t$Bu, $^i$Pr, Et, 2,6-$Me_2C_6H_3$), and $Ru(^tBuNc)_5$ and $Ru_2(^iPrNC)_9$ are known for Fe and Ru.[4–6] For osmium, however, no binary complex has so far been reported. Stone and coworkers, in attempting to prepare $Os(^tBuNC)_5$ by reduction of $[Os(COD)Cl_2]_n$ with K/Hg, isolated $Os(^tBuNC)_3$(COD) in 81% yield.[5] We attempted the synthesis of $Os(^tBuNC)_5$ via Na/Hg reduction of $(NH_4)_2OsBr_6$ in THF, in the presence of excess $^t$BuNC; however, the product from this reaction is *trans*-$OsBr_2(CNBu^t)_4$ (**1**). Isocyanides of this type are well known for Fe and Ru[1–3] but few have been reported for Os.[7] Since relatively few isocyanide complexes of osmium have been structurally characterised we have determined the molecular structure of this complex by a single crystal X-ray diffraction study. We report here details of the synthesis, characterisation and X-ray structure of (**1**) as its bis-dichloromethane solvate (**2**).

*Authors to whom correspondence should be addressed.

## EXPERIMENTAL

All operations were performed under oxygen-free argon. Microanalytical data were by the Schwarzkopf Microanalytical Laboratory, Woodside, New York. THF was dried over sodium and distilled from sodium/benzophenone under nitrogen before use. Dichloromethane was dried over $CaH_2$ and distilled under nitrogen before use. Instruments: IR Perkin–Elmer 1330, $^1$H NMR Varian EM-390 (90 MHz). $(NH_4)_2OsBr_6$[8] and $^t$BuNC[9] were prepared by published procedures.

*trans*-$OsBr_2(^tBuNC)_4 \cdot 2CH_2Cl_2$ (**1**)

THF (50 cm$^3$) was added to a flask containing $(NH_4)_2OsBr_6$ (0.77 g, 1.09 mmol), tert-butylisocyanide (1.29 g, 15.6 mmol) and sodium amalgam (1%, 11.62 mmol Na) at −78°C. The reaction mixture was stirred (24 hr) while the temperature was allowed to warm to room temperature. The stirring was stopped and the mixture separated into a grey solid and a clear light yellow solution. The solution was filtered and volatile materials were removed under vacuum (4 hr). Dichloromethane (20 cm$^3$) was added and the solution filtered. Evaporation to *ca.* 5 cm$^3$ and cooling (−20°C) yielded yellow crystals of trans-$OsBr_2(CNBu^t)_4 \cdot 2CH_2Cl_2$ after 24 h. Yield 0.56 g, 60%. M.p. 150–5°C (dec). IR (KBr disc), 2987*m*,

2937*w*, 2115*s*, 2065*sh*, 1620*w.br*, 1480*w*, 1458*w*, 1400*m*, 1371*m*, 1265*m*, 1237*m*, 1209*s* ($cm^{-1}$). In MeCN (matched $CaF_2$ cells), 2985*m*, 2940*w*, 2122*s*, 2067*sh*, 1629*w.br*, 1476*w.br*, 1390*w*, 1364*w*, 1263*w*, 1237*w*, 1209*m* ($cm^{-1}$). $^1H$ NMR (in $C_6D_6$, at 35°C, $\delta$ values in ppm rel. $Me_4Si$ $\delta 0.0$) $\delta 1.17s$ ($^tBu$NC). Samples of the dichloromethane solvate which had been subjected to high vacuum (10 h) had reproducible microanalytical data (C, H, N) which indicated only partial loss of $CH_2Cl_2$.

The dichloromethane solvate ($OsBr_2(^tBuNC)_4 \cdot 2CH_2Cl_2$) rapidly loses crystallinity under argon or vacuum. It is soluble in benzene, toluene, dichloromethane and acetonitrile but insoluble in hexane. It is air stable for short periods in the solid state but considerably more sensitive in solution.

*X-Ray experimental*

Single crystals of the bis-dichloromethane solvate $OsBr_2CN^tBu)_4 \cdot 2CH_2Cl_2$ were grown from $CH_2Cl_2$ solutions at $-20$°C and mounted in thin-walled glass capillaries under an argon atmosphere saturated with $CH_2Cl_2$ vapour. *Crystal Data*: $C_{22}H_{40}Br_2Cl_4N_4Os$, M = 852.40, monoclinic, space group $P2_1/c$, $a = 9.702(3)$ Å, $b = 10.143(5)$ Å, $c = 18.497(5)$ Å, $\beta = 104.28(3)°$, $U = 1764(1)$ Å$^3$, $Z = 2$ for $D_c = 1.60$ gcm$^{-3}$. $\lambda(MoK_\alpha) = 0.71069$ Å (graphite monochromator), $\mu(MoK_\alpha) = 65.44\,cm^{-1}$. Crystal dimensions (mm) $0.40 \times 0.20 \times 0.15$. Decay of standards (400, 040, 004) $< 3\%$. Data collected ($\theta/2\theta$ mode) = 1777 for $1° < 2\theta < 40°$. Observed data 1105 ($I > 2\sigma(I)$).

*Structure solution and refinement*

An absorption correction (psi scan) was applied and the structure was solved using standard heavy atom methods and refined (full matrix least squares) to final $R = \Sigma|\Delta F|/\Sigma|F_0| = 0.044$, $R_w = [\Sigma(\omega\Delta F_0)^2/\Sigma\omega F_0^2]^{1/2} = 0.056$. Non-hydrogen atoms were refined anisotropically; hydrogen atoms were not located. Data were collected on an Enraf–Nonius CAD-4 diffractometer at 25°C. Details of data collection, computer programs and sources of scattering factor data are given in Ref. 10.

Final atomic coordinates tables of anisotropic thermal parameters, bond lengths and angles and lists of $F_0/F_c$ have been deposited with the Editor as supplementary material.†

†Atomic coordinates for these structures have also been deposited with the Cambridge Crystallographic Data Centre for inclusion in their Data Base. Copies are also available on request from the Editor at Queen Mary College.

Table 1. Key bond lengths (Å) and angles (°) for *trans*-$OsBr_2(CN^tBu)_4 \cdot 2CH_2Cl_2$

| Atoms | Distance |
|---|---|
| Os----Br | 2.558(3) |
| Os----C(6) | 2.00(3) |
| C(2)--C(3) | 1.51(3) |
| Os----C(1) | 1.99(2) |
| C(1)--N(1) | 1.19(2) |
| C(2)--N(1) | 1.44(2) |
| C(6)--N(2) | 1.16(3) |
| **Atoms** | **Angle** |
| Br----Os----C(1) | 90.9(6) |
| C(1)--Os----C(6) | 88.9(8) |
| C(4)--C(2)--C(5) | 110(3) |
| C(4)--C(2)--N(1) | 107(2) |
| Os----C(6)--N(2) | 176(2) |
| C(1)--N(1)--C(2) | 174(2) |
| Br----Os----C(6) | 89.6(6) |
| Os----C(1)--N(1) | 174(2) |

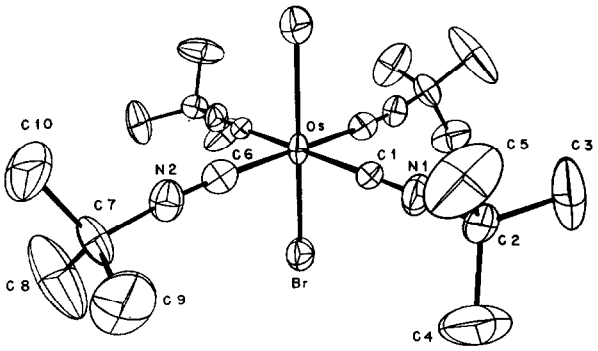



Fig. 1. Ortep view of *trans*-$OsBr_2(CNBu^t)_4$. Key bond lengths and angles are given in Table 1. A view of the unit cell showing the dichloromethane of solvation is available as supplementary material.

## RESULTS

The reduction of $(NH_4)_2(OsBr_6)$ with excess Na/Hg in THF in the presence of excess $^t$BuNC yields pale yellow *trans*-$OsBr_2(CNBu^t)_4$ (**1**) in 60% yield. The bis-dichloromethane solvate of (**1**) may be obtained by crystallisation from $CH_2Cl_2$ solution at $-20°C$. Spectroscopic data from (**1**) (see Experimental) is in accord with the solid state structure as determined by a single crystal X-ray diffraction study. Each Os(II) atom has four terminal, linear isocyanide ligands in a plane and two *trans* bromine atoms.

A view of the molecule with the atom numbering scheme is shown in Fig. 1. Each osmium atom lies on a crystallographic centre of inversion and all bond lengths and angles in the molecules are normal. Thus the Os–Br and Os–C(1) distances are 2.558(3) and 1.99(2) Å, respectively. The angles about Os are very close to those expected for an octahedron indicating that there are no major distortions from this geometry (C(1)–Os–C(6) = 88.9(8)° and C(1)–Os–Br = 90.9(6)°). Key bond lengths and angles for the osmium containing moiety of the structure are given in Table 1. A view of the unit cell packing showing the dichloromethane molecules of solvation is available as supplementry material.†

*Acknowledgements*—We thank the University Research Institute of the University of Texas at Austin, the Robert A. Welch Foundation and the Research Corporation for support.

## REFERENCES

1. L. Malatesta and F. Bonati, *Isocyanide Complexes of Metals*. Wiley, New York (1969).
2. P. M. Treichel, *Adv. Organomet. Chem.* 1973, **11**, 21.
3. Y. Yamamoto, *Coord. Chem. Rev.* 1980, **32**, 193.
4. G. K. Barker, A. M. R. Galas, M. Green, J. A. K. Howard, F. G. A. Stone, T. W. Turney, A. J. Welch and P. Woodward, *J. Chem. Soc. Chem. Commun.* 1977, 256.
5. J. M. Bassett, D. E. Berry, G. K. Barker, M. Green, J. A. K. Howard and F. G. A. Stone, *J. Chem. Soc. Dalton Trans.* 1979, 1003.
6. J. M. Bassett, M. Green, J. A. K. Howard and F. G. A. Stone, *J. Chem. Soc. Chem. Comm.* 1977, 853.
7. R. D. Adams and J. P. Selegue, In *Comprehensive Organometallic Chemistry* (Edited by G. Wilkinson, E. W. Abel and F. G. A. Stone), Vol. 4, p. 981. Pergamon Press, Oxford (1982).
8. F. P. Dwyer and J. W. Hogarth, *Inorg. Syn.* 1957, **5**, 204.
9. G. W. Gokel, R. P. Widera and W. P. Weber, *Org. Syn.* 1975, **55**, 96.
10. J. Holton, M. F. Lappert, D. G. H. Ballard, R. Pearce, J. L. Atwood and W. E. Hunter, *J. Chem. Soc. Dalton Trans.* 1979, 45.

*Polyhedron* Vol. 3, No. 3, pp. 388, 1984
Printed in Great Britain.

0277-5387/84 $3.00 + .00
Pergamon Press Ltd.

# ANNOUNCEMENT

## INTERNATIONAL SYMPOSIUM ON RARE EARTHS SPECTROSCOPY 10–15 September 1984, Wrocław, Poland

We are kindly informing you that the International Symposium on Rare Earths Spectroscopy will be held on 10–15 September 1984 in Wrocław.

### ORGANIZERS

Wrocław Branch of the Polish Academy of Sciences; Institute for Low Temperature and Structure Research, Polish Academy of Sciences; Institute of Chemistry, University of Wrocław; Institute of Inorganic Chemistry and Metallurgy of Rare Elements, Technical University of Wrocław.

### SPONSORS

Polish Academy of Sciences, Technical University of Wrocław.

### SCOPE

The Symposium is addressed to physicists and chemists interested in rare earths spectroscopy. The objective of the Symposium will be the presentation of the latest results concerning electronic structure and spectroscopic properties of rare earth ions and the possibilities of their applications in the field of laser technology.

### TOPICS

1. Spectroscopy methods in structural study of lanthanide compounds.
2. Intensities of $f$–$f$ transitions, $f$–$d$ transitions, hypersensitivity, environment effects.
3. Luminescence of lanthanide ions.
4. Non-radiative processes in luminescent materials.
5. Energy transfer (cross-relaxation, up-conversion, phonon-assisted energy transfer, concentration quenching).
6. Rare earth lasers (technology and materials).

Lectures will be presented in English. Contributed papers will be presented orally or during poster sessions.

The deadline for submission of abstracts will be 28 February 1984.

Those interested in attending the Conference, are requested to return the Preliminary Application Form* as soon as possible.

The Second Circular, containing a list of invited speakers, titles of plenary lectures and additional information concerning the organization of the Symposium will be forwarded at the beginning of 1984.

*All correspondence concerning the Symposium should be addressed to:

Dr. J. Legendziewicz
Institute of Chemistry
University of Wrocław
Joliot-Curie 14
50-383 Wrocław
Poland

*Polyhedron* Vol. 3, No. 4, pp. 389–432, 1984
Printed in Great Britain.

0277–5387/84 $5.00 + .00
Pergamon Press Ltd.

# POLYHEDRON REPORT NUMBER 6

# DOUBLE BONDING BETWEEN THE HEAVIER MAIN-GROUP ELEMENTS: FROM REACTIVE INTERMEDIATES TO ISOLABLE MOLECULES

ALAN H. COWLEY
Department of Chemistry, The University of Texas at Austin, Austin, TX 78712, U.S.A.

## CONTENTS

I. INTRODUCTION . . . . . 389
II. TRANSIENT MOLECULES WITH DOUBLE BONDS . . . . . 390
1. Diphosphenes (RP=PR) . . . . . 390
2. Disilenes ($R_2Si=SiR_2$) . . . . . 390
3. Miscellaneous double-bonded compounds . . . . . 396
III. PREPARATION AND STRUCTURES OF STABLE MOLECULES WITH DOUBLE BONDS . . . . . 396
1. Disilenes ($R_2Si=SiR_2$) . . . . . 396
2. Digermenes ($R_2Ge=GeR_2$) . . . . . 398
3. Distannenes ($R_2Sn=SnR_2$) . . . . . 398
4. Diphosphenes (RP=PR) . . . . . 398
5. Phospha-arsenes and phosphastibenes (RP=AsR and RP=SbR). . . . . 403
6. Diarsenes (RAs=AsR) . . . . . 405
IV. REACTIVITIES OF DOUBLE-BONDED MOLECULES . . . . . 406
1. Disilenes . . . . . 406
2. Diphosphenes, phospha-arsenes and diarsenes . . . . . 408
V. COORDINATION CHEMISTRY OF DOUBLE-BONDED COMPOUNDS . . . . 412
VI. MOLECULAR ORBITAL CALCULATIONS ON DOUBLE-BONDED COMPOUNDS 418
1. Disilenes, digermenes and distannenes . . . . . 418
2. Diphosphenes . . . . . 418
VII. ELECTRONIC SPECTRAL DATA FOR DOUBLE-BONDED COMPOUNDS. . . 420
1. Disilenes . . . . . 420
2. Diphosphenes, phospha-arsenes and diarsenes . . . . . 421
VIII. NMR AND VIBRATIONAL SPECTROSCOPIC DATA FOR DOUBLE-BONDED COMPOUNDS . . . . . 423
IX. ADDENDUM . . . . . 432

## I. INTRODUCTION

The history of the present subject starts in the last century when Köhler and Michaelis[1] isolated a substance of empirical composition $C_6H_5P$ which they formulated as $C_6H_5P=PC_6H_5$ and dubbed "phosphobenzene" by analogy with azobenzene. However, subsequent X-ray diffraction studies[2] revealed that "phosphobenzene" adopts a cyclic pentameric or hexameric structure in the solid state. A similar picture has emerged in arsenic and silicon chemistry. Thus, Erlich,[3] the originator of the chemotherapeutic drug "Salvarsan" formulated his compound as a diarsene, ArAs=AsAr, and Kipping[4] reported that the sodium coupling of ethylphenyldichlorosilane resulted in "diphenyldiethylsilicoethylene". Once again, however, the cyclic oligomeric nature of these types of compounds was demonstrated by X-ray crystallography.[5,6]

From these beginnings, the consensus developed that compounds featuring double bonds between the heavier main-group elements would not be stable because of weak $(p-p)\pi$ bonding. Such a view is sometimes referred to as the "classical double-bond rule".[7]

Starting in the 1960's, transient molecules with implied double bonds between the heavier Group 4A and/or Group 5A elements have been detected spectroscopically or deduced from trapping experiments. The past few years have witnessed the actual isolation of such compounds. This exciting development has been made possible by the use of bulky ligands. Interestingly, despite the requisite steric blockades, most of the kinetically stabilized compounds are able to undergo a wide variety of chemical reactions at the double bond.

## II. TRANSIENT MOLECULES WITH DOUBLE BONDS

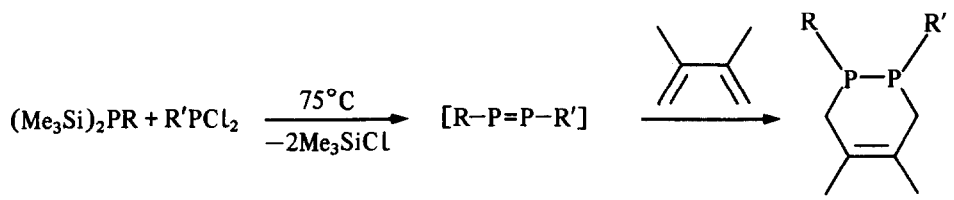
### 1. *Diphosphenes (RP=PR)*

The parent diphosphene, HP=PH, was first detected in 1966[8] as a product of thermal decomposition of $P_2H_4$. Diphosphene is unstable and undergoes decomposition to $P_4$ and $PH_3$ as shown below:

$$P_2H_4 \xrightarrow{\Delta} PH_3 + \tfrac{1}{2}P_2H_2 \longrightarrow [1/6]P_4 + [2/6\ PH_3].$$

Other studies have shown that diphosphene is formed from $P_2H_4$ at room temperature and low temperature[9] using a nearly static system and by photolysis of $P_2H_4$.[10]

More recently, the existence of the *t*-butyl- and mesityl-substituted diphosphenes, (Bu$^t$)P=P(Bu$^t$) and (Bu$^t$)P=P(Mes) has been implied from the following reaction sequence.[11]

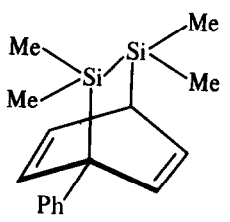



R = R′ = Bu$^t$

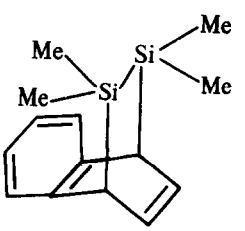
R = Bu$^t$; R′ = Mes

### 2. *Disilenes ($R_2Si$=$SiR_2$)*[12]

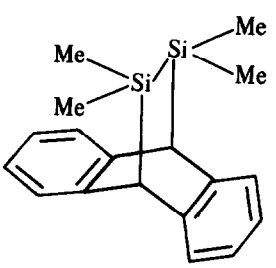
Pioneering work in the area was reported by Roark and Peddle.[13] These authors synthesized the tetramethyldisilene precursors, **1–3**, by treatment of the anion radicals of biphenyl, naphthalene, and anthracene with the disilane, $Me_2(Cl)SiSi(Cl)Me_2$. The relative temperatures required




**1**

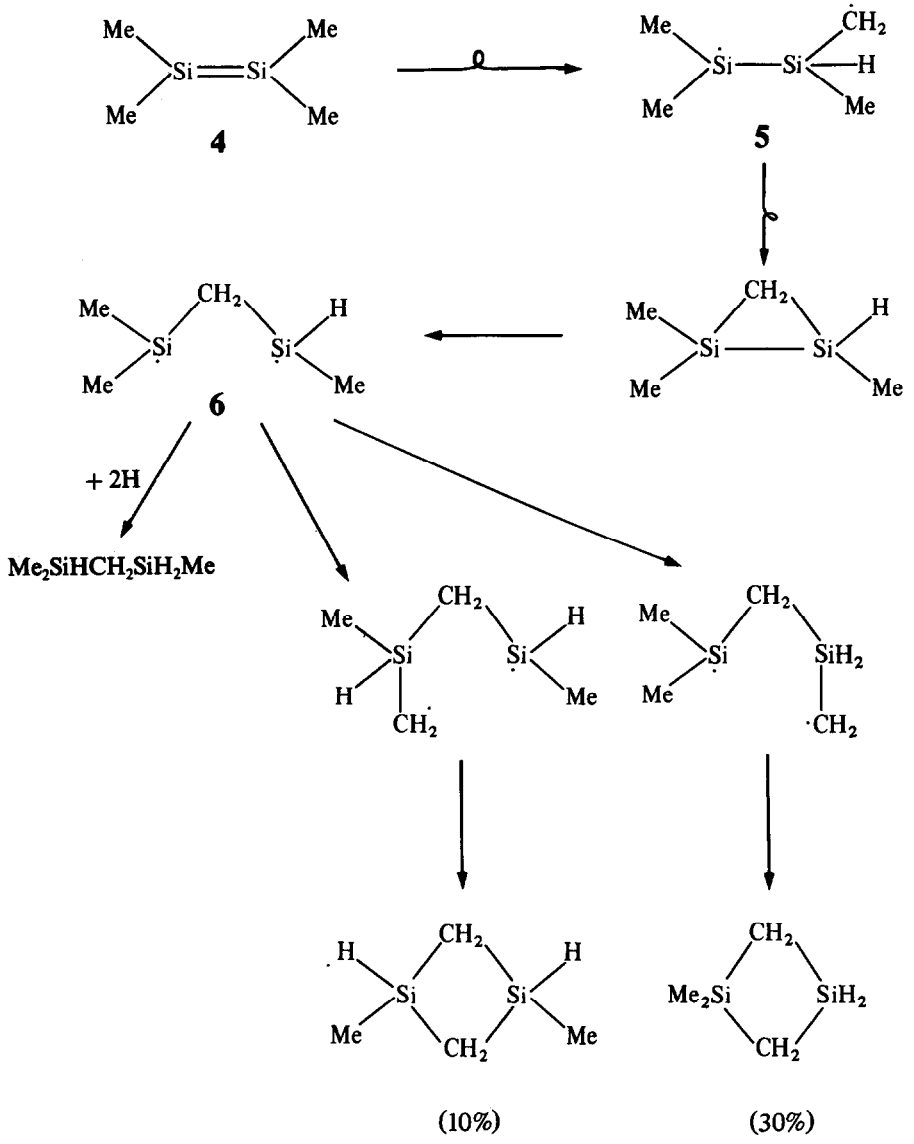



**2**



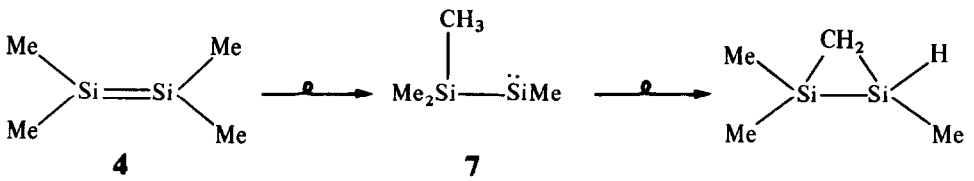

**3**

for thermal decompositions of **1** (260°C), **2** (360°C), and **3** (500°C), are consistent with a retro Diels–Alder production of tetramethyldisilene (**4**). Originally, it was suggested that the products of low-pressure pyrolysis (Scheme I) are consistent with the rearrangement of **4** to diradicals **5** and **6**.

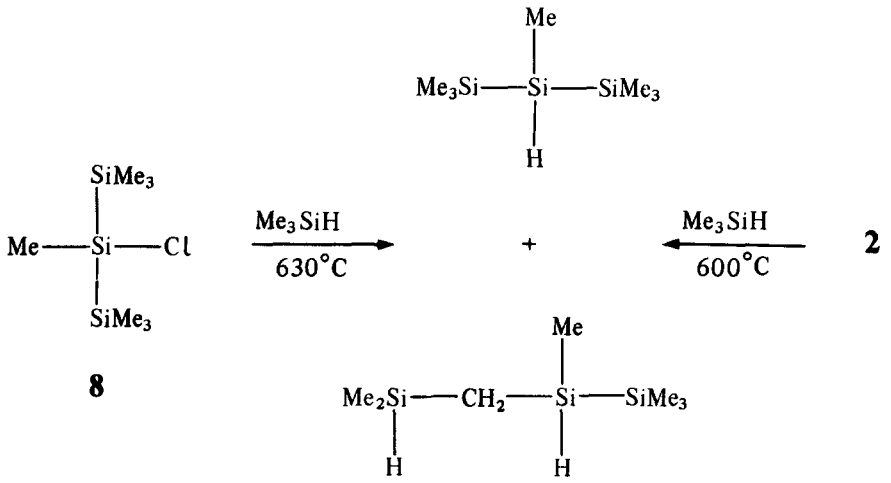



Scheme I.

However, subsequently Barton *et al.*[14] pointed out that the same products could arise if tetramethyldisilene rearranged first into trimethylsilylmethylsilylene, **7**, which then underwent an intramolecular C–H insertion to produce the same disilacyclopropane proposed by Roark and Peddle,[13] i.e.

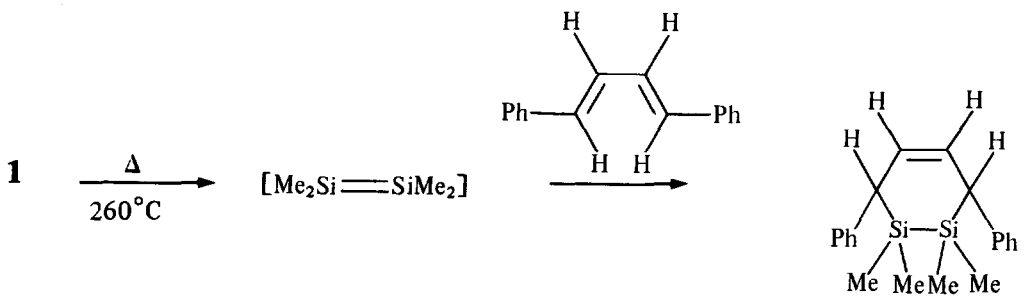


Strong support for the suggestion of Barton *et al.* was provided by the fact that co-pyrolysis of **8** (a silylene precursor) with $Me_3SiH$ (an excellent silylene trap) resulted in the same products as the co-pyrolysis of **2** and $Me_3SiH$.



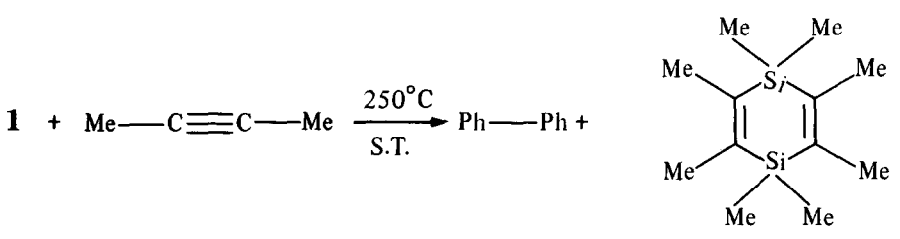

Recent work by Gaspar *et al.*[15] has shown that the rearrangement of the silylene, $(Me_3Si)_2Si$ is even more complicated.

More direct evidence for the intermediacy of tetramethyldisilene was obtained both from mass spectroscopy and Diels–Alder trapping experiments.[13] Thus, pyrolysis of **1** or **2** with anthracene produced a virtually quantitative yield of **3** and, likewise, the reaction of **1** with naphthalene produced **2**. Roark and Peddle[13] also established the reactivity of **4** toward dienes as shown below.



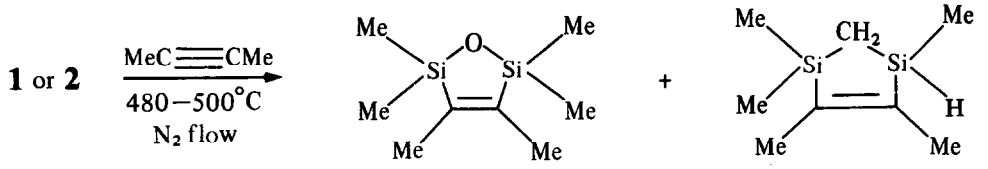

The above mode of addition indicated that $Me_2Si{=}SiMe_2$ is formed initially in a singlet state which therefore implies a $(p{-}p)\pi$ bond between the silicon atoms. Further evidence on this point stemmed from subsequent work of Sakurai *et al.*[16] Using the Roark and Peddle approach,[13] these authors generated *cis* and *trans*-1,2-dimethyl-1,2-diphenyldisilene and found that the additions of these isomers to anthracene were remarkably stereospecific.

Barton and Kilgour[17] reported that tetramethyldisilene is reactive towards other dienes and alkynes. However, the nature of the products depended on the reaction conditions. Thus, heating **1** with 2-butyne at 250°C in a sealed tube produced biphenyl and disilin, **9**, whereas co-pyrolysis of




**9**

**1** or **2** with 2-butyne in a flow system at 480°C resulted in **10** (4–8%) and the disilacyclopentene, **11** (26–28%) as isolated products. Presumably, **11** arises from the diradical, **5** and **10** *via*



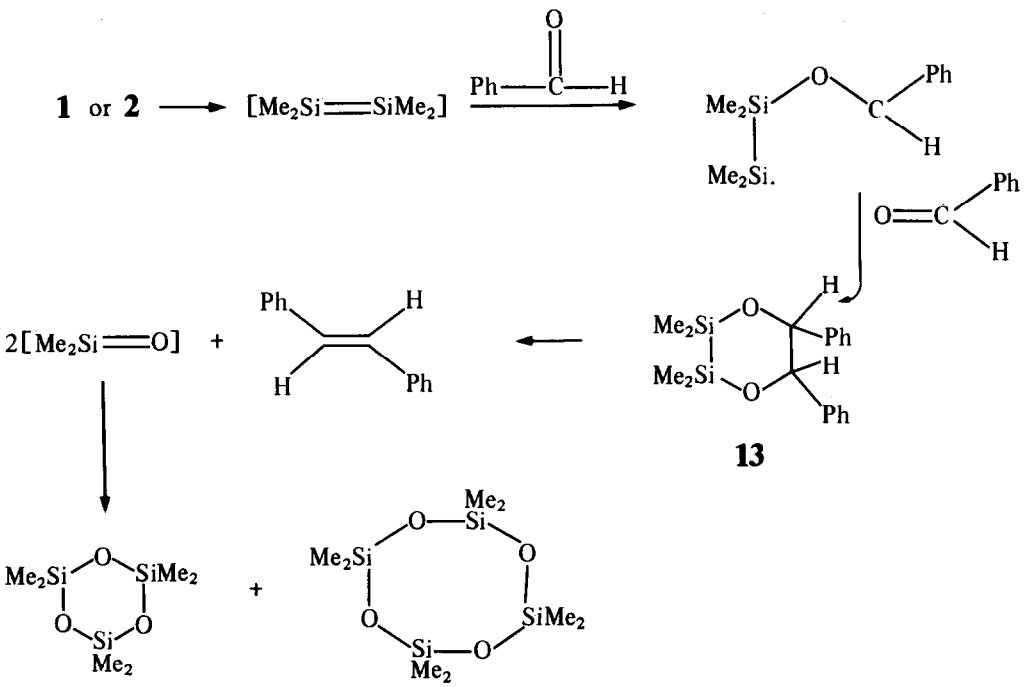

**10** **11**

atmospheric oxidation of permethyl-3,4-disilacyclobutene.[18] Sakurai *et al.*[19] have reported that tetramethyldisilene reacts with diphenylacetylene or phenyltrimethylsilylacetylene to give disilacyclobutenes, **12**.




**12**

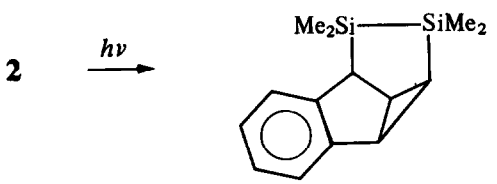
Barton and Kilgour[20] also discovered that **1** and **2** react with benzaldehyde in a flow system at 480–500°C to produce *trans*-stilbene and cyclic siloxanes. One plausible mechanism involves the concerted decomposition of a disiladioxane, **13**, as indicated in Scheme II.




**13**

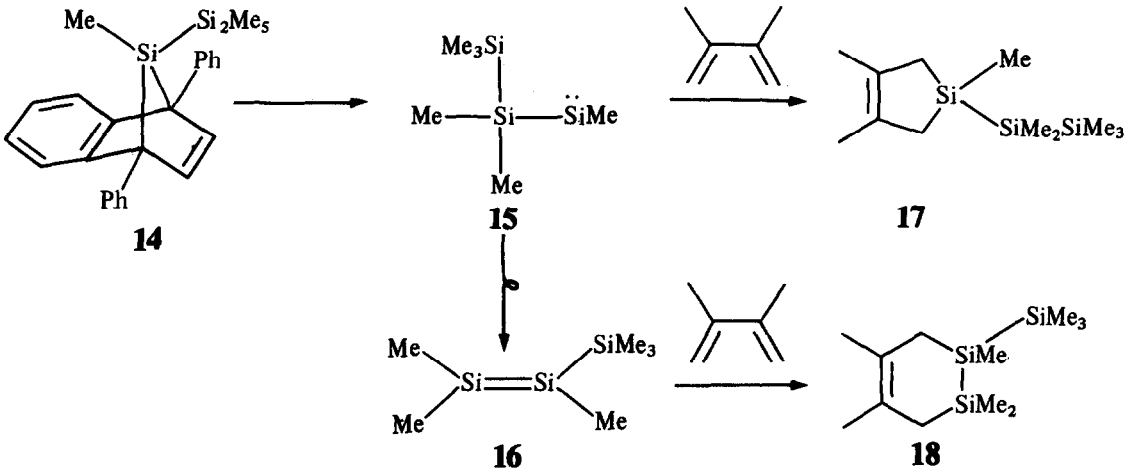
Scheme II.

Recent experiments[21] have demonstrated that the low-temperature photolysis of **2** results in the following rearrangement.




Ambient temperature photolysis, however, resulted in tetramethyldisilene production.[21,22]

We now turn to other means of disilene synthesis. For example, Sakurai *et al.*[23] have presented recent evidence that indicates that a disilene can be produced from a silylsilylene by means of silyl shift.

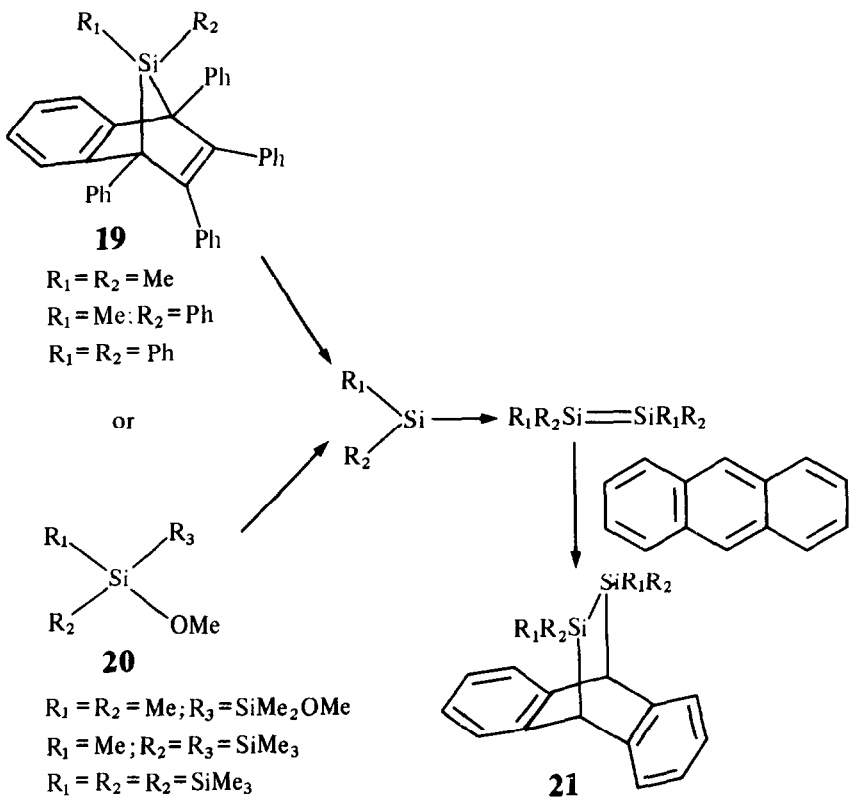



The fact that both **17**, the anticipated silylene addition product, and **18**, the anticipated disilene addition product, were formed competitively suggested that the rearrangement of the silylene to disilene is a rapid process.

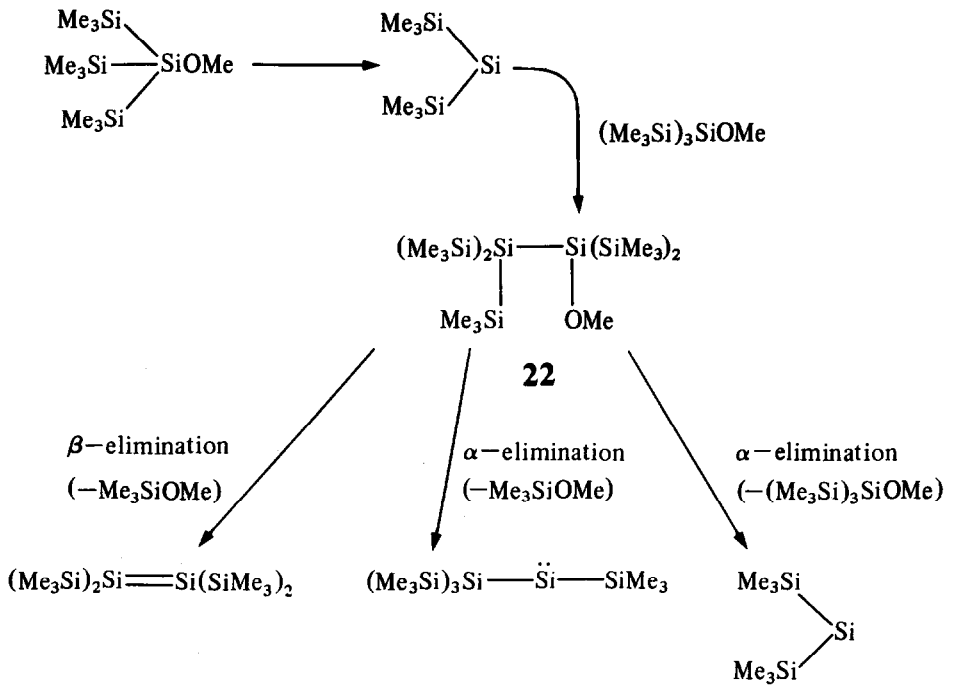
In principle, the rearrangement could occur via a $Me_3Si$ or Me shift. However, since no rearrangement occurred with the silylenes $Me(Me_3Si)Si$ and $(Me_3Si)_2Si$, it is clear that a Me shift was not involved.

Conlin and Gaspar[24] noted that the pyrolysis of $Me_2(MeO)SiSi(OMe)Me_2$, a $Me_2Si$ precursor, produced *inter alia* the same disilacyclobutanes that were isolated from the pyrolysis of the disilene precursor, **1**. On this basis, these authors suggested that dimerization of $Me_2Si$ to $Me_2Si{=}SiMe_2$ had occurred.

The idea of silylene→disilene dimerization has also been advanced by Sakurai *et al*[25] to explain the observation that the silylene generators **19** and **20** produce **21**, the disilene Diels–Alder addition product (rather than the silylene addition product) when co-thermolyzed with anthracene, viz.



However, the thermal reactions of **19** or **20** with 2,3-dimethyl-1-3 butadiene afforded silacyclopentenes, the anticipated silylene addition products. The difference in the diene and anthracene trapping experiments was explained by postulating that the former traps the silylene so efficiently that dimerization was precluded. However, as noted by e.g. Sakurai *et al.*[25] it is not *a priori* necessary to postulate silylene dimerization since stepwise reaction of the silylene with anthracene is possible. Chen and Gaspar[26] have suggested that a silylene such as $(Me_3Si)_2Si$ could insert into its precursor, $(Me_3Si)_3SiOMe$, to produce **22** which is capable of undergoing three different types of eliminations as indicated below:

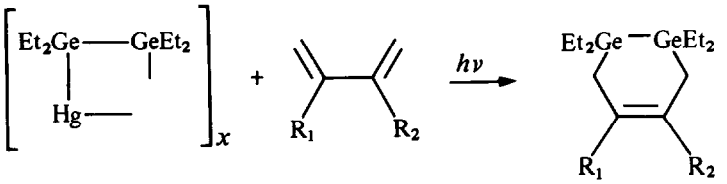



Thus, $\beta$-elimination of $Me_3SiOMe$ would produce a disilene which could, e.g. dimerize to give the observed cyclotetrasilane $(Me_3Si)_4Si_4$. $\alpha$-elimination of $Me_3SiOMe$ would produce a silylene which is presumably capable of rearranging to a disilene, while $\alpha$-elimination of $(Me_3Si)_3SiOMe$ would regenerate bis(trimethylsilyl)silylene.

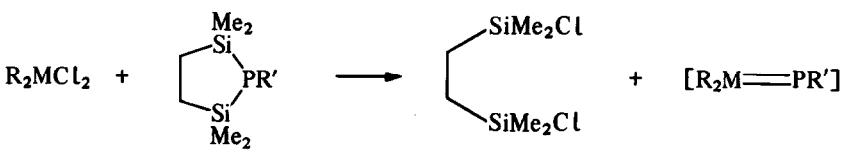
Tetrafluorodisilene, $F_2Si{=}SiF_2$, has been proposed as a short-lived intermediate in the reaction of $SiF_2$ with, e.g. acetylene.[27]

3. *Miscellaneous double-bonded compounds*

Evidence for digermenes ($R_2Ge{=}GeR_2$) as reactive intermediates is much more sparse. It is possible, for example, that $Et_2Ge{=}GeEt_2$ is involved in photolytic reactions such as[28,29]

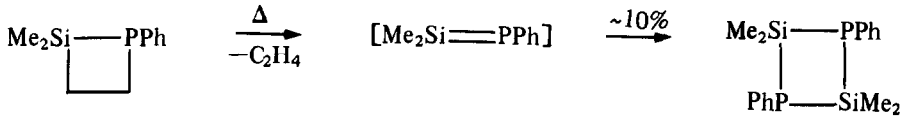



Similarly, species such as $R_2Ge{=}PR'$ and $R_2Sn{=}PR'$ have been postulated as intermediates in reactions of the type[28,29]




M = Ge,Sn; R = Me, R′ = Ph

A silaphosphene has also been proposed[29,31] on the basis of the following thermolysis of a 2-silaphosphetane

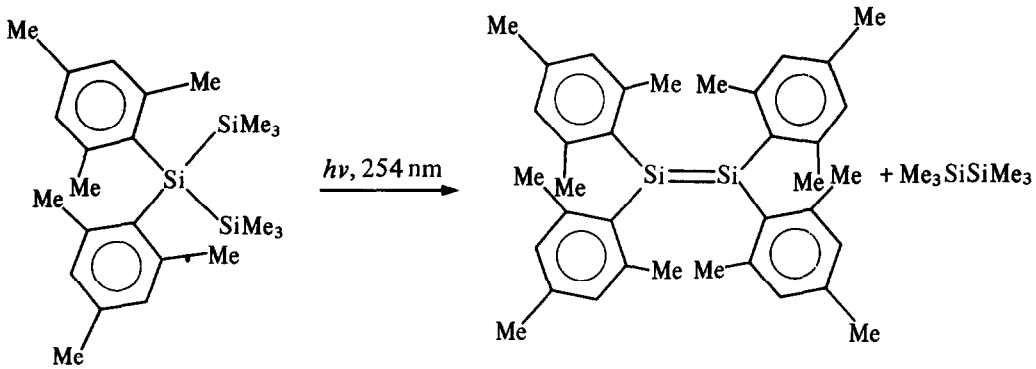



Mention should also be made of the novel sulfur dication, $[S_2I_4]^{2+}$, with a sulfur–sulfur bond length of 1.828(1) Å which corresponds to a bond order of over two.[32]

## III. PREPARATION AND STRUCTURES OF STABLE MOLECULES WITH DOUBLE BONDS

1. *Disilenes* ($R_2Si{=}SiR_2$)

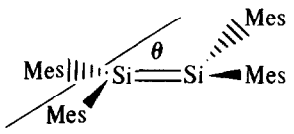
The first stable disilene was prepared by West *et al.*[33] Bright orange–yellow tetramesityldisilene (**24**) was prepared by the photochemical elimination of hexamethyldisilane from bis(-mesityl)hexamethyltrisilane in, e.g. hexane at − 100°C.




**23** **24**

Tetramesityldisilene is stable at room temperature providing air is excluded, and hydrocarbon solutions survive brief heating to 160°C. The reaction chemistry of disilenes will be discussed in a subsequent section. Tetramesityldisilene is probably formed via dimerization of dimesitylsilene since photolysis of **23** in 3-methylpentane at − 196°C produces the matrix—isolated blue silylene. Dimesitylsilylene can be trapped by, e.g. insertion into the Si–H bond of trimethylsilane. If no trapping agent is present, the dimesitylsilylene dimerizes to the disilene.

A recent X-ray crystal structure determination shows that tetramesityldisilene (**24**) adopts a slightly *trans*-bent geometry in the solid state.[34]

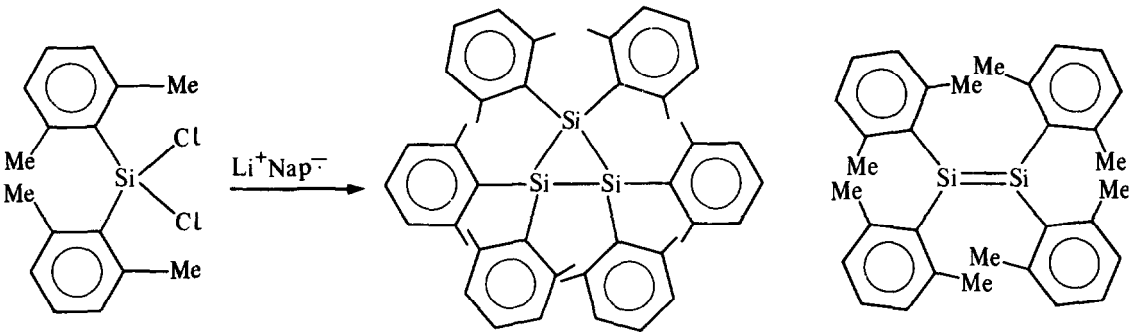



**24**

Si–Si = 2.160 Å
∠C–Si–Si = 113.9, 126.9°
∠C–Si–C = 115.5°

The angle between each C–Si–C plane and the line joining the two silicon atoms ($\theta$) is 18° and the twist angle is 5°. The silicon–silicon double bond length (2.160 Å) is 8–9% shorter than that of a typical silicon–silicon single bond.

Hard on the heels of the West *et al.* work, Masamune *et al.*[35] discovered a new disilene synthesis. Treatment of bis(2,6-dimethylphenyl)dichlorosilane, with lithium naphthalenide in dimethoxyethane afforded the first cyclotrisilane, **25**, photolysis of which resulted in a near quantitative conversion to the corresponding disilene, **26**, a yellow crystalline compound.

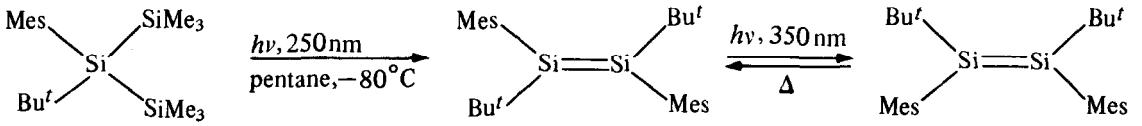



**25** **26**

Subsequently Boudjouk *et al.*[36] have reported that tetramesityldisilene can be produced from dimesityldichlorosilane either sonochemically or electrochemically. Thus, irradiation of a THF solution of dimesityldichlorosilane with ultrasonic waves in the presence of lithium metal produced ~ 90% yields of tetramesityldisilene within 20 min. Likewise, tetramesityldisilene can be produced from tetramesityldichlorosilane by controlled-potential reduction in a batch cell ( − 3.2V vs $Ag/Ag^+$).

Evidence for the first alkylated disilene has been presented very recently by Watanabe *et al.*[37] Reductive coupling of $(Bu^tCH_2)_2SiCl_2$ afforded the cyclotrisilane, $[(Bu^tCH_2)_2Si]_3$, which upon photolysis yielded solutions of the disilene, $(Bu^tCH_2)_2Si{=}Si(CH_2Bu^t)_2$. The disilene was not isolated, but was characterized spectroscopically and by an EtOH trapping experiment.

*Cis* and *trans* disilene isomers have now been isolated.[38] Photolysis of the trisilane, **27**, produces mostly the *trans* isomer, **28a**. Irradiation of




**27** **28a** **28b**

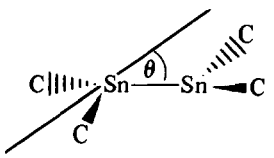
**28a** with 350 nm light resulted in a photostationary equilibrium mixture containing 63% of the *trans* (**28a**) and 37% of the *cis* (**28b**) isomer. The *cis* isomer **28b** is thermodynamically unstable and reverts to the equilibrium mixture of **28a** and **28b** (98 : 2 at 25°C). Photolysis of 2-mesityl-2-bis(trimethylsilylamino)hexamethyldisilane in pentane at − 60°C resulted mainly in the unstable *cis* isomer of $((Me_3Si)_2N)(Mes)Si{=}Si(Mes)(N(SiMe_3)_2)$ (**29**) which isomerized to a 88 : 12 *trans* : *cis* equilibrium mixture at 25°C. Possibly the more facile *cis–trans* interconversion for **29** is due to weaking of the silicon–silicon $\pi$-bond via conjugation from the amido groups.

2. *Digermenes* ($R_2Ge{=}GeR_2$)

A marginally stable digermene has been reported by Masamune *et al.*[39] using a virtually identical methodology to that employed for the disilene synthesis. Thus, reductive cyclization of bis(2,6–dimethylphenyl)dichlorogermane using lithium naphthalenide in DME afforded hexakis (2,6–dimethylphenyl)cyclotrigermane, the first example of a three-membered Ge ring. Irradiation of the cyclo trigermane with 254 nm light produced a yellow solution of tetrakis(2,6-dimethylphenyl)digermene. The digermene undergoes a slow photoinduced polymerization, its concentration reaching a maximum when 75% of the cyclotrigermane is consumed. The digermene was characterized by UV and $^1H$ NMR spectroscopy. Earlier, Lappert *et al.*[40] reported $[(Me_3Si)_2CH]_2Ge$ which probably has a digermene structure in the solid state.

3. *Distannenes*

The novel tin(II)alkyl, $[(Me_3Si)_2CH]_2Sn$ (**30**) was prepared by Lappert *et al.*[40] several years ago. This compound is monomeric in cyclohexane or benzene solution according to cryoscopic molecular weight determinations. An electron diffraction study[40c] revealed that **30** is also monomeric in the gas phase with an Sn–C bond length of 2.24(1) Å, and C–Sn–C, Sn–C–Si, and Si–C–Si bond angles of 96(1), 109(1) and 113(1)°, respectively. Interestingly, an X-ray diffraction study[40a,b] showed **30** to be dimeric in the solid state. The dimer possesses a *trans*-folded geometry, **31**, and the tin–tin distance of 2.764(2) Å is close to that of a typical Sn–Sn single bond and



**31**

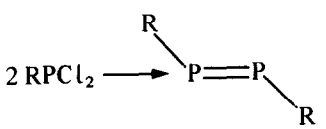
Sn–C = 2.28(3) Å (av)
Sn–Sn = 2.764(2) Å
∠C–Sn–C = 112° (av)
∠C–Sn–Sn = 115° (av)
$\theta = 41°$

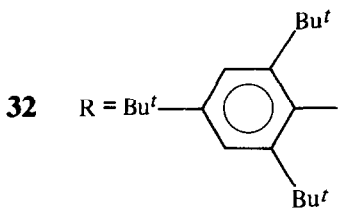
considerably longer than the sum of double-bond covalent radii (2.6 Å).[41] Moreover, the dimeric structure is not formed when the $(Me_3Si)_2CH$ ligand is replaced by the isoelectronic $(Me_3Si)_2N$ ligand, i.e. $[(Me_3Si)_2N]_2Sn$ is monomeric in both the solid and vapor phases.[42] Two theories have been advanced to explain the bonding in **31**: (i) a double bond exists between the tin atoms, i.e. it is a true distannene,[40] and (ii) a single bond exists between the tin atoms and an unshared electron pair resonates between the two metal centers,[43] viz.



4. *Diphosphenes (RP=PR)*

The first stable arylated diphosphene was prepared by Yoshifuji *et al.*[44] This was followed by the synthesis of the first alkylated diphosphene by our group[45] and Escudié *et al.*[46] Yoshifuji *et al.* prepared bis(2,4,6-tri-*tert*-butylphenyl) diphosphene (**32**) by treatment of 2,4,6-tri-*tert*-butylphenyldichlorophosphine with magnesium in THF, while our preparation of bis(tristrimethylsilyl) diphosphene (**33**) involved the reductive coupling of tristrimethylsilyldichlorophosphine with sodium naphthalenide of $(Me_3Si)_3CLi$ in THF.





**32** R = $Bu^t$

**33** $R = (Me_3Si)_3C$

The diphosphenes **32** (red–orange) and **33** (yellow–orange) are crystalline solids and their structures have been established by X-ray diffraction. Both molecules adopt a *trans* conformation in the solid state[44,46,47] (Fig. 1). For **32** the P–P bond length is 2.034(2) Å, while those for the two

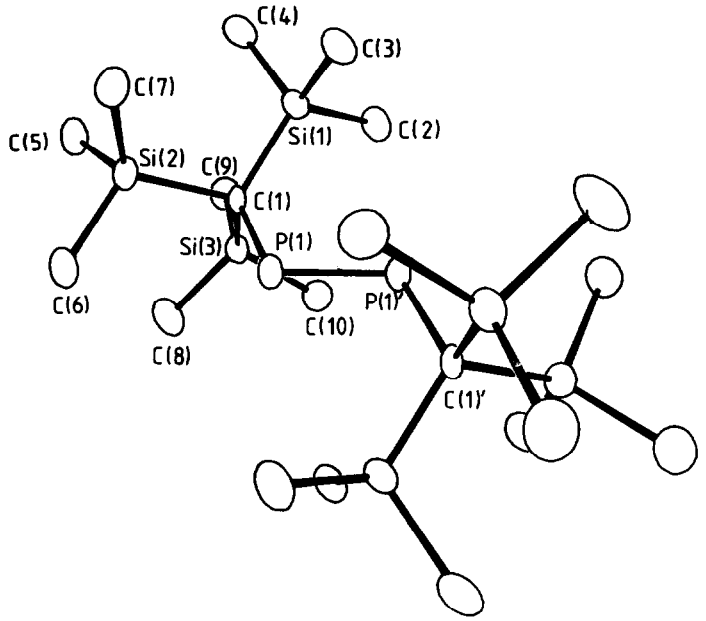
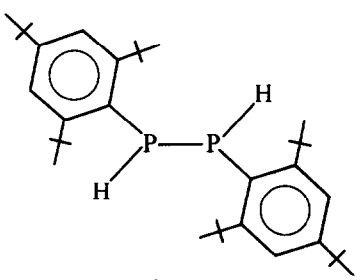


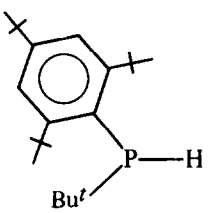

Fig. 1. View of the $(Me_3Si)_3CP{=}PC(SiMe_3)_3$ (**33**) molecule showing the atom numbering scheme. Important parameters for molecule A: P(1)–P(1)′ 2.014(6), P(1)–C(1) 1.85(1) Å; P(1)′–P(1)–C(1) 108.2(4)°. For molecule B: P(1)–P(1)′ 2.004(6), P(1)–C(1) 1.87(1) Å; P(1)′–P(1)–C(1) 108.9(4)°.

crystallographically independent molecules of **33** are 2.014(6) and 2.004(6) Å. These bonds lengths are close to the sum of double bond covalent radii (2.00 Å)[41] and thus indicative of double bond character. The P–P–C bond angles in **33** (av. 108.5(4)°) are considerably wider than those in **32** (102.8(1)°) indicating that the $(Me_3Si_3)C$ group is more sterically demanding than the 2,4,6-tri-*tert*-butylphenyl group. This size trend will have consequences for the reactivities of the two molecules (*vide infra*).

As will be discussed later, one of the characteristics of diphosphenes is a pronounced downfield $^{31}P$ NMR chemical shift, e.g. **33** ($\delta_P + 599.6$).[45,46] The shift originally reported by Yoshifuji *et al.* ($-59$ ppm)[44] was thus in an unanticipated region. The unusual shift prompted the interest of several workers who reported that the Yoshifuji *et al.* shift was in error and should be $+494$ ppm.[45,48–50] Our group reinvestigated the reaction of $(2,4,6\text{-}(Bu^t)_3C_6H_2)PCl_2$ with Mg in THF and found that it is not a straightforward reaction. Two other products are produced in addition to **32**: the diphosphine, **34**, and secondary phosphine, **35**.




**34**



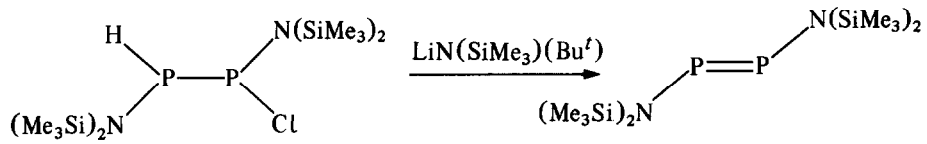

**35**

The isolation of **34** and **35** is suggestive of the intermediacy of free radicals. (The anion radical, $[ArP{=}PAr]^{\cdot-}$, has been produced by chemical or electrochemical reduction of **32**.)[49]

In view of the complexity of the $ArPCl_2$/Mg reaction, other preparations of ArP=PAr have been sought. Alternative routes which have been reported include (i) the dechlorination of $ArPCl_2$ with $(Me_3Si)_3SiLi$ or $Me_2Si(NBu^t)_2Sn$,[48] (ii) the coupling of $ArPCl_2$ with $(Me_3Si)_3CLi$,

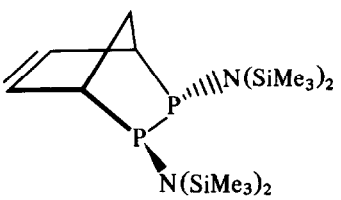
(iii) desulfurization of the trimer, $(ArPS)_3$ with $Ph_3P$[49], (iv) dehydrochloronation of a mixture of $(2,4,6\text{-}(Bu^t)_3C_6H_2)PH_2$ and $(2,4,6\text{-}(Bu^t)_3C_6H_2)PCl_2$.[51]

The amido-substituted diphosphene $(Me_3Si)_2NP{=}PN(SiMe_3)_2$, **36** has been prepared by Niecke and Rüger.[52] Red liquid **36** was prepared by dehydrochlorination of diphosphine **37**. As expected, due to the more modest bulk of the $(Me_3Si)_2N$ (compared with, e.g. $(Me_3Si)_3C$), compound **36**



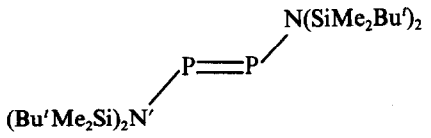

**37** **36**

dimerizes to the corresponding cyclotetraphosphine $[(Me_3Si)_2NP]_4$. Diphosphene **36** is conveniently stored as the cyclopentadiene adduct, **38**, but can be reobtained above 40°C as the retro Diels–Alder product.

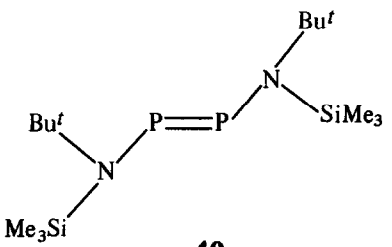



**38**

Since then, Niecke *et al.*[53] have reported that **36** and two additional diphosphenes, **39** and **40**, can be prepared by treatment of the appropriate lithium amide, $R_1R_2NLi$, with the sequence of reagents (i) $PCl_3$, (ii) $LiAlH_4$, (iii) $Et_3N$. As might be expected, the tendency toward dimerization




**39**

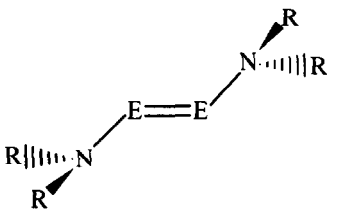



**40**

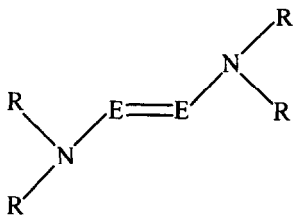
P–P = 2.034; P–N = 1.769 Å
∠NPP = 102.2°

decreases in the order **36** > **40** > **39**. In fact, **39** was sufficiently thermally stable to permit an X-ray crystal structure determination. Interestingly, **39** adopts an almost bisorthogonal comformation, **A**. By contrast, the isovalent molecule, $(Me_3Si)_2N{-}N{=}N{-}N(SiMe_3)_2$ adopts the coplanar conformation **B**.[54] Repulsion between the nitrogen and phosphorus lone pairs is presumably responsible for

the unusually long P–N bond length (1.769 Å) in **39**. MO calculations[53] on the parent compound $(H_2N)P{=}P(NH_2)$ indicate that conformation **B** is more stable than conformation **A** by 53 kJ/mol.

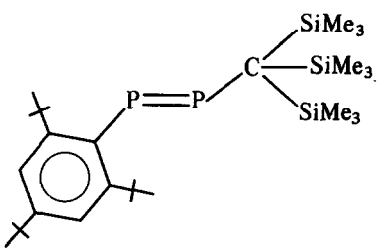


**A**



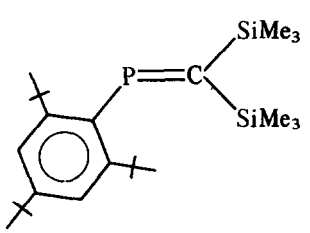
**B**

Diphosphene **41**, the first unsymmetrically-substituted compound featuring multiple bonding between the heavier main-group elements, was synthesized[56] by the action of sodium naphthalenide

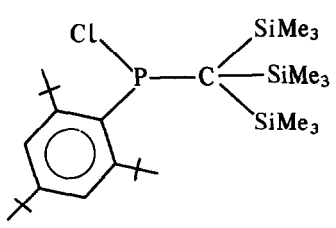


**41**

on a 2 : 1 mixture of $(Me_3Si)_3CPCl_2$ and $(2,4,6\text{-}(Bu^t)_3C_6H_2)PCl_2$ in THF at $-78°C$. The yields of **41** were only modest ($\sim 20\%$) because of the concomitant production of the symmetrical diphosphenes **32** and **33**. Moreover, **41** is not as stable as its symmetrical counterparts **32** and **33** and undergoes decomposition in $\sim 2$ days at ambient temperature to afford $(2,4,6\text{-}(Bu^t)_3C_6H_2)PH_2$ as the major product. Interestingly, the reaction of $(Me_3Si)_3CPCl_2/(2,4,6\text{-}(Bu^t)_3C_6H_2)PCl_2$ mixtures with $(Me_3Si)_3CLi$ does not produce **41**, but the phosphaalkene, **42**. Presumably, **42** arises via $Me_3SiCl$ elimination from **43**.

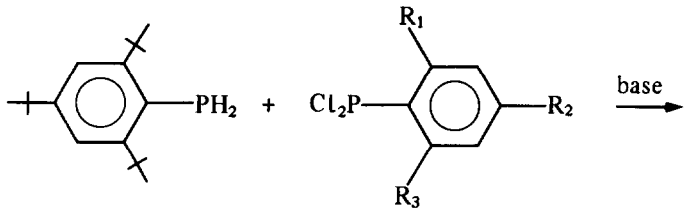


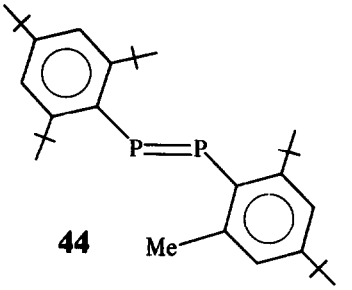
**42**



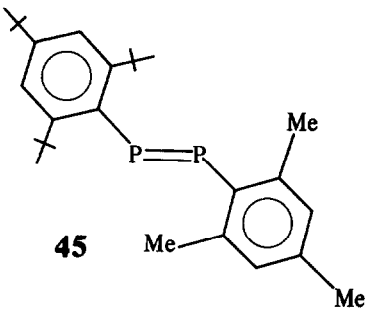
**43**

Yoshifuji *et al.*[56] have also reported the synthesis of unsymmetrical disphosphenes (**44–46**) but by a different route, viz. a primary phosphine and a dichlorophosphine (a route which is also viable for the synthesis of the symmetrical diphosphene, **32**). As expected, diphosphene **46** was the least stable of the three since it involves the smallest steric blockade.

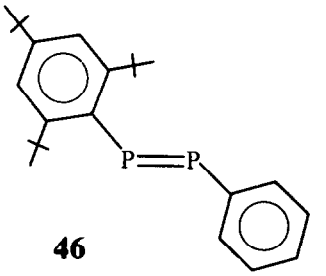



**44**

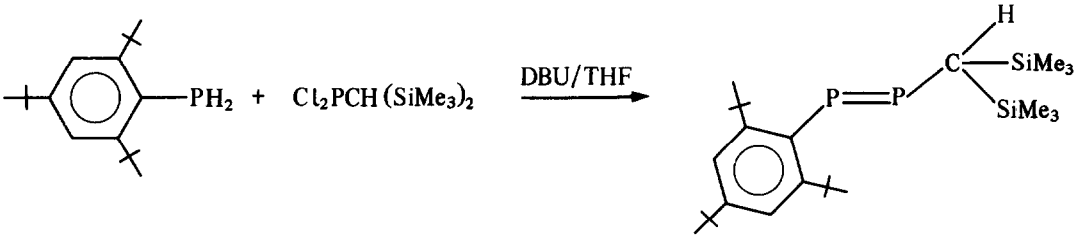



**45**



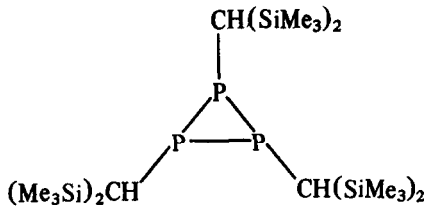

**46**

Independently, we have used the base-induced phosphine/dichlorophosphine coupling methodology to prepare the unsymmetrical diphosphene, **47**.[57]

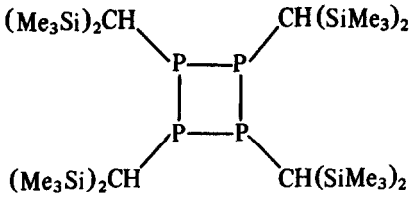



**47**

In our hands, the choice of base is critical and only DBU (1,5-diazabicyclo[5.4.0]undec-5-ene) functions satisfactorily. Interestingly, the reaction of $(2,4,6\text{-}(Bu^t)_3C_6H_2)PH_2$ with $((Me_3Si)_3CPCl_2$ in the presence of DBU results in **47** rather than **41**. Although we do not have any specific evidence on this point, we presume that the initially formed **41** is converted to **47** via $Cl^-$ attack on a $Me_3Si$ group followed by protonation of the resulting carbanion. Although it is possible to isolate a diphosphene with one $(Me_3Si)_2CH$ group, this moiety is not sufficiently bulky to permit isolation of the symmetrical diphosphene, $(Me_3Si)_2CHP{=}PCH(SiMe_3)_2$, since the reaction of $(Me_3Si)_2CHPCl_2$ with Mg or sodium naphthalenide in THF results in a mixture of the oligomerized products **48** and **49**.

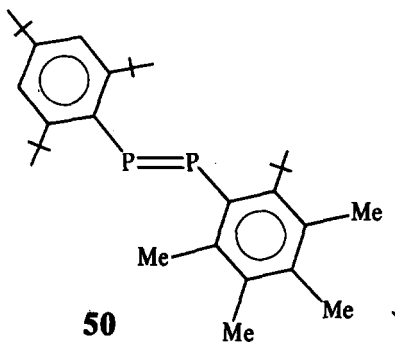


48

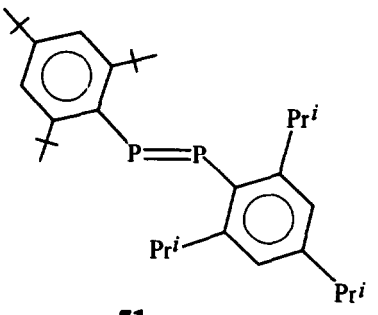


49

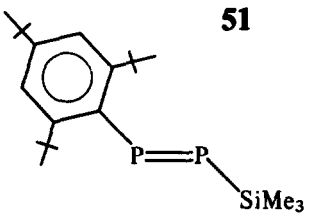
Unsymmetrical diphosphenes have also been reported more recently by two groups. Bickelhaupt *et al.*[58] prepared **45**, **50**, **51** and **52** using the Mg coupling of the respective dichlorides



50

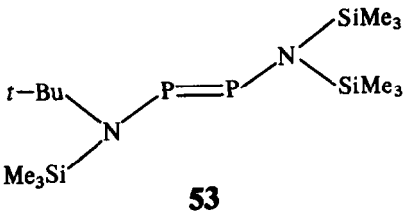


51



52

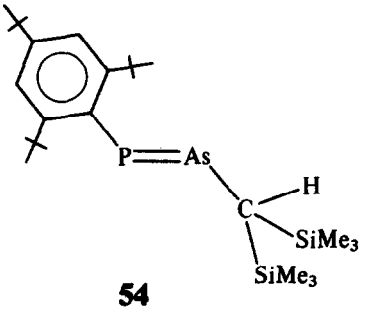
while Niecke *et al.*[53] discovered that treatment of a mixture of the lithium amides $(Me_3Si)_2NLi$ and $(Bu^t)(Me_3Si)NLi$ with (i) $PCl_3$, (ii) $LiAlH_4$, (iii) $Et_3N$ produced **53**.



53

5. *Phospha-arsenes and phosphastibenes* (RP=AsR *and* RP=SbR)

It was recognized that the dehydrochlorination approach might make available the first compounds with heteronuclear double bonding between the heavier main-group elements. Indeed, the reaction of $(2,4,6\text{-}(Bu^t)_3C_6H_2)PH_2$ with $(Me_3Si)_2CHAsCl_2$ in THF in the presence of DBU affords the phospha-arsene, **54**, as a stable orange crystalline material[59]



54

The phospha-arsene exhibits a low-field $^{31}P$ NMR chemical shift (+575 ppm), a feature also characteristic of diphosphenes. An X-ray crystal structure of **54** (Fig. 2) reveals that, like diphosphenes, the phospha-arsene adopts a *trans* planar structure (mean deviation of the central atoms, C(01), As(1), P(1), and C(1), 0.10(7) Å). The P–As distance in **54** is 2.124(2) Å. This distance

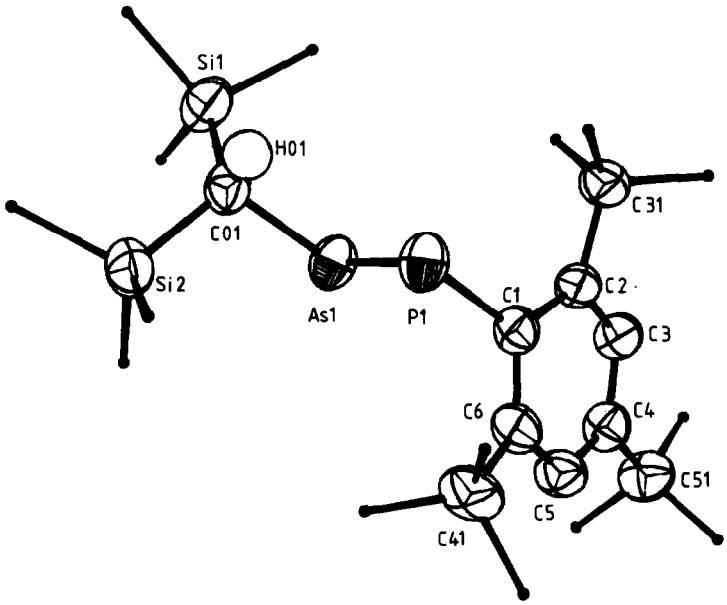
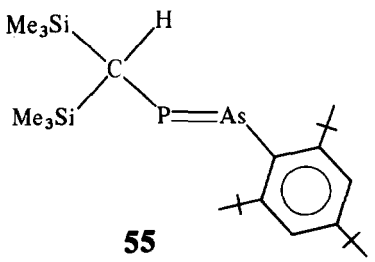


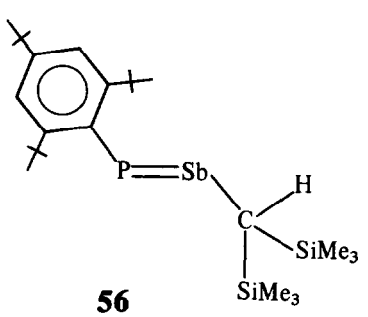

Fig. 2. View of the $\{2,4,6\text{-}(Bu^t)_3C_6H_2\}P{=}AsCH(SiMe_3)_2$ (**54**) molecule showing the atom numbering scheme. Important parameters: As(1)–P(1) 2.124(2), As(1)–C(01) 1.995(5), P(1)–C(1) 1.847(5) Å; C(01)–As(1)–P(1) 101.2(2), As(1)–P(1)–C(1) 96.4(2)°.

is close to the sum of double-bond covalent radii of P and As (2.11 Å)[41] and thus consistent with some double bond character. The bond angle at phosphorus in **54** (96.4(2)°) is much smaller than that in **32** (102.8(1)°) due to (i) replacement of a $2,4,6\text{-}(Bu^t)_3C_6H_2$ group by a less sterically demanding $(Me_3Si)_2CH$ group, and (ii) the longer central bond. Subsequently, the availability of $(2,4,6\text{-}(Bu^t)_3C_6H_2)AsH_2$ (*vide infra*) has permitted the synthesis of **55** via a DBU-induced coupling reaction with $(Me_3Si)_2CHPCl_2$




**55**

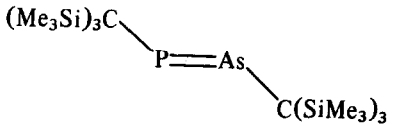
Extension of the above principles allowed us to synthesize the phosphastibene, **56**, via the reaction of $(2,4,6\text{-}(Bu^t)_3C_6H_2)PH_2$ with $(Me_3Si)_2CHSbCl_2$.[59] The phosphastibene, which exhibits a




**56**

very low-field $^{31}P$ NMR chemical shift (+620.0 ppm) is significantly less stable than the corresponding phospha–arsene and in solution undergoes decomposition to the symmetrical diphosphene, in approx. 2 hr at ambient temperature. This decomposition reaction can be followed by $^{31}P$ NMR and we are following up on the implication that **56** might represent a source of free phosphinidene, $(2,4,6\text{-}(t\text{-}Bu)_3C_6H_2)_2P$.

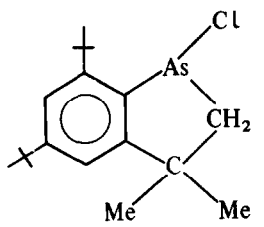
Escudié *et al.*[60] have independently synthesized phospha-arsene, **57**, by Bu$^t$Li coupling of a mixture of $(Me_3Si)_3CPCl_2$ and $(Me_3Si)_3CAsCl_2$.




**57**

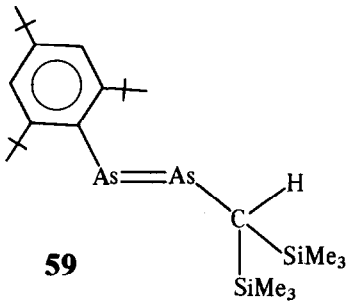
6. *Diarsenes* (RAs=AsR)

Our initial approach to the synthesis of a diarsene was frustrated by the fact that the reaction of $2,4,6\text{-}(Bu^t)_3C_6H_2Li$ with one equivalent of $AsCl_3$ in THF at −78°C afforded the heterocycle **58**[61] rather than $\{2,4,6\text{-}(Bu^t)_3C_6H_2\}AsCl_2$ due to elimination of HCl. (A similar cyclization occurs upon thermolysis of $\{2,4,6\text{-}(Bu^t)_3C_6H_2\}PCl_2$.)[62]




**58**

The difluoroarsine, $\{2,4,6\text{-}(Bu^t)_3C_6H_2\}AsF_2$, can be isolated from the corresponding $AsF_3$ reaction. Unfortunately, $\{2,4,6\text{-}(Bu^t)_3C_6H_2\}AsF_2$ fails to yield a diarsene upon treatment with sodium naphthalenide. However, $LiAlH_4$ reduction of the difluoroarsine affords $\{2,4,6\text{-}(Bu^t)_3C_6H_2\}AsH_2$ and treatment of the latter with $(Me_3Si)_2CHAsCl_2$ in THF at −78°C using a 5% excess of DBU produced the orange crystalline diarsene, **59**.[61] An X-ray diffraction study (Fig. 3) indicates that,




**59**

like the lighter congeneric diphosphenes, the diarsene **59** adopts a *trans* geometry and that the C–As–As–C skeleton is planar within experimental error (0.017 Å). The arsenic–arsenic bond length in **59** (2.224(2) Å) is considerably shorter than the As–As single-bond length (2.43–2.46 Å),[63] but close to the sum of double-bond covalent radii (2.22 Å).[41] The bond angles in diarsene **59** (99.9(3)° at As(1) and 93.6(3)° at As(2)) are significantly smaller than the range found for diphosphenes. Such an angle decrease is anticipated however due to lengthening of the central bond and to the increased valence p character in As bonds compared with P bonds.

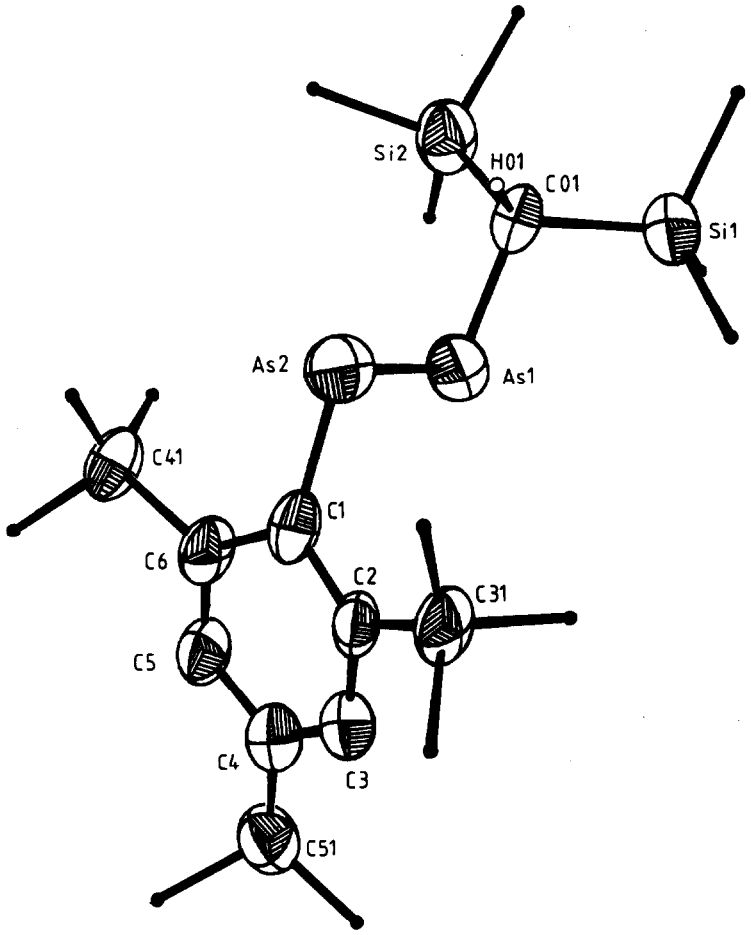
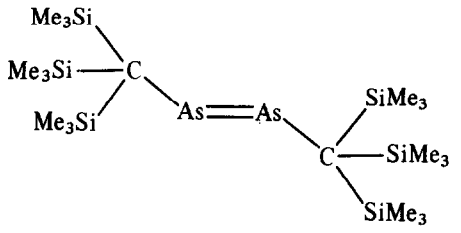



Fig. 3. View of the $\{2,4,6\text{-}(Bu^t)_3C_6H_2\}As{=}AsCH(SiMe_3)_2$ (**59**) molecule showing the atom numbering scheme. Important parameters: As(1)–As(2) 2.224(2), As(1)–C(01) 1.976(10), As(2)–C(1) 1.946(10) Å; As(2)–As(1)–C(01) 99.9(3), As(1)–As(2)–C(1) 93.6(3)°.

Couret *et al.*[64] have independently reported the synthesis of a diarsene (**60**) via Bu$^t$Li coupling of the new chloroarsine, $(Me_3Si)_3CAsCl_2$.




**60**

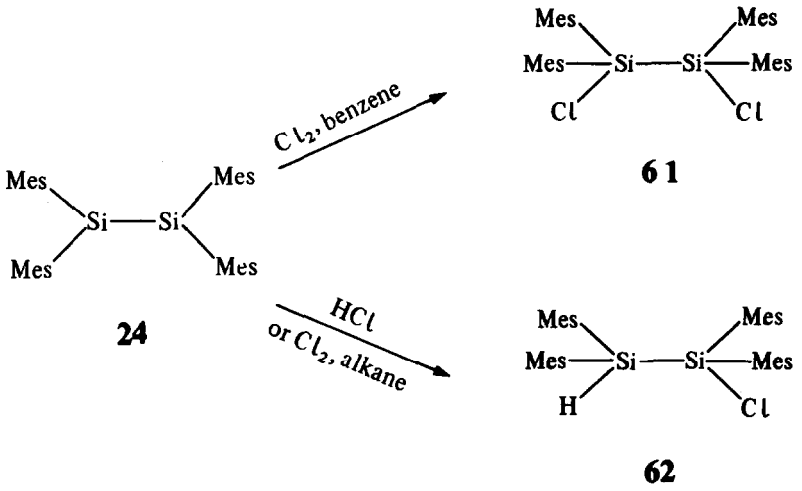
## IV. REACTIVITIES OF DOUBLE-BONDED MOLECULES

The reactions of transient molecules were dealt with in Section II. The present section is concerned with the reactivities of the kinetically stabilized species.

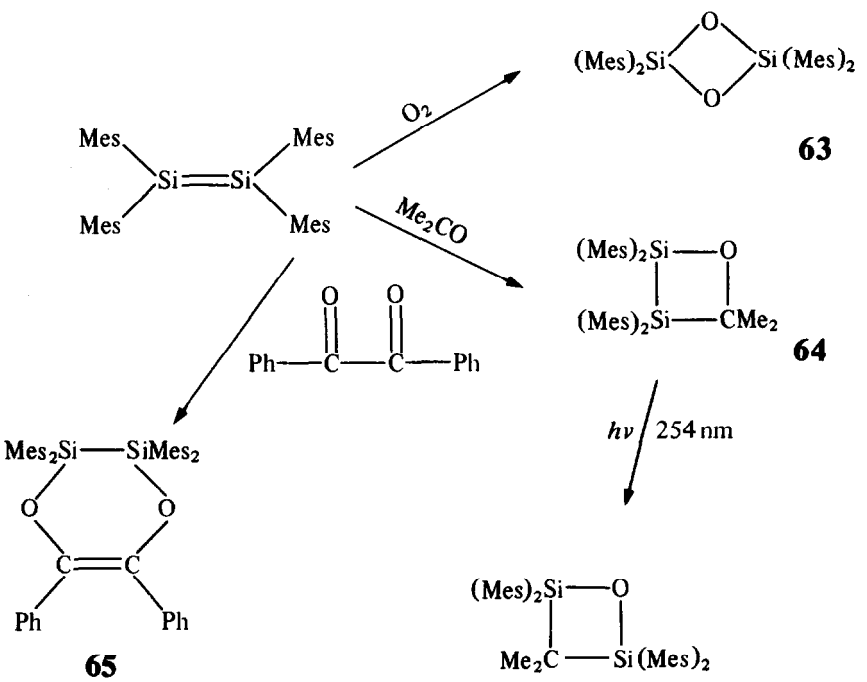
### 1. *Disilenes*

Given the fact that the electronegativity of silicon is less than that of carbon, the reactivity of disilenes is expected to resemble that of an electron rich olefin. Thus, it has been found[65] that tetramesityldisilene reacts with $Cl_2$ or HCl in benezene, to give the anticipated addition products

**61** and **62**, respectively. Likewise Masamune *et al.*[35] have found that tetrakis 2,6-dimethylphenyl)-disilene reacts with $Br_2$ to afford the corresponding dibromide.

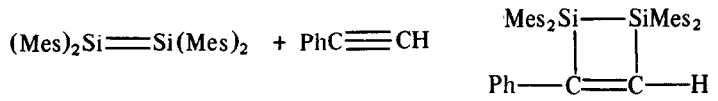



Interestingly, the reaction of **24** with $Cl_2$ in hydrocarbon solvents results in the HCl rather than the $Cl_2$ addition product. A radical-chain mechanism has been suggested to explain this observation. Unlike normal olefins, **24** reacts readily with alcohols[36,65] and water[65] to afford the adducts, $(Mes)_2Si(OR)SiH(Mes)_2$(R = Alkyl, H). The oxophilicity of silicon is also apparent in the addition reactions of **24** with $O_2$, acetone, and benzil which results in cyclic compounds **63**, **64** and **65** respectively.[65]




An X-ray crystal structure of **63**[66] revealed an unusually short silicon–silicon distance (2.31 Å) and an acute bond angle at oxygen (86°). Disilenes **28** and **29** also react with oxygen to give 1,3 cyclodisiloxanes analogous to **63**[38] Photolysis of the acetone adduct, **64**, causes rearrangement to the 1,3 isomer. It is possible that this rearrangement involves the intermediacy of $(Mes)_2Si{=}O$ and $(Mes)_2Si{=}CMe_2$ which undergo closure in the opposite sense. Support for this argument is provided by trapping experiments.

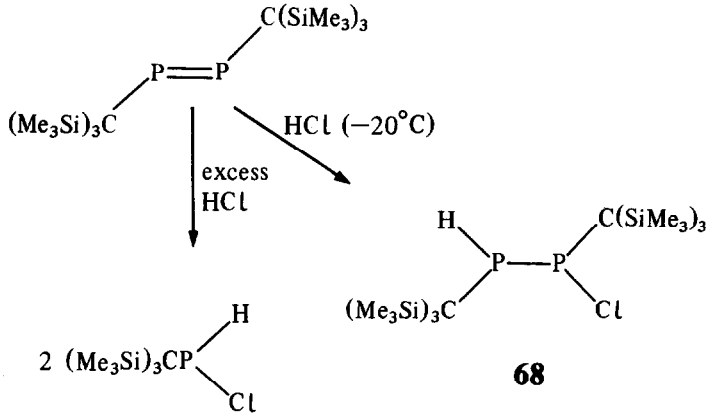
The steric bulk of the mesityl ligand is presumably responsible for the fact that **24** is unreactive toward anthracene, 2,3-dimethyl-1,3-butadiene, 1,4-diphenyl-1,3-butadiene, and phenyl(trimethylsilyl)acetylene since, as pointed out earlier, molecules such as these are employed as traps for transient disilenes such as $Me_2Si{=}SiMe_2$. However, **24** will, in fact react with phenylacetylene to give the disilacyclobutene, **66**.[65]




**66**

2. *Diphosphenes, phospha-arsenes, and diarsenes*

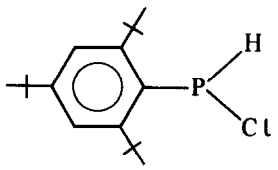
Like disilenes, the group 5A double-bonded compounds are reactive toward electrophiles. While much remains to be discovered, it is already clear that the reactivies of these compounds are rather dependent on ligand bulk and the length of the central double bond. These points can be illustrated by considering the reactions of $(Me_3Si)_3CP{=}PC(SiMe_3)_3$ (**33**) and $\{2,4,6\text{-}(Bu^t)_3C_6H_2\}P{=}P\{2,4,6\text{-}(Bu^t)_3C_6H_2\}$ (**32**) with HCl and $HBF_4 \cdot Et_2O$. In the case of **33** it is possible, using a stoichiometric quantity of HCl in $Et_2O$ at $-20°C$ to isolate **68**, the product of addition of HCl across a phosphorus-phosphorus double bond.[47] An excess of HCl at ambient temperature results in cleavage of the phosphorus–phosphorus double bond and formation of **67**. By contrast, it was not possible to isolate an addition product analogous to **68** when **32** was treated with a




**68**

**67**

stoichiometric quantity of HCl at low temperature. Instead, P=P cleavage was observed, resulting in **69**.

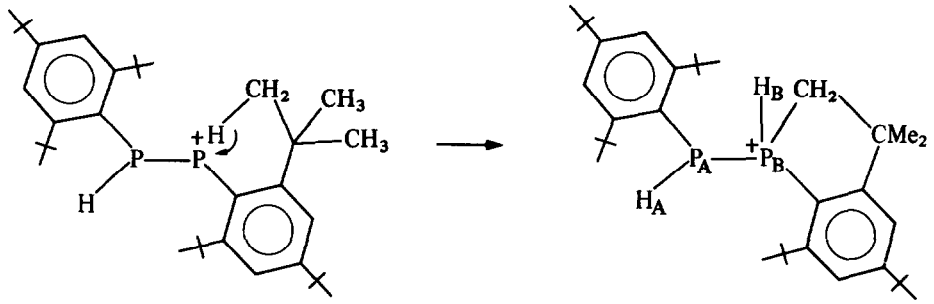



**69**

Phosphines of the type RP(H)(halogen) are remarkable because normally uncoordinated compounds of this type undergo facile dehydrohalogenation to $(RP)_n$ oligomers.

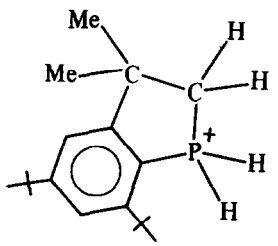
Differences of reactivity of **32** and **33** were also clear form protonation experiments using $HBF_4 \cdot Et_2O$. Treatment of **33** with excess $HBF_4 \cdot Et_2O$ results in the phosphonium salt

$[(Me_3Si)_3CPH_3][BF_4]$. On the other hand, treatment of **32** with excess $HBF_4 \cdot Et_2O$ results in a product which is formulated as the phosphonium salt, **70** on the basis of $^{31}P\{^1H\}$ NMR evidence.[47] It is proposed that the formation of **70** results from an intermediate, **71**, formed by initial



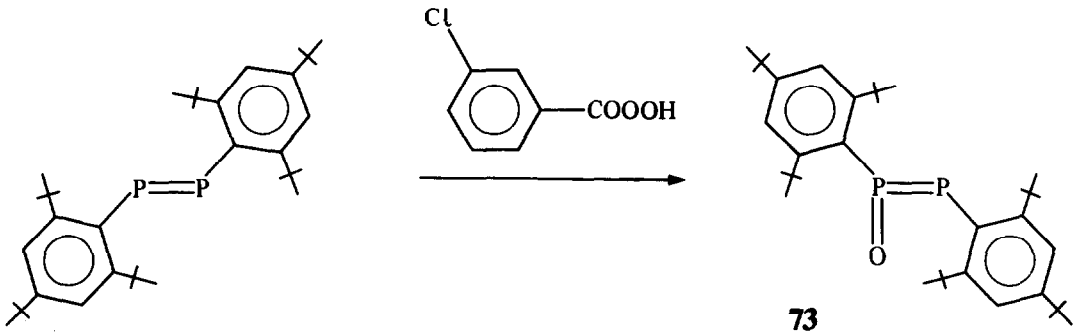
**71** **70**

protonation of **32** and containing a two-coordinate phosphenium cation. This cationic center inserts into a methyl C–H bond of an ortho Bu$^t$ group of the aryl ligand by an intramolecular oxidative addition reaction similar to that observed for other phosphenium ions.[67] When the solution of **32** and $HBF_4$ etherate containing **70** is allowed to warm to room temperature a single new product, **72**, is observed.



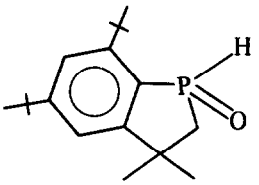
**72**

There is a lively interest in the oxidation of diphosphenes. Thus, **32** reacts with *m*-chloroperbenzoic acid to yield the diphosphene monoxide, **73**, as the initial product.[68] While **73** is not isolable from this particular reaction, it is possible to isolate this material from the

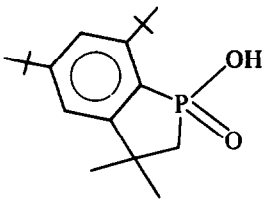


**73**

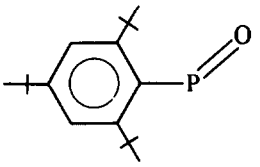
ultrasonic-assisted reaction of $\{2,4,6\text{-}(t\text{-}Bu)_3C_6H_2\}P(0)Cl_2$ with Mg in THF.[68] Photolytic oxidation of **32** in THF results in the known[62] bicyclic compounds **74** and **75** in 90% and 10% yields, respectively.[69] It is believed that **74** and **75** arise via intramolecular C–H insertion reactions of **76** and **77**, respectively.



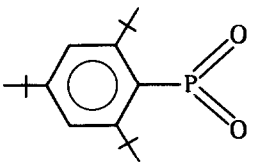
74



75

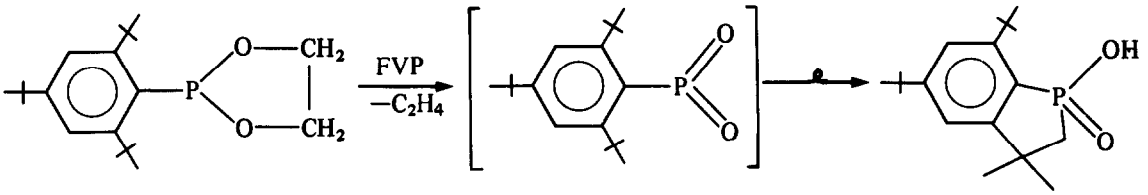


76



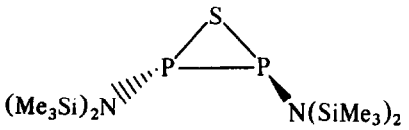
77

Support for this suggestion is provided by the fact that flash vacuum pyrolysis[69] of **78** affords **75**, a reaction that may imply the intermediacy of the metaphosphonate, **77**, viz.

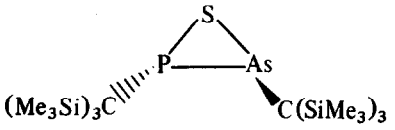


78 77 75

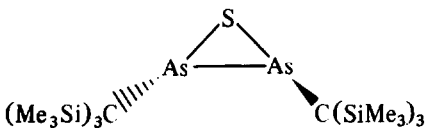
Examples of the formation of thiirans from the addition of elemental sulfur to the respective double-bonded compounds are provided by **79**,[52] **80**,[60] and **81**.[64]



79

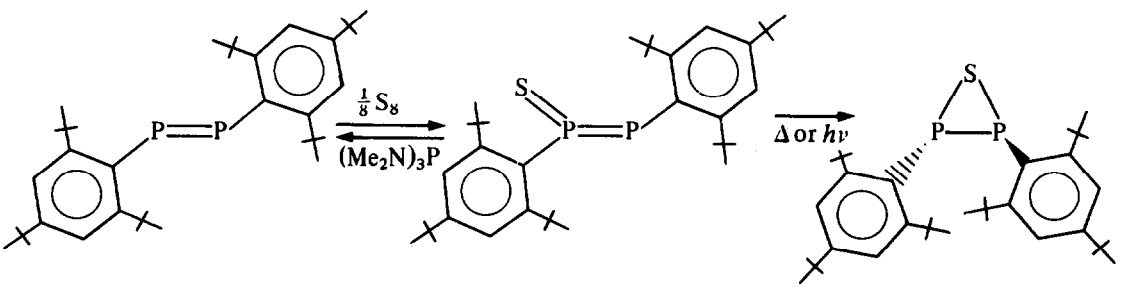


80



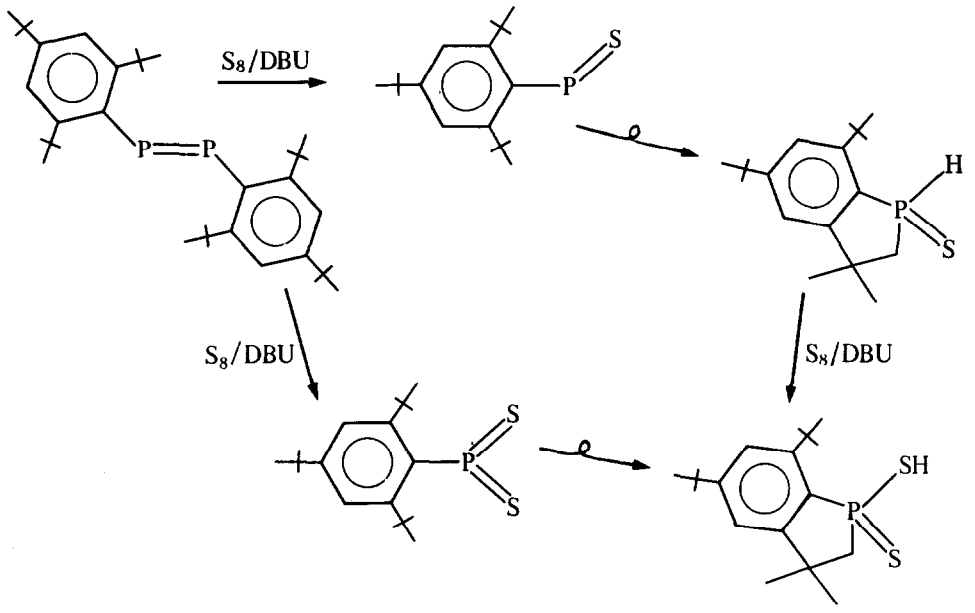
81

The sulfurization of **32** in $Et_3N$ is particularly interesting since it leads to the diphosphene monosulfide, **82**, rather than the thiiran.[70] The thiiran, **83**, can, however, be formed by heating or



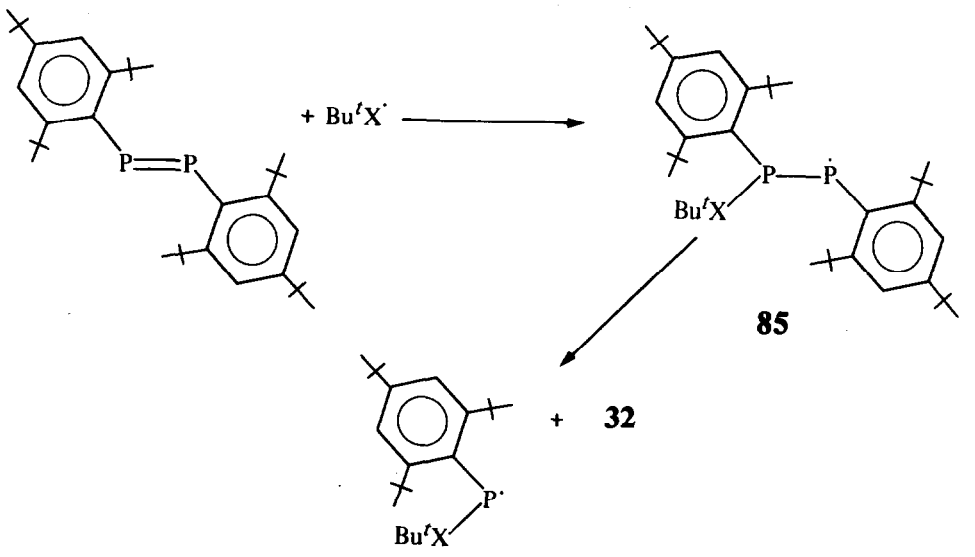
32 82 83

irradiating **82**. Interestingly, the diphosphene monosulfide, **82**, can be desulfurized with $(Me_2N)_3P$ whereas the thiiran, **83**, cannot. X-Ray crystallographic studies have demonstrated that the P–P bond orders in **82** (2.054(2)) Å[70] and **83** (2.249(3)) Å[71] are approx. 2 and 1 respectively. When **32** is treated with an excess of elemental sulfur in the presence of DBU in refluxing toluene, cleavage of the double bond occurs.[72] The isolated product, **84**, could arise via either of the pathways suggested below




**84**

Further examples of the reactivity of diphosphenes toward electrophiles is provided by the reaction of **32** with Bu$^t$O$^\cdot$ and Bu$^t$S$^\cdot$ radicals which results in novel phosphinyl radicals, **85** and **86**, respectively.[73]

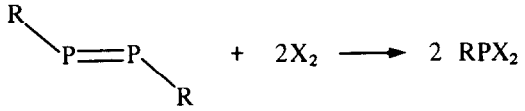



**85**

**86**

One electrophilic reaction that differentiates disilenes from diphosphenes is halogenation. As pointed out earlier, it is possible to add halogens across the Si=Si bond in a manner reminiscent

of alkenes. However, in the case of diphosphenes all halogenations reported thus far results in double bond cleavage.[44]



R = 2,4,6−$(Bu^t)_3C_6H_2$, $(Me_3Si)_3C$
X = Cl

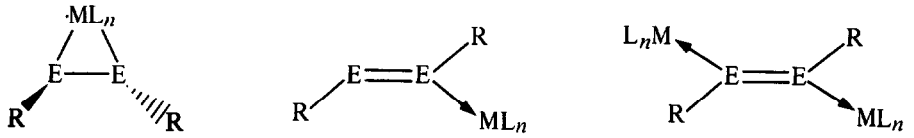
Diphosphenes and diarsenes are expected to be reactive toward alkenes, dienes and alkynes. However, so far the only example of this type of reaction is the production of the amido-substituted diphosphene, **36**, with cyclopentadiene monomer to produce **38**.[52]

MO calculations on the model diphosphene, HP=PH (*vide infra*), reveal the existence of a low-lying LUMO. Moreover, a cyclic voltammetry experiment on diphosphene **32** shows a reversible one-electron reduction at $E_{\frac{1}{2}} = -1.74$ V,[49] suggesting that diphosphenes should undergo facile reduction. In fact, **32** reacts with sodium naphthalenide in THF to produce the anion radical $[\{2,4,6\text{-}(Bu^t)_3C_6H_2\}_2P_2]^-$ (the same anion radical is also detectable in the magnesium coupling of $\{2,4,6\text{ - }(Bu^t)_3C_6H_2\}PCl_2$).[49]

## V. COORDINATION CHEMISTRY OF DOUBLE-BONDED COMPOUNDS

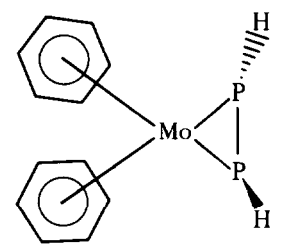
Even though the group IVA double bonded compounds are potentially capable of acting as $\eta^2$ ligands, so far there have been no reports of the reactions of disilenes or digermenes with organometallic reagents.

Several modes of coordination are possible for the Group 5A double-bonded compounds including $\eta^2$ (Type I), $\eta^1$ (Type II), or bis-$\eta^1$ (Type III). All three types of coordination behavior (and combinations of these) have now been recognized.



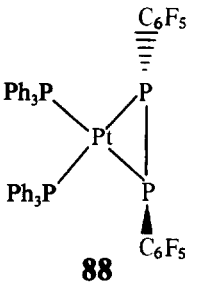
Type I Type II Type III

Thus far, the most common diphosphene complex is of Type I. Interestingly, **87** which is a complex of the parent diphosphene, HP=PH, was prepared by the reaction of $(\eta^5\text{-}C_5H_5)_2MoH_2$ with white phosphorus.[74]



**87**

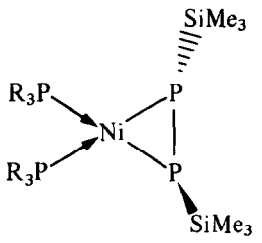
P−P=2.14 Å
∠ P−Mo−P=49.9; ∠ P−P−Mo=65.1°



**88**

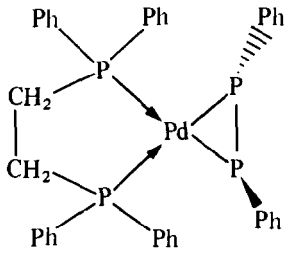
P−P=2.156(7) Å
∠ P−Pt−P=54.8(2)
∠ P−P−Pt=61.5 (2), 63.6 (2)°

The $\eta^2$ coordination geometry was confirmed by a subsequent X-ray diffraction study.[75] The perfluorophenyl compound **88** was isolated from the reaction of the cyclotetraphosphine, $(C_6F_5P)_4$ with $(Ph_3P)_3Pt$[76] and the $\eta^2$ silylated derivative, **89** was isolated from a complex condensation reaction of the labile bis(phosphido) complex $(Me_3P)_2Ni[P(SiMe_3)_2]_2$.[77] A more general route to $\eta^2$




R=Me,Et,Bu$^n$ **89**

R=Me: P—P=2.149(2)Å
∠ P—Ni—P=57.13(5)
∠ P—P—Ni=60.93(6), 61.95(7)°

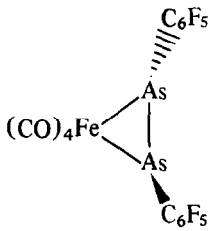



**90**

P—P=2.121(4)Å

diphosphene complexes has been reported recently.[78] The method involves treatment of the dilithium salt, $Li_2(PhPPPh)$ with *cis*-$[MCl_2L_2]$ in THF solution (M = Pt, $L_2 = Ph_3P$ or $Ph_2P(CH_2)_2PPh_2$; M = Pd, $L_2 = Ph_2P(CH_2)_2PPh_2$). The structure of the palladium derivative, **90**, has been determined by single-crystal X-ray diffraction.[78]

Two examples of $\eta^2$ diarsene coordination are known, $(C_6F_5AsAsC_6F_5)Fe(CO)_4$ (**91**) and $(C_6F_5AsAsC_6F_5)Pt(PPh_3)_2$ (**92**).[79] These compounds were synthesized via the reaction of the cyclotetraarsine, $(C_6F_5As)_4$, with $Fe(CO)_5$ and $(Ph_3P)_3Pt$, respectively.

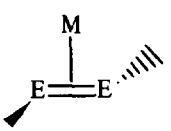



**91**

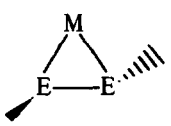
As—As=2.388(7) Å,
∠ As—Fe—As=56.8(3),
∠ Fe—As—As=61.6(1)°

In each of the complexes, **87–91**, the diphosphene or diarsene ligand adopts a *trans* conformation. The P–P bond lengths in the $\eta^2$ complexes **87–91** ( ~ 2.12–2.16 Å) fall between the values of ~ 2.2 reported for P–P single bonds[80] and the value of ~ 2.0 Å measured for the unsupported phosphorus–phosphorus double bonds in the diphosphenes **32**,[44] **33**,[46,47] and **39**.[53] Likewise, the As–As bond length in **91** falls between the range of 2.43–2.46 Å reported for arsenic–arsenic single bonds[63] and that of the arsenic–arsenic double bond length in **59**. Alkenes[81] and phospha-alkenes[82] undergo comparable increases of C=C or P=C bond length upon $\eta^2$ ligation.

In valence bond terminology, the bonding in **87–92** can be described as a resonance hybrid of $\pi$-bonded (**I**) and metallacyclic (**II**) canonical forms.



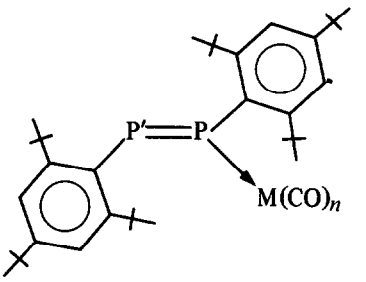

**I**




**II**

From a molecular orbital standpoint, the bonding in $\eta^2$ complexes is probably best represented as a dative $\pi$ interaction. For example, calculations on the model complex $Ni(PH_3)_2(C_2H_4)$ have revealed that the major contributor to ethene bonding is back donation from a filled Ni 3d AO to the vacant olefinic $\pi^*$ MO.[83] Since MO calculations on HP=PH (*vide infra*) indicate the existence of a low-lying $\pi^*$ MO, it seems reasonable to suggest retro $\pi$-bonding as the primary interaction in $\eta^2$ diphosphene and diarsene complexes.

The diphosphene **32** reacts with $Ni(CO)_4$ or $Fe_2(CO)_9$ to afford the Type II ($\eta^1$) complexes, **93**.[84] The X-ray structure of the iron complex, **93b**, (Fig. 4) reveals a P–P bond length of 2.050(1) Å which corresponds to a double bond. Furthermore, within experimental error the $C_2P_2Fe$ framework is planar. The P–P–C bond angles in **93b** are 6° wider than those in the free ligand, **32**. Steric crowding is also evidenced by the fact that the P(1)–C(1) bond is ~0.03 Å longer than the P(2)–C(7) bond.




**93a** M = Ni, $n = 3$
**93b** M = Fe, $n = 4$

P–P = 2.050(1), P–Fe = 2.215(1) Å
∠P–P'–C = 108.4(1), ∠P'–P–C = 109.3(1),
∠P'–P–Fe = 134.42(6)°

Steric crowding is also responsible for the observation that only one $Ni(CO)_3$ or $Fe(CO)_4$ unit attaches even when excess metal carbonyl is employed. In fact, the very bulky diphosphene, $(Me_3Si)_3CP{=}PC(SiMe_3)_3$ (**33**) fails to react with $Ni(CO)_4$ at 25°C.

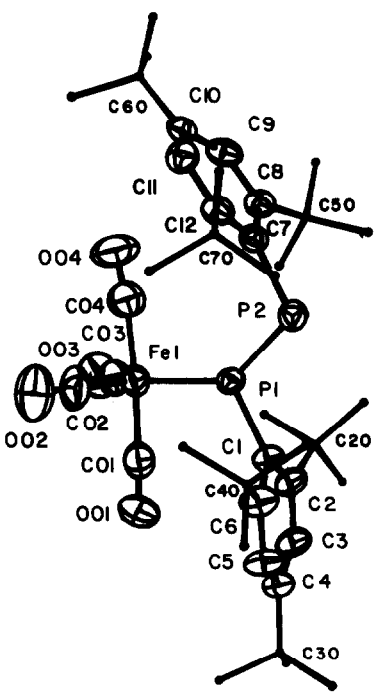
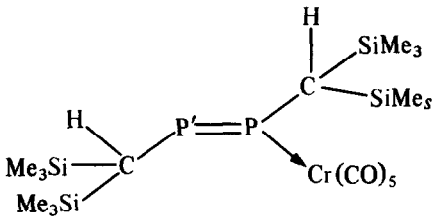



Fig. 4. View of the $\{2,4,6\text{-}(Bu^t)_3C_6H_2\}_2P_2Fe(CO)_4$ (**93b**) molecule showing the atom numbering scheme. Important parameters: P(1)–P(2) 2.050(1), P(1)–Fe(1) 2.215(1), P(1)–C(1) 1.893(4), P(2)–C(7) 1.859(4) Å; P(1)–P(2)–C(7) 108.4(1), P(2)–P(1)–Fe(1) 135.52(6), P(2)–P(1)–Fe(1) 135.52(6), P(2)–P(1)–C(1) 109.3(1), C(1)–P(1)–Fe(1)115.1(1)°.

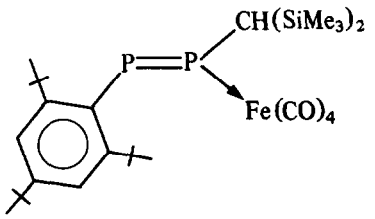
Power *et al.*[85] have independently prepared the Type II complex, **94**, via the reaction of $(Me_3Si)_2CHPCl_2$ with $[Cr(CO)_5]^{2-}$. It has also been found that the unsymmetrical diphosphene, **47**,



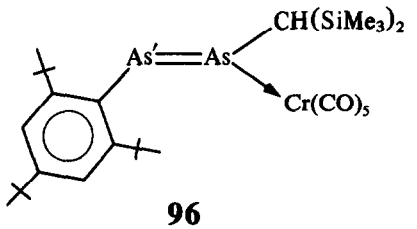

**94**

P–P = 2.027(3), P–Cr = 2.360(2) Å
∠P–P'–C = 105.9,(2) ∠P'–P–C = 105.6(2), ∠Cr–P–P' = 134.2(1)°

will react with $Fe_2(CO)_9$ to afford the $(Me_3Si)_2CH$-bound (Type II) complexes **95**.[84] An analogous Type II diarsene complex **96**, can likewise be prepared by treatment of the uncoordinated ligand, **59**, with $(THF)Cr(CO)_5$.[86] An X-ray crystal structure analysis of **96** (Fig. 5) reveals that the $C_2As_2Cr$



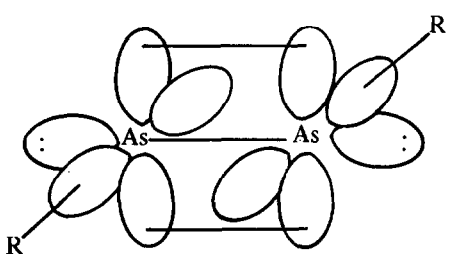

**95**



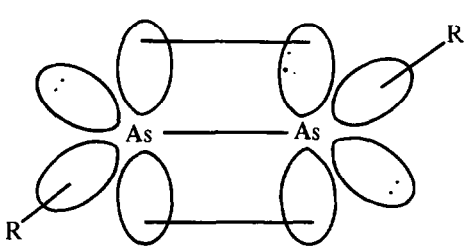

**96**

As–As = 2.246(1), As–Cr = 2.454(1) Å
∠ As'–As–C = 105.2(2), As–As'–C = 104.0(1), As'–As–Cr = 138.48(3)
∠ Cr–As–C = 116.3(2)°

framework is planar. All the skeletal bond lengths of **96** are longer than those of the uncoordinated diarsene **59** due to the steric demands of the $Cr(CO)_5$ group. However, the largest increase occurs at the arsenic–arsenic double bond ( ~ 0.02 Å). Interestingly, *both* C–As–As angles increase upon coordination. The bond angle increase at As(2) is not ascribable to steric effects and is presumably due to rehybridization of arsenic from approx. *sp*(III) to $sp^2$(IV).




III




IV

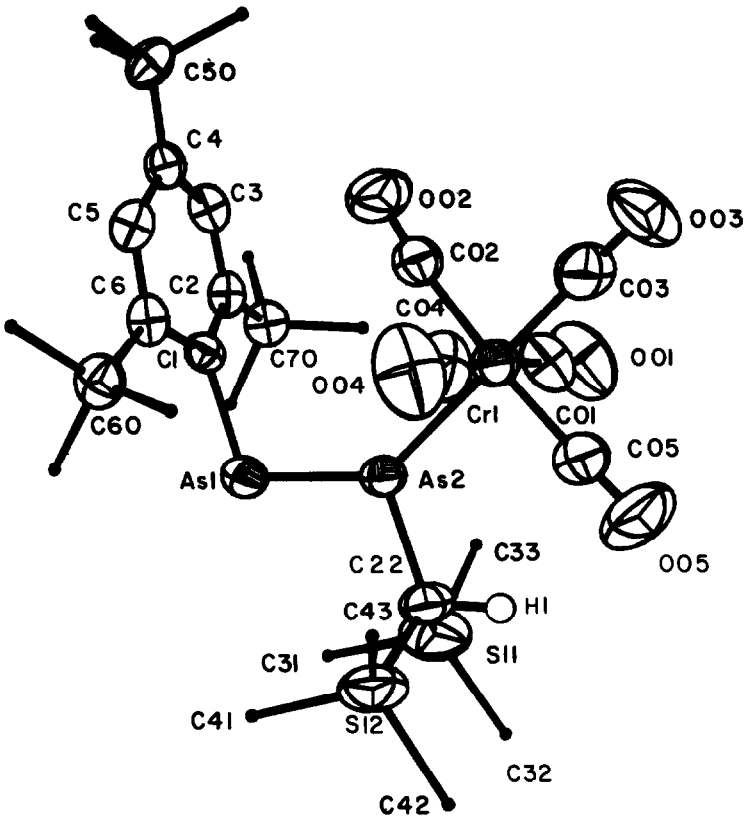
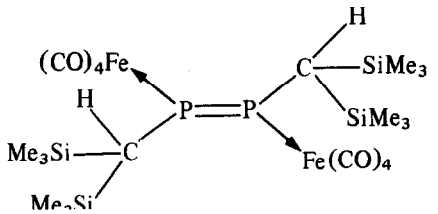



Fig. 5. View of the [{2,4,6 - $(Bu^t)_3(C_6H_2)$}As=AsCH$(SiMe_3)_2$]$Cr(CO)_5$ (**96**) molecule showing the atom numbering scheme. Important parameters: As(1)–As(2) 2.246(1), As(1)–C(1) 1.964(5), As(2)–C(22) 1.989(5), As(2)–Cr(1) 2.454(1) Å; As(2)–As(1)–C(1) 104.0(1), As(1)–As(2)–C(22) 105.2(2), As(1)–As(2)-Cr(1) 138.48(3), Cr(1)–As(2)–C(22) 116.3(2)°.

The only examples of a Type III complex, **97a,b** were prepared by Power *et al.*[87] via the reaction of $(Me_3Si)_2CHPCl_2$ or $(Me_3Si)_2NPCl_2$ with $Fe(CO)_4^{2-}$. The geometry at each phosphorus is planar and the phosphorus–phosphorus bond length of 2.038(1) Å is in the normal range for an unsupported double bond. Clearly, in Type II and Type III complexes, donation of the diphosphene or diarsene lone pair(s) to a transition metal leaves the E=E distance essentially unchanged. This view is supported by the fact that such complexes exhibit UV-visible spectra typical of the E=E chromophore, and the diphosphene or phospha-arsene complexes display characteristic low field $^{31}P$ chemical shifts.

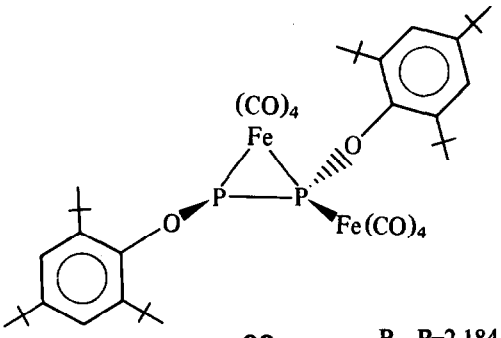



**97a**

P–P = 2.039(1), P–Fe = 2.226(1) Å
∠P–P–C = 107.1(1), ∠P–P–Fe = 126.6(1)°

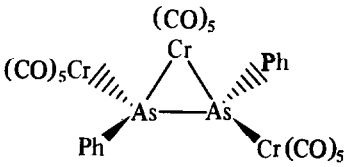
Combinations of Type I, II and III behavior become possible when (i) ligand bulk is reduced, (ii) the steric demands of the organometallic moiety are diminished, and (iii) the E=E bond length

is increased. Thus, treatment of $\{2,4,6\text{-}(Bu^t)_3C_6H_2O\}PCl_2$ with $Fe(CO)_4^{2-}$ results in **98**[85] which represents a combination of Type I and Type II coordination behavior. The diphosphene ligand maintains the *trans* conformation and the O–P–P–O and P–Fe–P planes are close to orthogonal. As expected, the P–P bond length (2.184(2) Å) is close to that observed for Type I complexes.




**98** P—P=2.184 (2) Å

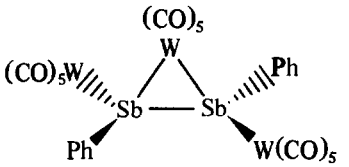
A diarsene complex exibiting a combination of Type I and Type III behavior, **99**, has been obtained[88] from the reaction of $PhAsCl_2$ with $Na_2[Cr_2(CO)_{10}]$ via the reaction of $(CO)_5CrAs(Ph)Li_2$




**99**

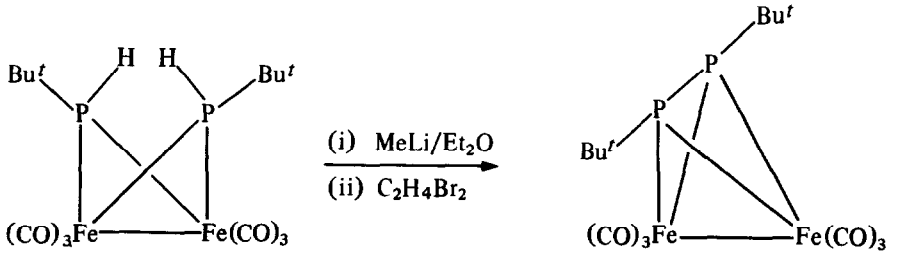
As—As = 2.371 Å

with $Cl_2(Ph)AsCr(CO)_5$. As expected, the arsenic–arsenic bond length is similar to that of the $\eta^2$ diarsene complex, **91**. The only known distibene derivative, **100**, was isolated from the reaction of $PhSbCl_2$ with $Na_2W_2(CO)_{10}$.[89]




**100**

One instance of six-electron donation by a diphosphene ligand has been reported recently.[90] The interesting derivative, **101**, which can be regarded as a tetrahedrane analogue, was prepared as indicated below:




**101**

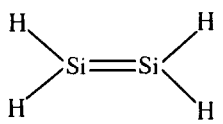
P—P = 2.059 (3), Fe—Fe = 2.740 (1) Å

A higher degree of clusterification has been reported by Power *et al.*[91] The novel derivative $[\{(Me_3Si)_2CHP{=}PCH(SiMe_3)_2\}_2Ni_5(CO)_6Cl]$ was isolated from the reaction of $(Me_3Si)_2CHPCl_2$ with $Na_2Ni_6(CO)_{12}$. Four of the five nickel atoms adopt a butterfly arrangement and one is bound to terminal carbonyls. Two additional carbonyls triply bridge the underside of each butterfly wing. The two diphosphene ligands (P–P = 2.085(4) and 2.098(4) Å) bridge two wingtips and hinge metal centers to the fifth nickel atom (which is also bonded to chlorine).

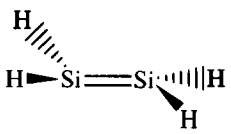
## VI. MOLECULAR ORBITAL CALCULATIONS ON DOUBLE BONDED COMPOUNDS

### 1. *Disilenes, digermenes and distannenes*

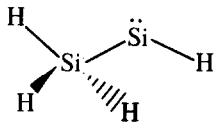
Significant interest has been generated in theoretical aspects of $Si_2H_4$. Much of the effort has been aimed at elucidation of the ground state of this molecule. By analogy with ethene, it might be thought that the planar structure, **102**, would be favored. However, some MO calculations indicated that the *trans*-bent conformation, **103**, is preferred. The silylsilylene structure, **104**, has also been considered partly because this species (rather than disilene) has been postulated[92] as an intermediate in the pyrolysis of trisilane. Moreover, as pointed out earlier, Barton *et al.*[14] have suggested the rearrangement of tetramethyldisilene into trimethylsilylmethylsilylene.



**102**



**103**



**104**

The first MO calculations on disilene were reported by Curtis[93] using CNDO and EHMO methods. Structure **102** and a silicon–silicon bond length of 2.20 Å were assumed. Two years later, Dewar *et al.*[94] reported that the MINDO/3 geometry-optimized structure was **102** with Si–Si = 2.023 Å and ∠H–Si–H = 111°. An FSGO calculation on disilene[95] indicated that the *trans*-bent structure, **103**, is the ground state. In the first *ab initio* (GAUSSIAN 70) calculation the planar structure **102** was assumed (with ∠H–Si–H = 120°) but with Si–Si optimized (2.1575 Å).[96] However, changing ∠H–Si–H by 2° resulted in an energy increase hence Daudel *et al.*[96] concluded that **102** did indeed represent the minimum. In another *ab initio* (POLYATOM) calculation[97] structure **102** with H–Si–H = 114.2 was assumed and Si–Si was optimized (2.15 Å). Using a 4–13G basis set, Snyder and Wasserman[98] found the silylsilylene structure, **104**, to be 8–9 kcal/mol more stable than the disilene structures **102** or **103**. These authors also concluded that the *trans*-bent forms (**103**) to be slightly more stable than the planar form (**102**). INDO-S calculations have since been performed using the Snyder and Wasserman optimized geometries.[99] Poirier and Goddard[100] also found the silylsilylene structure, **104**, to be favored by ~2 kcal/mol at the Hartree–Fock level. However, when correlation energy contributions were included, the order was reversed and the disilene structure became favored by 8–10 kcal/mol. Lischka and Köhler[101] found that when *d*-functions were included on silicon (Si[10*s*6*p*1*d*], H[3*s*]) the silylsilylene structure **104** was 8.0 kcal/mol more stable than the disilene structures. Using this same basis set, the *trans*-bent structure, **103** was very slightly favored (0.08 kcal/mole) over the planar structure. However, when additional polarization functions were employed (*d* on Si, *p* on H), the silylene–disilene energy gap decreased to 5.6 kcal/mol and **102** became more stable than **103** by 0.18 kcal/mol. Further calculations at the HF level by Krogh-Jespersen[102] revealed that the silylsilylene is 2–3 kcal/mol more stable than the *trans*-bent disilene. However, correlation energy corrections reversed this order, the best value for the **103**/**104** energy gap being 5.0 kcal/mol in favor of the *trans*-bent geometry. Planar disilene was not a local minimum at any calculational level employed. Calculational work on the heavier congeners, $Ge_2H_4$ and $Sn_2H_4$ is limited to one report. Lappert *et al.*[40c] concluded on the basis of SCF calculations that the *trans*-bent form represents the preferred geometry.

### 2. *Diphosphenes*

The first calculation on the parent diphosphene was performed by Issleib and Grundler[103] using the EHMO method. More recently *ab initio* calculations[56,104] have been reported on this molecule

and the results are summarized in Table 1. Regardless of the basis set employed, or whether configuration interaction is included, the *trans* isomer is more stable than *cis* by 3–5 kcal/mol. Note that the most satisfactory agreement between the computed bond length for *trans*-$P_2H_2$ and that observed for the sterically encumbered diphosphenes occurs when the 44–31G* and 6–31G** basis sets are employed, i.e. phosphorus *d*-type functions are included. As anticipated, the PPC bond angles in the bulky diphosphenes **32**, **33** and **39** are longer than those in *trans*-$P_2H_2$ due to steric effects.

Attention is now turned to the MO's of *trans*-$P_2H_2$. The $2b_g$ MO is the LUMO and possesses appreciable P–P $\pi^*$ character. The calculation of a low-lying LUMO (+ 0.24 eV) is consistent with the observation that **32** undergoes facile one-electron reduction to the anion radical[49] and supports the postulate of metal $nd$–$\pi^*$ back donation in the $\eta^2$ bonding of diphosphenes (and heavier congeners) to transition metals. The two highest occupied MO's $2a_u$ (−9.72 eV) and $7a_g$ (−9.92 eV) are closely spaced and correspond to the P–P $\pi$-bond and $n_+$ phosphorus lone pair combination respectively (Fig. 6). *Xα* scattered-wave calculations,[105] on *trans*-$P_2H_4$, on the other hand, reverse the order of the $7a_g$ (− 6.41 eV) and $2a_u$ (− 6.55 eV) MO's. The conclusion that the $n_+$ lone pair combination represents the HOMO is supported by UV PES data for **32**[49,106] and **33**.[106]

Table 1. Summary of *ab initio* results on diphosphene

| | STO-3G[a] | 44-31G[a,b] | 44-31G(CI)[b] | 44-31G*[a,b] |
|---|---|---|---|---|
| | | Trans | | |
| P–P | 1.961 | 2.121 | 2.187 | 1.992 |
| P–H | 1.387 | 1.444 | 1.469 | 1.415 |
| ∠PPH | 95.9 | 95.4 | 93.9 | 95.3 |
| $E_T$ | -674.9227 | -681.7413 | -681.90186 | -681.85935 |
| | | Cis | | |
| P–P | 1.964 | 2.122 | 2.191 | 1.9974 |
| P–H | 1.387 | 1.445 | 1.470 | 1.4123 |
| ∠PPH | 99.7 | 100.4 | 98.9 | 100.4 |
| $E_T$ | -674.9166 | -681.73705 | -681.89744 | -681.85356 |
| | | $\Delta_E$ = 2.77 kcal/mol | | $\Delta_E$ = 3.63 kcal/mol |

| | 6-31G**[b] | |
|---|---|---|
| | Trans | Cis |
| P–P | 2.0047 | 2.0120 |
| P–H | 1.4083 | 1.4079 |
| ∠HPH | 96.1 | 101.0 |
| | -682.57398 | -682.56845 |
| | $\Delta_E$ = 3.47 kcal/mol | |

[a] Data from reference 56.

[b] Data from reference 104.

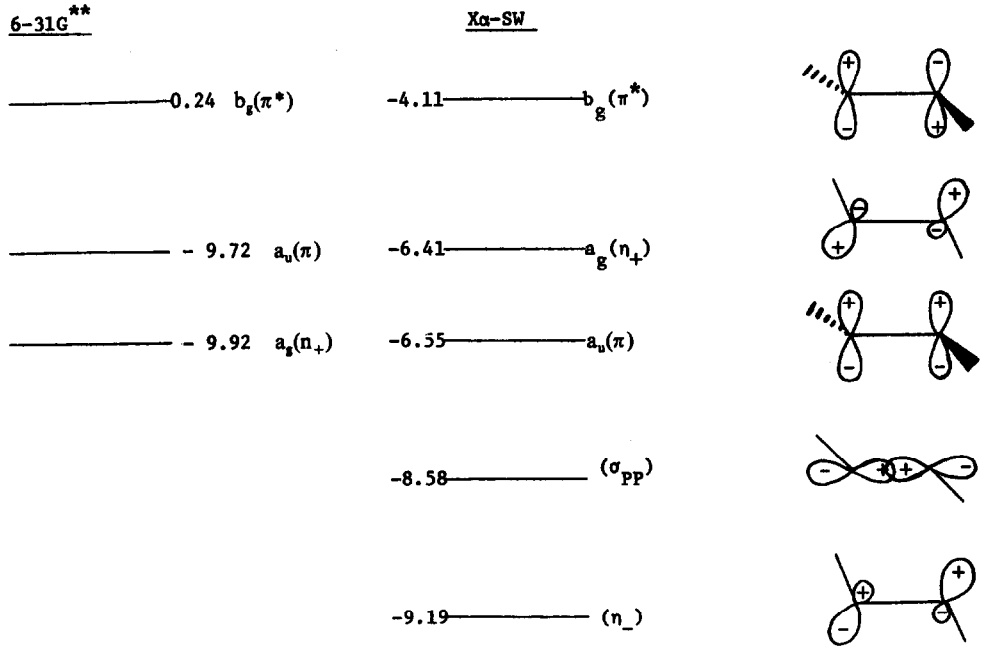



Fig. 6. Higher-lying Mo's of *trans*-$P_2H_2$.

Although the spectral interpretation is complicated by the occurrence of overlapping bands, both spectra exhibit a low intensity first ionization at $\sim 7$ eV which has the appearance of a lone pair peak.

## VII. ELECTRONIC SPECTRAL DATA FOR DOUBLE-BONDED COMPOUNDS

### 1. *Disilenes*

Electronic spectral data for the disilenes have been assembled in Table 2. Each compound exhibits a maximum at $\geq 400$ nm which is assignableto the $\pi \rightarrow \pi^*$ transition of the silicon–silicon double bond.

Table 2. Electronic spectral data for disilenes

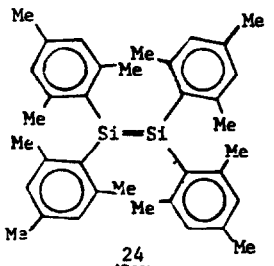
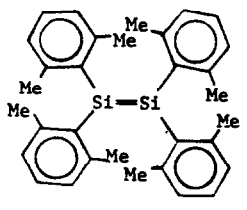
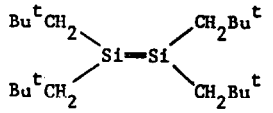
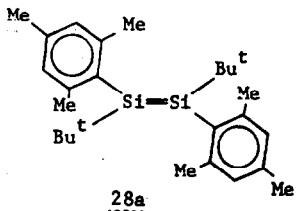
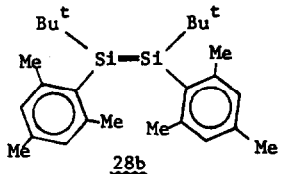
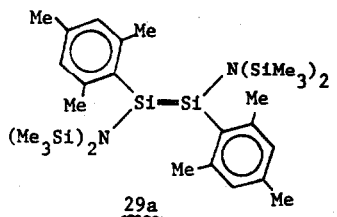
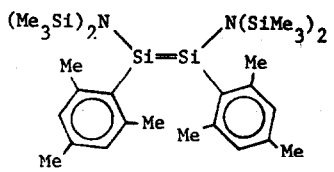
| Compound | $\lambda_{max}$ (nm) | Reference |
|---|---|---|
|  24 | 420 | 33 |
|  26 | 422 (log ε = 3.85)<br>~340 (log ε = 3.44)<br>272 (log ε = 3.85) | 35 |

Table 2. (*Contd*)

| Compound | $\lambda_{max}$ (nm) | Reference |
|---|---|---|
|  | 400 | 37 |
|  28a | 338<br>400 (sh) | 38 |
|  28b | ~332 | 38 |
|  29a | 468<br>362 | 38 |
|  29b | 480<br>350 | 38 |

2. *Diphosphenes phospa-arsenes and diarsenes*

Electronic spectral data for these compounds have been compiled in Table 3. Each compound exhibits two UV–VIS maxima at wavelengths > 300 nm, i.e. in the region outside aromatic $\pi \rightarrow \pi^*$ transitions. Note that for all the molecules listed, $\lambda_1$ is considerably less intense than $\lambda_2$. This observation is consistent with the view that the $n_+$ lone pair combination is the HOMO and the $\pi$ orbital is the HOMO-1, since the $n_+ \rightarrow \pi^*$ transition is symmetry forbidden, while the $\pi \rightarrow \pi^*$ transition is symmetry allowed.

Some other points are worthy of comment regarding the electronic spectral data. First, note the $\lambda_1$ and $\lambda_2$ are very similar for the arylated and alkylated diphosphenes, see **32** and **33**. This observation suggests that there is little conjugation between the aryl residues and the P=P chromophore. Secondly, note that $\lambda_1$ and $\lambda_2$ appear at longer wavelengths for diarsenes than for the corresponding diphosphenes. This occurs because the $\pi$-bonding is less strong in the diarsenes hence the $n_+ \rightarrow \pi^*$ and $\pi \rightarrow \pi^*$ energy gaps are diminished.

Table 3. Electronic spectral data ($\lambda_{max}$) for diphosphenes, phospha-arsenes and diarsenes

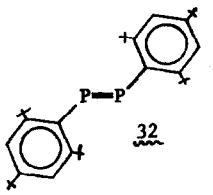
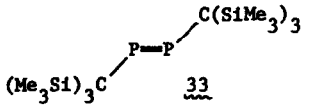
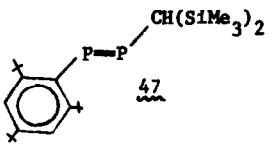
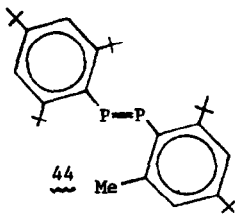
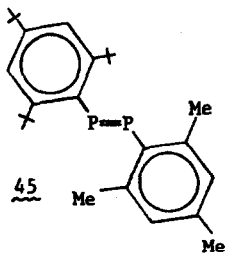
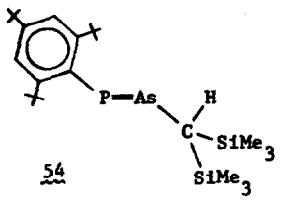
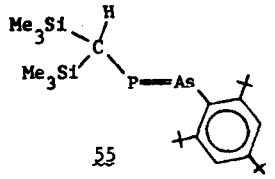
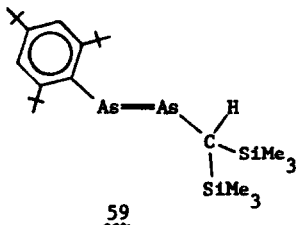
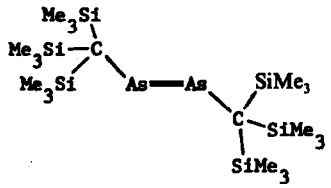
| Compound | $\lambda_1$ (nm) | $\lambda_2$ (nm) | $\lambda_3$ (nm) | Reference |
|---|---|---|---|---|
|  32 | 460 (ε=1,360) | 340 (ε=7,690) | 284 (ε=15,660) | 44 |
|  33 | 484 (ε=62.8) | 353 (ε=9,474) | 241 (ε=8,532) | 45,46 |
|  47 | 427 (ε=370) | 325 (ε=13,000) | 261 (ε=15,500) | 57 |
|  44 | 461 (ε=468) | 330 (ε=5,080) | 279 (ε=13,800) | 56 |
|  45 | 456 (ε=220) | 326 (ε=2,500) | 273 (ε=9,830) | 56 |
|  54 | 454 (ε=280) | 353 (ε=7,500) | 263 (ε=10,320) | 59 |
|  55 | 431 (ε=220) | 354 (ε=8,400) | 254 (ε=10,440) | 61 |

Table 3. (*Contd*)

| Compound | $\lambda_1$ (nm) | $\lambda_2$ (nm) | $\lambda_3$ (nm) | Reference |
|---|---|---|---|---|
|  59 | 449 (ε=180) | 368 (ε=6,900) | 255 (ε=12,660) | 61 |
|  60 | 505 (ε=10) | 380 (ε=5,000) | | 64 |

## VIII. NMR AND VIBRATIONAL SPECTROSCOPIC DATA FOR DOUBLE-BONDED COMPOUNDS

The $^{29}Si$ NMR chemical shifts of disilenes (Table 4) are deshielded compared to those of saturated (disilane)[107] analogues. This trend parallels that observed in $^{13}C$ NMR spectroscopy[108] where alkenes resonate at lower fields than alkanes. This deshielding effect is due to the importance of the paramagnetic shielding term ($\sigma_P$) which is caused by the existence of low-lying excited states of alkenes and disilenes. The parallel between alkenes and disilenes is further demonstrated by the observation that the solid-state $^{29}Si$ NMR spectrum of **24** shows anisotropy comparable to that of ethene.[109]

The $^{31}P$ NMR chemical shifts of diphosphenes, phospha-arsenes and the phosphastibene (Table 5) are among the lowest field known in $^{31}P$ NMR spectroscopy,[110] falling typically in the range 500–670 ppm. Note also that the $^1J_{PP}$ values, obtained from the spectra of unsymmetrically substituted diphosphenes, are also large ($\sim$ 550–650 Hz). These effects parallel, although are greater than those observed in $^{13}C$ NMR spectroscopy.[108] As with the disilenes, it seems reasonable to invoke the paramagnetic shielding term to explain the low field $^{31}P$ chemical shift. However, it is interesting that there is no apparent relationship between the $\eta_+ \rightarrow \pi^*$ or $\pi \rightarrow \pi^*$ transition energies and the $^{31}P$ NMR chemical shifts of the Group 5A double bonded compounds. The larger $^1J_{PP}$

Table 4. $^{29}Si$ NMR data for disilenes

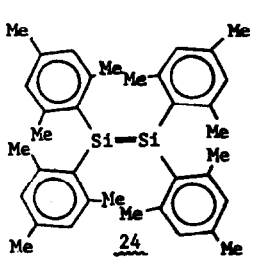
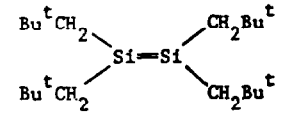
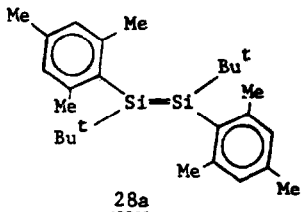
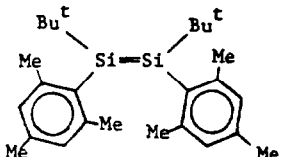
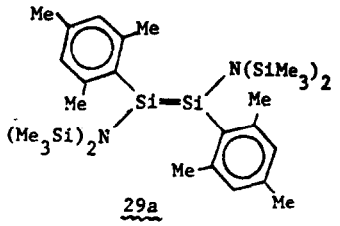
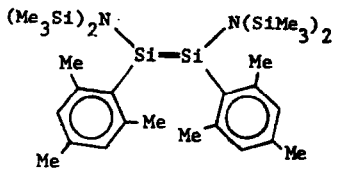
| Compound | Chemical Shift[a] | Reference |
|---|---|---|
|  24 | 63.6 | 33 |

Table 4. (*Contd*)

| Compound | Chemical Shift[a] | Reference |
|---|---|---|
|  | 81.68 | 37 |
|  28a | 90.3 | 38 |
|  28b | 94.7 | 38 |
|  29a | 61.9 | 38 |
|  29b | 49.4 | 38 |

[a]Relative to $Me_4Si$. All shifts positive (deshielded).

values for double-bonded compounds stem principally from increases in the Fermi contact term which in turn, result from changes in valence *s* character at phosphorus in proceeding from diphosphines to diphosphenes.

Finally, note that the $\eta^2$ transition metal complexes of diphosphenes are upfield compared to those of the free ligand. Upfield $^{13}C$ NMR chemical shifts also occur when alkenes are $\eta^2$-bonded to transition metals.[111]

The few vibrational spectroscopic data that are available for disilenes and diphosphenes have been collected in Table 6.

*Acknowledgement*—The author thanks the National Science Foundation (Grant CHE-8205871) and the Robert A. Welch Foundation for generous financial support.

Table 5. $^{31}P$ chemical shifts for diphosphenes, phospha-arsenes and phospha–stibenes and their transition metal complexes

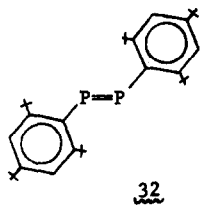
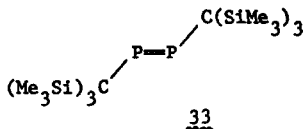
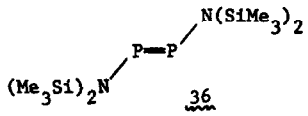
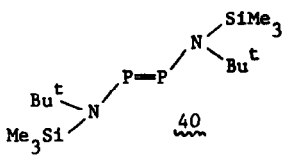
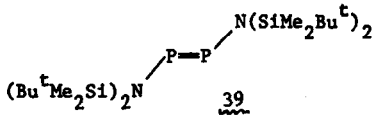
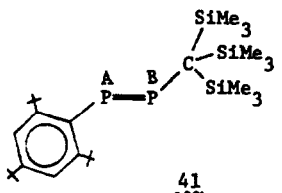
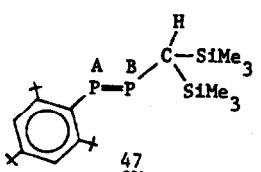
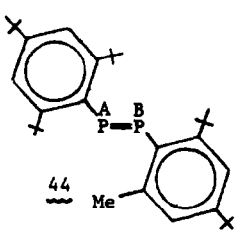
| Compound | Chemical Shift[a] | Coupling Constant (Hz) | Reference |
|---|---|---|---|
|  32 | 494 | — | 45,48,49,50 |
|  33 | 599 | — | 45,46 |
|  36 | 572 | — | 52 |
|  40 | 499 | — | 53 |
|  39 | 561 | — | 53 |
|  41 | $P_A$: 533.1<br>$P_B$: 530.0 | $^1J_{P_AP_B}$ = 619.7 | 55 |
|  47 | $P_A$: 495.0<br>$P_B$: 508.3 | $^1J_{P_AP_B}$ = 575.0<br>$^2J_{P_BCH}$ = 10.5 | 57 |
|  44 | $P_A$: 480.1<br>$P_B$: 517.0 | $^1J_{P_AP_B}$ = 583.5 | 56 |

Table 5. (*Contd*)

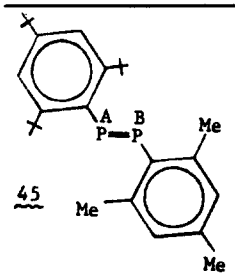
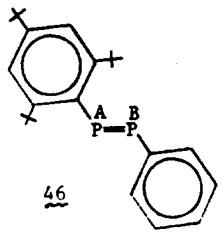
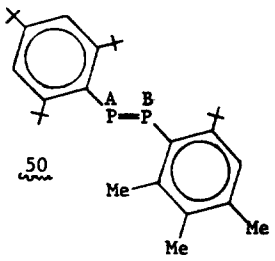
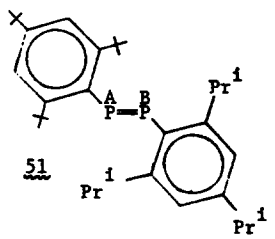
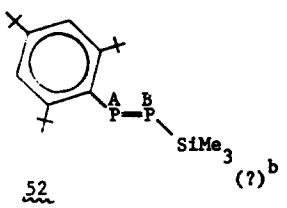
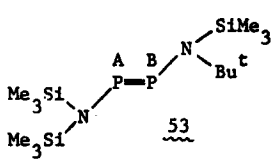
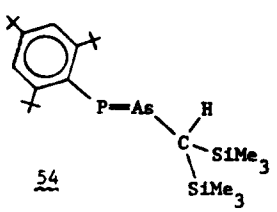
| Compound | Chemical Shift[a] | Coupling Constant | Reference |
|---|---|---|---|
|  45 | $P_A$: 467.6, 463<br>$P_B$: 540.4, 541 | $^1J_{P_AP_B}$ = 573.7<br>$^1J_{P_AP_B}$ = 571 | 56 |
|  46 | $P_A$: 455.5<br>$P_B$: 525.5 | $^1J_{P_AP_B}$ = 548.7 | 56 |
|  50 | $P_A$: 470<br>$P_B$: 535 | $^1J_{P_AP_B}$ = 572 | 58 |
|  51 | $P_A$: 463<br>$P_B$: 541 | $^1J_{P_AP_B}$ = 571 | 58 |
|  52 | $P_A$: 486.8<br>$P_B$: 628.2 | $^1J_{P_AP_B}$ = 575 | 58 |
|  53 | $P_A$: 544<br>$P_B$: 507 | $^1J_{P_AP_B}$ = 670 | 53 |
|  54 | 575 | $^3J_{PAsCH}$ = 8.9 | 59 |

Table 5. (*Contd*)

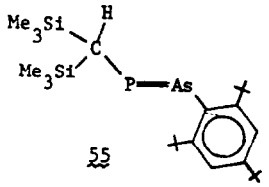
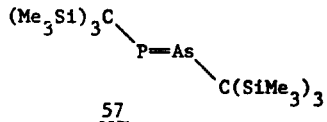
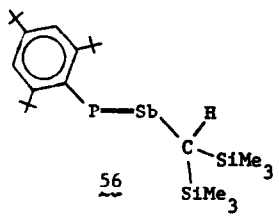
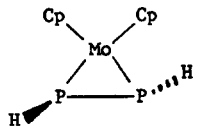
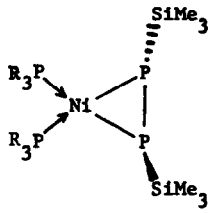
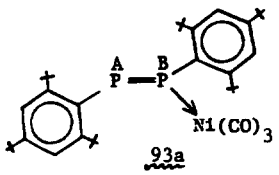
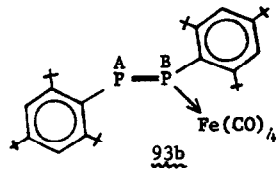
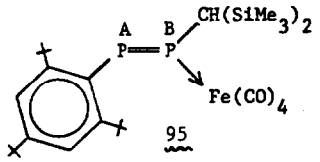
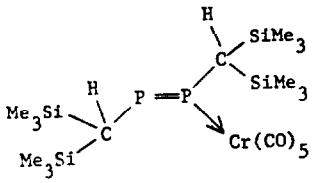
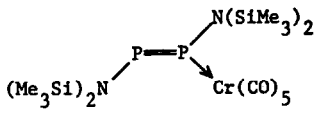
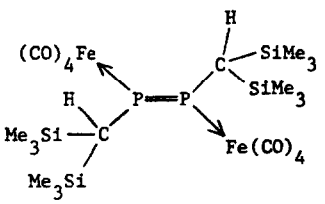
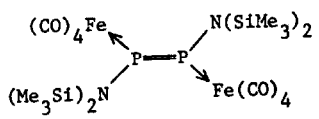
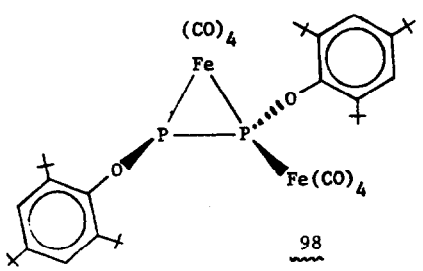
| Compound | Chemical Shift[a] | Coupling Constant | Reference |
|---|---|---|---|
|  55 | 533 | — | 61 |
|  57 | 668 | — | 60 |
|  56 | 620 | — | 59 |
|  87 | 203 | | 74 |
|  89 | 71.5 (R = Me)<br>62.0 (R = Et)<br>61.5 (R = $Bu^n$) | | 77 |
|  93a | $P_A$: 449.0<br>$P_B$: 422.0 | $^1J_{P_AP_B}$ = 540.3 | 84 |
|  93b | $P_A$: 423.6<br>$P_B$: 396.4 | $^1J_{P_AP_B}$ = 578.0 | 84 |

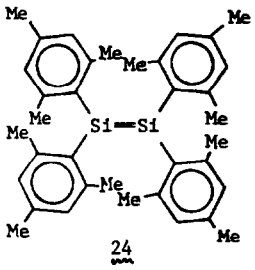
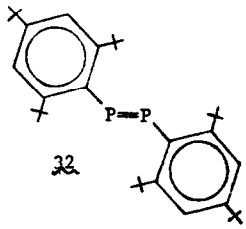
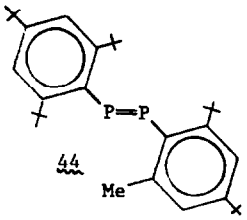
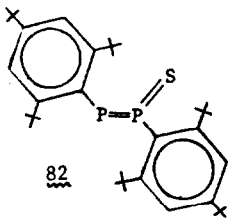
Table 5. (*Contd*)

| Compound | Chemical Shift[a] | Coupling Constant | Reference |
|---|---|---|---|
|  95 | $P_A$: 424<br>$P_B$: 416 | $^1J_{P_AP_B}$ = 517 | 84 |
|  94 | $P_A$: 480.4<br>474.1<br>$P_B$: 449.4<br>443.0 | $^1J_{P_AP_B}$ = 516 | 85 |
|  | $P_A$: 564.3<br>556.5<br>$P_B$: 534.5<br>542.3 | $^1J_{P_AP_B}$ = 631 | 85 |
|  97 | 384.6 | | 87 |
|  | 403.9 | | 87 |
|  98 | $P_A$: 237.1<br>230.4<br>$P_B$: 196.8<br>190.0 | $^1J_{P_AP_B}$ = 543 | 85 |

[a] Relative to external 85% $H_3PO_4$. All shifts positive (deshielded).

[b] Identity of compound not certain.

Table 6. Double bond stretching frequencies for disilenes and diphosphenes

| Compound | M=M Stretch ($cm^{-1}$) | Method | Reference |
|---|---|---|---|
|  24 | 529 | Raman | 33 |
|  32 | 610 | Raman | 56 |
|  44 | 620 | IR | 56 |
|  82 | 624 | IR | 70 |

## REFERENCES


1. H. Köhler and A. Michaelis, *Ber Dtsch. Chem. Ges.* 1877, **10**, 807.
2. J. J. Daly and L. Maier, *Nature (London)* 1964, **203**, 1167; *Ibid.* 1965, **208**, 383. J. J. Daly, *J. Chem. Soc.* 1964, 6147. J. J. Daly *Ibid.* 1965, 4789.
3. P. Erlich, *Lancet* 1907, **173**, 351.
4. F. S. Kipping, *Proc. Chem. Soc.* 1911, **27**, 143.
5. K. Hedberg, E. W. Hughes and J. Waser, *Acta Crystallogr.* 1961, **14**, 369. A. L. Rheingold and P. J. Sullivan, *Organometallics* 1983, **2**, 327.
6. See, for example, R. West, In *Comprehensive Organometallic Chemistry* (Edited by G. Wilkinson, F. G. A. Stone and E. W. Abel), Vol. 2, Chap. 9.4. Pergamon Press, Oxford (1982).
7. L. E. Gusel'nikov and N. S. Nametkin, *Chem. Rev.* 1979, **79**, 529.
8. T. P. Fehlner, *J. Am. Chem. Soc.* 1966, **88**, 1819; *Ibid.* 1967, **89**, 6477.
9. T. P. Fehlner and R. B. Callan, *Advances in Chemistry Series No.* 72, pp. 181–190. American Chemical Society, Washington, D.C. (1968).
10. T. P. Fehlner, *J. Am. Chem. Soc.* 1968, **90**, 6062.
11. J. Escudié, C. Couret, J. D. Andriamizaka and J. Satgé, *J. Organometal. Chem.* 1982, **228**, C76.

12. For a review, see P. P. Gaspar, *Reactive Intermediates* (Edited by M. Jones and R. S. Moss), Vol. 1, Chap. 7. Wiley, New York (1978).
13. D. N. Roark and G. J. D. Peddle, *J. Am. Chem. Soc.* 1972, **94**, 5837.
14. W. D. Wulff, W. F. Goure and T. J. Barton, *J. Am. Chem. Soc.* 1978, **100**, 6236.
15. Y. -S. Chen, B. H. Cohen and P. P. Gaspar, *J. Organometal. Chem.* 1980, 195, Cl.
16. H. Sakurai, Y. Nakadaira and T. Kobayashi, *J. Am. Chem. Soc.* 1979, **101**, 487.
17. T. J. Barton and J. A. Kilgour, *J. Am. Chem. Soc.* 1974, **96**, 7150; *Ibid.* 1976, **98**, 7746.
18. W. H. Atwell and J. G. Uhlman, *J. Organometal. Chem.* 1973, **52**, C21.
19. H. Sakurai, T. Kobayashi and Y. Nakadaira, *J. Organometal. Chem.* 1978, **162**, C43.
20. T. J. Barton and J. A. Kilgour, *J. Am. Chem. Soc.* 1976, **98**, 7231.
21. J. D. Rich, T. D. Drahnak, R. West and J. Michl, *J. Organometal. Chem.* 1981, **212**, Cl.
22. Y. Nakadaira, T. Otsuka and H. Sakurai, *Tetrahedron Lett.* 1981, **22**, 2417.
23. H. Sakurai, H. Sakaba and Y. Nakadaira, *J. Am. Chem. Soc.* 1982, **104**, 6156.
24. R. T. Conlin and P. P. Gaspar, *J. Am. Chem. Soc.* 1976, **98**, 868.
25. Y. Nakadaira, T. Kobayashi, T. Otsuka, and H. Sakurai, *J. Am. Chem. Soc.* 1979, **101**, 486.
26. Y. -S. Chen and P. P. Gaspar, *Organometallics* 1982, **1**, 1410.
27. J. L. Margrave and D. L. Perry, *Inorg. Chem.* 1977, **16**, 1820.
28. P. Mazerolles, M. Joanny and G. Turrou, *J. Organometal. Chem.* 1973, **60**, C3. See also P. Riviére, A. Castel and J. Satgé, *J. Organometal. Chem.* 1981, **212**, 351.
29. For a review, see J. Satgé, *Adv. Organometal. Chem.* 1982, **21**, 241.
30. C. Couret, J. Satgé, J. D. Andriamizaka and J. Escudié, *J. Organometal. Chem.* 1978, **157**, C35. C. Couret, J. D. Andriamizaka, J. Escudié and J. Satgé, *Ibid.* 1981, **208**, C3.
31. C. Couret, J. Escudié, J. Satgé, J. D. Andriamizaka and B. Saint-Roch, *J. Organometal. Chem.*1979, **182**, 9.
32. J. Passmore, G. Sutherland, T. Whidden and P. S. White, *J. Chem. Soc. Chem. Commun.*, 1980, 289.
33. R. West, M. J. Fink and J. Michl, *Science* (Washington, D.C.) 1981, **214**, 1343.
34. M. J. Fink, M. J. Michalczyk, D. J. Haller, R. West and J. Michl, *J. Chem. Soc. Chem. Commun.*, 1983, 1010.
35. S. Masamune, Y. Hanzawa, S. Murakami, T. Bally and J. F. Blount, *J. Am. Chem. Soc.* 1982, **104**, 1150.
36. P. Boudjouk, B. -H. Han and K. R. Anderson, *J. Am. Chem. Soc.* 1982, **104**, 4992.
37. H. Watanabe, T. Okawa, M. Kato and Y. Nagai, *J. Chem. Soc. Chem. Commun.*, 1983, 781.
38. M. J. Michalczyk, R. West and J. Michl, *J. Am. Chem. Soc.* in press.
39. S. Masamune, Y. Hanzawa and D. J. Williams, *J. Am. Chem. Soc.* 1982, **104**, 6136.
40. (a) D. E. Goldberg, D. H. Harris, M. F. Lappert and K. M. Thomas, *J. Chem. Soc. Chem. Commun.*, 1976, 261. (b) P. J. Davidson, D. H. Harris and M. F. Lappert, *J. Chem. Soc. Dalton Trans.* 1976, 2268. (c) T. Fjeldberg, A. Haaland, M. F. Lappert, B. E. R. Schilling, R. Seip and A. J. Thorne, *J. Chem. Soc. Chem. Commun.*, 1982, 1407.
41. L. Pauling, *The Nature of the Chemical Bond*, 3rd Edn. Cornell University Press, Ithaca, New York (1960).
42. T. Fjeldberg, H. Hope, M. F. Lappert, P. P. Power and A. J. Thorne, *J. Chem. Soc. Chem. Commun.*, 1983, 639.
43. L. Pauling, *Proc. Natl. Acad. Sci. USA*, 1983 **80**, 3871. This valence-bond representation was suggested earlier by Lappert *et al.* (Ref. 40b).
44. M. Yoshifuji, I. Shima, N. Inamoto, K. Hirotsu and T. Higuchi, *J. Am. Chem. Soc.* 1981, **103**, 4587.
45. A. H. Cowley, J. E. Kilduff, T. H. Newman and M. Pakulski, *J. Am. Chem. Soc.* 1982, **104**, 5820.
46. C. Couret, J. Escudié and J. Satgé, *Tetrahedron Lett.* 1982, **23**, 4941. J. Jaud, C. Couret and J. Escudié, *J. Organometal. Chem.* 1983, **249**, C25.
47. A. H. Cowley, J. E. Kilduff, N. C. Norman, J. L. Atwood, M. Pakulski and W. E. Hunter, *J. Am. Chem. Soc.* 1983, **105**, 4845.
48. G. Bertrand, C. Couret, J. Escudié, S. Majid and J. -P. Majoral, *Tetrahedron Lett.* 1982, 3567. M. Veith, V. Huch, J. -P. Majoral, G. Bertrand and G. Manuel, *Ibid.* 1983, 4219.
49. B. Cetinkaya, P. B. Hitchcock, M. F. Lappert, A. J. Thorne and H. Goldwhite, *J. Chem. Soc. Chem. Commun.*, 1982, 691.
50. The error was also corrected by the original authors: M. Yoshifuji, I. Shima, K. Inamoto, K. Hirotsu and T. Higuchi, *J. Am. Chem. Soc.* 1982, **104**, 6167.
51. M. Yoshifuji, K. Shibayama and N. Inamoto, *J. Am. Chem. Soc.* 1983, **105**, 2495.
52. E. Niecke and R. Rüger, *Angew. Chem. Int. Ed. Engl.* 1983, **22**, 155.
53. E. Niecke, R. Rüger, M. Lysek, S. Pohl and W. Schoeller, *Angew. Chem. Int. Ed. Engl.* 1983, **22**, 486.
54. M. Veith, *Acta Cryst.* 1975, **B32**, 678.
55. A. H. Cowley, J. E. Kilduff, M. Pakulski and C. A. Stewart, *J. Am. Chem. Soc.* 1983, **105**, 1655.

56. M. Yoshifuji, K. Shibayama, N. Inamoto, T. Matsushita and K. Nishimoto, *J. Am. Chem. Soc.* 1983, **105**, 2495.
57. A. H. Cowley, J. E. Kilduff, S. K. Mehrotra, N. C. Norman and M. Pakulski, *J. Chem. Soc. Chem. Commun.*, 1983, 520.
58. C. N. Smit, Th. A. van der Knaap and F. Bickelhaupt, *Tetrahedron Lett.* 1983, **24**, 2031.
59. A. H. Cowley, J. G. Lasch, N. C. Norman, M. Pakulski and B. R. Whittlesey, *J. Chem. Soc. Chem. Commun.*, 1983, 881.
60. J. Escudié, C. Couret, H. Ranaivonjatovo and J. -G. Wolf, *Tetrahedron Lett.* 1983, **24**, 3625.
61. A. H. Cowley, J. G. Lasch, N. C. Norman and M. Pakulski, *J. Am. Chem. Soc.*1983, **103**, 5506.
62. M. Yoshifuji, I. Shima, K. Ando and N. Inamoto, *Tetrahedron Lett.* 1983, **24**, 933.
63. A. L. Rheingold and P. J. Sullivan, *Organometallics* 1983, **2**, 327, and references therein.
64. C. Couret, J. Escudié, Y. Madule, H. Ranaivonjatovo and J. -G. Wolf, *Tetrahedron Lett.* 1983, **24**, 2769.
65. M. J. Fink, D. J. De Young, R. West and J. Michl, *J. Am. Chem. Soc.* 1983, **105**, 1070.
66. M. J. Fink, K. J. Haller, R. West and J. Michl, *J. Am. Chem. Soc.* in press.
67. A. H. Cowley, R. A. Kemp and C. A. Stewart, *J. Am. Chem. Soc.* 1982, **104**, 3239. A. H. Cowley and S. K. Mehrotra, *J. Am. Chem. Soc.* 1983, **105**, 2074.
68. M. Yoshifuji, K. Ando, K. Toyota, I. Shima and N. Inamoto, *J. Chem. Soc. Chem. Commun.*, 1983, 419.
69. J. I. G. Cadogan, A. H. Cowley, I. Gosney, M. Pakulski and S. Yaslek, *J. Chem. Soc. Chem. Commun.*, 1983, 1408.
70. M. Yoshifuji, K. Shibayama, N. Inamoto, K. Hirotsu and T. Higuchi, *J. Chem. Soc. Chem. Commun.*, 1983, 862.
71. M. Yoshifuji, K. Ando, N. Shibayama, N. Inamoto, K. Hirotsu and T. Higuchi, *Angew. Chem. Int. Ed. Engl.* 1983, **22**, 418.
72. A. H. Cowley and M. Pakulski, to be published.
73. B. Cetinkaya, A. Hudson, M. F. Lappert and H. Goldwhite, *J. Chem. Soc. Chem. Commun.*, 1982, 609.
74. J. C. Green, M. L. H. Green and G. E. Morris, *J. Chem. Soc. Chem. Commun.*, 1974, 212.
75. E. Cannillo, A. Coda, K. Prout and J. -C. Daran, *Acta Cryst.* 1977, **B33**, 2608.
76. P. S. Elmes, M. L. Scudder and B. O. West, *J. Organometal. Chem.* 1976, **122**, 281.
77. B. Deppisch and H. Schäfer, *Acta Cryst.* 1982, **B38**, 748. H. Schäfer, *Z. Naturforsch. B* 1979, **34b**, 1358.
78. J. Chatt, P. B. Hitchcock, A. Pidcock, C. P. Warrens and K. R. Dixon, *J. Chem. Soc. Chem. Commun.*, 1982, 932.
79. P. S. Elmes, P. Leverett and B. O. West, *J. Chem. Soc. Chem. Commun.*, 1971, 747.
80. A. H. Cowley, *Compounds Containing Phosphorus–Phosphorus Double Bonds.* Dowden, Hutchinson and Ross, Stroudsburg, PA (1973).
81. For a review of $\eta^2$-alkene complexes of e.g. Ni, see, P. W. Jolly and G. Wilke, *The Organic Chemistry of Nickel Organonickel Complexes*, Vol. I, Chap. 5. Academic Press, New York (1974).
82. A. H. Cowley, R. A. Jones, C. A. Stewart, A. L. Stuart, J. L. Atwood, W. E. Hunter and H.-M. Zhang, *J. Am. Chem. Soc.* 1983, **105**, 3737.
83. K. Kitaura, S. Sakaki and K. Morokuma, *Inorg. Chem.* 1981, **20**, 2292.
84. A. H. Cowley, J. E. Kilduff, J. G. Lasch, N. C. Norman, M. Pakulski, F. Ando and T. C. Wright, *J. Am. Chem. Soc.* in press.
85. K. M. Flynn, H. Hope, B. Murray, M. M. Olmstead and P. P. Power, *J. Am. Chem. Soc.* in press.
86. A. H. Cowley, J. G. Lach, N. C. Norman and M. Pakulski, *Angew. Chem.*, in press.
87. K. M. Flynn, M. M. Olmstead and P. P. Power, *J. Am. Chem. Soc.* 1983, **105**, 2085; K. M. Flynn, B. D. Murray, M. M. Olmstead and P. P. Power, *J. Am. Chem. Soc.* 1983, **105**, 7460.
88. G. Huttner, H. -G. Schmid, A. Frank and O. Orama, *Agnew. Chem. Int. Ed. Engl.* 1976, **15**, 234.
89. G. Huttner, U. Weber, B. Sigwarth and O. Scheidsteger, *Angew. Chem. Int. Ed. Engl.* 1982, **21**, 215.
90. H. Vahrenkamp and D. Wolters, *Angew. Chem. Int. Ed. Engl.* 1983, **22**, 154.
91. M. M. Olmstead and P. P. Power, submitted for publication.
92. M. D. Sefcik and M. A. Ring, *J. Am. Chem. Soc.* 1973, **95**, 5168.
93. M. D. Curtis, *J. Organometal. Chem.* 1973, **60**, 63.
94. M. J. S. Dewar, D. H. Lo and C. A. Ramsden, *J. Am. Chem. Soc.* 1975, **97**, 1311.
95. P. H. Blustin, *J. Organometal. Chem.* 1976, **105**, 161.
96. R. Daudel, R. E. Kari, R. A. Poirier, J. D. Goddard and I. G. Csizmadia, *J. Mol. Struct.* 1978, **50**, 115.
97. F. F. Roelandt, D. F. Van de Vandel and G. P. Van der Kelen, *J. Organometal. Chem.* 1979, **165**, 151.
98. L. C. Snyder and Z. R. Wasserman, *J. Am. Chem. Soc.* 1979, **101**, 5222.
99. J. Sauer, P. Carsky, and R. Zhradnik, *Collect. Czech. Chem. Commun.* 1982, **47**, 1149.
100. R. A. Poirier and J. D. Goddard, *Chem. Phys. Lett.* 1981, **80**, 37.
101. H. Lischka and H. -J. Koehler, *Chem. Phys. Lett.* 1982, **85**, 467.
102. K. Krogh-Jespersen, *J. Phys. Chem.* 1982, **86**, 1492.

103. K. Issleib and W. Grundler, *Theo. Chim. Acta* 1968, **11**, 107.
104. J. -G. Lee, A. H. Cowley and J. E. Boggs, *Inorg. Chim. Acta* 1983, **77**, L61.
105. M. Lattman and A. H. Cowley, to be published.
106. D. Gonbeau, G. Pfister-Guillouzo, J. Escudié, C. Couret and J. Satgé, *J. Organometal. Chem.* 1983, **247**, C17.
107. See, for example, E. A. Williams and J. D. Cargioli, In *Annual Reports on NMR Spectroscopy* (Edited by G. A. Webb), Vol. 9. Academic Press, New York (1979).
108. See, e.g. J. B. Stothers *Carbon*-13 *NMR Spectroscopy*. Academic Press, New York (1972).
109. K. W. Zilm, D. M. Grant, J. Michl, M. J. Fink and R. West, *Organometallics* 1983, **2**, 193.
110. Larger $^{31}P$ chemical shifts are observed for paramagnetic compounds, e.g. $OsCl_4(PMe_2Ph)_2$. J. Chatt, G. J. Leigh, D. M. P. Mingos, E. W. Randall, and D. Shaw, *J. Chem. Soc., Chem. Commun.* 1968, 419.
111. B. E. Mann and B. F. Taylor, *$^{13}C$ NMR Data for Organometallic Compounds*. Academic Press, New York (1981).
112. B. Cetinkaya, M. F. Lappert, J. G. Stamper and R. J. Suffolk, *J. Electron Spectrosc. Relat. Phenom.* 1983, **32**, 133.
113. M. Yoshifuji and N. Inamoto, *Tetrahedron Lett.* 1983, **24**, 4855.
114. J. Navech, J.-P. Majoral and R. Kraemer, *Tetrahedron Lett.* 1983, **24**, 5885.
115. S. Masamune, S. Murakami and H. Tobita, *Organometallics*, 1983, **2**, 1464.
116. S. Masamune, H. Tobita and S. Murakami, *J. Am. Chem. Soc.* 1983, **105**, 6524.

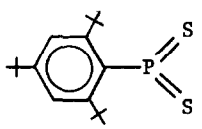
## IX. ADDENDUM

Several important developments have occurred since the submission of this Report.

He(I) and He(II) photoelectron spectroscopic data have been reported for $(2,4,6\text{-}(Bu^t)_3C_6H_2)_2P_2$ (**32**) and STO–3G MO calculations have been performed on the model diphosphenes, $H_2P_2$, $Me_2P_2$, and $(CH_2{=}CH)_2P_2$.[112]

Mono- and bis-$\eta^6$-$Cr(CO)_3$ complexes of $(2,4,6\text{-}(Bu^t)_3C_6H_2)_2P_2$ (**32**) have been produced by treatment of the diphosphene with $Cr(CO)_6$ in refluxing dioxane.[113]

The metadithiophosphonate, **105**, which was postulated as an intermediate in the reaction of **32** with excess $S_8$, has now been isolated.[114]




105

The thermally unstable disilene, $(Bu^t)_2Si{=}Si(Bu^t)_2$ has been produced by a retro Diels–Alder reaction,[115] and photolysis of hexakis(1-ethylpropyl) cyclotrisilane resulted in the corresponding disilene and silylene, both of which were trapped.[116]

103. K. Issleib and W. Grundler, *Theo. Chim. Acta* 1968, **11**, 107.
104. J. -G. Lee, A. H. Cowley and J. E. Boggs, *Inorg. Chim. Acta* 1983, **77**, L61.
105. M. Lattman and A. H. Cowley, to be published.
106. D. Gonbeau, G. Pfister-Guillouzo, J. Escudié, C. Couret and J. Satgé, *J. Organometal. Chem.* 1983, **247**, C17.
107. See, for example, E. A. Williams and J. D. Cargioli, In *Annual Reports on NMR Spectroscopy* (Edited by G. A. Webb), Vol. 9. Academic Press, New York (1979).
108. See, e.g. J. B. Stothers *Carbon*-13 *NMR Spectroscopy*. Academic Press, New York (1972).
109. K. W. Zilm, D. M. Grant, J. Michl, M. J. Fink and R. West, *Organometallics* 1983, **2**, 193.
110. Larger $^{31}P$ chemical shifts are observed for paramagnetic compounds, e.g. $OsCl_4(PMe_2Ph)_2$. J. Chatt, G. J. Leigh, D. M. P. Mingos, E. W. Randall, and D. Shaw, *J. Chem. Soc., Chem. Commun.* 1968, 419.
111. B. E. Mann and B. F. Taylor, *$^{13}C$ NMR Data for Organometallic Compounds*. Academic Press, New York (1981).
112. B. Cetinkaya, M. F. Lappert, J. G. Stamper and R. J. Suffolk, *J. Electron Spectrosc. Relat. Phenom.* 1983, **32**, 133.
113. M. Yoshifuji and N. Inamoto, *Tetrahedron Lett.* 1983, **24**, 4855.
114. J. Navech, J.-P. Majoral and R. Kraemer, *Tetrahedron Lett.* 1983, **24**, 5885.
115. S. Masamune, S. Murakami and H. Tobita, *Organometallics*, 1983, **2**, 1464.
116. S. Masamune, H. Tobita and S. Murakami, *J. Am. Chem. Soc.* 1983, **105**, 6524.

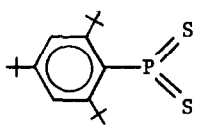
## IX. ADDENDUM

Several important developments have occurred since the submission of this Report.

He(I) and He(II) photoelectron spectroscopic data have been reported for $(2,4,6\text{-}(Bu^t)_3C_6H_2)_2P_2$ (**32**) and STO–3G MO calculations have been performed on the model diphosphenes, $H_2P_2$, $Me_2P_2$, and $(CH_2{=}CH)_2P_2$.[112]

Mono- and bis-$\eta^6$-$Cr(CO)_3$ complexes of $(2,4,6\text{-}(Bu^t)_3C_6H_2)_2P_2$ (**32**) have been produced by treatment of the diphosphene with $Cr(CO)_6$ in refluxing dioxane.[113]

The metadithiophosphonate, **105**, which was postulated as an intermediate in the reaction of **32** with excess $S_8$, has now been isolated.[114]




105

The thermally unstable disilene, $(Bu^t)_2Si{=}Si(Bu^t)_2$ has been produced by a retro Diels–Alder reaction,[115] and photolysis of hexakis(1-ethylpropyl) cyclotrisilane resulted in the corresponding disilene and silylene, both of which were trapped.[116]

*Polyhedron* Vol. 3, No. 4, pp. 433–442, 1984
Printed in Great Britain.

0277-5387/84 $3.00 + .00
© 1984 Pergamon Press Ltd.

# LIGAND EXCHANGE REACTIONS BETWEEN COPPER(II)- AND NICKEL(II)- CHELATES OF DIFFERENT SULPHUR- AND SELENIUM-CONTAINING LIGANDS—III

## SINGLE-CRYSTAL ESR STUDY ON THE MIXED-LIGAND CHELATE ($n$-$Bu_4N$) [$^{63}$Cu(mnt) ($et_2$dsc)]† AND CRYSTAL AND MOLECULAR STRUCTURE OF ($n$-$Bu_4N$) [Ni(mnt) ($et_2$dsc)]

JOACHIM STACH, REINHARD KIRMSE, ULRICH ABRAM and WOLFGANG DIETZSCH
Department of Chemistry, Karl–Marx–University, 7010 Leipzig Liebigstr. 18, G.D.R.

and

JAN H. NOORDIK, KAREL SPEE and KEES P. KEIJZERS
Crystallography Laboratory and Department of Physical Chemistry, University of Nijmegen, 6525 ED Nijmegen, The Netherlands

(*Received* 11 *January* 1983; *accepted* 10 *October* 1983)

**Abstract**—A single-crystal ESR study of the mixed-ligand complex tetra - *n* - butylammonium - (maleonitriledithiolato)(diethyl - di - selenocarbamato)cuprate(II) diamagnetically diluted by the corresponding Ni(II) complex, and the crystal and molecular structure of the host complex determined by a single-crystal X-ray diffraction study, is reported. ($n$-$Bu_4N$)[Ni(mnt)($et_2$dsc)] is monoclinic, space group C2/c, with eight molecules in the unit cell; $a = 19.932(9)$ Å, $b = 9.597(3)$ Å, $c = 37.580(13)$ Å and $\beta = 101.32(3)°$. Based on the structure the spin Hamiltonian parameters have been calculated from the results of extended Hückel molecular orbital calculations and compared with the experimentally obtained values. The principal axes of the $\tilde{g}$ and the metal hyperfine tensor do not coincide reflecting the large influence of the $et_2dsc^-$ ligand for which this behaviour was found to be typical. A comparison between the ESR parameters and the Mulliken spin densities of the mixed-ligand chelate and the corresponding parent complexes shows that in the former one spin density appears to be transfered from the S atoms to the Se atoms of the $et_2dsc^-$ part of the complex resulting in an increased Cu–Se covalency. Back-bonding effects were considered in discussing the bonding properties.

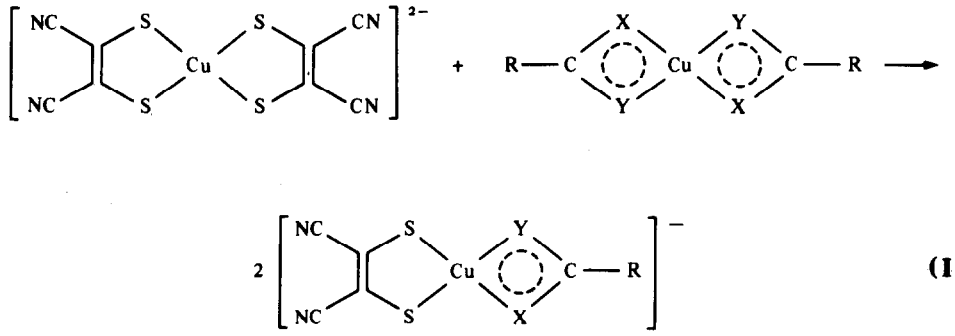
As a result of several studies on ligand exchange reactions between planar copper(II) complexes with different bidentate dichalcogeno ligands it has been established that mixed-ligand complexes are formed quantitatively if the parent compounds contain four-membered and five-membered chelate rings, respectively (I).[1,2]

The same was found for the corresponding nickel(II) compounds.

The formation of the copper(II) mixed-ligand complexes in solution can be established successfully by ESR spectroscopy, if the parent chelates and, therefore, the mixed-ligand chelate also consist of different donor atom sets because the isotropic $g$ value and the intensity of the $^{77}$Se ligand-hyperfine satellite lines ($^{77}$Se, $I = 1/2$, natural abundance $\approx 7.5\%$) depend on the various $CuS_{4-n}Se_n$ coordination spheres in a characteristic manner.[1,3]

We were interested in answering the question why quantitative formation of the mixed-ligand chelates took place for reactions of type (I). Among the reasons responsible for the sta-

†Tetra - *n* - butylammonium - (maleonitrile - dithiolato)(diethyl - di - selenocarbamato)cuprate(II).



(I)

bilization of the mixed-ligand systems changes in the electronic structure should be taken into account. These are expected to result in differences concerning the overall spin density distribution and, therefore, in some changes in the corresponding hyperfine splitting parameters of the mixed-ligand chelate with respect to those of parent chelates. Although some evidence can be obtained from solution ESR studies,[1,4] single-crystal ESR and ENDOR studies provide a much more reliable picture because the complete tensor parameters will be available. Recently, we studied the single-crystal ESR spectra of the mixed-ligand complex ($n$-$Bu_4N$)[Cu(mnt)($et_2$dtc)] ($et_2$dtc = diethyl - dithiocarbamate).[5] For this system, however, ($^{33}S$) ligand hyperfine parameters could not be obtained, and the changes in the $\tilde{g}$ and the $^{63}Cu$ hyperfine tensor components measured for the mixed-ligand and the parent complexes are too small to be used for discussion. The only mixed-ligand system studied in detail by ESR-ENDOR up to now is tetra - $n$ - butylammonium - (maleonitrile - dithiolato)(monoethyl - dithiophosphato)-copper(II), ($n$-$Bu_4N$)[Cu(mnt)(H(et)dtp)].[6,7]

In this paper we report the single-crystal ESR spectra of tetra - $n$ - butylammonium - (maleonitrile - dithiolato)(diethyl - diselenocarbamato)-copper(II), ($n$-$Bu_4N$)[$^{63}$Cu(mnt)($et_2$dsc)] (II), together with the crystal and molecular structure of the corresponding Ni(II) chelate which has been used as diamagnetic host. Apart from ($n$-$Bu_4N$)[Ni(mnt)(H(et)dtp)] recently characterized structurally[8] the structure of ($n$-$Bu_4N$)[Ni(mnt)-($et_2$dsc)] is the only known one of a bivalent Ni mixed-ligand complex containing unsaturated dichalcogeno ligands exclusively. This is of particular interest because during the preparation of the Ni mixed-ligand complexes ligand donor atom exchange may occur[2] and, therefore, the isolated compounds may not necessarily be pure products. In many cases the latter is difficult to be detected by such methods as UV/VIS, IR and NMR spectroscopy or by elemental analytical data.

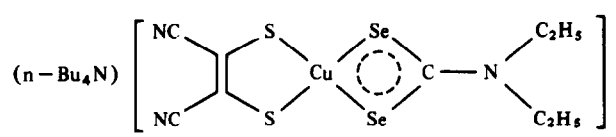
Based on the structure of ($n$-$Bu_4N$)[Ni(mnt)-($et_2$dsc)] the ESR parameters will be discussed in comparison with those of the corresponding parent chelates. Furthermore, extended Hückel MO calculations were made to confirm the experimental results.

## EXPERIMENTAL

*Preparation of compounds and single-crystals*

The complexes tetra - $n$ - butylammonium - bis(maleonitrile - dithiolato)Ni(II)($n$-$Bu_4N)_2$-[Ni(mnt)$_2$] and bis(diethyl - diselenocarbamato)-Ni(II) Ni($et_2$dsc)$_2$ were prepared by standard literature methods. The mixed-ligand complex was obtained by refluxing equimolar amounts of the parent compounds in an acetone/chloroform solution for 3–4 hr. The reaction mixture was reduced *in vacuo* and the reaction product was precipitated using isopropanol.[1,2] The corresponding Cu(II) mixed-ligand complex was obtained in a similar way. The ligand exchange reaction between ($n$-$Bu_4N)_2$[Cu(mnt)$_2$] and Cu($et_2$dsc)$_2$ takes place spontaneously. The complexes were recrystallized from acetone/isopropanol in the above described manner.

Suitable single-crystals of ($n$-$Bu_4N$)[Ni(mnt)-($et_2$dsc)] doped with the Cu chelate can be grown by slow evaporation of an acetone/ethanol solution (ratio 5 : 1) containing the diamagnetic host and approx. 1% of $^{63}$Cu enriched (98.7%) ($n$-$Bu_4N$)[$^{63}$Cu(mnt)($et_2$dsc)].



(II)

Table 1. Selected bond lengths (Å) and angles (°) for ($n$-$Bu_4N$)[Ni(mnt)($et_2$dsc)]

| Bond Lengths | | Angles | |
|---|---|---|---|
| Ni-S1 | 2.15(3) | S1-Ni-S2 | 94.0(12) |
| Ni-S2 | 2.08(4) | C1-S1-Ni | 101.0(11) |
| Ni-Se1 | 2.37(2) | C2-S2-Ni | 105.5(13) |
| Ni-Se2 | 2.31(2) | S1-C1-C2 | 119.2(8) |
| | | S2-C2-C1 | 117.9(9) |
| S1-C1 | 1.80(3) | S1-C1-C3 | 106.9(9) |
| S2-C2 | 1.74(3) | C2-C1-C3 | 123.6 |
| C1-C2 | 1.37 | N3-C3-C1 | 166.4 |
| C1-C3 | 1.50 | S2-C2-C4 | 111.2(9) |
| C3-N3 | 1.12 | C1-C2-C4 | 130.8 |
| C2-C4 | 1.58 | C2-C4-N4 | 146.7 |
| C4-N4 | 1.13 | Se1-Ni-Se2 | 80.6(6) |
| | | Ni-Se1-C5 | 83(4) |
| Se1-C5 | 1.80(12) | Ni-Se2-C5 | 84(4) |
| Se2-C5 | 1.86(12) | Se1-C5-N2 | 128(9) |
| C5-N2 | 1.40(18) | Se2-C5-N2 | 117(9) |
| N2-C6 | 1.36(15) | C5-N2-C6 | 128(11) |
| C6-C7 | 1.58(17) | C5-N2-C8 | 117(9) |
| N2-C8 | 1.49(16) | C6-N2-C8 | 115(10) |
| C8-C9 | 1.47(16) | C7-C6-N2 | 110(10) |
| | | C9-C8-N2 | 119(10) |
| | | Se1-C5-Se2 | 112(7) |

*Intensity data, structure determination and refinement*

Intensity data were measured with a CAD-4 diffractometer (Mo$K_\alpha$ radiation; $\lambda = 0.7093$ Å), using $\theta - 2\theta$ scans up to $2\theta = 28.6°$. During data collection severe crystal decay was observed resulting in a rather poor set of reflection data. The intensities were corrected for Lorentz and polarisation effects, but not for absorption.

Multiple measured reflections were averaged and of the 1247 independent reflections collected 528 were treated as observed ($I > 3.0\,\sigma(I)$).

The Ni, Se and S atoms were found using MULTAN. The other atoms were located in subsequent difference Fourier maps. Refinement was by block diagonal - least - squares with anisotropic thermal parameters for the Ni, Se and S atoms, and isotropic thermal parameters for the other atoms. Probably because of the poor intensity data some of the C and N atoms "refined" to chemically unacceptable positions. Final coordinates for those atoms were taken from a difference-Fourier map, and only the thermal parameters were refined.

Hydrogen atom positions were calculated and a final full matrix refinement cycle with weights $\sigma^2 = \sigma^2(\text{Fobs}) + 0.0005\,\text{Fobs} + 0.0005\,\text{Fobs}^2$, resulted in a R index of 0.101. The atomic scattering factors were taken from The International Tables Vol. IV (1974). Calculations were performed using X-RAY-72. Tables of atomic coordinates, temperature factors and $F_0/F_c$ values have been deposited with Editor as Supplementary Data and are available on request. Atomic co-ordinates have also been submitted to the crystallographic Data Centre, Cambridge.

*ESR spectra*

The single-crystal ESR spectra were recorded using an "E-112" spectrometer (VARIAN) in the X-band at room temperature. The tensor parameters of the spin Hamiltonian were obtained by studying the angular dependence of the ESR spectra in three planes spanned by the principal axes ($x$, $y$, $z$) of the Cu hyperfine structure tensor.

## RESULTS AND DISCUSSION

*Crystal and molecular structure*

($n$-$Bu_4N$)[Ni(mnt)($et_2$dsc)] is monoclinic, space group C2/c with $Z = 8$. The cell constants are $a = 19.932(9)$ Å, $b = 9.597(3)$ Å, $c = 37.580(13)$ Å and $\beta = 101.32(3)°$ ($V = 7049$ Å$^3$, $d_{(calc)} = 1.288$ g cm$^{-3}$).

Important interatomic distances and angles are listed in Table 1. A stereo view of the unit cell is given in Fig. 1; Fig. 2 shows the structure of the ions. The first coordination sphere of the complex

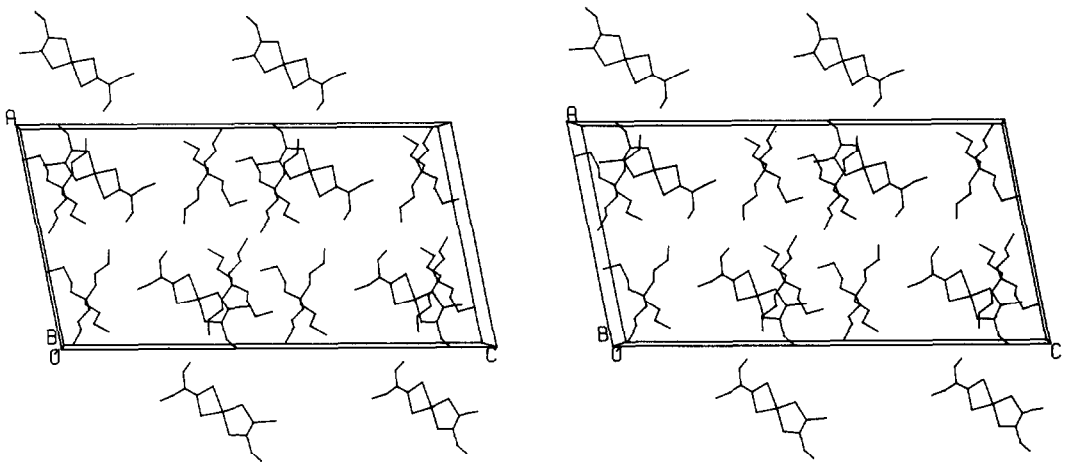



Fig. 1. Stereo view of the unit cell of ($n$-$Bu_4N$)[Ni(mnt)($et_2$dsc)].

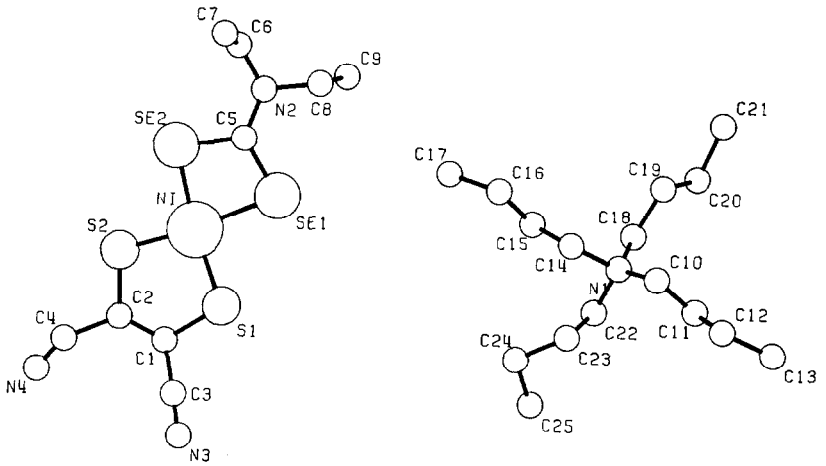



Fig. 2. Structures and numbering of the ions.

anion has low symmetry: the metal–donor atom bond distances are different from each other. The Ni, Se1, Se2, S1, C1, C2 and C5 atoms are coplanar with a maximum distance to the plane of 0.12 Å. For a least squares plane through the atoms Ni, Se1, Se2 and C5 the maximum deviation from the plane is 0.09 Å and for a plane through the atoms Ni, S1, S2, C1 and C2 this deviation is 0.11 Å.

The tetra - *n* - butylammonium cation shows C–C distances varying from 1.43 Å to 1.60 Å and C–C–C angles varying from 102° to 118°.

Comparing the bonding distances obtained for the first coordination sphere of $[Ni(mnt)(et_2dsc)]^-$ with those of the corresponding parent chelates[9,10] one can deduce a shortening of the Ni–S bond and a lengthening of the Ni–Se bond in the mixed-ligand chelate. The same tendency was found for the mixed-ligand chelate $[Ni(mnt)(H(et)dtp)]^-$.[8] In this complex the Ni–$S_{mnt}$ bonding distances are also shortened and the Ni–$S_{dtp}$ distances are longer than those obtained for the parent chelates, respectively.[9,11,12] The values are given in Table 2 for comparison.

*ESR measurements*

In accordance to the crystal structure of the host complex the signals of two magnetically non-equivalent $[^{63}Cu(mnt)(et_2dsc)]^-$ anions are observed in the single-crystal spectra. Each Cu hfs line (hfs = hyperfine structure) is flanked symmetrically by two doublets and two quartets which arise from the interaction of the unpaired electron with the $^{77}Se$ and $^{33}S$ nuclei of the Cu mixed-ligand complexes ($^{77}Se$, I = 1/2, natural abundance 7.54%; $^{33}S$, I = 3/2, natural abundance 0.74%). The in-

Table. 2. Bond distances (Å) and angles (°) of the first coordination sphere for ($n$-$Bu_4N$)[Ni(mnt)($et_2$dsc)], ($n$-$Bu_4N$)[Ni(mnt)(H(et)dtp)],[8] ($n$-$Bu_4N$)$_2$[Ni(mnt)$_2$][9], Ni($et_2$dtp)$_2$[12] and Ni($et_2$dsc)$_2$[10]

| | $Ni(mnt)_2^{2-}$ | $Ni(mnt)(H(et)dtp)^-$ | | $Ni(et_2dtp)_2$ |
|---|---|---|---|---|
| Ni-$S_1$ | 2.176(1) | 2.135(2) | 2.248(3) | 2.236(1) |
| Ni-$S_2$ | 2.173(1) | 2.151(2) | 2.265(3) | 2.230(1) |
| $S_1$-Ni-$S_2$ | 92.2(1) | 93.1(1) | 87.7(1) | 88.5(1) |
| | $Ni(mnt)_2^{2-}$ | $Ni(mnt)(et_2dsc)^-$ | | $Ni(et_2dsc)_2$ |
| Ni-S(e)$_1$ | 2.176(1) | 2.15(3) | 2.37(2) | 2.318(1) |
| Ni-S(e)$_2$ | 2.173(1) | 2.08(4) | 2.31(2) | 2.316(2) |
| S(e)$_1$-Ni-S(e)$_2$ | 92.2(1) | 94.0(12) | 80.6(6) | 81.8(1) |

tensity of the $^{33}S$ hfs peaks is approx. 0.2% and that of the $^{77}Se$ hfs lines approx. 4% of the major peaks. Due to the very low intensity and line overlappings with $^{77}Se$ sattellites the $^{33}S$ hfs signals could be detected in small intervals of the recorded angular dependencies using very high gains only. Therefore, the principal values of the $^{33}S$ hfs tensors could not be obtained experimentally. In addition to the ligand hfs signals the $^{63}Cu$ hfs lines are flanked by spin-flip satellites caused by protons of the ($n$-$Bu_4N$)$^+$ cation and the ethyl groups of the $et_2$dsc ligand which come close to the copper atom.[13–15] In some orientations $\Delta m_I^{Cu} \geqslant 1$ transitions could be detected. A typical ESR spectrum is shown in Fig. 3.

The principal values of all tensors derived from the ESR spectra are listed in Table 3. As has been found for other Cu complexes containing selenium donor atoms, the principal axes of the $\tilde{g}$ and the metal hfs tensor do not coincide. The reasons for this effect can be attributed to the low symmetry of the complex, the large spin-orbit coupling of the Se donor atoms and participation of the Se 4d orbitals in the bonding.[16–20] The location of the principal axes in the molecular frame as well as the angles between the corresponding axes are shown in Fig. 4. The maximum $g$ value $g_3$ bisects approximately the S2–Cu–Se1 angle, whereas the Cu hfs components $A_2^{Cu}$ and $A_3^{Cu}$ are rotated around $A_1^{Cu}$. The angle between $g_3$ and $A_3^{Cu}$ was found to be 11°;

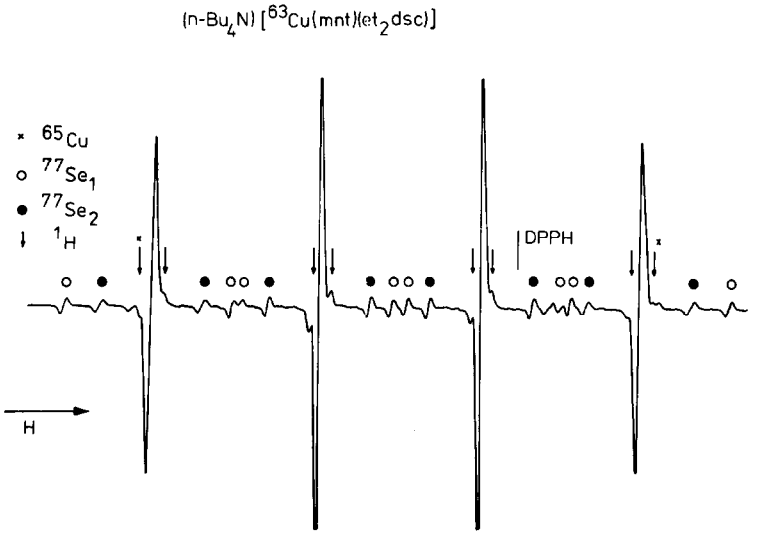



Fig. 3. X-band single-crystal ESR spectrum of ($n$-$Bu_4N$)[$^{63}$Cu/Ni(mnt)($et_2$dsc)] recorded at T = 295 K. The magnetic field lies in the ac plane for which the complex anions are magnetically equivalent.

Table 3. Experimentally obtained and calculated spin Hamiltonian parameters for ($n$-$Bu_4N$)[$^{63}$Cu/Ni(mnt)($et_2$dsc)]. Hyperfine coupling parameters in $10^{-4}$ cm$^{-1}$

| | observed[a] | calculated[b] | calculated[c] |
|---|---|---|---|
| $g_1$ | 2.014(8) | 1.9272 | 1.9783 |
| $g_2$ | 2.037(7) | 2.0549 | 2.0606 |
| $g_3$ | 2.043(8) | 2.0416 | 2.0446 |
| Copper | | | |
| $A_1 - A_{av}$ | -70.0 | -63.8 | -65.6 |
| $A_2 - A_{av}$ | 33.3 | 27.2 | 30.2 |
| $A_3 - A_{av}$ | 36.8 | 36.6 | 35.5 |
| $A_{av}$ | -79.2 | | |
| Selenium 1 | | | |
| $A_1 - A_{av}$ | 70.9 | 78.7 | 70.0 |
| $A_2 - A_{av}$ | -34.5 | -34.7 | -33.9 |
| $A_3 - A_{av}$ | -36.3 | -44.0 | -36.1 |
| $A_{av}$ | 53.4 | 52.9 | 44.7 |
| Selenium 2 | | | |
| $A_1 - A_{av}$ | 64.0 | 66.4 | 62.3 |
| $A_2 - A_{av}$ | -30.6 | -32.7 | -30.3 |
| $A_3 - A_{av}$ | -33.5 | -33.6 | -32.1 |
| $A_{av}$ | 51.5 | 54.7 | 44.3 |
| Sulphur 1 | | | |
| $A_1 - A_{av}$ | | 6.1 | 6.5 |
| $A_2 - A_{av}$ | | -2.9 | -3.2 |
| $A_3 - A_{av}$ | | -3.2 | -3.3 |
| $A_{av}$ | | 16.5 | 17.3 |
| Sulphur 2 | | | |
| $A_1 - A_{av}$ | | 5.8 | 6.1 |
| $A_2 - A_{av}$ | | -3.3 | -3.2 |
| $A_3 - A_{av}$ | | -2.5 | -2.9 |
| $A_{av}$ | | 18.7 | 18.2 |

[a] Experimental errors: $g_i \pm 0.001$; $A_1^{Cu}$, $A_1^{Se} \pm 0.5$; $A_{2,3}^{Cu(Se)} \pm 1.0$.

[b] Calculated using the structure of the Ni complex

[c] mnt shifted by 0.1 Å

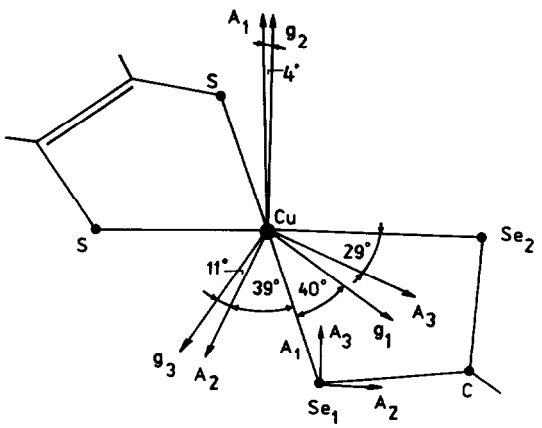



Fig. 4. Location of the principal axes of $\tilde{g}$. $\tilde{A}^{Cu}$ and $\tilde{A}^{Se}$ in the molecular frame of [Cu/Ni(mnt)($et_2$dsc)]$^-$.

$g_2$ and $A_1^{Cu}$ do nearly coincide. The largest Cu hfs component $A_1^{Cu}$ lies parallel to the normal of the molecular plane. The maximum components of the $^{77}$Se hfs point in the direction of the copper atom. The angle between $A_1^{Se1}$ and $A_1^{Se2}$ was found to be $(80 \pm 2)°$ and agrees well with the crystallographic Se1–Ni–Se2 angle which is 80.6°. The large difference in the Ni–Se1 and Ni–Se2 bonding distances is reflected by the corresponding $A_1^{Se1}$ and $A_1^{Se2}$ values which differ by about $9 \times 10^{-4}$ cm$^{-1}$. A rotation of the small $^{77}$Se hfs components $A_2^{Se}$ and $A_3^{Se}$ around the Cu–Se bonding axes could not be detected.

*MO calculations*

In order to obtain more detailed information

about the bonding properties especially on the Cu–S bonding—the $^{33}S$ could not be analyzed in the spectra—we calculated the spin Hamiltonian parameters by means of the extended Hückel MO method. Details concerning this method, the calculation of the ESR parameters and the used computer programme are described elsewhere.[17]

Two calculations were carried out: the first one using the structure of the Ni host complex and the second with the mnt ligand shifted by 0.1 Å. The calculated spin Hamiltonian parameters are listed in Table 3. Table 3 shows good agreement between calculated and experimentally obtained data especially for the second calculation. This is not surprising because the guest molecules are not expected to accept perfectly the structure of the host molecules.

The values listed in Table 3 refer to calculations which do not include Se 4*d* orbitals. Therefore, the poor agreement between calculated and experimentally obtained $\tilde{g}$ tensor components is not surprising.[17] As expected the calculated value for $g_2$ as well as the $\tilde{g}$ anisotropy in the coordination plane is too large. The experimentally observed rotation of the principal axes of the $\tilde{g}$ tensor is not reproduced.

The calculated anisotropic part of the Cu hfs agrees well with the experimental values. Because spin polarization of inner-shell s electrons dominates the isotropic Cu hfs splitting it is not possible to calculate this parameter by the extended Hückel MO method.[17]

In the calculation which uses the structure of the host complex the anisotropic Se hfs coupling constants are larger than the experimental values. Shifting the mnt ligand by 0.1 Å an excellent agreement could be obtained for the anisotropic couplings. However, the isotropic part of the Se hfs' is reduced by $\approx 17\%$. As pointed out this behaviour suggests that the differences between calculated and experimental ligand hfs parameters can be attributed to uncertainties in the structure of the incorporated guest molecule.

The anisotropic coupling constants predicted for $^{33}S$ by the extended Hückel MO calculations are in the expected order. Since the $^{77}Se$ hfs for $[Cu(mnt)(et_2dsc)]^-$ as well as the ligand hfs parameters for similar Cu complexes[8,13,17,19] are satisfactorally reproduced by extended Hückel MO calculations the calculated $^{33}S$ hfs tensors should be reliable. Nevertheless, the isotropic parts of the calculated $^{33}S$ hfs tensors appeared to be too large in comparison with those observed for the parent chelate $[Cu(mnt)_2]^{2-}$,[14] and other reliable complexes.[6,13,21]

*Bonding properties*

From the experimental and theoretical results obtained for the system $(n\text{-}Bu_4N)[Cu/Ni(mnt)(et_2dsc)]$ some conclusions about the bonding properties can be drawn. The MO of the unpaired electron mainly consists of the copper $3d_{xy}$ orbital with large participation of $3p_x$, $3p_y$, $4p_x$ and $4p_y$ orbitals of sulphur and selenium, respectively. The corresponding calculated MO coefficients are listed in Table 4. The $3d_{xy}$ character of this MO amounts to 39% (first calculation) and 42% (second calculation) indicating very strong covalent interactions with the ligands.

More insight in the bonding properties of the mixed-ligand chelate will be obtained from a comparison of the MO calculations made for the parent chelates and $[Cu(mnt)(et_2dsc)]^-$. In Table 5 the metal parts of those MO's of the three systems are listed in which at least one *d*-function of Cu has a coefficient larger than 0.25. The first one contains the unpaired electron. Furthermore, in Table 5 the Mulliken net spin densities of Cu, S and Se are given. As compared to the parent compounds, in the mixed-ligand complex Se gained spin density

Table 4. MO coefficients of the MO of the unpaired electron

| | Cu | | $Se_1$ | | | $Se_2$ | |
|---|---|---|---|---|---|---|---|
| | xy | s | x | y | s | x | y |
| (a) | 0.63 | 0.11 | -0.46 | +0.25 | -0.11 | +0.43 | +0.27 |
| (b) | 0.65 | 0.10 | -0.45 | +0.26 | -0.10 | +0.42 | +0.28 |
| | | | $S_1$ | | | $S_2$ | |
| | | s | x | y | s | x | y |
| (a) | | -0.14 | -0.26 | -0.21 | 0.15 | +0.22 | -0.21 |
| (b) | | -0.14 | -0.27 | -0.22 | 0.14 | +0.24 | -0.22 |

(a) Calculated using the structure of the Ni complex
(b) Mnt ligand shifted by 0.1 Å

Table 5. (A) Metal parts of the most important MO's for $Cu(mnt)(et_2dsc)^-$ and the corresponding parent chelates[17] in which at least one d-function has a coefficient larger than 0.25 (B) Mulliken net spin densities of Cu, S and Se

(A) Metal parts of most important MO's[a, b]

| $Cu(mnt)_2^{2-}$ | | $Cu(mnt)(dsc)^-$ | | $Cu(dsc)_2$ | |
|---|---|---|---|---|---|
| Energy (eV) | Orbitals of Cu | Energy (eV) | Orbitals of Cu | Energy (eV) | Orbitals of Cu |
| -5.7 | $0.71xy$ | -4.3 | $0.63xy$ | -4.4 | $0.64xy$ |
| -9.0 | $0.51xz$ | -8.9 | $0.36yz$ | -8.9 | $0.51yz$ |
| -10.2 | $0.43z^2-0.78x^2-y^2$ | -9.5 | $0.63xz$ | -10.0 | $0.82xz$ |
| -10.3 | $0.93yz$ | -9.8 | $0.27xy$ | -10.3 | $0.47z^2-0.83x^2-y^2$ |
| -10.5 | $0.84z^2+0.51x^2-y^2$ | -10.1 | $0.35z^2-0.73x^2-y^2$ | -10.4 | $0.80z^2+0.53x^2-y^2$ |
| -11.0 | $0.85xz$ | -10.4 | $0.54z^2+0.38x^2-y^2$ $-0.39yz$ | -10.5 | $0.42xy$ |
| -11.9 | $0.29z^2-0.33x^2-y^2$ | -10.5 | $0.41z^2+0.41x^2-y^2$ $+0.65yz$ | -11.1 | $0.86yz$ |
| -12.1 | $0.36xy$ | -10.6 | $0.57z^2-0.23yz$ | -11.8 | $0.55xz$ |
| -12.6 | $0.58xy$ | -11.1 | $0.64xz$ | -11.9 | $0.31z^2$ |
| -13.0 | $0.31yz$ | -11.9 | $0.32xz$ | -12.3 | $0.66xy$ |
| | | -12.3 | $0.20yz+0.59xy$ | | |
| | | -12.8 | $0.29yz-0.32xy$ | | |

(B) Mulliken net spin densities per atom

| $Cu(mnt)_2^{2-}$ | | $Cu(mnt)(dsc)^-$ | | $Cu(dsc)_2$ | |
|---|---|---|---|---|---|
| Cu | 0.510 | Cu | 0.409 | Cu | 0.404 |
| $S_1 = S_3$ | 0.18 | $Se_1$ | 0.29 | $Se_1 = Se_3$ | 0.24 |
| $S_2 = S_4$ | 0.17 | $Se_2$ | 0.26 | $Se_2 = Se_4$ | 0.24 |
| | 1.21 | $S_1$ | 0.13 | | 1.36 |
| | | $S_2$ | 0.12 | | |
| | | | 1.21 | | |

[a] The first one contains the unpaired electron

[b] The structures of the corresponding Ni chelates have been used

and S has lost some. Cu has nearly the same spin density in $[Cu(mnt)(et_2dsc)]^-$ and $Cu(et_2dsc)]_2$, but much less than in the mnt-parent chelate. These results are found to be in good agreement with the $^{77}Se$ and $^{63}Cu$ hfs' obtained experimentally. From Table 6 which compares the experimentally derived hfs parameters for the mixed-ligand and the parent chelates, it is seen that the isotropic and anisotropic parts of the $^{77}Se$ hfs' are considerably larger than those reported for $Cu(et_2dsc)_2$.[17] Also, as predicted the $^{63}Cu$ hfs tensor found for $[Cu(mnt)(et_2dsc)]^-$ resembles much more that reported for $Cu(et_2dsc)_2$ than that observed for $[Cu(mnt)_2]^{2-}$.

Interestingly, the bonding angles determined for the $NiSe_2C$ part of the mixed-ligand chelate are almost the same as those reported for $Ni(et_2dsc)_2$.[10] Therefore, structural differences could not account for the large differences observed for the $^{77}Se$ couplings. The latter are the result of increased $s$, $p_x$ and $p_y$ MO coefficients and hence an enlarged covalency of the Cu–Se bonds in $[Cu(mnt)(et_2dsc)]^-$. However, it should be noted, that the summed spin densities show that in the $Cu(et_2dsc)_2$ complex the spin is much more concentrated in the centre of the molecule than in the other two.

The results obtained suggest a comparison of the spin density distribution with the gross charges derived for Cu, S and Se from a Mulliken orbital population analysis for the complexes under consideration. The gross charges (not listed because

Table 6. Experimentally found principal values of the $^{63}Cu$ and $^{77}Se$ hyperfine tensors for $(n\text{-}Bu_4N)_2[^{63}Cu/Ni(mnt)_2]$,[14] $(n\text{-}Bu_4N)[^{63}Cu/Ni(mnt)(et_2dsc)]$ and $Cu/Ni(et_2dsc)_2$[16]

| | $Cu(mnt)_2^{2-}$ | $Cu(mnt)(et_2dsc)^-$ | $Cu(et_2dsc)_2$ |
|---|---|---|---|
| Copper | | | |
| $A_1 - A_{av}$[a] | -81.7 | -70.0 | -64.6 |
| $A_2 - A_{av}$ | +40.4 | +33.3 | +29.0 |
| $A_3 - A_{av}$ | +41.4 | +36.8 | +35.6 |
| $A_{av}$ | -79.4 | -79.2 | -79.6 |
| Selenium 1 | | | |
| $A_1 - A_{av}$ | | +70.9 | +57.2 |
| $A_2 - A_{av}$ | | -34.5 | -26.1 |
| $A_3 - A_{av}$ | | -36.3 | -31.1 |
| $A_{av}$ | | +53.4 | +48.0 |
| Selenium 2 | | | |
| $A_1 - A_{av}$ | | +64.0 | +58.0 |
| $A_2 - A_{av}$ | | -30.6 | -25.5 |
| $A_3 - A_{av}$ | | -33.5 | -32.5 |
| $A_{av}$ | | +51.5 | +45.0 |

[a]Principal values are given in $10^{-4}$ $cm^{-1}$

the differences between the chelates under study are small) show that there is very little effect on the atomic charges only. Interestingly, for $[Cu(mnt)(et_2dsc)]^-$ the charge of Se appears to be somewhat decreased, as opposed to the spin density (Table 5). The copper charge, however, is almost the same in all three systems. This indicates that back-bonding has been taken into account. This effect is clearly to be seen if one compares the density in "*xy*" of $[Cu(mnt)]^{2-}$ and $[Cu(mnt)(et_2dsc)]^-$. In the former the spin density is larger but the charge density is smaller (*xy*-charges: $[Cu(mnt)_2]^{2-} = 1.55$, $[Cu(mnt)(et_2dsc)]^- = 1.62$), due to the bonding in lower lying orbitals.

Unfortunately, $^{33}S$ hyperfine tensors (which would be very helpful for the spin density distribution analysis) could not be obtained experimentally for the mixed-ligand complex. Attempts have been made to determine the $^{13}C$ hfs coupling tensors of the $mnt^{2-}$ double bond and the chelate ring carbon atoms of the $et_2dsc^-$ ligand by ENDOR measurements. The crystals, however, burst asunder if cooled to temperatures necessary for ENDOR experiments ($T \approx 27$ K). The analysis of the angular dependencies of the $^{13}C$ ENDOR transitions for $[Cu(mnt)(et_2dsc)]^-$, as far as they could be followed, indicates some loss of electron spin density of the $mnt^{2-}$ part compared with the data recently obtained for the parent chelate ($n$-$Bu_4N)_2[Cu(mnt)_2]$.[22] This suggests—in agreement with the $^{77}Se$ couplings found — that spin density is transfered from "$mnt^{2-}$" to the Se atoms of the $et_2dsc^-$ ligand. For the mixed-ligand system $[Cu(mnt)(H(et)dtp)]^-$ spin density transfer from $(H(et)dtp)^-$ to $mnt^{2-}$ has been observed.[6,7] The direction of spin density transfer in the mixed-ligand complexes seems to be determined by the ligand which is able to form the more covalent metal-ligand bonds. Based on EHMO and experimental data obtained for several parent chelates[13,17,19,23] the dichalcogeno ligands can be arranged as follows concerning their ability to form covalent metal-ligand bonds ($dsp^-$ = O,O′-dialkyl-dialkyl-diselenophosphate):

$$dtp^- < dtc^- \lesssim mnt^{2-} < dsp^- < dsc^-.$$

This relation is also reflected by the mixed-ligand chelates studied.

Finally, it should be noted that a comparison of the total electron energies obtained by EHT calculations for the parent chelates and the mixed-ligand chelate results in an energy gain of $\Delta E = -36.22$ kJ/mole[2] for the reaction (I). Therefore, the formation of the mixed-ligand complex appears to be energetically favoured. The above-dicussed back-bonding effects should be considered as a possible factor in this stabilization.

## REFERENCES


1. W. Dietzsch, J. Reinhold, R. Kirmse, E. Hoyer, I. N. Marov and V. K. Beljaeva, *J. Inorg. Nucl. Chem.* 1977, **39**, 1377.
2. W. Dietzsch, J. Lerchner, J. Reinhold, J. Stach, R. Kirmse, G. Steimecke and E. Hoyer, *J. Inorg. Nucl. Chem.* 1980, **42**, 509.
3. R. Kirmse, R. Heber and E. Hoyer, *Z. Chem.* 1973, **13**, 385.
4. G. Krishnamoorthy and B. S. Prabhananda, *J. Magn. Reson.* 1978, **30**, 273.
5. J. Stach, W. Dietzsch, R. Kirmse and E. Hoyer, *Inorg. Nucl. Chem. Letts* 1978, **14**, 143.
6. J. Stach, R. Kirmse and W. Dietzsch, *Inorg. Chim. Acta* 1979, **36**, L 395.
7. R. Kirmse, R. Böttcher and C. P. Keijzers, *Chem. Phys. Lett.* 1982, **87**, 467.
8. R. Kirmse, R. Böttcher, C. P. Keijzers, L. Golic, W. Dietzsch, W. Brunner and J. Stach, to be published.
9. A. Kobayashi and Y. Sasaki, *Bull. Chem. Soc. Japan* 1977, **50**, 2650.
10. M. Bonamico and G. Dessy, *J. Chem. Soc. A* 1971, 264.
11. Q. Fernando and C. D. Green, *J. Inorg. Nucl. Chem.* 1967, **29**, 647.
12. J. F. McConnel and V. Katalsky, *Acta Cryst* 1967, **B 22**, 853.
13. D. Attanasio, C. P. Keijzers, J. P. van de Berg and E. de Boer, *Mol. Phys.* 1976, **31**, 501.
14. R. Kirmse, J. Stach, W. Dietzsch and E. Hoyer, *Inorg. Chim. Acta* 1978, **26**, L 53.
15. D. Snaathorst, C. P. Keijzers, A. A. K. Klaassen, E. de Boer, V. P. Chacko and R. Gomperts, *Mol. Phys.* 1980, **40**, 585.
16. C. P. Keijzers, G. F. M. Paulussen and E. de Boer, *Mol. Phys.* 1975, **29**, 973.
17. C. P. Keijzers and E. de Boer, *Mol Phys.* 1975, **29**, 1007.
18. C. P. Keijzers, P. L. A. Chr. M. van der Meer and E. de Boer, *Mol. Phys.* 1975, **29**, 1733.
19. C. P. Keijzers and E. de Boer, *Mol. Phys.* 1975, **29**, 1743.
20. J. Stach, R. Kirmse, E. Hoyer and S. Wartewig, *J. Inorg. Nucl. Chem.* 1978, **40**, 1529.
21. R. Kirmse and B. V. Solovev, *J. Inorg. Nucl. Chem.* 1977, **39**, 41. The carbon splitting cited herein is actually a hydrogen spin-flip transition.
22. R. Kirmse, R. Böttcher, C. P. Keijzers, J. Stach, U. Abram and W. Dietzsch, to be published.
23. C. P. Keijzers and D. Snaathorst, *Chem. Phys. Letts* 1980, **69**, 348.

*Polyhedron* Vol. 3, No. 4, pp. 443–449, 1984
Printed in Great Britain.

0277-5387/84 $3.00 + .00
Pergamon Press Ltd.

# THE FERRIC CHLORIDE α-DI-IMINE SYSTEM—VI

## ELECTRONIC STRUCTURE OF THE DIMETHYL FORMAMIDE ADDUCT OF MONO-1,10-PHENANTHROLINE FERRIC CHLORIDE AND THE BY-PRODUCT, TRIS-1,10-PHENANTHROLINE FERROUS μ-OXO-BIS[TRICHLORO FERRATE(III)]; FIELD INDUCED SLOW PARAMAGNETIC RELAXATION IN MONOMERIC FERRIC COMPLEXES

**W. M. REIFF* and E. H. WITTEN**
Department of Chemistry, Northeastern University, Boston, MA 02115, U.S.A.

(*Received* 25 *January* 1983; *accepted* 25 *April* 1983; *revised* 1983)

**Abstract**—Magnetic susceptibility (1.45–300 K), zero and high field Mössbauer spectroscopy, IR and solution conductivity measurements were used to characterize the title DMR adduct, $Fe(phen)Cl_3 \cdot DMF$. The absence of magnetic hyperfine splitting in zero external field is correlated with $D$ positive corresponding to an isolated, rapidly relaxing ground ($M_S = \pm 1/2$) Kramers doublet. X-ray data show that the ferric ion centres are apparently sufficiently close ($\sim 7$ Å) to allow for rapid spin–spin relaxation via dipolar interactions. The application of longitudinal magnetic fields (0–5 Tesla for 1.7–4.2 K) slows relaxation and results in fully resolved Zeeman split Mössbauer spectra for which the effective internal field, $H_n = 354$ kG at 1.7 K for $H_0 = 5$T. The complex $[Fe(phen)_3][O(FeCl_3)_2]$ contains an unusual binuclear anion based on tetrahedral $FeOCl_3$ units as recently found in $[pyridinium]_2[O(FeCl_3)_2]$ and is obtained as a trace by-product in our preparation of $Fe(phen)Cl_3 \cdot DMF$. Further magnetic characterization of the latter pyridinium compound is presented.

As part of our study of chlorine bridged iron(III) polymers of α-diimine ligands such as 1,10-phenanthroline and 2,2′-bipyridine, we had need of comparative spectroscopic, magnetic and structural data for monomeric ferric complexes of these ligands. This prompted our interest in and study of the title complex, $Fe(phen)Cl_3 \cdot DMF$. The compound was first prepared by Broomhead and Dwyer[1] and the single crystal structure determination of the chromium(III) analog was reported subsequently.[2] The latter exhibits a *meridional* pseudo-octahedral $CrCl_3N_2O$ chromophore as found in the present work for iron(III). We have been unable to isolate the *facial* isomer. We now present the details of our magnetic and spectroscopic characterization of $Fe(phen)Cl_3 \cdot DMF$ as well as the trace binuclear by-product $[Fe(phen)_3][O(FeCl_3)_2]$. Particular emphasis is placed on the extent and nature of slow paramagnetic relaxation for the DMF complex and its relation to the observed structure.

*Author to whom correspondence should be addressed.

## EXPERIMENTAL

The DMF adduct was prepared by the method of Broomhead and Dwyer.[1] Found: C, 43.83; H, 3.77; N, 10.19. Calc.: C, 43.36; H, 3.63; N, 10.11%. The details of the experimental methods used for the determination of magnetic susceptibility and zero field Mössbauer spectra have been described previously.[3] Temperature measurement and control involved the use of calibrated silicon and gallium arsenide diodes. IR spectra were determined using a Perkin–Elmer model 567 spectrometer using both KBr pellets and mineral oil mulls. Conductivity measurements were performed with an Industrial Instruments model RC 16B2 bridge.

The super-conducting solenoid for high field Mössbauer spectra was wound with a compensating coil such that the γ-ray source was always maintained in a fringing field (of the main coil) of $< 0.1$ T. The applied field was longitudinal, i.e. parallel to the direction of γ-ray propagation.

### *Magnetic susceptibility*

The temperature dependence of the corrected

molar susceptibility ($\chi'_M$), reciprocal susceptibility ($\chi'^{-1}_M$) and magnetic moment ($\mu$) for a powder sample are shown in Fig. 1 while some sample moment data are given in Table 1. No field dependence was observed over the range 1.6–5.1 kG. The material clearly obeys a Curie–Weiss law over essentially the entire temperature range. The following parameters are the result of a least squares fit of $\chi'^{-1}_M$ to $\chi'^{-1}_M = (T - \theta/C)$: $C = 4.30$(emu/mole), $\mu_{\text{eff}} = 5.93$, and the paramagnetic Curie temperature, $\theta = -0.62$ K. The absence of magnetic exchange interaction and ordering is expected in view of the structure,[4,5] i.e. there are no pathways for either direct of superexchange and the temperature dependence of $\chi'_M$ is unremarkable. The only remaining mechanism for exchange is then delocalization of metal ion spin density to the chloro ligands concommitant with reduction of the ferric ion charge. There could then be a weak exchange interaction between the spin densities at such chloro ligands via nonbonded (Cl–Cl) contacts between different coordination polyhedra. Hôwever, the shortest of such Cl–Cl

Table 1

| T(K) | $\mu(\mu_B)$ |
|---|---|
| 302.9 | 5.94 |
| 228.2 | 5.91 |
| 147.7 | 5.89 |
| 79.8 | 5.88 |
| 69.2 | 5.88 |
| 58.0 | 5.89 |
| 49.8 | 5.85 |
| 45.2 | 5.85 |
| 41.4 | 5.85 |
| 38.0 | 5.87 |
| 34.9 | 5.89 |
| 31.8 | 5.87 |
| 28.9 | 5.87 |
| 27.2 | 5.88 |
| 25.3 | 5.87 |
| 23.3 | 5.86 |
| 21.0 | 5.84 |
| 18.4 | 5.83 |
| 16.2 | 5.79 |
| 13.8 | 5.78 |
| 10.6 | 5.67 |
| 8.2 | 5.67 |
| 7.0 | 5.67 |
| 5.7 | 5.58 |
| 4.2 | 5.38 |
| 3.9 | 5.43 |
| 3.6 | 5.37 |
| 3.2 | 5.29 |
| 2.8 | 5.18 |
| 2.4 | 5.00 |
| 2.1 | 4.89 |
| 1.9 | 4.75 |
| 1.4 | 4.30 |

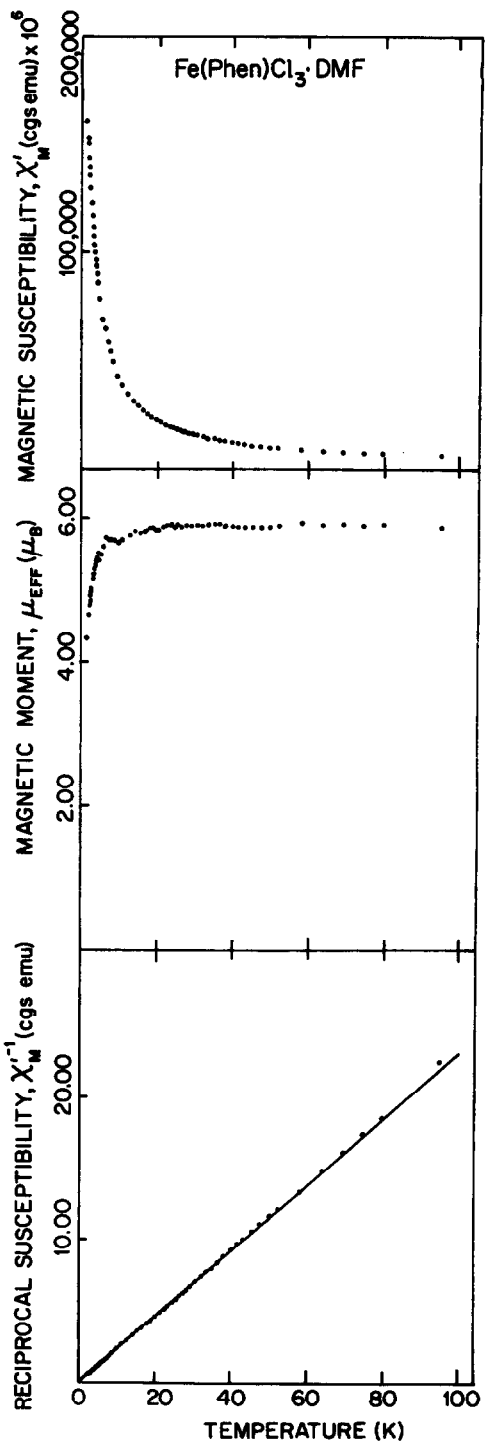



Fig. 1. Temperature dependence of the magnetic susceptibility, reciprocal susceptibility and magnetic moment for a powder sample for Fe(phen)$Cl_3 \cdot$ DMF, $H_0 = 5.1$ kG.

distances in the unit cell are > 4 Å thus ruling out significant exchange interaction via this route. However, as will be seen in the analysis of the Mössbauer results the metal ions are apparently not sufficiently isolated to prevent weak dipolar interactions and rapid spin–spin relaxation.

The temperature dependence of $\mu$ exhibits a large decrease in moment below ~ 20 K, and we attribute this effect to a large zero field splitting of the $^6$A ground term. For axial zero-field splitting, the limiting value of the average powder moment as $T \rightarrow 0$ is $\sqrt{19} \sim 4.38 \mu_\beta$ when $D$ is > 0.[6] The low temperature moment of Fe(phen)$Cl_3 \cdot$ DMF is quite close to this value indicating $D$ is in fact positive. The gross magnetic behavior of Fe(phen)$Cl_3 \cdot$ DMF is very similar to that of ferric hemin chloride and certain high spin ferric porphyrin compounds[7] whose axial zero field splittings ($D$) have been variously estimated from ~ +5 $cm^{-1}$ via far IR,[7] Mössbauer spectroscopy,[8] and susceptibility measurements[9] as to as large as +12 $cm^{-1}$, again by powder susceptibility measurements.[10] In any event, the electronic ground state of the system is thus relatively well isolated $M_S = \pm 1/2$ Kramers doublet as pictured in Fig. 2.

Before concluding this section, we consider rhombicity for the ligand field environment experienced by the central ferric ion. Such a possibility is certainly suggested by the local coordination[5] (metal–ligand bond distances) shown in Fig. 3. A large effect of this type is expected to result in $E \neq 0$ and an ESR spectrum with $g_{effective} = 4.3$, i.e. typical of rhombicly distorted high-spin iron(III). Here $E$ is the non-axial zero-field splitting parameter of the conventional spin Hamiltonian. However, the spectrum observed at ambient temperature was poorly defined while at ~ 4.2 K broad resonances centered at $g_{effective} = 2$ and 6 were apparent. The latter observation is again consistent with essentially *axial symmetry, with* $D > 0$ and a *ground* $M_S = +1/2$ Kramers doublet, i.e. $E \sim 0$.

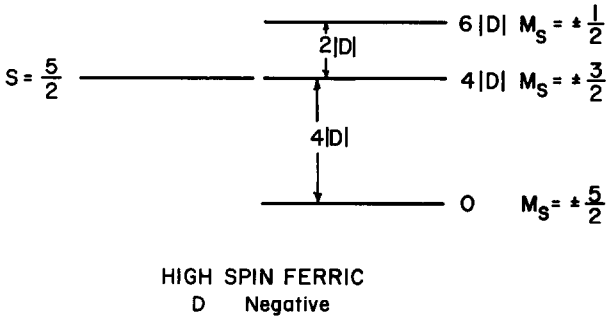



Fig. 2. Axial zero field splitting diagram for a $^6$A ground term, D negative.

Recall that the $M_s \pm 3/2$ and $\pm 5/2$ Kramers doublets are effectively ESR silent in usual $X$-band measurements. This aspect of the electronic symmetry of the $Fe^{3+}$ in Fe(phen)$Cl_3 \cdot$ DMF, i.e. the question of a very small $E$ value must await a more detailed investigation of the full temperature dependence of its ESR spectrum. This study is not possible with the equipment available to us at this time. In any event, the idea of whether $E$ is or is not zero does not change the conclusions and primary thrust of the present study.

*IR spectra and conductivity data*

The IR spectrum of Fe(phen)$Cl_3 \cdot$ DMF is generally similar to that of the isomorphous chromium(III) analogue. In particular, intense far IR bands are observed at 386 and 330 $cm^{-1}$ corresponding to terminal Fe(III)–Cl stretching vibrations and consistent with the X-ray structure determination.[2,5] The local coordination found in the structure determination is shown in Fig. 3. In nitrobenzene solution (0.0001 M) Fe(phen)$Cl_3 \cdot$ DMF has a molar conductivity of 13 MHO $cm^2$/mole as compared to 28 MHO $cm^2$/mole for the same concentration of the 1:1 electrolyte $[(CH_3CH_2CH_2CH_2)_4N]I$ used as a conductivity standard. This suggests essentially

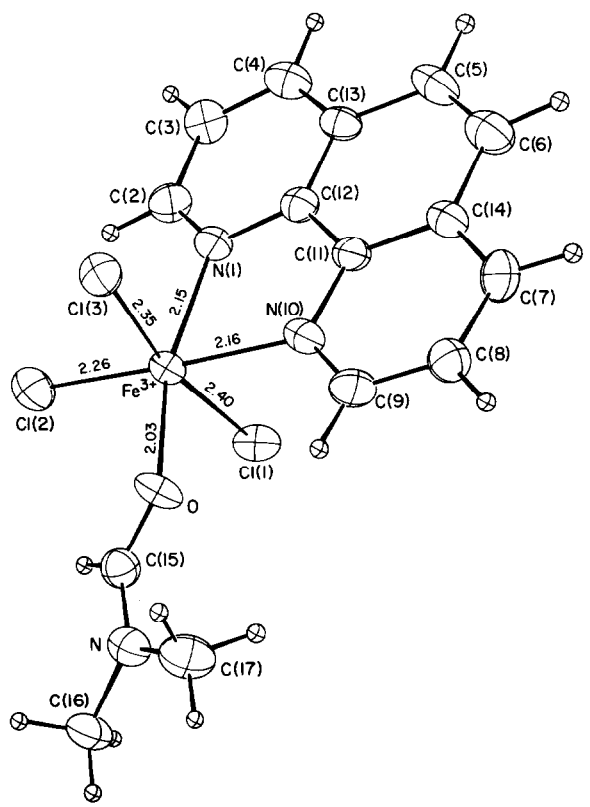



Fig. 3. Local coordination for Fe(phen)$Cl_3 \cdot$ DMF as determined from single crystal X-ray study.

non-electrolyte character for the ferric complex and maintenance of the iron-chloride coordination in solution. However, it is not clear that the DMF is still coordinated. This has relevance to the meaning of possible frozen solution–dilution Mössbauer spectroscopy studies of slow paramagnetic relaxation to be discussed subsequently.

*Zero-field Mössbauer spectra*

The temperature dependence of the zero-field Mössbauer spectra is shown in Fig. 4 with sample data given in Table 2. These parameters are the result of least-squares Lorentzian fitting to an asymmetric quadrupole doublet and are typical[11] of slightly distorted 6-coordinate, high-spin $Fe^{3+}$. Below 4.2 K, we are no longer able to fit the Mössbauer spectra to such a doublet; a single broad transition is now observed. We attribute this to probable hyperfine interaction and coupling of the nuclear spin levels of $^{57}Fe$ with those of the coordination $^{14}N$ ($I = 1$) and $^{35,37}Cl$ ($I = 3/2$) ligands. It is not likely that the broadening has its origin in a hyperfine field from interaction with the ground $M_S = \pm 1/2$ electronic spin level of the ferric ion as intralevel relaxation for the $M_S = \pm 1/2$ Kramers doublet is rapid[12] in zero field.

Although there is incipient broadening, we do not observe resolved magnetic hyperfine splitting of zero-field Mössbauer spectra for neat powder samples of $Fe(phen)Cl_3 \cdot DMF$. At low temperatures, it is usually assumed that the predominant relaxation mechanism for *high spin* $Fe^{3+}$ is spin–spin as opposed to spin–lattice. In this circumstance, in order to observe magnetic hyperfine splitting, one must not only have progressive population of a slowly relaxing Kramer's doublet ($M_S = \pm 5/2$ or $M_S = \pm 3/2$) corresponding to

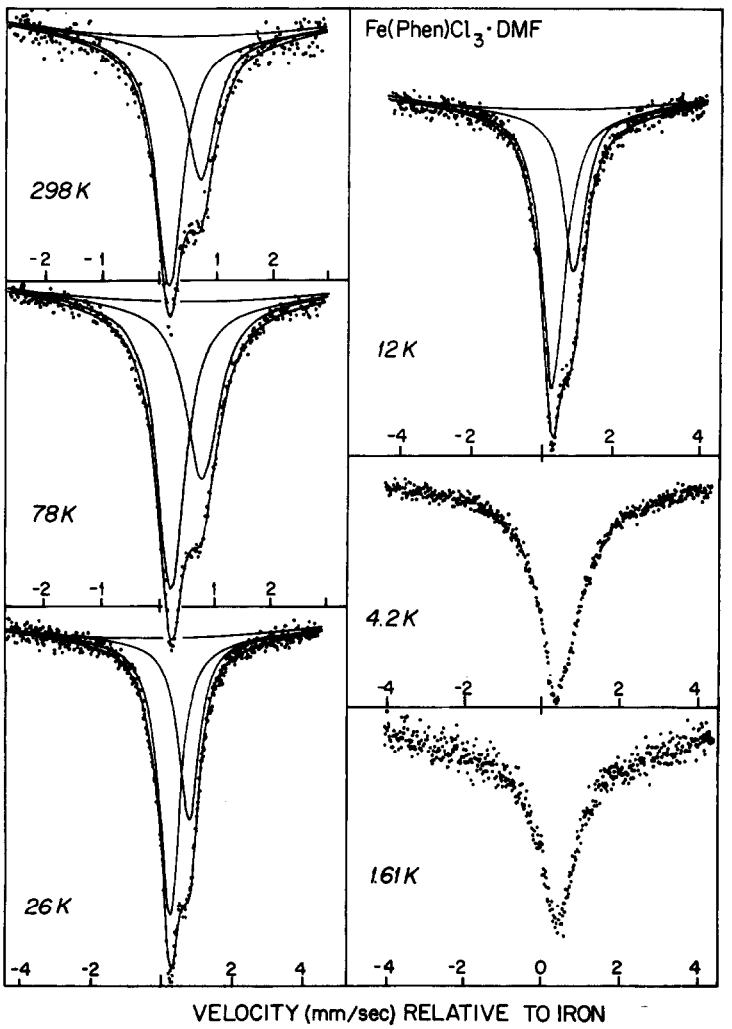



Fig. 4. Zero-field Mössbauer spectra of $Fe(phen)Cl_3 \cdot DMF$ from 298 to 1.61 K.

$D < 0$. The preceding doublets will also result in broadening effects with *increasing temperature* and population when $D$ is *positive* as in hemin.[13] It is also *necessary* that there be sufficient dilution of the paramagnetic metal ion centres so that the time for spin-spin relaxation via direct dipolar interactions is long. In one of the earlier Mössbauer spectroscopy studies of slow paramagnetic relaxation of simple monomeric high-spin ferric complexes, Wignal[14] has shown that the ferric ion centres have to be separated by $\geqslant 10$ Å before fully resolved hyperfine splitting is observed in low temperature, *zero-field* spectra. Thus, for instance, iron-(III)-(acetylacetonate) is a soluble neutral complex for which the iron–iron separation is $\sim 7.6$ Å in its neat form. This form of the complex exhibits a single broad transition to as low as 1.8 K. Dilution and glass formation in ether–alcohol mixtures ($\sim 1\%$ of $^{57}$Fe enriched complex) results in resolved hyperfine splitting of Fe(acac)$_3$ with $H_n \sim 530$ kG. For the present Fe(phen)Cl$_3 \cdot$ DMF complex, the shortest nearest neighbor iron–iron separations we observe are $\sim 7$ Å. Hence, it is not surprising that we do not observe hyperfine splitting in addition to the fact that the ground state is the rapid relaxing $M_S = \pm 1/2$ level. Although neutral, the present complex is not particularly soluble and in addition, we have no simple way of knowing whether the DMF remains coordinated in frozen solution. Thus we have not attempted $^{57}$Fe enrichment and dilution studies of the relaxation.

*High field Mössbauer spectroscopy*

An alternative approach to the preceding study is to slow the relaxation rate in the *neat powder* by applying external fields. This is shown in Fig. 5 for longitudinal fields of 25 and 50 kG at 1.7 K. The spectrum at 50 kG corresponds to an effective internal hyperfine field of 354 kG or an internal field of 404 kG where $H_{effective} = H_0 + H_{internal}$. The latter[14] value of internal field is reasonable for the contribution from an $M_S = \pm 1/2$ doublet in the limit of large external $H_0$.[15] In addition to inducing slow electron spin relaxation, the external field also decouples the weakly interacting $^{57}$Fe and ligand nuclear spin moments. Only *one* hyperfine pattern is evident in these spectra and the spectra exhibit four instead of the usual six transitions expected for nuclear Zeeman splitting of $^{57}$Fe. This is the result of polarization of the sample moments and internal hyperfine fields along the direction of $H_0$ and therefore parallel to the $\gamma$-ray since $H_0$ is longitudinal. In this situation the angular components of the selection rules for the $\Delta M_I = 0$ transitions (transitions 2 and 5) of a six line spectrum predict zero intensity.[11] These are precisely the transitions absent in Fig. 5. The spectra are consistent with population of a *single* relatively isolated Kramers doublet, namely $M_S = \pm 1/2$. This accords with a large positive $D$ value $\sim 15\,\text{cm}^{-1}$ suggested by our $\mu$ vs $T$ data. That is, the first excited Kramers doublet ($M_S = \pm 3/2$) at $2D$ is $\sim 30\,\text{cm}^{-1}$ above the ground state and is

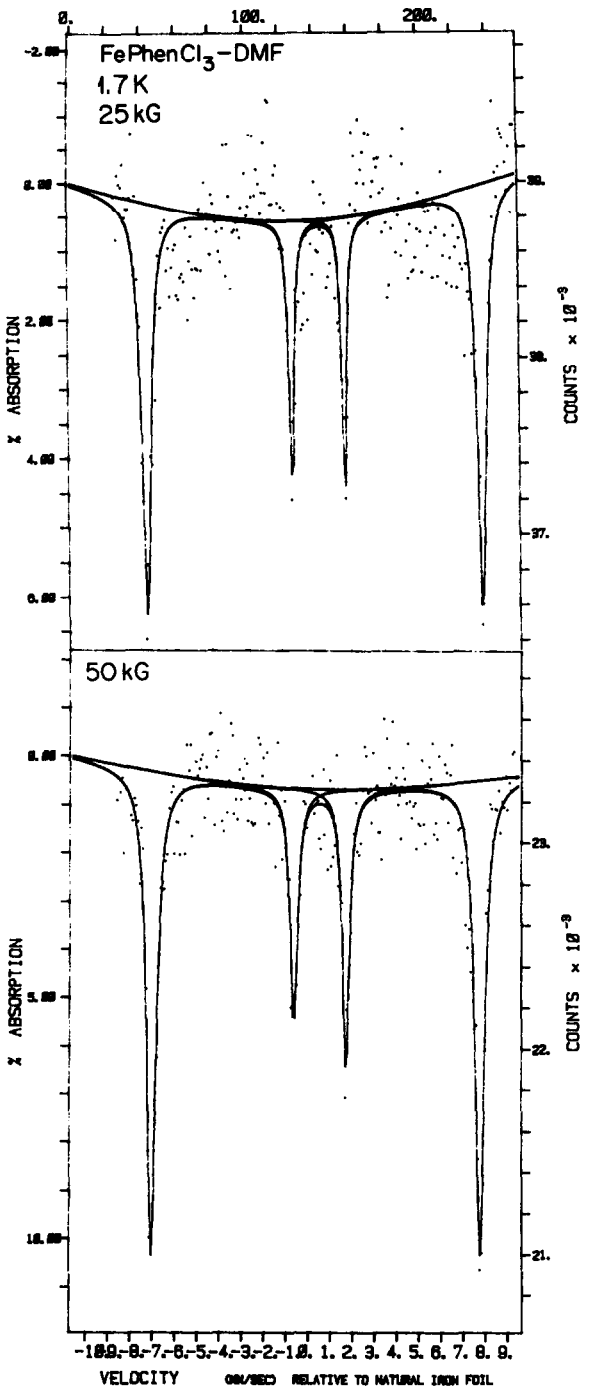



Fig. 5. Mössbauer spectra of Fe(phen)Cl$_3 \cdot$ DMF at 1.7 K for longitudinal applied fields of 25 and 50 kG.

Table 2. Mössbauer parameters for $Fe(phen)Cl_3 \cdot DMF$ from least squares computer fits of the spectra to Lorentzians

| Compound | T°K | $\chi^2$ | $\Gamma_1$ | $\Gamma_2$ | $\Gamma_1/\Gamma_2$ | $\delta$ (mm/sec) | $\Delta Eq$ (mm/sec) |
|---|---|---|---|---|---|---|---|
| $Fe(phen)Cl_3 \cdot DMF$ | 298 | 76.30 | 0.555 | 0.595 | 0.933 | 0.446 | 0.554 |
| | 78 | 207.32 | 0.573 | 0.683 | 0.839 | 0.492 | 0.545 |
| | 26 | 308.48 | 0.691 | 0.712 | 0.971 | 0.550 | 0.567 |
| | 12 | 281.87 | 0.777 | 0.731 | 1.063 | 0.568 | 0.575 |

therefore little populated at 1.7 K and not expected to contribute significantly to the limiting low temperature spectra.[15] The behavior of the present system contrasts strongly with that observed for the aforementioned Fe(acetylacetonate)$_3$. Through principal susceptibility measurements of single crystal samples in the range 300 K to 80 K, Gerloch and Slade[16] estimate a very small negative $D$ value ($\sim -0.2\,cm^{-1}$). Thus, the total energy separation of the three Kramers doublets of Fig. 5, $6|D|$, is $\sim 1\,cm^{-1}$ for Fe(acetylacetonate)$_3$ and all three Kramers doublets are populated at 4.2 K. Consistent with this is Bancroft's and Sham's observation[17] of relaxation broadening and resolved magnetic hyperfine splitting for Fe(acetylacetonate)$_3$ diluted in Al(acetylacetonate)$_3$ in zero applied field at 4.2 K. Contributions from all the Kramers doublets are evident in the spectra.

*Magnetic properties of the* $O(FeCl_3)_2^{2-}$ *anion*

We conclude this investigation with brief consideration of the magnetic properties of the binuclear $[O(FeCl_3)_2]^{2-}$ anion. As mentioned earlier the double salt $[Fe(phen)_3][O(FeCl_3)_2]$ containing this unusual anion was obtained as a by-product with $Fe(phen)Cl_3 \cdot DMF$ and its structure determined by X-ray diffraction.[18] It was found to be contaminated with the latter preventing meaningful detailed magnetic study and characterization of the expected anti-ferromagnetic exchange. However, at the time that we isolated this species, Drew *et al.*,[19] reported the isolation, magnetic, spectroscopic and structural characterization of the foregoing anion in the *pyridinium salt*. In addition, Fernandopulle *et al.*,[20] have also apparently isolated the same binuclear anion with di- and tripyridylammonium cations and report ambient temperature magnetic moments of $\sim 2\mu_\beta$/Fe. In an effort to further investigate the exchange in this anion, we have extended the results of Drew *et al.* for the pyridinium salt from their lowest temperature $\sim 131$ K to $\sim 50$ K, Table 3 and Fig. 6. Our data over comparable temperature ranges agree reasonably well with those of Drew and can be fitted to anti-ferromagnetic exchange $J \approx -90\,cm^{-1}$. As can be seen, although $\mu$ continues to show a steady and considerable decrease from the lowest value observed by Drew *et al.* ($1.17\mu\beta$) to our lowest value of $0.66\mu_\beta$ at 51.7 K

Table 3

| T(K) | $\mu$/Fe($\mu_\beta$) |
|---|---|
| 302.9 | 1.87 |
| 293.7 | 1.84 |
| 283.5 | 1.80 |
| 265.5 | 1.74 |
| 247.2 | 1.67 |
| 228.4 | 1.60 |
| 216.6 | 1.54 |
| 204.6 | 1.48 |
| 192.5 | 1.44 |
| 180.5 | 1.38 |
| 172.5 | 1.34 |
| 164.4 | 1.30 |
| 156.1 | 1.25 |
| 147.8 | 1.21 |
| 143.4 | 1.18 |
| 139.4 | 1.16 |
| 135.1 | 1.13 |
| 131.1 | 1.10 |
| 126.7 | 1.07 |
| 123.4 | 1.06 |
| 120.4 | 1.03 |
| 113.9 | 0.99 |
| 109.7 | 0.96 |
| 104.9 | 0.93 |
| 77.7 | 0.75 |
| 74.6 | 0.74 |
| 71.1 | 0.73 |
| 68.5 | 0.72 |
| 64.7 | 0.70 |
| 62.5 | 0.69 |
| 58.7 | 0.68 |
| 56.9 | 0.67 |
| 55.1 | 0.67 |
| 51.7 | 0.66 |

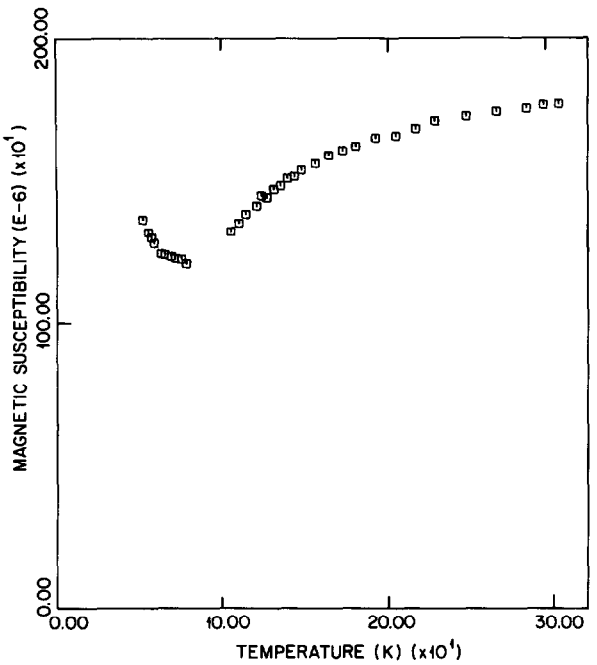



Fig. 6. Temperature dependence of the magnetic susceptibility of [pyridinium]$_2$[O(FeCl$_3$)$_2$] at 5.1 kG.

(obtained by pumping on nitrogen), $\chi'_M$ begins to rise at $\sim$70 K. We attribute this to monomeric $Fe^{3+}$ impurity whose presence often complicates the low temperature magnetic behaviour of binuclear iron(III) complexes. Hence, we have elected not to study the system to even lower temperatures.

*Acknowledgements*—The authors wish to thank the National Science Foundation for its support of this work under Grant No. DMR-80-12625 from the Division of Materials Research, Solid State Chemistry Program. We are grateful to Dr. Karoly Lázár for determination of high field Mössbauer spectra and Dr. Arthur Heiss (Brucker Co.) and Prof. William Hatfield (University of North Carolina) for ESR spectra. Finally, they are greatly indebted to Professor Hollis Wickman for helpful discussions on ESR data and the implications of our low temperature susceptibility moment data.

## REFERENCES

1. J. A. Broomhead and F. P. Dwyer, *Austral. J. Chem.* 1961, **14**, 250.
2. J. A. Broomhead, J. Evans, W. D. Grumley and M. Sterns, *J. Chem. Soc. Dalton* 1973, 173.
3. W. M. Reiff and C. Cheng, *Inorg. Chem.* 1977, **16**, 2097.
4. W. M. Reiff, E. Witten, T. Brennan, A. Garafalo and Kent Mottle, Abstracts, American Cryst. Assoc. Meeting, August 1979, Boston, Mass.
5. W. M. Reiff, E. Witten, T. Brennan, A. Garafalo and K. Mottle, *Inorgan. Chim. Acta.* 1983, **77**, L27.
6. M. Kotani, *Supplement Progr. Theo. Phys.* 1961, **17**, 4.
7. P. L. Richards, W. S. Caughey, H. Eberspaecher, G. Feher and M. Malley, *J. Chem. Phys. Lett.* 1967, **47**, 1187.
8. C. E. Johnson, *Phys. Lett.* 1966, **21**, 491.
9. V. R. Marathe and S. Mitra, *Chem. Phys. Lett.* 1973, **19**, 140.
10. C. Maricondi, W. Swift and D. K. Straub, *J. Am. Chem. Soc.* 1969, **91**, 5205.
11. N. N. Greenwood and T. C. Gibb, *Mössbauer Spectroscopy*. Chapman & Hall, London (1972).
12. G. K. Wertheim and J. P. Remeika, *Phys. Lett.* 1964, **10**, 14.
13. R. G. Shulman and G. K. Wertheim, *Rev. Mod. Phys.* 1964, **36**, 459.
14. J. W. G. Wignall, *J. Chem. Phys.* 1968, **44**, 2462.
15. H. H. Wickman and G. K. Wertheim, In *Chemical Applications of Mössbauer Spectroscopy* (Edited by R. H. Herber and V. I. Goldanskii), p. 554. Academic Press, New York (1968).
16. M. Gerloch, J. Lewis and R. C. Slade, *J. Chem. Soc. A*, 1969, 1422.
17. G. M. Bancroft and T. K. Sham, *J. C. S. Faraday II* 1976, **72**, 1706.
18. W. M. Reiff, E. Witten, T. Brennan, A. Garafalo and K. Mottle, *Inorganica Chimica* 1983, **77**, L83.
19. M. C. B. Drew, V. McKee and S. M. Nelson, *J. Chem. Soc. Dalton* 1978, 80.
20. M. E. Fernandopulle, P. A. Gillespie and W. R. McWhinnie, *Inorg. Chim. Acta* 1978, **29**, 197.

*Polyhedron* Vol. 3, No. 4, pp. 451–456, 1984
Printed in Great Britain.

0277-5387/84 $3.00 + .00
© 1984 Pergamon Press Ltd.

# IR SPECTRA AND THERMAL DECOMPOSITION/ DEHYDRATION OF DOUBLE COMPLEX SALTS OF LANTHANUM(III) SULPHATE COMPLEX ANIONS WITH SEVERAL COBALT(III) AMMINE COMPLEX CATIONS

MASATOMI SAKAMOTO
Department of Industrial Chemistry, Faculty of Engineering, Ehime University, Bunkyo-cho, Matsuyama-shi, Ehime-ken, Japan

(*Received* 5 *May* 1983; *accepted* 10 *October* 1983)

**Abstract**—Double complex salts of lanthanum(III) sulphate complex anions with several cobalt(III) ammine complex cations, $[Co(NH_3)_6][La(SO_4)_3]\cdot H_2O$ (**1**), $(NH_4)_3[Co(NH_3)_5H_2O]$-$[La(SO_4)_3]_2\cdot 2H_2O$ (**2**), and $(NH_4)_3[Co(NH_3)_4(H_2O)_2][La(SO_4)_3]_2\cdot 2H_2O$ (**3**), were prepared by the addition of hexaamminecobalt(III), pentaammineaquacobalt(III), and *cis*-tetra-amminediaquacobalt(III) complexes to the solution containing lanthanum(III) ion and excess ammonium sulphate. The IR spectra of sulphate groups of these double complex salts were much more complicated than those of the almost free sulphate groups such as $(NH_4)_2SO_4$ and $[Co(NH_3)_6]_2(SO_4)_3\cdot 5H_2O$. Furthermore, values of activation energy in the dehydration process of **1**, **2** and **3** were estimated using modified Doyle's and Wiedemann's method. They were $95.6 \pm 4.3$, $157.1 \pm 15.5$ and $163.2 \pm 20.8$ kJ mol$^{-1}$, respectively. Here, one molecule water is released per molecule of **1**, **2** and **3**.

It has been well known that lanthanide(III) ions form double salts such as $Na_2SO_4\cdot Ln_2(SO_4)_3\cdot 8H_2O$ with alkali metal sulphate.[1] There are several studies on the lanthanide(III) sulphate complex anions.[2–5] Recently, the crystal structure,[2,3] IR spectra,[2] and thermal properties[4] of $Cs[Ln(SO_4)_2(H_2O)_3]\cdot H_2O$ have been reported by Bukovec *et al.* According to these studies, Pr(III) atom, for example, is coordinated by nine oxygens. Six of them belong to tridentate sulphate ligands which are chelating and bridging at the same time, while three other oxygens belong to water molecules. Furthermore, IR spectra of sulphate groups are much more complicated and two DTG peaks corresponding to dehydrations are observed for all complexes except for $Cs[Lu(SO_4)_2(H_2O)_3]\cdot H_2O$ where only a single DTG effect appears. Saito and Ueno[5] have studied the precipitation behaviour of lanthanide(III) sulphate complexes from ammonium sulphate, sodium sulphate, and sulphuric acid solution with addition of hexaamminecobalt(III) complex as a precipitant. They obtained the double complex salts such as $[Co(NH_3)_6][Ln(SO_4)_3]\cdot nH_2O$($n$: 2–4) and $(NH_4)_3[Co(NH_3)_6][Ce(SO_4)_3]_2\cdot 6H_2O$. The solubility decreases from La to Sm where there is a minimum. Then it increases rapidly with increasing atomic number.

In the present work, it is shown that lanthanum(III) sulphate complex anion can also be precipitated from ammonium sulphate solution using pentaammineaquacobalt(III) and *cis*-tetraamminediaquacobalt(III) complexes as precipitants and that the compositions of the precipitates are $(NH_4)_3[Co(NH_3)_5H_2O][La(SO_4)_3]_2\cdot 2H_2O$ (**2**) and $(NH_4)_3[Co(NH_3)_4(H_2O)_2][La(SO_4)_3]_2\cdot 2H_2O$ (**3**), respectively. The double complex salt, $[Co(NH_3)_6][La(SO_4)_3]\cdot H_2O$ (**1**), was also prepared by a conventional method[5] with slight modifications. Furthermore, the discussions on the IR absorption and thermal properties will be given.

## EXPERIMENTAL

The stock solution of lanthanum(III)(*ca.* 0.1 mol dm$^{-3}$): After commercial $La_2O_3$ (purity of 99.99%) was dissolved in conc. HCl, the solution was evaporated almost to dryness on a water bath. The residue was dissolved in *ca.* 0.05 N HCl.

All the double complex salts were precipitated from the solution adjusted to *ca.* pH 2.

$[Co(NH_3)_6][La(SO_4)_3]\cdot H_2O$ (**1**) was prepared by a similar method as described in the literature.[5] In the present work, the precipitates were filtered, washed with water, alcohol, and ether successively, and air-dried at room temperature.

$(NH_4)_3[Co(NH_3)_5H_2O][La(SO_4)_3]\cdot 2H_2O$ (**2**):

40 $cm^3$ of $[Co(NH_3)_5H_2O]_2(SO_4)_3 \cdot 3H_2O$ solution containing $1.5 \times 10^{-3}$ mole of $[Co(NH_3)_5H_2O]^{3+}$ was added to the mixture of 10 $cm^3$ of a solution containing $5 \times 10^{-2}$ mole of $(NH_4)_2SO_4$ and 10 $cm^3$ of La(III) stock solution prepared above. After standing overnight, the precipitates which are reddish orange and needle-like were washed with water, alcohol, and ether successively, and air-dried at room temperature.

$(NH_4)_3[Co(NH_3)_4(H_2O)_2][La(SO_4)_3]_2 \cdot 2H_2O$ (**3**): The procedure was similar as described for **2** except for the use of 10 $cm^3$ of *cis*-$[Co(NH_3)_4(H_2O)_2]_2(SO_4)_3 \cdot 3H_2O$ solution containing $2.0 \times 10^{-3}$ mole of $[Co(NH_3)_4(H_2O)_2]^{3+}$. The precipitates are pale violet and needle-like.

*Analyses*

La(III) was determined as follows: Each compound was dissolved in 0.5 N HCl. Lanthanum(III) hydroxide was precipitated by adding aqueous ammonia to the solution. A small amount of conc. $HNO_3$ was added to dissolve the precipitates. After the solution was concentrated, the solution saturated with oxalic acid was added. The ignition product, $La_2O_3$, of lanthanum(III) oxalate was weighed.

Water was analyzed by heating each compound to about 300°C at the heating rate of 0.7°C per minute and collecting the desorbed water in glass "U" tube packed with granular sodium hydroxide. The determinations of cobalt(III) of **1**, **2** and **3** were carried out by measuring the absorbances at 475, 490 and 500 nm which are absorption maxima for $[Co(NH_3)_6]^{3+}$, $[Co(NH_3)_5H_2O]^{3+}$, and *cis*-$[Co(NH_3)_4(H_2O)_2]^{3+}$, respectively. Sulphate ion was analyzed by the method of $BaSO_4$ precipitation. Analytical results are given in Table 1.

*Measurements*

IR spectra were measured with a Shimazu IR 420 Spectrophotometer. Potassium bromide disk method was employed. The TG curves were recorded under an atmosphere of air with a Cahn 2000 Recording Electrobalance. About 10 mg of samples were used for each measurement. The particle size of the samples was within the range between 80 and 300 mesh. The heating rate was about 0.7°C per minute unless otherwise stated.

## RESULTS AND DISCUSSIONS

From the equilibrium constant for $SO_4^{2-} + H^+ = HSO_4^-$,[6] more than 50% of total sulphate ions exist in the form of $SO_4^{2-}$ at pH 2. Although the values of the formation constant for $La(SO_4)_3^{3-}$ are not available, the reasoning based on the analogy with the formation constants for $Ce(SO_4)_3^{3-}$ [7] and $Lu(SO_4)_3^{3-}$ [8] leads to the following conclusion, namely that it seems likely that a significant amount of La(III) exists as $La(SO_4)_3^{3-}$ under the condition in this work. As can be seen from Table 1, the compositions are in good agreement with those calculated, so that it can be proposed that the compositions of **1**, **2** and **3** are $[Co(NH_3)_6][La(SO_4)_3] \cdot H_2O$; $(NH_4)_3[Co(NH_3)_5H_2O][La(SO_4)_3]_2 \cdot 2H_2O$; and $(NH_4)_3[Co(NH_3)_4(H_2O)_2][La(SO_4)_3]_2 \cdot 2H_2O$, respectively. It is of interest that the compounds **2** and **3** contain ammonium cations whereas **1** does not. Furthermore, in these double complexes, all or some of the water molecules

Table 1. Analytical results

| Complex | | | Co | La | $NH_3$ | $SO_4$ | $H_2O$ |
|---|---|---|---|---|---|---|---|
| **1** | % | Found | 9.76 ± 0.08 | 22.64 ± 0.18 | 17.21 ± 0.09 | 46.90 ± 0.90 | 3.34 ± 0.42 |
| | | Calcd.[a] | 9.72 | 22.91 | 16.86 | 47.54 | 2.97 |
| | Molar ratio* | | 1.00 | 0.98 ± 0.01 | 6.09 ± 0.05 | 2.94 ± 0.06 | 1.11 ± 0.13 |
| **2** | % | Found | 5.36 ± 0.03 | 25.03 ± 0.28 | 12.42 ± 0.17 | 52.81 ± 0.69 | 5.03 ± 0.15 |
| | | Calcd.[b] | 5.33 | 25.11 | 12.31 | 52.09 | 4.88 |
| | Molar ratio* | | 1.00 | 1.98 ± 0.02 | 8.02 ± 0.04 | 6.05 ± 0.08 | 3.07 ± 0.09 |
| **3** | % | Found | 5.22 ± 0.03 | 24.59 ± 0.55 | 10.63 ± 0.17 | 51.28 ± 0.23 | 6.82 ± 0.60 |
| | | Calcd.[c] | 5.32 | 25.09 | 10.77 | 52.05 | 6.51 |
| | Molar ratio* | | 1.00 | 2.00 ± 0.05 | 7.04 ± 0.12 | 6.03 ± 0.04 | 4.27 ± 0.38 |

a) Values for $[Co(NH_3)_6][La(SO_4)_3] \cdot H_2O$. b) Values for $(NH_4)_3[Co(NH_3)_5H_2O][La(SO_4)_3]_2 \cdot 2H_2O$.

c) Values for $(NH_4)_3[Co(NH_3)_4(H_2O)_2][La(SO_4)_3]_2 \cdot 2H_2O$.

* Taking Co = 1.00.

Table 2. IR spectral data

| Complex | $\tilde{\nu}$/cm$^{-1}$ | | |
|---|---|---|---|
| | $\nu_4$ | $\nu_1$ | $\nu_3$ |
| 1 | 603(s),615(m,sh) | 968(m) | 1058(s),1098(s) |
| | 651(s),660(m,sh) | 993(m) | 1123(s,sh),1165(s,sh) |
| 2 | 607(s),627(m) | 967(m) | 1050(s,sh),1070(s,sh) |
| | 647(s),657(m,sh) | 982(m) | 1097(s),1120(s) |
| | | | 1150(s,sh),1182(s,sh) |
| 3 | 606(s),621(m) | 966(m) | 1039(s),1081(s,sh) |
| | 643(s),653(m,sh) | 981(m,sh) | 1096(s),1121(s) |
| | | | 1150(s,sh),1180(s,sh) |

outside the square brackets may coordinate to lanthanum(III) ion, because the coordination number of rare earth metal ions is generally greater than six.

*IR spectra*

The data for sulphate groups in the range of 500 to 1300 cm$^{-1}$ are summarized in Table 2. The double complex salts **1**, **2** or **3** give more complicated spectra than those of $K_2SO_4$; $(NH_4)_2SO_4$; $[Co(NH_3)_6]_2(SO_4)_3\cdot 5H_2O$; $[Co(NH_3)_5H_2O]_2(SO_4)_3\cdot 3H_2O$; or *cis*-$[Co(NH_3)_4(H_2O)_2]_2(SO_4)_3\cdot 3H_2O$. These sulphate groups have probably Td symmetry. As shown in Table 3, one $\nu_1$, one $\nu_2$, three $\nu_3$, and three $\nu_4$ vibrational modes are IR active in $C_{2v}$ symmetry. According to Postmus and Ferraro,[9] sulphate groups in $La_2(SO_4)_3\cdot 9H_2O$ and $La_2(SO_4)_3\cdot 4H_2O$ appear to be in $C_{2v}$ symmetry. Such lowering of symmetry must be chiefly caused by the effect of water–hydrogen bonding. On the other hand, the spectra of $Cs[La(SO_4)_2(H_2O)_3]\cdot H_2O$[3] and $CsLa(SO_4)_2$[10] are more complicated than those expected in $C_{2v}$ symmetry. The spectra of **1**, **2** and **3** are very similar to those of these compounds. Vibrations due to sulphate groups may split by the site group symmetry and in more detail, factor group analysis must be considered. Most simply, such complicated spectra would be due to the result that the sulphate groups of **1**, **2** and **3** may have the lower symmetry than $C_{2v}$, or all surroundings of the sulphate groups may not be equal.

*Thermal properties*

The TG and DTG curves of **1**, **2** and **3** are shown in Fig. 1. The components of evolved gas were analyzed using a mass spectrometer. The dehydration of $[Co(NH_3)_6]_2(SO_4)_3\cdot 5H_2O$ and $[Co(Nh_3)_5H_2O]Cl_3$ was completed at about 60 and 100°C, respectively. *cis*-$[Co(NH_3)_4(H_2O)_2]Cl_3$ lost its water in two steps in the temperature range of about 30 and 150°C. On the other hand, in the case of **1**, **2** and **3**, only dehydration was found to occur below 200, 190 and 180°C, respectively. Above those temperatures, ammonia was detected and dehydration was not still completed. Thus, the dehydration of all the double complex salts in this work is more difficult than that of $[Co(NH_3)_6]_2(SO_4)_3\cdot 5H_2O$; $[Co(NH_3)_5H_2O]Cl_3$; and *cis*-$[Co(NH_3)_4(H_2O)_2]Cl_3$. Lanthanide(III) malonate hydrates,[11] in which five or six molecules of water are known to coordinate to $Ln^{3+}$, release water more easily than the double complex salts in the present work. Therefore, as described above, **1**, **2** and **3** should be represented as $[Co(NH_3)_6][La(SO_4)_3H_2O]$; $(NH_4)_3[Co(NH_3)_5H_2O][La(SO_4)_3H_2O]_2$; and $(NH_4)_3$-$[Co(NH_3)_4(H_2O)_2][La(SO_4)_3H_2O]_2$, respectively. It is interesting to estimate the activation energies of dehydration. As can be seen from Fig. 1, since dehydration of the double complex salts do not

Table 3. Correlation table for Td, $C_{3v}$, and $C_{2v}$

| Point group | $\nu_1$ | $\nu_2$ | $\nu_3$ | $\nu_4$ |
|---|---|---|---|---|
| Td | $A_1$(R) | E(R) | $T_2$(I,R) | $T_2$(I,R) |
| $C_{3v}$ | $A_1$(I,R) | E(I,R) | $A_1$(I,R)+E(I,R) | $A_1$(I,R)+E(I,R) |
| $C_{2v}$ | $A_1$(I,R) | $A_1$(I,R)+$A_2$(R) | $A_1$(I,R)+$B_1$(I,R)+$B_2$(I,R) | $A_1$(I,R)+$B_1$(I,R)+$B_2$(I,R) |

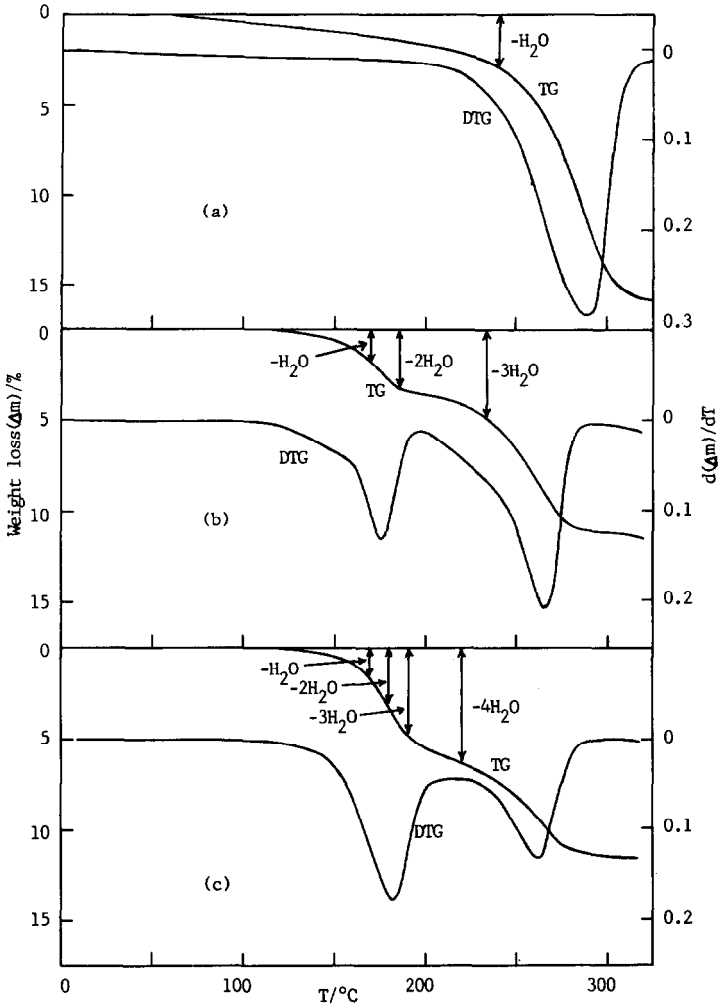



Fig. 1. TG and DTG curves. Weight losses(%) by only dehydrations are indicated by the symbol (↔). (a) Double complex salt **1**. (b) Double complex salt **2**. (c) Double complex salt **3**.

occur step-by-step even in a range of relatively low temperature, only the activation energy of the dehydration process, eqn (1), was estimated using a modified Doyle's[12] (named below as Doyle's method) and Wiedemann's method.[13]

$$\mathbf{1}, \mathbf{2} \text{ or } \mathbf{3} \rightarrow \mathbf{1}', \mathbf{2}' \text{ or } \mathbf{3}', \text{ respectively} + H_2O. \quad (1)$$

Where **1**′, **2**′ and **3**′ represent the species which are formed after one molecule of water is released from **1**, **2** and **3**, respectively.

All TG curves shift to higher temperature with increasing heating rate. $\alpha$-$T$ curves for dehydration process (1) are given as Fig. 2 by measuring TG curves with several different heating rates $\phi_i$. $\alpha$ is degree of dehydration in eqn (1) defined as $W\Delta m/(100w)$. Here, $W$, $\Delta m$ and $w$ are molecular weight of **1**, **2** or **3**, weight loss(%), and molecular weight of water, respectively. When log $\phi_i$ are plotted on the ordinate and the reciprocal of

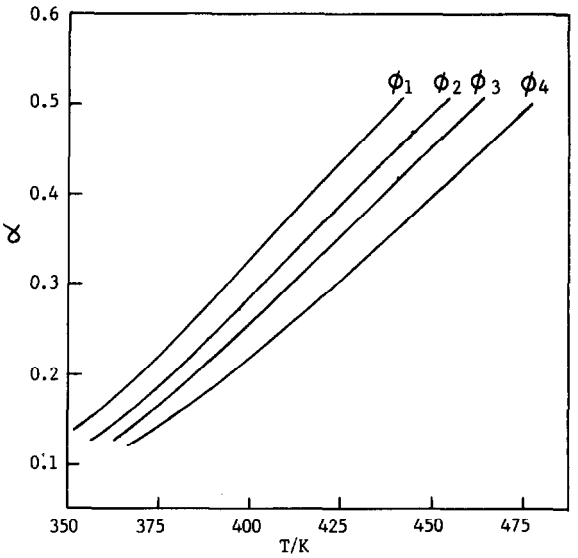



Fig. 2. Effect of heating rate ($\phi$) on $\alpha$ for the double complex salt **1**. Heating rate (°C min$^{-1}$): 0.70 ($\phi_1$), 1.43 ($\phi_2$), 2.89($\phi_3$), 6.04 ($\phi_4$).

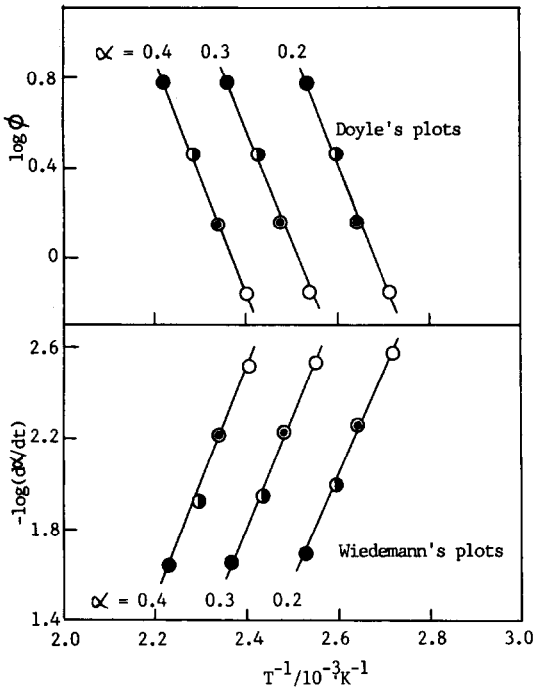



Fig. 3. The Doyle's and Wiedemann's plots for the double complex salt **1**. Heating rate ($\phi$/°C min$^{-1}$): 0.70 (○), 1.43 (⊙), 2.89 (◑), 6.04 (●).

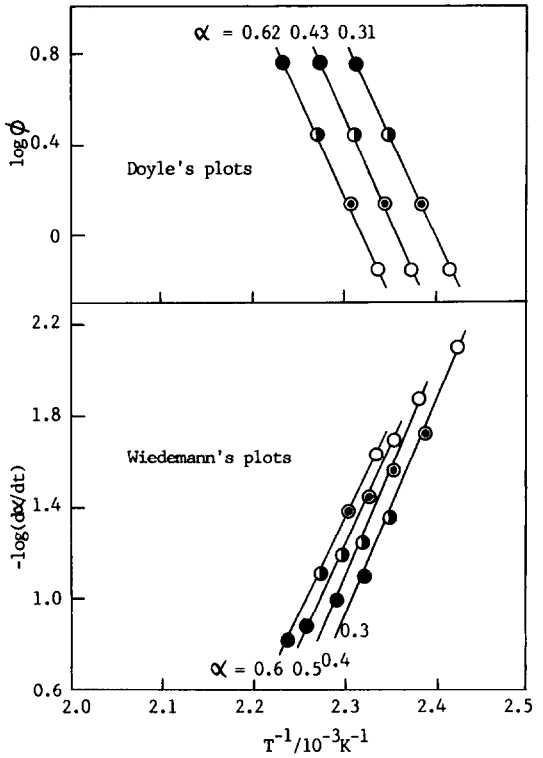



Fig. 5. The Doyle's and Wiedmann's plots for the double complex salt **3**. Heating rate ($\phi$/°C min$^{-1}$): 0.71 (○), 1.43 (⊙), 2.84 (◑), 5.84 (●).

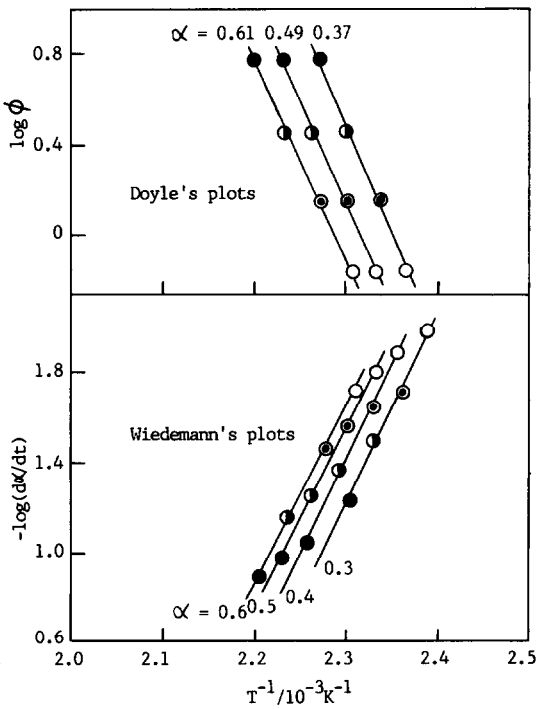



Fig. 4. The Doyle's and Wiedemann's plots for the double complex salt **2**. Heating rate ($\phi$/°C min$^{-1}$): 0.69 (○), 1.42 (⊙), 2.84 (◑), 5.97 (●).

absolute temperature, at which values of $\alpha$ are equal, are plotted on the abscissa, their plots form a straight line. From the slope, 0.4567E*/R, the activation energy, $E^*$, can be calculated.[12] On the other hand, from $\alpha$-time($t$) curves which are given by measuring TG curves with several different heating rates, it is possible to determine graphically the dehydration rate $d\alpha/dt$ in each curve. When values of $-\log(d\alpha/dt)$ are plotted on the ordinate and reciprocal of absolute temperature, at which values of $\alpha$ are equal one another, are plotted on the abscissa, their plots form a straight line. According to Wiedemann *et al.*, from the slope, $E^*/(2.303R)$, activation energy, $E^*$, can be calculated.[13] Figures 3–5 show the Doyle's and Wiedemann's plots for **1**, **2** and **3**. In all cases, these plots gave a good linearity. Slopes for different $\alpha$ are almost constant in each compound. Activation energies calculated from the slopes of these straight lines are summarized in Table 4. Values calculated by Doyle's method are in good agreement with those calculated by Wiedemann's method. Furthermore, values calculated by both methods for $[Co(NH_3)_5H_2O]Cl_3$ are also in good agreement with the value reported by Mori *et al.*[14] From these

Table 4. Activation energy

| Complex | $E^*$ / kJ mol$^{-1}$ | |
|---|---|---|
| **1** | 96.2 ± 2.1[a] | 95.0 ± 3.8[b] |
| **2** | 163.2 ± 14.2[a] | 151.0 ± 6.3[b] |
| **3** | 160.2 ± 8.8[a] | 166.1 ± 18.8[b] |
| $[Co(NH_3)_5H_2O]Cl_3$ | 104.6 ± 4.2[a] | 102.9 ± 9.2[b] |
| | 89.8[c] | |
| cis-$[Co(NH_3)_4(H_2O)_2]Cl_3$ | 102.9 ± 2.9[a] | 100.0 ± 4.6[b] |

a) Values estimated using the Doyle's method. b) Values estimated using the Wiedemann's method. c) Value from Ref. 14.

results, although isothermal work was not undertaken, $E^*$ values estimated in this study seem reasonable. **1** gives a smaller value than those for **2** and **3**. **2** gives a larger value than that for $[Co(NH_3)_5H_2O]Cl_3$. The value for **3** is also larger than that for *cis*-$[Co(NH_3)_4(H_2O)_2]Cl_3$. It is suggested that the de-aquation-anation reaction of pentaamminechromium(III) complexes is influenced by the ionic radii of counter anions.[15] The bromide, sulphate, and sulphite complexes give the high activation energies because of their larger ionic radii. Accordingly, if the water molecule coordinating to cobalt(III) ion in **2** and **3** is initially released, the higher activation energies than those for $[Co(NH_3)_5H_2O]Cl_3$ and *cis*-$[Co(NH_3)_4(H_2O)_2]Cl_3$ may be partially attributed to the large lanthanum(III) sulphate complex anion. However, it is not clear which water molecule would be initially released. Of course, substitution of sulphate into the first co-ordination sphere of cobalt(III) on dehydration must take place and this could affect both the kinetics and thermodynamics of dehydration.

*Acknowledgements*—The author is greatly thankful to Prof. Dr. Tomitaro Ishimori of Ehime University for his encouragement and discussion.

## REFERENCES

1. N. E. Topp, *Chemistry of the Rare-Earth Elements*. Elsevier, Amsterdam (1965). (Translation into Japanese by J. Shiokawa and G. Adachi, *Kagakudojin*, p. 63. Kyoto (1974).)
2. P. Bukovec and L. Golic, *Vestn. Slov. Kem. Drus.* 1975, **22**, 19.
3. N. Bukovec, P. Bukovec, L. Golic and J. Siftar, *Monatsh. Chem.* 1977, **108**, 997.
4. N. Bukovec, P. Bukovec and J. Siftar, *Vestn. Slov. Kem. Drus.* 1979, **26**, 103.
5. A. Saito and K. Ueno, *J. Inorg. Nucl. Chem.* 1979, **41**, 503.
6. L. G. Sillén and A. E. Martell, *Stability Constants of Metal-Ion Complexes*, pp. 232–235. The Chemical Society, London (1964).
7. L. G. Sillén and A. E. Martell, *Stability Constants of Metal-Ion Comlexes*, p. 237. The Chemical Society, London (1964).
8. L. G. Sillén and A.E. Martell, *Stability Constants of Metal-Ion Complexes*, Supplement No. 1, p. 138. The Chemical Society, London (1964).
9. C. Postmus and J. R. Ferraro, *J. Chem. Phys.* 1968, **48**, 3605.
10. N. Bukovec, P. Bukovec and J. Siftar, *Monatsh. Chem.* 1980, **111**, 957.
11. K. Muraishi, K. Nagase, M. Kikuchi, K. Sone and N. Tanaka, *Bull. Chem. Soc. Jpn.*, 1982, **55**, 1845.
12. C. D. Doyle, *J. Appl. Polym. Sci.* 1961, **5**, 285; C. D. Doyle, *Techniques and Methods of Polymer Evaluation* (Edited by P. E. Slade, Jr. and L. T. Jenkins, p. 113. Marcel Dekker, New York (1966), H. Kanbe, *Netsubunseki*, pp. 96–99. Kodansha, Tokyo (1975).
13. H. G. Wiedemann, A. V. Tets and H. P. Vaughan, *Presented at the Conf. on Analytical Chemistry and Applied Spectroscopy*. Pittsburgh, PA, 21 February (1966).
14. M. Mori, R. Tsuchiya and Y. Okano, *Bull. Chem. Soc. Jpn.* 1959, **32**, 1029.
15. R. Tsuchiya, Y. Kaji, A. Uehara and E. Kyuno, *Bull. Chem. Soc. Jpn.* 1969, **42**, 1881.

*Polyhedron* Vol. 3, No. 4, pp. 457–461, 1984
Printed in Great Britain.

0277–5387/84 $3.00 + .00
© 1984 Pergamon Press Ltd.

# DISSOCIATION OF URANIUM(III) AND URANIUM(IV) BOROHYDRIDES IN SOLUTION: $^{11}B$, $^{1}H$ NMR STUDY

**G. V. FAZAKERLEY†, G. FOLCHER* and H. MARQUET-ELLIS**
Département de Physico-chimie, SCM/LRMCI (LA 331), CEN-Saclay, 91191 Gif-sur-Yvette, Cedex, France

(*Received* 13 *June* 1983; *accepted* 1 *November* 1983)

**Abstract**—Uranium(III) borohydride, which can be prepared in THF solution, and uranium(IV) borohydride are found to undergo dissociation to give cationic and anionic species:

$$3\,U(BH_4)_3 \rightarrow U(BH_4)_5^{2-} + 2\,U(BH_4)_2^{+}$$
$$3\,U(BH_4)_4 \rightarrow U(BH_4)_6^{2-} + 2\,U(BH_4)_3^{+}$$

these species are identified by their $^{1}H$ and $^{11}B$ NMR spectra. $BH_4^-$ is found to be in exchange between the three species in both cases.

The structure of $U(BH_4)_4$ has been thoroughly investigated. In the solid a polymeric form with both terminal and bridging borohydrides has been observed[1,2] although more than one crystalline form is known.[3] In the gaseous phase the compound is monomeric with approximately tetrahedral symmetry.[4,5] Spectroscopic studies of $U(BH_4)_4$ dissolved in aromatic solvents, show it to be monomeric and having $T_d$ symmetry.[6]

The crystal structures of ether adducts (U/ether = 1/2) have been reported; with tetrahydrofuran[7] the structure is a distorted octahedron with the two THF molecules *trans* to each other. With other ethers[8,9] polymeric structures or unsymmetrical dimers have been found.

No solution studies have been reported.

The solid $U(BH_4)_4$ decomposes to the involatile brown $U(III)(BH_4)_3$[10] near 400 K and to U metal and $B_2H_6$ and $H_2$ at higher temperatures.

Neither its structure nor any reactions with coordinating ligands have been reported.

The uranium borohydrides of oxidation states IV and III are potentially good starting materials for subsequent chemistry, $BH_4^-$ being an easy leaving group, and reactions with potentially coordinating ligands are expected, even for weak bases, especially in non-polar solvents.

Moreover the structure and the dynamic behaviour is particularly interesting in the case of borohydride compounds owing to their lability. As in previous studies[6] the shift reagent effect induced by U(IV) as well as by U(III) provides readily such information.

Preliminary experiments in various solvents showed some complicated features and prompted us to study in some detail the species in solution; the effect of an added basic ligand was investigated with THF (tetrahydrofuran) well known for its high stability in a reducing medium.

## EXPERIMENTAL

$U(BH_4)_4$ was prepared by a literature method[11] and subsequently sublimed under vacuum. The green crystalline solid shows only a little decomposition over a period of several weeks. It was then resublimed into the reaction vessel. THF, thoroughly degassed was distilled from lithium–aluminium hydride into the vessel; the resulting solution was sealed in a NMR tube. All transfers were carried out under high vacuum. Alternatively the excess THF was pumped off and the THF adduct pumped dry for several hours. The adduct was redissolved in toluene and sealed in a NMR tube.

$U(BH_4)_3$ can be prepared in solution: $U(BH_4)_4$ was first dissolved in toluene and completely decomposed to U(III) by a cycle of heating to 400 K, cooling and pumping to remove the diborane and hydrogen evolved several times, followed by pumping to dryness.

The solutions were then prepared as above.

*Author to whom correspondence should be addressed.

†Present address: Service de Biochimie, CEN-Saclay, 91191 Gif-sur-Yvette Cedex, France.

Table 1. $^1$H Chemical shift, ppm * and line width (Hz) (in brackets)

| Temp. K | $BH_4$ | | | THF | |
|---|---|---|---|---|---|
| | | $U(BH_4)_4$ in THF | | | |
| 300 | | -160 (330) | | | |
| 233 | -434, (2150) | -204, (2090) | +54, (2400) | | |
| 203 | -521 | -217 | +80 | | |
| 193 | -538, (260) | -220, (170) | +84, (180) | +26 | +55 |
| | | $U(BH_4)_4$. xTHF in toluene | | | |
| 300 | | -165, (270) | | | |
| 223 | -465,(V.broad) | -210, (500) | +68, (V.broad) | | |
| 193 | -556, (190) | -220, (65) | +90, (102) | +28 | +56 |
| | | $U(BH_4)_3$ in THF | | | |
| 290 | -246, (280) | -160, (280) | -86, (380) | | |
| 233 | -288 | -180 | -80 | | |
| 193 | - | - | - | | |
| | | $U(BH_4)_3$. xTHF in toluene | | | |
| 290 | -230, (320) | -150, (300) | -90, (980) | | |
| 233 | -298 | -184 | -76 | | |
| 193 | - | -193, (80) | - | | |

* the chemical shifts are measured relative to TMS. Negative shifts are to low field. All the experiments were performed with a Bruker WP60 spectrometer.

## RESULTS

$U(BH_4)_4$

The $^1$H NMR spectrum of $U(BH_4)_4$ dissolved in THF shows at 300 K a single borohydride resonance at $-160$ ppm of line width *ca.* 330 Hz with no multiplet structure, the observed line width is however slightly larger than that expected for $^1J(H-^{11}B) = ca.$ 90 Hz.[6] The coordinated and free THF are in fast exchange. On cooling to 250 K the borohydride resonance becomes very broad and at 233 K it splits into three resonances (Table 1), each of line width greater than 2 KHz. As the temperature is further decreased all three resonances become narrower and two of them (at $\delta -220$ ppm and $+84$ ppm at 193 K, Fig. 1) have line widths significantly less than expected for $^{11}B-^1H$ coupling of *ca.* 90 Hz. In all preparations the integrated intensity ratio of the resonances at $-538$ ppm and $+84$ ppm (193 K) is 1:1 although their ratio respective to the third resonance changes slightly with the concentration of $U(BH_4)_4$. The average ratio observed for the three borohydride resonances was 1:1.66:1. At 240 K two broad resonances appear to high field of free THF and these are sharp at 193 K (Fig. 1, Table 1). These correspond to the $\alpha$ and $\beta$ protons of coordinated THF. This is confirmed by spectra in $d_8$-THF where they are almost absent.

$U(BH_4)_4$-THF adduct redissolved in toluene shows at 300 K a borohydride resonance at $-165$ ppm (Table 1) with resolvable coupling $^{11}B-^1H = 80$ Hz. The two THF resonances are observed shifted to high field.

On cooling, the borohydride resonance broadens and at 223 K is seen to be split into three resonances. Their chemical shifts correspond to those observed in THF solution but the upfield and furthest downfield resonances are of relatively low intensity. At 193 K all three are very narrow and again the resonances at $-220$ ppm and $+90$ ppm appear to have lost $^{11}B-^1H$ coupling. The two outer resonances are again found in the ratio 1/1 although they now account for only 4.4% of the total borohydride, the average ratio for the three resonances being 1:44.4:1.

The THF resonances follow a similar behaviour becoming broad at 260 K and consequently narrowing on lowering the temperature, their relative

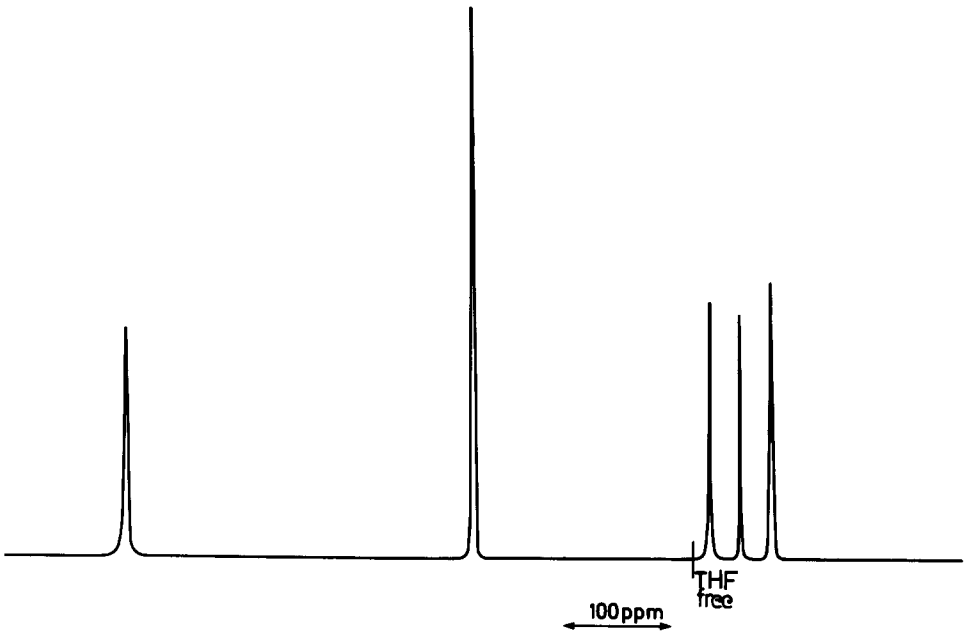



Fig. 1. $^1H$ spectrum of $U(BH_4)_4$ in THF at 193 K.

ratio is always 1/1, integration relatively to total borohydride gives a formula $U(BH_4)_4$. $2.4 \pm 0.1$ THF.

In order to confirm that the proton resonances correspond to discrete borohydride species and not to, for example, bound (or bridging) protons and non-bound protons, the $^{11}B$ spectra were measured. Exchange is slow on a $^{11}B$ time scale at 200 K and the spectra show the identical pattern to that observed in the $^1H$ NMR spectra, Table 2. All three resonances are found to low field (taking $LiBH_4$ in diethylether as a diamagnetic reference) two of which ($\delta$ 117 and 561 ppm) have the same integrated intensity.

For reference we have observed the $^{11}B$ spectrum of $U(BH_4)_4$ in toluene and obtain a quintuplet at ambient temperature: Fig. 2.

While several equilibria involving ionization of $U(BH_4)_4$ giving ionic species: $U(BH_4)_6^{2-}$, $U(BH_4)_5^-$, $U(BH_4)_3^+$ or $U(BH_4)_2^{2+}$ can be written as only one balanced equation satisfying the observation that for each product the *total* number of $BH_4$ groups are the same as found, i.e.

$$3\,U(BH_4)_4 \rightleftharpoons U(BH_4)_6^{2-} + 2\,U(BH_4)_3^+.$$

The neutral species account for 45% of the total uranium in THF solution. The relative assignment

Table 2. $^{11}B$ Chemical shifts ppm * (relative to $LiBH_4$ $(C_2H_5)_2O$) and line widths (Hz) (in brackets)

| Temp. K | $U(BH_4)_4$ in THF | | |
|---|---|---|---|
| 300 | 238, (250) | | |
| 200 | 561, (470) | 300, (480) | 117, (480) |
| | $U(BH_4)_3$ in THF | | |
| 270 | 734, (280) | 477, (350) | 452, (440) |

* Chemical shifts were measured relative to a saturated solution of $B(OH)_3$ in $^2H_2O$ at 300K. The correction for $LiBH_4$ as a diamagnetic reference for borohydride spectra is given in réf. 12.

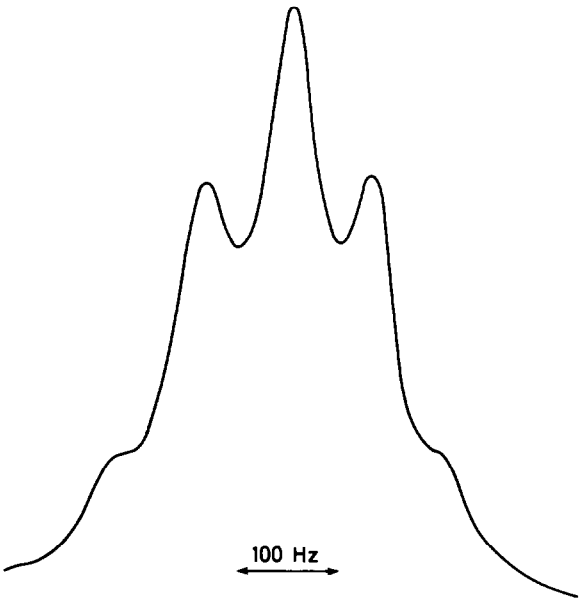



Fig. 2. $^{11}B$ spectrum of $U(BH_4)_4$ in toluene at 300 K.

of the $^1H$ resonances at $\delta - 538$ ppm and $\delta + 84$ ppm to $U(BH_4)_6^{2-}$ or $U(BH_4)_3^+$ cannot be made from the above results. The former species is probably not solvated whereas the latter would be. Addition of a more strongly coordinated ligand could result in a chemical shift change for the latter and of course of $U(BH_4)_4$. In the presence of 3 moles of pyridine per uranium at 193 K in THF we observed the coordinated pyridine resonances in the region $\delta + 5$ to 20 ppm, but the equilibrium was shifted totally to the left with only one species being observed.

Although intermolecular change of borohydride is slow on the NMR scale at 193 K, the shifted THF resonances correspond to an average for all bound environments.

$U(BH_4)_3$

At 290 K borohydride exchange is slow on the $^1H$ NMR time scale and three resonances are observed, shifted to low field, Fig. 3, Table 1, $A^1J(H-^{11}B) = 87$ Hz is found for the central resonance and integration gives a ratio of 4/5/1.8. Apart from changes in the chemical shifts there is no significant change in the spectrum on lowering the temperature to 230 K, the middle resonance retains its multiplet structure. Below 220 K all three broaden rapidly such that they disappear at 200 K. At 220 K two THF resonances are observed at $-20$ and $-16$ ppm although very broad and no accurate integration relative to borohydride is possible.

The $^{11}B$ NMR spectra, Table 2, show the same pattern of three resonances at low field with relative intensities very similar to those observed in the $^1H$ spectra, the resonances at $\delta$ 477 and 452 ppm are in the ratio 4:5.1.

For the THF adduct in toluene, borohydride exchange is not quite in the limit of slow exchange on a $^1H$ time scale at 290 K. The least shifted resonance has a line width of 980 Hz but this decreases to *ca.* 300 Hz at 270 K. The ratio of the integrals was found to be 4:5:7.2. The spectra are similar to those obtained in THF down to 230 K. Below this temperature the most and the least shifted resonances disappear but the third one remains and loses the $^1J$ coupling and at 195 K has a line width of only 80 Hz. The integration of the borohydride resonances again establishes the equilibrium present, for only one fits the observed data, i.e.

$$3\,U(BH_4)_3 \rightleftharpoons U(BH_4)_5^{2-} + 2\,U(BH_4)_2^+.$$

The least shifted $^1H$ resonance corresponds to the neutral species and the most shifted one to $U(BH_4)_2^+$. The different behaviour observed at very low temperature in THF and in toluene for $U(BH_4)_5^{2-}$ we are not able to explain. There may be a difference in the degree of solvation in the two cases due to drying under vacuum before redissolving in toluene.

In THF we find that *ca.* 18% of the total uranium is found in the neutral species at 300 K

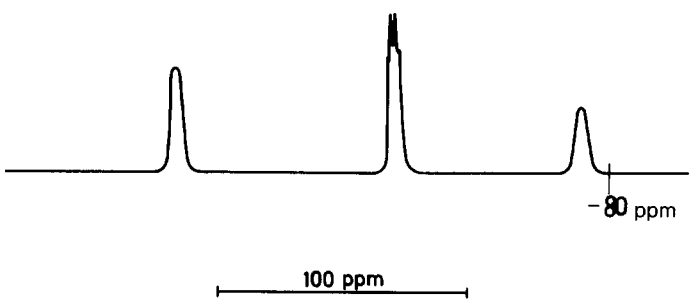



Fig. 3. $^1H$ spectrum of $U(BH_4)_3$ in THF at 290 K.

and *ca.* 44% for the THF adduct in toluene, these figures change very little over a 60° temperature range.

## DISCUSSION

The results clearly show that in a coordinating solvent uranium borohydrides disproportionate.

Three uranium borohydride species can be found for both U(III) and U(IV) oxidation states; two of them are assumed to be electrically charged (eqns 1 and 2). If we consider these equilibria from a kinetic point of view, the $BH_4$ groups are in a rapid exchange for U(IV) between the three species, neutral, anionic, and cationic, at room temperature and on a $^1H$ NMR time scale. Taking into account the paramagnetic induced shifts: 30.000 Hz for U(IV), the lifetime $\tau$ of $BH_4$ on each site can be evaluated at the collapse temperature, about $5 \times 10^{-6}$ sec for U(IV) by the condition: $\Delta\nu \cdot \tau \sim 1/2\pi$.

The same value can also be inferred from the line width of the $^{11}B$ resonance of 1000 Hz at 260 K where the $^{11}B$ are still in a rapid exchange.

These very short life times for U(IV) can be measured owing to the large paramagnetic induced shifts.

U(III) is in slow exchange for $^1H$ and $^{11}B$ at 290 K even with a lower shift. This means that $\tau > 1.5\ 10^{-5}$ sec and shows that U(III) is somewhat less labile than the U(IV) complexes.

The coupling between $^1H$ and $^{11}B$ could give some information on the molecular structure in solution.

The loss of the coupling at low temperature cannot be due to any chemical exchange process such as proton exchange because if this exchange is not observed at 300 K it seems unlikely that it would be evident at 200 K.

The disappearance of this coupling that we observed in many spectra is generally explained by the relaxation of the $^{11}B$ spin ($I = 3/2$) by the interaction of nuclear quadruple moments with the fluctuating electric field gradients.[13,14,16] This effect depends upon the rate of rotation $\tau_R$ of the $BH_4$ groups which is the most efficient process and upon the asymmetry parameter of the molecule. In the case of $U(BH_4)_4$ in toluene at room temperature, the splitting of the $^1H$ resonance (4 lines) and $^{11}B$ resonance (5 lines) (Fig. 2) reveals the symmetrical structure of the four $BH_4$ groups and the slow spin relaxation. $U(BH_4)_3$ under the same conditions, exhibits no structure on the $^{11}B$ resonance and the coupling to the $^1H$ resonance is only poorly resolved. This difference can be explained by a less symmetrical structure in the case of U(III).

In THF, unfortunately, most of the observed resonances are broad and no splitting is detected except in the $^1H$ spectrum of $U(BH_4)_5^{2-}$. In some cases the line width is less than 100 Hz and shows that the spin relaxation has completely removed the $^{11}B$, $^1H$ coupling. The chemical exchange can play a role in this effect but the asymmetry factor in molecules such as the THF adducts increases the efficiency of the interactions between the quadrupole moment and the electric field gradient.

## CONCLUSIONS

This study shows the tendency of uranium borohydrides to form ionic species in the presence of coordinating ligands. These species are in rapid exchange for $BH_4^-$ groups between the various species neutral and ionic.

The cationic species formed by the loss of $BH_4^-$ appear to interact strongly with coordinating ligand.

## REFERENCES


1. E. R. Berstein, T. A. Keiderling, S. J. Lippard and J. J. Mayerle, *J. Am. Chem. Soc.* 1972, **94**, 2552.
2. E. R. Berstein, W. C. Hamilton, T. A. Keiderling, S. J. La Placa, S. J. Lippard and J. J. Mayerle, *Inorg. Chem.* 1972, **11**, 3009.
3. P. Charpin, H. Marquet-Ellis and G. Folcher, *J. Inorg. Nucl. Chem.* 1979, **41**, 1143.
4. B. D. James, B. E. Smith and M. G. H. Wallbridge, *J. Mol. Structure*, 1972, **14**, 327.
5. N. Davies, M. G. H. Wallbridge, B. E. Smith and B. D. James, *J. Chem. Soc. Dalton*, 1973, 162.
6. G. Folcher, J. Lambard and H. Marquet-Ellis, *Nouv. J. Chimie*, 1980, **4**, 737.
7. R. R. Rietz, N. M. Edelstein, H. W. Ruben. D. H. Templeton and A. Zalkin, *Inorg. Chem.* 1978, **17**, 658.
8. R. R. Rietz, A. Zalkin, D. H. Templeton, N. M. Edelstein and L. K. Templeton, *Inorg. Chem.* 1978, **17**, 653.
9. A. Zalkin, R. R. Rietz, D. H. Templeton and N. M. Edelstein, *Inorg. Chem.* 1978, **17**, 661.
10. M. J. Schlesinger and H. C. Brown, *J. Am. Chem. Soc.*, 1953, **75**, 219. N. Ghiasseg and P. G. Walton, *J. Inorg. Nucl. Chem.* 1981, **11**, 2909.
11. V. Volkor and K. Myakislev, *Radiokkimiya*, 1976, **8**, 512.
12. T. P. Onak, H. Landesman and R. E. Williams, I. Shapiro, *J. Phys. Chem.* 1959, **63**, 1533.
13. A. Abragham, *Principles of Nuclear Magnetism.* Oxford University Press, Oxford (1961).
14. T. J. Marks, W. J. Kennelly, R. Kolb and L. A. Shimp, *Inorg. Chem.* 1972, **11**, 2540.

*Polyhedron* Vol. 3, No. 4, pp. 463–467, 1984
Printed in Great Britain.

0277–5387/84 $3.00 + .00
© 1984 Pergamon Press Ltd.

# SYNTHESIS AND SPECTROSCOPIC STUDIES OF DIMERIC COPPER(II) COMPLEXES CONTAINING IMIDAZOLES AND DIPEPTIDES

**S. V. DESHPANDE and T. S. SRIVASTAVA***
Department of Chemistry, Indian Institute of Technology, Powai, Bombay 400 076, India

(*Received* 28 *June* 1983; *accepted* 10 *October* 1983)

**Abstract**—Six dimeric copper(II) complexes of the type $Na[Cu_2(D)(L)]$, where D = glycylglycinate dianion, and HL = imidazole and 2-methylimidazole; D = glycyl-L-tyrosinate dianion, HL = imidazole and benzimidazole; D = glycyl-L-phenylalaninate dianion, and HL = imidazole; and D = glycyl-L-tryptophenate dianion, and HL = benzimidazole, have been prepared. They were characterized by IR, visible absorption, and EPR spectroscopy. The EPR data indicated their complete dimeric behaviour in basic solution with two Cu(II) ions in close proximity of <7Å with imidazolate, 2-methylimidazolate, and benzimidazolate bridges.

X-Ray structural studies of the bovine erythrocyte superoxide dismutase (BESOD) enzyme have shown that the $Zn^{2+}$ and $Cu^{2+}$ ions are bridged by an imidazolate ion of its histidine residue,[1] and its superoxide dismutase activity has been a major focus of the recent research.[2] The copper(II) has also been substituted for zinc(II) in this enzyme and the resulting enzyme exhibits catalytic activity as native enzyme and antiferromagnetic exchange interaction integral, $-J$, of 26 $cm^{-1}$.[3] This study has stimulated considerable recent research on imidazolate bridged model copper(II) and other metal complexes.[4–10] In addition, the study of these complexes in solution gives an explanation for the unusual pH dependent property of native and metal substituted BESOD[2,5] In this report, we describe the synthesis and spectroscopic studies of several new dimeric copper(II) complexes with imidazole, 2-methylimidazole or benzimidazole and dipeptides.

## EXPERIMENTAL

### *Materials*

Glycylglycine(glygly), glycyl-L-tyrosine(glytyr), glycyl-L-tryptophan(glytrp) and glycyl-L-phenylalanine(glyphe) were bought from Sigma (U.S.A.). Imidazole(imH), 2-methylimidazole(2-MeimH), and benzimidazole(BzimH) were purchased from SISCO, India. Other commercially available reagent grade chemicals were used without further purification.

### *Synthetic procedures*

Cu(glygly).$3H_2O$(**Ia**), Cu(glygly)(imH).$2H_2O$ (**Ib**), Cu(glygly)(2-MeimH).$2H_2O$(**Ic**), Cu(glytyr). $4H_2O$(**IIa**), Cu(glytyr)(lmH).$2H_2O$(**IIb**), Cu(glytyr)(BzlmH).$3.5H_2O$(**IIc**), Cu(glyphe)(lmH). $2H_2O$(**IIIa**), Cu(glytrp).$3H_2O$(**IVa**), and Cu(glytrp)(BzimH)(IVb) were prepared by known methods.[11–15]

$Na[Cu_2(glygly)_2(im)].6H_2O$(**Id**). The blue copper(II) hydroxide was first prepared by adding excess of 6N NaOH to a solution of 0.340 g (0.002 M) of cupric chloride in 20 $cm^3$ of water. The precipitate was filtered and washed with distilled water to free it from chloride ions. It is then suspended in 25 $cm^3$ of water to which 0.262 g (0.002 M) of glycylglycine, 0.069 g (0.001 M) of imidazole and 2 $cm^3$ of 0.5 N NaOH were added. The resulting solution of pH 10 was stirred for 1 hr and heated on a water bath for 5 min. After cooling it to room temperature, it was filtered and the deep blue filtrate was concentrated to a small volume using a rotary evaporator at 60°C. The blue crystals, obtained after cooling the solution for 1 day, were separated by filtration. This prod-

*Author to whom correspondence should be addressed.

Table 1. Elemental analyses of Cu(II) dimeric complexes

| Complex No. | Complex | Colour | % Calc. | | | % Found | | |
|---|---|---|---|---|---|---|---|---|
| | | | C | H | N | C | H | N |
| Id | $Na[Cu_2(glygly)_2(im)].6H_2O$ ($C_{11}H_{27}N_6O_{12}NaCu_2$) | blue | 22.56 | 4.62 | 14.36 | 22.3 | 4.7 | 14.9 |
| Ie | $Na[Cu_2(glygly)_2(2\text{-}Meim)].2H_2O$ ($C_{12}H_{21}N_6O_8NaCu_2$) | deep blue | 27.32 | 3.98 | 15.94 | 27.6 | 4.0 | 15.4 |
| IId | $Na[Cu_2(glytyr)_2(im)].3H_2O$ ($C_{25}H_{35}N_6O_{11}NaCu_2$) | sky blue | 40.26 | 4.69 | 11.28 | 40.8 | 4.4 | 11.5 |
| IIb | $Na[Cu_2(glyphe)_2(im)].3H_2O$ ($C_{25}H_{33}N_6O_9NaCu_2$) | deep blue | 42.19 | 4.64 | 12.81 | 42.9 | 4.8 | 12.1 |

uct was recrystallized from 80% alcohol. $Na[Cu_2(glygly)_2(2\text{-Meim})].2H_2O$(**Ie**), $Na[Cu_2)glytyr)_2(im)].3H_2O$(**IId**), and $Na[Cu_2(glyphe)_2(lm)].3H_2O$(**IIIb**) were prepared by the same method as described for the complex **Id** by using appropriate dipeptide and imidazole. The analysis of these complexes is given in Table 1.

$Na[Cu_2(glytyr)_2(Bzim)]$(**IIe**). The complex **IIa** (0.074 g), benzimidazole (0.012 g), and sodium hydroxide (1 $cm^3$, 0.1 N) were mixed in 15 $cm^3$ water in the molar ratio of 2 : 1 : 1. The resulting solution was stirred for 1 hr and heated on water bath for 10 min. This solution was diluted five fold with ethanol and used for recording EPR spectra.

Na[Cu(glytrp)(Bzim)](**IVc**). 0.076 (0.2 mM) of **IVa**, 0.024 g (0.2 mM) of benzimidazole and NaOH(1 $cm^3$, 0.1 N) were mixed in 20 $cm^3$ of water. The solution was stirred for half an hour and then heated on water bath for 5 min. It was filtered and the filterate was diluted to five fold with ethanol and this solution was used for recording EPR spectra.

*Physical measurements*

The electronic absorption spectra of the complexes were recorded using Perkin–Elmer model-402 spectrophotometer. The IR spectra of the complexes in Nujol mull were recorded using Perkin–Elmer model-577 spectrophotometer. The EPR spectra of the complexes in 60% ethanolic solution and in solid (frozen solution at 77 K) were recorded on a Varian E-112 ESR spectrometer (X-band) by using TCNE ($g = 2.00277$) as $g$ marker.

## RESULTS AND DISCUSSION

The four dimeric copper(II) complexes, out of six reported here, were isolated and their chemical analyses are given in Table 1. These complexes such as **Id**, **Ie**, **IId** and **IIIb** show characteristic IR spectra in the range of 1000–400 $cm^{-1}$. Some of characteristic features in their spectra are briefly discussed below. These complexes invariably show a strong band between 1580 and 1600 $cm^{-1}$. This band is assigned to the dipeptide carbonyl stretching vibration with ionization of peptide N–H hydrogen[16]. The N–H stretching vibrations due to coordinated $-NH_2$ group of dipeptides have been observed between 3040 and 3290 $cm^{-1}$. The OH stretching vibration of **IIb** which contains glycyl-L-tyrosine is observed at 3600 $cm^{-1}$.[17]

The absorption maxima for the *d–d* transition of these dimeric Cu(II) complexes are listed in Table 2. For the purpose of comparision, the electronic spectral data for Cu(II) dipeptides and their adducts with imidazoles are also given in Table 2. The dimeric Cu(II) complexes show a broad band in the range of 610–623 nm between pH 8 and 9.[18] The band maxima are blue shifted compared to their corresponding monomeric binary complexes such as **Ia**, **IIa** and **IVa**. These blue shifts are comparable to the corresponding monomeric imidazole, 2-methylimidazole and benzimidazole derivatives of **Ia**, **IIa** and **IVa** where the base seems to substitute the equatorial water molecule.[13] The shorter wavelength of the absorption maxima of dimeric Cu(II) complexes can be interpreted in terms of replacement of oxygen donors by nitrogen in square plane Cu(II) complexes.[4] The absorption spectra of the dimeric Cu(II) complexes between pH 9 and 10 obey Beer's law in the concentration range of $1.3 \times 10^{-2}$ to $2 \times 10^{-3}$ M/Cu, suggesting that virtually no dissociation of the dimeric structures occurs in the above concentration range. Similar observation was observed earlier[4] regarding the **Id** obeying Beer's law in the concentration range of $1.3 \times 10^{-2}$ to $2 \times 10^{-3}$ M/Cu.

The absorption maxima are red shifted when the

Table 2. Visible absorption spectral data of copper(II) complexes in aqueous solution

| Complex | pH | $\lambda_{max}$ in nm(ε) | Complex | pH | $\lambda_{max}$ in nm(ε) |
|---|---|---|---|---|---|
| Ia | 6.7-7.1 | 640(85) | IIc | 6.7 | 620 |
| Ib | 6.7-7.1 | 613(87) | IId | 8.0 | 610(179) |
| Ic | 6.7-7.1 | 630(87) | IIe | 8.2 | 625 |
| Id | 9.0 | 616(178) | IIIa | 6.7-7.1 | 615(87) |
| | 6.8 | 618 | IIIb | 8.2 | 610(192) |
| | 5.2 | 630 | | 6.4 | 620(164) |
| | 4.8 | 638 | IVa | 6.5 | 630(93) |
| Ie | 8.4 | 623(155) | IVb | 6.7 | 620 |
| | 6.1 | 632 | IVc | 7.9 | 623 |
| | 4.9 | 640 | | | |
| IIa | 6.8 | 635(75) | | | |
| IIb | 6.7-7.1 | 620(74) | | | |

pH of the dimeric Cu(II) complexes is decreased from 10 to 4.8 (see Table 2) indicating that the imidazolates bridges are broken at low pH.[4] Thus, there is an equilibrium between dimer and Cu(II) dipeptide and its imidazole complex at low pH. Depending on the pH, the equilibrium is expected to shift in the direction of monomers or dimer by breaking or forming an imidazolate bridge.

The EPR spectra of the dimeric Cu(II) complexes were obtained at various pH values between 5 and 10. At pH 10, the complexes **Id, Ie, IId, IIe, IIIb** and **IVc** show a broad peak due to $\Delta M_s = \pm 1$ transition. They also show an additional peak due to $\Delta M_s = \pm 2$ transition at $g \simeq 4$. A typical spectrum of **IId** is shown in Figs. 1(A) and (B). The $g$ values calculated along with peak to peak width

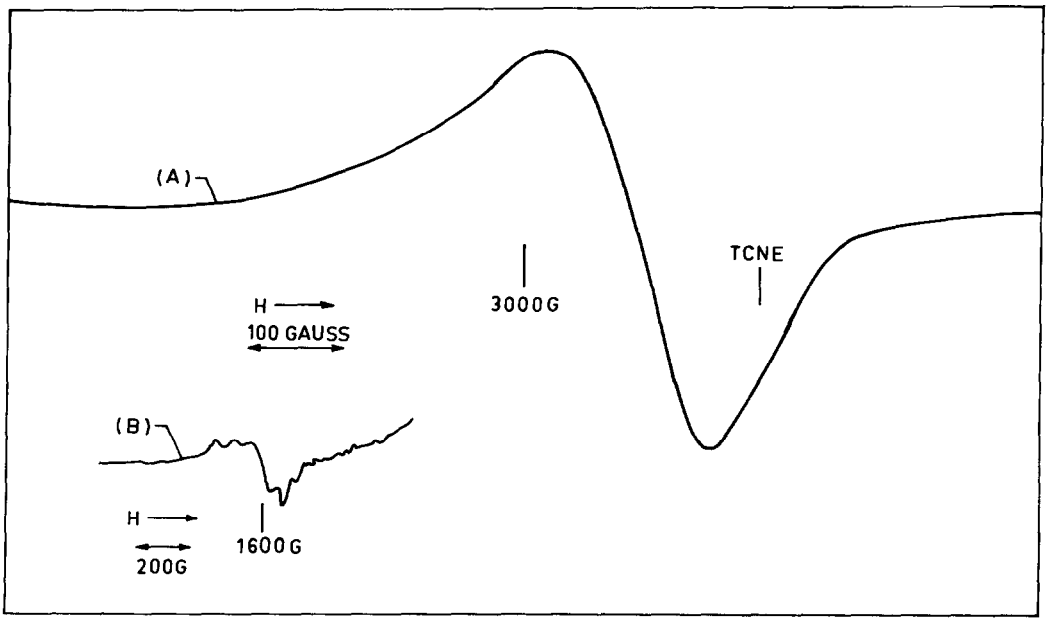



Fig. 1. Frozen solution EPR spectrum of $Na[Cu_2(glytyr)_2\text{-}(im)].3H_2O$(**IId**) at 77 K; solvent used:60% alcohol; pH = 9.2; (A) $\Delta M_s = \pm 1$ transition, (B) $\Delta M_s = \pm 2$ transition.

Table 3. Frozen solution (77 K) EPR spectral data for dimeric copper(II) complexes

| Complex | pH | $\Delta M_s = 1$ transition $g_o$ | Peak to peak width for $\Delta M_s = 1$ signal in gauss | $\Delta M_s = 2$ transition at g value |
|---|---|---|---|---|
| Id | 10.1 | 2.078 | 135 | 4.129 |
| Ie | 10.1 | 2.080[A)] | 230 | 4.26[C)] |
| IId | 9.2 | 2.085 | 155 | 4.075 |
| IIe | 10.0 | 2.102 | 180 | 4.22 |
| IIIb | 10.1 | 2.069[B)] | 160 | 4.052 |
| IVc | 10.0 | 2.107 | 190 | 4.27 |

[A)] Two weak broad signals were also observed at g = 2.292 and g = 2.434.

[B)] Two very weak broad signals were also observed at g = 2.291 and g = 2.428.

[C)] Very sharp and intense signal is observed in $\Delta M_s = 2$ region.

are given in Table 3. Similar broad peak due to $\Delta M_s = \pm 1$ transition of **Id** in 50% aqueous ethanol at 77 K was also observed earlier.[4] In addition, the aqueous solutions of 1 : 1 complexes of Cu(II) with glycylglycine, N-(2-aminoethyl)-1,2-ethanediamine and related tridentate lignads in presence of imidazole (0.1 mole) at pH $\geq$ 9 show a single broad peak due to $\Delta M_s = \pm 1$ transition, which is superimposed by weak monomer peak.[19] They[4, 19] were not able to observe a weak peak at $g \simeq 4$ in **Id**, and related complexes. However, the 1 : 1 complexes of Cu(II) with aminocarboxylates in the presence of imidazole (0.5 mole) at pH $\geq$ 9 behave very similar to **Id**, **Ie**, **IId**, **IIe** and **IVc**. They show a broad peak due to $\Delta M_s = \pm 1$ transition and an additional weak peak due to $\Delta M_s = \pm 2$ transition. Addition of 1-methylimidazole instead of imidazole does not lead to appearance of dimeric Cu(II) complexes.[19] In addition the 1 : 1 complex of **Ia** with 1-methylimidazole does not show EPR spectra corresponding to dimeric Cu(II) complex at basic pH.[4] All these results are consistent with the formation of imidazolate bridged dimeric Cu(II) complexes.

The imidazolate-bridged dimeric Cu(II) complexes have characteristic EPR spectra that arise from the thermally populated triplet state.[5] The $\Delta M_s = \pm 2$ transition at $g \simeq 4$ (see: Fig. 1(B) and Table 3) is a forbidden transition and so low intensity of this transition consists of seven lines due to the hyperfine interaction with the two copper nuclei (I = 3/2). The dimeric Cu(II) complexes such as **Id**, **Ie**, **IId**, **IIe** and **IVc** show seven lines (see Fig. 1(B), one lowest field peak is not resolved). The triplet state in the above complexes arises due to coupling between two Cu(II) ions with a coupling constant $|J| \geq 20\,cm^{-1}$. Here the distance between two copper centres is less than 7 Å (*ca.* 6 Å).[19, 20]

At low pH, i.e. 5–6, the EPR spectra of the dimeric Cu(II) complexes such as **Id**, **Ie**, **IId**, **IIe** and **IVc** show well resolved peaks due to $\Delta M_s = \pm 1$ transition and they do not show peaks corresponding to $\Delta M_s = \pm 2$ transition. Thus they correspond to monomeric Cu(II) complexes. Yokoi *et al.*[19] have investigated the pH dependence of formation of the imidazolate bridged complexes from the intensity variation of $\Delta M_s = \pm 2$ transition with pH. The plot of the relative spectral intensity of $\Delta M_s = \pm 2$ transition vs pH for the case of 1 : 1 complex of Cu(II) and N,N-ethylenediglycine in presence of imidazole (0.5 mole) has given a S-shaped curve with an apparent $pK_a$ of *ca.* 8.3. This property strongly resembles the pH-dependent migration of $Cu^{2+}$ to the empty zinc-binding site in zinc-free BESOD, with apparent $pK_a$ of 8.2 to form an imidazolate-bridged binuclear copper centres. These workers have also

measured the formation constants (K) of the imidazole-bridged Cu(II) complexes at *ca.* 0°C by comparing between the real integrated spectra intensities of monomer and dimer species at $g \simeq 2$. These K values are of the order of $10^7$ and it suggests virtually no dissociation of the dimeric Cu(II) complexes in basic solution. This supports the earlier conclusion obtained from electronic absorption spectroscopy.

The dimeric Cu(II) complexes containing imidazoles and dipeptides seem to be good models for the active site of BESOD with respect to pH and EPR behaviour.

*Acknowldegement*—We are grateful to Dr. R. K. Sharma for fruitful discussions.

## REFERENCES

1. J. S. Richardson, K. A. Thomas, B. H. Rubin and D. C. Richardson, *Proc. Natl. Acad. Sci. (USA)* 1975, **72**, 1349.
2. J. A. Fee, In *Metal ion Activation of Dioxygen* (Edited by T. G. Spiro), pp. 209–237. Wiley-Interscience, New York (1980)
3. J. A. Fee and R. G. Briggs, *Biochim. Biophys. Acta* 1975, **400**, 438.
4. Y. Nakao, W. Mori, T. Sakurai and A. Nakahara, *Inorg. Chim. Acta* 1981, **55**, 103 and references cited therin.
5. K. G. Strothkamp and S. J. Lippard, *Acc. Chem. Res.* 1982, **15**, 318 and references cited therein.
6. M. S. Haddad and D. N. Hendrickson, *Inorg. Chem.* 1978, **17**, 2622.
7. M. S. Haddad, E. N. Duesler and D. N. Hendrickson, *Inorg. Chem.* 1979, **18**, 141.
8. H. M. J. Hendriks, P. J. M. W. L. Birker, G. C. Uersckoor and J. Reedijk, *J. Chem. Soc. Dalton.* 1982, 623.
9. M. Suzuki, H. Kanatomi, H. Koyama and H. Murase, *Inorg. Chim. Acta* 1980, **44**, L41.
10. J. A. Ibers and R. H. Holms, *Science* 1980, **209**, 223.
11. A. R. Manyak, C. B. Murphy and A. E. Martell, *Arch. Biochem. Biophys.* 1955, **59**, 373.
12. R. Driver and W. R. Walker, *Austr. J. Chem.* 1968, **21**, 671.
13. S. V. Deshpande and T. S. Srivastava, *Polyhedron.* 1983, **2**, 761.
14. J. Dehand, J. Jordanov and F. Keck, *Inorg. Chim. Acta.* 1977, **21**, L-13.
15. M. B. Hursthouse, S. A. A. Jayaweera, A. Milburn and A. Quick, *J. Chem. Soc. Dalton.* 1975, 2569.
16. K. Nakamoto, *Infrared and Raman Spectra of Inorganic and Coordination Compounds*, 3rd Edn, pp. 314–317. Wiley, New York (1978).
17. J. R. Dyer, *Applications of Absorption Spectroscopy of Organic Compounds*, pp. 33–38. Prentice-Hall, New Jersey (1965).
18. B. J. Hathaway, *J. Chem. Soc. Dalton.* 1972, 1196.
19. H. Yokoi, M. Chikara, *J. Chem. Soc. Chem. Comm.* 1982, 1125.
20. K. Matsumoto, S. Ooi, Y. Nakao, W. Mori and A. Nakahara, *J. Chem. Soc. Dalton.* 1981, 2045.

*Polyhedron* Vol. 3, No. 4, pp. 469–474, 1984
Printed in Great Britain.

0277–5387/84 $3.00 + .00
© 1984 Pergamon Press Ltd.

# COMPLEX FORMATION OF PEROXOURANYL (AND URANYL) WITH POLYAMINOCARBOXYLATE LIGANDS

**MOHAMMED BRIGHLI, JANINE LAGRANGE and PHILIPPE LAGRANGE***
ERA 166, Ecole Nationale Superieure de Chimie, 1 rue Blaise Pascal, 67000 Strasbourg, France

(*Received* 12 *July* 1983; *accepted* 23 *September* 1983)

**Abstract**—Complexation of the uranyl ion ($UO_2^{2+}$) and of the peroxouranyl species ($UO_4$) by some polyaminocarboxylate ligands has been investigated in solution (3M $NaClO_4$) at 25°C. The logarithms of the cumulative formation constants of the $UO_2^{2+}$ chelates formed are: $UO_2edta^{2-}$ (15.65), $UO_2Hedta^-$ (18.59), $(UO_2)_2edta$ (20.24); $UO_2edda$ (16.02); $UO_2Hnta$ (12.19); $UO_2ida$ (9.63), $UO_2H_2(ida)_2$ (23.80). The equilibrium $UO_2^{2+} + H_2O_2 \rightleftharpoons UO_4 + 2H^+$ has a stability of $\log K = -3.99$. The peroxocomplexes formed are $UO_4Hedda^-$ (14.81, expressed from $UO_2^{2+}$ and $H_2O_2$) and $UO_4Hnta^{2-}$ (8.50). Solution structures of the chelates are proposed.

The determination of the stability constants of the uranyl ion ($UO_2^{2+}$) with polyaminocarboxylate ligands has been the subject of many investigations,[1-14] but few studies[15-17] have been carried out on the complexation of the peroxouranyl species ($UO_4$). The present paper describes the formation of $UO_4$ from $UO_2^{2+}$ and $H_2O_2$, and the complexation of $UO_2^{2+}$ and $UO_4$ with ethylenediaminetetraacetic acid ($H_4edta$), ethylenediamine-N,N′-diacetic acid ($H_2edda$), nitrilotriacetic acid ($H_3nta$), and iminodiacetic acid ($H_2ida$). The equilibria were studied at 25°C with 3 mol $dm^{-3}$ sodium perchlorate as ionic medium. Comparisons between the different complexes of $UO_2^{2+}$ or $UO_4$ obtained and between their stability constants allow us to speculate on their solution structure and to estimate the number of available sites of coordination in the plane perpendicular to the O–U–O axis.

## EXPERIMENTAL

### *Reagents*

Sodium perchlorate, perchloric acid, sodium hydroxide, ethylenediaminetetraacetic acid and nitrilotriacetic acid were obtained from MERCK as analytical reagent grade materials and were used without any purification. Iminodiacetic and ethylenediamine-N,N′-diacetic acids, purchased from FLUKA, were recrystallized twice from distilled water. Their concentrations were checked by pH titrations. $UO_2(ClO_4)_2,xH_2O$ purchased from VENTRON was titrated by polarography in 0.5 M HCl[18] and standardized vs a $UO_2(NO_3)_2$ standard solution. $H_2O_2$ purchased from PROLABO was titrated by $KMnO_4$.

### *Measurements*

All measurements were carried out at 25.0 ± 0.1°C. The ionic strength was kept constant at 3 M with sodium perchlorate. A TACUSSEL Aries 20000 pH-meter was used for pH measurements. The hydrogen ion concentration was measured with TACUSSEL TB/HA glass electrode in the following cell using an Ag/AgCl reference electrode:[19]

| Glass electrode | Test solution | 3M $NaClO_4$ | 2.9 M $NaClO_4$ / 0.1 M NaCl | AgCl | Ag. |
|---|---|---|---|---|---|

A $10^{-2}$ M perchloric acid solution containing 2.99 M $NaClO_4$ was employed as a standard:

*Author to whom correspondence should be addressed.

$-\log[H^+] = pH = 2.000$. Spectrophotometric measurements were performed with a CARY 17 spectrophotometer, interfaced to a data acquisition system.

Stability constants were found by applying Sillen's generalized least squares method in its spectrophotometric version: LETAGROP–SPEFO.[20] This program is available for three components. We have extended it to four components to study the complexes of $UO_4$. Formation curves of the complexes were calculated with the HALTAFALL program.[21]

## RESULTS AND DISCUSSION

### $UO_4$ *formation*

The literature[22–23] indicates that the action of $H_2O_2$ on $UO_2^{2+}$ gives essentially, in acidic medium, the species $UO_4{,}xH_2O$. The solubility of $UO_4$, $xH_2O$ is low, but increases with the presence of 3M $NaClO_4$. Solutions containing down to $[U(VI)] = 10^{-4}$ M, $[H_2O_2] = 2 \times 10^{-2}$ M at pH = 3 can be easily prepared. The equilibrium between $UO_2^{2+}$ and $H_2O_2$ as a function of pH, between 1 and 3, was spectrophotometrically studied. The wavelength studied range was 250 to 310 nm. Computations with LETAGROP program lead to only one equilibrium if $[H_2O_2]$ is as low as $2 \times 10^{-2}$M:

$$UO_2^{2+} + H_2O_2 \rightleftarrows UO_4 + 2H^+ \qquad (1)$$

with

$$K = \frac{[UO_4][H^+]^2}{[UO_2^{2+}][H_2O_2]}$$

and $\log K = -3.99 \pm 0.08$.

Uncertainty limit quoted is twice the computed standard deviation. In our experimental conditions, Fig. 1 shows the distribution of the two

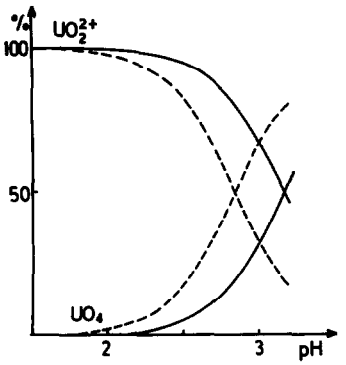



Fig. 1. Distribution of the U(VI) species as a function of pH; ———, $[U(VI)] = 10^{-4}$ M; $[H_2O_2] = 5 \times 10^{-3}$ M; – – –, $[U(VI)] = 10^{-4}$ M; $[H_2O_2] = 2 \times 10^{-2}$ M.

U(VI) species as a function of pH, calculated from program HALTAFALL. Figure 3 gives the calculated spectra of the $UO_4$ and $UO_2^{2+}$ species. As the pH must be limited down to 3 in order to avoid the $UO_2^{2+}$ hydrolysis,[24] $UO_4$ formation is never complete. Thus the two coordinating centres $UO_2^{2+}$ and $UO_4$ will take place simultaneously in acidic solutions in the study of the complexation of $UO_4$ with polyaminocarboxylate ligands. Firstly, a study of polyaminocarboxylate complexes of $UO_2^{2+}$ must be undertaken.

### $UO_2^{2+}$-*polyaminocarboxylate complexes*

Protonation constants ($K_i$) of the studied polyaminocarboxylic acids ($H_4$edta, $H_3$nta, $H_2$edda and $H_2$ida) are known[25] in the same medium (3M $NaClO_4$) and at the same temperature (25°C). In the pH range of interest (1.0–3.0), absorbance (250–300 nm) and pH were measured for solutions containing U(VI) ($5 \times 10^{-4}$ to $5 \times 10^{-3}$ M), and ligand ($10^{-3}$ to $10^{-2}$ M). The following equilibria were considered, where $L^{n-}$ represents the fully dissociated ligand (and $H_{n+n'}L^{n'+}$ the fully protonated ligand):

$$H_{i-1}L^{(n+1-i)-} + H^+ \rightleftarrows H_iL^{(n-i)-} \quad (1 \leqslant i \leqslant n+n')$$

$$xUO_2^{2+} + yH^+ + zL^{n-} \rightleftarrows (UO_2)_xH_yL_z^{(nz-2x-y)-} \qquad (2)$$

with

$$K_i = \frac{[H_iL^{(n-i)-}]}{[H_{i-1}L^{(n+1-i)-}][H^+]}$$

and

$$\beta_{xyz} = \frac{[(UO_2)_xH_yL_z^{(nz-2x-y)-}]}{[UO_2^{2+}]^x[H^+]^y[L^{n-}]^z}.$$

In the pH range studied, no hydrolysed complex was observed. Table 1 summarizes the different complexes formed and their stability constants which give the best fit with the LETAGROP program. In our experimental conditions, Fig. 2 shows the distribution of the various species in solution as a function of pH (HALTAFALL program), and Fig. 3 gives their molar absorption coefficients calculated with the LETAGROP program.

### $UO_4$-*polyaminocarboxylate complexes*

In the pH range (1.0–3.0), absorbance (250–300 nm) and pH were simultaneously measured for solutions containing U(VI) ($3.85 \times 10^{-4}$ M), polyaminocarboxylate ligand

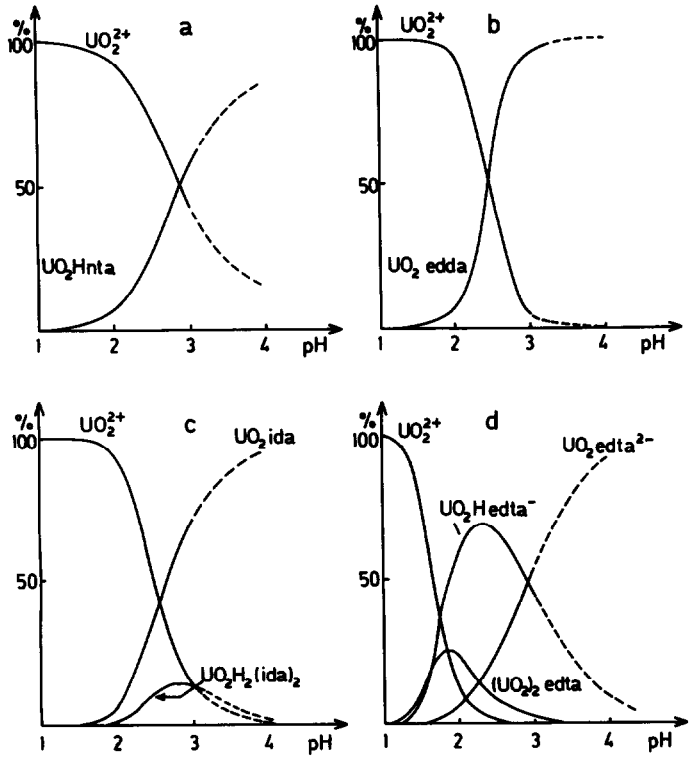



Fig. 2. Distribution of the U(VI) species as a function of pH. (a) $[U(VI)] = 1.08 \times 10^{-3}$ M; $[nta] = 10^{-2}$ M. (b) $[U(VI)] = 5.00 \times 10^{-4}$ M; $[edda] = 5 \times 10^{-3}$ M. (c) $[U(VI)] = 5.00 \times 10^{-4}$ M; $[ida] = 10^{-2}$ M. (d) $[U(VI)] = 3.85 \times 10^{-4}$ M; $[edta] = 2 \times 10^{-3}$ M.

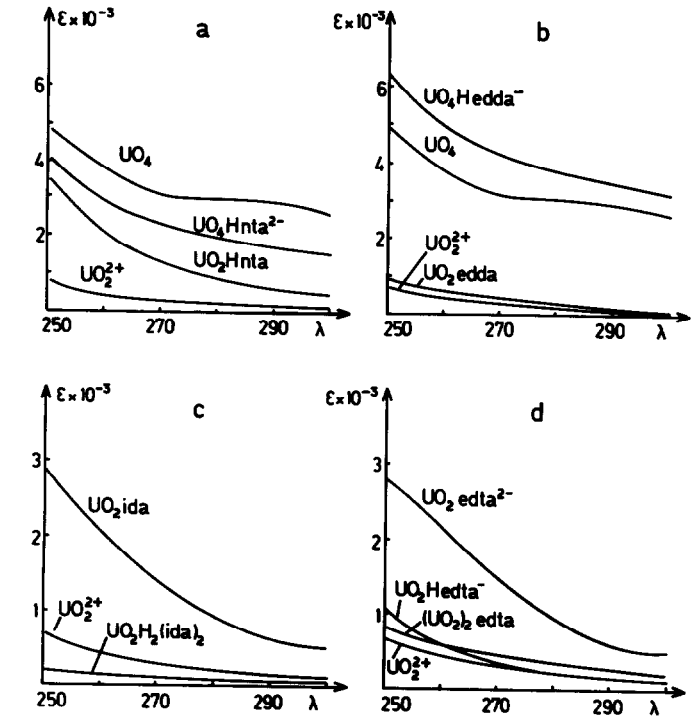



Fig. 3. Molar absorption coefficients of the U(VI) species in solution, (a) nta; (b) edda; (c) ida; (d) edta.

Table 1. Stability constants of $UO_2^{2+}$-polyaminocarboxylate chelates in 3 M $NaClO_4$ at 25°C. Uncertainty limits quoted are twice the computed standard deviations

| LIGAND | CHELATE | STABILITY CONSTANT |
|---|---|---|
| $edta^{4-}$ | $UO_2edta^{2-}$ | $\log\beta_{101} = 15.65 \pm 0.07$ |
| | $UO_2Hedta^-$ | $\log\beta_{111} = 18.59 \pm 0.07$ |
| | $(UO_2)_2edta$ | $\log\beta_{201} = 20.24 \pm 0.19$ |
| $edda^{2-}$ | $UO_2edda$ | $\log\beta_{101} = 16.02 \pm 0.18$ |
| $nta^{3-}$ | $UO_2Hnta$ | $\log\beta_{111} = 12.19 \pm 0.05$ |
| $ida^{2-}$ | $UO_2ida$ | $\log\beta_{101} = 9.63 \pm 0.09$ |
| | $UO_2H_2(ida)_2$ | $\log\beta_{122} = 23.8 \pm 0.2$ |

($5 \times 10^{-4}$ to $2 \times 10^{-2}$ M), and $H_2O_2$ ($4.6 \times 10^{-3}$ M). The following superposition of equilibria must be taken into account:

Equations (1), (2) and

$$xUO_2^{2+} + yH^+ + zL^{n-} + xH_2O_2 \rightleftarrows (UO_4)_xH_yL_z^{(nz-y)-} + 2xH^+ \quad (3)$$

with

$$\beta'_{xyzx} = \frac{[(UO_4)_xH_yL_z^{(nz-y)-}][H^+]^{2x}}{[UO_2^{2+}]^x[H^+]^y[L^{n-}]^z[H_2O_2]^x}.$$

Only two polyaminocarboxylate ligands were studied: $H_3nta$ and $H_2edda$ which give only 1:1 complex with $UO_2^{2+}$. $K_i$ and $\beta_{xyz}$ constants have been before determined. The values $\beta'_{xyzx}$ (Table 2) and molar absorption coefficients (Fig. 3) of the different species in solution have been calculated by the program LETAGROP–SPEFO extended by us to four component systems. Figure 4 gives the distribution of the various species in solution in our experimental conditions, as a function of pH.

## DISCUSSION

In Fig. 5 are the proposed solution structures of the 1:1 polyaminocarboxylate complexes of U(VI) (metal coordinating unit $UO_2^{2+}$ or $UO_4$).

The uranyl ion has a linear structure in which uranium has a formal $5f^\circ 6d^\circ$ configuration. In its complexes with *trans* geometry, four, five or six secondary coordinations may occur in an equatorial plane perpendicular to the main O–U–O axis.[26] For the $UO_4$ coordinating unit, peroxo group should occupy two coordination positions in the equatorial plane[23] or $UO_2^{2+}$.

*Complexes of* $UO_2^{2+}$. Molecular models of the studied complexes show that four available sites of coordination of $UO_2^{2+}$ are occupied by two nitrogen atoms of the amine functions and two oxygen atoms of the carboxylate functions in edta and edda complexes: stability constants of $UO_2edda$ and $UO_2edta^{2-}$ have the same order of magnitude. For edta complexes, the two other acetate groups are not bonded to the metal and are free to rotate around the C–N bond. Protonation of only one non-bonded acetate group is shown in the formation of the $UO_2Hedta^-$ chelate in acidic medium. The value of the logarithm of the protonation constant of $UO_2edta^{2-}$ (18.59–15.65 = 2.94) is this usually found for the protonation of polycarboxylic acids. The protonation of the second acetate group is not observed and may be explained by stabilization of the $UO_2Hedta^-$ species in the equilibrium:

$$UO_2H_2edta \rightleftarrows UO_2Hedta^- + H^+$$

Table 2. Stability constants of $UO_4$-polyaminocarboxylate chelates in 3 M $NaClO_4$ at 25°C. Uncertainty limits quoted are twice the computed standard deviations

| LIGAND | CHELATE | STABILITY CONSTANT |
|---|---|---|
| $edda^{2-}$ | $UO_4Hedda^-$ | $\log\beta_{1111} = 14.81 \pm 0.12$ |
| $nta^{3-}$ | $UO_4Hnta^{2-}$ | $\log\beta_{1111} = 8.50 \pm 0.17$ |

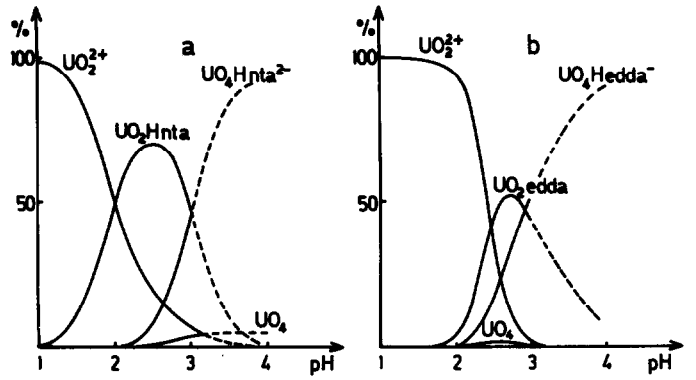



Fig. 4. Distribution of the U(VI) species as a function of pH. (a) $[U(VI)] = 3.85 \times 10^{-4}$ M; $[nta] = 10^{-2}$ M; $[H_2O_2] = 4.6 \times 10^{-3}$ M. (b) $[U(VI)] = 3.85 \times 10^{-4}$ M; $[edda] = 5 \times 10^{-3}$ M; $[H_2O_2] = 4.6 \times 10^{-3}$ M.

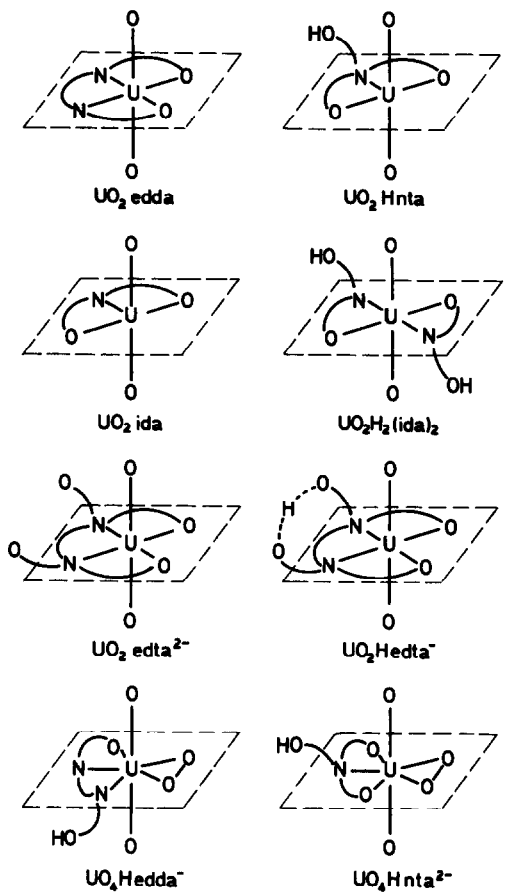



Fig. 5. Solution structure of the mononuclear complexes.

by formation of an internal hydrogen bond in the $UO_2Hedta^-$ chelate ($H^+$ linked between the carboxyl and the free carboxylate group). This second protonation could be observed in more acidic medium, but decomplexation occurs before protonation. A binuclear chelate is observed with edta: each iminodiacetate group of the edta ligand can complex a metal coordination unit $UO_2^{2+}$. We expect that $(1/2 \log \beta((UO_2)_2edta))$ and $(\log \beta(UO_2ida))$ should therefore have roughly the same value: $(1/2 \times 20.24 = 10.12) \simeq (9.63)$.

In nta and ida complexes, three available sites of coordination of $UO_2^{2+}$ are occupied by one nitrogen atom of the amine function and by two oxygen atoms of the carboxylate functions. For nta complex, molecular models show the impossibility to bond the third acetate group in the equatorial plane of the $UO_2^{2+}$ coordinating unit, thus a tridendate protonated nta complex is observed. The difference between $\log \beta(UO_2Hnta)$ and $\log \beta(UO_2ida)$: $(12.19–9.63) = 2.56$, is the value usually found for the protonation of polycarboxylic acids. The existence of $UO_2H_2(ida)_2$ confirms that the studied polyaminocarboxylate ligands cannot coordinate $UO_2^{2+}$ more than four times.

*Complexes of* $UO_4$. Complexation of $UO_4$ by nta and edda ligands confirms the previous observations. The stability of $UO_4Hnta^{2-}$ is similar to this of $UO_2Hnta$; the $UO_4Hnta^{2-}$ chelate formation may be written as:

$$UO_4 + H^+ + nta^{3-} \rightleftharpoons UO_4Hnta^{2-}$$

with

$$\log K' = 12.49.$$

The presence of the peroxo-bridge in the plane perpendicular to the O–U–O axis allows to obtain a coordination number of five in this plane for the $UO_4Hnta^{2-}$ chelate: two oxygen atoms of the peroxo-bridge and three chelating groups of the ligand bonded to U(VI) (two oxygen atoms of the

carboxylate groups and one nitrogen atom of the amine group as in the $UO_2Hnta$ chelate). The edda chelate which is singly protonated, appears also like a tridendate ligand (one oxygen atom of the carboxylate group and two nitrogen atoms of the amine groups bonded to U(VI)). The stability of $UO_4Hedda^-$ is greater than the stability of $UO_4Hnta^{2-}$. Thus, the nitrogen-U(VI) bond seems more stable than the oxygen–U(VI) bond.

In conclusion, the stability of the $UO_2^{2+}$ and $UO_4$ polyaminocarboxylate complexes is analogous to that of the other oxometals as $VO_2^+$, $MoO_3$, and $WO_3$.[25] Uranium has a greater affinity for nitrogen of the amine functions than for oxygen of the carboxylate functions of the ligand. The limitation of the coordination in the plane perpendicular to the O–U–O axis is mainly due to steric effects of the polycoordinating ligand. In this equatorial plane a maximum of four coordinating sites of U(VI) could be occupied by polyaminocarboxylate ligand in case of $UO_2^{2+}$ chelates and only three coordinating sites of U(VI) in case of $UO_4$ chelates.

## REFERENCES


1. A. G. Kozlov and N. N. Krot, *Russ. J. Inorg. Chem.* 1960, **5**, 954.
2. T. R. Bhat and M. Krishnamurthy, *J. Inorg. Nucl. Chem.* 1964, **26**, 587.
3. A. E. Klygin, I. D. Smirnova and N. A. Nikol'skaya, *Russ. J. Inorg. Chem.* 1959, **4**, 1209.
4. K. S. Rajan and A. E. Martell, *J. Inorg. Nucl. Chem.* 1964, **26**, 789.
5. L. Cattalini, U. Croatto, S. Degetto and E. Tondello, *Inorg. Chim. Acta Rev.* 1971, **5**, 19.
6. V. Kumari and G. K. Chaturvedi, *J. Indian Chem. Soc.* 1979, **56**, 854.
7. K. K. Kamble, V. S. Jatkar, S. S. Tamhankar, G. D. Shahapure and V. Damodaran, *J. Inorg. Nucl. Chem.* 1980, **42**, 1067.
8. P. Di Bernardo, G. Tomat, A. Bismondo, O. Traverso and L. Magon, *J. Chem. Res.* 1980, 234.
9. A. Napoli, *Ann. Chim.* 1982, **72**, 567.
10. M. Nourmand, I. Bayat and S. Yousefi, *Polyhedron* 1982, **1**, 827.
11. P. A. Overvoll and W. Lund, *Analyt. Chim. Acta* 1982, **143**, 153.
12. S. Koch and G. Ackermann, *Z. Anorg. Allg. Chem.* 1982, **494**, 196.
13. J. Stary, *Coll. czech. Chem. Comm.* 1960, **25**, 2630.
14. J. J. R. F. Da Silva and M. L. S. Simoes, *Talanta* 1968, **15**, 609.
15. K. L. Cheng and P. F. Lott, *Anal. Chem.* 1956, **28**, 462.
16. L. P. Polozhenskaya, L. F. Solntseva and A. M. Gurevich, *Radiokhimiya* 1966, **8**, 658.
17. A. M. Gurevich, L. P. Polozhenskaya and L. F. Solntseva, *Radiokhimiya* 1968, **10**, 195.
18. I. M. Kolthoff, J. J. Lingane, *Polarography*. Interscience, London (1952).
19. A. S. Brown, *J. Am. Chem. Soc.* 1934, **56**, 646.
20. L. G. Sillen, B. Warnqvist, *Arkiv Kemi* 1968, **31**, 377.
21. N. Ingri, W. Kakolowicz, L. G. Sillen and B. Warnqvist, *Talanta* 1967, **14**, 1261.
22. K. H. Gayer and L. C. Thompson, *Canad. J. Chem.* 1958, **36**, 1649.
23. G. G. Novitskii, D. S. Umreiko and R. I. Shamanovskaya, *Russ. J. Inorg. Chem.* 1969, **14**, 1216.
24. H. S. Dunsmore, S. Hietanen and L. G. Sillen, *Acta Chem. Scand.* 1963, **17**, 2644.
25. K. Zare, P. Lagrange and J. Lagrange, *J. Chem. Soc., Dalton* 1979, 1372.
26. K. Tatsumi and R. Hoffmann, *Inorg. Chem.* 1980, **19**, 2656.

*Polyhedron* Vol. 3, No. 4, pp. 475–478, 1984
Printed in Great Britain.

0277–5387/84 $3.00 + .00
Pergamon Press Ltd.

# OCTAHEDRAL $Mo_6$ CLUSTERS SUPPORTED BY METHOXIDE LIGANDS

MALCOLM H. CHISHOLM*, JOSEPH A. HEPPERT and JOHN C. HUFFMAN
Department of Chemistry and Molecular Structure Center Indiana University, Bloomington, IN 47405, U.S.A.

(*Received* 4 *August* 1983; *accepted* 15 *August* 1983)

**Abstract**—The structures of the $[Mo_6(\mu_3\text{-}Cl)_8(OMe)_6]^{2-}$ and $[Mo_6(\mu_3\text{-}OMe)_8(OMe)_6]^{2-}$ anions have been determined and reveal interesting comparisons of M–M and M–O distances with related $Mo_6(\mu_3\text{-}X)_8^{4+}$ containing compounds and polynuclear alkoxides of molybdenum.

A recent report[1] emphasized the importance of metal–metal bonding in the chemistry of molybdenum and tungsten alkoxides and noted that the only examples of alkoxides of molybdenum(II) were described[2] in 1968 as products obtained from the reactions between molybdenum(II) halides and NaOMe in methanol. Depending upon the reaction conditions, two types of compounds were isolated, namely, $Na_2Mo_6X_8(OMe)_6$ and $Na_2Mo_6(OMe)_{14}$. These were suggested to be structurally related to other well known $Mo_6(\mu_3\text{-}X)_8^{4+}$ containing compounds which have a 24 electron octahedral $Mo_6$ cluster inscribed within a cube of triply bridging halide ligands.[3] We report here a structural study which confirms this original suggestion and reveals some fascinating structural effects.

Following the literature procedure,[2] crystals of $2Na^+(MeOH)_{10}[Mo_6Cl_8(OMe)_6]^{2-}$ were obtained from methanol solution and one crystal was transferred to the goniostat of the diffractometer and cooled to −160°C in a liquid–nitrogen boil-off cold stream.[4] The following cell parameters were determined: $a = 12.218(4)$ Å, $b = 10.603(7)$ Å, $c = 10.673(3)$ Å, $\alpha = 59.46(2)°$, $\beta = 76.80(2)°$, $\gamma = 84.70(2)°$, $Z = 1$, $d_{calc} = 2.023$ g cm$^{-3}$ and space group $P\bar{1}$. Using 2915 reflections having $F > 2.33\sigma(F)$ out of a total of 3051 unique intensities (collected by scan techniques, Mo $K\alpha$, $6° < 2\theta < 45°$), the structure was readily solved by Patterson techniques and Fourier syntheses. All atoms, including hydrogen atoms, were located and refined. Final residuals are R(F) = 0.026 and Rw(F) = 0.036. The structure consists of $[Mo_6(\mu_3\text{-}Cl)_8(OMe)_6]^{2-}$ anions within a lattice of extensively hydrogen bonded MeOH with each $Na^+$ ion being surrounded by five MeOH molecules. An ORTEP view of the centrosymmetric molecule is given in Fig. 1.

Crystals of $2Na^+(MeOH)_{10}[Mo_6(OMe)_{14}]^{2-}$ were similarly obtained from methanol and examined at −160°C. Crystal data: $a = 12.199(2)$ Å, $b = 11.500(3)$ Å, $c = 18.689(5)$ Å, $\beta = 88.47(1)°$, $Z = 2$, $d_{calc} = 1.744$ g cm$^{-3}$ and space group $P2_1/n$. Using 2687 reflections having $F > 2.33\sigma(F)$ from a total of 3416 unique intensities (collected by scan techniques Mo$K\alpha$, $6° < 2 < 45°$), the structure was solved by a combination of direct methods and Fourier syntheses. Hydrogen atoms for all methyl groups were located in a difference Fourier phased on the refined non-hydrogen atom parameters. While several possible peaks in the final difference Fourier could be assigned to hydroxyl hydrogens, they were questionable at best and were thus ignored. Final residuals are R(F) = 0.045 and Rw(F) = 0.045. The structure consists of $[Mo_6(\mu_3\text{-}OMe)_8(OMe)_6]^{2-}$ anions within a lattice of extensively hydrogen bonded methanol and solvated $Na^+$ ions.

In the $[Mo_6(\mu_3\text{-}Cl)_8(OMe)_6]^{2-}$ structure, O(9) and O(10) are H bonded to one MeOH each, while O(8) is bonded with two MeOH molecules. In the

*Author to whom correspondence should be addressed.

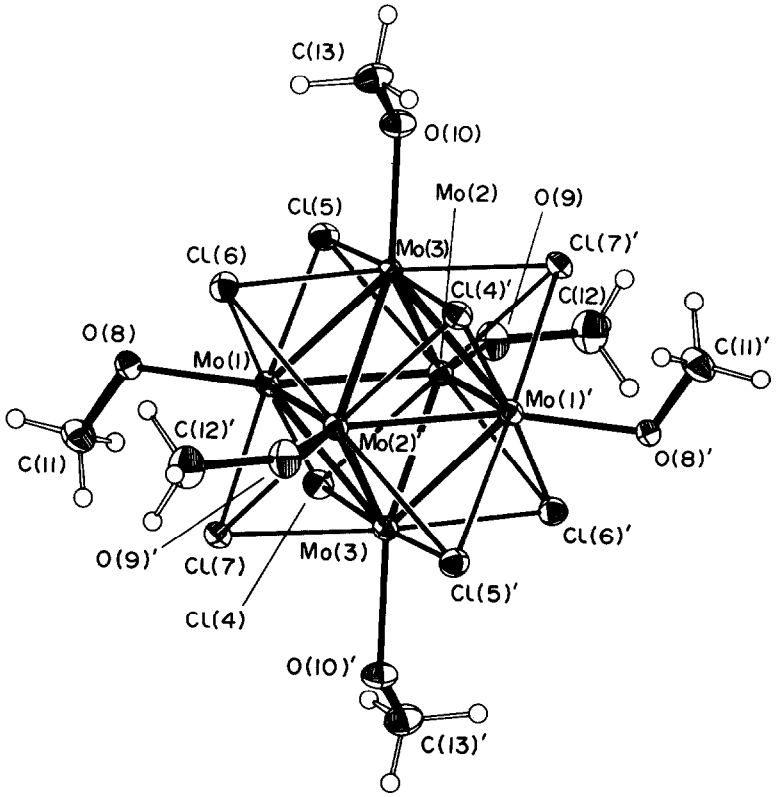



Fig. 1. An ORTEP view of the $[Mo_6(\mu_3\text{–}Cl)_8(OMe)_6]^{2-}$ anion found in the salt $2Na^+ \cdot 10MeOH \cdot Mo_6Cl_8(OMe)_6^{2-}$ showing the atom number scheme. Pertinent bond-distances (Å) are Mo(1)–O(8) = 2.080(3), Mo(2)–O(9) = 2.032(3), Mo(3)–O(10) = 2.038(3).

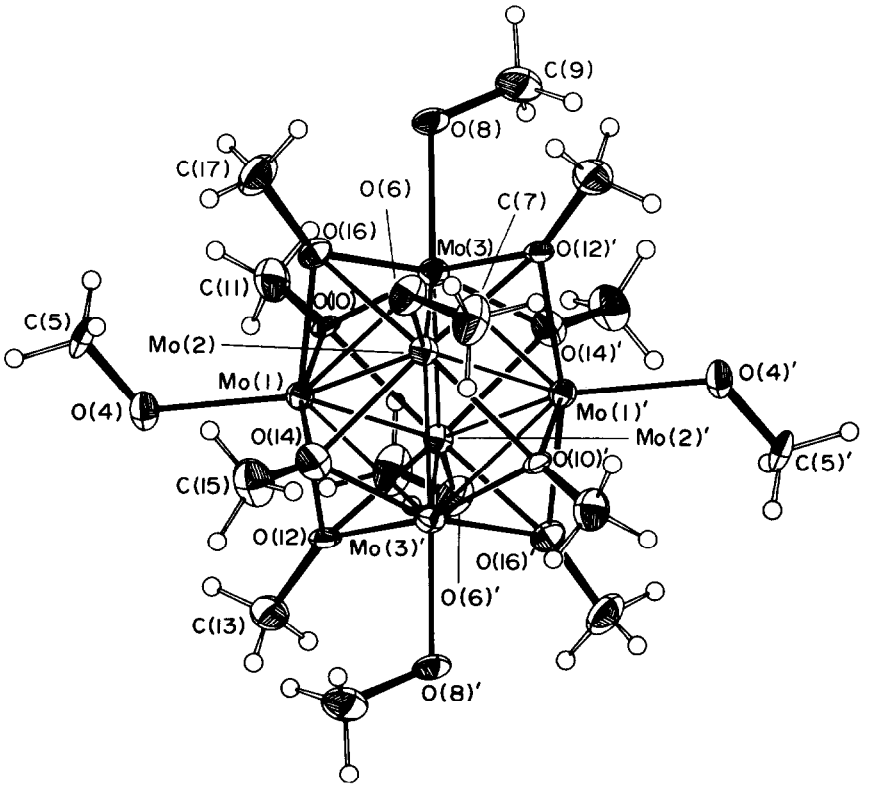



Fig. 2. An ORTEP view of the $[Mo_6(\mu_3\text{–}OMe)_8(OMe)_6]^{2-}$ anion in the salt $2Na^+ \cdot 10MeOH \cdot Mo_6(OMe)_{14}^{2-}$ showing the atom number scheme. Pertinent bond distances (Å) are Mo(1)–O(4) = 2.150(6), Mo(2)–O(6) = 2.092(6), Mo(3)–O(8) = 2.149(6).

Table 1. Comparison of some pertinent structural parameters in octahedral $Mo_6$ halide and alkoxide clusters

| Compound | Mo-Mo Distance Å | Mo-X Distance Å (terminal) | Mo-X Distance Å ($\mu_3$) | Mo-O-R Angle (°) | Mo-X-Mo Angle (°) | Ref |
|---|---|---|---|---|---|---|
| $HgMo_6(\mu_3\text{-}Cl)_8Cl_6$ | 2.620 ± 0.010 | 2.500 ± 0.020 | 2.480 ± 0.020 | --- | --- | 1 |
| $Na_2Mo_6(\mu_3\text{-}Cl)_8(OMe)_6$ | 2.607 ± 0.004 | 2.051 ± 0.029 | 2.490 ± 0.006 | 126.0 | 63.0 | this work |
| $Na_2Mo_6(\mu_3\text{-}OMe)_8(OMe)_6$ | 2.536 ± 0.008 | 2.130 ± 0.038 | 2.173 ± 0.013 | 119.9 | 71.3 | this work |
| $Mo_6(\mu_3\text{-}Br)_8Br_4(H_2O)_2$ | 2.640 ± 0.002 (2.630 ± 0.002) | 2.587 ± 0.002 (Mo-Br) | 2.606 ± 0.002 | --- | --- | 2 |

(1) Schnering, H.G. Zeit. Anorg. Chem. 1971, 385, 75. (2) Guggenberger, L.J.; Sleight, A.W. Inorg. Chem. 1969, 8, 2041.

$[Mo_8(\mu_3\text{-}OMe)_8(OMe)_6]^{2-}$ structure where the hydroxyl hydrogens were not located and refined, one may infer the existence of hydrogen bonds based on O---O separational distances.[5] Specifically, an O---O separation of 3.0 Å or less implies an O--H---O interaction. In this way we infer that O(4) and O(8) are both H bonded to two MeOH molecules while O(6) is H bonded with only one.

Pertinent averaged structural data for the $Mo_6$-methoxide anions are presented in Table 1 along with those for related halo species. A number of fascinating features emerge. (1) The substitution of terminal OMe ligands for terminal chlorides causes little change in M–M distances, but replacement of the $\mu_3$-Cl group by $\mu_3$-OMe causes a substantial shortening. This is expected as MO distances are substantially shorter (by *ca.* 0.3 Å) than MCl distances. (2) The terminal M–X bond distances are only marginally longer than the bridging ($\mu_3$) M–X distances. This is true for the $Mo_6Cl_{14}^{2-}$ and the $Mo_6(OMe)_{14}^{2-}$ anions. Generally one observes that M–X bridging distances are significantly longer than terminal distances.[6] For example in the compounds $Mo_3(\mu_3\text{-}O)(\mu_3\text{-}OR)(\mu_2\text{-}OR)_3(OR)_6$, where R = *i*-Pr or ($CH_2$-*t*-Bu), one finds Mo–O < Mo–$\mu_2$–O < Mo–$\mu_3$–O with roughly 0.1 Å difference between each type of alkoxide.[7] (3) The substitution of $\mu_3$-Cl by $\mu_3$-OMe causes the Mo–O terminal distances to increase by close to 0.1 Å. (4) An inspection of the individual terminal Mo–O distances (see captions to figures) shows that oxygen atoms which are hydrogen bonded to two MeOH molecules have longer Mo–O bonds, by roughly 0.05 Å, than those which are only hydrogen bonded to one MeOH molecule.

It should also be noted that these are the longest Mo–O distances seen thus far in the chemistry of molybdenum alkoxides.[6] In part, this may be attributable to the fact that the terminal ligands are H bonded with solvent MeOH molecules. However, we believe that there are electronic factors operating between the radial (terminal) RO ligands and the 24 election $Mo_6$ cluster[8] which also causes these Mo–O bonds to be unusually long. First, there is competition for use of molybdenum $d_{z^2}$ and $p_z$ atomic orbitals in a $\sigma$ bonding sense, i.e. a mutual trans-influence, between strong cluster bonding and strong metal–ligand bonding. Second, the molybdenum $d_{xz}$ and $d_{yz}$ atomic orbitals are extensively used in M–M bonding and are thus not available for RO-to-Mo $\pi$-bonding.[9] Indeed the latter becomes a repulsive effect. In going from $\mu_3$-Cl to $\mu_3$-OMe, the M–M interactions become stronger as a result of the contraction of the $Mo_6$ cluster and thus the Mo–O terminal bond distances are lengthened.

Clearly a more quantitative examination of the bonding in these $Mo_6$-alkoxide clusters is warranted. Also, their electrochemical and photoexcited state chemistry is of interest, if only to provide a comparison with the unusual properties already noted for the $Mo_6X_{14}^{2-}$ anions (X=Cl, Br).[10] Finally, the high reactivity of the alkoxy ligands toward ligand substitution reactions leads us to suggest that these alkoxides should be good materials for syntheses and exploration of new $Mo_6$-cluster chemistry. These studies are underway.

*Acknowledgements*—We thank the Office of Naval Research and the Wrubel Computing Center for support.

*Supplementary Materials Available.* Tables of fractional coordinates and thermal parameters have been deposited with the Cambridge Crystallographic Data Centre. Complete structural information is available, from the Editor at Queen Mary College and, in microfiche form, from the Indiana University Chemistry Library, Bloomington, Indiana 47405, at a cost of $2.50 per structural report. For $2Na^+[Mo_6(\mu_3\text{-}Cl)_8(OMe)_6]^{2-}$

·10MeOH, request MSC No. 83047, and for $2Na^+[Mo_6(\mu_3\text{-}OMe)_8(OMe)_6]^{2-}\cdot 10MeOH$, request MSC No. 83053.

## REFERENCES


1. M. H. Chisholm, *Polyhedron* 1983, **2**, 681.
2. P. Nannelli and B. P. Block, *Inorg. Chem.* 1968, **7**, 2423.
3. F. A. Cotton and G. Wilkinson, *Advanced Inorganic Chemistry*, 4th Edn (1980).
4. For general procedures, see J. C. Huffman, L. N. Lewis, and K. G. Caulton, *Inorg. Chem.* 1980, **19**, 2755.
5. W. C. Hamilton and J. A. Ibers, In *Hydrogen Bonding in Solids*. W. A. Benjamin, New York (1968).
6. For listings of Mo–O terminal and bridging ($\mu_2$ and $\mu_3$), see Ref. 1.
7. M. H. Chisholm, J. C. Huffmann and C. C. Kirkpatrick, *J. Am. Chem. Soc.* 1981, **103**, 5967.
8. For two leading references, two theoretical treatments of the M–M bonding in 24 electron $Mo_6(\mu_3\text{–}X)_8$ clusters, see (i) T. Hughbanks and R. Hoffmann, *J. Am. Chem. Soc.* 1983, **105**, 1150 and (ii) B. Bursten, F. A. Cotton and G. G. Stanley, *Isr. J. Chem.* 1980, **19**, 132.
9. The six molybdenum ($d_{xz}$, $d_{yz}$) atomic orbitals make significant contributions to the filled molecular orbitals $t_{1u}$, $t_{2g}$ and $t_{2u}$, all having cluster bonding character, and one unfilled low lying $t_{1u}$ anti-bonding orbital. While the interaction of the six radial (terminal) ligands with the $Mo_6(\mu_3\text{–}X)_{8\pi}^+$ moiety greatly destabilizes the $a_{1g}$ bonding orbital and the $e_g$ and $t_{1u}$ antibonding orbitals, which have significant $d_{z^2}$ contributions, it has little apparent effect on bonding orbitals having ($d_{xz}$, $d_{yz}$) character. However, the latter have appropriate symmetry to interact with p$\pi$ orbitals on the radial ligands. If the ligand p$\pi$ orbitals are filled, there would be a destabilization of the M–M bonding $t_{1u}$ and $t_{2u}$ orbitals.
10. A. W. Maverick, J. S. Najclzionck, D. Mackenzie, D. G. Nocera and H. B. Gray, *J. Am. Chem. Soc.* 1983, **105**, 1879.

*Polyhedron* Vol. 3, No. 4, pp. 479–484, 1984
Printed in Great Britain.

0277-5387/84 $3.00 + .00
Pergamon Press Ltd.

# EXTRACTION OF COPPER(II) AND NICKEL(II) BY CYCLIC TRIOXIMES AND CYCLIC FURAZAN OXIMES

**L. R. M. PAPING, T. P. M. BEELEN, M. MOLS and R. PRINS***
Laboratory of Inorganic Chemistry, Eindhoven University of Technology, P.O. Box 513, 5600 MB Eindhoven, The Netherlands

(*Received* 25 *August* 1983; *accepted* 1 *November* 1983)

**Abstract**—The extraction properties of 1,2,3-cyclopentanetrione trioxime ($H_3CPT$) and its furazan, and of 4-*t*-butyl-1,2,6-cyclohexanetrione trioxime ($H_3BHT$) and its furazan are described. $H_3CPT$ was found to be too soluble in water and was therefore of no use in extraction but $H_3BHT$ was satisfactory. The extracted copper and nickel chelates of $H_3BHT$ precipitate by agglomeration caused by intermolecular hydrogen bonding and/or coordination of the third oxime group. This precipitation blocked back extraction. The furazan oximes derived from these trioximes did not form copper or nickel chelates under extraction conditions.

In order to find an extractant that is selective for nickel with respect to copper a number of organic compounds have been synthesized and studied for their extraction properties. Because of the great affinity of nickel for dioximes this investigation is limited to organic groups containing oxime groups. From previous work[1,2] it became clear that the use of strained instead of unstrained dioximes makes the extraction more convenient because of a higher extraction rate, but the selectivity for nickel above copper disappears. In this article two new kinds of ligands will be examined, viz. the cyclic trioximes (Fig. 1) and the cyclic furazan oximes (Fig. 2).

Frierson and Marable[3] discovered that 1,2,3-cyclohexanetrione trioxime instantaneously forms a $NiL_2$ chelate with nickel(II) salts in an ethanol/water mixture but they did not investigate the extraction capacities. They postulated a $NiN_2O_2$ chromophore to be formed which is unexpected because there is not much strain in the cyclic hexane ring. Furthermore, it is unknown what the influence will be of the third oxime group on the stability of the copper and nickel chelates, because now additional hydrogen bridging is possible. This makes the cyclic trioximes very interesting to study. Besides, the cyclic trioxime is a precursor of the cyclic furazan oxime. In previous work[2] it was found that nopinoquinone dioxime could easily be converted into a furazan, but this furazan was not active in extraction, probably because no

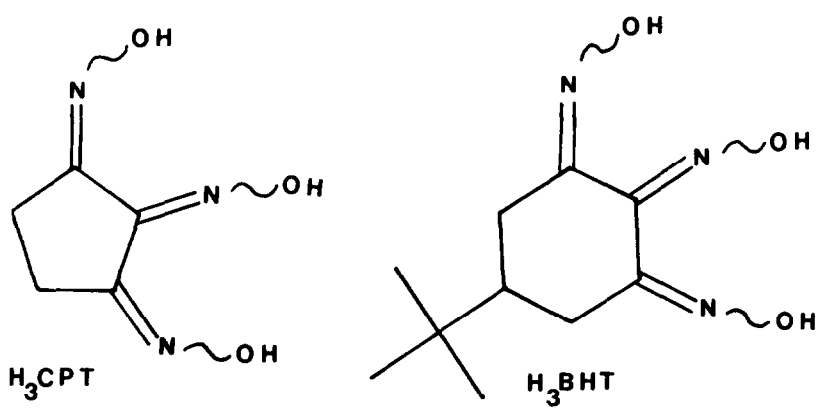



Fig. 1. Schematic structures of 1,2,3-cyclopentanetrione trioxime ($H_3CPT$) and 4-*t*-butyl-1,2,6-cyclohexanetrione trioxime ($H_3BHT$).

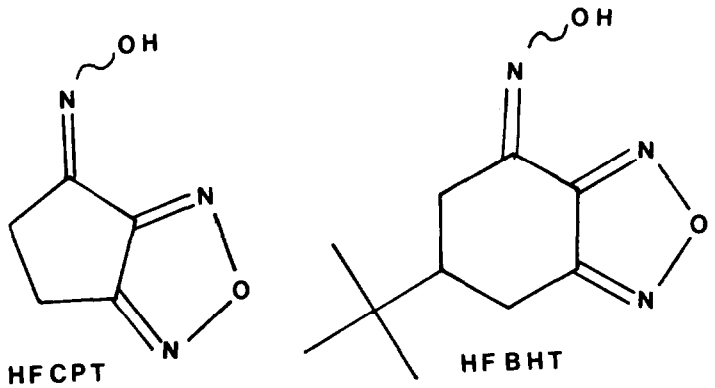



Fig. 2. Schematic structures of the furazan derived from 1,2,3-cyclopentanetrione trioxime (HFCPT) and the furazan derived from 4-*t*-butyl-1,2,6-cyclohexanetrione trioxime (HFBHT).

acidic hydrogen atom is present. The cyclic furazan oxime has such an acidic hydrogen and furthermore this molecule can react as a bidentate ligand.

For these reasons 1,2,3-cyclopentanetroine trioxime ($H_3CPT$) and 4-*t*-butyl-1,2,6-cyclohexanetrione trioxime ($H_3BHT$) were synthesized and examined. In addition, these two trioximes were converted into the furazan of 1,2,3-cyclopentanetrione trioxime (HFCPT) and the furazan of 4-*t*-butyl-1,2,6-cyclohexanetrione trioxime (HFBHT).

## EXPERIMENTAL

$^1$H NMR spectra were obtained at room temperature on a 60 MHz Varian EM 360 A spectrometer, while ESR measurements were made with a Varian E15 spectrometer at room temperature and UV-visible spectra were obtained on a Unicam Sp. 800D. Aqueous metal ion concentrations were measured with the Perkin–Elmer 300 Atomic Absorption Spectrophotometer.

The extraction experiments were carried out in a three stoppered flask with a stirring device and continuous pH measurements. The starting volumes of water and organic solvent were both 250 cm$^3$. Stirring was stopped when no further change of the pH was noticed, indicating that equilibrium was reached. For analysis equally small volumes of water layer and organic layer were withdrawn from the system. To measure the distribution coefficient as a function of pH thereafter a small quantity of 4N acid or base was added, and the process of stirring until equilibrium and withdrawal of small portions of the aqueous and organic solutions was repeated at a different pH. Care was taken to keep the volumes of the aqueous and organic solutions equal. Although in this procedure the electrolyte concentration does not stay constant we preferred this method because it is convenient to execute and because in a separate experiment it was shown that in the applied concentration range the influence of the electrolyte concentration is negligible. Pentanol was used as organic solvent and as inorganic salt we used metal nitrate. We used NaOH as base and $HNO_3$ as acid.

## SYNTHESIS

*1,2,3-Cyclopentanetrione trioxime* ($H_3CPT$)

Following the method of Ferris[4] using *n*-butylnitrite crude 1,2,3-cyclopentanetrione 1,3-dioxime was obtained as a brown compound from cyclopentanone (E. Merck A. G., Darmstadt, zur synthese).

IR: 1725 cm$^{-1}$ (C=O); and new bands at 1625 cm$^{-1}$ (C=N) and 3250 cm$^{-1}$ broad (OH).

The crude trione dioxime was dissolved in ethanol and treated with an aqueous solution of $NH_2OH \cdot HCl$ and NaOAc under reflux. The product was washed with ethanol and extracted with boiling ethanol and after that washed with water. A brown product was obtained in small quantity (because of the good solubility in water) which could not be decolourized. Found: C, 36.67; H, 4.23; N, 27.06. Calc. for $C_5H_7N_3O_3$: C, 38.22; H, 4.49; N, 26.74%.

IR: 1725 cm$^{-1}$ (C=O) disappeared; 1625 cm$^{-1}$ broad absorption (C=N) and 3300 cm$^{-1}$ broad absorption.

*The furazan of 1,2,3-cyclopentanetrione trioxime* (HFCPT)

Crude 1,2,3-cyclopentanetrione 1,3-dioxime (0.07 mol) (see synthesis $H_3CPT$) dissolved in a solution of 0.3 mol NaOH in 50 cm$^3$ water was treated with a solution of $NH_2OH \cdot HCl$ (0.18 mol) in 75 cm$^3$ water during several days at 60°C. After filtration the filtrate was acidified till pH = 2 and filtered. The filtrate was extracted with ether and evaporating the ether layer after drying ($Na_2SO_4$) gave 1 g of a yellow solid. Found: C, 43.22; H,

3.90; N, 30.11. Calc. for $C_5H_5N_3O_2$: C, 43.17; H, 3.62; N, 30.21%.

IR 3300 $cm^{-1}$ sharp (OH), 1520 $cm^{-1}$ (furazan) 1600–1650 $cm^{-1}$ broad (C=N).

*4-t-butyl-1,2,6-cyclohexanetrione trioxime* ($H_3BHT$)

Following the method of Ferris[4] using *n*-butylnitrite crude 4-*t*-butyl-1,2,6-trione-2,6-dioxime was obtained as a light brown compound from 4-*t*-butylcyclohexanon (Janssen Chimica, Beerse, Belgium, 95 + %). Found: C, 56.19; H, 7.51; N, 12.92. Calc. for $C_{10}H_{16}N_2O_3$: C, 56.60; H, 7.55; N, 13.21%.

IR: 3230 $cm^{-1}$ broad (OH), 1620 and 1590 $cm^{-1}$ (C=N) as new absorptions, 1710 $cm^{-1}$ (C=O).

Crude 4-*t*-butyl-1,2,6-trione 2,6-dioxime was converted into $H_3BHT$ by the same method as for $H_3CPT$. The reaction mixture was filtered and the filtrate was evaporated. The solid thus obtained was washed with ethylacetate resulting in a white product. Found: C, 53.00; H, 7.66; N, 18.77. Calc. for $C_{10}H_{17}N_3O_3$: C, 52.86; H, 7.49; N, 18.50%.
IR: 3230 $cm^{-1}$ broad (OH), 1650, 1610, 1580 $cm^{-1}$ weak (C=N); the C=O absorption at 1710 $cm^{-1}$ had disappeared. $^1H$ NMR DMSO-d6: $\delta$0.9 (s, 9H), $\delta$1.6–3.2 (m.c, 5H), $\delta$11.4, 11.7 en 12.6 (s, OH).

*The furazan of 4-t-butyl-1,2,6-cyclohexanetrione trioxime* (HFBHT)

Crude 4 - *t* - butyl - 1,2,6 - cyclohexanetrione - 2,6 - dioxime (see synthesis $H_3BHT$) was converted into the furazan of $H_3BHT$ by using the same method as for the synthesis of HFCPT. The reaction mixture was filtered and acidified till pH = 7. The solid thus obtained was filtered, washed with water and dried with silica to yield a white product. Found: C, 57.15; H, 7.33; N, 19.93. Calc. for $C_{10}H_{15}N_3O_2$: C, 57.42; H, 7.18; N, 20.10%.

IR: 3290 $cm^{-1}$ sharp (OH); 1635 and 1582 $cm^{-1}$(C=N), 1510 $cm^{-1}$ (furazan). $^1H$ NMR DMSO-d6: $\delta$0.9 (s, 9H), $\delta$ 1.6–3.5 (m.c, 5H), $\delta$ 12.1 (s, OH).

## RESULTS

$H_3CPT$ appeared to be fairly soluble in water. The only organic solvent in which we could dissolve $H_3CPT$ was tri-*n*-butyl phosphate (tbp) but when this solution was mixed with water the $H_3CPT$ was transported to the water layer. When adding metal sulphates the copper and nickel chelates formed were not transported to the organic layer, but precipitated in the water layer. The isolated brown copper chelate had an elemental analysis of C, 27.26; H. 2.55; N, 17.69; Cu, 19.34%. The isolated red brown nickel chelate had an elemental analysis of C, 28.78; H, 3.02; N, 18.48; Ni, 17.21%. No ESR signal could be measured for this copper chelate, while the NMR spectrum of the nickel chelate could not be obtained because of its insolubility in organic solvents.

HFCPT dissolved very well in tbp, pentanol, ether and water but it possessed no extraction capacity for Cu(II) and Ni(II).

$H_3BHT$ dissolved very well in pentanol and only slightly in water. Extraction experiments in pentanol with Ni(II) gave a fine red precipitate in the organic layer. At pH = 2.86 99.4% of the nickel was extracted, when using 0.025 mol/l $H_3BHT$ in pentanol and 0.002 mol/l $Ni(NO_3)_2$ in water with equal volumes. Equilibrium was reached in about 1 hr. Back extraction could not be observed down to pH = 1. The isolated nickel chelate had an elemental analysis of C, 47.74; H, 6.52; N, 16.60; Ni, 10.67% which points in the direction of a $Ni(H_2BHT)_2$ chelate: Calc. for $NiC_{20}H_{32}N_6O_6$: C, 46.99; H, 6.50; N, 16.45; Ni, 11.49%.

The extraction of a 0.001 mol/l $Cu(NO_3)_2$ solution in water by 0.025 mol/l $H_3BCT$ in pentanol gave the same results as with $Ni^{2+}$: a light brown suspension in the organic layer at pH = 2.91 and no back extraction till pH = 1. The isolated copper chelate had an elemental analysis of C, 45.41; H, 6.12; N, 15.91; Cu, 12.15% which is in good agreement with a $Cu(H_2BHT)_2 \cdot 2H_2O$ chelate. Calc. for $CuC_{20}H_{36}N_6O_8$: C, 44.99; H, 6.37; N, 15.75; Cu, 11.90%.

No proper solvent could be found to enable an ESR solution spectrum to be measured. A "powder" ESR spectrum from this compound was not recorded, because in such a spectrum anisotropy will not be averaged out (see (5)) and therefore it is unlikely that the total number of nitrogen atoms coordinated to the copper can be established.

An extraction experiment with excess $Cu^{2+}$ gave a surprising effect. The organic layer became dark brown and the suspension disappeared. The filtered organic layer was evaporated which yielded a dark brown solid with an elemental analysis of C, 40.07; H, 5.25; N, 17.74; Cu, 19.04%, which is not completely in agreement with a $Cu_n(HBHT)_n \cdot 2nH_2O$ chelate: Calc. Cu, 20.72; C, 39.15; H, 5.55; N, 13.70%. No ESR signal could be detected for this chelate in solution at room temperature.

HFBHT was very soluble in organic solvents, but did not possess extraction capacities for Cu(II) or Ni(II).

## DISCUSSION

### 1,2,3-*cyclopentanetrione trioxime* ($H_3CPT$)

$H_3CPT$ is fairly soluble in water. The origin of this behaviour is that the three oxime groups, which can form hydrogen bridges with water, make the molecule hydrophilic, and that the relatively small organic part ($-CH_2-CH_2-$) causes only a small hydrophobic effect. The relatively small organic part and the large polarity, caused by the three oxime groups, make this ligand almost insoluble in organic solvents, which do not form homogeneous solutions with water. The $H_3CPT$ ligand will therefore be of limited value as an extractant, because most of the $H_3CPT$ will be transported to the water layer, which will lead to undesired ligand losses. Furthermore, the chelates formed with Cu(II) and Ni(II) are not transported to the organic layer but precipitate in the water layer. It is therefore recommended to use branched cyclic rings to enlarge the organic hydrophobic part. In that way the resulting ligand will be more soluble in organic solvents and less in water. The elemental analysis of the copper $H_3CPT$ chelate shows that if a $Cu : H_3CPT = 1 : 2$ chelate is formed at all, it is not the only chelate. The $Cu : C = 1 : 7.5$ ratio and the $Cu : N = 1 : 4.15$ ratio point in the direction of $Cu : L = 2 : 3$ chelate.

The fact that no ESR spectrum is observed, which can be explained by a copper–copper interaction, confirms the hypothesis that at least one copper ion is present nearby each copper (II). For the nickel $H_3CPT$ chelate almost the same values are observed as for Cu: $Ni : C = 1 : 8.2$ and $Ni : N = 1 : 4.5$. So here also a $Ni : L = 2 : 3$ molecule is the most probable chelate. The $C : N = 5 : 2.78$ ratio in both chelates shows that some oxime must be lost. Too low hydrogen values (2.55 and 3.02) and the high other values (100%–Cu–C–H–N = 33.16%, 100%–Ni–C–H–N = 32.51%) are pointing in the direction of some inorganic part. Therefore no great significance must be given to the composition of these chelates in relation to extraction chemistry.

### *The furazan of* 1,2,3-*cyclopentanetrione trioxime* (HFCPT)

HFCPT can also be called 3,4-trimethylene furazan-6-oxime in analogy with the furazan oxide of Barnes.[6] This ligand is more soluble in organic solvents than $H_3CPT$ because two of the three polar oxime groups have now formed an organic aromatic furazan ring. The fact that no extraction capacities were found for this ligand is not surprising when we look at a molecular model of the ligand. The estimated N–N distance is about 3.2 Å, which is far too large for N,N-coordination and also makes N,O-coordination unattractive. It cannot be excluded that other furazan oximes with a smaller N–N distance may be good extractants for nickel and copper. If we compare HFCPT with $H_3CPT$ we can conclude that the solubility capacities have improved, but that the chelating capacities have disappeared.

### 4-*t-butyl*-1,2,6-*cyclohexanetrione trioxime* ($H_3BHT$)

The solubility properties of $H_3BHT$ for extraction are much better than those of $H_3CPT$. Differences between $H_3BHT$ and $H_3CPT$ are the increase of the carbon ring by one carbon atom and the *t*-butyl group. We suggest that most of the increased solubility originates from the large *t*-butyl group which makes the molecule hydrophobic. It is unlikely that enlargement of the ring with only one atom can cause such a change. $H_3CPT$ has a good extraction capacity (99.4% extraction at pH = 2.86) for nickel, but the extracted chelate was not soluble in the organic layer and precipitated in this phase. The reason for the precipitation in the organic layer (the pentanol layer is the upper phase, the water layer the lower phase) instead of in the water layer must be the strong hydrophobic effect of the *t*-butyl group. Because no such insolubility has been found for the bis(cyclohexaneglyoximato) nickel(II) chelate[7] the reason for the precipitation must be the third oxime group of $H_3BHT$. Elemental analysis showed that presumably a $Ni(H_2BHT)_2$ chelate is formed, which means that the third oxime group is likely to be involved in intermolecular coordination or hydrogen bridge formation between chelate molecules. As a result the chelate molecules agglomerate and precipitate. This precipitation also means that the extraction is no longer an equilibrium reaction, but a termination reaction. The back extraction is blocked, so the only way to free the nickel ions again is to break the chelate with strong acids, but these acids will also attack and possibly destroy the ligand. As a result this ligand is unattractive for use in a continous process.

The estimated N-N distance of 2.8 Å for $H_3BHT$ is comparable with that of $\beta$-$H_2NQD$ (see (2)), which formed N,N-coordinated chelates. The red colour of $Ni(H_2BHT)_2$ is also found for unstrained aliphatic dioxime nickel chelates and $Ni(\beta\text{-HNQD})_2$, while N,O-coordinated chelates, like $Ni(\alpha\text{-HCQD})_2$ and $Ni(\delta\text{-HCQD})_2$, are green.[8,9] This makes N,N-coordination the most reasonable structure, rather than N,O-coordination as suggested by Frierson and Marable.[3] In Fig. 3 some possible structures are presented.

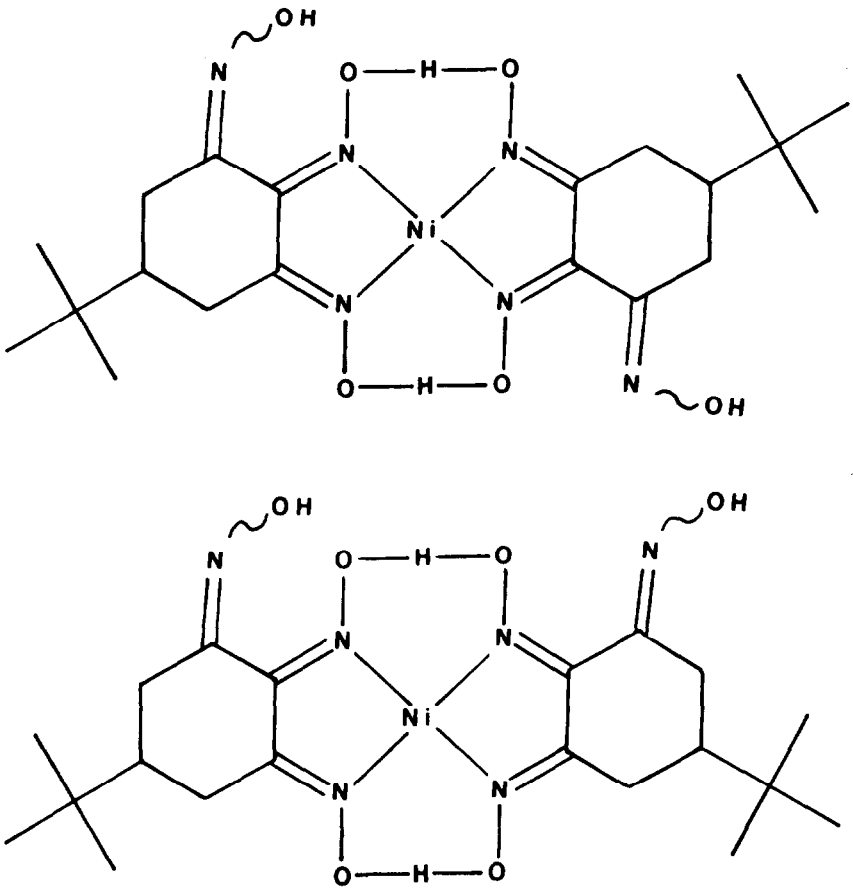



Fig. 3. Two possible structures of the $Ni(H_2BHT)_2$ chelate assuming N,N-coordination.

The copper extraction by $H_3BHT$ in pentanol gives the same picture as the nickel extraction when excess $H_3BHT$ is used. Elemental analysis showed that $Cu(H_2BHT)_2 2H_2O$ precipitated in the organic layer. This means that probably copper forms a distorted octahedral chelate with two additional waters in the axial position, while nickel forms a square planar chelate. This is in analogy with $\beta$-$H_2NQD$ chelates (see (2)). "Powder" ESR spectroscopy can perhaps confirm that the copper ion has an octahedral environment.[10]

When using excess copper in the extraction a new chelate is formed that is soluble in the organic layer. From the elemental analysis of the isolated chelate the ratio's Cu : C = 1 : 11.1 and Cu : N = 1 : 3.51 are calculated. This means that a Cu : L = 1 : 1 chelate is formed (Cu : C = 1 : 10 and C : N = 1 : 3) presumably with some organic impurities. The solubility of this chelate in the organic layer can now be explained by the fact that the third oxime group is involved in the chelation with copper, and therefore is no longer available for intermolecular hydrogen bridge formation or intermolecular coordination. The fact that no ESR spectrum can be found for this chelate points in the direction of a strong antiferromagnetic coupling between at least two copper ions, which is well known for binuclear copper complexes.[11-14] The chelate must be of the type $Cu_nL_n$ (with $n$ = even).

The phenomenon that with excess copper different chelates are formed was also observed with $\delta$-$H_2NQD$ (see (1)) where a Cu : L = 2 : 3 chelate was formed.

*The furazan of* 4-*t*-*butyl*-1,2,6-*cyclohexanetrione trioxime* (HFBHT)

HFBHT can also be called 6 - *t* - butyl - 4 - hydroxyimino - 4,5,6,7 - tetrahydrobenzofurazan in analogy with Lewis[15] (the same molecule without *t*-butyl group) or 6,7-dihydro-6-*t*-butylbenzofurazan-4(5H)-one oxime in similarity with Calleri[16] (the same molecule with a dimethyl group instead of a *t*-butyl group). Other names for this compound could use a 1,2,5-oxadiazole ring as basis.

HFBHT is not very soluble in water, but dissolves very well in organic solvents like ethanol and ether. This can be explained by the hydrophobic *t*-butyl group and by the fact that two of the three polar oxime groups are now transformed in an

organic furazan ring. The N–N distance between the nitrogen of the oxime group and the nitrogen of the furazan can be calculated from the values of the atomic coordinates found by Calleri[16] for a similar molecule. The N–N distance is calculated to be 2.835 Å and such a distance makes N,N-coordination the most likely one. Furthermore Calleri's X-ray analysis showed that the oxime group is *anti* in respect to the furazan. Nevertheless no extraction properties are found for this ligand. The reason for this is, most likely, that the furazan possesses such a poor complexing capacity (Driessen[17] found poor complexing capacities for furazans) that even with a strong complexing neighbour as the oxime group no bidentate reaction with metal ions takes place under extraction conditions. Another reason may be that a furazan oxime chelate cannot have hydrogen bridge stabilization, like dioxime chelates, because the oxime group will be deprotonated by the extraction reaction:

$$M^{2+} + 2HFBHT \rightleftarrows M(FBHT)_2 + 2H^+.$$

The conclusion that can be drawn from these results is that furazan oximes are of no use for extraction of Cu(II) and Ni(II).

## CONCLUSIONS

$H_3CPT$ is more soluble in water than in organic solvents, which makes this compound of no use as an extractant. This ligand is able to form chelates with copper and nickel which precipitate in the water layer. The introduction of a large hydrophobic group into the aliphatic ring, like *t*-butyl in $H_3BHT$, provides an answer to this solubility problem.

Ni(II) was extracted by $H_3CBHT$ as $Ni(H_2BHT)_2$, but this chelate precipitated in the organic layer and therefore blocked the back extraction. This is caused by intermolecular hydrogen bridge formation and/or coordination of the third oxime group, which is not primarily involved in the chelation with nickel. The Cu(II) extraction by excess $H_3BHT$ showed the same picture with the precipitation of $Cu(H_2BHT)_2 \cdot 2H_2O$. When the extraction is performed with excess copper ions a $Cu : H_3BHT = 1 : 1$ chelate is formed which is soluble in the organic layer. The third oxime group is now directly involved in the chelation with copper and no intermolecular hydrogen bridge formation can occur. These results show that the use of trioximes for the extraction of Cu(II) and Ni(II) is not an improvement with respect to the dioximes but, on the contrary, is a step backwards because new problems, like precipitation and blocked back extraction, are introduced.

The experiments with the two furazan oximes confirm the conclusion that a large hydrophobic group like *t*-butyl changes the solubility properties in the desired direction. Furthermore, it is shown that this type of ligand is not suitable for extraction of copper and nickel ions because under extraction conditions no chelates with copper and nickel are formed. The reasons for this are that furazan is too weak a ligand and that no hydrogen bridge stabilization is possible after chelation.

## REFERENCES

1. L. R. M. Paping, T. P. M. Beelen, C. P. J. Rummens and R. Prins, *Polyhedron* 1982, **1**, 503.
2. L. R. M. Paping, T. P. M. Beelen, M. Mols and R. Prins, *Polyhedron*, submitted for publication.
3. J. W. Frierson and N. Marable, *Anal. Chem.* 1962, **34**, 210.
4. A. F. Ferris, G. S. Johnson, F. E. Gould and H. K. Latourette, *J. Org. Chem.* 1960, **25**, 492.
5. H. M. Swartz, J. R. Bolton and D. C. Borg, *Biol. appl. of Elect. Spin Reson.* 1972.
6. J. F. Barnes, M. J. Barrow, M. M. Harding, R. M. Paton, P. L. Ashcroft, J. Crosby and C. J. Joyce, *J. Chem. Research (S)* 1979, 314.
7. V. Peshkova, V. Savostina and E. Astakhova-Ivanova, *Solvent Extraction Chem. Proc. Int. Conf. Goteborg*, p.66 (1966).
8. A. Nakamura, A. Konishi and S. Otsuka, *J.C.S. Dalton* 1979, 488.
9. M. S. Ma and R. J. Angelici, *Inorg. Chem.* 1980, **19**, 363.
10. B. J. Hathaway and D. E. Billing, *Coord. Chem. Rev.* 1970, **59**, 143.
11. J. A. Bertrand, J. H. Smith and P. G. Eller, *Inorg. Chem.* 1975, **13**, 1649.
12. D. E. Fenton and R. L. Lindtvedt, *J. Am. Chem. Soc.* 1978, **100**, 6367.
13. J. Reedijk and R. W. M. ten Hoedt, *Rec. Trav. Chim.* 1982, **101**, 49.
14. O. Kahn, *Inorg. Chim. Acta* 1982, **62**, 3.
15. J. J. Lewis, *J. Heterocycl. Chem.* 1975, **12**, 601.
16. M. Calleri and G. Chiari, *Acta Cryst.* 1978, **B34**, 2953.
17. W. L. Driessen and P. L. A. Everstijn, *Z. Naturforsch.* 1978, **33B**, 1120.

*Polyhedron* Vol. 3, No. 4, pp. 485–490, 1984
Printed in Great Britain.

0277–5387/84 $3.00 + .00
© 1984 Pergamon Press Ltd.

# DIORGANOTIN(IV) *BIS*(O,O-ALKYLENEDITHIOPHOSPHATES)

**R. J. RAO, G. SRIVASTAVA and R. C. MEHROTRA***
Chemical Laboratories, University of Rajasthan, Jaipur, India

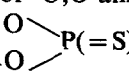
**and**

**B. S. SARASWAT and J. MASON**
The Open University, Milton Keynes, MK 7 6AA, England

(*Received* 13 *September* 1983; *accepted* 10 *October* 1983)

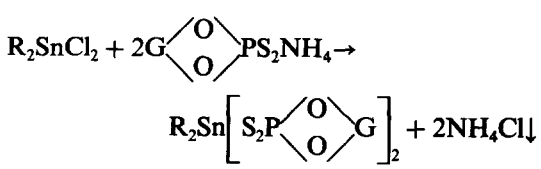
**Abstract**—O,O-Alkylenedithiophosphates of diorganotin(IV) of the type $R_2Sn[SP(S)O_2G]_2$ (R = Me, Et, *n*-Bu, Ph; G = $-CH_2-CMe_2-CH_2$, $-CMe_2-CMe_2$, $-CMe_2-CH_2-CHMe-$) have been synthesized by the reactions of diorganotin(IV) dichlorides with ammonium O,O-alkylenedithiophosphates or that of diorganotin(IV) oxides with O,O-alkylenedithiophosphoric acids in 1:2 molar ratio in benzene. These new complexes are white solids which are soluble in common organic solvents and are monomeric in refluxing benzene; and they have been characterized by elemental analysis and by different spectroscopic (IR, $^1H$, $^{13}C$, $^{31}P$ and $^{119}Sn$ NMR) studies, on the basis of which a six coordinated octahedral structure has been suggested in solution.

Dialkyldithiophosphoric acids, $(RO)_2P(S)SH$ form an important class of ligands, which give stable complexes with various metals including organotin(IV) moieties and show both monodentate[1–3] and bidentate behaviour.[4–6]

Compared to the extensive literature on metal complexes of O,O-dialkyldithiophosphoric acids[7,8] there are only a few references to the corresponding complexes of O,O-alkylenedithiophosphoric acids,[9–11]  Synthesis of O,O-alkylenedithiophosphate ligands[12] and their derivatives with nickel(II)[13] and trialkyltin[14] have been reported only recently from our laboratories.

## RESULTS AND DISCUSSION

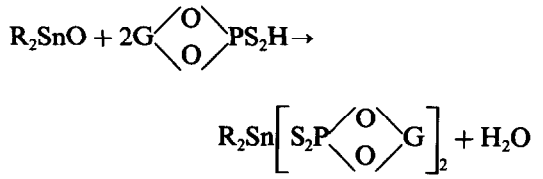
Diorganotin(IV)O,O-alkylenedithiophosphates have been synthesized by the reaction of ammonium O,O-alkylenedithiophosphates with diorganotin(IV) dichlorides in 1:2 molar ratio in benzene:



R = $C_6H_5$, *n*-$C_4H_9$, $C_2H_5$, $CH_3$:
G = $-CH_2-C(CH_3)_2-CH_2$, $-C(CH_3)_2-C(CH_3)_2-$ and $-C(CH_3)_2-CH_2-CHCH_3-$

These reactions, carried out at room temperature by stirring the reactants in benzene, were completed in 2–3 hr, after which ammonium chloride was removed by filtration and the product was isolated by stripping off the solvent from the filtrate.

These derivatives can also be synthesized by refluxing diorganotin(IV) oxide and O,O-alkylenedithiophosphoric acid in benzene and removing the water formed during the reaction azeotropically



R = $C_6H_5$, *n*-$C_4H_9$;
G = $-C(CH_3)_2-C(CH_3)_2-$ and $-CH_2-C(CH_3)_2-CH_2-$

All the derivatives are white crystalline powders, soluble in common organic solvents like benzene, chloroform, carbon tetrachloride and carbon disulphide etc. These solids were crystallised from

*Author to whom correspondence should be addressed.

Table 1. Reactions of diorganotin(IV) dichlorides with ammonium O,O-alkylenedithiophosphates in 1:2 molar ratio

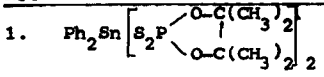
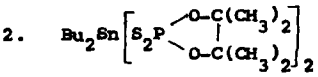
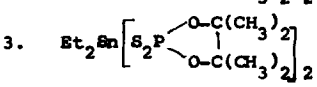
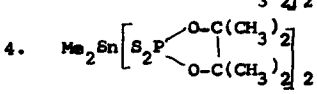
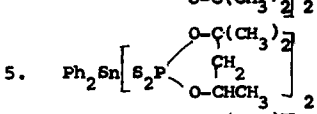
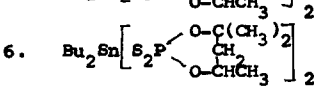
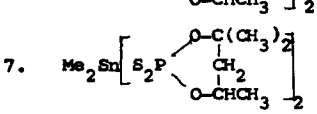
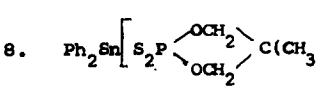
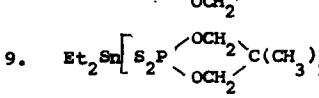
| Sl. No. | Reactants $R_2SnCl_2$ R = (g) | $G\langle^{O}_{O}\rangle P(S)SNH_4$ G = (g) taken (Calc) | Product (g) Found (Calc) | Weight of $NH_4Cl$ (g) Found (Calc) | Physical state (m.p.) | Analysis % Sn | % S | Molecular weight |
|---|---|---|---|---|---|---|---|---|
| 1. | $C_6H_5$ 1.07 | $-C(CH_3)_2-C(CH_3)_2-$ 1.44(1.42) | $(C_6H_5)_2Sn[S_2P(O-C(CH_3)_2-C(CH_3)_2-O)]_2$ 2.04 (2.16) | 0.31 (0.33) | White solid (70°) | 16.94 (17.09) | 18.58 (18.42) | 647 (695) |
| 2. | $C_6H_5$ 0.84 | $-C(CH_3)_2-CH_2-CHCH_3-$ 1.21(1.12) | $(C_6H_5)_2Sn[S_2P(O-C(CH_3)_2-CH_2-O-CHCH_3)]_2$ 1.68(1.69) | 0.24 (0.26) | White solid (165-166 ) | 17.06 (17.09) | 18.19 (18.42) | - |
| 3. | $C_6H_5$ 0.84 | $-CH_2-C(CH_3)_2-CH_2-$ 1.09(1.06) | $(C_6H_5)_2Sn[S_2P(OCH_2-C(CH_3)_2-CH_2O)]_2$ 1.44(1.63) | 0.25 (0.26) | White solid (80°) | 17.74 (17.82) | 19.12 (19.21) | - |
| 4. | n-$C_4H_9$ 1.69 | $-C(CH_3)_2-C(CH_3)_2-$ 2.55(2.53) | $(C_4H_9)_2Sn[S_2P(O-C(CH_3)_2-C(CH_3)_2-O)]_2$ 3.53(3.62) | 0.57 (0.59) | White solid (125°) | 18.17 (18.12) | 19.74 (19.54) | 697 (655) |
| 5. | n-$C_4H_9$ 2.08 | $-C(CH_3)_2-CH_2-CHCH_3$ 3.17(3.15) | $(C_4H_9)_2Sn[S_2P(O-C(CH_3)_2-CH_2-O-CHCH_3)]_2$ 4.40(4.48) | 0.74 (0.74) | White solid (96°) | 18.71 (18.12) | 19.33 (19.54) | - |
| 6. | n-$C_4H_9$ 2.81 | $-CH_2-C(CH_3)-CH_2$ 4.23(3.99) | $(C_4H_9)_2Sn[S_2P(OCH_2-C(CH_3)-CH_2O)]_2$ 5.41(5.82) | 0.94 (0.99) | White solid (146°) | 19.73 (19.94) | 20.29 (20.43) | - |
| 7. | $C_2H_5$ 1.21 | $-C(CH_3)_2-C(CH_3)_2-$ 2.23(2.23) | $(C_2H_5)_2Sn[S_2P(O-C(CH_3)_2-C(CH_3)_2-O)]_2$ 2.82(2.92) | 0.49 (0.51) | White solid (119-122°) | 19.75 (19.80) | 21.10 (21.36) | - |
| 8. | $C_2H_5$ 1.51 | $-C(CH_3)_2-CH_2-CHCH_3-$ 2.80(2.79) | $(C_2H_5)_2Sn[S_2P(O-C(CH_3)_2-CH_2-O-CHCH_3)]_2$ 3.60(3.62) | 0.63 (0.65) | White solid (144°) | 19.63 (19.80) | 21.63 (21.36) | - |
| 9. | $C_2H_5$ 1.63 | $-CH_2-C(CH_3)_2-CH_2$ 2.89(2.84) | $(C_2H_5)_2Sn[S_2P(OCH_2-C(CH_3)_2-CH_2O)]_2$ 3.66(3.71) | 0.65 (0.70) | White solid (148-150°) | 21.10 (21.14) | 22.69 (22.78) | - |
| 10. | $CH_3$ 1.46 | $-C(CH_3)_2-C(CH_3)_2-$ 3.43(3.42) | $(CH_3)_2Sn[S_2P(O-C(CH_3)_2-C(CH_3)_2-O)]_2$ 3.30(3.42) | 0.77 (0.79) | White solid (195-196°) | 21.34 (20.80) | 22.38 (22.42) | 533 (570) |
| 11. | $CH_3$ 1.06 | $-C(CH_3)_2-CH_2-CHCH_3-$ 2.31(2.31) | $(CH_3)_2Sn[S_2P(O-C(CH_3)_2-CH_2-O-CHCH_3)]_2$ | 0.51 (0.51) | White solid (148-150°) | 20.93 (20.80) | 22.26 (22.42) | 561 (570) |

benzene–petroleum ether (40–60°) mixture. These are stable in air and found to be monomeric in refluxing benzene.

*IR spectral data*

In the IR spectra (4000–400 $cm^{-1}$) of diorganotin(IV) *bis*(O,O-alkylenedithiophosphates), a sharp band in the region 670–705 $cm^{-1}$ appears to be due to $\nu(P=S)$[15] stretching vibrations which overlap with tin–phenyl vibrations in diphenyltin compounds. The bands present in the region 580–620 $cm^{-1}$ are due to $\nu(P-S)$[4,10] symmetric and asymmetric vibrations while those present in the region 1020–1100 and 825–890 $cm^{-1}$ could be ascribed[16–19] to $\nu((P)-O-C)$ and $\nu(P-O-(C))$ stretching vibrations respectively. The bands present in the region 930–1000 $cm^{-1}$ are due to dioxaphospholanes and dioxaphosphorinane ring

Table 2. IR spectral frequencies of the diorganotin(IV) *bis*(O,O-alkylenedithiophosphate), $R_2Sn[S_2PO_2G]_2$) derivative

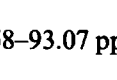
| Sl. No. | Compound | Infrared Absorptions ($cm^{-1}$) |
|---|---|---|
| 1. |  | 1170, 1150, 1100, 970, 930, 865, 830, 800, 740, 700, 680, 655, 610, 460, 440 |
| 2. |  | 1175, 1145, 1020, 960, 930, 890, 870, 800, 760, 725, 700 675, 610, 500, 450, 445 |
| 3. |  | 1260, 1222, 1090, 1020, 965, 930, 892, 800, 760, 728, 705 680, 610, 500, 465, 450 |
| 4. |  | 1175, 1100, 1020, 960, 930, 865, 830, 810, 785, 695, 670 605, 570, 525, 500, 460, 445. |
| 5. |  | 1220, 1155, 1135, 1100, 1050, 1000, 970, 890, 750, 720, 705 590, 515, 500, 460. |
| 6. |  | 1230, 1205, 1195, 1120, 1090, 1040, 950, 880, 770, 695, 650 620, 580, 490, 430. |
| 7. |  | 1150, 1100, 1090, 1040, 975, 960, 940, 880, 790, 725, 690 510, 500, 510. |
| 8. |  | 1105, 1055, 995, 860, 835, 740, 670, 620, 525, 460. |
| 9. |  | 1180, 1198, 1020, 961, 920, 862, 794, 730, 700, 615, 480 |

vibrations.[20,21] The $\nu$(Sn–C)[4,22] vibrations appear in the range 460–525 $cm^{-1}$ which are obscured by the $\nu$(P–S) vibrations. All these assignments are tentative due to the complexity of the spectra.

*NMR spectral data*

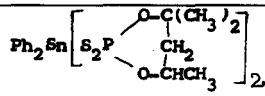
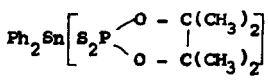
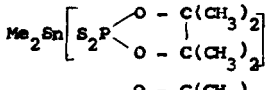
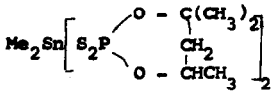
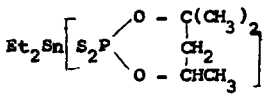
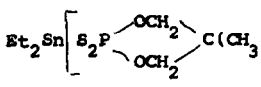
The relevant data on $^1H$, $^{31}P$, $^{13}C$ and $^{119}Sn$ NMR spectra of these complexes are summarized in tables three, four and five respectively. The $^1H$ NMR spectra (Table 3) show the characteristic proton resonances of the corresponding alkylene as well as alkyl (or aryl) tin groups. The signals due to protons of methyl, butyl, ethyl and phenyl groups attached to tin appear as singlet in the first case and as multiplets in other cases and alkyltin protons overlap with the resonances due to alkylene protons of the ligand moieties. In the dimethyltin(IV) derivatives, the position of signal of methyl protons bonded to tin appear at lower field ($\delta$ 1.4 ppm) compared to that found in corresponding trimethyltin(IV)–O,O-alkylenedithiophosphates.[14] This may be due to strong deshielding effects of dithio ligands.[23]

The $^{117}Sn$–$CH_3$ and $^{119}Sn$–$CH_3$ coupling constants in these derivatives are in the range 76 and 80 Hz respectively. These values are higher than the values for dimethyltin(IV) dichloride[24] and are in the range of six coordinated dimethyltin(IV) *bis*(dialkyldithiophosphates).[4]

$^{31}P$ NMR chemical shifts of these complexes as well as ligands occur in the range $\delta$87.09–109.82 and 78.58–93.07 ppm for  P(S)SM (where G = $-C(CH_3)_2-C(CH_3)_2-$ and $-CH_2-C(CH_3)_2-CH_2-$, M = $R_2Sn$ or H) respectively. Appearance of only one signal in these compounds and downfield of about 5–15 ppm from the respective chemical shift in corresponding ligand, indicate that both the O,O-alkylenedithiophosphate moieties on these compounds are behaving in a similar fashion and are bidentate in nature.[25]

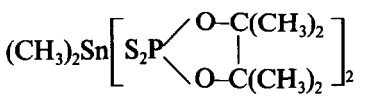
$^{13}C$ NMR spectra of three representative complexes were recorded and the data are summarized in Table 4. The value of coupling constants are strongly indicative of coordination state of tin atom in the present complexes. Recently $^1J$ ($^{119}Sn$–$^{13}C$) for six-coordinated dimethyltin compounds has been found in the range 618–977 Hz.[26,27] The observed values of $^1J$

Table 3. $^1$H NMR spectral data for some diorganotin(IV) *bis*(O,O-alkylenedithiophosphates)

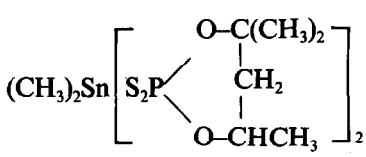
| Sl. No. | Compound | δ (ppm) |
|---|---|---|
| 1. |  | 7.1–8.4, m, 10H(Sn-$C_6H_5$)<br>4.5–5.0, m, 2H( OCH)<br>1.2–2.0, m, 22H($CH_2$, $CH_3$) |
| 2. |  | 7.0–8.1, m, 10H(Sn-$C_6H_5$)<br>1.0, s, 24H($CH_3$) |
| 3. |  | 1.7, s, 6H(Sn-$CH_3$)<br>1.4, s, 24H ($CH_3$) |
| 4. |  | 4.6–5.0, m, 2H(CHO)<br>1.3–1.8, m, 28H ($CH_3$Sn, $CH_3$, $CH_2$)<br>J($^{119}$Sn-C-H)= 80Hz, J($^{117}$Sn-C'H) = 76Hz |
| 5. |  | 1.5–2.4, m, 32H($C_2H_5$Sn, $CH_2$, $CH_3$)<br>5.5–6.0, m, 2H(-CHO) |
| 6. |  | 0.8–2.4 m, 22H($C_2H_5$Sn, $CH_3$)<br>4.0–4.2, d, 8H ($OCH_2$) |

S = Singlet, m = multiplet, d = doublet.

($^{119/117}$Sn–$^{13}$C) 588, 558 and 558, 534 for compounds



and



respectively are slightly lower than those for six coordinate compounds. However, it is suggested that they indicate hexa-coordination of the tin atom in these complexes, in which the ligand moieties are weakly coordinated to tin.

Hexacoordinated structure for diorganotin(IV) *bis*(O,O-alkylenedithiophosphates) gets further support from observed $^{119}$Sn NMR chemical shifts (Table 4) of these compounds. These shifts occur at much lower frequencies than that of four coordinated dimethyltin(IV) dichloride or dimethyltin(IV)dithiolates, $Me_2Sn(SR')_2$ (δ 122–144 ppm). This indicates that these diorganotin(IV) *bis*(O,O-alkylenedithiophosphate) do not contain four coordinated tin with ester type structure. The δ($^{119}$Sn) chemical shifts are observed at higher field than in the triorganotin(IV) O,O-alkylenedithiophosphates.

Recently $^{119}$Sn chemical shifts[28] in the range δ −125 to 501 ppm have been reported for a number of six coordinated complexes $R_2SnL_2$ (in which L is bidentate ligand of the type acetylacetonate, tropolonate, oxinate and dithiocarbamate). Thus the observed values of δ($^{119}$Sn) for diorganotin(IV)*bis*(O,O-alkylenedithiophosphate) δ(−155 to −220 ppm) can therefore be interpreted in terms of six coordinated tin compounds in which the Sn–S–P interactions are weak probably due to ring strain.

Replacement of methyl groups attached to tin by phenyl groups in these complexes induces an upfield shift in δ($^{119}$Sn) parallel to those found in other six coordinated compounds: this is comparable with the shift observed between $Me_2SnCl_2$ and $Ph_2SnCl_2$[29] which is probably due to increased shielding.

In conclusion, the $^{119}$Sn NMR chemical shift and $^1$J ($^{117/119}$Sn–$^{13}$C) and $^2$J ($^{119}$Sn–$^1$H) of diorganotin(IV)–*bis*(O,O-alkylenedithiophosphates) suggest that these contain weakly coordinated ligand moieties leading to six coordinated tin in solution.

## EXPERIMENTAL

Diorganotin(IV) dichlorides were used after purification. The O,O-alkylenedithiophosphoric acids and their ammonium salts were prepared by recently reported method[12] from our laboratories. Sulphur was estimated as barium sulphate and tin as oxide.

Table 4. $^{119}Sn$ and $^{31}P$ NMR data for diorganotin(IV) *bis*(O,O-alkylenedithiophosphates)

| Sl. No. | Compound | $^{119}Sn$ a,b (ppm) | $^{31}P$ ppm | Solvent |
|---|---|---|---|---|
| 1. | $Me_2Sn[S_2P(O-C(CH_3)_2-CH_2-O)]_2$ | -206.79 | 102.10 | $CDCl_3$ |
| 2. | $Me_2Sn[S_2P(O-C(CH_3)_2-CH_2-O-CHCH_3)]_2$ | -155.87 | 91.19 | " |
| 3. | $Et_2Sn[S_2P(O-C(CH_3)_2-CH_2-O)]_2$ | -223.2 | 109.97 | " |
| 4. | $Et_2Sn[S_2P(O-CH_2-C(CH_3)_2-CH_2-O)]_2$ | - 220.82 | - | " |
| 5. | $Bu_2Sn[S_2P(O-C(CH_3)_2-CH_2-O-CHCH_3)]_2$ | - 168.79 | 87.09 | " |
| 6. | $Ph_2Sn[S_2P(O-C(CH_3)_2-CH_2-O)]_2$ | - 178.59 | 107.82 | " |

a In ppm downfield from external $Me_4Sn$(neat).
b Chemical shifts depends upon concentration.
Me = Methyl, Et = Ethyl, Bu = n-butyl and Ph = phenyl.

Molecular weights were determined ebullioscopically with Gallenkamp ebulliometer equipped with thermistor sensor. $^1H$, $^{13}C$ and $^{31}P$ NMR spectra in $CDCl_3$ were recorded using TMS and $H_3PO_4$ as internal standards. $^{119}Sn$ NMR spectra were recorded in $CDCl_3$ using tetramethyltin as standard. IR spectra (4000–400 $cm^{-1}$) have been recorded as Nujol mull.

*Reaction of diphenyltin(IV) dichloride with ammonium O,O-hexylenedithiophosphate in* 1:2 *molar ratio*

To a suspension of ammonium O,O-hexylenedithiophosphate (0.84 g) in benzene was added weighed quantity of diphenyltin(IV) dichloride (1.21 g) in benzene. The contents were stirred for 3–4 hr and allowed to settle. The ammo-

Table 5. $^{13}C$ NMR data for some diorganotin(IV), O,O-alkylenedithiophosphates in ppm

| Sl. No. | Compound | $(\underline{C}H_3)_2Sn$ | $(\underline{C}_6H_5)_2Sn$ | $C(\underline{C}H_3)_2$ & $\underline{C}H_3CH$ | $\underline{C}H_2$ | $\underline{C}(CH_3)_2$ | $\underline{C}HCH_3$ | $J(Sn^{119}-{}^{13}C)$ $J(^{117}Sn-{}^{13}C)$ |
|---|---|---|---|---|---|---|---|---|
| 1. | $Me_2Sn[S_2P(O-C(CH_3)_2-CH_2-O)]_2$ | 16.55 | - | 24.12<br>23.89<br>J'=5.18Hz | - | 90.24<br>90.36<br>J'=2.59Hz | - | 588<br>558 |
| 2. | $Me_2Sn[S_2P(O-C(CH_3)_2-CH_2-O-CHCH_3)]_2$ | 14.99 | - | 22.11<br>22.51<br><br>31.32<br>32.17<br><br>44.06<br>44.40 | 71.80<br>71.46<br>J'=7.77Hz | 84.67<br>85.19<br>J'=11.65Hz | 75.71<br>77.15<br>J'=31.30Hz | 558<br>534 |
| 3. | $Ph_2Sn[S_2P(O-C(CH_3)_2-CH_2-O)]_2$ | | 137.01($C_\alpha$)<br>135.68($C_\beta$)<br>128.85($C_\gamma$)J'=5.18Hz | 24.01<br>23.78 | - | 88.41<br>90.30<br>J'=42.71Hz | - | - |

$J' = (^{31}P - {}^{13}C)$

nium chloride was filtered out and the solvent was evaporated under reduced pressure to get a white crystalline solid (1.68 g) which was recrystallised from benzene–petroleum ether (40–60°) mixture.

Details regarding other compounds synthesized by similar method are given in Table 1 for brevity.

*Reaction of dibutyltin(IV) oxide with O,O-neopentylene dithiophosphoric acid in* 1:2 *molar ratio*

A suspension of dibutyltin(IV) oxide (1.31 g) and the dithiophosphoric acid (2.10 g) in benzene (50 $cm^3$) was allowed to reflux for 1 hr and the water formed in the reaction was separated azeotropically on fractionating column. The cooled solution was filtered to remove trace amount of solid and concentrated to 20 $cm^3$. The solid that separated was redissolved in toluene, recrystallised at 0°C filtered and washed with petroleum ether to yield white solid.

*Acknowledgements*—One of the authors (R.J.R.) is grateful to U.G.C. New Delhi for financial assistance.

## REFERENCES

1. B. P. Singh, G. Srivastava and R. C. Mehrotra, *J. Organometal Chem.* 1979, **171**, 35.
2. J. L. Lefferts, K. C. Molloy, J. J. Zuckerman, I. Haiduc, C. Guta and D. Ruse, *Inorg. Chem.* 1980, **19**, 1662.
3. K. C. Molloy, M. B. Hossain, D. Vander Helm, J. J. Zuckerman and I. Haiduc, *Inorg. Chem.* 1979, **18**, 3507.
4. B. P. Singh, G. Srivastava and R. C. Mehrotra, *Synth. React. Inorg. Met. Org. Chem.* 1980, **10**, 359.
5. J. L. Lefferts, K. C. Molloy, J. J. Zuckerman, I. Haiduc, M. Curtui, C. Guta and D. Ruse, *Inorg. Chem.* 1980, **19**, 2861.
6. K. C. Molloy, M. B. Hossain, D. Van der Helm, J. J. Zuckerman and I. Haiduc, *Inorg. Chem.* 1980, **19**, 2041.
7. J. R. Wasson, G. M. Woltermann and H. J. Stoklosa, *Fortaschritte Chem. Forsch.* 1973, **35**, 65.
8. H. Schumann, and I. Schumann-Ruidish, *Organotin Compounds* (Edited by A. K. Sawyer), Vol. 2, Chap. 6. Marcel Dekker, New York (1971).
9. V. F. Toropova, R. A. Cherkasov, N. J. Saveleva and F. I. Petrova, *Zh. Obshch. Khim.* 1974, **44**, 531.
10. A. N. Pudovik, R. A. Cherkasov and R. M. Kondrat'leva, *Zh. Obshch. Khim.* 1968, **38**, 307.
11. V. V. Ouchinnikov, R. A. Karifanov, N. J. Savel'eva, V. F. Toropova, *Izv. Vyssh Uchebn Zaved Khim. Khim-Technol.* 1979, **22**, 654.
12. H. P. S. Chauhan, C. P. Bhasin, G. Srivastava and R. C. Mehrotra, *Phosphorus and Sulfur* 1983, **15**, 99.
13. C. P. Bhasin, G. Srivastava and R. C. Mehrotra, *Inorg. Chim. Acta* 1983, **77**, L131.
14. R. J. Rao, G. Srivastava and R. C. Mehrotra, *J. Organometal. Chem.* 1983, **258**, 155.
15. L. J. Bellamy, *Infrared Spectra of Complex Molecules*, p. 311. London (1966).
16. J. R. Wasson, G. M. Wolterman and H. J. Stoklosa, *Topics in Current Chem.* 1973, **35**, 65.
17. D. S. C. Corbridge, *Topics in Phosphorus Chem.* 1969, **6**, 235.
18. B. Wather, *Z. Anorg. Chem.* 1972, **211**, 395.
19. D. M. Adams and J. B. Cornell, *J. Chem. Soc.* 1968, 1299.
20. J. Cason, W. N. Baxter and W. De Aceter, *J. Org. Chem.* 1959, **24**, 247.
21. R. A. Y. Jones and A. R. Katritzky, *J. Chem. Soc.* 1960, 4376.
22. T. N. Srivastava, V. Kumar and R. B. Rastogi, *J. Inorg. Nucl. Chem.* 1978, **40**, 399.
23. E. W. Abel and D. B. Brady, *J. Organometal. Chem.* 1968, **11**, 145.
24. J. R. Holmes and H. D. Haerz, *J. Amer. Chem. Soc.* 1961, **83**, 3903.
25. C. Glidewell, *Inorg. Chim. Acta* 1977, **25**, 159.
26. J. Otera, T. Hinoishi, Y. Kawabe and R. Okawara, *Chem. Lett.* 1981, 273.
27. T. N. Mitchell, *J. Organometal. Chem.* 1973, **59**, 189.
28. J. Otera, *J. Organometal. Chem.* 1981, **221**, 57.
29. P. J. Smith and A. P. Tupciauskas, *Ann. Rep. NMR Spec.* 1978, **8**, 291.

*Polyhedron* Vol. 3, No. 4, pp. 491–496, 1984
Printed in Great Britain.

0277-5387/84 $3.00 + .00
© 1984 Pergamon Press Ltd.

# CHELATION OF MANGANESE(II) WITH QUINALDIC ACIDS. AN NMR RELAXATION STUDY

**CHRISTINA MOBERG and MICHAEL WEBER***
Royal Institute of Technology, Department of Organic Chemistry, S–100 44 Stockholm, Sweden

(*Received* 16 *September* 1983; *accepted* 24 *October* 1983)

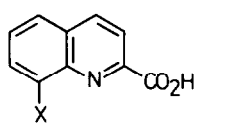
**Abstract**—Manganese(II) enhanced spin-lattice relaxation rates ($1/T_{1p}$) of $^1H$ and $^{13}C$ nuclei in quinoline-2-carboxylic acid, 8-methoxyquinoline-2-carboxylic acid, 8-hydroxyquinoline-2-carboxylic acid, 8-aminoquinoline-2-carboxylic acid, and 6-(hydroxymethyl)pyridine-2-carboxylic acid were measured in aqueous solution at various temperatures. Relative metal–nucleus distances were calculated from the $r^{-6}$ dependence of $1/T_{1p}$. The results indicate that the $Mn^{2+}$ ion in the 8-methoxyquinaldic acid chelate is coordinated to the carboxyl oxygen atom and the nitrogen atom but not to the methoxyl oxygen atom.

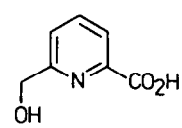
Quinoline-2-carboxylic acid (quinaldic acid) is a chelating agent with applications in gravimetric determinations of metals.[1] Alkylated and alkoxylated quinaldic acids have been found useful in solvent extraction and liquid membrane extraction.[2-4] In connection with a study of such extractants we were interested in the structure of metal complexes with quinaldic acids. The metal selectivity of some of our reagents may be influenced by the coordination geometry.[5]

Manganese(II) has been widely used as a paramagnetic probe in NMR spectroscopy in studies of the metal binding sites in large molecules of biological interest.[6] Recently detailed structure determinations of $Mn^{2+}$–amino acid complexes have also been published.[7-9]

Structural information from relaxation enhancement studies can be obtained using the Solomon–Bloembergen equations. If there is fast exchange between free and complexed ligands, the paramagnetic contribution to the relaxation rate ($1/T_{1p}$) is proportional to $r^{-6}$, where $r$ is the metal–nucleus distance and $1/T_{1p}$ is the difference between the spin-lattice relaxation rate in the presence and in the absence of manganese(II).

To gain further information about the complexing properties of quinaldic acids, we have studied $^1H$ and $^{13}C$ NMR spin-lattice relaxation enhancement of the ligands **1–5** in aqueous solution using $Mn^{2+}$ as a paramagnetic probe.





| | X |
|---|---|
| 1 | H |
| 2 | $OCH_3$ |
| 3 | OH |
| 4 | $NH_2$ |

5

## RESULTS

Paramagnetic ($Mn^{2+}$) enhanced spin-lattice relaxation times of protons in the quinaldic acids **1–4**, as well as relaxation times of the $^{13}C$ nuclei in compounds **1** and **2** and the picolinic acid **5** were measured with the objective to locate $Mn^{2+}$ in the chelates. The assignments of the $^1H$ and $^{13}C$ NMR spectra are shown in Table 1. The $1/T_1$ values for protons and $^{13}C$ nuclei in **2** are given as examples of relaxation rates in Table 2. From the ratios of the paramagnetic contributions to the relaxation rates (Table 3) relative proton–$Mn^{2+}$ distances were calculated. Absolute distances were calculated from the experimental relative distances by assuming the $Mn^{2+}$–H(4) distance to be 6.08 Å, which is a reasonable value derived from the known crystal structure of a Mn(II)–picolinic acid derivative[10] and from the known structure of quinoline-2-carboxamide[11] (Table 4). Table 5

*Author to whom correspondence should be addressed.

Table 1. $^{1}H$ and $^{13}C$ NMR data for **1–5**. Chemical shifts in ppm

| | 1 | 2 | 3 | 4 | 5 |
|---|---|---|---|---|---|
| H(3) | 7.88 | 7.84 | 7.90 | 7.93 | |
| H(4) | 8.32 | 8.08 | 8.18 | 8.18 | |
| H(5) | 7.87 | 7.23 | 7.26 | 7.25 | |
| H(6) | 7.61 | 7.36 | 7.44 | 7.41 | |
| H(7) | 7.79 | 6.98 | 7.05 | 7.07 | |
| H(8) | 8.04 | | | | |
| C(2) | 154.8 | 152.5 | | | 153.9 |
| C(3) | 121.3 | 121.8 | | | 123.7[a] |
| C(4) | 138.8 | 137.6 | | | 139.5 |
| C(5) | [b] | 120.0 | | | 123.2[a] |
| C(6) | [b] | 128.3 | | | 160.0 |
| C(7) | 131.1 | 108.7 | | | |
| C(8) | [b] | 154.6 | | | |
| C(8a) | 146.5 | 138.2 | | | |
| C(4a) | 128.9 | 129.5 | | | |
| $CO_2^-$ | 173.2 | 173.0 | | | 173.8 |
| $CH_2$ | | | | | 65.0 |

[a]Assignment may be reversed. [b]Three peaks at 128.3, 128.4 and 128.7 ppm.

Table 2. Spin-lattice relaxation rates ($s^{-1}$) for 8-methoxyquinaldic acid, **2**. $T_{1D}$ and $T_{1,obs}$ are the observed relaxation times in the absence and in the presence of $Mn^{2+}$

| | H(3) | H(4) | H(5) | H(6) | H(7) |
|---|---|---|---|---|---|
| $1/T_{1D}$ | 0.461 | 0.744 | 0.789 | 0.714 | 0.814 |
| $1/T_{1,obs}$ | 7.25 | 6.00 | 4.24 | 3.90 | 7.05 |
| | C(3) | C(4) | C(5) | C(6) | C(7) |
| $1/T_{1D}$ | 2.68 | 2.63 | 2.51 | 2.75 | 2.72 |
| $1/T_{1,obs}$ | 7.35 | 4.78 | 4.30 | 4.61 | 5.56 |

$^{1}H$ : $c_L/c_{Mn} = 2.79\ 10^3$ pH 8.0

$^{13}C$ : $c_L/c_{Mn} = 1.51\ 10^3$ pH 9.6

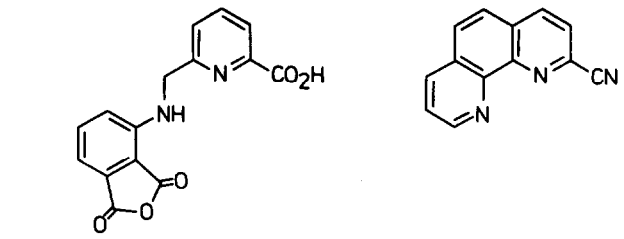
$c_L$ and $c_{Mn}$ are total concentrations of ligand and Mn respectively

shows the ratios of paramagnetic contributions to the relaxation rates of $^{13}C$ nuclei. The resulting $Mn^{2+}$–carbon distances are listed in Table 6.

The temperature dependence of $T_{2p}$ can be used to establish whether there is fast exchange of ligands in the manganese complexes. The $Mn^{2+}$-induced line-broadening of proton resonances in the quinaldic acids **1**, **2** and **4** decreased with increasing temperature (21–77°C), which indicates a fast ligand exchange. This was not the case for 8-hydroxyquinaldic acid, where the linewidth of the H(3) and H(4) peaks increased with increasing temperature. This suggests that the exchange rate of this ligand is slow.

## DISCUSSION

$^{1}H$ NMR spectra were assigned by comparison with a spectrum of quinoline and using additive



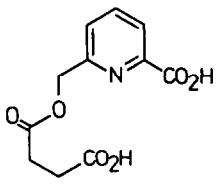
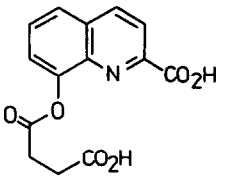
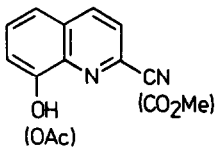




Table 3. Ratios of the paramagnetic contributions to relaxation rates of protons. $T_{1p}(i)/T_{1p}(4)$

| Ligand | Temp./°C | pH | $1/T_{1p}(4)$[a] | H(3) | H(5) | H(6) | H(7) | H(8) |
|---|---|---|---|---|---|---|---|---|
| 1[b] | 21 | 7.0 | 2.8 | [c] | 1.11(8) | 1.83(18) | 0.87(6) | |
| 1 | 21 | 7.1 | 2.59 | | 1.06(6) | 2.02(9) | 0.83(5) | 0.098(4) |
| 1 | 70 | 7.1 | 0.938 | | | 1.83(23) | 0.705(4) | |
| 2 | 21 | 8.0 | 2.97 | 0.745(31) | 1.50(2) | 1.71(7) | 0.853(45) | |
| 2 | 70 | 8.0 | 0.917 | 0.691(5) | 1.53(1) | 1.69(5) | 0.836(47) | |
| 3 | 29 | 7.6 | 3.15 | 1.21 | 1.11 | 1.51 | 0.748 | |
| 4 | 29 | 8.1 | 2.15 | 1.12 | 1.03 | 1.31 | 0.667 | |

[a]Normalized to $c_L/c_{Mn} = 5 \cdot 10^3$ where $c_L$ and $c_{Mn}$ are total conc. of ligand and Mn respectively. [b]$MnCl_2$ was used instead of $Mn(ClO_4)_2$. [c]Overlapping H(3) and H(5) peaks.

Table 4. Proton–$Mn^{2+}$ distances, $r$ (Å), calculated from $T_{1p}$ ratios. $r_4$ is assumed to be 6.08 Å

| Ligand | Temp./°C | $r_3$ | $r_5$ | $r_6$ | $r_7$ | $r_8$ |
|---|---|---|---|---|---|---|
| 1[a] | 21 | | 6.19 | 6.72 | 5.94 | |
| 1 | 21 | | 6.14 | 6.84 | 5.89 | 4.13 |
| 1 | 70 | | | 6.72 | 5.74 | |
| 2 | 21 | 5.79 | 6.50 | 6.65 | 5.92 | |
| 3 | 29 | 6.28 | 6.19 | 6.51 | 5.79 | |
| 4 | 29 | 5.83 | 6.21 | 6.30 | 5.72 | |
| Calc. distances[b] | | 5.24 | 6.64 | 6.78 | 5.28 | 2.92 |

[a]$MnCl_2$ was used instead of $Mn(ClO_4)_2$. [b]Calculated distances for a complex where Mn–N = 2.31 Å and Mn–O = 2.16 Å.[10]

Table 5. Ratios of paramagnetic contributions to relaxation rates of $^{13}C$ nuclei, $T_{1p}(i)/T_{1p}(4)$ or $T_{1p}(i)/T_{1p}(2)$

| Ligand | pH | C(2) | C(3) | C(4) | C(5) | C(6) | C(7) | C(8) | $CH_2$ | $CO_2H$ |
|---|---|---|---|---|---|---|---|---|---|---|
| 1 | 7.8 | | 0.466 | 1 | | | 1.01 | | | |
| 2 | 9.6 | | 0.501 | 1 | 1.38 | 1.32 | 0.83 | | | |
| 2[a] | 7.1 | 1 | | | | | | 2.05 | | |
| 5 | 6.9 | 0.0463 | 0.386[b] | 1 | 0.374[b] | 0.0537 | | | 0.0790 | 0.0368 |

[a]Temp. 60 °C. [b]Assigment may be reversed.

Table 6. Carbon–$Mn^{2+}$ distances (Å) calculated from $T_{1p}$ ratios. C(4)–$Mn^{2+}$ is assumed to be 5.16 Å

| Ligand | C(2) | C(3) | C(5) | C(6) | C(7) | $CH_2$ | $CO_2H$ |
|---|---|---|---|---|---|---|---|
| 1 | | 4.54 | | | 5.17 | | |
| 2 | | 4.60 | 5.44 | 5.40 | 5.00 | | |
| 5 | 3.09 | 4.4 | 4.4 | 3.19 | | 3.41 | 3.00 |
| quinoline[a] | | 4.56 | 5.78 | 5.82 | 4.84 | | |
| pyridine[a] | 3.16 | 4.56 | 4.72 | 3.44 | | 3.50 | 3.08 |

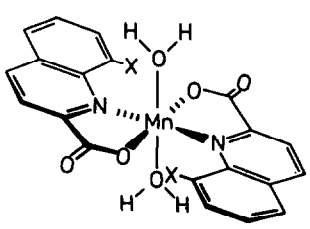
[a]Calculated distances for a complex where Mn-N = 2.31 Å and Mn-O = 2.16 Å.[10]

chemical shifts. The coupling constants $J_{5,6}$ and $J_{6,7}$ (ranging from 8.1–8.3 Hz and from 6.9–7.6 Hz, respectively) could also be used for assignment of H(5) and H(7). $^{13}C$ signals were assigned from chemical shifts and selective decoupling.

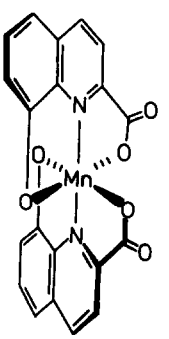
The relaxation times were measured by the inversion-recovery technique. For protons the major peak in a multiplet was used. The four peaks in the AB system of H(3) and H(4) protons in 8-methoxyquinaldic acid, for example, had different apparent $T_1$ values (Fig. 1), which made the $T_1$ measurements on proton somewhat ambiguous. At high $Mn^{2+}$ concentration some of the multiplets had become broad singlets, so that only one $T_1$ value was obtained for each proton.

Most of the $Mn^{2+}$–proton distances were within 10% from the estimated distances (Table 4). $^1H$ NMR relaxation enhancement could locate the $Mn^{2+}$ ion in an approximate position in the quinaldic acid complexes. Finer details of the complexing sites were revealed by $^{13}C$ NMR.

In complexes with 8-substituted quinaldic acids




A




B

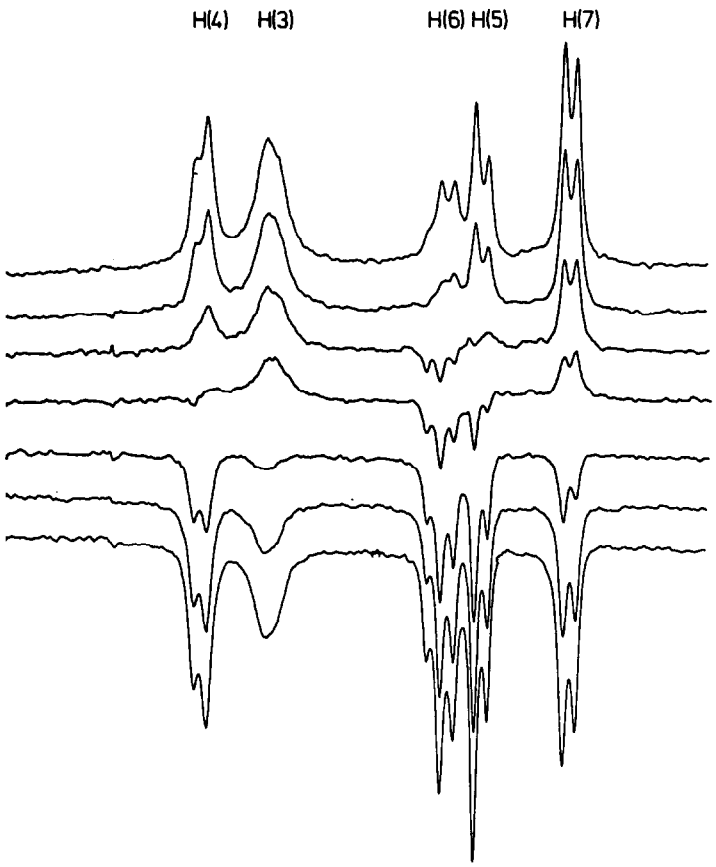



Fig. 1. $^1$H NMR measurements on 8-methoxyquinoline-2-carboxylic acid (**2**) in the presence of $Mn(ClO_4)_2$.

a metal ion may be coordinated by the 8-substituent and the quinoline nitrogen or by the quinoline nitrogen and the carboxyl oxygen or by all three heteroatoms. The first type of coordination has been assumed for 4,8-dihydroxyquinaldic acid.[12] The second situation seems plausible for weakly coordinating 8-substituents like a methoxy group, whereas 2-carboxyl-1,10-phenanthroline[13] and possibly 8-aminoquinaldic acid[14] are tridentate ligands.

The results from the $^{13}$C relaxation time measurements on **2** were used in an attempt to distinguish between a *trans*-planar complex A and a bisected octahedral structure B. When the Mn–N distance is assumed to be 2.31 Å and the Mn–O distances are taken to be 2.16 Å in A and equal (2.46 Å) in B, it is found that structure A gives a better fit (least squares) of the data (R = 0.16) than structure B (R = 0.27). We also measured $T_{1\rho}$ for the quaternary carbons C(2) and C(8) in compound **2**. The distance ratio $r_8/r_2$ is 1.10 in structure A and 0.99 in structure B. The measured ratio $T_{1\rho}(8)/T_{1\rho}(2)$ was 2.05 (Table 5), which corresponds to a metal–carbon distance ratio $r_8/r_2 = 1.13$, which further supports structure A.

The picolinic acid **5** was also examined by $^{13}$C NMR. The relaxation time ratio $T_{1\rho}(CH_2)/T_{1\rho}(CO_2H)$ was found to be 2.15 (Table 5), which corresponds to a distance ratio $r_{CH_2}/r_{CO_2H} = 1.14$. This value can be compared to the estimated distance ratio in a 6-(hydroxymethyl)picolinic acid $Mn^{2+}$ chelate. If we assume that the $Mn^{2+}$ ion is located as in 4-amino-3,5,6-trichloro-picolinic acid[10] and that the C–$CH_2$ distance is 1.50 Å, the C–O distance is 1.43 Å and the N–C–$CH_2$ angle is 114°, we obtain $r_{CH_2}/r_{CO_2H} = 1.14$. The hydroxymethyl oxygen–Mn distance would then be 2.25 Å, which is significantly longer than the carboxyl oxygen–Mn distance (2.16 Å).

Finally, it should be noted that the coordinating behaviour of quinaldic acids is of interest also in connection with studies on metal-catalyzed hydrolysis of 2,8-substituted quinoline compounds and of pyridine and phenanthroline derivatives with a similar disposition of ligand atoms.[15–19] The catalyzing metal ion (e.g. $Cu^{2+}$, $Ni^{2+}$ or $Zn^{2+}$) may be coordinated by two or three ligand atoms. These reactions are related to enzymatic processes of the zinc containing enzyme, carboxypeptidase.

The paramagnetic probe method appears to be

useful tool in structure elucidations of chelating agents. Future studies may establish whether it is possible to obtain information on the rate of complexation and the number of water molecules in the coordination sphere.

## EXPERIMENTAL

NMR spectra were run at 200 MHz ($^1$H) and 50.3 MHz ($^{13}$C) on a Bruker model WP 200 spectrometer. $^{13}$C Spectra were recorded in 0.8 M $D_2O$ solutions of the ligands. For $^1$H NMR 0.1 M solutions were used. Small amounts of 10 mM or 0.1 mM $Mn(ClO_4)_2$ in $H_2O$ were added in 2–3 portions. pH Values are uncorrected for deuterium isotope effects.

*Quinoline-2-carboxylic acid*, **1**, was purchased from Merck.

*8-Methoxyquinoline-2-carboxylic acid*, **2**,[20] was prepared from 8-hydroxyquinoline-2-carbonitrile[21] (1.7 g, 10 mmol), $K_2CO_3$ (1.4 g, 10 mmol) and iodomethane (1.7 g, 12 mmol) in DMF (50 cm$^3$) at room temperature for 6 h. Work-up by extraction with dichloromethane afforded 8-methoxyquinoline-2-carbonitrile. Alkaline hydrolysis of the nitrile (1.37 g, 7.4 mmol) in KOH (2.8 g), EtOH (56 cm$^3$) and $H_2O$ (3 cm$^3$) at reflux overnight yielded the carboxylic acid.

Ligands **3–5** were prepared by literature procedures.[17b,14,19]

*Acknowledgements*—This work was supported by the Swedish Board for Technical Development. A generous grant from the Knut and Alice Wallenbergs Stiftelse for the NMR instrumentation is gratefully acknowledged.

## REFERENCES

1. I. M. Kolthoff and E. B. Sandell, *Textbook of Quantitative Inorganic Analysis*, MacMillan, New York (1952).
2. *U. S. Patents* 3, 637, 476 (1972); 3, 697, 400 (1972); 3, 787, 418 (1974).
3. *Ger. Offen.* 2, 339, 240 (1974).
4. M. Muhammed, personal communication.
5. S. Högberg, B. Elman, D. H. Liem, K. Madan, C. Moberg, M. Muhammed, B. Sjöberg and M. Weber, to be published.
6. For reviews see: T. L. James, *Nuclear Magnetic Resonance in Biochemistry*. Academic Press, New York (1975). D. R. Burton, S. Forsén, G. Karlström and R. A. Dwek, *Progress in Nuclear Magnetic Resonance* 1979, **13**, 1. N. Niccolai, E. Tiezzi and G. Valensin, *Chem. Rev.* 1982, 359.
7. J. J. Led and D. M. Grant, *J. Am. Chem. Soc.* 1975, **97**, 6962.
8. B. Henry, M. Rappenau, J-C. Boubel and J-J. Delpuech, *Adv. Mol. Relax. Process.* 1980, **16**, 29.
9. B. Henry, J-C. Boubel and J-J. Delpuech, *Polyhedron* 1982, **1**, 113.
10. G. Smith, E. J. O'Reilly and C. H. L. Kennard, *Aust. J. Chem.* 1981, **34**, 891.
11. M. Gdaniec, M. Jaskólski and Z. Kosturkiewicz, *Acta Cryst.* 1977, **B33**, 2284.
12. S. P. Bag, Q. Fernando and H. Freiser, *Inorg. Chem.* 1964, **3**, 93.
13. H. A. Goodwin and R. N. Sylva, *Aust. J. Chem.* 1967, **20**, 217.
14. R. Roth and H. Erlenmeyer, *Helv. Chim. Acta* 1954, **37**, 1064.
15. R. Breslow, R. Fairweather and J. Keana, *J. Am. Chem. Soc.* 1967, **89**, 2135.
16. R. Breslow, D. E. McClure, R. S. Brown and J. Eisenach, *J. Am. Chem. Soc.* 1975, **97**, 194.
17[a-c] C. R. Clark and R. W. Hay, *J. Chem. Soc. Dalton Trans.* 1974, 2148; C. R. Clark and R. W. Hay, *Ibid.*, 1977, 1866; C. R. Clark and R. W. Hay, *Ibid.* 1977, 1993.
18. T. H. Fife, T. J. Przystas and V. L. Squillacote, *J. Am. Chem. Soc.* 1979, **101**, 3017.
19. T. H. Fife and T. J. Przystas, *J. Am. Chem. Soc.* 1982, **104**, 2251.
20. H. Irving and A. R. Pinnington, *J. Chem. Soc.* 1954, 3782.
21. I. A. Krasavin, V. M. Dziomko and Y. P. Radin, *Metody Polucheniya Khim. Reaktivov i Preparatov* 1965, **13**, 68, 94; *Chem. Abstr.* 1966, **65**, 5437b, 7139a.

*Polyhedron* Vol. 3, No. 4, pp. 497–501, 1984
Printed in Great Britain.

0277–5387/84 $3.00 + .00
© 1984 Pergamon Press Ltd.

# NOTE

# RHODIUM(I) AND RHODIUM(III) ARENE COMPLEXES WITH *N*-CARBAZOLYLTRIPHENYLPHOSPHINEGOLD(I) AND OTHER POLYCYCLIC ARENE LIGANDS

**R. USÓN, L. A. ORO* and J. A. CABEZA**
Departamento de Química Inorgánica, Universidad de Zaragoza, Zaragoza, Spain

(*Received* 25 *July* 1983; *accepted* 23 *September* 1983)

**Abstract**—The new heteronuclear arene complexes $[(COD)Rh(\mu\text{-cbz})AuPPh_3]ClO_4$, $[\{(COD)Rh\}_2(\mu\text{-cbz})AuPPh_3](ClO_4)_2$, $[(C_5Me_5)Rh(\mu\text{-cbz})AuPPh_3](ClO_4)_2$ and $[\{(C_5Me_5)Rh\}_2(\mu\text{-cbz})AuPPh_3](ClO_4)_4$ (COD = 1,5-cyclooctadiene, cbz = carbazolyl), and the mononuclear arene complexes $[(COD)Rh(arene)]ClO_4$ (arene = tetralin, biphenyl, fluorene, indene, 9,10-dihydroanthracene or carbazole) have been prepared by reaction of the acetone solvated complexes $[(COD)Rh(Me_2CO)_x]ClO_4$ or $[(C_5Me_5)Rh(Me_2CO)_3](ClO_4)_2$ with $(cbz)AuPPh_3$ or the appropriate polycyclic arene ligand.

Though the chemistry of rhodium(I) arene complexes has undergone a considerable development in recent years,[1–5] few examples containing polycyclic arene ligands have been reported.[4,5] Concerning rhodium(III) only indene, fluorene, indole,[6] and *N*-indolylgold(I) derivatives[7] have been used as polycyclic arene ligands. The lability of this type of ligand has been previously noted.[6,8,9] We now report the synthesis of rhodium complexes with *N*-carbazolyltriphenylphosphinegold(I), tetralin, biphenyl, fluorene, indene, 9,10-dihydroanthracene, and carbazole as arene ligands.

## EXPERIMENTAL

C, H and N analysis were carried out with a Perkin–Elmer 240-B microanalyzer. IR spectra were recorded on a Perkin–Elmer 599 spectrophotometer, using Nujol mulls between polyethylene sheets, and were calibrated with polystyrene. $^1H$ NMR spectra were recorded on a Varian FT-80A apparatus. Conductivities were measured with a Philips 9501/01 conductimeter.

$[(COD)Rh(\mu\text{-Cl})]_2$[10] and $[(C_5Me_5)RhCl(\mu\text{-Cl})]_2$[11] were prepared as described elsewhere. All the arene ligands (Merck, EGA) were used as received. All the reactions were carried out at room temperature, under argon and with dry solvents. Since the methods used to prepare the compounds were very similar only typical procedures are given. The analytical data, molar conductivities and yields for the isolated compounds are listed in Table 1.

*Preparation of* $[(COD)Rh(indene)]ClO_4$

$[(COD)Rh(\mu\text{-Cl})]_2$ (152 mg, 0.308 mmole) and $AgClO_4$ (127.8 mg, 0.616 mmole) in acetone (15 $cm^3$) were stirred for 20 min whereupon the formed AgCl was filtered off and the yellow solution containing the solvated complex $[(COD)Rh(Me_2CO)_x]ClO_4$ collected over a solution of freshly distilled indene (0.5 $cm^3$) in dichloromethane (10 $cm^3$). After stirring for 15 min the solvent was removed *in vacuo* precipitating yellow crystals. Then diethyl ether (5 $cm^3$) was added and the crystals were filtered off, washed with diethyl ether and vacuum-dried.

*Preparation of* $[(COD)Rh(fluorene)]ClO_4$

A solution of $[(COD)Rh(Me_2CO)_x]ClO_4$ (0.689 mmole) in acetone (15 $cm^3$) (prepared as above) was added to a solution of fluorene (114.6 mg, 0.689 mmole) in dichloromethane (10 $cm^3$). After stirring for 15 min, the solvent was vacuum-evaporated to *ca.* 2 $cm^3$ to leave yellow crystals. Then diethyl ether (5 $cm^3$) was added and

*Author to whom correspondence should be addressed.

Table 1. Analytical data, molar conductivities and yields

| Compound | Found C | (Calc) H | (%) N | $\Lambda_M$[a] ($Ohm^{-1}cm^2mol^{-1}$) | Yield (%) |
|---|---|---|---|---|---|
| [(COD)Rh(tetralin)]$ClO_4$ | 48.60 (48.85) | 5.70 (5.45) | | 126 | 93 |
| [(COD)Rh(biphenyl)]$ClO_4$ | 50.55 (51.70) | 4.65 (4.75) | | 131 | 78 |
| [(COD)Rh(fluorene)]$ClO_4$ | 52.05 (52.90) | 4.95 (4.65) | | 131 | 81 |
| [(COD)Rh(indene)]$ClO_4$ | 47.75 (47.85) | 5.05 (4.70) | | 137 | 95 |
| [(COD)Rh(DHA)]$ClO_4$ [b] | 53.55 (53.85) | 5.05 (4.95) | | [c] | 94 |
| [(COD)Rh(carbazole)]$ClO_4$ | 50.45 (50.30) | 4.35 (4.45) | 3.15 (2.95) | 138 | 82 |
| [($C_5Me_5$)Rh(carbazole)]$(ClO_4)_2$ | 43.80 (43.75) | 3.75 (4.00) | 2.50 (2.30) | 212 | 93 |
| (cbz)$AuPPh_3$ | 57.45 (57.60) | 4.00 (3.70) | 2.30 (2.25) | - | 87 |
| [(COD)Rh(μ-cbz)$AuPPh_3$]$ClO_4$ | 48.75 (48.75) | 3.90 (3.75) | 1.75 (1.50) | 131 | 89 |
| [($C_5Me_5$)Rh(μ-cbz)$AuPPh_3$]$(ClO_4)_2$ | 44.85 (45.20) | 3.65 (3.60) | 1.55 (1.30) | 207 | 90 |
| [{(COD)Rh}$_2$(μ-cbz)$AuPPh_3$]$(ClO_4)_2$ | 43.65 (44.35) | 4.00 (3.80) | 1.05 (1.10) | 205 | 95 |
| [{($C_5Me_5$)Rh}$_2$(μ-cbz)$AuPPh_3$]$(ClO_4)_2$ | 39.75 (40.05) | 3.70 (3.55) | 1.05 (0.95) | 338 | 96 |

[a] *ca.* $4\times10^{-4}$ *M* acetone solutions. [b] DHA= 9,10-dihydroanthracene. [c] Not enough soluble for determination.

the crystals were filtered off, washed with diethyl ether and vacuum-dried.

*Preparation of* [($C_5Me_5$)Rh(carbazole)]$(ClO_4)_2$

[($C_5Me_5$)RhCl(μ-Cl)]$_2$ (110 mg, 0.178 mmole) and $AgClO_4$ (147.7 mg, 0.712 mmole) were stirred in acetone (15 $cm^3$) for 20 min, whereupon the precipitated AgCl was removed by filtration. Addition of carbazole (59.6 mg, 0.356 mmole) to the filtered solution containing the solvated complex [($C_5Me_5$)Rh($Me_2CO$)$_3$]$(ClO_4)_2$ led to the immediate precipitation of yellow crystals. The suspension was vacuum-concentrated to *ca.* 2 $cm^3$ and diethyl ether (6 $cm^3$) was added. The solid was filtered off, washed with diethyl ether and vacuum-dried.

*Preparation of* (cbz)$AuPPh_3$

A solution of potassium hydroxide (8.1 ml, 0.1*M* in methanol) and carbazole (135.3 mg, 0.809 mmole) in chloroform (10 $cm^3$) was stirred for 30 min whereupon a solution of $ClAuPPh_3$ (400 mg, 0.809 mmole) in chloroform (10 $cm^3$) was added. After 30 min of stirring, the solvent was removed *in vacuo*. The oily residue was extracted with chloroform (15 $cm^3$) and the precipitated KCl was removed by filtration. Addition of *n*-hexane (8 $cm^3$) to the colourless solution and vacuum-concentration to *ca.* 2 $cm^3$ led to the precipitation of a white solid, that was filtered off, washed with diethyl ether and vacuum-dried.

*Preparation of* [(COD)Rh(μ-cbz)$AuPPh_3$]$ClO_4$

A solution of [(COD)Rh($Me_2CO$)$_x$]$ClO_4$ (0.088 mmole) in acetone (10 $cm^3$), prepared as above, was added to a solution of (cbz)$AuPPh_3$ (65.1 mg, 0.088 mmole) in dichloromethane (10 $cm^3$). The solution was stirred for 15 min and the solvent was removed *in vacuo* to leave a yellow oil. Addition of diethyl ether (8 $cm^3$) with vigorous stirring led to the precipitation of a yellow solid, that was filtered off, washed with diethyl ether and vacuum-dried.

[{(COD)Rh}$_2$(μ-cbz)$AuPPh_3$]$(ClO_4)_2$ was similarly prepared using a 2:1 molar ratio of the starting materials.

*Preparation of* [($C_5Me_5$)Rh(μ-cbz)$AuPPh_3$]$(ClO_4)_2$

A solution of [($C_5Me_5$)Rh($Me_2CO$)$_3$]$(ClO_4)_2$ (0.113 mmole) in acetone (15 $cm^3$), prepared as above, was added to a suspension of (cbz)$AuPPh_3$ (70.8 mg, 0.113 mmole) in the same solvent (8 $cm^3$). 15 min of stirring caused the formation of a clear orange solution that was vacuum-concentrated to *ca.* 1 $cm^3$. Addition of diethyl ether (5 $cm^3$) led to the precipitation of an orange solid, that was filtered off, washed with diethyl ether and vacuum-dried.

[{($C_5Me_5$)Rh}$_2$(μ-cbz)$AuPPh_3$]$(ClO_4)_4$ was prepared similarly using a 2:1 molar ratio of the starting materials.

## RESULTS AND DISCUSSION

The acetone solvated complex [(COD)Rh($Me_2CO$)$_x$]$ClO_4$ has proved to be an excellent starting material to prepare rhodium(I) arene complexes,[12] thus it reacts with the polycyclic arene ligands tetralin, biphenyl, fluorene, indene, 9,10-dihydroanthracene, and carbazole giving rise

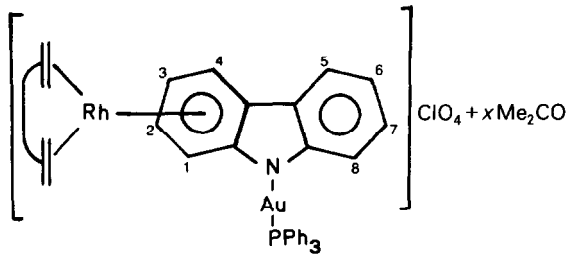
to the following equilibrium

$$[(COD)Rh(Me_2CO_x]ClO_4 + arene \rightleftharpoons [(COD)Rh(arene)]ClO_4 + x Me_2CO.$$

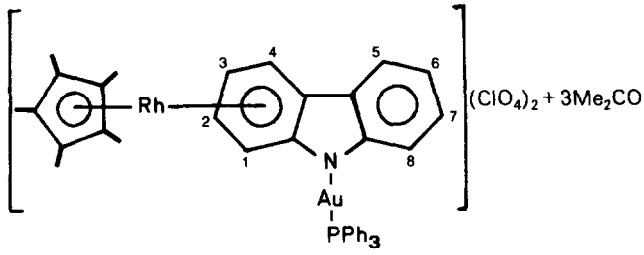
In acetone solution this equilibrium is mainly displaced to the left, but when these solutions are taken to dryness the rhodium(I) polycyclic arenes precipitate or form oils that can be resolved by adding diethyl ether. In solid state they are moisture sensitive, especially the tetralin and biphenyl derivatives. Their IR spectra confirm the presence of the diolefin and the arene ligands as well as the uncoordinated perchlorate anion ($T_d$). The measured conductivities show that they are 1:1 electrolytes.[13] Attempts to isolate complexes with other polycyclic arene ligands such as anthracene, pyrene, benzo[b]furan, dibenzofuran, benzo [b]thiophen or dibenzothiophen were unsuccessful, the reactions giving rise to hygroscopic solids which did not give satisfactory analysis, or oils that we were unable to precipitate.

On the other hand, the reaction of $ClAuPPh_3$ with the potassium salt of carbazole led to the formation of the *N*-carbazolyl complex $(cbz)AuPPh_3$ as a white air-stable solid. The six-membered rings of the carbazolyl ligand in this complex can potentially be used as arene ligands by other metal complexes. Thus, its reaction with acetone solvated rhodium(I) or rhodium(III) complexes lead to the formation of heteronuclear rhodium(I)–gold(I) or rhodium(III)–gold(I) arene complexes as yellow [Rh(I)] or orange [Rh(III)] air-stable solids whose stability towards moisture contrasts with the hygroscopicity of the above described mononuclear arene derivatives.

$$[(COD)Rh(Me_2CO)_x]ClO_4 + (cbz)AuPPh_3 \longrightarrow$$




$$[(C_5Me_5)Rh(Me_2CO)_3](ClO_4)_2 + (cbz)AuPPh_3 \longrightarrow$$




When in these types of reactions a 2:1 molar ratio of the starting materials is used, the two six-membered rings of the carbazolyl ligand attach to the rhodium atoms giving rise to the heterotrinuclear compounds $[\{(COD)Rh\}_2(\mu\text{-cbz})AuPPh_3](ClO_4)_2$ or $[\{(C_5Me_5)Rh\}_2(\mu\text{-cbz})AuPPh_3](ClO_4)_4$ as yellow [Rh(I)] or orange [Rh(III)] moisture-sensitive solids.

Table 2. $^1H$ NMR data for the soluble mononuclear arene complexes and the free ligands[a]

| Compound | Arene | | COD[b] | |
|---|---|---|---|---|
| | Aromatic Protons | Other | =CH- | Other |
| tetralin | 7.07(m,br,4H) | 2.77(m,4H)<br>1.79(m,4H) | | |
| $[(COD)Rh(tetralin)]ClO_4$ | 7.20(m,2H)<br>6.32(m,2H) | 2.90(m,4H)<br>2.02(m,4H) | 4.72(m,4H) | 2.35(m,8h) |
| biphenyl | 7.59(m,4H)<br>7.41(m,6H) | | | |
| $[(COD)Rh(biphenyl)]ClO_4$ | 7.90(m,2H)<br>7.65(m,4H)<br>7.16(m,4H) | | 4.77(s,br,4H) | 2.26(m,8H) |
| fluorene[c] | 7.58(m,2H)<br>7.23(m,6H) | 3.70(s,2H) | | |
| $[(COD)Rh(fluorene)]ClO_4$ | 7.92(m,3H)<br>7.65(m,3H)<br>7.45(m,2H) | 4.56(s,2H) | 3.89(s,br,4H) | 1.69(m,8H) |
| carbazole[c] | 8.08(m,2H),7.16(m,2H)<br>6.37(m,2H),6.49(m,2H) | 9.75(s,1H) | | |
| $[(COD)Rh(carbazole)]ClO_4$ | 8,20(d,1H),7.80(d,1H)<br>7.56(m,4H),6.68(t,1H)<br>6.30(t,1H) | 10.26(s,1H) | 3.95(m,4H) | 1.95(m,8H) |

[a] Unless otherwise stated spectra were recorded at 80 MHz in $CDCl_3$ solutions at room temperature. Chemical shifts (δ) are refered to i.TMS. [b] Uncoordinated COD exhibit broad peaks at 5.59(4H) and 2.37(8H) p.p.m. [c] Determined in $CCl_4$ (ref. 14).

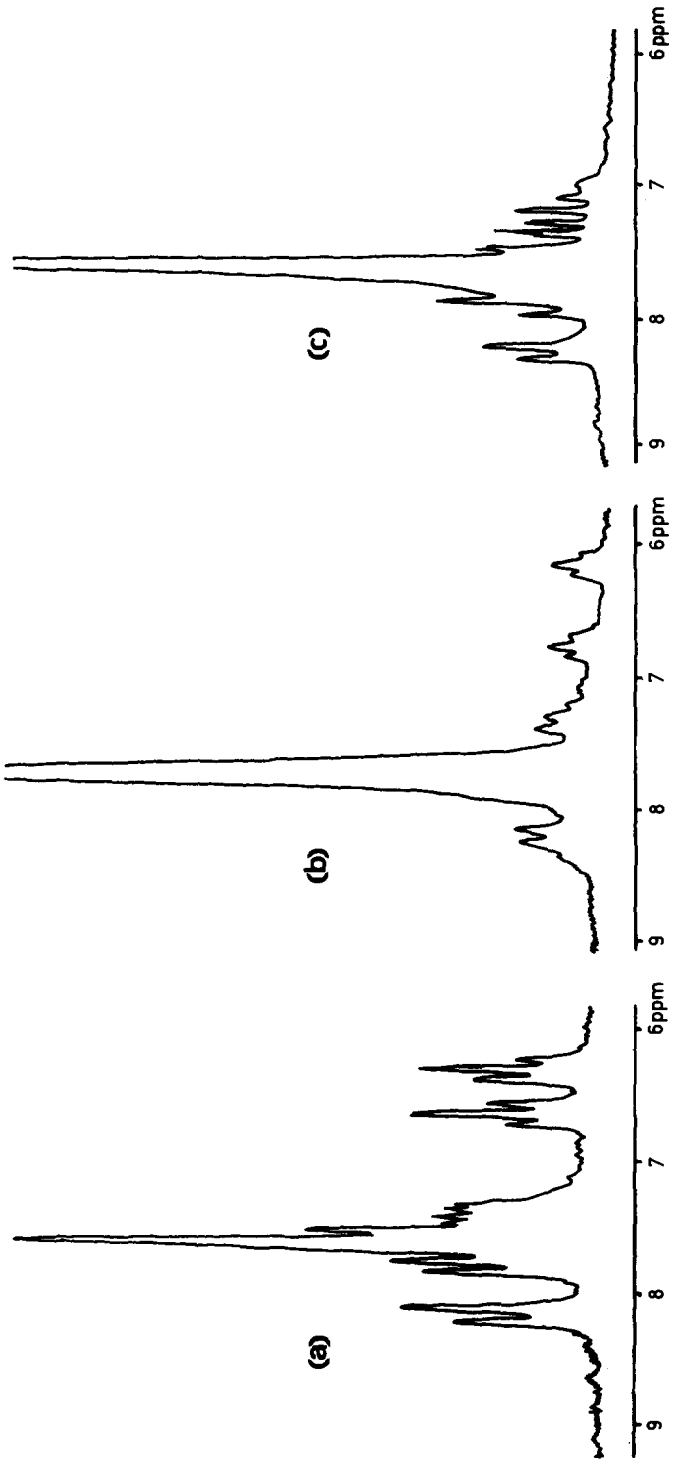



Fig. 1. $^1H$ NMR spectra in the aromatic region of (a) [(COD)Rh(carbazole)]$ClO_4$. (b) [(COD)Rh ($\mu$-cbz)$AuPPh_3$]$ClO_4$. (c) (cbz)$AuPPh_3$.

The IR spectra of all the herein described heteronuclear compounds show the presence of all the expected ligands and the uncoordinated perchlorate anion. Their molar conductivities in acetone solution confirm the presence of species that behave as 1:1, 1:2 or 1:4 electrolytes.[13]

The proposed bonding for all the herein described complexes is supported by their $^1$H NMR spectra[14] (see Table 2). In the case of the complex [(COD)Rh(carbazole)]$ClO_4$ a significant shift is experienced by the H(2) and H(3) protons of the carbazole ligand on coordination, that appear as two pseudotriplets at 6.68 and 6.30 ppm ($J_{1,2} \simeq J_{2,3} \simeq J_{3,4} \simeq 7$ Hz, $J_{1,3} \simeq J_{2,4} < 1$ Hz). The N–H proton, situated at 10.26 ppm readily interchanges with deuterium when a drop of deuterium oxide is added to the NMR tube. The only heteronuclear arene complex soluble in deuterochloroform proved to be [(COD)Rh($\mu$-cbz)$AuPPh_3$]$ClO_4$. The $^1$H NMR spectrum of the coordinated ring protons (Fig. 1) in this complex is very similar to that of [(COD)Rh(carbazole)]$ClO_4$, showing the H(2) and H(3) resonances as two pseudotriplets shifted at 6.80 and 6.20 ppm, but the most of the carbazolyl ligand protons, as occurs for the complex (cbz)$AuPPh_3$, are obscured by the triphenylphosphine ligand.

*Acknowledgement*—We thank Dr. J. Gimeno (University of Oviedo, Spain) for assistance in the $^1$H NMR measurements.

## REFERENCES

1. M. Valderrama and L. A. Oro, *Can. J. Chem.* 1982, **60**, 1044, and references therein.
2. M. Green and T. A. Kuc, *J. Chem. Soc. Dalton Trans.* 1972, 832.
3. R. Usón, L. A. Oro, C. Foces-Foces, F. H. Cano, S. García-Blanco and M. Valderrama, *J. Organomet. Chem.* 1982, **229**, 293. L. A. Oro, C. Foces-Foces, F. H. Cano and S. García-Blanco, *J. Organomet. Chem.* 1982, **236**, 385.
4. R. Usón, L. A. Oro, J. A. Cabeza and M. Valderrama, *J. Organomet. Chem.* 1982, **231**, C81. R. Usón, L. A. Oro, J. A. Cabeza, C. Foces-Foces, F. H. Cano and S. García-Blanco, *J. Organomet. Chem.* 1983, **246**, 73.
5. M. Valderrama, R. Ganz and R. Sariego, *Transition Met. Chem.* 1983, **8**, 160.
6. C. White, S. J. Thompson and P. M. Maitlis, *J. Chem. Soc. Dalton Trans.* 1977, 1654.
7. A. Tiripicchio, M. Tiripicchio-Camellini, R. Usón, L. A. Oro and J. A. Cabeza, *J. Organomet. Chem.* 1983, **224**, 165.
8. M. A. Bennett and T. W. Matheson, *J. Organomet. Chem.* 1979, **175**, 87.
9. A. C. Sievert and E. L. Muetterties, *Inorg. Chem.* 1981, **20**, 489.
10. J. Chatt and L. M. Venanzi, *J. Chem. Soc.* 1957, 4753.
11. J. W. Kang, K. Moseley and P. M. Maitlis, *J. Am. Chem. Soc.* 1969, **91**, 5970.
12. R. R. Schrock and J. A. Osborn, *J. Am. Chem. Soc.* 1971, **93**, 3089.
13. W. J. Geary, *Coord. Chem. Rev.* 1971, **7**, 81.
14. E. O. Fischer, H. A. Goodwin, C. G. Kreiter, H. D. Simmons Jr., K. Sonogashira and S. B. Wild, *J. Organomet. Chem.* 1968, **14**, 359.

*Polyhedron* Vol. 3, No. 4, pp. 503–504, 1984
Printed in Great Britain.

0277–5387/84 $3.00 + .00
© 1984 Pergamon Press Ltd.

# NOTE

## TRIMETHYLSILYLATION OF SERICITE BY VARIOUS METHODS

MEISETSU KAJIWARE

Department of Applied Chemistry, Faculty of Engineering, Nagoya University, Nagoya 464, Japan

(*Received* 2 *August* 1983; *accepted* 10 *August* 1983)

**Abstract**—Trimethylsilylation studies on sericite by various methods show that octahedral or tetrahedral aluminium can easily be isolated by Lentz and Masson's methods.

Trimethylsilylation of silicates, glasses or gel was reported by Lentz,[1] Masson,[2] Tamas,[3] Milestone[4] and Kajiwara,[5] respectively. The degree of trimethylsilylation of sericite using different methods and the yield of the silylated derivative or the coordination of aluminium is described in this report.

### EXPERIMENTAL

Sericite $KNaO{\cdot}3Al_2O_3{\cdot}6SiO_2{\cdot}2H_2O$ belongs to the mica group and was available from Murakami Clay Co. in Japan. The particle size was under 0.2 $\mu$m. This sericite is produced in nature, and contains a trace of impurities such as $Fe_2O_3$. The commercial reagent such as hexamethylsiloxane, isopropanol and hydrogen chloride was used. The product was separated and purified after the reaction was carried out under the same experimental conditions as previously described.[1-4]

### RESULTS AND DISCUSSION

The relation between the yield of the silylated derivative and the method of silylation is summarized in Table 1. It is found that Tamas's method shows the highest yield in comparison with the other methods. After the distribution of the molecular weight of the product was determined by gel permeation chromatography (g.p.c.), the weight or number average molecular weight was estimated by g.p.c. curves and the results of chemical analysis of the product are shown in Table 2.

The product having the highest molecular weight was formed using Lentz's and Masson's methods, but the degree of the dispersion is similar even if the reaction is in the different conditions. Both Lentz's and Masson's methods can effect silylation of sericite because of the higher $SiMe_3$/OH ratio, and only aluminium located in octahedral layers interacts with trimethylsilyl group since the Si/Al ratio of the product is three. In case of Tamas's method and Milestone's method, aluminium located in octahedral and tetrahedral layers may interact with trimethyl silyl group because Si/Al ratio shows the highest value. That is, the skeleton constructed back-bone of sericite is broken down.

Table 1. The yield of silylated derivative and the method of silylation

| Method | Yield (g) | $\overline{Mw}$ | $\overline{Mn}$ | $\overline{Mw}/\overline{Mn}$ |
|---|---|---|---|---|
| Lentz | 0.15 | 2140 | 1480 | 1.50 |
| Masson | 0.14 | 1710 | 910 | 1.90 |
| Tamas | 0.61 | 1250 | 740 | 1.70 |
| Milestone | 0.02 | 2180 | 780 | 2.78 |

Table 2. The results of chemical analysis of the product

| Method | Elemental analysis (Weight %) | | | | Si/Al (Mol %) | $SiMe_3$/OH (Mol%) |
|---|---|---|---|---|---|---|
| | Si | Al | C | H | | |
| Lentz | 27.8 | 2.5 | 23.7 | 6.2 | 3 | 3.3 |
| Masson | 19.7 | 2.6 | 11.8 | 3.6 | 3 | 0.7 |
| Tamas | 30.9 | 2.7 | 2.2 | 3.2 | 14 | 0.03 |
| Milestone | 22.9 | 2.1 | 8.4 | 4.0 | 10 | 0.1 |

Usually octahedral or tetrahedral aluminium occupied in aluminosilicates has been determined by X-ray diffraction or infrared absorption. However, it is assumed that octahedral or tetrahedral aluminium can easily be isolated by Lentz's and Masson's method. Currell[6] reported that no aluminium contained in trimethylsilylated derivatives of biotite, phlogophite or muscovite, but in this study aluminium in trimethylsilylated derivatives is detected by chemical analysis.

## REFERENCES

1. C. W. Lentz, *Inorg. Chem.* 1964, **3**, 574.
2. T. Gotz and W. D. Masson, *J. Chem. Soc.* 1970, 28.
3. F. D. Tamas, A. K. Sarkar and D. M. Roy, *Hung. J. Ind. Chem.* 1977, **5**, 115.
4. N. B. Milestone, *Cement and Concr Rev.* 1977, **7**, 345.
5. M. Kajiwara and N. Yamamoto, *Polymer Comm.* 1983, **24**, 151.
6. B. R. Currell, H. G. Midgley, M. A. Seaborne and C. P. Thakur, *Br. Polym. J.* 1974, **6**, 229.

*Polyhedron* Vol. 3, No. 4, pp. 505–507, 1984
Printed in Great Britain.

0277-5387/84 $3.00 + .00
Pergamon Press Ltd.

# NOTE

## SYNTHESIS OF TERT-BUTYL MERCAPTO COMPLEXES OF TITANIUM(IV). X-RAY CRYSTAL STRUCTURE OF Ti(diars)$Cl_2$ ($^t$BuS)$_2$

**RICHARD A. JONES,* STUART T. SCHWAB and BRUCE R. WHITTLESEY**
Department of Chemistry, The University of Texas at Austin, Austin, TX 78712, U.S.A.

(*Received* 4 *August* 1983; *accepted* 15 *August* 1983)

**Abstract**—The new class of tert-butyl mercapto compounds, Ti(L)$Cl_2$($^t$BuS)$_2$ (L = diars, dmpe, dppe), has been synthesized and characterized. The X-ray crystal structure of Ti(diars)$Cl_2$($^t$BuS)$_2$ (**1**) shows that the Ti(IV) atom has a distorted octahedral geometry with *trans* chlorides and *cis* tert-butyl mercapto units. The structures of the other complexes are similar based on spectroscopic (NMR, IR) evidence. Crystal data for (**1**): $C_{18}H_{34}As_2Cl_2S_2Ti$, M = 583.24, trigonal space group $P3_121$ (No. 152), $a = b = 16.892(5)$ Å, $c = 8.492(2)$ Å, U = 2098.4 Å$^3$, Z = 3, $D_c = 1.389$ gcm$^{-3}$, $\mu = 29.841$ cm$^{-1}$, $\lambda(MoK_\alpha) = 0.71069$ Å (graphite monochromator). Refinement of 948 observed (1371 unique measured; $I > 3\sigma(I)$ reflections gave a final R = 0.0462 and $R_w = 0.0597$.

The structure and bonding in transition metal mercapto or thiolate ($SR^-$) complexes[1] is of current interest since they are relevant to catalysis[2] (e.g. dehydrosulfurization) and enzymology (e.g. Fe–S cubane clusters and molybdenoenzymes).[3]

For the Group IV transition metals (Ti, Zr, Hf) relatively few different types of thiolate complexes are known.[4] They include mono- or dicyclopentadienyl (Cp) stabilized derivatives such as $CpTiCl_2(SPh)$[5] and $Cp_2Ti(SR)_2$.[6] Also known are some dianionic derivatives such as $[Me_4N]_2[Zr(S_2C_6H_4)_3]$,[7] and the binary complexes $Ti(SC_6F_5)_4$[8] and $M(SPh)_4$,[9] and dialkylamide derivatives such as $Ti(NMe_2)_3(SEt)$.[10]

In order to further investigate the chemistry of the early transition metals we have attempted the synthesis of group IV thiolate complexes which are stabilized with phosphine or arsine ligands. Although the group IV transition metals are normally considered "hard" acceptors and unlikely to coordinate strongly with soft donors such as phosphorus, arsenic or sulfur, we have succeeded in synthesizing and characterizing several members of a new class of complexes of general formula $M(L)Cl_2(SR)_2$ (M = Ti, Zr, Hf, L = chelating diphosphine or diarsine, R = alkyl or aryl). We report here the initial results of our investigations with M = Ti, R = $^t$Bu and L = diars (**1**), dmpe (**2**) or dppe (**3**).[11] The X-ray crystal structure of Ti(diars)$Cl_2$($^t$BuS)$_2$ (**1**) has been determined and the structures of the dmpe and dppe analogs (**2**) and (**3**) are similar based on spectroscopic evidence (NMR, IR).[11]

In the presence of one equivalent of the chelating bidentate ligand, diars, dmpe or dppe(L), $TiCl_4$ reacts immediately with two equivalents of $^t$BuSLi in hexane at −78°C. The complexes Ti(L)$Cl_2$($^t$BuS)$_2$ can be isolated in *ca.* 70% yield from the resulting deep red homogeneous solutions.[12] The use of four equivalents or more of $^t$BuSLi gives only (**1**) and unreacted $^t$BuSLi. The dark red complexes decompose immediately on exposure to the air, either in the solid state, or in solution.

All three compounds give straightforward NMR spectra. Thus for (**1**) (L = diars), both the $^t$*Bu*S and *Me*$_2$As resonances are sharp singlets ($\delta$ 1.88 and 1.35, respectively). In hydrocarbon or ether ($Et_2O$, THF) solvents the diphosphine or diarsine ligands are labile. Thus in the presence of excess dmpe the diars ligand of (**1**) is readily replaced to give Ti(dmpe)$Cl_2$($^t$BuS)$_2$ (**2**). In the absence of excess diphosphine or diarsine all three complexes slowly decompose in solution at room temperature to give intractable light brown materials plus free diars, dmpe, or dppe. This decomposition is most rapid for (**1**). Solutions are considerably more stable when a slight excess of chelating ligand is present.

The X-ray crystal structure[13] of (**1**) shows that

*Author to whom correspondence should be addressed.

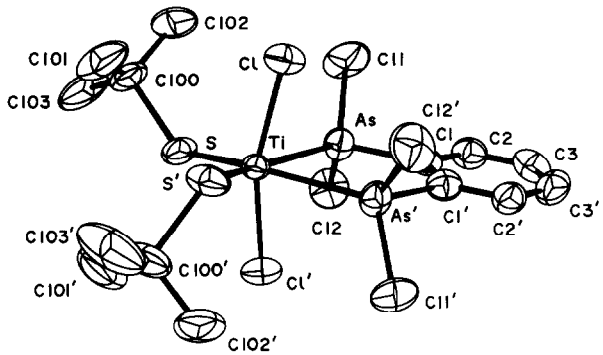



Fig. 1. A general view of (1); key bond lengths and angles are listed in Ref. 14.

the coordination geometry about the Ti(IV) atom is a distorted octahedron.[14] The ligands are arranged so that the two chloride and two 'BuS ligands occupy roughly *trans* and *cis* positions, respectively. A general view of the molecule is shown in Fig. 1. The compound crystallizes in the trigonal space group $P3_121$ with three molecules in the unit cell. There is a crystallographically imposed two-fold axis lying in the S–S′–Ti–As–As′ plane and which bisects the S–Ti–S′ and As–Ti–As′ angles. Thus the asymmetric unit contains half the molecule. The sulfur, titanium and arsenic atoms are all virtually coplanar[14] while the angles subtended at titanium reflect the notable distortions from an idealized octahedral geometry. Thus the As–Ti–As′ angle is 75.71(7°) which can be compared with that found in $TiCl_4(diars)_2$[15] (72.6°). The As–Ti–Cl and As–Ti–S angles are also acute (82.97° (av.) and 85.86(8)°, respectively). Interestingly the two *trans* chloride ligands are markedly bent back from the side of the molecule occupied by the two 'BuS ligands (Cl–Ti–Cl = 162.2(2)°). This distortion is no doubt due to the steric bulk of the 'BuS ligands. The S–Ti–S′ angle is much larger than 90° (113.7(2)°) and the 'Bu groups bend to opposite sides of the S–S′–Ti–As–As′ plane. The resulting geometry thus minimizes the steric interactions between the 'BuS groups. The Ti–Cl and Ti–As bond lengths are all normal while the Ti–S distance (2.332(3) Å) is considerably shorter than that found in $Cp_2Ti(SPh)_2$[16] (2.41 Å). In addition the Ti–S–C(100) angle of 119.5(4)° is similar to that observed in $Mo('BuS)_4$[17] (117.5° (av.)). Both of these effects may be due to substantial S→Ti $\pi$ bonding. The chemistry of these and related complexes is currently under investigation.

*Acknowledgements*—We thank the Research Corporation, the Robert A. Welch Foundation and the University of Texas at Austin for support. The X-ray diffractometer was purchased with funds from the National Science Foundation (CHE82-05871) and the University of Texas at Austin.

*Supplementary Materials*—Tables of bond lengths and angles, positional and thermal parameters and observed and calculated structure factors for (1) (14 pages) are available.

Atomic co-ordinates for the structure have been deposited with the Cambridge Crystallographic Data Centre for inclusion in their Data Base. Copies are also available on request from the Editor at Queen Mary College.

## REFERENCES

1. F. A. Cotton and G. Wilkinson, *Advanced Inorganic Chemistry*, 4th Edn, p. 178. Wiley, New York (1980).
2. F. E. Massoth, *Adv. Catal.* 1978, **27**, 265; S. C. Schumann and H. Shalit, *Catal. Rev.* 1970, **4**, 245; O. Weisser and S. Landa, *Sulfide Catalysts, Their Properties and Applications*. Pergamon Press, New York (1973).
3. For leading references see, E. I. Stiefel, *Prog. Inorg. Chem.* 1977, **22**, 1; W. E. Newton and S. Otsuka, (Editors), *Molybdenum Chemistry of Biological Significance*. Plenum Press, New York (1980).
4. M. Bottrill, P. D. Gavens, J. W. Kelland and J. McMeeking, In *Comprehensive Organometallic Chemistry*, Vol. 3, p. 384. (Edited by G. Wilkinson, F. G. A. Stone and E. W. Abel), Pergamon Press, 1982.
5. R. S. P. Coutts and P. C. Wailes, *J. Organometal. Chem.* 1974, **73**, C5; H. Kopf and B. Block, *Z. Naturforsch. B.* 1968, **23**, 1534.
6. G. Fachinetti and C. Floriani, *J. Chem. Soc. Dalton* 1974, 2433.
7. M. Cowie and M. J. Bennet, *Inorg. Chem.* 1976, **15**, 1595.
8. R. J. H. Clark and D. Kaminaris, *Inorg. Chim. Acta* 1974, **11**, L8.
9. H. Funk and M. Hesselbarth, *Z. Chem.* 1966, **6**, 227.
10. D. C. Bradley and P. A. Hammersley, *J. Chem. Soc. A*, 1967, 1894.
11. diars = *o*-phenylene bis(dimethylarsine), dmpe = bis(dimethylphosphino)ethane, dppe = bis(diphenylphosphino)ethane.
12. (1)–(3) were prepared similarly. Details of the synthesis of (1) are given here. $TiCl_4$ (0.30 $cm^3$, 2.72 mmol) was added to a solution of *o*-phenylene bis(dimethylarsine) (diars) (2.72 mmol) in hexane

($100\ cm^3$) at $-78°C$. The orange suspension was stirred (0.5 h) at $-78°C$, and $^tBuSLi$ ($9.91\ cm^3$ of a 1.1 M THF solution, 10.9 mmol) was added dropwise. The mixture was allowed to warm to room temperature over 5.0 hr. Volatile materials were removed under vacuum, and the dark red residue extracted into hexane ($2 \times 30\ cm^3$). The solution was filtered and evaporated to *ca.* $20\ cm^3$ under vacuum. Cooling ($-25°C$) yielded dark red crystals of (**1**) after *ca.* 12 hr. They were collected and dried under vacuum at room temperature. Yield 1.10 g, 70%, m.p. 72–78°C (dec), IR (nujol mull, NaCl plates) 3020 *w*, 1355 *m*, 1260 *m*, 1145 *s*, 1080 *w.br.*, 1010 *m.br.*, 900 *w*, 860 *w*, 795 *m.br.*, 745 *m*, and 665 *vw* ($cm^{-1}$). $^1H$ NMR ($C_6D_6$ at 25°C, 90 MHz, relative to $Me_4Si$ $\delta 0.0$) $\delta$ 7.10 *m* (4H) (*o*-$C_6H_4(AsMe_2)_2$), $\delta$ 1.88 *s*, (18 *H*) ($^tBuS$), $\delta$ 1.35 *s* (12 *H*), (*o*-$C_6H_4(AsMe_2)_2$). Microanalysis: calcd for $C_{18}H_{34}As_2Cl_2S_2Ti$; C 37.07, H 5.88, Cl 12.16, S 10.99, %. Found C 36.94, H 5.45, Cl 11.55, S 9.98, %. (**2**): Yield 70%, m.p. 97–110°C (dec), IR (nujol, NaCl plates), 1460 *s*, 1410 *s*, 1350 *s*, 1285 *w*, 1265 *w*, 1200 *w*, 1130 *s.br.*, 1080 *s*, 1015 *m*, 990 *w*, 920 *s*, 910 *s*, 880 *m*, 860 *w*, 830 *w*, 790 *w.br.*, 725 *m*, 705 *m*, ($cm^{-1}$); NMR (conditions as for (**1**))[1] $\delta$ 2.25 *m* (4 *H*), $Me_2PCH_2$, $\delta$ 2.05 *s* (18 *H*) $^tBuS$, $\delta$ 1.50 *d* (12 *H*) $J_{P-H} = 7.0$ Hz ($Me_2PCH_2$-), $^{31}P\{^1H\}$ (in $C_6D_6$ at ambient temperature, 32.384 MHz, in ppm rel. $H_3PO_4$ $\delta$ 0.0) $\delta$ 1.39 *s*. (**3**): Yield 70%, m.p. 89–94°C (dec.), IR (nujol, NaCl plates) 1475 *m*, 1445 *w*, 1385 *w*, 1265 *s*, 1220 *w*, 1150 *s*, 1100 *m*, 1020 *m*, 865 *vw*, 800 *m*, 665 *vw* ($cm^{-1}$). NMR (in $d_8$-PhMe as for (**1**)) $^1H$ $\delta$ 7.30 *m* (20 H), $Ph_2P$–$CH_2$, $\delta$ 2.31 *m* (4 *H*), ($Ph_2P$–$CH_2$) $\delta$ 1.35 *s* (18 *H*) $^tBuS$ $^{31}P\{^1H\}$ $\delta$ 11.00 *s*.

13. Crystals of (**1**) were mounted under nitrogen in thin-walled glass capillaries. Data were collected on an Enraf–Nonius CAD-4 diffractometer at $23 \pm 2°C$. Crystal data: formula $C_{18}H_{34}As_2Cl_2S_2Ti$, M = 583.24, trigonal, space group $P3_121$ (No. 152), $a = b = 16.892(5)$ Å, $C = 8.492(2)$ Å, $U = 2098.4$ Å$^3$, $Z = 3$, $D_c = 1.389\ gcm^{-3}$, $\lambda(MoK_\alpha) = 0.71069$ Å (graphite monochromator), $\mu = 29.841\ cm^{-1}$, crystal dimensions (mm), $0.50 \times 0.50 \times 0.50$, scan width (deg) $0.8 + 0.2 \tan\theta$. Standard reflections; 312, 13$\bar{2}$. Decay of standards < 1.2%. Data were collected in the $\theta/2\theta$ mode ($2.0 < 2\theta < 50.0°$). A psi scan showed that an absorption correction was unnecessary and none was applied. Equivalent reflections were averaged to give 1371 unique measured reflections of which 948 were considered observed ($I > 3\sigma(I)$). The structure was solved using standard heavy atom techniques (Patterson and difference Fourier). Final refinement with anisotropic thermal parameters for the non-hydrogen atoms and unit weights converged smoothly to give a final $R = 0.0462$ and $R_w = 0.0597$. Parameters varied = 114; data:parameter ratio = 8.32. Hydrogen atoms were not located.
14. A complete listing of bond distances and angles is provided as supplementary material (see paragraph at end of paper for details). For convenience the key bond lengths (Å) and angles (°) are as follows. Lengths: Ti–As = 2.691(2), As–C(1) = 1.937(9), As–C(11) = 1.995(9), Ti–Cl = 2.319(2), Ti–S = 2.332(3), S–C(100) = 1.887(9). Angles: As–Ti–As′ = 75.71(7), As–Ti–Cl = 83.60(9), As–Ti–Cl′ = 82.34(9), As–Ti–S = 85.86(8), As–Ti–S′ = 159.3(1), Cl–Ti–Cl′ = 162.2(2), S–Ti–S′ = 113.7(2). For the S–S′–Ti–As–As′ plane the maximum deviations from the least squares plane through these atoms is ± 0.2 Å by each of the two S atoms. The Cl–Ti–Cl′ plane is tilted at 87.8° (dihedral angle) from this plane.
15. R. J. H. Clark, J. Lewis and R. S. Nyholm, *J. Chem. Soc.* 1962, 2460.
16. E. G. Muller, S. F. Watkins and L. F. Dahl, *J. Organometal. Chem.* 1976, **111**, 73.
17. S. Otsuka, M. Kamata, K. Hirotsu and T. Higuchi, *J. Am. Chem. Soc.* 1981, **103**, 3011.

*Polyhedron* Vol. 3, No. 4, pp. 509–512, 1984
Printed in Great Britain.

0277–5387/84 $3.00 + .00
Pergamon Press Ltd.

# COMMUNICATION

## NEW TWO- AND THREE-COORDINATE CADMIUM(II) DIALKYLAMIDES

(Received 1 March; accepted 5 January 1984)

Abstract – Some adducts of the known two-coordinate cadmium disilylamide, $Cd[N(SiMe_3)_2]_2$, have been studied by $^1H$, $^{29}Si$, and $^{113}Cd$ nuclear magnetic resonance spectroscopy. The physical and spectral properties of three new $Cd(NR_2)_2$ species are also described.

The ability of the bulky bis(trimethylsilyl)amido-ligand $[N(SiMe_3)_2]^-$ to stabilize low coordination numbers is well established, though most studies have focused on transition metal compounds.[1,2] During their pioneering work[3] with this disilylamido-ligand, Bürger and Wannagat showed that $Cd[N(SiMe_3)_2]_2$ was monomeric[4], and one of us has previously performed calorimetric measurements on adduct formation by this unique cadmium(II) compound[5]. We have now extended the range of cadmium dialkylamides and characterized them and some adducts of $Cd[N(SiMe_3)_2]_2$ by multinuclear NMR spectroscopy. In particular, recent demonstrations of the sensitivity of the $^{113}Cd$ chemical shift, which has a range of ca. 900 ppm, to coordination geometry[6] and to ligand substituent effects[7] prompts this preliminary report of our results on low-coordinate cadmium(II) species.

Syntheses of the $Cd(NR_2)_2$ and $Cd[N(SiMe_3)_2]\cdot L$ compounds were readily accomplished in high yields by previously published methods.[4,5] The liquids or low-melting solids were purified by distillation or sublimation (near 70° at 0.2 mm Hg except for $Cd(NC_9H_{18})_2$ (115° at 0.35 mm Hg) and $Cd[N(SiPhMe_2)_2]_2$ (recrystallized from cyclohexane, m.p. 119°)] and gave satisfactory Cd analysis (atomic absorption). The ability of the adducts to survive sublimation attests to the strength of the ligand interaction with $Cd[N(SiMe_3)_2]_2$ and is in contrast to the weak binding displayed by ligands to transition metal disilylamides.[1,2] The volatility of the compounds is compatible with their expected monomeric nature, as proved for several divalent Group 4 disilylamides of similar molecular weight.[8]

Table 1 summarizes the chemical shift data for the cadmium(II) dialkylamides and the adducts of $Cd[N(SiMe_3)_2]_2$. The single resonances in the $^{113}Cd$ spectra of all the complexes except $Cd[NBu^t(SiMe_3)]_2$ indicate that in each case only one species is present both in the neat liquids and in solution. The similarity of the chemical shifts for $Cd[N(SiMe_3)_2]_2$ and $Cd[N(SiPhMe_2)_2]_2$ agrees with the conclusion that both are monomeric, as shown for $Cd[N(SiMe_3)_2]_2$[4]. The $^{113}Cd$ chemical shift for the latter complex is independent of concentration and state, showing that benzene has no significant interaction with the two-coordinate species; in contrast, a large concentration dependence was observed for dimethylmercury in benzene solution.[9] Because of the many factors that may influence the chemical shift position, the observed chemical shifts cannot yet be directly related to two- and three-coordination (e.g. $\delta(^{113}Cd)$ for four- and six-coordinate complexes with pyridyl-type ligands also occur in the range 250-450 ppm).[7,10] We note nevertheless that two-coordinate species $[Cd(PR_3)_2]^{2+}$ ($R=C_6H_{11}, Bu^n$) and $Cd[EP(o\text{-}C_6H_4Me)_3]_2^{2+}$ (E=S,Se) have $\delta(^{113}Cd)$ values of ca. 350 ppm[6b] and 242, 195[6c], respectively. Most importantly, it was demonstrated with the latter complexes[6b,c] that chemical shifts move downfield (by up to 310 ppm) upon an increase in coordination number. We thus assign three-coordination to the adducts with monodentate nitrogen donor ligands, though exchange processes leading to chemical shift averaging may be present.

The $^{113}Cd$ NMR spectra of the compounds $Cd[NC_9H_{18}]_2$ and $Cd[NBu^t(SiMe_3)]_2$ merit further discussion. The chemical shift of the tetramethylpiperidine complex is in the range found for the adducts and thus association cannot be ruled out. In the case of the $Cd[NBu^t(SiMe_3)]_2$ complex, the two $^{113}Cd$ signals are interpretable in terms of both monomer and dimer species being present. However, only one $^{29}Si$ signal was observed and neither the $^{113}Cd$ nor the $^{29}Si$ peaks shift significantly from the neat liquid to solution or with a change in temperature. Further characterization of these two dialkylamides are underway via NMR concentration studies, adduct formation and molecular weight measurements.

The $^{29}Si$ NMR chemical shifts of the cadmium(II) dialkylamides and of the

Table 1. NMR spectral data of the cadmium(II) dialkylamides[a]

| Compound[b] | Solvent(concentration) | δCd(ppm) | δSi(ppm)[c] | δH(ppm) |
|---|---|---|---|---|
| $Cd[N(SiMe_3)]_2$ | neat liquid | 294 | -0.97 | 0.05 |
| | $C_6H_6$ (0.87M) | 294 | (0.80) | -0.14 |
| | $C_6H_6$ (0.26M) | 294 | | -0.14 |
| $Cd[NBu^t(SiMe_3)]_2$ | neat liquid | 430 | -5.52 | 0.00 |
| | | 324[d] | (-3.87) | 1.15 |
| | $MeC_6H_{11}$ (0.4M) | 417 | -5.60 | |
| | | 325[d] | | |
| $Cd[N(SiPhMe_2)_2]_2$ | $C_6H_6$ (0.2M) | 264 | -7.20 | -0.15 |
| | | | (-5.22) | 7.03 |
| $Cd[NC_9H_{18}]_2$ | $C_6H_6$ (0.35M) | 362 | - | 0.80 |
| $Cd[N(SiMe_3)_2]\cdot py$ | $C_6H_6$ (0.65M) | 337 | -3.62 | -0.10[e] |
| $Cd[N(SiMe_3)_2]\cdot 4\text{-Mepy}$ | $C_6H_6$ (0.62M) | 344 | -4.04 | -0.25[e] |
| | | | | 1.83 |
| $Cd[N(SiMe_3)_2]\cdot 4\text{-}Bu^t py$ | $C_6H_6$ (0.64M) | 340 | -4.20 | -0.23[e] |
| | | | | 0.35 |
| $Cd[N(SiMe_3)_2]\cdot N\text{-MeIm}$ | $C_6H_6$ (0.74M) | 363 | -4.54 | -0.12[e] |
| | | | | 2.22 |

[a]Spectra were obtained on naturally abundant samples with a multinuclear WH-400 spectrometer operating in the pulsed Fourier Transform mode at 88.75 MHz ($^{113}Cd$) or 79.50 MHz ($^{29}Si$) or on a Varian T-60 spectrometer ($^1H$). Chemical shifts are expressed as δ values in ppm (positive values at higher frequency) relative to 0.1M $Cd(ClO_4)_2$ aqueous solutions ($^{113}Cd$), and TMS ($^{29}Si$, $^1H$). Linewidths varied from 150-300 Hz ($^{113}Cd$), or were about 15 Hz ($^{29}Si$).

[b]Abbreviations: $C_9H_{18}$ = 2,2,6,6-tetramethylpiperidine, py = pyridine, 4-Mepy = 4-methylpyridine, 4-$Bu^t$py = 4-t-butylpyridine, N-MeIm = N-methylimidazole.

[c]Chemical shift of free amine given in parenthesis.

[d]Intensity is 0.9 of peak at higher frequency.

[e]Peaks at high field are due to $SiMe_3$ protons. The multiplets due to ligand ring protons are not recorded.

$Cd[N(SiMe_3)_2]_2$ adducts all represent a more shielded environment than shown by the respective free amine or by $Cd[N(SiMe_3)_2]_2$ itself (Table 1). Whether these upfield $^{29}Si$ chemical shifts (3.5 ppm for the N-methylimidazole adduct), and the corresponding downfield $^{113}Cd$ chemical shifts can be correlated to the enthalpy of formation[5] awaits studies of a wider range of adducts.

Acknowledgements - Support of this research via an operating grant to E.C.A. and funding for the Southwestern Ontario NMR Centre by the Natural Sciences and Engineering Research Council of Canada is gratefully acknowledged.

KEITH J. FISHER
Faculty of Education
University of Khartoum
Republic of Sudan

ELMER C. ALYEA
(GWC)[2], Guelph Campus,
University of Guelph,
Guelph, Ontario, Canada
N1G 2W1

REFERENCES

1 (a) D.C. Bradley and M.H. Chisholm, Accounts Chem. Res. 1976, 9, 273; (b) D.C. Bradley, Chem. in Britain 1975, 11, 393.

2 M.F. Lappert, P.P. Power, A.R. Sanger and R.C. Srivastava, "Metal and Metalloid Amides", Ellis Horwood Ltd., England, 1980.

3 U. Wannagat, Adv. Inorg. Chem. Radiochem. 1964, 6, 225.

4 H. Bürger and U. Wannagat, Monatsh. Chem. 1963, 94, 1007.

5 R.S. Drago and K.J. Fisher, Inorg. Chem. 1975, 14, 2804.

6 (a) P.F. Rodesiler and E.L. Amma, J. Chem. Soc. Chem. Commun. 1982, 182; (b) D. Dakternieks, Aust. J. Chem. 1982, 35, 469; (c) P.A.W. Dean, Can. J. Chem. 1981, 59, 3221.

7 E.C. Alyea, Inorg. Chim. Acta 1983, 76, L696.

8 M.J.S. Gynane, D.H. Harris, M.F. Lappert, P.P. Power, P. Rivière and M. Rivière-Baudet, J. Chem. Soc., Dalton Trans. 1977, 2004.

9 A.J. Brown, O.W. Howarth and P. Moore, J. Chem. Soc. Dalton Trans. 1976, 1589.

10 P.F. Rodesiler, E.H. Griffith, P.D. Ellis and E.L. Amma, J. Chem. Soc. Chem. Commun. 1980, 492.

*Polyhedron* Vol. 3, No. 4, pp. 513–514, 1984
Printed in Great Britain.

0277–5387/84 $3.00 + .00
© 1984 Pergamon Press Ltd.

# COMMUNICATION

## DIOXYGEN ADDUCT COMPLEX OF BIS(ETHYLENE)PLATINUM(0) : FORMATION AND CHARACTERIZATION

Wen-Shu Hwang

Department of Chemistry, National Sun Yat-Sen University,
Kaohsiung, Taiwan, Republic of China.

(Received 20 September 1983; accepted 3 January 1984)

ABSTRACT—The existence of the dioxygen adduct $Pt(O_2)(C_2H_4)_2$ has been concretely proven, and its ability to act as a catalyst for ethylene-oxide formation in both homogeneous and heterogeneous phase was studied.

The primary objective of this research was to study a feasible catalytic autoxidation of ethylene *via* the tris(ethylene)platinum(0) complex. Tris(ethylene)platinum(0) was prepared according to literature methods.[1]

The dioxygen adduct $Pt(O_2)(C_2H_4)_2$ was prepared [2] by introducing gaseous oxygen into a solution of tris(ethylene)platinum(0) at -46°C and its existence established from its spectra and physical data obtained in solution. Attempts to isolate the dioxygen adduct from the solution by recrystallization were not successful.

The complex in ether or chloroform is stable under an oxygen and ethylene atmosphere at low temperature. This complex was found to reacts with iodine[3] to produce an almost quantitative amount of oxygen (0.92 mole/mole complex). This finding strongly implied the formation of a dioxygen adduct with the platinum complex and indicated that a strong d-electron acceptor can further replace the oxygen ligand.

The low temperature infrared spectrum of the dioxygen adduct complex in chloroform showed two groups of characteristic absorption bands at $\nu_{max.}$ 814; 1481 and 1498 $cm^{-1}$. These could be assigned as the O-O and C=C stretching mode respectively. Similar O-O band has been shown by numerous other side-on dioxygen adduct of $d^{10}$ complexes from isotopic studies by Otsuka *et. al.*[4,5] This band might not be solely due to a pure O-O stretching motion, but also an indication of charge transfer from metal to the dioxygen. Therefore, the oxygen molecule coordinated to the platinum centre as a bidentate ligand. For comparison, some known side-on coordinated dioxygen complexes were prepared in our laboratory and their infrared spectra were recorded under the same condition. The O-O stretching frequencies are listed in Table I. Relative to nickel(0), the peroxo stretching frequencies for platinum(0) complexes are generally lower, which implied a stronger bonding between metal and oxygen. Electrons from the platinum(0) are considered to delocalize through the platinum-oxygen bond and the degree of electron transfer to the dioxygen is such that the formal oxidation state of the platinum is near that of a divalent state. Among the platinum complexes listed in Table I, the O-O stretching frequency for the ethylene complex is lower than that of phosphine complexes , which implied poor back π-bonding of ethylene ligands. The moderately intense C=C stretching absorption of tris(ethylene)platinum(0) occurs at 1468 $cm^{-1}$. This

Table I. Infrared O-O stetching absorption of peroxo complexes in $CHCl_3$.

| COMPOUNDS | $\nu_{O-O}$ $cm^{-1}$ |
|---|---|
| $Pt(PPh_3)_2O_2$ | 828 |
| $Pt(PEt_3)_2O_2$ | 824 |
| $Pt((P(Cy\text{-}C_6H_{11})_3)_2O_2$ | 818 |
| $Pt(PPhMe_2)_2O_2$ | 825 |
| $Pt(C_2H_4)_2O_2$ | 814 |
| $Ni(t\text{-}BuNC)_2O_2$ | 882 |

band was shifted slightly and split into two features of equal intensity at 1481 $cm^{-1}$ and 1498 $cm^{-1}$ upon replacing one ethylene ligand with a dioxygen ligand. This result indicated a cis ligation of the two ethylene ligands ($C_{2v}$).

The evidence from the reaction of the dioxygen adduct with iodine, releasing a near quantitative molar equivalent of oxygen and the infrared spectra point clearly to the existence of such a dioxygen platinum adduct in solution at low temperature having the molecular formula $Pt(O_2)(C_2H_4)_2$. The coplanarity of dioxygen and two ligands of an analogous complex, $Pt(PPh_3)_2O_2$ had been demonstrated by X-ray diffraction [6] studies. The structure of $Pt(O_2)(C_2H_4)_2$ complex may thus be tentatively assigned as having a similar square-planar geometry (Fig).

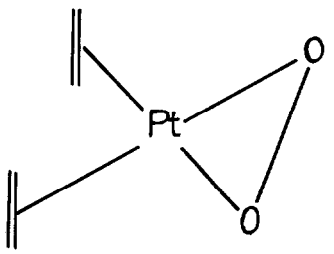



Fig.

In the absence of ethylene and oxygen, decomposition to metallic platinum and platinum(II) oxide was observed to occur within minutes at temperature above -20°C. Thermal decomposition of the complex, under vacuum was also found to release 2.11 moles of ethylene when one mole of complex was used. This is why the experiments with tris(ethylene)platinum(0) were carried out under a ethylene atmosphere in which it is stable.

The scope of utilising the dioxygen platinum complex $Pt(O_2)(C_2H_4)_2$ in insertion reaction of oxygen to an additional electron rich ligand within the coordinated sphere to give rise to coordinated epoxide are currently under investigation. In the homogeneous liquid phase, with ethylene as the additional electron rich ligand, no formation of ethylene oxide has so far been detected. We are however encouraged by the detection of 6-10% yield of ethylene oxide during several trials in heterogeneous phase reaction between solid tris(ethylene)platinum(0) complex under ethylene atmosphere and gaseous oxygen. Further experimental manipulation on the homogeneous liquid phase will be carried out.

ACKNOWLEDGEMENT:

I am indebted to Prof. C. W. Ong for valuable discussions and corrections.

REFERENCES.

1. T. L. Spencer, Inorg. Syn. 1979, 19, 213.
2. Dioxygen adduct complex. Excess oxygen gas 0.5 atm. were introduced to a vacuum line initially. In a Schlenk tube, which was attatched to the vacuum line, a petroleum ether (b.p.30-40°) or chloroform solution of tris(ethylene)platinum(0) under 1 atm. of ethylene at -46°C was stirred for about 4 h. At the end of the reaction, the pressure dropping of the oxygen gas stopped and the solution turned brown.
3. A chloroform solution of the dioxygen adduct complex in a Schlenk tube, on which a bent tube containing an excess amount of iodine was attached, cooled to -196°C and the appartus evacuated. After warming up the appartus to -46°C, the $N_2$ gas was introduced and iodine added to the solution. Upon mixing, the colour of the solution changed from brown to dark violet with concomitant evolution of oxygen (92%).
4. K. Hirota, M. Yamamoto, S. Otsuka, A. Nakamura, Y. Tatsuno, J. Chem. Soc. Chem. Commun., 1968, 583.
5. S. Otsuka, A. Nakamura, Y. Tatsuno, J. Am. Chem. Soc., 1969, 91, 6996.
6. C. D. Cook, P-T. Chen, S. C. Nyburg, J. Am. Chem. Soc., 1969, 91, 2123.

*Polyhedron* Vol. 3, No. 4, p. 515, 1984
Printed in Great Britain.

0277-5387/84 $3.00 + .00
Pergamon Press Ltd.

# BOOK REVIEW

**Reactions of molybdenum metal. Gmelin Handbook of Inorganic Chemistry**. 8th Edn. **Mo-Molybdenum**. Supplement Volume **A.3: Metal. Chemical Reactions**. Published by the Gmelin Institute for Inorganic Chemistry of the Max Planck Society for the Advancement of Science. Springer–Verlag, Berlin. 1983. xv + 227. DM 905. U.S. approx. $323.

This volume describes the chemical reactions of metallic Mo and is a welcome addition to the Gmelin Handbooks. It covers the literature through 1979 and is in English. Gmelin's "Molybdän;" (System No. 53) was published in 1935 and a Supplementary Volume, Al, covering the preparation and technology of Mo metal, in 1977. A Supplementary Volume, A2, on the physical properties and electrochemistry of Mo metal is promised. Supplementary Volumes on Mo compounds, mostly oxides and molybdates, were published in 1975 (B1) and 1976 (B2).

The volume under review is a comprehensive listing of the chemical reactions of Mo metal. Topics covered are reactions of Mo metal with elementary particles, with metals and non-metals and their compounds, including water and aqueous solutions of acids, alkalis and salts and with organic compounds. The treatment of each topic follows a pattern: chemisorption, reaction products, kinetics and thermodynamics. The accounts of chemisorption, the first step towards chemical reaction, are especially well done. The section on carbon monoxide chemisorption, for example, includes evaporated Mo films, powders, polycrystalline samples and oriented crystals and summarises work function measurements, electron and ion impact processes and surface spectroscopic studies (LEED, SIMS, AES, XPS, UPS). This volume, like all Gmelin volumes, is compendious rather than critical or interpretative. The authors conscientiously report contradictory literature statements occasionally allowing themselves an exclamation mark. A researcher seeking a problem would find much to excite his curiosity in this volume.

What impression of Mo metal chemistry does one get from this volume of Gmelin? Mo metal is rather easily passivated and so seems to be chemically inert, having the character almost of a noble metal. A layer of molybdenum dioxide protects Mo metal from aerial oxidation under ambient conditions. At high temperatures ($\gtrsim 600°C$) Mo oxidises rapidly as the molybdenum *tri*oxide formed sublimes off. When freshly polished Mo is contacted with water, the *di*oxide is formed. This is probably why Mo metal is resistant to mineral acids, except nitric, in the absence of air or other oxidants. Mo metal dissolves in dilute nitric acid and in hot concentrated nitric acid, forming $MoO_3$, but is apparently passivated by cold concentrated $HNO_3$. Mo is also apparently inert to aqueous alkalis in the absence of oxidising agents. When exposed to sulphur or $H_2S$, Mo becomes covered by an adherent, low-friction layer of $MoS_2$.

The ability of Mo metal surfaces to chemisorb dissociatively hydrocarbons, CO and $CO_2$, $N_2$, $NH_3$, $O_2$, $H_2O$, $H_2S$ is noteworthy. The reactions reflect the stability of the surface compounds formed (carbide, nitride, oxide or sulfide). Consequently the surface chemistry of Mo is that of the surface compound and not the metal. A Mo carbide, for example, is the catalyst in reactions of $CO + H_2$ and hydrocarbon over Mo metal.

The coverage is deliberately restricted to *chemical* reactions of Mo metal. Not included are the electrochemistry of Mo (not even Mo electrode potentials) and reactions of vaporised Mo atoms from the vapour. This is a pity because they represent ways of entering Mo chemistry using Mo metal as a starting point.[1,2] The catalytic chemistry of Mo metal is also excluded.

This volume of Gmelin is an important work of reference which should be on the shelves of institutional libraries. It will be consulted by corrosion scientists, surface and catalytic chemists and inorganic chemists who wish to venture beyond the familiar terrain of Group VIII.

The literature coverage is, as one would expect of Gmelin, comprehensive. Many of the sources are obscure or not easily accessible and certainly not familiar to the average chemist. The authors have done a most useful service in collecting all this material together.

In conclusion, then, this volume is a thorough compilation of chemical reactions of Mo metal, a work of reference but also well worth browsing through. Even in the age of electronic information retrieval, this type or readable compendium still has a place. I regret that the price, no doubt justified by research and production costs, will exclude this volume (and other Gmelin volumes) from the personal libraries of all but the most affluent chemists.

*Department of Chemistry*
*University of Reading*
*Whiteknights*
*Reading*
*Berks., RG6 2AD*
*England*

**P. C. H. MITCHELL**

## REFERENCES

1. For example, M. L. H. Green, In *Proc. Climax 4th Int. Conf. Chem. and Uses Molybdenum, Climax Molybdenum Co.* (Edited by H. F. Barry and P. C. H. Mitchell), p. 74. Ann Arbor, U.S.A. (1982).
2. J. J. Habeeb, C. Oldham and D. G. Tuck, *J. Inorg. Nucl. Chem.* 1981, **43**, 2087.

*Polyhedron* Vol. 3, No. 5, pp. 517–522, 1984
Printed in Great Britain.

0277–5387/84 $3.00 + .00
© 1984 Pergamon Press Ltd.

# TRANSITION METAL COMPLEXES OF FURFURAL AND BENZIL SCHIFF BASES DERIVED FROM S-BENZYLDITHIOCARBAZATE

**M. AKBAR ALI***
Department of Chemistry, University of Chittagong, Chittagong, Bangladesh

**and**

**R. N. BOSE†**
Department of Chemistry, Dhaka University, Dhaka, Bangladesh

(*Received* 11 *April* 1983; *accepted* 10 *October* 1983)

**Abstract**—New nickel(II), copper(II), cobalt(III) and rohdium(III) complexes of two Schiff base ligands formed by condensation of furfural and benzil with S-benzyldithiocarbazate have been synthesized and characterized by elemental analysis and magnetic and spectroscopic measurements. The nickel(II) complexes, $Ni(N–S)_2$ and $Ni(O–N–S)_2$ (N–S and O–N–S stand for the uninegatively charged furfural and benzil Schiff bases, respectively) are square-planar and octahedral, respectively. The Cu(N–S)Cl complex is paramagnetic with a magnetic moment of 1.73 B.M. A halogen-bridged dimeric structure is proposed for this complex. The copper(II) complex, Cu(O–N–S)Cl is diamagnetic, suggesting strong antiferromagnetic interactions between a pair of copper(II) ions in a thiolo sulphur-bridged dimeric or polymeric structure. Cobalt(II) ions are oxidized in the presence of the Schiff bases with the concomitant formation of cobalt(III) complexes of empirical formulae, $Co(N–S)_3$, $Co(O–N–S)_2ClO_4$ and $Co(O–N–S)_2Cl$, respectively, which are spin-paired and octahedral. The rhodium(III) complex of the furfural Schiff base, $Rh(N–S)_2Cl$ is tentatively assigned a halogen-bridged dimeric structure.

Metal complexes of ligands derived from S-alkyldithiocarbazic acid have received considerable attention over the past few years.[1–7] Aside from showing interesting physico-chemical properties, some of the complexes have been found to display carcinostatic activities.[1] As part of our general study of metal complexes of ligands containing oxygen, nitrogen and sulphur as the donor atoms, we report herein data on some new metal complexes of two Schiff base ligands formed by condensation of furfural and benzil with S-benzyldithiocarbazate.

## EXPERIMENTAL

*Physical measurements.* Electronic spectra were recorded with either a Beckman Model 24 or a Perkin–Elmer Model 402 UV-visible spectrophotometer. IR spectra were obtained with a Perkin–Elmer 577 IR spectrophotometer. $^1H$ NMR spectra were obtained with a Bruker WP 80 spectrometer with tetramethylsilane or its sodium salt as the internal standard. Magnetic susceptibilities were measured by the Gouy method. Molar susceptibilities were corrected for diamagnetism of the constituent atoms using Pascal's constants.[8] Molar conductances were measured with a Beckman Conductivity Bridge. Microanalyses for carbon, hydrogen and nitrogen were performed at the Microanalytical Laboratory, University of Stirling, England. All other physical measurements and analytical procedures employed in the present work were similar to those described previously.[3]

*Preparation of the ligands*

*Preparation of the furfural Schiff base.* S-Benzyldithiocarbazate was prepared as described

*Author to whom correspondence should be addressed.

†Present address: Chemistry Department, Wichita State University, Wichita, KS 67208, U.S.A.

before.[2] To a hot solution of S-benzyldithiocarbazic acid (0.8 g) in abs. ethanol (50 $cm^3$) was added with stirring, a solution of furfural (1.0 g) in ethanol (50 $cm^3$). The mixture was heated on a water-bath for *ca.* 15 min and then left to cool, whereupon the pale yellow crystals which had formed were filtered off and recrystallised from benzene. Yield, 1.2 g; M.P. 168°C. Found: C, 56.8; H, 4.05; N, 10.0; S, 23.3. Calc. for $C_{13}H_{12}N_2OS_2$: C, 56.7; H, 4.4; N, 10.1; S, 22.9%.

*Preparation of the benzil Schiff base.* S-Benzyldithiocarbazate (2.0 g) in abs. ethanol (150 $cm^3$) was mixed with a solution of benzil (1.6 g) in the same solvent (100 $cm^3$). The mixture was heated on a water-bath for about 10 min during which time the solution changed its colour from pale yellow to yellowish-brown. The solution was then rotary evaporated to obtain an oily substance. Several attempts to crystallise the oil did not meet with success. However, solution of the oil in ethanol reacted readily with metal salts producing crystalline compounds which were found to be pure and consequently, an ethanolic solution of the oil was used for the preparation of metal complexes.

*General method for the preparation of metal complexes.* All the complexes isolated in the present study were prepared by the same general method: A filtered solution of the appropriate metal salt (0.005 mole) in abs. ethanol (*ca.* 25 $cm^3$) was mixed with a solution of the Schiff base (0.005 or 0.01 mole wherever appropriate) in the same solvent (50 $cm^3$) and the resulting mixture was heated on a water-bath for about 10 min and then left to cool down to room temperature. The crystals which had formed were then filtered off, washed thoroughly with ethanol and then dried in a vacuum desiccator over $P_4O_{10}$.

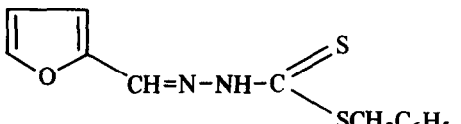
## RESULTS AND DISCUSSION

*Complexes of the furfural Schiff base* (HN–S). The reaction of furfural and S-benzyldithiocarbazate in ethanol yields the Schiff base (**1A**), the formulation of which is supported by analytical and spectral data. Its mass spectrum shows the molecular ion peak at 276 and its $^1H$ NMR spectrum in dmso-$d_6$ shows signals at 7.29; 4.48 and 8.20 ppm. corresponding to the phenyl, $-CH_2-$ and $-CH=N-$ protons, respectively.[9] The signals due to the furan ring protons were observed at 6.70, 7.20 and 7.90 ppm. The IR spectrum of the Schiff base displays the $\nu C=N$[10] and $\nu N-N$[11] bands at 1610 and 938 $cm^{-1}$, respectively. The IR spectrum does not display the $\nu N-H$ at 3100 $cm^{-1}$, suggesting that in the solid state, the Schiff base remains in the thioketo form (**1A**), but in solution it may remain as an equilibrium mixture of both the thioketo (**1A**) and thiolo (**1B**) tautomeric forms.

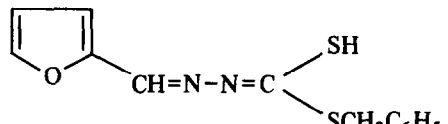
Reaction of the Schiff base with metal salts yielded crystalline complexes which were found to be quite stable in the atmosphere. The complexes which were isolated in the present study are listed in Table 1 along with some of their physical properties. The IR spectra of the complexes (Table 2) do not contain the $\nu N-H$ band of the free ligand indicating that the proton on the $\alpha$-nitrogen atom is lost upon complexation with metal ions. The $\nu C=N$ band of the free ligand is lowered by *ca.* 20 $cm^{-1}$ in the spectra of the complexes suggesting coordination via the azomethine nitrogen atom. The occurrence of the $\nu N-N$ band at a higher frequency in the IR spectra of the complexes compared to that in the ligand suggests a reduction of the repulsion between the lone pairs of the nitrogen atoms[11] as a result of coordination via the azomethine nitrogen. The downfield shift of the $-CH-N-$ proton signal in the $^1H$ NMR spectrum of the cobalt (III) complex (Table 1) compared to that in the free ligand further supports coordination through the nitrogen atom.

The IR spectra of the complexes do not contain any band attributable to the $\nu M-O$, suggesting that the furan oxygen does not participate in coordination. A medium to weak band at *ca.* 315 $cm^{-1}$ in the IR spectra of the complexes is assigned to the $\nu M-S$.[12] From the foregoing discussions it can be assumed that the Schiff base behaves as an NS bidentate rather than an ONS tridentate. The diamagnetism of the nickel(II) complex (Table 1) is strong evidence that coordination occurs through the thiolo sulphur atom and not through the thioether sulphur, since thiols but not thioethers, cause spinpairing in complexes of nickel(II).[13]

Reaction of nickel(II) salts with the ligand yields a brown compound, $Ni(N-S)_2$, which is a non-electrolyte in nitrobenzene. Its diamagnetism and




**(1A)**




**(1B)**

Table 1. Colour, conductivity, magnetic moment, analytical and $^1H$ NMR spectral data

| Compound | Colour | $\Lambda^a$ ($\Omega^{-1}cm^2mole^{-1}$) | $\mu_{eff}^e$ (B.M.) at 298 K | Analytical data[d] C | H | N | S | $^1H$ n.m.r. spectra[e] (D.D.M.) $\delta$(CH) | $\delta(CH_2)$ | $\delta$ (heterocyclic H) |
|---|---|---|---|---|---|---|---|---|---|---|
| HN-S | Pale Yellow | - | - | 56.8 (56.7) | 4.05 (4.4) | 10.1 (10.1) | 23.3 (22.9) | 8.20 | 4.48 | 6.70, 7.20, 7.90. |
| $[Ni(N-S)_2]$ | Brown | 0 | Diam. | 51.3 (51.3) | 3.6 (3.6) | 9.1 (9.2) | 20.6 (21.0) | 7.80[f] | 4.60[f] | 6.50[f], 722, 7.60. |
| $[Cu(N-S)Cl]$ | Greenish Black | 0.7[b] | 1.73 | 41.9 (41.7) | 2.5 (3.0) | 7.4 (7.5) | - | | | |
| $[Co(N-S)_3]$ | Brown | 1.0 | Diam. | 52.9 (52.4) | 3.8 (3.7) | 9.5 (9.5) | 21.7 (21.7) | 8.55 | 4.45 | 6.75, 7.05, 8.10. |
| $[Rh(N-S)_2Cl]$ | Yellow Orange | 5.0[b] | Diam. | 45.7 (45.2) | 3.55 (3.5) | 8.4 (8.05) | - | - | - | - - - |
| $[Ni(O-N-S)_2]$ | Brownish Green | 0 | 2.94 | 62.8 (63.1) | 3.8 (4.1) | 6.6 (6.7) | 15.5 (15.3) | - | - | - - - |
| $[Cu(O-N-S)Cl]$ | Red | 1.0[b] | 0.2 | 54.1 (54.1) | 3.2 (3.1) | 5.8 (5.75) | 6.85 (7.25) | - | 4.50 | - - - |
| $[Co(O-N-S)_2]ClO_4$ | Brown | 22.0 | Diam. | 57.3 (56.4) | 3.7 (3.7) | 6.3 (6.0) | - | - | 4.42 | - - - |
| $[Co(O-N-S)_2]Cl$ | Brown | 19.3 | Diam. | 60.5 (60.5) | 3.8 (3.9) | 6.1 (6.4) | 14.2 (14.7) | - | 4.55 | - - - |

a. Molar conductivity of ca. $10^{-3}M$ - $5 \times 10^{-4}M$ solutions in nitrobenzene.

b. measured in DMF.

c. $\mu_{eff} = 2.83\sqrt{\chi_M' T}$ ; average of two measurements, ± 0.05 B.M.

d. Calculated values are given in parentheses

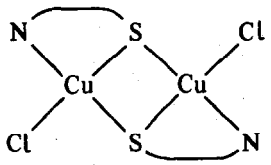
e. Spectra measured in dmso - $d_6$

f. measured in $CDCl_3$.

Table 2. IR and electronic spectral data

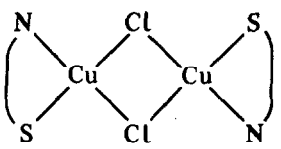
| Compound | IR Spectra[a] ($cm^{-1}$) $\nu$(N-H) | $\nu$(C=N) | $\nu$(N-N) | $\nu$(C=O) | $\nu$(M-S) | State | Electronic spectra Band maxima in nm ($\epsilon$ $mole^{-1}$ $liter$ $cm^{-1}$) |
|---|---|---|---|---|---|---|---|
| HN-S | 3130sh 3100 S | 1610 S | 938 S | - | - | - | - |
| $[Ni(N-S)_2]$ | - | 1590 s | 960 s | - | 315 m | Nujol | 600, 490, 330 |
| | | | | | | $CH_2Cl_2$ | 588(214), 458($1.2 \times 10^4$), 330($4.0 \times 10^4$), 283($4.0 \times 10^4$), 241($2.8 \times 10^5$). |
| [Cu(N-S)Cl] | - | 1592 S | 970 s | - | 305 m | Nujol | 730, 400. |
| $[Co(N-S)_3]$ | - | 1588 s | 958 s | - | 310 w | Nujol | 470 sh, 390, 310. |
| | | | | | | $CH_2Cl_2$ | 384($4.0 \times 10^4$), 324($5.4 \times 10^4$), 287($5.3 \times 10^4$), 246($4.3 \times 10^4$). |
| $[Rh(N-S)_2Cl]$ | - | 1608 S | 970 S | - | 300 w | Nujol | 350, 230. |
| $[Ni(O-N-S)_2]$ | - | 1592 S | 980 S | 1672 S | 315 S | Nujol | 530 sh, 385, ca. 300 |
| | | | | | | $CH_2Cl_2$ | 540 sh, 393($6.2 \times 10^4$), 290($2.2 \times 10^4$), 255($2.6 \times 10^4$). |
| [Cu(O-N-S)Cl] | - | 1580 S | 980 s | 1660 S | 340 m | Nujol | ca. 500 |
| $[Co(O-N-S)_2]ClO_4$ | - | 1590 s | 995 s | 1670 S | - | Nujol | 530 sh, 470, 298, 260 · |
| $[Co(O-N-S)_2]Cl$ | - | 1580 S | 970 S | 1660 S | - | Nujol | 532 sh, 475, 290, 260 · |

the presence of a single band at 600 nm in its electronic spectrum suggest that it has a square-planar structure.[14] With copper(II) chloride, the ligand yields, Cu(N–S)Cl which behaves as a non-electrolyte in DMF (Table 1). Its insolubility in non-polar and weakly polar solvents suggest that it might possess a dimeric or a polymeric structure. A sulphur-bridged dimeric structure (II) is unlikely, since such a bridging arrangement generally




(II)

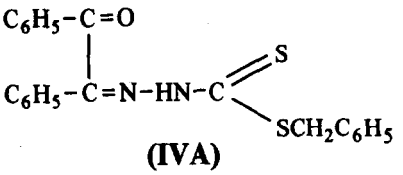
leads to strong antiferromagetic interactions resulting in complete diamagnetism.[15] The room-temperature magnetic moment of 1.73 B.M. suggests that structure III is more likely. The



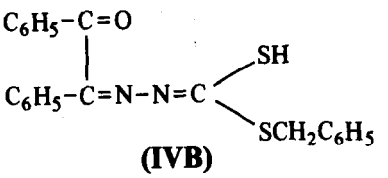

(III)

electronic spectrum of the compound shows a broad band at 730 nm indicative of a square-planar structure.[16] Cobalt(II) nitrate hexahydrate reacts with the Schiff base producing a brown compound, $Co(N–S)_3$ which behaves essentially as a non-electrolyte in nitrobenzene (Table 1). The diamagnetic nature of the compound suggests that it is a cobalt(III) rather than a cobalt(II) complex. This observation is in keeping with the findings of other workers that ligands with thiol groups generally oxidize cobalt(II) ions to produce cobalt(III) complexes.[17,18] The electronic spectrum of the compound was not well resolved because of the presence of the tail of a very intense charge-transfer band extending up to the visible portion of the spectrum. With rhodium(III) chloride, the ligand yields an orange compound of composition, $Rh(N–S)_2Cl$, which behaves as a non-electrolyte in DMF. Its very poor solubility in non-donor solvents suggests that it does not possess a monomeric structure. A chlorine-bridged dimeric or polymeric structure is likely for the complex.

*Complexes of the benzil Schiff base.* Benzil reacts with S-benzyldithiocarbazate producing an oily product, which, however, reacts with metal salts producing pure metal complexes. The compounds which were isolated are listed in Table 1 and their IR and electronic spectral data are presented in Table 2. The IR spectra of the complexes do not show $\nu$N–H band at *ca.* 3100 $cm^{-1}$ indicating that the ligand is present as the mercaptide form as shown in IVB.




(IVA)




(IVB)

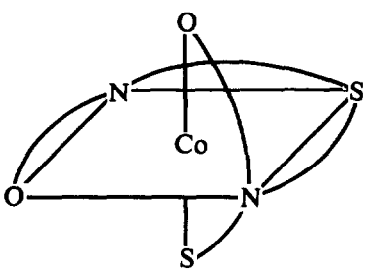
The $\nu C=O$ band was discernible at *ca.* 1658 $cm^{-1}$ in the IR spectra of the metal complexes (Table 2). The position of this band is about 70 $cm^{-1}$ lower than that found for free carbonyl groups in α-diketones.[19] This is an indication that the carbonyl group is coordinated to the metal ions. Similarly a strong peak at about 1590 $cm^{-1}$ in the IR spectra of the metal complexes may be assigned to the $\nu C=N$ of the coordinated azomethine group.[10]

The Schiff base, hereinafter abbreviated as O–N–SH reacts with nickel(II) yielding a greenish brown compound, $Ni(O–N–S)_2$, which behaves essentially as a non-electrolyte in nitrobenzene. Its room-temperature magnetic moment of 2.94 B.M. suggests that it has an octahedral configuration. Its electronic spectrum displays several bands in the range 1000–250 nm (Table 2) of which the band at 540 nm may be assigned to the $^3A_{2g} \rightarrow {}^3T_{1g}$ transition of octahedral nickel(II). The band corresponding to the transition $^3A_{2g} \rightarrow {}^3T_{2g}$ could not be measured with the available spectrophotometer. The third expected band is presumably hidden beneath intense charge-transfer transitions.

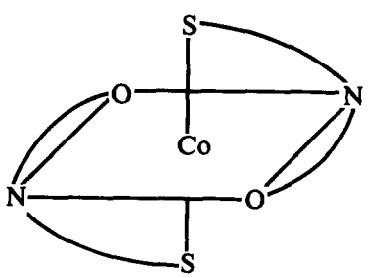
The Schiff base reacts with copper(II) chloride producing a red compound, Cu(O–N–S)Cl which is a non-electrolyte in DMF. Its very poor solubility in non-polar and weakly polar solvents suggests that it might possess a dimeric or a polymeric structure. Its stoichiometry and colour indicate the presence of copper(II) rather than copper(I), since copper(I) compounds are usually yellow or colourless. Its near diamagnetism suggests a strong spin-spin interaction[14,15,20] involving a sulphur-bridged dimeric or polymeric structure. Oxygen

bridging seems unlikely, since such bridging arrangements generally do not lead to complete diamagnetism at room-temperature.[21]

Cobalt(II) ion is rapidly oxidized in the presence of the Schiff base with the concomitant formation of cobalt(III) complexes of general formula, $Co(O–N–S)_2X(X = Cl^-, ClO_4^-)$ which are diamagnetic. Molar conductance data in nitrobenzene (Table 1) suggest that the counter ions are not coordinated to the cobalt(III) ion. The IR spectrum of the perchlorate complex shows strong bands at 1082 and 616 $cm^{-1}$ indicating the presence of ionic perchlorate.[22] The electronic spectra of the complexes are not very well resolved owing to the intrusion of the tail of a very strong charge-transfer band to the visible portion of the spectrum. However, a shoulder is discernible at 530 nm which may be assigned to the $^1A_{1g} \rightarrow {}^1T_{1g}$ transition of octahedral symmetry. A *cis*-octahedral structure (V) is suggested for these complexes. Since the ligand is planar it will be quite strenuous for them to span *trans*- octahedral positions as shown in VI.




(V)




(VI)

Similar *cis*-octahedral structures were also assigned to the cobalt(III) complexes of salicylaldehyde thiosemicarbazone[23] and salicylaldehyde Schiff base of S-methyldithiocarbazate[24] which have the analogous chromophores $CoO_2N_2S_2$.

*Acknowledgements*—We thank Mrs. M. Berry and Mr. D. F. Dance of the Chemistry Department, University of Stirling, U.K. for helping us with some microanalyses and NMR spectroscopic measurements.

## REFERENCES

1. M. Akbar Ali and S. E. Livingstone, *Coord. Chem. Rev.* 1974, **13**, 101 and references cited therein.
2. M. Akbar Ali and M. T. H. Tarafder, *J. Inorg. Nucl. Chem.* 1977, **39**, 1785.
3. M. Akbar Ali and R. Bose, *J. Inorg. Nucl. Chem.* 1977, **39**, 265.
4. M. Akbar Ali and S. G. Teoh, *J. Inorg. Nucl. Chem.* 1978, **40**, 451.
5. M. Akbar Ali and S. G. Teoh, *J. Inorg. Nucl. Chem.* 1978, **40**, 2013.
6. M. T. H. Tarafder and M. Akbar Ali, *Can. J. Chem.* 1978, **56**, 2000.
7. M. Akbar Ali, *Can. J. Chem.* 1980, **58**, 727.
8. B. N. Figgis and J. Lewis, In *Modern Coordination Chemistry* (Edited by J. Lewis and R. G. Wilkins), p. 403. Interscience, New York, (1959).
9. A. Saxena, J. P. Tandon, K. C. Molloy and J. J. Zuckerman, *Inorg. Chim. Acta* 1982, **63**, 71.
10. J. E. Kovacic, *Spectrochim Acta* 1967, **23A**, 183.
11. A. Monaci and F. Trali, *J. Chem. Soc. Dalton*, 1977, 417.
12. D. M. Adams, *Metal-Ligand and Related vibrations*, p. 319. Arnold, London (1967).
13. S. E. Livingstone, *Quart. Rev.* 1965, **19**, 386.
14. H. B. Gray and C. J. Ballhausen, *J. Am. Chem. Soc.* 1963, **85**, 260.
15. R. S. Nyholm, *Proc. Chem. Soc.* 1961, 273.
16. L. Sacconi and M. Ciampolini, *J. Chem. Soc.* 1964, 276.
17. M. Akbar Ali, S. E. Livingstone and D. J. Phillips, *Inorg. Chim. Acta* 1973, **7**, 179.
18. S. H. H. Chaston and S. E. Livingstone, *Aust. J. Chem.* 1967, **20**, 1079.
19. L. J. Bellamy, *The Infrared Spectra of Complex Molecules*, p. 132. Methuen, New York (1954).
20. B. Singh, M. Lakshmi and U. Agarwala, *Inorg. Chem.* 1969, **8**, 2341.
21. M. Kato, H. B. Jonassen and J. C. Manning, *Chem. Rev.* 1964, **64**, 99.
22. B. J. Hathaway and A. E. Underhill, *J. Chem. Soc.* 1961, 3091.
23. A. V. Ablov and N. V. Gerbeleu, *Russ. J. Inorg. Chem.* 1964, **9**, 1260.
24. M. Akbar Ali, S. E. Livingstone and D. J. Phillips, *Inorg. Chim. Acta* 1973, **7**, 531.

*Polyhedron* Vol. 3, No. 5, pp. 523–526, 1984
Printed in Great Britain.

0277–5387/84 $3.00 + .00
© 1984 Pergamon Press Ltd.

# POTENTIOMETRIC INVESTIGATION MIXED LIGAND COMPLEXES OF Ni(II) WITH DL-METHIONINE AND DL-ETHIONINE IN AQUEOUS SOLUTION

J. MASŁOWSKA* and L. CHRUŚCIŃSKI
Institute of General Food Chemistry, Technical University 90–924 Łódź, Gdańska 162/168, Poland

(*Received* 16 *May* 1983; *accepted* 5 *August* 1983)

**Abstract**—The formation of mixed ligand complexes of Ni(II) with DL-methionine in aqueous solution was investigated. The composition and stability constants of the complexes were determined by the potentiometric method.

The growing importance of mixed complexes, particularly of biologically active compounds with transition metal ions, is a strong incentive for intensive studies in this field. There have been available in the literature papers on mixed complexes of aminoacids in aqueous solutions mainly complexes of Ni(II), Cu(II), Zn(II) and Co(II) with such aminoacids as serine, alanine, glycine, histidine, threonine and others.[1–10] Considerably less papers have been on mixed complexes of metal ion with aminoacids containing sulphur.[11–14] Chang and Martin[12] have studied mixed complexes in system Ni(II)-cysteine-ethylenediamine. Complexes of Cd(II), Hg(II) and Cu(I) with D-penicilamine and other ligands containing sulphur have been examined by Sugiura and Tanaka.[14] Sovago *et al.*[11] have determined stability constants of complexes of Ni(II) and Zn(II) with L-cysteine and D-penicilamine and other ligands such as glycine, histamine and L-histidine.

The aim of the present paper was the electrochemical examinations of the composition and properties of mixed complexes in the system Ni(II)-DL-methionine-DL-ethionine including the determination of their stability constants.

## EXPERIMENTAL

### *Reagents*

DL-methionine (Fluka) and DL-ethionine (Fluka) were purified by crystallization from water–ethanol solutions. Nickel perchlorate was prepared by treating basic nickel carbonate with perchloric acid. $Ni(ClO_4)_2$ solution was standardized by complexometric method.[15] The pH-metric titrations were carried out with carbonate-free NaOH with a concentration of 2.9976 M. To maintain a constant ionic strength $\mu = 0.5$, a solution of $NaClO_4$ was used.

## APPARATUS

The pH-metric titrations were carried out under nitrogen in a special vessel described in paper.[16] pH measurements were made with a OP-208 pH-meter Radelkis equipped with a glass OP-0718P and OP-0830P calomel electrodes. The glass electrode was calibrated with 0.05 M potassium hydrogen phthalate solution pH = 4.008, and a phosphate buffer 0.025 M $KH_2PO_4$ and 0.025 M $Na_2HPO_4$ pH = 6.865, at 25°. The NaOH solution was added from microburette.

### *Measurement method and calculation procedure*

The measurements were carried out as described in paper.[3] Several series of titration curves were made. In each series, a constant concentration of two components was kept while the concentration of third component was varied. The concentration of Ni(II) was varied from $1 \times 10^{-2}$ to $6 \times 10^{-2}$ M. The sample volume was 40 cm$^3$. Figure 1 shows the titration curves for the system Ni(II)-DL-methionine-DL-ethionine. From particular series of titration curves, the concentration of free uncomplexed component $[H_2A]$ or [M] was found using formulae (1, 2):

$$p[H_2A] = p[H_2A]_0 - \int_{pH_0}^{pH} \left(\frac{\partial c_H}{\partial c_A}\right)_{c_M, pH} d\text{pH} \quad (1)$$

$$p[M] = p[M]_0 - \int_{pH_0}^{pH} \left(\frac{\partial c_H}{\partial c_M}\right)_{c_A, pH} d\text{pH} \quad (2)$$

where $c_H = 2c_A + c_{HClO_4} - c_{NaOH}$ is a concentration of titrated protons; $c_A$ and $c_M$—total concentration

*Author to whom correspondence should be addressed.

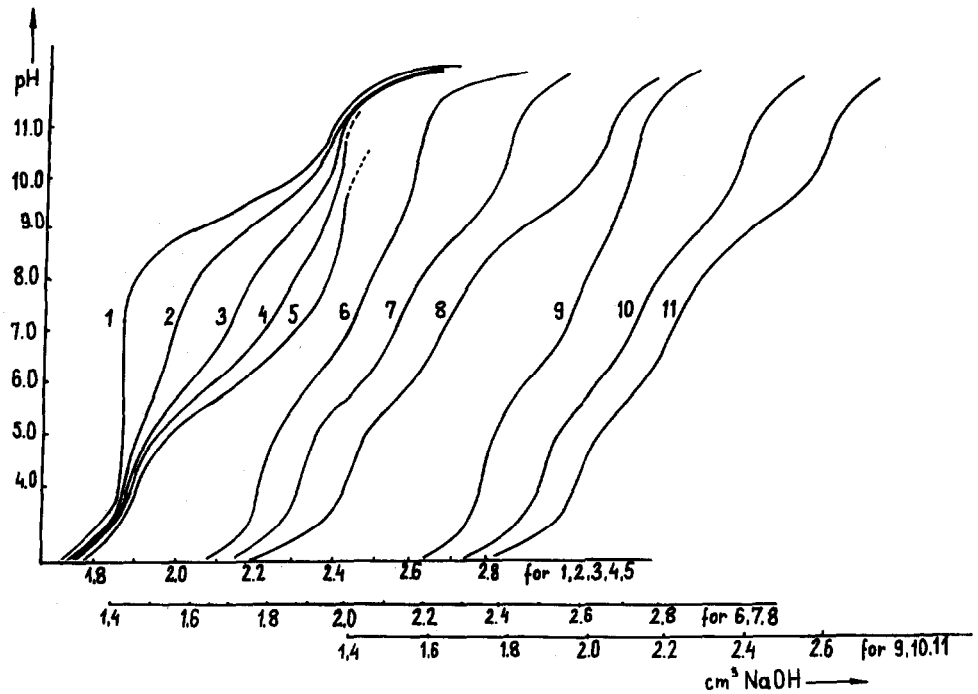



Fig. 1. Titration curves for the system: Ni(II)-DL-methionine-DL-ethionine

| | | | |
|---|---|---|---|
| 1. | $c_{Ni} = 0$ | $c_A = 0.02$ | $c_B = 0.02$ M |
| 2. | $c_{Ni} = 0.005$ | $c_A = 0.02$ | $c_B = 0.02$ M |
| 3. | $c_{Ni} = 0.010$ | $c_A = 0.02$ | $c_B = 0.02$ M |
| 4. | $c_{Ni} = 0.015$ | $c_A = 0.02$ | $c_B = 0.02$ M |
| 5. | $c_{Ni} = 0.020$ | $c_A = 0.02$ | $c_B = 0.02$ M |
| 6. | $c_{Ni} = 0.010$ | $c_A = 0.01$ | $c_B = 0.02$ M |
| 7. | $c_{Ni} = 0.010$ | $c_A = 0.02$ | $c_B = 0.02$ M |
| 8. | $c_{Ni} = 0.010$ | $c_A = 0.03$ | $c_B = 0.02$ M |
| 9. | $c_{Ni} = 0.010$ | $c_A = 0.02$ | $c_B = 0.01$ M |
| 10. | $c_{Ni} = 0.010$ | $c_A = 0.02$ | $c_B = 0.02$ M |
| 11. | $c_{Ni} = 0.010$ | $c_A = 0.02$ | $c_B = 0.03$ M. |

of metal ion and ligand; $H_2A$ and M—concentration of free components; $c_{HClO_4}$—total concentration of perchloric acid; $c_{NaOH}$—concentration NaOH in volume sample; $[H_2A]_0$ at the initial point of the titration curve was calculated from formula (3)

$$[H_2A]_0 = \frac{c_A}{1 + \text{antilog}\,(pH - pK_a)} \tag{3}$$

where $pK_a$—dissociation constant of corresponding aminoacid p[A] at each point of the titration curve can be calculated from formula (4):

$$p[A] = p[H_2A] + pK_1 + pK_2 - 2pH. \tag{4}$$

Having the concentration of free uncomplexed components stability constants of the complexes can be calculated from eqns (5)–(9) by means of ODRA 1305 computer:

$$\beta_{pqrs} = \frac{[M_pH_qA_rB_s]}{[M]^p[H]^q[A]^r[B]^s} \tag{5}$$

$$c_M - [M] = \sum_p (\beta_{pqrs} = [M]^p[H]^q[A]^r[B]^s) \tag{6}$$

$$c_A - [A] = \sum_r (\beta_{pqrs}[M]^p[H]^q[A]^r[B]^s) \tag{7}$$

$$c_B - [B] = \sum_s (\beta_{pqrs}[M]^p[H]^q[A]^r[B]^s) \tag{8}$$

$$c_H - [H] = \sum_q (\beta_{pqrs}[M]^p[H]^q[A]^r[B]^s) \tag{9}$$

## RESULTS AND DISCUSSION

Figure 2 shows relationships $c_H = f(c_A)_{c_M}$ and $c_H = f(c_M)_{c_A}$ which were used to calculate the deriv-

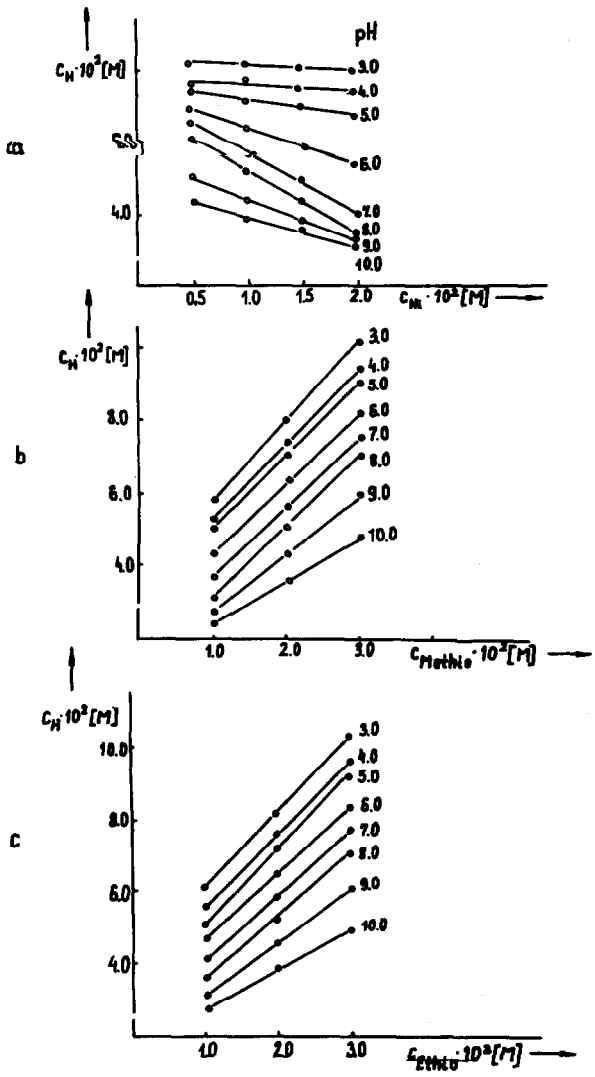



Fig. 2. Plots of the relationships. (a) $c_H = f(c_M)c_A$, $c_B$, pH. (b) $c_H = f(c_A)c_M$, $c_B$, pH. (c) $c_H = f(c_B)c_A$, $c_M$, pH.

atives appearing in eqns (1) and (2). Figure 3 shows the dependence of concentration of free uncomplexed components on pH. Numerical values of log for 1:1 and 1:2 complexes of Ni(II) with methionine Table 1, $\log\beta_1 = 5.10$, $\log\beta_2 = 9.68$, are in good agreement with those given for these complexes by Lenz and Martell:[17] $\log\beta_1 = 5.19$ and $\log\beta_2 = 9.94$ at $\mu = 0.1$ $KNO_3$. The comparison of stability constants of simple complexes of Ni(II) with methionine and ethionine determined in the present study with these for other complexes of Ni(II) with aminoacid free of sulphur, e.g. Ni(II)-alanine $\log\beta_1 = 5.95$, $\log\beta_2 = 10.66$; Ni(II)-valine $\log\beta_1 = 5.30$, $\log\beta_2 = 9.52$,[18] shows that Ni(II) coordinates methionine and ethionine via oxygen of carboxyl group and nitrogen of amine group. The same type of coordination takes place in mixed complexes. The values of stability constants of complexes of Ni(II) with ethionine are slightly lower than those of Ni(II) complexes with methionine which can be due to the presence of the ethyl group in ethionine, being bigger than the methyl group. The formation of mixed complexes, types MAB and MHAB, has been found. The value of stability constants of the mixed complex is between the values of stability constants for complexes $MA_2$ and $MB_2$.

Perrin and Sharma[4] have found that in the case of the formation of complexes of Ni(II) (metal with coordination number 6) can be simple complexes MA, $MA_2$, $MA_3$ and mixed complexes MAB, $MA_2B$, $MAB_2$. In the case of Ni(II) complexes with DL-methionine and DL-ethionine, complexes $MA_2B$ and $MAB_2$ are not formed, which can be due to the presence of a big functional group in the aminoacid under investigation.

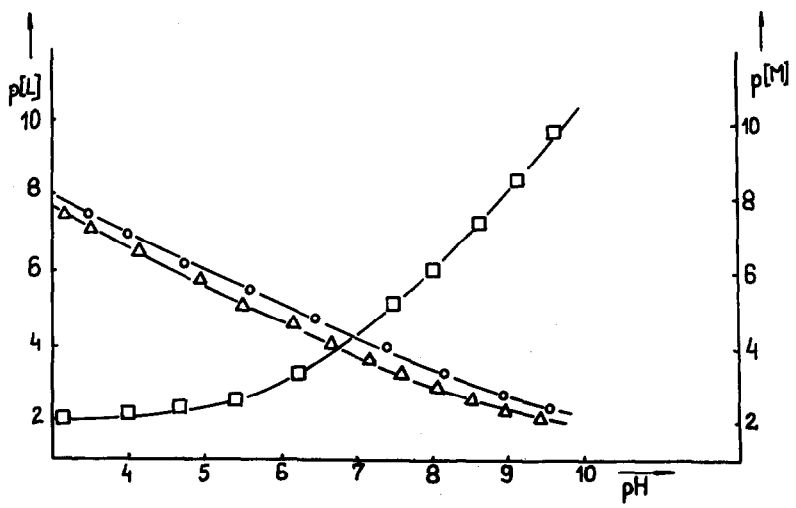



Fig. 3. Dependence of the concentration of free uncomplexed on pH. ○, DL-methionine; △, DL-ethionine; □, $Ni^{2+}$.

Table 1. Log of stability constants $\log \beta_{pqrs}$ of $M_pH_qA_rB_s$ complexes, M = Ni(II), A = DL-methionine, B = DL-ethionine $\mu = 0.5$ ($NaClO_4$), 25°C

| p | q | r | s | $\log \beta_{pqrs}$ |
|---|---|---|---|---|
| 0 | 2 | 1 | 0 | 11.47 (0.01) |
| 0 | 1 | 1 | 0 | 9.15 (0.01) |
| 0 | 2 | 0 | 1 | 11.15 (0.01) |
| 0 | 1 | 0 | 1 | 8.94 (0.01) |
| 1 | 0 | 1 | 0 | 5.10 (0.04) |
| 1 | 0 | 2 | 0 | 9.88 (0.06) |
| 1 | 0 | 0 | 1 | 4.98 (0.05) |
| 1 | 0 | 0 | 2 | 9.46 (0.07) |
| 1 | 0 | 1 | 1 | 9.50 (0.09) |
| 1 | 1 | 1 | 1 | 12.07 (0.05) |

## REFERENCES


1. H. C. Freeman and R. P. Martin, *J. Biol. Chem.* 1969, **244**, 4823.
2. D. D. Perrin and I. G. Sayce, *J. Chem. Soc.* (A) 1967, 1755.
3. T. P. A. Kruck and B. Sarkar, *Can. J. Chem.* 1973, **51**, 3555.
4. D. D. Perrin and V. S. Sharma, *J. Chem. Soc.* (A) 1968, 446; 1969, 2060.
5. R. C. Tewawi and M. N. Srivastava, *J. Inorg. Nucl. Chem.* 1973, **35**, 2441.
6. M. K. Singh and M. N. Srivastava, *J. Inorg. Nucl. Chem.* 1973, **35**, 2433.
7. N. E. Jackobs and D. W. Margerum, *Inorg. Chem.* 1967, **6**, 2038.
8. V. S. Sharma and J. Schubert, *J. Chem. Educ.* 1956, **46**, 506.
9. A. V. Ablov, *Zh. Neorg. Chim.* 1975, **20**, 722.
10. J. Nagypal, A. Georgely and E. Farkas, *J. Inorg. Nucl. Chem.* 1974, **36**, 699.
11. J. Sovago, A. Georgely, B. Harman and T. Kiss, *J. Inorg. Nucl. Chem.* 1979, **41**, 1629.
12. J. W. Chang and R. B. Martin, *J. Phys. Chem.* 1969, **73**, 4277.
13. H. C. Freeman and M. L. Golomb, *Chem. Commun.* 1970, 1523.
14. Y. Sugiura and H. Tanaka, *Chem. Pharm. Bull.* 1970, **18**, 746.
15. F. J. Welcher, *The Analytical Uses of Ethylenediamine Tetraacetic Acid.* Van Nostrand, Amsterdam (1958).
16. D. D. Perrin and I. G. Sayce, *Chem. and Ind.* 1966, 661.
17. G. R. Lenz and A. E. Martell, *Biochemistry* 1964, **3**, 745.
18. K. B. Yatsimirskii, E. E. Kriss and V. L. Gviasdovskaya, *Constanti ustoichivosti metalov s bioligandami.* Naukova Dumka Kiiev (1979).

*Polyhedron* Vol. 3, No. 5, pp. 527–534, 1984
Printed in Great Britain.

0277-5387/84 $3.00 + .00
© 1984 Pergamon Press Ltd.

# ETHYLENEDIAMINE-N,N,N′,N′-TETRAKIS(METHYLENEPHOSPHONIC) ACID AS COMPLEXING AGENT

NEELAM PALTA, B. V. RAO, S. N. DUBEY and D. M. PURI*
Department of Chemistry, Kurukshetra University, Kurukshetra-132119, Haryana, India

(*Received* 20 *June* 1983; *accepted* 15 *August* 1983)

**Abstract**—Metal derivatives of ethylenediamine-N,N,N′,N′-tetrakis(methylenephosphonic) acid (EDTMP, $H_8L$) with some bivalent ions—Mn(II), Co(II), Ni(II), Cu(II), Zn(II), Cd(II) and Pb(II) have been isolated in various stoichiometric ratios from aqueous medium. Electronic spectra indicate them to be six-coordinated. EPR studies of Cu(II) complexes show that they are tetragonally elongated. Magnetic moments of $M_4L$ derivatives are very low due to antiferromagnetic exchange interactions, but the moments go on increasing for $M_3Na_2L$ and $M_2Na_4L$ and are normal for $MNa_6L$ derivatives, due to isolation of paramagnetic centres by diamagnetic sodium ions. IR spectra and thermal stability of the complexes have also been studied.

The structural similarities of ethylene-diaminetetrakis(methylenephosphonic) acid (EDTMP) to ethylenediaminetetraacetic acid (EDTA) has led many research workers to study its complex forming properties.[1–6] The replacement of carboxylic group by organophosphonic acid groups makes it more selective towards cations with an enhanced coordination capacity.[7,8] The specific nature of such chelating agents is due to the presence of tetrahedral phosphonic group as compared to planar carboxylic group and greater polarisability of P–O bond. In the present work, the complexes of EDTMP with some bivalent metal ions in various stoichiometric ratios have been isolated and their structure studied.

## EXPERIMENTAL

The ligand, ethylenediaminetetrakis(methylenephosphonic) acid (EDTMP), was prepared by the method of Dennis and Derek.[9] The thick oily product, so obtained, was crystallised from water giving a white solid. Bivalent metal salts (BDH, Analar) were used as such.

The complexes of 1:1 metal to ligand ratio were prepared by adding 0.002 mole of metal salt solution to 0.002 mole of aqueous solution of the ligand dropwise with constant stirring at room temperature, followed by the addition of 8 $cm^3$ of 2N NaOH. Only in the case of lead, immediate precipitation occurred, whereas for cadmium and cobalt, addition of methanol was required to get good yields of the resulting complexes. Addition of acetone facilitated the precipitation in the case of zinc. With the addition of acetone, nickel and copper complexes separated as coloured liquids, which when vigorously shaken with a glass rod under methanol gave solid products. The solid products in all these cases were washed with 75% acetone until free from $Cl^-$, $CH_3COO^-$ or $SO_4^{2-}$ ions (depending upon the salt used for preparation) and then dried at 50–60°C.

The complexes with 2:1 and 3:1 metal-to-ligand ratio were also prepared by the same method. For isolation of 2:1 complexes of cadmium and copper methanol was added. In the case of nickel, a green liquid separated out after the addition of acetone which was then solidified by adding MeOH with constant grinding.

In 3:1 complexes immediate precipitation occurred after the addition of NaOH solution, but the yield was increased by the addition of acetone or methanol.

For the preparation of 4:1 complexes, 8 $cm^3$ of 2N NaOH were first added to 0.002 moles of ligand which was then added dropwise to 0.008 moles of metal salt solution. Addition of NaOH was essential, as the yields were poor at lower pH. However, once isolated these complexes were insoluble in water and did not melt even up to 250°C.

*Author to whom correspondence should be addressed.

It was observed that manganese did not form 1:1, 2:1 and 3:1 ratio complexes. Only 4:1 complex could be isolated. An attempt to prepare complexes of other molar ratios resulted in solids with much higher percentage of manganese, indicating thereby the greater stability of the 4:1 complex. Similarly, 3:1 complex of nickel, 2:1 and 3:1 complexes of lead and 2:1 complexes of zinc and cobalt could not be isolated in the pure form.

The complexes were stable in air and non-hygroscopic. All the complexes were analysed for the metal and phosphorus by conventional methods.[10,11]

IR spectra in the form of KBr pellets were recorded on Beckman IR-20 spectrophotometer. Diffuse transmittance spectra were run on DMR-21 spectrophotometer in 200–2000 nm region and solution spectra were recorded in 200–2000 nm region on Beckman DU-2 spectrophotometer. The EPR spectra (X-band) were obtained in Varian E-4 spectrophotometer (working frequency 9.5 GHz) at room temperature in the powder form. Magnetic measurements were made on a Gouy balance. Thermal analyses were done on Derivatograph Mom-Budapest, Hungary, Type Paulik–Paulik–Erdey, OD-102. The specimens were heated at the rate of 10°/min in 200–1000° range and heated alumina was used as standard.

## RESULTS AND DISCUSSION

Ethylenediaminetetrakis(methylenephosphonic) acid, being an octabasic acid, could be written as $H_8L$. The elemental analyses showed the general formula of the products to be $M_nNa_{8-2n}L.xH_2O$ where $n = 1, 2, 3$ and 4, when metal salt and ligand are taken in 1:1, 2:1, 3:1 and 4:1 molar ratio respectively (Table 1). The structure of these complexes was studied from IR, electronic spectra, magnetic moment data, ESR spectra and thermal analyses.

### *IR spectra*

The presence of intense absorptions at 1160 $cm^{-1}$ [$\nu_{as}$ ($PO_2$)] and 1050 $cm^{-1}$ [$\nu_s(PO_2)$], corresponding to the vibrations of bonds in the $PO_3H^-$ group, showed the acid to be a zwitterion.[12] In addition to this $\nu_{as}$ P–OH and $\nu_s$ P–OH absorptions corresponding P–$(OH)_2$ were also observed at

Table 1. Analytical and magnetic moment data of EDTMP complexes

| Complex | Colour | Found (Calc.) % M | P | $\mu_{eff}$ (BM) at room temp. |
|---|---|---|---|---|
| $Mn_4L.8H_2O$ | Almost white | 28.82(27.77) | 15.18(15.62) | 2.85 |
| $CoNa_6L.H_2O$ | Purple | 9.19 (9.17) | 19.40(19.29) | 4.52 |
| $Co_3Na_2L.12H_2O$ | Blue-violet | 20.35(20.39) | 14.82(14.27) | 2.83 |
| $Co_4L.8H_2O$ | Blue-violet | 28.67(29.77) | 15.18(15.62) | 2.47 |
| $NiNa_6L.6H_2O$ | Green | 8.12 (8.02) | 15.93(16.07) | 3.43 |
| $Ni_2Na_4L.16H_2O$ | Green | 12.18(12.69) | 13.34(13.36) | 2.39 |
| $Ni_4L.16H_2O$ | Light green | 24.75(24.67) | 12.15(13.01) | 1.72 |
| $CuNa_6L.6H_2O$ | Deep blue | 8.26(8.61) | 16.64(16.77) | 2.12 |
| $Cu_2Na_4L.2H_2O$ | Deep blue | 18.92(18.61) | 18.20(18.11) | 1.48 |
| $Cu_3Na_2L.6H_2O$ | Blue | 24.92(24.67) | 15.18(16.01) | 1.19 |
| $Cu_4L.12H_2O$ | Blue | 28.25(28.29) | 13.85(13.77) | 1.01 |
| $ZnNa_6L.H_2O$ | White | 10.25(10.07) | 19.32(19.11) | - |
| $Zn_3Na_2L.6H_2O$ | White | 26.90(25.75) | 15.81(15.89) | - |
| $Zn_4L.10H_2O$ | White | 29.55(30.09) | 14.04(14.23) | - |
| $CdNa_6L.4H_2O$ | White | 14.65(14.95) | 16.34(16.48) | - |
| $Cd_2Na_4L.4H_2O$ | White | 28.76(27.54) | 15.03(15.14) | - |
| $Cd_3Na_2L.3H_2O$ | White | 40.30(38.99) | 13.62(14.29) | - |
| $Cd_4L.8H_2O$ | White | 43.09(44.02) | 12.65(12.10) | - |
| $PbNa_6L.H_2O$ | White | 26.40(26.20) | 15.44(15.68) | - |
| $Pb_4L.2H_2O$ | White | 65.38(64.13) | 9.60(9.59) | - |

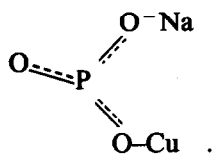
Table 2. Principal bands ($cm^{-1}$) in the IR spectra of EDTMP and its copper derivatives

| EDTMP | $CuNa_6L.6H_2O$ | $Cu_2Na_4L.2H_2O$ | $Cu_3Na_2L.6H_2O$ | $Cu_4L.12H_2O$ | Assignments |
|---|---|---|---|---|---|
| 3400 | 3440 br | 3400 br | 3400 br | 3370 br | $\nu$(O-H) |
| 2960 | - | - | - | - | $\nu(\overset{+}{N}\text{-H})$ |
| 1610 | 1650 | 1640 | 1630 | 1630 | $\delta(\overset{+}{N}\text{-H})$, $\delta$(O-H) |
| 1570 | - | - | - | - | $\delta(\overset{+}{N}\text{-H})$ |
| 1430 | 1470<br>1445<br>1400 | 1460<br>1430 | 1460<br>1420 | 1460<br>1430 | $\nu$(C-N), $\delta$(C-H) |
| 1320 | 1295<br>1265 | 1315<br>1285 | 1315<br>1285 | 1315<br>1290 | $\delta$(O-H) |
| 1200 | 1200<br>1140 | 1110 | 1100 | 1100 | $\nu$(P=O) |
| 1160 | - | - | - | - | $\nu_{as}(PO_2)$ |
| 1050 | - | - | - | - | $\nu_{s}(PO_2)$ |
| | 1115<br>1060<br>1030 | 1070<br>1055 | 1060br | 1065 | $\nu_{as}$ $(PO_3)$ |
| 1030 | - | - | - | - | $\nu_{as}$P-$(OH)_2$ |
| | 980 sh<br>920<br>880 sh | 980<br>920 Sh | 990<br>920 sh | 980 | $\nu_{s}(PO_3)$ |
| 920 | - | - | - | - | $\nu_{s}$ P-$(OH)_2$ |
| 750 | 765 | 770 | 770 | 770 | $\nu$(P-C), $\delta$ (C-CH), $\delta$ (OPO) |
| | 640 | 640 | 640 | 640 | |

1030 and 920 $cm^{-1}$.[13] The characteristic stretching mode of phosphoryl group appeared at 1200 $cm^{-1}$. $N^+$–H showed absorption due to stretching vibrations at 2960 $cm^{-1}$, and at 1610 and 1570 $cm^{-1}$ due to bending vibrations.[14] The corresponding increase in absorptions of $\nu$(C–H) and $\nu$(C–N) have been pointed out by Dyatlova *et al.*[13] but could not be observed in this case probably due to the weakness of bands in this region.

The IR spectra of all the complexes with the same general formula are quite similar and hence only the spectra of various copper complexes is discussed here (Table 2).

In the IR spectrum of $CuNa_6L{\cdot}6H_2O$, the $\nu$(P=O) band split into two with maxima at 1200 and 1140 $cm^{-1}$. This may probably be due to the fact that all the phosphoryl groups do not coordinate to the central metal ion. Appearance of large number of bands in the regions of absorption of $\nu_{as}(PO_3)$ and $\nu_s(PO_3)$ further indicated the presence of more than one type of such groups. The band at 1115 $cm^{-1}$ was assigned to asymmetric stretching of fully ionised $PO_3^{2-}$ group and a doublet with maxima at 1060 and 1030 $cm^{-1}$ to the coordinated phosphonic group. The splitting of the latter band could be due to non-symmetric coordination




Almost same intensity of these bands further indicated the presence of equal number of these groups. In the region of symmetric stretching of $PO_3$ group, the main band at 920 $cm^{-1}$ had shoulders at 980 $cm^{-1}$ and 880 $cm^{-1}$.

In $Cu_2Na_4L{\cdot}2H_2O$, unsplit $\nu$(P=O) band was observed at 1110 $cm^{-1}$. Such a large shift in the position of the band could be due to the formation of the coordination bond with the central metal ion.[15] In $\nu_{as}(PO_3)$ band only a small split of 10 $cm^{-1}$ was observed and may be due to unsymmetric coordination of phosphonic group. From IR spectra there appeared to be only one type of phosphonic group. The symmetric stretching vibration

$\nu_s(PO_3)$ was found at 980 $cm^{-1}$ with a shoulder at 920 $cm^{-1}$.

The IR spectrum of $Cu_3Na_2L{\cdot}6H_2O$ was characterized by an intense band at 1100 $cm^{-1}$ which could be assigned to stretching vibrations of coordinated P=O bond. There is a single broad band in the region of $\nu_{as}(PO_3)$ at 1060 $cm^{-1}$ and $\nu_s(PO_3)$ band at 980 $cm^{-1}$ showed a shoulder at 920 $cm^{-1}$.

In the case of $Cu_4L{\cdot}12H_2O$, the bands at 1065 $cm^{-1}$ and 980 $cm^{-1}$ have been assigned to $\nu_{as}(PO_3)$ and $\nu_s(PO_3)$ respectively. There was no splitting in either of the bands. This may be expected, since all the acidic hydrogens have been replaced by copper ions and thus phosphonic groups coordinated symmetrically. The characteristic band of coordinated P=O bond appeared at 1110 $cm^{-1}$. The $\nu$(O–H) shifted to lower frequency by another $\sim$70 $cm^{-1}$ as compared to $\nu$(OH) band at 3440 $cm^{-1}$ in $CuNa_6L{\cdot}6H_2O$ which is an evidence of $H_2O$ being coordinated to metal ion.

*Electronic spectra and magnetic moments*

Except $CuNa_6L{\cdot}6H_2O$, $NiNa_6L{\cdot}6H_2O$, $Ni_2Na_4L{\cdot}16H_2O$ and $CoNa_6L{\cdot}H_2O$, all other metal derivatives of EDTMP are insoluble in water as well as other common organic solvents. Therefore, the electronic absorption spectra were recorded as diffuse transmittance spectra. However, for $CuNa_6L{\cdot}6H_2O$, $NiNa_6L{\cdot}6H_2O$, $Ni_2Na_4L{\cdot}16H_2O$ and $CoNa_6L{\cdot}H_2O$ solution spectra in 200–1000 nm range have also been recorded, since they are soluble in water.

*Manganese(II) derivatives.* The colour of the complex $Mn_4L{\cdot}8H_2O$ being almost white, the electronic spectra showed no clear band. The magnetic moment of the complex was found to be 2.85 BM at room temperature, whereas for both tetrahedral and octahedral complexes of manganese(II), the expected range for dilute systems is 5.65–6.10 BM.[16] This low value of magnetic moment indicates the presence of interaction between manganese ions, resulting in antiferromagnetic exchange.

*Cobalt(II) derivatives.* In solution spectra, $CoNa_6L{\cdot}H_2O$ showed an intense band at 19,230 $nm^{-1}$ ($\epsilon$ = 101 l $cm^{-1}$ $mole^{-1}$) and a weak band at 15,630 $cm^{-1}$ ($\epsilon$ = 10 l $cm^{-1}$ $mole^{-1}$). The intensity of the bands clearly indicated it to be a six coordinate complex. The enhancement in the intensity of band at 19,230 $cm^{-1}$ may be due to distorted form of regular octahedral structure.[17] In diffuse transmittance spectra, three main bands are observed at 19,420, 15,630 and 7360 $cm^{-1}$ and the following assignments have been made in accordance with the reported literature.[18–20]

7360 $cm^{-1}$ $^4T_{2g}(F) \leftarrow {}^4T_{1g}(F)$ ($\nu_1$)

15,630 $cm^{-1}$ $4A_{2g}(F) \leftarrow 4T_{1g}(F)$ ($\nu_2$)

19,420 $cm^{-1}$ $^4T_{1g}(P) \leftarrow {}^4T_{1g}(F)$ ($\nu_3$).

The visible band at 19,420 $cm^{-1}$ is asymmetric in nature with shoulders both at low and high energy side, i.e. at 17,540 and 21,510 $cm^{-1}$. These could be assigned to spin-forbidden transitions. The crystal field stabilization energy for the complex was found to be 8110 $cm^{-1}$ and Racah parameter in the complex ion (863 $cm^{-1}$) is reduced to about 95% of the free ion value for $Co^{+2}$ (1120 $cm^{-1}$).[21]

The magnetic moment, 5.20 BM, is well within the range (4.30–5.20 BM)[16] for $sp^3d^2$ spin free complexes. This showed that the system is magnetically dilute and there is no interaction between neighbouring cobalt ions.

In the case of $Co_3Na_2L{\cdot}12H_2O$ bands are observed in the same region (7200, 15,380, 17,700 (sh) and 19,050 $cm^{-1}$) and indicate the cobalt ion to be six coordinated. The magnetic moment 2.93 BM indicates the presence of appreciable Co–Co interaction.

With the increasing number of paramagnetic centres per molecule in $Co_4L{\cdot}8H_2O$, metal–metal interaction seemed to become stronger and $\mu_{eff}$ value further decreased to 2.43 BM. The position of absorption bands (7560, 16,000; 17,390 (sh) and 19,050 $cm^{-1}$) does not differ much from $CoNa_6L{\cdot}H_2O$ and $Co_3Na_2L{\cdot}12H_2O$ which implied that the crystal field environments remained practically the same.

*Nickel(II) derivatives.* $NiNa_6L{\cdot}6H_2O$ showed one band in the near IR region at 9520 $cm^{-1}$ and was assigned to $^3T_{2g}(F) \leftarrow {}^3A_{2g}(F)$ ($\nu_1$) transition. In the visible region, two bands at 16,260 and 26,670 $cm^{-1}$ were observed corresponding to the transitions $^3T_{1g}(F) \leftarrow {}^3A_{2g}(F)$ ($\nu_2$) and $^3T_{1g}(P) \leftarrow {}^3A_{2g}(F)$($\nu_3$) respectively. A shoulder at 21,280 $cm^{-1}$ also appeared which could be attributed to the lower symmetry.[22] In the solution spectra, the visible bands shifted to 24,390 (= 14.23 l $cm^{-1}$ $mole^{-1}$) and 15,150 ($\epsilon$ = 6.71 l $cm^{-1}$ $mole^{-1}$). There is a reduction of about 24% of the free ion value (1040 $cm^{-1}$) for the inter-electronic repulsion parameter upon incorporation of the ion into the complex ($B$ = 793.3 $cm^{-1}$). The crystal field stabilization energy was found to be 9524 $cm^{-1}$.

The magnetic moment of this complex 3.43 BM at room temperature further confirmed the existence of six-coordinated species.[16]

In $Ni_2Na_4L{\cdot}16H_2O$ also, all the three spin allowed transitions were observed at 9090, 15,380 and 26,670 $cm^{-1}$ and also a shoulder at

21,280 $cm^{-1}$. In the solution spectra $\nu_2$ and $\nu_3$ bands are observed at 14,930 and 25,000 $cm^{-1}$ respectively. The magnitude of $B$ derived from the spectra was 757 $cm^{-1}$ and the value of 10 Dq as 9090 $cm^{-1}$. The magnetic moment at room temperature 2.39 BM in this case is somewhat lower than the spin only value and suggests that a spin coupling may be operating.

The antiferromagnetic exchange seemed to be much more pronounced in $Ni_4L{\cdot}16H_2O$ from observed magnetic moment 1.72 BM at room temperature. The electronic spectra for this complex showed bands at 9090, 14,930 and 19,530 (sh) and 25,970 $cm^{-1}$.

*Copper(II) derivatives.* Electronic spectra of $CuNa_6L{\cdot}6H_2O$ in water showed a sharp band at 31,650 $cm^{-1}$ having 2378.41 $cm^{-1}$ $mole^{-1}$ molar extinction coefficient. From the intensity of band, it could be suggested that it is charge transfer in nature. In the visible region, a band observed at 13,330 $cm^{-1}$ (120.51 $cm^{-1}$ $mole^{-1}$) with three more components at 15,630, 11,360 and 9260 $cm^{-1}$ is typical of a six coordinated species, visible band being attributed to $^2T_{2g} \leftarrow {}^2E_g$ transition.

The EPR spectra of the copper complex indicated it to be elongated along the Z axis, since $g_\parallel > g_\perp > 2$ ($g_\parallel = 2.22$, $g_\perp = 2.043$). This would stabilize the $dz^2$ orbital leaving the unpaired electron in $dx^2$–$y^2$ orbital. Thus components of the visible band in electronic spectra may be assigned as transitions from the $d_{xy}$, $d_{z^2}$ and $d_{xz}$, $d_{yz}$ pair to the $\sigma$-antibonding and half filled $d_{x^2-y^2}$ level.[22] The relative order of these transitions depends upon the extent of axial metal–ligand interaction. The splitting of the band at 13,330 by ~200 $cm^{-1}$ may be because of the actual site symmetry being still lower.

With the magnetic moment of the complex being 2.12 BM (normal $\mu_{eff}$ range 1.73–2.20 BM) absence of metal–metal exchange interactions could be inferred.

$Cu_2Na_4L{\cdot}2H_2O$ showed a band at 32,260 $cm^{-1}$ and a single broad band in the visible region at 13,330 $cm^{-1}$. Similar spectra have also been observed in case of $Cu_3Na_2L{\cdot}6H_2O$ and $Cu_4L{\cdot}12H_2O$ with their bands at 32,260; 13,330 and 30,770; 13,330 respectively.

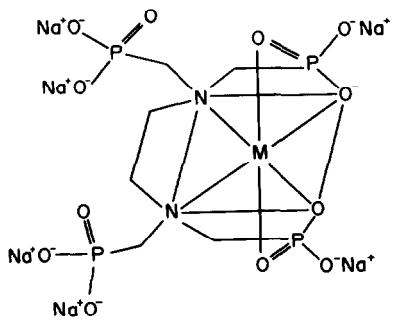
The EPR spectra indicated $Cu_2Na_4L{\cdot}2H_2O$ and $Cu_3Na_2L{\cdot}6H_2O$ also to be tetragonally elongated having the following $g$ values:

| | $g_\parallel$ | $g_\perp$ |
|---|---|---|
| $Cu_2Na_4L{\cdot}2H_2O$ | 2.22 | 2.04 |
| $Cu_3Na_2L{\cdot}6H_2O$ | 2.22 | 2.07 |

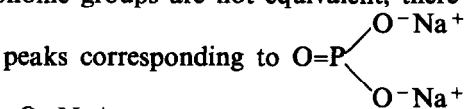
The EPR spectrum of $Cu_4L{\cdot}12H_2O$ was not so simple. The splitting in this may perhaps be due to dipole dipole interaction between copper ions.

The trend in the values of magnetic moments continued to be the same as for other metals. $Cu_2Na_4L{\cdot}2H_2O$ has $\mu_{eff}$ 1.48 BM which showed that in binuclear species metal ions do interact. 1.19 BM and 1.01 BM values for $Cu_3Na_2L{\cdot}6H_2O$ and $Cu_4L{\cdot}12H_2O$ respectively showed the increasing anti-ferromagnetic exchange interactions with the increase in number of metal ions per molecule.

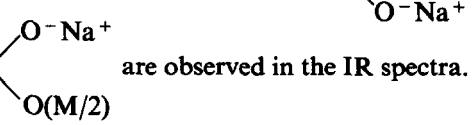
From electronic spectral data, the metal ion seems to be six coordinated in all the complexes. Using this information along with the IR data, the following structure may be proposed for complexes with formula $MNa_6L.xH_2O$. In this case, coordination of both the nitrogen atoms to the same metal ion has been suggested: similar to 1:1 complexes of EDTA. This structure explained the split




in $\nu$(P=O) band as all the phosphoryl oxygens are not engaged in coordination to the metal ion. All the phosphonic groups are not equivalent, therefore two peaks corresponding to




and




are observed in the IR spectra.

The absence of polymeric chains is indicated from their general solubility in water and normal magnetic moments.

For $M_2Na_4L{\cdot}xH_2O$ complexes, it is suggested that the two nitrogen atoms coordinate to different metal ions and are probably arranged in a trans-manner due to steric factors. In the cis-form, the negatively charged phosphonic ions come very close and repulsion between them could make it less stable. Martell *et al.*[23] have also explained the stability constants on this basis.

Polymeric structure for $M_3Na_2L$ and $M_4L$ complexes could be suggested through coordinated phosphoryl groups. The abnormal magnetic mo-

ments arise from an exchange interaction which tends to align the magnetic moments of neighbouring atoms antiparallel. The antiferromagnetism of $M_4L$ complexes, due to the interaction between metal ions operates throughout the polymeric structures. With the replacement of M by diamagnetic sodium ions, the interactions are weakened and magnetic moments increase so that $MNa_6L$ has normal value. Diamagnetic metal ions magnetically isolate the central metal ions. Such isolation has been proved in case of calcium tetraacetatocuperate.[24]

*Thermal analyses*

Thermal analyses of $NiNa_6L{\cdot}6H_2O$ and $Cu_2Na_4L{\cdot}2H_2O$ compounds have been carried out. As is obvious from thermogram of $NiNa_6L{\cdot}6H_2O$ (Fig. 1) five molecules of water were lost in two clear steps. The first step has been shown on the differential mass loss curve between 60–100°C with an endothermic effect at 80°C corresponding to loss of two molecules of water. (Theoretical loss in mass 4.8%, observed loss in mass 4.9%.) The next three molecules of water lost slowly up to 250°C (theoretical mass loss 12.15%, obs. 11.90%). The minimum of endothermic peak corresponding to this loss was observed at 220°C. The loss of sixth molecule is not indicated through a clear step in mass loss curve but DTA curve has an inflexion at 270°C and mass loss of another 2.4% is observed. The anhydrous complex is unstable, as is shown by the absence of a horizontal part on the TG curve.

The second stage of thermolysis of the complex is very rapid with exothermic decomposition of the specimen and a sudden mass loss of 11.00%. The decomposition of anhydrous complex began at about 340°C and is characterized by exothermic peaks concentrated at 470° and 540°C and proceeded in steps at different rates. The total mass loss in the process of thermal decomposition is 39%.

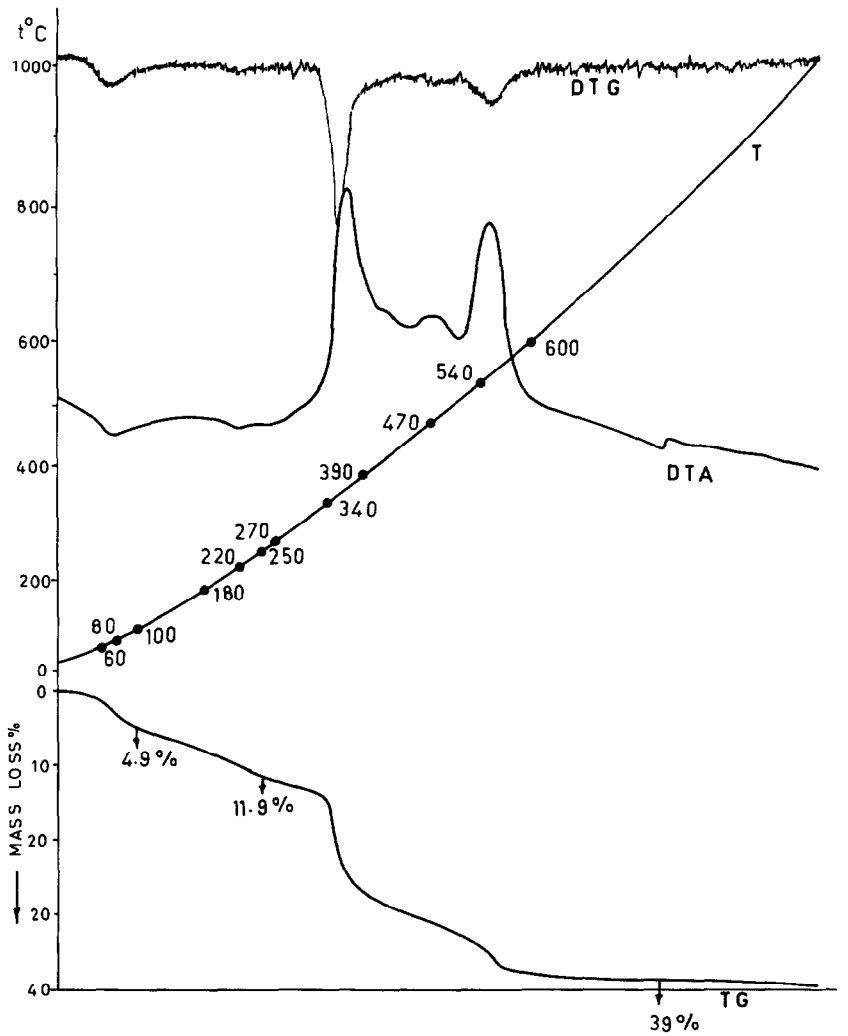



Fig. 1. Derivatogram of $NiNa_6L{\cdot}6H_2O$ (100 mg specimen).

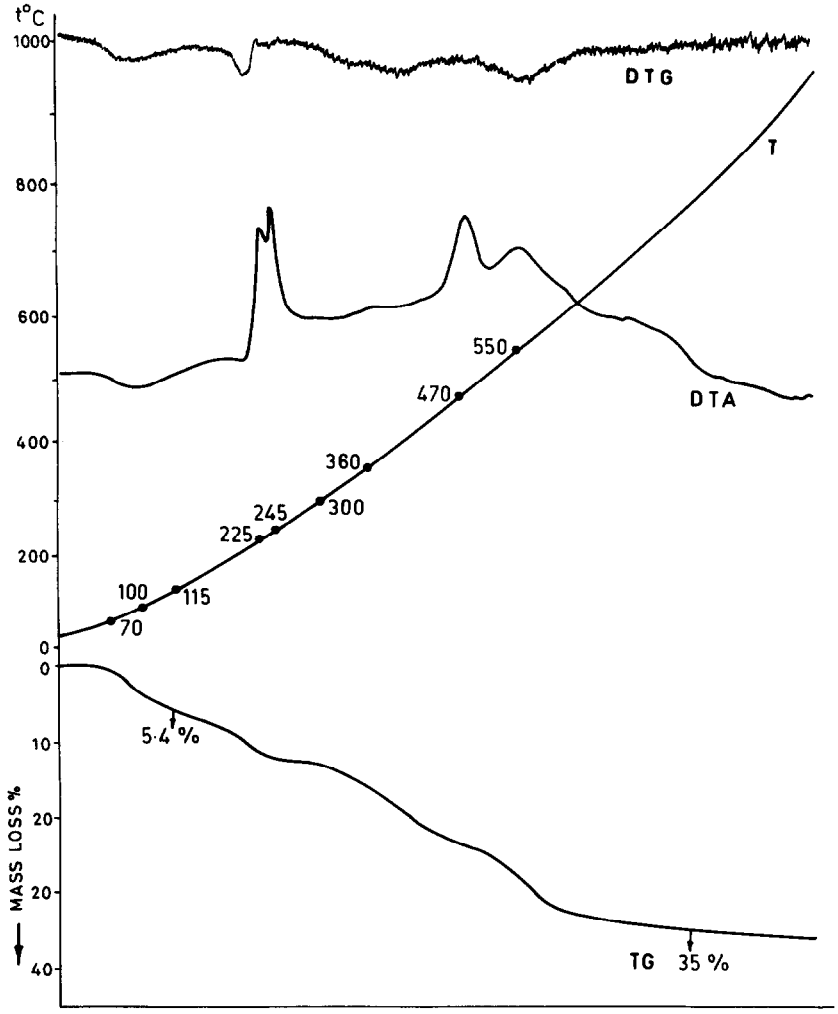



Fig. 2. Derivatogram of $Cu_2Na_4L{\cdot}2H_2O$ (100 mg specimen)

Figure 2 shows the thermal decomposition of $Cu_2Na_4L{\cdot}2H_2O$. Two molecules of water are lost in the temperature range 70–115°C. The dehydration takes place in a single step with a mass loss of 5.4% (theoretical 5.3%). The corresponding endothermic peak has a minima at 100°C. In this complex, the mass loss curve is difficult to divide into definite stages, and only at 250°C can a small horizontal section be distinguished. In the initial part of the DTG–DTA curves, two mass loss stages are observed to which correspond exothermic effects at 225 and 245°C and subsequently there are three stages of mass loss with exothermic effects at 360, 470 and 550°C. The complex suffered a total mass loss of 35%.

*Acknowledgements*—We are thankful to Prof. V. Yatirajam, Chairman of the Department for laboratory facilities and one of us (BVR) is thankful to INSA (New Delhi) for financial assistance.

## REFERENCES

1. S. Westerback, K. S. Rajan and A. E. Martell, *J. Am. Chem. Soc.* 1965, **87**, 2567.
2. M. Dyatlova, T. Ya. Medved, Yu. F. Belugin and V. V. Sidorenko, *Dokl. Akad. Nauk SSR* 1967, **175**, 351.
3. L. I. Tikhonova, *Radiokhimya* 1970, **12**(3), 519.
4. R. I. Motekaitis, Ichiro Murase and A. E. Martell, *Inorg. Chem.* 1976, **15**, 2303.
5. E. N. Rizkalla and M. T. M. Zaki, *Talanta* 1979, **26**, 507.
6. L. V. Ruzaikina, V. A. Ryabukhin, A. N. Ermakov, I. N. Marov, L. S. Davydova and E. B. Krutka, *Russ. J. Inorg. Chem.* 1980, **25**, 1783.
7. M. I. Kabachnik, T. Ya. Medved, N. M. Dyatlova, O. G. Arkhipova and M. V. Rudomino, *Russ. Chem. Rev.* 1968, **37**, 503.
8. M. I. Kabachnik, T. Ya. Medved, N. M. Dyatlova and M. V. Rudomino, *Russ. Chem. Rev.* 1974, **43**, 733.
9. Dennis R. Peck and Derek Hudson, *Chem. Abstr.* 1969, **70**, 106650x.
10. A. I. Vogel, *A Text Book of Quantitative Inorganic Analysis*, (1961) Longmans, London.

11. Laszlo Erdey, *Gravimetric Analysis*, Part II. Pergamon Press, Oxford (1965).
12. B. V. Zhadanov and N. M. Dyatlova, *Russ. J. Phys. Chem.* 1969, **43**, 406.
13. A. Yu. Kireeva, N. F. Shugal and N. M. Dyatlova, *Russ. J. Inorg. Chem.* 1973, **18**, 1426.
14. J. R. Dyer, *Applications of Absorption Spectroscopy of Organic Compounds*. Prentice-Hall, New Jersey (1978).
15. V. P. Khramov and A. A. Koltsov, *Russ. J. Inorg. Chem.* 1973, **18**, 1567.
16. J. Lewis and R. G. Wilkins, *Modern Coordination Chemistry*. Interscience, New York (1967).
17. A. B. P. Lever, *Inorg. Chem.* 1965, **4**, 1042.
18. J. Ferguson, D. L. Wood and K. Knox, *J. Chem. Phys.* 1963, **39**, 881.
19. R. W. Kiser and T. W. Lapp, *Inorg. Chem.* 1962, **1**, 401.
20. A. Ludi and W. Feitknecht, *Helv. Chim. Acta* 1963, **46**, 2226.
21. B. N. Figgis, *Introduction of Ligand Fields*. Wiley, New York (1976).
22. A. B. P. Lever, *Inorganic Electronic Spectroscopy*. Elsevier, Amsterdam (1968).
23. S. Westerback, K. S. Rajan and A. E. Martell, *J. Am. Chem. Soc.* 1965, **87**, 2589.
24. G. A. Barclay and A. Cooper, *J. Chem. Soc.* 1965, 3746.

*Polyhedron* Vol. 3, No. 5, pp. 535–544, 1984
Printed in Great Britain.

0277–5387/84 $3.00 + .00
© 1984 Pergamon Press Ltd.

# THE FORMATION AND STRUCTURAL CHEMISTRY OF THE HEXA($\mu$-*t*-BUTYLTHIOLATO) PENTACUPRATE(I) CAGE ANION WITH TRIETHYLAMMONIUM AND TETRAETHYLAMMONIUM CATIONS

**GRAHAM A. BOWMAKER, GEORGE R. CLARK* and JEFFREY K. SEADON**
Department of Chemistry, University of Auckland, Auckland, New Zealand

and

**IAN G. DANCE**
School of Chemistry, University of New South Wales, Kensington, NSW 2033, Australia

(*Received* 28 *June* 1983; *accepted* 2 *August* 1983)

**Abstract**—Yellow $(Et_4N)[Cu_5(SBu^t)_6]$ crystallises from solutions prepared from Cu(II), Bu$^t$SH, $Et_3N$ and $Et_4NBr$ in acetone/ethanol, while $(Et_3NH)[Cu_5(SBu^t)_6]$ crystallises from solutions of CuSBu$^t$ and Bu$^t$SH in $Et_3N$. Crystal structure determinations reveal that both compounds contain the molecular cage $[Cu_5(\mu\text{-}SBu^t)_6]^-$, in which two copper atoms are three-coordinate ($Cu_{trig}$), three copper atoms are two-coordinate ($Cu_{dig}$), and all thiolate ligands are doubly-bridging. The polyhedral stereochemistry of the core is *trigonal bipyramido*-$Cu_5$-*trigonal antiprismo*-$S_6$. The complete $[Cu_5(\mu\text{-}SBu^t)_6]^-$ cage in the $Et_4N^+$ compound closely approaches $D_3$ symmetry, but in the $Et_3NH^+$ compound one SBu$^t$ ligand is inverted at the sulphur bridge, causing angular distortions in the cage.

Two structural features, the antiprismatic twist of the $S_6$ polyhedron and the bending of $Cu_{dig}$ towards the cage centroid (S–$Cu_{dig}$–S = 171(1)°), provide evidence for weak Cu-Cu attractive interactions within the cage. Infrared data are discussed. Crystal data: $(Et_4N)[Cu_5(SBu^t)_6]$, $C_{32}H_{74}Cu_5NS_6$, $a = 45.500$ (3), $b = 11.805(1)$, $c = 20.168(2)$ Å, $\beta = 117.81$ (1)°, $C2/c$, $Z = 8$, $R = 0.078$ (2953 observed $F$); $(Et_3NH)[Cu_5(SBu^t)_6]$, $C_{30}H_{70}Cu_5NS_6$, $a = 10.519(1)$, $b = 21.457(1)$, $c = 20.065(1)$, $\beta = 95.11(1)$, $P2_1/c$, $Z = 4$, $R = 0.072$ (3093 observed $F$). $(Et_4N)[Ag_5(SBu^t)_6]$ is isostructural with $(Et_4N)[Cu_5(SBu^t)_6]$.

Although binary metal thiolates $M(SR)_n$ have been long known,[1] it is only in recent years that significant advances have been made in the synthetic and structural chemistry of homoleptic metal thiolate complexes.[2] Newly discovered structures for copper(I) and silver(I) include the molecular cages $[M_4(SR)_6]^{2-}$,[3,4] $[M_5(SR)_6]^-$,[5,6] $[M_5(SR)_7]^{2-}$,[7] and $[Ag_6(SR)_8]_p^{2p-}$, $p = 1, 2$,[8] and the molecular cycle $(AgSR)_{12}$.[9,10] A one-dimensionally non-molecular structure has been confirmed in only one compound, $AgSC(CH_3)_2CH(CH_3)_2$.[10]

This paper deals with the $[M_5(SBu^t)_6]^-$ cage, M = Cu, Ag, providing previously unreported synthesis information, and giving full details and analysis of the cage structure and stereochemistry.

## RESULTS

*Synthesis.* The yellow compounds $(Et_4N)[M_5(SBu^t)_6]$, M = Cu, Ag, crystallise from solutions prepared by dissolution of the metal(I) oxide in solutions containing Bu$^t$SH, Bu$^t$S$^-$, and $Et_4N^+$.[6] The copper compound can also be prepared by reaction of copper(II) nitrate in ethanol with excess of an acetone solution of Bu$^t$SH and equimolar tertiary amine, and crystallised by addition of $Et_4N^+Br^-$. At room temperature the reduction of

*Author to whom correspondence should be addressed.

copper(II) to copper(I) by excess thiolate occurs in less than one second, and there is no evidence that solutions containing $Bu^tS^-$-Cu(I) complexes are not at equilibrium. Although it is expected that a range of anionic complexes $[Cu_x(SBu^t)_y]^{x-y}(y > x)$ may exist in solution, the only crystalline compounds isolated so far are those containing the $[Cu_5(SBu^t)_6]^-$ ion. Solutions from which $(Et_4N)[Cu_5(SBu^t)_6]$ has been crystallised in yield > 50% have possessed a $Bu^tS^-$/Cu(I) molar ratio of *ca.* 2. Acetone solutions in which this ratio is much higher (> 10) are more intensely yellow, and probably contain higher proportions of species such as $[Cu(SBu^t)_2]^-$, $[Cu(SBu^t)_3]^{2-}$. When this ratio is < *ca.* 1.8 (depending on solvent) $CuSBu^t$ crystallises. The presence of halide ion in solution has not interfered with the crystallisation of $(Et_4N)[Cu_5(SBu^t)_6]$.

The compound $(Et_3NH)[Cu_5(SBu^t)_6]$ was obtained during experiments aimed at preparing crystals of $CuSBu^t$ suitable for X-ray diffraction studies. It was found that $CuSBu^t$ could be dissolved in $Et_3N$ containing a small amount of $Bu^tSH$. While it is clear that the solubility is probably due to complexation of $CuSBu^t$ by $Bu^tS^-$ produced by deprotonation of the thiol, elemental analysis of the product which crystallised from such solutions was not consistent with its formulation as an $Et_3NH^+$ salt of an anionic $[Cu_x(SBu^t)_y]^{x-y}$ complex, and seemed to suggest that it was an adduct of $Et_3N$ with $CuSBu^t$. The IR spectrum showed only a very weak band at 2380 $cm^{-1}$ in the region expected for $\nu$(NH) of $Et_3NH^+$. The $^1H$ NMR spectrum of the compound dissolved in $[D_5]$ pyridine showed no signal which could be assigned to an NH proton, but the integrals of the signals assigned to the *t*-butyl and ethyl protons (see Experimental) yielded a value of $2.0 \pm 0.1$ for the number of *t*-butyl groups per ethyl group. This is consistent with the formula $(Et_3NH)[Cu_5(SBu^t)_6]$ found for this compound from the crystal structure analysis (see below).

*Crystal and molecular structures.* The molecular cage anion $[Cu_5(SBu^t)_6]^-$ (see Figs. 1 and 2) occurs in crystals with $Et_4N^+$ and with $Et_3NH^+$, and the molecular cage anion $[Ag_5(SBu^t)_6]^-$ occurs in $(Et_4N)[Ag_5(SBu^t)_6]$ which is isostructural with the copper analogue. There is no structural evidence for cation-anion association, nor for the inter-anion M–S secondary bonding which is known in some related silver–thiolate compounds.[8,9] The lattice packing of $(Et_3NH)[Cu_5(SBu^t)_6]$ is shown in Fig. 3.

In both $[Cu_5(SBu^t)_6]^-$ compounds the $Cu_5S_6$ core of the cage may be described as a trigonal bipyramid of metal atoms, each axial-equatorial edge of which is bridged by a thiolate sulphur atom (see Fig. 3). The equatorial–equatorial edges of the trigonal bipyramid are not bridged by sulphur atoms, and so the equatorial metal atoms are only two-coordinate, whereas the axial metal atoms are trigonally coordinated. Therefore the axial and equatorial copper atoms willl be denoted as $Cu_{trig}$ and $Cu_{dig}$ respectively. The sulphur atoms of the six doubly-bridging thiolate ligands are located at the vertices of a trigonal antiprism. Accordingly, the cage structure is best described in terms of the interpenetrating metal and sulphur polyhedra,[2] as *trigonal bipyramido*-$Cu_5$-*trigonal antiprismo*-$S_6$. It should be noted that the $S_6$ polyhedron does not approximate an octahedron.

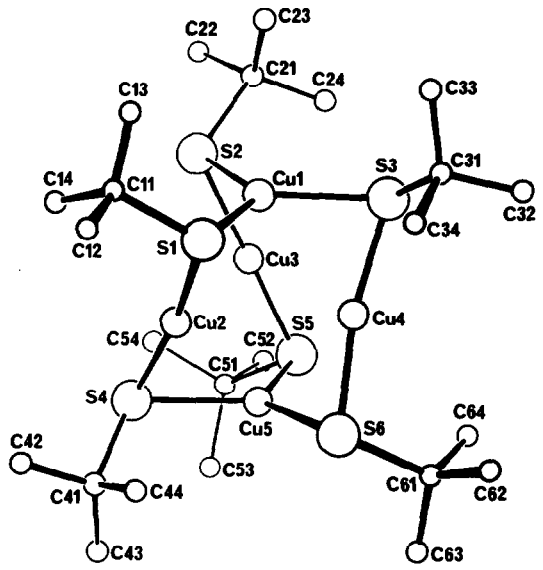



Fig. 1. The $[Cu_5(\mu\text{-}SBu^t)_6]^-$ molecular cage (excluding hydrogen atoms) in $(Et_4N)[Cu_5(SBu^t)_6]$: carbon atoms are presented as arbitrary spheres.

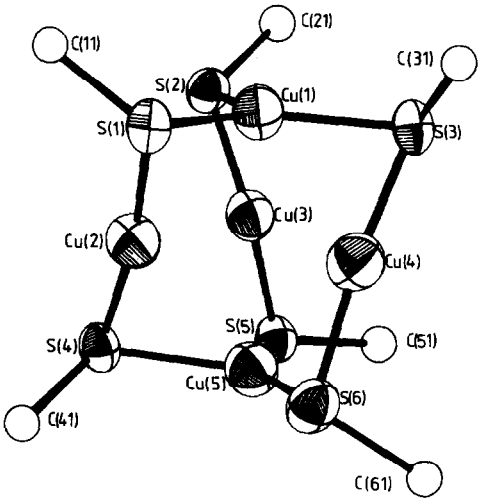



Fig. 2. The $[Cu_5(\mu\text{-}SBu^t)_6]^-$ molecular cage (excluding methyl groups) in $(Et_3NH)[Cu_5(SBu^t)_6]$.

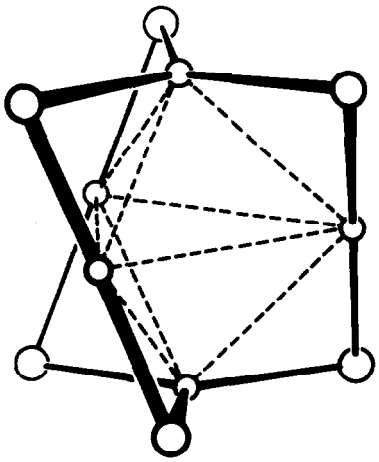


Fig. 3. The *trigonal-bipyramido*-$M_5$-*trigonal-antiprismo*-$S_6$ core of $[Cu_5(SBu^t)_6]^-$.

Although the essential cage structure and atom connectivity in the anion is the same in both the $Et_4N^+$ and $Et_3NH^+$ compounds of $[Cu_5(SBu^t)_6]^-$, some differences occur in the *t*-butyl substituents, the pseudosymmetry of the cage, and in geometric details. The cage in the $Et_4N^+$ compound has the higher pseudosymmetry, which is approximately that of point group $D_3$, and therefore presentation of the stereochemistry and geometrical details of both compounds will be made with reference to the $D_3$ idealisation. One atom labelling scheme is used for both compounds, as defined in Figs. 1 and 2, and consistent atom labelling is adopted for the carbon atoms of all Bu$^t$ groups with respect to rotamerism about the S–C bonds, as defined in Fig. 4. Selected intramolecular distances and angles are presented in Table 1.

The $Et_4N^+$ crystal is slightly distorted, to the extent that 12% of the anionic cage sites are occupied by a similar cage which is approximately the enantiomer of the predominant cage. The positions of the copper and sulphur atoms in the alternative cage have been refined (see Experimental section) and the core dimensions are included in Table 1. Figure 5 compares pseudo-threefold views of the three cages in the two crystals.

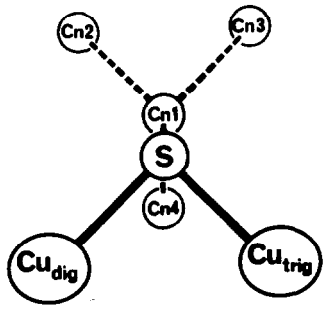



Fig. 4. Definition of the SBu$^t$ atom labelling scheme in terms of the projection along the S–C bond.

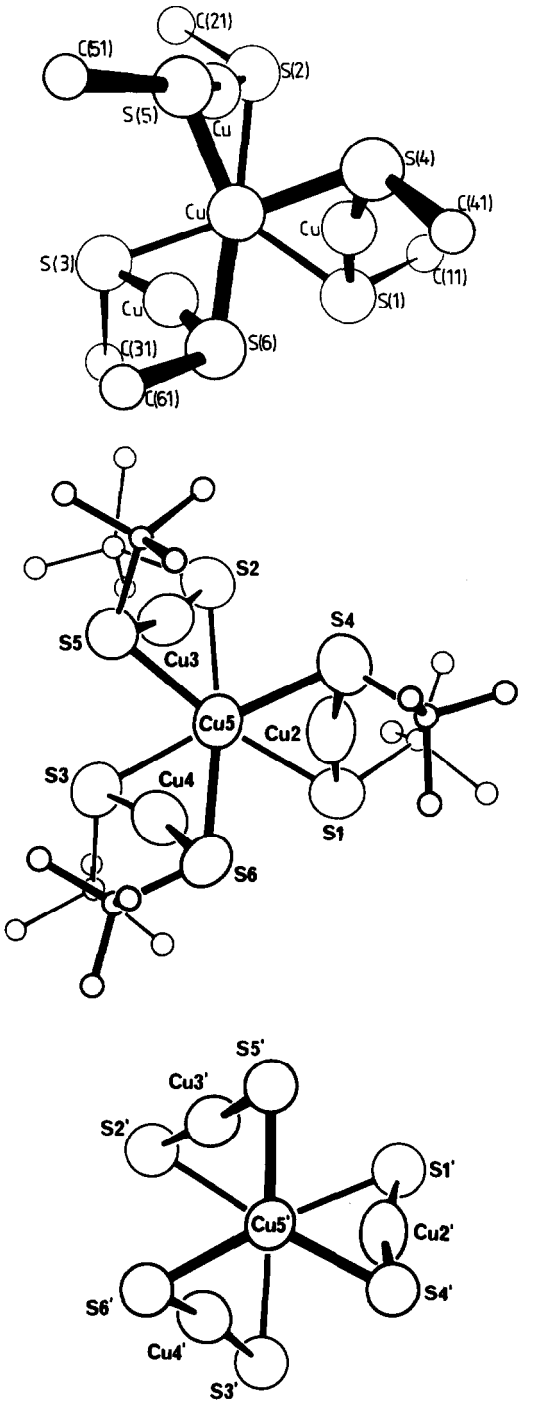



Fig. 5. Pseudo-threefold views of the $[Cu_5(SBu^t)_6]^-$ molecular cages: (a) in the $Et_3NH^+$ compound (excluding methyl groups); (b) the predominant cage of the $Et_4N^+$ compound; (c) the less abundant cage of the $Et_4N^+$ compound ($Cu_5S_6$ only). The cages in (b) and (c) populate virtually the same locations with the same pseudo-threefold axis.

The close approach to $D_3$ symmetry by the $[Cu_5(SBu^t)_6]^-$ cage in the $Et_4N^+$ compound is

Table 1. Selected intramolecular dimensions of (cation) $[Cu_5(SBu^t)_6]$, cation = $Et_4N^+$, $Et_3NH^+$, with estimated standard deviations in parentheses

| Dimension | Cation | | |
|---|---|---|---|
| | $Et_4N^+$ | | $Et_3NH^+$ |
| | $Cu_{dig}$-S (Å) | | |
| Cu2-S1 | 2.196(11) | [2.186(19)][a] | 2.158(4) |
| Cu2-S4 | 2.136(11) | [2.127(18)] | 2.153(4) |
| Cu3-S2 | 2.164(9) | [2.166(18)] | 2.152(4) |
| Cu3-S5 | 2.162(8) | [2.157(19)] | 2.178(4) |
| Cu4-S3 | 2.163(9) | [2.166(20)] | 2.166(4) |
| Cu4-S6 | 2.163(9) | [2.165(17)] | 2.160(4) |
| | $Cu_{trig}$-S (Å) | | |
| Cu1-S1 | 2.271(7) | [2.286(17)] | 2.303(4) |
| Cu1-S2 | 2.287(6) | [2.299(19)] | 2.265(4) |
| Cu1-S3 | 2.277(6) | [2.283(17)] | 2.272(4) |
| Cu5-S4 | 2.281(6) | [2.289(17)] | 2.371(4) |
| Cu5-S5 | 2.270(6) | [2.272(16)] | 2.251(4) |
| Cu5-S6 | 2.283(6) | [2.291(16)] | 2.239(5) |
| | S-C (Å) | | |
| S1-C11 | 1.80(2) | | 1.85 |
| S2-C21 | 1.91(1) | | 1.85 |
| S3-C31 | 1.90(1) | | 1.85 |
| S4-C41 | 1.88(2) | | 1.85 |
| S5-C51 | 1.92(1) | | 1.85 |
| S6-C61 | 1.89(1) | | 1.85 |
| | S-$Cu_{dig}$-S (deg) | | |
| S1-Cu2-S4 | 170.9(4) | [167(3)] | 170.7(2) |
| S2-Cu3-S5 | 169.2(4) | [175(3)] | 170.8(2) |
| S3-Cu4-S6 | 170.3(4) | [171(3)] | 173.4(2) |
| | S-$Cu_{trig}$-S (deg) | | |
| S1-Cu1-S2 | 124.3(2) | [124(2)] | 118.5(1) |
| S2-Cu1-S3 | 114.6(3) | [118(2)] | 120.9(2) |
| S3-Cu1-S1 | 120.9(2) | [117(2)] | 120.6(2) |
| S4-Cu5-S5 | 115.5(2) | [116(2)] | 95.1(1) |
| S5-Cu5-S6 | 124.5(2) | [120(2)] | 147.5(2) |
| S6-Cu5-S4 | 119.7(3) | [123(2)] | 117.2(2) |
| | Cu-S-Cu (deg) | | |
| Cu1-S1-Cu2 | 74.8(2) | [74.6(7)] | 73.3(1) |
| Cu1-S2-Cu3 | 75.9(2) | [75.4(8)] | 79.3(1) |
| Cu1-S3-Cu4 | 74.7(2) | [74.6(7)] | 75.7(1) |
| Cu5-S4-Cu2 | 75.7(2) | [75.6(7)] | 77.1(1) |
| Cu5-S5-Cu3 | 76.4(2) | [76.5(7)] | 80.9(1) |
| Cu5-S6-Cu4 | 75.1(2) | [74.9(7)] | 75.4(1) |
| | $Cu_{dig}$-S-C (deg) | | |
| Cu2-S1-C11 | 106.2(5) | | 108.3(5) |
| Cu3-S2-C21 | 106.1(5) | | 111.0(4) |
| Cu4-S3-C31 | 106.8(4) | | 106.7(3) |
| Cu2-S4-C41 | 108.7(6) | | 105.6(4) |
| Cu3-S5-C51 | 106.9(5) | | 107.9(4) |
| Cu4-S6-C61 | 103.9(5) | | 107.0(4) |

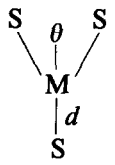
Table 2 (*Contd*)

| Dimension | Cation | | |
|---|---|---|---|
| | $Et_4N^+$ | | $Et_3NH^+$ |
| | $Cu_{trig}$-S-C (deg) | | |
| Cu1-S1-C11 | 110.8(6) | | 111.2(5) |
| Cu1-S2-C21 | 111.3(4) | | 112.4(4) |
| Cu1-S3-C31 | 113.9(5) | | 109.4(4) |
| Cu5-S4-C41 | 114.3(6) | | 115.8(4) |
| Cu5-S5-C51 | 111.1(5) | | 119.7(4) |
| Cu5-S6-C61 | 113.3(5) | | 115.4(5) |
| | $Cu_{dig}$--$Cu_{dig}$ (Å) | | |
| Cu2--Cu3 | 3.271(12) | [3.27(9)] | 3.202(3) |
| Cu3--Cu4 | 3.258(12) | [3.22(9)] | 3.554(3) |
| Cu4--Cu2 | 3.168(13) | [3.17(9)] | 3.255(3) |
| | $Cu_{trig}$--$Cu_{dig}$ (Å) | | |
| Cu1--Cu2 | 2.715(4) | [2.72(2)] | 2.667(3) |
| Cu1--Cu3 | 2.735(4) | [2.74(2)] | 2.820(3) |
| Cu1--Cu4 | 2.691(3) | [2.69(2)] | 2.724(3) |
| Cu5--Cu2 | 2.717(4) | [2.72(2)] | 2.825(3) |
| Cu5--Cu3 | 2.749(4) | [2.75(2)] | 2.874(3) |
| Cu5--Cu4 | 2.718(3) | [2.72(2)] | 2.691(3) |
| | S--S (Å) | | |
| S1--S2 | 4.029(6) | [4.07(4)] | 3.926(6) |
| S2--S3 | 3.848(6) | [3.93(4)] | 3.947(6) |
| S3--S1 | 3.949(7) | [3.88(4)] | 3.973(6) |
| S4--S5 | 3.848(7) | [3.89(4)] | 3.413(6) |
| S5--S6 | 4.028(6) | [3.91(4)] | 4.312(6) |
| S6--S4 | 3.944(6) | [4.04(4)] | 3.937(6) |
| S1--S4 | 4.317(6) | [4.31(3)] | 4.296(6) |
| S2--S5 | 4.311(6) | [4.32(2)] | 4.316(6) |
| S3--S6 | 4.309(6) | [4.31(2)] | 4.318(6) |
| S1--S6 | 4.537(6) | [5.91(4)] | 4.520(6) |
| S2--S4 | 4.602(7) | [5.97(3)] | 4.545(6) |
| S3--S5 | 4.604(6) | [5.83(3)] | 5.044(6) |
| Torsional angles (deg) | $Cu_{dig}$-Sn-Cn1-Cn4 | | |
| Cu2-S1-C11-C14 | -13.9(1.7) | | 9.3 |
| Cu3-S2-C21-C24 | -12.2(1.2) | | -18.5 |
| Cu4-S3-C31-C34 | -25.4(1.2) | | -21.1 |
| Cu2-S4-C41-C44 | -26.6(1.6) | | -29.8 |
| Cu3-S5-C51-C54 | -10.0(1.2) | | -75.2 |
| Cu4-S6-C61-C64 | -36.2(1.4) | | -5.4 |
| Twist angles (deg) | S(n)-$Cu_{trig}$--$Cu_{trig}$-S(n+3) | | |
| S1-Cu1--Cu5-S4 | 54.9(2) | [-50.0(1.5)] | 54.7 |
| S2-Cu1--Cu5-S5 | 45.9(2) | [-58.3(1.5)] | 31.2 |
| S3-Cu1--Cu5-S6 | 56.0(2) | [-58.8(1.5)] | 57.8 |

[a] Dimensions in square brackets are for the alternative cage in the $Et_4N^+$ crystal.

substantiated by the small *sample* standard deviations of each of the following sets of six dimensions: $Cu_{dig}$–S, 0.02 Å; $Cu_{trig}$–S, 0.007 Å; $Cu_{dig}$–$Cu_{trig}$, 0.02 Å; S–S(via $Cu_{trig}$), 0.08 Å; Cu–S–Cu, 0.7°; S–$Cu_{trig}$–S, 4.2°. The largest deviations from threefold equivalence occur in the angles S–$Cu_{trig}$–S which range 115–124°. This close approach to $D_3$ symmetry extends also to the locations and conformations of the Bu$^t$ groups in the $Et_4N^+$ compound, as shown by the following *sample* standard deviations for sets of six comparable dimensions: $Cu_{dig}$–Sn–Cnl, 1.6°; $Cu_{trig}$–Sn–Cnl, 1.6°; $Cu_{dig}$–Sn–Cnl–Cn4 torsional angles, 10.3°; $Cu_{dig}$–Cn4, 0.06 Å.

In the $Et_3NH^+$ compound the high pseudo-symmetry of the cage does not occur because one of the Bu$^t$ groups, that on S5, has been inverted through the $Cu_{dig}$–S5–$Cu_{trig}$ plane as shown in Fig. 5. This conformational change at S5 leads to increased steric repulsion with the Bu$^t$ group on S6, which is relieved by a 27° rotation of the Cu5–S5 bond about the $Cu_{trig}$–$Cu_{trig}$ axis within the Cu5 coordination plane. Concomitant with this is a lengthening of the Cu5–S4 bond, an effect which is electronic rather than steric, and which has been observed in related silver thiolate complexes.[2,9] In distorted three coordination




the distance $d$ increases as the opposite angle $\theta$ increases, in regular transition from trigonal to linear coordination.

The effects of the distortions due to the irregular ligand 5 in the $Et_3NH^+$ compound are also apparent (see Table 1) in the secondary dimensions S–S (long S5–S6, short S4–S5) and, to a lesser extent, Cu–Cu (long Cu3–Cu4). No specific cause for the reversal of ligand 5 can be identified from a study of the crystal packing nor are any intermolecular contacts abnormally short. It is assumed that subtle and relatively low-energy crystal packing forces are responsible. It may be noted that inversion at sulphur atoms allows a total of ten stereoisomers for the $[M_5(SR)_6]$ cage.[2]

Two small but regular features appear in the copper atom positions of both structures. The $Cu_{trig}$ atoms are displaced slightly outward from their $S_3$ coordination planes, by 0.06, 0.09 Å (Cu1, Cu5) for the $Et_4N^+$ compound and 0.02, 0.04 Å (Cu1, Cu5) for the $Et_3NH^+$ compound. Also, all $Cu_{dig}$ atoms are displaced from their S–S lines towards the centroid of the cage, by distances of 0.17 Å (Cu2), 0.21 Å (Cu3), 0.18 Å (Cu4) in the $Et_4N^+$ compound, and 0.18 Å (Cu2), 0.17 Å (Cu3), 0.13 Å (Cu4) in the $Et_3NH^+$ compound. The mean S–$Cu_{dig}$–S angle is 170.9°.

The orientations of the Bu$^t$ groups on the minor alternative cage in the disordered $Et_4N^+$ crystal could not be determined, but there is virtual $D_3$ symmetry in the dimensions of the $Cu_5$–$S_6$ core, indicating a similarly symmetrical $(Bu^t)_6$ set. There is one significant difference between the major and minor component $Cu_5S_6$ cages in the $Et_4N^+$ crystal, in the angle of antiprismatic twist of the $S_6$ polyhedron. In the minor component the mean S(n)–Cu1–Cu5–S($n$ + 3) torsional angle is 55.7°, and the mean distance between $S$ atoms *not* connected by $Cu_{dig}$ or $Cu_{trig}$ is 5.90 Å, in contrast to values of 52.3° and 4.58 Å respectively in the major component.

The distinct change in Cu–S bond length with coordination number[2,3] is again apparent, the mean values $Cu_{dig} - (\mu\text{-SBu}^t) = 2.163$, $\sigma_{mean} = 0.004$ Å (12 values) and $Cu_{trig} - (\mu\text{-SBu}^t) = 2.273$, $\sigma_{mean} = 0.005$ Å (11 values, excluding Cu5–S4 in the $Et_3NH^+$ crystal) compares well with the previously reported values[7] $Cu_{dig} - (\mu\text{-SPh}) = 2.160$ Å, $Cu_{trig} - (\mu\text{-SPh}) = 2.270$ Å.

In the pyramidal geometry at the sulphur atoms the Cu–S–C angles fall into two distinct classes, $Cu_{dig}$–S–C, mean 106.3, $\sigma_{mean}$, 0.5° (12 values), being less than $Cu_{trig}$–S–C, mean 113.2, $\sigma_{mean}$ 0.8° (12 values).

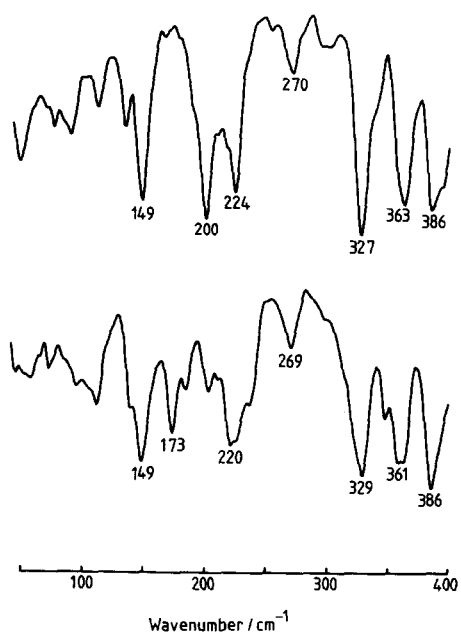



Fig. 6. Far-infrared spectra (at *ca.* 125 K) of (a) $(Et_4N)]Cu_5(SBu^t)_6]$; (b) $(Et_3NH)[Cu_5SBu^t)_6]$.

In both the $Et_3NH^+$ and $Et_4N^+$ cations there exist planar $C_2NC_2$ units, with maximum deviations from the three best atomic planes of 0.05, 0.03 and 0.03 Å. Mean values of C–N and C–C bond lengths in the cations are 1.55, $\sigma_{mean}$ 0.01 Å and 1.55, $\sigma_{mean}$ 0.02 Å, respectively.

*IR spectra.* The far IR spectra of $(Et_4N)[Cu_5(SBu^t)_6]$ and $(Et_3NH)[Cu_5(SBu^t)_6]$ (Figure 6) show some evidence of the structural differences found for the anions in these compounds. As discussed previously,[6] the bands in the range 300–400 $cm^{-1}$ are due to the coordinated thiolate ligand and these occur at similar frequencies in both spectra. The band at about 270 $cm^{-1}$ is assigned to the antisymmetric stretching mode of the diagonal S–Cu–S units in the anion,[6] and this has virtually the same frequency and intensity in both spectra. The region 150–250 $cm^{-1}$ presumably includes bands due to the trigonal Cu–S bonds, and here there are marked differences between the two spectra. No specific assignments are possible, but the greater complexity of the spectrum of $(Et_3NH)[Cu_5(SBu^t)_6]$ in this region is probably a consequence of the more distorted structure of the anion in this compound.

## DISCUSSION

The $[Cu_5(SBu^t)_6]^-$ molecular cage is easily crystallised, and easily decomposed by visible- and X-radiation. It is presumed that the decomposition is initiated by S–C homolysis, generating copper sulphides. At room temperature atomic thermal motions in the crystals, particularly at the cation and the Bu$^t$ groups, are relatively large.

The cage structure, a trigonal bipyramid of metal atoms within a trigonal antiprism of doubly-bridging thiolate ligands, is unprecedented. A structural relationship can be drawn with the $[M_5(SPh)_7]^{2-}$ (M = Cu, Ag) molecular cage **1** as shown in Fig. 7. If the thiolate group opposite the two-coordinate metal in **1** is removed, and both of the two-coordinate metals so generated drop into linearity, the *trigonal bipyramido*-$M_5$-*trigonal prismo*-$S_6$ structure, **2**, results and may be twisted to the *antiprismo* form **3**.

The predominance of two- over three-coordinate metal in $[M_5(SBu^t)_6]^-$ further accents the general tendency to low metal coordination numbers with thiolate ligands.[2] As the electrophilicity of copper(I) and silver(I) can be satisfied with two double-bridging alkylthiolate ligands, it could be postulated that a complex $[M(SR)_3]^{2-}$ with non-bridging alkylthiolate ligands would be electron excessive at the metal and unstable with respect to dissociation to $[M(SR)_2]^-$.

The $[M_5(SBu^t)_6]^-$ cage is clearly held together by the bridging thiolate ligands, but the question arises as to the possibility of some direct metal–metal bonding. Several structural properties bear on this question.

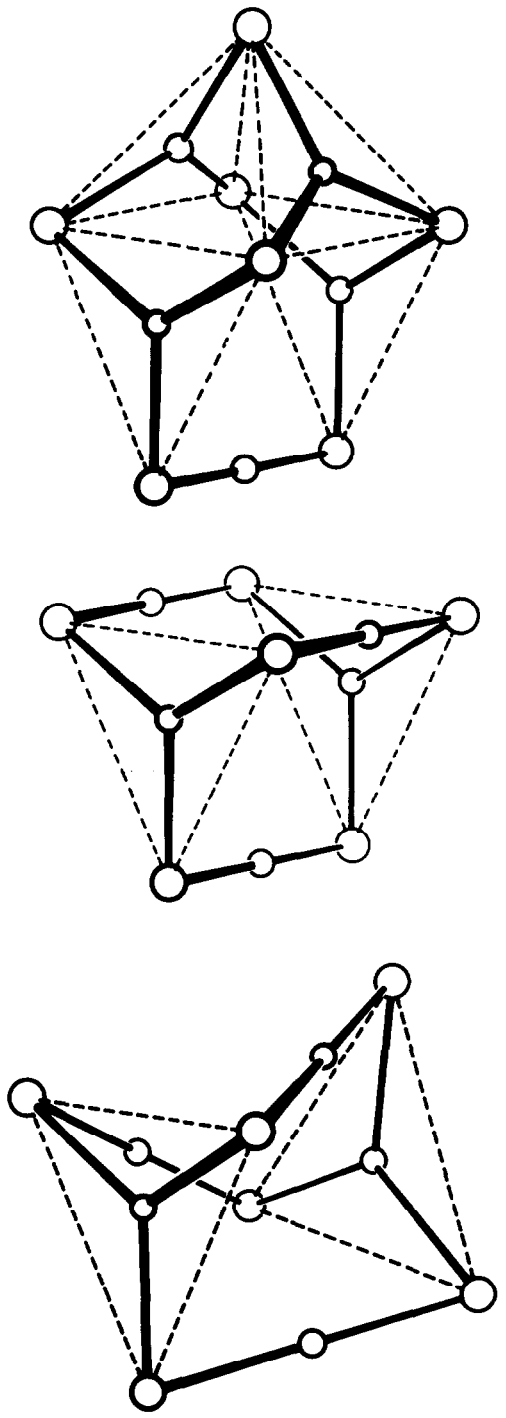


Fig. 7. $M_xS_y$ polyhedra in thiolate cages $M_5(SR)_7$, **1**, *trigonal-prismo*-$M_5(SR)_6$, **2**, and *trigonal-antiprismo*-$M_5(SR)_6$, **3**.

(a) The $Cu_{dig}$–$Cu_{trig}$ and $Cu_{dig}$–$Cu_{dig}$ distances, averaging 2.74 and 3.28 Å respectively, are substantially greater than the Cu–Cu distance (2.55 Å)

in copper metal. It can be argued[7] that the Cu–Cu bonding of order one would not be longer than this.

(b) The $Cu_{dig}$ atoms are systematically displaced from linear coordination towards the centroid of the cage, decreasing Cu–Cu distances slightly.

(c) The $Cu_{trig}$ atoms are systematically displaced away from the centroid of the cage, increasing the $Cu_{trig}$–$Cu_{dig}$ distances slightly.

(d) The $S_6$ polyhedron is antiprismatic (**3**), with an antiprismatic twist angle of *ca.* 50°. Lesser twists, or even prismatic $S_6$ (**2**) appear to be feasible geometries. One consequence of the antiprismatic twist is substantially reduced Cu–Cu distances (assuming unchanged Cu–S distances). For instance, in structure **2** the $Cu_{dig}$–$Cu_{trig}$ distance would be 3.14 Å, rather than the 2.74 Å observed for structure **3**.

These structural properties may be the consequence of electronic factors other than copper–copper bonding. The antiprismatic twist and the inwards displacement of the $Cu_{dig}$ atoms both reduce the Cu–S–Cu angles from 90° to an average value of 75°. Angles M–S–M at doubly-bridging thiolate are known over a wide range,[2] but values of 76–80° predominate where the metal is copper or silver. It is not yet clear whether these acute values are a consequence of the cage structure, or whether details of the cage structure are determined by a preference for M–S–M angles at 75°. Therefore, the available structural data do not permit unequivocal conclusions about the bonding in the $Cu_5S_6$ core of $[Cu_5(SBu^t)_6]^-$, although it appears that some $Cu_{trig}$–$Cu_{dig}$ attractive forces be present.

There exist patterns in two aspects of the $SBu^t$ group conformations which appear not to be caused by steric effects, and for which bonding explanations could be sought. First, the S–C bonds are closer to S–$Cu_{dig}$ than to S–$Cu_{trig}$, and second the $Cu_{dig}$–Sn–Cnl–Cn4 torsional angle is consistently smaller than the $Cu_{trig}$–Sn–Cnl–Cn4 torsional angle. Neither of these effects appears to be due to methyl–methyl group repulsions on the surface of the cage, and in fact the second effect results in unusually short Cn4–$Cu_{dig}$ contacts which average 3.21 A° ($\sigma_{sample}$ 0.06 Å) in the $Et_4N^+$ compound.

All interligand $CH_3$–$CH_3$ distances on the surface of the cage are greater than 4 Å, and the Cn3–$Cu_{trig}$ distances over the trigonal faces are all greater than 3.5 Å. The positions of the $Bu^t$ groups on the surface of the cage are determined also by the magnitude of the antiprismatic twist.

It can be concluded from the two structures reported here that the $[Cu_5(SBu^t)_6]^-$ is angularly non-rigid. An irregular position of one $Bu^t$ group in the $Et_3NH^+$ compound causes large angular distortions. This is consistent with the general notion that cage structures are floppy when connectivities are low,[2] and supports the contention that any secondary interactions such as Cu–Cu bonding on Cn4–$Cu_{dig}$, Cn3–$Cu_{trig}$ repulsions are not pronounced.

A relevant comparison structure is $[CuOBu^t]_4$,[11] which contains a planar square of copper atoms, situated at the midpoints of a coplanar square of oxygen atoms. All four $Bu^t$ groups are directed to the same side of the $Cu_4O_4$ plane. There is a simple relationship between the $[CuXBu^t]_4$ structure (X = 0) and the prismatic $[Cu_5(XBu^t)_6]^-$ structure (X = S), **2**, namely addition/elimination of a $[Bu^tX–Cu–XBu^t]$ moiety across opposite copper atoms.

The structure of $[CuOBu^t]_4$ is also pertinent to the question of direct Cu–Cu bonding in these $XBu^t$ bridged compounds. The facts that the Cu–Cu distances in $[CuOBu^t]_4$ (range 2.65–2.77 Å) are slightly less than the Cu–Cu distance in $[Cu_5(SBu^t)_6]^-$, and the lack of evidence of significant contraction of the $Cu_4$ square, indicate that any direct Cu–Cu bonding is at best weak.

A species $[Cu_5Ph_6]^-$ has recently been characterized, and has been shown to have a structure similar to that of $[Cu_5(SBu^t)_6]^-$. The size of the $Cu_5$ cage is smaller by about 10% in the former complex. In this species, too, the presence of a weak $Cu_{dig}$–$Cu_{trig}$ bonding interaction has been suggested.[12]

## EXPERIMENTAL

All preparative solutions containing *t- butylthiol* and its metal complexes were maintained under an atmosphere of dinitrogen. All reagents and solvents were laboratory grade, and were used as received. Infrared spectra were obtained on a Perkin–Elmer 397 spectrometer. Spectra were run on Nujol mulls between KBr plates, and were calibrated by using the spectrum of polystyrene. Far IR spectra were obtained on a Grubb–Parsons Cube Mk II interferometer fitted with a 6.25 $\mu$m Mylar-film beam splitter. Far IR spectra were run on petroleum jelly mulls between polythene plates at *ca.* 125 K and were calibrated by using the spectrum of water vapour. $^1$H NMR spectra were run at *ca.* 308 K on a Varian T60 spectrometer.

*Tetraethylammonium hexa-t-butylthiolatopentacuprate(I),* $(Et_4N)[Cu_5(SBu^t)_6]$

A solution of $Cu(NO_3)_2 3H_2O$ (4.8 g, 20 mmol) in absolute ethanol (55 cm$^3$) was added slowly to a solution of *t*-butylthiol (5.4 g, 60 mmol) and tri-

ethylamine (6.0 g, 60 mmol) in acetone (90 $cm^3$) at room temperature. To the resulting bright yellow solution was added a solution of tetraethylammonium bromide (7.5 g, 36 mmol) in ethanol (75 $cm^3$). This solution, sealed and protected from light, was allowed to stand at *ca.* 0°C for several days, while large multifaceted crystals grew. The product was filtered, washed with 2-propanol, and vacuum dried in the dark.

Found: C, 39.65; H, 7.77; N, 1.23. $Cu_5S_6NC_{32}H_{74}$ requires C, 39.09; H, 7.59; N, 1.42.

This compound is easily soluble in acetone and in acetonitrile, appreciably soluble in ethanol and less so in methanol or 2-propanol. On exposure to light, solutions of this compound become green, while the solid becomes orange then brown.

*Tetraethylammonium hexa-t-butylthiolatopentaargentate(I)*, $(Et_4N)[Ag_5(SBu^t)_6]$

The preparation of this compound has been described previously.[6] Powder diffraction patterns ($CuK_\alpha$ radiation) reveal that it is isostructural with the copper analogue.

*Triethylammonium hexa-t-butylthiolatopentacuprate* (I) $(Et_3NH)[Cu_5(SBu^t)_6]$

*t*-butylthiol (2 $cm^3$) was added to triethylamine (200 $cm^3$), and the mixture degassed. $CuSBu^t$ (0.5 g) was added, and the mixture was heated to 67°C to produce a yellow solution which was filtered while hot. Fine yellow needles were obtained by preparing the yellow solution as above and seeding it with crystals of $(Et_3NH)[Cu_5(SBu^t)_6]$. No satisfactory elemental analysis could be obtained for this compound.

Found: C, 46.7; H, 9.0; Cu, 31.5. $C_{30}H_{70}Cu_5NS_6$ requires C, 37.7; H, 7.4; Cu, 33.3%. $^1H$ NMR ([$D_5$] pyridine solution) $\delta$/p.p.m. from t.m.s. (multiplicity, integral, assignment): 1.0 (triplet (J = 7 Hz), 13.5, ethyl $CH_3$), IR (nujol mull): 2720 m, 2680 sh, 2380 vw, 1360 s, 1300 vw, 1216 w, 1074 vw, 1050 vw, 1023 w, 1017 sh, 841 w, 819 w, 782 vw, 577 m [ν(CS)], 435 w. The $^1H$ NMR and the X-ray crystal structure determination show conclusively that this compound is $(Et_3NH)[Cu_5(SBu^t)_6]$. Other crystals chosen at random gave identical diffraction patterns.

*X-Ray crystallography*. The following general information applies to the two crystals. Data were collected at 293 ± 1 K; scattering factors for uncharged atoms, corrected for dispersion, were from International Tables;[13] residuals quoted are $R = \Sigma \| Fo| - |Fc\| / \Sigma |Fo|$, $Rw = [\Sigma w(|Fo| - |Fc|)^2 / \Sigma w|Fo|^2]^{1/2}$. Full matrix least-squares weights were $w = [\sigma(F)]^{-2}$.

$(Et_3NH)[Cu_5(SBu^t)_6]$. $C_{30}H_{70}Cu_5NS_6$, M = 954.96, yellow needles. The direction of elongation is always along (1 0 0), but the cross sectional shape varies depending on the relative development of the [0 *k l*] faces. Monoclinic, space group $P2_1/c$ (No. 14), $a = 10.519(1)$, $b = 21.457(1)$, $c = 20.065(1)$ Å, $\beta = 95.11(1)°$, $U = 4511$ Å$^3$; $D_m = 1.39$ g $cm^{-3}$ (flotation in *n*-hexane/1,3-dibromopropane), $Z = 4$, $D_c = 1.41$ g $cm^{-3}$; $F(0\,0\,0) = 1992$. Nickel-filtered Cu-$K_\alpha$ radiation, $\lambda = 1.5418$ Å; $\mu = 51.86$ $cm^{-1}$; Crystal faces: (a) (100, $\bar{1}00$, 0$\bar{1}$0, 001, 011, 0$\bar{2}$1, 03$\bar{4}$, 0$\bar{2}\bar{3}$), (b) (100, $\bar{1}00$, 010, 01$\bar{4}$, 0$\bar{2}\bar{1}$, 0$\bar{2}$1, 01$\bar{4}$, 021). Crystal dimensions: (a) 0.34 × 0.14 × 0.20 mm; (b) 0.34 × 0.25 × 0.30 mm. Mosaic spreads 0.11°. Intensity data (Nonius CAD-4) to $\theta_{max}$ 57° ($\sin\theta/\lambda$ 0.54) were collected by a symmetric $2\theta$-$\omega$ scan of 70 steps of 0.01° in theta. The background was counted for 15 s at each end of the scan range. After every 200 measurements, three standard reflections were remeasured to monitor crystal alignment and stability. It was found that the crystals suffered radiation damage on prolonged exposure to X-rays, and it was necessary to employ two crystals to complete the data collection. The first crystal was used to collect data in the theta range 0–45° (the intensities of its standard reflections had then declined by approx. 17%). The second crystal underwent a similar degree of decomposition during the collection of the high-theta data. The combined data set comprised 3093 unique reflections with $I > 2.58\ \sigma(I)$ [where $\sigma(I) = \{T + t^2B + (pI)^2\}^{1/2}$ $T$ = integrated peak count, $B$ = average background count, $t$ = ratio of scan to background times, $p$ was assigned a value of 0.04]. The data were corrected for intensity decay and for absorption.

The positions for the copper and sulphur atoms were determined using direct methods (MULTAN), with carbon and nitrogen atoms being located from subsequent "difference" electron density syntheses.

After refinement (SHELX) with copper and sulphur atoms anisotropic and all other non-hydrogen atoms isotropic, $R = 0.073$, the temperature factors of the methyl-carbon atoms attached to C(11) were high, indicating a considerable degree of disorder in that *t*-butyl group. Accordingly, these atoms were placed in positions such that the geometry of the group equated with the average geometry of the other five *t*-butyl groups. Thereafter, all *t*-butyl groups were refined as groups with bond length and angle constraints. The final values of $R$ and $Rw$ were 0.072 and 0.082 respectively.

$(Et_4N)[Cu_5(SBu^t)_6]$. $C_{32}H_{74}Cu_5NS_6$, M = 983.04; equi-dimensional multifaceted triangular or hexag-

onal prisms, which are decomposed by X-rays (Cu$K_\alpha$) at room temperature. Monoclinic, $C2/c$ (No. 15), $a = 45.500(3)$, $b = 11.805(1)$, $c = 20.168(2)$ Å, $\beta = 117.81(1)°$; $U = 9582$ Å$^3$; $Z = 8$, $D_c = 1.37$ g cm$^{-3}$, $D_m = 1.37(2)$ g cm$^{-3}$; Cu($K_\alpha$), $\lambda = 1.5418$ Å, $\mu = 37.3$ cm$^{-1}$. The crystal was bounded by 14 faces in the zones {100}{101}{102}{211}{311}, with maximum and minimum crystal dimensions 0.42 and 0.25 mm. Intensity data (Siemens AED) to $\theta_{max} = 50°$ by $\theta/2\omega$ scan; intensity loss due to radiation damage of up to 50%, for which appropriate corrections were made. Data reduction, including absorption corrections, was performed as for the $Et_3NH^+$ compound, yielding 3965 independent reflections of which 2953 have $I > 2.58\ \sigma(I)$. The crystal decay limited the quality of these data.

Structure solution by Patterson and Fourier methods proceeded normally. During the least-squares refinement two scale factors were included to account for some of the effect of crystal decay. Hydrogen atoms were not included. At convergence of refinement (temperature factors anisotropic for Cu, S, isotropic for C, N) based on 2629 observed reflections wih $\sin\theta/\lambda > 0.2$, $R = 0.096$, $Rw = 0.087$. However, a difference map at this stage revealed slight disorder of the $[Cu_5(SBu^t)_6]^-$ cage, appearing as weak additional peaks (3 e Å$^{-3}$) for sulphur atoms related to the predominant atoms by reflection through the $(Cu_{dig})_3$ plane. Further refinement (RAELS) therefore included an alternative $Cu_5S_6$ cage, slack constrained to the predominant cage with occupancies refined to sum to unity. The alternative cage was unconstrained in location, but slack constrained to the main cage by means of Cu–S and Cu–Cu distances, and fully constrained to the Cu, S thermal parameters of the major cage. In addition the C–C distances of each Bu$^t$ group were slack constrained, as were the C–C and C–N distances of the cation, and TLX thermal motion was refined for the Bu$^t$ groups.

This refinement proceeded well, to $R$, $Rw = 0.078$, 0.088 for all 2953 observed data, and $R$, $Rw = 0.072$, 0.068 for data with $\sin\theta/\lambda > 0.2$. The occupancy for the alternative cage refined to 0.117(2). A final difference map gave some evidence (*ca.* 1 e Å$^{-3}$) of the $\alpha$-carbon atoms of the alternative cage, in positions which maintained the mirror relationship with the predominant cage. Some evidence of Bu$^t$ hydrogen atoms for the main cage also appeared, but as it was clear that no new information could be extracted from the diffraction data no further refinement was undertaken.

The estimated standard deviations in atomic parameters and derived quantities are influenced by the atomic (Cu) overlap in the disordered model, and by the constraints used during matrix inversion.

Atomic coordinates and thermal parameters for the two structures have been deposited with the Editor as supplementary material; copies are available on request. Atomic coordinates have also been deposited with the Cambridge Crystallographic Data Centre.

*Acknowledgements*—We thank the ARGC for financial support, D. C. Craig for assistance with diffraction data collection, and Dr. A. D. Rae for the constrained least-squares refinement.

## REFERENCES

1. E. E. Reid, *Organic Chemistry of Bivalent Sulfur*, Vol. I, Chap. 2. Chemistry Publishing Co., New York (1958).
2. I. G. Dance, *Coord. Chem. Rev.*, to be published.
3. I. G. Dance and J. C. Calabrese, *Inorg. Chim. Acta* 1976, **19**, L41.
4. G. A. Bowmaker, G. R. Clark, J. K. Seadon and I. G. Dance, *Polyhedron*, in press.
5. I. G. Dance, *J. C. S. Chem. Comm.* 1976, 68.
6. G. A. Bowmaker and L.-C. Tan, *Aust. J. Chem.* 1971, **32**, 1443.
7. I. G. Dance, *Aust. J Chem.* 1978, **31**, 2195.
8. I. G. Dance, *Inorg. Chem.* 1981, **20**, 1487.
9. I. G. Dance, *Inorg. Chim. Acta* 1977, **25**, L17.
10. S. Hong, A. Olin and R. Hesse, *Acta Chem. Scand.* 1975, **A29**, 583.
11. T. Greiser and E. Weiss, *Chem. Ber.* 1976, **109**, 3142.
12. P. G. Edwards, R. W. Gellert, M. W. Marks and R. Bau, *J. Am. Chem. Soc.* 1982, **104**, 2072.
13. *International Tables for X-Ray Crystallography*, Vol. IV, Tables 2.2A and 2.3.1. Kynoch Press, Birmingham (1974).

*Polyhedron* Vol. 3, No. 5, pp. 545–549, 1984
Printed in Great Britain.

0277–5387/84 $3.00 + .00
© 1984 Pergamon Press Ltd.

# INFLUENCE OF THE CARBON–CARBON DOUBLE BOND ON THE COORDINATIVE ABILITY OF UNSATURATED BICARBOXYLIC LIGANDS IN AQUEOUS SOLUTION. A THERMODYNAMIC STUDY

**ROBERTO ARUGA**
Institute of Analytical Chemistry, University of Turin, via Giuria 5, 10125 Turin, Italy

(*Received* 12 *July* 1983; *accepted* 10 *October* 1983)

**Abstract**—Enthalpies of complex formation of fumarate, itaconate, maleate and succinate with calcium have been determined by direct calorimetry. By using the stability constants of the literature, Gibbs function and entropy were also obtained. The present data refer to the aqueous medium at $T = 25°C$ and $I = 0.5$ mol $l^{-1}$. In spite of the *trans*-configuration of fumarate, examination of the present thermodynamic results indicates a probable bidentate behaviour for this ligand, as a consequence of a charge-transmission due to the carbon–carbon double bond. The lower stability of the fumarate complexes in comparison with those of its *cis*-isomer seems due to different solute–solvent interactions, while the metal–ligand bond strength seems similar in both cases. On the other hand the present results seem to indicate for the itaconate complexes a structure similar to that of maleate and succinate, without charge transmission.

It has for a time been known that the complexes of uni- or bi-carboxylic ligands containing a carbon–carbon double bond with certain metal ions of *b* class, such as Cu(I), owe their fairly high stability to a metal-double bond $\pi$ interaction, while the carboxylate groups do not seem to contribute to complex formation.[1–3]

More recently[4] an interesting behaviour has been observed in the case of fumarate (which is of the same type as that of the above ligands) with lanthanide cations. In spite of its *trans*-conformation, the behaviour of fumarate in these complexes seems more similar to that of bidentate than of unidentate ligands. The abnormally high stability of these complexes does not seem explainable as above suggested for Cu(I), as lanthanides are typical "class *a*" metals. A possible charge transmission by the double bond has been suggested in this case.[4] The values of the stability constants seem to indicate an abnormal behaviour of fumarate with calcium too.[5] Moreover, in order to justify the high stability constant values of itaconic acid with some bivalent metals, an abnormal behaviour caused by the double bond was suggested for this ligand in a previous paper.[6]

Various conformational studies on the metal salts of the above ligands, particularly of fumaric acid, are available in the literature, but they refer, almost exclusively, to the crystalline state, and are of little use for clarifying the structures present in solution. These studies appear especially inadequate in the present case, as the charge transmission to one end of the bicarboxylate anion is difficult in the crystal structure, where each end of the anion (as results from an X-ray study of calcium fumarate trihydrate[7]) is in contact with a metal ion.

There have been few conformational as well as thermodynamic studies in solution.

Taking these observations into account, and also considering the contribution of thermodynamic parameters in elucidating the structures of complexes in solution, it was thought of interest, in the present work, to determine by calorimetry the enthalpy and entropy of association of the anions of fumaric, itaconic (or methylenebutanedioic), maleic and succinic acids with the calcium ion. No calorimetric data were previously reported for these complexes in solution.[8] The present results refer to the aqueous medium, at $T = 25°C$ and ionic strength $I = 0.5$ mol $l^{-1}$.

## EXPERIMENTAL

### *Reagents*

Calcium nitrate C. Erba RPE was used. The metal concentration was determined by complexometric titration with EDTA (0.1 mol $l.^{-1}$ solution, C. Erba RPE). Ligand solutions were prepared by using analytical grade reagents (C. Erba RPE). Their purity was checked by potentiometric ti-

tration. The background electrolyte was sodium nitrate C. Erba RPE.

*Equipment*

Calorimetric measurements were performed at 25°C by an LKB 8700-2 Precision Calorimetry System and an LKB 8726–1 100 $cm^3$ titration vessel, provided with a standard resistor (50 Ω) and a thermistor (2000 Ω). The accuracy of the instrument was checked by measuring the molar enthalpy of the reaction between *tris*-(hydroxymethyl)methylamine and HCl in aqueous solution. Greater details on the instrument calibration were reported previously.[9] The temperature of the titrant was kept at the temperature of the calorimeter by immersing (at least 12 hr before the measurement) the Teflon reservoir of the titrant in the same thermostatic bath containing the calorimetric cell. The calorimeter was also equipped with a Radiometer ABU 12b autoburet for the titrant addition. The calorimetric experiments were performed in a room whose temperature was kept constant within $\pm 0.3$°C.

*Procedure*

At least three series of measurements of the reaction and dilution heats were carried out for each metal–ligand system, each series being performed in the following manner. Successive amounts of $2.507 \pm 0.002$ $cm^3$ of ligand solution were added to 88.00 $cm^3$ of calcium nitrate in the calorimetric cell, and the heat for each addition was measured (for the metal and ligand concentrations, see Table 1). The ionic strength in the cell had been previously brought to 0.5 mol $l.^{-1}$ by $NaNO_3$, and pH of all solutions to $8.5 \pm 0.2$ by NaOH. The corresponding heat of dilution was measured by adding the same amounts of ligand solution to 88.00 $cm^3$ of 0.5 mol $l.^{-1}$ $NaNO_3$, at pH = 8.5, without the metal. Under these conditions the following results were obtained: (a) the presence of only 1:1 complex species;[6] (b) a negligible ionic strength variation in the cell during the measurement; (c) no interaction between ligand (in the form of the bivalent anion) and proton; (d) absence of neutralization heat between $H^+$ and $OH^-$; (e) no hydrolysis process of the calcium ion. It must also be observed that an attempt was made to extend the present determinations to the corresponding associations of Cu(II) which was unsuccessful, as precipitation took place when this metal was mixed with fumarate ion.

Table 1. Experimental data for the mixing of calcium nitrate and bicarboxylic ligand aqueous solutions, at 25°C†

| Ligand | $C_L$ (mol $l^{-1}$) | $\Sigma V_T$ (ml) | $[CaL] \times 10^3$ (mol $l^{-1}$) | $[L^{2-}] \times 10^3$ (mol $l^{-1}$) | $-\Sigma Q_c$ (cal) |
|---|---|---|---|---|---|
| Succinate | 0.550 | 2.507 | 4.24 | 11.0 | 0.718 |
| | | 5.014 | 7.78 | 21.8 | 1.345 |
| | | 7.521 | 10.7 | 32.5 | 1.894 |
| | | 10.028 | 13.2 | 43.0 | 2.372 |
| Maleate | 0.300 | 2.507 | 4.21 | 4.05 | 0.466 |
| | | 5.014 | 7.86 | 8.21 | 0.891 |
| | | 7.521 | 11.0 | 12.4 | 1.280 |
| | | 10.028 | 13.7 | 16.7 | 1.638 |
| Itaconate | 0.400 | 2.507 | 4.38 | 6.69 | 0.540 |
| | | 5.014 | 8.10 | 13.4 | 1.028 |
| | | 7.521 | 11.2 | 20.2 | 1.471 |
| | | 10.028 | 13.9 | 26.9 | 1.867 |
| Fumarate | 0.550 | 2.507 | 4.24 | 11.0 | 0.440 |
| | | 5.014 | 7.78 | 21.8 | 0.845 |
| | | 7.521 | 10.7 | 32.5 | 1.204 |
| | | 10.028 | 13.2 | 43.0 | 1.523 |

†Initial concentration of metal in the cell: 0.080 mol $l^{-1}$.

*Treatment of the experimental data*

The following experimental data, which refer to one of the series of measurements for each metal–ligand system, are collected in Table 1: initial concentration of ligand in the titrant solution ($C_L$); cumulative volume of titrant added ($\Sigma V_T$); complex and free-ligand concentration after each addition ([CaL], ($L^{2-}$]); cumulative heat corrected for the dilution ($\Sigma Q_c$). (See Table 1.)

The molar enthalpies of the association were determined from the experimental heats ($\Sigma Q_c$) and the complex species concentrations. The latter were obtained by means of the corresponding stability constants of Topp and Davies[10] and of Schubert and Lindenbaum,[11] previously corrected to $I = 0.5$ mol l.$^{-1}$ by Davies' equation: $-\log f = Az^2[I^{1/2}/(1 + I^{1/2}) - 0.2I]$ ($A = 0.509$ for water at 25°C). The $\Delta H^\circ$ values and the corresponding standard deviations were calculated by the numerical method of minimization of the error square sum;[12] the entropy values by the equation: $\Delta G^\circ = \Delta H^\circ - T\Delta S^\circ$.

## RESULTS AND DISCUSSION

The molar thermodynamic quantities are collected in Table 2.

The positive entropy values of Table 2 may be justified considering the following processes: (a) the solvent–destructuring process deriving from the charge neutralization during the association; (b) the release of water molecules from the first hydration sphere of the metal by the carboxylate groups. The not very endothermic values of enthalpy may also be justified by the above (a) and (b) processes, but their influence on $\Delta H^\circ$ is probably weaker. In fact the bonds between solvent molecules are weak, and, on the other hand, the crystal-fields produced by oxygen-coordinating groups are very similar to those of the water molecules,[13] so that the breaking of the water–metal bond is approximately counterbalanced by the metal–carboxylate bond formation. It is interesting to note, in this connection, that for maleate ion with calcium a $\Delta H^\circ$ value of opposite sign that for the present ligands was obtained in a previous study[14] ($\Delta H^\circ = -0.44$ kcal mol$^{-1}$). This value is in accordance with a tridentate behaviour of malate. Furthermore, it could indicate that a different type of bond (probably of outer-sphere type) is formed by the alcoholic hydroxyl of maleate, as compared to that of the carboxylate groups. In other words, for this type of interaction the exothermic formation of the metal–ligand bond is not counterbalanced by water–metal bond breaking.

The magnitude of the thermodynamic quantities of Table 2 is in accordance, for succinate and maleate, with the structures generally assigned to their metal complexes. The lower stability of the succinate complex is due to enthalpy factors, i.e. to the different metal–ligand bond strength. In fact, a better steric adjustment of the two carboxylate groups with the metal is permitted by the planar configuration of maleate. On the contrary, the conformation of succinate, which is not planar because of the smaller bond angles and the stronger repulsion between the two carboxylate groups, has greater difficulty in forming stable bonds with the metal.[15,16] On the other hand the $\Delta S^\circ$ values are very similar (9.5 and 9.4 cal K$^{-1}$ mol$^{-1}$), as a consequence of similar solvent–destructuring processes.

The abnormal behaviour of fumarate with calcium may be pointed out if one considers the quantity $\log K_{Ca}/pK_a$, which relates the metal–ligand complex stability with the stability of the proton–ligand association.[17,18] By using the literature values of $\log K_{Ca}$ and $pK_a$ for various

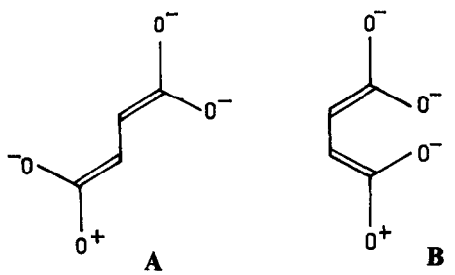
Table 2. Molar thermodynamic quantities for the complex-formation reaction: $Ca^{2+} + L^{2-} \rightarrow CaL$ in aqueous solution, at $T = 25$°C and $I = 0.5$ mol l$^{-1}$

| L | log K | $-\Delta G^\circ$ (kcal mol$^{-1}$) [b] | $\Delta H^\circ$ (kcal mol$^{-1}$) | $\Delta S^\circ$ (cal K$^{-1}$mol$^{-1}$) |
|---|---|---|---|---|
| Succinate | 0.72±0.08 [a] | 0.98±0.11 | 1.84±0.01 | 9.5±0.4 |
| Maleate | 1.15±0.02 | 1.57±0.02 | 1.22±0.01 | 9.4±0.1 |
| Itaconate | 0.95 | 1.29 | 1.37±0.01 | 9.0 |
| Fumarate | 0.72±0.04 | 0.98±0.06 | 1.17±0.01 | 7.2±0.2 |

[a] The uncertainty in each case is given as the estimated standard deviation. The log K values for itaconate were reported[11] without standard deviation.

[b] The results are expressed by means of the thermochemical calorie, equal to 4.1840 abs J.

anions,[6,10,11,19] a constant value of 0.11 is obtained for the above ratio in the case of acetate, propionate and butyrate unicarboxylic ligands, while for fumarate the above ratio is 0.46. This value is different from the preceding ones, but is similar to those obtained for phtalate, itaconate, maleate and succinate (0.45; 0.43; 0.39; 0.36, respectively). In order to investigate the possible bidentate behaviour of fumarate, it is useful to consider the $\Delta H^{\circ}$ and $\Delta S^{\circ}$ values of Table 2. The $\Delta H^{\circ}$ of fumarate is similar to that of maleate, while $\Delta S^{\circ}$ is considerably less positive than in the case of maleate and succinate. This seems to suggest that similar metal–anion bonds, but different solvent–destructuring processes are present in the complexes of fumarate and maleate. The charge transmission in the fumarate complexes can give rise to the following conformations for this ligand:



A B

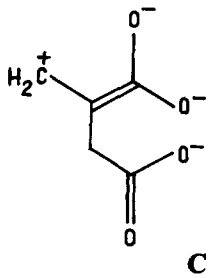
The existence of the above **A** and **B** conformations had already been suggested in the past,[21] in order to explain the behaviour of some substances, which catalyze the isomerization of maleic acid to fumaric acid. Regarding structures **A** and **B** and the structure of maleate, the following observations can be made: (a) from the lengths and the angles of the bonds of maleate in its crystalline potassium salt,[20] a distance of *ca.* 2.4 Å is obtained between the two negative oxygen atoms, i.e. between the two coordinating sites; (b) similar considerations in the case of the carboxylate group[20] give a probable distance of *ca.* 2.2 Å between the two negative oxygen atoms of structure **A**, this distance being very similar to that above calculated; (c) in structure **B** the bond angles are similar to those of maleate, so that the distance between the two negative oxygen atoms of the two carboxylate groups of structure **B** should be similar to that of maleate. Therefore it is clear that structures **A** and **B**, as regards both coplanarity and distance of the two bonding sites, should have the same coordinating ability as maleate. This conclusion is in complete accordance with the previous considerations on the $\Delta H^{\circ}$ values of maleate and fumarate. On the other hand, as concerns the solvent–destructuring external processes, maleate and fumarate seem to behave differently. In the case of the association of maleate an almost complete charge neutralization takes place, while for fumarate (**A** or **B** configuration) two free charges are present in the final structure which has, consequently, a remarkable solvent-ordering ability. In this case too the experimental entropy data are in agreement with the configurations above suggested.

In the above cited paper[4] a comparison is made between the $\Delta H^{\circ}$ and $\Delta S^{\circ}$ of fumarate with lanthanide metals, and of sulphate with the same metals, in order to confirm the charge-transmission process in fumarate (no indication regarding the possible structure of fumarate was given in that paper, but structure **A** was probably taken into consideration). The comparison between the $\Delta H^{\circ}$ values (i.e. between the metal–oxygen bond strength) seems justified. In fact a distance of *ca.* 2.4 Å between the oxygen atoms of sulphate is obtained from the literature data,[22] which is very similar to that above calculated for the negative oxygen atoms of **A** and **B** structures. As regards the present case, the enthalpy calorimetric data of the literature for calcium and sulphate (0.81 and 1.50 kcal $mol^{-1}$)[23,24] are in good accordance with the value of 1.17 kcal $mol^{-1}$ of Table 2 for calcium with fumarate. On the contrary, the comparison proposed[4] between the $\Delta S^{\circ}$ values does not seem to be equally valid, as the solvent–destructuring process is very different in the association of sulphate and fumarate (see above).

As regards the prevailing **A** or **B** conformation in the present complexes of fumarate, it may be observed that form **A** is entropy-favoured, as it associates with smaller loss of conformational freedom. In any case the thermodynamic data of the present work do not seem sufficient to clarify this point.

In the case of itaconate it must be observed that, as a consequence of the methylene group in the side chain, the bond angles give rise to a repulsion between the carboxylate groups which is intermediate to that of succinate and maleate (see the initial part of the Discussion). The enthalpy of association of this ligand, which is intermediate to the enthalpy of succinate and maleate (Table 2) may be justified with this assumption. In the same manner, the $\Delta S^{\circ}$ of itaconate is similar to those of succinate and maleate (9.0 vs 9.5 and 9.4 cal $K^{-1}$ $mol^{-1}$), while it is more distant from the value of fumarate (7.2 cal $K^{-1}$ $mol^{-1}$). Therefore the present data seem to suggest for the calcium-itaconate complexes a structure similar to that of succinate and maleate, and, on the other hand, tend to discard the hypothesis of charge transmission. This fact may be justified in terms of

entropy, since an only partial charge neutralization should take place in the presence of charge transmission (conformation C), while a complete neutralization is obtained with the usual structure of itaconate.



C

## REFERENCES


1. L. J. Andrews and R. M. Keefer, *J. Am. Chem. Soc.* 1949, **71**, 2379.
2. R. M. Keefer, L. J. Andrews and R. E. Kepner, *J. Am. Chem. Soc.* 1949, **71**, 2381.
3. J. K. Hurst and R. H. Lane, *J. Am. Chem. Soc.* 1973, **95**, 1703.
4. G. R. Choppin, A. Dadgar and R. Stampfli, *J. Inorg. Nucl. Chem.* 1973, **35**, 875.
5. L. G. Sillén and A. E. Martell, *Stability Constants of Metal–Ion Complexes—Special Publication No.* 17. The Chemical Society, London, 1964.
6. M. Yasuda, K. Yamasaki and H. Ohtaki, *Bull. Chem. Soc. Jap.* 1960, **33**, 1067.
7. M. P. Gupta, S. M. Prasad, R. G. Sahu and B. N. Sahu, *Acta Cryst.* 1972, **B28**, 135.
8. J. J. Christensen, D. J. Eatough and R. M. Izatt, *Handbook of Metal Ligand Heats.* Marcel Dekker, New York (1975).
9. R. Aruga, *Aust. J. Chem.* 1981, **34**, 501.
10. N. E. Topp and C. W. Davies, *J. Chem. Soc.* 1940, 87.
11. J. Schubert and A. Lindenbaum, *J. Am. Chem. Soc.* 1952, **74**, 3529.
12. L. G. Sillén, *Acta Chem. Scand.* 1962, **16**, 159.
13. G. H. Nancollas, *Interactions in Electrolyte Solutions.* Elsevier, Amsterdam (1966).
14. R. Aruga, *Inorg. Chem.* 1980, **19**, 2895.
15. I. R. Desai and V. S. K. Nair, *J. Chem. Soc.* 1962, 2360.
16. R. E. Dodd, R. E. Miller and W. F. K. Wynne-Jones, *J. Chem. Soc.* 1961, 2790.
17. J. Bjerrum, *Chem. Rev.* 1950, **46**, 381.
18. D. E. Goldberg and W. C. Fernelius, *J. Phys. Chem.* 1959, **63**, 1246.
19. R. K. Cannan and A. Kibrick, *J. Am. Chem. Soc.* 1938, **60**, 2314.
20. *Molecular Structures and Dimensions*, Vol. A1. Crystallographic Data Centre, Cambridge (1972).
21. K. Nozaki and R. Ogg, Jr., *J. Am. Chem. Soc.* 1941, **63**, 2583.
22. L. Pauling, *The Nature of the Chemical Bond*, 2nd Edn. Cornell University Press, London (1945).
23. R. M. Izatt, D. Eatough, J. J. Christensen and C. H. Bartholomew, *J. Chem. Soc.* (*A*) 1969, 45.
24. J. W. Larson, *J. Phys. Chem.* 1970, **74**, 3392.

*Polyhedron* Vol. 3, No. 5, pp. 551–558, 1984
Printed in Great Britain.

0277-5387/84 $3.00 + .00
Pergamon Press Ltd.

# METAL COMPLEXES OF SOME ASYMMETRIC DIAMINODIAMIDE LIGANDS—II[1]. STABILITIES OF COMPLEXES OF NICKEL(II) IN AQUEOUS SOLUTION[2]

**MARIEL M. MUIR,* JOSE A. DIAZ[3] and LYDIA OYOLA**
Department of Chemistry, University of Puerto Rico, Rio Piedras, Puerto Rico 00931

(*Received* 27 *July* 1983; *accepted* 23 *September* 1983)

**Abstract**—Equilibria between a series of asymmetric diaminodiamides and Ni(II) in aqueous solution have been studied by potentiometric and spectrophotometric methods. The ligands were S,R,S– and S,S,S–N,N′-dialanylpropylenediamine (DAPN), S,S–N,N′-dialanylethylenediamine (DAEN), R–N,N′-diglycylpropylenediamine (DGPN), and N,N′-diglycylethylenediamine (DGEN). At lower values of pH the complexes $NiL^{2+}$ and in some cases $NiL_2^{2+}$ were formed. Spectral data indicated that both of these were octahedral. At higher pH the two amide protons were lost and square planar complexes were formed. The diastereomeric DAPN ligands showed stereoselectivity in the equilibrium constants for deprotonation and formation of the square planar complexes. Comparison of optical rotatory dispersion curves and absorption spectra for the various complexes permits partial assignment of structures.

The importance of deprotonated planar peptide linkages in the metal complexes of peptides and other amides has been amply demonstrated.[4–17] Studies have been made of the complexes of the diaminodiamide, N,N′-diglycylethylenediamine (DGEN),[18–25] and several of its methyl C-substituted derivatives,[1] in which the presence of two amino groups can provide additional stabilization for the complexes. The previous paper in this series[1] reported the equilibria in aqueous solution between Cu(II) and a series of asymmetric diaminodiamides, $H_2N$–CHR–CO–NH–CHR′–$CH_2$–NH–CO–CHR–$NH_2$. The ligands used included S,R,S– and S,S,S–N,N′-dialanylpropylenediamine (DAPN, R = R′ = $CH_3$), S,S–N,N′-dialanylethylenediamine (DAEN, R = $CH_3$, R′ = H), R–N,N′-diglycylpropylenediamine (DGPN, R = H, R′ = $CH_3$), and DGEN (R = R′ = H). The methyl groups on the carbon chains were found to affect the equilibrium constants. The greatest effect was observed for the deprotonation of the dimer $[(CuH_{-1}L)_2]$ when the central carbon chain was substituted (R′ = $CH_3$). Some stereoselectivity was observed for the diastereomeric SRS– and SSS–DAPN systems.

It seemed of interest to study the same ligands with Ni(II) in aqueous solution. Previous studies[19,23,24] on the Ni(II)–DGEN system showed that as the pH was increased there was a slow interconversion from the blue, octahedral complex to a yellow, square planar complex. It was expected there should be steric effects on both the equilibria and the rates for the complexes of Ni(II) with the same series of methyl substituted ligands. The determinations of the equilibrium constants for the SRS–DAPN, SSS–DAPN, SS–DAEN, and R–DGPN complexes of Ni(II) are reported here. The rate studies will be reported in a subsequent paper.

## RESULTS AND CALCULATIONS

### *Potentiometric titrations*

In all titrations, NaOH was added to solutions containing Ni(II) and the dihydrochloride salt of the diaminodiamide, $[H_2L]Cl_2$. Constants and corrections to the values of pH and the analytical concentrations of ligand, metal and base, $C_L$, $C_M$ and $C_B$, respectively, were as described previously,[1] as were the values of the acid protonation constants, $K_1^H$ and $K_2^H$:

$$K_1^H = \frac{[HL^+]}{[H^+][L]} \quad (1)$$

$$K_2^H = \frac{[H_2L^{2+}]}{[H^+][HL^+]}. \quad (2)$$

*Author to whom correspondence should be addressed.

Typical curves obtained from the potentiometric titrations with NaOH of the diaminodiamides in the presence and absence of Ni(II) are shown in Figs. 1 and 2. In each figure, curve *A* is for the titration of the dihydrochloride salt of the diaminodiamide in which the two ammonium protons dissociate from the ligand salt, $H_2L^{2+}$, in overlapping steps. Curve *B* is for titration of a mixture with a 1 : 1 ligand to metal ratio and curve *C* is for a 2 : 1 ligand to metal ratio.

For titrations in which the ligand to metal ratio is 1 : 1, it can be seen that four protons dissociate, two from the ammonium groups of the ligand hydrochloride salt and two from the amide groups of the ligand. The presence of two breaks in curve *B* of Fig. 1, which is for the titration of R–DGPN and Ni(II) in a 1 : 1 ratio, indicates that the two ammonium protons dissociate in overlapping steps and that the two amide protons then dissociate, also in overlapping steps. A similar curve was

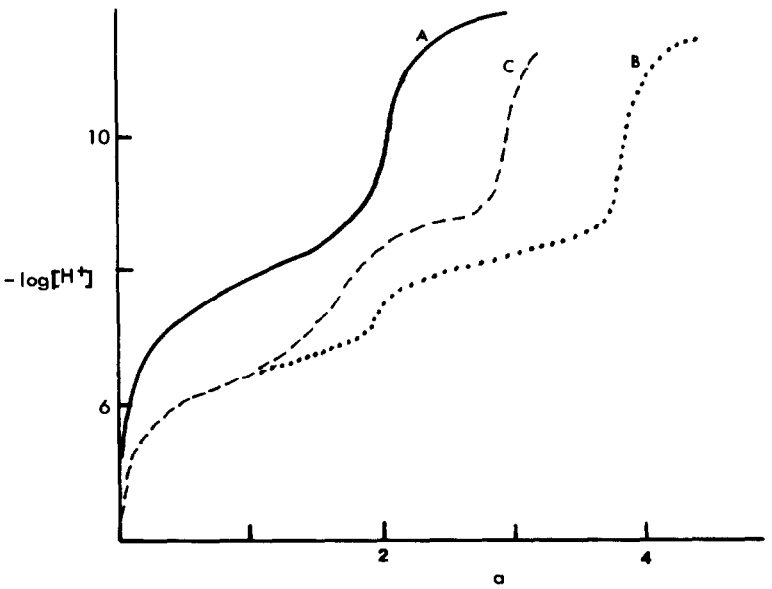



Fig. 1. Potentiometric titration curves for R–DGPN and its nickel(II) complexes. Solution concentrations: (A), $1.00 \times 10^{-3}$ M DGPN; (B), $1.00 \times 10^{-3}$ M DGPN and $Ni(NO_3)_2$; (C), $2.00 \times 10^{-3}$ M DGPN and $1.00 \times 10^{-3}$ M $Ni(NO_3)_2$. All solutions were 0.10 M in $KNO_3$.

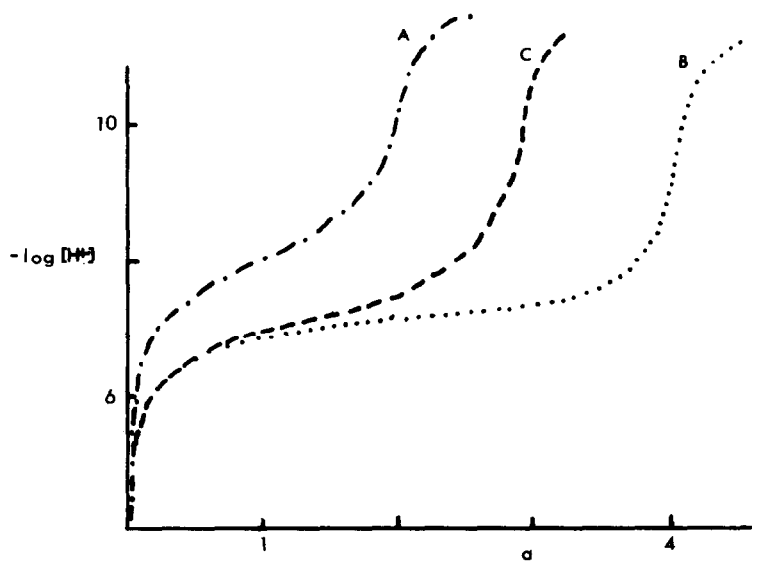



Fig. 2. Potentiometric titration curves for SRS–DAPN and its nickel(II) complexes. Solution concentrations: (A), $1.00 \times 10^{-3}$ M DAPN; (B), $1.00 \times 10^{-3}$ M DAPN and $Ni(NO_3)_2$; (C), $2.00 \times 10^{-3}$ M DAPN and $1.00 \times 10^{-3}$ M $Ni(NO_3)_2$. All solutions were 0.10 M in $KNO_3$.

reported for DGEN.[19] The breaks in curve *C* of Fig. 1 show similar pairs of overlapping steps for the 2:1 case for DGPN.

However, for the other diaminodiamides, SS–DAEN, SRS–DAPN, and SSS–DAPN, only one break was observed in the titration curves, as shown for SRS–DAPN in Fig. 2.

The attainment of equilibrium was slow in the region from $a = 1.5$–4 for all the 1 : 1 titrations, where $a$ is the molar ratio of base added to ligand. For $a > 4$, the systems reached equilibrium rapidly. The equilibria considered by Martell for the DGEN–Ni(II) system[19] were found by iterative calculations to give consistent values of the constants at several different concentrations, with the exception of $K_2$ in the cases to be discussed below. The equilibrium expressions were:

$$M^{2+} + L \rightleftharpoons ML^{2+} \qquad K_1 = \frac{[ML^{2+}]}{[M^{2+}][L]} \quad (3)$$

$$ML^{2+} + L \rightleftharpoons ML_2^{2+} \qquad K_2 = \frac{[ML_2^{2+}]}{[ML^{2+}][L]} \quad (4)$$

$$ML^{2+} \rightleftharpoons MH_{-2}L + 2H^+ \quad K_{1AB} = \frac{[MH_{-2}L][H^+]^2}{[ML^{2+}]} \quad (5)$$

where M = Ni and L = diaminodiamide.

Below $a = 2$ for the 1 : 1 titration, reaction (3) is the major reaction, and reactions (4) and (5) can be neglected for DGEN and R–DGPN. However even for $a < 2$, reaction (5) must be considered for L = SS–DAEN, SRS–DAPN, and SSS–DAPN. Initial estimates of the constants were obtained by making simplifying assumptions for limited titration ranges. $K_1$ was approximated from data in the range $a = 0.5$–1.6 for 1 : 1 titrations by assuming the concentrations $[ML_2^{2+}]$ and $[MH_{-2}L]$ to be negligible. $K_{1AB}$ was estimated for the range $a = 2.3$–3.8 by assuming $[ML_2^{2+}]$ and $[M^{2+}]$ were negligible. For 2 : 1 titrations, estimates of $K_1$ and $K_2$ were obtained from modified Bjerrum plots of $[L](2 - \bar{n})/(1 - \bar{n})$ as a function of $\bar{n}/((1 - \bar{n})[L])$.

The values of $K_1$, $K_2$ and $K_{1AB}$ were then refined by minimization of

$$S = (T_H^{obs} - T_H^{calc})^2 \quad (6)$$

from $a = 0.05$ to 2.9 for 2 : 1 or from $a = 0.05$ to 3.9 for 1 : 1 titrations, where

$$T_H^{obs} = 4C_L - C_B \quad (7)$$

$$T_H^{calc} = 4[H_2L^{2+}] + 3[HL^+] + 2[L] + 2[ML^{2+}] + 4[ML_2^{2+}] + [H^+] - [OH^-]. \quad (8)$$

The values obtained for the equilibrium constants are listed in Table 1. For SS–DAEN, SRS–DAPN, and SSS–DAPN only an upper limit is given for $K_2$. In these cases the loss of the amide protons and formation of the yellow, square planar complex occurred at a low value of $a$ and no consistent value for $K_2$ could be obtained.

*Spectrophotometric titrations*

The absorption spectra of the 1 : 1 diaminodiamide–Ni(II) systems are shown in Figs. 3–5. Before the addition of base, essentially no complex formation can be observed. As base is added, until $a = 1$, the absorption maximum shifts toward shorter wavelength, with a small increase in intensity, which indicates the formation of the blue octahedral complex. A rather pronounced change in the spectrum for R–DGPN with Ni(II) could be observed near $a = 2$, as shown in Fig. 3. The DGEN system gave a very similar change. This

Table 1. Average values of equilibrium constants for the interaction of diaminodiamides with Ni(II)

| Ligand | Log $K_1^H$ | Log $K_2^H$ | Log $K_1$ | Log $K_2$ | Log $K_{1AB}$ |
|---|---|---|---|---|---|
| DGEN[a] | 8.22 | 7.48 | 5.38 | 3.04 | -16.04 |
| DGEN[b] | | | 5.32 | | -16.46 |
| DGEN | 8.22(2) | 7.48(2) | 5.04(5) | d | -16.06(4) |
| R-DGPN | 8.23(3)[c] | 7.50(6) | 5.46(4) | 4.31(8) | -15.64(5) |
| SS-DAEN | 8.30(4) | 7.34(3) | 4.52(6) | <3 | -15.02(7) |
| SRS-DAPN | 8.26(3) | 7.38(4) | 4.64(7) | <3 | -14.76(7) |
| SSS-DAPN | 8.31(3) | 7.37(4) | 4.66(7) | <3 | -15.04(8) |

a) Data taken from ref. 19.
b) Data taken from ref. 25.
c) Values in parentheses represent the average deviations in the final digit of the numbers
d) Not measured in this work.

change was not observed for SS–DAEN, SRS–DAPN, or SSS–DAPN. In fact, for SS–DAPN, shown in Fig. 5, no trace of the band with $\lambda_{max} < 400$ nm could be observed. The spectra for the SS–DAEN system were nearly identical to those shown in Fig. 4 for SRS–DAPN. The absorption spectra for 2 : 1 mixtures were quite similar to the corresponding 1 : 1 spectra. For R–DGPN, a band at 365 nm was observed when $a = 1.5$ in the 2 : 1 mixture, as has been reported for DGEN.[19] This was attributed to $NiL_2^{2+}$ in the solution, which is consistent with the concentrations calculated from the equilibrium constants for DGEN and R–DGPN. No evidence for this band could be found for the other diaminodiamide systems. The final spectra in all the systems are very similar and can be assumed to belong to the square planar complex formed in all the systems upon loss of the amide protons.

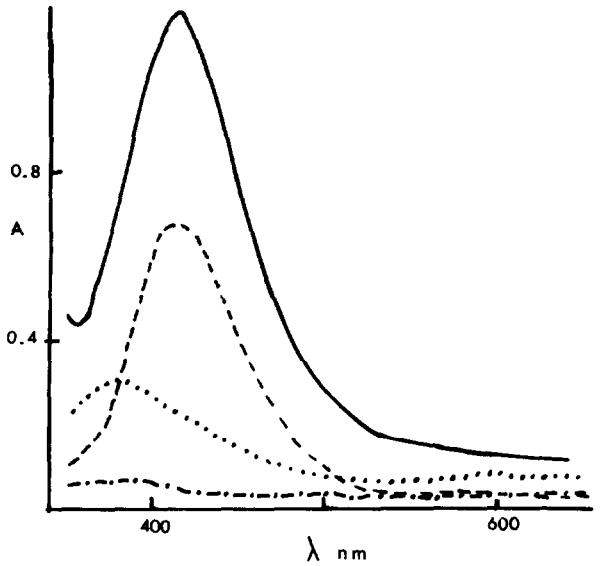



Fig. 3. Absorption spectra for 1:1 reaction mixtures of R–DGPN and Ni(II) after equilibrium. $C_M = 0.00974$ M, $C_L = 0.0117$ M. –·–·–·– $a = 1$, pH = 7.039; ····· $a = 2$, pH = 7.565; ----- $a = 3$, pH = 8.034; ——— $a = 4$, pH = 9.925.

The qualitative observations made during the titrations are consistent with these spectral data. Gradual colour changes were observed on addition of base to the DGEN–Ni(II) mixtures, from the initial pale green, to blue, and finally to yellow. The blue colour was most intense just before the molar ration of base to ligand reached a value of 2. However, no blue colour was observed during the titrations of the other ligands, DAEN and DAPN, with Ni(II).

Optical rotatory dispersion curves were obtained for the same solutions of Ni(II) with the diaminodiamides. The curves for R–DGPN at values of $a < 2$, shown in Fig. 6, were different than those for the other three optically active ligands. This is consistent with the potentiometric and visible absorption data. Only the DGPN and DGEN maintain a substantial concentration of the blue octahedral complex up to $a = 2$. In the other systems, the square planar complex forms to a significant extent below $a = 2$. For larger values of $a$, the Cotton effect is similar in shape and negative

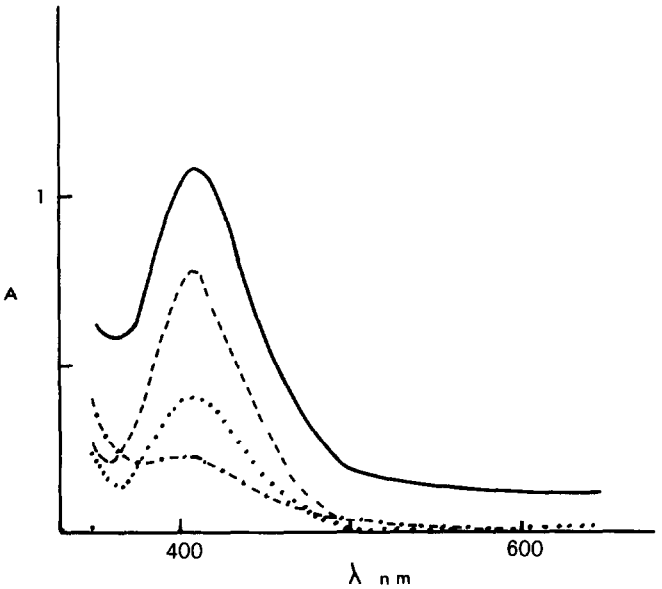



Fig. 4. Absorption spectra for 1 : 1 reaction mixtures of SRS–DAPN and Ni(II) after equilibrium. $C_M = 0.00974$ M, $C_L = 0.0126$ M. –·–·–·– $a = 1$, pH = 6.975; ····· $a = 2$, pH = 7.306; ------ $a = 3$, pH = 7.527; ——— $a = 4$, pH = 9.232.

for solutions of Ni(II) with R–DGPN (Fig. 6), SS–DAEN, and STS–DAPN (Fig. 7). However, the Cotton effect for the more basic solutions of SSS–DAPN with Ni(II) is positive and almost the mirror image of the curve for the diastereomeric SRS–DAPN, as can be seen in Fig. 8. The increase in the molar rotation with increasing $a$ corresponds to the increase in the concentration of the yellow, planar species.

## DISCUSSION

The relative stabilities of the octahedral complexes, based on the values of $K_i$ can be summarized as:

$$\text{R–DGEN} > \underset{\simeq}{\text{DGEN}} > \text{SSS–DAPN} \simeq \text{SRS–DAPN} > \underset{\simeq}{\text{SS–DAEN}}.$$

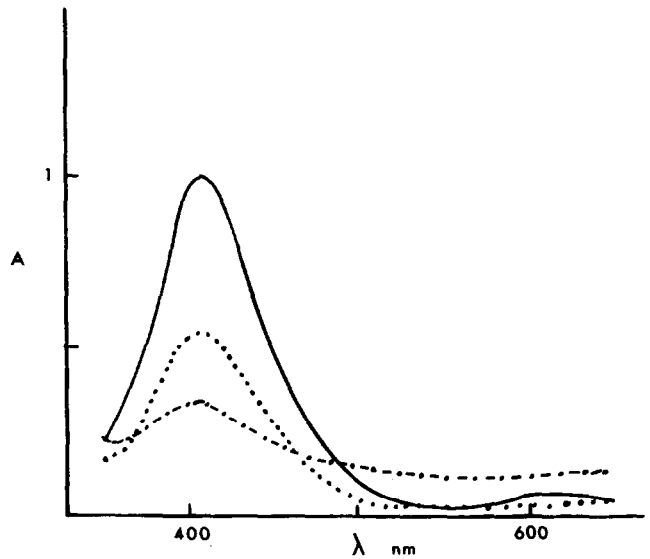



Fig. 5. Absorption spectra for 1 : 1 reaction mixtures of SSS–DAPN and Ni(II) after equilibrium. $C_M = 0.00974$ M, $C_L = 0.0123$ M. –·–·–·– $a = 1$, pH = 7.205; ····· $a = 2$, pH = 7.462; ——— $a = 4$, pH = 10.128.

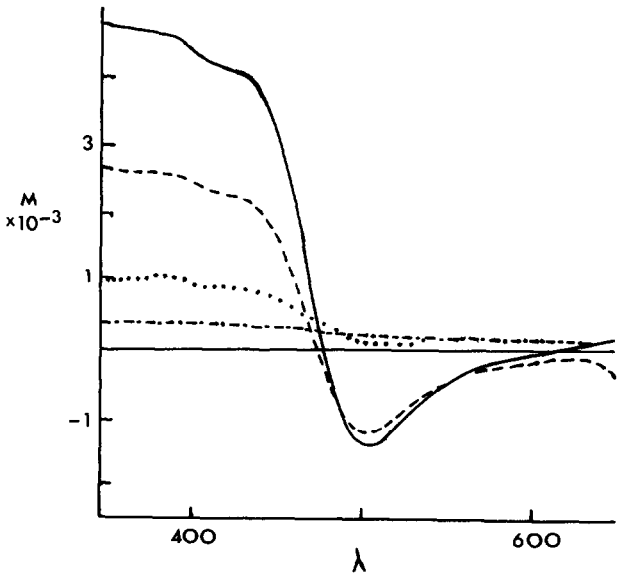



Fig. 6. Optical rotatory dispersion for 1 : 1 reaction mixtures of R–DGPN and Ni(II) after equilibrium. $C_M = 0.00974$ M, $C_L = 0.0117$ M. –·–·–·– $a = 1$, pH = 7.039; ····· $a = 2$, pH = 7.565; – – – – – $a = 3$, pH = 8.034; ——— $a = 4$, pH = 9.925.

The relative stabilities of the square planar complexes, based on the values of $K_{1AB}$ are:

$$\text{SRS–DAPN} > \text{SSS–DAPN} \simeq \text{SS–DGPN} > \text{R–DGPN} > \text{DGEN}.$$

These differences in stability can be rationalized by considering two types of steric effect, those due to methyl substituents on the side arms near the terminal amino groups and those due to methyl substituents on the central chain next to an amido nitrogen.

For the octahedral complexes, substituents on the side arms decrease the stability, while substituents on the central chain seem to increase the stability. Thus, the octahedral R–DGPN complex is slightly more stable than the corresponding DGEN complex of Ni(II). A similar effect has been observed in the relative stabilities of the glycylglycine and glycyl-L-alanine complexes.[26] Log K for the glycylglycine copper(II) complex was reported to be 5.43 whereas the corresponding value for the glycyl-L-alanine complex was 5.31.[26]

Much larger differences occur for the de-

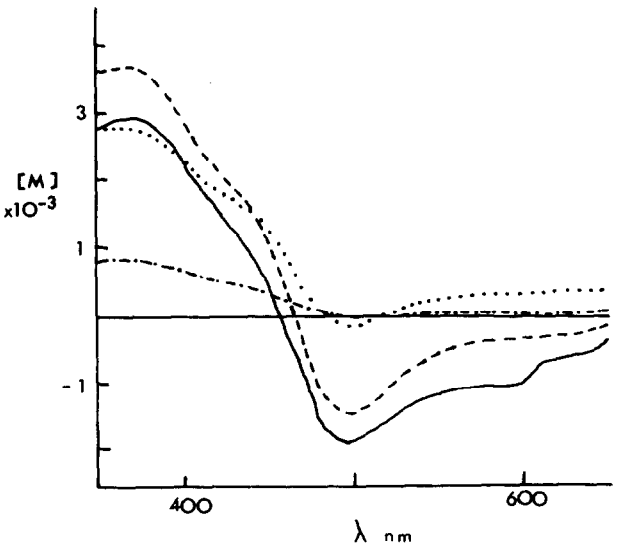



Fig. 7. Optical rotatory dispersion for 1 : 1 reaction mixtures of SRS–DAPN and Ni(II) after equilibrium. $C_M = 0.00974$ M, $C_L = 0.0126$ M. –·–·– $a = 1$, pH = 6.975; ····· $a = 2$, pH = 7.306; ––––– $a = 3$, pH = 7.527; ——— $a = 4$, pH = 9.232.

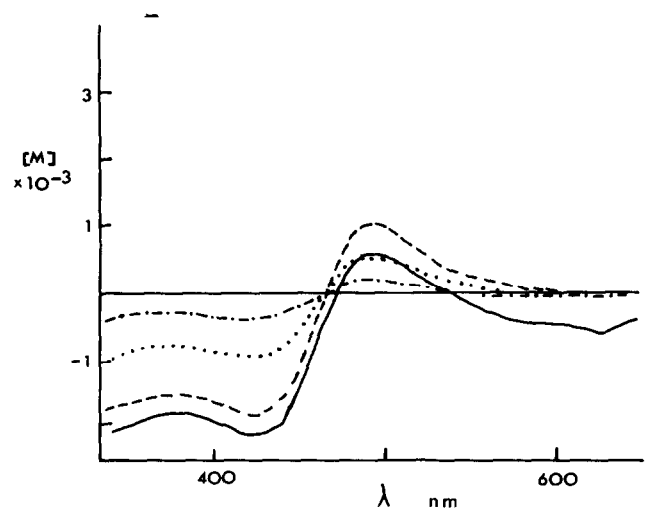



Fig. 8. Optical rotatory dispersion for 1 : 1 reaction mixtures of SSS–DAPN and Ni(II) after equilibrium. $C_M = 0.00974$ M, $C_L = 0.0117$ M. –·–·– $a = 1$, pH = 7.205; ····· $a = 2$, pH = 7.476; ––––– $a = 3$, pH = 8.045; ——— $a = 4$, pH = 10.128.

protonation and rearrangement to the square planar complex. The shapes of the titration curves suggest that the loss of the amide protons is a cooperative process, that is, once one of these protons has been released, the other is lost rapidly and there is a transition from the octahedral form to the square planar form of the complex. There are never any appreciable amounts of $NiH_{-1}L$ present in the solution. This kind of behaviour has been observed before with polypeptides[7] containing more than one ionizable peptide hydrogen. It has also been confirmed in the nickel(II) diglycylethylenediamine system by magnetic susceptibility measurements.[23] Including separate deprotonation steps in the calculations of the equilibrium constants did not give any improvement in the fit of the data. Methyl substituents on the side arms cause a marked increase in the tendency for deprotonation and rearrangement in the complexes studied here. There is also an increase in this tendency with methyl substituents in the central chain, as can be seen by comparison of the $K_{\lambda AB}$ values for *R–DGPN* and *DGEN*.

Although the formation constants for a series of 1 : 2 complexes of Ni(II) with carbon substituted ethylenediamine ligands are very similar,[26] the formation constants of the 1 : 3 complexes decrease with increasing carbon substitution, probably because of steric factors. Thus, carbon substitution has been found to increase the stability of the square planar complexes relative to the six coordinate octahedral complexes to the extent that only a square planar, yellow form was found[26] for tetramethylethylendiamine complexes of Ni(II). This tendency could explain the reduced stability of the $ML_2^{2+}$ complexes of SS–DAEN, SRS– and SSS–DAPN relative to the analogous complexes of DGEN and R–DGPN, so that the 1 : 2 complexes with the former ligands were not observed.

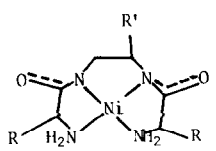
Although there are differences in stabilities, a comparison of the potentiometric curves, the absorption spectra, and the ORD curves suggests that the same structural changes are occurring in all of these systems as base is added. An examination of molecular models for the deprotonated square planar complexes of nickel(II) with these ligands shows that the steric requirements of the deprotonated peptide bond force the side chelate rings to be almost planar, while the central chelate ring adopts a gauche form. In order for the methyl group of the central ring to have the more stable equatorial conformation in the planar complexes with the ligands R–DGPN and SRS–DAPN, it is necessary that this ring adopt the $\lambda$ conformation. Since the SS–DAEN planar complex has an ORD curve almost identical to that of the SRS–DAPN complex, the central ring in the SS–DAEN complex must also have the $\lambda$ conformation. Thus, it can be concluded that the chirality found for the central ring conformation in the planar complexes determines the shape of the ORD curves. This is confirmed by the ORD curve observed for the SSS–DAPN complex, shown in Fig. 6. In order for the methyl group in the central ring of this complex to adopt an equatorial position, the conformation of the chelate ring must be $\delta$, which is opposite to that of the other planar complexes. The ORD curves for solutions containing the planar complex of SSS–DAPN are nearly mirror images of those observed for the complexes with all the other diaminodiamides. The structures of these planar complexes should all be like that proposed for DGEN,[18] as shown in structure **I**.

Two different structures have been proposed[18] for the 1 : 1 octahedral complex of DGEN in aqueous solution. These are shown in structures **II** and **III**. Molecular models do not allow an easy choice to be made between the two, and the equilibrium constants do not help with this choice. Structure **II** in which both carbonyl oxygens and both amino nitrogens are coordinated gives a rather distorted octahedron. Structure **III**, in which only one of the carbonyl oxygens is coordinated, gives a more regular geometry for the donor atoms, but has a very large chelate ring. No choice can be made between the two on the basis of this work.

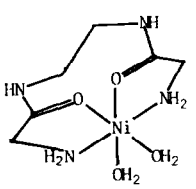
## EXPERIMENTAL

### *Materials*

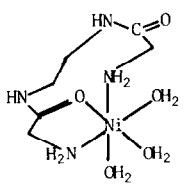
The syntheses and characterization of the ligands have been reported previously.[1,28] The ligands were obtained as the dihydrochloride salts. The purity of each sample was established by titration with standard NaOH. All other chemicals were reagent grade. Solutions of Ni(II) were standardized by addition of excess standardized EDTA




I




II




III

and back-titration with magnesium ion with Eriochrome Black T as indicator.

*Potentiometric titrations*

Potentiometric titrations were carried out with a Corning model 12 pH meter equipped with a micro combination electrode, which was standardized using standard buffer solutions. The ionic strength was maintained relatively constant by using a supporting electrolyte of 0.10 M $KNO_3$. All experiments were carried out at $25.0 \pm 0.1$ °C.

The dissociation of the amide protons and rearrangement was a slow process, so a batch titration method was used in which aqueous solutions of $Ni(NO_3)_2 \cdot 6H_2O$ and $[H_2L]Cl_2$ to which different amounts of NaOH had been added were allowed to equilibrate in a constant temperature water bath until a constant pH was attained. The titration vessel was a 50 $cm^3$ filter flask fitted with a syringe cap through which a glass tube was inserted. This tube and the sidearm were stoppered while the solution was allowed to equilibrate. To obtain measurements, the stoppers were removed, the micro combination electrode was inserted through the glass tube and $N_2$ was introduced with a needle through the syringe cap. The sidearm served as the $N_2$ outlet. After equilibrium was reached for a solution with a given quantity of base, an additional increment of base could be introduced through the glass tube. From five to ten flasks were kept in the bath. This system permitted the use of the same electrode for all the readings without removing the samples from the bath.

*Spectrophotometric titrations*

Visible absorption spectra were obtained on a Perkin–Elmer 202 or Hitachi 139 spectrophotometer after solutions reached the equilibrium pH values. Values of optical rotation were obtained with a Perkin–Elmer 141 polarimeter equipped with a Bausch and Lomb grating monochromator and Xenon source. The visible spectra were obtained with matched quartz 1.00 cm cells and rotation measurements in a 10 cm cell. The ionic strength was adjusted with KCl instead of with $KNO_3$ for these measurements.

*Acknowledgements*—This work was supported in part by the NIH Division of Reasearch Resources through grant RR-8102. We thank the University of Puerto Rico Computer Center for generous grants of time and Lourdes M. Torres and Ruben Saez for help with measurements.

## REFERENCES

1. Part I: M. M. Muir and P. R. Rechani, *Inorg. Chim. Acta* 1974, **11**, 137.
2. Presented in part at the *Int. Symposium on Biological Aspects of Inorganic Chemistry*, Vancouver, B.C., Canada (June 1976).
3. Taken from the thesis submitted by J. A. D. to the University of Puerto Rico in partial fulfillment of the requirements for the degree Ph.D. (1977).
4. H. C. Freeman, In *The Biochemistry of Copper* (Edited by J. Peisach, P. Aisen and W. E. Blumberg), p. 77. Academic Press, New York (1966).
5. M. K. Kim and A. E. Martell, *Biochem.* 1964, **3**, 1169.
6. M. K. Kim and A. E. Martell, *J. Am. Chem. Soc.* 1966, **88**, 914.
7. M. K. Kim and A. E. Martell, *J. Am. Chem. Soc.* 1967, **89**, 5138.
8. H. C. Freeman, In *Inorganic Biochemistry* (Edited by G. I. Eichhorn), pp. 121–166. Elsevier, Amsterdam (1973).
9. S. Linskog, *Struct. Bonding* 1970, **8**, 153.
10. M. Llinas, *Struct. Bonding* 1974, **17**, 135.
11. A. S. Mildvan and C. M. Grisham, *Struct. Bonding* 1975, **20**, 1.
12. J. A. Fee, *Struct. Bonding* 1975, **23**, 1.
13. M. F. Dunn, *Struct. Bonding* 1975 **23**, 61.
14. F. P. Bossu, K. L. Chellappa and D. W. Margerum, *J. Am. Chem. Soc.* 1977, **99**, 2195.
15. J. C. Cooper, L. F. Wong and D. W. Margerum, *Inorg. Chem.* 1978, **17**, 261.
16. Y. Sugiura and Y. Mino, *Inorg. Chem.* 1979, **18**, 1336.
17. G. D. Owens, K. L. Chellappa and D. W. Margerum, *Inorg. Chem.* 1979, **19**, 960.
18. K. S. Bai and A. E. Martell, *Inorg. Chem.* 1970, **9**, 1126.
19. K. S. Bai and A. E. Martell, *J. Am. Chem. Soc.* 1969, **91**, 4412.
20. P. Pfeiffer and S. Saure, *J. Prakt. Chem.* 1941, **157**, 97.
21. A. K. Chakraburtty, N. N. Ghosh and P. Ray, *J. Indian Chem. Soc.* 1953, **30**, 185.
22. A. Zuberbuehler and S. Fallab, *Helv. Chim. Acta* 1967, **50**, 889.
23. K. S. Bai and A. E. Martell, *J. Inorg. Nucl. Chem.* 1973, **35**, 1313.
24. T. D. Smith and A. E. Martell, *J. Am. Chem. Soc.* 1972, **94**, 4123.
25. T. Kaden, *Helv. Chim. Acta* 1971, **54**, 625.
26. J. L. Biester and P. M. Ruoff, *J. Am. Chem. Soc.* 1959, **81**, 6517.
27. F. Basolo, Y. T. Chen and R. K. Murmann, *J. Am. Chem. Soc.* 1954, **76**, 956.
28. M. M. Muir, P. R. Rechani and J. A. Diaz, *Synth. React. Inorg. Met. -Org. Chem.* 1981, **11**, 317.
29. J. Bjerrum, *Chem. Rev.* 1950, **46**, 381.

*Polyhedron* Vol. 3, No. 5, pp. 559–566, 1984
Printed in Great Britain.

0277–5387/84 $3.00 + .00
© 1984 Pergamon Press Ltd.

# COPPER(II) COMPLEXES OF DIAMINODIAMIDES IN AQUEOUS SOLUTION

**SI-HAN LIU and CHUNG-SUN CHUNG***
Department of Chemistry, National Tsing Hua University, Hsinchu, Taiwan 300, Republic of China

(*Received* 15 *August* 1983; *accepted* 24 *October* 1983)

**Abstract**—The basicity constants of N,N′-bis(β-carbamoylethyl)ethylenediamine, N,N′-bis(β-carbamoylethyl)trimethylenediamine, N,N′-bis(β-carbamoylethyl)-1,2-propylenediamine, and N,N′-bis-(β-carbamoylethyl)-2-hydroxyltrimethylenediamine were determined potentiometrically in 0.10 mol dm$^{-3}$ $NaNO_3$ at 25.0°C. The formation of Cu(II) complexes of these ligands and the Cu–O to Cu–N bond rearrangements at the two amide sites of these complexes were investigated quantitatively by potentiometric and spectrophotometric techniques under the same conditions. Electronic spectra of the Cu(II) complexes of these ligands and their deprotonated species formed in aqueous solution were measured and discussed.

In our previous studies of Cu(II) complexes of N,N′-bis(β-carbamoylethyl)ethylenediamine, bcen[1] and N,N′-bis(β-carbamoylethyl)trimethylenediamine, bctn,[2] it was noted that Cu(II), after complexation with each of these ligands, can induce ionization of the amide protons, and the Cu–O to Cu–N bond rearrangements at the two amide sites occur with an increase in pH. The result of an X-ray crystallographic study[3] has shown unequivocally displacement of the amide proton in the solid $[CuH_{-2}L]$ and the coordination of the resulting negative amide groups to metal ion. We now report an extension of the previous investigations to include a study of the interactions of Cu(II) with the four closely related diaminodiamides depicted in Chart I at 25.0°C and 0.1 mol dm$^{-3}$, the detailed stepwise reactions which precede the formation of the Cu(II) complex with each of these ligands, and the Cu–O to Cu–N bond rearrangements at the two amide sites have now been studied by potentiometric and spectrophotometric techniques.

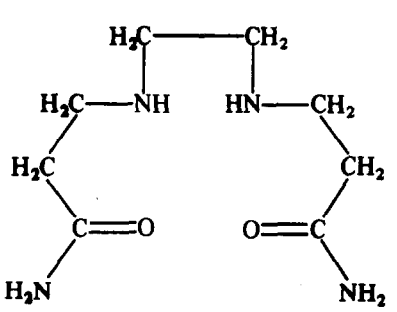
## EXPERIMENTAL

*Reagents.* The ligands, bcen and bctn, were the same as those reported previously.[1,2] The ligand, bchtn, was prepared from 2-hydroxytrimethylenediamine (18.0 g; 0.2 mol) and acrylamide (28.4 g; 0.4 mol) in acetonitrile (100 cm$^3$) by heating under reflux for 2 hr. The solution was cooled and the product filtered off, washed with cold chloroform, recrystallized from chloroform, and dried in air, m.p. 141–142.5°C (Found: C, 45.95; H, 8.80; N, 23.72. Calc. for $C_9H_{20}N_4O_3$: C, 46.54; H, 8.68; N, 24.12%). The compound was 99.9% pure as determined by titration with standard base. The ligand, bcmen, was prepared from 1,2-propylenedimaine (17.1 cm$^3$; 0.2 mol) and acrylamide (28.4 g; 0.4 mol) in acetonitrile (100 cm$^3$) by heating under reflux for 2 hr. The solution was cooled and the product filtered off, washed with cold N,N-dimethylformamide, recrystallized from N,N-dimethylformamide, and dried in air, m.p. 124–126°C. (Found: C, 50.00; H, 9.20; N, 25.55. Calc. for $C_9H_{20}N_4O_2$: C, 49.98; H, 9.32; N, 25.90%). The compound was 99.9% pure as determined by titration with standard base. All other chemicals used were of GR grade from Merck or Fluka.

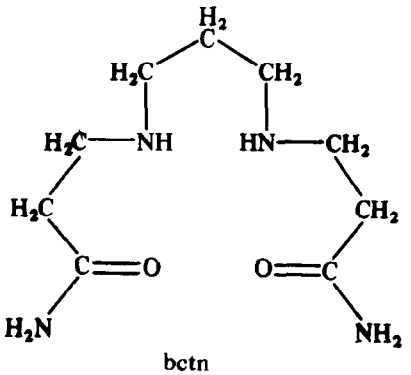
*Measurements.* For pH measurements a Radiometer PHM 64 equipped with a GK 2401B combined electrode was used. The pH was standardized with NBS buffers. The hydrogen-ion and hydroxide-ion concentrations in 0.1 mol dm$^{-3}$ $NaNO_3$ were calculated from $-\log[H^+] = pH - 0.11$ and $K_w = 10^{-13.78}$.[4]

Appropriate aliquots of standard solutions of ligand or ligand and metal were titrated with a standard sodium hydroxide solution. In all ti-

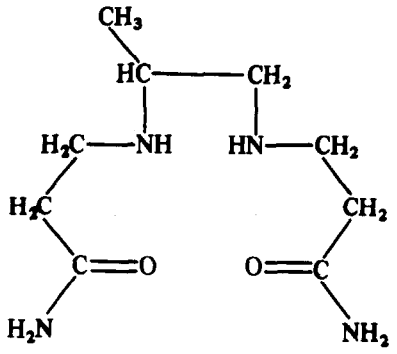
*Author to whom correspondence should be addressed.



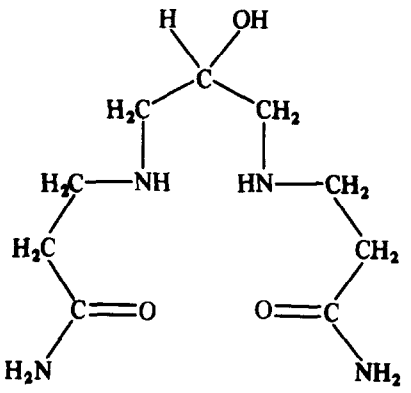
bcen



bctn



bcmen



bchtn

Chart I.

trations the ionic strength was maintained relatively constant by using 0.10 mol dm$^{-3}$ $NaNO_3$ as supporting electrolyte. The solutions were protected from air by a stream of humidified prepurified nitrogen and were maintained at 25.0 ± 0.1°C during measurements. The equilibrium constants were obtained by a linear least-squares fit of the data by using the CDC Cyber-172 computer. A Cary 17 spectrophotometer with a thermostated cell compartment was used to record absorption spectra.

*Calculations.* The methods of calculations are the same as reported previously.[1,2]

## RESULTS AND DISCUSSION

*Protonation constants.* A potentiometric titration of the nitrate salts of diprotonated ligands with standard base yielded the experimental data shown in Figs. 1–4. The values of the protonation constants of these four ligands obtained from these experimental data are listed in Table 1.

The sequence for $K_1^H$, bchtn < bcen, bcmen < bctn, is mainly due to the inductive effects of the constituent groups in the ligand. The values of the protonation constants of these diaminodiamides are all significantly lower than the corresponding constants of their parent diamines[5] in accord with the base-weakening effect of the neighboring amide group.[6]

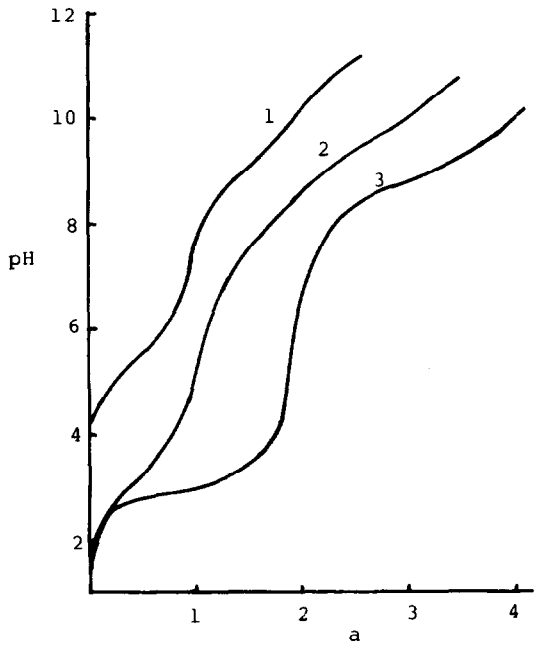



Fig. 1. Titration curves for bcen in the presence and absence of Cu(II) at 25.0 ± 0.1°C and in 0.10 mol dm$^{-3}$ sodium nitrate. Test solutions: (1) 20.0 cm$^3$, 0.00425 mol dm$^{-3}$ $[H_2bcen][NO_3]_2$; (2) 30.0 cm$^3$, 0.00331 mol dm$^{-3}$ $Cu[NO_3]_2$ and 0.00660 mol dm$^{-3}$ $[H_2bcen][NO_3]_2$; (3) 20.0 cm$^3$ 0.00500 mol dm$^{-3}$ in both $Cu[NO_3]_2$ and $[H_2bcen][NO_3]_2$. Titrant: 0.1025 mol dm$^{-3}$ sodium hydroxide; $a$ = number of moles of sodium hydroxide added per mol of ligand.

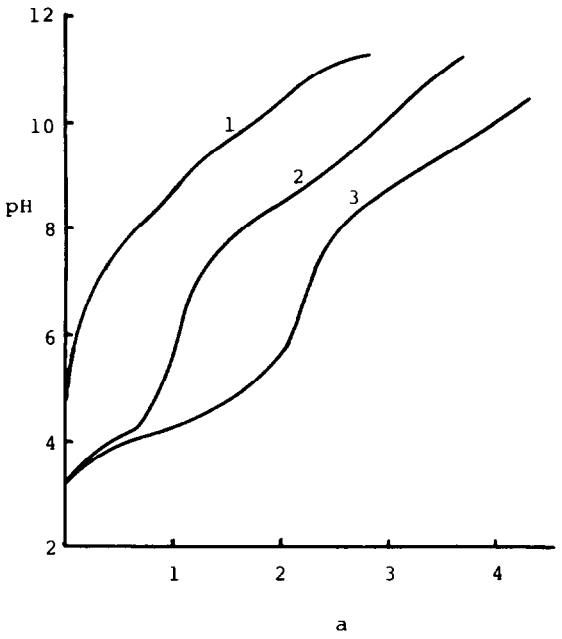



Fig. 2. Titration curves for bctn in the presence and absence of Cu(II) at 25.0 ± 0.1°C and in 0.10 mol dm$^{-3}$ sodium nitrate. Test solutions (1) 20.0 cm$^3$, 0.00365 mol dm$^{-3}$ $[H_2bctn][NO_3]_2$; (2) 30.0 cm$^3$, 0.00266 mol dm$^{-3}$ $Cu[NO_3]_2$ and 0.00532 mol dm$^{-3}$ $[H_2bctn][NO_3]_2$; (3) 20.0 cm$^3$, 0.00400 mol dm$^{-3}$ in both $Cu[NO_3]_2$ and $[H_2bctn][NO_3]_2$. Titrant: 0.1025 mol dm$^{-3}$ sodium hydroxide; $a$ = number of moles of sodium hydroxide added per mol of ligand.

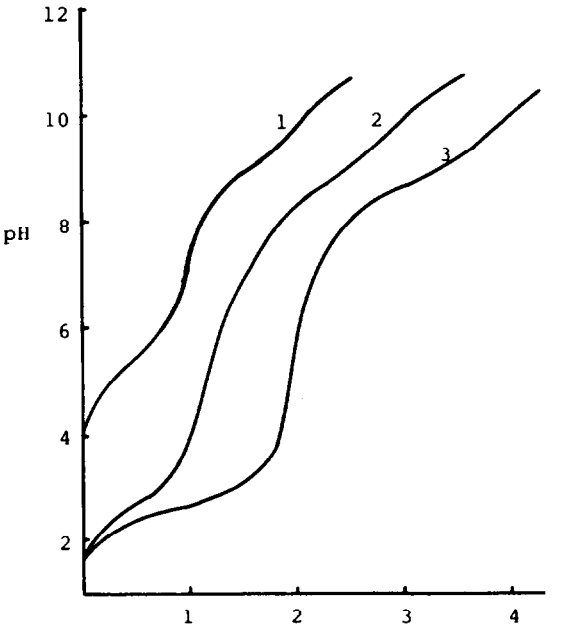



Fig. 3. Titration curves for bcmen in the presence and absence of Cu(II) at 25.0 ± 0.1°C and in 0.10 mol dm$^{-3}$ sodium nitrate. Test solutions: (1) 20.0 cm$^3$, 0.00424 mol dm$^{-3}$ $[H_2bcmen][NO_3]_2$; (2) 30.0 cm$^3$, 0.00340 mol dm$^{-3}$ $Cu[NO_3]_2$ and 0.00680 mol dm$^{-3}$ $[H_2bcmen][NO_3]_2$; (3) 20.0 cm$^3$, 0.00502 mol dm$^{-3}$ in both $Cu[NO_3]_2$ and $[H_2bcmen][NO_3]_2$. Titrant: 0.1025 mol dm$^{-3}$ sodium hydroxide; $a$ = number of moles of sodium hydroxide added per mol of ligand.

*Compositions of Cu(II) complexes.* Job's method of continuous variations was adopted for the determination of the composition of the complex. The results indicated that copper(II) forms a 1:1 complex with each of these four ligands.

*Equilibrium constants for the interactions of Cu(II) with diaminodiamides.* The complexation reactions of Cu(II) with these ligands are fast. During titration the colour of the solutions changed from blue to deep blue and finally to violet. The titration curves for these systems are shown in Figs. 1–4 (curves 2 and 3).

For the 1:1 Cu(II)–ligand solution (curve 3) a definite break at $a = 2$ is seen for each of these four

Table 1. Basicity constants of diaminodiamides and equilibrium constants of their Cu(II) complexes at 25.0 ± 0.1° and I = 0.10 mol dm$^{-3}$ ($Na[NO_3]$)

| logK | bcen | bctn | bcmen | bchtn |
|---|---|---|---|---|
| $\log K_1^H$ | 8.79±0.03 | 9.27±0.05 | 8.80±0.04 | 8.52±0.06 |
| $\log K_2^H$ | 5.80±0.03 | 7.01±0.04 | 5.47±0.04 | 6.58±0.06 |
| $\log K_f$ | 12.56 | 10.25 | 12.61 | 10.04 |
| $\log K_A$ | -7.98 | -8.53 | -8.12 | -8.31 |
| $\log K_B$ | -9.25 | -10.02 | -9.38 | -9.78 |

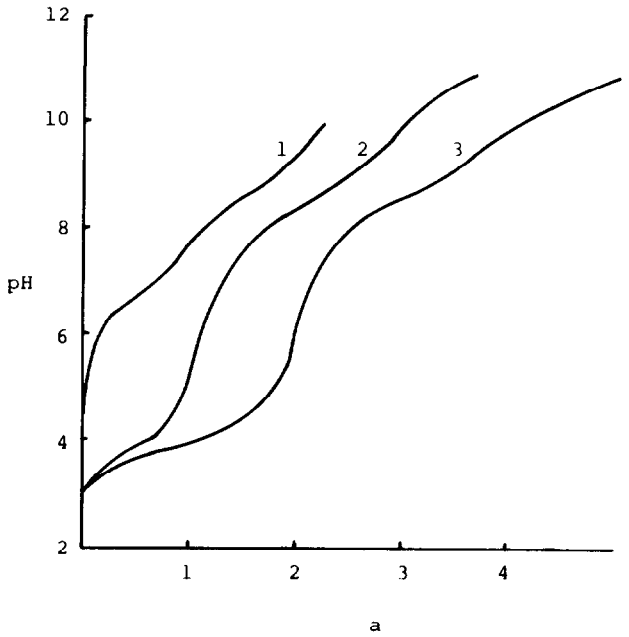



Fig. 4. Titration curves for bchtn in the presence and absence of Cu(II) at 25.0 ± 0.1°C and in 0.10 mol $dm^{-3}$ sodium nitrate. Test solutions: (1) 20.0 $cm^3$, 0.00393 mol $dm^{-3}$ $[H_2bchtn][NO_3]_2$; (2) 30.0 $cm^3$, 0.00261 mol $dm^{-3}$ $Cu[NO_3]_2$ and 0.00522 mol $dm^{-3}$ $[H_2bchtn][NO_3]_2$; (3) 20.0 $cm^3$, 0.00393 mol $dm^{-3}$ in both $Cu[NO_3]_2$ and $[H_2bchtn][NO_3]_2$. Titrant: 0.1025 mol $dm^{-3}$ sodium hydroxide; $a$ = number of moles of sodium hydroxide added per mol of ligand.

ligands. In the first (sloping) buffer region the two protons attached to the amine groups of the ligand are dissociated by the Cu(II) ion. In the second (sloping) buffer region the two amide protons are dissociated in overlapping steps. The equilibria (1)–(3) were found to describe the reactions of Cu(II) with each of these ligands,

$$Cu^{2+} + L \rightleftarrows [CuL]^{2+};$$
$$K_f = [CuL^{2+}]/[Cu^{2+}][L] \quad (1)$$

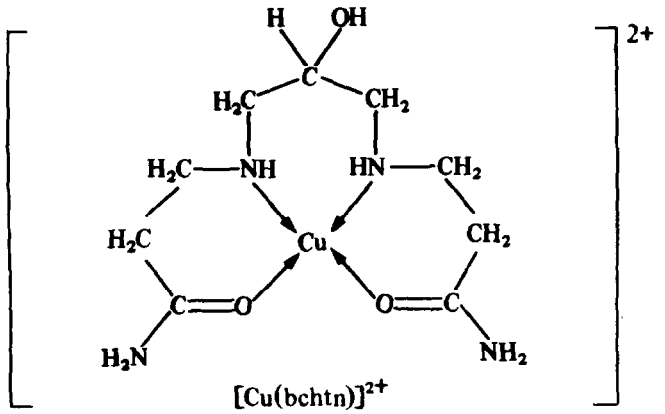
$$[CuL]^{2+} \rightleftarrows [CuH_{-1}L]^{+} + H^{+};$$
$$K_A = [CuH_{-1}L^{+}][H^{+}]/[CuL^{2+}] \quad (2)$$

$$[CuH_{-1}L]^{+} \rightleftarrows [CuH_{-2}L] + H^{+};$$
$$K_B = [CuH_{-2}L][H^{+}]/[CuH_{-1}L^{+}] \quad (3)$$

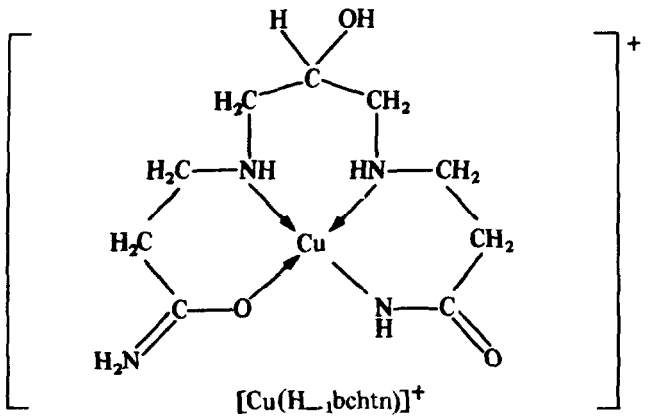
where L represents the unprotonated ligand and the negative subscript to H represents the number of amide protons removed from the complex. The three complexes $[CuL]^{2+}$, $[CuH_{-1}L]^{+}$, and $[CuH_{-2}L]$, where L is bchtn, are depicted in Chart II. The equilibrium constants obtained are listed in Table 1.

The stability constant varies in the order $[Cu(bcmen)]^{2+}$, $[Cu(bcen)]^{2+} > [Cu(bctn)]^{2+} > [Cu(bchtn)]^{2+}$. These sequence reflects that the most important factor influencing the stability of these Cu(II) complexes is the steric strains among the three linked chelate rings. Analogous to the transition-metal complexes of the linear quadridentate ligand N,N′-bis(3-aminopropyl)propane-1,3-diamine and macrocyclic quadridentate ligand 6,7,8,9,10,11,18,19-octahydro-5H,17H-dibenzo[f,o][1,5]dioxa-[9,13]diaza–cyclohexadecine,[7–9] the extremely large girdle strains in the three consecutive six-membered chelate rings significantly hinders the formation of metal complex and an alternating sequence of five- and six-membered rings increases complex stability.[9,10] In addition to the steric strains among the three linked chelate rings, the basicity of the ligand also influences the stabilities of these Cu(II) complexes. The very low stability constant for $[Cu(bchtn)]^{2+}$ is attributed to both the large steric strains among the three linked six-membered chelate rings and the low basicity of the ligand.

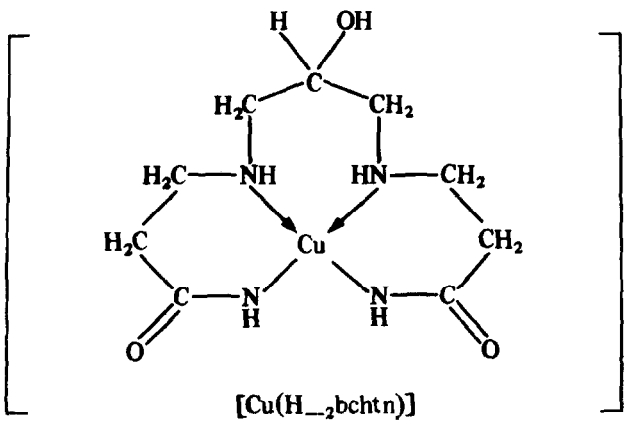
As pointed out previously,[1,2] Cu(II) can induce ionization of the amide protons, and the Cu–O to Cu–N bond rearrangements at the two amide sites occur with an increase in pH (eqns 2 and 3). These reactions take place in the region from $a$ = 2–4 of the 1:1 titration curve (curve 3) or in the region from $a$ = 1–3 of the 1:2 titration curve (curve 2). The values of the equilibrium constants for these reactions, obtained by using Schwarzenbach's




[Cu(bchtn)]$^{2+}$




[Cu(H$_{-1}$bchtn)]$^{+}$




[Cu(H$_{-2}$bchtn)]

Chart II.

method,[11] are listed in Table 1. The equilibrium constants, $K_A$, varies in the order $[Cu(bcen)]^{2+} > [Cu(bcmen)]^{2+} > [Cu(bchtn)]^{2+} > [Cu(bctn)]^{2+}$; and $K_B$ varies in the analogous order $[Cu(H_{-1}bcen]^{+} > [Cu(H_{-1}bcmen)]^{+} > [Cu(H_{-1}bchtn)]^{+} > [Cu(H_{-1}bctn)]^{+}$. These orders indicate that the steric strains in the three consecutive six-membered chelate rings increase in the order $[CuL]^{2+} < [CuH_{-1}L]^{+} < [CuH_{-2}L]$. In other words, the steric strains among three entirely saturated six-membered rings is larger than those when one or more double bonds are present in these rings.

Above $a = 4$ for the 1:1 solution and above

$a = 3$ for the 1:2 solution the titration curves are the same as those calculated assuming no further reaction between $[CuH_{-2}L]$ and hydroxide ion.

*Electronic spectra.* The electronic spectra of Cu(II)–bcmen solutions are shown in Fig. 5. At pH = 1.48 (curve 1), practically no complex formation takes place. As the concentration of base is increased, the band maximum increases in intensity (curves 2–4). Curve 4, at $a = 2$, is almost entirely due to the species $[Cu(bcmen)]^{2+}$. As the base concentration is further increased beyond $a = 2$ (curves 5–7) the band maximum shifts to shorter wavelengths. That curve 8 is identical with curve 9 confirms the potentiometric observation that no further reaction takes place between $[Cu(H_{-2}bcmen)]$ and $OH^-$.

The concentrations of all species present in the solution can be calculated by using the equilibrium constants listed in Table 1. Then, with eqn (4),

$$A = l(\epsilon_{Cu^{2+}}[Cu^{2+}] + \epsilon_{CuL^{2+}}[CuL^{2+}] + \epsilon_{CuH_{-1}L^{+}}[CuH_{-1}L^{+}] + \epsilon_{CuH_{-2}L}[CuH_{-2}L]) \quad (4)$$

the spectra in Fig. 5 can be resolved into their components. The absorption characteristics of all species so obtained are listed in Table 2.

The electronic spectra of Cu(II)–bchtn solutions are shown in Fig. 6. The same method was used to obtain the absorption characteristics of $[Cu(bchtn)]^{2+}$, $[Cu(H_{-1}bchtn)]^{+}$, and $[Cu(H_{-2}bchtn)]$. The results are given in Table 2, along with the reported values for the Cu(II)–bcen and Cu(II)–bctn systems.

As preliminary observations on the absorption maxima listed in Table 2, the following trends are particularly noteworthy.

1. For each of these ligands, the absorption maximum varies in the order $[CuL]^{2+} > [CuH_{-1}L]^{+} > [CuH_{-2}L]$.

2. For $[CuL]^{2+}$, the absorption maximum varies in the order $[Cu(bctn)]^{2+}$, $[Cu(bchtn)]^{2+} > [Cu(bcen)]^{2+}$, $[Cu(bcmen)]^{2+}$.

3. For $[CuH_{-1}L]^{+}$, the absorption maximum varies in the order $[Cu(H_{-1}bchtn)]^{+} > [Cu(H_{-1}bctn)]^{+} > [Cu(H_{-1}bcen)]^{+}$, $[Cu(H_{-1}bcmen)]^{+}$.

4. For $[CuH_{-2}L]$, the absorption maximum varies in the order $[Cu(H_{-2}bchtn)] > [Cu(H_{-2}bctn)] > [Cu(H_{-2}bcen)]$, $[CuH_{-2}bcmen)]$.

The potentiometric observations show two protons of $[CuL]^{2+}$ are dissociated as the base concentration is beyond $a = 2$ for the 1:1 solution. The sequence of absorption maximum, $[CuL]^{2+} > [CuH_{-1}L]^{+} > [CuH_{-2}L]$, indicates that it is the amide protons, not those of coordinated water molecules, which are dissociated. The results of an

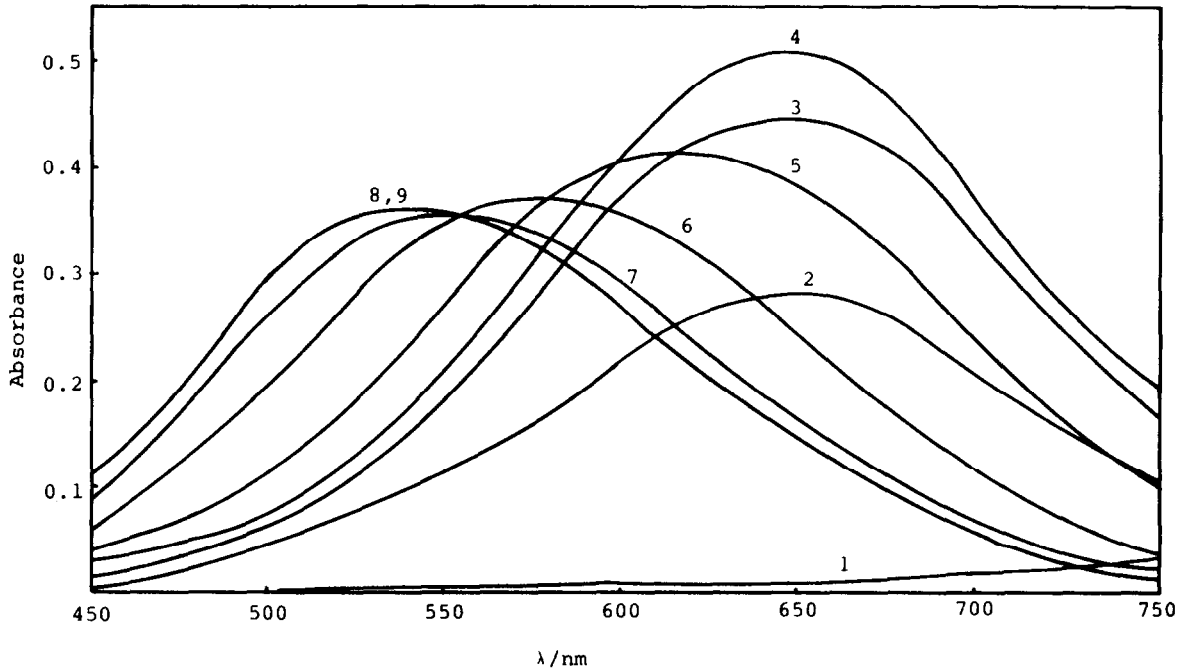



Fig. 5. Visible absorption spectra of Cu(II)–bcmen solutions. All solutions contain $8.1 \times 10^{-4}$ mol dm$^{-3}$ in both $Cu[NO_3]_2$ and $[H_2bcmen][NO_3]_2$ with 0.10 mol dm$^{-3}$ sodium nitrate. The pH values of the solution are: (1) 1.48; (2) 2.62; (3) 3.26; (4) 5.58; (5) 8.12; (6) 8.98; (7) 10.10; (8) 11.50; and (9) 11.94.

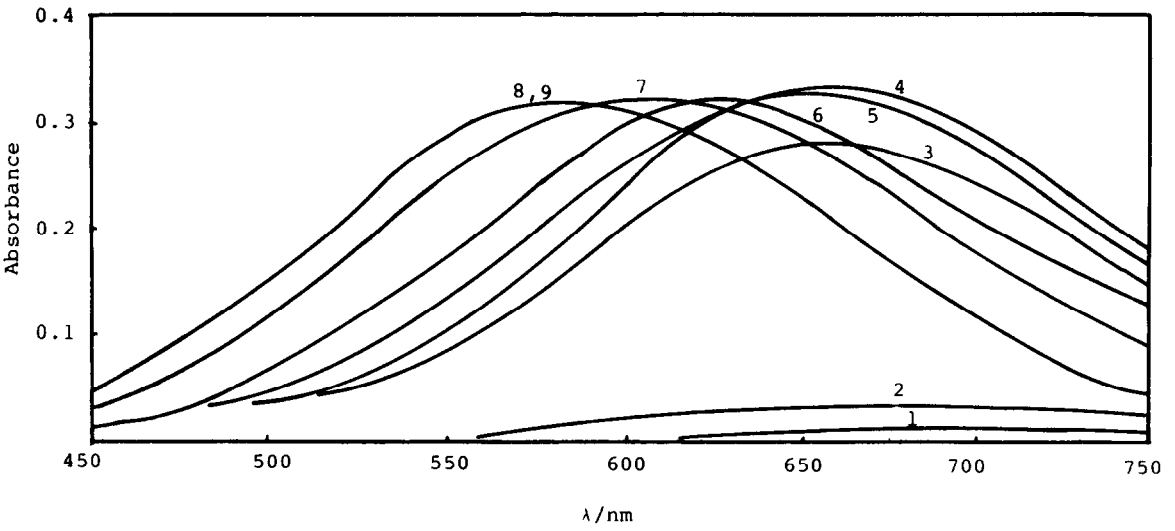



Fig. 6. Visible absorption spectra of Cu(II)–bchtn solutions. All solutions contain $8.0 \times 10^{-4}$ mol dm$^{-3}$ in both $Cu[NO_3]_2$ and $[H_2bchtn][NO_3]_2$ with 0.10 mol dm$^{-3}$ sodium nitrate. The pH values of the solution are: (1) 2.85; (2) 3.35; (3) 4.85; (4) 6.38; (5) 7.31; (6) 8.54; (7) 9.27; (8) 11.60; and (9) 12.01.

X-ray crystallographic study[3] have also shown unequivocally the displacement of the amide proton in the solid $[CuH_{-2}L]$ and the coordination of the resulting negative amide groups to Cu(II).

As pointed out previously,[2] the larger the degree of distortion from a square–planar structure, the larger is $\lambda_{max}$. The absorption maximum for each of the Cu(II)–bchtn or Cu(II)–bctn complexes is larger than that of the corresponding Cu(II)–bcen or Cu(II)–bcmen species. These differences reflect the distorted structures of the Cu(II)–bchtn and Cu(II)–bctn complexes. The results of X-ray crystallographic study[12,3] have also indicated that the degree of tetrahedral distortion from a square–planar structure of $[Cu(bchtn)]^{2+}$ is larger than that of $[Cu(bcen)]^{2+}$. These distortions are mainly attributed to the steric constraints in the three linked chelate rings.

Table 2. Absorption maxima for Cu(II) complexes in the visible region

| Species | $\lambda_{max}$/nm |
|---|---|
| $[Cu(bcen)]^{2+}$ | 645 |
| $[Cu(H_{-1}bcen)]^{+}$ | 580 |
| $[Cu(H_{-2}bcen)]$ | 535 |
| $[Cu(bctn)]^{2+}$ | 658 |
| $[Cu(H_{-1}bctn)]^{+}$ | 595 |
| $[Cu(H_{-2}bctn)]$ | 555 |
| $[Cu(bcmen)]^{2+}$ | 645 |
| $[Cu(H_{-1}bcmen)]^{+}$ | 578 |
| $[Cu(H_{-2}bcmen)]$ | 535 |
| $[Cu(bchtn)]^{2+}$ | 658 |
| $[Cu(H_{-1}bchtn)]^{+}$ | 605 |
| $[Cu(H_{-2}bchtn)]$ | 575 |

*Acknowledgements*—This work was supported by the Chemistry Research Center, National Science Council of the Republic of China, to which the authors wish to express their thanks. We are also grateful to Dr. Chi-Chao Wan and Mr. Yuan-Chung Hsieh for elemental analyses and for providing laboratory facilities.

## REFERENCES

1. L.-W. Wei, M.-S. Chao and C.-S- Chung, *J. Chin. Chem. Soc. (Taipei)* 1979, **26**, 145.
2. M.-S. Chao and C.-S. Chung, *J. Chem. Soc., Dalton Trans.* 1981, 683.
3. T.-J. Lee, T.-H. Lu and C.-S. Chung, unpublished work.
4. B.-F. Liang, D. W. Margerum and C.-S. Chung, *Inorg. Chem.* 1979, **18**, 2001.
5. R. M. Smith and A. E. Martell, *Critical Stability Constants—Amines*, Vol. 2. Plenum Press, New York (1975).
6. J. Clark and D. D. Perrin, *Quart. Rev., Chem. Soc.* 1964, **18**, 295.
7. R. Barbucci, L. Fabbrizzi and P. Paoletti, *Coord. Chem. Rev.* 1972, **8**, 31.

8. R. Barbucci, L. Fabbrizzi and P. Paoletti, *J. Chem. Soc., Dalton Trans.* 1972, 745.
9. B. Wang and C.-S. Chung, *J. Chem. Soc., Dalton Trnas.* 1982, 2565.
10. P. Paoletti, L. Fabbrizzi and R. Barbucci, *Inorg. Chem.* 1973, **12**, 1861.
11. J. Inczedy, *Analytical Applications of Complex Equilibria*, p. 97. Ellis Horwood, Chichester (1976).
12. J.-Y. Hurng, M. S. Thesis. Tsing Hua University (1983).

*Polyhedron* Vol. 3, No. 5, pp. 567–573, 1984
Printed in Great Britain.

0277–5387/84 $3.00 + .00
Pergamon Press Ltd.

# SYNTHESIS AND MOLECULAR STRUCTURE OF $[Au_3Ru_4(\mu_3\text{-}H)(CO)_{12}(PPh_3)_3]$

JUDITH A. K. HOWARD, IAN D. SLATER and F. GORDON A. STONE*
Department of Inorganic Chemistry, The University of Bristol, Bristol BS8 1TS, England

(*Received* 5 *September* 1983; *accepted* 24 *October* 1983)

**Abstract**—The title compound can be prepared in good yield by heating either $[Ru_4(\mu\text{-}H)_4(CO)_{12}]$ or $[Au_2Ru_4(\mu_3\text{-}H)_2(CO)_{12}(PPh_3)_2]$ with $[AuMe(PPh_3)]$ in toluene. The related compound $[Au_3Ru_4(\mu_3\text{-}H)(\mu\text{-}dppm)(CO)_{12}(PPh_3)]$ has also been prepared. Both trigoldtetraruthenium clusters undergo dynamic behaviour in solution, involving intramolecular rearrangement of the metal core, as revealed by variable temperature NMR studies. The crystal structure of $[Au_3Ru_4(\mu_3\text{-}H)(CO)_{12}(PPh_3)_3]$ has been established by an X-ray diffraction study. The metal atom core comprises a trigonal bipyramidal $AuRu_4$ unit with two $AuRu_2$ faces capped by gold atoms.

Heteronuclear metal carbonyl clusters containing $AuPR_3$ (R = alkyl or aryl) groups are currently attracting attention and many such complexes have now been prepared.[1–8] If only one $AuPR_3$ unit is present in the cluster, it occupies either an edge- or face-bridging position. For this class of compound the molecular structures are generally the same as those of isolobally related[6a] hydrido polynuclear metal carbonyl compounds. However, once more than one $AuPR_3$ fragment is present in a cluster, the stereochemical and bonding analogy with H fades.[9] Thus, digold species are known with and without gold–gold bonds, and for some structures the internuclear separations are such that whether or not a direct gold–gold linkage is present is arguable. Indeed, there may be little to gain in energy for these species upon forming gold–gold bonds.[1f] As yet the title compound[2c] and the compounds $[Au_3Ru_3(\mu_3\text{-}COMe)(CO)_9(PPh_3)_3]$,[2c,f] $[Au_3V(CO)_5(PPh_3)_3]$,[5] and $[Au_3CoRu_3(CO)_{12}(PPh_3)_3]$[7a] are the only structurally characterised species reported containing three gold atoms in a heteronuclear cluster, and in all three compounds gold–gold bonds are present. In this paper we describe the synthesis and structure of $[Au_3Ru_4(\mu_3\text{-}H)(CO)_{12}(PPh_3)_3]$ (**1**), following our preliminary communication.[2c]

## RESULTS AND DISCUSSION

An initial observation[2a] that a $AuPPh_3$ group could be introduced into the cluster $[Os_3(\mu\text{-}H)_2(CO)_{10}]$ by treating the triosmium compound with $[AuMe(PPh_3)]$ led us to develop this type of reaction as a general method for the synthesis of heteronuclear clusters containing gold. Thus, the triruthenium compound $[Ru_3(\mu\text{-}H)_3(\mu_3\text{-}COMe)(CO)_9]$ reacts with $[AuMe(PPh_3)]$ in diethyl ether at room temperature affording a chromatographically separable mixture of $[AuRu_3(\mu\text{-}H)_2(\mu_3\text{-}COMe)(CO)_9(PPh_3)]$, $[Au_2Ru_3(\mu\text{-}H)(\mu_3\text{-}COMe)(CO)_9(PPh_3)_2]$, and $[Au_3Ru_3(\mu_3\text{-}COMe)(CO)_9(PPh_3)_3]$.[2c,f]

Extending this method of cluster synthesis, we investigated the reaction between $[Ru_4(\mu\text{-}H)_4(CO)_{12}]$[10] and $[AuMe(PPh_3)]$. At 50°C, in toluene solution, these reactants gave (**1**) in *ca.* 60% yield. Compound (**1**) was the only gold–ruthenium species observed, even when an excess of $[AuMe(PPh_3)]$ was used. Moreover, no complexes containing one or two gold atoms could be isolated. It would thus appear that (**1**) is the thermodynamically most stable of the possible products. In this context, it is interesting that Lewis *et al.*[1b] report that the reaction between $[Os_4(\mu\text{-}H)_4(CO)_{12}]$ and $[AuMe(PPh_3)]$ gives only the mono-gold complex $[AuOs_4(\mu\text{-}H)_3(CO)_{12}(PPh_3)]$ in moderate yield.

At ambient temperatures, the $^1H$ NMR spectrum of (**1**) shows a very broad high-field signal ($\delta$, *ca.* −13), but at −60°C this hydrido-ligand resonance is a sharp doublet [$\delta$ −12.70, J(PH) 16 Hz], indicating coupling to only one $PPh_3$ group. In the temperature range 50–100°C the hydrido signal sharpens, but remains somewhat broad, probably

*Author to whom correspondence should be addressed.

due to unresolved $^{31}P$ couplings. The $^{31}P$-$\{^1H\}$ NMR spectrum at room temperature is a singlet ($\delta$ 61.3 ppm) with the chemical shift typical for a $AuPPh_3$ moiety in a gold–ruthenium cluster.[2f] A singlet is also observed for the CO ligands in the room temperature $^{13}C$–$\{^1H\}$ NMR spectrum of (1), indicating complete site-exchange of these groups at ambient temperatures. Poor solubility prevented low temperature $^{13}C$ NMR measurements. Since the NMR data did not unambiguously define the structure of (1), we carried out an X-ray diffraction study on the cluster. However, since our original communication,[2c] others[7b] have reported compound (1) and also carried out an X-ray diffraction study. Compound (1) was isolated in 15% yield as one product of a mixture obtained by treating $K[Ru_4(\mu\text{-}H)_3(CO)_{12}]$ with $[\{Au(PPh_3)\}_3O][BF_4]$. These workers[7b] did not carry out variable temperature NMR studies and so failed to observe the dynamic behaviour of (1) in solution. Our description of the structure of (1) is abbreviated in view of the lengthy discussion elsewhere,[7b] and attention is directed to comparisons with our previously determined[2c,f] structure of the related compound $[Au_3Ru_3(\mu_3\text{-}COMe)(CO)_9(PPh_3)_3]$.

The molecular structure of (1) is shown in Fig. 1, and selected bond lengths and angles are given in Table 1. The metal atom core of (1) can be regarded as a trigonal bipyramid [Au(3), Ru(1), Ru(2), Ru(3), Ru(4)] with two faces capped by Au(1) and Au(2). The hydrido ligand, the presence of which was revealed by the $^1H$ NMR data, was not located in the X-ray diffraction study. However, potential energy minimisation calculations[11] suggest that it triply bridges the Au(3)Ru(2)Ru(4) face of the trigonal bipyramid, and this position accords with the $^{31}P$–$^1H$ coupling observed in the $^1H$ NMR spectrum, mentioned above. With the hydrido ligand lying on the pseudo-mirror plane through Au(3)Ru(1)Ru(3) coupling would only be expected witht the *transoid* P(3) nucleus.

The structure of (1) is closely related to that of $[Au_3Ru_3(\mu_3\text{-}COMe)(CO)_9(PPh_3)_3]$,[2c,f] with a $Ru(CO)_3$ group in the former replaced by a $\mu_3$-COMe group in the latter. However, although both groups provide three orbitals for cluster bonding they do not contribute the same number of electrons; two $[Ru(CO)_3]$ and three ($\mu_3$-COMe), respectively.[12] Hence, a hydrido ligand must be present in (1). Evidently, the isolobal analogy between H and $AuPPh_3$ groups does not hold for either (1) or $[Au_3Ru_3(\mu_3\text{-}COMe)(CO)_9(PPh_3)_3]$, as the geometries of both clusters bear no resemblance to the structures of their hydrido precursors $[Ru_4(\mu\text{-}H)_4(CO)_{12}]$[10] and $[Ru_3(\mu\text{-}H)_3(\mu_3\text{-}COMe)(CO)_9]$,[2f] respectively.

The two Au–Au distances in (1) [Au(1)–Au(3) 2.822(2), and Au(2)–Au(3) 2.838(2) Å] are similar, and lie at the lower end of the range [2.784(1)–3.176(1)Å][2f] previously observed. They are also significantly shorter than the Au–Au distances [2.930(1) and 3.010(1) Å] in $[Au_3Ru_3(\mu_3\text{-}COMe)(CO)_9(PPh_3)_3]$.

Whereas in (1), the Au(3)–Ru(2) vector is the longest, for the related complex $[Au_3Ru_3(\mu_3\text{-}COMe)(CO)_9(PPh_3)_3]$ the largest gold–ruthenium

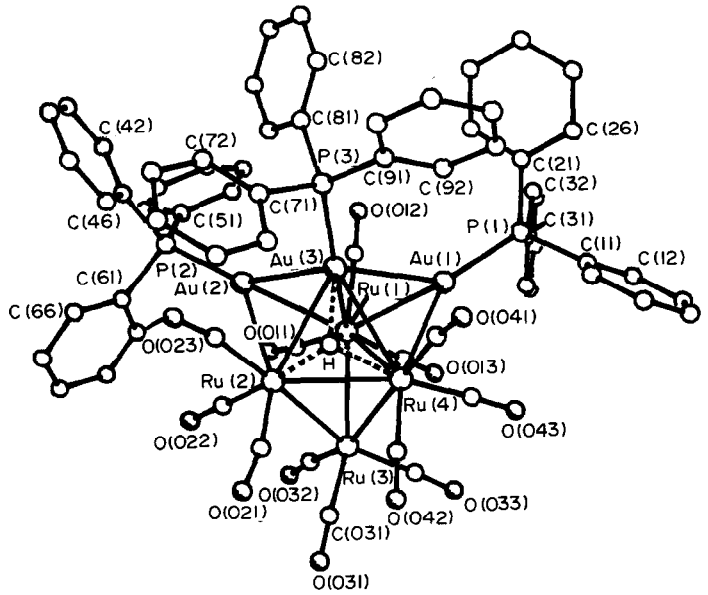



Fig. 1. The molecular structure of $[Au_3Ru_4(\mu_3\text{-}H)(CO)_{12}(PPh_3)_3]$ (1) with the crystallographic numbering scheme.

Table 1. Selected internuclear separations (Å) and angles (°) for $[Au_3Ru_4(\mu_3\text{-}H)(CO)_{12}(PPh_3)_3]$ (1)

| | | | |
|---|---|---|---|
| (a) Distances | | | |
| Au(3)-Au(1) | 2.822(2) | Au(3)-Au(2) | 2.838(2) |
| Au(3)-Ru(1) | 2.832(2) | Au(3)-Ru(2) | 3.011(2) |
| Au(3)-Ru(4) | 2.961(3) | Au(1)-Ru(1) | 2.834(2) |
| Au(1)-Ru(4) | 2.825(2) | Au(2)-Ru(1) | 2.831(3) |
| Au(2)-Ru(2) | 2.844(2) | Ru(1)-Ru(2) | 2.978(3) |
| Ru(1)-Ru(4) | 3.001(3) | Ru(2)-Ru(4) | 2.960(4) |
| Ru(3)-Ru(1) | 2.822(3) | Ru(3)-Ru(2) | 2.801(3) |
| Ru(3)-Ru(4) | 2.805(3) | | |
| P(1)-Au(1) | 2.279(7) | P(2)-Au(2) | 2.289(9) |
| P(3)-Au(3) | 2.276(6) | | |
| Ru-H | 1.95* | Ru-CO | 1.84(3)-1.97(3) |
| (b) Angles | | | |
| Au(3)-Au(1)-Ru(1) | 60.1(1) | Au(3)-Au(1)-Ru(4) | 63.3(1) |
| Ru(1)-Au(1)-Ru(4) | 64.1(1) | Au(3)-Au(1)-P(1) | 140.6(2) |
| Ru(1)-Au(1)-P(1) | 142.5(2) | Ru(4)-Au(1)-P(1) | 146.0(2) |
| Au(3)-Au(2)-Ru(1) | 59.9(1) | Au(3)-Au(2)-Ru(2) | 64.0(1) |
| Ru(1)-Au(2)-Ru(2) | 63.3(1) | Au(3)-Au(2)-P(2) | 146.6(2) |
| Ru(1)-Au(2)-P(2) | 143.9(2) | Ru(2)-Au(2)-P(2) | 139.2(2) |
| Au(1)-Au(3)-Au(2) | 115.90(5) | Au(1)-Au(3)-Ru(1) | 60.2(1) |
| Au(2)-Au(3)-Ru(1) | 59.9(1) | Au(1)-Au(3)-Ru(2) | 107.9(1) |
| Au(2)-Au(3)-Ru(2) | 58.1(1) | Ru(1)-Au(3)-Ru(2) | 61.2(1) |
| Au(1)-Au(3)-Ru(4) | 58.4(1) | Au(2)-Au(3)-Ru(4) | 108.7(1) |
| Ru(1)-Au(3)-Ru(4) | 62.4(1) | Ru(2)-Au(3)-Ru(4) | 59.4(1) |
| Au(1)-Au(3)-P(3) | 116.0(2) | Au(2)-Au(3)-P(3) | 110.6(2) |
| Ru(1)-Au(3)-P(3) | 157.7(1) | Ru(2)-Au(3)-P(3) | 133.8(2) |
| Ru(4)-Au(3)-P(3) | 137.0(2) | Au(1)-Ru(1)-Au(2) | 115.8(1) |
| Au(1)-Ru(1)-Au(3) | 59.70(5) | Au(2)-Ru(1)-Au(3) | 60.2(1) |
| Au(1)-Ru(1)-Ru(2) | 108.5(1) | Au(2)-Ru(1)-Ru(2) | 58.6(1) |
| Au(3)-Ru(1)-Ru(2) | 62.4(1) | Au(1)-Ru(1)-Ru(3) | 108.2(1) |
| Au(2)-Ru(1)-Ru(3) | 110.3(1) | Au(3)-Ru(1)-Ru(3) | 108.8(1) |
| Ru(2)-Ru(1)-Ru(3) | 57.7(1) | Au(1)-Ru(1)-Ru(4) | 57.8(1) |
| Au(2)-Ru(1)-Ru(4) | 107.8(1) | Au(3)-Ru(1)-Ru(4) | 60.9(1) |
| Ru(2)-Ru(1)-Ru(4) | 59.4(1) | Ru(3)-Ru(1)-Ru(4) | 57.5(1) |
| Au(2)-Ru(2)-Ru(1) | 58.1(1) | Au(2)-Ru(2)-Au(3) | 57.90(5) |
| Au(2)-Ru(2)-Ru(3) | 110.5(1) | Au(3)-Ru(2)-Ru(1) | 56.4(1) |
| Ru(1)-Ru(2)-Ru(3) | 58.4(1) | Au(3)-Ru(2)-Ru(3) | 104.5(1) |

Table 1 (*Contd*)

| | | | |
|---|---|---|---|
| (b) Angles | | | |
| Au(3)-Ru(2)-Ru(4) | 59.5(1) | Au(2)-Ru(2)-Ru(4) | 108.6(1) |
| Ru(3)-Ru(2)-Ru(4) | 58.2(1) | Ru(1)-Ru(2)-Ru(4) | 60.7(1) |
| Ru(1)-Ru(3)-Ru(4) | 64.5(1) | Ru(1)-Ru(3)-Ru(2) | 63.9(1) |
| Au(1)-Ru(4)-Au(3) | 58.3(1) | Ru(2)-Ru(3)-Ru(4) | 63.8(1) |
| Au(3)-Ru(4)-Ru(1) | 56.7(1) | Au(1)-Ru(4)-Ru(1) | 58.1(1) |
| Au(3)-Ru(4)-Ru(2) | 61.1(1) | Au(1)-Ru(4)-Ru(2) | 109.2(1) |
| Au(1)-Ru(4)-Ru(3) | 109.0(1) | Ru(1)-Ru(4)-Ru(2) | 59.9(1) |
| Ru(1)-Ru(4)-Ru(3) | 58.0(1) | Au(3)-Ru(4)-Ru(3) | 105.7(1) |
| | | Ru(2)-Ru(4)-Ru(3) | 58.1(1) |
| Ru-C-O(mean) | 173 (3) | | |

* Constrained, see text.

separation is the vector equivalent to Au(3)–Ru(1) in (**1**). The three Ru–Ru distances [2.960(4)–3.001(3) Å] of the Au(3)Ru(1)Ru(2)Ru(4) tetrahedron of (**1**) are significantly longer than the analogous separations in $[Au_3Ru_3(\mu_3\text{-}COMe)(CO)_9(PPh_3)_3]$, and, as expected in view of the capping H and $AuPPh_3$ groups, they are also larger than the Ru(3)–Ru(1) [2.822(3)], Ru(3)–Ru(2) [2.801(3)], and Ru(3)–Ru(4) [2.805(3) Å] distances.

Subsequent to our preliminary report[2c] of (**1**), Bruce and Nicholson[7a] have described the synthesis and molecular structure of $[Au_3CoRu_3(CO)_{12}(PPh_3)_3]$ which also has a bicapped trigonal bipyramidal metal atom core (Fig. 2). The Au–Au separations in $[Au_3CoRu_3(CO)_{12}(PPh_3)_3]$ [2.836(1) and 2.784(1) Å] are similar to those in (**1**), and like the latter, the trigold–cobalt–triruthenium cluster shows a wide variation in the metal–metal separations of the metal core.[7]

Another structure related to (**1**) is that of the bicapped tetrahedral cluster $[Au_2Ru_4(\mu_3\text{-}H)_2(CO)_{12}(PPh_3)_2]$.[2e] Formal replacement of a $\mu_3$-H ligand in the latter by the isolobal $AuPPh_3$ group produces (**1**). It is, therefore, interesting that (**1**) can be prepared by treating $[Au_2Ru_4(\mu_3\text{-}H)_2(CO)_{12}(PPh_3)_2]$ with $[AuMe(PPh_3)]$.

Both (**1**) and $[Au_3CoRu_3(CO)_{12}(PPh_3)_3]$ are 96 valence electron clusters.[12] The bonding in these clusters is perhaps best viewed[6,9] in terms of the $AuPPh_3$ groups partaking in four-centre two-electron interactions. Thus in (**1**) the $Au(3)PPh_3$ group caps the Ru(1)Ru(2)Ru(4) triangle using its $hy(s-z)$ molecular orbital in a four-centre two-electron bond. The other two $AuPPh_3$ groups are then attached to $AuRu_2$ faces in similar four-centre two-electron bonding modes.

In view of the relative weakness of the proposed bonding between the $AuPPh_3$ fragments in (**1**), it is not surprising that in solution the cluster undergoes a facile intramolecular rearrangement of the metal core on the NMR time-scale. A similar dynamic process has been observed in homonuclear gold clusters,[9] in certain heteronuclear clusters containing two Group 1b metals,[2e] in $[Au_2Ru_3(\mu_3\text{-}S)(CO)_8(L)(PPh_3)_2]$ (L = CO or $PPh_3$),[2d] and in $[Au_3Ru_3(\mu_3\text{-}COMe)(CO)_9(PPh_3)_3]$.[2f]

As mentioned above, the $^{31}P\text{-}\{^1H\}$ NMR spectrum of (**1**) shows only a singlet at ambient temperatures, which is clearly inconsistent with the structure in the solid state (Fig. 1). However, at − 60°C, the low temperature limiting spectrum is observed, consisting of two resonances of relative

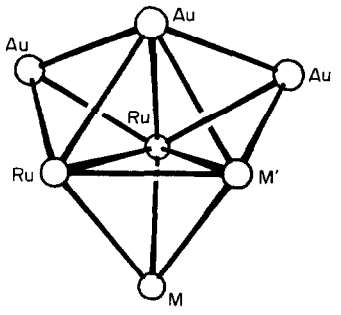



Fig. 2. For compound (**1**), M = M′ = Ru; for $[Au_3Ru_3(\mu_3\text{-}COMe)(CO)_9(PPh_3)_3]$, M = $\mu_3$-COMe, M′ = Ru; for $[Au_3CoRu_3(CO)_{12}(PPh_3)_3]$, M = Ru, M′ = Co.

intensity 1:2 at $\delta$ 53.5 and 62.3 ppm, respectively. Addition of free $PPh_3$ does not change the $^{31}P\text{–}\{^1H\}$ NMR spectrum of (**1**), apart from the appearance of a peak due to free triphenylphosphine. Hence, a dissociative mechanism can be eliminated as a possible explanation of the apparent equivalence of the $PPh_3$ groups at room temperature. A polytopal rearrangement of the metal atom core[2d] would seem the most likely explanation of the data. The value of $\Delta G^{\ddagger}_{T_c}$ for the process is $46 \pm 1$ kJ mol$^{-1}$, as estimated from the coalescence temperature ($-30 \pm 5$°C) in the $^{31}P\text{–}\{^1H\}$ NMR spectrum. Interestingly, the $^{31}P\text{–}\{^1H\}$ NMR spectrum of $[Au_3Ru_3(\mu_3\text{-}COMe)(CO)_9(PPh_3)_3]$ consists[2f] of a sharp singlet even at $-90$°C, corresponding to $\Delta G^{\ddagger}_{T_c} < 34$ kJ mol$^{-1}$. This value is estimated by assuming that the difference in chemical shift between the two separate $^{31}P$ resonances in the limiting low temperature $^{31}P\text{–}\{^1H\}$ NMR spectrum of $[Au_3Ru_3(\mu_3\text{-}COMe)(CO)_9(PPh_3)_3]$ is comparable with that observed for (**1**), since the magnitude of $\Delta G^{\ddagger}_{T_c}$ is not very sensitive to the chemical shift difference.

To gain further insight into the dynamic behaviour of the trigold heteronuclear clusters, the green-brown compound $[Au_3Ru_4(\mu_3\text{-}H)(\mu\text{-}dppm)(CO)_{12}(PPh_3)]$ (dppm = $Ph_2PCH_2PPh_2$) (**2**) was prepared by heating $[Au_2Ru_4(\mu_3\text{-}H)_2(\mu\text{-}dppm)(CO)_{12}]$[13] with $[AuMe(PPh_3)]$ in toluene at 60°C. A close resemblance between the IR spectra of (**1**) and (**2**) in the carbonyl stretching region implies that the $Au_3Ru_4$ metal core geometries are similar. For steric reasons the dppm ligand in (**2**) will be bridging adjacent gold sites. In the $^1H$ NMR spectrum of (**2**) at ambient temperatures the $\mu_3$-H resonance is sharp [$\delta$ $-14.37$], and occurs as a doublet of triplets [J(PH) 3 Hz (dppm), 2 Hz ($PPh_3$)]. The room temperature $^{31}P\text{–}\{^1H\}$ NMR spectrum consists of a triplet and a doublet (rel. int. 1:2). Hence both the $^1H$ and $^{31}P\text{–}\{^1H\}$ NMR spectra indicate that the two phosphorus nuclei of the dppm ligand are equivalent on the NMR time scale. Clearly, the data are not consistent with the proposed solid state structure. As the temperature is lowered both the $\mu_3$-H resonance in the $^1H$ NMR spectrum and the dppm signal in the $^{31}P\text{–}\{^1H\}$ spectrum broaden, becoming very broad at the experimental limit ($-90$°C). However, the signal for the triphenylphosphine group in the $^{31}P\text{–}\{^1H\}$ NMR spectrum is relatively sharp even at $-90$°C, although the $^{31}P\text{–}^{31}P$ coupling is lost.

Evidently (**2**), like (**1**), undergoes dynamic behaviour in solution, but the limiting low temperature spectrum is not reached at $-90$°C. The observed $^1H\text{–}^{31}P$ and $^{31}P\text{–}^{31}P$ couplings show that the process does not involve dissociation or intermolecular exchange of ligated phosphine groups, and as for (**1**), must take the form of a skeletal rearrangement, a process seen also in $[Au_3Ru_3(\mu_3\text{-}COMe)(CO)_9(PPh_3)_3]$.[2f] It is interesting that a polytopal rearrangement can occur in (**2**) even though two of the three gold atoms are linked by dppm. Indeed, compared with (**1**), $\Delta G^{\ddagger}_{T_c}$ for the process is actually lowered by replacing two $PPh_3$ groups by dppm. The coalescence temperature for (**2**) is *ca.* $-90$°C implying a $\Delta G^{\ddagger}_{T_c}$ value of $\sim 34$ kJ mol$^{-1}$. The $^1H$ NMR spectra of (**2**) show that the hydrido ligand signal is broadened at a much lower temperature than the same signal in the spectra of (**1**), suggesting that the broadening of these peaks is connected with the intramolecular rearrangement of the cores of these two clusters, rather than any additional independent fluxional process.

Unfortunately, there is insufficient evidence to determine whether or not the $AuPPh_3$ unit of (**2**) is involved in the skeletal rearrangement. The observed results can be explained by assuming that only the two gold atoms bonded to the dppm ligand exchange environments. The slight broadening of the $AuPPh_3$ peak observed in the $^{31}P\text{–}\{^1H\}$ NMR spectrum of (**2**) at $-90$°C can be attributed to the coupling between the dppm ligand and the $PPh_3$ group. However, the mechanism of the dynamic process may additionally involve the $AuPPh_3$ fragment in (**2**) changing its position between two equivalent gold environments [i.e. Au(1) and Au(2) for (**1**) (Fig. 1)]. In this case, no further broadening of the $AuPPh_3$ peak in the spectrum of (**2**) would be expected at the coalescence temperature for the dppm signals, because the $AuPPh_3$ moiety would only be switching between equivalent environments with the same chemical shift. We conclude that the mechanism of the dynamic process which rearranges the metal atom cores of (**1**), (**2**) and $[Au_3Ru_3(\mu_3\text{-}COMe)(CO)_9(PPh_3)_3]$[2c,f] may involve either the exchange of only two gold atoms at any given time, or all three gold atoms may rearrange at once.

## EXPERIMENTAL

All reactions were performed using Schlenk tube techniques under oxygen-free nitrogen, and all solvents were rigorously dried before use. Light petroleum had b.p. 40–60°C. Established methods were used to prepare $[Ru_4(\mu\text{-}H)_4(CO)_{12}]$,[14] $[AuMe(PPh_3)]$,[15] and $[Au_2Ru_4(\mu_3\text{-}H)_2(CO)_{12}(PPh_3)_2]$.[2e] The compound $[Au_2Ru_4(\mu_3\text{-}H)_2(\mu\text{-}dppm)(CO)_{12}]$[13] was obtained from $[Au_2(\mu\text{-}dppm)Cl_2]$ and $[N(PPh_3)_2][Ru_4(\mu\text{-}H)_2(CO)_{12}]$ in a similar manner to that previously described.[2e] Yields are based on the amount of

ruthenium cluster compound taken for reaction. Alumina for chromatography was BDH Brockman Activity II.

*Synthesis of the compound* $[Au_3Ru_4(\mu_3\text{-}H)(CO)_{12}(PPh_3)_3]$

In a typical experiment, a mixture of $[Ru_4(\mu\text{-}H)_4(CO)_{12}]$ (0.16 g, 0.22 mmol) and $[AuMe(PPh_3)]$ (0.32 g, 0.68 mmol) in toluene (80 $cm^3$) was placed in a Schlenk tube fitted with a Young's high-pressure stopcock. The reactants were frozen with liquid nitrogen and the reaction vessel was evacuated, sealed, and heated at 50°C for *ca.* 15 hr. The reaction mixture was reduced in volume *in vacuo* to *ca.* 15 $cm^3$, and then chromatographed (25 × 3 cm column). Elution with toluene afforded a green fraction. Removal of solvent *in vacuo*, and crystallisation of the residue from dichloromethane–light petroleum gave very dark green *microcrystals* of $[Au_3Ru_4(\mu_3\text{-}H)(CO)_{12}(PPh_3)_3]$ (**1**) (0.27 g, 59%), m.p. 169–173°C (decomp.); (Found: C, 37.4; H, 2.2%; M (FAB mass spectrometry), 2 120.$C_{66}H_{46}Au_3O_{12}P_3Ru_4$ requires C, 37.4; H, 2.2%; M, 2 120). $\nu_{max}$ (CO), 2 053 vs, 2013 (sh), 2007 vs, 1989 s, 1967 w, 1951 m, and 1 920 w $cm^{-1}$ ($CH_2Cl_2$). NMR: $^1H$ ($CDCl_3$), $\delta \sim -13$ (s vbr, 1 H, $\mu_3$-H) and 7.12–7.37 (m, 45 H, Ph); at −60°C, $\delta$ −12.70 [d, 1 H, $\mu_3$-H, J(PH) 16 Hz] and 7.01–7.34 (m, 45 H, Ph); $^{31}P\text{-}\{^1H\}$ ($CDCl_3$), $\delta$ (rel. 85% $H_3PO_4$ external) 61.3 ppm; at −60°C, $\delta$ 62.3 (s, 2 P) and 53.5 ppm (s, 1 P); $^{13}C\text{-}\{^1H\}$ ($CD_2Cl_2$–$CH_2Cl_2$), $\delta$ 203.3 (CO), 134.3 [d, $C^2$(Ph), J(PC) 14], 132.4 [d, $C^1$(Ph), J(PC) 48], 131.0 [s, $C^4$(Ph)], and 129.1 ppm [d, $C^3$(Ph), J(PC) 12 Hz].

The use of less than three equivalents of $[AuMe(PPh_3)]$ in the reaction with $[Ru_4(\mu\text{-}H)_4(CO)_{12}]$ resulted only in a lower yield of (**1**). Use of larger amounts of $[AuMe(PPh_3)]$ did not produce an $Au_4Ru_4$ cluster.

Compound (**1**) was prepared in a similar manner from $[Au_2Ru_4(\mu_3\text{-}H)_2(CO)_{12}(PPh_3)_2]$ (0.20 g, 0.12 mmol) and $[AuMe(PPh_3)]$ (0.06 g, 0.13 mmol) in toluene (50 $cm^3$). The reaction mixture was heated at 50°C for 5 hr. Chromatography led to the isolation of dark green microcrystals of (**1**) (0.16 g, 63%), after removal of solvent under reduced pressure and crystallisation from dichloromethane–light petroleum. A reduced yield (*ca.* 40%) of (**1**) is obtained by stirring a mixture of $[Au_2Ru_4(\mu_3\text{-}H)_2(CO)_{12}(PPh_3)_2]$ and $[AuMe(PPh_3)]$ in diethyl ether at room temperature for 15 hr.

*Synthesis of the compound* $[Au_3Ru_4(\mu_3\text{-}H)(\mu\text{-dppm})(CO)_{12}(PPh_3)]$

A mixture of $[Au_2Ru_4(\mu_3\text{-}H)_2(\mu\text{-dppm})(CO)_{12}]$ (0.20 g, 0.13 mmol) and $[AuMe(PPh_3)]$ (0.06 g, 0.13 mmol) in toluene (50 $cm^3$) was placed in a Schlenk tube fitted with a Young's high-pressure stopcock. The reaction vessel was cooled with liquid nitrogen, evacuated, sealed and heated at 60°C (*ca.* 15 hr). The reaction mixture was reduced to a volume of *ca.* 15 $cm^3$ under reduced pressure. Chromatography (25 × 3 cm column), eluting with toluene, afforded one green-brown fraction. After removal of solvent *in vacuo*, crystallisation of the residue from dichloromethane–light petroleum gave greenish-brown *microcrystals* of $[Au_3Ru_4(\mu_3\text{-}H)(\mu\text{-dppm})(CO)_{12}(PPh_3)]$ (**2**) (0.14 g, 54%), m.p. 184–187°C (decomp.); (Found: C, 33.2; H, 1.8%. $C_{55}H_{38}Au_3O_{12}P_3Ru_4$ requires C, 33.4; H, 1.9). $\nu_{max}$ (CO) at 2 053 vs, 2 014 s, 2 003 s, 1 986 (sh), 1 969 m, 1 944 m and 1 908(sh) $cm^{-1}$ ($CH_2Cl_2$). NMR: $^1H$ ($CD_2Cl_2$), $\delta$ −14.37 [d of t, 1 H, $\mu_3$-H, J(PH) 2 and 3 Hz for $PPh_3$ and dppm, respectively], 3.61 [t, 2 H, $Ph_2PCH_2PPh_2$, J(PH) 11 Hz], and 7.11–7.53 (m, 35 H, Ph); at −90°C, $\delta$ −15 (vbr, s); $^{31}P\text{-}\{^1H\}$ ($CD_2Cl_2$), $\delta$ 61.3 [t, 1 P, $PPh_3$, J(PP) 7] and 42.0 ppm [d, 2 P, $Ph_2PCH_2PPh_2$, J(PP) 7 Hz]; at −90°C, $\delta$ 60.3 (s, $PPh_3$) and ~40 ppm (vbr, s, $Ph_2PCH_2PPh_2$).

*Crystallographic studies*

A small black crystal of (**1**) was grown from dichloromethane–light petroleum. Data were collected at room temperature on a Nicolet *P*3*m* four-circle diffractometer, operating in the $\omega/2\theta$ scan mode in the range $2.9 \leqslant 2\theta \leqslant 45°$. Of the total 5 510 independent intensities, 4 322 for which $I \geqslant 3\sigma(I)$ were used in the solution and refinement of the structure. An empirical absorption correction was applied after the data had been corrected for Lorentz and polarisation effects.

*Crystal data.* $C_{66}H_{46}Au_3O_{12}P_3Ru_4$, $M = 2119.2$, monoclinic, $a = 22.31(1)$, $b = 18.54(4)$, $c = 18.76(1)$ Å, $\beta = 113.33(5)°$, $U = 7125.8$ Å$^3$, $Z = 4$, $D_c = 1.98$ g $cm^{-3}$, $F(000) = 3979$, space group $P2_1/n$, Mo–$K_\alpha$ *X*-radiation (graphite monochromator), $\bar{\lambda} = 0.71069$ Å, $\mu$(Mo–$K_\alpha$) = 70.7 $cm^{-1}$.

The structure was solved by heavy atom methods and refined by blocked-cascade least squares, with anisotropic thermal parameters for all non-hydrogen atoms, except the phenyl C atoms which were refined isotropically as rigid hexagons (C–C 1.395 Å). Their hydrogen atoms were calculated to be in idealised positions (C–H 0.960 Å) "riding" on the C atoms to which they were attached. Using weights of the form $w = [\sigma^2(F_0) + 0.00175\,|F_0|^2]^{-1}$, which gave a reasonable weight analysis, the final residual indices were R 0.055 (R′ 0.056). Scattering factors were from Ref. 16. All computations were carried out on an Eclipse S230 (Data General) computer with the SHELXTL system of programs.[17]

Tables of atomic co-ordinates, thermal parame-

ters, bond lengths and angles, and observed and calculated structure factors have been deposited as supplementary data with the Editor, from whom copies are available on request. Atomic coordinates have also been deposited with the Cambridge Crystallographic Data Centre.

*Acknowledgements*—We thank the S.E.R.C. for a research studentship (I.D.S.) and the U.S.A.F. Office of Scientific Research (Grant 82-0070) for support.

## REFERENCES

1. (a) B. F. G. Johnson, D. A. Kaner, J. Lewis, P. R. Raithby and M. J. Taylor, *J. Chem. Soc., Chem. Commun.* 1982, 314. (b) B. F. G. Johnson, D. A. Kaner, J. Lewis, P. R. Raithby and M. J. Taylor, *Polyhedron* 1982, **1**, 105. (c) B. F. G. Johnson, J. Lewis, W. J. H. Nelson, J. Puga, P. R. Raithby, D. Braga, M. McPartlin and W. Clegg, *J. Organomet. Chem.* 1983, **243**, C13. (d) B. F. G. Johnson, J. Lewis, W. J. H. Nelson, J. N. Nicholls and M. D. Vargas, *J. Organomet. Chem.* 1983, **249**, 255. (e) K. Burgess, B. F. G. Johnson, D. A. Kaner, J. Lewis, P. R. Raithby and S. N. A. B. Syed-Mustaffa. *J. Chem. Soc., Chem. Commun.* 1983, 455. (f) B. F. G. Johnson, J. Lewis, W. J. H. Nelson, P. R. Raithby and M. D. Vargas, *J. Chem. Soc., Chem. Commun.* 1983, 608.
2. (a) L. J. Farrugia, J. A. K. Howard, P. Mitrprachachon, J. L. Spencer, F. G. A. Stone and P. Woodward, *J. Chem. Soc., Chem. Commun.* 1978, 260. (b) M. Green, K. A. Mead, R. M. Mills, I. D. Salter, F. G. A. Stone and P. Woodward, *J. Chem. Soc., Chem. Commun.* 1982, 51. (c) L. W. Bateman, M. Green, J. A. K. Howard, K. A. Mead, R. M. Mills, I. D. Salter, F. G. A. Stone and P. Woodward, *J. Chem. Soc., Chem. Commun* 1982, 773. (d) L. J. Farrugia, M. J. Freeman, M. Green, A. G. Orpen, I. D. Salter and F. G. A. Stone, *J. Organomet. Chem.* 1983, **249**, 273. (e) M. J. Freeman, M. Green, A. G. Orpen, I. D. Salter, and F. G. A. Stone, *J. Chem. Soc., Chem. Commun.* 1983, 1332. (f) L. W. Bateman, M. Green, K. A. Mead, R. M. Mills, I. D. Salter, F. G. A. Stone and P. Woodward, *J. Chem. Soc., Dalton Trans.* 1983, 2599.
3. (a) P. Braunstein, G. Predieri, A. Tiripicchio and E. Sappa, *Inorg. Chim. Acta*, 1982, **63**, 113. (b) P. Braunstein, J. Rose, Y. Dusausoy and J-P. Mangeot, *C. R. Acad. Sci. Paris, Serie II* 1982, **294**, 967.
4. J. W. Lauher and K. Wald, *J. Am. Chem. Soc.* 1981, **103**, 7648.
5. J. E. Ellis, *J. Am. Chem. Soc.* 1981, **103**, 6106.
6. (a) D. G. Evans and D. M. P. Mingos, *J. Organomet. Chem.* 1982, **232**, 171. (b) C. E. Briant, K. P. Hall, and D. M. P. Mingos, *J. Chem. Soc., Chem. Commun.* 1983, 843.
7. (a) M. I. Bruce and B. K. Nicholson, *J. Chem. Soc., Chem. Commun* 1982, 1141; (b) *idem, J. Organomet. Chem.* 1983, **252**, 243.
8. E. Roland, K. Fischer, and H. Vahrenkamp, *Angew. Chem., Int. Ed. Engl.* 1983, **22**, 326.
9. K. P. Hall and D. M. P. Mingos, *Prog. Inorg. Chem.* in press.
10. R. D. Wilson, S. M. Wu, R. A. Love, and R. Bau, *Inorg. Chem.* 1978, **17**, 1271.
11. A. G. Orpen, *J. Chem. Soc., Dalton Trans.* 1980, 2509.
12. K. Wade, in *Transition Metal Clusters* (Edited by B. F. G. Johnson), Chap. 3. Wiley, New York (1980). *Adv. Inorg. Chem. Radiochem.* 1976, **18**, 1.
13. I. D. Salter, Ph.D. Thesis. Bristol University (1983).
14. S. A. R. Knox, J. W. Koepke, M. A. Andrews, and H. D. Kaesz, *J. Am. Chem. Soc.* 1975, **97**, 3942.
15. G. E. Coates and C. Parkin, *J. Chem. Soc.* 1962, 3220.
16. *International Tables for X-ray Crystallography*, Vol. 4. Kynoch Press, Birmingham (1975).
17. G. M. Sheldrick, SHELXTL programs for use with the Nicolet *P3m* X-ray system. University of Cambridge, (1976) updated Gottingen (1981).

*Polyhedron* Vol. 3, No. 4, pp. 575–580, 1984
Printed in Great Britain.

0277-5387/84 $3.00 + .00
© 1984 Pergamon Press Ltd.

# STUDIES OF GLYCINE ACETOPHENONE COMPLEXES OF COPPER(II), COBALT(II) AND OXOVANADIUM(IV)

**N. S. BIRADAR, V. L. RODDABASANAGOUDAR and T. M. AMINABHAVI***
Department of Chemistry, Karnatak University, Dharwad 580003, India

(*Received* 15 *September* 1983; *accepted* 17 *October* 1983)

**Abstract**—Complexes of copper(II), cobalt(II) and oxovanadium(IV) with glycine acetophenone Schiff bases were synthesized and characterized by elemental analyses, conductivity measurements, magnetic and spectral data. The complexes were shown to have 1:2 (metal:ligand) stoichiometry and were found to be non-electrolytes in solution.

Although metal complexes of Schiff bases derived from substituted salicylaldehydes and various amines have been studied extensively,[1,2] comparatively little attention has been given to systems in which the Schiff base is obtained from salicylaldehyde and amino acids.[3–7] These salicylidene aminoacid complexes may serve as models for N-pyridoxyledene amino acid systems which are considered to be the intermediates in biologically important amination processes.[8–10] It was therefore decided to synthesize transition metal complexes like copper(II), cobalt(II) and oxovanadium(IV) with ligands derived from the condensation of 5-methyl-2-hydroxyacetophenone and glycine. The complexes were characterized by conductivity measurements, magnetic measurements, IR and electronic spectral results.

## EXPERIMENTAL

All the chemicals used in this work were of reagent grade and used without further purification. Glycine-5-methyl-2-hydroxy acetophenone Schiff base was prepared by mixing a hot aqueous solution of glycine (0.1 mole) with a hot alcoholic solution of 5-methyl-2-hydroxyacetophenone (0.1 mole) with constant stirring. The mixture was refluxed on water bath for 2 hr and the excess of solvent was removed by slow evaporation. The separated pale yellow coloured silky needles were dried under vacuum over $P_2O_5$.

The complexes were prepared by adding warm alcoholic solution of the ligand to a hot solution of metal chloride (namely, cobalt(II) chloride, copper(II) chloride, and oxovanadium(IV) chloride) in equimolar proportions. The mixture was refluxed for 15–20 min and allowed to cool to room temperature. The precipitate formed was filtered, dried over fused calcium chloride and finally under vacuum over $P_2O_5$.

Elemental analyses were carried out by a procedure as outlined in Vogel's Text Book.[11] Cobalt and copper were estimated as its pyridine thiocyanate, nitrogen was determined by Kjeldahl's method. Carbon and hydrogen were estimated by microanalytical techniques.

Conductivities were measured in dimethylformamide (DMF) using an Elico-CM-82 conductivity bridge with a cell having a cell constant of 0.829 $cm^{-1}$. All conductivity measurements were performed at room temperature using $10^{-3}$ M solutions of complex.

Effective magnetic moments ($\mu_{eff}$) were measured using a Gouy balance at room temperature. The infrared (IR) spectra were obtained from 4000–400 $cm^{-1}$ using a Carl–Zeiss UR-10 IR spectrometer. Samples were prepared as KBr pellets. Electronic spectra were obtained on Perkin–Elmer 492–5000 spectrophotometer in the region 200–850 nm using 1 cm quartz cells.

## RESULTS AND DISCUSSION

### *Analytical data*

The complexes are coloured, amorphous in nature, insoluble in common organic solvents and soluble in DMF and DMSO. Their insolubility in nitrobenzene precluded the possibility of determining the molecular weights cryoscopically. The elemental analyses as given in Table 1 clearly show that they have a 1:2 stoichiometry. The molar conduc-

*Author to whom correspondence should be addressed.

Table 1. Analytical and physical data of glycine-acetophenone complexes of cobalt(II), copper(II) and oxovanadium(IV)

| Serial No. | Empirical formula of complex | Color | % Metal [a] | % Nitrogen [a] | % Carbon [a] | % Hydrogen [a] | Molar Cond. $ohm^{-1}cm^2$ $mole^{-1}$ | Mag. moment eff (B.M) |
|---|---|---|---|---|---|---|---|---|
| 1 | $Cu(C_{11}H_{11}O_3N)_2$ | Green | 13.60 (13.41) | 5.88 (5.91) | 55.63 (55.76) | 4.37 (4.65) | 23.48 | 1.76 |
| 2 | $Co(C_{11}H_{11}O_3N)_2$ | Brown | 12.33 (12.58) | 5.90 (5.97) | 55.98 (56.29) | 4.36 (4.69) | 31.76 | 4.5 |
| 3 | $VO(C_{11}H_{11}O_3N)_2$ | Green | 10.49 (10.69) | 5.80 (5.87) | 55.42 (55.35) | 4.66 (4.61) | 46.31 | 1.72 |

a - Values in the parenthesis are the theoretical yields.

tance values are in the range of 10–30 $\Omega^{-1}$ cm$^2$ mole$^{-1}$ indicating their non-electrolytic behaviour in solution.

## MAGNETIC PROPERTIES

(a) *Copper(II) complexes*

The four coordinated complex exhibits magnetic moment of 1.80 B.M. which is normal for S = 1/2 copper(II) complexes. As is well known, Pauling's valence bond theory[12] assumes that the tetrahedral complexes of copper(II) owing to their low symmetry have a greater orbital contribution to the magnetic moments than the square planar complexes. Ray and Sen[13] divided tetracoordinated complexes of copper(II) into two groups, one having the $\mu_{eff}$ values between 1.72–1.82 B.M. attributed to a planar $dsp^2$ structure, and the other having $\mu_{eff}$ values in the range of 1.9–2.2 B.M. corresponding to the tetrahedral $sp^3$ or planar $sp^2d$ configuration. Figgis[14] has shown that in a regular tetrahedral environment copper(II) should have magnetic moments of about 2.2 B.M. The crystal field theory predicts that copper(II) complexes have a marked orbital contribution to the magnetic moments only when the ground state is orbitally degenerate.[15] Since the square planar is not a degenerate one it should possess a value $\mu_{eff}$ close to the "spin-only" value of 1.73 B.M. In the present investigation the copper complex has a magnetic moment of 1.80 B.M. which is in line with the preconceived values[16,17] for square planar copper(II) complexes. These considerations suggest a square-planar configuration in the copper(II) complex.

(b) *Oxovanadium(IV) complex*

The $3d^1$ oxovanadium(IV) ion belongs to $S = \frac{1}{2}$ system and the coupling of the two $S = \frac{1}{2}$ spins of interacting pair of oxovanadium(IV) ions may lead to both antiferromagnetic and ferromagnetic spin–spin couplings. Many terdentate dibasic ONO or ONS donor Schiff base ligands have been utilised for the syntheses of dimeric or polymeric oxovanadium(IV) complexes with antiferromagnetic properties.[18] The terdentate dibasic character of the ligands force the oxovanadium(IV) ion to dimerise or polymerise, leading to complexes with subnormal magnetic moments. The oxovanadium(IV) complexes of the bidentate monobasic, terdentate monobasic, quadridentate dibasic, Schiff bases are usually magnetically dilute.[19] The non-participation of the vanadyl oxygen atom is responsible for the absence of out-of-plane magnetic interaction in oxovanadium(IV) complexes.

In the present investigation the complex has the magnetic moment of 1.72 which is very close to the spin only value expected for oxovanadium(IV) complexes.[20] Most quadrivalent vanadium(IV) complexes showing normal magnetic moments contain the vanadyl ion, ($VO^{2+}$) and acquire square pyramidal stereochemistry.[21] However, there are reports on oxovanadium(IV) complexes of ON donor bidentate monobasic Schiff bases which possess a magnetic moment of 1.54 B.M. at 297 K indicating the presence of antiferromagnetic exchange.[22] Recently, Kuge *et al.*[23] and Syamal[24] have prepared vanadium(IV) Schiff base complexes and attributed the low magnetic moment

Table 2. Electronic transitions (nm) and their assignments of copper(II), cobalt(II) and oxovanadium(IV) complexes

| Bis(2-OH-5-Me-acph-glycinato) copper(II) | | Bis(2-OH-5-Me-acph-glycinato) cobalt(II) | Bis(2-OH-5-Me-acph-glycinato) oxovanadium(IV) | |
|---|---|---|---|---|
| $^2A_{1g} \leftarrow {}^2B_{1g}$ | $^2E_g \leftarrow {}^2B_{1g}$ | $^4A_2 \longrightarrow {}^4T_1(P)$ ($\nu_3$) | $^2B_2 \longrightarrow {}^2B_1$ | $^2B_2 \longrightarrow {}^2A_1$ |
| 550 | 360 | 685 | | |
| | | 646 | 590 | 390 |
| | | 636 | | (Obscured by Charge transfer band) |

not to the antiferromagnetic exchange but to the magnetically dilute nature of the complex. On the basis of the above mentioned reports a monomeric square pyramidal geometry is suggested for this complex.

(c) *Cobalt(II) complex*

The ground state for tetrahedral cobalt(II) is $4A_2$ and a low magnetic moment is usually observed. But the magnetic moments in the range 4.00–5.00 B.M. have been found experimentally.[25] These are higher than the anticipated "spin only" value of 3.89 B.M. for tetrahedral cobalt(II). This can be attributed to the mixing of the excited triplet state with the ground state.

The cobalt(II) acetophenone-glycinato complex under consideration has a magnetic moment of 4.5 B.M. which is concurrent with the reported values[26,27] for high spin-tetrahedral cobalt(II) complexes.

## ELECTRONIC SPECTRA

Electronic spectral transitions and their assignments of complexes are summarized in Table 2.

(a) *Copper(II) complex*

It is observed that the spectrum of the copper(II) complex does not resemble those of the standard tetrahedral ones,[28,29] which rules out the tetrahedral arrangement of copper(II). Octahedral copper(II) complexes usually have two equally intense bands at 1100 nm and 710 nm.[30] A comparison of the spectrum of this complex with the above mentioned ones, eliminates the possibility of six coordinated octahedral geometry.

In the present investigation the copper(II) complex exhibits two low energy bands at 550 nm and 360 nm. These have been assigned as $2A_{1g} \leftarrow 2B_{1g}$ and $2E_g \leftarrow 2B_{1g}$ transitions for square planar copper(II). The high intensity of the second band is probably due to intensity stealing from the adjacent charge transfer band. The spectrum of this complex is comparable with the known square planar copper(II) complexes.[31]

(b) *Oxovanadium(IV) complex*

A system containing quadrivalent oxovanadium(IV) is expected to exhibit three *d–d* transitions.[32] The first absorption band occurring in the region 770–740 nm can be assigned to the transition $2B_2 \rightarrow 2E$, the second around 590 nm to $2B_2 \rightarrow 2B_1$ and the last one around 390 nm to $2B_2 \rightarrow 2A_1$ transitions.[33–35]

The spectrum in the present work does not show three distinct bands as expected. The band at 390 nm is obscured by the charge transfer bands and the first one around 770 nm is not very clearly resolved. Nevertheless it is concluded from the electronic spectral data that vanadium(IV) in this complex has a square pyramidal geometry.

(c) *Cobalt(II) complex*

The electronic spectrum of tetrahedral cobalt(II) complex is characterised mainly by two transitions which appear as multiple absorptions in the near IR and visible regions respectively. They are considered to be due to $\nu_2(4T_1(F) \leftarrow 4A_2)$ and $\nu_3(4T_1(P) \leftarrow 4A_2)$ transitions.[36,37] In the spectrum of the complex under consideration only the band in the visible region is noticed. It is a multicomponent band of high intensity centred around 625 nm which is assigned as $\nu_3$ arising from $4A_2 \rightarrow 4T_1(P)$ transition. This spectrum closely resembles the spectra of known typical tetrahedral complexes.[38,39] Thus the electronic spectral data suggests that cobalt(II) in this complex exists in the tetrahedral environment.

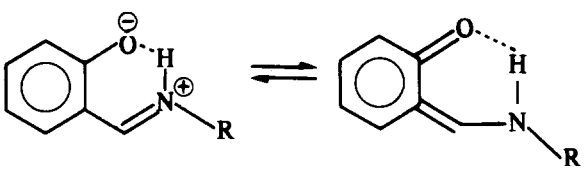
*IR spectra*

The IR frequencies, of ligands and complexes and their assignments are given in Table 3.

Table 3. IR frequencies ($cm^{-1}$) and their assignments for 2-hydroxy-5-methyl-acetophenone and its copper(II), cobalt(II) and oxovanadium(IV) complexes

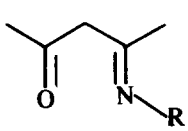
| Assignments | 2-OH-5-Me-acph Gly | Cu(II) complex | Co(II) complex | VO(IV) complex |
|---|---|---|---|---|
| -NH stretch | 3400 | 3335 | 3340 | 3340 |
| -COO assymetric stretch | 1675 | 1620 | 1625 | 1630 |
| -C=C/C=N stretch | 1610 | | | |
| -COO symmetric stretch | 1380 | 1400 | 1410 | 1410 |
| Phenolic $\nu$ (C-O) | 1280 | 1280 | 1280 | 1280 |
| -OCO wagging | 690 | 740 | 730 | 750 |
| -$\gamma$(C=O) out-of-plane | - | 630 | 640 | 635 |
| -$CH_2$ bending vibrations of trans type complex | - | 1450 | 1420 | 1435 |
| $\nu$V=O stretch | - | - | - | 1000 |
| $\nu$ (M-N) | - | 525 | 520 | 540 |
| $\nu$ (M-O) | - | 450 | 440, | 445 |

In the spectra of the ligands, it seems probable that carbonyl stretching vibration of an amide is the origin for the absorption band in the region of the imine stretching frequency, while the new band at 1500 $cm^{-1}$ is assigned to the C=C stretching vibration observed in amide vinylogs. Consequently, the structure of this compound is interpreted as a tautomeric amide form(I) in equilibrium with the smaller fractions of the imine form (II).

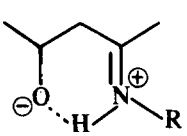


I II

This tautomerism was first noticed by Metzler.[40] A number of spectroscopic investigations[41] of acetylacetone imines and bis(acetylacetone) ethylenediamines and their NMR spectra[42] proved the absence of non-enolised ketimine form (III) and the existence of the enamine tautomeric form (IV).

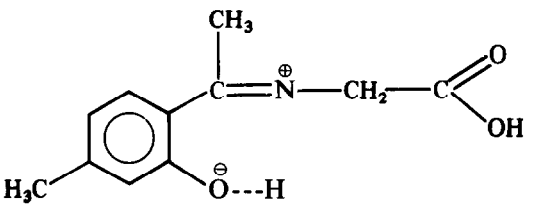


III



IV

Hence it was concluded that in the present investigation, the Schiff base ligands derived from amino acid and 5-methyl, 2-hydroxy acetophenone exist predominently in keto enamine form (IV).



A medium intensity band around 3400 $cm^{-1}$ assignable to –NH vibration[43] also confirms the observation that the ligand is in the keto-enamine form. Instead of the carbonyl stretching vibration, two bands at 1675 and 1610 $cm^{-1}$ are observed and are assigned to the –COO asymmetric stretch and the C=C/C=N ring stretching bands. Another symmetric –COO vibration appears at 1380 $cm^{-1}$. As mentioned earlier, the broad band around 1500 $cm^{-1}$ may be attributed to the C=C/C=N stretching vibration of the conjugated amide.

In the spectra of complexes, the band at 3400 $cm^{-1}$ is shifted towards lower frequency region, i.e. 3340–3300 $cm^{-1}$, indicating that the coordination has taken place through the amide nitrogen. The antisymmetric –COO stretch is shifted to lower frequency as a single wide band spreading over the region 1640–1620 $cm^{-1}$, which could be accounted as a combination of C=C/C=N ring stretching vibrations. The symmetric stretch of

–COO group suffers high frequency shift from a well defined sharp peak at 1380 $cm^{-1}$ to a broad band at around 1410 $cm^{-1}$ which is split, indicating the possibility of metal-oxygen bond formation through the –COO group. Furthermore, the separation between antisymmetric and symmetric vibrations is about 220 $cm^{-1}$, indicating the covalent nature of the metal–oxygen bond.[44]

The band which could be assigned for phenolic $\nu$(C–O) stretch at 1280 $cm^{-1}$ did not change which rules out the possible bond formation between the oxygen of the *o*-hydroxy group and the metal moiety. The spectrum of the oxovanadium(IV) complex is characterised by an intense single band at 1000 $cm^{-1}$, which is unambiguously assigned to the $\nu$(V=O) stretch[45] indicating the monomeric nature of the oxovanadium(IV) complex.

In accordance with the earlier reports[46] on platinum glycinato complexes, a strong band in the region 550–500 $cm^{-1}$ is assigned to metal–nitrogen vibrations [Cu–N:525 $cm^{-1}$, Co–N:520 $cm^{-1}$, V–N; 540 $cm^{-1}$]. A band between 450–400 $cm^{-1}$ is attributed to metal-oxygen vibrations [Cu–O:450 $cm^{-1}$, Co–O:440 $cm^{-1}$, V–O:445 $cm^{-1}$].[47] Based on the observations made earlier,[46] the $-CH_2$ bending vibration is assigned to a band at 1440 $cm^{-1}$. Another band at 1333 $cm^{-1}$ is attributed to the $-CH_2$ wagging, which corresponds to the trans complex. The –CO wagging vibration of the ligand was observed at 690 $cm^{-1}$ and these vibrations have been assigned at 740 $cm^{-1}$ for the complexes. A strong band invariably present in all the complexes in the region 640–600 $cm^{-1}$ is assigned to $\nu$(C=O) out of plane vibrations.[46]

In conclusion, the foregoing results clearly imply that all the three complexes possess different configurations. A square planar structure for the copper(II) complex, tetrahedral environment for the cobalt(II) complex and square-pyramidal geometry for the oxovanadium(IV) complex are suggested.

## REFERENCES


1. R. H. Holm, G. W. Everett Jr. and A. Chakravorty, *Progr. Inorg. Chem.* 1966, **7**, 83.
2. R. H. Holm and M. J. O'Conner, The stereochemistry of bis-chelate metal(II) complexes. *Progress in Inorganic Chemistry* (Edited by S. J. Lippard), Vol. 14, pp. 241–401. Wiley-Interscience, New York (1971).
3. J. B. Hodgson and G. C. Percy, *Spectrochim. Acta.* 1976, **32(A)**, 1291.
4. G. C. Percy and H. C. Streton, *J. Inorg. Nucl. Chem.* 1976, **38**, 1255.
5. F. L. Bowden, R. P. Carpenter, R. V. Parrish and R. D. Pollock, *Inorg. Chim. Acta.* 1977, **23**, 35.
6. G. C. Percy, *J. Inorg. Nucl. Chem.* 1975, **37**, 2071.
7. R. C. Burrows and J. C. Bailar Jr., *J. Am. Chem. Soc.* 1966, **88**, 4150.
8. G. L. Eichorn and N. D. Marchand, *J. Am. Chem. Soc.* 1956, **78**, 2688.
9. H. N. Christensen and S. Collins, *J. Biol. Chem.* 1956, **220**, 279.
10. E. Willsstadter, T. A. Hamor and J. L. Hoard, *J. Am. Chem. Soc.* 1963, **85**, 1205.
11. A. I. Vogel, *Text Book of Quantitative Inorganic Analysis.* Longmans Green, New York (1969).
12. L. Pauling, *Nature of Chemical Bonds.* Cornell University Press, New York (1940).
13. P. Ray and D. N. Sen, *J. Indian Chem. Soc.* 1948, **25**, 473.
14. B. N. Figgis, *Nature* 1958, **182**, 1568.
15. K. Ito and T. Ito, *Aust. J. Chem.* 1958, **1**, 406.
16. W. Byers, A. B. P. Lever and R. V. Parrish, *Inorg. Chem.* 1968, **7**, 1835.
17. R. Whyman, W. E. Hatfield and J. S. Paschal, *Inorg. Chim. Acta.* 1967, **1**, 113.
18. A. Syamal, *Coord. Chem. Rev.* 1975, **16**, 309.
19. J. Selbin, *Chem. Rev.* 1965, **65**, 153; *Coord. Chem. Rev.* 1966, **1**, 293.
20. B. N. Figgis and J. Lewis, *Progr. Inorg. Chem.* 1964, **6**, 37.
21. A. Kapahi, K. B. Pandeya and R. P. Singh, *J. Inorg. Nucl. Chem.* 1976, **38**, 2121.
22. R. L. Dutta and G. P. Sengupta, *J. Indian Chem. Soc.* 1967, **44**, 738; 1971, **48**, 33.
23. U. Kuge and S. Yamada, *Bull. Chem. Soc.* (*Jap.*) 1972, **45**, 799.
24. A. Syamal, *Bull. Chem. Soc.* (*Jap.*) 1977, **50(2)**, 557.
25. B. N. Figgis and J. Lewis, The magnetochemistry of complex compounds, In *Modern Coordination Chemistry* (Edited by J. Lewis and R. G. Wilkins). Interscience, New York (1960).
26. R. L. Carlin and S. L. Holt, Jr., *Inorg. Chem.* 1963, **2**, 849.
27. M. A. Weiner, *Inorg. Chem.* 1975, **14**, 1714.
28. J. Denuynck, A. Viellard and U. Wahlgren, *J. Am. Chem. Soc.* 1973, **95**, 5563.
29. D. W. Smith, *J. Chem. Soc., A.* 1970, 2900.
30. M. C. Styka, R. C. Smierciak, E. L. Blinn, R. E. Desimone and J. V. Passariello, *Inorg. Chem.* 1978, **17**, 82.
31. R. H. Holm, *J. Am. Chem. Soc.* 1960, **82**, 5632.
32. C. J. Ballhausen and H. B. Gray, *Inorg. Chem.* 1962, **1**, 111.
33. J. Bernal and P. H. Reiger, *Inorg. Chem.* 1963, **2**, 256.
34. J. Selbin, G. Mause and D. L. Johnson, *J. Inorg. Nucl. Chem.* 1967, **29**, 1735.
35. L. I. Boucher, E. C. J. Tynan and T. F. Yen, *Inorg. Chem.* 1968, **7**, 731.
36. A. B. P. Lever, *Inorganic Electronic Spectroscopy.* Elsevier, New York (1968).
37. P. P. Singh, U. P. Shukla and A. K. Srivatsava, *Aust. J. Chem.* 1976, **29**, 79.
38. F. A. Cotton, D. M. L. Goodgame and R. H. Soderberg, *Inorg. Chem.* 1962, **2**, 1162.

39. B. B. Garrett, *J. Am. Chem. Soc.* 1970, **93**, 489.
40. D. E. Metzler, *J. Am. Chem. Soc.* 1957, **79**, 485.
41. A. E. Martell, R. L. Belford and M. Calvin, *J. Inorg. Nucl. Chem.* 1958, **5**, 170.
42. G. O. Dudek and R. H. Holm, *J. Am. Chem. Soc.* 1961, **83**, 2099.
43. G. Marcotrigiano, L. Menabue and G. C. Pellacani, *J. Inorg. Nucl. Chem.* 1978, **40**, 165.
44. K. Nakamoto, Y. Morimoto and A. E. Martell, *J. Am. Chem. Soc.* 1961, **83**, 4528.
45. N. S. Biradar and V. H. Kulkarni, *Rev. Roum. Chim.* 1971, **16**, 1203; 1972, **17**, 481; 1973, **18**, 63.
46. R. A. Condrate and K. Nakamoto, *J. Chem. Phys.* 1965, **42**, 2590.
47. C. N. R. Rao, *Chemical Applications of Infrared Spectroscopy*. Academic Press, London (1963).

*Polyhedron* Vol. 3, No. 5, pp. 581–584, 1984
Printed in Great Britain.

0277–5387/84 $3.00 + .00
© 1984 Pergamon Press Ltd.

# SYNTHESIS AND CHARACTERIZATION OF DIETHYLPHOSPHINO Ga(III) AND In(III) COMPLEXES WITH COVALENT METAL–PHOSPHORUS BONDS

**F. MAURY* and G. CONSTANT**
Laboratoire de Cristallochimie, Réactivité et Protection des Matériaux, ERA 263, Ecole Nationale Supérieure de Chimie, 118 route de Narbonne, 31077 Toulouse Cedex, France

(*Received* 22 *September* 1983; *accepted* 1 *November* 1983)

**Abstract**—The covalent derivatives $[Et_2M–PEt_2]_3$ (M = Ga, In) have been prepared from Lewis acid-base complexes, $R_3M.PHEt_2$, by alkane elimination and characterized by elemental analyses, IR, $^1H$ and $^{31}P$ NMR spectroscopy. Features of the mass spectra reveal a trimeric form and the strength of the $[M–P]_n$ ring. For the compound $[ClMeGa–PEt_2]_n$, spectral data are consistent with a weakening of the $[Ga–P]_n$ chain, in good agreement with the pyrolysis results.

Group III organometallic trialkyls, $MR_3$(M = Al, Ga, In; R = Me, Et) and group V hydrides ($AsH_3$, $PH_3$) are generally used to elaborate III–V semiconductor materials by the organometallic Chemical Vapour Deposition process.[1] The formation of intermediates such as Lewis acid-base complexes and covalent compounds in the chemical mechanisms[2,3] led us to use directly these species to simplify and sometimes to improve the process.[4,5]

The goal of our investigations is to foresee whether organometallic compounds can be used as precursors in this process from their physicochemical properties. The principal adduct limitation, as source of III and V elements, seems to be the relative fragility of the donor-acceptor bonds.[4] Consequently, molecules with covalent bonds between the III and V elements were interesting to test since covalent bond strength is generally more important than donor–acceptor bond strength.

The reaction of group III trialkyls with ligands containing acidic hydrogen yields adducts which readily eliminate alkanes to produce unsaturated covalent intermediates. Usually, cyclization occurs to give dimeric or trimeric more stable compounds.

$$R_3M + HXR'_2 \rightarrow R_3M.XR'_2H \rightarrow RH\uparrow + [R_2M - XR'_2]_n$$

Such nitrogen-derivatives are very numerous and various[6–9] whereas related dialkyl phosphino compounds were essentially studied only by Coates *et al.*[10,11]

In this paper we describe the preparation and the characterization of the cyclic compounds $[Et_2M–PEt_2]_3$ (M = Ga, In) and $[ClMeGa–PEt_2]_n$ and discuss the stability of the $[M–P]_n$ ring.

## EXPERIMENTAL

### *Starting materials*

All compounds were handled under purified nitrogen or argon atmosphere. Solvents were purified by conventional means.[12] Triethylgallium (b.p. 140°C/745 mm; lit. 143°C/760 mm) was prepared from the $Ga_2Mg_3$ alloy by a Grignard reaction.[13] Triethylindium was obtained by reaction between $InCl_3$ and an excess of ethyllithium in diethyl ether and purified by distillation (b.p. 64°C/4 mm; lit. 53°C/3 mm). The chlorodimethylgallium (Ventron) and diethylphosphine (Stream Chemical, Inc.) were not purified prior to use. All complexes were prepared by following the same procedure.

### *Preparation of complexes*

(1) $[Et_2Ga–PEt_2]_3$. A slight excess of $HPEt_2$ (52.6 mmoles) was slowly added to $GaEt_3$ (49.0 mmoles) and cooled to −20°C. The mixture was stirred 15 min at this temperature before being warmed. The temperature was increased and ethane was slowly evolved from 100°C. Heating was progressively increased and controlled in such a way that a regular ethane evolution was observed in the bubbler at the outlet of the apparatus. The volume of alkane was measured with a gas burette

*Author to whom correspondence should be addressed.

Table 1. Analytical and IR data

| Compound | Analysis found (calcd.) (%) C | H | P | Ga/In | Cl | degree of association | Sublimation temperature | IR bands ($cm^{-1}$) |
|---|---|---|---|---|---|---|---|---|
| $[Et_2Ga - PEt_2]_3$ | 43.6 (44.3) | 9.3 (9.2) | 13.6 (14.3) | 32.9 (32.2) | - | 3[a] | 100-110°C/0.05 mm | 1418, 1243, 1184, 1040, 1029, 990, 973, 959, 930, 889, 754, 739, 646, 527, 498 |
| $[ClMeGa - PEt_2]_n$ | 27.6 (28.6) | 5.7 (6.2) | 13.9 (14.8) | 30.7 (33.4) | 16.6 (16.9) | 2.6[b] | 150-160°C/0.05 mm | 1420, 1250, 1195, 1040, 1030, 970, 945, 920, 890, 850, 815, 755, 660, 580, 560 |
| $[Et_2In - PEt_2]_3$ | 38.2 (36.7) | 8.0 (7.6) | 12.6 (11.9) | 40.8 (43.8) | - | 3[a] | visc. liq. | 1418, 1242, 1160, 1040, 1025, 995, 970, 952, 919, 886, 754, 735, 620, 467, 450 |

a) obtained by mass spectrometry ; b) in benzene solution, by cryoscopic measurements.

connected to the apparatus and heating was maintained until the theoretical volume corresponding to quantitative reaction was obtained (required: 1098 $cm^3$). In these conditions, the reaction mixture was heated at 100–150°C for 5 hr. After cooling to room temperature, the remaining white solid mass was dissolved in dry benzene, filtered to remove insoluble particles due to some decomposition, recrystallized and dried under vacuum.

(2) The reaction between $HPEt_2$ and $GaMe_2Cl$, led to methane elimination in the range 100–180°C during 24 hr (volume evolved, found: 1180 $cm^3$, required: 1228 $cm^3$). The white solid compound $[ClMeGa–PEt_2]_n$ was obtained by recrystallization from methylene chloride.

(3) The formation of $[Et_2In–PEt_2]_3$ was easier since ethane was briskly evolved from 20°C. Heating for 2 hr was necessary and the maximum temperature reached at the end of the reaction was 100°C. Removal under vacuum of diethyl ether traces, coming from triethylindium, led to a viscous oil which was subjected to physical measurements (Table 1).

*Spectra*

IR spectra were recorded as Nujol mulls by using KBr plates in the range 4000–400 $cm^{-1}$ by means of a Perkin–Elmer model 457 spectrometer. Proton magnetic resonance spectra were recorded at 250 MHz on a Cameca spectrometer and $^{31}P$

Table 2. $^1H$ and $^{31}P$ NMR data[a]

| Compound | Metal $CH_2$ | Metal $CH_3$ | Phosphine $CH_2$ | Phosphine $CH_3$ | $\delta^{31}P$ |
|---|---|---|---|---|---|
| $[Et_2Ga - PEt_2]_3$ | 0.50 m (J(GaH)2) | 1.15 t (8.0) | 1.75 q (7.2) | 1.13 m (J(PH)14) | - 71.5 s |
| $[Et_2In - PEt_2]_3$ | 0.63 q | 1.29 t (7.8) | 1.83 q (7.5) | 1.22 m (J(PH)14.5) | - 74.3 s |
| $[ClMeGa - PEt_2]_n$ | - | 0.54 s<br>0.65 s | 2.44 m | 1.64 m | - 68.2 m |

Solvent $CDCl_3$ ;a) chemical shift (ppm, relative to TMS for $^1H$ and to $H_3PO_4$ for $^{31}P$ spectra), multiplicity (s = singlet, t = triplet, q = quartet, m = multiplet), (coupling constant (Hz)).

NMR spectra were obtained at 36.44 MHz on a Brucker instrument. Mass spectra were recorded either on a VG micro mass 70–70 or 305 F mass spectrometer at a ionizing potential of 70 eV, a source temperature of 180–200°C and using direct insertion into the ion source.

## RESULTS AND DISCUSSION

According to previous works,[7,11] the alkane elimination was easier with indium than gallium as metal atom. Moreover, a chlorine atom in place of an alkyl group on the gallium atom seems to increase the difficulty of alkane elimination since the quantitative formation of $[ClMeGa–PEt_2]_n$ requires 24 hr at 100–180°C but only 5 hr at 100–150°C for $[Et_2Ga–PEt_2]_3$ derivative. Thermal decomposition in a sealed tube, at high pressure of reactants, leads frequently to polymer formation[11] whereas our procedure led to the isolation of crystalline compounds, as indicated by X-ray powder diffraction pattern of the two gallium derivatives.

IR spectra of these compounds were recorded (Table 1) and the quantitative elimination of alkane from adducts, $R_3M \leftarrow PHEt_2$, was verified by the absence of P–H stretching vibrations in the range 2350–2450 $cm^{-1}$. The characteristic bands of $PEt_2$, $MEt_2$ (M = Ga, In) and GaMeCl groups were identified on the basis of previous studies.[6,11] Thus, two intense bands are found at 1040 and 1029 $cm^{-1}$ for P–$CH_2$ rocking vibrations and a sharp doublet at 754 and 739 $cm^{-1}$ for the P–C stretching modes. Furthermore, the symmetrical and antisymmetrical metal–carbon stretching vibrations require more energy in the case of $[ClMeGa–PEt_2]_n$ than for $[Et_2Ga–PEt_2]_3$, 560 and 580 $cm^{-1}$ and 498 and 527 $cm^{-1}$, respectively. This probably correlates with the difference between the bond strengths of Ga–Me and Ga–Et and is in good agreement with the difficulty to eliminate the methyl groups without breaking of the Ga–P bond in the thermal decomposition experiments.[3]

NMR data of these compounds are reported in Table 2. The $^{31}P$ NMR spectra of $[Et_2M–PEt_2]_3$ (M = Ga, In) are constituted by just one peak whereas a complicated multiplet is obtained in the same range for $[ClMeGa–PEt_2]_n$. The integrations in the $^1H$ NMR spectra conformed to the the-

Table 3. Mass spectra data

| $[Et_2Ga - PEt_2]_3$ | | | $[Et_2In - PEt_2]_3$ | | |
|---|---|---|---|---|---|
| m/e | rel. intensity | assignment | m/e | rel. intensity | assignment |
| 625, 623, 621, 619 | 2; 6; 9; 4 | $Ga_3P_3Et_{11}^+$ | 757 | 5 | $In_3P_3Et_{11}^+$ |
| 565, 563, 561, 559 | 1; 2; 3; 1 | $Ga_3P_2Et_{10}^+$ | 555 | 4 | $In_2P_3Et_8^+$ |
| 467, 465, 463 | 2; 4; 3 | $Ga_2P_3Et_8^+$ | 527 | 2 | $In_2P_3Et_7H^+$ |
| 407, 405, 403 | 17; 47; 35 | $Ga_2P_2Et_7^+$ | 523 | 7 | $In_2P_2Et_8^+$ |
| 379, 377, 375 | 1; 3; 2 | $Ga_2P_2Et_6H^+$ | 511 | 3 | $In_2P_3Et_6CH_2^+$ |
| 367, 365, 363 | 1; 3; 2 | $Ga_2P_2Et_5CH_6^+$ | 495, 493 | 47; 4 | $In_2P_2Et_7^+$ |
| 347, 345, 343 | 14; 31; 21 | $Ga_2PEt_6^+$ | 467 | 1 | $In_2P_2Et_6H^+$ |
| 337, 335, 333 | 1; 3; 2 | $Ga_2P_2Et_4CH_5^+$ | 437 | 7 | $In_2P_2Et_5^+$ |
| 319, 317, 315 | 1; 2; 2 | $Ga_2PEt_5H^+$ | 435, 433 | 13; 1 | $In_2PEt_6^+$ |
| 289, 287, 285 | 2; 5; 4 | $Ga_2PEt_4^+$ | 409 | 1 | $In_2P_2Et_4H^+$ |
| 249, 247 | 5; 7 | $GaP_2Et_4^+$ | 405 | 1 | $In_2PEt_5^+$ |
| 221, 219 | 3; 4 | $GaP_2Et_3H^+$ | 377 | 11 | $In_2PEt_4^+$ |
| 189, 187 | 23; 36 | $GaPEt_3^+$ | 319 | 9 | $In_2PEt_2^+$ |
| 160, 158 | 4; 6 | $GaPEt_2^+$ | 233 | 12 | $InPEt_3^+$ |
| 129, 127 | 32; 51 | $GaEt_2^+$ | 204 | 4 | $InPEt_2^+$ |
| 101, 99 | 6; 10 | $GaEtH^+$ | 201 | 12 | $InEt_3^+$ (-H) |
| 90 | 17 | $PEt_2H^+$ | 173, 171 | 75; 3 | $InEt_2^+$ |

oretical ratios of the different types of proton on the basis of simple monomers. The coupling between gallium (I = 3/2) and hydrogen atoms bound to the alpha carbon appears in the spectra of $[Et_2Ga–PEt_2]_3$ (J(GaH) 2.0 Hz) whereas for the others a broadening of the quartet peaks, at about 0.6 ppm, is only observed. The peaks assigned to $CH_2$–M with $[Et_2In–PEt_2]_3$ are shifted downfield compared to those of $[Et_2Ga–PEt_2]_3$, which indicates that the size of the metal atom is more important than its electronegativity.[14] Furthermore, the substitution of an alkyl group on gallium atom by a chlorine atom enhance, by inductive effect, the deshielding of $CH_2$–P.

The $^1H$ NMR spectra of $[Et_2M–PEt_2]_3$ are consistent with a trimer cyclic structure with, in solution rapid inversion at room temperature between two chair forms of a six-membered ring. On the contrary, for $[ClMeGa–PEt_2]_n$, the two peaks in the intensity ratio 1/2 assigned to $CH_3$–Ga and the complexity of the other signals can be interpreted from a mixture, in solution, of two compounds in the ratio 1/2. Cryoscopic molecular weight measurements in benzene solution of this compound give M = 556, 533 and a mean degree of association equal to 2.6 that corresponds exactly to a mixture of dimer and trimer in the ratio 1/2 according to the proton NMR results.

The mass spectroscopic data are summarized in Table 3. Those of $[Et_2M–PEt_2]_3$ (M = Ga, In) show that the primary ions are always fragments derived from trimeric molecules by loss of one Ethyl group followed by competitive loss of either $MEt_3$ or PEt groups. In both spectra the more important peaks are those of $M^+$ and $MEt_2^+$ followed by $M_2P_2Et_7^+$, $M_2PEt_6^+$, $M_2PEt_4^+$ and $MPEt_3^+$. The ion-fragments obtained by M–Et and P–Et cleavage are numerous and their abundances suggest a relatively simple fragmentation pattern due to the stability of $[M–P]_n$ ring.

The mass spectrum of $[ClMeGa–PEt_2]_n$ is more complicated and ions derived from trimeric molecule are not detected. Fragments arising from dimeric species are observed ($Ga_2\ Cl_2\ P_2\ Et_3\ Me^+$ $Ga_2\ Cl_2\ PEt_4^+$ ...) but also ions such as $Ga\ Cl_2\ P\ C_5\ H_{15}^+$ due to ion-molecule side reactions, and several ions containing bromine and coming from impurities in $GaMe_2Cl$. A Negative Chemical Ionization mass spectrum with methane displays characteristic quintuplets at m/e = 623 and 491 assigned to $[ClMeGa–PEt_2]_3$–H and $[Ga_3\ Cl_3\ P_2\ Et_3\ Me_2]$, respectively. Next to these trimeric species, this spectrum reveals ions containing bromine and $Ga_x\ Cl_{x+1}$ entities which are very enhanced and numerous corroborating a recent work on this spectrometry.[15]

In conclusion, the trimeric covalent compounds $[Et_2M–PEt_2]_3$ (M = Ga, In) have a similar fragmentation pattern and the preferential process, which involves M–Et and P–Et bond cleavage, implies considerable stability of the $[M–P]_n$ ring. The fragility of this chain seems to increase with the number of polar functions. Thus, with $[ClMeGa–PEt_2]_n$ a weakening of the Ga–P $\sigma$ bond strength is assumed to explain the complexity of the fragmentation. These results are in good agreement with the pyrolysis study of these organometallic molecules[3] since no GaP coating was obtained from $[ClMeGa–PEt_2]_n$, probably because the Ga–P $\sigma$ bonds are broken in the vapour phase, whereas the two other compounds led to III–V semiconductor layers.

*Acknowledgements*—We wish to thank the Centre de Spectrométrie de Masse (Lyon) and the Service de RMN á Haut Champ (UPS, Toulouse) for recording spectra.

## REFERENCES

1. H. M. Manasevit and W. I. Simpson, *J. Electrochem. Soc.* 1969, **116**, 1725.
2. R. Didchenko, J. E. Alix and R. H. Toeniskoetter, *J. Inorg. Nucl. Chem.* 1960, **14**, 35.
3. F. Maury and G. Constant, Proc. of IV European Conference on CVD (Edited by J. Bloem, G. Verspui and L. R. Wolff), p. 257, Eindhoven (1983).
4. A. Zaouk, E. Salvetat, J. Sakaya, F. Maury and G. Constant *J. Cryst. Growth*, 1981, **55**, 135.
5. F. Maury and G. Constant, *J. Cryst. Growth* 1983, **62**, 568.
6. O. T. Beachley, G. E. Coates and G. Kohnstam, *J. Chem. Soc.* 1965, 3248.
7. A. Storr and B. S. Thomas, *J. Chem. Soc.* (*A*) 1971, 3850.
8. J. Muller, K. Margiolis and K. Dehnicke, *J. Organometal. Chem.* 1972, **46**, 219.
9. J. R. Jennings, I. Pattison, K. Wade and B. K. Wyatt, *J. Chem. Soc.* (*A*) 1967, 1608.
10. G. E. Coates and J. Graham, *J. Chem. Soc.* 1963, 233.
11. O. T. Beachley and G. E. Coates, *J. Chem. Soc.* 1965, 3241.
12. D. D. Perrin, W. L. F. Armarego and D. R. Perrin, In *Purification of Laboratory Chemicals*, 2nd Edn. Pergamon Press, Oxford (1980).
13. L. M. Goloubinsdkaia, V. I. Bregadze, B. I. Kozirkin and B. G. Gribov, UDK 547–256–81 (1976).
14. B. Sen and G. L. White, *J. Inorg. Nucl. Chem.* 1973, **35**, 2207.
15. J. Tirouflet, J. Besancon, B. Gautheron, F. Gomez and D. Fraisse, *J. Organometal. Chem.* 1982, **234**, 143.

*Polyhedron* Vol. 3, No. 5, pp. 585–588, 1984
Printed in Great Britain.

0277-5387/84 $3.00 + .00
© 1984 Pergamon Press Ltd.

# A NEW EXAMPLE OF LIGAND-TO-METAL ELECTRON-TRANSFER PROCESS : ONE-ELECTRON REDUCTION PRODUCTS OF NICKEL(II)-TETRADENTATE SCHIFF BASE COMPLEXES

G. CROS*, J.-P. COSTES and D. de MONTAUZON
Laboratoire de Chimie de Coordination du CNRS
associé à l'Université Paul Sabatier, 205 route de Narbonne,
31400 Toulouse, France

(Received 3 October 1983; accepted 16 February 1984)

Abstract - The reduction of three nickel(II) complexes involving two symmetrical N,N'-ethylenebis (acetylacetoneiminato) and N,N'-ethylenebis (salicylideneiminato) and one non-symmetrical N,N'-ethylene(acetylacetoneiminatosalicylideneiminato) Schiff bases has been investigated by electrochemistry and ESR spectroscopy. In all cases, exhaustive reduction results in the formation of nickel(I) complexes. However, ESR data support the formation of a nickel(II)-stabilized ligand radical species at the early stage of the reduction of the non-symmetrical Schiff base complex.

As part of a continuing study of the Schiff base metal complexes, we report here some findings on the electrochemical reduction of three nickel(II) complexes incorporating two symmetrical (BAE, Salen)** and one non-symmetrical (AESalen)** Schiff bases.

Reduction of cyclic-tetraaza Ni(II) complexes is well documented.[1-3] The species produced were found to be either $d^9$ nickel(I) complexes or nickel(II) stabilized radical anions. These two cases were distinguished on the basis of their electron spin resonance spectra. In one instance,[4] an equilibrium between two species was demonstrated and attributed to a valence isomerization between a nickel(I) complex and the isomeric nickel(II) radical anion. More recently,[5] another example of a reversible ligand-to-metal electron-transfer has been given. However, the works devoted to electrochemical reduction of Schiff base nickel(II) complexes are rather limited. One may note a recent paper by Jager et al.[6] where the reduction process of some Ni(II) complexes with BAE derivatives is shown to correspond to the formation of Ni(I) complexes.

## RESULTS AND DISCUSSION

In the -1.6, -2.0 V range (versus the SCE), the three complexes show a cathodic wave. The gradient of the plot of E versus log $i/(i_d-i)$ is as expected for a reversible (or quasi reversible) and diffusion-controlled monoelectronic process. Coulometric measurements at a controlled potential confirm that a one-electron transfer occurs in each case.

The trend of the $E_{1/2}$ values reported in Table 1 is similar to that previously observed[7] for the cobalt complexes, i.e. the non-symmetrical complex lies between the two symmetrical ones.

---

* Author to whom correspondence should be addressed.

** BAE = N,N'-ethylenebis(acetylacetoneiminato)
Salen = N,N'-ethylenebis(salicylideneiminato)
AESalen = N,N'-ethylene(acetylacetoneiminatosalicylideneiminato)

To probe definitively the nature of the species responsible of the g = 2.003 signal, we have performed the reduction of the nickel(II) complexes in the presence of trace of air. Exhaustive electrolysis at 230 K followed by rapid freezing of the sample (120 K) leads to spectra identical to those of the $Ni^{I}L$ complexes obtained in an argon atmosphere. However warming the samples to 245 K causes the appearance of new signals attributable to $Ni^{II}LO_2^-$ species.

From these experiments and, more particularly, from the effects of varying the temperature, it is obvious that the three species, ($Ni^{I}L$), ($Ni^{II}L^{\cdot}$) and ($Ni^{II}LO_2^-$) may be easily distinguished. Without any doubt, the two species observed during the early stage of the electrolysis of NiAESalen are actually the corresponding nickel(i) complex and nickel(II)-stabilized radical anion. Since the radical is no longer discernible at the end of the reduction process, we may reasonably assume the occurrence of rapid ligand-to-metal electron transfer ($Ni^{II}L^{\cdot} \rightarrow Ni^{I}L$). However, we did not succeed in determining reliably the relative intensities of the two sets of signals at various temperatures in the range 120-245 K so that we cannot conclude in favour of a reversible process ($Ni^{II}L^{\cdot} \rightleftharpoons Ni^{I}L$).

## EXPERIMENTAL

Ni(BAE) was prepared according to the procedure of McCarthy.[16] The synthesis of Ni(Salen) and Ni(AESalen) has been described elsewhere.[17]

Voltammetric measurements and controlled potential electrolysis were carried out under argon with a Tacussel PRT 20-2X polarograph, according to the procedure previously described.[18] Rigorously deaerated acetonitrile was used as solvent and $Et_4NBF_4$ (0.1 M) as supporting electrolyte. Coulometry was performed at 230 K on a large area electrode (Hg or Pt) and at -2.2 V (NiBAE), -2.0 V (NiAESalen) and -1.8 V (NiSalen), respectively. ESR spectra of reduced species in acetonitrile glass were recorded on a Bruker ER-200D instrument with a conventional X-band (9.63 GHz) accessory.

Due to the experimental requirements (temperature and atmosphere control), a particular electrolysis cell allowing combined coulometry-ESR studies has been used (Figure 1).

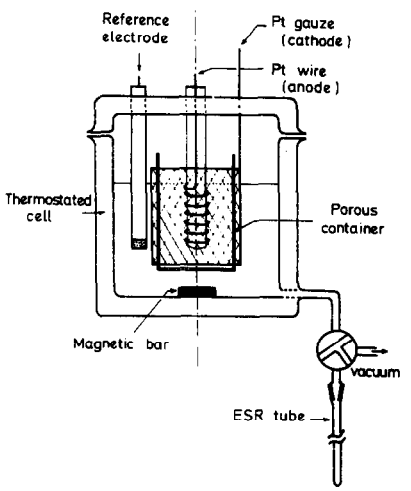



Fig. 1. Electrolytic cell.

While determining the nature of the reduced species, surprisingly we found that, for the systems involving the AESalen ligand, the sight of the ESR spectra depends on the stage at which the electrolysis is stopped. Thus, exhaustive electrolysis at 230 K of the three nickel(II) complexes results in green solutions which give rhombic spectra (Cf. Table I) at 120 K. The g-values reported in Table 1 are similar in magnitude to those observed earlier for various nickel(I) complexes so that one may conclude that for the three nickel(II) complexes $Ni^{II}L$ (with L = BAE, Salen, or AESalen), it is primarily the metal which is reduced to afford nickel(I) complexes ($Ni^{I}L$). However, in the case of $Ni^{II}$AESalen, an electrolysis limited at ca. 0.2 Faraday affords a sample which, rapidly frozen to 120 K, exhibits a supplementary signal with a g-value (2.003) very nearly equal to the free-electron value. This strongly suggests that the unpaired electron responsible for this signal is delocalized onto the ligand and the corresponding species would be considered as a nickel(II)-stabilized ligand radical species ($Ni^{II}L^{\cdot}$). Warming the glassy sample causes the g = 2.003 signal to disappear at ca. 220 K. At intermediate temperatures, other supplementary signals are discernible. They are ill-resolved and they are likely attributable to some exchange process[8] which has not been studied further.

Table 1. Half-wave potentials related to the one-electron reduction of the $Ni^{II}L$ (L = BAE, Salen, AESalen) complexes and g-values characterizing the "$Ni^{I}L$", "$Ni^{II}L^{\cdot}$" and "$Ni^{II}LO_2^{-}$" species.

| | $E_{1/2}$ | g-values | | |
|---|---|---|---|---|
| | (volts vs. SCE) | ($Ni^{I}L$) | ($Ni^{II}L^{\cdot}$) | ($Ni^{II}LO_2^{-}$) |
| BAE | -1.95* | 2.264, 2.124, 2.058 | - | - |
| Salen | -1.63** | 2.242, 2.132, 2.051 | - | 2.101, 2.009 |
| AESalen | -1.77** | 2.268, 2.083, 2.048 | 2.003 | 2.113, 2.007 |

* dropping mercury electrode
** rotating platinum electrode (2000 rpm)

Due to the fact that the supposed $Ni^{II}L^{\cdot}$ species has never been observed alone, its real nature remains controversial. For instance, one may suspect that traces of $O_2$ would be present during the electrolysis and, therefore, the extra signal at g = 2.003 would be attributable to oxygenated ESR-active species, such as superoxide ions. It is known[9] that this type of complex ($Ni^{II}LO_2^{-}$) may be prepared by reacting nickel(II) complexes with superoxide ions. The $O_2^{-}$ electrogenerated at 230 K in acetonitrile is characterized by an ESR spectrum which shows two g values ($g_{\perp}$ = 2.009, $g_{\parallel}$ = 2.094) at 120 K. It is noteworthy that these data are not exactly identical with the values reported in the literature.[9-15] The discrepancy is likely due to an interaction between the solvent and the superoxide ions which is known to affect primarily the $g_{\parallel}$ component. In fact, addition of $Ni^{II}L$ does not induce any modification of the spectrum as long as the temperature of the mixture remains low (ca. 200 K). However, when the temperature rises above 240 K the two g-values are slightly affected (cf. Table 1) due to the formation of the superoxo complexes ($Ni^{II}LO_2^{-}$). These values remain unchanged when the sample warmed to room temperature is frozen again to 120 K.

Acknowledgement - Dr. J.-P. Laurent is greatly acknowledged for the interest he has taken in this problem.

REFERENCES

1 F.V. Lovecchio, E.S. Gore and D.H. Busch, J. Am. Chem. Soc. 1974, 96, 3109.

2 S.M. Peng, J.A. Ibers, M. Millar and R.H. Holm, J. Am. Chem. Soc. 1976, 98, 8037.

3 D.P. Rillema, J.F. Endicott and E. Papaconstantinou, Inorg. Chem. 1971, 10, 1739. L. Fabrizzi and A. Poggi, Inorg. Chim. Acta 1980, 39, 207.

4 R.G. Gagné and D.M. Ingle, J. Am. Chem. Soc. 1980, 102, 1444, and Inorg. Chem. 1981, 20, 420.

5 J. Lewis and M. Schröder, J. Chem. Soc. Dalton 1982, 1085.

6 E.J. Jäger and M. Rudolph, Z. Chem. 1981, 21, 371.

7 J.-P. Costes, G. Cros, M.-H. Darbieu and J.-P. Laurent, Trans. Met. Chem. 1982, 7, 219.

8 D. Suryanarayana, L. Kevan and S. Schlick, J. Am. Chem. Soc. 1982, 104, 668.

9 M. Rudolph and E.G. Jäger, Z. Chem. 1982, 22, 67.

10 D.L. Marick and W.G. Hodgson, Anal. Chem. 1965, 37, 1562.

11 J.H. Lunsford, Catalysis Rev. 1973, 8, 135.

12 J.A. Fee and P.G. Hildebrand, FEBS Lett. 1974, 39, 79.

13 R.C. Bray, G.N. Mautner, E.M. Fielden and C.I. Carle in "Superoxide and Superoxide Dismutases", Academic Press, New York, 1977.

14 T. Ozawa, A. Hanaki and H. Yamamoto, FEBS Lett. 1977, 74, 99.

15 B.H.J. Bielski and J.M. Gebicki, J. Am. Chem. Soc. 1982, 104, 796.

16 P.J. McCarthy, R.J. Hovey, K. Dewo and A.E. Martell, J. Am. Chem. Soc. 1955, 77, 5820.

17 J.-P. Costes, G. Cros, M.-H. Darbieu and J.-P. Laurent, Inorg. Chim. Acta 1982, 60, 111.

18 M.-H. Darbieu, G. Cros, D. de Montauzon and J.-P. Laurent, Trans. Met. Chem. 1982, 7, 149.

*Polyhedron* Vol. 3, No. 5, pp. 589–594, 1984
Printed in Great Britain.

0277-5387/84 $3.00 + .00
© 1984 Pergamon Press Ltd.

# SPIROBORATES DERIVED FROM CATECHOLBORANE AND EPHEDRINE TYPE AMINOALCOHOLS - MODEL COMPOUNDS FOR THE STUDY OF INTRAMOLECULAR N→B COORDINATION BY DYNAMIC $^{1}H$-, $^{11}B$- AND $^{13}C$-NMR.

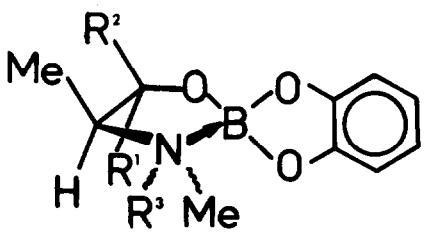
FERNANDO SANTIESTEBAN, MARCO ANTONIO CAMPOS, HILDA MORALES and ROSALINDA CONTRERAS*.
Centro de Investigación y de Estudios Avanzados del I.P.N. Departamento de Química.
Apartado Postal 14-740. 07000-México, D.F.

BERND WRACKMEYER
Institut für Anorganische Chemie der Universität München, 8000 München 2,
Meiserstrasse 1, Germany

(Received 15 November 1983; accepted 16 January 1984)

Abstract. A convenient synthesis of the title compounds is reported. These serve as models to study intramolecular N→B coordination by means of dynamic NMR spectroscopy ($^{1}H$, $^{11}B$, $^{13}C$). Steric interactions between substituents at the boroxazolidine ring (C(5)Ph, C(4)Me, NMe) determine the stability of the N→B bond and the nitrogen configuration.

Introduction. Esters of boric and boronic acids form readily adducts with Lewis bases and intramolecular N→B coordination is wellknown [1a-1f]. Very often these compounds have been characterized only by elemental analysis and I.R.,U.V. or mass spectra measurements[1a-1c]. Sometimes, $^{1}H$-[1d-1e] or $^{11}B$-NMR data[1f] have been reported. However, little is known about their dynamic properties in solution. In this work we report the preparation of the spiroborates I-IV derived from catecholborane and ephedrine type aminoalcohols:




| | $R^1$ | $R^2$ | $R^3$ |
|---|---|---|---|
| I | H | Ph | H |
| II | H | Ph | Me |
| III | Ph | H | H |
| IV | Ph | H | Me |

The dynamic behavior of these compounds in solution was studied by $^{1}H$-, $^{11}B$- and $^{13}C$-NMR spectroscopy.

The compounds I to IV have been selected for the following reasons:

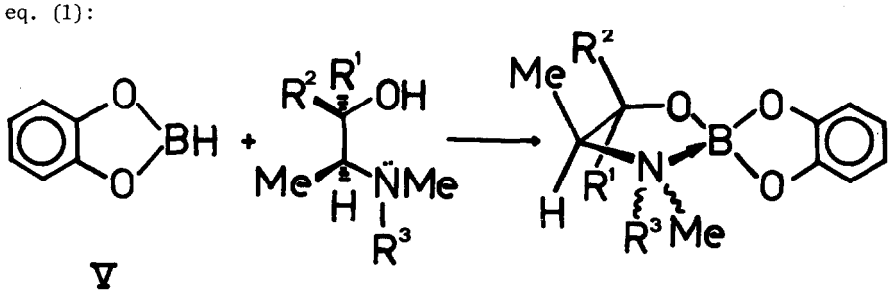
(i) The catecholborane unit guarantees a rigid structure in this part of the molecule.

(ii) The Lewis-acidity of the catecholborane unit is high as result of the bond angle strain in the corresponding three-coordinate borane. Therefore, dynamic processes involving bond breaking at the boron atom should be sufficiently slow to be studied conveniently by NMR techniques.

(iii) Observation of fixation of nitrogen configuration by N→B coordination. The ephedrine type amino alcohols used here lead either a pair of diastereomers (N-epimers) for each compound I and III or two isomer compounds II and IV in which the nitrogen becomes a prochiral center with two diastereotopic N-methyl groups. Therefore, NMR will show readily if fixation of the configuration at the nitrogen atom takes place.

(iv) The energy of activation $\Delta G_c^{\neq}$ for N→B bond breaking can be obtained from dynamic NMR studies of compounds I to IV.

Results and Discussion. The spiroborates I to IV were prepared in yields of 25 to 40% according to eq. (1):



eq. (1)

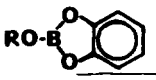
V

The compounds I to IV are crystalline, colorless solids which are only slowly hydrolized in moist air. They are slightly soluble in ether or benzene and better soluble in chlorinated hydrocarbons.

$^{11}$B-NMR (Table 1). All compounds I to IV show a single $^{11}$B-resonance near to $\delta$ $^{11}$B + 12. This corresponds to a low frequency shift of ca. 11 ppm with respect to catecholborane esters[2]. This, together with the observation that the $^{11}$B-resonance in I to IV is independent of the temperature (till +60°C) indicates a strong intramolecular N→B coordination in I to IV[3] as implied from their stability and solubility.

The constancy of the $\delta$ $^{11}$B-values, irrespective of an NHMe- or $NMe_2$-donor, can be traced to the absence of steric interactions between groups at the nitrogen and at the boron atom as a consequence of the spiro-structure.

TABLE 1 $^{11}$B-NMR OF SPIROBORATES I-IV

| Compound | $\delta$ $^{11}$B[a] |
|---|---|
| I | +11.8 |
| II | +12.2 |
| III | +12.0 |
| IV | +12.2 |
|  VI | ∿+23[b] |

a) Constant between 25 and 65°C
b) Ref. 2,3.

$^{13}$C-NMR (Table 2). The assignment of the $^{13}$C-NMR spectra is based upon $^{1}$H-coupled spectra, selective $^{13}$C {$^{1}$H-off resonance} spectra and on the magnitude of accepted substituent effects[5]. The $\delta$ $^{13}$C values of the catechol unit are fairly constant and correspond closely to the $\delta$ $^{13}$C-values of catecholborane-amine adducts[4]. Similarly, there is not much variation in the $\delta$ $^{13}$C(Ph) values of the ephedrine unit. The $^{13}$C(7)-resonances are hardly affected by methyl substitution at the nitrogen atom. The $^{13}$C(8)-resonance are shifted to higher frequencies upon N-methyl substitution (Ia, Ib to II: 4.6 and 6.6 ppm respectively; III to IV 3.5 ppm).

The NMe- and OMe-$^{13}$C-resonances reflect the steric interactions if they are in cis or in trans-position. There is a shift to lower frequencies for the $^{13}$C(Me)resonance if another methyl group is in cis-position[5] (see Ib with respect to Ia (NMe, OMe), II, IV (NMe), IV with respect to III (OMe)).

Since the $^{1}$H-NMR of compound I was unsuitable for the $\Delta G_C^{\neq}$ values to be obtained (vide infra), $^{13}$C-NMR spectra were recorded between -30 and +60 °C. The compounds Ia and Ib

(Fig. 1) are present at -30°C in a ratio of ca. 3:1. The coalescence temperature for the two OMe-resonances was 33±4°C. Since this is just a moderately biased two site exchange case we evaluate[6] $\Delta G_c^{\neq}$ without line shape analysis to 61±4 kJ/M.

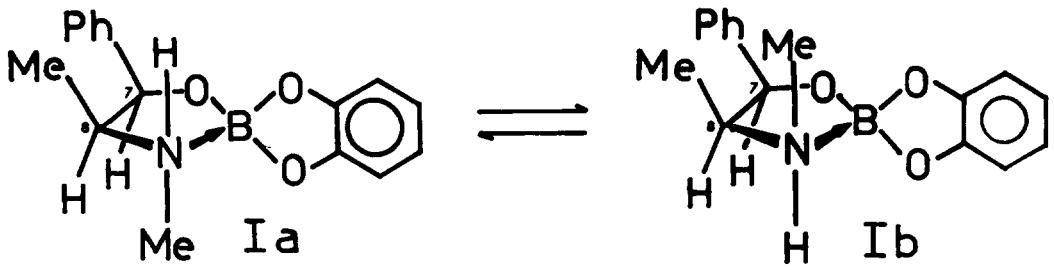
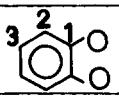
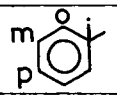



Fig. 1. Structures of compound I as proved by $^{1}H$- and $^{13}C$-NMR. At -30°C Ia and Ib are present in a 3:1 ratio.

TABLE 2 $^{13}C$ NMR OF SPIROBORATES I-IV

| Compound | Temperature (solvent) | C(7) | C(8) | N-Me | C-Me |  |  |
|---|---|---|---|---|---|---|---|
| Ia[a] | -30°C ($CDCl_3$) | 77.2 | 61.4 | 32.0 | 13.8 | 150.7, 151.1(1)<br>109.6, 109.7(2)<br>119.3(3) | 138.4(i), 126.3(o)<br>128.6(m), 128.1(p) |
| Ib[a] | -30°C ($CDCl_3$) | 76.9 | 59.4 | 29.6 | 9.1 | 150.5, 151.0(1)<br>109.4, 109.9(2)<br>119.0, 119.3(3) | 138.4(i), 125.7(o)<br>128.1(m), 127.9(p) |
| II | | 75.1 | 66.1 | 45.5(a)[b]<br>40.4(b) | 10.8 | 151.0, 151.1(1)<br>109.8 (2)<br>119.1, 119.2(3) | 139.5(i), 126.4(o)<br>128.2(m), 127.6(p) |
| III[c] | +27°C ($CDCl_3$) | 80.8 | 65.3 | 30.9 | 12.3 | 150.4, 151.2(1)<br>108.6, 110.2(2)<br>118.9, 120.0(3) | 140.6(i), 126.9(o)<br>128.6(m), 128.2(p) |
| IV | +27°C ($CDCl_3$) | 79.4 | 68.9 | 37.2(b)[b]<br>42.8(a) | 7.9 | 151.5, 151.4(1)<br>109.8, 109.7(2)<br>119.1, 119.4(3) | 140.5(i), 126.9(o)<br>128.6(m), 128.2(p) |

a) 70-30% ratio of Ia-Ib respectively, for structural assignment, see Figure 1.
b) See text. c) Only one isomer, for structural assignment, see Figure 2.

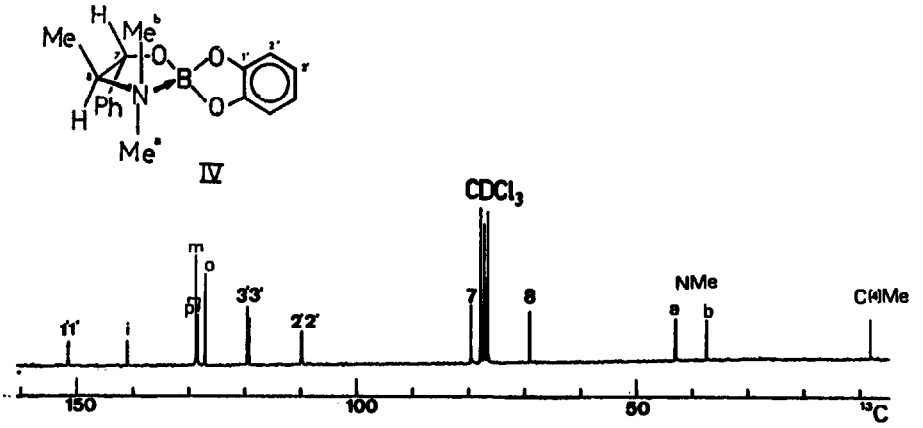
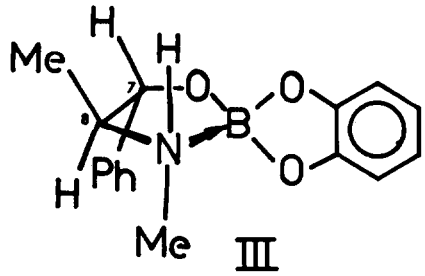



Fig. 3. The $^{13}C$-NMR spectrum (50.3 MHz, 27°C) of compound IV give for the N-$CH_3$ diastereotopic groups two well separated signals.

$^1$H-NMR (Table 3). The $^1$H-NMR of compounds I to IV at 200 MHz are readily assigned. There are multiplets for the $C_6H_4$- and for the $C_6H_5$- groups at high frequencies. The other resonances are clearly defined owing to their splitting pattern due to $^3$J (HH) (e.g. H(8,7), C(8)Me) and their relative intensities (NMe). The NH- resonances are shifted to lower frequencies and become broader with increasing temperature. In case of Ia, b some of the $^1$H-resonances are broad and ill defined even at -60°C as the consequence of a coupled unequally populated two-site exchange process.

The $^1$H-NMR spectrum of compound II at ambient temperature shows two $^1$H-resonances for the diastereotopic NMe-groups. Heating the sample to 55°C caused coalescence of these signals. From this $\Delta G_c^{\neq}$ for the N→B bond breaking process can be evaluated[6] as 68.0±0.5 kJ/M.

In contrast to compound I the $^1$H-NMR spectrum of III shows that in the range between -40° and +120°C only one isomer is present. Above 120°C the line shape of the NMe-resonances (doublet) changes. At 130°C an asymmetric doublet structure is just resolved. This behavior is ascribed to the increase in the rate of N→B bond breaking. Rapid exchange of the NH-proton is unlikely since the coupling $^3$J(HNC(8)H) is still present. From these observations it follows that $\Delta G_c^{\neq}$ (N→B) is presumably >80 kJ/M. The structure of compound III (Fig. 2) follows from appropriate nuclear Overhauser effect (NOE) difference spectra[7] (e.g. saturation of the C(8)Me-resonances gives no appreciable NOE for the NMe-resonances; saturation of the NMe-resonances gives a NOE for the C(8)H-resonance).




III

Fig. 2. Structure of compound III as proved by $^1$H- and $^{13}$C-NMR, and by NOE difference spectra.

In case of compound IV there is no appreciable change in the $^1$H-NMR spectra in $CDCl_3$-solution until +60°C. In $C_2D_2Cl_4$-solution the sample was heated to 120°C. Coalescence of the NMe-signals occurred at 108°C. This corresponds to a $\Delta G_c^{\neq}$ value of 80.2±0.5 kJ/M.

Conclusions. The N→B bond energy in the compounds I and II is significantly smaller than in III and IV. This is attributed to the steric interaction between the C(8)Me and the C(7)Ph-group in I and II which destabilizes the N→B bond in the boroxazolidine ring. The slightly greater N→B bond energy in II with respect to I may be due to the greater basicity of the tertiary nitrogen atom. Since there is no steric crowding at the boron atom the NMe-groups can avoid a close contact to the C(8)Me-group. However, the preferred formation of Ia and the selective formation of III shows that the nitrogen configuration is controlled mainly by steric effects.

Experimental. NMR spectra were recorded on a BRUKER WP 200 FT spectrometer in 5 mm tubes from diluted (2 to 5% W/V) solutions in dry $CDCl_3$ or $C_2D_2Cl_4$. TMS served as an internal standard ($^1$H, $^{13}$C) and $BF_3$-$OEt_2$ as external reference. The temperature control was achieved using a standard BRUKER VT unit with the thermocouple element placed directly underneath the tube. The $^1$H-NOE difference spectra were obtained using a saturation time of 10 s with an R.F. power setting of 40L (to build up the NOE). Mass spectra were recorded at 15 eV with a Hitachi-Perkin-Elmer PMU-7H spectrometer. Elemental analysis were obtained in the institute's (Munich) Analytical Laboratory.

TABLE 3 $^1$H-NMR OF SPIROBORATES I-IV

| Compound | Temperature (solvent) | H(7) | H(8) | N-Me | C(7)Me | NH | $C_6H_4$ | $C_6H_5$ |
|---|---|---|---|---|---|---|---|---|
| Ia[a] | -60°C ($C_2D_2Cl_4$) | 5.11 (d; 6.4) | 3.57(d,d,q; 11.9, 6.4, 6.7) | 2.41 (d,5.2) | 0.90 (d; 6.7) | 3.94 (m)[c] | 6.6-6.9 (m) | 7.1-7.6 (m) |
| Ib[a] | | 4.79 broad | 3.06(m) broad | 2.51 broad | 0.81 (d; 6.7) broad | | | |
| fast Ia⇌Ib | +60°C ($C_2D_2Cl_4$) | 5.22 (d; 5.8) | 3.52(d,d,q; 6.4) | 2.44 (d,4.5) | 0.91 (d; 6.7) | | | |
| II | | 5.43 (d,7.0) | 3.60(d,q, 7.0,7.0) | 2.39(s) 2.62(s) | 0.98 (d;7.0) | | 6.66-6.84 (m) | 7.20-7.45 (m) |
| III[b] | 0°C $CDCl_3$ | 4.94 (d,10) | 3.03(d,d,q) | 2.55 (d,6.0) | 1.25 (d;7,0) | 6.38 (m)[d] | 6.52-6.94 (m) | 7.20-7.48 (m) |
| IV | +27°C $CDCl_3$ | 4.65 (d,9.7) | 3.26(d,q, 9.7,6.8) | 2.42(s) 2.60(s) | 1.15 (d;6.8) | | 6.65-6.85 (m) | 7.25-7.55 (m) |

a) 3:1 ratio of Ia-Ib respectively, for structural assignment see Figure 1.
b) Only one isomer, see Figure 2.
c) $^1$H {$^1$H (NMe)} d, 11.9 Hz.
d) $^1$H {$^1$H (NMe)} d, 11.0 Hz.

Catecholborane was prepared as described[8] and the ephedrine and pseudoephedrine were used as commercially (Sigma Chemical Company) available. N-methylephedrine and N-methyl-pseudoephedrine were prepared as described in the literature[9].

Preparation of (benzo-1',2') methyl-8 phenyl-7 trioxa-1,4,6 aza-9 bora-5 spiro[4,4]nonane derivatives I to IV. (Table 4)

This procedure is representative for all spiroborate derivatives prepared. 2 g (12.1 mM) of (-)ephedrine dissolved in 2.5 ml of THF were placed in a dry 50 ml round bottom flask equipped with a magnetic stirrer under nitrogen atmosphere. The flask was immersed in an ice-water bath and with the aid of a hypodermic syringe 1.45 g (12.1 mM) of catecholborane were added. Hydrogen was rapidly evolved. The reaction mixture was allowed to stir for two h at room temperature. A colourless precipitate was formed and filtered off at the end of the reaction. The filtrate was evaporated in vacuo and a crystalline compound was obtained in each case.

Table 4. PROPERTIES AND ANALYTICAL DATA FOR THE COMPOUNDS I TO IV

| Compound | Yield[c] % | m.p. | MS(m/e $M^+$) | MW | C % found / required | H | N |
|---|---|---|---|---|---|---|---|
| I[a] | 30 | 215-218 | 284 | 283.13 | 67.75<br>67.87 | 6.35<br>6.41 | 4.82<br>4.95 |
| II[b] | 25 | 158-164 | 297 | 297.16 | 68.52<br>68.71 | 6.61<br>6.78 | 4.62<br>4.71 |
| III[b] | 40 | 239-243 | 284 | 283.13 | 67.72<br>67.87 | 6.40<br>6.41 | 4.90<br>4.95 |
| IV[b] | 32 | 238-242 | 297 | 297.16 | 68.62<br>68.71 | 6.65<br>6.78 | 4.55<br>4.71 |

a) Recrystallized from $CHCl_3$.
b) Recrystallized from THF.[3]
c) Isolated compounds.

Acknowledgment.

One of us (M.A.C.) thanks Avon Co. for a scholarship. F.S. thanks Conacyt Mexico for a scholarship. The authors thank L. Velasco and H. Bojórquez from the Instituto de Química de la Universidad Autónoma de México for the mass spectra.

B.W. acknowledges the support by the Deutsche Forschungsgemeinschaft and by the Fonds der Chemischen Industrie.

References

1a) R.C. Mehrotra and G. Srivastava, J. Chem. Soc., 4045 (1961).
b) R.L. Letsinger and D.B. Maclean, J. Am. Chem. Soc., 85, 2230 (1963).
c) J.C. Catlin and H. R. Snyder, J. Org. Chem., 34 1660 (1968).
d) J.R. Kuszewski, W.J. Lennarz and H.R. Snyder, J. Org. Chem. 33 4479 (1968).
e) H.G. Dunn, J.C. Catlin and H.R. Snyder, J. Org. Chem. 33, 4483 (1968).
f) E. Hohaus, Z. Anorg. Allg. Chem., 484, 41 (1982).

2) E.F. Mooney and M.G. Anderson, Ann. Rep. NMR Specrosc. 2, 219 (1969).

3) H. Nöth and B. Wrackmeyer, NMR Spectroscopy of Boron Compounds, in NMR - Basic Principles and Progress, eds. P. Diehl, E. Fluck and R. Kosfeld, Vol. 14, Springer Verlag, Berlin, Heidelberg, New York, 1978.

4) R. Goetze, H. Nöth, H. Pommerening, D. Sedlak, and B. Wrackmeyer, Chem. Ber., 114, 1884 (1981).

5a) J.B. Stothers, Carbon-13 Nuclear Magnetic Resonance Spectroscopy, Academic Press, New York, 1972.
b) F.W. Wehrli and T. Wirthlin, Interpretation of Carbon-13 NMR Spectra, Heyden, London, 1976.

6) J. Sandström, Dynamic NMR Spectroscopy, Academic Press, New York, 1982, p. 93-123.

7a) J.H. Noggle and R.E. Schirmer, The Nuclear Overhauser Effect, Chemical Applications, Academic Press, New York, 1971.
b) K. Nakanishi, D.A. Shoolery, M. Koreeda, and I. Miura, J. Am. Chem. Soc., 94, 2865 (1972).
c) W.E. Hull, Aspect 2000 Application Note No. 1, Bruker Report, 1, 40 (1978).
d) F. Santiesteban, C. Grimaldo, R. Contreras and B. Wrackmeyer, J. Chem. Soc. Chem. Commun., in print.

8) H.C. Brown, G.W. Kramer, A.D. Levy, and M.M. Midland, Organic Synthesis via Boranes, Wiley, New York, 1975, p. 63.

9) H.T. Clarke and H.B. Gillespie and S.Z. Weisshaus, J. Am. Chem. Soc., 55, 4571 (1933).

*Polyhedron* Vol. 3, No. 5, pp. 595–598, 1984
Printed in Great Britain.

0277-5387/84 $3.00 + .00
© 1984 Pergamon Press Ltd.

# NOTE

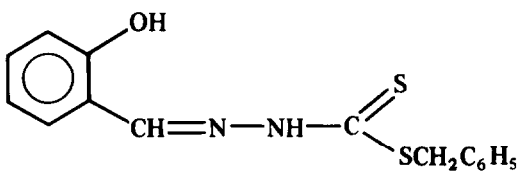
## FOUR- AND FIVE-COORDINATE COPPER(II) COMPLEXES CONTAINING MIXED LIGANDS

**M. AKBAR ALI*, D. A. CHOWDHURY-I and M. NAZIM UDDIN**
Department of Chemistry, University of Chittagong, Chittagong, Bangladesh

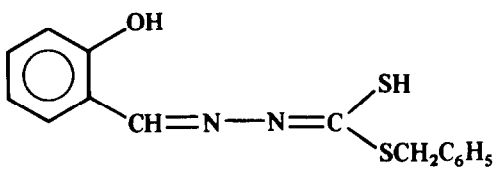
(*Received* 26 *April* 1983; *accepted* 15 *October* 1983)

**Abstract**—New copper(II) complexes of general formula, Cu(ONS)B (ONS = the di-negatively charged Schiff base, S-benzyl-β-N-(2-hydroxyphenyl) methylendithiocarbazate; B = pyridine, 2,2′-dipyridyl or 1,10-phenanthroline) have been synthesized and characterised by magnetic and spectroscopic measurements. The complex, Cu(ONS)py is four-coordinate and square-planar. Magnetic and spectroscopic data support a five-coordinate, presumably, a trigonal-bipyramidal structure for the [Cu(ONS)dipy] and (Cu(ONS)phen] complexes.

The preparation and characterisation of the salicylaldehyde Schiff base of S-benzyldithiocarbazate were initially reported by Akbar Ali and Bose[1]. From IR spectroscopic evidence, the authors postulated that in the solid-state, the Schiff base remains in the thioketo form (**Ia**), but in solution, it might remain as an equilibrium mixture of both the thioketo and thioenol (**Ib**) forms.



(**1a** HONS)



(**1b** $H_2$ONS)

In all its reactions with metal ions, the Schiff base was found to coordinate as a dinegatively charged tridentate ligand. The copper (II) complex, (Cu(ONS)] was found to possess an anomalously low magnetic moment of 1.02 B.M. This was thought to be due to the presence of antiferromagnetic interactions between a pair of copper(II) ions in an oxygen-bridged binuclear structure.[1] Since the subject Schiff base satisfies three coordination positions whilst simultaneously satisfying the dipositive charge of the copper(II) ion, we thought it worthwhile to study complexes of the type, [Cu(ONS)B], where ONS stands for the dinegatively charged tridentate ligand and B stands for the heterocyclic bases such as pyridine, 2,2′-dipyridyl (dipy) and 1,10-phenanthroline (phen). Thus, with pyridine, a monomeric four-coordinate copper(II) complex is expected, whereas with dipy and phen, five-coordination should result. Our results, shown below, indicate that the compounds do in fact form in this manner.

## EXPERIMENTAL

*Physical measurements.* The solid reflectance spectra were obtained with an SP 500 spectrophotometer. IR spectra as KBr discs were recorded on a Perkin–Elmer 577 spectrophotometer. All other physical measurements and analytical procedures employed in the present investigation were similar to those described previously.[2]

*Preparation of S-benzyl-β-N-(2-hydroxyphenyl)-methylendithiocarbazate.* This compound was prepared according to the method of Akbar Ali and Bose.[1] (Found: C, 60.0; H, 4.8; N, 9.3; S, 21.0.

*Author to whom correspondence should be addressed.

$C_{15}H_{15}N_2OS_2$ requires: C, 59.6; H, 4.7; N, 9.3; S, 21.2%).

*General method for the preparation of the copper(II) complexes.* The Schiff base (1.0 g) and the appropriate heterocyclic base (0.5-0.6 g) were dissolved in a 1 : 1 mixture of abs. ethanol (100 $cm^3$) and 2,2-dimethoxypropane (100 $cm^3$). To this was added a hot and filtered solution of copper(II) acetate dihydrate (0.9 g) in the same solvent (100 $cm^3$). The mixture was heated on a water-bath for *ca.* 30 min whereupon the volume of the reaction mixture was reduced to about 100 $cm^3$ by slow heating. On cooling to ambient temperature, crystals of the complexes precipitated and were removed by filtration, washed with ethanol and then dried in a vacuum desiccator over $P_4O_{10}$.

## RESULTS AND DISCUSSION

The Schiff base, hereinafter abbreviated as $H_2ONS$ was obtained as beautiful long needles. Its relevant IR spectral bands with their tentative assignments are shown in Table 2. The positions of these bands agree well with those reported by Akbar Ali and Bose.[1] Reaction of the Schiff base with copper(II) acetate in the presence of heterocyclic bases such as pyridine, dipy and *o*-phen yields crystalline complexes of empirical formula, Cu(ONS)B. The complexes which were isolated are listed in Table 1 along with their physical properties. The molar conductance data of the complexes (Table 1) indicate that these compounds behave essentially as non-electrolytes in nitrobenzene. The ligand, therefore, must be behaving as a dinegatively charged species. Comparison of the IR spectrum of the ligand with those of the metal complexes (Table 2) reveals the following facts: (i) the phenolic and N–H protons of the ligand are lost on complex formation with copper(II), (ii) the $\nu C = S$ band at 782 $cm^{-1}$ of the free ligand[3,4] disappears in the spectra of the complexes, (iii) the $\nu C = N$ band is lowered and a new band at 343 $cm^{-1}$ attributable to the metal–sulphur stretching frequency[5,6] appears in the spectra of the complexes. The foregoing facts suggest that the present Schiff base behaves as a tridentate chelating agent coordinating via the phenolic oxygen atom, the azomethine nitrogen atom and the thiolo sulphur atom. The IR spectrum of [Cu(ONS)phen] shows bands at 420, 840 and 1522 $cm^{-1}$ due to the coordinated phenanthroline molecule.[7,8] In a similar manner the IR spectra of [Cu(ONS)dipy] and [Cu(ONS)py] (Table 2) are indicative of dipy and pyridine coordination[9].

The colour ofthe [Cu(ONS)B] complexes is green in contrast with the red brown colour of the dimeric $Cu_2(ONS)_2$ complex reported by Akbar

Table 1. Colour, conductivity, magnetic moments and analytical data for the complexes

| Compound | Colour | $\Lambda_M$[a] | $\mu_{eff}$[b] | Analytical data[d] C | H | N | S | M |
|---|---|---|---|---|---|---|---|---|
| [Cu(ONS)py][d] | Pale-green | 1.7 | 1.88 | 54.2 (54.2) | 3.9 (3.9) | 9.0 (9.5) | 14.1 (14.5) | 14.4 (14.3) |
| [Cu(ONS)dipy][e] | Green | 0.8 | 1.76 | 57.5 (57.7) | 3.9 (3.9) | 10.8 (10.8) | 12.3 (12.3) | 12.0 (12.2) |
| [Cu(ONS)phen][f] | Green | 0.9 | 1.99 | 59.2 (59.6) | 3.2 (3.7) | 10.7 (10.3) | 11.8 (11.8) | 11.2 (11.7) |

a. Molar conductivity of ca. $10^{-3}$M solutions in nitrobenzene, $ohm^{-1}cm^2mole^{-1}$;

b. $\mu_{eff} = 2.83 \sqrt{\chi_M \cdot T}$ at 298°K;

c. Calculated values are given in parentheses.

d. S - Benzyl-β-N-(2-hydroxyphenyl)methylendithiocarbazato(pyridine)copper(II);

e. S - Benzyl-β-N-(2-hydroxyphenyl)methylendithiocarbazato(2,2'-dipyridyl)copper(II).

f. S - Benzyl-β-N-(2-hydroxyphenyl)methylendithiocarbazato(1,10-phenanthroline)copper(II).

Table 2. Selected IR absorption bands and electronic spectral data

| Compound | IR bands[a] ($cm^{-1}$) $\nu$ O–H | $\nu$ N–H | $\nu$ C=N | $\nu$ C=S | $\nu$ C–O | $\nu$ M–S | Bands due to the heterocyclic bases | Electronic spectra[b] ($\lambda_{max}$ in nm) |
|---|---|---|---|---|---|---|---|---|
| $H_2ONS$[c] | 3110s | 2970m | 1618s | 782s | 1520s | - | - | - |
| [Cu(ONS)py] | - | - | 1602s | - | 1535s | 343w | 425w, 627s, 1250m | 550, 430, 365 |
| [Cu(ONS)dipy] | - | - | 1596 | - | 1520s | 332w | 410w, 755s, 1020s, 1435s | 725, 430 |
| [Cu(ONS)phen] | - | - | 1595 | - | 1523 | 340w | 420w, 632m, 840s, 1422s | 675, 520sh, 360 |

a. $\nu$ denotes stretching frequency; s, m, w and sh. mean strong, medium, weak and shoulder, respectively.

c. S - Benzyl-$\beta$-N-(2-hydroxyphenyl)methylenedithiocarbazate.

Ali and Bose.[1] The room-temperature magnetic moments (Table 1) of the copper complexes suggest that these have normal magnetic moments for a $3d^9$ ion. The position of the *d–d* band at 530 nm in the electronic spectrum [Cu(ONS)py] is very similar to that displayed by other known square-planar copper(II) species.[10] Therefore, a square-planar structure is assigned to [Cu(ONS)py]. Intercomparison of the electronic spectrum of [Cu(ONS)py] with that of [Cu(ONS)phen] (Table 2) shows that the latter has a different structure than the former. The tendency of 1,10-phenanthroline and 2,2'-dipyridyl to act as bidentates and the Schiff base as an ONS tridentate is expected to impose a five-coordinate configuration on the [Cu(ONS)dipy] and [Cu(ONS)phen] complexes. An oxygen-bridged or a sulphur-bridged diemric or polymeric structure is very unlikely since such bridging arrangements generally lead to antiferromagnetic interactions causing a reduction in the room-temperature magnetic moments.[10,11]

The [Cu(ONS)dipy] and [Cu(ONS)phen] complexes are most probably associated with a five-coordinate configuration. Five-coordinate complexes may have either a square-pyramidal or a trigonal-bipyramidal geometry, but the choice between these two configurations is not clearcut. The electronic spectrum of [Cu(ONS)phen] displays two incompletely resolved bands at 675 and 520 nm (Table 2). Similar incompletely resolved bands in the same region were also observed in the electronic spectrum of bis(N-methylsalicylaldiminato) copper(II) for which a trigonal-bipyramidal structure has been proposed.[12] Furthermore, Cu(1,2-dimethylimidazole)$_3$Cl$_2$, for which a slightly distorted trigonal-bipyramidal structure has been proposed has been shown to display the main ligand-field band at 757 nm.[13] The electronic spectra of the present copper(II) complexes do not resemble those of other square-planar or octahedral copper(II) species, but are very similar to those displayed by five-coordinate trigonal-bipyramidal copper(II) complexes.[12-13]

## REFERENCES


1. M. Akbar Ali and R. Bose, *J. Inorg. Nucl. Chem.* 1977, **39**, 265.
2. M. Akbar Ali and M. T. H. Tarafder, *Ibid.* 1977, **39**, 1785.
3. M. Mashima, *Bull. Chem. Soc., Japan* 1974, **37**.
4. M. J. M. Campbell and R. Grezeskowiak, *J. Chem. Soc. A* 1967, 396.
5. D. M. Adams *Metal–Ligand and Related Vibrations*, p. 319. Arnold, London (1967).
6. S. H. H. Chaston and S. E. Livingstone, *Aust. J. Chem.* 1967, **20**, 1965.

7. R. G. Inskeep, *J. Inorg. Nucl. Chem.* 1962, **24**, 763.
8. A. A. Schilt and R. C. Taylor, *Ibid.* 1959, **9**, 217.
9. M. Monoyama, *Inorg. Chim. Acta.* 1975, **13**, 5.
10. M. Akbar Ali, S. E. Livingstone and D. J. Phillips, *Inorg. Chim. Acta.* 1973, **7**, 531.
11. R. S. Nyholm, *Proc. Chem. Soc.* 1964, 273.
12. L. Sacconi, M. Ciampolini and G. Speroni, *J. Am. Chem. Soc.* 1965, **87**, 3102.
13. D. M. L. Goodgame, M. Goodgame and G. W. Rayner Canham, *J. Chem. Soc.* A 1971, 1923.

Polyhedron Vol. 3, No. 5, pp. 599–602, 1984
Printed in Great Britain.

0277–5387/84 $3.00 + .00
© 1984 Pergamon Press Ltd.

# NOTE

## ALKALI–METAL TRIFLUOROMONOSULPHATOMANGANATES (III) $A_2[MnF_3(SO_4)]$ (A = $NH_4$, Li, Na or K)

M. N. BHATTACHARJEE and M. K. CHAUDHURI*
Department of Chemistry, North-Eastern Hill University, Shillong 793003, India

(*Received* 19 *May* 1983; *accepted* 10 *October* 1983)

**Abstract**—Pink–brown crystalline alkali–metal trifluoromonosulphatomanganates(III), $A_2[MnF_3(SO_4)]$ (A = $NH_4$, Li, Na or K), have been synthesised in high yields by reacting $KMnO_4$ or MnO(OH) with 40% HF and $A_2SO_4$ or by the reaction of MnO(OH) with 40% HF and $A_2S_2O_8$ (A = $NH_4$ or K). The chemically estimated oxidation state of manganese occurs between 2.9 and 3.1, and the room temperature magnetic moments lie in the range 4.0–4.2 BM. $(NH_4)_2[MnF_3(SO_4)]$ on being pyrolysed at 340°C yields $MnSO_4$.

Although the tripositive oxidation state is quite common for many first-row transition metals, manganese presents a different story probably because of its strong oxidising power and photolytic instability.[1] However, the known compounds of manganese(III) have received widespread attention primarily because of their interesting structural,[2–10] photochemical[1] and magnetic properties.[10,11] Our interest in this area involves synthesis, characterization and structural assessment of compounds of manganese(III). In two previous reports[12,13] we presented the direct synthesis and structural assessment of alkali–metal pentafluoromanganates(III). Their limitation is that all Mn-ligand interactions are only between Mn and F. This paper reports the synthesis, characterization and structural assessment of the mixed fluorosulphato compounds of manganese(III) and presents a set of internally consistent data concerning the effect of sulphate ligand on the magnetic properties of fluoromanganates(III).

### EXPERIMENTAL

Reagent grade chemicals were used. MnO(OH) was prepared by the literature method.[14] IR spectra were recorded on a Perkin–Elmer model 125 spectrophotometer. Reflectance spectra were recorded against MgO using a Carl Zeiss Jena VSU 2–P instrument. Magnetic susceptibility measurements were made by the Gouy method. $Hg[Co(NCS)_4]$ was the calibrant.

*Synthesis of alkali–metal trifluoromonosulphatomanganates(III)*, $A_2[MnF_3(SO_4)]$(A = $NH_4$, Li, Na or K)

*Method I.* Reaction of $KMnO_4$ with $A_2SO_4$ (A = $NH_4$, Li, Na or K), 40% HF and formaldehyde—an intimately mixed powder of $KMnO_4$ and $A_2SO_4$ (mole ratio 1:1) was dissolved in a minimum amount of water by gentle warming, followed by the addition of 40% hydrofluoric acid maintaining the molar ratio between $KMnO_4$ and HF at 1:4. The resultant solution was then cooled to room temperature and 38% formaldehyde solution was added dropwise with stirring until a deep-brown solution (A) was obtained. The solution (A) was concentrated, over a steam-bath, to nearly one-third of its original volume, and then allowed to cool in a freezer for 2–3 hr to obtain crystallised pink–brown $A_2[MnF_3(SO_4)]$. The compound was separated by filtration, washed with heptane and finally dried *in vacuo*. While in the case of the sodium salt the solution (A) was concentrated by about 50%, in the case of the lithium salt it was not concentrated at all, instead a small amount of alcohol was added to initiate precipitation.

*Method II.* Reaction of MnO(OH) with $A_2SO_4$ (A = $NH_4$, Li, Na or K) and 40% HF—freshly prepared MnO(OH) was dissolved in 40% HF and a concentrated solution of $A_2SO_4$ was added to it (mole ratio of MnO(OH):HF:$A_2SO_4$ at 1:4:1) under stirring. The mixture was heated over a steam-bath for *ca.* 25 min. The dark brown solution thus obtained was worked up in a manner analogous to that described under Method I to obtain pink-brown $A_2[MnF_3(SO_4)]$ (A = $NH_4$, Li, Na or K).

*Author to whom correspondence should be addressed.

*Method III.* Reaction of MnO(OH) with $A_2S_2O_8$ (A = $NH_4$ or K) and 40% HF—This reaction was done in a similar manner as described under Method II maintaining the molar ratio of MnO(OH):HF:$A_2S_2O_8$ as 1:4:1.

The yields of $NH_4^+$, $Li^+$ and $K^+$ salts of trifluoromonosulphatomanganate(III), $[MnF_3(SO_4)]^{2-}$, lie between 80 and 90%, while that of $Na^+$ salt is around 60%.

Elemental analysis and chemical determination of oxidation state of manganase—Manganese was determined by complexometric titration with EDTA using Erio T as the indicator,[15(a)] fluoride was estimated volumetrically,[15(b)] and sulphate gravimetrically as barium sulphate.[15(c)]

The oxidation state of manganese was determined chemically by the reduction of a known amount of the compound with aqueous acidic iron(II) solution followed by the estimation of unoxidized $Fe^{2+}$ in the solution.

Analytical data, estimated oxidation states of manganese, magnetic moment values and ir bands are summarized in Table 1, while reflectance spectral band positions and their assignments are set out in Table 2.

Pyrolysis of $(NH_4)_2[MnF_3(SO_4)]$—An amount of 0.5 g of $(NH_4)_2[MnF_3(SO_4)]$ was heated at 340 ± 5°C until a constant weight was reached. The white pyrolysis product was found to be $MnSO_4$. Yield 0.31 g (weight loss 37.9%). (Found: Mn, 36.4; $SO_4$, 63.7. Calc for $MnSO_4$: Mn, 36.38; $SO_4$, 63.62%. Estimated oxidation state of Mn, 2.1).

## RESULTS AND DISCUSSION

It was reported recently that alkali-metal pentafluoromanganates(III) could by synthesized either by the reduction of $KMnO_4$ with acetylacetone[12] in the presence of alkali-metal bifluorides, $AHF_2$, through the oxidation of acetylacetone[16] to α, α, β, β-tetra-acetylethane, or by the reaction of MnO(OH), 40% HF and $AHF_2$.[13] The reaction of $KMnO_4$ with 40% HF and alkali-metal sulphates, $A_2SO_4$, in the presence of formaldehyde, or the reaction of MnO(OH), 40% HF and $A_2SO_4$ has now led to the synthesis of trifluoromonosulphatomanganates(III) of alkali-metals in very high yields. The role of formaldehyde was to reduce Mn(VII). It is evident from the results that, under the conditions de-

Table 1. Analytical data, magnetic moments, estimated oxidation states, and structurally significant IR bands of $A_2[MnF_3(SO_4)]$ (A = $NH_4$, Li, Na or K)

| Compound | μ in B.M. (288 K) | Estimated oxidation state of Mn | Analysis[a] (%) A | Mn | F | $SO_4$ | $\bar{\nu}$/cm$^{-1}$ | Assignments |
|---|---|---|---|---|---|---|---|---|
| $(NH_4)_2[MnF_3(SO_4)]$ | 4.1 | 3.1 | 11.4[b] (11.48) | 22.6 (22.51) | 23.2 (23.35) | 39.4 (39.35) | 1225(s), 1145(s), 1025(s) | $\nu_3$ SO |
| | | | | | | | 970(s) | $\nu_1$ SO |
| | | | | | | | 680(s), 635(s), 605(s) | $\delta$ SO |
| | | | | | | | 525(s) | $\nu$ (Mn-F) |
| | | | | | | | 3158(m) | $\nu_3$ (N-H |
| | | | | | | | 3040(s) | $\nu_1$ (N-H |
| | | | | | | | 1400(s) | $\nu_4$ (N-H |
| $Li_2[MnF_3(SO_4)]$ | 4.2 | 3.0 | | 24.8 (24.76) | 25.4 (25.69) | 43.4 (43.29) | 1230(s), 1145(s), 1030(s) | $\nu_3$ SO |
| | | | | | | | 975(s) | $\nu_1$ SO |
| | | | | | | | 685(s), 630(s), 608(s) | $\delta$ SO |
| | | | | | | | 530(s) | $\nu$ (Mn-F) |
| $Na_2[MnF_3(SO_4)]$ | 4.1 | 2.9 | 18.2 (18.1) | 21.8 (21.63) | 22.6 (22.44) | 37.6 (37.82) | 1230(s), 1140(s), 1030(s) | $\nu_3$ SO |
| | | | | | | | 975(s) | $\nu_1$ SO |
| | | | | | | | 680(s), 630(s), 605(s) | $\delta$ SO |
| | | | | | | | 530(s) | $\nu$ (Mn-F) |
| $K_2[MnF_3(SO_4)]$ | 4.0 | 3.1 | 27.5 (27.32) | 19.5 (19.2) | 20.1 (19.92) | 33.6 (33.56) | 1230(s), 1145(s), 1030(s) | $\nu_3$ SO |
| | | | | | | | 975(s) | $\nu_1$ SO |
| | | | | | | | 680(s), 635(s), 605(s) | $\delta$ SO |
| | | | | | | | 525(s) | $\nu$ (Mn-F) |

a, Calculated values in parentheses; b, Analysis for N.

Table 2. Electronic Spectral Data of $(NH_4)_2[MnF_3(SO_4)]$ and $K_2[MnF_3(SO_4)]$

| Compound | Band I $^5B_{1g} \rightarrow {}^5A_{1g}$ cm$^{-1}$ | Band II $^5B_{1g} \rightarrow {}^5B_{2g}$ cm$^{-1}$ | Band III $^5B_{1g} \rightarrow {}^5E_g$ cm$^{-1}$ |
|---|---|---|---|
| $(NH_4)_2[MnF_3(SO_4)]$ | 13,500 | 17,850 | 21,300 |
| $K_2[MnF_3(SO_4)]$ | 13,700 | 18,200 | 21,700 |

scribed, manganese is reduced not below $Mn^{3+}$, and that a maximum of one $SO_4^{2-}$ is coordinated to the $Mn^{3+}$ centre since a higher amount of $A_2SO_4$ did not alter the results. The fact, that the reaction of MnO(OH), 40% HF and $A_2S_2O_8$ (A = $NH_4$ or K) also afforded only $A_2[MnF_3(SO_4)]$, enables us to conclude that peroxydisulphate cannot oxidise $Mn^{3+}$ in the presence of $F^-$ ions. The process $S_2O_8^{2-} + 2e \rightarrow 2SO_4^{2-}$, as a consequence of electron-transfer between $S_2O_8^{2-}$ and water, must be the origin of $SO_4^{2-}$ in this case.

Characterisation and Assessment of Structures—$A_2[MnF_3(SO_4)]$ are all pink–brown crystalline compounds, stable for prolonged periods. They are relatively more stable than the corresponding $A_2MnF_5$ compounds and the enhanced stability must owe its origin to the presence of $SO_4^{2-}$ ligand. The $A_2[MnF_3(SO_4)]$ compounds are insoluble in organic solvents, and in water they decompose, thus precluding molar conductance measurements. The chemically estimated oxidation state of manganese, falling between 2.9 and 3.1 (Table 1), supports the contention that manganese, in each of the compounds, is in its +3 state. It is interesting to note that while the mangnetic moments of $A_2MnF_5$ compounds occur at *ca.* 3.2 BM (strong antiferromagnetic case)[11-13] and those of sulphato compounds of manganese(III) fall at *ca.* 4.8 BM (normal),[17] the magnetic moments of $A_2[MnF_3(SO_4)]$ compounds lie between 4.0 and 4.2 BM. It is evident that the degree of antiferromagnetic exchange interaction can be controlled by the replacement of two $F^-$ ligands by an $SO_4^{2-}$ ligand in going from $[MnF_5]^{2-}$ to $[MnF_3(SO_4)]^{2-}$.

The IR spectra of the compounds show the SO frequencies at *ca.* 1230, *ca.* 1145, *ca.* 1030, *ca.* 975, *ca.* 684, *ca.* 635 and at *ca.* 605 cm$^{-1}$, and the $\nu_{Mn-F}$ at *ca.* 525 cm$^{-1}$. The pattern suggest a lowering of symmetry [18] of the $SO_4^{2-}$ group from $T_d$ to $C_2$ and rule out the presence of an ionic $SO_4^{2-}$. Further the splitting of the $\nu_3$ and $\delta$ modes of SO into three bands each (Table 1) enables us to assign a $C_{2v}$ symmetry[19] to the $SO_4^{2-}$ group. Although the $\nu_{SO}$ modes appear at relatively higher frequencies than those usually observed for a bridging[19,20] $SO_4^{2-}$, the possibility of inter molecular sulphato bridging cannot be ruled out. The reflectance spectra of $A_2[MnF_3(SO_4)]$ (A = $NH_4$ or K) exhibit three bands at ~ 21,500, ~ 17,900 and ~ 13,600 cm$^{-1}$, which have been assigned to the transitions[21] $^5B_{1g} \rightarrow {}^5E_g$, $^5B_{1g} \rightarrow {}^5B_{2g}$ and $^5B_{1g} \rightarrow {}^5A_{1g}$ respectively. This suggests an appreciable splitting of $^5E_g$ ground state of $Mn^{3+}$ ion in $[MnF_3(SO_4)]^{2-}$ as a consequence of the Jahn–Teller effect. Pyrolysis of $(NH_4)_2[MnF_3(SO_4)]$ at *ca.* 340°C loses 37.9% weight to yield $MnSO_4$.

*Acknowledgement*—We thank the University for award of a U.G.C. fellowship to M.N.B., and the Department of Atomic Energy, Government of India, for the financial assistance (Grant No. 37/16/82–G).

## REFERENCES

1. A. Harriman, *Coord. Chem. Rev.* 1979, **28**, 147.
2. D. R. Sears and J. L. Hoard, *J. Chem. Phys.* 1969, **50**, 1066.
3. A. J. Edwards, *J. Chem. Soc., A* 1971, 2653.
4. M. Bartlett and G. J. Palenik, *J. Chem. Soc. D*, 1970, 416.
5. P. C. Healy and A. H. White, *J. Chem. Soc. Dalton Trans.* 1972, 1883.
6. A. Avdeef, J. A. Costamagna and J. P. Fackler, Jr., *Inorg. Chem.* 1974, **13**, 1854.
7. J. P. Fackler, Jr., and A. Avdeef, *Inorg. Chem.* 1974, **13**, 1864.
8. R. J. Butcher and E. Sinn, *J. Chem. Soc., Dalton Trans.* 1975, 2517.
9. B. Stults, R. S. Marianelli and V. W. Day, *Inorg. Chem.* 1979, **18**, 1853.
10. H. Aghabozorg, G. J. Palenik, R. C. Stoufer and J. Summers, *Inorg. Chem.* 1982, **21**, 3903.
11. S. Emori, M. Inoue, M. Kishita and M. Kubo, *Inorg. Chem.* 1969, **8**, 1385.
12. M. N. Bhattacharjee, M. K. Chaudhuri, H. S. Dasgupta and D. T. Khathing, *J. Chem. Soc., Dalton Trans.* 1981, 2587.
13. M. N. Bhattacharjee, M. K. Chaudhuri, H. S.

Dasgupta, A. Kathipri and D. T. Khathing, *Synth. React,. Inorg. Met.-Org. Chem.* 1982, **12**, 485.
14. G. Brauer (Editor) *Handbook of Preparative Inorganic Chemistry*, Vol. 2. p. 1457. Academic Press, London (1965).
15. A. I. Vogel, *A Text Book of Quantitative Inorganic Analysis*, (a) p. 434; (b) p. 296; (c) p. 462. Longman Green, London (1964).
16. M. N. Bhattacharjee, M. K. Chaudhuri, S. K. Ghosh, Z. Hiese and N. Roy, *J. Chem. Soc., Dalton Trans.* in press.
17. B. N. Figgis and J. Lewis, *Progr. Inorg. Chem.* 1964, **6**, 37.
18. K. Nakamoto, *Infrared Spectra of Inorganic and Coordination Compounds*, 2nd Edn, p. 123. Wiley-Interscience, London (1970).
19. C. G. Barraclough and M. L. Tobe, *J. Chem. Soc.* 1961, 1993.
20. R. Eskenazi, J. Raskovan and R. Levitus, *J. Inorg. Nucl. Chem.* 1966, **28**, 521.
21. T. S. Davis, J. P. Fackler, Jr., and M. J. Weeks, *Inorg. Chem.* 1968, **7**, 1994.

*Polyhedron* Vol. 3, No. 5, pp. 603–606, 1984
Printed in Great Britain.

0277–5387/84 $3.00 + .00
© 1984 Pergamon Press Ltd.

# NOTE

# BINUCLEAR COMPLEXES OF SILICON(IV) CHLORIDE WITH NICKEL(II) SALICYLALDOXIMATES

**N. S. BIRADAR, V. L. RODDABASANAGOUDAR and T. M. AMINABHAVI***
Department of Chemistry, Karnatak University, Dharwad 580003, India

(*Received* 13 *June* 1983; *accepted* 10 *October* 1983)

**Abstract**—Some binuclear complexes of silicon(IV) chloride and nickel(II) salicylaldoximates were synthesized and characterized by elemental analyses, conductivity measurements, magnetic and spectral data. The complexes were proved to be 1:1 $SiCl_4$ adducts. The resulting complexes were amorphous in nature and electrolytes in solution.

In recent years there has been a continuing interest in the synthesis and characterization of binuclear, bimetallic complexes.[1] In a previous study,[2] nickel(II) aldoximates and tin(IV) chloride were shown to form 1:1 adducts. In this continuing study bimetallic complexes of nickel(II) salicyaldoximate and silicon tetrachloride were prepared. The complexes were characterized by elemental analysis, conductivity measurements, magnetic measurements, electronic and IR spectra.

## EXPERIMENTAL

All the chemicals used in this work were of reagent grade and were used without further purification. The substituted salicylaldoximines were prepared by dissolving hydroxylamine hydrochloride (0.1 mole) in the minimum amount of water, then adding this solution to a hot ethanolic solution of the substituted salicylaldehyde (0.1 mole). The mixture was then mixed with nickel(II) chloride and refluxed for 30 min. Upon cooling, crystals corresponding to nickel(II) salicylaldoximates were obtained with a yield of 80%. These were washed repeatedly with ethanol, filtered, then dried over anhydrous calcium chloride. The nickel(II) salicylaldoximates of the type $Ni[O(HON\overline{CH})C_6H_3R]_2$ were prepared.

Where,

| Ligand | R | Name |
|---|---|---|
| A | H | Bis(Salicylaldoximato)nickel(II) |
| B | 3-$CH_3$ | Bis(3-methylsalicylaldoximato)nickel(II) |
| C | 4-$CH_3$ | Bis(4-methylsalicylaldoximato)nickel(II) |
| D | 5-$CH_3$ | Bis(5-methylsalicylaldoximato)nickel(II) |
| E | 5-Cl | Bis(5-chlorosalicylaldoximato)nickel(II) |

The binuclear complexes were prepared by the reaction of nickel(II) salicylaldoximates with silicon(IV) tetrachloride. Equimolar quantities (0.01 mole) of both nickel(II) salicylaldoximates and silicon(IV) tetrachloride were taken in 100 $cm^3$ of dry benzene in a 250 $cm^3$ round bottom flask. The reaction mixture was refluxed for 12 hr. The solid precipitate formed was filtered, washed repeatedly with dry benzene and dried under vacuum over $P_2O_5$. Approximately 75–80% yields of the complexes were obtained in all reactions. Table 1 correlates each nickel(II) salicylaldoximate (A–E) with its corresponding $SiCl_4$ adduct (I–V).

Elemental analyses were carried out by a procedure described elsewhere.[3] Gravimetric technique was used to estimate silicon as its oxide and nickel(II) as its dimethylglyoximate; chloride was determined as silver chloride and nitrogen by micro-Kjeldahl method.

Conductivities were measured in dimethylformamide (DMF) using an Elico-CM-82 conductivity bridge with a cell having a cell constant of 0.829 $cm^{-1}$. All conductivity measurements were performed at room temperature using $10^{-3}$ M solutions of complex. Magnetic susceptibility measurements were made using a Gouy balance. At least three measurements were averaged for each compound at 298 K, the observed susceptibilities

*Author to whom correspondence should be addressed.

Table 1. Physical, spectroscopic and analytical data of complexes

| Ligand | Empirical formula of complex | % Ni[a] | % Si[a] | % N[a] | % Cl[a] | Molar cond. $ohm^{-1}cm^2$ $mole^{-1}$ | Electronic spectral transitions (b) | (c) | $\mu_{eff}$ B.M. |
|---|---|---|---|---|---|---|---|---|---|
| A | $(C_{14}H_{12}N_2O_4Ni)SiCl_4$ | 11.52 (11.60) | 5.62 (5.60) | 5.46 (5.60) | 28.66 (28.40) | 87 | 690 | 485 | 3.62 |
| B | $(C_{16}H_{16}N_2O_4Ni)SiCl_4$ | 10.76 (10.98) | 5.27 (5.30) | 5.23 (5.30) | 25.52 (26.89) | 92 | 680 | 470 | 3.90 |
| C | $(C_{16}H_{16}N_2O_4Ni)SiCl_4$ | 11.03 (10.98) | 5.41 (5.30) | 5.29 (5.30) | 27.06 (26.89) | 78 | 695 | 480 | 4.00 |
| D | $(C_{16}H_{16}N_2O_4Ni)SiCl_4$ | 11.30 (10.98) | 5.06 (5.30) | 5.33 (5.30) | 26.77 (26.89) | 97 | 680 | 465 | 3.55 |
| E | $(C_{16}H_{10}N_2O_4Cl_2Ni)SiCl_4$ | 9.67 ( 9.78) | 4.68 (4.72) | 4.91 (4.72) | 23.88 (23.95) | 79 | 700 | 480 | 3.42 |

(a) - Values in the parenthesis are the calculated numbers

(b) - $^3T_1 \rightarrow {}^3T_1(P)$

(c) - $^3T_1 \rightarrow {}^1A_1(G)$

were corrected for diamagnetic contributions[4] and $\mu_{eff}$ was derived assuming the Curie law applied.

The IR spectra were obtained using a Carl–Zeiss UR-10 IR spectrometer. Samples were prepared as KBr pellets. UV-visible spectra were obtained on a Perkin–Elmer, 492–5000 spectrophotometer.

## RESULTS AND DISCUSSION

*Analytical data*

All the complexes (I–V) are coloured, amorphous and insoluble in common organic solvents. The complexes were soluble in dimethylformamide (DMF) and dimethylsulphoxide (DMSO). The elemental analyses (see Table 1) indicate a 1:1 $SiCl_4$ adduct formation. The molar conductivities are in the range 90–102 $\Omega^{-1}$ $cm^2$ $mole^{-1}$ indicating a 1:1 electrolytic behaviour.

*Magnetic properties*

For nickel(II) in a regular tetrahedral field, the ground state is an orbitally degenerate T state and a large orbital contribution is expected giving, $\mu^{eff}$ in the range 3.5–4.0 B.M.[5] In the present study the effective magnetic moments are in the range of 3.4–4.01 B.M. (see Table 1) suggesting a tetrahedral configuration. It therefore appears that the nickel stereochemistry has changed from square planar to tetrahedral configuration.

*Electronic spectra*

The spectra of square planar four coordinated nickel(II) compounds exhibit a consistent medium intensity band at 470 nm which is typical of square planar nickel[6] and the presence of no bands above 1000 nm is a further proof of the planarity of the ligand.[7] The data presented in Table 1 suggest that the $SiCl_4$ adducts reported here are pseudo-tetrahedral nickel(II) compounds. The band at 700–650 nm is assigned to $^3T_1 \rightarrow {}^3T_1(P)$ transition while a band at 500–450 nm may be assigned to a $^3T_1 \rightarrow {}^1A_1(G)$ transition or charge transfer.

These data taken together with the high values of magnetic moments (3.6–4.0 B.M.) suggest that the complexes are of tetrahedral nature.[8,9]

*IR spectra*

The important IR frequencies and their assignments are reported in Tables 2 and 3. An intense band at 1640–1635 $cm^{-1}$ observed in the nickel(II) salicylaldoximate complexes (A–E) is ascribed to the O–H deformation vibration of the oxime moiety. The band is shifted to 1650 $cm^{-1}$ on formation of the binuclear complexes (I–V) thus indicating the formation of a Si←OH linkage.[2] The strong absorption bands in the range 1225–1185 $cm^{-1}$ and 925–910 $cm^{-1}$ are assigned to $\nu$(N–O).[10,11] One of the bands at 915 $cm^{-1}$ in the spectra of nickel(II) salicylaldoximates splits when the complexes react with silicon(IV) chloride to form binuclear complexes. This evidence corroborates the fact that the oxygen of the oxime moiety bonds to the silicon. This bonding is further confirmed by the presence of a band at 800–780 $cm^{-1}$ assigned to $\nu$(Si–O).[13] The bands observed at 550 $cm^{-1}$ and 470 $cm^{-1}$ in the bis-complexes are assigned to $\nu$(Ni–N) and

Table 2. IR frequencies (in $cm^{-1}$) of nickel(II) salicylaldoximates and their assignments

| S.No. | Assignments | Ligands | | | | |
|---|---|---|---|---|---|---|
| | | A | B | C | D | E |
| 1 | Intramolecular hydrogen bonded OH | 3225br.m | 3250br.m | 3230br.w | 3225br | 3238br.w |
| 2 | -OH deformation | 1640s | 1640s | 1640s | 1640s | 1635s |
| 3 | ν(C=N) | 1605s | 1602s | 1608s | 1610s | 1600s |
| 4 | ν(C=C) aromatic stretch | 1550s<br>1500s | 1575s<br>1510s | 1550s<br>1525s | 1540s<br>1500s | 1540s<br>1495s |
| 5 | Phenolic ν(C-O) | 1320s | 1325s | 1320s | 1320s | 1320s |
| 6 | ν(N-O) | 1210s<br>920br | 1225s<br>915br | 1205s<br>910br | 1190s<br>915br | 1185s<br>920br |
| 7 | ν(Ni-N) | 540s | 535m | 550m | 540s | 535s |
| 8 | ν(Ni-O) | 470m | 465m | 465m | 465m | 465m |

s = strong; br.m. = broad medium; br.w = broad weak; br = broad; m = medium

Table 3. IR frequencies (in $cm^{-1}$) of silicon(IV) chloride complexes with nickel(II) salicylaldoximates and their assignments

| S.No. | Assignments | Complexes | | | | |
|---|---|---|---|---|---|---|
| | | I | II | III | IV | V |
| 1 | -OH stretching | 3433br.w | 3340s | 3350br.s | 3400s | 3400br.m |
| 2 | -OH deformation | 1650 | 1643 | 1647 | 1633 | 1652 |
| 3 | ν(C=N) and aromatic C=C stretch | 1616s<br>1604s<br>1490m | 1620s<br>1572br.m<br>1500br.m | 1612s<br>1590br.m<br>1486br.m | 1618s<br>1550s<br>1500m | 1615s<br>1542s<br>1483s |
| 4 | Phenolic ν(C-O) | 1310s | 1300s | 1305s | 1295s | 1310s |
| 5 | ν(N-O) | 1215w<br>920spl | 1210w<br>910spl | 1210w<br>920spl | 1220w<br>925spl | 1215w<br>915spl |
| 6 | ν(Si-O) | 800s | 785s | 790s | 800s | 780s |
| 7 | ν(Si-Cl) | 620m | 615m | 610m | 620m | 630m |
| 8 | ν(Ni-N) | 540m | 560br.m | 545m | 565m | 550br.m |

s = strong; br.m. = broad medium; w = weak; spl = splitted; br = broad

ν(Ni–O) respectively. These bands do not shift on formation of the binuclear complexes. A strong band observed around 610–630 $cm^{-1}$ is assigned to ν(Si–Cl).[14] A medium intensity band observed around 1510 $cm^{-1}$ is ascribed to *o*-disubstituted benzene ring vibrations. The bands observed at 1610 $cm^{-1}$ due to azomethine group in nickel(II) salicylaldoximate have been shifted to 1620 $cm^{-1}$ on complexation with silicon(IV) tetrachloride; the split in this band is further evidence of the fact that the symmetry around nickel(II) might have changed. This change in symmetry is further supported by the shift of phenolic ν(C–O) stretch from 1325 $cm^{-1}$ in nickel(II) salicylaldoximate to

1305 $cm^{-1}$ in the binuclear complexes. Finally, in the spectra of the complexes I–V a shallow broad band at 3400 $cm^{-1}$ is attributed to $\nu$(O–H).

*Acknowledgements*—We gratefully extend our thanks to the referees for constructive comments on this work.

## REFERENCES

1. N. Voiculescu, *Rev. Roum. Chim.* 1977, **22**, 237.
2. N. S. Biradar, B. R. Patil and V. H. Kulkarni, *J. Inorg. Nucl. Chem.* 1975, **37**, 1901.
3. A. I. Vogel, *Textbook of Quantitative Inorganic Analysis*, 3rd Edn. Longmans Green, New York (1969).
4. C. J. O'Connor, *Magnetochemistry–advances in theory and instrumentation*, In *Progress in Inorganic Chemistry* (Edited by S. J. Lippard), Vol. 29. Wiley, New York (1982).
5. M. A. Weiner and P. Schwartz, *Inorg. Chem.* 1975, **14**, 1715.
6. F. A. Cotton and G. Wilkinson, *Advanced Inorganic Chemistry*, 3rd Edn, Wiley Eastern, New Delhi (1976).
7. A. B. P. Lever, *Inorganic Electronic Spectroscopy* (Edited by Lappert). Elsevier, Amsterdam (1968).
8. N. S. Gill and R. S. Nyholm, *J. Chem. Soc.* 1959, 3997.
9. F. A. Cotton and R. Francis, *J. Am. Chem. Soc.* 1960, **82**, 2986.
10. R. Blinc and H. Hadzi, *J. Chem. Soc.* A, 1958, 4536.
11. A. Palm and H. Werbin, *Can. J. Chem.* 1953, **31**, 1004.
12. K. K. Ramaswamy, C. J. Jose and D. N. Sen, *Ind. J. Chem.* 1967, **5**, 156.
13. A. L. Smith, *Spectrochim. Acta.* 1963, **19**, 849.

*Polyhedron* Vol. 3, No. 5, pp. 607–610, 1984
Printed in Great Britain.

0277–5387/84 $3.00 + .00
© 1984 Pergamon Press Ltd.

# NOTE

# CATALYSIS BY HETEROPOLYACID—VII. CATALYTIC OXIDATION OF CYCLOHEXANOL BY DODECAMOLYBDATE

**KENJI NOMIYA, MAKOTO MIWA* and YOSHIO SUGAYA**
Department of Industrial Chemistry, Faculty of Engineering, Seikei University, Musashino, Tokyo 180, Japan

(*Received* 12 *July* 1983; *accepted* 23 *September* 1983)

**Abstract**—In the oxidation of cyclohexanol to cyclohexanone and the further oxidation to adipic acid, a dodecamolybdo-heteropolyanion (HPA) functions catalytically in the presence of aqueous hydrogen peroxide, whereas the HPA without hydrogen peroxide reacts only stoichiometrically. Air- or oxygen-passing through the refluxing system of cyclohexanone and the HPA in the presence of active charcoal, without hydrogen peroxide, has also promoted the oxidation catalytically. Since both hydrogen peroxide and aeration in the presence of active charcoal convert the reduced-form (blue) of the HPA produced by the oxidation of substrate to the oxidized-form (yellow), they play a role as a promoter or a reoxidizing reagent for the oxidation by the HPA. The reoxidizing effect of the aqueous hydrogen peroxide is much the more effective.

Keggin-type dodecamolybdo-HPA, $[XMo_{12}O_{40}]$ (X = Si, P), shows the typical colour change from yellow to blue in the presence of organic compounds. This has been attributed to the reduction of some of twelve sexivalent-molybdenum ions in the HPA to quinquevalent ions.[1] The reduced HPA is protonated, that is, one of the oxygens coordinating to a reduced molybdenum ion is protonated. Thus, the oxidation function of the HPA can be considered as the oxidative dehydrogenation arising from its electron-withdrawing property. The oxidizability of HPA, implied from the high sensitivity of the colour change, has been expected to be powerful, however, the yields of oxidation products are usually very low. For instance, the refluxing (16-hr) of 10 g (0.1 mol) cyclohexanol and 3 g ($1.18 \times 10^{-3}$ mol) $Y_3[PMo_{12}O_{40}]$ (Y is tetrabutylammonium) gives cyclohexanone (36.2 mg; $3.7 \times 10^{-4}$ mol) and a trace of adipic acid, and the refluxing (15-hr) of 10 g (0.093 mol) benzyl alcohol and 2 g ($7.84 \times 10^{-4}$ mol) $Y_3[PMo_{12}O_{40}]$ gives benzaldehyde (23.1 mg; $2.2 \times 10^{-4}$ mol) and benzoic acid (10.6 mg; $8.7 \times 10^{-5}$ mol). The apparent low efficiency of oxidation by the HPA probably stems from the fact that only a fraction of the twelve molybdenum ions is involved stoichiometrically. Since the yellow-to-blue process of HPA is irreversible, the reverse process should be attained by other more powerful oxidants. If the oxidant does not react with the substrate, or does not give the undesired products, the catalytic oxidation by HPA can be performed. In this work, hydrogen peroxide (30% aqueous solution) was used as a reoxidizing reagent for the catalytic oxidation of cyclohexanol by HPA. Furthermore, the aeration of the refluxing system of substrate and HPA in the presence of active charcoal, instead of hydrogen peroxide, has also been examined. The aeration in the presence of charcoal has been traditionally used, instead of hydrogen peroxide, for the preparation of Co(III) complexes from Co(II) salts in coordination chemistry.[2]

## EXPERIMENTAL

Guaranteed hydrogen peroxide (30% aqueous solution) was purchased from Mitsubishi Gas Chem., sodium molybdate and sodium tungstate from Wako Pure Chem., and granular active charcoal from Kokusan Chemical Works. The charcoal was thoroughly washed with hot water and dried before use. Dodecamolybdo-HPA, $[PMo_{12}O_{40}]^{3-}$, dodecatungsto-HPA, $[PW_{12}O_{40}]^{3-}$, and $[\alpha\text{-}Mo_8O_{26}]^{4-}$ were prepared as tetrabutylammonium salts according to the usual methods.[3–5]

The oxidation reaction of cyclohexanol in the

*Author to whom correspondence should be addressed.

presence of aqueous hydrogen peroxide as a reoxidizing reagent was tried using two methods; (A) refluxing a mixture of substrate, HPA and hydrogen peroxide for an appropriate time, and (B) refluxing a mixture of substrate and HPA, where into one drop of hydrogen peroxide was added whenever the HPA showed a colour change. The reaction time was determined to be a time, in the method (A), in which the yellow HPA has been converted to the blue HPA and, in the method (B), in which an appropriate amount of hydrogen peroxide in the dropping funnel had been consumed. After the reaction was finished, the HPA was filtered off and water contained in the filtrate was evaporated. One of oxidation products was isolated as crystals and the other obtained by distillation under reduced pressure of the solvent extract with ether or benzene. These products were identified by IR and $^1$H-NMR spectra.

The reaction by the aeration in the presence of ative charcoal as a reoxidizing reagent was performed for the oxidation of cyclohexanone. Three neck flask was equipped with a thermometer, an air-inlet capillary tube and a condenser, the top of which was linked with rubber tube to an aspirator by way of the trap with cock to adjust the air current. 2 g of charcoal, 500 mg ($1.96 \times 10^{-4}$ mol) of $Y_3[PMo_{12}O_{40}]$ and 20 g (0.2 mol) of cyclohexanone were heated to 50°C with air passed. After an appropriate time, 100 cm$^3$ ethanol was added, stirred thoroughly, and charcoal and HPA were filtered off. Ethanol and unreacted substrate were removed by distillation. Upon cooling, crystals were produced.

Reoxidizing by the aeration for the reduced blue HPA in acetonitrile solution was monitored spectrophotometrically. 500 mg of the reduced-form of $Y_3[PMo_{12}O_{40}]$, which was obtained by the oxidation, was dissolved in 50 cm$^3$ acetonitrile, 2 g of charcoal was added, and air passed through at room temperature. After an appropriate time, charcoal was filtered off and thoroughly washed with acetonitrile. The absorbance at *ca.* 700 nm of the solution adjusted to a constant volume was measured, which was due to the absorption of the Mo(V)→Mo(VI) transition within the reduced HPA. A small loss of HPA by the adsorption on charcoal was observed from the absorbance at *ca.* 300 nm which was due to the charge transfer transition of O→Mo(VI) in the $Mo_{12}O_{40}$ lattice.

## RESULTS AND DISCUSSION

Large excess amounts of hydrogen peroxide relative to the dodecamolybdo-HPA exist in the system of the method (A), while only small excess amounts of it were present in the system of the (B). In the former, only while hydrogen peroxide remains in the system, the HPA apparently keeps yellow, and in the latter the change of the blue HPA to the yellow, by each addition of one drop of hydrogen peroxide, is observed during the reaction. The methods showed no marked difference in products or yields, except that the reaction time of method (B) was comparatively longer than that of the method (A).

The conditions and results obtained by method (A) are presented in Table 1. Cyclohexanol was

Table 1. Oxidation of cyclohexanol catalyzed by various molybdenum (tungsten) compounds in the presence of 30% aqueous hydrogen peroxide

| Substrate (mol) | Catalyst: Mo or W compound (mol) | 30% $H_2O_2$ (g) | Reflux Time (hr) | Results: Products | Yields g | (%) |
|---|---|---|---|---|---|---|
| cyclohexanol 10 g (0.1) | $Y_3[PMo_{12}O_{40}]$ 50 mg ($1.96 \times 10^{-5}$) | 11 | 17 | cyclohexanone<br>adipic acid | 1.58 g<br>1.30 g | 25% |
| | $Y_3[PW_{12}O_{40}]$ 50 mg ($1.39 \times 10^{-5}$) | 11 | 16 | cyclohexanone | 0.97 g | 10% |
| | $Y_4[\alpha\text{-}Mo_8O_{26}]$ 50 mg ($2.32 \times 10^{-5}$) | 11 | 15 | cyclohexanone<br>adipic acid | 0.80 g<br>0.20 g | 10% |
| | $Na_2MoO_4 \cdot 2H_2O$ 50 mg ($2.07 \times 10^{-4}$) | 11 | 20 | cyclohexanone | 0.67 g | 7% |
| | $Na_2WO_4 \cdot 2H_2O$ 50 mg ($1.52 \times 10^{-4}$) | 11 | 16 | cyclohexanone | 1.19 g | 12% |

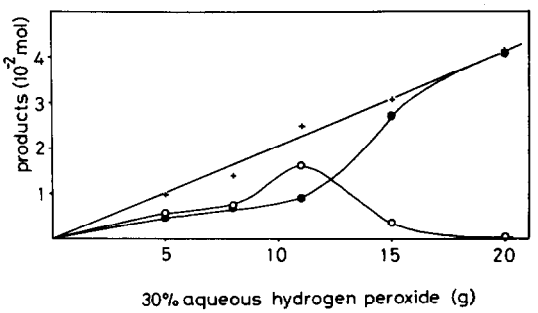



Fig. 1. Distribution of oxidation products of cyclohexanol depending upon varied amounts of 30% aqueous hydrogen peroxide. Open circle is the mole number of produced cyclohexanone, dark circle is that of the produced adipic acid, and cross mark is the sum of them. Conditions; 10 g (0.1 mol) of cyclohexanol and 50 mg ($1.96 \times 10^{-5}$ mol) of $Y_3[PMo_{12}O_{40}]$ were used. Reflux time is 17 hr.

converted to cyclohexanone by oxidative dehydrogenation and furthermore to adipic acid by oxidative cleavage of C–C bond. In the absence of HPA, such oxidation products were not obtained. In the reaction of cyclohexanone with hydrogen peroxide, the formation of monomeric and/or dimeric hydro-peroxides has been known.[6] The amounts of hydrogen peroxide influence the reaction time, the yields, and the distribution of products (Fig. 1). In order to examine the specific interaction between the HPA and hydrogen peroxide, e.g. the formation of the peroxide such as Mo-OOH, the aqueous hydrogen peroxide solution containing the HPA was evaporated to dryness and the IR spectrum of the residue was measured.[7] It was coincident with the spectrum of original HPA and no evidence for the formation of such a peroxide was obtained. During the course of reaction, the HPA is structurally stable. The reduced blue HPA, obtained after the reaction, can be reused for the same reaction by addition of hydrogen peroxide. Thus, it has been suggested that the HPA functions catalytically by a re-oxidizing effect of hydrogen peroxide, whereas the HPA alone reacts only stoichiometrically.

Further justification was obtained from the experiments of aeration through the refluxing system of cyclohexanone and HPA in the presence of active charcoal, instead of hydrogen peroxide. Adipic acid was practically produced. The results are shown in Table 2. Turn-over number, or a ratio of the mole number of product to that of the HPA, shows the catalysis by HPA. The reoxidizing effect for the blue HPA by the aeration in the presence of charcoal was assured by the time-dependent decrease of the absorbance at *ca.* 700 nm, which is based on the Mo(V)→Mo(VI) intervalence transition within the blue HPA. By the aeration for about 4 hr at room temperature, more than 95% of the blue HPA could be converted to the yellow HPA, on the other hand, by addition of one drop of hydrogen peroxide it could be immediately converted to the yellow HPA. Thus, the re-oxidizing effect of hydrogen peroxide is much stronger than that of aeration.

In Table 1, the results of $Y_3[PW_{12}O_{40}]$ in the presence of hydrogen peroxide are also listed. The catalysis by this HPA is more selective than that by the dodecamolybdo-HPA; the product is only cyclohexanone, although the yield is not so high. This may be related to the comparatively low oxidizability of the dodecatungsto-HPA.

The oxidation of cyclohexanol was also promoted by isopolyanion of $Y_4[\alpha\text{-}Mo_8O_{26}]$, sodium molybdate and sodium tungstate in the presence of hydrogen peroxide. The results are presented in Table 1. However, there are some remarks distinct from the HPA-hydrogen peroxide system; (1) these compounds have no oxidizability, although the molybdenum (or tungsten) are in oxidation state VI (2) their oxidizing power is generated only by the coexistence of hydrogen peroxide, and (3) after the reaction, these compounds do not retain their original structure. Thus, these compounds form active intermediates with hydrogen peroxide, which may promote the oxidation.

Table 2. Oxidation of cyclohexanone by air-passing through the system in the presence of active charcoal[a]

| Substrate (mol) | Catalyst (mol) | Reaction Temp. (°C) | Air-passing Time (hr) | Product (mol) | Molar ratio of Product to HPA |
|---|---|---|---|---|---|
| cyclohexanone 20 g (0.2) | $Y_3[PMo_{12}O_{40}]$ 500 mg ($1.96 \times 10^{-4}$) | 50 | 15 | adipic acid 199 mg ($1.36 \times 10^{-3}$) | 6.9 |
| | | 50 | 30 | adipic acid 907 mg ($6.21 \times 10^{-3}$) | 31.7 |

a Active charcoal of 2 g is used.

## REFERENCES

1. K. Nomiya, T. Ueno and M. Miwa, *Bull. Chem. Soc. Jpn.* 1980, **53**, 827.
2. F. Basolo and R. Johnson, *Coordination Chemistry*, p. 90. Benjamin, New York (1964).
3. E. O. North and W. Haney, *Inorganic Syntheses* Vol. I, p. 127 (1939).
4. H. Wu, *J. Biol. Chem.* 1920, **43**, 189.
5. M. Filowitz, R. K. C. Ho, W. G. Klemperer and W. Shum, *Inorg. Chem.* 1979, **18**, 93.
6. L. F. Fieser and M. Fieser, *Reagents for Organic Synthesis*, Vol. I, p. 459. Wiley, New York (1967).
7. Y. Kurusu, *Bull. Chem. Soc. Jpn.* 1981, **54**, 293.

*Polyhedron* Vol. 3, No. 5, pp. 611–613, 1984
Printed in Great Britain.

0277–5387/84 $3.00 + .00
© 1984 Pergamon Press Ltd.

# NOTE

## MONO- AND BISPHENOXY DERIVATIVES OF BIS(INDENYL)ZIRCONIUM(IV)

**B. KHERA and N. K. KAUSHIK***
Department of Chemistry, University of Delhi, Delhi, 110007, India

(*Received* 12 *July* 1983; *accepted* 23 *September* 1983)

**Abstract**—A series of $(C_9H_7)_2Zr(OAr)Cl$ and $(C_9H_7)_2Zr(OAr)_2$ complexes, where $Ar = C_6H_5$, $p$-$ClC_6H_4$, $\alpha$-$C_{10}H_7$, or $\beta$-$C_{10}H_7$, have been synthesised by the reaction of bis(indenyl)zirconium(IV)-dichloride with an appropriate phenol in a 1:1 and 1:2 molar ratio in refluxing benzene in the presence of triethylamine. These complexes have been characterised by elemental analyses, conductance measurements and spectral (IR, $^1$H NMR and electronic) studies.

The organometallic chemistry of titanium has been extensively developed over the past three decades, while that of zirconium is only now beginning to be developed. Organo-titanium compounds are known as catalysts for the polymerisation[1,2] and hydrogenation[3,4] of olefins and dienes. Transition metal phenoxides on the other hand have been used as olefin polymerisation catalysts in many organic reactions.[5] Some phenoxo and diphenoxo derivatives of bis(cyclopentadienyl)/(methyl cyclopentadienyl)titanium(IV) and zirconium(IV) have been reported.[6–11] However, reactions of bis-(indenyl)zirconium(IV)dichloride with phenols have not been reported previously. The present work describes the preparation and characterisation of such compounds.

## EXPERIMENTAL

*Reagents and general techniques*

All the reagents used were of analytical grade. Bis(indenyl)zirconium(IV) dichloride, $(C_9H_7)_2ZrCl_2$ was prepared by the reaction of indenyl thallium(I)[12] and zirconium tetrachloride in anhydrous tetrahydrofuran in a 2:1 molar ratio. THF (Baker, AR) was dried over sodium metal and then boiled under reflux until it gave a blue colouration with $Ph_2CO$. It was finally dried by distillation from $LiAlH_4$. Benzene and triethylamine were dried as reported in the literature.[13] Nitrobenzene for conductance measurements was purified by the method described by Fay *et al.*[14] Zirconium was determined gravimetrically as its oxide whereas chlorine was estimated as silver chloride.

Conductance measurements were made in nitrobenzene at $30 \pm 0.05$°C using a Systronic Digital Direct Reading Conductivity Meter Type 304. IR spectra in the region 4000–200 cm$^{-1}$ were recorded as KBr discs using a Perkin–Elmer 621 spectrophotometer. The proton NMR spectra were determined using Perkin–Elmer R-32 spectrometer (with TMS as internal standard). Electronic spectra of the complexes in chloroform were recorded on a Perkin–Elmer UV-visible spectrophotometer, Model 554.

*Preparation of the complexes*

(1) $(C_9H_7)_2Zr(OAr)Cl$. All operations were carried out under strictly anhydrous conditions. An appropriate phenol (5 mmol) in 20 cm$^3$ benzene was added to a solution containing bis(indenyl)-zirconium(IV)dichloride, $(C_9H_7)_2ZrCl_2$ (5 mmol) and $Et_3N$ (8 mmol) in 40 cm$^3$ benzene. The reaction mixture was refluxed for 4 hr and then allowed to cool at room temperature. The precipitate of $Et_3N \cdot HCl$ was filtered and the filtrate so obtained was concentrated to about 1/3 of the initial volume under reduced pressure. An excess of petroleum ether (40–60°C) was added to the concentrated filtrate and the mixture was allowed to stand for some time when crystals of the product separated out. These were filtered, washed with ether and dried under vacuum.

(2) $(C_9H_7)_2Zr(OAr)_2$. A solution of $(C_9H_7)_2ZrCl_2$ and an appropriate phenol in a 1:2 molar ratio in benzene containing $Et_3N$ was refluxed for 4 hr and

*Author to whom correspondence should be addressed.

the product was isolated by a similar method as described for $(C_9H_7)_2Zr(OAr)Cl$.

## RESULTS AND DISCUSSION

Dichlorobis(indenyl)zirconium(IV), reacts with phenols in a 1:1 and 1:2 molar ratio to yield complexes of the type I and II, respectively according to the following equations:

$$(C_9H_7)_2ZrCl_2 + ArOH + Et_3N \xrightarrow[80°C]{\text{benzene}} (C_9H_7)_2Zr(OAr)Cl + Et_3N \cdot HCl \qquad \mathbf{I} \quad (1)$$

$$(C_9H_7)_2ZrCl_2 + 2ArOH + 2Et_3N \xrightarrow[80°C]{\text{benzene}} (C_9H_7)_2Zr(OAr)_2 + 2Et_3N \cdot HCl \qquad \mathbf{II} \quad (2)$$

where Ar = $C_6H_5$, $p$–$ClC_6H_4$, $\alpha$-$Cl_{10}H_7$ or $\beta$–$C_{10}H_7$.

All the complexes form yellow to yellowish-brown crystals. The compounds so obtained decompose slightly in air to brown amorphous solids over a period of several days. These are soluble in common organic solvents, viz. benzene, nitrobenzene, dichloromethane, chloroform, carbon disulphide, ethanol and acetone. It is evident from

Table 1. Analytical and physical data

| Complex | Yield (%) | Dec. temp.[a] (°C) | Conductance[b] M x $10^3$= 0.5 | Elemental analyses % Found(Calc.) Zr | Cl |
|---|---|---|---|---|---|
| $(C_9H_7)_2Zr(OC_6H_5)Cl$ | 60 | 159-162 | 0.32 | 20.19(20.28) | 7.80(7.89) |
| $(C_9H_7)_2Zr(OC_6H_4Cl)Cl$ | 64 | 117-119 | 0.24 | 18.72(18.84) | 14.75(14.66) |
| $(C_9H_7)_2Zr(\alpha\text{-}OC_{10}H_7)Cl$ | 70 | 97-99 | 0.28 | 18.20(18.25) | 7.16(7.10) |
| $(C_9H_7)_2Zr(\beta\text{-}OC_{10}H_7)Cl$ | 68 | 103-105 | 0.22 | 18.12(18.25) | 7.06(7.10) |
| $(C_9H_7)_2Zr(OC_6H_5)_2$ | 65 | 170-172 | 0.30 | 17.84(17.98) | - |
| $(C_9H_7)_2Zr(OC_6H_4Cl)_2$ | 62 | 130-132 | 0.24 | 15.73(15.83) | 12.37(12.32) |
| $(C_9H_7)_2Zr(\alpha\text{-}OC_{10}H_7)_2$ | 66 | 85-87 | 0.30 | 15.06(15.02) | - |
| $(C_9H_7)_2Zr(\beta\text{-}OC_{10}H_7)_2$ | 70 | 135-137 | 0.26 | 14.95(15.02) | - |

a) Uncorrected values; b) in $ohm^{-1}$ $cm^2$ $mole^{-1}$

Table 2. Characteristic IR bands

| Complex | $\nu$(Zr-Cl) | $\nu$(Zr-O-C) | $\nu$(C-H) stretching band | $\nu$(C-C) asymmetric ring breathing | $\nu$(C-H) in plane bending | $\nu$(C-H) bending out of plane deformation |
|---|---|---|---|---|---|---|
| $(C_9H_7)_2Zr(OC_6H_5)Cl$ | 380(m) | 620(m) | 3090(s) | 1450(m) | 1020(m) | 820(w) |
| $(C_9H_7)_2Zr(OC_6H_4Cl)Cl$ | 390(m) | 625(m) | 3110(s) | 1440(m) | 1010(m) | 835(m) |
| $(C_9H_7)_2Zr(\alpha\text{-}OC_{10}H_7)Cl$ | 385(m) | 630(m) | 3100(s) | 1450(m) | 1025(m) | 830(w) |
| $(C_9H_7)_2Zr(\beta\text{-}OC_{10}H_7)Cl$ | 380(m) | 630(m) | 3080(s) | 1445(m) | 1015(m) | 840(m) |
| $(C_9H_7)_2Zr(OC_6H_5)_2$ | - | 635(m) | 3085(s) | 1450(m) | 1020(m) | 840(m) |
| $(C_9H_7)_2Zr(OC_6H_4Cl)_2$ | - | 620(m) | 3080(s) | 1460(m) | 1010(m) | 820(w) |
| $(C_9H_7)_2Zr(\alpha\text{-}OC_{10}H_7)_2$ | - | 625(m) | 3100(s) | 1440(m) | 1015(m) | 830(m) |
| $(C_9H_7)_2Zr(\beta\text{-}OC_{10}H_7)_2$ | - | 630(m) | 3085(s) | 1455(m) | 1010(m) | 825(m) |

(s) = strong, (m) = medium, (w) = weak

conductance measurements in nitrobenzene that the compounds are non-electrolytes. The analytical and physical data of the complexes are given in Table 1.

The assignment of characteristic IR frequencies for the complexes are listed in Table 2. The C–H stretching frequency at $\sim 3080\,cm^{-1}$ in the complexes is indicative of the indenyl group.[15] The perpendicular hydrogen wagging vibration around $840\,cm^{-1}$, the parallel hydrogen wagging mode at $\sim 1015\,cm^{-1}$, the band due to C–C stretching and ring breathing mode of $\pi$-bond at $\sim 1450$ and $\sim 1160\,cm^{-1}$, respectively, further confirm the presence of the indenyl group.[15] The bands occurring at $\sim 630\,cm^{-1}$ may be assigned to the Zr–O–C group.[16] Besides these, the $(C_9H_7)_2Zr(OAr)Cl$ complexes also absorb at $\sim 380\,cm^{-1}$ due to Zr-Cl band.

Proton magnetic resonance spectra of the complexes were taken in deutero-chloroform. The resonance signals due to indenyl protons overlap with that of phenoxy ring protons. Thus, a complex multiplet appeared in the region $\delta 6.70$–$7.80$ ppm and these groups could not be identified separately.

The electronic spectra of all the complexes recorded in chloroform exhibit a single band in the region 24775–24225 $cm^{-1}$. Absence of a *d–d* transition rules out the presence of any unpaired electron in the zirconium ion confirming the quadrivalent state of zirconium.[17,18]

*Acknowledgement*—We take this opportunity to thank the Council of Scientific and Industrial Research, New Delhi (India) for awarding Research Fellowship to B.K.

## REFERENCES

1. K. Ziegler and H. Martin, *Makromol. Chemie* 1956, **18**, 186.
2. K. S. Pitzer and H. S. Gutowsky, *J. Am. Chem. Soc.* 1946, **68**, 2204.
3. G. H. Olivé and S. Olivé, *Angew. Chemie* 1967, **79**, 764.
4. R. Sonogashira and H. Hapihara, *Bull. Chem. Soc. Japan* 1966, **39**, 1178.
5. K. Taniguchi and T. Arakawa, *Japan Kokai* 1971, **73**, 1046.
6. K. Andrä, *J. Organometal. Chem.* 1968, **11**, 567.
7. J. Besancon, F. Huq and M. Collette, *J. Organometal. Chem.* 1975, **96**, 63.
8. K. Andrä and E. Hille, *Z. Chem.* 1968, **8**, 65.
9. K. Andrä and E. Hille, *Z. Naturforsch* 1969, **24b**, 169.
10. A. K. Sharma and N. K. Kaushik, *Synth. React. Inorg. Met.-Org. Chem.* 1982, **12**, 827.
11. A. K. Sharma and N. K. Kaushik, *J. Chinese Chem. Soc.* 1983 (accepted for publication).
12. K. Chandra, R. K. Sharma, A. K. Garg and B. S. Garg, *Chem. Ind.* 1980, 537.
13. A. I. Vogel, *A Text Book of Practical Organic Chemistry, 4th Edn.* Longmans Green, London (1978).
14. R. C. Fay and R. N. Lowry, *Inorg. Chem.* 1967, **6**, 1512.
15. N. K. Kaushik, R. P. Singh, H. S. Sangari and G. S. Sodhi, *Synth. React. Inorg. Met-Org. Chem.* 1980, **10**, 617.
16. N. S. Biradar and V. H. Kulkarni, *Z. Anorg. Allg. Chem.* 1972, **387**, 275.
17. N. K. Kaushik, B. Bhushan and G. R. Chhatwal, *J. Inorg. Nucl. Chem.* 1980, **42**, 457.
18. A. K. Sharma and N. K. Kaushik, *Synth. React. Inorg. Met.-Org. Chem.* 1981, **11**, 685.

*Polyhedron* Vol. 3, No. 5, pp. 615–617, 1984
Printed in Great Britain.

0277–5387/84 $3.00 + .00
© 1984 Pergamon Press Ltd.

# NOTE

# SOLVENT EXTRACTION OF Fe(III) BY DI-(2-ETHYLHEXYL)PHOSPHORIC ACID FROM PHOSPHORIC ACID SOLUTIONS

**S. MELEŠ and M. V. PROŠTENIK***
INA, Research and Development Division, 41000 Zagreb, Yugoslavia

(*Received* 23 *August* 1983; *accepted* 10 *October* 1983)

**Abstract**—The extraction of iron(III) from aqueous phosphoric acid was studied using di-(2-ethylhexyl)phosphoric acid and trioctylphosphine oxide in nonaromatic hydrocarbon diluent. Distribution ratios have been investigated as a function of concentration of iron(III), phosphoric acid concentration, extractant concentration and extraction temperature. The apparent enthalpy change for the extraction reaction has been calculated from the temperature dependence data. It was found that the extractant dependency for iron(III) is first power indicating hydrolysis of iron(III) in the aqueous phase.

Di(2-ethylhexyl)phosphoric acid (abbreviated as HDEHP or simply HA) is widely used in hydrometallurgical processes for the separation and purification of a number of metals such as uranium, rare earth, copper, cobalt and nickel.[1–6] Iron is a very common impurity in raw industrial acid metal solutions in either the divalent or trivalent states and, therefore, it is of importance to know its properties in a given extraction system.

The extraction of Fe(III) with HDEHP from sulphuric, hydrochloric, perchloric and nitric acid solutions has been studied in detail.[7–13] On the contrary, the extraction of Fe(III) from phosphoric acid solutions has received little attention, although iron is associated with uranium in the wet process phosphoric acid and is coextracted during the uranium recovery by HDEHP-TOPO[14,15] (TOPO = trioctylphosphine oxide).

Kletenik[16] has reported extraction of iron(III) from phosphoric acid with a crude reaction mixture of 2-ethyl-1-hexanol with $P_2O_5$ (comprising the undetermined ratio of mono- and di-(2-ethylhexyl)phosphoric acid and di-(2-ethylhexyl)pyrophosphoric acid). The extraction is characterised by unusually high distribution coefficients. Bunus *et al.*[17] studied the influence of iron, particularly Fe(II) in uranium(IV) extraction from phosphoric acid and with HDEHP and HDEHP–TOPO mixtures but no details on Fe(III) extraction were given.

Therefore, the purpose of the present investigation was to define in some detail the Fe(III) extraction by HDEHP and HDEHP–TOPO from phosphoric acid solutions.

## EXPERIMENTAL

*Reagents.* Analytical grade phosphoric acid and $FeCl_3 \cdot 6H_2O$ ("Kemika"–Zagreb) were used. HDEHP and TOPO were used as purchased from Mobil Co.

*Procedure.* Aqueous solutions were prepared by dissolving Fe(III) chloride in phosphoric acid of selected concentrations. Organic solutions were prepared from HDEHP and TOPO and nonaromatic hydrocarbon diluent Mobil 190/210. Distribution ratio measurements were performed at 20°C in the thermostated bath with the exception of temperature studies. Equal volumes of aqueous and organic solutions were mixed mechanically for 20 min to ensure thermal and chemical equilibrium. Preliminary experiments had shown that the equilibrium is reached after 10 min. Phases were disengaged by centrifugation and the aqueous phase was analysed for iron content by atomic-absorption spectrophotometry or spectrophotometrically with 2,2′-bipyridine.

## RESULTS AND DISCUSSION

Typical isotherms for the extraction of Fe(III) by 0.3 M and 0.5 M HDEHP in kerosene from 1.5 M and 5.1 M $H_3PO_4$ as well as with the mixture of 0.3 M HDEHP 0.075 M TOPO are presented in Fig. 1.

The values of distribution coefficient obtained for Fe(III) as a function of $H_3PO_4$ concentration are presented in Fig. 2.

The distribution coefficient decreases rapidly with increasing concentration of phosphoric acid.

*Author to whom correspondence should be addressed.

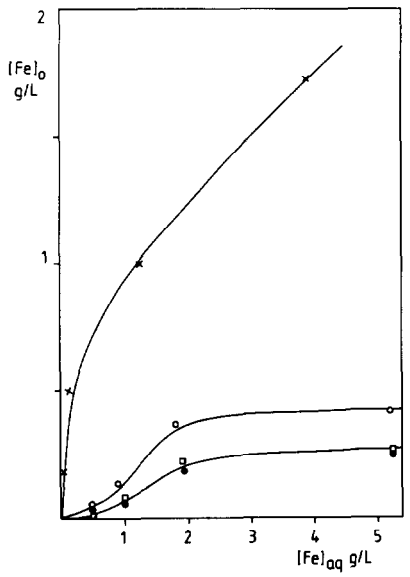



Fig. 1. Equilibrium loading isotherms for Fe(III) extraction at 20°C; ● 0.3 M HDEHP, 5.1 M $H_3PO_4$; □ 0.3 M HDEHP + 0.075 M TOPO, 5.1 M $H_3PO_4$; ○ 0.5 M HDEHP, 5.1 M $H_3PO_4$; × 0.5 M HDEHP, 1.5 M $H_3PO_4$.

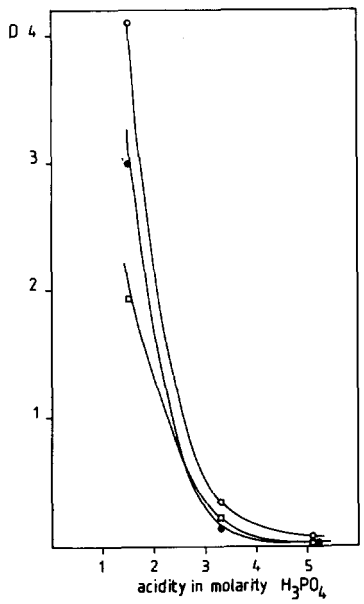



Fig. 2. Distribution ratios as a function of acidity in aqueous phase: ● with 0.3 M HDEHP at 20°C; □ with 0.3 M HDEHP + 0.075 M TOPO at 20°C; ○ with 0.3 M HDEHP + 0.075 M TOPO at 0°C.

TOPO alone (examined in the concentration range from 0.075 M to 0.75 M) shows no detectable extraction of iron(III) from 1.5 and 5.1 M $H_3PO_4$. In the mixtures with HDEHP, TOPO had only a slightly negative effect on Fe(III) extraction similar to the effect observed earlier by Blake *et al.*[18] that

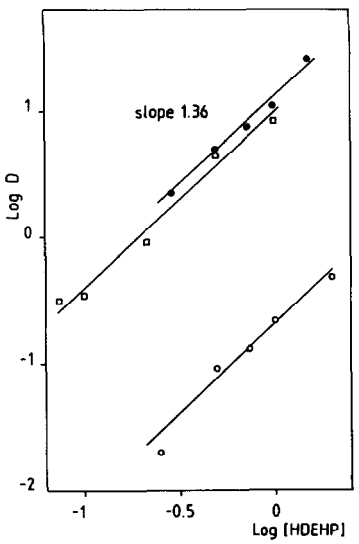



Fig. 3. Dependence of the extraction of Fe(III) on HDEHP concentrations; ○ in 5.1 M $H_3PO_4$ at 20°C; □ in 1.5 M $H_3PO_4$ at 20°C; ● in 1.5 M $H_3PO_4$ at 20°C with TOPO (HDEHP/TOPO molar ratio 4).

neutral organophosphorus compounds such as tributylphosphine oxide (TBPO) in combination with HDEHP had a negative influence on the extraction of Fe(III) from nitric acid solutions.

The variations of the distribution coefficients as a function of extractant concentration are shown in Fig. 3.

The extractant dependency was performed at low and high acidity.

It has been shown by Baker and Baes[19] that HDEHP is a dimer ($H_2A_2$) in *n*-octane and this is probably the same in a hydrocarbon diluent such as Mobil 190/210. The results show slopes of about 1.4 at 1.5 M and 5.1 M $H_3PO_4$ respectively, with and without the presence of TOPO. This may be considered as a first power dependence on the extractant concentration. For the extraction of Fe(III), the third power dependence is expected with following equilibrium reaction

$$Fe^{+3} + 3H_2A_2 \rightleftharpoons Fe(HA_2)_3 + 3H^+.$$

Islam *et al.*[20] have shown that Fe(III) hydrolyzes in aqueous phase

$$Fe^{+3} + H_2O \rightleftharpoons Fe(OH)^{+2} + H^+$$

and that the extraction of Fe(III) with HDEHP in benzene from sulphate solutions is first power dependent on extractant concentration. That could be accepted also for extraction of Fe(III) with HDEHP from phosphoric acid

$$Fe(OH)^{+2} + H_2A_2 \rightleftharpoons Fe(OH)A_2 + 2H^+.$$

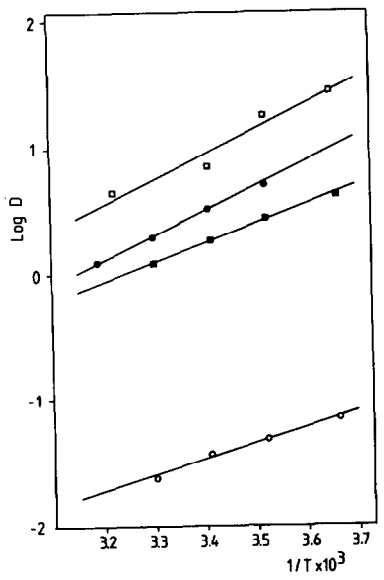



Fig. 4. Dependence of the extraction of Fe(III) with HDEHP on temperature; ○ 0.3 M HDEHP + 0.075 M TOPO from 5.1 M $H_3PO_4$; ■ 0.3 M HDEHP + 0.075 M TOPO from 1.5 M $H_3PO_4$; ● 0.3 M HDEHP from 1.5 M $H_3PO_4$; □ 0.5 M HDEHP from 1.5 M $H_3PO_4$.

Enthalpy changes associated with the extraction reaction at constant phosphoric acid and extractant concentration were calculated according to Van't Hoff's equation

$$\frac{\log D}{(1/T)} = -\frac{\Delta H}{2.303R}$$

The plots of $\log D$ vs $1/T$ for HDEHP and HDEHP–TOPO shown in Fig. 4 are linear with slopes of $-\Delta H/2.303R$, the values of which, along with their precision were computed by linear regression using a UNIVAC 1100 computer.

The extraction of Fe(III) was found to be exothermic and $\Delta H$ values for the extraction reaction have been found to be in $kJmol^{-1}$:

$-35.05 \pm 1.3$ for 0.3 M HDEHP and 1.5 M $H_3PO_4$;

$-40.32 \pm 11.6$ for 0.5 M HDEHP and 1.5 M $H_3PO_4$;

$-27.66 \pm 1.23$ for 0.3 M HDEHP + 0.075 M TOPO and 1.5 M $H_3PO_4$;

$-24.43 \pm 1.95$ for 0.3 M HDEHP + 0.075 M TOPO and 5.1 M $H_3PO_4$,

in the temperature range 20–60°C. The above study indicates that there is a difference in enthalpy between HDEHP and HDEHP–TOPO extraction of about 10 $kJmol^{-1}$ from which may be concluded that Fe(III) forms a stronger complex with HDEHP than with HDEHP–TOPO mixture.

## REFERENCES


1. G. M. Ritcey, A. W. Ashbrook and B. H. Lucas, CIM Bulletin, 111 (Jan. 1975), U.S. Pat. 3,399,055 (1968).
2. C. J. Bouboulis, *CIM Special Volume* 1979, **21**, 32.
3. J. A. Golding, S. Fouda and V. Saleh, *Ibid.* 1979, **21**, 227.
4. A. K. De, S. M. Khopkar and R. A. Chalmers, *Solvent Extraction of Metals*, Chap. 9. Van Nostrand, Reinhold, New York (1970).
5. R. J. Leimala and B. G. Nyman, *CIM Special Volume*, 1979, **21**, 475.
6. A. S. Kertes, *Recent Advances in Liquid–Liquid Extraction* (Edited by C. Hanson), Chap. 2. Pergamon Press, Oxford (1971).
7. C. F. Baes and H. T. Baker, *J. Phys. Chem.* 1960, **64**, 89.
8. S. N. Karapacheva and L. V. Ilozheva, *Radiokhimiya*, 1969, **11**, 37.
9. J. W. Roddy and C. F. Coleman and Sumio Arai, *J. Inorg. Nucl. Chem.* 1971, **33**, 1099.
10. J. E. Barnes, J. H. Setchfield and G. O. R. Williams, *J. Inorg. Nucl. Chem.* 1976, **38**, 1065.
11. F. Islam, H. Rahman, N. Ali, *J. Inorg. Nucl. Chem.* 1979, **41**, 217.
12. V. L. Bykhovtsov, *Radiokhimiya* 1970, **12**, 792.
13. T. Sato and T. Nakaumura, *Proc. Int. Solvent. Ext. Conf.* 1971, **1**, 238.
14. F. J. Hurst and D. J. Crouse, *Ind. Eng. Chem. Proc. Des. Develop.* 1974, **13**, 3; 286.
15. W. W. Berry and A. V. Henrickson, US. Pat. 4, 302, 427 (1981).
16. Yu. B. Kletenik, *Izv. Sib. Otd. Akad. Nauk SSSR, Ser. Khim. Nauk.* 1964, **8**, 109.
17. F. T. Bunus, V. C. Domocos and P. Dimitresen, *J. Inorg. Nucl. Chem.* 1978, **40**, 117.
18. C. A. Blake, D. E. Horner and J. M. Schmitt, Rep. ORNL 2259 (1959).
19. H. T. Baker and C. F. Baes, *J. Inorg, Nucl. Chem.* 1962, **24**, 1277.
20. F. Islam, H. Rahman and M. Ali, *J. Inorg. Nucl. Chem.* 1979, **41**, 217.

*Polyhedron* Vol. 3, No. 5, pp. 619–621, 1984
Printed in Great Britain.

0277-5387/84 $3.00 + .00
© 1984 Pergamon Press Ltd.

# NOTE

## CREATININE COMPLEXES OF ZINC, CADMIUM AND MERCURY

S. MURALIDHARAN, K. S. NAGARAJA and M. R. UDUPA*
Department of Chemistry, Indian Institute of Technology, Madras 600036 India

(*Received* 20 *September* 1983; *accepted* 24 *October* 1983)

**Abstract**—Zinc, cadmium and mercury(II) complexes of creatinine of the composition $M(Creat)_2X_2$ (X = Cl, Br or I) are prepared. The complexes are characterized by analytical and spectral methods. The increase in cyclic NH stretching frequency in the case of complexes (3350 $cm^{-1}$) from that of the free ligand (3300 $cm^{-1}$) suggested that secondary nitrogen is involved in coordination. The shift in the resonances of cyclic NH proton in the $^1H$ NMR and carbonyl and imine carbons in $^{13}C$ NMR when compared to the ligand indicated that cyclic nitrogen coordinates. Conductivity measurements in N, N-dimethylformamide suggested that the complexes are non-electrolytes. Thermal decomposition behaviour of the complexes is also discussed.

Creatinine is an important end product of creatine metabolism[1,2] in physiological systems. Knowledge of metal creatinine complexes may be helpful in understanding certain biological aspects of creatine metabolism. In this connection we have communicated[3] the potentiometric studies of the systems Zn, Cd and Hg(II) with creatinine. The studies revealed the formation of 1:1 and 1:2 complexes in aqueous solution. We hereby report the preparation, characterization and thermal behaviour of Zn, Cd and Hg(II) complexes with creatinine.

## EXPERIMENTAL

Creatinine was purchased from Fluka and used without any further purification. Metal halides were of Laboratory grade or were prepared by neutralising the metal carbonate or metal oxide with the hydrohalic acid.

*Preparation of dichlorodicreatininezinc*

Anhydrous zinc chloride (5 mM) and creatinine (10 mM) were dissolved in water (10 $cm^3$) separately. The solutions were mixed together and methanol was added and stirred. The precipitated white complex was filtered, washed with acetone and dried. Yield: 1.2 g.

Other complexes were also prepared by using a similar procedure. In some cases, the metal salts were dissolved in methanol instead of water. The analytical data of the complexes are given in Table 1. The IR, far IR and NMR spectra were recorded on Perkin–Elmer 257, Polytec IR 12 and Varian XL 100 spectrometers respectively. The NMR spectra were recorded in $d_6$-DMSO using TMS as internal reference. The thermogravimetric studies were carried out on Stanton recording thermobalance in air at a linear heating rate of 6°C $min^{-1}$.

## RESULTS AND DISCUSSION

Creatinine is a cyclic compound (Fig. 1) with cyclic, imine and tertiary nitrogen atoms. The IR spectrum of creatinine exhibited bands at 3300, 3180, 1710 and 1590 $cm^{-1}$, which are assigned[4,5] to cyclic NH, imine NH, C = O and C = N stretching frequencies respectively. The IR spectra of the complexes (Table 2) indicated shift in cyclic $\nu_{NH}$ and other frequencies are unaffected. The $\nu_{M-N}$ and $\nu_{M-X}$ (X = Cl, Br, I) are given[6] in Table 2. $^1H$ NMR spectrum of creatinine (Table 2) has resonances at 7.3, 3.6, 3.2 and 2.8 $\delta$, which are due to cyclic NH, imine NH, $-CH_2-$ and $-NCH_3$ protons. The assignments were made on comparison with the substituted guanidines.[7] The comparison of the spectra of the complexes with that of creatinine revealed that there is a shift in $\delta$ value of cyclic NH (7.8 $\delta$) proton and the resonating positions of the other protons are unaltered. $^{13}C$ NMR spectra of creatinine and $Cd(Creat)_2Cl_2$ were recorded in $d_6$-DMSO. The resonances of the $C_1$, $C_2$, $C_3$ and $C_4$ for creatinine occur[8] at 32.1, 55.1, 173.3 and 157.8 ppm. The corresponding chemical shift values for the complex are 33.7, 52.5, 187.2 and

*Author to whom correspondence should be addressed.

Table 1. Analytical data for $M(creat)_2X_2$ complexes

| Complex | Found (calc.) % C | H | N | X | M |
|---|---|---|---|---|---|
| $Zn(Creat)_2Cl_2$ | 26.1 (26.5) | 4.3 (3.9) | 23.5 (23.2) | 19.1 (19.6) | 18.4 (18.0) |
| $Zn(Creat)_2Br_2$ | 21.7 (21.3) | 3.5 (3.1) | 18.9 (18.6) | 34.9 (35.4) | 14.9 (14.5) |
| $Zn(Creat)_2I_2$ | 17.1 (17.6) | 2.9 (2.6) | 15.8 (15.4) | 47.0 (46.5) | 12.5 (12.0) |
| $Cd(Creat)_2Cl_2$ | 23.1 (23.5) | 3.9 (3.5) | 20.9 (20.5) | 16.8 (17.3) | 27.1 (27.5) |
| $Cd(Creat)_2Br_2$ | 19.8 (19.3) | 2.4 (2.8) | 16.5 (16.9) | 32.4 (32.1) | 22.1 (22.66) |
| $Cd(Creat)I_2$ | 16.7 (16.2) | 2.1 (2.4) | 14.7 (14.2) | 42.4 (42.8) | 18.6 (19.0) |
| $Hg(Creat)_2Cl_2$ | 19.6 (19.3) | 2.3 (2.8) | 16.4 (16.9) | 13.7 (14.2) | 39.9 (40.3) |
| $Hg(Creat)_2Br$ | 16.8 (16.4) | 2.7 (2.4) | 14.8 (14.3) | 26.8 (27.2) | 33.8 (34.2) |
| $Hg(Creat)_2I_2$ | 14.6 (14.1) | 2.6 (2.1) | 12.9 (12.4) | 37.8 (37.3) | 29.9 (29.5) |

Table 2. Principal IR ($cm^{-1}$) and $^1H$ NMR spectral data

| Compound | NH(cyclic) | M–N | M–X | Chemical shift of cyclic NH($\delta$) |
|---|---|---|---|---|
| Creatinine | 3300 | — | — | 7.3 |
| $Zn(Creat)_2Cl_2$ | 3320 | 245 | 300 | 7.7 |
| $Zn(Creat)_2Br_2$ | 3340 | 230 | 215 | 7.5 |
| $Zn(Creat)_2I_2$ | 3340 | 240 | 185 | 7.6 |
| $Cd(Creat)_2Cl_2$ | 3350 | 250 | 215 | 7.8 |
| $Cd(Creat)_2Br_2$ | 3360 | 255 | 195 | 7.7 |
| $Cd(Creat)_2I_2$ | 3340 | 245 | 180 | 7.5 |
| $Hg(Creat)_2Cl_2$ | 3340 | 380 | 230 | 8.1 |
| $Hg(Creat)_2Br_2$ | 3350 | 380 | 190 | 7.8 |
| $Hg(Creat)_2I_2$ | 3380 | 390 | 175 | 8.0 |

Table 3. TG data of creatinine complexes

| Complex | Temp. range (°C) | Weight Found % | loss (calcd.) | Metal halide | Temp. range (°C) | Found % | loss (calcd.) | Metal oxide |
|---|---|---|---|---|---|---|---|---|
| $Zn(Creat)_2Cl_2$ | 260–320 | 62 | (62.4) | $ZnCl_2$ | 580–680 | 77 | (77.6) | ZnO |
| $Zn(Creat)_2Br_2$ | 220–320 | 50 | (50.1) | $ZnBr_2$ | 500–660 | 82 | (82.0) | ZnO |
| $Zn(Creat)_2I_2$ | 220–340 | 42 | (41.5) | $ZnI_2$ | 480–670 | 85 | (85.1) | ZnO |
| $Cd(Creat)_2Cl_2$ | 230–320 | 55 | (55.7) | $CdCl_2$ | 580–690 | 68 | (68.7) | CdO |
| $Cd(Creat)_2Br_2$ | 210–320 | 45 | (45.4) | $CdBr_2$ | 480–680 | 74 | (74.2) | CdO |
| $Cd(Creat)_2I_2$ | 230–340 | 38 | (38.2) | $CdI_2$ | 440–680 | 78 | (78.3) | CdO |
| $Hg(Creat)_2Cl_2$ | — | — | — | — | 190–340 | 57 | (56.5) | HgO |
| $Hg(Creat)_2Br_2$ | — | — | — | — | 190–380 | 63 | (63.1) | HgO |
| $Hg(Creat)_2I_2$ | — | — | — | — | 180–380 | 68 | (68.2) | HgO |

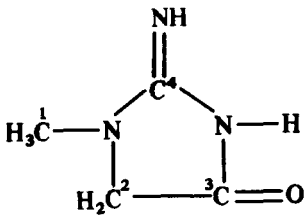



Fig. 1. Creatinine.

169.3 ppm. $^{13}C$ NMR studies indicate that there is shift in $C_3$ and $C_4$ and so the coordination occurs through the cyclic nitrogen. If it were through imine nitrogen or tertiary nitrogen, shifts in $C_4$ (imine) or $C_1(N–CH_3)$ would have been observed. IR and NMR spectra of the complexes indicate that cyclic NH is involved in coordination and the halide ions complete four coordination around the metal atom. The electrical conductivity values of the complexes in DMF are in the range 10–30 mho $cm^2$ $mol^{-1}$, which suggests that the complexes are non-electrolytes.

TG data of the complexes are presented in Table 3. Zinc and cadmium complexes undergo decomposition in two steps. The first step is due to the loss of creatinine yielding the corresponding metal halides. The second step involves the conversion of metal halide to metal oxide. In the case of mercury complexes it was observed the loss of creatinine and the formation of oxide are simultaneous and a single step decomposition was observed. At higher temperature (500°C), the sublimation of mercuric oxide takes place. The intermediate and end products were characterized by chemical analysis and "$d_{hkl}$" values.

## REFERENCES

1. H. H. Beard, *Ann. Rev. Biochem.* 1941, **10**, 245.
2. H. Brainerd, S. Margen and M. Shatton, *Current Diagnosis and Treatment*, p. 502. Lang Medical Publications, California (1968).
3. S. Muralidharan, K. S. Nagaraja and M. R. Udupa, Trans SAEST, In Press.
4. M. Padmanabhan, Ph.D. Thesis. Indian Institute of Technology. Madras, India (1976).
5. A. J. Canty, M. Fyfe and B. M. Gatehouse, *Inorg. Chem.* 1978, **17**, 1467.
6. D. M. Adams, *Metal–Ligand and Related Vibrations.* Edward Arnold, London (1967).
7. V. N. Shafranskii, A. A. Stratulat and I. V. Dranka, *Russ. J. Inorg. Chem.* 1981, **26**, 975.
8. R. F. Dietrich, M. A. Marletta and G. L. Kenyon, *Org. Mag. Res.* 1980, **13**, 79.

*Polyhedron* Vol. 3, No. 5, pp. 623–626, 1984
Printed in Great Britain.

0277–5387/84 $3.00 + .00
© 1984 Pergamon Press Ltd.

# NOTE

## DINITROGEN COMPLEXES OF IRON(II) WITH CHELATING AGENTS AS LIGANDS

J. M. LOPEZ-ALCALA*, M. C. PUERTA and F. GONZALEZ-VILCHEZ
Departamento de Química Inorgánica, Facultad de Ciencias, Universidad de Cádiz, Cádiz, Spain

(*Received* 26 *September* 1983; *accepted* 24 *October* 1983)

**Abstract**—Two new dinitrogen compounds of formulae $Na_2[Fe(EDTA)N_2].2H_2O$ and $Na_2[Fe(CDTA)N_2].2H_2O$ have been synthesized from $[Fe(H–EDTA)H_2O]$ and $[Fe(H–CDTA)–H_2O]$, respectively, and $NaN_3$. Both complexes have been characterized by IR and electronic spectra. The thermal behaviour has been studied by TG and DTA techniques.

Since the first report of a dinitrogen complex by Allen and Senoff in 1965,[1] many papers have been published dealing with the study of dinitrogen complexes with a simple amine ligand, $[M(NH_3)_5(N_2)]^{+2}$. However, the interest for analogous compounds with chelating agents of the EDTA family has been much less. In a recent paper, Diamantis[2] synthesized the species $[Ru(EDTA)N_2]^{+2}$ and $[(EDTA)–Ru–N_2–Ru(EDTA)]^{+4}$ showing the ability of EDTA to act as a pentadentate ligand in dinitrogen complexes.

In previous papers, we described a general method of synthesis for these compounds based on the conversion to coordinated dinitrogen of a ligand with a N–N bond. This method has been successfully applied to the syntheses of $Na_2[Fe(PDTA)N_2].H_2O$,[3] $Na_2[Ru(PDTA)N_2].H_2O$,[4] and $Na[Cr(PDTA)N_2].2H_2O$.[5] In this paper, we report the synthesis in aqueous solution and using sodium azide of $Na_2[Fe(EDTA)N_2].2H_2O$ and $Na_2[Fe(CDTA)N_2].2H_2O$ from $[Fe(H–EDTA)H_2O]$ and $[Fe(H–CDTA)H_2O]$.

## EXPERIMENTAL

$Fe(NO_3)_3.9H_2O$, $NaN_3$, EDTA–$H_4$, and CDTA–$H_4$ were obtained from Merck. All compounds were used without further purification.

C, H and N analyses were performed at the Departamento de Microanalisis of the Instituto de Química Orgánica General, C.S.I.C., Madrid. The water content of the samples was determined from the TG curves.

IR spectra were recorded in the 4000–200 $cm^{-1}$ region using a Pye–Unicam, SP3-300 spectrophotometer. The samples were prepared as KBr pellets. TG and DTA curves were obtained with a Mettler TA–HE–20 system.

*Synthesis of* $Na_2[Fe(EDTA)N_2].2H_2O$

0.500 g of $[Fe(H–EDTA)H_2O]$[6] were dissolved in 75 $cm^3$ of water at 70°C. 0.500 g of $NaN_3$ were added to the resulting solution, precipitating then a reddish compound that dissolved almost immediately. The mixture was heated at 70°C for 60 min, and was cooled in the refrigerator. When the precipitation began to occur, 50 $cm^3$ of absolute ethanol were added to the solution, producing an orange–brown product that was filtered and washed with absolute ethanol and dried over $P_2O_5$. Found: C, 26.6; H, 3.6; N, 11.4; $H_2O$, 8.0. Calc: C, 26.5; H, 3.6; N, 12.3; $H_2O$, 7.9%.

*Synthesis of* $Na_2[Fe(CDTA)N_2].2H_2O$

This product was obtained from 0.500 g of $[Fe(H–CDTA)H_2O]$[7] using the same procedure as described above for the analogous compound with EDTA. The conditions were the same except the time of heating at 70°C (120 min). The solid product obtained was also orange–brown coloured. Found: C, 33.2; H, 4.6; N, 8.5; $H_2O$, 9.0. Calc: C, 33.1; H, 4.4; N, 11.0; $H_2O$, 7.1%.

## RESULTS

*UV and visible spectra*

The ion Fe(II) in these compounds is a low-spin $d^6$ system with fundamental term $^1A_{1g}$. The formation of this type of complex is favoured by

*Author to whom correspondence should be addressed.

ligands causing an intense field, in conjunction with the reduction of the electronic density on the metal by means of the back-bonding from the "*d*" orbitals of the metal to the empty $\pi^*$ orbitals of the dinitrogen ligand.

The absorption spectra of both compounds in aqueous solution (Fig. 1) shows an intense charge-transfer band at 196 nm and a band at 470 nm (EDTA complex) or 460 nm (CDTA complex) which can be assigned to the $^1T_{1g} \leftarrow {}_1A_{1g}$ transition. Other bands appear in both spectra at 250 or 270 nm (EDTA and CDTA complexes, respectively) and can be assigned to the $^1T_{2g} \leftarrow {}_1A_{1g}$ transition.

*IR spectra*

Figures 2 and 3 shows the IR spectra of both compounds and the numerical values for the positions of the most significant bands are listed in Table 1.

Both compounds show a band in the characteristic region for dinitrogen complexes, i.e. 2100–1900 $cm^{-1}$. This band corresponds to the N–N stretching vibration and appears at 2040 and 2060 $cm^{-1}$ for the EDTA and CDTA complexes, respectively. The position and intensity of this band is normally used as a measure of the covalent character of the metal–dinitrogen bond. For these complexes, the medium intensity can be considered indicative of a moderate covalent character of the bond.

The broad band observed in both spectra at *ca.* 3400 $cm^{-1}$ corresponds to the stretching of O–H bonds of the water of crystallization. Two bands appear in the C–H stretching region for both compounds. The intensity of these bands is

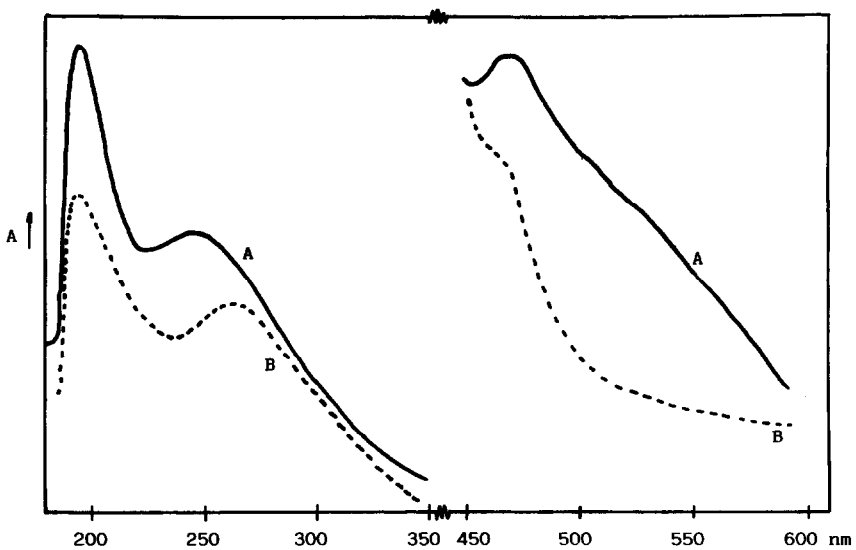



Fig. 1. UV and visible spectra of $Na_2[Fe(EDTA)N_2].2H_2O$ (A) and $Na_2[Fe(CDTA)N_2].2H_2O$ (B).

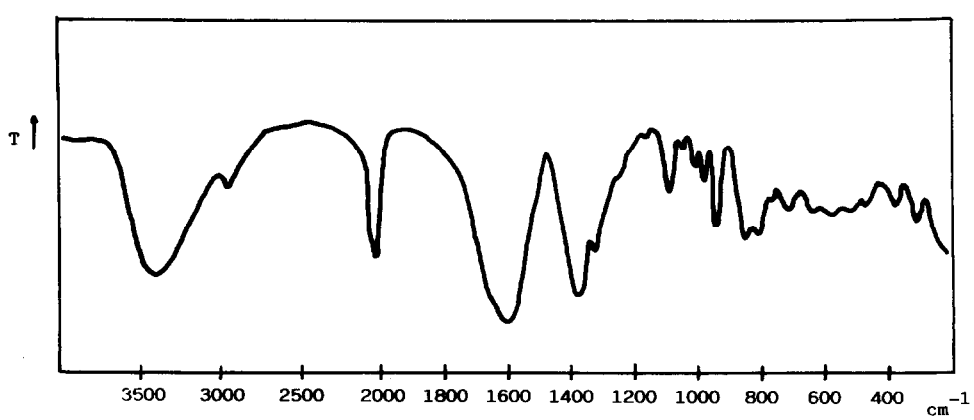



Fig. 2. IR spectrum of $Na_2[Fe(EDTA)N_2].2H_2O$.

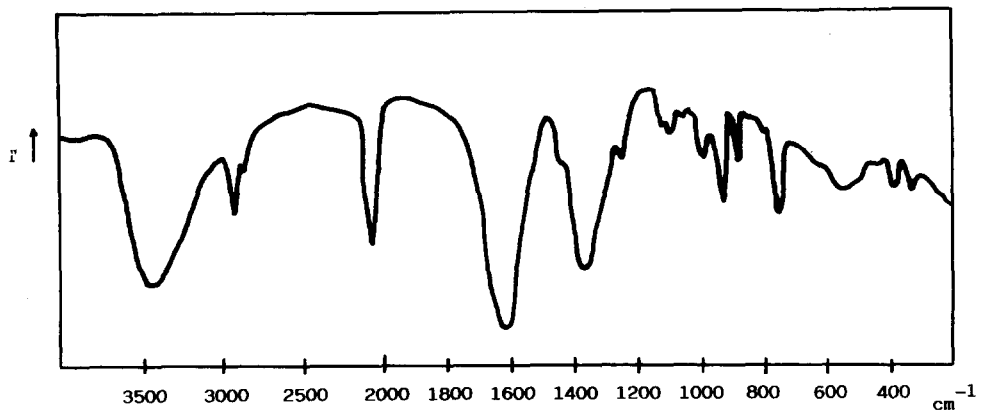



Fig. 3. IR spectrum of $Na_2[Fe(CDTA)N_2].2H_2O$.

Table 1. Main IR absorption bands of dinitrogen complexes

| | $\nu_{O-H}$ | $\nu_{-CH_2}$ | $\nu_{(N\equiv N)}$ | $\nu_{(COO^-)}$ assym. | $\nu_{(COO^-)}$ sym. | $\nu_{(C-N)}$ |
|---|---|---|---|---|---|---|
| $Na_2[Fe(EDTA)N_2].2H_2O$ | 3400 | 2970<br>2930 (sh) | 2040 | 1600 | 1380 | 1090 |
| $Na_2[Fe(CDTA)N_2].2H_2O$ | 3400 | 2940<br>2860 | 2060 | 1620 | 1390 | 1095 |

different in each case as a consequence of the different central backbone of both ligands, although a contribution of minor differences between the $CH_2$ groups of the glycinate rings cannot be ignored.

The symmetrical stretching vibration of carboxylate groups appears at 1380 $cm^{-1}$ for both compounds, but the position of the asymmetrical one is somewhat different, 1600 and 1620 $cm^{-1}$ for the EDTA and CDTA complexes, respectively. However, for both compounds, the separation between the asymmetrical and symmetrical bands suggests a moderately covalent character of the metal–carboxylate bonds.[8]

*Thermal behaviour*

The DTA and TG curves obtained in air atmosphere of static air for both compounds are given in Figs. 4 and 5.

Between 50 and 200°C, there is an initial weight loss associated with an endothermic effect, both corresponding to the elimination of the water of crystallization. The theoretical values for the elimination of two water molecules are in accordance with the experimental values.

The weight loss between 180 and 250°C is also an endothermic process and can be associated with

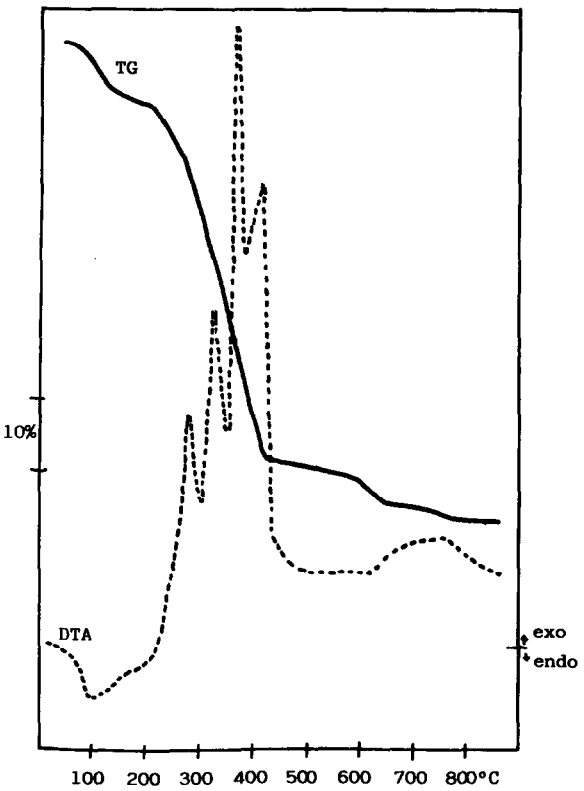



Fig. 4. TG (———) and DTA (– – – –) curves for $Na_2[Fe(EDTA)N_2].2H_2O$.

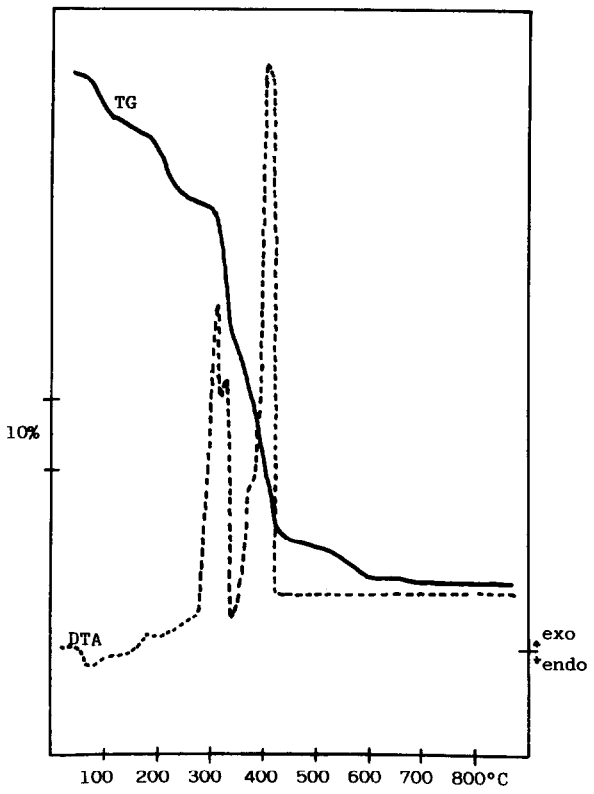



Fig. 5. (———) and DTA (– – – –) curves for $Na_2[Fe(CDTA)N_2].2H_2O$.

the loss of the coordinated dinitrogen molecule, although the theoretical values (6.77 and 5.54% for the EDTA and CDTA complexes) are somewhat lower than the experimental one (7% for both cases). This fact can be explained having in mind that the elimination of coordinated dinitrogen overlaps with the following stages in the thermal decomposition of the compounds.

The exothermic effects between 280 and 500°C in the DTA curves are similar to those found for analogous complexes[9] except in the temperature range, and correspond to the decarboxylation and further decomposition of the complexes with formation of $Na_2CO_3$ and FeO. This results in a great weight loss in the TG curves, corresponding in the total values for the anhydrous compounds of 52.3 (EDTA complex) and 56.5% (CDTA complex). The theoretical values for the formation of $Na_2CO_3$ and FeO are 52.97 and 57.87% for the EDTA and CDTA complexes, respectively. At higher temperatures, decomposition of $Na_2CO_3$ causes the formation of $Na_2O_3$ and FeO as final products at 900°C.

## REFERENCES

1. A. D. Allen and C. V. Senoff, *J. Chem. Soc. Chem. Comm.* 1965, 621.
2. A. A. Diamantis and J. V. Dubrawsky, *Inorg. Chem.* 1981, **20**, 1942.
3. M. C. Puerta, M. F. Gargallo and F. González-Vílchez, *Polyhedron* 1983, **2**, 397.
4. M. C. Puerta, M. F. Gargallo and F. González-Vílchez, *Trans. Met. Chem.* 1982, **7**, 355.
5. M. C. Puerta, M. F. Gargallo and F. González-Vílchez, *Rev. Chem. Min.* 1983, **20**, 149.
6. J. L. Lambert, C. E. Godsey and L. M. Seitz, *Inorg. Chem.* 1963, **2**, 127.
7. G. H. Cohen and J. L. Hoard, *J. Am. Chem. Soc.* 1966, **88**, 3228.
8. D. T. Sawyer and J. M. McKinnie, *J. Am. Chem. Soc.* 1960, **82**, 4191.
9. F. González-Vílchez, J. M. López-Alcalá and M. García-Basallote, *Thermochim. Acta* 1982, **58**, 317.

*Polyhedron* Vol. 3, No. 5, pp. 627–630, 1984
Printed in Great Britain.

0277–5387/84 $3.00 + .00
© 1984 Pergamon Press Ltd.

# NOTE

## *DIMETHYLFORMAMIDE AND DIMETHYLSULPHOXIDE ADDUCTS OF TIN(II) PERCHLORATES*

A.R.Bassoteli, A.C.D.Ângelo, E.Tfouni*, and N.R.Stradiotto*

Departamento de Química
Faculdade de Filosofia, Ciências e Letras de Ribeirão Preto
Universidade de São Paulo
14.100 - Ribeirão Preto (SP) - Brasil

(Received 4 November, 1983; accepted 16 February 1984)

*ABSTRACT - The synthesis and some properties of dimethylformamide and dimethylsulphoxide adducts of tin(II) perchlorates are described. Coordination is discussed from molar conductance measurements, infrared and nmr spectra.*

Dimethylformamide (dmf) and dimethylsulphoxide (dmso) form adducts and complexes with several metal cations[1,2], including tin(II). In these latter compounds, tin(II) acts as acceptor[3], as showed by $SnCl_2$.2dmf, $SnCl_2$.2dmso, $SnCl_2$.1.5dmso, and $SnF_2$.dmso, where in addition, the anions are also coordinated.

Here are described the synthesis and properties of dmf and dmso adducts of tin(II) perchlorates in which the anions are not coordinated. Besides this aspect, the perchlorates, dmf, and dmso are chemical species which are used in electrochemical measurements.

## EXPERIMENTAL

*Dmf adduct synthesis* - $Sn(ClO_4)_2.3H_2O$ was prepared, according to published procedure[4], by dissolution of 2g of SnO (Baker) in 40 $cm^3$ of 70% $HClO_4$ (Merck) with gentle heating. After filtration, the solid was washed with 30 $cm^3$ of chloroform and dissolved in 10 $cm^3$ of ethanol. 2 $cm^3$ of dmf (Merck) where then added, along with triethylorthoformate (Merck), with stirring, till precipitation occurred. After filtration, the white precipitate was washed with 30 $cm^3$ ethanol and dried in a vacuum desiccator over calcium chloride. All manipulations were run under nitrogen atmosphere in a glove bag.

*Dmso adduct synthesis* - $Sn(ClO_4)_2.3H_2O$ (0.015mol), prepared as above, was dissolved in 35 $cm^3$ ethanol, and 0.06 mol of dmso (Fisher) was added. After filtration, the white precipitate was washed with ethanol, and then dried in a vacuum desiccator over calcium chloride. All manipulations were run under nitrogen atmosphere in a glove bag.

*Analysis* - C and H were analysed in a model 240 Perkin-Elmer analyser. Sulfur was determined by the method of Schöniger. Tin was determined by back-titration with EDTA.

Conductance measurements were made at 25ºC using a model 'E 365B Metrohm conductoscope.

*Authors to whom correspondence should be addressed.

Infrared spectra were recorded using a model 467 Perkin-Elmer spectrophotometer in nujol mulls between KBr plates, in the 4000-400 $cm^{-1}$ region.

NMR spectra in deuterated methanol were recorded with a model EM-360, 60 MHz, nmr spectrometer from Varian Instruments.

## RESULTS AND DISCUSSION

Addition of dmf or dmso to an ethanolic solution of $Sn(ClO_4)_2.3H_2O$, in inert atmosphere, leads to the formation of white precipitates. These solids are only formed with the addition of the dehydrating agent triethylorthoformate, which was added in the amount required to start precipitation. The hygroscopic solids were analysed (Table 1), and correspond to $Sn(ClO_4)_2.3dmf$ and $Sn(ClO_4)_2.4dmso$. Addition of ligands in excess of the stoichiometric amount leads to an oily product, or prevents the solid formation. Both compounds melt with decomposition (Table 1). $Sn(ClO_4)_2.3dmf$ is soluble in water, dmf, acetonitrile, nitromethane, and acetone, and insoluble in ethyl acetate, methanol, ethanol, propanol, tetrahydrofuran, chloroform, dioxane, carbon tetrachloride, and benzene. $Sn(ClO_4)_2.4dmso$ is soluble in water, dmf, acetonitrile, dmso, ethyl ether, and nitromethane, slightly soluble in dioxane and methanol, and insoluble in benzene, carbon tetrachloride, toluene, chloroform, ethanol, tetrahydrofuran, and acetone.

TABLE 1. Analytical data and melting points of $Sn(ClO_4)_2.3dmf$ and $Sn(ClO_4)_2.4dmso$

| Compound | Sn(%) | | C (%) | | H (%) | | N (%) | | S (%) | | m.p |
|---|---|---|---|---|---|---|---|---|---|---|---|
| | calc. | obs. | calc. | obs. | calc. | obs. | calc. | obs. | calc. | obs. | ºC |
| $Sn(ClO_4)_2.3dmf$ | 22.11 | 22.39 | 20.13 | 20.30 | 3.94 | 4.31 | 7.83 | 8.16 | - | - | 220dec. |
| $Sn(ClO_4)_2.4dmso$ | 18.89 | 19.17 | 15.24 | 15.43 | 3.81 | 3.93 | - | - | 20.32 | 20.75 | 95dec. |

### Conductance measurements

Millimolar solutions of $Sn(ClO_4)_2.4dmso$ and of $Sn(ClO_4)_2.3dmf$ in acetonitrile have molar conductances of 273 $ohm^{-1}.cm^2.mol^{-1}$ and 288 $ohm^{-1}.mol^2.cm^{-1}$, respectively. These values show that the adducts behave as 1:2 electrolytes in this solvent[5], and indicate the non-coordination of the perchlorate ions to tin(II) in these solutions.

### Infrared spectrum of dmso adduct

The fundamental vibrations of coordinated dmso were assigned by comparison with those reported for the free ligand[6] and some dmso complexes[7-12].

The shift of the S-O frequency to lower wavelength ($\sim$990 $cm^{-1}$), compared with the value of 1058 $cm^{-1}$ in free sulphoxide, suggest that coordination is through oxygen. Accordingly, the 698 $cm^{-1}$ band of the free sulphoxide, assigned to C-S-C asymmetric stretching, is shifted to higher energy ($\sim$725$cm^{-1}$) in the complex.

The weak band at 1040 $cm^{-1}$ in the adduct can be assigned to $r(CH_3)A'$, which appears at 1022 $cm^{-1}$ in the free ligand. This band could also originate from a second S-O stretching vibration, and implying in two different kinds of dmso in the adduct, a situation not uncommon for Sn(II) adducts. On the other

hand, the remaining spectral features do not lead to definite identification of that second kind of dmso ligand. Assignment of that band as a coordinated perchlorate is unlikely, since there are no further bands in the high energy side of the perchlorate band in the 1100 $cm^{-1}$ region[13].

The narrow band at 625 $cm^{-1}$ and the broad band at 1090 $cm^{-1}$ are indicative of non-coordinated perchlorate[13-15].

The rather broad band located at 930 $cm^{-1}$ may originate from the 931 and 953 $cm^{-1}$ rocking bands of the free ligand, shifted in the adducts, and eventually from a perchlorate vibration. A perchlorate band in that region could be due to either a $\nu_1(T_d)$ or $\nu_2(C_{3v})$ vibration from a coordinated or a distorted perchlorate. However, the presence of a perchlorate band in this region is not definite evidence for perchlorate coordination[15,16]. Thus, if perchlorate is contributing in this region, it could be through a distorted non-coordinated perchlorate, since no further coordinated perchlorate bands appear in the spectrum.

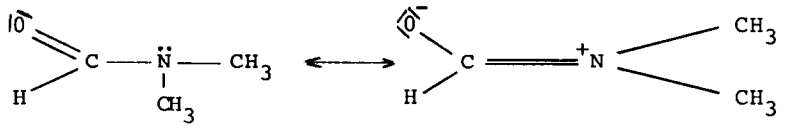
Infrared and nmr spectra of dmf adduct

The bands located at 620 $cm^{-1}$ and 1070 $cm^{-1}$ are assigned as $\nu_4$ and $\nu_3$ Td perchlorate bands, indicating ionic perchlorates.

The bands located at 1675, 1255, and 658 $cm^{-1}$ in the free ligand are shifted in the adduct to 1640 $cm^{-1}$, 1240, and $\sim$ 700 $cm^{-1}$, respectively.

The 1675 $cm^{-1}$ band in the free amide is assigned to a mainly carbonyl stretching vibration, but coupled with a CN vibration[17], and its shift to lower energy could indicate coordination through oxygen, but, since there is not a definite assignment for the fundamental vibrations of the ligand[17], assignment of dmf bands in the adduct was not made, and thus, in order to determine the coordination site of dmf, a nmr spectrum of the complex was run.

In free dmf, the nmr spectrum shows one signal at 8.10$\delta$, assigned to the carbonyl proton, which in the complex is shifted to 7.80$\delta$ . Two further signals, assigned to the methyl groups, appear in the complex, at 3.01 and 2.87$\delta$, as in free dmf. Dmf can be represented by two resonance structures:



I II

Bonding through nitrogen favors structure I, and thus rotation through HOC-$N(CH_3)_2$ bond, rendering the methyl groups equivalent, and, then, only one signal should be observed. On the other hand, bonding through oxygen favors structure II, which due to the double bond character, renders the methyl groups non-equivalent, and thus two signals appear in the nmr spectrum, as is the present case. Thus ir and nmr spectra suggest that dmf is bonded through the oxygen atom.

Therefore, the perchlorate anions are ionic in both adducts, and the ligands are coordinated through their oxygen atoms. In the dmf adduct, this implies $sp^3$ hybridization for Sn(II)[3]. In the dmso adduct, Sn(II) should be in $dsp^3$ hybridization; however, the possibility cannot be ruled out that the

three dmso molecules are coordinated to a $sp^3$ Sn(II), with the fourth molecule held trapped in the lattice, as is the case in some Sn(II) adducts[3].

Acknowledgment - support from FAPESP and CNPq is gratefully acknowledged.

REFERENCES

1. S.S.KRISHNAMURTHY and S.SOUNDARARAJAN, Can.J.Chem., 1969, 47, 995.
2. W.L.REYNOLDS, Prog.Inorg.Chem., 1970, 12, 1.
3. J.D.DONALDSON, Prog.Inorg.Chem., 1967, 8, 287.
4. C.G.DAVIES and J.D.DONALDSON, J.Inorg.Nucl.Chem., 1968, 30, 2635.
5. W.J.GEARY, Coord.Chem.Rev., 1971, 7, 81.
6. M.T.FOREL and M.TRANQUILLE, Spectrochim. Acta. A, 1970, 26, 1023.
7. A.IWASE and S.TADA, Nippon Kagaku Kaishi, 1973, 60.
8. V.N.KRISHNAMURTHY and S.SOUNDARARAJAN, J.Inorg.Nucl.Chem., 1967, 29, 517
9. J.SELBIN, W.E.BULL, and L.H.HOLMES, Jr., J.Inorg.Nucl.Chem., 1961, 16, 219.
10. F.A.COTTON and R.FRANCIS, J.Amer.Chem.Soc., 1960, 82, 2986.
11. M.K.KUYA, O.A.SERRA, and V.K.LAKATOS OSÓRIO, J.Inorg.Nucl.Chem., 1975, 37, 1998.
12. V.K.LAKATOS OSÓRIO, Y.KAWANO, M.K.KUYA and M.PERRIER, An.Acad.Bras.Ciên. 1980, 52, 273.
13. B.J.HATHAWAY and A.E.UNDERHILL, J.Chem.Soc., 1961, 3091.
14. F.A.MILLER and C.H.WILKINS, Anal.Chem., 1952, 24, 1253.
15. S.D.ROSS, Spectrochim, Acta, 1962, 18, 225.
16. A.HEZEL and S.D.ROSS, Spectrochim. Acta, 1966, 22, 1949.
17. T.C.JAO, I.SCOTT, and D.STEELE, J.Mol.Spectrosc. 1982, 92, 1.

*Polyhedron* Vol. 3, No. 5, pp. 631–634, 1984
Printed in Great Britain.

0277–5387/84 $3.00 + .00
© 1984 Pergamon Press Ltd.

# COMMUNICATION

## On the Formation of Arseno Aminoxyls (Nitroxides) by Spin Trapping of Arseno Radicals

Detlef Rehorek† and Edward G. Janzen‡

Department of Chemistry and Biochemistry
Guelph-Waterloo Centre for Graduate Work in Chemistry
Guelph, Ontario, N1G 2W1 Canada

(Received 15 August, 1983; accepted 16 January 1984)

Abstract

The $\cdot AsO_2$ radical is detected by spin trapping using 2-methyl-2-nitrosopropane producing a new aminoxyl spin adduct. $AsO_4\cdot^{2-}$ is trapped as an oxygen-centered radical by phenyl tert-butyl nitrone.

Paramagnetic As(IV) species are assumed to be short-lived intermediates in the one-electron oxidation of arsenites.[1-3] Although radicals generated by low temperature radiolysis of arsenites and arsenates are well characterized by ESR in the solid state,[4-7] attempts to detect arseno radicals directly by ESR in liquid solutions have failed.[8] However using nitromethane aci-anion as a spin trap, Fessenden et. al.[9] were able to establish the formation of $\cdot AsO_2$ radicals during the reaction of $AsO_2^-$ with either $\cdot OH$ or $SO_4^{\bar{\cdot}}$ in aqueous solutions.

The use of nitromethane as a spin trap suffers from the shortcoming that solutions with relatively high pH are required and the nitro-anion addition products are not persistent radicals. On the other hand no arseno radical spin adducts of the widely used nitroso and nitrone spin traps have been reported so far. Since the use of these spin traps is not restricted to basic solutions, a wider application range is expected, provided the spin adducts are persistent.

Following Fessenden's work,[9] $SO_4^{\bar{\cdot}}$ radicals, formed in the photolysis of $Na_2S_2O_8$, were used to react with $NaHAsO_2$ and $Na_2HAsO_4$ to produce the arseno radicals by electron transfer oxidation:

$$SO_4^{\bar{\cdot}} + AsO_2^- \rightarrow SO_4^{2-} + \cdot AsO_2 \qquad (1)$$

$$SO_4^{\bar{\cdot}} + \underset{(HAsO_4^{2-})}{AsO_4^{3-}} \rightarrow SO_4^{2-} + AsO_4\cdot^{2-} \qquad (2)$$

The spin traps used were phenyl tert-butyl nitrone (PBN),[10] 2-sulphonatophenyl tert-butyl nitrone (2-SSPBN),[11] 5,5-dimethyl-1-pyrroline-1-oxide (DMPO),[12] and 2-methyl-2-nitrosopropane (MNP)[13].

It is well established that aromatic compounds react rapidly (e.g. $5\times10^9$ $M^{-1}sec^{-1}$ for anisole and $1.2\times10^8$ $M^{-1}sec^{-1}$ for benzonitrile[14,15]) by electron transfer to $SO_4^{\bar{\cdot}}$ to produce the aromatic radical cation. Accordingly the following reaction should be fast (~$5\times10^8$ $M^{-1}sec^{-1}$ perhaps),

$$PBN + SO_4^{\bar{\cdot}} \rightarrow PBN^{\dagger} + SO_4^{2-} \qquad (3)$$

and the reaction of $PBN^{\dagger}$ with $H_2O$ to produce the hydroxy adduct should always be expected as a side reaction:

---

‡ Author for correspondence

† On sabbatical leave from Sektion Chemie der Karl-Marx Universität, Leipzig, DDR.

$$[Ph\text{-}CH{=}N(O)\text{-}CMe_3]^{+\cdot} + H_2O \rightarrow Ph\text{-}CH(OH)\text{-}N(O\cdot)\text{-}CMe_3 + H^+ \quad (4)$$

Also in some instances $SO_4^{-\cdot}$ adds directly to the spin trap[16] and the hydrolysis of this adduct could also yield the hydroxy adduct:

$$Ph\text{-}CH{=}N(O)\text{-}CMe_3 + SO_4^{-\cdot} \rightarrow Ph\text{-}CH(OSO_3^-)\text{-}N(O\cdot)\text{-}CMe_3 \quad (5)$$

$$Ph\text{-}CH(OSO_3^-)\text{-}N(O\cdot)\text{-}CMe_3 + H_2O \rightarrow Ph\text{-}CH(OH)\text{-}N(O\cdot)\text{-}CMe_3 \quad (6)$$

Thus it is not too surprising that aqueous solutions of sodium persulphate become quite acidic and the hydrolysis of PBN to produce benzaldehyde and tert-butyl hydroxylamine leads to the detection of tert-butyl aminoxyl:

$$Me_3C(OH)NH + S_2O_8^{2-} \rightarrow Me_3C\text{-}N(O\cdot)\text{-}H + SO_4^{-\cdot} + HSO_4^- \quad (7)$$

Another route to the hydroxylamine might be scission of the $SO_4^{-\cdot}$ adduct of the nitrone:

$$Ph\text{-}CH(OSO_3^-)\text{-}N(O\cdot)\text{-}CMe_3 \xrightarrow{H_2O} Ph\text{-}CHO + Me_3C\text{-}N(O\cdot)\text{-}H + HSO_4^- \quad (8)$$

When $SO_4^{-\cdot}$ radicals were reacted with $NaAsO_2$ in the presence of PBN or 2-SSPBN the same spectrum was obtained consisting of a triplet of 1:1:1:1 quartets ($a_N$ = 1.410, $a_{As}$ = 0.772 mT; $I_{As} = \frac{3}{2}$). The appropriate triplet of doublets for the hydroxy adduct ($a_N$ = 1.546, $a_\beta^H$ = 0.272 mT)[17] and the tert-butyl aminoxyl ($a_N$ = 1.458, $a_\alpha^H$ = 1.390 mT) are also present. When it was found that DMPO gave a weak triplet of quartets with only slightly different hyperfine splitting constants (hfsc's) ($a_N$ = 1.444, $a_{As}$ = 0.749 mT) it was realized that the spectra being observed were not due to the simple addition products of the nitrone. Indeed experiments with MNP proved that the triplets of quartets was due to the spin adducts of the nitroso compounds (see Figure 1) formed in the oxidation of the hydroxylamines resulting from the hydrolysis of the spin traps:

$$R\text{-}N{=}O + \cdot AsO_2 \rightarrow R\text{-}N(O\cdot)\text{-}AsO_2 \quad (9)$$

$Me_3C\text{-}N(O\cdot)\text{-}AsO_2$ (I) $a_N$ = 1.410, $a_{As}$ = 0.772

$X\text{-}(CH_2)_2\text{-}C(MeO\cdot)(Me)\text{-}N\text{-}AsO_2$ (II) $a_N$ = 1.444, $a_{As}$ = 0.749 mT (X = CHO or COOH)

The magnitude of the hfsc's of I deserves comment. Firstly the N-hfsc is relatively small which rules out an oxy adduct of $\cdot AsO_2$ and MNP since the N-hfsc should be 2.0-2.6 mT if the triplet of quartets was due to this type of function. In addition it is interesting to note that although the N-hfsc's for the arsenic and phosphorous aminoxyls of similar structure (and the same oxidation state) are not too different (compare I and III[18]), the As-hfsc is somewhat smaller than expected from a comparison of the isotropic coupling constants calculated for the $^{75}As$ and $^{31}P$ nuclei[19] ($a_{As}$ = 1.13 mT calculated based on III):

$Me_3C\text{-}N(O\cdot)\text{-}PO(OH)_2$ (III) $a_N$ = 1.34, $a_P$ = 1.20 mT

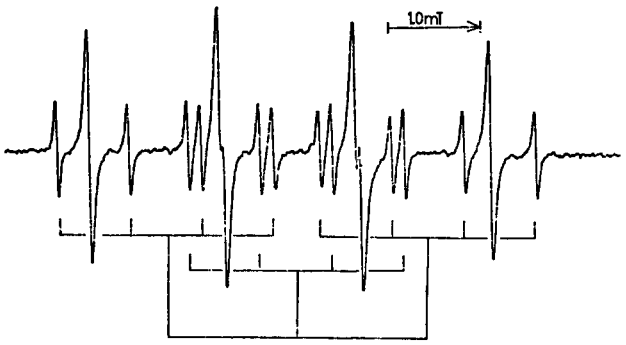



FIGURE 1: ESR spectrum of $Me_3C-\overset{O^{\bullet}}{\underset{|}{N}}-AsO_2$ (1:1:1 triplet of 1:1:1:1 quartets, marked) and $Me_3C-\overset{O^{\bullet}}{\underset{|}{N}}-H$ (1:1:1 triplet of doublets) in aqueous solution made by reaction of $SO_4^{\bullet-}$ from photolysis of $Na_2S_2O_8$ with $NaAsO_2$ in the presence of $Me_3C-N=O$.

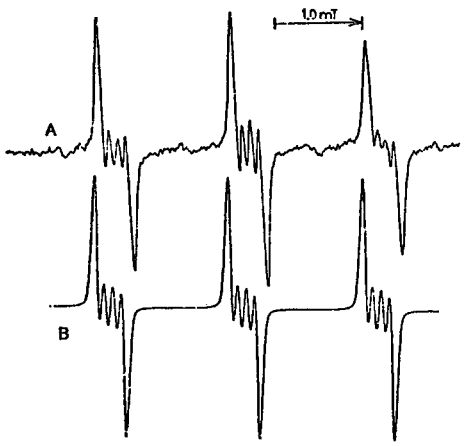
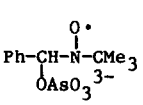



FIGURE 2A: ESR spectrum of $AsO_4^{\bullet-}$ adduct of PBN produced from $SO_4^{\bullet-}$ radicals formed in the photolysis of $Na_2S_2O_8$, and $Na_2HAsO_4$ in aqueous solutions of PBN.

2B: Computer simulated spectrum using the following parameters: $a_N = 1.531$, $a_{As} = 0.096$, $a_{\beta}^{H} = 0.047$, with line width = 0.065 mT. The spectrum could not be simulated without introducing a small doublet splitting of approximately 0.047 mT.

The reaction of $SO_4^{\cdot-}$ with $Na_2HAsO_4$ in the presence of PBN gave the spectrum shown in Figure 2 ($a_N$ = 1.531, $a_{As}$ = 0.096, $a_\beta^H$ = 0.047 mT) but no spin adducts could be observed with MNP. The spectrum is assigned to the oxy adduct of $AsO_4^{\cdot 2-}$:



IV

$a_N$ = 1.531, $a_\gamma^{As}$ = 0.096, $a_\beta^H$ = 0.047 mT

The formation of this spin adduct is visualized as simple trapping of $AsO_4^{\cdot 2-}$ radicals although the reaction of $PBN^{\pm\cdot}$ with $AsO_4^{3-}$ cannot be ruled out at this time.

REFERENCES


1. R. Woods, I.M. Kolthoff and E.J. Meehan, J. Am. Chem. Soc., 1963, 85, 2385.
2. L.J. Csanyi, Disc. Faraday Soc., 1960, 29, 146.
3. L.J. Csanyi, Talanta, 1958, 1, 359.
4. I.S. Ginns, S.P. Misra and M.C.R. Symons, J. Chem. Soc., Dalton Trans., 1973, 2509.
5. A. Reuveni and Z. Luz, J. Magn. Reson., 1974, 16, 339.
6. B. Lamotte, J. Gaillard and O. Constantinescu, J. Chem. Phys., 1972, 57, 3319.
7. W.C. Linand and C.A. McDowell, Mol. Phys., 1964, 7, 223.
8. D. Behar and R.W. Fessenden, J. Phys. Chem., 1972, 76, 1706.
9. D. Behar and R.W. Fessenden, J. Phys. Chem., 1972, 76, 1710; O.P. Chawla and P.W. Fessenden, J. Phys. Chem., 1975, 79, 2693.
10. E.G. Janzen and B.J. Blackburn, J. Am. Chem. Soc., 1968, 90, 5909.
11. E.G. Janzen and R.V. Shetty, Tetrahedron Lett., 1979, 3229.
12. E.G. Janzen and J. I-P. Liu, J. Magn. Reson., 1973, 9, 510.
13. G.R. Chalfont, M.J. Perkins and A. Horsfield, J. Am. Chem. Soc., 1968, 90, 7141.
14. P. Neta, V. Madhavan, H. Zemel and R.W. Fessenden, J. Am. Chem. Soc., 1977, 99, 163.
15. F. Minisci, A. Citterio and C. Giordano, Accounts Chem. Res., 1983, 16, 27.
16. E.G. Janzen and G.A. Coulter, J. Am. Chem. Soc., submitted; E.G. Janzen, R.L. Dudley and R.V. Shetty, J. Am. Chem. Soc., 1979, 101, 243.
17. E.G. Janzen, D.E. Nutter, E.R. Davis, B.J. Blackburn, J.L. Poyer and P.B. McCay, Can. J. Chem., 1978, 56, 2237.
18. H. Karlsson and C. Lagercrantz, Acta Chem. Scand., 1970, 24, 3411.
19. J.R. Morton, J.R. Rowlands and D.H. Whiffen, Natl. Phys. Lab., Gr. Brit., Circ. No. BPR 13. (from P.W. Atkins and M.C.R. Symons, "The Structure of Inorganic Radicals", Elsevier, Amsterdam, 1967, p.21).

*Polyhedron* Vol. 3, No. 5, pp. 635–638, 1984
Printed in Great Britain.

0277–5387/84 $3.00 + .00
Pergamon Press Ltd.

# COMMUNICATION

## A NEW FACILE SYNTHESIS OF CHELATE REAGENT VIA 2-AMINOMETHYLPYRIDINE-Co(III) COMPLEX: 2,3,5,6-TETRA(2-PYRIDYL)PYRAZINE

Yoshihisa Okamoto*, Kuniyoshi Ogura, and Toshio Kinoshita

School of Pharmaceutical Sciences, Kitasato University, 5-9-1, Shirokane, Minato-ku, Tokyo 108, Japan

(Received 4 October 1983; accepted 16 January, 1984)

Abstract: 2-Aminomethylpyridine (1) readily reacted with Co(II) ion to give a chelate complex which reacted with oxygen to form, presumably, a μ-peroxodicobalt(III) complex or a Co(III)-(1) complex, and finally it was transformed to 2,3,5,6-tetra(2-pyridyl)pyrazine.

As a reagent for $Fe^{2+}$ ion, an excellent tridentate chelate compound, 2,3,5,6-tetra(2-pyridyl)pyrazine (2) has been reported which was synthesized in 32% yield by the reaction of α-pyridoin with ammonium acetate at 180°C without using solvent.[1] Also, the compound (2) is of interest because of its stereochemistry of the chelate compound.[1] We report here a new facile synthesis of (2) from 2-aminomethylpyridine (1) using cobaltous chloride and oxygen (air).

### EXPERIMENTAL[2]

A solution of (1) (1 g, 9.2 mmol) in 50 $cm^3$ of water was heated on a water-bath in the presence of cobaltous chloride (1 g, 4.2 mmol) for 3 h. The colour of the solution changed during the reaction; first, blue and finally to reddish-brown, of which the solution contained Co(II) complex of the product (2). The solution was extracted with chloroform (5 times). [The extraction was also carried out from the solution which was made alkaline (above pH 12) by addition of 10% NaOH solution]. The eluate was washed with a small amount of water, and dried over sodium sulphate. The solution was evaporated to dryness under reduced pressure. Chromatography was carried out on silica gel with chloroform-methanol (9:1) as eluent, and (2) was obtained in 48% yield (0.43 g), mp 280–282°C, with 2,4,5-tri-(2-pyridyl)oxazole (3) (a trace amount), mp 140–141°C. It is worth noting that the extracted solution contained only these two products, and also (2) was recrystallized from ethanol-water.

Found: C, 73.93; H, 4.03; N, 21.37. Calc. for $C_{24}H_{16}N_6$ (2): C, 74.21; H, 4.15; N, 21.64%. MS: m/e 388 ($M^+$). For $C_{18}H_{12}N_4O$ (3): Found: C, 71.87; H, 4.23; N, 18.58. Calc. C, 71.99; H, 4.03; N, 18.66%. MS: m/e 300.100 ($M^+$) [Calc. m/e 300.101 ($M^+$)].

RESULTS AND DISCUSSION

The formation of (2) from (1) should depend on intermolecular carbon-carbon bond formation which might be brought about by oxidation of (1). In fact, when the reaction was carried out under a nitrogen stream, the blue colour appeared, but it never changed during the reaction, and the starting amine (1) was recovered after the reaction. Moreover, when 3-aminomethyl-pyridine (and 4-aminomethylpyridine) was employed in this reaction under normal conditions, the starting amine was also recovered. Oxidation of (1) with potassium ferricyanide under a nitrogen stream gave a trace of (2) with many other by-products (checked by TLC), and the starting amine (1) was mostly recovered. These results strongly indicated that chelation between (1) and Co(II) ion, and participation of oxygen are essential to produce (2).

Since it is well known that Co(II)-amino acids (or ammonia) complexes readily react with oxygen to form $\mu$-peroxodicobalt(III) complexes,[3,4] and also it has recently been reported that Ortego and Seymour[5] prepared a series of $\mu$-peroxodicobalt(III) complexes containing pyridyl ligands, it may naturally be accepted that Co(II)-(1) chelate complex (4) readily reacts with oxygen to give (5) which reacts with (4) to give $\mu$-peroxo complex (6). The complex (6) undergoes irreversible reaction to give the cation radical (7) of the ligand as shown in eq. 1.[6] On the other hand, Hammershøi and Sargeson[7] pointed out that the tightness and steric bulk of the ligand structures prevent access of $O_2$ to the hindered Co(II) center. This would suggest that there is a possibility of the formation of Co(III)-(1) complex (8), produced directly from the Co(II) intermediate (4). From this point of view, cation (7) may also generate from (8) where the redoxes are accompanied by stereochemical change involving loss of axial ligands (eq. 2).[8]

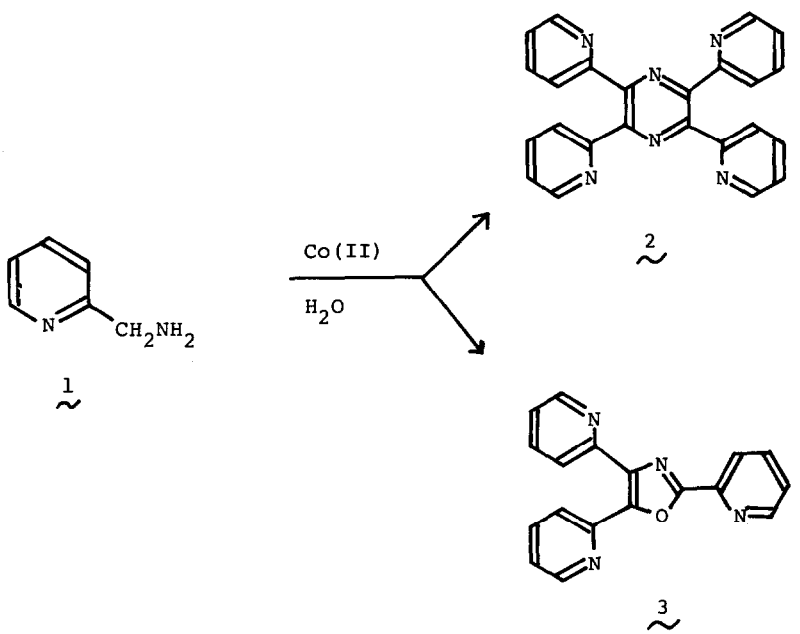
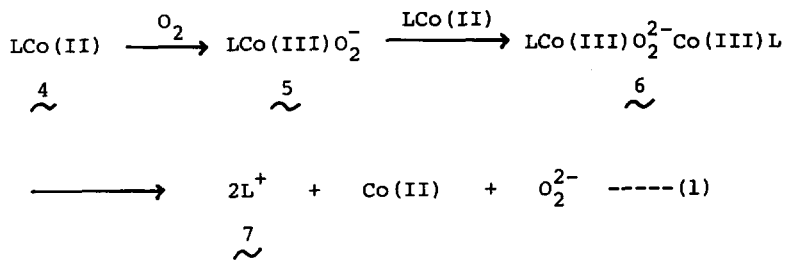
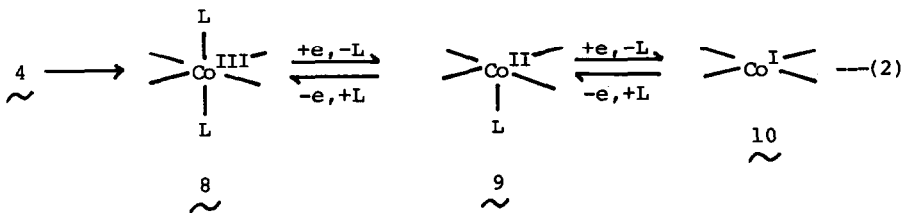



Chart 1


LCo(II)
O2
LCo(III)O2-
LCo(II)
LCo(III)O2 2-Co(III)L
4
5
6
2L+ + Co(II) + O2 2- -----(1)
7


4
L
Co III
L
+e,-L
-e,+L
Co II
L
+e,-L
-e,+L
Co I
---(2)
8
9
10

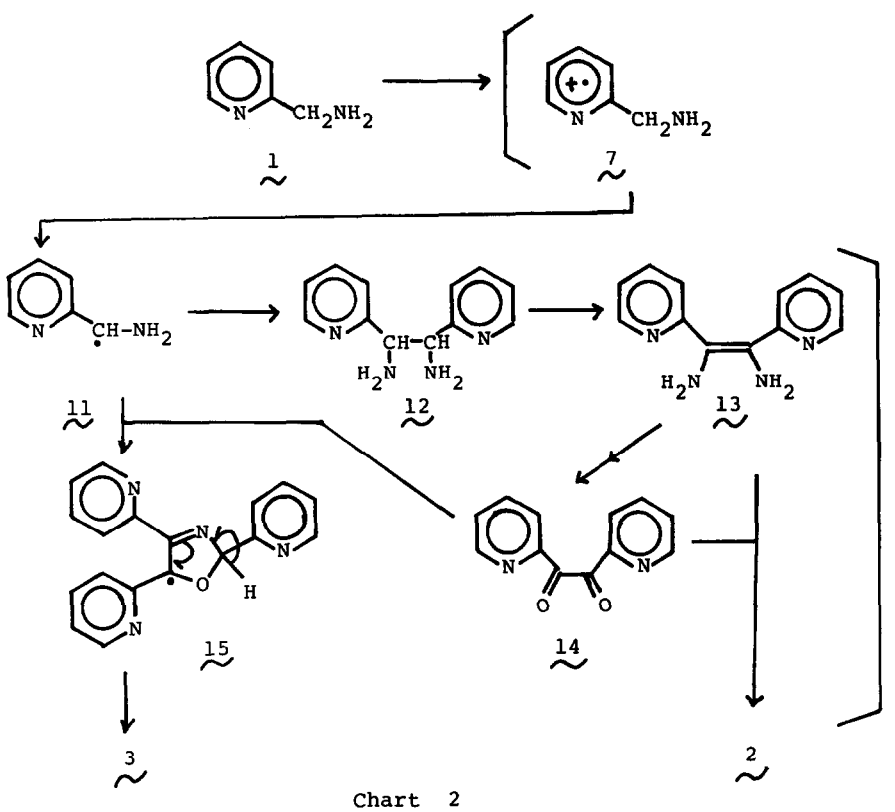
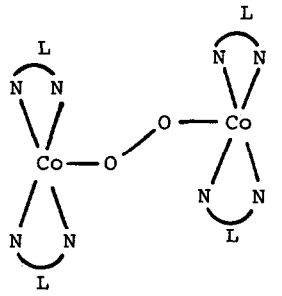

CH2NH2
1
7
CH-NH2
CH-CH
H2N NH2
12
13
11
15
14
3
2

Chart 2



L: 2-Aminomethylpyridine

A Possible Structure of 6

We propose the reaction mechanism in Chart 2. The ligand (1) was oxidized to (7) which was converted to radical (11) by deprotonation. Intermolecular coupling of (11) gave (12) which was again oxidized to (13). Oxidation followed by hydrolysis of (13) gave (14) which reacted with (13) to give (2), while (14) reacted with (11) to give (15) which was dehydrogenated to give (3).

REFERENCES AND NOTES


1. H. A. Goodwin and F. Lions, J. Am. Chem. Soc., 1959, 81, 6415.
2. Melting points were determined using a Yamato Scientific stirred liquid apparatus and uncorrected. Mass spectra were obtained on JMS-01S and DX-300 (equipped with JMA-3100) spectrometers (Japan Electron Optics Laboratory Co., Ltd.). Elementary analyses were performed on a Perkin-Elmer model 240B machine. H-NMR spectra were obtained on a Varian EM-390 spectrometer with tetramethylsilane as an internal standard. Both (2) and (3) in $CDCl_3$ showed signals (multiplets) at 7.10-8.50 ppm and 6.90-10.25 ppm, respectively, due to pyridine ring protons.
3. W. P. Schaefer and R. E. Marsh, J. Am. Chem. Soc., 1966, 88, 178.
   N. G. Vannerberg, Acta Cryst., 1965, 18, 449.
4. D. Burk, J. Z. Hearon, L. Caroline, and A. L. Schade, J. Biol. Chem., 1946, 165, 723.
   J. Z. Hearon, and D. Burk, J. Natl. Cancer Inst., 1949, 9, 337.
   L. Michaelis, Arch. Biochem., 1947, 14, 17.
5. J. D. Ortego and M. Seymour, Polyhedron, 1982, 1, 21.
6. F. Basolo and R. G. Pearson, "Mechanisms of Inorganic Reactions," ed. by John Wiley and Sons, Inc., 1967, p. 641-648.
7. A. Hammershøi and A. M. Sargeson, Inorg. Chem., 1983, 22, 3554.
8. A. M. Bond, G. A. Lawrance, P. A. Lay, and A. M. Sargeson, Inorg. Chem., 1983, 22, 2010, and references therein.

*Polyhedron* Vol. 3, No. 5, p. 639, 1984
Printed in Great Britain.

0277-5387/84 $3.00 + .00
© 1984 Pergamon Press Ltd.

# COMMUNICATION

## EVIDENCE FOR ABSENCE OF AN INVERTED REGION FOR Ru(III)–Ti(III) OUTER-SPHERE ELECTRON-TRANSFER REACTION

**RATHINDRA N. BOSE and JOSEPH E. EARLEY***
Department of Chemistry, Georgetown University, Washington, DC 20057, U.S.A.

(*Received* 18 *August* 1983; *accepted* 10 *October* 1983)

**Abstract**—A lower limit of $10^8\ M^{-1}\ s^{-1}$ was obtained for the 2nd-order rate constant at 25°C for the reduction of $Ru(bpy)_3^{3+}$ by Ti(III) in an aqueous medium of ionic strength 1.0 M and pH range 0–2. The theoretical implications of this result are discussed.

We have previously shown that both $Ti^{3+}$ and $TiOH^{2+}$ reduce certain Ru(III) oxidants by outer-sphere electron-transfer reactions, and that these reactions follow a linear free energy relationship (LFER).[1] On theoretical grounds, [2] it is expected that, as driving force for such reactions increases, an "inverted region" might be reached in which reaction rate decreases as driving force increases. There is some evidence of curvature in the Ru(III)–Ti(III) data previously reported. $Ru(bpy)_3^{3+}$ is a Ru(III) oxidant of the class that exhibits the LFER, and is an oxidant of sufficient potential (1.26 V vs n.h.e.) that its reactions would be expected to be in the inverted region. On the basis of the linear free energy relationship, a 25° rate constant of *ca.* $10^9\ M^{-1}\ sec^{-1}$ is expected for this reaction. If curvature towards an inverted region were to exist, a value of $< 10^6\ M^{-1}\ sec^{-1}$ would be expected.

*tris*-Bipyridylruthenium(III) trichloride was prepared by chlorine oxidation of tris-bipyridylruthenium(III) dichloride in perchloric acid. The extinction coefficient at 418 nm, $3.1 \times 10^3\ cm^{-1}\ M^{-1}$, is in good agreement with the literature.[3] Kinetic studies were performed on a computer-linked Durrum stopped-flow spectrometer. The reaction was followed at 450 nm, by means of increase in absorbance due to formation of $Ru(bpy)_3^{2+}$ in media of ionic strength 1 M and $0.01\ M < [H^+] < 1\ M$. The reaction was >95% complete within the time of mixing (4 ms) both when psuedo-first-order conditions were used at room temperature, and also when second-order conditions were used at 10°C.

On the basis of an upper limit of 1 ms as the half-time of the reaction with each reagent at a concentration of 0.5 mM at 10°C, a lower limit of $10^8\ M^{-1}\ s^{-1}$ is obtained for the 25°C second-order rate constant for reaction of $Ti^{3+}$ or ($TiOH^{2+}$) with $Ru(pby)_3^{3+}$. This high value of the rate constant for this reaction leads to the unexpected conclusion that Ru(III)–Ti(III) reactions of driving force of 1.36 V have not entered an inverted region.

*Author to whom correspondence should be addressed.

## REFERENCES

1. J. E. Earley, R. N. Bose and B. H. Berrie, *Inorg. Chem.* 1983, **22**, 1836.
2. P. Siders and R. A. Marcus, *J. Am. Chem. Soc.* 1979, **103**, 748.
3. J. N. Braddock and T. J. Meyer, *J. Am. Chem. Soc.* 1973, **95**, 158.

*Polyhedron* Vol. 3, No. 5, p. 640, 1984. Pergamon Press Ltd. Printed in Great Britain.

# ERRATUM

G. A. RODLEY, The crystal and molecular structure of bis(*o*-phenylenebisdimethylarsine) cobalt(II) perchlorate. *J. Inorg. Nucl. Chem.* 1967, **29**, 347.

When this result was reported the compound (an orthorhombic form for which only a small amount was available) was thought to have been a cobalt complex. Subsequently it was found that the corresponding nickel compound could be isolated in the same orthorhombic form (as well as in a monoclinic form) but several additional attempts to obtain the orthorhombic form for the cobalt complex failed. This indicated, although it did not prove, that the original sample was a nickel complex. I apologise for reporting the identity and preparation of this crystalline product (for which I was responsible) when neither were as completely documented as indicated in the publication.

*Polyhedron* Vol. 3, No. 6, pp. 641–649, 1984
Printed in Great Britain.

0277–5387/84 $3.00 + .00
Pergamon Press Ltd.

# SYNTHESIS AND CHARACTERIZATION OF COPPER AND NICKEL COMPLEXES OF LIX63 OXIME

**M. E. KEENEY and K. OSSEO-ASARE***
Department of Materials Science and Engineering, The Pennsylvania State University, University Park, PA 16802, U.S.A.

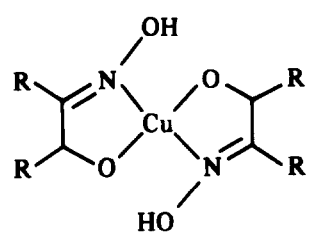
(*Received* 4 *January* 1983; *accepted* 10 *October* 1983)

**Abstract**—Several complexes of 5,8-diethyl-7-hydroxy-6-dodecanone oxime [$H_2L$] with Cu(II) and Ni(II) have been synthesized and characterized by means of a number of techniques including elemental analysis, IR spectra, magnetic susceptibility measurements, electronic absorption spectra, NMR spectra, and mass spectra. The results indicate that Cu(II) and Ni(II) generally form analogous, isomorphous complexes, although no bis-[$H_2L$] complex with Cu(II) has been isolated. $[Cu(L)]_n$ and $[Ni(L)]_n$ are oligomeric complexes with pseudo-octahedral geometry. $[Ni(HL)_2]$ is *cis*-square-planar ($C_{2v}$) with bifurcated hydrogen bridges. $[Ni(H_2L)_3SO_4]$ and $[Cu(H_2L)_3SO_4]$ have octahedral symmetry in which the sulphate is coordinated as a unidentate ligand and the oxime is functioning as a neutral ligand.

The chemical properties of transition metal hydroxyoxime solvent extraction systems have received a considerable amount of attention in recent years. However, most of the studies have been concerned with kinetic and equilibrium extraction properties, and relatively little work has been reported on the characterization of the extracted metal species. Of the reports that have appeared in the literature in which transition metal complexes of hydroxyoxime extractants have been characterized, few have used direct analytical or spectroscopic techniques, rather, the emphasis has been on the use of slope analysis.

In a previous study,[1] it was proposed on the basis of metal distribution and limited spectrophotometric data, that nickel and cobalt form a variety of complexes with 5,8-diethyl-7-hydroxy-6-dodecanone oxime, [$H_2L$], (the active extractant in the commerical solvent extraction reagent **LIX63**, a proprietary product of Henkel Corp.). The suggested complexes contained two or three oxime ligands. It was further proposed that the deprotonated oxime molecules as well as the neutral molecules could serve as ligands. However, none of the complexes were isolated. Accordingly, a study has been initiated on the synthesis and characterization of hydroxyoxime complexes in order to elucidate their full chemical properties. In this paper structures are proposed for the Cu(II) and Ni(II) complexes of [$H_2L$] on the basis of data derived from spectroscopic techniques and several types of physical measurements (e.g. molecular weight determination by vapour pressure osmometry, conductivity and viscosity determinations). Some preliminary results were presented previously.[2]

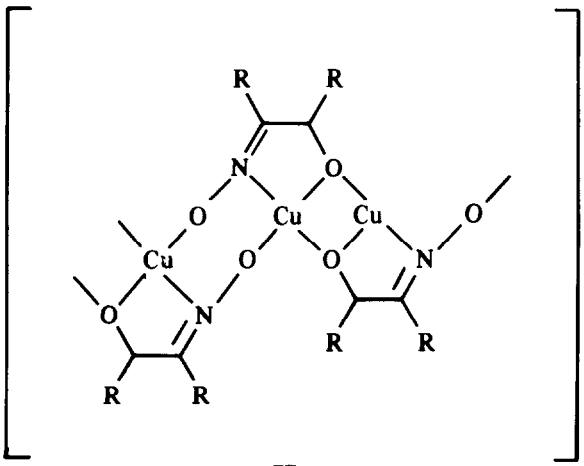
Fritz *et al.*[3] have proposed structures for the Cu(II) complexes of [$H_2L$]. As a result of graphical analyses, it was reported that two complexes are formed depending upon the extraction conditions. The complexes $[Cu(HL)_2]$ and [Cu(L)] were proposed as the preferred species at high and low oxime concentrations respectively. Based on the results of PMR studies, Fritz *et al.*[3] assigned structure (I) to $[Cu(HL)_2]$. In the case of [Cu(L)], a monomeric structure with [O–Cu–O] bonds was suggested in which the oxime functions as a dibasic ligand.




I

*Author to whom correspondence should be addressed.

However, no explanation was given for this unusual bonding in [Cu(L)]. It is well known that Cu(II)-acyloin oxime complexes can have a polymeric structure (II), i.e. $[Cu(L)]_n$.[4]



II

Preston[5] examined the structure of [Cu(L)] in more detail by a variety of analytical and spectroscopic techniques and suggested that the complex is oligomerized according to structure (II) with *n* approximately equal to 10. With the exception of Cu(II), no other polymeric transition metal complexes with $[H_2L]$ have been reported.

Most of the metal complexes of $[H_2L]$ that have been characterized appear to exhibit the typical bidentate five-member ring structure as depicted by (I).[5-7] For example, Flett *et al.*[7] and Preston[5] have examined the Ni(II)–$[H_2L]$ extraction system and concluded that only square-planar $[Ni(HL)_2]$ is formed. However, Tammi[8,9] isolated $[Ni(HL)_2(H_2L)]$ and a complex sulphate salt but did not propose structures for any of the complexes.

## EXPERIMENTAL

5,8-diethyl-7-hydroxy-6-dodecanone oxime, $[H_2L]$, was prepared as described previously.[10] Spectral measurements were made in spectroquality solvents and all other chemicals were reagent grade. Elemental analyses were performed by Galbraith Laboratories, Inc., Knoxville, Tennessee.

*Preparation of metal complexes*

$[Ni(HL)_2]$. An ethanolic solution of $[H_2L]$ (24 $cm^3$; 1.5 g) was added gradually with stirring to an aqueous ammoniacal solution of nickel nitrate (250 $cm^3$; 35.0 g). The orange viscous oil that formed was decanted and extracted with diethyl ether. The organic solution was washed repeatedly with water, dried over anhydrous sodium sulphate and rotary evaporated to give an orange viscous liquid. Found: C 64.66, H 10.77, O 10.36, N 4.53, Ni 9.47%; $C_{32}H_{64}O_4N_2Ni$ requires: C 64.05, H 10.68, O 10.68, N 4.67, Ni 9.80%.

$[Ni(L)]_n$. An acetone solution of $[Ni(HL)_2]$ (100 $cm^3$; 1.0 g) was refluxed under nitrogen purge for 5 min. Water was slowly added (3.5 $cm^3$) and the solution refluxed for an additional 15 min. The dark green precipitate was filtered, washed with acetone and dried under vacuum. Found: C 55.43, H 9.04, N 3.52, Ni 16.38%; $C_{16}H_{31}O_2NNi$ requires: C 58.39, H 9.42, N 4.25, Ni 17.84%.

$[Ni(H_2L)_3SO_4]$. An absolute methanolic solution of $[H_2L]$ (25 $cm^3$; 1.0 g) was added to a refluxing methanolic solution of nickel sulphate (50 $cm^3$; 0.8 g). The pale blue precipitate was filtered, washed alternately with water, methanol and acetone and dried under vacuum. Found: C 59.46, H 10.27, O 16.73, N 4.04, S 3.48, Ni 5.87%; $C_{48}H_{99}O_{10}N_3SNi$ requires: C 59.48, H 10.29, O 16.51, N 4.33, S 3.31, Ni 6.05%.

$[Cu(L)]_n$. A hexane solution of $[H_2L]$ (100 $cm^3$; 2.5 g) was used to extract an aqueous ammoniacal cupric nitrate solution (100 $cm^3$; 50.0 g). The organic layer was washed with water and the volume reduced to 10 $cm^3$ by rotary evaporation. Acetone was added (100 $cm^3$) and the dark green precipitate was filtered, washed with hot acetone and ethanol and dried under vacuum. Found: C 58.8, H 9.36, O 6.80, N 3.96, Cu 20.93%; $C_{16}H_{31}O_2NCu$ requires: C 57.72, H 9.31, O 9.61, N 4.21, Cu 19.07%.

$[Cu(H_2L)_3SO]$. A quantity of finely ground copper sulphate (5.0 g) was added to a hexane solution of $[H_2L]$ (25 $cm^3$; 1.0 g) and refluxed for 2 hr. The organic solution was filtered and acetonitrile added (30 $cm^3$). The pale blue precipitate was filtered, washed alternately with water and acetonitrile and dried under vacuum. Found: C 58.91, H 10.30, O 16.02, N 4.30, S 3.37, Cu 6.59%; $C_{48}H_{99}O_{10}N_3SCu$ requires: C 59.21, H 10.17, O 16.43, N 4.31, S 3.29, Cu 6.52%.

*Physical measurements*

High pressure liquid chromatographic analyses (HPLC) were made with a Waters M-6000A liquid chromatograph equipped with an ultraviolet (254 nm) detector. The packing was Poropac Q in a 61 cm X 0.64 cm O.D. column. A hexane/$CH_2Cl_2$ (90/10) solvent system was used at a flow rate of 1 $cm^3$ $min^{-1}$. Samples injected were 10 $\mu$l of an approx. 10 wt.% solution. Thin layer chromatographic analyses (TLC) were made with Gelman ITLC-SA plates using 2,2,4-trimethylpentane for developing.

Molecular weights were determined in toluene at 37°C by vapour pressure osmometry (VPO) using a Wescan 200 molecular weight apparatus. Selected complexes were analyzed by Galbraith Laboratories, Inc. for verification of the VPO results.

Differential scanning calorimetric measurements (DSC) were conducted using a Perkin–Elmer DSC-1B calorimeter. Thermal gravimetric analyses (TGA) were recorded with an Ainsworth RV automatic semi-microbalance coupled with a tube furnace equipped with a Leeds and Northrup Series 60 temperature controller.

Conductance measurements on $1 \times 10^{-3}$ mol dm$^{-3}$ nitrobenzene solutions were made at room temperature using a YSI 31 conductivity bridge with a YSI 3400 conventional closed type conductivity cell.

Viscosity measurements were made using hexane solutions in a Cannon 75-K461 or a Cannon 100-F841 viscometer thermostatted at 25°C in a constant temperature bath.

Magnetic susceptibilities were determined at 25°C using a Gouy apparatus consisting of a Mettler H-16 balance combined with a Varian V-4005 electromagnet and a Varian V-2900 power supply. All samples were measured as powdered solids or neat liquids.

*Spectral measurements*

IR spectra were recorded on a Perkin–Elmer 283B grating spectrophotometer using 0.1 mm pathlength NaCl cells or in KBr discs prepared from IR spectroquality powder. X-Ray powder diffraction patterns were recorded as thin films on glass slides on a Rigaku Geigerflex diffractometer with monochromated CuKα radiation using a Ni filter.

Electronic absorption spectra were recorded with a Cary 17 spectrophotometer using 1 cm pathlength quartz cells. NMR spectra were recorded at 24°C on either a Varian EM360 (60 MHz), a JOEL-PS-100-FT (100 MHz) or a Bruker WP-200 (200 MHz) spectrometer. All samples were referenced internally to TMS and downfield chemical shifts are reported as positive. $^2$HNMR spectra utilized hexafluorobenzene as the internal lock substance. Mass spectra were recorded with an AEI MS902 or a Finnigan 3200 GC–MS mass spectrometer. ESR spectra were recorded with a Varian Century E4 spectrometer at room temperature and at 77K. Samples were run either as powders or in hexane solution.

## RESULTS AND DISCUSSION

*Physical properties*

A few selected physical properties of the isolated metal hydroxyoxime complexes are listed in Table 1. As indicted, Cu(II) and Ni(II) form analogous isomorphic complexes with [$H_2$L]. However, despite previous reports[3,5] and repeated efforts, it was not possible to isolate the bis-[$H_2$L] complex with Cu(II), [Cu(HL)$_2$]. The purity of the complexes was confirmed by TLC or HPLC. With the exception of [Ni(HL)$_2$], all the complexes are stable in air and are quite soluble in chloroform, benzene, toluene and hexane. [Ni(HL)$_2$] slowly hydrates in moist air to form the bis-aquo adduct.[13] [Cu(L)]$_n$ and [Ni(L)]$_n$ are oligomerized in solution with association numbers of seven and five respectively in

Table 1. Selected physical properties of metal oxime complexes

| Complex | Color | Form | MW[a] | mp(°C) | λ[e] |
|---|---|---|---|---|---|
| [Cu(L )]$_n$ | green | amorphous solid | 2350[b] (333) | 202 | 1.63 |
| [Ni(L)]$_n$ | olive | amorphous solid | 1642[c] (329) | | 1.56 |
| [Ni(HL)$_2$] | orange | viscous liquid | 606 (599) | -20 | 11.76 |
| [Cu(H$_2$L)$_3$SO$_4$] | pale blue | amorphous solid | 1009 (973)[d] | 110 | 9.21 |
| [Ni(H$_2$L)$_3$SO$_4$] | pale blue | amorphous solid | 1044 (969) | 220 dec | |

a VPO results in toluene. Calculated values (for monomers) in parentheses.

b n∿7

c n∿5

d Determined as 997 by Galbraith Laboratories, Inc.

e Molar conductance (λ; ohm$^{-1}$ cm$^2$ mol$^{-1}$) as 1 x 10$^{-3}$ mol dm$^{-3}$ nitrobenzene solution at 25°C.

toluene. This is consistent with previous reports on the solution polymerization of $[Cu(L)]_n$.[5] The other complexes essentially are monomeric in solution, however, $[Ni(H_2L)_3SO_4]$ and $[Cu(H_2L)_3SO_4]$ form extremely viscous solutions indicative of intermolecular association as shown by the viscosity results in Fig. 1 for the Ni(II) complex. Molar conductance values in nitrobenzene were all in the range 1–13 $\Omega^{-1}$ cm$^2$ mol$^{-1}$ indicating the complexes are all non-electrolytes.

*Thermal analyses*

The thermal analyses of the metal oxime complexes indicate that generally there is decomposition, or melting followed by decomposition (Table 1) in which the oxime ligands are oxidized initially in the temperature range of approx. 150–500°C. Above 500°C the complexes eventually convert to either $Ni_2O_3$ or CuO as verified by the X-ray powder patterns of the thermal residues following acetone wash. These results are in reasonable agreement with the thermoanalytical results listed in Table 2 for several of the complexes.

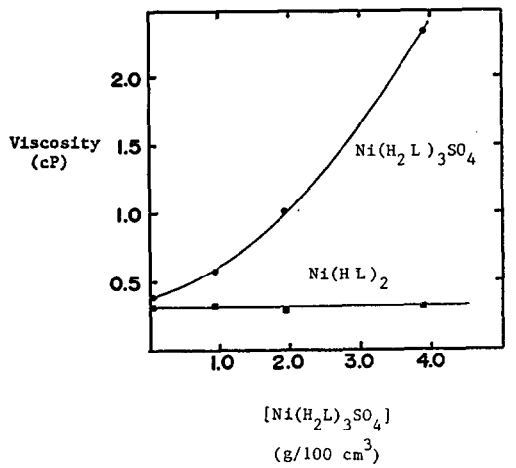



Fig. 1. Viscosities of hexane solutions of $[Ni(HL)_2]$ and $[Ni(H_2L)_3SO_4]$ at 25°C.

Table 2. Thermolysis data for metal–oxime complexes

| Temperature °C | % Weight Loss[a] Found | Calculated | Composition[b] |
|---|---|---|---|
| 25 | ---- | ---- | $[Cu(L)]_n$ |
| 600 | 80.9 | 76.1 | CuO |
| 25 | ---- | ---- | $[Ni(HL)_2]$ |
| 600 | 81.4 | 87.5 | $Ni_2O_3$ |
| 25 | ---- | ---- | $[Cu(H_2L)_3SO_4]$ |
| 600 | 90.2 | 91.8 | ---- |
| 25 | ---- | ---- | $[Ni(H_2L)_3]SO_4$ |
| 600 | 88.7 | 92.3 | ---- |

[a] Samples approximately 100 mg.
[b] Oxide determined by X-ray analysis.

Similar results have been reported for other hydroxyoxime complexes with transition metals.[12] $[Ni(H_2L)_3SO_4]$ and $[Cu(H_2L)_3SO_4]$ appear to convert to the inorganic sulphate salt and free $[H_2L]$ shortly after melting as observed during melting point determinations. Washing of the residue with hot water results in either $[Cu(aq)]^{2+}$ or $[Ni(aq)]^{2+}$ as determined by atomic absorption measurements. DTA and TGA analyses of $[Ni(HL)_2]$ indicate a structural rearrangement prior to decomposition. Thermal studies of $[Ni(HL)_2]$ are described in detail elsewhere.[11]

*IR spectra*

The IR spectra of the analogous Cu(II) and Ni(II) complexes are virtually identical suggesting similar structural symmetry. The frequencies of some significant bands of the free ligands and of the metal complexes are reported in Table 3. The assignments are made on the basis of literature data for other metal–hydroxyoxime complexes.[10,11,13–17]

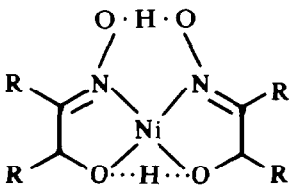
Examination of the IR spectral results (Table 3) for the metal complexes shows that the hydroxyl proton generally is lost upon coordination to the metal and the band at 3320 cm$^{-1}$ due to the

Table 3. IR spectral data[a] (cm$^{-1}$)

| Complex | $\nu_{NO-H}$ | $\nu_{CO-H}$ | $\nu_{C=N}$ | $\nu_{N-O}$ | $\nu_{C-O}$ | $\delta_{O-H}$ |
|---|---|---|---|---|---|---|
| $[H_2L]$ | 3320 st br | 3600 sp | 1650 br | 950 w | 1105 s | 1270 m |
| $[Cu(L)]_n$ | ---- | ---- | 1590 m | 960 w | 1110 s | ---- |
| $[Ni(L)]_n$ | ---- | ---- | 1580 m | 950 w | 1115 s | ---- |
| $[Ni(HL)_2]$ | ---- | ---- | 1570 m | 920 w | 1115 s | 1250 m |
| $[Cu(H_2L)_3SO_4]$ | 3000 st br | 3600 sp | 1645 br | 910 w | 1105 s | 1250 m |
| $[Ni(H_2L)_3SO_4]$ | 2900 st br | 3600 sp | 1645 br | 915 w | 1105 s | 1250 m |

[a] Spectra in $CCl_4$ (4000–600 cm$^{-1}$)
st = strong; m = medium; w = weak; sp = sharp; br = broad

hydroxyl proton of the oxime group is shifted considerably, indicative of strong hydrogen bridging.[14] Both hydroxyl protons are lost from $[Cu(L)]_n$ and $[Ni(L)]_n$ as a result of the polymerization of the complexes; however, neither of the hydroxyl protons is lost in $[Ni(H_2L)_3SO_4]$ and $[Cu(H_2L)_3SO_4]$, confirming that the hydroxyoxime is coordinating to the metals as a neutral ligand. $[Ni(HL)_2]$ is unusual in that both the $\nu_{NO-H}$ and $\nu_{CO-H}$ bands disappear completely suggesting that the OH vibrational modes have become infrared inactive. This can be explained by considering a complex of structure (III) ($C_{2v}$ symmetry) in which vibrations of the bifurcated hydrogen bridges result in no net change in the dipole moment of the complex.

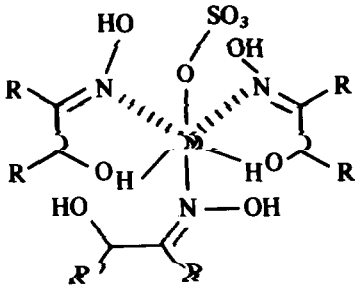


III

The presence of two non-equivalent hydroxyl protons is confirmed by the PMR spectrum of $[Ni(HL)_2]$ (discussed below) which shows two sharp singlets at 12.4 and 17.5 ppm.

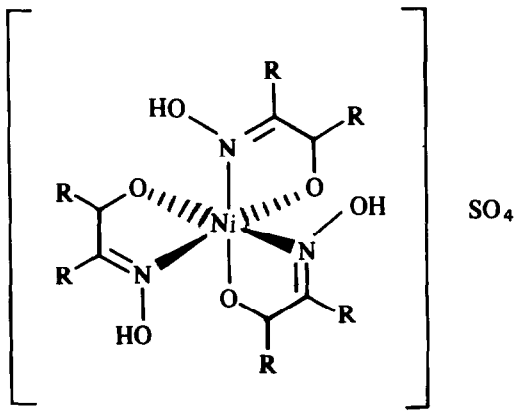
The C=N stretching frequency in the ligand generally is shifted to lower wave numbers upon coordination to the metal. This shifting is a result of metal to ligand ($d \rightarrow \pi$) back bonding stabilizing the nitrogen–metal $\sigma$-bond.[12,14,18] However, the shifting is only observed in the complexes in which the hydroxyl proton is lost. No significant shift in the $\nu_{CN}$ band is observed in $[Cu(H_2L)_3SO_4]$ or $[Ni(H_2L)_3SO_4]$ in which the oxime is functioning as a neutral ligand. This indicates that the $d \rightarrow \pi$ back bonding is not occuring in the protonated ligand complexes, suggesting that there is a bonding electronic problem inhibiting the metal to ligand charge transfer in $[Ni(H_2L)_3SO_4]$ and $[Cu(H_2L)_3SO_4]$ upon protonation of the oxygen of coordinated $[H_2L]$. This is reflected by a loss of the charge transfer bands in the electronic absorption spectra of these complexes (see below).

The solubility of $[Ni(H_2L)_3SO_4]$ and $[Cu(H_2L)_3SO_4]$ in nonpolar solvents and their nonelectrolyte properties in nitrobenzene indicate that in both complexes the sulphate ion is coordinated directly to the metal. The presence of three S–O stretching modes at 1120 ($\nu_{3a}$), 1025 ($\nu_{3b}$) and 980 ($\nu_1$) in the infrared spectra of these complexes confirms that the sulphate is functioning as a unidentate ligand[19] and suggests that $[Ni(H_2L)_3SO_4]$ and $[Cu(H_2L)_3SO_4]$ have octahedral structures (IV).



IV

This complex structure has a large number of hydroxyl groups capable of intermolecular hydrogen bonding and fully explains the significant shifting of the $\nu_{OH}$ IR bands and the increased viscosity of solutions of these complexes. However, it is observed that $[Ni(H_2L)_3SO_4]$ is insoluble in the more polar organic solvents such as acetone, methyl ethyl ketone and acetonitrile. Once the complex is precipitated it will not redissolve in the nonpolar organic solvents even under reflux conditions. The IR spectrum (KBr disc) of the insoluble form of $[Ni(H_2L)_3SO_4]$ has a single broad band at 950 $cm^{-1}$ characteristic of uncoordinated sulphate ion.[20] This suggests that the sulphate has been displaced from the metal to give a complex salt of structure (V) in which the unidentate hydroxyoxime ligand has chelated to achieve a coordinately saturated complex. The refractive indices of $[Ni(H_2L)_3SO_4]$ and $[Ni(H_2L)_3]SO_4$ are the same (1.495) but the measured densities are slightly different as shown in Table 4 listing some of the physical properties of the complexes. The X-ray powder patterns indicate that both complexes are



V

Table 4. Physical properties of $[Ni(H_2L)_3SO_4]$ and $[Ni(H_2L)_3]SO_4$

| | |
|---|---|
| $[Ni(H_2L)_3SO_4]$ - $C_{48}H_{99}O_{10}N_3SNi$ | |
| Anal. C 59.46, H 10.49, O 16.73, N 4.04, S 3.48, Ni 5.87% | |
| ρ = 1.01; n = 1.495; BCC: a = 18.6 A° | |
| $[Ni(H_2L)_3]SO_4$ - $C_{48}H_{99}O_{10}N_3SNi$ | |
| Anal. C 60.58, H 10.50, O 16.68, N 4.11, S 2.66, Ni 5.30% | |
| ρ = 1.04; n = 1.495; BCC: a = 18.7 A° | |

BCC structured in the solid state with only a slight difference in the dimensions and volume of the unit cell. Elemental analyses for both complexes are in agreement with the calculated values.

*Magnetic and electronic spectral studies*

The magnetic and electronic spectral properties of the metal oxime complexes are given in Tables 5 and 6 respectively along with the probable assignments for the electronic transitions based on available literature data.[12,18-21] The electronic spectra in the UV region generally show bands characteristic of intraligand $\pi \rightarrow \pi^*$ transitions and charge transfer bands[12,18] and the spectra of all the complexes obey Beer's Law over large concentration regions.

Table 5. Magnetic susceptibilities (X) and magnetic moments ($\mu_{eff}$)[a]

| Complex | X(x10$^6$cgs) | $\mu_{eff}$ (B.M.) |
|---|---|---|
| $[Cu(L)]_n$ | 173 | 0.65 |
| $[Ni(L)]_n$ | 1425 | 1.87 |
| $[Ni(HL)_2]$ | diamagnetic | 0 |
| $[Cu(H_2L)_3SO_4]$ | 1835 | 2.10 |
| $[Ni(H_2L)_3SO_4]$ | 4360 | 3.24 |

[a] 298 K

$[Cu(L)]_n$ and $[Ni(L)]_n$ exhibit anomalously low magnetic moments indicative of anti-ferromagnetic interaction as a result of their oligomeric behaviour. The electronic absorption spectra suggest octahedral geometry for the complexes. This result is consistent with the expected axial interactions with neighboring ligands in order to achieve a coordinately saturated structure. The intense bands near 350 nm have been tentatively assigned to metal-to-ligand charge transfer (MLCT) since $[H_2L]$ exhibits only very weak bands in the UV region.

Octahedral geometry also is indicated for $[Ni(H_2L)_3SO_4]$ by the presence of three principal bands of low intensity in the electronic absorption spectrum.[21] Their assignments, shown in Table 6, are in agreement with those predicted for the energy level diagram for Ni(II) in octahedral symmetry.[21,22] Furthermore, the calculated $\nu_1/\nu_2$ ratio of 1.72 for $[Ni(H_2L)_3SO_4]$ is a distinguishing feature of octahedral Ni(II) complexes.[12,18] The magnetic moment (3.24 B.M.) is above the spin only value of 2.83 B.M. indicating an orbital contribution to the octahedral $^3A_{2g}$ ground state or a spin orbit coupling of the $^3A_{2g}$ and $^3T_{2g}$ terms. However, we have been unable to obtain an ESR spectrum of this complex in order to more closely examine this phenomenon.

The diamagnetism of $[Ni(HL)_2]$ indicates that this complex is square-planar. The electronic ab-

Table 6. Electronic absorption spectral data

| Complex | $\lambda_{max}$(nm) | ε(1 mole$^{-1}$cm$^{-1}$) | Probable Assignment |
|---|---|---|---|
| $[Cu(L)]_n$ | 610 | 344 | $^2B_{1g} \rightarrow {}^2A_{1g}$ |
| | 425 | 3280 | $^2B_{1g} \rightarrow {}^2E_{1g}$ |
| | 350 | 1390 | MLCT |
| $[Ni(L)]_n$ | 595 | 30 | $^3A_{2g} \rightarrow {}^3T_{1g}(F)$ |
| | 510 sh | 46 | $^3A_{2g} \rightarrow {}^3T_{1g}(P)$ |
| | 350 | 480 | MLCT |
| $[Ni(HL)_2]$ | 530 sh | 48 | $^3T_{1g} \rightarrow {}^3A_{2g}$ (see text) |
| | 455 | 143 | $^1A_{1g} \rightarrow {}^1A_{2g}$ |
| | 305 sh | 4080 | MLCT |
| | 295 | 4620 | MLCT |
| $[Cu(H_2L)_3SO_4]$ | 775 | 65 | $d_{z^2} \rightarrow d_{x^2-y^2}$ |
| | 290 sh | 99 | |
| $[Ni(H_2L)_3SO_4]$ | 1050 | 8 | $^3A_{2g} \rightarrow {}^3T_{2g}(F)$ |
| | 608 | 8 | $^3A_{2g} \rightarrow {}^3T_{1g}(F)$ |
| | 360 | 25 | $^3A_{2g} \rightarrow {}^3T_{1g}(P)$ |

sorption spectrum for this complex is typical of square-planar Ni(II) as indicated by the assignments in Table 6. However, the shoulder observed at 530 nm in $[Ni(HL)_2]$ is extremely sensitive to solvation effects and appears to be due to tetrahedral distortion of the square-planar structure as a result of steric hindrance in the complex.[23] This band is probably assignable to the $^3T_{1g} \rightarrow {}^3A_{2g}$ ligand field transition as a result of the tetrahedral distortion of nickel (II). The strong band at 295 nm in $[Ni(HL)_2]$ is probably due to metal to ligand charge transfer through $\pi$-bonding of the $d\pi$–$p\pi$ type previously described in the discussion of the IR spectra.

The magnetic moment of $[Cu(H_2L)_3SO_4]$ is typical for Cu(II) complexes. The electronic absorption spectrum of $[Cu(H_2L)_3SO_4]$ exhibits a single broad band of weak intensity at 775 nm suggesting a tetragonally distorted octahedral geometry. Unlike the other transition metal complexes, however, both $[Cu(H_2L)_3SO_4]$ and $[Ni(H_2L)_3SO_4]$ have very weak bands in the 300–400 nm region characteristic of $d_\pi \rightarrow p_\pi$ charge transfer for chelated hydroxyoxime ligands. It appears that the protonation of the oximic oxygen of the coordinated hydroxyoxime ligand results in a rehybridization of oxime orbitals eliminating the $\pi^*$ antibonding orbital which is responsible for the $\pi$-acceptor properties of the deprotonated ligand. As a result no $d \rightarrow \pi$ back bonding is possible.

*PMR and mass spectra*

The proton magnetic resonance and mass spectral data for the metal oxime complexes are presented in Table 7. The data for $[H_2L]$ were presented previously.[10] The paramagnetism of the Cu(II) complexes and the Ni(II) octahedral complexes (Table 5) generally results in the proton peaks being broad and poorly resolved while the mass spectra of the Ni(II) and Cu(II) complexes with $[H_2L]$ do not show a parent peak. However, significant structural information is provided by the PMR and mass spectra.

The PMR spectra of $[Cu(H_2L)_3SO_4]$ and $[Ni(H_2L)_3SO_4]$ clearly indicate that both the hydroxyl and oxime protons are retained upon coordination of the oxime to the metal and the broad oximic proton at 38 ppm in $[Ni(H_2L)_3SO_4]$ is split into a triplet ($J_{N\text{-}H} \sim 4$Hz) as a result of proton coupling with the adjacent nitrogen atom.[24] The similarity of the mass spectra of the Cu(II) and Ni(II) tris-oximato complexes supports the isostructural symmetry previously suggested based on their IR spectra. Furthermore, the absence of significant mass fragments above *m/e* 270 (corresponding to $[HL]^+$) suggests that a significant portion of the observed mass fragments is due to fracture of the coordinated ligand as indicated by the similarity of the chemical ionization mass spectra of $[H_2L]$ and $[Ni(H_2L)_3SO_4]$ shown in Fig. 2.

Table 7. PMR and mass spectral data

| Complex | $^1$HNMR [a] | | Mass Spectral Data [b] |
|---|---|---|---|
| | N-O(H) | C-O(H) | |
| $[H_2L]$ | [c] | 6.1 | [d] |
| $[Cu(L)]_n$ | ------ | ------ | 269(80); 253(25); 235(25); 223(100) |
| $[Ni(L)]_n$ | ------ | ------ | 269(80); 253(20); 235(20); 223(100) |
| $[Ni(HL)_2]$ | 17.5 s | 12.4 s | 270(25); 173(40); 126(100); 99(30); 69(75); 57(95) |
| $[Cu(H_2L)_3SO_4]$ | 38 br | 17 br | 270(5); 173(100); 157(20); 142(10); 127(100) |
| $[Ni(H_2L)_3SO_4]$ | 38 t br | 17 br | 270(5); 173(100); 157(20); 139(10); 127(100) |

a Values given are in ppm measured in $CDCl_3$ solution. Samples are referenced to $(CH_3)$ Si. s = singlet; t = triplet, br = broad.

b Values in parenthesis are relative intensities. Values in brackets are isotopic distribution of parent ion from electron impact mass spectrum

c Proton resonance unobserved.

d See Reference 10.

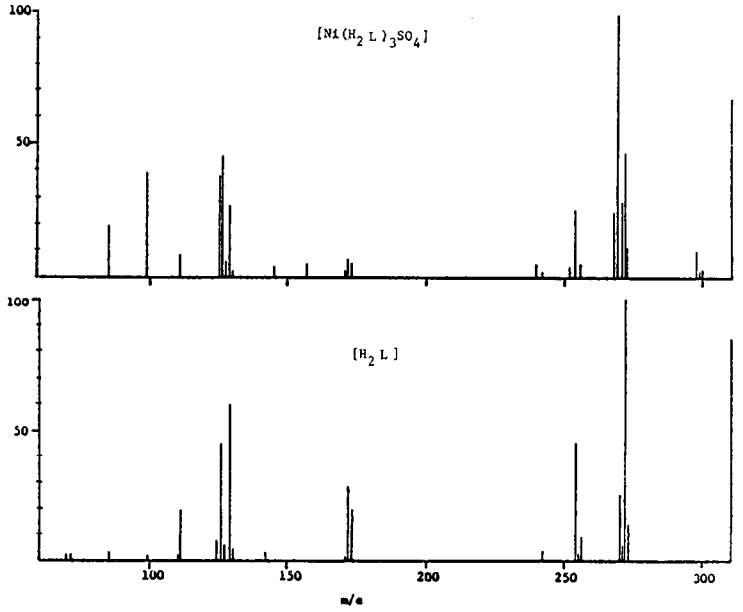
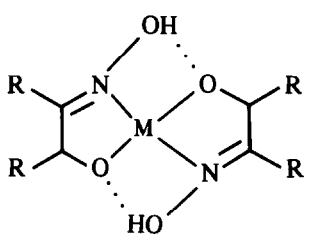



Fig. 2. Chemical ionization mass spectra of $[H_2L]$ and $[Ni(H_2L)_3SO_4]$.

$[Cu(L)]_n$ and $[Ni(L)]_n$ show no hydroxyl protons in the PMR spectra confirming the loss of both the N–OH and C–OH protons upon coordination of $[H_2L]$ to the metal and oligomerization of the complexes. As with the tris-oxime complexes mentioned above, the mass spectra of $[Cu(L)]_n$ and $[Ni(L)]_n$ are nearly identical, suggesting similar structures for the complexes.

The PMR spectrum of $[Ni(HL)_2]$ has two sharp singlets at 12.4 and 17.5 ppm attributable to non-equivalent hydroxyl protons. The large downfield chemical shift of these proton resonances indicates that they are very strongly hydrogen bonded.[24] No proton exchange occurs upon contacting concentrated solutions of $[Ni(HL)_2]$ in hexane with $D_2O$ for 2 hr; however, both protons are immediately replaced by $CD_3OD$ in $CCl_4$. Solvation effects on the bridging protons are discussed in more detail elsewhere.[23] The strength of the hydrogen bridges and the extent of the proton deshielding support the bifurcated hydrogen bridged structure (**III**) proposed above for $[Ni(HL)_2]$. The complex appears to have a distorted square-planar structure in which the ligands are coordinated in a *cis*-configuration ($C_{2v}$ symmetry). In contrast to structure (**III**), *trans*-configuration of the ligands ($D_{2h}$ symmetry) should result in the hydroxyl protons being equivalent and a single downfield proton resonance would be expected (**VI**).




**VI**

*Acknowledgements*—This research was supported by the National Science Foundation under Grant No. CPE8110756. M.E.K. acknowledges fellowship support by the Mining and Mineral Resources Research Institute, The Pennsylvania State University.

## REFERENCES

1. D. R. Renninger and K. Osseo-Asare, *Metall. Trans. B* 1983, **14**, 41.
2. M. E. Keeney and K. Osseo-Asare, Proc. Int. Solvent Extr. Conf., 1980, **1**, Paper 80–53, Assoc. Ing. Univ. Liege, Liege, Belgium.
3. J. S. Fritz, D. R. Beuerman and J. J. Richard, *Talanta* 1971, **18**, 1095.
4. G. Rindorf, *Acta Chem. Scand.* 1971, **25**, 774.
5. J. S. Preston, *J. Inorg. Nucl. Chem.* 1975, **37**, 1235.
6. D. S. Flett, M. Cox and J. D. Heels, *J. Inorg. Nucl. Chem.* 1975, **37**, 2533.
7. D. S. Flett, M. Cox and J. D. Heels, *Proc. Int. Solvent Extr. Conf.* 1974 **3**, 2560.
8. T. T. Tammi, *Tutkimus Tek.* 1976, **4**, 44.
9. T. T. Tammi, *Hydrometallurgy* 1977, **2**, 371.
10. M. E. Keeney and K. Osseo-Asare, *Hydrometallurgy*, in press.

11. M. E. Keeney, Ph.D. Thesis. The Pennsylvania State University, University Park, Pennsylvania (1981).
12. K. S. Bhave and R. B. Kharat, *J. Inorg. Nucl. Chem.* 1980, **42**, 977.
13. K. Burger and I. Egyed, *J. Inorg. Nucl. Chem.* 1965, **27**, 2361.
14. K. Burger, F. Ruff, I. Ruff and I. Egyed, *Acta Chim.* 1965, **46**, 1.
15. K. K. Ramaswamy, C. I. Jose and D. N. Sen, *Indian J. Chem.* 1967, **5**, 156.
16. K. Nakamoto, M. Margoshes and R. E. Rundel, *J. Am. Chem. Soc.* 1955, **77**, 6480.
17. R. E. Rundel and M. Parasol, *J. Chem. Phys.* 1952, **20**, 1487.
18. V. D. Khanolkar and D. D. Khanolkar, *Indian J. Chem.* 1979. **184**, 315.
19. F. A. Cotton and G. Wilkinson, *Advanced Inorganic Chemistry*. Wiley, New York (1972).
20. F. Holmes, G. Lee and A. E. Underhill, *J. Chem Soc.* 1971, 999.
21. L. Sacconi, *Trans. Met. Chem.* 1968, **4**, 199.
22. A. D. Liehr and C. J. Ballhausen, *Ann Phys.* 1969, **6**, 134.
23. M. E. Keeney and K. Osseo-Asare, *Polyhedron*, summitted.
24. R. M. Silverstein, G. C. Bassler and T. C. Morrill, *Spectrometric Identification of Organic Compounds*. Wiley, New York (1974).

*Polyhedron* Vol. 3, No. 6, pp. 651–659, 1984
Printed in Great Britain.

0277–5387/84 $3.00 + .00
© 1984 Pergamon Press Ltd.

# PENTACOORDINATE IRON(III) PORPHYRIN CARBOXYLATES: SYNTHESIS, PHYSICOCHEMICAL CHARACTERISTICS AND X-RAY CRYSTAL STRUCTURE OF ACETATO(5, 10, 15, 20-TETRAPARATOLYLPORPHYRINATO) IRON(III)

**HASSAN OUMOUS, CLAUDE LECOMTE and JEAN PROTAS**
Laboratoire de Minéralogie et Cristallographie (ERA 162), Faculté des Sciences, Centre de 2ème Cycle, B. P. 239, 54506 Vandoeuvre les Nancy, France

**and**

**PANAYOTIS COCOLIOS and ROGER GUILARD***
Laboratoire de Synthèse et d'Electrosynthèse Organométallique associé au C.N.R.S. (LA 33), Faculté des Sciences "Gabriel", 6, Bd Gabriel, 21100 Dijon, France

(*Received* 3 *May* 1983; *accepted* 10 *October* 1983)

**Abstract**—Carboxylatoiron(III) porphyrins have been synthesised by the action of carboxylic acids on the $[(por)Fe]_2O$ dimers. $^1H$ NMR and ESR data of the isolated products are in accordance with pentacoordinate high spin 5/2 ferric complexes, the iron atom being displaced out of the plane of the porphyrin ligand. IR spectra show $\nu(C{=}O)$ and $\nu(C{-}O)$ bands separated by 356–409 $cm^{-1}$. The magnitude of this separation suggests coordination between the metal centre and the carboxylate group via one oxygen atom. Magnetic susceptibility measurements from 5 to 120 K lead to the value of $\mu = 5.88$ B.M.. The X-ray structure of acetato (5, 10, 15, 20-tetra *p*-tolyporphyrinato) iron(III) confirms the above deductions. (t*p* MePP) $Fe(CO_2CH_3)$. 0.5 $CH_3COOH$ crystallises in the *I*2/c space group with unit cell parameters $a = 24.464(8)$, $b = 9.332(3)$, $c = 37.174(4)$ Å, $\beta = 90.49(2)°$, $V = 8485$ Å$^3$, $D_c = 1.27$ g·cm$^{-3}$ and $Z = 8$. The crystal structure was refined to a conventional $R(F) = 0.0584$ and $R_w(F) = 0.0653$ for 5132 unique reflections with $F_0 > 3\sigma(F_0)$. The iron atom is pentacoordinated by the four nitrogen atoms and one oxygen atom of the acetate group. It lies at 0.520(1) Å out of the porphinato plane and 0.485(1) Å out of the four nitrogen plane. The Fe–O bond length is 1.898(4) Å.

Synthesis, solution study and solid state structural characterisation of metalloporphyrins with oxygenated axial ligands are of great current interest. Such model compounds provide a structural framework for understanding the nature of the iron–oxygen bonding in various biological systems and in particular in the hemoproteins.[1–3]

One of the aims of our research has been the synthesis and characterisation of metalloporphyrins with various metallic ions coordinated to several oxygenated ligands: $(por)Ti(O_2)$,[4,5] $(por)Nb(O)(CO_2CH_3)$,[6,7] $[(por)Nb]_2O_3$,[7] (por)Nb(O)(F),[8] (por)In$[SO_2R(Ar)]$,[9] (por)In$[SO_3R(Ar)]$,[9] (por)In$(CO_2CH_3)$[10] and (por)Fe$[SO_2R(Ar)]$.[11]

During the last decade iron(III) porphyrin complexes possessing the oxyanionic axial ligands $ClO_4^-$,[12,13] $NO_3^-$,[14,15] $CF_3SO_3^-$,[12] $ArSO_3^-$,[14,15] $SO_4^{2-}$[14,15] $ArO^-$,[16–19] $RO^-$,[17,19–23] $CH_3CO_2^-$,[17,24,25] $CF_3CO_2^-$[24] have been reported. In most cases[12–23] solution behaviour and molecular stereochemistry have been well established, however only partial data concerning the acetato derivatives[17,24,25] are available.

In this paper we report the synthesis and physicochemical measurements of a series of carboxylato iron(III) porphyrins, (por)Fe$[CO_2R(Ar)]$

*Author to whom correspondence should be addressed.

(por = oep, tpp, *tm*Mepp, *tp*Mepp†) and describe the X-ray structure of acetato(5, 10, 15, 20-tetra *p*-tolylporphyrinato)iron(III).

## EXPERIMENTAL

The carboxylato-iron(III) porphyrins were prepared by acid hydrolysis of the $\mu$-oxo bridged dimers [(por)Fe]$_2$O with the appropriate acid according to the following reaction:

$$\underset{\mathbf{1}}{[(\text{por})\text{Fe}]_2\text{O}} + 2\text{R(Ar)CO}_2\text{H} \xrightarrow{\Delta} \underset{\mathbf{2}}{2(\text{por})\text{Fe}[\text{CO}_2\text{R(Ar)}]} + \text{H}_2\text{O}$$

*Preparation of the* (por)Fe($CO_2$R) *compounds,* $\mathbf{2}_a$ *and* $\mathbf{2}_b$

A solution of 0.35 mmol of [(por)Fe]$_2$O, **1**, in 50 cm$^3$ of $RCO_2H$ was heated under reflux for 20 min and then concentrated under reduced pressure. The resulting solution was left at room temperature. Crystals were collected by filtration, washed with methanol and dried at 120°C under vacuum.

*Preparation of the* (por)Fe($CO_2$Ar) *compounds,* $\mathbf{2}_c$

A mixture of 4.4 mmol of benzoic acid and 0.35 mmol of $\mu$-oxo dimer [(por)Fe]$_2$O was heated at 250°C for 15 min. After cooling the mixture was washed several times with 50 cm$^3$ of hot diisopropyl ether. The residual solid was recrystallised and the obtained product dried under vacuum.

The reaction yields vary according to the nature of both the porphyrin ligand and the R or Ar group. The isolated products are stable in the solid state but they rapidly hydrolyse in diluted solution.

The reaction conditions, yields and elemental analyses for complexes **2** are summarised in Table 1.

*Physical measurements*

Elemental analyses were performed by the "Service de Microanalyse du C.N.R.S.". Mass spectra were recorded in the electron-impact mode with a Finnigan 3300 spectrometer: ionising energy, 35–70 eV‡; ionizing current, 0.4 mA; source temperature, 250–400°C. $^1$H NMR spectra were recorded on a Jeol FX 100 spectrometer. Samples (6 mg) were dissolved in $C_6D_6$ or $CDCl_3$ (0.5 cm$^3$) with tetramethylsilane as internal reference; one hundred scans over 16 K points were accumulated for each spectrum at 21 ± 1°C. ESR spectra were obtained in frozen toluene solution (115 K) on a Varian E4 spectrometer operating in the *Q*-band frequency and equipped with liquid nitrogen cooling system. IR spectra were performed on a Perkin–Elmer 580B apparatus. Samples were 1% dispersions in CsI pellets or Nujol mulls. Visible and UV spectra were recorded on a Perkin–Elmer 559 spectrophotometer using $5 \times 10^{-3}$ mol . l$^{-1}$ benzene (or toluene) solutions. Magnetic measurements[26] were performed on a Squid magnetometer using a field of 10000 Oersted.

*Determination of crystal and molecular structure*

*Crystal data.* (*tp*Mepp)Fe($CO_2CH_3$) · 0.5 $CH_3COOH$, $\mathbf{2}_{4a}$, F.W. = 843, Monoclinic, $a$ = 24.464(8), $b$ = 9.332(3), $c$ = 37.174(4) Å, $\beta$ = 90.49(2)°, $V$ = 8485 Å$^3$, Z = 8, $D_c$ = 1.27 g . cm$^{-3}$, space group $I2/0c$, $\mu$(Cu-$K\alpha$) = 32.47 cm$^{-1}$, F(000) = 3302 $\bar{e}$.

*X-Ray data collection and crystal structure determination.* Prismatic blue crystals of (*tp*Mepp)Fe($CO_2CH_3$) · 0.5 $CH_3COOH$ were obtained by recrystallisation of the complex from acetic acid. A crystal of dimensions 0.19 × 0.15 × 0.30 mm$^3$ was mounted on an Enraf–Nonius CAD4 diffractometer. Unit cell dimensions were obtained by least squares refinement on the observed setting angles of the K$\alpha$1 peaks of 25 reflections. Scans for systematically absent reflections ($hkl$: $h + k + l = 2n + 1$, $hol$: $l = 2n + 1$) verified the space group preliminarily deduced from Weissenberg photographs.

X-Ray intensities were collected with monochromatised Cu-$K\alpha$ radiation using a $\omega$-$2\theta$ scan technique. Three standard reflections were used for periodic checking on the alignment of the crystal (every 150 reflections) and three others for testing the possible deterioration of the crystal. No statistically significant deviations were observed. A total of 9505 reflections was collected and 5132 having $\sigma(I)/I < 0.33$ were used to solve and refine the structure. Each reflection was corrected for Lorentz and polarisation effects. Absorption corrections were not applied ($\mu R_{max}$(Cu-$K\alpha$) = 0.97).

The structure was solved by MULTAN[27] which gave all the non hydrogen atoms of the structure. Hydrogen atoms were located from difference Fourier maps. All positional and thermal parameters were refined with the full matrix least squares programme SHELX[28] to an R index of $R(F)$ = 0.086. A difference electron density map

†Abbreviations: por = porphyrinate (2–); oep = 2, 3, 7, 8, 12, 13, 17, 18-octaethylporphyrinate (2–); tpp = 5, 10, 15, 20-tetraphenylporphyrinate (2–); *tm* Mepp = 5, 10, 15, 20-tetra*m*-tolylporphyrinate (2–); *tp*Mepp = 5, 10, 15, 20-tetra*p*-folylporphyrinate (2–).

‡Throughout this paper: 1 eV = 1.60 × 10$^{-19}$ J.

Table 1. Experimental data and yields

| Complex | Reaction solvent | Recrystallisation solvent | Yield (%) | Molecular formula | Analysis (%) C | H | N | Fe |
|---|---|---|---|---|---|---|---|---|
| $\underset{\sim}{2}_{1a}$ (oep)Fe($CO_2CH_3$) | A[a] | A | 60 | $C_{38}H_{47}N_4O_2Fe$ | 70.0 (70.45)[b] | 7.3 (7.35) | 8.5 (8.65) | 8.4 (8.6) |
| $\underset{\sim}{2}_{1b}$ (oep)Fe($CO_2CH_2CH_3$) | B | B | 65 | $C_{39}H_{49}N_4O_2Fe$ | 70.8 (70.8) | 7.5 (7.5) | 8.5 (8.45) | 8.4 (8.45) |
| $\underset{\sim}{2}_{1c}$ (oep)Fe($CO_2C_6H_5$) | C | D | 30 | $C_{43}H_{49}N_4O_2Fe$ | 72.5 (72.75) | 6.9 (6.95) | 7.9 (7.9) | 7.8 (7.85) |
| $\underset{\sim}{2}_{2a}$ (tpp)Fe($CO_2CH_3$) | A | A | 70 | $C_{46}H_{31}N_4O_2Fe$ | 76.1 (75.95) | 4.3 (4.3) | 7.8 (7.7) | 7.6 (7.7) |
| $\underset{\sim}{2}_{2b}$ (tpp)Fe($CO_2CH_2CH_3$) | B | B | 35 | $C_{47}H_{33}N_4O_2Fe$ | 75.7 (76.1) | 4.6 (4.5) | 7.6 (7.55) | 7.3 (7.55) |
| $\underset{\sim}{2}_{2c}$ (tpp)Fe($CO_2C_6H_5$) | C | D | 60 | $C_{51}H_{33}N_4O_2Fe$ | 76.7 (77.55) | 4.1 (4.2) | 7.0 (7.1) | 6.9 (7.1) |
| $\underset{\sim}{2}_{3a}$ (t*m*Mepp)Fe($CO_2CH_3$) | A | A | 35 | $C_{50}H_{39}N_4O_2Fe$ | 76.8 (76.6) | 5.0 (5.05) | 7.2 (7.15) | 7.1 (7.15) |
| $\underset{\sim}{2}_{4a}$ (t*p*Mepp)Fe($CO_2CH_3$). 1/2 $CH_3COOH$ | A | A | 62 | $C_{51}H_{41}N_4O_3Fe$ | 75.2 (75.25) | 5.0 (5.1) | 6.9 (6.9) | 6.8 (6.85) |

[a] A = acetic acid, B = propionic acid, C = benzoic acid, D = toluene.
[b] Calculated values are given in parentheses.

revealed a statistically disordered solvent molecule ($CH_3COOH$) around the two-fold axis and three residual peaks of 0.8, 0.7 and 0.5 e/Å$^3$. These latter could be obtained from the acetate ligand atoms C(70), C(71) and O(2) by a rotation of 180° around the Fe–O(1) axis. Each solvent atom was given a site occupation factor of 0.5 and a second acetate ligand [O(1), C′(70), C′(71), O′(2)] sharing the oxygen atom O(1) with the main ligand was included in the least squares calculation. The sum of the occupancies of the two $CH_3COO^-$ groups was constrained to 1. The refinement then converged to $R(F) = 0.0584$ and $R_w(F) = 0.0653$ ($w = 1/\sigma^2(F)$, $\sigma^2(F) = \sigma^2$ count + 0.005 $F^2$). The fractional occupancy of the second ligand site was found to be 0.166(4).

## RESULTS AND DISCUSSION

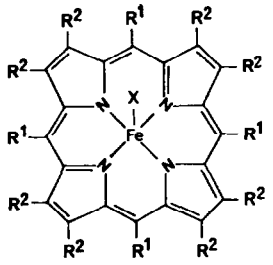
The proposed formula (por)Fe[$CO_2R(Ar)$] for compounds **2** is in accordance with the analytical results (Table 1) and spectral mass data (Table 2). In all of the mass spectra—compound $\mathbf{2}_{3a}$ omitted—the molecular peak is observed (4.16–87.17%). The parent peak corresponds to $[(por)Fe]^+$ or $[(por)Fe + H]^{+\cdot}$ resulting from the fission between the metal ion and the axial ligand without previous fragmentation of the $[R(Ar)CO_2]$ moiety. This should be in agreement with a monodentate ligation between the iron atom and the carboxylate anion.

Complexes **2** exhibit typical $^1$H NMR features of high spin 5/2 iron(III) porphyrins[29] (Table 3). For tetraaryl complexes, $\mathbf{2}_2$–$\mathbf{2}_4$, pyrrole protons resonance signal appears at 80 ppm downfield from internal $Me_4Si$ (line width ~320 Hz). The *meta*-phenyl protons of the macrocycle are highly anisotropic giving rise to two singlets around 10.8 and 11.8 ppm vs $Me_4Si$. In the case of acetato (5, 10, 15, 20-tetra*m*-tolylporphyrinato) iron(III), $\mathbf{2}_{3a}$, one observes two different peaks for the *m*–$CH_3$

Table 2. Characteristic mass-spectral and IR data

| Complex | Mass spectra | | | I. R. ($cm^{-1}$) | | | |
|---|---|---|---|---|---|---|---|
| | m/e | relative intensity | Fragmentation pattern | ν(C=O) | ν(C–O) | Δν | ν(M–O) |
| $\mathbf{2}_{1a}$ | 647<br>588 | 86.17<br>100.00 | $[(oep)Fe(CO_2CH_3)]^{+\cdot}$<br>$[(oep)Fe]^+$ | 1658 | 1285 | 373 | 531 |
| $\mathbf{2}_{1b}$ | 661<br>589 | 4.16<br>100.00 | $[(oep)Fe(CO_2CH_2CH_3)+H]^+$<br>$[(oep)Fe+H]^{+\cdot}$ | 1663 | 1260 | 403 | |
| $\mathbf{2}_{1c}$ | 710<br>589 | 66.33<br>100.00 | $[(oep)Fe(CO_2C_6H_5)+H]^+$<br>$[(oep)Fe+H]^{+\cdot}$ | 1651 | 1295 | 356 | 588 |
| $\mathbf{2}_{2a}$ | 727<br>668 | 33.30<br>100.00 | $[(tpp)Fe(CO_2CH_3)]^{+\cdot}$<br>$[(tpp)Fe]^+$ | 1665 | 1276 | 389 | 530 |
| $\mathbf{2}_{2b}$ | 741<br>668 | 13.51<br>100.00 | $[(tpp)Fe(CO_2CH_2CH_3)]^{+\cdot}$<br>$[(tpp)Fe]^+$ | 1666 | 1275 | 391 | |
| $\mathbf{2}_{2c}$ | 790<br>668 | 18.44<br>100.00 | $[(tpp)Fe(CO_2C_6H_5)]^{+\cdot}$<br>$[(tpp)Fe]^+$ | 1663 | 1275 | 388 | 570 |
| $\mathbf{2}_{3a}$ | 724 | 100.00 | $[(tmMepp)Fe]^+$ | 1670 | 1270 | 400 | 535 |
| $\mathbf{2}_{4a}$ | 783<br>724 | 18.82<br>100.00 | $[(tpMepp)Fe(CO_2CH_3)]^{+\cdot}$<br>$[(tpMepp)Fe]^+$ | 1668 | 1259 | 409 | |

Table 3. $^1$H NMR data




| Compound | $R^1$ | $R^2$ | R(Ar) | Protons of $R^1$ | | | Protons of $R^2$ | | | Protons of R(Ar) | | |
|---|---|---|---|---|---|---|---|---|---|---|---|---|
| | | | | multiplicity, intensity | | δ | multiplicity, intensity | | δ | multiplicity, intensity | | δ |
| $^2_{\equiv}$1a | H | $CH_2CH_3$ | $CH_3$ | | | ~ 59* | β-$CH_3$<br>α-$CH_2$ | s/24<br>s/16 | 5.9<br>38.6 | | (a) | |
| $^2_{\equiv}$1a** | H | $CH_2CH_3$ | $CH_3$ | | (a) | | β-$CH_3$<br>α-$CH_2$<br>α'-$CH_2$ | s/24<br>s/8<br>s/8 | 6.1<br>39.0<br>42.6 | | (a) | |
| $^2_{\equiv}$1b | H | $CH_2CH_3$ | $CH_2CH_3$ | | | - 58.5* | β-$CH_3$<br>α-$CH_2$ | s/24<br>s/16 | 6.4<br>37.4 | | (a) | |
| $^2_{\equiv}$1c | H | $CH_2CH_3$ | $C_6H_5$ | | | - 58* | β-$CH_3$<br>α-$CH_2$ | s/24<br>s/16 | 5.7<br>38.6 | *o*-H<br>*m*-H<br>*p*-H | s/2 | (a)<br>11.8<br>(a) |
| $^2_{\equiv}$2a | $C_6H_5$ | H | $CH_3$ | *o*-H<br>*m*-H<br>*m'*-H<br>*p*-H | s/4<br>s/4<br>s/4 | (a)<br>10.81<br>11.91<br>6.34 | | s/8 | 79.2 (b) | | (a) | |
| $^2_{\equiv}$2b | $C_6H_5$ | H | $CH_2CH_3$ | *o*-H<br>*m*-H<br>*m'*-H<br>*p*-H | s/4<br>s/4<br>s/4 | (a)<br>10.86<br>11.70<br>6.33 | | s/8 | 80.2 (b) | | (a) | |
| $^2_{\equiv}$2c | $C_6H_5$ | H | $C_6H_5$ | *o*-H<br>*m*-H<br>*m'*-H<br>*p*-H | s/4<br>s/4<br>s/4 | (a)<br>11.44<br>12.38<br>6.66 | | s/8 | 80.1 (b) | | (a) | |
| $^2_{\equiv}$3a | *m*-$CH_3C_6H_4$ | H | $CH_3$ | *o*-H<br>*m*-H<br>*m'*-H<br>*m*-$CH_3$<br>*m'*-$CH_3$<br>*p*-H | s/2<br>s/2<br>s/6<br>s/6<br>s/4 | (a)<br>10.71<br>11.72<br>2.20<br>2.49<br>6.35 | | s/8 | 79.4 (b) | | (a) | |
| $^2_{\equiv}$4a | *p*-$CH_3C_6H_4$ | H | $CH_3$ | *o*-H<br>*m*-H<br>*m'*-H<br>*p*-$CH_3$ | s/4<br>s/4<br>s/12 | (a)<br>10.88<br>11.72<br>5.75 | | s/8 | 79.6 (b) | | (a) | |

s = singulet ; (a) non observed signal ; (b) line width ~ 320 Hz.

*Approximate position of the very broad signals observed for meso protons.

**solvent : $CDCl_3$.

protons resonance at 2.20 and 2.49 ppm. These splittings result from the magnetic non-equivalence between the two sides of the porphyrin ligand induced by both an out-of-plane displacement of the iron atom and the asymmetry of the axial ligand.[30] *Ortho*-phenyl proton resonances are not observed. Strong dipolar interactions should be the cause of the important broadening of their peaks.

Carboxylato-iron(III)octaethylporphyrins, $\mathbf{2}_1$, also exhibit characteristic spectra of high spin iron(III) species. Very broad signals are observed around 58 ppm upfield from $Me_4Si$ for meso protons and 6 ppm downfield vs $Me_4Si$ for $\beta$–$CH_3$ protons; α–$CH_2$ protons surprisingly show a singlet near 38 ppm downfield from $Me_4Si$. This result is unexpected for metallooctaethylporphyrins with

Table 4. ESR and UV-visible spectroscopic data

| Compound | E.S.R. | | UV-visible | | | | | | |
|---|---|---|---|---|---|---|---|---|---|
| | $g_{\perp}$ | $g_{//}$ | I | Soret ou II | | | | | |
| $\underline{2}_{1a}$ | 6.01 | 2.07 | 359 (53.4) [b] | 399 (124) | 503 (7.6) | 544 (7.4) | | 616 (4.5) | |
| $\underline{2}_{1b}$ | 6.05 | 1.97 | 360 (56.9) | 397 (85.1) | | | 559 (7.6) | 590 (6.5) | 620 (3.5) |
| $\underline{2}_{1c}$ | 6.11 | 2.05 | 364 (60.6) | 398 (89.8) | 489 (8.7) | 532 (7.8) | 555 (5.9) | 612 (4.6) | |
| $\underline{2}_{2a}$ | 6.00 | (a) | 346 (34.1) | 410 (112) | | | | 570 (7.4) | 612 (3.3) |
| $\underline{2}_{2b}$ | 6.04 | 2,00 | 343 (34.9) | 414 (113) | | | | 570 (7.0) | 613 (3.2) |
| $\underline{2}_{2c}$ | 6.09 | (a) | 345 (34.3) | 413 (107) | 500 (9.3) | | | 570 (5.7) | 613 (2.3) 667 (0.9) |
| $\underline{2}_{3a}$ | 6.08 | (a) | 342 (36.7) | 411 (117) | | | | 570 (7.9) | 610 (3.4) |
| $\underline{2}_{4a}$ | 6.08 | (a) | 374 (45.5) | 419 (114) | 507 (10.3) | | | 570 (3.0) | 610sh [c] 685 (0.4) |

[a] non observed signal ; [b] values given are of λ/nm with $10^{-3}\varepsilon/mol^{-1}.l.cm^{-1}$ ; [c] sh = shoulder.

the metal ion displaced out-of-the plane and could only be explained by a solvent effect. The fact that in $CDCl_3$ two different peaks are obtained for these protons (Table 3) is in accordance with the former suggestion.

Resonance signals of the axial ligand protons are not observed. However a broad peak at 11.8 ppm downfield from $Me_4Si$ in the case of the benzoatooctaethyl - porphyrinatoiron(III), $\underline{2}_{1c}$, might be attributed to the meta protons of the phenyl group.

The ESR spectra of compounds **2** are characteristic of high spin iron(III) complexes[31]. Two peaks are observed (Table 4) at $g \sim 6$ and $g \sim 2$ attributed respectively to the orthogonal and parallel components of the $g$-factor suggesting an axial symmetry. The lack of rhombicity is quite surprising for such complexes possessing asymmetric anions bonded to the metal centre. This phenomenon has however been observed for the iron (III)porphodimethenes $(oeptBu_2)Fe(OH)$ and $(oeptBu_2)Fe(OC_6H_5)$.[19]

As expected for porphyrins with metal ions in the $d^5$ configuration porphyrinatoiron(III) carboxylates exhibit electronic absorption spectra belonging to the hyper class.[32,33] One or two extra bands are observed in the visible region and another one appears blue shifted compared to the Soret band (Table 4).

The IR spectra of the whole isolated complexes show two intense bands around 1660 and 1260–1295 $cm^{-1}$ respectively assigned to $\nu$(C=O) and $\nu$(C–O) (Table 2). The extent of the peaks' separation (356–409 $cm^{-1}$) allows us to predict mono-ligation for the carboxylate anion. An absorption of medium intensity located between 531 and 588 $cm^{-1}$ is attributed to the Fe–O stretch-

Table 5. Main interatomic distances and angles

| *Iron Coordination polyhedron* | | *Macrocycle* | |
|---|---|---|---|
| Angles (in degree) | | | |
| N(1) - Fe - O(1) | 103.2(2) | N(1) - C(1) | 1.386(5) |
| N(2) - Fe - O(1) | 107.9(1) | N(1) - C(4) | 1.385(5) |
| N(3) - Fe - O(1) | 104.2(1) | N(2) - C(6) | 1.372(5) |
| N(4) - Fe - O(1) | 98.9(2) | N(2) - C(9) | 1.380(5) |
| N(1) - Fe - N(2) | 87.2(1) | N(3) - C(11) | 1.384(5) |
| N(1) - Fe - N(4) | 87.4(1) | N(3) - C(14) | 1.382(5) |
| N(2) - Fe - N(3) | 86.4(1) | N(4) - C(16) | 1.380(5) |
| N(3) - Fe - N(4) | 86.3(1) | N(4) - C(19) | 1.388(5) |
| N(4) - N(1) - N(2) | 90.2(2) | C(1) - C(2) | 1.429(6) |
| N(1) - N(2) - N(3) | 89.6(2) | C(2) - C(3) | 1.354(6) |
| N(2) - N(3) - N(4) | 90.6(2) | C(3) - C(4) | 1.420(6) |
| N(3) - N(4) - N(1) | 89.5(2) | C(4) - C(5) | 1.390(5) |
| distances | | C(5) - C(6) | 1.409(6) |
| Fe - O(1) | 1.898(4) | C(6) - C(7) | 1.432(6) |
| Fe - N(1) | 2.051(3) | C(7) - C(8) | 1.350(7) |
| Fe - N(2) | 2.073(3) | C(8) - C(9) | 1.436(6) |
| Fe - N(3) | 2.072(3) | C(9) - C(10) | 1.382(6) |
| Fe - N(4) | 2.072(3) | C(10) - C(11) | 1.400(5) |
| N(1) - N(2) | 2.843(4) | C(11) - C(12) | 1.418(6) |
| N(2) - N(3) | 2.838(4) | C(12) - C(13) | 1.346(6) |
| N(3) - N(4) | 2.835(4) | C(13) - C(14) | 1.440(6) |
| N(1) - N(4) | 2.850(4) | C(14) - C(15) | 1.399(5) |
| *Acetate ligand* | | C(15) - C(16) | 1.391(6) |
| O(1) - C(71) | 1.242(8) | C(16) - C(17) | 1.445(6) |
| O(2) - C(71) | 1.211(10) | C(17) - C(18) | 1.328(8) |
| C(70) - C(71) | 1.495(12) | C(18) - C(19) | 1.418(6) |
| | | C(19) - C(20) | 1.392(6) |
| Fe - O(1) - C(71) | 129.6(4) | C(20) - C(1) | 1.396(5) |
| O(1) - C(71) - O(2) | 121.6(7) | C(30) - C(5) | 1.487(5) |
| O(1) - C(71) - C(70) | 118.8(7) | C(40) - C(10) | 1.497(5) |
| O(2) - C(71) - C(70) | 119.4(7) | C(50) - C(15) | 1.486(6) |
| | | C(60) - C(20) | 1.503(6) |

ing. Such absorptions have already been reported for several methoxymetalloporphyrins (530–540 $cm^{-1}$)[16,34] and some trinuclear iron(III) acetates (~520 $cm^{-1}$).[35]

In order to confirm the previous conclusions and to correlate spectroscopic data of compounds **2** and other iron(III) porphyrins coordinated with oxyanions we determined the molecular configuration of acetato (5, 10, 15, 20-tetra*p*-tolylporphyrinato)iron(III) by X-ray diffraction methods.

Table 5 gives the main distances and angles of the molecule. Figure 1 is an ORTEP view of the complex with the main acetato ligand and gives the numbering scheme used. Fractional coordinates, thermal parameters, other distances, angles and details of the least squares planes have been deposited as supplementary data with the Editor.†

The iron atom is five coordinated and the resulting polyhedron is a slightly deformed square pyramid with the oxygen atom in the axial position. The Fe–N(2), Fe–N(3) and Fe–N(4) distances are equal (2.072(3) Å) and a little longer than the Fe–N(1) distance (2.051(3) Å); the Fe–0(1) distance (1.898(3) Å) is greater than the Fe–O bond length of 1.815(1) Å found in the crystal structure of tetraphenylporphinato iron(III) methoxide[23] (tpp)Fe($OCH_3$) and is curiously equal to that observed in a dioxygen complex of the iron(II)

†Atomic coordinates have also been deposited with the Cambridge Crystallographic Data Centre.

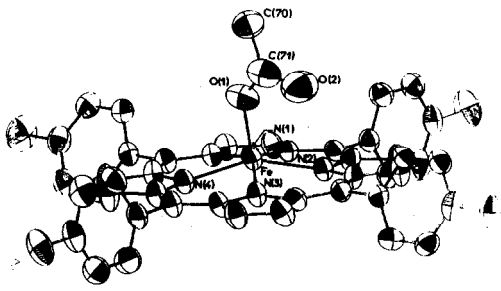



Fig. 1. ORTEP view of (tpMepp)Fe($CO_2CH_3$)·0.5 $CH_3COOH$.

"picket fence porphyrin".[36] The Fe–O–C angle (129.6(4)) is close to that found in (tpp)Fe($OCH_3$) (129.10(9) Å).

The iron atom lies 0.520(2) Å above the least squares mean plane of the porphyrin and 0.485(2) Å above the four nitrogen plane. The corresponding distances in (tpp)Fe($OCH_3$) are 0.562(1) Å and 0.484(1) Å. A relation between the spin state of the iron atom and its distance from the four nitrogen plane is now well established.[37] The value found in (*tp*Mepp)Fe($CO_2CH_3$) agrees with a high spin state. This assumption was verified by a thermomagnetic study of the same complex which follows a Curie law between 5 and 120 K leading to $\mu_{eff} = 5.88$ B.M.

The oxygen atom is slightly displaced from the ideal position resulting in unequal N(4)–Fe–O(1) and N(2)–Fe–O(1) angles (98.9(2)° and 107.9(1)°) while the N(1)–Fe–O(1) and N(3)–Fe–O(1) are almost equal (103.2(2)° and 104.2(1)°).

The acetate ligand is planar within 0.03 Å; the oxygen–carbon distances are different (C(71)–O(1) = 1.245(7), C(71)–O(2) = 1.210(9) Å) suggesting a slight covalent character of the iron oxygen bond which is consistent with the end on coordination of the acetate group: a pure ionic bond would lead to a bidentate coordination.

The bond distances and angles in the macrocycle are normal. Least squares planes calculations indicate a small doming of the porphyrin (0.035 Å). The solvent molecule is disordered around the binary axis. All inter-porphyrin distances are greater than 3.62(1) Å. The solvent molecule hydrogen bonds with the ligand (O(4)–O(1) = 3.12(4) Å), helping to increase the stability of the crystal.

## REFERENCES

1. J. P. Collman, *Acc. Chem. Res.* 1977, **10**, 265.
2. H. B. Dunford and J. S. Stillman, *Coord. Chem. Rev.* 1976, **19**, 187.
3. G. R. Moore and R. J. P. Williams, *Coord. Chem. Rev.* 1976, **18**, 125.
4. R. Guilard, M. Fontesse, P. Fournari, C. Lecomte and J. Protas, *J. Chem. Soc., Chem. Commun.* 1976, 161.
5. R. Guilard, J. M. Latour, C. Lecomte, J. C. Marchon, J. Protas and D. Ripoll, *Inorg. Chem.* 1978, **17**, 1228.
6. C. Lecomte, J. Protas, R. Guilard, B. Fliniaux and P. Fournari, *J. Chem. Soc., Chem. Commun.* 1976, 434.
7. C. Lecomte, J. Protas, R. Guilard, B. Fliniaux and P. Fournari, *J. Chem. Soc., Dalton* 1979, 1306.
8. C. Lecomte, J. Protas, P. Richard, J. M. Barbe and R. Guilard, *J. Chem. Soc. Dalton* 1982, 247.
9. P. Cocolios, P. Fournari, R. Guilard, C. Lecomte, J. Protas and J. C. Boubel, *J. Chem. Soc. Dalton* 1980, 2081.
10. P. Cocolios, R. Guilard, D. Bayeul and C. Lecomte, submitted to *Inorg. Chem.*
11. P. Cocolios, G. Lagrange, R. Guilard, H. Oumous and C. Lecomte, *J. Chem. Soc.* Dalton, in press.
12. C. A. Reed, T. Mashiko, S. P. Bentley, M. E. Kastner, W. R. Scheidt, K. Spartalian and G. Lang, *J. Am. Chem. Soc.* 1979, **101**, 2948.
13. H. Masuda, T. Taga, K. Osaki, H. Sugimoto, Z. I. Yoshida and H. Ogoshi, *Inorg. Chem.* 1980, **19**, 950.
14. M. A. Phillipi, E. T. Shimomura and H. M. Goff, *Inorg. Chem.* 1981, **20**, 1322.
15. M. A. Phillippi, N. Baenziger and H. M. Goff, *Inorg. Chem.* 1981, **20**, 3904.
16. N. Sadavisan, H. I. Eberpaecher, W. H. Fuchsman and W. S. Caughey, *Biochemistry* 1969, **8**, 534.
17. J. W. Buchler and H. H. Schneehage, *Z. Naturforsch.* 1973, **B28**, 433.
18. E. W. Ainscough, A. W. Addison, D. Dolphin and B. R. James, *J. Am. Chem. Soc.* 1978, **100**, 7585.
19. A. Botulinski, J. W. Buchler, K. L. Lay, J. Ensling, H. Twilfer, J. Billecke, H. Leuken and B. Tonn, *Electrochemical and Spectrochemical studies of Biological Redox components*, (Edited by K. M. Kadish). Advances in Chemistry series, p. 253 Washington (1982).
20. J. L. Hoard, M. J. Hamor, T. A. Hamor and W. S. Caughey, *J. Am. Chem. Soc.* 1965, **87**, 2312.
21. J. O. Alben, W. H. Fuchsman, D. A. Beaudreau and W. S. Caughey, *Biochemistry* 1968, **7**, 624.
22. J. C. Maxwell and W. S. Caughey, *Biochemistry* 1976, **15**, 388.
23. C. Lecomte, D. L. Chadwick, P. Coppens and E. D. Stevens, *Inorg. Chem.* 1983, **22**, 2982.
24. M. A. Torrens, D. K. Straub and L. M. Epstein, *J. Am. Chem. Soc.* 1972, **94**, 4162.
25. D. Lexa, M. Momenteau, J. Mispelter and J. M. Lhoste, *Bioelec. Bioenerg.* 1974, **1**, 108.
26. Magnetic behavior of the complex was established by J. Hubsch.
27. P. Main, A system of computer programm for the automatic solution of crystal structure from X-ray diffraction data. University of York, England, 1980.
28. G. M. Sheldrick, Programme for crystal structure determination, University of Cambridge, England (1976).

29. G. N. La Mar and F. A. Walker (Jensen), *The Porphyrins* (Edited by D. Dolphin), Vol. IV, Chap. 2. Academic Press, New York (1979).
30. G. N. La Mar, G. R. Eaton, R. H. Holm and F. A. Walker, *J. Am. Chem. Soc.* 1973, **95**, 63.
31. G. Palmer, *The Porphyrins* (Edited by D. Dolphin), Vol. IV, Chap. 6. Academic Press, New York (1979).
32. J. W. Buchler, *The Porphyrins* (Edited by D. Dolphin), Vol. I, Chap. 10. Academic Press, New York (1978).
33. M. Gouterman, *The Porphyrins* (Edited by D. Dolphin), Vol. III, Chap. I. Academic Press, New York (1978).
34. J. W. Buchler, L. Puppe, K. Rohbock and H. H. Schneehage, *Chem. Ber.* 1973, **106**, 2710.
35. G. L. Long, W. T. Robinson, W. P. Tappmeyer and D. L. Bridges, *J. Chem. Soc. Dalton* 1973, 573.
36. G. B. Jameson, F. S. Molinaro, J. A. Ibers, J. P. Collman, J. I. Brauman, E. Rose and K. S. Suslick, *J. Am. Chem. Soc.* 1980, **102**, 3224.
37. W. R. Scheidt and C. A. Reed, *Chem. Rev.* 1981, **81**, 543.

*Polyhedron* Vol. 3, No. 6, pp. 661–665, 1984
Printed in Great Britain.

0277–5387/84 $3.00 + .00
© 1984 Pergamon Press Ltd.

# $^{121}$Sb MÖSSBAUER SPECTRAL AND RELATED STUDIES ON Sb(III) COMPLEXES

**ANIL SAXENA† and JAGDISH P. TANDON**
Department of Chemistry, University of Rajasthan, Jaipur, India

**THOMAS BIRCHALL***
Department of Chemistry, McMaster University, Hamilton, Ontario, Canada L85 4M1

**and**

**BERNARD DUCOURANT and GUY MASCHERPA**
U.S.T.L., Montpellier, France

(*Received* 12 *July* 1983; *accepted* 23 *September* 1983)

**Abstract**—The bonding and structural features of antimony(III) complexes of the type, ($Pr^iO$)SbL and $Sb_2L_3$ are described (where L is the dianion of semicarbazone or thiosemicarbazone). The Mössbauer spectra are typical of Sb(III) complexes in which the non-bonding pair of electrons is stereochemically active. The thiosemicarbazone complexes show more negative isomer shifts compared to the semicarbazone complexes.

In recent years, there has been considerable interest in the chemistry of organoantimony (III) and (V) complexes with various nitrogen and sulphur donor ligands.[1,2] Thiosemicarbazone and semicarbazone can function as either bifunctional or monofunctional ligands depending on the reaction conditions. Complexes of these ligands with many different central metal ions have been extensively studied.[3,4] However, little information on the bonding and structural properties is available for complexes with antimony.[5] It was therefore, considered worthwhile to synthesize antimony (III) derivatives by reacting $Sb(OPr^i)_3$ with semicarbazones and thiosemicarbazones of the following type.

Comparative studies have been carried out on these complexes using IR, NMR and $^{121}$Sb Mössbauer spectroscopies.

## EXPERIMENTAL

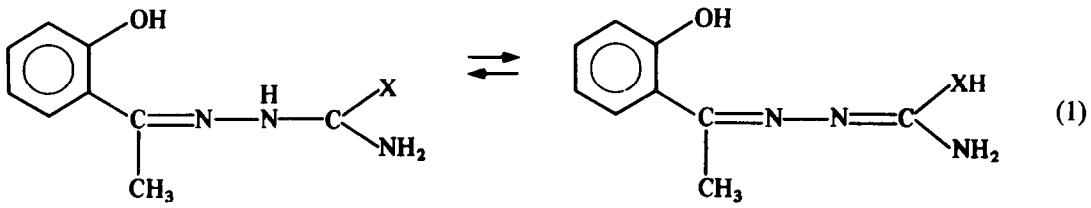
Chemicals and solvents used were dried and purified by standard methods, and moisture was excluded from the glass apparatus using $CaCl_2$ drying tubes. The ligands and antimony isopropoxide were prepared by standard literature methods.[6,7] All the manipulations were carried out under absolutely dry conditions. The complexes were prepared by mixing antimony tris-isopropoxide and the ligands in 1:1 and 2:3 molar ratios. The contents were refluxed on a fractionating column with benzene as the solvent. The isopropanol liberated was removed azeotropically and the completion of the reaction was followed by monitoring the isopropanol produced. The excess solvent was removed and the compounds dried in vacuo. The details of these reactions together with the physical properties of the products are given in Table 1.

The complexes were analyzed by literature methods. Molecular weights were determined by the Rast camphor method. Infrared spectra, as Nujol mulls or in chloroform solution, were obtained using a Perkin–Elmer 577 grating spectrophotometer. NMR spectra were recorded on a Perkin–Elmer RB 12 spectrometer in DMSO-$d_6$ using TMS as an internal standard.

Antimony-121 Mössbauer spectra were recorded using an Elscint drive system in conjunction with a Promeda multichannel analyzer. The source was a nominally 0.5 mCi. $Ba^{121m}SnO_3$, purchased from New England Nuclear and was cooled, together with the sample to 4.2 K in a cryostat designed by

*Author to whom correspondence should be addressed.

†Present address: School of Molecular Sciences, University of Sussex, Brighton, BNI 9QJ, England.



(1)

Table 1.

| Sl. No. | Reactants (g) $Sb(OPr^i)_3$ | Ligands | Molar Ratio | Yield % | Product and Characteristics (colour and state) | M.P. °C | $Pr^iOH$ in Azeotrope Found (Calcd.) | Analyses % Sb Found (Calcd. | C Found Calcd. | H Found Calcd.) |
|---|---|---|---|---|---|---|---|---|---|---|
| 1. | 0.78 | 0.50 | 1:1 | 93 | $Sb(OPr^i)(C_9H_9N_3O_2)$ | 260* | 0.29 | 36.59 | 37.05 | 4.95 |
| | | $C_9H_{11}N_3O_2$ | | | Yellow solid | | 0.31 | 32.52 | 38.73 | 4.30 |
| 2. | 1.01 | 0.98 | 2:3 | 85 | $Sb_2(C_9H_9N_3O_2)_3$ | 198 | 0.43 | 31.35 | 39.68 | 3.34 |
| | | $C_9H_{11}N_3O_2$ | | | Yellow solid | | 0.48 | 29.82 | 39.06 | 5.60 |
| 3. | 1.63 | 1.14 | 1:1 | 92 | $Sb(OPr^i)(C_9H_9N_3OS)$ | 239 | 0.59 | 35.61 | 38.52 | 4.90 |
| | | $C_9H_{11}N_3OS$ | | | Orange solid | | 0.65 | 31.39 | 37.13 | 4.12 |
| 4. | 1.76 | 1.85 | 2:3 | 82 | $Sb_2(C_9H_9N_3OS)_3$ | 252 | 0.95 | 30.59 | 37.30 | 3.90 |
| | | $C_9H_{11}N_3OS$ | | | Brick red solid | | 1.05 | 28.16 | 37.48 | 3.13 |

* Decomposition temperature.

B. Ducourant and manufactured by Aire Liquide. The window of the single channel analyzer was set on the escape peak of the 37 KeV $\gamma$-ray. Samples contained $\sim 15$ mg Sb cm$^{-2}$ and all isomer shifts were measured with respect to InSb. The velocity range was calibrated periodically using a $^{57}$Co source and a standard iron foil. About $10^5$ counts per folded channel were accumulated and the data were computer fitted using the program described by Ruebenbauer and Birchall[8] which incorporated the full transmission integral procedures which are necessary for the successful refinement of $^{121}$Sb Mössbauer spectra.

## RESULTS AND DISCUSSION

The reactions of $Sb(OPr^i)_3$ with these bifunctional tridentate ligands have been carried out in 1 : 1 and 2 : 3 molar ratios in refluxing benzene. The reactions proceed with the liberation of isopropanol, which was removed azeotropically with benzene until the reaction was complete.

$$Sb(OPr^i)_3 + LH_2 \rightarrow Sb(OPr^i)L + 2Pr^iOH \quad (2)$$

$$2Sb(OPr^i)_3 + 3LH_2 \rightarrow Sb_2L_3 + 6Pr^iOH \quad (3)$$

[where L = $C_9H_9N_3OS$ or $C_9H_9N_3O_2$].

These reactions are quite facile and are completed after refluxing for 15–25 hr. The resulting complexes are yellow to brick red coloured solids and their physical properties are recorded in Table 1. Molecular weight measurements show these to be monomeric complexes which are partially soluble in most of the common organic solvents; they are susceptible to moisture.

In the IR spectra of these complexes (Table 2) two bands are observed at $\sim 3440$ and 3310 cm$^{-1}$ due to the symmetric and antisymmetric modes of the primary amino group.[9] These vibrational modes are in the same positions as in the free ligands suggesting that the $NH_2$ group is not involved in chelation to the antimony. The region 3300–2850 cm$^{-1}$ is that where one would normally expect $\nu_{OH}$ and $\nu_{NH}$ vibrations to occur but no bands are visible in this region indicating that the O–H and N–H protons have been removed in reactions (2) and (3) making these sites available for coordination to the antimony.[10] A sharp strong band is observed in all complexes in the region 1595–1580 cm$^{-1}$ and this is assigned to the $\nu_{C=N}$ stretching mode. The position of this band is lower than the corresponding band in the free ligand strongly suggesting that the nitrogen of the azomethine moiety is coordinated to antimony. Similar shifts on coordination to Sb(V) have been observed for the oximate ligand by Mehrotra *et al.*[11]

Table 2. $^{121}$Sb Mössbauer (mms$^{-1}$) and IR (cm$^{-1}$) spectral data of antimony complexes

| | Compound | $\delta^a$ | $e^2qQ^b_g$ | $\eta^c$ | $\nu$(C=N) | $\nu$(Sb←N) | $\nu$(Sb-O) | $\nu$(Sb-S) |
|---|---|---|---|---|---|---|---|---|
| | | mm s$^{-1}$ | | | cm$^{-1}$ | | | |
| 1. | $Sb(OPr^i)(C_9H_9N_3O_2)$ | -3.65 | 17.31 | 1.52 | 1595 | 410 | 518 | - |
| 2. | $Sb_2(C_9H_9N_3O_2)_3$ | -3.54 | 17.45 | 1.42 | 1580 | 405 | 520 | - |
| 3. | $Sb(OPr^i)(C_9H_9N_3OS)$ | -4.42 | 15.48 | 1.65 | 1587 | 412 | 510 | 350 |
| 4. | $Sb_2(C_9H_9N_3OS)_3$ | -4.56<br>7.20 | 12.88<br>-- | 1.88<br>2.20 | 1585 | 405 | 517 | 342 |
| InSb | | -8.73 | -- | -- | | | | |

a ± 0.01 mms$^{-1}$

b ± 0.13 mms$^{-1}$

c ± 0.04 mms$^{-1}$

In the region $\sim 520 - 350\,cm^{-1}$ new bands are observed in the complexes which are not present in the free ligands. There have been assigned to $\nu_{Sb-O}$, $\nu_{Sb-N}$ and $\nu_{Sb-S}$ vibrations (Table 2). This is based on the results of Olera and Okawara,[12] who have suggested that bands in the region 380–360 cm$^{-1}$ may be attributed to Sb–S vibrations, and those of Chremos and Zingaro[13] who have assigned bands in the 430 cm$^{-1}$ region to $\nu_{Sb-N}$ vibrations. All of our complexes show bands in the 405–412 cm$^{-1}$ region and suggests the presence of Sb–N bands in these compounds. The bands in the range 510–520 cm$^{-1}$ indicate the presence of Sb–O interactions.

Proton NMR spectra of the free ligands and of the $Sb_2L_3$ complexes have been recorded in DMSO-$d_6$ using T.M.S. as an internal standard. The free ligands show bands at $\delta = 12.10$ ppm and $\delta = 9.81$ ppm which are assigned to the OH and secondary amino protons respectively. These bands are absent in the complexes, confirming the IR evidence that these protons are removed in the complexation process. The $CH_3$ protons on the carbon adjacent to the =N are shifted from $\delta = 1.70$ ppm and $\delta = 1.62$ ppm to $\delta = 2.48$ ppm and $\delta = 2.25$ ppm in the semicarbazone and thiosemicarbazone complexes respectively. This is further evidence that the nitrogen of the $CH_3$–C=N– group is coordinated to the antimony. The multiplet arising from the aromatic protons remains essentially unchanged in the $\delta = 6.58$–$7.75$ ppm region. However those peaks due to the $NH_2$ protons undergo a downfield shift to $\delta = 3.58$ ppm and 3.22 ppm in the semicarbazone and thiosemicarbazone respectively. This is consistent with



presence of the =C–$NH_2$ group in the complexes



compared to the predominant –C–$NH_2$ grouping in the free ligand. The downfield shift being the result of the proximity of the N=C group to the primary amino protons.

$^{121}$Sb Mössbauer spectra were recorded and these data are summarised in Table 2: typical spectra are shown in Fig. 1. These data are characteristic of antimony(III) complexes since they show large negative isomer shifts. Since $\delta R/R$ is negative for antimony these shifts indicate a high s electron density at the antimony nucleus, typical of Sb(III). These shifts may be compared with those of the $Sb(OR)_3$ series.[14] The complexes examined in this study all have isomer shifts that are more negative than the $Sb(OR)_3$ compounds, indicating that there is a higher s electron density at the antimony in the complexes than in the alkoxy compounds. It is also noted that the thiosemicarbazone complexes have much more negative isomer shifts than their oxo analogues. This strongly suggest that the X-(X = 0, S) is bound to the antimony. More negative isomer shifts are found for Sb(III)-S species than for the oxo analogues.[14,15] We note also that the sulphur containing complexes have smaller quadruple coupling constants than their oxo analogues. This, taken with the trend in isomer shifts, indicates a less active participation of the antimony 5*s* electrons in the bonding scheme of the thio complexes than in the oxo species.

Based upon the evidence suggested above we propose the following structures, **I** and **II**, for those complexes with the semicarbazone behaving as a tridentate ligand. The antimony then has four ligands and a non-bonding electron pair in its immediate environment, an example of the $AX_4E$

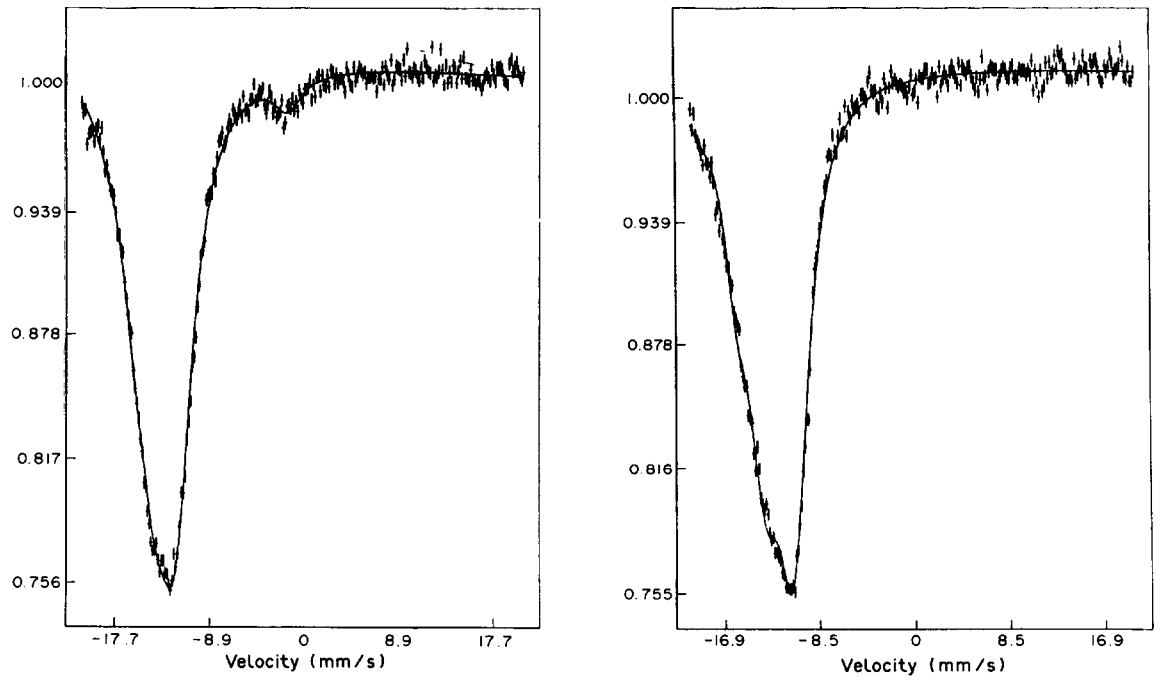
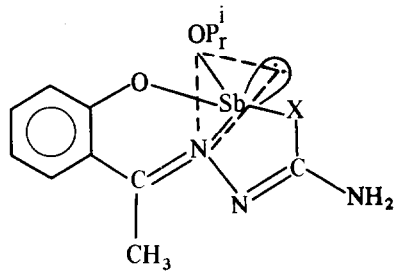
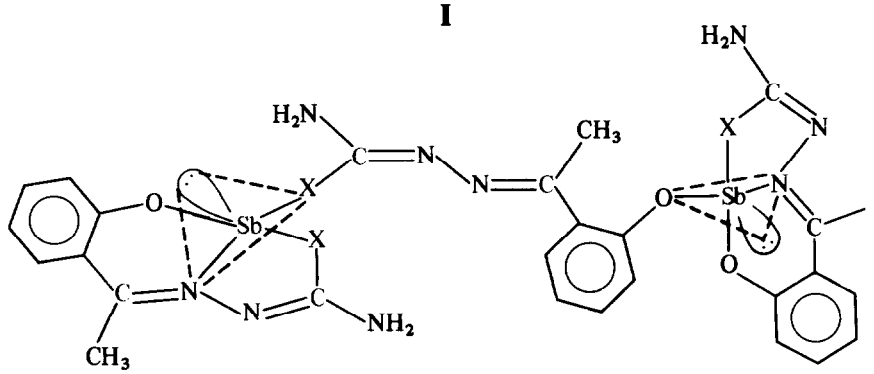



Fig. 1(a). The $^{121}$Sb Mössbauer spectrum of $Sb(OPr^i)(C_9H_9N_3O_2)$ at 4.2 K. (b) The $^{121}$Sb Mössbauer spectrum of $Sb_2(C_9H_9N_3OS)_3$ at 4.2 K.

type. For Pr$^i$OSbL there are two likely arrangements of the ligands, the first having the non-bonding electron pair, the O and atom X in the equatorial plane, while the N and the OPr$^i$ group would occupy the axial positions of a trigonal bipyramid. This arrangement would have considerable strain and would lead to a very distorted structure. The alternative arrangement which is shown as I has the OPr$^i$ group, the N and the non-bonding electron pair in the equatorial plane while the O and X atoms occupy the axial positions of a virtually strain free idealised trigonal bipyramid. This latter is the structure that we favour. In II the equatorial OPr$^i$ groups in Pr$^i$OSbL have been replaced in one case by an O and in the other by an X of a semicarbazone ligand which bridges




I




II

two SbL units. Other structures are possible in which the semicarbazone bridges different antimony atoms, but polymeric structures are not likely in view of the solubility of the complexes in common solvents and are ruled out by the molecular weight measurements. For the $Sb_2L_3$ complex when X=S there will actually be two different antimony (III) environments: one [:$Sb(O)_2SN$] and the other [:$Sb(O)(S)_2N$]. These should have different $^{121}$Sb Mössbauer parameters. Unfortunately it is not possible to resolve these two sites but their presence manifests itself in the increased line width for $Sb_2L_3$ when X=S (Table 2). It is also noted that the $^{121}$Sb Mössbauer spectrum of this complex shows evidence of the presence of a small amount of an Sb(V) species. Presumably the thio analogue of $Sb_2L_3$ is much more easily oxidised than the other complexes where no Sb(V) is visible in the Mössbauer spectrum.

*Acknowledgements*—One of us (A. S.) is thankful to the C.S.I.R., New Delhi for the award of P.D.F. and (T.B.) is grateful to N.S.E.R.C. of Canada and C.N.R.S. France for the opportunity to participate in the Canada–France Cultural Exchange Scheme.

## REFERENCES

1. C. L. Raston and A. H. White, *J. Chem. Soc. Dalton* 1976, 791.
2. P. J. H. A. M. Van de Leemput, J. A. Cras and J. Willemse, *Rec. Trav. Chim.* 1977, **96**, 288.
3. B. A. Gingras, R. W. Harnal and C. H. Bayley, *Can. J. Chem.* 1960, **38**, 712.
4. M. Mathew and C. J. Palenik, *J. Am. Chem. Soc.* 1969, **91**, 6310.
5. A. Saxena, S. K. Sinha and J. P. Tandon, *J. Antifung. Antibact. Agents* 1981, **9**, 337.
6. A. I. Vogel, *A Text Book of Practical Organic Chemistry*, p. 722. Longmans, London (1963).
7. O. D. Dubrovina, *Uchenye Zapiski Kazau, Gof-udarst. Univ. in V. I. Ul' Yanova-Lenine* 1956, **116**, 3; *Chem. Abstr.* 1957, **51**, 6534.
8. K. Ruebenbauer and T. Birchall, *Hyperfine Interact.* 1979, **7**, 125.
9. A. V. Ablov and N. V. Gerbelau, *Russ. J. Inorg. Chem.* 1964, **9**, 46.
10. A. K. Saxena, J. K. Koacher and J. P. Tandon, *J. Inorg. Nucl. Chem.* 1981, **43**, 3091.
11. V. K. Jain, R. Bohra and R. C. Mehrotra, *J. Ind. Chem. Soc.* 1980, **57**, 408.
12. J. Olera and R. Okawara, *J. Organometal Chem.* 1968, **11**, 299.
13. G. N. Chremos and R. A. Zingaro, *J. Organometal Chem.* 1970, **22**, 647.
14. L. H. Bowen, G. G. Long, J. G. Stevens, N. C. Cambell and T. B. Brill, *Inorg. Chem.* 1974, **13**, 1787.
15. G. G. Long, J. G. Stevens, H. Lawrence and S. L. Ruby, *Inorg. Nucl. Chem. Lett.* 1969, **5**, 21.
16. T. Birchall and B. Della Valle, *J. C. S. Chem. Commun.* 1970, 675.

*Polyhedron* Vol. 3, No. 6, pp. 667–673, 1984
Printed in Great Britain.

0277–5387/84 $3.00 + .00
Pergamon Press Ltd.

# COMPLEXATION OF NEPTUNIUM(V) BY SALICYLATE, PHTHALATE AND CITRATE LIGANDS IN A pH 7.5 PHOSPHATE BUFFERED SYSTEM

**TERRY F. REES* and STEPHEN R. DANIEL**
Department of Chemistry and Geochemistry, Colorado School of Mines, Golden, CO 80401, U.S.A.

(*Received* 15 *July* 1983; *accepted* 23 *September* 1983)

**Abstract**—Conditional stability constants, enthalpies and entropies of complexation at pH 7.5 and ionic strength 0.1 have been determined for neptunium(V) complexes of phosphate, salicylate, phthalate and citrate. Phosphate forms a complex with $\log \beta = 2.36 \pm 0.42$ at 25°C, $\Delta H_c^\circ = -69.9$ kJ/mole and $\Delta S_c^\circ = -188$ J/mole-K. At pH 7.5 salicylate does not form a complex with neptunium(V) due to the low charge density of the $NpO_2^+$ ion and incomplete ionization of the salicylate ion. Phthalate forms a complex with $\log \beta = 3.43 \pm 0.33$ at 25°C, $\Delta H_c^\circ = 33.5$ kJ/mole and $\Delta S_c^\circ = 182$ J/mole-K. Citrate forms a complex with $\log \beta = 4.84 \pm 0.72$ at 25°C, $\Delta H_c^\circ = 14.0$ kJ/mole and $\Delta S_c^\circ = 140$ J/mole-K. In all cases, only 1:1 complexes were identified.

In recent years, interest in the geochemical behaviour of neptunium has increased due to the large amount of that element produced in nuclear power reactors and the relative hazard of neptunium compared to other components of nuclear waste. As of the end of 1981, over 2000 metric tons of $^{237}Np$ were contained in the waste.[1] Serne *et al.*[2] estimated that the hazard index of neptunium, based on half-life, mobility and biological activity, equals that of plutonium. In order to develop models which will predict the geochemical behaviour of neptunium, certain thermodynamic parameters such as stability constants or the enthalpy and entropy of complexation are required. Virtually no data exist for neptunium complexes under environmental conditions, i.e. near neutral pH and low ionic strength. This paper reports complexation data for neptunium with phosphate, salicylate, phthalate and citrate under these conditions. These organic ligands contain functional groups representative of naturally-occurring organic materials.

A convenient procedure for determining stability constants, based on the distribution of metal ions between the aqueous phase and an ion-exchange resin was developed by Schubert.[3] The assumptions of the procedure are as follows. (1) The complex-forming ions are swamped by excess neutral salts which maintain an essentially constant ionic strength. (2) The total concentration of the metal ion under study is negligible as compared to that of the complex-forming ligand. (3) All pairs of solutions which are compared have the same pH, volume of solution and weight of exchanger. (4) The exchanger used has been previously saturated with the cation component of the bulk electrolyte. (5) No adsorption on the resin of the complex-forming ligand or of the complex ion takes place. (6) The metal ion concentrations allow the work to be carried out on the linear portion of the ion-exchange isotherm.

We will define the distribution coefficient ($D_0$) as the equilibrium concentration [in Becquerel/g resin (Bq/g)] of metal ion on the resin ([M,]) divided by the equilibrium concentration (Bq/ml) of uncomplexed metal ion in the aqueous phase ($[M_{aq}^{n+}]$):

$$D_0 = \frac{[M,]}{[M_{aq}^{n+}]}. \quad (1)$$

As complexing ligand ($L_{aq}^{m-}$) is added to an aqueous solution of $M^{n+}$ equilibrated with resin, the total concentration of metal ion in the aqueous phase will increase relative to that in the resin due to a shift in the distribution of metal between the resin and aqueous phases caused by complexation of the metal ion. The measured distribution ratio

*Author to whom correspondence should be addressed. Present address: U.S. Geological Survey, Lakewood, Colorado, U.S.A.

($D$) in the presence of complexing agent, is the equilibrium concentration of metal ion on the resin divided by the total concentration of metal ion in the aqueous phase, which includes both free metal ion and complexed metal ion.

$$D = \frac{[M_r]}{[M_{aq}^{n+}] + [ML_{aq}^{(n-m)+}]}. \quad (2)$$

If we define $\beta$ as the conditional stability constant at the pH and ionic strength being studied, and assume only 1:1 complexes:

$$\beta = \frac{[ML_{aq}^{(n-m)+}]}{[M_{aq}^{n+}][L_{aq}^{m-}]} \quad (3)$$

by combining eqns (2) and (3) we obtain

$$D = \frac{[M_r]}{[M_{aq}^{n+}] + [M_{aq}^{n+}]\beta[L_{aq}^{m-}]}. \quad (4)$$

Combining this equation with eqn (1) gives

$$D = \frac{D_0}{1 + \beta[L_{aq}^{m-}]}. \quad (5)$$

Rearranging and taking the logarithm of both sides yields

$$\log((D_0/D) - 1) = \log\beta + \log[L_{aq}^{m-}]. \quad (6)$$

A plot of $\log((D_0/D) - 1)$ vs $\log[L_{aq}^{m-}]$ is a straight line of unit slope with intercept of $\log\beta$.

A similar derivation can be followed for simple systems involving a total of $r$ ligands. The denominator in eqn (2) includes all complexes in the system. Thus, eqn (4) becomes

$$D = \frac{[M_r]}{\{[M_{aq}^{n+}] + \beta_1[M_{aq}^{n+}][L1_{aq}] + \beta_2[M_{aq}^{n+}][L2_{aq}] + \cdots + \beta_r[M_{aq}^{n+}][Lr_{aq}]\}} \quad (4a)$$

and eqn (5) becomes

$$D = \frac{D_0}{1 + \beta_1[L1_{aq}] + \beta_2[L2_{aq}] + \cdots + \beta_r[Lr_{aq}]} \quad (5a)$$

which yields

$$\log((D_0/D) - 1 - \sum_{i=1}^{r-1} \beta_i[Li_{aq}]) = \log\beta_r + \log[Lr_{aq}]. \quad (6a)$$

Thus if the stability constants of all complexes except one ($\beta_r$) are known, and if the concentrations of all ligands are known, $\beta_r$, may be determined from the intercept of a plot of

$$\log(D_0/D) - 1 - \sum_{i=1}^{r-1} \beta_i[Li_{aq}] \text{ vs } \log[Lr_{aq}].$$

If stability constants are determined at various temperatures, the free energy of complexation ($\Delta G_c^\circ$), enthalpy of complexation ($\Delta H_c^\circ$), and entropy of complexation ($\Delta S_c^\circ$) can be determined (4) by plotting $R \ln\beta$ vs $1/T$ (slope $= -\Delta H_c^\circ$ and intercept $= \Delta S_c^\circ$).

## EXPERIMENTAL

All reagents used in these studies were either commercially available, ultra-high purity reagents, or were recrystallized before use from reagent grade chemicals. Solutions were made by dissolving purified reagents in triply distilled water which had been treated with activated carbon to remove trace organic contaminants.

The perchloric acid ($HClO_4$) was Baker Ultrex grade with a certified assay of 69.8%. Low-carbonate sodium hydroxide (NaOH) solutions were prepared by dissolving dry (110°C to constant weight) Baker reagent grade NaOH in triply distilled water. The solutions were then heated to boiling, placed in glass bottles, tightly sealed, and cooled. The solutions were exposed to air only for very short periods to minimize carbon dioxide absorption. Merck reagent grade sodium perchlorate ($NaClO_4$), was recrystallized twice from a prepared aqueous solution of that salt by saturation at 90°C, followed by cooling in an ice bath. The crystals from the second crystallization were first air dried, then dried at 110°C to constant weight. The purified $NaClO_4$ was stored in a desiccator until needed.

Disodium hydrogen phosphate ($Na_2HPO_4$) and sodium dihydrogen phosphate ($NaH_2PO_4 \cdot H_2O$) were both Baker reagent grade chemicals. They were dried at 110°C to constant weight and stored in a desiccator over $CaCl_2$.

The pH 7.5 buffer was prepared by dissolving 18.93 g $Na_2HPO_4$ and 9.20 g $NaH_2PO_4 \cdot H_2O$ in 1 l. of the deionized water. The pH was adjusted using $HClO_4$ and NaOH solutions.

The sodium salicylate, sodium phthalate and sodium citrate were initially prepared by dissolution of the respective acid in dilute NaOH. Sufficient reagent was added to nearly saturate the solution. The sodium salts were then precipitated by adding triply-distilled ethanol. The supernate was removed by filtration, and the salts were used

for a second recrystallization. The salts were then air dried followed by drying at 50°C to constant weight. The dried crystals were stored in a desiccator.

The carrier-free neptunium ($^{237}Np$) solution was prepared by dissolving neptunium oxide ($NpO_2$) in 16 *N* $HNO_3$ with 1 $cm^3$ $HClO_4$ added. The resulting solution was evaporated to dryness and the residue was dissolved in approx. 2 $cm^3$ 0.001 *M* $HClO_4$–0.001 *M* HF. This solution was loaded onto a Biorad AG50WX8 hydrogen form resin (100–200 mesh) column with a resin bed 20 mm deep by 7 mm dia. The column was pretreated with approx. 10 $cm^3$ 0.001 *M* $HClO_4$–0.001 *M* HF. After loading, the column was rinsed with 5 $cm^3$ 0.001 *M* $HClO_4$. The neptunium was then eluted from the column using 1 *M* $HClO_4$. This neptunium-rich eluate was evaporated to dryness and dissolved in 0.1 *M* $HClO_4$.

The sodium-form resin was prepared by pouring a slurry of Biorad AG50WX8 hydrogen form resin (100–200 mesh) in deionized water into a large preparative column. A 5 *M* NaCl solution was passed through the column until the pH of the effluent was greater than 5. The resin was removed from the column into a large beaker and was repeatedly rinsed with the triply distilled water until all chloride was removed as shown by a negative silver chloride precipitation test. The resin was then air dried to constant weight and packaged in an air tight jar until use.

*Procedure*

The following experiments were run at 10°, 25° and 35°C in a Hetofridge constant temperature water bath capable of maintaining a preset temperature to ±0.5°C. A weighed aliquot of prepared ion exchange resin was placed in a 20 $cm^3$ glass liquid scintillation vial. Appropriate volumes of either $HClO_4$ or $NaClO_4$, ligand, buffer (pH 7.5) (as appropriate) and $^{237}Np$ solutions were added to give, upon dilution, an ionic strength (I) of 0.1 and the proper metal and ligand concentrations for study. The mixture was then diluted to 10 $cm^3$ using organic-free triply distilled water. The vial was capped and placed in the controlled-temperature water bath equipped with a sample shaker, and allowed to equilibrate for at least 12 hr (24 hr for the 10°C runs). Longer-term experiments established that equilibrium was attained in these times. At the end of the equilibration, the resin was allowed to settle and an aliquot of the solution was transferred to a new liquid scintillation vial containing liquid scintillation cocktail (Scinti-verse II, Fisher Scientific Co.). The sample was mixed to achieve a homogeneous gel, and the neptunium content was determined by counting the alpha decay using a Beckman LS-100 liquid scintillation counter. The count time was selected to give a counting precision of ±1% and a detection limit of 3 Bq/L. The resulting data were then subjected to the analysis described previously to obtain the conditional stability constants, and the conditional $\Delta G_c^\circ$, $\Delta H_c^\circ$, and $\Delta S_c^\circ$.

## RESULTS AND DISCUSSION

In order to satisfy the assumptions of the Schubert method, it is necessary to buffer all solutions at a specific pH during equilibration. The solution therefore contains competing ligands, namely hydroxide and the anions of the buffer. To correct the measured thermodynamic values for any competitive reactions, the stability constants, enthalpy, entropy, and free energy of reaction for these additional complexes must be known.

The ion exchange sorption isotherm for neptunium(V) was determined by independently varying, in 10 $cm^3$ of a 0.1 *M* $HClO_4$ solution, the neptunium concentration between $10^{-7}$ and $10^{-6}$ *M*, and the ion exchange resin weight between 0.10 and 1.0 g. No ligands other than $ClO_4^-$ were present in the solutions and the hydroxide concentration was low enough ($10^{-13}$ M) to be ignored. The results of this study (Table 1) indicate that within these ranges, the resin is not saturated and an average distribution constant ($D_0$) of 11.52 ± 0.04 is obtained.

The effect of hydrolysis was evaluated by repeating the above study substituting 0.1 *M* $NaClO_4$ for the perchloric acid and adjusting the pH between pH 5.5 and 9.5 with dilute $HClO_4$ and carbonate-free NaOH. (Hydrolysis constants were not determined since the hydroxide concentration at pH 7.5 is $3.2 \times 10^{-7}$ *M* while the neptunium concentration was also about $3 \times 10^{-7}$ *M*. The assumptions of the Schubert method are not met under these conditions.) The results, shown in Table 2, indicate a slight diminution in distribution coefficient at pH 7.5 as compared to 0.1 *M* $HClO_4$. Approximately 3.2% of the neptunium is hydrolyzed at this pH. Baes and Messmer[5] report a hydrolysis constant of $1.4 \times 10^{-9}$ at 25° and I = 0.1 which is equivalent to about 5% hydrolysis at pH 7.5.

The phosphoric acid system was chosen as the buffer system for our studies. At pH 7.5, the $[HPO_4^{2-}]/[H_2PO_4^-]$ ratio is 2:1, and buffer capacity was found sufficient at total phosphate concentrations of $10^{-3}$ *M*. Complexation of neptunium by phosphate at 10°, 25° and 35°C was studied at pH 7.5 and total phosphate concentrations between $10^{-3}$ and $10^{-2}$ *M* with a constant initial neptunium concentration of $3 \times 10^{-7}$ *M*.

Table 1. Distribution coefficient vs Np(V) concentration and vs resin weight at 25°C*

| $[NpO_2^+]_{Total}$ (M) | Resin Weight (g) | $D_o$ |
|---|---|---|
| $1.0 \times 10^{-7}$ | 0.500 | 11.58 |
| $3.0 \times 10^{-7}$ | 0.100 | 11.48 |
| $3.0 \times 10^{-7}$ | 0.500 | 11.52 |
| $3.0 \times 10^{-7}$ | 1.00 | 11.50 |
| $7.0 \times 10^{-7}$ | 0.500 | 11.48 |
| $1.0 \times 10^{-6}$ | 0.500 | 11.56 |

* in 10 mL 0.1 M $HClO_4$

Table 2. Neptunium hydrolysis study

$[NpO_2^+]_T = 3.2 \times 10^{-7}$ M

10 mL solution

*Ionic Strength = 0.1 M

0.500 g resin

| | D | | |
|---|---|---|---|
| pH | 10° | 25° | 35° |
| 0.1 M $HClO_4$ | | 11.52 | |
| 5.5 | | 11.51 | |
| 6.5 | | 11.49 | |
| 7.5 | 11.12 | 11.16 | 11.18 |
| 8.5 | | 8.37 | |
| 9.5 | | 2.02 | |

Table 3. Neptunium(V)—phosphate Schubert plot data

| Temperature | Log $[HPO_4^{2-}]$ | D | Log$[(D_o/D)-1-0.032]^1$ |
|---|---|---|---|
| 10° | -3.00 | 5.41 | 0.04 |
| | -2.83 | 4.53 | 0.18 |
| | -2.68 | 3.69 | 0.32 |
| | -2.47 | 2.70 | 0.51 |
| | -2.28 | 1.66 | 0.77 |
| | -2.00 | 0.94 | 1.05 |
| 25° | -3.00 | 8.06 | -0.40 |
| | -2.83 | 7.63 | -0.32 |
| | -2.68 | 7.34 | -0.27 |
| | -2.47 | 5.54 | +0.02 |
| | -2.28 | 4.21 | 0.23 |
| | -2.00 | 2.61 | 0.53 |
| 35° | -3.00 | 6.61 | -0.88 |
| | -2.83 | 6.37 | -0.70 |
| | -2.68 | 6.28 | -0.65 |
| | -2.47 | 5.53 | -0.32 |
| | -2.28 | 5.14 | -0.20 |
| | -2.00 | 4.02 | 0.10 |

[1]This is the left side of Equation 6a which includes the hydrolysis of $NpO_2^+$.

For purposes of this research, it was not necessary to determine which species ($H_2PO_4^-$, $HPO_4^{2-}$, or both) was responsible for complexing the neptunium. As long as the total phosphate concentration and pH are kept constant the $\beta$ value determined represents the composite complexation of $NpO_2^+$ by all phosphate species. Moskvin and Peretrukhin[6] identified both $[NpO_2(HPO_4)]^-$ and $[NpO_2(H_2PO_4)]$ in their studies, between pH 4.8 and 6.7, and phosphate concentrations from 0 to 0.2 *M*. However, in the total phosphate concentration range of $5 \times 10^{-3}$ to $5 \times 10^{-2}$ *M*, they only found $[NpO_2(HPO_4)]^-$. Their data, taken with ours suggest that $[NpO_2(HPO_4)]^-$ is the predominant complex present in our studies.

The data for the $[NpO_2(HPO_4)]^-$ Schubert plots at the three temperatures studied are given in Table 3. These data are representative of the type and precision seen in our other studies. The results, and those of the organic ligand studies, are given in Table 4.

The plots in Fig. 1 for the neptunium–phthalate system are representative of the types of curves the Schubert approach gives. The abscissa is the loga-

Table 4. Thermodynamic data for neptunium complexation

| Ligand | Temperature | log β | $\Delta G_C^{\circ}$(1) | $\Delta H_C^{\circ}$(1) | $\Delta S_C^{\circ}$(2) |
|---|---|---|---|---|---|
| $HPO_4^{2-}$ | 10° | 3.11±0.19 | -16.7 | -69.9 | -188 |
| | 25° | 2.36±0.42 | -13.4 | | |
| | 35° | 2.06±0.39 | -12.1 | | |
| Salicylate | 10° | * | 0 | - | - |
| | 25° | * | 0 | | |
| | 35° | * | 0 | | |
| Phthalate | 10° | 3.32±0.22 | -18.0 | 33.5 | 182 |
| | 25° | 3.43±0.33 | -19.7 | | |
| | 35° | 3.83±0.19 | -22.6 | | |
| Citrate | 10° | 4.70±0.53 | -25.6 | 14.0 | 140 |
| | 25° | 4.84±0.72 | -27.6 | | |
| | 35° | 4.93±0.11 | -29.0 | | |

1 units = kJ/mole
2 units = J/mole-°K
* no complex formed

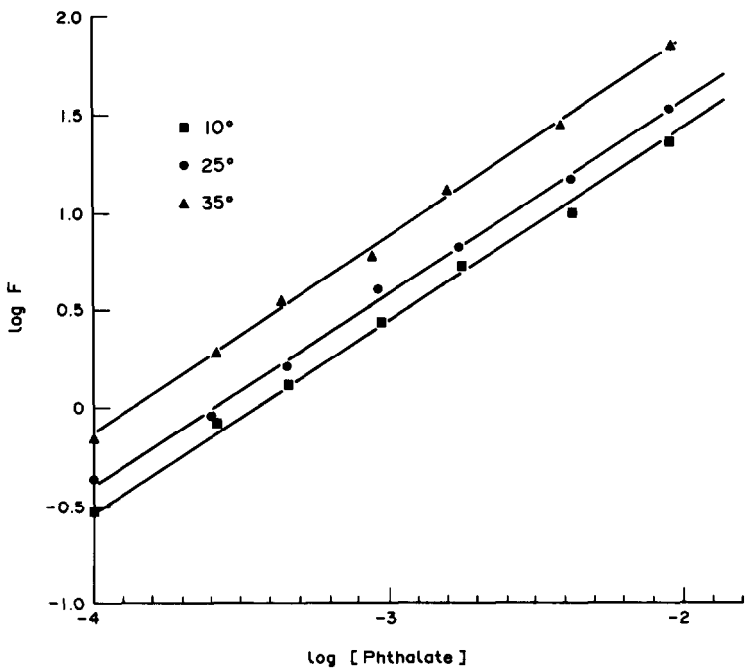



Fig. 1. $NpO_2$—phthalate Schubert plot.

rithm of the total ligand concentration while the ordinate is the logarithm of the function $F$:

$$F = [(D_0/D) - R] \quad (7)$$

where $R$ is the sum of constants from eqn (6a), in this case:

$$R = 1 + \beta_{OH^-}[OH^-] + \beta_{HPO_4^{2-}}[HPO_4^{2-}]. \quad (8)$$

Using the phosphate stability constants determined earlier, the values for $R$ and $F$ at the three temperatures are:

$$R_{10} = 1 + 0.032 + 6.6 = 7.19 \quad (9)$$

$$F_{10} = [(D_0/D) - 7.19] \quad (10)$$

$$R_{25} = 1 + 0.032 + 1.38 = 2.41 \quad (11)$$

$$F_{25} = [(D_0/D) - 2.41] \quad (12)$$

$$R_{35} = 1 + 0.032 + 0.58 = 1.61 \quad (13)$$

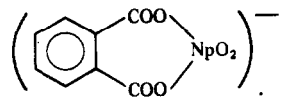
$$F_{35} = [(D_0/D) - 1.61]. \quad (14)$$

These values were verified to within 5% by runs at the three temperatures with only the phosphate buffer being present.

The Schubert plots for salicylate at 10°, 25° and 35°C in the ligand concentration range $10^{-4}$ to $10^{-2}$ M yielded slopes of zero, indicating that salicylate does not significantly complex neptunium(V) at pH 7.5. Stober[7] found a stability constant of $\sim 10^7$ for salicylate complexation of neptunium(V) under conditions where the phenolic group of salicylate was nearly totally ionized. At pH 7.5 only the carboxylate group is ionized [$Ka_1 = 1 \times 10^{-3}$, $Ka_2 = 4 \times 10^{-14}$].[8] Apparently salicylate does not complex neptunium(V) unless the additional stabilization from chelation is available, and a bidentate complex does not form due to the low charge density of $NpO_2^+$ until the phenolic group is ionized.

The Schubert plots for phthalate (Fig. 1) are linear with slope of about unity between $10^{-4}$ and $10^{-2}$ $M$ phthalate. The results of the Schubert and van't Hoff analyses are given in Table 4.

The large positive $\Delta S_C^\circ$ is probably due to reduction in the number of charged species in solution and resulting extensive dehydration of the phthalate and neptunyl ions upon complexation. Since the reaction is endothermic, as shown by the increase in stability at elevated temperatures, the entropy change provides the driving force for the formation of the complex. Taken together, the $\Delta H_C^\circ$ and $\Delta S_C^\circ$ imply that the neptunium(V)-phthalate is an inner sphere complex.[9–12] The $\beta$ value at 25°C found in this study is about twice that reported for oxalate at pH 4.8 [$\beta_1 = 2000$][13] suggesting the phthalate forms a bidentate complex with neptunium(V) of the form:




The citrate Schubert plots are also linear with slopes approximately equal to unity from citrate concentrations of about $2 \times 10^{-6}$ $M$ to $10^{-4}$ $M$. A summary of the thermodynamic data determined for the citrate system is also given in Table 4. Since $\Delta S_C^\circ$ is smaller for citrate than for phthalate, the $NpO_2^+$-citrate complex is apparently less dehydrated than the phthalate complex. This is to be expected due to the relatively smaller hydration sphere associated with the exposed benzene ring in the phthalate complex compared to the hydration sphere of the citrate complex. Even so, the large $\Delta S_c^\circ$ is indicative of some dehydration even in the citrate system. This fact, and the large positive heat of reaction suggest, as for the phthalate system, an inner sphere complex. The very high stability of the neptunium(V)-citrate complex strongly suggests a chelate, probably bidentate. The slope of unity in the Schubert plots suggests a 1:1 complex.

The stability constants are much smaller than for Pu(IV) complexes with the same ligands. Comparisons are with Pu(IV) rather than with Np(IV) since only a few Np(IV) complexes have been studied. The Pu(IV)-citrate 1:1 complex at $I = 0.5$ has a reported stability constant of $10^{15}$ (10). The lower stability of the Np(V) complexes is expected due to its lower charge density and thus lower Lewis acidity.

## SUMMARY

Several observations regarding neptunium(V) complexation by organic ligands seem warranted. Only 1:1 complexes were observed for the ligands studied. Salicylate fails to complex neptunyl due to the low degree of ionization of the ligand at the pH studied. The other organic ligand complexes studied here appear to form inner sphere complexes with substantial dehydration of the ligand and neptunyl ions. The stability constants are much smaller than for corresponding Pu(IV) complexes.

*Acknowledgements*—The support of the U.S. Geological Survey in providing facilities essential for conducting this research is gratefully ackowledged.

## REFERENCES

1. G. Z. Oertel and F. E. Coffman, *Spent Fuel and Radioactive Waste Inventories, Projections and*

*Characteristics*, U.S. Department of Energy Report DOE/NE-0017-1 (October 1982).
2. R. J. Serne and J. F. Relyea, *The Status of Radionuclide Sorption–desorption Studies Performed by the WRIT Program*, U.S. Department of Energy Report PNL-3997 Battelle Pacific Northwest Laboratory (April 1982).
3. J. Schubert, *J. Phys. and Coll. Chem.*, 1948, **52**, 340.
4. G. N. Lewis and M. Randall, *Thermodynamics*, Chap. 15. McGraw–Hill, New York (1961).
5. F. Baes, Jr., and R. E. Mesmer, *The Hydrolysis of Cations*. Wiley, New York (1976).
6. A. I. Moskvin and V. F. Peretrukhin, *Sov. Radiochem.* (Eng. Trans.) 1964, **6**, 198.
7. H. Stober, German Report KFK-1657 (1972).
8. R. C. Weast (Editor), *Handbook of Chemistry and Physics*, 49th Edn, D90. The Chemical Rubber Company, Cleveland (1968).
9. G. N. Lewis and M. Randall, *Thermodynamics*, Chap. 32. McGraw-Hill, New York (1961).
10. F. J. C. Rossotti, In *Modern Coordination Chemistry* (Edited by J. Lewis and R. G. Wilkins). Interscience, New York (1960).
11. G. R. Choppin and W. F. Strazik, *Inorg. Chem.* 1965, **4**, 1254.
12. S. Ahrland, *Coord. Chem. Rev.* 1972, **8**, 21.
13. D. M. Gruen and J. J. Katz, *J. Am. Chem. Soc.* 1953, **75**, 3772.

*Polyhedron* Vol. 3, No. 6, pp. 675–679, 1984
Printed in Great Britain.

0277-5387/84 $3.00 + .00
Pergamon Press Ltd.

# THE ISOLATION AND X-RAY CRYSTAL STRUCTURE OF A COMPLEX BETWEEN SODIUM HEXAFLUOROPHOSPHATE AND DIBENZO-36-CROWN-12

**JOHN M. MAUD and J. FRASER STODDART***
Department of Chemistry, The University, Sheffield S3 7HF, England

**HOWARD M. COLQUHOUN**
New Science Group, Imperial Chemical Industries PLC, The Heath, Runcorn WA7 4QE, England

**and**

**DAVID J. WILLIAMS**
Chemical Crystallography Laboratory, Department of Chemistry, Imperial College, London SW7 2AY, England

(*Received* 19 *July* 1983; *accepted* 15 *August* 1983)

**Abstract**—The crystal structure of $2NaPF_6$·dibenzo-36-crown-12 was determined by X-ray diffraction methods. The 2:1 (metal:ligand) complex crystallises in the monoclinic system, space group $P2_1/n$ with cell constants of $a = 14.189(2)$, $b = 9.372(1)$, $c = 16.750(3)$ Å, and $\beta = 108.98(1)°$. The two $NaPF_6$ units are each coordinated through five oxygen atoms to opposite faces of the macrocycle in a centrosymmetric manner.

During some recent investigations[1,2] on 1:1 complexes involving dibenzo-3*n*-crown-*n* ethers ($n = 6$–12) as hosts and $[Pt(bipy)(NH_3)_2][PF_6]_2$ and $[Diquat][PF_6]_2$ as guests, we isolated inadvertently a crystalline 2:1 complex between $NaPF_6$ (present as an impurity in one of the $[Diquat][PF_6]_2$ samples) and dibenzo-36-crown-12† (DB36C12). Since there are relatively few examples[3–7] of crown ether-like receptor molecules which give rise to complexes containing *two* metal cations bound simultaneously by *one* ligand, we decided to pursue this chance observation to a satisfactory conclusion. This paper describes the preparation, characterisation, and X-ray structural investigation of $2NaPF_6$·DB36C12. Comparisons are drawn between the coordination properties of this 2:1 complex and the crystalline 1:1 complex formed[8] between NaI and benzo-15-crown-5 (B15C5). In addition, the implications of this new result for the future design of binary and ternary metal complexes involving crown ether hosts is explored.

## EXPERIMENTAL

The stepwise synthesis of DB36C12 has been described briefly elsewhere.[1] A full account of the synthesis will be published shortly.[9]

*Preparation of* $2NaPF_6$·DB36C12

Dibenzo-36-crown-12 (58.4 mg, 93.4 μmol) and sodium hexafluorophosphate (31.4 mg, 187 μmol) were dissolved in methanol-dichloromethane (3:1, 2 $cm^3$). Ether (3 $cm^3$) was layered on top of the solution, and *n*-pentane (3 $cm^3$) was layered on top of the ether layer. After 24 hr, the mixture contained small transparent crystals of a size and quality suitable for X-ray crystallography. After a further 4 days, the crystals were collected by filtration, washed with *n*-pentane, and dried *in vacuo*. Yield 76 mg, 85%; m.p. 186–188°C with softening from *ca.* 170°C. Found: C, 40.3; H, 5.0. $C_{32}H_{48}F_{12}Na_2O_{12}P_2$ requires C, 40.0; H, 5.0%.

*X-Ray structural analysis of* $2NaPF_6$·DB36C12

*Crystal data.* $C_{32}H_{48}O_{12}Na_2(PF_6)_2$, colourless prisms, monoclinic, $a = 14.189(2)$, $b = 9.372(1)$,

*Author to whom correspondence should be addressed.

†The trivial name for 6, 7, 9, 10, 12, 13, 15, 16, 18, 19, 26, 27, 29, 30, 32, 33, 35, 36, 38, 39-eicosahydrodibenzo[*b*, *t*][1, 4, 7, 10, 13, 16, 19, 22, 25, 28, 31, 34]dodecaoxacyclohexatriacontin.

$c = 16.750(3)$ Å, $\beta = 108.98(1)°$, $U = 2106$ Å$^3$, space group $P2_1/n$, $Z = 2$, $M = 960.6$, $D_c = 1.52$ g cm$^{-3}$, $\mu$Cu-$K_a = 21$ cm$^{-1}$.

*Measurements.* Refined unit cell parameters were obtained by centering 22 reflections on a Nicolet R3m diffractometer. 2841 Independent reflections ($\theta \leqslant 57°$) were measured with Cu-$K_\alpha$ radiation (graphite monochromator) using the omega-scan measuring routine. Of these, 2662 had $|F_0| > 3\sigma(|F_0|)$ and were considered to be observed. Lorentz, polarisation, and an empirical absorption correction, based upon 320 azimuthal scans, were applied.

*Structure analysis.* The structure was solved by direct methods. An $E$ map computed with 423 $E$'s > 1.52 for the phase solution with the highest "figure of merit" gave the positions of all non-hydrogen atoms. All hydrogen atoms were placed at idealised positions (C–H = 0.96 Å) and allowed to ride on their parent carbon atoms. The non-hydrogen atoms were refined anisotropically. The hydrogen atoms were assigned isotropic thermal parameters, $U(\mathrm{H}) = 1.2U_{eq}$ (C).

Refinement was by block-cascade least-squares to $R = 0.078$, $R_\omega = 0.098$, $[\omega^{-1} = \sigma^2(F) + 0.0014F^2]$. Computations were carried out on an Eclipse S140 computer using the SHELXTL program system.[10] Scattering factors were taken from the International Tables for X-ray crystallography.[11]

Final atomic coordinates, including those of the hydrogen atoms, and thermal parameters have been deposited with the Editor as supplementary data.†

†Atomic coordinates have also be deposited with the Cambridge Crystallographic Data Centre.

## RESULTS AND DISCUSSION

Tables 1 and 2 record the bond lengths and bond angles respectively for $2NaPF_6 \cdot DB36C12$. Torsional angles for the C–C and C–O bonds in macrocyclic ring are shown in the Figure of the crystal structure of the 2:1 complex. The macrocycle possesses a crystallographic centre of symmetry and is twisted such that it presents two complexing faces at opposite ends of the molecule. One of these is directed upwards and the other downwards and each accommodates a bound $NaPF_6$ unit. This arrangement can be likened to that of two linked 15-crown-5 units, though the non-covalently bonded O(4)–O(16) distance (3.33 Å) is somewhat longer than that (2.71 and 2.79 Å) for the oxygen atoms joined by bismethylene units. Each sodium ion is seven coordinate, with bonding to five oxygen atoms at distances ranging from 2.419(3) to 2.544(2) Å, and the two fluorine atoms of a hexafluorophosphate anion at 2.424(4) and 2.528(4) Å. The sodium ion is displaced 0.45 Å from the mean plane of these five oxygen atoms towards the phosphorus atom. The Na–O distances in $2NaPF_6 \cdot DB36C12$ are, on average, larger than those (2.35–2.43 Å) observed in the crystalline $NaI \cdot B15C5 \cdot H_2O$ complex.[8] Also, in that structure, the sodium ion is displaced 0.75 Å from the mean plane of the five oxygen atoms. In $2NaPF_6 \cdot DB36C12$, the angles of approach of the Na–O bond vectors to the COC planes vary from 15.6° for O(16) to 45.4 for O(7) (see the caption to Fig. 1). Although the approach closest to a trigonal geometry [15.6° at O(16)] results in the largest coordinated COC angle [117.2(4)°], there is no apparent correlation between the angle of approach and the COC angles at the other coordinated oxygen atoms. Even in the case of O(16), the

Table 1. Bond lengths (Å)

| | | | |
|---|---|---|---|
| P–F(1) | 1.600(4) | P–F(2) | 1.553(4) |
| P–F(3) | 1.579(4) | P–F(4) | 1.546(4) |
| P–F(5) | 1.576(4) | P–F(6) | 1.592(4) |
| F(1)–Na | 2.528(4) | F(6)–Na | 2.424(4) |
| Na–O(4) | 2.544(2) | Na–O(7) | 2.420(3) |
| Na–O(10) | 2.447(4) | Na–O(13) | 2.419(3) |
| Na–O(16) | 2.449(4) | O(1)–C(2) | 1.416(5) |
| O(1)–C(22a) | 1.363(5) | C(2)–C(3) | 1.498(6) |
| C(3)–O(4) | 1.403(5) | O(4)–C(5) | 1.422(5) |
| C(5)–C(6) | 1.489(7) | C(6)–O(7) | 1.433(5) |
| O(7)–C(8) | 1.413(6) | C(8)–C(9) | 1.509(7) |
| C(9)–O(10) | 1.408(7) | O(10)–C(11) | 1.424(6) |
| C(11)–C(12) | 1.510(8) | C(12)–O(13) | 1.399(6) |
| O(13)–C(14) | 1.420(9) | C(14)–C(15) | 1.302(8) |
| C(15)–O(16) | 1.440(6) | O(16)–C(17) | 1.402(5) |
| C(17)–C(18) | 1.362(7) | C(17)–C(22) | 1.404(6) |
| C(18)–C(19) | 1.395(7) | C(19)–C(20) | 1.365(8) |
| C(20)–C(21) | 1.378(7) | C(21)–C(22) | 1.379(5) |
| C(22)–O(1a) | 1.363(5) | O(1a)–C(22) | 1.363(5) |

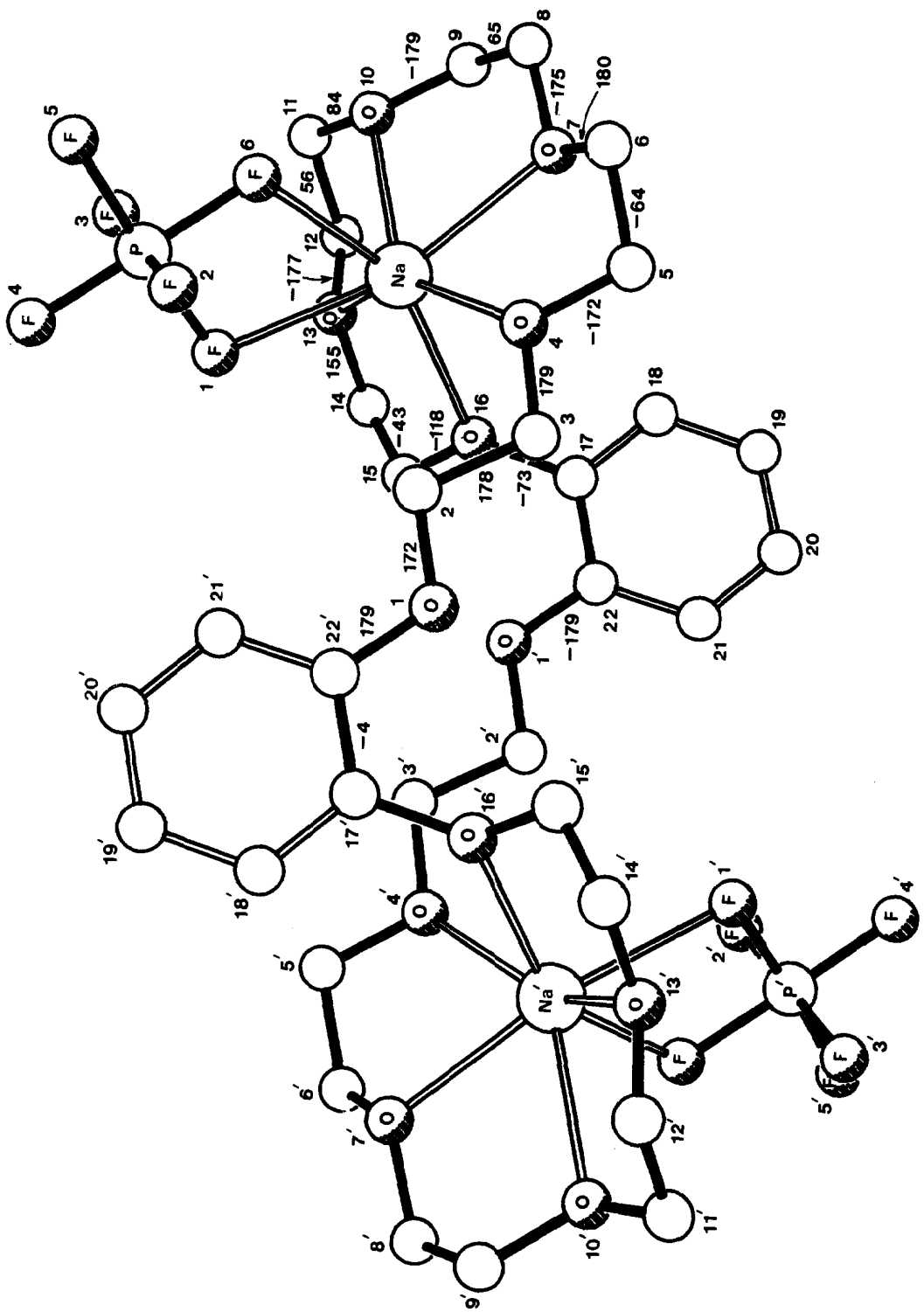



Fig. 1. Crystal structure of $2NaPF_6{\cdot}DB36C12$. Torsional angles (°) are indicated beside the relevant C–C and C–O bonds. Coordination distances, R[Na . . . . O] (Å), angles (°) between COC planes and Na–O vectors: O(4), 2.544(2), 34.1; O(7), 2.420(3), 45.4; O(10), 2.447(4), 46.9; O(13), 2.419(3), 39.0; O(16), 2.449(4), 15.6. Coordination distances, R[Na . . .F] (Å) F(1), 2.528(4); F(6), 2.424(4).

Table 2. Bond lengths (deg)

| | | | |
|---|---|---|---|
| F(1)-P-F(2) | 92.4(2) | F(1)-P-F(3) | 88.3(2) |
| F(2)-P-F(3) | 178.7(3) | F(1)-P-F(4) | 92.5(2) |
| F(2)-P-F(4) | 90.6(2) | F(3)-P-F(4) | 90.4(2) |
| F(1)-P-F(5) | 176.7(2) | F(2)-P-F(5) | 88.2(2) |
| F(3)-P-F(5) | 91.1(2) | F(4)-P-F(5) | 90.7(2) |
| F(1)-P-F(6) | 87.2(2) | F(2)-P-F(6) | 89.3(2) |
| F(3)-P-F(6) | 89.7(2) | F(4)-P-F(6) | 179.7(3) |
| F(5)-P-F(6) | 89.6(2) | P-F(1)-Na | 106.9(2) |
| P-F(6)-Na | 112.0(2) | F(1)-Na-F(6) | 52.7(1) |
| F(1)-Na-O(4) | 98.9(1) | F(6)-Na-O(4) | 92.6(1) |
| F(1)-Na-O(7) | 151.9(1) | F(6)-Na-O(7) | 101.4(1) |
| O(4)-Na-O(7) | 68.4(1) | F(1)-Na-O(10) | 111.4(1) |
| F(6)-Na-O(10) | 80.0(1) | O(4)-Na-O(10) | 133.7(1) |
| O(7)-Na-O(10) | 68.5(1) | F(1)-Na-O(13) | 85.7(1) |
| F(6)-Na-O(13) | 112.1(1) | O(4)-Na-O(13) | 151.2(1) |
| O(7)-Na-O(13) | 117.8(1) | O(10)-Na-O(13) | 67.9(1) |
| F(1)-Na-O(16) | 98.4(1) | F(6)-Na-O(16) | 150.1(2) |
| O(4)-Na-O(16) | 83.6(1) | O(7)-Na-O(16) | 104.7(1) |
| O(10)-Na-O(16) | 123.3(1) | O(13)-Na-O(16) | 67.6(1) |
| C(2)-O(1)-C(22a) | 117.6(3) | O(1)-C(2)-C(3) | 106.1(3) |
| C(2)-C(3)-O(4) | 108.4(3) | Na-O(4)-C(3) | 124.5(2) |
| Na-O(4)-C(5) | 110.2(2) | C(3)-O(4)-C(5) | 112.2(3) |
| O(4)-C(5)-C(6) | 108.3(3) | C(5)-C(6)-O(7) | 108.7(4) |
| Na-O(7)-C(6) | 112.6(3) | Na-O(7)-C(8) | 113.0(2) |
| C(6)-O(7)-C(8) | 113.0(4) | O(7)-C(8)-C(9) | 107.8(5) |
| C(8)-C(9)-O(10) | 106.1(4) | Na-O(10)-C(9) | 111.4(2) |
| Na-O(10)-C(11) | 112.2(3) | C(9)-O(10)-C(11) | 114.1(4) |
| O(10)-C(11)-C(12) | 111.2(4) | C(11)-C(12)-O(13) | 105.9(4) |
| Na-O(13)-C(12) | 117.5(3) | Na-O(13)-C(14) | 115.4(3) |
| C(12)-O(13)-C(14) | 110.0(5) | O(13)-C(14)-C(15) | 115.6(7) |
| C(14)-C(15)-O(16) | 115.0(6) | Na-O(16)-C(15) | 109.4(3) |
| Na-O(16)-C(17) | 130.7(3) | C(15)-O(16)-C(17) | 117.2(4) |
| O(16)-C(17)-C(18) | 120.6(4) | O(16)-C(17)-C(22) | 118.5(4) |
| C(18)-C(17)-C(22) | 120.8(4) | C(17)-C(18)-C(19) | 120.0(5) |
| C(18)-C(19)-C(20) | 119.6(5) | C(19)-C(20)-C(21) | 120.6(4) |
| C(20)-C(21)-C(22) | 120.7(4) | C(17)-C(22)-C(21) | 118.3(4) |
| C(17)-C(22)-O(1a) | 116.0(3) | C(21)-C(22)-O(1a) | 125.7(4) |

correlation may be illusory as there is evidence for some disorder (large thermal anisotropy) in the adjacent C(14)–C(15) bond. On the other hand, an approximately trigonal approach of the electrostatic bond to O(16) in its unique capacity as the only phenolic representative of the five coordinated oxygen atoms, is not unreasonable (see Refs. 3 and 4). By utilising a lone pair of electrons in an $sp^2$ orbital for coordination, the $Na^+$ ion leaves the other line pair of electrons in the *p* orbital on O(16) to interact conjugatively with the $\pi$ system of the aromatic ring. It is also noteworthy that there is a significant difference in lengths of the two aryl–O bonds [1.363(5) and 1.402(5) Å], the shorter one being associated with the non-coordinated oxygen atom, O(1).

At the crystal packing level, the structure is loosely packed with slight overlap in geometrically parallel fashion of the aromatic rings in symmetry related molecules. The inter-ring plane separation between these aromatic rings is 3.55 Å.

Not surprisingly, the stoichiometry of metal cationic complexes with benzo and dibenzo crown ethers appears to exhibit some dependence upon the size of the macrocyclic ring. Thus, B15C5 forms[12] a sandwich-like crystalline 2:1 (ligand:metal) complex with KI, whereas the 18-membered ring of DB18C6 is just the right size, judging from stability constant measurements,[13] to form Saturn-like 1:1 complexes with $K^+$ ions. Also, DB30C10 appears to prefer forming 1:1 complexes, as evidenced by the fact that single crystals have been isolated and characterised by X-ray crystallography in the case of at least three examples,[14–16] KI·DB30C10, KSCN·DB30C10, and RbSCN·DB30C10.$H_2O$. In all these complexes, the ligand clearly seeks to maximise its interactive role by wrapping itself around the metal ion adopting a conformation reminiscent of the seam on a tennis ball. However, with a ligand such as DB24C8, which is too large to form Saturn-like 1:1 complexes, yet not flexible enough to wrap itself around a metal cation, the 2:1 (metal:ligand) complex is a compromise (Ref. 3), judging from the crystal structures of 2KSCN·DB24C8[3] and 2Na(*o*-nitrophenolate)·DB24C8.[4] The question of what would happen at even larger ring sizes has now begun to be resolved with realisation that DB36C12 forms a 2:1 (metal:ligand) complex with $NaPF_6$. In retrospect, the formation of a binary

metal complex by this ligand is probably hardly surprising. Importantly, however, it does raise the further question of the possibility of isolating crystalline ternary metal complexes when the size of the macrocyclic ring is increased even further.

*Acknowledgements*—We thank Imperial Chemical Industries PLC and the Science and Engineering Research Council for support. DB36C12 was prepared by Mr. J. B. Wolstenholme in connection with a project financed by the Agricultural Research Council.

## REFERENCES

1. H. M. Colquhoun, J. F. Stoddart, D. J. Williams, J. B. Wolstenholme and R. Zarzycki, *Angew. Chem. Int. Ed. Engl.* 1980, **20**, 1051.
2. H. M. Colquhoun, E. P. Goodings, J. M. Maud, J. F. Stoddart, D. J. Williams and J. B. Wolstenholme, *J. Chem. Soc., Chem. Commun.* 1983, 1140.
3. M. Mercer and M. R. Truter, *J. Chem. Soc., Dalton Trans.* 1973, 2469.
4. D. L. Hughes, *J. Chem. Soc., Dalton Trans.* 1975, 2374.
5. M. Mellinger, J. Fischer and R. Weiss, *Angew. Chem. Int. Ed. Engl.* 1973, **12**, 771; R. Wiest and R. Weiss, *J. Chem. Soc., Chem. Commun.* 1973, 678; J. Fischer, M. Mellinger and R. Weiss, *Inorg. Chim. Acta* 1977, **21**, 259; R. Louis, Y. Agnus and R. Weiss, *J. Am. Chem. Soc.* 1978, **100**, 3604.
6. R. Iwamoto, *Bull. Soc. Chem. Japan* 1973, **46**, 1123.
7. G. Weber and W. Saenger, *Angew. Chem. Int. Ed. Engl.* 1979, **18**, 227.
8. M. A. Bush and M. R. Truter, *J. Chem. Soc., Perkin Trans. II* 1972, 341.
9. H. M. Colquhoun, E. P. Goodings, J. M. Maud, J. F. Stoddart, D. J. Williams and J. B. Wolstenholme, *J. Chem. Soc., Perkin Trans. II*, to be submitted.
10. G. M. Sheldrick, SHELXTL, *An Integrated System for Solving, Refining, and Displaying Crystal Structures from Diffraction Data*, University of Göttingen, Federal Republic of Germany (1978).
11. *International Tables for X-ray Crystallography*, Vol. IV, pp. 99–149. Kynoch Press, Birmingham, England.
12. P. R. Mallinson and M. R. Truter, *J. Chem. Soc., Perkin Trans. II* 1972, 1818.
13. H. K. Frensdorff, *J. Am. Chem. Soc.* 1971, **93**, 600.
14. M. A. Bush and M. R. Truter, *J. Chem. Soc., Perkin Trans. II* 1972, 345.
15. J. Hašek, D. Hlavatá and K. Huml, *Acta Cryst.* 1980, **B36**, 1782.
16. J. Hašek, K. Huml and D. Hlavatá, *Acta Cryst.* 1979, **B35**, 330.

*Polyhedron* Vol. 3, No. 6, pp. 681–688, 1984
Printed in Great Britain.

0277–5387/84 $3.00 + .00
© 1984 Pergamon Press Ltd.

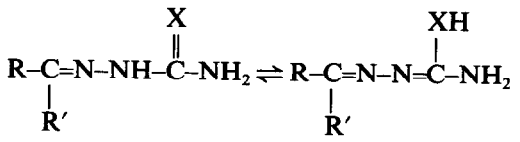
# STRUCTURAL FEATURES OF SOME ORGANOTIN(IV) COMPLEXES OF SEMI- AND THIO-SEMICARBAZONES‡

**ANIL SAXENA† and J. P. TANDON***
Department of Chemistry, University of Rajasthan, Jaipur 302004, India

(*Received* 17 *August* 1983; *accepted* 23 *September* 1983)

**Abstract**—Some five- and six-coordinated di and tri-*n*-butyl tin(IV) semi- and thio-semi carbazates have been synthesized. The characterization of these complexes, by IR, NMR ($^1$H, $^{13}$C, $^{119}$Sn), $^{119}$Sn Mössbauer and Mass spectroscopies along with X–ray diffraction, reveals that complexes of biionic ligands of the type $Bu_2Sn\,L''$ are five-coordinated having trigonal bipyramidal geometry. However, complexes of monoionic ligands of the type $Bu_2SnL'_2$ are six-coordinated in a distorted *cis*-octahedral geometry and $Bu_3SnL'$ are five-coordinated with a trigonal bipyramidal structure. X-ray structural studies on the compound $Bu_2Sn(O.C_6H_4.CH{:}N.N.CS.NH_2)$, show that it crystallizes in a monoclinic lattice with $a = 16.90$ Å, $b = 9.71$ Å, $c = 8.60$ Å, and $\beta = 103°45'$.

Semicarbazones and thiosemicarbazones are amongst the most important nitrogen–oxygen/sulphur donor ligands.[1] Both of these ligands are capable of acting as neutral or charged ligand moieties. During the past few years, a plethora of references describing the transition metal complexes of these ligands have appeared in the literature.[2,3] However, little is known about the complexing behaviour of non-transition elements with these ligands.[4] Amongst the non-transition elements, tin occupies an important position as a number of modern physicochemical techniques can be applied for the detailed structural study of its compounds. It was, therefore considered of interest to react organotin oxides with semi– and thio-semicarbazones;



(where X = O or S)

and carry out detailed systematic studies of the resulting compounds.

## EXPERIMENTAL

Chemicals and solvents used were dried and purified by standard methods, and moisture was excluded from the glass apparatus using $CaCl_2$ drying tubes. The ligands were prepared by the literature method[5] and all the manipulations were carried out under absolutely dry conditions. The complexes were prepared by a method similar to that reported in an earlier publication.[6] The details are given in Table 1.

The complexes were analyzed by the literature methods and the molecular weights were determined by the Gallenkamp ebulliometer or cryoscopically in freezing benzene. $^{119}$Sn Mössbauer spectra were recorded with $Ba^{119}SnO_3$ source at 77 K and the isomer shift values are relative to $SnO_2$. The X-ray powder diffractogram of the compound was obtained on a Phillips PM 9929/05 automatic diffractometer with Fe$K_a$ target. The structure was solved by Ito's method.[7] The details of spectroscopic measurements are similar to those reported earlier.[6]

## RESULTS AND DISCUSSION

Reaction of di-*n*-butyl and tri-n-butyl tin oxides with these ligands have been carried out in 1 : 1 and 1 : 2 molar ratios in refluxing benzene. These reactions proceed with the liberation of water, which is

*Author to whom correspondence should be addressed.

†Present address: School of Chemistry and Molecular Sciences, University of Sussex, Brighton, BN1 9QI, England.

‡Presented at XXII Int. Conf. Coord. Chem., Hungary, 1982.

Table 1. Analyses and physical characteristics of organotin complexes

| Compound | | Mol. wt. Found (Calcd.) | M.P. °C | Colour and State (Yield %) | Analyses % Found (Calcd.) S % | Sn % | C % | H % |
|---|---|---|---|---|---|---|---|---|
| $Bu_2Sn(C_9H_9N_3OS)$ | $A_1$ | 430 (440) | 81 | Yellow solid (94) | 6.52 (7.27) | 26.92 (27.03) | 45.87 (46.37) | 5.58 (6.13) |
| $Bu_2Sn(C_8H_7N_3OS)$ | $A_2$ | 405 (426) | 87 | Dark yellow solid (92) | 7.05 (7.51) | 27.48 (27.98) | 46.95 (45.07) | 6.32 (5.86) |
| $Bu_2Sn(C_{12}H_9N_3OS)$ | $A_3$ | 495 (478) | - | Red semi-solid (90) | 5.91 (6.72) | 24.72 (25.02) | 48.23 (50.42) | 6.81 (6.09) |
| $Bu_2Sn(C_8H_8N_3S)_2$ | $A_4$ | 565 (589) | - | Orange semi-solid (92) | 10.13 (10.86) | 20.36 (20.18) | 47.12 (48.89) | 6.06 (5.77) |
| $Bu_3Sn(C_8H_8N_3S)$ | $A_5$ | 484 (468) | - | Brown yellow semi solid (88) | 6.23 (6.88) | 25.00 (25.45) | 50.10 (51.61) | 7.83 (7.52) |
| $Bu_3Sn(C_9H_{10}N_3S)$ | $A_6$ | 498 (482) | - | Yellow semi solid (86) | 5.88 (6.65) | 24.05 (24.73) | 53.21 (52.39) | 7.05 (7.69) |
| $Bu_2Sn(C_9H_9N_3O_2)$ | $A_7$ | 400 (424) | 91 | Light green yellow solid (92) | - | 27.82 (28.05) | 47.05 (48.11) | 5.80 (6.36) |
| $Bu_2Sn(C_8H_7N_3O_2)$ | $A_8$ | 402 (410) | - | Yellow semi-solid (90) | | 28.52 (29.00) | 47.82 (46.83) | 6.52 (6.09) |
| $Bu_2Sn(C_9H_{10}N_3O)_2$ | $A_9$ | 572 (585) | 185 | Brown yellow-solid (94) | | 21.05 (20.33) | 51.88 (53.35) | 5.91 (6.49) |
| $Bu_2Sn(C_8H_8N_3O)_2$ | $A_{10}$ | 578 (557) | 192 | Cream yellow-solid (90) | | 21.12 (21.43) | 50.05 (51.89) | 6.63 (6.12) |
| $Bu_3Sn(C_9H_{10}N_3O)$ | $A_{11}$ | 480 (466) | - | Brown semi-solid (90) | | 25.81 (25.57) | 55.83 (54.19) | 7.32 (7.95) |
| $Bu_3Sn(C_8H_8N_3O)$ | $A_{12}$ | 440 (452) | - | Cream yellow semi-solid (90) | | 26.05 (26.38) | 51.59 (53.21) | 7.05 (7.76) |

Note: These complexes were also analyzed for the nitrogen contents.

removed azeotropically with benzene.

$$Bu_2SnO + N\begin{matrix}OH\\XH\end{matrix} \rightarrow Bu_2Sn(\widehat{O\,N\,X}) + H_2O$$

$$Bu_2SnO + 2\widehat{N\,X}H \rightarrow Bu_2Sn(\widehat{N\,X})_2 + H_2O$$

$$(Bu_3Sn)_2O + 2\widehat{N\,X}H \rightarrow 2Bu_3Sn(\widehat{N\,X}) + H_2O.$$

(where X = O or S)

The above reactions were found to be quite facile and could be completed in 8–10 hr of refluxing. The resulting complexes are obtained in good yields in the form of yellow to dark red coloured solids, semi-solids and viscous oils. These monomeric, low melting solids are soluble in most of the common organic solvents and susceptible to moisture.

In the IR spectra of ligands, a broad band is observed in the region, 3300–2850 $cm^{-1}$ . This band attributable to $\nu$OH and/or $\nu$NH does not appear in the complexes and in its place two sharp bands are observed at $\sim$ 3310 and 3130 $cm^{-1}$ due to the symmetric and asymmetric modes of $NH_2$ group.[8]

A sharp and strong band at 1635 $cm^{-1}$ in these complexes compared to one at $\sim$ 1620 $cm^{-1}$ in the ligands may be assigned to $\nu$C=N. The shifting of this band to higher frequency is probably due to an increase in the C=N bond order due to the coordination of nitrogen with the metal atom. The Sn–C stretching vibration gives two bands, one near 600 $cm^{-1}$ due to the *trans* form and the other one around 510 $cm^{-1}$ due to the *gauche* form. Several new bands in the complexes at $\sim$ 550, 425 and 340 $cm^{-1}$ are probably due to $\nu$Sn.O, $\nu$Sn←N and $\nu$Sn–S respectively.[6]

The proton magnetic resonance spectral data of these complexes have been recorded in Table 2. The protons of –OH and –SH groups of the ligands give signals at $\delta$ 12.10 and 9.81 ppm and which are absent in the metal complexes indicating the coordination of tin with oxygen as well as sulphur atoms. The protons of the $NH_2$ group appear at $\delta$ 5 ppm in $Bu_2SnL$, whereas in the case of $Bu_3SnL$ these are observed at $\delta$ 3.5 ppm. The protons of the aldehyde or ketonic –C̈–R group show marked shifting due to the coordination of > C=N with the tin atom. The protons of the butyl groups appear in the range of $\delta$ 0.5–1.9 ppm.

$^{119}$Sn Mössbauer parameters for two of these complexes have been derived and are recorded in Table 3.

The isomer shift values indicate the presence of tin in the +4 oxidation state and the presence of quadruple splitting shows that the EFG around the tin nucleus is produced by the inequalities in the

Table 2. $^1$H NMR data ($\delta$ ppm) of ligands and organotin semi- and thiosemicarbazates

| Compound | | -OH | -NH | $-C_6H_4$* | -H, $-CH_3$ | $-NH_2$ | Sn($C_4H_9$) |
|---|---|---|---|---|---|---|---|
| $OH.C_6H_4.CH{:}N.\overset{H}{\underset{\diagdown}{N}}{:}C.O.NH_2$ | | 11.46 | 9.81 | 6.93 | 8.22 | 2.72 | - |
| $n\text{-}Bu_2Sn(O.C_6H_4.CH{:}N.N{:}C.O.NH_2$ | $A_8$ | - | - | 7.01 | 8.35 | 4.95 | 0.7-1.8 |
| $OH.C_6H_4.CH{:}N.\overset{H}{\underset{\diagdown}{N}}{:}C.S.NH_2$ | | 11.40 | 10.02 | 6.86 | 8.20 | 2.65 | - |
| $n\text{-}Bu_2Sn(O.C_6H_4.CH{:}N,N{:}C.S.NH_2)$ | $A_2$ | - | - | 6.92 | 8.34 | 4.90 | 0.6-1.65 |
| $OH.C_6H_4.C(CH_3){:}N.\overset{H}{\underset{\diagdown}{N}}.C.S.NH_2$ | | 12.10 | 9.81 | 7.11 | 1.62 | 2.32 | - |
| $n\text{-}Bu_2Sn(O.C_6H_4.C(CH_3){:}N.N.C.S.NH_2$ | $A_1$ | - | - | 7.02 | 2.6 | 5.05 | 0.7-1.75 |
| $n\text{-}Bu_2Sn(O.C_{10}H_6.CH{:}N.N.C.S.NH_2)$ | $A_3$ | - | - | 7.42 | 9.35 | 4.85 | 0.75-1.70 |
| $n\text{-}Bu_3Sn(O.C_6H_5.CH{:}N.N.C.O.NH_2)$ | $A_{12}$ | - | - | 7.51 | 9.46 | 3.45 | 0.7-2.1 |
| $n\text{-}Bu_3Sn(C_6H_5.CH{:}N.N.C.S.NH_2)$ | $A_5$ | - | - | 7.63 | 9.40 | 3.55 | 0.58-2.0 |

* Center of multiplet.

tin-ligand $\sigma$ bonds.[9] These compounds give a $\rho$ value of 2.2 which indicates a coordination number greater than four. The monomeric six-coordinate structures seem to be most probable for these compounds, as the isomeric shift and quadrupole splitting values are well within the range (1.63–2.56) prescribed for octahedral geometries with *cis*–R groups.[10] The point charge calculations predict a $\Delta$Eq value of 2 $mm^{-1}$ for the *cis*-isomer and 4 $mms^{-1}$ for the *trans* isomer with no distortion. A slightly higher value of $\Delta$Eq may be accounted for by considering a slight distortion from the ideal symmetry.[11] The isomer shift values are also somewhat lower than *trans* analogues due to a decrease in the 5 *s*-character of the Sn–C $\sigma$ bonds. Naik *et al.*[12] have reported $\delta$ values (0.92 and 1.45 $mms^{-1}$) for *cis*- and *trans* octahedral $Bu_2Sn$ complexes.

The mass spectra of $Bu_2Sn(OC_6H_4.C(CH_3){:}NNCSNH_2)$ and $Bu_2Sn(OC_6H_4CH.NNCSNH_2)$ are typical of Schiff base metal complexes. The fragmentation pattern for the former compound is given in Fig. 1 while for the latter, it has been reported by us.[13] The $^{13}$C NMR spectral data of a few representative complexes relative to TMS have been recorded in Table 4. The large change in $^{13}$C chemical shifts in the spectra of the complexes compared to the ligands clearly shows the coordination of the azomethine nitrogen to the metal atom. Compounds $A_8$, $A_2$ and $A_1$ show $^1$J values of 607,565.2 and 598.2 Hz respectively and these are characteristic of 5-coordinate tin. James *et al.*[14] have reported a value of 586 Hz for dibutyl tin bis (*p*-ethoxy-benzoate), while a $^1$J ($^{119}$Sn–$^{13}$C) value equal to 614 Hz has been reported by Smith *et al.*[15] for compounds having five coordination around tin. The observation of two $\nu(SnC_2)$ bands in the IR spectra rules out a strictly linear array.

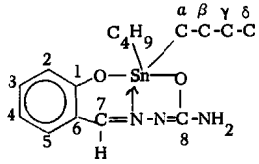
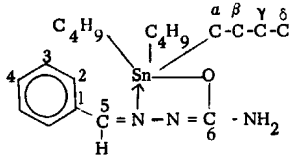
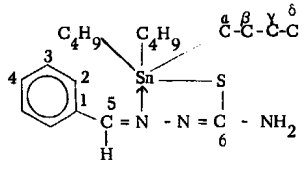
Table 3. $^{119}$Sn Mössbauer data of organotin semicarbazates

| Compound | I.S. $mms^{-1}$ | Q.S. $mms^{-1}$ |
|---|---|---|
| $Bu_2Sn(C_8H_8N_3O)_2$ | 1.08 | 2.36 |
| $Bu_2Sn(C_9H_{10}N_3O)_2$ | 0.98 | 2.23 |

The compounds, $BuSn(OC_6H_4.CH{:}NNCONH_2)$, $Bu_3Sn(C_6H_5.CH{:}NNCONH_2)$ and $Bu_2Sn(OC_6H_4.C(CH_3{:}NNCONH_2)$ give sharp signals in the $^{119}$Sn spectra at $\delta$-189.1, $\delta$-104 and $\delta$-142.4 ppm respectively and these are in accordance with the proposed five coordinated structures. Smith *et al.*[16] have reported a value of $\delta$-149.2 ppm for five coordinated $Ph_3SnONPhCOPh$ while a value of $\delta$-92 ppm has been reported by Otera[17] for $Me_2SnCl$ (Oxin).

X-Ray powder diffraction studies have been carried out on $Bu_2Sn(OC_6H_4.CH{:}NNCSNH_2)$ in

Table 4. $^{13}C$ NMR data of ligands and organotin complexes

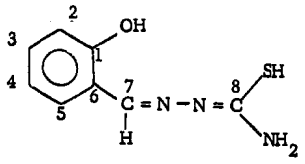
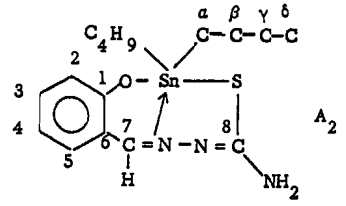
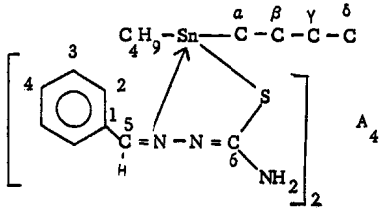
| Structure | | Chemical shifts in δ, ppm | | | | | | | | | | | |
|---|---|---|---|---|---|---|---|---|---|---|---|---|---|
| | | 1 | 2 | 3 | 4 | 5 | 6 | 7 | 8 | α | β | γ | δ |
|  | $A_8$ | 165.4 | 116.9 | 113.3 | 121.4 | 132.9 | 117.7 | 167.0 | 153.6 | 21.9 | 27.0 | 26.5 | 13.5 |
|  | $A_{12}$ | 137.6 | 129.5 | 126.0 | 128.2 | 144.6 | 156.7 | - | - | 16.9 | 27.6 | 26.5 | 13.3 |
|  | $A_5$ | 134.3 | 128.6 | 127.2 | 129.8 | 142.7 | 170.5 | | | 17.4 | 27.9 | 26.3 | 13.4 |

Contd. ---

Note: For $A_8$ $^1J(^{119}Sn-^{13}C) = 607.7$ Hz $^2J(^{119}Sn-^{13}C) = 33.3$ Hz

$^1J(^{117}Sn-^{13}C) = 570.2$ Hz $^3J(^{119}Sn-^{13}C) = 83.5$ Hz

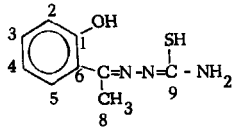
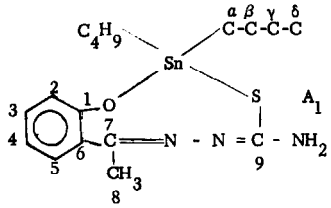
Table 4 (*Contd*)

| Structure | 1 | 2 | 3 | 4 | 5 | 6 | 7 | 8 | 9 | α | β | γ | δ |
|---|---|---|---|---|---|---|---|---|---|---|---|---|---|
|  | 155.2 | 115.9 | 129.0 | 118.52 | 127.2 | 117.4 | 175.74 | 179.32 | | | | | |
|  $A_2$ | 163.8 | 115.02 | 130.50 | 119.10 | 128.0 | 119.90 | 163.18 | 162.42 | | 21.25 | 26.51 | 26.15 | 13.02 |
|  $A_4$ | 133.8 | 128.0 | 126.7 | 130.1 | 143.4 | 171.0 | | | | 21.72 | 27.3 | 26.5 | 13.1 |

contd. ...

Note: For $A_2$ $^1J(^{119}Sn-^{13}C) = 598.2$Hz; $^2J(^{119}Sn-^{13}C) = 32.1$Hz; $^3J(^{119}Sn-^{13}C) = 80.6$Hz.

Table 4 (*Contd*)

| Structure | Chemical shifts in δ, ppm | | | | | | | | | | | | |
|---|---|---|---|---|---|---|---|---|---|---|---|---|---|
| | 1 | 2 | 3 | 4 | 5 | 6 | 7 | 8 | 9 | α | β | γ | δ |
|  | 155.67 | 115.30 | 128.91 | 119.03 | 126.58 | 116.94 | 176.03 | 12.61 | 178.71 | | | | |
|  | 162.29 | 114.87 | 130.10 | 119.89 | 127.85 | 119.12 | 164.79 | 18.31 | 161.92 | 21.56 | 25.33 | 24.10 | 11.55 |

For $A_1$ $^{1}J(^{119}Sn-^{13}C) = 565.2$ Hz

$^{2}J(^{119}Sn-^{13}C) = 30.9$ Hz

$^{3}J(^{119}Sn-^{13}C) = 84.3$ Hz

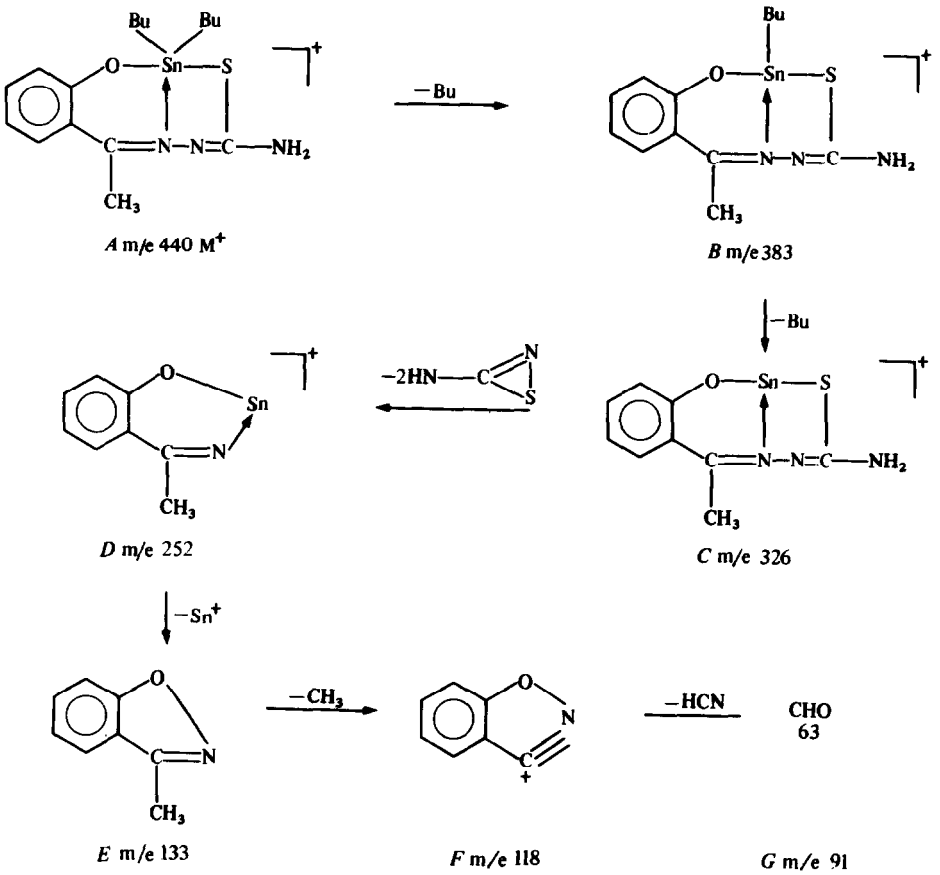



Fig. 1. Mass fragmentation of $Bu_2Sn(O.C_9H_9N_3S)$

Table 5. X-Ray powder diffraction data for $n$-$Bu_2Sn(C_8H_7N_3OS)$ [$A_2$]

| Sl. No. | $d_{obsd.}$ | $d_{calcd.}$ | hkl | Sl. No. | $d_{obsd.}$ | $d_{calcd.}$ | hkl |
|---|---|---|---|---|---|---|---|
| 1. | 16.83 | 16.90 | 100 | 21 | 3.07 | 3.07 | 0.31 |
| 2. | 9.71 | 9.71 | 010 | 22 | 3.02 | 3.02 | 230 |
| 3. | 8.71 | 8.60 | 007 | 23 | 2.89 | 2.91 | 511 |
| 4. | 8.42 | 8.45 | 200 | 24 | 2.85 | 2.86 | 003 |
| 5. | 7.72 | 7.65 | 101 | 25 | 2.81 | 2.81 | 600 |
| 6. | 6.39 | 6.39 | 210 | 26 | 2.77 | 2.75 | 013 |
| 7. | 6.06 | 6.02 | 201 | 27 | 2.74 | 2.73 | 113 |
| 8. | 5.62 | 5.63 | 300 | 28 | 2.68 | 2.70 | 610 |
| 9. | 4.91 | 4.87 | 310 | 29 | 2.54 | 2.55 | 611 |
| 10. | 4.72 | 4.71 | 301 | 30 | 2.38 | 2.38 | 700 |
| 11. | 4.24 | 4.23 | 311 | 31 | 2.34 | 2.34 | 710 |
| 12. | 3.96 | 3.93 | 012 | 32 | 2.30 | 2.31 | 141 |
| 13. | 3.85 | 3.83 | 112 | 33 | 2.25 | 2.26 | 711 |
| 14. | 3.75 | 3.79 | 401 | 34 | 2.15 | 2.15 | 004 |
| 15. | 3.69 | 3.67 | 320 | 35 | 2.11 | 2.11 | 800 |
| 16. | 3.50 | 3.53 | 411 | 36 | 2.06 | 2.06 | 810 |
| 17. | 3.45 | 3.41 | 302 | 37 | 2.04 | 2.05 | 801 |
| 18. | 3.37 | 3.38 | 500 | 38 | 1.94 | 1.94 | 050 |
| 19. | 3.23 | 3.23 | 030 | 39 | 1.88 | 1.88 | 151 |
| 20. | 3.14 | 3.18 | 510 | 40 | 1.84 | 1.80 | 911 |

order to determine the lattice dimensions of the compound. The indexed 'd' values are reported in Table 5. The compound crystallizes in a "Monoclinic' type of lattice with the unit cell dimensions as under:

$$a = 16.90\,\text{Å} \quad \beta = 103°.45'$$
$$b = 9.71\text{Å} \quad Z = 6$$
$$c = 8.60\,\text{Å}.$$

The unit cell of the compound is made up of 6 molecules.

*Acknowledgements*—The authors are highly thankful to Prof. T. N. Mitchell (W. Germany) for very kindly recording the $^{13}C$ and $^{119}Sn$ NMR spectra. Thanks are also due to Dr. Prithviraj (B.A.R.C., Bombay) for kindly recording the X-ray diffractogram and Mössbauer spectra. A. Saxena is grateful to the C.S.I.R., New Delhi for the award of P.D.F.

## REFERENCES

1. B. A. Gingras, R. W. Hornal and C. H. Baylay, *Canad. J. Chem.* 1960, **38**, 712.
2. V. K. Arora, K. B. Pandeya and R. P. Singh, *J. Indian Chem. Soc.* 1979, **LV1**, 656.
3. P. L. Maurya, B. V. Agarwala and A. K. Dey, *J. Indian Chem. Soc.* 1980, **LV11**, 275.
4. A. K. Saxena, J. K. Koacher and J. P. Tandon, *J. Inorg. Nucl. Chem.* 1981, **43**, 3091.
5. A. I. Vogel, *A Text Book of Practical Organic Chemistry*, p. 722. Longmans, London (1963).
6. A. K. Saxena and T. P. Tandon, *Polyhedron* 1983, **2**, 443.
7. T. Ito, *X-ray Studies of Polymorphism*, p. 187. Maruzen Co. Ltd., Japan (1950).
8. P. K. Singh, J. K. Koacher and J. P. Tandon, *J. Inorg. Nucl. Chem.* 1981, **43**, 1755.
9. A. K. Saxena, J. J. Zuckerman, K. C. Molloy and J. P. Tandon, *Inorganica Chimica Acta*, 1982, **63**, 71.
10. B. W. Fitzsimmons, N. J. Seeley and A. W. Smith, *J. Chem. Soc., A* 1969, 143.
11. R. R. Berrett and B. W. Fitzsimmons, *J. Chem. Soc. A* 1967, 525.
12. D. V. Naik and C. Curran, *Inorg. Chem.* 1971, **10**, 1017.
13. A. K. Saxena, J. K. Koacher and J. P. Tandon, *Inorg. Nucl. Chem. Lett.* 1981, **17**, 229.
14. G. Domazetis, R. J. Magee and B. D. James, *J. Organometal. Chem.* 1978, **148**, 339.
15. S. J. Blunden, P. J. Smith, P. J. Beynon and D. G. Gillies, *Carbohydrate Res.* 1981, **88**, 9.
16. S. J. Blunden and P. J. Smith, *J. Organometal. Chem.* 1982, **226**, 157.
17. J. Otera, *J. Organometal. Chem.* 1981, **221**, 57.

*Polyhedron* Vol. 3, No. 6, pp. 689–693, 1984
Printed in Great Britain.

0277–5387/84 $3.00 + .00
© 1984 Pergamon Press Ltd.

# METAL-PHENOXYALKANOIC ACID INTERACTIONS—12†

## THE CRYSTAL AND MOLECULAR STRUCTURE OF μ-AQUA-DI-μ-[(2-CHLOROPHENOXY)ETHANOATO-(*O*, *O'*)]-bis[(2-CHLOROPHENOXY)-ETHANOATO-BIS(PYRIDINE)NICKEL(II)]-WATER (1/1)

COLIN H. L. KENNARD*
Department of Chemistry, University of Queensland, Brisbane 4067, Australia

and

ERIC J. O'REILLY and GRAHAM SMITH
Department of Chemistry, Queensland Institute of Technology, Brisbane 4000, Australia

(*Received* 29 *August* 1983; *accepted* 24 *October* 1983).

**Abstract**—The crystal structure of the pyridine adduct of nickel (2-chlorophenoxy)-ethanote, $\{[Ni_2(2\text{-}CPA)_4(py)_4(H_2O)] \cdot H_2O\}$, has been determined from three dimensional X-ray data at 293 K. Crystals of the complex are triclinic, space group $P\bar{1}$, with two dimers in a unit cell of dimensions $a = 21.740(5)$, $b = 14.312(7)$, $c = 9.044(2)$Å, $\alpha = 96.69(4)$, $\beta = 84.99(4)$, $\gamma = 101.20(3)°$. The structure was solved by direct methods and refined to 0.059 for 2682 'observed' reflections. The dimer consists of two face-to-face $NiO_4N_2$ octahedra joined at their apical positions by a bridging water molecule [Ni(1)–Ow; 2.14(1)Å; Ni(2)–Ow, 2.10(1)Å; Ni(1)–Ôw–Ni(2), 116.9(4)°]. Two bidentate carboxyl groups of the 2–CPA molecules bridge the other two corners of the triangular face while the other two 2–CPA ligands are unidentate [Ni–O, 2.05(1)Å (mean)]. The coordination about each Ni is completed by two *cis*-related pyridine nitrogens [Ni–N; 2.11(1)Å (mean)]

Structural studies on the mode of interaction of univalent and divalent metal ions with the phenoxyalkanoic acids, which include the commercial auxin herbicides (2,4-dichlorophenoxy)ethanoic acid (2,4-D), (2,4,5-trichlorophenoxy)ethanoic acid (2,4,5-T) and (4-chloro-2-methylphenoxy)-ethanoic acid (MCPA), have shown a diversity of complex types.[1-3] Nickel(II) phenoxyalkanoates appear to be relatively stereotypical, as found in the only known X-ray examples, tetraaquabis-(phenoxyethanoato)nickel(II),[4] which has octahedral co-ordination with *trans*-related phenoxy ligands. However, reaction of an ethanolic solution of (2-chlorophenoxy)ethanoic acid (2-CPAH) with excess nickel(II) carbonate gave a pale green complex which appears (from elemental analysis, IR spectroscopy and DTA/TGA) to be atypical [empirical formula $Ni(2\text{-}CPA)_2(H_2O)_3$]. Poor crystallinity obviated a single crystal X-ray structure determination on this compound. In contrast, the pyridine adduct of this complex is a dark blue crystalline solid with empirical formula $Ni(2\text{-}CPA)_2(py)_2(H_2O)$. Since the IR spectrum and DTA/TGA did not resolve the anomaly of the sterochemistry for this formula, and preliminary X-ray photographs suggested the possibility of a dimeric structure (four formula units per triclinic cell), the X-ray structure determination was completed. The conformational aspects of the bonded 2-CPA ligands are also of interest since the structure of the parent acid (2-chlorophenoxy)ethanoic acid is known.[5]

## EXPERIMENTAL

*Preparation of* $[Ni_2(2\text{-}CPA)_4(py)_4(H_2O)] \cdot H_2O$

The complex was prepared by treating an aqueous ethanolic solution of nickel(II) (2-chlorophenoxy)ethanoate, $[Ni(2\text{-}CPA)_2(H_2O)_3]$ (preparation, Ref. 1), with a dilute solution of pyridine in ethanol. The crystals grew from the solution as blue prisms after allowing some of the solvent to evaporate at room temperature. The compound was quite stable in air and in the X-ray beam even after 70 hr exposure. Analyses and structure work were completed on the air dried crystals without prior recrystallization. Elemental analyses (C, H,

†Part 11.[1]

*Author to whom correspondence should be addressed.

Cl) were done by the University of Queensland Microanalytical Laboratory while Ni was determined titrimetrically using complexometric methods. IR spectra were determined on the samples as thin films in Nujol mulls using a Perkin–Elmer 598 spectrophotometer. A Rigaku instrument was used for thermogravimetric differential thermal analyses.

*Analyses*

(a) $[Ni(2\text{-}CPA)_2(H_2O)_3]$. Found: C, 39.7; H, 3.96; Cl, 14.5% Calculated for $C_{16}H_{38}Cl_2Cu_2O_9$: C, 39.7: H, 4.02; Cl, 14.1%.

(b) $[Ni(2\text{-}CPA)_4(py)_4(H_2O)] \cdot H_2O$. Found: C, 51.7; H, 4.04; Cl, 11.8; Ni, 9.87%. Calculated for $C_{52}H_{48}Cl_4N_4Ni_2O_{14}$; C, 51.5; H, 3.95; Cl, 11.6; Ni, 9.69%.

*Crystallography for* $[Ni_2(2\text{-}CPA)_4(py)_4(H_2O)] \cdot H_2O$

*Crystal data.* $C_{52}H_{48}Cl_4N_4Ni_2O_{14}$, $M = 1212.2$, triclinic, $a = 21.740(5)$, $b = 14.312(7)$, $c = 9.044(2)$Å, $\alpha = 96.69(4)$, $\beta = 84.99(4)$, $\gamma = 101.20(3)°$, $U = 2735$Å$^3$, $D_f = 1.48$, $D_c = 1.47$ g cm$^{-3}$, $Z = 2$, Mo-$K\alpha$ radiation, $\lambda = 0.7107$Å $\mu$(Mo-$K\alpha$) $= 9.52$ cm$^{-1}$, $F(000) = 1248$, space group $P\bar{1}$.

*Data collection, structure solution and refinement*

Three thousand nine hundred and eighty four reflections were collected from a single crystal ($0.20 \times 0.18 \times 0.08$ mm) mounted about the prism axis on an Enraf–Nonius CAD 4 automatic diffractometer ($2\theta_{max} = 50°$; graphite monochromated Mo-$K\alpha$ radiation, $\lambda = 0.7107$Å). Of these, 2682 with $I > 2.5\sigma(I)$ were considered observed and were used in structure refinement. The data were not corrected for absorption. The structure was solved using the multi-solution $\Sigma_2$ sign expansion direct methods procedure of SHELX[6] which provided the positions of the Ni atoms, while subsequent difference-Fourier syntheses gave all other heavy atoms. Blocked matrix least-squares refinement with only Ni and Cl atoms anisotropic reduced $R[= \Sigma \| Fo| - |Fc\| / \Sigma |Fo|]$ to 0.059 and $Rw$ $[= (\Sigma w(\| Fo| - |Fc\|^2 / \Sigma w |Fo|^2)^{\frac{1}{2}}]$ to 0.061, with $w = 1.68/(\sigma^2 Fo + 0.00076 Fo^2)$ found to be suitable. Some disorder was evident in the lattice water and in one of the pyridine rings. Allowance was made for the latter by including the atoms of this ring in the refinement with their site occupancy factors fixed at values determined from least-squares refinement. The maximim peak in the final difference-Fourier was 0.21 eÅ$^{-3}$. Neutral atom scattering factors were used.[7] Hydrogens were located in difference-Fourier syntheses and included in the refinement at fixed positions with their isotropic thermal parameters set invariant at 0.05Å$^2$.

Atomic coordinates, thermal parameters, observed and calculated structure factors and intra-ligand bond distances and angles have been deposited with the Editor as supplementary material; copies are available on request. Atomic coordinates have also been deposited with the Cambridge Crystallographic Data Centre. Bond distances and angles about the coordination polyhedron are given in Table 1.

## DISCUSSION

The complex species in the title compound consist of two slightly distorted octahedra facially linked by two carboxylate (*0, 0'*) bridges [Ni–O, 2.026(9)–2.066(9)Å; mean 2.040(9)Å] from two 2-CPA ligands, and an almost symmetrical bridge from a single aqua ligand [Ni(1)–Ow(1), 2.137(8)Å; Ni(2)–Ow(1), 2.097(8)Å, Ni(1)–Ôw(1)–Ni(2), 116.9(4)Å] (Fig. 1). The remaining three coordination positions about each Ni are occupied by a carboxyl oxygen of a unidentate 2-CPA ligand [Ni-O, 2.058(8), 2.080(9)Å] and two pyridine nitrogens [Ni–N, 2.102(14)–2.113(14)Å; mean, 2.108(14)Å]. The structure is stabilized by intramolecular hydrogen bonding involving the bridging water molecule [Ow(1)] and the uncomplexed oxygens of the carboxyl groups [O(10)a, 2.56Å and O(10)b, 2.65Å]. The lattice water Ow(2) is also associated with the carboxyl oxygen [O(10)] of one of these ligands [a] via a single hydrogen bond (2.83Å). No inter-dimer contacts less than 3Å, involving either lattice water, or carboxylate oxygens are found, indicating that the complex units are quite discrete in their packing mode (Fig. 2). Differential thermal/thermogravimetric analysis of the compound shows a two-step weight loss. The first, corresponding to the loss of a single water and two pyridines, takes place over the temperature range 80–120°C, while the second results in a further two-pyridine loss, occurring at 200°C. The low-temperature water loss represents the removal of the lattice water, the lability of which was indicated in the structure analysis. In contrast, the bridging water molecule, together with the 2-CPA ligands remain coordinated up to the decomposition point of the complex. A parallel analysis of $[Ni(2\text{-}CPA)_2(H_2O)_3]$ showed a one-step loss of all three water molecules over the range 70–110°C, followed by progressive decomposition up to *ca.* 230°C. The IR spectrum for this compound indicates at least two different water environments, so it may be concluded that a water bridged system comparable to $[Ni_2(2\text{-}CPA)_4(py)_4(H_2O)] \cdot H_2O$ is not present. Al-

Table 1. Bond distances (Å) and angles (deg.) about the coordination sphere for $[Ni_2(2\text{–}CPA)_4(py)_2(H_2O)] \cdot H_2O$*

| | | | |
|---|---|---|---|
| a. *Distances* | | | |
| N(1)-N(1)ap | 2.104(14) | Ni(2)-N(1)bp | 2.112(15) |
| Ni(1)-N(1)cp | 2.113(14) | Ni(2)-N(1)dp | 2.106(13) |
| Ni(1)-O(11)a | 2.058(8) | Ni(2)-O(11)b | 2.080(9) |
| Ni(1)-O(11)c | 2.026(9) | Ni(2)-O(10)c | 2.037(8) |
| Ni(1)-O(11)d | 2.031(9) | Ni(2)-O(10)d | 2.066(9) |
| Ni(1)-Ow(1) | 2.137(8) | Ni(2)-Ow(1) | 2.097(8) |
| b. *Angles* | | | |
| N(1)ap-Ni(1)-N(1)cp | 91.3(5) | N(1)bp-Ni(2)-N(1)dp | 90.6(5) |
| N(1)ap-Ni(1)-O(11)a | 87.3(5) | N(1)bp-Ni(2)-O(11)b | 91.9(5) |
| N(1)ap-Ni(1)-O(11)c | 85.9(5) | N(1)bp-Ni(2)-O(10)c | 87.3(5) |
| N(1)ap-Ni(1)-O(11)d | 89.7(5) | N(1)bp-Ni(2)-O(10)d | 177.3(5) |
| N(1)ap-Ni(1)-Ow(1) | 174.7(4) | N(1)bp-Ni(2)-Ow(1) | 90.9(4) |
| N(1)cp-Ni(1)-O(11)a | 89.6(4) | N(1)dp-Ni(2)-O(11)b | 88.0(4) |
| N(1)cp-Ni(1)-O(11)c | 176.4(5) | N(1)dp-Ni(2)-O(10)c | 89.3(4) |
| N(1)cp-Ni(1)-O(11)d | 88.3(4) | N(1)dp-Ni(2)-O(10)d | 86.7(4) |
| N(1)cp-Ni(1)-Ow(1) | 93.5(4) | N(1)dp-Ni(2)-Ow(1) | 177.6(4) |
| O(11)a-Ni(1)-O(11)c | 87.9(3) | O(11)b-Ni(2)-O(10)c | 177.2(3) |
| O(11)a-Ni(1)-O(11)d | 176.3(3) | O(11)b-Ni(2)-O(10)d | 88.3(3) |
| O(11)a-Ni(1)-Ow(1) | 90.5(3) | O(11)b-Ni(2)-Ow(1) | 90.1(3) |
| O(11)c-Ni(1)-O(11)d | 93.9(3) | O(10)c-Ni(2)-O(10)d | 92.4(3) |
| O(11)c-Ni(1)-Ow(1) | 89.2(3) | O(10)c-Ni(2)-Ow(1) | 92.6(3) |
| O(11)d-Ni(1)-Ow(1) | 92.7(3) | O(10)d-Ni(2)-Ow(1) | 91.8(3) |
| Ni(1)-Ow(1)-Ni(2) | 116.9(4) | | |

* Intraligand bond distances and angles have been deposited with the Editor and are also available from the authors.

though carboxylate bridged Ni(II) dimers are known, e.g. in the acetate bridged $[Ni_2(phensal\dagger)_4CH_3CO_2]^-$ complex,[8] a monoaqua bridge of the type found in the present example appears to be without precedence in the complex chemistry of nickel(II). The carboxylate (*0, 0'*) bridges allow the two complex units to open out, increasing the Ni–Ni distance to 3.607(5)Å, which compares with 3.101(1)Å in the phensal complex and 3.161(3)Å in $[Ni_2(TFDAA\ddagger)_2(py)_4]$,[9] where bis-oxo bridges are found in more symmetrical edge-shared octahedral dimers.

The four independent 2-CPA ligands show similar conformations in the dimer complex (Table 2). The parent acid (2-CPAH) is essentially planar,[5] the preferred conformation in the solid state of all phenoxyethanoic acids except those with both 2-*and* 6- substituents in the benzene ring. Furthermore, the free acids, without exception adopt the conformation of the side-chain with the "carbonyl" oxygen (rather than the "hydroxyl" oxygen) adjacent to and presumably interactive with the ether oxygen.[10] This O–O distance ranges from 2.605 to 2.775Å (mean, 2.771Å) for 19 examples of phenoxyalkanoic acids[10] (including propanoic acid analogues) and compares with 2.64(1)Å for the parent acid 2-CPAH. Also associated with this preferred conformation is a discrete angle difference between C–C–O (hydroxyl) and C–C–O (carbonyl) (usually $< 120°$ and $> 120°$ respectively), as is shown in 2-CPAH [mean for the two independant molecules in the asymmetric unit, 114.5(8) and 125.2(8)°]. It has also been found that the interactive O–O distance and the angle difference in the carboxyl group is usually retained with deprotonation, i.e. with complexation.[11] This does not depend on the type of metal involved or the nature of the mode of complexation (unidentate, bidentate, bridging). The C–O bond length

†phensal = phenylsalicylaldimine.
‡TFDAA = 1,1,1-trifluoro-2,4,6-heptanetrionato.

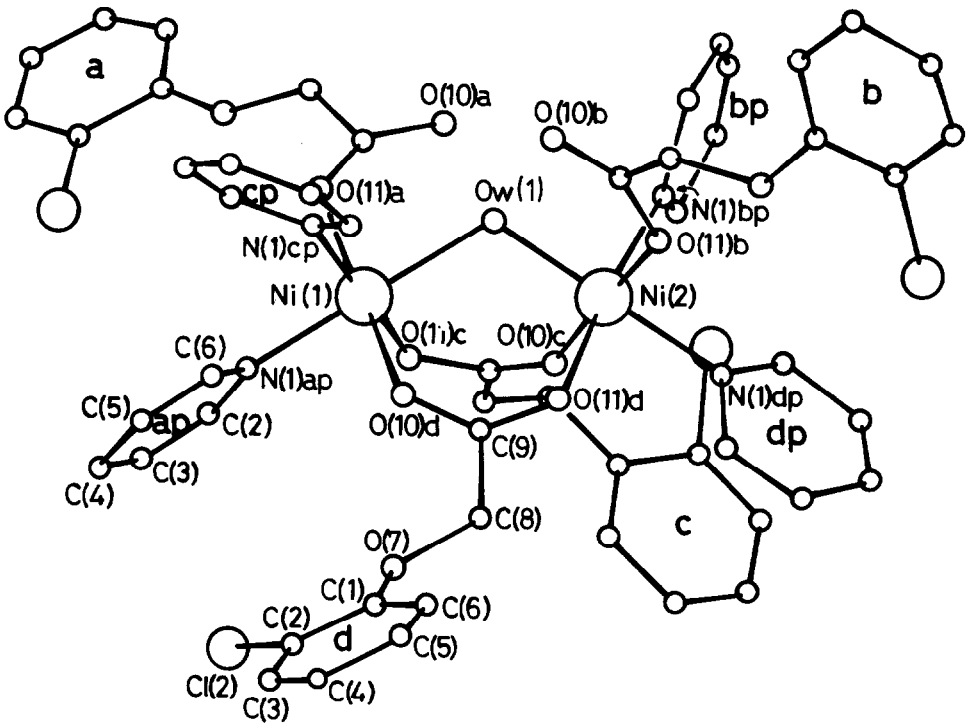



Fig. 1. Molecular configuration and atom naming scheme for $[Ni_2(2\text{–}CPA)_4(py)_4(H_2O)]$. Hydrogens are omitted for clarity.

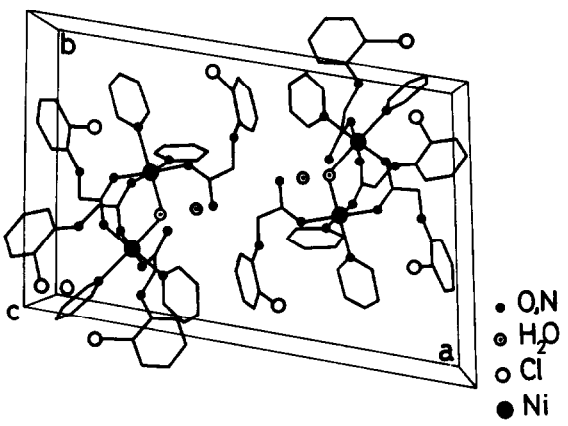



Fig. 2. Perspective view of the packing of the two molecular dimers in the unit cell viewed down the *c* axis.

difference is also a quantity which tends to be retained in proceeding from the acid to the anion, although it tends to be more susceptible to differences in the mode of complexation. It has generally been possible to determine the origin of the carboxyl oxygen as "carbonyl" or "hydroxyl" and hence ascertain if the side-chain conformation of the parent is retained or lost. In considering $[Ni_2(2\text{-}CPA)_4(py)_2(H_2O]$, the classification is less definite than any previously considered examples,[1,2] possibly because of the lesser precision in this determination but assignments have been made on the basis of the following data.

For ligand (a), the conformation has changed [O(7)–O(11) (unidentate bonded), 2.69(1)Å; C(8)–C(9)–O(10), 116(2)°; C(8)–C(9)–O(11),

Table 2. Comparative torsion angles within the oxo-ethanoate ligands in $[Ni_2(2\text{–}CPA)_4(py)_4(H_2O)] \cdot H_2O$ and for the parent acid (2–CPAH)[5] (ESD's for angles are *ca.* 1°)

| | a | b | c | d | 2-CPAH* |
|---|---|---|---|---|---|
| C(2)-C(1)-O(7)-C(8) | -168 | -166 | -179 | -177 | -179, 180 |
| C(1)-O(7)-C(8)-C(9) | +71 | +68 | +82 | +72 | -175, -173 |
| O(7)-C(8)-C(9)-O(10) | +177 | -165 | +164 | -162 | -179, 180 |
| O(7)-C(8)-C(9)-O(11) | -4 | +15 | -15 | +21 | -179, 180 |
| C(8)-C(9)-O(11)-Ni(1)/(2) | +166 | +170 | +167 | +166 | - |

* 2-CPAH has two crystallographically independent molecules in the asymmetric unit.

117(2)°; C(9)–O(11), 1.26(2)Å; C(9)–O(10), 1.22(2)Å]

For ligand (b), the conformation is retained. [O(7)–O(11) (bonded unidentate), 2.71(1)Å; C(8)–C(9)–O(11), 119(1)°; C(8)–C(9)–O(10), 114(1)°; C(9)–O(11), 1.24(2)Å; C(9)–O(10), 1.27(2)Å].

For ligand (c), the conformation has changed. [O(7)–O(11) (bridging), 2.75(1)Å; C(8)–C(9)–O(11), 112(1)°; C(8)–C(9)–O(10), 120(1)°; C(9)–O(11), 1.25(1)Å; C(9)–O(10), 1.25(1)Å].

For ligand (d), the conformation has probably changed. [O(7)–O(10) (bridging 2.66(1)Å; C(8)–C(9)–O(10), 114(1)°; C(8)—C(9)–O(11), 116(1)°; C(9)–O(10), 1.22(2)Å; C(9)–O(11), 1.24(2)Å].

*Acknowledgements*—The authors thank Professor Mary Truter of the Molecular Structures Department, Rothamsted Experiment Station, Harpenden, Herts. who made facilities available for CHLK to complete this work while on a special study programme supported by the Joint Committee for X-ray Powder Diffraction and the University of Queensland. G.S. and E.J.O'R thank the Queensland Institute of Technology for leave to work on this project.

## REFERENCES

1. C. H. L. Kennard, G. Smith and E. J. O'Reilly, *Inorg. Chim. Acta* 1983, **77**, 181.
2. G. Smith, E. J. O'Reilly and C. H. L. Kennard, *J. Chem. Soc Dalton Trans.* 1980, 2462; G. Smith, E. J. O'Reilly, C. H. L. Kennard, K. Stadnicka and B. Oleksyn, *Inorg. Chim. Acta* 1981, **47**, 111; C. H. L. Kennard, G. Smith, E. J. O'Reilly and K. E. Brown, *Inorg. Chim. Acta* 1981, **52** 55; G. Smith, E. J. O'Reilly and C. H. L. Kennard, *Inorg. Chim. Acta* 1981, **49**, 54; G. Smith, E. J. O'Reilly and C. H. L. Kennard, *Cryst. Struct. Commun.* 1981, **10**, 1397; C. H. L. Kennard, G. Smith, E. J. O'Reilly, K. M. Stadnicka and B. J. Oleksyn, *Inorg. Chim. Acta* 1982, **59**, 241; G. Smith, E. J. O'Reilly and C. H. L. Kennard, *Inorg. Chim. Acta* 1982, **62**, 241; G. Smith, E. J. O'Reilly, C. H. L. Kennard and T. C. W. Mak, *Inorg. Chim. Acta* 1982, **65**, L219; C. H. L. Kennard, G. Smith, E. J. O'Reilly and W. Chiangjin, *Inorg. Chim. Acta* 1983, **69**, 53; C. H. L. Kennard, G. Smith, E. J. O'Reilly, and P. T. Manohoran, *Inorg. Chim. Acta* 1984, in press.
3. C. K. Prout, R. A. Armstrong, J. R. Carruthers, J. G. Forrest, P. Murray-Rust and F. J. C. Rossotti, *J. Chem. Soc. A.* 1968, 2791; C. K. Prout, C. Walker and F. J. C. Rossotti, *J. Chem. Soc. A* 1971, 556; C. K. Prout, R. M. Dunn, O. J. R. Hodder and F. J. C. Rossotti, *J. Chem. Soc. A* 1971, 1986; C. K. Prout, P. J. Grove, B. D. Harridine and F. J. C. Rossotti, *Acta Cryst. Sect. B* 1975, **31**, 2047; J. R. Carruthers, C. K. Prout and F. J. C. Rossotti, *Acta Cryst. Sect. B* 1975, **31**, 2044; C. V. Goebel and R. J. Doedens, *Inorg. Chem.*, 1971, **10**, 2607; G. Reck and W. Jahnig, *J. prakt. Chemie*, 1979, **321**, 549.
4. C. K. Prout, C. Walker and F. J. C. Rossotti, *J. Chem. Soc. A* 1971, 556.
5. C. H. L. Kennard and G. Smith, *Acta Cryst. Sect. B* 1981, **37**, 1456.
6. G. M. Sheldrick, *SHELX*-76, *Program for Crystal Structure Determination.* Cambridge University, England (1976).
7. *International Tables for X-ray Crystallography*, Vol. IV. Kynoch Press, Birmingham (1974).
8. R. J. Butcher, J. W. Overman and E. Sinn, *J. Am. Chem. Soc.* 1980, **102**, 3276.
9. J. W. Guthrie, R. L. Lintvedt and M. D. Glick, *Inorg. Chem.* 1980, **19**, 2949.
10. C. H. L. Kennard, G. Smith and A. H. White, *Acta Cryst. Sect. B* 1982, **36**, 868.
11. G. Smith, C. H. L. Kennard, E. J. O'Reilly, K. Stadnicka and B. Oleksyn, *Inorg. Chim. Acta* 1981, **47**, 111.

*Polyhedron* Vol. 3, No. 6, pp. 695–699, 1984
Printed in Great Britain.

0277–5387/84 $3.00 + .00
© 1984 Pergamon Press Ltd.

# MONOCYCLOPENTADIENYL TITANIUM(IV) ALKYL XANTHATE COMPLEXES

**O. P. PANDEY, S. K. SENGUPTA and S. C. TRIPATHI***
Department of Chemistry, University of Gorakhpur, Gorakhpur 273001, India

(*Received* 6 *September* 1983; *accepted* 16 *November* 1983)

**Abstract**—Titanium(IV) alkyl xanthates of the types $CpTi(S_2COR)Cl_2$, $CpTi(S_2COR)_2Cl$ and $CpTi(S_2COR)_3$, where R = $CH_3$, $C_2H_5$, $C_3H_7$, $C_4H_9$ and $C_5H_{11}$, have been prepared by the reaction of monocyclopentadienyl titanium(IV) trichloride with potassium alkyl xanthates in anhydrous dichloromethane. Conductance and infrared studies suggest that these complexes are non-electrolytes in which all of the xanthate ligands are bidentate. Proton nmr spectra of these complexes indicate that there is rapid rotation of the cyclopentadienyl ring about the metal-ring axis and for the $CpTi(S_2COR)_3$ complexes non-equivalence of the alkylxanthate ligands was observed.

There is a continuing interest in the preparation of metal complexes of higher coordination number with nitrogen, oxygen and sulphur donor ligands.[1,2] The bidentate xanthate ligand by virtue of its low charge and relatively small bite ($\sim 3$ Å) is particularly well suited for stabilisation of higher coordination states of metals.[3,4] Although the literature of metal xanthates is quite extensive, very few complexes with titanium have been reported. Coutts *et al.* have reported the preparation of xanthates of titanium(III) by reacting stoichiometric quantities of biscyclopentadienyl titanium(III) chloride with sodium salts of alkyl xanthates.[5] In these complexes, the xanthate groups are supposed to behave as bidentate ligands. Dina Nath *et al.* have prepared xanthates of titanium(IV) of the type $Cp_2Ti(S_2COR)_2$ where R = $CH_3$,$C_2H_5$,$C_3H_7$.[6] However, there is no mention in the literature about the titanium(IV) complexes of the types $CpTi(S_2COR)Cl_2$, $CpTi(S_2COR)_2Cl$ and $CpTi(S_2COR)_3$. The method of preparation of these complexes also differ from that reported by Coutts *et al.* or by Dina Nath *et al.*

## EXPERIMENTAL

*Reagents and general techniques*

Potassium alkyl xanthates were prepared as mentioned in the literature.[3] Monocyclopentadienyl titanium(IV) trichloride was prepared from $Cp_2TiCl_2$ and $TiCl_4$ in *p*-xylene.[7] Dichloromethane was dried by refluxing it for 30 hr over calcium hydride. All experimental operations were carried out in strictly anhydrous conditions.

Titanium was determined gravimetrically as $TiO_2$ and chloride as AgCl. Sulphur was estimated as $BaSO_4$.

The details of physical measurements are the same as described earlier.[2,8]

*Preparation of complexes*

The complexes were prepared by taking monocyclopentadienyl titanium(IV) trichloride and the respective ligand in 1:1, 1:2 and 1:3 molar ratios separately and adding 60 $cm^3$ of dichloromethane followed by a reflux time 20–40 hr. The solutions were then filtered and their volume reduced to 20 $cm^3$. Further, addition of dry petroleum ether (60–80°, $\sim 20$ $cm^3$) to each of the above solutions and allowing them to stand overnight resulted yellow–brown crystals of the products which were filtered and dried at 80°C.

The details of the amounts of reactants taken for the preparation of complexes, refluxing time, yield and colour of the products are given in Table 1.

## RESULTS AND DISCUSSION

The analytical data of the complexes are given in Table 2. The methods used for the preparation and isolation of these compounds gave materials of

*Author to whom correspondence should be addressed.

Table 1. Physical data of the complexes

| Reactants taken(gm) $CpTiCl_3$ | $KS_2COR$ | Refluxing time(hr) | Product, Colour, % yield | Decomp. temp. | Conductance* $Mx10^3$ = 0.5 |
|---|---|---|---|---|---|
| 1.1 | R= $CH_3$, 0.75 | 32 | $CpTi(S_2COCH_3)Cl_2$ yellow, 53 | 204 | 0.50 |
| 1.0 | R= $CH_3$, 1.5 | 40 | $CpTi(S_2COCH_3)_2Cl$ yellow, 60 | 212 | 0.40 |
| 0.58 | R= $CH_3$, 1.12 | 40 | $CpTi(S_2COCH_3)_3$ Light brown, 46 | 196 | 0.26 |
| 1.0 | R= $C_2H_5$, .80 | 22 | $CpTi(S_2COC_2H_5)Cl_2$ yellow, 49 | 184 | 0.58 |
| 1.0 | R=$C_2H_5$, 1.6 | 31 | $CpTi(S_2COC_2H_5)_2Cl$ yellow, 60 | 265 | 0.30 |
| 0.5 | R=$C_2H_5$, 1.2 | 39 | $CpTi(S_2COC_2H_5)_3$ brown, 48 | 162 | 0.15 |
| 1.1 | R=$C_3H_7$, 0.85 | 37 | $CpTi(S_2COC_3H_7)Cl_2$ yellow, 57 | 192-194 | 0.45 |
| 1.0 | R=$C_3H_7$, 1.75 | 39 | $CpTi(S_2COC_3H_7)_2Cl_2$ light brown, 71 | 222 | 0.40 |
| 0.52 | R= $C_3H_7$, 1.25 | 40 | $CpTi(S_2COC_4H_9)Cl_2$ dark brown, 52 | 210 | 0.30 |
| 1.0 | R=$C_4H_9$, 0.95 | 20 | $CpTi(S_2COC_4H_9)Cl_2$ light brown, 75 | 198 | 0.68 |
| 1.1 | R=$C_4H_9$, 1.8 | 35 | $CpTi(S_2COC_4H_9)_2Cl$ light yellow, 67 | 202-203 | 0.65 |
| 0.54 | R=$C_4H_9$, 1.4 | 40 | $CpTi(S_2COC_4H_9)_3$ brown, 65 | 206 | 0.60 |
| 1.0 | R=$C_6H_{11}$, 1.0 | 22 | $CpTi(S_2COC_5H_{11})Cl_2$ yellow, 48 | 208 | 0.48 |
| 1.0 | R=$C_5H_{11}$, 2.0 | 25 | $CpTi(S_2COC_5H_{11})_2Cl$ yellow, 46 | 187 | 0.45 |
| 0.5 | R=$C_5H_{11}$, 1.5 | 40 | $CpTi(S_2COC_5H_{11})_3$ brown, 48 | 244 | 0.38 |

* in $ohm^{-1}$ $cm^2$ $mole^{-1}$

good purity as supported by their analyses and TLC. All these complexes are yellow–brown in colour. They are thermally stable but decompose above ~ 160°C without melting. They are quite stable in air but their solutions are hydrolysed on standing. Conductance measurements showed that they are essentially non-electrolytes ($0.5 \times 10^3 \Omega^{-1} cm^2$ $mole^{-1}$). Magnetic susceptibility values at room temperature show they are all diamagnetic. The electronic spectra of all these complexes exhibit a single intense charge transfer band in the region 24000–25000 $cm^{-1}$.

Table 2. Analytical data of the complexes

| Complex | Found ( calc ) % of | | | | |
|---|---|---|---|---|---|
| | C | H | S | M | Cl |
| $CpTi(S_2COCH_3)Cl_2$ | 28.6 (28.8) | 2.6 (2.74) | 21.7 (21.99) | 16.4 (16.49) | 24.0 (24.39) |
| $CpTi(S_2COCH_3)_2Cl$ | 29.5 (29.8) | 3.0 (3.03) | 35.1 (35.3) | 13.0 (13.24) | 9.6 (9.80) |
| $CpTi(S_2COCH_3)_3$ | 30.1 (30.4) | 3.0 (3.2) | 44.0 (44.2) | 11.0 (11.05) | - |
| $CpTi(S_2COC_2H_5)Cl_2$ | 31.2 (32.47) | 3.2 (3.27) | 20.6 (20.98) | 15.4 (15.73) | 23.0 (23.27) |
| $CpTi(S_2COC_2H_5)_2Cl$ | 33.5 (33.8) | 3.6 (3.8) | 32.4 (32.7) | 12.0 (12.29) | 8.8 (9.09) |
| $CpTi(S_2COC_2H_5)_3$ | 35.0 (35.29) | 4.0 (4.20) | 40.1 (40.3) | 9.9 )10.08) | - |
| $CpTi(S_2COC_3H_7)Cl_2$ | 31.0 (31.2) | 3.5 (3.9) | 20.4 (20.8) | 15.6 (15.6) | 23.0 (23.1) |
| $CpTi(S_2COC_3H_7)_2Cl$ | 37.0 (37.2) | 4.2 (4.6) | 30.3 (30.5) | 11.2 (11.5) | 8.5 (8.5) |
| $CpTi(S_2COC_3H_7)_3$ | 39.1 (39.3) | 5.0 (5.0) | 36.8 (37.0) | 9.0 (9.3) | - |
| $CpTi(S_2COC_4H_9)Cl_2$ | 36.0 (36.0) | 4.0 (4.2) | 19.2 (19.2) | 14.2 (14.4) | 21.0 (21.02) |
| $CpTi(S_2COC_4H_9)_2Cl$ | 40.1 (40.3) | 5.0 (5.1) | 28.5 (28.7) | 10.4 (10.7) | 7.7 (7.95) |
| $CpTi(S_2COC_4H_9)_3$ | 42.5 (42.8) | 5.4 (5.7) | 34.1 (34.3) | 8.2 (8.5) | - |
| $CpTi(S_2COC_5H_{11})Cl_2$ | 39.1 (39.4) | 4.5 (4.77) | 19.1 (19.1) | 14.0 (14.3) | 21.0 (21.19) |
| $CpTi(S_2COC_5H_{11})_2Cl$ | 42.7 (42.9) | 5.3 (5.69) | 26.8 (26.97) | 10.1 (10.1) | 7.5 (7.48) |
| $CpTi(S_2COC_5H_{11})_3$ | 45.6 (45.8) | 6.3 (6.3) | 31.7 (31.8) | 8.0 (7.97) | - |

*IR spectra*

The important IR frequencies are given in Table 3. Absorption bands occurring at $\sim 3000\,cm^{-1}$ $\nu$(C–H) $\sim 1430\,cm^{-1}$ $\nu$(C–C) and $\sim 1000\,cm^{-1}$ $\delta$(–CH) in the complexes indicate the presence of cyclopentadienyl ring. All these bands are similar to those of mono(cyclopentadienyl) titanium(IV).[9] Davision and Rakita have pointed out that at $3000\,cm^{-1}$ $\eta^1$–$C_5H_5$ should show four bands whereas $\eta^5$–$C_5H_5$ should show only one.[10] In the complexes reported in this paper, a single band near $3000\,cm^{-1}$ indicated the pentahapto nature of cyclopentadienyl ring. However, in some areas of the spectrum, there is considerable overlap between bands due to cyclopentadienyl, alkyl and xanthate groups and care must be taken in making some assignments. Our conclusions are based on the data reported for $[Cp_2V(Xan)]^+$ complex ion.[11]

The subject of chief interest in the preparation of these complexes is the attachment of xanthate ligands. Xanthate can behave as monodentate or bidentate ligand. However, assignment of structure of metal xanthates from infrared is not always reliable. All the xanthate ligands exhibit four characteristic bands around 1250, 1100, 1060 and $550\,cm^{-1}$, which according to Watt and McCormick, are assigned to $\nu(C=S)$, $\nu$(C–S), $\nu$(C–O) and $\nu$(R–O) vibrations.[12] These bands are highly

Table 3. Characteristic IR spectral bands ($cm^{-1}$)

| Complex | $\nu$(C-O-C) | $\nu$(C — O) | $\nu$(C=S) | $\nu$(R-O) | $\nu$(Ti-$C_5H_5$) | $\nu$(Ti-S) |
|---|---|---|---|---|---|---|
| $CpTi(S_2COCH_3)Cl_2$ | 1230sb | 1150sb | 1030s | 530m | 460w | 350m |
| $CpTi(S_2COCH_3)_2Cl$ | 1225sb | 1140sb | 1035s | 510 m | 450w | 380w |
| $CpTi(S_2COCH_3)_3$ | 1230sb | 1132sb | 1040s | 525m | 460m | 370w |
| $CpTi(S_2COC_2H_5)Cl_2$ | 1240sb | 1165sb | 1040s | 530m | 460m | 370mb |
| $CpTi(S_2COC_2H_5)_2Cl$ | 1230sb | 1160sb | 1038s | 535m | 450w | 360m |
| $CpTi(S_2COC_2H_5)_3$ | 1220sb | 1140sb | 1040s | 525m | 440w | 355m |
| $CpTi(S_2COC_3H_7)Cl_2$ | 1235sb | 1160sb | 1030s | 520m | 445w | 350m |
| $CpTi(S_2COC_3H_7)_2Cl$ | 1235sb | 1150sb | 1035s | 520m | 448w | 355mb |
| $CpTi(S_2COC_3H_7)_3$ | 1228sb | 1148sb | 1030s | 520m | 450w | 360w |
| $CpTi(S_2COC_4H_9)Cl_2$ | 1230sb | 1130sb | 1035s | 535m | 460w | 380m |
| $CpTi(S_2COC_4H_9)_2Cl$ | 1225sb | 1130sb | 1040s | 532m | 440w | 385m |
| $CpTi(S_2COC_4H_9)_3$ | 1220sb | 1140sb | 1030s | 525m | 440w | 400m |
| $CpTi(S_2COC_5H_{11})Cl_2$ | 1230sb | 1165sb | 1038s | 530m | 455w | 360m |
| $CpTi(S_2COC_5H_{11})_2Cl$ | 1235sb | 1150sb | 1035s | 530m | 450w | 370w |
| $CpTi(S_2COC_5H_{11})_3$ | 1230sb | 1140sb | 1040s | 525m | 440w | 390mb |

s = strong, m = medium, w = weak, b = broad.

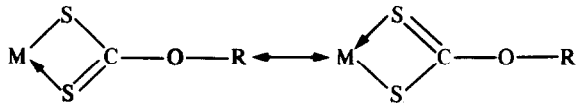
coupled and sensitive to the environmental changes. A normal coordinate analysis of nickel(II) ethyl xanthate by Agarwala *et al.* indicated that the 1250 $cm^{-1}$ band has about 90% contribution from C–O–R stretch and 10% from C = S stretch.[13] The band around 1100 $cm^{-1}$ is mainly a contribution of C–O, R–O and C = S stretching modes. The band around 1060 $cm^{-1}$ has a single major contribution of 60% from C = S stretch.[13] From a detailed investigation of IR spectra of various xanthate derivatives, Little *et al.* also assigned[14] the band at 1060–1070 $cm^{-1}$ to $\nu$(C = S) and proposed that resonance forms (a) and (b) describe the most probable structure of metal

Table 4. $^1H$ NMR data of complexes

| Complex | $\eta^5$- $C_5H_5$ | -CH | $-CH_2$ | $-CH_3$ |
|---|---|---|---|---|
| $CpTi(S_2COCH_3)Cl_2$ | 6.50(s) | - | - | 3.00(s) |
| $CpTi(S_2COCH_3)_2Cl$ | 6.62(s) | - | - | 3.00(s) |
| $CpTi(S_2COCH_3)_3$ | 6.55(s) | - | - | 3.22(d) J= 6.6 $H_z$ |
| $CpTi(S_2COC_2H_5)Cl_2$ | 6.55(s) | - | 3.20(q) J= 7.2$H_z$ | 1.10(t) J= 6.68 $H_z$ |
| $CpTi(S_2COC_2H_5)_2Cl$ | 6.60(s) | - | 3.22(q) J= 7.0$H_z$ | 1.00(t) J= 6.68 $H_z$ |
| $CpTi(S_2COC_2H_5)_3$ | 6.62(s) | - | 3.2-3.4(d) each split into (q) | 1.00-1.18(d) each split into (t) |
| $CpTi(S_2COC_3H_7)Cl_2$ | 6.50(s) | 4.00(sep) J= 7.0 $H_z$ | - | 1.40(d) J = 6.2 $H_z$ |
| $CpTi(S_2COC_3H_7)_2Cl$ | 6.60(s) | 4.12 (sep) J= 6.2$H_z$ | - | 1.44(d) J= 6.6 $H_z$ |
| $CpTi(S_2COC_3H_7)_3$ | 6.65(s) | 4.2-4.5(d) each split into sep. | - | 1.48(q) J= 7.0 $H_z$ |

(s) = singlet, (d)= doublet, (t) = triplet, (q) = quadret, (sep) = septet

xanthates which was further supported by Chatt *et al.*[15]



(a) (b)

In our complexes, the C = S stretching band appears at about 1030–1040 $cm^{-1}$. The lowering of the frequency of C=S band ($\sim$ 30–20 $cm^{-1}$) in titanium(IV) complexes as compared to free ligands indicate involvement of sulphur in bonding with the metal. The bands observed around 350–400 $cm^{-1}$ in the IR spectra of the complexes may be assigned to $\nu$(M–S).[16]

*Proton NMR spectra*

The proton NMR spectra of some of these complexes have been recorded in deuterated chloroform and dimethylformamide. Chemical shifts for protons in different chemical environments are indicated in Table 4. The intensities of all the resonance lines were determined by planimetric integration. The resonance line for the protons on the $C_5H_5$ ring always falls near $\delta$6.5 ppm. The appearance of a single sharp signal for protons of the cyclopentadienyl ring indicates the rapid rotation of the ring about the metal-ring axis. The two kinetic possibilities, viz. metal-centred rearrangement is slow or fast, can be distinguished by the analysis of NMR spectra. In the NMR spectra of $CpTi(S_2COR)_3$ complexes, two distinct methyl, ethyl and propyl resonances are observed which must result from non-equivalent environments for these groups. However, in bis-xanthato derivatives, $CpTi(S_2COR)_2Cl$, the xanthate groups are equivalent since only one signal was observed for methyl, ethyl or propyl groups. The integrated proton ratios correspond to the formulae.

*Acknowledgements*—The authors are thankful to Indian National Science Academy for financial grant and to Dr. Nizamuddin, East Carolina University, U.S.A. for recording the spectra.

## REFERENCES

1. M. G. B. Drew, *Coord. Chem. Rev.* 1977, **24**, 179.
2. S. K. Sengupta, S. K. Sahni and R. N. Kapoor, *J. Coord. Chem.* 1982, **12**, 113 and references therein.
3. S. Ramachandra Rao, *Xanthates and Related Compounds*. Marcel Dekker, New York (1971).
4. V. K. Jain, R. K. Sharma and B. S. Garg, *Inorg. Chim. Acta* 1978, **26**, 51.
5. R. S. P. Coutts, P. C. Wailes and J. V. Kingston, *Aust. J. Chem.* 1970, **23**, 469.
6. Dina Nath and A. N. Bhat, *Indian J. Chem.* 1976, **14A**, 281.
7. R. D. Gorsich, *J. Am. Chem. Soc.* 1960, **82**, 4211.
8. S. K. Sengupta, S. K. Sahni and R. N. Kapoor, *Polyhedron* 1983, **2**, 317.
9. H. P. Fritz, *Adv. Organometal. Chem.* 1964, **1**, 262.
10. A. Davision and P. E. Rakita, *Inorg. Chem.* 1970, **9**, 289.
11. A. J. Casey and J. R. Thakeray, *Austral. J. Chem.* 1972, **25**, 2085.
12. G. W. Watt and B. J. McCormick, *Spectrochim Acta* 1965, **21**, 753.
13. U. Agarwala, Lakshmi and P. B. Rao, *Inorg. Chim. Acta* 1968, **2**, 337.
14. L. H. Little, G. W. Poling and J. Leja, *Can. J. Chem.* 1961, **39**, 754.
15. J. Chatt, L. A. Duncanson and L. M. Venanzi, *Nature* 1956, **177**, 1042; *Suomen Kemi* 1956, **29B**, 75.
16. S. Kumar and N. K. Kaushik, *J. Inorg. Nucl. Chem.* 1981, **43**, 2679.

*Polyhedron* Vol. 3, No. 6, pp. 701–705, 1984
Printed in Great Britain.

0277–5387/84 $3.00 + .00
© 1984 Pergamon Press Ltd.

# SPECTRAL AND KINETIC EVIDENCE FOR ATTACK AT COORDINATED PHENANTHROLINE IN THE REACTION BETWEEN ALIPHATIC AMINES AND TRANSITION METAL COMPLEXES OF 5-NITRO-1,10-PHENANTHROLINE

A. BARTOLOTTA, M. CUSUMANO*, G. DI MARCO, A. GIANNETTO and G. GUGLIELMO

Dipartimento di Chimica Inorganica e Struttura Molecolare, University of Messina, Italy

(*Received* 13 *September* 1983; *accepted* 28 *November* 1983)

**Abstract**—Various transition metal complexes of 5-nitro-1,10-phenanthroline react with aliphatic amines in dipolar aprotic solvents to give deeply coloured species. The spectral changes, which can be reversed upon addition of acid or of the appropriate protonated amine, do not depend either on the nature of the metal and the ancillary ligands or on the geometry of the complexes; this has been taken as evidence that the colour forming process is due to a specific interaction of aliphatic amines with coordinated phenanthroline. While the rate of reaction of $[Pt(5\text{-}NO_2phen)Cl_2]$ and $[Pd(5\text{-}NO_2phen)Cl_2]$ with $Br^-$, which is known to displace $Cl^-$ in the substrates, depends strongly on the nature of the central atom, the second order rate constant at 25°C being $3.2 \times 10^{-4}$ $dm^3mol^{-1}s^{-1}$ and 1.35 $dm^3mol^{-1}s^{-1}$ for the platinum and the palladium derivative respectively, the rate of reaction with *n*-propylamine has a comparable value for both substrates. This is further evidence that amines attack the coordinated phenanthroline, rather than the central atom. On the basis of the spectral features and the reaction stoicheiometry, the adducts of metal complexes of $5\text{-}NO_2phen$ and aliphatic amines are presumably Meisenheimer-like complexes.

Gillard and others[1] have interpreted many reactions of transition metal-polypyridine complexes with nucleophiles in terms of mechanisms involving the formation of covalent hydrates or pseudo-bases by attack of the nucleophile at the coordinated ligand. This interpretation has been very controversial;[2-4] alternative explanations implying the usual attack at the central atom have in some cases been given and the existence of pseudo-bases, so far not unambiguously proved, has been challenged.[5,7] In this context we wish to describe some experimental observations which show how in the reaction of metal complexes of 5-nitro-1,10-phenanthroline ($5\text{-}NO_2phen$) nucleophilic attack of amines at coordinated phenanthroline occurs. In this paper we report the results of a spectrophotometric investigation on the reaction of the complexes $[M(5\text{-}NO_2phen)_3](ClO_4)_2$ (M = Co(II), Ni(II), Cu(II)), $[M(5\text{-}NO_2phen)Cl_2]$ (M = Pt(II) or Pd(II)) and $[Pd(5\text{-}NO_2phen)_2](ClO_4)_2$ with *n*-propylamine or piperidine in dimethylformamide (dmf) or dimethylsulphoxide (dmso). Kinetic data relative to the reactions of $[Pt(5\text{-}NO_2phen)Cl_2]$ and $[Pd(5\text{–}NO_2phen)Cl_2]$ with $Br^-$ in dmf at 25°C and to the reactions of the same substrates with n-propylamine in dmf at −30°C are given.

## EXPERIMENTAL

The complexes $[M(5\text{-}NO_2phen)_3](ClO_4)_2$ (M = Ni(II), Co(II), Cu(II)) were prepared[8] on treating the appropriate metal perchlorate, dissolved in methanol, with the stoicheiometric amount of $5\text{-}NO_2phen$. The substances thus precipitated were crystallised from acetone–ethanol.

$[Pd(5\text{-}NO_2phen)_2](ClO_4)_2$ was obtained as a microcrystalline precipitate by treating the solvo-complex $[Pd(5\text{-}NO_2phen)(solvent)_2]Cl_2$, freshly prepared in acetone from $[Pd(5\text{-}NO_2phen)Cl_2]$ and $AgClO_4$, with the stoicheiometric amount of $5\text{-}NO_2phen$.

*Author to whom correspondence should be addressed.

$[M(5\text{-}NO_2phen)Cl_2]$ (M = Pt or Pd) were prepared following essentially the procedure reported in the literature.[9] The substituted complexes $[Pd(5\text{-}NO_2phen)X_2]$ (X = Br, I, SCN, $NO_2$, $N_3$) were prepared either from the respective tetrahalopalladite by reaction with excess of $5\text{-}NO_2$phen in ethanol or by reaction of the solvocomplex in acetone with the stoicheiometric amount of the appropriate salt NaX.

All the complexes were characterized by elemental analysis.

Amines were refluxed over potassium hydroxide pellets and then distilled under reduced pressure. Amine perchlorates were obtained on mixing equimolar amounts of the appropriate amine and perchloric acid in ethanol. The resulting solutions were evaporated under reduced pressure and the oily substances obtained were crystallised twice from absolute ethanol.

*Caution!* Although we have never experienced explosions with perchlorates in organic solvents, other workers have reported accidents; due precaution against this possibility must be taken.

Dimethylformamide and dimethylsulphoxide were of spectrophotometric grade. The use of dmf distilled under reduced pressure did not lead to significant changes in the spectral and kinetic results.

The other products were of reagent grade.

Electronic spectra were recorded by means of a Cary 219 spectrophotometer. Slower kinetics were followed spectrophotometrically in the u.v.-visible region by recording spectra of the reaction mixtures at various times. For faster kinetics the stopped-flow technique was adopted. A HI-TECH SF-3 stopped-flow spectrophotometer was used; the oscilloscope traces, stored on a Gould Advance 054100 oscilloscope were recorded on a Radiometer REC 61 potentiometric recorder. In both cases good linear plots were obtained on plotting $\ln(A_{00} - A_t)$ vs time. $A_{00}$ represents the mixture absorbance at six to seven half-lives and $A_t$ that at various times. The $k_{obs}$ values were reproducible to better than $\pm 5\%$.

## RESULTS AND DISCUSSION

Solutions of the complexes $[M(5\text{-}NO_2phen)_3](ClO_4)_2$ (M = Cu(II), Ni(II), Co(II)) in the presence of aliphatic amines in dmso, dmf or other dipolar aprotic solvent, turn immediately red orange. The spectra of the reaction mixtures are in all cases characterized by two maxima (Fig. 1) at 395–406 and 470–486 nm, the absorbance at the lower wavelength having the higher intensity. The complexes $[M(5\text{-}NO_2phen)X_2]$ (M = Pt(II) or Pd(II); X = Cl, Br, I, $N_3$, SCN, $NO_2$) and $[Pd(5\text{-}NO_2phen)_2](ClO_4)_2$ undergo a similar reaction and the electronic spectra of the reaction mixtures are directly comparable, for position and intensity, to those relative to the nickel(II), copper(II) and cobalt(II) trisnitrophenanthroline cations (Fig. 2). In the case of the latter complexes, however, the colour forming reactions with aliphatic amines proceed in two steps both associated to spectral variations. The first spectral variation is very fast and only the second one can be recorded by means of a conventional spectrophotometer; nevertheless, the first spectral change can be detected by lowering the rate of the second process. This can be done taking advantage of the large dependence of this reaction on the ionic strength of the reacting solution; in the presence of large amounts of $NaClO_4$ (0.3 mol dm$^{-3}$) the second reaction is almost inhibited and the first spectral variation can be conveniently recorded (Fig. 2). The spectral features of mixtures of the complexes here studied and piperidine in dmf and dmso are reported in Table 1. Precise quantitative measurements of the relative intensities of the two absorption bands are difficult in that in all cases the red orange colour produced is unstable and fades slowly. Nevertheless an approximate estimation affords an intensity ratio of the absorbance at the lower and the higher wavelengths in all cases of 2–3. It appears, therefore, that the electronic spectra of the substances formed by reaction of metal complexes of $5\text{-}NO_2$phen with aliphatic amines in dipolar aprotic solvents, do not depend on the nature of the central metal, ancillary ligands

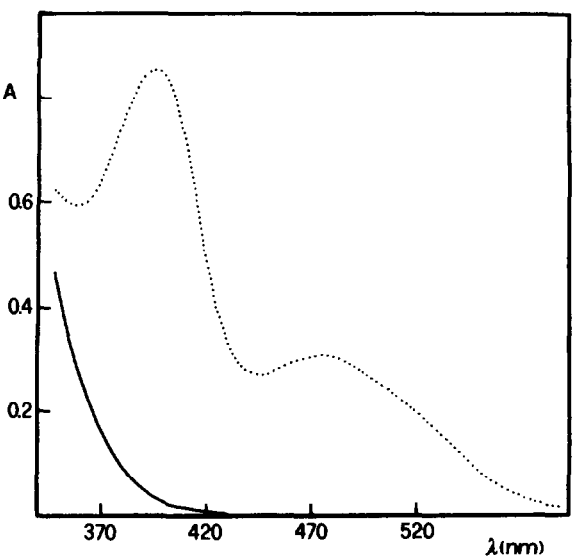



Fig. 1. Spectral variations, in the UV and visible region, on additon of piperidine to $[Co(5\text{-}NO_2phen)_3](ClO_4)_2$ in dmso. ———, complex $1 \times 10^{-4}$ mol dm$^{-3}$. · · · · ·, complex + piperidine 0.2 mol dm$^{-3}$.

and geometry of the substrates. This is an obvious indication that the red colour development is the result of a specific interaction of aliphatic amines with coordinated 5-$NO_2$phen.

Kinetic data relative to the four-coordinate complexes [Pt(5-$NO_2$phen)$Cl_2$] and [Pd(5-$NO_2$phen)$Cl_2$] are in agreement with this suggestion. Among the factors influencing the rate of substitution of one of the groups coordinated in a square planar complex, the nature of the central atom is of primary importance. Thus, palladium(II) substrates are much more labile[10] than the platinum(II) analogues, the rate of substitution of a group X being larger by a factor of $10^4$–$10^6$ for the former. While the complexes here studied conform to such a trend as regards the reaction with bromide, in the reaction with n-propylamine the platinum and the palladium substrates exhibit comparable reactivity. We have actually studied both the reaction of [Pd(5-$NO_2$phen)$Cl_2$] and [Pt(5-$NO_2$phen)$Cl_2$] with $Br^-$ at 25°C in dmf and the reaction between the same substrates and *n*-propylamine at −30°C in dmf. The first reaction is known[11] to proceed in two steps leading to the formation of the disubstituted derivative [M(5-$NO_2$phen)$Br_2$] according to the scheme

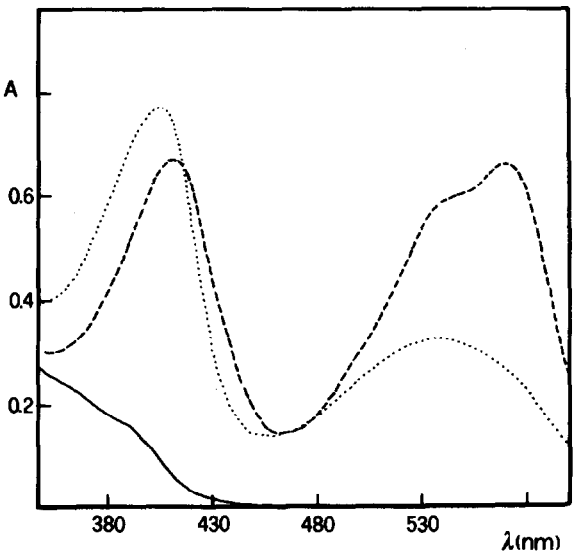



Fig. 2. Spectral variations, in the UV and visible region, on addition of piperidine to [Pt(5-$NO_2$phen)$Cl_2$] in dmso. ———, complex $1 \times 10^{-4}$ mol $dm^{-3}$. – – – –, complex + piperidine 0.2 mol $dm^{-3}$. ·····, complex + piperidine in the presence of $LiClO_4$ 0.3 mol $dm^{-3}$.

$$[M(5\text{-}NO_2phen)Cl_2] + Br^- \longrightarrow [M(5\text{-}NO_2phen)ClBr] + Cl^-$$

$$[M(5\text{-}NO_2phen)ClBr] + Br^- \xrightarrow{\text{fast}} [M(5\text{-}NO_2phen)Br_2] + Cl^- \quad (1)$$

Table 1. Electronic spectra of mixtures of metal complexes of 5-$NO_2$phen and excess of piperidine in dimethylsulphoxide or dimethylformamide

| Complex | $\lambda_{1,max}$ (nm) | $\lambda_{2,max}$ (nm) |
|---|---|---|
| [Co(5-$NO_2$phen)$_3$] $(ClO_4)_2$ | 475 | 396 |
| [Ni(5-$NO_2$phen)$_3$] $(ClO_4)_2$ | 485 (494) | 406 (408) |
| [Cu(5-$NO_2$phen)$_3$] $(ClO_4)_2$ | 485 | 403 |
| [Pd(5-$NO_2$phen)$_2$] $(ClO_4)_2$ | 520 | 393 |
| [Pd(5-$NO_2$phen)$Cl_2$] | 520 | 400 |
| [Pd(5-$NO_2$phen)$(NO_2)_2$] | 520 | 398 |
| [Pd(5-$NO_2$phen)$(SCN)_2$] | 520 | 402 |
| [Pt(5-$NO_2$phen)$Cl_2$] | 536 | 412 |

values in brackets refer to dimethylformamide.

We have followed the kinetic course of these reactions spectrophotometrically under pseudo-first-order conditions with respect to the complex and found that the usual two-term rate law

$$k_{obs} = k_1 + k_2[Br^-] \quad (2)$$

is obeyed. $k_1$, the rate constant for the solvolytic path, refers to the attack of the solvent at the central atom; $k_2$ is the rate constant relative to the direct entry of the nucleophile. In our case $k_1$ is negligible for [Pt(5-$NO_2$phen)$Cl_2$] and has a value of 0.02 $dm^3mol^{-1}s^{-1}$ for [Pd(5-$NO_2$phen)$Cl_2$]. As expected on the basis of the large difference in lability between platinum(II) and palladium(II) analogues, the values of $k_2$ are respectively $3.2 \times 10^{-4}$ $dm^3mol^{-1}s^{-1}$ and 1.35 $dm^3mol^{-1}s^{-1}$ for the former and the latter complex. The colour forming reaction has also been followed spectrophotometrically at low temperature using a large excess of amine both to get pseudo-first-order conditions and to force the reactions to completion. The processes have all stopped-flow rates and their kinetics obey the equation

$$k_{obs} = k_2[n\text{-propylamine}]. \quad (3)$$

The $k_2$ values (Table 2) are almost identical for the two complexes, being 115 $dm^3mol^{-1}s^{-1}$ for [Pt(5-$NO_2$phen)$Cl_2$] and 137 $dm^3mol^{-1}s^{-1}$ for [Pd(5-$NO_2$phen)$Cl_2$]. Furthermore, one can note that these values are much larger than those relative to the reaction of the same substrates with $Br^-$, though these latter refer to a higher temperature. This is especially true for [Pt(5-$NO_2$phen)$Cl_2$]; the difference in reactivity, which is over a factor of $10^5$ is not certainly explainable on the basis of the different nucleophilicity of $Br^-$ and *n*-propylamine. Our findings, which should be very unusual if referred to substitution reactions at square planar complexes, strongly suggest that in the colour forming reactions between aliphatic amines and the platinum(II) and palladium(II) complexes studied the amines do not attack the central metal but rather the coordinated ligand 5-$NO_2$phen.

It is very difficult to establish the nature of the red species formed by interaction of aliphatic amines with 5-$NO_2$phen coordinated to a transition metal. These substances are in fact unstable both thermodynamically and kinetically and decompose, inevitably, more or less rapidly. Any attempt to isolate one of these species so far has failed. On the other hand their characterization by NMR measurements is hampered by spectral broadening observed either in dmf or dmso solu-

Table 2. Values of observed rate constants $k_{obs}$ ($s^{-1}$) and second order rate constants $k_2$ ($dm^3mol^{-1}s^{-1}$) for reaction of the substrates [M(5-$NO_2$phen)$Cl_2$] (M = Pt(II) or Pd(II) with $Br^-$ and *n*-propylamine in dimethylformamide

| | [nucleophile] | T/C | Pt | | Pd | |
|---|---|---|---|---|---|---|
| | | | $k_{obs}$ | $k_2$ | $k_{obs}$ | $k_2$ |
| | 0.1 | | $3.26 \times 10^{-5}$ | | | |
| | 0.2 | | $6.04 \times 10^{-5}$ | | | |
| $Br^-$ | 0.3 | 25 | $9.24 \times 10^{-5}$ | $3.2 \pm 0.1 \times 10^{-4}$ | | 1.35[a] |
| | 0.4 | | $12.5 \times 10^{-5}$ | | | |
| | 0.5 | | $16.1 \times 10^{-5}$ | | | |
| | 0.05 | | 6.4 | | 9.0 | |
| | 0.1 | | 13.3 | | 15.0 | |
| $n\text{-prNH}_2$ | 0.2 | -30 | 23.0 | 115±3 | 26.7 | 137±4 |
| | 0.3 | | 34.6 | | 42.6 | |
| | 0.5 | | 59.0 | | 70.0 | |

a values from ref. 10.

tions of the complexes[12,13] or in their mixtures with amines. Various suggestions have been advanced in order to account for the nature of the adducts between nucleophiles and diimines coordinated to metal atoms. Gillard and others[14] have proposed that the effect on the reactivity of heterocycles caused by coordination to metal ions are similar to quaternization of N-heterocycles by charge acceptors such as alkyl or aryl groups. The last process is known to lead to activation of some positions in the aromatic ring to nucleophilic addition and to a facile formation of pseudo-bases, or Meisenheimer complexes in the case of nitroaromatics. Our reactions conform to Gillard's suggestion. In fact, addition at room temperature of metal ions such as $Ni^{2+}$, $Cu^{2+}$, $Ag^{+}$, etc. to a mixture of 5-$NO_2$phen and piperidine in dmf, produces a rapid red colour development. The electronic spectrum of the solution is characterized by two twin maxima, the one at the lower wavelength having the higher intensity, typical of Meisenheimer complexes.[15] Free 5-$NO_2$phen, under the same experimental conditions, interacts with piperidine only to a very small extent, as indicated by the lack of significant spectral variations in a solution of these substances.

The spectral changes produced on mixing aliphatic amines and dipolar aprotic solvents solutions of metal complexes of 5-$NO_2$phen are reversed either by addition of acid or addition of the appropriate protonated amine. The red colour can be restored by further addition of amine and in most cases this operation can be repeated indefinitely provided it is performed quickly with respect to the decomposition of the adduct. In the case of the reaction between $[Ni(5\text{-}NO_2phen)_3](ClO_4)_2$ and piperidine the product is stable enough to allow the determination of the equilibrium constant of the process and its stoicheiometry[13] which can be summarized as in (4).

$$\text{Complex} + 2 \text{ piperidine} \rightleftarrows \text{adduct}^{-} + \text{pipH}^{+}. \quad (4)$$

This scheme is identical with that relative to the formation of the well known Meisenheimer adducts formed in the reaction of nitroaromatics with aliphatic amines.[15]

The alternative explanation that ion pairs can form between substrate and nucleophile is to be ruled out because at least for the Pt(II) and Pd(II) derivatives, a reaction between neutral species is involved. Likewise, proton transfer by amine from one of the positions of the ring to give a carbanion, as proposed by Burgess and Prince[16] to explain the exceptional reactivity of $[Fe(5\text{–}NO_2phen)_3]^{2+}$ with $OH^{-}$, is also unlikely. In fact, while proton transfer are usually diffusion controlled,[17] we have been able to follow in all cases the rate of the colour forming reactions by stopped-flow technique.

## REFERENCES


1. R. D. Gillard, D. W. Knight and P. A. Williams, *Trans. Met. Chem.* 1980, **5**, 321 and preceding papers of this series.
2. E. D. Constable, *Polyhedron* 1983, **7**, 551.
3. N. Serpone, G. Ponterini, M. A. Jamieson, F. Bolletta and M. Maestri, *Coord. Chem. Rev.* 1983, **50**, 209.
4. R. D. Gillard, *Coord. Chem. Rev.* 1983, **50**, 303.
5. O. Farver, O. Monsted and G. Nord, *J. Am. Chem. Soc.* 1979, **101**, 6118.
6. G. Nord, *Acta Chem. Scand., Sect. A* 1975, **29**, 270.
7. O. Wernberg and A. Hazell, *J. Chem. Soc., Dalton Trans.* 1980, 973.
8. G. B. Kaufman and L. K. Takahashi, *Inorg. Synth.* 1966, **VIII**, 227.
9. R. C. Conrad and J. V. Rund, *Inorg. Chem.* 1972, **11**, 129.
10. F. Basolo and R. G. Pearson, *Mechanisms of Inorganic Reactions*. Wiley, New York (1967).
11. M. Cusumano, G. Guglielmo and V. Ricevuto, *J. Chem. Soc., Dalton Trans.* 1980, 2044.
12. D. W. Anderson, P. Roberts, M. W. Twigg and M. B. Williams, *Inorg. Chim. Acta* 1979, L281.
13. A. Bartolotta, M. Cusumano, A. Giannetto and V. Ricevuto, *J. Chem. Soc. Dalton Trans.* in press.
14. R. D. Gillard, *Coord. Chem. Rev.* 1975, **16**, 67.
15. M. Strauss, *Chem. Rev.* 1970, **70**, 667.
16. J. Burgess and R. H. Prince, *J. Chem. Soc.* 1965, 4697.
17. M. Eigen, *Angew. Chem., Int. Ed. Engl.* 1966, **3**, 1.

*Polyhedron* Vol. 3, No. 6, pp. 707–711, 1984
Printed in Great Britain.

0277–5387/84 $3.00 + .00
© 1984 Pergamon Press Ltd.

# REACTIONS OF DIAZOLES WITH MANGANESE AND IRON CARBONYLS

V. V. GUMENYUK,* V. N. BABIN, YU. A. BELOUSOV, N. S. KOCHETKOVA and I. V. DOBRYAKOVA

A. N. Nesmeyanov Institute of Organo-Element Compounds, Academy of Sciences of the U.S.S.R., Vavilov st.28,II7813, Moscow V-312, U.S.S.R.

(*Received* 14 *September* 1983; *accepted* 10 *October* 1983)

**Abstract**—The compounds of two types were isolated in the reactions of dimanganese decacarbonyl with diazoles. The compounds with an unaltered oxidation state of the metal were formed as a result of nucleophilic substitution of a carbonyl ligand of $Mn_2(CO)_{10}$. The compounds with an altered oxidation state of the central atom were produced in redox-transformations of $Mn_2(CO)_{10}$. The substances were characterized by the data of mass-, IR-, $^1$H-NMR -spectra. The EPR-data were obtained for paramagnetic $Mn^{2+}$ salts. The reactions of $Mn_2(CO)_{10}$ with diazoles are compared with those of iron carbonyls.

Until recently researchers were interested in azoles as merely ligands. In reactions with metal compounds azoles were regarded as nucleophilic reagents. It was shown for the first time in our laboratory in a series of papers[1–4] (exemplified by the reactions with iron compounds) that the nitrogen-containing heterocycles, as well as their anions, are able to react as redox reagents. With this in mind, taking into account the fact that manganese carbonyl undergoes redox disproportionation in reactions with nitrogen bases[5] (similarly to iron carbonyls), we decided to study the redox aspects of the reactions of manganese carbonyl with pyrazole, imidazole and their salts, and to compare these reactions with those of iron carbonyls.

## DISCUSSION

When studying the interaction of manganese and iron carbonyls with diazoles and their sodium salts, it was established that the common feature for the reactions studied is the occurrence of two reaction paths, namely, the nucleophilic substitution of a carbonyl ligand, and the reduction-oxidation transformations. During the studies both the compounds with the initial oxidation state of the central atom, and the compounds with altered oxidation state of the metal ion, were isolated and characterized. The reactions of iron carbonyls with azoles were reported in detail in our previous publications.[6]

In the present paper we studied for the first time the reactions of manganese carbonyl with diazoles and their salts from the reduction-oxidation standpoint. In this case the new compounds were obtained, which were not described previously, namely, $Mn_2(CO)_9(AzH)$ (nonacarbonyldimanganese diazole, with AzH = pyrazole PzH and imidazole ImH). The formation of compounds of such a type is the result of the nucleophilic substitution of a carbonyl group in $Mn_2(CO)_{10}$ by the diazole. In the case of the heterocyclic anion the reaction mixture contains, probably, the anion $[Mn_2(CO)_9Az]^-$, with $Na^+$ acting as a counter-ion. The latter assumption confirmed by the absence of N–H bands in the 3200–3500 $cm^{-1}$ region in the IR spectrum of the ether solution of the reaction mixture. Nevertheless, after chromatography on $Al_2O_3$ (Brockman II) the diazole anion captures a proton and turns into a neutral molecule. That is why the compounds of the $Mn_2(CO)_9(AzH)$ type were also isolated in the reaction of $Mn_2(CO)_{10}$ with sodium pyrazolide and sodium imidazolide.

Nonacarbonyldimanganese-diazoles were obtained as highly air-sensitive compounds although it was possible to record the mass spectra prior to their decomposition. The molecular ion with $m/e = 430$ loses successively either nine carbonyl groups, or the $[Mn(CO)_5]^+$ fragment with $m/e = 195$. The presence of the $[Mn_2]^+$ ion with $m/e = 110$ evidences in favour of the binuclear structure of the compounds studied. The fragment

*Author to whom correspondence should be addressed.

ion with $m/e = 68$ corresponds to a free heterocycle.

A large number of bands in the IR spectra of $Mn_2(CO)_9(AzH)$ in the region of stretching vibrations of the terminal carbonyl ligands (see Table 1) indicates the low symmetry of the complex. The heterocyclic ligand is likely to occupy the equatorial position. Similar complexes of the $Mn_2(CO)_9(L)$ type (L = acetonitrile, propionitrile) with nitrogen ligand in the equatorial position are reported in literature.[7] The PMR spectrum (in THF) in the case of the pyrazole complex contains three signals with ratio 1:1:1—two doublets with chemical shifts of $\delta$7.61 and 7.25 ppm, corresponding to the 3 and 5-protons of the heterocyclic ligand, and the multiplet at $\delta$6.48 p.p.m. corresponding to the 4-proton. It had not been possible to detect the N–H proton at room temperature.

On the basis of the data obtained the compounds $Mn_2(CO)_9AzH$ were attributed the structure of binuclear $\sigma$-complexes with diazoles coordinated through the pyridine nitrogen atom.

It is known that the "pure" substitution takes place also in the reactions of dodeca- and nonacarbonyls of iron with diazoles. Unstable red crystals of $Fe(CO)_3(AzH)$ and $Fe(CO)_4(AzH)$ were reported previously.[6] The compounds of the $Fe(CO)_4(AzH)$ type are distinguished by the axial position of the heterocycle.

Thus, the nucleophilic substitution reactions in bi- and tri-nuclear carbonyls, $Fe_2(CO)_9$ and $Fe_3(CO)_{12}$, occur with the Fe–Fe bond breaking, whereas manganese carbonyl retains its metal–metal bond to form the binuclear complexes.

The reduction–oxidation transformations of manganese carbonyl, accompanying the substitution of carbonyl ligands, yield the compounds of two types: the complex salts, $[Mn(AzH)_4 \cdot solv]^{2+}[Mn(CO)_5]_2^-$, solv = $C_2H_5OH$, THF, and the tetraethylammonium salt of the binuclear anion tris-$\mu$-pyrazolide-bis-[tricarbonylmanganese(I)]: $[Mn_2(CO)_6(Az)_3]^-NEt_4^+$ (where Az is the anion of L). The latter salt is not produced in the case of imidazole, probably due to the steric overcrowding. Previously, the pyrazole-containing complex was obtained through the reaction of $Mn(CO)_5Br$ with the excess of sodium pyrazolide. Therefore, we identified the salt by comparing the IR spectrum data (Table 1) and the PMR spectra (see Experimental) with those reported in the literature.[8]

The salts $[Mn(AzH)_4 \cdot C_2H_5OH]^{2+}[Mn(CO)_5]_2^-$ obtained in the reactions of manganese carbonyl with both pyrazole and imidazole, and sodium pyrazolide and imidazolide, were isolated by chromatography on $Al_2O_3$ followed by the crystallization from $C_2H_5OH$. In the case of azole salts the reaction proceeds at the rate of reactants' mixing, and the yield of complex salts of bivalent manganese with the manganese carbonyl–anion, in this case, is well above that for the reaction of free heterocycles. The latter fact is accounted for by the azole anions being much stronger reducing agents than the neutral ligand[1] and, hence, by the more appreciable contribution of the anions into the redox processes.

The isolated dark-red solids of $[Mn(AzH)_4 \cdot C_2H_5OH][Mn(CO)_5]_2$ are soluble in polar solvents, non-volatile, and decomposed at temperatures about 100°C. Elemental analysis yields (see Experimental) the overall formula $Mn_3C_{24}H_{22}N_8O_{11}$. The salts obtained are paramagnetic. The ESR spectrum of the imidazole complex salt contains the broad signal (the line width of 700 G) with a g

Table 1. IR spectra of products of the reaction of manganese carbonyl with diazoles

| | Compound | $\nu_{CO}$ $cm^{-1}$ | Solvent |
|---|---|---|---|
| I. | Nonacarbonyldimanganesepyrazole | 2093,2020,2000,1990,1970,1940 | Ether |
| 2. | Nonacarbonyldimanganeseimidazole | 2092,2020,2005,1988–1982,1963, 1941 | Hexane |
| 3. | μ-Tripyrazolide-bis-(tricarbonylmanganese)tetraethylammonium | 1910,2010 | Acetone |
| 4. | $[Mn(PzH)_4][Mn(CO)_5]_2$ | 1865,1910,1980,2015 | Acetone |
| 5. | $[Mn(ImH)_4][Mn(CO)_5]_2$ | 1870,1910,1980,2030 | Ethanol |

PzH - pyrazole;

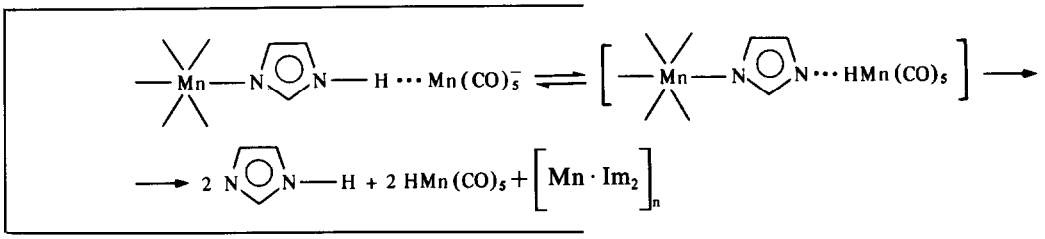
ImH - imidazole.

factor equal to 1.9834, i.e. the outline is typical for high-spin $d^5$-complexes of bivalent manganese ($Mn^{2+}$).[9-11]

In the $^1$H-NMR spectrum (with THF as a solvent) the proton signals of the heterocyclic ring were absent, whereas the solvent's signals were broadened. As the paramagnetic ion $Mn^{2+}$ is the coordination unsaturated species (elemental analysis yields four AzH molecules), it is reasonable to suppose that the solvent's molecules enter the coordination sphere of the metal ion. A similar phenomenon was reported for the salts of the $MnX_2(ImH)_4$ type with X = Br, I. The above phenomenon results in the rapid exchange between the coordinated and free solvent's molecules. The exchange with the paramagnetic species leads to the essential broadening of the THF $\alpha$- and $\beta$-protons, and to the shift of signals.

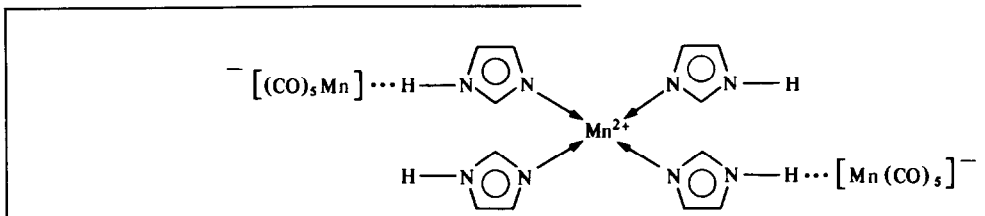
The IR spectrum (recorded in acetone) contains four bands in the region of CO-group vibrations: 1860, 1910, 1980 and 2015 $cm^{-1}$, which fact is typical for the $[Mn(CO)_5]^-$ anion since, as is well known, the negative charge results in the decrease of the CO-group vibration frequences as compared with neutral molecules.

The IR spectrum of the pyrazolyl salt (recorded in THF) contains, along with the bands attributed to the CO-group stretching vibrations of the $[Mn(CO)_5]^-$ anion, the bands corresponding to manganese pentacarbonyl hydride $\nu$Mn–H = 1718 $cm^{-1}$; $\nu_{CO}$ = 2035, 2051, 2095 $cm^{-1}$. In addition, $HMn(CO)_5$ was identified through its mass spectrum among the decomposition products when the salts were heated in an inert atmosphere. The free heterocycle and an insoluble residue are also formed upon thermal decomposition, the latter corresponding, apparently, to the coordination polymer $[Mn(Az)_2]_n$. From these considerations it can be suggested that the proton transfer from the cation to the anion occurs in the process of the thermal decomposition:

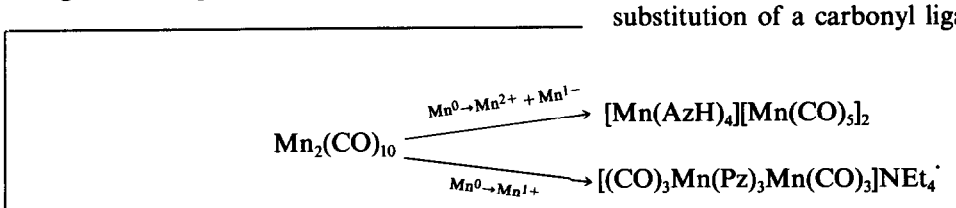


The heating shifts the equilibrium to the side of volatile manganese carbonyl hydride.

Summing up the reported data we attributed the salts obtained to the following structure:



Thus, in the reactions of $Mn_2(CO)_{10}$ with diazoles and their salts the reduction–oxidation transformations take place along with the nucleophilic substitution of a carbonyl ligand.



It is well known[6] that the redox reactions of iron carbonyls with diazoles yield: (i) the salts of the $[(AzH)_6Fe]^{2+}B^{2-}$ type, where $B = Fe_2(CO)_8$ for pyrazole, and $B = Fe_3(CO)_{11}$ in the case of imidazole, and (ii) the binuclear complex $Pz_2Fe_2(CO)_6$.

To summarize, all the compounds formed in the reactions of diazoles and their salts with manganese and iron carbonyls can be arranged in Table 2. It should be noted that, using the ESR technique in the reactions of diazoles with iron carbonyls, we recorded, previously, the paramagnetic species[4] and suggested the mechanism of one-electron transfer from diazoles to $Fe_3(CO)_{12}$ or other carbonyls. In the case of manganese carbonyl, the radical species failed to be detected in the

Table 2. Types of species, which are formed in reactions of manganese and iron carbonyls with azoles and their salts

| Types of species | | | | Metal oxidation state |
|---|---|---|---|---|
| $[Mn(AzH)_4]^{2+}$ | $d^5$ | $[Fe(AzH)_6]^{2+}$ | $d^6$ | 2 |
| $[Mn_2(CO)_6Az_3]^-$ | $d^6$ | $Fe_2(CO)_6Az_2$ | $d^7$ | I |
| $Mn_2(CO)_9AzH$ | $d^7$ | $Fe(CO)_4AzH$<br>$Fe(CO)_3AzH$ | $d^8$ | 0 |
| $[Mn(CO)_5]^-$ | $d^8$ | $[Fe_2(CO)_8]^-$<br>$[Fe_3(CO)_{12}]^-$ | $d^9$ | -I |
| ——— | $d^9$ | $[Fe_3(CO)_{11}]^{2-}$<br>$[Fe_2(CO)_8]^{2-}$ | $d^{10}$ | -2 |

AzH - pyrazole, imidazole

reaction mixture, which fact corresponds, most likely, to the two-electron transfer in the systems studied. Subsequently we intend to carry out the electrochemical investigation to arrive at a definite conclusion.

## EXPERIMENTAL

Most of compounds obtained by us were unstable in the air. Therefore the synthesis of the compounds and their subsequent isolation and purification were performed in an atmosphere of argon. The same holds for the preparation of samples for spectral studies and elemental analysis. Prior to the experiment the solvents were distilled over a suitable drying agent in an atmosphere of argon.

*Reaction of manganese carbonyl with pyrazole.* 1.95 g (0.005 mol) of manganese carbonyl and 0.68 g (0.01 mol) of pyrazole were placed in a three-necked quartz flask equipped with a magnetic stirrer. Then, 50 $cm^3$ of THF was added and the reaction mixture was stirred upon irradiation with the PRK-4 lamp for 4 hr. When the stirring was terminated, the solution was concentrated and siphonated into the chromatographic column filled with $Al_2O_3$. A lemon–yellow band was eluted by hexane, which band (after the solvent was distilled off) represented initial $Mn_2(CO)_{10}$ (m.p. 150°C, yield 0.27 g). The yellow–orange compound, nonacarbonyldimanganesepyrazole, was eluted by ether (yield 0.32 g). Molecular weight: mass spectrum $-m/e = 430$, calculated for $C_{12}H_4N_2O_9Mn_2$-430. The IR spectrum is given in Table 1.

A dark-orange band was eluted by ethanol. After the solvent was distilled off, a reddish solid of the complex salt, $[Mn(PzH)_4]^2+[Mn(CO)_5]_2^- C_2H_5OH$, was obtained (decomposition point 100°C) (yield 1.14 g). Found: C-37.81; H-2.79; Mn-22.03. Calc. for $C_{14}H_{22}N_8O_{11}Mn_2$: C-37.74; H-2.83; Mn-21.62%.

A dark-yellow band was eluted by the acetone:water mixture with ratio 1:1; tetraethylammonium chloride precipitated from the former a yellow solid of the tetraethylammonium salt of tris-($\mu$-pyrazolide)-bis-(tricarbonylmanganese), $[Mn_2(CO)_6(Pz)_3]NEt_4$, m.p. 381°C (lit. data:[8] m.p. 380–382°C), yield 0.48 g.

The $^1$H-NMR data: $\delta H_{C_3H_3N_2} = 7.45$ ppm, 5.80 ppm, $\delta H_{CH_2-} = 2.73$ ppm, $\delta H_{CH_3-} = 0.79$ ppm.

*Reaction of manganese carbonyl with imidazole.* The reaction was carried out as the previous one from 1 g of $Mn_2(CO)_{10}$ and 0.408 g of imidazole in 40 $cm^3$ of THF. By chromatography on $Al_2O_3$ the following compounds were isolated:

(i) manganese carbonyl.

(ii) nonacarbonyldimanganeseimidazole, $Mn_2(CO)_9ImH$, yield ~15% Molecular weight: mass spectrum—$m/e = 430$, calculated for $C_{12}H_4N_2O_9Mn_2$—430. The IR spectrum see in Table 1.

(iii) complex salt of the pentacarbonylmanganate anion, $[Mn(ImH)_4][Mn(CO)_5]_2 \cdot C_2H_5OH$, yield ~30%.

Found: C-37.64; H-2.85; N-14.53; Mn-22.01. Calc. for $C_{24}H_{22}N_8O_{11}Mn_2$: C-37.74; H-2.83; N-14.68; Mn-21.62%.

*Reaction of manganese carbonyl with sodium pyrazolide*

To 0.75 g of manganese carbonyl dissolved in 20 $cm^3$ of THF a solution of 0.34 g of sodium pyrazolide in 35 $cm^3$ of THF was added dropwise. After addition, the reaction mixture was stirred at room temperature for another 20 min. Further, the solution was concentrated and separated by chro-

matography on $Al_2O_3$. The following products were isolated:

(i) manganese carbonyl 0.08 g,

(ii) nonacarbonyldimanganesepyrazole (yield ~ 7%),

(iii) tetraethylammonium salt of $\mu$-tripyrazolide-bis-(tricarbonyl-manganese), yield 12%,

(iv) $[Mn(PzH)_4][Mn(CO)_5]_2 \cdot C_2H_5OH$, yield 21.5%.

*Reaction of manganese carbonyl with sodium imidazolide*

Starting from the solution of 1.5 g of manganese carbonyl in 20 $cm^3$ of THF and the suspension of 0.69 g of sodium imidazolide in 30 $cm^3$ of THF, the following products were isolated through the procedure described above:

(i) manganese carbonyl 0.16 g, (10.7%).

(ii) nonacarbonyldimanganeseimidazole 0.11 g, (6.8%).

(iii) $[Mn(ImH)_4][Mn(CO)_5]_2 \cdot C_2H_5OH$ (decomposition point 115–120°C).

## REFERENCES


1. V. N. Babin, V. V. Gumenyuk, S. P. Solodovnikov and Yu. A. Belousov, *Z. Naturforsch.* 1981, **36b** 400.
2. V. N. Babin, Yu. A. Belousov, I. R. Lyatifov, R. B. Materikova, V. V. Gumenyuk, *J. Organometal. Chem.* 1981, **214**, C11.
3. V. N. Babin, Yu. A. Belousov, V. V. Gumenyuk, R. B. Materikova, R. M. Salimov, N. S. Kochetkova, *J. Organometal. Chem.* 1981, **214**, C13.
4. V. N. Babin, Yu. A. Belousov, V. V. Gumenyuk, R. M. Salimov, R. B. Materikova and N. S. Kochetkova, *J. Organometal. Chem.* 1983, **241**, C41.
5. W. Hieber, W. Beck, G. Zeitler, *Angew. Chem.* 1961, **73**, 364.
6. V. N. Babin, Thesis, Inst. Org. -Elem. Comp., USSR Acad. Sci., 1971.
7. L. Manfred Ziegler, Heinz Haas and Raymond K. Sheline, *Chem. Ber.* 1965, **98**, 2454.
8. S. Trofimenko, *J. Am. Chem. Soc.* 1969, **91**, 5410.
9. J. Reedijk, *Rec. Trav. Chim.* 1969, **88**, 1451.
10. J. Reedijk, *Inorg. Chim. Acta* 1969, **3**, 517.
11. J. Reedijk, *Rec. Trav. Chim.* 1970, **89**, 605.

*Polyhedron* Vol. 3, No. 6, pp. 713–720, 1984
Printed in Great Britain.

0277–5387/84 $3.00 + .00
© 1984 Pergamon Press Ltd.

# STUDIES ON NOVEL UNSYMMETRICAL AZOMETHINES—III

## COPPER(II) COMPLEXES OF UNSYMMETRICAL TETRADENTATE AZOMETHINES

**R. P. SHARMA and R. N. PRASAD***
Department of Chemistry, University of Rajasthan, Jaipur 302004, India

(*Received* 15 *September* 1983; *accepted* 12 *October* 1983)

**Abstract**—Copper(II) complexes of unsymmetrical bifunctional tetradentate azomethines having the general formulae, (–$OC_{10}H_6CH$:N–X–N:C(R)$C_6H_4O$–)Cu, (–$OC_{10}H_6CH$:N–X–N:C($CH_3$)CHC($CH_3$)O–)Cu, (–$OC_6H_4CH$:N–X–N:C($CH_3$)$C_6H_4O$–)Cu, (–$OC_6H_4$C(R):N–X–N:C($CH_3$)CHC($CH_3$)O–)Cu (where R = H or $CH_3$, X = –$(CH_2)_3$–, –$(CH_2)_4$–, –$(CH_2)_6$– or –*o*–$C_6H_4$–) have been synthesized by the reactions of preformed mixed imine complexes of the type, CuLL′ (where L and L′ are two different imines such as 2-hydroxy-1-naphthaldimine, salicylaldimine, *o*-hydroxyacetophenonimine or acetylacetonimine) with diamines such as 1,3-diaminopropane, 1,4-diaminobutane, 1,6-diaminohexane or *o*-phenylenediamine. These complexes have been characterized by elemental analyses, TLC, conductance, magnetic measurements, IR and electronic spectra.

Metal complexes of symmetrical tetradentate azomethines have been widely studied. However, during recent years a few complexes of unsymmetrical azomethines have also been reported.[1–5] These studies are confined to the unsymmetrical ligands derived from ethylenediamine or propylenediamine and those derived from long chain diamines or aromatic diamines have not yet been studied. In our earlier communications[6,7] Ni(II) complexes of unsymmetrical tetradentate azomethines derived from long chain diamines or aromatic diamines have been described. In the present paper similar complexes (**I–IV**) of copper with the unsymmetrical azomethines are reported.

## RESULTS AND DISCUSSION

### *Complex formation*

Addition of ammonia to an ethanolic solution of $CuCl_2 \cdot 2H_2O$ or $Cu(NO_3)_2 \cdot 3H_2O$ gives copper ammine complex which on treatment with a 1:1 mixture of two different carbonyl compounds results in the formation of the mixed imine complex. The reaction with 2-hydroxy-1-naphthaldehyde and salicylaldehyde or *o*-hydroxyacetophenone may be represented by Scheme I.

The reactions of mixed imine complexes with diamines such as 1,3-diaminopropane, 1,4-diaminobutane, 1,6-diaminohexane or *o*-phenylenediamine yield the unsymmetrical complexes (**I–IV**). The synthesis of the complexes **I** may be represented by Scheme II.

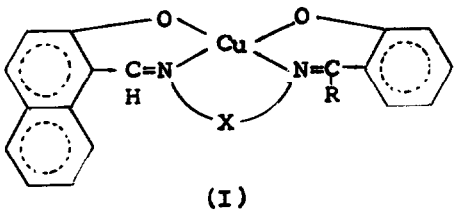
The mixed imine complexes are green solids soluble in chloroform and insoluble in water. The complexes of unsymmetrical tetradentate azomethines are also green solids except those derived from *o*-phenylenediamine which are of brown colour. These are soluble in common organic solvents such as chloroform, methanol and ethanol and insoluble in water. The solubility of the unsymmetrical complexes in organic solvents decreases in the following order:

$$-(CH_2)_3- > -o-C_6H_4- > -(CH_2)_4- > -(CH_2)_6-.$$

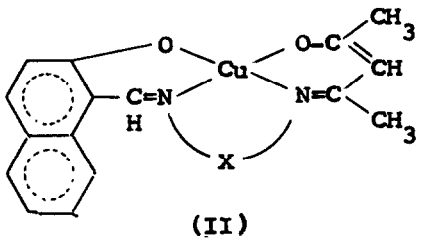
### *Thin layer chromatography*

TLC of the unsymmetrical complexes was performed on silica gel G using chloroform–ether (3:2) mixture as a solvent. Single spots were observed for all the complexes. $R_f$ values of a few representative unsymmetrical and corresponding

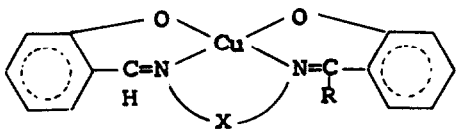
*Author to whom correspondence should be addressed.



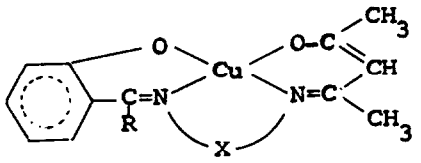
(I)



(II)



(III)



(IV)

R = H or $CH_3$

X = $-(CH_2)_3-$, $-(CH_2)_4-$,

$-(CH_2)_6-$ or $-O-C_6H_4-$

symmetrical complexes are recorded in Table 3. The $R_f$ values of the unsymmetrical complexes were found to be intermediate between those of the corresponding symmetrical complexes. This indicates that they are single unsymmetrical complexes and not mixtures of the corresponding symmetrical complexes.

*Magnetic measurements*

The magnetic moments of mixed imine and a few unsymmetrical complexes are recorded in Tables 1 and 4 respectively. The data are consistent with square planar geometry. Magnetic moment values higher than expected for a single unpaired electron (1.73 BM) may be attributed to the incomplete quenching of the orbital contribution to the magnetic moment[8] or spin orbit coupling.[9]

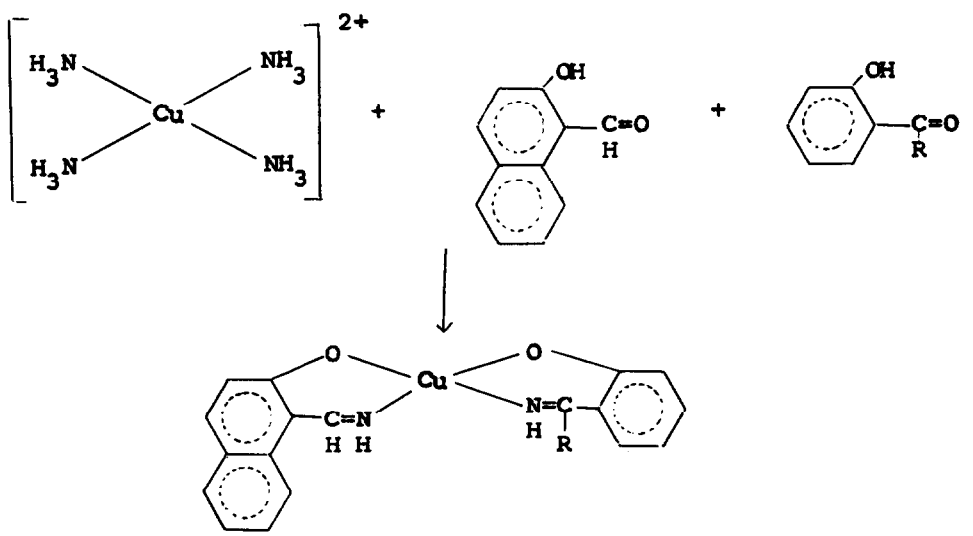
*Conductivity measurements*

Molar conductances of the mixed imine and unsymmetrical complexes were determined in nitrobenzene. Molar conductance values range from 0.40 to 0.85 $\Omega^{-1}\,cm^2\,mole^{-1}$ indicating them to be non-electrolytes.

*IR spectra*

The mixed imine complexes of Cu(II) exhibit a strong band at $\sim 3300\,cm^{-1}$ due to the presence of –NH– group. A strong broad or split band at $\sim 1630\,cm^{-1}$ indicates the presence of two different azomethine groups.

Cu(II) complexes of unsymmetrical tetradentate azomethines do not exhibit bands in the region 3600–3100 $cm^{-1}$ indicating the absence of $H_2O$,



(V)

R = H or $CH_3$

Scheme I.

Table 1. Analyses and characteristics of mixed imine complexes of Cu(II)

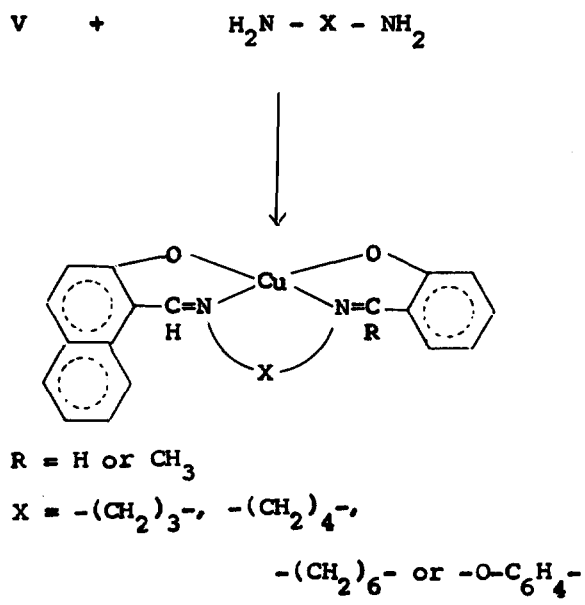
| S. No. | Complex | Characteristics | Yield (%) | Analyses (%) C Found (Calcd.) | H Found (Calcd.) | N Found (Calcd.) | Cu Found (Calcd.) | $\mu_{eff}$ (BM) |
|---|---|---|---|---|---|---|---|---|
| 1. | $Cu(-OC_{10}H_6CH{:}N-)(-N{:}CHC_6H_4O-)$ (H, H) | Green solid 290°C, d | 93 | 61.21 (61.10) | 4.17 (3.99) | 7.80 (7.92) | 18.02 (17.96) | 1.78 |
| 2. | $Cu(-OC_{10}H_6CH{:}N-)(-N{:}C(CH_3)C_6H_4O-)$ (H, H) | Green solid 315°C, d | 88 | 61.94 (62.03) | 4.42 (4.38) | 7.55 (7.62) | 17.48 (17.46) | 1.81 |
| 3. | $Cu(-OC_{10}H_6CH{:}N-)(-N{:}C(CH_3)CHC(CH_3)O-)$ (H, H) | Green solid 261°C, d | 87 | 58.10 (57.91) | 5.00 (4.86) | 8.37 (8.44) | 19.09 (19.15) | 1.80 |
| 4. | $Cu(-OC_6H_4CH{:}N-)(-N{:}C(CH_3)C_6H_4O-)$ (H, H) | Green solid 260°C, d | 90 | 56.66 (56.69) | 4.59 (4.44) | 8.80 (8.81) | 19.93 (20.00) | 1.83 |
| 5. | $Cu(-OC_6H_4CH{:}N-)(-N{:}C(CH_3)CHC(CH_3)O-)$ (H, H) | Green solid 205°C, d | 81 | 51.10 (51.15) | 4.95 (5.01) | 10.03 (9.94) | 22.51 (22.55) | 1.77 |
| 6. | $Cu(-OC_6H_4C(CH_3){:}N-)(-N{:}C(CH_3)CHC(CH_3)O-)$ (H, H) | Green solid 260°C, d | 77 | 52.88 (52.78) | 5.44 (5.45) | 9.60 (9.47) | 21.39 (21.48) | 1.85 |

d = decomposed

Table 2. Analyses and characteristics of Cu(II) complexes of unsymmetrical tetradentate azomethines

| S.No. | Complex | Characteristics | Yield (%) | Analyses (%) N Found (Calcd.) | Analyses (%) Cu Found (Calcd.) |
|---|---|---|---|---|---|
| 1. | Cu(-$OC_{10}H_6CH{:}N(CH_2)_3N{:}CHC_6H_4O$-) | Dark green solid 205°C, d | 78 | 7.08 (7.11) | 16.22 (16.13) |
| 2. | Cu(-$OC_{10}H_6CH{:}N(CH_2)_3N{:}C(CH_3)C_6H_4O$-) | Green solid 255°C, d | 74 | 7.01 (6.87) | 15.55 (15.85) |
| 3. | Cu(-$OC_{10}H_6CH{:}N(CH_2)_3N{:}C(CH_3)CHC(CH_3)O$-) | Green solid 225°C, d | 71 | 7.40 (7.53) | 16.98 (17.08) |
| 4. | Cu(-$OC_6H_4CH{:}N(CH_2)_3N{:}C(CH_3)C_6H_4O$-) | Green solid 300°C, d | 77 | 7.91 (7.83) | 17.80 (17.75) |
| 5. | Cu(-$OC_6H_4CH{:}N(CH_2)_3N{:}C(CH_3)CHC(CH_3)O$-) | Green solid 200°C, d | 73 | 8.72 (8.70) | 19.66 (19.74) |
| 6. | Cu(-$OC_6H_4C(CH_3){:}N(CH_2)_3N{:}C(CH_3)CHC(CH_3)O$-) | Dark green solid 240°C, d | 67 | 8.39 (8.34) | 19.01 (18.92) |
| 7. | Cu(-$OC_{10}H_6CH{:}N(CH_2)_4N{:}CHC_6H_4O$-) | Green solid 245°C, | 85 | 6.92 (6.87) | 15.55 (15.58) |
| 8. | Cu(-$OC_{10}H_6CH{:}N(CH_2)_4N{:}C(CH_3)C_6H_4O$-) | Green solid 200°C, d | 81 | 6.66 (6.64) | 14.97 (15.06) |
| 9. | Cu(-$OC_{10}H_6CH{:}N(CH_2)_4N{:}C(CH_3)CHC(CH_3)O$-) | Green solid 247°C, d | 77 | 7.30 (7.26) | 16.52 (16.46) |
| 10. | Cu(-$OC_6H_4CH{:}N(CH_2)_4N{:}C(CH_3)C_6H_4O$-) | Green solid 305°C, d | 82 | 7.50 (7.53) | 17.21 (17.09) |
| 11. | Cu(-$OC_6H_4CH{:}N(CH_2)_4N{:}C(CH_3)CHC(CH_3)O$-) | Green solid 280°C, d | 79 | 8.41 (8.34) | 19.03 (18.92) |

| | | | | | |
|---|---|---|---|---|---|
| 12. | $Cu(-OC_6H_4C(CH_3):N(CH_2)_4N:C(CH_3)CHC(CH_3)O-)$ | Dark green solid<br>242°C, d | 68 | 7.94<br>(8.01) | 18.22<br>(18.16) |
| 13. | $Cu(-OC_{10}H_6CH:N(CH_2)_6N:CHC_6H_4O-)$ | Green solid<br>160°C, d | 87 | 6.40<br>(6.43) | 14.59<br>(14.57) |
| 14. | $Cu(-OC_{10}H_6CH:N(CH_2)_6N:C(CH_3)C_6H_4O-)$ | Green solid<br>230°C, d | 83 | 6.30<br>(6.23) | 14.10<br>(14.12) |
| 15. | $Cu(-OC_{10}H_6CH:N(CH_2)_6N:C(CH_3)CHC(CH_3)O-)$ | Green solid<br>270°C, d | 78 | 6.86<br>(6.77) | 15.46<br>(15.35) |
| 16. | $Cu(-OC_6H_4CH:N(CH_2)_6N:C(CH_3)C_6H_4O-)$ | Green solid<br>190°C, d | 83 | 6.93<br>(7.00) | 16.00<br>(15.89) |
| 17. | $Cu(-OC_6H_4CH:N(CH_2)_6N:C(CH_3)CHC(CH_3)O-)$ | Green solid<br>182°C, d | 75 | 7.74<br>(7.70) | 17.39<br>(17.46) |
| 18. | $Cu(-OC_6H_4C(CH_3):N(CH_2)_6N:C(CH_3)CHC(CH_3)O-)$ | Bluish green solid<br>235°C, d | 73 | 7.37<br>(7.41) | 16.75<br>(16.81) |
| 19. | $Cu(-OC_{10}H_6CH:N(O-C_6H_4)N:CHC_6H_4O-)$ | Brown solid<br>310°C, d | 80 | 6.50<br>(6.55) | 14.91<br>(14.85) |
| 20. | $Cu(-OC_{10}H_6CH:N(O-C_6H_4)N:C(CH_3)C_6H_4O-)$ | Brown solid<br>320°C, d | 77 | 6.26<br>(6.34) | 14.43<br>(14.38) |
| 21. | $Cu(-OC_{10}H_6CH:N(O-C_6H_4)N:C(CH_3)CHC(CH_3)O-)$ | Brown solid<br>300°C, d | 73 | 6.86<br>(6.90) | 15.71<br>(15.65) |
| 22. | $Cu(-OC_6H_4CH:N(O-C_6H_4)N:C(CH_3)C_6H_4O-)$ | Brown solid<br>295°C, d | 78 | 7.08<br>(7.15) | 16.22<br>(16.21) |
| 23. | $Cu(-OC_6H_4CH:N(O-C_6H_4)N:C(CH_3)CHC(CH_3)O-)$ | Brown solid<br>240°C, d | 70 | 7.94<br>(7.87) | 17.80<br>(17.85) |
| 24. | $Cu(-OC_6H_4C(CH_3):N(O-C_6H_4)N:C(CH_3)CHC(CH_3)O-)$ | Greenish brown solid<br>250°C, d | 68 | 7.61<br>(7.57) | 17.09<br>(17.18) |




Scheme II.

$NH_2$, NH or OH groups. A strong split absorption band at about 1600 $cm^{-1}$ supports the presence of two different azomethine groups. The bands in the region 600–525 $cm^{-1}$ may be assigned to $\nu_{Cu-O}$ and $\nu_{Cu-N}$.[10]

*Electronic spectra*

The absorption bands in the electronic spectra of a few representative unsymmetrical complexes are recorded in Table 5. The mixed imine complexes exhibit three absorption bands at ~366, 270 and 246 nm. In addition to these bands a band at ~560 nm with very low extinction coefficient was also observed. Unsymmetrical complexes exhibit five or six absorption bands in the region 244–424 nm with an additional band at ~600 nm.

The absorption bands at ~560 nm ($\epsilon = 0.006 \times 10^4$) in mixed imine complexes and at ~600 nm ($\epsilon = 0.02 \times 10^4$) in unsymmetrical complexes may be assigned to a combination of $^2B_{1g} \rightarrow {}^2A_{1g}$, $^2B_{1g} \rightarrow {}^2B_{2g}$ and $^2B_{1g} \rightarrow {}^2E_{1g}$ transitions in $D_{4h}$ symmetry probably square planar for these complexes.[11,12] The higher extinction coefficient of this band for unsymmetrical complexes as compared to mixed imine complexes may be due to the change of the geometry from *trans* to *cis*-planar.

## EXPERIMENTAL

*Materials*

Salicylaldehyde (E.Merck), *o*-hydroxyacetophenone (John Baker), acetylacetone (IDPL), 1,3-diaminopropane (Fluka), 1,4-diaminobutane (Fluka), 1,6-diaminohexane (Fluka) and ethanol were purified by distillation before use. 2-Hydroxy-1-naphthaldehyde (Fluka) and *o*-phenylenediamine (Fluka) were recrystallized before use. $CuCl_2 \cdot 2H_2O$ (BDH) and $Cu(NO_3)_2 \cdot 3H_2O$ (BDH) were of AR grade.

*Analytical methods*

Carbon and hydrogen were analysed on a Coleman C,H analyser model 33. Copper was estimated volumetrically by hypo and nitrogen by Kjeldahl's method. IR spectra were recorded as Nujol mulls in the region 4000–200 $cm^{-1}$ on a Perkin–Elmer 577 Grating IR Spectrophotometer. The electronic spectra in the region 200–800 nm were recorded in chloroform on a Pye–Unicam model SP8-100 spectrophotometer at room temperature using 1 cm quartz cell.

Molar conductances were determined in nitrobenzene by a conductivity meter, type 302 (Systronics) with a cell of cell constant 1.39 $cm^{-1}$. Magnetic susceptibilities were determined by Gouy method at room temperature using Bruker B-M6 magnet.

*Preparation of complexes*

*Synthesis of mixed imine complex* (2 - *hydroxy* - 1 - *naphthaldiminato*) (*salicylaldiminato*)Cu(*II*). To the ethanolic solution of $CuCl_2 \cdot 2H_2O$ (3.92 g) ammonia (1 : 1) was added drop by drop with constant stirring until the precipitate of metal hydroxide formed redissolved forming the metal–ammine complex. It was heated to ~80°C and to the hot solution an ethanolic solution of 2-hydroxy-1-naphthaldehyde (3.96 g) and salicylaldehyde (2.81 g) (1 : 1 : 1 molar ratio) was added with constant stirring. The reaction mixture was refluxed for about half an hour and the green solid obtained was filtered, washed with ethanol and dried *in vacuo*.

The mixed imine complexes, (2 - hydroxy - 1 - naphthaldiminato) (*o*-hydroxyacetophenoniminato)Cu(II), (2 - hydroxy - 1 - naphthaldiminato) (acetylacetoniminato)Cu(II), (salicylaldiminato)(*o*-hydroxyacetophenoniminato)Cu(II), (salicylaldiminato)(acetylacetoniminato)Cu(II) and (*o* - hydroxyacetophenoniminato)(acetylacetoniminato Cu(II) were synthesized following the same procedure. These were recrystallized from chloroform and analysed (Table 1).

*Syntheses of* Cu(*II*) *complexes of unsymmetrical tetradentate azomethines derived from* 1,3-*diaminopropane*. About 1.0 g of the mixed imine complex was suspended in ~50 $cm^3$ of ethanol and to this ethanolic solution 1,3-diaminopropane was added in slight excess than 1 : 1 molar ratio. The reaction mixture was stirred for ~1 hr and refluxed for ~30 min. The crystalline solid sepa-

Table 3. $R_f$ values of Cu(II) complexes of unsymmetrical tetradentate azomethines and corresponding symmetrical complexes

| S.No. | Complex | Rf value |
|---|---|---|
| 1. | $Cu\{(-OC_{10}H_6CH{:}N)_2(CH_2)_3\}$ | 0.59 |
| 2. | $Cu\{(-OC_6H_4CH{:}N)_2(CH_2)_3\}$ | 0.69 |
| 3. | $Cu(-OC_{10}H_6CH{:}N(CH_2)_3N{:}CHC_6H_4O-)$ | 0.65 |
| 4. | $Cu\{(-OC_6H_4C(CH_3){:}N)_2(CH_2)_3\}$ | 0.66 |
| 5. | $Cu(-OC_{10}H_6CH{:}N(CH_2)_3N{:}C(CH_3)C_6H_4O-)$ | 0.62 |
| 6. | $Cu(-OC_6H_4CH{:}N(CH_2)_3N{:}C(CH_3)C_6H_4O-)$ | 0.67 |
| 7. | $Cu\{(-OC(CH_3)CHC(CH_3)O-)_2(CH_2)_3\}$ | 0.72 |
| 8. | $Cu(-OC_{10}H_6CH{:}N(CH_2)_3N{:}C(CH_3)CHC(CH_3)O-)$ | 0.65 |
| 9. | $Cu(-OC_6H_4CH{:}N(CH_2)_3N{:}C(CH_3)CHC(CH_3)O-)$ | 0.70 |
| 10. | $Cu(-OC_6H_4C(CH_3){:}N(CH_2)_3N{:}C(CH_3)CHC(CH_3)O-)$ | 0.70 |

Table 4. Magnetic moments of a few representative Cu(II) complexes of unsymmetrical tetradentate azomethines

| S.No. | Complex | $\mu_{eff}$ (BM) |
|---|---|---|
| 1. | $Cu(-OC_{10}H_6CH{:}N(CH_2)_3N{:}CHC_6H_4O-)$ | 1.98 |
| 2. | $Cu(-OC_{10}H_6CH{:}N(CH_2)_4N{:}CHC_6H_4O-)$ | 1.91 |
| 3. | $Cu(-OC_{10}H_6CH{:}N(CH_2)_6N{:}CHC_6H_4O-)$ | 1.83 |
| 4. | $Cu(-OC_{10}H_6CH{:}N(O-C_6H_4)N{:}CHC_6H_4O-)$ | 1.89 |
| 5. | $Cu(-OC_{10}H_6CH{:}N(CH_2)_3N{:}C(CH_3)C_6H_4O-)$ | 1.94 |
| 6. | $Cu(-OC_{10}H_6CH{:}N(CH_2)_4N{:}C(CH_3)C_6H_4O-)$ | 1.85 |
| 7. | $Cu(-OC_{10}H_6CH{:}N(CH_2)_6N{:}C(CH_3)C_6H_4O-)$ | 1.74 |
| 8. | $Cu(-OC_{10}H_6CH{:}N(O-C_6H_4)N{:}C(CH_3)C_6H_4O-)$ | 1.89 |
| 9. | $Cu(-OC_{10}H_6CH{:}N(CH_2)_3N{:}C(CH_3)CHC(CH_3)O-)$ | 2.03 |
| 10. | $Cu(-OC_{10}H_6CH{:}N(CH_2)_4N{:}C(CH_3)CHC(CH_3)O-)$ | 1.88 |
| 11. | $Cu(-OC_{10}H_6CH{:}N(CH_2)_6N{:}C(CH_3)CHC(CH_3)O-)$ | 1.75 |
| 12. | $Cu(-OC_{10}H_6CH{:}N(O-C_6H_4)N{:}C(CH_3)CHC(CH_3)O-)$ | 1.92 |

rated was filtered, washed with ethanol and dried *in vacuo*. These were recrystallized from chloroform and analysed (Table 2).

*Syntheses of* Cu(*II*) *complexes of unsymmetrical tetradentate azomethines derived from* 1,4-*diaminobutane*. These complexes were synthesized following the same general procedure as described for 1,3-diaminopropane. These were recrystallized from chloroform and analysed (Table 2).

*Syntheses of* Cu(*II*) *complexes of unsymmetrical tetradentate azomethines derived from* 1,6-*diaminohexane*. To the ethanolic suspension of the mixed imine complex an ethanolic solution of 1,6-diaminohexane was added in slight excess than

Table 5. Absorption bands in the electronic spectra of a few Cu(II) complexes of unsymmetrical tetradentate azomethines

| S.No. | Complex | $\lambda_{max}$ ($\epsilon$) ($\times 10^4$) |
|---|---|---|
| 1. | Cu(-$OC_{10}H_6CH{:}N(CH_2)_3N{:}CHC_6H_4O$-) | 244(5.05), 268(3.32), 320(2.60), 382(1.23), 404(1.03) |
| 2. | Cu(-$OC_{10}H_6CH{:}N(CH_2)_4N{:}CHC_6H_4O$-) | 244(4.00), 266(2.53), 314(1.63), 386(0.98), 404(0.82) |
| 3. | Cu(-$OC_{10}H_6CH{:}N(CH_2)_6N{:}CHC_6H_4O$-) | 244(4.63), 262(2.62), 272(2.36), 302(1.88), 316(1.75), 372(0.96) |
| 4. | Cu(-$OC_{10}H_6CH{:}N(O\text{-}C_6H_4)N{:}CHC_6H_4O$-) | 246(4.03), 268(2.83), 280(2.67), 314(1.76), 348(1.42), 424(2.15) |

1:1 molar ratio. The reaction mixture was stirred for ~3 hr at room temperature (25°C) and the green solid obtained was filtered, washed with ethanol and dried *in vacuo*. These were recrystallized from chloroform and analysed (Table 2).

Syntheses of Cu(II) complexes of unsymmetrical tetradentate azomethines derived from o-phenylenediamine. These complexes were synthesized following the same procedure as discussed in case of 1,3-diaminopropane. These were recrystallized from chloroform and analysed (Table 2).

*Acknowledgements*—The authors are thankful to the Head of Chemistry Department, University of Rajasthan, Jaipur, for providing laboratory facilities. One of us (R. P. Sharma) is thankful to University of Rajasthan, Jaipur for the award of a Research Fellowship.

## REFERENCES

1. H. A. Kuska, M. F. Farona, P. Pappas and P. Potterton, *J. Coord. Chem.* 1971, **1**, 259.
2. R. C. Elder, *Aust. J. Chem.* 1978, **31**, 35.
3. P. J. Burke and D. R. McMillin, *J.C.S. Dalton* 1980, 1794.
4. E. Kwiatkowski and M. Kwiatkowski, *Inorg. Chim. Acta* 1980, **42**, 197.
5. B. Chiswell, J. P. Crowford and P. J. O. Reilly, *Inorg. Chim. Acta* 1980, **40**, 223.
6. R. P. Sharma and R. N. Prasad, *Synth. React. Inorg. Metal-Org. Chem.* 1982, **12**, 347.
7. R. P. Sharma and R. N. Prasad, *Acta Chim.* (In press).
8. M. Calvin and C. H. Berkelew, *J. Am. Chem. Soc.* 1946, **68**, 2267.
9. A. Earnshaw, *Introduction to Magnetochemistry*, p. 35. Academic Press, New York (1969).
10. C. P. Gupta, P. K. Kamingo and R. K. Mehta, *J. Indian Chem. Soc.* 1979, **LVI**, 826.
11. R. L. Carlin, *Transition Metal Chemistry*, p. 51. Marcel Dekker, New York (1969).
12. C. J. Ballahausen, *Introduction to Ligand Field Theory*, p. 268. McGraw-Hill, New York (1962).

*Polyhedron* Vol. 3, No. 6, pp. 721–728, 1984
Printed in Great Britain.

0277–5387/84 $3.00 + .00
© 1984 Pergamon Press Ltd.

# ALKYLXANTHATES OF PHENYLARSENIC(III)

**RAJESH K. GUPTA, A. K. RAI and R. C. MEHROTRA***
Department of Chemistry, University of Rajasthan, Jaipur 302004, India

**and**

**V. K. JAIN**
Department of Chemistry, University of Guelph, Guelph, Ontario, Canada NIG 2W1

(*Received* 10 *October* 1983; *accepted* 28 *November* 1983)

**Abstract**—*Bis*-xanthates of phenylarsenic(III), having the general formula, $PhAs(S_2COR)_2$ (where R = Me, Et, Pr$^n$, Pr$^i$, allyl and Bu$^n$), have been synthesized and characterized by elemental analysis, molecular weight, IR, NMR ($^1H$ and $^{13}C$) and mass spectral data which have been discussed in relation to plausible structures for these arsenic derivatives.

Although xanthates of arsenic(III) have long been known and the crystal structure of $As(S_2COEt)_3$ was elucidated in 1960,[1] yet the studies on the corresponding organo-arsenic complexes do not appear to have received much attention except their mention as biologically active substances.[2,3]

The synthesis of phenylantimony *bis*-xanthates has been reported by us recently.[4] In the present paper, the synthesis of the corresponding phenylarsenic(III) complexes is reported and an attempt has been made to investigate the effect of size and electronegativity of the central metal atom on the properties of these xanthate complexes. On the basis of IR and NMR ($^1H$ and $^{13}C$) as well as mass spectral studies, a square pyramidal structure is proposed for these derivatives and the probable fragmentation pattern, based on mass spectral studies of some representative compounds is discussed.

## RESULTS AND DISCUSSION

Phenyldichloroarsine reacts with potassium alkyl xanthates (KL) in 1:2 molar ratios to afford the complexes of the type $PhAsL_2$ at room temperature:

$$PhAsCl_2 + 2KS_2COR \xrightarrow{CS_2} PhAs(S_2COR)_2 + 2KCl\downarrow$$

where R = Me, Et, Pr$^n$, Pr$^i$, allyl and Bu$^n$.

These reactions are quite facile and the potassium chloride is precipitated readily on mixing the reactants.

Alternatively, these complexes may be prepared by the insertion of carbon disulphide across the As–O bond by refluxing the corresponding phenyl alkoxyarsines in carbon disulphide:

$$PhAs(OR)_2 \xrightarrow{CS_2} PhAs(S_2COR)_2$$

R = Et and Pr$^i$.

These derivatives are crystalline solids (except R = allyl; liquid), soluble in common organic solvents like benzene, chloroform, carbon disulphide etc. and found to be monomeric in refluxing chloroform solutions.

Similar to the corresponding phenylantimony *bis*-xanthates,[4] these complexes are non-volatile and tend to decompose on heating, even under reduced pressure. On heating the phenylarsenic *bis*-xanthates at ~120°C, phenylarsenic sulphide is obtained:

$$PhAs(S_2COR)_2 \xrightarrow{\Delta} PhAsS + \text{Volatile products}$$

R = Me, Pr$^n$.

The volatile products appear to $CS_2$, COS,

Table 1. Reactions of $PhAsCl_2$ with potassium alkylxanthates in 1:2 molar ratios

| Sl No. | Reactants $PhAsCl_2$ (g) | $KS_2COR$ R | (g) | KCl (g) Found (Calcd.) | Yield % | Physical State (m.p.) °C | Analysis (%) Found (Calcd.) As | S | Mol. wt. Found (Calcd.) |
|---|---|---|---|---|---|---|---|---|---|
| 1. | 1.18 | Me | 1.58 | 0.70 (0.79) | 87 | Whitecrystals (70-72) | 20.32 (20.47) | 34.67 (34.98) | 350 (366) |
| 2. | 1.24 | Et | 1.80 | 0.76 (0.83) | 98 | Colourless crystals (45-46) | 18.80 (19.02) | 32.29 (32.49) | 387 (394) |
| 3. | 1.28 | $Pr^n$ | 2.03 | 0.78 (0.86) | 91 | White crystals (42-43) | 17.69 (17.76) | 30.16 (30.34) | - |
| 4. | 0.94 | $Pr^i$ | 1.48 | 0.58 (0.62) | 91 | White crystals (103-104) | 17.48 (17.76) | 30.07) (30.34) | 401 (422) |
| 5. | 1.11 | Allyl | 1.72 | 0.68 (0.74) | 94 | Light yellow liquid | 17.79 (17.93) | 30.36 (30.63) | - |
| 6. | 0.76 | $Bu^n$ | 1.30 | 0.45 (0.51) | 92 | Colourless crystals (48-50) | 16.48 (16.65) | 28.34 (28.45) | 446 (450) |

hydrocarbons and thioester, etc. as indicated by mass spectral studies.

*IR spectra*

IR spectra of these complexes (Table 2) have been recorded in the region 4000–200 $cm^{-1}$ and the assignments are made on the basis of previous reports.[5] The bands around 1220 and 1140 $cm^{-1}$ have been assigned to the $\nu$(C–O–C) and $\nu$(C–O) vibrations respectively, while C ⋯ S stretching, vibrations have been observed around 1040 $cm^{-1}$ in these complexes. The appearance of only one strong band around 1040 $cm^{-1}$ indicates the bidentate nature of the ligands.[6]

The bands observed around 470 and 350–400 $cm^{-1}$ may be assigned to $\nu$As–C[7] and As–S stretchings[8] respectively in these complexes.

*NMR spectra*

The $^1H$ NMR spectra of these complexes show (Table 2) the characteristic resonances due to the alkyl groups present. The signals are sharp and do not exhibit splitting, indicating the equivalence of both xanthate ligands on the NMR timescale.

The aromatic protons appear in the region $\delta$7.1–8.2 in two sets of multiplets, having integration of 2:3 ratio; it suggests that ortho-proton signals appear down-field compared to meta- and para-protons.[9]

The signals of the protons, bonded to carbon in $S_2C$–O–C< group in phenylarsenic complexes appear downfield (3–9 Hz) as compared to the signals of the same protons in the corresponding antimony complexes. On the other hand, the $^{13}C$ signals for the $S_2C$–O–C< group appear upfield in the arsenic complexes in comparison to antimony complex (Table 3). A possible explanation may be in terms of more intense $\pi$-back donation to vacant 3*d* orbitals of sulphur in the arsenic compared with antimony complexes; this should cause shielding of carbon atom in S⋯S>C–O group. However, in the antimony complexes, a lower electron density at this carbon might be expected to impart some $\pi$-character to $S_2C$–O bond which may affect the protons adjacent to it via its shielding cone,[10] causing an upfield shift and giving a relative deshielding to the protons of arsenic complexes.

The $^{13}C$ NMR spectral data of some of the complexes, presented in Table 3, seem to display some discernible trends. The carbon bonded to oxygen in O–$CH_3$ group (complex 1) absorbs at $\delta$61.27 and tends to deshield on further substitution of its hydrogens by methyl groups (complex 2, 3): the same effect of substitution is also experienced to a much less extent by the carbon atom of phenyl ring (Cx) bonded to the metal atom. However, conversely, the more substituted alkoxy group causes shielding of the carbon atom of $S_2C$–O group which may be attributed to the increasing electron releasing capacity of the alkoxy group on substitution. Finally, the corrected chemical shifts, $\delta'$, for mono-substituted benzene derivatives ($C_6H_5$–X), defined as $\delta' = \delta(Cp) - \delta(Cm)$ (where $\delta$(Cp) and $\delta$(Cm) are the chemical shifts value of the para and meta carbon atoms of phenyl ring), are found to be a linear measure of the resonance effects of the substituent, X.[11] This corrected chemical shift $\delta'$, may be related to the Hammett–Taft constant $\sigma_R^\circ$, by the equation;[12] $\sigma' = 22.06\,\sigma_R^\circ$ (where downfield shifts relative to TMS have been given positive values).

The values of $\delta'$ and $\sigma_R^\circ$, calculated according to the above equations, are shown in Table 3. These negative values suggest an electron release from the metal towards the phenyl ring by $p\pi$–$p\pi$ conjugation. A higher value of $\sigma_R^\circ$ is obtained for the antimony complex in comparison to corresponding arsenic complex and is in agreement with the fact that the antimony has a poorer donor capacity than the arsenic.

*Mass spectra*

Some relevant mass spectral peaks of a few complexes, along with their relative intensities and assignments, are summarized in Table 4. As expected from the appearance of a strong $|CS_2|^+$ peak, molecular ion peaks for the complexes were not observed; this may be attributed to the pyrolytic decomposition of these complexes.[13] Analysis of the mass spectral data suggests two prominent decomposition pathways in which phenyl or one of the ligand moieties is lost. One of the important features of the iso-propyl-compounds is the sequential loss of the alkene from xanthate group. On the other hand, the methyl-compound cannot eliminate alkene and it fragments by the loss of methyl groups.

The arsenic and antimony complexes show almost identical fragmentation patterns but the ions of the high *m/e* values are less abundant in the mass spectra of the antimony complex indicating its greater decomposition tendency.

Arsenic is a mono-isotopic species while antimony has two isotopes of mass numbers 121 and 123, having natural abundance of about 57 and 43% respectively; any species containing antimony may, therefore, be identified by appearance of two sister peaks at two mass numbers apart, with their relative intensities in approx. 5.7:4.3 ratio.

Table 2. Some IR and $^1H$ NMR spectral assignments for the $PhAs(S_2COR)_2$ complexes

| Sl No. | COMPLEX | IR Frequencies ($cm^{-1}$) | | | | | $^1H$ NMR Chemical shifts ($\delta$, ppm) | | | |
|---|---|---|---|---|---|---|---|---|---|---|
| | | $\nu$C-O-C | $\nu$C-O | $\nu$C=S | $\nu$As-C | $\nu$As-S | $CH_3$- | -$CH_2$- | -CH< | Aromatic |
| 1. | $PhAs(S_2COMe)_2$ | 1220m | 1150m | 1055m | 465m | 385m | 4.20(s) | - | - | 7.23-8.10(m) |
| 2. | $PhAs(S_2COEt)_2$ | 1225s | 1150w | 1040m | 470m | 350m | 1.50(t) | 4.60(q) | - | 7.20-8.03(m) |
| 3. | $PhAs(S_2COPr^n)_2$ | 1220s | 1140m | 1040s | 470s | 375s | 1.00(t) | 1.80(h)<br>4.48(t) | - | 7.26-7.94(m) |
| 4. | $PhAs(S_2COPr^i)_2$ | 1230s | 1140w | 1030s | 470s | 400m | 1.45(d) | - | 5.60(m) | 7.13-8.13(m) |
| 5. | $PhAs(S_2COBu^n)_2$ | 1220s,b | 1140m | 1050m | 480m | 395m | 1.00(t) | 1.00-2.10(m)<br>4.55(t) | - | 7.10-8.10(m) |

s = strong, m = medium, w = weak and b = broad

(s) = singlet, (d) = doublet,
(t) = triplet, (q) = quartet,
(h) = hextet and (m) = multiplet.

Table 3. Some $^{13}C$ NMR* spectral data of xanthate complexes

| Sl. No. | COMPLEX | Types of carbon atoms | | | Chemical shifts ($\delta$, ppm) | | | | $\delta'$ | $\sigma_R^o$ |
|---|---|---|---|---|---|---|---|---|---|---|
| | | | | | Aromatic | | | | | |
| | | $>C-\underline{C}H_3$ | $O-\underline{C}<$ | $S>\underline{C}-O$ (S) | C(x) | C(o) | C(m) | C(p) | | |
| 1. | $PhAs(S_2COMe)_2$ | - | 61.27 | 215.42 | 138.40 | 133.00 | 130.15 | 128.56 | -1.59 | -0.072 |
| 2. | $PhAs(S_2COEt)_2$ | 13.70 | 71.34 | 214.63 | 138.50 | 132.99 | 130.01 | 128.48 | -1.53 | -0.069 |
| 3. | $PhAs(S_2COPr^i)_2$ | 21.18 | 79.67 | 213.83 | 138.63 | 132.92 | 129.93 | 128.46 | -1.47 | -0.067 |
| 4. | $PhSb(S_2COPr^i)_2$ | 21.30 | 80.46 | 220.13 | 145.85 | 135.19 | 129.22 | 128.56 | -0.66 | -0.030 |

* in $CDCl_3$ solutions relative to TMS, downfield shifts given positive values

C(x) = Carbon bonded to metal

C(o), C(m) and C(p) are the carbon atoms at ortho, meta and para positions in phenyl ring.

Table 4. Mass spectral analysis of some of the xanthate complexes

| $PhAs(S_2COPr^i)_2$ | | | $PhSb(S_2COPr^i)_2$ | | | $PhAs(S_2COMe)_2$ | | |
|---|---|---|---|---|---|---|---|---|
| R.I*(%) (1) | m/e (2) | Assignments (3) | R.I.(%) (1) | m/e (2) | Assignments (3) | R.I.(%) (1) | m/e (2) | Assignments (3) |
| 5.8 | 346 | $\|HAs(S_2COPr^i)_2\|^+$ | 0.4 | 410 | $\|PhSb(S_2CH)(S_2COPr^i)\|^+$ | 2.5 | 336 | $\|PhAs(S_2CO)_2\|^+$ |
| 6.2 | 336 | $\|PhAs(S_2CO)_2\|^+$ | 0.6 | 392 | $\|HSb(S_2COPr^i)_2\|^+$ | 17.0 | 290 | $\|HAs(S_2COMe)_2\|^+$ |
| 23.8 | 287 | $\|As(S_2CH)(S_2COPr^i)\|^+$ | 0.8 | 350 | $\|HSb(S_2COPr^i)(S_2COH)\|^+$ | 6.7 | 261 | $\|As(S_2COH)_2\|^+$ |
| | | or $\|PhAs(S_2COPr^i)\|^+$ | 7.1 | 333 | $\|PhSb(S_2COPr^i)\|^+$ | 6.7 | 260 | $\|As(S_2CO)_2H\|^+$ |
| 6.5 | 246 | $\|As_2S_3\|^+$ | 2.6 | 307 | $\|Sb(S_2COH)_2\|^+$ | 65.7 | 259 | $\|As(S_2COMe)(S_2CH)\|^+$, |
| 61.4 | 245 | $\|PhAs(S_2COH)\|^+$ | 4.4 | 301 | $\|Sb(SCH)(S_2COPr^i)\|^+$ | | | $\|PhAs(S_2COMe)\|^+$, $\|As(S_2CO)_2\|^+$ |
| 9.0 | 244 | $\|PhAs(S_2CO)\|^+$ | 16.0 | 291 | $\|PhSb(S_2COH)\|^+$ | 6.1 | 229 | $\|As(S_2CH)_2\|^+$, $\|PhAs(S_2CH)\|^+$ |
| 9.9 | 243 | $\|As(SH)(S_2COPr^i)\|^+$ | 7.9 | 275 | $\|PhSb(S_2CH)\|^+$ | 3.1 | 227 | $\|As(S_2C)_2\|^+$ |
| 14.0 | 229 | $\|PhAs(S_2CH)\|^+$, $\|As(S_2CH)_2\|^+$ | 5.4 | 273 | or $\|Sb(S_2CH)_2\|^+$ $\|Sb(S_2C)_2\|^+$ | 9.8 | 215 | $\|AsS_2(S_2C)\|^+$ |
| 9.8 | 227 | $\|As(S_2C)_2\|^+$ | 5.9 | 258 | $\|PhSb(SCO)\|^+$ | 5.6 | 214 | $\|As_2S_2\|^+$ |
| 19.0 | 211 | $\|HAs(S_2COPr^i)\|^+$ | 14.2 | 257 | $\|HSb(S_2COPr^i)\|^+$ | 22.5 | 184 | $\|PhAsS\|^+$ |
| 6.5 | 201 | $\|HSAs(S_2COH)\|^+$ | 4.8 | 231 | $\|PhSbSH\|^+$ | 62.1 | 183 | $\|AsS(S_2C)\|^+$ |
| 13.5 | 185 | $\|PhAsSH\|^+$ | 9.8 | 230 | $\|PhSbS\|^+$, $\|SSb(S_2CH)\|^+$ | 100.0 | 153 | $\|PhAsH\|^+$ |
| 52.7 | 184 | $\|PhAsS\|^+$, $\|SAS(S_2CH)\|^+$ | 1.2 | 229 | $\|SSb(S_2C)\|^+$ | | | |

| | | | | | | | | |
|---|---|---|---|---|---|---|---|---|
| 49.0 | 169 | $\lvert HAs(S_2COH)\rvert^+$ | 11.8 | 215 | $\lvert HSb(S_2COH)\rvert^+$ | 10.4 | 152 | $\lvert PhAs\rvert^+$, $\lvert As(S_2CH)\rvert^+$ |
| 47.5 | 153 | $\lvert PhAsH\rvert^+$, $\lvert HAs(S_2CH)\rvert^+$ | 25.6 | 199 | $\lvert PhSbH\rvert^+$ | 8.3 | 151 | $\lvert As(S_2C)\rvert^+$ |
| 8.7 | 152 | $\lvert PhAs\rvert^+$, $\lvert As(S_2CH)\rvert^+$ | 7.3 | 198 | $\lvert PhSb\rvert^+$, $\lvert SbS_2CH\rvert^+$ | 8.5 | 137 | $\lvert HAs(SCOH)\rvert^+$ |
| 3.0 | 151 | $\lvert As(S_2C)\rvert^+$ | 3.7 | 197 | $\lvert Sb(S_2C)\rvert^+$ | 6.3 | 121 | $\lvert As(SCH_2)\rvert^+$ |
| 3.6 | 137 | $\lvert HAs(SCOH)\rvert^+$ | 5.5 | 181 | $\lvert SbSOC\rvert^+$ | 27.6 | 107 | $AsS^+$ |
| 16.8 | 107 | $AsS^+$ | 8.2 | 154 | $\lvert SbSH\rvert^+$ | 23.8 | 78 | $\lvert H_2CO_2S\rvert^+$ |
| 9.1 | 78 | $\lvert H_2CO_2S\rvert^+$ | 10.3 | 153 | $SbS^+$ | 12.8 | 77 | $C_6H_5^+$ |
| 5.1 | 77 | $C_6H_5^+$ | 2.1 | 123 | $Sb^+$ | 79.6 | 76 | $CS_2^+$ |
| 100.0 | 76 | $CS_2^+$ | 2.9 | 121 | $Sb^+$ | 61.0 | 75 | $As^+$ |
| 4.0 | 60 | $COS^+$ | 8.8 | 78 | $\lvert H_2CO_2S\rvert^+$ | 15.9 | 44 | $CS^+$ |
| 4.6 | 59 | $OC_3H_7^+$ | 4.2 | 77 | $C_6H_5^+$ | 9.1 | 32 | $S^+$ |
| 9.4 | 44 | $CS^+$ | 100.0 | 76 | $CS_2^+$ | | | |
| 50.2 | 43 | $C_3H_7^+$ | 5.1 | 60 | $COS^+$ | | | |
| 6.1 | 41 | $C_3H_5^+$ | 2.9 | 59 | $OC_3H_7^+$ | | | |
| 7.9 | 32 | $S^+$ | 10.3 | 44 | $CS^+$ | | | |
| | | | 17.1 | 43 | $C_3H_7^+$ | | | |
| | | | 7.6 | 32 | $S^+$ | | | |

Mass based upon most abundant isotopes i.e., $^{1}H$, $^{12}C$, $^{16}O$, $^{32}S$, $^{75}As$ and $^{121}Sb$

* R.I. = Relative intensity

## CONCLUSIONS

The IR spectra reveal the bidentate nature of the xanthate group in these monomeric complexes, resulting in a co-ordination number of five for the central arsenic atom. These complexes may, therefore, have either a square pyramidal (SP) or trigonal bipyramidal (TBP) structure presumably distorted by the lone pair on As. The appearance of sharp and unsplit signals in the $^1H$ and $^{13}C$ NMR spectra favour the SP structure, although a rapid exchange between the two structures can also not be ruled out on this basis. Moreover, according to Furlani[14] the $\pi$-back donation favours the SP structure rather than TBP. The SP structure has also been established for a similar dithiocarbamate complex, $PhAs(S_2CNEt_2)_2$, by X-ray crystallographic studies.[15]

A stereochemically active lone pair of electrons present in As(III) complexes[16] would also influence the geometry, occupying one of the hybrid (probably $sp^3d^2$) orbitals and giving rise to a pseudo-octahedral geometry for these complexes with the phenyl group *trans* to the lone pair of electrons.

## EXPERIMENTAL

Phenyl dichloroarsine was prepared by the reduction of phenylarsonic acid[17] and potassium alkylxanthates were synthesized by the reported method.[18] The phenyldialkoxyarsines were prepared by the reaction of phenyl dichloroarsine and sodium alkoxides.[19]

Arsenic was estimated iodometrically[20] after converting it into arsenic (V) and sulphur was estimated gravimetrically[21] as barium sulphate. The molecular weights were determined ebullioscopically in chloroform, using a Gallenkamp Ebulliometer, fitted with a thermistor sensor. IR spectra were recorded (4000–200 $cm^{-1}$) as nujol mulls and NMR ($^1H$ and $^{13}C$) spectra were recorded in $CDCl_3$ solutions, using TMS as an internal standard.

*Reactions of phenyldichloroarsine with potassium alkylxanthates in* 1:2 *molar ratios*

A carbon disulphide solution of phenyldichloroarsine (0.5 mole) was added dropwise to the suspension of potassium alkylxanthate (1.0 mole), in carbon disulphide solution. The reaction mixture was stirred for ~4 hr and the potassium chloride formed during the reaction was filtered off. The solvent was removed under vacuum and the product, if solid, was recrystallized from $CS_2$/hexane mixture.

A similar method was followed in the synthesis of all of these complexes and the results are all summarized in Table 1, for brevity.

*Insertion reactions of carbon disulphide with phenyl alkoxyarsines*

Phenyl diethoxyarsine (1.13 g) was taken in ~20 $cm^3$ of carbon disulphide solution. The reaction mixture was refluxed for about half an hour and solvent was removed under vacuum, giving the product which was recrystallized from $CS_2$/Hexane mixture. Found: As, 18.91; S, 32.34; Calc. for $PhAs(S_2COEt)_2$: As, 19.02; S, 32.49%; Yield, 82%.

Similarly compound $PhAs(S_2COPr^i)_2$ Found: As, 17.44; S, 30.17; Calc. for $PhAs(S_2COPr^i)_2$: As, 17.76; S, 30.34%; Yield, 84%.

*Acknowledgement*—The authors thank the U.G.C. for the sanction of a Special Assistance Programme under which the present investigations have been carried out.

## REFERENCES

1. G. Carrai and G. Gottardi, *Z. Krist.* 1960, **113**, 373.
2. C. A. Peri, *Gazz. Chim. Ital.* 1959, **89**, 1315.
3. H. Oda, H. Sumi and Y. Tanaka, *Tokamine Kenkyusho Nempo* 1959, **11**, 193.
4. R. K. Gupta, V. K. Jain, A. K. Rai and R. C. Mehrotra, *Indian J. Chem.* 1983, **22A**, 708.
5. A. Ray, D. N. Sathyanarayana, G. D. Prasad and C. C. Patel, *Spectrochim. Acta* 1973, **29**, 1579.
6. F. Bonati and R. Ugo, *J. Organometal. Chem.* 1967, **10**, 257.
7. G. B. Deacon and R. A. Jones, *Aust. J. Chem.* 1963, **16**, 499.
8. T. B. Brill and N. C. Campbell, *Inorg. Chem.* 1973, **12**, 1884.
9. A. C. Sau and R. R. Holmes, *J. Organometal. Chem.* 1981, **217**, 157.
10. G. J. Karabatsos, G. C. Sonnichsen, N. Hsi, D. J. Fenoglio, *J. Am. Chem. Soc.* 1967, **89**, 5067.
11. G. M. Bodner and L. J. Todd, *Inorg. Chem.* 1974, **13**, 360.
12. L. F. Wuyts, D. F. Van de Vondel and G. P. Van der Kelen, *J. Organometal. Chem.* 1977, **129**, 163.
13. F. M-N. Kheiri, C. A. Tsipis, C. L. Tsiamis and G. E. Manoussakis, *Can. J. Chem.* 1979, **57**, 767.
14. C. Furlani, *Coord. Chem. Rev.* 1968, **3**, 141.
15. R. Bally, *Acta Cryst.* 1967, **23**, 295.
16. S. L. Lawton, C. J. Fuhrmeister, R. G. Haas, C. S. Jarman, Jr. and F. G. Lohmeyer, *Inorg. Chem.* 1974, **13**, 135.
17. E. Booth, W. E. Jones, A. F. Millidge and F. N. Woodward, *J. Soc. Chem. Ind. (London)* 1949, **68**, 289.
18. S. R. Rao, *Xanthates and Related Compounds*, pp. 7–18. Marcel Dekker, New York (1971).
19. G. Kamai and V. M. Zoroastrova, *J. Gen. Chem. (USSR)* 1940, **10**, 921.
20. H. P. S. Chauhan, G. Srivastava and R. C. Mehrotra, *Synth. React. Inorg. Metal-Org. Chem.* 1981, **11**, 565.
21. B. P. Singh, G. Srivastava and R. C. Mehrotra, *J. Organometal. Chem.* 1979, **171**, 35.

*Polyhedron* Vol. 3, No. 6, pp. 729–734, 1984
Printed in Great Britain.

0277-5387/84 $3.00 + .00
© 1984 Pergamon Press Ltd.

# SYNTHESIS AND STUDIES OF SOME BIVALENT METAL CHELATES OF 1,2-DIHYDROXY-9,10-ANTHRACENEDIONE AND 5-HYDROXY-1,4-NAPHTHALENEDIONE

MARIA N. BAKOLA-CHRISTIANOPOULOU
Department of Chemical Engineering, Organic Chemistry, Aristotle University of Thessaloniki, Greece

(*Received* 10 *October* 1983; *accepted* 28 *November* 1983)

**Abstract**—The chelates of 1,2-dihydroxy-9,10-anthracenedione and 5-hydroxy-1,4-naphthalenedione have been prepared and studied. The structure and bonding of these compounds are discussed in relation to their spectroscopic and magnetic data.

Quinones and their substituted derivatives have long been known to possess numerous chemically and biologically significant properties with many important applications in several areas.[1-3] For example 5-hydroxy-1,4-naphthalenedione (juglone) has been used as antitubercular and antibacterial agent as well as for the determination of nickel(II).[4] 1,2-dihydroxy-9,10-anthracenedione (alizarin) and its derivatives have been used as analytical agents for the determination of molybdenum[5] as well as for the production of dyes and pigments.

Since in most of the above applications of hydroxy-quinones their chelating ability plays an important role, the study of their metal chelates would be of great value in understanding the mechanisms of their chemical and biological activity.

In the last few years a number of papers concerning the synthesis, characterization, thermal stability and biological function of some metal chelates of hydroxybenzoquinones, hydroxynaphthoquinones and hydroxyanthraquinones have been published.[6-9]

Continuing our interest on the study of the structure and bonding of metal chelates of hydroxy-quinones[10] we present in this paper our results concerning the chelates of 5-hydroxy-1,4-naphthalenedione (5-HNQ) and 1,2-dihydroxy-9,10-anthracenedione (1,2-DHAQ) with some bivalent metal ions such as Fe(II), Ni(II), Cu(II), Zn(II), Pd(II) and Pt(II).

## RESULTS AND DISCUSSION

The analytical data for the new compounds their colours and yields are shown in Table 1. All the compounds were fine powders or microcrystalline materials, stable in air, which do not melt up to 300°C.

They were insoluble in most of the common organic solvents and water, but were soluble in DMF and DMSO and slightly soluble in methylene chloride and/or EtOH. Most of the isolated compounds contain also molecules of water either as coordinated and/or as crystalline water. By heating the chelates at 50°C under vacuum (2 mmHg) over $P_2O_5$ we found that only the chelates III and IV showed weight changes. The weight changes observed correspond to the loss of two water molecules per molecule of each of the above chelates. Hence, two molecules of water are present as crystalline water in these chelates.

The structures of the new chelates as well as the bonding properties of the ligands were determined on the basis of spectroscopic (IR, UV–Vis) and magnetic measurements.

### *IR spectra*

The most relevant absorption bands in the IR spectra of the studied chelates and their tentative assignments are shown in Table 2.

Band assignments were based on the comparison method by considering the IR spectra of the new chelates as well as of the free ligands and their parent compounds anthraquinone and naphthoquinone.

In the IR spectra of all the 1,2-DHAQ chelates a distinct intense band occurs with a maximum at 3,430 $cm^{-1}$, like that of 2-hydroxy-anthraquinone.[12-13] Therefore the 2-hydroxyl group of alizarin is preserved in the structure of the chelates and consequently provides evidence for form **I**.

In the region 1700–1200 $cm^{-1}$ all the chelates showed a number of intense bands, which are due to normal modes of vibration of the ligand affected by its coordination.

The stretching frequency $\nu(C\cdots O)_1$ of the

Table 1. Analytical and some physical data of 1,2-DHAQ and 5-HNQ chelates

| | Compound | Yield % | Color | % C | % N | % H | % M |
|---|---|---|---|---|---|---|---|
| I | $Ni(C_{14}H_7O_4)_2(OH_2)_2$ | 70 | dark-brown | 58,22 (58,67)* | — | 2,89 (3,16) | 11,01 (10,24) |
| II | $Cu(C_{10}H_7O_4)_2(OH_2)_2$ | 75 | dark-purple | 57,81 (58,18) | — | 2,94 (3,14) | 9,46 (10,99) |
| III | $\|Zn(C_{14}H_7O_4)\|\cdot 2H_2O$ | 68 | navy-blue | 58,43 (58,00) | — | 2,69 (3,12) | 10,83 (11,27) |
| IV | $[Pd(C_{14}H_7O_4)_2]\cdot 2H_2O$ | 65 | dark-brown | 54,48 (54,17) | — | 2,67 (2,92) | 16,73 (17,14) |
| V | $Mn(C_{14}H_7O_4)_2(OH_2)_2$ | 60 | brown | 58,31 (59,06) | — | 3,41 (3,18) | 10.02 (9,64) |
| VI | $Fe(C_{10}H_5O_3)_2$ | 75 | brown | 60,21 (59,73) | — | 1,92 (2,50) | 13,46 (13,88) |
| VII | $Ni(C_{10}H_5O_3)_2(OH_2)_2$ | 95 | blue | 54,99 (54,47) | — | 3,29 (3,20) | 13,06 (13,31) |
| VIII | $Pt(C_{10}H_5O_3)_2$ | 80 | brown-yellow | 44,36 (44,36) | — | 1,91 (1,86) | 36,01 (36,03) |
| IX | $Pt(C_{10}H_5O_3)Cl(NH_3)_2$ | 40 | black | 27,01 (27,44) | 6,47 (6,39) | 2,53 (2,53) | 44,01 (44,56) |
| X | $Pd(C_{10}H_5O_3)_2(NH_3)_2$ | 70 | brown-red | 49,24 (49,34) | 5,83 (5,75) | 3,01 (3,31) | 20,49 (21,85) |

* Figures in parentheses are the calculated values.

uncoordinated carbonyl group in all chelates is similar to that of the free ligand.[14] In contrast the coordinated carbonyl group in all chelates gave a strong band with frequency $\nu(C\cdots O)_2$ at lower energy. This observation could be easily explained on the basis of the expected **I** and **II** structures for the 1,2-DHAQ and 5-HNQ chelates respectively. In these structures every ligand acts through its monoanionic form, as a chelating bidentate ligand, forming with the metal ion a chelated ring. This ring is expected to be stabilized by a considerable delocalization of the $\pi$-electron density.

This type of coordination is established as will be seen later from the study of the absorption bands with frequencies $\nu_{sym}(M–O)$ and $\nu_{asym}(M–O)$.

Of interest and considerable importance is also the region 600–300 cm$^1$. This region contains several absorption bands with medium or weak intensities. Some of them are typical absorptions of the free ligands while the rest, which are sensitive to the central metal ion and the structure of the chelates, are attributed to the normal modes of vibration of the $MO_4$ moiety of the chelates.

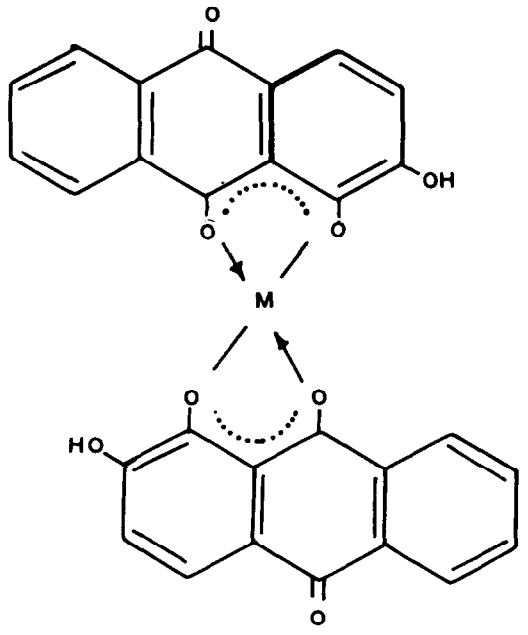
In order to make a reasonable assignment of these bands we used the comparison method. Thus, we have compared the IR spectra of the studied compounds with those of the corresponding acetylacetonate complexes for which the absorption bands have been fully characterised on the basis of theoretical treatment.[15,16]

A similar pattern has been observed for the absorption bands in the region 600–300 cm$^{-1}$. The only difference being the shifts of the bands. Such a shift must be expected on the basis of the different electron donor and acceptor abilities of the 1,2-DHAQ, 5-HNQ and the acetylacetonato ligands.

The number and form of the bands due to M–O stretching for the 1:2 chelates are similar to those of the corresponding 1:2 metal acetylacetonates. Hence, since the 1:2 metal acetylacetonates have $D_{2h}$ symmetry, we can conclude that our 1:2 chelates adopt structure **I** and **II**, which also has $D_{2h}$ symmetry. On the basis of $D_{2h}$ symmetry we can assign the band in the region 599–421 cm$^{-1}$ to $\nu_{sym}(M–O)$ stretching vibration (symmetry species

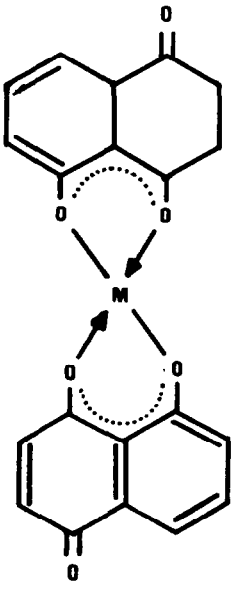
Table 2. Relevant IR frequencies ($cm^{-1}$) of the 1,2-DHAQ and 5-HNQ chalates with divalent metal ions and their assignments

| | Compound | $\nu(C{=}O)_1$ | $\nu(C{=}O)_2$ | $\nu(C{=}O)_3$ | $\nu_s$ (M—O) | $\nu_{as}$ (M—O) |
|---|---|---|---|---|---|---|
| | $C_{14}H_8O_4$(1,2-DHAQ) | 1665m | 1640vs | 1262vs | — | — |
| I | $Ni(C_{14}H_7O_4)_2(OH_2)_2$ | 1650m | 1585vs | 1270vs | 435w | 360w |
| II | $[Zn(C_{14}H_7O_4)_2]\cdot 2H_2O$ | 1648m | 1600vs | 1269vs | 575w | 355w |
| III | $Cu(C_{14}H_7O_4)_2(OH_2)_2$ | 1670m | 1535vs | 1272vs | 599w | 360w |
| IV | $[Pd(C_{14}H_7O_4)_2]\cdot 2H_2O$ | 1657m | 1602vs | 1265vs | 464w | 318w |
| V | $Mn(C_{14}H_7O_4)_2(OH_2)_2$ | 1648m | 1602vs | 1267vs | 421w | 335w |
| | $C_{10}H_6O_3$(5-HNQ) | 1670s | 1647vs | 1222m | — | — |
| VI | $Fe(C_{10}H_5O_3)_2$ | 1635s | 1605vs | 1250m | 450w | 320w |
| VII | $Ni(C_{10}H_5O_3)(OH_2)_2$ | 1675m | 1602vs | 1251m | 549w | 318w |
| VIII | $Pt(C_{10}H_5O_3)_2$ | 1700m | 1648vs | 1272vs | 479w | |
| IX | $Pt(C_{10}H_5O_3)Cl(NH_3)_2$ | 1650vs | 1650vs | 1270s | 471w | |
| X | $Pd(C_{10}H_5O_3)_2(NH_3)_2$ | 1650vs | 1630vs | 1260s | 490w | 385w |




I

Local symmetry of group $MO_4$, $D_{2h}$.




II

Local symmetry of group $MO_4$, $D_{2h}$.

$B_{1u}$) and the band in the region 385–318 $cm^{-1}$ to $\nu_{asym}$(M–O) stretching vibration (symmetry species $B_{2u}$). The third IR-active vibration (symmetry species $B_{3u}$) occurs at a lower frequency (below 300 $cm^{-1}$) and could not be observed in the present study. The $\nu_{sym}$(M–O) and $\nu_{asym}$(M–O) are sensitive to the nature of the central metal ion.

The Zn(II) chelate gave a different pattern for the $\nu$(M–O) bands. This is no doubt due to the ability of Zn(II) to adopt a tetrahedral and not a square planar geometry. Also for the Pt(II) and Pd(II) chelates the group M–O gave the most strong IR active bands in the region below 300 $cm^{-1}$.[17]

*Electronic spectra and magnetic data*

Table 3 shows the positions of the band maxima and of discernible shoulders as well as their log $\epsilon_{mol}$ values of the 1,2-DHAQ and 5-HNQ chelates. Also in Table 3 we present the room temperature magnetic moments of the new chelates that were calculated.

In the region 50–35 kK a composite band(band I) occurs in the UV spectra of the free ligands, which is not included in Table 3, because it is obscured from the absorption of the solvent DMF. This band is also observed in the spectra of the I, VI and VIII chelates in EtOH solution. This band is attributed to a composite band resulting from the overlap of two bands, one with benzenoid and the other one with quinonoid character of the type $\pi^* \leftarrow \pi ({}^1B_{1u} \leftarrow {}^1A_{1g})$.[18,19]

In the region 31–27 kK band II occurs, which is shifted in the UV–Vis spectra of the chelates to

Table 3. Electronic spectral (DMF solution) and magnetic data of 1,2-DHAQ and 5-HNQ chelates with bivalent metal ions

| Compound | Band II $\nu$(kK)($\log\epsilon_{mol}$) | Band III $\nu$(kK)($\log\epsilon_{mol}$) | Band IV $\nu$(kK)($\log\epsilon_{mol}$) | Band V $\nu$(kK)($\log\epsilon_{mol}$) | $\mu_{eff}$, BM |
|---|---|---|---|---|---|
| 1,2-DHAQ | 27,02sh† (3,58) | 23,25 (3,70)†† | | | — |
| I* | 28,98 (4,05) | 23,64 (3,84) | 17,24 (4,05)<br>15,64sh (3,89) | 10,23 (1,35)<br>8,86 (1,40) | 3,29††† |
| II | 29,44 (3,42) | 23,25 (3,97)<br>22,07sh† (3,96) | 18,51 (3,96)<br>16,52sh (3,77) | | 2,08 |
| III | 29,07 (3,99) | 20,01sh (4,09) | 18,35 (4,18)<br>17,09sh (4,09) | | — |
| IV | 28,57 (3,47) | 24,27 (3,36) | 18,51 (3,59)<br>16,68sh (3,44) | | — |
| V | 29,06 (3,44) | 22,02 (3,89) | 18,46 (3,95)<br>16,09sh (3,81 | | 6,02 |
| 5-HNQ | 30,30 (3,31) | 24,03 (4,87) | | | — |
| VI* | | 24,69 (4,65) | 19,34 (4,52) | 7,93 (2,53)<br>7,24sh (2,41) | 5,01 |
| VII | 27,77 (4,30) | | 18,45sh (4,59)<br>17,71 (5,38)<br>15,79sh (4,28) | 10,21sh (1,31)<br>8,85 (1,76) | 3,16 |
| VIII* | 28,09 (3,46) | 25,31 (3,43) | 19,80sh (3,03)<br>14,38sh | | — |
| IX | 28,16 (4,06) | 25,31 (4,05) | 19,99sh (3,75)<br>14,38sh (3,42) | | — |
| X | ——— | 25,00 (4,31) | 19,56sh (3,72 | | — |

* The spectra were also obtained in EtOH solution in order to investigate the 35–41 kK region of the spectra. In this region the band I exists.

† sh = shoulder

†† Figures in parentheses are the values of $\log\epsilon_{mol}$.

††† Magnetic field strength 11.700 Gauss.

lower energies. This band is attributed to intraligand quinonoid E.T. transition of the type $\pi^* \leftarrow \eta$.[18]

Band III is also attributed to an intraligand E.T. transition of the type $\pi^* \leftarrow \eta$.

In the region 19–15 kK band IV occurs which is absent in the spectra of the free ligands, but exists in the spectra of their anions (solution of 1,2-DHAQ or 5-HNQ in NaOH).[2] Consequently this band can be attributed to an intraligand transition. Except for the band IV in all chelates a shoulder exists at $\simeq$ 18–15 kK with intensity ($\log \epsilon_{mol} \simeq 3$–4) very close to that of CT. transition, and hence can be assigned to a CT. transition. The presence of this shoulder in the spectrum of the Zn(II) chelate indicates that this band must be of the $M \rightarrow L$ type.

The two $d$–$d$ transitions expected in this region for the nickel(II) chelates of type $A_{2g} \leftarrow B_{1g}$ and $E_g \leftarrow B_{1g}$ are obscured by the intense CT. transitions. For the same reason the $d$–$d$ transitions of the copper(II) chelate could not be observed.

Finally, in the region 11–7 kK, in the spectra of the nickel(II) and iron(II) chelates band V occurs, which, only for the nickel(II) chelates, splits into two well separated bands at $\simeq$ 10 and 8 kK. These correspond to $^3B_{2g} \leftarrow {}^3B_{1g}$ and $^3E_g \leftarrow {}^3B_{1g}$ transitions.[20] The observed splitting of the band V support the distorted octahedral geometry for the nickel(II) chelate.

The room temperature magnetic moments of the 1,2-DHAQ and 5-HNQ chelates (Table 3) are normal and in accordance with the proposed structures of the chelates,[21] while the Zn(II), Pd(II) and Pt(II) chelates, as expected, are diamagnetic.

## EXPERIMENTAL

*Physical measurements*

IR spectra were recorded, in the region of 4000–250 $cm^{-1}$, on a Perkin–Elmer 467 spectrophotometer using KBr discs or Nujol mulls. Electronic spectra were obtained on a Perkin–Elmer Hitachi 200 spectrophotometer and on a Cary 17D spectrophotometer, using both freshly prepared solutions in DMF and Nujol mulls. Magnetic susceptibility measurements were done by the Faraday technique at different magnetic field strengths using $Hg[Co(SCN)_4]$ as the calibrant. Diamagnetic corrections were made using Pascal's constants. Carbon, hydrogen and nitrogen were determined using a Perkin–Elmer 240 Elemental Analyzer. The metal analyses were performed on a Perkin–Elmer 503 Atomic Absorption spectrophotometer.

*Starting materials*

All solvents were of reagent grade and were used without further purification in synthetic work. The 1,2-DHAQ and 5-HNQ ligands were obtained commercially from Sarsyntex and used without further purification.

*Preparation of the 1,2-DHAQ complexes*

All chelates of 1,2-DHAQ were prepared by direct mixing of a solution of potassium alizarinate with the solution of the appropriate metal acetate or chloride according to the following general method. 2 mmoles of potassium alizarinate prepared according to previously described method[11] were dissolved in 150 $cm^3$ of water. To this solution an aqueous of ethanolic solution of 1 mmole of the appropriate metal salt was added slowly under continuous stirring. The mixture was left stirring at room temperature for 3 hr and then was kept in a refrigerator overnight before filtering.

In all cases the precipitate was washed several times with warm water, ethanol and finally with diethyl ether, until the washings were colourless, and was dried in a vacuum desiccator over $P_2O_5$.

*Preparation of the 5-HNQ complexes*

$Ni(C_{10}H_5O_3)_2(OH_2)_2$ (VII). This compound was prepared as follows: In 100 $cm^3$ of warm water 0.58 g (2,9 mmoles) nickel acetate monohydrate were dissolved. To this solution 1.00 g (5.8 mmoles) of 5-HNQ dissolved in 100 $cm^3$ of boiling ethanol were added slowly under continuous magnetic stirring. The pH was adjusted to 5 with 25% $NH_3$ solution.

The mixture was left stirring at room temperature for 3 hr and then was kept in a refrigerator overnight. The precipitate was washed several times with warm water, ethanol and finally with diethyl ether and was dried in a vacuum desiccator over $P_2O_5$.

$Fe(C_{10}H_5O_3)_2$(VI) and $Pt(C_{10}H_5O_3)_2$(VIII). These chelates were prepared by mixing of an ethanolic solution of 5-HNQ with an aqueous solution of $FeCl_2 \cdot 4H_2O$ of $K_2PtCl_4$ respectively using a metal to ligand ratio 1:2. Then an excess of potassium acetate was added and following the same procedure, as described before, the pure compounds were isolated. $Pt(C_{10}H_5O_3)Cl(NH_3)_2$(IX). 0.174 g (1 mmole) of 5-HNQ dissolved in 100 $cm^3$ of water was mixed with an excess of 25% $NH_3$ solution.

To this solution an aqueous solution containing 0.415 g (1 mmole) $K_2PtCl_4$ was added slowly under continuous magnetic stirring. The resulting mixture was left stirring for 2 hr at room temperature. The black precipitate was washed alternatively with water, ethanol and diethyl ether and dried in a vacuum desiccator over $P_2O_5$.

$Pd(C_{10}H_5O_3)_2(NH_3)_2$(X). 0.348 g (2 mmoles) of

5-HNQ dissolved in 100 $cm^3$ of ethanol were mixed with a solution of 0.326 g (1 mmole) $K_2PdCl_4$ in 30 $cm^3$ water under continuous magnetic stirring. Then an excess of 25% $NH_3$ solution was added. After 3 hr the reaction mixture was left in a refrigerator for one day and the resulting precipitate was isolated by filtration, washed several times with small portions of water, ethanol and diethyl ether and dried under vacuum.

## REFERENCES


1. R. A. Morton, *Biochemistry of Quinones* (Edited by R. A. Morton). Academic Press, New York (1965).
2. R. H. Thomson, *Naturally Occurring Quinones*. Academic Press, New York, (1971).
3. S. Patai, *The Chemistry of the quinoid compounds*, (Edited by S. Patai), Part 2. Wiley, London (1974).
4. R. S. Bottei and C. P. McEachern, *J. Inorg. Nucl. Chem.* 1970, **32**, 2653.
5. M. Krizan and J. Nozaki, *Microchim, Acta* 1975, **2(4–5)**, 435.
6. R. S. Bottei and P. L. Gerace, *J. Inorg. Nucl. Chem.* 1961, **23**, 245.
7. R. S. Bottei and D. Quane, *Ibid.* 1964, **26**, 1919.
8. H. D. Coble and H. F. Holtzclaw Jr., *J. Inorg. Nucl. Chem.* 1974, **36**, 1049.
9. R. M. Issa, Y. Z. Ahmed and A. H. Zewail, *Egypt. J. Chem.* 1972, **15**, 1.
10. C. Tsipis, E. Bakalbassis, V. Papageorgiou and M. Bakola-Chritianopoulou, *Can. Jour. of Chem.* 1982, **60**, 2477.
11. R. Weinland and K. Binder, *Ber.* 1914, **47**, 984.
12. S. E. Sheppared and P. T. Newsome, *J. Am. Chem. Soc.* 1942, **64**, 2.937.
13. I. M. Issa, R. M. Issa, M. S. El-Ezaby and Y. Z. Ahmed, *Z. Physik. Chem.* 1969, **242**, 169.
14. R. S. Bottei and P. L. Gerace, *J. Chem. Educ.* 1961, **38**, 568.
15. K. Nakamoto, P. L. McCarthy and A. E. Martell, *J. Am. Chem. Soc.*, 1961, **83**, 1272.
16. M. Mikami, J. Nakagawa and T. Shimanouchi, *Spectrochim. Acta* 1967, **23A**, 1037.
17. M. Textor und H. Oswald, *Z. Anorg. Allg. Chem.* 1974, **407**, 244.
18. I. Singh, R. Ogata, R. Moore, C. Chang and P. Scheuer, *Tetrahedron* 1968, **24**, 6053.
19. A. I. Scott, *Interpretation of the Ultraviolet Spectra of Natural Products*. Macmillan, New York, (1964).
20. A. B. P. Lever, *Coord. Chem. Rev.* 1968, **3**, 119.
21. B. N. Figgis and J. Lewis, *Progress in Inorganic Chemistry* (Edited by S. Lippard), Vol. 6, p. 37. Wiley, New York (1967).

*Polyhedron* Vol. 3, No. 6, pp. 735–742, 1984
Printed in Great Britain.

0277-5387/84 $3.00 + .00
© 1984 Pergamon Press Ltd.

# FOUR-COORDINATED PALLADIUM(II) AND PLATINUM(II) COMPLEXES CONTAINING THE LEWIS-ACID $\{M(S_2CNHR)(PR_3')\}$ GROUP COMBINED WITH A VARIETY OF OTHER LIGANDS

**G. A. KATSOULOS, G. E. MANOUSSAKIS and C. A. TSIPIS***
Laboratory of Inorganic Chemistry, University of Thessaloniki, Thessaloniki, Greece

(*Received* 17 *October* 1983; *accepted* 28 *November* 1983)

**Abstract**—A new series of four-coordinated Pd(II) and Pt(II) complexes in which the Lewis-acid (14-electron) $\{M(S_2CNHR)(PR_3')\}$ group is combined with a variety of other ligands (such as $RHNCS_2^-$, $I^-$, $SCN^-$, $SnCl_2I^-$) has been synthesised and studied. The structures of the new compounds are discussed in relation to their specroscopic, magnetic and thermal properties. In the case of $[M(S_2CNHR)_2(PR_3')]$ complexes both the spectroscopic data (IR, $^1H$ NMR, UV-Vis) and their thermal behaviour strongly suggest the coexistence of two kinds of *gem*-disulphide ligands, one acting as a bidentate ligand and the other one as a unidentate. Also it was confirmed that the chemical behaviour of the bis(N-alkyldithiocarbamato) complexes of Pd(II) and Pt(II) towards tertiary phosphines is similar to that of the isoelectronic xanthate complexes rather than to the bis(N,N-dialkyldithiocarbamato) complexes.

The continued interest in the behaviour of planar $d^8$ complexes with sulphur-containing ligands in the presence of Lewis bases has motivated us to investigate further the reactions of bis(N-monosubstituted-dithiocarbamato)palladium(II) and platinum(II) complexes with tertiary phosphines. Consequently, the results of our attempts to find a general synthetic route to palladium(II) and platinum(II) complexes of the types $[M(S_2CNHR)_2(PR_3')]$ and $[MI(S_2CNHR)(PR_3')]$ as well as the study of some reactions of these complexes are reported in this paper. Their synthesis was planned after considering that square planar $[M(S–S)_2]$ complexes [M = Pd or Pt; $(S–S)^- = R_2NCS_2^-$, $ROCS_2^-$, $(RO)_2PS_2^-$ and $R_2PS_2^-$] easily form adducts with various tertiary phosphines[1–7] and that the reaction of halide-bridged dimers $[\{MX_2(PR_3')\}_2]$ with various alkali-metals dithioacid salts leads to the formation of the $[MX(S–S)(PR_3')]$ complexes.[8–10] However, in a previous communication[11] we have reported some preliminary results concerning the reactions with iodine of bis(N-alkyldithiocarbamato)phosphine-platinum(II) complexes. These reactions gave high yields of the required $[PtI(S_2CNHR)(PR_3')]$ by replacement of the unidentate N-alkyldithiocarbamato ligand by $I^-$ under mild conditions. An investigation of the reaction mechanism by CNDO/2 quantum chemical calculations showed that the electrophilic centre on the unidentate N-alkyldithiocarbamato ligand is located on the $NCS_2$ moiety.[12] Hence, the attack by the nucleophile $I^-$ results in the substitution of the unidentate $\{RHNCS_2\}^-$ group and the formation of the corresponding iodo-complexes. Furthermore, we have found that the behaviour of the $\{RHNCS_2\}^-$ ligands is similar to that of the isoelectronic xanthate ligands,[5] since reacting the N-alkyldithiocarbamato complexes with excess $PMe_2Ph$ nucleophilic attack by anionic $RHNCS_2^-$ on a coordinated bidentate dithio-ligand can occur to give the novel N-alkyliminodithiocarbonato complexes.[12] A possible mechanism has also been proposed for the formation of these complexes with respect to the results of quantum chemical CNDO/2 calculations.

*Author to whom correspondence should be addressed.

## EXPERIMENTAL

*Physical measurements*

IR spectra were recorded in the 4000–250 $cm^{-1}$ region on a Perkin–Elmer 467 spectrophotometer using KBr pellets or Nujol mulls. $^1H$ NMR spectra were recorded on a Varian A 60A (60 Mc/s) instrument in DMSO-$d_6$ solutions using TMS as an internal standard. Electronic spectra were obtained on a Cary 17DX spectrophotometer using freshly prepared chloroform solutions. Mass spectra were measured on a RMU–6L Hitachi Perkin–Elmer mass spectrometer with ionisation source of T–2*p* type operating at 70 eV. The thermogravimetric curves were obtained on a Q-Derivatograph using nitrogen furnace atmosphere; sample sizes of 20–40 mg were used at the conventional furnace heating rate of 4°C per minute. Magnetic susceptibility measurements in solid state were done by the Faraday technique using $Hg[Co(SCN)_4]$ as the calibrant. Molecular weights were determined using a Perkin–Elmer molecular weight apparatus Model 115 in $CHCl_3$ solutions. Melting points were determined with a Büchi apparatus and are uncorrected. The elemental analysis of carbon, nitrogen and hydrogen was performed on a Perkin–Elmer 240 Elemental Analyser. Platinum and palladium were determined according to published methods.[13]

*Preparation of the complexes*

*Bis*(N-*benzyldithiocarbamato*)*platinum*(*II*). This was prepared as described previously.[11] A similar method was also employed for the preparation of the corresponding *bis*(N-*benzyldithiocarbamato*)-*palladium*(*II*), m.p. 224–226°C (decomp.).

*Bis*(N - *t* - *butyldithiocarbamato*)*platinum*(*II*). Platinum (II) chloride was suspended in acetone and treated with a 1:1 mole ratio of ($Bu^tNH_3^+$)($Bu^tNHCS_2^-$) dissolved in ethanol. In the resulted clear solution ethanol–aqua solution (1:1) was added and an orange precipitate was formed which was filtered off, washed with ethanol and dried under vacuum. Recrystallisation was carried out from acetone, m.p. 220–222°C (decomp.). In a similar manner *bis*(N-*t-butyldithiocarbamato*)-*palladium*(*II*) was prepared, m.p. 218–220°C (decomp.).

*Bis*(N - *benzyldithiocarbamato*)*triphenylphosphineplatinum*(*II*). A suspension of the complex $[Pt(S_2CNHBz)_2]$ in a small amount of toluene was treated with triphenylphosphine (1:1 mole ratio). A clear solution was obtained which, on addition of light petroleum (b.p. 50–60°C), precipitated the white product which was filtered off, washed with diethyl ether and dried under vacuum. The complex was recrystallised from chloroform, m.p. 189–191°C. A similar method was also employed for the preparation of *bis*(N-*t-butyldithiocarbamato*)*triphenylphosphineplatinum*(*II*), m.p. 186–188°C.

*Bis*(N - *benzyldithiocarbamato*)*tricyclohexylphosphineplatinum*(*II*). This was prepared as described elsewhere.[11] The same synthetic route was also followed for the preparation of the complexes *bis*(N - *benzyldithiocarbamato*)*tricyclo* - *hexylphosphinepalladium*(*II*), m.p. 153–155°*C*, *bis*(N - *t* - *butyldithiocarbamato*) *tricyclohexylphosphineplatinum*(*II*), m.p. 211–213°C (decomp.), and *bis*(N - *t* - *butyldithiocarbamato*) *tricyclohexylphosphinepalladium*(*II*), m.p. 208–210°C (decomp.).

*Iodo*(N - *benzyldithiocarbamato*)*triphenylphosphineplatinum*(*II*). The complex $[Pt(S_2CNHBz)_2(PPh_3)]$ (1 mmol) was suspended in toluene and treated with iodine (0.5 mmol) dissolved in the same solvent. To the resulting clear solution light petroleum was added and an orange solid was precipitated which was filtered off, washed with diethyl ether and dried under vacuum. The complex was recrystallised from acetone, m.p. 77–79°C. In a similar manner *iodo*(N-*t-butyldithiocarbamato*)*triphenylphosphineplatinum*(*II*) was prepared, m.p. 130–132°C.

*Iodo*(N - *benzyldithiocarbamato*)*tricyclohexylphosphineplatinum*(*II*). This was prepared as described previously.[11] A similar method was also employed for the preparation of *iodo*(N-*benzyldithiocarbamato*)*tricyclohexylphosphinepalladium*-(*II*), m.p. 117–119°C, *iodo*(N-*t-butyldithiocarbamato*)*tricyclohexylphosphineplatinum*(*II*), m.p. 156–158°C, and *iodo*(N-*t-butyldithiocarbamato*)-*tricyclohexylphosphinepalladium*(*II*), m.p. 148–150°C.

*Isothiocyano*(N-*benzyldithiocarbamato*)*triphenylphosphineplatinum*(*II*). A solution of 0.76 g (1 mmol) of $[PtI(S_2CNHBz)(PPh_3)]$ in 20 $cm^3$ of acetone was treated with 0.16 g (1 mmol) of silver thiocyanate and the mixture was left at room temperature under continuous magnetic stirring. After a period of half an hour a yellow precipitate of silver iodide was formed which was removed by filtration. The filtrate was condensed up to a small volume (*ca.* 2 $cm^3$) under reduced pressure and then 20 $cm^3$ of light petroleum (b.p. 50–60°C) were added to give an orange solid which was filtered off, washed with diethyl ether and dried under vacuum. Recrystallisation was carried out by dissolving the orange solid in acetone and reprecipitating with aqueous ethanol solution (1:1), m.p. 190–192°C (decomp.). The same synthetic route was also followed for the preparation of *isothiocyano*(N-*benzyldithiocarbamato*)*tricyclo*-

*hexylphosphineplatinum(II)*, m.p. 103–105°C (decomp.).

*Dichloroiodotin(N-benzyldithiocarbamato)triphenylphosphineplatinum(II)*. A solution of 0.76 g (1 mmol) of the $[PtI(S_2CNHBz)(PPh_3)]$ complex in 20 $cm^3$ of acetone was treated with 0.22 g (1 mmol) of $SnCl_2 \cdot 2H_2O$. The reaction mixture was left for 1 hr at room temperature under continuous magnetic stirring and then the solvent was removed by evaporation under reduced pressure. The resulted solid material was dissolved in a minimum volume of toluene and reprecipitated with light petroleum to give an orange solid which was filtered off, washed with diethyl ether and dried under vacuum. Recrystallisation was carried out from acetone, m.p. 153–155°C (decomp.). In a similar manner *dichloroiodotin(N-benzyldithiocarbamato)tricyclohexylphosphineplatinum(II)* was prepared, m.p. 116–118°C (decomp.).

## RESULTS AND DISCUSSION

Reaction of a suspension of $[M(S_2CNHR)_2]$ (M = Pt or Pd; R = Bz or Bu$^t$) in toluene with tertiary phosphines (1 : 1 molar ratios) rapidly gave clear solutions from which white solid compounds of stoicheiometry $[M(S_2CNHR)_2(PR_3')]$ ($PR_3'$ = $PPh_3$ or $PCy_3$) were isolated, either by precipitation with light petroleum or by removal of solvent under reduced pressure. These are non-conducting, diamagnetic, and quite stable both in solid and solution state.

The phosphine adducts $[M(S_2CNHR)_2(PR_3')]$ were found to react easily with iodine to give the corresponding $[MI(S_2CNHR)(PR_3')]$ complexes. The overall reaction for the preparation of these compounds may be represented by the following general equation:

$$[M(S_2CNHR)_2(PR_3')] + \tfrac{1}{2}I_2 \rightarrow [MI(S_2CNHR)(PR_3')] + \tfrac{1}{2}[RHNCSS]_2.$$

Possibly, in this reaction dithiocarbamate radicals are formed through an homolytic rupture of M–S bonds which, in succession, are dimerized into alkylthiuramdisulphides.[14] This seems likely, because it is well known that the alkylthiuramdisulphides and the corresponding free dithiocarbamate radicals are in equilibrium in solution.[15] However, this reaction is a very simple general synthetic route to palladium(II) and platinum(II) iodo-complexes which can be also prepared in one step by treating a suspension of the dithiocarbamate complex in toluene with phosphine followed by the addition of the halogen. Molecular weight measurements in chloroform show them to be monomeric.

Under the experimental conditions, though at times an excess of iodine was used, the isolated products were always iodo(N-alkyldithiocarbamato)phosphinemetal(II) complexes. The facile substitution of one of the two dithiocarbamato ligands of the bis(N-alkyldithiocarbamato)phosphineplatinum(II) and palladium(II) complexes by an iodine atom shows that one of the two ligands is more weakly bonded to the central atom. This fact has been ascertained by spectroscopic and thermal studies of these complexes as well as by X-ray data for the bis(N-*t*-butyldithiocarbamato)tricyclohexylphosphineplatinum(II) complex[16] and the results of quantum chemical CNDO/2 calculations on the dithio-ligands.[12]

Finally, it was found that iodo-complexes are useful starting materials for a number of reactions which lead to products containing the Lewis-acid $\{M(S_2CNHR)(PR_3')\}$ group. For example, they react with carbene like molecules, such as $SnCl_2$, to give the insertion products into the Pt–I bond which contain Pt–Sn bonds. They also give a number of substitution reactions of the iodide with other nucleophiles.

All these complexes were characterised by elemental analyses (Table 1), spectroscopic methods (IR, $^1H$ NMR, UV–Vis), magnetic measurements, and in several instances the monomeric nature of the products was established by mass spectroscopy and/or osmometric molecular-weight measurements in chloroform. The volatility characteristics and thermogravimetric analysis data for the new compounds were also studied.

The IR spectra (Table 2) of the bis(N-alkyldithiocarbamato) complexes show one broad band in the 3100–3300 $cm^{-1}$ region due to the N–H stretching frequency.[17] This is an indication for the equivalence of the two dithio-ligands in these complexes. The bidentate bonding mode of the dithio-ligands is established by the position of the band in the 1450–1550 $cm^{-1}$ region. This region is associated primarily with the "thioureide" vibration and is attributed to the $\nu(C\cdots N)$ vibration of the $S_2C\cdots NHR$ bond. An increase in the double-bond character of the $C\cdots N$ bond results in higher frequencies for this vibration.[18] The position of this band is affected by the nature of the central atom and is shifted to lower frequencies in the Pd(II) complexes. This is a reflection of the higher electron acceptor ability of Pt(II) than Pd(II). The band in the region between 950 and 1050 $cm^{-1}$ is attributed to the stretching vibration of the $C\cdots S$ bonds. In the case of phosphine adducts, the Ugo–Bonati criterion[19] that distinguishes unidentate from bidentate bind-

Table 1. Analytical data for some Pt(II) and Pd(II) dithio-compounds

| Compound | %C | %N | %H | %I | %M† | M.W. |
|---|---|---|---|---|---|---|
| $\|Pt(S_2CNHBz)_2\|$ | 34.31 (34.34)‡ | 4.92 (5.00) | 2.85 (2.88) | | 34.21 (34.86) | 563 (559.7) |
| $\|Pt(S_2CNHBu^t)_2\|$ | 24.69 (24.43) | 5.81 (5.70) | 4.12 (4.10) | | 39.28 (39.68) | 504 (491.6) |
| $\|Pd(S_2CNHBz)_2\|$ | 40.68 (40.80) | 5.92 (5.95) | 3.35 (3.42) | | 22.47 (22.59) | 495 (470.9) |
| $\|Pd(S_2CNHBu^t)_2\|$ | 29.79 (29.81) | 6.52 (6.95) | 4.77 (5.00) | | 26.33 (26.41) | 418 (402.9) |
| $\|Pt(S_2CNHBz)_2(PPh_3)\|$ | 49.85 (49.68) | 3.21 (3.41) | 3.89 (3.80) | | 23.65 (23.73) | 821 (821.9) |
| $\|Pt(S_2CNHBz)_2(PCy_3)\|$ | 48.87 (48.61) | 3.21 (3.33) | 5.76 (5.88) | | 23.08 (23.22) | 828 (840.1) |
| $\|Pt(S_2CNHBu^t)_2(PPh_3)\|$ | 44.38 (44.61) | 3.59 (3.72) | 4.93 (4.68) | | 25.67 (25.88) | 770 (753.9) |
| $\|Pt(S_2CNHBu^t)_2(PCy_3)\|$ | 43.76 (43.56) | 3.43 (3.63) | 6.41 (6.92) | | 25.13 (25.27) | 746 (772.1) |
| $\|Pd(S_2CNHBz)_2(PCy_3)\|$ | 54.41 (54.35) | 3.69 (3.73) | 6.55 (6.57) | | 14.03 (14.16) | 765 (751.4) |
| $\|Pd(S_2CNHBu^t)_2(PCy_3)\|$ | 49.17 (49.21) | 4.18 (4.10) | 7.87 (7.82) | | 15.23 (15.57) | 662 (683.4) |
| $\|PtI(S_2CNHBz)(PPh_3)\|$ | 40.81 (40.74) | 1.89 (1.83) | 3.10 (3.02) | 16.45 (16.55) | 25.28 (25.45) | 776 (766.6) |
| $\|PtI(S_2CNHBz)(PCy_3)\|$ | 39.81 (39.80) | 1.80 (1.78) | 5.28 (5.27) | 16.11 (16.17) | 24.40 (24.86) | 754 (784.7) |
| $\|PtI(S_2CNHBu^t)(PPh_3)\|$ | 37.83 (37.71) | 1.78 (1.91) | 3.46 (3.44) | 17.28 (17.32) | 26.32 (26.63) | 725 (732.5) |
| $\|PtI(S_2CNHBu^t)(PCy_3)\|$ | 36.94 (36.80) | 1.92 (1.86) | 5.70 (5.77) | 16.87 (16.90) | 25.63 (25.99) | 740 (750.7) |
| $\|PdI(S_2CNHBz)(PCy_3)\|$ | 44.63 (44.87) | 1.98 (2.01) | 5.75 (5.94) | 18.30 (18.23) | 15.20 (15.29) | 671 (696.0) |
| $\|PdI(S_2CNHBu^t)(PCy_3)\|$ | 41.53 (41.73) | 2.17 (2.12) | 6.48 (6.55) | 19.24 (19.17) | 16.26 (16.07) | 657 (662.0) |
| $\|Pt(NCS)(S_2CNHBz)(PPh_3)\|$ | 46.57 (46.48) | 4.10 (4.01) | 3.28 (3.32) | | 27.80 (27.96) | 682 (697.7) |
| $\|Pt(NCS)(S_2CNHBz)(PCy_3)\|$ | 45.12 (45.30) | 3.85 (3.91) | 5.81 (5.77) | | 27.51 (27.25) | 698 (715.9) |
| $\|Pt(SnCl_2I)(S_2CNHBz)(PPh_3)\|$ | 32.46 (32.66) | 1.58 (1.46) | 2.58 (2.42) | 13.17 (13.27) | 20.56 (20.40) | 910 (956.2) |
| $\|Pt(SnCl_2I)(S_2CNHBz)(PCy_3)\|$ | 31.98 (32.05) | 1.50 (1.44) | 4.18 (4.24) | 12.93 (13.02) | 19.77 (20.02) | 933 (974.3) |

†M=Pt or Pd. ‡Figures in parentheses are the calculated values.

ing by the number of bands in the 950–1050 $cm^{-1}$ region was shown to be valid and is further supported from the observed splittings of the $\nu$(N–H) and $\nu$(C⋯⋯N) bands.[18,20] Hence, it can be deduced for these complexes that one of the dithio-ligands acts as a bidentate ligand and the other one as a unidentate. Finally, the M–S stretching frequencies were observed in the 300–400 $cm^{-1}$ region indicating the coordination of the *gem*-disulphide ligands. In the case of [Pt(NCS)($S_2$CNHBz)($PR_3'$)] complexes the linkage isomerism of the thiocyanate ion was determined on the basis of the C–S stretching frequency (835 $cm^{-1}$), since this band is shifted to higher frequency in the spectra of M–NCS complexes[21] relative to $\nu$(C–S) of the free ion (749 $cm^{-1}$). This type of bonding is further confirmed by the $\delta$(SCN) frequency[22,23] which appears as a single band at *ca.* 475 $cm^{-1}$. Furthermore, it seems that $\pi$-bonding ligands, such as phosphines, favour the isothiocyanato linkage which is also promoted by bulky ligands, since the bending M–S–C thiocyanato linkage has a larger steric requirement than does the linear structure M–NCS.

The IR data, the diamagnetic nature of the complexes under investigation and their stoicheiometry allowed us to suggest a square planar configuration. This structure was further sup-

Table 2. Relevant IR frequencies ($cm^{-1}$) for some Pt(II) and Pd(II) dithio-compounds with their assignments (KBr discs)

| Compound | ν(N-H) | ν(C···N) | ν(C···S) | ν(CSS) | ν(M-S) |
|---|---|---|---|---|---|
| $\|Pt(S_2CNHBz)_2\|$ | 3257m,br† | 1538vs,br | 980m | 934s | 377m<br>280w |
| $\|Pt(S_2CNHBu^t)_2\|$ | 3220m,br | 1535vs,br | 970s | 925m | 370m<br>275w |
| $\|Pd(S_2CNHBz)_2\|$ | 3245m,br | 1532vs,br | 968m | 922s | 361m<br>268sh |
| $\|Pd(S_2CNHBu^t)_2\|$ | 3210m,br | 1530vs,br | 965m | 920w | 355m |
| $\|Pt(S_2CNHBz)_2(PPh_3)\|$ | 3305m<br>3125m,br | 1545vs,br<br>1493s | 1008m<br>988m | 943s<br>900m | 400m<br>300w |
| $\|Pt(S_2CNHBz)_2(PCy_3)\|$ | 3300m<br>3130m,br | 1538vs,br<br>1490s | 1012m<br>990w | 945s<br>910m | 395m<br>295w |
| $\|Pt(S_2CNHBu^t)_2(PPh_3)\|$ | 3255m<br>3110m,br | 1535vs,br<br>1490s | 990w<br>970m | 917w | 385w<br>292sh |
| $\|Pt(S_2CNHBu^t)_2(PCy_3)\|$ | 3240m<br>3085m,br | 1528vs,br<br>1488s | 995m<br>972s | 919sh<br>910m | 380m<br>285sh |
| $\|Pd(S_2CNHBz)_2(PCy_3)\|$ | 3310m<br>3130m,br | 1532vs,br<br>1495s | 1003m<br>975w | 935sh<br>928s | 375m<br>288sh |
| $\|Pd(S_2CNHBu^t)_2(PCy_3)\|$ | 3250m<br>3090m,br | 1530vs,br<br>1492s | 998w<br>975m | 921sh<br>912m | 368m<br>275sh |
| $\|PtI(S_2CNHBz)(PPh_3)\|$ | 3130m,br | 1535vs,br | 995m | 928m | 388m |
| $\|PtI(S_2CNHBz)(PCy_3)\|$ | 3125m,br | 1530vs,br | 1008m | 925w | 385w |
| $\|PtI(S_2CNHBu^t)(PPh_3)\|$ | 3135m,br | 1528vs,br | 968m | 922w | 378w |
| $\|PtI(S_2CNHBu^t)(PCy_3)\|$ | 3130m,br | 1522vs,br | 990m | 912m | 375w |
| $\|PdI(S_2CNHBz)(PCy_3)\|$ | 3140m,br | 1530vs,br | 965w | 921m | 360m |
| $\|PdI(S_2CNHBu^t)(PCy_3)\|$ | 3115m,br | 1528vs,br | 955m | 910s | 362m |
| $\|Pt(NCS)(S_2CNHBz)(PPh_3)\|$ | 3170m,br | 1540vs,br | 980m | 918m | 385w |
| $\|Pt(NCS)(S_2CNHBz)(PCy_3)\|$ | 3160m,br | 1535vs,br | 965w | 910m | 380w |
| $\|Pt(SnCl_2I)(S_2CNHBz)(PPh_3)\|$ | 3180m,br | 1528vs,br | 992w | 928w | 378w |
| $\|Pt(SnCl_2I)(S_2CNHBz)(PCy_3)\|$ | 3150m,br | 1520vs,br | 970w | 922w | 375w |

†vs=very strong, s=strong, m=medium, w=weak, sh=shoulder, br=broad.

ported by the $^1H$ NMR data (Table 3) of the new compounds. Thus, although the $^1H$ NMR spectra of the bis(N-benzyldithiocarbamato) complexes show one sharp peak for the N–$CH_2$ protons, their corresponding phosphine adducts exhibit two broad signals at the N–$CH_2$ proton region, a fact which is consistent with the coexistence of one unidentate and one bidentate dithio-ligand. The line broadening of the N–$CH_2$ proton signals of the phosphine adducts could be explained on the basis of their fluxional behaviour. Such dynamic processes for analogous compounds which interconvert the two kinds of the dithio-ligands have been already observed and studied by low-temperature $^1H$ NMR spectroscopy.[5]

The electronic spectra (Table 4) of the complexes are also consistent with the proposed square planar configuration. The most intense band I is due to an intraligand $\pi^* \leftarrow \pi$ transition located on the N···C···S group.[24,25] The position of this band is slightly affected by the nature of the central atom as well as by the electron releasing ability of the amine group. Band II, which appears as a shoulder, is also attributed to a $\pi^* \leftarrow \pi$ transition of the S···C···S group[26] and is associated with the inequivalence of the C···S bonds of the ligands.

Table 3. $^1$H NMR data for various Pt(II) and Pd(II) dithio-compounds in DMSO-$d_6$

| Compound | τ Value |
|---|---|
| $\|Pt(S_2CNHBz)_2\|$ | 5.45(s, 4H, N-$CH_2$)*; 2.62(s, 10H, $C_6H_5$) |
| $\|Pt(S_2CNHBu^t)_2\|$ | 8.47(s, 18H, C-$CH_3$) |
| $\|Pd(S_2CNHBz)_2\|$ | 5.46(s, 4H, N-$CH_2$); 2.63(s, 10H, $C_6H_5$) |
| $\|Pd(S_2CNHBu^t)_2\|$ | 8.46(s, 18H, C-$CH_3$) |
| $\|Pt(S_2CNHBz)_2(PPh_3)\|$ | 5.04(s, 2H, N-$CH_2$); 4.90(s, 2H, N-$CH_2$); 2.38(m, 25H, $C_6H_5$) |
| $\|Pt(S_2CNHBz)_2(PCy_3)\|$ | 8.85-7.97(mu, 33H, $C_6H_{11}$); 5.33(s, 2H, N-$CH_2$); 5.17(s, 2H, N-$CH_2$); 2.57(s, 10H, $C_6H_5$) |
| $\|Pt(S_2CNHBu^t)_2(PPh_3)\|$ | 8.37(s, 18H, C-$CH_3$); 2.43(m, 15H, $C_6H_5$) |
| $\|Pt(S_2CNHBu^t)_2(PCy_3)\|$ | 8.14(s, 18H, C-$CH_3$); 8.04-7.53(mu, 33H, $C_6H_{11}$) |
| $\|Pd(S_2CNHBz)_2(PCy_3)\|$ | 8.52-8.10(mu, 33H, $C_6H_{11}$); 5.40(s, 2H, N-$CH_2$); 5.28(s, 2H, N-$CH_2$); 2.51(s, 10H, $C_6H_5$) |
| $\|Pd(S_2CNHBu^t)_2(PCy_3)\|$ | 8.25(s, 18H, C-$CH_3$); 8.18-7.85(mu, 33H, $C_6H_{11}$) |
| $\|PtI(S_2CNHBz)(PPh_3)\|$ | 4.82(s, 2H, N-$CH_2$); 2.38(m, 20H, $C_6H_5$) |
| $\|PtI(S_2CNHBz)(PCy_3)\|$ | 8.77-7.86(mu, 33H, $C_6H_{11}$); 5.12(s, 2H, N-$CH_2$); 2.57(s, 5H, $C_6H_5$) |
| $\|PtI(S_2CNHBu^t)(PPh_3)\|$ | 8.35(s, 9H, C-$CH_3$); 2.44(m, 15H, $C_6H_5$) |
| $\|PtI(S_2CNHBu^t)(PCy_3)\|$ | 8.14(s, 9H, C-$CH_3$); 8.06-7.80(mu, 33H, $C_6H_{11}$) |
| $\|PdI(S_2CNHBz)(PCy_3)\|$ | 8.45-8.29(mu, 33H, $C_6H_{11}$); 5.28(s, 2H, N-$CH_2$); 2.58(s, 5H, $C_6H_5$) |
| $\|PdI(S_2CNHBu^t)(PCy_3)\|$ | 8.22(s, 9H, C-$CH_3$); 8.18-7.81(mu, 33H, $C_6H_{11}$) |
| $\|Pt(NCS)(S_2CNHBz)(PPh_3)\|$ | 4.85(s, 2', N-$CH_2$); 2.37(m, 20H, $C_6H_5$) |
| $\|Pt(NCS)(S_2CNHBz)(PCy_3)\|$ | 8.75-7.87(mu, 33H, $C_6H_{11}$); 5.14(s, 2H, N-$CH_2$); 2.57(s, 5H, $C_6H_5$) |
| $\|Pt(SnCl_2I)(S_2CNHBz)(PPh_3)\|$ | 4.88(s, 2H, N-$CH_2$); 2.38(m, 20H, $C_6H_5$) |
| $\|Pt(SnCl_2I)(S_2CNHBz)(PCy_3)\|$ | 8.78-7.84(mu, 33H, $C_6H_{11}$); 5.20(s, 2H, N-$CH_2$); 2.56(s, 5H, $C_6H_5$) |

*s=singlet, m=multiplet, mu=multiplet unresolved.

Table 4. Electronic spectra of some Pt(II) and Pd(II) dithio-compounds in $CHCl_3$

| Compound | Band I | | Band II | | Band III | | Band IV | | Band V | |
|---|---|---|---|---|---|---|---|---|---|---|
| $\|Pt(S_2CNHBz)_2\|$ | 39.5† | (4.92)†† | 35.1sh‡ | (4.16) | 28.8 | (4.24) | 25.1 | (3.38) | 23.9sh | (3.25) |
| $\|Pt(S_2CNHBu^t)_2\|$ | 39.6 | (4.63) | 34.5sh | (4.03) | 28.9 | (4.17) | 25.3 | (3.36) | 24.1sh | (3.31) |
| $\|Pd(S_2CNHBz)_2\|$ | 37.1 | (4.89) | 33.2sh | (4.12) | 28.6 | (4.11) | 24.3 | (2.57) | 21.1 | (2.48) |
| $\|Pd(S_2CNHBu^t)_2\|$ | 37.4 | (4.58) | 32.9sh | (4.01) | 28.7 | (4.08) | 24.4 | (2.51) | 21.7 | (2.50) |
| $\|Pt(S_2CNHBz)_2(PPh_3)\|$ | 39.1 | (4.69) | 33.7 | (4.56) | 28.9 | (3.87) | 24.1 | (2.22) | | |
| $\|Pt(S_2CNHBz)_2(PCy_3)\|$ | 39.7 | (4.43) | 34.2 | (4.48) | 30.1sh | (3.97) | 24.7 | (2.85) | | |
| $\|Pt(S_2CNHBu^t)_2(PPh_3)\|$ | 39.3 | (4.49) | 33.4 | (4.18) | 29.5 | (3.81) | 24.1 | (2.93) | | |
| $\|Pt(S_2CNHBu^t)_2(PCy_3)\|$ | 39.8 | (4.39) | 34.2 | (4.66) | 30.3sh | (3.73) | 24.6 | (2.83) | | |
| $\|Pd(S_2CNHBz)_2(PCy_3)\|$ | 37.2 | (4.43) | 33.3 | (3.96) | 28.8 | (3.98) | 23.5 | (1.23) | | |
| $\|Pd(S_2CNHBu^t)_2(PCy_3)\|$ | 37.8 | (4.40) | 33.4 | (4.85) | 29.5sh | (3.95) | 23.8 | (1.20) | | |
| $\|PtI(S_2CNHBz)(PPh_3)\|$ | 38.2 | (4.52) | 31.5sh | (3.97) | 27.3 | (3.61) | 23.8 | (2.13) | | |
| $\|PtI(S_2CNHBz)(PCy_3)\|$ | 38.5 | (4.38) | 32.2sh | (3.75) | 28.8 | (3.77) | 24.1 | (2.55) | | |
| $\|PtI(S_2CNHBu^t)(PPh_3)\|$ | 38.7 | (4.63) | 30.9sh | (3.65) | 28.7 | (3.76) | 24.1 | (2.94) | | |
| $\|PtI(S_2CNHBu^t)(PCy_3)\|$ | 38.9 | (4.31) | 31.8sh | (3.84) | 28.9 | (3.63) | 24.3 | (2.86) | | |
| $\|PdI(S_2CNHBz)(PCy_3)\|$ | 37.0 | (4.36) | 30.5sh | (3.89) | 28.4 | (3.24) | 23.2sh | (1.95) | | |
| $\|PdI(S_2CNHBu^t)(PCy_3)\|$ | 37.3 | (4.30) | 30.6sh | (3.92) | 28.8 | (3.20) | 23.6sh | (1.88) | | |

†$\tilde{\nu}$/kK ††log $\varepsilon_{mol}$ ‡sh=shoulder

Band II of the bis(N-alkyldithiocarbamato) complexes is less characteristic than that of the corresponding phosphine adducts, and tends to disappear. This may be attributed to the fact that in these cases the bonding mode of the dithiocarbamato ligands is similar, in agreement with their IR and $^1$H NMR spectra. Band III may be assigned to a $\pi^* \leftarrow n$ electronic transition located on the sulphur atom,[27,28] since its frequency is slightly increased as the electron releasing ability of amine group increases. The assignments of bands I, II and III as intraligand transitions are also consistent with the results of CNDO/2 quantum chemical calculations.[29] Bands IV and V are due to charge transfer (CT) transitions of type M→L. These bands are analogous to the CT bands observed in square planar Pt(II) and Pd(II) complexes of $D_{2h}$ symmetry and are assigned to $^1B_{1u}$, $^1B_{2u}$, $^1B_{3u} \leftarrow {}^1A_g$ transitions.[30]

Finally, the coexistence of two different kinds of dithiocarbamato ligands in the molecules of the phosphine adducts as well as their square planar configuration was definitely established by an X-ray structure determination[16] of a representative complex, namely the $[Pt(S_2CNHBu^t)_2(PCy_3)]$ complex.

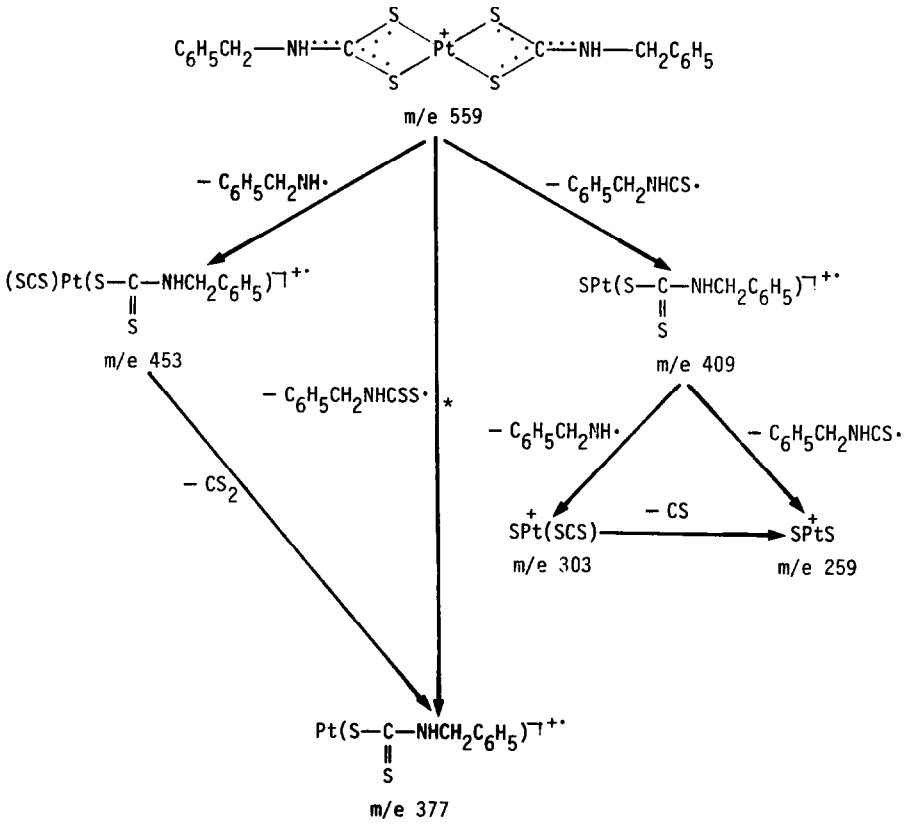
The molecular ions of the studied compounds were not detected in the mass spectra, except in the cases of bis(N-alkyldithiocarbamato) complexes. The absence of molecular ions can be attributed either to pyrolytic decomposition, in the direct inlet, under the high temperature which was used (200–280°C), or to electron impact. The fragments corresponding to higher $m/e$ values can be regarded as direct fragments of the molecular ions, while those at lower m/e values may be regarded as daughter fragments of the phosphine and N-alkyldithiocarbamato ligands. In most cases the base peak of the spectra corresponds to the $RP_3^{+\cdot}$ ion. In the case of the $[Pt(S_2CNHBz)_2]$ complex the existence of a metastable peak at $m^* = 254.3$ confirms the following fragmentation:

$$P^+t(S_2CNHBz)_2 \xrightarrow{-BzNHCSS\cdot} Pt(S_2CNHBz)^{+\cdot}$$

$m/e$ 559 $m/e$ 377

A possible fragmentation mechanism of the molecular ion of this complex is represented by Scheme 1.

Finally, the thermogravimetric study of both the bis(N-alkyldithiocarbamato) complexes and their phosphine adducts further confirms the bonding mode of the dithio-ligands to the central atom. For example, the thermograms of the $[Pt(S_2CNHBu^t)_2(PCy_3)]$ complex show two endothermic decom-




Scheme 1.

positions corresponding to a two-stage weight loss of 31%. The two weight losses occur at 180 and 220°C and can be attributed to loss of $\{Bu^tNHCS_2\}$ (Found: 21.0%; Calc.: 21.7%) and $\{Bu^tNH\}$ (Found: 10.0%; Calc.: 10.6%) respectively. The easy rupture of the Pt–S bond of the one dithiocarbamato ligand strongly suggests its unidentate bonding mode. On the contrary, the thermograms of $[Pt(S_2CNHBz)_2]$ are composed of three weight losses, all of them endothermic at 187, 227 and 245°C which can be attributed to loss of {BzNH} (Found: 18.0%; Calc.: 18.9%), {SC} (Found: 8.0% Calc.: 7.9%) and {S} (Found: 6.5%; Calc.: 5.7%) respectively.

## REFERENCES


1. J. P. Fackler Jr., W. C. Seidel and J. A. Fetchin, *J. Am. Chem. Soc.* 1968, **90**, 2707.
2. J. P. Fackler Jr., J. A. Fetchin and W. C. Seidel, *J. Am. Chem. Soc.* 1969, **91**, 1217.
3. J. P. Fackler Jr. and W. C. Seidel, *Inorg. Chem.* 1969, **8**, 1631.
4. J. M. C. Alison, T. A. Stephenson and R. O. Gould, *J. Chem. Soc., A* 1971, 3690.
5. J. M. C. Alison and T. A. Stephenson, *J. Chem. Soc., Dalton* 1973, 254.
6. J. Zagal and J. A. Costamagna, *Inorg. Nucl. Chem. Lett.* 1977, **13**, 411.
7. M. C. Cornock, R. O. Gould, C. L. Jones, J. O. Owen, D. F. Steele and T. A. Stephenson, *J. Chem. Soc., Dalton* 1977, 496.
8. N. Sonoda and T. Tanaka, *Inorg. Chim. Acta* 1975, **12**, 261.
9. M. C. Cornock and T. A. Stephenson, *J. Chem. Soc., Dalton* 1977, 501.
10. J. P. Fackler Jr., I. J. B. Lin and J. Andrews, *Inorg. Chem.* 1977, **16**, 450.
11. G. A. Katsoulos, G. E. Manoussakis and C. A. Tsipis, *Inorg. Chim. Acta* 1978, **30**, L295.
12. G. A. Katsoulos and C. A. Tsipis, *Inorg. Chim. Acta*, accepted for publication.
13. A. Vogel, *Quantitative Inorganic Analysis*, p. 510. Longmans, London (1964); *Ibid*, p. 512.
14. C. A. Tsipis and G. E. Manoussakis, *Inorg. Chim. Acta* 1976, **18**, 35.
15. H. P. Koch, *J. Chem. Soc.* 1949, 401.
16. P. C. Christidis and P. J. Rentzeperis, *Acta Cryst.* 1979, **B35**, 2543.
17. K. J. Rao and M. L. Venkataragha, *Can. J. Chem.* 1961, **39**, 1757.
18. D. A. Brown, W. K. Glass and M. A. Burke, *Spectrochim. Acta* 1976, **32A**, 137.
19. F. Bonati and R. Ugo, *J. Organomet. Chem.* 1967, **10**, 257.
20. E. C. Alyea and B. C. Ramaswamy, *Inorg. Nucl. Chem. Lett.* 1970, **6**, 441.
21. J. L. Burmeister and F. Basolo, *Inorg. Chem.* 1964, **3**, 1587.
22. A. Sabatini and I. Bertini, *Inorg. Chem.* 1965, **4**, 959; 1665.
23. J. Lewis, R. S. Nyholm and P. W. Smith, *J. Chem. Soc.* 1961, 4590.
24. C. K. Jörgensen, *J. Inorg. Nucl. Chem.* 1962, **24**, 1571.
25. F. Takami. S. Wakahara and T. Maeda, *Tetrahedron Lett.* 1971, **28**, 2645.
26. M. J. Janssen, *Rec. Trav. Chim.* 1960, **79**, 1066.
27. M. J. Janssen, *Rec. Trav. Chim.* 1960, **79**, 454.
28. M. L. Shankaranarayana and C. C. Patel, *Acta Chem. Scand.* 1965, **19**, 1113.
29. G. A. Katsoulos, Ph.D. Thesis. University of Thessaloniki (1983).
30. A. R. Latham, V. C. Hascall and H. B. Gray, *Inorg. Chem.* 1965, **4**, 788.

*Polyhedron* Vol. 3, No. 6, pp. 743–747, 1984
Printed in Great Britain.

0277–5387/84 $3.00 + .00
© 1984 Pergamon Press Ltd.

# PHOTOCHEMISTRY OF AQUEOUS $[W(CN)_8]^{4-}$

**A. E. NYA* and HARI MOHAN**
Department of Chemistry, University of Calabar, P.M.B. 115, Calabar, Nigeria

(*Received* 22 *October* 1982; *accepted* 16 *May* 1983)

**Abstract**—Aqueous $[W(CN)_8]^{4-}$ undergoes photoaquation when irradiated at ~ 365 nm with pH independent quantum yield. The yield for aquoheptacyanotungstate (IV) ion production is 0.8 at 0.5°C. If added alkali is present a wide variety of products $[W(CN)_7(OH)]^{4-}$, $[WO_2(CN)_4]^{4-}$, $[WO(OH)(CN)_4]^{3-}$ $[W(OH)_2(CN)_4]^{2-}$ are formed.

Extensive photochemical studies of the $[W(CN)_8]^{4-}$ system have been carried out[1–15] in several laboratories but the issue has not been fully clarified. On irradiation with ultraviolet light, neutral aqueous solution of octacyanotungstate (IV) become alkaline[1] and the yellow colour of the solution changes, first to red and then violet.[5] The primary photochemical reaction is believed to be one of photo-aquation.

$$[W(CN)_8]^{4-} + 2H_2O \overset{h\nu}{\rightleftharpoons} [W(CN)_7(H_2O)]^{3-} + HCN + OH^- . \quad (1)$$

Balzani *et al.*[4,5] and Mitra *et al.*[7] think that the red species is $[W(CN)_7H_2O]^{3-}$ while according to Jakoh *et al.*[8,9] it is a decacoordinated species $[W(CN)_8(H_2O)_2]^{4-}$. Mohan[10] precipitated this species as the silver salt $Ag_3[W(CN)_7(H_2O)]$. According to Samotus and Sieklucka,[14,15] three primary photoproducts, viz. $[HW(CN)_7(H_2O)]^{2-}$, $[W(CN)_7(H_2O)]^{3-}$ and $[W(CN)_7(OH)]^{4-}$ are formed. The quantum yield of the primary photochemical reaction has been determied,[2,4,7,15] values ranging from 0.07 to 1.0 have been reported. In what follows it will be shown that starting from a mixture of acid $H_4[W(CN)_8]$ and $K_4[W(CN)_8]$, when the $[W(CN)_8]^{4-}$ anion is photolysed, the red anion $[W(CN)_7(H_2O)]^{3-}$ is obtained as a stable species and no violet[11,12] or brown compounds[7] are formed by secondary reactions. To eliminate thermal reaction as far as possible, photolysis was done at 0.5°C. Calculated amount of alkali was added to convert $[W(CN)_7(H_2O)]^{3-}$ into $[W(CN)_7(OH)]^{4-}$ from this tetracyano-oxo-, or hydroxo-complexes were obtained.

*Author to whom correspondence should be addressed.

## EXPERIMENTAL

$K_4[W(CN)_8]2H_2O$ was prepared by a known method.[16] The absorption spectra agreed with those previously reported.[17] $H_4[W(CN)_8]$ was obtained by ion exchange with the hydrogen form of Amberlite IR 120 resin.

A high pressure Philips mercury arc lamp with a Watten 18A filter provided radiation in the 365 nm region. Photolysis was done in standard spectrophotometric cells and absorption spectra were taken immediately after photolysis using a recording spectrophotometer.

Potassium was determined as potassium tetraphenylborate.[18] Carbon, hydrogen and nitrogen were determined by microanalyses.[19] Tungsten was determined by boiling an aqueous solution of the complex with concentrated nitric acid and perchloric acid, and then weighing the precipitated tungsten (VI) oxide. The water in a complex was determined by heating in vacuum at 110°C, to constant weight. Ferric oxalate was used for actinometry[20,21] with a quantum yield of 1.2 at ~ 365 nm. The intensity of the light used was $\sim 9 \times 10^{19}$ photons/m$^2$/sec.

## RESULTS AND DISCUSSION

When an ice cold mixture of 0.005 M $H_4[W(CN)_8]$ and 0.005 M $K_4[W(CN)_8]$ 1:3 was irradiated with ultraviolet light in a closed cell the solution became red. During irradiation a peak at 516 nm synchronizing with the appearance of the

red colour was observed. When the irradiation of the acid was stopped and the solution was kept in the dark, the red colour disappeared to give back the original yellow solution.

$$[W(CN)_7(H_2O)]^{3-} + HCN \rightarrow [W(CN)_8]^{4-}. \quad (2)$$

A fresh solution of the mixture was irradiated with UV light with nitrogen gas bubbling through the solution to remove HCN as fast as it was formed. When the absorption peak at 516 nm characteristic of the red complex reached its maximum value pH and conductometric titration of an aliquot of the solution showed that it had lost the hydrogen ions as HCN. Redox titration of aliquots of the irradiated solution with $KMnO_4$ indicated that the oxidation state of W did not change. Molar extinction coefficient $\epsilon_{max}$ of the complex was determined by measuring the optical density at 516 nm. An $\epsilon_{max}$ of $92 \pm 1$ was observed at 0.5°C. Mitra *et al.*[7] reported a much higher value $114 \pm 1$ at 0°C. Samotus and Sieklucka[14] reported a value of 78.2 at 520 nm. Our results are in general consistent with them as they also observed the peak at 516 nm/520 nm for the red complex. The photolysed solution can be kept at 0.5°C for several days with decomposition.

When a calculated amount of KCN was added to the red complex. The yellow anion $[W(CN)_8]^{4-}$ was formed as can be seen by the spectra. This suggested that the red anion is susceptible to $CN^-$ substitution. When KOH solution was added to the red complex the red colour faded to a yellow species, probably the hydroxy complex $[W(CN)_7(OH)]^{4-}$. A yellow solid separated out on the addition of alcohol, its analysis gave: K, 28.8; W, 33.8; C, 15.0; N, 17.5. These results agree with the formula $K_4[W(CN)_7(OH)]$

$$[W(CN)_7(H_2O)]^{3-} + OH^- \rightarrow [W(CN)_7(OH)]^{4-} + H_2O. \quad (3)$$

When the exactly calculated amount of KOH was added to the red complex a slow change was observed. Figure 1 shows the spectral variations. The colour of the solution changed from red to yellow. This change from red to yellow by the action of alkali was not reversible. The solution remained yellow when kept in the dark at room temperature (25°C). The red colour did not return even on acidification. Figure 1 shows an isosbestic point at 468 nm this clearly indicates that the species $[W(CN)_7(H_2O)]^{3-}$ is converted to $[W(CN)_7OH]^{4-}$ only. Such spectra evidence showing the conversion of heptacyno-aquo complex of tungsten (IV) to heptacyano-hydroxo complex has not been reported before.

By the photolysis of neutral aqueous solutions of $K_4[W(CN)_8]$ at 25°C first the red species was formed. The observation of an isosbestic point at 464 nm produced from the spectra of $[W(CN)_8]^{4-}$ and $[W(CN)_7(H_2O)]^{3-}$ was convincing proof that only $[W(CN)_7(H_2O)]^{3-}$ was formed (Fig. 2). After photolysis when the solution was kept in dark spectral variations at different time intervals showed a slow change. The $[W(CN)_7(H_2O)]^{3-}$ spe-

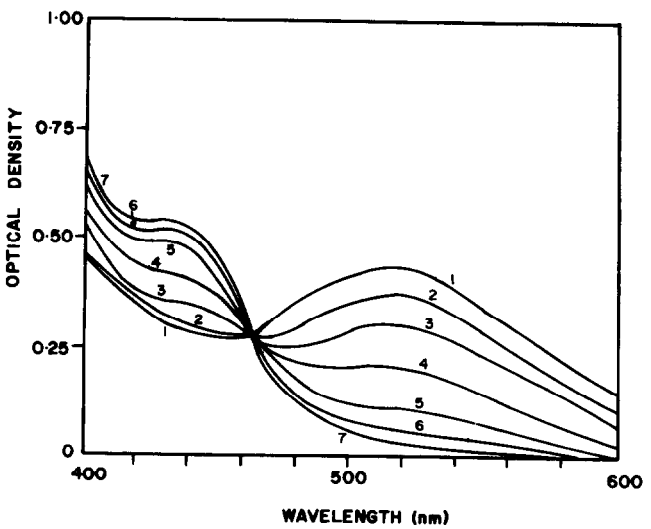



Fig. 1. Spectral variations showing the conversion of $[W(CN)_7H_2O]^{3-}$ to $[W(CN)_7OH]^{4-}$ curves numbers 1 to 7 recorded after 1, 2, 5, 7, 10, 15 and 20 min respectively $5 \times 10^{-3}$ M heptacyanoaquo tungstate (IV) was used.

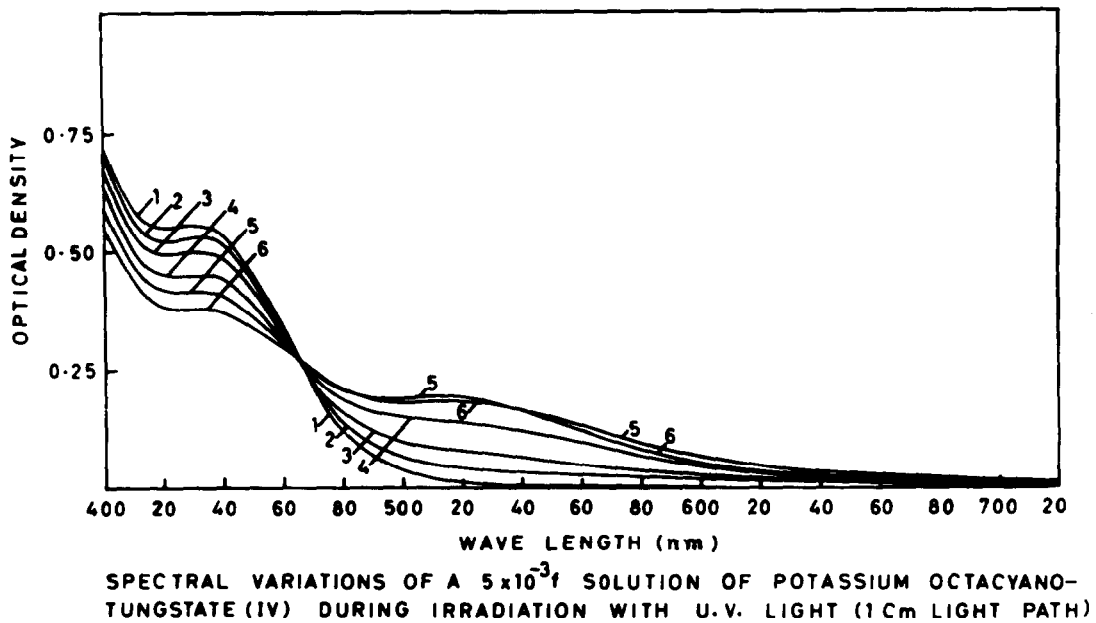



Fig. 2. Spectral variations of a $5 \times 10^{-3}$ M solution of $K_4[W(CN)_8]$ during irradiation (1 cm light path). Curve numbers 1, 2, 3, 4, 5 and 6 refer to irradiation times of 1, 2, 4, 7, 10 and 12 min respectively.

cies faded to yellow species. Probably the reactions 3 and 4

$$[W(CN)_7(H_2O)]^{3-} + CN^- \rightarrow [W(CN)_8]^{4-} + H_2O \quad (4)$$

are competing kinetically.

We also found that the lower the temperature of the neutral aqueous solution of $[W(CN)_8]^{4-}$ other conditions remaining constant, the greater was the 516 nm peak produced. On photo-irradiation at 25°C the yellow solution of $[W(CN)_8]^{4-}$ became red within 2 min and the characteristic absorption peak of the red species appeared, the maximum optical density of 0.2 for a solution of 0.005 M observed. At 0.5°C for the same solution on irradiation a value of 0.46 was obtained. The red species disappeared at a much slower rate than at 25°C when light was cut off. The pH of the solution increased from 6.2 to 9.5 as a result of irradiation in agreement with previous work.[1] Photolysis was next done under alkaline conditions to see if the same red species is formed. The secondary reactions could be eliminated at low temperature. At 0.5°C the optical density was 0.19 for a highly alkaline solution (pH—12.5) of 0.005 M $K_4[W(CN)_8]$. The spectral variations are presented in Fig. 3. The red species was formed at this pH also. When after necessary irradiation to produce maximum red anion the solution was kept in dark at 0.5°C the red species disappeared at a much slower rate than at 25°C when light was cut off.

Mitra *et al.*[7] has shown that if the solution of $H_4[W(CN)_8]$ was photolysed the red species was first formed and then on prolonged irradiation the red species were replaced by a brown species. We found that the mixture of acid and the salt on prolonged irradiation at 0.5°C did not show any appreciable change once the maximum optical density at 516 nm is reached. Calculated amount of KOH was added to convert $[W(CN)_7(H_2O)]^{3-}$ into $[W(CN)_7(OH)]^{4-}$ as indicated above and the solution was further photolysed it immediately turned blue and a broad absorption peak at 640 nm appeared. As photolysis was continued the peak at 640 nm grew in height. The blue species was precipitated by the addition of alcohol and after repeated recrystallization, its analysis gave: K, 19.8; W, 46.0; C, 11.8; N, 13.8. These results agree with the formula $K_2[W(OH)_2(CN)_4]$. The IR spectrum of the solid indicated strong bands at 2100 $cm^{-1}$ and 920 $cm^{-}$.

The blue compound when dissolved in alkaline solution gave an absorption peak at 540 nm instead of 640 nm. As the solution was diluted the peak shifted towards the longer wave length side. When to a dilute solution more and more solid KOH was added three different peaks at 640, 540 and 480 nm could be observed. No further shift in the 480 nm peak occurred on the addition of more solid KOH: on keeping at this stage a dark solid separated out. The latter on analysis gave: K, 26.1; W, 31.5; C, 8.2; N, 9.6; $H_2O$, 18.4; $[K_4(WO_2(CN)_4]$

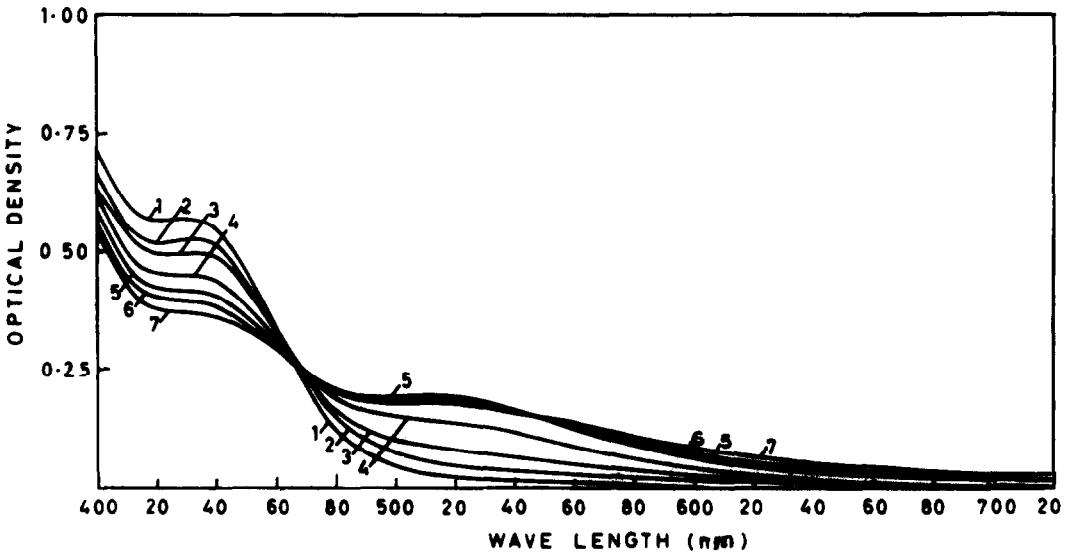



Fig. 3. Spectral variations of a $5 \times 10^{-3}$ M solution of $[W(CN)_8]^{4-}$ at pH 12.5 (Buffer) during irradiation curve numbers 1–7 refer to irradiation times of 1, 2, 4, 6, 10, 12 and 15 min respectively.

$6H_2O$ would require K, 26.76; W, 31.46; C, 8.24; N, 9.57; $H_2O$, 18.48%. The dark solid when dissolved in concentrated solution of KOH gave light pinkish brown solution. The absoption spectrum showed a peak at 480 nm. The infrared spectrum of the solid indicated strong bands at 2060 $cm^{-1}$ and a broad band at 800 $cm^{-1}$.

Peaks at 640 and 540 nm apparently indicate the

Table 1. Values of quantum yields for $[W(CN)_8]^{4-}$ system at different pH and temperatures

| Concentration of $[W(CN)_8]^{4-}$ | pH | Temperature °C | $\phi$ $[W(CN)_7H_2O]^{3-}$ |
|---|---|---|---|
| 0.005 | 2.0(Buffer) | 0.5 | 0.82 ± 0.05 |
| 0.005 | 3.8(Buffer) | 0.5 | 0.82 ± 0.05 |
| 0.005 | 3.8 | 0.0 | 0.80 ± 0.05.⁂ |
| 0.005 | 6.4 | 0.5 | 0.82 ± 0.05 |
| 0.005 | (neutral) | 0.0 | 0.78 ± 0.05.⁂ |
| 0.005 | 8.2(Buffer) | 0.5 | 0.80 ± 0.05 |
| 0.005 | 9.2(Buffer) | 0.5 | 0.80 ± 0.05 |
| 0.005 | 10.3(Buffer) | 0.5 | 0.80 ± 0.05 |
| 0.005 | 12.5(Buffer) | 0.5 | 0.78 ± 0.05 |
| 0.005 | 13.0 (Buffer) | 0.5 | 0.74 ± 0.05 |
| 0.005 | 2.0 (Mixture) | 0.5 | 0.80 ± 0.05 |
| 0.010 | 2.0 (Mixture) | 0.5 | 0.80 ± o.05 |
| 0.005 | 2.0 (Mixture) | 10.0 | 0.80 ± 0.05 |
| o.005 | 2.0 (Mixture) | 20.0 | 0.80 ± 0.05 |
| 0.005 | 2.0 (Mixture) | 30.0 | 0.76 ± 0.05 |
| 0.005 | 2.0 (Mixture) | 40.0 | 0.60 + 0.05 |
| 0.010 | 2.0(Mixture) | 40.0 | 0.58 ± 0.05 |
| | 6 to 8 | 20.0 | 0.98 ± 0.05 .⁂. .⁂. |

.⁂; Ref. 7 Mitra , Sharma and Mohan

.⁂. .⁂. Ref. 15 Sieklucka and Samotus

two products of hydrolysis of the $[WO_2(CN)_4]^{4-}$ species, viz. $[WO(OH)CN_4]^{3-}$ and $[W(OH)_2(CN)_4]^{4-}$ respectively.

When the solid $K_4[WO_2(CN)_4]$ was dissolved in dilute alkali it gave a violet solution with a peak at 540 nm, a violet solid separated out on the addition of alcohol to it which after recrystallization could be identified as $K_3[WO(OH)(CN)_4]$.

The latter when dissolved in pH-Buffer (pH = 10.7) showed a peak at 540 nm. The infrared spectrum of the solid indicated strong bands at 2070, 1060, 920 and 850 $cm^{-1}$.

The formation of a red anion in a mixture of $H_4[W(CN)_8]$ and $K_4[W(CN)_8]$ clearly shows that, aquo-heptacyanotungstate (IV) is the only photo-aquation product of octocyanotungstate (IV) ion. This is quite stable at low temperature. When the pH of the solution is high it reacts with $OH^-$ ions to produce hydroxo-heptacyanotungstate (IV). The latter is the precursor of the tetracyano complexes of W(IV).

$$[W(CN)_8]^{4-} \xrightarrow[H_2O]{h\nu} \underset{\text{Red}}{[W(CN)_7(H_2O)]^{3-}} \quad (5)$$

$$[W(CN)_7(H_2O)]^{3-} + OH^- \longrightarrow \underset{\text{Yellow}}{[W(CN)_7(OH)]^{4-}} \quad (6)$$

$$[W(CN)_7(OH)]^{4-} \xrightarrow[H_2O]{h\nu} \underset{\text{Blue}}{[W(OH)_2(CN)_4]^{2-}} \quad (7)$$

$$[W(OH)_2(CN)_4]^{2-} + OH^- \rightleftharpoons \underset{\text{Violet}}{[WO(OH)(CN)_4]^{3-}} + H_2O \quad (8)$$

$$[WO(OH)(CN)_4]^{3-} + OH^- \rightleftharpoons \underset{\text{Brown}}{[WO_2(CN)_4]^{4-}} + H_2O. \quad (9)$$

The quantum yield for the primary photochemical reaction was determined by estimation of the red anion spectrophotometrically. Values of the quantum yield are given in Table 1. We have calculated the quantum yield for the primary photochemical reaction by direct estimation of $[W(CN)_7(H_2O)]^{3-}$ rather than computing indirectly, e.g. by determining $OH^-$ ions generated by the hydrolysis of $CN^-$ ions, as has been done by Balzani *et al.*[5] Balzani *et al.*[5] realized that if secondary reactions also gave $CN^-$ and hence $OH^-$ ions determination of the primary reaction by their method would give erroneous results.

## REFERENCES


1. E. L. Goodenow and C. S. Garner, *J. Am. Chem. Soc.* 1955, **77**, 5268.
2. V. Carassiti, A. M. Marinangeli and V. Balzani *Ann. Chim. (Rome)* 1960, **50**, 790.
3. A. Berloluzza, V. Carassiti and A. M. Marinangeli *Ann. Chem. (Rome)* 1960, **50**, 806.
4. V. Carassiti and V. Balzani *Ann. Chim. (Rome)* 1960, **50**, 630.
5. V. Balzani and V. Carassiti, *Photochemistry of Coordination Compounds*. Academic Press, New York (1970).
6. V. M. Litvinehuk and K. N. Mikhalevich, *UKr. Khim. Zh.* 1959, **25**, 563.
7. R. P. Mitra, B. K. Sharma and H. Mohan, *Austr. J. Chem.* 1972, **25**, 499.
8. W. Jakob, A. Kosinska–Samotus and Z. Stasieka, *Roczniki Chem.* 1962, **36**, 165.
9. W. Jakob, A. Samotus and Z. Stasicka, *Roczniki Chem.* 1966, **40**, 1383.
10. M. Mohan, *J. Inorg. Nucl. Chem.* 1976, **38**, 1303.
11. S. J. Lippard H, Nozaki and B. J. Russ, *J. Chem. Soc. Chem. Commun.* 1967, 118.
12. S. J. Lippard and B. J. Russ, *Inorg. Chem.* 1967, **6**, 1943.
13. A. Samotus, *Roczniki Chem.* 1973, **47**, 251.
14. A. Samotus and B. Sieklucka, *J. Inorg. Nucl. Chem.* 1978, **40**, 315.
15. B. Sieklucka and A. Samotus, *J. Inorg. Nucl. Chem.* 1980, **42**, 1003.
16. E. A. Heintz, *Inorg. Synth.* 1963, **7**, 142.
17. J. R. Perumareddi, A. D. Liehr and A. W. Adamson, *J. Am. Chem. Soc.* 1963, **85**, 249.
18. L. E. Dey, *Gravimetric Analysis*, p. 730, Part 1. Pergamon Press, Oxford (1965).
19. C. L. Wilson and D. W. Wilson *Comprehensivve Analytical Chemistry*, Vol. 1, p. 466. Elsevier, New York (1960).
20. C. G. Hatchard and C. A. Parker, *Proc. Roy. Soc(A)* 1956, **235**, 518.
21. C. A. Parker, *Photoluminescence of Solutions*, p. 210. Elsevier, New York (1968).

*Polyhedron* Vol. 3, No. 6, pp. 749–752, 1984
Printed in Great Britain.

0277-5387/84 $3.00 + .00
© 1984 Pergamon Press Ltd

# NOTE

# CRYSTAL AND MOLECULAR STRUCTURE OF COMPLEX COMPOUND $(C_5H_5)_2Re(H)Cu(\mu\text{-}I)_2CuRe(H)(C_5H_5)_2$: A FIRST DIRECT PROOF OF THE FORMATION OF THE Cu(I)–Cu(I) BOND

**VITALY K. BEL'SKY**
The L. Ya. Karpov Physico-Chemical Research Institute, 107120, Moscow, U.S.S.R.

**VICTOR M. ISHCHENKO and BORIS M. BULYCHEV***
The Lomonosov Moscow State University, Chemistry Department, 117234, Moscow, U.S.S.R.

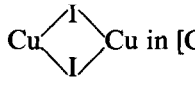
**and**

**GRIGORY L. SOLOVEICHIK**
The Institute of New Problems in Chemistry, U.S.S.R. Academy of Sciences, 142432, Chernogolovka, Moscow District, U.S.S.R.

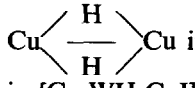
(*Received* 9 *March* 1983; *accepted* 23 *September* 1983)

**Abstract**—The structure of the bimetallic dimer complex $[(\eta^5\text{-}C_5H_5)_2Re(H)CuI]_2$ has been investigated. The crystals are monoclinic: $a = 16.070(4)$ Å, $b = 7.788(2)$Å, $c = 17.439(5)$ Å; $\beta = 96.62(2)°$; the space group $I2/a$; $z = 4$. The bond between rhenium and copper atoms (2.60 Å) is of the donor–acceptor type; dimerization occurs by the way of formation of the double bridge Cu–$I_2$–Cu and the direct inter-metal bond Cu–Cu(2.55 Å). The hydride hydrogen atom is the terminal one. The cyclopentadienyl rings form a bent sandwich with the angle between the ring centres and rhenium atom being equal to 158°. It is suggested that the Cu–Cu inter-metal bonding takes place on account of the transition of the non-bonding *d*-electrons of copper atoms to a high-spin state.

Monovalent copper halogenides form rather stable complexes with Lewis *d*-bases, viz. bis-cyclopentadienyl hydrides of molybdenum,[1–3] tungsten[4] and rhenium.[5] As investigations of the structure of bimetallic complexes between CuX and $Cp_2MH_2$, where X=Cl, I; $Cp = \eta^5\text{-}C_5H_5$; M=Mo, W[2,3] have shown, the nature of bonding between the copper atoms in the dimer molecules $[Cp_2MH_2CuX]_2$ is sensitive to the nature of the transition metal or halogen, that is, depends both on the basicity of $Cp_2MH_2$ and the acidity of CuX and can vary from the usual bridge bond



Cu in $[Cp_2MoH_2CuI]_2$[2] to the mixed bond



Cu in $[Cp_2MoH_2CuCl]_2$ and, perhaps, in $[Cp_2WH_2CuI]_2$.[3]

Since $Cp_2ReH$ is a Lewis $d^4$-base, one would expect that its reaction with CuI would yield a compound of a different structure type than the earlier investigated compounds formed by $d^2$-bases.

## EXPERIMENTAL

The compound of composition $Cp_2Re(H)CuI(I)$ was obtained by direct synthesis from $Cp_2ReH$ and copper(I) iodide in acetonitrile according to a procedure described elsewhere.[5] Brownish-coloured single crystals of I weakly susceptible to the attack of atmospheric oxygen were obtained in the form of tetragonal pyramids by slowly cooling its hot saturated solution in acetonitrile.

Intensity data of a $Cp_2Re(H)CuI$ single crystal sealed in a capillary were taken using a "Syntex P$\bar{1}$" diffractometer (Mo-$K_\alpha$-radiation, graphite monochromator) by scanning to $2\theta_{max} = 46°$. The crystals are monoclinic, $a = 16.070(4)$ Å, $b = 7.788(2)$ Å, $c = 17.439(5)$ Å, $\beta = 96.62(2)°$; $z = 4$ (for the dimeric unit); the space group is $I2/a$; $V = 2168$ Å$^3$; $\rho = 3.11$ g/cm$^3$. The total number of

*Author to whom correspondence should be addressed.

reflexions taken into account in the calculations was 1426 with $I > 3\sigma(I)$, and a correction for absorption was made ($\mu_{Mo} = 166.6\,cm^{-1}$).

The structure was solved by the heavy atom (Patterson synthesis) technique. Hydrogen atom coordinates in the cyclopentadienyl rings were calculated from geometric considerations. The structure was refined by the full-matrix least-squares method using anisotropic thermal parameters for non-hydrogen atoms. The final R-factor is 0.044. The structure of the complex $Cp_2Re(H)CuI$ is shown in Fig. 1.

## DESCRIPTION OF STRUCTURE AND DISCUSSION OF RESULTS

The crystal structure of **I** is built up of dimer molecules $[Cp_2Re(H)CuI]_2$ (Fig. 1) spaced by distances corresponding to the standard van der Waals contacts. The fragments $Cp_2Re(H)CuI$ are interconnected via the double bridge Cu–$I_2$–Cu and the metal-metal Cu–Cu bond. The resultant is a four-nucleus chain cluster Re-Cu-Cu-Re in which the Re–Cu–Cu angles are 140.5° (Table 1).

The fragment $Cp_2Re(H)Cu$ has a configuration which is standard for the bent-metal sandwiches $Cp_2ML_2$ with $\eta^5$-$C_5H_5$ groups.[6] Taking into account the difference in the atomic radii of Mo and Re (0.02 Å), the average Re–C bond length (2.24 Å) is comparable with that of the Mo–C bond in the complex $(Cp_2MoH_2)_2Cu(CuCl_2)$ (2.28 Å).[3]

The fragment $(\eta^5\text{-}C_5H_5)_2Re$ is in an eclipsed conformation and the average C–C distance is 1.44 Å and, considering the strong thermal vibrations of the atoms in the complex under study, is comparable with the counterparts in complexes of CuI and CuCl with $Cp_2MoH_2$ (1.40[2] and 1.41 Å[3], respectively). Cyclopentadienyl rings are planar. The angle between the centres of the $C_5H_5$-groups and the rhenium atom (158°) is much

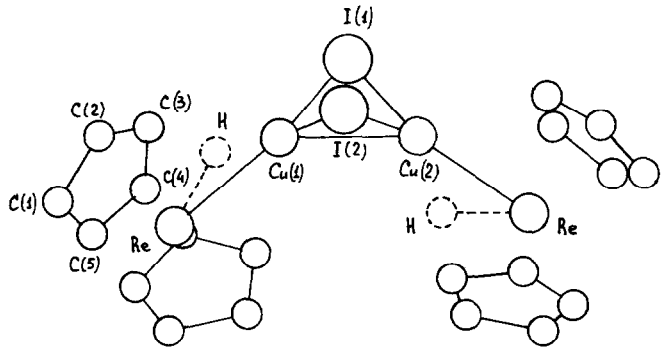



Fig. 1. The structure of the complex $[Cp_2Re(H)CuI]_2$.

Table 1. Main interatomic distances and valence angles in the $[Cp_2Re(H)CuI]_2$ molecule

| Distance | d, Å | Angle | ω, ° |
|---|---|---|---|
| Re - Cu | 2.599(3) | Re-Cu-I(1) | 134.04(12) |
| Cu - I(1) | 2.582(4) | Re-Cu-I(2) | 122.99(12) |
| Cu - I(2) | 2.745(3) | Cu(1)-Cu(2)-Re | 140.51(14) |
| Cu(1)-Cu(2) | 2.552(4) | Cu(1)-I-Cu(2) | 57.2(1) |
| Re - C (aver.) | 2.24 | I(1)-Cu-I(2) | 102.95(11) |
| C - C (aver.) | 1.44 | Cu(1)-Cu(2)-I(1) | 64.64(10) |
| I(1)···I(2) | 4.169(2) | Cu(1)-Cu(2)-I(2) | 58.20(10) |
| Cu ··· C(3) | 2.628(28) | Ctr*(1)-Cu(2)-I(2) | 96.7 |
| | | Ctr(2)-Re-Cu | 105.3 |
| | | Ctr(1)-Re-Ctr(2) | 158.0 |
| | | pl.[I(1)-Cu-I(2)]-[Re-Cu] | 91.0 |
| | | pl.[Ctr(1)-Re-Ctr(2)]-[Re-Cu] | 124.5 |

Ctr*—is the centre of the corresponding *cyclopentadienyl* ring.

larger than in a similar complex $[Cp_2MoH_2CuI]_2$ (141.3°)[2] which, in general is what one would expect, because the *d*-orbitals of metal are filled.[7]

It was not possible to locate the H atom bonded to the rhenium atom, although its existence in the molecule of I had been unambiguously proved by the NMR technique and reaction with carbon tetrachloride which yields chloroform[5] and, besides, follows from crystal chemistry considerations. In fact, a copper atom located in the bisector plane of the bent sandwich is directly bonded to the rhenium atom. The angle between the direction of the Re–Cu bond and the imaginary symmetry plane of the bent sandwich $Cp_2Re$ is 55.1° which is typical of $Cp_2ML_2$ molecules[6] and unambiguously demonstrates the presence in the molecule of I a second ligand—the hydrogen atom in our case.

The Re–Cu distance in I equal to 2.60 Å is 0.06 Å shorter than the Mo–Cu distance in the complex $(Cp_2MoH_2)_2Cu(CuCl_2)$ for which absence of a bond of the Mo–Cu type or, at any rate, an insignificant contribution of this type of bond in the formation of a bimetallic complex has been postulated.[3] No published data for the Re–Cu bond lengths are available, but the distance observed in I is close to that predictable for a single bond (2.65 Å). Since, according to the NMR data, the hydride atom is a terminal one,[5] i.e. no bridge bond Re–H–Cu is formed, one may assume with a high degree of certainty that the Re–Cu bond is a donor–acceptor metal–metal bond.

The question of the nature of the very unusual coordination polyhedron of the copper atom in the molecule of I is of considerable interest. Apart from the rhenium atom donating an electron pair, the coordination sphere of the copper atom also includes two iodine atoms. They form a slightly assymetrical double iodine bridge which bonds two copper atoms as in the case of CuI complexes with nitrogen-containing Lewis bases[8] and $Cp_2MoH_2$.[2] However, in the molecule of I, the $CuI_2Cu$ unit is folded along the I–I vector (Fig. 1), whereas it is planar in the above-mentioned complexes of CuI.[2,8] This tends to decrease the CuICu angles (by 18.3° as compared with the $CuI_2Cu$ unit in $[Cp_2MoH_2CuI]_2$[2] but does not affect the ICuI angle (102.9° and 104.6°,[2] respectively). The Cu–Cu distance is thereby decreased from 3.33 Å in $[Cp_2MoH_2CuI]_2$[2] to 2.55 Å in $[Cp_2Re(H)CuI]_2$. The latter value almost coincides with the sum of the covalent radii of two copper atoms (2.56 Å).[9] It should be stressed that unlike all multi-nuclear copper(I) complexes with a short Cu–Cu distance described in the literature,[10] in the molecule of I the disposition of the bridge ligands—iodine atoms—is such that a closer distance between copper atoms is unnecessary. Therefore, the short Cu–Cu distance in I may only be attributed to a direct chemical bond Cu(I)–Cu(I).

It is known that in many copper(I) complex associates the Cu–Cu distance is close to or even smaller than the sum of covalent radii (2.42 Å in $(CuCH_2SiMe_3)_4$[11] and $(CuCN–NH_3)_n$).[12] For this reason the question of whether or not the direct copper–copper bond is possible in these compounds has been much discussed in the literature. Most authors assume that there is no such thing as Cu–Cu bond and the short Cu–Cu distance is due only to the steric requirements of the bridge ligands themselves. This opinion is based on classical precepts, according to which a chemical bond between metal atoms in an electronic configuration of the $d^{10}$-type, e.g. in complexes of Cu(I) or Pt(O), is impossible[10] (although this suggestion does not explain the existence of Pt(O) carbonyl clusters, e.g. $Pt_3(CO)_3R_n$, $n = 3, 4$[13]). These assumptions are corroborated by MO studies of the clusters $Cu_8S_{12}^{4-}$ that have shown that electron density is almost entirely concentrated on the Cu–S bonds and is almost absent between the copper atoms.[14] Using the extended Hückel technique which takes into account only the *d*-orbitals it has been shown that the populated $d^{10}$-shells are subject to repulsion in systems of $Cu_n^{n+}$ $(n = 2–4)$[15] or $Pt_2$ (in $[Pt(Bu^t)_2P(CH_2)_3P(Bu^t)_2]_2$[16]). However, the mixing of *s*- and *p*-functions with *d*-functions results in a relatively weak bonding of metal atoms.[15,16] Considering that formally (i.e., without taking into account the direct Cu–Cu bond) the copper atoms in the complex $[Cp_2Re(H)CuI]_2$ have a 16-electron environment, one may assume that a strong Lewis base, such as $Cp_2ReH$, causes unpairing of one pair of *d*-electrons of copper atom and their transition to the lower 4*s*- and 4*p*-orbitals of this atom which will then be transferred to a high-spin state. The rather low value of *ds*-hybridization energy[17] is consistent with this hypothesis. It is the subsequent pairing of these electrons which is responsible for the formation of the metal–metal bond between copper atoms which formally produces the 18-electron environment of the copper atom. However the more simple way of interaction between the filled *d*-orbitals of one of the copper atoms with vacant *d*-orbitals of another ( and vice versa) may not be excluded. It leads also to 18-electron environment of each copper atom. Nevertheless it seems to us that the nature of this interaction is not clear so far and one may need quantum chemical calculations. Since normally electron pairing and or formation of a metal–metal bond results in diamagnetism of the binuclear complexes, one

might expect that, like other copper(I) compounds, the complex I should be diamagnetic.

Thus the X-ray analysis of the complex compound $[Cp_2Re(H)CuI]_2$ has shown with certainty the existence of the direct Cu–Cu bond. This supports the assumption of the authors of the review[10] that the metal–metal bond makes a considerable contribution into the bonding strength in multi-nuclear organometallic copper(I) complexes.

## REFERENCES


1. A. V. Aripovsky, B. M. Bulychev and V. B. Polyakova, *Zh. Neorg. Khimii* 1981, **26**, 2722.
2. V. K. Bel'sky, E. B. Fomicheva, A. V. Aripovsky and B. M. Bulychev, *Dokl. AN SSSR* 1981, **258**, 1137.
3. E. B. Lobkovsky, A. V. Aripovsky, V. K. Bel'sky and B. M. Bulychev, *Koordin. Khimiya* 1982, **8**, 104.
4. A. V. Aripovsky, B. M. Bulychev, L. B. Krivdin and V. B. Polyakova, *Zh. Neorg. Khimii* 1981, **26**, 2109.
5. V. M. Ishchenko, B. M. Bulychev and G. L. Soloveichik, *Koordin. Khimiya* 1983, **9**, 622.
6. K. Prout, T. S. Kameron, R. A. Forder and S. R. Critchley, *Acta Cryst.* 1974, **B30**, 2290.
7. J. W. Lauer and R. Hoffmann, *J. Am. Chem. Soc.* 1976, **98**, 1729.
8. R. G. Wilkins and A. R. Burkin, *J. Chem. Soc.* 1950, 127.
9. S. A. Semiletov, *Kristallografiya* 1976, **21**, 752.
10. A. Camus, N. Marsich, G. Nardin and L. Randaccio, *Inorg. Chim. Acta* 1977, **23**, 131.
11. J. A. Jarvis, B. T. Kilbourn, R. Pearce and M. F. Lappert, *J. Chem. Soc. Chem. Commun.* 1973, 475.
12. D. T. Cromer, A. C. Larson and R. B. Roof, *Acta Cryst.* 1965, **19**, 192.
13. J. Chatt and P. Chini, *J. Chem. Soc. A* 1970, 1538.
14. A. Avdeef and J. P. Fackler, *Inorg. Chem.* 1978, **17**, 2182.
15. P. K. Mehrotra and R. Hoffmann, *Inorg. Chem.* 1978, 17, 2187.
16. A. Dedin and R. Hoffmann, *J. Am. Chem. Soc.* 1978, **100**, 2074.
17. C. Day and J. Selbin, *Theoretical Inorganical Chemistry*, p. 446. Moscow, "Khimiya" (1976).

*Polyhedron* Vol. 3, No. 6, pp. 753–755, 1984
Printed in Great Britain.

0277-5387/84 $3.00 + .00
© 1984 Pergamon Press Ltd.

# COMMUNICATION

## SYNTHESIS AND CRYSTAL STRUCTURE OF [N,N′-BIS(2,3,5,6-TETRAFLUOROPHENYL)-ETHANE-1,2-DIAMINATO(2-)]DIPYRIDINEPLATINUM(II)

**G. B. DEACON*, B. M. GATEHOUSE, I. L. GRAYSON and M. C. NESBIT**
Chemistry Department, Monash University, Clayton, Victoria 3168, Australia

(*Received* 3 *October* 1983; *accepted* 21 *November* 1983)

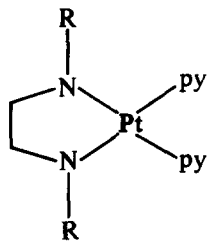
**Abstract**—The reaction of $PtCl_2en$ (en = ethane-1,2-diamine) with $TlO_2CC_6F_5$ in boiling pyridine unexpectedly yielded a polyfluorophenyl-stabilized ethane-1,2-diaminatoplatinum(II) complex, $Pt[N(p\text{-}HC_6F_4)CH_2]_2(py)_2$, **1a**, the structure of which has been established by X-ray crystallography.

Decarboxylation reactions between $PtCl_2L_2$ [e.g. $L_2$ = 2,2′-bipyridyl(bpy) or *trans*-(pyridine)$_2$] complexes and thallous polyfluorobenzoates in boiling pyridine yield $R_2PtL_2$ (e.g. R = $C_6F_5$ or *p*-$HC_6F_4$) and $RPtClL_2$ organometallics,[1] e.g. $PtCl_2L_2 + 2TlO_2CR \rightarrow R_2PtL_2 + 2CO_2 + 2TlCl$. We now report that the corresponding reaction of $PtCl_2en$ (en = ethane-1,2-diamine) with thallous pentafluorobenzoate does not give $(C_6F_5)_2Pten$ or $C_6F_5PtClen$, but surprisingly an N-(2,3,5,6-tetrafluorophenyl) substituted ethane-1,2-diaminatoplatinum(II) complex is obtained.

$$PtCl_2en + 2TlO_2CC_6F_5 + 4py \rightarrow \mathbf{1a} + 2TlCl + 2CO_2 + 2pyHF.$$

Reaction of stoichiometric amounts of the reagents in boiling pyridine for 60 min under nitrogen gave carbon dioxide (95%). Evaporation of the reaction mixture to dryness, extraction with acetone, filtration to remove thallous chloride, and crystallization from acetone/petroleum ether gave **1a** as the air-stable, yellow, 1 : 1 acetone solvate in 37% yield, m.p. 170–171° (dec.)†. The structure (Fig. 1) was established by X-ray crystallography.

*Crystal data* **1a**.$Me_2CO$: $C_{27}H_{24}N_4OF_8Pt$,




**1a** R = *p*−$HC_6F_4$
**1b** R = H
**1c** R = $C_6F_5$

M = 767.59, monoclinic, $a$ = 19.044(8), $b$ = 14.006(7), $c$ = 11.223(6) Å, $\beta$ = 110.73(5)°, $U$ = 2800Å$^3$. $D_m$(flotation) = 1.82(1), $D_c$ = 1.82 g cm$^{-3}$ for $z$ = 4. Mo$K_\alpha$, $\lambda$ = 0.7107 Å, $\mu$ = 48.7 cm$^{-1}$, $F(000)$ = 1487.64, 298 K. Space group C2/c or Cc, the former confirmed by successful refinement. The molecule possesses a 2-fold axis of symmetry. Tabular crystal (0.20 × 0.06 × 0.11 mm), Philips PW1100 diffractometer (graphite monochromator); cell parameters from 25 reflections $\theta$ 8–15°; absorption correction applied, transmission maximum 0.7449, minimum 0.5926. Sin $\theta/\lambda$ max. 0.704, $\pm hkl$, ± 23, 18, 14. Three standard reflections (2hr intervals) showed no significant intensity variation. 4274 reflections measured ($\omega$-scans, scan width ± 1.5° in 2$\theta$ + dispersion allowance), 4083 unique reflections ($R_{int}$ 0.038) with 2806 unobserved ($I \geqslant 3\sigma(I)$). Structure solution by Patterson and Fourier methods, full-matrix least

*Author to whom correspondence should be addressed.

†New complexes **1a**.$Me_2CO$ and **1c** were obtained analytically pure with satisfactory 1H and 19F NMR spectra.

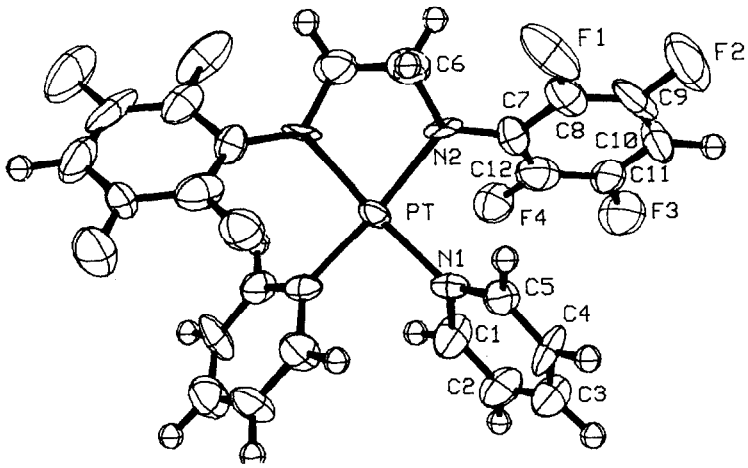



Fig. 1. Structure of $C_{24}H_{18}N_4F_8Pt.C_2H_6O$ (1a.$Me_2CO$)—Acetone not located (see text). Selected bond lengths (Å) and angles (°) are:

| | | | |
|---|---|---|---|
| Pt–N(1) | 1.98(2) | N(1)–Pt–N(1) | 90(1) |
| Pt–N(2) | 2.08(2) | N(1)–Pt–N(2) | 95(1) |
| N(2)–C(6) | 1.45(3) | N(2)–Pt–N(2) | 80(1) |
| N(2)–C(7) | 1.35(2) | C(6)–N(2)–C(7) | 126(2) |
| C–N(py) | 1.36–1.40 | C(6)–N(2)–Pt | 109(1) |
| C–C(py) | 1.31–1.37 | C(7)–N(2)–Pt | 123(1) |
| C–C(arom) | 1.34–1.42 | C(6)–C(6)–N(2) | 116(2) |
| C–F(arom) | 1.33–1.36 | | |

squares refinement (F magnitudes), 175 parameters refined (all non-hydrogen atoms anisotropic), $R$ 0.054, $wR$ 0.047 ($w = 1/\sigma^2(F)$). Maximum shift to E.S.D. ($U_{12}$ of N(1)) was 0.026; maximum and minimum peak heights in final difference Fourier synthesis were $2eÅ^{-3}$ and $1eÅ^{-3}$ respectively in vicinity of disordered acetone molecule positions. Atomic scattering factors (neutral atoms) from Ref. 2. Programs used were SHELX[3] and ORTEP[4]; data reduction methods were as described previously[5].†

The molecule is illustrated in the figure with the numbering scheme used and selected bond lengths. The disordered acetone molecule, whose presence was inferred from analytical, spectroscopic [$\nu_{CO}$: 1709 $cm^{-1}$], and density measurements was not located. Peaks in the difference Fourier synthesis implied that it was situated about the centre of symmetry at 1/2 0 1/2. A cavity of radius 3.372 Å exists around 1/2 0 1/2 providing ample space for an acetone molecule in any orientation.

It is of interest to note that Pt–N(2) (anionic) is longer than Pt–N(1) (neutral) and this may be attributed to the electron withdrawing character of the polyfluorophenyl substituent. This is supported by the ($p$-$HC_6F_4$)–N distance which is closer to that of an aromatic C=N distance than a single C–N bond.

The reaction path to **1a** is considered to involve formation of $[Pten(py)_2](O_2CC_6F_5)_2$ **2** by substitution and metathesis,

$$PtCl_2en + 2py + 2TlO_2CC_6F_5 \rightarrow \mathbf{2} + 2TlCl \quad (1)$$

followed by decarboxylation and proton abstraction by the highly carbanionic $C_6F_5$ groups giving pentafluorobenzene and the ethane-1,2-diaminatoplatinum(II) intermediate **1b**,

$$\mathbf{2} \rightarrow \mathbf{1b} + 2C_6F_5H + 2CO_2 \quad (2)$$

and then nucleophilic attack by the secondary amine nitrogens of **1b** on pentafluorobenzene.

$$\mathbf{1b} + 2C_6F_5H + 2py \rightarrow \mathbf{1a} + 2pyHF. \quad (3)$$

Support for this path is provided by the following observations: The complex $[Pten(py)_2]Cl_2$, obtained from $PtCl_2en$ in boiling aqueous pyridine,[6], reacts with thallous pentafluorobenzoate in pyridine at room temperature to give **2**, which yields **1a** in

†Atomic and thermal parameters, observed and calculated structures together with a list of bond lengths and angles have been deposited with the Editor, from whom copies are available on request. Atomic Co-ordinates have also been deposited with the Cambridge Crystallographic Data Centre.

boiling pyridine [reactions (2) and (3)]. Monitoring reaction (1) by $^{19}F$ NMR spectroscopy reveals the presence of pentafluorobenzene in the reaction mixture as required by reactions (2) and (3). Reaction of $PtCl_2en$ with thallous 2,3,5,6-tetrafluorobenzoate in boiling pyridine yields 1,2,4,5-tetrafluorobenzene, which is much less reactive than $C_6F_5H$ to nucleophilic attack,[7] and an air-sensitive intermediate, plausibly **1b**, which reacts with added pentafluorobenzene and hexafluorobenzene to give **1a** and **1c** respectively.

The present reactions provide a convenient synthesis of air-stable ethane-1,2-diaminatoplatinum-(II) complexes, which are stabilised by polyfluorophenyl substitution on nitrogen. Previous ethane-1,2-diaminatoplatinum(II) complexes, e.g. $Pt(NHCH_2)_2bpy$,[8] have been prepared under forcing conditions, viz. deprotonation of ethane-1,2-diamineplatinum(II) complexes by potassium amide in liquid ammonia, and are highly moisture sensitive (e.g. Refs. 8 and 9). Analogous decarboxylation reactions may provide a route to stabilised diorganoamido derivatives of other precious metals.

*Acknowledgement*—We are grateful for assistance from the Australian Research Grants Scheme, for C.P.R.A. assistance to I.L.G. and an M.G.S. for M.C.N.

## REFERENCES

1. G. B. Deacon and I. L. Grayson, *Trans. Met. Chem.* 1982, **7**, 97.
2. D. T. Cromer and J. T. Waber; D. T. Cromer and J. A. Ibers, In *International Tables for X-ray Crystallography*, Vol. IV. Kynoch Press, Birmingham (1974).
3. G. M. Sheldrick, "SHELX-76" (A Program for Crystal Structure Determination). Cambridge University (1976).
4. C. K. Johnson, "ORTEP". Report ORNL-3794. Oak Ridge National Laboratory, Tennessee.
5. B. M. Gatehouse, T. Negas and R. S. Roth, *J. Solid State Chem.* 1976, **18**, 1.
6. *Gmelin Handbook of Inorganic Chemistry*, Main Series, Vol. 68D, p. 173. Verlag Chemie, Weinheim (1957).
7. R. D. Chambers, W. K. R. Musgrave, J. S. Waterhouse, D. L. H. Williams, J. Burdon, W. B. Hollyhead and J. C. Tatlow, *J. Chem. Soc., Chem. Commun.* 1974, 239.
8. G. W. Watt and D. G. Upchurch, *J. Am. Chem. Soc.* 1968, **90**, 914.
9. G. W. Watt and J. E. Cuddeback, *Inorg. Chem.* 1971, **10**, 947.

*Polyhedron* Vol. 3, No. 6, pp. 757–758, 1984
Printed in Great Britain.

0277–5387/84 $3.00 + .00
© 1984 Pergamon Press Ltd.

# COMMUNICATION

## SYNTHESIS OF *cis*-$(Me_3Sn)_2Fe(CO)_4$ BY REACTION OF $(Me_3Sn)_3Sb$ WITH $Fe_2(CO)_9$. FORMATION OF $(Me_3E)_3SbFe(CO)_4$ (E = Si, Ge)

**H. J. BREUNIG**
University Bremen FB 2, Leobener Straße, D 2800 Bremen 33,
Federal Republic of Germany

(*Received* 10 *October* 1983; *accepted* 28 *November* 1983)

**Abstract**—$(Me_3Sn)_3Sb$ and $Fe_2(CO)_9$ reacted to form $(Me_3Sn)_2Fe(CO)_4$ in 79% yield. From $(Me_3E)_3Sb$(E = Si or Ge) and $Fe_2(CO)_9$ the complexes $(Me_3E)_3SbFe(CO)_4$ were obtained

Reactions of tris(trimethylsilyl-, -germyl-, and -stannyl)- stibines with oxygen,[1] alkylhalides,[2] and halogens,[3] result in the transfer of the organoelement (IVB) substituents to the non-metal atoms. In contrast the organoelement(IVB)stibine molecule remains intact, when it reacts with carbonyl complexes of the metals Cr, Mo, W, Ni, and coordination compounds of the type $(Me_3E)_3Sb$-$M(CO)_n$ (E = Si, Ge, Sn; M = Cr, Mo, W; $n = 5$; M = Ni, $n = 3$)[4] are obtained.

We report now the first example of a organoelement(IVB) group migration from antimony to a transition metal.

Equimolar amounts of $(Me_3Sn)_3Sb$ and $Fe_2(CO)_9$ react in *n*-pentane at room temperature to form *cis*-$(Me_3Sn)_2Fe(CO)_4$[5] in 80% yield, together with $Fe(CO)_5$ and a dark precipitate, which contains antimony.

The first step of this reaction, where $(Me_3Sn)_3Sb$ serves as stannylating agent, is presumably the formation of $(Me_3Sn)_3SbFe(CO)_4$. This assumption is supported by the reactions of $(Me_3Si)_3Sb$ and $(Me_3Ge)_3Sb$ with $Fe_2(CO)_9$, which result in the formation of the derivatives $(Me_3E)_3SbFe(CO)_4$ (E = Si or Ge) as colourless crystals, soluble in common organic solvents. These iron complexes are thermally much less stable, than analogous compounds of VI A metals or Ni.[4] They decompose even at −25°C with formation of dark solids and they ignite spontaneously in the air. Structural evidence is based mainly on the ir spectra The frequencies in the $\nu$(CO) region are typical for the axial isomers of $LFe(CO)_4$ complexes.[6] The observation of the characteristic absorptions of the $(Me_3E)_3Sb$ skeleton including the $E_3Sb$ valence vibrations proves, that the ligands are coordinated without fragmentation. The $^1$H-NMR spectra show the expected singlet signal for each complex at positions which, as in other organoelement-stibine carbonyl complexes,[4] are close to the resonance frequencies of the free ligands.

### EXPERIMENTAL

Reactions are carried out in Ar atmosphere. *cis*-Tetracarbonylbis(trimethylstannyl)iron 6.13 g (10 mmol) $(Me_3Sn)_3Sb$ and 3.64 g (10 mmol) $Fe_2(CO)_9$ were stirred in 50 cm$^3$ *n*-pentane for 12 hr. After filtration the solvent was removed *in vacuo* leaving 3.6 g of $(Me_3Sn)_2Fe(CO)_4$. $^1$H-NMR ($C_6H_6$): $\delta = 0.45$ ppm, $^1J_{HC}$ 117/119$_{Sn}$ = 50 Hz. IR (Nujol): 2056, 1996, 1985, 1974 cm$^{-1}$ (Lit.[7]: identical data). MS (EI, 30 eV, 25°C) m/z (r.i.%): 481 (10) $M^+ - Me$, 453 (2) $M^+ - Me - CO$, 452 (2), 397 (2), 369 (2), 318 (100)$M^+ - Me_4Sn$, 290 (30), 262 (8), 234 (3), 206 (7), 165 (3) $Me_3Sn$; only the most intense signal of each ion is given, isotopic abundances agreed with those expected. $C_{10}H_{18}FeO_4Sn_2$ (495.5). Found: C, 24.24 (24.22); H, 3.59 (3.66)%.

Tetracarbonyl(tristrimethylsilylstibine)iron 3.4 g (10 mmol) $(Me_3Si)_3Sb$ and 3.6 g (10 mmol) $Fe_2(CO)_9$ were stirred in 50 cm$^3$ *n*-pentane for 12 hr. Work up as described above and recrystallization at −25°C from pentane gives 1.5 g (30%) of $(Me_3Si)_3SbFe(CO)_4$. $^1$H-NMR ($C_6H_6$) $\delta$ = 0.26 ppm (S). IR (Nujol): 2040 st, 1945 w, 1910 m $\nu$(CO), 318 m $\nu Si_3Sb$, cm$^{-1}$.

Tetracarbonyl(tristrimethylgermylstibine) iron 0.7 g (1.5 mmol) $(Me_3Ge)_3Sb$ and 0.5 g (1.5 mmol) $Fe_2(CO)_9$ were stirred in 20 cm$^3$ *n*-pentane for 12 hr. Filtration and crystallization gives 0.15 g (15%) $(Me_3Ge)_3SbFe(CO)_4$. $^1$H-NMR ($C_6H_6$)

$\delta = 0.35$ ppm (S). IR (Nujol): 2040 st, 1950 w, 1915 m $\nu$(CO), 230 w $\nu Ge_3Sb$; $cm^{-1}$.

## REFERENCES


1. H. Schumann, *Angew. Chem.* 1969, **81**, 970.
2. H. J. Breunig, *Z. Naturforsch. B.* 1978 **33**, 990.
3. H. J. Breunig and V. Breunig-Lyriti, *Z. Naturforsch. B* 1979, **34**, 926.
4. H. Schumann, H. J. Breunig and U. Frank, *J. Organometal. Chem.* 1973, **60**, 279. H. Schumann and H. J. Breunig, *J. Organometal. Chem.* 1974, **76**, 225. H. J. Breunig and W. Fichtner, *J. Organometal. Chem.* 1981, **222**, 97.
5. *Gmelin Handbuch der Anorganischem Chemie, Eisen-Organische Verbindungen* (Edited by U. Krüerke), p. 134. Springer-Verlag, Berlin (1978).
6. P. S. Braterman, *Metal Carbonyl Spectra.* Academic Press, London, (1975).
7. E. W. Abel, S. Moorhouse, *Inorg. Nucl. Chem. Lett.* 1971, **7**, 905.

*Polyhedron* Vol. 3, No. 6, pp. 759–760, 1984
Printed in Great Britain.

0277-5387/84 $3.00 + .00
Pergamon Press Ltd.

# COMMUNICATION

## A GENERAL SYNTHESIS FOR DITUNGSTEN TETRACARBOXYLATES. PREPARATION OF W–W QUADRUPLE BONDS BY REDUCTIVE-ELIMINATION (ALKYL GROUP DISPROPORTIONATION) FROM 1,2-DIETHYL COMPOUNDS WITH W–W TRIPLE BONDS

**M. H. CHISHOLM,* H. T. CHIU and J. C. HUFFMAN**
Department of Chemistry and Molecular Structure Center, Indiana University, Bloomington, IN 47405, U.S.A.

(*Received* 14 *November* 1983; *accepted* 6 *December* 1983)

**Abstract**—A general high yield synthesis for $W_2(O_2CR)_4$ compounds is proposed based on eqn (1), wherein a W–W triple bond is converted to a quadruple bond, and this has been established for R=Me, Et and *t*-Bu.

$$W_2Et_2(NMe_2)_4 + 4RCOOCOR \rightarrow W_2(O_2CR)_4 + 4RCONMe_2 + C_2H_4 + C_2H_6 \quad (1)$$

The search for compounds containing W–W quadruple bonds, particularly ditungsten tetracarboxylates, is one of the fascinating stories in the development of the chemistry of compounds containing multiple bonds between metal atoms.[1,2] At this time there are two reports of the preparation and characterization of $W_2(O_2CR)_4$ compounds. Sattelberger and McLaughlin[3] reported in 1981 that reduction of $W_2Cl_6(THF)_4$ with 2 equivalents of sodium amalgam in THF at −20°C, followed by addition of sodium trifluoroacetate (4 equiv) gave, upon work up, $W_2(O_2CCF_3)_4$ in 20% yield based on tungsten. More recently Cotton and Wang[4] reported a higher yield synthesis (*ca.* 55% based on W) for the benzoate, $W_2(O_2CPh)_4.2THF$, from Na/Hg reduction of $WCl_4$ in THF followed by treatment with sodium benzoate. We wish to report a general high yield synthesis for $W_2(O_2CR)_4$ (M≡M) compounds based on reductive elimination (alkyl group disproportionation) from W≡W containing compounds.

Hydrocarbon solutions of 1,2-$W_2Et_2(NMe_2)_4$[5] react quickly at room temperature with acid anhydrides RCOOCOR, where R=Me, Et and *t*-Bu, according to eqn (1). These reactions appear quantitative when they are carried out in sealed NMR tubes and followed by $^1H$ NMR spectroscopy and, by crystallization, have given yields in the range

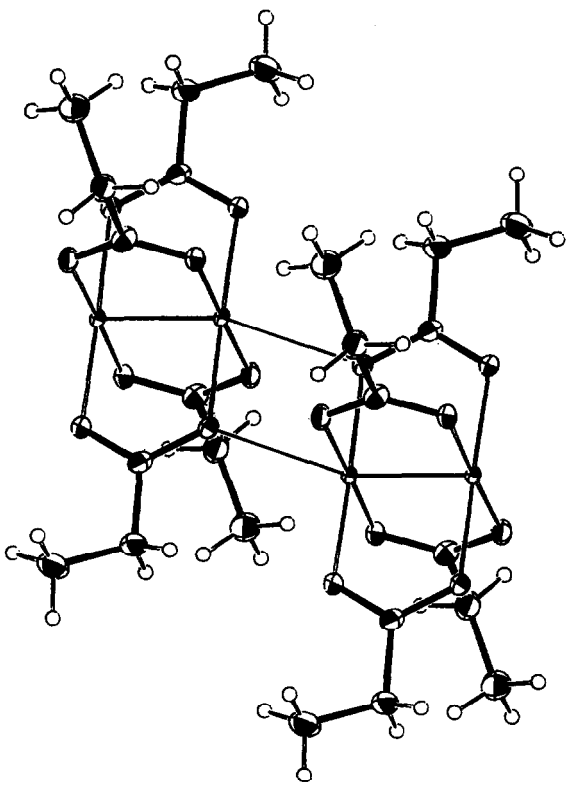


Fig. 1. An ORTEP view of the centrosymmetric $W_2(O_2CEt)_4$ molecule showing the connectivity in the infinite chain $[W_2(O_2CEt)_4]_n$. Pertinent distances (Å) and angles (°) (averaged where appropriate), are W–W = 2.189(1), W–O = 2.08(2), W—O = 2.665(4), W–W–O = 91(1), W–W—O = 161.6(1).

*Author to whom correspondence should be addressed.

40–65%. In the absence of oxygen donor solvents, the tetracarboxylates are isolated either as weakly ligated polymers $[W_2(O_2CR)_4]_n$, where R=Me or Et,[6] as shown in Fig. 1, or as the $RCONMe_2$ adduct $W_2(O_2C\text{-}t\text{-}Bu)_4.2t\text{-}BuCONMe_2$, by crystallization from benzene or hexane. These new bright-yellow, crystalline, volatile, air-sensitive compounds appear analogous to the two previously reported related compounds. An extension of eqn (1) to include other R groups seems obvious.

$$W_2Et_2(NMe_2)_4 + 4RCOOCOR \rightarrow W_2(O_2CR)_4 + 4RCONMe_2 + C_2H_6 + C_2H_4. \quad (1)$$

The present finding is of interest and worthy of note because it reveals that by appropriate synthetic strategy W–W triple bonds can be converted to W–W quadruple bonds.[7] This is the first observation of this transformation.

*Acknowledgement*—We thank the Office of Naval Research and the Wrubel Computing Center for support.

†Full details of this structure analysis including all relevant tables have been deposited as supplementary data with the Editor, from whom copies are available on request. Atomic co-ordinates have also been deposited with the Cambridge Crystallographic Data Centre.

## REFERENCES

1. F. A. Cotton and R. A. Walton, *Multiple Bonds Between Metal Atoms*. Wiley, New York (1982).
2. F. A. Cotton, *Chem. Soc. Rev.* 1983, **12**, 35.
3. A. P. Sattelberger, K. W. McLaughlin and J. C. Huffman, *J. Am. Chem. Soc.* 1981, **103**, 2880.
4. F. A. Cotton and W. Wang, *Inorg. Chem.* 1982, **21**, 3860.
5. M. H. Chisholm, D. A. Haitko and J. C. Huffman, *J. Am. Chem. Soc.* 1981, **103**, 4046.
6. Crystal data for $W_2(O_2CEt)_4$ at $-160°C$: $a = 9.377(2)$ Å, $b = 8.271(2)$ Å, $c = 5.527(1)$ Å, $\alpha = 102.49°$; $\beta = 84.61(1)°$; $\gamma = 89.45(2)$, $Z = 1$, $d_{calc} = 2.631$ gcm$^{-3}$ and space group $P\bar{1}$. Data collection was performed using standard moving crystal-moving detector techniques (Mo$K\alpha$ $6° < 2\theta < 50°$. Of 1477 unique intensities, 1464 having $F > 2.33\sigma(F)$ were used in the refinement. The W atom position was located in a Patterson and all remaining atoms, including H atoms, were located in the Fourier synthesis. A final difference Fourier was featureless, the largest peak being 0.83e/Å$^3$, located near the W position. Final residuals are $R(F) = 0.016$ and $R_w(F) = 0.015$.†
7. Reactions between $W_2Et_2(NMe_2)_4$ and each of $CO_2$ and ArNNNHAr do not appear to parallel reactions wherein Mo–Mo triple bonds are converted to Mo–Mo quadruple bonds. These reactions are under continuing investigation: M. J. Chetcuti, M. H. Chisholm, K. Folting, D. A. Haitko and J. C. Huffman, *J. Am. Chem. Soc.* 1982, **104**, 2138.

*Polyhedron* Vol. 3, No. 6, pp. 761–762, 1984
Printed in Great Britain.

0277–5387/84/$3.00 + .00
Pergamon Press Ltd.

# COMMUNICATION

## PLUTONIUM UNIQUENESS

G. L. Silver

Monsanto Research Corp., Mound Plant*, Miamisburg, Ohio 45342

(Received 11 January 1984; accepted 2 March 1984)

Abstract - A standard is suggested against which the putative uniqueness of plutonium may be tested.

It is a common folklore that plutonium is unique among the chemical elements because its four common oxidation states can coexist in the same solution.[1] Whether this putative uniqueness appears only during transit to equilibrium,[2] or only at equilibrium, or all of the time, is not generally made clear. But while the folklore may contain some truth, it cannot be put to test until some measure of "uniqueness" is agreed upon so that quantitative comparisons are possible. One way of measuring uniqueness is as the magnitude of the product of the mole fractions of the element at equilibrium. A "coexistence index" can be defined as

$$\text{C.I.} = (P^P) \prod_{i=1}^{P} [OX_i] \tag{1}$$

in which "P" is the number of different forms of the element being considered, and $\prod [OX_i]$ represents the product of these mole fractions. The term $P^P$ normalizes the C.I. so that its value is unity when all P mole fractions are equal. Arbitrarily inserting braces into the C.I. for plutonium (P = 4) yields.

$$\text{C.I.} = 256 \left\{[Pu^{3+}][PuO_2^{2+}]\right\} \left\{[Pu^{4+}][PuO_2^{+}]\right\} \tag{2}$$

The C.I. is maximized when the quantities in braces are maximized.

For plutonium, Equation (3) is always maintained at equilibrium, and is nearly maintained even in some nonequilibrium circumstances.[2]

$$K_2 = \frac{[Pu^{3+}][PuO_2^{2+}]}{[Pu^{4+}][PuO_2^{+}]} \tag{3}$$

If the numerator of Equation (3) is maximized, then the denominator is also maximized, by virtue of their ratio being the constant $K_2$. Therefore maximization of the product $[Pu^{3+}][PuO_2^{2+}]$ alone is sufficient to maximize the C.I. This product is

$$\left\{\frac{K_2^2 H^4 [PuO_2^{+}]}{K_1 M^2}\right\} \left\{M[PuO_2^{+}]\right\} = F(M,H) \tag{4}$$

in which $K_1$ is also an equilibrium constant, H is the acidity in moles per cubic decimeter (molar, M, units), and M is the equilibrium ratio $[PuO_2^{2+}]/[PuO_2^{+}]$. The expression for $[PuO_2^{+}]$ is given as Equation (1) in Reference 3.

The coexistence index is maximized when Equations (5) and (6) are simultaneously satisfied

$$\frac{\partial F}{\partial M} = 0; \quad \frac{\partial F}{\partial H} = 0 \qquad (5;6)$$

Solving these equations yields $M = \sqrt{K_2}$ and $H = 0.118M$. (This calculation has neglected all forms of complexation, including hydrolysis. The assumption of unity for all values of the alpha coefficients in the C.I. is arbitrary. It seems reasonable because any desired value of the C.I. ($\leq 1.0$) can be obtained if selective complexation is permitted.[4-6] This assumption does not imply that the alpha coefficients are unity in the solution, however.) At these values of M and H, the calculated fractions of $Pu^{3+}$ and $PuO_2^{2+}$ are both about 0.392, and the fractions of $Pu^{4+}$ and $PuO_2^{+}$ are both about 0.108. The oxidation number of the uncomplexed plutonium is therefore 4.5 when the C.I. is maximized, and its value at maximum is about 0.458. This value is much larger than the maximum values of the C.I. for uranium ($\sim 10^{-11}$) and neptunium ($\sim 10^{-16}$). But whether plutonium has the highest value of the C.I. of all the elements has not been settled, and it should be pointed out that one of the halogens, sulfur, or nitrogen may have a C.I. value greater than the maximum C.I. value for plutonium. The values of the C.I. in metastable ("false") equilibrium should also be considered; it is to be remembered that plutonium itself is metastable with respect to helium and lead.

## REFERENCES

1. J. M. Cleveland, The Chemistry of Plutonium, Gordon and Breach Science Publishers, New York, 1970, p. 21.
2. G. L. Silver, Polyhedron (1983), 2, 835-838.
3. G. L. Silver, J. Inorg, Nucl. Chem. (1973), 35, 1369-1372.
4. G. L. Silver, J. Inorg. Nucl. Chem. (1972), 34, 1857-1860.
5. R. A. Penneman in Plutonium Chemistry, W. T. Carnall and G. R. Choppin (Eds.), A.C.S. Symposium Series 216, American Chemical Society, Washington, D.C., 1983, pp. 453-458.
6. G. L. Silver, Marine Chemistry (1983), 12, 91-96.

*Mound Plant is operated by Monsanto Research Corporation for the U. S. Department of Energy under contract No. DE-AC04-76-DP00053.

*Polyhedron* Vol. 3, No. 6, p. 763, 1984
Printed in Great Britain.

0277-5387/84 $3.00 + .00
Pergamon Press Ltd.

# BOOK REVIEW

**Gmelin Handbuch der Anorganischen Chemie. Technetium Supplement Volume 2. Metal, Alloys, Compounds and the Chemistry in Solution.** This supplementary volume covering the literature up to the end of 1981 contains a systematic description of the metal technetium, its alloys and its compounds. Additionally, there is a large special chapter devoted to the solution chemistry of technetium. In keeping with current Gmelin policy, the volume is entirely written in English.

There is only limited data available on the physical properties of Tc metal and associated alloys. However, with the increasing use of nuclear reactors with higher burn-up of fuel, then the properties of the so-called "dissolver insolubles", which are fission product alloys, will become increasingly important.

The major portion of the volume deals with the compounds of technetium and the solution chemistry. In recent years there has been an upsurge in the number of papers of technetium due to the increased availability of the long-lived isotope $^{99}$Tc and the extensive use of $^{99m}$Tc in nuclear medicine. Nevertheless there is still considerably less information on technetium than its congener rhenium.

As expected from Gmelin the volume is comprehensive in its treatment of the literature although, because of the chapter on solution chemistry, there is a considerable amount of repetition, which is sometimes confusing. One criticism of the volume, however, is that when describing the complexes prepared no differentiation is made between those reactions carried out using $^{99}$Tc and those using $^{99m}$Tc. Using the former, standard chemical techniques may be employed whereas using $^{99m}$Tc at carrier-free or very low $^{99}$Tc levels absolute species identification is impossible except in exceptional circumstances, where the $^{99}$Tc complex is identical to the $^{99m}$Tc complex prepared under pharmaceutical conditions. Since there is now considerable evidence that in many cases the complexes prepared under radiopharmaceutical ($^{99m}$Tc) conditions are different from those prepared under chemical conditions ($^{99}$Tc), more details of the actual conditions used when discussing particularly redox reactions, should have been included.

The remaining chapters are concerned with the separation of technetium from either molybdenum or fission products. The latter is of particular interest with the development of new reprocessing plants, and is well documented except that the replacement of $NO_3^-$ by $TcO_4^-$ during extraction of thorium and plutonium is not mentioned although the formation of $UO_2(NO_3)(TcO_4).2TBP$ is discussed in detail.

In summary, this volume will be proved to be an extremely useful reference to those in both the nuclear power and medical research fields.

*Chemistry Department* JOHN THORNBACK
*Loughborough University of Technology*
*Loughborough*
*Leicestershire LE*11 3*TO*
*England*

*Polyhedron* Vol. 3, No. 7, pp. 765–769, 1984
Printed in the U.S.A.

0277-5387/84 $3.00 + .00
© 1984 Pergamon Press Ltd.

# CRYSTAL AND MOLECULAR STRUCTURE OF HYDRIDO(TRICHLOROSTANNYL)BIS-CYCLOPENTADIENYL MOLYBDENUM($\eta^5$-$C_5H_5)_2$Mo(H)$SnCl_3$

**ALEKSEY I. GUSEV and NATALIA I. KIRILLOVA**
The State Research Institute for Chemistry and Technology of Organoelemental Compounds, 111123, Moscow, U.S.S.R.

**ALEKSEY N. PROTSKY and BORIS M. BULYCHEV***
Chemistry Department, Lomonosov Moscow State University, 117234 Moscow, U.S.S.R.

**and**

**GRIGORIY L. SOLOVEICHIK**
The Institute of New Problems in Chemistry, USSR Academy of Sciences, 142432 Chernogolovka, Moscow District, U.S.S.R.

(*Received* 10 *May* 1983; *accepted* 21 *November* 1983)

**Abstract**—On the basis of X-ray analysis the crystal and molecular structures of ($\eta^5$-$C_5H_5)_2$Mo(H)$SnCl_3$ have been determined. The compound crystallizes in the monoclinic system with parameters: $a = 8.313(3)$, $b = 13.109(4)$, $c = 6.384(2)$ Å, $\beta = 106.52(2)°$, space group $P2_1/m$, $R = 0.028$. The conformation occurring in $Cp_2$Mo(H)$SnCl_3$ is that with the maximum repulsion between the chloride atoms and the cyclopentadienyl rings. The hydride H atom is shielded by the cyclopentadienyl groups and chlorine atoms, which accounts for the compound's stability to oxygen and hydrolysis.

Transition metal bis-cyclopentadienyl hydrides are very convenient test compounds for the study of the reactivity of metal–hydrogen bonds and *d*-basicity of transition metal atoms, as well as useful intermediates for the production of bis-cyclopentadienyl complexes with other ligands.[1,2] In this connection it is interesting to investigate compounds which contain, apart from the hydrido-ligand, bulky substituents which considerably affect the geometry of the $Cp_2M$ wedge-sandwich.

The present work reports the results of an X-ray analysis of the bis-cyclopentadienyl hydride complex of molybdenum containing a molybdenum–tin bond, viz. $Cp_2$Mo(H)$SnCl_3$.

## EXPERIMENTAL

Compound $Cp_2$Mo(H)$SnCl_3$ (**1**) was prepared by reacting $Cp_2MoH_2$ with an excess of tin chloride pentahydrate in diethyl ether.[3] The single crystals of (**1**) were grown by slow evaporation of the solution in acetonitrile.

The X-ray experiment was carried out using an automatic X-ray difractometer (R-3m Nicolet; Mo-$K\alpha$, graphite monochromator, $2\theta \leqslant 52°$).

The crystals of **1** are monoclinic, $a = 8.313(3)$ Å, $b = 13.109(4)$ Å, $c = 6.384(2)$ Å, $\beta = 106.52(2)°$, with space group $P2_1/m$. The structure was refined by the least-squares method in the full-matrix anisotropic approximation to an $R = 2.8\%$. A difference Fourier synthesis revealed all the hydrogen atoms and these were included with a fixed $B_{iso} = 5.0$ Å$^2$.

## RESULTS AND DISCUSSION

Crystals **1** are composed of isolated $Cp_2$Mo(H)$SnCl_3$ molecules separated by the normal van der Waals contacts. The molecule of **1** possesses a crystallographic mirror plane contain-

*Author to whom correspondence should be addressed.

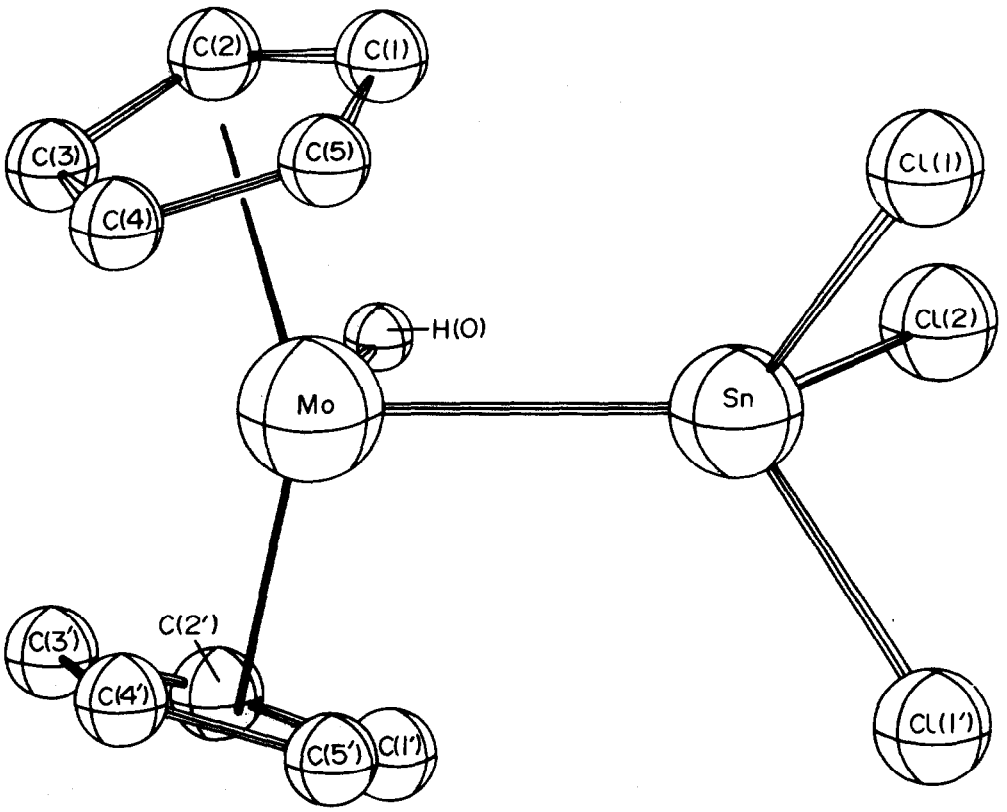



Fig. 1.

ing the atoms Mo,H,Sn and Cl(2) (Fig. 1). Its structure is typical of $Cp_2MXX'$ molecules in which the bound atoms of the substituent X, X' are located in the plane bisecting the wedge-sandwich.

The cyclopentadienyl rings are planar and are disposed in an eclipsed configuration.

The hydride hydrogen atom bonded to the molybdenum atom is a terminal atom (the H(O)... Sn distance = 2.88 Å is only 0.14 Å shorter than the sum of the van der Waals radii), which is in good agreement with IR data ($\nu_{Mo-H} = 1840\ cm^{-1}$).[3] The length of the Mo–H bond in **1** (Table 1) is practically the same as the Mo–H bond length in $Cp_2MoH_2$ (1.685 Å)[4] and in the binuclear complex $Cp_2\overline{Mo(H)}\text{–}C_5H_4\overline{M}oCp_2$ (1.72 Å).[5]

The Mo–Sn bond length (Table 1) is close to that in the related complex $Cp_2Mo(Br)SnBr_3$ (2.691 Å).[6] In the complex $[(bipy)(CO)_3\ MoCl(SnCl_3)]$ the Mo–Sn distance is 0.1 Å longer than in **1**, which is apparently due to the formation of the bridge bond $Mo\overset{Cl}{\diagup\!\!\diagdown}Sn$.[7] The Sn–Cl distance in **1** is practically the same as that usually observed in transition metal complexes containing the groups $SnCl_3$ or $SnCl_2$.[7-9] At the same time the valence angles Mo–Sn–Cl and Cl–Sn–Cl (Table 2) are markedly different from the tetrahedral angle, although their average is close to 109°. The reason is apparently the repulsion between the chlorine atoms Cl(1) and Cl(1)' and the cyclopentadienyl rings (the Cl(1)... C(5) contact length is 3.719 Å within the molecule itself and 3.644 Å with C(5) of the neighbouring molecule).

The angle Cp–$\hat{M}$o–Cp (Table 2) is much larger than in the complex $Cp_2Mo(Br)SnBr_3$ (128°).[6]

The value of the valence angle H(o)–$\hat{M}$o–Sn (Table 2), which is one of the most important structural characteristics of complexes of the type $Cp_2MXX'$, lies within the range typical of compounds having an electron configuration of the $d^2$ type.[10,11] As one would expect, this value is higher than it is for the dihydride (75.5°)[4] but is just slightly higher than for the complex containing bulkier halogen atoms $Cp_2Mo(Br)SnBr_3$ (80.16°)[6] or a wedge-shaped arene complex with a $d^2$-configuration $(PhMe)_2Hf(SnMe_3)_2$ containing two tin atoms bonded to the hafnium atom (81.14°).[12]

In general, the structure of **1** is very similar to that of the related tin-containing complex $Cp_2Mo(X)SnX'_3$ (X = X' = Br);[6] however, there is a very essential difference as well. In a molecule of **1**, the Cl(2)–Sn bond lying in the bisector plane of the

Table 1. Bond lengths, d (Å)

| Bond | d | Bond | d |
|---|---|---|---|
| Mo-Sn | 2.652(1)* | Sn-Cl(1) | 2.382(2) |
| Mo-C(1) | 2.297(5) | Sn-Cl(2) | 2.380(2) |
| Mo-C(2) | 2.332(6) | aver. | 2.381(2) |
| Mo-C(3) | 2.287(7) | Mo-H(0) | 1.74(7)* |
| Mo-C(4) | 2.262(7) | | |
| Mo-C(5) | 2.278(7) | C(1)-H(1) | 0.91(6) |
| aver. | 2.291(7) | C(2)-H(2) | 0.95(6) |
| | | C(3)-H(3) | 0.87(6) |
| C(1)-C(2) | 1.38(1) | C(4)-H(4) | 0.69(7) |
| C(2)-C(3) | 1.35(1) | C(5)-H(5) | 0.92(7) |
| C(3)-C(4) | 1.43(1) | aver. | 0.87(7) |
| C(4)-C(5) | 1.39(1) | | |
| C(1)-C(5) | 1.38(1) | | |
| aver. | 1.39(1) | | |

* Bond lengths for atoms in special position.

wedge-sandwich is directed towards the second substituent (the hydride hydrogen atom), whereas in $Cp_2Mo(Br)SnBr_3$ the bromine atom bonded to the molybdenum atom and lying in the same plane of symmetry is located on the opposite side[6] (Figs. 2a and b).

From general considerations, the complexes containing a ligand $EX'_3$ with local symmetry $C_{3v}$ most probably have two configurations in which one of the X′ atoms lies in the mirror symmetry plane of the wedge-sandwich $Cp_2M$ and the E–X′ bond is directed either towards the second substituent (conformation **A** occurring in complex **1**) or away from it (conformation **B**) (Figs. 2a and b). The repulsion of the X′ atoms (groups) in $EX'_3$ and the pentadienyl rings is weaker in conformation **A**, but the mutual repulsion of the atoms (groups) X and X′ is, as a rule, much stronger, and the conformation occurring in all the known compounds of this type: $Cp_2Mo(Br)SnBr_3$,[6] $Cp_2Zr(Cl)SiPh_3$,[13] $(PhMe)_2Hf(SnMe_3)_2$ [12] is always of the type **B**. Indeed, in the molecule of $Cp_2Mo(Br)SnBr_3$ having conformation **A** the distance Br···Br should be 0.7 Å smaller than the sum of the van der Waals radii. At the same time, since the dimensions of the hydrogen atom as the second substituent are small, it is configuration **A** which is more favorable for **1** (the H(o)... Cl(2) distance is only 0.2 Å smaller than the sum of the van der Waals radii).

The observed conformation of the molecule $Cp_2Mo(H)SnCl_3$ is responsible for the inertness of this compound; its crystals stay unaffected by air even after exposure for several months. The reason apparently lies with the fact that the Cl(2) atom blocks the coordination site which is necessary for an electrophilic attack on the molybdenum atom (Fig. 2). Really, in the known structures of $Cp_2MXX'$-based compounds (M = Mo,W) with a bonding pair of *d*-electrons, for example, in the complex $Cp\overline{Mo(H)\mu\text{-}C_5H_4)M}oCp_2$ [5], the acceptor atom becomes coordinated along the direction lying in the bisector plane between the substituent X and X′.

Table 2. Valence angles, w(°)

| Angle | w |
|---|---|
| SnMoH(0) | 79(2) x |
| CpMoCp xx | 141.3 |
| MoSnCl(1) | 121.79(4) |
| MoSnCl(2) | 118.92(5) x |
| Cl(1)SnCl(2) | 95.33(6) |
| Cl(1)SnCl(1') | 97.46(6) x |
| aver. | 108.44(6) |
| C(1)C(2)C(3) | 108.8(6) |
| C(2)C(3)C(4) | 106.7(7) |
| C(3)C(4)C(5) | 108.8(8) |
| C(4)C(5)C(1) | 105.6(7) |
| C(5)C(1)C(2) | 110.1(6) |
| aver. | 108.0(7) |

x Angle between atoms in special positions.

xx Cp = $\eta^5$-$C_5H_5$.

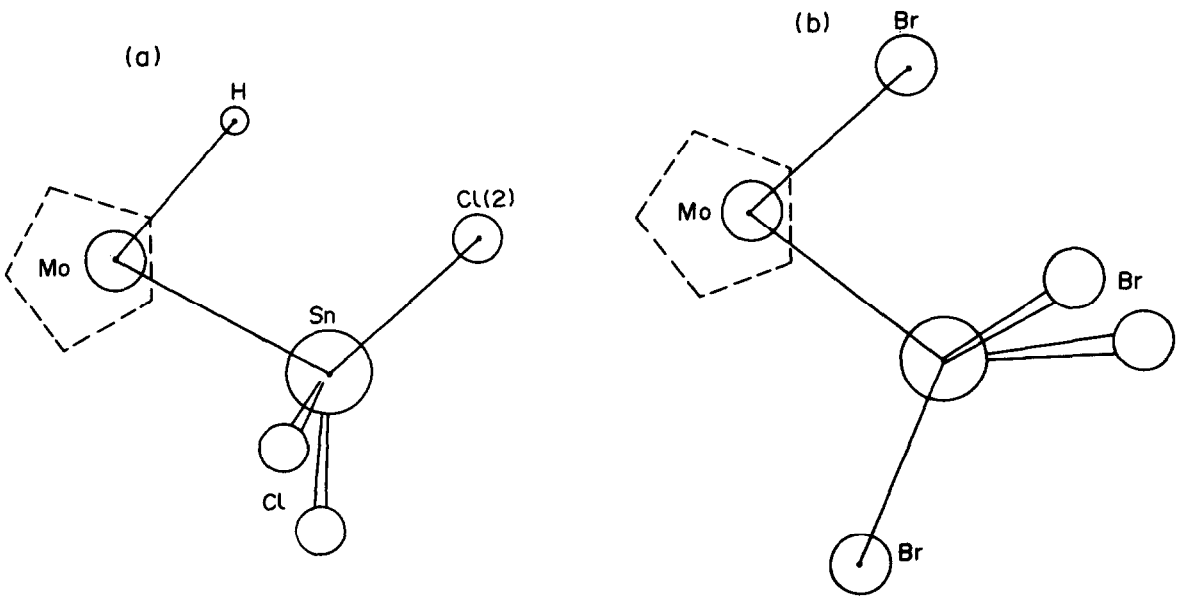



Fig. 2.

## REFERENCES


1. M. M. Kubicki, R. Kergoat, S. E. Guerchais, C. Bois and P. L'Haridon, *Inorg. Chim. Acta* 1980, **43**, 17.
2. G. A. Soloveichik and B. M. Bulychev, *Uspekhi Khimii* 1982, **51**, 507.
3. A. N. Protsky, B. M. Bulychev and G. L. Soloveichik, *Inorg. Chim. Acta* 1983, **71**, 35.
4. A. J. Schultz, K. L. Stearby, J. M. Williams, R. Mink and G. B. Stucky, *Inorg. Chem.* 1977, **16**, 3303.
5. M. L. N. Green, M. L. Poveda, J. Bashkin and K. Prout, *Chem. Commun.* 1982, 30.
6. T. S. Cameron and C. S. Prout, *J. Chem. Soc. Dalton Trans.* 1972, 1447.
7. M. Elder, W. A. G. Graham, D. Hall and R. Kummer, *J. Am. Chem. Soc.* 1968, **90**, 2189.
8. J. E. O'Connor and E. R. Corey, *Inorg. Chem.* 1967, **6**, 968.
9. P. T. Green and R. F. Bryan, *J. Chem. Soc. (A)*, 1970, 1696.
10. K. Prout, T. S. Cameron, R. A. Forder, S. R. Critchley, B. Denton and G. V. Rees, *Acta Cryst. B.* 1974, **30**, 2290.
11. J. W. Laucher and R. Hoffmann, *J. Am. Chem. Soc.* 1976, **98**, 1729.
12. F. G. N. Cloke, K. P. Cox, M. L. H. Green, J. Baskin and K. Prout, *Chem. Commun.* 1981, 117.
13. K. W. Muir, *J. Chem. Soc. A* 1971, 2663.

*Polyhedron* Vol. 3, No. 7, pp. 771–774, 1984
Printed in the U.S.A.

0277–5387/84 $3.00 + .00
© 1984 Pergamon Press Ltd.

# REDUCTION OF COPPER (II) CHLORIDE BY MOLYBDENUM AND RHENIUM BISCYCLOPENTADIENYL HYDRIDES. INVESTIGATION OF THE CRYSTAL AND MOLECULAR STRUCTURE OF $[(\eta^5\text{-}C_5H_5)_2Re]^+[CuCl_2]^-$

**VICTOR M. ISHCHENKO and BORIS M. BULYCHEV***
Department of Chemistry, M. V. Lomonosov Moscow State University, Moscow 117234, U.S.S.R.

**GRIGORI L. SOLOVEICHIK**
Institute of New Chemical Problems, Academy of Sciences of the U.S.S.R., Chernogolovka 142432, U.S.S.R.

**VITALI K. BEL'SKY**
L. Ya. Karpov Scientific Research Institure of Physical Chemistry, Moscow 107120, U.S.S.R.

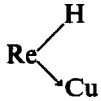
**and**

**OLGA G. ELLERT**
N. S. Kurnakov Institute of General and Inorganic Chemistry, Moscow 117071, U.S.S.R.

(*Received* 27 *July* 1983; *accepted* 16 *November* 1983)

**Abstract**—The reduction of copper (II) chloride by molybdenum and rhenium biscyclopentadienyl hydrides upon their interaction in donor-type solvents has been studied by NMR, X-ray diffraction, and magnetic methods. It is established that the ionic complex $[(\eta^5\text{-}C_5H_5)_2Re]^+[CuCl_2]^-$ forms ortho rhombic crystals with $a = 13.696(2)$ Å, $b = 7.317(1)$ Å, $c = 5.969(1)$ Å, space group $Pm2_1n$, $Z = 2$. The cyclopentadienyl rings make a bent-sandwich with an angle between the ring centres and Re atom of 150.1°;the Cl–Cu–Cl angle being 174.8° anf the Re–Cu minimum distance 4.346(29) Å. The solution of $[(\eta^5\text{-}C_5H_5)_2Re]^+[CuCl_2]^-$ seems to activate the C–H bond of the $C_5H_5$ rings, which results in the addition of the $[(C_5H_5)(C_5H_4)ReH]^+$ hydride ion.

Previous work[1–3] has shown that biscyclopentadienyl hydrides of Group VI and VII metals (Mo, W, Re) form stable complex compounds with copper (II) chloride. On the basis of IR spectral data, showing the preservation of M–H bonds, these compounds were suggested to be simple adducts containing hydrogen bridges M–H–Cu(M = Mo, W)[1,2] or donor–acceptor bond



[3] The oxidation level of copper in these compounds remains +2. At the same time $^1$H NMR data on the one hand and a low $Cu^{2+}/Cu^+$ redox potential on the other, along with the data obtained in investigating the products formed in the interaction of $HgX_2$ and $CpMoH_2$,[4] strongly contradict the conclusions previously made.[1–3] In this connection we undertook a detailed investigation of the interaction of $[(\eta^5\text{-}C_5H_5)_2ReH]$ and $[(\eta^5\text{-}C_5H_5)_2MoH_2]$ with copper (I) and (II) halides.

## EXPERIMENTAL

$Cp_2ReCuCl_2$, $Cp_2ReHCuI$, $(Cp_2Mo)_2H_3CuCl_2$ and $[(Cp_2MoH_2)_2CuCuCl_2]$ were obtained via direct synthesis from $Cp_2ReH$ or $Cp_2MoH_2$(Cp = $\eta^5\text{-}C_5H_5$) and the corresponding cooper halide in acetonitrile as previously described.[1–3]

*Author to whom correspondence should be addressed.

The static magnetic susceptibility was measured in the 298–77 K temperature range by the Faraday technique. The measurements were performed with a device designed at the Institute of General and Inorganic Chemistry, Academy of Sciences of the USSR.

$^1$H NMR-spectra were recorded on a Varian XL-100 spectrometer sperating at 100 MHz. The samples were run as deuteriated dimethylformamide-$d_7$ solutions

*Determination of the crystal and molecular structure of* $Cp_2ReCuCl_2$(I).

A hot saturated solution of I in acetonitrile was slowly cooled to give brown pyramidal single crystals stable to the air.

Crystals of I are orthorhombic, $a = 13.696(2)$ Å, $b = 7.317(1)$ Å, $c = 5.969(1)$ Å, $V = 588.2$ Å$^3$, space group $Pm2_1n$, $Z = 2$, $d_{calc} = 2.50$ g/cm$^3$. 717 reflections were collected with a Syntex $P\bar{1}$ diffractometer (Mo – $K\alpha$ radiation, graphite monochromator, $\theta/2\theta$ scan, $2\theta < 50°$, and corrected for absorption, $\mu_{Mo} = 129.4$ cm$^{-1}$).

The structure was solved by direct methods to give the positions of Re, Cu and Cl atoms. The C atom positions were determined by sequential Fourier syntheses. The cyclopentadienyl ring hydrogen atom positions were calculated from geometrical considerations. Full-matrix least-squares refinement with an anisotropic approximation for the heavy atoms only gave an R-factor of 4.7%. A projection of the structure on the (010) plane is given in Fig. 1. Table 1 lists the main bond lengths and valence angles.†

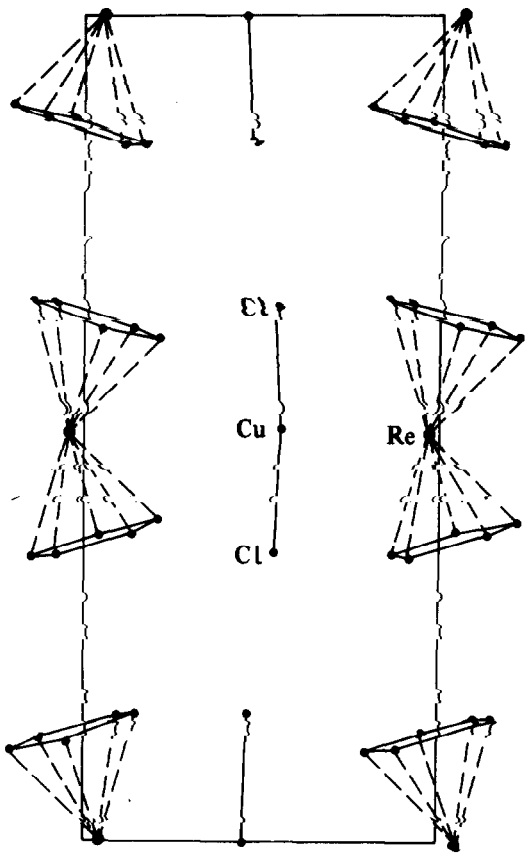



Fig. 1. Projection of the structure on the (010) plane.

## RESULTS AND DISCUSSION

The crystal structure of $Cp_2ReCuCl_2$ comprises two distinct fragments, $Cp_2Re$ and $CuCl_2$ each of which have mirror symmetry, (see Fig. 1). Significant distances between the metallic atoms of the structure point to the ionic nature of their bonding ( > 4.3 Å). The difference in the distances between the Cu atom and the two neighbouring Re atoms is insignificant (see Table 1) which is an indication of a high degree of the charge distribution. As we expected the $CuCl_2^-$ ion has a linear configuration with the Cl–Cu–Cl angle equal to 174.8°($[\{N_6P_6(NMe_2)_{12}\}Cu^{II}Cl]^+[Cu^ICl_2]^-$ with the same anion gives an angle of 179.5°[5]). The Cu–Cl distance in this anion is similar to that in $[\{N_6P_6(NMe_2)_{12}\}Cu^{II}Cl]^+[Cu^ICl_2]^-$ (2.11Å[5]) and $[(Cp_2MoH_2)_2Cu]CuCl_2$ (2.17 Å[6]) complexes and somewhat less than the sum of the covalent metal radii (2.17 Å[5]).

It is noteworthy, that the linear $CuCl_2^-$ ions are parallel to the plane passing through the centres of cyclopentadienyl rings and the atom, although the position of the $CuCl_2$ fragment in the bisector plane of the sandwiches would ensure their minimum contact. This coordination of the ions causes the maximum repulsion of the cyclopentadienyl rings and chlorine atoms in the closest anion $CuCl_2^-$ and so, instead of the expected structure with planar parallel rings similar to that of the cation complex $Cp_2Fe^+$[7] and chromocene[8] a previously unknown type is realized of the ionic sandwich compounds with slanted rings. The strong repulsion of the cyclopentadienyl rings and the Cl atoms in I leads to a significant increase in the dihedral angle between the ring planes (32.5°) compared with a similar angle in the sterically hindered complex of the composition ($Cp_2ReHCuI$) (II) (22°).[9] The most reasonable explanation of the unusual coordination of $CpRe^+$ and $CuCl_2^-$ in relation to each other is in our view a consequence of the weak hydrogen bond between the chlorine atoms and positive hydrogen atoms of

*Atomic co-ordinates, Kiernal parameters and lists of $F_o/F_c$ values have been deposited with the Editor as supplementary material. Copies are available on request. Atomic Co-ordinates have also been deposited with the Cambridge Crystallographic Data Centre.

Table 1. The main bond lengths $d$(Å) and valence angles (°) in $Cp_2ReCuCl_2$ molecule

| Bond | d | angle | ω |
|---|---|---|---|
| Re - Cu | 4.346(29) | Cl - Cu - Cl | 174.80(15) |
| | 4.382(29) | Ctr*(1) - Re - Ctr(2) | 150.10 |
| Cu - Cl | 2.097(5) | α | 32.5 |
| Re - Ctr | 1.898 | C - C - C | 107.99 |
| C - $C_{(aver.)}$ | 1.471 | | |
| C - H | 0.960 | | |
| Cl ··· H | 2.62 | | |
| Re - $C_{(aver.)}$ | 2.275 | | |

Ctr* - a center of the corresponding cyclopentadienyl ring

the cyclopentadienyl rings ($r_{Cl..H} = 2.62$ Å). This hydrogen bond is weaker than Van der Waals contacts and is assumed to lead to stabilization of molecule **I**. The shift of the electron density on the Cl atoms seems to account for the absence of the $\nu$(Cu–$Cl^{term.}$) absorption band in the IR spectra of this compound in the 280–320 $cm^{-1}$ range[3] which is observed in the IR spectra of $CuCl_2$ complexes with organic ligands[10]. This effect in combination with the removal of an electron from the binding $d^{10}$-orbital of the Re atom in the $Cp_2Re$ fragment causes weakening of Re–C bonds (2.28 Å as compared to 2.24 Å in **II**[9]) and C–C bonds (1.47 Å as compared to 1.44 Å[9]).

The eclipsed conformation of the cyclopentadienyl rings in complex **I** is similar to that previously observed in complex **II**.[9] Their geometry is distorted as shown by the lack of coincidence between the angle between the normals to their planes (147.5°) and the C(I)–Re–C(2) angle 150.1°) (where C(1) and C(2)–are the ring centres).

The presence of $CuCl_2^-$ ions in structure **I** unambiguously indicates that in the course of reaction with $Cp_2ReH$ the valence of copper is reduced from II to I. This conclusion is also confirmed by magnetic susceptibility data which revealed that complex **I** is diamagnetic. At the same time these data point to the absence of the unpaired electrons in the Re atom, which means that the level of rhenium oxidation is maintained at +3. That is why in this case copper (II) is reduced by the hydride's hydrogen and the reaction can be described as follows:

$$Cp_2ReH + CuCl_2 \longrightarrow Cp_2Re^+CuCl_2^- + 1/2H_2. \quad (1)$$

The X-ray data and diamagnetism of complex **1** strongly suggest the absence of a metal–hydrogen bond in the crystalline state. At the same time the treatment of **I** in acetonitrile by $CCl_4$ leads to the formation of chloroform[3] which is characteristic of compounds with a transient metal–hydrogen bond.[11] In order to explain the reasons causing this phenomenon we studied the reaction of **I** with $CCl_4$ in a deuteriated solvent, $d_7$-DMFA. The NMR spectrum of the solution of **I** in $d_7$-DMFA treated with an excess $CCl_4$ was recorded in 1 h. after the preparation and demonstrated a weak chloroform signal ($\tau = 7.3$). The intensity of the signal increases with time and a few days later, becomes comparable with the intensity of the cyclopentadienyl signals. Simultaneously we observed the signal splitting of these groups. Since $d_7$-DMFA was used as a solvent only the cyclopentadienyl rings can be the source of protons in the formation of chloroform in the reaction of $[Cp_2Re]^+[CuCl_2]^-$ with $CCl_4$, while the reaction mechanism seems to involve a C–H bond activation step via oxidative addition of hydrogen to Re atom followed by Re–H bond interaction with $CCl_4$. The equilibrium (eqn 2) is obviously shifted to the left as evidenced by a slow accumulation of $CHCl_3$ with time. It is true, however, that this process is somewhat accelerated when the reaction is conducted in the usual (non-deuteriated) solvent:

$$[(C_5H_5)_2Re]^+ \rightleftarrows [(C_5H_5)(C_5H_4)ReH]^+. \quad (2)$$

It may well be that the ease of the C–H bond activation in the cyclopentadienyl rings is due to the above-mentioned properties of the complex **I** structure, i.e. to the "forced" coordination of the chlorine atoms among $C_5H_5$-groups, which brings about the loosening of Re–C, C–C and apparently

C–H bonds. The removal of hydrogen from the "hydride" complex on interaction with $CCl_4$ results in the formation of compounds with substituted cyclopentadienyl rings in $[(C_5H_5)(C_5H_4X)Re]^+$ rather than in the decomposition of the complex as it is the case with **II**.[3] The mechanism of this substitution is unclear but it seems to be of a radical nature. Since in the usual solvent the rate of $[(C_5H_5)(C_5H_4)ReH]^+$ accumulation in the solution increases it can be assumed that the solvent's protons contribute to the process.

The fact that we observed the formation of chloroform on interaction of $CCl_4$ with a compound whose initial structure lacks a metal–hydrogen bond indicates that one should be more cautious while using this reaction as a traditional test for M–H bonds in transition metal compounds.

Since metal–hydrogen bonds in $Cp_2MoH_2$ and $Cp_2WH_2$ as well as in $Cp_2ReH$ are of hydridic nature[12] these compounds were also likewise expected to reduce $CuCl_2$. Indeed the Mo : Cu : Cl = 2 : 1 : 2 complex generated upon the interaction of $Cp_2MoH_2$ with $CuCl_2$ exhibits diamagnetism as in complex **I**. In addition the $^1H$ NMR spectrum of this compound shows two signals at 4.8 and 20.6 $\tau$ with the intensity ratio near 20 : 3. Since the amount of chlorine in the final product remains unchanged then in this case too the reaction proceeds only with hydrogen evolution. This differentiates the reaction of $CuCl_2$ with $Cp_2MoH_2$ from a similar reaction of $HgX_2$ with a dihydride, which results in the evolution of the hydrogen halide and formation of Mo–Hg-bond.[4]

An unusual ratio Mo:Cu = 2:1 in the compound obtained can be apparently explained by the formation of $(Cp_2MoH)_2H^+$ bi-nuclear cation similar to $[(Cp_2WH)_2H]^+$ cation detected on electrochemical oxidation of $Cp_2WH_2$.[13] Taking into account the tendency of $CuCl_2$ to form anion complexes its compound with $Cp_2MoH_2$ can be represented as $[(Cp_2MoH)_2H]^+[CuCl_2]^-$ salt **(III)**. Indeed complex **III** reacts with the salts of large anions, (e.g. sodium tetraphenylborate), to give the $[(Cp_2MoH)_2H]^+[BPh_4]^-$ salt.

The $CuX_2$ group appears to be widely spread in the chemistry of bimetallic complexes, since it can be formed not only as the result of $CuCl_2$ reduction but also in the reactions of copper (I) chloride (I) addition to dihydride of molybdenocene and the iodide of copper (I) to tungstenocene dihydride, although the details of this interaction may differ from that mentioned above. Thus, in the unique T-shaped cluster of $[\{Cp_2Mo(\mu_2\text{-}H)(\mu_3\text{-}H)\}_2Cu][CuCl_2]$ **(IV)** composition the Cu–Cu interatomic bond length is only 2.72 Å[6]. Formally the Cu atoms in **IV** can be considered as having various valencies from 0 to 2. In this case the complex should be paramagnetic. Actually this complex is diamagnetic, i.e. the level of oxidation of the both copper atoms is +1. Due to a short Cu–Cu bond length comparable with the sum of the covalent radii (2.56 Å) the **IV** molecule can not be considered as a purely contact ion pair $[(Cp_2MoH_2)_2Cu]^+[CuCl_2]^-$ too especially since the Cu atom in the $CuCl_2$ fragment is bonded to hydrogen bridges.[6] Thus we are not in the position to give an unambiguous answer as to the nature of Cu–Cu bonding in the molecule **IV**. We can only assume that as with complex **II** in this case the action of the strong base—$Cp_2MoH_2$—promotes one $d^{10}$-electron to a higher S-level to yield a high spin configuration of the copper atoms $3d^9 4s^1$ with the electron coupling in Cu–Cu bond formation.

On interaction of $Cp_2MoH_2$ with a weaker Lewis acid—CuI—the shift of electron density from molybdenocene dihydride to the Cu atom in $[Cp_2Mo(\mu\text{-}H)_2CuI]_2$ appears to be inadequate to promote *ds*-hybridization and a Cu–Cu bond is not formed. At the same time the crystals of CuI complex with a stronger base—$Cp_2WH_2$—are isostructural to that of complex **IV** which seems to indicate that in this case there is a direct bond Cu(I)–Cu(I), leading to formation of $[CuI_2]$ fragment.

## REFERENCES


1. A. V. Aripovsky, B. M. Bulychev and V. B. Polyakova, *Zh. Neorg. Khimii* 1981, **26**, 2722.
2. A. V. Aripovsky, B. M. Bulychev, L. B. Krivdin and V. B. Polyakova, *Zh. Neorg. Khimii* 1981, **26**, 2109.
3. V. M. Ishchenko, B. M. Bulychev and G. L. Soloveichik, *Koordin. Khimiya* 1983, **9**, 622.
4. M. M. Kubicki, P. Kergoat, J. E. Guerchais, C. Bois and P. L.'Haridon, *Inorg. Chim. Acta* 1980, **43**, 17.
5. W. C. March and J. Trotter, *J. Chem. Soc., A* 1971, 1482.
6. E. B. Lobkovsky, A. V. Aripovsky, V. D. Bel'sky and B. M. Bulychev, *Koordin. khimiya* 1982, **8**, 104.
7. M. R. Churchill, A. G. Landers and A. L. Rheingold, *Inorg. Chem.* 1981, **20**, 849.
8. E. Weis and E. O. Fisher, *J. Anorg. Allgem. Chem.* 1956, **284**, 69.
9. V. K. Bel'sky, V. M. Ishchenko, B. M. Bulychev and G. L. Soloveichik, *Polyhedron*, 1984, **3**, 749.
10. C. W. Frank and L. B. Rogers, *Inorg. Chem.* 1966, **5**, 615.
11. M. L. H. Green, L. Prat and G. Wilkinson, *J. Chem. Soc.* 1958, 3916.
12. J. A. Labinger and K. H. Kamadina, *J. Organomet. Chem.* 1978, **155**, C25.
13. R. J. Klinger, J. C. Huffman and J. K. Kochi, *J. Am. Chem. Soc.* 1980, **102**, 208.
14. V. K. Bel'sky, E. V. Fomicheva, A. V. Aripovsky and B. M. Bulychev, *Dokl. AN SSSR* 1981, **258**, 1137.

*Polyhedron* Vol. 3, No. 7, pp. 775–780, 1984
Printed in the U.S.A.

0277–5387/84 $3.00 + .00
© 1984 Pergamon Press Ltd.

# SYNTHESIS AND STRUCTURE OF THE HETEROTRINUCLEAR CHROMIUM–PALLADIUM CLUSTERS $(RC_5H_4CrCl)_2$-$(\mu_3\text{-}S)(\mu\text{-}SCMe_3)_2Pd(PPh_3)$ WITH FERROMAGNETIC EXCHANGE INTERACTIONS OVER THE CrSCr SYSTEM

A. A. PASYNSKII,* I. L. EREMENKO, G. Sh. GASANOV, O. G. ELLERT, V. M. NOVOTORTSEV, Yu. V. RAKITIN, T. Kh. KURBANOV and V. T. KALINNIKOV

The N. S. Kurnakov Institute of General and Inorganic Chemsitry, Academy of Sciences of the U.S.S.R., Moscow V-71, 31 Leninskii Pr., U.S.S.R.

and

Yu. T. STRUCHKOV and V. E. SHKLOVER

The A. N. Nesmeyanov Institute of Organoelement Compounds, Academy of Sciences of the U.S.S.R., Moscow V-312, 28 Vavilov St., U.S.S.R.

(*Received* 6 *June* 1983; *accepted* 28 *November* 1983)

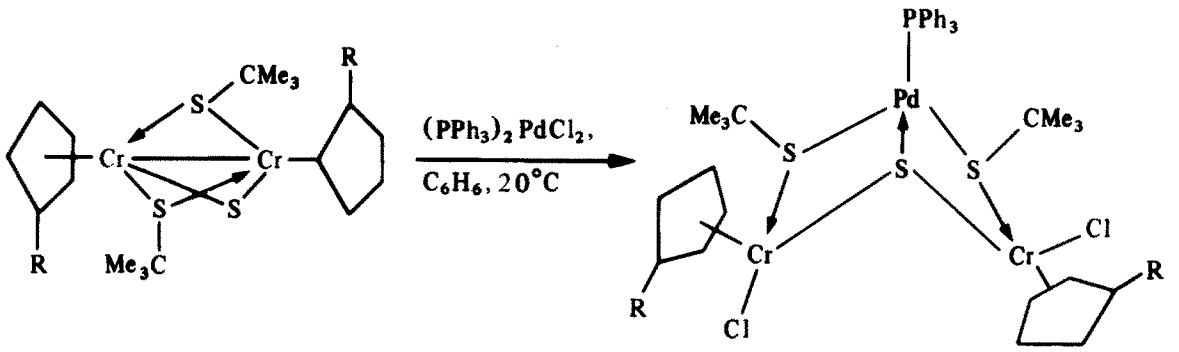
**Abstract**—Reactions of $(RC_5H_4)_2Cr_2(SCMe_3)_2S$(**I**, R = H; **II**, R = Me) with $(PPh_3)_2PdCl_2$ in benzene at 20°C gives trinuclear complexes $(RC_5H_4)_2Cr_2Cl_2(\mu_3\text{-}S)(\mu\text{-}SCMe_3)_2Pd(PPh_3)$(**III**, R = H; **IV**, R = Me). The structure of **IV** as a monobenzene solvate is established by an X-ray analysis (black–green triclinic crystals space group $P\bar{1}$ with $a = 11.403(4)$, $b = 14.933(5)$, $c = 14.131(5)$ Å, $\alpha = 99.13(3)$, $\beta = 112.72(3)$, $\gamma = 95.65(3)°$, $V = 2201.6$ Å, $Z = 2$; IV·$C_6H_6$). The structure was solved by direct methods and refined in an anisotropic approximation to $R = 0.046$, $R_w = 0.058$ for 7643 reflections with $I \geqslant 2\sigma(I)$. In the molecule of **IV** metal atoms are separated by non-bonding distances (Cr . . . Cr 4.079(I), Cr . . . Pd 3.230(I) and 3.380(I) Å) but linked by the bridging tridentate sulphur atom (Cr–S 2.339(2) and 2.329(2), Pd–S 2.327(2) Å), and two $SCMe_3$ groups between Pd and Cr (Cr–S 2.396(2) and 2.403(2), Pd–S 2.350(2) and 2.381(2) Å, CrŜPd 85.14(6) and 89.92(6)°). The Cl atoms are transferred from Pd to Cr atoms (Cr–Cl 2.308(2) Å) and being terminally coordinated are in *trans*-positions to each other (as well as $\eta\text{-}CH_3C_5H_4$ rings) with respect to the $Cr_2Pd$ plane. Cr atoms in **III** and **IV** exhibit ferromagnetic exchange interactions over the CrŜCr system ($+2J = 28$ and 11 $cm^{-1}$, respectively).

Earlier we have proposed the method of synthesis of the heteronuclear high-spin clusters on the basis of metal-containing Lewis acids LM(CO) and antiferromagnetic complexes $[(RC_5H_4)Cr(SCMe_3)]_2S$ with the short Cr–Cr bond (2.689 Å, R = H).[1] The reaction course is defined by the coordination number (CN) of M in the Lewis acid. With CN = 6 only an adduct $(RC_5H_4CrSCMe_3)_2S{\cdot}ML$ is formed but when CN = 5 a heterometallic cluster is produced with new Cr–M bonds and elimination of one or both tert-butyl groups. Mono- and binuclear metal carbonyls and cyclopentadienylcarbonyls were used as Lewis acids also with CN's varying from 5 to 7.[2] It seemed of interest to investigate reactions of **I** and **II** with the square-planar complex $(PPh_3)_2PdCl_2$, in which the CN of the metal is equal to 4 and the $PPh_3$ molecule is readily substitutable.

## EXPERIMENTAL

All operations were carried out under pure argon. The starting $(RC_5H_4CrSCMe_3)_2S$ (R = H[1] and $CH_3$[3]) and $(PPh_3)_2PdCl_2$ were prepared by the methods described earlier. Dry benzene and saturated hydrocarbons were prepared by distillation over Na sand under argon. The IR spectra were measured in KBr pellets with a "Specord IR-75" instrument. The magnetic measurements were performed using Faraday's method with an apparatus at the Institute of General and Inorganic Chemistry of the Academy of Sciences of the U.S.S.R.[4] 8217 reflections were measured with a Syntex $P2_1$ automatic four-circle X-ray diffractometer at −120°C (Mo$K\alpha$, $\lambda = 0.7107$ Å, $\theta$–$2\theta$ scan, $\theta \leqslant 52°$). 7643 reflections with $I \geqslant 2\sigma(I)$ were used

*Author to whom correspondence should be addressed.




**I** R = H

**II** R = $CH_3$

**III** R = H

**IV** R = $CH_3$

Scheme 1.

in the structure determination. The structure was solved by direct methods using the MULTAN program and refined to $R_1 = 0.046$ ($R_w = 0.058$) by the block-diagonal anisotropic least squares method for all non-hydrogen atoms (except carbon atoms fo a disordered fragments which were treated isotropically).† Crystals of the complex **IV** are triclinic, space group $P\bar{1}$, at $-120°C$; $\alpha = 99.13(3)$, $\beta = 112.72(3)$, $\gamma = 95.65(3)°$, $\alpha = 99,13(3)$, $\beta = 112.72(3)$, $\gamma = 95.65(3)°$, $V = 2201(6)$ Å$^3$, $Z = 2$; IV·$C_6H_6$. Atomic coordinates, anisotropic thermal parameters and lists of $F_c/F_0$ factors have been deposited with the Editor as Supplementary material and are available on request. Atomic coordinates have also been deposited with the Cambridge Crystallographic Data Centre.

$(RC_5H_4CrCl)_2(\mu_3\text{-}S)(\mu\text{-}SCMe_3)_2PdPPh_3 \cdot C_6H_6$(**III**, R = H; **IV**, R = $CH_3$)

The light yellow solution of $(PPh_3)_2PdCl_2$ (0.7 g, 1 mmole) in 35 cm$^3$ of hot benzene was added to the violet solution of 2.426 mmole of $(RC_5H_4CrSCMe_3)_2S$ (R = H, $CH_3$) in 40 cm$^3$ of benzene. The reaction mixture changed its colour from violet to dark green. The solution was evaporated to dryness at 80°/10 Torr, and the solid extracted with 60 cm$^3$ of benzene–heptane (I : I) mixture. The dark green solution obtained was cooled to $-10°C$. Large dark green prisms precipitated which were separated from the solution, washed with benzene and pentane and dried *in vacuo*. Yield; (R = H) 2.16 g (92.6%); (R = $CH_3$) 2.23 g (92.9%). Found (R = H): C, 52.06; H, 4.92. $C_{42}H_{49}Cl_2Cr_2\text{–}PPdS_3$, requires, C, 52.45; H, 5.10%.

IR spectrum ($\gamma$, cm$^{-1}$): **III**, R = H: 405w, 430w, 475w, 490s, 505s, 550w, 675s, 728s, 730sh, 785s, 905sh, 995s, 1075s, 1140s, 1290sh, 1338m, 1425s, 1435m, 1450m, 2800–2910br. m, 3025w. **IV**, R = $CH_3$: 405w, 440w, 478m, 490m, 509m, 590w, 666s, 725m, 795s, 850w, 915w, 980w, 1015m, 1080s, 1153s, 1135s, 1170w, 1270sh, 1290sh, 1338m, 1370m, 1420s, 1435w, 1455m, 2800–2890br. m, 3040br. m.

## RESULTS

As is noted above the choice of $(PPh_3)_2PdCl_2$ as the metal containing Lewis acid with CN = 4 and square planar environment of the Pd atom was governed first by a possible replacement of the phosphine ligand by a sulphide atom of the dichromium complex $(RC_5H_4)Cr_2\text{–}(SCMe_3)_2S$ (**I** or **II**). On the other hand on such replacement the Pd atom coordination sphere retains its vacant fifth position which can be used for additional coordination of a sulphur atom of the thiolate bridge between chromium atoms. Thus the conditions previously proposed[2] and required for deep transformation of the starting binuclear complex **I** and **II** were fulfilled. Actually the reactions of complexes **I** and **II** with $(PPh_3)_2PdCl_2$ in benzene at room temperature were almost instantaneous with the colour of reaction mixture changing from black–violet to dark green. Further recrystallization afforded the products $(RC_5H_4)_2Cr_2Cl_2(S)\text{-}(SCMe_3)_2Pd(PPh_3)\cdot C_6H_6$, i.e. only one $PPh_3$ molecule was lost (Scheme I).

The IR spectra of **III** and **IV** isolated in the form of dark green prisms are identical differing only by the band at 1370 cm$^{-1}$ in the case of the **IV** which

†The EXTL programs modified by A. I. Yanovskii and R. G. Gerr (Institute of Organoelement Compounds of the U.S.S.R. Acad. Sci.) were used.

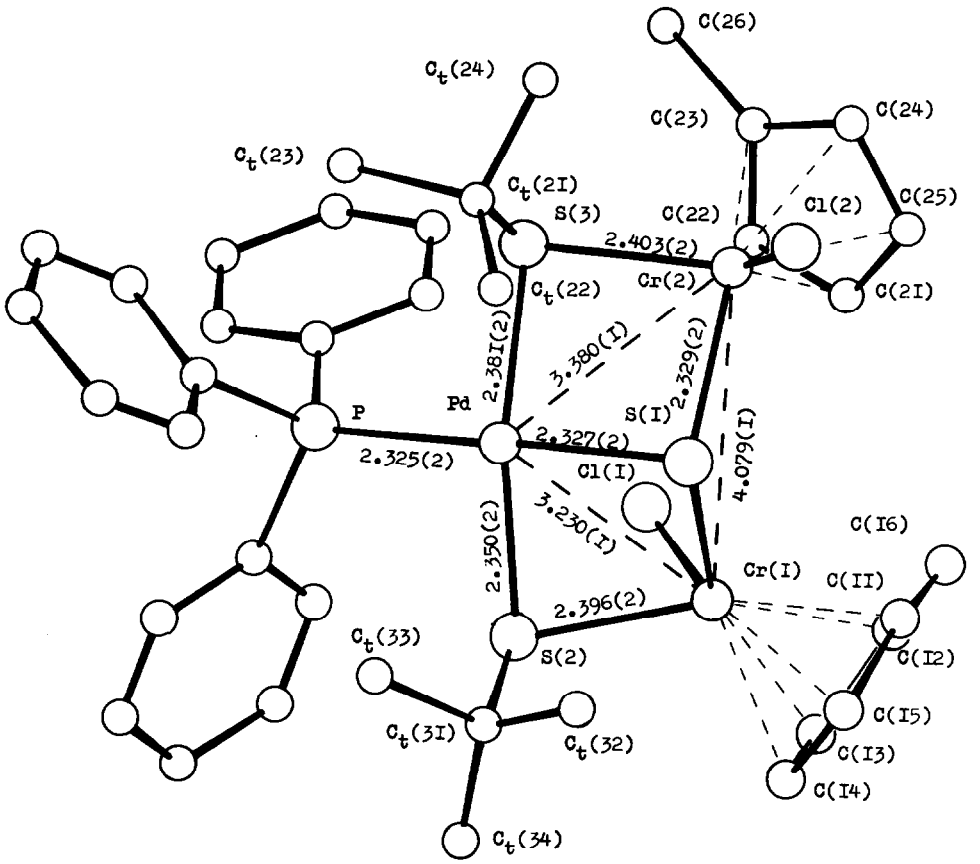



Fig. 1.

is due to the stretching modes of $CH_3$ in cyclopentadienyl ligand. It is to be noted that the same differences was observed in the spectra of pairs of complexes $(RC_5H_4CrS)_4$(R = H, $CH_3$)[3] and $(RC_5H_4)_2Cr_2(SCMe_3)S_2Co(CO)_2$ studied by us recently.

Unlike the starting complexes I and II displaying antiferromagnetic exchange interactions ($-2J$ = 430 and 480 $cm^{-1}$ respectively,[3] the complexes III and IV have positive exchange parameters (III, $\mu_{eff.}$ (B.M.) = 4.11(296K), 4.26(197K), 4.57(79K); IV, $\mu_{eff.}$ (B.M.) = 3.87(296K), 4.00(213K), 4.20(95K)). Temperature dependences of the static magnetic susceptibility are described in terms of HDVV model[5] of two chromium(III) atoms with spin 3/2. The ferromagnetic exchange parametefs are $+2J = 28$ and 11 $cm^{-1}$ for III and IV respectively.

Formally the composition of complexes III and IV corresponds to the adducts $(RC_5H_4CrSCMe_3)_2S{\cdot}PdCl_2(PPh_3)$ similar to the complexes $(RC_5H_4CrSCMe_3)_2S{\cdot}ML$, formed when CN is equal to 6.[2] However, all of these complexes are antiferromagnetic ($-2J \simeq 400\ cm^{-1}$). Moreover in them the structure of molecules I or II remains practically unchanged and the treatment of complexes with dipyridyl yields I or II. In the case of complexes III and IV such treatment gives neither I or II. Therefore for unequivocal determination of the structure of III and IV we carried out an X-ray study of the latter which crystallized with one benzene molecule (Fig. 1). It was shown that an addition of the $PPh_3PdCl_2$ moiety to the sulphide bridge of II (Pd–S(I) 2.327(2) Å) results in transfer of Cl atoms from Pd to Cr atoms (Cr–Cl 2.308(2) Å). The chlorine atoms as well planar methylcyclopentadienyl ligands $\pi$-bonded to Cr (mean Cr–C 2.256(6), mean C–C 1.427(9) Å) are in *trans*-position to each other in respect to the $Cr_2Pd$ plane. The thiolate groups become bridges between the Pd atom and each Cr atom (Pd–S 2.350(2) and 2.381(2), Cr–S 2.396(2) and 2.403(2) Å). The Pd atom retains in fact its square planar environment supplemented by coordination of the $PPh_3$ ligand (Pd–P 2.325(2) Å). Thus an unusual chelate ligand $PPh_3Pd(SCMe_3)_2$ is formed. The distances between metal atoms are nonbonding (Cr ... Cr 4.079(1), Cr(1) ... Pd 3.230(1), Cr(2) ... Pd 3.380(1) Å) and the exchange interactions between Cr atoms are achieved mainly via the sulphide bridge shared with the Pd atom (Cr(1)–S(1) 2.339(2), Cr(2)–S(1)

Table 1. Bond lengths d (Å)

| Bond | d(Å) | Bond | d(Å) | Bond | d(Å) |
|---|---|---|---|---|---|
| Pd–S(1) | 2.327(2) | Cr(2)–C(24) | 2.275(6) | $C_t$(21)–$C_t$(23) | 1.537(9) |
| Pd–S(2) | 2.350(2) | Cr(2)–C(25) | 2.234(6) | $C_t$(21)–$C_t$(24) | 1.534(9) |
| Pd–S(3) | 2.381(2) | S(2)–$C_t$(31) | 1.880(7) | $C_t$(31)–$C_t$(32) | 1.56(1) |
| Pd–P | 2.325(2) | S(3)–$C_t$(21) | 1.872(6) | $C_t$(31)–$C_t$(33) | 1.52(1) |
| Cr(1)–S(1) | 2.339(2) | P–$C_p$(11) | 1.822(6) | $C_t$(31)–$C_t$(34) | 1.55(1) |
| Cr(1)–S(2) | 2.396(2) | P–$C_p$(17) | 1.825(6) | $C_t$(31)–$C_t$(32') | 1.54(2) |
| Cr(1)–Cl(1) | 2.308(2) | C(11)–C(12) | 1.428(9) | $C_t$(31)–$C_t$(33') | 1.54(2) |
| Cr(1)–C(11) | 2.248(6) | C(11)–C(15) | 1.429(9) | $C_t$(31)–$C_t$(34') | 1.50(2) |
| Cr(1)–C(12) | 2.286(6) | C(12)–C(13) | 1.424(9) | $C_b$(1)–$C_b$(2) | 1.39(1) |
| Cr(1)–C(13) | 2.264(6) | C(12)–C(16) | 1.501(9) | $C_b$(1)–$C_b$(3) | 1.41(1) |
| Cr(1)–C(14) | 2.244(7) | C(13)–C(14) | 1.432(9) | $C_b$(2)–$C_b$(3) | 1.38(1) |
| Cr(1)–C(15) | 2.216(7) | C(14)–C(15) | 1.420(9) | $C_b$(1')–$C_b$(2') | 1.42(2) |
| Cr(2)–S(1) | 2.329(2) | C(21)–C(22) | 1.42(1) | $C_b$(1')–$C_b$(3') | 1.46(2) |
| Cr(2)–S(3) | 2.403(2) | C(21)–C(25) | 1.399(9) | $C_b$(2')–$C_b$(3') | 1.39(2) |
| Cr(2)–Cl(2) | 2.308(2) | C(22)–C(23) | 1.428(9) | $C_b$(1'')–$C_b$(2'') | 1.32(2) |
| Cr(2)–C(21) | 2.225(6) | C(23)–C(24) | 1.426(7) | $C_b$(1'')–$C_b$(3'') | 1.40(2) |
| Cr(2)–C(22) | 2.241(7) | C(24)–C(25) | 1.425(9) | $C_b$(2'')–$C_b$(3'') | 1.34(2) |
| Cr(2)–C(23) | 2.298(7) | $C_t$(21)–$C_t$(22) | 1.527(7) | | |

2.329(2) Å, CrSCr angle 121.77(7)°). A notable displacement of the S(1) atom (0.94 Å) from the $Cr_2Pd$ plane and slight deviations of two S atoms of the thiolate bridges and the P atom of $PPh_3$ ligand in the opposite direction give rise to the dihedral angle of 148° between the $S_3PdP$ and $Cr_2Pd$ planes. In this situation the Pd–S(1) bond is normal to the $Cr_2S(1)$ plane. It is to be noted that one of the tert-butyl groups (at the S(2) atom) is disordered and of carbons the methyl groups occupy two nearly equally populated positions. A similar disorder is found for one of the crystallization molecules of benzene (only three atoms are independent as in the case of the second but ordered benzene molecule, both benzene molecules being situated in the symmetry centres).

## DISCUSSION OF RESULTS

Formation of the complexes **III** and **IV** in the reactions of **I** and **II** with $(PPh_3)_2PdCl_2$ probably starts with a substitution of one $PPh_3$ ligand by a lone electron pair of the sulphide bridge of dichromium fragment. Further rearrangement of an intermediate adduct $(RC_5H_4Cr–SCMe_3)_2S·Pd(PPh_3)Cl_2$ seems to be due to an additional coordination of the thiolate sulphur atoms in sites axial of the Pd atom. The formation of RS–Pd bonds is accompanied by a transfer of Cl atoms from Pd to both Cr atoms. Probably this rearrangement is governed by the Pearson principle,[6] i.e. $Cl^-$ ions, being hard Lewis bases, are bonded preferably with Cr(III) ions as hard Lewis acids. At the same time the Pd(II) atom as a soft acid prefers binding with thiolate groups acting as soft bases.

Probably a transformation of Cr–SR–Cr bridges to Pd–SR–Cr ones explains also an elongation of the Cr...Cr distances from 2.689 Å in **I** to a non-bonding value (4.079(1) Å) in **IV** although formally the number of electrons donated by ligands to each Cr atom has not changed. Here it should be stressed that the axial position of the system $RC_5H_4Cr–CrC_5H_4R$ in **I** and probably in **II** provided an efficient overlap of $d_{z^2}$ orbitals responsible mainly for Cr–Cr bonding. On the other hand in **IV** the Cp′ĈrCr angles are equal to 124.5° (Cp′–centroid of the $RC_5H_4$ ring) so that the $d_{z^2}$ orbitals have almost no overlap and thus $S...C_{C_5H_4R}$ and $Cl...C_{C_5H_4R}$ repulsion effects become decisive.

A disappearance of direct Cr–Cr bonding is

Table 2. Bond angles (degrees)

| Angle | (deg.) | Angle | (deg.) | Angle | (deg.) |
|---|---|---|---|---|---|
| S(I)PdS(2) | 84.I8(5) | $PdPC_p(23)$ | II6.0(2) | $S(3)C_t(2I)C_t(22)$ | I07.6(4) |
| S(I)PdS(3) | 86.00(5) | $C_p(II)PC_p(I7)$ | I07.4(3) | $S(3)C_t(2I)C_t(23)$ | I09.8(4) |
| S(I)PdP | I72.57(6) | $C_p(II)PC_p(23)$ | I00.3(3) | $S(3)C_t(2I)C_t(24)$ | I06.4(5) |
| S(2)PdS(3) | I68.39(6) | $C_p(I7)PC_p(23)$ | I03.5(3) | $C_t(22)C_t(2I)C_t(23)$ | III.I(5) |
| S(3)PdP | 95.60(6) | C(I2)C(II)C(I5) | I07.6(6) | $C_t(22)C_t(2I)C_t(24)$ | I08.9(5) |
| S(2)PdP | 93.37(6) | C(II)C(I2)C(I3) | I08.I(5) | $C_t(23)C_t(2I)C_t(24)$ | II2.8(5) |
| S(I)Cr(I)Cl(I) | I04.56(6) | C(II)C(I2)C(I6) | I26.9(6) | $S(2)C_t(3I)C_t(32)$ | III.6(5) |
| S(2)Cr(I)Cl(I) | 88.47(6) | C(I3)C(I2)C(I6) | I25.9(6) | $S(2)C_t(3I)C_t(33)$ | I05.0(6) |
| S(I)Cr(I)S(2) | 82.92(6) | C(I3)C(I4)C(I5) | I08.5(6) | $S(2)C_t(3I)C_t(34)$ | I08.9(5) |
| S(I)Cr(2)Cl(2) | 9I.09(6) | C(I2)C(I3)C(I4) | I08.0(6) | $S(2)C_t(3I)C_t(32')$ | I04.5(8) |
| S(3)Cr(2)Cl(2) | I07.58(7) | C(II)C(I5)C(I4) | I08.5(6) | $S(2)C_t(3I)C_t(33')$ | I05.0(9) |
| S(I)Cr(2)S(3) | 85.46(6) | C(22)C(2I)C(25) | I08.8(6) | $S(2)C_t(3I)C_t(34')$ | II4(I) |
| PdS(I)Cr(I) | 86.95(6) | C(2I)C(22)C(23) | I07.2(6) | $C_t(32)C_t(3I)C_t(33)$ | III.3(8) |
| PdS(I)Cr(2) | 93.I0(6) | C(22)C(23)C(24) | I08.2(6) | $C_t(32)C_t(3I)C_t(34)$ | I09.0(7) |
| Cr(I)S(I)Cr(2) | I2I.77(7) | C(22)C(23)C(26) | I26.4(6) | $C_t(33)C_t(3I)C_t(34)$ | II0.8(8) |
| PdS(2)Cr(I) | 85.I4(6) | C(23)C(24)C(25) | I07.0(6) | $C_t(32')C_t(3I)C_t(33')$ | I08(I) |
| $PdS(2)C_t(3I)$ | I09.8(3) | C(2I)C(25)C(24) | I07.0(6) | $C_t(32')C_t(3I)C_t(34')$ | II0(I) |
| $Cr(I)S(2)C_t(3I)$ | II7.3(2) | $PC_p(II)C_p(I2)$ | II8.9(5) | $C_t(33')C_t(3I)C_t(34')$ | II5(I) |
| PdS(3)Cr(2) | 89.92(6) | $PC_p(II)C_p(I6)$ | I20.6(5) | $C_b(2)C_b(I)C_b(3)$ | II9.2(8) |
| $PdS(3)C_t(2I)$ | II3.0(2) | $PC_p(I7)C_p(I8)$ | I23.5(5) | $C_b(I)C_b(2)C_b(3)$ | I20.5(8) |
| $Cr(2)S(3)C_t(2I)$ | I09.5(2) | $PC_p(I7)C_p(22)$ | II6.7(5) | $C_b(I)C_b(3)C_b(2)$ | I20.7(7) |
| $PdPC_p(II)$ | III.4(2) | $PC_p(23)C_p(24)$ | II6.3(5) | $C_b(2')C_b(I')C_b(3')$ | I22(I) |
| $PdPC_p(I7)$ | II6.7(2) | $PC_p(23)C_p(28)$ | II9.6(5) | $C_b(I')C_b(2')C_b(3')$ | I22(I) |
| | | | | $C_b(I')C_b(3')C_b(2')$ | II6(I) |

probably a cause of the change of both value and sign of exchange interaction parameters on going from I and II to III and IV. As was previously shown[1] the high value of antiferromagnetic exchange parameter for I ($-2J = 430\,cm^{-1}$) and its derivatives (e.g. for $(Cp_2Cr_2SCMe_3)(\mu_3\text{-}S)_2Fe(CO)_3$ $-2J_{Cr\text{-}Fe} = 2600\,cm^{-1}$)[7] is explained by direct Cr–M bonding whereas an indirect exchange via sulphide bridges is smaller by an order of magnitude ($-2J_{Cr\text{-}S\text{-}Fe} = 170\,cm^{-1}$).[7] In the absence of direct Cr–Cr bonding the character of superexchange via the bridging ligands L would be determined by contributions of antiferro- and ferromagnetic exchange interactions depending on the value of M–L̂–M angle.

As was shown in[8,9] the angular dependence of antiferromagnetic exchange contribution $-2J^{af}$ to the superexchange parameter $-2J$ via monoatomic bridging ligands is described by the equation:

$$-2J^{af} = 4(a + b\cos\theta)^2 \qquad (1)$$

here $\theta$ is the M–L̂–M angle, $a$ and $b$ are contributions into a superexchange due to interaction of unpaired electrons via $s$- and $p$-orbitals of a bridged atom respectively.

Since the antiferromagnetic contribution to superexchange as a rule essentially exceeds the ferromagnetic term[10] the maximum of the latter is attained when $-2J^{af} = 0$, i.e.

$$\theta = \arccos(-a/b) \qquad (2)$$

With electronegative ligands ($O^{2-}$, $F^-$, $Cl^-$ ...) an interaction of unpaired electrons via $s$-orbitals is considerably weaker then via the $p$-orbitals. For

instance with NiO the angular dependence of superexchange has the form:[11]

$$-2J = 770\cos^2\theta + 222\cos\theta - 25(\text{cm}^{-1}). \quad (3)$$

From (3) and (1) it follows that $a/b = 0.144$ and substitution of this value in (2) gives $\theta = 98.5°$ corresponding to maximum of ferromagnetism.

On going to the donor ligand $S^{2-}$ one should observe the stronger interaction of unpaired electrons via *s*-orbitals of a bridging atom, i.e. an increase of the $a/b$ ratio. In accordance with (2) this should increase essentially the value of $\theta$ which is in agreement with experimental data (in **IV** the $Cr\hat{S}Cr$ angle is 121.77°).

As to the decrease of $+2J$ from 28 to 11 $cm^{-1}$ on going from **III** to **IV** this effect can be due to an enhancing of antiferromagnetic exchange interaction of electron–donor methyl group into the cyclopentadienyl ring. In particular, this effect was observed on going from **I** to **II** ($-2J$ increased from 430 to 480 $cm^{-1}$).[3]

In conclusion it should be stressed that the complexes **III** and **IV** are the first examples of ferromagnetic exchange interactions via a sulphur-containing bridging ligand. This is of great interest for better understanding of the role of exchange interactions in magnetic materials with spinel type structure.[12]

## REFERENCES


1. A. A. Pasynskii. I. L. Eremenko, Yu. V. Rakitin, V. M. Novotortsev, V. T. Kalinnikov, G. G. Aleksandrov adn Yu. T. Struchkov, *J. Organometal. Chem.* 1979, **165**, 57.
2. A. A. Pasynskii, I. L. Eremenko, V. T. Kalinnikov and Yu. A. Buslaev, *Izv. Sibirsk. Otd. Akad. Nauk. SSSR, ser. khim.* 1982, **9**, 88.
3. A. A. Pasynskii, I. L. Eremenko, Yu. V. Rakitin, V. M. Novotortsev, O. G. Ellert, V. T. Kalinnikov, V. E. Shklover, Yu. T. Struchkov, S. V. Lindemann, T. Kh. Kurbanov and G. Sh. Gasanov, *J. Organometal. Chem.* 1983, **248**, 309.
4. V. M. Novotortsev, Dr. Ph. Thesis. Moscow (1974).
5. J. H. VanVleck, *The Theory of Electric and Magnetic Susceptibilities*. Oxford University Press, Oxford (1932).
6. R. G. Pearson, *J. Am. Chem. Soc.* 1963, **85**, 3533.
7. A. A. Pasynskii, I. L. Eremenko, B. Orazsakhatov, Yu. V. Rakitin, V. M. Novotortsev, O. G. Ellert, G. G. Aleksandrov and Yu. T. Struchkov, *J. Organometal. Chem.* 1981, **210**, 385.
8. A. S. Moskvin, N. S. Oganesyan and V. A. Trukhtanov, *Hyperfine Interactions* 1975, **I**, 265.
9. Yu. V. Rakitin, V. V. Volkov and V. T. Kalinnikov, *Koordinatsionnaya Khimiya* 1981, **7**, 1622.
10. P. W. Anderson, *Phys. Rev.* 1950, **115**, 2.
11. K. Motida, *J. Phys. Soc. Japan* 1978, **44**, 1498.
12. S. V. Vonsovskii, *Magnetism*, p. 385. "Nauka", Moscow (1971).

*Polyhedron* Vol. 3, No. 7, pp. 781–785, 1984
Printed in the U.S.A.

0277-5387/84 $3.00 + .00
© 1984 Pergamon Press Ltd.

# KINETIC STUDIES OF SOLVENT EXTRACTION OF METAL COMPLEXES—IX. RATE OF COMPLEX FORMATION OF CHROMIUM(III) WITH ACETYLACETONE IN AQUEOUS PERCHLORATE SOLUTIONS AND IN TWO POLAR ORGANIC SOLVENTS

TATSUYA SEKINE,* KAZUHO INABA and OSAMU TAKAHASHI
Department of Chemistry, Science University of Tokyo, Kagurazaka, Shinjuku-ku, Tokyo, Japan

(*Received* 14 *June* 1983; *accepted* 6 *December* 1983)

**Abstract**—The rate of complex formation of chromium(III) with acetylacetone in aqueous perchlorate solutions was determined by a solvent extraction method in 4-methyl-2-pentanone and 4-methyl-2-pentanol. The rate of complex formation in the organic solvents was also studied by a spectrophotometric method. On the basis of the results that the rate of complex formation was nearly the same in these three media, a mechanism for the extraction of the metal ions in aqueous perchlorate solutions with acetylacetone into these polar organic solvents was proposed.

In a previous study,[1] the rate of solvent extraction of chromium(III) with acetylacetone into 4-methyl-2-pentanone and 4-methyl-2-pentanol was studied. A possible extraction mechanism, in which the metal ions in the aqueous phase were first extracted as perchlorate and then formed the complexes in the organic phase, was suggested. In order to explain the results obtained, the rate of complex formation was supposed in this previous paper to be much higher in the organic solutions than in the aqueous solutions in the same solvent extraction system.[2] In the present paper, the rate of this complex formation in the aqueous perchlorate solutions has been measured by a solvent extraction method and the rates of formation in these two organic solvents has also been measured by a spectrophotometric method. The rates in the organic solvents were concluded, on the contrary to this previous assumption, to be similar with that in the aqueous solutions. For this reason, another mechanism for the solvent extraction of the metal ions in the above liquid–liquid systems has been proposed.

*Author to whom correspondence should be addressed.

## EXPERIMENTAL

All the reagents were of a reagent grade. Acetylacetone(HA) and tris(acetylacetonato)chromium(III) were supplied by Dojindo Laboratories, Kumamoto, Japan. Purification of the organic solvents and preparation of the aqueous perchlorate solutions were carried out as reported previously.[1] All the procedures were performed in a thermostatted room at 298 K. An aqueous 4 mol $dm^{-3}$ sodium perchlorate solution containing acetylacetone was prepared and left standing overnight before the use. The solution was mixed with an aqueous sodium perchlorate solution containing chromium(III) and the resulting sample was kept in the dark. The concentration of acetylacetone in the sample was in a range from $3 \times 10^{-3}$ to $8 \times 10^{-2}$ mol $dm^{-3}$ and that of chromium(III) was $1.5 \times 10^{-3}$ mol $dm^{-3}$. After a certain time interval, which was longer than 5 min, a portion of the sample was transferred into another stoppered glass tube and vigorously agitated with the same volume of a fresh organic solution containing acetylactone and the acid for 5 sec by hand. The amount of chromium(III) in the organic phase after this extraction was measured by an atomic absorption method.

A portion of one of the organic solvents was agitated with an amount of aqueous 4 mol $dm^{-3}$

sodium perchlorate solution containing chromium(III) and perchloric acid and the solvent which extracted the metal perchlorate was mixed up with the same solvent containing a certain amount of acetylacetone. The concentration of chromium(III) in the mixed sample was $1 \times 10^{-3}$ mol dm$^{-3}$ and that of acetylacetone was in a range from $1.0 \times 10^{-2}$ to $2.0 \times 10^{-1}$ mol dm$^{-3}$. The acid concentration in the organic solution was obtained by separate experiments. The concentration of acetylacetone in these organic solutions was supposed to be high enough to convert the whole chromium(III) into the tris(acetylacetonato) complex at equilibrium. The absorption was measured on the reagent blank and measurements were repeated after certain time intervals. The calibration curve was obtained by measuring the absorption of standard solutions prepared from weighed amounts of the tris-(acetylacetonato)chromium(III).

## STATISTICAL

In this paper, the subscript "org" denotes chemical species in an organic solution while lack of it denotes those in an aqueous solution.

Since the rate was found in all cases to be first order with respect to $Cr^{3+}$, the rate of complex formation can generally be represented by;

$$-d[Cr^{3+}]/dt = k[Cr^{3+}][HA]^a[H^+]^b. \quad (1)$$

The dependence on each component, "$a$" or "$b$" can be determined by measuring the rate at several concentrations but keeping the others constant. The equations for the rate in the aqueous solutions can be written as;

$$\log q_{(HA)} = \log k^*(h)^b + a \log[HA] \quad (2a)$$

$$\log q_{(H^+)} = \log k^*(ha)^a + b \log[H^+] \quad (2b)$$

where $(h)$ or $(ha)$ is the concentration of $H^+$ or HA in the aqueous solution which is kept at a certain value in a series of experiments and $k^*$ is $k/\log_e 10$. From the slope of the log $q_{(HA)}$ vs log[HA] plot, the dependence "$a$" can be obtained and in the same way, "$b$" can also be determined. The rate constant $k$ can be calculated from these data by eqn (1).

The amount of complexes formed in the aqueous solution was calculated from that of the extracted chromium(III) as written in the experimental section. When the distribution equilibrium is established among the metal species in both phases, the following equations can be written;

$$MA_n^{(3-n)} + (3-n)ClO_4^- \rightleftharpoons MA_n(ClO_4)_{3-n}(org)$$

$$R = \Sigma[MA_n(ClO_4)_{3-n}]/\Sigma[MA_n^{3-n}] \quad (3)$$

where $n$ may be 1–3.

$$R = ([M(m)]_{org.total} - R_0[M^{3+}])/\Sigma[MA_n^{3-n}]. \quad (4)$$

Thus when the distribution ratio of the $M(ClO_4)_3$ species, $R_0$, is determined in the absence of HA, the distribution ratio of the complexes, R, can be calculated by eqn (3). Equation (3) should be applied only when both the distribution and complex formation equilibria are established. However, if the rate of complex formation is low and a transient distribution equilibrium is established within a very short time interval, it is possible to calculate an approximate amount of complex formed in the aqueous phase on the basis of eqn (4).

The rate of complex formation in the organic phase can also be written as;

$$-d[Cr^{3+}]_{org}/dt = k_{org}[Cr^{3+}]_{org}[HA]^a_{org}[H^+]^b_{org} \quad (5)$$

$$\log q_{(HA)org} = \log k^*_{org}(h)^b_{org} + a \log[HA]_{org} \quad (6a)$$

$$\log q_{(H^+)org} = \log k^*_{org}(ha)^a_{org} + b \log[H^+]_{org} \quad (6b)$$

where $[H^+]_{org}$ is the stoichiometric concentration of perchloric acid in these solvents and $k^*_{org}$ is $k_{org}/\log_e 10$. The rate constant $k_{org}$ can also be calculated by the same way as above.

## RESULTS

(1) *Liquid–liquid distribution equilibria of acetylacetone and perchloric acid*

The distribution constants of acetylacetone and perchloric acid between each organic solvent and the aqueous 4 mol dm$^{-3}$ sodium perchlorate solution;

$$K_d = [HA]_{org}[HA]^{-1} \quad (7)$$

$$D_{H^+} = ([HClO_4]_{org} + [H^+]_{org})/[H^+] \quad (8)$$

which are necessary for the analysis of the kinetic data were obtained at 298 K as:

(i) 4-methyl-2-pentanone-aqueous system

$$\log K_d = 0.4 \quad \log D_{H^+} = -0.2$$

(ii) 4-methyl-2-pentanol-aqueous system

$$\log K_d = 0.1 \quad \log D_{H^+} = 0.5.$$

(2) *Rate of complex formation in aqueous perchlorate solutions*

No marked change in the absorption was found either in the visible or in the UV region after acetylacetone was added to the aqueous perchlorate solution containing $Cr^{3+}$ and thus spectrophotometry of the complexes in the aqueous solutions could not be made. This should be due to that the molar extinction coefficients of the acetylacetonato complexes were too low and the amounts formed were too small to allow such measurements.

As already described, a certain amount of chromium(III) was extracted into the organic phase by an agitation of a portion of the sample aqueous solution with a portion of an 4-methyl-2-pentanone- or 4-methyl-2-pentanol-acetylacetone solution. A part of the extracted metal species was chromium perchlorate but since the amount extracted increased by an increase in the standing time of the aqueous solution, the rest was concluded to be acetylacetonato complexes. In order to determine the distribution ratio of the complexes, a portion of the aqueous phase was transferred into another tube after this extraction and agitated with the same volume of a fresh 4-methyl-2-pentanone- or 4-methyl-2-pentanol-acetylacetone solution. The net distribution ratio of chromium complexes, R, obtained from these data on the basis of eqn (3), was 0.4 when the solvent was 4-methyl-2-pentanone and was 0.6 when the solvent was 4-methyl-2-pentanol. These values were affected neither by pH nor by the concentration of the extractant. From these values of R and eqn (1), the rate of complex formation in the aqueous solution was calculated and the values of $\log q_{(HA)}$ and $\log Q_{(H^+)}$ in eqns (2a) and (2b) were obtained as given in Figs. 1(a), (b), 2(a) and (b).

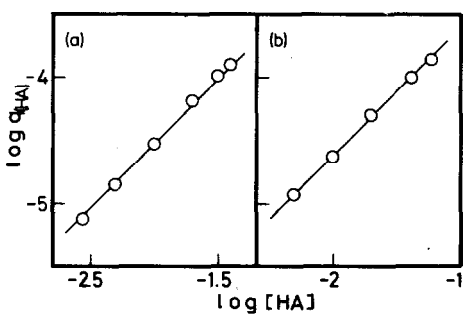



Fig. 1. Dependence of the rate of formation of acetylacetonato chromium(III) complexes on the ligand concentration in 4 mol dm$^{-3}$ (H, Na)$ClO_4$ constant ionic media; (a) determined by 4-methyl-2-pentanone extraction method and (b) by 4-methyl-2-pentanol extraction method. The hydrogen-ion concentration was kept at $10^{-3.8}$ mol dm$^{-3}$ in the both systems.

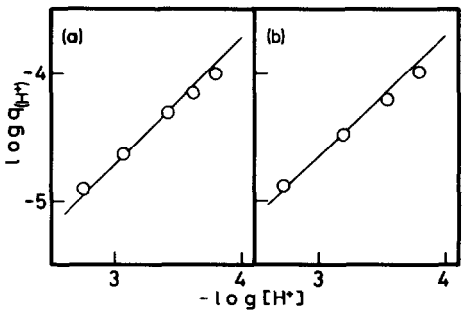



Fig. 2. Dependence of the rate of formation of acetylacetonato chromium(III) complexes on hydrogen-ion concentrations in 4 mol dm$^{-3}$ (H, Na)$ClO_4$ ionic media; (a) determined by 4-methyl-2-pentanone extraction method and (b) by 4-methyl-2-pentanol extraction method. The acetylacetone concentration in the aqueous solutions were 0.028 mol dm$^{-3}$ in the former system and 0.042 mol dm$^{-3}$ in the latter system.

As seen from these figures, the rate of complex formation in the aqueous solutions was first order with respect to the total ligand and inverse first order to the hydrogen-ion. The $-\log [H^+]$ vs $\log q_{(H^+)}$ plot slightly deviates from a slope of $+1$ (see Figs. 2a and b). This may be explained in terms that the hydrolyzed species of chromium(III) are not negligible in this pH range.

(3) *Rate of complex formation in organic solutions*

The molar extinction coefficient of the tris-(acetylacetonato)chromium(III) in 4-methyl-2-pentanone containing acetylacetone and perchloric acid was found to be $1.60 \times 10^4$ at 336 nm while that in 4-methyl-2-pentanol was $1.50 \times 10^4$ at 331 nm. The amount of tris-complex formed in the organic solution was calculated from the absorbance at these wave lengths assuming that the tris-complex was dominant. The rate of complex formation was always first order with respect to chromium(III). When the hydrogen-ion concentration was kept constant, the rate was first order with respect to the total reagent concentration. However, the dependence on the acid concentration was not an integer as can be seen from Figs. 3(a) and (b).

## DISCUSSION

From the results in Figs. 1(a)–2(b), the following equation can be introduced for the rate of complex formation in the aqueous perchlorate solutions;

$$-d[Cr^{3+}]/dt = k[Cr^{3+}][HA][H^+]^{-1}. \quad (9)$$

Both of the following reactions may explain the

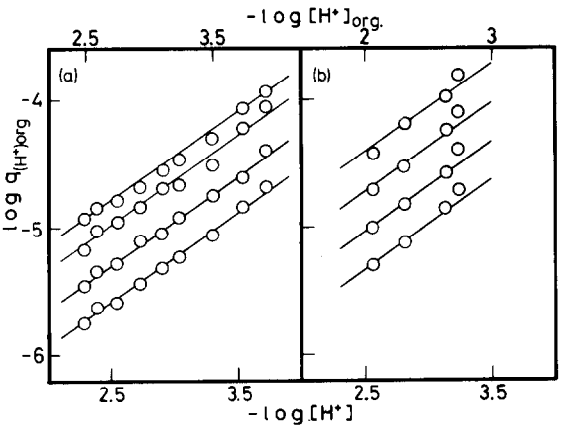



Fig. 3. Dependence of the rate of formation of acetylacetonato chromium(III) complexes on hydrogen-ion concentration, (a) in 4-methyl-2-pentanone and (b) in 4-methyl-2-pentanol. The organic solutions were prepared by equilibrating with aqueous solutions whose pH is given on the bottom line. The concentration of the ligand in the organic solutions is (a) 0.15, 0.10, 0.05 and 0.025 mol $dm^{-3}$, and (b) 0.20, 0.10, 0.05 and 0.025 mol $dm^{-3}$ from the top to the bottom. The figures on the top line give the stoichiometric acid concentration in the organic solutions. The straight lines in figures indicate a slope of +0.7.

rate in eqn (9);

$$Cr^{3+} + A^- \rightarrow CrA^{2+}$$

$$-d[Cr^{3+}]/dt = k_{(A)}[Cr^{3+}][A^-]$$

$$k_{(A)} = k \times K_a^{-1} \qquad (10)$$

$$Cr(OH)^{2+} + HA_{(enol)} \rightarrow CrA^{2+} + H_2O$$

$$-d[CrOH^{2+}]/dt = k_{(HAenol)}[CrOH^{2+}][HA]_{enol}$$

$$k_{(HAenol)} = k(1 + K_e)K_e^{-1}K_h^{-1} \qquad (11)$$

where $K_a$ is the acid dissociation constant, $K_e$ is the keto-enol equilibrium constant ($K_e = [HA]_{enol}[HA]_{keto}^{-1}$), and $K_h$ is the hydrolysis constant ($K_h = [CrOH^{2+}][H^+][Cr^{3+}]^{-1}$).

The rate constant, $k$, in eqn (9) is calculated from the data in Figs. 1(a)–2(b) to be about $10^{-6.2} - 10^{-6.0}$ ($sec^{-1}$). From this and the values $10^{-10.09}$ for $K_a$ (unpublished data by the authors), $10^{-0.63}$ for $K_e$ (Ref. 3), and $10^{-4}$ for $K_h$ (in the literature it is in a range of $10^{-3.5} - 10^{-4.2}$ (Ref. 4)), the value of $k_{(A)}$ in eqn (10) obtained was about $10^{3.9}$ ($mol^{-1}\,dm^3\,sec^{-1}$) and $k_{(HAenol)}$ for eqn (11) was about $10^{-1.5}$ ($mol^{-1}\,dm^3\,sec^{-1}$). Since the values used for the analysis of the present data were to some extent erroneous, the value of $k_{(A)}$ and $k_{(HAenol)}$ should also be somewhat erroneous. There have been several reports on the rate constants of hydrated $Cr^{3+}$ ion with several ligands;[5-7] they are in a range of $10^{-5}$–$10^{-7}$ ($mol^{-1}dm^3\,sec^{-1}$) and the value of $k_{(A)}$ obtained in the present study is obviously too high. Thus it seems to be reasonable to conclude that the complex formation is controlled by the reaction between the hydrolyzed chromium(III) species, $CrOH^{2+}$, and the ligand in the undissociated enol form, HA, although the value of $k_{(HAenol)}$ in eqn (11) is still a little higher than the values in the literature (they are in a range of $10^{-3}$–$10^{-5}$ ($mol^{-1}\,dm^3\,sec^{-1}$)).[5-7]

Since the dependence of the rate in the organic solutions on hydrogen-ions was not an integer, the rate in the aqueous and organic solutions cannot be compared directly on the basis of eqns (1) and (3). However, when the hydrogen-ion concentration in the aqueous phase is $10^{-2.4}$ mol $dm^{-3}$ and the total acetylacetone concentration in the aqueous phase at equilibrium is 0.028 mol $dm^{-3}$, the rates of complex formation in these aqueous and organic solutions were nearly the same though there should be a small difference if the acid concentration is higher or lower than this.

This dependence of the rate on the hydrogen-ions in the organic solvents does not seem to be explained only by a change in the activity coefficient of the ions due to changes in their concentrations. It was reported that chromium(III) was extracted together with trichloroacetate ions into several polar organic solvents rapidly and the absorption of the extracted organic phase was similar to that of hexahydrated chromium(III).[8] From these previous and present results, it may be assumed that the chromium(III) extracted as ion-pairs into the two polar solvents was hydrated even in the organic phase and the exchange of the hydrating water molecules with the solvent molecules may be rather slow. The complex formation may take place by an exchange of the ligand molecules with the solvating water and/or organic solvent molecules.

It was assumed in the previous study[1] that the rate of complex formation should be much higher in 4-methyl-2-pentanone or 4-methyl-2-pentanol than in the aqueous 4 mol $dm^{-3}$ sodium perchlorate solutions. However, from the direct rate measurements in the present study, such a higher rate of complex formation in the organic solvents was not found. On the contrary, it can be concluded that the solvent extraction of chromium(III) in the liquid–liquid system treated previously should be controlled mainly by the formation of the first complex in the aqueous phase and the rate of extraction into the polar solvents

observed should give the rate of extraction of the charged complexes, $CrA^{2+}$ and $CrA_2^+$, as ion-pairs with perchlorate ions. At the same time, since the extraction of the metal perchlorate into the organic phase was rather poor, the contribution of the complex formation in the organic phase to the rate of the metal extraction should be only small. In the previous study,[1] a second order dependence of the extraction rate on the aqueous perchlorate concentration was found and although this was explained to be due to an extraction of the $Cr(OH)^{2+}$ species as ion-pairs with perchlorate ions, it would be more reasonable to assume it to be due to the extraction of the $(CrA^{2+})(ClO_4^-)_2$ species. At the same time, it should also be affected by changes in the extraction of the other species such as the extractant and so on.

There have been several methods reported to measure the rate of complex formation in aqueous solutions and the solvent extraction method has been proposed as one of them.[9] However, this method is not always applicable for this purpose because knowledge of the chemical equilibria involved in the liquid–liquid system is sometimes indispensable for a reasonable analysis of the kinetic data as was pointed out by the present authors previously.[10] In other words, the rate of solvent extraction of certain metal ions is not identical with that of complex formation in the aqueous phase even when the extraction is controlled by this complex formation. In the present study, a solvent extraction technique was found to be useful for the measurements of the rate of complex formation of chromium(III) in the aqueous solutions even when the spectrophotometric method was not applicable. This technique should also be useful when the complexes are colourless and the rate of complex formation is very low if the charged complexes are extractable.

## REFERENCES


1. T. Sekine and H. Inagaki, *J. Inorg. Nucl. Chem.* 1980, **42**, 115.
2. T. Sekine, *Proc. Int. Solvent Extraction Conf.*, pp. 80–46. Liege (1980).
3. O. Kammori, K. Sato, K. Takimoto and K. Arakawa, *Bunseki Kagaku* 1966, **15**, 561.
4. L. G. Sillen and A. E. Martell, *Stability Constants*, Special Publications Nos. 17 and 24. The Chemical Society, London (1964) and (1972).
5. C. Postmus and E. L. King, *J. Phys. Chem* 1955, **59**, 1208 and 1217.
6. R. E. Hamm, R. L. Johnson, R. H. Perkins and R. E. Davis, *J. Am. Chem. Soc.* 1958, **80**, 4469.
7. M. Kimura and J. Shirai, *J. Inorg. Nucl. Chem.* 1978, **40**, 1085.
8. T. Kiba, H. Imura and T. Honjo, *Chem. Lett.* 1977, 805.
9. H. Freiser, *Solvent Extraction Chemistry, Proc. Int. Solvent Extraction Conf.*, p. 85. North-Holland, Gothenburg (1967).
10. T. Sekine and K. Inaba, *Bull. Chem. Soc. Jpn.* 1982, **55**, 3773.

*Polyhedron* Vol. 3, No. 7, pp. 787–797, 1984
Printed in the U.S.A.

0277-5387/84 $3.00 + .00
© 1984 Pergamon Press Ltd.

# MIXED LIGAND COMPLEXES INVOLVED IN THE SYSTEM PYRIDOXAMINE–GLYCYLGLYCINE–IMIDAZOLE COPPER(II)

**HAYAT M. MARAFIE, MOHAMED S. EL-EZABY* and MOUSTAFA RASHAD**
Department of Chemistry, University of Kuwait, Kuwait

**and**

**NAGUIB M. MOUSSA**
Department of Biochemistry, University of Kuwait, Kuwait

(*Received* 1 *July* 1983; *accepted* 16 *November* 1983)

**Abstract**—Ternary as well as quaternary complexes involved in the system pyridoxamine–glycylglycine–imidazole–copper(II) have been studied by pH-metric titration at 37°C and I = 0.15 M ($NaNO_3$). The data were assessed by program MINIQUAD 75. The formation constants were compared with those obtained from the system of pyridoxamine–glycine–imidazole with some bivalent metal ions previously reported. They are ~2.5 log units less. In addition, the enhancement of quaternary complex formation has been described in terms of binary and ternary complex formation reactions. It has been also found that deprotonation of the peptidic proton of glycylglycine took place in the presence of more than one different ligand.

Pyridoxamine (Pm), a vitamin $B_6$ compound, may act as coenzyme for reactions of carbonyl compounds.[1] It forms stable binary complexes with many metal ions, Cu(II) in particular.[2,3] It has been involved in some ternary metal complex systems as one of the ligands.[4,5] Quite recently, quarternary metal complex systems involving pyridoxamine glycine (Gly), and imidazole (Imd) have been investigated.[6] In the binary, ternary and quaternary systems, pyridoxamine behaves as a monodentate as well as a bidentate ligand. In addition, the presence of Pm in the vicinity of the metal ions in the quaternary system enhanced their ligation to glycine and imidazole moieties.

The importance of such a study is to prove that not only binary and ternary complex species but also quaternary species may exist in biological systems. Besides, these complex equilibria may serve as models for vitamin $B_6$-dependent enzymatic reactions. The enzymes usually contain clusters of carboxylate, imidazole or other groups which provide the sites for vitamin $B_6$ compounds to interact through specific metal ions.

The aim of this work was to determine the stoichiometry and the formation constants of the ternary and quaternary Cu(II) complexes involved in the system pyridoxamine, glycylglycine, and imidazole and to correlate the results with previously reported pertinent systems.

*Author to whom correspondence should be addressed.

## EXPERIMENTAL

### *Materials*

Glycylglycine (Glygly) (> 99%; BDH) and pyridoxamine–dihydro chloride (Pm.2HCl) (> 99%; Merck) were used without further purification. Imidazole (Imd) (Aldrich) was crystallized from benzene and dried under reduced pressure. The stock solutions of the ligands were kept at 5°C in dark.

Copper(II) nitrate (> 99%; BDH) was used as provided. The concentration of the stock solution was checked by potentiometric methods. The method is essentially EDTA titration of the metal ions using Radiometer pH meter model pH M62 provided with Radiometer cupric selectrode type 1112 Cu as indicator electrode and Radiometer calomel electrode type K401 as a reference electrode.[7]

### *Measurements*

The titrimetric data were acquired using Orion Research Microprocessor Ionalyzer type 901, using

Radiometer combined glass electrode type GK 2301 C. The ionalyzer in the pH mode was calibrated using two Radiometer buffers at pH's 6.98 and 4.03 at 37°C. All pH-metric titrations were carried out as previously described.[6] The ionic strength of all titration solutions was adjusted to 0.15 M $NaNO_3$. The temperature of the titration cell was kept constant at 37°C. The titrant in most cases was a solution of 0.1 M carbonate-free NaOH which was 0.15 M in $NaNO_3$ and in few cases was 0.1 M $HNO_3$. In all titrations, purified nitrogen was surged in the solution before and during the titration time. The metal ion concentration was in the range $(0.6–2.0)10^{-3}$ M. The ligand concentrations did not exceed four times the concentration of metal ions in the binary systems. In ternary systems, the concentrations of each ligand were not more than twice the concentration of metal ions except in case of imidazole where its concentration did not exceed four times that of the metal ions. In the quaternary systems, the concentrations of each ligand was identical to that of metal ions except imidazole where its concentration was not more than four times that of the metal ions. Multiple titrations were carried out for each system. The hydrogen-ion concentration was taken as $10^{-pH}$

*Methods*

Titration data were analyzed by using the MINIQUAD-75 Program.[8] Different equilibrium models have been tested. The results were assessed by observing the values of Chi square $(Xi)^2$, reliability factor (R) and sum of squared residuals (S). The model which gave the lowest R values, $Xi^2$ value (or both) and S value has been adopted taking into consideration the errors in experimental quantities and rules for propagation of errors.

The conditions of measurements for the determination of the stability constants of the binary, ternary and quaternary complex species were the same as previously described.[6] The composition ratios of ligands to Cu ions were always 1:1, 2:1 and 3:1 in case of Glygly and Pm binary systems whereas 2:1 and 4:1 in case of Imd binary systems. Table 1 lists the values of stability constants of the binary systems. In the ternary systems, the ratios of Pm:Glygly:$Cu^{2+}$ were 1:1:1, 1:2:1, 2:1:1 while the ratios of Pm:Imd:$Cu^{2+}$ and Glygly:Imd:$Cu^{2+}$ were 1:2:1 and 1:4:1. Table 2 depicts the values of the ternary stability constants obtained in this work. In the quaternary systems, the ratios of Pm:Glygly:Imd:$Cu^{2+}$ were 1:1:2:1 and 1:1:4:1. The values of the stability constants are listed in Table 3.

In calculating the stability constants of the binary complexes using the MINIQUAD-75 program, the protonation constants were kept invariant while varying the values of the binary species. In the case of ternary systems, the values of protonation constants of ligands and the sta-

Table 1. Protonation constants of Glygly, Pm, Gly and Imd at I = 0.15 M and T = 37°C, $n$ = number of titration points and $\sigma$ = S.D.

| System | l p q r s[(a)] | log$\beta$ ($\sigma$) | n | pH range | literature values | Ref.I,T. |
|---|---|---|---|---|---|---|
| Glygly | 0 1 0 0 1 | 7.981(0.005) | 138 | 7.2-9.6 | 7.97 | (b),0.06,35° |
| | 0 1 0 0 2 | 11.090(0.005) | 124 | 4.1-2.9 | 11.16 | (b),0.06,35° |
| Pm | 1 0 0 0 1 | | | | 10.407 | 6,0.15,37° |
| | 1 0 0 0 2 | | | | 18.562 | 6, " , " |
| | 1 0 0 0 3 | | | | 22.063 | 6, " , " |
| Gly | 0 1 0 0 1 | | | | 9.335 | 6, " , " |
| | 0 1 0 0 2 | | | | 11.868 | 6, " , " |
| Imd | 0 0 1 0 1 | | | | 7.090 | 6, " , " |

(a) l,p,q,r,s, are the stoichiometric coefficients corresponding to $Pm^-$, $Gly^-$ or $Glygly^-$, Imd, $M^{2+}$ and $H^+$, respectively.

(b) S. Morazzini-Pelletier, J. Chim. Phys., 66, 1434 (1969).

Table 2. Formation constants of the binary Cu(II) complexes of Glygly together with those reported for Pm, Gly and Imd at I = 0.15 M and T = 37°C

| L | l p q r s | logβ ( σ ) | n | pH range |
|---|---|---|---|---|
| Glygly | 0 1 0 1 0 | 5.633 (.019) | 170 | 4.1 - 5.3 |
| | 0 1 0 1 -1 | 1.274 (.004) | | |
| | 0 2 0 1 0 | 11.716 (.047) | 187 | 7.1 - 9.5 |
| | 0 1 0 1 -2 | -8.763 (.031) | | |
| | 0 2 0 2 -1 | 11.856 (.075) | | |
| Pm[a] | 1 0 0 1 0 | 10.805 | | |
| | 1 0 0 1 1 | 17.225 | | |
| | 1 0 0 1 2 | 21.337 | | |
| | 2 0 0 1 0 | 17.471 | | |
| | 2 0 0 1 1 | 25.458 | | |
| | 2 0 0 1 2 | 32.535 | | |
| | 2 0 0 1 3 | 38.914 | | |
| Gly[a] | 0 1 0 1 0 | 7.832 | | |
| | 0 2 0 1 0 | 13.870 | | |
| Imd[a] | 0 0 1 1 0 | 4.015 | | |
| | 0 0 2 1 0 | 7.550 | | |
| | 0 0 3 1 0 | 10.079 | | |
| | 0 0 2 1 -2 | -8.487 | | |
| | 0 0 8 2 0 | 29.666 | | |

(a) Ref.(6). I = 0.15M and T = 37°C

bility constants of binary complex species were kept invariant while varying those of ternary complex species. In the case of the quaternary system the values of protonation constants of ligands, the stability constants of 1:1 binary complex species and those of 1:1:1 ternary complex were not varied while changing those of the quaternary complex species.

The ionization of water ($pK_w$) was taken to be 13.38 at I = 0.15 and 37°C.[9]

## RESULTS AND DISCUSSIONS

### *Binary* Cu(II) *complexes*

Binary complexes of pyridoxamine and imidazole and Glygly were extensively studied in the last two decades.[10] Various equilibria for their formation constants were reported. The formation constants of the first two ligands as well as glycine with Cu(II) complexes were recently re-evaluated at the ionic strength, $I = 0.15$ M and temperature of 37°C.[11] In the present work the formation constants of binary complexes of Cu(II) with glycylglycine are also re-evaluated under the same conditions. Table 2 depicts these constants together with those previously reported for other pertinent systems. Glycylglycine is noticed to form unique complexes with Cu(II) ions of various stoichiometric coefficients in which the peptidic linkage has probably lost its proton and the ligand acts as a tridentate ligand. Being a tridentate ligand does not prevent it from acting as a bidentate ligand utilizing either the carboxylate and the peptidic groups or the carboxylate and the amino

Table 3. Formation constants of the ternary and quaternary complexes of Cu(II) involving Pm, Glygly (or Gly) and Imd at I = 0.15 M and 37°C

| L, L', L" | l | p | q | r | s | logβ (σ) | L, L', L" | l | p | q | r | s | logβ (σ) |
|---|---|---|---|---|---|---|---|---|---|---|---|---|---|
| Pm,Glygly[a] | 1 | 1 | 0 | 1 | -1 | 5.719(.002) | Pm,Gly[c] | 1 | 1 | 0 | 1 | 0 | 16.605 |
| | 1 | 1 | 0 | 1 | 0 | 13.877(.019) | | 1 | 1 | 0 | 1 | 1 | 25.394 |
| | 1 | 1 | 0 | 1 | 1 | 22.089(.003) | | 1 | 1 | 0 | 1 | 2 | 31.515 |
| | 1 | 1 | 0 | 1 | 2 | 27.267(.005) | | 1 | 1 | 0 | 1 | 3 | 35.930 |
| | 1 | 1 | 0 | 1 | 3 | 31.727(.003) | | 1 | 2 | 0 | 1 | 1 | 30.078 |
| | 1 | 2 | 0 | 1 | 0 | 18.272(.001) | | 1 | 2 | 0 | 1 | 2 | 37.946 |
| Glygly,Imd[b] | 0 | 1 | 1 | 1 | 0 | 11.682(.003) | | 2 | 1 | 0 | 1 | 2 | 39.490 |
| | 0 | 1 | 1 | 1 | -1 | 5.551(.001) | Pm,Glygly,Imd[d] | 1 | 1 | 1 | 1 | 3 | 39.032(.004) |
| | 0 | 1 | 2 | 1 | -1 | 8.021(.001) | | 1 | 1 | 1 | 1 | 2 | 33.406(.005) |
| Pm,Imd[c] | 1 | 0 | 1 | 1 | 1 | 21.049 | | 1 | 1 | 1 | 1 | -1 | 10.004(.005) |
| | 1 | 0 | 2 | 1 | 0 | 16.788 | | 1 | 1 | 2 | 1 | 2 | 36.867(.005) |
| | 1 | 0 | 2 | 1 | 1 | 24.060 | | 1 | 1 | 2 | 1 | 1 | 30.260(.003) |
| | 2 | 0 | 2 | 1 | 1 | 31.388 | | 1 | 1 | 2 | 1 | 0 | 22.511(.003) |
| Gly,Imd[c] | 0 | 1 | 1 | 1 | 0 | 11.860 | Pm,Gly,Imd[c] | 1 | 1 | 1 | 1 | 0 | 21.575 |
| | 0 | 1 | 3 | 1 | 0 | 18.080 | | 1 | 1 | 1 | 1 | 3 | 42.510 |
| | 0 | 2 | 1 | 1 | 0 | 16.856 | | 1 | 1 | 2 | 1 | 3 | 46.341 |
| | | | | | | | | 1 | 1 | 2 | 1 | 2 | 39.966 |
| | | | | | | | | 1 | 1 | 2 | 1 | 1 | 32.861 |

(a) n=328, pH range = 3.3-10.2, R = 0.007, $Xi^2$=130 and S=2.2x$10^{-7}$.

(b) n=140, pH range = 5.6-8.2, R=0.009, $Xi^2$=90 and S = 1.7x$10^{-7}$.

(c) Ref. (6). I=0.15M and T = 37°C .

(d) n=170, pH range = 4.9-9.9, R = 0.006, $Xi^2$ = 66 and S =1.2x$10^{-7}$.

terminal groups. These complexes are weaker than the corresponding glycine complexes.

*Ternary and quaternary* Cu(II) *complexes*

The stability constants of ternary and quaternary Cu(II) complexes listed in Tables 3 and 4 are for the following equilibrium reaction:

$$l\mathrm{Pm}^- + p\mathrm{Glygly}^- + q\mathrm{Imd} + r\mathrm{Cu}^{2+} + sH^+ \rightleftharpoons (\mathrm{Cu}_r\mathrm{Pm}_l\mathrm{Glygly}_p\mathrm{Imd}_q\mathrm{H}_s)^z \quad (1)$$

where $l$, $p$, $q$, $r$, and $s$ are the stoichiometric coefficients and $z = (2r + s) - (l + p)$.

At least 20 sets of complexes for each system were examined using MINIQUAD-75. Many were rejected whenever the values of Chi square ($Xi^2$), reliability factor (R) and sum of squared residuals (S) are larger or when the calculated constants had large standard deviations. Furthermore, the effect of variations in the values of protonation and binary constants of the chosen ternary model (and also ternary constants in the case of the chosen quarternary model) were examined and it was concluded that the choices were correct with errors in the values of the stability constants within the standard deviations depicted in Table 3.

(i) *Ternary complexes.* The formation constants of ternary complexes of Cu(II) with Pm–Glygly and Glygly–Imd system together with those reported for the systems: Cu(II)–Pm–Gly, Pm–Imd and Gly–Imd are given in Table 3. In

Table 4. The values of log $K^I$ and log $K^{II}$ defined by eqns (2) and (3) for the other ternary complexes of Cu(II)

| System | l | p | q | r | s | log $K^I$ | log $K^{II}$ |
|---|---|---|---|---|---|---|---|
| Pm-Glygly | 1 | 1 | 0 | 1 | 0 | -2.56 | -1.43 |
| | 1 | 1 | 0 | 1 | 1 | -0.77 | +0.56 |
| Glygly-Imd | 0 | 1 | 1 | 1 | 0 | -0.17 | +4.10 |
| Pm-Gly[a] | 1 | 1 | 0 | 1 | 0 | -2.03 | +1.87 |
| | 1 | 1 | 0 | 1 | 1 | -1.62 | +0.48 |
| Pm-Imd[a] | 1 | 0 | 1 | 1 | 0 | -0.82 | +3.00 |
| | 1 | 0 | 1 | 1 | 1 | -0.09 | +2.01 |
| Gly-Imd[a] | 0 | 1 | 1 | 1 | 0 | +0.01[b] | +2.24 |

(a) Ref. (6).

(b) M. Mohan et al* obtained a value of -0.28.

* M. Mohan, D. Bancroft and E.H. Abott, Inorg. Chem., 18, 6, 1527 (1979).

those systems involving Pm as one of the ligands the ternary Cu(II) complexes are mostly protonated. Since Glygly forms unprotonated complexes with Cu(II), Table 2, one would expect that it behaves similarly in the formation of ternary complexes. In such cases the proton may be located on the Pm moiety, such as in 1:1:0:1:1 and 1:1:0:1:2 complex species. However, in the species 1:1:1:1:3 Glygly may also be protonated, Table 3. Unprotonated ternary complexes in both systems are also formed where deprotonation of the peptidic linkage in Glygly takes place, such as 1:1:0:1:−1, 0:1:1:1:−1 and 0:1:2:1:−1 species. The presence of the monodentate ligand, Imd seems to add extra strength to the Cu(II) bonding in the peptidic linkage.

The formation of 1:1:0:1:$s$ or 0:1:1:1:$s$ (Pm:Glygly or Glygly:Imd:Cu:$sH$) ternary complex species from binary species may result from either one (or both) of the following reactions:

$$CuLH_m + CuL'H_n \rightleftarrows CuLL'H_s + Cu$$

$$K^I = \beta_{1TH_s}/\beta_{1CuLH_m}\beta_{1CuL'H_n} \quad (2)$$

$$Cu(LH_m)_2 + Cu(L'H_n)_2 \rightleftarrows 2CuLL'H_s$$

$$K^{II} = \beta^2_{1TH_s}/\beta_{2CuLH_m}\beta_{2CuL'H_n} \quad (3)$$

where $\beta_{1TH_s}$, $\beta_{1CuLH_m}$, $\beta_{2CuLH_m}$, $\beta_{1CuL'H_n}$ and $\beta_{2CuL'H_n}$ are the formation constants of the ternary complex, first and second binary complex species of $LH_m$ and first and second binary complex species of $L'H_n$ and $s = m + n$. Table 4 lists the values of log $K^I$ and log $K^{II}$ ($\Delta$ log K and log X used by Sigel)[11] for 1:1:0:1:$s$ and 0:1:1:1:$s$ (Pm:Glygly or Glygly:Imd:Cu:$sH$) complex species whenever binary formation constants were available. It is quite obvious that the formation of the ternary complex species 1:1:0:1:$s$ and 0:1:1:1:$s$ are favoured over the formation of the binary species $Cu(LH_m)_2$ and $Cu(L'H_n)_2$ but less favoured over the binary species $CuLH_m$ and $CuL'H_n$ (log $K^{II}$ > log $K^I$). It is worth mentioning also that the magnitude of log $K^I$ and log $K^{II}$ are strongly influenced by the statistical differences in the formation of each complex as well as differences in bonding. The statistical values of log $K^I$ and log $K^{II}$ for tetragonal complexes of Cu(II) with bidentate ligands is −0.6 log units.[12,13] For other configurations the statistical values may be less. Values greater than −0.6 indicate that ternary metal complex formation is more favoured than the corresponding binary complexes. The values for Glygly–Imd–Cu(II) system are noticed to be greater than −0.6 indicating that enhancement of ternary complex formation is due to reasons other than statistical. Again comparison of

Table 5. The values of log $K^{III}$ and log $K^{IV}$ for the ternary Cu(II) complexes involving Glygly and Pm or Imd expressed by eqns (4a) and (4b), together with the reported values[6] for the other ternary systems Pm–Gly–, Pm–Imd– and Gly–Imd–Cu(II)

| Stoichiometry l p q r s* | log $K^{III}$ | log $K^{IV}$ |
|---|---|---|
| | 2 fused five-(Glygly),six-membered(Pm) chelate | Six-(Pm),2 fused five-membered(Glygly)chelate |
| 1 1 0 1 0 | 3.07 | 8.24 |
| 1 1 0 1 1 | 4.86 | - |
| | Five-(Gly),six-membered (Pm) chelate | Six-(Pm), five-membered (Gly) chelate |
| 1 1 0 1 0 | (5.80) | (8.78) |
| 1 1 0 1 1 | (8.17) | (17.56) |
| | Monodentate(Imd), 2 fused five-membered(Glygly)chelate | 2 fused five-(Glygly),monodentate(Imd) complexes |
| 0 1 1 1 0 | 6.05 | 7.67 |
| | Monodentate(Imd), five-membered (Gly)chelate | Five-(Gly), monodentate (Imd) ligand |
| 0 1 1 1 0 | (4.03) | - |
| | Monodentate (Imd),, six-membered (Pm) chelate | Six-(Pm),monodentate (Imd) complexes |
| 1 0 1 1 0 | - | - |
| 1 0 1 1 1 | (3.83) | (17.03) |

* l,p,q,r, and s are stoichiometric coefficients for Pm, Glygly (or Gly) Imd, $Cu^{2+}$ and $H^{+}$, respectively.

( ) log$K^{III}$ from the equilibria: $CuPmH_n + LH_m \rightleftarrows CuPmLH_s$

log$K^{IV}$ from the equilibria: $CuLH_m + PmH_m \rightleftarrows CuPmH_s$

log $K^{II} = +4.098$ values for the system(1:1:1:0) with those of the other systems such as Pm–Glygly (log $K^{II} = -1.43$) or Gly–Imd–Cu(II) (log $K^{II} = 2.24$) show other factors (e.g. the steric hindrance in the second system and strengthening of the Cu(II) bonding with peptidic linkage in presence of Imd in the first system) may be also involved, Table 4.

The formation of 1:1:1:3 (Pm:Glygly or Gly-gly:Imd:Cu:*s*H) ternary complex species may also be visualized through the following equilibria:

$$CuLH_m + L'H_n \rightleftarrows CuLL'H_s$$

$$K''' = \beta_{1TH_s}/\beta_{1CuLH_m} \qquad (4a)$$

$$CuL'H_n + LH_m \rightleftarrows CuLL'H_s$$

$$K^{IV} = \beta_{1TH_s}/\beta_{1CuL'H_n} \qquad (4b)$$

where $LH_m$ and $L'H_n$ denote the first and the second ligand respectively. Table 5 lists the values of log $k^{III}$ and log $K^{IV}$ for 1:1:1:0 and 1:1:1:1 complex species.

It is quite clear that the log $K^{IV}$ values are almost greater than log $K^{III}$ for the ternary complexes of Pm–Glygly and Glygly–Imd–Cu(II), a trend which is in agreement with the results obtained in a previous report for Pm–Gly–, Pm–Imd– and Gly–Imd–Cu(II) ternary complexes, Table 5. Again the presence of Pm may increase the electron

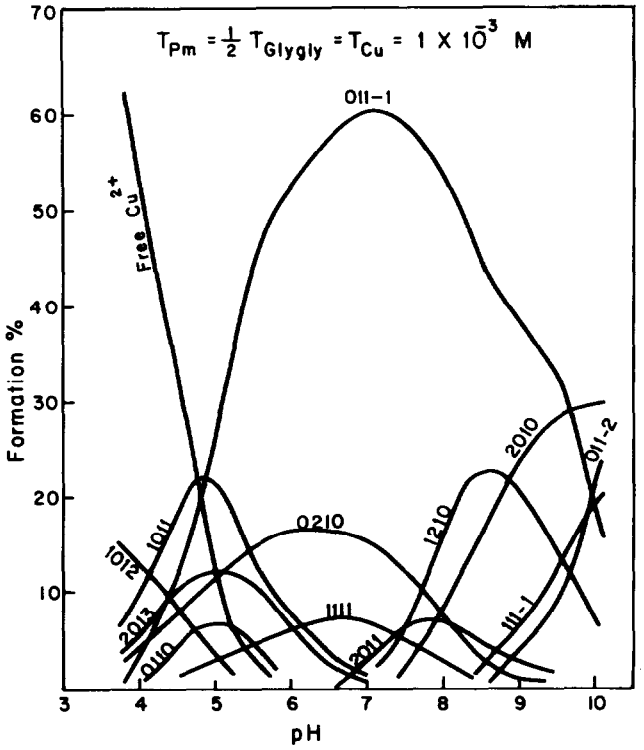



Fig. 1. Distribution diagram of the ternary system Pm–Glygly–Cu(II).

density in the vicinity of Cu(II) ion rendering the binary complex less reactive towards the other ligands, Glygly, Gly or Imd. The stability increasing effect due to Imd seems to be more pronounced in case of Glygly containing ternary species ($\log K^{III} = 6.05$) than those containing PmH ($\log K^{III} = 3.83$) and Gly ($\log K^{III} = 4.03$).

Figures 1 and 2 show the distribution curves of the various Cu(II) species at different pH's for the ternary systems Pm–Glygly–Cu(II) and Glygly–Imd–Cu(II). These distribution curves are actually dependent on the initial concentrations of the reactants, and their selection here has been made on the basis of showing the distribution of the greatest number of the species mentioned in Table 3. In Fig. 1 it is observed that at pH $\simeq 7.4$ (which is isotonic with blood pH) $\sim 80\%$ of the $Cu^{2+}$ is in the form of binary complex species. The major binary species (which is $\sim 66\%$) is the monobinary species of Glygly (0:1:1:−1). However, this species is also present in a wide pH range (4–10) with maximum formation at a pH of $\sim 7$. The contribution of the ternary complexes (1:1:1:1 and 1:2:1:0) seems to be of minor importance at pH 7.4 but at higher pH's (>8) the species 1:2:1:0 and 1:1:1:−1 increase in formation to some extent ($\sim 20\%$). The other ternary species (1:1:1:0, 1:1:1:2 and 1:1:1:3) listed in Table 3 do not appear in the distribution curves which indicate that their formation is less favored than the binary complexes, (Fig. 1). On the other hand, in case of the ternary system Glygly–Imd–Cu(II) all the ternary complexes listed in Table 3 show appreciable degrees of formation at different pH's. At pH of $\simeq 7.4$ the contribution of these complexes reaches $\sim 88\%$ the predominant complex species is 1:1:1:−1 ($\sim 70\%$) which is contrary to the Pm–Glygly system. This may be attributed to the greater steric hindrance exhibited by the latter system (pentacoordinated) than the former (tetra-coordinated) species. It is also noticed that the binary complexes in Fig. 2 are mostly those of Glygly.

(ii) *Quaternary complexes.* Table (3) lists the formation constants of the quaternary system Pm–Glygly–Imd–Cu(II) together with those of the system involving Gly. It is clear from this table that the quaternary complexes containing Glygly are less stable than those containing Gly as indicated by a decrease in the magnitude of the formation constants of the various quaternary species by $\sim 3$ log units. This may be ascribed to the steric hindrance exerted by glycyl–glycine or that the latter ligand forms seven-membered ring chelates which are less stable than the five-membered ones,

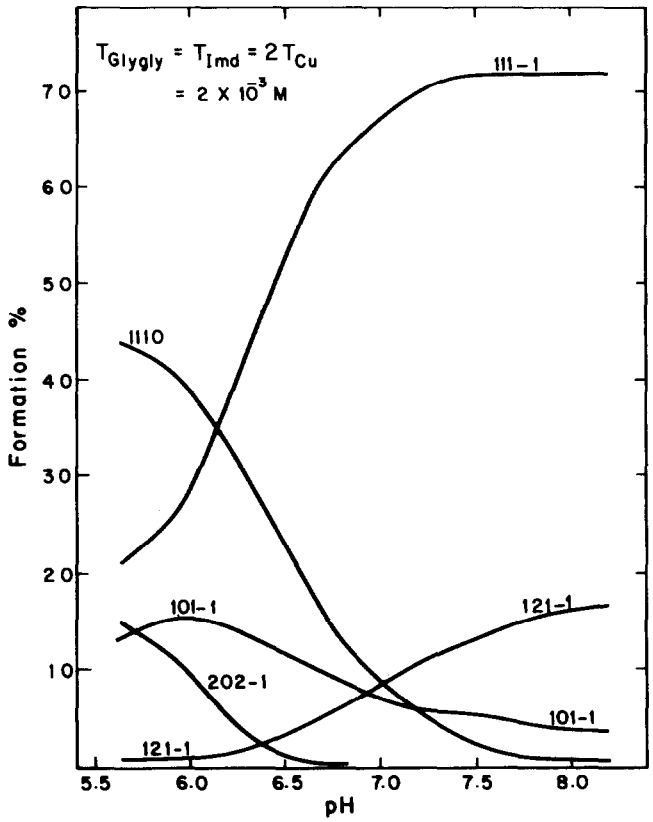



Fig. 2. Distribution diagram of the ternary system Glygly–Imd–Cu(II).

involving Gly. Furthermore, most of these complexes are protonated in a pH range of 5–8. As one may expect from the previous discussion, the proton may be located again on the Pm-moiety especially in mono- and diprotonated species. In case of triprotonated species Glygly may also be protonated. In such case the three ligands may act as monodentate.

One may also notice that the peptidic protons are lost in the case of Glygly containing quaternary complexes (1:1:1:1:−1) a situation which is also found in the corresponding ternary and binary systems containing Glygly. This suggests that the complexing ability of protein is not much affected by the presence of ligands of low molecular weight. Complexes containing two Imd molecules are also proved to exist (which is similar to the previously reported results for Gly systems)[6] (1:1:2:1:2, 1:1:2:1:1 and 1:1:2:1:0) which indicates that Pm and Glygly do not hinder the imidazole from attacking the Cu ions. As long as coordination sites are available one may expect penta- and hexa-coordinated structures to be formed. The formation constants $\beta_{1QH_r}$ and $\beta_{2QH_r}$ of these complexes (1:1:1:1:$s$ and 1:1:2:1:$s$) may be explained through the equilibrium reactions (5 and 6) shown in Table 6.

Comparison of the $\log K^{V}$ values for the 1:1:1:1:2 and 1:1:1:1:3 (6.41 and 7.31 respectively) with the $\log \beta$ for the mono-binary species of imidazole (0:0:1:1:0), shows that they are greater by approximately two log units. Similar results are observed with the 1:1:2:1:2 species ($\log K^{VI} = 9.60$) in comparison with the di-binary species of imidazole (0:0:2:1:0), Table 2. However, in the case of less protonated complexes (1:1:2:1:1 and 1:1:2:1:0) the difference is $\sim$ one log unit. From this, one can conclude that the electron density of the other ligands in the vicinity of the central metal ion is an important factor in the nucleophilic attack of imidazole molecules.

Since the previous results show the existence of binary species in equilibrium with the ternary species (Figs. 1 and 2 and Tables 2 and 4) one can predict that the formation of quaternary complex species may take place through the interaction of binary species with ternary species, two different ternary species or three binary species. These equilibria are summarized in Table 6 together with their $\log K$ values (whenever the formation con-

Table 6. Formation of quaternary complex species $MLL'L''H_s$ and $MLL'L''_2H_s$ through various equilibrium reactions with their corresponding log K values. M, L. L′, L″ and H denote $Cu^{2+}$, pyridoxamine, glycylglycine, imidazole and proton respectively

| | Reaction | K | | Stoichiometric coefficients l p q r s | log K |
|---|---|---|---|---|---|
| 5 | $MLL'H_s + L'' \rightleftharpoons MLL'L''H_s$ | V | $\beta_{1QH_s}/\beta_{1MLL'H_s}$ | 1 1 1 1 2 | 6.14 |
| | | | | 1 1 1 1 3 | 7.31 |
| 6 | $MLL'H_s + 2L'' \rightleftharpoons MLL'L''_2H_s$ | VI | $\beta_{2QH_s}/\beta_{1MLL'H_s}$ | 1 1 2 1 0 | 8.64 |
| | | | | 1 1 2 1 2 | 9.60 |
| 7 | $ML' + MLL''H_s \rightleftharpoons MLL'L''H_s + M$ | VII | $\beta_{1QH_s}/\beta_{1ML'}\beta_{1MLL''H_s}$ | 1 1 1 1 2 | - |
| | | | | 1 1 1 1 3 | - |
| 8 | $ML'' + MLL'H_s \rightleftharpoons MLL'L''H_s + M$ | VIII | $\beta_{1QH_s}/\beta_{1ML''}\beta_{1MLL'H_s}$ | 1 1 1 1 2 | 2.12 |
| | | | | 1 1 1 1 3 | 3.29 |
| 9 | $MLH_s + ML'L'' \rightleftharpoons MLL'L''H_s + M$ | IX | $\beta_{1QH_s}/\beta_{1MLH_s}\beta_{1ML'L''}$ | 1 1 1 1 2 | -0.39 |
| 10 | $MLL'H_s+ML'L'' \rightleftharpoons MLL'L''H_s+ML'$ | X | $\beta_{1QH_s}\beta_{1ML'}/\beta_{1MLL'H_s}\beta_{1ML'L''}$ | 1 1 1 1 2 | 0.09 |
| | | | | 1 1 1 1 3 | 1.26 |
| 11 | $MLL''H_n+ML'L''H_m \rightleftharpoons MLL'L''H_s+ML''$ | XI | $\beta_{1QH_s}\beta_{1ML''}/\beta_{1MLL''H_n}\beta_{1ML'L''H_m}$ | 1 1 1 1 2 | - |
| 12 | $MLL''H_n+MLL'H_m \rightleftharpoons MLL'L''H_s+MLH_t$ | XII | $\beta_{1QH_s}\beta_{1MLH_t}/\beta_{1MLL''H_n}\beta_{1MLL'H_m}$ $(n + m = s + t)$ | 1 1 1 1 2 (n=1, m=1 t=0, s=2) | 1.07 |
| | | | | 1 1 1 1 2 (n=1, m=2 s=2, t=1) | 2.32 |
| | | | | 1 1 1 1 2 (n=1, m=3 t=2, s=2) | 1.98 |
| | | | | 1 1 1 1 3 (n=1, m=2 t=0, s=3) | 1.52 |
| | | | | 1 1 1 1 3 (n=1, m=3 t=1, s=3) | 3.48 |
| | | | | l p q r s | |
| 13 | $MLH_s+ML'+2ML'' \rightleftharpoons MLL'L''_2H_s+3M$ | XIII | $\beta_{2QH_s}/\beta_{1MLH_s}\beta_{1ML'}\beta^2_{1ML''}$ | 1 1 2 1 0 | -4.16 |
| | | | | 1 1 2 1 1 | -2.83 |
| | | | | 1 1 2 1 2 | -0.33 |
| 14 | $ML'+MLL''_2H_s \rightleftharpoons MLL'L''_2H_s+M$ | XIV | $\beta_{2QH_s}/\beta_{1ML'}\beta_{2MLL''_2H_s}$ | 1 1 2 1 0 | 0.09 |
| | | | | 1 1 2 1 1 | 0.57 |
| | | | | 1 1 2 1 2 | - |
| 15 | $2ML''+MLL'H_s \rightleftharpoons MLL'L''_2H_s+2M$ | XV | $\beta_{2QH_s}/\beta^2_{1ML''}\beta_{1MLL'H_s}$ | 1 1 2 1 0 | 0.60 |
| | | | | 1 1 2 1 1 | 0.14 |
| | | | | 1 1 2 1 2 | 1.57 |
| 16 | $MLH_n+ML'L''_2H_m \rightleftharpoons MLL'L''_2H_s+M$ | XVI | $\beta_{2QH_s}/\beta_{1MLH_n}\beta_{2ML'L''_2H_m}$ | 1 1 2 1 0 | - |
| | | | | 1 1 2 1 1 | - |
| | | | | 1 1 2 1 2 | - |

Table 6 (Contd.)

| | Reaction | K | | Stoichiometric coefficients | log K |
|---|---|---|---|---|---|
| 17 | $ML'L''H_m+MLL''H_n \rightleftharpoons MLL'L''_2H_s+M$ | XVII | $\beta_{2QH_s}/\beta_{1ML'L''H_n}\beta_{1MLL''H_m}$ | 1 1 2 1 0 | - |
| | | | | 1 1 2 1 1 | -2.47 |
| | | | | (n=1, m=0) | |
| | | | | 1 1 2 1 2 | - |
| 18 | $MLH_s+ML'+ML'' \rightleftharpoons MLL'L''H_s+2M$ | XVIII | $\beta_{1QH_s}/\beta_{1MLH_s}\beta_{1ML'}\beta_{1ML''}$ | 1 1 1 1 2 | 2.42 |
| 19a | $M(LH_s)_2+ML'_2+ML''_2 \rightleftharpoons 2MLL'L''H_n+M$ | XIXa | $\beta^2_{1QH_n}/\beta_{2MLH_s}\beta_{2ML'}\beta_{2ML''}$ | 1 1 1 1 2 (s = n) | 15.01 |
| 19b | $M(LH_s)_2+ML'_2+ML''_2 \rightleftharpoons MLL'L''H_n+ML'+ML''+LH_m$ | XIXb | $\beta_{1QH_n}\beta_{1ML'}\beta_{1ML''}/\beta_{2MLH_s}\beta_{2ML'}\beta_{2ML''}$ | 1 1 1 1 2 (2s=m+n, m=0) | -8.75 |
| 19c | $M(LH_s)_2+ML'_2+ML''_2 \rightleftharpoons MLL'L''H_n+MLH_m+ML''+L'$ | XIXc | $\beta_{1QH_n}\beta_{1MLH_m}\beta_{1ML''}/\beta_{2MLH_s}\beta_{2ML'}\beta_{2ML''}$ | 1 1 1 1 2 (2s=m+n, m=0) | -3.58 |
| 19d | $M(LH_s)_2+ML'_2+ML''_2 \rightleftharpoons MLL'L''H_n+MLH_m+ML'+L''$ | XIXd | $\beta_{1QH_n}\beta_{1MLH_m}\beta_{1ML'}/\beta_{2MLH_s}\beta_{2ML'}\beta_{2ML''}$ | 1 1 1 1 2 (2s=m+n, m=0) | -1.96 |
| 19e | $M(LH_s)_2+ML'_2+ML''_2 \rightleftharpoons MLL'L''H_n+ML'L''+MLH_m$ | XIXe | $\beta_{1QH_n}\beta_{1MLL''}\beta_{1MLH_m}/\beta_{2MLH_s}\beta_{2ML'}\beta_{2ML''}$ | 1 1 1 1 2 (2s=m+n, m=0) | 4.09 |
| 19f | $M(LH_s)_2+ML'_2+ML''_2 \rightleftharpoons MLL'L''H_n+MLL''H_m+ML'$ | XIXf | $\beta_{1QH_n}\beta_{1MLL''H_m}\beta_{1ML'}/\beta_{2MLH_s}\beta_{2ML'}\beta_{2ML''}$ | 1 1 1 1 2 (2s=m+n,m=0) | - |
| 19g | $M(LH_s)_2+ML'_2+ML''_2 \rightleftharpoons MLL'L''H_n+MLL'H_m+ML''$ | XIXg | $\beta_{1QH_n}\beta_{1MLL'H_m}\beta_{1ML''}/\beta_{2MLH_s}\beta_{2ML'_2}\beta_{2ML''}$ | 1 1 1 1 2 (2s=m+n,n=0) | -0.50 |

stants of the necessary species were available for calculation). Equilibrium reaction 8 seems to be more favoured than 9 (some values for reaction 7 were not available), as indicated by the difference in their log K values, i.e. $\log K^{VIII} = 2.12$ and $\log K^{IX} = -0.39$ for 1:1:1:1:2 species. The greater $\log K^{VIII}$ (+3.29) for the quaternary species 1:1:1:1:3 containing Glygly than that containing Gly (2.56)[6] may be explained as due to steric hindrance exerted by Glygly molecule in the ternary systems which enhances interaction with imidazole molecule to form the quaternary species. Table 6 shows that the possible interaction of two different ternary complex species is also favoured (eqns 10–12). In such cases the formation of the quaternary complex species depends also on the location of the proton(s) on any of the ternary species. This is quite exemplified in eqn (12), which shows the greatest $\log K^{XII}$ values when all the species involved in the equilibrium reaction are protonated, e.g. $\log K^{XII}$ for 1:1:1:1:2 and 1:1:1:1:3 are 2.32 and 3.48 respectively. Formation of quaternary complex species (1:1:1:1:2) through interaction of three binary species seem also to be of appreciable contribution in some cases as shown by their positive log K values, e.g. $\log K^{XVIII} = 2.42$, $\log K^{XIXa} = 15.01$ and $\log K^{XIXe} = 4.09$. The formation of quaternary complex species involving two imidazole molecules (1:1:2:1:*s*) may be explained through equilibrium reactions 14–17. It is unfortunate that the log K values for some of these quaternary species were not possible to be determined due to unavailability of the formation constants of the binary and ternary species. The coordination of a second imidazole molecule to glycylglycine containing quaternary complexes is more favoured than to those containing glycine as shown by the more positive $\log K^{XIV}$ and $\log K^{XV}$

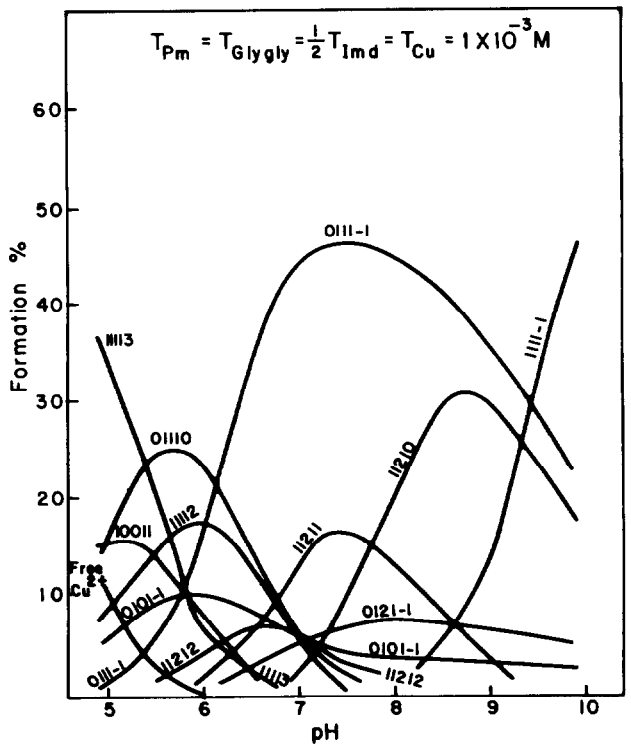



Fig. 3. Distribution diagram of the quaternary system Pm–Glygly–Imd–Cu(II).

values of the former system, e.g. these values for 1:1:2:1:1 species are −0.56 and −0.97 for the former system and 0.57 and 0.14 for the latter system.[6] This may be rationalized in terms of electrostatic effects, where repulsion of Glygly with imidazole molecules are expected to be less than that of Gly with imidazole. The distribution curve in Fig. 3 shows that a large number of species are in equilibrium at various pH ranges. At pH 7.4, it is obvious that only ~ 30% of Cu is present in the form of quaternary complexes, whereas twice as much is found in the form of ternary complexes. The major contributing ternary species at this pH seems to be that of Glygly–Imd–Cu(II) system (0:1:1:1:−1; ~46%). Similar result is also found for the quaternary complex species (1:1:1:1:−1) where also the peptidic proton is lost, but with maximum formation at ~ pH = 10. The presence of the quaternary species 1:1:1:1:3 and 1:1:1:1:2 together with the binary species Cu–PmH in the distribution curve also gives a confirmation to reaction 12, when the reacting species are protonated ($\log K^{XII} = 3.48$ and 2.32 respectively). Again the presence of the quaternary species 1:1:2:1:0, 1:1:2:1:1 and 1:1:2:1:2 in appreciable amount shows that the existence of a second imidazole molecule is not hindered.

*Acknowledgement*—The authors thank Kuwait University for provision of SC21 Grant.

## REFERENCES

1. D. E. Metzler, *Biochemistry*. Academic Press, New York (1977).
2. R. I. Gustafson and A. E. Martell, *Arch. Biochem. Biophys.* 1957, **68**, 485.
3. M. S. El-Ezaby and F. R. El-Eziri, *J. Inorg. Nucl. Chem.* 1976, **38**, 1901.
4. M. S. El-Ezaby, H. M. Marafie and S. Farid, *J. Inorg. Biochem.* 1979, **11**, 317.
5. M. S. El-Ezaby and T. E. El-Khalafawy, *J. Inorg. Nucl. Chem.* 1981, **43**, 831.
6. M. S. El-Ezaby, M. Rashad and N. M. Moussa, *Polyhedron* 1982, **1**, 791.
7. Instruction Manual for Cupric Selectrode Type F1112Cu, Radiometer A/S, Copenhagen, 1972.
8. P. Gans, A. Sabatini and A. Vacca, *Inorg. Chim. Acta*, 1976, **18**, 237.
9. G. Berthon, P. M. May and D. R. Williams, *J. Chem. Soc. Dalton*, 1978, 1433.
10. L. G. Sillen and A. E. Martell, *Stability Constants of the Metal Ion Complexes, Spec. Publ.* No. 17 (1964), and *Supplement* No. 1, *Spec. Publ.* No. 25 (1971). The Chemical Society, London. D. D. Perrin, *Stability Constants of Metal Ion Complexes, Part B, Organic Ligands*. I.U.P.A.C. Chemical Data Series No. 22. Pergamon Press, Oxford (1979).
11. H. Sigel, *J. Inorg. Nucl. Chem.* 1975, **37**, 507.
12. B. Sen, *Anal. Chim. Acta.* 1962, **27**, 515.
13. V. S. Sharma, T. J. Schubert, *J. Chem. Ed.* 1969, **46**, 506.

*Polyhedron* Vol. 3, No. 7, pp. 799–804, 1984
Printed in the U.S.A.

0277-5387/84 $3.00 + .00
© 1984 Pergamon Press Ltd.

# CARBONYL RHODIUM(I) COMPLEXES WITH α-DIIMINES LIGANDS

**E. DELGADO-LAITA* and E. SANCHEZ-MUñOYERRO**
Dpto. Quimica Inorganica and Insto. Quimica Inorganica "ELHUYAR", Facultad de Quimicas, Universidad Complutense, Madrid, Spain

(*Received* 7 *July* 1983; *accepted* 6 *December* 1983)

**Abstract**—The reactions of $[Rh(CO)_2Cl]_2$ with α-diimines, RN=CR′-CR′=NR (R = *c*-Hex, $C_6H_5$, *p*-$C_6H_4OH$, *p*-$C_6H_4CH_3$, *p*-$C_6H_4OCH_3$, R′ = H; R = *c*-Hex, $C_6H_5$, *p*-$C_6H_4OH$, *p*-$C_6H_4OCH_3$; R′ = Me) in 2:1 Rh/R-dim ratio gave rise to ionic compounds $[(CO)_2Rh.R\text{-}dim(R',R')][Rh(CO)_2Cl_2]$ which have been characterized by elemental analyses, electrical conductivity, $^1H$–NMR and electronic and IR spectroscopy. Some of these complexes must involve some kind of metal–metal interaction. The complex $[Rh(CO)_2Cl.c\text{-}Hex\text{-}dim(H,H)]$ has been obtained by reaction of $[Rh(CO)_2Cl]_2$ with the *c*-Hex-dim(H,H) ligand in 1:1 Rh/R-dim ratio. The reactions between $[(CO)_2Rh.R\text{-}dim(H,H)][Rh(CO)_2Cl_2]$(R = *c*-Hex or *p*-$C_6H_4OCH_3$) with the dppe ligand have been studied. The known complex $RhCl(CO)(PPh_3)_2$ has been isolated from the reaction of $[(CO)_2Rh.R\text{-}dim(H,H)]$–$[Rh(CO)_2Cl_2]$ (R = *c*-Hex or *p*-$C_6H_4OCH_3$) with $PPh_3$ ligand.

The bridge-splitting reactions of $[Rh(CO)_2Cl]_2$ with monodentate N-donor ligands such as amines or nitriles have been intensively investigated[1–3] and it is well known that the reactions between $[Rh(CO)_2Cl]_2$ and N-heterocyclic ligands, 2,2-bipyridyl or 1,10-phenanthroline give rise to the formation of ionic compounds.[4] Some of these dark coloured complexes may involve some kind of metal–metal interaction.[5] In spite of the extensive investigations that have been carried out with bipy and phen as ligands it is only in the past few years that the chemistry of transition metal complexes with α-diimines has been developed.[6–10] The α-diimines, RN=CR′–CR″=NR, (R–DAB) have a versatile coordination chemistry because they may contribute via their σ(N) and additionally via their π(C=N) electron system a varying number of electrons to the metal.[11] To date only a limited number of rhodium complexes with α-diimines have been described.[12,13] H. van der Poel *et al.* reported the syntheses and studies of some four- and five-coordinate Rh(I) complexes with these ligands. The nature of the R-imine substituent seems to influence the coordination mode. The study of carbonyl rhodium(I) complexes is interesting because they may play an important role as catalysts in the hydroformylation reactions.[14] In this paper we report the isolation and characterization of some carbonylrhodium(I) complexes with R-dim ligands which are chelated bonded.

## EXPERIMENTAL

### *Materials*

The starting complex $[Rh(CO)_2Cl]_2$ was prepared by a published method.[15] α-Diimines, RN=CR′–CR′=NR, R-dim(R′,R′) being R = *c*-Hex, $C_6H_5$, *p*-$C_6H_4OH$, *p*-$C_6H_4CH_3$, *p*-$C_6H_4OCH_3$, R′ = H; R = *c*-Hex, $C_6H_5$, *p*-$C_6H_4OH$, *p*-$C_6H_4OCH_3$, R′ = Me; were prepared by standard methods.[16,17] The preparation of the new metal complexes were carried out in a dry, oxygen-free, nitrogen atmosphere at room temperature. Solvents were dried and distilled before use.

### *Physical measurements*

Elemental analyses for C, H, and N were performed by Elemental Microanalyses Ltd. Laboratories, Amberley, Winsford Drive, Halwill Junction, Beaworthy, Devon, England, and Insto. Q. Organica. CSIC, Madrid, Spain. Infrared spectra in the 4000–200 $cm^{-1}$ region were recorded as KBr

*Author to whom correspondence should be addressed.

discs on a Perkin–Elmer 325 spectrometer. Electronic spectra were recorded with a Kontron–Uvikon 620 spectrophotometer. Conductivity measurements were carried out with a Radiometer Copenhagen CDM2e apparatus and a Radiometer Copenhagen CDC 104 cell in methanol solution at 25°C. Proton NMR spectra were recorded at room temperature with a Varian T–60–A spectrometer with tetramethylsilane (TMS) as internal standard, using deuterochloroform or deuteroacetone as solvent.

$[(CO)_2Rh.R\text{-}dim(R',R')][Rh(CO)_2Cl_2]$

A suspension of R-dim(R′,R′)(1 mmol) in hexane (50 $cm^3$) was added to a stirred solution of $[Rh(CO)_2Cl]_2$ (1 mmol) in hexane (30 $cm^3$). An immediate precipitation of the products occurred in all cases (except with *c*-Hex-dim (Me, Me) that it was necessary to leave the solution stirring overnight to obtain a precipitate). The mixture was left aside for 30 min, then the resulting products were filtered off, washed with hexane (in order to romove the excess of $[Rh(CO)_2Cl]_2$ and free ligand) and dried *in vacuo* (yields 60–90%).

$Rh(CO)_2Cl.c\text{-}Hex\text{-}dim(H,H)$

A stirred solution of $[Rh(CO)_2Cl]_2$ (0.39 g, 1 mmol) in hexane (25 $cm^3$) was treated with a solution of *c*-Hex-dim(H,H) (0.22 g, 2 mmol) in the same solvent (35 $cm^3$). The solution turned dark purple and after 5 min a yellow compound started to precipitate which was filtered off. The complex was washed with hexane (3 × 10 $cm^3$) and dried *in vacuo* (yield 75%).

*Reaction of* $[Rh(CO)_2Cl]_2$ *with diacetyl and cyclohexylamine*

To a stirred solution of $[Rh(CO)_2Cl]_2$ (0.39 g, 1 mmol) in hexane (15 $cm^3$) was added diacetyl (0.08 g, 1 mmol) and cyclohexylamine (0.18 g, 2 mmol), respectively. The solution turned quickly orange and then a green solid began to precipitate which was filtered off, washed with hexane several times and dried *in vacuo* (yield 70%).

*Reactions of* $[(CO)_2Rh.R\text{-}dim(H,H)][Rh(CO)_2Cl_2]$ (R = *c*-Hex or p-$C_6H_4OCH_3$) *with* $PPh_3$

The complexes $[(CO)_2Rh.R\text{-}dim(H,H)][Rh(CO)_2Cl_2]$ (R = *c*-Hex or p-$C_6H_4OCH_3$) (0.5 mmol) dissolved in dichloromethane (25 $cm^3$) were treated with $PPh_3$ (1.5 mmol) dissolved in the same solvent. Immediately a pale yellow compound began to precipitate in both cases. The mixture was left aside for 15 min and after the compound was filtered off, washed with diethyl ether and dried *in vacuo* (yield 70–80%).

*Reactions of* $[(CO)_2Rh.R\text{-}dim(H,H)][Rh(CO)_2Cl_2]$ (R = *c*-Hex or p-$C_6H_4OCH_3$) *with* dppe

A solution of dppe ligand (1.5 mmol) in dichloromethane was added to a solution of $[(CO)_2Rh.R\text{-}dim(H,H)][Rh(CO)_2Cl_2]$ (R = *c*-Hex or P-$C_6H_4OCH_3$) (1 mmol) in the same solvent. The mixture was stirred for 3 hr, evaporated until dryness, washed with diethyl ether several times and dried *in vacuo* (yield 50–60%).

## RESULTS AND DISCUSSION

The $[(CO)_2Rh.R\text{-}dim(R',R')][Rh(CO)_2Cl_2]$ compounds were obtained by reaction of $[Rh(CO)_2Cl]_2$ with the corresponding α-diimines in 2:1 Rh/R-dim ratio using hexane or diethyl ether as solvent.

The reaction between $[Rh(CO)_2Cl]_2$ and the *c*-Hex-dim(H,H) or *p*-$C_6H_4OCH_3$-dim(H,H) ligand in 1:1 Rh/R-dim ratio gave rise to a new compound $Rh(CO)_2Cl.c\text{-}Hex\text{-}dim(H,H)$ and the 1:1 stoichiometry $[(CO)_2Rh.p\text{-}C_6H_4OCH_3\text{-}dim\text{-}(H,H)][Rh(CO)_2Cl_2]$ compound. In the last case only 50% of the starting diazabutadiene ligand reacts.

Colour, decomposition temperature, analytical data and conductivity measurements of the complexes are listed in Table 1. In general the $[(CO)_2Rh.R\text{-}dim(R',R')][Rh(CO)_2Cl_2]$ solid compounds are dichroic, dark coloured, soluble in dichloromethane, methanol, chloroform, and acetone, sparingly soluble in benzene, diethyl ether and hexane, and insoluble in water. These compounds are stable in the solid state but most of them decompose in solution. It has been difficult to obtain very pure compounds.

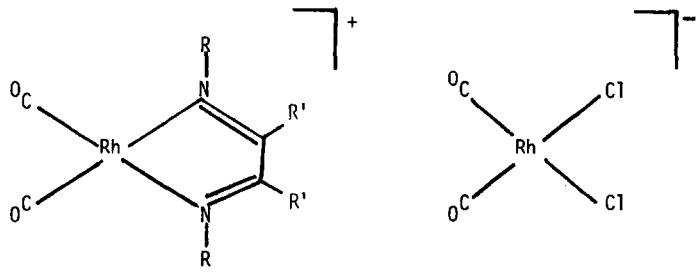
All $Rh_2(CO)_4Cl_2.R\text{-}dim(R',R')$ compounds obtained show ionic structures, $[Rh(CO)_2R\text{-}dim(R',R')]^+[Rh(CO)_2Cl_2]^-$ (Structure **I**) as has been demonstrated by electrical conductivities in $10^{-3}$ M methanol solution. These values are comparable with other 1:1 electrolytes with large complex ions.[18] The IR spectra (Table 2) of the $[(CO)_2Rh.R\text{-}dim(R',R')][Rh(CO)_2Cl_2]$ complexes in the solid state and in solution show four intense $\nu$(CO) bands in the 2100–1980 $cm^{-1}$ region, due to two $Rh(CO)_2$ fragments with *cis*-CO ligands. All complexes show similar spectra in this region, this fact leads us to think that the varying natures of parasubstituted phenyl rings do not seem to play an important role.

Assignments of the $\nu$(C=N) stretching vibrations in the range 1630–1550 $cm^{-1}$ were attempted. The strong absorption of phenyl rings made it difficult. The IR spectra show, in the range 350–270 $cm^{-1}$ two Rh–Cl stretching vibrations at higher frequencies than the $Rh\text{–}Cl_{bridging}$ of the dimeric rhodium(I) complexes.[19]

Table 1. Analytical and physical data of the complexes

| Compound | Colour | M.p.[a] (°C) | % C Found.(Calcd.) | % H Found.(Calcd.) | % N Found.(Calcd) | $\lambda m$[b] $ohm^{-1}cm^2mol^{-1}$ |
|---|---|---|---|---|---|---|
| $\|(CO)_2Rh.c\text{-}Hex\text{-}dim(H, H)\|\|Rh(CO)_2Cl_2\|$ | brown | 95 | 35.09(35.47) | 4.00(3.94) | 4.55(4.59) | 73.2 |
| $Rh(CO)_2Cl.c\text{-}Hex\text{-}dim(H, H)$ | yellow | 117 | 45.95(46.32) | 6.08(5.79) | 6.30)(6.75) | - |
| $\|(CO)_2Rh.c\text{-}Hex\text{-}dim(Me, Me)\|\|Rh(CO)_2Cl_2\|$ | red | 91 | 37.15(37.68) | 4.01(4.39) | 3.97(4.39) | 77.4 |
| $\|(CO)_2Rh.C_6H_5\text{-}dim(H, H)\|\|Rh(CO)_2Cl_2\|$ | purple | 106 | 36.01(36.18) | 2.06(2.01) | 4.42(4.69) | 57.4 |
| $\|(CO)_2Rh.C_6H_5\text{-}dim(Me, Me)\|\|Rh(CO)_2Cl_2\|$ | purple | 103-105 | 38.92(38.40) | 2.63(2.56) | 4.15(4.48) | 75.6 |
| $\|(CO)_2Rh.C_6H_4OH\text{-}dim(H, H)\|\|Rh(CO)_2Cl_2\|$ | purple | > 300 | 34.60(34.34) | 2.15(1.90) | 4.20(4.45) | 56.3 |
| $\|(CO)_2Rh.C_6H_4OH\text{-}dim(Me, Me)\|\|Rh(CO)_2Cl_2\|$ | blue | 93-95 | 36.76(36.50) | 2.62(2.43) | 4.01(4.26) | 61.8 |
| $\|(CO)_2Rh.p\text{-}C_6H_4CH_3\text{-}dim(H, H)\|\|Rh(CO)_2Cl_2\|$ | brown | 94 | 38.72(38.40) | 2.45(2.56) | 4.76(4.48) | 63.8 |
| $\|(CO)_2Rh.p\text{-}C_6H_4OCH_3\text{-}dim(H, H)\|\|Rh(CO)_2Cl_2\|$ | brick-red | > 300 | 36.14(36.52) | 2.28(2.43) | 4.32(4.26) | 62.6 |
| $\|(CO)_2Rh.p\text{-}C_6H_4OCH_3\text{-}dim(Me, Me)\|\|Rh(CO)_2Cl_2\|$ | purple | 118-120 | 38.92(38.54) | 3.16(2.92) | 4.24(4.08) | 87.2 |

[a] Decomp. temp., [b] The conductivity measurements have been carried out in MeOH solutions $10^{-3}$ M at 25 °C.



Structure 1.

The $^1$H-NMR spectra of the complexes (Table 3) are characterized by one multiplet at $\delta$ *ca.* 2.10 ppm ($C_6H_{11}$) or 7 ppm (phenyl derivatives). The $CH_3$–C=H protons appear as singlets at $\delta$ 2.2 ppm. The N=CH protons were not observed.

The electronic spectra in dichloromethane solution and in the solid state are detailed in Table 4. The bands are essentially due to charge-transfer transitions between the d levels of Rh(I) and the antibonding orbitals of the R-dim and CO ligands.[18] The spectra in the solid state of these complexes differ from the solution spectra. The bands in solid state appear at lower energies than in solution. Many authors who have investigated carbonylrhodium(I) complexes have observed it. They suggested that the dark coloured complexes must involve some kind of metal–metal interaction. Those compounds have a columnar structure with alternate square planar cations and anions.[3,5] It is possible that some of the compounds here described may involve some metal–metal interaction. We are trying to obtain some suitable crystals to carry out a structural study by X-ray diffraction but until now all attempts have been unsuccessful.

Investigations on the structure of the [$Rh(CO)_2Cl$.*c*-Hex-dim(H,H)] compound shows, in less polar solvents, a weak interaction between the chloride and rhodium resulting in a five-coordinate rhodium complex (structure **II**). In a highly polar solvent such as methanol the equilibrium between the structures **II** and **III** is completely displaced to the right. The analogous [$Rh(CO)_2Cl$.phen] displayed a similar behaviour.[4] The IR spectrum (Table 1) shows two $\nu$(CO) stretching vibrations at 2050 and 1985 cm$^{-1}$. The $\nu$(Rh–Cl) stretching vibrations appear at 315 cm$^{-1}$, the $^1$H-NMR spectrum shows one singlet at $\delta$

Table 2. IR spectra of the complexes (cm$^{-1}$)

| Compound | $\nu$(CO) | $\nu$(CN) | $\nu$(Rh-Cl) |
|---|---|---|---|
| $\|(CO)_2Rh$.c-Hex-dim(H, H)$\|\|Rh(CO)_2Cl_2\|$ | 2080s, 2050s, 2020s, 1980s. | 1615w, 1550m. | 318s, 290m. |
| $Rh(CO)_2Cl$.c-Hex-dim(H, H) | 2050s, 1985s. | 1610w. | 315m. |
| $\|(CO)_2Rh$.c-Hex-dim(Me, Me)$\|\|Rh(CO)_2Cl_2\|$ | 2070s, 2050s, 2010s, 1985s. | 1570-1530br. | 315s, 285m. |
| $\|(CO)_2Rh.C_6H_5$-dim(H, H)$\|\|Rh(CO)_2Cl_2\|$ | 2090s, 2070s, 2030s, 2000s. | 1600m, 1570m. | 310m, 290w. |
| $\|(CO)_2Rh.C_6H_5$-dim(Me, Me)$\|\|Rh(CO)_2Cl_2\|$ | 2090s, 2060s, 2040s, 1990s. | 1615w, 1585w. | 315s, 285m. |
| $\|(CO)_2Rh.p\text{-}C_6H_4OH$-dim(H, H)$\|\|Rh(CO)_2Cl_2\|$ | 2100s, 2065s, 2040s, 2025s. | 1605m, 1570m. | 310m, 285w. |
| $\|(CO)_2Rh.p\text{-}C_6H_4OH$-dim(Me, Me)$\|\|Rh(CO)_2Cl_2\|$ | 2080s, 2020s, 2005s, 1995(sh), 1985(sh). | 1630m, 1605m. | 310m, 295w. |
| $\|(CO)_2Rh.p\text{-}C_6H_4CH_3$-dim(H, H)$\|\|Rh(CO)_2Cl_2\|$ | 2090s, 2060s, 2025s, 1995s. | 1615w, 1570w. | 310m, 280w. |
| $\|(CO)_2Rh.p\text{-}C_6H_4OCH_3$-dim(H, H)$\|\|Rh(CO)_2Cl_2\|$ | 2080s, 2060s, 2030s, 1990s, 2005(sh). | 1600m, 1565w. | 318s, 290m. |
| $\|(CO)_2Rh.p\text{-}C_6H_4OCH_3$-dim(Me, Me)$\|\|Rh(CO)_2Cl_2\|$ | 2080s, 2050s, 2010s, 1990s. | 1625w, 1600m. | 310m, 295w. |

s = strong, w = weak, m = medium.

Table 3. $^1$H NMR spectra

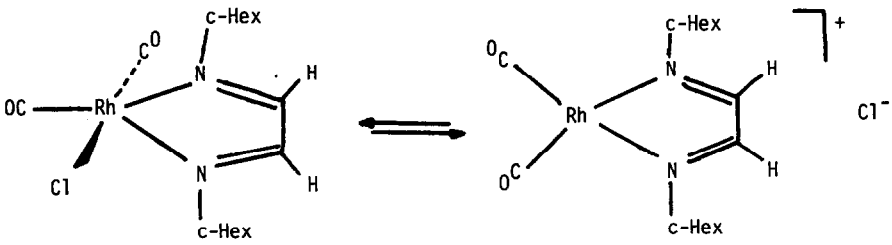
| Compound | δ(ppm) | Assignments | Solvent |
|---|---|---|---|
| $\|(CO)_2Rh.c\text{-}Hex\text{-}dim(H, H)\|\|Rh(CO)_2Cl_2\|$ | 2.05m | $C_6H_{11}$ | $CDCl_3$ |
| $Rh(CO)_2Cl.c\text{-}Hex\text{-}dim(H, H)$ | 8.3s | CH=N | $CDCl_3$ |
| | 1.63m | $C_6H_{11}$ | |
| $\|(CO)_2Rh.c\text{-}Hex\text{-}dim(Me, Me)\|\|Rh(CO)_2Cl_2\|$ | 2.1s | $CH_3$-C=N | $CDCl_3$ |
| | 1.5m | $C_6H_{11}$ | |
| $\|(CO)_2Rh.C_6H_5\text{-}dim(H, H)\|\|Rh(CO)_2Cl_2\|$ | 7.18m | $C_6H_5$ | $CD_3$-CO-$CD_3$ |
| $\|(CO)_2Rh.C_6H_5\text{-}dim(Me, Me)\|\|Rh(CO)_2Cl_2\|$ | 7.1m | $C_6H_5$ | $CDCl_3$ |
| | 2.25s | $CH_3$-C=N | |
| $\|(CO)_2Rh.p\text{-}C_6H_4OH\text{-}dim(H, H)\|\|Rh(CO)_2Cl_2\|$ | 6.9m | $C_6H_4$ | $CD_3$-CO-$CD_3$ |
| $\|(CO)_2Rh.p\text{-}C_6H_4OH\text{-}dim(Me, Me)\|\|Rh(CO)_2Cl_2\|$ | 6.7m | $C_6H_4$ | $CD_3$-CO-$CD_3$ |
| | 2.15s | $CH_3$-C=N | |
| $\|(CO)_2Rh.p\text{-}C_6H_4CH_3\text{-}dim(H, H)\|\|Rh(CO)_2Cl_2\|$ | 7.3m | $C_6H_4$ | $CDCl_3$ |
| | 2.3s | $CH_3$ | |
| $\|(CO)_2Rh.p\text{-}C_6H_4OCH_3\text{-}dim(H, H)\|\|Rh(CO)_2Cl_2\|$ | 6.9m | $C_6H_4$ | $CDCl_3$ |
| | 3.8s | $OCH_3$ | |
| $\|(CO)_2Rh.p\text{-}C_6H_4OCH_3\text{-}dim(Me, Me)\|\|Rh(CO)_2Cl_2\|$ | 6.85m | $C_6H_4$ | $CDCl_3$ |
| | 3.79s | $OCH_3$ | |
| | 2.3s | $CH_3$-C=N | |

m = medium, s = singlet.

Table 4. Electronic spectra of the complexes in solid state and in dichloromethane solution (900–250 nm)

| Compound | $\lambda^a$ (nm, | $\lambda^b$ (nm) |
|---|---|---|
| $\|(CO)_2Rh.c\text{-}Hex\text{-}dim(H, H)\|\|Rh(CO)_2Cl_2\|$ | 570, 415. | 900, 610, 415. |
| $Rh(CO)_2Cl.c\text{-}Hex\text{-}dim(H, H)$ | 565, 410 | 560, 430 |
| $\|(CO)_2Rh.c\text{-}Hex\text{-}dim(Me, Me)\|\|Rh(CO)_2Cl_2\|$ | 430, 330 | 615, 330 |
| $\|(CO)_2Rh.C_6H_5\text{-}dim(H, H)\|\|Rh(CO)_2Cl_2\|$ | 625, 330. | 900, 580, 340. |
| $\|(CO)_2Rh.C_6H_5\text{-}dim(Me, Me)\|\|Rh(CO)_2Cl_2\|$ | 569, 335. | 680, 350. |
| $\|(CO)_2Rh.p\text{-}C_6H_4OH\text{-}dim(H, H)\|\|Rh(CO)_2Cl_2\|$ | 400, 325. | 590, 460. |
| $\|(CO)_2Rh.p\text{-}C_6H_4OH\text{-}dim(Me. Me)\|\|Rh(CO)_2Cl_2\|$ | 340, 290. | 600, 340. |
| $\|(CO)_2Rh.p\text{-}C_6H_4CH_3\text{-}dim(H, H)\|\|Rh(CO)_2Cl_2\|$ | 630, 370, 330. | 900, 610, 505, 345. |
| $\|(CO)_2Rh.p\text{-}C_6H_4OCH_3\text{-}dim(H, H)\|\|Rh(CO)_2Cl_2\|$ | 450, 330. | 620, 330. |
| $\|(CO)_2Rh.p\text{-}C_6H_4OCH_3\text{-}dim(Me, Me)\|\|Rh(CO)_2Cl_2\|$ | 435, 355, 335. | 615, 330. |

a = solution. b = solid state ($BaSO_4$).




Structure II. Structure III.

8.3 ppm (CH=N) and one multiplet at $\delta$ 1.63 ppm ($C_6H_{11}$).

Attempts to obtain the [$(CO)_2$Ph.*c*-Hex-dim-(H,H)][$Rh(CO)_2Cl_2$] compound by reaction of [$Rh(CO)_2Cl]_2$ with $\alpha$-diimine ligand prepared "in situ" (diacetyl and cyclohexylamine) gave rise to the amine complex [$Rh(CO)_2$Cl.*c*-Hex-$NH_2$] which was characterized by elemental analysis and IR spectroscopy.[3]

The reactions between [$(CO)_2$Rh.R-dim-(H,H)][$Rh(CO)_2Cl_2$] (R-*c*-Hex or *p*-$C_6H_4OCH_3$) and $PPh_3$ gave rise in both cases to the same compound which was characterized by analysis elemental, IR spectroscopy and conductivity measurement as the known [$RhCl(CO)(PPh_3)_2$] compound.

The reactivity of [$(CO)_2$Rh.R-dim(H,H)]-[$Rh(CO)_2Cl_2$] (R-*c*-Hex or *p*-$C_6H_4OCH_3$) with dppe ligand has been studied. In both cases two CO ligands have been displaced by one dppe ligand. The IR spectra show only two $\nu$(CO) at *ca.* 2060 and 1970 $cm^{-1}$. The stretching vibrations of the free dppe ligand are shifted by coordination. Two $\nu$(Rh–Cl) bands appear in the range 350–290 $cm^{-1}$. We did not observe appreciable modifications in the $\nu$(C=N) stretching vibrations in respect to the starting complex [$(CO)_2$Rh.R-dim(H,H)][$Rh(CO)_2Cl_2$].

## REFERENCES

1. L. M. Vallarino, *Int. Conf. Coordination Chemistry*, Special Publication, No. 13. The Chemical Society, London (1959).
2. R. Ugo, F. Bonati and S. Cenini, *Inorg. Chem. Acta* 1969, **2**, 220.
3. L. M. Vallarino and S. W. Sheargold, *Inorg. Chim. Acta* 1979, **36**, 243.
4. R. D. Gillard, K. Harrison and I. H. Mather, *J. Chem. Soc., Dalton Trans.* 1975, 133.
5. F. Pruchnik and K. Wajda, *J. Organomet. Chem.* 1979, **164**, 71.
6. P. L. Sandrini, A. Mantovani, B. Crociani and P. Uguagliati, *Inorg. Chim. Acta* 1981, **51**, 71.
7. B. Crociani and R. L. Richards, *J. Organomet. Chem.* 1978, **154**, 65.
8. L. Maresca, G. Natile and L- Cattalini, *Inorg. Chim. Acta* 1975, **14**, 79.
9. H. van der Poel, G. van Koten and K. Vrieze, *Inorg. Chem.* 1980, **19**, 1145.
10. C. Barral, E. Dalgado, E. Gutierrez-Puebla, R. Jimenez-Aparicio, A. Monge, C. del Pino and A. Santos, *Inorg. Chim. Acta* 1983, **74**, 101.
11. G. van Koten and K. Vrieze, *Advanced Organomet. Chemistry* Vol. 21. Academic Press, New York (1982).
12. H. van der Poel, G. van Koten and K. Vrieze, *Inorg. Chim. Acta* 1981, **51**, 241.
13. H. van der Poel, G. van Koten and K. Vrieze, *Inorg. Chim. Acta* 1981, **51**, 253.
14. L. Markó, *Aspects of Homogeneous Catalysis*, Vol. 2. Reidel, Dordrecht (1974).
15. J. A. McCleverty and G. Wilkinson, *Inorg. Syntheses*, Vol. VIII (1966).
16. H. tom Diek and I. W. Renk, *Chem. Ber.* 1971, **104**, 110.
17. B. Crociani, T. Boschi and P. Uguagliati, *Inorg. Chim. Acta* 1981, **48**, 9.
18. B. Crociani, U. Belluco and P. Sandrini, *J. Organomet. Chem.* 1979, **177**, 385.
19. A. L. Balch, *J. Am. Chem. Soc.* 1976, **98**, 8049.

*Polyhedron* Vol. 3, No. 7, pp. 805–810, 1984
Printed in the U.S.A.

0277–5387/84 $3.00 + .00
© 1984 Pergamon Press Ltd.

# KINETICS AND MECHANISM OF OXIDATION OF ARSENIOUS ACID BY TETRACHLOROAURATE(III) IN HYDROCHLORIC ACID MEDIUM

**KALYAN KALI SENGUPTA* and BISWANATH BASU**
Department of Chemistry, Jadavpur University, Calcutta 700 032, India

(*Received* 12 *July* 1983; *accepted* 6 *December* 1983)

**Abstract**—Kinetics of the oxidation of arsenious acid by tetrachloroaurate(III) have been studied spectrophotometrically in hydrochloric acid medium. Initial complex formation between As(III) and Au(III) followed by the decomposition of the intermediate complex to give products of the reaction is suggested. The empirical rate law is

$$-\frac{d[\text{Au(III)}]}{dt} = \frac{k\,K[\text{Au(III)}][\text{As(III)}]}{1 + K[\text{As(III)}]}$$

$k$ and K are found to be $13.9 \times 10^{-4}\,s^{-1}$ and $24.2\,M^{-1}$ respectively at 30°C and $\mu = 1.0$ M. $\Delta H^{\ddagger}$ and $\Delta S^{\ddagger}$ for $k$ are found to be 49.2 kJ mol$^{-1}$ and $-137.2$ JK$^{-1}$ mol$^{-1}$ whereas $\Delta H$ and $\Delta S$ associated with K are $-6.75$ kJ mol$^{-1}$ and 4.14 JK$^{-1}$ mol$^{-1}$ respectively.

The kinetics of oxidation of arsenious acid by some metal ion oxidants have been published[1–5] but the oxidation of arsenic(III) by gold(III) has not been studied. Since halides of gold(III) are partially hydrolysed[6] at lower acidities $(1.1–12.6) \times 10^{-7}$ M, the oxidation of arsenious acid by tetrachloroaurate(III) has been studied in hydrochloric acid (1.0M). Au(III) as an oxidant is of interest because it may behave as one equivalent or a two equivalent oxidant in the reaction with As(III). The present reaction was studied in view of the results obtained earlier with other oxidants.[2,3]

## EXPERIMENTAL

*Reagents.* All inorganic materials were of AnalaR (BDH) grade. Sodium arsenite was of E. Merck (G.R.) grade. Chloroauric acid (Johnson Mathey) was used to prepare solutions of Au(III). The concentration of Au(III) was determined gravimetrically.[7] Solutions were stored in the dark and used under subdued lighting conditions. All solutions were made in doubly distilled water.

*Absorption spectra.* The absorption spectrum of Au(III) solution in hydrochloric acid was recorded in the ultraviolet region (220–380) nm. The spectra showed two very strong bands at 227 and 315 nm.[8a] The extinction coefficients at the respective wavelengths were $(35{,}750 \pm 50)$ and $(5400 \pm 20)$ in (0.1–2.0)M hydrochloric acid. Beer's law was obeyed in the concentration range of Au(III) = $(0.25–1.5) \times 10^{-4}$ M studied.

*Kinetic measurements.* The reaction was studied in the presence of a large excess of As(III). The course of the reaction was followed spectrophotometrically using a cell of path length 1 cm at 315 nm in the thermostated cell compartment of a Perkin–Elmer digital (Hitachi 200) spectrophotometer as mentioned earlier.[8b] The rate of decrease of Au(III) concentration was followed for at least one half life, a higher conversion was noted at higher temperatures. Generally 10–14 absorbance vs time readings were taken for each run. The pseudo-first order rate constants ($k_{obs}$) were calculated as usual. The rate constants were reproducible to within $\pm 5\%$.

## RESULTS

### *Stoichiometry*

The stoichiometry of the reaction was studied in excess As(III) and unreacted As(III) was determined volumetrically.[9] The reaction takes place

*Author to whom correspondence should be addressed.

according to the following equation.

$$H_3AsO_3 + Au(III) + H_2O \rightarrow H_3AsO_4 + Au(I) + 2H^+. \quad (1)$$

*Effect of reactant concentration.* The reaction was studied at varying concentrations of Au(III) but at constant As(III) concentration, acidity and temperature of $2.0 \times 10^{-2}$ M, 1.0 M and 30°C respectively. The observed pseudo-first order rate constants were found to be $4.6 \times 10^{-4}$, $4.4 \times 10^{-4}$, $4.55 \times 10^{-4}$, $4.7 \times 10^{-4}$ and $4.5 \times 10^{-4}$ ($s^{-1}$) at [Au(III)] of $0.5 \times 10^{-4}$, $0.75 \times 10^{-4}$, $1.0 \times 10^{-4}$, $1.25 \times 10^{-4}$ and $1.5 \times 10^{-4}$ M respectively. These results confirm that the order with respect to Au(III) is unity. The rate of oxidation, on the other hand, increases with increase in As(III) concentrations and $1/k_{obs}$ is linear in 1/[As(III)] (Table 1 and Fig. 1).

*Effect of pH.* The effect of changing [$H^+$] was studied at constant [Au(III)], [As(III)] and ionic strength ($\mu$) of $1.0 \times 10^{-4}$, $2.0 \times 10^{-2}$ and 1.0 M (adjusted by the addition of $NaClO_4$) respectively. The values of pseudo-first order rate constants are $4.5 \times 10^{-4}$, $4.62 \times 10^{-4}$, $4.60 \times 10^{-4}$, $4.58 \times 10^{-4}$ and $4.55 \times 10^{-4}$ ($s^{-1}$) at [$H^+$] of 0.1, 0.3, 0.5, 0.7 and 1.0 M respectively. Hydrogen ion has no effect on the rate of reaction in this concentration range of acidity.

*Effect of salts.* Lithium chloride, sodium chloride and potassium chloride were used. The pseudo-first order rate constant increases with the increase in salt concentration (Table 2) and in these experiments no attempts were made to keep ionic strength constant. Although when the reaction was studied at constant [$H^+$] and ionic strength of 0.5 and 1.0 M (adjusted by the addition of sodium perchlorate) respectively but at different [NaCl] in the region (0.1–0.5)M, the pseudo–first order rate constant was independent of [$Cl^-$]. This indicates that increase in pseudo-first order rate constant with increase in salt concentrations (Table 2) may be due to the variation of ionic strength or nature and concentration of the cations. However, the results of the pseudo-first order rate constants at different concentrations of the salts indicate that cations rather than the ionic strength play significant role otherwise the rates would have been the same at the similar concentrations of the different salts. The effectiveness of the cations

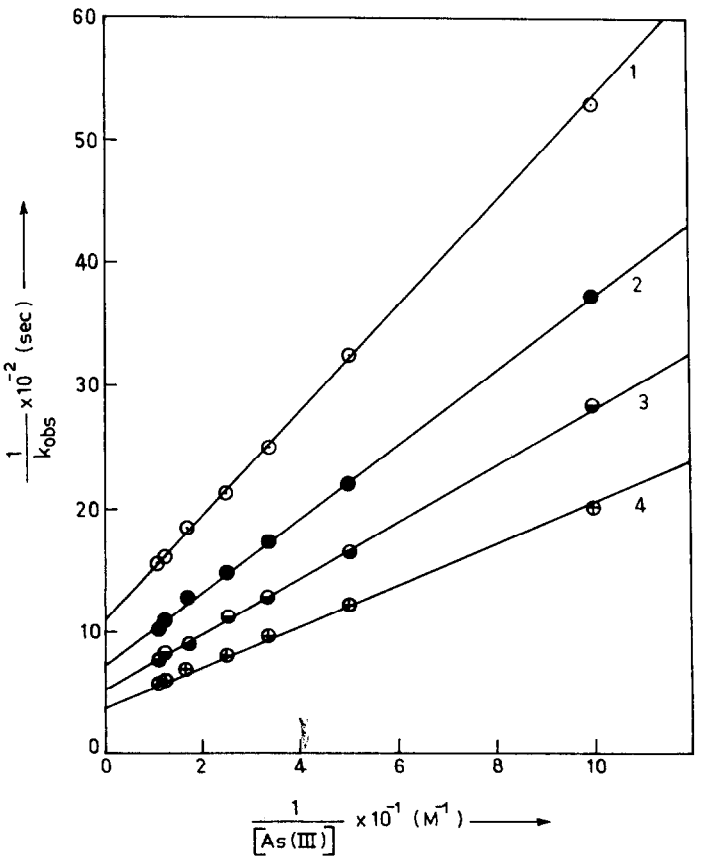



Fig. 1. Effect of substrate concentrations on pseudo first order rate constant. Plots of $1/k_{obs}$ vs 1/[As(III)] at different temperatures. [As(III)] = $1.0 \times 10^{-4}$, [$H^+$] = 1.0 M. (1) 24°C. (2) 30°C. (3) 35°C. (4) 40°C.

Table 1. Effect of arsenic(III) concentration of pseudo-first order rate constants. [Au(III)] = $1.0 \times 10^{-4}$ M, [$H^+$] = 1.0 M

| Temp. °C | [As(III)] x $10^{-2}$ M | $k_{obs}$ x $10^4$ ($s^{-1}$) | $k_{cal}$ x $10^4$ ($s^{-1}$) |
|---|---|---|---|
| 24 | 1.0 | 1.89 | 1.88 |
| | 2.0 | 3.12 | 3.13 |
| | 3.0 | 4.03 | 4.01 |
| | 4.0 | 4.72 | 4.68 |
| | 6.0 | 5.46 | 5.60 |
| | 8.0 | 6.17 | 6.21 |
| | 9.0 | 6.44 | 6.5 |
| 30 | 1.0 | 2.69 | 2.71 |
| | 2.0 | 4.55 | 4.53 |
| | 3.0 | 5.82 | 5.85 |
| | 4.0 | 6.76 | 6.84 |
| | 6.0 | 7.83 | 8.23 |
| | 8.0 | 9.12 | 9.16 |
| | 9.0 | 9.76 | 9.52 |
| 35 | 1.0 | 3.52 | 3.59 |
| | 2.0 | 6.06 | 6.05 |
| | 3.0 | 7.82 | 7.84 |
| | 4.0 | 9.01 | 9.2 |
| | 6.0 | 11.3 | 11.1 |
| | 8.0 | 12.5 | 12.4 |
| | 9.0 | 13.2 | 12.9 |
| 40 | 1.0 | 5.02 | 4.91 |
| | 2.0 | 8.13 | 8.3 |
| | 3.0 | 10.4 | 10.8 |
| | 4.0 | 12.5 | 12.7 |
| | 6.0 | 14.45 | 15.4 |
| | 8.0 | 16.7 | 17.3 |
| | 9.0 | 17.8 | 18.0 |

follow the order, $K^+ > Na^+ > Li^+$. It has been shown in the oxidations of some inorganic compounds[8a,8b] by gold(III) in hydrochloric acid medium that the added salts had no effect on the rate of reaction. This suggests that ion-pairing between the cations and $AuCl_4^-$ does not take place. On the other hand, the catalytic effect of the cations possibly arises from the formation of less stable complexes between the cations and the {Au(III). As(III)} intermediate because of the increased size of the cations.

*Effect of acrylamide.* The reaction was also studied in the presence of different concentrations of acrylamide. The pseudo-first order rate constant decreases to the extent of 73% in 12% (w/v) acrylamide (Table 3). The reaction mixture containing [Au(III)], [As(III)] and [$H^+$] of $1.0 \times 10^{-4}$, $2.0 \times 10^{-2}$ and 1.0M respectively was also polymerised in the presence of 12% (w/v) acrylamide. No such polymerisation was observed in control experiments when either Au(III) or As(III) was excluded. The results indicate that free radicals are produced in solution.

*Effect of temperature.* The values of $k$ (step 3) (calculated from the intercepts of Fig. 1) are found to be $9.26 \times 10^{-4}$, $13.9 \times 10^{-4}$, $19.2 \times 10^{-4}$ and $27.0 \times 10^{-4}$ ($s^{-1}$) at 24, 30, 35 and 40°C respectively. The values of $K$ (step 2) which have

Table 2. Effect of different salts on pseudo-first order rate constants at 30°C. [Au(III)] = $1.0 \times 10^{-4}$ M, [As(III)] = $2.0 \times 10^{-2}$ M, [$H^+$] = 1.0 M

| [Salt] | $k_{obs} \times 10^4$ ($s^{-1}$) | | |
|---|---|---|---|
| M | LiCl | NaCl | KCl |
| 0 | 4.55 | 4.55 | 4.55 |
| 0.04 | - | - | 7.62 |
| 0.08 | - | - | 10.3 |
| 0.12 | - | - | 13.2 |
| 0.16 | - | - | 18.0 |
| 0.20 | - | - | 21.2 |
| 0.25 | 5.05 | 6.65 | 28.0 |
| 0.50 | 5.51 | 9.08 | 60.5 |
| 0.75 | 5.62 | 10.0 | - |
| 1.0 | 5.75 | 11.6 | - |
| 1.25 | 5.97 | 13.4 | - |
| 1.75 | 6.23 | 17.1 | - |

Table 3. Effect of acrylamide on pseudo-first order rate constants at 30°C. [Au(III)] = $1.0 \times 10^{-4}$ M, [As(III)] = $2.0 \times 10^{-2}$ M, [$H^+$] = 1.0 M

| % Acrylamide (w/v) | 0 | 2 | 4 | 6 | 8 | 12 |
|---|---|---|---|---|---|---|
| $k_{obs} \times 10^4$ ($s^{-1}$) | 4.55 | 2.55 | 1.95 | 1.70 | 1.47 | 1.22 |

been calculated from the intercepts and slopes of the above plots are 25.5, 24.2, 23.0 and 22.2 at the respective temperatures. The least squares plot of log $k$ vs 1/T was used to calculate the energy of activation ($E_a$) followed by the calculation of enthalpy of activation ($\Delta H\ddagger$ and $\Delta S\ddagger$ are 49.2 kJ $mol^{-1}$ and $-137.2$ $JK^{-1}$ respectively. The enthalpy change ($\Delta H$) associated with the equilibrium step was also calculated from the least squares plot of log $K$ vs 1/T and was used to calculate $\Delta S$. The values are $-6.75$ kJ $mol^{-1}$ and 4.14 $JK^{-1}$ $mol^{-1}$ respectively. The calculations of $\Delta H\ddagger$, $-\Delta S\ddagger$ and $\Delta S$ were done at 303 K.

## DISCUSSION

The reactive species of As(III) is thought[4] to be $H_3AsO_3$ or $HAsO_2$ in hydrochloric acid medium employed in the present study. The hydrate $As(OH)_3$ behaves as a weak acid with a dissociation constant[11a] of about $6.0 \times 10^{-10}$ at 25°C. Though $As(OH)_3$ behaves in some ways like a weak base[2], the basic character is extremely feeble and hence unlike Sb(III)[11b] it gives no cations of this type $As^+(OH)_2$. Au(III) is invariably complexed in all solutions, usually as an anionic species. According to Robb[6c] the $AuCl_4^-$ anion in aqueous medium undergoes thermal hydrolysis reactions which can be quite complex leading to the formation of no less and perhaps more than five species. Again, in hydrochloric acid medium $HAuCl_4$ remains in equilibrium[8c] with $H^+$ and $AuCl_4^-$ as follows.

$$HAuCl_4 \rightleftharpoons H^+ + AuCl_4^-.$$

Hydrogen ion has no effect in the present reaction. Since the dissociation constant[8a] of $HAuCl_4$ is nearly 1 and the reaction has been studied at 1.0 M, the results indicate that both $HAuCl_4$ and $AuCl_4^-$ react with the substrate at the same speed. The reaction may take place between $HAuCl_4$ or $AuCl_4^-$ {hereafter referred to as Au(III)} and arsenious acid or its anion. Since the reaction was studied at [$H^+$] = 1.0 M, it is suggested that undissociated substrate reacts with the oxidant. The results plotted in Figure 1 indicate the formation of 1:1 intermediate complex between As(III) and Au(III). The formation of a transient intermediate complex is also indicated by the increase in optical density to the extent of 20% over that of initial

Au(III) and by the shift of the $\lambda_{max}$ of the oxidant from 315 to 320 nm on mixing with the As(III) at temperature ($\sim 5°C$). The reaction between a metal ion and a ligand thus prefers an initial complex formation[10] rather than the simple second order mechanism as has been observed in the oxidation of hypophosphorous acid[8b] by this oxidant. The energy of activation of the former process is lower than that of the latter one.[10] The much lower activation enthalpy of 49.2 kJ $mol^{-1}$ as compared to the value of 125.5 kJ $mol^{-1}$ obtained in the oxidation of hypophosphorous acid[8b] justifies further that the present reaction occurs through intermediate complex formation. A kinetic $Cl^-$ dependence would require additional chlorides in the activated complex. Since there is no $Cl^-$ dependence (at constant ionic strength) it can be explained by a bridge between the oxidant and the substrate (assuming significant amounts of $AuCl_3$ species are not present). It is suggested that a chloride from chloro complex of Au(III) acts as a bridge[12] between Au(III) and one of the $-OH$ groups of arsenious acid.

The complex decomposes to give the products of reaction. The steps of the reaction are,

$$\text{As(III)} + \text{Au(III)} \overset{K}{\rightleftharpoons} \{\text{As(III). Au(III)}\} \quad (2)$$

$$\{\text{As(III). Au(III)}\} \overset{k}{\rightarrow} \text{products.} \quad (3)$$

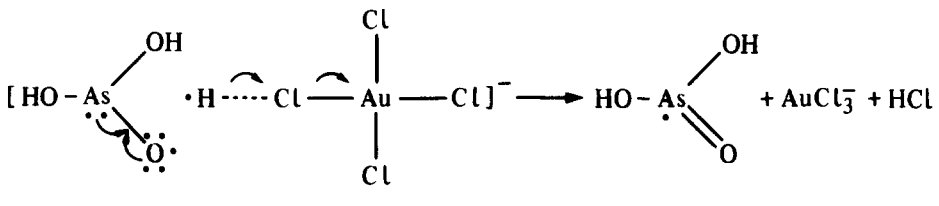
The rate expression would then be

$$-\frac{d[\text{Au(III)}]}{dt} = \frac{kK[\text{Au(III)}][\text{As(III)}]}{1 + K[\text{As(III)}]} \quad (4)$$

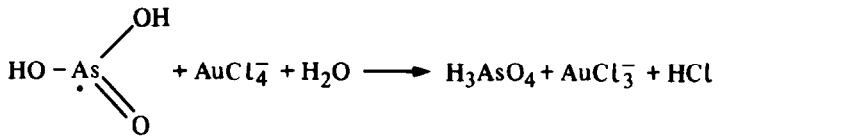
$$k_{obs} = \frac{kK[\text{As(III)}]}{1 + K[\text{As(III)}]}. \quad (5)$$

The values of $k$ and K at different temperatures were determined. With the use of these values the pseudo-first order rate constants were then calculated for various sets of experiments from the eqn (5). The agreement between the experimental and calculated values (Table 1) confirms the adequacy of eqn (5).

It is proposed that the oxidation of As(III) to As(V) goes by the univalent change[13,14] through the formation of intermediate free radicals. Since both Au(II) and $H_2\dot{A}sO_3$ are unstable intermediates, the reaction between these two species to give Au(I) and $H_3AsO_4$ can easily be ruled out. On the other hand, it is possible that the free radical reacts with another Au(III) to give products as shown below (step 7). Au(II) then disproportionates[15] to give Au(III) and Au(I) as in step (8). The steps of the reaction are



(6)



(7)



(8)

The mechanism predicts a 50% decrease in pseudo-first order rate constant although the loss is higher (73%) in excess acrylamide. It may be that some other factor is responsible for the decrease of pseudo-first order rate constant in excess acrylamide. However, a two electron transfer mechanism which has been proposed earlier[2] is not favourable in the present reaction. Au(I) is formed by the disproportionation of Au(II). Again, Au(0) can be generated by further reduction of Au(I) by excess of reductant and/or by disproportionation of Au(I).[16] There is no evidence for metallic gold under the condition at which the present reaction was carried out.

## REFERENCES

1. K. S. Gupta and Y. K. Gupta, *J. Chem. Soc.* (*A*), 1970, 256.
2. B. B. Pal, D. C. Mukherjee and K. K. Sen Gupta, *J. Inorg. Nucl. Chem.* 1973, **34**, 3433.

3. K. K. Sen Gupta and J. K. Chakladar, *J. Chem. Soc. (Dalton)* 1974, 222.
4. P. D. Sharma and Y. K. Gupta, *J. Chem. Soc. (Dalton)* 1972, 52.
5. K. K. Sen Gupta and P. K. Sen, *J. Inorg. Nucl. Chem.* 1978, **40**, 1657.
6. (a) F. H. Fry, G. A. Hamilton and J. Turkevich, *Inorg. Chem.* 1966, **5**, 1943. (b) R. L. Rich and H. Taube, *J. Phys. Chem.* 1954, **58**, 1. (c) W. Robb, *Inorg. Chem.* 1967, **6**, 382.
7. S. C. Soundar Rajan and N. Appala Raju, *J. Ind. Chem. Soc.* 1973, **50**, 110.
8. (a) K. K. Sen Gupta and B. Basu, *Trans. Metal Chem.*, 1983, **8**, 3. (b) K. K. Sen Gupta, B. Basu, S. Sen Gupta and S. Nandi, *Polyhedron* 1983, **2**, 983. (c) K. G. Moodley and M. J. Nicol, *J. Chem. Soc., (Dalton)* 1977, 993.
9. A. I. Vogel, *A Text Book of Quantitative Inorganic Analysis*, 3rd Edn, p. 376. E.L.B.S. and Longmans Green, London (1962).
10. H. Taube, *J. Chem. Educ.* 1968, **45**, 452.
11. (a) *Hand Book of Chemistry and Physics.* 52nd Edn p. D–121, The Chemical Rubber Co., Cleaveland, Ohio (1971). (b) B. B. Pal and K. K. Sen Gupta, *Inorg. Chem.* 1975, **14**, 2268.
12. (a) G. Annibale, L. Canovess, L. Cattalini, G. Natile, M. Biagini-Cingi, A. M. Lanfredi and A. Tiripicchio, *J. Chem. Soc. (Dalton)*, 1981, 2280. (b) G. Annibale, L. Canovese, L. Cattalini and G. Natile: *J. Chem. Soc. (Dalton)* 1980, 1017.
13. R. Woods, I. M. Kolthoff and E. J. Meehan, *J. Am. Chem. Soc.* 1963, **85**, 2385.
14. (a) L. J. Csayni and M. Szabo, *Talanta* 1958, **1**, 359. (b) L. J. Csayni, *Disc. Farad. Soc.* 1960, **29**, 145.
15. F. Basalo and R. G. Pearson, *Mechanism of Inorganic Reactions*, 2nd Edn, p. 414. Wiley Eastern Limited (New Delhi) (1977).
16. L. G. Sillen and A. E. Martell, *Stability Constants of Metal Complexes*, Special Publication, No. 17. The Chemical Society, London (1964).

*Polyhedron* Vol. 3, No. 7, pp. 811–819, 1984
Printed in the U.S.A.

0277–5387/84 $3.00 + .00
© 1984 Pergamon Press Ltd.

# EFFECT OF ACIDITY ON CHELATE RING CLOSURE OCCURRING BY CHLORO, NITRO OR AZIDO GROUP DISPLACEMENT IN RHODIUM(III) COMPLEXES

**G. FAVERO and A. PELOSO***
Istituto di Chimica Analitica, Universita' di Padova, Padua, Italy

**and**

**L. VOLPONI**
Istituto di Chimica Generale, Universita' di Padova, Padua, Italy

(*Received* 29 *July* 1983; *accepted* 15 *December* 1983)

**Abstract**—The effect of $CH_3COOH$, $ClCH_2COOH$, $Cl_2CHCOOH$, $Cl_3CCOOH$ and of $ClCH_2COOH$–$ClCH_2COO^-$ buffers on the rates of the conversion of *mer*-$[Rh(L)(L')Cl_2X]$ into *trans*-$[Rh(L)_2Cl_2]^+ + X^-$ has been investigated in methanol [L and L′ = (*o*-dimethylaminophenyl)dimethylarsine–*NAs* and –*As*, respectively; $X^- = Cl^-$, $NO_2^-$, $N_3^-$]. The rates have been found to depend only on the hydrogen ion concentration and not on the particular concentration or strength of the acid used. The observed rate constant of *mer*-$[Rh(L)(L')Cl_3]$ is decreased by increasing the hydrogen ion concentration. Conversely, $k_{obs}$ for *mer*-$[Rh(L)(L')Cl_2N_3]$ increases smoothly up to a maximum limiting value by increasing the hydrogen ion concentration. A similar behaviour is shown by *mer*-$[Rh(L)(L')Cl_2NO_2]$, but in this case the rate constant achieves a maximum value and then it decreases towards a limiting value as the hydrogen ion concentration is increased further. The dependence of $k_{obs}$ on $[H^+]$ for the acid-dependent reaction path of the *mer*→*trans* conversion of *mer*-$[Rh(L)(L')Cl_3]$ and *mer*-$[Rh(L)(L')Cl_2N_3]$ is explained in terms of protonation at the $-NMe_2$ free end of L′, whereas also diprotonation of the complex is tentatively invoked to explain the kinetic effect of acidity on the reactions of *mer*-$[Rh(L)(L')Cl_2NO_2]$.

In a previous paper[1] we attempted to establish the effect of hydrogen ion on the rate of substitution reactions of the type (1), where the $-NMe_2$ free end of a chelating ligand (L′) is the entering group [L and L′ = (*o*-dimethylaminophenyl)dimethylarsine–*NAs* and –*As*, respectively; $X^- = NO_2^-$ or $N_3^-$]. It was found that the reactions are much faster in toluene-*p*-sulphonic acid methanolic solutions than in neutral methanol. However, the dependence of the rates on the hydrogen ion concentration could not be established, since a limiting rate constant was observed even at the smallest acid concentration that could be reliably employed (*ca.* $1.5 \times 10^{-4}$ mol dm$^{-3}$). On the other hand, the detailed knowledge of this dependence is required to elucidate the course of the acid-dependent path of reactions (1) for such complexes, owing to the presence of two potentially basic sites, i.e. the entering $-NMe_2$ end of L′ and the nitro or azido groups, which are known to exhibit a basic character also after coordination.[2]

*mer*-$[Rh(L)(L')Cl_2X] \rightarrow$ *trans*-$[Rh(L)_2Cl_2]^+ + X^-$ (1)†

In this paper we report the results of a kinetic investigation of reactions (1) ($X^- = NO_2^-$ or $N_3^-$) at 25.0°C in $ClCH_2COOH$–$ClCH_2COO^-$ buffered methanolic solutions at $I = 5.14 \times 10^{-2}$ mol dm$^{-3}$. The reactions have been investigated also in

*Author to whom correspondence should be addressed.

†The prefix *mer* is appropriate only when $X^-$ is a chloride ion. Here it is used to emphasize that $X^-$ and the two *trans* chlorides lie on the same meridional plane.

unbuffered methanolic solutions containing variable concentrations of weak acids of known $pK_a$ [acid ($pK_a$ in methanol): $CH_3COOH$ (9.7), $ClCH_2COOH$ (7.8), $Cl_2CHCOOH$ (6.3), $Cl_3CCOOH$ (4.9)].[3] An analogous kinetic investigation has been carried out with the trichloro complex, *mer*-[Rh(L)(L′)$Cl_3$], whose leaving group does not exhibit any basic character and whose reaction rates are already known to decrease with increasing acidity of the medium.[4]

## EXPERIMENTAL

*Materials.* Rhodium(III) complexes were prepared as described elsewhere.[1,5] Acids, sodium monochloroacetate and sodium toluene-*p*-sulphonate were reagent grade and were used without further purification. Dried methanol was cautiously distilled in the presence of small amounts of toluene-*p*-sulphonic acid.

*Preparation and analysis of the reaction mixtures.* Stock solutions of acids and sodium monochloroacetate were standardized by titration, whereas those of sodium toluene-*p*-sulphonate were prepared by weight. Stock solutions of the complexes were prepared by weighing immediately before use since reactions (1) start just on dissolution of the complexes. The reactions were followed spectrophotometrically and the acid-dependent reaction path was initiated by mixing appropriate volumes of thermostatted stock solutions in 1 cm silica cells maintained in the thermostatted cell compartment of the spectrophotometer. The starting concentration of the complexes was usually *ca.* $2.5 \times 10^{-5}$ mol dm$^{-3}$, though concentrations in the range $1 \times 10^{-5}$–$5 \times 10^{-5}$ have been sometimes used. The reactions in $ClCH_2COOH$–$ClCH_2COO^-$ buffered methanolic solutions were carried out at $I = 5.14 \times 10^{-2}$ mol dm$^{-3}$, using sodium toluene-*p*-sulphonate to adjust the ionic strength. In these cases the concentrations of acid and conjugate base were changed in the following ranges: (i) $ClCH_2COOH$, $2.94 \times 10^{-2}$ [$5.88 \times 10^{-2}$ for $X^- = Cl^-$)]–$4.41 \times 10^{-1}$; (ii) Na($ClCH_2COO$), $1.51 \times 10^{-3}$–$4.69 \times 10^{-2}$ ($Cl^-$); $7.51 \times 10^{-4}$–$4.38 \times 10^{-2}$ mol dm$^{-3}$ ($NO_2^-$ or $N_3^-$). No strong electrolytes were added to the reaction mixtures for the reactions carried out in unbuffered methanolic solutions of weak acids. The acid concentrations employed in these cases are listed in Tables 1–3.

The progress of the reaction was followed by scanning the absorption spectrum of the reaction mixture in the wavelength range 360–290 nm at suitable time intervals. Fast reactions were followed by recording the absorbance at a selected wavelength vs time. The reactions of *mer*-[Rh(L)(L′)$Cl_3$] exhibited an isosbestic point at a wavelength which decreased from 315 to 300 nm by increasing the acid content of the reaction medium. The reactions of *mer*-[Rh(L)(L′)$Cl_2NO_2$] and *mer*-[Rh(L)(L′)$Cl_2N_3$] did not exhibit isosbestic points in the wavelength range explored. The only rhodium(III) complex obtained in the reactions was *trans*-$[Rh(L)_2Cl_2]^+$, in agreement with stoicheiometry (1). The progress of the reactions was usually found to obey a pseudo-first-order rate law. The observed rate constants, $k_{obs}$, were determined with a reliability better than $\pm 3\%$ from the slopes of plots of $\log|A_t - A_\infty|$ vs time, where $A_t$ and $A_\infty$ are the absorbances at time $t$ and at the end of the reaction, respectively. When the reactions of *mer*-[Rh(L)(L′)$Cl_2NO_2$] or *mer*-[Rh(L)(L′)$Cl_2N_3$] were carried out in acid concentrations lower than *ca.* $1 \times 10^{-4}$ mol dm$^{-3}$, the gradient of $\log|A_t - A_\infty|$ vs time decreased with the progress of the reaction. In these cases the observed rate constant was evaluated by taking into account only the first 10–15% of the progress of the reaction.

## RESULTS AND DISCUSSION

The observed rate constants, $k_{obs}$, of reactions (1) ($X^- = Cl^-$, $NO_2^-$, $N_3^-$) carried out in $ClCH_2COOH$–$ClCH_2COO^-$ buffered methanolic solutions are found to depend on the concentration ratio [HA]/[$A^-$] (Figs. 1–3) and not on the particular concentration of acid or of its conjugate base used. This behaviour suggests that these species are not directly involved in the reaction mechanism, their actual function being essentially to buffer the hydrogen ion concentration to the value $[H^+] = K_a[HA]/[A^-]$.

The observed rate constant of the *mer*→*trans* conversion for *mer*-[Rh(L)(L′)$Cl_3$] is related to the [HA]/[$A^-$] ratio by relationship (2), where $K_1$ is the protonation constant of the complex [see reaction scheme (4)]. From a set of 32 runs (Fig. 1), the value of $k_{(m\to t)}$ and $K_1K_a$ obtained were $2.78 \times 10^{-3}$ s$^{-1}$ and $8.03 \times 10^{-3}$, respectively ($r = 0.982$). The value of $k_{(m\to t)}$ agrees fairly well with that ($2.86 \times 10^{-3}$ s$^{-1}$) obtained previously in neutral methanol at the same ionic strength.[4] Moreover, since the value of $K_1$ in methanol at $I = 5.14 \times 10^{-2}$ mol dm$^{-3}$ is already known ($4.78 \times 10^4$ dm$^3$ mol$^{-1}$),[4] one can derive a value of $1.68 \times 10^{-7}$ mol dm$^{-3}$ for the dissociation constant of monochloroacetic acid in methanol at $I = 5.14 \times 10^{-2}$ mol dm$^{-3}$, which may be compared with that found at zero ionic strength ($1.6 \times 10^{-8}$ mol dm$^{-3}$).[3] Kinetic measurements of the reaction of this complex, carried out in unbuffered solutions containing different weak

Table 1. Acid concentrations and observed rate constants for the chelate ring-closure substitution reactions of *mer*-[Rh(L)(L′)$Cl_3$] in methanol at 25.0°C

| ACID | [HA] (mol $dm^{-3}$) | $k_{obs}$ ($s^{-1}$) | ACID | [HA] (mol $dm^{-3}$) | $k_{obs}$ ($s^{-1}$) |
|---|---|---|---|---|---|
| $CH_3COOH$ | $4.41\times10^{-1}$ | $1.58\times10^{-3}$ | $Cl_2CHCOOH$ | $1.00\times10^{-2}$ | $3.26\times10^{-4}$ |
| | $3.82\times10^{-1}$ | $1.46\times10^{-3}$ | | $6.77\times10^{-3}$ | $4.03\times10^{-4}$ |
| | $2.61\times10^{-1}$ | $1.82\times10^{-3}$ | | $3.81\times10^{-3}$ | $4.95\times10^{-4}$ |
| | $2.35\times10^{-1}$ | $1.74\times10^{-3}$ | | $2.06\times10^{-3}$ | $6.42\times10^{-4}$ |
| | $8.82\times10^{-2}$ | $2.01\times10^{-3}$ | | $6.77\times10^{-4}$ | $1.10\times10^{-3}$ |
| | $4.41\times10^{-2}$ | $2.10\times10^{-3}$ | | $3.82\times10^{-4}$ | $1.33\times10^{-3}$ |
| | | | | $2.35\times10^{-4}$ | $1.66\times10^{-3}$ |
| $ClCH_2COOH$ | $5.68\times10^{-1}$ | $2.43\times10^{-4}$ | | | |
| | $3.34\times10^{-1}$ | $3.11\times10^{-4}$ | $Cl_3CCOOH$ | $4.63\times10^{-4}$ | $3.98\times10^{-4}$ |
| | $1.84\times10^{-1}$ | $4.14\times10^{-4}$ | | $3.09\times10^{-4}$ | $4.41\times10^{-4}$ |
| | $1.10\times10^{-1}$ | $5.02\times10^{-4}$ | | $1.84\times10^{-4}$ | $5.86\times10^{-4}$ |
| | $8.24\times10^{-2}$ | $6.13\times10^{-4}$ | | $9.26\times10^{-5}$ | $7.97\times10^{-4}$ |
| | $6.18\times10^{-2}$ | $7.07\times10^{-4}$ | | $7.18\times10^{-5}$ | $9.02\times10^{-4}$ |
| | $2.65\times10^{-2}$ | $9.76\times10^{-4}$ | | $5.58\times10^{-5}$ | $1.02\times10^{-3}$ |
| | $1.47\times10^{-2}$ | $1.24\times10^{-3}$ | | | |
| | $8.82\times10^{-3}$ | $1.44\times10^{-3}$ | No acid added | | $2.41\times10^{-3}$ |
| | $6.68\times10^{-3}$ | $1.61\times10^{-3}$ | | | $2.31\times10^{-3}$ |
| | $4.34\times10^{-3}$ | $1.71\times10^{-3}$ | | | $2.46\times10^{-3}$ |
| | $2.00\times10^{-3}$ | $1.93\times10^{-3}$ | | | |

acids, show that the observed rate constants are decreased when the strength of the acids or their concentration is increased (Table 1). In this case an analysis of the dependence of $k_{obs}$ on [$H^+$] has been made by evaluating the actual hydrogen ion concentration by means of a quartic equation[6] which included the equilibrium concentrations of protonated and unprotonated *mer* complex, and those of the acid (of known $pK_a$) and its conjugate base. Only hydrogen ion concentrations higher than about $5\times10^{-6}$ mol $dm^{-3}$ may be considered reliable since trace impurities and small changes of the actual concentration of the *mer* complex strongly affect the hydrogen ion concentration for unbuffered solutions close to neutrality. However, this limitation has not important consequences in processing the data since the reactivity of *mer*-[Rh(L)(L′)$Cl_3$] at very low hydrogen concentrations is practically the same as that observed in neutral methanol (e.g. Fig. 1). If the set of data collected in Table 1 is worked out according to eqn (2), one finds that the observed rate constant is dependent on the hydrogen ion concentration only, whereas it is independent of the nature of the acid involved, thus showing that such acids are not intrinsically active in affecting the rates of the reaction. The values of $k_{(m\to t)}$ and $K_1$ which have been obtained are reported in Table 4 ($r = 0.993$).

$$k_{obs} = \frac{k_{(m\to t)}}{1 + K_1K_a[HA]/[A^-]} = \frac{k_{(m\to t)}}{1 + K_1[H^+]} \quad (2)$$

A different effect of the acidity is observed for the *mer*→*trans* conversions of *mer*-[Rh(L)(L′)$Cl_2N_3$] and *mer*-[Rh(L)(L′)$Cl_2NO_2$]. In these cases an increase of acidity gives rise to an increase of the rate, though a somewhat different behavior is observed at high acidities according to the particular leaving group involved in the reaction. The dependence of the observed rate constant on [HA]/[$A^-$] for the reactions of *mer*-[Rh(L)(L′)$Cl_2N_3$] carried out in $ClCH_2COOH$–$ClCH_2COO^-$ buffered solutions is consistent with relationship (3) ($K_a$ =

Table 2. Acid concentrations and observed rate constants for the chelate ring-closure substitution reactions of *mer*-[Rh(L)(L′)$Cl_2N_3$] in methanol at 25.0°C

| ACID | [HA] (mol $dm^{-3}$) | $k_{obs}$ ($s^{-1}$) | ACID | [HA] (mol $dm^{-3}$) | $k_{obs}$ ($s^{-1}$) |
|---|---|---|---|---|---|
| $CH_3COOH$ | $4.27\times10^{-1}$ | $1.23\times10^{-2}$ | $Cl_2CHCOOH$ | $3.53\times10^{-3}$ | $6.56\times10^{-2}$ |
| | $2.65\times10^{-1}$ | $1.06\times10^{-2}$ | | $2.06\times10^{-3}$ | $5.96\times10^{-2}$ |
| | $1.32\times10^{-1}$ | $6.30\times10^{-3}$ | | $1.47\times10^{-3}$ | $4.66\times10^{-2}$ |
| | $5.88\times10^{-2}$ | $3.61\times10^{-3}$ | | $9.18\times10^{-4}$ | $3.75\times10^{-2}$ |
| | $2.94\times10^{-2}$ | $2.17\times10^{-3}$ | | $5.88\times10^{-4}$ | $3.03\times10^{-2}$ |
| | | | | $2.94\times10^{-4}$ | $1.89\times10^{-2}$ |
| $ClCH_2COOH$ | $4.57\times10^{-1}$ | $1.01\times10^{-1}$ | | | |
| | $2.96\times10^{-1}$ | $9.35\times10^{-2}$ | $Cl_3CCOOH$ | $3.24\times10^{-3}$ | $1.06\times10^{-1}$ |
| | $1.48\times10^{-1}$ | $7.92\times10^{-2}$ | | $2.06\times10^{-3}$ | $1.09\times10^{-1}$ |
| | $7.32\times10^{-2}$ | $6.32\times10^{-2}$ | | $1.03\times10^{-3}$ | $1.00\times10^{-1}$ |
| | $3.10\times10^{-2}$ | $4.52\times10^{-2}$ | | $7.66\times10^{-4}$ | $9.38\times10^{-2}$ |
| | $2.07\times10^{-2}$ | $3.33\times10^{-2}$ | | $5.93\times10^{-4}$ | $9.91\times10^{-2}$ |
| | $1.33\times10^{-2}$ | $2.62\times10^{-2}$ | | $5.47\times10^{-4}$ | $8.96\times10^{-2}$ |
| | $7.39\times10^{-3}$ | $1.90\times10^{-2}$ | | $4.45\times10^{-4}$ | $8.72\times10^{-2}$ |
| | $4.49\times10^{-3}$ | $1.41\times10^{-2}$ | | $3.53\times10^{-4}$ | $8.47\times10^{-2}$ |
| | $3.63\times10^{-3}$ | $1.33\times10^{-2}$ | | $3.46\times10^{-4}$ | $8.15\times10^{-2}$ |
| | $2.61\times10^{-3}$ | $1.06\times10^{-2}$ | | $2.22\times10^{-4}$ | $7.24\times10^{-2}$ |
| | | | | $1.76\times10^{-4}$ | $6.17\times10^{-2}$ |
| $Cl_2CHCOOH$ | $8.35\times10^{-2}$ | $1.05\times10^{-1}$ | | $1.48\times10^{-4}$ | $6.57\times10^{-2}$ |
| | $6.47\times10^{-2}$ | $1.08\times10^{-1}$ | | $9.88\times10^{-5}$ | $5.47\times10^{-2}$ |
| | $4.12\times10^{-2}$ | $1.08\times10^{-1}$ | | $9.88\times10^{-5}$ | $5.31\times10^{-2}$ |
| | $2.06\times10^{-2}$ | $1.00\times10^{-1}$ | | $7.41\times10^{-5}$ | $5.02\times10^{-2}$ |
| | $9.12\times10^{-3}$ | $8.70\times10^{-2}$ | | | |
| | $5.88\times10^{-3}$ | $7.75\times10^{-2}$ | No acid added | | $1.50\times10^{-5}$ |

$1.68 \times 10^{-7}$ mol $dm^{-3}$). The related protonation and specific rate constants, obtained from a set of 32 runs most of which are plotted in Fig. 2, are reported in Table 4 ($r = 0.999$). A less satisfactory analysis can be done for the same reactions carried out in unbuffered solutions of weak acids (Table 2) owing to the previously mentioned poor reliability of the hydrogen ion concentrations calculated for reaction mixtures close to neutrality. Nevertheless, such an analysis enables one to infer that the general behaviour observed is consistent with relationship (3) and that the weak acids involved are not intrinsically active in affecting the rates, just as found above for the reactions of *mer*-[Rh(L)(L′)$Cl_3$]. In the case of the *mer*→*trans* conversions of *mer*-[Rh(L)(L′)$Cl_2NO_2$] in $ClCH_2COOH$–$ClCH_2COO^-$ buffered solutions, the observed rate constant increases rather sharply with the acidity (i.e. with increasing the [HA]/[$A^-$] ratio; Fig. 3), achieving a maximum value of about $9.7 \times 10^{-2}$ $s^{-1}$. However, a further increase of the acidity causes a progressive decrease of $k_{obs}$ to the limiting value of $6.89 \times 10^{-2}$ $s^{-1}$, which can be attained only by using concentrations of toluene-*p*-sulphonic acid ranging from $6.05 \times 10^{-3}$ and $4.38 \times 10^{-2}$ mol $dm^{-3}$. Such a behaviour is displayed also in unbuffered solutions of weak acids (Table 3), where the inability of the undissociated acids to affect the rates can be once again envisaged.

$$k_{obs} = \frac{k_{(m\to t)} + k^{H}_{(m\to t)} K_1 K_a [HA]/[A^-]}{1 + K_1 K_a [HA]/[A^-]}$$

Table 3. Acid concentrations and observed rate constants for the chelate ring-closure substitution reactions of *mer*-$[Rh(L)(L')Cl_2NO_2]$ in methanol at 25.0°C

| ACID | [HA] (mol $dm^{-3}$) | $k_{obs}$ ($s^{-1}$) | ACID | [HA] (mol $dm^{-3}$) | $k_{obs}$ ($s^{-1}$) |
|---|---|---|---|---|---|
| $CH_3COOH$ | $4.27\times10^{-1}$ | $4.76\times10^{-2}$ | $Cl_2CHCOOH$ | $5.88\times10^{-4}$ | $7.58\times10^{-2}$ |
| | $2.94\times10^{-1}$ | $3.67\times10^{-2}$ | | $3.82\times10^{-4}$ | $6.56\times10^{-2}$ |
| | $1.47\times10^{-1}$ | $2.33\times10^{-2}$ | | $2.35\times10^{-4}$ | $4.98\times10^{-2}$ |
| | $7.35\times10^{-2}$ | $1.39\times10^{-2}$ | | $5.88\times10^{-5}$ | $1.13\times10^{-2}$ |
| | $2.94\times10^{-2}$ | $6.42\times10^{-3}$ | | | |
| | $1.47\times10^{-2}$ | $3.52\times10^{-3}$ | $Cl_3CCOOH$ | $8.78\times10^{-2}$ | $7.62\times10^{-2}$ |
| | | | | $7.66\times10^{-2}$ | $7.05\times10^{-2}$ |
| $ClCH_2COOH$ | $5.41\times10^{-1}$ | $8.47\times10^{-2}$ | | $8.18\times10^{-2}$ | $7.48\times10^{-2}$ |
| | $4.57\times10^{-1}$ | $8.99\times10^{-2}$ | | $2.54\times10^{-3}$ | $8.47\times10^{-2}$ |
| | $2.94\times10^{-1}$ | $9.66\times10^{-2}$ | | $2.00\times10^{-3}$ | $8.69\times10^{-2}$ |
| | $1.77\times10^{-1}$ | $1.03\times10^{-1}$ | | $1.36\times10^{-3}$ | $8.28\times10^{-2}$ |
| | $8.82\times10^{-2}$ | $1.07\times10^{-1}$ | | $7.66\times10^{-4}$ | $8.55\times10^{-2}$ |
| | $7.21\times10^{-2}$ | $1.06\times10^{-1}$ | | $5.93\times10^{-4}$ | $8.93\times10^{-2}$ |
| | $5.41\times10^{-2}$ | $1.04\times10^{-1}$ | | $5.47\times10^{-4}$ | $9.12\times10^{-2}$ |
| | $4.41\times10^{-2}$ | $1.04\times10^{-1}$ | | $3.53\times10^{-4}$ | $9.48\times10^{-2}$ |
| | $3.24\times10^{-2}$ | $8.99\times10^{-2}$ | | $3.46\times10^{-4}$ | $9.66\times10^{-2}$ |
| | $2.16\times10^{-2}$ | $8.93\times10^{-2}$ | | $3.14\times10^{-4}$ | $9.80\times10^{-2}$ |
| | $1.44\times10^{-2}$ | $7.21\times10^{-2}$ | | $2.51\times10^{-4}$ | $1.00\times10^{-1}$ |
| | $7.58\times10^{-3}$ | $5.98\times10^{-2}$ | | $2.22\times10^{-4}$ | $1.02\times10^{-1}$ |
| | $2.94\times10^{-3}$ | $2.39\times10^{-2}$ | | $1.88\times10^{-4}$ | $1.04\times10^{-1}$ |
| | | | | $1.77\times10^{-4}$ | $1.06\times10^{-1}$ |
| $Cl_2CHCOOH$ | $9.33\times10^{-2}$ | $7.24\times10^{-2}$ | | $1.48\times10^{-4}$ | $1.01\times10^{-1}$ |
| | $6.67\times10^{-2}$ | $8.33\times10^{-2}$ | | $9.88\times10^{-5}$ | $1.04\times10^{-1}$ |
| | $4.76\times10^{-2}$ | $8.07\times10^{-2}$ | | $7.41\times10^{-5}$ | $1.02\times10^{-1}$ |
| | $1.33\times10^{-2}$ | $8.41\times10^{-2}$ | | $6.27\times10^{-5}$ | $8.60\times10^{-2}$ |
| | $9.52\times10^{-3}$ | $1.00\times10^{-1}$ | | $4.94\times10^{-5}$ | $8.76\times10^{-2}$ |
| | $9.12\times10^{-3}$ | $1.02\times10^{-1}$ | | | |
| | $4.76\times10^{-3}$ | $1.05\times10^{-1}$ | $p\text{-}CH_3C_6H_4SO_3H$ | $6.21\times10^{-3}$ | $7.24\times10^{-2}$ |
| | $1.43\times10^{-3}$ | $1.02\times10^{-1}$ | | $8.70\times10^{-4}$ | $7.24\times10^{-2}$ |
| | $8.82\times10^{-4}$ | $1.02\times10^{-1}$ | | $6.21\times10^{-4}$ | $7.32\times10^{-2}$ |
| | | | No added acids | | $4.41\times10^{-4}$ |

$$= \frac{k_{(m\to t)} + k^{H}_{(m\to t)}[H^+]}{1 + K_1[H^+]} \qquad (3)$$

Reversible protonation of the *mer* complex and slow conversion to *trans*-$[Rh(L)_2Cl_2]^+$ of both unprotonated and protonated complexes [reactions scheme (4)] can explain the kinetic results observed for both *mer*-$[Rh(L)(L')Cl_3]$ and *mer*-$[Rh(L)(L')Cl_2N_3]$ complexes. Accordingly, the observed rate constant related to reaction scheme (4) [eqn (5)] is fully consistent with relationship (3) operating for

$$mer + H^+ \overset{K_1}{\rightleftharpoons} mer\ H^+ \qquad (4a)$$

$$mer \xrightarrow{k_{(m\to t)}} trans^+ + X^- \qquad (4b)$$

$$mer\ H^+ \xrightarrow{k_{(m\to t)}} trans^+ + (HX \rightleftharpoons X^- + H^+) \qquad (4c)$$

the azido complex. The fact that step (4c) is operative with the azido complex may be ascribed to the occurrence of an hydrogen bond or a proton transfer between the protonated $-NMe_2H^+$ end of L′ and the outgoing azido group which is then released as $N_3H$. The inability of an outgoing chloro group to give to any extent such interactions is consistent with the lack of evidence of a

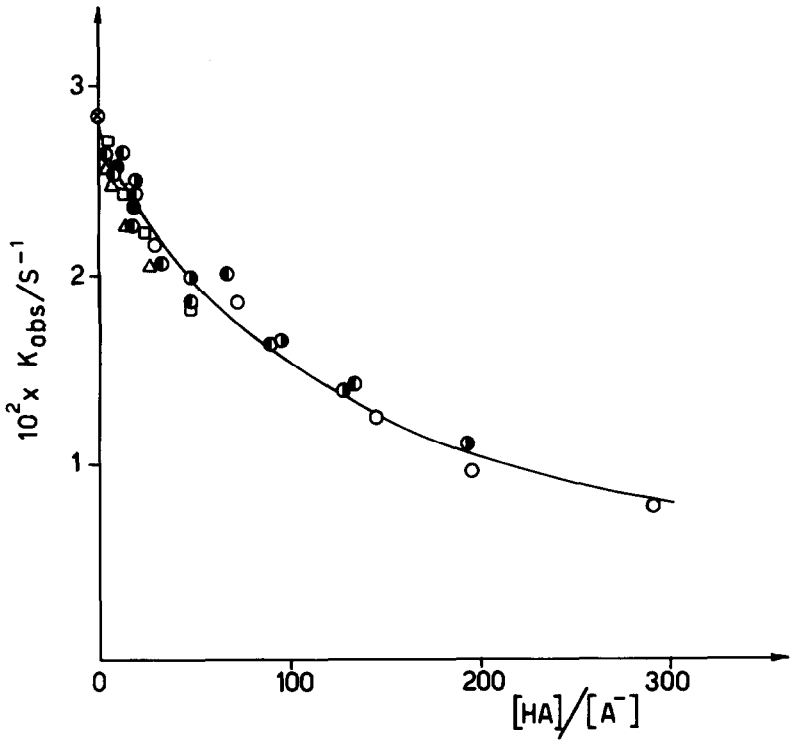



Fig. 1. Dependence of $k_{obs}$ on $[ClCH_2COOH]/[ClCH_2COO^-] = [HA]/[A^-]$ for reaction (1) ($X^- = N_3^-$) in methanol at 25.0°C and $I = 5.14 \times 10^{-2}$ mol dm$^{-3}$. $[ClCH_2COOH] = 2.94 \times 10^{-2}$ (▲), $1.47 \times 10^{-1}$ (□), $2.06 \times 10^{-1}$ (◐), $2.94 \times 10^{-1}$ (◑), $4.41 \times 10^{-1}$ (○) mol dm$^{-3}$.

$k^H_{(m\to t)}$ rate term for the *mer*→*trans* conversion of *mer*-[Rh(L)(L′)$Cl_3$].

$$k_{obs} = \frac{k_{(m\to t)} + k^H_{(m\to t)} K_1[H^+]}{1 + K_1[H^+]} \qquad (5)$$

The basic character preserved by a coordinated nitro group[2] would suggest the occurrence of an acid-catalysed reaction step for the *mer*→*trans* conversions of *mer*-[Rh(L)(L′)$Cl_2NO_2$] similar to that envisaged for the azido analogous. Indeed, the observed catalytic effect of the acidity would find a qualitative rationalization. However, the reaction schemes (4a)–(4c) is not fully adequate since it cannot explain the decrease of $k_{obs}$ observed when the hydrogen ion concentration is strongly increased (Fig. 3). Such different behaviour between the azido and the nitro complex has not a straightforward explanation. On the other hand, it is noteworthy that analogous kinetic behaviours have been previously reported for other nitro and azido complexes. Thus, a maximum rate followed by a decrease upon further increase of the acidity of the medium has been observed in the acid-catalysed hydrolysis of transition metal nitro complexes,[2,7,8] whereas the rates of the acid-catalysed hydrolysis of analogous azido complexes have been found to increase up to a limiting value which did not appear to change using higher acidities.[2] However, such acid-catalysed hydrolysis were carried out in highly concentrated acidic solutions (usually more than 2 mol dm$^{-3}$ in acid) and without any ionic strength control so that the different kinetic behaviour observed by changing the leaving group could be ascribed to different effects connected with changes of activity coefficients caused by changes of the acid content.[2,7] Such an explanation can hardly account for the differences here observed in the effect of hydrogen ion on the reaction rates of *mer*-[Rh(L)(L′)$Cl_2NO_2$] and *mer*-[Rh(L)(L′)$Cl_2N_3$]. In fact, these reactions were carried out either at a constant or nearly zero ionic strength so that the activity coefficients are expected to remain practically constant in the acid concentration ranges explored.

A tentative explanation of the observed kinetic behaviour of *mer*-[Rh(L)(L′)$Cl_2NO_2$] would involve invoking the occurrence of a further protonation of the monoprotonated complex. Poliprotonation is rather common in the

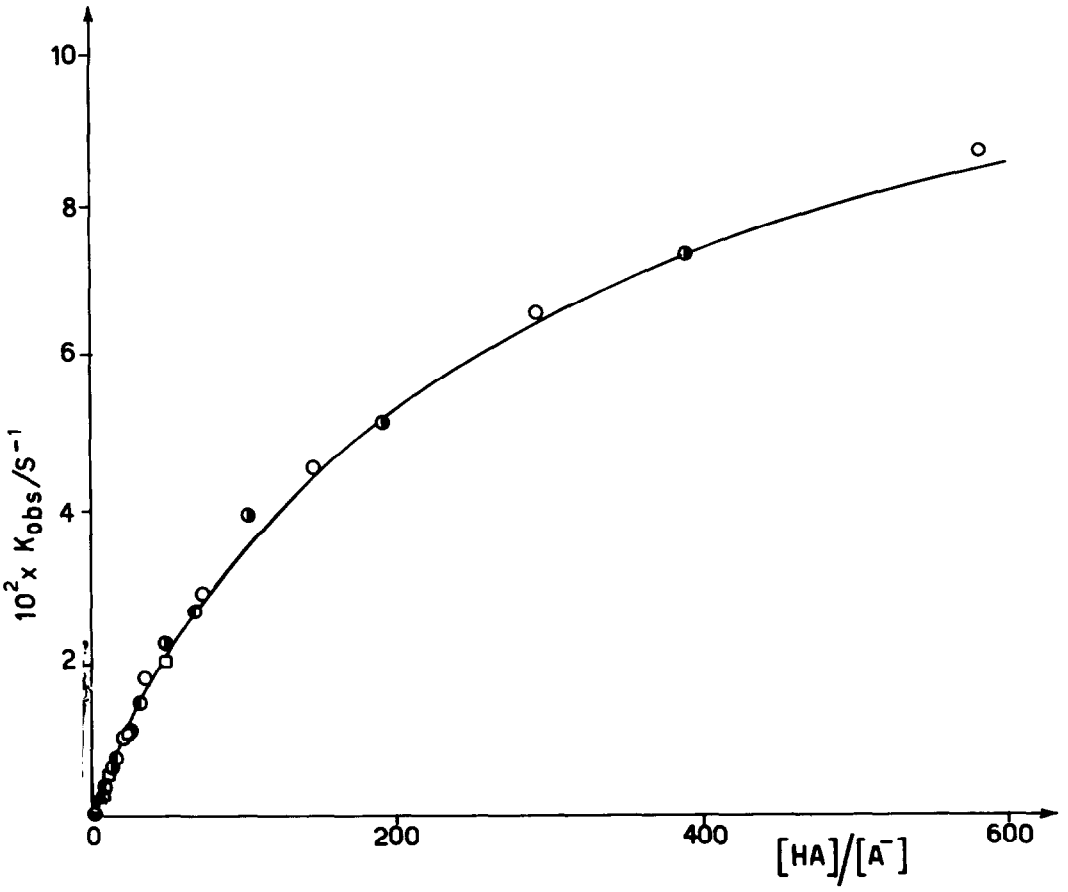



Fig. 2. Dependence of $k_{obs}$ on $[ClCH_2COOH]/[ClCH_2COO^-] = [HA]/[A^-]$ for reaction (1) ($X^- = N_3^-$) in methanol at 25.0°C and $I = 5.14 \times 10^{-2}$ mol dm$^{-3}$. $[ClCH_2COOH] = 2.94 \times 10^{-2}$ (▲), $5.88 \times 10^{-2}$ (●), $8.82 \times 10^{-2}$ (■), $1.47 \times 10^{-1}$ (□), $2.06 \times 10^{-1}$ (◐), $2.94 \times 10^{-1}$ (◑), $4.4i \times 10^{-1}$ (○) mol dm$^{-3}$.

*acid-catalysed dissociation of many complexes and* it has also been invoked to account for the form of the rate law found for the acid-catalysed hydrolysis of $[Co(NH_3)_4(NO_2)_2]^+$ carried out at a constant ionic strength.[9] Diprotonation of *mer*-$[Rh(L)(L')Cl_2NO_2]$ is possible, at least in principle, for the presence of two basic sites, i.e. the $-NMe_2$ free end of L′ and the nitro group (according to this hypothesis also the azido complex is expected to undergo diprotonation). In such a case eqns (4d) and (4e) must also be considered. The observed rate constant

$$mer\ H^+ + H^+ \overset{K_2}{\rightleftharpoons} mer\ H_2^{2+} \qquad (4d)$$

$$mer\ H_2^{2+} \xrightarrow{k_{(m\to t)}^{2H}} trans^+ + H^+ + (HX \rightleftharpoons H^+ + X^-) \qquad (4e)$$

for the overall reaction scheme (4a)–(4e) has the *form (6). Such a relationship is consistent with the* experimental results found for the nitro complex. Thus, processing the data for 43 runs carried out in buffered solutions, most of which are reported in Fig. 3, the values of protonation and specific rate constants reported in Table 4 ($r = 0.980$) can be obtained. Obviously, relationship (6) includes as special cases the expressions for the observed rate constants found for *mer*-$[Rh(L)(L')Cl_3]$ and *mer*-$[Rh(L)(L')Cl_2N_3]$. If reaction scheme (4a)–(4e) is reliable, a question which remains unanswered is the reason why a contribution to the rate due to a diprotonated complex was not detected for the azido complex. However, it must be noticed that a relatively low value of $K_2$ for this complex would make it difficult to detect experimentally such a contribution.

$$k_{obs} = \frac{k_{(m\to t)} + k_{(m\to t)}^{H} K_1 H^+] + k_{(m\to t)}^{2H} K_1 K_2 [H^+]^2}{1 + K_1[H^+] + K_1 K_2 [H^+]^2} \qquad (6)$$

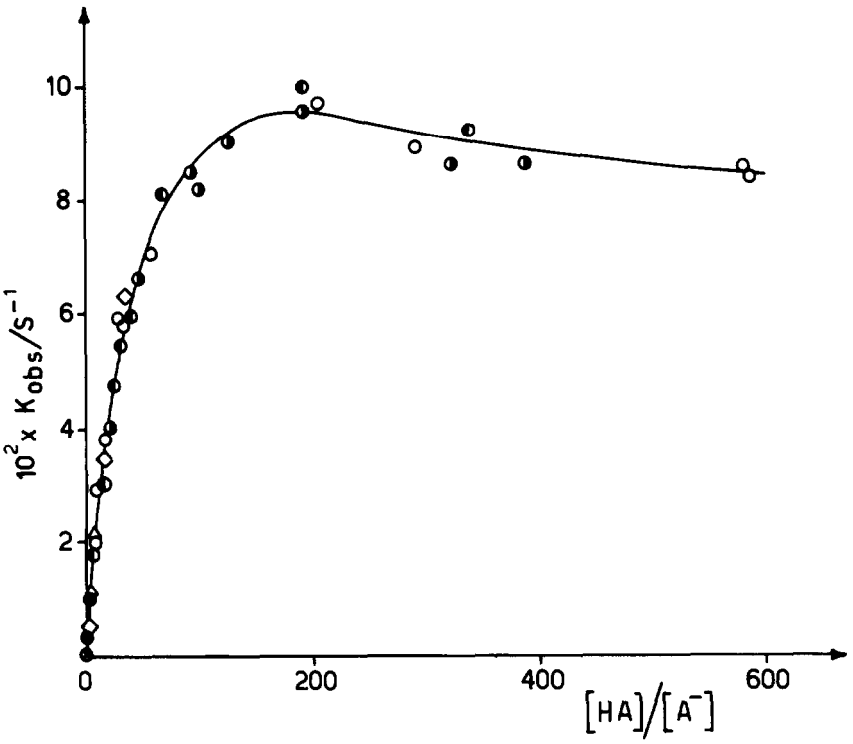



Fig. 3. Dependence of $k_{obs}$ on $[ClCH_2COOH]/[ClCH_2COO^-] = [HA]/[A^-]$ for reaction (1) ($X^- = NO_2^-$)in methanol at 25.0°C and $I = 5.14 \times 10^{-2}$ mol dm$^{-3}$. $[ClCH_2COOH] = 5.88 \times 10^{-2}$ (●), $8.47 \times 10^{-2}$ (△), $1.18 \times 10^{-1}$ (◇), $2.06 \times 10^{-1}$ (◐), $2.94 \times 10^{-1}$ (◑), $4.41 \times 10^{-1}$ (○) mol dm$^{-3}$.

Table 4. Rate constants for the chelate ring-closure substitution reactions and protonation constants of *mer*-$[Rh(L)(L')Cl_2X]$ complexes in methanol at 25.0°C according to reaction scheme (4a–e)

| $X^-$ | $I$(mol dm$^{-3}$) | $k_{(m\to t)}$($s^{-1}$) | $k^H_{(m\to t)}$($s^{-1}$) | $k^{2H}_{(m\to t)}$($s^{-1}$) | $K_1$(dm$^3$ mol$^{-1}$) | $K_2$(dm$^3$ mol$^{-1}$) |
|---|---|---|---|---|---|---|
| $Cl^-$ | $5.14\times10^{-2}$ | $2.78\times10^{-3}$ | - | - | $4.78\times10^4$(a) | - |
| | 0 | $2.40\times10^{-3}$ | - | - | $1.05\times10^5$ | - |
| $NO_2^-$ | $5.14\times10^{-2}$ | $4.81\times10^{-4}$(b) | $1.78\times10^{-1}$ | $6.89\times10^{-2}$ | $7.2\times10^4$ | $5.5\times10^4$ |
| | 0 | $4.41\times10^{-4}$ | - | $7.05\times10^{-2}$ | - | - |
| $N_3^-$ | $5.14\times10^{-2}$ | $1.95\times10^{-5}$(b) | $1.22\times10^{-1}$ | - | $2.25\times10^4$ | - |
| | 0 | $1.50\times10^{-5}$ | $1.08\times10^{-1}$ | - | - | - |

(a) Data taken from Ref. 4 (b) Data taken from Ref. 1

make it difficult to detect experimentally such a contribution.

An inspection to the data collected in Table 4 show that the protonation constants of the three *mer* complexes, $K_1$, considered in this paper are rather similar. This fact suggests that in each case the same basic site is likely involved in the protonation, i.e. the $-NMe_2$ free end of L'. Moreover, it is found that the $k^H_{(m\to t)}$ rate term for the azido complex is rather close to that related to the nitro complex. Since the $Rh-N_3$ bond appears to be much stronger than the $Rh-NO_2$ bond,[1] close rate

constants for the reactions of the related protonated complexes would be hardly explained in terms of a bond breaking as rate determining step. A better explanation would be that the release of the protonated leaving group is a fast step so that the chelate ring closure, which is a common step for the reactions of both complexes, becomes rate determining.

## REFERENCES

1. A. Peloso, *J. Chem. Soc., Dalton.* 1981, 2429.
2. P. J. Staples, *Coord. Chem. Rev.* 1973, **11**, 277 and references therein.
3. L. Šůcha and St. Kotrlý, *Solution Equilibria in Analytical Chemistry*, p. 111. Van Nostrand, Reinhold, London (1972).
4. A. Peloso, *J. Chem. Soc., Dalton*, 1979, 2033.
5. L. Volponi, C. Panattoni, R. Graziani and G. Bombieri, *Gazz. Chim. Ital.* 1966, **96**, 1158.
6. H. Freiser and Q. Fernando, *Ionic Equilibria in Analytical Chemistry*, p. 116. Wiley, New York (1963).
7. B. E. Crossland and P. J. Staples, *J. Chem. Soc., A* 1970, 1305.
8. D. Humpherey and P. J. Staples, *J. Chem. Soc., A* 1970, 2708.
9. U. D. Gomwalk and A. McAuley, *J. Chem. Soc., A* 1966, 1692.

*Polyhedron* Vol. 3, No. 7, pp. 821–831, 1984
Printed in the U.S.A.

0277-5387/84 $3.00 + .00
© 1984 Pergamon Press Ltd.

# EXTRACTION OF COPPER(II) AND NICKEL(II) BY NOPINOQUINONE DIOXIME

**L. R. M. PAPING, T. P. M. BEELEN, M. MOLS, J. H. M. C. van WOLPUT and R. PRINS***

Department of Inorganic Chemistry, Eindhoven University of Technology, P. O. Box 513, 5600 MB Eindhoven, The Netherlands

(*Received* 25 *August* 1983; *accepted* 16 *November* 1983)

**Abstract**—In the research for a selective extractant for nickel a strained dioxime, β-nopinoquinone dioxime, has been studied in its extraction properties for copper(II) and nickel(II). Spectroscopic investigations (ESR and NMR) showed that both copper and nickel are extracted as a N,N-coordinated chelate. The extraction studies showed that the use of strained instead of aliphatic dioximes makes the extraction more convenient because of the higher extraction rate, but the selectivity for nickel above copper disappears.

δ-nopinoquinone dioxime is easily converted into its furazan by treatment with 1N NaOH. This furazan is a rather weak ligand without significant extraction capacities.

Vicinal dioximate ligands usually form stable N,N-chelated complexes containing a conjugated N = C–C = N system (Fig. 1a).

In previous work[1] it became clear that camphorquinone dioxime cannot form a stable N,N-coordinated chelate with copper and nickel. The rigid bicyclic skeleton is responsible for a larger N–N distance than in aliphatic α-dioximes and makes the N,O-coordination, with a six-membered ring metal–N = C–C = N–O– more attractive (Fig. 1b).

*Author to whom correspondence should be addressed.

Nopinoquinone dioxime $H_2$NQD(6,6-dimethylbicyclo[3.1.1]-heptane-2,3-dione dioxime), also a bicyclic molecule, is therefore of interest because the strain in this structure is somewhat less and so the N–N distance will be shorter than in camphorquinone dioxime. This may have consequences for the way of coordination and may lead to different complexes for copper and nickel. By using the right isomer (Fig. 2) there might be a chance that a selective ligand will be found for nickel. For this reason we tried to synthesize β- and δ-nopinoquinone dioxime, studied the extraction properties and tried to determine the structure of the chelates formed during the extraction.

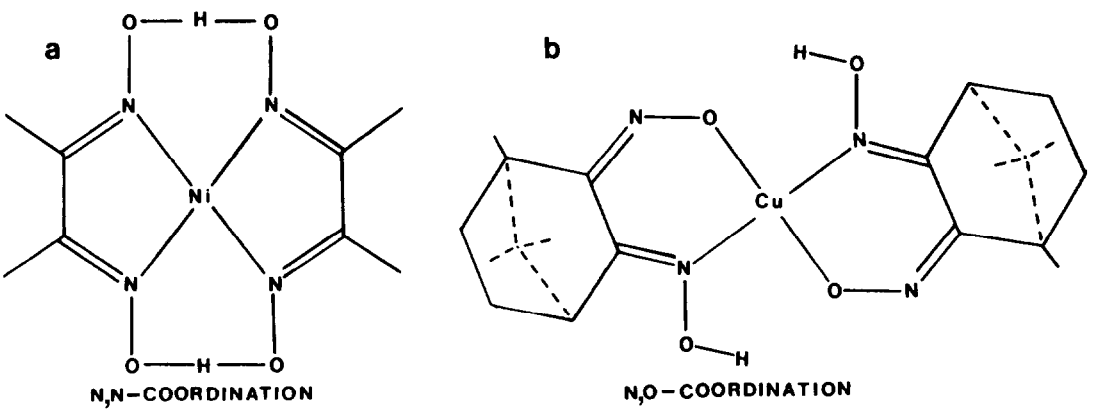



Fig. 1. (a) The N,N-coordinated bis(dimethylglyoximato)nickel(II) chelate. (b) The N,O-coordinated bis(camphorquinonedioximato) copper(II) chelate.

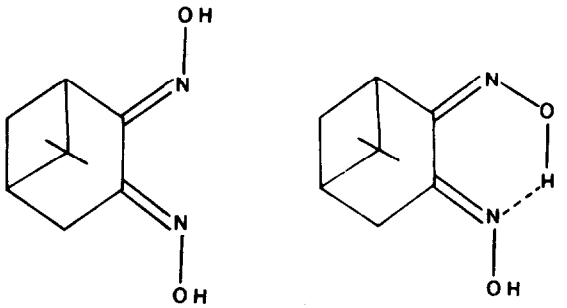



Fig. 2. Two isomeric forms of nopinoquinone dioxime.

## EXPERIMENTAL

$^1$H NMR spectra were obtained at room temperature on a 60 MHz Varian EM 360 A spectrometer, while ESR measurements were done with a Varian E15 spectrometer at room temperature and UV-visible spectra were obtained on a Unicam SP.800D. Aqueous metal ion concentrations were measured with the Perkin–Elmer 300 Atomic Absorption Spectrophotometer.

The extraction experiments were carried out in a three stoppered flask with a stirring device and continuous pH measurements. The starting volumes of water and organic solvent were both 250 cm$^3$. Stirring was stopped when no further change of the pH was noticed, indicating that equilibrium was reached. For analysis equally small volumes of water layer and organic layer were withdrawn from the system. To measure the distribution coefficient as a function of pH thereafter a small quantity of 4N acid or base was added, and the process of stirring until equilibrium and withdrawal of small portions of the aqueous and organic solutions was repeated at a different pH. Care was taken to keep the volumes of the aqueous and organic solutions equal. Although in this procedure the electrolyte concentration does not stay constant we preferred this method because it is convenient to execute and because in a separate experiment it was shown that in the applied concentration range the influence of the electrolyte concentration was negligible. Pentanol was used as organic solvent and as inorganic salt we used metal nitrate. We used NaOH as base and $HNO_3$ as acid.

## SYNTHESIS

*β-Nopinoquinonedioxime*

Nopinone(6,6-dimethylbicyclo[3.1.1]heptane-2-one) was prepared by ozonolysis of β-pinene (J. T. Baker chemicals B. V. Deventer, Baker grade) according to a published method.[2] The decrease in intensity of the sharp C–H band of alkenes at 3070 cm$^{-1}$ in the IR spectrum was a useful indication how much pinene was converted. Following the conventional method[3] using *n*-butyl nitrite, isonitrosonopinone was obtained in 30% yield from nopinone. Following the procedures of Nakamura[4], crude isonitrosonopinone (0.18 mol) dissolved in 50 cm$^3$ ethanol was treated with an aqueous solution of $NH_2OH.HCl$ (0.48 mol) and NaOAc (0.51 mol) at 90°C for 3 days. A solid white inorganic product precipitated. The mother liquid was concentrated *in vacuo* to 50% of the original volume and filtered. Further concentration, removing ethanol completely gave the crude β-isomer. Extraction with boiling ethyl acetate removed the δ-isomer completely and gave the pure β-$H_2$NQD. Found: C,59.3; H,7.9; N,15.5. Calc.: C,59.3; H,7.7; N,15.4%. IR: OH stretching vibrations at 3360 and 3180 cm$^{-1}$ C = N absorptions at 1585 and 1615 cm$^{-1}$. These values are in perfect agreement with Nakamura.[5] $^1$H NMR (DMSO-d6): δ0.74 (*s*, 3H), 1.03 (*s*, 3H), 2.05 (*m.c*, 1H), 2.41 (*t*, 1H), 2.64 (*d*, 1H), 3.41 (*t*, 1H), 10.74 (*s*, 1H), 11.18 (*s*, 1H) confirms the β structure.[4]

*The furazan of nopinoquinone dioxime (Fig. 3)*

The yellow oil, which was obtained in the above synthesis by the evaporation of the ethylacetate from the extract, was treated with 1N NaOH and extracted with ether. The ether layer was dried and evaporated. A yellow pleasantly smelling oil was obtained. After distillation a white powder was produced with a melting point of 30°C. IR: 1510 cm$^{-1}$ (furazan) 1550 and 1615 cm$^{-1}$ (C = N); no OH stretchings present. Found: C,65.5; H,7.5; N,16.9. Calc. for $C_9H_{12}N_2O$: C,65.8; H,7.3; N,17.1%. $^1$H NMR (DMSO-d6): see Fig. 4.

*Bis(β-nopinoquinonedioximato)nickel(II)*

Ni(β-HNQD)$_2$ was synthesized by the reaction of β-nopinoquinone dioxime and $NiCl_2.6H_2O$ in ethanol with NaOH in a minimum amount of water. After stirring for two hours water was added and the orange–red chelate precipitated.The chelate was washed with water and dried at 50°C in the presence of silica.

IR: No absorption in the 3100–3600 cm$^{-1}$ region. 1585 and 1560 cm$^{-1}$ (shoulder) (C=N) Found: C,51.9; H,6.26; N,13.51. Calc. for $NiC_{18}H_{26}N_4O_4$: C,51.35; H,6.25; N.13.31%.

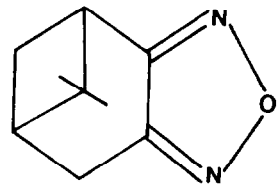



Fig. 3. The structure of the furazan derived from nopinoquinone dioxime.

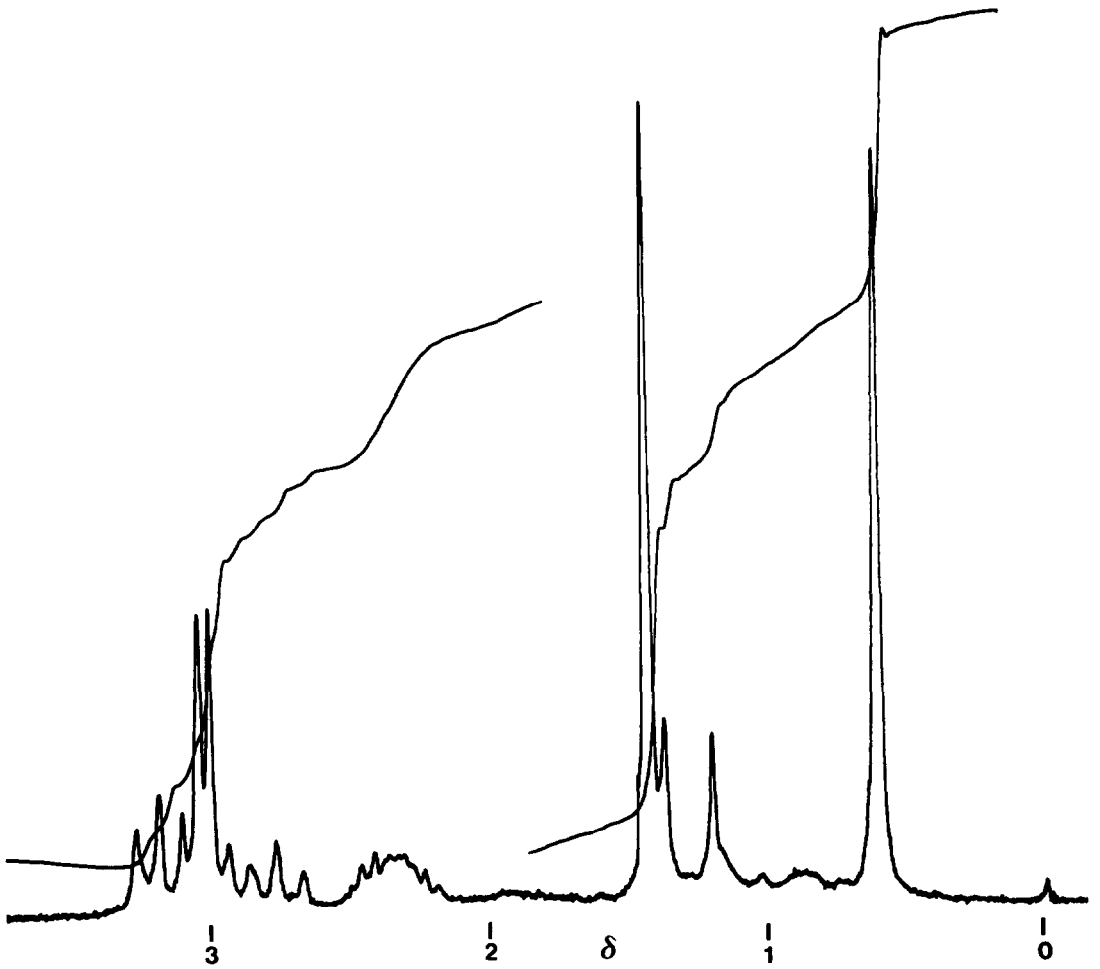



Fig. 4. 60 MHz $^1$H NMR spectrum of the furazan of nopinoquinone dioxime.

## TREATMENT OF EXTRACTION DATA

The extraction is expected to follow eqn (1):

$$Me^{2+} + \overline{2H_2NQD} \rightleftharpoons \overline{Me(HNQD)_2} + 2H^+ \quad (1)$$

where $Me^{2+}$ represents the aquo metal ion, $Me(HNQD)_2$ the extractable complex and bars indicate the organic layer. The equilibrium constant $K_E$ and the distribution coefficient D are defined as:

$$K_E = \frac{[Me(HNQD)_2][H^+]^2}{[Me^{2+}][H_2NQD]^2} \quad (2)$$

$$D = \frac{[Me(HNQD)_2]}{[Me^{2+}]}. \quad (3)$$

Combination of (2) and (3) gives

$$\log D = \log K_E + 2pH + 2\log[H_2NQD]. \quad (4)$$

When taking a large excess $H_2NQD$, so that $H_2NQD$ is constant, it follows that

$$\left(\frac{\partial \log D}{\partial pH}\right)_{[H_2NQD]} = 2. \quad (5)$$

Introducing $pH_{1/2}$ as the pH value at which 50% of the metal is extracted ($\log D = 0$) eqn (4) leads to:

$$\log K_E = -2\log[H_2NQD] - 2pH_{\frac{1}{2}}. \quad (6)$$

Finally the value of $pH_{\frac{1}{2}}$ at 1.0 M equilibrium concentration of extractant in the organic phase, denoted by $(pH_{\frac{1}{2}})_{1.0}$ can be obtained from eqn (6) as

$$(pH_{1/2})_{1.0} = -\frac{\log K_E}{2}. \quad (7)$$

Figure 5 shows the results for the extraction of $Cu^{2+}$ and $Ni^{2+}$ with an excess of $\beta$-$H_2NQD$. The $pH_{\frac{1}{2}}$ value of 1.85 for $Cu^{2+}$ corresponds with

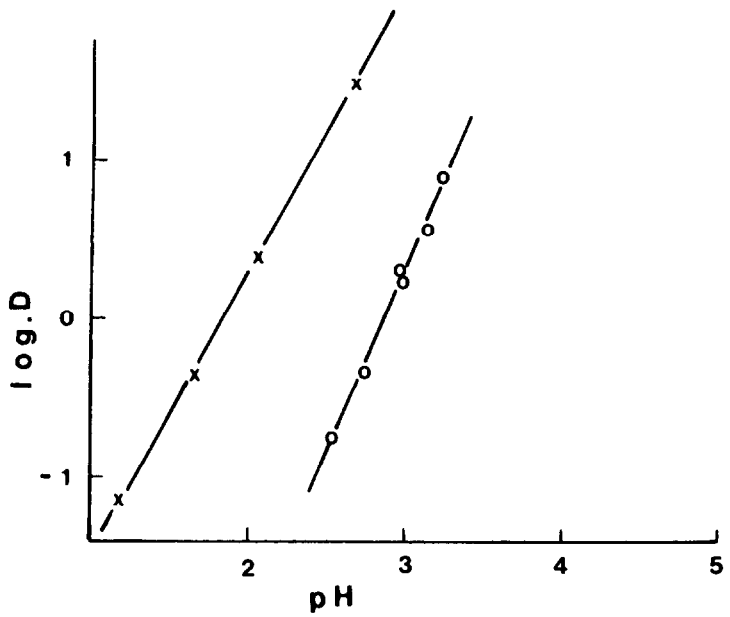



Fig. 5. Log D as a function of pH for the extraction of Cu(II) (X) and Ni(II) (O) by nopinoquinone dioxime. Concentration of $\beta$-$H_2$NQD is pentanol 0.025 M. Initial metal nitrate concentration 0.001 M.

$(pH_{\frac{1}{2}}^{1})_{1.0} = 0.25$. For $Ni^{2+}$ these values are somewhat higher: $pH_{\frac{1}{2}}^{1} = 2.88$ and $(pH_{\frac{1}{2}}^{1})_{1.0} = 1.28$. For the nickel extraction equilibrium was reached within ten minutes.

The slopes of the log $D$ – pH curves are 1.75 for copper and 2.22 for nickel, both values deviate from the theoretically expected value of 2 for a meatal:ligand ratio of 1:2. No change in the extraction behaviour of $\beta$ – $H_2$NQD could be observed after 2 days of contact.

To find out if copper only forms a 1:2 chelate with $\beta$-$H_2$NQD an experiment was done with equimolar amounts of copper and $\beta$-$H_2$NQD (Fig. 6). Maximum copper extraction was 50%, in excellent agreement with the formation of Cu·$\beta$-$H_2$NQD = 1:2. The shape of the UV/visible spectrum of the pentanol solution with the extracted chelate did not change during this experiment. The spectrum showed two maxima below 37.500 $cm^{-1}$, one at 35.700 $cm^{-1}$ ($\epsilon = 9000$) and

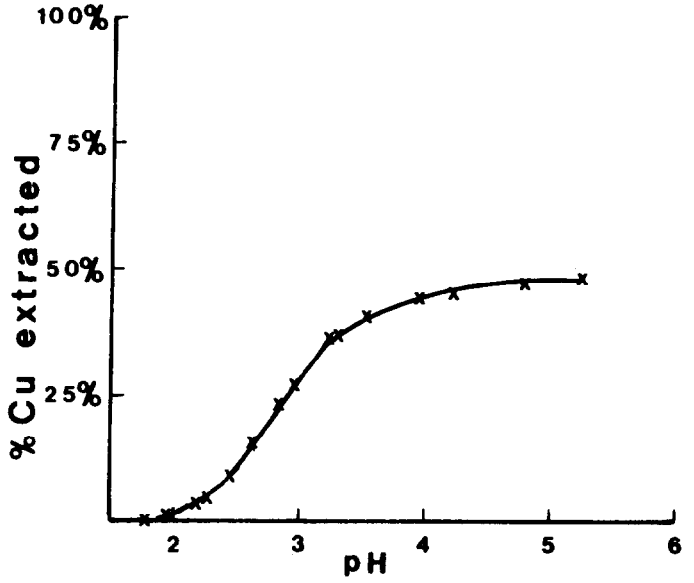



Fig. 6. % Copper extraction as a function of pH for the extraction of Cu(II) by $\beta$- nopinoquinone dioxime. The initial concentration of $\beta$-$H_2$NQD in pentanol and the initial copper concentration in water are both 0.002 M.

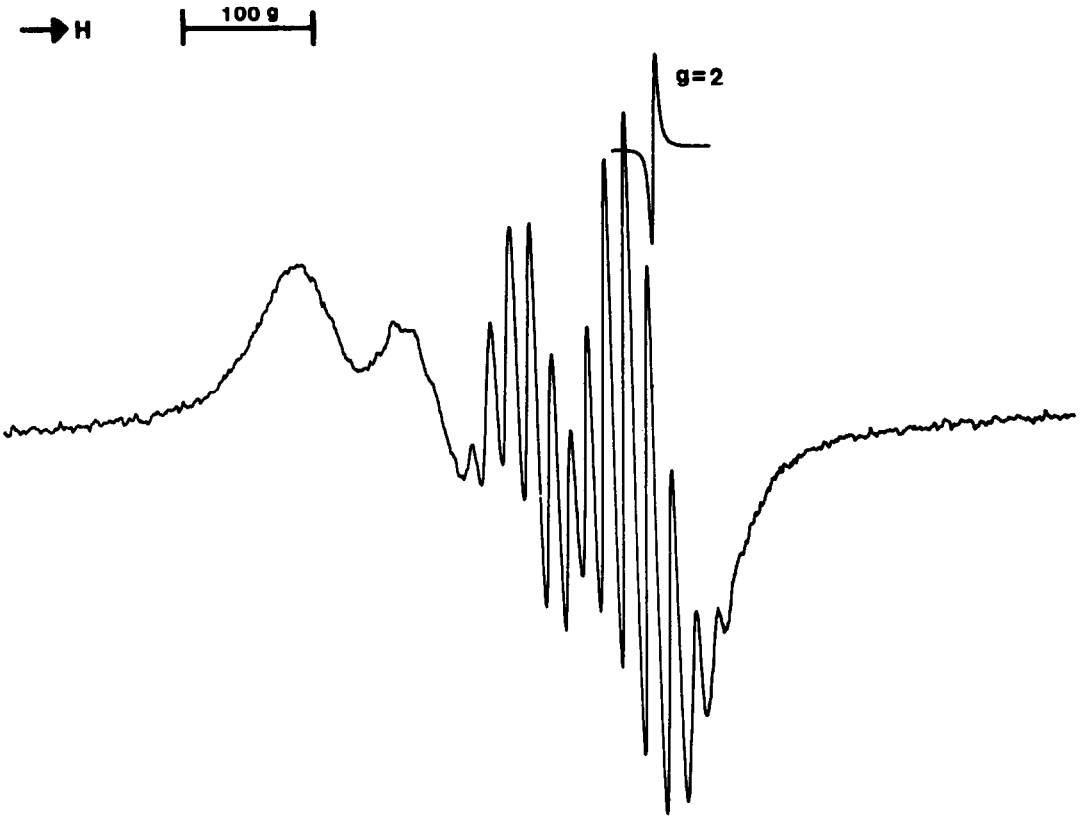



Fig. 7. ESR spectrum of the copper chelate formed during the extraction of $Cu^{2+}$ by $\beta$-$H_2$NQD in chloroform at room temperature.

the other at 27.000 $cm^{-1}$ ($\epsilon = 2300$). The elemental analysis from the isolated chelate is: C,48.61; H,6.32; N,11.29; Cu,12.98; O,20.8%. This leads to a chelate with formula $CuC_{20}H_{31}N_4O_6$ indicating that the chelate has two additional water molecules and also that some pentanol is retained. The expected elemental analysis for $Cu(HNQD)_2.2H_2O$ containing 6½% pentanol ($C_5H_{11}OH$) is: C,48.19; H,6.96; N,11.34; Cu,12.88; O,20.63%. The ESR spectrum of the chelate in $CHCl_3$ is presented in Fig. 7.

The nickel $H_2$NQD chelate isolated from the extraction was examined by NMR (Fig. 8). The elemental analysis gave: C,54.4; H,7.0; N,12.6; Ni,11.7% which was different from the expected for $Ni(HNQD)_2$: C,51.3; H,6.2; N,13.3; Ni,13.9%. The IR spectrum was almost identical with that from the synthesized Ni($\beta$-HNQD)$_2$. Only one extra absorption appeared at 3400 $cm^{-1}$, probably due to the OH from pentanol that was not completely removed at 60°C.

The furazan of nopinoquinone dioxime did not have any extraction capacities at all.

## DISCUSSION

*Extraction*

If we compare the extraction results of $\beta$-$H_2$NQD with those of $\beta$-$H_2$CQD clearly a lowering of the $(pH_{\frac{1}{2}})_{1.0}$ value for both copper and nickel is observed (Table 1). This lowering cannot completely be explained by the fact that different solvents are used. In previous work[1] it was proven that $\beta$-$H_2$CQD isomerizes to $\delta$-$H_2$CQD and that this is coupled with a lowering of the $pH_{\frac{1}{2}}$ value. So $pH_{\frac{1}{2}}(\beta\text{-}H_2CQD) > pH_{\frac{1}{2}}(\delta\text{-}H_2CQD)$. In Table 1 it is observed that the $pH_{\frac{1}{2}}$ value of $\delta$-$H_2$CQD is larger than that of $\beta$-$H_2$NQD in pentanol. The conclusion can be drawn that the $pH_{\frac{1}{2}}$ value of $\beta$-$H_2$NQD is smaller than that of $\beta$-$H_2$CQD. Another difference between $\beta$-$H_2$NQD and $\beta$-$H_2$CQD is that with the former compound no change in the extraction behaviour is seen after a contact time of two days. Isomerization of $\beta$-$H_2$NQD is therefore very unlikely. To confirm this the isolated copper chelate was investigated with ESR spectroscopy and the isolated nickel chelate was examined with NMR spectroscopy.

*The structure of the copper* $H_2$NQD *chelate*

Figure 6 shows that copper forms a 1:2 chelate with $\beta$-$H_2$NQD under extraction conditions. From the elemental analysis of the extracted Cu($\beta$-HNQD)$_2$ it became clear that the chelate is extracted with two additional water molecules. It

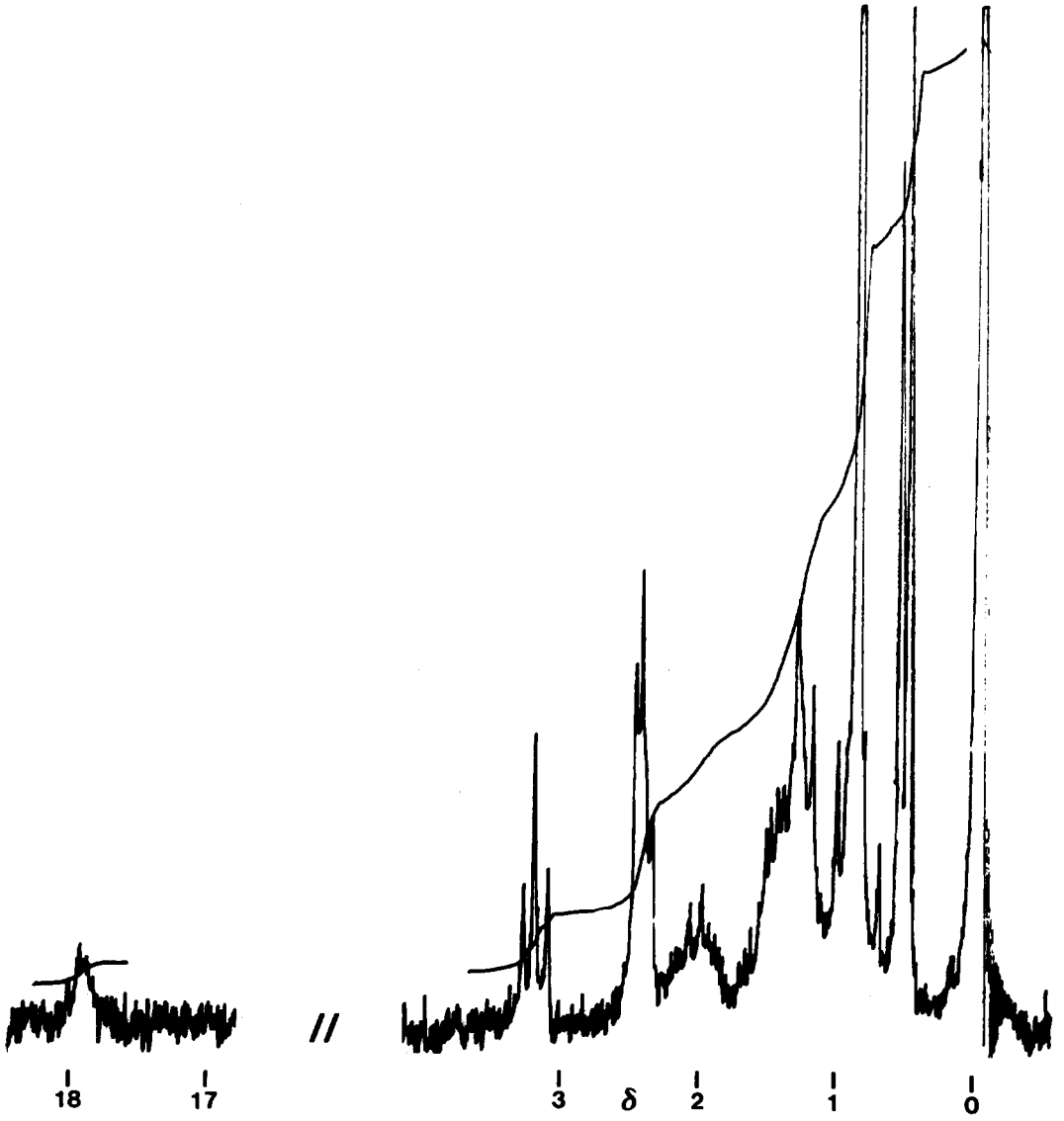



Fig. 8. 60 MHz $^1$H spectrum of the nickel chelate formed during the extraction of $Ni^{2+}$ by $\beta$-$H_2$NQD in benzene at room temperature.

Table 1. Extraction of copper(II) and nickel(II) by some vic-dioximes

| compound | solvent | $(pH_{\frac{1}{2}})_1$. Cu | $(pH_{\frac{1}{2}})_1$. Ni | reference |
|---|---|---|---|---|
| α-$H_2$CQD* | pentanol | +1.48 | +3.43 | (1) |
| β-$H_2$CQD* | t.b.p. | +2.61 | +4.73 | (1) |
| δ-$H_2$CQD | pentanol | +1.15 | +3.60 | (1) |
| β-$H_2$NQD | pentanol | +0.25 | +1.28 | this study |
| $C_5H_{11}$-C(NOH)-C(NOH)-$C_5H_{11}$ | toluene | +0.62 | -0.42 | (6) |
| $C_7H_{15}$-C(NOH)-C(NOH)-$C_7H_{15}$ | toluene | +0.54 | -0.36 | (6) |
| C-C-C-C-C(NOH)-C(NOH)-C-C-C-C | toluene | +0.59 | -0.14 | (6) |

*Isomerization occurs to δ-$H_2$CQD under extraction conditions.

is reasonable to expect that these two water molecules are weakly bound in the axial position of a distorted octahedron. $Cu^{2+}$ is a $d^9$ system with one unpaired electron which will be located in the $d(x^2-y^2)$ orbital to minimize the electronic repulsion of the other electrons with the ligand electrons. The ESR spectrum (Fig. 7) shows four main lines which are due to copper ($^{63}Cu$, $^{65}Cu$: I = 3/2) and extra lines superimposed on it due to nitrogen ($^{14}N$: I = 1) superhyperfine interaction. If copper forms a $CuN_4$ species then the $d(x^2-y^2)$ orbital will have overlap with 4N's which results in a superhyperfine structure with nine equidistant lines with an intensity ratio of 1:4:10:16:19:16:10:4:1. If on the other hand copper forms a $CuN_2O_2$ chromophore, only 2 N's are coupled to copper, and given the fact that O does not have a magnetic moment, five equidistant lines with an intensity ratio of 1:2:3:2:1 are expected. In Fig. 7 it is hard to see how many lines are superimposed on one copper line because there is some overlap between the two copper lines on which nitrogen superhyperfine splitting is noticeable. In contrast with the spectrum of Cu($\delta$-HCQD)$_2$ (Ref. 1 Fig. 9) there are now no equidistant extra lines with strange intensities due to $^{65}Cu$, visible on the high field side of the spectrum. This can be explained in two days. Firstly, the Cu($\delta$-HCQD)$_2$ spectrum has more narrow lines as deduced from the fact that the nitrogen superhyperfine splitting is clearly visible on the second low-field copper line. Furthermore, the $^{63}Cu$ splitting is smaller in Cu($\beta$-HNQD)$_2$: 77.5 G instead of 90.5 G. The splitting of $^{65}Cu$ can now be calculated from the difference in magnetic moment ($0.70904 \times 10^{-4}$ for $^{63}Cu$ vs $0.75958 \times 10^{-4}$ rad sec$^{-1}$ G$^{-1}$ for $^{65}Cu$). The expected separation between $^{63}Cu$ and $^{65}Cu$ on the high field side of the ESR spectrum is 3/2. ((0.75958/0.70904) − 1).77.5 = 8.3 G instead of the 9.6 G for Cu($\delta$-HCQD)$_2$. In Fig. 9 the two high-field lines of copper are seen, and the nitrogen superhyperfine lines are numbered. The intensities cannot be measured exactly, because of the superposition on the copper lines. The rough values can be obtained by taking the so-called up–down distance, but these values are too low if the copper line goes up and too high if the copper line goes down.

Table 2 shows that the intensities are in reasonably good correlation with a $CuN_4$ chromophore, especially the lines 8–13 where no overlap occurs with the other nitrogen superhyperfine splitting. The $CuN_2O_2$ chromophore can be rejected because the lines 1, 12 and 13 cannot be explained. Furthermore the calculated intensities of the lines 7, 8, 10 and 11 deviate from the observed intensities. It is concluded from the ESR spectrum that Cu($\beta$-HNQD)$_2$ has N,N-coordination.

*The structure of the nickel* $H_2$NQD *chelate*

The elemental analysis of Ni($\beta$-HNQD)$_2$ from extraction deviates from the expected values, while the synthesized Ni($\beta$-HNQD)$_2$ had a very good elemental analysis. Nevertheless the IR spectra of these two species are identical, except for an extra absorption of the extracted chelate at 3400 cm$^{-1}$, probably due to the OH group of pentanol that was not completely removed at 60°C. That is why the C and H percentages are raised and as a consequence the N and Ni percentages are lowered. No additional water molecules were found by the elemental analysis. This makes a square planar structure the most probable configuration as is often seen for $Ni^{2+}$ $d^8$ systems. This system will

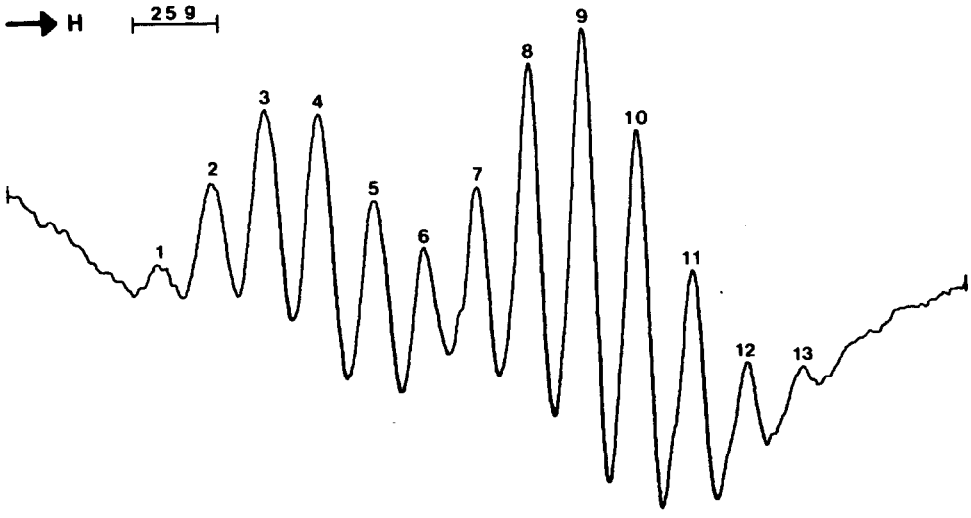



Fig. 9. The two high-field lines of copper from Fig. 7.

Table 2. Up-down values of the nitrogen superhyperfine splittings of Fig. 9 and the expected values for $CuN_4$ and $CuN_2O_2$ chromophores

| line number | up-down value | $CuN_4$ expectation | $CuN_2O_2$ expectation |
|---|---|---|---|
| 1 | 1.2 | 2.3 | 0 |
| 2 | 4.4 | 5.8 | 3.7 |
| 3 | 9.1 | 9.3 | 7.4 |
| 4 | 11.1 | 11.1 | 11.1 |
| 5 | 8.4 | 9.3/1.0* | 7.4 |
| 6 | 4.4 | 5.8/4.1* | 3.7 |
| 7 | 8.1 | 2.3/10.3* | 6.5 |
| 8 | 15.2 | 0.6/16.4* | 13.0 |
| 9 | 19.5 | 19.5 | 19.5 |
| 10 | 15.7 | 16.4 | 13.0 |
| 11 | 9.6 | 10.3 | 6.5 |
| 12 | 3.2 | 4.1 | 0 |
| 13 | 0.8 | 1.0 | 0 |

*The superhyperfine splitting of the two copper lines are overlapping in this region.

Table 3. $^1H$ NMR spectra of $\beta$- and $\delta$-nopinoquinone dioxime and their nickel(II) chelates

| compound | $C^9H_3$ | $C^8H_3$ | Hf | He | Hd | Hb,c | Ha | OH | solvent | reference |
|---|---|---|---|---|---|---|---|---|---|---|
| Ni(δ-HNQD)$_2$ | 0.80 | 1.35 | 1.21 | 2.16 | 2.60 | 2.82 | | 11.16 | $CDCl_3$ | (5) |
| Ni(β-HNQD)$_2$ | 0.56 | 0.94 | 1.17 | 1.52 | 2.20 | 2.45 | 3.29 | 17.90 | $C_6D_6$ | (5) |
| | 0.63 | 0.94 | 0.86 | 1.52 | 2.09 | 2.38 | 3.29 | 18.14 | | |
| Ni(β-HNQD)$_2$ | 0.53 | 0.89 | 1.16 | * | 2.15 | * | 3.28 | 17.87 | $C_6H_6$ | this |
| extraction | 0.60 | 0.89 | 0.82 | * | 2.05 | * | 3.28 | | | study |
| β-$H_2$NQD | 0.74 | 1.30 | 1.07 | 2.05 | 2.48-2.74 | | 3.47 | 11.09/10.72 | DMSO-$d_6$ | (4) |
| δ-$H_2$NQD | 0.74 | 1.31 | 1.20 | 2.10 | 2.44- - - | | 2.78 | 12.30/12.08 | DMSO-$d_6$ | (4) |
| β-$H_2$NQD | 0.74 | 1.30 | 1.03 | 2.05 | 2.40-2.80 | | 3.41 | 11.18/10.74 | DMSO-$d_6$ | this |
| | | | | | | | | | | study |

The chemical shifts are given in ppm from $SiMe_4$.
*The chemical shifts of these protons could not be determined because of the presence of some pentanol.

therefore have a low-spin state, which means that the electrons are paired in the $d(z^2)$ orbital—the orbitals $d(xy)$, $d(xz)$ and $d(yz)$ are also filled with paired electrons—and the $d(x^2-y^2)$ orbital, which has a large electron repulsion with the ligand electrons, is empty. As a consequence Ni($\beta$-HNQD)$_2$ is diamagnetic and NMR spectroscopy might give useful information.

The NMR spectrum of Ni($\beta$-HNQD)$_2$ is of a bad quality probably due to the presence of some paramagnetic traces. This is not strange for such a strong complexant as $\beta$-$H_2$NQD. According to Nakamura[5] Ni($\beta$-HNQD)$_2$ can have two possible ligand alignments, *anti* and *syn*. This can also be observed in the NMR spectrum of the extracted Ni($\beta$-HNQD)$_2$. The values of the chemical shifts are given in Table 3 together with the literature values. The proton numbering can be found in Fig. 10.

Daniel and Pavia[7,8] have studied in detail the effect of the oxime group on the chemical shift of the neighbouring proton. If the oxime group is *anti*, as is the case in Ni($\beta$-HNQD)$_2$ the chemical

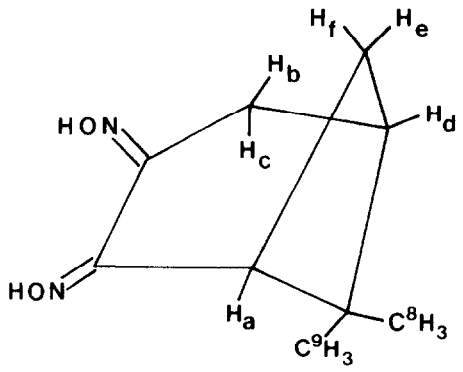



Fig. 10. The nopinoquinone dioxime molecule with hydrogen numbering.

shift of Ha will move to higher field. The origin of this effect is not known with certainty. Phillips[9] explains the shift by the interaction of the hydroxyl group with the Ha proton. Saitô[10] suggests an interference of the free electron pair of nitrogen in the *syn* structure. The observed $\delta$ of 3.28 for the extracted Ni($\beta$-HNQD)$_2$ proves that the neighbouring oxime group has the *anti* configuration. Furthermore, the observed $\delta$ of 17.87 of the OH group is in very good agreement with the Ni($\beta$-HNQD)$_2$ compound synthesized by Nakamura.

In N,O-coordination another kind of hydrogen bridging occurs (see Fig. 1) and this leads to a different chemical shift, such as Ni($\delta$-HNQD)$_2$: $\delta = 11.16$, Ni($\alpha$-HCQD)$_2$: $\delta = 11.07$[5] and Ni($\delta$-HCQD)$_2$: $\delta = 10.80$[5]. The conclusion drawn from this NMR study is that the extracted nickel chelate indeed has N,N-coordination. The spectrum gives some extra lines in the $\delta = 1.4$ region because of the presence of some pentanol. From the NMR integral the quantity of pentanol is calculated to be about 6%, which is in good agreement with that estimated by elemental analysis.

*The influence of the* N–N *distance*

The fact that both $Cu^{2+}$ and $Ni^{2+}$ form N,N-bonding chelates with $\beta$-$H_2$NQD confirms the theory that the N–N distance is an important factor in the chelation. Camphorquinone dioxime $H_2$CQD, an analogous molecule with a N–N distance of about 3.0 Å instead of the 2.8 Å of $H_2$NQD, cannot form stable N,N-coordinated chelates. From the fact that copper and nickel have smaller $pH_{\frac{1}{2}}$ values with $\beta$-$H_2$NQD than with $\delta$-$H_2$CQD (see Table 1) the conclusion may be drawn that N,N-coordinated chelates are thermodynamically more stable, but that with $H_2$CQD the critical boundary for the N–N distance is passed.

Comparing $\beta$-$H_2$NQD with the unstrained aliphatic dioximes in Table 1 it is remarkable that the order of stability for copper and nickel is reversed. For copper it does not seem to matter that the N–N distance is enlarged and even a slight decrease of the $pH_{\frac{1}{2}}$ value can be observed. For nickel the greater N–N distance is coupled with a striking increase of the $pH_{\frac{1}{2}}$ value. Furthermore, the nickel extraction rate is raised enormously. Equilibrium is reached within 10 min using $\beta$-$H_2$NQD as extractant instead of several days, when using unstrained aliphatic dioximes. To understand this difference the crystal structure of some known copper and nickel dioxime chelates have to be discussed. If we compare the results of the crystal structure analysis of bis(methylethylglyoximato)nickel(II) of Bowers *et al.*[11] with the crystal structure analysis of bis-(dimethylglyoximato)copper(II) from Vaciago and Zambonelli[12] there are some clear differences. Nickel forms a square planar structure with a nickel to nitrogen distance of 1.86 Å and a dioxime N–N distance of 2.426 Å, while copper is five coordinated in a square-pyramidal configuration with a copper to nitrogen distance of 1.95 Å and a dioxime N–N distance of 2.52 Å. Shannon[13] has calculated the ionic radii for different kinds of configurations. The values for copper(II) are 0.57 Å for a four cooordinated square complex, 0.65 Å for a five coordinated complex and 0.73 Å for a six coordinated complex. For nickel(II) these values are 0.49 Å for a four coordinated square complex, 0.63 Å for a five coordinated complex and 0.69 Å for a six coordinated complex. The difference between the copper and nickel radius in the structure analysis of the glyoxime chelate, however, is 0.09 Å. In the unstrained glyoxime chelate the N–N distance will be determined by the metal ion radius. That elucidates the difference in N–N distance between the two complexes in the crystal structure. In the $\beta$-$H_2$NQD complex the N–N distance is determined by the strained carbon skeleton to be about 2.8 Å. This is far from the ideal N–N distance for a $NiN_4$ chromophore which is 2.426, so the chelate will be destabilized and the $pH_{\frac{1}{2}}$ value will rise. For Cu($\beta$-HNQD)$_2$ elemental analysis shows that there are two additional water molecules associated to the chelate. It is not unlikely that these water molecules are located in the axial position of octahedral copper ($d(z^2)$) so that a (distorted) octahedral configuration exists. The six coordinated copper has according to Shannon a much greater ionic radius than the four coordinated nickel: 0.73 Å vs 0.49 Å. Furthermore the copper coordination sphere possesses some plasticity[14] i.e. the stronger the axial ligands are bonded, the weaker the equatorial ligands are bonded (which means in this case the larger the Cu–N distance). So less destabilization is to be expected for copper.

Good kinetics of nickel(II) extraction are to be expected whenever substitution of water takes place within an octahedral paramagnetic complex, which is directly followed by the elimination of the surplus monodentate ligands to a square planar diamagnetic complex.[15] No octahedral complexes of the type Ni($H_2O$)$_2$ (LL)$_2$ are formed by unstrained aliphatic dioximes. The weakening of the ligand by enlargement of the N–N distance makes it energetically more favourable to form this kind of paramagnetic octahedral intermediate. This could explain why $\beta$-$H_2$NQD has such good kinetics relative to unstrained aliphatic dioximes.

Table 4. The chemical shifts in ppm and the coupling constants in *cps* from the furazan of nopinoquinone dioxime. NMR spectrum see Fig. 7. Proton numbering see Fig. 10

| | | | | | |
|---|---|---|---|---|---|
| Ha | = 3.20 | triplet | $^2J$(He, Hf) | = 10.5 |
| Hb,c | = 3.04 | doublet | $^3J$(Ha, He) | = 5.0 |
| Hd | = 2.35 | multiplet | $^3J$(Ha, Hf) | = 0 |
| He | = 2.87 | doublet | $^3J$(Hd, He) | = 5.0 |
| Hf | = 1.27 | multiplet | $^3J$(Hd, Hf) | = 0 |
| $C^9H_3$ | = 0.58 | singlet | $^3J$(Hd, Hb,c) | = 2.5 |
| $C^8H_3$ | = 1.42 | singlet | $^4J$(Ha, Hd) | = 5.0 |

*The furazan of nopinoquinone dioxime*

The yellow oil which was obtained in the synthesis of $\beta$-$H_2$NQD by evaporation of ethylacetate probably consists for the major part of $\delta$-$H_2$NQD. To remove the impurities the oil was treated with 1N NaOH and extracted with ether. Acidifying of the water layer did not give much product, but evaporation of the ether layer gave a compound that is probably the dehydrated form of nopinoquinone dioxime. Wolff[16] made such a furazan—also called 1,2,5-oxadiazole—by refluxing dimethylglyoxime with sodium hydroxide in water. This compound had a low melting point $-7$°C and a sweet smell. Also other furazans could be synthesized from dioximes. Behr[17] found that especially the *amphi* forms ($\delta$-$H_2$NQD is *amphi*) are most easily dehydrated. To prove whether the compound really is the furazan the NMR spectrum (Fig. 4) was studied in detail. The compound gave a very clear spectrum. Chemical Shifts and coupling constants are given in Table 4. Because furazan is a six electron system, $4\pi$ electrons from the two CN double bonds and two from the oxygen, the five membered ring is aromatic. The field of this aromatic ring causes a deshielding effect for the protons on the pinene skeleton. Comparing the chemical shifts of $\beta$-$H_2$NQD with those of the furazan it is notable that almost all chemical shifts are shifted downfield. This confirms the aromatic character of the furazan ring. The chemical shift of Ha is somewhat smaller, which was to be expected because in the furazan no *anti* OH group exists. The chemical shift of $C^9H_3$ is changed in the opposite direction because the methyl group is placed partly above the aromatic ring where lines of the induced field are opposite to the applied field.

It is known that theoretical treatments of the magnitude of coupling constants such as the Karplus[18] equation (vicinal couplings) must be treated with reserve.[19] Nevertheless the use of the equation of Karplus:

$$^3J(H, H) = 4.22 - 0.5\cos\phi + 4.5\cos 2\phi$$

in which $\phi$ is the dihedral angle between the two H's, gives dihedral angles which are in good agreement with the scale model made from the furazan of nopinoquinone dioxime. $^3J$(H*a*, H*e*) = 5.0 *cps* leads to an angle of 37° between H*a* and H*e*. The expected angle between H*a* and H*f* now is 120° − 37° = 83°. A dihedral angle of 83° leads to a coupling constant $^3J$(H*a*, H*f*) = − 0.21 *cps*, a coupling that will not be observed. The same holds for $^3J$(H*d*, H*f*). The coupling constants are almost equal to the values found by Abraham[20] for some other pinane derivatives. The long-range coupling $^4J$(H*a*, H*d*) is remarkable but not unknown in bicyclic molecules.[20,21] Meinwald[21] explained this long-range interaction by assuming a fairly extensive overlap between the small lobes of the orbitals directed 180° away from the direction of the CH bonds, which are pointed towards each other. This explanation appears reasonable when a scale model is examined. This proves that the pinane skeleton is still preserved. Elemental analysis also leaves no doubt on the compound being the furazan of nopinoquinone dioxime.

The furazan of nopinoquinone dioxime shows no extraction capacities at all. The main reason for this is that there is no acidic H atom present. Also no hydrogen bridge stabilization of the complex can occur. Furthermore the bidentate character of the ligand is lost. Driessen[22] did make some metal furazan complexes with $SbCl_6^-$ as anion. All the complexes decomposed when in contact with water which means that furazan is a rather weak ligand.

The aromaticity of the furazan ring makes the molecule very stable. It is therefore not possible to convert the furazan into $\beta$- or $\delta$-$H_2$NQD.

## REFERENCES

1. L. R. M. Paping, T. P. M. Beelen, C. P. J. Rummens and R. Prins, *Polyhedron* 1982, **1**(6), 503.
2. J. Grimshaw, J. T. Grimshaw and H. R. Juneja, *J. Chem. Soc. Perkin Trans.* 1972, **1**, 50.
3. L. Claisen and O. Manassa, *Liebigs Ann.* 1883, **274**, 71.
4. A. Nakamura, A. Konishi, R. Tsujitani, M. Kudo and S. Otsuka, *J. Am. Chem. Soc.* 1978, **100**, 3449.

5. A. Nakamura, A. Konishi and S. Otsuka, *J. Chem. Soc. Dalton* 1979, 488.
6. A. R. Burkin and J. S. Preston, *J. Inorg. Nucl. Chem.* 1975, **37**, 2187.
7. A. Daniel and A. A. Pavia, *Tetrahedron Lett.* 1967, **13**, 1145.
8. A. Daniel and A. A. Pavia, *Compt. Rend. C* 1966, **263**, 634.
9. W. D. Phillips, *Ann. N.Y. Acad. Sci.* 1958, **70**, 817.
10. H. Saitô, K. Nukada and M. Ohno, *Tetrahedron Lett.* 1964, 2124.
11. R. H. Bowers, C. V. Banks and R. A. Jacobson, *Acta Cryst.* 1972, **B28**, 2318.
12. A. Vaciago and L. Zambonelli, *J. Chem. Soc. A* 1970, 218.
13. R. D. Shannon, *Acta Cryst.* 1976, **A32**, 751.
14. J. Gažo, J. B. Bersuker, J. Garaj, M. Kabešová, J. Kohout, H. Langfelderová, M. Melník, M. Serátor and F. Valack, *Coord. Chem. Rev.* 1976, **19**, 253.
15. E. Uhlig, *Coord. Chem. Rev.* 1982, **43**, 299.
16. Wolff, *Chem. Ber.* 1895, **28**, 70.
17. L. C. Behr, *Heterocyclic Compounds* 1962, **17**, 283
18. M. Karplus, *J. Chem. Phys.* 1959, **30**, 11.
19. M. Karplus, *J. Am. Chem. Soc.* 1963, **85**, 2870.
20. R. J. Abraham, F. H. Bottom, M. A. Cooper, J. R. Salmon and D. Whittaker, *Org. Magn. Res.* 1969, **1**, 51.
21. J. Meinwald and A. Lewis, *J. Am. Chem. Soc.* 1961, **83**, 2769.
22. W. L. Driessen and P. L. A. Everstyn, *Z. Naturforsch.* 1978, **33B**, 1120.

*Polyhedron* Vol. 3, No. 7, pp. 833–838, 1984
Printed in the U.S.A.

0277-5387/84 $3.00 + .00
© 1984 Pergamon Press Ltd.

# ON THE pH DEPENDENCE OF Cu(II) BINDING TO INSULIN: ESR AND ELECTRONIC STUDIES

**R. P. FERRARI* and P. MICHELIN LAUSAROT**
Istituto di Chimica Generale ed Inorganica dell'Università di Torino, Corso Massimo d'Azeglio 48, 10125 Torino, Italy

**and**

**T. BERINGHELLI and F. MORAZZONI**
Dipartimento di Chimica Inorganica e Metallorganica dell'Università di Milano e Centro CNR, Via Venezian 21, Milano, Italy

(*Received* 29 *August* 1983; *accepted* 6 *January* 1984)

**Abstract**—The ESR and electronic absorption spectra have been used to investigate co-ordination of Cu(II) to insulin in aqueous solutions at different pH. Two series of complexes with low- and high copper content were examined and the values of the magnetic tensor components and the shape of the diffuse reflectance transitions suggested that these copper–insulin derivatives have tetragonal symmetry with Cu(II) in a $(N_xO_y)$ ligand field, where oxygen donor groups are predominant at low pH and nitrogenous ligands at high pH. Such a trend was further supported by the presence of superhyperfine structure at pH = 13. Oxygen of the carboxylato groups, nitrogen of $\alpha$- and $\epsilon$-amino groups and of imidazoles, all contribute to the coordinations field. At very high pH only, a preferential binding site for Cu(II) is found, which probably involves deprotonated peptide nitrogens.

Spectroscopic measurements, if associated with labelling techniques by transition metal ions, can provide information on the bonding groups in natural proteins even when they do not contain paramagnetic ions.[1] The widespread use of Cu(II) as a probe is justified both by its high co-ordinating power to proteins and by the fact that a great number of model compounds in which Cu(II) is co-ordinated to aminoacids and peptides has been described in literature.[1-3]

As part of our studies on the interaction of transition metal ions with nucleic acids, proteins and their monomeric units,[4,5] aimed at identifying the specific binding sites for the ions, we describe in this paper the co-ordination of Cu(II) to insulin in aqueous solution. It is well known that several transition metal ions play an important role in crystallization of insulin.[6] However, detailed structural and spectral analyses on their binding sites to the protein have been performed only on some crystalline metal(II) insulin derivatives.[6]

In the present paper, co-ordination of Cu(II) to insulin in aqueous solution was investigated at different pH values in order to clarify the influence of a change of the surroundings on the interaction of the protein with the metal ion. Two series of complexes were examined, differing from each other as regards insulin/Cu(II) molar ratio: a first series (low copper content) having a 1/1 insulin/Cu(II) ratio, was meant to reproduce biological conditions in which very low metal concentrations are likely to be present whilst a second series (high copper content) having a 1/57 insulin/Cu(II) ratio better reproduces the conditions found in low molecular weight model compounds.

## EXPERIMENTAL

### *Materials*

Crystalline insulin was purchased from Hoechst. $CuCl_2$, NaOH and HCl were Merk pure reagents. Metal-free insulin was obtained according to literature.[7]

*Author to whom correspondence should be addressed.

*Apparatus*

ESR spectra were recorded on a Varian E 109X band spectrometer; the $g$ values were standardised by DPPH. Electronic spectra were recorded in a Pye Unicam Mod. 1700 UV/Visible spectrophotometer. Diffuse reflectance spectra on a Beckman DK-2A spectrophotometer.

*Preparation of samples*

Appropriate volumes of an aqueous solution of metal-free insulin ($1.8\,10^{-4}$ M) and of $CuCl_2$ (1M) were mixed to give either a 1/1 or a 1/57 insulin/Cu(II) molar ratio. Solutions were adjusted to the desired pH by dropwise addition of hydrochloric acid (1N) or of sodium hydroxide (1N). The mixtures were allowed to stand at room temperature for at least 10 min before the spectroscopic measurements were taken. pH was checked after ESR spectra has been recorded. Samples in which a precipitate formed following the addition of HCl or NaOH, were centrifuged and dried under vacuum, after having checked the pH of the supernatant solution. In no case was it found that precipitation of the protein was accompanied by a change of the pH of the solution.

## RESULTS AND DISCUSSION

*ESR results*

The values of $g$ and $A$ tensor components for the two series of samples are collected in Tables 1 and 2.

Features common to both series are: (a) isotropic resonance lines similar to those observed in aqueous solutions of $CuCl_2$, at low pH values; (b) a change of the resonance shape and detection of Cu(II) centres having axial magnetic symmetry at pH values higher than a starting value, which is slightly different in the two series of samples: pH = 4 for series I and pH = 5 for series II. The trend of $g$ components $g_\parallel > g_\perp > 2$ is characteristic of the $(xz)^2(yz)^2(xy)^2(z^2)^2(x^2-y^2)$ ground state of Cu(II) and no triplet state transitions were observed; (c) the presence, in all samples, of hyperfine structure due to interaction with Cu nucleus, in the region of parallel resonances lines. Only few samples, mainly those containing a mixture of different Cu(II) derivatives (see later), do not show clearly detectable hyperfine structure.

The main differences between the two series of samples are due to the variations of ESR parameters with pH.

*Series I samples* (1/1 *insulin/Cu(II) molar ratio*). Increase of the pH value induces variations of the observed paramagnetic species; specifically, the broad shape of the hyperfine components suggests that at any defined pH value more than one paramagnetic species is present. The paramagnetic species can be grouped in a low pH form, stable in

Table 1. ESR parameters for series I samples (1/1 insulin/Cu(II) molar ratio) at 77 K

| pH[a] | $g_\parallel$ | $A_\parallel$ (Gauss) | $g_\perp$ |
|---|---|---|---|
| 4.0[b] | 2.26 | 160 | 2.08 |
| 4.5[b] | 2.27 | 160 | 2.08 |
| 5.1[b] | 2.27 | 160 | 2.08 |
| 5.5[b] | 2.28 | 160 | 2.07 |
| 6.5[b] | 2.26 | 160 | 2.08 |
| 8.5[c] | 2.20 | 200 | 2.05 |
| 9.7[c] | 2.20 | 200 | 2.06 |
| 10.5[c] | 2.17 | 200 | 2.06 |
| 12.3[c] | 2.17 | 200 | 2.06 |
| 12.7[c] | 2.17 | 200 | 2.05 |
| 13.3[c] | 2.17 | 200 | 2.05 |

a) ESR parameters for samples at pH 7.2, 7.5 and 8.0 are not reported in the table since the spectra correspond to a superimposition of the low and high pH forms.

b) Powders.

c) Solution.

Table 2. ESR parameters for series II samples (1.57 insulin/Cu(II) molar ratio) at 77 K

| pH[a] | $g_\parallel$ | $A_\parallel$ (Gauss) | $g_\perp$ |
|---|---|---|---|
| 5.1[b] | 2.30 | 160 | 2.09 |
| 7.1[b] | 2.17 | 200 | 2.07 |
| 8.5[b] | 2.17 | 200 | 2.07 |
| 10.5[b] | 2.17 | 200 | 2.07 |
| 12.0[c] | 2.18 | 200 | 2.05 |
| 13.1[c] | 2.18 | 200 | 2.06 |

a) ESR parameters for samples at pH 4.0 and 4.5 are not reported due to superimposition of major amounts of Cu(II) not bound to the protein. At pH 5.5, 6.0 and 6.6 the spectra correspond to a superimposition of the low and high pH forms.

b) Powders.

c) Solutions.

the 4.0–7.0 pH range (Fig. 1a) and in a high pH form stable above pH 8.5 (Fig. 1c). In the pH region between 7 and 8 there is a mixing of the two forms (Fig. 1b). At pH 13.3 the resonances become sharper (Fig. 2) and the superhyperfine interaction with N nuclei is observed. The number of lines and the value of the N coupling constant are not warranted since we cannot exclude the overlap with hyperfine perpendicular splitting by Cu nucleus. The number of lines is not less than 7 nor more than 9 but they are surely attributable to a single paramegnetic species. Therefore, three or four nitrogens are involved in this co-ordination.

*Series II samples* (*1/57 insulin/Cu(II) molar ratio*). Series II samples gave good evidence for two paramagnetic forms discussed in series I samples (Figs. 3a and c). More evident was the overlap of the two forms in the 5–7 pH range (Fig. 3b). It is worth noting that the change of the resonance shape from the isotropic to the axially symmetric one becomes evident at higher pH than in series I, probably because at high Cu(II) concentration the spectrum of Cu(II) not bound to the protein, overlaps that of insulin Cu(II) derivatives over a more extended range of pH values.

ESR spectra of series II samples were much more similar to those observed for the Cu(II)–tetrapeptide model compounds[3] than those of series I. In fact, both the sharper shapes of the two paramagnetic species and the pH range showing overlap between the two species reproduce the corresponding behaviour of model compounds. On the other hand, there is a correspondence of the magnetic parameters for the low and high pH species observed in series I and II of Cu(II) insulin derivatives also as far as the hyperfine structure is concerned. Thus, it can be assumed that the change of insulin/Cu(II) ratio influences only the pH region where the two paramagnetic species overlap.

The values of the magnetic tensor components observed for the low and high pH forms of Cu(II) insulin derivatives, in both series I and II samples, indicate that, though the ground state of the metal remains the same, large variations of the ligand field strength are present. The strength increases upon going from the species stable at lower pH values to that stable at higher values, in agreement with the decrease of the $g$ tensor components. The similarity between the ESR behaviour of series I samples (low Cu content) and those of series II (high Cu content) allows comparison between $g_\parallel$ and $A_\parallel$ values of series I samples with those of the model tetrapeptide Cu(II) complexes. On these bases it can be suggested that the copper–insulin derivatives stable at lower pH values contain Cu(II) in a ligand field of N and O mixed donor ($N_xO_y$) with a predominant contribution from oxygen donor group. However, we cannot specify $x$ and $y$ from the ESR data. The broad shape of the lines is not necessarily due to the coexistence of chromophores with different $x$ and $y$ but is more likely to be due to differences of the surroundings of the ligands. This condition is a consequence of the complexity of the macromolecule. At higher pH values there is a predominant contribution from the nitrogenous ligands, taking for granted that the broadening of the lines can be explained as detailed above. The predominance of N with respect to O in the ligand field is further evidenced at pH 13.3 by the superhyperfine splitting. At this

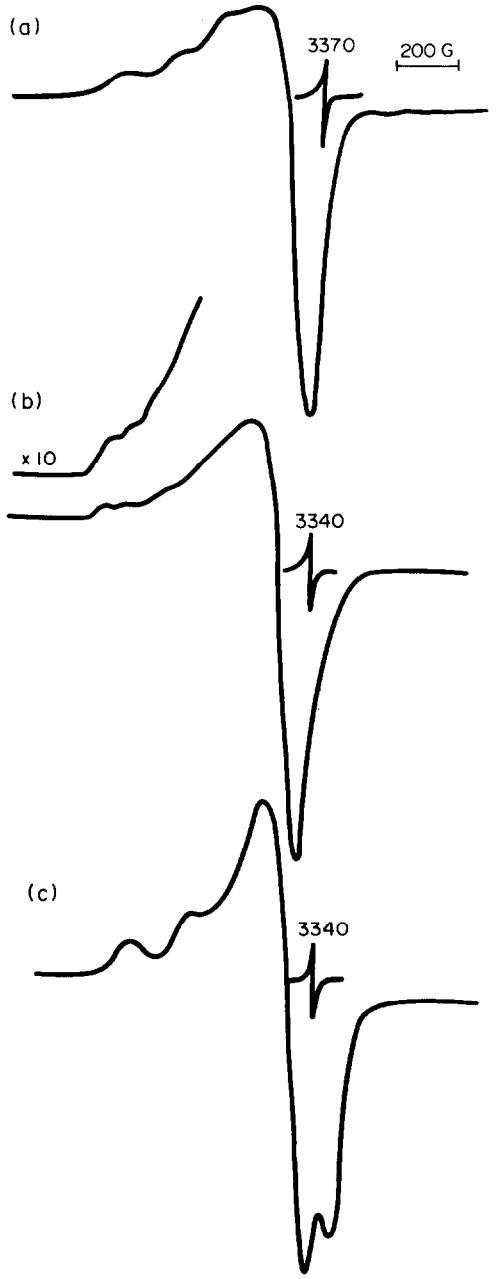



Fig. 1. ESR spectra for series I samples (1/1 insulin/Cu(II) molar ratio) recorded at 77 K. (a) pH 4.0. (b) pH 7.2. (c) pH 9.7.

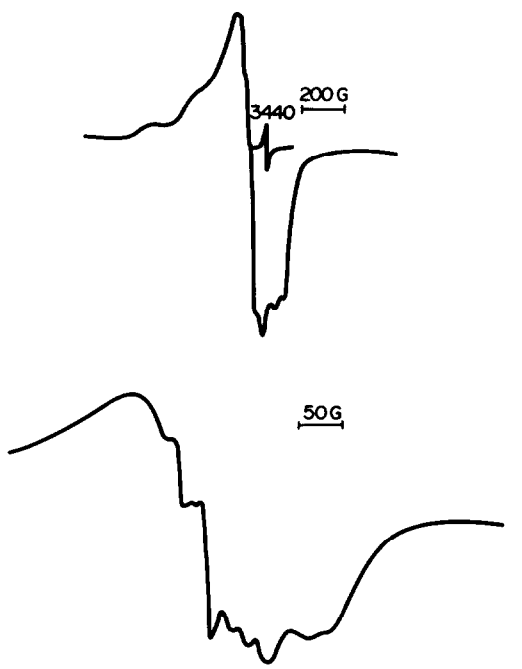



Fig. 2. ESR spectrum of series I samples at pH 13.3 recorded at 77 K. Bottom part: expanded magnetic field axis.

pH value, the main contribution comes from peptide nitrogens and the narrowing of the lines can be related to a presumable higher uniformity of the ligands.

*Electronic and diffuse reflectance spectra*

Electronic spectral analysis was performed in solution or in the solid state. Comparison between the spectra at pH 10.5 before and after liophylisation shows that the physical state does not affect the shape of the spectra. The spectral data are collected in Table 3.

The reported bands are all assignable to transitions derived from the octahedral $^2E_g \rightarrow {}^2T_{2g}$, broadened or split by the low symmetry components. By considering the shape of the diffuse reflectance transitions reported in Fig. 4, we observe that: (i) the spectrum of Cu(II) aquo ion and that of the precipitate from the Cu(II)–insulin mixture at pH 4 have identical shape. This confirms that, at lower pH values, nitrogen is not involved in the coordination; (ii) the spectrum at pH 5.1 (Fig. 4b) is characteristic of tetragonal Cu(II) compounds. The splitting of the broad band can be considered as predominantly due to lowering of the symmetry, but we cannot exclude that besides the effect of the low symmetry field, also the presence of different Cu(II)–insulin derivatives can play an important rôle. Really, the second effect becomes evident in the spectra at pH 6.5 and even more so at pH 7.5, in agreement with the ESR analysis; (iii) though the broad shape of the bands does not allow easy identification of the Cu(II)–insulin derivatives, Cu(II) chromophores are responsible for the absorptions. Transitions centred around 12,000 $cm^{-1}$ are predominantly due to chromophores containing O atoms, these centred between 17,000 and 19,000 $cm^{-1}$ predominantly to chromophores containing N atoms. It is worth noting that the ligand field variations in the higher frequency region

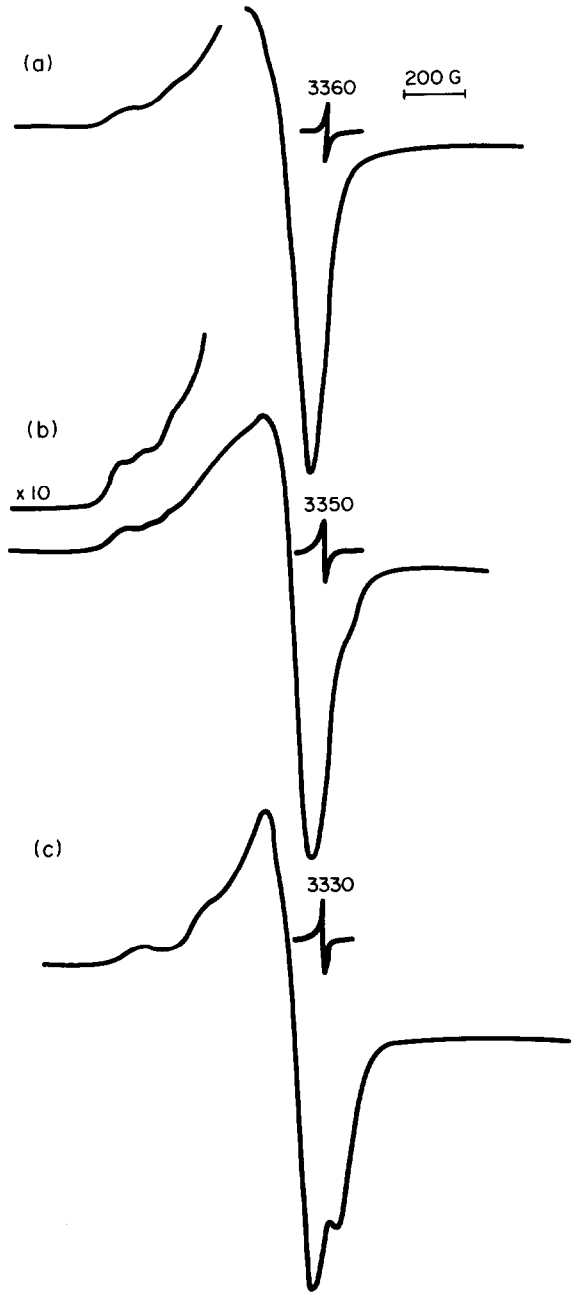



Fig. 3. ESR spectra for series II samples (1/57 insulin/Cu(II) molar ratio) recorded at 77 K. (a) pH 5.1. (b) pH 6.0. (c) pH 10.5.

Table 3. Electronic absorption for series I samples (1/1 insulin/Cu(II) molar ratio)

| pH | 4.0[b] | 4.5[b] | 5.1[b] | 6.5[b] | 7.5[b] | 8.0[b] | 8.5[a] | 10.5[a,c] | 12.5[c] | 13.3[c] |
|---|---|---|---|---|---|---|---|---|---|---|
| $\mu$ ($cm^{-1}$) | 11700 | 11700 | 12000 | 12000 | 12000 | 12000 | | | | |
| | | | | 16600 | 17200 | 17200 | 17800 | 18500 | 18500 | 18500 |

a) Liophylized solutions.
b) Powders.
c) Solutions.

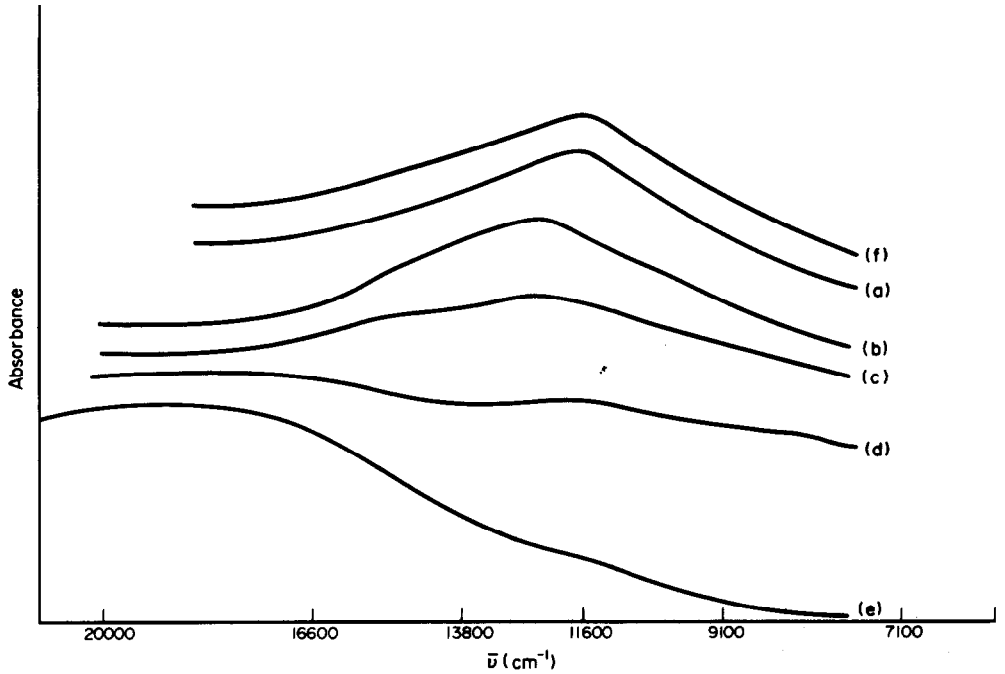



Fig. 4. Reflectance absorption spectra for series I samples. (a) pH 4.0. (b) pH 5.1. (c) pH 6.5. (d) pH 7.5. (e) pH 10.5. (f) Cu(II) aquo complex at pH 4.4.

cause larger shifts of the absorption maximum, probably as a consequence of the existence in the protein molecule of several different nitrogen containing ligands.

## CONCLUSIONS

From the results reported above, the following conclusions can be drawn—

(a) Binding of Cu(II) to insulin at pH 5 in aqueous solution differs from what was found for insulin single crystals by Brill and Venable.[6] It is very likely that, in the pH range studied, oxygen of the carboxylato groups, nitrogen of α- and ε-amino groups and of imidazoles contribute to the co-ordination field. The contribution by each one of the ligands mentioned is different at different pH values and binding specificity of the crystalline Cu(II)–insulin derivatives is lacking.

(b) Only at very high pH values is the field strength increased to such an extent that a preferential binding site for Cu(II) is found, and it probably involves deprotonated peptide nitrogens. At these pH values the Cu(II)–N bonding becomes much more covalent, as detected by the N coupling in the ESR spectrum.

The fact that strong covalent binding of Cu(II) to insulin does not occur in the physiological pH range could be of biological significance.

## REFERENCES

1. J. Peisach and W. E. Blumberg, *Arch. Biochem. Biophys.* 1974, **165**, 691.
2. G. Formicka-Kozlowska, H. Kozlowski and B. Jezowska-Trzebiatowska, *Inorg. Chim. Acta* 1977, **24**, 1.
3. H. Kozlowski, *Inorg. Chim. Acta* 1978, **31**, 135.
4. P. Michelin Lausarot and R. P. Ferrari, *Inorg. Chim. Acta* 1979, **33**, 145.
5. M. Freni, A. Gervasini, P. Romiti, T. Beringhelli and F. Morazzoni, *Spectrochim. Acta* 1983 **39A**, 85.
6. A. S. Brill and J. H. Venable, Jr., *J. Mol. Biol.* 1968, **36**, 343: and references therein.
7. J. Schlichtkrull, *Acta Chem. Scand.* 1956, **10**, 1455.

*Polyhedron* Vol. 3, No. 7, pp. 839–843, 1984
Printed in the U.S.A.

0277-5387/84 $3.00 + .00
© 1984 Pergamon Press Ltd.

# METAL COMPLEXES OF MERCAPTOAMINES—I. SYNTHESIS AND CRYSTAL AND MOLECULAR STRUCTURE OF TETRAKIS (3-AMINO-1-PROPANETHIOLATO) TRINICKEL(II)CHLORIDE

**H. BARRERA and J. SUADES***
Departament de Química Inorgànica, Universitat Autònoma de Barcelona, (Bellaterra) Barcelona, Spain

**M. C. PERUCAUD**
Departement de Minéralogie et Cristallographie, Université Pierre et Marie Curie, Paris, France

**and**

**J. L. BRIANSÓ**
Departament de Cristal.lografia, Universitat Autònoma de Barcelona, (Bellaterra) Barcelona, Spain

(*Received* 28 *September* 1983; *accepted* 15 *December* 1983)

**Abstract**—The reaction of nickel(II)chloride with $\gamma$-mercapto-propylamine in ethanolic solution gives the complex $[Ni_3(MPA)_4]Cl_2$(MPA=$NH_2$–$(CH_2)_3$–S). The complexes $[Ni_3(MPA)_4]X_2$(X=Br, I, $ClO_4$) can be synthesized from the chloride complex by addition of the sodium salt in aqueous solution. The crystal structure consists of discrete divalent trinuclear cations and chloride anions. Each sulphur atom of the ligand acts as a bridge between two nickel atoms, and the nitrogen atoms complete the coordination around the terminal nickel atoms. The geometry around the metal atoms is square-planar. The electronic and IR spectra of the complexes $[Ni_3(MPA)_4]X_2$(X=Br, I, $ClO_4$) indicate that all these compounds are composed of the $[Ni_3(MPA)_4]^{2+}$ and $X^-$ ions.

While metal complexes of $\beta$-mercaptoamine ligands have been widely studied,[1–5] many of them being stable chelates, those of $\gamma$-mercaptoamines have received little attention up to now. Several metal complexes of 1 - methyl - 4 - mercapto-piperidine, 2 - (2-mercaptoethyl) - 1 - methyl-piperidine, and 3 - (mercaptomethyl) - 1 - methyl-piperidine have been synthesized in this Department and reported in recent papers.[6–9] In all these cases the $\gamma$-mercaptopiperidines behave as unidentate ligands coordinating only through the sulphur atom. In order to investigate whether this different coordinating behaviour of $\beta$- and $\gamma$-mercaptoamines has to be attributed to the piperidine ring, or to the presence of another $-CH_2-$ group, or to the nature of the metal atom we have undertaken a wider study, part of which includes the complexes formed by aliphatic linear $\gamma$-mercaptoamine ligands.

In this paper we report the synthesis of the following complexes: $[Ni_3(MPA)_4]X_2$ (MPA=$NH_2$–$(CH_2)_3$–S; X=Cl, Br, I, $ClO_4$) and the crystal and molecular structure of $[Ni_3(MPA)_4]Cl_2$.

The choice of $\gamma$-mercaptopropylamine has been based on the simplicity of the ligand together with the fact that, as a ligand, it has been poorly studied.

## EXPERIMENTAL

### *Preparations*

MPAH was synthesized from 3-amino-1-propanol, with HBr and thiourea, according to B. C. Cossat *et al.*[10] The compound was purified by sublimation (MPAH=$NH_2$–$(CH_2)_3$–SH).

$[Ni_3(MPA)_4]Cl_2$

A solution of MPAH (8.0 mmols) in ethanol

*Author to whom correspondence should be addressed.

Table 1. Analytical data

| Compound | % Ni | | % C | | % H | | % N | | % X | |
|---|---|---|---|---|---|---|---|---|---|---|
| | Found | Calc. | Found | Calc. | Found | Calc. | Found | Calc. | Found | Calc. |
| | | | | | | | | | X= Cl | |
| $[Ni_3(MPA)_4]Cl_2$ | 29.02 | 29.02 | 23.38 | 23.72 | 5.13 | 5.27 | 8.94 | 9.23 | 11.60 | 11.68 |
| | | | | | | | | | X= Br | |
| $[Ni_3(MPA)_4]Br_2$ | 24.58 | 25.31 | 20.25 | 20.69 | 4.64 | 4.60 | 7.67 | 8.05 | 23.22 | 22.96 |
| | | | | | | | | | X= I | |
| $[Ni_3(MPA)_4]I_2$ | 21.93 | 22.29 | 18.40 | 18.23 | 4.21 | 4.05 | 7.29 | 7.09 | 31.90 | 32.13 |
| $[Ni_3(MPA)_4](ClO_4)_2$ | 24.11 | 23.95 | 19.67 | 19.58 | 3.98 | 4.35 | 7.32 | 7.61 | | |

(50 $cm^3$) was cooled to 0°C, and triethylamine (7.6 mmols) was added with stirring. This solution was added, slowly and with stirring, to a solution of $NiCl_2 \cdot 6H_2O$ (6.0 mmols) in ethanol (50 $cm^3$). A red powder was immediately formed, which was filtered and washed with ethanol. The crude product was recrystallized from methanol–water. Deep red crystals of the complex were slowly formed. They were collected by filtration, washed with methanol and dried under vacuum (yield 40%). This method yielded crystals of suitable size and quality for X-ray analysis.

$[Ni_3(MPA)_4]X_2$ (X=Br, I, $ClO_4$)

To a solution of the chloride complex $[Ni_3(MPA)_4]Cl_2$ in water at room temperature, was added with stirring, a solution of the sodium salt NaX, in water. An orange precipitate was always formed almost immediately, which was filtered off, washed with cold water and dried under vacuum.

*X-Ray data collection and reduction*

Weissenberg photographs were used for preliminary cell and space group determination. Final cell parameters and intensity data were obtained using a Philips four circle diffractometer PW-1100 (Department of Mineralogy and Crystallography of Paris VI University). The intensities were corrected only for the Lorentz-polarization factors.

*Crystal data*

$[Ni_3(SC_3H_8N)_4]Cl_2$, monoclinic, $a = 8.136(4)$, $b = 10.666(5)$, $c = 13.150(6)$ Å, $\beta = 103.32(7)°$, space group $P21/a$, $Z = 2$.

*Data collection*

Philips PW 1100 diffractometer, graphite monochromated Cu$K_\alpha$ radiation, $\theta$–$2\theta$ scan mode, scan speed of 2°/min in $2\theta$, 2084 reflections collected, 1909 observed [$Fo^2 > 2\sigma(Fo^2)$].

*Structure solution and refinement*

The structure was solved by direct methods using the basic set chosen by the program MULTAN,[11] using 150 reflections with $E \geq 1.33$.

In the $E$ map all the non-hydrogen atoms were located and their coordinates refined by the least-squares method to $R = 0.177$ with isotropic temperature factors. With anisotropic temperature factors $R$ reduced to 0.100 with all the $F_{hkl}$. Because of the low accuracy of the structure determination, no attempt was made to locate the H atoms. The refinement was carried out using the program AFFINE.[12] All calculations were performed on a IBM 370–168 computer (C.I.R.C.E. Orsay, France). Bond lengths and angles are given in Table 2. Final atomic coordinates, thermal parameters and a list of Fo/Fc values have been deposited with the Editor as supplementary data.

## RESULTS AND DISCUSSION

*Preparative*

By reacting a Ni(II) salt with MPAH in ethanolic solution, at different molar metal to ligand ratios ($r$), the following complexes have been obtained:

$$\text{Ni(II)} + \text{(MPA)} \xrightarrow{r=\frac{1}{3}} \text{Ni(MPA)}_2$$

$$\text{Ni(II)} + \text{(MPA)} \xrightarrow{r=\frac{3}{4}} [Ni_3(MPA)_4]^{2+}.$$

The complex $Ni(MPA)_2$[13] reacts with Ni(II) in the same way as does the homologous complex with $\beta$-mercaptoethylamine (MEA) (MEA=

Table 2.

| | | |
|---|---|---|
| **Bond lengths(A)** | | |
| Ni(1)–Ni(2) | 3.104 | ( 2) |
| Ni(1)–S(1) | 2.185 | ( 5) |
| Ni(1)–S(2) | 2.202 | ( 5) |
| Ni(2)–S(1) | 2.182 | ( 6) |
| Ni(2)–S(2) | 2.182 | ( 6) |
| Ni(2)–N(1) | 1.956 | (17) |
| Ni(2)–N(2) | 1.982 | (17) |
| S(1)–C(3) | 1.843 | (22) |
| S(2)–C(6) | 1.861 | (25) |
| N(1)–C(1) | 1.509 | (28) |
| N(2)–C(4) | 1.514 | (30) |
| C(3)–C(2) | 1.506 | (31) |
| C(2)–C(1) | 1.520 | (32) |
| C(5)–C(6) | 1.503 | (34) |
| C(5)–C(4) | 1.530 | (34) |
| S(1)–S(2) | 2.839 | ( 6) |
| **Angles(deg.)** | | |
| S(1)Ni(1)S(2) | 80.6 | (0.3) |
| S(1)Ni(2)S(2) | 81.2 | (0.3) |
| S(1)Ni(2)N(1) | 4.8 | (0.9) |
| S(1)Ni(2)N(2) | 177.1 | (1.7) |
| S(2)Ni(2)N(1) | 174.9 | (1.6) |
| S(2)Ni(2)N(2) | 96.7 | (0.9) |
| N(1)Ni(2)N(2) | 87.2 | (1.1) |
| Ni(1)S(1)Ni(2) | 90.7 | (0.3) |
| Ni(1)S(1)C(3) | 109.7 | (1.4) |
| Ni(2)S(1)C(3) | 106.2 | (1.4) |
| Ni(1)S(2)Ni(2) | 90.2 | (0.3) |
| Ni(1)S(2)C(6) | 110.9 | (1.6) |
| Ni(2)S(2)C(6) | 110.2 | (1.6) |
| Ni(2)N(1)C(1) | 121.5 | (2.8) |
| Ni(2)N(2)C(4) | 121.2 | (2.9) |
| S(1)C(3)C(2) | 110.9 | (3.0) |
| C(3)C(2)C(1) | 115.7 | (3.8) |
| C(6)C(5)C(4) | 114.8 | (4.0) |
| S(2)C(6)C(5) | 112.9 | (3.4) |
| N(1)C(1)C(2) | 111.4 | (3.5) |
| N(2)C(4)C(5) | 110.7 | (3.6) |

$NH_2$–$(CH_2)_2$–S) giving the trinuclear complex.[1]

$$2NiL_2 + Ni(II) \longrightarrow [Ni_3L_4]^{2+}$$

$$L = MPA, MEA.$$

When L=MPA, electronic spectroscopy shows that this reaction, analogously to that with MEA, is almost quantitative.

On the contrary, there are some interesting differences in behaviour between $Ni(MPA)_2$ and $Ni(MEA)_2$. The $Ni(MPA)_2$ complex dissolves in polar solvents giving $[Ni_3(MPA)_4]^{2+}$, while $Ni(MEA)_2$ remain practically insoluble. Furthermore, the aqueous solutions of trinuclear $[Ni_3(MPA)_4]^{2+}$ complex are less stable than those of the homologous trinuclear complex $[Ni_3(MEA)_4]^{2+}$.

The $[Ni_3(MPA)_4]^{2+}$ solutions decompose slowly in cold water, and very quickly in hot water. The colour fades and a nickel hydroxide precipitate appears. This different behaviour can be assigned to the lower stability of the compounds with six membered chelate rings with respect to compounds with five membered chelate rings.[14]

The complexes $[Ni_3(MPA)_4]X_2$, X = Br, I, $ClO_4$ can be obtained either by adding to the ligand the corresponding nickel(II) salt, or by mixing aqueous solutions of the corresponding sodium salt with that of $[Ni_3(MPA)_4]Cl_2$.

*Description of the structure of* $[Ni_3(MPA)_4]Cl_2$

Intramolecular bond lengths and bond angles are listed in Table 2. The numbering system employed is displayed in Fig. 1.

The crystal structure consists of discrete tri-

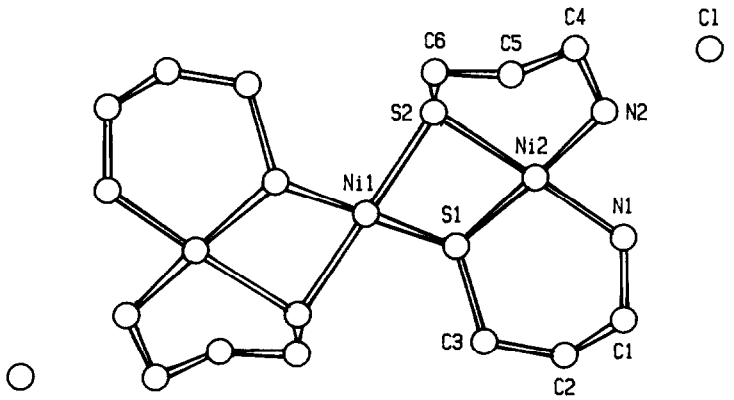



Fig. 1. Structure of $[Ni_3(MPA)_4]Cl_2$.

Table 3. Intermolecular Cl–N distances

| | Å |
|---|---|
| $Cl^{i} - N(1)^{ii}$ | 3.33(2) |
| $Cl^{i} - N(1)^{iii}$ | 3.26(2) |
| $Cl^{i} - N(2)^{i}$ | 3.23(2) |
| $Cl^{i} - N(2)^{iii}$ | 3.21(2) |

i= $-x + {}^{3}/_{2}$, $y - \frac{1}{2}$, $-z + 2$

ii= $-x + 2$, $-y + 2$, $-z + 2$

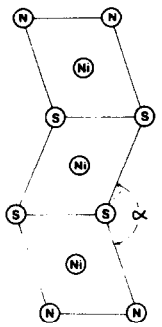
iii= $x - \frac{1}{2}$, $-y + {}^{3}/_{2}$, $z - 1$

nuclear $[Ni_3(MPA)_4]^{2+}$ cations and chloride anions. The hydrogen bond distances between chloride and nitrogen atoms are listed in Table 3. These lengths are in the usual range 2.91–3.41 Å expected for NH · · · Cl hydrogen bonds,[15] and they essentially determine the packing of the structure. The cations have the Ni(1) atom placed in plane (001) and chloride anions are near plane (002).

Crystal packing can be described as alternative layers of cations and anions bound by NH · · · Cl hydrogen bonds.

The central nickel atom Ni(1) is located on a crystallographic inversion centre and imposes on the cation $C_i$ symmetry. The Ni(1) atom is surrounded by four bridging sulphur atoms which are also bonded to terminal Ni(2) atoms. The five atoms of the square-planar unit $Ni(1)S_4$ are rigorously in a plane due to the crystallographic symmetry.

Terminal Ni(2) atoms are surrounded by two nitrogen and two sulphur atoms; the five atoms of the unit *cis*-$Ni(2)S_2N_2$ also lie in a plane within experimental error. Both S–Ni(2) distances are practically equal to those between S–Ni(1). All S–Ni and N–Ni bond lengths are in accordance with literature data.[4]




| Compound | α (deg.) |
|---|---|
| $[Ni_3(MPA)_4]Cl_2$ | 139 |
| $[Ni_3(MEA)_4]Cl_2$ | 109 |

Fig. 2. The dihedral angle between the planes $NiS_4$ and $NiS_2N_2$.

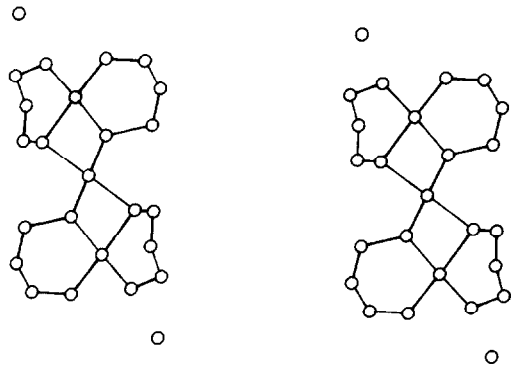


Fig. 3. A stereoscopic view of $[Ni_3(MPA)_4]Cl_2$.

The deviation of the four coordinated sulphur atoms of Ni(1) from square geometry is revealed from the S(1)–Ni(1)–S(2) angle of 80.6°. The same deviation takes place around the Ni(2) atoms, average S–Ni(2)–N angles are 14.6 and 8.6° higher than SNi(2)S and NNi(2)N respectively.

There are two crystallographically independent chelate rings. One of them is in chair conformation and the other one in skew-boat as can be seen in the stereoscopic view of the cation (Fig. 3).

It is particularly informative to relate the structural features of the $Ni[NiS_2N_2]_2$ fragment of the $[Ni_3(MPA)_4]Cl_2$ complex with that of the homologous $[Ni_3(MEA)_4]Cl_2$ complex.[4]

In both cases, the fragment possesses $C_{2h}$ symmetry and bond lengths are very similar. The most striking difference between the structures of these two complexes is the dihedral angle ($\alpha$) determined by the planes $NiS_4$ and $NiS_2N_2$ along the S–S edge (Fig. 2).

This angle $\alpha$, is 30° greater in the complex with MPA than in the complex with MEA. It has to be noted that in metal complexes of thiol ligands the folding of the $M_2S_2$ ring has been attributed to three different causes:[16]

(1) Ni–Ni interactions; (2) S–S interactions; (3) steric requirements of the ligands.

In the $Ni_3(MPA)_4Cl_2$ complex a Ni–Ni interaction cannot probably be considered because the distance between Ni(1)–Ni(2) atoms is too long.

As in several thiol complexes, the S–S bond distance in this complex is also shorter than a typical nonbonded S–S distance ($\sim 3.2$ Å),[17] so a weak S–S interaction may be considered.

On comparing the structures of $[Ni_3L_4]Cl_2$ complexes (L=MPA, MEA), we can see that as a result

Table 4.

Electronic Spectra

$\lambda$ max (nm) ( $\epsilon$ )

| $[Ni_3(MEA)_4]Cl_2$ | $[Ni_3(MPA)_4]Cl_2$ |
|---|---|
| 574 (800) sh | |
| 492 (1450) | 480 (1500) |
| 377 (3600) | 398 (7500) |
| 303 (10000) | 325 (9320) |

$\nu$(N–H) stretching frequencies ($cm^{-1}$)

| Ligand (MPAH) | Complexes $[Ni_3(MPA)_4]X_2$ | | | |
|---|---|---|---|---|
| | Cl | Br | I | $ClO_4$ |
| 3400 | 3030 | 3090 | 3130 | 3260 |
| 3325 | 3100 | 3150 | 3200 | 3300 |
| | 3170 | | | |

of the presence of another $-CH_2-$ group in the MPA complex, the angle $\alpha$ is opened by 30°. It is reasonable to think, that it can be attributed essentially to the steric requirements of the enlargement of the chelate ring size.

Consequently, this structure shows that the steric requirements of the ligands are probably one of the most important reasons for the folding of $Ni_2S_2$ ring in thiol complexes.

*IR spectra*

A significant shift of the $\gamma$(N–H) bands to lower frequencies was observed in the spectra of all the $[Ni_3(MPA)_4]X_2$ complexes with respect to that of the free ligand (Table 4), and that agrees well with the coordination of the nitrogen atom to nickel atoms in all these complexes.[18] Furthermore, the $\gamma$(N–H) stretching frequency decreases along the series $Cl^- < Br^- < I^- < ClO_4^-$ showing that the strength of the hydrogen bond N–H···X decreases from $Cl^-$ to $ClO_4^-$.

*Electronic spectra*

It is interesting to relate the electronic spectrum of the complex $[Ni_3(MPA)_4]Cl_2$ with that of its homologue $[Ni_3(MEA)_4]Cl_2$ (Table 4).

As is shown in Table 4, there are some important differences between these spectra. Thus, while there are little changes in the position of the bands, the intensity of the band at 398 nm is practically doubled in the MPA complex, and a new band at 574 nm appears only in the spectrum of the MEA complex. Those differences could be attributed to the different bond lengths and angles of the chromophores of these complexes. However it seems that the Ni–Ni interaction in the MEA complex (Ni–Ni 2.733 Å) and the very weak interaction, if any, in the MPA complex (Ni–Ni 3.104 Å) offers a much better explanation for the differences observed in the electronic spectra.

There is not any significative difference between the electronic spectra of the aqueous solutions of $[Ni_3(MPA)_4]X_2$ (X=Cl, Br, I, $ClO_4$) complexes, for this reason all these compounds are probably composed of $[Ni_3(MPA)_4]^{2+}$ and $2X^-$ ions.

## REFERENCES


1. D. C. Jicha and D. H. Busch, *Inorg. Chem.* 1962, **1**, 872.
2. D. C. Jicha and D. H. Busch, *Inorg. Chem.* 1962, **1**, 878.
3. D. C. Jicha and D. H. Busch, *Inorg. Chem.* 1962, **1**, 884.
4. C. H. Wei and L. F. Dahl, *Inorg. Chem.* 1970, **9**, 1878.
5. D. H. Busch, J. A. Burke, D. C. Jicha, M. C. Thompson and M. L. Morris, *Adv. Chem. Ser.* 1963, **37**, 125.
6. J. C. Bayon, M. C. Briansó, J. L. Briansó and P. González, *Inorg. Chem.* 1979, **18**, 3478.
7. W. Gaete, J. Ros, J. Suñer, M. C. Briansó and J. L. Briansó, *J. Chem. Soc. Dalton* 1981, 852.
8. W. Gaete, J. Ros, X. Solans, M. Font-Altaba, J. L. Briansó, *Inorg. Chem.* in press.
9. H. Barrera, J. C. Bayon, P. González, J. Sola, J. M. Viñas, J. L. Briansó, M. C. Briansó and X. Solans, *Polyhedron* 1982, **1**, 647.
10. B. C. Cossar, J. O. Fournier, D. L. Fields and D. D. Reynolds, *J. Org. Chem.* 1962, **27**, 93.
11. P. Main, M. M. Woolfson, L. Lessinger, G. Germain and J. P. Declercq, *MULTAN 76, A System of Computer Programs for the Automatic Solution of Crystal Structures from X-Ray Diffraction Data.* York, England (1976).
12. R. Bally, J. Delettre and J. P. Mornon, "AFFINE 1973". Laboratoire de Mineralogié-Cristallographie Associé au C.N.R.S., Université de Paris VI, France.
13. C. W. Schläpfer and K. Nakamoto, *Inorg. Chim. Acta* 1972, **6**, 177.
14. G. J. McDougall, R. D. Hancock and J. C. A. Boeyens, *J. Chem. Soc., Dalton* 1978, 1438.
15. G. C. Pimentel and A. L. McClellan, *The Hydrogen Bond*, p. 290. W. Freeman, San Francisco, CA (1960).
16. J. P. Fackler Jr., *Prog. Inorg. Chem.* 1976, **21**, 55.
17. R. L. Girling and E. L. Amma, *Acta Cryst.* 1976, **B32**, 2903.
18. D. Segnini, C. Curran and J. V. Quagliano, *Spectrochim. Acta* 1960, **16**, 540.

*Polyhedron* Vol. 3, No. 7, pp. 845–851, 1984
Printed in the U.S.A.

0277–5387/84 $3.00 + .00
© 1984 Pergamon Press Ltd.

# FLUORIDE COMPLEXES OF THE ALKALI METAL IONS

**C. B. CHAN and N. H. TIOH**
Chemistry Department, University of Malaya, Kuala Lumpur 22-11, Malaysia

**and**

**G. T. HEFTER***
School of Mathematical and Physical Sciences, Murdoch University, Murdoch, W.A. 6150, Australia

(*Received* 3 *October* 1983; *accepted* 16 *November* 1983)

**Abstract**—Measurements by fluoride ion-selective electrode potentiometry on the very weak monofluoride complexes of the alkali metal ions in aqueous solution at 25°C and an ionic strength of 1*M* indicate their stability constants lie in the order $Li^+ > Na^+ > K^+ > Rb^+ \simeq Cs^+$. Data at varying ionic strengths and temperatures were used to calculate infinite dilution stability constants and enthalpies and entropies of complexation for LiF and NaF.

Although the alkali metal halide salts are usually considered to be fully dissociated in aqueous solution there is increasing evidence that this is not strictly true for the fluoride salts.

Thus, Robinson *et al.*[1,2] have shown from conductivity and activity measurements that NaF is appreciably more associated than KF and have consequently recommended that the latter be adopted as a fluoride activity standard.[1] Butler and Huston,[3] and Miller and Kester,[4] have also found NaF to be significantly associated in NaCl media. Hefter[5] has shown that abnormally low values of the association constant of HF in $LiClO_4$ media are consistent with the association of LiF. In very dilute solutions, precise conductivity measurements by Pethybridge and Spiers[6] indicated that the degree of association of the alkali metal ion–fluoride complexes falls in the sequence $LiF > NaF > KF \simeq RbF > CsF$, although, as is usual for very weakly associated electrolytes, the association constants were rather dependent on the nature of the conductivity equation assumed.[6]

The greatest interest in these very weak complexes derives from their role in chemical speciation in solutions of relatively high ionic strength such as seawater,[7] geological brines,[8] etc. Hence a study of the alkali metal ion-fluoride complexes was undertaken to provide reliable association constants at ionic strengths relevant to practical applications.[7,8] The method employed was potentiometry with a fluoride ion-selective electrode (ISE). This technique is both simple to use and is capable of excellent accuracy.[9,10] It is also especially suited to the study of very weak fluoride complexes.[11]

## EXPERIMENTAL

*Reagents*

All chemicals used were of reagent grade purity. All solutions were prepared using glass distilled water and calibrated volumetric glassware. Lithium and sodium perchlorates and lithium nitrate were prepared by reacting the appropriate carbonates and acids. The crystals so obtained were purified twice by recrystallization from hot water then vacuum dried ($10^{-2}$ mm Hg) at 110–120°C for several days. Sodium fluoride was further purified by the method of Lingane.[12] Potassium fluoride (NBS, Standard Reference Material 2203) and rubidium and cesium fluoride (Alfa Inorganics, 99.9% stated purity) were used as supplied.

All fluoride solutions were stored in pre-leached air-tight polyethylene containers. The pH of all solutions was maintained at 5.0–6.0. At this pH the formation of HF and $HF_2^-$[10] and metal

*Author to whom correspondence should be addressed.

ion–hydroxy species[13] may be neglected, as may $OH^-$ interference with the fluoride ISE.[14]

All measurements were made at 25.00 ± 0.02°C maintained with a circulating thermostat (Haake FE) which was itself cooled by thermostatted (20.0 ± 0.2°C) water. Free fluoride concentrations were determined by a commercial fluoride ISE (Orion Model 94–09). Potentials were measured to 0.1 mV with an Orion Model 801A or 901 digital voltmeter, relative to a Ag|AgCl electrode consisting of a silver wire in contact with solid AgCl.[9] Titrations were performed with 5 cm³ Metrohm Micro Hand Burette (Model E457). The technique of *in situ* calibration was employed.[9]

*Calculations*

Equilibria in aqueous metal ion-fluoride solutions can be represented by the equation

$$M^+(aq) + nF^-(aq) \overset{\beta_n}{\rightleftharpoons} MF_n^{(1-n)+}(aq). \quad (1)$$

If $[M^+]_T \gg [F^-]_T$ (where the subscript T denotes the total or analytical concentration) the following equation may be readily derived

$$\frac{1}{[M]}\left[\frac{[F^-]_T}{[F^-]} - 1\right] = F_0(X) = \Sigma\, n\beta_n[F^-]^{n-1} \quad (2)$$

where $\beta_n$ are the overall concentration stability constants corresponding to the equilibria in eqn (1) and $F_0(X)$ is introduced to represent the experimetally determinable left hand side of eqn (2). As the alkali metal fluorides are very weakly associated, only the first complex is formed and $F_0(X)$ reduces to $\beta_1$. Existence of high order complexes would be indicated by a dependence of $F_0(X)$ on $[F^-]$ (eqn 2).

*Liquid junction potentials*

Cells used for this study may be represented in general terms as

| | reference half cell | | salt bridge | indicating half cell | | |
|---|---|---|---|---|---|---|
| Ag | AgCl | 0.1I *M* ACl<br>0.9I *M* AB | I *M* (AB) | *x M* MB<br>*y M* AF<br>(I − *x* − *y*)*M* AB | FE | (3) |
| | | | $E_{j1}$ | $E_{j2}$ | | |

where FE represents the fluoride ISE, I ($= \frac{1}{2}\Sigma[i]z_i^2$) is the total ionic strength which is maintained constant throughout by the addition of a supposedly inert (non-complexing) "swamping electrolyte" AB[13] and $E_{j1\&2}$ are liquid junction potentials (LJPs).

Because the $MF^0(aq)$ complexes are very weak it is necessary to use exceptionally high metal ion concentrations and thus careful consideration must be given to LJPs. It has been shown in detail elsewhere[15] that LJPs for the "constant ionic medium junctions" used in cell (3) may be calculated with considerable reliability from the Henderson equation. Under typical experimental conditions $E_{j1}$ is essentially constant and may be incorporated into the "standard" cell potential and the Henderson eqn for $E_{j2}$ has the form (at 25°C):[15]

$$E_{j2} = -59.16 \log\left\{1 - \frac{[M^+](\lambda_{M^+} - \lambda_{A^+})}{I\,\Lambda_{AB}}\right\}. \quad (4)$$

The necessary conductivity and transference data for the calculation of $E_{j2}$ were obtained by appropriate interpolation and extrapolation of literature data[16–20] and, in some cases, by direct measurement.[21]

## RESULTS AND DISCUSSION

A typical set of experimental data is shown in Table 1. The constancy of $F_0(X)$ indicates only the $MF^0(aq)$ complex is detectable over the concentration ranges employed (eqn 2). $F_0(X)$ was independent of both $[M^+]$ and $[F^-]$ for all the ions studied indicating no appreciable formation of "polynuclear" or higher order fluoride complexes respectively.

As these complexes are exceedingly weak, their stability constants are very difficult to measure reliably. When feasible therefore, determinations were made in a number of swamping electrolytes to assess likely errors and medium effects. Table 2 summarizes the stability constants obtained at I = 1 *M*. All values are the average of at least three, and usually more than five, independent titrations. The stability constants of the complexes decrease in the order $Li^+ > Na^+ > K^+ > Rb^+ \simeq Cs^+$. This sequence parallels that found by Pethybridge and Spiers[6] at infinite dilution and is consistent with the increasing ionic radius of the metal ion, assuming an "inner sphere" complex (rather than a solvent-

Table 1. Typical potentiometric data for the determination of alkali metal ion-fluoride complexes. System: $Li^+/F^-$, I = 1.000 *M*($KNO_3$), T = 25.00°C

| $-E_{obs}$ [a] | $E_j$ [b] | $[F^-]_T$ [c] | $[F^-]$ [d,e] | $[Li^+]$ [e] | $F_o(X)$ [e,f] |
|---|---|---|---|---|---|
| mV | mV | $10^4 M$ | $10^4 M$ | *M* | $M^{-1}$ |
| 34.4 | 0.38 | 6.769 | 6.477 | 0.0540 | 0.83 |
| 32.8 | 0.56 | 6.591 | 6.129 | 0.0789 | 0.96 |
| 31.5 | 0.73 | 6.422 | 5.853 | 0.1025 | 0.95 |
| 30.1 | 0.89 | 6.262 | 5.589 | 0.1249 | 0.96 |
| 27.1 | 1.27 | 5.893 | 5.047 | 0.1764 | 0.95 |
| 24.5 | 1.61 | 5.566 | 4.622 | 0.2221 | 0.92 |
| 19.6 | 2.20 | 5.009 | 3.908 | 0.2999 | 0.94 |
| 15.4 | 2.69 | 4.554 | 3.383 | 0.3635 | 0.95 |
| 12.0 | 3.10 | 4.174 | 3.011 | 0.4166 | 0.93 |
| 8.7 | 3.46 | 3.853 | 2.685 | 0.4614 | 0.94 |
| 6.1 | 3.77 | 3.578 | 2.459 | 0.4999 | 0.91 |
| 3.4 | 4.04 | 3.339 | 2.235 | 0.5332 | 0.93 |
| -0.1 | 4.50 | 2.947 | 1.985 | 0.5881 | 0.82 |

Average: $\beta_1(LiF^o(aq)) = 0.92 \pm 0.04\ M^{-1}$.

*a.* Observed potential of cell (3): A = $K^+$, B = $NO_3^-$, M = $Li^+$

*b.* Calculated from eq.(4)

*c.* Total fluoride concentration, corrected for background fluoride impurities[9].

*d.* Calculated from Nernst eq: $E_{corr} = E^{o'} - 59.16 \log [F^-]$, where $E_{corr} = E - E_j$ and $E^{o'} = -223.42 \pm 0.12$ mV determined by *in situ* calibration (data not shown).

*e.* Calculated iteratively[9]

*f.* As defined in eq.(2)

Table 2. Summary of present results for the stability constants of fluoride complexes of the alkali metal ions at I = 1 *M* and T = 25°C

| Ion | $\beta_1(M^{-1})$ | Ionic Medium |
|---|---|---|
| $Li^+$ | 0.75 ± 0.05 | $NaClO_4$ |
| | 0.58 ± 0.06 | $NaNO_3$ |
| | 0.93 ± 0.07 | $KNO_3$ |
| | 1.02 ± 0.04 | $RbNO_3$ |
| | 1.17 ± 0.06 | $CsNO_3$ |
| $Na^+$ | 0.20 ± 0.02 | $KNO_3$ |
| | 0.21 ± 0.01 | $RbNO_3$ |
| | 0.33 ± 0.02 | $CsNO_3$ |
| $K^+$ | 0.02 ± 0.01 | $RbNO_3$ |
| | 0.07 ± 0.01 | $CsNO_3$ |
| $Rb^+$ | see text | $CsNO_3$ |

separated ion pair) and an essentially electrostatic interaction between $M^+$ and $F^-$. It is, however, interesting to note that the strength of association is somewhat stronger than would be predicted on the basis of the well known[23] linear correlations between fluoride stability constants and metal ion properties as shown in Fig. 1. The reasons for this are not clear but may be due to covalency effects.[23,24] Not surprisingly, association constants for the alkali metal-fluorides which have been estimated[25] from this type of correlation differ markedly, from the experimental values.

The equality, $\beta_1$ ($RbF^0(aq)$) $\simeq \beta_1$ ($CsF^0(aq)$), is based on our inability to quantitatively detect complex formation of RbF in I = 1 $M$($CsNO_3$). Despite considerable experimental effort (employing $Rb^+/F^-$ ratios of up to 500 : 1) the only reasonable conclusion was that the results were consistent with $\beta_1$ ($RbF^0(aq)$) = 0.00 ± 0.01 $M^{-1}$ in this medium. This finding is still consistent with that of Pethybridge and Spiers[6] given the extreme weakness of the complexes. Failure to detect RbF association is probably a reflection of errors involved in the assumptions made in calculating LJPs via the Henderson equation.[15] It might also be due to minor changes in the electrode response or activity coefficients when appreciable amounts of $Rb^+$ replace $Cs^+$ in the ionic medium[13] (although in respect to the latter it should be noted that $RbNO_3$ and $CsNO_3$ have almost identical activity coefficients at I = 1 $M$[22]).

It is interesting in passing to consider the present limits of detection of complexation ($\beta_1 \simeq 0.01\ M^{-1}$) with those reported previously[11] ($\beta_1 \simeq 0.2\ M^{-1}$). The improvement can be ascribed to the *in situ* calibration of the fluoride electrode[9] and the reliable calculation of LJPs.[15]

*Variation of stability constants with the ionic medium*

The dependence of the $\beta_1$ values on the nature of the swamping electrolyte (Table 2) arises from differences in activity coefficients between each medium. Minor differences in association of the various electrolytes present in the measuring solutions may also exert a significant effect. This can be seen by remembering that eqn (1) in the presence of a swamping electrolyte AB is more realistically represented as a competition reaction

$$M\text{–}B^0(aq) + A\text{–}F^0(aq) \rightleftharpoons M\text{–}F^0(aq) + A\text{–}B^0(aq). \quad (5)$$

Clearly, depending on the relative strengths of the competing equilibria, the desired stability constant (eqn 1) may differ significantly from the apparent measured constant (eqn 5). These effects are discussed more fully elsewhere.[26]

Determination of the stability constants at

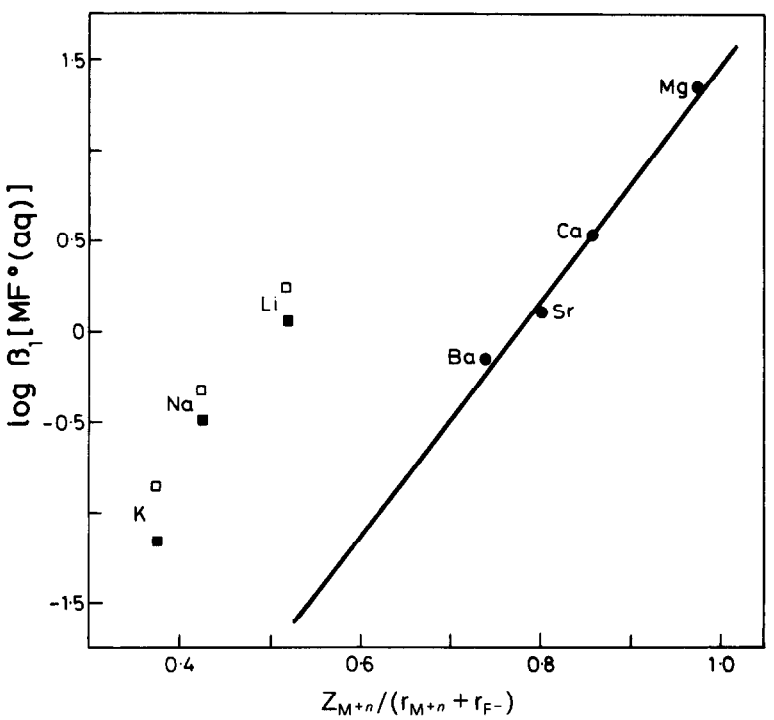



Fig. 1. Electrostatic correlation of metal ion properties with fluoride stability constants (see text however): □, Ref. 6, I = 0; ●, Ref. 1, I = 1 $M$ ($NaClO_4$): (■) present work, I = 1 $M$ ($CsNO_3$).

Table 3. Stability constants of LiF and NaF at various ionic strengths and temperatures

| Ion | Swamping Electrolyte | Ionic Strength ($M$)[a] | | | | | | |
|---|---|---|---|---|---|---|---|---|
| | | 1.0 | 0.5 | 0.2 | 0.1 | 0.05 | 0.02 | 0 |
| $Li^+$ | $NaClO_4$ | 0.75 ± 0.05 | 0.63 ± 0.02 | 0.95 ± 0.02 | 1.08 ± 0.03 | 1.12 ± 0.26 | 1.35 ± 0.07 | 1.7 ± 0.2[b] |
| $Na^+$ | $KNO_3$ | 0.20 ± 0.02 | 0.21 ± 0.02 | 0.32 ± 0.05 | n.d. | n.d. | n.d. | 1.0 ± 0.3[c] |

| | | Temperature ($^oC$)[d] | | |
|---|---|---|---|---|
| | | 15 | 25 | 35 |
| $Li^+$ | $NaClO_4$ | 0.68 ± 0.08 | 0.75 ± 0.05 | 0.80 ± 0.05 |
| $Na^+$ | $KNO_3$ | 0.17 ± 0.05 | 0.20 ± 0.02 | 0.24 ± 0.02 |

a. At 25°C; n.d. = not detected
b. Obtained by non-linear regression; see text
c. Estimated graphically
d. At I = 1 $M$

Table 4. Enthalpies and entropies of association of LiF and NaF at 25°[a]

| Complex | Ionic Medium $M$ | $\Delta H$ kJ mol$^{-1}$ | $\Delta S$ JK$^{-1}$ mol$^{-1}$ |
|---|---|---|---|
| $LiF^0(aq)$ | $1(NaClO_4)$ | 6.0 ± 0.6 | 18 ± 7 |
| $NaF^0(aq)$ | $1(KNO_3)$ | 13 ± 1 | 30 ± 5 |

a. Data refer to eq.(1)

infinite dilution ($\beta_1^0$), whilst of less practical relevance, has the advantage of removing such effects. Unfortunately, evaluation of $\beta_1^0$ by the usual extrapolation or correction procedures[22] is problematic because the weakness of the complexes makes reliable stability constant determination extremely difficult by potentiometry, especially at low I. In fact, satisfactory data could only be obtained (Table 3) for LiF, although incomplete results were also gathered for NaF. Extrapolation to zero ionic strength using non-linear regression techniques[27] and an extended form of the Debye–Huckel equation (Ref. 22, eqn (9.11)) gave $\beta_1$ ($LiF^0(aq)$) = 1.7 ± 0.2. This is in excellent agreement with the values 1.78 and 2.45 (depending on the conductance equation assumed) given by Pethybridge and Spiers.[6]

Insufficient data were obtained for NaF for regression analysis but a graphical extrapolation gave a value of $\beta_1^0$ ($NaF^0(aq)$) ≃ 1.0 which is again in reasonable agreement with Pethybridge and Spiers' values of 0.47 and 1.04[6] and the value of 1.88 reported by Robinson *et al.*[1,2] All of these results are somewhat higher than the value $\beta_1^0$ ($NaF^0(aq)$) = 0.11 calculated from the data of Miller and Kester using their recommended activity coefficients (Ref. 4, p. 77). It should be noted, however, that Miller and Kester's experimental value $\beta_1$ ($NaF^0(aq)$) = 0.045 ± 0.006 at I = 0.7 $m$ (NaCl) is in marked disagreement with the value of 0.16 ± 0.02 at I = 1 $M$ (NaCl)[3] and the interpolated value of 0.21 ± 0.02 at I = 0.7 $M$ ($KNO_3$) from the present work (Table 3). The reasons for this discrepancy are unclear (the differences in units should be negligible[13]) but might be due to small errors arising from the use of a glass membrane sodium -ISE fluoride rich solutions.[4] Clearly, further work is required on this matter.

*Variation of stability constants with temperature*

The dependence of $\beta_1$ for LiF and NaF on temperature is shown in Table 3. The enthalpies and entropies of complexation (eqn 1) calculated by linear regression of log $\beta_1$ vs $T^{-1}$ data are given in Table 4. Since concentrations were expressed in molarities it is strictly necessary to correct these values for changes in solvent density.[28] However, in view of the experimental difficulties in measuring $\beta_1$ and the consequently large uncertainties in $\Delta H_1$ and $\Delta S_1$ this relatively minor correction was not considered to be justified at this stage (see below).

Like almost all known fluoride complexation reactions in aqueous solution[10,23] the present enthalpies are small and positive ($\beta_1$ increases with $T$). That is, the complexes owe their stability to the increase in entropy arising from charge neutralization. The present results are, however, again markedly different from those of Miller and Kester[4] who found $\beta_1$ ($NaF^0(aq)$ *decreased* with increasing temperature with $\Delta H_1 = -15.4\,kJ\,mol^{-1}$. Although it is not possible at this stage to decide which of these values is more realistic the value reported by Miller and Kester is more exothermic than any other fluoride complexation in aqueous solution[10] which seems unlikely. In view of the well known deficiencies of determining $\Delta H$ from log $\beta$ vs $T^{-1}$ data this discrepancy would be best resolved by direct calorimetry.

## REFERENCES

1. R. A. Robinson, W. C. Duer and R. G. Bates, *Anal. Chem.* 1971, **43**, 1852.
2. W. C. Duer, R. A. Robinson and R. G. Bates, *J. Chem. Soc. Faraday Trans. I* 1972, **68**, 716.
3. J. N. Butler and R. Huston, *Anal. Chem.* 1970, **42**, 1308.
4. G. R. Miller and D. R. Kester, *Marine Chem.* 1976, **4**, 67.
5. G. T. Hefter, *J. Soln. Chem.*, in press.
6. A. D. Pethybridge and D. J. Spiers, *J. Chem. Soc. Faraday Trans. I* 1977, **73**, 768.
7. J. P. Riley and G. Skirrow (Editors) *Chemical Oceanography*, 2nd Edn, Vol. 1. Academic Press, London (1975).

8. See for example, C. K. Richardson and H. D. Holland, *Geochem. Cosmochim. Acta*, 1979, **43**, 1327.
9. G. T. Hefter, *J. Soln. Chem.* 1982, **11**, 45.
10. A. M. Bond and G. T. Hefter, *Critical Survey of Stability Constants and Related Thermodynamic Data of Fluoride Complexes in Aqueous Solution.* IUPAC Chemical Series No. 27. Pergamon Press, Oxford (1980).
11. A. M. Bond and G. T. Hefter, *J. Inorg. Nucl. Chem.* 1971, **33**, 429.
12. J. J. Lingane, *Anal. Chem.* 1967, **39**, 881.
13. C. F. Baes and R. E. Mesmer, *The Hydrolysis of Cations.* Wiley-Interscience, New York (1976).
14. M. S. Frant and J. W. Ross, *Science* 1966, **154**, 1553.
15. G. T. Hefter, *Anal. Chem.* 1982, **54**, 2518.
16. E. M. Kartzmark, *Can. J. Chem.* 1972, **50**, 2845.
17. J. H. Jones, *J. Amer. Chem. Soc.* 1945, **67**, 855.
18. M. L. Miller, *J. Phys. Chem.* 1956, **60**, 189.
19. R. Haase, G. Lehnert and H. J. Jansen, *Z. Phys. Chem. Neue Folge* 1964, **42**, 32.
20. A. N. Campbell, G. H. Debus and E. M. Kartzmark, *Can J. Chem.* 1955, **33**, 1508.
21. C. B. Chan, G. T. Hefter and N. T. Tioh, unpublished observations, University of Malaya (1980–81).
22. R. A. Robinson and R. H. Stokes, *Electrolyte Solutions*, 2nd Edn. Butterworths, London (1970).
23. G. T. Hefter, *Coord. Chem. Rev.* 1974, **12**, 221.
24. D. F. C. Morris, *Structure & Bonding* 1968, **4**, 63.
25. J. V. Leyendekkers, *Anal. Chem.* 1971, **43**, 1835.
26. G. T. Hefter, C. B. Chan and N. H. Tioh, *Anal. Chem.*, in press.
27. N. R. Draper and H. Smith, *Applied Regression Analysis.* Wiley, New York (1968).
28. L. G. Hepler, *Thermochim. Acta* 1981, **50**, 69.

*Polyhedron* Vol. 3, No. 7, pp. 853–859, 1984
Printed in the U.S.A.

0277-5387/84 $3.00 + .00
© 1984 Pergamon Press Ltd.

# ON THE PAULING ELECTRONEGATIVITY SCALES—II

**KEN OHWADA**
Division of Chemistry, Japan Atomic Energy Research Institute, Tokai-mura, Naka-gun, Ibaraki-ken, Japan

(*Received* 4 *October* 1983; *accepted* 16 *November* 1983)

**Abstract**—From the analysis of the electrostatic potential near the core-valence boundary in an atom, it is shown that the Pauling electronegativity scale $\chi_P$ is approximately given by the formula,

$$\chi_P = \frac{(N_v + 1)}{2} f(n),$$

where $N_v$ is the valence electron number and $f(n)$ is some function of the periodic number in the periodic table. It is also shown in detail that the Pauling electronegativity scale is closely related to the Wang–Parr electronegativity scale which is determined as the negative of the chemical potential in density functional theory. Correlation between the Pauling and Mulliken electronegativities is briefly discussed.

Recently, the renewed interest in the concept of electronegativity[1] as applied to atoms, molecules and even alloys, has led to several interesting papers.[2–10] Especially, we take an interest in some studies[2–4, 9, 10] which have dealt with the electronegativity from the point of view of density functional theory by Hohenberg and Kohn.[11] The density functional theory provides an exact route to the theoretical electronegativity. That is, variation with respect to the density of the Hohenberg–Kohn energy functional yields the chemical potential $\mu$ as given by

$$\mu = \frac{\delta E[\rho]}{\delta \rho(\mathbf{r})}, \qquad (1)$$

where $E[\rho]$ is the ground state energy of a many electron system and is a function of the electron density $\rho(\mathbf{r})$. It is important to note here the recent proposal of Parr *et al.*[2] equating the electronegativity to the negative of the chemical potential $\mu$. By virtue of this, we are now able to attack electronegativity precisely on a reliable theoretical basis.

In the present work, we start with considerations of the historic Pauling electronegativity scales[1] which have played an important role in chemical binding studies. From the detailed analysis of the electrostatic potential near the core-valence boundary in an atom, it is shown that the Pauling electronegativity scale[1] can be well reproduced with the valence electron number and some function of the periodic number in the periodic table. Next, we discuss the correlations between the Pauling and the Mulliken,[12] other[4] electronegativity scales. It is emphasized that the Mullken[12] and other[4] electronegativity scales are nearly proportional to the Pauling electronegativity scales.[1] Finally, we show that the pauling electronegativity scale is closlely related to the Wang–Parr[13] electronegativity scale which is the negative of the chemical potential derived from the density functional theory.

## PAULING ELECTRONEGATIVITY

As is well known, the Pauling electronegativity scale[1] is based on thermochemical data and depends on the electronic configuration of the atom in question. In this section, we try to reproduce the Pauling scales, without using any thermochemical data, from considerations of the electrostatic potential near the core-valence boundary in an atom. In a previous report,[14] we have already discussed in detail the reproduction of the Pauling scales. Here, brief arguments will be repeated for the sake of a better understanding of this problem.

Politzer and Parr[15] have shown that the outermost minimum in the radial density defines a physically meaningful boundary between the core and valence regions of a ground state atom. It

seems worthwhile to investigate in detail the electrostatic potential near such a boundary. To make this, we expand the electrostatic potential $V$ with the radial distance $r$ from the nucleus;

$$V(r_m+\Delta r)=V(r_m)+\left(\frac{\partial V}{\partial r}\right)_{r_m}(\Delta r)+\frac{1}{2}\left(\frac{\partial^2 V}{\partial r^2}\right)_{r_m}(\Delta r)^2+\cdots \quad (2)$$

where $r_m$ is the radial distance at which the radial density function $4\pi r^2\rho(r)$ has the outermost minimum, and the partial differentials with respect to $r$ are evaluated at the position $r_m$. In eqn (2), we may take, to a first approximation, the first and second terms and ignore the higher order terms:

$$V(r_m+\Delta r)=V(r_m)+\left(\frac{\partial V}{\partial r}\right)_{r_m}(\Delta r). \quad (3)$$

Here, we note the useful relationships derived by Politzer[16,17] who has studied in detail the electrostatic potential-electronic density relationships in an atom:

$$\left(\frac{\partial V}{\partial r}\right)_{r_m}=-\frac{2V(r_m)}{r_m}, \quad (4)$$

and

$$V(r_m)=\int_{r_m}^{\infty}\frac{\rho(\mathbf{r}')}{|\mathbf{r}_m-\mathbf{r}'|}\,d\mathbf{r}'=\frac{N_m e}{2r_m}, \quad (5)$$

where $\rho(\mathbf{r}')$ is the electron density, $e$ is the electronic charge, and $N_m$ is the electron number which is located beyond the radial distance $r_m$ from the nucleus. substituting eqns (4) and (5) into eqn (3), we have

$$V(r_m+\Delta r)=\frac{N_m e}{2r_m}\left[1-\frac{2(\Delta r)}{r_m}\right], \quad (6)$$

this being the approximate electrostatic potential produced near the outermost minimum by the nucleus and the electrons $N_m$. Since the electronegativity depends upon the outermost electronic configuration of an atom, substantially valence electrons, there is no doubt that this potential is a good measure of the electronegativity in an atom.

We now define conveniently the electronegativity $\chi$ from eqn (6) as

$$\chi=\int\frac{r_m}{e}V(r_m+\Delta r)\,dr=\int_{-\Delta r_m}^{\Delta r_m}\frac{N_m}{2}\left[1-\frac{2(\Delta r)}{r_m}\right]dr, \quad (7)$$

and, to reproduce the Pauling electronegativity scale $\chi_P$, we take the following integration range:

$$\Delta r_m=\frac{N_m+1}{2N_m}. \quad (8)$$

The integration result is that

$$\chi_P=\int\frac{r_m}{e}V(r_m+\Delta r)\,dr=\frac{N_m+1}{2}. \quad (9)$$

Since $r_m$ and $N_m$ in eqn (9) may be replaced by the core radius $r_c$ and the valence electron number $N_v$,[15,17] eqn (9) becomes

$$\chi_P=\int\frac{r_c}{e}V(r_c+\Delta r)\,dr=\frac{N_v+1}{2}, \quad (10)$$

which means that the Pauling electronegativity scale can be expressed with the valence electron number of the valence electronic charge.

Now, we can easily verify that eqn (10) completely reproduces the Pauling electronegativity values for atoms (Li, Be, B, C, N, O, F) in the first period in the periodic table. However, for atoms belonging to the other periods, eqn (10) should be modified slightly taking into account the periodicity. Such a modification may be accomplished by slightly varying the integration range of eqn (8). Introducing a correction factor $f(n)$ into eqn (8),

$$\Delta r_m=\frac{(N_m+1)}{2N_m}f(n), \quad (8a)$$

and then integrating similarly eqn (7), we have

$$\chi_P=\int\frac{r_c}{e}V(r_c+\Delta r)\,dr=\frac{(N_v+1)}{2}f(n). \quad (11)$$

This is the desired result which we were looking for. Here, $f(n)$ may be assumed empirically as

$$f(n)=\left[1-\frac{2}{9}(n-1)^{1/2}\right];\ n\geq 1, \quad (12)$$

$n$ being the periodic number. Derivation of eqn (12) has not yet been made theoretically and remains as a problem to be solved in the future.

It can easily be confirmed by numerical calculations that eqn (11) combined with eqn (12) reproduces well the Pauling electronegativity scales for most atoms except for the hydrogen atom as shown in Table 1. It may therefore be concluded that the electrostatic potential near the physical meaningful boundary between the core and valence regions in an atom is closely related to the Pauling electronegativity scale.

Table 1. Calculated Pauling electronegativities.[a,b] (a) Calculated values in parentheses. (b) Electronegativity values for noble gas elements were taken from L. C. Allen and J. E. Huheey, *J. Inorg. Nucl. Chem.* 1980, **42**, 1523

| | | | | | | | |
|---|---|---|---|---|---|---|---|
| H 2.1 | | | | | | | He 5.2 |
| Li 1.0 (1.0) | Be 1.5 (1.5) | B 2.0 (2.0) | C 2.5 (2.5) | N 3.0 (3.0) | O 3.5 (3.5) | F 4.0 (4.0) | Ne 4.5 (4.5) |
| Na 0.9 (0.8) | Mg 1.2 (1.2) | Aℓ 1.5 (1.6) | Si 1.8 (1.9) | P 2.1 (2.3) | S 2.5 (2.7) | Cℓ 3.0 (3.1) | Ar 3.2 (3.5) |
| K 0.8 (0.7) | Ca 1.0 (1.0) | Sc 1.3 (1.4) | Ge 1.8 (1.7) | As 2.0 (2.1) | Se 2.4 (2.4) | Br 2.8 (2.7) | Kr 2.9 (3.0) |
| Rb 0.8 (0.6) | Sr 1.0 (0.9) | Y 1.2 (1.2) | Sn 1.8 (1.5) | Sb 1.9 (1.8) | Te 2.1 (2.2) | I 2.5 (2.5) | Xe 2.4 (2.8) |
| Cs 0.7 (0.6) | Ba 0.9 (0.8) | La-Lu 1.1-1.2 (1.1) | Pb 1.8 (1.4) | Bi 1.9 (1.7) | Po 2.0 (1.9) | At 2.2 (2.2) | Rn 2.1 (2.5) |
| Fr 0.7 (0.5) | Ra 0.9 (0.8) | Ac 1.1 (1.0) | | | | | |

## CORRELATION BETWEEN PAULING AND MULLIKEN ELECTRONEGATIVITIES

The purpose of this section is to discuss briefly the relation between the Pauling and Mulliken and other electronegativity scales. As is well known, the Mulliken scale $\chi_M$[12] is based on both the ionization potential ($IP$) and electron affinity ($EA$) of a neutral atom, and is defined by the arithmetic mean of them, i.e.

$$\chi_M = \frac{IP + EA}{2}. \tag{13}$$

As Coulson[18] argued, there is no doubt that the scale has, in its simplicity, a precise experimental and theoretical foundation. Recently, Parr *et al.*[2] have shown that the Mulliken electronegativity is immediately connected with the chemical potential in the density functional theory through the following relation,

$$\chi_M = \frac{IP + EA}{2}$$

$$= -\mu + \frac{\delta^2 F(\Delta\rho_-) - \delta^2 F(\Delta\rho_+)}{2} + \ldots, \tag{14}$$

where $\mu$ is of course the chemical potential and $\delta^2 F$ is given by

$$\delta^2 F(\Delta\rho) = \frac{1}{2}\int\int \frac{\delta^2 F}{\delta\rho(1)\delta\rho(2)} \Delta\rho(1)\Delta\rho(2)\, d\tau_1\, d\tau_2. \tag{15}$$

Here, $F$ is the universal functional of the density $\rho$. Therefore, we can say that the Mulliken scale which has a precise theoretical basis is a good measure for the atomic electronegativity.

By the way, we are able to find from comparisons of the Pauling and Mulliken scales that there is a simple relationship as given by the formula,

$$\chi_M = \alpha\chi_P = \frac{\alpha(N_v + 1)}{2} f(n), \tag{16}$$

where $\alpha$ is the proportionality constant as is approximately given by 2.47 eV. The property of the constant $\alpha$ is not so simple and will be discussed in the next section. By the use of eqn (16), we can easily calculate the Mulliken values from those of Pauling. The results are listed in Table 2, in which the calculated values from eqn (16) agree well with those from eqn (13).

Table 2 also includes new atomic electronegativity scales $\chi_{BGP}$ by Bartolotti, Gadre and Parr,[4] who have calculated systematically those by a known density functional technique, namely the spin non-polarized $X\alpha$ transition-state method. The key formula used by them is that

$$\left(\frac{\partial E}{\partial n_i}\right)_{n_j} = \epsilon_i, \tag{17}$$

where $E$ is the ground state energy functional of the density $\rho$, $n_i$ is the occupation number in the $i$th orbital and $\epsilon_i$ is the $i$th orbital energy. From equation (17), the $\chi_{BGP}$ is defined for two cases:

$$\chi_{BGP} = -\epsilon_i^t \text{ (Case A, one orbital involved)}, \tag{18}$$

and

$$\chi_{BGP} = -\frac{1}{2}(\epsilon_i^t + \epsilon_j^t) \text{ (Case B, two orbitals involved)}. \tag{19}$$

The superscript $t$ denotes the transition state, which may or may not be the same as the ground state. As seen from Table 2, the values of $\chi_{BGP}$[4] are very similar to those of $\chi_M$. This suggests that the transition-state method as described above may correctly reproduce the Mulliken electronegativity scale.

From the foregoing discussions, we have ultimately

$$\chi_M = \chi_{BGP} = \alpha\chi_P = \frac{\alpha(N_v + 1)}{2} f(n), \tag{20}$$

which is the approximate relationship connecting mutually three electronegativity scales, $\chi_M$, $\chi_{BGP}$ and $\chi_P$ in question.

Table 2. Comparisons of electronegativity scales, $\chi_M$[a], Calc. $\chi_M$[b] and $\chi_{BGP}$[c] (in units of eV)

| Atom | Electronegativity scale $\chi_M$ | Calc. $\chi_M$ | $\chi_{BGP}$ |
|---|---|---|---|
| Li | 3.00 | 2.47 | 2.58 |
| Be | — | 3.71 | 3.80 |
| B | 4.29 | 4.94 | 3.40 |
| C | 6.26 | 6.18 | 5.13 |
| N | 7.23 | 7.41 | 6.97 |
| O | 7.54 | 8.65 | 8.92 |
| F | 10.42 | 9.88 | 11.00 |
| Na | 2.84 | 1.93 | 2.32 |
| Mg | — | 2.89 | 3.04 |
| Al | 3.22 | 3.85 | 2.25 |
| Si | 4.78 | 4.79 | 3.60 |
| P | 5.61 | 5.76 | 5.01 |
| S | 6.22 | 6.72 | 6.52 |
| Cl | 8.33 | 7.68 | 8.11 |

a: Mulliken electronegativity scale calculated from equation (13).

b: Calculated from the Pauling electronegativity scale using equation (16).

c: Bartolotti-Gadre-Parr electronegativity scale in reference (4).

## ELECTRONEGATIVITY FROM DENSITY FUNCTIONAL THEORY

There is no doubt that the density functional theory is currently one of the most powerful tools in elucidating theoretically the physical and chemical phenomena. In this section, we note the chemical potential whose determination is one of the main subjects in the development of the density functional theory, and try to relate it to the Pauling electronegativity.

According to the density functional theory of Hohenberg and Kohn,[11] the ground state energy of a many electron system is a functional of the electron density $\rho$,

$$E = E[\rho]. \tag{21}$$

It is here appropriate to express $E[\rho]$ with the sum of six traditional energy functionals,[13,19,20]

$$E[\rho] = T_\theta[\rho] + E_{ne}[\rho] + E_{ee}[\rho] + E_{ex}[\rho] + E_c[\rho] + T_w[\rho], \tag{22}$$

where $T_\theta$ denotes the Thomas–Fermi kinetic energy of the electrons, $E_{ne}$ the attractive (Coulomb) interaction energy between the nucleus and electrons, $E_{ee}$ the repulsive (Coulomb) energy among the electrons, $E_{ex}$ the so-called exchange energy, $E_c$ the correlation energy and $T_w$ the lowest order gradient correction, in other words, the Weizsacker correction.[21]

The kinetic energy is approximately given by the sum of the Thomas–Fermi term[22] and the modified Weizacker correction[21] as follows (atomic units are used throughout this work),

$$T_\theta[\rho] + T_w[\rho] = \frac{3(3\pi^2)^{2/3}}{10}\int \rho^{5/3}\,\mathrm{d}\mathbf{r} + \frac{1}{72}\int \frac{(\nabla\rho)^2}{\rho}\,\mathrm{d}\mathbf{r}. \tag{23}$$

In Weizsacker's work[21] the coefficient 1/72 was given as 1/8. The electron–nucleus and electron–electron interaction energies are also

given by

$$E_{ne}[\rho]+E_{ee}[\rho]=\int\left(V_n+\frac{1}{2}V_e\right)\rho\,\mathrm{d}\mathbf{r}, \quad (24)$$

$V_n$ and $V_e$ being the nuclear potential and the Coulombic potential due to the electrons. The exchange energy is of the form

$$E_{ex}[\rho]=\frac{3}{4}(3/\pi)_{1/3}\int\rho^{4/3}\,\mathrm{d}\mathbf{r}, \quad (25)$$

which was first introduced by Dirac.[23] The last correlation energy may be represented by some formula such as the Wigner's low density expression.[24]

The chemical potential $\mu$ in question is derived as the Euler equation by variation of $E$ (eqn 22) with respect to the electron density $\rho(\mathbf{r})$ as follows:

$$\mu=\frac{\delta E[\rho]}{\delta\rho(\mathbf{r})}=\frac{1}{2}(3\pi^2)^{2/3}\rho^{2/3}+\frac{1}{72}\left(\frac{\nabla\rho}{\rho}\right)^2-\frac{1}{36}\left(\frac{\nabla^2\rho}{\rho}\right)$$
$$+(V_nV_e)+(3/\pi)^{1/3}\rho^{1/3}+\frac{\delta E_c}{\delta\rho}. \quad (26)$$

For the ground state of the neutral atom, the chemical potential $\mu$ is a constant independent of the distance $\mathbf{r}$ from the nucleus. Then we can evaluate $\mu$ in the asymptotic region of the atom, i.e. at large $\mathbf{r}$. As has been pointed out by Alonso and Girifalco,[10] the only terms which give a contribution to $\mu$ different from zero at the boundary of the free atom are the gradient terms in eqn (26). All the other terms vanish for the limit $\mathbf{r}\to\infty$, i.e. $\rho\to 0$.

If we here recall an excellent proposition of Parr

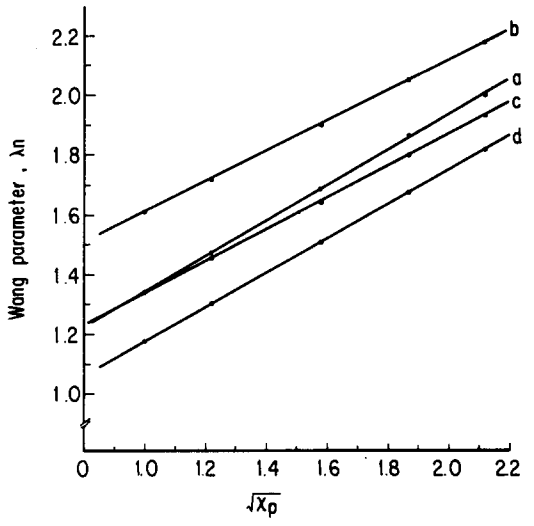



Fig. 1. Wang parameter $\lambda_n$ vs root of Pauling electronegativity scale. Curves, *a*, *b*, *c*, *d*: data taken from Tables II, IV, VI, VIII in Ref. 29.

*et al.*[2] that the electronegativity is equal to the negative of the chemical potential, the theoretical electronegativity can be related to the asymptotic behaviour of the electron density which has been investigated in detail by several authors.[13,25–28] Let us focus our attention particularly on the work of Wang and Parr[13] and hereafter discuss the correlation between the Wang–Parr and the Pauling electronegativities.

Wang and Parr[13] have shown that the shell structure of an atom can be introduced to the energy-density functional formalism by constraining the atomic electron density to be piecewise exponentially decaying, and have proposed the atomic electron density of the following form;

$$\rho(r)=\begin{cases}A_1\exp(-2\lambda_1 r), & 0\le r\le R_1\ (K\text{ shell}),\\ A_2\exp(-2\lambda_2 r), & R_1\le r\le R_2\ (L\text{ shell}),\\ A_3\exp(-2\lambda_3 r), & R_2\le r\le R_3\ (M\text{ shell}),\\ \cdots\cdots\cdots\cdots\cdots\end{cases} \quad (27)$$

with $0<R_1<R_2<R_3$, etc. and $\lambda_1\le\lambda_2\le\lambda_3=$ etc. It is assumed that $\rho$ is continuous but $\mathrm{d}\rho/\mathrm{d}r$ not necessarily so. Wang and Parr[13] have tried to determine the parameters: $A_1, A_2, \ldots; \lambda_1, \lambda_2, \ldots; r_1, r_2, \ldots$; by minimization of the approximate energy functional similar to eqns (22)–(25). Recently, Wang[29] has recalculated the parameters described above and determined their exact values. In this work, we note such parameters[29] and shall proceed with the discussion of electronegativities.

In evaluating the electronegativity, we may take only the electron density of the outermost electronic shell as that in the asymptotic region. Then, from eqns (26) and (27), we have, at the boundary of the atom,

$$\chi_{WP}=\frac{1}{72}(2\lambda_n)^2, \quad (28)$$

this being none other than the Wang–Parr atomic electronegativity.

At this stage, we intend to investigate the correlation of the Pauling scale with the parameter $\lambda_n$ in the electron density of the outermost electronic shell. Plotting the Wang $\lambda_n$[29] vs the root of the Pauling scale $\sqrt{\chi_P}$ as shown in Fig. 1, we find that there is an excellent linearlity between them. Therefore, we can replace the Wang $\lambda_n$ with the Pauling $\sqrt{\chi_P}$ by the relationship:

$$\lambda_n=C\sqrt{\chi_P}+D, \quad (29)$$

or recalling eqn (11),

$$\lambda_n=C\sqrt{\frac{(N_v+1)}{2}f(n)}+D, \quad (30)$$

where $C$ and $D$ are the correlation constants. Equations (29) or (30) is an important result because such a relationship plays the role connecting the Pauling electronegativity with that from the density functional theory. Some numerical tests of eqn (29) for the first-row atoms in the periodic table are given in Tables 3 and 4. The constants in eqn (29) are determined using the Wang $\lambda_n$ by minimizing the average percentage error. As seen from these tables, the agreement

Table 3. Wang parameter $\lambda_n$ calculated from the Pauling electronegativity scale

| Atom | $\lambda_2^a$ | Calc. $\lambda_2^b$ | Error (%) |
|---|---|---|---|
| Li | 1.341 | 1.343 | -0.149 |
| Be | 1.476 | 1.476 | 0 |
| C | 1.689 | 1.686 | 0.178 |
| O | 1.859 | 1.858 | 0.054 |
| Ne | 2.003 | 2.006 | -0.150 |

a: Parameter of piecewise exponentially decaying electron density; data taken from Table II in reference (29).

b: Calculated from equation (29); C = 0.591018, D = 0.751844.

Table 4. Wang parameter $\lambda_n$ calculated from the Pauling electronegativity scale

| Atom | $\lambda_2^a$ | Calc. $\lambda_2^b$ | Error (%) |
|---|---|---|---|
| Li | 1.609 | 1.606 | 0.186 |
| Be | 1.719 | 1.721 | -0.116 |
| C | 1.901 | 1.903 | -0.105 |
| O | 2.052 | 2.052 | 0 |
| Ne | 2.181 | 2.180 | 0.046 |

a: Parameter of piecewise exponentially decaying electron density; data taken from Table IV in reference (29).

b: Calculated from equation (29); C = 0.511401, D = 1.094815.

Table 5. Wang–Parr electronegativity $\chi_{WP}$ calculated from the Pauling electronegativity scale (in units of eV)

| Atom | $\lambda_2$ | $\chi_{WP}^a$ | Calc. $\lambda_2$ | Calc. $\chi_{WP}^b$ | Error (%) |
|---|---|---|---|---|---|
| Li | 1.341 | 2.72 | 1.343 | 2.73 | -0.368 |
| Be | 1.476 | 3.29 | 1.476 | 3.29 | 0 |
| C | 1.689 | 4.31 | 1.686 | 4.30 | 0.232 |
| O | 1.859 | 5.22 | 1.858 | 5.22 | 0 |
| Ne | 2.003 | 6.07 | 2.006 | 6.08 | -0.165 |

a: Calculated from equation (28) using $\lambda_2$ taken from Table II in reference (29).

b: Calculated from equation (31).

Table 6. Wang–Parr electronegativity $\chi_{WP}$ calculated from the Pauling electronegativity scale (in units of eV)

| Atom | $\lambda_2$ | $\chi^a_{WP}$ | Calc. $\lambda_2$ | Calc. $\chi^b_{WP}$ | Error (%) |
|---|---|---|---|---|---|
| Li | 1.609 | 3.91 | 1.606 | 3.90 | 0.256 |
| Be | 1.719 | 4.47 | 1.721 | 4.48 | -0.224 |
| C | 1.901 | 5.46 | 1.903 | 5.48 | -0.366 |
| O | 2.052 | 6.37 | 2.052 | 6.36 | 0.157 |
| Ne | 2.181 | 7.19 | 2.180 | 7.18 | 0.139 |

a: Calculated from equation (28) using $\lambda_2$ taken from Table IV in reference (29).

b: Calculated from equation (31).

between the Wang $\lambda_n$ and the calculated $\lambda_n$ are very good and the percentage error is within only about 0.2%.

Combining eqn (28) with eqns (29) or (30), we obtain finally the relationship between the Wang–Parr and the Pauling electronegativities:

$$\chi_{WP} = \frac{1}{18}(C\sqrt{\chi_P} + D)^2$$

$$= \frac{1}{18}\left[C\sqrt{\frac{(N_v+1)}{2}f(n)} + D\right]^2. \quad (31)$$

Some examples of the numerical calculations are listed in Tables 5 and 6, in which the $\chi_{WP}$ values are obtained from the Wang $\lambda_n$ using eqn (28) and the calculated $\chi_{WP}$ values are from the Pauling scales $\chi_P$ using eqn (31). Again, the agreement between the $\chi_{WP}$ and the Calc. $\chi_{WP}$ are satisfactory.

We further develop eqn (31) into

$$\chi_{WP} = \frac{1}{18}(C^2\chi_P + 2CD\sqrt{\chi_P} + D^2), \quad (32)$$

and, to a drastic approximation, we may write as

$$\chi_{WP} \approx \alpha\chi_P, \quad (33)$$

where $\alpha$ is the proportionality constant. It should be noted that the form of eqn (33) just corresponds to eqn (20) in the preceding section.

## REFERENCES


1. L. Pauling, *The Nature of the Chemical Bond.* Cornell University Press, Ithaca, New York (1960).
2. R. G. Parr, R. A. Donnelly, M. Levy and W. E. Palke, *J. Chem. Phys.* 1978, **68**, 3801.
3. N. K. Ray, L. Samuels and R. G. Parr, *J. Chem. Phys.* 1979, **70**, 3680.
4. L. J. Bartolotti, S. R. Gadre and R. G. Parr, *J. Am. Chem. Soc.* 1980, **102**, 2945.
5. J. Chelikowsky and J. C. Phillips, *Phys. Rev.* 1978, **B17**, 2453.
6. R. E. Watson and L. H. Bennett, *J. Phys. Chem. Solids* 1978, **39**, 1235.
7. R. E. Watson and L. H. Bennett, *Phys. Rev.* 1978, **B18**, 6439.
8. J. A. Alonso and L. A. Girifalco, *Phys. Rev.* 1979, **B19**, 3889.
9. N. H. March, *J. Chem. Phys.* 1979, **71**, 1004.
10. J. A. Alonso and L. A. Girifalco, *J. Chem. Phys.* 1980, **73**, 1313.
11. P. Hohenberg and W. Kohn, *Phys. Rev.* 1964, **B136**, 864.
12. R. S. Mulliken, *J. Chem. Phys.* 1934, **2**, 782; 1935, **3**, 573.
13. W.-P. Wang and R. G. Parr, *Phys. Rev.* 1977, **A16**, 891.
14. K. Ohwada, *Polyhedron* 1983, **2**, 423.
15. P. Politzer, *J. Chem. Phys.* 1980, **72**, 3027.
16. P. Politzer, *J. Chem. Phys.* 1980, **73**, 3264.
17. C. A. Coulson, *Valence.* Oxford University Press, London (1952).
18. N. H. March, *Adv. Phys.* 1957, **6**, 1.
19. E. H. Lieb, *Rev. Mod. Phys.* 1981, **53**, 603.
20. C. F. von Weizsacker, *Z. Phys.* 1935, **96**, 431.
21. L. H. Thomas, *Proc. Camb. Phil. Soc.* 1927, **23**, 542; E. Fermi, *Z. Phys.* 1928, **48**, 73.
22. P. A. M. Dirac. *Proc. Roy. Soc. Lond.* 1926, **A112**, 661.
23. E. P. Wigner, *Trans. Faraday Soc.* 1938, **34**, 678.
24. N. C. Handy, M. T. Marron and H. J. Silverstone, *Phys. Rev.* 1969, **180**, 45.
25. M. M. Morrell, R. G. Parr and M. Levy, *J. Chem. Phys.* 1975, **62**, 549.
26. M. Hoffman-Ostenhof and T. Hoffmann-Ostenhof, *Phys. Rev.* 1977, **A16**, 1782.
27. Y. Tal. *Phys. Rev.* 1978, **A18**, 1781.
28. W. P. Wang, *Phys. Rev.* 1982, **A25**, 2901.

Polyhedron Vol. 3, No. 7, pp. 861–866, 1984
Printed in the U.S.A.

0277-5387/84 $3.00 + .00
© 1984 Pergamon Press Ltd.

# CYCLIC VOLTAMMETRIC STUDIES OF COPPER(II) DIPEPTIDE COMPLEXES. EVIDENCE FOR COPPER(I) DIPEPTIDE COMPLEXES IN AQUEOUS MEDIA

**GEORGE THOMAS and P. S. ZACHARIAS***
School of Chemistry, University of Hyderabad, Hyderabad 500134, India

(*Received* 14 *October* 1983; *accepted* 6 *December* 1983)

**Abstract**—The reduction of the title complexes was studied by cyclic voltammetry in aqueous media. It proceeds through a one-electron process generating intermediate copper(I) dipeptide complexes. The copper(I) dipeptide complexes are found to be short-lived and undergo transformations eventually generating $Cu^0$ at the mercury electrode. The unchanged fraction of the copper(I) species is re-oxidised to the copper(II) complexes. The $Cu^0$ generated undergoes a two-electron oxidation at a more anodic potential than the copper(I) complexes. pH-dependence of the title complexes is also investigated by cyclic voltammetry.

During the last two decades intensive investigations have been carried out on the copper(II) di- and oligo-peptide complexes to elucidate and interpret their thermodynamic and structural characteristics.[1–3] Dipeptides coordinate to copper(II) at physiological pH values using deprotonated peptide nitrogen, amino nitrogen, and the carboxyl oxygen.[4–6] Copper(I) complexes involving deprotonated-peptide-nitrogen coordination are of much current interest.[7–10] Very recently Margerum *et al.*[11] observed copper(I) diglycine complex with dmp (2,9-dimethyl-1,10-phenanthroline). However, no copper(I) species could be detected during cyclic voltammetric studies of the reduction of copper(II) triglycine complexes.[11] Our studies on the reduction of copper(II) amino acid complexes by cyclic voltammetry[12] showed the generation of copper(I) complexes as an intermediate in aqueous media. Encouraged by this result we extended our studies to copper(II) dipeptide complexes and our results are presented and discussed in the following sections.

## EXPERIMENTAL

### *Chemicals*

Copper(II) dipeptide complexes were prepared from basic copper carbonate and the corresponding dipeptides. Basic copper carbonate was used after estimating the copper content gravimetrically.[13] The dipeptides, glycylglycine (Gly Gly), glycyl-L-serine (Gly Ser), glycyl-L-isoleucine (Gly Ile), glycyl-L-phenylalanine (Gly Phe), glycyl-L-tryptophan (Gly Trp), glycyl-L-tyrosine (Gly Tyr), glycyl-L-threonine (Gly Thr), etc. were obtained from Sigma Chemicals Co. Analar grade sodium perchlorate was used throughout the work. Mercury was purified and distilled twice. Doubly distilled water was used always.

The copper(II) dipeptide complexes were prepared by employing the method reported earlier.[6d] Stoichiometric amounts of the dipeptide and basic copper carbonate were mixed in water and stirred for about 1–2 hr at about 50–60°C and the resultant bluish–violet solution was filtered to remove unreacted copper carbonate and concentrated. The pH of the solution was 6.8–7.2. The bluish–violet crystals were separated by filtration, washed with water and dried at 100–110°C in vacuum.

Copper(I) bathocuproin complex was prepared by adding a solution of bathocuproin reagent in amyl alcohol, to an aqueous solution of copper(I) ions (obtained by reducing $Cu(NO_3)_2$ with sodium metabisulphite). The resulting yellow organic layer was separated, washed several times with water to remove bisulphite ions. This solution was used to record CV after adding TEAP (tetraethyl ammonium perchlorate) in acetone to it. The electro-

*Author to whom correspondence should be addressed.

lytically generated copper(I) ions were complexed with bathocuproin reagent as described below. A few $cm^3$ of the bathocuproin reagent solution in amyl alcohol was added to the aqueous solution of the copper complex in the electrolytic cell and stirred well to mix the two immiscible layers intimately. This was then subjected to controlled potential electrolysis at $-0.5$ V over mercury pool electrode with stirring. After the completion of the electrolysis a deep yellow organic layer was separated from the aqueous layer and was used for recording the electronic spectra and cyclic voltammograms.

Cyclic voltammetric experiments were carried out in a three-electrode cell with a metrohm E 410 hanging mecury drop electrode (HMDE) as working electrode and a platinum-wire auxiliary electrode. All the potentials reported here are referred to saturated calomel electrode (SCE) and are uncorrected for liquid-junction potentials. Cyclic voltammograms (CV) were recorded using PAR 175 universal programmer, PAR 174 A polarographic analyzer, and a PAR RE0074 XY recorder. Controlled potential coulometry was carried out using PAR179 digital coulometer over mercury pool electrode. Electronic spectra were recorded on a Shimadzu 2000S spectrometer and ESR on a JEOL-FE 3X spectrometer.

## RESULTS AND DISCUSSION

A series of copper(II) dipeptide complexes of the general formula, Cu(II)L, ($H_2L = H_3N^+$–CHR–CO–NH–CHR′–$COO^-$; R,R′ = alkyl or H) were isolated from aqueous solutions at pH about 7. The identity of the complexes was established by elemental analysis and spectral methods. Cyclic voltammograms were recorded in the potential range $+0.1$ to $-0.6$ V in aqueous solution (*ca.* $1 \times 10^{-3}$M) with $NaClO_4$ as supporting electrolyte at the dissolution pH (pH is not adjusted after dissolving the samples in water) of about 7.0. All complexes show reasonably similar cyclic voltammetric behaviour. Sample cyclic voltammograms of Cu(II) Gly Ser and Cu(II) Gly Gly are shown in Fig. 1. The relevant CV data for all complexes are collected in Table 1. There are no peaks in the positive potential range for any of the copper(II) complexes. None of the dipeptides in the absence of metal ions shows any peak in the potential range $+1.0$ to $-1.0$ V.

The general features of the cyclic voltammograms are summarised below and they constitute the basis for the discussion.

(i) Only the cathodic peak C at about $-0.3$ V is observed in the first cathodic scan.

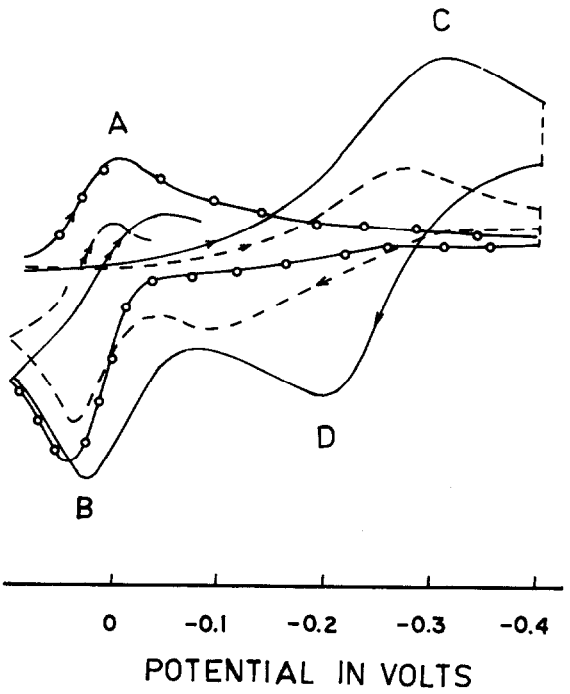



Fig. 1. Cyclic voltammograms of Cu(II) Gly Ser (——); Cu(II) Gly Gly (---); and free $Cu^{2+}$ ions (–O–O–) in aqueous media.

(ii) During the reverse scan an anodic peak D at about $-0.18$ V appears along with another anodic peak B at about $+0.03$ V.

(iii) A new cathodic peak A at about $-0.03$ V is apparent from second scan onwards.

(iv) A substantial decrease in the current function values of A and B is observed with an increase in the scan rate.

(v) Holding the potential at a point well past the peak C for a few minutes and on scanning back, the peak heights of A and B increase considerably while that of C and D remain unaffected. Similar effects are also observed on multiscans in the full potential range ($+0.1$ to $-0.6$ V).

(vi) If the potential scan is reversed after the peak A in the second and subsequent scans, the heights of A and B decrease.

(vii) Peaks A and B do not appear if the potential scan is reversed before the appearance of the peak C, in the first scan itself.

It is known that in diglycine and many other dipeptide copper(II) complexes, the dipeptide is tridentate and coppper(II) ion is five coordinate with water molecules occupying two coordination sites. It is well documented that the copper(II) dipeptide complexes retain their structure on dissolution in water at neutral pH conditions.[6b,14] Hence the CV recorded in aqueous solutions at pH about 7 corresponds solely to the species of composition Cu(II)L. Then the peak C can arise due to

Table 1. Cyclic voltammetric data[a] on copper(II) dipeptide complexes

| Compound | Sweep rate $Vs^{-1}$ | $E_p$,A[b] | $E_p$,B | $E_p$,C | $E_p$,D | $\Delta E_p$ C,D | $\bar{E}_p$ C,D |
|---|---|---|---|---|---|---|---|
| Cu Gly Ser | 0.02 | -0.050 | +0.020 | -0.310 | -0.195 | 0.115 | -0.253 |
| (pH=7.53; | 0.04 | -0.055 | +0.020 | -0.320 | -0.190 | 0.130 | -0.255 |
| 1.02 mM) | 0.10 | -0.055 | +0.020 | -0.320 | -0.185 | 0.135 | -0.253 |
| Cu Gly Gly | 0.02 | -0.005 | +0.045 | -0.335 | -0.130 | 0.205 | -0.233 |
| (pH=7.38; | 0.04 | -0.005 | +0.050 | -0.345 | -0.120 | 0.225 | -0.233 |
| 1.11 mM) | 0.10 | 0.000 | +0.050 | -0.350 | -0.110 | 0.280 | -0.230 |
| Cu Gly Phe | 0.02 | -0.005 | +0.045 | -0.325 | -0.110 | 0.215 | -0.217 |
| (pH=6.67; | 0.04 | -0.005 | +0.040 | -0.330 | -0.110 | 0.230 | -0.215 |
| 1.22 mM) | 0.10 | 0.000 | +0.040 | -0.340 | -0.090 | 0.250 | -0.215 |
| Cu Gly Ile | 0.02 | -0.010 | +0.040 | -0.305 | -0.100 | 0.205 | -0.200 |
| (pH=6.86; | 0.04 | -0.005 | +0.050 | -0.310 | -0.070 | 0.240 | -0.190 |
| 1.08 mM) | 0.10 | c | c | -0.335 | -0.050 | 0.285 | -0.193 |
| Cu Gly Trp | 0.02 | -0.010 | +0.040 | -0.340 | c | - | - |
| (pH=7.32; | 0.04 | -0.005 | +0.050 | -0.350 | c | - | - |
| 1.02 mM) | 0.10 | c | c | -0.365 | c | - | - |
| Cu Gly Tyr | 0.02 | -0.005 | +0.045 | -0.315 | -0.115 | 0.195 | -0.215 |
| (pH=7.39; | 0.04 | 0.000 | +0.050 | -0.325 | -0.075 | 0.215 | -0.217 |
| 1.15 mM) | 0.10 | c | c | -0.325 | -0.070 | 0.250 | -0.203 |
| Cu Gly Thr | 0.02 | -0.005 | +0.040 | -0.370 | -0.100 | 0.270 | -0.235 |
| (pH=7.22; | 0.04 | 0.000 | +0.050 | -0.360 | -0.100 | 0.260 | -0.230 |
| 1.25 mM) | 0.10 | c | c | -0.355 | -0.070 | 0.285 | -0.215 |

[a] All potentials are in volts.

[b] Peak appears only in the second and subsequent scans.

[c] Broad peak, difficult to measure precisely.

either a one-electron process ($Cu(II) \xrightarrow{1e} Cu(I)$) or a two-electron process ($Cu(II) \xrightarrow{2e} Cu(O)$) of the Cu(II)L species. If peak C originates due to the latter process, then the appearance of the anodic peak D (~200 mV anodic to C) is difficult to explain. But if the peak C is due to the one-electron reduction process, D can result from the re-oxidation of the [Cu(I)L] species. [Cu(I)L] complex, being an unstable species,[11] undergoes decomposition and/or disproportionation generating Cu(O) in aqueous media. Then peak B results from a two-electron oxidation of the Cu to $Cu^{2+}$ ions and peak A will correspond to the reduction of the electrogenerated $Cu^{2+}$ ions. Cyclic voltammograms of the free copper(II) ions in aqueous media under identical experimental conditions show peaks similar to A and B at comparable potentials and is shown in Fig. 1 for comparison. The absence of peak A in the first scan shows the absence of free copper(II) ions in the solution to start with. The

overall electrode processes can be represented by eqns (1)–(3).

$$Cu(II)L \overset{1e}{\rightleftharpoons} [Cu(I)L] \quad (1)$$

$$[Cu(I)L] \xrightarrow[\text{reactions}]{\text{Chemical}} Cu(O)(Hg) + L^{2-} \quad (2)$$

$$Cu(O)(Hg) \overset{2e}{\rightleftharpoons} Cu^{2+}aq. \quad (3)$$

Equation (1) represents the most imoprtant step in the overall processes which generate the copper(I) dipeptide complexes. They are stable only in tetrahedral[15] or pseudo-tetrahedral geometries. The copper(I) complexes generated, can be expected to have a geometry distorted towards tetrahedral since the parent copper(II) complexes possess a distorted square pyramidal geometry.[6] The extent of stability of the copper(I) species depends on the degree of tetragonality. The transient existence of copper(I) complexes, which retain the peptide nitrogen coordination, demonstrated by the CV pattern (presence of Peak D) shows that it has a life-time long enough to be detected by cyclic voltammetry. This is one of the few examples where copper(I) dipeptide complexes are identified electrochemically.

Further proof for the generation of copper(I) species was obtained by trapping the short-lived copper(I) species using bathocuproin which is a highly specific reagent towards $Cu^+$ ions in forming stable complexes.[13,16,17] The electrochemically generated copper(I) bathocuproin complex is identical with chemically generated bathocuproin complex in their spectral and cyclic voltammetric behaviour (both gave an irreversible reduction peak at $-0.595$ V in amyl alcohol/TEAP medium at HMDE). These results prove that the reduction of copper(II) depeptide complexes proceed through a one-electron process generating the copper(I) dipeptide complexes as mentioned in eqn (1). The peak D is observed only at scan rates higher than 100 mV $s^{-1}$ and at about 200 mV anodic to peak C in the case of dipeptide complexes other than Cu(II) Gly Ser indicating the process in eqn (1) to be quasi-reversible. However, the behaviour of Cu(II) Gly Ser is very similar to the reversible behaviour of copper(II) amino acid complexes reported earlier.[12]

It is to be noted that copper(I)peptide nitrogen coordination does not occur readily[7–10] and even if it occurs it undergoes decomposition immediately.[11] Thus the process in eqn (2) may involve the steps 4 and 5.

$$[Cu(I)L] \rightleftharpoons Cu^+ + L^{2-} \quad (4)$$

$$2Cu^+ \rightleftharpoons Cu + Cu^{2+}. \quad (5)$$

Under the cathodic potential prevailing in the experimental conditions the predominant species in eqn (5) will be Cu(O) which is continuously removed as Cu(Hg) at the mercury electrode.[18] Cu(O) thus generated undergoes the process in eqn (3) giving the peaks B and A.

Reaction sequences 1–3 is consistent with an ECE mechanism.[19] A decrease in $i_B/v^{1/2}$ value is observed with an increase in the scan rate (Fig. 2). This shows that at rapid scan rates, Cu(O) generation by the interposed chemical reaction decreases which in turn reduces the $i_B/v^{1/2}$ value. As noted earlier the peaks C and D are not affected by holding the potential at $-0.5$ V whereas peaks B and A increase considerably. Such a situation can arise only when a steady concentration of [Cu(I)L] species is maintained. This happens when the process in eqn (1) is faster than that in (2). On the other hand if the process in eqn (2) is faster than that in (1), the peak D would have decreased on holding the potential or at slow scan rates as observed by earlier workers.[11,20] The comparison of the effect of scan rates on peaks B, C and D shown in Fig. 2 illustrate these facts.

*Protonation*

It has been clearly shown by different methods that in aqueous media copper(II) ions can form complexes with dipeptides with different stoichiometries depending on the pH conditions and the

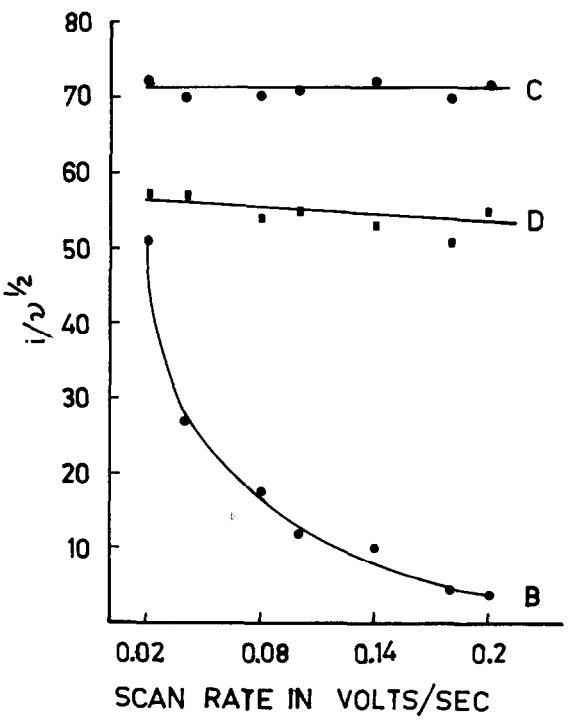



Fig. 2. Effect of scan rates on peaks B, C and D.

metal to ligand ratio.[21] Because of the interesting observations on the copper(II) dipeptide complexes it seemed appropriate to investigate the cyclic voltammetric behaviour of these complexes in various pH conditions. Our emphasis was more on the acid pH ranges (protonation).

The pH of the solution was decreased gradually by the addition of small amounts ($\mu$l) of a protonic acid, $HClO_4$, to the aqueous solution of the copper(II) complexes. All dipeptide complexes behaved in a similar fashion on protonation. Cyclic voltammograms of Cu(II) Gly Ser at various pH conditions are shown in Fig. 3 and the relevant data are collected in Table 2. The major changes on the CV profile occurring on protonation are the following.

(1) Heights of peaks C and D decrease gradually and finally disappear at low pH values.

(2) Peak A begins to appear in the first scan itself as a broad peak.

(3) Peaks A and B increase in heights accompanied by a decrease in "peak-broadening" of A as pH decreases.

(4) Peaks A and B shifts anodically as pH decreases and at very low pH values ($<3.0$) the peaks A and B become very similar to the corresponding peaks of free copper(II) ions.

(5) At intermediate pH values (5.3–4.1) an overlapping cathodic peak A*, close to A, is apparent in Cu(II) Gly Ser.

Observation (1) can result because of the decrease in concentration of Cu(II)L species due to its conversion to other forms on protonation. It is well documented that protonation first occurs at the peptide nitrogen followed by a rearrangement which ultimately results in the formation of the protonated species $[Cu(II)LH]^+$. On further protonation it dissociates to free copper(II) ions. Thus the peaks A and B at low pH region correspond to the reduction and the re-oxidation of the liberated free copper(II) ions. The presence of peak A from the first scan itself shows the availability of free copper(II) ions in solution liberated on protonation. In neutral pH conditions they have to be generated electrochemically and hence peak A appears only from the second scan onwards. $[Cu(II)LH]^+$ can undergo reduction at a potential less cathodic to peak C. The initial "peak-broadening" observed can be due to the overlap of the reduction wave (A) of free copper(II) ions and that (A*) of the $[Cu(II)LH]^+$ when both are at relatively low concentrations. At the intermediate pH region (5.3–4.1) the concentration of $[Cu(II)LH]^+$ increases as the pH goes down which in turn helps the broad peak A, to get resolved into peaks A and A*. A further decrease in pH catalyses the dissociation of $[Cu(II)LH]^+$ to free copper(II) ions, and is reflected in the increased peak heights of A and B. The peak A* is clearly observable only in the case of Cu(II) Gly Ser whereas other dipeptides show only the "peak-broadening". The entire processes of protonation can be reversed by increasing the pH by adding small amounts of NaOH solution. This cycle can be repeated several times showing the reversibility of protonation.

*Controlled potential coulometry*

To distinguish between one or two-electron reduction of the starting complex Cu(II)L, con-

Table 2. Cyclic voltammetric data[a] on protonation of copper(II) Gly Ser at scan rate 0.02 $Vs^{-1}$

| pH | $E_p$,A | $E_p$,B | $E_p$,C | $E_p$,D | $i_p$,A | $i_p$,B | $i_p$,C | $i_p$,D |
|---|---|---|---|---|---|---|---|---|
| 7.10 | -0.060 | 0.010 | -0.315 | -0.205 | 0.0 | 9.5 | 18.5 | 11.0 |
| 6.51 | -0.055 | 0.015 | -0.315 | -0.205 | 3.5 | 12.5 | 16.0 | 10.5 |
| 6.38 | -0.050 | 0.020 | -0.310 | -0.205 | 4.5 | 13.5 | 14.0 | 10.0 |
| 5.32 | -0.040 | 0.025 | -0.310 | -0.200 | 8.0 | 18.0 | 10.0 | 8.0 |
| 4.81 | -0.030 | 0.025 | -0.310 | -0.200 | 11.0 | 23.0 | 9.5 | 6.0 |
| 4.23 | -0.023 | 0.030 | -0.310 | -0.200 | 18.5 | 31.0 | 2.5 | 1.5 |
| 3.77 | -0.020 | 0.035 | b | b | 19.5 | 37.0 | 0.0 | 0.0 |

[a] All potentials are in volts and current in microampers.

[b] Peak absent.

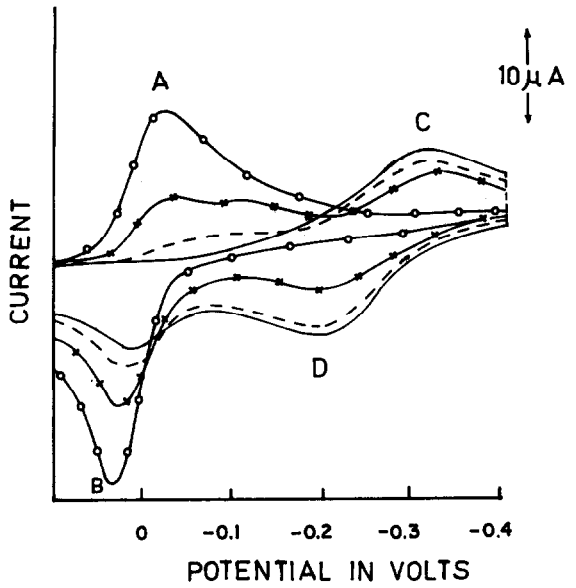



Fig. 3. Cyclic voltammograms of Cu(II) Gly Ser at various pH values. Scan rate, $0.10\,Vs^{-1}$. (——), pH = 7.1; (---), pH = 6.38; (-×-×-), pH = 4.81; (-O-O-), pH = 3.77.

trolled potential coulometry (CPC) was carried out at a potential −0.5 V, well past the peak C over mercury pool electrode. CPC yielded coulombs which corresponded to $n = 2$. This value is contrary to the experimental observations discussed earlier for $n = 1$. This difference can be understood in the following way. Under the continued influence of the cathodic potential the copper(I) species generated by the first electron-transfer undergo further reduction to Cu which immediately forms amalgam with the mercury electrode. Thus the overall processes involve two electrons. The absence of $Cu^{2+}$ ions in the electrolysed solution is confirmed by the disappearance of ESR signals and the absorption band.

## CONCLUSION

The cyclic voltammetric studies on the reduction of copper(II) dipeptide complexes showed clearly the transient existence of copper(I) dipeptide complexes where deprotonated-peptide-nitrogen coordination is intact. The CV pattern corresponds to an ECE reaction path way. The final product of the interposed chemical reactions is identified as Cu. The composition of the peptide complexes are dependent on the pH conditions. The protonation process is found to be reversible.

*Acknowledgements*—Financial assistance for this scheme from Department of Science and Technology, New Delhi, is gratefully acknowledged.

## REFERENCES

1. H. C. Freeman, *The Biochemistry of Copper*, p. 77. Academic Press, New York (1966); H. C. Freeman, *Inorganic Biochemistry* (Edited by G. L. Eichhorn), Chap. 4. Elsevier, New York (1973).
2. D. W. Margerum and G. D. Owens, *Metal Ions in Biological Systems* (Edited by H. Sigel), Vol. 12, Chap. 3. Marcel Dekker, New York (1981) and references therein.
3. A. Kaneda and A. E. Martell, *J. Coord. Chem.* 1975, **4**, 137.
4. A. Gergely and I. Nagypal, *J. Chem. Soc. Dalton Trans.* 1977, 1104.
5. G. Brookes and L. D. Pettit, *J. Chem. Soc. Dalton. Trans.* 1975, 2106.
6. (*a*) B. Strandberg, I. Lindqvist and R. Rosenstein, *Zeit. Krist.* 1961, **116**, 266; (*b*) J. F. Blount, K. A. Fraser, H. C. Freeman, J. T. Szymanski and C. H. Wang, *Acta. Cryst.* 1967, **22**, 396; (*c*) H. C. Freeman and J. T. Szymanski, *Ibid.* 1967, **22**, 406; (*d*) H. C. Freeman, M. J. Healy and M. L. Scudder, *J. Biol. Chem.* 1977, **252**, 8840.
7. T. Kaden and A. Zuberbuhler, *Helv. Chim. Acta* 1966, **49**, 2189.
8. P. A. Temussi and A. Vitagliano, *J. Am. Chem. Soc.* 1975, **97**, 1572.
9. Y. Suguiro, *Eur. J. Biochem.* 1977, **78**, 431.
10. Y. Suguiro, *Inorg. Chem.* 1978, **17**, 2176.
11. M. P. Youngblood and D. W. Margerum, *J. Coord. Chem.* 1981, **11**, 103.
12. George Thomas and P. S. Zacharias, *J. Chem. Soc. (Dalton)*, Communicated.
13. A. I. Vogel, *A Text Book of Quantitative Inorganic Analysis*, 4th Edn. Longmans, London (1978).
14. H. C. Freeman, *Adv. Protein Chem.* 1967, **22**, 235.
15. G. S. Patterson and R. H. Holm, *Bioinorg. Chem.* 1975, **4**, 257.
16. W. H. McCurdy, Jr. and G. F. Smith, *Analyst* 1952, **77**, 846.
17. L. G. Borchardt and J. D. Butler, *Anal. Chem.* 1957, **29**, 415.
18. J. A. Altermatt and S. E. Manahan, *Anal. Chem.* 1968, **40**, 655.
19. R. S. Nicholson and I. Shain, *Anal. Chem.* 1965, **37**, 178; 190.
20. G. N. Coleman, J. W. Gesler, F. A. Shirley and J. R. Kuempel, *Inorg. Chem.* 1973, **12**, 1036.
21. W. S. Kittl and B. M. Rode, *J. Chem. Soc. Dalton Trans.* 1983, 409 and references therein.

*Polyhedron* Vol. 3, No. 7, pp. 867–870, 1984
Printed in the U.S.A.

0277–5387/84 $3.00 + .00
© 1984 Pergamon Press Ltd.

# $^{35}Cl$ NQR IN $N_3P_3Cl_4Ph_2$ AND $N_3P_3Cl_4(NMe_2)_2$

**K. R. SRIDHARAN and J. RAMAKRISHNA***
Department of Physics, Indian Institute of Science, Bangalore 560 012, India

**and**

**K. RAMACHANDRAN and S. S. KRISHNA MURTY**
Department of Inorganic and Physical Chemistry, Indian Institute of Science, Bangalore 560 012, India

(*Received* 24 *October* 1983; *accepted* 12 *December* 1983)

**Abstract**—$^{35}Cl$ NQR has been investigated in two cyclotriphosphazene derivatives $N_3P_3Cl_4Ph_2$ and $N_3P_3Cl_4(NMe_2)_2$. The observed frequencies are assigned to the various chlorines and the temperature variation of the NQR frequencies studied in the range from 77 K to 300 K. The results are analysed using the Bayer–Kushida–Brown approach. Torsional (librational) frequencies are found to fall in the range 10–25 $cm^{-1}$ and are found to be only slightly temperature dependent.

Recently there have been several reports of chlorine nuclear quadrupole resonance studies on cyclophosphazene derivatives which constitute an interesting family of inorganic ring compounds. In this paper, the variable temperature $^{35}Cl$ NQR studies for two cyclophosphazene derivatives, 2,2 - diphenyl - 4,4,6,6 - tetrachlorocyclotriphosphazene, $N_3P_3Cl_4Ph_2$ (Compound **I**) and 2 - *trans*-4 - bis - (dimethylamino) - 2,4,6,6 - tetrachlorocyclotriphosphazene, $N_3P_3Cl_4(NMe_2)_2$ (Compound **II**), in the range from 77 to 300 K are presented. The experiments have been performed using a home-made super-regenerative NQR spectrometer employing lock-in detection. The resonance frequencies and the temperature are accurate to within $\pm 1$ kHz and $\pm 0.5$ K respectively. The compounds were prepared by literature methods.[1]

## NQR FREQUENCIES AND ASSIGNMENT

The chlorine NQR spectrum of $N_3P_3Cl_4Ph_2$ was first reported by Whitehead[2] who observed at 77 K, two broad signals, one at 27.4 MHz and the other at 27.8 MHz. On the other hand, Keat *et al.*[3] observed, again at 77 K, four signals at 27.091, 27.619, 28.079 and 28.248 MHz. There are no reports of NQR measurements at room temperature for this compound.

In the present study, a four-line spectrum has been observed at all temperatures between 77 K and room temperature (~298 K). The signals are all equally intense and the lines are 1.5–2 KHz wide. The frequencies at 77 K and at room temperature are given in Table 1. The observation of four signals shows that there are four inequivalent chlorines in the crystallographic unit cell. The crystal is monoclinic belonging to the space group $P2_{1/n}$ with four molecules in the unit cell.[4] The four molecules are symmetry related and hence the four NQR signals belong to the four chlorines in a molecule. The 4 P–Cl bonds are approximately of the same length, differing within 0.02 Å.

It would be interesting to "assign" the frequencies to the different chlorines in the molecule. On mapping the "co-ordination" around the chlorine atoms in the crystallographic unit cell, it is found that the four chlorines in the molecule have different environments making them inequivalent. The values of the electron density maxima at the four chlorine sites are available from X-ray crystal structure data.[4] Assuming that the core electron orbitals of all the four chlorines are similar, we ascribe the differences in the electron density maxima to the differences in the occupation of the $3p$ valence shells of the chlorines. Cyclophosphazenes are expected to have negligible $\pi$ character[5,6] and we can therefore, assume the electron populations of the $3p_x$ and $3p_y$ orbitals to be 2 for all of the chlorines. Hence, the differences in the electron density maxima at the various chlorine sites may be attributed to differences in the $3p_z$ ($\sigma$ bond) populations. Townes and Dailey[7] have shown that the

*Author to whom correspondence should be addressed.

Table 1. $^{35}Cl$ NQR frequencies of $N_3P_3Cl_4(Ph)_2$

| Line | Frequency (MHz) | |
|---|---|---|
| | 77K | RT+ |
| I | 28.253 | 27.655 |
| II | 28.080 | 27.246 |
| III | 27.619 | 26.994 |
| IV | 27.097 | 26.524 |

+Room temperature ( ~ 298K)

greater the $p_z$ population the lower the NQR frequency. The corresponding assignment of the frequencies is shown in Table 2. The errors in the estimation of electron densities, in the X-ray work, seem to be well within the differences between the sites.

The $^{35}Cl$ NQR spectrum of $N_3P_3Cl_4(NMe_2)_2$, at room temperature, as first reported by Dalgleish *et al.*[8] consisted of two lines in the 26–27 MHz range and two lines in the 23–24 MHz range. At 77 K, they observed only one line in the 26–27 MHz range and two lines near 24 MHz. Recently Connelly *et al.*[9] also reported the $^{35}Cl$ NQR spectrum of this compound. They observed four signals at room temperatures as well as at 77 K. The intensities were reported to be equal. We have observed four room temperature signals at 26.540, 26.250, 23.859 and 23.395 MHz respectively. The lines were not of equal intensity. Line-I (26.540 MHz) was about triple the intensity of each of the other three equally intense lines. Also, the line widths in this compound (3–4 kHz) are clearly broader than those in $N_3P_3Cl_4Ph_2$ (1.5–2 kHz).

The higher frequency pair of lines (26–27 MHz) are characteristic of $PCl_2$ type of chlorines whereas the low frequency pair (23–24 MHz) signify the presence of PClR type of chlorines (R = $NMe_2$ in the present case). The NQR spectrum is thus consistent with a non-*geminal* disposition of the $NMe_2$ groups in this molecule. Such trends, characteristic of *geminal* and non-*geminal* substitutions, have already been recognised in the literature.[3] The crystal structure study of this compound[10] has shown the crystal to be triclinic with $Z = 2$ and belonging to the space-group $P1$. There are 4 inequivalent sites for the chlorines in the unit cell and the sites are equally populated. The NQR signal intensity anomaly we have observed is probably ascribable to non-equivalent nuclear spin relaxation times. A similar intensity anomaly has been reported for the tris-derivative, $N_3P_3Cl_3(NMe_2)$.[11] As already mentioned, the NQR signals observed in compound II are rather broad (3–4 kHz). Such broad lines have also been observed in the other aminocyclophosphazenes which we have studied and was ascribed to indirect spin–spin interaction between phosphorus and chlorine.[11]

## THE TEMPERATURE DEPENDENCE OF NQR AND TORSIONAL MODE ANALYSIS

It is well known that the temperature dependence of the nuclear quadrupole interaction, in a molecular solid, is mainly due to the low lying librational (torsional) modes of the molecules. The Bayer expression for the temperature dependence of NQR frequency is based on the assumption that the torsional motions about the EFG principal axes are normal modes (harmonic). This approximation is valid only when the EFG axes coincide with the principal axes of the moment of inertia tensor of the molecule. If they do not coincide, the expression for the temperature dependence takes the form.[12]

$$\nu(T) = \nu_0\left[1 - \frac{3h}{8\pi_2 c}\sum_i \frac{\sin^2\alpha_i}{A_i f_i}\left\{\frac{1}{2} + \frac{1}{e^{(hcf_i/kT)} - 1}\right\}\right]$$

Table 2. Frequency assignment

| Bond+ | Bond length (Å) | Electron density (e Å$^{-3}$) | $^{35}$Cl NQR frequency (RT) (MHz) |
|---|---|---|---|
| P(4)-Cl(1) | 1.990 | 23.3 | 27.655 |
| P(4)-Cl(2) | 2.002 | 26.5 | 26.994 |
| P(6)-Cl(3) | 1.989 | 27.2 | 26.524 |
| P(6)-Cl(4) | 2.006 | 24.3 | 27.246 |

+The numbering is as given in Ref.(4).

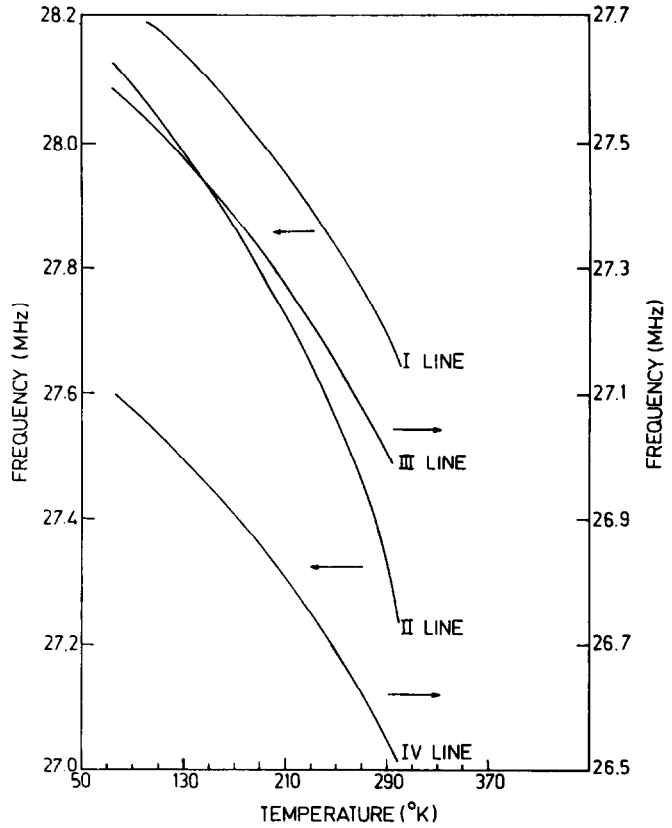



Fig. 1.

where $v_0$ is the NQR frequency for the stationary molecule, $f_i$ is the frequency ($cm^{-1}$) of the $i$th torsional mode, $A_i$ is the corresponding moment of inertia, $\alpha_i$ is the angle between the axis of the $i$th torsional mode and the principal $Z$-axis of the EFG tensor, and $T$ is the absolute temperature.

In principle, a three mode analysis would be ideal, but the numerical evaluation becomes complicated. Hence, only two modes have been included in the analysis based on the consideration that the larger the $(\sin^2\alpha_i/A_i)$ ratio, the more important the corresponding mode. A numerical method similar to the one employed by Vijaya *et al.*[13] has been used to evaluate the two torsional frequencies $f_1$ and $f_2$.

Table 3. Torsional frequencies from NQR data

| Line | $f_1$ ($cm^{-1}$) | | $f_2$ ($cm^{-1}$) | |
|---|---|---|---|---|
| | RT | 77K | RT | 77K |
| I | 14 | 18 | 15 | 20 |
| II | 12 | 22 | 16 | 27 |
| III | 12 | 13 | 17 | 19 |
| IV | 12 | 15 | 17 | 20 |

RT = Room Temperature.

The NQR frequency vs temperature plots (for $N_3P_3Cl_4Ph_2$) are shown in Fig. 1. The torsional frequencies were found to be in a characteristically low range and exhibit a rather small temperature dependence (Table 2).

Line II differs from the other signals (Fig. 1). The temperature coefficient of the NQR frequency for this line is small at low temperatures, then increases more rapidly for $T > 150$ K, unlike the other lines.

A plausible explanation could be as follows. An estimate of the net angular displacement of a given bond direction has been made using the thermal amplitudes of the atoms. It is found that P–Cl bond containing Cl(4) suffers the highest mean-square angular displacement at room temperature. From Bayer's theory, the higher the mean square angular displacement, the higher is the temperature coefficient. Thus line II with the highest temperature coefficient at room temperature should

correspond to Cl(4). This is consistent with the assignment we have made based on change density data. Further assuming that the angular displacements, $\langle\theta^2\rangle$, are mainly due to the torsional modes, the corresponding torsional frequencies are found to agree fairly well with those obtained from NQR data.

Regarding the temperature dependence of the torsional frequencies themselves, one can assume, following Brown,[14] a linear temperature dependence described by

$$f_i = f_i^0(1 - g_i t)$$

where $g_i$ characterises the temperature coefficient of the $i$th torsional mode frequency and "$t$" is the temperature measured with respect to a reference temperature $T_0$ ($t = T - T_0$). By introducing this approximation into the Kushida high temperature expression,[15] Brown relates the first and second derivatives of $\nu_Q$ vs $T$ ($\delta\nu_Q/\delta T$, $\delta^2\nu_Q/\delta T^2$) to an average temperature coefficient $\langle g\rangle$ of the torsional frequencies.[16] By a suitable curve-fitting of the experimental points ($\nu_Q$ vs $T$), $\delta\nu_Q/\delta t$ and $\delta^2\nu_Q/\delta t^2$ can be obtained and hence $\langle g\rangle$ can be estimated. Any temperature in the high temperature region can be chosen as $T_0$. $\langle g\rangle$ was evaluated at $T_0 = 250$ K and was found to be 0.0009, 0.002, 0.0006 and 0.0009 for lines I, II, III and IV respectively. These values are in agreement with those obtained from Bayer's equation and are similar to the values obtained in other phosphazenes.[11]

In the case of compound **II**, the dimethylamino derivative, the $\nu_Q$ vs temperature data of the NQR signals have been analysed using a two-torsional-mode approximation following the same procedure as outlined for compound **I**. The calculated torsional frequencies for this compound also are in the range 10–25 $cm^{-1}$. Line II was not clearly observed at temperatures below 250 K due to a decrease in its intensity and due to its proximity to the more intense line I which had strong side-bands associated with it. Thus, at 77 K, we could locate clearly only three lines. The $\langle g\rangle$ values were also estimated as in the earlier case and were found to be in the range 0.0002–0.0004 indicating that the torsional frequencies are less temperature dependent in this case. Our results for $N_3P_3Cl_4(NMe_2)_2$ generally agree with those reported by Connelly *et al.*

*Acknowledgements*—K.R.S. thanks CSIR, New Delhi for a fellowship while K.R. and S.S.K. thank UGC, New Delhi for support. The authors thank Prof. R. A. Shaw for helpful comments and for his kind interest in this work.

## REFERENCES

1. V. B. Desai, R. A. Shaw and B. C. Smith, *J. Chem. Soc.* (*A*), 1969, 1977. R. Keat, S. K. Ray and R. A. Shaw, *J. Chem. Soc.* 1965, 2215.
2. M. A. Whitehead, *Can. J. Chem.* 1964, 1212.
3. R. Keat, A. L. Porte, D. A. Tong and R. A. Shaw, *J. Chem. Soc.* (*Dalton*) 1972, 1648.
4. N. V. Mani, F. R. Ahmed and W. H. Barnes, *Acta Cryst.* 1965, **19**, 693.
5. L. Pauling, *The Nature of the Chemical Bond*, p. 126. Cornell University Press, Ithaca, New York (1948).
6. E. A. C. Lucken in *Proc. XI Colloque Ampere* (Edited by J. Smidt), p. 678. North Holland, Amsterdam 1963).
7. C. H. Townes and B. P. Dailey, *J. Chem. Phys.* 1949, **17**, 782.
8. W. H. Dalgleish, R. Keat, A. L. Porte, D. A. Tong, Masood-Ul-Hasan and R. A. Shaw, *J. Chem. Soc.* (*Dalton*), 1975, 309.
9. A. Connelly, W. H. Dalgleish, P. Harkins, R. Keat, A. L. Porte, I. Raitt and R. A. Shaw, *J. Magn. Resonance*, 1978, **30**, 439.
10. F. R. Ahmed and S. Fortier, *Acta Cryst.* 1980, **B36**, 1454.
11. K. R. Sridharan, J. Ramakrishna, K. Ramachandran and S. S. Krishna Murthy, *J. Mol. Structure*, 1980, **69**, 105.
12. I. Tatsuzaki and Y. Yokozawa, *J. Phys. Soc., Japan*, 1957, **12**, 802.
13. M. S. Vijaya and J. Ramakrishna, *Mol. Phys.* 1970, **19**, 131.
14. R. J. C. Brown, *J. Chem. Phys.* 1960, **32**, 116.
15. T. Kushida, *J. Sci. Hiroshima Univ.* 1955, **A19**, 327.

*Polyhedron* Vol. 3, No. 7, pp. 871–877, 1984
Printed in the U.S.A.

0277-5387/84 $3.00 + .00
© 1984 Pergamon Press Ltd.

# EQUILIBRIUM STUDY OF THE SYSTEMS OF ALUMINIUM(III), GALLIUM(III) AND INDIUM(III) WITH MERCAPTOACETATE, 3-MERCAPTOPROPIONATE AND 2-MERCAPTOBENZOATE

**IMRE TÓTH,* LÁSZLÓ ZÉKÁNY and ERNÖ BRÜCHER**
Department of Inorganic and Analytical Chemistry, Lajos Kossuth University, H-4010 Debrecen, Hungary

(*Received* 26 *October* 1983; *accepted* 28 *November* 1983)

**Abstract**—Equilibrium studies were carried out by pH-potentiometry on the systems of aluminium(III), gallium(III) and indium(III) with mercaptoacetate ($MerAc^{2-}$), 3-mercaptopropionate ($MerPr^{2-}$) and 2-mercaptobenzoate ($MerBe^{2-}$). It was found that the complex-forming properties of the $Al^{3+}$ ion towards these mercaptocarboxylic acid ligands differ from those of $Ga^{3+}$ and $Al^{3+}$. Under the conditions of the study, $Al^{3+}$ forms only hydroxo complexes, while $Ga^{3+}$ and $In^{3+}$ form relatively stable complexes involving the simultaneous coordination of the carboxylate and the deprotonated mercapto group. In all cases the equilibrium systems can be described without the assumption of polynuclear complexes. The complexes $Ga(MerAc)_2$ and $Ga(MerBe)_2$ show marked stability; this was interpreted in terms of back-coordination and of interaction between the $d^{10}$ electrons of the $Ga^{3+}$ ion and the empty $d$ orbitals of the S donor atom. Complexes of composition $ML_i$ are not formed in the $Ga^{3+}$–$MerPr^{2-}$ system; this points to the important roles of the number of atoms in the chelate ring and the higher stability of the Ga(III)–hydroxo complexes.

Interest in the solution chemistry of gallium(III) has increased in recent years; there are two basic reasons for this. The development of the semiconductor industry has increased the demand for high-purity gallium and its compounds,[1] and liquid–liquid extraction procedures are gaining in importance in recovering gallium.[2] This requires a knowledge of the differences in the coordination properties of $Al^{3+}$ and $Ga^{3+}$. The other field of interest is connected with the application of salts and complexes of $Ga^{3+}$ (and to a lesser extent $In^{3+}$) in tumour diagnostics and tumour therapy.[3]

$Al^{3+}$, $Ga^{3+}$ and $In^{3+}$ are all Class A metal ions[4] but the $d^{10}$ outer electron shell of the latter two ions means that they are potentially class B in character towards appropriately selected ligands.[5–8]

The results relating to the complexes of $Ga^{3+}$ and $In^{3+}$ with ligands containing the SH group are fairly contradictory. Kojima *et al.*[6,7] have made detailed studies of the complexes of $Ga^{3+}$ and $In^{3+}$ with peptides and aliphatic carboxylic acids containing one or two SH groups. They found that $Ga^{3+}$, in contrast with $In^{3+}$, does not form complexes with peptide ligands containing one SH group.[6c] The formation of polynuclear species was described in the $In^{3+}$–$MerAc^{2-}$ system.[6b] Sarin and Munshi reported the stability sequence–SH ≫ –OH > $-NH_2$ for the complexes of $In^{3+}$ with substituted carboxylic acids, and interpreted this by the formation of a $d\pi$–$d\pi$ bond between the metal ion and the S donor atom.[8] The fact that the $MerPr^{2-}$ complexes of $In^{3+}$ are less stable than the $MerAc^{2-}$ complexes was explained by the different numbers of ring atoms and by entropy factors.[8b]

We have made a pH-potentiometric study of the equilibrium systems of $Al^{3+}$, $Ga^{3+}$ and $In^{3+}$ with $H_2MerAc$, $H_2MerPr$ and $H_2MerBe$. The choice of $H_2MerBe$ as ligand was justified by the fact that, similarly to $H_2MerPr$, it is capable of forming a six-membered chelate ring and can therefore be

*Author to whom correspondence should be addressed.

regarded as an analogue of $H_2$MerPr containing an aromatic ring. It appeared interesting to make a comparison with the ligand salicylic acid ($H_2$Sa) too, as $Al^{3+}$ and $Ga^{3+}$ form very stable complexes with phenolate-type ligands.[9] Due to the low solubility of $H_2$MerBe in water, and in the interest of comparability with $H_2$MerPr and $H_2$MerBe, the investigations were carried out in 50% (v/v) aqueous ethanol solutions.

## EXPERIMENTAL

The $Ga(NO_3)_3$ and $Al(NO_3)_3$ solutions were prepared by the dissolution of metallic gallium (5N, Ajka Aluminium Works) and aluminium (highest analytical purity, Reanal) in $HNO_3$ (Carlo Erba). The $In(NO_3)_3$ solution was prepared by the dissolution of $In(NO_3)_3 \cdot 5H_2O$ (Schuchardt) in doubly distilled water. The metal ion concentrations of the stock solutions were determined by complexometry, and the free acid content by the method proposed by Harris and Martell.[10]

$H_2$MerAc and $H_2$MerPr (Merck) were purified by vacuum-distillation,[11] and $H_2$MerBe (Fluka) by recrystallization from glacial acetic acid. The solutions used for the investigations were freshly prepared with boiled doubly distilled water. The concentrations of the ligand stock solutions were determined pH-metrically, by titration with KOH solution. Concentration determination was also carried out by iodometric measurement of the SH group,[11a] and the agreement was within 1%.

The pH-potentiometric studies were made at $25 \pm 0.2$°C in a medium of constant ionic strength: 0.5 mol $dm^{-3}$ $KNO_3$ (highest analytical purity, Reanal, recrystallized). Radiometer PHM 84 and Radelkis OP-208/1 pH-meters were used for the measurements, with Radiometer GK 2401B combined, G 202B glass and K 401 calomel electrodes. The pH-meters were standardized with KH-phthalate (Merck, pH = 4.008) and $KH_2PO_4$–$Na_2HPO_4$ (Reanal, pH = 6.865) buffer solutions. The stoichiometric equilibrium constants were calculated by the method proposed by Irving *et al.*[12] The stoichiometric ionic product of water was determined: in 0.5 mol $dm^{-3}$ $KNO_3$ solution: $pK_w = 13.76 \pm 0.01$.

The ethanolic solutions were prepared by mixing one volume of 96% (m/m) ethanol (Reanal, distilled, $g = 0.797$ g $cm^{-3}$) with the added stock solutions and distilled water so as to give two volumes; the density of the alcohol–water mixture used as solvent was thus approximately 0.92 g $cm^{-3}$. The stoichiometric equilibrium constants were calculated with the method used in the study of aqueous solutions.[12] The ionic product of water was $14.29 \pm 0.01$.

The concentration of the KOH solution was determined by pH-metric titration of KH-phthalate solution. Argon freed from oxygen with alkaline pyrogallol was used as protective gas during the titrations.

In the potentiometric titrations, the total metal ion concentration ($T_M$) was $3 \times 10^{-4}$, $5 \times 10^{-4}$ or $7 \times 10^{-4}$ mol $dm^{-3}$, and the ligand:metal ion ratio was 4:1. For the gallium(III)–$MerAc^{2-}$ system, $T_{Ga}$ was $3 \times 10^{-3}$ mol $dm^{-3}$, and the measurements were made at $T_L/T_{Ga}$ values of 2, 3 and 5. (Formation of the aluminium(III) and indium(III) complexes cannot be examined under such conditions, because of the slowness with which equilibrium is established.) Conditions differing from those given above are indicated in the text and in the Table.

The protonation and stability constants were calculated with the PSEQUAD programme.[13]

## RESULTS AND DISCUSSION

### (a) *Protonation constants of ligands*

The constants determined by means of the potentiometric titrations are presented in Table 1, with the $\Delta v$ [$cm^3$] values characterizing the goodness of the computer fitting. The error in the constants is the S.D. ($\sigma$). Literature data too are given in the Table 1 for comparison purposes.

When the slightly different ionic strengths and temperatures are taken into consideration, the agreement between the literature data in Table 1 and the results of our own measurements can be said to be good. The $\log \beta_1^H$ value of 9.52 for the ligand $MerBe^{2-}$ was measured by a polarographic method,[15] while the $\log K_2^H$ value of 5.44 was the result of potentiometric measurement;[16] the considerably different ionic strengths and temperatures mean that it is difficult to compare the results of our measurements with the constants $\log \beta_1^H = 9.69$ and $\log \beta_2^H = 12.97$.[17]

### (b) *Mercaptoacetate complexes*

Table 2 gives the equilibrium constants calculated from the best fitting of the potentiometric titration results. The constants relate to the following equilibrium processes (M = Al, Ga, In):

$$M^{3+} + iL^{2-} \rightleftharpoons ML_i^{(3-2i)+} \quad (1)$$

$$\beta_i^L = \frac{[ML_i]}{[M][L]^i} \quad (2)$$

$$M^{3+} \cdot aq + iH_2O \rightleftharpoons M(OH)_i^{(3-i)+} \cdot aq + iH_3O^+ \quad (3)$$

$$\beta_i^{OH} = \frac{[M(OH)_i][H_3O^+]}{[M]}. \quad (4)$$

Table 1. Protonation constants of the ligands mercaptoacetate ($MerAc^{2-}$), 3-mercaptopropionate ($MerPr^{2-}$) and 2-mercaptobenzoate ($MerBe^{2-}$)

| | $\log\beta_1^H$ | $\log\beta_2^H$ | $\overline{\Delta v}$ [cm$^3$] |
|---|---|---|---|
| $MerAc^{2-}$ | 9.92 | [a]13.45[8b] | - |
| | 10.048 | [b]13.596[14] | - |
| | 10.01±0.005 | 13.48±0.006 | 0.0071 |
| $MerPr^{2-}$ | 10.15 | [c]14.16[8a] | - |
| | 10.31 | [d]14.51[6b] | - |
| | 10.09±0.005 | 14.30±0.008 | 0.0042 |
| | [*]10.71±0.007 | [*]15.61±0.008 | 0.0024 |
| $MerBe^{2-}$ | [*] 9.52[15] | [*,e]14.96[16] | - |
| | [*] 9.69 | [*,f]12.97[17] | - |
| | [*] 9.07±0.01 | [*]13.41±0.01 | 0.0081 |

*: in 50 % (v/v) ethanol

a: 0.2 mol dm$^{-3}$ $NaClO_4$, 25 °C

b: 0.5 mol dm$^{-3}$ $KNO_3$, 25 °C

c: 0.4 mol dm$^{-3}$ $NaClO_4$, 25 °C

d: 0.5 mol dm$^{-3}$ $KNO_3$, 20 °C

e: $\log\beta_2^H$ calculated from $\log\beta_1^H$ [15] + $\log K_2^H$ ($\log K_2^H = 5.44$)

f: 0.05 mol dm$^{-3}$ $HClO_4$+$NaClO_4$, 17 °C

The data in Table 2 show that an interaction cannot be demonstrated between $Al^{3+}$ and $MerAc^{2-}$ under the concentration conditions employed. $H_2MerAc$ can therefore be used to mask $Fe^{3+}$ in the photometric determination of $Al^{3+}$.[18] The failure of $Al^{3+}$ to interact with the SH group is also indicated by the fact that maleonitriledithiolate is likewise suitable for the masking of heavy metals in the extraction enrichment of $Al^{3+}$.[19] Although their uncertainty is fairly high, the constants characterizing the hydrolysis of the $Al^{3+}$ ion reveal that the titration curves can be described with constants close to the literature values,[20] without the assumption of the formation of polynuclear hydroxo complexes. A method suitable for the elimination of the difficulties caused by the slow reactions in the study of the hydrolysis of metal ions is to use a ligand forming a comparatively weak complex with the metal ion; with the decrease of the ligand excess, the formation of the hydroxo complexes then comes progressively into prominence.[21] A slight interaction between $Al^{3+}$ and $MerAc^{2-}$ is indicated by our experience that establishment of equilibrium during the titration was fast, whereas we could not carry out pH-metric measurements under similar concentration conditions in the $Al^{3+}$–AcOH system, for example, at pH > 4.

$Ga^{3+}$ forms relatively stable complexes with $MerAc^{2-}$. Determination of $\log\beta_1^L$ was hampered by the fact that formation of the complex $ML_2$ became predominant at ligand:metal ion ratios of 2:1 or higher, as did the formation of hydroxo complexes at a ratio of 1:1. $\log\beta_1^L = 11.2$ can be regarded as the maximum value which (calculating with independently determined and fixed $\log\beta_2^L$) does not spoil the goodness of the fit. From the values obtained in this way, $\log K_1^L \leqslant 11.2$ and $\log K_2^L \geqslant 11.14$. The difference in favour of $\log K_2^L$ from the values to be expected on the basis of statistical considerations can be interpreted by the phenomenon of back-coordination. The charge density of the appropriately directed $d^{10}$ electrons of $Ga^{3+}$ may shift slightly in the direction of the

Table 2. Equilibrium constants for mercaptoacetate systems of aluminium(III), gallium(III) and indium(III) in aqueous medium

| complex | log $\beta_i$ | | |
|---|---|---|---|
| | $^{a}Al^{3+}$ | $^{b}Ga^{3+}$ | $^{a}In^{3+}$ |
| ML | - | $^{c}11.20\pm0.08$ | $12.10^{8b}$<br>$12.57\pm0.02$ |
| $ML_2$ | - | $22.34\pm0.01$ | $22.43^{8b}$<br>$23.53\pm0.02$ |
| $ML_3$ | - | $29.67\pm0.05$ | $28.78^{8b}$<br>$31.21\pm0.07$ |
| $ML_4$ | | $31.91\pm0.08$ | $36.3\pm0.2$ |
| MOH | $-4.60^{20}$<br>$-5.5\pm0.6$ | $-2.41^{20}$<br>$-2.46\pm0.02$ | $-3.3^{20}$<br>- |
| $M(OH)_2$ | $-9.09^{20}$<br>$-9.8\pm0.1$ | $-5.92^{20}$<br>- | $-7.1^{20}$<br>- |
| $M(OH)_3$ | $-14.94^{20}$<br>$-15.0\pm0.1$ | $-10.63^{20}$<br>$-8.2\pm0.07$ | $-11.9^{20}$<br>$-11.0\pm0.2$ |
| $M(OH)_4$ | $-23.08^{20}$<br>$-23.4\pm0.1$ | $-16.87^{20}$<br>$-17.3\pm0.04$ | $-21.7^{20}$<br>- |
| No. of titration curves | 6 | 9 | 7 |
| No. of experimental points | 145 | 275 | 161 |
| pH range | 2.1-10.8 | 1.5-10.8 | 2.1-11.0 |
| $\bar{\Delta v}$[cm$^3$] | 0.0085 | 0.0064 | 0.0046 |

a: $T_M$ = $3\times10^{-4}$, $5\times10^{-4}$, $7\times10^{-4}$ mol dm$^{-3}$, $T_L/T_M$ = 4

b: $T_{Ga}$ = $3\times10^{-3}$ mol dm$^{-3}$, $T_L/T_M$ = 2, 3 and 4

c: $T_{Ga}$ = $5\times10^{-4}$ and $1\times10^{-3}$ mol dm$^{-3}$, $T_L/T_{Ga}$ = 1, 6 titration curves, 137 experimental points, pH = 2.2-3.7, $\bar{\Delta v}$=0.0081 cm$^{-3}$, MOH and $M(OH)_3$ are also formed: $\log\beta_1^{OH} = -3.2\pm0.5$, $\log\beta_3^{OH} = -10.0\pm0.15$.

empty d orbitals of the S donor atom, which may make coordination of the second ligand favoured. Leussing[22] gave a similar interpretation for the values of the equilibrium constants found in the $Co^{2+}$–$MerAc^{2-}$ system.

The equilibrium conditions in the $Ga^{3+}$–$MerAc^{2-}$ system are illustrated in Fig. 1. It can be seen that the concentration of the species $HL^-$ passes through a minimum at pH ~ 6 as a function of pH. In a study of the unusual concentration distributions, Nagypál *et al.*[23] consider that the appearance of even 5 extrema are possible in a three-component (M, L and $H^+$) system if the associations $H_2L$, HL, $ML_2$ and $M(OH)_4$ are

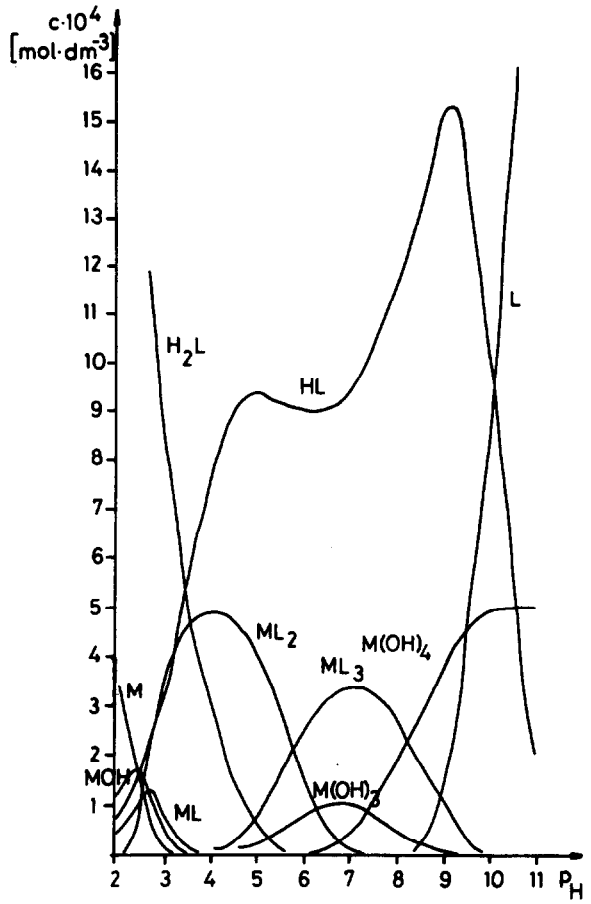



Fig. 1. Concentration distribution of species in gallium(III)-mercaptoacetate system ($T_{Ga} = 5 \times 10^{-4}$, $T_L = 2 \times 10^{-3}$ mol dm$^{-3}$).

formed. In the system we examined, the unusual variation in the HL concentration is caused by the fact that in the pH interval in which the reaction $H_2L \rightleftharpoons HL^- + H^+$ occurs, the concentration of the $HL^-$ ion is decreased appreciably by the following reaction, because of the outstandingly high stability of the complex $ML_2$:

$$M^{3+} + 2HL^- \rightleftharpoons ML_2^- + 2H^+. \qquad (5)$$

The presence of $Ga^{3+}$-hydroxo complexes too must be reckoned with in the system, to an extent depending on the metal ion:ligand ratio. The agreement of the found equilibrium constants with the literature values is satisfactory (Table 2), which indicates that the assumption of the formation of polynuclear, or possibly mixed hydroxo complexes is not justified.

The constants obtained in the $In^{3+}$–$MerAc^{2-}$ system are closer to the values determined by Sarin and Munshi.[8b] These authors did not identify the complex $ML_4$ even at a ligand:metal ion ratio of 5:1 ($T_{In} = 1 \times 10^{-3}$ mol dm$^{-3}$), whereas our measurements suggest that this complex is formed even at a ratio of 4:1, together with a small amount of $M(OH)_3$. The assumption of the complexes $InL_3$ and $In_2L_6$ described by Kojima *et al.*[6b] may be justified at $T_{In} = 0.5 \times 10^{-3}$–$4.0 \times 10^{-3}$ mol dm$^{-3}$ and a ligand:metal ion ratio of 5:1, as in their case, but it was not necessary to assume polynuclear complexes to describe the titration curves we obtained at lower $In^{3+}$ concentrations.

(c) *3-Mercaptopropionate complexes*

On the basis of the measurements in 50% (v/v) ethanolic medium, complex formation was experienced only in the $In^{3+}$–$MerPr^{2-}$ system; the values of the stability constants found in the pH interval 2.4–5.0 were $\log \beta_1^L = 13.35 \pm 0.03$ and $\log \beta_2^L = 22.8 \pm 0.1$ ($\Delta v = 0.0080$ cm$^3$, 6 titration curves, 120 experimental points). Literature data are known only for aqueous medium; under essentially not different experimental conditions, only the formation of mononuclear[8a] or, among other alternatives, polynuclear and mixed hydroxo complexes too[6b] is assumed. In our experience, pH-potentiometric measurements cannot be carried out in 50% (v/v) ethanolic medium at pH > 5, because of the slow, presumably hydrolytic reactions.

Metal ion-ligand interactions were not observed in the $Al^{3+}$–$MerPr^{2-}$ and $Ga^{3+}$–$MerPr^{2-}$ systems. The formation of complexes $ML_i$ could not be demonstrated when measurements were made at $T_{Ga} = 5 \times 10^{-4}$ mol dm$^{-3}$ and $T_L/T_{Ga} = 10$ in either alcoholic or aqueous solution. Our findings relating to the $Ga^{3+}$–$MerAc^{2-}$ system (Table 2) indicate that though $Ga^{3+}$ is able to form a stable complex with ligands containing an SH group (in contrast with the literature data[6c]), the strength of the interaction depends to a large extent on the number of ring atoms in the resulting chelate ring.

(d) *2-Mercaptobenzoate complexes*

The stability constants found are listed in Table 3.

A metal ion-ligand interaction could not be detected in the $Al^{3+}$–$MerBe^{2-}$ system. The $\log \beta_1^L$ value for $Ga^{3+}$ was determined at a ligand:metal ion ratio of 1:1, as described in connection with the $Ga^{3+}$–$MerAc^{2-}$ system. From the values $\log K_1^L \leqslant 10.3$ and $\log K_2^L \geqslant 10.62$, it is seen that $\log K_1^L < \log K_2^L$; this again points to the higher stability of the complex $ML_2$, suggesting back-coordination. The $\log \beta_1^L$ and $\log \beta_2^L$ values for the $In^{3+}$–$MerBe^{2-}$ complexes are smaller than those for the corresponding $MerPr^{2-}$ complexes. Although the structures of the two ligands differ

Table 3. Equilibrium constants for 2-mercaptobenzoate systems of gallium(III) and indium(III) in 50% (v/v) ethanolic medium

| complex | $\log \beta_i$ | |
|---|---|---|
| | $Ga^{3+}$ | $In^{3+}$ |
| ML | [a]10.3±0.06 | 12.03±0.02 |
| $ML_2$ | 20.92±0.04 | 21.56±0.04 |
| MOH | -2.92±0.03 | - |
| No. of titration curves | 6 | 6 |
| No. of experimental points | 107 | 134 |
| pH range | 2-4 | 2-6 |
| $\overline{\Delta v}$ [$cm^3$] | 0.0073 | 0.0047 |

a: $T_{Ga}$ = 1x10$^{-3}$ and 3x10$^{-3}$ mol dm$^{-3}$; $T_L/T_{Ga}$ = 1; 5 titration curves, 148 experimental points, pH = 2.4-3.2, $\overline{\Delta v}$= 0.0074, $\log \beta_1^{OH}$= 3.09±0.03, $\log \beta_2^{OH}$ = -5.58±0.02.

substantially, such a ratio of the complex stabilities corresponds to the values of the ligand basicities (for $H_2$MerPr and $H_2$MerBe, $\log \beta_2^H = 15.61$ and 13.41, respectively). Our measurements show that this regularity does not hold for the complexes of $Ga^{3+}$. One reason for this may be that the higher stability of the hydroxo complexes of $Ga^{3+}$ compared to those of $In^{3+}$ at higher pH, and the higher protonation constants of $MerPr^{2-}$ at lower pH, decrease the apparent stability constants so much that demonstration of the complexes $ML_i$ in the $Ga^{3+}$–$MerPr^{2-}$ system is not possible under the experimental conditions employed.

Literature data are known only for $Tl^{3+}$–$MerBe^{2-}$ complexes:[16] $\log K_1^L = 8.964$, $\log L_2^L = 8.647$ and $\log K_3^L = 5.420$. Ramakrishnan and Fernandopulle make no mention of the formation of hydroxo complexes, though the values $\log \beta_1^{OH} = -0.62$, $\log \beta_2^{OH} = -1.52$ and $\log \beta_3^{OH} = -3.3$ in the case of $Tl^{3+}$ [20] point to the high stability of such complexes. With the use of the above constants, we have calculated[13] the concentration distribution in the $Tl^{3+}$–$MerBe^{2-}$–$H^+$ system at $T_{Tl} = 2.5 \times 10^{-5}$ and $5 \times 10^{-5}$ mol dm$^{-3}$ and a $T_L/T_{Tl}$ ratio of 10:1 in the pH interval 0–11. Our calculations showed that the complexes $ML_i$ are not formed under such conditions; only $M(OH)_i$ is obtained. (Besides hydrolysis, Ramakrishna and Fernandopulle do not discuss redox reactions, though in acidic medium $Tl^{3+}$ is able to oxidize iodide ion to iodine, and iodine is suitable for iodometric measurement of the SH group.) On the above basis, the lower stability constants of the Class B metal $Tl^{3+}$ compared with those of $In^{3+}$ do not appear realistic.

The group IIIB metal ions $Al^{3+}$, $Ga^{3+}$, $In^{3+}$ and $Tl^{3+}$ form salicylate complexes with $\log \beta_1^L$ stability constant values of 12.9,[9] 14.5,[9] 2.59[9,24] and 12.7,[9] respectively. The constant for $In^{3+}$ in 75% (v/v) alcoholic medium is an unrealistically low value, since the ions of this group form fairly stable complexes with ligands containing OH groups.[9,21,25] Although the stabilities of the complexes of $Ga^{3+}$ and $In^{3+}$ with $MerBe^{2-}$ are somewhat lower than those of the salicylate complexes, the $\log \beta_1^L$ values of 10.3 and 12.03 for $MerBe^{2-}$ indicate that "exchange" of the phenolic OH group for the SH group does not decrease the stability considerably.

On the above basis, it may be stated that the complex-forming properties of $Al^{3+}$ differ substantially from those of $Ga^{3+}$ and $In^{3+}$ in their reactions with mercaptocarboxylic acid ligands. The

compositions of the species formed in the equilibrium systems permit the assumption that the $Al^{3+}$ ion does not interact with the SH group of the ligands, whereas relatively stable complexes of $Ga^{3+}$ and $In^{3+}$ may be produced by the simultaneous coordination of the carboxylate group and the deprotonated mercapto group. With regard to the probable coordination number of 4 in the species $ML_4$ formed at high pH, coordination is also conceivable only via S donor atoms.[6b] The phenomenon of back-coordination result in the favoured formation of complexes $GaL_2$ ($L = MerAc^{2-}$ and $MerBe^{2-}$). The non-occurrence of complex formation in the $Ga^{3+}$–$MerPr^{2-}$ system points to the important roles of the number of ring atoms and the apparent stability ratios.

Of the metal ions $M^{3+}$ of group IIIB, $Al^{3+}$ did not display Class B character, but $Ga^{3+}$ and $In^{3+}$, formed relatively stable complexes with aliphatic or aromatic carboxylic acids containing the SH group in an appropriate position.

## REFERENCES


1. I. G. Lossmann and H. F. Repko, *Metall* 1978, **38**, 713.
2. C. M. Wang, L. Q. Zang, J. G. Xu, J. H. Li, S. Q. Sun and J. Z. He, *Abst. Paper Am. Chem. Soc.* 1981, **182**, 148.
3. *Metal Ions in Biological Systems* (Edited by H. Sigel), Vol. 10, Chap. 10, Vol. 11, Chap. 1. Basel, New York (1980).
4. S. Ahrland, *Structure and Bonding*, Vol. 1, p. 207. Springer-Verlag, Berlin (1966).
5. I. Tóth, L. Zékány and E. Brücher, *Magy. Kém. Foly.* 1983, **90**, 33.
6. N. Kojima, Y. Sugiura and H. Tanaka, (a) *Bull. Chem. Soc. Japan* 1976, **49**, 3023; (b) *Chem. Pharm. Bull.* 1978, **26**, 440; (c) *Chem. Pharm. Bull.* 1978, **26**, 579.
7. Y. Sugiura, N. Kojima and H. Tanaka, *Chem. Pharm. Bull.* 1977, **25**, 2263.
8. R. Sarin and K. N. Munshi, (a) *Aust. J. Chem.* 1972, **25**, 929. (b) *J. Inorg. Nucl. Chem.* 1973, **35**, 201.
9. A. E. Martell and R. M. Smith, *Critical Stability Constants*, Vol. 3. Plenum Press, New York (1977); Vol. 5 (1982).
10. W. R. Harris and A. E. Martell, *Inorg. Chem.* 1976, **15**, 713.
11. (a) D. L. Leussing and I. M. Kolthoff, *J. Electrochem. Soc.* 1953, **100**, 334. (b) K. Yamaguchi and K. Ueno, *Talanta* 1963, **10**, 1195.
12. H. M. Irving, M. G. Miles and L. P. Pettit, *Anal. Chim. Acta* 1967, **38**, 475.
13. L. Zékány and I. Nagypál, PSEQUAD program, XXII. I.C.C.C. Abstracts of Papers, Vol. 1, p. 450. Budapest (1982).
14. H. F. DeBrabander, L. C. Van Poucke and Z. Eeckhaut, *Anal. Chim Acta* 1974, **70**, 401.
15. A. N. Kumar, H. L. Nigam and R. D. Seth, *J. Polarograph. Soc.* 1966, **3**, 83.
16. R. S. Ramakrishna and M. E. Fernandopulle, *J. Inorg. Nucl. Chem.* 1971, **33**, 1940.
17. M. V. Reddy and P. K. Bhattacharya, *J. Inorg. Nucl. Chem.* 1970, **32**, 2321.
18. F. Cabrera, L. Madrid and P. de Arambarri, *Analyst*, 1981, **106**, 1296.
19. F. Ikeda, H. Matsunaga and T. Yotsuyanagi, *Bunseki Kagaku*, 1982, **31**, 407.
20. C. F. Baes and R. E. Mesmer, *The Hydrolysis of Cations*, pp. 112–123, 313–335. Wiley, New York (1976).
21. L. Öhman, Thesis, p. 7. University of Umeå (1983).
22. D. L. Leussing, *J. Am. Chem. Soc.* 1958, **80**, 4180.
23. I. Nagypál, M. T. Beck and A. D. Zuberbühler, *Talanta* 1983, **30**, 593.
24. R. Sarin and K. N. Munshi, *J. Ind. Chem. Soc.* 1973, **50**, 307.
25. P. Letkeman, A. E. Martell and R. J. Motekaitis, *J. Coord. Chem.* 1980, **10**, 47.

*Polyhedron* Vol. 3, No. 7, pp. 879–882, 1984
Printed in the U.S.A.

0277–5387/84 $3.00 + .00
Pergamon Press Ltd.

# $^{1}H$- AND $^{13}C$-NMR SPECTRA OF PALLADIUM AND PLATINUM MESO-TETRAPHENYLPORPHYRINS

Lionel R. Milgrom

Imperial College of Science and Technology,
Department of Chemistry,
Exhibition Rd., London, SW7 2AZ.

**(Received 7 February 1984; accepted 27 March 1984)**

Abstract: The $^{1}H$- and $^{13}C$-NMR spectra of palladium and platinum meso-tetraphenylporphyrins (TPP) are reported. PtTPP demonstrates spin-spin coupling between platinum and the pyrrole β-protons and carbons. There is some evidence for spin-spin coupling between platinum and the pyrrole α-carbons. PdTPP and PtTPP also demonstrate upfield shifting of their pyrrole α-carbon $^{13}C$-resonances. Structural and electronic arguments are advanced to explain this behaviour.

Spectroscopic studies on metalloporphyrins are of continuing interest because of their biological[1] and increasing technological importance.[2–4] For example, palladium and platinum porphyrins are being considered as photosensitisers in photochemical electron-transfer systems for solar-energy conversion,[2,5] and as novel one-dimensional 'molecular metals'.[3] While characterising PdTPP and PtTPP for experiments along these lines, several unusual (for metalloporphyrins) features were observed in their $^{1}H$- and $^{13}C$-NMR spectra. As there is little NMR data on palladium[6–8] and platinum[6] porphyrins, this paper reports $^{1}H$- and $^{13}C$-NMR spectra for PdTPP and PtTPP.

## Results and Discussion

The metalloporphyrins were prepared according to literature methods.[9,10] Significant improvement in the yield of PtTPP, following the method of Thomas and Martell,[9] was achieved using column chromatography on acidified silica gel. Unmetallated TPP, previously reported as a hindrance to clean PtTPP separation,[9,11] was left on the top of the column as a green band of the dication. The yield of PtTPP was comparable to that obtained by the method of Eisner and Harding.[12]

The $^{1}H$-NMR spectra of PdTPP and PtTPP are typical of diamagnetic metalloporphyrins.[13] Three sets of peaks are observed in the aromatic region ($\delta$ = 7.5 - 9 ppm). These are assigned to the phenyl meta- and para-hydrogens ($H_m$ and $H_p$), the phenyl ortho-hydrogens ($H_o$), and the pyrrole β-hydrogens ($H_\beta$), respectively (see Figure 1 and Table 1).

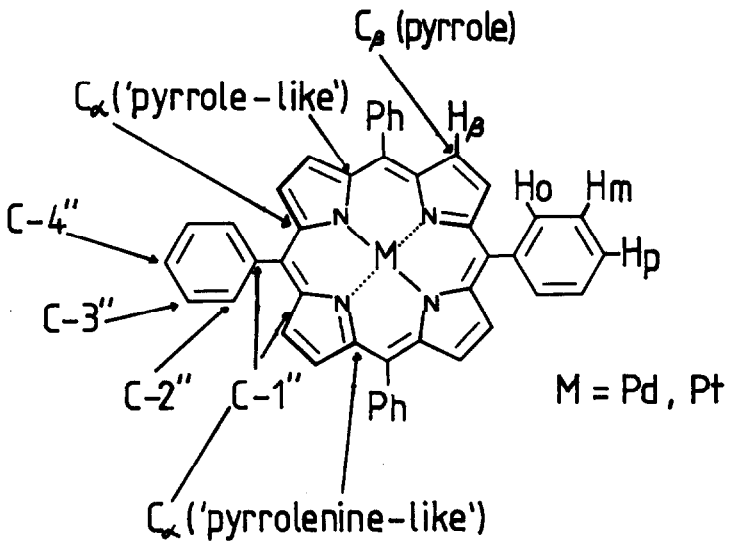



FIGURE 1

With PtTPP, however, the usual β-proton singlet (at δ = 8.74 ppm) is flanked by two satellites 6.25 Hz either side of the central peak. The relative intensity ratios of the peaks (1:4:1) is concommitant with the superimposition of a $^{1}H - ^{195}Pt$ spin-doublet ($^{195}Pt$ has spin of ½, natural abundance = 34%) on the β-proton singlet. The coupling constant, $^{4}J_{(^{1}H-^{195}Pt)}$ is 12.5 Hz, consistent with long-range $^{1}H - ^{195}Pt$ coupling over four bonds, reported elsewhere.[14] A previous observation of the $^{1}H$-NMR spectrum of platinum octaethylporphyrin,[6] failed to report long-range, four-bond coupling between porphyrin meso-protons and platinum.

| | Pyrrole β-H | Phenyl-$H_o$ | Phenyl-$H_m$ and $H_p$ |
|---|---|---|---|
| TPP[a] | 8.75[b] | 8.30 | 7.80 |
| PdTPP | 8.81 | 8.17 | 7.73 |
| PtTPP | 8.74[c] | 8.14 | 7.72 |

a) See reference 23; b) Chemical shifts in δ ppm

c) Satellites are 6.25 Hz either side of this peak.

$^{4}J_{(^{1}H-^{195}Pt)}$ = 12.5 Hz compared to 8 - 17 Hz.[14]

TABLE 1

The $^{13}C$-NMR spectra of PdTPP and PtTPP are also typical of diamagnetic metalloporphyrins.[13] The $^{13}C$-resonances were assigned by comparison with the work of Abraham et. al.[15] (see Table 2). For PtTPP, the pyrrole β-carbon resonance at 130.7 ppm, is flanked by two satellites 12.6 Hz either side of the main peak. The relative intensity ratios of the peaks (1:4:1) indicates $^{13}C - ^{195}Pt$ spin-spin coupling. The coupling constant, $^{3}J_{(^{13}C-^{195}Pt)}$, is 25.2 Hz and is of the order of magnitude consistant with long-range $^{13}C - ^{195}Pt$ coupling over three bonds, reported elsewhere.[16,17] There is some evidence that the pyrrole α-carbons, at 140.9 Hz are also spin-coupled to platinum. The expected satellites, however, are poorly

resolved. This does not seem to be due to $^{14}$N-line broadening as the pyrrole α-carbon peaks have a similar line width to the other peaks in the spectrum. The coupling constant, $^{2}J_{(^{13}C-^{195}Pt)}$, is 12.6 Hz and, although tentative, is of the order of magnitude found in previously reported long-range $^{13}$C - $^{195}$Pt coupling over two bonds.[16,17] It also follows the pattern whereby three-bond $^{13}$C - $^{195}$Pt coupling constants are larger than two-bond.

| | $C_\alpha$ | $C_\beta$ | $C_{meso}$ | C-1" | C-2" | C-3" | C-4" |
|---|---|---|---|---|---|---|---|
| TPP[a] | 145.8[b] | 130.6 | 119.6 | 141.7 | 134.0 | 126.1 | 127.5 |
| PdTPP | 141.7 | 131.0 | 121.7 | 141.9 | 134.1 | 126.7 | 127.7 |
| PtTPP | 140.9[c] | 130.7[d] | 122.3 | 141.5 | 133.9 | 126.8 | 127.8 |
| ZnTPP[a] | 150.8 | 132.5 | 121.6 | 143.3 | 134.9 | 127.5 | 128.0 |

a) See reference 15; b) Chemical shifts in δ ppm; c) Satellites are 6.3 Hz either side of this peak. $^{2}J_{(^{13}C-^{195}Pt)}$ = 12.6 Hz compared to 16 - 30 Hz.[16,17] d) Satellites are 12.6 Hz either side of this peak. $^{3}J_{(^{13}C-^{195}Pt)}$ = 25.2 Hz compared to 34 - 70 Hz.[16,17]

TABLE 2

With the exception of the porphyrin meso-carbons, all the $^{13}$C-resonances show an upfield shift compared to other metallo-TPPs.[15] The greatest effect is observed for the pyrrole α-carbon resonances (141.7 and 140.9 ppm for PdTPP and PtTPP, respectively). This may be due to steric 'ruffling'[18] of the porphyrin nucleus caused by square-planar coordination to large central cations. Ring-strain and angle deformations are thought to play a dominant role in determining the positions of $^{13}$C-resonance signals.

An alternative view is based on the observation by Abraham et. al.,[15] of large chemical shift differences between 'α-pyrrole' and 'α-pyrrolenine' (see Figure 1) resonances in TPP at low temperatures. They argue that 'pyrrolenine-like' carbons, which are conjugated to nitrogen, can be shifted downfield by 22 - 33 ppm.

In porphyrin free-bases, the two inner protons stabilise an 18-membered conjugation pathway,[20] with four α-carbons conjugated to β-carbons (i.e. 'pyrrole-like') and four α-carbons conjugated to nitrogens (i.e. 'pyrrolenine-like'). Because of tautomerism at ambient temperatures, the position of the pyrrole α-carbon $^{13}$C-resonances is an average of the two. Metalloporphyrin formation generates a formal porphyrin dianion which stabilises a 16-membered conjugation pathway. This excludes the β-carbons which means that all the pyrrole α-carbons are conjugated to nitrogen atoms and are, therefore, of the 'pyrrolenine' type. Consequently, a downfield shift in the position of these resonances is expected. This prediction is confirmed in the $^{13}$C-NMR spectra of the Group IIb metallo-TPPs[15] (see Table 2) which show a downfield shift of the pyrrole α-carbon resonances to 150 - 152 ppm.

In PdTPP and PtTPP, there is strong evidence from UV/visible spectroscopy,[21] for increasing back-bonding from metal d-atomic orbitals into porphyrin $\pi^*$-molecular orbitals.

Inspection of the porphyrin HOMOs and LUMOs, generated by Gouterman's 4-orbital theory[20], indicates that $d \rightarrow \pi^*$ back-bonding would increase electron density over conjugated pairs of α- and β-carbons at the expense of downfield-shifting C-N conjugation. This would make the α-carbons less 'pyrrolenine-like', shifting their $^{13}C$-resonances upfield to an extent depending on metal-to-porphyrin back-bonding. Non-planar Group IIb metal cations, with their lower-lying d-orbitals, cannot do this. These electronic interactions and/or steric ruffling should have a greater upfield-shifting effect on the pyrrole carbons than the phenyl C-1"s, hence their reversed assignment compared to TPP (see Table 2).

## Experimental

$^1H$- and $^{13}C$-NMR spectra were obtained in the FT mode on a Bruker WM 250 using $CDCl_3$ as solvent and TMS as internal reference. UV/ visible spectra were recorded on a Pye-Unicam SP8-400 spectrophotometer. PdTPP was prepared by a literature method[10] from TPP[22] and $PdCl_2$ Aldrich). PtTPP was prepared by the method of Thomas and Martell[9] from TPP (100 mg) and $K_2PtCl_4$ (Aldrich; 1gm). PtTPP, free of TPP, was achieved by column chromatography on silica gel (Kieselgel 60, Merck). The column was prepared as a slurry in $CHCl_3$, acidified with TFA (1%, v/v). The metalloporphyrin was eluted, with $CHCl_3$ containing TFA (1%, v/v), as an orange band, leaving green TPP dication at the top of the column. The eluant was concentrated and crystallised with methanol to yield PtTPP (49 mg; 37%) as orange-red microcrystals (Found: C = 64.20; H = 3.56; N = 6·76. $C_{44}H_{28}N_4Pt.H_2O$ requires C = 64.0; H = 3.6; N = 6.8%). $\lambda_{max}$nm (ε mmol $l^{-1}$) in $CHCl_3$: 402(264), 510(25), 539(5).

The author wishes to thank Dr. R. Shepherd, Ms. S. Johnson and Mr. P. Booth for running NMR spectra, and Dr. G.B. Young for helpful discussions. Support by the SERC (post-doctoral fellowship) is gratefully acknowledged.

## References

1) "The Porphyrins", ed. D. Dolphin, Vols. I - VII, Academic Press, New York, N.Y., 1978 - 1979.

2) J.R. Darwent, P. Douglas, A. Harriman, G. Porter, M.-C. Richoux, Coord. Chem. Rev., 1982, 44, 83.

3) B.M. Hoffman, J.A. Ibers, Acc. Chem. Res., 1983, 16, 15.

4) L.R. Milgrom, J. Chem. Soc., Perkin I, 1983, 2535.

5) W.J. Albery, Acc. Chem. Res., 1982, 15, 242.

6) J.W. Buchler, L. Puppe, Justus Liebig's Ann. Chem., 1974, 1046.

7) W.S. Caughey, W.S. Koski, Biochemistry, 1962, 1, 923.

8) K. Wuthrich, R. Baumann, Helv. Chim. Acta., 1973, 56, 585.

9) D.W. Thomas, A.E. Martell, J. Amer. Chem. Soc., 1959, 81, 5111.

10) A.D. Adler, F.R. Longo, F. Kampas, J. Kim, J. Inorg. Nucl. Chem., 1970, 32, 2443.

11) J.A. Mercer-Smith, D.G. Whitten, J. Amer. Chem. Soc., 1978, 100, 2620.

12) U. Eisner, M.J.C. Harding, J. Chem. Soc., 1964, 489.

13) See reference 1, Vol IV, pp 1 - 59.

14) F. Bonati, H.C. Clark, C.S. Wong, Can. J. Chem., 1980, 58, 1435.

15) R.J. Abraham, G.E. Hawkes, M.F. Hudson, K.M. Smith, J. Chem. Soc. Perkin II, 1975, 204.

16) H.C. Clark, J.E.H. Ward, J. Amer. Chem. Soc., 1974, 96, 1741.

17) C.A. Wilkie, D.T. Haworth, J. Inorg. Nucl. Chem., 1978, 40, 195.

18) E.B. Fleischer, C.K. Miller, L.E. Webb, J. Amer. Chem. Soc., 1964, 86, 2342.

19) H. Gunther, H. Schmickler, H. Königshofen, K. Recker, E. Vogel, Angew. Chem. Int. Ed., 1973, 12, 243.

20) M. Gouterman, J. Mol. Spectrosc., 1961, 6, 138.

21) D. Eastwood, M. Gouterman, J. Mol. Spectrosc., 1970, 35, 359.

22) A.D. Adler, F. Longo, J. Finarelli, J. Goldmacher, J. Assour, L. Korsakoff, J. Org. Chem., 1967, 32, 476.

23) H. Scheer, J.J. Katz in "Porphyrins and Metallo-porphyrins, ed. K.M. Smith, Elsevier, N.Y., 1974, p 413.

*Polyhedron* Vol. 3, No. 7, pp. 883–887, 1984
Printed in the U.S.A.

0277–5387/84 $3.00 + .00
© 1984 Pergamon Press Ltd.

# NOTE

## HALIDE AND COMPLEX HALOGENO ANIONS AS SALTS OF OXINATO BIS($\eta^5$-INDENYL)TITANIUM(IV)/ ZIRCONIUM(IV) CHELATES†

**RAJESH K. BAJAJ, GURVINDER S. SODHI, NARENDER K. KAUSHIK and KRISHAN N. JOHRI***
Department of Chemistry, University of Delhi, Delhi 110007, India

(*Received* 25 *July* 1983; *accepted* 6 *December* 1983)

**Abstract**—Bis($\eta^5$-indenyl)titanium(IV) dichloride and bis($\eta^5$-indenyl)zirconium(IV) dichloride, when treated with 8-hydroxyquinoline (oxine) in aqueous medium form ionic derivatives of the type $[(\eta^5\text{-}C_9H_7)_2ML]^+Cl^-$ (M = Ti(IV), Zr(IV), L is the conjugate base of oxine). A number of halide and complex halogeno anions present in aqueous solution were isolated as salts of these ionic complexes giving derivatives of the type, $[(\eta^5\text{-}C_9H_7)_2ML]^+X^-$ ($X = Br^-$, $I^-$, $ZnCl_3(H_2O)^-$, $CdCl_4^{2-}$, $HgCl_3^-$). Conductivity measurements in nitrobenzene indicate that these complexes are electrolytes. Both the IR and $^1H$ NMR spectral studies demonstrate that the ligand L is chelating. Consequently there is tetrahedral coordination about the titanium(IV) or zirconium(IV) ion.

During the course of our recent investigations, we have elucidated that the coordination of two nitrogen and two oxygen atoms to the $(\eta^5\text{-R})(\eta^5\text{-R}')M(IV)$ moiety would lead to the weakening of the metal-ring bonds[1–3] [R = $C_4H_4N$, R′ = $C_5H_5$, $C_9H_7$; R = $C_5H_5$, R′ = $C_9H_7$; M = Ti, Zr]. In order to investigate whether or not the coordination of two nitrogen and two oxygen atoms around the $(\eta^5\text{-}C_9H_7)_2M(IV)$ moiety (M = Ti, Zr) would produce a similar weakening of metal-ring bonds, we studied the interaction of $(\eta^5\text{-}C_9H_7)_2MCl_2$ with oxine in aqueous medium. We failed to isolate a derivative in which two oxinate groups coordinated to the $(\eta^5\text{-}C_9H_7)_2M(IV)$ moiety. However, ionic complexes of the type $[(\eta^5\text{-}C_9H_7)_2ML]^+Cl^-$ (L is the conjugate base of oxine), in which only one bidentate oxinate ligand is coordinated to the metal ion were readily obtained. Such complexes possess low solvation energies, as is evident from the ease of their preparation. This suggested that a number of halogeno anions present in aqueous solution might be isolated as salts of these complexes. The present communication describes the preparation and characterisation of these complexes.

## EXPERIMENTAL

Nitrobenzene was purified for conductance measurements by the method described by Fay *et al.*[4] Conductance measurements were made on a Digital Direct Reading Conductivity Meter 304. Solid state IR spectra were recorded in KBr pellets in the 4000–200 $cm^{-1}$ range using a Perkin–Elmer 621 grating spectrophotometer. $^1H$ NMR spectra were recorded at a sweep width of 900 Hz with a Perkin–Elmer R-32 spectrometer. Chemical shifts are expressed relative to an internal reference of TMS (1% by volume). Bis($\eta^5$-indenyl)titanium(IV) dichloride and bis($\eta^5$-indenyl)zirconium(IV) dichloride were prepared by the reaction of titanium(IV) chloride or zirconium(IV) chloride with sodium indenide in THF.[5]

### *Preparation of complexes*

An aqueous solution of $[(\eta^5\text{-}C_9H_7)_2ML]^+Cl^-$ was obtained by stirring an aqueous solution of $(\eta^5\text{-}C_9H_7)_2MCl_2$ with a slight excess of solid oxine

†Presented at Fifty-third Annual Session of National Academy of Sciences, India, 27–29 Oct. 1983, Goa.

*Author to whom correspondence should be addressed.

Table 1. Analytical data and physical characteristics

| Complex[a] | Dec. temp.[b] (°C) | Conductivity data $\Lambda_c$ ($C = 1.5\times10^{-3}$ M) | Analysis Found (Calc.)% | |
|---|---|---|---|---|
| | | | Cl | N |
| $[(\eta^5\text{-}C_9H_7)_2TiL]^+Br^-$ | 178 | 26.6 | - | 2.70(2.73) |
| $[(\eta^5\text{-}C_9H_7)_2TiL]^+I^-$ | 220 | 30.2 | - | 2.65(2.55) |
| $[(\eta^5\text{-}C_9H_7)_2TiL]^+ZnCl_3(H_2O)^-$ | 232 | 26.2 | 17.53(17.40) | 2.35(2.29) |
| $[(\eta^5\text{-}C_9H_7)_2TiL]_2^+CdCl_4^{2-}$ | 106 | 56.2 | 12.91(12.93) | 2.48(2.55) |
| $[(\eta^5\text{-}C_6H_7)_2TiL]^+HgCl_3^-$ | 178 | 28.2 | 14.75(14.61) | 1.91(1.92) |
| $[(\eta^5\text{-}C_9H_7)_2ZrL]^+Br^-$ | 183 | 30.4 | - | 2.48(2.57) |
| $[(\eta^5\text{-}C_9H_7)_2ZrL]^+I^-$ | 204 | 24.8 | - | 2.49(2.36) |
| $[(\eta^5\text{-}C_9H_7)_2ZrL]^+ZnCl_3(H_2O)^-$ | 260 | 26.4 | 16.40(16.26) | 2.28(2.13) |
| $[(\eta^5\text{-}C_9H_7)_2ZrL]_2^+CdCl_4^{2-}$ | 275 | 55.6 | 11.81(11.98) | 2.46(2.36) |
| $[(\eta^5\text{-}C_9H_7)_2ZrL]^+HgCl_3^-$ | 174 | 28.6 | 13.63(13.79) | 1.69(1.81) |

[a] L = conjugate base of oxine ($C_9H_6NO$); [b] uncorrected value; [c] in $ohm^{-1}$ $cm^2$ $mole^{-1}$

Table 2. Relevant IR data ($cm^{-1}$)

| Complex | $\nu$(C≡N) | $\nu$(M-Cl) | $\nu$(C-O) | $\nu$(C-H) in plane deformation | $\nu$(C-H) out of plane deformation |
|---|---|---|---|---|---|
| $[(\eta^5\text{-}C_9H_7)_2TiL]^+Br^-$ | 1330(s) | - | 1110(s) | 1070(w),1220(m) | 825(w),780(m) |
| $[(\eta^5\text{-}C_9H_7)_2TiL]^+I^-$ | 1335(s) | - | 1120(s) | 1075(w),1215(m) | 835(w),775(m) |
| $[(\eta^5\text{-}C_9H_7)_2TiL]^+ZnCl_3(H_2O)^-$ | 1335(s) | 325(w),375(m) | 1110(s) | 1070(w),1215(m) | 830(m),785(m) |
| $[(\eta^5\text{-}C_9H_7)_2TiL]_2^+CdCl_4^{2-}$ | 1330(s) | 340(w),375(m) | 1115(s) | 1080(w),1230(m) | 840(w),790(m) |
| $[(\eta^5\text{-}C_9H_7)_2TiL]^+HgCl_3^-$ | 1320(s) | 330(m),350(m) | 1115(s) | 1065(w),1220(m) | 855(m),780(m) |
| $[(\eta^5\text{-}C_9H_7)_2ZrL]^+Br^-$ | 1325(s) | - | 1125(s) | 1070(w),1220(m) | 850(w),795(m) |
| $[(\eta^5\text{-}C_9H_7)_2ZrL]^+I^-$ | 1330(s) | - | 1105(s) | 1075(w),1210(m) | 860(w),775(m) |
| $[(\eta^5\text{-}C_9H_7)_2ZrL]^+ZnCl_3(H_2O)^-$ | 1325(s) | 335(m),380(m) | 1110(s) | 1090(w),1215(m) | 860(w),790(m) |
| $[(\eta^5\text{-}C_9H_7)_2ZrL]_2^+CdCl_4^{2-}$ | 1325(s) | 325(w),365(m) | 1110(s) | 1095(w),1205(m) | 860(w),775(m) |
| $[(\eta^5\text{-}C_9H_7)_2ZrL]^+HgCl_3^-$ | 1330(s) | 330(w),380(m) | 1115(s) | 1080(w),1220(m) | 850(m),775(m) |

(s) strong, (m) medium, (w) weak

in about 100 $cm^3$ double-distilled water. After about 3 hr, the contents were filtered and the aqueous solution was shaken with about 25 $cm^3$ benzene. The aqueous phase was collected and added separately to an aqueous solution of KBr, KI, $ZnCl_2$, $CdCl_2$ or $HgCl_2$. The green precipitate was filtered and washed with water followed by petroleum ether. The compounds were reprecipitated from acetone solution by the addition of petroleum ether.

## RESULTS AND DISCUSSION

The method used for preparing and isolating $[(\eta^5\text{-}C_9H_7)_2ML]^+X^-$ complexes yields materials of good purity as judged from satisfactory elemental analysis and spectroscopic data. The complexes are green in colour and thermally stable. They are soluble in acetone, THF and partially soluble in halogenated hydrocarbons. With $ZnCl_2$, an aquotrichloro zincate(II) anion is precipitated and coordinated water can be identified by intense infrared absorptions. Conductivity measurements reveal that the complexes are 1:1 electrolytes in nitrobenzene. However, in the case of cadmium(II) derivatives, the results are consistent with those of 1:2 electrolytes, indicating that dinegative anions are precipitated. The analytical data and physical characteristics of the complexes are given in Table 1.

The C⋯N bond in the oxinate group shows a very intense IR absorption frequency at $\sim 1330\ cm^{-1}$. Since this bond possesses partial double bond character, it is expected that its vibrational frequency should occur in the 1450–1500 $cm^{-1}$ range.[6] In fact free oxine shows an intense absorption in this region. The occurrence of this band at lower energy in the present complexes indicates considerably less double bond character of C—N bond in the oxinate group.[2]

The complexes show medium intensity absorption bands in the 345–365 $cm^{-1}$ region due to the metal–chlorine stretching vibrations.[7,8] No halide bridging is involved, since with the exception of bands assigned to the anions, the IR spectra are virtually the same for all the complexes. The $\nu$(C–H) and $\nu$(C–C) aromatic stretching vibrations occur at the same frequencies as reported earlier.[2]

The C–O stretching frequency shows an intense absorption centred around the 1110 $cm^{-1}$ region.[7] A doublet is observed at $500 \pm 40\ cm^{-1}$. The absorption at higher frequency is attributed to the C–O in-plane bending[9] and that at lower frequency to M–O stretching vibrations.[7] The characteristic IR frequencies, together with their assignments are presented in Table 2.

The $^1$H NMR spectra of the complexes were recorded in deuterated acetone. The C(2) proton of the oxinate group, in the case of metal complexes, gave a signal at $\delta$ 9.08 ppm ($q$, J = 4 and 1.8 Hz). This is downfield as compared to the value of $\delta$ 8.73 ppm for the free oxine. Hence, it supports the conclusion that the oxinate group is chelating. The signals due to the remaining protons of the oxinate group results in a complex multiplet in the range $\delta$ 7.4–8.2 ppm. The spectra of the zinc(II) derivatives show an additional resonance signal (a broad peak at $\delta$ 4.20 ppm) due to the presence of a coordinated water molecule.

The possibility of oxinate ligand bonding by simple hard sphere coulombic interaction to $(\eta^5\text{-}C_9H_7)_2M(IV)$ moiety is ruled out because in such a case a bis-oxinate complex may be isolated, such a structure would maximise the coordination number of the metal ion and simultaneously maximise the total metal-ring overlap. Since the $\pi$-clouds are used in the formation of metal-ring bands and would exert less of a steric effect as the equatorial ligands, this configuration cannot be described as unstable on the basis of steric effects. However, applying Ballhausen and Dahl's[10] theory to the present complexes, it can be assumed that two strongly directed metal hybrids, which are used in $(\eta^5\text{-}C_9H_7)_2MCl_2$ are binding on oxinate ligands. Coordination of two oxygen and two nitrogen atoms in the $xy$ plane by strong covalent bonds would result in the weakening of the metal-ring bonds and would be energetically unfavourable. The Ti–O and Ti–N bonds have appreciable covalent character, since only one oxinate ligand interacts.

*Acknowledgement*—We take this opportunity to thank the Council of Scientific and Industrial Research, New Delhi for awarding senior research fellowships to R.K.B. and G.S.S.

## REFERENCES

1. G. S. Sodhi and N. K. Kaushik, *Inorg. Nucl. Chem. Lett.* 1981, **17**, 211.
2. G. S. Sodhi, A. K. Sharma and N. K. Kaushik, *J. Organomet. Chem.* 1982, **238**, 177.
3. G. S. Sodhi and N. K. Kaushik, *Bull. Soc. Chim., France* 1982, 45.
4. R. C. Fay and R. N. Lowry, *Inorg. Chem.* 1967, **6**, 1512.
5. E. Samuel and R. Setton, *J. Organomet. Chem.* 1967, **10**, 257.
6. J. Chatt, L. A. Duncanson, L. M. Venanzi, *Suomen Kemi* 1956, **29B**, 75; C.A. 1957, **51**, 5559.

7. G. Doyle and R. S. Tobias, *Inorg. Chem.* 1967, **6**, 1111; 1968, **7**, 2484.
8. K. Chandra, R. K. Sharma, B. S. Garg and R. P. Singh, *Transition Met. Chem.* 1979, **4**, 367.
9. J. E. Tackett and O. T. Sawyer, *Inorg. Chem.* 1964, **3**, 692.
10. C. J. Ballhausen and J. P. Dahl, *Acta Chim. Scand.* 1961, **15**, 1333.

*Polyhedron* Vol. 3, No. 7, pp. 889–894, 1984
Printed in the U.S.A.

0277–5387/84 $3.00 + .00
© 1984 Pergamon Press Ltd.

# NOTES

## REACTIONS OF COLLMAN COMPLEX WITH TIN(IV) AND GERMANIUM(IV) PORPHYRINS. FORMATION OF [TIN(II) AND GERMANIUM(II) PORPHYRINS] TETRACARBONYLIRON AND CRYSTAL STRUCTURE OF [2,3,7,8,12,13,17,18-OCTAETHYLPORPHINATO TIN(II)] TETRACARBONYLIRON

JEAN-MICHEL BARBE[(a)], ROGER GUILARD[(a)]*, CLAUDE LECOMTE[(b)] and RENE GERARDIN[(c)].

[(a)]Laboratoire de Synthèse et d'Electrosynthèse Organométallique associé au C.N.R.S. (LA 33), Faculté des Sciences "Gabriel", 6, Bd Gabriel, 21100 DIJON, FRANCE.

(b)Laboratoire de Minéralogie et Cristallographie (ERA 162), Faculté des Sciences, Centre de 2ème Cycle, B. P. N° 239, 54506 VANDOEUVRE LES NANCY, FRANCE.

[(c)]Laboratoire de Chimie du Solide Minéral associé au C.N.R.S. (n° 158), Service de Chimie Minérale, Université de NANCY 1, B. P. N° 239, 54506 VANDOEUVRE LES NANCY, FRANCE.

*(Received 25 November 1983: accepted 2 April 1984)*

Abstract - The action of $Na_2Fe(CO)_4$ with tin(IV) and germanium(IV) porphyrins affords metal(II) porphyrin complexes $[(por)M(II)Fe(CO)_4]$ (por = porphyrinate, M = Sn(II) or Ge(II)). The molecular structure of $[(oep)Sn(II)Fe(CO)_4]$ was solved by X-ray diffraction techniques. The molecular structure of $[(oep)Sn(II)Fe(CO)_4]$ was solved by X-ray diffraction techniques : the Sn coordination is square pyramidal with the iron in axial position (Sn-Fe = 2.492(1)Å) whereas the Fe coordination is trigonal bipyramidal. Mössbauer parameters provide convincing evidence for the formal zero oxidation state of the iron atom.

*Author to whom correspondence should be adressed.

Metal-metal interactions in metalloporphyrins have been shown to be an effective strategy for the synthesis of metal-chain complexes. Some of these complexes exhibit high or unusual electric conductivities[1]. Although much work has been devoted to metalloporphyrin chemistry[2], there are very few studies of porphyrin compounds containing metal-metal bonds[3,4]. In this note we report one approach to synthesize linear metal-chain derivatives in which metallomacrocycles would be linked in a "face to face" orientation by the ion $Fe(CO)_4^{2-}$. Reaction of $[(por)M(IV)Cl_2]$ with $Na_2Fe(CO)_4$ gives M(II) porphyrins possessing a binuclear framework instead of the expected metal-chain complexes. (Abbreviations used : por = porphinato ; oep = octaethylporphinato ; tptp = meso-tetra-*p*-tolylporphinato).

All operations were carried out in Schlenk tubes under purified argon and with dried oxygen free solvents. To a solution of 0.67 mmol (0.23 g) of $Na_2Fe(CO)_4$ in THF (180 $cm^3$) was added 0.67 mmol (0.479 g) of $[(oep)Sn(IV)Cl_2]$ and the mixture, with stirring, was allowed to room temperature over a period of 24 h. Next, the solution was evaporated to dryness under vacuum and the residual solid was purified by chromatography on an aluminium oxide column (eluent : toluene). Evaporation of the eluate resulted in an orange-red solid which was recrystallized in toluene (25 $cm^3$) (0.25 g, 46 % yield of $[(oep)Sn(II)Fe(CO)_4]$). The conditions, yields and spectroscopic data for this reaction and reactions of other porphyrins are summarized in Table 1.

Elemental analyses of the compounds obtained are consistent with the molecular formula $[(por)M(II)Fe(CO)_4]$. Electronic spectra of octaethylporphyrin complexes belong to the hyperclass[2b,5]. They show two bands in the Soret region (370 - 450 nm) and two other blue shifted with respect to the Soret range (560 - 630 nm). Absorption spectra of tetraaryl derivatives are normal. In the carbonyl stretching region, the IR spectra of all the compounds exhibit three bands of which two are sharp (2020 - 1940 $cm^{-1}$) whilst the band at lowest energy (1920-1905 $cm^{-1}$) is very broad and intense. On the basis of "local" $C_{3v}$ symmetry for the $M(CO)_4$ fragment, three infrared active carbonyl stretching frequencies are predicted by group theoretical considerations. The proton NMR data[6] for $[(oep)M(II)Fe(CO)_4]$ complexes show that the methylene protons are diastereotopic. Both the out-of-the porphyrin plane displacement of the tin atom and the asymmetry of the axial ligand can render the two sides of the macrocycle magnetically non-equivalent[7].

The above assumptions were fully confirmed by the X-ray diffraction results carried out on the complex $[(oep)Sn(II)Fe(CO)_4]$. The crystal is triclinic $\bar{P}1$ with cells constants : a = 12.253(4),

$b$ = 13.910(5), $c$ = 15.087(5) Å, $\alpha$ = 59.53(3), $\beta$ = 61.14(3), $\gamma$ = 68.88(3)°, V = 1918 Å$^3$, Z = 2, $F_{000}$ = 840 $\bar{e}$. A total of 7330 reflections were collected with MoKα radiation to give 5965 unique structure factors ($\sigma(I)/I < 0.3$). These reflections were corrected from Lorentz and polarisation effects. The structure was solved by the heavy atom method and refined to a R index of R(F) = 0.0409 and $R_w(F)$ = 0.0482 with the SHELX Program[8]. Atomic coordinates, thermal parameters and lists of Fo/Fc values have been deposited as supplementary material with the Editor, from whom copies are available on request. Copies have also been sent to the Cambridge Data Centre.

The figure is an ORTEP[9] view of the complex ; table 2 gives the main bond distances and angles in the coordination spheres of the tin and iron atoms. The tin atom is coordinated by the four nitrogen atoms of the porphinato group (< Sn - N > = 2.187(3)Å) and in axial position by the iron atom (Sn - Fe = 2.492(1) Å, Sn - Fe - C(52) = 179.1(1)°). The tin atom lies 0.818(9)Å from the plane of the four nitrogens and the radius of the central hole is 2.028(3)Å. The resulting polyhedron is a square pyramid. The iron atom possesses a pseudo-symmetry $C_{3v}$ and its coordination polyhedron is a trigonal bipyramid with three equatorial carbonyl ligands and two different axial ligands : a carbonyl group and the tin porphinato rest. The iron carbonyl distances are statistically equal (< Fe - C > = 1.754(5)Å). The bond distances are normal in the porphinato ring.

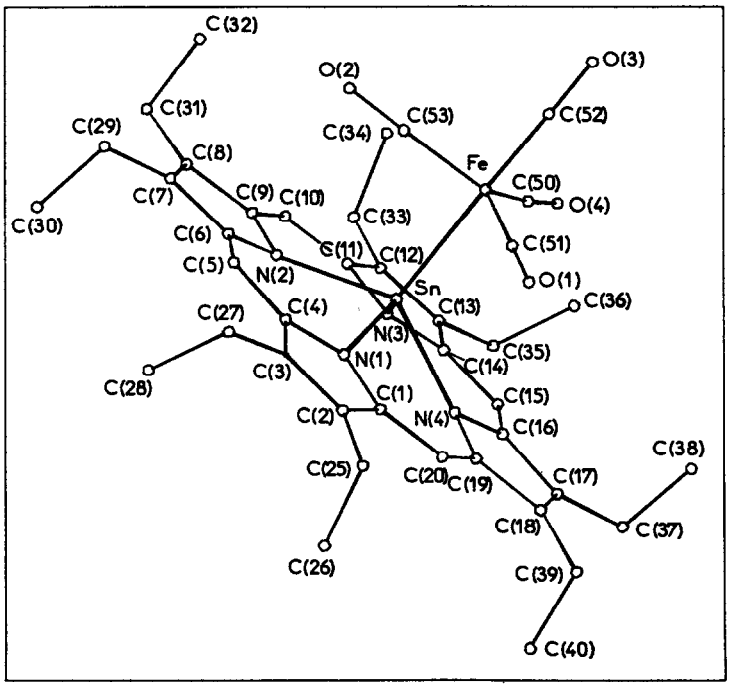



Fig. 1 : ORTEP view of $[(oep)Sn(II)Fe(CO)_4]$.

Table 1 : Experimental conditions, yields and spectroscopic data for the complexes $[(por)M(II)Fe(CO)_4]$.

| Complex | Recryst. solvent* | % yield | UV-visible $\lambda_{max/nm}$ ($10^{-4}$ $\varepsilon/dm^3.mol^{-1}.cm^{-1}$) | IR $\nu_{cm}^{-1}$ |
|---|---|---|---|---|
| $[(oep)Sn(II)Fe(CO)_4]$ | A | 46 | 368(7.25) 441(9.44) 558(1.46) 592(0.51) | 2019 1938 1905 |
| $[(tptp)Sn(II)Fe(CO)_4]$ | A-B (1/1) | 48 | 350(6.51) 453(20.30) 540(0.47) 585(0.92) 630(1.1) | 2023 1943 (1917-1905) |
| $[(oep)Ge(II)Fe(CO)_4]$ | A | 14 | 366(7.12) 442(9.52) 557(1.38) 591(0.49) | 2023 1940 (1912-1904) |
| $[(tptp)Ge(II)Fe(CO)_4]$ | A-B (2/1) | 29 | 350(6.42) 452(20.26) 540(0.47) 582(1.00) 625(1.05) | 2026 1945 (1919-1905) |

* A : toluene ; B : heptane.

Table 2 : Important bond lengths(Å) and angles(°) of $[(oep)Sn(II)Fe(CO)_4]$.

| | | | | | |
|---|---|---|---|---|---|
| Sn - N(1) | 2.185 (5) | Sn - N(2) | 2.202 (3) | Sn - N(3) | 2.171 (4) |
| Sn - N(4) | 2.193 (3) | Sn - Fe | 2.492 (1) | Fe - C(50) | 1.767 (6) |
| Fe - C(51) | 1.755 (5) | Fe - C(52) | 1.751 (6) | Fe - C(53) | 1.745 (7) |

| | | | |
|---|---|---|---|
| N(1) - Sn - Fe | 112.2 (1) | N(2) - Sn - Fe | 110.5 (1) |
| N(3) - Sn - Fe | 111.6 (1) | N(4) - Sn - Fe | 113.8 (1) |
| Sn - Fe - C(50) | 88.0 (1) | Sn - Fe - C(51) | 86.5 (1) |
| Sn - Fe - C(52) | 179.1 (1) | Sn - Fe - C(53) | 87.0 (1) |

Two $^{57}Fe$ Mössbauer spectra of $[(oep)Sn(II)Fe(CO)_4]$ were recorded at 95 and 297 K using an ELSCINT spectrometer with constant acceleration. These spectra were refined by a least squares method with Lorentzian line shapes[10]. They show a quadrupole splitting and the hyperfine parameters are given in Table 3. The Lamb-Mössbauer factor decreases significantly when the temperature increases, the relative absorption varies from about 4 % at 95 K to less than 1 % at room temperature. COLLINS and PETIT[11] have found a quasi linear correlation between the quadrupole splitting and the isomer shift for some $L\text{-}Fe(CO)_4$ complexes where the iron atom possesses a $C_{3v}$ symmetry. $\Delta$ and $\delta$ parameters agree with this linear relation. Hence the iron atom is at formal zero oxidation state and $[(oep)Sn(II)]$ can be considered as a $\sigma$-donor ligand which enhances 4s electron occupation of the iron atom.

Table 3 : Mössbauer data for $[(oep)Sn(II)Fe(CO)_4]$.

| T(K) | $\delta(mm.s^{-1})$ | $\Delta(mm.s^{-1})$ | $\Gamma_1(mm.s^{-1})$ | $\Gamma_2(mm.s^{-1})$ | $I_1$ | $I_2$ |
|---|---|---|---|---|---|---|
| 297 | - 0.154 | 2.23 | 0.22 | 0.24 | 0.45 | 0.55 |
| 95 | - 0.081 | 2.27 | 0.31 | 0.32 | 0.46 | 0.54 |

$\delta$ : relative to metal iron at 297 K

$I_1$ : relative intensity of the lower energy line

$I_2$ : relative intensity of the upper energy line

Such an arrangement would be expected since the reduction of diorganometal dichlorides $R_2M(IV)Cl_2$ (M = Ge, Sn, Pb) by $Na_2Fe(CO)_4$ produced dimeric $[R_2M(II)Fe(CO)_4]_2$ complexes[12,13,14]. These compounds undergo ring fission in strong bases (B) affording the base stabilized B $[R_2M(II)Fe(CO)_4]$ species which contain trigonal bipyramidally coordinated iron. The $\sigma$-donor and $\pi$-acceptor properties of diaryl and dialkylgermylenes and -stannylenes when coordinated to a transition metal are also well established and comparable to those of $[(oep)M(II)]$ ligands.

Acknowledgement :

We thank Mr M. SOUSTELLE for his technical assistance.

## References

[1] J. A. Ibers, L. J. Pace, J. Martinsen and B. M. Hoffman, *Structure and Bonding (Berlin)*, 1982, 50, 1.

[2] (a) J. W. Buchler, in "*Porphyrins and Metalloporphyrins*", K. M. Smith, Ed. Elsevier Scientific Publishing Company, Amsterdam, 1975, p. 157.

(b) J. W. Buchler, in "*The Porphyrins*", D. Dolphin, Ed., Vol. I, Chap. 10, Academic Press, New York, 1978, p. 390.

[3] S. Onaka, Y. Kondo, K. Toruimi and T. Ito, *Chemistry Letters*, 1980, 1605.

[4] P. Cocolios, C. Moïse and R. Guilard, *J. Organometal. Chem.*, 1982, 228, C 43.

[5] M. Gouterman, in "*The Porphyrins*", D. Dolphin, Ed., Vol. III, Chap. I, Academic Press, New York, 1978, p. 1.

[6] NMR data : $[(oep)Sn(II)Fe(CO)_4]$ ($C_5D_5N$), δ 1.95 (24 H, triplet, methylic H), 4.26 (16 H, multiplet, methylenic H), 10.88 (4 H, singlet, meso H) ; $[(tptp)Sn(II)Fe(CO)_4]$ ($C_6D_6$), 2.40 (12 H, singlet, *p*-methylic H), 7.24 (4 H, singlet, meta H), 7.32 (4 H, singlet, meta'H), 8.10 (8 H, massive, ortho H), 9.25 (8 H, singlet, pyrrolic H) ; $[(oep)Ge(II)Fe(CO)_4]$ ($C_6D_6$), 1.80 (24 H, triplet, methylic H), 3.94 (16 H, multiplet, methylenic H), 10.42 (4 H, singlet, meso H) ; $[(tptp)Ge(II)Fe(CO)_4]$ ($C_6D_6$), 2.38 (12 H, singlet, *p*-methylic H), 7.22 (4 H, singlet, meta H), 7.30 (4 H, singlet, meta'H), 8.06 (4 H, singlet, ortho H), 8.14 (4 H, singlet, ortho'H), 9.18 (8 H, singlet, pyrrolic H).

[7] C. A. Busby and D. Dolphin, *J. Magn. Res.*, 1976, 23, 211.

[8] G. M. Sheldrick, SHELX 76, Program for Crystal Structure Determination, University of Cambridge, England, 1976.

[9] C. K. Johnson, *ORTEP Report ORNL-30794*, Oak Ridge National Lab. Tennessee, USA, 1965.

[10] G. Lecaer, private communication.

[11] R. L. Collins and R. Petit, *J. Chem. Phys.*, 1963, 39, 3433.

[12] T. J. Marks and A. R. Newman, *J. Amer. Chem. Soc.*, 1973, 95, 769.

[13] A. R. Cornwell, P. C. Harrison and J. A. Richards, *J. Organometal. Chem.*, 1976, 108, 47.

[14] R. A. Burnham, M. A. Lyle and S. R. Stobart, *J. Organometal. Chem.*, 1977, 125, 179.

*Polyhedron* Vol. 3, No. 7, pp. 895-896, 1984
Printed in the U.S.A.

0277-5387/84 $3.00 + .00
© 1984 Pergamon Press Ltd.

# COMMUNICATION

## KINETIC AND COMPETITION STUDIES OF SUBSTITUTION REACTIONS OF THE TRANS-AQUOSULPHITOTETRACYANOCOBALT COMPLEX, $Co(CN)_4(SO_3)(OH_2)^{3-}$

MOUSTAFA H.M. ABOU-EL-WAFA and MICHAEL G. BURNETT*

Department of Chemistry, The Queen's University of Belfast,
Belfast, BT9 5AG, N. Ireland

(Received 23 February; accepted 9 April 1984)

Abstract--The relative nucleophile efficiencies predicted for $NH_3$, $CH_3NH_2$ and $CN^-$ from their rates of reaction with trans-$Co(CN)_4(SO_3)(OH_2)^{3-}$ are confirmed by competition experiments with similar nucleophiles ($NH_3$-$CH_3NH_2$) but not by experiments with contrasting nucleophiles ($NH_3$-$CN^-$). This system, though substantially dissociative in mechanism, (D), possesses some interchange properties, ($I_d$).

Recently, we have shown by kinetic and competition experiments[1] that the substitution of $[Co(CN)_5X]^{n-}$, X = $H_2O$, $Cl^-$, and $N_3H$ by the nucleophiles $N_3^-$, $NCS^-$, and $Me_2SO$, (dimethylsulphoxide), takes place via a dissociative interchange mechanism, ($I_d$), and not by the limiting dissociative mechanism, (D), initially proposed.[2-3] The study presented here has been designed to apply a similar test to the limiting D-type mechanism suggested[4-6] for the replacement of the water ligand in trans-$Co(CN)_4(SO_3)(OH_2)^{3-}$ complex.

The rate constants for the displacement of water in trans-$Co(CN)_4(SO_3)(OH_2)^{3-}$ by nucleophiles $CN^-$, $NH_3$, and $CH_3NH_2$ were measured spectroscopically at 25°C, unit ionic strength ($NaClO_4$) and in presence of 0.5M sodium hydroxide. Two series of competition experiments were carried out using the mixtures $NH_3$-$CH_3NH_2$, and $NH_3$-$CN^-$. These systems were chosen because the spectra of the reactants and products were sufficiently different to allow them to be analysed by U.V. spectroscopy, and also because they showed limiting dissociative kinetics. Three wavelengths were found for each system, at each of which one pair of the complexes present had identical extinction coefficients. The absorbance change at each wavelength was then proportional to the concentration of the third complex only. Thus the concentrations of the reactant and both products could be measured independently using spectroscopy alone. The sum of the concentrations remained constant during a run thereby confirming the absence of secondary reactions. The ratio of the product concentrations was extrapolated to zero time to eliminate the effects of secondary substitution.

The kinetic and competition behaviour is broadly consistent with the dissociative mechanism proposed earlier.[4]

$$Co(CN)_4(SO_3)(OH_2)^{3-} \underset{k_{-1}}{\overset{k_1}{\rightleftharpoons}} Co(CN)_4(SO_3)^{3-} + H_2O \qquad \ldots (1)$$

$$Co(CN)_4(SO_3)^{3-} + X^- \xrightarrow{k_{3,X}} Co(CN)_4(SO_3)X^{4-} \qquad \ldots (2)$$

$$Co(CN)_4(SO_3)^{3-} + Y^- \xrightarrow{k_{3,Y}} Co(CN)_4(SO_3)Y^{4-} \qquad \ldots (3)$$

$$Co(CN)_4(SO_3)(OH_2)^{3-} + OH^- \underset{}{\overset{K_4}{\rightleftharpoons}} Co(CN)_4(SO_3)(OH)^{4-} + H_2O \qquad \ldots (4)$$

Assuming a steady state concentration for $Co(CN)_4(SO_3)^{3-}$ and the earlier result[4] that negligible substitution occurs via $Co(CN)_4(SO_3)(OH)^{4-}$, the first order constant k follows,

$$k = \frac{k_1(k_{3,X}[X^-] + k_{3,Y}[Y^-])}{(1 + K_4[OH^-])(k_{-1} + k_{3,X}[X^-] + k_{3,Y}[Y^-])} \qquad \ldots (5)$$

*Author to whom correspondence should be addressed

All the rate data fit equation (5) and the numerical values of $k_1$ and $k_3/k_{-1}$ are listed in table (1). The concentration ratios of the $CN^-$ or $CH_3NH_2$ products to the $NH_3$ product were plotted against the concentrations of $CN^-$ and $CH_3NH_2$ respectively. The slopes of the resulting linear plots interpreted according to equation (5) gave the data shown in column 5 of the table (1).

The small but significant variation of $k_1$ confirms the slight degree of nucleophile participation in the initial dissociative step. It suggests that the variation in the values of $k_1$ for different nucleophiles reported earlier[6] is a real effect and not due to the uncertainty of the rate data. The major discrepancy in the constants for $CH_3NH_2$ arises from a disagreement in the actual rate measurements. However, the internal consistency of our data seems superior to that of the original measurements, and we therefore have based our conclusions on our results alone.

The change in k found for a nucleophile mixture of $NH_3$ and CN points to quite unexpected nucleophile-substrate interactions. It seems very likely that the dramatic difference between the calculated and observed values of $k_{3,CN}/k_{3,NH_3}$ arises from the same cause. The existence of these discrepancies is clearly nucleophile dependent since for the chemically similar pair, competition and kinetic data are in accord.

In short, we may conclude that the evidence supports the hypothesis that the nucleophilic substitution of trans-$Co(CN)_4(SO_3)(OH_2)^{3-}$ takes place predominantly via a D-type mechanism but that nucleophile participation in the dissociative transition state does occur at least in the case of the cyanide ion. Even for this family of complexes a spectrum of behaviour seems possible ranging from the purely dissociative, (D), to the interchange dissociative, ($I_d$), depending on the nucleophile reaction system used.

Acknowledgement – We thank the Arab Republic of Egypt for the award of a post-graduate scholarship and the C.V.C.P. for an Overseas Research Student award (to M.H.M.A.-El-W.).

Table 1

| X | $k_1$[a] ($s^{-1}$) | $k_{3,X}/k_{-1}$ (M) | $k_{3,X}/k_{3,NH_3}$ | |
|---|---|---|---|---|
| | | | calc. | obs. |
| $CN^-$ | 1.963 ± 0.035(1.73 ± 0.07)[b] | 34.0 ± 2.2( 35.2)[b] | 0.236 ± 0.016 | 0.066 ± .009[c] |
| $NH_3$ | 2.116 ± 0.012(2.1 ± 0.1)[b] | 143.7 ± 3.7(142.9)[b] | 1 | 1 |
| $CH_3NH_2$ | 2.07 ± 0.025(3.2 ± 0.1)[b] | 149 ± 14 (104.2)[b] | 1.034 ± 0.099 | 0.970 ± .056[d] |

[a] $k_1$ calculated using $K_4$ = 807, (ref. 6). [b] Data from ref. 6.

[c] $[NH_3]$ = 0.05M, 0.50 < [CN] < 0.1M; k, measured using $NH_3$–CN mixtures rises from $4.57 \times 10^{-3}$, ($[CN^-] = 0$), to $5.94 \times 10^{-3}$ $s^{-1}$, ($[CN^-]$ = 0.5M). Values calculated from eq (5): $4.59 \times 10^{-3}$ to $4.77 \times 10^{-3}$ $s^{-1}$.

[d] $[NH_3]$ = 0.513M, 0.25M < $[CH_3NH_2]$ < 0.02M, k using $NH_3$–$CH_3NH_2$ mixtures is constant, $(5.164 \pm .018) \times 10^{-3}$ $s^{-1}$. Value calculated from eq (5): $5.166 \times 10^{-3}$ $s^{-1}$.

REFERENCES

1. M.H.M. Abou-El-Wafa and M.G. Burnett, J. Chem. Soc., Chem. Commun., 1983, 833.
2. A. Haim, Inorg. Chem., 1982, 21, 2887.
3. M.G. Burnett and W.M. Gilfillan, J. Chem. Soc., Dalton Trans., 1981, 1578.
4. P.H. Tewari, R.W. Gaver, H.K. Wilcox and W.K. Wilmarth, Inorg. Chem., 1967, 6, 611.
5. J.E. Byrd and W.K. Wilmarth, Inorg. Chim. Acta Rev., 1971, 5, 7.
6. W.K. Wilmarth, J.E. Byrd, H.N. Po, H.K. Wilcox and P.H. Tewari, Coord. Chem. Rev., 1983, 51, 181. W.K. Wilmarth, J.E. Byrd and H.N. Po, ibid, 1983, 51, 209.

*Polyhedron* Vol. 3, No. 7, pp. 897–900, 1984
Printed in the U.S.A.

0277–5387/84 $3.00 + .00
© 1984 Pergamon Press Ltd.

# COMMUNICATION

## FIRST NMR OBSERVATION OF $^{47}$Ti AND $^{49}$Ti IN CYCLOPENTADIENYL COMPLEXES

A. DORMOND, M. FAUCONET, J. C. LEBLANC and C. MOISE*

Laboratoire de Synthèse et d'Electrosynthèse Organométalliques
associé au C. N. R. S. (L. A. 33), Faculté des Sciences "Gabriel",
6, bd Gabriel 21100 Dijon (France)

**(Received 2 March 1984; accepted 9 April 1984)**

Abstract. $^{47}$Ti and $^{49}$Ti NMR spectra of some mono and biscyclopentadienyl complexes are reported for the first time. The resonances span a relatively large range : electron donating substituents on the cyclopentadienyl ring causes an unexpected downfield shift.

High magnetic field strengths and pulse-FT techniques make possible the direct observation of transition metal nuclei at natural abundance[1,2] ; this ability has opened up a new field of investigations in organic and inorganic chemistry. At this time, no application of titanium organometallic complexes has been yet reported. In this paper, we report the first direct observation of $^{47}$Ti and $^{49}$Ti NMR spectra of a representative series of substituted mono and biscyclopentadienyl titanium(IV) halides. These compounds have been synthetized according literature procedures[3]. Spectra were obtained on naturally abundant samples with a Bruker 400 WM spectrometer operating in the Fourier Transform mode at 22.55 MHz. The solvent was $CDCl_3$ and the concentrations were approximately 0.15 M.

Table 1 summarizes the chemical shifts relative to the two isotopes $^{47}$Ti (I = 5/2, 7.28 %) and $^{49}$Ti (I = 7/2, 5.51 %) for the species studied in this preliminary work (Table 1).

Some general conclusions can be made from the spectral data.

- A large chemical shifts range is observed for these organometallic species ; the $^{49}$Ti resonance exhibits a shielding effect of c.a 266 ppm relative to $^{47}$Ti signal which, futhermore, gives always the most narrow bandwidth.

* Author for correspondence.

Table 1 : $^{47}Ti$ and $^{49}Ti$ NMR parameters[a)]

| Compound | $\delta\ ^{47}Ti$ | $\Delta\nu 1/2(H_2)$ | $\delta\ ^{49}Ti$ | $\Delta\nu 1/2(H_2)$ | $\Delta\delta$ |
|---|---|---|---|---|---|
| $Cp_3TiCl_3$ | - 394 | 36 | - 660 | 80 | 266 |
| $C_5Me_4EtTiCl_3$ | - 104 | 18 | - 371 | 20 | 267 |
| $Cp_2TiCl_2$[c)] | - 773 | 24 | - 1039 | 48 | 266 |
| $Cp_2TiBr_2$ | - 670 | 36 | - 936 | 97 | 266 |
| $Cp_2TiI_2$ | - 517 | 150 | b) | - | - |
| $Cp_2TiBrCl$ | - 723 | 50 | - 990 | 200 | 267 |
| $Cp_2TiICl$ | - 660 | 150 | - 966 | - | 266 |
| $(C_5H_4Me)CpTiCl_2$ | - 745 | 60 | - 1012 | 220 | 267 |
| $(C_5H_4\text{-}CHMe_2)CpTiCl_2$ | - 743 | 122 | - 1011 | 400 | 268 |
| $(C_5H_4\text{-}CHMePh)CpTiCl_2$ | - 741 | 146 | - 1012 | 550 | 271 |
| $(C_5H_4\text{-}CMe_3)CpTiCl_2$ | - 728 | 230 | b) | - | - |
| $(C_5H_4\text{-}Me)_2TiCl_2$ | - 720 | 61 | - 986 | 232 | 266 |
| $(C_5H_4\text{-}CHMePh)_2TiCl_2$[d)] | - 709 | 550 | b) | - | - |
| $(C_5Me_5)_2TiCl_2$ | - 443 | 40 | - 710 | 146 | 267 |
| $(C_5Me_4Et)_2TiCl_2$ | - 443 | 48 | - 710 | 170 | 267 |

a)Chemical shifts are expressed as $\delta$ values in ppm (negative values are highfield) relative to $^{47}TiCl_4$ (neat). Samples were measured at ambient temperature in 10 mm diameter cylindrical tubes. Digital resolution was 6.104 Hz per data point. b)The signal is very broadened. c)$CD_3COCD_3$ : $\delta$ (ppm) $^{47}Ti$ = - 775 ; $^{49}Ti$ = - 1041. d)Mixture of meso and racemic forms.

- The chemical shifts are relative to the number of σ bonded halides and as expected, monocyclopentadienyl trihalides are less shielded (c.a 450 ppm) as biscyclopentadienyl dihalides. In the biscyclopentadienyl series, the chemical shifts are strongly dependant of the nature of the σ bonded halogen. The deshielding increase in the order Cl < Br < I against the electronegativity of the halogen and the mixed dihalides compounds show intermediate resonances with respect to the symmetrical complexes. A similar trend has been also noted in $^{1}H$ NMR for the ring proton shifts[4]. This deshielding can be attributed to some degree of double bond character in the halogen-titanium bond due to pπ-dπ overlap between ligand and $1a_1$ empty metal orbitals[5].

- The chemical shifts are also sensitive to the cyclopentadienyl ring substitution. Replacement of ring hydrogens by electron donnor substituents causes an unexpected deshielding effect of the titanium resonance : especially, a dramatic downfield shift is observed in the $C_5Me_5$ or $C_5Me_4Et$ complexes. These unexpected results can be interpreted by considering the electron density around the titanium nucleï : the increase of the negative charge on the substituted Cp ring allows an enhancement of the ionic character of the Cp-Ti bond, concurrently raising a partial positive charge on the metal atom. This interpretation can be related to the lengthening of the Ti-Cp centroïds distances increasing in the order[6] : $C_5H_5 < C_5H_4Me < C_5Me_5$.

- It is also noteworthy that the bulk of the substituents affects strongly the bandwidths : the broader lines are observed in monosubstituted complexes with the tertiobutyl group and in disubstituted complexes with the asymetric group -CHMePh (with tertiobutyl, the signal is to broad to be clearly detected). This broadening is responsible for the failure to detect the two diastereoisomeric forms present in the $(C_5H_4\text{-}CH(Me)(Ph))_2TiCl_2$ complex. In contrast, the peralkylcyclopentadienyl compounds show narrow signals : this fact suggests an important contribution of the molecular cyclopentadienyl symmetry to the resonance linewidths.

The relatively narrow signals and the spectrum simplicity provide optimism for applications of $^{47}Ti$ and $^{49}Ti$ NMR to a wide variety of cyclopentadienyl titanium complexes.

Acknowledgement

We thank Dr. B. Hanquet for his assistance in using the spectrometer.

References

[1] R. G. Kidd and R. J. Goodfellow, *NMR and the Periodic Table*, Academic Press, New York, 1978.
[2] C. Brevard and P. Franger, *Handbook of high resolution multinuclear NMR*, John Wiley and Sons, New York, 1981.
[3] J. C. Leblanc, C. Moïse and J. Tirouflet, *Nouv. Journal de Chimie*, 1977, **1**, 211 and ref. therein. A. Dormond, F. Le Moigne and J. Tirouflet, *J. Organomet. Chem.*, 1975, **101**, 71. M. F. Sullivan and W. F. Little, ibid., 1967, **8**, 277.
[4] M. C. Beachell and S. A. Butter, *Inorg. Chem.*, 1965, **4**, 1133.
[5] J. W. Lauher and R. Hoffmann, *J. Amer. Chem. Soc.*, 1976, **98**, 1729.
[6] *Comprehensive Organometallic Chemistry*, G. Wilkinson, Pergamon Press, New York, 1982, **3**, 363-4.

*Polyhedron* Vol. 3, No. 7, pp. 901–904, 1984
Printed in the U.S.A.

0277-5387/84 $3.00 + .00
© 1984 Pergamon Press Ltd.

# COMMUNICATION

## A NOVEL *CLOSO*-TYPE METALLAUNDECABORANE, $[1,1\text{-}(PPh_3)_2\text{-}2,5\text{-}(OEt)_2\text{-}1\text{-}RuB_{10}H_8]$, AND ITS RELATIONSHIP TO THE *'ISOCLOSO'* SERIES OF METALLABORANE CLUSTERS

JANET E. CROOK, MARGARET ELRINGTON, NORMAN N. GREENWOOD, JOHN D. KENNEDY, AND J. DEREK WOOLLINS

Department of Inorganic and Structural Chemistry, The University of Leeds, Leeds LS2 9JT, England

(Received 19 March 1984; accepted 9 April 1984)

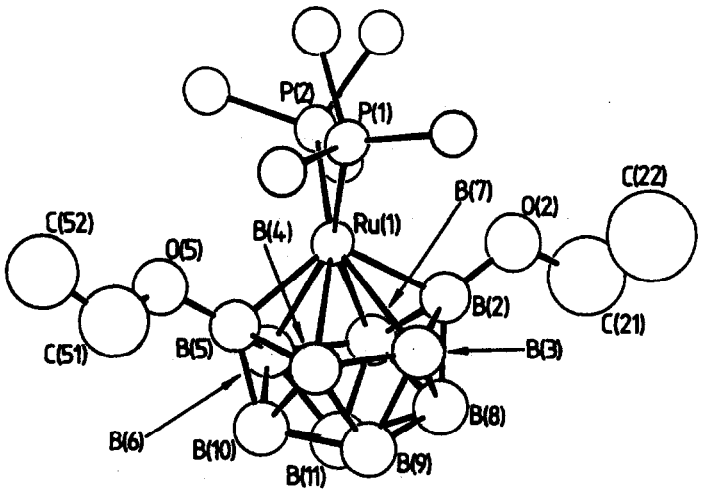
Abstract - The new ruthenaundecaborane $[(PPh_3)_2RuB_{10}H_8(OEt)_2]$ may be considered as an eleven-vertex member of a previously unrecognised series of metallaboranes which are formally derived by the single capping of an *arachno*-type (rather than a *nido*-type) cluster geometry with a metal centre which can be thought of as contributing four orbitals to the cluster bonding schemes.

We wish to report preliminary findings about an interesting new eleven-vertex *closo*-type metallaborane $[(PPh_3)_2RuB_{10}H_8(OEt)_2]$. The compound, an air-stable yellow solid, is prepared in reasonable yield (at present ca. 40%, unoptimized) by the reaction of the *closo*-decaborane anion $B_{10}H_{10}^{2-}$ with $[RuCl_2(PPh_3)_3]$ in ethanol/chloroform solution. The structure as determined by single-crystal X-ray diffraction analysis is given in the Figure.[1] Hydrogen atoms were not locatable in this analysis, but multiple resonance n.m.r. spectroscopy shows that the only cluster hydrogen atoms are the eight *exo*-terminal ones on the non-ethoxy-substituted boron atoms. In particular there are no terminal or bridging hydrogen atoms associated with the metal centre or with the oxygen atoms. The cluster structure conforms closely to an idealized $C_{2v}$ symmetry, and is seen to have the closed deltahedral eleven-vertex 1:2:4:2:2-stack structure as typified by the *closo* binary boron hydride anion $B_{11}H_{11}^{2-}$.

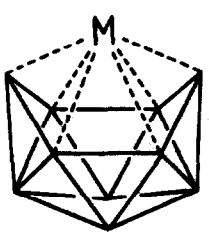
Although this compound is the first structurally characterized polyhedral ruthenaborane, the principal novelty resides in the implications that this structure has for the continuing development of polyhedral skeletal bonding schemes and electron-counting rules.

Two views of the cluster bonding are possible. If the ruthenium atom retains a $d^6$ core, and contributes three orbitals and two electrons to the cluster bonding in the same manner as presumed for the unique capping neutral {BH} moiety in $B_{11}H_{11}^{2-}$, then it is a formal $d^6$ ruthenium(II) centre with an overall five-fold bonding-orbital geometry.

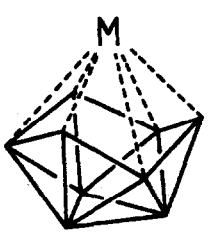
In this case, however, the $\{RuB_9\}$ cluster would then be deficient by two electrons for a formal *closo* bonding-electron count. An alternative view would be that the ruthenium metal vertex supplies four electrons to the cluster bonding, which would imply a full *closo* electron count: the metal would then have a four-orbital contribution to the cluster resulting in a sixteen electron $d^4$ ruthenium(IV) centre with a quasi-octahedral or related disposition of six bonding orbitals.



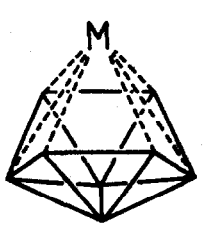

ORTEP drawing of the molecular structure of $[(PPh_3)_2RuB_{10}H_8(OEt)_2]$, with all but the *ipso* carbon atoms of the P-phenyl groups omitted for clarity. Hydrogen atoms were not located by X-ray diffraction but n.m.r. spectroscopy shows that each boron atom except B(2) and B(5) has an *exo* terminal hydrogen atom bound to it, and that there are no other hydrogen atoms associated with the metallaborane cluster. Distances from Ru(1) are as follows, to P(1) 253.6(3) to P(2) 251.3(3), to B(2) 205.7(13), to B(5) 205.2(13), to B(3) 238.5(14), to B(4) 241.5(13), to B(6) 238.3(13) and to B(7) 240.8(13) ppm. B(3)-B(4) and B(6)-B(7) are 170.1(19) and 171.6(18) pm respectively and B(2)-B(3) B(2)-B(7) B(4)-B(5) B(5)-B(6) are in the range 175.2(19)-183.7(18) pm. The angle P(1)-Ru(1)-P(2) is 96.9(1)°.




I




II




III

In terms of this latter interpretation the ruthenaundecaborane reported here would be an eleven-vertex analogue (I) of the previously reported ten-vertex and nine-vertex *isocloso* metallaboranes of the type $[(PR_3)_2HIrB_9H_9]$ (II), and $[(PR_3)_2HIrB_8H_8]$ (III) respectively.[2,3] These formally derive geometrically by the capping of an open *arachno*-tupe cluster geometry to produce a closed deltahedron. This contrasts with conventional *closo* structures which are formally derived by the capping of an open *nido*-type geometry with a three-orbital contributor. In the *isocloso* structures, the capping atom would contribute four orbitals to the cluster bonding scheme and, conversely, the *arachno*-type borane fragment would have one more orbital available than the *nido*-type fragment in the metal/borane frontier region. In the present case the *nido* and *arachno* ten-vertex clusters happen to have mutually similar gross geometries, so that the corresponding derived *closo* and *isocloso* eleven-vertex clusters also have mutually similar gross geometries (I). In the ten- and nine-vertex *isocloso* species (II and III), however, the geometries are quite different from those of the straightforward *closo* species.

The overall principles implicit in these considerations may be quite general, for example in the interpretation of the so-called *'hypercloso'* metallacarboranes such as $[(C_5H_5)_2Fe_2C_2B_6H_8]$ [4] and $[(PPh_3)_2RuC_2B_7H_9]$ [5], and in their extension to the interpretation of the *'isonido'* clusters typified by $[(Ph_3P)_2(Ph_2PC_6H_4IrC(OH)B_8H_7OMe]$ [6] and $[(Ph_3P)_2HIrB_9H_9(PPh_3)]$. The "interstitial" ferraborane $[(CO)_{12}HFe_4BH_2]$ [8] may also be interpreted on this basis; the *arachno* $\{Fe_4\}$ fragment is capped by a $\{BH_2\}$ unit of which all four orbitals are involved in cluster bonding, thus resulting in a *closo* five-vertex trigonal bipyramidal geometry.

We thank SERC for support, Dr D. Reed (Edinbrugh University) for services in high-field n.m.r. spectroscopy, Dr M.A. Beckett for useful discussions, and Johnson Matthey Ltd. for the loan of chemicals.

## References

1. Crystal data: $C_{40}H_{48}B_{10}O_2P_2Ru$, $M$ = 831.94, monoclinic, $a$ = 1.3090(4), $b$ = 2.3335(4), $c$ = 1.3902(4) nm, $\beta$ = 93.63(2)°, $U$ = 4.238(2) $nm^3$, $Z$ = 4, $D_c$ = 1.304 g $cm^{-3}$, $F(000)$ = 1.712, space group $P2_1/n$, Mo-$K_\alpha$ graphite-monochromatised radiation, $\lambda$ = 71.069 pm. Atomic coordinates, thermal parameters, interatomic distances and angles have been deposited with the Cambridge Crystallographic Data Centre.

2. J. Bould, J.E. Crook, N.N. Greenwood, J.D. Kennedy, and W.S. McDonald, *J. Chem. Soc., Chem. Commun.*, 1982, 346.

3. J. Bould, N.N. Greenwood, J.D. Kennedy, and W.S. McDonald, *J. Chem.Soc., Chem. Commun.*, 1982, 465.

4. K.P. Callahan, W.J. Evans, F.Y. Lo, C.E. Strouse, and M.F. Hawthorne, *J. Amer. Chem. Soc.*, 1975, 97, 296; E. Nishimura, *J. Chem. Soc., Chem. Commun.*, 1978, 858.

5. C.W. Jung, R.T. Baker, C.B. Knobler, and M.F. Hawthorne, *J. Amer. Chem. Soc.*, 1980, 102, 5782; C.W. Jung, R.T. Baker, and M.F. Hawthorne, *J. Amer. Chem. Soc.*, 1981, 103, 810.

6. J.E. Crook, N.N. Greenwood, J.D. Kennedy, and W.S. McDonald, *J. Chem. Soc., Chem. Commun.*, 1981, 933.

7. J. Bould, Thesis, University of Leeds, 1983, cited by N.N. Greenwood and J.D. Kennedy in *Metal Interactions with Borane Clusters*, ed. R.N. Grimes. Plenum, 1982, Chapter 2, pp. 108-109.

8. T.P. Fehlner, C.E. Housecroft, W.R. Scheidt, and K.S. Wong, *Organometallics*, 1983, 2, 825.

*Polyhedron* Vol. 3, No. 7, p. 905, 1984 0277-5387/84 $3.00 + .00 Printed in the U.S.A.

# ANNOUNCEMENT

## MOLYBDENUM

The 5th International Mo conference will be held at the University of Newcastle upon Tyne from 1 to 5 July, 1985. The conference is intended to provide a forum for the discussion of recent research in Mo chemistry, to stimulate progress and produce cross fertilization between areas, and to foster new ideas and concepts with particular reference to their possible technological usage. Lecture sessions will include consideration of the following: multiple metal bonds, metal clusters, Mo–S complexes, organometallic compounds, polymeric forms, complexes with special ligands, solution chemistry, Mo in enzymes, solid-state compounds, catalysis, techniques and applications.

The Proceedings will be published as Vol. 5, No. 1 of *Polyhedron* 1986.

Further information can be obtained from:

Professor A. G. Sykes,
Department of Inorganic Chemistry,
The University,
Newcastle upon Tyne, NE1 7RU, England.

*Polyhedron* Vol. 3, No. 8, pp. 907–909, 1984
Printed in the U.S.A.

0277–5387/84 $3.00 + .00
© 1984 Pergamon Press Ltd.

# SPECTRAL AND ELECTROCHEMICAL STUDIES ON OXOISOTHIOCYANATOBIS(PYRROLIDINYLDITHIOCARBAMATO)MOLYBDENUM(V)

**K. S. NAGARAJA and M. R. UDUPA***
Department of Chemistry, Indian Institute of Technology, Madras 600 036, India

(*Received* 4 *March* 1983; *accepted* 17 *January* 1984)

**Abstract**—The complex, oxoisothiocyanatobis(pyrrolidinyldithiocarbamato)molybdenum(V), MoO(NCS) (pyrroldtc)$_2$ was prepared. The IR spectra of the complex suggest that the thiocyanate group is attached through nitrogen and the presence of $MoO^{3+}$ moiety. The voltammograms of the complex in acetonitrile exhibited a pronounced cathodic wave at −0.23 V vs S.C.E. which was attributed to Mo(V)/Mo(IV) couple. The magnetic, epr and electrochemical studies indicate that the compound is mononuclear and molybdenum is in +5 oxidation state.

In spite of the extensive development in the chemistry of binuclear molybdenum(V) complexes in recent years, the properties of molybdo-enzymes are generally interpreted on the basis of a mononuclear molybdenum(V) centre.[1] Few examples of $MoO^{3+}$ complexes with halide and dithiocarbamate ligands such as $MoOCl(Et_2dtc)_2$ and $MoOBr(Et_2dtc)_2$ have been reported.[2] The interesting ambidentate nature[3] of the pseudohalide thiocyanate ligand led to the study[4] of mononuclear oxoisothiocyanatomolybdenum(V) complexes. In the present paper, the synthesis, characterization and voltammetric behaviour of oxoisothiocyanatobis (pyrrolidinyldithiocarbamato)molybdenum(V), MoO(NCS) (Pyrroldtc)$_2$, are discussed.

## EXPERIMENTAL

*Preparation of* MoO(NCS) (Pyrroldtc)$_2$

Molybdenum trioxide (1.0 g) was dissolved in Conc. HCl (1 cm$^3$) containing water (10 cm$^3$). To the resultant solution, hydrazine (2 cm$^3$) was added and warmed over water bath. The solution obtained was cooled and to which ammonium thiocyanate (1.0 g) in water (30 cm$^3$) was added and filtered. To the filtered solution sodium pyrrolidinyldithiocarbamate (1.2 g) in water (200 cm$^3$) was added. The complex thrown out was filtered, washed with water and finally with methanol and dried. Found C, 28.6; H, 3.4; N, 9.1; S, 34.5; Mo, 20.5. Calc. for MoO(NCS) (Pyrroldtc)$_2$: C, 28.5; H, 3.48; N, 9.16; S, 34.7; Mo, 20.7%

The IR and far IR spectra were recorded on Perkin–Elmer 257 and Polytech IR 12 respectively. The electronic spectra were recorded on Carl Zeiss DMR–21 recording spectrophotometer. The EPR spectra were obtained on a Varian E-4 X-band spectrometer. Magnetic measurements were made at room temperature using Gouy balance.

The voltammograms of the complex were recorded in acetonitrile using $NaClO_4$ as the supporting electrolyte. The voltammetric measurements were carried out by a three electrode McKee–Pedersen potentiostatic circuit constructed from operational amplifiers. The working electrode was a Pt foil and Pt wire served as auxillary electrode along with a saturated calomel electrode as reference electrode. The non-aqueous solution under investigation and the reference electrode were separated by non-aqueous salt bridge. Sweep rates varied between 0.01 and 5 V/sec. De-aeration of the solution was performed before commencing the experiment by a stream of purified nitrogen gas. The gas was passed above the solution throughout the experiment.

## RESULTS

The measured magnetic moment of the complex was found to be 1.71 B.M. The powder EPR spectrum at room temperature has a single line with $g$ value 1.968. The EPR spectrum of the

*Author to whom correspondence should be addressed.

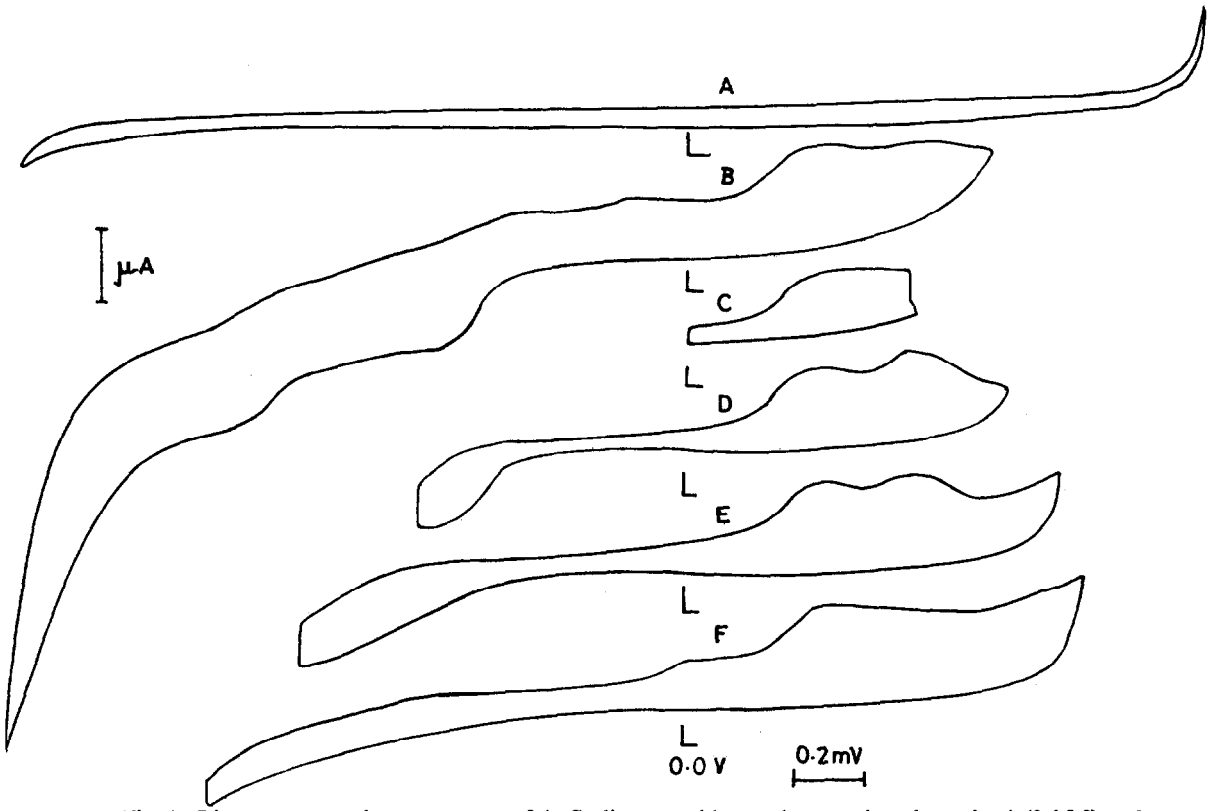



Fig. 1. Linear sweep voltammograms of A. Sodium perchlorate (supporting electrolyte) (0.1 M) and B. MoO(NCS)(pyrroldtc)$_2$ ($1 \times 10^{-3}$ M) + $NaClO_4$ in acetonitrile. Voltammograms C, D and E are recorded after baising the potentials at −0.40, +0.75, +1.05 and +1.02 V respectively. Sweep rate: 0.1 V/sec.

complex in dichloromethane at room temperature exhibits a six line pattern with a strong zero field centre line, which is expected[5] since the nuclear spins of $^{95}$Mo and $^{97}$Mo are 5/2. The $g_{av}$ and $A_{av}$ values, 1.961 and 40 G, are in good agreement with the reported[2] values for similar type of complexes. The electronic spectrum recorded in methanol exhibits shoulders at 730(100), 465(5200) and 270(13760) nm. The first two absorptions are assigned[6] to $d \rightarrow d$ and $\pi(S) \rightarrow d(Mo)$ charge-transfer transitions. The third absorption is assigned to $\pi \rightarrow \pi^*$ internal ligand transition. The infrared spectral bands at 2020 m, 830 m, 480 m and 340 m are assigned[7,8] to $\nu_{NCS}$, $\nu_{C=S}$, $\delta_{NCS}$ and $\nu_{Mo-N}$ respectively, which suggest that thiocyanate group is attached to molybdenum through nitrogen and not through sulphur. The strong band at 930 cm$^{-1}$ is characteristic[2] of Mo=O stretching mode. The bands at 1525 and 1005 cm$^{-1}$ suggest[9,10] that the dithiocarbamate act as univalent bidentate ligand. The Mo–S(dtc) stretching is observed around 365 cm$^{-1}$.

The voltammograms of the complex MoO(NCS)(Pyrroldtc)$_2$ are given in Fig. 1 and the electrochemical data are given in Table 1. As seen from the Fig. 1, an irreversible wave is observed at −0.23 V when the sweep rate was 0.1 V/sec. The wave position did not change when sweep rates from 40 to 200 mV/sec were employed. During the anodic sweep rates, three waves were observed. The potentials were biased at both cathodic and anodic potentials and the voltammograms were recorded. When the potential at −0.30 V was biased, the voltammogram gave no further information. However, biasing at the first anodic potential (+0.60 V) showed a pronounced wave at −0.55 V along with the wave at −0.23 V. The voltammogram recorded after biasing at +1.05 V and a well defined wave at −0.55 V. But biasing the potential at +1.20 V, the wave at −0.55 V completely disappeared and only one cathodic wave was observed at −0.23 V.

## DISCUSSION

The magnetic moment value of 1.71 B.M. indicates that the complex is mononuclear and molyb-

Table 1. Electrochemical data of MoO(NCS)(Pyrroldtc)$_2$

| | | | $E_{1/2}$ Volts vs S.C.E. |
|---|---|---|---|
| $Mo^{V}O(NCS)(pyrroldtc)_2 + 1e^-$ | → | $Mo^{IV}O(NCS)(pyrroldtc)_2$ | -0.23 |
| $Mo^{V}O(NCS)(pyrroldtc)_2$ | → | $Mo^{VI}O(NCS)(pyrroldtc)_2 + 1e^-$ | +0.55 |
| $2MoO(NCS)(pyrroldtc)_2$ | ⇌ | $Mo_2O_2(NCS)_2(pyrroldtc)_4$ | |
| $Mo_2O_2(NCS)_2(pyrroldtc)_4$ | → | $Mo^{VI}Mo^{V}O_2(NCS)_2(pyrroldtc)_4 + 1e^-$ | +0.92 |
| Oxidation of dithiocarbamate ligand | | | +1.15 |

denum has the $d^1$ configuration. The EPR studies further reveal that the complex is mononuclear. The electronic spectrum also suggests a $d^1$ configuration for the Mo atom in the complex. The infrared spectral studies unequivocally point out that the thiocyanate group is attached to molybdenum through nitrogen and the presence of $MoO^{3+}$ moiety. The complex may assume a distorted octahedral geometry with the bidentate chelation of the ligand.

The complex showed a cathodic wave at −0.23 V. The complex, MoO(OH) (Oep) (Oep = octaethylporphyrin) is found[11] to undergo reduction from Mo(V) to Mo(IV) at −0.21 V vs S.C.E. in DMSO medium. Thus the reduction in the present complex is assigned[12] to Mo(V)/Mo(IV) couple which strongly indicates that the complex is monomeric and molybdenum is in +5 oxidation state. The first anodic wave at +0.55 V is attributed to the oxidation[13] of Mo(V) to Mo(VI). The wave observed at +0.92 V is assigned to the oxidation of dimeric Mo(V) species in solution to Mo(VI). Such types of electrochemical processes are not uncommon in the chemistry of molybdenum.[12,13] The third wave at +1.15 V is due to the oxidation of the ligand, which is also observed[4] in the voltammogram of $Mo(NO)_2(Pyrroldtc)_2$. The voltammograms recorded after biasing the potentials indicate that the first two anodic waves are dut to oxidation of Mo(VI). Biasing at the potentials + 0.60 V and +1.05 V, Mo(VI) species are stored in solution and in the reverse cycle undergo reduction to Mo(V) at −0.55 V vs S.C.E. The third oxidation step raptures the coordinated molybdenum(VI) species by the oxidation of the ligand and thus on the reverse cycle no reduction wave is observed.

The electrochemical studies support the conclusion that the complex is mononuclear and molybdenum is in the +5 oxidation state, which is also confirmed by the magnetic and EPR studies.

*Acknowledgement*—We are grateful to the Council of Scientific and Industrial Research (India) for the financial support.

## REFERENCES

1. K. B. Swedo and J. H. Enemark, *J. Chem. Educ.* 1979, **56**, 70.
2. G. J. J. Chen, J. W. McDonald and W. E. Newton, *Inorg. Chim. Acta*, 1980, **41**, 49.
3. A. H. Norbury, *Adv. Inorg. Radiochem.* 1975, **17**, 231.
4. K. S. Nagaraja, Ph.D. Thesis. Indian Institute of Technology, Madras (1982).
5. H. Carrington, *Electron Paramagnetic Resonance.* Academic Press, New York (1974).
6. H. Sabat, M. F. Rudolf and B. J. Jezowska-Trzebiatowska, *Inorg. Chim. Acta*, 1973, **7**, 365.
7. P. C. H. Mitchell and R. J. P. Williams, *J. Chem. Soc.* 1960, 1912.
8. J. Lewis, R. S. Nyholm and P. W. Smith, *J. Chem. Soc.* 1961, 4590.
9. D. Coucouvanis, *Prog. Inorg. Chem.* 1969, **11**, 233.
10. K. Nakamoto, J. Fujita, R. A. Condrate and Y. Mormoto, *J. Chem. Phys.* 1963, **39**, 423.
11. J. H. Fuhrhop, K. M. Kadish and D. G. Davis, *J. Am. Chem. Soc.* 1973, **95**, 5140.
12. L. J. Dehayes, H. C. Faulkner, W. H. Doub and D. T. Sawyer, *Inorg. Chem.* 1975, **14**, 210.
13. J. K. Howie and D. T. Sawyer, *Inorg. Chem.* 1976, **15**, 1892.

Polyhedron Vol. 3, No. 8, pp. 911–916, 1984
Printed in the U.S.A.

0277–5387/84 $3.00 + .00
© 1984 Pergamon Press Ltd.

# CHEMISTRY OF IRON COMPLEXES—III. X-RAY DIFFRACTION, ESR AND OTHER SPECTRAL STUDIES OF NEW IRON(II) AND IRON(III) COMPLEXES WITH TRI-*p*-TOLYLARSINE OXIDE

T. S. LOBANA,* H. S. CHEEMA and S. S. SANDHU
Department of Chemistry, Guru Nanak Dev University, Amritsar 143005, India

(*Received* 7 *June* 1983; *accepted* 17 *January* 1984)

**Abstract**—Reactions of iron(II) and iron(III) salts with tri-*p*-tolylarsine oxide(L) in suitable organic solvents yield complexes of formulas: (i) $[FeL_2Cl_2(OH_2)_2]$ $[FeCl_4].2H_2O$, $[FeL_2Br_2]$ $[FeBr_4].2H_2O$; (ii) $[Fe(NCS)_3L_2].H_2O$; (iii) $[FeL(O_2ClO_2)_2(OH_2)]$ $(ClO_4).0.25C_6H_6$; (iv) $[FeL_3I]$ $[FeI_3].H_2O$ and (v) $[Fe(CO)_3LI]I$. Characterization has been done through elemental analyses, IR, far IR, ESR, and reflectance spectra, molar conductance, magnetic moments, t.g.a. and X-ray diffraction (powder) data. The species $[FeL_2Cl_2(OH_2)_2]^+$, $[FeL_2Br_2]^+$, $[Fe(NCS)_3L_2]$, $[FeL(O_2ClO_2)_2OH_2]^+$, $[FeL_3I]^+$ and $[Fe(CO)_3LI]^+$ have been assigned *trans*-octahedral, *trans*-square planar, *trans*-trigonal bipyramid, *trans*-octahedral, tetrahedral and *cis*-trigonal bipyramid structures respectively.

Triphenylphosphine (arsine) oxides form complexes with iron(III) salts possessing 1:2 (metal to ligand) stoichiometry for halide, thiocyanate and nitrate anions and 1:4 for perchlorate anion.[1] There has been very little work on ditertiaryphosphine oxides and none at all with ditertiaryarsine oxides.[1] In order to study the effect of ring size on nature and stereochemistry of complexes, we have investigated a number of iron(II) and iron(III) complexes.[2–4] Techniques such as ESR and far IR have been helpful in structure elucidation in these complexes. In continuation of our studies on the chemistry of iron complexes, this paper describes the synthesis and characterization of complexes of iron(II) and iron(III) with a monodentate ligand tri-*p*-tolylarsine oxide. Various physico-chemical techniques have been employed for the characterization of the complexes. The complexes exhibit a variety of geometries.

## EXPERIMENTAL

*Ligand.* The ligand, tri-*p*-tolylarsine and its oxide were prepared by the method reported by Shriner and Wolf.[5]

*Complexes.* Iron(III) complexes were obtained by the addition of a hot solution of the ligand in chloroform to a hot solution of the metal salt in 5:1 acetone–benzene mixture. The complexes either separated out as white solid (perchlorate), yellow (chloride), reddish brown (bromide) or red viscous liquid (thiocyanate). The latter was converted into a solid using pet-ether (40–60°C). The complexes were recrystallized from the solvents employed for the preparation of the complexes. Similarly, the complex with iron(II) iodide was obtained (except that it required refluxing for half an hour). Mixed ligand complex of iron(II) tetracarbonyl iodide was obtained in dark at low temperature. (In all the above reactions, the metal salts and the ligand were taken in 1:1 mole ratio).

*Analytical data and techniques used.* Carbon and hydrogen were analyzed from the University College of Sciences, Calcutta (India). Iron was estimated spectrophotometrically.[6] The molar conductances of millimolar solutions of complexes in nitrobenzene were measured with Toshniwal conductivity Bridge type CLOI/02 A. The IR spectra were recorded with Spectromom-2000 in 4000–650 $cm^{-1}$ region (using Nujol mull) and PYE-UNICHEM in the region 4000–200 $cm^{-1}$. The far IR spectra in the range 600–200 $cm^{-1}$ were recorded by the University of Surrey, Surrey (England), I.I.T. Madras, Defence R and D Centre, Gwalior and Chemistry Department, B.H.U. Varanasi. The reflectance spectra of the

*Author to whom correspondence should be addressed.

Table 1. Analytical data, melting points, molar conductance and magnetic moments of the complexes

| S.No. | Complex | Found (Required) C% | H% | Fe% | M.p °C | Colour | $\Lambda_m$ ohm$^{-1}$cm$^2$mole$^{-1}$ | $\mu_{eff}$ B.M. |
|---|---|---|---|---|---|---|---|---|
| 1. | $[FeL_2Cl_2(OH_2)_2][FeCl_4].2H_2O$ | 44.68 (44.92) | 3.88 (4.45) | 10.31 (10.00) | 94 | Greenish yellow | 16 | 5.92 |
| 2. | $[FeL_2Br_2][FeBr_4].2H_2O$ | 37.79 (37.17) | 4.05 (3.30) | 8.90 (8.26) | 196-7 | Red | 16 | 5.94 |
| 3. | $[Fe(NCS)_3L_2].H_2O$ | 55.93 (55.33) | 3.84 (4.50) | 5.18 (5.73) | 128 | Red | 9 | 5.40 |
| 4. | $[FeL(O_2ClO_2)_2(OH_2)](ClO_4).0.25C_6H_6$ | 35.42 (35.70) | 3.88 (3.25) | 6.95 (7.42) | 96 | Light brown | 31 | 5.82 |
| 5. | $[FeL_3I][FeI_3].H_2O$ | 43.26 (43.69) | 3.22 (3.75) | 5.66 (6.45) | 168 | Yellow | 24 | 4.90 |
| 6. | $[FeL(CO)_3I]I$ | 36.57 (36.41) | 3.05 (2.77) | 7.30 (7.48) | - | Brown | 33 | 3.95 |

complexes were recorded with spectrophotometer VSU-2P type. Magnetic susceptibility measurements were carried out at room temperature using Gouy's method [$HgCo(NCS)_4$ as the calibrant]. Diamagnetic corrections were made by using Pascal's constants.[7] X-Ray photographs of the powder samples were taken using Debye–Scherrer camera of radius 57.3 mm. The Cu$K_\alpha$-X-rays from Phillips generator type PW 1720 were used. The X-band (9.3 GHz) ESR spectra of iron(III) complexes have been recorded from Hyderabad University, Hyderabad (India).

## RESULTS AND DISCUSSION

The complexes of tri-*p*-tolylarsine oxide with iron(III) chloride, bromide and perchlorate correspond to 1:1 metal to ligand ratio, while the complex with iron(III) thiocyanate has 1:2 metal to ligand ratio. The iron(II) iodide complex has an unusual stoichiometry, viz. 2:3 and iron(II) tetracarbonyl iodide also forms a 1:1 complex by replacing one CO group (Table 1). Molar conductance values of the chloride and bromide complexes ($\sim 16.00\ ohm^{-1}\ cm^2\ mole^{-1}$) show their electrolytic character and are formulated as $[FeL_2X_2]\ [FeX_4].nH_2O$ (X=Cl,Br). In the literature there have been reported complexes also of the type $[FeL_4X_2]\ [FeX_4]$ (X=Cl,Br), but having lower $\Lambda_M$ values than expected for a 1:1 electrolyte.[1,2] The thiocyanate complex has $\Lambda_M$ value of 9 $ohm^{-1}\ cm^2\ mole^{-1}$ indicating its nonelectrolytic structure, $[Fe(NCS)_3L_2]$. The perchlorate complex is a 1:1 electrolyte ($\Lambda_M$ 31 $ohm^{-1}\ cm^2\ mole^{-1}$) formulated as $[FeL(O_2ClO_2)_2(OH_2)]\ (ClO_4).0.25C_6H_6$. Similarly, iron(II) iodide and iron(II) tetracarbonyl iodide complexes shows 1:1 electrolytic behaviour and formulated as $[FeL_3I][FeI_3]$ and $[Fe(CO)_3LI]I$ respectively. It may be noted here that the analogous ligand $Ph_3AsO$ formed 1:2 complexes with iron(III) halides and 1 : 4 (metal : ligand) with iron-(III) perchlorate (Table 1).[1,8]

In the IR spectra, $\nu As=O$ of the free ligand at 880 $cm^{-1}$ records a low-energy shift of 15–65 $cm^{-1}$ in its complexes. The chloride complex shows the largest decrease. The other significant band, $\nu(As–C)_{aromatic}$ as usual remains unaffected[3,4] probably because it is away from the site of coordination or is due to the presence of bulky polarisable arsenic which may help to satisfy the acidic nature of iron(III) through oxygen donor atom (Table 2). The latter possibility appears to be more plausible in view of the fact that the phosphine oxide complexes show a decrease in $\nu(P=O)$.[2-4] In the far IR spectra of the halide complexes, a strong band at 360 $cm^{-1}$ occurs in the case of the chloride complex and at 285 $cm^{-1}$ in the bromide complex.[1,9] These bands are characteristic $\nu_3$ modes of the $FeX_4^-$ moiety observed in $FeL_2X_3$ (L=$Ph_3PO$, $Ph_3AsO$, X=Cl, Br) type of complexes in the literature which have *trans*-$[FeL_4X_2]\ [FeX_4]$ structures with low conductance values. The $\nu_{as}$(Fe–Cl) at 280 $cm^{-1}$ is attributed to *trans*-$[FeL_2Cl_2(OH_2)_2]^+$ cation.[1]

The IR spectrum of the thiocyanate complex shows coordination via nitrogen because $\nu(C\equiv N)$ band occurs at 2060 $cm^{-1}$ (s) and $\delta$(NCS) at 490 $cm^{-1}$ (s).[10] The other $\nu$(C–S) band has been obscured by the ligand band. In far IR, $\nu$(Fe–NCS) occurs at $\sim 250\ cm^{-1}$.[3,4,8] The IR spectrum of the perchlorate complex is somewhat complex in view of the fact that $\nu(As–C)_{aromatic}$ and $\nu(ClO_4)$ bands fall in the same region. However, there is a strong evidence to prove that the perchlorate groups are coordinated because the strong $\nu_3$ mode of the ionic perchlorate has undergone splitting showing bands at 1135 sh, 1115 s and 1085 s $cm^{-1}$ (s). This is further supported by the appearance of $\nu_1$ and $\nu_2$ bands at 925 m $cm^{-1}$ and 435 w $cm^{-1}$ which are inactive in the case of an ionic perchlorate group.[11,12]

*Cis*-$Fe(CO)_4I_2$ has $C_{2v}$ symmetry and its IR spectrum shows two bands at 2135 and 2190 $cm^{-1}$. Its complex with *p*-TAO also shows two bands at 2090 (s) and 1900 (s) $cm^{-1}$. Reckziegel and Bigorgne[13] report similar behaviour for $[Fe(CO)_3(EDP)]$ complex in $CHCl_3$ solution (EDP-1,2-ethylenebis (diphenylphosphine)). The expected decrease in $\nu$(CO) is due to extensive $\pi$-bonding from metal to $\pi^*$-orbital of CO.[14]

The complexes show $\nu$(O–H) and $\delta$(HOH) bands at 3400–3500 and 1620–35 $cm^{-1}$ (Table 2). The chloride and perchlorate complexes in addition show wagging and rocking modes at 780 $cm^{-1}$ and 775 $cm^{-1}$ respectively. This indicates that water is coordinated in these two complexes. Such modes do occur in the region 785–805 $cm^{-1}$.[15] The other complexes, thus, do not contain coordinated water but only lattice water. The t.g.a. of latter complexes also shows loss of water below 120°C. However, the chloride complex does not lose all the water below 120°C indicating that half of the water is present as lattice water and the other half as coordinated. The high water content in case of chloride complex is understandable due to the greater Lewis acidity of the ferric chloride. The presence of benzene in the perchlorate complex is shown by elemental analysis and it is not surprising in view of the fact that other analogous perchlorate complexes also showed the presence of solvent employed in the preparation of the complexes.[4] It may be worth remarking here that in an analogous complex, $[Na(MDPO)_3]I2H_2O.C_6H_6$,

Table 2. The IR spectra of the complexes (4000–200 $cm^{-1}$)

| S.No. | Complex | $\nu$(As=O) | $\nu$(As-C) Ar | $\nu$(Fe-X) | $\nu$(CH) | $\delta$(HCH) |
|---|---|---|---|---|---|---|
| 1. | $[FeL_2Cl_2(OH_2)_2]$-$[FeCl_4]$[a]. $2H_2O$ | 815s,b | 1065m,sp | 360s,sp 280wb | 3400mb | 1630wb |
| 2. | $[FeL_2Br_2][FeBr_4]\cdot 2H_2O$ | 845s,b | 1085m,sp | 285s,sp 250s,sp | 3400wb | 1630wb |
| 3. | $[Fe(NCS)_3L_2].H_2O$ | 855sb | 1085m,sp | 250m | 3500wb | 1620vwb |
| 4. | $[FeL(O_2ClO_2)_2(OH_2)]$-$(ClO_4)\cdot 0.25C_6H_6$ | 845m,b | -[b]- | - | 3400sb | 1635mb |
| 5. | $[FeL_3I][FeI_3].H_2O$ | 840s,sp | 1090m,sp | - | 3400wb | 1630vwb |
| 6. | $[FeL(CO)_3I]I$ | 845s,sp | 1095m,sp | - | - | - |

a) $\delta$(C-$CH_3$) mode at 805–810 $cm^{-1}$ has merged with $\nu$(As=O) absorption.

b) $\nu$(As-C) is obscured by the very strong absorption due to perchlorate aromatic group.

(MDPO=$Ph_2P(O)CH_2P(O)Ph_2$), the presence of water and benzene has been established using single crystal X-ray method.[16]

Magnetic moments for halide and perchlorate complexes lie in the range 5.82–5.94 B.M. conforming the high-spin $d^5$- configuration of iron(III) having $^6A_1$ as the ground state (Table 1).[1,8] The sulphocyanide complex shows a lower value (5.40 B.M.) implying that this complex with a chromophore $FeN_3O_2$ might show the spin-crossover phenomenon if studied at lower temperatures. This expectation is based on two factors.

Table 3. The reflectance spectra of the complexes ($cm^{-1}$)

| S.No. | Complex | d-d bands | Transition | Charge transfer bands |
|---|---|---|---|---|
| 1. | $[FeL_2Cl_2(OH_2)_2][FeCl_4]$-$2H_2O$ | 13890w,15625w, 17240w | $^6A_1 \rightarrow {}^4T_1$(G)<br>$^6A_1 \rightarrow {}^4T_2$(G) | 27,027s,sp |
| 2. | $[FeL_2Br_2][FeBr_4]2H_2O$ | 12195w,13157w, 15625w | $^6A_1 \rightarrow {}^4T_1$(G)<br>$^6A_1 \rightarrow {}^4T_2$(G) | 25,640s,sp |
| 3. | $[Fe(NCS)_3L_2].H_2O$ | 10,870w | $^6A_1 \rightarrow {}^4T_1$(G) | 20833s,b |
| 4. | $[FeL(O_2ClO_2)_2(OH_2)]$-$(ClO_4).0.25\ C_6H_6$ | 10,870w<br>15150w<br>20,000sh | $^6A_1 \rightarrow {}^4T_1$(G)<br>$^6A_1 \rightarrow {}^4T_1$(G)<br>$^6A_1 \rightarrow {}^4T_2$(D) | 26,315s,sp |
| 5. | $[FeL_3I][FeI_3].H_2O$ | 10,638w<br>11,110w<br>14,150w<br>17,240w | - | 25,975s,sb<br>23,255m,sp<br>21,276s,b |

Table 4. The ESR data of the complexes

| Complex | g-values | | Intensity of lines |
|---|---|---|---|
| | $g_\perp$ | $g_\parallel$ | |
| 1. $[FeL_2Br_2][FeBr_4]\cdot 2H_2O$ | 6.04 | 2.07 | 1100s, sp, 3200wb |
| 2. $[Fe(NCS)_3L_2].H_2O$ | 4.35 | 2.03 | 1525mb, 3275sb |
| 3. $[FeL(O_2ClO_2)_2(OH_2)](ClO_4)\cdot\frac{1}{4}C_6H_6$ | 4.09 | 2.007 | 1625wb, 3312sb |

s-strong, sp-sharp, w-weak, b-broad, m-medium

Firstly, phenanthroline ligands (or bipyridines and related N-donors) usually exert stronger ligand.[17-20] Secondly, spin-crossover has been observed in $[Fe(L\text{–}L)_3]^{3+}$ cation (L–L=mono-N-oxide of 1,10-phenanthroline; L–L=mono-N-oxide of 2,2′-bipyridine) possessing the chromophore $FeN_3O_3$.[17-20] Iron(II) iodide complex shows a value of 4.90 B.M., expected for high-spin $d^6$-configuration but, iron(II) carbonyl iodide complex shows a value of 3.95 B.M. in accord with similar behaviour observed for ditertiaryphosphine (arsine) dioxides.[3,4] Thus, iron(II) has a triplet ground state and $\mu_{eff}$ value corresponds to the moment expected for two unpaired electrons (~2.83 B.M.) with an additional contribution of about 1.00 B.M. from the second order Zeeman effect. The high-second order contribution is commonly observed in $d^6$ compounds of low-spin type. König and Madeja[21] have observed $\mu_{eff}$ value of ~3.90 B.M. for iron(II) complexes with N-donors.

Table 5. Main bands in X-ray diffraction powder patterns of complexes

| S.No. | complex | d-lines Å | | | |
|---|---|---|---|---|---|
| 1. | $[FeL_2Cl_2(OH_2)_2][FeCl_4]\cdot 2H_2O$ | 7.63(30) | 6.74(10) | 6.11(20) | 4.97(30) |
| | | 4.50(40) | 2.62(90) | 2.37(80) | 2.23(60) |
| | | 2.03(30) | 1.74(10) | 1.61(80) | 1.45(50) |
| | | 1.32(30) | | | |
| 2. | $[FeL_2Br_2][FeBr_4]2H_2O$ | 6.72(20) | 5.50(20) | 2.64(70) | 2.39(60) |
| | | 2.22(30) | 2.16(30) | 1.92(10) | 1.61(60) |
| | | 1.45(30) | 1.32(20) | 1.23(20) | 1.24(20) |
| 3. | $[Fe(NCS)_3L_2].H_2O$ | 3.06(40) | 2.77(40) | 2.68(30) | 2.40(50) |
| | | 2.21(70) | 2.08(30) | 1.89(50) | |
| 4. | $[FeL(O_2ClO_2)_2(OH_2)](ClO_4)\cdot 0.25C_6H_6$ | 8.66(80) | 6.88(70) | 5.35(75) | 4.84(60) |
| | | 4.64(50) | 4.30(90) | 4.14(40) | 3.85(40) |
| | | 3.67(50) | 3.56(50) | 3.23(30) | 2.95(20) |
| | | 2.64(70) | 2.46(30) | 2.39(60) | 2.24(30) |
| | | 2.13(20) | 1.61(60) | 1.45(30) | 1.34(30) |
| | | 1.23(40) | | | 1.31(20) |
| 5. | $[FeL_3I][FeI_3].H_2O$ | 2.36(60) | 2.19(70) | 2.06(30) | 1.97(30) |
| | | 1.87(40) | 1.71(30) | | |

The reflectance spectra of the high-spin iron(III) complexes show charge-transfer bands in the range 20833–27027 $cm^{-1}$ (Table 3). Various *d–d* bands from $^6A_1$ to $^4T_1(G)$, $^4T_2(G)$, $^4T_2(D)$ have been assigned as weak[1,22–27] bands. The anions $[FeCl_4]^-$ and $[FeBr_4]^-$ show their characteristic *d–d* transitions. The spectrum of the iron(II) iodide complex, $[FeL_3I][FeI_3]$ is complicated, however, weak *d–d* bands occur in the range 10638–17240 $cm^{-1}$, while charge-transfer bands lie in the range 21276–25975 $cm^{-1}$.

The ESR, X-band (9.3 GHz) spectrum of the bromide complex shows a sharp and strong signal at 1100 g ($g_\perp$ 6.04). Another weak and broad signal occurs at 3200 g ($g_\parallel$ 2.07) (Table 4). The latter value is characteristic of $[FeBr_4]^-$ ion in conformity with literature data.[1,2] The $g_\perp$ value of 6.04 is indicative of a *trans*-square planar structure for the cation rather than tetrahedral. In the literature, ion(III) perchlorate complexes, $[FeL_4](ClO_4)_3$ (L=$Ph_3PO$, $Ph_3AsO$) have also been assigned square planar structure on the basis of ESR studies.[1,8] The ESR spectrum of the thiocyanate complex gave two signals, one of strong intensity at $g_\parallel$ value of 2.03 and the other of medium intensity at $g_\perp$ value of 4.35. This datum is consistent with a trigonal–bipyramidal structure having arisine ligands in the *trans*-positions. The ESR spectrum of the perchlorate complex, shows two major bands, one with $g_\perp$ value of 4.09 and the other $g_\parallel$ value of 2.007. This datum supports an axially symmetric octahedral *trans*-$[FeL(O_2ClO_2)_2(OH_2)]^+$ structure for the perchlorate complex. The chloride complex, presumably has *trans*-octahedral structure.

X-ray powder diffraction data show that the complexes are crystalline, but not isomorphous with one another (Table 5). It may be appropriate to remark that none of the complexes showed Mössbauer absorption at room temperature, probably due to heavy atom absorption like arsenic, iodide and bromide. However, low-temperature Mössbauer study might give absorption.

*Acknowledgement*—One of us (HSC) is thankful to the UGC, India for teacher fellowship and to the Guru Nanak Dev University for research facilities. We are also grateful to Professor G. Mehta for recording ESR spectra at the University of Hyderabad, Hyderabad (AP).

## REFERENCES

1. S. A. Cotton, *Coord. Chem. Rev.* 1972, **5**, 185.
2. T. S. Lobana, H. S. Cheema and S. S. Sandhu, *J. Chem. Soc. Dalton Trans.* 1983, 2039.
3. T. S. Lobana, H. S. Cheema and S. S. Sandhu, Unpublished work.
4. H. S. Cheema, Ph.D Thesis submitted to Guru Nanak Dev University, Amritsar, India.
5. R. L. Shriner and C. W. Wolf, *Org. Synth.* 1950, **30**, 95.
6. A. I. Vogel, *A Text Book of Quantitative Inorganic Analysis*, p. 787. ELBS and Longman (1973).
7. A. Earnshaw, *Introduction of Magnetochemistry*, p. 5. Academic Press, London (1966).
8. S. A. Cotton and J. F. Gibson, *J. Chem. Soc. (A)* 1971, 859.
9. J. S. Avery, C. D. Burbridge and D. M. L. Goodgame, *Spectrochim Acta* 1968, **24A**, 1721.
10. J. L. Burmeister, *Coord. Chem. Rev.* 1968, **3**, 225. Ibid. 166, **1**, 205.
11. N. M. Karayannis, C. M. Mikulski, L. L. Pytlewski and M. M. Labes, *Inorg. Chem.* 1970, **9**, 582.
12. B. J. Hathaway and A. E. Underhill, *J. Chem. Soc.* 1961, 3091.
13. A. Reckziegel and M. Bigorgne, *J. Organomet. Chem.* 1965, **3**, 341.
14. R. C. Taylor and W. D. Horrocks (Jr.), *Inorg. Chem.* 1964, **3**, 584.
15. H. Meider and P. Bronzan, *Polyhedron* 1983, **2**, 69.
16. T. S. Lobana and S. S. Sandhu, *J. Chem. Sci. (GNDU)* 1979, **5**, 102.
17. A. N. Speca, N. M. Karayanis and L. L. Pytlewski, *Inorg. Chim. Acta* 1974, **9**, 87.
18. A. N. Speca, N. M. Karayanis and L. L. Pytlewski, *J. Inorg. Nucl. Chem.* 1974, **36**, 1227.
19. A. N. Speca, L. L. Pytlewski, C. Owens and N. M. Karayanis, *J. Inorg. Nucl. Chem.* 1976, **38**, 1119.
20. P. Gütlich, *Structure and Bonding* 1981, **44**, 85.
21. E. König and K. Madeja, *Inorg. Chem.* 1968, **7**, 1848.
22. F. A. Cotton and E. Bannister, *J. Chem. Soc.* 1960, 1878.
23. S. A. Cotton and J. F. Gibson, *J. Chem. Soc. (A)* 1971, 879.
24. R. Bembi, *Indian J. Chem.* 1977, **15A**, 316.
25. A. P. Ginsberg and M. B. Robin, *Inorg. Chem.* 1963, **2**, 817.
26. H. Yamatera and A. Kato, *Bull. Chem. Soc. Jpn.* 1968, **41**, 2220.
27. C. K. Jörgensen, *Discuss. Faraday Soc.* 1958, **26**, 110.

*Polyhedron* Vol. 3, No. 8, pp. 917–920, 1984
Printed in the U.S.A.

0277–5387/84 $3.00 + .00
© 1984 Pergamon Press Ltd.

# KINETICS OF THE REACTION OF ALUMINUM EDTA AND COBALT(II) EDTA WITH CALMAGITE

MARIA HUFFMAN and DEAN C. LUEHRS*
Department of Chemistry and Chemical Engineering, Michigan Technological University, Houghton, MI 49931, U.S.A.

(*Received* 25 *July* 1983; *accepted* 17 *January* 1984)

**Abstract**—The reaction of aluminum EDTA with calmagite was found to be first-order in calmagite, half-order in aluminum EDTA, and zero-order in excess EDTA. The three-halves-order apparent rate constant at pH 9.48 and 20°C with ionic strength 0.30 was $0.232 \pm 0.0141^{1/2} \cdot mol^{1/2} \cdot s^{-1}$. The activation energy was 3.2 ± 0.3 kcal/mol. The pH dependence was complex between 8 and 10. The mechanism proposed is a rapid dissociation of a dimer of aluminum EDTA to a monomer followed by a rate-determining displacement of the EDTA by calmagite. The reaction of Co(II) EDTA with calmagite was confirmed to be first-order in Co(II) EDTA and first-order in calmagite with an activation energy of 7.5 ± 0.6 kcal/mol.

A number of metal ions may be determined by adding an excess of ethylenediaminetetraacetic acid (EDTA), ammonia buffer, a few drops of Eriochrome Black T (BT) 3-hydroxy-7-nitro-4-(2-hydroxy-phenylazo)-1-naphthalenesulfonic acid) solution as an indicator, and back-titrating the excess EDTA with standard zinc, manganese, or magnesium ion solution.[1] It is mentioned that there are slow, irreversible color changes with $Al^{3+}$, $Co^{2+}$, $Ni^{2+}$, and a number of other metal ions. To titrate these ions, it is recommended that the solution be cooled, the amount of metal to be determined be limited, and the back titration be done rapidly although these details are not always mentioned.[1,2] All this is understandable if it is realized that for some metal ions, including $Al^{3+}$, $Co^{2+}$, $Ni^{2+}$ and $Hg^{2+}$ the reaction (disregarding charges)

$$M(EDTA) + BT = M(BT) + EDTA \quad (1)$$

has an equilibrium constant greater than one and the apparent pseudo-first-order rate constant will be increased by an increase in temperature or an increase in the concentration of M(EDTA).

In order to determine the effects of temperature and concentration of metal ion more precisely, this study of the kinetics of reaction (1) was carried out with M = Al(III) or Co(II). Calmagite [3-hydroxy-4-(2-hydroxy-5-methylphenyl-azo)-1-naphthalene-sulfonic acid] was used as the indicator because it is chemically similar to BT but more generally used now.[3] The kinetics of the reaction of calmagite or BT with a variety of aminocarboxylates of Ni(II) or Co(II) have been studied by Kodama.[4–9] The reactions are first-order in calmagite or BT, first-order in metal complex, and zero-order in excess aminocarboxylate if it is hexadentate. The pH dependence was studied and discussed in detail, but few activation energies were determined. Since the effect of temperature on reaction (1) is of great importance in the determination of aluminum or cobalt by EDTA titration with a back titration,[1] the activation energy of reaction (1) with M = Co(II) was determined as well as several aspects of the kinetics of reaction (1) with M = Al(III).

## EXPERIMENTAL

A standard aluminum solution was prepared by dissolving Fisher aluminum metal in hydrochloric acid and diluting to volume. Fisher certified di-sodium EDTA was standardized with standard zinc chloride. Mallinckrodt reagent Co(II) chloride was standardized by the method of Harris and Sweet.[2] The ionic strength of all solutions was maintained at 0.31 with lithium perchlorate which was re-crystallized from water and dried under vacuum at 110°C. Aldrich Chemical Co. calmagite was purified by the method of Lindstrom and Isaac,[10] which was not very effective in this laboratory. Others have also reported lack of success with this

*Author to whom correspondence should be addressed.

method.[11] The concentration of calmagite was determined using the literature value of 20,400 for $\epsilon_{610}$.[3,11]

The pH measurements were by a Sargent–Welch 6050 pH meter. A Perkin–Elmer Lamda 3 spectrophotometer with a 561 recorder was used for absorbance measurements. All absorbance values obtained in kinetics runs were read directly from the spectrophotometer at 640 nm. A MGW Lauda unit controlled the temperature to within 0.2°C.

All reactions were followed for at least two half-lives. Following the reaction up to three half-lives did not significantly change the value or confidence interval of the rate constant. All values are reported to the 95% confidence level except the slope of $\log k$ vs $\log[Al]_T$ which was at the 90% confidence level. Calmagite concentrations were around $1.5 \times 10^{-5}$ M, total EDTA varied from $4.7 \times 10^{-4}$ to $4.7 \times 10^{-3}$ M, aluminum varied from $4.1 \times 10^{-5}$ to $1.6 \times 10^{-3}$ M and Co(II) was $1.2 \times 10^{-3}$ M. Ammonia buffers were used to control the pH in the aluminum series. In the reactions with Co(II) the pH was adjusted with dilute sodium hydroxide to avoid any mixed ligand complexes of EDTA and ammonia with Co(II).[12]

## RESULTS

*Aluminum EDTA and calmagite.* Good pseudo-first-order plots were obtained on all runs.[13] The pseudo-first-order rate constant and its confidence interval were obtained by a standard program. The confidence limits averaged 4.6% of the rate constants for the aluminum series and 2.2% for the Co(II) series. A plot of absorbance vs wavelength during the reaction showed an isosbestic point at 575 nm indicating no significant accumulation of any intermediate. There was no dependence of the rate on excess EDTA concentration in the range studied. A preliminary plot of $\log k_{ps}$ vs $\log [Al]_T$ (Table 1) where $k_{ps}$ is the pseudo-first-order rate constant and $[Al]_T$ is the total concentration of aluminum at pH 9.48 gave a slope of 0.43 which was interpreted as being close to 0.5. Replotting the data as $k_{ps}$ vs $[Al]_T^{1/2}$ gave a straight line with an intercept of $3.6 \times 10^{-4}$. A plot of $\log(k_{ps} - 3.6 \times 10^{-4})$ vs $\log[Al]_T$ now gave a slope of $0.50 \pm 0.10$ indicating that the reaction is half-order in aluminum. The pH dependence of the rate (Table 2) shows an increase in rate and then a decrease between pH 9 and 10.

A plot of $\log k_{ps}$ at pH 9.48 vs $1/T$ for temperatures from 278.2 K to 298.2 K gave an activation energy of 3.2 ± 0.3 kcal/mol (Table 3). No entropy of activation was calculated since the pH dependence has not been established.

By measuring the absorbances at 500 and 650 nm of the solution before and after reaction (1) with M = Al(III) was completed, a value of 64 for the value of the apparent equilibrium constant at pH 9.25 was found.

Co(II) *EDTA and calmagite.* Preliminary experiments confirmed the result of Kodama[4] that reaction (1) with M = Co(II) was first-order in Co(II), first-order in calmagite, and zero-order in excess EDTA. The activation energy at pH 9.25 was determined to be 7.5 ± 0.7 kcal/mol (Table 4). The second-order rate constant at pH 9.25 and 15°C was $2.94 \pm 0.03$ which was in poor agreement with the value of 7.1 calculated from Kodama's data with sodium perchlorate to maintain the ionic strength at 0.30.[4]

Table 1. Kinetic results for the $AlEDTA^-$ + calmagite reaction at pH 9.48 and 20°C with various concentrations of aluminum

| $10^4[AlEDTA^-]$ | $10^3 k_{ps}$ |
|---|---|
| 0.410 | $1.24 \pm 0.01$ |
| 0.820 | $1.99 \pm 0.03$ |
| 4.10 | $4.12 \pm 0.25$ |
| 8.20 | $4.68 \pm 0.34$ |
| 16.0 | $6.37 \pm 0.69$ |

Table 2. pH dependence of the rate of reaction of aluminum EDTA with calmagite at 20°C

| pH | Three-halves-order overall rate constant |
|---|---|
| 10.05 | $0.194\ L^{1/2}/M^{1/2} \cdot s$ |
| 9.68 | 0.216 |
| 9.48 | 0.232 |
| 9.35 | 0.199 |
| 9.25 | 0.164 |
| 9.09 | 0.157 |
| 8.94 | 0.045 |

Table 3. Kinetic results for the $AlEDTA^-$ + calmagite reaction at pH 9.48 with $4.10 \times 10^{-4}$ M $AlEDTA^-$ at various temperatures

| $T$, °C | $10^3 k_{ps}$ |
|---|---|
| 25.0 | $4.72 \pm 0.28$ |
| 20.0 | $4.12 \pm 0.25$ |
| 17.0 | $3.90 \pm 0.25$ |
| 15.0 | $3.73 \pm 0.19$ |
| 12.0 | $3.58 \pm 0.19$ |
| 10.0 | $3.42 \pm 0.15$ |
| 5.0 | $3.12 \pm 0.18$ |

Table 4. Kinetic results for the $CoEDTA^{2-}$ + calmagite reaction at pH 9.25 with $1.20 \times 10^{-3}$ M $CoEDTA^{2-}$

| $T$, °C | $10^3 k_{ps}$ |
|---|---|
| 30.0 | $6.68 \pm 0.28$ |
| 25.0 | $5.33 \pm 0.11$ |
| 20.0 | $4.53 \pm 0.09$ |
| 15.0 | $3.53 \pm 0.04$ |
| 10.0 | $2.74 \pm 0.03$ |

## DISCUSSION

*Aluminum EDTA and calmagite.* The limited number of activation energies that have been reported for exchange reactions of multidentate ligands are in a range of 10–20 kcal/mol.[8,14-17] The value of 3.2 kcal/mol obtained in this study is very low compared to similar reactions with other metal ions and indeed is in the range of diffusion controlled reactions. Since it is unlikely that such a slow reaction is diffusion controlled, it is likely that there is an exothermic pre-equilibrium reaction.[18,19] The half-order dependence on $[Al]_T$ is also unusual for a nonradical reaction.

Both the low value for the activation energy and the half-order dependence on $[Al]_T$ may be rationalized with the mechanism:

$$2H^+ + Al_2(EDTA)_2(OH)_2^{4-} \underset{k_{-2}}{\overset{k_2}{\rightleftharpoons}} 2Al(EDTA)^- + 2H_2O \quad (2)$$

and

$$Al(EDTA)^- + Hcalmagite^{2-} \xrightarrow{k_3} Al(calmagite) + HEDTA^{3-}. \quad (3)$$

Aluminum-EDTA is known to be a dimer with a value of $K_{eq}$ of $2.4 \times 10^{10}$ for the equilibrium constant of reaction (2) at a pH below 7.[20,21] It is known that the interconversion of the corresponding dimer and monomer of Fe(III) EDTA occurs with a half-life of less than 1 s.[22]

Treating $Al(EDTA)^-$, the monomer, as a steady-state intermediate with $k_3 \ll k_{-2}$ leads to: Rate $= 2^{1/2} k_3 K_{eq}^{1/2} [H^+][Al_2(EDTA)_2(OH)_2^{4-}]^{1/2}$ [Hcalmagite$^{2-}$] which is half-order in $[Al]_T$ and first-order in calmagite, as observed. The dependence on $[H^+]$ has been simplified in this treatment because the actual aluminum-EDTA species is not known in this pH range.

The pH dependence of the rate from pH 9 to 10 (Table 2) cannot be explained in the same way that Kodama[4-9] explained his results. He had a regularly increasing rate with increasing pH which is explained by the 3-ion of calmagite being more reactive than the 2-ion. Here we have a maximum around pH 9.5. A possible explanation of the maximum is that a species of the aluminum-EDTA dimer with additional hydroxyl group is formed in this pH region and the species with an additional hydroxyl group is not as reactive. The exact species of aluminum-EDTA present in this pH range is not known and would be difficult to study because the solutions are metastable with respect to aluminum hydroxide. All measurements in this study were carried out before any aluminum hydroxide precipitated.

This mechanism also rationalizes the low value observed for the activation energy. The observed enthalpy of reaction would be $(1/2)\Delta H_2 + \Delta H_3^{\ddagger}$.[19] If $\Delta H_3^{\ddagger}$ was around 12 kcal/mol as is the case for many reactions similar to reaction (3), $(1/2)\Delta H_2$ could be a negative value large enough to bring the combination to the observed enthalpy of activation of 2.7 kcal/mol ($\Delta H^{\ddagger} = E_{act} - RT$). Usually dissociations have a positive enthalpy of reaction, but in this case the neutralization of the hydroxyl groups by hydrogen ions would lead to a negative enthalpy of reaction for reaction (2).

Thus, the proposed mechanism account for the usual half-order with respect to aluminum concentration and the unusually low value of the activation energy while retaining the first-order dependence on calmagite concentration and zero-order dependence on the concentration of excess EDTA.

Co(II) *EDTA and calmagite.* The enthalpy of activation of 6.9 kcal/mol observed for this reaction is comparable to the observed for other multidentate ligand exchange reactions although at the low end of the range.[8,14-17]

The reactions observed in this study are much faster than the complete dissociation of the very stable metal EDTA complexes to free metal ion and free ligand. It is expected that there is an intermediate with the incoming and outgoing ligands each occupying at least two positions of the coordination sphere of the metal. Such intermediates are well established for similar reactions.[4-8,17,23,24]

In conclusion, it is recommended that in the determination of Ni(II), Co(II), Al(III) or Hg(II) by adding an excess of EDTA and back titrating with standard zinc solution with BT or calmagite indicator that the solution be cooled first in an ice bath, the concentration of the metal ion should not be too high, and the titration should be done as rapidly as possible. In addition, when aluminum is

to be determined, the solution should be boiled after the EDTA is added to the aluminum ion solution before the indicator is added. The reaction of the EDTA with aluminum ion to form the complex is sluggish at room temperature.[1] If even 1% of the free aluminum ion is not converted to the EDTA complex, the indicator will be converted to the aluminum complex within a minute with a change of color of the indicator.

*Acknowledgement*—The preliminary work of Elizabeth L. Kennell and Joan M. Hawn is greatly appreciated. Joshua Kawai translated Ref. 4. Drs. Terrell Warrington and Dale W. Margerum gave several helpful suggestions.

## REFERENCES

1. F. J. Welcher, *The Analytical Uses of Ethylenediaminetetraacetic Acid*, pp. 35, 166, 173. Van Nostrand, Princeton, N.J. (1958).
2. W. F. Harris and T. R. Sweet, *Anal. Chem.* 1954, **26**, 1649.
3. F. Lindstrom and H. Diehl, *Anal. Chem.* 1960, **32**, 1123.
4. M. Kodama, *Nippon Kagaku Zasshi* 1970, **91**, 134.
5. M. Kodama, C. Sasaki and K. Miyamoto, *Bull. Chem. Soc. Jpn.* 1969, **42**, 163.
6. M. Kodama, T. Sato and S. Karasawa, *Bull. Chem. Soc. Jpn.* 1972, **45**, 2757.
7. M. Kodama, C. Sasaki and T. Noda, *Bull. Chem. Soc. Jpn.* 1968, **41**, 2033.
8. M. Kodama, C. Sasaki and M. Murata, *Bull. Chem. Soc. Jpn.* 1968, **41**, 1333.
9. M. Kodama, *Bull. Chem. Soc. Jpn.* 1967, **40**, 2575.
10. F. Lindstrom and R. Isaac, *Talanta* 1966, **13**, 1003.
11. B. Kratochvil, J. Nolan and F. F. Cantwell, *Can. J. Chem.* 1981, **59**, 2539.
12. M. Kodama and K. Miyamoto, *Bull. Chem. Soc. Jpn.* 1969, **42**, 1596.
13. M. Huffman, M.S. Dissertation. Michigan Technological University, Houghton, Michigan (1982).
14. M. Kodama, *Bull. Chem. Soc. Jpn.* 1969, **42**, 2532.
15. M. Kodama, *Bull. Chem. Soc. Jpn.* 1969, **42**, 3330.
16. J. C. Cassalt and R. G. Wilkins, *J. Am. Chem. Soc.* 1968, **90**, 6045.
17. D. W. Margerum, G. R. Cayley, D. C. Weatherburn and G. K. Pagenkopf, In *Coordination Chemistry* (Edited by A. E. Martell), Vol. 2, p. 1. American Chemical Society, Washington, D.C. (1978).
18. J. P. Jones and D. W. Margerum, *Inorg. Chem.* 1969, **8**, 1486.
19. R. D. Cannon, *J. Chem. Soc. A*, 1968, 1098.
20. D. T. Sawyer and J. E. Tackett, *J. Am. Chem. Soc.* 1963, **85**, 2390.
21. R. R. Das, T. R. Bhat and J. Shankar, *J. Inorg. Nucl. Chem.* 1968, **30**, 1691.
22. R. G. Wilkins and R. E. Yelin, *Inorg. Chem.* 1969, **8**, 1470.
23. D. B. Rorabacher and D. W. Margerum, *Inorg. Chem.* 1964, **3**, 382.
24. D. W. Margerum, In *Mechanistic Aspects of Inorganic Reactions* (Edited by D. B. Rorabacher and J. F. Endicott), p. 26. American Chemical Society, Washington, D.C. (1982).

*Polyhedron* Vol. 3, No. 8, pp. 921–927, 1984
Printed in the U.S.A.

0277–5387/84 $3.00 + .00
© 1984 Pergamon Press Ltd.

# SYNTHESIS AND STRUCTURE OF TETRAKIS(PHENYLENETHIOUREA)TELLURIUM(II) CHLORIDE DIHYDROCHLORIDE, $C_{28}H_{26}N_8S_4Cl_4Te$

**G. C. ROUT and M. SESHASAYEE***
Department of Physics, Indian Institute of Technology, Madras 600 036, India

**and**

**G. ARAVAMUDAN and S. SOWRIRAJAN**
Department of Chemistry, Indian Institute of Technology, Madras 600 036, India

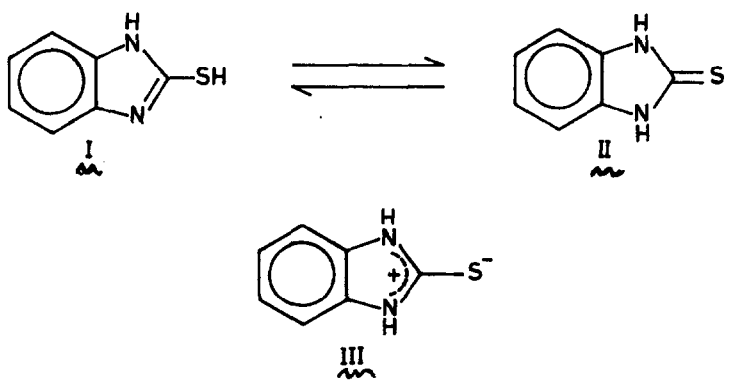
(*Received* 2 *August*, 1983; *accepted* 10 *January* 1984)

**Abstract**—Reaction of tellurium(IV) with excess phenylenethiourea(2-mercaptobenzimidazole) in aqueous methanolic hydrochloric acid leads to the formation of Te(II) complex, tetrakis(phenylenethiourea)tellurium(II) chloride dihydrochloride. The characterisation and crystal structure of the complex are reported. The crystals are monoclinic, space group $P2_1/c$, $a$ = 13.939(5), $b$ = 26.523(9), $c$ = 4.873(2) Å, $\beta$ = 100.29(4)°, $V$ = 1772.6 Å$^3$, $M$ = 872.4, $D_c$ = 1.651 g cm$^{-3}$, $Z$ = 2, $F(000)$ = 868, $\mu(MoK_\alpha)$ = 1.298 mm$^{-1}$. Final $R = 0.055$ and $R_W = 0.056$ for 918 independent reflections. The tellurium atom in the molecule lies at the crystallographic centre of symmetry and is bonded to four phenylenethiourea sulphur atoms in a square planar arrangement with Te–S(1) = 2.678(6), Te–S(2) = 2.674(5) Å and S(1)–Te–S(2) is 90.5(3)°. The ligand behaves as a thione. Chlorine atoms remain outside the coordination sphere of the Te and stabilise the packing arrangement in the unit cell through hydrogen bondings to nitrogen atoms.

Tellurium(II) is a typical soft acid and a large number of complexes of Te(II) with sulphur ligands have been reported.[1] The most extensively studied unidentate sulphur containing ligands are thiourea and its substituted derivatives.[2–11] The condensation product of *o*-phenylenediamine with carbon disulphide is referred to as 2-mercaptobenzimidazole (I). However, photoelectron spectroscopy[12] and X-ray structure determination[13] have shown that the compound in the crystalline state occurs only as the thione, phenylenethiourea (ptu) (II).

Deuton *et al.*[14] have recently reported a Te(IV) complex, cis-bis(phenylenethiourea)tetrachlorotellurium(IV)–dioxane. We have found that when

*Author to whom correspondence should be addressed.

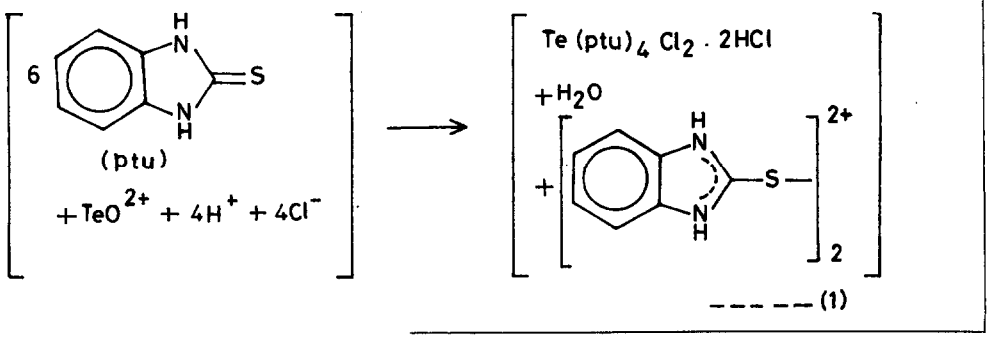


Te(IV) is reacted with methanolic solutions of ptu under acid conditions, complexes of either Te(IV) or Te(II) or both are formed depending on the acid used. In hydrochloric and hydrobromic acid media, exclusively Te(II) complexes result. In $H_2SO_4$, exclusively Te(IV) complex results. In $HClO_4$, both Te(IV) and Te(II) complexes result. A novel mixed ligand complex of Te(II), *trans*-bis-thiourea-bis(phenylenethiourea)tellurium(II) dichloride [$Te(tu)_2(ptu)_2Cl_2$, where tu = thiourea] has been reported and its structure determined.[15] An interesting aspect in these cases is the nature of Te–S interaction. If complexes with Te(II) were to be formed with the ligand in two tautomeric forms (I) and (II), the Te–S lengths are expected to be very much different. Te–S interaction with the ligand in the thiol form (I) is expected to be stronger leading to a shortening of the Te–S bonds as compared to Te–S interaction with the ligand in form (II). Bonding via mercaptan sulphur with attendant deprotonation would involve inequivalence of the two C–N distances. The thione structure could, through the delocalised form (III), offer greater electron density on the sulphur atom while still preserving the equivalence of C–N bonds.

In view of the extensive literature available on sulphur ligated complexes of Te(II), it was considered interesting to find out the mode of ligation of the compound towards Te(II) namely either as a thione sulphur or as a mercaptan sulphur after deprotonation. In the present paper are reported the synthesis and structural details of the complex, tetrakis (phenylenethiourea) tellurium(II) chloride dihydrochloride (hereafter called $Te(ptu)_4Cl_2 \cdot 2HCl$), wherein interestingly we have observed, that there are two hydrogen chloride molecules in the molecular composition.

## EXPERIMENTAL

*Isolation of the complex*: The reaction scheme is written as




1 mM (0.16 g) of tellurium dioxide (BDH) was taken in 60 $cm^3$ of 8 N hydrochloric acid (by dissolving in conc. HCl and diluting suitably). This solution was added slowly with stirring to a solution of 10 mM (1.50 g) of ptu (Aldrich 99% pure) dissolved in 60 $cm^3$ of methanol. It turned yellow and on allowing the methanol to evaporate at room temperature, fibrous yellow needles of the Te(II) complex crystallised out. This was recrystallised by dissolving in 1:1 conc. HCl and methanol containing a small amount of ptu and evaporating at room temperature. Found (Calc.) C 38.4 (38.55), H 3.02 (3.00), N 12.62 (12.84), Cl 16.41 (16.28), S 14.34 (14.70) and Te 14.50 (14.63)%.

*Collection and reduction of intensity data*

The unit cell parameters were refined on a Nonius CAD-4 diffractometer using graphite monochromated Mo$K_\alpha$ radiation ($\lambda = 0.71069$ Å). The crystal data are as follows: $C_{28}H_{26}N_8S_4Cl_4Te$, $Te(ptu)Cl_2 \cdot 2HCl$, space group $P2_1/c$, $a$ = 13.939(5), $b$ = 26.523(9), $c$ = 4.873(2) Å, $\beta$ = 100.29(4)°, $V$ = 1772.6 Å$^3$, $M$ = 872.4, $D_c$ = 1.651 g cm$^{-3}$, $Z$ = 2, $F(000)$ = 868.

The intensity data were collected by $\omega - 2\theta$ scan technique. In the range $2 < \theta < 28°$, 4550 reflections ($\pm h, k, l$) were collected. 918 reflections satisfied the criterion $I > 3\sigma(I)$. As better crystals could not be grown, a tiny needle shaped crystal (0.08 × 0.12 × 0.35 mm) was used for data collection. Intensity data were corrected for Lorentz and polarisation effects but no absorption correction was deemed necessary with $\mu(MoK_\alpha) = 1.298$ mm$^{-1}$.

*Structure refinement.* Structure was solved using heavy atom techniques. The final refinement converged to a $R = 0.055$ and $R_w = 0.056$. The following weighting scheme was used: $W = k/[\sigma^2(F_0) + g|F_0|^2]$ where $k = 1.0$ and $g = 2.5530$. The maximum shift/ESD observed for any parameter was 0.674, the final difference Fourier map showed a peak maximum of 1.07 eÅ$^{-3}$ near the Te atom. All the calculations were carried out using SHELX-76 program.[16] The atomic scattering factors for non-hydrogen atoms were taken

from Cromer and Mann[17] for hydrogen atoms from Stewart *et al.*,[18] the anomalous dispersion correction factors for non-hydrogen atoms were taken from Cromer and Liberman.[19]

## RESULTS AND DISCUSSION

The complex, tetrakis(phenylenethiourea)-tellurium(II) chloride dihydrochloride is yellow in colour and this is attributed to the characteristic charge transfer processes in Te(II)–S complexes. The Te:Cl atomic ratio is 1:4 which might imply an oxidation state of +4 for tellurium. However, the oxidation state of tellurium is concluded to be +2 on the following considerations.

(i) Diethyldithiocarbamate test:[20] Treatment of the complex with methanolic solution of sodium diethyldithiocarbamate gave only bis(diethyl-dithiocarbamato)tellurium(II) as the product and not tetrakis(diethyldithiocarbamato)tellurium(IV).

(ii) The disulphide oxidation product of ptu in the reaction scheme (1), was identified by suitable chemical procedures.

(iii) The stereochemistry of ligand arrangement around tellurium in the crystal structure (see below) is characteristic of tellurium(II) and not of tellurium(IV).

Therefore, the two extra chlorides in the complex, figure as two hydrogen chloride molecules. Using lower concentrations of hydrochloric acid, it has been possible to isolate other Te(II) complexes of composition $Te(ptu)_4Cl_2$ and $Te(ptu)_2Cl_2$. The stability of the phenylenethiourea complexes of Te(II) and their reactivity patterns are similar to those reported for thiourea complexes of Te(II).[1] The IR spectrum of the complex $Te(ptu)_4Cl_2 \cdot 2HCl$ in the fingerprint region was identical with that of the neat ligand. The Te–S interactions in these types of complexes (see below) are not very strong and therefore the C=S stretching frequency is not perceptibly altered.

Figure 1 gives the ORTEP[21] plot of the molecule. The bond lengths and bond angles† are given in Tables 1 and 2. The structure consists of $[Te(ptu)_4]^{2+}$ cation and chloride anions. The $Te^{2+}$ has an $S_4$ ligand coordination which is very nearly square planar. Although the average Te–S bond length of 2.676(4) Å is considerably larger than

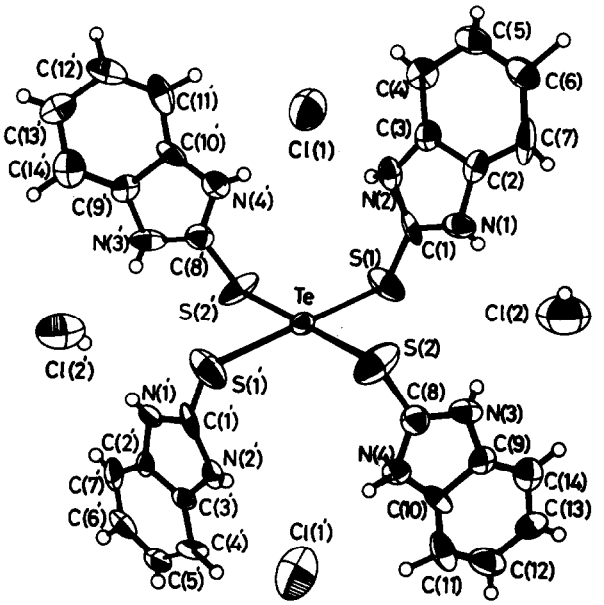



Fig. 1. ORTEP plot of the molecule $Te(ptu)_4Cl_2 \cdot 2HCl$, showing 50% probability thermal-vibration ellipsoids.

2.36 Å,[22] the sum of the covalent single bond radii of Te and S, it is typical for such bondings found in numerous Te(II) complexes[6] with monodentate sulphur containing ligands. Following the notation given by Elder *et al.*,[2] ligands in the cation are arranged in the + + − − conformation. Thus, the spatial arrangement of the planar ligand molecules with respect to $TeS_4$ plane is such that one adjacent pair of them lies above and the other pair below the $TeS_4$ plane providing an inversion symmetry to the entire molecular fragment. This is the common conformation found in similar compound[4–11] with the sole exception of $Te(etu)_4Cl_2^2$. The same arrangement is displayed in the complexes, $Te(tu)_2(ptu)_2Cl_2$[15] and the selenium analogue[23] of the title compound.

It can be seen (Tables 3) that Te–S bond lengths in various Te(II) complexes featuring coordination to four unidentate sulphur ligands are intriguingly inequivalent. This effect could perhaps be attributed either due to the proximity of the counter ions to the two lone pairs of electrons on Te(II) (II, III, IV) or to the proximity of the counter ions to the sulphur ligands (I). In the present case (VII), the chloride ions are quite away from the lone pairs of electrons and also from the sulphur atoms and hence induce no distortions to the square planar $TeS_4$ chromophore. Similar situation arises in compounds (V, VI). The molecular parameters of the ptu group in the complex are nearly the same as observed in crystalline ptu.[13] This is in keeping with the thione and not the mercaptan formulation for the ligand in the complex. A much larger C–S distance of 1.79 Å has been quoted in *cis*-bis(benz-

†Final position coordinates, anisotropic thermal parameters, and a list of observed and calculated structure factors have been deposited as supplementary material with the Editor and with the Cambridge Crystallographic Data Centre.

Table 1. Bond lengths (Å) with their ESD's in parentheses Te–S(1) 2.678(6) Te–S(2) 2.674(5)

| | | | |
|---|---|---|---|
| S(1)-C(1) | 1.67(2) | S(2)-C(8) | 1.73(2) |
| C(1)-N(1) | 1.34(2) | C(8)-N(3) | 1.31(3) |
| C(1)-N(2) | 1.38(2) | C(8)-N(4) | 1.32(2) |
| N(1)-C(2) | 1.41(2) | N(3)-C(9) | 1.38(2) |
| N(2)-C(3) | 1.39(2) | N(4)-C(10) | 1.37(2) |
| C(2)-C(3) | 1.37(2) | C(9)-C(10) | 1.39(2) |
| C(3)-C(4) | 1.38(2) | C(10)-C(11) | 1.36(3) |
| C(4)-C(5) | 1.41(2) | C(11)-C(12) | 1.35(3) |
| C(5)-C(6) | 1.37(3) | C(12)-C(13) | 1.39(3) |
| C(6)-C(7) | 1.40(3) | C(13)- C(14) | 1.38(3) |
| C(2)-C(7) | 1.36(2) | C(9)-C(14) | 1.37(3) |

Table 2. Bond angles (°) with ESD's in parentheses, S(1)–Te–S(2) 90.5(3)

| | | | |
|---|---|---|---|
| Te-S(1)-C(1) | 104.0(8) | Te-S(2)-C(8) | 104.2(8) |
| S(1)-C(1)-N(1) | 126(1) | S(2)-C(8)-N(3) | 125(1) |
| S(1)-C(1)-N(2) | 129(1) | S(2)-C(8)-N(4) | 127(1) |
| N(1)-C(1)-N(2) | 105(1) | N(3)-C(8)-N(4) | 108(1) |
| C(1)-N(1)-C(2) | 113(1) | C(8)-N(3)-C(9) | 111(1) |
| C(1)-N(2)-C(3) | 109(1) | C(8)-N(4)-C(10) | 110(1) |
| N(1)-C(2)-C(3) | 103(1) | N(3)-C(9)-C(10) | 105(1) |
| N(1)-C(2)-C(7) | 131(1) | N(3)-C(9)-C(14) | 133(1) |
| N(2)-C(3)-C(2) | 110(1) | N(4)-C(10)-C(9) | 107(1) |
| N(2)-C(3)-C(4) | 123(1) | N(4)-C(10)-C(11) | 135(1) |
| C(2)-C(3)-C(4) | 122(1) | C(9)-C(10)-C(11) | 118(1) |
| C(3)-C(4)-C(5) | 114(1) | C(10)-C(11)-C(12) | 120(1) |
| C(4)-C(5)-C(6) | 122(1) | C(11)-C(12)-C(13) | 122(1) |
| C(5)-C(6)-C(7) | 124(1) | C(12)-C(13)-C(14) | 118(1) |
| C(6)-C(7)-C(2) | 112(1) | C(13)-C(14)-C(9) | 119(1) |
| C(7)-C(2)-C(3) | 125(1) | C(14)-C(9)-C(10) | 122(1) |

Table 3. Comparison of Te–S bond lengths (Å)

| Compounds | | Te–S | Reference |
|---|---|---|---|
| I | Tetra(thiourea)tellurium(II) perchlorate | 2.638(3), 2.573(4) 2.845(4), 2.707(3) | 3 |
| II | Tetrakis(ethylthiourea)tellurium(II)-chloride | 2.654(3) 2.702(3) | 2 |
| III | Tetrakis(dimethylthiourea)tellurium(II)-chloride | 2.674(1) 2.690(1) | 3 |
| IV | Trans-dithioureabis(tetraethylthiourea)-tellurium chloride | 2.688(3) 2.710(3) | 4 |
| V | Trans-bisthioureabis(phenylenethiourea)-tellurium(II) chloride | 2.685(1) 2.694(2) | 15 |
| VI | Tetra(thiourea)tellurium(II) dichloride | 2.685(10) 2.690(10) | 5 |
| VII | Tetrakis(phenylenethiourea)tellurium(II)-chloride dihydrochloride | 2.674(5) 2.678(6) | present work |

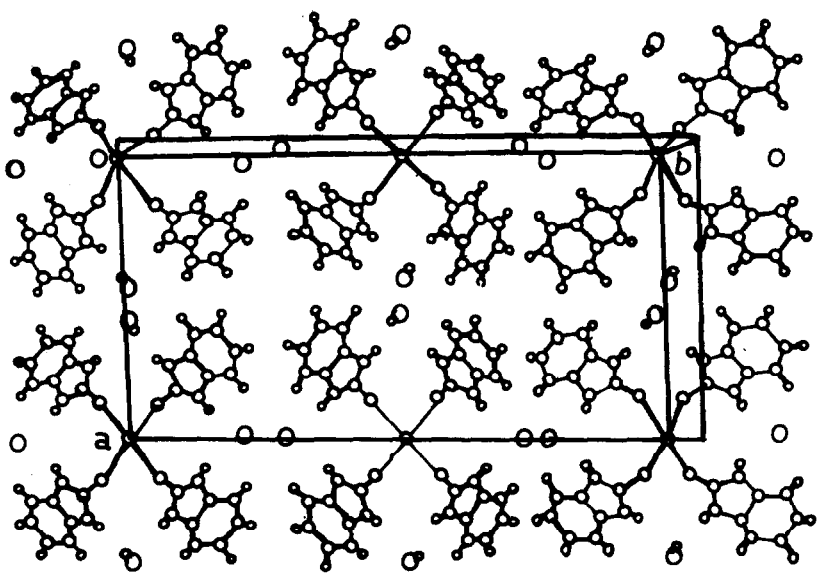



Fig. 2. Projection of the structure of $Te(ptu)_4Cl_2 \cdot 2HCl$ along the $C$-axis.

Table 4. Plane equations and deviations (Å) of the atoms from the least squares planes. The atoms not included in the plane calculations are denoted by an asterisk *

| | |
|---|---|
| I | $TeS_4$ group (exact plane) |
| | 0.134x - 0.651y -0.748 z = 0 |
| | Te 0.0 S(1) 0.0 S(2) 0.0 |
| II | Phenylenethiourea group I |
| | 0.580x + 0.547y - 0.604z = 2.485 |
| | S(1) 0.041(5), C(1)-0.007(16), N(1)-0.033(14) |
| | N(2)-0.029(13), C(2) 0.017(15), C(3) 0.001(15), |
| | C(4)-0.014(16), C(5) 0.024(17), C(6) 0.017(18), |
| | C(7)-0.018(18), Cl(1)* 0.577(8), Cl(2)* 0.321(7) |
| III | Phenylenethiourea group II |
| | -0.343x + 0.539y -0.770z = -2.488 |
| | S(2)-0.041(5), C(8) 0.004(18), N(3) 0.023(14), |
| | N(4) 0.039(14), C(9) 0.010(16), C(10) -0.001(17), |
| | C(11) - 0.021(20), C(12) 0.011(19), C(13) -0.034(19), |
| | C(14) 0.011(19), Cl(2)* - 0.345 (7). |
| | The angles between the planes (deg) |
| | (I)-(II) 80.014(2), (I)-(III) 79.703(8) and |
| | (II)-(III) 55.879(7) |

imidazolethione–S)tetrachlorotellurium(IV) Dioxane.[14]

The four chlorides remain outside the coordination sphere of Te, two at 5.714(8) Å and the other two 6.018(7) Å from Te. Chlorine atoms remain approximately in the least squares planes of the ptu group. This facilitates hydrogen bonding of Cl. .H–N type. All the chlorine atoms in the molecules are involved in hydrogen bonding with NH groups of ptu ligand as revealed by the distances N(1)... Cl (2) = 3.111(17) Å, N(2)... Cl(1) = 3.149(16) Å, N(3)... Cl(2) = 3.099(16) Å and N(4) ... Cl(1) $(-x, -y, -z)$ = 3.166(17) Å. It is interesting to note that there are unusual short contacts of type Cl(1)... Cl(1) $(x, 1/2-y, 1/2+z)$ = 3.050(13) and Cl(2)... Cl(2) $(1-x, -y, -z)$ = 2.944(11) Å. The position of hydrogen chloride (two per formula unit) molecules needs comment. The difference Fourier maps do show electron density peaks indicating location of two HCl moieties in the lattice, each with a spacing of 1.47 Å. This is in order when compared with the bond length in gaseous hydrogen chloride, viz. 1.275 Å, wherein, the interaction is localized. Based, on X-ray evidence only, this is of course, a tentative suggestion. Compounds featuring hydrohalides of crystallization have been reported[24] previously, even though only a few in number. The $TeS_4$ planes in the unit cell are stacked nearly parallel to the *a*-axis. The crystal packing (Fig. 2) seems to be mainly dictated by the hydrogen bonding network involving Cl and N atoms.

## REFERENCES

1. O. Foss, *Pure and Appl. Chem.* 1970, **24**, 31.
2. R. C. Elder, T. Marcuso and P. Boolchand, *Inorg. Chem.* 1977, **16**, 2700.
3. P. W. C. Barnard, J. D. Donaldson, R. M. A. Grimsey, G. Dennes, U. Russo and S. Calogero, *Inorg. Chim. Acta* 1981, **51**, 217.
4. O. P. Anderson, *Acta Chem. Scand.* 1971, **25**, 3593.
5. K. Fosheim, O. Foss, A. Scheie and S. Solheimsnes, *Acta Chem. Scand.* 1965, **19**, 2336.
6. H. K. Ault and S. Husebye, *Acta Chem. Scand.* 1978, **A32**, 157.

7. O. Foss, K. Maroy and S. Husebye, *Acta Chem. Scand.* 1965, **19**, 2361.
8. K. Ase, K. M. Moe and J. O. Solheim, *Acta Chem. Scand.* 1971, **25**, 2467.
9. K. Ase, *Acta Chem. Scand.* 1969, **23**, 3206.
10. O. Foss, N. Lyssandtrae, K. M. Moe and M. Tysseland, *Acta Chem. Scand.* 1973, **27**, 218.
11. K. Ase and I. Roti, *Acta Chem. Scand.* 1974, **A28**, 104.
12. Y. Takahashi and K. Yabe, *Bull. Chem. Soc. Japan*, 1969, **42**, 3064.
13. G. R. Form, E. S. Raper and T. C. Downie, *Acta Cryst.* 1976, **B32**, 345.
14. K. V. Deuton, W. Schnabel and G. Klar, *Cryst. Struct. Commun.* 1979, **8**, 679.
15. G. C. Rout, M. Seshasayee, G. Aravamudan and S. Sowrirajan, *Acta Cryst.* **40C** (1984), in press.
16. G. M. Sheldrick, *SHELX Program for Crystal Structure Determination*. University of Cambridge, England (1976).
17. D. T. Cromer and J. B. Mann, *Acta Cryst.* 1968, **A24**, 321.
18. R. F. Stewart, E. R. Davidson and W. T. Simpson, *J. Chem. Phys.* 1965, **42**, 3175.
19. D. T. Cromer and D. G. Liberman, *J. Chem. Phys.* 1970, **53**, 1891.
20. G. Aravamudan, P. R. Sethuraman and M. R. Udupa, *J. Inorg. Nucl. Chem.* 1973, **35**, 3291.
21. C. K. Johnson, *ORTEP Report ORNL*–3794. Oak Ridge National Laboratory, Tennessee (1965).
22. N. W. Alcock, *Adv. Inorg. Chem. Radiochem.* 1972, **15**, 1.
23. S. Sowrirajan, G. Aravamudan, M. Seshasayee and G. C. Rout (under communication).
24. A. F. Wells, *Structural Inorganic Chemistry*, 4th Edn, pp. 312, 319. The English Language Book Society (1979).

*Polyhedron* Vol. 3, No. 8, pp. 929–937, 1984
Printed in the U.S.A.

0277–5387/84 $3.00 + .00
© 1984 Pergamon Press Ltd.

# SYNTHESIS AND STRUCTURAL ELUCIDATION OF SOME NEW HETEROCYCLIC β-DIKETONE DERIVATIVES OF BORON

**YASH PAL SINGH and A. K. RAI***
Department of Chemistry, University of Rajasthan, Jaipur 302004, India

(*Received* 29 *August* 1983; *accepted* 10 *January* 1984)

**Abstract**—Some new β-diketone derivatives of boron having the general formula $\{B_2O(OAc)_{4-n}[OC(R)\overline{C:CON(Ph)N:C}CH_3]_n\}$ (where $n = 1$ or 2; R = $CH_3$, $C_2H_5$, $C_6H_5$ and $p$-$ClC_6H_4$) have been synthesised by the reactions of oxy-*bis*(diacetatoborane) and substituted pyrazolones, such as 4-acyl-3-methyl-1-phenyl-2-pyrazolin-5-ones (acyl = acetyl, propionyl, benzoyl and $p$-chlorobenzoyl) in dry toluene solution in 1:1 and 1:2 molar ratios. These derivatives have been characterised by elemental analysis, molecular weight measurements. Structures have been proposed on the basis of chemical reactions, IR, $^1H$ and $^{11}B$ NMR spectral studies.

In the derivatives $\{B_2O(OAc)_3[OC(R)\overline{C:CON(Ph)N:C}CH_3]\}$ two of the three acetate groups are unidentate and the third is bridged between two boron atoms along with B–O–B linkage. Whereas the derivatives $B_2O(OAc)_2[OC(R)\overline{C:CON(Ph)N:C}CH_3]_2$ are the mixture of geometrical isomers.

The chemistry of oxy-*bis*(diacetatoborane) has been of continuing interest[1–6] from the date of its synthesis in 1903. This compound is quite stable and a report dealing with its Schiff's base derivatives appeared recently.[7] An extensive survey of the literature reveals that no attempt has been made to study its reaction with monofunctional bidentate ligands. In continuation of our work on heterocyclic β-diketone derivatives of some group III elements[8–10] we have synthesised some new heterocyclic β-diketonates of boron and established their probable structures on the basis of chemical reactions and spectroscopic evidence.

## RESULTS AND DISCUSSION

The reactions of oxy-*bis*(diacetato)borane with 4-acyl-3-methyl-1-phenyl-2-pyrazolin-5-ones (AcMPPOH) (acyl = acetyl, propionyl, benzoyl and $p$-chlorobenzoyl) have been carried out in molar ratios 1:1 and 1:2 in refluxing toluene solution.

$$O[B(OAc)_2]_2 + n\,AcMPPOH \xrightarrow[n=1 \text{ and } 2]{} B_2O(OAc)_{4-n}(OPPMAc)_n + n\,AcOH.$$

Acetic acid liberated was fractionated off azeotropically and the progress of reaction was checked periodically. The synthesised derivatives are summarised in Table 1 along with their physical properties, analysis and molecular weights.

### *IR spectra*

The characteristic IR absorption bands of these compounds are summarised in Table 2. The comparison of the IR absorption bands of the boron complexes with those of the corresponding ligands provide the following useful information regarding the mode of bonding.

(1) The absorption band observed in the region 1510–1520 $cm^{-1}$ in these complexes may be assigned to C⋯O stretching frequency. In free ligands this band was observed at $1540 \pm 5$ $cm^{-1}$.[8–10] The shift of 20–30 $cm^{-1}$ indicates that coordination is through the carbonyl oxygen of the ligand to the boron atom.

(2) The spectra of the derivatives $B_2O(OAc)_2(OPPMAc)_2$ also exhibit a broad band consisting of two absorption bands at 1710–1720 $cm^{-1}$ which may be assigned to free carbonyl stretching frequency of the acetate moieties.[11] The appearance of two very close absorption bands in this region indicate the existence of two unidentate acetate groups in different environment in these complexes. The absence of any absorption band in the region 1610–1630 $cm^{-1}$ ruled out the possibility of any bridging acetate group.

*Author to whom correspondence should be addressed.

Table 1. Synthetic and physical data for substituted pyrazolone derivatives of boron

| Sr. No. | Reactants gms $B_2O(OAc)_4$ | $OC(R)C{:}C(OH)N(Ph)N{:}CCH_3$ R = | Molar ratios | Product % Yield | Physical State mp °C | AcOH in azeotrope Found (Calcd) | % Analysis Found (Calcd.) B | % Analysis Found (Calcd.) OAc | Mol. Wt. Found (Calcd.) |
|---|---|---|---|---|---|---|---|---|---|
| 1. | 0.99 | Me 1.65 | 1:2 | $B_2O(OAc)_2[OC(Me)C{:}CON(Ph)N{:}CCH_3]_2$ 86 | Red crystalline solid 118 | 0.46 (0.45) | 3.72 (3.78) | 20.10 (20.14) | - |
| 2. | 1.02 | Et 1.79 | 1:2 | $B_2O(OAc)_2[OC(Et)C{:}CON(Ph)N{:}CCH_3]_2$ 85 | Brown sticky solid - | 0.46 (0.44) | 3.59 (3.62) | 19.01 (19.22) | |
| 3. | 1.04 | Ph 2.22 | 1:2 | $B_2O(OAc)_2[OC(Ph)C{:}CON(Ph)N{:}CCH_3]_2$ 88 | Yellow powder 125 | 0.46 (0.48) | 2.96 (3.09) | 16.41 (16.62) | 710 (736) |
| 4. | 0.66 | ClPh 1.99 | 1:2 | $B_2O(OAc)_2[OC(ClPh)C{:}CON(Ph)N{:}CCH_3]_2$ 86 | Orange yellow powder 121 | 0.31 (0.31) | 2.83 (2.84) | 14.99 (15.14) | 779 (796) |
| 5. | 1.52 | Me 1.25 | 1:1 | $B_2O(OAc)_3[OC(Me)C{:}CON(Ph)N{:}CCH_3]$ 85 | Pink powder 87 | 0.36 (0.35) | 5.17 (4.98) | 26.98 (27.44) | - |
| 6. | 1.47 | Et 1.29 | 1:1 | $B_2O(OAc)_3[OC(Et)C{:}CON(Ph)N{:}CCH_3]$ 84 | Light yellow powder 93 | 0.34 (0.33) | 4.91 (5.01) | 26.46 (26.58) | 444 (472) |
| 7. | 1.50 | Ph 1.59 | 1:1 | $B_2O(OAc)_3[OC(Ph)C{:}CON(Ph)N{:}CCH_3]$ 85 | Light yellow powder 144 | 0.35 (0.34) | 4.48 (4.50) | 23.80 (23.98) | 492 (468) |
| 8. | 1.76 | ClPh 2.11 | 1:1 | $B_2O(OAc)_3[OC(ClPh)C{:}CON(Ph)N{:}CCH_3]$ 81 | Yellow powder 116 | 0.41 (0.40) | 4.19 (4.18) | 22.16 (22.43) | - |

Table 2. IR spectral data ($cm^{-1}$) for substituted pyrazolone derivatives of boron

| Sl. No. | Compound | ν C=O (Acetate terminal) | ν C=O (acetate bridging) | νC=O (Ligand) | νC - O (Acetate) | νB—O | νB←O |
|---|---|---|---|---|---|---|---|
| 1. | $B_2O(OAc)_3[OC(Ph)C{:}CON(Ph)N{:}CCH_3]$ | 1710s | 1615m | 1510m | 1260m | 1110m | 730m |
| 2. | $B_2O(OAc)_3[OC(ClPh)C{:}CON(Ph)N{:}CCH_3]$ | 1700s | 1610m | 1520m | 1250m | 1120m | 720m |
| 3. | $B_2O(OAc)_3[OC(C_2H_5)C{:}CON(Ph)N{:}CCH_3]$ | 1730s | 1620m | 1520m | 1270m | 1110m | 730m |
| 4. | $B_2O(OAc)_3[OC(CH_3)C{:}CON(Ph)N{:}CCH_3]$ | 1720s | 1630m | 1520m | 1250m | 1115m | 720m |
| 5. | $B_2O(OAc)_2[OC(Ph)C{:}CON(Ph)N{:}CCH_3]_2$ | 1700s, 1710s | - | 1520m | 1260m | 1125m | 730m |
| 6. | $B_2O(OAc)_2[OC(ClPh)C{:}CON(Ph)N{:}CCH_3]_2$ | 1710s, 1720s | - | 1500m | 1280m | 1110m | 730m |
| 7. | $B_2O(OAc)_2[OC(C_2H_5)C{:}CON(Ph)N{:}CCH_3]_2$ | 1710s, 1720s | - | 1510m | 1260m | 1120m | 720m |
| 8. | $B_2O(OAc)_2[OC(CH_3)C{:}CON(Ph)N{:}CCH_3]_2$ | 1710s, 1720s | - | 1510m | 1280m | 1120m | 725m |
| 9. | $OC_6H_4OBOB(OAc)[OC(Ph)C{:}CON(Ph)N{:}CCH_3]_2$ | - | 1610m | 1510 | 1260m | 1120m | 720m |
| 10. | $HOCH_2CH_2OBOB(OAc)[OC(Ph)C{:}CON(Ph)N{:}CCH_3]_2$ * | 1710s | | 1510m | 1260m | 1110m | 720m |
| 11. | $(HOCH_2CH_2O)_2B_2O[OC(Ph)C{:}CON(Ph)N{:}CCH_3]_2$ * | - | - | 1510m | - | 1110m | 720m |

* νOH was observed at ∼ 3450 $cm^{-1}$; s = strong, m = medium.

Table 3. $^1$H NMR data ($\delta$ ppm) of substituted pyrazolone derivatives of boron

| Sr. No. | Compound | $-CH_3$ ligand | $-CH_3$ (Unidentate acetate) | $-CH_3$ (bridging acetate) | $OC_2H_5$ (Ligand) | Phenyl |
|---|---|---|---|---|---|---|
| 1. | $B_2O(OAc)_3[OC(C_6H_5)C{:}CON(Ph)N{:}CCH_3]$ | 2.26s | 2.06s | 1.98s | - | 7.40-7.83m |
| 2. | $B_2O(OAc)_3[OC(C_2H_5)C{:}CON(Ph)N{:}CCH_3]$ | 2.46s | 2.10s | 2.00s | 1.04-1.4t<br>2.65-2.92q | 7.36-7.80m |
| 3. | $B_2O(OAc)_3[OC(ClC_6H_4)C{:}CON(Ph)N{:}CCH_3]$ | 2.56s | 2.08s | 2.00s | - | 7.30-7.90m |
| 4. | $B_2O(OAc)_2[OC(C_6H_5)C{:}CON(Ph)N{:}CCH_3]_2$ | 2.23s | 2.01s<br>2.07s | - | - | 7.35-7.80m |
| 5. | $B_2O(OAc)_2[OC(C_2H_5)C{:}CON(Ph)N{:}CCH_3]_2$ | 2.40s | 1.94s<br>1.04s | - | 1.05-1.40t<br>2.60-2.90q | 7.20-7.80m |
| 6. | $B_2O(OAc)_2[OC(ClC_6H_4)C{:}CON(Ph)N{:}CCH_3]_2$ | 2.60s | 2.00s<br>2.28s | - | - | 7.20-7.90m |

(3) In the spectra of the derivatives $B_2O(OAc)_3(OPPMAc)$ the presence of a sharp absorption band at 1720 $cm^{-1}$ and a medium intensity band at 1600–1610 $cm^{-1}$ may be attributed to the C=O stretching vibration of the unidentate and bridging acetate groups respectively.[11]

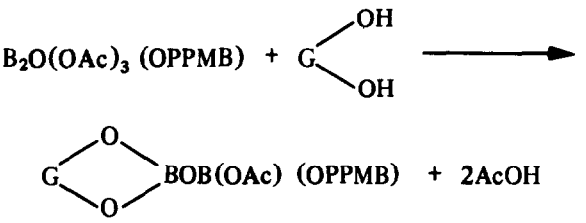
The absorption bands at 1260–1280, 1120–1140 and 720–730 $cm^{-1}$ observed in these derivatives may be assigned to C–O(acetate),[11] B–O[12] and B←O[13] vibrations respectively.

*$^1$H NMR spectra*

The $^1$H NMR spectra of some representative compounds have been recorded and are summarised in Table 3. The singlet due to the –OH proton ($\delta$ 12.1) which was observed in the $^1$H NMR spectrum of the ligand disappears from the spectra of all the boron derivatives showing that deprotonation of –OH proton occurs during complexation. The other proton signals (due to $CH_3$, $OC_2H_5$ and phenyl) remained unaffected on chelation.

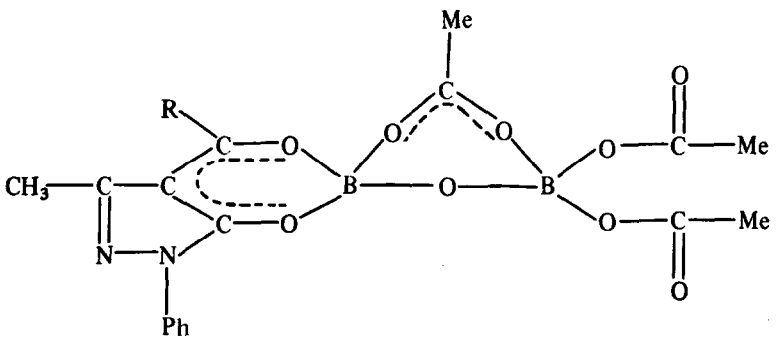
In the spectra of $B_2O(OAc)_3(OPPMAc)$, three singlets at $\delta$ 1.98, 2.06 and 2.20 ppm were observed and may be assigned to methyl protons. A comparison of the spectra of the two reactants viz. $B_2O(OAc)_4$[11] and AcMPPOH with the derivatives $B_2O(OAc)_3(OPPMAc)$ indicates that the above three singlets were due to the methyl protons of the bridging acetoxy, terminal acetoxy and of the other ligand moiety respectively. The integration of the signal at $\delta$ 2.06 ppm (due to terminal acetoxy methyl protons) corresponded to six protons whereas the signal at $\delta$ 1.98 ppm corresponded to three protons only. This indicated that the two acetate groups out of three were unidentate and the remaining one was bridging the two boron atoms along with B–O–B bond. Thus on the basis of IR and $^1$H NMR spectral data the following plausible structure may be assigned to $B_2O(OAc)_3(OPPMAc)$ derivatives:

The presence of one bridging and two terminal acetate groups has further been confirmed by the reaction of these derivatives with catechol in a 1:1 molar ratio in toluene solution where two moles of acetic acid were fractionated off azeotropically with toluene and estimated.




In the IR spectrum of the above derivative the absence of any absorption band in the region 1710–1730 $cm^{-1}$ which was earlier observed in the IR spectrum of $B_2O(OAc)_3(OPPMB)$ ruled out the presence of unidentate acetate groups. However, the medium intensity band at 1610 $cm^{-1}$ which was earlier assigned to $\nu C\cdots O$ of the bridging acetate group[11] was found to be intact.

The $^1$H NMR spectra of $B_2O(OAc)_2(OPPMAc)$, derivatives exhibited two singlets at $\delta$ 2.01 and 2.07 ppm which were assigned to the $CH_3$ protons of the acetate groups.[11] The presence of any bridging acetate group in these derivatives was ruled out by their IR spectra and therefore the two acetate groups occupy the terminal positions on the two boron atoms in the molecule. The appearance of two sharp singlets for the methyl protons of the terminal acetate groups instead of one singlet clearly indicates that the two acetate groups are present in different environments. The appearance of two singlets for the methyl protons of the two acetate groups may indicate their existence in the *trans*-positions assuming restricted rotation about the B–O–B system. When their reactions were carried out with glycols in 1:1 molar ratios in refluxing toluene, only one mole of acetic acid could



be fractionated off even after prolonged refluxing. The second acetoxy group could only be replaced by carrying out the reactions in 1:2 molar ratios.

$$B_2O(OAc)_2(OPPMB)_2 + HOGOH \longrightarrow B_2O(OAc)(HOGO)(OPPMB) + AcOH$$

$$B_2O(OAc)_2(OPPMB)_2 + 2HOGOH \longrightarrow B_2O(OGOH)_2(OPPMB)_2 + 2AcOH$$

$$G = -CH_2-CH_2- \text{ and } (CH_3)_2C-C(CH_3)_2$$

These reactions show that the glycols are constrained to react in the monofunctional mode probably due to the steric effect of ligand moiety as compared to a very small size of boron (0.48 Å). One explanation of this behaviour is that the two acetate groups are present in *trans*-geometry due to restricted rotation about the B–O–B bond. That means that most of the molecules in these compounds prefer to stay in *trans*-geometry as in *trans*-geometry the boron atom experiences less steric hindrance as compared to *cis*-geometry.

*$^{11}$B NMR spectra*

The $^{11}$B NMR spectra of two representative compounds were recorded at the Indian Institute of Sciences, Bangalore, in $CDCl_3$ solution with reference to $BF_3 \cdot O(C_2H_5)_2$.

In the $^{11}$B NMR spectrum of the derivative $B_2O(OAc)_3[OC(Ph)C:CON(Ph)N:C\,CH_3]$ two singlets were observed at $\delta$ 4.02 and 4.49 ppm. The appearance of two singlets clearly indicates the presence of two types of tetracoordinated[14–17] boron atoms in this compound. Contrary to the above, the spectrum of $B_2O(OAc)_2[OC(ClPh)C:CON(Ph)N:C\,CH_3]_2$ exhibited four singlets at $\delta$ 2.42, 2.84, 3.23 and 3.94ppm. A perusal of the structure proposed for the derivatives $B_2O(OAc)_2[OC(R)C:CON(Ph)N:C\,CH_3]_2$ clearly indicated that the following configurations of these derivatives are possible.

The two configurations *cis-cis* and *trans-trans* are centro-symmetric and give two signals (one from each). Whereas in the structure *cis-trans* there is no such centre of symmetry hence the two boron atoms are different. Thus four different boron atoms (geometrically as well as magnetically) result in the appearance of four singlets in $^{11}$B NMR spectra. Hence we conclude that these derivatives are mixture of above isomers.

## EXPERIMENTAL

Care was taken to exclude moisture from the apparatus during the experiments. Toluene was dried by distillation twice over sodium wire. Oxy-*bis*(diacetatoborane) was synthesised by the reaction of boric acid and acetic anhydride[1] whereas the ligands were prepared by Jensen's method.[18]

Boron was estimated as methyl borate.[19] Acetic acid/acetoxy group was estimated by titrating azeotrope/compound against standard N/10 NaOH solution. IR spectra were recorded as Nujol mull on Perkin–Elmer Model-577 grating IR spectrophotometer while $^1$H NMR spectra were recorded on a Varian S-100 spectrometer in $CDCl_3$ solution using TMS as an internal standard.

*Synthesis of 4-acyl-3-methyl-1-phenyl-2-pyrazolin-5-one derivatives of boron*

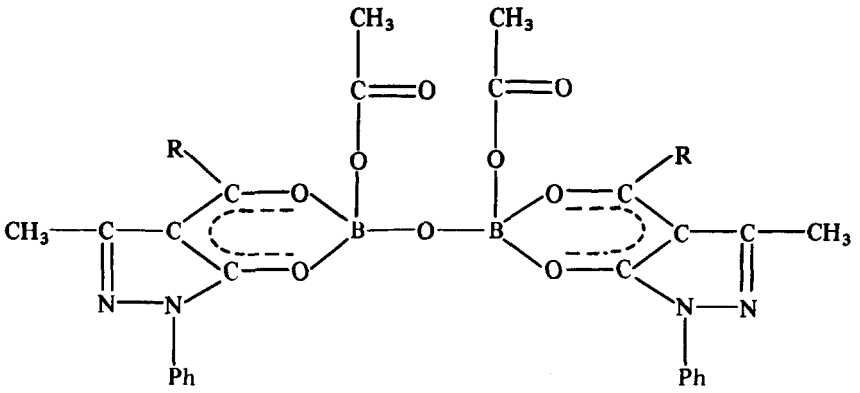
The reactions of oxy-*bis*(diacetatoborane) with 4-acyl-3-methyl-1-phenyl-2-pyrazolin-5-ones have been carried out in 1:1 and 1:2 molar ratios in refluxing toluene solutions. The reactions of these derivatives have also been carried out with glycols. Since similar methods were followed, the synthesis and reaction of only one derivative is given in detail and the results of the other derivatives are summarised in Tables 1 and 4.

*Synthesis of oxy - bis(acetatoborane)bis(4 - benzoyl - 2,4 - dihydro - 5 - methyl - 2 - phenyl - 5H - pyrazolonato O'O')*

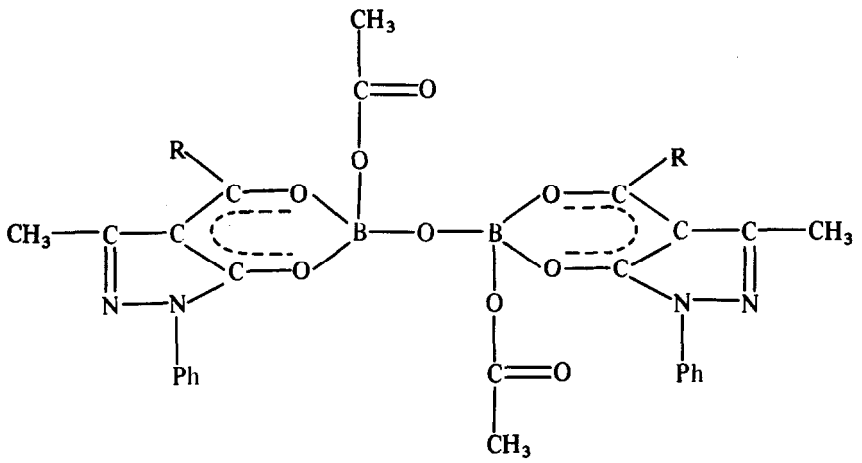
To a toluene solution of oxy-*bis*(diacetatoborane)(1.04 g, 3.79 mM), a weighed amount of 4-benzoyl-3-methyl-1-phenyl-2-pyrazolin-5-one (2.11 g, 7.58 mM) was added and the mixture was refluxed under fractionating column. The acetic acid thus liberated was fractionated off azeotropically with toluene. The progress of the reaction was checked by estimating the acetic acid in the azeotrope periodically (Found, acetic acid, 0.31 g, Calc. 0.31 g). After the completion of reaction, the excess solvent was removed by distillation and the compound was dried under reduced pressure. The compound was recrystallised from toluene. Found, B, 2.96; OAc, 16.14; Calc. for $B_2O_7C_{38}H_{32}N_4$, B, 3.09; OAc, 16.62%.

*Reaction between oxy-bis(acetatoborane)bis(4-benzoyl 2,4-dihydro-5-methyl-2-phenyl-5H-pyrazolonato O'O') with ethane 1,2-diol in 1:1 molar ratio*

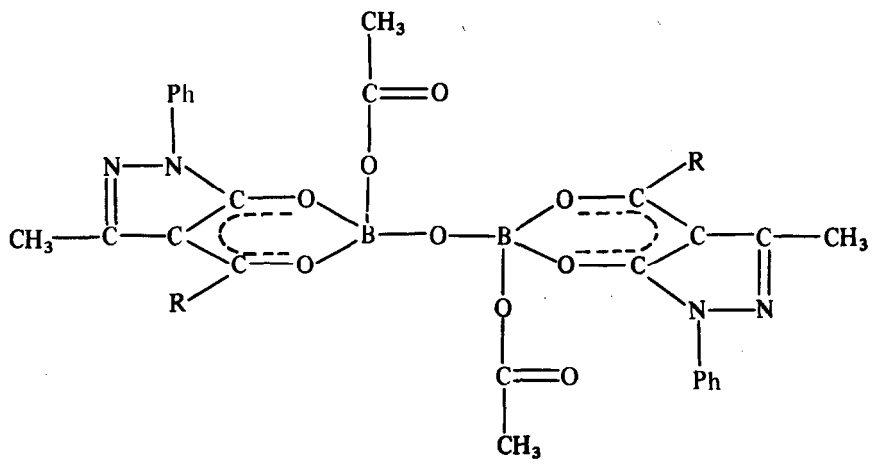
A calculated amount of ethane 1,2-diol (0.11 g, 1.83 mM) was mixed with a toluene solution ($\sim$50 cm$^{-3}$) of oxy-*bis*(acetato-borane) pyrazolone derivative (1.33 g, 1.87 mM). The reaction contents were refluxed. The acetic acid liberated during the course of the reaction was removed azeotropically with toluene and was estimated to check the progress of the reaction (Found, acetic acid, 0.16 g; Calc. 0.16 g). On completion of the reaction the excess solvent was distilled off and the compound



(*cis–cis*)



(*cis–trans*)



(*trans–trans*)

Table 4. Reactions of boroacetate pyrazolonate derivatives with glycols

| Sl. No. | Reactants gms: Boroacetate Complex | Reactants gms: Glycol | Molar ratio | Product % Yield | Physical state m.p. °C | Acetic acid Found (Calcd) gms | % Analysis Found (Calcd): B | % Analysis Found (Calcd): OAc | Molecular weight Found (Calcd.) |
|---|---|---|---|---|---|---|---|---|---|
| 1. | $B_2O(OAc)_3OPPMB$ 1.54 | $HOC_6H_4OH$ 0.35 | 1:1 | $\overline{OC_6H_4OB}(OAc)OB(OPPMB)$ 90 | Yellow powder 205 | 0.37 (0.38) | 4.65 (4.84) | 21.65 (21.81) | - |
| 2. | $B_2O(OAc)_2(OPPMB)_2$ 1.21 | HOGOH 0.20 | 1:1 | $(HOGO)(OAc)OB_2(OPPMB)_2$ 86 | yellow powder 66 | 0.11 (0.10) | 2.76 (2.88) | 15.43 (15.60) | 789 (756) |
| 3. | $B_2O(OAc)_2(OPPMB)_2$ 0.74 | HOGOH 0.25 | 1:2 | $(HOGO)_2OB_2(OPPMB)_2$ 85 | Yellow powder 80 | 0.10 (0.12) | 2.58 (2.64) | - | - |
| 4. | $B_2O(OAc)_2(OPPMB)_2$ 1.33 | HOG'OH 0.17 | 1:1 | $(HOG'O)(OAc)OB_2(OPPMB)_2$ 85 | Yellow sticky solid | 0.16 (0.16) | 3.11 (3.08) | 16.02 (16.29) | 756 (724) |
| 5. | $B_2O(OAc)_2(OPPMB)_2$ 0.71 | HOGOH 0.17 | 1:2 | $(HOG'O)_2OB_2(OPPMB)_2$ 86 | Yellow sticky solid | 0.15 (0.17) | 2.86 (2.95) | - | - |

$BMPPO^- = \bar{O}C(C_6H_5)\overline{C{:}CON(Ph)N{:}C}CH_3$

$G = (CH_3)_2\overset{|}{C}-\overset{|}{C}(CH_3)_2$

$G' = -CH_2-CH_2-$

was dried under reduced pressure. Found, B, 3.26; OAc, 16.02; Calc. for $C_{38}H_{34}O_9B_2N_2$, B, 3.16; OAc, 16.29%.

*Acknowledgement*—One of the authors (Y.P.S.) is thankful to CSIR, New Delhi for financial assistance.

## REFERENCES

1. A. Pictet and A. Geleznoff, *Chem. Ber.* 1903, **36**, 2219.
2. O. Dimroth, *Annals* 1925, **446**, 97.
3. W. Gerrard and M. Wheelans, *Chem. and Ind.* 1954, 758.
4. M. F. Lappert, *Chem. Rev.* 1956, **56**, 959.
5. R. G. Hayter, A. W. Laubengayer and P. G. Thompson, *J. Am. Chem. Soc.* 1957, **79**, 4243.
6. A. D. Negro, L. Urigaretti and A. Perotto, *J. Chem. Soc. Dalton Trans.* 1972, 1639.
7. H. B. Singh and J. P. Tandon, *J. Inorg. Nucl. Chem.* 1980, **42**, 793.
8. Y. P. Singh and A. K. Rai, *Synth. React. Inorg. Met-Org. Chem.* 1982, **12**, 85.
9. Y. P. Singh, S. Saxena and A. K. Rai, *J. Indian Chem. Soc.* 1982, **59**, 273.
10. Y. P. Singh, S. Saxena and A. K. Rai, *Indian J. Chem. A* 1983, **22**, 298.
11. N. W. Alcock, V. M. Tracy and T. C. Waddinton, *J. Chem. Soc. Dalton Trans.* 1976, 2243.
12. A. Barbas, E. Isfan, M. Roman, M. Paraschiv, E. Romas and A. T. Balaban, *Tetrahedron* 1968, **24**, 1133.
13. P. N. Gates and E. F. Mooney, *J. Inorg. Nucl. Chem.* 1968 **30**, 839.
14. J. P. Onak, H. Landensman, R. E. William and I. Shapiro, *J. Phys. Chem.* 1959, **63**, 1533.
15. N. M. D. Crown and P. Bladon, *J. Chem. Soc. A* 1969, 526.
16. E. Hohaus and W. Riepe, Z. *Naturforsch* 1973, **28B**, 440.
17. E. Hohaus and W. Riepe, *Z. Naturforsch* 1976, **31B**, 324.
18. B. S. Jensen, *Acta Chem. Scand.* 1959, **13**, 1068.
19. I. H. Thomas, *J. Chem. Soc.* 1946, 820.

*Polyhedron* Vol. 3, No. 8, pp. 939–945, 1984
Printed in the U.S.A.

0277–5387/84 $3.00 + .00
© 1984 Pergamon Press Ltd.

# PREPARATION AND COMPLEXATION PROPERTIES OF POLYSTYRENE RESINS CONTAINING DIETHYLENETRIAMINE DERIVATIVES

**TOSHISHIGE M. SUZUKI* and TOSHIRO YOKOYAMA**
Government Industrial Research Instutite, Tohoku 4–2–1 Nigatake, Sendai, Japan

(*Received* 4 *November* 1983; *accepted* 17 *January* 1984)

**Abstract**—Styrene-divinylbenzene copolymer resins containing a series of diethylenetriamine derivatives have been prepared and characterized. The multidentate ligands are covalently bound to the polymer matrix without causing inter- and intrastrand bridging structures. The properties of the present chelating resins have been examined with respect to the uptake of transition metal ions.

Chelating polymer resins have the potential utilities for recovery of metal ions from industrial effluents and mine tailings.[1] Since the stability of a metal complex increases with the number of chelate rings,[2] it is desirable to immobilize multidentate ligands into polymer matrix rather than unidentate ligands. Polyazaalkane-$\alpha,\omega$-diamines $[\{H_2N(CH_2)_nNH\}_n(CH_2)_n\text{-}(NH_2)]$ are those ligands which can form stable metal complexes with a wide variety of metal ions. In addition, they are convenient starting materials for preparing further multidentate ligands, for example, amine-*N*-polycarboxylates,[3] amine-*N*-polyalcohols,[4] and amine-*N*-polyphosphonates.[5]

Polymer-bound polyazaalkane-$\alpha,\omega$-diamines have been prepared by the reaction of the amines with chloromethylated styrenedivinylbenzene copolymer.[6,7] However intra- and interstrand bridging reactions are inevitable due to *N*-alkylation at different amino and imino groups in the ligand. These bridging reactions which occur at the expense of available chloromethyl groups should decrease the number of immobilized ligand.[8] Moreover complicated cross-linkings by the ligand should bring about steric restrictions on metal chelate formation. So far several attmepts have been carried out to immobilize multidentate ligands as discrete units,[9–11] but they require long steps and result in rather low yield.

In the present paper, we report a simple method to introduce diethylenetriamine into polystyrene beads without causing undesirable bridging reactions. The preliminary results have been reported briefly.[12] The resin containing diethylenetriamine was afforded for the starting material to prepare amine-*N*-derivatives including amine-*N*-polycarboxylate and amine-*N*-polyphosphonate. The complexation properties of the present chelating resins were compared with those of the resins prepared by the conventional method.

## EXPERIMENTAL

*General procedures.* The pH from 3.0 to 6.0 was adjusted with acetate buffer and below 3.0 with hydrochloric acid. IR spectra were recorded with a Hitachi 285 grating infrared spectrophotometer. Metal ion concentration was determined with a Shimadzu atomic absorption/flame photometer Model AA-610S.

### *Preparations*

*Chloromethylated polystyrene beads* **1**. Styrene-2%-divinylbenzene copolymer beads (200–400 mesh, Kodac Chemical Co.) were chloromethylated with chloromethyl methylether and tin(IV) chloride according to the published method.[13] The chloromethylated resin **1** was throughly extracted with dioxane and dried at 50°C under vacuum. Cl, 20.8%. The chlorine content corresponds to chloromethylation 86% of the available benzene rings.

*Author to whom correspondence should be addressed.

*Bis*[2-(*salicylideneamino*) *ethyl*] *amine* **2.** This ligand was prepared by the method described in the literature[14] and was identified via $^1$H NMR analysis.

*Schiff base resin* **3.** Resin **1** (26 g) in dioxane (400 cm$^3$) was stirred for 1 hr at room temperature to allow full swelling. To this suspension was added the Schiff base **2** (93 g) and heated at 100°C for 48 hr with continuous stirring. Excess ligand acts as an acceptor of hydrogen chloride which was produced by the alkylation. Hydrochloride of the free ligand deposited as yellow crystals during the reaction. The solid materials were filtered off, washed well with water to remove the crystalline compound and then with dioxane and transferred to a Soxhlet extractor. After extraction with dioxane for 48 hr, the resin was collected, washed with diethyl ether and dried at 50°C under vacuum. Yield: 50.4 g.

*Diethylenetriamine resin* **4.** The resin **3** (49.1 g) was stirred with 6 M (M = mol dm$^{-3}$) HCl (600 cm$^3$) at 60°C for 24 hr. Salicylaldehyde was liberated as an oil during the hydrolysis. Brown polymer beads which are the hydrochloride form of resin **4** were filtered off, washed with ethanol and diethylether, and dried under vacuum. The resin in the free amine form was obtained by treatment with 2 M sodium hydroxide followed with water unitl the washings were neutral. Yield: 30.5 g.

*Diethylenetriamine resin* **4′**. Diethylenetriamine was directly introduced into polymer resin by the reaction with chloromethylated polystyrene **1**. A mixture of chloromethylated polystyrene beads **1** (51.2 g) and diethylenetriamine (61.8 g) in dioxane (600 cm$^3$) was refluxed for 48 hr with continuous stirring. The resin beads were filtered off, washed well with water, and then dioxane in a Soxhlet extractor. After 48 hr extraction, the resin was collected, washed with diethyl ether and dried at 50°C under vacuum. Yield: 58.0 g.

*Amine-N-polycarboxylate resin* **5.** Chloroacetic acid (94.5 g in 100 cm$^3$ of water) was neutralized with sodium carbonate at 0°C. To this solution was added polymer resin **4** (30.0 g) and stirred at 70°C for 12 hr. The reaction solution was maintained basic (pH 9–10) with sodium carbonate. The resin was filtered off, washed with 2 M HCl and then water unitl the washings were neutral and dried at 50°C under vacuum. Yield: 49.9 g.

*Amine-N-polycarboxylate resin* **5′**. This resin was prepared according to a method similar to that for resin **5** using resin **4′** in place of **4**. Carboxymethylation of resin **4′** (15 g) yielded 19.5 g of resin **5′**.

*Amine-N-poly*(*methylphosphonate*) *resin* **6.** To a refluxed mixture of resin **4** (15 g), phosphorous acid (33 g) and 6 M HCl (80 cm$^3$) was added dropwise 37% aqueous formaldehyde solution (64 cm$^3$) in the course of *ca.* 2 hr. The reaction mixture was kept at reflux temperature for additional 3 hr. The resin was filtered, washed well with water, ethanol and then diethyl ether and dried under vacuum. Yield: 25.3 g.

*Amine-N-poly*(*methylphosphonate*) *resin* **6′**. This resin was prepared according to a method similar to that for resin **6** using resin **4′** in place of resin **4**. Phosphonomethylation of resin **4′** (15 g) yielded 24.1 g of resin **6′**.

The analytical data of the resins are summarized in Table 1 along with the ligand capacity (the concentration of ligand in one gram of dry resin) and the reaction conversion.

*Determination of capacity for metal ion uptake*

The amount of metal ion adsorbed on one gram of dry resin was determined as a function of pH by the following procedure.

A 500 mg of dry resin was added to 100 cm$^3$ of buffered metal ion solution (0.2 M). After 15 hr stirring at room temperature the resin was filtered off and washed with water. The adsorbed ion was stripped from the resin by elution with 2 M HCl. The amount of metal ion in the eluate was determined with an atomic absorption spectrometer.

In the case of resin **3** the experiments were carried out in dimethylformamide (DMF). The rate of metal ion uptake is significantly slow in an aqueous solution, while in DMF and dimethylsulphoxide (DMSO) the equilibrium can be attained within 1 hr.

*Chromatographic separation of metal ion mixture*

*Separation of* $Ni^{2+}$, $Cu^{2+}$ *and* $Zn^{2+}$. A glass column ($\phi$ 1.0 cm) was packed with 5 g of resin **4** which was fully swollen in advance. One cm$^3$ of metal ion mixture ($NiCl_2 \cdot 6H_2O$, $CuCl_2 \cdot 2H_2O$, $ZnCl_2 \cdot 2H_2O$; 1 g of each salt was dissolved in 100 cm$^3$ of water) was poured onto the column and the adsorbed band was eluted at a flow rate of 1.1 cm$^3$ min$^{-1}$ with desired eluent: 0.1 M acetate buffer (pH 4.6) for $Zn^{2+}$; 0.1 M HCl for $Ni^{2+}$; and 2 M HCl for $Cu^{2+}$. The eluate was fractionated into 10 cm$^3$ portions and the amount of metal ion was determined.

*Separation of* $Co^{2+}$ *and* $Ni^{2+}$. The procedure was very similar to that described above using the resin **5** in place of resin **4**. One cm$^3$ of metal ion mixture ($CoCl_2 \cdot 6H_2O$, $NiCl_2 \cdot 6H_2O$; 1 g of each salt was dissolved in 100 cm$^3$ of water) was poured onto the

Table 1. Analytical data and amount of ligand incorporated into polystyrene resin

| Resin | Analytical data/% | | Amount of ligand incorporated[a] (mmol/g-resin) | Conversion/%[b] |
|---|---|---|---|---|
| | Cl | N | | |
| 3 | 1.33 | 8.6 | 2.01 | 89 |
| 4 | 0 | 12.7 | 3.02 | 72 |
| 4' | 0.4 | 9.5 | 2.30 | 54 |
| 5 | 0 | 7.9 | 1.84 | - |
| 5' | 0 | 6.6 | 1.57 | - |
| 6 | 0 | 6.5 | 1.55 | - |
| 6' | 0 | 5.5 | 1.31 | - |

a) Calculated from the nitrogen content.[1d] Amount of ligand incorporated (mmol/g-resin)= $\frac{\% N}{14n}$ X 10, where % N= % nitrogen in product and n= number of nitrogen in the ligand.

b) Based on the ratio of the actual ligand content to the theoretical value calculated from the total displacement of chlorine by the ligand.[1d] % Conversion= $\frac{\% N}{14n} \times \frac{(L-35.5)\%Cl/100 + 35.5}{\%Cl/100}$, where %Cl = % chlorine in the original chloromethylated polystyrene, L = ligand molecular weight minus 1.

column and eluted at a flow rate 1.4 $cm^3 min^{-1}$. Cobalt(II) ion was stripped from the column by elution with a solution of pH 1.3–1.5 (HCl) while $Ni^{2+}$ was eluted by 0.2 M HCl.

## RESULTS AND DISCUSSION

*Preparation and characterization of the chelating resins*

Reaction of diethylenetriamine with chloromethylated polystyrene should lead to a wide range of products as a result of *N*-alkylation at different amine groups in the ligand.[6,7] It is known that diethylenetriamine readily forms 1 : 2 Schiff base with salicylaldehyde,[14] and the original amine can be regenerated by acid hydrolysis. Thus we intended to protect the primary amine groups of the ligand by Schiff base formation prior to immobilization.

The synthetic scheme for the preparation of present polymer-bound ligands is given in Fig. 1. The Schiff base **2** was introduced into polymer matrix by the reaction with chloromethylated styrenedivinylbenzene copolymer beads **1**. The resulting yellow resin **3** is presumed to have a structure as depicted in Fig. 1 in which the ligand is linked to polystyrene uniquely through the imino nitrogen. Bis(salicylideneiminate)ethylenediamine which has no imino group did not react with resin **1** indicating that *O*-alkylation at the hydroxide group must be less significant. From the elemental analysis (Table 1), the amount of Schiff base attached to the polymer beads was *ca.* 2.0 mmol per gram resin or roughly 89% conversion with respect to the available chloromethyl groups. The resin **3** gave IR absorption band at around 1630 $cm^{-1}$ due to (C=N) stretching vibration of the introduced ligand. Acid hydrolysis of resin **3** followed by neutralization yielded resin **4** where the $\nu$(C=N) band entirely disappeared. The resin **4** was shown to contain 3 mmol of diethylenetriamine per gram of dry resin on the basis of the nitrogen analysis which corresponds to approx. 72% of the original chlorine atoms in the resin **1** are replaced by the ligand. The resin **4** contains pendant primary amine groups and was afforded for the preparation of amine-*N*-derivatives. Treatment of resin **4** with sodium chloroacetate yielded amine-*N*-polycarboxylate resin **5** in which strong IR band assignable to $\nu$(C=O) was observed at around 1730 $cm^{-1}$. Amine-*N*-poly(methylphosphonate) resin **6** was obtained by refluxing a mixture of resin **4**, 6 M HCl, $H_2PHO_3$ and aqueous formaldehyde solution. Nitrogen analysis indicates that resin **5** and resin **6** contain formally 1.84 and 1.60 mmol of the ligand per gram resin, respectively. These resins

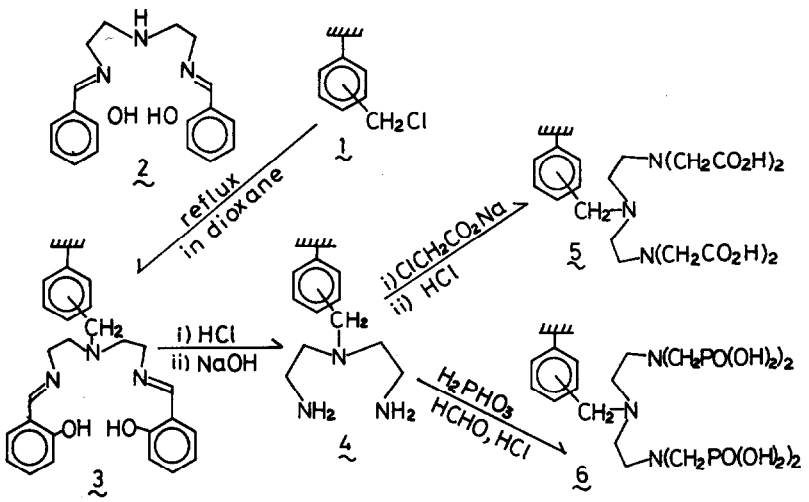



Fig. 1. Reaction scheme for the preparation of the chelating resins containing pendant multidentate ligands.

probably contain some incompletely carboxymethylated or phosphonomethylated functional groups, i.e. from zero to three *N*-substituted derivatives.

In order to compare the complexing properties of the above resins with those obtained by conventional method,[6,7] analogous resins (**4′**, **5′**, and **6′**) were prepared by direct reaction of diethylenetriamine with resin **1** followed by *N*-carboxymethylation and *N*-phosphonomenthylation. Two-fold excess of diethylenetriamine with respect to chloromethyl groups was used for the preparation of resin **4′** in analogy with the case of resin **4**. The nitrogen content therefore amount of ligand in the resin **4′** is rather lower than that of resin **4** (Table 1). In the case of resin **4′**, complicated cross-linkings between amine groups and polymer matrix must have taken place at the expence of available chloromethyl groups giving rise to a decrease in the ligand capacity.

*Complexation properties of the chelating resins*

The metal ion adsorption capacities of the chelating resins were determined by batch type equilibrium procedure in the presence of excess amount of metal ion.

Schiff base resin **3** readily forms metal complexes with many kinds of transition metal ions including $Cu^{2+}$, $Ni^{2+}$, $Co^{2+}$ and $Zn^{2+}$ in polar organic solvents such as DMF and DMSO. However complex formation is significantly slow in aqueous solution presumably due to hydrophobic character of the functional group as well as the polymer matrix. The amount of metal ion adsorbed on resin **3** in DMF are 1.23, 1.12, 1.25 and 0.92 mmol per gram resin for $Cu^{2+}$, $Ni^{2+}$, $Co^{2+}$ and $Zn^{2+}$, respectively. Assuming that the functional group of resin **3** forms 1 : 1 complex with these metal ions, nearly half of the introduced ligands are effectively used for chelation. Most of the adsorbed ions can be released from the resin by treatment with 1 M HCl. However gradual hydrolysis of Schiff base moiety inevitably takes place by this procedure and hence the adsorption capacities are not reproducible on repeated use. In the case of $Co^{2+}$, a part of the ion was strongly retained on the resin so that it could not be eluted even by use of concd HCl. Schiff base-cobalt(II) complexes are known to form adducts with molecular oxygen.[15] The dark-brown colour of the resin suggests the formation of such adduct which is subject to acid hydrolysis by treatment with HCl to give an inert $Co^{3+}$ complex and $Co^{2+}$ ion. The former ion must be retained on the resin while the latter ion is liberated.

The maximum adsorption capacity of the resins **4–6** are given in Table 2 along with those of the analogous resins **4′–6′**. The resins **4–6** revealed much higher adsorption capacities regardless of feeded metal ions than the corresponding resins **4′–6′**. As mentioned before, our resins contain rather discrete ligand units, whereas the functional group of resin **4′** and its derivatives are sterically much hindered due to cross-linking. Such cross-linking around the ligand would bring about unfavourable steric environments on metal complex formation. The adsorption capacity vs. pH curves of resin **4** are given in Fig. 2. The maximum capacity for $Cu^{2+}$ is *ca.* 2.8 mmol per gram resin which is close to the ligand content (3 mmol/g-resin). Thus, most of the functional

Table 2. Maximum amount of metal ion adsorbed on 1 g of dry resin (mmol metal/g-resn)

| Resin | $Cu^{2+}$ | $Ni^{2+}$ | $Co^{2+}$ | $Zn^{2+}$ |
|---|---|---|---|---|
| 4 | 2.9 | 1.0 | | 1.7 |
| 4' | 1.6 | 0.4 | | 0.5 |
| 5 | 3.0 | 2.2 | 1.9 | 2.3 |
| 5' | 1.2 | 1.0 | 1.0 | 0.6 |
| 6 | 2.8 | 2.7 | 2.6 | 1.8 |
| 6' | 1.7 | 1.2 | 1.3 | 0.5 |

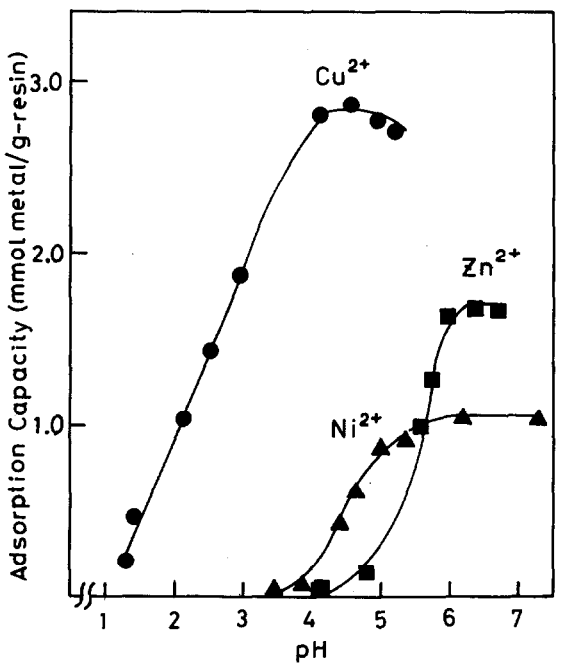



Fig. 2. Metal ion adsorption capacity vs pH curves of resin 4. ●, $Cu^{2+}$; ▲, $Ni^{2+}$; ■, $Zn^{2+}$.

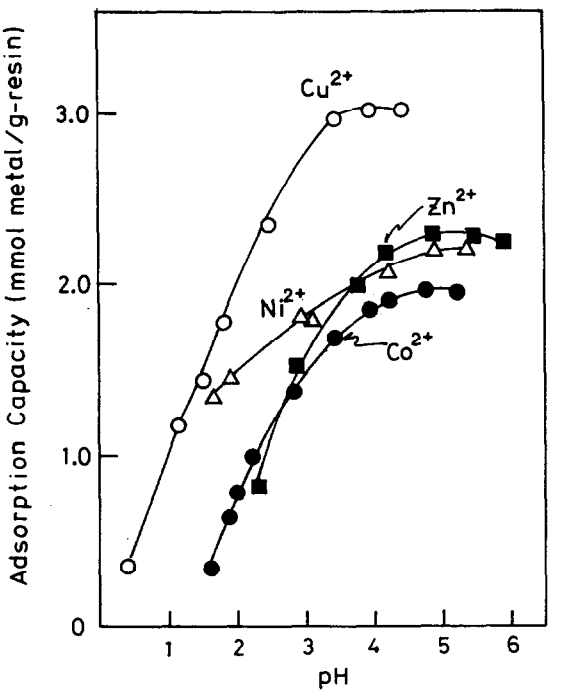



Fig. 3. Metal ion adsorption capacity vs pH curves of resin 5, ○, $Cu^{2+}$; △, $Ni^{2+}$; ●, $Co^{2+}$; ■, $Zn^{2+}$.

groups of resin 4 seems to form 1 : 1 complex with $Cu^{2+}$. On the other hand, the adsorption capacity for $Ni^{2+}$ and $Zn^{2+}$ is lower than $Cu^{2+}$presumably because more than two sets of functional group are required to retain $Ni^{2+}$ and $Zn^{2+}$. The pH dependence curves clearly imply that the order of affinity toward resin 4 is $Cu^{2+} \gg Ni^{2+} > Zn^{2+}$, which is in good agreement with the order of formation constants of the free diethylenetriamine.[16] This result suggests the possibility of quantitative separation of the metal ions by the column process (*vide infra*).

The resins 5 and 6 can adsorb various kinds of transition metal ions at wide pH ranges as given in Figs. 3 and 4. Since the functional group of resin 5 and resin 6 consists of two sets of iminodiacetic acid and iminodiphosphonic acid, respectively, they can form 1 : 1 or even 1 : 2 (ligand : metal) complexes. In fact the maximum capacities of resin 5 for $Cu^{2+}$ and resin 6 for $Cu^{2+}$, $Ni^{2+}$ and $Co^{2+}$ are 2.8–3.0 mmol per gram resin, which are approximately twice as much as the amount of the functional groups suggesting the formation of 1 : 2 complexes.

The selectivity order toward the resins is in accord with the order of their respective formation constants of ethylenediamine - *N,N,N',N'* - tetraacetic acid [17] and ethylenediamine - *N,N,N',N'* - tetra(methylenephosphonic acid)[18] which are structurally analogous to the functional groups of the

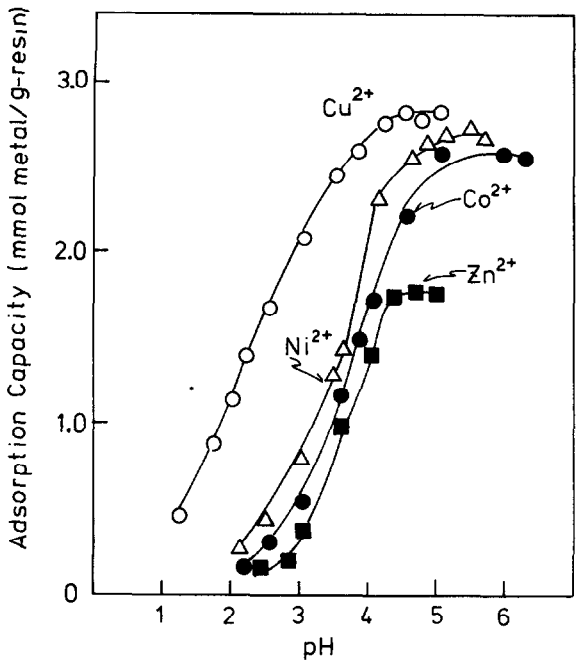



Fig. 4. Metal ion adsorption capacity vs pH curves of resin **6**. ○, $Cu^{2+}$; △, $Ni^{2+}$; ●, $Co^{2+}$; ■, $Zn^{2+}$.

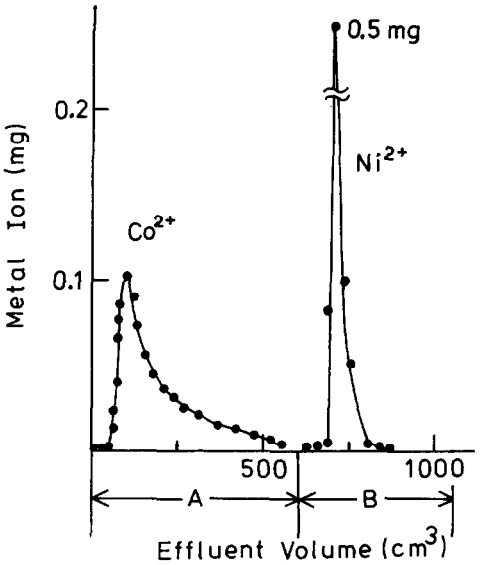



Fig. 6. Chromatographic separation of $Co^{2+}$ and $Ni^{2+}$ by the column of resin **5**. (A) HCl (pH 1.5). (B) 0.2 M HCl.

resin **5** and resin **6**, respectively. Both of the resins showed a reproducible capacities for most of metal ions on repeated adsorption and desorption cycles.

*Separation of metal ions.* Resin **4** showed an apparent selectivity toward $Cu^{2+}$, $Ni^{2+}$ and $Zn^{2+}$ which suggested the possibility of chromatographic separation of metal ion mixture. A solution containing $Cu^{2+}$, $Ni^{2+}$ and $Zn^{2+}$ was poured onto a column loaded with resin **4** and the adsorbed band was eluted sequentially with 0.1 M acetate buffer (pH 4.6), 0.1 M HCl and 2 M HCl. Three metal ion components were well separated depending on their affinity order as given in Fig. 5. In a similar manner, a separation of $Co^{2+}$ from $Ni^{2+}$ was carried out by the column of resin **5** (Fig. 6). The pH of the eluent must be very strictly adjusted in the case because the affinity of the two ions toward the resin does not much differ. Cobalt(II) was stripped off by elution with a solution of pH 1.3–1.5, while $Ni^{2+}$ retained on the column at this pH range. Small changes in pH greatly disturb the clear separation.

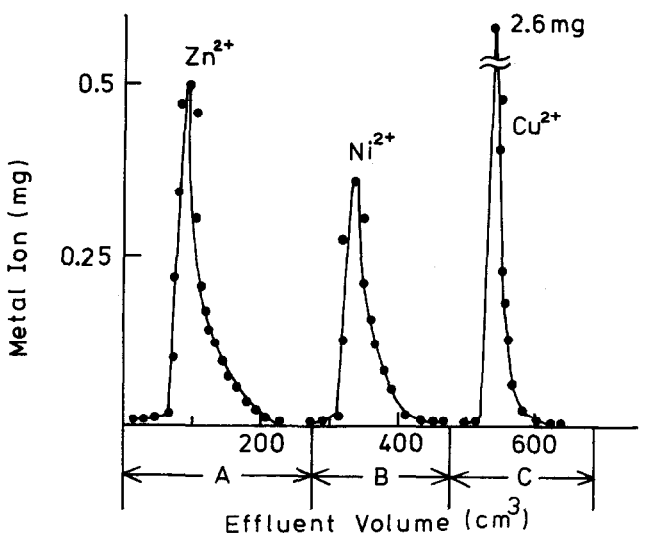



Fig. 5. Chromatographic separation of $Cu^{2+}$, $Ni^{2+}$ and $Zn^{2+}$ by the column of resin **4**. (A) 0.1 M Acetate buffer (pH 4.6). (B) 0.2 M HCl. (C) 2 M HCl.

## REFERENCES


1. (a) F. Vernon, *Chem. Ind.* (*London*) 1977, 634. (b) H. F. Walton, *Anal. Chem.* 1978, **50**, 36R. (c) J. H. Hodgkin, *Chem. Ind.* (*London*) 1979, 153. (d) L. R. Melby, *J. Am. Chem. Soc.* 1975, **97**, 4044. (e) A. Akalah and D. C. Sherrington, *Chem. Rev.* 1981, **81**, 557. (f) T. Yokoyama, A. Kikuchi, T. Kimura, and T. M. Suzuki, *Bull. Chem. Soc. Jpn.* 1983, **56**, 463. (g) M. Nishizawa, T. Yokoyama, T. Kimura, and T. M. Suzuki, *Chem. Lett.* 1983, 1413.
2. G. Schwarzenbach, *Helv. Chim. Acta* 1952, **35**, 2344.
3. G. Schwarzenbach and H. Ackermann, *Helv. Chim. Acta* 1949, **32**, 1682.
4. L. Knorr and H. W. Brownsdon, *Ber.* 1902, **35**, 4470.
5. K. Moedritzer and R. R. Irani, *J. Org. Chem.* 1966, **31**, 1603.
6. E. Blasius and I. Bock, *J. Chromatogr.* 1964, **14**, 224.
7. H. Egawa and H. Saeki, *Kogyo Kagaku Zasshi* 1971, **74**, 772.
8. J. Dingman Jr., S. Siggia, C. Barton, and K. B. Hiscook, *Anal. Chem.* 1972, **44**, 1351.
9. R. S. Drago, J. Gaul, A. Zombeck, and D. K. Straub, *J. Am. Chem. Soc.* 1980, **102**, 1033.
10. E. M. Moyers and J. S. Fritz, *Anal. Chem.* 1977, **49**, 418.
11. K. Kaeriyama and Y. Shimura, *Makromol. Chem.* 1979, **180**, 2499.
12. T. M. Suzuki and T. Yokoyama, *Polyhedron* 1983, **2**, 127.
13. K. W. Pepper, H. M. Paisiey, and M. A. Young, *J. Chem. Soc.* 1953, 4097.
14. W. M. Coleman and L. T. Taylor, *Inorg. Chem.* 1971, **10**, 2195.
15. L. H. Vogt, H. M. Faigenbaum, and S. E. Wiberley, *Chem. Rev.* 1963, **63**, 269.
16. J. Bjerrum Ed., *Spec. Publ.-Chem. Soc. Suppl.* 1971, No. 25, 334.
17. J. Bjerrum Ed., *Spec. Publ.-Chem. Soc. Suppl.* 1971, No. 25, 623.
18. R. J. Motekaitis, I. Murase, and A. E. Martell, *Inorg. Nucl. Chem. Lett.* 1971, **7**, 1103.

*Polyhedron* Vol. 3, No. 8, pp. 947–955, 1984
Printed in the U.S.A.

0277–5387/84 $3.00 + .00
© 1984 Pergamon Press Ltd.

# COPPER(II) COMPLEXES OF THIOSEMICARBAZONES DERIVED FROM 2-ACETYLPYRIDINE AND ITS N-OXIDE

**DOUGLAS X. WEST* and ROBERT M. MAKEEVER**
Department of Chemistry, Illinois State University, Normal, IL 61761, U.S.A.

**and**

**JOHN P. SCOVILL and DANIEL L. KLAYMAN**
Division of Experimental Therapeutics, Walter Reed Army Institute of Research, Washington, DC 20307, U.S.A.

(*Received* 11 *November* 1983; *accepted* 17 *January* 1984)

**Abstract**—A series of Cu(II) complexes of the thiosemicarbazone, 3-azabicyclo[3.2.2]-nonene-3-thiocarboxylic acid 2-[1-(2-pyridinyl)ethylidene]hydrazide(HL) and the corresponding N-oxide (HLO) have been prepared and characterized. Both ligands undergo deprotonation and appear to coordinate via the thione sulfur, the imine nitrogen and the pyridyl nitrogen (or N-oxide oxygen). A single anionic ligand such as $Cl^-$, $Br^-$, $NCS^-$ and $N_3^-$ completes the bonding to the Cu(II) center of these 4-coordinate complexes. When the complexes are prepared using Cu(II) perchlorate, the solids isolated contain a neutral thiosemicarbazone ligand as well as the deprotonated ligand. The solids were primarily characterized by IR, electronic and electron spin resonance spectroscopy. In addition, electronic and ESR spectra of their chloroform solutions were recorded. Most of the solids (except the nitrates) were unaltered upon dissolution. Simulation of the solution ESR spectra was used to estimate the coupling constants of the various coordinated nuclei.

Thiosemicarbazones of 2-acetylpyridine possess a broad spectrum of potentially useful chemotherapeutic properties and have been evaluated for their antimalarial, antitumor and antibacterial activities.[1] Transition metal complexes of several of these thiosemicarbazones have also been screened for their medicinal properties.[2] However, the characterization of these new metal complexes has been limited because of the interest in screening large numbers of this class of compounds. Therefore, we report here the preparation and spectral characterization of a series of Cu(II) complexes of the thiosemicarbazone, 3-azabicyclo[3.2.2]nonane-3-thiocarboxylic acid 2-[1-(2-pyridinyl)ethylidene]-hydrazide (HL).[1] Most recently there has been a report[3] of the electronic and ESR spectra of three of these same Cu(II) complexes (Cl, Br, and $NO_3$ solids) and results obtained in the two different laboratories will be compared.

In addition, the N-oxide (HLO) of this ligand (see Fig. 1) has also been synthesized[4] and a study of some of its complexes prepared by employing different Cu(II) salts are also included.

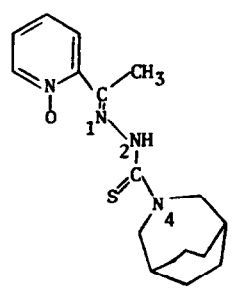



Fig. 1. 3-Azabicyclo[3.2.2]nonane-3-thiocarboxylic acid 2[1-(2-pyridinyl N-oxide)ethylidene]hydrazide.

## EXPERIMENTAL

The complexes were generally prepared in warm ethanolic solution using equimolar amounts of either of the two ligands (i.e. HL and HLO) and the appropriate copper(II) salt. An exception was the two perchlorate solids, for which a 2:1 ligand to salt molar ratio was required to obtain a suitable solid. Also, the complexes contining thiocyanato

*Author to whom correspondence should be addressed.

and azido groups were derived from the corresponding chloro solids by the method described previously. The spectral and physical measurements were carried out on these compounds in an analogous manner to our previous studies on 2-substituted pyridine N-oxides.[5]

## RESULTS AND DISCUSSION

The colors, decomposition temperatures and partial elemental analyses as well as the stoichiometry of the new complexes that have been isolated are compiled in Table 1. Other than for the perchlorate solids, both series of complexes appear to have the thiosemicarbazone coordinating as a deprotonated tridentate ligand with the further coordination position being occupied by the anion derived from the Cu(II) salt. Previously, thiosemicarbazones have been found to coordinate via the sulfur and the amine nitrogen[6] so that we can envision HL to have to $N_2S$ set of donor atoms and HLO to have ONS donor atoms. Reports[7] on a related 2-formylpyridine thiosemicarbazone showed it to coordinate as a neutral ligand with Co(II) and Ni(II), but also as a deprotonated tridentate chelating agent with Ni(II).

The two perchlorate solids have both a deprotonated thiosemicarbazone, presumably bound in a tridentate manner, and a neutral thiosemicarbazone which is likely to be attached to the Cu(II) either as a mono- or bidentate ligand. The molar conductivities in methanol (*ca.* $10^{-3}$ M) for both of the perchlorate solids were found to be consistent with them being 1:1 electrolytes[8] as might be expected from their chemical formulas. However, somewhat surprisingly, both of the nitrate solids also were found to be 1:1 electrolytes while the remaining complexes in this study are nonelectrolytes. The electrolytic behavior of the nitrate solids could be due to dissociation of a nitrate ligand on dissolution and the IR spectra should prove useful in establishing the nature of the nitrate ion in both solids.

The colors of both series indicate that the thiosemicarbazone functional group dominates the color of the solids rather than the particular ligand occupying the fourth position. The decomposition temperatures are typical of Cu(II) solids having complex organic ligands.[9] The lower values for the perchlorate solids are probably due to the greater steric hindrance provided by the coordination of two large ligands.

In Table 2 we have compiled the band assignments of the HLO ligand and its Cu(II) complexes which are most useful in determining the nature of ligand bonding to Cu(II). The NO stretching frequency in the spectrum of the ligand is considerably lower in energy than the analogous band in the spectrum of the unsubstituted pyridine N-oxide.[10] This is probably due to some hydrogen bonding as well as the electron withdrawing effect of the 2-substituent. The hydrogen bonding may be intramolecular as found for a sulfonic acid derivative of 2-pyridine N-oxide[11] as well as 2-picolinamine N-oxides.[12] In the spectra of the

Table 1. Partial elemental analyses, colors and decomposition temperatures of various Cu(II) complexes of a 2-acetylpyridine and a 2-acetylpyridine N-oxide thiosemicarbazone, HL and HLO, respectively

| Compound | Color | Dec Pt. (°C) | Calculated C | H | N | Found C | H | N |
|---|---|---|---|---|---|---|---|---|
| [Cu(HL)L)](ClO$_4$) | olive green | 189 | 39.99 | 5.90 | 14.57 | 39.87 | 5.68 | 14.23 |
| [Cu(L)Cl] | olive green | 259 | 47.98 | 5.29 | 13.99 | 48.05 | 5.24 | 14.02 |
| [Cu(L)Br] | olive green | 259 | 43.10 | 4.97 | | 43.06 | 4.79 | |
| [Cu(L)(NCS)] | yellow green | 229 | 48.26 | 5.00 | 15.16 | 48.26 | 5.07 | 15.17 |
| [Cu(L)(N$_3$)] | dark green | 184 | 47.22 | 5.20 | 24.09 | 47.18 | 5.32 | 24.08 |
| [Cu(L)(NO$_3$)] | olive green | 222 | 45.01 | 4.96 | | 45.95 | 5.16 | |
| [Cu(HLO)(LO)]ClO$_4$•4H$_2$O | brown | 198 | 44.13 | 5.90 | | 43.71 | 5.88 | |
| [Cu(LO)Cl] | yellow-brown | 244 | 46.15 | 5.08 | 13.45 | 46.36 | 5.25 | 13.52 |
| [Cu(LO)Br] | yellow-brown | 227 | 41.61 | 4.80 | 12.13 | 41.53 | 4.65 | 12.04 |
| [Cu(LO)NCS] | yellow-brown | 217 | 46.51 | 4.82 | 15.95 | 46.57 | 4.76 | 15.95 |
| [Cu(LO)NO$_3$] | yellow-brown | 210 | 43.38 | 4.79 | | 42.49 | 4.49 | |

Table 2. IR band assignments ($cm^{-1}$) of a 2-pyridyl N-oxide thiosemicarbazone (HLO) and its Cu(II) complexes

| Compound | $\nu_{C=N}$ | $\nu_{C-S}$* | $\nu_{NO}$ | $\nu_{NN}$ | $\nu_{NO}$ | $\nu_{C-S}$* | $\nu_{CuO}$ | $\nu_{Cu-N}$ | $\nu_{Cu-S}$ | $\nu_{Cu-X}$ |
|---|---|---|---|---|---|---|---|---|---|---|
| HLO | (1565) | 1316s | 1214s | 1006m | 828m | 860m | - | | | |
| $[Cu(HLO)(LO)](ClO_4)\ 4H_2O$ | 1609 | 1298s | 1210s<br>1201m | 1013m<br>1009 | 824m | 850m<br>742w | 431m<br>393m | 366w<br>362w | 270m | |
| Cu(LO)Cl | 1604m | 1294s | 1201s | 1012m | 824m | 747w | 420m | 362w | 272s | 309m |
| Cu(LO)Br | 1601w | 1291s | 1200s | 1010m | 822m | 752w | 420m | 266w | 269s | 227w |
| Cu(LO)NCS | 1609m | 1293s | 1210s | 1013m | 822m | 860m<br>752w | 428m<br>408w | 376m | 272m | 309m |
| $Cu(LO)NO_3$ | 1601m | 1290s | 1202s | 1011m | 820m | 745w | 429m | 352m | 271m | 298s |

*Bands considered to have significant contributions from the C-S bond.

complexes the $\nu_{NO}$ is shifted to lower energy and, although the shift is small, its position is similar to that found for the 2-acetylpyridine N-oxide complex of Cu(II),[13] confirming coordination by the N-oxide oxygen. It is noteworthy that the perchlorate solid appears to have two bands assignable to this mode which is indicative of two types of N-oxide, either one coordinated and one not, or both coordinated, but having different bond lengths due to differences in their coordination. The bending mode of an aromatic N-oxide quite often provides little information concerning its coordination because it is affected by two factors:[14] the loss in double bond character which would shift it to lower energy and a metal ion effect similar to protonation which shifts the band to higher energy. The former effect is the more significant for these complexes and only one band is observable.

Both bands considered to have a significant contribution from the CS bond are shifted to lower energy in the complexes compared to the free ligand which indicates coordination via the sulfur atom.[15] Given the similarity of the colors of the solid complexes it would seem likely that a second indication of the bonding of the sulfur atom is the color arising from a sulfur to copper(II) charge transfer band. The bonding of the imine nitrogen is indicated by the shift in frequency in the spectra of the complexes of the $\nu_{C-N}$ band to *ca.* 16 $cm^{-1}$. While $\nu_{C-N}$ is observed at *ca.* 1620 $cm^{-1}$ in the IR spectra of other thiosemicarbazones of pyridines and quinolines,[16] as well as in our HL (*vide infra*), no band is observable in this region of the spectrum of HLO. However, careful inspection of the spectrum of HLO shows a band at *ca.* 1565 $cm^{-1}$ that we tentatively assign to $\nu_{C-N}$. It is not unexpected that this band would be found at somewhat lower energy because of the greater electron-withdrawing ability of the N-oxide ring. The increase of the $\nu_{N-N}$ energy in the spectra of the complexes is due to the increase in double bond character offsetting the loss of electron density via donation and is a further indication of coordination by the sulfur atom. Therefore, the deprotonated LO ligand coordinates via the O, N and S atoms to give a 6,5 tridentate ligand as depicted in Fig. 2.

Prior to discussion of the Cu(II)-ligand bands as well as the bands assignable to the various anions, the bonding of the deprotonated L ligand will be considered based on its band assignments as shown in Table 3. As has already been indicated, the imine nitrogen is bound to the Cu(II) with the expected decrease of 10–20 $cm^{-1}$ in $\nu_{C-N}$ in the spectra of the complexes.[16] The three bands identified as being indicative of sulfur bonding in the $LO^-$ complexes are shifted in the same manner for these L complexes confirming its coordination although the shift in the lowest energy band is not nearly as large. This may be the result of somewhat weaker

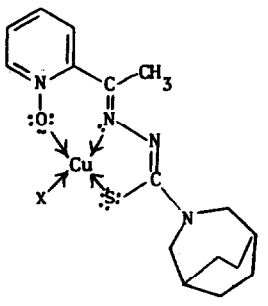



Fig. 2. Proposed bonding of HLO in the Cu(II) complexes.

Table 3. IR band assignments ($cm^{-1}$) of a 2-pyridyl thiosemicarbazone (HL) and its Cu(II) complexes

| Compound | $\nu_{C=N}$ | $\nu_{CS}$* | $\nu_{N-N}$ | $\nu_{CS}$* | $\nu_{CC(o.p.)}$ | $\nu_{CC(i.p.)}$ | $\nu_{Cu-N}$ | $\nu_{Cu-N(Py)}$ | $\nu_{Cu-S}$ | $\nu_{Cu-X}$ |
|---|---|---|---|---|---|---|---|---|---|---|
| HL | 1616m | 1322m | 1006sh | 861m,sh | 600m | 395m | | | | |
| $CuL(HL)ClO_4$ | 1600m<br>1591sh | 1311sh<br>1301m | 1016sh<br>1009m | 860sh<br>823m | 632sh<br>601m | 433m<br>394w | 393m | 340s | 270w | 323s |
| CuLCl | 1596m | 1294m | 1012m | 829m | 631m | 425m | 391m | 341m | 270w | 329s |
| CuLBr | 1599m | 1293m | 1009m | 825m | 624m | 423m | 400m | 335w | 264w | 225m |
| CuL(NCS) | 1600m | 1299m | 1017m | 831s | 628sh | 428m | 391w | 336m | 270w | 317s |
| $CuL(NO_3)$ | 1603m | 1299m | 1013s | 829m | 630m | 439m | 394w | 342m | 270w | 320m |
| $CuL(N_3)$ | 1601m | 1300m | 1017m | 828m | 627m | 430m | 398m | 340m | 269m | 382m |

bonding of the sulfur atom in these compounds compared to the LO series. Finally, bonding of the pyridine nitrogen can be shown by shifts in a number of bands and we have used the two low energy ring deformations[17] because of the multitude of bands in the higher energy portion of our spectra. Both are shifted to higher energy by *ca.* 30 $cm^{-1}$ confirming bonding by the pyridine nitrogen and showing that this deprotonated ligand is also bonded in a tridentate manner. In this case there are two 5-membered chelate rings and the bonding is NNS, and analogous to that shown in Fig. 2.

Bands assignable to the polyatomic anions of both series of complexes are shown in Table 4. The two perchlorate solids have bands associated with the presence of ionic perchlorate anions exclusively and no strong bands assignable to $\nu_1$ (*ca.* 930 $cm^{-1}$) or $\nu_2$ (*ca.* 460 $cm^{-1}$) are observable in their spectra. Therefore, the additional coordination arises from the neutral ligand that is present in both solids and its bonding will be considered later. The thiocyanato ligand in each solid appears to be bound via the nitrogen as would be expected for the hard Cu(II) ion and our assignments are in excellent agreement with those of previous authors.[18]

As opposed to the other compounds of polyatomic anions the spectral richness of the thiosemicarbazone moieties makes complete assignment of the bands attributable to the nitrato ligands difficult. Included in Table 4 are a partial assignment[19,20] of the bands and most importantly the bands in the combination area considered to be diagnostic for the type of nitrate present.[21] For

Table 4. IR band assignments for the polyatomic anions in the Cu(II) complexes of HL and HLO

| Compounds | | | | |
|---|---|---|---|---|
| **Perchlorate Solids** | $\nu_3$ | $\nu_4$ | $\nu_1$ | |
| $CuL(HL)(ClO_4)$ | 1090vs | 623s | - | |
| $Cu(LO(HLO)(ClO_4)\cdot 4H_2O$ | 1108vs | 621s | 931w | |
| **Thiocyanate Solids** | $\nu_{CN}$ | $\nu_{CS}$ | $\delta_{NCS}$ | |
| CuL(NCS) | 2080vs | 831s | 466m | |
| CuLO(NCS) | 2090vs | 848s | 467s | |
| **Nitrate Solids** | **Combination Bands** | | **Other Observable Bands** | |
| $CuL(NO_3)$ | $\nu_1 + \nu_4 = 1720$ | | $\nu_1 = 1013$ | $\nu_2 = 822,811$ |
| $CuLO(NO_3)$ | $\nu_1 + \nu_4 = 1722$ | | $\nu_1 = 1011$ | $\nu_2 = 812,807$ |
| **Azide Solid** | $\nu_a$(NNN) | | | |
| $CuL(N_3)$ | 2040vs | | | |

both solids only a single band was observable indicating that strong coordination by the nitrate ions is unlikely. However, some splitting of $\nu_2(NO_3)$ exists and $\nu_1(NO_3)$ is evidently present in combination with $\nu_{NN}$ since the band at this energy is much stronger relative to other bands than in the spectra of other members of both series. The $\nu_a$ vibration of the azide group is observed at 2040 $cm^{-1}$ as compared to the ionic sodium azide value of 2128 $cm^{-1}$ indicative of azide coordination.[22] Other bands due to $N_3$ such as $\nu_{s(NNN)}$ and $\delta_{(NNN)}$ are difficult to assign because of richness of the spectra of the complex.

The Cu(II)-ligand stretching frequency assignments are included in both Tables 2 and 3. In general, the LO complexes have bands at somewhat lower energies than their L counterparts. Evidently the tridentate 6,5-membered rings of LO causes a greater steric effect on the bonding of the various anions to the Cu(II) than does the 5,5-membered ring system of L. The $\nu_{Cu-O}$ band in each of the complexes is found in the 420–430 $cm^{-1}$ range and its assignment is consistent with that of the complex of 2-acetylpyridine N-oxide[13] as well as other pyridine N-oxides with bulky substituents.[12] Bands assignable to $\nu_{Cu-N}$ for the imine nitrogen are found at *ca.* 390 $cm^{-1}$ for the L complexes and *ca.* 360 $cm^{-1}$ for the complexes of LO. These assignments compare favorably with that of 370 $cm^{-1}$ reported by other authors.[23] For both series of complexes the $\nu_{Cu-S}$ band is assigned at approximately 270 $cm^{-1}$ which is consistent with the reports of others.[23] Finally, we have assigned the $\nu_{Cu-N}$ of the pyridine ring in the 340 $cm^{-1}$ region of the spectrum which is somewhat higher in energy than the 250–270 $cm^{-1}$ range usually assigned for this band.[24] However, this very bulky ligand would be expected to limit interaction from adjacent Cu(II) sites and its 4-coordinate character would feature stronger copper–pyridine bonding.

As previously indicated there is a general trend for the $LO^-$ complexes to have the copper–ligand bands at lower energy compared to the L complexes. This is also true for the bands assigned to the copper–anion stretching frequencies for the various members of the two series. The $\nu_{Cu-Cl}$ bands are consistent with terminal rather than bridging chlorines[25] as are the assignments for $\nu_{Cu-Br}$.[26] Assignment for $\nu_{Cu-N}$ for the azido ligand is based on the assignment of Forster and Horrocks:[27] They assigned bands for Co(II) and Zn(II) complexes at 368 $cm^{-1}$ and 351 $cm^{-1}$, respectively, and the $\nu_{Cu-N(N_3)}$ band would be expected at somewhat higher energy. Similarly, copper (II) nitrogen stretching frequencies for thiocyanato ligands have been reported in the 325 $cm^{-1}$ region.[28] If coordination of the nitrate ion occurs, then the assignments fall in the range of 250–350 $cm^{-1}$ reported previously,[29] but these bands could be due to other Cu(II)–ligand bonds.

For the two perchlorate solids the bonding of the neutral ligand needs to be considered in that both solids show that the perchlorate groups are present as uncomplexed ions in their spectra. In the HLO case a band at 3410 $cm^{-1}$ is assignable to $\nu_{N-H}$ and there appears to be two $\nu_{N-O}$ bands, unshifted $\nu_{N-N}$ and $\nu_{C-S}$ bands compared to the ligand spectrum and two bands assignable to $\nu_{Cu-O}$ which all suggest coordination of the N-oxide oxygen of the neutral ligand. There is a possibility that a second atom of this ligand, the imine nitrogen, also coordinates since the $\nu_{N-N}$ is shifted somewhat and there appears to be a second band assignable to $\nu_{Cu-N}$ and the possibility of chelation will be considered during the discussion of the other spectral results for this compound. For $[Cu(HL)L]ClO_4$ neither the pyridine nitrogen (unshifted ring deformation bands are present) nor the sulfur atom (unshifted thioamide bands) appear to bond to copper for the neutral ligand. However, the $\nu_{N-N}$ band is split with both peaks shifted from their position in the ligand's spectrum and it is likely that the neutral HL coordinates via the imine nitrogen. A relatively strong band at 323 $cm^{-1}$ is assigned to $\nu_{Cu-N}$ for this bond in Table 3.

The electronic spectra (Table 5) of both series of complexes are dominated by intense intraligand and charge transfer bands. The assignments of the energies of the *d–d* bands are shoulders on the more intense, higher energy bands. Therefore, the accuracy of the energies shown in Table 5 is questionable and comparisons of the different solids will to be kept to a minimum. It appears that charge transfer bands for the LO ligands are somewhat lower energy than for the L complexes. Recall that the latter solids have 5,5-membered tridentate ring system and it is probably a more planar arrangement making charge transfer more difficult than for the more distorted 6,5-membered tridentate system of LO. The opposite relationship is found for the *d–d* bands with the planar L ligand having the higher ligand field. Cu(II) complexes of 2-acetylpyridine-4-phenyl-3-thiosemicarbazone showed *d–d* bands between 18.6 and 17.6 kK with a lower energy shoulder at *ca.* 15 kK.[30] The lower energy of our *d–d* envelope probably obscures any shoulder and also suggests a weaker ligand field due most likely to greater steric hindrance.

Although it is a divalent ligand, 2-hydroxynaphthalidine thiosemicarbazone complexes[31] like Cu(ONS)X (X–$NH_3$ or py) are brown like our LO solids and have their *d–d* maxima at 13 kK, which

Table 5. Electronic spectral results (kK) of Cu(II) complexes of a 2-acetylpyridine and a 2-acetylpyridine N-oxide thiosemicarbazone HL and HLO, respectively

| Compound | Solid State Reflectance C.T. | d-d | Solution ($CHCl_3$) C.T. | d-d[3] |
|---|---|---|---|---|
| $[Cu(HL)L](ClO_4)$ | 25.5<br>24.1sh | 18.7<br>13.9sh | 24.1sh<br>23.4 | 18.2<br>16.8sh |
| [CuLCl] | 26.3<br>23.8sh | 17.0sh<br>14.1sh | 27.0<br>22.3 | 17.0sh |
| [CuLBr] | 26.2<br>22.8sh<br>21.1sh<br>19.1 | 13.7sh | 26.7<br>22.8 | 16.7sh |
| $[CuL(NO_3)]$ | 26.2<br>23.2sh | 17.5sh<br>14.2sh | 26.6<br>22.8 | 17.9sh |
| [CuL(NCS)] | 25.1<br>22.2sh | 17.9sh | 27.2<br>22.8 | 17.2sh |
| $[CuL(N_3)]$ | 27.0<br>23.9 | 19.1sh | 26.3<br>23.1 | 17.5sh |
| $[Cu(HLO)(LO)]ClO_4 \cdot 4H_2O$ | 25.2<br>20.0 | 15.8sh | 25.7sh<br>23.9<br>20.2 | 15.6sh |
| [CuLOCl] | 24.3<br>18.9 | 13.9sh | 27.4<br>23.8<br>19.4 | 15.4sh |
| [CuLOBr] | 23.7<br>21.0sh<br>18.4 | 13.8sh | 26.0sh<br>23.2<br>18.9 | 14.6sh |
| $[CuLO(NO_3)]$ | 25.8<br>22.6<br>19.6 | 15.9sh | 26.0sh<br>23.5<br>20.0 | 15.6sh |
| [CuLO(NCS)] | 22.6<br>19.2 | 15.0sh | 26.0sh<br>24.5<br>20.2 | 15.7sh |

is at lower energy than is found for our LO complexes. Finally, for both series of complexes the species remain unchanged upon dissolution in $CHCl_3$ as would be expected.

Cu(II) complexes having a sulfur coordinated generally have $g_\perp$ close to 2.03 and $g_\parallel$ in the range of 2.08 to 2.15.[32] The ESR parameters for the solid powders are compiled in Table 6 and the $g$- values suggest coordination by sulfur for both series of complexes in agreement with the IR results discussed earlier. Additionally, when the spectra are resolved they show an axial $d_{x^2-y^2}$ ground state with small exchange coupling ($G$ in the range of 3–5).[33] Assuming the L complexes to be planar, the position of $g_\parallel$ may be taken as a measure of the ligand field strength of the X's: $NO_3 < Cl$,NCS, $N_3 <$ Br. The $Br^-$ position is somewhat surprising and is indicative of a substantial contribution to $\pi$-bonding[34] due to its greater nephelauxetic effect, but otherwise the order is reasonable. In the LO series both the perchlorate and Cu(LO)(NCS) solids appear to have different stereochemistries than the remainder of the series based on the $g_\parallel$ values. It should be noted that the latter solid has some extra bands in its IR spectrum suggesting structural differences and that the perchlorate solid's bonding was unclear with respect to the nature of the bonding of the protonated ligand. Note that there is little change in the value of $g_\parallel$ in either series upon lowering the temperature indicating no significant change in the planarity of these 4-coordinate species.

The ESR parameters obtained from chloroform–toluene solutions are collected in Table 7. As opposed to the powder spectra there are considerable differences between compounds not only due to the resolved hyperfine coupling of the $^{63}Cu$ and $^{65}Cu$ nuclei but also the superhyperfine coupling of the various ligand atoms. In order to better interpret the results we have simulated the spectra and show the derived coupling constants in Table 7. In addition, an example of

Table 6. ESR spectral parameters of solid powders of some Cu(II) thiosemicarbazone complexes

| Compound | Room Temperature $g_{\parallel}$ | $g_{\perp}$ | $g_{av}$ | 77K $g_{\parallel}$ | $g_{\perp}$ | $g_{av}$ |
|---|---|---|---|---|---|---|
| [Cu(HL)L](ClO$_4$) | $g_{iso}$ = 2.057 | | | $g_{iso}$ = 2.052 | | |
| [CuLCl] | 2.140 | 2.038 | 2.072 | 2.135 | 2.039 | 2.071 |
| [CuLBr] | 2.126 | 2.041 | 2.069 | 2.121 | 2.037 | 2.065 |
| [CuL(NO$_3$)] | 2.164 | 2.048 | 2.087 | 2.161 | 2.051 | 2.088 |
| [CuL(NCS)] | 2.138 | 2.047 | 2.077 | 2.140 | 2.042 | 2.075 |
| [CuL(N$_3$)] | 2.139 | 2.041 | 2.074 | 2.137 | 2.040 | 2.072 |
| [Cu(HLO)(LO)]ClO$_4$·4H$_2$O | 2.278 | 2.046 | 2.123 | ? | 2.047 | ? |
| [CuLOCl] | 2.135 | 2.051 | 2.079 | 2.137 | 2.051 | 2.080 |
| [CuLOBr] | $g_{iso}$ = 2.099 | | | $g_{iso}$ = 2.105 | | |
| [CuLO(NO$_3$)] | 2.126 | 2.060 | 2.082 | 2.133 | 2.063 | 2.086 |
| [CuLO(NCS)] | 2.176 | 2.053 | 2.094 | 2.189 | 2.056 | 2.100 |

Table 7. Solution ($CHCl_3$-toluene) ESR spectral parameters for Cu(II) complexes of some thiosemicarbazones

| | RT | | | | | 77K | | | |
|---|---|---|---|---|---|---|---|---|---|
| | $g_o$ | $A_o$[1] | A(N)[2] | A(N)[3] | A(X) | $g_{\parallel}$ | $g_{\perp}$ | $g_{av}$ | $A_{\parallel}$ |
| Cu(L)(HL)ClO$_4$ | 2.077 | 75 | 12 | 10 | -- | 2.145 | 2.035 | 2.072 | 175 |
| Cu(L)Cl | 2.077 | 88 | 15.5 | 10 | 0 | 2.154 | 2.037 | 2.076 | 182 |
| Cu(L)Br | 2.072 | 84 | 12 | 10 | 50 | 2.161 | 2.040 | 2.080 | 185 |
| Cu(L)NO$_3$ | 2.085 | 86.3 | 16 | 10 | -- | 2.177 | 2.048 | 2.091 | 188 |
| Cu(L)NCS | 2.081 | 90 | 12 | 10 | 11 | 2.162 | 2.042 | 2.082 | 189 |
| Cu(L)N$_3$ | 2.075 | 90 | 12 | 10 | 7 | 2.154 | 2.036 | 2.075 | 184 |
| | | | | A(N)[4] | | | | | |
| Cu(LO)(HLO)CLO$_4$ 4H$_2$O | 2.101 | 75 | 16.5 | 4 | -- | 2.209 | 2.041 | 2.097<br>A(N) = 12 | 175 |
| Cu(LO)Cl | 2.086 | 84 | 13 | -- | 10 | 2.211 | 2.050 | 2.104<br>A(N) = 14 | 175 |
| Cu(LO)Br | 2.086 | 80 | 14 | -- | 50 | 2.202 | 2.046 | 2.098<br>A(N) = 16 | 172 |
| Cu(LO)NO$_3$ | 2.098 | 80 | 15.5 | 4 | -- | 2.201 | 2.048 | 2.099 | 183 |
| Cu(LO)NCS | 2.130 | 68.5 | 16.5 | 4 | -- | 2.207 | 2.042 | 2.097<br>A(N) = 15 | 173 |

1. A-values are in Gauss
2. Imine nitrogen
3. Pyridine nitrogen
4. Another nitrogen

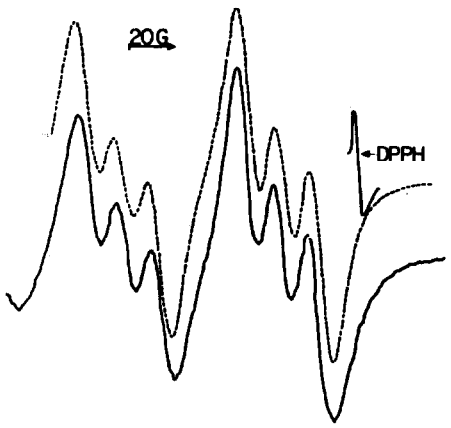



Fig. 3. The two high field features of the recorded (——) and simulated (· · · · · ·) spectra of Cu(LO)(HLO)$(ClO_4)_4$).

the recorded and simulated spectra are shown in Fig. 3. It should be noted that our program did not allow for variation of linewidth in these isotropic spectra so that reasonable simulation of only the two narrowest features was possible.

The isotropic spectra of the N-oxide (LO) series generally have larger values of $g_0$ and lower values for $A_0$ due to the weaker $\pi$-bonding of the oxygen compared to the pyridine nitrogen. Within the series the lowest values for $g_0$ and largest $A_0$'s occur for Cu(LO)Cl followed by Cu(LO)Br suggesting that greater steric effects predominate in the remaining complexes which reduces their in-plane coordination. Note that all complexes have a strong interaction with one nitrogen ($A(N)$ = 13–16.5G) which we have assigned to the imine nitrogen (see Fig. 2). In the non-halogen solids a second nitrogen ($A(N)$ = 4G) needs to be included in order to achieve a reasonable simulation of the recorded spectra. For the perchlorate solid this was expected because of the presence of the HLO ligand. The low value of the coupling constant may be indicative of a rather weak bond due to steric crowding. The $CuLO(NO_3)$ compound was a 1:1 electrolyte and some interaction with a nitrogen from an adjacent coordination site must occur. For CuLO(NCS) the weakly coordinating nitrogen is likely to be the thiocyanato nitrogen, but its coupling is weaker than for CuL(NCS).

The superhyperfine coupling constants for the halogen atoms in the isotropic spectra are also included in Table 7. For both series best fits of the simulated spectra to the recorded spectra were obtained by using essentially the same coupling constant with each halogen. The strong coupling to bromine atoms gives an unusual six-feature spectrum, which has been depicted elsewhere.[3]

The frozen spectral parameters included in Table 7 show the stronger in-plane bonding for the L series. For example the $g_\parallel$ values are substantially lower for this series and this is probably due to the greater planarity of the chelate ring involving the pyridine nitrogen as opposed the N-oxide oxygen. Pavkovic *et al.*[35] have shown that, while both the coordinating oxygen and nitrogen are found in the same plane as the Cu(II) ion in both 5- and 6-membered chelating rings, only for the 5-membered case is the entire chelate ring in the same plane with the Cu(II). Therefore, even though steric hindrance might not be significantly greater in the HLO complexes, the tridentate ligand is unlikely to retain complete planarity in its complexes. The lower values for the $A_\parallel$ are consistent with this proposal and, in addition, probably indicate reduced $\pi$-bonding in the HLO complexes. In the latter series of complexes greater resolution of nitrogen superhyperfine coupling does occur in the +3/2 parallel and perpendicular region of the frozen solution spectra. The lack of observable nitrogen hyperfine coupling in the spectra of the HL series is probably due to the additional coupling of the pyridine nitrogen which broadens the superhyperfine lines of both types of nitrogen. Simulation of spectra with a number of coupling nuclei with small $A$-values combined with the coupling of the two copper isotopes demonstrates this phenomenon.

In conclusion, small variations occur in the electronic spectral parameters of the HL complexes reported on previously[3] (i.e. CuLCl, CuLBr and $CuLNO_3$), but no major differences. In addition, there is general agreement in the majority of the ESR results. We are able, because of inclusion of LO complexes, to suggest that the nitrogen with the smaller coupling constant (*ca.* 10G) is the pyridine nitrogen. Also, because of simulation we have tested the Bhoon *et al.*[3] $A_{Br} - = 3/4\ A_{Cu}$ statement. There is no reason to suspect a simple relationship between the two coupling constants and their suggested values do not simulate the recorded spectrum.

*Acknowledgement*—The authors thank Drs. G. J. Clark and R. C. Reiter for the ESR simulation programs.

## REFERENCES

1. D. L. Klayman, J. P. Scovill, J. F. Bartosevich and J. Bruce, *J. Med. Chem.* 1983, **26**, 35 and references contained therein.
2. J. P. Scovill, D. L. Klayman and C. F. Franchino, *J. Med. Chem.* 1982, **25**, 1261.
3. Y. K. Bhoon, J. P. Scovill and D. L. Klayman, *Ind. J. Chem.* 1983, **22A**, 267, and private communication.

4. J. P. Scovill, D. L. Klayman, C. Lambros, G. E. Childs and J. D. Notsch, *J. Med. Chem.* 1984, **27**, 87.
5. D. X. West and W-H. Wang, *J. Inorg. Nucl. Chem.* 1979, **41**, 1719; *Ibid.*; 1981, **43**, 1511.
6. V. B. Rana, P. C. Jain, M. P. Swami and A. K. Srivastava, *J. Inorg. Nucl. Chem.* 1975, **37**, 1826.
7. M. F. Iskander, L. El-Sayed and K. I. Zaki, *Trans. Met. Chem.* 1979, **4**, 225; A. V. Ablov and N. I. Belichuk, *Russ. J. Inorg. Chem.* 1969, **14**, 93.
8. W. L. Geary, *Coord. Chem. Rev.* 1971, **1**, 81.
9. B. G. Saha, R. P. Bhatnagar and S. K. Banerji, *J. Ind. Chem. Soc.* 1982, **59**, 927.
10. J. V. Quagliano, J. Fujita, G. Franz, D. J. Phillips, J. A. Walmsley and S. Y. Tyree, *J. Am. Chem. Soc.* 1961, **83**, 3770.
11. B. Brzezinski and G. Zundel, *J. Mol. Struct.* 1980, **68**, 315.
12. D. X. West and K. D. Mariam, *J. Inorg. Nucl. Chem.* 1981, **43**, 2343 and references therein.
13. V. S. Hagley, R. E. Kohrman and D. X. West, *J. Inorg. Nucl. Chem.* 1977, **39**, 1959.
14. S. Kida, J. V. Quagliano, J. A. Walmsley and S. Y. Tyree, *Spectrochim. Acta* 1963, **1**, 189.
15. Y. K. Bhoon, *Polyhedron* 1983, **2**, 365.
16. M. Mohan and Manmohan, *Synth. React. Inorg. Met-Org. Chem.* 1982, **12**, 761.
17. M. A. Ali and R. Bose, *J. Inorg. Nucl. Chem.* 1977, **39**, 265.
18. I. Bertini and A. Sabatini, *Inorg. Chem.* 1966, **4**, 1025; K. Mukhanti, K. B. Pandeya and R. P. Singh, *Ind. J. Chem.* 1982, **21A**, 641; B. Balaiah, B. A. Sastry, M. N. Chary, G. Ponticelli and M. Massacesi, *J. Mol. Struct.* 1982, **78**, 289.
19. L. Ramakrishnan and S. Soundararajan, *Monatsh. Chem.* 1976, **107**, 1095.
20. G. Vicentini and W. De Oliveira, *J. Inorg. Nucl. Chem.* 1975, **37**, 2018.
21. N. F. Curtis and Y. M. Curtis, *Inorg. Chem.* 1965, **3**, 804; A. B. P. Lever, E. Mantovani and B. S. Ramaswamy, *Can. J. Chem.* 1976, **49**, 1957.
22. R. Raina and T. S. Srivastava, *Inorg. Chem. Acta* 1982, **67**, 83.
23. N. C. Mishra, B. B. Mohapatra and S. Guru, *J. Inorg. Nucl. Chem.* 1979, **41**, 408.
24. J. Kohout, M. Kabesova, M. Hvastijova and J. Gazo, *Coll. Czech. Chem. Comm.* 1978, **43**, 379. A. Brown, G. Butler and W. R. McWhinnie, *Inorg. Chim. Acta* 1977, **25**, 121.
25. I. S. Ahuja, R. Singh and C. R. Rai, *Trans. Met. Chem.* 1977, **2**, 257.
26. A. C. Fabretti, G. C. Franchini and G. Peyronel, *Trans. Met. Chem.* 1978, **3**, 363.
27. D. Forster and W. D. Horrocks, *Inorg. Chem.* 1966, **5**, 1510.
28. S. Delgado, M. Moran and V. Fernandez, *J. Coord. Chem.* 1982, **12**, 105.
29. R. H. Nuttall and D. W. Taylor, *J. Chem. Soc., Chem. Commun.* 1968, 1417; A. C. Fabretti, G. Peyronel and G. C. Fanchini, *J. Coord. Chem.* 1979, **9**, 111; and N. M. Karayannis, C. M. Mikulski, L. L. Pytlewski and M. M. Labes, *Inorg. Chem.* 1974, **13**, 1146.
30. S. K. Jain, B. S. Garg, J. K. Bhoon, D. L. Klayman and J. P. Scovill, to be published.
31. Y. Thakur and B. N. Jha, *J. Inorg. Nucl. Chem.* 1980, **42**, 449.
32. U. Sakaguchi and A. W. Addison, *J. Chem. Soc., Dalton* 1979, 600.
33. M. J. Bew, B. J. Hathaway and R. J. Fereday, *J. Chem. Soc., Dalton* 1972, 1229.
34. J. Casabo, M. Izquierdo, J. Ribas and C. Diaz, *Trans. Met. Chem.* 1983, **8**, 110.
35. S. F. Pavkovic, J. N. Brown and D. X. West, *Acta Cryst.* 1980, **B36**, 143; S. F. Pavkovic and J. N. Brown, *Acta Cryst.* 1982, **B38**, 274.

*Polyhedron* Vol. 3, No. 8, pp. 957–962, 1984
Printed in the U.S.A.

0277–5387/84 $3.00 + .00
© 1984 Pergamon Press Ltd.

# THE REACTIONS OF SOME ORGANOTIN(IV) CHLORIDES WITH ANTIMONY(V) CHLORIDE AND BORON(III) CHLORIDE

**KEITH B. DILLON* and GEOFFREY F. HEWITSON**
Chemistry Department, University of Durham, South Road, Durham DH1 3LE, England

(*Received* 14 *November* 1983; *accepted* 10 *January* 1984)

**Abstract**—The reactions of the organotin chlorides $R_nSnCl_{4-n}$ ($R = Me$ or Ph; $0 \leqslant n \leqslant 4$) with the Lewis acids $SbCl_5$ and $BCl_3$ have been investigated by $^{119}Sn$ and (where appropriate) $^{11}B$ NMR spectroscopy. The results show that transfer of organo-groups to antimony or boron usually takes place rather than chloride abstraction to give cationic tin(IV) species, and this process is more facile for phenyl than methyl groups. These conclusions have been confirmed in some instances by isolation of the non-volatile reaction products.

The reactions of strong Lewis acids such as antimony(V) chloride, boron trichloride or aluminium trichloride with chloroorgano-derivatives of some main group elements including phosphorus(V)[1] and arsenic(V)[2] have been used to prepare cationic derivatives, eqns (1) and (2), which could then be identified by spectroscopic techniques as well as by elemental analysis of the isolated products.

$$R_nPCl_{5-n} + SbCl_5 \rightarrow [R_nPCl_{4-n}]^+ SbCl_6^- \quad (1)$$

$$R_nAsCl_{5-n} + BCl_3 \rightarrow [R_nAsCl_{4-n}]^+ BCl_4^-. \quad (2)$$

In certain instances, however, $SbCl_5$ is capable of undergoing exchange reactions with organometallic compounds, resulting in the formation of organoantimony(V) chlorides. Thus the preparation of $Ph_2SbCl_3$ has been described by reaction of $Ph_4Pb$ with $SbCl_5$.[3] Organoboron halides are also well-established, and $^{11}B$ NMR shifts have been reported for the phenyl and methyl compounds.[4–7] The reaction of $Ph_4Sn$ with $BCl_3$ in various solvents has been used to prepare $PhBCl_2$,[8] but the tin-containing product varied with the solvent. $PhSnCl_3$ was identified in the residues from reaction in $CH_2Cl_2$, but $SnCl_4$ was found in $CCl_4$ or in the absence of a solvent.[8] Similarly the methyl boron bromides have been prepared by reaction of $Me_4Sn$ with $BBr_3$,[9] but in contrast with the phenyl system not more than two of the alkyl groups could be transferred from tin to boron, and the tin-containing product was found to be $Me_2SnBr_2$. It was therefore of considerable interest to investigate the reactions of organotin(IV) chlorides with $SbCl_5$ and $BCl_3$, using $^{119}Sn$ NMR spectroscopy to identify the main tin-containing species present in solution. Formation of a cationic three-coordinate tin(IV) species was expected to cause a large downfield shift of the $^{119}Sn$ resonance from the position of the starting material,[10,11] while the occurrence of exchange reactions should also be observable. In the case of $BCl_3$, $^{11}B$ NMR spectroscopy could also be used to follow the progress of the reactions. The results obtained have been confirmed in some instances by isolation and analysis of the non-volatile reaction products.

## EXPERIMENTAL

All manipulations including NMR sample preparation were carried out in an inert atmosphere of dry nitrogen. Chemicals of the best available commercial grade were used, in general without further purification. For reactions with $SbCl_5$, the organotin compound was usually dissolved in $CH_2Cl_2$ and the requisite amount of $SbCl_5$ diluted with the same solvent was added. The non-volatile products were isolated as required by removing $CH_2Cl_2$ and any excess $SbCl_5$ *in vacuo*, adding a small amount of low-boiling petroleum ether, and again pumping *in vacuo* to remove the last traces of solvent. Some reactions were carried out with neat $SbCl_5$, as described in the Results section, by cautiously adding $SbCl_5$ dropwise to the organotin compound in an NMR tube. The exothermic reactions which resulted were allowed to subside before the $^{119}Sn$ NMR spectra of the resultant clear solutions were recorded.

*Author to whom correspondence should be addressed.

For reactions with $BCl_3$, a preweighed amount of the tin(IV) compound was dissolved in $CH_2Cl_2$ in a thick-walled NMR tube of 8.4 mm outside diameter, which was connected to the vacuum line via a modified socket joint. This section of the line was isolated, and the required amount of $BCl_3$ condensed into a graduated cold finger attached to the line at 77K. The NMR tube was then cooled to 77K while the cold finger was allowed to warm up slowly to room temperature, resulting in the condensation of $BCl_3$ into the NMR tube. When this process was complete, the tube was sealed, and allowed to warm up gradually to room temperature.

$^{119}Sn$ NMR spectra were recorded at 307.2K on a Fourier transform multinuclear spectrometer constructed by Dr. A. Royston, which utilises the permanent magnet (1.4T) from a Perkin–Elmer R10 spectrometer, a Racal 9061/2 frequency synthesiser as the frequency source, a Dec pdp 11/34 computer, and a HIPLOT digital plotter. Samples were contained in 8.4 mm o.d. stationary sample tubes. Chemical shifts were measured relative to external $Me_4Sn$, with the downfield direction taken as positive. $^{11}B$ spectra were similarly obtained relative to external $(MeO)_3B$. IR spectra between 650 and 250 $cm^{-1}$ were recorded on a Perkin–Elmer 457 instrument. C, H and Cl microanalyses were determined as described previously,[12] and Sn and Sb microanalyses by atomic absorption spectroscopy.

## RESULTS AND DISCUSSION

### (a) *Reactions with antimony(V) chloride*

Initially reactions were carried out in $CH_2Cl_2$ as solvent by adding slightly more than an equimolar amount of $SbCl_5$ to the organotin species $R_nSnCl_{4-n}$ (R = Me or Ph; $0 \leq n \leq 4$). When reaction had subsided the $^{119}Sn$ NMR spectra of samples of the resultant solutions were recorded; the results are given in Table 1, together with literature values for the chemical shifts of the starting materials in this solvent where available.[10,11] Chemical shifts of four-coordinate tin compounds are known to be markedly concentration- and solvent-dependent,[11] and the species formed could be readily identified when this was taken into account, as shown in Table 1. There was no evidence for formation of cationic tin(IV) species, but transfer of organo-groups to antimony(V) appeared to occur with all the phenyltin compounds and with $Me_4Sn$ and $Me_3SnCl$, whereas $Me_2SnCl_2$, $MeSnCl_3$ and $SnCl_4$ did not react under these conditions. ($Me_2SnCl_2$ reacted with an excess of $SbCl_5$ to give $MeSnCl_3$, although some starting material was still present.) The reactions were repeated (except for $SnCl_4$) using a larger excess of $SbCl_5$, and the non-volatile products were isolated after any effervescence had subsided (Experimental section). The results of $^{119}Sn$ NMR investigations and elemental analyses of the products are shown in Table 2, and indicate that under these more forcing conditions $Me_2SnCl_2$ also transfers one methyl

Table 1. $\delta^{119}Sn$ (ppm) for reaction of some organotin chlorides with $SbCl_5$ in $CH_2Cl_2$

| Compound | $\delta$ $^{119}Sn$ (p.p.m.) in $CH_2Cl_2$[11] | $\delta$ $^{119}Sn$ (p.p.m.) after reaction with $SbCl_5$ | Assignment |
|---|---|---|---|
| $Ph_4Sn$ | -140[a] | -29.7 | $Ph_2SnCl_2$ |
| $Ph_3SnCl$ | -48 | -62.9 | $PhSnCl_3$ |
| $Ph_2SnCl_2$ | -32 | -62.8 | $PhSnCl_3$ |
| | | -162.3[b] | $SnCl_4$ |
| $PhSnCl_3$ | -63 | -150.1 | $SnCl_4$ |
| $SnCl_4$ | -150 | -150.1 | $SnCl_4$ |
| $Me_4Sn$ | 0 | 171.3 | $Me_3SnCl$ |
| | | 131.7[b] | $Me_2SnCl_2$ |
| $Me_3SnCl$ | 155 to 169 | 143.2 | $Me_2SnCl_2$ |
| $Me_2SnCl_2$ | 137 | 139.6 | $Me_2SnCl_2$ |
| $MeSnCl_3$ | 21[c] | 17.5 | $MeSnCl_3$ |

a estimated value

b major peak

c $CHCl_3$ solvent

Table 2. Products isolated from reactions with $SbCl_5$

| Starting material | Product Appearance | $\delta^{119}Sn$ (p.p.m.) | Product | Analysis found (%) | Analysis required (%) |
|---|---|---|---|---|---|
| $Me_4Sn$ | white powdery solid | 130.3[a] | $Me_2SnCl_2$ + $Me_2SbCl_3$ (1:1) | Sn, 22.7; Sb, 25.9; Cl, 35.2; C, 10.8; H, 3.3. | Sn, 24.9; Sb, 25.5; Cl, 37.1; C, 10.0; H, 2.5. |
| $Me_3SnCl$ | a) off-white crystals | 132.6[b] | $Me_2SnCl_2$ $Me_2SbCl_3$ (2:1) | Sn, 33.3; Sb, 16.7; Cl, 33.7; C, 10.3; H, 2.9. | Sn, 34.1; Sb, 17.5; Cl, 35.7; C, 10.3; H, 2.6. |
| | b) orange-red crystals | 235.1[b] | see text | Sn, 35.7; Sb, 16.1; Cl, 35.3; C, 9.2; H, 2.8 | |
| $Me_2SnCl_2$ | red liquid | 14.0[b] | $MeSnCl_3$ | | |
| $MeSnCl_3$ | red liquid | 17.5[b] | $MeSnCl_3$ | | |
| $Ph_4Sn$ | white solid | - | $Ph_2SbCl_3$ | Sn, -; Sb, 28.7; Cl, 26.7; C, 37.5; H, 2.6. | Sn, -; Sb, 31.9; Cl, 27.8; C, 37.6; H, 2.6. |
| $Ph_3SnCl$ | off-white solid | - | $Ph_2SbCl_3$ | Sn, -; Sb, 32.0; Cl, 29.7; C, 37.3; H, 2.6. | Sn, -; Sb, 31.9; Cl, 27.8; C, 37.6; H, 2.6. |
| $Ph_2SnCl_2$ | off-white solid | - | $Ph_2SbCl_3$ | Sn, -; Sb, 29.5; Cl, 26.9; C, 35.9; H, 3.0. | Sn, -; Sb, 31.9; Cl, 27.8; C, 37.6; H, 2.6. |
| $PhSnCl_3$ | grey solid | - | $PhSbCl_4$ | Sn, -; Sb, 35.1; Cl, 41.6; C, 21.1; H, 1.5. | Sn, -; Sb, 35.8; Cl, 41.6; C, 21.1; H, 1.5. |

a $CH_2Cl_2$ solvent. b Solid state or neat liquid

group to antimony but $MeSnCl_3$ does not react. No tin was detected in any of the products isolated from reaction of the phenyltin compounds, and these appear to be converted completely to $SnCl_4$, which is then removed with the volatiles. The elemental analyses confirm that the non-volatile product is $Ph_2SbCl_3$ from $Ph_4Sn$, $Ph_3SnCl$ and $Ph_2SnCl_2$, and $PhSbCl_4$ from $PhSnCl_3$. The reaction of $SbCl_5$ with $Ph_4Sn$ thus parallels that with $Ph_4Pb$.[3] The IR spectra of the products from $Ph_4Sn$, $Ph_3SnCl$ and $Ph_2SnCl_2$ were also virtually identical, and differed from that of the reaction product with $PhSnCl_3$, as expected. These reactions may indeed provide a useful route for preparation of the phenylantimony chlorides. The white or off-white products from the $Me_4Sn$ and $Me_3SnCl$ reactions were readily identified as 1:1 and 2:1 mixtures of $Me_2SnCl_2$ and $Me_2SbCl_3$ respectively, eqns (3) and (4), and may similarly be suitable for preparation of $Me_2SbCl_3$.

$$Me_4Sn + SbCl_5 \rightarrow Me_2SnCl_2 + Me_2SbCl_3 \quad (3)$$

$$2Me_3SnCl + SbCl_5 \rightarrow 2Me_2SnCl_2 + Me_2SbCl_3. \quad (4)$$

In one reaction of $Me_3SnCl$ with $SbCl_5$, however, a crystalline product was obtained which gave a solid state signal at very low field (Table 2), as expected for a three-coordinate cationic species. Nevertheless the analysis of the solid was similar to that of the "normal' product, as shown, and the experiment was not reproducible. Assignment of this signal to a cationic tin(IV) species such as $Me_3Sn^+$ is thus very tentative, but is supported by some of the results from reactions of $Me_4Sn$ with neat $SbCl_5$, described below. $Me_2SnCl_2$ and $MeSnCl_3$ both gave liquid products, the $^{119}Sn$ NMR of which indicated the presence of $MeSnCl_3$ as the only tin-containing species. These liquids were not analysed.

Similar reactions were also carried out with neat $SbCl_5$, as indicated previously. A single $^{119}Sn$ NMR signal was obtained in most cases from the resultant solutions (Table 3), and the species formed could then be readily identified. $Me_3SnCl$ and $Me_2SnCl_2$ both appear to lose one methyl group under these conditions while $MeSnCl_3$ and $SnCl_4$ do not react. All the phenyltin compounds form $SnCl_4$ exclusively, however, in agreement with the results from excess $SbCl_5$ in $CH_2Cl_2$. No attempt was made to isolate the products from these

Table 3. $\delta$ $^{119}Sn$ (ppm) of some organotin chlorides in neat $SbCl_5$

| Starting Material | $\delta$ $^{119}Sn$ (p.p.m.) | Assignment |
|---|---|---|
| $Me_3SnCl$ | 137.4 | $Me_2SnCl_2$ |
| $Me_2SnCl_2$ | 20.9 | $MeSnCl_3$ |
| $MeSnCl_3$ | 21.0 | $MeSnCl_3$ |
| $SnCl_4$ | -150.1 | $SnCl_4$ |
| $Ph_4Sn$ | -150.1 | $SnCl_4$ |
| $Ph_3SnCl$ | -150.1 | $SnCl_4$ |
| $Ph_2SnCl_2$ | -153.6 | $SnCl_4$ |
| $PhSnCl_3$ | -150.1 | $SnCl_4$ |

reactions since the NMR data appeared quite conclusive.

The most unusual results were obtained from $Me_4Sn$, where the shifts ascribed to the tri- and dimethyltin species which form the reaction products differed markedly with the relative concentrations of the reagents (Table 4). When a large excess of $Me_4Sn$ was used, the signals were at 160.6 ($Me_3SnCl$), 97.8 and 0.0 ($Me_4Sn$) ppm. A 2:1 molar ratio of $Me_4Sn$ to $SbCl_5$ similarly gave resonances at 160.6, 104.7 and 0.0 ppm. A 1:1 ratio of reagents led to peaks at 208.0, 131.2 ($Me_2SnCl_2$) and −5.0 ppm. Other solutions with an excess of $Me_4Sn$, but where this was not measured quantitatively, gave signals in positions intermediate between those for the 1:1 and 2:1 mixtures, as shown, while an excess of $SbCl_5$ yielded only one strong signal at 136.4 ppm, readily assigned to $Me_2SnCl_2$. Thus the resonance for $Me_3SnCl$ has a normal shift value when excess $Me_4Sn$ (≥2:1) is present, but moves progressively to lower field and decreases in intensity as the Sn:Sb ratio falls. The downfield movement could be due to partial ionisation, facilitated by the increasing concentration of $SbCl_5$, eqn (5),

$$Me_3SnCl + SbCl_5 \rightleftharpoons Me_3Sn^+SbCl_6^- \quad (5)$$

with rapid exchange on the NMR time scale between the covalent and ionic tin(IV) species.

The more difficult data to explain are those for the dimethyltin derivatives, since the shift is initially to higher field of the normal position, which is only reached at Sn:Sb ratios of 1:1 or less. Association of $Me_2SnCl_2$ molecules might increase the shielding about each tin nucleus and thus cause an upfield shift, but aggregation would seem to be more likely at higher concentrations of $Me_2SnCl_2$, the opposite trend to that observed. $Me_2SnCl_2$ is known to be associated in the solid state, with a distorted octahedral arrangement about each tin atom and asymmetric chlorine bridges in a linear chain polymer.[13] $Me_3SnCl$ is also polymeric at 135K, with five-coordinate tin and an asymmetric chlorine bridge, but the intermolecular association is apparently disrupted by melting or dissolution in $CS_2$.[14] An alternative possibility is the formation of octahedral aggregates between $SbCl_5$ and $Me_2SnCl_2$ such as $Cl_4SbCl_2Me_2SnCl_2SbCl_4$, but formation of such species would appear more likely at high rather than low $SbCl_5$ concentrations. In any event there seems no reason to postulate ionisation of dimethyltin species, since no shifts downfield from the values in organic solvents[10,11] were found.

Table 4. $\delta$ $^{119}$Sn (ppm) for reaction products from $Me_4Sn$ and $SbCl_5$

| Molar Ratio | $\delta$ $^{119}$Sn (p.p.m.) | | |
|---|---|---|---|
| $Me_4Sn$: $SbCl_5$ | $Me_3SnCl$ | $Me_2SnCl_2$ | $Me_4Sn$ |
| Large xs $Me_4Sn$ | 160.6* | 97.8 | 0.0 |
| 2:1 | 160.6* | 104.7 | 0.0 |
| xs $Me_4Sn$[a] | 172.8* | 113.5 | not recorded |
| xs $Me_4Sn$[a] | 179.2* | 117.7 | not recorded |
| xs $Me_4Sn$[a] | 186.8 | 124.0* | not recorded |
| 1:1 | 208.0 | 131.2* | -5.0 |
| xs $SbCl_5$ | | 136.4* | |

* major peak  a not measured quantitatively

(b) *Reactions with boron trichloride*

The solutions were prepared as described in the Experimental section and their $^{119}$Sn and $^{11}$B NMR spectra were recorded. The results are shown in Table 5, and indicate that organogroup transfer rather than chloride abstraction again takes place. Since $BCl_3$ is a weaker Lewis acid than $SbCl_5$, and $R_4Sn$ compounds have been used to prepare organoboron derivatives,[8,9] this behaviour is not unexpected. Interpretation of the results for the methyltin compounds is quite straightforward and the $^{11}$B NMR shifts for $MeBCl_2$ and $Me_2BCl$, where formed, are in good agreement with literature data.[7] Reaction between an excess of $Me_4Sn$ and $BCl_3$ was also carried out to see whether $Me_3B$ ($\delta^{11}$B 68.9 ppm[7]) would be formed. The $^{11}$B spectrum contained no $BCl_3$ resonance, showing that it had reacted completely. The major peak present was due to $MeBCl_2$, with a smaller signal from $Me_2BCl$, and there was no evidence for formation of $Me_3B$. $Me_2SnCl_2$ and $MeSnCl_3$ did not react under these conditions, even with excess $BCl_3$.

The results for the phenyltin compounds require more discussion. A small peak at 13.4 ppm was seen in the $^{11}$B NMR spectrum from reaction of $Ph_4Sn$ with excess $BCl_3$, which cannot be ascribed to any of the phenylboron chlorides.[7] The shift is quite close to that reported for $PhB(OH)_2$[4], which could have been formed if a leakage of air or moisture into the tube had occurred, but no hydrolysis products of $BCl_3$ were detected. This signal was not present when a higher proportion of $Ph_4Sn$ was used, but a broad hump at 38.7 ppm was apparent, intermediate in shift between $PhBCl_2$ (37.7 ppm) and $Ph_2BCl$ (43.0 ppm).[7] Since an exchanging system between $PhBCl_2$ and $Ph_2BCl$ is unlikely, this hump is presumably a composite with contributions from both species and overlapping peaks. A similar signal was observed in the $^{11}$B spectrum from the reaction of $Ph_2SnCl_2$ with excess

Table 5. $^{119}Sn$ and $^{11}B$ shifts of products from reactions between organotin chlorides and $BCl_3$

| System | $\delta$ $^{119}Sn$ (p.p.m.) | Tin-Containing product | $\delta$ $^{11}B$ (p.p.m.) | Boron-Containing product |
|---|---|---|---|---|
| $Me_4Sn$ + excess $BCl_3$[a] | 146.7 | $Me_2SnCl_2$ | 29.6* | $BCl_3$ |
| | | | 45.8 | $MeBCl_2$ |
| $Me_4Sn$ + $BCl_3$ (~1.1) | 140.5 | $Me_2SnCl_2$ | 45.8* | $MeBCl_2$ |
| | | | 60.5 | $Me_2BCl$ |
| $Me_3SnCl$ + $BCl_3$ (≥1:0.7) | 167.2* | $Me_3SnCl$ | 44.1 | $MeBCl_2$ |
| | 128.7 | $Me_2SnCl_2$ | 59.3* | $Me_2BCl$ |
| $Me_2SnCl_2$ + excess $BCl_3$[a] | 142.0 | $Me_2SnCl_2$ | 29.4 | $BCl_3$ |
| $MeSnCl_3$ + excess $BCl_3$[a] | 19.8 | $MeSnCl_3$ | 28.6 | $BCl_3$ |
| $Ph_4Sn$ + excess $BCl_3$[a] | -64.0 | $PhSnCl_3$ | 13.4 | See text |
| | | | 29.4 | $BCl_3$ |
| | | | 38.3* | $PhBCl_2$ |
| $Ph_4Sn$ + $BCl_3$ (~1:2) | -62.7 | $PhSnCl_3$ | 38.7 | $PhBCl_2/Ph_2BCl$ |
| $Ph_3SnCl$ + excess $BCl_3$[a] | -153.7 | $SnCl_4$ | 29.6 | $BCl_3$ |
| | | | 37.7* | $PhBCl_2$ |
| $Ph_2SnCl_2$ + excess $BCl_3$[a] | -62.9 | $PhSnCl_3$ | 29.6 | $BCl_3$ |
| | | | 39.4* | $PhBCl_2/Ph_2BCl$ |
| $PhSnCl_3$ + excess $BCl_3$[a] | -146.6 | $SnCl_4$ | 28.6 | $BCl_3$ |
| | | | 37.7* | $PhBCl_2$ |

* major peak

a Excess $BCl_3$ means > 1:1 molar ratio

of $BCl_3$. The other unexpected feature was that the reactions of $Ph_4Sn$ with $BCl_3$ (~1:2), and $Ph_2SnCl_2$ with excess $BCl_3$, both showed $PhSnCl_3$ as the tin-containing product, even though $PhSnCl_3$ (and $Ph_3SnCl$) clearly react with excess $BCl_3$ to form $SnCl_4$. This result is in agreement with the previous report of $PhSnCl_3$ as the reaction product from $Ph_4Sn$ and $BCl_3$ in $CH_2Cl_2$.[8] The reactions are probably still continuing but at a slow rate, and the products observed ($PhSnCl_3$ or $SnCl_4$) may well depend on the relative concentrations of $BCl_3$ and the organotin compound, as well as the solvent. The ultimate product is presumably $SnCl_4$ in each case, corresponding to the reactions of the phenyltin compounds with $SbCl_5$ under forcing conditions.

It is thus evident that both $SbCl_5$ and $BCl_3$ usually react with the organotin compounds $R_nSnCl_{4-n}$ (R = Me or Ph; $0 \leqslant n \leqslant 4$) to give organoantimony- and -boron-derivatives respectively, rather than cations by halogen abstraction. The only evidence for formation of cationic species is from systems with $Me_3SnCl$ and $SbCl_5$ present. The exchange of phenyl groups is more facile than that of methyl groups, and $MeSnCl_3$ does not react with either reagent, even under forcing conditions. $Me_2SnCl_2$ similarly does not react with $BCl_3$, or with $SbCl_5$ in a 1:1 ratio in $CH_2Cl_2$, but does form $MeSnCl_3$ when excess $SbCl_5$ is used. The reactions with $SbCl_5$ may provide a useful preparative route to $PhSbCl_4$ and $Ph_2SbCl_3$, which have been isolated successfully, and possibly to $Me_2SbCl_3$ also.

We thank Dr. A. Royston for assistance with the NMR spectrometer, J. Lincoln for recording some of the NMR spectra, and the University of Durham for the award of a Research Studentship (to G.F.H.).

## REFERENCES

1. K.B. Dillon, R.J. Lynch, R.N. Reeve and T.C. Waddington, *J. Chem. Soc., Dalton Trans.* 1976, 1243.
2. K.B. Dillon, R.J. Lynch and T.C. Waddington, *J. Chem. Soc., Dalton Trans.*1976, 1478.

3. A.E. Goddard, J.N. Ashley and R.B. Evans, *J. Chem. Soc.* 1922, **121**, 978.
4. J.E. de Moor and G.P. van der Kelen, *J. Organomet. Chem.* 1976, **6**, 235.
5. W.D. Phillips, H.C. Miller and E.L. Muetterties, *J. Am. Chem. Soc.* 1959, **81**, 4496.
6. H. Nöth and H. Vahrenkamp, *Chem. Ber.* 1966, **99**, 1049.
7. H. Nöth and B. Wrackmeyer, *Chem. Ber.* 1976, **109**, 1075.
8. J.E. Burch, W. Gerrard, M. Howarth and E.F. Mooney, *J. Chem. Soc.* 1960, 4916.
9. W. Gerrard, E. F. Mooney and R. G. Rees, *J. Chem. Soc.* 1964, 740.
10. P.J. Smith and L. Smith, *Inorg. Chim. Acta Rev.* 1973, **7**, 11.
11. P.J. Smith and A. P. Tupčiauskas, *Ann. Rep. NMR Spectroscopy* 1978, **8**, 291.
12. K.B. Dillon, R.N. Reeve and T.C. Waddington, *J. Chem. Soc. Dalton Trans.* 1977, 1410.
13. A.G. Davies, H.J. Milledge, D.C. Puxley and P.J. Smith, *J. Chem. Soc.(A)* 1970, 2862.
14. M. Bilayet Hossain, J.L. Lefferts, K.C. Molloy, D. van der Helm and J.J. Zuckerman, *Inorg. Chim. Acta* 1979, **36**, L409.

*Polyhedron* Vol. 3, No. 8, pp. 963–968, 1984
Printed in the U.S.A.

0277–5387/84 $3.00 + .00
© 1984 Pergamon Press Ltd.

# NICKEL(II) COMPLEXES OF ETHYLENEDIPHOSPHINETETRA-ACETIC ACID†

J. PODLAHOVÁ,* L. KAVAN,‡ J. ŠILHA and J. PODLAHA
Department of Inorganic Chemistry, Charles University, 12840 Prague, Czechoslovakia

(*Received* 21 *November* 1983; *accepted* 17 *January* 1984)

**Abstract**—Ethylenediphosphinetetraacetic acid ($H_4L$) coordinates nickel(II) preferentially as a chelating di(tertiary phosphine). The two complexes identified in non-aqueous solutions are *cis*-square planar $NiBr_2(H_4L)$ and square-pyramidal $[NiBr_2(H_4L)_2]Br$; both structures are retained in the solid state. The square planar anion $NiL_2^{6-}$ is the predominant complex in a neutral aqueous solution. A number of its solid salts $M_6NiL_2 \cdot aq$ (M = Na, 1/2 divalent metal) has the same square planar $NiP_4$ core. The compound $Ni_2L \cdot 8H_2O$ also belongs to this series and should be formulated as $Ni_3[NiL_2] \cdot 16H_2O$: one nickel(II) is located in the $NiP_4$ core and the remaining three are coordinated by the carboxyl group oxygen atoms and water molecules in a roughly octahedral environment. The results are based on preparative, X-ray powder, magnetic susceptibility, conductometric, UV–VIS, NMR, IR (both normal and $^{62}Ni$) and XPS spectral studies.

Ethylenediphosphinetetraacetic acid, $(HO_2CCH_2)_2PCH_2CH_2P(CH_2CO_2H)_2$, $H_4L$, as a phosphorus analogue of the familiar EDTA, belongs to the class of hybrid ligands containing both hard and soft donor atoms. The synthesis,[1,2] protonation[2] and stability constants of its metal complexes[3] have been described. This work deals with the interaction of the ligand with nickel(II) as a typical representative of borderline class metal ions with comparable affinity for both donor functions of the ligand. Nickel(II) complexes of simpler phosphineacetic acids have been studied previously[4–7] and have shown that three types of coordination can take place: monodentate through P, bidentate through $PCH_2CH_2P$ (PP) and bidentate through $PCH_2COO$, the actual mode being critically dependent on the structure of the ligand and on the experimental conditions such as acidity and solvent.

## EXPERIMENTAL

All manipulations with the solutions were carried out in the absence of oxygen; solid samples are air-stable.

### *Materials*

The synthesis of the ligand has been described.[1,2] The salt, $Ba_2L \cdot 12H_2O$, was prepared by neutralization of $H_4L \cdot 2HBr$ with the calculated amount of a $Ba(OH)_2$ solution and crystallization from water. $^{62}NiBr_2 \cdot 3H_2O$ was obtained from $^{62}NiO$ (99.5% isotopic purity, Tekhsnabexport, USSR) by treating with hydrobromic acid and crystallization. Other chemicals were of reagent grade and were used as received. Solvents were purified, degassed and dried using standard procedures.

### *Measurements*

*Conductivity.* Radiometer CDM 3 with a cell calibrated vs KCl solutions to 0.5 rel.%. X-Ray powder patterns: Micrometa 2 (Chirana, Czechoslovakia), Fe-radiation, film recording. Magnetic susceptibility: Faraday balance calibrated with $Co[Hg(SCN)_4]$ for solids and Evans' NMR method

*Author to whom correspondence should be addressed.

†Part XXIV in the series *Compounds Structurally Related to Complexones*—XXIII. *Coll. Czech. Chem. Commun.* 1984, **48**, 586.

‡J. Heyrovský Institute of Physical Chemistry and Electrochemistry, Czechoslovak Academy of Sciences, 10200 Prague.

for solutions. IR spectra: Perkin–Elmer 684, 200–4000 $cm^{-1}$, solid samples in Nujol and Kel-F mulls and in KBr pellets. UV–VIS spectra: Unicam SP 800 for solutions and VSU 2 (Zeiss, Jena) for solid diffuse reflectance. NMR: Varian XL-200, 23°C, $\delta$ scale, J in Hz, downfield shifts positive, internal TMS for $^1H$ and external 85% $H_3PO_4$ for $^{31}P$ respectively.

*XPS spectra.* ESCA 3 Mk II (VG Scientific) interfaced to Nicolet 1072 multichannel analyzer, Al $K_\alpha$ non-monochromated source; the composition of the surface of the samples was approximately identical with the bulk chemical composition except for a high content of the aliphatic carbon originating from the pump oil and oxygen adsorbed on the surface. Samples were exposed as thin layers by evaporating an acetone solution of suspension on a copper holder connected electrically with the spectrometer; control samples adhered on Scotch-tape were measured in order to obtain accurate data about surface stoicheiometry. The binding energies of photoelectrons were normalized to the aliphatic C 1*s* (285.0 eV); the spectra are averages of 2–4 independent runs using both methods, yielding a reproducibility better than ±0.2 eV.

## SYNTHESIS OF THE COMPLEXES

$NiBr_2(H_4L)$. 1 mmole $H_4L \cdot 2HBr$ and 1 mmole $NiBr_2 \cdot 3H_2O$ were dissolved by heating in 75% aqueous acetic acid. After removing water by repeated vacuum evaporation with acetic acid, the complex was crystallized from acetic acid and dried at 50°/0.1 kPa. Yield 0.47 g, m.p. 225–228° (dec.), soluble in acetone, $CH_3CN$, THF, hot acetic acid. Analysis of this and all subsequent complexes for C, H, P, Ni and Na, Mn, Br (where appropriate) agreed within 0.4 rel.% with the calculated values.

$NiBr(H_4L)_2$ Br. 2 mmoles $H_4L \cdot 2HBr$, 4 mmoles $CH_3CO_2Na$ and 1 mmole $NiBr_2 \cdot 3H_2O$ were dissolved by heating in 75% aqueous acetic acid. Water was thoroughly removed by repeated vacuum evaporation with acetic acid/benzene; the complex was crystallized twice from acetic acid to remove traces of NaBr and dried at 80°/0.1 kPa. Yield 0.39 g, m.p. 123–125° (dec.), soluble in THF, acetonitrile and hot acetic acid.

$Na_6NiL_2 \cdot 6H_2O$. 2 mmoles $H_4L \cdot 2HBr$, 1 mmoles $NiBr_2 \cdot 3H_2O$ and 12 mmoles $NaHCO_3$ were stirred with 5 $cm^3$ warm water until dissolution and expelling $CO_2$. The complex crystallized after adding 20 $cm^3$ methanol and cooling to −5°; it was filtered when cool, washed with a little cold methanol and dried at 25°/0.1 kPa. Yield 0.45 g, m.p. 258° (dec.), soluble in water and warm methanol.

$Ni_2L \cdot 8H_2O$. 1 mmoles $H_4L \cdot 2HBr$, 12 $cm^3$ 0.5M–NaOH, 3 mmoles $CH_3CO_2Na$ and 2 mmoles $NiBr_2 \cdot 3H_2O$ were mixed, filtered and allowed to stand undisturbed for 2 months at room temperature. The crystals were filtered, washed with water and dried at 50°/0.1 kPa. Yield 0.35 g, insoluble in all common solvents except concentrated aqueous $CH_3CO_2Na$.

$Mn_3NiL_2 \cdot 16H_2O$. 1 mmole $H_4L \cdot 2HBr$, 20 $cm^3$ 0.3M–NaOH, 0.5 mmole $CH_3CO_2Na$, 0.5 mmole $NiBr \cdot 3H_2O$ and 20 $cm^3$ 0.1M–$MnBr_2$ are mixed in that order, filtered and allowed to stand undisturbed at room temperature. The crystals are filtered, washed with water and dried at 25°/0.1 kPa. Yield 0.48 g, insoluble in all common solvents. Salts containing other divalent metals in places of Mn (Mg, Ca, Sr, Ba, Fe, Co, Zn, Cd, Pb) can be prepared similarly by changing the solvent volume according to the solubility of the product which roughly decreases along the given series.

The complexes with $^{62}Ni$ were prepared by appropriately scaling down the procedures outlined above.

## RESULTS AND DISCUSSION

The properties of the complexes prepared are summarized in Tables 1–4.

It follows from the properties that the structures of the complexes can be conveniently discussed depending on whether the protonized or the dissociated form of the ligand is involved.

The complex $NiBr_2(H_4L)$ belongs to the familiar type of nickel(II) complexes with a $NiBr_2(PP)$ core.[8] It is formed easily even from the bis-(quaternized) form of the ligand.[2] The *cis*-square planar structure of the complex in solution and in the solid state clearly follows from the UV-VIS, IR, conductivity and magnetic susceptibility data. The complex is labile on a NMR-time scale and both the $^1H$ and $^{31}P$ spectra display marked low field coordination shifts. In the IR spectra, some bands in the 450–250 $cm^{-1}$ region are strongly affected by the $^{62}Ni$ substitution. The number of these bands corresponds[9] to the $C_{2v}$ local microsymmetry of the $NiBr_2(PP)$ core. The XPS spectrum is also in agreement with this structure: The ligand group shifts of the Ni $2p_{1/2}$ and Ni $2p_{3/2}$ bands relative to the bare nickel atom is −1.2 eV, which is typical for tertiary phosphine ligands;[10] both these energies and the absence of shake-up satellites[11] clearly indicate a *cis*-square planar structure; in accordance with the IR spectra, the binding energies of C 1*s* and O 1*s* correspond to the undissociated and uncoordinated carboxyl groups.[12]

Similarly to other di(tertiary phosphines) with electronegative substituents,[13] forcing conditions

Table 1. Properties of the complexes. (a) *ca.* $10^{-3}$M solutions; (b) THF; (c) diffuse reflectance; (d) acetonitrile; (e) water; (f) per 1 Mn; (g) per 4/3 Ni

| Complex | Formula (m.w.) | Colour | UV-VIS spectrum $10^{-3}cm^{-1}(\varepsilon_M)$ | Magnetic moment, B.M. | $\Lambda$ [a] $Scm^2mole^{-1}$ |
|---|---|---|---|---|---|
| $NiBr_2(H_4L)$ | $C_{10}H_{16}Br_2NiO_8P_2$ (544.71) | deep red | b: 21.6(1530),28.1(770), 33.1(1720),37.0(4650), 41.1(21600)<br>c: 21.5,28sh,33sh,37sh,42.0 | dia | 0.2[b],0.9[d] |
| $[NiBr(H_4L)_2]Br$ | $C_{20}H_{32}Br_2NiO_{16}P_4$ (870.89) | brown | b: 17.4(90),22.1(1150), 32.2(2800),35.1(3200), 39.7(19000)<br>c: 17.9sh,22.8,32sh,35sh,38.9 | dia | 4.3[b],126[d] |
| $Na_6NiL_2.6H_2O$ | $C_{20}H_{36}Na_6NiO_{22}P_4$ (949.04) | orange | e: 25.0(438),31.7(2800),34.6 (7000),38.2(35300)<br>c: 25.0,30sh,35sh,38.5 | dia | see text |
| $Mn_3NiL_2.16H_2O$ | $C_{20}H_{56}Mn_3NiO_{32}P_4$ (1156.08) | orange-yellow | c: 25.0,31sh,35sh,38.1 | 5.94[f] | |
| $Ni_3NiL_2.16H_2O$ | $C_{20}H_{56}Ni_4O_{32}P_4$ (1167.39) | lemon yellow | c: 8.7,13.3,14.7,24.9, 31sh,35sh,38.5 | 3.18[g] | |

Table 2. Selected bands in the IR spectra. (a) bands sensitive to $^{62}Ni$ substitution ($\Delta\tilde{\nu} = \tilde{\nu}_{Ni} - \tilde{\nu}_{62Ni}$); other bands in this region fluctuate within 0.5 $cm^{-1}$

| Complex | $\nu$(OH) | $\nu_{as}$(COO), $\nu$(C=O) | a |
|---|---|---|---|
| $NiBr_2(H_4L)$ | 2880s,vb | 1712vs | 443.1m(3.9)<br>358.9w(7.7)<br>301.8w(3.0)<br>288.9s(2.7) |
| $[NiBr(H_4L)_2]Br$ | 2860s,vb | 1695vs | 370.7s(2.8)<br>345.0s(2.8)<br>304.4m(2.9) |
| $Na_6NiL_2.6H_2O$ | 3240vs,b | 1578vs | 390.7w(5.6) |
| $Mn_3NiL_2.16H_2O$ | 3110s,vb | 1602vs | 399.6w(3.8) |
| $Ni_3NiL_2.16H_2O$ | 3170s,vb | 1593vs | 399.1w(7.3)<br>519.2m(6.2) |

Table 3. NMR spectra of the compounds studied. (a) centre of gravity; (b) see[2]; (c) apparent triplet; (d) filled-in-doublet

| Compound (solvent) | $^1H$ $PCH_2CH_2P$ | $^1H$ $CH_2CO_2$ | $^{31}P\{^1H\}$ |
|---|---|---|---|
| $NiBr_2(H_4L)$ (acetone-$d_6$) | 2.60bs | 3.63bs | 66.11s |
| $[NiBr(H_4L)_2]Br$ (THF-$d_8$) | 2.21m | 3.45m | see text |
| $Na_6NiL_2.6H_2O$ ($D_2O$) | 2.40bs | 3.14bs | 45.72s |
| $H_4L$ [b] ($D_2O$) | 1.87[c] | 2.78bs | -23.65s |
| $Ba_2L.12H_2O$ | 1.71[d] | 2.52s | -24.27s |

Table 4. XPS spectra of the compounds studied. Binding energies in eV, sat—satellite. (a) carbon in the carboxyl groups

| Compound | P 2p | C 1s[a] | O 1s | Ni $2p_{1/2}$ | Ni $2p_{3/2}$ | Other |
|---|---|---|---|---|---|---|
| $Ba_2L.12H_2O$ | 131.2 | 288.4 | 531.4 | | | |
| $NiBr_2(H_4L)$ | 131.8 | 289.3 | 532.5 | 872.0 | 854.7 | Br $3p_{3/2}$ 182.0 |
| $[NiBr(H_4L)_2]Br$ | 131.6 | 289.3 | 532.4 | 872.8 | 855.4 | Br $3p_{3/2}$ 181.3sh,181.9 |
| $Na_6NiL_2.6H_2O$ | 131.5 | 288.0 | 531.2 | 872.2 | 854.8 | |
| $Mn_3NiL_2.16H_2O$ | 131.7 | 288.5 | 531.7 | 872.4 | 855.2 | Mn $2p_{3/2}$ 642.0 sat.+3.5 |
| $Ni_3NiL_2.16H_2O$ | 132.3 | 288.4 | 531.6 | 873.3 | 856.2 | Ni $2p_{1/2}$ sat.+6.3 |
| | | | | | | Ni $2p_{3/2}$ sat.+4.4 |

must be employed to synthesize the 1:2 complex, $[NiBr(H_4L)_2]Br$. In this particular case, the neutralization of the phosphonium protons of the ligand functioned well. A square pyramidal pentacoordinate structure with the $Ni(PP)_2$ base and the apical Br atom can be assigned for the product in the solid state and in solution. The UV–VIS spectrum[14] and the 1:1 electrolyte behaviour in acetonitrile[15] strongly support the suggested structure. The NMR spectra show that the complex is rigid, as usual for this structural type;[16] while the $^1H$ spectrum consists of two multiplets which were not interpreted but merely characterized by the mean value of the coordination shifts, the $^{31}P\{^1H\}$ spectrum (Fig. 1) is clearly the $A_2B_2$ pattern with $\delta_A = 43.76$, $\delta_B = 56.77$, $J_{AA} = 49$, $J_{BB} = -71$, $J_{A_1B_1} = 210$, $J_{A_1B_2} = -59$ (the location of $P_A$ and $P_B$ relative to Br as well as the relative signs of the J's cannot be determined and are arbitrary). The spectrum can be interpreted as reflecting the usual distortion of the $Ni(PP)_2$ plane, which is forced by the steric bulk of the diphosphine ligands;[17,18] the nonequivalence of the pairs of phosphorus atoms is then caused by the axial bromide. As expected, the P, P coupling constants clearly reflect the chemical bonding of the pairs of phosphorus atoms through the carbon backbone. The IR spectra indicate undissociated carboxyl groups in agreement with the C 1*s* and O 1*s* bands in the XPS spectrum. Again, the number of $^{62}Ni$-substitution-sensitive bands agrees with the local $C_{4v}$ microsymmetry of the $NiBr(PP)_2$ core: the $\nu_{as}(NiP)$, $\nu_s(NiP)$ and $\nu(NiBr)$ vibrations are expected to be IR-active. While the main features of the XPS spectrum are similar to those of $NiBr_2(H_4L)$ and consistent with the proposed structure,[11] the Br $3p_{3/2}$ band is split into two components which agrees nicely with the presence of one coordinated and one ionic bromide in the complex.

Complexes containing dissociated ligand $L^{4-}$ are present in Ref. 3 and can be prepared from neutral aqueous solutions. The complex $NiL_2^{6-}$ bonds up to six protons in solution[3] but none of these protonized complexes could be isolated. The hexakis (sodium) salt and the salts with a number of divalent metal ions (the manganese salt was further characterized because its crystal habit makes it the obvious candidate for X-ray crystal structure analysis) were isolated. They all contain the square planar $Ni(PP)_2$ core as follows from the UV–VIS spectra, magnetic susceptibility and the solution behaviour of the sodium salt. The molar conductance of dilute solutions of the sodium salt can be interpreted[19] in terms of the relatively stable ion pair $Na^+NiL_2^{6-}$ characterized with $\lambda(1/6NiL_2) = 106.2(3)$ $Scm^2\,mole^{-1}$, $\lambda(1/5NaNiL_2) = 90(1)$ $Scm^2\,mole^{-1}$ and $\log \beta_{NaNiL_2} = 2.64(7)$, all at $I \to 0$ and 25°C. The NMR spectra of the sodium salt possess marked coordination shifts and suggest that the $NiL_2^{6-}$ anion is labile on the NMR-time scale. The presence of dissociated carboxyl groups and water is apparent from the IR spectra; only one IR band is sensitive to $^{62}Ni$ substitution which corresponds to the square planar $Ni(PP)_2$ core. The main features of the XPS spectra are similar to the diamagnetic structures discussed previously but, moreover, the paramagnetic and probably octahedral environment of the Mn(II) (and also of the Co(II)) ion is evident from the shake-up satellites associated with the metal 2*p* bands.

On mixing a nickel(II) salt with $L^{4-}$ in a 1:1 molar ratio, the $NiL_2^{6-}$ anion remains in solution and a new complex separates as an amorphous precipitate: $3Ni^{2+} + 3L^{4-} \rightarrow NiL_2^{6-} + Ni_2L$. This complex can be prepared as the crystalline octahydrate by depressing the precipitation rate by adding weakly coordinating anions such as acetate or sulphate. According to the X-ray powder patterns, the complex belongs to the isostructural

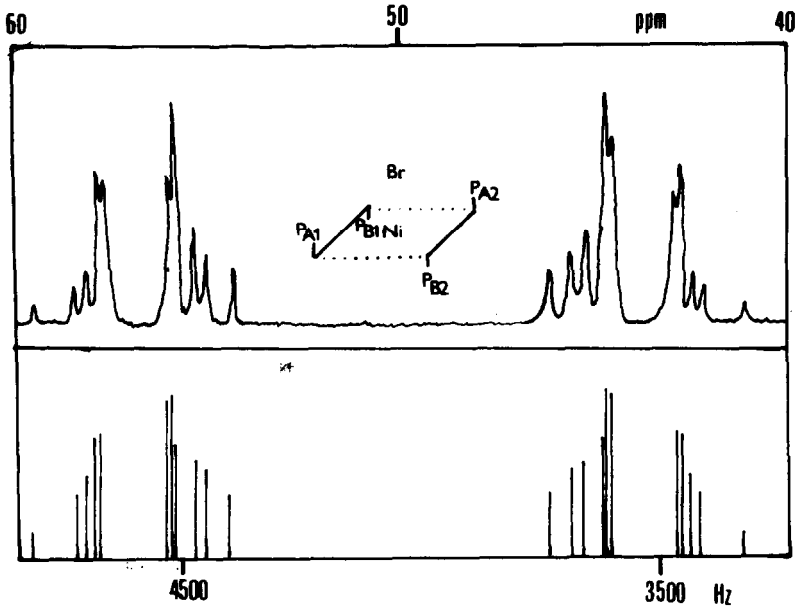



Fig. 1. The $^{31}P\{^1H\}$-NMR spectrum of $[NiBr(H_4L)_2]Br$ in THF-$d_8$ (top) and the spectrum simulated using parameters given in the text (bottom).

series, $M^{II}_3NiL_2 \cdot 16H_2O$ (M = Mn, Fe, Co, Ni, Zn, Cd) and hence should—in agreement with all its other properties—be formulated as $Ni_3[NiL_2] \cdot 16H_2O$. The magnetic susceptibility corresponds to the presence in the formula unit of three high spin Ni(II) ions and one low spin Ni(II). In the VIS–NIR spectrum the maxima attributable to an approximately octahedral Ni(II) are clearly discernible; the values of Dq = 870 and B = 690 $cm^{-1}$ suggest[20] a $NiO_6$ core, probably with carboxyl groups and water molecules as donors. The IR spectrum, in addition to giving information about dissociated and weakly coordinated[21] carboxyl groups, displays two $^{62}$Ni-isotopic substitution-sensitive bands: one evidently belongs to the $\nu_{as}$(NiP) in $D_{4h}$ symmetry (very similar to that in $Mn_3NiL_2$) and the second at 519 $cm^{-1}$ can be attributed to $\nu$(NiO) of the high spin nickel(II). Interestingly, when the complex is prepared from $Na_6NiL_2$ and $3NiBr_2$ as either $^{62}Ni_3[NiL_2]$ and $Ni_3[^{62}NiL_2]$, the respective isotopic shifts vanish, which indicates slow exchange of Ni(II) ions and hence conformational character of the NMR lability. The octahedral environment of the high spin Ni(II) ion as well as of the other divalent metal ions comprising the isostructural series can most probably be assumed to be formed through both intramolecular and intermolecular bonding of carboxyl groups, which should be responsible for the low solubility of the complexes. However, the solubility of $Ni_3NiL_2$ in solutions of sodium acetate indicates that this intermolecular interaction can be easily broken. The two types of Ni(II) ions reflect in the XPS spectrum as broad Ni 2*p* bands ($\Delta E_{FWHM}$ = 3.5 eV in contrast to the average value of 2.4 eV in the other complexes). The bands are characterized by a satellite structure and by a bonding energy typical of octahedral complexes. It seems likely that the bonds originating from octahedral and square planar Ni(II) overlap in this particular case, which causes broadening.

In summary, the coordinating behaviour of ethylenediphosphinetetraacetic acid towards nickel(II) differs from that of its analogue, EDTA, mainly in that it is dictated primarily by the very stable Ni(PP) chelate bonding; the acetate groups possess no appreciable tendency to form additional bonds to the same Ni(II). Hence, divalent nickel behaves towards the ligand as a typically soft metal ion.

## REFERENCES

1. J. Podlahová and J. Podlaha, *Coll. Czech. Chem. Commun.* 1980, **45**, 2049.
2. J. Podlahová, B. Kratochvíl, V. Langer, J. Šilha and J. Podlaha, *Coll. Czech. Chem. Commun.* 1981, **46**, 3063.
3. J. Podlahová and J. Podlaha, *Coll. Czech. Chem. Commun.* 1982, **47**, 1078.
4. T. Jarolím and J. Podlahová, *J. Inorg. Nucl. Chem.* 1976, **38**, 125.
5. J. Podlahová, *Coll. Czech. Chem. Commun.* 1978, **43**, 64.
6. J. Podlahová, *Coll. Czech. Chem. Commun.* 1980, **45**, 1477.

7. J. Ludvík and J. Podlahová, *J. Inorg. Nucl. Chem.* 1978, **40**, 1045.
8. For a review, see W. Levason and C. A. McAuliffe, *Adv. Inorg. Chem. Radiochem.* 1972, **14**, 173.
9. C. Udovich, J. Takemoto and K. Nakamoto, *J. Coord. Chem.* 1971, **1**, 89.
10. R. D. Feltham and P. Brant, *J. Am. Chem. Soc.* 1982, **104**, 641.
11. L. J. Matienzo, L. I. Yin, S. O. Grim and W. E. Swartz, *Inorg. Chem.* 1973, **12**, 2762; C. A. Tolman, W. M. Riggs, W. J. Linn, C. M. King and R. C. Wendt, *Inorg. Chem.* 1973, **12**, 2770; A. Furlani, G. Polzonetti, M. V. Russo and G. Mattogno, *Inorg. Chim. Acta* 1978, **26**, 239; V. I. Nefedov, Y. V. Salyn, R. Wather, B. Messbauer and R. Schöps, *Inorg. Chim. Acta* 1980, **45**, L103; T. Yoshida and K. Yamasaki, *Bull. Chem. Soc. Jpn* 1981, **54**, 935; M. Scrocco, *J. Electron Spectr. Rel. Phen.* 1980, **19**, 311.
12. V. Gelius, P. F. Hedén, J. Hedman, B. J. Lindberg, R. Manne, R. Nordberg, C. Nordling and K. Siegbahn, *Phys. Scripta* 1970, **2**, 70.
13. G. R. Van Hecke and W. deW. Horrocks Jr., *Inorg. Chem.* 1966, **5**, 1968; M. J. Hudson, R. S. Nyholm and M. H. B. Stiddard, *J. Chem. Soc. A* 1968, 40.
14. C. A. McAuliffe and D. W. Meek, *Inorg. Chem.* 1969, **8**, 904; K. Issleib and H. Weichmann, *Z. Anorg. Allgem. Chem.* 1968, **362**, 33; R. B. King, R. N. Kapoor, M. S. Saran and P. N. Kapoor, *Inorg. Chem.* 1971, **10**, 1851; M. Bacci, S. Midollini, P. Stoppioni and L. Sacconi, *Inorg. Chem.* 1973, **12**, 1801; W. Levason and C. A. McAuliffe, *Inorg. Chim. Acta* 1974, **11**, 33; K. K. Chow and C. A. McAuliffe, *Inorg. Chim. Acta* 1974, **10**, 197.
15. W. J. Geary, *Coord. Chem. Rev.* 1971, **7**, 81.
16. N. K. Roberts and S. B. Wild, *Inorg. Chem.* 1981, **20**, 1892.
17. A. C. Alyea and D. W. Meek, *Inorg. Chem.* 1972, **11**, 1029.
18. J. Podlahová, B. Kratochvíl and V. Langer, *Inorg. Chem.* 1981, **20**, 2160.
19. J. C. James, *Trans. Farad. Soc.* 1949, **45**, 855.
20. A. B. P. Lever, *Inorganic Electronic Spectroscopy*, p. 334. Elsevier, Amsterdam (1968).
21. K. Nakamoto, Y. Morimoto and A. E. Martell, *J. Am. Chem. Soc.* 1962, **84**, 2081; 1963, **85**, 309.

*Polyhedron* Vol. 3, No. 8, pp. 969–975, 1984
Printed in the U.S.A.

0277–5387/84 $3.00 + .00
© 1984 Pergamon Press Ltd.

# METAL COMPLEXES OF MERCAPTOAMINES—III. DIFFERENT BEHAVIOUR OF β- AND γ-(N,N-DIMETHYL)-MERCAPTOAMINES

**H. BARRERA, J. C. BAYÓN and J. SUADES***
Departament de Química Inorgànica, Facultat de Ciències, Universitat Autònoma de Barcelona, (Bellaterra), Spain

**and**

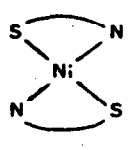
**C. GERMAIN and J. P. DECLERQ**
Unité CRIS, Université de Louvain, Louvain-la-Neuve, Belgium

(*Received* 24 *November* 1983; *accepted* 10 *January* 1984)

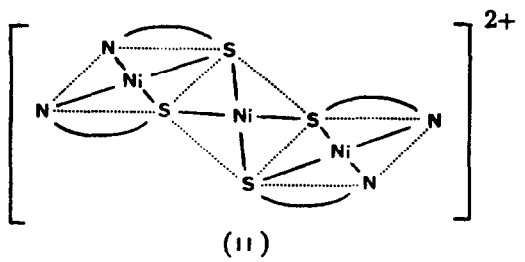
**Abstract**—The complexes $Ni_6(MPDMA)_{12}$, $[Ni_6(MPDMAH)_{12}]X_{12}$ $X = (I, ClO_4)$ and $Pd_2(MPDMA)_2Cl_2$ ($MPDMA = {}^-S{-}(CH_2)_3{-}N(CH_3)_2$) have been prepared and characterized. An X-ray diffraction study shows that the structure of $[Ni_6(MPDMAH)_{12}]$ $(ClO_4)_{12}$ consists of a cyclic hexanuclear array of nickel atoms linked by sulphur bridging ligands. Infrared and electronic spectra show that there is no chelation in any of the nickel complexes. However, coordination through the nitrogen atoms occurs in the palladium complex. This behaviour differs from that of the homologous β-mercaptoamine, which forms monomeric chelate complexes with both nickel and palladium.

γ-Mercaptoamines as ligands and particularly the different behaviour between these and the homologous β-mercaptoamines has been subject of study in this laboratory.[1–3]

The reaction of β-mercaptoethylamine with Ni(II) yields two complexes of stoichiometry $[Ni_3(MEA)_4]X_2$ ($MEA = H_2N{-}(CH_2)_2{-}S^-$; X = halogen) and $Ni(MEA)_2$.[4] Their structure has been solved by X-ray diffraction.[2,5]




(I)




(II)

Analogously, by reacting the γ-mercaptopropylamine with Ni(II) the complexes $Ni(MPA)_2$ and $[Ni_3(MPA)_4]X_2$ ($MPA = H_2N{-}(CH_2)_3{-}S^-$) can be prepared.[1,2] The green complex $Ni(MPA)_2$ has probably the same structure as its homologous $Ni(MEA)_2$. The X-ray analysis of $[Ni_3(MPA)_4]Cl_2$ has a structure similar to $[Ni_3(MEA)_4]Cl_2$. The main difference lies in the angle between the planes $[NiS_4]$ and $[NiS_2N_2]$, which is wider in the former complex because of the steric requirement of the ligand.[1] Consequently, the difference in behaviour of MEA and MPA as ligands is very small.

Tertiary aliphatic amines seldom coordinate to metal salts but their coordinating power is enhanced if the group forms part of a molecule having a second coordinating group in such a position that the two groups can form a chelate unit. This is the case of N,N - dimethyl - β - mercaptoethylamine[6] in the complex $Ni(MEDMA)_2$ (Structure I) ($MEDMA = (CH_3)_2N{-}(CH_2)_2{-}S^-$). It seems then interesting to know whether chelation occurs when the thiol and the $-N(CH_3)_2$ groups are in the γ position.

*Author to whom correspondence should be addressed.

## EXPERIMENTAL

*Preparations*

The ligand was obtained from N,N - Dimethyl-3 - amino - 1 - propanol)[7] according to previously published procedures.[8]

$Ni_6(MPDMA)_{12}\cdot 3H_2O$

To a suspension of the ligand (8.4 mmols) in 100 $cm^3$ of water, a solution of nickel chloride (4.2 mmols) in 30 $cm^3$ of 2 M ammonia was slowly added with stirring. The red–brown solution formed was further stirred for 15 min. and then extracted with four portions of 20 $cm^3$ of chloroform each. The chloroform solution was dried with anhydrous potassium carbonate and evaporated to dryness yielding a viscous liquid which crystallized in a desiccator over silica gel after a few weeks. Found: Ni, 18.84; C, 39.45; H, 8.14; N, 9.08. Calc. for $Ni_6C_{60}H_{150}N_{12}S_{12}O_3$: Ni, 19.32; C, 39.51; h, 8.23; N, 9.21%.

$[Ni_6(MPDMAH)_{12}][ClO_4]_{12}\cdot 2H_2O$ (MPDMAH = $(CH_3)_2\overset{+}{N}H-(CH_2)_3-S^-$)

*Method* 1. The complex $Ni_6(MPDMA)_{12}$ (3 mmols) was dissolved in 50 $cm^3$ of water and mixed with 33 $cm^3$ of 0.2 M perchloric acid. The red–brown solid was isolated by adding a large excess of $NaClO_4$ and cooling in ice for 4–6 hr. Single crystals were obtained by recrystallization from methanol.

*Method* 2. The complex was also prepared by direct reaction of nickel perchlorate (4.2 mmols) and the ligand 8.4 mmols) in 100 $cm^3$ of water and adding an excess of $NaClO_4$. Found: Ni, 11.32; C, 23.60; H, 5.19; N, 5.37; S, 12.35. Calc. for $Ni_6C_{60}H_{162}N_{12}S_{12}Cl_{12}O_{51}$: Ni, 11.74; C, 23.91; H, 5.31; N, 5.58; S, 12.75%.

$[Ni_6(MPDMAH)_{12}]I_{12}\cdot 10H_2O$

The complex can be obtained by the two methods described above but replacing perchlorate by iodide. It can be recrystallized from ethanol. Found: Ni, 10.09; C, 20.60; H, 4.47; N, 4.80. Calc. for $Ni_6C_{60}H_{176}N_{12}S_{12}O_{10}I_{12}$: Ni, 10.11; C, 20.66; H, 5.05; N, 4.82%.

$[Ni_6(MPTMA)_{12}]I_{12}\cdot 3H_2O$ (MPTMA = $(CH_3)_3\overset{+}{N}-(CH_2)_3-S^-$)

To a solution in chloroform of $Ni_6(MPDMA)_{12}$ (3 mmols), methyl iodide (6 mmols) was added very slowly and with vigorous stirring. Further stirring for 15 min. produced a red–brown precipitate. The product was filtered and washed with chloroform. Found: Ni, 9.87; C, 24.01; H, 5.11; N, 4.62; S, 10.58. Calc. for $Ni_6C_{72}H_{136}N_{12}S_{12}O_3I_2$: Ni, 9.99; C, 24.51; H, 5.28; N, 4.77; S, 10.89%.

$Pd_2(MPDMA)_2Cl_2$

A solution of the ligand (0.2 mmols) in methanol (2 $cm^3$) was added to a mixture of concentrated ammonia and methanol (1:3). Then, an aqueous solution of sodium tetrachloropalladate (0.3 mmols) was added with vigorous stirring. If a precipitate had appeared it was dissolved by heating and adding more water. The solution was allowed to evaporate and single crystals were formed after a few days. Found: C, 23.34; H, 4.56; N, 5.36. Calc. for $Pd_2C_{10}H_{24}N_2S_2Cl_2$: C, 23.09; H, 4.62; N, 5.39%.

*Physical measurements*

IR spectra were recorded as KX (X = Br, I) pellets using a Beckman IR-20A spectrophotometer. Electronic spectra were recorded on a Beckman Acta-III spectrophotometer.

*X-Ray data collection*

Diffraction data were collected on a Syntex four-circle diffractometer using $MoK_\alpha$ radiation. Fifteen accurately centered reflections were used to obtain an orientation matrix for data collection and cell dimensions. Intensities of 6177 independent reflections were measured and of these only 3387 were used for structural determination, having $|F| > 5 \times \sigma(F)$. The crystals are monoclinic, with $a = 36.842(6)$, $b = 16.077(2)$, $c = 25.403(3)$ (Å) and $\beta = 118.36°(4)$, and space group Cc or C2/c. The latter group was chosen and subsequent refinement of the structure showed that the choice had been correct.

*Solution and refinement of the structure*

The Ni and S positions were found by direct methods.[9] The SHELX 76 program system[10] was used in the subsequent structure development and refinement. Non-hydrogen atoms were located on successive difference Fourier maps. Isotropic refinement converged to R = 13.02 and Rw = 13.46.[11] All the heavy atoms except for the O atoms, which showed large isotropic thermal parameters, were refined anisotropically leading to values of R = 10.14 and Rw = 10.76.

The perchlorate anions appeared to be highly disordered. Since a final difference Fourier showed only one peak higher than 1e/$A^3$, which occurred in the vicinity of the perchlorate labelled as 3, disorder was considered in this case. No other attempts were made along this line since all the remaining peaks in the neighbourhood of the anions had electronic densities smaller than 0.8 e/$A^3$.

A complete list of bond lengths within the ligands, final atomic coordinates, thermal para-

maters and a list of Fo/Fc values have been deposited with the Editor as supplementary data. Atomic coordinates have also been deposited with the Cambridge Crystallographic Data Centre.

## RESULTS AND DISCUSSION

*Preparative*

The hygroscopic complex $Ni_6(MPDMA)_{12}$ is soluble in both polar and non-polar solvents. The protonation of the dimethylamino group accounts for its solubility in polar sovents. In a mixture of chloroform and water the following equilibrium takes place:

$$\underset{\text{(chloroform)}}{Ni_6(MPDMA)_{12}} \underset{+nH^+}{\overset{-nH^+}{\rightleftharpoons}} \underset{\text{(water)}}{[Ni(MPDMA)_{12-n}(MPDMAH)_n]^{n+}}$$

and thus it can be displaced to the left or to the right by changing the pH.

On reacting a metal chelate mercaptoamine complex with methyl iodide, the sulphur atom is methylated.[12] However, the nitrogen atom is methylated when the $Ni_6(MPDMA)_{12}$ complex reacts in the same conditions. This fact is in agreement with the non-coordination of the nitrogen atom in $Ni_6(MPDMA)_{12}$.

*Description of the structure of* $[Ni_6(MPDMAH)_{12}][ClO_4]_{12}$

The most significant bond lengths and angles are listed in Table 1. The numbering system employed is displayed in Fig. 1.

The crystal structure consists of hexanuclear cations $[Ni_6(MPDMAH)_{12}]^{12+}$ and perchlorate anions. The ligand is coordinated to metal atoms only by bridging sulphur atoms, so there is no chelation.

The structure of the cation can be described as a cyclic hexanuclear array of nickel atoms, all of them lying rigorously in a plane, as a consequence of the presence of a crystallographic inversion centre placed in the centre of the cation. The geometry around the nickel atoms is approximately square planar. The $[NiS_4]$ units form the rectangular faces of a hexagonal prism, where the sulphur atoms are located at the corners, and they lie on least square planes 1.45 Å above and below the plane of the nickel atoms. All the Ni–S bond distances are in the interval 2.212–2.178 Å in agreement with literature data.[5] The units $[Ni(1)S_4]$ and

Table 1. Intramolecular distances and angles in the unit $[Ni_6S_{12}]$

| Distances (Å) | | Angles (Deg.) | |
|---|---|---|---|
| Ni(1) – S(1) | 2.215(7) | S(1)Ni(1)S(2) | 81.2(2) |
| Ni(1) – S(2) | 2.187(5) | S(1)Ni(1)S(3) | 97.9(2) |
| Ni(1) – S(3) | 2.195(5) | S(2)Ni(1)S(4) | 98.8(2) |
| Ni(1) – S(4) | 2.211(8) | S(3)Ni(1)S(4) | 82.2(2) |
| Ni(2) – S(1) | 2.208(6) | S(1)Ni(2)S(2) | 81.4(2) |
| Ni(2) – S(2) | 2.183(7) | S(1)Ni(2)S(6) | 98.6(3) |
| Ni(2) – S(5) | 2.198(7) | S(2)Ni(2)S(5) | 97.9(3) |
| Ni(2) – S(6) | 2.188(7) | S(5)Ni(2)S(6) | 82.0(2) |
| Ni(3) – S(3) | 2.188(8) | S(3)Ni(3)S(4) | 82.4(3) |
| Ni(3) – S(4) | 2.212(7) | S(3)Ni(3)S(5) | 97.7(3) |
| Ni(3) – S(5) | 2.203(7) | S(4)Ni(3)S(6) | 98.3(3) |
| Ni(3) – S(6) | 2.177(8) | S(5)Ni(3)S(6) | 82.1(3) |
| S(1) – S(2) | 2.864(9) | | |
| S(3) – S(4) | 2.898(10) | | |
| S(5) – S(6) | 2.879(9) | | |
| Ni(1) – Ni(2) | 2.840(2) | | |
| Ni(1) – Ni(3) | 3.018(2) | | |
| Ni(2) – Ni(3) | 2.931(2) | | |

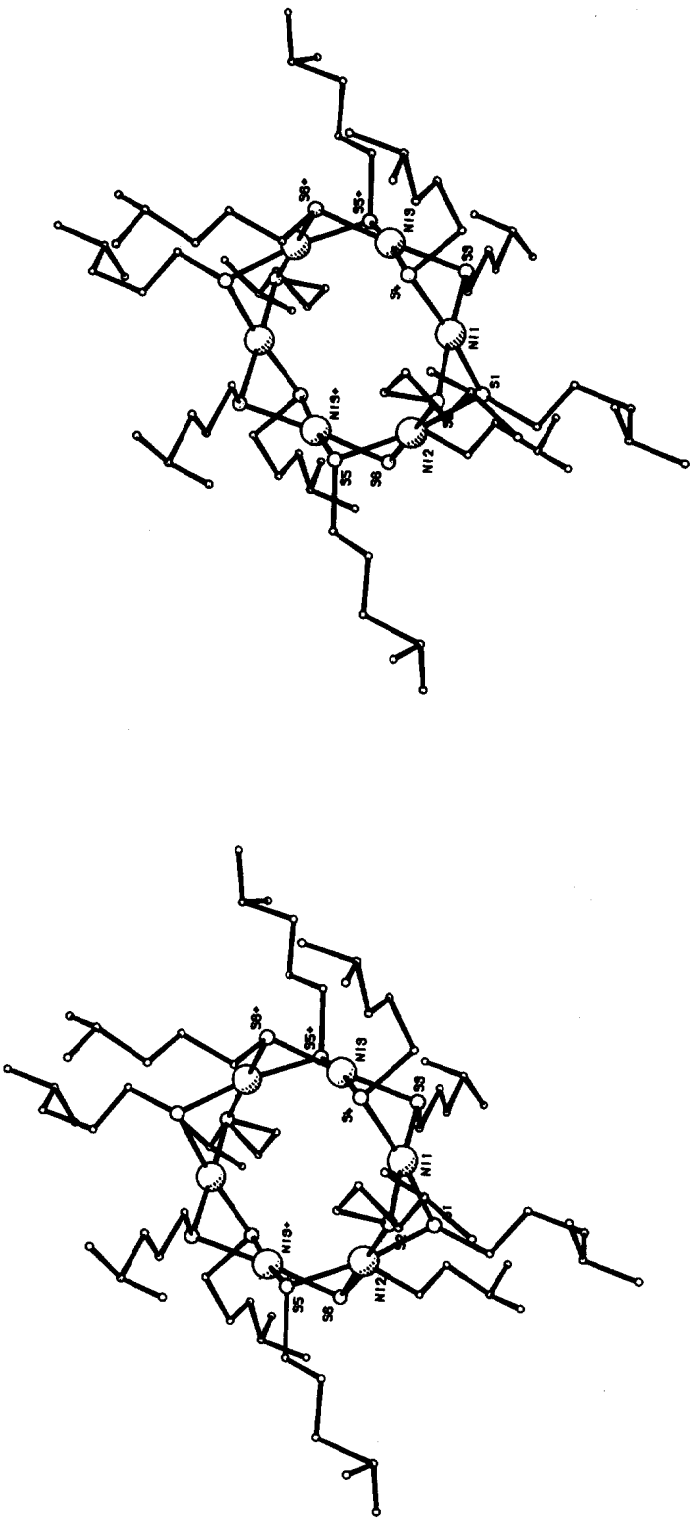



Fig. 1. A stereoscopic view of the cation $[Ni_6(MPDMAH)_{12}]^{12+}$.

[Ni(3)$S_4$] are approximately planar (Table 2), but [Ni(2)$S_4$] is folded along the axis determined by the atoms S(6)–S(2). The S–Ni–S angles for which both the sulphur atoms lie on the same side of the plane defined by the nickel atoms average 98.0(3)° and are 16° greater than those for which the sulphur atoms lie on the opposite sides of the plane (81.9(3)°).

The [$NiS_4$] planes are perpendicular, within experimental error, to those formed either by the nickel atoms or by any of the two sets of sulphur atoms. The hexagonal prism is not exactly regular, the dihedral angles between [$NiS_4$] planes deviating from the theoretical value of 120° (Table 2). The Ni–Ni distances average 2.930(2) Å which are probably long enough to prevent any Ni–Ni interaction.

There are two ranges of S–S distances. For the sulphur atoms placed in the same hexagonal face of the prism the S–S distances average 3.320(10) Å, while for the sulphur atoms lying on opposite sides of the nickel plane they average 2.881(10) Å, 0.32 Å shorter than S–S non-bonded distance.[13] Attractive S–S forces have been considered in thiolate metal complexes in order to explain S–S short contacts.[14]

All the $Ni_2S_2$ rings show an anti isomerism.[14] Half of the S–C bonds are approximately parallel to the plane of nickel atoms (axial), while the other half is approximately normal to that plane (equatorial).

Similar cyclic polynuclear complexes have been prepared with ethanethiol[15] and 2-hydroxyethanethiol.[16] The structure of their nickel complexes have been solved by X-ray diffraction, the unit [$Ni_6S_{12}$] being nearly the same in all of them. The crystal structure of a cyclic tetranuclear complex of Ni(II) with the ligand N-methyl-4-mercaptopiperidine has been reported recently.[17] The different degree of polymerization in thiolate complexes has been attributed to steric requirements of the ligands.[17]

*IR spectra*

On comparing the spectra (4000–2000 $cm^{-1}$) of the complex $Ni_6$(MPDMA)$_{12}$ with that of the ligand (Fig. 2), no significant difference can be observed. The bands at 2940 and 2860 $cm^{-1}$ are assigned to $\gamma$(C–H) stretching vibrations of the $-CH_2-$ groups. The bands at 2810 and 2780 $cm^{-1}$ are characteristic of the $\gamma$(C–H) vibrations of the methyl group bonded to a nitrogen atom which retains its lone pair of electrons.[18] Therefore, in this complex the amine group is not coordinated to the metal atom. The absence of the $\gamma$(S–H) in the spectrum of the complex agrees well with the coordination only through the sulphur atom. The same argument can be used on comparing the

Table 2. Selected least-squares planes and deviations (in Å) of individual atoms from these planes

| Plane 1 | | Plane 2 | |
|---|---|---|---|
| Ni(1) | 0.055 | Ni(3) | 0.017 |
| S(1) | −0.083 | S(3) | 0.109 |
| S(2) | 0.053 | S(4) | −0.111 |
| S(3) | 0.080 | S(5) | −0.086 |
| S(4) | −0.103 | S(6) | 0.072 |

| Plane 3 | | Plane 4 | |
|---|---|---|---|
| Ni(2) | 0.014 | Ni(2) | −0.163 |
| S(1) | 0.002 | S(2) | 0.179 |
| S(2) | −0.008 | S(5) | −0.143 |
| S(6) | −0.008 | S(6) | 0.126 |

Angles between planes (deg.)

1–2: 128.5; 1–3: 114.3; 2–4: 124.9; 3–4: 12.1

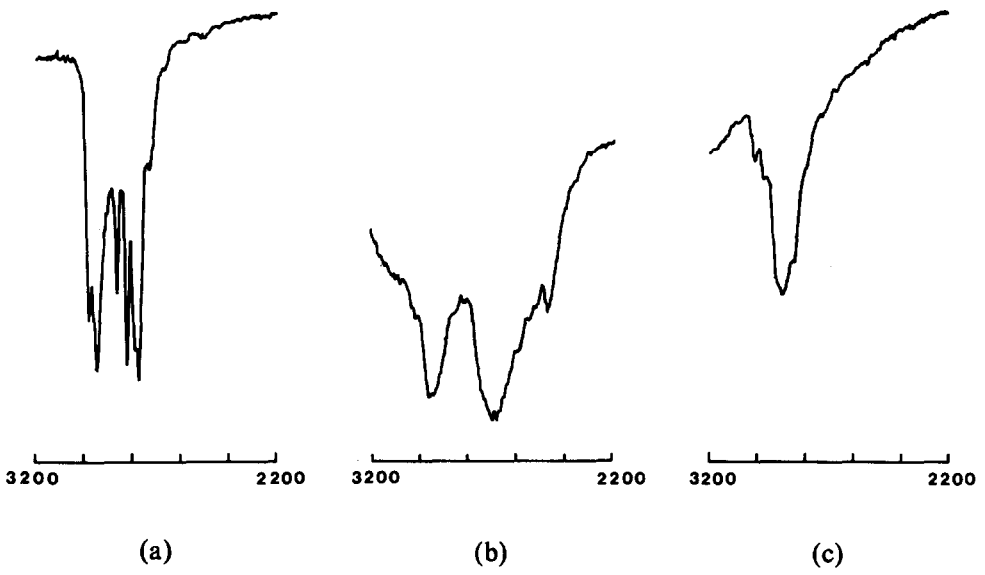



Fig. 2. IR spectra ($\bar{\nu}$ in $cm^{-1}$). (a) $Ni_6(MPDMA)_{12}$. (b) $[Ni_6(MPDMAH)_{12}]$ $(ClO_4)_{12}$. (c) $Pd_2(MPDMA)_2Cl_2$.

spectra of $[Ni_6(MPDMAH)_{12}]X_{12}$ (X = I, $ClO_4$) and $(MPDMAH_2)I$ (Fig. 2). The spectra show clearly two bands at 2940 $cm^{-1}$ and 2700 $cm^{-1}$ assigned respectively to $\gamma$(C–H) and $\gamma$(N–H). On the other side the spectrum of the $[Ni_6(MPTMA)_{12}]I_{12}$ shows a sharp band at 3000 $cm^{-1}$ characteristic of the $-\overset{+}{N}-(CH_3)_3$ group.[19] Therefore, in these complexes there is no coordination through the nitrogen atom.

Finally, the spectrum of $Pd_2(MPDMA)_2Cl_2$ shows a broad band at 2900 $cm^{-1}$ assigned to $\gamma$(C–H) vibrations. The absence of the bands at 2810 and 2780 $cm^{-1}$ ($-N(CH_3)_2$), and 2700 $cm^{-1}$ ($\gamma$(N–H)) is characteristic of coordinated dimethylamine groups.[18]

*Electronic spectra*

There is not any significant difference between the electronic spectra (800–300 nm) of methanolic solutions of $Ni_6(MPDMA)_{12}$, $[Ni_6(MPDMAH)_{12}]X_{12}$ (X = I, $ClO_4$) and $[Ni_6(MPTMA)_{12}]I_{12}$. The spectral bands (absorption maxima in nm($\epsilon$)) appear at 530(1050), 407(3370) and 335(8760). Therefore it seems reasonable to propose for all the nickel complexes here reported a cyclic hexanuclear structure analogous to that of $Ni_6(MPDMAH)_{12}(ClO_4)_{12}$. The fact that the positions of the absorption band maxima for the complex cyclotetrakis bis($\mu$ - N - methylpiperidine-4 - thiolato)nickel(II)[17] are somewhat shifted if compared to the previous ones supports the above conclusion.

## CONCLUSIONS

The X-ray analysis of $[Ni_6(MPDMAH)_{12}][ClO_4]_{12}$ together with the infrared and electronic spectra of all nickel complexes indicate that all of them have essentially the same structure, which consists of a toroid of six metal atoms bridged by twelve sulphur atoms. In all cases, the nitrogen atoms do not coordinate, and they are present either as a free base, or protonated, or methylated, depending on the complex. However, with Ni(II) the homologous $\beta$-mercaptoamines always coordinate through the nitrogen atom forming a chelate. This can be attributed to the higher stability of a five atoms chelate ring versus a six-membered ring. This is, to our knowledge, the first difference reported between the behaviour as ligands of a $\beta$-mercaptoamines and the corresponding $\gamma$-derivates.

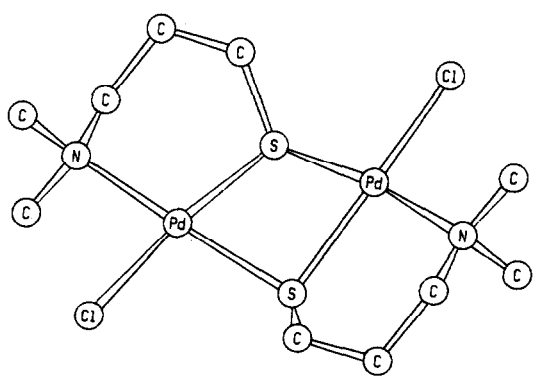



Fig. 3. The structure of $Pd_2(MPDMA)_2Cl_2$.

However, MPDMA forms a dimeric complex with Pd(II). The structure of the complex shows that the ligand behaves as a chelate[3] (Fig. 3).

Apparently, the greater size of Pd(II) can make the chelate stable in spite of the slight tendency of the tertiary amine to coordinate through the nitrogen atom. Furthermore, the dimeric structure is favoured by the higher stability of chloropalladate complexes versus chloronickelates.

Summarizing, while MPDMA has a selective behaviour towards Ni(II) and Pd(II), forming a chelate only with the latter metal atoms, MEDMA chelates both, Ni(II) and Pd(II).

## REFERENCES


1. H. Barrera, J. Suades, M. C. Perucaud and J. L. Briansó, Submitted for publication in Polyhedron.
2. J. Suades, X. Solans and M. Font-Altaba, Submitted for publication in Polyhedron.
3. X. Solans, M. Font-Altaba, J. L. Briansó, J. Sola, J. Suades and H. Barrera, *Acta Cryst.* 1983, **C39**, 1653.
4. D. C. Jicha and D. H. Busch, *Inorg. Chem.* 1962, **1**, 872.
5. C. H. Wei and L. F. Dahl, *Inorg. Chem.* 1970, **9**, 1878.
6. C. A. Root and D. H. Busch, *Inorg. Chem.* 1968, **7**, 789.
7. A. Kaluszyner and A. B. Galun, *J. Org. Chem.* 1960, **26**, 3536.
8. B. C. Cossar, J. O. Fournier, D. L. Fields and D. D. Reynolds, *J. Org. Chem.* 1962, **27**, 93.
9. M. M. Wolfson, P. Main, L. Lessinger, C. Germain and J. P. Declerq, (1976) MULTAN. *A System of Computer Programs for Crystal Structure Determination From X-Ray Diffraction Data.* University of York, England and University of Louvain, Belgium.
10. G. M. Sheldrick, (1976). SHELX. *A Computer Program For Crystal Structure Determination.* University of Cambridge, England.
11. The function minimized was $w\|Fo| - |Fc\|^2$ where $w = (\sigma^2(Fo) + 0.00367|F|^2)^{-1}$.
12. D. H. Busch, J. A. Burke, D. C. Jicha, M. C. Thompson and M. L. Morris *Adv. Chem. Ser.* 1963, **37**, 125.
13. R. L. Girling and E. L. Amma, *Acta Cryst.* 1976, **B-32**, 2903.
14. J. P. Fackler, *Progr. Inorg. Chem.* 1976, **21**, 55.
15. P. Woodward, L. F. Dahl, E. W. Abel and B. C. Crosse, *J. Am. Chem. Soc.* 1965, **87**, 5251.
16. R. O. Gould and M. M. Harding, *J. Chem. Soc.* (*A*) 1970, 875.
17. W. Gaete, J. Ros, X. Solans, M. Font-Altaba and M. C. Briansó, *Inorg. Chem.* 1984, **23**, 39.
18. J. T. Braunholtz, E. A. V. Ebsworth, F. G. Mann and N. Sheppard, *J. Chem. Soc.* 1958, 2780.
19. N. B. Colthup, L. H. Dahl and S. L. Wiberley, *Introduction to IR and Raman Spectroscopy.* Academic Press, New York (1964).

*Polyhedron* Vol. 3, No. 8, pp. 977–982, 1984
Printed in the U.S.A.

0277–5387/84 $3.00 + .00
© 1984 Pergamon Press Ltd.

# ELECTRON TRANSFER REACTION WITH AMIDE—ONE ELECTRON OXIDANT SYSTEM IN SOLUTION

**FIROZ AHMAD and VIKRAM SINGH BASWANI***
Department of Chemistry, Aligarh Muslim University, Aligarh 202001, India

(*Received* 10 *May* 1981†; *accepted* 28 *November* 1983)

**Abstract**—The kinetics of reduction of Mn(III) by acetamide, formamide (F), N-methylformamide (NMF), and N,N-dimethylformamide (DMF) have been measured spectrophotometrically at 50°C in aqueous acid perchlorate media. Four moles of Mn(III) are consumed for formamides and two moles of Mn(III) are consumed per mole of acetamide, leading in each case to the formation of the respective amines. All rates were first order in each reactant and were independent of $[Mn^{2+}]$ and $[NaClO_4]$. The reciprocals of observed rate constants are inversely dependent on acidity. A free radical mechanism consistent with these results has been proposed for the reactions. Activation energies and entropies are calculated for each reaction.

Amides are favoured solvent media for carrying out synthesis and investigating the kinetics of organic reactions, but electron transfer processes involving amides have been neglected. Kinetic studies of the oxidation of amides by Tl(III), persulphate and Ce(IV) have been reported and different mechanisms suggested.[1–3] Our observations on these oxidations are different from those of earlier researches. Here we propose a probable mechanism which satisfies the kinetic behaviour of oxidation of amides by manganese(III) in perchloric acid. The use of manganese(III) in perchloric acid simplifies the interpretation of the oxidation processes as uncomplexed manganic ions exist in significant concentration in perchloric acid solutions.[4,5] The interpretation of kinetic data is further simplified by the use of the well characterized Mn(III)–Mn(II) system in the presence of a large excess of Mn(II) in perchloric acid medium.[6] In the present paper we report a study of the stoichiometry and kinetics of the reactions between manganese(III) and acetamide, formamide, N-methylformamide (NMF) and N,N-dimethylformamide (DMF) in aqueous perchloric acid solutions.

## EXPERIMENTAL

*Chemicals.* Manganese(II) perchlorate was prepared by dissolving manganese(II) carbonate in perchloric acid. The manganese(III) was prepared by slow electrolysis of manganese(II).[15] Total concentrations of manganese(III) were determined by addition of aliquots of acidic ferrous perchlorate followed by the spectrophotometric determination of Fe(III) at 260 nm ($\epsilon = 2.9 \times 10^3$).[7] Fresh solutions of Mn(III) were always prepared and used immediately after cessation of the electrolysis, as slow irreversible changes occur due to the tendency of manganese(III) to disproportionate to manganese(II) and $MnO_2$.

All chemicals used were of Analar grade, or of the purest class available and triply distilled water was used throughout. Sodium perchlorate (Koch Light Laboratories, England) was used to maintain the ionic strength at 3.8–5.4 M. The acid content of solutions was determined by titrating against standard alkali.

*Kinetics.* The kinetic studies were made spectrophotometrically using a Bausch and Lomb Spectronic-20. Solutions of Mn(III) and other reactants were thermostated separately in a temperature controlled (±0.1°C) water bath. The reaction was started by addition of the temperature equilibrated Mn(III) to the reaction mixture. The progress of the reaction was followed by determining Mn(III) spectrophotometrically at 470 nm after suitable intervals of time and the concentration of Mn(III) was directly read from the calibration curve obtained by plotting [Mn(III)] against absorbance. In most of the cases the reaction was followed to well over 80% completion. All rate measurements described here were made at 50°C unless otherwise stated. Pseudo first order rate

*Author to whom correspondence should be addressed.

†Delay caused by loss of manuscript in the mail—Editor.

constants reported here are the slopes of the log[Mn(III)] against time plots. Duplicate rate measurements were reproducible to ±5%.

The rate of oxidation of all the amides was inhibited in the presence of acrylonitrile, which indicates the presence of free radicals. In the present investigation the involvement of free radicals in the reaction mixture was also indicated by the addition of traces of iodine[8] which was found to accelerate the reaction rate in all cases. An increase in the ionic strength from 3.8–6.3 M ($NaClO_4$) had no effect on any of the reaction rates.

*Identification of product.* With formamide, N-methylformamide and N,N-dimethylformamide as reductants the final products are ammonia,[9] methylamine[10] and dimethylamine,[11] respectively, while, with acetamide, ammonia and acetic acid are the final products and these products did not undergo oxidation under the conditions employed. The presence of $CO_2$ was confirmed in each case except acetamide and was measured gasometrically, the results were in agreement with the proposed stoichiometry.

*Stoichiometry.* The stoichiometry of the reaction was determined by adding a standardized solution of Mn(III) to excess of amide. At the end of the reaction the excess of perchloric acid was neutralized with standard sodium hydroxide and then the amount of unreacted amide in the reaction mixture was determined by Bergman's method.[12] Reproducible results could be obtained only when the test was employed at pH = 5–6. The $\Delta$[Mn(III)]/$\Delta$[amide] ratio was found to be 4.1 for formamides and 2.1 for acetamides. The slightly higher values of moles of oxidant consumed over the stoichiometric requirements as given by equations (a) and (b) may be due to a minor reaction path involving oxidation of water. The reactions may be presented according to the equations

$$HCONR_1R_2 + 4Mn(III) + 2H_2O \rightarrow 4Mn^{2+} + HNR_1R_2 + CO_2 + \tfrac{1}{2}O_2 + 4H^+ \quad (a)$$

(where $R_1$ and $R_2$ = H or $CH_3$).

For acetamide the total reaction is:

$$CH_3CONH_2 + 2Mn(III) + 2H_2O \rightarrow 2Mn^{2+} + CH_3COOH + NH_3 + \tfrac{1}{2}O_2 + 2H^+. \quad (b)$$

## RESULTS AND DISCUSSION

The plot of log[Mn(III)] against time indicates a first order dependence of rate on [Mn(III)] in all cases. The slopes of these plots gave $k_{obsd}(s^{-1})$ as reported in the tables at different amide concentrations.

The order of the reaction with respect to amide was determined by varying the amide concentration while keeping other variable constant. Plots of $k_{obsd}$ against [amide] indicate a first order dependence of reaction rate on [amide]; Table 1 collects the data for all the amides. Additional measurements were performed at different $Mn^{2+}$ concentrations by varying manganous perchlorate. $Mn^{2+}$ does not seem to affect the rate constant upto a concentration of 0.60 M which is nearly 100 times of the concentration of Mn(III) in the reaction mixture.

Hydrogen ion concentration was varied with perchloric acid in the range 2.0–5.0 M at constant $\mu$ = 5.0 adjusted with sodium perchlorate. The reaction rates increase with the increase of [$HClO_4$] and the plots of $1/k_1'$ vs $1/[H^+]$ is linear, Table 2 (where $k_1' = k_{obs}/[amide]$).

Oxidation of amides is complicated by the possi-

Table 1. Pseudo first order rate constants $10^{-6}\ k_{obs}\ s^{-1}$ for the oxidation of amides by Mn(III) at 50°C; [Mn(III)] = 0.005 M; [$HClO_4$] = 3.75 M and $\mu$ = 3.78 M for all the amides

| [AMIDE] (M) | $CH_3CONH_2$ | $HCONH_2$ | HCONHMe | $HCONMe_2$ |
|---|---|---|---|---|
| 0.025 | 6.5 | 35.0 | 18.0 | 20.0 |
| 0.05 | 14.0 | 76.6 | 40.0 | 52.0 |
| 0.10 | 20.0 | 133.3 | 62.0 | 85.3 |
| 0.15 | 26.6 | 191.6 | 100.0 | 133.3 |
| 0.20 | 35.0 | 264.0 | 135.0 | 183.3 |

Table 2. Kinetic data for reactions of $Mn^{III}$ with amides at different acidities and temperatures, $k_1'$ in $M^{-1} \times 10^{-4}$ [Mn(III)] = 0.005 M; [Amide] = 0.05; $\mu$ = 5.0 M

| AMIDE | T (K) | $[HClO_4]$, M | | | | | | |
|---|---|---|---|---|---|---|---|---|
| | | 2.0 | 2.5 | 3.0 | 3.5 | 4.0 | 4.5 | 5.0 |
| $MeCONH_2$ | 313 | - | 0.78 | 0.87 | 0.97 | 1.10 | - | - |
| | 323 | 1.67 | 2.30 | 2.40 | 2.76 | 3.10 | 3.53 | 3.60 |
| | 333 | - | 3.33 | 4.00 | 4.66 | 5.33 | - | - |
| $HCONH_2$ | 313 | - | 7.33 | 8.66 | 9.33 | 10.00 | - | - |
| | 323 | 10.33 | 12.00 | 12.66 | 14.33 | 16.33 | 18.33 | 19.00 |
| | 333 | - | 22.66 | 25.33 | 28.00 | 30.33 | - | - |
| HCONHMe | 313 | - | 4.00 | 4.66 | 5.66 | 6.33 | - | - |
| | 323 | 5.66 | 6.66 | 7.33 | 8.33 | 10.00 | 11.33 | 12.00 |
| | 333 | - | 12.66 | 14.33 | 16.66 | 18.33 | - | - |
| $HCONMe_2$ | 313 | - | 5.66 | 7.33 | 9.00 | 10.50 | - | - |
| | 323 | 8.00 | 9.00 | 9.66 | 11.00 | 12.66 | 14.66 | 15.33 |
| | 333 | - | 16.66 | 20.00 | 23.33 | 26.66 | - | - |

bility that the reaction may simply be,

(a) $HCONHR + H_2O \rightarrow HCOOH + NH_2R$

(b) $HCOOH + M^{n+} \rightarrow$ product

(where $M^{n+}$ is an oxidant).

However, if step (a) is the rate determining step then the reaction rate should be independent of $[M^{n+}]$. On the other hand if step (b) determines the rate then $k_{obs}$ and activation parameters for the reaction under study should not be different from those obtained for the oxidation of formic acid.

It appears that the oxidation of amides by Mn(III) is taking place by the interaction of protonated amide with the oxidant. We do not favour the route involving Mn(III)-amide complex as suggested with Co(III).[13] In the oxidation of alcohols it was demonstrated by Waters that the oxidation by cobalt(III) always involves a Co(III)-substrate complex whereas oxidation by Mn(III) does not favour such complex formation.[14] However, as amides are basic there are two equilibria and four possible rate determining steps involved.

$$A + H^+ \overset{K_a}{\rightleftharpoons} AH^+ \text{ (A = unprotonated amide)} \quad (1)$$

$$Mn^{3+}_{aq} \overset{K_h}{\rightleftharpoons} MnOH^{2+}_{aq} + H^+_{aq} \text{ (Ref. 14(a) and (b))}$$

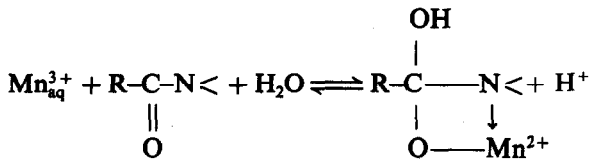
$$Mn^{3+}_{aq} + A \xrightarrow{k_1} \text{product} \quad (3)$$

$$Mn^{3+}_{aq} + AH^+ \xrightarrow{k_2} \text{product} \quad (4)$$

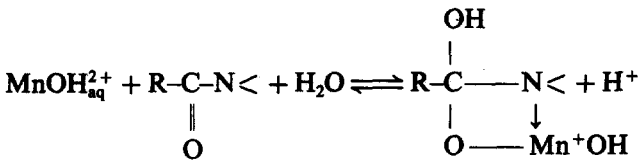
$$MnOH^{2+}_{aq} + A \xrightarrow{k_3} \text{product} \quad (5)$$

$$MnOH^{2+}_{aq} + AH^+ \xrightarrow{k_4} \text{product.} \quad (6)$$

Our kinetic data favour step (4) as the most significant path through which oxidation is taking place. Interaction of the oxidant with unprotonated amide may result in the formation of stable complexes (I) and (II) whose decomposition into product may be insignificant. A slight shift in the absorption of manganese(III) spectra is observed in the presence of amides at very low temperature.

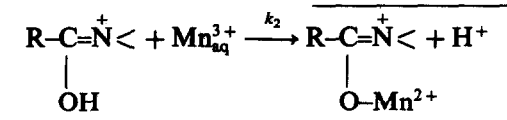


(I)

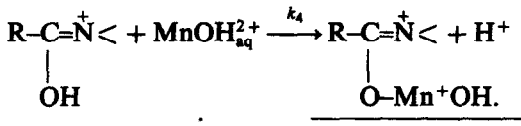


(II)

But the interaction of $Mn^{3+}_{aq}$ and $MnOH^{2+}_{aq}$ with protonated amide should be considered.



(III)



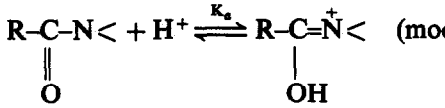
(IV)

Because of linear dependence of $1/k_1'$ vs $1/[H^+]$, we favour interaction of protonated amide with $Mn^{3+}_{aq}$ as the major reaction path. Gasometric results indicate that in the total gas produced there is one mole of oxygen for two moles of $CO_2$. Moreover, there is no change in the total moles of gas produced or $CO_2/O_2$ with the change in acid concentration. This fact also suggests that there is probably only one major reaction path. Therefore, the most probable mechanism of the reaction is,

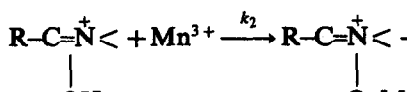
which gives the following rate law,

$$\text{rate} = n\{k_2 + k_4K_h/[H^+]\}\frac{[Mn^{3+}]_T}{(1 + K_h/[H^+])} \times \frac{[\text{amide}]_T}{(1 + 1/K_a[H^+])}$$

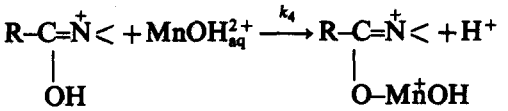
where subscript T indicates analytical concentration. As $[H^+] > 1$, a value of $K_a = 0.6$ at 50°C[19] will make $(1 + 1/K_a[H^+])$ almost constant.



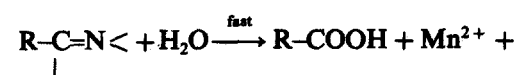
(moderate) (Ref. 15) (1)



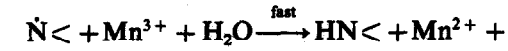
(slow) (2)



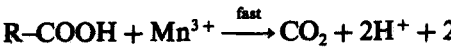
(minor reaction path) (2a)



(Ref. 16) (3)



(Ref. 17) (4)



(Ref. 18) (5)

(when R=H)

$$\text{rate} = n\left(\frac{k_2 + k_4K_h/[H^+]}{1 + K_h/[H^+]}\right) \cdot [Mn^{3+}]_T[\text{amide}]_T.$$

$K_h$ is 1.30 at 34.5°C[20] and should have larger value at 50°C, it is evident that $K_h/[H^+]$ is not insignificant. Therefore, the above equation gives,

$$\text{rate} = n\left(\frac{k_2[H^+] + k_4K_h}{[H^+] + K_h}\right)[Mn^{3+}]_T[\text{amide}]_T.$$
$$= k_{obs}[Mn^{3+}]_T$$

where

$$k_{obs} = n\left(\frac{k_2[H^+] + k_4K_h}{[H^+] + K_h}\right)[\text{amide}]_T.$$

giving

$$k_1' = \frac{k_{obs}}{[\text{amide}]_T} = \left(\frac{k_2[H^+] + k_4K_h}{[H^+] + K_h}\right)n. \qquad (1)$$

For formamides $n = 4$ and for acetamide $n = 2$, where $k_1'$ is the second order rate constant for the oxidation of an amide. If $k_2 > k_4K_h$, we get

$$k_1'(1 + K_h/[H^+]) = k_2.$$

Using kinetic data for the oxidation of formamide we calculated mean value of $K_h$ as $1.1 \pm 0.2$ M at 50°C. $K_h$ is 1.30 at 34.5°C as reported by Davies.[21] Using our value of $K_h$ we calculated $k_2$ for the oxidation of all the amides at different $[H^+]$. The mean of $k_2'$s for each amide is reported in Table 3. With these mean values of $K_h$ and $k_2$ evaluation of $k_4$ was done by using eq (1) at different $[H^+]$. The mean values of $k_4$ for each amide is also reported. The relative values of $k_2$ and $k_4$ indicate that $k_2 > k_4$ and justifies our earlier assumption. $k_1'$ at different $[H^+]$ at 40, 50 and 60°C are known. This was utilized to evaluate the activation parameters associated with $k_2$ and $k_4$. Plots of $1/k_1'$ vs $1/[H^+]$ did give the expected straight lines obeying,

$$1/k_1' = \frac{1}{k_2} + \frac{K_h}{k_2[H^+]}$$

$K_h$ was evaluated from the values of slope and the intercept obtained by least square method using the data for formamide reaction. However, when $K_h$ was used to evaluate $k_2$ from the intercept ($1/k_2$) and slopes ($K_h/k_2$) for other amides, erratic results were obtained. Knowing that both $K_h$ and $k_2$ have rather low precision, ± 15%, larger deviations are not unexpected.

Comparisons of $k_{obs}$ for different amides shows that the reaction is slowest in the case of acetamide.

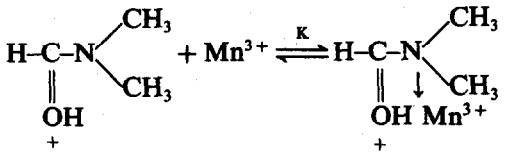
Table 3. Rate constants[a] and activation parameters[b] for the oxidation of amides

| AMIDE | T (K) | $k_2 \times 10^4$ | $\Delta E^*$ | $\Delta S^*$ | $k_4 \times 10^5$ | $\Delta E^*$ | $\Delta S^*$ |
|---|---|---|---|---|---|---|---|
| $MeCONH_2$ | 333 | 1.67 | 14.6 ± 0.8 | −34.1 ± 2.5 | 0.64 | 11.0 ± 1.8 | −51.7 ± 5.7 |
| | 323 | 0.97 | | | 0.28 | | |
| | 313 | 0.41 | | | 0.22 | | |
| $HCONH_2$ | 333 | 19.58 | 14.9 ± 1.9 | −28.4 ± 2.0 | 2.90 | 9.1 ± 1.3 | −63.5 ± 4.3 |
| | 323 | 7.00 | | | 1.50 | | |
| | 313 | 4.60 | | | 1.20 | | |
| HCONHMe | 333 | 7.00 | 15.2 ± 0.4 | −39.3 ± 1.2 | 2.43 | 10.4 ± 2.5 | −50.8 ± 7.9 |
| | 323 | 3.20 | | | 0.97 | | |
| | 313 | 1.60 | | | 0.88 | | |
| $HCONMe_2$ | 333 | 7.90 | 14.8 ± 1.4 | −30.4 ± 4.4 | 3.90 | 11.3 ± 1.7 | −56.2 ± 5.5 |
| | 323 | 5.05 | | | 1.70 | | |
| | 313 | 1.91 | | | 1.30 | | |

a - Units of Rate constants are $M^{-1}$ $sec^{-1}$.

b - Units of $\Delta E^*$ in Kcal $mol^{-1}$ and $\Delta S^*$ in cal $K^{-1}$ $mol^{-1}$.

This could be the case if the rate determining step (2) involves ionization of hydroxy group. As the rate determining step involves deprotonation of the amide it is expected that the presence of methyl group at carbon will discourage the process (acetic acid is a weak acid). The presence of methyl group at nitrogen may favour a minor secondary reaction path as shown below,



The K for DMF will be larger as compared to NMF.

The presence of free radical is indicated by the fact that the addition of traces of iodine enhances the reaction rate which could be due to the formation of hydroxylamine which reacts rapidly with manganese(III).[21] The formation of free radical $\dot{N}<$ has been reported.[16]

$$\dot{I} + \dot{N}< + H_2O \rightarrow OHN< + I^- + H^+$$

$$OHN< + 6Mn^{3+} + 3H_2O \rightarrow$$

$$6Mn^{2+} + NO_3^- + 7H^+.$$

This side reaction is strongly indicated by the fact that the total stoichiometry of the reaction is completely changed in the presence of iodine, almost 10 moles of manganese(III) are consumed per mole of amide.

*Acknowledgements*—The authors thank the referee for making some very useful and positive suggestions. VSB is grateful to CSIR for financial assistance.

## REFERENCES

1. S. S. Krishnamurthy and S. Sundarajan, *Proc. 1st Chemistry Symp. A.E.C., Bombay* 1969, **2**, 261; *C.A.* 1971, **74**, 3513d.
2. H. Singh and S. P. Srivastava, *J. Ind. Chem. Soc.* 1971, **48**, 725.
3. S. D. Saxena and K.S. Gupta, *J. Inorg. Nucl. Chem.* 1977, **39**, 329.
4(a). E. Mentasti, E. Pelizzetti, E. Pramauro and G. Giraudi, *Inorg. Chim. Acta.* 1975, **12**, 61. (b). G. Davies, *Inorg. Chem.* 1972, **11**, 2488. (c). C. F. Wells and D. Fox, *J. Inorg. Nucl. Chem.* 1976, **38**, 107. (d). D. R. Rosseinsky and R. J. Hill, *J. Chem. Soc.* 1972, 715.
5. G. Davies, *Coord. Chem. Rev.* 1969, **4**, 119.
6. E. Pelizzetti, E. Mentasti and C. Baiocchi, *J. Inorg. Nucl. Chem.* 1976, **38**, 557.
7. R. Bastian, R. Weberling and F. Palilla, *Anal. Chem.* 1956, **28**, 459.
8. R. M. Noyes and D. J. Sibbett, *J. Am. Chem. Soc.* 1953, **75**.
9. A. I. Vogel, *Quantitative Inorganic Analysis*, p. 643. Longmans, London (1951).
10. E. L. Stanley, H. Baum and J. L. Gove, *Anal. Chem.* 1951, **23**, 1779.
11. H. C. Dower, *Bio. Chem. J.* 1938, **32**, 455.
12. John Metchell, Jr. *et al., Organic Analysis*, Vol. 3, p. 188. Interscience, New York (1956).
13. F. Ahmad and Vikram S. Baswani, *Aust. J. Chem.* 1979, **32**, 537.
14(a). C. F. Wells and G. Davies, *Trans. Faraday Soc.* 1967, **63**, 2737. (b). C. F. Wells, C. Barnes and G. Davies, *Trans. Faraday Soc.* 1968, **64**, 3069. (c). D. G. Hoare and W. A. Waters, *J. Chem. Soc.* 1962, 965. (d). D. G. Hoare and W. A. Waters, *J. Chem. Soc.* 1964, 2552.
15. W. D. Philips, *J. Chem. Phys.* 1955, **23**, 1363.
16. P. Neta, P. Maruthamutha, P. M. Carton and R. W. Fessenden, *J. Phys. Chem.* 1978, **83**, 1875.
17. F. Ahmad and V. S. Baswani, *Int. J. Chem. Kinetics*, 1981, **13**, 565.
18. C. F. Wells and D. Whately, *J. Chem. Soc. Faraday Trans. I* 1972, 434.
19. M. Liler, *J. Chem. Soc. B* 1969, 385.
20. C. F. Wells and G. Davies, *J. Chem. Soc. A* 1967, 1858.
21. G. Davies and K. Kustin, *Inorg. Chem.* 1969, **8**, 484.

*Polyhedron* Vol. 3, No. 8, pp. 983–990, 1984
Printed in the U.S.A.

0277–5387/84 $3.00 + .00
© 1984 Pergamon Press Ltd.

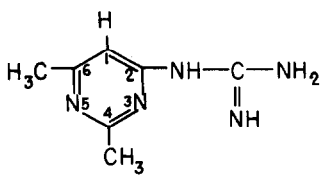
# METAL COMPLEXES OF PYRIMIDINE-DERIVED LIGANDS—IV.† SYNTHESIS, CHARACTERISATION AND COORDINATING PROPERTIES OF TWO GUANIDINO PYRIMIDINES: Ni(II) COMPLEXES WITH 2-GUANIDINO-4,6-DIMETHYL PYRIMIDINE AND 2-PHENYL GUANIDINO-4,6-DIMETHYL PYRIMIDINE—POTENTIAL LIGANDS OR BIOLOGICAL INTEREST

NITYANANDA SAHA* and DURGADAS MUKHERJEE
Department of Chemistry, University College of Science, 92, A.P.C. Road, Calcutta 700009, India

(*Received* 7 *June* 1983; *accepted* 15 *December* 1983)

**Abstract**—Synthesis and spectroscopic characterisation (IR, mass, PMR) of 2-guanidino 4,6-dimethyl pyrimidine (GPym) and 2-phenyl guanidino 4,6-dimethyl pyrimidine (PG-Pym) are reported. Complexation of the title ligands with nickel(II) salts in moisture-free condition furnish complex species of the type: $Ni(GPym)_2X_2$[X = Cl, Br, SCN and $NO_3$] and $Ni(PGPym)_2X_2$ [X = Cl, Br, I and SCN]. Physico-chemical characterisation of the complex species have been made from molar conductance data, magnetic susceptibility measurements, electronic and vibrational spectra. Magnetic and electronic spectral features suggest a pseudo-octahedral environment of the central Ni(II) ion in all these complexes. IR spectra have furnished positive information regarding the bonding sites of the ligand molecules (namely, the pyrimidyl nitrogen and the imino nitrogen of the guanidine residue) and the mode of the attachment of the counterion(X) to the metal ion.

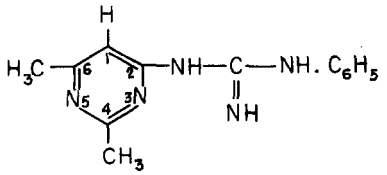
It is well-documented that pyrimidine derivatives play a significant role in many biological systems, the ring system being a component of nucleic acids, several vitamins, co-enzymes etc. and provide potential binding sites for metal ions. Moreover, pyrimidine analogues have the capacity to impede the bio-synthesis of pyrimidine nucleotides. Certain of the drugs with pyrimidine ring are employed in the treatment of neoplastic diseases and infections caused by fungi and DNA containing viruses. On the other hand, biguanides and guanyl ureas which have attracted much attention because of their well-acclaimed medicinal values (e.g. anti-malarial activity of paludrine) are also well established as coordinated agents. In the living systems, biguanide is known to undergo cyclisation to form triazine which is the active substance to act as anti-malarial drug. It was, therefore, considered necessary to have pyrimidine derivatives containing the guanidine moiety as a side chain, with the hope that the resulting compounds might have biological potency and with a view to study the coordination pattern of such ligands by complexation with metal ions in order to understand more precisely the role of such metal ions in living systems. As a part of our programme [1,2] of investigating the interaction of biologically potent pyrimidine-based ligands with metal ions, the present communication is intended to report the synthesis, characterisation and coordinating behaviour of the title ligands viz. the guanidino pyrimidines, together with preparation and physico-chemical characterisation of a few bis-Ni(II) complexes with the title ligands (**1a** and **1b**).




**1a**

*Author to whom correspondence should be addressed.

†For Part III: see Ref 2b.



**1b**

## EXPERIMENTAL

The title ligands viz. 2-guanidino 4,6-dimethyl pyrimidine and 2-phenyl guanidino 4,6-dimethyl pyrimidine were prepared by condensation reactions of free biguanide/phenyl biguanide with acetyl acetone according to similar but somewhat modified methods of Poddar *et al.*[3] Normal biguanide sulphate was prepared according to the method of Ray *et al.*[4] On recrystallisation from hot water the product melted at 230°C (lit. m.p 231°C). Free normal biguanide was obtained according to known methods.[5,6]

*Preparation of 2-guanidino-4,6-dimethyl pyrimidine.* 1.2 g (0.05 mole) clean and dried sodium dissolved in perfectly dry alcohol (50 $cm^3$) was refluxed with 5 g (0.025 mole) powdered biguanide sulphate for 1 hr with usual precautions. The resulting alcoholic solution of free biguanide was mixed thoroughly with freshly distilled acetyl acetone [3 g, 0.03 mole] and the resulting mixture was refluxed for 2 hr at water-bath temperature. The reaction mixture, upon cooling to room temperature (25°C) deposited fine needle-shaped white crystals; these were filtered off and recrystallised from boiling methanol to remove a little of triazine which might have been formed due to a side reaction. The recrystallised product was dried in a vacuum desiccator over fused $CaCl_2$.

The compound is insoluble in water but soluble in alcohol, DMSO, acetone and dilute mineral acids. It melted with decomposition at 242 ± 2°C. Found: C, 50.83; H, 6.69; N, 42.21. Calc. for $C_7H_{11}N_5$: C, 50.91; H, 6.67; N, 42.42%.

*Preparation of 2-phenyl guanidino-4,6-dimethyl pyrimidine.* Phenyl biguanide hydrochloride[7] (10 g, 0.045 mole) was converted to free base in the usual manner. An alcoholic solution of the free phenyl biguanide base was refluxed with 4.7 $cm^3$ [4.7 g, 0.047 mole] distilled acetyl acetone for 2 hr. Upon cooling at room temperature, fine needle-shaped white cyrstals were deposited. These were recrystallised from boiling ethanol to remove any triazine that might have formed. The compound was insoluble in water but soluble in alcohol, acetone and dilute mineral acids. It melted with decomposition at 200 ± 2°C. Found: C, 64.64; H, 6.26; N, 28.92. Calc. for $C_{13}H_{15}N_5$: C, 64.51; H, 6.20; N, 29.05%.

*Preparation of Ni(II) complexes.* The Ni(II) complexes of the title ligands could not be isolated in the pure state starting with hydrated Ni(II) salts. However, successful synthesis of the desired complexes was made using anhydrous Ni(II) salts as detailed below:

*Preparation of anhydrous Ni(II) salts.* About 2 gms of $NiX_2.nH_2O$ [X = Cl/Br/I/$NO_3$, n = 3 to 6] taken in suspension with 5 $cm^3$ triethyl orthoformate [b.p. 146°C] were refluxed for about 2 hr on a hot plate at regulated temperature in moisture free condition. The resultant mixture was distilled on an oil bath at 80°C at reduced pressure [0.4 mm of Hg]. The left-out residue was kept in a vacuum desiccator over fused $CaCl_2$ for 48 hours. Anhydrous $Ni(NO_3)_2$, $NiCl_2$ and $NiBr_2$ were obtained as golden yellow micro-crystalline solid compounds. Anhydrous $NiI_2$ was obtained as iron-black solid.

*Preparation of Ni(II) chelates.* The Ni(II) chelates with GPym and PGPym were prepared by refluxing anhydrous Ni(II) salt [0.001 mole] with the corresponding ligand [0.002 mole] in dry alcohol on a hot plate at 60–80°C for 14–16 hr maintaining anhydrous conditions. The yellowish green solution obtained after the reflux, on cooling to room temperature, deposited micro crystals of the desired complex species in each case.

The product, in each case, was filtered off, washed with ice-cold dry alcohol and finally dried in a desiccator over fused $CaCl_2$.

Nickel(II) thiocyanate complexes of both the ligands GPym and PGPym were obtained by refluxing the corresponding chloro complex with potassium thiocyanate in dry ethanol medium for 15 min and filtering off the precipitated potassium chloride. The bluish green solution on concentration at water-bath temperature followed by cooling to *ca.* 25°C deposited a blue–violet product in each case.

Elemental analyses and physico-chemical measurements like equivalent conductances, magnetic susceptibilities and the electronic [both in solid and in solution] and the vibrational spectra of the complexes were carried out as described earlier.[2] The mass spectra of the ligands were recorded on an AEIMS 12 spectrometer at 70 eV. The PMR spectra of the guanidino pyrimidines (GPym and PGPym) were recorded in DMSO-$d_6$ solvent in a Varian CFT-I 60 MHz NMR spectrometer using TMS as internal standard reference.

## RESULTS AND DISCUSSION

*Characterisation of the ligands.* The electron impact mass spectra of the ligands showed molecular ion peaks at m/z 165 for GPym and 241 for PGPym confirming the synthesised ligands to have

molecular formulae $C_7H_{11}N_5$ (GPym [**1a**] and $C_{13}H_{15}N_5$ (PGPym) [**1b**] respectively. The important ion peaks for both the ligands with percentage of relative intensity are given in Table 1 showing most plausible formulations of the species. The fragmentation peaks are in well agreement with Structures (**1a**) and (**1b**) proposed for 2-guanidino-4,6-dimethyl pyrimidine and 2-phenyl guanidino-4,6-dimethyl pyrimidine respectively.

The 60 MHz PMR spectra of GPym and PGPym show 6-protons singlet around $\delta$ 2.22 which might be ascribed to the methyl groups at C-4 and C-6 positions of pyrimidine ring.[8] The lone pyrimidine proton (at C-1), in both the cases appear as a singlet at $\delta$ 6.6. In case of PGPym, the aromatic protons of the phenyl component appear as a complex signal in the region $\delta$ 7.2–7.6. The triplet at $\delta$ 1.04 could be ignored since the compound has been recrystallised from ethanol which might be retained as alcohol of crystallization. The corresponding methylene signals merged with noise of the base line. However, the protons bonded to the nitrogens of the guanidine moiety of the molecules do not appear in the spectra and they might have undergone exchange with HOD present in the solvent. Thus the mass spectra and the PMR data rightly characterise the synthesised compounds as 2-guanidino-4,6-dimethyl pyrimidine and 2-phenyl guanidino-4,6-dimethyl pyrimidine.

*Characterisation of the Ni(II) complexes.* The analytical results for the Ni(II) complexes of GPym and PGPym along with other pertinent data are given in Table 2. All the bis-complexes are soluble in low molecular weight alcohols, acetone and in coordinating solvents like DMF, DMSO, etc. All the Ni(II) complexes are magnetically normal 6-coordinate complexes [$\mu_{eff}$ = 2.74–2.98]. The molar conductance values of 121.9–142.4 mho $cm^2$ $mole^{-1}$ in DMF [Table 2] indicate their 1 : 2 electrolytic nature in the said solvent.[9] The following schematic formulation may be represented to express the extensive solvolysis which might be responsible for the observed conductance data.

$$[Ni(N\text{–}N)_2X_2] \xrightarrow{DMF} [Ni(N\text{–}N)_2(DMF)_2]^{2+} + 2X^-$$

where N–N represents one molecule of ligand viz. GPym/PGPym, X = Cl/Br/I/SCN/$NO_3$.

Electronic spectral data (Table 3) indicate that most of the Ni(II) complexes probably belong to $O_h$ or $D_{4h}$ or a group of lower symmetry.[10] The diffuse reflectance spectra of the complexes were characterised by three main bands appearing in the region 8500–10,400, 14,200–15,800 and 21,200–25,000 $cm^{-1}$ which may be assigned to $[^3A_{2g}(F) \rightarrow {}^3T_{2g}(F)]$, $[^3A_{2g}(F) \rightarrow {}^3T_{1g}(F)]$ and $[^3A_{2g}(F) \rightarrow {}^3T_{1g}(P)]$ transitions respectively in an idealised $O_h$ symmetry. For the complexes $Ni(GPym)_2X_2$ [X = Cl, SCN] and $Ni(PGPym)_2X_2$ [X = Br, I, SCN] and $\nu_2/\nu_1$ ratio lying between 1.53 and 1.68 characterise them as essentially pseudo-octahedral in the solid state. However, $\nu_2/\nu_1$ values for the rest of the Ni(II) species are found to fall in the range 1.78–1.85 indicating appreciable degree of tetragonal distortion in these octahedral species.[11] Electronic spectral data of most of the complexes recorded in DMF solutions suggest that no gross change occurs in the electronic or geometric structures of the complexes on dissolution in the said solvent and show three principal bands in the range 8900–9400 $cm^{-1}$ ($\nu_1$), 14,000–16,500 $cm^{-1}$ ($\nu_2$) and 23,200–25,000 $cm^{-1}$ ($\nu_3$). The low values of molar extinction coefficients ($\epsilon$ = 2.21–6.1) for the observed spectral bands are consistent with a pseudo-octahedral arrangements of the ligands,[12] in these species. In case of electronic spectra of the DMF solutions of $Ni(GPym)_2Br_2$, $Ni(GPym)_2(NO_3)_2$ and $Ni(PGPym)_2Cl_2$, it is observed that the respective $\nu_2/\nu_1$ ratios (Table 3) have come down to the pseudo-octahedral range ($\sim$ 1.55–1.58). The data reasonably suggest that there might be an effective change from $D_{4h}$ to $O_h$ summetry due to solvation effects.

Construction of molecular models suggest that the formation of a stable six-membered ring system with the central Ni(II) ion having N–N donor function taking one of the pyrimidyl ring nitrogens and the imino nitrogen (> NH) of the guanidine residue as bonding sites is the most probable proposition; this substantiated through the present IR spectral studies recorded down to 200 $cm^{-1}$.

In the IR spectra of all the Ni(II) complexes, the bands in the 3$\mu$ region arising due to $\nu_{asy}$(N–H) (3300–3390 $cm^{-1}$) and $\nu_{sy}$(N–H) (3100–3140 $cm^{-1}$) modes of vibration of the guanyl group[13] are observed almost in the same positions as those in the original ligand molecules with slight decrease in intensities suggesting participation of ligands in complex formation without deprotonation. The $\nu$(C=N) stretching bands of the guanidine part of both the ligand [Schemes 1(a) and 1(b)] appearing around 1650 $cm^{-1}$ [14–16] has been found to experience a negative shift of (10 ± 5) $cm^{-1}$ pointing to the probable participation of the imino nitrogen of the guanidine moiety of the ligands in complex formation with Ni(II). IR bands due to diazine (pyrimidine) system appearing around 1540 ($\nu$ C—C) and 1590 $cm^{-1}$ ($\nu$ C—N)[17] in the free ligand have been found to experience shifts in the higher energy side ($\Delta\nu \sim 15 \pm 5$ $cm^{-1}$) in the metal complexes indicat-

Table 1. Field desorption mass spectral data of the ligand molecules

| Ligands | Important ion peaks (m/z) | % of Relative intensity | Plausible formulation |
|---|---|---|---|
| | 165 | 65.21 | $C_7H_{11}N_5$ ($M^+$) |
| GPym($L_1$) | 148 | 22.86 | $C_7H_8N_4$ [$M^+$-$NH_3$ (17 unit)] |
| | 123 | 100.00 | $C_6H_9N_3$ [$M^+$-$H_2N.C \equiv N$ (42 unit)] |
| | 96 | 30.00 | $C_5H_8N_2$ [m/z 123-HCN (27 unit)] |
| | 241 | 77.63 | $C_{13}H_{15}N_5$ [$M^+$] |
| PGPym($L_2$) | 224 | 22.37 | $C_{13}H_{12}N_4$ [$M^+$-$NH_3$ (17 unit)] |
| | 147 | 100.00 | $C_7H_7N_4$ [m/z 224-$C_6H_5$ (77 unit)] |
| | 117 | 19.74 | $C_5H N_4$ [m/z 147-$2CH_3$ (30 unit)] |

Table 2. Physical properties and the analytical data of the complexes

| Complex | Colour | % Metal | | Found (%) | | | Calc. (%) | | | Magnetic moment $\mu_B$ at 301°K | Molar conductance conc. $1.0\times10^{-3}$M in DMF at 30°C (mho $cm^2$ $mole^{-1}$) |
|---|---|---|---|---|---|---|---|---|---|---|---|
| | | Found | Calc. | C | N | X | C | N | X | | |
| $Ni(L_1)_2Cl_2$ | green | 12.75 | 12.77 | 36.29 | 30.84 | 15.36 | 36.35 | 30.96 | 15.45 | 2.92 | 140.7 |
| $Ni(L_1)_2Br_2$ | green | 10.60 | 10.68 | 30.48 | 25.43 | 29.12 | 30.58 | 25.52 | 29.17 | 2.90 | 132.8 |
| $Ni(L_1)_2(SCN)_2$ | blue violet | 11.54 | 11.61 | 33.24 | 33.18* | - | 33.33 | 33.27 | - | 2.88 | 126.4 |
| $Ni(L_1)_2(NO_3)_2$ | blue violet | 11.34 | 11.43 | 32.62 | 32.82** | - | 32.77 | 32.77 | - | 2.96 | 138.2 |
| $Ni(L_2)_2Cl_2$ | green | 9.52 | 9.58 | 49.92 | 22.79 | 11.52 | 50.01 | 22.89 | 11.61 | 2.74 | 142.4 |
| $Ni(L_2)_2Br_2$ | green | 8.29 | 8.36 | 44.32 | 19.92 | 22.76 | 44.41 | 19.98 | 22.84 | 2.89 | 127.7 |
| $Ni(L_2)_2I_2$ | blue violet | 7.29 | 7.37 | 39.19 | 17.52 | 32.03 | 39.26 | 17.61 | 31.96 | 2.98 | 121.9 |
| $Ni(L_2)_2(SCN)_2$ | violet blue | 8.86 | 8.93 | 47.50 | 25.43* | | 47.52 | 25.54 | - | 2.84 | 123.6 |

$L_1$ = 2-Guanidino-4,6-dimethyl pyrimidine; $L_2$ = 2-Phenyl guanidino-4,6-dimethyl pyrimidine.

*Including nitrogen present in thiocyanate; **Including nitrogen present in nitrate.

Table 3. Electronic spectral data of the complexes

| Complexes | State | Absorption maxima kK ($\epsilon_{max}$) | $\nu_2/\nu_1$ |
|---|---|---|---|
| $Ni(L_1)_2Cl_2$ | Reflectance | 9.2, 15.6, 21.2 | 1.68 |
| | DMF (green) | 8.9 (2.21), 14.1(2.46), 23.2(5.71) | |
| $Ni(L_1)_2Br_2$ | Reflectance | 8.5, 15.8, 21.3 | 1.85 |
| | DMF (green) | 8.9(2.43), 14.0(2.51), 23.5(5.6) | 1.57 |
| $Ni(L_1)_2(SCN)_2$ | Reflectance | 9.2, 15.1, 25.3 | 1.64 |
| | DMF (pale blue) | 9.3(2.46), 16.5(2.62), 24.6(6.1) | |
| $Ni(L_1)_2(NO_3)_2$ | Reflectance | 8.9, 15.6, 25.4 | 1.74 |
| | DMF (blue violet) | 8.9(2.27), 14.1(2.32), 23.6(5.3) | 1.58 |
| $Ni(L_2)_2Cl_2$ | Reflectance | 8.6, 15.3, 25.0 | 1.78 |
| | DMF (green) | 9.0(3.21), 14.0(4.26), 23.6(5.37) | 1.55 |
| $Ni(L_2)_2Br_2$ | Reflectance | 8.5, 14.2, 23.8 | 1.67 |
| | DMF (green) | 8.9(2.26), 14.2(4.29), 23.5(5.33) | |
| $Ni(L_2)_2I_2$ | Reflectance | 10.4, 14.6, 24.3 | 1.55 |
| | DMF (pale blue) | 8.9(2.61), 14.08(4.21), 23.5(6.1) | |
| $Ni(L_2)_2(SCN)_2$ | Reflectance | 10.0, 15.3, 24.0 | 1.53 |
| | DMF (blue) | 9.0(2.71), 16.4(4.92), 25.0(6.0L) | |

$L_1$ = 2-Guanidino-4,6-dimethyl pyrimidine; $L_2$ = 2-Phenyl guanidino-4,6-dimethyl pyrimidine.

Table 4. Some characteristic IR bands (550–200 $cm^{-1}$) of the ligands together with the complexes

| Compounds | $\nu$ M-N (guanidine) | $\nu$ M-N (Pym ring) | $\nu$ M-X | Other bands |
|---|---|---|---|---|
| GPym | - | - | - | 550s, 470s, 400ms, 380w, 360w, 300w, 265ms, 240s, 230ms, 205s. |
| PGPym | - | - | - | 555s, 530w, 500s, 481w, 460w, 435w, 410m, 380ms, 350w, 250s, 225ms, 210s, 205m. |
| $Ni(L_1)_2Cl_2$ | 540s | 248s,240w | 290s | 570s, 460w, 440s, 400s, 370w, 310s, 245s, 230m, 220s. |
| $Ni(L_1)_2Br_2$ | 535s | 245ms | 265s | 560ms, 520w, 480w, 435ms, 380w, 355w, 305m, 245w, 220w, 215w. |
| $Ni(L_1)_2(SCN)_2$ | 530s | 245s | 275ms | 540w,510ms,480w,465w,410ms,380ms,260w,230ms,215w. |
| $Ni(L_1)_2(NO_3)_2$ | 535s | 250ms | - | 560ms,500w,440w,390ms,320ms,300w,270w,230ms,210w. |
| $Ni(L_2)_2Cl_2$ | 525ms | 280ms | 285s | 590w, 560m, 470w, 420m, 370w, 240m, 210w. |
| $Ni(L_2)_2Br_2$ | 528s | 275ms | 260s | 560m, 520w, 450w, 400m, 340ms, 290w, 260m, 210m. |
| $Ni(L_2)_2(SCN)_2$ | 540ms | 245ms | 270ms | 550ms, 490w, 410w, 380ms, 310w, 230ms, 205w. |

s = strong; m = medium; w = weak

$L_1$ = 2-Guanidino-4,6-dimethyl pyrimidine; $L_2$ = 2-Phenyl guanidino-4,6-dimethyl pyrimidine.

ing, thereby, the expected involvement of the pyrimidyl ring nitrogen in complexation.

The above proposition has been further substantiated by far IR spectra of the metal complexes (Table 4) through the appearance of new bands in the range of 280–240 $cm^{-1}$ and 525–540 $cm^{-1}$ which may safely be assigned to $\nu_{M-N}$ (Pym)[18] and $\nu_{M-N}$ (guanidine).[19-21]

A monodentate nitrate in $C_{2v}$ symmetry is present in $Ni(GPym)_2(NO_3)_2$ as is evidenced by three IR bands at 1415(ms), 1310(s) (components of $\nu_3$) and 827(ms) $cm^{-1}$ ($\nu_2$).

The IR spectra of thiocyanate complexes have three bands at 2100–2110, 790 and 480 $cm^{-1}$ in the regions of $\nu_{C\equiv N}$, $\nu_{C-S}$ and $\delta$ NCS vibrations respectively indicating the presence of N-bonded[23] thiocyanate group.

The diagnostic band frequencies of the other counterions (X), (X = Cl/Br) $\nu_{M-Cl}$ 285–290 $cm^{-1}$ and $\nu_{M-Br}$ 260–265 $cm^{-1}$[24], indicate the coordinated nature of $Cl^-$ and $Br^-$ ions respectively.

*Acknowledgements*—The authors are thankful to Sri Subhas Maikup, R.S.I.C., Eastern Zone, India, for providing d.r.s. and solution spectra of the Ni(II) complexes.

## REFERENCES

1. N. Saha and S. K. Kar, *J. Inorg. Nucl. Chem.* 1977, **39**, 195.
2. (a). N. Saha and S. K. Kar, *J. Inorg. Nucl. Chem.* 1979, **41**, 1233. (b). N. Saha and D. Mukherjee, *Polyhedron* 1983, **2**, 47.
3. S. N. Poddar and A. Sarkar, Private communication.
4. P. Ray, *Chem. Rev.* 1961, **61**, 313.
5. K. H. Slotta and R. Tschesche, *Ber.* 1929, **62**, 1390.
6. L. Birkoffer and A. Ritter, *Chem. Ber.* 1960, **93**, 424.
7. A. Smolka and A. Friedrich, *Monatsh Chem.* 1888, **9**, 227.
8. *High Resolution NMR Catalog*, compiled by N. S. Bhacca, D. P. Hollis, L. F. Johnson and E. A. Pier of the Instrument Division of Varian Associates.
9. W. J. Geary, *Coord. Chem. Rev.* 1971, **7**, 81.
10. A. B. P. Lever, J. Lewis and R. S. Nyholm, *J. Chem. Soc.* 1964, 4761.
11. A. B. P. Lever, *Coord. Chem. Rev.* 1968, **3**, 119.
12. K. C. Patel and D. E. Goldberg, *J. Inorg. Nucl. Chem.* 1972, **34**, 637.
13. A. Albert and E. Spinner, *J. Chem. Soc.* 1960, 1221.
14. N. Nakanishi and P. H. Solomon, *Infrared Absorption Spectroscopy*, 2nd Edn, p. 257. Holden-Day, San Francisco (1977).
15. S. P. Ghosh and P. Bhattacharjee, *J. Inorg. Nucl. Chem.* 1970, **32**, 573.
16. S. P. Ghosh, P. Bhattacharjee, L. Dubey and L. K. Mishra, *J. Ind. Chem. Soc.* 1977, **LIV**, 234.
17. I. A. Brownlie, *J. Chem. Soc.* 1950, 3062.
18. I. A. Dorrity and K. G. Orrel, *J. Inorg. Nucl. Chem.* 1974, **36**, 230.
19. J. R. During and D. W. Wertz, *Appl. Spectros.* 1968, **22**, 63.
20. I. R. During, L. Layton, D. Link and B. Mitchel, *Spectrochim. Acta* 1965, **21**, 1367.
21. A. D. Alien and T. Theophanides, *Can. J. Chem.* 1964, **42**, 1551.
22. N. F. Curtis and Y. M. Curtis, *Inorg. Chem.* 1965, **4**, 804.
23. I. Berlini and A. Sabatini, *Inorg. Chem.* 1966, **5**, 1025.
24. D. M. Adams, *Metal-Ligand and Related Vibrations*, p. 248. Edward Arnold, London (1968).

*Polyhedron* Vol. 3, No. 8, pp. 991–995, 1984
Printed in the U.S.A.

0277–5387/84 $3.00 + .00
© 1984 Pergamon Press Ltd.

# MANGANESE(II) AND COPPER(II) COMPLEXES OF SOME NITROGEN–OXYGEN AND NITROGEN–SULPHUR DONOR LIGANDS

S. CHANDRA* and K. K. SHARMA
Department of Chemistry, Zakir Husain College, Ajmeri Gate, Delhi 110006, India

(*Received* 8 *July* 1983; *accepted* 15 *December* 1983)

**Abstract**—Manganese(II) and copper(II) complexes of the type M(ligand–H)$_2$ with some nitrogen–oxygen and nitrogen–sulphur donor ligands (HL) viz. phenylpyruvic acid semicarbazone (ppysc), 4-methylphenylpyruvic acid semicarbazone (4-mppysc), phenylpyruvic acid thiosemicarbazone (ppytsc) and 4-methylphenyl pyruvic acid thiosemicarbazone (4-ppytsc), have been synthesised. All the complexes have been characterised by magnetic moment measurements, IR electronic and electron spin resonance spectral studies. All the ligands behave as tridentate.

The study of transition metal complexes of thiosemicarbazones is of great interest due to their pharmacological activities.[1,2] In many cases it has been observed that the pharmacological activities of thiosemicarbazones are enhanced in the presence of a transition metal ion.[3] The corresponding semicarbazones on the other hand appear to be inactive. Chromium(III) and iron (II) complexes with these ligands have been reported recently.[4,5] Manganese(II) and copper(II) complexes have now been synthesised by using ligands (HL) viz. phenylpyruvic acid semicarbazone (**Ia**), phenylpyruvic acid thiosemicarbazone (**Ib**), 4-methyl phenylpyruvic acid semicarbazone (**Ic**) and 4-methylphenyl thiosemicarbazone (**Id**). All the complexes have been characterised by various physicochemical investigations. The complexes are six-coordinate octahedral.

## EXPERIMENTAL

(a) *Preparation of ligands*

All ligands were prepared by the methods reported earlier.[4,5]

(b) *Preparation of complexes*

A general method has been used for the preparation of complexes. Hot ethanolic solution of hydrated metal salts ($MnCl_2.2H_2O$ or $CuCl_2.2H_2O$) (0.05 mole) and the corresponding ligand (0.1 mole) were mixed together. The contents were refluxed on a water-bath for about 3–4 hr. On cooling the contents coloured precipitates separated out in each case. The same were filtered, washed with ethanol and dried at ~60°C.

*Physical measurements*

Magnetic moments of the complexes at room temperature were measured on a Gouy balance using $Hg[Co(NCS)_4]$ ($\chi_g = 16.44 \times 10^{-6}$ cgs unit) as a calibration agent. IR spectra were recorded (4000–200 cm$^{-1}$) on a Perkin–Elmer 621 automatic recording spectrophotometer in KBr medium. Electronic spectra were recorded on DMR–21 automatic recording spectrophotometer. Electron spin resonance measurements were carried out on Varian $E_4$ EPR spectrometer operating at ~9.4 GHz and 100 kHz field modulation and phase-sensitive detection.

The analyses for carbon and hydrogen were performed in the departmental microanalytical laboratory. Nitrogen was estimated by Kjeldahl's method. The content of manganese and copper in the complexes were determined gravimetrically as $Mn_2P_2O_7$ and Cu(CNS) respectively.

## RESULTS AND DISCUSSION

The elemental analysis of the complexes reveal that all are of the general composition M(ligand–H)$_2$ (M = Mn or Cu) (Table 1).

*Author to whom correspondence should be addressed.

Table 1. Colour and composition of the complexes

| Complex | Colour | M.P. °C | Elemental Analysis (Found/(Calcd). %M | %C | %H | %N |
|---|---|---|---|---|---|---|
| $Mn(ppysc-H)_2$ | Light yellow | 210 | 13.54 (13.51) | 53.90 (53.87) | 4.82 (4.91) | 20.58 (20.64) |
| $Mn(ppytsc-H)_2$ | Light yellow | 225 | 12.48 (12.53) | 49.16 (49.20) | 4.52 (4.55) | 19.10 (19.13) |
| $Mn(4-mppysc-H)_2$ | Yellow-ish pink | 205 | 12.62 (12.64) | 55.08 (55.17) | 5.58 (5.52) | 19.34 (19.31) |
| $Mn(4-mppytsc-H)_2$ | Light yellow | 202 | 11.76 (11.78) | 51.48 (51.39) | 5.09 (5.14) | 17.98 (17.94) |
| $Cu(ppysc-H)_2$ | Bluish green | 208 | 15.30 (15.28) | 51.88 (51.98) | 4.85 (4.81) | 20.18 (20.22) |
| $Cu(ppytsc-H)_2$ | Bluish | 215 | 14.25 (14.19) | 48.38 (48.27) | 4.60 (4.67) | 18.72 (18.77) |
| $Cu(4-mppysc-H)_2$ | Greenish blue | 225 | 14.38 (14.32) | 54.16 (54.11) | 5.48 (5.41) | 19.89 (18.94) |
| $Cu(4-mppytsc-H)_2$ | Greenish blue | 220 | 13.38 (13.35) | 50.42 (50.47) | 5.09 (5.05) | 17.60 (17.66) |

Table 2. Important IR bands of their assignment

| Complex | $\nu_{C=O}$ Semicarbazide moety | $\nu_{C=O}$ Carboxylic group | $\nu_{C=N}$ | $\nu_{C=S}$ |
|---|---|---|---|---|
| ppysc | 1680(s) | 1750(s) | 1620(s) | - |
| $Mn(ppysc-H)_2$ | 1650(s) | 1730(s) | 1610(s) | - |
| $Cu(ppysc-H)_2$ | 1650(s) | 1735(s) | 1610(s) | - |
| Ppytsc | - | 1700(s) | 1600(s) | 1090(m) 1030(m) 1085(m) |
| $Mn(ppytsc-H)_2$ | - | 1680(s) | 1605(s) | 1010(m) 1085(m) |
| $Cu(ppytsc-H)_2$ | - | 1680(s) | 1600(s) | 1015(m) |
| 4-mppysc | 1680(s) | 1750(s) | 1620(s) | - |
| $Mn(4-mppysc-H)_2$ | 1650(s) | 1730(s) | 1610(s) | - |
| $Cu(4-mppysc-H)_2$ | 1650(s) | 1735(s) | 1605(s) | - |
| 4-mppytsc | - | 1700(s) | 1620(s) | 1090(m) 1020(m) |
| $Mn(4-mppytsc-H)_2$ | - | 1680(s) | 1608(s) | 1080(m) 1015(m) |
| $Cu(4-mppytsc-H)_2$ | - | 16800(s) | 1605(s) | 1082(m) 1010(m) |

Table 3(a). Electronic spectral bands and ligand field parameters for the complexes

| Complex | $\mu_{eff}$ B.M. | $\lambda_{max} \times 10^{-3}$ ($cm^{-1}$) | Dq ($cm^{-1}$) | g | B ($cm^{-1}$) | C ($cm^{-1}$) | $\beta$ |
|---|---|---|---|---|---|---|---|
| Mn(ppysc-H)$_2$ | 5.9 | 32200<br>29500<br>24500<br>20600 | 745 | 1.982 | 700 | 3520 | 0.89 |
| Mn(ppytsc-H)$_2$ | 6.0 | 31900<br>29400<br>24400<br>20500 | 760 | 1.992 | 714 | 3452 | 0.91 |
| Mn(4-mppysc-H)$_2$ | 6.0 | 3200<br>29400<br>24500<br>20600 | 745 | 1.984 | 700 | 3500 | 0.89 |
| Mn(4-mppytsc-H)$_2$ | 5.92 | 31900<br>29400<br>24400<br>20500 | 760 | 1.988 | 714 | 3452 | 0.91 |

Table 3(b).

| Complex | $\mu_{eff}$ B.M. | $\lambda_{max} \times 10^{-3}$ ($cm^{-1}$) | $g_{\parallel}$ | $g_{\perp}$ | $g_{av}$ |
|---|---|---|---|---|---|
| Cu(ppysc-H)$_2$ | 1.92 | 13200,<br>15200 | 2.254 | 2.086 | 2.142 |
| Cu(ppytsc-H)$_2$ | 1.95 | 13600,<br>15700 | 2.268 | 2.092 | 2.151 |
| Cu(4-mppysc-H)$_2$ | 2.03 | 13300,<br>15400 | 2.256 | 2.086 | 2.143 |
| Cu(4-mppytsc-H)$_2$ | 2.00 | 14000,<br>16600 | 2.262 | 2.089 | 2.147 |

*IR spectra*

IR spectra of the complexes (Table 2) provide direct information about the coordination of ligands. IR spectra of semicarbazones (ppysc and 4-mppysc) show bands at 1750, 1680 and 1620 $cm^{-1}$ (Table 2) due to $\nu_{C-O}$ of carbonyl group, $\nu_{C-O}$ of semicarbazide moiety and $\nu_{C-N}$ vibrations respectively. On complex formation these bands are shifted towards lower wave numbers. The possibility of a bond between the semicarbazone group and metal through the nitrogen atom of the amido group must be excluded, however since the frequencies of the N–H stretching vibration in the complexes are slightly higher than in the free ligand. The formation of a metal–ligand bond through the nitrogen atom of the amino group leads to the opposite effect.[6–8]

Infrared spectra of thiosemicarbazones (ppytsc and 4-mppytsc) show bands at 1620 and 1700 $cm^{-1}$ (Table 2). The bands may be assigned to $\nu_{C-N}$ and $\nu_{C-O}$ of the carboxyl group respectively.[9] On complex formation these bands are shifted to lower wave numbers. Although definite assignment for the $\nu_{C-S}$ vibration is difficult, it appears that the bands ~ 1100 $cm^{-1}$ in the free ligands are due to the $\nu_{C-S}$ vibration is suggested by earlier workers.[9] This band also shifted towards lower wave numbers on the formation of the coordinate bond. This indicates that all the ligands behave as tridentate, coordinating through O/S, oxygen of carboxyl group and nitrogen of hydrazinic residue.

*Manganese(II) complexes*

The magnetic moments of these complexes were found to be in the 5.9–6.01 B.M., ranges, corresponding to five unpaired spins[10] (Table 3a).

The electronic spectra (Table 3a) of these complexes display four very weak bands in the range of 32,000–33,000, 29,000–30,000, 24,500–25,000 and 19,500–20,000 $cm^{-1}$. These bands may be assigned[11] as $^6A_{1g} \rightarrow {}^4T_{1g}$ ($^4G$) (10B + 5C), $^6A_{1g} \rightarrow {}^4E_g$, $^4A_{1g}$ ($^4G$), (10B + 5C), $^6A_{1g} \rightarrow {}^4E_g$ ($^4D$), (17B + 5C) and $^6A_{1g} \rightarrow {}^4T_{1g}$ (4P) transitions respectively. Various ligand field parameters have been calculated and presented in Table 3(a).

The values of B and C were calculated by using,[12,13] the transitions $^6A_{1g} \rightarrow {}^4E_g$, $^4A_{1g}$ ($^4G$) and $^6A_{1g} \rightarrow {}^4E_g$ ($^4D$). The value Dq has been calculated by using the Orgel energy level diagram.[14] The values for the nephelauxetic parameter $\beta$ have been calculated by using [B complex/B free ion] where B for the free ion is 786 $cm^{-1}$. The values of $\beta$ indicate that the complexes under study have substantial ionic character.[15]

The esr spectra on polycrystalline powders of the manganese(II) compounds were isotropic and showed one broad signal in each case. The $g$-values have been calculated and are presented in Table 3(a). The broadness is probably the result of low symmetry and consequent anisotropy of $g$ and possibly D and E. Such type of broadening has already been observed in a number of manganese(II) complexes.[16,17]

*Copper(II) complexes*

These complexes gave magnetic moments in the range of 1.88–1.92 B.M., corresponding to one unpaired spin.[10] Irrespective of stereochemistry involved, bivalent copper(II) complexes contain one unpaired spin per copper atom, unless there is antiferromagnetic exchange interaction between copper pairs, in which case lower magnetic moments or even diamagnetism may result.[18]

The absorption spectra of six-coordinate copper(II) complexes exist in $D_4$ or $C_{4v}$ symmetry, the $e_g$ and $t_{2g}$ levels of the $^2D$ free ion term will further split into $B_{1g}$, $A_{1g}$, $B_{2g}$, and $E_g$ levels respectively. Thus three spin allowed transitions are expected in the visible and near IR region of copper(II) complexes, but there are very few copper(II) complexes in which such bands are resolved either by Gaussian analysis or single crystal polarisation studies and are assigned to the $^2B_{1g} \rightarrow {}^2A_{1g}$ ($d_{z^2} \leftarrow d_{x^2-y^2}$); $^2B_{1g} \rightarrow {}^2B_{2g}$ ($d_{xy} \leftarrow d_{x^2-y^2}$) and $^2B_{1g} \rightarrow {}^2B_g$ ($d_{xz}$, $d_{yz} \leftarrow d_{x^2-y^2}$) transitions in order of increasing energy. The energy level sequence will depend on the amount of distortion due to ligand field and Jahn–Teller effect.[20] The electronic spectra of the present complexes display a sharp band in the range 12,500–13,000 $cm^{-1}$ and a well defined shoulder at 15,000–16,000 $cm^{-1}$ range. The main band and shoulder may be assigned to the $^2B_{1g} \rightarrow {}^2E_g$ and $^2B_{1g} \rightarrow {}^2A_{1g}$ transitions respectively. Because of the low intensity of $^2B_{1g} \rightarrow {}^2B_{2g}$, this band is usually not observed as a separate band in tetragonal field.

All the complexes show anisotropic esr spectra characteristic of tetragonal copper(II) complexes. $g$-Tensor values have been calculated by Kneübuhl's[21] method and results are presented in Table 3(b).

The $g$-tensor values of copper(II) complexes can be used to derive the ground state.[22] In an elongated octahedron the $3d$ unpaired electron for $Cu^{2+}$ ion lies in $d_{x^2-y^2}$ orbital ($^2B_1$ as ground state). The $g$-values are then given by $g_\parallel = 2(1 - (4\lambda/\Delta_1))$ and $g_\perp = 2(1 - (\lambda/\Delta_2))$. In a compressed octahedron, on the other band, the $3d$ unpaired electron lies in $d_{z^2}$ orbital ($^2A_1$ ground state) and so gives the $g$ value expressions: $g_\parallel = 2$ and $g_\perp = (1 - (3\lambda/\Delta_3))$. Here $\Delta_1$, $\Delta_2$ and $\Delta_3$ are $d_{x^2-y^2} \rightarrow d_{xy}$, $d_{x^2-y^2} \rightarrow d_{xz}$, $d_{yz}$ and $d_{x^2-y^2} \leftarrow d_{z^2}$ excitation energies, respectively. From the observed $g$ values it is evident that the unpaired electron lies predominantly in the $d_{x^2-y^2}$ orbital with the possibility of some $d_{z^2}$ character being mixed with it because of low symmetry.

A parameter G has been calculated (Table 3b) by using the expression[20]: $G = (g_\parallel - 2)/(g_\perp - 2)$. The value of G measure the exchange interaction between copper centres in the polycrystalline solid. According to Hathaway[18,23–25] if the value of G is larger than four exchange interaction is negligible while the value of G less than four indicates considerable exchange interaction in solid complexes. In the present study such interaction is negligible.

## REFERENCES


1. M. A. Ali and S. E. Livingston, *Coord. Chem. Rev.* 1974, **13**, 101 and references therein.
2. M. J. M. Campbell, *Coord. Chem. Rev.* 1975, **15**, 279 and references therein.
3. K. Liebermeister, *Z. Naturforsch* 1950, **B5**, 79.
4. S. Chandra and K. B. Pandeya, *Gazz. Chim. Ital.* 1981, **111**, 419.
5. G. L. Sawhney, J. S. Baijal, S. Chandra and K. B. Pandeya, *Acta. Chim. Acad. Sci. Hung* 1981, **108**, 325.
6. A. V. Ablov, N. I. Belichuk, L. F. Chapurina, *Russ. J. Inorg. Chem.* 1970, **15**, 57.
7. A. V. Ablov and N. V. Gerbeleu, *Russ. J. Inorg. Chem.* 1970, **15**, 952.
8. L. J. Bellamy and P. I. Rogash, *J. Chem. Soc.* 1960, 2218.
9. A. Yama Guchi, R. B. Penland, S. Mizushima, J. J. Lane, C. Curran and J. B. Quaglino, *J. Am. Chem. Soc.* 1958, **80**, 527.
10. B. N. Figgis and J. Lewis, *Prog. Inorg. Chem.* 1964, **6**, 37.

11. L. J. Heidt, G. F. Koster and M. A. Johnson, *J. Am. Chem. Soc.* 1958, **80**, 6471.
12. C. Preti and G. Tosi, *Aust. J. Chem.* 1976, **20**, 543.
13. S. Chandra and K. K. Sharma, *Syn. React. Inorg. Met-Org. Chem.* 1982, **12**, 123.
14. L. E. Orgel, *J. Chem. Phys.* 1955, **23**, 1004.
15. C. K. Jorgensen, *Oxidation Number and Oxidation States*, p. 106. Springer Verlag, New York (1969).
16. G. M. Woltermann and J. R. Wasson, *Inorg. Chem.* 1973, **12**, 2366.
17. S. Chandra, K. B. Pandeya, S. K. Sindhwani and R. P. Singh, *Gazz. Chim. Ital.* 1980, **110**, 207.
18. B. J. Hathaway, *Essay in Chemistry* (Edited by J. N. Bradley and R. D. Gillard), p. 61. Academic Press (1971).
19. A. B. P. Lever, *Inorganic Electronic Spectroscopy*, p. 204. Elsevier, Amsterdam (1968).
20. I. M. Procter, B. J. Hathaway and P. Nicholls, *J. Chem. Soc. A* 1968, 1678.
21. F. K. Kneübuhl, *J. Chem. Phys.* 1960, **33**, 1074.
22. C. J. Ballhausen, *Introduction to Ligand Field Theory*, p. 134. McGraw-Hill, New York (1962).
23. B. J. Hathaway and D. E. Billing, *Coord. Chem. Rev.* 1970, **5**, 143.
24. B. J. Hathaway, R. J. Dudley and P. Nicholls, *J. Chem. Soc. A* 1968, 1845.
25. R. J. Dudley and B. J. Hathaway, *J. Chem. Soc. A* 1970, 1725.

*Polyhedron* Vol. 3, No. 8, pp. 997–1000, 1984
Printed in the U.S.A.

0277-5387/84 $3.00 + .00
© 1984 Pergamon Press Ltd.

# A NEW IRON(II) THIOCYANATO THIOCYANOGEN COMPLEX

**S. K. TOBIA* and W. G. HANNA**
Chemistry Department, Faculty of Science, Ain Shams University, Abbassia, Cairo, Egypt

(*Received* 18 *August* 1983; *accepted* 25 *December* 1983)

**Abstract**—The reaction between $Fe^{3+}$ and $SCN^-$, in glacial acetic acid medium, gave a dark red solution which differs from the classical $FeSCN^{2+}$, prepared in aqueous medium, with regard to stability and composition. In contrast to $[FeSCN]^{2+}$ which undergoes photochemical decomposition and is bleached by light and reduced by hydroxylammonium chloride, the new complex is stable towards these agents, but it reacts with water. In addition to the charge transfer band at 480 nm exhibited by both solutions, the new complex exhibits a sharp strong band at 253 nm characteristic of the trithiocyanate ion, $[SCN^- + NCS–SCN]$; thiocyanogen being produced by oxidation of $SCN^-$ by $Fe^{3+}$. The reaction with water is attributed to the hydrolysis of thiocyanogen mainly into sulphate. The presence of thiocyanogen in the new complex enhanced polymerization and subsequent deposition of solid complex. On the basis of chemical, spectral, and thermal analyses the formula $K_2[Fe(SCN)_4(NCS–SCN)]$, is assigned to the new compound.

The reaction of thiocyanate and ferric ion to yield an intensely red solution has been known for a long time and used for the qualitative and quantitative determination of either ion. Previous studies were carried with the objective of elucidating the nature and stability of the complex species in the coloured solution. Because of the high sensitivity of the reaction, most of these studies were carried out in very dilute solutions in aqueous or in non-aqueous media or in a mixture of both. A solid complex has never been obtained, and it has been assumed that a complex species is present in solution containing iron(III) bonded to one thiocyanate ion.

The red solution resulting from the reaction in aqueous medium was found to fade after a period of time depending on the composition of the solution. The fading was attributed to thermal and photochemical oxidation of $SCN^-$ by $Fe^{3+}$ in the complex $[FeSCN]^{2+}$. The results of thermal bleaching studied by Betts and Dainton,[1] and photochemical bleaching studied by Ellis and Lawrence[2] suggested the formation of thiocyanogen which undergoes hydrolysis giving mainly sulphate and other products.[3]

The study of the reaction in media in which thiocyanogen would be stable provided direct evidence for its production by oxidation of $SCN^-$ by $Fe^{3+}$. For example, Kratochvil and Lang[4] titrated potentiometrically thiocyanate with ferric perchlorate, in acetonitrile. Two inflections were obtained at Fe/SCN ratios of 0.19 and 1.00, the latter was attributed to oxidation of $SCN^-$ to thiocyanogen by $Fe^{3+}$. In molten thiocyanate, the reduction of $Fe^{3+}$ to $Fe^{2+}$ and oxidation of $SCN^-$ to parathiocyanogen (polymerized thiocyanogen) has been confirmed by Metzger,[5a] Eluard and Tremillon,[5b] and Kerridge and Mosley.[5c]

Although a non-aquous $Fe^{3+}$–$SCN^-$ system has been shown also to involve thiocyanogen, no attempt has been made before to investigate the possibility of its cooordination to the metal ion to form a complex containing both thiocyanate and thiocyanogen. The present investigation has been undertaken to study this possibility. The formation of a complex containing both the pseudohalide and its oxidation product has been previously demonstrated in the $Cu^{2+}$–$CN^-$ system.[6] Since thiocyanogen is known to be most stable in glacial acetic acid,[7] the latter was used as a reaction medium in this study.

## EXPERIMENTAL

*Solutions.* Stock solutions of iron(III) and thiocyanate were prepared by saturating respectively, a

*Author to whom correspondence should be addressed.

certain volume of glacial acetic acid (AR 99.7%) by anhydrous ferric chloride and potassium thiocyanate, at 25°C. The concentration of these solutions was over 3M. Each of the saturated solutions was suitably diluted by the acid to give solutions that are 3 and 0.1 M with respect to each ion.

*Preparation of the complexes.* The iron solution was run from a burette into the thiocyanate solution contained in a 50 $cm^3$ conical flask mounted on a magnetic stirrer. Any Fe/SCN ratio can be attained by mixing the suitable volumes of the two solutions.

The 0.1 M solutions were used to prepare the complex solution, while the 3M solutions were used to prepare the solid complex. The latter precipitated when the mixed solutions at an Fe/SCN molar ratio of 1:2, were left to stand overnight. The dark brown solid was separated by filtration, washed with acetic acid, and dried over $P_2O_5$.

*Analytical.* The iron(III) solutions were standardized after being diluted with water by direct complexometric titration at pH 2–3 using EDTA and sulphosalicylic acid as indicator.[8] The thiocyanate solutions were standardized after dilution with water by the Volhard's method.

The solid complex was analyzed as follows: Treatment of the solid with dilute sulphuric acid (0.5 M) resulted in the production of (i) an orange precipitate which proved to be parathiocyanogen, and (ii) a colourless clear solution containing $K^+$, $Fe^{2+}$ and $SCN^-$. Parathiocyanogen was separated using a Grade 4 sintered glass crucible, washed with water, dried at 80°C, and weighed. Aliquots of the clear solution were used for the determination of the three ions. Iron was determined by complexometric titration,[8] after oxidation of $Fe^{2+}$ to $Fe^{3+}$ by nitric acid. Potassium was determined gravimetrically as cobaltinitrite after removal of iron. For the determination of thiocyanate, iron was first precipitated as hydroxide by NaOH and removed by filtration. The thiocyanate in the alkaline filtrate was determined by using an ion-selective electrode.

*Elemental analysis.* Carbon and nitrogen were determined by the usual microanalytical methods at The National Research Centre in Cario. Sulphur was determined by a $Na_2CO_3$–$KNO_3$ fusion method using a gravimetric method for the determination of the sulphate formed.[9]

*Tests for thiocyanogen.* Thiocyanogen in glacial acetic acid was tested by addition of water which produced sulphate by hydrolysis.

Thiocyanogen produced by thermal treatment of the solid was identified by a test based on its decomposition into sulphur and cyanogen. The latter was detected by the sensitive oxine–sodium cyanide test.[10]

*Physical measurements.* The VIS–UV spectra were examined by a Pye Unicam SP 1800 double beam spectrophotometer. The IR spectra were examined using Nujol mulls or KBr discs by a Beckman IR 9 Spectrophotometer (4000–400 $cm^{-1}$). Differential thermal analysis (DTA) was carried out on a conventional apparatus using alumina as a reference. The rise in temperature was kept linear at a rate of 12°/min. by an Ether transistoral programme temperature controller type 994/2. The temperature difference was recorded by means of a Cambridge temperature recorder model B. Thermogravimetric analysis (TG) was carried out by a Stanton–Redcroft thermo-balance type 750 connected to a BD 9 two-channel automatic recorder "Kipp and Zonnen", at a heating rate of 10°C per minute.

Magnetic measurements were made using a Varian Electromagnet Model V 2300 A, by the kind permission of the American University in Cairo.

The X-ray diffraction pattern of the solid was recorded with a Philips diffractometer (30 Kv, 20 mA).

## RESULTS AND DISCUSSION

In the discussion that follows, the red complex solution and the solid complex will be dealt with separately.

(1) *The red complex solution.* The red complex solution formed by mixing $Fe^{3+}$ and $SCN^-$ in glacial acetic acid, at any molar ratio was found to differ from that prepared in aqueous medium. Simple chemical tests indicated that the first is a complex of $Fe^{2+}$ coordinated to thiocyanate and thiocyanogen, while the second is a complex of $Fe^{3+}$ coordinated to thiocyanate only and is usually formulated as $[FeSCN]^{2+}$. Evidence for this conclusion has been inferred from the following observations:

(a) *Action of water.* Addition of water to the freshly prepared complex solution caused instantaneous and complete bleaching of colour with production of sulphate ion (tested by $Ba^{2+}$). This is explained as being due to the hydrolysis of coordinated thiocyanogen.

(b) *Action of reducing agents.* Addition of a reducing agent such as few crystals of hydroxylammonium chloride had no effect on colour, whereas this reagent bleaches the red solution prepared in aqueous medium. This indicated that the new complex contains ferrous iron. This was

confirmed by bleaching the colour with water followed by the addition of potassium hexacyanoferrate (III), when a blue colour appeared.

(c) *Spectroscopic characteristics.* Both solutions exhibit the charge transfer band at 480 nm. However, on standing, the intensity of the band decreases and its position is unchanged in the case of the red complex prepared in aqueous medium. In the case of the new complex, on the other hand, the position shifts to a higher wave length (494 nm), and the intensity increases. This is explained as being due to polymerization of the complex species, the molecule of thiocyanogen may act as a bridging ligand. This explanation is supported by the fact that, on standing, the solution becomes gradually resistant to the bleaching action of water. In the UV region, the new complex exhibits a sharp strong band at 253 nm, which has been ascribed to the thrithiocyanate ion $(SCN)_3^-$ or to some other condensed species with a large extinction coefficient.[11]

(2) *The solid complex.* Preliminary experiments indicated that on mixing solutions of $Fe^{3+}$ and $SCN^-$, in glacial acetic acid, a solid is deposited only if the original concentration is relatively high (3M), and the nature of the solid depends on the SCN/Fe ratio. When this ratio is above 2, the solid deposited is almost pure parathiocyanogen containing only traces of iron. When the ratio is between 1 and 2, the solid has a constant composition and contains about 10% of iron. On decreasing the SCN/Fe ratio below one, the percentage of iron in the deposit increases, In this investigation, the solid examined is that obtained at an SCN/Fe ratio of 2.

The solid deposited is dark brown, insoluble in water and most organic solvents. It is diamagnetic and its X-ray diffraction pattern differs from any of the known Fe(II) thiocyanato complexes. The principal lines are found at 3.151 (100%), 2.231 (50%) and 1.818 (12%). Treatment with dilute sulphuric acid (0.5 M) caused partial dissolution, the insoluble portion coloured orange was proved by analysis to be pure parathiocyanogen. The resulting solution is colourless and contains $Fe^{2+}$, $K^+$ and $SCN^-$. The separation of parathiocyanogen on acid treatment may mean that either (i) the solid is a mixture of parathiocyanogen and Fe(II) thiocyanato complex or (ii) the solid is an Fe(II) thiocyanato thiocyanogen complex, and acid treatment caused decomposition and subsequent polymerization of coordinated thiocyanogen into parathiocyanogen. The following observations favour (ii) over (i).

(a) Gentle heating of the solid, in a micro test tube produced a sublimate of sulphur which deposited on the cold part of the tube and evolution of cyanogen gas which was identified by the oxinecyanide test. Sulphur and cyanogen are the decomposition products of thiocyanogen:

$$(SCN)_2 = 2S + (CN)_2$$

Parathiocyanogen does not give sulphur and cyanogen on heating.

(b) The IR spectrum exhibited a strong relatively wide band between 1990 and 2180 $cm^{-1}$ and centred at 2080 $cm^{-1}$. This band may embrace the –C≡N asymmetric stretching of both the thiocyanate and thiocyanogen. It is known that the latter exhibits a sharp strong band at 2175 $cm^{-1}$.[11] Parathiocyanogen, on the other hand was found to exhibit a band at 1620 $cm^{-1}$ assigned to =C=N– stretching. This band is also exhibited by the solid complex, but because it is rather weak, may be due to an impurity of parathiocyanogen in the complex. The infrared spectrum of the solid complex is shown in Fig. 1.

(c) Thermal analysis of the solid showed a weight loss of about 12% at 280°C, accompanied by an endothermic peak on the DTA curve. The observed weight loss corresponds to cyanogen that

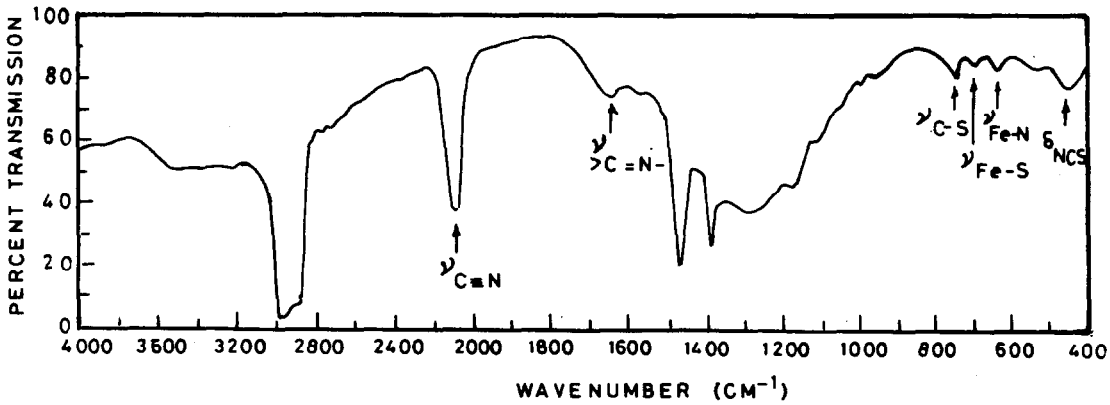


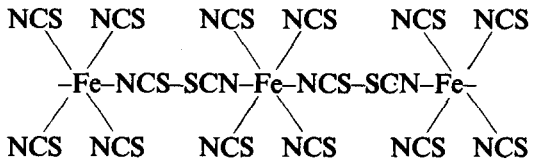

Fig. 1. IR spectrum of the solid complex (Nujol Mull).

Table 1. Analytical data for the solid complex, %

| Component sought | Observed | Calculated from: $K_2[Fe(SCN)_4(NCS\text{-}SCN)]$ |
|---|---|---|
| C | 15.00 | 14.93 |
| N | 17.11 | 17.43 |
| S | 40.21 | 39.83 |
| $Fe^{2+}$ | 10.00 | 11.61 |
| $K^+$ | 16.20 | 16.18 |
| $SCN^-$ | 48.00 | 48.13 |
| $(NCS)_2$ | 27.12 | 24.07 |

would be produced by the decomposition of the coordinated thiocyanogen.

The results of chemical analysis of the solid complex are shown in Table 1. These results correspond to the formula: $K_2[Fe(SCN)_4(NCS\text{–}SCN)]$, where Fe(II) is coordinated to four thiocyanate anions and a molecule of thiocyanogen. Since, in solution, the complex tends to polymerize, it may be inferred that polymerization may be brought about by thiocyanogen bridges. A possible structure which may account for these observations is:




in which the iron is in an octahedral environment. It was not easy to decide the mode of bonding of thiocyanate to the metal ion, but since the C–S stretching frequency is relatively low, (740 $cm^{-1}$), it is probable that the iron is bonded through the thiocyanate sulphur, in addition to the thiocyanogen nitrogen. The bands at 630 and 690 $cm^{-1}$, in the infrared spectrum may correspond to Fe–N stretching frequencies.

## REFERENCES

1. R. H. Betts and F. S. Dainton, *J. Am. Chem. Soc.* 1953, **75**, 5721.
2. K. J. Ellis and G. S. Lawrence, *Trans. Farad. Soc.* 1967, **63**, 91.
3. N. J. Bjerrum and A. Kirschner, *Kgl. Danske Videnskab. Math. Fys. Series* 8.5.57 (*C.A.* 1919, **13**, 1057).
4. B. Kratochvil and R. Lang, *Anal. Chem.* 1970, **42**, 43.
5. (a) G. Metzger, Rapp. CEA-T 2566 Comissarial a l'Energie Atomique, Centre d'Edudes Nucleaires, Saclay, France (1964); (b) A. Eluard and B. Tremillon, *J. Electroanal. Chem.* 1967, **13**, 208; (c) D. H. Kerridge and M. Mosley, *J. Chem. Soc* (*A*) 1969, 2211.
6. S. K. Tobia and M. F. El-Shahat, *J. Chem. Soc.* (*A*) 1968, 2444.
7. P. Mesnard and A. Liermain, *Bull. Soc. Pharm. Bordeaux*, 1952, **90**, 87.
8 T. S. West, *Complexometry with EDTA and Related Reagents*, p. 187. BDH Chemicals Ltd., Poole, England (1969).
9. A. I. Vogel, *Elementary Practical Organic Chemistry*, Part III, 2nd Edn., p. 659. Longmans, London (1958).
10. A. S. Kamarowsky and N. S. Polueklow, *Z. Anal. Chem.* 1934, **96**, 23.
11. C. E. Vanderzee and A. S. Quist, *Inorg. Chem.* 1966, **5**, 1238.

*Polyhedron* Vol. 3, No. 8, pp. 1001–1011, 1984
Printed in the U.S.A.

0277–5387/84 $3.00 + .00
© 1984 Pergamon Press Ltd.

# SPECTROSCOPIC AND SCATTERING INVESTIGATION OF ISOPOLY-MOLYBDATE AND TUNGSTATE SOLUTIONS

KA YUEN SIMON NG and ERDOGAN GULARI*
Department of Chemical Engineering, The University of Michigan, Ann Arbor, MI 48109, U.S.A.

(*Received* 6 *October* 1983; *accepted* 21 *November* 1983)

**Abstract**—Detailed spectroscopic and scattering investigations of isopoly-molybdate and -tungstate solutions as a function of concentration and pH were made. From scattering results the apparent molecular weights were determined as a function of time and concentration. We find that the results agree with the aggregation scheme of simple → hepta → octa → $[Mo_{36}O_{112}]^{-8}$ → protonated polymeric species, for molybdate solutions. Tungstate solutions aggregate according to simple → Y-polytungstate → paratungstate-A → paratungstate-B → Ψ-metatungstate. The molybdate solutions exhibited very rapid equilibration, but the tungstate solutions required several days to reach equilibrium. From the discrete changes in the Raman spectra of both systems we find that the formation of isopoly anions is not a continuous process and that only certain species are present in solution. Our results do not rule out the formation of significant quantities of the octamolybdate anion as suggested by previous investigators.

The isopoly-molybdates and -tungstates constitute a large class of inorganic compounds and have been the subjects of two reviews[1,2] and numerous investigations.[3–8] These compounds consist of a simple cation and a condensed molybdate or tungstate anion. Solutions of these compounds are the starting point for molybdate and tungstate-based supported catalysts for hydrodesulfurization and hydrodenitration. Supported molybdates and tungstates are also good candidates to become sulfur tolerant methanation and water gas shift reaction catalysts. As a part of our efforts to develop high activity, high dispersion catalysts, we investigated the formation of isopoly species in solution as a function of concentration and pH.

The following is a brief review of the conditions for the existence of the various isopoly species studied in this work.

*Author to whom correspondence should be addressed.

(a) *Isopolymolybdates in solution*

Whilst there has been confusion and contradictory findings[9] regarding the existence of polynuclear species such as $Mo_4O_{13}^{2-}$, at present the following species appear to be generally accepted (1): $MoO_4^{2-}$ ion is the stable species above pH 6.5; for $4.5 < pH < 6.5$, the paramolybdate $(Mo_7O_{24})^{6-}$ exists in equilibrium with $MoO_4^{2-}$.

$$7(MoO_4)^{2-} + 8H^+ \rightleftharpoons (Mo_7O_{24})^{6-} + 4H_2O. \quad (1)$$

Further acidification leads to the formation of the octamolybdate anion $(Mo_8O_{26})^{4-}$ between pH 2.9 and 1.5. Formation of larger aggregates at lower pH values was initially postulated by Jahr[10] but not proven. From an analysis of Raman spectra, Tytko and Schonfeld[15] showed that the anion $Mo_{36}O_{112}^{8-}$ is also present in solution below a pH of 2.0. At pH 0.9, molybdic acid ($MoO_3 \cdot H_2O$) precipitates from solution and redissolves with further increases in the hydrogen ion concentration. Below pH 0.9,

positively-charged species such as $MoO_2^{+}$ and $MoO^{4+}$, $HMo_2O_6^{4+}$ have been reported.[11] In concentrated HCl solutions, the presence of $MoO_2Cl_2$ species was also deduced from the Raman spectra.[7]

(*b*) *Isopolytungstates in solution*

In the highly alkaline region (pH > 8), the tungstate ion exists as the normal tungstate species $WO_4^{2-}$. Upon acidification to a pH of 5–6, the paratungstate-A ion $[HW_6O_{21}]^{5-}$ is formed by the reaction (1):

$$6WO_4^{2-} + 7H^+ \rightleftharpoons [HW_6O_{21}]^{5-} + 3H_2O. \quad (2)$$

The paratungstate-A ion is in slow equilibrium with the paratungstate-B ion $[W_{12}O_{36}(OH)_{10}]^{10-}$.

$$2[W_6O_{20}(OH)]^{5-} + 4H_2O \rightleftharpoons [W_{12}O_{36}(OH)_{10}]^{10-}. \quad (3)$$

At high concentrations, the B ion is predominant.[12] Aging solutions of paratungstate ions result in the formation of $\Psi$-metatungstate $[W_{24}O_{72}(OH)_{12}]^{12-}$. Polytungstate-Y has been obtained shortly after acidification of the normal tungstate solution to a $H^+$ to $WO_4^{2-}$ ratio of 2.00 and has been formulated as (5):

$$[W_{12}O_x(OH)_y]^{-72-(2x+y)}. \quad (4)$$

When the concentration of $WO_4^{2-}$ is less than $5 \times 10^{-5}$ M, no isopoly anions are formed; instead, the insoluble tungstic acid $H_2WO_4$ is formed by direct protonation.[13]

## EXPERIMENTAL

(*a*) *Materials*

All the solutions were prepared from certified ACS grade (Fisher) Ammonium molybdate, sodium tungstate and doubly-distilled deionized water.

(*b*) *Methods*

(1) *Light scattering.* Light scattering measurements were made with a laser light scattering spectrometer consisting of a 2 W argon-ion laser, a 64 channel multibit Malvern correlator, an HP 5300B counter, and an HP 9835 computer. All the optics were mounted on a vibration isolation table to eliminate the effect of building vibrations. Intensity measurements were made by photon counting at 90° scattering angle. By using pure benzene as a reference, molecular weights were computed from the intensity measurements. Diffusion coefficients were obtained from the autocorrelation function of the scattered light using:[14]

$$g(\tau) = A^* \exp(-D K^2 \tau) \quad (5)$$

where $g$ is the field autocorrelation function, $D$ is the diffusion coefficient, $K$ is the scattering vector ($= 4\pi n/\lambda \sin \theta/2$) at an angle $\theta$ with an incident light wavelength of $\lambda$, and $\tau$ is the delay time.

(2) *Raman spectroscopy.* Raman spectra were obtained with a SPEX Triplemate spectrograph coupled to a Tracor Northern 1024 large area intensified diode array detector. The 514.5 line of a 4W Argon ion laser was used as the excitation source. Typical power at the sample was on the order of 100 mW. 5 mm dia. NMR tubes were used as sample cells. Since the detector simultaneously measured a 1300 $cm^{-1}$ region, all the spectra were obtained without moving any of the gratings. Spectra were taken either with 2 or 4 $cm^{-1}$ resolution. Typically, each spectrum consisted of 512 co-added scans taking the total time of ten minutes. Since the spectrum is totally digital and no gratings were moved, spectral subtraction could be used very reliably to eliminate the background without increasing the noise.

## RESULTS

(*a*) *Light and X-ray scattering*

The results of the scattering experiments are shown in Table 1. We emphasize that all the molecular weights and the hydrodynamic radii calculated from the diffusion coefficient using the Stokes–Einstein relationship are apparent values:

$$D = kT/6\eta r\pi \quad (6)$$

$D$ is the diffusion coefficient, $k$ is the Boltzmann constant, $T$ is the absolute temperature, $\eta$ is the viscosity of the solvent, and $r$ is the hydrodynamic radius.

This is due to the fact that these values were determined using solutions of finite concentrations, and the scattering theory is rigorous only at the limit of infinite dilution. Since the degree of association is concentration dependent, the standard technique of making a Zimm plot to eliminate the concentration dependence is not possible. The apparent molecular weights of polymeric molybdates are 1260 at pH 2.6, 660 at pH 5.5 and 260 at pH 9.0 for a 0.2 M solution. The value $1260 \pm 100$ is low compared to MW = $2500 \pm 1000$ reported by Kestigian *et al.*,[3] but in excellent agreement with a formula weight of 1183.5 for the octa-molybdate anion $[Mo_8O_{26}]^{4-}$. MW = 660 at pH 5.5 indicates that at this pH and concentration, significant amounts of both the simple molybdate $(MoO_4)^{2-}$ and the heptamolybdate $(Mo_7O_{24})^{6-}$ exist in equilibrium. If we

Table 1. Scattering results of molybdates and tungstates

| Sample | Conc. wt.% | pH | X-Ray | Laser | | |
|---|---|---|---|---|---|---|
| | | | Rg(A) | Apparent MWT | Rh(A) | Diff. Coeff. ($\times 10^6$ cm$^2$/sec.) |
| Ammonium Molybdate | 5 | 2.5 | 4.71 | 1260 ± 100 | 7.3205 | 3.1266 |
| | 5 | 5.4 | 4.15 | 660 ± 100 | 5.3376 | 4.2881 |
| | 12.5 | 9.0 | 2.95 | 470 ± 100 | - | - |
| Sodium Tungstate | 2.5 | 2.4 | 6.03 | 2760 ± 100 | 13.063 | 1.8757 |
| | 2.5 | 5.5 | 4.36 | 660 ± 100 | 6.9732 | 3.5138 |
| | 2.5 | 9.2 | 3.33 | 220 ± 100 | - | - |

assume simple and heptamolybdate are the only anions present, a rough estimate based on the weight average molecular weight of 660 indicates that about 30% is in the hepta form, in good agreement with the Raman results discussed later. We also followed the change in the apparent molecular weight of polymeric species as a function of pH. The results are shown in Fig. 1 for 0.1 M solution. Starting from a pH of 2.4, the pH of the solution in a light scattering cell was slowly lowered by dropwise addition of 2 M or 10 M HCl. The apparent molecular weight as computed from the intensity of the scattered light started at MW = 350, pH = 2.4 and increased to a maximum of 5200 at a pH of 1.1; it then decreased to a local minimum of MW = 800 around the isoelectric point (pH = 0.9). The apparent MW continued increasing with further lowering of the pH reaching MW = 2500 at pH = 0.80. We should note that all the changes were very rapid; even the dramatic increase in MW observed when going from a pH of 2.5–1.10 occurred over a period of three minutes. The molecular weight of the pH 2.5 species is lower than the corresponding value obtained with a 0.2 M solution by a factor of about three, indicating significant concentration dependence.

For the tungstate solutions, we find that MW = 220 ± 50, 660 ± 100, 2760 ± 100 at pH 9.2, 5.5 and 2.4 respectively. MW = 220 ± 50 is in very good agreement with the formula weight of the simple tungstate anion $WO_4^{2-}$, MW = 247.8. MW = 660 at pH 5.5 indicates an equilibrium between the simple anion and the polymeric species. MW = 2760 ± 100 at pH of 2.4 is in very good agreement with the formula weights of $[W_{12}O_{36}(OH)_{10}]^{10-}$, FW = 2952 of paratungstate-B and $[W_{12}O_{38}(OH)_2]^{6-}$, FW = 2848 of metatungstate. However, under the conditions of our experiments, the most likely species is either the paratungstate-B species or polytungstate-Y species because our samples were relatively fresh.

In order to study the time dependent kinetics of the transition from paratungstate-A to paratungstate-B to $\Psi$-metatungstate, we first prepared a 0.07 M sodium tungstate solution, acidified it to a pH of 5.0 and then heated it to 80°C. The changes in the molecular weight were followed by measuring the intensity of the scattered light as a function of time. Figure 2 shows the results of our measurements. The starting point on the time axis corresponds to 1 hr after the preparation of the sample because of the time consumed by the centrifugation of the sample to remove dust. At the start, there is already a small amount of paratungstate-B as evidenced by the molecular weight of MW = 1800. In a period of 6 hr, the measured molecular weight more than doubles and reaches a value of MW = 4500.

Also shown in Table 1 are the radii of gyration values determined from the angular dependence of the scattered X-ray intensity. Since these values are at the lower end of the measurable values by SAXS, their accuracy is low (± 0.5A); however, they parallel changes in the molecular weight measurements. The hydrodynamic radii of the isopoly species are larger for the tungstates than the molybdates, in agreement with the molecular weight measurements.

It is interesting to note that if we use our values of the molecular weight and the diffusion coefficient to test Riecke's Law $D\sqrt{M}$ = constant, we find that the law seems to be holding: [pH 5.4] $(3.13 \times 10^{-6})\sqrt{1260} = 1.11 \times 10^{-4} \simeq (4.29 \times 10^{-6})\sqrt{660}$ [pH 2.5] $= 1.10 \times 10^{-4}$ for the isopolymolybdates and [pH 2.4] $(1.88 \times 10^{-6})\sqrt{2760} = 9.88 \times 10^{-5} \simeq (3.51 \times 10^{-6})\sqrt{660}$ [at pH 5.5] $= 9.02 \times 10^{-5}$ for the tungstates.

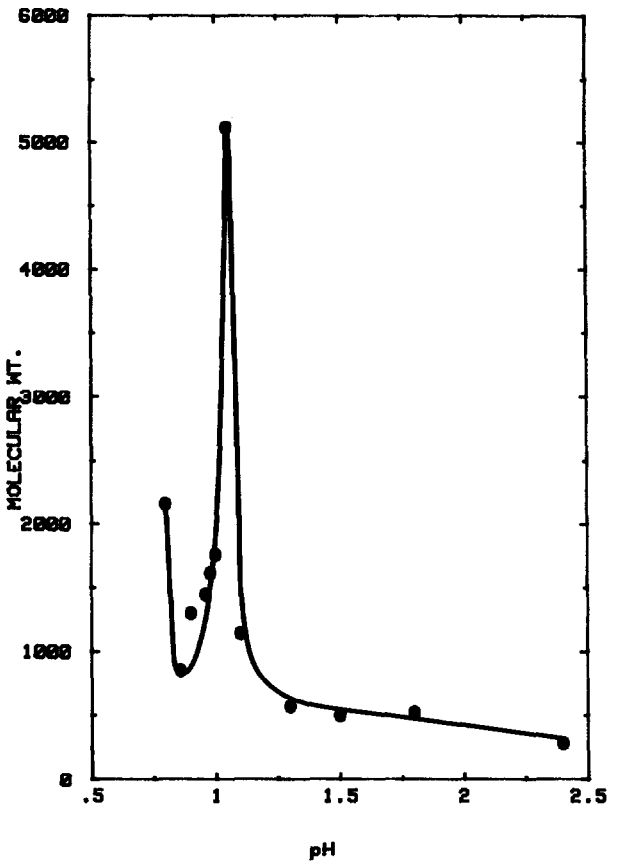



Fig. 1. Apparent molecular weights of the polymeric species as a function of pH for 0.1 M ammonium heptamolybdate solution.

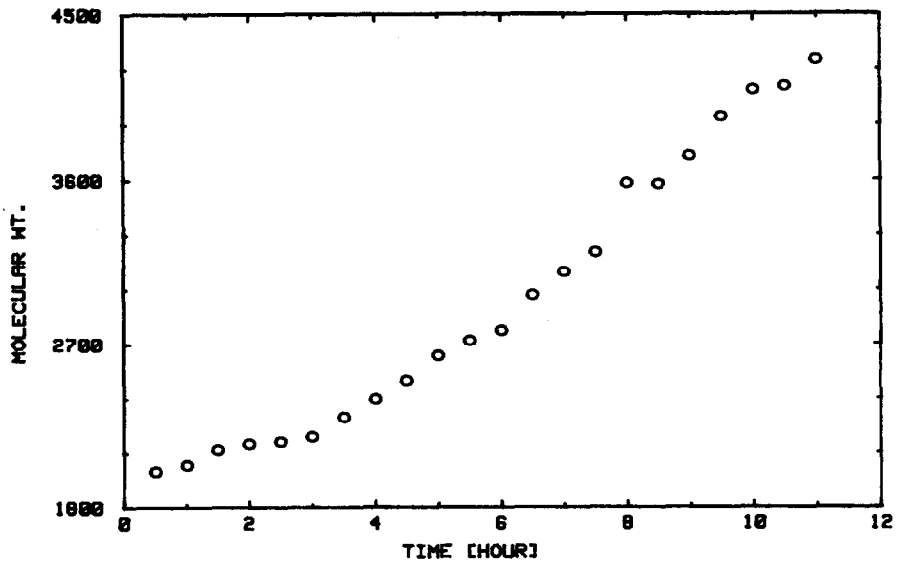



Fig. 2. Dynamic study of molecular weight of 0.07 M sodium tungstate solution as a function of time at 80 C. The molecular weights obtained show the aggregation behaviour of tungstates with respect to time as Y-Polytungstate → Paratungstate-A → Paratungstate-B → Ψ-Metatungstate.

(*b*) *Raman spectroscopy*

(1) *Raman spectra of the isomolybdates in solution.* Raman spectra of isopolymolybdates were obtained as a function of pH and concentration. Figure 3 shows the pH dependence for 5% by weight of ammonium paramolybdate solution in the wavenumber range of 750 to 1000 $cm^{-1}$. We see that at pH 9 there are only two peaks: a sharp peak at 896 $cm^{-1}$ and a broader peak at 854 $cm^{-1}$. These are due to the Mo=O stretch. Upon acidification to a pH of 6.6, both of the peaks decrease in intensity but a new strong peak at 939 $cm^{-1}$ appears. This new peak is due to the formation of the heptamolybdate species in solution, which as seen from the Raman spectra exists in equilibrium with the $(MoO_4)^{2-}$ anion. The fact that there is a sudden shift is proof that there are no appreciable intermediates between the simple and the heptamolybdate anions. At pH 5.4, the heptamolybdate series is the primary species but there is still a significant concentration of $(MoO_4)^{2-}$ anion present. Further acidification to pH 2.2 leads to the appearance of two new peaks (one at 973 $cm^{-1}$ and one at 844 $cm^{-1}$), and the shifting of the two major Mo=O stretch peaks to 958 and 913 $cm^{-1}$. This is the first investigation in which the 973 and 844 $cm^{-1}$ bands have been observed. At this pH and concentration (0.2 M) we expect the dominant isopoly species to be the octamolybdate anion $(Mo_8O_{26})^{4-}$. It is possible that the new peaks are due to the formation of the more highly aggregated species such as the $Mo_{36}O_{112}^{8-}$ anion. The time between the preparation of the sample and obtaining the Raman spectrum was less than half an hour, thus there should not be significant amounts of slow-forming aggregates. At

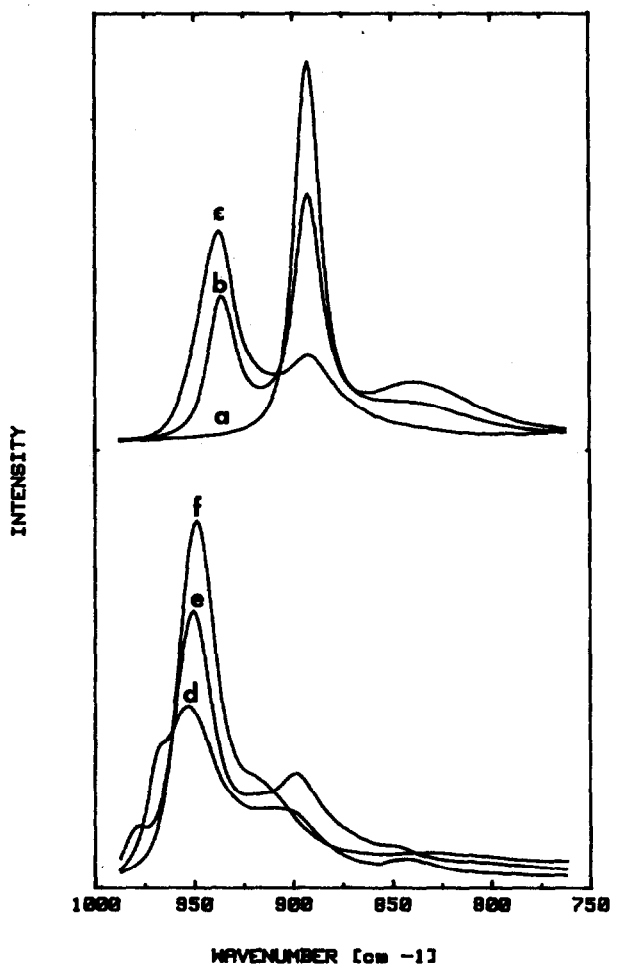



Fig. 3. Raman spectra of 0.2 M AHM solution in high wavenumber region, as a function of pH; (a) pH 9, (b) pH 6.6, (c) pH 5.4, (d) pH 2.2, (e) pH 0.95, (f) pH 0.3. The sudden shift of the 896 $cm^{-1}$ peak to the 939 $cm^{-1}$ peak shows that there are no appreciable intermediates between the simple and the heptamolybdate anions.

pH 0.95, just above the isoelectric point of molybdic acid, there are still four peaks: the two major peaks at 954 and 911 $cm^{-1}$ and the peaks at 835 and 982 $cm^{-1}$. The final set of spectra at pH = 0.3 was taken with a lower concentration (0.1 M) in order to prevent any precipitate formation. The spectrum of the pH 0.3 sample is significantly different than the others. At pH 0.3, the high frequency band at 982 $cm^{-1}$ completely disappears. Instead, the 953 $cm^{-1}$ band is sharp and strong and a second peak at 933 $cm^{-1}$ is observed. There is also a weak and broad third peak at 827 $cm^{-1}$. All the wavenumbers given above were obtained after curve fitting the M=O stretch region with a sum of Gaussian bands.

The Raman spectra for pH's of 6.6, 2.2 and 0.95 show two weak and broad peaks between 400 and 600 $cm^{-1}$. At pH 0.3, there is only single asymmetric peak at 450 $cm^{-1}$.

Figure 4 shows the Raman bands in the frequency range of 150–500 $cm^{-1}$. A single strong peak at 318 $cm^{-1}$ is observed for pH 9 solutions. At pH 6.6, two strong peaks at 318 and 208 $cm^{-1}$ are observed; the stronger of the two is the 318 $cm^{-1}$. As the pH is lowered to 2.2, the intensity of the 318 $cm^{-1}$ band decreases and its position shifts to 363 $cm^{-1}$. The intensity and position of the 208 $cm^{-1}$ band stays constant but the frequency is shifted to 200 $cm^{-1}$. Further acidification to pH 0.95 shifts the 208–225 $cm^{-1}$ and the peak structure indicates a possible splitting. At pH 0.3, the 363 and 210 $cm^{-1}$ peaks are still present and a third weak band at 300 $cm^{-1}$ appears.

We also obtained the Raman spectra as a function of concentration at a pH of 5 for 0.2, 0.04 and 0.008 molar molybdate solutions. The only significant change was the appearance of the 844 $cm^{-1}$ band at the lower concentrations. The relative ratio of the 896 $cm^{-1}$ to the 939 $^{-1}$ bands also increased by about 10–15% with decreasing concentration.

(2) *Raman spectra of the isopolytungstates in solution.* Raman spectra of the tungstate solutions were obtained as a function of time, pH and concentration in order to elucidate the complex equilibrium processes present in isopolytungstate solutions. We followed the changes occurring in the solution by taking the spectra at $t = 0$, $t = 1$

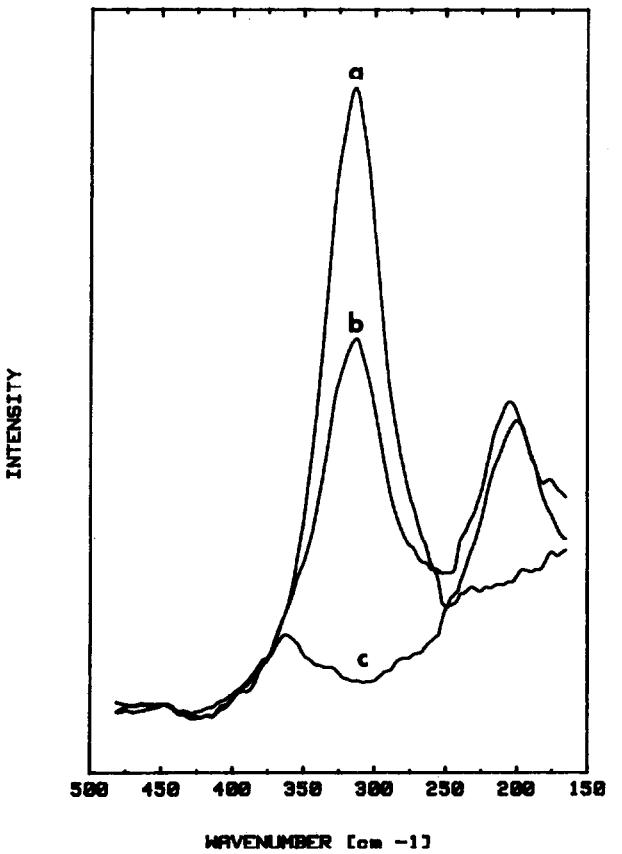



Fig. 4. Raman spectra of 0.2 M AHM solution in low wavenumber region as a function of pH; (a) pH 9, (b) pH 6.6, (c) pH 2.2.

day and $t = 6$ days. Figure 5 shows the Raman spectra of a 0.1 M solution (pH 7.3) taken at $t = 0$ and $t = 6$ days. We see that there is a significant difference between the two spectra. After equilibration, the ratio of the 960–931 $cm^{-1}$ peak has decreased. This decrease is accompanied by a slight broadening and upshift of the 931 $cm^{-1}$ peak. The spectrum obtained after 1 day of aging is essentially the same. Time dependent changes were observed for the other solutions with different pH's. All the other Raman spectra shown in Fig. 6 were obtained after the samples had aged for 6 days. At pH 9, there is a sharp peak at 930 $cm^{-1}$ (W=O stretch) and a broad peak at 834 $cm^{-1}$ (W–O–W asymmetric stretch) characteristic of the monomeric $WO_4^{2-}$ anion. As the pH is lowered to 7.3, aggregation starts and two more peaks appear at 960 and 927 $cm^{-1}$. These are due to the polymeric tungstate species in solution (most likely the paratungstate-B anion). In order to make more quantitative measurements we assumed that the scattering cross sections of all the Raman peaks in the W=O stretch region remained the same (according to our measurements this assumption holds to within 10%) and performed Gaussian deconvolution of the complex peaks. Judging from the results of Gaussian curve deconvolution, at pH 7.3, 16% of the tungstate is in polymeric form. We should note that around this pH the relative ratios of the monomeric and polymeric species are very pH sensitive. As the pH is decreased to 4.9, the intensity of the 960 $cm^{-1}$ band increases at the expense of the 930 $cm^{-1}$ band and curve deconvolution tells us that 80% of the tungstate is in the polymeric form. The fact that the frequency of the W=O band at 960 $cm^{-1}$ has not shifted to higher frequencies indicates that the polymeric species present at pH 4.9 are identical to those of pH 7.3 (paratungstate-B). The W–O–W asymmetric stretching frequency for the polymeric species is shifted to directly under the W=O stretching peak of the monomeric species at 930 $cm^{-1}$. Further decrease of the pH to 3 results in a small shift of 5 $cm^{-1}$ to 965 $cm^{-1}$ for the W=O vibration; the other peaks are at 933 and 894 $cm^{-1}$, respectively. The width of the W=O stretching peak increases with decreasing pH from 8 $cm^{-1}$ at pH 9 to 13 $cm^{-1}$ at pH 3.0. Further acidification of the solution results in the precipitation of tungstic acid at a pH of 2.0. By decreasing the solution concentration we were able to get Raman spectra of solutions with pH's as low as 1.7. At a pH of 2.2, strong peaks at 990 $cm^{-1}$, 975 $cm^{-1}$, 890 $cm^{-1}$ and 838 $cm^{-1}$ were observed.

Figure 7 shows the tungstate solution spectra at pH = 6.6 for 0.24, 0.06 and 0.015 M solutions. For all three concentrations, there are three peaks: 960, 930 and 895 $cm^{-1}$. However, the relative intensities change drastically. The relative ratio of the 930 $cm^{-1}$ peak (due to the simple anion ($WO_4^{2-}$) to 960 $cm^{-1}$ (due to the polymeric species A, B and Y polytungstates) decreases with increasing concentration, and changes by almost a factor of twenty. The low frequency Raman peaks for the tungstate solutions are given in Table 2.

## DISCUSSION

### (a) *Light and X-ray scattering results*

The apparent molecular weight measurements we obtained in this study are in good agreement

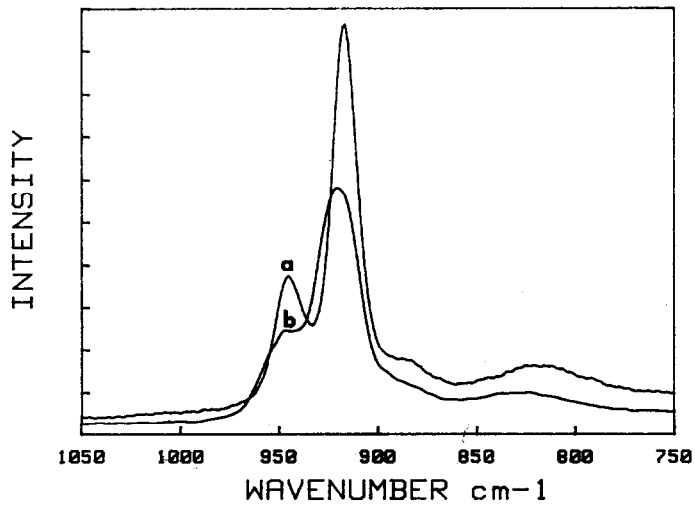



Fig. 5. Raman spectra of 0.1 M sodium tungstate solution as a function of time; (a) $t = 0$, (b) 6 days. After equilibration, the ratio of the 960–931 $cm^{-1}$ peak has decreased.

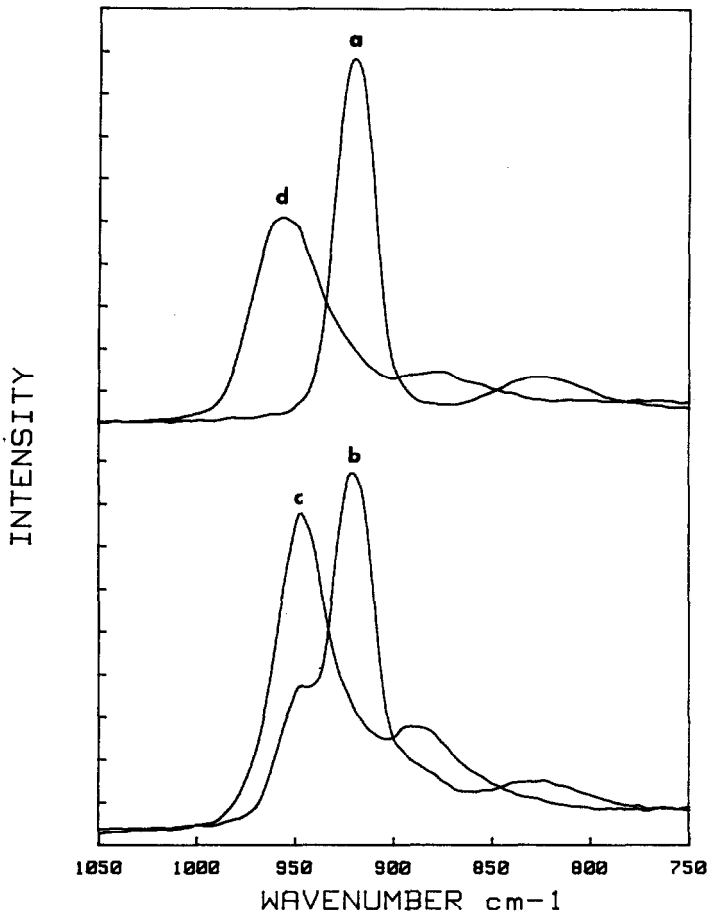



Fig. 6. Raman spectra of 6 day old 0.1 M sodium tungstate solution as a function of pH; (a) pH 9, (b) pH 7.3, (c) pH 4.9, (d) pH 3.

with those determined by the sedimentation equilibrium method.[2] Unfortunately, there is a significant concentration dependence and the resolution is not high enough to distinguish between the hepta- and octa-molybdate species in order to resolve the question whether or not octamolybdate is the dominant species at pH's below 4.5. However, our light scattering measurements as a function of pH definitely show the rapid transition from the normal molybdate to hepta-(or octa-) molybdate, followed by the $(Mo_{36}O_{112})^{8-}$ anion at a pH of 1.3, reaching complete conversion at pH 1.10. These pH's are low compared to Tytko and Glemser,[2,15] but these authors did not give the concentration of their solutions. As a result, the comparisons in pH are only approximate. We have also observed a phenomenon that has not been observed before: a decrease in aggregation as pH is lowered from 1.1, reaching to a minimum molecular weight of 800 at a pH of 0.86, and then rapidly increasing to MW = 2200 at a pH of 0.8. This result indicates that below the isoelectric point of molybdic acid (pH 0.9), there is a different polymeric species (possibly positively charged) existing in very acidic solution. This finding is in good agreement with the Raman spectra which show a significant change at a pH of 0.95. At the moment, we do not know the exact formula of this new species.

Our time-dependent studies of the changes in the molecular weight of the isopolymolybdates and isopolytungstates dramatically show the difference in the kinetics of aggregation between the two systems. For the isopolymolybdates, the aggregation is very fast. Upon acidification to pH of 1.0, the molecular weight increased and reached a steady value of MW = 5200 in a few minutes. This indicates an almost complete conversion to $(Mo_{36}O_{112})^{8-}$ anion, in agreement with the previous findings of Tytko *et al.*[15] In the isopolytungstates, the formation of paratungstate-A (MW = 1490) is fast. At room temperature, aggregation to paratungstate-B (MW = 2952) also proceeds relatively fast. As seen in Fig. 2, at 80°C, further

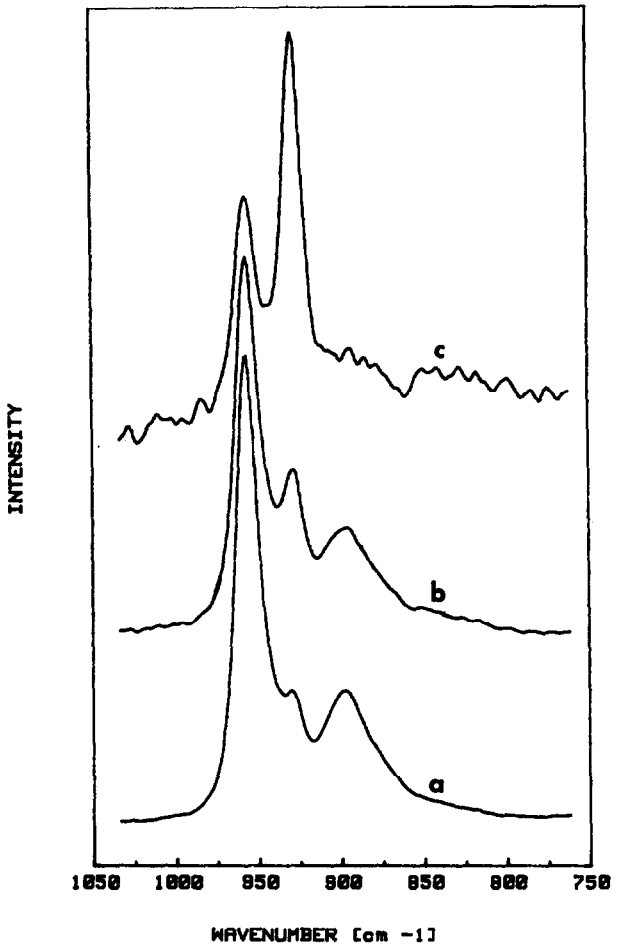



Fig. 7. Raman spectra of sodium tungstate solution at pH 6.6 as a function of concentration; $a = 0.24$ M, $b = 0.06$ M, $c = 0.015$ M. The relative ratio of the 930 $cm^{-1}$ peak (due to the simple anion $WO_4^{2-}$) to 960 $cm^{-1}$ peak (due to the polymeric species) decreases with increasing concentration.

aggregation of the present paratungstate-B to $\Psi$-metatungstate is going on simultaneously with the aggregation of paratungstate A to B. At the end of the 12 hr period, the average molecular weight of the isopoly species is about 4500, showing that the polymeric species are mostly $\Psi$-metatungstate. After standing for another week, this solution contained large suspended crystallites of 2000–3000 Å size, indicating that sodium-$\Psi$-metatungstate was precipitating out of solution even though there was no visible precipitate at the bottom.

Since our Rh and Rg values are the only data of their kind, it is not possible to make any comparisons with past work.

*(b) Raman results*

(1) *Isopolymolybdates.* Our measurements were made with very dilute solutions compared to previous investigators.[7,15,16] As a result, it is possible that some band frequencies are shifted slightly due to the concentration effect. The Raman spectrum of isopolymolybdates contains the following bands: around 900 $cm^{-1}$, Mo=O stretching; 840–750 $cm^{-1}$, Mo–O–Mo asymmetric stretching, 600–400 $cm^{-1}$, Mo–O–Mo symmetric stretching, Mo=O bending at 350 $cm^{-1}$, and Mo–O–Mo deformations at 200 $cm^{-1}$. The pH 9 spectrum has three strong bands at 896, 854 and 318 $cm^{-1}$. These frequencies are in very good agreement with the reported literature values.[7,15,16] According to Tytko and Glesmer,[2] the first stable polymeric species that is formed in appreciable quantities is the hepta $(Mo_7O_{24})^{6-}$ molybdate. According to our measurements, this species is first detectable at a pH of 7.5 for 0.2 M solutions. We also see no gradual shift in the frequencies of any of the Mo=O and Mo–O–Mo bands; rather, the changes in Raman

Table 2. Low frequency Raman peaks of the 0.10 M sodium solution as a function of pH

| pH | Peak Position ($cm^{-1}$) | |
|---|---|---|
| 9 | 330 | s |
| | 475 | w |
| | 575 | w |
| | 480 | w |
| 7.1 | 360 | s |
| | 310 | s |
| | 200 | s |
| | 625 | w |
| | 450 | w |
| 4.7 | 360 | w |
| | 310 | w |
| | 200 | s |

s = strong; w = weak

spectrum are discrete. As soon as the pH is lowered to 7.0, we observe the presence of new bands at 939, 450, 208 and 180 $cm^{-1}$, along with the bands of $(MoO_4)^{2-}$ given above. These new bands are due to the formation of the heptamolybdate anion as has been correctly assigned before.[7] We have, however, for the first time demonstrated that the equilibrium between the simple and the heptamolybdate anions result in significant amounts of both over a wide pH range if we assume that the Raman cross sections are the same. Quantitative deconvolution of the Raman spectra show that even at pH 6.6, almost half of all molybdate is in hepta form. This transformation is complete at a pH of 4.5 for 0.2 M solutions but for more dilute solutions the transformation is complete at lower pH values. All the Raman band frequencies for molybdates are in good agreement (within a few $cm^{-1}$) with the previous measurements.

Perhaps the most significant controversy regarding isopolymolybdate solutions has been about the existence of the octamolybdate anion. Until 1976, it was assumed that lowering of the pH (or increasing the degree of protonation below pH 4.5) resulted in the transformation of the heptamolybdate anion into the octamolybdate anion. This conclusion was reached after comparing the structure of the crystalline octamolybdate Raman spectra to that of a concentrated solution of lithium or ammonium molybdate at a protonation ratio of 1.5.[7] Tytko and Schonfeld[15] have argued strongly against this and have proposed a different aggregation scheme where the octamolybdate occurs in very small quantities and a new species $(Mo_{36}O_{112})^{8-}$ is the main polymeric anion between pH 2.5 and pH 1.0 ($p = 1.5$–$1.78$). A close inspection of our Raman spectra does not show any bands at 700 $cm^{-1}$, thus ruling out the polyoctamolybdate anion as a major component.[15] These is, however, a distinct shift in the Mo=O stretching frequency from 936 to 954 $cm^{-1}$ as the pH goes from 5.4 to 2.2. Quantitative comparisons with the spectra given by Tytko and Schonfeld[15] are impossible due to the lack of a table of peak frequencies in their paper. However, a qualitative comparison shows agreement with their $p = 1.67$ (pH 2.0) spectra. Most of the peak frequencies we observe are very close to those reported by Anacker and Johnson,[7] with the exception of the bands at 973 $cm^{-1}$ and the ones at 450 and 600 $cm^{-1}$. Qualitative agreement is also found with the Raman spectrum of tetrabutylammonium isooctamolybdate given by Fuchs and Brudgam,[17] who had listed strong peaks at 957, 917, 857, 531, 481, 367, 307 and 217 $cm^{-1}$. These values, however, were obtained in an organic solvent and some of the bands may not be due to the octamolybdate anion. Our peak frequencies of 973, 958, 913, 844, 363 and 200 $cm^{-1}$ for the pH 2.2 solution are in quantitative agreement with the results of Griffith and Lesniak[16] for crystalline ammonium octamolybdate and solution spectra for pH 1.8. Thus, contrary to the arguments of Tytko,[15] it is not possible to rule out the presence of significant amounts of octamolybdate anion on the basis of Raman and light scattering measurements alone. The Raman spectrum of pH 0.95 solution is significantly different than that of pH 2.2 solution. If we take the shift toward higher wavenumbers to be an indication of more aggregation, then the 982 $cm^{-1}$, Mo=O stretching band definitely shows the presence of aggregates much larger than the hepta and octamolybdate species. Qualitatively, our pH 0.95 spectrum is in good agreement with the spectrum given by Tytko[15] for the $(Mo_{36}O_{112})^{8-}$ anion. No quantitative comparisons are possible because of a lack of quantitative intensity and frequency information in Tytko's paper.

Since there are no other existing quantitative solution spectra below the isoelectric point, it is not possible to have a comparison of our pH 0.3 spectrum. This spectrum is very different than

those above the isoelectric point. If we again use the shift in the Mo=O stretching frequency as an indication of the degree of aggregation, we arrive at the conclusion that the species in solution has a degree of aggregation less than the 36 anion (in agreement with the light scattering measurements). At present, we do not have enough information to propose a formula for the isopoly species present in this strongly acidic solution.

(2) *Isopolytungstates.* The only other comprehensive Raman spectroscopy investigation of isopolytungstates is by Griffith.[16] For pH 9 solution, our peak frequencies fo 930, 834 and 330 $cm^{-1}$ are in exact agreement with their values. At a pH of 7.4, they observe a new band at 908 $cm^{-1}$ which is not present in our spectrum; however, we observed many more Raman bands due to the polymeric species in the low wavenumber region (as shown in Table 2). For pH 4.9 solution, our peak frequencies of 957, 927, 900, 625, 450, 360, 310 and 200 $cm^{-1}$ can be compared to Griffith's[16] 980, 966, 941, 902, 650, 460, 420, 348, 200 and 164 $cm^{-1}$. The bands at 980, 941 and 420 $cm^{-1}$ that they observed are probably due to the polytungstate A or Y species which are present in large amounts only for a short period after the acidification of the solution. We also observe these bands when our solutions are fresh. A further possibility may be due to the tenfold difference in concentration (1.0 M versus our 0.1 M solutions). Our spectra for the highly acidic solutions contain additional peaks at 838 and 875 $cm^{-1}$ that they did not observe.

*Acknowledgements*—Financial support of this research by the National Science Foundation (DMR 81–00130 and CPE 79–20818) and ACS–PRF(13210–AC7–C) is gratefully acknowledged. All the spectrometers used were bought by equipment grants from the National Science Foundation and The Dreyfus Foundation.

## REFERENCES

1. G. A. Tsigdinos and C. J. Hallada, Climax Molybdenum Co. Bulletin, Cdb–14, (1969).
2. K. H. Tytko and O. Glemser, *Adv. Inorg. Chem. Radio Chem.* 1976, **19**, 239.
3. M. Kestigian, P. Colodny and R. S. Stein, *J. Chem. Phys.* 1958, **21**, 952.
4. Y. Sasaki, I. Lindquist and L. G. Sillen, *J. Inorg. Nucl. Chem.* 1959, **9**, 93.
5. O. Glemser, W. Holznagel, W. Holtje and E. Schwarzmann, *Zeit Naturforsch* 1965, **20b**, 725.
6. A. Bartecki and D. Dembicka, *J. Inorg. Nucl. Chem.* 1967, **29**, 2907.
7. J. Aveston, E. W. Anacker and J. S. Johnson, *Inorg. Chem.* 1964, **3**, 735.
8. P. Souchay, *Talanta* 1965, **12**, 1187.
9. C. Heitner-Wirguin and R. Cohen, *J. Inorg. Nucl. Chem.* 1964, **26**, 161.
10. K. F. Jahr and J. Fuchs, *Angew. Chem. Int. Edn.* 1966, **5**, 689.
11. Y. Sasaki, *Acta Chem. Scand.* 1961, **15**, 75.
12. J. Aveston, *Inorg. Chem.* 1964, **3**, 981.
13. G. Schwarzenbach, G. Geier, and J. Meier, *J. Inorg. Nucl. Chem.* 1958, **8**, 302.
14. B. Chu, *Laser Light Scattering.* Academic Press, New York (1974).
15. K. H. Tytko and B. Schonfeld, *Z Naturforsch* 1975, **30b**, 471.
16. W. P. Griffith and P. J. B. Lesniak, *J. Chem. Soc. (A)*, 1969, 1066.
17. J. Fuchs and I. Brudgam, *Z Naturforsch* 1977, **32b**, 853.

*Polyhedron* Vol. 3, No. 8, pp. 1013–1015, 1984
Printed in the U.S.A.

0277–5387/84 $3.00 + .00
© 1984 Pergamon Press Ltd.

# NOTES

## REDUCTION OF IRIDIUM IN SOLUTION

**P. J. MAYNE**
Process Development Department, Matthey Rustenburg Refiners (UK) Limited,
Orchard Road, Royston, Herts, SG8 5HE, England

(*Received* 25 *August* 1983; *accepted* 10 *January* 1984)

**Abstract**—Iridium(IV) in solution may be reduced to metal via the intermediate Ir(I). Reduction of Ir(III) has not been detected. The current efficiency for metal deposition is low because: (1) The (IV)–(I) reduction is competing with the (IV) to (III) reduction, and hydrogen evolution in aqueous solution. (2) Ir(I) is very easily oxidised to (III), even by hydrogen. (3) Some iridium salts are not stable in the (IV) state (e.g. triaquotrichloroiridate in molar chloride).

Reduction of iridium metal from aqueous solution is desirable for decorative plating, analytical, and metal winning processes. Previous attempts to study voltammetrically the deposition of iridium metal have been unsuccessful, only recording the (IV)–(III) reduction and concluding that hydrogen evolution occurs before metallic deposition. Plating of the metal from fused cyanide baths[1,2] has been reported.

MacNamara,[3,4] Tyrrell[5] and Conn[6] examined the plating of iridium from aqueous baths. Each author favoured a different iridium salt and generally the (IV) oxidation state, rather than the (III). There was some indication that freshly dissolved iridium was more easily plated than stock solution. Even so, the bulk of the iridium (90%) remained in solution in an unplatable form, so that a fresh solution was required for a thick coating. In the absence of a separator reoxidation of Ir(III) to (IV) would occur at the anode, so that even if Ir(III) is itself inactive, as MacNamara proposed, it should be reoxidised and plated under the conditions of the experiments.

The hexachloroiridate (III) anion loses chloride ions in aqueous solution, and the coordination sites are filled with water molecules. Delépine[7] described the preparation of the aquopentachlorosalts by repeated evaporation to dryness with oxalic acid of the hexachloro-salt. Garner *et al.*[8] isolated diaquo- and triaquo-complexes by ion exchange chromatography and in one paper claimed to separate a *cis*- and *trans*-diaquo and a 1,2,3 and a 1,2,6 triaquo-salt.[9] By use of two-dimensional chromatography and electrophoresis Van Ooij[10] claimed evidence for cationic tetra- and penta-aquo ions.

Using a rotating platinum electrode, Pshenitsyn *et al.*[11] found a cationic wave for hexachloroiridate (IV) reduction and an anodic wave for (III) oxidation. The aquopentachloroiridate (III) was found to give a separate wave at more positive potential, but the more highly aquated ions were not examined.

The reports of the electroplaters indicate that deposition of metallic iridium from aqueous solution is possible, though not with complete recovery. Therefore, the aquated iridates were examined in aqueous solution at a rotating platinum electrode, and evidence for further reduction sought using a dropping mercury electrode (DME) in dimethyl formamide (DMF) where the hydrogen evolution reaction would be avoided.

### RESULTS AND DISCUSSION

Table 1 shows the half wave potential vs a saturated calomel electrode at a rotating platinum electrode for the (IV)–(III) reduction and (III)–(IV) oxidation for the isolable aquoiridium salts. For all but the triaquosalt the oxidation and reduction potentials are the same, within experimental error, so the reductions are reversible.

With increasing aquation the wave moves to more positive potentials, i.e. the (IV) state becomes a stronger oxidising agent. The triaquo is so

Table 1. $E_{1/2}$ for aquated iridium salts at a rotating platinum disc electrode

| Salt | Supporting Electrolyte | $E_{\frac{1}{2}}$ with Respect to Saturated Calomel |
|---|---|---|
| Hexachloroiridate III | 0.6M HCl | + 0.69V |
| Hexachloroiridate IV | 0.6M HCl | + 0.68V |
| Aquopentachloroiridate III | M HCl | + 0.82V |
| Aquopentachloroiridate IV | M HCl | + 0.83V |
| Trans Diaquotetrachloroiridate III | M HCl | + 0.94V |
| Trans Diaquotetrachloroiridate IV | M HCl | + 0.93V |
| 1,2,6 Triaquotrichloroiridate III | M HCl | Beyond anodic limit |
| 1,2,6 Triaquotrichloroiridate IV* | M HCl | i.e. > 1.03 |
| 1,2,6 Triaquotrichloroiridate III | 0.5M $HClO_4$ | + 1.05 |
| 1,2,6 Triaquotrichloroiridate III | 0.5M $H_2SO_4$ | + 1.05 |
| 1,2,6 Triaquotrichloroiridate IV | 0.5M $HClO_4$ | + 0.7 |
| 1,2,6 Triaquotrichloroiridate IV | 0.5M $H_2SO_4$ | Broad irreversible |

* Reduction wave of IV → III visible.

difficult to oxidise in hydrochloric acid that chlorine is evolved preferentially, and the waves were only detectable in perchloric and sulphuric acids. Thus the triaquotrichloriridate (IV) is unstable in molar chloride and will evolve chlorine and itself be reduced to the (III) state.

In perchloric or sulphuric acids oxidation of the triaquo also gave a pink solution, but this rapidly turned blue/black (24 hr). On prolonged standing all colour was lost, but analysis showed the colourless solution maintained the original iridium concentration. Similar colour changes have been reported by Fine[12] who interpreted them in terms of the formation of aquoiridium polymers.

Table 2 shows the recovery by zinc cementation of iridium in the aquated forms; with increasing aquation the recovery decreases. If MacNamara[3] is correct that only the (IV), but not the (III), oxidation state may be reduced to metal, Table 2 is readily explained with the results of Table 1. The further iridium is aquated, the more readily the (IV) state is reduced to the (III), which is not then further reducible.

Working in dimethyl formamide (DMF) with $2.10^{-2}$M tetramethyl ammonium chloride as the supporting electrolyte, the (IV)–(III) reduction was observed as in aqueous solution, and also a wave at $-1.65$ V at 0°C, with wave height 3.05 times the (IV)–(III) reduction. The half wave potential was temperature dependent moving to more positive potentials with increasing temperature at $+3.9$ mV/°C suggesting an irreversible reduction.

Both the $-1.65$ V wave and the (IV)–(III) reduction varied with the mercury column height in a manner compatible with diffusion controlled reductions. Page[13] also found the (IV)–(III) reduction diffusion controlled in aqueous solution.

Plots of $\log_{10}(i/id - i)$ for the waves at 0 and 100°C gave slopes of 50 and 65 mV/decade respectively. Coupled with the high temperature coefficient of the half wave potential the slopes indicate an irreversible reduction involving more that one electron. That the two reductions are diffusion controlled and the wave at $-1.65$ V three times the height of the one electron reduction gives evidence for a three electron reduction.

Reductions of ammonium hexachloroiridate (IV)–(III) in DMF with tetramethyl ammonium chloride present gave a hazy solution from which the iridium was removed by filtration. It was

Table 2. Percentage recovery by zinc cementation of aquated iridium salts

| Salt | ppm | | % Recovered by Zn |
|---|---|---|---|
| | ICP | Zn + AA | |
| Aquopentachloroiridate | 92 | 70 | 76 |
| Trans Diaquotetrachloroiridate | 230 | 180 | 78 |
| 1,2,6 Triaquotrichloroiridate | 150 | 80 | 53 |

concluded that the tetramethyl ammonium salt of hexachloroiridate (III) was insoluble in DMF. When lithium chloride was used as the supporting electrolyte the yellow solution characteristic of Ir(III) was produced. This solution showed no sign of the three electron reduction.

The polarographic evidence indicated a (IV)–(I), three electron, reduction of hexachloroiridate in DMF.

Attempts were made to reduce DMF solutions of ammonium hexachloroiridate (IV) to metal at $-2.9$ V at a 1.5 $cm^2$ platinum cathode with the anode separated from the bulk of the solution by a sintered glass disc. Reductions at $-0.5$ V, the (IV)–(III) reduction, gave a yellow solution characteristic of the (III) oxidation state. A similar yellow solution was produced by reduction at $-1.9$ V in the presence of air, or in a hydrogen purged solution, with no evidence for metal deposition. No absorption maximum was detectable in the UV/visible spectrum, only the tail of a band lying to shorter wavelength than 350 mm. DMF is effectively opaque below this wavelength.

However, in a nitrogen purged solution a black deposit appeared on the cathode, and this was enhanced by the addition of ten times the iridium concentration of triphenyl phosphine. Analysis of the solution revealed that 20% of the iridium has been deposited.

Iridium(IV) in solution may be reduced to metal via the intermediate Ir(I). Ir(I) is very unstable, being oxidised to Ir(III) by any dissolved oxygen, or even hydrogen. Ir(I) is known to undergo oxidative addition reactions with hydrogen.[14] Both rhodium[15] and ruthenium[16] have been shown to be reduced via lower oxidation state intermediates. Reduction of Ir(III) has not been detected.

The current efficiency for metal deposition will always be low because it proceeds through the very easily oxidised Ir(I) intermediate. The selection of different bath compositions by the electroplaters may be explained by the varying degree of aquation of the different preparations. The aquated species may be identified from their reduction potential, and this would permit the determination of the components of a mixture.

## EXPERIMENTAL

A Princeton Applied Research PAR 174A was used in conjunction with either a dropping mercury electrode or a rotating platinium electrode. In aqueous solution a saturated calomel electrode was used as reference and in the organic solvent a Ag/AgCl electrode in a solution of 100 mgm tetramethyl ammonium chloride per 100 $cm^3$ of dimethyl formamide separated by a sintered glass disc from the solution under examination. A Thompson Associates ministat was used for the bulk reductions at a 1.5 $cm^2$ platinum electrode.

Potassium aquopentachloroiridate was prepared according to Delépine,[7] and used according to Garner *et al.*[9] to isolate the *cis*- and *trans*-diaquotetrachloroiridates and the 1,2,6- and 1,2,3-triaquotrichloroiridates. However, the $E_{1/2}$ values indicated that the *cis*-diaquo was a weak solution of the aquopentachloro and the 1.2.3-triaquo a mixture of 1,2,6-triaquo and the *trans*-diaquo. Hence, it appeared doubtful whether the *cis*-diaquo or the 1,2,3-triaquo species had been prepared, and these results have been excluded from Table 1.

*Acknowledgements*—I am grateful to the management of Matthey Rustenburg Refiners for the provision of facilities and permission to publish this work.

## REFERENCES

1. D. R. Flinn and C. L. Manger, Rep. of Investigation 8656, U.S. Bureau of Mines.
2. J. C. Withers and P. E. Ritt, Tech. Proc. Am. Electroplaters Soc. 44th Ann. Conv. 1957, pp. 124–129.
3. E. L. MacNamara, *J. Electrochem. Soc.* 1962, **109**, 61.
4. E. L. MacNamara, U.S.P. 3,207,680.
5. C. J. Tyrrell, *Trans. Inst. Met. Finish.* 1965, **43**, 161.
6. G. A. Conn, *Plating* 1965, **52**, 1258.
7. M. Delépine, *Bull. Soc. Chim. Fr.* 1908, **4**, 901.
8. J. C. Chang and C. S. Garner, *Inorg. Chem.* 1965, **4**, 209.
9. A. A. El-Awady, E. J. Bounsall and C. S. Garner, *Inorg. Chem.* 1967, **6**, 79.
10. W. J. Van Ooij, *J. Chromatogr.* 1973, **81**, 190.
11. N. K. Pshenitsyn, N. A. Ezerskaya and V. D. Ratnikova, *J. Inorg. Chem. U.S.S.R.* 1958, **8**, 1791 (99 in trans.).
12. D. A. Fine, *J. Inorg. Nucl. Chem.* 1970, **32**, 2731.
13. J. A. Page, *Talanta* 1962, **9**, 365.
14. S. A. Cotton and F. A. Hart, *The Heavy Transition Elements*, p.99. MacMillan, London (1975).
15. R. D. Gillard, J. A. Osborn and G. Wilkson, *J. Chem. Soc.* 1965, 4107.
16. D. Rose and G. Wilkinson, *J. Chem. Soc. A.* 1970, 1791.

*Polyhedron* Vol. 3, No. 8, pp. 1017–1019, 1984
Printed in the U.S.A.

0277-5387/84 $3.00 + .00
© 1984 Pergamon Press Ltd.

# NOTE

# NOVEL SYNTHESIS OF A POTENTIALLY TRINUCLEATING LIGAND: 1,3-BIS-(2-HYDROXYPHENYL)-1,3-PROPANEDIONE

**FRANCESC TEIXIDOR, ANTONI LLOBET, LUIS ESCRICHE and JAUME CASABO***
Departament de Química Inorgànica, Facultat de Ciències, Universitat Autònoma de Barcelona, Barcelona, Spain

(*Received* 15 *September* 1983; *accepted* 10 *January* 1984)

**Abstract**—Reaction of 1,3-bis-(2-hydroxyphenyl)-1,3-propanedione ($H_3L$), a ligand with three possible sites of coordination acting as a chelating agent, with metal acetates results in the formation of mononuclear species $M(H_2L)_2 \cdot S,S'$ (M = Zn, Cu, Co; S,S' = solvent or water molecules). A compound of general formula $NEt_4[Li(H_2L)_2]$ is obtained upon reaction of $Zn(H_2L)_2 \cdot S,S'$ with excess of lithium ethanolate. Further reaction of the mononuclear species with excess of the appropriate metal acetate yielded di- or trinuclear complexes depending upon the metal used. Due to the different coordination sites of $H_3L$ it is expected that trinuclear complexes of the types $A_3$, $A_2B$ or $AB_2$ will be obtained. Examples of the types $A_3$ and $A_2B$ are reported.

The area of polynuclear complexes has grown extensively, stimulated by interest in their application to physico-chemical studies, catalysis and bio-inorganic chemistry.[1-4] The early 1970's saw the first reports of metal complexes of binucleating ligands and since then a considerable amount of information about these systems has appeared.[2] However, only a few systematic studies involving trinucleating ligands have been reported.[2]

Whereas the compound 1,3-bis-(2-hydroxyphenyl)-1,3-propanedione (Fig. 1) ($H_3L$) has been already synthesized several years ago, it had not been used as a ligand for metal complexes. To our understanding, this compound presents some remarkable possibilities as a ligand. It presents three possible sites of coordination acting as a chelating agent; two of them equivalent and one, the $\beta$-diketone moiety, different and the most reactive.

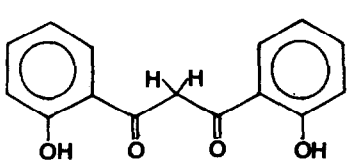



Fig. 1.

This is expected to permit the formation of discrete molecules with even three metal atoms each, with all these aligned. In addition, the synthesis can be directed to the formation of trinuclear complexes of the type $A_3$, $A_2B$ or $AB_2$.

In an attempt to test the aforementioned possibilities, $H_3L$ was synthesized according to the published method.[5] Mononuclear complexes of general formula $M(H_2L)_2 \cdot S,S'$ (M = Zn, Cu, Co; S,S' = solvent or water molecules) were synthesized[6] by mixing stoichiometric amounts of $H_3L$ and the corresponding hydrated metal acetate in alcohol. The chemical shift ($^1$H-NMR) of the methine (=CH–) proton (7 ppm) is a very good indication that the coordination of the $H_3L$ to metal takes place preferentially via the $\beta$-diketone moiety in the Zn complex. This coordination has been further corroborated by an X-ray study of the $Zn(H_2L)_2 \cdot 2$ EtOH complex.[7] The high reactivity of the $\beta$-diketone versus the $\beta$-ketophenol moiety toward metals is a good basis for obtaining pure mononuclear complexes contrarily to tri-ketones where different isomers are expected (Fig. 2).[8]

The almost identical IR spectra shown by all the mononuclear complexes led us to believe that the coordination around the metal centre is the same in all these compounds.

*Author to whom correspondence should be addressed.

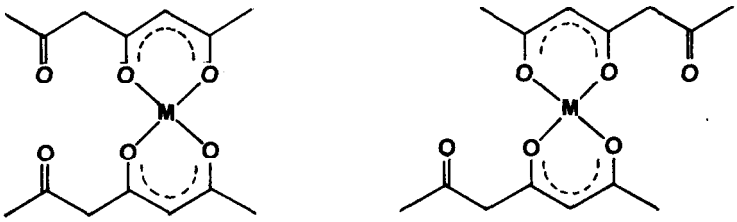


Fig. 2.

The solvent or water molecules (S,S′ in the formula) have been shown to be easily replacable, e.g. the solid material obtained when M = Zn and S = methanol has the general formula $Zn(H_2L)_2 \cdot MeOH \cdot H_2O$,[9] however upon recrystallization of this solid in a tetrahydrofuran/ethanol mixture a compound with general formula $Zn(H_2L)_2 \cdot EtOH$ has been obtained.[10] A Zn–O (ethanol) distance of 2.177 A(average) has been found in this latter compound,[7] with *trans* ethanol and the $H_2L$ Amoieties lying in the equatorial plane.

The Zn is readily displaced in the compound $Zn(H_2L)_2 \cdot 2$ EtOH by an excess of lithium ethanolate in the presence of tetraethylammonium chloride. The resulting compound has the formula $NEt_4[Li(H_2L)_2]$.[11] The aromatic region of the $^1$H-NMR of this compound is very much comparable to that of the $Zn(H_2L)_2 \cdot S \cdot S'$ precursor. As stated by Holm and Cotton[12] the chemical shift of the methine proton is nearly independent of the size, charge and $\pi$-bonding ability of the metal ion. Consequently, it is believed that this compound (Li) consists of an anionic complex with the Li chelated by two $\beta$-diketone moieties. Attempts are being made to get suitable crystals for an X-ray diffraction study of this compound.

Reaction of the mononuclear complex $Cu(H_2L)_2$ with excess of hydrated copper acetate in ammonia solution yielded the homodinuclear copper complex $Cu_2(HL)_2$. Based on the expected stability of the $\beta$-diketone/metal ring the proposed structure consists of two nonequivalent copper centres as indicated in Fig. 3.

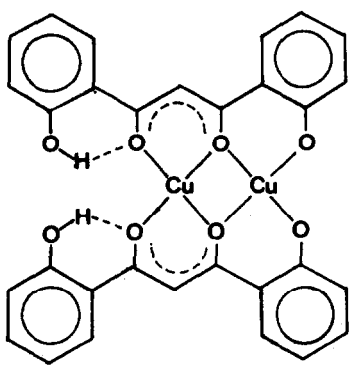


Fig. 3.

It is interesting to note that the copper complexes (mono and homodinuclear) do not have solvent or water molecules to complete their coordination sphere. This is probably fulfilled with the oxygen atoms of molecules placed above and below the copper atoms in the lattice.

Reaction of the mononuclear complex $Co(H_2L)_2$ with excess of hydrated cobalt acetate in ammonia solution produces the homotrinuclear complex $Co_3(L)_2 \cdot EtOH \cdot 3H_2O$ ($A_3$ type). In a similar fashion, reaction of $Co(H_2L)_2$ with a slight excess of nickel and zinc acetates yields $Ni_2Co(L)_2 \cdot 5{,}5\ H_2O$ and $Zn_2Co(L)_2 \cdot 2\ H_2O$ respectively ($A_2B$ type). Most plausible, in these complexes the three compartments are occupied by three metal atoms, two equivalent and one different.

These results show the expected great versatility of the ligand $H_3L$ which may be valuable to get considerable information in the fields above mentioned. It has been observed that the mono, di and trinuclear complexes display considerable differences in the 1650–1400 $cm^{-1}$ IR region. It permits a distinction between mono, di or trinuclear complexes.

Attempts to obtain crystals suitable for X-ray structure determination are underway and a considerable effort is being made to explore the different metal combinations that this ligand permits.

*Acknowledgements*—This work was supported in part by "Comisión Asesora de Investigación Científica y Técnica" through Grant 360/81.

## REFERENCES

1. D. E. Fenton, C. M. Regan, U. Casellato, P. A. Vigato and M. Vidali, *Inorg. Chim. Acta* 1982, **58**, 83.
2. U. Casellato, P. A. Vigato and M. Vidali, *Coord. Chem. Rev.* 1977, **23**, 31.
3. J. E. Groh, *Israel J. Chem.* 1976–1977, **15**, 277.
4. U. Casellato, P. A. Vigato, D. E. Fenton and M. Vidali, *Chem. Soc. Rec.* 1979, **8**, 199.
5. F. Eiden and H. D. Schweiger, *Synth. Commun.* 1978, 511.
6. The Cu complex has the general formula $M(H_2L)_2$. Satisfactory elemental analyses have been found for all complexes presented in the text.

7. X. Solans, M. Font-Altaba, J. L. Briansó, A. Llobet, F. Teixidor and J. Casabó, *Acta Cryst.* 1983, **C39**, 1512.
8. U. Casellato, S. Tamburini, P. A. Vigato and A. De Stefani, M. Vidali and D. E. Fenton, *Inorg. Chim. Acta* 1983, **69**, 45–51.
9. This formula has been proved by elemental analyses and $^1$H-NMR ($d_6$-DMSO) (doublet at 3.2 ppm, intensity 3 and quadruplet at 4.2 ppm, intensity 1).
10. This formula has been proved by elemental analyses, $^1$H-NMR ($d_6$-DMSO) and X-ray structure determination. See Ref. 7.
11. In addition to the analyses, $^1$H-NMR spectrum of this compound is in accordance with this formula.
12. R. H. Holm and F. A. Cotton, *J. Am. Chem. Soc.* 1958, **80**, 5658.

*Polyhedron* Vol. 3, No. 8, pp. 1021–1024, 1984
Printed in the U.S.A.

0277–5387/84 $3.00 + .00
© 1984 Pergamon Press Ltd.

# NOTE

## TUNGSTEN(V) DIMERIC THIO-COMPLEXES WITH DITHIOCARBAMATE LIGANDS

**R. LOZANO,* E. ALARCON, J. ROMAN and A. DOADRIO**
Departamento de Química Inorgánica, Facultad de Farmacia, Universidad Complutense de Madrid, Madrid (3), Spain

(*Received* 25 *November* 1983; *accepted* 17 *January* 1984)

**Abstract**—The syntheses of four new tungsten(V) dimeric thio-complexes with disulphido bridge are reported. The complexes have been identified by IR and electronic spectra, magnetic susceptibilities and analytical data. On the basis of the physical measurements we propose these complexes the following formula $W_2S_4(Rdtc)_2$, where dtc = dithiocarbamate and R = morpholine, piperidine, N-ethylaniline and N,N-methylcyclohexyl. The low values of magnetic moments show a W–W interaction. IR spectral results support a bidentate ligand behaviour and show a band in the 550–525 $cm^{-1}$ region, that we attribute to a W = S bond.

In contrast to the large amount of work which has centred on the chemistry of molybdenum(V) dimeric complexes with dithiocarbamates, xanthates, oxines, etc.[1–6] much less attention has been drawn to the chemistry of tungsten(V) dimeric complexes.

Recently, we have reported the synthesis and study of several tungsten(V) dimeric oxo-complexes with dithiocarbamates as ligands.[7–10] Herein, we describe the preparation and spectral characterization of new dinuclear tungsten(V) thio-complexes, in which the tungsten atoms are bound only by sulphur atoms.

Also, we have compared the thio-complexes obtained with the tungsten(V) dimeric oxo-complexes previously obtained by us.[7,8] The results permit us to assign to the tungsten(V) dimeric thio-complexes a similar structure to the one found for the oxo-complexes of W(V).

### EXPERIMENTAL

(a) *Materials.* $Na_2WO_4 \cdot 2H_2O$ and $P_4S_{10}$ were Merck commercial products. Sodium morpholine dtc, piperidine dtc, N-ethylaniline dtc and N,N-methylcyclohexyl dtc, where dtc is dithiocarbamate, were prepared as previously reported[11] and characterised by IR spectroscopic and elemental analyses. The solvents used to prepare and to purify the complexes were Carlo Erba or Merck. The solutions for absorption spectra were prepared using $CH_2Cl_2$ or dimethylsulphoxide (DMSO) spectral grade Merck–Uvasol.

(b) *Analytical.* Elemental analyses were performed on a Perkin–Elmer Analyser 240 B model. Tungsten was determined by Atomic Absorption with a Perkin–Elmer model 430 Absorption Spectrophotometer, after decomposing the complexes with concentrated NaOH. Analytical data are collected in Table 1.

(c) *Methods.* Magnetic susceptibilities were measured by the Gouy method at room temperature on a Mettler H-51 A. R. balance and a type C Oxford electromagnet. Molar susceptibilities given have been corrected for the diamagnetism of the constituent molecules[12]

The IR spectra have been registered on a Perkin–Elmer recording spectrophotometer model 283. Important IR absorption peaks for the complexes prepared in this study are listed in Table 2.

The visible near UV spectra of the compounds, were measured in the range 200–900 nm on a Perkin–Elmer recording spectrophotometer model 554, using solutions of the complexes in DMSO or $CH_2Cl_2$. We have registered the same peaks for

*Author to whom correspondence should be addressed.

Table 1. Elemental analyses (%) of tungsten(V) thio-complexes

| COMPOUND | % Cald. | | | | | % Found | | | | |
|---|---|---|---|---|---|---|---|---|---|---|
| | C | H | N | S | W | C | H | N | S | W |
| $W_2S_4(S_2CNC_4H_8O)_2$ | 14.63 | 1.95 | 3.41 | 31.22 | 44.88 | 14.85 | 2.08 | 3.40 | 30.50 | 44.61 |
| $W_2S_4(S_2CNC_5H_{10})_2$ | 17.64 | 2.45 | 3.43 | 31.37 | 45.10 | 17.52 | 2.25 | 3.65 | 31.40 | 45.36 |
| $W_2S_4(S_2CNC_8H_{10})_2$ | 24.32 | 2.25 | 3.15 | 28.82 | 41.44 | 24.75 | 2.47 | 3.19 | 28.09 | 41.72 |
| $W_2S_4(S_2CNC_7H_{14})_2$ | 22.01 | 3.21 | 3.21 | 29.35 | 42.20 | 22.20 | 3.35 | 3.05 | 29.06 | 42.25 |

Table 2. IR absorption maxima, in $cm^{-1}$, of tungsten(V) thio-complexes

| COMPOUND | ν C-N | ν C-S | $\nu_s$ W=S | $\nu_a$ W-$S_b$ | $\nu_s$ W-$S_b$ |
|---|---|---|---|---|---|
| $W_2S_4(S_2CNC_4H_8O)_2$ | 1523 | 1090 | 550 | 460 | 365 |
| $W_2S_4(S_2CNC_5H_{10})_2$ | 1520 | 1105 | 540 | 463 | 370 |
| $W_2S_4(S_2CNC_8H_{10})_2$ | 1517 | 1110 | 525 | 462 | 370 |
| $W_2S_4(S_2CNC_7H_{14})_2$ | 1519 | 1090 | 535 | 460 | 368 |

Table 3. Electronic absorption spectra of tungsten(V) thio-complexes

| COMPOUND | $\tilde{\nu}$ (kk) |
|---|---|
| $W_2S_4(S_2CNC_4H_8O)_2$ | 16.9(205); 20.4(2510); 21.8(4785); 26.6(7325); 29.0(12065); 33.4(19180); 38.1(31405) |
| $W_2S_4(S_2CNC_5H_{10})_2$ | 16.8(170); 20.6(2915); 21.7(5230); 26.8(9185); 28.7(14320); 33.3(22010); 37.9(40090) |
| $W_2S_4(S_2CNC_8H_{10})_2$ | 17.1(490); 20.3(2145); 21.9(5100); 26.5(8715); 28.9(15360); 33.4(19990); 38.2(36065) |
| $W_2S_4(S_2CNC_7H_{14})_2$ | 17.0(370); 20.4(1870); 21.8(4115); 26.4(8095); 28.8(14900); 33.5(25155); 38.2(50240) |

both solvents, however, we give in Table 3 the results obtained in DMSO as solvent, because the complexes have a limited solubility in $CH_2Cl_2$.

(d) *Preparation of the complexes.* All the complexes prepared in this study were susceptible to aerial oxidation, therefore all manipulations and reactions were carried out in a nitrogen atmosphere dry-box on a vacuum line.

The complexes were isolated by two methods:

(1) Beginning with W(V) oxo-complexes with disulphido bridge $W_2O_2S_2(Rdtc)_2$, previously obtained.[7,8]

(2) Beginning with W(V) oxo-complexes with oxo-sulphido bridge $W_2O_3S(Rdtc)_2$, previously obtained.[7,8]

We have compared the results of the analyses obtained by two methods and we observe that both results are very similar. For this reason we describe only the isolation of these thio-complexes using W(V) oxo-complexes with disulphido bridge.

$W_2S_4(S_2CNC_4H_8O)_2$: $W_2S_4(S_2CNC_5H_{10})_2$

$W_2O_2S_2(S_2CNC_4H_8O)_2$ (4g), phosphorus pentasulphide (4.4 g) and xylene (100 $cm^3$) as solvent were stirred for 30 min at room temperature, then refluxed at 140°C for 3 hr. The yellow reaction mixture soon became brown in colour. After cooling to room temperature a brown solid was filtered *in vacuo*, washed with benzene and petroleum ether, and dried over $P_4O_{10}$. The brownish product was insoluble in benzene and chloroform, and dissolved in DMF at 100–120°C. After 1 week, red crystals were precipitated. Yield: 55%. $\chi'_m = 4.19 \cdot 10^{-6}$ cgs (where $\chi'_m$ is corrected molar susceptibility).

A similar preparation was realised for the corresponding thio-complexes with piperidine dithiocarbamate as ligand. Yield: 63%. $\chi'_m = 3.39 \cdot 10^{-6}$ cgs.

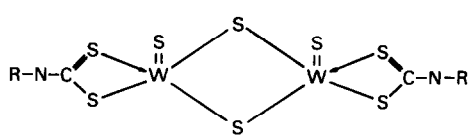
$W_2S_4(S_2CNC_8H_{10})_2$: $W_2S_4(S_2CNC_7H_{14})_2$

$W_2O_2S_2(S_2CNC_8H_{10})_2$ (4.5 g), phosphorus pentasulphide (6.6 g) and xilene (150 $cm^3$) as solvent were stirred for 30 min at room temperature then refluxed for 3 hr. After filtration while hot the solvent was removed under reduced pressure and a brown reaction product was recrystallized from benzene–petroleum ether mixture (50%), obtaining red crystals. Yield: 60%. $\chi'_m = 2.05 \cdot 10^{-6}$ cgs.

A similar preparation was realised for the corresponding thio-complexes with N,N-methylcyclohexil dithiocarbamate as ligand. Yield: 42%. $\chi'_m = 6.03 \cdot 10^{-6}$ cgs.

## DISCUSSION

In this study, we have synthesised four different complexes of tungsten(V) with morpholine dtc, piperidine dtc, N-ethylaniline dtc and N,N-methylcyclohexyl as ligands, in which, the tungsten atoms are only bound to sulphur atoms. The complexes obtained present a disulphido bridge, the stoichiometry is 1 : 1 and the tungsten is 5-coordinated. The formula which most closely fits the analyses is $W_2S_4(Rdtc)_2$ and we suggest that the structure for these complexes should be as follows:




We now discuss the analogy between these complexes and the tungsten(V) oxo-complexes with disulphido and oxo-sulphido bridges previously obtained by us,[7,8] and we assign the band for the stretching mode of the terminal W = S bond in the new complexes.

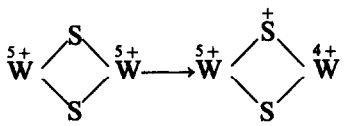
The low values of magnetic susceptibilities, suggest the presence of dimeric species for these thio-complexes. This is due to the possible formation of a direct metal–metal bond or a spin–spin interaction between the two tungsten atoms through the bridging atoms.

The IR spectra of these thio-complexes show a band in the 550–525 $cm^{-1}$ region, which we attribute to the vibration of the symmetric stretching mode of the terminal W = S bond. No bands appeared in the region between 900 and 1000 $cm^{-1}$, which is indicative of the absence of the terminal W = O bond. The terminal W = S bond, appears in the same region that the terminal Mo = S bond in thio-complexes of Mo(V) with the same structure and ligand.[4]

We assign the bands corresponding to the W–S–W bridge, over 370 and 460 $cm^{-1}$, which we attribute to the vibration of the symmetric and antisymmetric stretching mode, respectively, of the W–S bridge bond. We observe no differences between the frequencies of these bands in tungsten(V) oxo-complexes with disulphido and oxo-sulphido bridge and the same ligands[7,8] previously obtained by us, and the frequencies of the complexes studied in the present paper.

The IR spectra of the complexes, show the vibration bands of the C–N and C–S bonds around 1520 and 1100 $cm^{-1}$ respectively. The displacement to greater frequencies to the first band (C–N) and to lower frequencies to the second band (C–S), in comparison with the sodium dithiocarbamates,[13] are indicative that the ligands are bidentates.

The electronic spectra of these tungsten(V) dimeric thio-complexes present a band at 590 nm (17,000 $cm^{-1}$) which we attribute to *d–d* transition $^2B_2 \rightarrow {}^2B_1$, according to the Ballhausen–Gray scheme[14] for a possible square-pyramidal structure. Two other bands, in the 490 nm (20,400 $cm^{-1}$) and 375 nm (26,500 $cm^{-1}$) region, we assign to a charge-transfer of the ligand to the metal. These thio-complexes showed one transition over 460 nm (21,850 $cm^{-1}$) that we assign to a charge-transfer:




as we have observed in dimeric molybdenum(V) and tungsten(V) oxo-complexes with disulphido and oxo-sulphido bridge.[6–8]

In ultraviolet region, three transitions were detected around 345 nm (28,900 $cm^{-1}$), 300 nm (33,400 $cm^{-1}$) and 265 nm (38,150 $cm^{-1}$). The electronic spectra of the sodium dithiocarbamates exhibit also three bands at the same wavelength[13] and differences are not significant. We attribute these bands to intraligand transitions. The first to a $n \rightarrow \pi^*$ transition the second to a $\pi \rightarrow \pi^*$ transition and the last to a $n \rightarrow \sigma^*$ transition.

## REFERENCES


1. A. Kay and P. C. H. Mitchell, *J. Chem. Soc.* (*A*) 1970, 2421.
2. F. A. Cotton, D. L. Hunter and R. Weiss, *J. Coord. Chem.* 1974, **3**, 259.
3. A. Doadrio, R. Lozano and A. L. Doadrio, *An. Quim.* 1980, **78B**, 193.
4. F. A. Schultz, V. R. Ott, D. S. Rolison, D. C. Braward, J. W. McDonald and W. E. Newton, *Inorg. Chem.* 1978, **17**, 1758.
5. R. Lozano, A. Doadrio and A. L. Doadrio, *Polyhedron* 1982, **1**, 163.
6. R. Lozano, J. Roman, E. Alarcón, A. L. Doadrio and A. Doadrio, *Revue de Chimie Minérale* 1983, **20**, 173.
7. R. Lozano, E. Alarcón, A. L. Doadrio and A. Doadrio, *Polyhedron* 1983, **2**, 435.
8. R. Lozano, E. Alarcón, A. L. Doadrio and A. Doadrio, *Polyhedron* 1984, **3**, 25.
9. R. Lozano, E. Alarcón, A. L. Doadrio and A. Doadrio, *An. Quim.* 1983, **79B**, 37.
10. R. Lozano, A. L. Doadrio, E. Alarcón, J. Roman and A. Doadrio, *Revue de Chimie Minérale* 1983, **20**, 109.
11. A. Doadrio and A. Doadrio Villarejo, *An. Quim.* 1978, **74**, 1504.
12. P. W. Selwood, *Magnetochemistry*. Interscience, New York (1956).
13. A. Doadrio and A. L. Doadrio, *An. Quim.* 1977, **73**, 959.
14. C. J. Ballhausen and H. B. Gray, *Molecular Orbital Theory*. W. Benjamin, New York (1965).

*Polyhedron* Vol. 3, No. 8, pp. 1025–1028, 1984
Printed in the U.S.A.

0277–5387/84 $3.00 + .00
© 1984 Pergamon Press Ltd.

# NOTE

# ALKYL COMPLEXES OF PALLADIUM(II) WITH TRIMETHYLPHOSPHINE AND 1,2-BIS-(DIMETHYLPHOSPHINO)ETHANE LIGANDS

**ROBERT TOOZE, KWOK W. CHIU and GEOFFREY WILKINSON***
Chemistry Department, Imperial College, London SW7 2AY, England

(*Received* 30 *January* 1984; *accepted* 17 *February* 1984)

**Abstract**—A number of neutral, mononuclear dialkylpalladium(II) tertiary phosphine complexes of geneal formula *cis* or *trans*-$PdR_2(PMe_3)_2$ and *cis*-$PdR_2$ (dmpe) [dmpe = 1,2-bis(dimethylphosphino)ethane], R = Me, $CH_2Ph$, $CH_2CMe_2Ph$, $CH_2SiMe_3$ have been obtained by interaction of magnesium reagents with palladium(II) acetate or *trans*-$Pd(O_2CMe)_2(PMe_3)_2$.

Since the original synthesis[1] of the palladium alkyls with tertiary phosphine ligands, $PdR_2(PR_3)_2$, which were the first of this type for any transition metal, many analogous palladium compounds have been obtained[2,3] by a variety of routes[3] but mostly from phosphine halide species. We have now made a number of new alkyls with $PMe_3$ and $Me_2PCH_2CH_2PMe_2$ ligands. These have been obtained either by alkylation of palladium(II) acetate in presence of the phosphine or from $Pd(O_2CMe)_2(PMe_3)_2$, which in turn was obtained from $[Pd(O_2CMe)_2]_3$[4] by interaction with $PMe_3$ [the reaction with dmpe yields the known[5] $[Pd(dmpe)_2]$]. Interaction of palladium(II) acetate with various mercury, tin or lead alkyls has been used by Heck[6] to alkylate alkenes, but the intermediate "alkylpalladium acetates" have not been characterised.

## RESULTS AND DISCUSSION

Interaction of palladium(II) acetate in tetrahydrofuran containing excess $PMe_3$ or three equivalents of dmpe with $MgR_2$(R = Me, $CH_2SiMe_3$, $CH_2Ph$) or MgClR, (R = $CH_2SiMe_3$, $CH_2CMe_2Ph$), gives the *cis* alkyls, $PdR_2(PMe_3)_2$, R = Me, $CH_2CMe_2Ph$, and $PdR_2$dmpe, R = Me, $CH_2SiMe_3$, $CH_2Ph$, $CH_2CMe_2Ph$, and *trans* alkyls, $PdR_2(PMe_3)_2$, R = $CH_2SiMe_3$, $CH_2Ph$. All the complexes are air-sensitive and are soluble in hydrocarbons. The assignment as *cis* or *trans* compounds is based on $^1H$ and $^{31}P$ spectra which are collected in Table 1.

(a) *Trimethylphosphine.* Compounds of the type *cis*-$PdMe_2(PR_3)_3$ are known[7] and *cis*-$PdMe_2(PMe_3)_2$ has previously been reported[8] no NMR or experimental details were given. The compound *cis*-$PdIMe(PMe_3)_2$ has been obtained from $Pd(Me_3)_4$.[9] The only previously known trimethylsilylmethyls (R) are *cis*-$PdR_2(PEt_3)_2$ and *trans*-$PdClR(PEt_3)_2$ but the neopentyl could not be isolated.[10]

(b) 1,2 *bis(dimethylphosphino)ethane complexes.* These compounds are all, necessarily, *cis*; no dmpe complexes are known but compounds with other chelate tertiary phosphines have been made.[11] Attempts to prepare compounds from $Ph_2Mg$ and alkyl magnesium bromide led only to biphenyl and $Pd(dmpe)_2$ in the first case and $Pd(dmpe)_2$ and a mixture of organic products in the second.

No cyclometallation reactions have been noted although some dppe palladium metallacycles have been reported.[12]

The $^1H$ NMR data for the compounds are collected in Table 1. Most assignments are straightforward with the exception of the alkyl methylene resonances, (i.e. those due to the protons on the $\alpha$ carbon atom). The multiplicity of these resonances arises from coupling with two magnetically inequivalent phosphorus atoms (*cis* and *trans*) which leads to a second order spectrum characteristic of an $AA'MX_2X_2'$ spin system[13] their overall appearance depending on the magnitude of the two coupling constants.

*Author to whom correspondence should be addressed.

Table 1. Nuclear magnetic resonance spectra of palladium alkyls

| Compound | $^1H$, J(Hz) | $^{31}P\{^1H\}$ |
|---|---|---|
| 1. cis-$PdMe_2(PMe_3)_2$ | 0.74d(6,Pd-Me), $^3J_{PH}$ = 3.3<br>0.93d(18,$PMe_3$), $^2J_{PH}$ = 5.8 | -22.4s |
| 2. trans-$Pd(CH_2SiMe_3)_2(PMe_3)_2$ | 0.31s(18,$CH_2SiMe_3$)<br>1.09"t"(18,$PMe_3$), $^2J_{PH}+^4J_{PH}$ = 6.0<br>-0.25t(4,$CH_2SiMe_3$) $^3J_{PH}$ = 8.3 | -15.5s |
| 3. cis-$Pd(CH_2CMe_2Ph)_2(PMe_3)_2$ | 0.69d(18,$PMe_3$), $^2J_{PH}$ = 5.8<br>1.10s(4,$CH_2CMe_2Ph$)<br>1.71s(12,$CH_2CMe_2Ph$)<br>7.00-7.80m(10, $CH_2CMe_2Ph$) | -32.8s |
| 4. trans-$Pd(CH_2Ph)_2(PMe_3)_2$ | 1.00"t"(18,$PMe_3$), $^2J_{PH}+^4J_{PH}$ = 6.6<br>2.60t(4,$CH_2Ph$), $^3J_{PH}$ = 7.6<br>7.00-7.60m(10,$CH_2Ph$) | -12.0s |
| 5. cis-$Pd(CH_2SiMe_3)_2$dmpe | 0.34s(18,$CH_2SiMe_3$)<br>0.53m(4,$CH_2SiMe_3$)<br>0.89d(12,$Me_2$-P), $^2J_{PH}$ = 8.1<br>0.86d(4,$CH_2$-P), $^2J_{PH}$ = 13.4 | 23.44s |
| 6. cis-$Pd(CH_2CMe_2Ph)_2$dmpe | 0.55d(12,$Me_2$-P), $^2J_{PH}$ = 7.2<br>0.74d(4,$CH_2$-P), $^2J_{PH}$ = 12.5<br>1.76s(12,$CH_2$-$CMe_2Ph$)<br>2.16"q"(4,$CH_2$-$CMe_2Ph$)<br>7.03-7.29m, 7.74-7.85m } (10,$CH_2$-$CMe_2Ph$) | 14.12s |
| 7. cis-$PdMe_2$dmpe | 0.81"t"(6,Pd-Me)<br>0.92d(12,$PMe_2$), $^2J_{PH}$ = 8.0<br>0.98s(2,$CH_2$-P) | 20.14s |
| 8. cis-$Pd(CH_2Ph)_2$dmpe | 0.59d(12,$Me_2$-P), $^2J_{PH}$ = 8.3<br>0.68d(4,$CH_2$-P), $^2J_{PH}$ = 16.17<br>3.11"q"(4,$CH_2Ph$)<br>6.91-7.41m(10,$CH_2$-Ph) | 20.87s |

The infrared spectra show only bands typical of the phosphine and alkyl concerned, all of which are well documented.

## EXPERIMENTAL

Microanalysis by Pascher, Bonn. Molecular weights were determined cryoscopically in benzene; m.p.'s are uncorrected in sealed tubes under vacuum.

All operations were carried out under nitrogen or argon or in vacuum. Solvents were dried over sodium–benzophenone and distilled before use. Petroleum used had b.p. 40–60°.

*Spectrometers.* NMR: Jeol FX 90Q and Bruker WM 250. Data are given in $\delta$ ppm referenced to $Me_4Si$($^1H$) and external 85% $H_3PO_4$($^{31}P$); spectra in $C_6D_6$ at 25°C unless otherwise noted.

IR: Perkin–Elmer 683; spectra in $cm^{-1}$ in Nujol mulls. Analytical data are collected in Table 2. The palladium(II) acetate used was from Johnson Matthey PLC.

Table 2. Analytical data for palladium alkyls

| Compound | m.p.,θ/°C | Found (required) % | | | |
|---|---|---|---|---|---|
| | | C | H | P | M |
| 1. cis-$PdMe_2(PMe_3)_2$ | 84–6 | 33.4 (33.3) | 8.4 (8.3) | 21.2 (21.5) | 270 (288) |
| 2. trans-$Pd(CH_2SiMe_3)_2(PMe_3)_2$ | 81–2 | 38.4 (38.5) | 9.2 (9.2) | 13.8[a] (14.3) | 420 (432) |
| 3. cis-$Pd(CH_2CMe_2Ph)_2(PMe_3)_2$ | 80–1 | 59.5 (59.5) | 8.4 (8.4) | 11.6 (11.8) | 510 (524) |
| 4. trans-$Pd(CH_2Ph))_2(PMe_2)_2$ | 98 | 54.2 (54.5) | 7.2 (7.3) | 14.0 (14.1) | 428 (440) |
| 5. cis-$Pd(CH_2SiMe_3)_2$dmpe | 77–80 | 39.1 (39.0) | 8.9 (8.9) | 14.4[b] (14.4) | 420 (430) |
| 6. cis-$Pd(CH_2CMe_2Ph)_2$dmpe | 118–121d | 59.3 (59.7) | 8.1 (8.1) | 11.9 (11.8) | 510 (523) |
| 7. cis-$PdMe_2$dmpe | 128–131 | 33.6 (33.5) | 7.6 (7.7) | 21.6 (21.6) | 270 (286) |
| 8. cis-$Pd(CH_2Ph)_2$dmpe | 98–101d | 54.9 (54.7) | 6.9 (6.9) | 14.3 (14.1) | 425 (439) |

[a] Si 12.7(12.9). [b] Si 13.0(12.6).

*Bis(acetato)bis(trimethylphosphine)palladium(II)*

To a solution of the acetate (0.7 g. 1.04 mmol) in toluene (70 $cm^3$) was added excess $PMe_3$ (1.0 $cm^3$, 10 mmol) and the mixture stirred for *ca.* 24 hr. The precipitate was collected and recrystallised from tetrahydrofuran (50 $cm^3$) as pale yellow crystals. Yield: 1.1 g, 95%; m.p., 157°C. [Found: C, 31.5 (31.9); H, 6.3 (6.4); P, 16.4 (16.5). *M*($CH_2Cl_2$), 350 (376).]

NMR: $^1H(CDCl_3)$: 0.47, *s*(6, $O_2CMe$); 0.12, *brs* (18, $PMe_3$).

IR: 1610 vs ($O_2CMe$ unidentate).

All of the alkyls were prepared by minor modifications of the same general procedure.

1. cis-*Bismethylbis(trimethylphosphine)palladium (II)*

To a suspension of palladium(II) acetate[4] (0.3 g, 0.45 mmol) in $Et_2O$ (50 $cm^3$) was added $PMe_3$ (1 $cm^3$, 10 mmol) and $Me_2Mg$ (4.0 $cm^3$, 0.35 M in $Et_2O$, 1.4 mmol) at −78°C. The mixture was allowed to warm to room temperature and stirred for *ca.* 12 hr after which, volatiles were removed in vacuum. The residue was extracted with petroleum (2 × 30 $cm^3$), the solution filtered reduced to *ca.* 15 $cm^3$ and cooled at −20°C to give white crystals. Yield: 0.3 g, 75%.

2. trans-*Bis(trimethylsilylmethyl)bis(trimethylphosphine)palladium(II)*

As (1) from $Pd(O_2CMe)_2$ (0.37 g, 0.55 mmol) in $Et_2O$ (50 $cm^3$), $PMe_3$ (1 $cm^3$, 10 mmol) and $Me_3SiCH_2MgCl$ (30 $cm^3$ of 1.24 M solution in $Et_2O$, 3.7 mmol).

Final solution concentrated to *ca.* 5 $cm^3$. Yield: 0.5 g, 70%.

3. cis-*Bis(neophyl)bis(trimethylphosphine)palladium(II)*

As above except residue extracted with 3 × 40 $cm^3$ petroleum, subsequently reduced to 40 $cm^3$ before cooling. Yield: 0.68 g, 72%.

4. trans-*Bis(benzyl)bis(trimethylphosphine)palladium(II)*

As above from $Pd(O_2CMe)_2$0.5 g in toluene (40 $cm^3$) and $(PhCH_2)_2Mg$ (6.5 $cm^3$ of 0.38 M solution in $Et_2O$, 2.5 mmol). Final petroleum extract concentrated to *ca.* 50 $cm^3$. Yield: 0.6 g, 60%.

5. cis-*Bis(trimethylsilymethyl)(dmpe)palladium(II)*

As above from 0.5 g (0.74 mmol) $Pd(O_2CMe)_2$ in thf (40 $cm^3$), dmpe (0.33 $cm^3$, 2.2 mmol) and $(Me_3SiCH_2)_2Mg$ (7.8 $cm^3$ of a 0.28 M solution in $Et_2O$). Final petroleum extract reduced to *ca.* 15 $cm^3$. Yield: 0.65 g, 68%.

6. cis-*Bis(neophyl)(dmpe)palladium(II)*

As above from $Pd(CO_2CMe)_2$ (0.5 g, 0.74 mmol) in THF (40 $cm^3$), dmpe (0.33 $cm^3$, 2.2 mmol) and neophylmagnesium chloride (25 $cm^3$ of a 0.09 m solution in $Et_2O$). Final petroleum extract reduced to *ca.* 20 $cm^3$. Yield: 0.93 g, 78%.

7. cis-*Bis(methyl)(dmpe)palladium(II)*

As for 5 and 6 but here using $Me_2Mg$ (12.7 $cm^3$ of a 0.35 M solution in $Et_2O$). The white product was slightly less soluble, crystallizing from *ca.* 40 $cm^3$ of petroleum. Yield: 0.49 g, 75%.

8. cis-*Bis(benzyl)(dmpe)palladium (II)*

The best yields were obtained by stirring $Pd(O_2CMe)_2$ (0.5 g, 0.74 mmol) and dmpe (0.33 $cm^3$, 2.2 mmol) in toluene (45 $cm^3$). To this was added bis(benzyl)magnesium (6 $cm^3$ of a 0.38 m solution in $Et_2O$). After allowing to warm to room temperature, the reaction was stirred for 2 days. After removal of volatile products the residue was extracted into a mixture of $Et_2O$ and petroleum (1 : 10 by volume). Concentration to *ca.* 10 $cm^3$ and cooling to −10°C yielded yellow crystals. Yield: 0.56 g, 58%.

*Acknowledgement*—We thank the S.E.R.C. for support R.P.T. and K.W.C.) and Johnson Matthey P.L.C. for loan of palladium.

## REFERENCES

1. G. Calvin and G. E. Coates, *Chem. Ind.* 1958, 160; *J. Chem. Soc.* 1961, 2768.
2. G. E. Coates, M. L. M. Green and K. Wade, *Organometallic Compounds—2. The Transition Elements*, 3rd Edn. Methuen, London (1968).
3. P. M. Maitlis, P. Espinet and M. J. H. Russel, In *Comprehensive Organometallic Chemistry*, Vol. 8. Pergamon Press, Oxford (1982).
4. T. A. Stephenson, S. M. Morehouse, A. R. Powell, J. P. Heffer and G. Wilkinson, *J. Chem. Soc.* 1965, 3632.
5. J. Chatt, F. A. Hart and H. R. Watson, *J. Chem. Soc.* 1962, 2537.
6. R. F. Heck, *J. Organomet. Chem.* 1972, **37**, 389.
7. T. Ito, H. Tsuchiya and A. Yamamoto, *Bull. Chem. Soc. Japan* 1977, **50**, 1319.
8. G. E. Coates and C. Parkin, *J. Chem. Soc.* 1963, 421.
9. H. Werner and W. Bertloff, *J. Chem. Res.* (S) 1978, 201.
10. B. Wozniak, J. D. Ruddick and G. Wilkinson, *J. Chem. Soc.* (*A*) 1971, 3116.
11. R. Uson, J. Fornies, J. Gimeno, P. Espinet and R. Navaro, *J. Organomet. Chem.* 1974, **81**, 115; G. Calum and G. E. Coates, *J. Chem. Soc.* 1960, 2008.
12. P. Diversi, G. Ingrosso and A. Lucherini, *J. Chem. Soc., Chem. Comm.* 1978, 735.
13. E. O. Greaves, R. Bruce and P. M. Maitlis, *J. Chem. Soc., Chem. Comm.* 1967, 860.

*Polyhedron* Vol. 3, No. 8, pp. 1029–1031, 1984
Printed in the U.S.A.

0277–5387/84 $3.00 + .00
© 1984 Pergamon Press Ltd.

# COMMUNICATION

## SOME NIOBIUM(V) COMPLEXES AND THEIR RELEVANCE TO THE UPTAKE OF NIOBIUM BY ASCIDIANS

G. W. RAYNER-CANHAM
Department of Chemistry, Sir Wilfred Grenfell College,
Memorial University of Newfoundland,
Corner Brook, Canada NF A2H 6P9

(*Received* 20 *September* 1983; *accepted* 17 *January* 1984)

**Abstract**—Ascidians have been reported to absorb many unusual elements, including niobium. A study of some aqueous niobium(V) chemistry is used to identify potential ligating systems. It is proposed from the inorganic chemical evidence that these marine organisms may concentrate other early second and third row transition elements.

Ascidians (sea squirts) are simple marine organisms which are found in most coastal waters. Several species of ascidians are known to utilize high concentrations of vanadium,[1,2] and there has been considerable interest in the role of this "exotic" element. The vanadium exists within vanadocytes[3] in the blood as a complex of low molecular weight.[4] Vanadium, which is present in seawater as the $HVO_4^{2-}$ and $H_2VO_4^-$ ions,[5] is reduced to the +4 oxidation state in some species of ascidian, but to the +3 state in others.[6,7] The biochemical role of the vanadium has been the subject of many studies, but the metal function is still not understood.[8] Model complexes have been proposed, the earlier discussion using a 2–O, 2–N donor species[9,10] while a later report invokes an EDTA-like ligand.[11]

Much less interest has been shown in the reports of accumulation of niobium by ascidians.[12,13] To an inorganic chemist, the absorption and possible utilization of niobium is a significant challenge, as the element has a very limited aqueous solution chemistry.[14]

This work consists of a study of potential ligating systems for niobium in its common aqueous oxidation state of +5, and a collation of the evidence from inorganic chemistry and from biochemistry as to a possible metal environment in the ascidians.

### EXPERIMENTAL

"Niobic acid" (hydrated niobium(V) oxide[14]) was prepared by addition of concentrated ammonia solution to a solution of sodium niobate. The gelatinous precipitate was centrifuged off and washed repeatedly with water.

To attempt complex formation, the "niobic acid" was refluxed in ethanol with an excess of the ligand for 24 hr. In the case where dissolution occurred, diethyl ether was added and the white product filtered off and dried. Identification was performed by infrared spectroscopy (Unicam SP 1000) and carbon–hydrogen elemental analysis (Chemalytics Inc.). Reaction was attempted using glycine, alanine, serine, tyrosine, cysteine, lactic acid, malic acid, glycollic acid, and tartaric acid. No reaction with the five amino-acids could be detected. The analyses of the complexes formed with the four α-hydroxy carboxylic acid match those previously reported for the formulation $Nb(acid)(OH)_3$[15,16,17] that is, with lactic acid, C = 15.29; H = 3.02 [for $Nb(C_3H_4O_3)(OH)_3$, C = 15.52; H = 3.02%], with malic acid, C = 17.12; H = 3.12 [for $Nb(C_4H_4O_5)(OH)_3$, C = 17.41; H = 2.56%], with glycollic acid, C = 11.76; H = 1.71 [for $Nb(C_2H_2O_3)(OH)_3$, C = 11.03; H = 2.32%], and with tartaric acid, C = 16.60; H = 2.89 [for $Nb(C_4H_4O_6)(OH)_3$, C = 16.46; H = 2.40%].

### RESULTS AND DISCUSSION

The infrared spectra show a very strong broad absorption at about 1660 $cm^{-1}$ which can be assigned as the asymmetric carbonyl stretching frequency. This is about 40–60 $cm^{-1}$ higher in energy than the analogous sodium salts, suggestive of coordination of the carbonyl function. Evidence for coordination of the hydroxyl functions is less

conclusive as the pair of bands at about 3300 and 3500 $cm^{-1}$ in the sodium salts are replaced by a single broader band at about 3400 $cm^{-1}$ in the niobium complex (these may also be due to hydroxide groups coordinated to the niobium). The absence of strong absorptions about 950 $cm^{-1}$ indicates the lack of a terminal Nb=O bond[18] while the presence of a strong absorption at about 710 $cm^{-1}$ in each case would indicate Nb–O–Nb bridges.[18] The compounds may therefore be dimeric (as suggested for an oxalato complex[19]) with two oxygen bridges. Alternatively, the complexes could be of the form $Nb_2O_2(acid)_2 \cdot 3H_2O$, as this particular structure is suggested for the oxysulfates and oxyselenites of niobium(V).[14] Unfortunately, the amorphous nature of these complexes precludes a crystal structure determination.

It is surprising that the usually tetradentate tartate ligand[20] should form a complex of the same stoichiometry as the tridentate malate ligand and as the bidentate glycollate and lactate ligands. However, the recent structure determination of a malatomolybdenum(VI) complex[21] has shown only one of the two carboxylate functions of the malate to be coordinated. Thus it is possible in the complexes here that the ligands are all acting as bidentate chelates, forming the stable five-membered rings. This would be consistent with the fact that no complexation occurs with $\beta$-hydroxy carboxylic acids,[15] which could only form six-membered rings.

Although niobium is ubiquitous in the environment,[22] its concentration is very low (about 0.1 ppb in seawater[23]) thus a strong ligating system must be present on the ascidian to concentrate the element to about 100 ppm.[12,13] From this work, amino-acids do not appear to be strong ligating systems for niobium(V). It is surprising in the case of cysteine, as molybdenum(VI), a somewhat analogous metal species, forms complexes readily with esters of this amino-acid.[24]

A strong ligating system is, however, provided by the $\alpha$-hydroxy carboxylate function. Solution studies[25] have shown significant complex stability with these ligands even at high hydrogen ion concentrations. It is of note that the efficiency of the $\alpha$-hydroxy carboxylic acids as ligands is such that they have been proposed as extraction agents of niobium from minerals.[26] These ligands do have biochemical relevance, for naturally-occurring $\alpha$-hydroxy carboxylic acids play important roles in biochemistry[27] particularly glucuronic acid,[28] an acid-carbohydrate.

The involvement of an acid mucopolysaccharide in metal uptake by ascidians has already been suggested.[29] Glucuronic acid residues may be part of the metal environment in the vanadocyte: in a vanadium-containing species, the vanadium(III) is reported to be surrounded by six oxygen atoms in a non-rigid ligand environment.[30] In addition, both carboxyl and carbohydrate functions have been identified in the cell[3,4,31] (it should be noted that Macara *et al.*[4] assigned an IR spectral peak at 1660 $cm^{-1}$ as being characteristic of vinyl C=C stretching, when alternatively it could be the C=O stretching mode of a carboxyl function, corresponding to the absorption at this frequency in the complexes reported here).

If $\alpha$-hydroxy carboxylic acid residues are involved in the metal complexation, then other metal ions which are also strongly complexed by this ligating system should be significantly concentrated by tunicates. Uncommon metals which do form strong complexes with such ligands are molybdenum,[21,32] tungsten,[33] zirconium[34,35] and hafnium.[35] It would therefore be of interest to analyze ascidians for the presence of significant concentrations of these metals (an unsubstantiated report of high concentrations of molybdenum, zirconium and tungsten has been made[12] and re-cited[1] but no confirmatory work has been reported).

*Acknowledgements*—J. S. Gillick and L. B. M. Carling of Bishop's University, Quebec are thanked for assistance with the experimental work. The work was supported by a President's Research Grant (Bishop's U.).

## REFERENCES

1. L. Botte and S. Scippa, *Annot. Zool. Jpn.* 1979, **52**, 188.
2. G. P. Danskin, *Can. J. Zool.* 1978, **56**, 547.
3. R. Endean, *Quart. J. Micr. Sci.* 1960, **101**, 177.
4. I. G. Macara, G. C. McLeod and K. Kustin, *Biochem J.* 1979, **181**, 457.
5. G. C. McLeod, K. V. Ladd, K. Kustin and D. L. Toppen, *Limnol. Oceanogr.* 1975, **20**, 491.
6. J. H. Swinehart, W. R. Biggs, D. J. Halko and N. C. Schroeder, *Biol. Bull.* 1974, **146**, 302.
7. I. G. Macara, G. C. McLeod and K. Kustin, *Comp. Biochem. Physiol.* 1979, **63B**, 299.
8. K. Kustin and I. G. Macara, *Comments Inorg. Chem.* 1982, **2**, 1.
9. D. B. Carlisle, *Proc. Roy. Soc. Ser. B* 1958, **171**, 31.
10. W. Rummel, H.-J. Bielig, W. Forth, K. Pfleger, W. Rudiger and E. Seifen, *Prot. Biol. Fluids* 1966, **205**, 14.
11. K. Kustin, K. V. Ladd and G. C. McLeod, *J. Gen. Physiol.* 1975, **65**, 315.
12. D. B. Carlisle, *Nature* 1958, **181**, 933.
13. N. Kokubu and T. Hidaka, *Nature* 1965, **205**, 1028.
14. R. J. H. Clark and D. Brown, *The Chemistry of Vanadium, Niobium and Tantalum.* Pergamon Press, New York (1973).

15. F. Fairbrother and J. B. Taylor, *J. Chem. Soc.* 1956, 4946.
16. L. L. Shevchenko and V. V. Grigor'eva, *Russ. J. Inorg. Chem.* 1969, **14**, 60.
17. N. Brnicevic and C. Djordjevic, *J. Less-Common Metals* 1971, **23**, 61.
18. V. Katovic and C. Djordjevic, *Inorg. Chem.* 1970, **9**, 1720.
19. M. Muller and J. Dehand, *Bull. Soc. Chim. Fra.* 1971, 2844.
20. R. E. Tapscott, R. L. Belford and I. C. Paul, *Coord. Chem. Rev.* 1969, **4**, 323.
21. C. B. Knobler *et al.*, *J. Chem. Soc. Dalton Trans.* 1983, 1299.
22. H. A. Schroeder and J. J. Balassa, *J. Chron. Dis.* 1965, **18**, 229.
23. D. B. Carlisle and L. G. Hummerstone, *Nature* 1958, **181**, 1002.
24. L. R. Melby, *Inorg. Chem.* 1969, **8**, 349.
25. Ct. Konecny, *Z. Phys. Chem.* 1966, **235**, 39.
26. S. N. Rossovskii and S. M. Urusova, *Tr. Tsentr. Nauchn-Issled Gornorazved. Inst.* 1964, 122; (*Chem. Abs.* 1965, **63**, 2664).
27. R. F. Boyer, M. E. Wernette, S. van Wylen, E. Faustman and R. Titus, *J. Inorg. Biochem.* 1979, **10**, 205.
28. G. J. Dutton, *Glucuronic Acid.* Academic Press, New York (1966).
29. M. Kalk, *Nature* 1963, **198**, 1010.
30. T. D. Tullius, W. O. Gillum, R. M. K. Carlson and K. O. Hodgson, *J. Am. Chem. Soc.* 1980, **102**, 5670.
31. M. Kalk, *Quart. J. Micr. Sci.* 1963, **104**, 483.
32. J. T. Spence and G. Kallos, *Inorg. Chem.* 1063, **2**, 710.
33. D. H. Brown and D. Neumann, *J. Inorg. Nucl. Chem.* 1975, **37**, 331.
34. C. G. Macarovici and L. Czegledi, *Rev. Roum. Chim.* 1971, **16**, 687.
35. K. F. Karlysheva, A. V. Koshel', J. A. Sheka and G. S. Semenova, *Russ. J. Inorg. Chem.* 1975, **20**, 932.

*Polyhedron* Vol. 3, No. 8, pp. 1033–1035, 1984
Printed in the U.S.A.

0277-5387/84 $3.00 + .00
© 1984 Pergamon Press Ltd.

# COMMUNICATION

## NOTABLE FEATURES IN THE MOLECULAR STRUCTURE OF $W_2(OCH_2$-*t*-Bu$)_6(NCNMe_2)_3$: THREE DIFFERENT MODES OF BONDING FOR $NCNMe_2$(2-) LIGANDS

MALCOLM H. CHISHOLM,* KIRSTEN FOLTING, JOHN C. HUFFMAN and NANCY S. MARCHANT
Department of Chemistry and Molecular Structure Center, Indiana University, Bloomington, IN 47405, U.S.A.

(*Received* 28 *November* 1983; *accepted* 14 *December* 1983)

**Abstract**—Hydrocarbon solutions of $W_2(OCH_2$-*t*-Bu$)_6(HNMe_2)_2$(M≡M) and $Me_2NCN$ (≥3 equiv) react at 0°C to give a compound of formula $W_2(OCH_2$-Bu-*t*$)_6(NCNMe_2)_3$. The crystal and molecular structure of the latter compound, deduced from an X-ray study, reveals the loss of the W–W triple bond (W–W = 3.85 Å) and the formal reduction of each $Me_2NCN$ molecule to a 2- ligand for which three different modes of bonding are seen.

Steric factors have been shown to be particularly important in determining the products obtained from the reactions between ditungsten hexaalkoxides and alkynes.[1–3] We now find that steric factors are similarly important in determining the products obtained from reactions involving dimethylcyanimide. Whereas $W_2(OBu$-*t*$)_6$(M≡M) and $Me_2NCN$ yield[4] a 1:1 mixture of (*t*-BuO)$_3$W≡N and (*t*-BuO)$_3$W≡CNMe$_2$, $W_2(OCH_2Bu$-*t*$)_6(HNMe_2)_2$, which by facile reversible loss of $HNMe_2$ provides a source of $W_2(OCH_2Bu$-*t*$)_6$,[5] reacts with $NCNMe_2$ under comparable conditions to yield a compound of formula $W_2(OCH_2Bu$-*t*$)_6(NCNMe_2)_3$.

Toluene solutions of $W_2(OCH_2Bu$-*t*$)_6(HNMe_2)_2$ react rapidly with $NCNMe_2$ at 0°C to give $W_2(OCH_2Bu$-*t*$)_6(NCNMe_2)_3$, which is isolated as tan crystals upon cooling to −15°C.[6] A rapid uptake of 3 equivalents of $NCNMe_2$ per $W_2$-neopentoxide is evident since addition of 1 or 2 equivalents of $NCNMe_2$ yields only $W_2(OCH_2$-Bu-*t*$)_6(NCNMe_2)_3$ and $W_2(OCH_2Bu$-*t*$)_6(HNMe_2)_2$ as the NMR-detectable or isolable crystalline products. It is noteworthy that $Mo_2(OCH_2Bu$-*t*$)_6$ and $Me_2NCN$ form only the 1:1 adduct $Mo_2(OCH_2Bu$-*t*$)_6(NCNMe_2)$,[4] even in the presence of excess $Me_2NCN$. The compound $W_2(OCH_2Bu$-*t*$)_6(NCNMe_2)_3$ reacts further at room temperature and the nature of this subsequent reaction is currently under investigation.

A stereoview of the $W_2(OCH_2Bu$-*t*$)_6(NCNMe_2)_3$ molecule[7] is shown in Fig. 1. The W–W distance, 3.85 Å, is a non-bonding distance and based on $Me_2NC$–*N* or W–N distances each $Me_2NCN$ molecule may be viewed as a 2- ligand. The six electrons in the W≡W bond in $W_2(OCH_2Bu$-*t*$)_6(HNMe_2)_2$ have been used to reduce three $Me_2NCN$ molecules by two electrons apiece, in contrast to the reaction between $W_2(OBu$-*t*$)_6$ and $Me_2NCN$ in which the six electrons of the W≡W bond are used to reduce, and hence cleave, only one –C≡N bond. A parallel is seen in the reactions involving MeC≡CMe which lead to (*t*-BuO)$_3$W≡CMe[2] or $W_2(OR)_6(\mu$-$C_4Me_4)(C_2Me_2)$ compounds (R = *i*-Pr and *t*-$BuCH_2$).[3]

The modes of (C–N)-to-metal bonding in $W_2(OCH_2Bu$-*t*$)_6(NCNMe_2)_3$ are shown pictorially in Fig. 2 where a comparison with pertinent structural parameters for those found in $Mo_2(OCH_2Bu$-*t*$)_6(NCNMe_2)$[4] is also given. The $\eta^2$-ligand provides a very rare example of a

*Author to whom correspondence should be addressed.

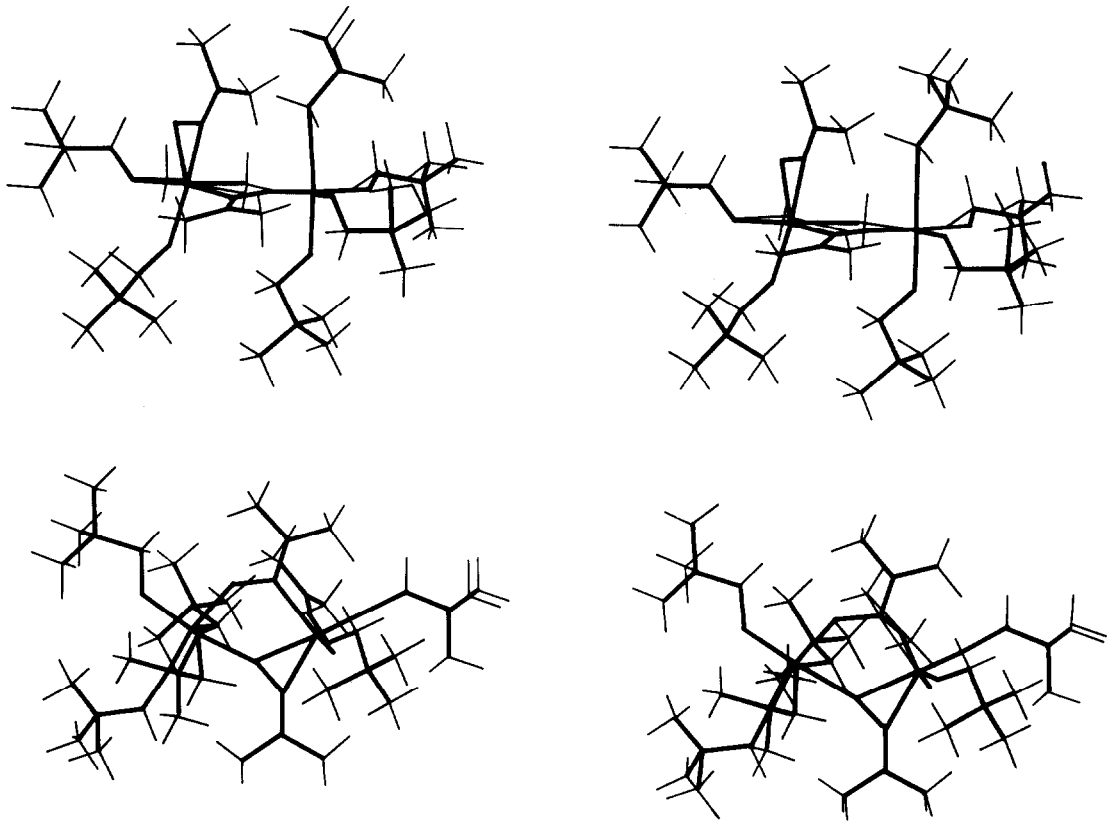
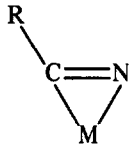
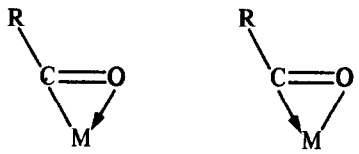


Fig. 1. Two stereoviews of the $W_2(OCH_2Bu\text{-}t)_6(NCNMe_2)_3$ molecule.

$\pi$-bonded –C≡N group.[8] The $Me_2NC$–*N*, M–C and M–N distances suggest that the $\eta^2$-ligand may be viewed as a 2- ligand, I, and bears a close resemblance to $\eta^2$-acyl ligands (1-), II, which have recently been well documented in early transition metal chemistry.[9]

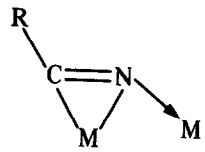


I



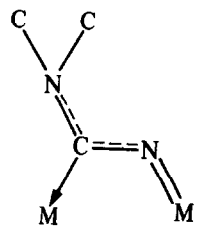
II

The bridging $\eta^2$, $\eta^1$-ligand is very similar to the non-bridging $\eta^2$-ligand but with an additional long, dative bond ($\eta^1$), III.



III

On the other hand the bridging $\eta^1$(C), $\eta^1$(N) ligand has a very short W–N distance, 1.84 Å, indicative of a W=N (imido) bond distance[10] and a rather long W–C distance, 2.17 Å. The latter may be viewed as a dative carbene ($sp^2$) to tungsten bond with the carbon carbene atom being stabilized by two amino groups, IV.



IV

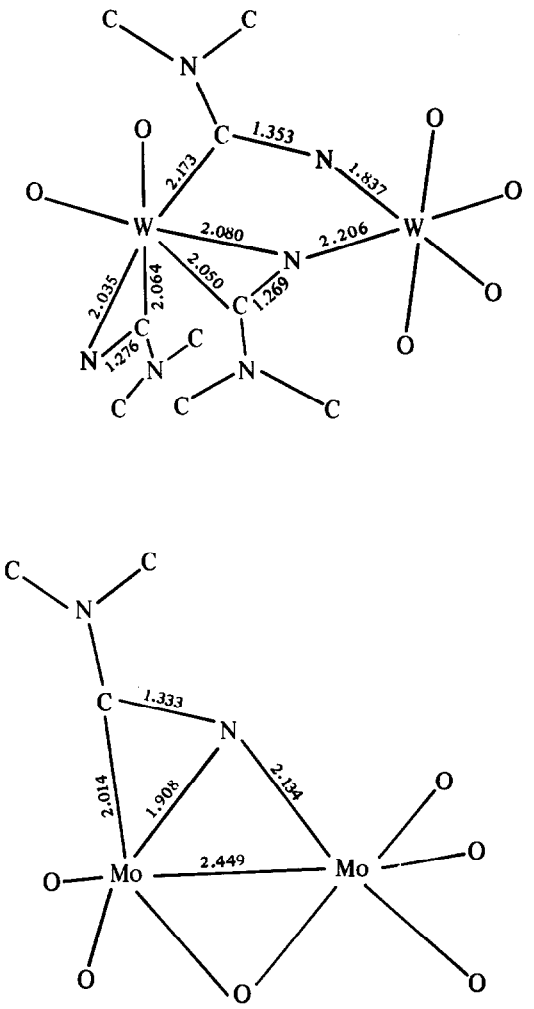
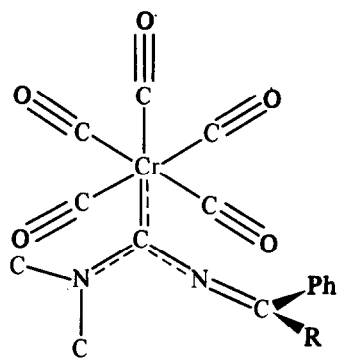



Fig. 2. Sketches of the $Me_2NCN$-to-metal bonding seen in the compounds $W_2(OCH_2Bu\text{-}t)_6(NCNMe_2)_3$ and $Mo_2(OCH_2Bu\text{-}t)_6(NCNMe_2)$.

A similarity with the bonding in IV may be seen in the structure of V which contains a long Cr–C(carbene) distance, 2.13 Å,[11] and is formed in the reaction between $(CO)_5CrC(Ar)(R)$ and $NCNMe_2$.




V

In each of the $Me_2NCN$ to W bonding modes the $C_2N$ unit is coplanar with the M(CN) moiety, which together with the $Me_2N$–CN distances, 1.34 Å (averaged), implies significant $Me_2N$ *p*-to-C *p* $\pi$-interaction. This coplanarity of the $C_2NCN$ moiety is also seen in the previously reported structures for $Cp_2Mo_2(CO)_4(NCNMe_2)$[12] and $Mo_2(OCH_2Bu\text{-}t)_6(NCNMe_2)$.[4] $Me_2N$ $\pi$-donation is presumably very important in stabilizing the $\eta^2$-CN bonding since this is not seen for RCN ligands where R=alkyl.[8]

Finally it may be noted that the central planar six membered ring in the present compound has some similarity with the central six membered planar ring in the $Cp(CO)Mo(\mu\text{-}\eta^1, \eta^2\text{-}CO)(\mu\text{-}\eta^1, \eta^1MeCO)ZrCp_2$ molecule.[13]

Further studies are in progress.

*Acknowledgements*—We thank the National Science Foundation and the Wrubel Computing Center for support.

## REFERENCES

1. M. H. Chisholm, K. Folting, D. M. Huffman, J. C. Huffman and J. Leonelli, *J. Chem. Soc. Chem. Commun.* 1983, 589.
2. R. R. Schrock, M. L. Listermann and L. G. Sturgeoff, *J. Am. Chem. Soc.* 1982, **104**, 4291.
3. F. A. Cotton, W. Schwotzer and E. S. Shamshoum, *Organometallics* 1983, **2**, 1167.
4. M. H. Chisholm, J. C. Huffman and N. S. Marchant, *J. Am. Chem. Soc.* 1983, **105**, 6162.
5. M. H. Chisholm, *Polyhedron* 1983, **2**, 681.
6. Dry and oxygen free atmospheres ($N_2$) were used throughout.
7. Crystal data for $W_2(OCH_2\text{-}t\text{-}Bu)_6(NCNMe_2)_3$ at −160°C: space group $P\bar{1}$, $a = 16.784(9)$ Å, $b = 15.959(9)$ Å, $c = 9.839(4)$ Å, $\alpha = 76.58(3)°$, $\beta = 97.61(3)°$, $\gamma = 82.28(3)°$, $Z = 2$, $d_{calc} = 1.460$ gm cm$^3$. Of the 12,540 reflections collected using MoK$\alpha$, $6 \leqslant 20 \leqslant 45°$, the number of unique reflection was 6562. The number with $F > 2.33\sigma(F)$ was 4993 and those were used in the full matrix refinement. Final residuals are $R(F) = 0.057$ and $Rw(F) = 0.054$.
8. For a general review of RCN complexes see: B. N. Storhoff and A. J. Infante, *Coord. Chem. Rev.* 1977, **23**, 1.
9. M. D. Curtis, K. B. Shiu and W. M. Butler, *Organometallics* 1983, **2**, 1475 and references therein.
10. W. A. Nugent and B. L. Haymore, *Coord. Chem. Rev.* 1980 **31**, 123.
11. H. Fischer and U. Schubert, *Angew. Chem. Int. Edit. Engl.* 1981, **20**, 461.
12. M. H. Chisholm, F. A. Cotton, M. W. Extine and L. A. Rankel, *J. Am. Chem. Soc.* 1978, **100**, 807.
13. J. A. Marsella, J. C. Huffman, K. G. Caulton, B. Longato and J. R. Norton, *J. Am. Chem. Soc.* 1983, **104**, 6360.

*Polyhedron* Vol. 3, No. 9/10, pp. 1037–1057, 1984
Printed in the U.S.A.

0277-5387/84 $3.00 + .00
Pergamon Press Ltd.

POLYHEDRON REPORT NUMBER 7

# CYCLOMETALLATED COMPLEXES INCORPORATING A HETEROCYCLIC DONOR ATOM; THE INTERFACE OF COORDINATION CHEMISTRY AND ORGANOMETALLIC CHEMISTRY

EDWIN C. CONSTABLE
University Chemical Laboratory, Lensfield Road, Cambridge, CB2 1EW, England

INTRODUCTION ..... 1037
1. CYCLOMETALLATION ..... 1038
1.1 General introduction ..... 1038
1.2 Synthesis of cyclometallated species ..... 1038
1.3 Mechanistic considerations ..... 1040
1.4 The ligands ..... 1040
2. SURVEY OF CYCLOMETALLATED COMPOUNDS ..... 1041
2.1 Scandium, yttrium and lanthanum ..... 1041
2.2 Titanium, hafnium and zirconium ..... 1041
2.3 Vanadium, niobium and tantalum ..... 1041
2.4 Chromium, molybdenum and tungsten ..... 1041
2.5 Manganese, technetium and rhenium ..... 1042
2.6 Iron, ruthenium and osmium ..... 1043
2.7 Cobalt, rhodium and iridium ..... 1046
2.8 Nickel, palladium and platinum ..... 1047
2.9 Copper, silver and gold ..... 1055
Acknowledgements ..... 1055
References ..... 1055

## INTRODUCTION

Coordination chemistry is concerned with the compounds which result from the donation of electrons into vacant orbitals on a metal. The new bond which is formed is known as a dative or coordinate bond, and the resulting compound as a complex. The species donating electrons to the metal is a ligand, the ligands may donate one, two or three electrons per donor atom.† Organometallic chemistry is concerned with those compounds which exhibit a significant bonding interaction between a metal and one or more carbon atoms. Compounds which are typically considered to be organometallic may contain $\sigma$-donor, $\pi$-acceptor ligands $[Ni(CO)_4]$, one-electron $\sigma$-donor ligands $[W(CH_3)_6]$, two-electron $\pi$-donor ligands $K[PtCl_3(H_2C{=}CH_2)]$, or multi-electron donor ligands $[Fe(cp)_2]$ or $[\{\eta^3\text{-}CH_2CHCH_2)Pd(\mu\text{-}Cl)\}_3]$.

It is evident that an organometallic compound is a special class of complex in which one or more of the ligands acts as a donor through carbon. In practice the ambiguity inherent in these definitions presents few problems, and a working empirical

†Throughout this review, ligands and metal atoms will be regarded as neutral or radical entities whenever this is possible. Thus, $[FeF_6]^{3-}$ is regarded as being derived from a neutral iron atom with eight available valence electrons and six one-electron donor $s^2p^5$ fluorine atoms, giving a total electron count about the metal of $8+6+3=17$. Alkyl and aryl groups are treated as one-electron donor radicals, and this is denoted $\eta^1$ or $\sigma$. Neutral ligands, such as phosphines, amines, olefins and carbon monoxide are two-electron donors. Occasionally ligands donating more than two electrons are encountered, and examples include $\eta^5$-$C_5H_5$ and $\eta^6$-$C_6H_6$. Species such as the allyl group can act as an $\eta^1$ (or $\sigma$) or an $\eta^3$ (or $\pi$) donor ligand.

distinction between organometallic and coordination chemistry exists. Organometallic compounds are frequently characterised by a high reactivity towards small molecules (e.g. dioxygen) associated with the metal–carbon bonding.

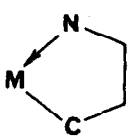
The *chelate* effect, by which complexes of a polydentate ligand are more stable than those containing an equivalent number of monodentate ligands containing the same donor atoms, is well known in coordination chemistry. It is possible to envisage a similar effect occurring in complexes of multidentate ligands in which one or more of the donor atoms is carbon. If such a ligand forms chelated complexes, then a new cyclic X–M–C system is formed. Such complexes represent the interface between classical coordination chemistry and organometallic chemistry, and are described variously as cyclometallated, *ortho*metallated or organometallic intramolecular coordination compounds.

A number of previous reviews have discussed the topic of cyclometallation, either in general terms,[1-3] or with special emphasis upon oxygen (*C, O*),[4] sulphur (*C, S*),[5] or nitrogen (*C, N*)[6] donor systems. This review is specifically concerned with those cyclometallated systems in which the non-carbon donor atom is contained in a heterocyclic ring, and in which a transition metal is involved. Such complexes are expected to combine the classical coordination chemistry of heterocyclic ligands with the useful reactivity of organometallic compounds.

## 1. CYCLOMETALLATION

### 1.1 *General introduction*

As defined above, a cyclometallated compound incorporates a X–M–C ring system, in which the donor atom *X* is not carbon. This review only considers those complexes in which *X* is incorporated into a heterocyclic ring, although it also considers non-cyclic and polynuclear complexes in which a heterocyclic ligand exhibits both *X* and *C* donor ability. The majority of examples of such cyclometallated systems are based on the pyridine nucleus, and are thus examples of the N–M–C type (Fig. 1).

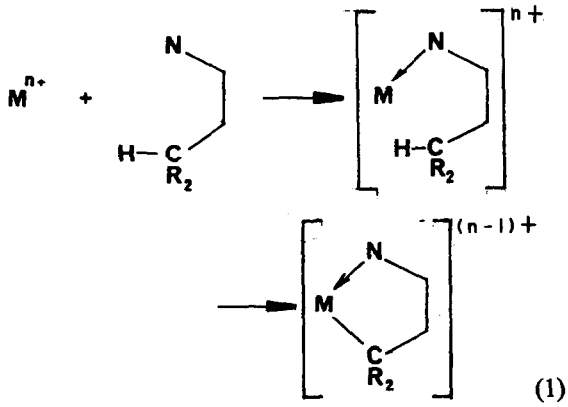



Early studies by Cope and Friedrich[7] on the formation of N–M–C cyclometallated systems established that the ring must contain a total of five atoms for the cyclic product to be formed (eqn 1). This observation holds for the vast majority of N–M–C cyclometallated systems, although a few exceptions are now known. The rule does not hold true, and indeed could not be expected to, for polynuclear complexes.

### 1.2 *Synthesis of cyclometallated species*

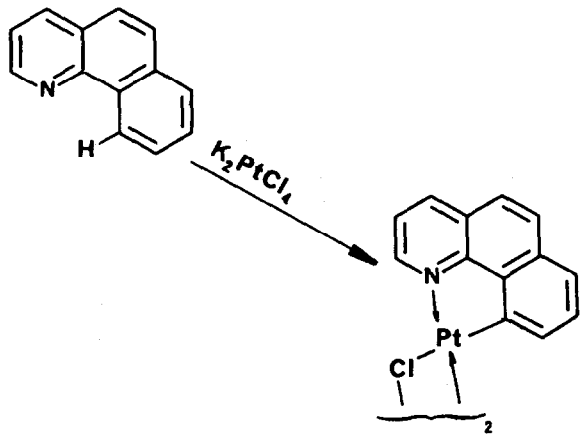
A number of synthetic approaches to cyclometallated complexes may be envisaged, and, although most have been investigated, the commonest method involves thermal activation of a C–H bond.

#### 1.2.1 *Activation of a* C–H *bond* (eqn 1)



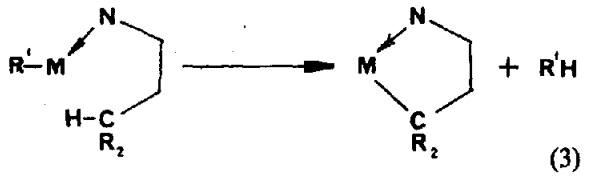

(1)

This is the commonest, and historically the earliest method for the preparation of cyclometallated complexes. The reaction is formally an electrophilic attack at the carbon atom which is involved in the M–C bonding and, as expected, this approach is most useful in the formation of M-aryl bonds (eqn 2).[8] However, it has also been successfully utilised in the formation of M-alkyl, M-acyl and M-iminoacyl (RN=C(R′)–) cyclometallated complexes. Variants upon the basic strategy involve the addition of a base (commonly pyridine or acetate) to abstract the proton from the site of attack, and buffer the system, or the use of metal




(2)

alkyls, which can eliminate an alkane in a coordination-assisted *trans*-alkylation reaction (eqn 3).



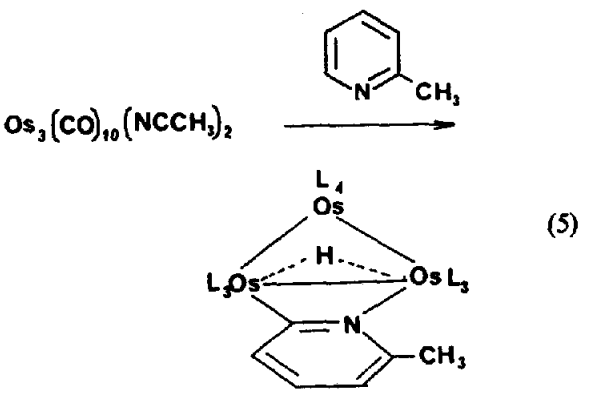

(3)

1.2.2 *Insertion into a* C–H *bond* (eqn 4)



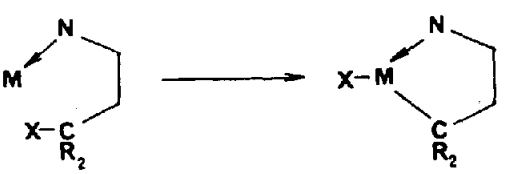

(4)

Although it is possible to envisage a mononuclear complex undergoing an insertion reaction into a C–H bond to give a hydridoalkyl compound, this mechanism for the formation of a cyclometallated compound is relatively uncommon. This may be, in part due to the ease with which a pyridine will accept a hydride ion from a metal hydride (i.e. the hydrido complex would be unstable with respect to reductive dissociation of the heterocycle). However, in polynuclear complexes this mechanism is more common, since the hydride may either be bonded to a *different* metal atom to the heterocycle, or it may adopt the bridging mode, which is less nucleophilic. This mechanism is commonly observed in the reactions of clusters with aromatics and heteroaromatics (eqn 5).[9]



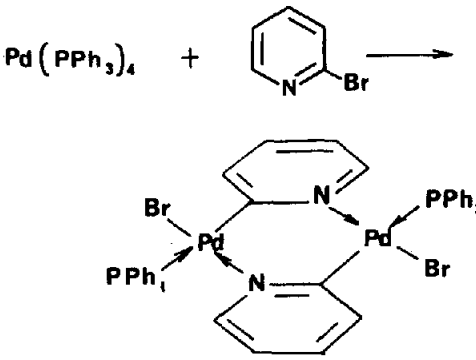

(5)

1.2.3 *Oxidative insertion into a* C–X *bond* (eqn 6)




(6)

This is a more generalised case of an insertion reaction than that into a C–H bond considered in 1.2.2, and is more commonly observed in mononuclear complexes. The method has been widely used for the formation of M-aryl and M-acyl bonds from the corresponding halides (eqn 7).[10]



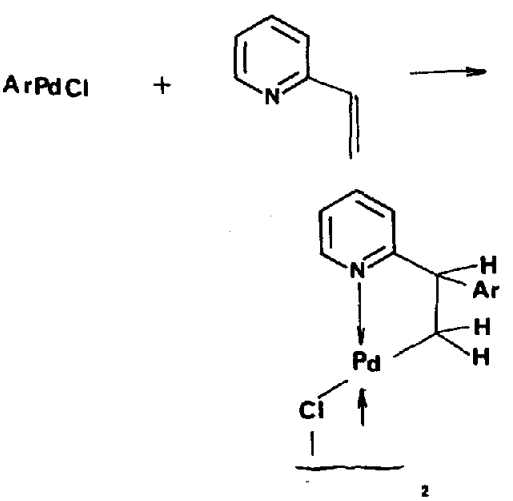

(7)

1.2.4 $\eta^2 - \eta^1(\pi - \sigma)$ *interconversion* (eqn 8)



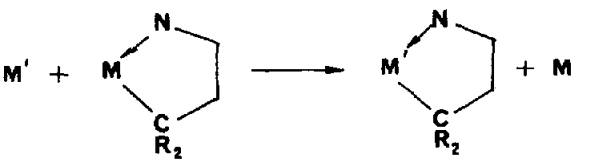

(8)

The conversion of an $\eta^2$-olefin to a $\eta^1$-alkyl donor involves the addition of M–R across the double bond of the olefin, or attack by an external nucleophile upon the double bond, and a number of reactions of this type are known (eqn 9).[11]



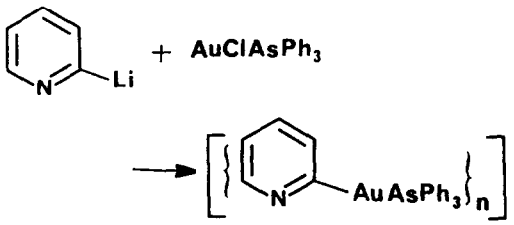

(9)

1.2.5 *Metal exchange reactions* (eqn 10)




(10)

The metal exchange reaction has been used for the preparation of cyclometallated complexes which are not directly accessible via the routes described above. The starting complexes are commonly cyclometallated palladium compounds or organolithium derivatives (eqn 11).[12]




(11)

### 1.3 *Mechanistic considerations*

Mechanistic studies concerning the formation of cyclometallated complexes incorporating a heterocyclic donor appear to be lacking, but there is little reason to expect these reactions to differ radically from those of other cyclometallation reactions. The cases which have been most widely investigated involve the formation of a cyclometallated M-aryl system from the reaction of an electrophilic complex (commonly of palladium(II) or platinum(II)) with a suitably substituted arene. The first step is thought to be the formation of a complex in which the non-carbon donor is coordinated to the metal. This then forms an $\eta^2$-arene ($\pi$-arene) complex, which undergoes an $\eta^2 - \eta^1$ ($\pi - \sigma$) interconversion to give a cyclohexadienylium system, which finally eliminates a proton to give the cyclometallated complex (eqn 12). Mechanisms involving nucleophilic attack upon the aromatic ring are proposed for the formation of cyclometallated products from the reaction of electron-rich, low-valent complexes with arenes, and must also be involved in reactions involving the formation of M–C bonds by the displacement of halide from a C–Hal bond.

### 1.4 *The ligands*

The commonest examples of metallation reactions involve the formation of M-aryl bonds, and this trend is reflected in those complexes incorporating a heterocyclic donor group. Numerous phenyl-substituted or benzo-fused heterocycles have been shown to form cyclometallated complexes, but the two ligands which have been most widely investigated are 2-phenylpyridine (Fig. 2) and benzo[h]quinoline (Fig. 3). In each case, the C–H bond which is broken is indicated, and it is evident that complexation involves the formation of a 5-membered metallocyclic ring. Indeed, with the proviso that a 5-membered ring is formed, almost any phenyl substituted heterocycle is expected to be able to form cyclometallated complexes.

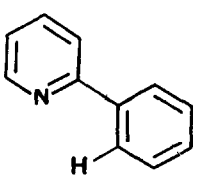



Fig. 2.

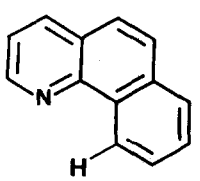
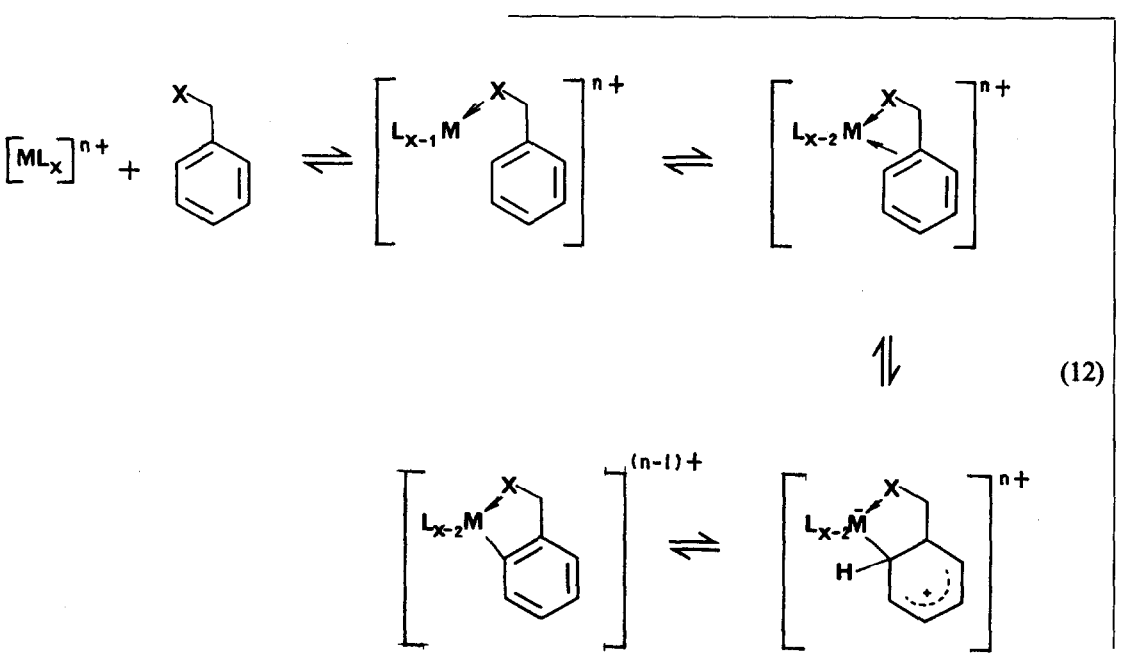



Fig. 3.




(12)

It follows from the above, that unsubstituted heterocycles would not be expected to form mononuclear cyclometallated products, and this is, in general, true. Thus pyridine forms *either* polynuclear or cluster complexes on cyclometallation *or*, in one instance, a 3-*membered* metallocycle.

The same constraints are applied to the formation of M-alkyl cyclometallated systems, which are only found if a 5-membered ring can be formed.

Ligands other than 2-phenylpyridine and benzo[h]quinoline are discussed at the appropriate section in the text.

## 2. SURVEY OF CYCLOMETALLATED COMPLEXES INCORPORATING A HETEROCYCLIC DONOR

The vast majority of cyclometallated complexes which have been described involve bonds from carbon to the nickel triad. This probably represents the high kinetic and thermodynamic stability of C–Ni, C–Pd and C–Pt bonds, as reflected in the ease of formation of such cyclometallated complexes. Indeed, it is sometimes difficult to obtain *non*-cyclometallated complexes with these metals.

An attempt is made here to give a comprehensive survey up to 1982, although there are undoubtedly a number of omissions.

### 2.1 *Scandium, yttrium and lanthanum*

To date, no compounds of these elements incorporating a cyclometallated ligand have been recognized.

### 2.2 *Titanium, hafnium and zirconium*

The reactions of $[Ti(cp)_2Me]$ or $[Ti(cp)_2Bu^n]$ with a range of substituted heterocycles expected to form cyclometallated products (2-methyl-, 2-phenyl and 2-vinylpyridines, quinoline and 8-methylquinoline) have been investigated. In each case, very air-sensitive, purple, paramagnetic solids of stoichiometry $[Ti(cp)_2L]$ ($HL$ = heterocycle) were obtained. The magnetic moment ($\mu_{eff}$ = 1.65 BM; *spin-only value for $d^1$ species = 1.73 BM*), *EPR spectrum ($g$ = 1.990) and molecular weights were* all consistent with a mononuclear formulation as titanium(III) aryl complexes. The quantitative formation of the appropriate 6-substituted pyridine or 2-substituted quinoline on deuteration or iodination according to:

$$[Ti(cp)_2L] + DCl \rightarrow [Ti(cp)_2Cl_2] + DL$$

$$[Ti(cp)_2L] + 1.5I_2 \rightarrow [Ti(cp)_2I_2] + DI$$

established the position of the bond between titanium and the heteroaryl ring. The stability of the complexes is not consistent with a simple coordinatively-unsaturated $\sigma$-aryl structure (for example, the complexes do not react with dinitrogen), and a three membered cyclic metallaazirane structure (Fig. 4) is proposed.[13,14] This bonding

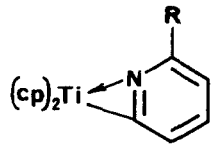
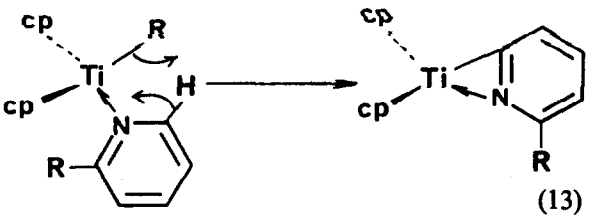



Fig. 4.

mode has been observed in other cyclometallated systems incorporating pyridine, and is not as unusual as originally thought. It is of interest that pyridines which do not bear substituents at the 2-position do not form cyclometallated complexes with $[Ti(cp)_2R]$, and it is suggested that steric interactions with the 2-substituent force the ligand into a suitable configuration for the elimination of RH and the formation of the $\sigma$-bonded production (eqn 13).




(13)

### 2.3. *Vanadium, niobium and tantalum*

To date no cyclometallated complexes incorporating heterocyclic donors have yet been identified.

### 2.4 *Chromium, molybdenum and tungsten*

2-(2-Lithiophenyl)pyridine, formed from the reaction of n-butyllithium with a 2-(2-halophenyl)-pyridine, is reported to react with $[Cr(thf)_3Cl_3]$ to give the cyclometallated product $[CrL_3]$ ($HL$ = 2-phenylpyridine).[15] The orange paramagnetic complex ($\mu_{eff}$ = 3.64 BM) was hydrolysed to give 2-phenylpyridine and $Cr^{3+}(aq.)$. This cyclometallated compound may be contrasted with the product from the reaction of ($\eta^6$-phenyllithium)tricarbonylchromium(0) with pyridine, which is formulated as [($\eta^6$-(2-pyridylphenyl)tricarbonylchromium(0))] (Fig. 5).[16]

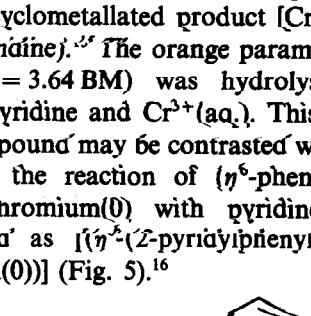



Fig. 5.

The reaction of $Na[Mo(CO)_3(cp)]$ with the complexes [PdLL'Cl] (HL = 8-methylquinoline; L' = $PPh_2Me$, 4-Mepy or CO) leads to the formation of heterodimetallic *Mo–Pd* bonded species (Fig. 6) rather than cyclometallated molybdenum complexes. The crystal structure of $[L(Ph_2MeP)PdMo(CO)_3(cp)]$ has been determined, and is discussed in Section 2.8.[17] The authentic cyclometallated product $[MoL(CO)_2(cp)]$ (HL = 8-methylquinoline) was prepared by the reaction of 8-bromomethylquinoline with $Na[Mo(CO)_3(cp)]$. The $^{13}C$ NMR spectrum of this, and related cyclometallated complexes, has been reported ($\delta$ $CH_2Mo$, −1.0, $CDCl_3$).[18] The reaction of $Na[Mo(CO)_3(cp)]$ with 2-chloromethylpyridine gives the cyclometallated acyl compound $[MoL(CO)_2(cp)]$ (HL = 2-(2-pyridyl)acetaldehyde) (Fig. 7), identified by infrared ($\nu$C=O, 1624 $cm^{-1}$) and $^1H$ NMR spectroscopy ($\delta$ $CH_2CO$, 6.0, $(CD_3)_2CO$).

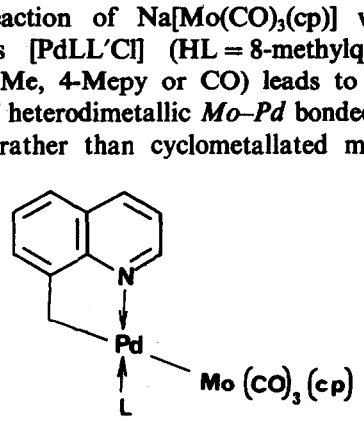



Fig. 6.

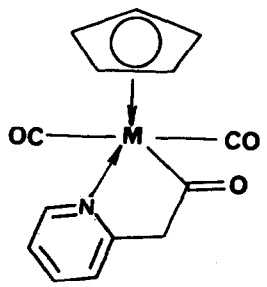



Fig. 7.

This reaction may be rationalised in terms of the formation of a 5-membered cyclometallated ring. In contrast, the corresponding reaction with $Na[W(CO)_3(cp)]$ gives only the $\eta^1$-alkyl complex $[W(CO)_3L(cp)]$ (L = $\eta^1$-2-pyridylmethyl) ($\nu$C=O, 1900 $cm^{-1}$; $\delta CH_2$, 7.09, $CS_2$).[19] The complex $[MoL(CO)_2(cp)]$ (HL = benzo[h]quinoline) has been characterised spectroscopically as the low yield product from the reaction of $[Mo(CO)_3(cp)Me]$ with benzo[h]quinoline.[20]

## 2.5 *Manganese, technetium and rhenium*

The cyclometallated complexes $[ML(CO)_4]$ (M = Mn; HL = benzo[h]quinoline, 2-phenylpyridine, 2,3-diphenyl-quinoxaline, 1-phenylpyrazole, 4-phenylpyrimidine, 1,4-diphenylphthalazine, 2,5-diphenylaxazole or ($\eta^6$-benzo[h]quinoline)tricarbonylchromium(0): M = Re; HL = benzo[h]quinoline or 2-phenylpyridine) are readily prepared by the reaction of $[M(CO)_5R]$ (M = Mn or Re; R = Me or $PhCH_2$) with HL.[20,21] The reaction of $[Mn(CO)_4L]$ (HL = benzo[h]quinoline) with $Ph_2MeP$ results in the formation of phosphine substituted complexes $[MnL(CO)_{4-n}(Ph_2MeP)_n]$ (HL = benzo[h]quinoline; n = 1 or 2).[21] The reaction of 2-vinylpyridine with $[Re(CO)_5Me]$ gave a very insoluble product of stoichiometry $[\{ReL(CO)_4\}_n]$ (HL = 2-vinylpyridine), for which the authors proposed a mononuclear structure (Fig. 8). In the absence of mass spectroscopic data, a polynuclear structure (e.g. Fig. 9) could not be discounted.

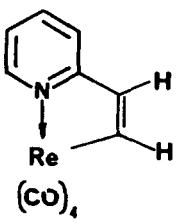



Fig. 8.

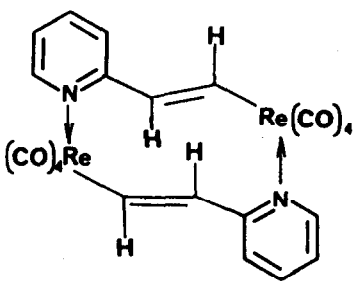



Fig. 9.

The complex $[MnL(CO)_4]$ (HL = 2-(bis-*tert*-butylphosphinomethyl)-8-methylquinoline is formed in the reaction of $[Mn(CO)_5Me]$ with HL, but the ligand is thought to be *C, P* rather than *C, N* bonded (Fig. 10).[22]

The reaction of 2-chloromethylpyridine with $Na[Mn(CO)_5]$ results in the formation of the cyclometallated acyl derivative $[Mn(CO)_4L]$ (HL = 2-

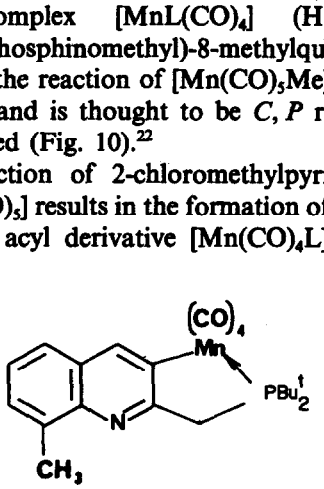



Fig. 10.

(2-pyridyl)acetaldehyde) ($\nu$C=O, 1668 cm$^{-1}$; $\delta$, $CH_2CO$, 6.00, $(CD_3)_2CO$) (see Section 2.4 for the corresponding molybdenum complex).[19]

The photolysis of *eq*-$[Re_2(CO)_9(py)]$ in thf leads to mixtures containing $[Re_2(CO)_7(C_5H_4N)H(py)]$ (Fig. 11), $[Re_2(CO)_{10}]$ and $[Re(CO)_3(py)_3]$

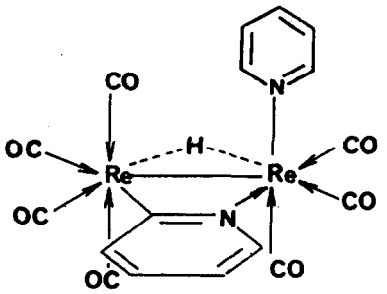



Fig. 11.

$[HRe_4(CO)_{16}]$. Flash photolysis has established that the primary photoproduct is 1,2-*eq*, *eq*-$[Re_2(CO)_8(py)_2]$, which then gives rise to the observed photoproducts in a secondary photochemical reaction. In a thermal reaction, $[Re_2(CO)_8(C_5H_5N)H]$ (Fig. 12) is formed from 2-*eq*, *eq*-$[Re_2(CO)_8(py)_2]$

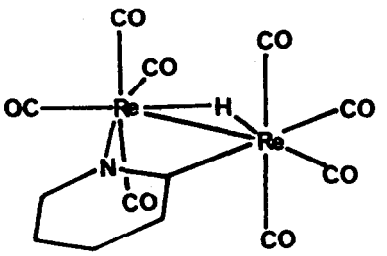



Fig. 12.

after thirty minutes at reflux in benzene solution.[23] Prolonged reaction times (28 h) result in the formation of $[Re_2(CO)_7(py)(C_5H_4N)H]$, which is converted to $[Re_2(CO)_8(C_5H_4N)H]$ on reaction with carbon monoxide, and to $[Re_2(CO)_7(C_5H_4N)H(Me_3NO)]$ (Fig. 13) with $Me_3NO$. Single crystal

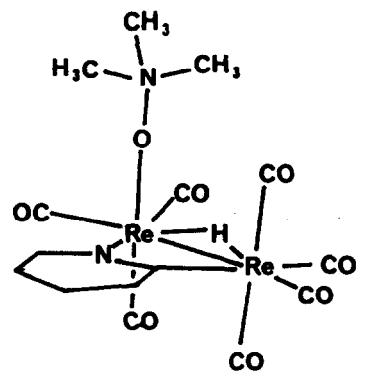



Fig. 13.

X-ray structural analyses of the complexes $[Re_2(CO)_7X(C_5H_4N)H]$ (X = CO or $Me_3NO$) have been reported.[24]

### 2.6 *Iron, ruthenium and osmium*

To date, there appears to have been no successful attempts at preparing a cyclometallated complex of iron, containing a heterocyclic donor atom. The reaction of $Na[Fe(CO)_2(cp)]$ with 2-chloromethylpyridine results in the formation of the alkyl complex $[Fe(CO)_2(cp)L]$ (L = 2-pyridylmethyl) ($\nu$ C=O, >1900 cm$^{-1}$; $\delta$, $CH_2$, 7.45, $CS_2$).[19] Similarly, attempted metal exchange reactions between $K[Fe(CO)_3(NO)]$ and [PdLCl(py)] (HL = 8-methylquinoline) lead to the metal–metal bonded complex $[L(py)PdFe(CO)_3(NO)]$ (Fig. 14).[17] The attempted reaction of benzo[h]quinoline with $[\{Fe(CO)_2(cp)\}_2]$ yielded only $[\{Fe(CO)(cp)\}_2]$.[20]

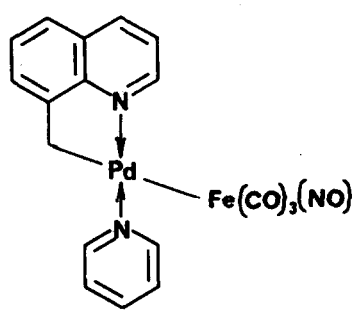



Fig. 14.

In contrast to these results, cyclometallated derivatives of ruthenium and osmium are relatively well-known. Thus, the reaction of benzo[h]quinoline with $[M_3(CO)_{12}]$ (M = Ru or Os) results in the formation of the mononuclear complexes $[M(CO)_2L_2]$ (HL = benzo[h]quinoline; M = Ru or Os) and $[\{HRu(CO)_3\}_4]$. These complexes exhibited two carbonyl stretching frequencies, characteristic of a *cis*-$M(CO)_2$ group, but it was not possible to determine the relative orientation of the cyclometallated ligands (i.e. axial-*N*, axial-*N*; axial-*C*, axial-*N* or axial-*C*, axial-*C*).[20] The $^1$H NMR spectra reported for the ruthenium complex indicate a symmetrical structure (i.e. *not* axial-*N*, axial-*C*). The crystal structural analysis of $[RuL_2(CO)_2]$ (HL = benzo[h]quinoline) has recently been reported; the carbonyl ligands are in the expected *cis* configuration, and are each *trans* to nitrogen.[110] Cyclometallated complexes $[\{RuL(CO)_2(\mu\text{-}Cl)\}_2]$ (HL = 1-phenylpyrazole, 2-phenylpyridine or benzo[h]quinoline) are readily prepared by the reaction of HL with $[Ru(CO)_nCl_m]$ (made *in situ* by the passage of carbon monoxide through a 2-methoxyethanol solution of "$RuCl_3.3H_2O$"). The configur-

ation of the chloro-bridged dimers has yet to be established, but they are readily converted to mononuclear complexes on reaction with Tl(acac), $PPh_3$ or 4-methylpyridine. The complexes $[RuL(CO)_2(acac)]$ exhibit two carbonyl stretching frequencies ($\nu$ C=O, $\simeq$1970, $\simeq$2040 $cm^{-1}$), consistent with *cis*-dicarbonyls in which one of the carbonyls is *trans* to nitrogen, and were thus assigned the structure shown in Fig. 15.[25] The reaction of

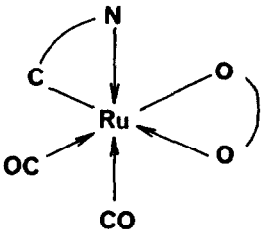



Fig. 15.

$[\{RuCl_2(CO)_3\}_2]$ with 2-thienylpyridine results in the formation of the chlorobridged dimer $[\{Ru(CO)_2L(\mu\text{-}Cl)\}_2]$ (HL = 2-thienylpyridine), which may be converted to the mononuclear complexes $[Ru(CO)_2L(Cl)L']$ (HL = 2-thienylpyridine; L' = py or $^nBu_3P$) on treatment with pyridine or tri-*n*-butylphosphine. The complexes are thought to possess the structure shown in Fig. 16.[26]

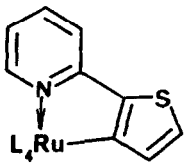



Fig. 16.

2-Vinylpyridine has been shown to insert into the Ru–H bond of $[RuCl(H)(CO)(PPh_3)_3]$ to form the cyclometallated complex $[RuCl(CO)(PPh_3)_2L]$ (L = 2-(2-pyridyl)ethyl). On the basis of IR ($\nu$ C=O, 1980 $cm^{-1}$), $^1H$ NMR ($\delta$, 1.8 and 2.6, $CDCl_3$) and $^{13}C$ NMR spectroscopic measurements ($\delta$, $\underline{C}H_2Ru$, 13.5; $\underline{C}H_2CH_2$, 42.5; $C_6$(py), 151.2; $C_2$(py), 166.9, $\underline{C}DCl_3$) and the known structure of the starting material, the product was thought to possess an equatorial 2-(2-pyridyl)ethyl group and *trans*-diaxial phosphines (Fig. 17).[27]

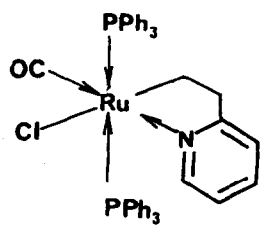



Fig. 17.

Although $[Os_3(CO)_{12}]$ reacts with benzo[h]quinoline to form mononuclear complexes, direct reaction with pyridine occurs to form a range of products, including $[HOs_3(CO)_{10}(C_5H_4N)]$ (Fig. 18), two isomers of $[HOs_3(CO)_9(py)(C_5H_4N)]$, $[H_2Os_3(CO)_8(C_5H_4N)_2]$ and two isomers of $[Os_2(C_5H_4N)_2(CO)_6]$ (Figs. 19 and 20).

Similar reactions occur with 4-methylpyridine, 4-benzylpyridine, quinoline (Fig. 21), 7-methylquinoline and isoquinoline (Figs. 22 and 23).[28] These complexes were all characterised on the basis of $^1H$ and $^{13}C$ NMR, IR and mass-spectroscopic studies. The complex

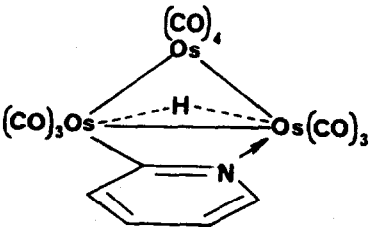



Fig. 18.

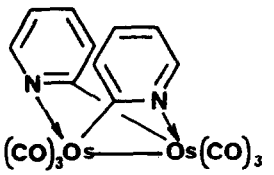



Fig. 19.

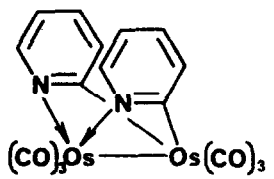



Fig. 20.

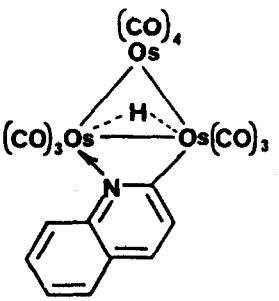



Fig. 21.

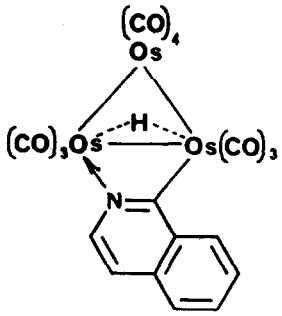



Fig. 22.

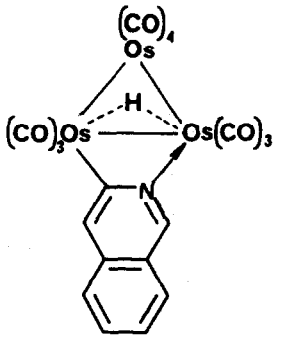



Fig. 23.

$[HOs_3(CO)_{10}(C_5H_4N)]$ may also be prepared by the reaction of $[Os_3(CO)_{10}L_2]$ (L = cyclooctene) or $[Os_3(CO)_{10}(NCMe)_2]$ with pyridine.[29] The reactions of 2-substituted pyridines are more complex, and

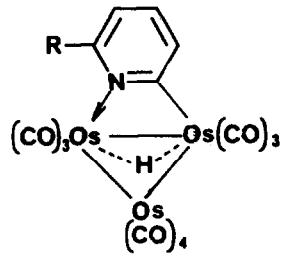



Fig. 24.

the products obtained depend upon the precise nature of the 2-substituent. 2(1H)-Pyridone, 2-aminopyridine and 2(1H)-pyridinethione all give the complexes $[HOs_3(CO)_{10}L]$ (L = $C_5H_4NO$, $C_5H_4NNH$ or $C_5H_4NS$), which rearrange on warming to form $\mu_3$-bridged systems; however none of these complexes contain a cyclometallated ligand.[30-33] The product from the reaction of 2-pyridinecarboxaldehyde with $[Os_3(CO)_{10}(NCMe)_2]$ is the complex $[Os_3(CO)_{10}H(\mu_2\text{-}C\text{-}, O\text{-}C_5H_4NCO)]$, which on warming eliminates carbon monoxide, to form the known cyclometallated complex $[HOs_3(CO)_{10}(C_5H_4N)]$.[30] The cyclometallated complexes $[HOs_3(CO)_{10}L]$ (HL = 2-methylpyridine, 2-cyanopyridine, 2-benzylpyridine or 2-chloropyridine) (Fig. 24) are formed in the reaction of HL with $[Os_3(CO)_{10}L_2]$ (L = cyclooctene) or $[Os_3(CO)_{10}(NCMe)_2]$.[30,34] Related complexes were obtained with a wide range of other 5- and 6-membered ring nitrogen-donor heterocycles.[30,34] A

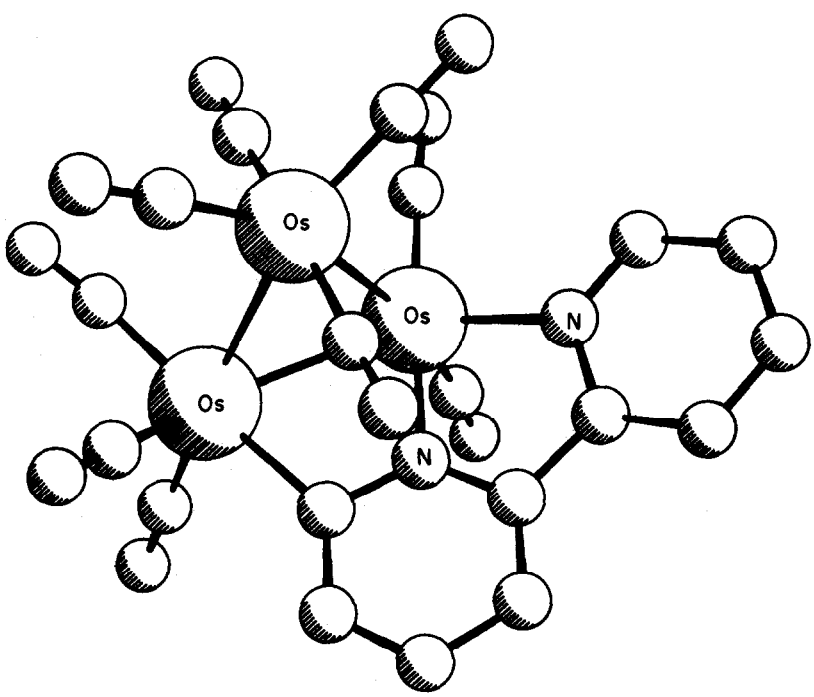



Fig. 25.

single crystal structural analysis of the complex $[Os_3H(CO)_9L]$ (HL = 2,2′-bipyridine) has revealed it to possess the related cyclometallated structure shown in Fig. 25 (see also Section 2.7 and Ref. 35).[34] The reactions of 2-benzylaminopyridine are anomalous, in that the novel cyclometallated complex $[H_2Os_3(CO)_9L]$ (HL = 2-benzylaminopyridine) (Fig. 26) may be prepared.[32,33] the pyrolysis of $[Os_3(CO)_{11}(py)]$ results in the formation of a range of high-nuclearity clusters, including the cyclometallated carbido-cluster $[Os_5C(CO)_{14}H(C_5H_4N)]$.[36] The molecular structure of this complex has been determined, and is shown in Fig. 27.[36]

### 2.7 *Cobalt, rhodium and iridium*

No mononuclear cyclometallated complexes of cobalt incorporating a heterocyclic donor atom have been described. The reaction of [PdL(Cl)L′] (HL = 8-methylquinoline; L′ = CO, py or $PPh_2Me$) with $Na[Co(CO)_4]$ results in the formation of metal–metal bonded systems $[LL'PdCo(CO)_4]$.[17] The complex $[Co(CN)_5L]$ (L = 2-pyridyl is formed in the reaction of 2-iodopyridine with $[Co(CN)_5]^{3-}$, but there is little evidence for the involvement of the pyridine nitrogen in bonding to the metal. 2,2′-Bipyridine is formed on thermolysis of the complex.[37]

Matsuda *et al.* have demonstrated the beneficial effect of pyridine upon the $[Co_2(CO)_8]$ catalysed hydroesterification reaction; but the role of the heterocycle in these transformations is not fully apparent.[38–44] the active catalytic species appears to be $[H_2Co_3(CO)_9(py)_5]$, which has been shown to react with 2-vinylpyridine to form a 1 : 1 complex.[44] This complex was thought to possess the cyclometallated 2-(2-pyridyl)ethyl structure (Fig. 28) on the basis of $^{13}C$ NMR spectroscopy ($\delta$, $\underline{C}H_2Co$, 60.00, triplet; $\underline{C}H_2CH_2$, 37.4, triplet, $C_6D_6$). The IR spectrum of the complex did not exhibit any absorptions which could be assigned to an acyl carbonyl group.

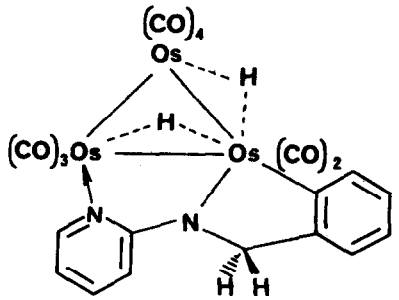



Fig. 26.

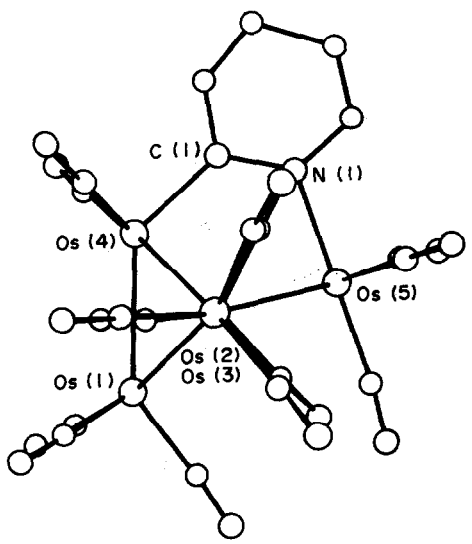



Fig. 27.

The simplest approach to cyclometallated rhodium complexes involves the reaction of HL with rhodium trichloride, to give the chloro-bridged dimers $[\{RhL_2(\mu\text{-}Cl)\}_2]$ (HL = 2-(4-tolyl)-4,5-dimethyltriazole,[45] 2-arylpyridines,[46] benzo[h]quinoline,[47,48] 2-phenylpyridine[48] or 1-phenylpyrazole.[49] These complexes are all thought to possess the *trans*-axial-*N*, *trans*-axial-*N* configuration (Fig. 29), and undergo the expected bridge-splitting reactions to give mononuclear complexes $[RhL_2(Cl)L']$ with phosphines, thioethers, sulphoxides, amines, thiolates and pyridines, and also with bidentate ligands such as dithiocarbamates, diphosphines, 2,2′-bipyridine and ethylenediamine ($[RhL_2L']^{n+}$). A variant on this preparative scheme involves the use of $[\{RhX_3(PR_3)_2\}_2]$ (X = halogen) in the preparation of $[RhLX_2(PR_3)_2]$ (HL = 1-phenylpyrazole,[50] 3,5-dimethyl-1-phenylpyrazole,[50] 2-phenylpyridine,[50] benzo[h]quinoline[50] or 1-(3-thienyl)pyrazole[51]) although 1-(2-thienyl)pyrazole, and 2-(2-thienyl)- or 2-(3-thienyl)pyridine also gave $[\{RhClL(PR_3)(\mu\text{-}Cl)\}_2]$.[51,52] The complexes are thought to contain *trans*-diaxial phosphine groups. Although benzo[h]quinoline reacts with $[\{Rh(CO)_2(\mu\text{-}Cl)\}_2]$ to give the cyclometallated complex $[\{RhL(CO)(\mu\text{-}Cl)\}_2]$ (HL = benzo[h]quinoline), 2-phenylpyridine only gave the nitrogen donor complex $[Rh(HL)_2(CO)Cl]$, which would not eliminate HCl to form the cyclometallated compound even on heating with base.[20,21]

Deeming *et al.* have investigated a series of rhodium(I) complexes of 2-substituted quinolines,

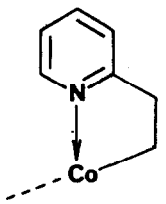



Fig. 28.

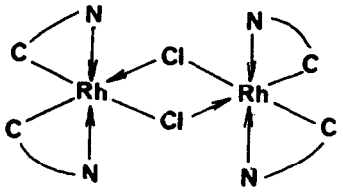



Fig. 29.

and have shown that the products are *not* cyclometallated.[53] Complexes with 2-(bis-*tert*-butylphosphinomethyl)-8-methylquinoline[22] and 8-alkyl-2-(*N*-methyliminoformyl)quinoline[54] have also been characterised, but these are either *not* cyclometallated, or cyclometallated without involvement of the ring donor atom.

Iridium complexes with 2-arylpyridines,[46] 1-phenylpyrazole,[49] 2-(4-tolyl)-4,5-dimethyltriazole,[45] 2-(2-thienyl)pyridine[55] and benzo[h]quinoline[56] have been prepared by the same general methods as the corresponding rhodium compounds.

The acyl complexes ($\nu$C=O, 1670 cm$^{-1}$) [Rh(PPh$_3$)$_2$(Cl)RL] (HL = 8-quinolinealdehyde; R = H or *tert*-butyl) (Fig. 30) have been prepared by the reaction of 8-quinolinealdehyde or 8-quinolyl *tert*-butyl ketone with [RhCl(PPh$_3$)$_3$].[57,58] The compound [Rh(PPh$_3$)$_2$Cl(R)H] represents an intermediate in the [Rh(PPh$_3$)$_3$Cl] promoted decarbonylation of aldehydes, and loses quinoline to form *trans*-[Pd(PPh$_3$)$_2$L(CO)] on heating. Iminoacyl complexes [Rh(PPh$_3$)$_2$H(Cl)L] (HL = (3-methyl-2-pyridyl)iminoacyl) ($\nu$C=N, 1598 cm$^{-1}$, $\delta$, Rh–H, −11.5, $J_{Rh-H}$, 13 Hz, $CD_2Cl_2$) (Fig. 31) are formed in the reaction of the appropriate aldimines with [Rh(PPh$_3$)$_3$Cl].[59] The related vinyl complexes [RhX$_2$(PBu$^n_3$)$_2$L] (X = halogen, XL = 2-vinylpyridine) (Fig. 32) are readily prepared from the reaction of 2-vinylpyridine with [{RhX$_2$(PBu$^n_3$)$_2$}$_2$].[60,61] The Rh–C bond was established by $^{13}$C NMR spectroscopy ($\delta$, CHRh, 179–197, $J_{Rh-C}$, 27–30 Hz, various R,R', $CDCl_3$), and it was shown that 2-allylpyridine did not undergo similar reactions.

There has been controversy over the nature of "[Ir(bipy)$_3$]$^{n+}$" complexes for some years, but it is now evident that cyclometallated 2,2'-bipyridines

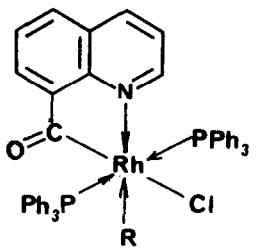



Fig. 30.

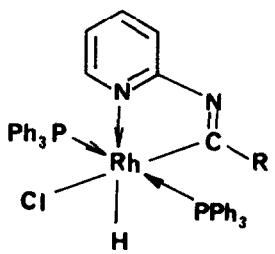



Fig. 31.

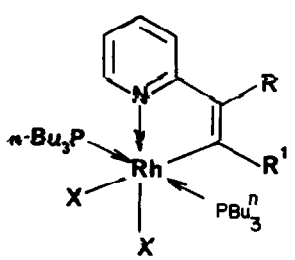



Fig. 32.

coordinated to iridium can be formed, and Serpone has reported the crystal structure of [Ir(bipy)$_2$(LH)][ClO$_4$]$_3$.H$_2$O (HL = 2,2'-bipyridine) (Fig. 33) in which one of the bipy ligands is cyclometallated, although it is protonated on nitrogen.[106] For a full discussion of this and related complexes, the reader is referred to Ref. 55.

### 2.8 *Nickel, palladium and platinum*

The use of transition metal salts (frequently nickel(II)) in the formation of dimeric RR, or RR' species from organometallic RLi or RMgHal complexes is well known. Such reactions almost certainly involve M–C bonded species, but will not be discussed further herein. Jolly has reviewed the use of nickel complexes in the coupling of alkyl and aryl halides,[62] and reactions of this type are only discussed where there is evidence for involvement of cyclometallated intermediates.

It is well-established that [Ni(PPh$_3$)$_4$] reacts with 2-halopyridines to form complexes of stoichi-

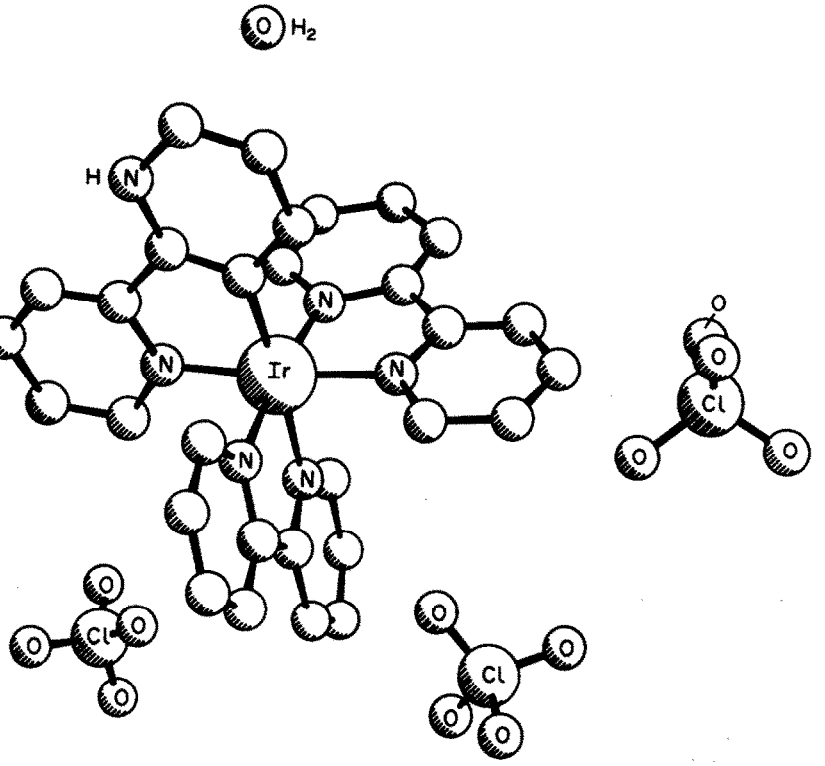



Fig. 33.

ometry $[\{NiX(PPh_3)L\}_2]$ (X = halogen; L = substituted 2-pyridyl), which react with Na(acac) or NaSCN to give $[\{Ni(PPh_3)LL'\}_2]$ (L' = SCN or acac).[63-65,116] The $^1H$ NMR of $[\{Ni(PPh_3)L(Cl)\}_2]$ (L = 6-chloro-2-pyridyl) ($\delta$, $H_3$, 6.45; $H_4$, 6.21; $H_5$, 6.65, $CD_2Cl_2$) is consistent with formulation as either a chloro-bridged dimer or a pyridyl-bridged dimer. Treatment of this complex with triphenylphosphite results in the formation of 6,6'-dichloro-2,2'-bipyridine in high (70%) yield. $[Pd(PPh_3)_4]$ undergoes similar reactions with 2-halopyridines to produce $[\{Pd(PPh_3)XL\}_2]$, which is converted to $[Pd(PEt_3)_2XL]$ (X = halogen; L = 2-pyridyl) on treatment with excess $PEt_3$.[10,64,115] The single crystal X-ray structure of $[Pd(PEt_3)_2Br(C_5H_4N)]$ has been determined, and the pyridyl group shown to be bonded to the metal through carbon only.[64] A range of 6-chloro-2-pyridyl complexes *trans*-$[MCl(L)_2(C_5H_3ClN)]$ (M = Pd or Pt; $(L)_2 = (PR_3)_2$, dppe or $Me_2NCS_2$ have been prepared.[107] These compounds have been shown to insert carbon monoxide to form 6-chloro-2-pyridylcarbonyl complexes of the type *trans*-$[PdCl(L)_2(ClC_5H_3NCO)]$.[107,115,117] A structural analysis of $[\{PdBr(PPh_3)(C_5H_4N)\}_2]$ (Fig. 34) (from the reaction of 2-bromopyridine with $[Pd(PPh_3)_4]$) has also been reported, and conclusively demonstrates the presence of a bridging pyridyl group, and terminal halide ions.[10,115] There is no evidence for metal–metal bonding in this compound (Pd–Pd, 3.194 Å). The reaction of $[\{PdBr(C_5H_4N)(PPh_3)\}_2]$ with RNC led to the formation of $[PdBr(PPh_3)L]$ (Fig. 35), whereas $[PdBr(PPh_2Me)_2(C_5H_4N)]$ gave the non-cyclometallated $[PdBr(PPh_2Me)_2L]$ (L = 2-$C_5H_4N$-C=NR).[66]

2-Vinylpyridine reacts with $Li_2[PdCl_4]$ in alcoholic medium to give $[\{PdL(\mu\text{-}Cl)\}_2]$ (HL = 2-(2-pyridyl)-2-alkoxyethyl) (Fig. 36) ($\delta$, $CH_2Pd$, 5.8, $CDCl_3$), which liberates the free ligands $(2\text{-}C_5H_4N)CH(OMe)CH_3$ or $(2\text{-}C_5H_4N)CH(OMe)CH_2D$ on treatment with $Li[AlH_4]$ or $Li[AlD_4]$.[67] The corresponding platinum complexes were prepared similarly.

The platinum(IV) complex $[Pt(PEt_3)Br_4(HL)]$ (HL = 2-vinylpyridine) reacts with water to give the acyl complex $[Pt(PEt_3)Br_3L]$ (HL = 2-acetylpyridine) (Fig. 37) ($\nu$C=O, 1695 $cm^{-1}$; $\delta$ $CH_2Pt$, 4.3, $J_{Pt-H}$, 56 Hz).[68] The complex could not be prepared directly from 2-acetylpyridine. The chloro-bridged dimers $[\{PdL(\mu\text{-}Cl)\}_2]$ (L = 2-(2-pyridyl, 2-arylethyl) are readily prepared by the reaction of [ArPdCl] with 2-vinylpyridine.[11] This is analogous to the formation of 2-(2-pyridyl)-2-alkoxyethyl complexes discussed above, but utilises the Pd-bonded aryl group as an internal nucleo-

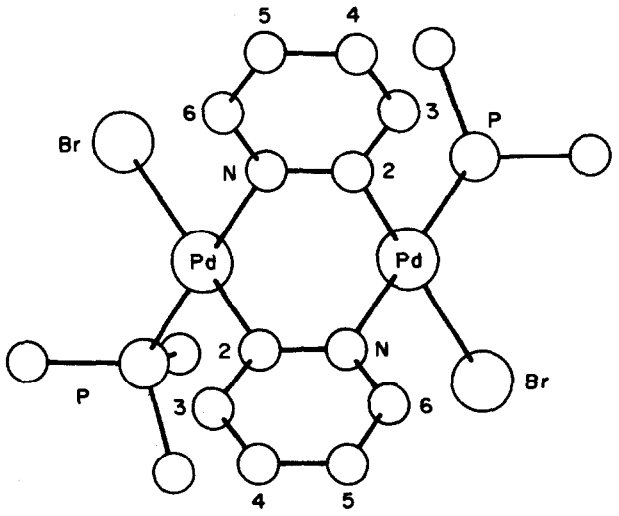



Fig. 34.

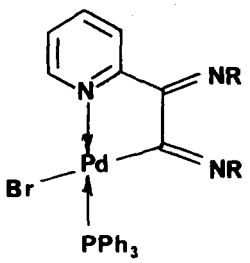



Fig. 35.

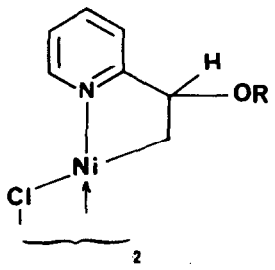



Fig. 36.

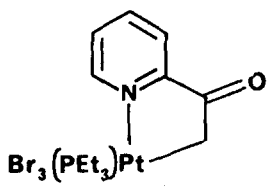



Fig. 37.

phile. It is worthy of note that in non-nucleophilic solvents, 2-vinylpyridine will form simple *N* donor complexes (e.g. $[PtBr_4(HL)(PEt_3)]$). The ylid complexes $[ML(Cl)_2]$, $[ML_2]^+$ and $[ML(bipy)]^{2+}$ ($M = Pd$ or Pt; $L = (2\text{-}C_5H_4N)\overset{-}{C}O\overset{+}{C}Hpy$) have been investigated by NMR techniques.[69] Newkome has reported a series of cyclometallated complexes in which resonance stabilised carbanions are bonded to palladium (Figs. 38 and 39). These complexes are the first examples of terdentate

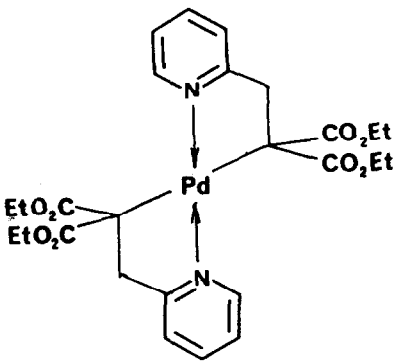



Fig. 38.

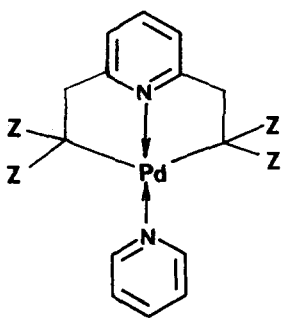



Fig. 39.

*C,C,N*-cyclometallated systems, and structural studies on two of these compounds have been reported (Figs. 40 and 41).[70–72] Newkome has also described the preparation and structural characterisation of the complex *trans*-[PdL$_2$] (HL = 2-{1, 1-bis(methoxycarbonyl)propyl}pyridine, (MeO)$_2$CHCH$_2$CH$_2$C$_5$H$_4$N); the compound is unusual in possessing two six-membered *N,C* chelate rings.[109]

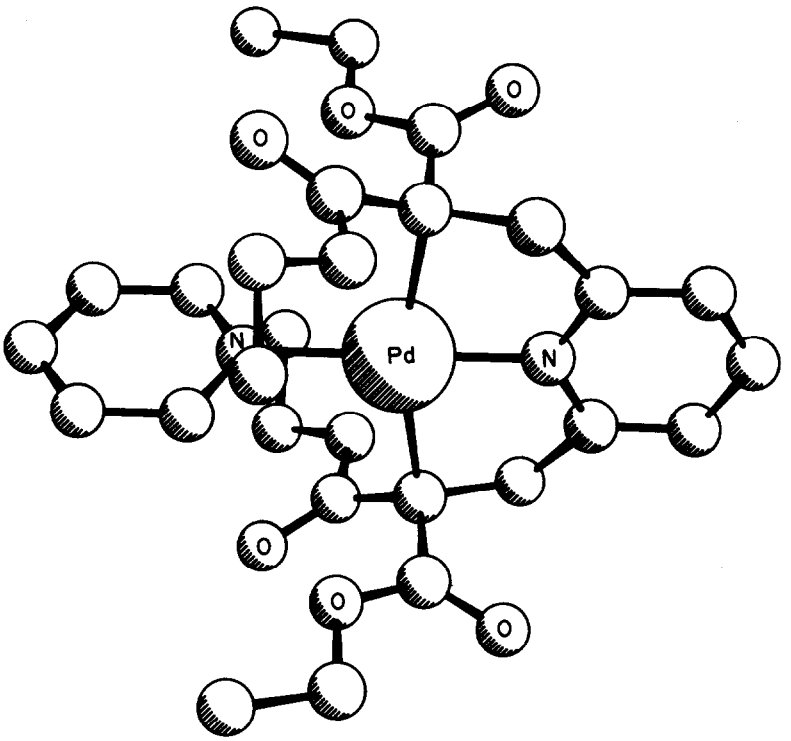



Fig. 40.

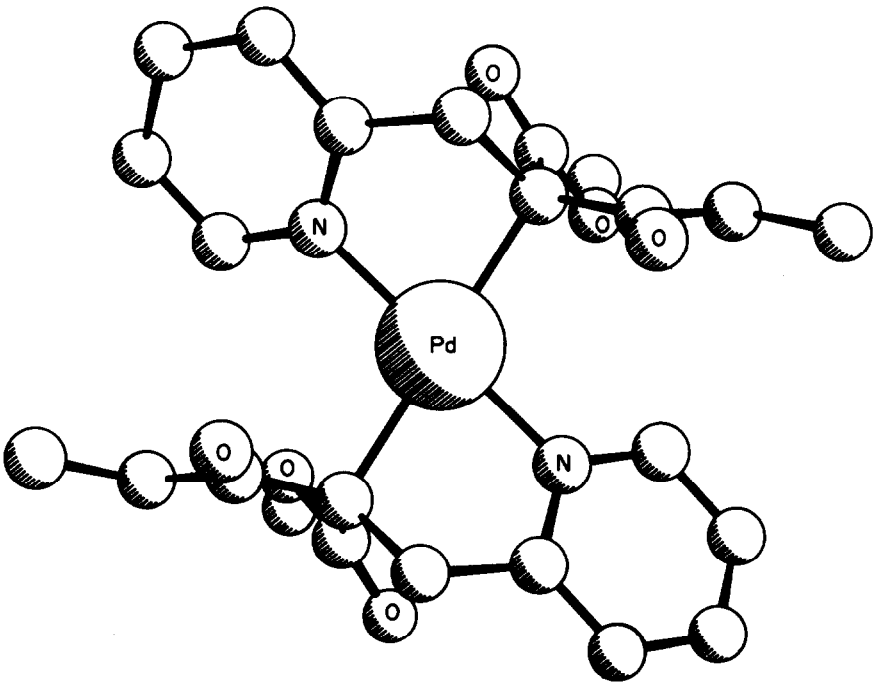
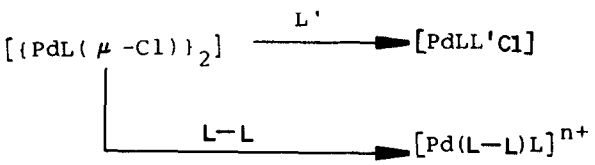
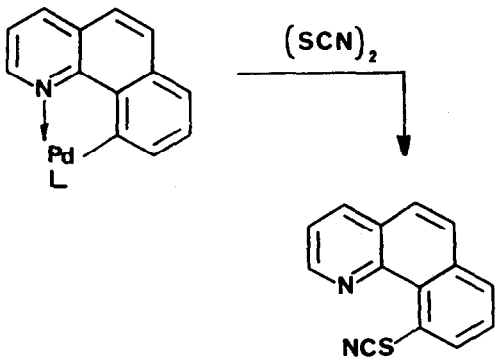



Fig. 41.

The complexes [{ML($\mu$-X)}$_2$] (M = Pt; HL = benzo[h]quinoline,[8] 8-methylquinoline,[73] 2-(4-tolyl)-4,5-dimethyltriazole,[45] 1-arylpyrazoles[74]: M = Pd; HL = benzo[h]quinoline,[20,46,73,75,76,79,80] 2-phenylpyridines,[8,75,77,78,81] 2-phenylquinoline,[81] 2-(2-thienyl)-pyridine,[52] 2-(3-thienyl)pyridine,[52] 2-phenylbenzothiazole,[82] 2-phenylbenzoxazole,[82] 1-phenylpyrazoles,[74,83] 2-phenylthiazole,[84] 2-aryl-4,5-dimethyltriazole,[45] 2-phenylimidazoles,[86] 2-pyridylferrocenes,[87,88] and 2-phenylisoxazoles[89] have been reported. The compounds [M(PPh$_3$)$_2$ClL] (L = 2-thienyl) (M = Pd or Pt) have been described, although the degree of M–S interaction is not clear.[113,118] It is sometimes found that the use of $[PdCl_4]^{2-}$ results in the formation of [Pd(HL)$_2$Cl$_2$] complexes (e.g. Ref. 51), rather than the desired cyclometallated complexes; in such cases the cyclometallated compound is frequently obtained with palladium acetate. The chloro- and acetato-bridged complexes undergo all the anticipated bridge splitting reactions with monodentate or polydentate ligands to give mononuclear species (eqn 14), which will not be discussed in any detail.

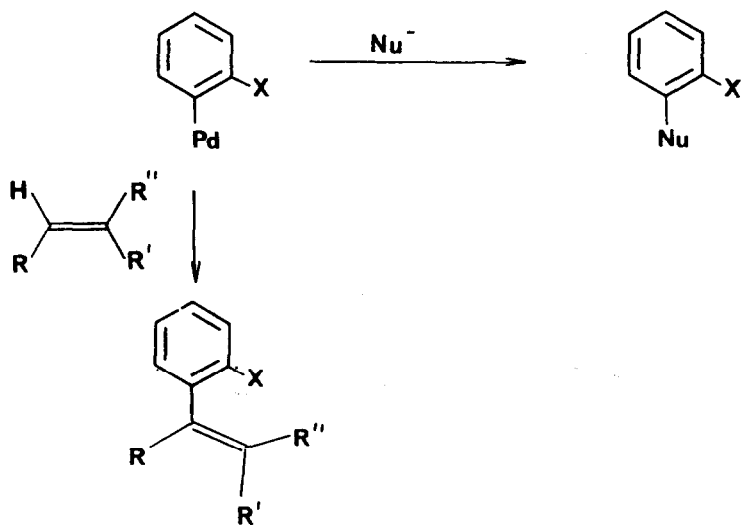



The reaction of the cyclopalladated complexes with nucleophiles (Li[AlH$_4$] or Li[AlD$_4$]) or electrophiles (PhCH=CH$_2$ or CH$_3$COCH=CH$_2$) results in the liberation of the free organic fragments LH, LD, LCH=CHPh or LCH=CHCOCH$_3$ respectively (eqn 15). A novel example of the reactivity of the cyclometallated ligand occurs on reaction with thiocyanogen. Although the dimers [{PdL($\mu$-X)}$_2$] (HL = 2-phenylpyridine or benzo[h]quinoline; X = Cl or OAc) do not react cleanly with (SCN)$_2$, treatment with dithiocarbamates gives mononuclear complexes [PdLL'] (HL = 2-phenylpyridine or benzo[h]quinoline; HL' = HSSCNR$_2$), which are more reactive. Thus [PdLL'] reacts with (SCN)$_2$ to give high yields of the appropriate 2-(2-S-thiocyanato)-substituted heterocycle (eqn 16).[104] A crystal structural analysis of the complex




[PdL(L')] (HL = 8-methyquinoline; HL' = 1-methoxynaphthalene) has recently been reported; both ligands are metallated, acting as *N,C* and *O,C* donors respectively.[108] The two Pd–C bonds are arranged *cis* to each other.

In those cases in which the heterocycle possesses more than one potential donor atom, the palladium commonly forms Pd–N bonded complexes. Thus, isoxazolines,[89] benzothiazoles[82] and benzoxazoles[82] all from cyclometallated complexes with the heterocyclic nitrogen atom coordinated to the metal. Single crystal structural analyses of the



complexes $[\{PdL(OAc)\}_2]$ (HL = 2-(4-tolyl)-5-methylbenzothiazole or (2-(4-tolyl)-5-methylbenzoxazole) (Figs. 42 and 43) have definitively established this bonding mode, and also demonstrate the folding about the acetato bridges.[82] This folding about the bridging groups is also observed in the single crystal X-ray structures of the complexes $[\{PdL(\mu\text{-}OAc)\}_2]$ (HL = 2-(3-nitrophenyl)-pyridine or 2,6-bis(4-chlorophenyl) pyridine).[78] The 2,6-diphenylpyridine complex is of interest, as only one of the phenyl groups is cyclometallated (Figs. 44 and 45). 2-Benzoylpyridine and 2-benzylpyridine react with $Pd(OAc)_2$ to form the unusual complexes $[\{PdL(\mu\text{-}OAc)\}_2]$, which contain a 6-membered cyclometallated ring.[90,91] These complexes show all the reactions expected of cyclometallated complexes, and suggest that other complexes containing such 6-membered cyclometallated rings should be preparable with a judicious choice of ligands. Cyclometallated compounds derived from 2-neopentylpyridine, $[\{PdL(\mu\text{-}L')\}_2]$ (HL = $CH_3Me_2CH_2C_5H_4N$; $\mu$-L = Cl or OAc) also contain 6-membered *N,C* chelate rings.[112] Six-membered *N,C* chelates are also found in the cyclopalladated derivatives of 2-benzylamino-, 2-benzyloxy-, 2-benzylthio- and 2-benzylmethyl-pyridines.[114]

8-Methylquinoline reacts with $Li_2[PdCl_4]$ to form the chloro-bridged complex $[\{PdL(\mu\text{-}Cl)\}_2]$.[17,73,92,93] 8-Ethylquinoline and 8-isopropylquinoline react similarly to give the chloro-bridged dimers (Fig. 46).[49,99] The 8-ethylquinoline complex was resolved by separating the diastereoisomers of $[PdL(Cl)(NH_2CHMePh)]$ (HL = 8-ethyl-quinoline) obtained upon reaction with optically active 1-(phenylethyl)amine.[94] The chiral platinum analogue $PtL(PPh_3)Br$ (HL = 8-ethylquinoline) was obtained in the stereoretentive reaction of $[Pt(PPh_3)_4]$ with chiral 8-(1-bromoethyl)quinoline.[95] Deeming has characterised a number of

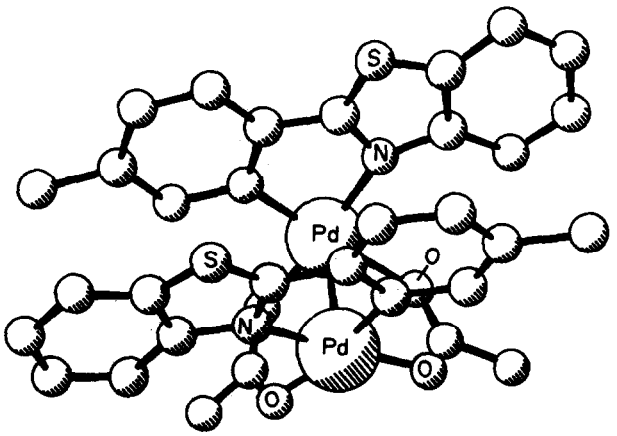



Fig. 42.

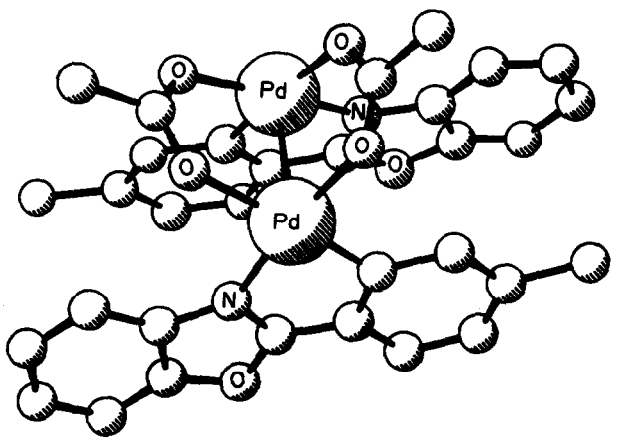



Fig. 43.

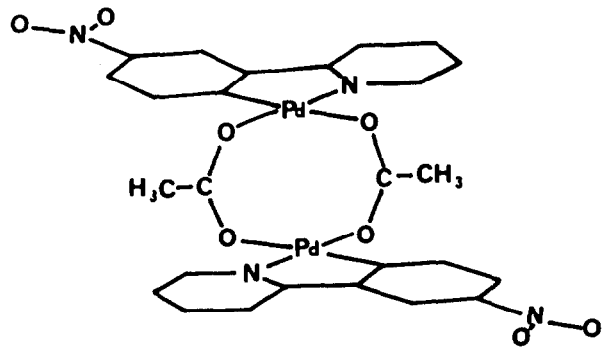


Fig. 44.

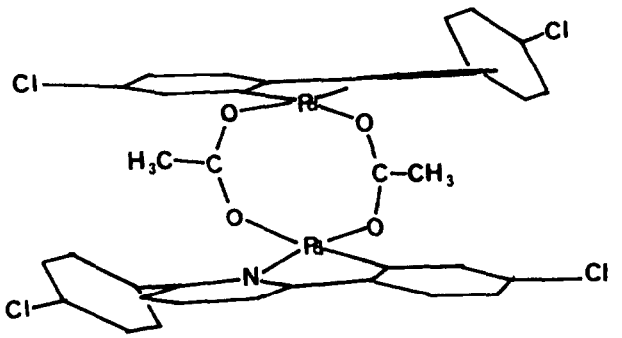


Fig. 45.

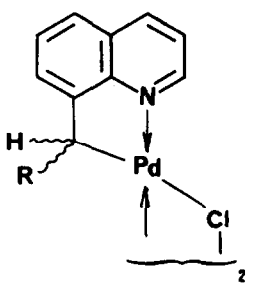


Fig. 46.

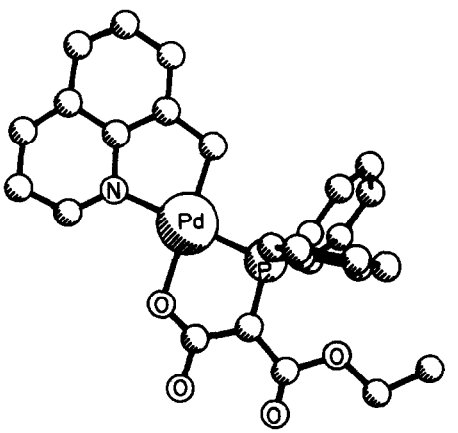


Fig. 47.

mixed ligand complexes containing 8-methylquinoline or benzo[h]quinoline in which the ligand is *not* cyclometallated, although the appropriate C–H bond is spatially close to the palladium atom.[96,97] A crystal structural analysis of the remarkable complex obtained from the reaction of [PdLL′] (HL = 8-methylquinoline; HL′ = $Ph_2PCH{=}C(OH)OEt$) has been reported (Fig. 47).[98] These compounds exhibit a facile, reversible insertion of carbon dioxide.

Deeming has demonstrated that the presence of a 2-substituent has a profound effect upon the cyclometallation of 8-methylquinolines. Thus, 8-methyl-2-(bis-*tert*-butylphosphinomethyl)quinoline metallated under forcing conditions to give complexes in which the ring nitrogen atom was not coordinated to the metal,[22] whereas 2-iminoacyl derivatives could metallate at either $C_3$ or the methyl group.[54,92,99]

8-Quinolinealdehyde reacts with $Na_2[PdCl_4]$ to form the acyl complex $[\{PdL(\mu\text{-}Cl)\}_2]$ (HL = 8-quinolinealdehyde) (Fig. 48), which has been characterised spectroscopically.[100] A number of re-

actions giving mononuclear cyclometallated complexes directly have been described, including the reactions of $[PdL'_2]$ with HL to give [PdLL'] (HL' = $CF_3COCH_2COCF_3$; HL = 2-phenylpyridine of 2,6-diphenylpyridine).[101,102] Only one ring of the 2,6-diphenylpyridine is metallated. A number of cyclometallated tris (1-pyrazoyl)methane complexes of platinum have been prepared, as shown in eqn (17),[102,111] The reaction of [PdLL'] (HL = 8-methylquinoline; L' = various) with a range of $[ML_x]^{n-}$ anions to form metal–metal bonded spe-

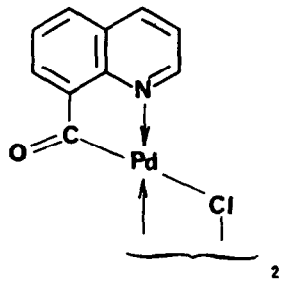
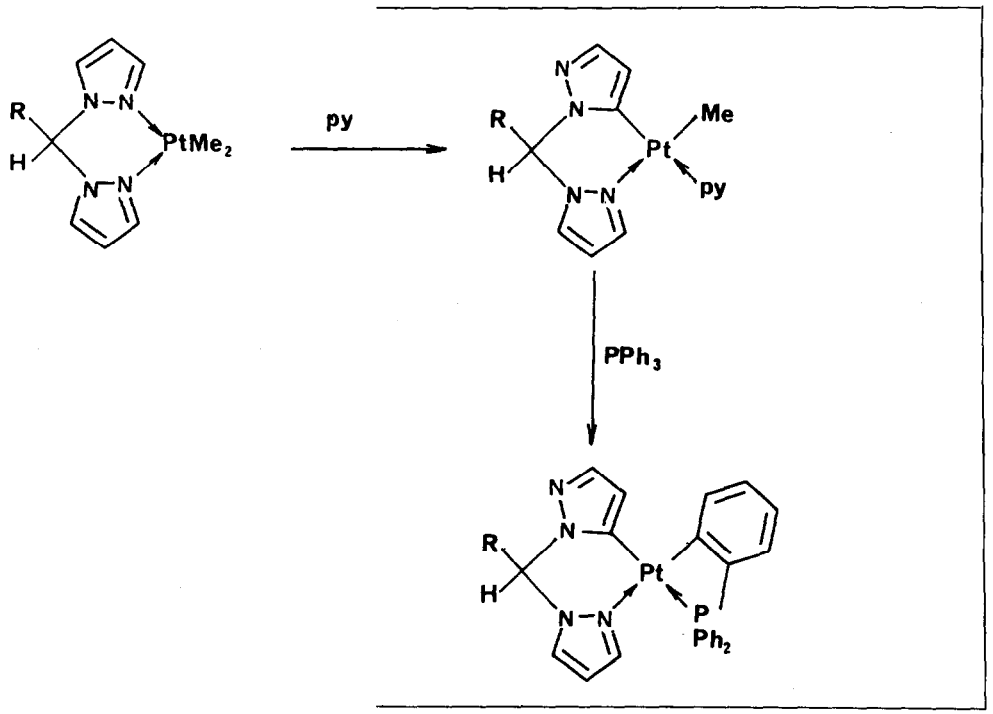



Fig. 48.



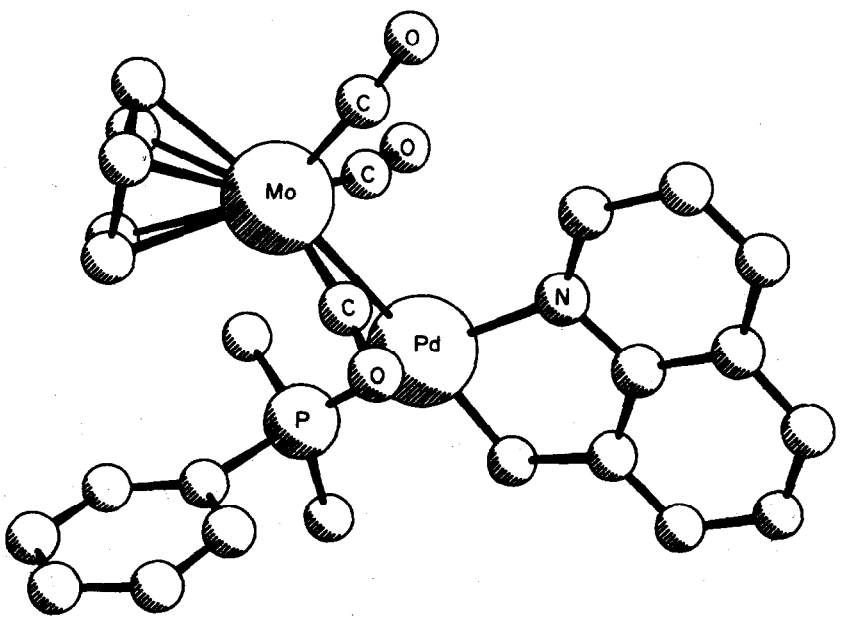




Fig. 49.

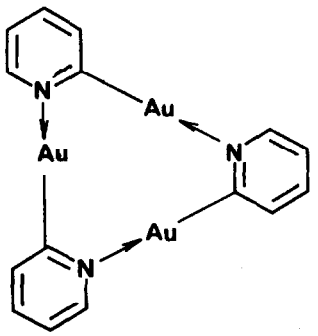



Fig. 50.

cies, rather than trans-metallation products has been described earlier. The single crystal structural analysis of a molybdenum complex has been reported (Fig. 49).[17]

### 2.9 *Copper, silver and gold*

The reaction of 2-pyridyllithium or 2-quinolyllithium with $[Au(Cl)AsPh_3]$ results in the formation of $[\{AuL\}_n]$ (L = 2-pyridyl or 2-quinolyl). These compounds are thought to be trimers (Fig. 50). A range of other heterocycles have been shown to behave similarly. In each case, the $[\{AuL\}_n]$ species are thermally unstable with respect to decomposition to gold and the dimer LL.[12,80] 2-Pyridylcopper probably has a related trimeric structure.

*Acknowledgements*—I should like to thank Dr. Sharon Bellard for obtaining structural data from the Crystallographic Data Centre, University Chemical Laboratory, and all my colleagues in the University Chemical Laboratory, for helpful discussions.

## REFERENCES

1. G. W. Parshall, *Acc. Chem. Res.* 1970, **3**, 139.
2. M. I. Bruce, *Angew. Chem. Int. Ed. Engl.* 1977, **16**, 73.
3. J. Dehand and M. Pfeffer, *Coord. Chem. Rev.* 1976, **18**, 327.
4. I. Omae, *Rev. on Silicon, Germanium, Tin and Lead Compounds* 1973, **1**, 59.
5. I. Omae, *Coord. Chem. Rev.* 1979, **28**, 97.
6. I. Oame, *Chem. Rev.* 1979, **79**, 287.
7. A. C. Cope and E. C. Friedrich, *J. Am. Chem. Soc.* 1968, **90**, 909.
8. B. N. Cockburn, D. V. Howe, T. Keating, B. F. G. Johnson and J. Lewis, *J. Chem. Soc., Dalton Trans.* 1973, 404.
9. K. Burgess, B. F. G. Johnson and J. Lewis, *J. Organomet. Chem.* 1982, **233**, C55.
10. K. Nakatsu, K. Kinoshita, H. Isobe, Y. Nakamura and S. Kawaguchi, *Chem. Lett.* 1980, 913.
11. A. Kasahara, T. Izumi, T. Takeda and H. Imamura, *Bull. Chem. Soc. Jpn.* 1974, **47**, 183.
12. L. G. Vaughan, *J. Am. Chem. Soc.* 1970, **92**, 730.
13. B. Klei and J. H. Teuben, *J. Chem. Soc., Chem. Commun.* 1978, 659.
14. B. Klei and J. H. Teuben, *J. Organomet. Chem.* 1981, **214**, 53.
15. K. Madeja, E. Husing and N. Ahrens, *Z. Chem.* 1967, **7**, 33.
16. M. D. Rausch and R. E. Gloth, *J. Organomet. Chem.* 1978, **153**, 59.
17. M. Pfeffer, D. Grandjean and G. Le Borgne, *Inorg. Chem.* 1981, **20**, 4426.
18. A. R. Garber, P. E. Garrou, G. E. Hartwell, M. J. Smas, J. R. Wilkinson and L. J. Todd, *J. Organomet. Chem.* 1973, **86**, 219.
19. R. B. King and M. B. Bisnette, *Inorg. Chem.* 1966, **5**, 293.
20. M. I. Bruce, B. L. Goodall and F. G. A. Stone, *J. Organomet. Chem.* 1973, **60**, 343.
21. M. I. Bruce, B. L. Goodall and I. Matsuda, *Aust. J. Chem.* 1975, **28**, 1259.
22. A. J. Deeming, I. P. Rothwell, M. B. Hursthouse and K. M. A. Malik, *J. Chem. Soc., Dalton Trans.* 1980, 1974.
32. D. R. Gard and T. L. Brown, *Organomet.* 1982, **1**, 1143.
24. P. O. Nubel, S. R. Wilson and T. L. Brown, *Organomet.* 1983, **2**, 515.
25. K. Hiraki, Y. Obayashi and Y. Oki, *Bull. Chem. Soc. Jpn.* 1979, **52**, 1372.
26. M. Nonoyama and S. Kajita, *Transition Met. Chem.* 1981, **6**, 163.
27. K. Hiraki, Y. Sasada and T. Kitamura, *Chem. Lett.* 1980, 449.
28. C. C. Yin and A. J. Deeming, *J. Chem. Soc., Dalton Trans.* 1975, 2091.
29. M. Tachikawa and J. R. Shapley, *J. Organomet. Chem.* 1977, **124**, C19.
30. K. Burgess, B. F. G. Johnson and J. Lewis, *J. Organomet. Chem.* 1982, **233**, C55.
31. B. F. G. Johnson, J. Lewis, T. I. Odiaka and P. R. Raithby, *J. Organomet. Chem.* 1891, **216**, C56.
32. A. J. Deeming, R. Peters, M. B. Hursthouse and J. D. Backer-Dirks, *J. Chem. Soc., Dalton Trans.* 1982, 1205.
33. A. J. Deeming and R. Peters, *J. Organomet. Chem.* 1980, **202**, C39.
34. A. J. Deeming, R. Peters, M. B. Hurethouse and J. D. Backer-Dirks, *J. Chem. Soc., Dalton Trans.* 1982, 787.
35. E. C. Constable, *Polyhedron* 1983, **2**, 551.
36. P. F. Jackson, B. F. G. Johnson, J. Lewis, W. J. H. Nelson and M. McPartlin, *J. Chem. Soc., Dalton Trans.* 1982, 2099.
37. J. Halpern and J. P. Maher, *J. Am. Chem. Soc.* 1965, **87**, 5361.
38. A. Matsuda and H. Uchida, *Bull. Chem. Soc. Jpn.* 1965, **38**, 710.

39. A. Matsuda, *Bull. Chem. Soc. Jpn.* 1967, **40**, 135.
40. A. Matsuda, *Bull. Chem. Soc. Jpn.* 1968, **41**, 1876.
41. A. Matsuda, *Bull. Chem. Soc. Jpn.* 1969, **42**, 571.
42. A. Matsuda, *Bull. Chem. Soc. Jpn.* 1969, **42**, 2590.
43. A. Matsuda, *Bull. Chem. Soc. Jpn.* 1973, **46**, 524.
44. S. Shin, A. Matsuda, J-I. Nakayama and K-I. Bando, *Chem. Lett.* 1977, 115.
45. M. Nonoyama and C. Hayata, *Transition Met. Chem.* 1978, **3**, 366.
46. J. Selbin and M. A. Gutierrez, *J. Organomet. Chem.* 1981, **214**, 253.
47. M. Nonoyama, *J. Organomet. Chem.* 1974, **82**, 271.
48. M. Nonoyama and K. Yamasaki, *Inorg. Nucl. Chem. Lett.* 1971, **7**, 943.
49. M. Nonoyama, *J. Organomet. Chem.* 1975, **86**, 263.
50. M. Nonoyama, *J. Organomet. Chem.* 1975, **92**, 89.
51. M. Nonoyama, *J. Organomet. Chem.* 1982, **299**, 287.
52. M. Nonoyama and S. Kajita, *Transition Met. Chem.* 1981, **6**, 163.
53. A. J. Deeming and I. P. Rothwell, *J. Chem. Soc., Dalton Trans.* 1980, 1259.
54. A. J. Deeming, I. P. Rothwell, M. B. Hursthouse and K. M. A. Malik, *J. Chem. Soc., Dalton Trans.* 1979, 1899.
55. M. Nonoyama, *Bull. Chem. Soc. Jpn.* 1979, **52**, 3749.
56. M. Nonoyama, *Bull. Chem. Soc. Jpn.* 1974, **47**, 767.
57. J. W. Suggs, *J. Am. Chem. Soc.* 1978, **100**, 641.
58. J. W. Suggs and S. D. Cox, *J. Organomet. Chem.* 1981, **221**, 199.
59. J. W. Suggs, *J. Am. Chem. Soc.* 1979, **101**, 489.
60. R. J. Foot and B. T. Heaton, *J. Chem. Soc., Chem. Commun.* 1973, 838.
61. R. J. Foot and B. T. Heaton, *J. Chem. Soc., Dalton Trans.* 1979, 295.
62. P. W. Jolly, *Comprehensive Organometallic Chemistry* (Edited by G. Wilkinson, F. G. A. Stone and E. W. Abel), Vol. 8, p. 713. Pergamon Press, Oxford (1982).
63. K. Isobe, Y. Nakamura and S. Kawaguchi, *Chem. Lett.* 1977, 1383.
64. K. Isobe, Y. Nakamura, E. Kai, K. Nishimoto, T. Miwa and S. Kawaguchi, *J. Am. Chem. Soc.* **102**, 2475.
65. T. Tsou and J. Kochi, *J. Am. Chem. Soc.* 1971, **93**, 5402.
66. A. Mantovani and B. Crociani, *J. Organomet. Chem.* 1982, **236**, C37.
67. A. Kasahara, K. Tanaka and T. Izumi, *Bull. Chem. Soc. Jpn.* 1969, **42**, 1702.
68. B. T. Heaton and K. J. Timmins, *J. Organomet. Chem.* 1978, **152**, 125.
69. G-E. Matsubayashi and Y. Kondo, *J. Organomet. Chem.* 1981, **219**, 269.
70. G. R. Newkome, V. K. Gupta and F. R. Fronczek, *Organomet.* 1982, **1**, 907.
71. G. R. Newkome and T. Kawato, *Inorg. Chim. Acta* 1979, **37**, 481.
72. G. R. Newkome, T. Kawato, D. K. Kohli, W. E. Puchett, B. D. Oliver, G. Chiari, F. R. Fronczek and W. A. Deutsch, *J. Am. Chem. Soc.* 1981, **103**, 3423.
73. G. E. Hartwell, R. V. Lawrence and M. H. Smas, *J. Chem. Soc., Chem. Commun.* 1970, 912.
74. M. Nonoyama and H. Takayanagi, *Transition Met. Chem.* 1975, **1**, 10.
75. M. Onishi, Y. Ohama, K. Sugimura and K. Hiraki, *Chem. Lett.* 1976, 955.
76. M. Nonoyama and K. Yamasaki, *Nippon Kagaku Zasshi* 1970, **91**, 1058.
77. M. A. Gutierrez, G. R. Newkome and J. Selbin, *J. Organomet. Chem.* 1980, **202**, 341.
78. J. Selbin, K. Abboud, S. F. Watkins, M. A. Gutierrez and F. R. Fronczek, *J. Organomet. Chem.* 1983, **241**, 259.
79. J. Selbin and M. A. Gutierrez, *J. Organomet. Chem.* 1983, **246**, 95.
80. M. Nonoyama, K. Suzuki and K. Yamasaki, *Proc. Jpn. Acad.* 1969, **45**, 605.
81. A. Kashara, *Bull. Chem. Soc. Jpn.* 1968, **41**, 1272.
82. M. R. Churchill, H. J. Wasserman and G. J. Young, *Inorg. Chem.* 1980, **19**, 762.
83. S. Trofimenko, *Inorg. Chem.* 1973, **12**, 1215.
84. K. Hiraki, Y. Fuchita and S. Takakura, *J. Organomet. Chem.* 1981, **210**, 273.
85. J. A. C. Allison, H. S. El Khadem and C. A. Wilson, *J. Heterocycl. Chem.* 1975, **12**, 1275.
86. K. Hiraki, Y. Fuchita, H. Nakaya and S. Takakura, *Bull. Chem. Soc. Jpn.* 1979, **52**, 2531.
87. A. Kasahara, T. Izumi and M. Maemura, *Bull. Chem. Soc. Jpn.* 1977, **50**, 1878.
88. T. Izumi, K. Endo, O. Saito, I. Shimizu, M. Maemura and A. Kasahara, *Bull. Chem. Soc. Jpn.* 1978, **51**, 663.
89. T. Izumi, H. Watabe and A. Kasahara, *Bull. Chem. Soc. Jpn.* 1981, **45**, 1771.
90. Y. Fuchita, K. Hiraki and Y. Kage, *Bull. Chem. Soc. Jpn.* 1982, **55**, 955.
91. K. Hiraki, Y. Fuchita and K. Takechi, *Inorg. Chem.* 1981, **20**, 4317.
92. A. J. Deeming and I. P. Rothwell, *J. Chem. Soc., Chem. Commun.* 1978, 340.
93. J. Dehand, M. Pfeffer and M. Zinsius, *Inorg. Chim. Acta* 1973, **13**, 299.
94. V. I. Sokolov, T. A. Sorokina, L. L. Troitskaya, L. I. Solovieva and O. A. Reutov, *J. Organomet. Chem.* 1972, **36**, 389.
95. V. I. Sokolov, *Inorg. Chim. Acta* 1976, **18**, L9.
96. A. J. Deeming, I. P. Rothwell, M. B. Hursthouse and L. New, *J. Chem. Soc., Dalton Trans.* 1978, 1490.
97. A. J. Deeming and I. P. Rothwell, *J. Chem. Soc., Dalton Trans.* 1978, 1497.
98. P. Braunstein, D. Matt, Y. Dusausoy, J. Fischer, A. Mitschler and L. Ricard, *J. Am. Chem. Soc.* 1981, **103**, 5115.
99. A. J. Deeming and I. P. Rothwell, *J. Organomet. Chem.* 1981, **205**, 177.
100. C. G. Anklin and P. S. Pregosin, *J. Organomet. Chem.* 1983, **101**, 243.
101. A. R. Siedle. *J. Organomet. Chem.* 1981, **108**, 115.

102. S. Okeya, H. Sazaki, M. Ogita, T. Takemoto, Y. Onuki, Y. Nakamura, B. K. Mohapatra and S. Kawaguchi, *Bull. Chem. Soc. Jpn.* 1981, **54**, 1978.
103. A. J. Canty and N. J. Minchin, *J. Organomet. Chem.* 1982, **226**, C14.
104. R. C. Davies, T. J. Grinter, D. Leaver and R. M. O'Neill, *Tetrahedron Lett.* 1979, **35**, 3339.
105. L. G. Vaughan, *J. Organomet. Chem.* 1980, **190**, C56.
106. W. A. Wickramasinghe, P. H. Bird and N. Serpone, *J. Chem. Soc., Chem. Commun.* 1981, 1284.
107. A. Mantovani, *J. Organomet. Chem.* 1983, **255**, 385.
108. J. Dehand, A. Mauro, H. Osser, M. Pfeffer, R. H. de A. Santos and J. R. Lechat, *J. Organomet. Chem.* 1983, **250**, 537.
109. G. R. Newkome, W. E. Puckett, V. K. Gupta and F. R. Fronczek, *Organometallics* 1983, **2**, 1247.
110. J. M. Patrick, A. H. White, M. I. Bruce, M. J. Beatson, D. St. C. Black, G. B. Deacon and N. C. Thomas, *J. Chem. Soc., Dalton Trans.* 1983, 2121.
111. A. J. Canty, N. J. Minchin, J. M. Patrick and A. H. White, *J. Chem. Soc., Dalton Trans.* 1983, 1253.
112. Y. Fuchita, K. Hiraki and T. Uchiyama, *J. Chem. Soc., Dalton Trans.* 1983, 897.
113. L-Y. Chia and W. R. McWhinnie, *J. Organomet. Chem.* 1980, **188**, 121.
114. M. Nonoyama, *Transitian Met. Chem.* 1982, **7**, 281.
115. K. Isobe and S. Kawaguchi, *Heterocycles*, 1981, **16**, 1603.
116. K. Isobe, Y. Nakamura and S. Kawaguchi, *Bull. Chem. Soc. Jpn.* 1980, **53**, 139.
117. H. Tanaka, K. Isobe and S. Kawaguchi, *Inorg. Chim. Acta* 1981, **54**, L201.
118. A. Mantovani, L. Calligaro and A. Pasquetto, *Inorg. Chim. Acta* 1983, **76**, L145.

*Polyhedron* Vol. 3, No. 9/10, pp. 1059–1063, 1984
Printed in the U.S.A.

0277-5387/84 $3.00 + .00
© 1984 Pergamon Press Ltd.

# PHOSPHINE CONTAINING RHENIUM(III) CARBONYL COMPLEXES. THE CRYSTAL AND MOLECULAR STRUCTURE OF TRIBROMODICARBONYLBIS(DIMETHYLPHENYLPHOSPHINE)RHENIUM(III)

MICHAEL G. B. DREW*
Department of Chemistry, The University, Whiteknights, Reading RG6 2AD, England

and

BRIAN J. BRISDON* and ANDREW M. WATTS
School of Chemistry, University of Bath, Bath BA2 7AY, England

(*Received* 4 *November* 1983; *accepted* 17 *January* 1984)

**Abstract**—Bromine oxidation of $[ReBr(CO)_3(PR_3)_2]$ [$PR_3 = PMe_2Ph$, $PEt_2Ph$, $PMePh_2$, $PPh_3$, $PPh_2C_6H_4Me$-4 or $P(C_6H_4OMe\text{-}4)_3$] yields stable seven-coordinate rhenium(III) complexes $[ReBr_3(CO)_2(PR_3)_2]$ only for the less sterically demanding phosphines $PMe_2Ph$, $PEt_2Ph$ and $PMePh_2$. Crystals of $[ReBr_3(CO)_2(PMe_2Ph)_2]$ (1) are triclinic, space group $P\bar{1}$, $Z = 2$, in a unit cell with lattice parameters $a = 9.575(8)$, $b = 14.705(11)$, $c = 9.629(12)$ Å, $\alpha = 77.71(7)$, $\beta = 109.06(8)$ and $\gamma = 115.02(8)°$. 2991 independent reflections above background were collected on a diffractometer and refined to R0.07. The metal atom has a capped octahedral environment with a carbonyl in the unique capping position [1.87(3) Å], two phosphines [2.456(13), 2.496(11) Å] and one carbonyl 1.85(5) Å in the capped face, and three bromine atoms in the uncapped face [2.589(5), 2.623(6), 2.622(5) Å]. Attempts to convert (1) to the six-coordinate $d^4$ cation $[ReBr_2(CO)_2(PMe_2Ph)_2]^+$ for structural comparison with the isoelectronic Group 6 analogues $[MBr_2(CO)_2(PR_3)_2]$ (M = Mo or W) were unsuccessful.

Recent calculations by Kubáček and Hoffmann[1] have accounted for the deformations from octahedral geometry observed in several diamagnetic $d^4$ complexes of molybdenum- and tungsten(II) of the type $M(CO)_2L_2'L_2''$. Such molecules containing *cis*-carbonyl ligands should be stabilised by either a substantial increase or decrease in the $M(CO)_2$ bond angle from the regular octahedral value of 90°, with the particular form of the distortion dependent upon the $\sigma$- and $\pi$- donor properties of the ligands L′ and L″.

Diamagnetic six-coordinate $d^4$ complexes are comparatively rare, but one such group of compounds has been prepared by the following route, with the final decarbonylation reaction critically dependent upon the halogen and phosphine ligands.[2,3]

$$M(CO)_6 \xrightarrow{X_2} M(CO)_4X_2 \xrightarrow{PR_3} M(CO)_3(PR_3)_2X_2$$

$$CO \uparrow\downarrow -CO$$

$$M(CO)_2(PR_3)_2X_2$$

(X = Cl or Br, M = Mo or W).

Both $[MoBr_2(CO)_2(PPh_3)_2]$ and $[WBr_2(CO)_2(PPh_3)_2]$ have been prepared by this procedure, and their structures determined.[4,5] Their degree of distortion was found to exceed that predicted by extended Hückel calculations on model compounds,[1] and in an attempt further to define factors which affect the deformations in this class of

*Authors to whom correspondence should be addressed.

molecule, we wished to synthesise $d^4$ analogues containing other metals in combination with the same basic ligand set. One possible route to the isoelectronic rhenium cation $[ReBr_2(CO)_2(PR_3)_2]^+$ is outlined below.

$$Re(CO)_5X \xrightarrow{2PR_3} Re(CO)_3(PR_3)_2X \xrightarrow{X_2} Re(CO)_2(PR_3)_2X_3 \downarrow -X^- [Re(CO)_2(PR_3)_2X_2]^+.$$

To date only one seven-coordinate rhenium(III)dicarbonyl complex containing monodentate phosphine ligands has been reported, namely $[ReCl_3(CO)_2(PMe_2Ph)_2]$ prepared by chlorine oxidation of chloro(tricarbonyl)bis(dimethylphenylphosphine)rhenium(I).[6] We have therefore sought to extend this reaction in order to prepare several $[ReBr_3(CO)_2(PR_3)_2]$ derivatives which we hoped would be of use in synthesising six-coordinate $d^4$ cationic rhenium complexes for direct structural comparison with their isoelectronic molybdenum and tungsten analogues.[4,5]

## RESULTS AND DISCUSSION

Treatment of *fac*-$[ReBr(CO)_3(PR_3)_2]$ ($PR_3$ = $PMe_2Ph$, $PEt_2Ph$ or $PMePh_2$) with bromine in carbon tetrachloride solution at room temperature affords diamagnetic seven-coordinate rhenium(III) complexes $[ReBr_3(CO)_2(PR_3)_2]$ in high yields. These complexes provide further examples of the well-known halogen oxidation reaction in which six-coordinate $d^6$ carbonyls are oxidised to seven-coordinate $d^4$ derivatives.[7] Although this type of reaction is a very common one for phosphine or arsine substituted Group 6 carbonyl derivatives, few reports of Group 7 examples have been published. Thus $[Re(CO)_2(diars)_2X]$ [diars = *o*-phenylenebis(dimethylarsine); X = Br or I] can be oxidised to the ionic derivative $[Re(CO)(diars)_2X_2]X_3$,[8] whilst $[ReX_3(CO)(PMe_2Ph)_3]$,[6] $[ReCl_3(CO)_2(PMe_2Ph)_2]$[6] and $[Re(CO)_2(dppm)X_3]$[9] [dppm = bis(diphenylphosphino)methane; X = Cl or Br] have also been prepared by oxidation of rhenium(I) precursors.

None of the three new rhenium(III) complexes formed appreciably conducting solutions at $10^{-3}$ molar in acetone, and consequently simple monomeric structures were expected. Variable temperature $^1H$ NMR measurements revealed that the complexes were stereochemically non-rigid in solution at ambient temperatures, and on cooling to −40°C, the broad aliphatic proton signals split into two components of unequal intensities indicating the formation of more than one isomeric form for each of the three complexes. In order to determine the solid-state stereochemistry of a representative example of this type of complex, a single crystal X-ray diffraction study was carried out on $[ReBr_3(CO)_2(PMe_2Ph)_2]$.

*Discussion of the structure*

The molecule $[ReBr_3(CO)_2(PMe_2Ph)_2]$ is shown in Fig. 1 together with the atomic numbering scheme. The rhenium environment is a capped octahedron with a carbonyl group in the unique capping position [1.87(3) Å]; two phosphines [2.456(13), 2.496(11) Å] and one carbonyl [1.85(5) Å] in the capped face, and three bromine atoms in the uncapped face [2.589(5), 2.623(6), 2.622(5) Å]. This is the expected geometry for such a stoichiometry. It has been shown previously[10] that seven-coordinate molecules with three halide ligands prefer to fall into two categories. They are either pentagonal pyramidal as in $[NbCl_3(bidentate)_2]$[11] in which three halogens fit into the *T* formation with two in axial positions and one in the equatorial plane, or alternatively capped octahedral with three halogens in the uncapped face as in $[WBr_3(CO)_4]^-$[12] and $[Mo(PMe_2Ph)_3X_4]$ (X = halide).[13] The one exception is $[ReBr_3(bipy)(CO)_2]$[14] where the bidentate ligand prevents either geometric form. This structure is still a capped octahedron but with one bromine in the capped face and two in the uncapped face; the bidentate ligand as is usual for this

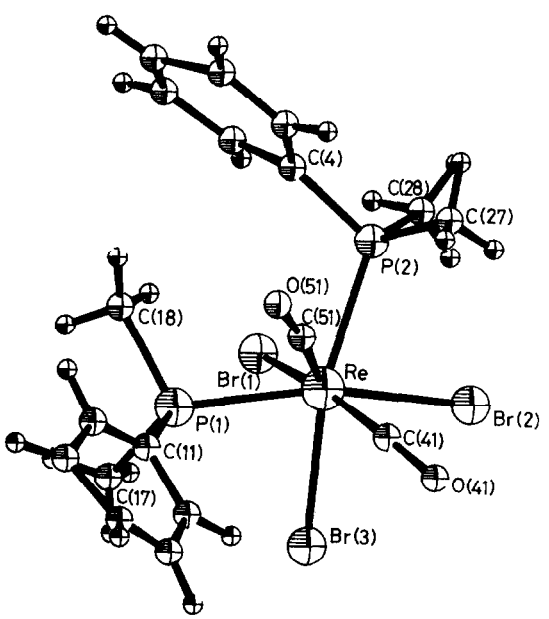



Fig. 1.

polyhedron occupying an edge between two faces. So the geometry of (1) is as predicted and is very close to an ideal capped octahedron, with an r.m.s. deviation[10] of 0.042 Å (0.115 Å for a capped trigonal prism) with $\delta$ angles (after normalisation) of 18.1, 15.1, 10.5°. A search of the Cambridge data files[15] shows that there are very few rhenium(III) structures that have been determined and no other halocarbonyl apart from $[ReBr_3(bipy)(CO)_2]$.[14]

One obvious asymmetry that is introduced is in the angles in the capped face of (1). Thus the P–Re–P angle (116.1°) is greater than the P–Re–C angles (110.8, 107.3°). The positions of the carbon atoms on the phosphorus atoms are such as to be staggered with respect to adjacent atoms. Thus P(1) has three adjacent neighbours Br(1), Br(3) and C(51) but there is no torsion angle of the type L–Re–P–C less than 37.3°. For P(2) the smallest torsion angle is 43.2°. The Re–Br distances in (1) [2.589(5), 2.623(6), 2.622(5) Å] are slightly longer than those in the uncapped face of $[ReBr_3(bipy)(CO)_2]$, namely 2.576(4), 2.551(5) Å. The shorter bond Re–Br(1) [2.589(5) Å] is unique in that Br(1) is *trans* to carbonyl while the others are *trans* to phosphine. It seems unlikely that this could be an electronic effect; steric constraints with the phosphines could cause such distortions. The three Br–Re–Br angles are irregular ranging from 84.5(2) to 90.7(2)°, and the two Re–P distances are also unequal at 2.453(13) and 2.496(11) Å, but there seems to be no obvious reason for the difference.

Repeated attempts to prepare other seven-coordinate complexes by bromine oxidation of *fac*-$[ReBr(CO)_3L_2]$ [L = $PPh_3$, $P(C_6H_4OMe)_3$ or $PPh_2C_6H_4Me$] in $CCl_4$ were unsuccessful. The reactions were monitored by infrared spectroscopy which showed that despite varying the amount of bromine used and the temperature of the bromination reaction, no significant concentration of dicarbonyl-products was evident in the course of the reaction. Under forcing conditions, oily solids containing non-carbonyl products were formed. The room temperature bromination of *fac*-$[ReBr(CO)_3(PPh_3)_2]$ in $CHCl_3$ did not cause oxidation, but rather resulted in the formation of the known[16] *mer-trans*-isomer [$\nu_{max}$(CO) 2060w, 1958s, 1908s]. Such isomerisation reactions have been reported previously for several phosphine substituted rhenium carbonyl bromides.[17,18] Thermal rearrangements are slow,[18] but in the presence of a strong oxidant, isomerisation is fast due to the intermediacy of kinetically labile 17-electron rhenium(II) species which are light sensitive and rapidly reform rhenium(I) derivatives in the presence of dichloromethane.[18] Bromine in chloroform appears to cause *fac* → *mer* isomerism in an analogous manner as the reaction did not proceed cleanly in the dark. Under these conditions several carbonyl containing species as well as unchanged starting material were revealed by infrared spectroscopy, indicating decompositon of the reactive intermediate(s) in the absence of a photochemically induced reaction with the solvent.

Steric constraints caused by the phosphine ligands are apparent in (1) and molecular models of $[ReBr_3(CO)_2L_2]$ (L = tertiary phosphine containing one or more phenyl groups) reveal considerable steric interactions for both capped octahedral and pentagonal bipyramidal geometries. The degree of steric hindrance is clearly related to the effective size of the phosphine and increases in the order L = $PMe_2Ph$ < $PMePh_2$ ≈ $PEt_2Ph$ < $PPh_3$ ≈ $PPh_2C_6H_4Me$ ≈ $P(C_6H_4OMe)_3$. It is noticeable that the only seven-coordinate tribromodicarbonyl complexes we have been able to prepare contain good $\sigma$-donor phosphorus ligands with relatively small cone angles ($PMe_2P$, 122°; $PMePh_2$, 132°; $PEt_2Ph$, 136°).[19]

*Cationic rhenium(III) species*

Attempts to isolate pure six-coordinate rhenium(III) species by halide abstraction from $[ReBr_3(CO)_2(PR_3)_2]$ were not successful. All three complexes reacted with an equimolar quantity of $MBF_4$ (M = Ag or Tl) to produce MBr, but only (1) yielded small quantities of a new rhenium dicarbonyl species containing borofluoride. The product was very unstable even in the solid state, and could not be obtained analytically pure. Attempts to recrystallise the material were also unsuccessful and resulted in the reformation of $[ReBr_3(CO)_2(PMe_2Ph)_2]$ together with traces of $[ReBr(CO)_3(PMe_2Ph)_2]$ and non-carbonyl products. However, in view of the relatively low carbonyl stretching modes observed for the original material it seems unlikely to contain the required cation $[ReBr_2(CO)_2(PMe_2Ph)_2]^+$.

## EXPERIMENTAL

All syntheses were carried out in an atmosphere of dry $N_2$ gas using solvents and liquid reagents freed from moisture and oxygen by standard procedures. Infrared spectra in the region 200–4000 $cm^{-1}$ were recorded on a Perkin–Elmer 597 spectrophotometer. Hydrogen-1 and $^{13}C$ NMR spectra were recorded on JEOL PS 100 and FX 90Q instruments respectively with $SiMe_4$ as internal standard. Microanalyses are by Butterworth Laboratories Limited.

Liquid phosphines were stored in an inert atmosphere over molecular sieves. The solid phosphines

were used as received. The complexes $[ReBr(CO)_5]$ and *fac*-$[ReBr(CO)_3L_2]$ ($L = PPh_3$, $PMePh_2$, $PMe_2Ph$ or $PEt_2Ph$) were prepared by literature procedures or simple extensions thereof.[18,20]

*Synthesis of fac*-$[ReBr(CO)_3\{P(C_6H_4OMe\text{-}4)_3\}_2]$. The compounds $[ReBr(CO)_5]$ (0.54 g, 1.3 mmol) and $P(C_6H_4OMe\text{-}4)_3$ (0.94 g, 2.7 mmol) were heated in refluxing benzene (20 $cm^3$) for 3 hr. The solution was cooled, evaporated to 5 $cm^3$ under reduced pressure, and treated with ethanol (25 $cm^3$) to precipitate the product. Recrystallisation was from chloroform/hexane (1:1). Yield 86%, m.p. 179–180°C. (Found: C, 49.9; H, 3.98% $C_{45}H_{42}O_6BrP_2Re$ requires C, 51.2; H, 3.98%); $\nu_{max}$(CO) 2032s, 1950s, 1895s $cm^{-1}$ (chloroform); NMR: $^{13}C\text{-}\{^1H\}$ (25°C, $CD_2Cl_2$), $\delta$ 31.8 (OMe), 113.9, 125.2, 136.2 and 161.6 (aromatics), 191.6 and 206.2 ppm (CO).

*Synthesis of fac*-$[ReBr(CO)_3\{PPh_2C_6H_4Me\text{-}4\}_2]$-$[ReBr(CO)_5]$ (0.35 g, 0.87 mmol) and $PPh_2C_6H_4Me$-4 (0.48 g, 1.7 mmol) were heated in refluxing benzene (20 $cm^3$) for 7 hr. The solution was evaporated to dryness and the residue recrystallised from dichloromethane/hexane (1:1), affording the product as white needles (78%), m.p. 180–181°C. (Found: C, 52.8; H, 3.84% $C_{41}H_{34}O_3BrP_2Re$ requires C, 54.4; H, 3.77%); $\nu_{max}$(CO) 2038s, 1952s, 1897s $cm^{-1}$ (chloroform); NMR: $^{13}C\text{-}\{^1H\}$ (25°C, $CD_2Cl_2$), $\delta$ 21.3 (Me), 128.4, 129.2, 130.6, 133.7, 134.7 and 141.1 (aromatics), 192.1 and 205.8 ppm (CO).

*Synthesis of* $[ReBr_3(CO)_2(PMePh_2)_2]$. A solution of $Br_2$ (0.22 g, 1.4 mmol) in anhydrous $CCl_4$ (25 $cm^3$) was stirred at room temperature with *fac*-$[ReBr(CO)_3(PMePh_2)_2]$ (1.0 g, 1.3 mmol) for 2 hr. The yellow product tribromodicarbonylbis(methyldiphenylphosphine)rhenium(III) precipitated during the course of the reaction and was finally collected, washed with $CCl_4$ and dried *in vacuo*. Recrystallisation was from dichloromethane/hexane (1:1). Yield 85%, m.p. 142–143°C. (Found: C, 37.7; H, 3.00; Br, 26.4% $C_{28}H_{26}O_2Br_3P_2Re$ requires C, 38.1, H, 2.94; Br, 27.2%); $\nu_{max}$(CO) 2036s, 1940s $cm^{-1}$ (chloroform); NMR: $^1H$ (25°C, $CD_2Cl_2$), $\delta$ 2.56 [6H, br d, $J$(PH) 11 Hz 2 Me], 7.38 ppm (20 H, br m, aromatics).

(a) In a similar way pale yellow *crystals* of tribromodicarbonylbis(dimethylphenylphosphine)rhenium(III), m.p. 148–149°C were isolated in a 92% yield. (Found: C, 28.0; H, 2.80; Br, 30.2% $C_{18}H_{22}O_2Br_3P_2Re$ requires C, 28.5; H, 2.90; Br, 31.6%); $\nu_{max}$(CO) 2046s, 1935s $cm^{-1}$ (chloroform); NMR: $^1H$ (25°C, $CD_2Cl_2$), $\delta$ 2.22 (12 H, vbr s, 4 Me), 7.42 (4 H, m, aromatics), 7.72 ppm (6H, m, aromatics).

(b) Reaction of bromine with $[ReBr(CO)_3(PEt_2Ph)_2]$ as above afforded yellow *crystals* of tribromodicarbonylbis(diethylphenylphosphine)rhenium(III), m.p. 138–140°C (dec), in 76% yield. (Found: C, 32.0; H, 3.91; Br, 29.3% $C_{22}H_{30}O_2Br_3Re$ requires C, 32.4; H, 3.72; Br, 29.5%); $\nu_{max}$(CO) 2050s, 1938s $cm^{-1}$ (chloroform); NMR: $^1H$ (25°C, $CD_2Cl_2$), $\delta$ 1.00 (12 H, vbr s, 4 Me), 2.90 (8 H, vbr s, 4 $CH_2$), 7.36 (6 H, m, aromatics), 7.61 ppm (4 H, m, aromatics); $^{13}C\text{-}\{^1H\}$ (25°C, $CD_2Cl_2$), $\delta$ 9.9 (Me), 20.7 (m, $CH_2$), 128.3, 128.5, 128.7, 129.2, 131.5, 132.6, 132.7 and 132.8 ppm (aromatics).

*Halide abstraction from* $[ReBr_3(CO)_2(PMe_2Ph)_2]$. A solution of $[ReBr_3(CO)_2(PMe_2Ph)_2]$ (0.39 g, 0.51 mmol) in anhydrous acetone (15 $cm^3$) was stirred at room temperature with $MBF_4$ (M = Ag or Tl, 0.51 mmol) dissolved in acetone (3 $cm^3$). After 0.5 hr, the precipitated MBr was filtered from the solution and the filtrate was concentrated to low bulk (5 $cm^3$) at 0°C, and treated dropwise with heptane to initiate crystallisation. On further cooling yellow microcrystals were deposited. Yield 0.067 g; $\nu_{max}$ (CO) 2028s, 1928 $cm^{-1}$; $\nu_{max}$ (BF) 1080 $cm^{-1}$ (Nujol).

*Crystal structure determination of* $[ReBr_3(CO)_2(PMe_2Ph)_2]$. Crystals of (**1**) were obtained as yellow needles by recrystallisation from $CH_2Cl_2$.

*Crystal data.* $C_{18}H_{27}O_2Br_3P_2Re$, M = 863.1, Triclinic, Spacegroup $P\bar{1}$, $Z = 2$, $a = 9.575(8)$, $b = 14.705(11)$, $c = 9.629(12)$ Å, $\alpha = 77.71(7)$, $\beta = 109.06(8)$, $\gamma = 115.02(8)°$, $U = 1\ 156.8$ Å$^3$, $D_m = 2.48$ g $cm^{-3}$, $F(000) = 722$, Mo-$K_\alpha$ radiation, $\lambda = 0.7107$ Å, $\mu = 141.4$ $cm^{-1}$.

*Structure solution and refinement.* The chosen crystal was mounted on a Stoe STADI-2 diffractometer and data was collected via variable width $\omega$ scan. Background counts were 20s and the scan rate of 0.033°/s was applied to a width of $(1.5 + \sin\mu/\tan\theta)$. 2991 independent reflections with $2\theta < 50°$ were measured of which 1957 with $I > 3\sigma(I)$ were used in subsequent refinement. An empirical absorption correction was applied. The structure was solved by the Patterson method. The positions of the remaining non-hydrogen atoms were obtained from Fourier syntheses. The phenyl hydrogen atoms were positioned in trigonal positions and those in the same ring were given a common thermal parameter. Those on methyl groups were located by rigid body refinement and each group was given a common thermal parameter which was refined.

The structure was then refined using full-matrix least-squares using SHELX76.[21] The weighting scheme used was chosen to give equivalent values of $w\Delta^2$ over ranges of $F_0$ and $(\sin\theta/\lambda)$. This was

Table 1.

DIMENSIONS IN THE COORDINATION SPHERE

DISTANCES, A, ANGLES, DEGREES

| | | | | | |
|---|---|---|---|---|---|
| RE | - | BR(1) | | 2.589( 5) | |
| RE | - | BR(2) | | 2.623( 6) | |
| RE | - | BR(3) | | 2.622( 5) | |
| RE | - | P(1) | | 2.454( 13) | |
| RE | - | P(2) | | 2.496( 11) | |
| RE | - | C(41) | | 1.85( 5) | |
| RE | - | C(51) | | 1.87( 3) | |
| BR(1) | - | RE | - | BR(2) | 90.68(18) |
| BR(1) | - | RE | - | BR(3) | 87.37(18) |
| BR(2) | - | RE | - | BR(3) | 84.52(18) |
| BR(1) | - | RE | - | P(1) | 77.85(29) |
| BR(2) | - | RE | - | P(1) | 160.8( 3) |
| BR(3) | - | RE | - | P(1) | 79.7( 3) |
| BR(1) | - | RE | - | P(2) | 80.1( 3) |
| BR(2) | - | RE | - | P(2) | 76.2( 3) |
| BR(3) | - | RE | - | P(2) | 156.8( 3) |
| P(1) | - | RE | - | P(2) | 116.1( 4) |
| BR(1) | - | RE | - | C(41) | 163.0(11) |
| BR(2) | - | RE | - | C(41) | 76.7(12) |
| BR(3) | - | RE | - | C(41) | 80.2(14) |
| P(1) | - | RE | - | C(41) | 110.8(14) |
| P(2) | - | RE | - | C(41) | 107.3(15) |
| BR(1) | - | RE | - | C(51) | 127.1(17) |
| BR(2) | - | RE | - | C(51) | 126.5(19) |
| BR(3) | - | RE | - | C(51) | 127.4(17) |
| P(1) | - | RE | - | C(51) | 72.4(19) |
| P(2) | - | RE | - | C(51) | 75.4(17) |
| C(41) | - | RE | - | C(51) | 69.9(21) |

$w^{1/2} = 1/(\sigma^2(F) + 0.003\,F^2)$ where $\sigma(F)$ was taken from counting statistics. The Re, Br and P atoms were refined anisotropically. Scattering factors were taken from International Tables.[22] Calculations were made using SHELX76 on the CDC 7600 computer at the University of Manchester Computer Centre.

Details of interatomic distances and angles are listed in Table 1. Atomic coordinates, anisotropic thermal parameters, observed and calculated structure factors and hydrogen atom positions are given in the Supplementary Publication.†

*Acknowledgements*—We thank S.E.R.C. for support and A. W. Johans for his assistance with the crystallographic investigations.

## REFERENCES

1. P. Kubácek and R. Hoffmann, *J. Am. Chem. Soc.* 1981, **103**, 4320.
2. M. W. Anker, R. Colton and I. B. Tomkins, *Aust. J. Chem.* 1967, **20**, 9.
3. R. Colton and I. B. Tomkins, *Aust. J. Chem.* 1966, **19**, 1519.
4. M. G. B. Drew and I. B. Tomkins, *Aust. J. Chem.* 1970, **23**, 2517.
5. M. G. B. Drew, B. J. Brisdon and A. G. Buttery, *Acta Cryst.* 1982, **38B**, 1598.
6. P. G. Douglas and B. L. Shaw, *J. Chem. Soc.* (*A*) 1969, 1491.
7. R. Colton, *Coord. Chem. Rev.* 1971, **6**, 269.
8. W. J. Kirkham, A. G. Osborne and R. S. Nyholm, *J. Chem. Soc.* 1965, 550.
9. D. A. Edwards and J. Marshalsea, *Transition Met. Chem.* 1979, **4**, 267.
10. M. G. B. Drew, *Progr. Inorg. Chem.* 1977, **23**, 67.
11. M. G. B. Drew and J. D. Wilkins, *J. Chem. Soc., Dalton Trans.* 1974, 198.
12. M. G. B. Drew and A. P. Wolters, *J. Chem. Soc., Chem. Commun.* 1972, 1278.
13. M. G. B. Drew, J. D. Wilkins and A. P. Wolters, *J. Chem. Soc., Chem. Commun.* 1976, 192.
14. M. G. B. Drew, K. M. Davis, D. A. Edwards and J. Marshalsea, *J. Chem. Soc., Dalton Trans.* 1978, 1098.
15. Cambridge Data Centre Files, July 1982 update.
16. J. Chatt, J. R. Dilworth and H. P. Gunz, *J. Organomet. Chem.* 1974, **64**, 245.
17. A. M. Bond, R. Colton and M. E. McDonald, *Inorg. Chem.* 1978, **17**, 2842.
18. R. H. Reinmann and E. Singleton, *J. Organomet. Chem.* 1973, **59**, 309.
19. C. A. Tolman, *Chem. Rev.* 1977, **77**, 313.
20. M. Freni, V. Valenti and D. Guisto, *J. Inorg. Nucl. Chem.* 1965, **27**, 2636.
21. SHELX 76, Program for Crystal Structure Determination, G. M. Sheldrick, Cambridge University, 1976.
22. *International Tables for X-ray Crystallography*, Vol. 4. Kynoch Press, Birmingham, (1974).

†Copies of supplementary data have been deposited with the Editor and with the Cambridge Data Centre.

*Polyhedron* Vol. 3, No. 9/10, pp. 1065–1069, 1984
Printed in the U.S.A.

0277-5387/84 $3.00 + .00
© 1984 Pergamon Press Ltd.

# $^{57}$Fe HYPERFINE INTERACTION AND ELECTRONIC STRUCTURE OF IRON NITROSYL COMPLEXES. ESR STUDY

**ADAM JEZIERSKI* and BOGUSŁAWA JEŻOWSKA-TRZEBIATOWSKA**
Institute of Chemistry, Wrocław University, Poland

(*Received* 4 *August* 1983; *accepted* 17 *January* 1984)

**Abstract**—The structure of mono- and dinitrosyl iron complexes with sulphur and nitrogen coordinating ligands was investigated by ESR method. On the basis of anisotropic hyperfine (for $^{57}$Fe) and superhyperfine (for $^{14}$N) parameters the influence of donor–acceptor properties of the ligands on electronic structure of the complexes was examined. The diminishing effect of the increased $d$–$\pi$ back bonding on isotropic contact parameter K($^{57}$Fe) and $p$-electron spin density on nitrosyl nitrogen ($^{14}$N) was found.

The very small value of the nuclear magnetic moment for $^{57}$Fe nucleus (+0.090 nm) prevents the observation of the hyperfine splitting in many iron complexes giving broad-line ESR spectra (e.g. $Fe^{3+}$ complexes). The mono- and dinitrosyl iron complexes of semi-radical character containing formally Fe(I) give, however, the narrow-line ESR spectra and it is possible to analyse the $^{57}$Fe splitting in liquid and frozen solution spectra.

## EXPERIMENTAL

The complexes of formula $Fe(NO)(chel)_2$ were obtained by direct reaction of $Fe(chel)_3$ with gaseous NO in toluene or chloroform solution;[1] the mono- and dinitrosyls were also obtained by "ascorbic" method in which $NO_2^-$ ion was the donor of NO group in presence of ascorbic acid.[2,3]

ESR spectra were obtained using a JES-ME X-band spectrometer with proton magnetometer, frequency meter and ESR standards. The calculation of hyperfine parameters and the simulation of the spectra were made on JEC-6 computer. Our $g$ values measured in liquid and frozen solution spectra are accurate to $\pm 0.001$ and the hyperfine values are accurate to $\pm 0.2 \times 10^{-4}\,cm^{-1}$. For preparation of the complexes the iron(III) oxide containing 90% of $^{57}$Fe isotope was used.

## RESULTS AND DISCUSSION

The hyperfine parameter $A_{ii}$ is the sum of iso- and anisotropic parts, $A_{xx} = A_{iso} + T_{xx}$; $A_{yy} = A_{iso} + T_{yy}$; $A_{zz} = A_{iso} + T_{zz}$. Using McGarvey's formulae[4] for anisotropic ESR data we can calculate the $K$ (isotropic contact) parameters. We postulate that $A_{iso}$ is negative as is usual for transition ions with positive nuclear magnetic moment and hence in McGarvey's notation the $K$ parameter is positive.

The superhyperfine splitting for $^{14}$N of nitrosyl group or additional organic ligand may be source of the spin density coefficients calculations, $c_s^2$ for $s$ electrons and $c_p^2$ for $p$ electrons.[5,6] For the superhyperfine coupling

$$A_{ii}(\text{experimental}) = A_{iso} + T_{ii} + A_{dipolar}.$$

If the value of 1.7 Å is used as an estimate of the Fe–N bond length, $A_{dipolar}$ can be calculated by use of a point-dipole approximation[6] to be about $+0.8 \times 10^{-4}\,cm^{-1}$. This must be subtracted from $A_{ii}$ (experimental). The additional equations

$$A_{iso} = \frac{1}{3}(A_{xx} + A_{yy} + A_{zz})$$

and

$$T_{xx} + T_{yy} + T_{zz} = 0$$

allow us to calculate the $A_{iso}$ and $T_{zz}$ as well as $c_s^2 = A_{iso}/A_{iso}^0$ and $c_p^2 = T_{zz}/T_{zz}^0$. The theoretically calculated values $A_{iso}^0$ and $T_{zz}^0$ are for $^{14}$N 557 G and 33.5 G, respectively.[6] We postulate that the $A_{iso}$ ($^{14}$N) is positive and $T_{zz}$($^{14}$N) is also positive as results from the ESR spectra which corresponds to positive spin density on nitrogen $p_\sigma$ orbital. The

*Author to whom correspondence should be addressed.

Table 1. ESR parameters for the class A complexes, $FeNO(chel)_2$

| chel | $g_x$ | $g_y$ | $g_z$ | $K$ ($^{57}Fe$) | $T_{zz}$ ($^{57}Fe$) | $c_s^2$ [%] | $c_p^2$ [%] | $g_{iso}$ | $A_{iso}$ ($^{57}Fe$) | $A_{iso}$ ($^{14}N$) |
|---|---|---|---|---|---|---|---|---|---|---|
| $S_2COR$ | 2.045 | 2.043 | 2.022 | 10.1 | 9.2 | 2.52 | 2.54 | 2.038 | -9.3 | 13.3 |
| $S_2CSR$ | 2.044 | 2.042 | 2.022 | 10.0 | 9.2 | 2.54 | 2.55 | 2.037 | -9.3 | 13.3 |
| $S_2CN(i\text{-}Pr)_2$ | 2.045 | 2.041 | 2.022 | 10.5 | 9.6 | 2.56 | 2.61 | 2.037 | -9.7 | 13.5 |
| $S_2CNPh_2$ | 2.045 | 2.041 | 2.022 | 10.6 | 9.6 | 2.58 | 2.90 | 2.037 | -9.7 | 13.7 |
| $S_2CNEtPh$ | 2.045 | 2.041 | 2.024 | 10.7 | 9.6 | 2.59 | 2.92 | 2.037 | -9.8 | 13.7 |
| $S_2CNEt_2$ | 2.045 | 2.041 | 2.025 | 10.8 | 9.8 | 2.60 | 2.99 | 2.037 | -9.9 | 13.8 |
| $S_2CNHR$ | 2.046 | 2.041 | 2.026 | 10.9 | 9.9 | 2.62 | 3.82 | 2.037 | -9.9 | 14.0 |
| $S_2P(OR)_2$ | 2.050 | 2.052 | 2.025 | 12.0 | 11.1 | 2.35 | 8.22 | - | - | - |

Note: All data for toluene solutions, $g_{x,y,z}$, $K, T_{zz}, c_s^2, c_p^2$ - at 130 K, $g_{iso}$, $A_{iso}$ - at 300 K.
Ph=phenyl, Et=ethyl, i-Pr=isopropyl, R=alkyl or aryl radical.
$K, T_{zz}$ and $A_{iso}$ in units of $10^{-4}cm^{-1}$.

$T_{zz}(^{57}Fe)$ must be positive for $d_z^2$, $d_{xz}$ and $d_{yz}$ electrons and negative for $d_{xy}$ and $d_{x^2-y^2}$ electrons;[6] it is proportional to the $P = g_e g_n \beta_e \beta_n \langle r^{-3} \rangle$. The $P$ parameter is assumed as $+25 \times 10^{-4}$ cm$^{-1}$. The $T_{zz} = -(T_{xx} + T_{yy})$; for the nearly axial symmetry $T_{xx} \cong -(1/2)\, T_{zz}$.

On the basis of the ESR spectra we have obtained three types of spectra characteristic of three types of compound: *A*, *B* and *C*.

*Class A.* The mononitrosyl complexes of formula $Fe(NO)(chel)_2$, where chel = dithiochelating ligand (see Table 1).

*Class B.* The dinitrosyl complexes of formula $Fe(NO)_2L_4$, where two or more L ligands are sulphur monodentate ligands (see Table 2).

*Class C.* The dinitrosyl iron complexes of formula $Fe(NO)_2L_4$, where two or more L ligands are monodentate nitrogen ligands (see Table 2).

Table 2. ESR parameters for classes B and C

| | $g_x$ | $g_y$ | $g_z$ | $K$ ($^{57}Fe$) | $T_{zz}$ ($^{57}Fe$) | $g_{iso}$ | $A_{iso}$ ($^{57}Fe$) | $A_{iso}$ ($^{14}N$) |
|---|---|---|---|---|---|---|---|---|
| class B - $Fe(NO)_2(RS)_2(H_2O)_2$ | | | | | | | | |
| 2-mercaptopyridine | 2.041 | 2.041 | 2.012 | 11.2 | 10.1 | 2.031 | -10.5 | 2.4 |
| 6-mercaptopurine | 2.042 | 2.042 | 2.012 | 11.5 | 10.2 | 2.032 | -10.8 | 2.4 |
| 6-mercaptoguanine | 2.042 | 2.042 | 2.012 | 11.7 | 10.4 | 2.032 | -10.9 | 2.4 |
| class C - $Fe(NO)_2(im)_2(H_2O)_2$ | | | | | | | | |
| imidazole | 2.021 | 2.013 | 2.039 | 14.1 | -13.2 | 2.024 | -13.5 | 2.5 |
| pyrazole | 2.022 | 2.013 | 2.039 | 14.3 | -13.5 | 2.025 | -13.7 | 2.5 |
| purine | 2.021 | 2.013 | 2.042 | 14.8 | -13.6 | 2.025 | -14.1 | 2.5 |
| histamine | 2.022 | 2.013 | 2.040 | 14.6 | -14.1 | 2.025 | -14.1 | 2.5 |

Note: All data for isoamyl alcohol solutions, $g_{x,y,z}$, $K, T_{zz}$ - at 130 K, $g_{iso}$, $A_{iso}$ - at 310 K.
$K, T_{zz}$ and $A_{iso}$ in units of $10^{-4}cm^{-1}$.

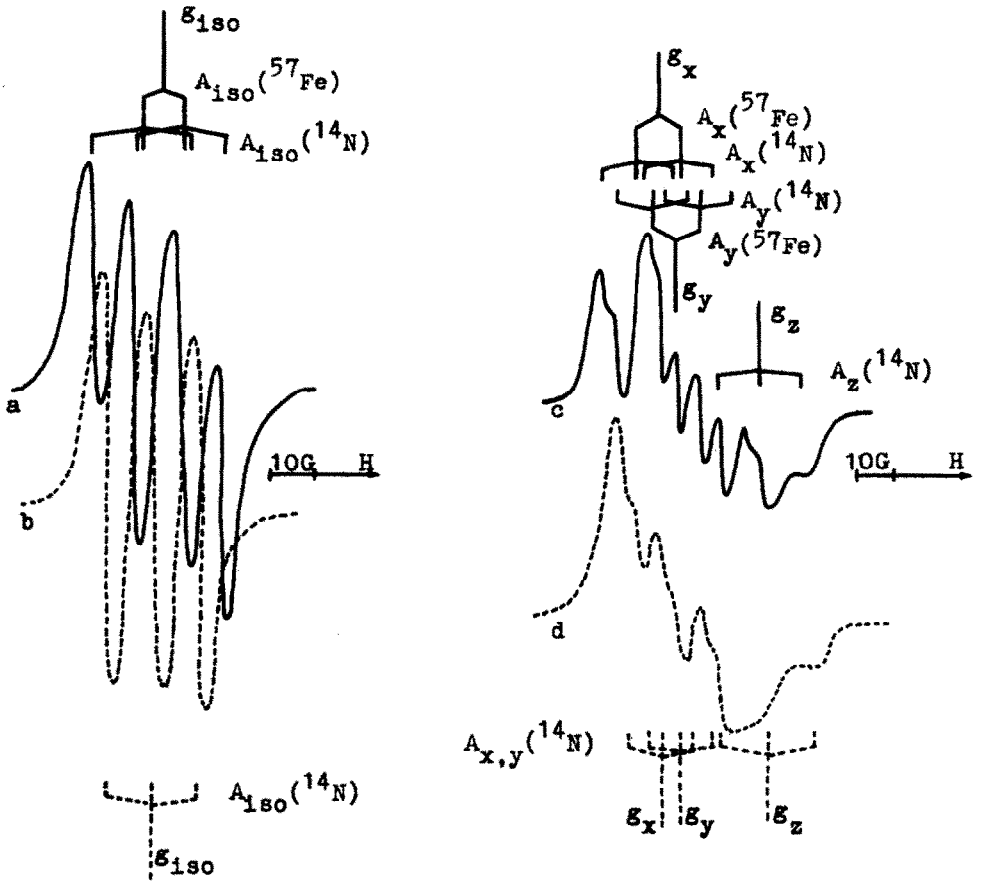



Fig. 1. ESR spectra of $FeNO(S_2CNEtPh)_2$ complex. Solvent—toluene. (a), (b) at 300 K; (c), (d) at 130 K. (a), (b) microwave frequency 9.215 GHz; (c), (d) 9.201 GHz. (a), (c) 90% of $^{57}$Fe isotope; (b), (d) normal (2.19%) abundance of $^{57}$Fe isotope.

The typical ESR spectra with the interpretation of hyperfine and superhyperfine splittings are shown in Figs. 1–3. On the basis of experimental and calculated ESR parameters, especially $^{57}$Fe hyperfine parameters, we postulate that the $(d_{z^2})^1$ configuration is suitable for the mononitrosyls A and dinitrosyls B. In case of the type C complexes the unpaired electron occupies the $(d_{x^2-y^2})$ orbital. The geometry of the complexes depends on the type of additional ligands coordinated by S or N; Enemark and Feltham's scheme[7] is adequate for the interpretation of the observed parameters.

For the series of mononitrosyls A the characteristic dependence of the ESR parameters on the sulphur chelate ligand properties is observed. This phenomenon is connected with donor–acceptor properties of the ligands,[3,8–14] in particular with the ESCA properties[13] and acid dissociation constants.[14] There is parallelism of the experimental hyperfine parameters (see Table 1) and other physicochemical data for the ligands. The $\pi$-levels of the sulphur ligands interact with $d_{xy}$ (in-plane) and $d_{xz,yz}$ (out-of-plane) orbitals; the last orbital is involved in $\pi$-bonding with $\pi^*$(NO). Increased $d$–$\pi$ back bonding results also in a shift of the $d_{z^2}$ electron density away from the NO ligand to the sixth vacant coordination position and this corresponds to the observed decrease of $K(^{57}Fe)$ and $c_p^2(^{14}N)$. This effect cannot be noticed on the basis of isotropic data only.[15] For the dinitrosyls the signs of $T_{zz}$ are connected with coordination atoms and geometry of the molecule; in this case ESR is the simplest analytical method for examination of coordination type.

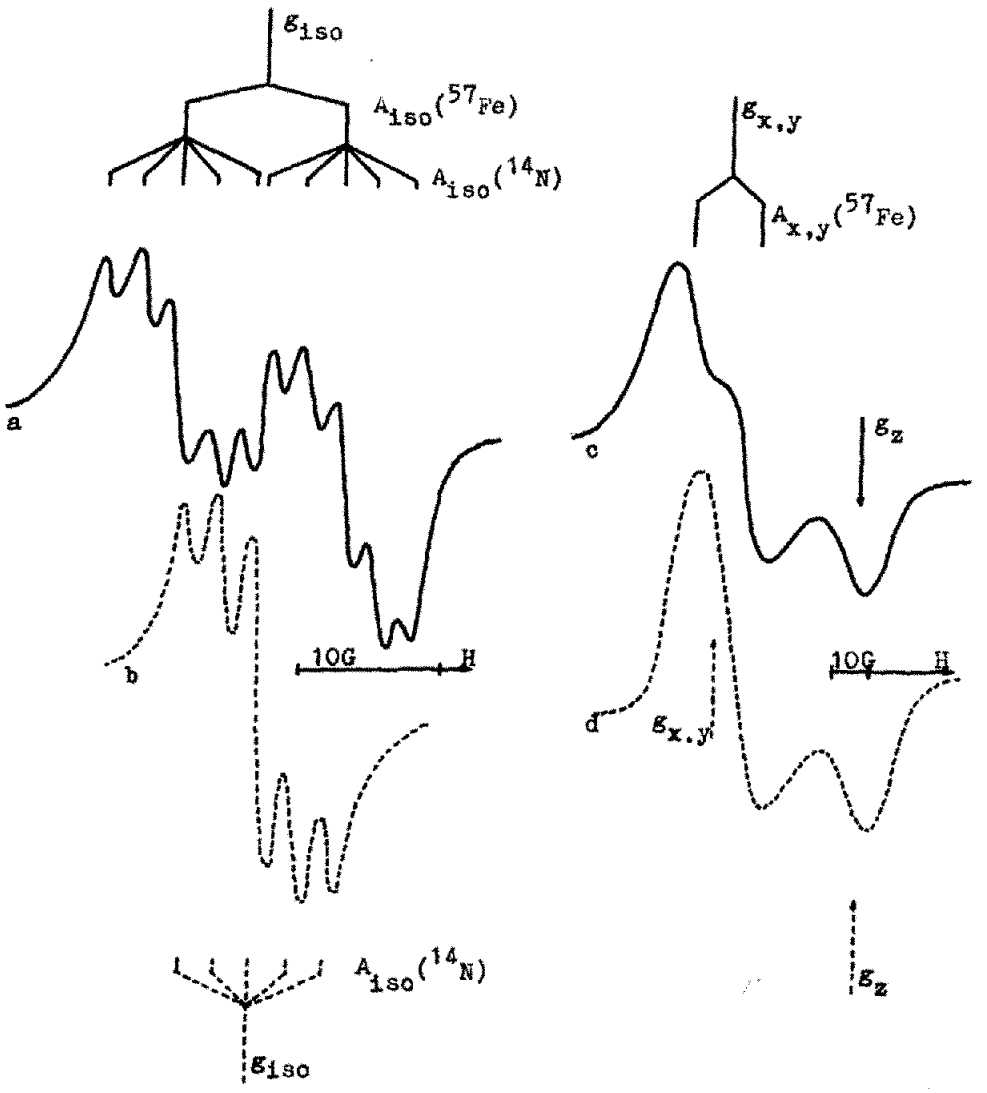



Fig. 2. ESR spectra of $Fe(NO)_2(2\text{-mercaptopyridine})_2(H_2O)_2$. Solvent—isoamyl alcohol. (a), (b) at 310 K; (c), (d) at 130 K. (a), (b) microwave frequency 9.221 GHz; (c), (d) 9.208 GHz. (a), (c) 90% of $^{57}Fe$ isotope; (b), (d) normal abundance of $^{57}Fe$ isotope.

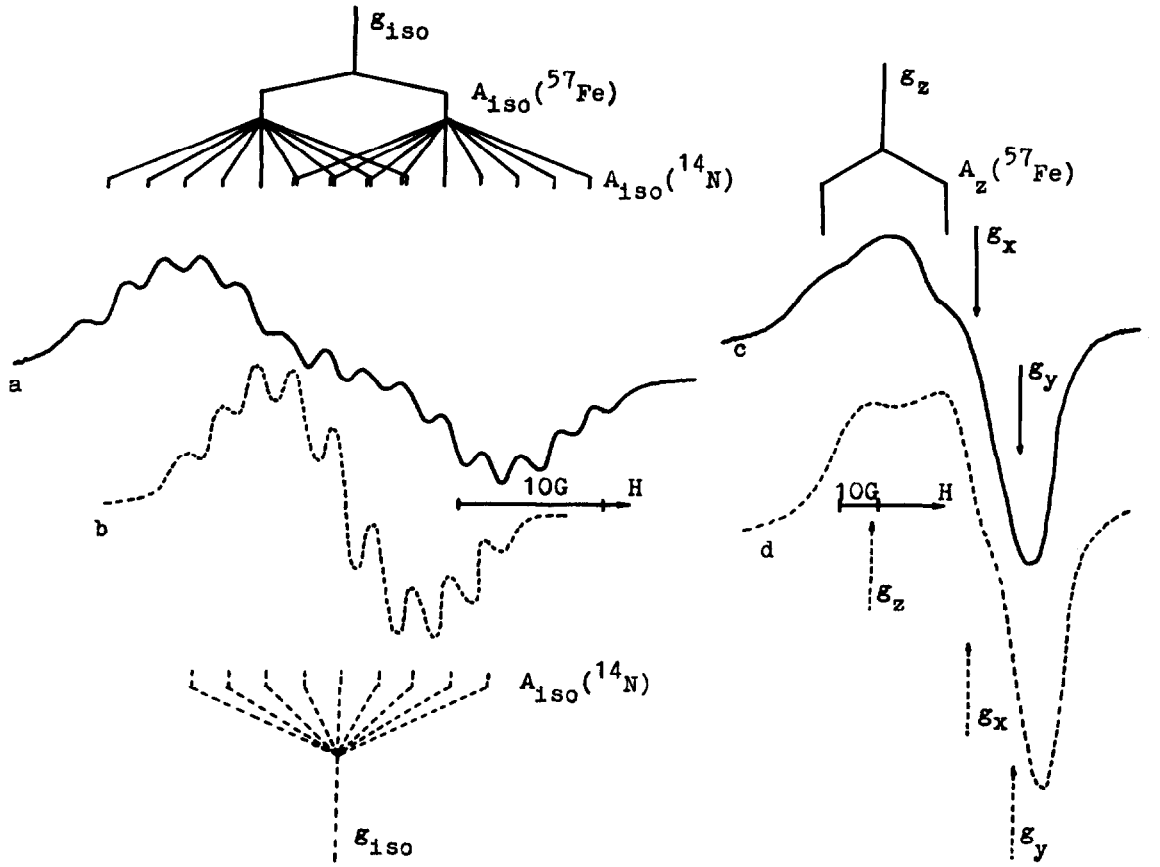



Fig. 3. ESR spectra of $Fe(NO)_2(purine)_2(H_2O)_2$. Solvent—isoamyl alcohol. (a), (b) at 310 K; (c), (d) at 130 K. (a), (b) microwave frequency 9.218 GHz; (c), (d) 9.206 GHz. (a), (c) 90% of $^{57}$Fe isotope; (b), (d) normal abundance of $^{57}$Fe isotope.

*Acknowledgement*—This work was supported by the Polish Academy of Sciences.

## REFERENCES

1. N. D. Yordanov, V. Iliev, D. Shopov, A. Jezierski and B. Jeżowska-Trzebiatowska, *Inorg. Chim. Acta* 1982, **60**, 9.
2. J. C. Woolum, E. Tiezzi and B. Commoner, *Biochim. Biophys. Acta* 1968, **160**, 311.
3. A. Jezierski and B. Jeżowska-Trzebiatowska, *Bull. Acad. Pol. Sci. Ser. Sci. Chim.* 1979, **27**, 481.
4. B. R. McGarvey, *J. Phys. Chem.* 1967, **71**, 51.
5. B. A. Goodman, J. B. Raynor and M. C. R. Symons, *J. Chem. Soc. A* 1969, 2572.
6. B. A. Goodman and J. B. Raynor, *Adv. Inorg. Chem. Radiochem.* 1970, **13**, 135.
7. J. Enemark and R. D. Feltham, *Coord. Chem. Rev.* 1974, **13**, 339.
8. B. Jeżowska-Trzebiatowska and A. Jezierski, *J. Mol. Struct.* 1973, **19**, 635.
9. B. Jeżowska-Trzebiatowska and A. Jezierski, *J. Mol. Struct.* 1978, **46**, 197.
10. B. Jeżowska-Trzebiatowska, A. Jezierski, H. Kozłowski, N. D. Yordanov and D. Shopov, *Inorg. Chim. Acta* 1978, **31**, 31.
11. A. Jezierski and B. Jeżowska-Trzebiatowska, *Nouv. J. Chem.* 1980, **4**, 599.
12. R. E. Eley, R. R. Myers and N. V. Duffy, *Inorg. Chem.* 1972, **11**, 1128.
13. C. Cauletti, N. V. Duffy and C. L. Furlani, *Inorg. Chim. Acta* 1977, **23**, 181.
14. K. I. Aspila, C. L. Chakrabarti and V. S. Sastri, *Anal. Chem.* 1973, **45**, 363.
15. B. Sarte, J. Stanford, W. J. LaPrice, D. L. Uhrich, T. E. Lockhart, E. Gelerinter and N. V. Duffy, *Inorg. Chem.* 1978, **17**, 3361.

*Polyhedron* Vol. 3, No. 9/10, pp. 1071–1076, 1984
Printed in the U.S.A.

0277-5387/84 $3.00 + .00
© 1984 Pergamon Press Ltd.

# INDUCED COTTON EFFECT OF KEGGIN-TYPE AND MIXED-COORDINATION-TYPE HETEROPOLYANIONS IN NONAQUEOUS MEDIA CONTAINING *l*-BRUCINE SULPHATE

KENJI NOMIYA, RYOICHI KOBAYASHI, MAKOTO MIWA* and TATSUHIKO HORI
Department of Industrial Chemistry, Faculty of Engineering, Seikei University, Musashino, Tokyo 180, Japan

(*Received* 23 *June* 1983; *accepted* 17 *January* 1984)

**Abstract**—The reactivities, or the interactions in nonaqueous media of the Keggin-type heteropolyanions $[XM_{12}O_{40}]^{n-}$ ($X = Co^{II}$, $Zn^{II}$, $Al^{III}$, Si, P, $2H^+$, M = W; X = P, Si, M = Mo) and the Fe(III)-substituted mixed-type polyanions $[PFeM_{11}O_{40}H_2]^{4-}$ (M = Mo, W) with a chiral organic compound such as *l*-brucine sulphate have been studied using the electronic absorption, differences absorption and CD spectra. Two types of the interaction of *l*-brucine with the polyanions have been indicated from the observed Cotton effect; one is an outer-sphere association of the brucinium ion with the surface bridged oxygens of dodecametallate and the other a coordination of brucine to the Fe(III) ion in the mixed-type polyanions. In the latter, an outer-sphere association between the $PM_{11}O_{39}^{7-}$ moiety and brucinium ion has been also suggested.

Keggin-type heteropolyacids have shown various catalyses for organic molecules, e.g. polycondensation of benzyl alcohol[1,2] and Friedel-Crafts-type reaction.[3] These reactions are primarily based on the strong Brønsted acidity of the polyacid. However, the roles of the polyanion-moiety have not been necessarily elucidated, although the structural factor may participate possibly in these reactions. In this work, using a chiral compound having N-coordinating site such as *l*-brucine sulphate, the interaction of various Keggin-type polyanions and their derivatives with an organic molecule has been studied spectrophotometrically. The behaviour of brucine molecule acting on the surface atoms of polyanions has been discussed on the basis of observed Cotton effect. The heteropoly compounds used here are tetrabutylammonium salts of Keggin-type polyanions $[XM_{12}O_{40}]^{n-}$ ($X = Co^{II}$, $Zn^{II}$, $Al^{III}$, Si, P, $2H^+$, M = W; X = P, Si, M = Mo) and the Fe(III)-substituted polyanions $[PFeM_{11}O_{40}H_2]^{4-}$ (M = Mo, W). The metatungstate anion of ($X = 2H^+$, M = W) has two protons instead of a heteroatom in the tetrahedral cavity of Keggin-structure. The Fe(III)-substituted polyanions can be readily derived from the corresponding parent anions in aqueous solution of an appropriate pH, where one M atom of the $[PM_{12}O_{40}]^{3-}$ compound is replaced by a Fe(III) ion with the original Keggin-unit retained and the Fe(III) ion is coordinated by one water molecule.[4]

*Author to whom correspondence should be addressed.

## EXPERIMENTAL

Electronic and differences absorption spectra were recorded by a Hitachi Model-340 spectrophotometer with an attached computer keyboard, and CD spectra by a JASCO J-40AS spectropolarimeter. These spectra were measured on varying molar concentration of *l*-brucine sulphate to a constant concentration of polyanion. Difference absorption spectra were measured according to the usual way.

Acetonitrile, DMF, DMAc and DMSO, purified before use, are used as solvent. Chiral compound, *l*-brucine, was obtained as sulphate from commercial source (Tokyo Kasei).

Tetrabutylammonium potassium salt of dodecatungstocobaltate, $K_2[(C_4H_9)_4N]_4$ $[CoW_{12}O_{40}]$, was

prepared according to the previous method.[5,6] Brucinium salt of the polyanion was also obtained by adding excess brucine sulphate to the aqueous solution of $K_6[CoW_{12}O_{40}]$ and purified by reprecipitation from the DMF solution with methanol. Found: C, 25.29; H, 3.13; N, 2.79. Calc. for $K_2(C_{23}H_{27}O_4N_2)_4$ $[CoW_{12}O_{40}]\cdot 3DMF$: C, 25.35; H, 2.72; N, 3.22%. Other dodecatungstopolyanions $[XW_{12}O_{40}]^{n-}$ (X = Zn, Al, Si, P and $2H^+$) and the dodecamolybdopolyanions $[XMo_{12}O_{40}]^{n-}$ (X = P and Si) were prepared by previous methods, isolated as tetrabutylammonium salts and recrystallized several times from acetonitrile.[7-9] Brucinium salt of the dodecatungstophosphate was obtained as above from the aqueous solution of the free acid. Found: C, 16.50; H, 2.06; N, 1.96. Calc. for $H(C_{23}H_{27}O_4N_2)_2[PW_{12}O_{40}] \cdot 2DMF$: C, 16.37; H, 1.83; N, 2.20%. The mixed-type polyanions, $[PFeM_{11}O_{40}H_2]^{4-}$ (M = Mo, W), were prepared as potassium salts from corresponding parent anions by the previous methods and its modification, and converted to tetrabutylammonium salts.[4,10] Found: C, 27.40; H, 5.22; N, 2.04. Calc. for $[(C_4H_9)_4N]_4[PFeMo_{11}O_{40}H_2]$: C, 27.90; H, 5.30; N, 2.03%. Found: C, 20.55; H, 4.20; N, 1.58. Calc. for $[(C_4H_9)_4N]_4[PFeW_{11}O_{40}H_2]$: C, 20.65; H, 3.92; N, 1.51%. The characteristic bands of the Keggin-structure for these compounds were confirmed by the IR spectra.

## RESULTS AND DISCUSSION

*Keggin-type dodecatungstopolyanions.* Electronic absorption spectra of the X = Co polyanion and of the increasing molar ratio of brucine to the polyanion are shown in Fig. 1(a). The absorption band with fine structure at *ca.* 626 nm is dominated by a spin-allowed transition to the third excited state $^4T_1(P)$ of the tetrahedral Co(II), which also includes some transitions to doublet excited states.[5] The absorbance increases with the molar ratio of brucine, but becomes nearly constant at the brucine ratio of more than 4. The tail of the charge transfer (CT) band of intra-lattice of $W_{12}O_{40}$ around 400 nm is also influenced largely by increasing the brucine concentration and saturates at the brucine ratio of more than 8. Difference absorption and CD spectra measured in the same region are shown in Fig. 1(b). The former reveals two explicit peaks at *ca.* 610 and *ca.* 400 nm, and the latter shows two negative Cotton effects, the intensities of which increase similarly to the spectral pattern. These are in accordance with the absorption and the CD of the brucinium salt, $K_2$(brucinium)$_4[CoW_{12}O_{40}]$. The induced CD in the near-UV region is due to a new chiral ligand,

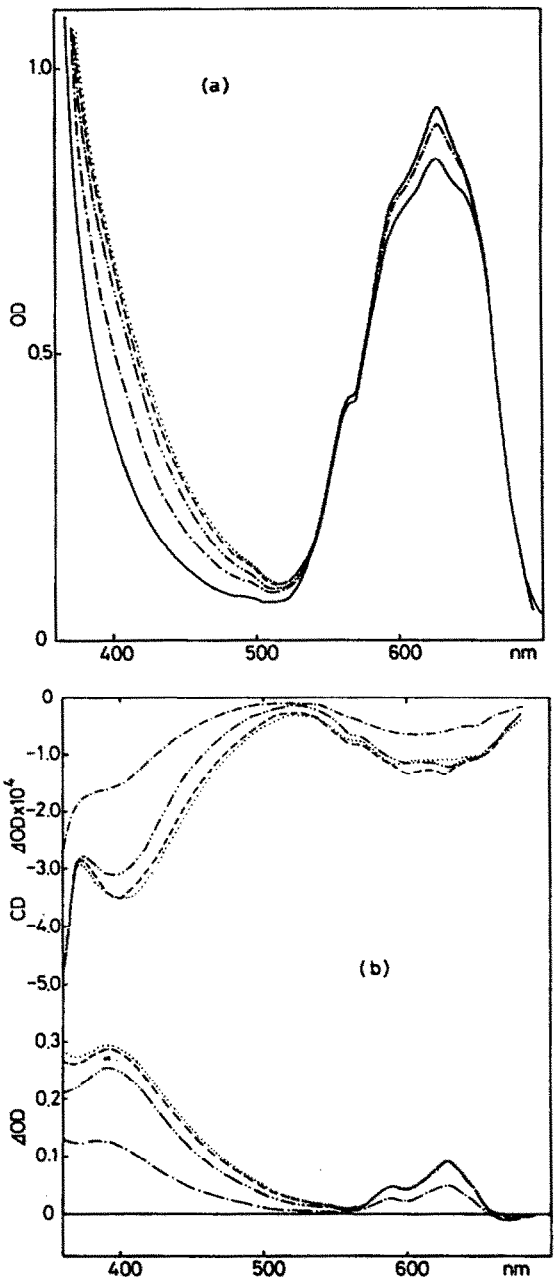



Fig. 1. Absorption spectra (a), and CD and difference absorption spectra (b) of tetrabutylammonium salt of $[CoW_{12}O_{40}]^{6-}$ anion in DMF media containing various molar ratios of *l*-brucine sulphate; the molar ratios of polyanion:brucine are 1:0 (———), 1:2 (—·—·—), 1:4 (—··—··—), 1:6 (------) and 1:8 (·····). [polyanion] = $3.91 \times 10^{-3}$ mol dm$^{-3}$.

"$W_{12}O_{40}$-brucinium", formed by the outer-sphere association. The CD in visible region has also fine structure like the original absorption structure and the saturated intensity ($\Delta\epsilon = -3.54 \times 10^{-2}$) is in good agreement with that of the brucinium salt. The Cotton effect induced in the region of the *d–d* transition of Co(II) by the chiral ligand may be

attributed to a kind of vicinal effect. The interaction of the dodecatungstate with brucine is significantly influenced by solvents, and the increasing order of saturated intensity of the induced CD in both visible and near-UV is DMF < DMAc < DMSO. This suggests that the association of the X = Co polyanion with brucine via hydrogen bonding provides an important contribution to the induced CD.

These facts suggest that the brucinium ion as counter cation in the $K_2$(brucinium)$_4$[$CoW_{12}O_{40}$] should be binding to the surface site of dodecatungstate. There are three possible sites on the surface oxygens: terminal oxygen and two bridging oxygens of W–O–W octahedral corner- and edge-sharings. The IR spectrum in the solid (KBr disk) of the Keggin-structure moiety of the brucinium salt was very similar to that of the tetrabutylammonium salt, except that the broad band at *ca.* 760 $cm^{-1}$, being overlapped of W–O–W corner-sharing band with tetrahedral Co–O stretching band,[5] was sharpened and its relative intensity was more increased. If the tetrabutylammonium ion is binding to the surface atom in the same site with the brucinium ion in the brucinium salt and can be easily replaced by the added brucinium ion in the solution, the bridging oxygen of corner-sharing may be proposed as a binding site. Recently Knoth and Harlow have reported the electrophilic O-alkylation of $[PM_{12}O_{40}]^{3-}$ (M = Mo, W) by a trimethyloxonium and the crystal structure of the alkylated product, and clarified that the preferred alkylation site is a bridging, rather than a terminal, oxygen atom.[11] This fact may support the proposed binding site of brucinium ion to the $W_{12}O_{40}$.

Analogous experiments with other polyanions, $[XW_{12}O_{40}]^{n-}$ (X = Zn, Al, Si and $2H^+$), showed the induced CD around 400 nm. These are also based on the new chiral ligand, "$W_{12}O_{40}$-brucinium", formed by the association. The maximal positions of the CD peaks are obscured except for the case of X = Zn compound, although they are observed in the similar regions around 400 nm. The electronic absorption, difference absorption and CD spectra in the system of the X = Zn compound are shown in Fig. 2. The replacing effect of heteroatom in the polyanion is markedly observed in the intensities, rather than the positions, of both the induced CD and the absorption. The least molar ratios of brucine, which should be added to give the saturated intensity of the CD under the constant molar concentration of each polyanion, were found to be 8 for X = Zn, 12 for X = Al, more than 12 for X = Si and 8 for X = $2H^+$. The magnitude of induced CD, estimated by dividing the saturated intensity of the induced CD at 400 nm of the brucine-polyanion solution with concentration of the polyanion, is presented in Table 1. The decreasing order is X = Co > Zn > $2H^+$ ~ Al > Si. The CD and absorption of the X = P compound in the DMF solution containing brucine gave rather different aspects from other cases; only a spectral shift of brucine itself was observed, and the new absorption and the induced CD could not be observed. The isolated brucinium salt, H(brucinium)$_2$[$PW_{12}O_{40}$], also did show neither new absorption nor induced CD in DMF. Analogous experiments in the acetonitrile media also gave no evidence of the association of brucinium ion with dodecatungstate. Thus, the X = P compound could be forcibly located in the last of the order.

The electronic interaction between the heteroatom and the dodecatungstate lattice can be proba-

Table 1. Intensity of induced CD at 400 nm of tetrabutylammonium salts of $[XW_{12}O_{40}]$ anions in DMF media containing *l*-brucine sulphate

| X | Intensity ($\Delta\varepsilon \times 10^2$) [a] |
|---|---|
| $Co^{II}$ | -9.0 |
| $Zn^{II}$ | -5.7 |
| $2H^+$ | -4.4 |
| $Al^{III}$ | -4.2 |
| Si | -1.9 |
| P | —— |

a Values estimated by dividing the saturated intensity of induced CD with the concentration of polyanion.

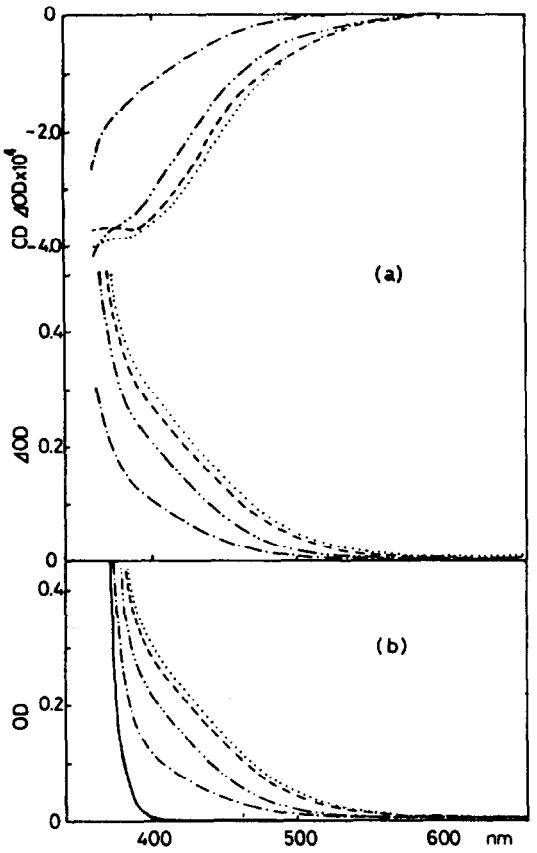



Fig. 2. CD and difference absorption spectra (a), and electronic absorption spectra (b) of tetrabutylammonium salt of $[ZnW_{12}O_{40}]^{6-}$ anion in DMF media containing various molar ratios of *l*-brucine sulphate; the molar ratios of polyanion:brucine are 1:0 (———), 1:2 (– – –), 1:4 (– – – –), 1:8 (— — —) and 1:12 (· · · · · · · · · ·). [polyanion] = $6.38 \times 10^{-3}$ mol dm$^{-3}$.

bly judged from the positions of two W–O–W stretching vibrations in the IR spectrum (Table 2). The polyanions used here have been classified to two groups; one is of X = Al, Si, P compounds and the other of X = Co, Zn compounds. The W–O–W stretching bands of the former are only slightly shifted to a higher frequency region, while those of the latter are shifted considerably to a lower one as compared with the W–O–W stretchings of $X = 2H^+$ compounds.[5,8] This suggests that there is a strong electronic interaction in the latter rather than the former. Thus, the interaction may affect the nucleophilicity of the bridging oxygen in the lattice, i.e. the reactivity at a specific site on the surface. This may lead to the change of the induced CD with the heteroatom.

*Keggin-type dodecamolybdopolyanions.* The absorption spectra in acetonitrile solution of the tetrabutylammonium salts of $[XMo_{12}O_{40}]^{n-}$ show broad bands at 307 nm ($\epsilon$ $2.39 \times 10^4$) for X = P and at 300 nm ($\epsilon$ $2.1 \times 10^4$) for X = Si, which are also due to the intra-lattice CT transition of the $Mo_{12}O_{40}$ unit. By the addition of brucine, the induced CD with negative sign was observed, although the bands are extremely broad and weak, at the longer wavelength region than 320 nm for the X = P compound and at the 330–350 nm region for the X = Si one. The saturated intensity was observed at a molar ratio of more than 3 in the former, while it was obscured in the latter. Since such a saturation is influenced by some polar solvents, the induced CD will be also due to the association via hydrogen bonding. As the association effect, the difference between the tungsto- and molybdo-polyanions is not so large, except the case of P heteroatom.

Fe(III)-*substituted polyanions.* In the mixed-type polyanions $[PFeM_{11}O_{40}H_2]^{4-}$ (M = Mo, W), one M•atom of the Keggin-type polyanions $[PM_{12}O_{40}]^{3-}$ is replaced by a Fe(III) ion, which is simultaneously coordinated by one water molecule. Thus, we can consider the mixed polyanions to be a hexa-coordination Fe(III) complex with the "quinquedentate" ligand $PM_{11}O_{39}^{7-}$ and unidentate water molecule.[12] The absorption spectrum in acetonitrile solution of the M = Mo compound shows a comparatively broad band ($\epsilon$ $2.58 \times 10^4$) due to the intra-lattice CT at 306 nm. This spectrum is very similar to that of the parent molybdopolyanion and the discrimination between their spectra is difficult. The absorptions based on the Fe(III) ion, possibly weak bands due to the spin-forbidden transition from the high-spin $d^5$ configuration, are completely masked by the tail of the CT band. Under the coexistence of brucine, a new absorption band appears at 360 nm (Fig. 3a). The absorbance of the band becomes intense with the ratio of brucine and saturates at the ratio of more than 5. The molar absorptivity of the new band is more than $1.5 \times 10^4$. This absorption may be caused by a Fe ← N(brucine) CT transition in the new complex formed by the replacement of the coordinating water molecule with brucine. This type of reaction has been suggested in the systems of pyridine and mixed polyanions such as $[PCo^{II}W_{11}O_{40}H_2]^{5-}$ and $[SiCo^{III}W_{11}O_{40}H_2]^{5-}$.[13,14] Correlating with the absorption spectra, the CD spectra show a negative Cotton effect at 365 nm (Fig. 3b). This is induced by the coordination of brucine to Fe(III) ion and is much more intense than the CD observed by the association between brucine and $Mo_{12}O_{40}$ unit aforementioned. The new absorption and induced CD due to the coordination of brucine can be observed in the much lower concentration of the polyanion than in the systems of the dodecametallates.

Table 2. IR data in the Keggin-structure stretchings of tetrabutylammonium salts of $[XW_{12}O_{40}]$ anions in the solid state[a,b]

| X = $Co^{II}$ | $Zn^{II}$ | $2H^+$ | $Al^{III}$ | Si | P | Assignment |
|---|---|---|---|---|---|---|
| | | | | | 1072s | ν(P–O tetrahedral) |
| 1017w | | | | 1010m | | |
| | | 956s | | | | ν(O–H tetrahedral) |
| 940s | 940s<br>918sh | 947s | 957s<br>922sh | 966s | 969s | ν(W–O terminal) |
| | | | | 920vs | | ν(Si–O tetrahedral) |
| 870vs | 874s | 880vs | 885s | 882m | 887s | ν(W–O–W octahedral edge-sharing) |
| | | 800vs | 810s | 805vs | 804vs | ν(W–O–W octahedral corner-sharing) |
| | | | 770s | | | ν(Al–O tetrahedral) |
| 760vs | 766vs | | | | | ν(W–O–W octahedral corner-sharing) |
| | | | | | | and ν(X–O tetrahedral) |
| 520–580<br>w(br) | 550w | 520–580<br>w(br) | 535w | | 584w | |
| | | | | 528m | | δ(O–Si–O) |
| | | | | | 505m | δ(O–P–O) |
| | | | | 477w | 460w | |
| 441m | 441m | | 476m | | | δ(O–X–O) |
| | | 410s | | | | ν(O–H tetrahedral) |

a Measured in KBr disk, $cm^{-1}$.
b Refs. 5, 6 and 8.

In Figs. 3(a) and (b), both absorption and induced CD at the molar ratios of 1 and 2 look very weak and broad, whereas they become remarkably intense and sharp at the ratios more than 3. This is unlike the aspect of usual 1:1 complex formation. As a matter of fact, when Lang's iteration method is applied to estimate the formation constant and the molar absorptivity on the assumption of the 1:1 complex,[15] only the plots at the ratios 1 and 2 markedly deviated from a straight line given by the plots at the ratios 3–6. This indicates that the brucine should also play another role other than the 1:1 complex formation. The possibility of brucine-polyanion (1:2) complex formation is ruled out on account of the dilute concentrations of polyanion studied here and the electrostatic repulsion of the highly charged polyanion. Rather, the outer-sphere association of some brucine molecules with the "quinquedentate" ligand $PMo_{11}O_{39}^{7-}$ can be possibly considered as observed in the dodecametallates.

Analogous experiments with the M = W compound (the intra-lattice CT band; $\epsilon$ $4.5 \times 10^4$ at 260 nm) and brucine showed a new absorption at 345 nm due to the coordination of brucine to the Fe(III) ion. The induced CD was observed at 340 nm. The molar absorptivity of new band is more than $6 \times 10^3$. The increasing aspect of both absorption and CD with the molar ratio of brucine is similar to the case of the M = Mo compound. The role of brucine playing on the polyanion has also been suggested not only as the coordination to the Fe(III) ion, but as the outer-sphere association with the $PW_{11}O_{39}^{7-}$ moiety. Since the association of brucine with the parent $[PW_{12}O_{40}]^{3-}$ anion could not be observed, the association with the $PW_{11}O_{39}^{7-}$ moiety may be caused by the substituted Fe(III) ion.

## CONCLUSION

Keggin-type dodecatungstopolyanions $[XW_{12}O_{40}]^{n-}$ (X = Co, Zn, Al, Si and $2H^+$) in DMF media containing various molar ratios of *l*-brucine

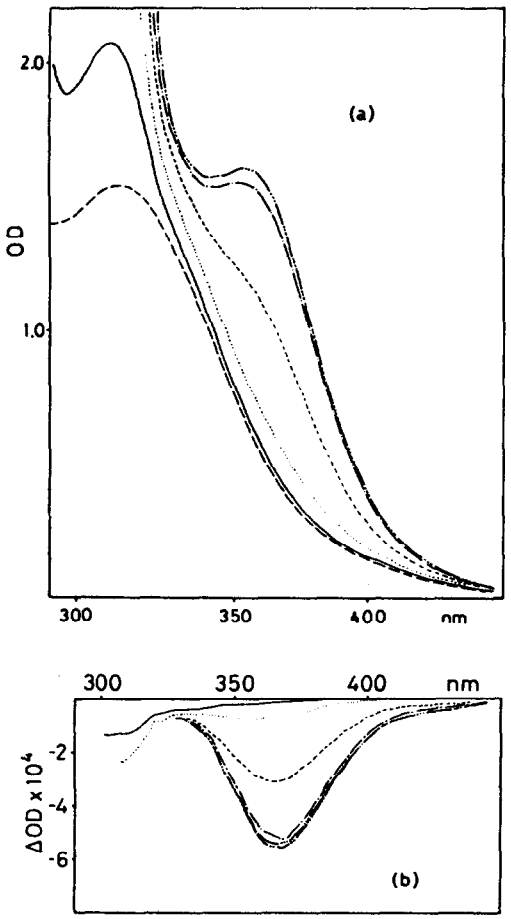



Fig. 3. Absorption spectra (a) and CD spectra (b) of tetrabutylammonium salt of $[PFeMo_{11}O_{40}H_2]^{4-}$ anion in the acetonitrile solution containing various molar ratios of *l*-brucine sulphate; the molar ratios of polyanion:brucine are 1:0 (———), 1:1 (———), 1:2 (·····), 1:3 (----------), 1:4 (—·—·—), 1:5 (—··—··—) and 1:6 (—···—···). [polyanion] = $6.0 \times 10^{-5}$ mol dm$^{-3}$.

sulphate show induced CD in near-UV region due to the association of brucinium ion with the surface oxygen of dodecatungstate. The binding site is proposed as a bridging oxygen of the surface. The X = Co compound also shows the induced CD in visible region, which is brought about in the *d–d* transition of tetrahedral Co(II) ion by the chiral ligand, "$W_{12}O_{40}$-brucinium". The X = P compound gives no evidence of outer-sphere association. The decreasing order of the induced CD in near-UV region is in the order: X = Co > Zn > $2H^+$ ~ Al > Si > P. The hetero-atom X significantly contributes to the nucleophilicity of the bridging oxygen, that is, to the reactivity at a specific site on the dodecatungstate lattice. As the association effect, the difference between the tungsto- and molybdo-polyanions is not so large. The mixed polyanions $[PFeM_{11}O_{40}H_2]^{4-}$ (M = Mo, W) show the intense absorption and induced CD in the visible region due to a coordination of brucine to the Fe(III) ion. In these cases, an outer-sphere association of the $PM_{11}O_{39}^{7-}$ moiety and brucine is also suggested.

## REFERENCES

1. K. Nomiya, T. Ueno and M. Miwa, *Bull. Chem. Soc. Jpn.* 1980, **53**, 827.
2. K. Nomiya, M. Miwa and Y. Sugaya, *Polyhedron* 1984, **3**, 381.
3. K. Nomiya, Y. Sugaya, S. Sasa and M. Miwa, *Bull. Chem. Soc. Jpn.* 1980, **53**, 2089.
4. K. Nomiya, M. Sugaya and M. Miwa, *Bull. Chem. Soc. Jpn.* 1979, **52**, 3107.
5. K. Nomiya, M. Miwa, R. Kobayashi and M. Aiso, *Bull. Chem. Soc. Jpn.* 1981, **54**, 2983.
6. K. Nomiya, R. Kobayashi and M. Miwa, *Bull. Chem. Soc. Jpn.* 1983, **56**, 2272.
7. E. O. North and W. Haney, *Inorg. Syntheses*, Vol. I, p. 127.
8. K. Nomiya and M. Miwa, *Polyhedron* 1983, **2**, 955.
9. H. Wu, *J. Biol. Chem.* 1920, **43**, 189.
10. F. Zonnevijlle, C. M. Tourné and G. F. Tourné, *Inorg. Chem.* 1982, **21**, 2751.
11. W. H. Knoth and R. L. Harlow, *J. Am. Chem. Soc.* 1981, **103**, 4265.
12. L. C. W. Baker, V. S. Baker, K. Eriks, M. T. Pope, M. Shibata, O. W. Rollins, J. H. Fang and L. L. Koh, *J. Am. Chem. Soc.* 1966, **88**, 2329.
13. T. J. R. Weakley, *J. Chem. Soc. Dalton Trans.* 1973, 341.
14. L. C. W. Baker and J. S. Figgis, *J. Am. Chem. Soc.* 1970, **92**, 3794.
15. R. P. Lang, *J. Am. Chem. Soc.* 1962, **84**, 1185.

*Polyhedron* Vol. 3, No. 9/10, pp. 1077–1081, 1984
Printed in the U.S.A.

0277-5387/84 $3.00 + .00
© 1984 Pergamon Press Ltd.

# SOLUTION CHEMISTRY OF SILVER-PORPHYRINS—3. SILVER(I) PORPHYRINS

**JOSEPH M. OKOH, NORMAN BOWLES and M. KRISHNAMURTHY***
Department of Chemistry, Howard University, Washington, DC 20059, U.S.A.

(*Received* 16 *December* 1983; *accepted* 17 *February* 1984)

**Abstract**—Complex formation reactions of Ag(I) with tetra(*p*-trimethylammoniumphenyl)porphyrin, ($H_2$TAPP), and with tetra(3-N-methylpyridinium)porphyrin, ($H_2$TMPyP), were investigated at 25°C and $\mu$ = 0.1 M($NaNO_3$). The composition of the complex was established to be 2:1 (metal:$H_2$TMPyP) by spectrophotometric titration. The equilibrium constant, K, was found to be $10^{-5.8}$. Binding of the first Ag(I) was found to be rate determining with rate constant, $k_1 = 2.28 \times 10^3$ and $4.17 \times 10^4$ $M^{-1}$ $s^{-1}$ for $H_2$TMPyP and $H_2$TAPP respectively. A plausible mechanism is discussed.

Stable Ag(I)porphyrins are usually synthesized by mixing a porphyrin solution with a Ag(I) salt such as nitrate or acetate.[1] On mixing the two, the red porphyrin solution becomes green momentarily then slowly changes to red, often accompanied by a silver mirror. The final red colour is due to Ag(II)porphyrin, formed as a result of disproportionation of Ag(I) ions. Continuing our interest in the chemistry of silver porphyrins, we investigated the green aqueous solution formed by mixing silver nitrate with tetra(3-N-methylpyridinium)porphyrin acetate ($H_2$TMPyP),[2] and with tetra(*p*-trimethylammoniumphenyl) porphyrin acetate ($H_2$TAPP). The results are presented here.

## EXPERIMENTAL

A Beckman model Acta CIII spectrophotometer equipped with a thermostatted sample compartment and a Radiometer model PHM 64 Research pH meter were used for titration studies. For kinetic studies a Durrum–Gibson stopped flow spectrometer was employed. Plots of log $(A_t - A_\infty)$ vs time were linear for over three half lives. Pseudo-first order rate constants were reproducible within 5%. There was no evidence of any other reaction within the life-time of these reactions.

Common chemicals such as silver nitrate (AR grade, Mallinckrodt), $NaNO_3$ (Reagent grade, Alfa Products) and buffers such as N-hydroxyethylpiperazine-N-2-ethanesulphonic acid (HEPES), morpholinoethanesulphonic acid (MES) (US Biochemicals) were used as obtained. The iodide salts of $H_2$TMPyP) and $H_2$TAPP were synthesized as described in the literature.[3,4] Hot solutions of these sparingly soluble salts were converted to the soluble acetate form by passing through a column of anion-exchange resin (Rexyn 202, Fisher) in acetate form and stored in amber colored bottles. Concentration of the stock solutions thus obtained were spectrophotometrically found to be $10^{-4}$ M employing known extinction coefficients. Concentration of silver nitrate stock solution was determined by standard procedures. All studies were carried out at 25.0 ± 0.1°C. For all studies the ionic strength was kept at 0.1 M in $NaNO_3$ except in the series where nitrate was substituted with fluoride. In this series the total inert salt concentration was 0.1 M.

Spectrophotometric titrations were carried out by placing 500 $cm^3$ of porphyrin solution, containing 5.0 $cm^3$ of stock porphyrin, 50.0 $cm^3$ of 0.1 M HEPES solution and 25 $cm^3$ of 2.0 M $NaNO_3$ in a jacketted vessel. The solution was thermal equilibrated for 30 min. Different aliquots of 0.1 M $AgNO_3$ solution were added employing a microburette. Before each addition, the spectrum of porphyrin sample was recorded. By returning this sample, the total volume was maintained close to 500 ± 50 $cm^3$ allowing for silver nitrate.

*Author to whom correspondence should be addressed.

## RESULTS AND DISCUSSION

Spectra of the porphyrin solutions during spectrophotometric titration are presented in Fig. 1. On addition of Ag(I) ion, the absorption of free-base at 515 nm decreases while the absorption at 585 and 635 nm increases with a shift in the maxima of each of these bands. A new band, with substantial intensity appears at 473 nm even at the very first addition of Ag(I). From the extent of increase in absorption at 473 nm and from the fact that the Soret of the free-base disappears at the end, this 473 nm band is assigned as the Soret band of Ag(I) porphyrin that is formed in solution. Though there are regions where apparently all curves pass through (regions of same absorbance) no clearcut isosbestic point was observed.

A plot of absorbance at 473 nm, the Soret of Ag(I)porphyrin, and at 515 nm, the major visible band of the free-base, as a function of the added silver ion concentrations is shown in Fig. 2. Each curve has only two inflections. This would mean that though there may be more than two absorbing species in solution probably the equilibria are coupled. Assuming a reaction of the type: $n\mathrm{Ag}^+ + \mathrm{H_2TMPyP} \rightleftharpoons \mathrm{H}_{2-n}\mathrm{Ag}_n\mathrm{TMPyP} + n\mathrm{H}^+$, where $n$ can be 1, 2 etc. one can derive the following:

$$\log[(A_i - A)/(A - A_f)] = n \log[\mathrm{Ag}^+] + \log \mathrm{K} - n \log[\mathrm{H}^+].$$

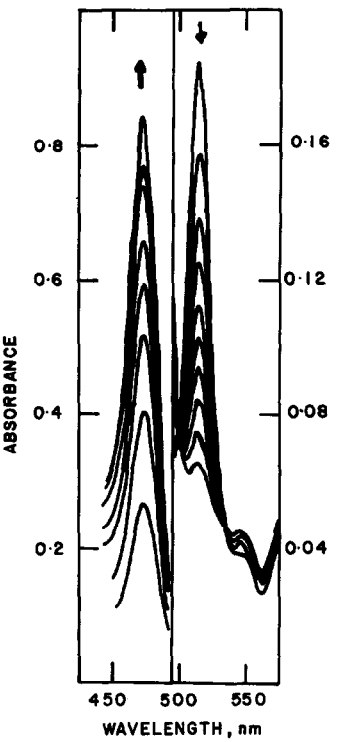



Fig. 1. Variation of spectrum in the range of 425 to 575 nm during the titration of $\mathrm{H_2TMPyP}$ with Ag(I). (Scale on the left ordinate for the left half of the figure and scale on the right ordinate is for the right half of the figure.)

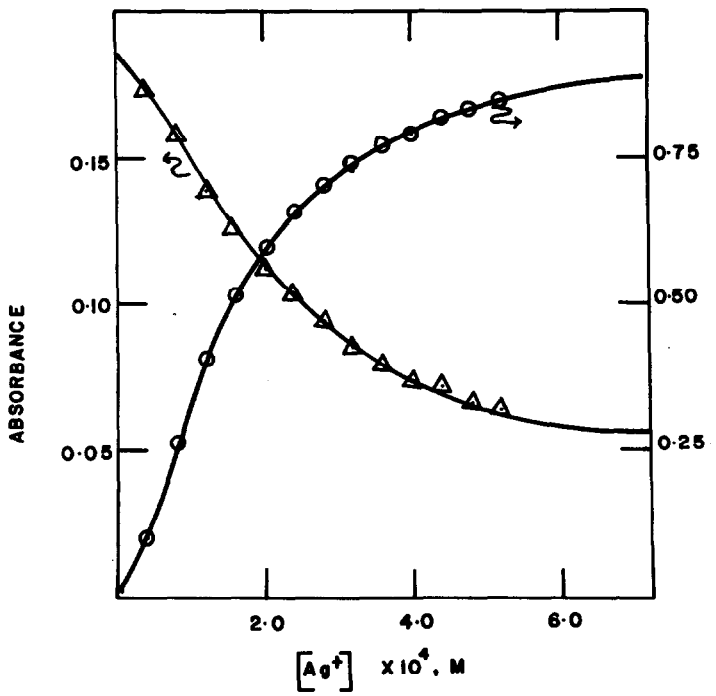



Fig. 2. Plot of absorbance vs $[\mathrm{Ag}^+]$ at 473 nm (-⊙-⊙-⊙-, right ordinate) and at 515 nm (-△-△-△-, left ordinate) during the spectrophotometric titration of $\mathrm{H_2TMPyP}$ with Ag(I).

In this $A_i$, $A$, $A_f$ and K represent absorbance at the beginning of the titration, absorbance during the titration corresponding to $[Ag^+]$, absorbance at the end of the titration and the equilibrium constant respectively. From this if one plots $\log[(A_i - A)/(A - A_f)]$ as a function of $\log[Ag^+]$, a straight line should result with a slope of "$n$". From the intercept one can extract a value for "K". Such a plot for the titration with $H_2$TMPyP at 473 and 515 nm did indeed yield straight lines with slopes of $1.8 \pm 0.03$ and $1.73 \pm 0.05$ respectively. From the intercept, log K values were extracted to be $-5.8 \pm 0.3$ and $-5.8 \pm 0.4$ at 473 and 515 nm respectively. Such a titration with $H_2$TAPP was not successful due to the faster rate of disproportionation of the Ag(I) complex.

The spectra of most synthetic tetraaryl porphyrins are very similar in their general characteristics. Such a resemblance is also noted for the same metal ion complex of different synthetic tetraarylporphyrins. Dorough and coworkers[1] reported the spectrum of disilver(I) tetraphenyl porphyrin. The spectrum of the final product of the titration agrees with the spectrum reported by Dorough *et al.* Analysis of the titration data also indicates that two Ag(I) ions are bound to the porphyrin molecule. Thus the following stoichiometry is formulated for the equilibrium: $2Ag^+ + H_2TMPyP \rightleftharpoons Ag_2TMPyP + 2H^+$.

Kinetics of the formation of Ag(I)porphyrin were monitored at 473 nm. This reaction was found to be first order in porphyrin. Under pseudo-first order conditions, keeping the pH constant, dependence on Ag(I) was investigated over a concentration range of $3.1 \times 10^{-4}$ M to $8.3 \times 10^{-3}$ M, and $1.25 \times 10^{-4}$ M to $2.50 \times 10^{-3}$ M in the case of $H_2$TMPyP and $H_2$TAPP respectively. In both cases the reaction was found to be first order in Ag(I). Studies to investigate the hydrogen ion dependence were inconclusive as no suitable buffers could be found for the relevant range and as the concentration of the base form of most buffers increase, they interfere by complexing with silver.

Most metal incorporation studies with $H_2$TMPyP analogues were found to be linearly dependent on nitrate ("inert ion") concentration.[5,6] To see any such catalysis occur in this reaction, nitrate concentrations were varied from 0 to 0.1 M keeping the ionic strength constant employing sodium fluoride. The observed rate constants remained the same over the entire series indicating the absence of any participation of nitrate in the reaction.

In accordance with the concept of stepwise complex formation the following mechanism is proposed for the silver porphyrin formation:

$$Ag^+ + H_2P \rightleftarrows HAgP + H^+ \qquad k_1, k_2$$

$$Ag^+ + HAgP \rightleftarrows Ag_2P + H^+ \qquad k_3, k_4.$$

For this mechanism, the ratelaw for attaining complex formation equilibrium can be derived as:

$$d[Ag_2P]/dt = (k_1k_3[Ag^+]^2 + k_2k_4[H^+]^2)/(k_2[H^+] + k_3[Ag^+])([Ag_2P]_{equ} - [Ag_2P]_t).$$
$$= k_{obs}([Ag_2P]_{equ} - [Ag_2P]_t).$$

thus $k_{obs}$, the pseudo-first order rate constant is equal to $(k_1k_3[Ag^+]^2 + k_2k_4[H^+]^2)/(k_2[H^+] + k_3[Ag^+])$. If $k_3 \gg k_2$, this can be simplified to

$$k_{obs}[Ag^+] = k_1[Ag^+]^2 + k_2k_4/k_3[H^+]^2.$$

A plot of $k_{obs}[Ag^+]$ vs $[Ag^+]^2$ should be linear with a slope of $k_3$ and intercept of $k_2k_4/k_3[H^+]^2$. Such a plot for the reaction of Ag(I) with $H_2$TMPyP and $H_2$TAPP are presented in Figs. 3 and 4, respectively. Linearity of Fig. 3 validates the assumption that $k_3$ is larger than $k_2$. But in the case of $H_2$TAPP, at lower Ag(I) concentrations there is some deviation indicating that the dropped term, $k_2[H^+]/[Ag^+]$ is also probably important. Values of $k_1$ for $H_2$TMPyP and $H_2$TAPP obtained from these plots are $2.28 \times 10^3\ M^{-1}\ s^{-1}$ and $4.17 \times 10^4\ M^{-1}\ s^{-1}$ respectively.

For the formation reaction of Ag(I) with *o*-phenanthroline, a rate constant of $\geqslant 10^7\ M^{-1}\ s^{-1}$ was reported by Holyer *et al.*[7] For the formation of monothiosulphato Ag(I), a rate constant of $3.5 \times 10^9\ M^{-1}\ s^{-1}$ was reported by Eyring *et al.*[8] Both these data were for monodentate complex formation. Significantly lower values obtained here may be because these rate constants are for chelation.

Of the numerous metalloporphyrin formation studies reported in the literature,[5,9-11] a general mechanism comprising the following steps has evolved in recent times: (1) formation of outer sphere complexes ($K_{os}$); (2) dissociation of ligands from the metal ion (multiple desolvation, may be) ($k_E$); (3) deformation of the porphyrin, $k_d$, and (4) deprotonation of porphyrin ($k_{N-H}$).

The contribution of porphyrin deformation to rate determining step has been suggested by earlier workers,[12] primarily based on the fact that N-alkylporphyrins bind metal ions faster than the parent free-base porphyrin. This is untenable since the observed increase in rate constant could also be due to increase in the rate of proton dissociation.

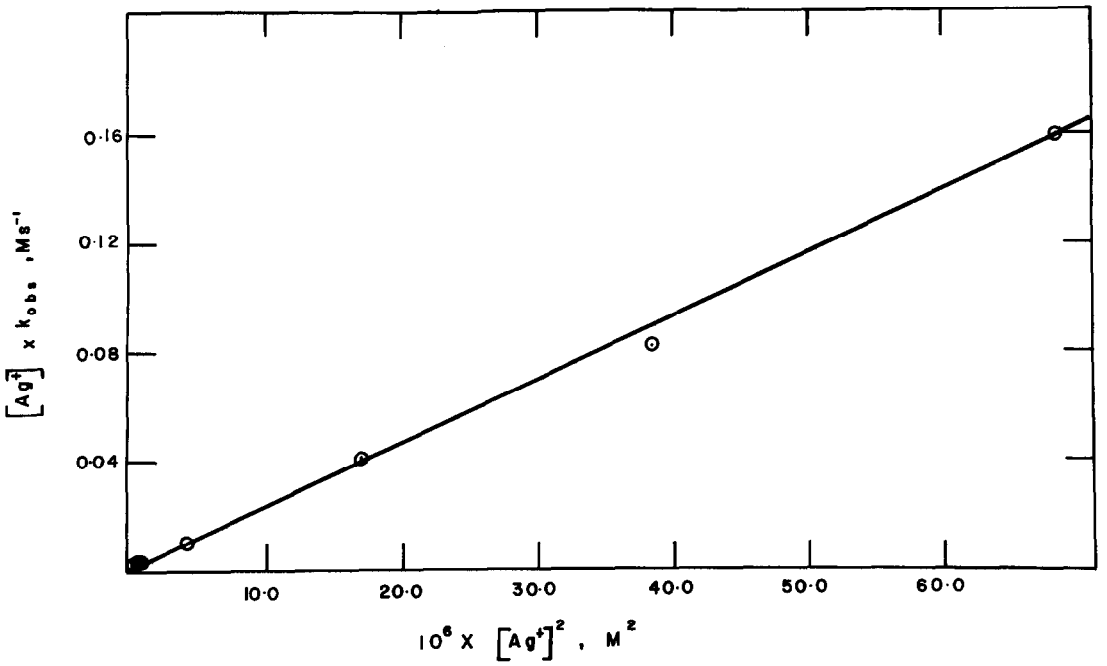



Fig. 3. Plot of $k_{obs} \times [Ag^+]$ vs $[Ag^+]^2$ for the reaction of Ag(I) with $H_2$TMPyP.

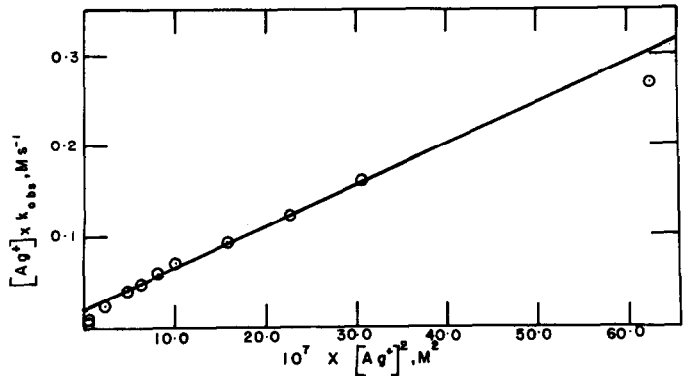



Fig. 4. Plot of $k_{obs} \times [Ag^+]$ vs $[Ag^+]^2$ for the reaction of Ag(I) with $H_2$TAPP.

But the binding of the first Ag(I) enhancing the rate of binding of second Ag(I) observed in this case strongly suggests the influence of porphyrin deformation. Similar enhanced rates have also been reported for Hg(II) catalyzed metalloporphyrin formations.[13,14]

Metal incorporation rates have been found to parallel water (or solvent) exchange rates of the parent metal ion.[5] The second-order rate constant for the reaction of Cu(II) with $H_2$TMPyP and $H_2$TAPP were found to be 12.4 $M^{-1}s^{-1}$ (at 39°C)[6] and 6.2 $M^{-1}s^{-1}$[15] respectively. Similar constants for the reaction of Ag(I) with $H_2$TMPyP and $H_2$TAPP determined in this study are $2.28 \times 10^3$ $M^{-1}s^{-1}$ and $4.17 \times 10^4$ $M^{-1}s^{-1}$ respectively.

Since all other relevant factors earlier suggested (such as $K_{os}$, $k_d$ and $k_{N-H}$), being the same, such large difference in the Cu(II) and Ag(I) metallation rates can only be partly attributed to the increased solvent exchange rates. An additional parameter, probably the nature of bonding in the product metalloporphyrin, also needs to be considered. The greater the ionic character of metal–porphyrin bonds, the faster the rate of formation. This parameter can also be quantified much as the others were by introducing an instability index (inverse of Buchler's stability index, $S_i$)[16] as an additional term as:

$$k_1 = 1/S_i \cdot K_{os} \cdot k_d \cdot k_E \cdot k_{N-H},$$

and

$$S_i = 100 \times E_n Z / r_i$$

where $E_n$, Z and $r_i$ represent electronegativity, charge and radius of the metal ion.

In conclusion, both $H_2$TMPyP and $H_2$TAPP form labile 2:1 (metal:ligand) complexes of low thermodynamic stability with Ag(I). Binding of the first Ag(I) catalyses the binding of the second Ag(I), supporting the concept of rate determining deformation of the porphyrin core. The large rate constant for the first Ag(I) binding suggests that in addition to well-known factors that influence metalloporphyrin formation one should also take into consideration the nature of bonding in the final product: more ionic metal–porphyrin bond resulting in a faster formation of the product.

*Acknowledgements*—Financial assistance from Grant No. 5 SORR08016-11 from the MBRS Program, DRR, NIH is gratefully acknowledged.

## REFERENCES

1. G. D. Dorough, J. R. Miller and F. M. Huennekens, *J. Am. Chem. Soc.* 1951, **73**, 4315.
2. Peripheral charges on the porphyrinic species were omitted for clarity.
3. B. P. Neri and G. S. Wilson, *Anal. Chem.* 1973, **45**, 442. P. Hambright, T. Gore and M. Burton, *Inorg. Chem.* 1976, **15**, 2314.
4. M. Krishnamurthy, *Ind. J. Chem.* 1977, **15B**, 964.
5. P. Hambright and P. B. Chock, *J. Am. Chem. Soc.* 1974, **96**, 3123.
6. J. Reid and P. Hambright, *Inorg. Chem.* 1977, **16**, 968.
7. R. H. Holyer, C. D. Hubbard, S. F. A. Kettle and R. G. Wilkins, *Inorg. Chem.* 1965, **4**, 929.
8. M. M. Farrow, N. Purdie and E. M. Eyring, *Inorg. Chem.* 1975, **14**, 1584.
9. W. Schneider, *Struct. Bonding* 1975, **23**, 123.
10. J. Turay and P. Hambright, *Inorg. Chem.* 1980, **19**, 562.
11. S. Funnahashi, K. Saito and M. Tanaka, *Bull. Chem. Soc. Japan* 1981, **54**, 2695.
12. B. Shah, B. Shears and P. Hambright, *Inorg. Chem.* 1971, **10**, 1685.
13. M. Tabata and M. Tanaka, *Anal. Lett.* 1980, **13**, 427.
14. A. Adeyemo and M. Krishnamurthy, Submitted.
15. J. Turay and P. Hambright, *Inorg. Chim. Acta.* 1979, **35**, L319.
16. J. W. Buchler, In *Porphyrins and Metalloporphyrins* (Edited by K. M. Smith), Chap. 5, p. 199. Elsevier, New York (1975).

Polyhedron Vol. 3, No. 9/10, pp. 1083–1085, 1984
Printed in the U.S.A.

0277-5387/84 $3.00 + .00
Pergamon Press Ltd.

# SYNTHESIS AND X-RAY STRUCTURE OF THE *TRANS*-DIOXOTETRAKIS(TRIMETHYLPHOSPHINE)RHENIUM(V) CATION

PETER G. EDWARDS, ANDRZEJ C. SKAPSKI,*
ALEXANDRA M. Z. SLAWIN and GEOFFREY WILKINSON*
Chemistry Department, Imperial College, London SW7 2AY, U.K.

(*Received* 30 *April* 1984; *accepted* 14 *June* 1984)

**Abstract**—Dirhenium heptaoxide, $Re_2O_7$, reacts with excess trimethylphosphine to give *trans*-$[ReO_2(PMe_3)_4]ReO_4$. The structure of the cation in the perrhenate and the tetraphenylborate salts has been determined.

During studies on reactions of dirhenium heptaoxide[1] it was observed that $Re_2O_7$ and excess trimethylphosphine in dichloromethane produced canary yellow solutions from which pale yellow crystals were formed. Analytical data indicated an empirical formula of $ReO_3(PMe_3)_2$ but conductivity measurements in acetonitrile showed the complex to be a 1:1 electrolyte. The IR spectrum had two intense bands in the Re=O stretching region[2] at 770 and 900 $cm^{-1}$, the former being consistent with the presence of a *trans*-dioxo group and the latter with $ReO_4^-$. X-ray crystallographic study (see later) showed the complex to be *trans*-$[ReO_2(PMe_3)_4]ReO_4$.† Both the $^1H$ and $^{31}P$-$\{^1H\}$ NMR spectra are singlets showing only a linear chemical shift dependence on cooling at −80°C.

Exchange of $ReO_4^-$ by $BPh_4^-$ in tetrahydrofuran gives the tetraphenylborate whose IR spectrum has only the *trans*-$ReO_2$ band at 778 $cm^{-1}$.

The perrhenate salt was the first to be examined by single-crystal X-ray methods. Although the structure was solved, the crystals were not of good quality and *R* reached only 0.098. In the case of the $[BPh_4]^-$ salt, the X-ray data were better ($R = 0.061$), but the cations showed disorder. Despite these problems, however, the essential structure of the $[ReO_2(PMe_3)_4]^+$ cation is clear.

Figure 1 shows two aspects of the cation. The two *trans* oxygen atoms form a linear (O—Re—O, 177°) system, with Re=O distances of 1.79(2) Å. These may be compared to 1.781(3) in $[ReO_2(CN)_4]^{3-}$,[3] 1.764(13) in $[ReO_2py_4]^{+4}$ and 1.765(7) in $[ReO_2en_2]^+$.[4] The four phosphorus atoms of the equatorial $PMe_3$ groups show an appreciable

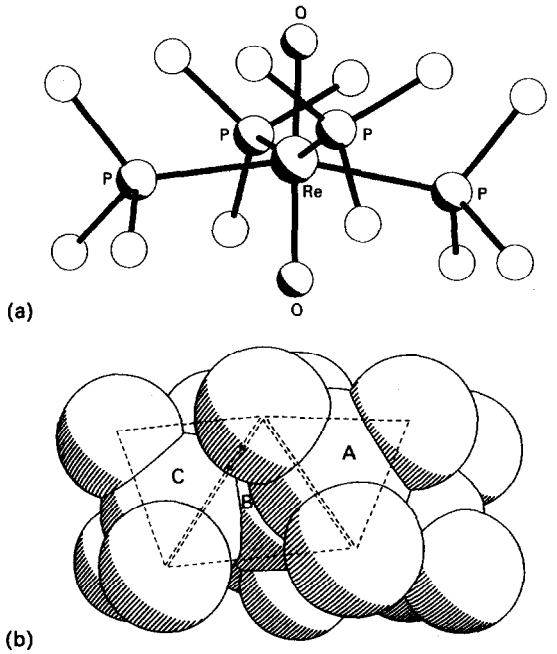



Fig. 1. (a) Structure of the *trans*-$[ReO_2(PMe_3)_4]^+$ cation in the perrhenate salt. (b) A space-filling diagram of the cation viewed as in (a). The three triangles marked A, B and C, relate to the disorder found in the tetraphenylborate salt. They indicate the approximate alternative positions of the methyl groups in the three orientations which the cation can adopt without seriously affecting its external appearance.

*Authors to whom correspondence should be addressed.

† A recent paper (J. W. Johnson, J. F. Brody, G. B. Ansell and S. Zents, *Inorg. Chem.* 1984, **23**, 2415) reports that $Re_2O_7$ in the presence of pyridines (py) is reduced by $PEt_3$ to give $[ReO_2py_4]ReO_4$ while $ReO_3$ reacts with pyridine to give the same pyridine compound.

tetrahedral distortion from planarity, such that the *trans* P—Re—P angles are 162(1)°. The mean Re—P bond length of 2.485(8) Å is on the long side, presumably because of bond weakening caused by the mutual *trans* influence and the steric repulsions of the $PMe_3$ groups. The cation approximates quite closely to $\bar{4}2m$ ($D_{2d}$) point symmetry.

In the $[BPh_4]^-$ salt, a curious form of disorder affects the cation in which it adopts three orientations about the O=Re=O axis, such that Re—P bonds appear to lie every 30°. It can be seen from Fig. 1(b) that the cation has a shape approximating to a flat cylinder, and that by rotation every 60° or so an arrangement of methyl groups can be obtained which leaves the external appearance of the cation relatively unchanged.

The reduction of rhenium(VII) in $Re_2O_7$ to rhenium(V) in the complex is clearly due to $PMe_3$, and $Me_3PO$ was identified in the reaction mixture by $^{31}P$ NMR in essentially the amount required by the quantitative reaction:

$$Re_2O_7 + 5PMe_3 = [ReO_2(PMe_3)_4]ReO_4 + Me_3PO$$

in which $Re_2O_7$ can be considered as $ReO_3^+ReO_4^-$.

The cation is analogous to other established *trans*-$Re^VO_2L_4$ species such as

$[ReO_2py_4]^+$,[4,5] $[ReO_2en_2]^+$,[4,6] $[ReO_2bipy_2]^+$,[4,7] and

$$[ReO_2(CN)_4]^{3-};[3,8]$$

it appears to be the first tertiary phosphine complex in the $MO_2L_4$ class for any transition metal.

## EXPERIMENTAL

Analyses were by Pascher (Bonn, F.R.G.). Instruments: NMR: JEOL FX90Q ($^1H$ 89.55 MHz, $^{31}P$ 36.2 MHz; $\delta$-values in ppm). IR: Perkin–Elmer 683 (spectra in nujol mulls in $cm^{-1}$). Conductivity: Data Scientific PT1-18 (in acetonitrile). All operations were performed under dry oxygen-free nitrogen or *in vacuo*. Solvents were purified by standard methods and were distilled immediately prior to use.

### trans-*Dioxotetrakis(trimethylphosphine)rhenium(V) perrhenate*

To a suspension of $Re_2O_7$[9] (3.52 g, 6.7 mmol) in dichloromethane (50 $cm^3$) was added, with vigorous stirring, trimethylphosphine (6.7 $cm^3$, 67 mmol). The oxide dissolved rapidly forming a yellow solution which was stirred (30 min). Hexane (150 $cm^3$) was added causing precipitation of the product which was filtered, washed with hexane (2 × 10 $cm^3$), extracted into dichloromethane (40 $cm^3$) and filtered. The product was isolated by addition of hexane (*ca* 5–10 $cm^3$ or until crystals appeared) followed by cooling (−78°C). The crystals were collected, washed with hexane (2 × 10 $cm^3$) and dried *in vacuo*. The supernatant provided a further crop. Combined yield: 4.86 g, 86% based on $Re_2O_7$; m.p. decomp. *ca* 120°C. [$C_{12}H_{36}O_6P_4Re_2$, *M*, 772: C, 18.6(18.6); H, 4.60(4.66); P, 16.4(16.1); O, 12.7 (12.4)%.] The compound is soluble in tetrahydrofuran, acetonitrile and chlorinated hydrocarbons and is insoluble in diethylether and hydrocarbons. Crystals suitable for X-ray crystallography were grown from $CH_2Cl_2$/hexane mixtures at −20°C. Conductivity: $\lambda_M = 179.5$ s $cm^{-1}$ $M^{-1}$.

IR: 1309m, 1288m, 1279m, 1170w, br, 950s, 900s, 849m, 770s, 727m, 670w, 362w, 335m, 267m. NMR ($CDCl_3$, 25°C): $^1H$: 1.63; $^{31}P$-{$^1H$}: −38.67 (−36.78 at −80°C).

### *The tetraphenylborate salt*

To a solution of $[ReO_2(PMe_3)_4]ReO_4$ (0.5 g, 0.6 mmol) in tetrahydrofuran (30 $cm^3$) was added tetraphenylboron sodium (0.22 g, 0.6 mmol). The solution was stirred (30 min), then it was homogeneous, filtered, concentrated (to *ca* 15 $cm^3$ or until crystals appeared) and cooled (−20°C). The pale yellow prisms were collected, washed with hexane (2 × 5 $cm^3$) and dried *in vacuo*. Yield: 0.39 g, 72%; m.p. decomp. *ca* 105°C. [$C_{36}H_{56}BO_2P_4Re$, *M* 842: C, 51.3(51.3); H, 6.6(6.6); P, 14.1(14.7%.] Conductivity; $\lambda_M = 182$ s $cm^{-1}$ $M^{-1}$. IR: 1580w, 1303w, 1287m, 1149w, 1065w, 1030w, 943s, 903m, 849m, 778s, 743m, 731m, 703m, 679w, 625w, 614w, 602m, 489w, 324w, 258m. NMR ($CDCl_3$, 25°C): $^1H$: 7.63–6.75(*m*, 5) $C_6H_5$; 1.67(*s*, 9) $P(CH_3)_3$; $^{31}P$-{$^1H$}: −39.8(*s*).

### *Crystallographic studies*

X-ray intensity data collection was carried out using a Nicolet R3m/Eclipse S140 diffractometer system. Graphite monochromated Cu-$K\alpha$ radiation was used. Calculations were performed with the SHELXTL program system,[10] and atomic scattering factors and the anomalous dispersion corrections were taken from Ref. 11.

*Crystal data for* $[ReO_2(PMe_3)_4]ReO_4$. $C_{12}H_{36}O_6P_4Re_2$, monoclinic, space group *Pc*, $a = 9.941(3)$, $b = 11.092(4)$, $c = 11.263(4)$ Å, $\beta = 90.55(3)°$, $U = 1241.9$ Å$^3$ (at 19°C), $Z = 2$, $\mu$(Cu-$K\alpha$) = 207.6 $cm^{-1}$.

Unit-cell dimensions based on 22 automatically centred reflections for a crystal sealed in a Lindemann tube under dry argon. The crystal was of poor quality, and a $\theta$–$2\theta$ scan technique was used to collect intensity data for 1906 reflections ($2 < 2\theta$

$< 114°$). Of these 683 were rejected on processing, and of the remainder 1102 were unique and 972 were observed [$I > 3\sigma(I)$]. An empirical absorption correction was applied[10] based on psi scan measurements for eight representative reflections.

The structure was solved by Patterson and Fourier methods, although early refinement was complicated by the fact that the rhenium positions nearly conform to space group $P2_1/c$ (consistent with only weak $0k0$, $k$ = odd, reflections being present). Refinement in space group $Pc$ with Re, P and O atoms anisotropic, and the carbon atoms isotropic reduced $R$ to 0.098, with the perrhenate ion showing some disorder. Because of the poor quality and the paucity of the data further refinement was discontinued. By this stage, however, the structure of the $[ReO_2(PMe_3)_4]^+$ cation was determined unambiguously.

*Crystal data for* $[ReO_2(PMe_3)_4]BPh_4$. $C_{36}H_{56}BO_2P_4Re$, monoclinic, space group $I2/a$ (no. 15), $a = 19.219(3)$, $b = 19.619(5)$, $c = 21.376(6)$ Å, $\beta = 97.19(2)$, $U = 7996.6$ Å$^3$ (at 20°C), $Z = 8$, $\mu$(Cu-$K\alpha$) = 74.7 cm$^{-1}$.

Unit-cell dimensions based on 25 automatically centred reflections for a crystal sealed in a Lindemann tube under dry argon. Intensity data collected with the $\omega$ scan technique for 4796 reflections ($2 < 2\theta < 104°$), 4469 unique, and 3908 observed [$I > 3\sigma(I)$]. An empirical absorption correction was applied[10] based on psi scan measurements for 10 representative reflections.

The structure was solved by Patterson and Fourier methods. It became clear that, while the $[BPh_4]^-$ anions could be seen easily, the cations were badly affected by disorder. This, however, was allowed for, and refinement with Re, P, O and the non-hydrogen atoms of the $BPh_4^-$ anisotropic, and the disordered methyl carbon atoms isotropic, gave $R = 0.061$.

*Acknowledgements*—We thank the SERC for the diffractometer system and support and the Somerset and Avon Education Authority for a maintenance grant (A.M.Z.S.).

## REFERENCES

1. P. G. Edwards and G. Wilkinson, *J. Chem. Soc., Dalton Trans.* 1984, in press.
2. N. P. Johnson, C. J. L. Lock and G. Wilkinson, *J. Chem. Soc.* 1964, 1054.
3. R. K. Murmann and E. O. Schlemper, *Inorg. Chem.* 1971, **10**, 2352.
4. C. J. L. Lock and G. Turner, *Acta Crystallogr.* 1978, **34B**, 923.
5. E. E. Burovaya, *Krist. Nauk. SSSR.* 1949, **5**, 197; J. H. Beard, J. Casey and R. K. Murmann, *Inorg. Chem.* 1965, **4**, 797.
6. V. V. Lebendinski and B. N. Ivanov-Emin, *Zh. Obshch. Khim.* 1943, **13**, 253; R. K. Murmann, *J. Inorg. Nucl. Chem.* 1961, **18**, 226.
7. M. C. Chakravorti, *J. Inorg. Nucl. Chem.* 1975, **37**, 1991.
8. J. H. Beard, C. Calhoun, J. Casey and R. K. Murmann, *J. Am. Chem. Soc.* 1968, **90**, 3389.
9. A. D. McLaven, J. N. Fowle, W. Bicknell and C. F. Hiskey, *Inorg. Synth.* 1950, **3**, 188.
10. G. M. Sheldrick, *SHELXTL—An Integrated System for Solving, Refining, and Displaying Crystal Structures from Diffraction Data. Revision* 3. Nicolet Instruments Ltd, Warwick, U.K. (1981).
11. *International Tables for X-ray Crystallography*, Vol. 4. The Kynoch Press, Birmingham, U.K. (1974).

*Polyhedron* Vol. 3, No. 9/10, pp. 1087–1092, 1984
Printed in the U.S.A.

0277–5387/84 $3.00 + .00
© 1984 Pergamon Press Ltd.

# STUDIES OF THE PFEIFFER EFFECT INDUCED IN TRIS(PYRIDINE-2,6-DICARBOXYLATE)Tb(III) BY HISTIDINE DERIVATIVES

**HARRY G. BRITTAIN* and LAUREN RISPOLI**
Department of Chemistry, Seton Hall University, South Orange, NJ 07079, U.S.A.

(*Received* 25 *May* 1984; *accepted* 14 *June* 1984)

**Abstract**—Optical activity has been induced in racemic mixtures of the title compound [$Tb(DPA)_3^{3-}$] upon formation of outer-sphere complexes with several derivatives of histidine, and this induced chirality has been studied by means of circularly polarized luminescence spectroscopy. The association of $Tb(DPA)_3^{3-}$ with the chiral environment substances was found to be dominated by electrostatic effects whenever possible, but hydrophobic and hydrogen-bonding contributions to the bonding were also found to be important in certain instances.

It is well known that optical activity may be developed in racemic mixtures of labile metal complexes upon addition of certain chiral substances,[1,2] a phenomenon which has been termed the Pfeiffer effect. A variety of explanations have been advanced to account for the observed effects,[3,4] but most investigations have been rationalized through the assumption that some sort of outer sphere association exists between the racemic metal complex and the chiral environment substance. For a labile metal complex, the enantiomeric interconversion process:

$$\Delta\text{-M(L)}_3 \rightleftharpoons \Lambda\text{-M(L)}_3$$

is rapid and the relative abundances of the two enantiomers would remain equal (since the equilibrium constant for the process must be unity). Addition of a compound capable of forming an outer-sphere complex with the racemic metal compound:

$$\Delta\text{-M(L)}_3 + \Lambda\text{-M(L)}_3 + \text{B} \rightleftharpoons \Delta\text{M(L)}_3\text{(B)} + \Lambda\text{-M(L)}_3\text{(B)}$$

will not shift the equilibrium position. However, should B be chiral, then the process of outer-sphere complexation will produce diastereomers. The stabilities of these will not generally be the same, and the diastereomer interconversion:

$$\Delta\text{-M(L)}_3\text{(B)} \rightleftharpoons \Lambda\text{-M(L)}_3\text{(B)}$$

would not be characterized by an equilibrium constant equal to unity. An unequal diastereomer population would yield observable chirality. Since the association is outer-sphere in nature, one may assume (to a first approximation) that the observed optical activity would correspond to that of the resolved metal complex. Thus, the Pfeiffer effect may be used to study the chirality of metal complexes too labile to be resolved by conventional means.

Only one Pfeiffer active system has been identified thus far for lanthanide compounds, and this consists of the tris lanthanide complexes of pyridine-2,6-dicarboxylic acid [dipicolinic acid (DPA)]. The $Ln(DPA)_3^{3-}$ complexes are somewhat unique in lanthanide chemistry in that the metal ion experiences trigonal symmetry in the solid state[5] and the $D_3$-symmetry is preserved in aqueous solution.[6] Each DPA ligand is known to bind lanthanide ions with such efficiency[7] that relatively few ligands (outside of the aminopolycarboxylates) are capable of displacing a bound DPA. Thus far, it has been demonstrated that optical activity may be induced in aqueous solutions of $Tb(DPA)_3^{3-}$ and $Eu(DPA)_3^{3-}$ upon outer-sphere coordination with L-ascorbic acid,[8] resolved tris(ethylenediamine)Cr(III),[9] proline-type amino acids,[10] monoamino and diamino carboxylic acids,[11] phenylalkylamines, phenylalkylamino alcohols and phenylalkylamino acids,[12,13] tartrate substrates[14] and simple aldose sugars.[15]

During earlier work involving amino acids, it was found that the Pfeiffer effects induced when using L-histidine as the environment substance disappeared with the first deprotonation of the imidazole ring.[10]

* Author to whom correspondence should be addressed.

Apparently, L-histidine in its zwitterionic form exhibited no affinity for the $Tb(DPA)_3^{3-}$ complex, unlike other amino acids containing aromatic ring systems.[12] As a means of probing these interactions further, the Pfeiffer effects induced in $Tb(DPA)_3^{3-}$ by a series of histidine derivatives have been obtained, and a discussion of these forms the basis of the present work. As in the earlier work[8-15] the study of induced chiralities was followed by means of circularly polarized luminescence (CPL) spectroscopy, as it has been shown that this particular chiroptical technique is most aptly suited to the study of chiral lanthanide compounds.[16,17]

## EXPERIMENTAL

The $Tb(DPA)_3^{3-}$ complexes were normally prepared by mixing stock solutions of Tb(III) and pyridine-2,6-dicarboxylic acid at a 1:3 stoichiometric ratio. The Tb(III) ions were obtained as the perchlorate salt by dissolving a suitable amount of $Tb_4O_7$ in a very slight excess of 5 *M* $HClO_4$, neutralizing to pH 3 with NaOH, and then diluting to the desired volume. The DPA ligand was used as received from Aldrich, and the histidine derivatives used as environment substances were obtained from Aldrich. In normal practice, a weighed amount of substrate was dissolved in 3.0 $cm^3$ of a 0.02 *M* $Tb(DPA)_3^{3-}$ solution. Excessive amounts of $NaClO_4$ were found to inhibit the development of the Pfeiffer effects, and consequently all work was carried out at an effective ionic strength of 0.05.

All CPL and total luminescence (TL) spectra were obtained on a medium-resolution spectrometer constructed in our laboratory. The $Tb(DPA)_3^{3-}$ complexes were excited at 295 nm, taking advantage of the fact that the DPA ligand absorbs strongly at this wavelength and thus will act as an excellent sensitizer of Tb(III) luminescence. The emission spectra were analyzed at 1-nm resolution by a 0.5-m grating monochromator. The TL and CPL spectra were obtained in proportional arbitrary units: the TL intensity ($I$) is given as:

$$I = 1/2(I_L + I_R)$$

and the CPL intensity ($\Delta I$) is given as:

$$\Delta I = I_L - I_R.$$

The unit dependencies of these quantities may be removed by computation of the luminescence dissymmetry ($g_{lum}$) factor:

$$g_{lum} = \Delta I/I.$$

$g_{lum}$ is thus dimensionless, and may be taken as a measure of the degree of optical activity exhibited within a particular emission band. It was found that $I$ was not normally affected by the outer-sphere association of the $Tb(DPA)_3^{3-}$ complex and the environment substances.

The pH of each solution was systematically varied between 3 and 12 in increments of 0.5 pH units, with both the TL and CPL spectra being recorded at each pH value. The solution pH values were obtained on an Orion 701A pH meter, employing a glass microcombination electrode which could be directly inserted into the fluorescence cuvettes. The system was calibrated daily with standard phosphate and phthalate buffers.

## RESULTS AND DISCUSSION

Upon binding three equivalents of DPA, the emission intensity of Tb(III) is greatly enhanced through a sensitization process in which excitation energy is absorbed by the coordinated DPA ligands and transferred nonradiatively to the metal ion.[18-20] The $Tb(DPA)_3^{3-}$ compound must be coordinatively saturated, since it has been shown that no water molecules are present at the inner sphere of the metal ion.[21] Nevertheless, it has been shown that a wide variety of materials will bind to the outer coordination sphere of $Tb(DPA)_3^{3-}$,[8-15] and there appears to be no direct interaction between the Tb(III) ion and the substrate.

When these materials are chiral in nature, optical activity may be observed in all the $Tb(DPA)_3^{3-}$ emission bands corresponding to emission from the $^5D_4$ excited state to the various components of the $^7F_J$ ($J$ = 1–6) ground state. The lineshapes of the TL and CPL spectra invariably are of the same form, and these have never been found to be a function of the nature of the chiral material inducing the chirality. Thus, it may be contended that the CPL lineshapes are characteristic of $Tb(DPA)_3^{3-}$ in a dissymmetric, trigonal environment. Thus, one may concentrate on the trends observed within a single Tb(III) emission band system, as the same trends must be duplicated in all other band systems. The $^5D_4 \rightarrow {}^7F_5$ transition (centered around 545 nm) is known to exhibit the strongest TL and CPL spectra,[22] and consequently all the work which shall be discussed in subsequent sections was obtained within this transition.

In all of the systems to be discussed, the concentration ratio of [substrate]/[$Tb(DPA)_3^{3-}$] was found to determine the magnitude of the observed dissymmetry factors. Such an effect is anticipated on the basis of association equilibria of the form:

$$Tb(DPA)_3^{3-} + \text{substrate} \rightleftharpoons Tb(DPA)_3(\text{substrate}).$$

The 1:1 stoichiometry associated with this equilibrium has been verified on several previous

occasions.[11] The equilibrium constant corresponding to this reaction would then be given by:

$$\frac{[Tb(DPA)_3(substrate)]}{[Tb(DPA)_3][substrate]} = K_1.$$

Complete formation of the $Tb(DPA)_3^{3-}$(substrate) complex would be evident in that a limiting dissymmetry factor would necessarily be reached at some point in the concentration studies. Knowledge of that factor then would permit a calculation of the association constant for the outer-sphere complex via the methods we have outlined.[11] In several earlier works, it was noted that a limiting dissymetry factor of $\pm 0.022$ [specifically for the 544-nm Tb(III) CPL peak] could be reached *independent* of the nature of the chiral environment substance.[10–14] Since this value has been reached so many times for such varied environment substrates, it is our contention that it does indeed represent the dissymmetry factor of the fully formed $Tb(DPA)_3$(substrate) complex. With the assumption that $\pm 0.022$ does represent the limiting dissymmetry factor for Pfeiffer optical activity induced in $Tb(DPA)_3^{3-}$, association constants may be calculated for any substrate. CPL data were obtained using a minimum of three [substrate]/[$Tb(DPA)_3^{3-}$] ratios in order to obtain reproducible results.

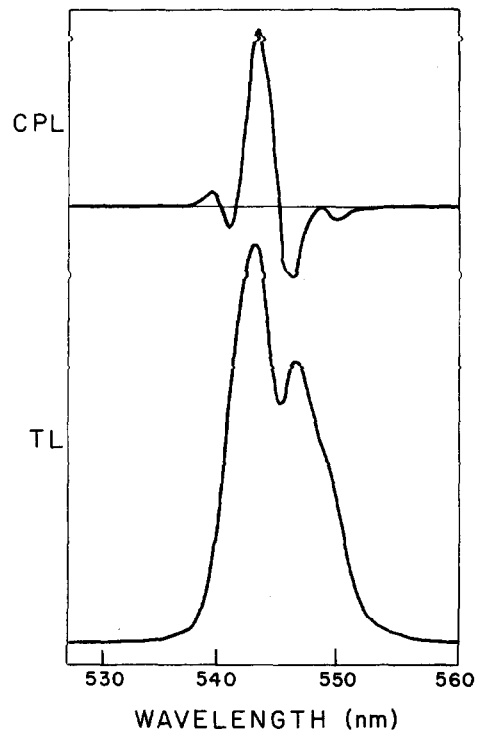



Fig. 1. Total luminescence (lower trace) and circularly polarized luminescence (upper trace) spectra for $Tb(DPA)_3^{3-}$/L-histidine, obtained within the $^5D_4 \rightarrow {}^7F_5$ Tb(III) transition at pH 3.0. The spectral lineshapes obtained for the $Tb(DPA)_3^{3-}$ complexes with the methyl ester of L-histidine, *N*-acetyl-L-histidine or L-histidinol are identical to the ones depicted here.

*Histidine*

When using L-histidine as the chiral environment substance, CPL could only be detected in the Tb(III) emission bands below pH 7.5.[10] An example of typical TL and CPL spectra as obtained within the 4–5 Tb(III) emission band system is shown in Fig. 1, where one should note that the major CPL component is positive in sign. It has been established that positively signed CPL within the 4–5 emission of a $Tb(DPA)_3$(substrate) complex implies that the Λ-Tb(III) enantiomer is present in the largest amount.[11,13]

The disappearance of optical activity above pH 7.5 may be explained upon consideration of the protonation equilibria associated with histidine. The various equilibrium constants have been determined,[23] and these have been correlated with the corresponding deprotonations in Fig. 2. It is clear that the loss of observable optical activity accompanies formation of the zwitterion, III. This observation implies that the determining interaction between histidine and $Tb(DPA)_3^{3-}$ is the positive charge associated with the protonated imidazole ring. While it has been shown that a variety of hydrogen-bonding and hydrophobic effects also contribute to the outer-sphere association,[11–14] it is clear that these forces are not sufficiently strong as to offset the loss of the electrostatic attractions which would exist as long as an overall positive charge resided on the histidine substrate.

Equilibrium constant values calculated at various pH values are to be found in Table 1.

*L-histidine, methyl ester*

With the methyl ester of L-histidine, the carboxyl position is effectively blocked and possible effects

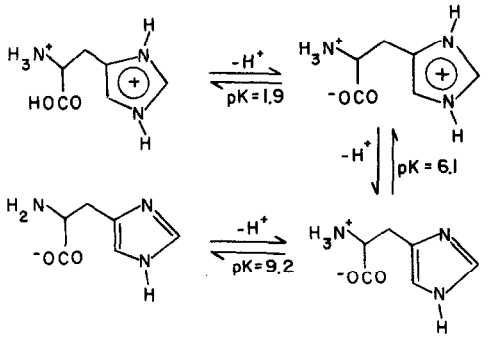



Fig. 2. Deprotonation equilibria assocated with L-histidine. The dissociation constants were taken from Ref. 23.

Table 1. Formation constants for the $Tb(DPA)_3^{3-}$/substrate adduct complexes

| pH | L-Histidine | L-Histidine, Methyl Ester | N-Acetyl-L-Histidine | L-Histidinol |
|---|---|---|---|---|
| 3.0 | 12.1 | 33.7 | 13.3 | 24.4 |
| 3.5 | 10.1 | 30.2 | 12.3 | 25.2 |
| 4.0 | 7.7 | 20.4 | 7.5 | 25.2 |
| 4.5 | 6.8 | 16.0 | 6.8 | 24.1 |
| 5.0 | 5.7 | 13.9 | 6.0 | 24.6 |
| 5.5 | 5.6 | 9.7 | 5.8 | 24.0 |
| 6.0 | 5.5 | 7.6 | 5.7 | 13.9 |
| 6.5 | 3.7 | 4.1 | 5.5 | 8.8 |
| 7.0 | 2.2 | 3.6 | 5.4 | 6.7 |
| 7.5 | 0.3 | 3.6 | 3.7 | 5.0 |
| 8.0 | * | 3.6 | 3.2 | * |
| 8.5 | * | 3.4 | 2.5 | 6.5 |
| 9.0 | * | 3.3 | 2.3 | 11.5 |
| 9.5 | * | 3.4 | 2.0 | 11.3 |
| 10.0 | * | 3.7 | 1.8 | 11.3 |
| 10.5 | * | 3.8 | 1.5 | 10.6 |
| 11.0 | * | 4.1 | 1.3 | 10.7 |
| 11.5 | * | 4.6 | 1.1 | 10.7 |

* The CPL intensities were too weak at this pH value to permit a computation of the association constant, which must be smaller than 0.1.

resulting from a negative charge at this group are eliminated. The protonation constants associated with this compound are known,[24] and are presented in Fig. 3 along with the appropriate reactions. It may be noted that esterification of the carboxyl group results in a general lowering of all p$K$ values.

The interaction between the methyl ester of L-histidine and $Tb(DPA)_3^{3-}$ was found to be strongest at pH 3, and was observed to decrease with increasing pH. As with L-histidine, the major 4–5 CPL peak was observed to be positive in sign, and thus it is inferred that the Λ-isomer of $Tb(DPA)_3^{3-}$ is the preferred enantiomer. However, the CPL was not found to disappear at neutral pH (as was the case with L-histidine), since measurable optical activity could be detected up to pH 11.5. Beyond pH 7, the degree of optical activity was found to be essentially constant, but was considerably reduced in magnitude relative to that observed at the lower pH values. These trends are reflected in the association constant values which are found in Table 1.

Comparison of the formation constant values with the protonation equilibria reveals a great deal about the nature of the outer-sphere interactions. Each substrate deprotonation led to a reduction in the association constant. The largest decrease was noted for the removal of a proton from the imidazole ring, as is the case with histidine. However, with the methyl ester the substrate retains its positive charge, and continues to associate with the $Tb(DPA)_3^{3-}$ complex. The second deprotonation is substantially complete by neutral pH, and here the degree of association is found to be quite small. The chiral substrate still is capable of binding to the Tb(III) complex, even though it does not possess any charge. This association must require the existence of substantial hydrogen-bonding or hydrophobic interactions.

### N-*acetyl*-L-*histidine*

Upon substitution at the ammonium group of the α-amino carboxylate functionality, this group cannot be considered as being protonated over the pH 3–12 range. The equilibrium constants for this substrate are also available in the literature,[25] and have been illustrated in the usual manner in Fig. 4. The effect of the acetyl substitution is to raise all p$K$ values (relative to those of histidine) by about 1 log unit.

As with L-histidine or its methyl ester, the major 4–5 Tb(III) CPL peak was found to be positive in sign.

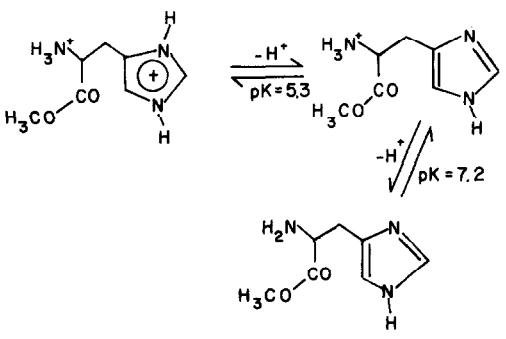



Fig. 3. Deprotonation equilibria associated with the methyl ester of L-histidine. The dissociation constants were taken from Ref. 24.

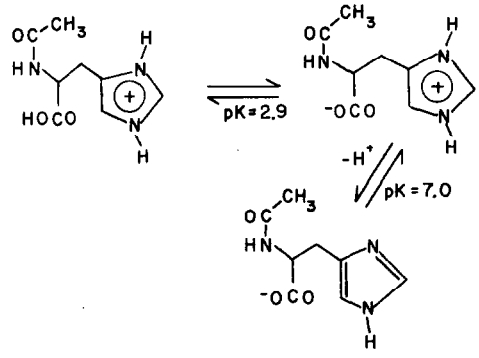



Fig. 4. Deprotonation equilibria associated with *N*-acetyl-L-histidine. The dissociation constants were taken from Ref. 25.

This observation again implies the predominance of the Λ-isomer. Unlike in the case of L-histidine, the CPL is not completely lost upon deprotonation of the imidazole ring, and optical activity could be measured over the entire range of pH values. Systematic variation of the substrate concentration permitted the calculation of association constant values, and these are also found in Table 1.

The carboxylate deprotonation takes place at very low pH values, and this process accompanies the rapid initial decrease in association. The imidazole ring still contains a net positive charge, but as this ring is deprotonated (around neutral pH) the degree of association is further decreased. With L-histidine as the environment substance, this process led to the complete loss of CPL. An association mechanism must still exist for *N*-acetyl-L-histidine, however, since it is still possible to observe optical activity up to pH 11.5. Since the only difference between L-histidine and its acetyl derivative is the presence of a carbonyl group on the amino group, it seems probable that the acetyl group might be hydrogen bonded to the DPA ring systems. Such hydrogen-bonding mechanisms are known in transition metal Pfeiffer effects.[1,2]

### L-*histidinol*

Replacement of the carboxyl group of L-histidine by a $-CH_2OH$ group produces a chiral substrate whose protonation equilibria are very similar to those of the histidine methyl ester. However, the dissociation constants are quite different,[26] and the corresponding equilibrium scheme is presented in Fig. 5.

While the protonation equilibria might be similar to previous substrates, the pH dependence of the observed CPL was found to be quite different. An example of the effect of pH on the observed CPL bands is shown in Fig. 6. While the sign of the 544-nm

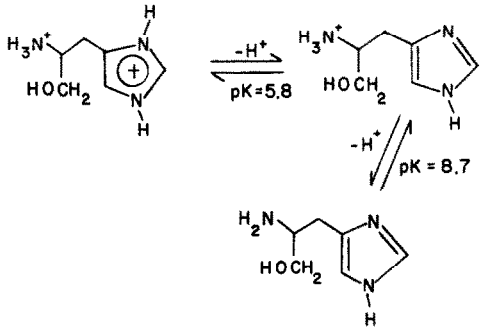



Fig. 5. Deprotonation equilibria associated with L-histidinol. The dissociation constants were taken from Ref. 26.

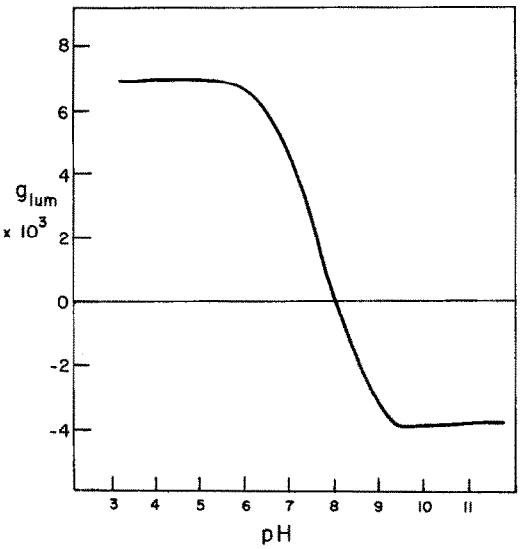



Fig. 6. Luminescence dissymmetry ($g_{lum}$) factor calculated for the 544-nm component of the $^5D_4 \rightarrow {}^7F_5$ Tb(III) transition. The $Tb(DPA)_3^{3-}$ concentration was 0.02 *M*, and the L-histidinol concentration was 0.028 *M*.

component of the 4–5 Tb(III) CPL was positive at low pH values, an inversion took place near pH 8. The new Tb(III) lineshapes were found to be the exact mirror images of the low-pH lineshapes, and this relationship held for the 4–6, 4–4 and 4–3 band systems. It is reasonable to conclude from these observations that a change in the association mechanism must take place around pH 8, and that the new interaction mode leads to the stabilization of the opposite $Tb(DPA)_3^{3-}$ enantiomer. Similar CPL sign inversions have been noted earlier[12] when employing phenylglycinol or phenylalaninol as chiral environment substances.

Association constants were calculated at each pH value following the usual procedures, and these may also be found in Table 1. The deprotonation of the imidazole ring (and consequent loss of positive charge at this group) leads to the largest decrease in the magnitude of the outer-sphere association. The deprotonation of the ammonium group would take place next, and during this process the association mode changes and one observes a CPL sign inversion. The neutral species produced in this fashion would appear to be quite similar to the analagous species produced at the end of the histidine methyl ester sequence, but the differences in the observed CPL lineshapes clearly demonstrate that the nature of the hydrogen-bonding or hydrophobic effects must be very different. The bonding mode existing with the histidinol must represent a slightly more favorable situation, as the association constants are nearly double with the amino alcohol relative to those of the ester.

## CONCLUSIONS

Further insight into the association mechanism of the Pfeiffer effect [at least as applied to the $Tb(DPA)_3^{3-}$ compound] has been obtained through the use of histidine derivatives as environment compounds. The forces leading to formation of the outer-sphere complexes were found to be dominated (when possible) by electrostatic effects. The presence of a net positive charge on the environment substances invariably led to the observation of the strongest optical activity. This effect is as would be expected, since the Tb(III) complex is anionic in nature. Hydrogen-bonding and hydrophobic forces were also found to play a role in the association process, but these were clearly weaker in magnitude than the electrostatic attraction. In most cases, the use of the *R*-isomer of the histidine derivatives[27] led to the predominance of the Λ-isomer of $Tb(DPA)_3^{3-}$, an observation which is consistent with the earlier amino acid work.[11] The sole exception to this general trend was found with histidinol, where at high pH values the Δ-isomer of $Tb(DPA)_3^{3-}$ was present in the largest amount.

The present work demonstrates that the Pfeiffer effect in lanthanide compounds can be more complicated than analagous effects in transition metal compounds. As in the earlier work,[8–15] the results can be readily explained through the assumption of an associative mechanism for the Pfeiffer effects.

*Acknowledgement*—This work was supported by the Camille and Henry Drefus Foundation, through a Teacher–Scholar award to HGB.

## REFERENCES

1. S. Kirschner, N. Ahmad, C. Munir and R. J. Pollock, *Pure Appl. Chem.* 1979, **51**, 913.
2. S. Kirschener and I. Bakkar, *Coord. Chem. Rev.* 1982, **43**, 325.
3. P. E. Schipper, *Inorg. Chim. Acta* 1975, **12**, 199.
4. P. E. Schipper, *J. Am. Chem. Soc.* 1978, **100**, 1079.
5. J. Albertsson, *Acta Chem. Scand.* 1972, **26**, 985, 1023.
6. H. Donato and R. B. Martin, *J. Am. Chem. Soc.* 1972, **94**, 4129.
7. I. Grenthe, *J. Am. Chem. Soc.* 1961, **83**, 360.
8. J. S. Madaras and H. G. Brittain, *Inorg. Chim. Acta* 1980, **42**, 109.
9. J. S. Madaras and H. G. Brittain, *Inorg. Chem.* 1980, **19**, 3841.
10. H. G. Brittain, *Inorg. Chem.* 1981, **20**, 3007.
11. F. Yan, R. A. Copeland and H. G. Brittain, *Inorg. Chem.* 1982, **21**, 1180.
12. H. G. Brittain, *Inorg. Chem.* 1982, **21**, 2955.
13. F. Yan, R. A. Copeland and H. G. Brittain, *Inorg. Chim. Acta* 1983, **72**, 211.
14. F. Yan and H. G. Brittain, *Polyhedron* 1982, **1**, 195.
15. H. G. Brittain, *J. Chem. Soc., Dalton Trans.* in press.
16. H. G. Brittain, *Coord. Chem. Rev.* 1983, **48**, 243.
17. F. S. Richardson and J. P. Riehl, *Chem. Rev.* 1977, **77**, 773.
18. T. D. Barela and A. D. Sherry, *Anal. Biochem.* 1976, **71**, 351.
19. H. G. Brittain, *Inorg. Chem.* 1978, **17**, 2762.
20. T. L. Miller and S. I. Senkfor, *Anal. Chem.* 1982, **54**, 2022.
21. W. D. Horrocks and D. R. Sudnick, *J. Am. Chem. Soc.* 1979, **101**, 334.
22. F. S. Richardson, *Inorg. Chem.* 1980, **19**, 2806.
23. A. E. Martell and R. M. Smith, *Critical Stability Constants*, Vol. 1, p. 61. Plenum Press, New York.
24. R. M. Smith and A. E. Martell, *Critical Stability Constants*, Vol. 2, p. 159. Plenum Press, New York.
25. A. E. Martell and R. M. Smith, *Critical Stability Constants*, Vol. 1, p. 80. Plenum Press, New York.
26. R. M. Smith and A. E. Martell, *Critical Stability Constants*, Vol. 2, p. 158. Plenum Press, New York.
27. W. Klyne and J. Buckingham, *Atlas of Stereochemistry*, 2nd edition, p. 24. Oxford University Press, New York (1974).

*Polyhedron* Vol. 3, No. 9/10, pp. 1093–1097, 1984
Printed in the U.S.A.

0277–5387/84 $3.00 + .00
© 1984 Pergamon Press Ltd.

# THE SYNTHESIS AND X-RAY CRYSTAL STRUCTURE OF THE HEXANUCLEAR METAL CLUSTER COMPLEX $[Ir_3Pt_3(\mu\text{-}CO)_3(CO)_3(\eta\text{-}C_5Me_5)_3]$

MARK J. FREEMAN, ANTHONY D. MILES, MARTIN MURRAY, A. GUY ORPEN and F. GORDON A. STONE*
School of Chemistry, The University of Bristol, Bristol BS8 1TS, U.K.

(*Received* 30 *May* 1984; *accepted* 14 *June* 1984)

**Abstract**—The compounds $[Ir(CO)_2(\eta\text{-}C_5Me_5)]$ and $[Pt(C_2H_4)_3]$ in diethyl ether at 0°C react to give the cluster complex $[Ir_3Pt_3(\mu\text{-}CO)_3(CO)_3(\eta\text{-}C_5Me_5)_3]$ in quantitative yield. The structure of the hexanuclear metal species was established by X-ray diffraction. The main feature is a near-planar array of metal atoms with a central triangle of platinum atoms [Pt—Pt (mean), 2.703(3) Å] each edge-bridged by an iridium atom [Ir—Pt (mean) 2.667(3) Å]. The iridium atoms are each ligated by an $\eta^5$-$C_5Me_5$ group and by two CO ligands. Three of the latter are essentially terminally bound to Ir and lie approximately orthogonal to the $Ir_3Pt_3$ plane, and three bridge between Pt and Ir and lie close to the hexametal plane. The $^{13}C$-$\{^1H\}$ NMR data for the cluster reveal that the carbonyl groups and $\eta^5$-$C_5Me_5$ ligands undergo dynamic behaviour in solution and possible mechanisms for ligand site exchange are discussed.

We have reported previously[1] that the unsaturated dirhodium compound $[Rh_2(\mu\text{-}CO)_2(\eta\text{-}C_5Me_5)_2]$, an inorganic analogue of ethylene,[2] reacts with $[Pt(C_2H_4)_3]$ to give the pentanuclear cluster complex $[PtRh_4(\mu\text{-}CO)_4(\eta\text{-}C_5Me_5)_4]$. The iridium analogue of the latter compound cannot at present be prepared by a similar synthesis since the unsaturated diiridium precursor has not as yet been described. We have, therefore, investigated the reaction between $[Ir(CO)_2(\eta\text{-}C_5Me_5)]$ and $[Pt(C_2H_4)_3]$ in the expectation that an iridium–platinum cluster species would be formed. No heteronuclear metal complexes of this type appear to have been previously well characterised,[3] apart from (R = H or Ph).[4] Recently we have employed $[Rh(CO)_2(\eta\text{-}C_5Me_5)]$ as a reagent for obtaining $(CO)_2(\eta\text{-}C_5Me_5)]$ as a reagent for obtaining heteronuclear clusters containing rhodium,[5] and it seemed probable that $[Ir(CO)_2(\eta\text{-}C_5Me_5)]$ would behave in a similar manner.

## RESULTS AND DISCUSSION

Addition of a mol equivalent of $[Ir(CO)_2(\eta\text{-}C_5Me_5)]$ in diethyl ether to $[Pt(C_2H_4)_3]$ in the same solvent at 0°C gave immediately an intense red-brown solution. Chromatography on an alumina column yielded a brown crystalline product. Since analytical and spectroscopic data for the compound did not establish its nature an X-ray diffraction study was carried out which showed that it was a hexanuclear metal species. There are two crystallographically independent molecules present in the solid-state structure and both are shown in Fig. 1. These two molecules are very similar in terms of their stereochemistry. The central feature of the molecule is a near-planar array of the six metal atoms, a central triangle of platinum atoms, each edge-bridged by an iridium atom. The iridium atoms each carry an $\eta$-$C_5Me_5$ group and are linked to two CO ligands. The latter may be broadly divided into two sets, three lie roughly orthogonal to the $Ir_3Pt_3$ plane and are essentially terminally bound to the iridium atoms, and three close to the $Ir_3Pt_3$ plane, bridging alternate outer Ir—Pt edges of the $Ir_3Pt_3$ core. The $Ir_3Pt_3$ $(\mu\text{-}CO)_3$ unit has approximate $C_3$-symmetry. The $\eta$-$C_5Me_5$ ligands are well out of the $Ir_3Pt_3$ plane, one above and two below this plane as viewed in Fig. 1.

The internuclear distances and angles are given in Table 1, from which it will be seen that the $Pt_3$ triangle is essentially equilateral, with the mean Pt—Pt distance [2.703(3) Å] within the range observed in other species having such triangles, viz.

* Author to whom correspondence should be addressed.

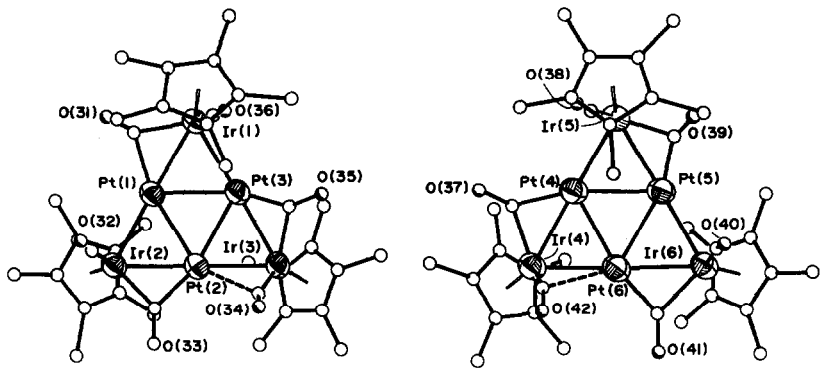



Fig. 1. The molecular structures of the two crystallographically independent molecules of $[Ir_3Pt_3(\mu\text{-}CO)_3(CO)_3(\eta\text{-}C_5Me_5)_3]$ showing the atom numbering scheme.

$[Pt_3(CNBu^t)_6]$ [2.632(2) Å],[6] $[Fe_3Pt_3(CO)_{15}]^{n-}$ [$n = 1$, 2.656(1) Å; $n = 2$, 2.750(1) Å],[7] $[Pt_3(SO_2)_3(PPh_3)_3]$ [2.703(1) Å],[8] and $[Pt_3(CO)_3\{P(C_6H_{11})_3\}_4]$ [2.708(1) Å].[9]

The Ir—Pt separations can be divided into two sets, those bridged by CO groups [av. 2.693(3)Å] and those unbridged [av. 2.640(3) Å], both distances being similar to that observed [2.687(2) Å] in $[IrPt(H)(Ph)(\mu\text{-}H)_2(PEt_3)_4][BPh_4]$.[4] The two sets of carbonyl groups show distinctly different metal–carbon bond lengths. Those bonded in a bridging mode showing the expected longer Ir—CO distance [mean Ir—C 2.06(4) Å] compared with those bonded terminally [mean Ir—C 1.80(4) Å]. There is evidence, however, of platinum–carbon interactions in one member of the latter set of carbonyl groups. This is reflected in the non-linearity of Ir(3)—C(34)—O(34) [155.3(56)°] and Ir(4)—C(42)—O(42) [161.8(46)°]. In the structurally related raft complexes $[Fe_3Pt_3(CO)_{15}]^{n-}$ ($n = 1$ or 2) the three Pt-bonded CO ligands in the 'plane' of the six metal atoms are essentially terminally bound to the platinums [$n = 1$, Pt—C—O av. 173.3°; $n = 2$, Pt—C—O av. 175.3°],[7] and also in contrast the Fe-bonded carbonyl ligands are entirely terminal and linear ($n = 1$, Fe—C—O av. 175.4°, $n = 2$, Fe—C—O av. 173.8°).

As in the $Fe_3Pt_3$ species, the hexametal $Ir_3Pt_3$ raft is not exactly planar. Two iridium atoms lie below and one above the $Pt_3$ plane. The deviations from the 'raft' plane range from 0.1 to 0.6 Å, similar to that in the $Fe_3Pt_3$ compounds. The dihedral angles between the $Ir_2Pt$ and $Pt_3$ planes are:

| | |
|---|---|
| Ir(1)—Pt(1)—Pt(3) | 13.4°, |
| Ir(3)—Pt(2)—Pt(3) | −8.6° |
| Ir(5)—Pt(5)—Pt(4) | 15.8°, |
| Ir(2)—Pt(1)—Pt(2) | −9.3°, |
| Ir(4)—Pt(4)—Pt(6) | −9.4°, |
| Ir(6)—Pt(5)—Pt(6) | −3.0°. |

These values compare with the all-positive angles of 8.6 and 16.1° found between the fused $Os_3$ triangles in $[Os_6(\mu_3\text{-}O)(\mu_3\text{-}CO)(CO)_{18}]$,[10] and the dihedral angles of 12.2, 19.1 and 23.5° between the three $Os_3$ planes and the $Hg_3$ plane in $[Hg_3Os_9(CO)_{33}]$.[11] The other osmium raft complex $[Os_6(CO)_{17}\{P(OMe)_3\}_4]$ has an approximately planar metal core, showing a maximum deviation of only 0.1 Å.

The compound $[Ir_3Pt_3(\mu\text{-}CO)_3(CO)_3(\eta\text{-}C_5Me_5)_3]$ is stable in air in the solid state, although solutions in organic solvents decompose slowly giving $[Ir(CO)_2(\eta\text{-}C_5Me_5)]$ and a black residue presumed to be platinum. In the IR spectrum CO bands occur at 1959 and 1768 $cm^{-1}$, corresponding to terminal and bridging modes, as established in the X-ray diffraction study. Examination of the $^{13}C\text{-}\{^1H\}$ NMR spectrum of the cluster revealed that it undergoes dynamic behaviour in solution. Although in the structure found in the solid state one $\eta\text{-}C_5Me_5$ ligand lies above the $Ir_3Pt_3$ plane and two below, and also there are terminal and bridging CO groups, at ambient temperatures in the 50.1-MHz spectrum there are only three resonances at 178.1 (CO), 99.1 ($\eta\text{-}C_5Me_5$) and 9.6 ppm ($\eta\text{-}C_5\mathit{Me}_5$). The observation of a single resonance for the carbonyl carbons indicates that these are undergoing a rapid exchange between the different bonding sites shown by the crystal structure, and the observation of single resonances for the $\eta\text{-}C_5Me_5$ groups indicates that they are undergoing exchange between sites on either side of the metal atoms.

The resonance at 178.1 ppm also shows satellite peaks due to coupling to $^{195}Pt$ nuclei. There are two sets of satellite peaks, a sharper pair [$J$(PtC) = 35 Hz] and a very broad pair [$J$(PtC) ~ 300 Hz]. That some of the broadening of the latter pair is due to platinum relaxation caused by chemical shift anisotropy is proved by the fact that when the spectrum was measured at 22.5 MHz these lines became somewhat sharper. However, the main cause

Table 1. Bond distances (Å) and angles (°) for the complex $[Ir_3Pt_3(\mu\text{-}CO)_3(CO)_3(\eta\text{-}C_5Me_5)_3]$

| | | | |
|---|---|---|---|
| Ir(1)-Pt(1) | 2.686(3) | Ir(1)-Pt(3) | 2.643(3) |
| Ir(1)-C(31) | 2.073(47) | Ir(1)-C(36) | 1.773(43) |
| Pt(1)-Pt(3) | 2.711(3) | Pt(1)-Ir(2) | 2.644(3) |
| Pt(1)-Pt(2) | 2.710(3) | Pt(1)-C(31) | 2.056(48) |
| Pt(3)-Ir(3) | 2.702(3) | Pt(3)-Pt(2) | 2.700(3) |
| Pt(3)-C(35) | 1.714(41) | Pt(5)-Pt(6) | 2.708(3) |
| Pt(5)-Ir(5) | 2.678(3) | Pt(5)-Ir(6) | 2.646(3) |
| Pt(5)-Pt(4) | 2.691(3) | Pt(5)-C(39) | 1.752(35) |
| Ir(4)-Pt(6) | 2.645(3) | Ir(4)-Pt(4) | 2.701(3) |
| Ir(4)-C(42) | 1.853(40) | Ir(4)-C(37) | 2.074(47) |
| Pt(6)-Ir(6) | 2.708(3) | Pt(6)-Pt(4) | 2.702(3) |
| Pt(6)-C(41) | 1.882(47) | Pt(6)-C(42) | 2.610(53) |
| Ir(2)-Pt(2) | 2.683(3) | Ir(2)-C(32) | 1.823(43) |
| Ir(2)-C(33) | 2.053(39) | Ir(5)-Pt(4) | 2.641(3) |
| Ir(5)-C(39) | 2.012(36) | Ir(5)-C(38) | 1.780(39) |
| Ir(3)-Pt(2) | 2.625(3) | Ir(3)-C(34) | 1.764(45) |
| Ir(3)-C(35) | 2.058(35) | Ir(6)-C(40) | 1.805(47) |
| Ir(6)-C(41) | 2.124(35) | Pt(2)-C(33) | 1.901(45) |
| Pt(2)-C(34) | 2.326(61) | Pt(4)-C(38) | 2.739(53) |
| Pt(4)-C(37) | 1.924(60) | C(32)-O(32) | 1.156(58) |
| C(31)-O(31) | 1.124(57) | C(33)-O(33) | 1.180(66) |
| C(34)-O(34) | 1.162(65) | C(35)-O(35) | 1.210(55) |
| C(36)-O(36) | 1.113(65) | C(39)-O(39) | 1.169(59) |
| C(40)-O(40) | 1.161(62) | C(38)-O(38) | 1.148(56) |
| C(41)-O(41) | 1.176(56) | C(42)-O(42) | 1.189(60) |
| C(37)-O(37) | 1.172(61) | | |
| Pt(1)-Ir(1)-Pt(3) | 61.1(1) | Pt(1)-Ir(1)-C(31) | 49.1(13) |
| Pt(3)-Ir(1)-C(31) | 106.5(13) | Pt(1)-Ir(1)-C(36) | 98.5(21) |
| Pt(3)-Ir(1)-C(36) | 77.7(22) | C(31)-Ir(1)-C(36) | 91.1(27) |
| Ir(1)-Pt(1)-Pt(3) | 58.6(1) | Ir(1)-Pt(1)-Ir(2) | 175.8(1) |
| Pt(3)-Pt(1)-Ir(2) | 119.3(1) | Ir(1)-Pt(1)-Pt(2) | 117.1(1) |
| Pt(3)-Pt(1)-Pt(2) | 59.8(1) | Ir(2)-Pt(1)-Pt(2) | 60.1(1) |
| Ir(1)-Pt(1)-C(31) | 49.7(13) | Pt(3)-Pt(1)-C(31) | 104.7(13) |
| Ir(2)-Pt(1)-C(31) | 133.6(13) | Pt(2)-Pt(1)-C(31) | 163.5(15) |
| Ir(1)-Pt(3)-Pt(1) | 60.2(1) | Ir(1)-Pt(3)-Ir(3) | 175.0(1) |
| Pt(1)-Pt(3)-Ir(3) | 117.7(1) | Ir(1)-Pt(3)-Pt(2) | 119.0(1) |
| Pt(1)-Pt(3)-Pt(2) | 60.1(1) | Ir(3)-Pt(3)-Pt(2) | 58.2(1) |
| Ir(1)-Pt(3)-C(35) | 130.7(12) | Pt(1)-Pt(3)-C(35) | 159.0(14) |
| Ir(3)-Pt(3)-C(35) | 49.6(12) | Pt(2)-Pt(3)-C(35) | 103.0(12) |
| Pt(6)-Pt(5)-Ir(5) | 117.2(1) | Pt(6)-Pt(5)-Ir(6) | 60.8(1) |
| Ir(5)-Pt(5)-Ir(6) | 169.1(1) | Pt(6)-Pt(5)-Pt(4) | 60.1(1) |
| Ir(5)-Pt(5)-Pt(4) | 58.9(1) | Ir(6)-Pt(5)-Pt(4) | 120.7(1) |
| Pt(6)-Pt(5)-C(39) | 162.9(13) | Ir(5)-Pt(5)-C(39) | 48.7(12) |
| Ir(6)-Pt(5)-C(39) | 135.2(12) | Pt(4)-Pt(5)-C(39) | 103.5(12) |
| Pt(6)-Ir(4)-Pt(4) | 60.7(1) | Pt(6)-Ir(4)-C(42) | 68.3(16) |
| Pt(4)-Ir(4)-C(42) | 89.4(16) | Pt(6)-Ir(4)-C(37) | 103.6(18) |
| Pt(4)-Ir(4)-C(37) | 45.2(17) | C(42)-Ir(4)-C(37) | 92.6(27) |
| Pt(5)-Pt(6)-Ir(4) | 119.7(1) | Pt(5)-Pt(6)-Ir(6) | 58.5(1) |
| Ir(4)-Pt(6)-Ir(6) | 169.1(1) | Pt(5)-Pt(6)-Pt(4) | 59.7(1) |
| Ir(4)-Pt(6)-Pt(4) | 60.7(1) | Ir(6)-Pt(6)-Pt(4) | 118.1(1) |
| Pt(5)-Pt(6)-C(41) | 107.3(11) | Ir(4)-Pt(6)-C(41) | 132.9(11) |
| Ir(6)-Pt(6)-C(41) | 51.4(11) | Pt(4)-Pt(6)-C(41) | 161.8(13) |
| Pt(5)-Pt(6)-C(42) | 125.6(12) | Ir(4)-Pt(6)-C(42) | 41.3(9) |
| Ir(6)-Pt(6)-C(42) | 149.4(9) | Pt(4)-Pt(6)-C(42) | 75.7(11) |
| C(41)-Pt(6)-C(42) | 106.9(16) | Pt(1)-Ir(2)-Pt(2) | 61.1(1) |
| Pt(1)-Ir(2)-C(32) | 76.2(15) | Pt(2)-Ir(2)-C(32) | 99.5(16) |
| Pt(1)-Ir(2)-C(33) | 99.7(12) | Pt(2)-Ir(2)-C(33) | 44.9(12) |
| C(32)-Ir(2)-C(33) | 87.8(20) | Pt(5)-Ir(5)-Pt(4) | 60.8(1) |
| Pt(5)-Ir(5)-C(39) | 40.9(10) | Pt(4)-Ir(5)-C(39) | 98.0(10) |
| Pt(5)-Ir(5)-C(38) | 99.5(19) | Pt(4)-Ir(5)-C(38) | 73.7(18) |
| C(39)-Ir(5)-C(38) | 95.7(22) | Pt(3)-Ir(3)-Pt(2) | 60.9(1) |
| Pt(3)-Ir(3)-C(34) | 95.1(20) | Pt(2)-Ir(3)-C(34) | 60.3(20) |
| Pt(3)-Ir(3)-C(35) | 39.4(11) | Pt(2)-Ir(3)-C(35) | 96.3(12) |
| C(34)-Ir(3)-C(35) | 100.0(23) | Pt(5)-Ir(6)-Pt(6) | 60.8(1) |
| Pt(5)-Ir(6)-C(40) | 74.5(15) | Pt(6)-Ir(6)-C(40) | 95.2(16) |
| Pt(5)-Ir(6)-C(41) | 102.2(13) | Pt(6)-Ir(6)-C(41) | 43.8(13) |
| C(40)-Ir(6)-C(41) | 93.9(21) | Pt(1)-Pt(2)-Pt(3) | 60.1(1) |
| Pt(1)-Pt(2)-Ir(2) | 58.7(1) | Pt(3)-Pt(2)-Ir(2) | 118.2(1) |
| Pt(1)-Pt(2)-Ir(3) | 120.5(1) | Pt(3)-Pt(2)-Ir(3) | 60.9(1) |
| Ir(2)-Pt(2)-Ir(3) | 164.6(1) | Pt(1)-Pt(2)-C(33) | 101.6(12) |
| Pt(3)-Pt(2)-C(33) | 155.9(13) | Ir(2)-Pt(2)-C(33) | 49.7(12) |
| Ir(3)-Pt(2)-C(33) | 137.1(12) | Pt(1)-Pt(2)-C(34) | 134.7(15) |
| Pt(3)-Pt(2)-C(34) | 83.4(14) | Ir(2)-Pt(2)-C(34) | 151.8(12) |
| Ir(3)-Pt(2)-C(34) | 41.2(12) | C(33)-Pt(2)-C(34) | 103.2(18) |
| Pt(5)-Pt(4)-Ir(4) | 118.3(1) | Pt(5)-Pt(4)-Pt(6) | 60.3(1) |
| Ir(4)-Pt(4)-Pt(6) | 58.6(1) | Pt(5)-Pt(4)-Ir(5) | 60.3(1) |
| Ir(4)-Pt(4)-Ir(5) | 173.9(1) | Pt(6)-Pt(4)-Ir(5) | 118.7(1) |
| Pt(5)-Pt(4)-C(38) | 78.9(11) | Ir(4)-Pt(4)-C(38) | 147.4(9) |
| Pt(6)-Pt(4)-C(38) | 134.6(12) | Ir(5)-Pt(4)-C(38) | 38.6(9) |
| Pt(5)-Pt(4)-C(37) | 165.0(18) | Ir(4)-Pt(4)-C(37) | 49.9(14) |
| Pt(6)-Pt(4)-C(37) | 106.0(16) | Ir(5)-Pt(4)-C(37) | 130.3(14) |
| C(38)-Pt(4)-C(37) | 116.1(21) | Ir(2)-C(32)-O(32) | 175.4(48) |
| Ir(1)-C(31)-Pt(1) | 81.2(16) | Ir(1)-C(31)-O(31) | 144.7(41) |
| Pt(1)-C(31)-O(31) | 134.0(40) | Ir(2)-C(33)-Pt(2) | 85.4(17) |
| Ir(2)-C(33)-O(33) | 139.1(39) | Pt(2)-C(33)-O(33) | 135.5(37) |
| Ir(3)-C(34)-Pt(2) | 78.5(20) | Ir(3)-C(34)-O(34) | 155.3(56) |
| Pt(2)-C(34)-O(34) | 119.9(45) | Pt(3)-C(35)-Ir(3) | 91.0(15) |
| Pt(3)-C(35)-O(35) | 141.2(36) | Ir(3)-C(35)-O(35) | 127.0(35) |
| Ir(1)-C(36)-O(36) | 178.0(72) | Pt(5)-C(39)-Ir(5) | 90.4(15) |
| Pt(5)-C(39)-O(39) | 136.0(40) | Ir(5)-C(39)-O(39) | 125.3(39) |
| Ir(6)-C(40)-O(40) | 170.6(44) | Ir(5)-C(38)-Pt(4) | 67.7(15) |
| Ir(5)-C(38)-O(38) | 175.4(46) | Pt(4)-C(38)-O(38) | 116.7(40) |
| Pt(6)-C(41)-Ir(6) | 84.8(15) | Pt(6)-C(41)-O(41) | 141.2(33) |
| Ir(6)-C(41)-O(41) | 134.0(36) | Ir(4)-C(42)-Pt(6) | 70.4(16) |
| Ir(4)-C(42)-O(42) | 161.8(46) | Pt(6)-C(42)-O(42) | 121.6(38) |
| Ir(4)-C(37)-Pt(4) | 84.9(18) | Ir(4)-C(37)-O(37) | 135.0(49) |
| Pt(4)-C(37)-O(37) | 138.5(49) | | |

of the broadening is chemical exchange, since a spectrum run at +60°C showed these lines to be considerably sharper. Also, on the 22.5-MHz spectrum, a further sharp pair of satellite peaks is observed [$J$(PtC) = 616 Hz]. Their intensity (approximately one-quarter of that of the peaks with $J$ = 35 Hz] corresponds to the expected abundance of molecules with two $^{195}$Pt nuclei, and their sharpness indicates that chemical shift anisotropy cannot be the cause of the broadness of the satellites with $J \sim 300$ Hz.

At −90°C, the spectrum at 50.1 MHz is more complicated. The ring and methyl carbon signals are now both split into two resonances, at $\delta$ 100.5 and 100.2 ppm (ring carbons, intensity ratio 1 : 2) and at 11.0 and 10.8 ppm (methyl carbons, intensity ratio 1 : 2). The splitting of these signals indicates that the location of the $\eta$-$C_5Me_5$ rings relative to the plane of the metal atoms indicated by the crystal structure (one above, two below) now has a sufficiently long lifetime for the separate signals to be observed. In the −90°C spectrum there are also three CO peaks at $\delta$ 181.2, 180.9 and 179.6 ppm. The observation of three, rather than six separate signals, together with the fact that two of the rings are equivalent, indicates that there is still an apparent $C_s$-symmetry in the molecule, as shown in Fig. 2.

The close similarity of the chemical shifts of all the carbonyls suggests that no distinction can be made in solution between bridging and terminal environments, though the observation of three signals shows that there is only slow exchange between different positions on each iridium atom, e.g. B⇌C or B′⇌C′ (Fig. 2). This is confirmed by the platinum satellite signals, which, though very broad, show a value of $J$(PtC) of approximately 600 Hz. The

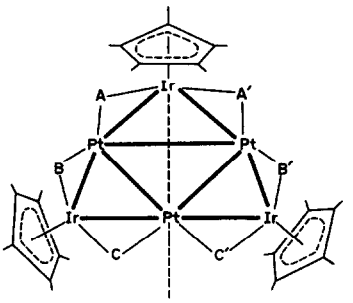



Fig. 2. Apparent structure of $[Ir_3Pt_3(CO)_6(\eta\text{-}C_5Me_5)_3]$ as indicated by $^{13}$C-{$^1$H} NMR studies at −90°C. Symmetry plane indicated by dotted line, one $\eta$-$C_5Me_5$ group above the metal plane, two below. At ambient temperatures slipping of the $C_5Me_5$ groups equilibrates chemical shifts of all CO groups and $^{195}$Pt coupling information also indicates a rapid pairwise exchange A⇌A′, B⇌C and B′⇌C′ (see cursive text).

exchange observed at ambient temperatures within pairs, A ⇌ A′, B ⇌ C and B′ ⇌ C′, then results in the broad platinum satellites observed at approximately 300 Hz, i.e. one half of $J$(PtC). If both platinum nuclei in an $IrPt_2(CO)_2$ fragment are $^{195}Pt$, then exchange will leave the resonance unchanged, with the satellite separation equal to $^1J(PtC)+{}^2J(PtC)$ (observed at 616 Hz). The observation of the second coupling to $^{195}Pt$ ($J = 35$ Hz) shows that even at ambient temperatures the carbonyls remain associated with two platinums and one iridium, *i.e.* there is no exchange of the type A ⇌ B, C ⇌ C′ or B′ ⇌ A′, although the chemical shifts are equilibrated by the flipping of the $\eta$-$C_5Me_5$ groups.

The structure of $[Ir_3Pt_3(\mu\text{-}CO)_3(CO)_3(\eta\text{-}C_5Me_5)_3]$ is of interest in view of a recent theoretical analysis[12] of bonding in raft clusters. The electronic requirements for triangulated rafts are evidently flexible since the total number of cluster valence electrons (CVEs) varies from 84 for the $Ir_3Pt_3$ species, through 85 in $[Fe_3Pt_3(CO)_{15}]^-$, 86 in $[Fe_3Pt_3(CO)_{15}]^{2-}$ to 90 in $[Os_6(CO)_{17}\{P(OMe)_3\}_4]$ and $[Os_6(\mu_3\text{-}O)(\mu_3\text{-}CO)(CO)_{18}]$. Evans and Mingos have postulated that there exists a low-lying empty metal-based orbital in the 90 CVE clusters which is anti-bonding with respect to the metal–metal interactions within the central triangle.[12] The electron count of 84 in $[Ir_3Pt_3(\mu\text{-}CO)_3(CO)_3(\eta\text{-}C_5Me_5)_3]$ can be related to the 90 CVEs in the $Os_6$ clusters if it is assumed that one valence orbital on each platinum is empty, and not involved in bonding, i.e. the platinums are 16 e centres. The $[Fe_3Pt_3(CO)_{15}]^{n-}$ ($n = 1$ or 2) anions are then also analogous to the $Os_6$ rafts with the low-lying orbital half and fully occupied for $n = 1$ and 2, respectively. An alternative view of the electronic structure of the three triplatinum species depends on an appreciation that the groups $Ir(CO)(\eta\text{-}C_5Me_5)$, $Fe(CO)_4$, $CR_2$, $SO_2$, and less exactly CO and CNR, are isolobal. This allows the stoichiometry of the $Ir_3Pt_3$ species and the $Fe_3Pt_3$ carbonyl anions to be related to the known compounds $[Pt_3(CNBu^t)_6]$, $[Pt_3(SO_2)_3(PPh_3)_3]$, $[Pt_3(CO)_3(PR_3)_3]$ and $[Pt_3(CR_2)_3(PR_3)_3]$, and also to the dianion $[Pt_3(CO)_6]^{2-}$, due allowance being made for any negative charge. For $[Ir_3Pt_3(\mu\text{-}CO)_3(CO)_3(\eta\text{-}C_5Me_5)_3]$ the bridging CO ligands render the closeness of the analogy arguable.

## EXPERIMENTAL

The compounds $[Pt(cod)_2]$[13] and $[Ir(CO)_2(\eta\text{-}C_5Me_5)]$[14] were prepared as described previously. Preparative work was carried out under oxygen-free nitrogen employing Schlenk tube techniques. Light petroleum refers to the fraction with b.p. 40–60°C. The NMR spectra were measured with JEOL FX90Q and FX200 instruments. Chemical shifts are positive to a high frequency of $SiMe_4$ ($^{13}C$-{$^1H$}) and $^{195}Pt$ [Ξ ($^{195}Pt$) 21.4 MHz].

### *Synthesis of the compound* $[Ir_3Pt_3(\mu\text{-}CO)_3(CO)_3(\eta\text{-}C_5Me_5)_3]$

Ethylene was bubbled into a solution of $[Pt(cod)_2]$ (0.5 g, 1.2 mmol) in diethyl ether (30 $cm^3$) at 0°C in order to generate $[Pt(C_2H_4)_3]$ *in situ*. This reagent was then treated with $[Ir(CO)_2(\eta\text{-}C_5Me_5)]$ (0.46 g, 1.2 mmol) in the same solvent (30 $cm^3$). The mixture became dark brown and after stirring for 30 min the solvent was removed *in vacuo*. The residue was transferred to the top of an alumina column (15 × 2 cm) and chromatographed, eluting initially with light petroleum to remove trace amounts of $[Ir(CO)_2(\eta\text{-}C_5Me_5)]$. Subsequent elution with diethyl ether-light petroleum (1:1) gave an orange-brown band. Removal of solvent *in vacuo* and crystallisation of the product from dichloromethane-light petroleum (1:2) afforded dark brown *crystals* of $[Ir_3Pt_3(\mu\text{-}CO)_3(CO)_3(\eta\text{-}C_5Me_5)_3]$ (0.66 g, *ca* 100%). Found: C, 24.8; H, 2.6%. $C_{36}H_{45}Ir_3O_6Pt_3$ requires C, 24.9; H, 2.6%. M.p. 234°C (with decomp.); $\nu_{CO}$ (tetrahydrofuran) at 1959s(br) and 1768s $cm^{-1}$. NMR: $^1H(CDCl_3)$, $\delta$ 2.15 [Me, $J$(PtH) 7 Hz]; $^{13}C$-{$^1H$} ($CD_2Cl_2$-$CH_2Cl_2$), $\delta$ 179.0 (*br*, CO), 100.1 ($C_5Me_5$) and 10.7 ppm ($C_5Me_5$); $^{195}Pt$-{$^1H$} ($CDCl_3$), $\delta$ −874.9 ppm.

### *Crystal structure determination*

A suitable crystal (0.4 × 0.25 × 0.15 mm) was grown from dichloromethane-light petroleum. Data were collected at 293 K on a Nicolet *P3m* diffractometer.

*Crystal data.* $C_{36}H_{45}Ir_3O_6Pt_3$, $M = 1639.7$, monoclinic, $a = 41.811(34)$, $b = 9.183(6)$, $c = 21.892(14)$ Å, $\beta = 90.99(6)°$, $U = 8404(10)$ Å$^3$, $Z = 8$, $D_c = 2.59$ g $cm^{-3}$, $F(000) = 5694$, space group $P2/n$, Mo-$K\alpha$ X-radiation (graphite monochromator), $\bar{\lambda} = 0.71069$ Å, $\mu$(Mo-$K\alpha$) = 130.9 $cm^{-1}$.

The structure was solved by direct methods, which located the 12 independent metal atoms; the remaining carbon and oxygen atoms being located from difference Fourier syntheses. Absorption effects were corrected by an empirical method via a six-parameter fit to 348 azimuthal scan data. Transmission coefficients varied between 0.013 and 0.002. Of 11,307 intensities measured in a unique

quadrant of reciprocal space for $4 \leqslant 2\theta \leqslant 45°$, 9740 unique data remained after averaging of repeat measurements, and deletion of mismeasured reflections. Of these data, 6549 with $I \geqslant 2\sigma(I)$ were retained for use in the structure solution and refinement. The C—C separations within the $\eta$-$C_5Me_5$ rings were fixed at 1.42 Å, and exocyclic C—C distances were constrained to be close to a common value which refined to 1.52(1) Å. Similar constraints were applied to the iridium–carbon distances of the bridging and terminal CO groups. The common values refined to 2.06(2) and 1.79(2) Å, respectively. The C—O bonds were constrained to average 1.15 Å. Final residuals were $R = 0.0903$ $(R' = 0.0915)$ $[R = \sum||F_o|-|F_c||/\sum|F_o|$; $R' = \sum w^{1/2}||F_o|-|F_c||/\sum w^{1/2}|F_o|$; $w = (\sigma^2(F_o)+0.002F_o^2)]$*. The weighting scheme adopted accounted satisfactorily for the variance in $|F_o|$ as shown by examination of $\sum w(|F_o|-|F_c|)^2$ as a function of sin $\theta$ and $|F_o|$. All computations were carried out on an Eclipse (Data General) computer with the SHELXTL system of programs.[15] Complex neutral atom scattering factors were from Ref. 16.

*Acknowledgements*—We thank the Air Force Office of Scientific Research USAF for support under grant AFOSR-82-0070, and the U.K. Science and Engineering Research Council for the award of a research studentship (to A.D.M.).

*The atomic positional and thermal parameters, together with lists of $F_o/F_c$ values have been deposited as supplementary material with the Editor, from whom copies are available on request. Atomic coordinates have also been deposited with the Cambridge Crystallographic Data Centre.

## REFERENCES

1. M. Green, J. A. K. Howard, G. N. Pain and F. G. A. Stone, *J. Chem. Soc., Dalton Trans.* 1982, 1327.
2. A. R. Pinhas, T. A. Albright, P. Hofmann and R. Hoffmann, *Helv. Chim. Acta* 1980, **63**, 29.
3. D. A. Roberts and G. L. Geoffroy, In *Comprehensive Organometallic Chemistry* (Edited by G. Wilkinson, F. G. A. Stone and E. W. Abel), Vol. 6, Section 40. Pergamon Press, Oxford (1982).
4. A. Immirzi, A. Musco, P. S. Pregosin and L. M. Venanzi, *Angew. Chem., Int. Ed. Engl.* 1980, **19**, 721.
5. M. Green, R. M. Mills, G. N. Pain, F. G. A. Stone and P. Woodward, *J. Chem. Soc., Dalton Trans.* 1982, 1309; L. J. Farrugia, J. C. Jeffery, C. Marsden and F. G. A. Stone, *ibid.* in press.
6. M. Green, J. A. K. Howard, M. Murray, J. L. Spencer and F. G. A. Stone, *J. Chem. Soc., Dalton Trans.* 1977, 1509.
7. G. Longoni, M. Manassero and M. Sansoni, *J. Am. Chem. Soc.* 1980, **102**, 7973.
8. D. C. Moody and R. R. Ryan, *Inorg. Chem.* 1977, **16**, 1054.
9. A. Albinati, G. Carturan and A. Musco, *Inorg. Chim. Acta* 1976, **16**, L3.
10. R. J. Goudsmit, B. F. G. Johnson, J. Lewis, P. R. Raithby and K. H. Whitmire, *J. Chem. Soc., Chem. Commun.* 1983, 246; *idem. ibid.* 1982, 640.
11. M. Fajardo, H. D. Holden, B. F. G. Johnson, J. Lewis and P. R. Raithby, *J. Chem. Soc., Chem. Commun.* 1984, 24.
12. D. G. Evans and D. M. P. Mingos, unpublished results; D. G. Evans, D.Phil. Thesis, University of Oxford (1984).
13. J. L. Spencer, *Inorg. Synth.* 1979, **19**, 213.
14. J. W. Kang and P. M. Maitlis, *J. Organomet. Chem.* 1971, **26**, 393.
15. G. M. Sheldrick, *SHELXTL Programs for Use with the Nicolet X-ray System.* Cambridge (1976), updated Göttingen (1981).
16. *International Tables for X-ray Crystallography*, Vol. 4. Kynoch Press, Birmingham (1974).

*Polyhedron* Vol. 3, No. 9/10, pp. 1099–1104, 1984
Printed in the U.S.A.

0277–5387/84 $3.00 + .00
© 1984 Pergamon Press Ltd.

# PREPARATION, PROPERTIES AND MOLECULAR STRUCTURE OF MONOHYDROGEN DIETHYLENETRIAMINEPENTAACETATOSTANNATE(IV) TRIHYDRATE—AN EIGHT COORDINATED 1:1 TIN(IV) CHELATE

**R. KRISHNA IYER* and S. G. DESHPANDE**
Chemistry Division

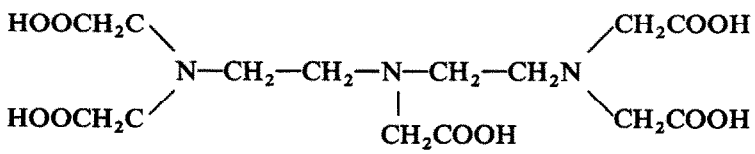
**and**

**V. AMIRTHALINGAM**
Water Chemistry Division, Bhabha Atomic Research Centre, Bombay 400 085, India

(*Received* 21 *December* 1983; *accepted* 23 *June* 1984)

**Abstract**—The properties and structural features of tin(IV) chelates with diethylenetriaminepentaacetic acid (DTPA) are reported. Potentiometric and IR data indicate that DTPA functions as an octadentate ligand in the hydrated acid chelate. The metal–oxygen bonds in the chelates have a high degree of covalency. Dehydration of the acid chelate occurs through the formation of the intermediate compound, $H(SnDTPA).0.5H_2O$. The anhydrous chelate contains a free carboxylate group. The acid chelate $H(SnDTPA).3H_2O$ crystallises in the orthorhombic system (space group *Pbca*) having cell constants $a = 13.92(2)$, $b = 12.09(2)$ and $c = 23.05(5)$ with $Z = 8$. Crystal structure data show that DTPA behaves as an octadentate ligand with five carboxyl oxygens and three nitrogens coordinating to tin forming a distorted dodecahedron. A very short hydrogen bond (2.43 Å) between the oxygens of two of the three water molecules leads to the appropriate formulation of the chelate as $(H_5O_2)^+(SnDTPA)^-H_2O$.

Diethylenetriaminepentaacetic acid ($H_5DTPA$) is a potentially octadentate ligand which chelates with metals with coordination number > 8 (e.g. lanthanides and actinides) more efficiently than the hexadentate ethylenediaminetetraacetic acid ($H_4EDTA$).[1] Possible structures of many chelates have been suggested based on potentiometric,[2–4] IR[5] and proton magnetic resonance[6,7] studies. Crystal structures of copper[8] and neodymium[9] chelates have been reported. During our attempts to prepare crystalline acid chelates of tetravalent metals with DTPA which do not contain an uncomplexed COOH group, a suitable candidate could be located in the tin(IV) chelate. This paper describes potentiometric, IR, thermal and X-ray diffraction studies of the acid chelate of tin(IV) with DTPA. IR studies of the monosodium salt and the anhydrous acid chelate are also reported.




$H_5DTPA$

* Author to whom correspondence should be addressed.

## EXPERIMENTAL

### *Reagents*

$H_5DTPA$ (Koch-Light Labs Ltd, Colnbrook, U.K.) with a purity of ~99% (determined by potentiometric and complexometric titrations) was used for preparation of the chelate. The tin tetrachloride used was of high purity.[10] An aqueous solution of $SnCl_4$ was prepared by adding little by little 50 $cm^3$ of $SnCl_4$ to 50 $cm^3$ of ice-cold water, with continuous stirring. The tin content in the solution was determined gravimetrically as $SnO_2$. All other chemicals were of analytical reagent grade.

### *Preparation of the chelates*

$SnCl_4$ (4.6 $cm^3$, 4.36 *M*) in water was added dropwise with stirring to $Na_3H_2DTPA$ (100 $cm^3$, 0.2 *M*) in water at 90°C. Turbidity was observed initially which increased during the course of the addition and subsequently decreased. Since the solution was not clear, it was filtered. Estimation of tin in the residue showed that ~99% of the added tin was retained in the solution. On keeping the filtrate over $P_2O_5$, white crystals were obtained which were filtered and washed with a small quantity of water. The chelate was purified by recrystallisation from hot water and dried over anhydrous $CaCl_2$. The anhydrous chelate was prepared by heating the hydrated one at 170°C for 2 h under vacuum. The product was hygroscopic.

For isolation of the sodium salt of the chelate, the pH of an aqueous solution of the chelate (0.1 g in 50 $cm^3$ water) was raised from 2.5 to 4.5 (for 95% conversion to the sodium salt) by dropwise addition of 0.05 *N* NaOH with continuous stirring. (Dilute NaOH was used to prevent precipitation of $Sn(OH)_4$. The pH was not raised above 4.5 to avoid hydrolysis.) On keeping the solution over $P_2O_5$, a dry mass was obtained after a few days (no crystals).

### *Analyses*

The tin content in the hydrated chelate was determined by ignition to $SnO_2$ at about 800°C. DTPA content in the chelate was estimated by complexometric titration in the filtrate after precipitating Sn as $SnS_2$ from a solution in hydrochloric acid. Kjeldahl's method was used for determination of nitrogen. Water content was estimated by thermogravimetry.

### *Analytical data*

Found: Sn, 21.0; DTPA, 68.4; N, 7.9; $H_2O$, 9.7%. Calc. for $HSnDTPA.3H_2O$: Sn, 21.13; DTPA, 69.07; N, 7.48; $H_2O$, 9.61%.

### *Measurements*

Potentiometric titration was carried out using an Elico Model LI-120 pH meter equipped with glass and saturated calomel electrodes. The ionic strength of the solution was adjusted to 0.1 with $KNO_3$ and this solution was titrated with standard 0.05 *N* NaOH solution. IR spectra were recorded with a Perkin–Elmer Model 577 double-beam spectrophotometer using KBr pellet and mull techniques. Since the anhydrous chelate was hygroscopic, preparation of the sample was carried out in a glove-box. A thermogram of 200 mg of the chelate was obtained using a Stanton self-recording thermobalance of $\pm 1$ mg sensitivity while that of a 10-mg sample in flowing air (21/h) was recorded using a microthermobalance (sensitivity $\pm 1$ $\mu$g) described earlier.[11]

### *X-ray data*

The chelate crystallises from aqueous solution as colourless transparent prisms and needles in the orthorhombic system, elongated along the "*b*"-axis. The unit cell parameters determined from Weissenberg photographs using Cu-$K_\alpha$ radiation were refined by least squares fitting of the indexed powder data. The values are: $a = 13.92(2)$, $b = 12.09(2)$, $c = 23.05(5)$ Å, $\rho_o = 1.87$, $\rho_c = 1.91$ g $cm^{-3}$, $Z = 8$. The space group is fixed as *Pbca* from systematic absences.

### *X-ray structure analysis*

Intensity data for 815 unique reflections were collected by visual estimation using Weissenberg techniques and they were corrected for Lorentz, polarisation and absorption effects. Scaling was carried out using Wilson's method together with common reflections obtained from photographs about other axes.

The structure was solved by the heavy-atom method. The tin atom was located using the Harker and non-Harker Sn—Sn vectors and all the lighter atoms were located by iterative Fourier methods. The structural parameters were refined by full-matrix least squares using Cruickshank's weighting scheme with $A = 5.0$ and $C = 0.015$. Only the tin atom was allowed to vibrate anisotropically and hydrogen atoms were ignored. The final *R*-factor is 10.7%.*

* Atomic coordinates, full lists of bond lengths and angles, thermal parameters and a table of $F_o/F_c$ values have been deposited with the Editor. Atomic coordinates have also been deposited with the Cambridge Crystallographic Data Centre.

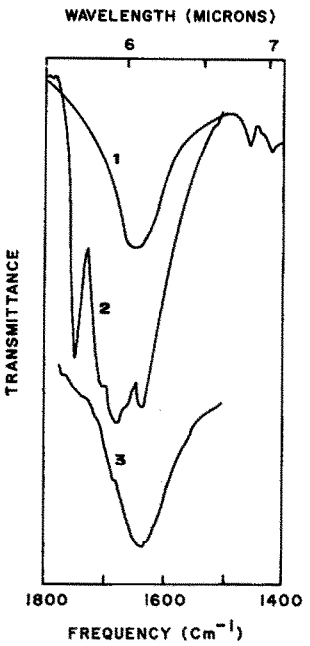



Fig. 1. IR spectra of Sn–DTPA chelates: (1) $HSnDTPA.3H_2O$ (KBr), (2) HSnDTPA (nujol) and (3) NaSnDTPA (nujol).

## RESULTS AND DISCUSSION

The acid Sn(IV)–DTPA chelate behaves as a strong acid, the pH of a $10^{-3}$ *M* solution being 3.05. The potentiometric titration curve showed a single buffer region in the pH range 3–4 corresponding to the neutralisation of an acidic proton. Above pH 6.5 addition of alkali did not raise the equilibrium pH. On the contrary, the pH decreased to 5.8–6.0, indicating the onset of hydrolytic reactions. Further addition of alkali resulted in the precipitation of $Sn(OH)_4$. The thermogram of the chelate in air showed a single step for dehydration which was complete at about 180°C. The weight loss corresponded to 3 moles of $H_2O$ per mole of complex. DTA in air indicated two endothermic peaks below 180°C. The dehydration step in the thermogram could be resolved into two stages by employing microthermogravimetry. The first step corresponded to the formation of $HSnDTPA.0.5H_2O$.

The IR spectra of the hydrated and anhydrous acid chelates and also of the sodium salt are shown in Fig. 1. In Table 1 assignments are given for absorption bands which are of diagnostic value in the studies of structure and nature of bonding in the chelates. In the spectrum of the hydrated chelate (curve 1) the peak at 1650 $cm^{-1}$ due to antisymmetric COO stretching is attributed to coordinated carboxylates. No peak is observed in the range 1700–1750 $cm^{-1}$ due to uncomplexed COOH group. The possibility of the presence of $NH^+—CH_2—COO^-$ cannot be completely ruled out since the carboxylate group in the zwitterion absorbs at 1620–1630 $cm^{-1}$. However, if the proton exists as $NH^+$, the solution of the chelate will not behave as a strong acid. Hence this possibility can be excluded. Absence of $NH^+$ even in the presence of a proton suggests that all the three nitrogens are coordinated to tin. The fact that the chelate does not contain uncomplexed COOH even though it contains a proton indicates that there is no free $COO^-$ group in the chelate. Thus it may be concluded that all the five carboxyl groups and all the three nitrogens of DTPA are coordinated to tin.

The IR spectrum of the anhydrous chelate shows a peak at 1750 $cm^{-1}$ due to a free COOH group. The manifestation of the COOH group after removal of the three water molecules indicates the association of the proton with the water molecules in the hydrated chelate. The number of carboxyl groups coordinated to tin decreases from five to four as a result of dehydration. The free $CH_2COOH$ group is likely to be bonded to one of the terminal nitrogens of DTPA

Table 1. IR spectroscopic data

| Frequency ($cm^{-1}$) | | | | |
|---|---|---|---|---|
| DTPA | $HSnDTPA.3H_2O$ | HSnDTPA | NaSnDTPA | Assignment |
| — | 3540 m<br>3410 m | — | — | Antisymmetric OH stretching |
| 1740 s<br>1695 s | — | 1750 s | — | C=O stretching in COOH |
| 1635 vs | 1650 vs | 1680 vs<br>1635 vs | 1640 vs | Antisymmetric COO stretching |
| 1400 s | 1350 s | — | 1350 s | Symmetric COO stretching |
| 1240 m | — | 1230 m | — | Unionized COOH |

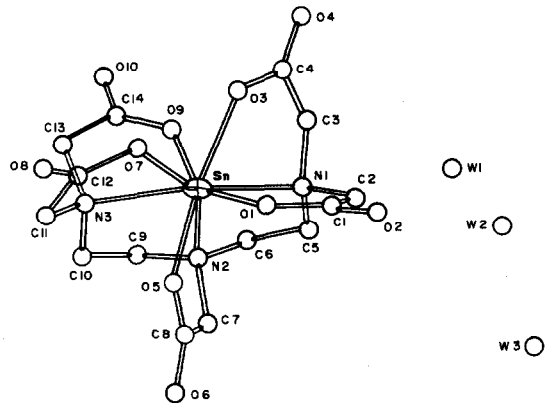



Fig. 2. Perspective view of the molecule together with three water molecules, structure as seen down the "*b*"-axis. Atoms are labelled as in the text.

since the p$K$ value of the second $CH_2COOH$ group attached to the two terminal nitrogens is much higher than those of the other three $CH_2COOH$ groups. The probable coordination number of tin in the anydrous chelate is 7 [heptacoordination is present is Sn(IV)EDTA.$H_2O$[12]].

The spectrum of the sodium salt of the tin(IV) chelate shows a single peak between 1500 and 1750 $cm^{-1}$. This peak observed at 1640 $cm^{-1}$ is symmetrical and no shoulder is present around 1600 $cm^{-1}$ due to free carboxylate. Hence it may be concluded that all the five carboxylates are coordinated to tin as in the case of the acid chelate.

Sievers and Bailar[5] have correlated the charge to size ratio ($q/r$) of the metal ion with the position of the carbonyl peak maximum for the EDTA and DTPA complexes of 33 metal ions. When $q/r$ is larger than 3.6, carbonyl absorption maxima occur in the 1625–1650 $cm^{-1}$ region and the metal carboxylate bonds have a high degree of covalency. The peaks due to antisymmetric COO stretching of the coordinated carboxylates in SnDTPA chelate are located at 1680 (with another peak at 1635), 1650 and 1640 $cm^{-1}$ in the spectra of anhydrous acid chelate, hydrated acid chelate and the sodium salt respectively. Sn—O bonds in all the chelates have a high degree of covalency [$q/r$ = 5.7 for Sn(IV)]. The degree of covalency varies in the order anhydrous acid chelate > hydrated acid chelate > sodium salt.

The conclusions drawn from potentiometric and IR studies of the hydrated acid chelate have been confirmed by the crystal structure data. The structure projected down the "*b*"-axis is shown in Fig. 2. The metal atom has an eight-fold coordination involving all the three nitrogen atoms and five oxygen atoms of the carboxylate groups of DTPA. All the metal–nitrogen distances are greater than the metal–oxygen bond lengths (see Table 2). These values are nearer to those reported for the seven coordinated Sn(IV)EDTA.$H_2O$[12] except that the length of one Sn—N bond in the EDTA chelate is shorter (2.296 Å). The angles subtended at the metal atom (the $\phi$-values) vary from 71 to 86°(1) (the acute angles) and from 103 to 122°(1) (the obtuse angles). The corresponding theoretical values are 73.70 and 110.54° for a regular dodecahedron. These results clearly indicate that the coordination geometry is a distorted dodecahedron (Fig. 3). The molecular dimensions of DTPA are quite normal.

The three water molecules fill the gap between the complex molecules and stabilise the structure by hydrogen bonding with the oxygen atoms of the carboxyl groups. While the hydrogen bond distances from $W_1$ are 2.80(2) and 2.95(2) Å, the distances from $W_2$ and $W_3$ are rather short: $W_2$—O, 2.51(2) and 2.45(2) and $W_3$—O, 2.70(2) and 2.66(2) Å. The distance $W_2$—$W_3$ is very short [2.43(2) Å], which indicates that the proton is located between the oxygens of these two water molecules.

There are a few interesting aspects in the crystal

Table 2. Bond distances and angles in the coordination sphere of tin in HSnDTPA.3$H_2O$

| Bond distance (Å) | | | Bond angle (°) | | |
|---|---|---|---|---|---|
| Sn—$O_1$ | 2.13(1) | $O_1$—Sn—$O_3$ | 76(1) | $O_5$—Sn—$N_2$ | 74(1) |
| Sn—$O_3$ | 2.15(1) | $O_1$—Sn—$O_5$ | 73(1) | $O_5$—Sn—$N_3$ | 76(2) |
| Sn—$O_5$ | 2.11(1) | $O_1$—Sn—$O_7$ | 79(2) | $O_7$—Sn—$N_3$ | 71(1) |
| Sn—$O_7$ | 2.08(1) | $O_1$—Sn—$N_1$ | 74(1) | $O_9$—Sn—$N_1$ | 86(2) |
| Sn—$O_9$ | 2.18(1) | $O_3$—Sn—$O_7$ | 77(2) | $O_9$—Sn—$N_2$ | 78(2) |
| Sn—$N_1$ | 2.35(1) | $O_3$—Sn—$O_9$ | 73(1) | $O_9$—Sn—$N_3$ | 70(1) |
| Sn—$N_2$ | 2.32(1) | $O_3$—Sn—$N_1$ | 71(1) | $N_1$—Sn—$N_2$ | 74(1) |
| Sn—$N_3$ | 2.40(2) | $O_5$—Sn—$O_7$ | 84(2) | $N_2$—Sn—$N_3$ | 76(1) |

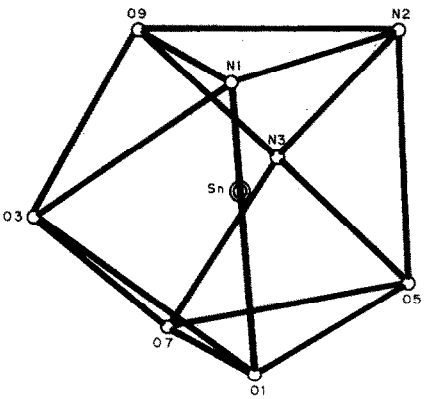



Fig. 3. The coordination polyhedra around $Sn^{4+}$—a distorted dodecahedron [the two interlocking trapezia are formed by the nearly planar groups: (1) $O_5N_2O_9O_3$ and (2) $O_1N_1N_3O_7$].

structure of $HSnDTPA.3H_2O$. These are discussed now.

(1) Coordination number 8 is relatively rare in tin(IV) compounds. Two excellent reviews[13,14] have appeared in the literature on eight-coordination chemistry and the structural chemistry of tin has also been reviewed extensively.[15] Although the preparation of some eight coordinate tin chelates have been reported, there are only two compounds for which crystal structure data are available [$Sn(NO_3)_4$[16] and Sn(phthalocyanine)$_2$[17]]. The present work appears to be the first case of a 1:1 Sn(IV) chelate with coordination number 8.

(2) Among the vast number of ligands employed for preparation of metal chelates, there are very few polydentate ligands with eight or more coordinating sites. DTPA and triethylenetetraminehexaacetic acid are two such ligands. However, instances reported earlier in which DTPA acts as an octadenate are very few. Sievers and Bailar[5] concluded from IR evidence that DTPA functions as an octadentate in the acid thorium chelate, $H(ThDTPA)H_2O$.

(3) Studies on hydrated proton complexes occurring in crystals by diffraction methods have been reviewed extensively.[18] Most of the compounds studied are acid hydrates (both inorganic and organic) while there are a few metal complexes with carboxylic acids [e.g. $MH(C_2O_4)_2.3H_2O$, where M = Er or Y].[19,20] There exists a symmetrical hydrogen bond (O...O bond length = 2.44 Å) between two of the three water molecules in $YH(C_2O_4)_2.3H_2O$ with the proton at the centre of the bond. Hoard *et al.*[21] have indicated that the acid hydrogens in $Mn[Mn(OH_2)HY].8H_2O$ are used in extraordinarily strong hydrogen bonds (2.46 Å) which tie the complex anion into infinite strings.

The situation in the present case is slightly different from that in $YH(C_2O_4)_2.3H_2O$. Though the length of the hydrogen bond between $W_2$ and $W_3$ is 2.43 Å, these two water oxygens have different environments. The hydrogen bond distance between the carboxylate oxygen ($O_2$) and $W_2$ is also short. Hence it is likely that the single negative charge on the DTPA chelate is concentrated on this carboxylate group. The positive charge of $(H_5O_2)^+$ is not uniformly distributed over the ion, but somewhat displaced towards the $W_2$-end.

From the results and discussions earlier, the appropriate formulation of the hydrated acid chelate is $(H_5O_2)^+(SnDTPA)^-H_2O$.

*Acknowledgements*—We sincerely thank Dr R. M. Iyer, Head, Chemistry Division and Associate Director, Chemical Group, Dr G. S. Rao, Head, Pure Materials Section, Chemistry Division and Dr K. S. Venkateswarlu, Head, Water Chemistry Division, B.A.R.C. for their keen interest and guidance.

## REFERENCES

1. V. Volf, *Treatment of Incorporated Transuranium Elements*, Technical Reports Series No. 184, p. 13. International Atomic Energy Agency, Vienna (1978).
2. S. Chaberek, A. E. Frost, M. A. Doran and N. J. Bicknell, *J. Inorg. Nucl. Chem.* 1959, **11**, 184.
3. R. Harder and S. Chaberek, *ibid.* 1959, **11**, 197.
4. J. Vandegaer, S. Chaberek and A. E. Frost, *ibid.* 1959, **11**, 210.
5. R. E. Sievers and J. C. Bailar, Jr, *Inorg. Chem.* 1962, **1**, 174.
6. B. B. Smith and R. H. Betts, *J. Am. Chem. Soc.* 1969, **91**, 7749.
7. A. R. Fried, Jr and A. E. Martell, *ibid.* 1971, **93**, 4695.
8. R. C. Seccombe, B. Lee and G. M. Henry, *Inorg. Chem.* 1975, **14**, 1147.
9. J. J. Stezowski, R. Countryman, M. O.'D. Julian, V. W. Day, R. E. Hughes and J. L. Hoard, Paper presented at the 14th International Conference on Coordination Chemistry, Toronto, Canada (1972).
10. G. S. Rao, Y. W. Gokhale, G. M. Phatak, S. S. Gupta and K. Gangadharan, B.A.R.C./I-732 (1982).
11. S. R. Dharwadkar, V. V. Deshpande and M. D. Karkhanavala, In *Thermal Analysis* (Edited by I. Buzas), Vol. 3; p. 759. Akademiai Kiado, Budapest (1975).
12. F. P. Van Remoortere, J. J. Flynn and F. P. Boer, *Inorg. Chem.* 1971, **10**, 2313.
13. S. J. Lippard, In *Progress in Inorganic Chemistry* (Edited by F. A. Cotton), Vol. 8, p. 109. Wiley, New York (1967).
14. D. L. Kepert, In *Progress in Inorganic Chemistry* (Edited by S. J. Lippard), Vol. 24, p. 179. Wiley, New York (1978).

15. J. A. Zubieta and J. J. Zuckerman, In *Progress in Inorgamic Chemistry* (Edited by S. J. Lippard), Vol. 24, p. 251. Wiley, New York (1978).
16. C. D. Garner, P. Sutton and S. C. Wallwork, *J. Chem. Soc. (A)* 1967, 1949.
17. W. E. Bennett, D. E. Broberg and N. C. Baenziger, *Inorg. Chem.* 1973, **12**, 930.
18. J. O. Lundgren and I. Olovsson, In *The Hydrogen Bond* (Edited by P. Schuster, G. Zundel and C. Sandorfy), Vol. 2, p. 471. North-Holland, Amsterdam (1976).
19. H. Steinfink and G. D. Brunton, *Inorg. Chem.* 1970, **9**, 2112.
20. H. R. Ryan and R. A. Penneman, *ibid.* 1971, **10**, 2637.
21. J. L. Hoard, B. Pedersen, S. Richards and J. V. Silverton, *J. Am. Chem. Soc.* 1961, **83**, 3533.

*Polyhedron* Vol. 3, No. 9/10, pp. 1105–1108, 1984
Printed in the U.S.A.

0277–5387/84 $3.00 + .00
© 1984 Pergamon Press Ltd.

# $^1H$ AND $^{31}P$ NMR STUDY OF THE COMPLEXES BETWEEN Cd(II) AND ADENOSINE-5′-TRIPHOSPHATE

**G. CRISPONI* and R. CAMINITI**
Istituto di Chimica Generale, Inorganica ed Analitica, Università di Cagliari, Via Ospedale 72, 09100 Cagliari, Italy

**and**

**S. BIAGINI, M. CASU and A. LAI**
Dipartimento di Scienze Chimiche, Università di Cagliari, Via Ospedale 72, 09100 Cagliari, Italy

(*Received* 6 *February* 1984; *accepted* 23 *June* 1984)

**Abstract**—The Cd(II)–adenosine-5′-triphosphate system was investigated by potentiometry and $^1H$ and $^{31}P$ NMR spectroscopy. Our results are consistent with the formation of three 1 : 1 complexes with different degrees of protonation and suggest a binding through $\beta$- and $\gamma$-phosphates and the N7 on the adenine ring.

It is well known that metal ions play a dominant role in the biological activity of nucleic acids and nucleotides. In particular different metal ions cause remarkable alterations in the normal properties of these molecular systems. Therefore the knowledge of the molecular mechanism responsible for the activity of metal ions is fundamental and a large amount of work has been carried out on this topic using NMR spectroscopy.[1–4] Adenosine-5′-triphosphate (ATP) is one of the most studied nucleotides; it is known that numerous metal ions form ATP adducts,[5,6] which can be involved in many enzymatic processes. In spite of the known biotoxic effects[7,8] of Cd(II) little attention has been paid to the interaction of this metal ion with ATP. Therefore, in this paper the ATP–Cd(II) system in aqueous solution has been investigated using $^1H$ and $^{31}P$ NMR spectroscopy and potentiometric titrations, in order to obtain some information about the structure and stability of the complexes. This work is part of a systematic study on the complex formation between biological ligands and metal ions in aqueous solution using different approaches (NMR structural and conformational investigations[9–12] and calculation of equilibrium constants).[13–15]

## EXPERIMENTAL

### *Materials*

ATP, $CdCl_2$, $D_2O$ and NaOD were purchased from Boehringer. The $^1H$-measurements were carried out on the samples dissolved in $D_2O$, while the $^{31}P$-measurements were made in $H_2O$ enriched with $D_2O$ (5%). Paramagnetic impurities were removed by a Chelex 100 (Calbiochem) resin bed and the purity was checked by $^1H$ and $^{31}P$ NMR spectra.

### *NMR measurements*

$^1H$ and $^{31}P$ NMR spectra were recorded on a Varian FT-80 A spectrometer utilizing a broad band probe at an operating frequency of 80 MHz for $^1H$ and 32.2 MHz for $^{31}P$.

Ten-millimetre sample tubes, equipped with a coaxial inner cell containing, as external reference, 1 *M* $H_3PO_4$, for the phosphorus spectra, were used. Proton resonances were referred to 4,4-dimethyl-4-silapentane sodium sulphonate used as the internal standard. Measurements were made at a probe temperature of about 32°C. The assignment of resonances was made on the basis of previously reported ones. $^1H$ and $^{31}P$ chemical shifts are reported as positive if more deshielded, and negative if more shielded. Various pH values were adjusted by adding NaOD; pH values in $D_2O$ were corrected for the deuterium isotope effect by adding 0.4 units to the pH-meter readings.[16]

### *Potentiometric titrations*

Numerous titrations with 0.1 *M* NaOH of different Cd(II)–ATP mixtures were performed; the ATP concentration was $3 \times 10^{-3}$ *M*, while the Cd(II) concentration ranged from $3 \times 10^{-4}$ to $3 \times 10^{-3}$ *M*. 50 $cm^3$ of the mixture solution were titrated at 30°C

* Author to whom correspondence should be addressed.

under a nitrogen atmosphere at a constant ionic strength obtained with 1 *M* $KNO_3$. pHs were measured on a pH-meter equipped with a 3-mm electrode (Wilmad).

### *Calculations*

The evaluation of the formation constants of the complexes formed between Cd(II) and ATP was made on a HP-85 computer by means of a BASIC program previously described.[17] By using the earlier formation constants it was possible to calculate the distribution of the various species as a function of pH at the concentrations of the reagents used in the NMR measurements. A least-squares program has been used to evaluate from these data and from the experimental chemical shifts the intrinsic chemical shifts of the various species in solution.

## RESULTS AND DISCUSSION

### *Potentiometric titrations*

The titration curve for the Cd(II)–ATP system at the 1 : 1 molar ratio is shown as an example in Fig. 1: its comparison with the free-ligand titration curve A is indicative of a strong interaction between the metal ion and ATP. The curve (A) was fitted by using $pK_{a_1} = 4.06$ and $pK_{a_2} = 6.53$ for ATP[18] and $pK_{M_1} = 7.7$ and $pK_{M_2} = 9.3$ for the formation of hydroxy compounds of cadmium (obtained as an average of different reported values[19]) and assuming the formation of $CdLH^-$ and $CdL^{2-}$ with relative formation constants log $K_1 = 2.70$ and log $K_2 = 5.41$.* These values were obtained by fitting the data of the titrations of five different solutions with ATP : Cd(II) ratios ranging from 1 : 1 to 10 : 1. The good fitting of all the data with the reported constants is indicative of the validity of the simple 1 : 1 model assumed. These constants are also in good agreement with previously reported constants for ATP with numerous divalent cations.[18] The distribution of the various forms is reported in Fig. 2(A) for a solution at a concentration of 0.5 *M* (both Cd(II) and ATP). Figure 2(A) shows the existence of $CdLH^-$ species up to a pH of $\simeq 5$ and of $CdL^{2-}$ species up to a pH of $\simeq 10$. Apart from this last value the Cd–ATP complex decomposes at the expense of the formation of various hydroxylated forms of $Cd^{2+}$.

* $K_1 = [CdLH^-]/([Cd^{2+}][LH^{3-}])$ and $K_2 = [CdL^{2-}]/([Cd^{2+}][L^{4-}])$, where $L^{4-}$ is the completely deprotonated form of ATP.

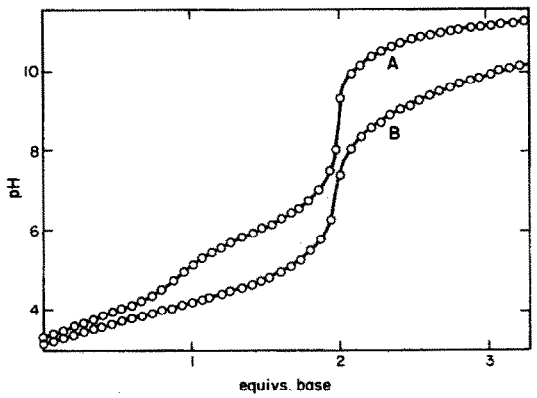



Fig. 1. Titration curves (pH vs the ratio mol of titrant/mol of ligand) of: (A) $3 \times 10^{-3}$ *M* ATP and (B) $3 \times 10^{-3}$ *M* ATP in the presence of $3 \times 10^{-3}$ *M* $Cd^{2+}$. The continuous lines are the calculated curves.

### *Proton NMR spectra*

The addition of $Cd^{2+}$ to ATP concentrated aqueous solutions induced significant shifts for the $H_2$ and $H_8$ resonances, relative to the free ligand shifts, while the ribose protons were practically unaffected. These changes indicate that $Cd^{2+}$ interacts with the ring adenine moiety whereas the

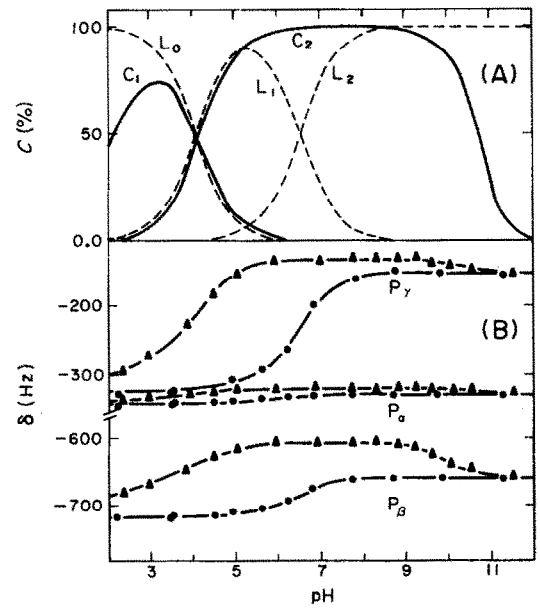



Fig. 2. (A) pH dependence of the concentration distribution of the various deprotonated species of 0.5 *M* ATP in the absence and in the presence of 0.5 *M* $Cd^{2+}$. Continuous lines representing the complex species ($C_1 = CdLH^-$ and $C_2 = CdL^{2-}$) and dotted lines, relative to the pure ATP species ($L_0 = LH_2^{2-}$, $L_1 = LH^{3-}$ and $L_3 = L^{4-}$), were calculated by using the pertinent parameters of Table 1. (B) pH dependence of $^{31}P$ chemical shifts ($\delta$) of 0.5 *M* ATP in the absence (●) and in the presence (▲) of 0.5 *M* $Cd^{2+}$.

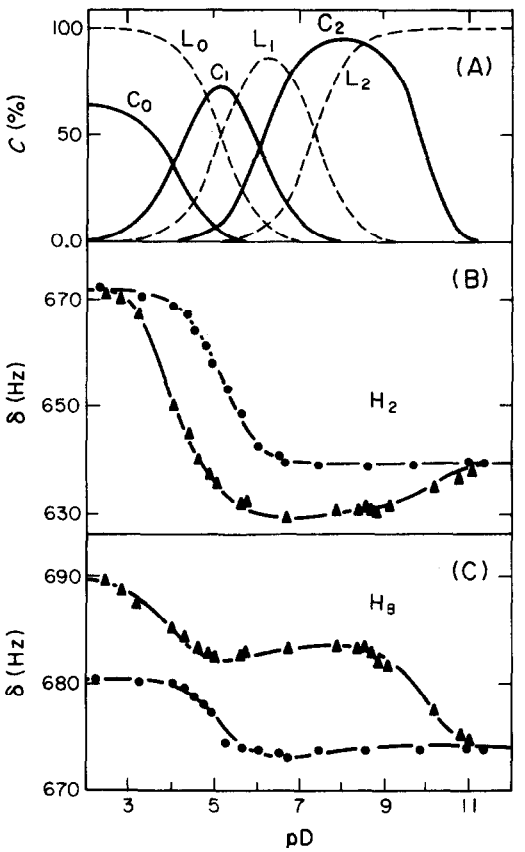



Fig. 3. (A) pD dependence of the concentration (c) distribution of the various deprotonated species of 0.5 M ATP in the absence and in the presence of 0.5 $M$ $Cd^{2+}$. (Continuous lines representing the complex species ($C_0 = CdLH_2$, $C_1 = CdLH^-$ and $C_2 = CdL^{2-}$) and dotted lines, relative to the pure ATP species ($L_0 = LH_5^{2-}$, $L_1 = LH^{3-}$ and $L_2 = L^{4-}$), were calculated by using the pertinent parameters of Table 1. (B) and (C) pD dependence of $^1H$ chemical shifts ($\delta$) of 0.5 $M$ ATP in the absence (●) and in the presence (▲) of 0.5 $M$ $Cd^{2+}$.

ribose protons are not likely involved in the binding. Furthermore, the variation of the chemical shifts, without the appearance of any new peak, is consistent with a rapid exchange (in the $^1H$ chemical shift time scale) among the various protonated and complexed forms of the ligand.

In Fig. 3(B) and (C) the $H_8$ and $H_2$ chemical shifts of ATP in the absence and in the presence of $Cd^{2+}$ are shown as a function of pD. The experimental trends of the pure ligand were analysed by a least-squares procedure to obtain the best estimates of chemical shifts for the species $ATPH_2^{2-}$, $ATPH^{3-}$ and $ATP^{4-}$, and of the acidity constants. The relative $pK_a$s (Table 1) are significatively higher than the corresponding ones for the aqueous solution reported earlier. A similar analysis was employed to investigate the trends in the presence of the metal ion using the p$K$ values obtained potentiometrically as starting parameters. The assumption of a further $CdLH_2$ species,* potentiometrically undetectable, allowed us to fit the experimental trends. The relative best-fitted parameters are reported in Table 2. Also, in this case, the p$K$s values are significatively different than those found by potentiometric measurements in dilute solutions. The simulated curves reported in Fig. 3(B) and (C) show an overall good agreement with the experimental points, while in Fig. 3(A) the relative deprotonated species are shown.

From Table 2 the $H_8$ chemical shifts of the three complexes are seen to move downfield in respect to the resonances of corresponding uncomplexed forms, indicating a reduction of the diamagnetic shielding. These findings are consistent with models where $Cd^{2+}$ binds to N7, such a hypothesis being supported by the shifts to a high field of the $H_2$ resonances which exclude possible bindings of the metal ion to N1.

### $^{31}P$ *spectra*

The $^{31}P$ NMR chemical shifts of ATP in the absence and in the presence of $Cd^{2+}$ at various pHs are shown in Fig. 2. The curves of pure ATP are consistent with acidity constants (Table 1) and with the chemical shift parameters (Table 2). The addition of $Cd^{2+}$ results in a specific downfield shift of $\beta$- and $\gamma$-phosphorus resonances, while those of $\alpha$-phosphorus are almost unaffected; the chemical shifts for the phosphorus atoms in the complexed forms are also reported in Table 2. These values and the trends in Fig. 2 clearly suggest that $Cd^{2+}$ binds $\beta$- and $\gamma$-phosphorus in agreement with the findings for complexes with other metal ions such as $Zn^{2+}$ and $Mg^{2+}$.[1] Furthermore, at pH values greater than 8.5 the occurrence of free ATP due to the formation of hydroxylated forms of $Cd^{2+}$ is evident, as is also pointed out by potentiometric measurements and $^1H$ resonances.

Table 1. Stability constants for interaction of ATP with $Cd^{2+}$ in $H_2O$ and $D_2O$ solutions

| $pK_{a_1}$ | $pK_{a_2}$ | $\log K_0$ | $\log K_1$ | $\log K_2$ |
|---|---|---|---|---|
| 4.06[a] | 6.53[a] | - | 2.7[b] | 5.41[b] |
| 4.9 [c] | 5.73[c] | 0.88[c] | 3.30[c] | 4.71[c] |

[a] From Ref. 18.
[b] Calculated from potentiometric data in $H_2O$ solutions.
[c] Calculated from $^1H$ NMR data in $D_2O$ solutions.

* $K_0 = [CdLH_2]/([Cd^{2+}][LH_2^{2-}])$.

Table 2. Chemical shift parameters for interaction of ATP with $Cd^{2+}$ in $H_2O$ and $D_2O$ solutions*

| | $LH_2^{2-}$ | $LH^{3-}$ | $L^{4-}$ | $CdLH_2$ | $CdLH^-$ | $CdL^{2-}$ |
|---|---|---|---|---|---|---|
| $^1H,\delta$ ($H_2$) | 671.4 | 639.6 | 639.3 | 672.3 | 625.9 | 629.7 |
| $\delta(H_8)$ | 680.2 | 672.8 | 674.2 | 695.0 | 682.5 | 684.0 |
| $^{31}P,\delta$ (Pα) | -351.0 | -344.5 | -334.9 | - | -338.1 | -328.4 |
| $\delta$(Pβ) | -714.8 | -705.2 | -653.7 | - | -650.4 | -608.6 |
| $\delta$(Pγ) | -331.7 | -315.6 | -151.3 | - | -270.5 | -132.0 |

* All $\delta$s are in Hz.

*Conclusion*

The combined analysis of potentiometric, $^1H$ and $^{31}P$ NMR measurements has demonstrated the formation only of 1:1 adducts between Cd(II) and ATP, with different degrees of protonation. While the potentiometry showed only the species $CdL^{2-}$ and $CdLH^-$, due to ATP deprotonation, the chemical shift changes of $H_2$ and $H_8$ and phosphorus resonances give additional evidence of a $CdLH_2$ species at lower pHs.

A comparison of the acid dissociation as well as complex formation constants obtained from the two methods (Table 1) shows remarkable differences in $pK_{a_1}$ and log $K_1$ when the deprotonation of N1 occurs, even when the isotopic effect of deuterium is accounted for. Therefore these discrepancies may be ascribed on the one hand to the inherently low thermodynamic reliability of the NMR data, due to neglecting the ionic strength effects coming from the high ATP concentration, and, on the other hand to the occurrence of ATP self-association phenomena. Particularly, in view of the extremely different experimental conditions used in the two methods (potentiometry: $3 \times 10^{-3}$ *M* ATP; NMR: 0.5 *M* ATP), the stacked ATP seems to cause the main differences. In fact the self-association phenomena affect both the deprotonation at the adenine moiety and the complex formation; obviously the use of only ATP monomers in the elaboration of equilibrium constants from NMR data necessarily introduces the aforementioned deviations.

Nevertheless our results in the actual NMR experimental conditions allowed us to obtain confident evidence of $\beta$- and $\gamma$-phosphates and the N-7 on the adenine moiety as binding sites for Cd–ATP complexes.

## REFERENCES


1. M. Cohn and T. R. Hughes, *J. Biol. Chem.* 1962, **237**, 176.
2. (a) H. Sternlicht, R. G. Shulman and E. W. Anderson, *J. Chem. Phys.* 1965, **43**, 3123; (b) *J. Chem. Phys.* 1965, **43**, 3133.
3. G. C. Levy and J. J. Dechter, *J. Am. Chem. Soc.* 1980, **102**, 6191.
4. V. Wee, I. Fieldman, P. Rose and S. Gross, *J. Am. Chem. Soc.* 1974, **96**, 103.
5. J. Granot and D. Fiat, *J. Am. Chem. Soc.* 1977, **99**, 4963.
6. J. Granot, *J. Am. Chem. Soc.* 1978, **100**, 2886.
7. K. Nomiyama, *Sci. Total Environ.* 1980, **14**, 199.
8. M. P. Verma, R. P. Sharma and D. R. Bourcier, *Biol. Trace Element Res.* 1982, **4**, 35.
9. A. Lai, M. Monduzzi, G. Saba, M. Casu and G. Crisponi, *Chem. Phys.* 1982, **71**, 27.
10. M. Monduzzi, A. Lai, G. Saba, M. Casu and G. Crisponi, *Adv. Mol. Relaxation Interact. Processes* 1982, **24**, 465.
11. S. Biagini, M. Casu, A. Lai, M. Monduzzi and G. Saba, *Chem. Phys. Lett.* 1983, **97**, 427.
12. L. Burlamacchi, A. Lai, M. Monduzzi and G. Saba, *J. Magn. Reson.* 1983, **55**, 39.
13. G. Carta, G. Crisponi and V. Nurchi, *Tetrahedron* 1981, **37**, 2115.
14. G. Carta and G. Crisponi, *J. Chem. Soc. Perkin* II 1982, 53.
15. G. Carta, G. Crisponi and A. Lai, *J. Magn. Reson.* 1982, **48**, 341.
16. P. K. Glasol and F. A. Long, *J. Phys. Chem.* 1960, **64**, 188.
17. G. Crisponi, A. Lai, M. Monduzzi and G. Saba, *Inorg. Chim. Acta, Bioinorg. Sect.* 1983, **80**, 85.
18. M. M. Taqui Khan and A. E. Martell, *J. Phys. Chem.* 1962, **66**, 10.
19. *Stability Constants of Metal–Ion Complexes.* Special Publication 17, The Chemical Society, London (1964).

*Polyhedron* Vol. 3, No. 9/10, pp. 1109–1119, 1984
Printed in the U.S.A.

0277-5387/84 $3.00 + .00
© 1984 Pergamon Press Ltd.

# FLEXIBILITY OF SILOXANE RINGS AND RIGIDITY OF LADDER-LIKE SILOXANE POLYMERS: INTERPRETATION ON THE BASIS OF ATOM–ATOM POTENTIAL FUNCTIONS

**T. V. TIMOFEEVA,* I. L. DUBCHAK, V. G. DASHEVSKY and YU. T. STRUCHKOV**

A. N. Nesmeyanov Institute of Organoelement Compounds, U.S.S.R. Academy of Sciences, Moscow V-334, 28 Vavilov St., U.S.S.R.

(*Received* 27 *February* 1984; *accepted* 23 *June* 1984)

**Abstract**—On the basis of geometrical data of small Si—O bond containing molecules in the gas phase and in crystals as well as of Allinger's parameters for the conformational calculations of siloxanes, parameters for the mechanical model have been obtained which are suitable for calculation of the conformation and energy of siloxane molecules. The geometry and energy of the isolated cyclotetrasiloxane ring were estimated and a considerable conformational flexibility of this fragment was shown. The calculation of the geometry and conformational energy of di- and tricyclic organosiloxane oligomers has led to the conclusion that the flexibility of a tetrasiloxane ring fused with two other rings is essentially restricted. On the basis of the conformational calculations of oligomeric molecules conclusions were drawn on the rigidity of cyclolinear (ladder-like) siloxane polymers.

Polyorganosiloxanes occupy the most important place among organosilicon polymers due to their unique physicochemical properties and wide scope for designing new types of structures. In recent years a great number of siloxane polymers with untraditional and specific structures have been synthesized, viz. cyclolinear, ladder-like, spirocyclic polymers and polymers with different units.[1] In this connection the problem of the elucidation of these new polymeric structures becomes rather important. In general, the solving of a polymer structure is extremely difficult. However, it can be essentially simplified if data are available on the structure of the fragments which build up a polymer chain.

Siloxane chains are highly flexible as a result of the ease of deformation of the Si—O—Si bond angles and rotation around Si—O bonds.[2] The cyclic siloxanes, $(R_2SiO)_n$, with $n = 4$ are also conformationally flexible, as testified by a great variety of ring conformations observed in crystals of cyclotetrasiloxanes (CTSs) with various substituents at the Si atoms.[3]

However, the ladder-like polyorganosiloxanes which are widely used nowadays are rigid-chain polymers. The equilibrium rigidity of a ladder-like polymer chain (defined as a Kuhn segment or a persistent length) is, by an order of magnitude higher than that of a linear polysiloxane and it is insensitive to the structure of side chains.[4] In this respect it is very interesting and important to find out which constraints are imposed on the conformation of the CTS fragments when they are included into a ladder-like system or, alternatively, why ladder-like polymers do not have a flexibility specific for siloxane chains.

In the present paper an attempt is made to get an answer, using conformational calculations of the fragments of polysiloxane chains, because the investigation of conformations of the building blocks of polymers, i.e. the oligomeric molecules, represents a first step in the elucidation of the structure of macromolecules.

Recently the geometrical and electronic characteristics of small molecules containing an Si—O bond were comprehensively analysed by means of quantum chemical (semiempirical and *ab initio*) techniques.[5–8] However, for the conformational analysis of more complicated molecules, viz. oligomers and corresponding polymers, the most

* Author to whom correspondence should be addressed.

applicable is an atom–atom potential-function technique or the molecular mechanics which are used in the present paper. According to that method, the conformational energy of a molecule, $U_{conf}$, is represented as a sum:

$$U_{conf} = U_{nb} + U_b + U_a + U_{tors}.$$

The energy of nonbonded interactions is calculated by the use of a 6-exp potential:

$$U_{nb} = \sum_m B_m \exp(-\alpha_m r_m) - A_m r_m^{-6},$$

where $r_m$ are nonbonded distances, and $A$, $B$ and $\alpha$ are empirical parameters of the potential. The energy of deformation of bonds and bond angles is calculated according to Hooke's law:

$$U_b = 1/2 \sum_i K_{l,i}(l_i - l_{o,i})^2,$$

$$U_a = 1/2 \sum_i K_{\theta,j}(\theta_j - \theta_{o,j})^2,$$

where $l$ and $\theta$ are bond lengths and bond angles, $l_o$ and $\theta_o$ are their "ideal" values, and $K_l$ and $K_\theta$ are empirical elastic constants of bonds and angles. The torsion energy is given by the formula:

$$U_{tors} = 1/2 \sum_k U_{o,k}(1 + \cos 3\phi_k),$$

where $\phi$ is the torsion angle and $U_o$ is the torsion constant.

The present investigation consists of the following three parts:

(1) Determination of the parameters of $U_{conf}$ (potential-function parameters), which was necessary because conformational calculations for the types of compounds considered have never been carried out previously.

(2) Study of the conformational properties of an isolated CTS ring representing an important part of various molecules and polymers.

(3) Calculation of conformations of particular oligomeric molecules and comparison with the conformations observed in a crystal.

## DETERMINATION OF THE POTENTIAL-FUNCTION PARAMETERS

Earlier Allinger and coworkers[9] proposed a set of parameters which allowed calculation of the structure and conformational energy of silane molecules. To apply their system of parameters to siloxane molecules, it was necessary to supplement them with the elastic and torsion constants for the molecular fragments containing Si—O bonds as well as with the parameters of nonbonded interactions involving oxygen atoms. Parameters of the O ··· O nonbonded interactions were taken from Ref. 10.

The experimental data on the energy difference between conformers or the barriers to internal rotation for siloxanes are, in fact, absent. Therefore the choice of the corresponding parameters was based only on the data on the geometry of five simple siloxane molecules in the gas phase and in crystals, viz. disiloxane [$H_3Si—O—SiH_3$ (I)], hexamethyldisiloxane [$Me_2Si—O—SiMe_3$ (II)], hexamethylcyclotrisiloxane [$(Me_2SiO)_3$ (III)], tetracyclosiloxane [$(H_2SiO)_4$ (IV)] and octamethyltetracyclosiloxane [$(Me_2SiO)_4$ (V)]. The parameters were chosen so that the calculated molecular geometry was in the best agreement with the experimental data. These parameters are given in Table 1. Application of these parameters together with those obtained by Allinger[9,10] leads to a satisfactory agreement between the calculated and experimental values of bond lengths and bond angles (Table 2), which allows the use of this set of parameters in calculations of conformations of more complicated molecules. The technique for the parameter choice and adjustment is described in detail in Ref. 11.

## THE CONFORMATIONAL CALCULATION OF THE CYCLIC TETRASILOXANE

Cyclosiloxanes with eight-membered rings (CTSs) are the fragments most frequently occurring in a polymer chain due to their small strain compared to the cyclotrisiloxanes and their availability compared to the larger rings. While a planar conformation or the conformation in which planarity is violated by various steric factors (bulky substituents or involvement of some groups in a polycyclic system) are typical for a six-membered siloxane ring, a variety of conformers is in principle possible for

Table 1. Parameters for calculation of the conformations of molecules containing fragments with Si—O bonds

| Si—O bond | $l_o$ (Å) 1.630 | $K_1$ (mdyn Å$^2$) 4.04 |
|---|---|---|
| Bond angle | $\theta_o$ (g) | $K_\theta$ (mdyn rad$^{-2}$) |
| Si—O—Si | 145.0 | 0.17 |
| O—Si—O | 109.5 | 0.45 |
| O—Si—C | 109.5 | 0.48 |
| O—Si—H | 109.5 | 0.27 |
| Torsion angle | | $U_o$ (kcal/mol) |
| X—O—Si—Y | | 0.0 |

Table 2. Comparison of experimental (XRSA, X-ray structure analysis; GE, gaseous electronography) and calculated parameters of molecules I–V*

| Molecule | | Bond length (Å) | | | | Bond angle | | | | | | | | Reference |
|---|---|---|---|---|---|---|---|---|---|---|---|---|---|---|
| | | Si—O | Si—C | C—H | Si—H | Si—O—Si | O—Si—O | O—Si—C | O—Si—H | H—Si—H | Si—C—H | C—Si—C | H—C—H | |
| I | XRSA | 1.631 | — | — | 1.307 | 142.2 | — | — | 105.0 | 113.0 | — | — | — | 12 |
| | GE | 1.634 | — | — | 1.486 | 144.1 | — | — | 109.9 | 109.1 | — | — | — | 13 |
| | Calc. | 1.629 | — | — | 1.484 | 144.2 | — | — | 109.3 | 109.5 | — | — | — | |
| II | XRSA | 1.626 | 1.851 | 0.970 | — | 148.8 | — | 108.8 | — | — | 110.2 | 110.1 | 108.8 | 12 |
| | GE | 1.631 | 1.865 | 1.102 | — | 148.0 | — | † | — | — | † | 109.6 | 108.3 | 14 |
| | Calc. | 1.630 | 1.873 | 1.094 | — | 147.2 | — | 109.4 | — | — | 110.7 | 109.6 | 108.2 | |
| III | XRSA | 1.61 | 1.82 | † | — | 131.9 | 105.3 | 110.8 | — | — | † | 107.1 | * | 15 |
| | GE | 1.635 | 1.845 | 1.086 | — | 131.6 | 107.8 | † | — | — | 113.7 | 114.6 | * | 16 |
| | Calc. | 1.628 | 1.869 | 1.094 | — | 133.6 | 106.3 | 110.0 | — | — | 108.8 | 110.3 | 110.1 | |
| IV | GE | 1.628 | — | — | 1.48 | 148.6 | 112.0 | — | † | † | — | — | — | 17 |
| | Calc. | 1.629 | — | — | 1.484 | 143.4 | 109.0 | — | 109.3 | 109.7 | — | — | — | |
| V | XRSA | 1.65 | 1.92 | † | — | 142.5 | 109.0 | † | — | — | † | 106.0 | † | 18 |
| | GE | 1.622 | 1.844 | 1.087 | — | 144.8 | 110.0 | 109.4 | — | — | 113.5 | 111.2 | † | 16 |
| | Calc. | 1.629 | 1.871 | ‡ | — | 143.9 | 109.1 | 109.5 | — | — | ‡ | 109.7 | ‡ | |

* Real accuracy of the bond length elucidation by XRSA and GE is within the limits of 0.002–0.005 Å and that of the bond angles is 0.2–0.7 (XRSA) and 1–3° (GE).

† Not given in the original paper.

‡ The methyl group was considered in the calculation as a spherical atom.[30]

eight-membered rings. Therefore we undertook calculations to determine the regions in the space of the geometrical parameters where various conformers of CTS exist and to estimate the relative energy of these conformers.

In the fundamental work of Hendrickson,[19,20] the conformations of the cycloalkanes, $C_nH_{2n}$, with $n$ = 6–10 were considered and the nomenclature for these rings was suggested. This nomenclature will be used later for the conformers of CTS.

CTS which is built of two kinds of atoms differs from cyclooctane considered by Hendrickson by its bond lengths and by the alternation of two different endocyclic bond angles at the Si and O atoms. It results in a geometric region of existence of CTS (the combination of the allowed values for torsion angles) different from that of cyclooctane and in some differences in conditions determining symmetric molecular forms. Eight canonical symmetric forms with the sequence of signs and values of the torsion angles which are necessary for the description of all CTS conformations are shown in Fig. 1.

On going from cyclooctane to CTS some forms retain all the symmetry elements. For instance, in cyclooctane the forms CC (chair–chair) and LB (long-boat, which is a special case of CC) have in both cases a $C_{2v}$-symmetry, while in CTS these conformations are represented by two families: with atoms of Si or, accordingly, O on the mirror planes through positions 1, 5 and 3, 7. In a similar way, forms LC (long-chair, $C_{2h}$-symmetry), BB (boat–boat, $D_{2d}$-symmetry) and BC (boat–chair, $C_s$-symmetry) retain the symmetry but become split into two families. In Fig. 1 all these conformations are shown for both types of rings. The coplanarity of six-ring atoms (in positions 2-4 and 6-3) should be noted for forms LC and LB.

In contrast to the forms mentioned earlier, conformation C (chair, its necessary feature being the existence of three planar fragments, 1-2-3-4, 1-4-5-8 and 5-6-7-8) reduces its symmetry from $C_{2h}$ to $C_i$ on going from cyclooctane to CTS. In the case of the B-form (boat with three planar fragments, 1-2-3-4, 1-4-5-8 and 5-6-7-8, atoms 2, 3, 6 and 7 also being in one plane) the symmetry is reduced from $S_4$ to $C_2$ (CTS).

In eight-membered rings with fixed values of bond lengths and angles only two torsion angles are independent[21,22] and others are determined by the ring closure conditions.[23] This gives an opportunity to estimate the extreme values of torsion angles in CTS. Calculation of the conformational energy with both independent torsion angles, $\phi_1$ and $\phi_2$, being varied has shown[24] that, within the isoenergy line of 10 kcal/mol, the allowed region is as follows: $\phi_1 = -90$ to $+90°$ and $\phi_2 = -120$ to $+120°$ (Fig. 2). The

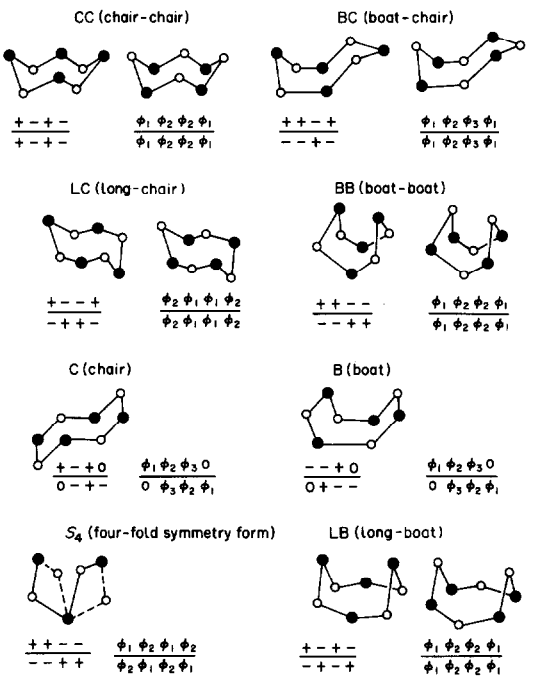



Fig. 1. The canonical symmetric forms of the tetrasiloxane cycle. The notation by Hendrickson, and the notation and sequence of signs and absolute values of torsion angles are given for each form. Signs and angles are separated by a horizontal line for the forms which have a symmetry plane. The shaded circles are the Si atoms, the empty ones the O atoms.

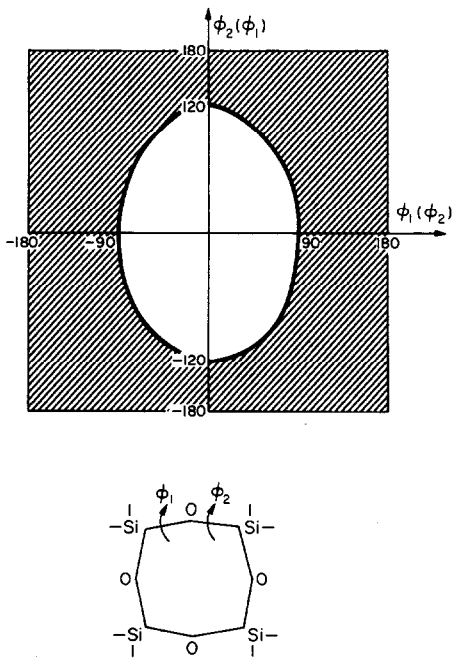


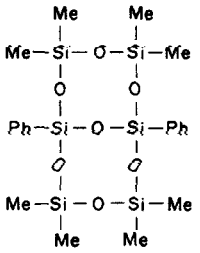

Fig. 2. The region of existence of an ideal tetrasiloxane cycle (the Si atoms without substituents) in the space of torsion angles $\phi_1$ and $\phi_2$. The forbidden region is shaded.

values of the other six torsion angles at any point, $\phi_1$, $\phi_2$, of the allowed region are also in the indicated intervals.

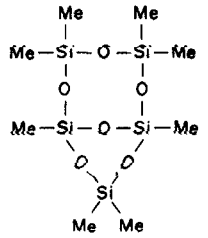
For some canonical forms of CTS the regions of existence and the energies of the most favourable conformers were calculated in more detail. This calculation was done by varying the angles $\phi_1$ and $\phi_2$, taking into account the symmetry conditions (alternation of signs and absolute values of the torsion angles) corresponding to each particular conformation. The Si—O bond lengths in the ring were assumed to be constant, and so only two components of $U_{conf}$ were taken into account, the nonbonded and bond angle energies ($U_{conf}$ is negligibly small owing to a low value of $U_0$).

For forms CC, BB and $S_4$ calculation of the conformational energy resulted in the low-energy regions in the form of ravines of practically the same depth in the $\phi_1$, $\phi_2$ coordinates. Therefore the torsion angles can continuously change within the same conformation. At the same time, for cyclooctane, quite definite values of torsion angles corresponding to the energy minimum were found in each family of forms.[19] This leads to an important general conclusion that CTS is much more flexible than cyclooctane.

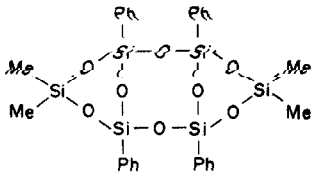
The torsion and bond angles for the canonical forms of CTS with the minimum conformational energy are listed in Table 3. For forms CC, BB and $S_4$ the listed values correspond to the lowest point on the line of the minimum energy though $U_{conf}$ remains practically constant along this line. Table 3 shows that the $U_{conf}$ of all conformers excluding the B and planar forms differs by no more than 0.1–0.2 kcal/mol. It is the energetic proximity that leads to unsymmetric conformations of CTS fragments which can be described as a superposition of various symmetrical forms and which are commonly observed in the majority of structural investigations. In a previous paper[3] the conformations of 43 molecules with CTS fragments in crystal structures were analyzed by the modified Cremer–Pople technique and the "pure" symmetrical forms were found to be practically absent.



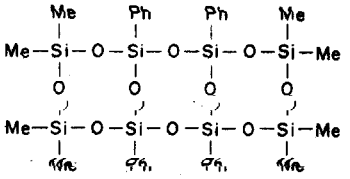
VI



VII



VIII (*cis*)
IX (*trans*)



X (*cis*)
XI (*trans*)

*Unlike CTS, all terms of the conformational* energy described earlier were taken into account in the calculation of the conformations of these molecules. As a starting point for minimization of the conformational energy the molecular geometry obtained by XRSA was used. In addition, for some molecules the other versions of the starting geometry were also used. Ph and Me substituents were treated as a single spherically symmetric atom. Parameters of the nonbonded interactions of this atom which correspond to an equilibrium distance of 3.8 Å were taken from Ref. 30 where it was shown that, when taking into account separate C and H atoms of the Me group, the results turned out to be close to those obtained for the spherically symmetric effective potential of this group. The elastic constants of the Me group were taken as being the same as for the C atom.

### *Results of the conformational calculations of oligosiloxanes*

With the use of the set of parameters proposed earlier we carried out the calculation of conformations of some oligomeric siloxane molecules (VI–XI) which represent the simplest fragments of polymer chains. Structures of these molecules in crystal (with the exception of VII) were studied by X-ray structure analysis (XRSA).[25–29]

### *Bicyclic molecules*

The bicyclic molecule VI (Fig. 3) does not realize its possible symmetry elements in the crystal. The conformations of the eight-membered cycles are different: for ring A it is close to boat (B), for ring B to BB. For this molecule minimization of $U_{conf}$ was performed from two starting points: (1) the conformation of the molecule in the crystal and (2) the model with planar rings. The experimental

Table 3. Results of the conformational calculations of the symmetric CTS forms

| Form of the ring | Ring symmetry | Atoms in 1, 3, 5, 7 positions | Torsion angle (g) | | | Bond angle (g) | | Relative energy $U_{conf}$ (kcal/mol) |
|---|---|---|---|---|---|---|---|---|
| | | | $\phi_1$ | $\phi_2$ | $\phi_3$ | Si—O—Si | O—Si—O | |
| CC | $C_{2v}$ | Si | 60.0 | 70.0 | — | 144.8 | 109.5 | 0.2 |
| CC | $C_{2v}$ | O | 80.0 | 50.0 | — | 144.8 | 109.5 | 0.2 |
| BB | $D_{2d}$ | Si | 32.5 | 34.2 | — | 144.7 | 109.4 | 0 |
| BB | $D_{2d}$ | O | 46.5 | 55.1 | — | 144.7 | 109.4 | 0.1 |
| LB | $C_{2v}$ | Si | 42.8 | 74.2 | — | 144.8 | 109.5 | 0.1 |
| LB | $C_{2v}$ | O | 18.3 | 87.2 | — | 144.7 | 109.4 | 0.1 |
| $S_4$ | $S_4$ | * | 32.1 | 34.5 | — | 144.7 | 109.5 | 0 |
| LC | $C_{2h}$ | Si | 74.2 | 42.8 | — | 144.8 | 109.5 | 0.1 |
| LC | $C_{2h}$ | O | 18.4 | 86.9 | — | 144.8 | 109.4 | 0.1 |
| C | $C_i$ | * | 78.4 | 89.8 | 36.6 | 144.8 | 109.4 | 0.1 |
| B | $C_2$ | * | 32.2 | 52.5 | 91.3 | 137.0<br>159.6 | 110.0<br>109.5 | 2.2 |
| BC | $C_s$ | Si | 74.2 | 44.1 | 41.5 | 144.8 | 109.5 | 0.1 |
| BC | $C_s$ | O | 30.6 | 5.9 | 85.7 | 144.8 | 109.4 | 0.1 |
| Planar form | $D_{4h}$ | * | 0 | 0 | — | 159.1 | 110.8 | 3.4 |

* No difference, Si or O.

geometrical parameters and the results of calculations are represented in Figs 3 (bond lengths and angles) and 4 (torsion angles).

As seen from Fig. 3, the calculated bond lengths and angles change insignificantly compared to the experimental data. At the same time the range of the experimental values of Si—O bond lengths is 1.595–1.645 Å, and of Si—O—Si and O—Si—O bond angles 141.4–147.4 and 108.9–111.4° respectively; the corresponding calculated ranges are 1.629–1.630 Å, and 142.5–145.7 and 108.8–109.6° which shows the equalization of the calculated chemically equivalent bond lengths and angles which is typical for the other considered molecules as well.

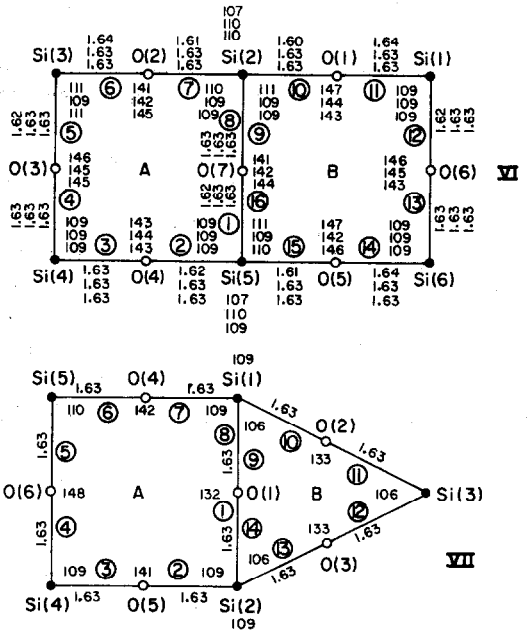



Fig. 3. The bond lengths (Å) and angles (°) in the cyclic fragments of molecules VI and VII. For molecule VI the upper, middle and lower figures are the experimental value, calculation 1 and calculation 2 respectively. For VII the calculated values are given. Numbering of torsion angles in the rings is given by the figures in circles.

The sequence of the signs and values of the torsion angles in the rings of molecules VI and VII is demonstrated in Fig. 4. The numbers of the torsion angles which are shown on the schemes of the corresponding molecules (Fig. 3) are plotted along the ordinate and the values of the angles along the abscissa. Such a representation of the torsion angles allows us to compare easily the results of experiments and calculations. According to calculation (1) both cycles have the same conformation, close to BB, and the whole molecule has $C_2$-symmetry. Calculation 2 results in quite different conformations of cycles A and B, viz. CB and LC respectively. Thus both calculations lead to a conformation which differs from that observed in the crystal.

The values of the contributions to the conformational energy according to both versions of the calculation are listed in Table 4. Molecules in conformations 1 and 2 are not strained and their conformational energies are close to each other. Thus, in a free state, compound VI seems to exist as a mixture of energetically close conformers (some of them can be symmetrical) and the conformations of

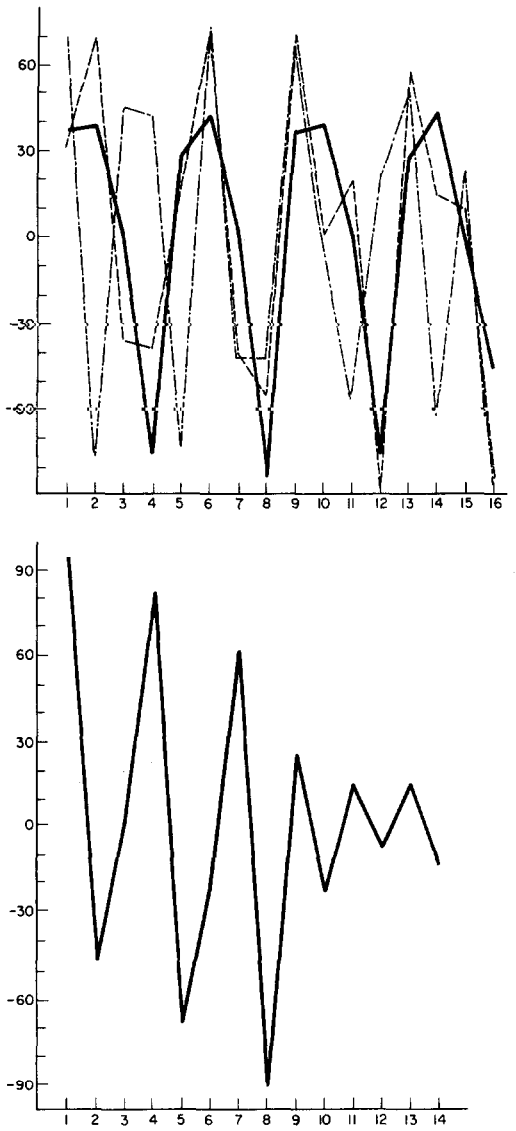



Fig. 4. The torsion angles in the rings of molecules **VI** (upper) and **VII** (lower). Unbroken line—calculation 1, dot-and-dash line—calculation 2, broken line—experiment. Numbering of the torsion angles is given in Fig. 3.

the rings of molecule **VI** in the crystals are determined by packing conditions.

To follow the changes of the structure of the eight-membered siloxane ring upon its involvement in a bicyclic system with the second six-membered cycle, calculation of the conformation of molecule **VII** was carried out. A planar conformation of both rings was taken as a starting point for minimization of conformational energy. Comparison of the contributions to the conformational energy of molecule **VII** (Table 4) shows it to be significantly more strained (see the value of $U_a$) than molecule **VI**. The strain arises mainly from the deviation of the

Table 4. Values of the potential-energy components (kcal/mol) of molecules **VI–XI** in the equilibrium conformation

| Molecule | | $U_b$ | $U_a$ | $U_{tors}$ | $U_{nb}$ | $U_{conf}$ |
|---|---|---|---|---|---|---|
| **VI** | Calculation 1 | 0.0 | 0.14 | 0.0 | −5.40 | −5.26 |
| | Calculation 2 | 0.0 | 0.04 | 0.0 | −5.60 | −5.56 |
| **VII** | | 0.0 | 2.39 | 0.0 | −3.77 | −1.38 |
| **VIII** | | 0.0 | 3.86 | 0.0 | −4.23 | −0.37 |
| **IX** | | 0.0 | 3.88 | 0.0 | −4.29 | −0.41 |
| **X** | | 0.0 | 0.22 | 0.0 | −7.97 | −7.75 |
| **XI** | | 0.0 | 0.06 | 0.0 | −8.23 | −8.17 |

Si—O—Si angles in the six-membered ring from their ideal value of 145°.

The calculated bond lengths and angles of molecule **VII** are represented in Fig. 3. The calculated values of the torsion angles are given in Fig. 4. Acccording to the calculations, the molecule is not symmetrical. The eight-membered ring has the CB conformation, the six-membered ring is a flattened boat.

Thus, involvement of the terasiloxane ring in a bicyclic system of two such eight-membered rings practically does not affect its conformational flexibility, while the fusion of this ring with a six-membered trisiloxane ring restrains the flexibility somewhat.

*Tricyclic molecules*

Molecules **VIII** and **IX** are the *cis*- and *trans*-isomers respectively: according to X-ray structure analysis (XRSA) the symmetry of these molecules in the crystal is $C_2$ and $C_i$. Both experimental and calculated geometrical parameters of these molecules are represented in Figs 5 and 6.

The calculated and experimental bond lengths are in good agreement. The largest deviations from an experimental value are observed in the bond angle Si(1)—O(1)—Si(2'), which is equal to 6.3 (**VIII**) and 5.8° (**IX**). It should be noted that the calculation leads to close values of this angle in molecules **VIII** and **IX**, which is decreased in comparison with the ideal value of 145° while this angle is ideal in crystals of **VIII** and decreased more in the crystal of **IX**. This difference seems to be caused by the steric influence of Ph substituents which are treated as pseudoatoms in our calculations, i.e. by the simplifications of the model. This assumption is confirmed by the fact that, according to XRSA data on the carbosiloxane molecule which is similar to the considered *trans*-isomer (**VIII**) and has Me substituents in the eight-membered ring, the corresponding Si—O—Si angle is 138.1° which is close to the calculated value of 139°.

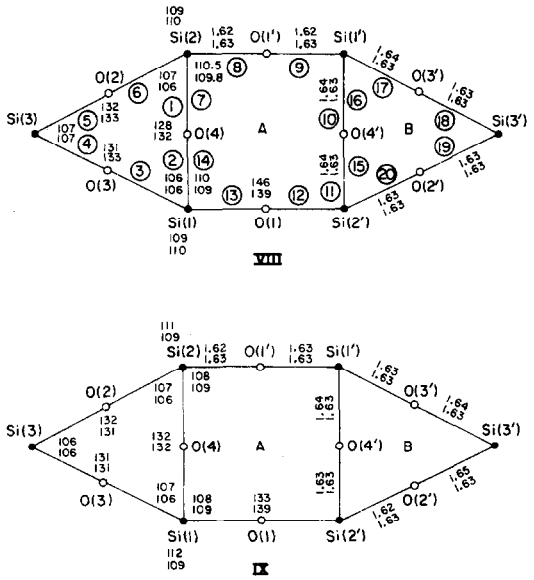
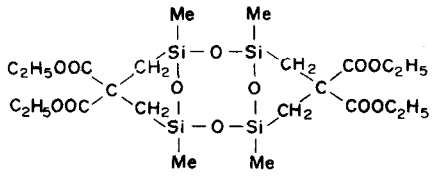



Fig. 5. The bond lengths and angles in the symmetrically independent parts of molecules **VIII** and **IX**; the upper and lower figures are the experimental and calculated values respectively. The figures in circles give the numbering of the torsion angles.

Comparison of the torsion angles in the cyclic fragments of molecules **VIII** and **IX** (Fig. 6) shows that the calculated and experimental conformations are close as a whole, though the calculated ones are of higher symmetry ($C_{2v}$ for **VIII**, $C_{2h}$ for **IX**). Both experimental and calculated conformations of the central cycle of **VII** can be described as **BB**. The difference in the signs of some calculated and experimental torsion angles which are small by their absolute values does not mean a change in the type of conformation in this case. The six-membered ring in **VIII** has a flattened conformation: deviations from planarity can be described as a twisted-boat conformation in the crystal and as a boat for the calculated data. According to both the experiment and the calculation, the eight-membered ring of **IX** has the LC conformation and the six-membered ring is a chair.

Isomers **VIII** and **IX** have equal conformational energies (Table 4).

Unlike **VIII** and **IX**, in which molecules of one eight-membered siloxane cycle is condensed with two six-membered cycles, the isomeric molecules, **X** and **XI**, consisting of three 1,3-fused eight-membered



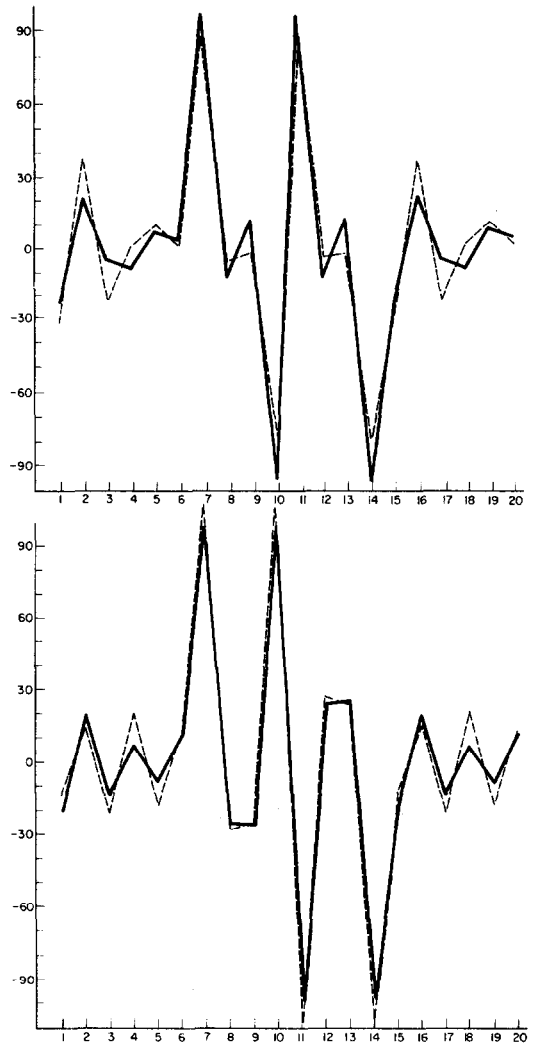




Fig. 6. The torsion angles in the rings of molecules **VIII** (upper) and **IX** (lower) (numbering of the torsion angles is given in Fig. 5).

rings, have no symmetry elements in the crystal according to XRSA data, though molecule **XI** has an approximate $C_i$-symmetry. The results of the conformational calculations of these molecules are represented in Figs 7 and 8. For molecule **X** the calculation leads to values of the bond lengths and angles which differ considerably from those found in the crystal. However, a wide range of experimental values for the chemically equivalent bond lengths and angles in this molecule should be noted. Though the $R$-factor is rather small in this case (0.062), the accuracy of the determination of the geometrical parameters of this molecule is not sufficiently high because of the complicated disorder of the crystal structure, where a number of conformers seem to coexist.[28] In this case the calculation probably gives a more correct geometrical picture.

The calculated and experimental values of the torsion angles in molecule **X** are compared in Fig. 8.

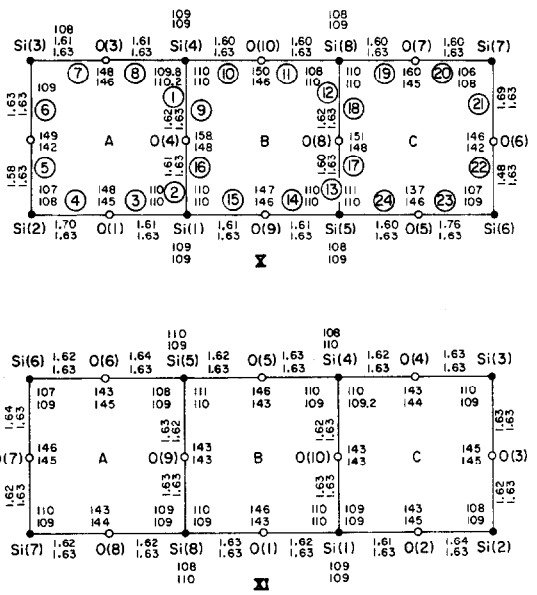


Fig. 7. The bond lengths and angles in the cyclic fragments of molecules X and XI. The upper figure is an experimental and the lower a calculated value.

Just as in **VIII**, the conformation of the central ring (**BB**) observed in the crystal coincides with the calculated one. On the contrary, the calculated confirmation of the side rings with a $C_2$-symmetry differs considerably from the experimental one.

For molecule **XI** (the *trans*-isomer) the calculated and experimental values of the geometrical parameters agree significantly better than for molecule **X**. As in the case of the *cis*-isomer, **X**, the largest conformational changes are observed in the side rings. According to the calculation, the central ring does not retain the LC conformation observed in the crystal, which can be seen from a comparison of the torsion angles (Fig. 3) but acquires a $C_i$-symmetry. This example confirms once more that the lowering of the molecular symmetry compared to the ideal one can serve as an indication of the influence of the crystal forces on the conformation.

The molecules of isomers **X** and **XI** are unstrained as is shown by the corresponding values of $U_{conf}$ (Table 5). The *trans*-isomer, **XI**, is somewhat more energetically favourable than the *cis*-isomer, **X**.

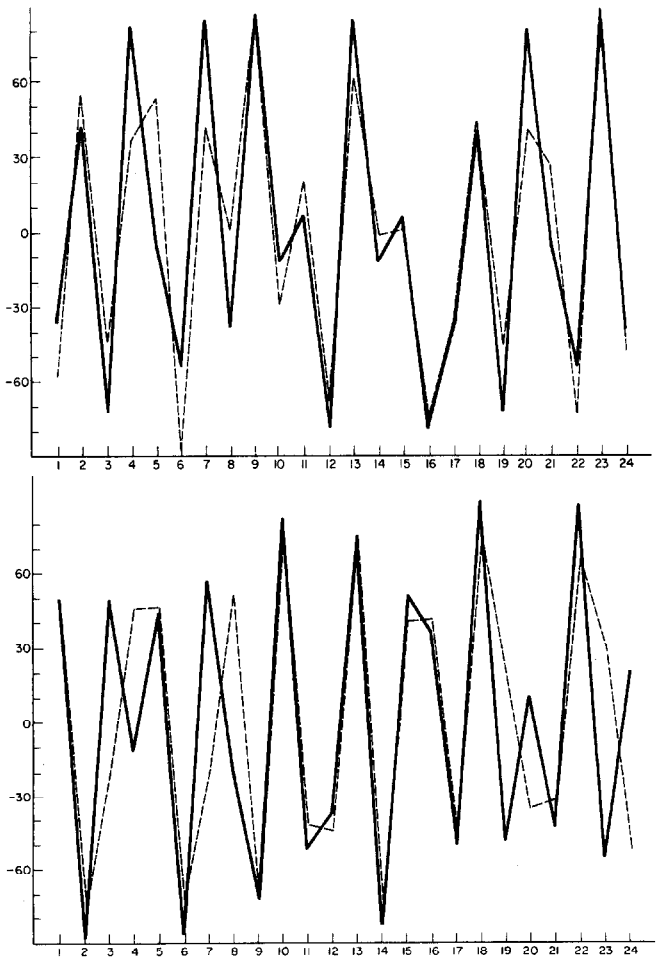


Fig. 8. The torsion angles in the rings of molecules **X** (upper) and **XI** (lower) (numbering of the torsion angles is given in Fig. 7).

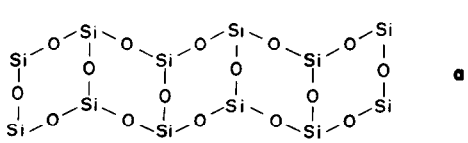
## CONCLUSION

The molecules of the majority of siloxanes are characterized by a formational non-rigidity in the free state. It is noteworthy that such a non-rigidity is observed also in crystals. As shown in Ref. 31, in crystalline siloxanes the intermolecular contacts are characteristically increased compared to the sums of van der Waals' radii typical for molecular organic crystals. The corresponding increase in the effective molecular volume seems to be caused by an intensive thermal motion of the molecules which, in its turn, is a consequence of the conformational non-rigidity.

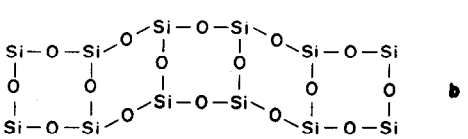
According to the earlier calculations, the tetrasiloxane ring is the most flexible. Its form in the monomer molecules is determined by the types of substituent and the influence of the crystal field. The fusion of two tetrasiloxane rings in the 1,3-position does not in fact restrict their conformational flexibility, while the fusion of the tetrasiloxane and trisiloxane cycles introduces some constraints on the mobility of the first one. The conformation of the central eight-membered ring in the 1,3-condensed tricyclic systems is determined unambiguously by the position (*cis* or *trans*) of the side rings, which do not lose their conformational flexibility on such fusion.

The qualitative results obtained can be transferred to the polymer molecules built of the oligomeric blocks considered. Various schemes of the fusion of the eight-membered rings in the ladder-like polyorgansiloxanes have been proposed, e.g. **a**, where only *trans*-fusion takes place, and **b**, where *cis*- and *trans*-fusion of cycles alternate.

The calculated data obtained allow us to suggest that the chains of type **a** are more favourable energetically since the aforementioned small differences between the energies of the *cis*- and *trans*-isomers of the oligomeric molecules (in favour of the latter) will accumulate in a polymer chain. The fragments in the *trans*- and *cis*-environment will probably have LC and BB conformations respectively. As an indirect confirmation of the preference of isomer **a** of the polymer chain there is the fact that the polymers to which such a structure is ascribed have a molecular weight and length of the Kuhn segment higher by at least an order of magnitude than the polymers for which the structure of type **b** is supposed.[32,33]



**a**



**b**

*Acknowledgements*—We are grateful to V. E. Shklover and N. N. Makarova for their interest in this work and a fruitful discussion of the results.

## REFERENCES

1. V. V. Korshak and A. A. Zhdanov, *Usp. Khim.* 1975, **44**, 468.
2. A. N. Lazarev, I. S. Ignatiev and T. F. Tenisheva, *Vibrations of Simple Molecules with* Si—O *Bonds* (in Russian). Leningrad, Nauka (1980).
3. V. A. Paliulin, N. S. Zefirov, V. E. Shklover and Yu. T. Struchkov, *J. Mol. Struct.* 1981, **70**, 65.
4. V. N. Tzvetkov, *Vysokomol. Sojed.* 1977, **19A**, 2171.
5. H. Oberhammer and J. E. Boggs, *J. Am. Chem. Soc.* 1980, **102**, 7241.
6. J. Z. Sauer, *Z. Phys. Chem.* 1982, **263**, 60.
7. D. Heidrich, D. Volkman and B. Zuravski, *Z. Phys. Chem.* 1982, **263**, 269.
8. B. F. Shchegolev and V. Ya. Bespalov, *Zh. Struk. Khim.* 1981, **22**, N 1, 149.
9. M. T. Tribble and N. L. Allinger, *Tetrahedron* 1972, **28**, 2174.
10. N. L. Allinger, I. A. Hirsh, M. A. Miller and I. J. Timinski, *J. Am. Chem. Soc.* 1969, **91**, 337.
11. T. V. Timofeeva, I. L. Dubchak, V. E. Shklover and Yu. T. Struchkov, *Teor. Eksp. Khim.* 1981, **17**, 674.
12. M. I. Borrow, E. A. V. Ebsworth and M. M. Harding, *Acta Crystallogr.* 1979, **B35**, 2093.
13. A. Almenningen, O. Bastiansen, V. Eving and K. Hedburg, *Acta Chem. Scand.* 1963, **17**, 2455.
14. B. Csanary, Z. Wagner, P. Gomory, F. C. Mijlnoff, B. Rozogondai and I. Hargitai, *J. Organomet. Chem.* 1976, **107**, 287.
15. R. P. Hernandes, *Acta Crystallogr.* 1978, **A34**, S 406.
16. N. Oberhammer, W. Zeil and G. Gogarasi, *J. Mol. Struct.* 1973, **18**, 309.
17. C. Glidewell, A. G. Robiette and G. M. Sheldrick, *J. Chem. Soc., Chem. Commun.* 1970, **15**, 931.
18. H. Steinfink, B. Post and I. Fankuchen, *Acta Crystallogr.* 1955, **8**, 420.
19. J. B. Hendrickson, *J. Am. Chem. Soc.* 1967, **89**, 7043.
20. J. B. Hendrickson, *J. Am. Chem. Soc.* 1967, **89**, 7047.
21. M. Bixon and S. Lifson, *Tetrahedron* 1967, **23**, 769.
22. J. D. Dunitz and J. Wasser, *J. Am. Chem. Soc.* 1972, **94**, 5645.
23. N. Go and A. Sheraga, *Macromolecules* 1973, **6**, 273.
24. I. L. Dubchak, V. G. Dachevskii and Yu. T. Struchkov, *Zh. Struk. Khim.* 1983, **24**, N5, 114.
25. V. E. Shklover, Yu. T. Struchkov, N. N. Makarova and A. A. Zhdanov, *Cryst. Struct. Commun.* 1980, **9**, 1.
26. V. E. Shklover, Yu. T. Struchkov, I. Yu. Klementiev, V. S. Tikhonov and K. A. Andrianov, *Zh. Struk. Khim.* 1979, 20, 302.
27. V. E. Shklover, I. Yu. Klementiev and Yu. T. Struchkov, *Zh. Struk. Khim.* 1981, **22**, N3, 76.
28. V. E. Shklover, A. N. Chekhlov, Yu. T. Struchkov, N.

N. Makarova and K. A. Andrianov, *Zh. Struk. Khim.* 1978, **19**, 1091.
29. V. E. Shklover, I. Yu. Klementiev and Yu. T. Struchkov, *Dokl. Akad. Nauk SSSR* 1981, **259**, 131.
30. V. G. Dashevskii, A. P. Baranov, T. Ya. Medved and M. I. Kabachnik, *Teor. Eksp. Khim.* 1977, **13**, 340.
31. I. L. Dubchak, T. V. Timofeeva, V. E. Shklover, Yu. T. Struchkov and A. A. Zhdanov, *Zh. Struk. Khim.* 1981, **22**, N6, 112.
32. K. A. Andrianov, S. V. Bushin, M. G. Vitkovskaya, V. N. Emel'yanov, P. N. Lavrenko, N. N. Makarova, A. M. Muzafarov, V. Ya. Nikolaev, G. F. Kolbina, I. N. Shtennikova and V. N. Tsvetkov, *Vysokomol. Sojed.* 1977, **19A**, 469.
33. K. A. Andrianov, I. I. Tverdokhlebova, N. N. Makarova, I. I. Mamaeva, A. K. Chekalov, V. M. Men'shov and S.-S. A. Pavlova, *Vysokomol. Sojed.* 1978, **20A**, 377.

*Polyhedron* Vol. 3, No. 9/10, pp. 1121–1124, 1984
Printed in the U.S.A.

0277–5387/84 $3.00 + .00
© 1984 Pergamon Press Ltd.

# SYNTHESIS OF STERICALLY DEMANDING PHENOXIDE DERIVATIVES OF Ti(IV) AND Zr(IV), M(*O*-2,4,6-(t-Bu)$_3$C$_6$H$_2$)$_2$X$_2$ (X = NMe$_2$, M = Ti, Zr; X = Cl, M = Ti): X-RAY CRYSTAL STRUCTURE OF Ti(*O*-2,4,6-(t-Bu)$_3$C$_6$H$_2$)$_2$(NMe$_2$)$_2$

**RICHARD A. JONES,* JOHN G. HEFNER and THOMAS C. WRIGHT**
Department of Chemistry, The University of Texas at Austin, Austin, TX 78712, USA

(*Received* 19 *March* 1984; *accepted* 23 *June* 1984)

**Abstract**—The interaction of M(NMe$_2$)$_4$ with excess 2,4,6-tri-t-butylphenol yields M{*O*-2,4,6-(t-Bu)$_3$C$_6$H$_2$}$_2$(NMe$_2$)$_2$[M = Ti (**1**) (82%); M = Zr (**2**) (88%)]. Further reaction of **1** with neat Me$_3$SiCl yields M{*O*-2,4,6-(t-Bu)$_3$C$_6$H$_2$}$_2$Cl$_2$ (**3**) (90% yield). The solid-state structure of **1** has been determined by a single-crystal X-ray diffraction study. The coordination geometry around Ti is a distorted tetrahedron.

The use of sterically demanding ligands is currently receiving considerable attention in all areas of chemistry. Several reports describing the chemistry of early transition metal complexes with bulky phenoxide ligands appeared while this work was in progress.[1] In particular Rothwell and coworkers have reported several studies involving the large 2,6-di-t-butylphenoxide ligand. Interesting observations have included intramolecular C—H activation via metallation of a t-butyl (tiBu) group of the phenoxide.[2]

We have investigated the synthesis and isolation of early transition metal complexes containing the 2,4,6-tri-t-butylphenoxide ligand. We studied the reaction of this bulky phenoxide with Ti(NMe$_2$)$_4$ and Zr(NMe$_2$)$_4$, since the interaction of free alcohols (or phenols) with early transition metal dialklyamides is a well-known route to alkoxide (or phenoxide) complexes via elimination of secondary amines[3a] [eqn (1)]:

$$M(NR_2)_x + xHOR \rightarrow M(OR)_x + xHNR_2. \quad (1)$$

We were interested in several aspects of these reactions. One question concerned the extent to which the dialkylamide ligands could be replaced by phenoxides. This should be limited by the steric bulk of the phenoxide ligand and give mixed dialkylamide/phenoxide species. We found that even in the neat molten phenol only two NMe$_2$ units could be replaced to give complexes **1** and **2** [eqn (2)]:

$$M(NMe_2)_4 + \text{excess H-}O\text{-2,4,6-(t-Bu)}_3C_6H_2 \xrightarrow[120°C]{\Delta}$$

$$M\{O\text{-2,4,6-(t-Bu)}_3C_6H_2\}_2(NMe_2)_2 + 2HNMe_2, \quad (2)$$

**1, 2**

where M = Ti (**1**) and Zr (**2**). Since few stable crystalline mixed dialkylamide/alkoxides of the group IV transition metals are known[3b] we determined the solid-state structure of **1** via a single-crystal X-ray diffraction study. We were also naturally interested in the possibility of C—H bond activation by metallation of one of the t-Bu groups of the phenoxide accompanied by further amine elimination. However, both **1** and **2** are unaffected by heating to 220 and 180°C respectively and failed to give clean isolable products when pyrolyzed and were unaffected by photolysis experiments. Conversion of **1** to the chloride derivative TiCl$_2${*O*-2,4,6-(t-Bu)$_3$C$_6$H$_2$}$_2$ (**3**) may be achieved cleanly in high yield (*ca* 90%) by refluxing **1** in neat Me$_3$SiCl.

We describe here the synthesis of **1**, **2** and **3** and the X-ray crystal structure of **1**.

## RESULTS AND DISCUSSION

The interaction of the binary dimethylamido derivatives of Ti(IV) or Zr(IV) [M(NMe$_2$)$_4$] with 2,4,6-tri-t-butylphenol at elevated temperatures (*ca* 120°C) results in rapid elemination of HNMe$_2$

* Author to whom correspondence should be addressed.

and gives high yields of the mixed bisphenoxide bisdimethylamide derivatives **1** and **2** [see eqn (2)]. These hydrocarbon soluble orange (**1**) or white (**2**) crystalline compounds are air-stable in the solid state and also in solution for prolonged periods. Spectroscopic data (IR, $^1H$ and $^{13}C$ NMR) are quite straightforward (see Experimental). We found that other attempts to prepare derivatives of the bulky phenoxide such as via lithiation reactions failed to give cleanly isolable products. However we were able to obtain $TiCl_2\{O\text{-}2,4,6\text{-}(t\text{-}Bu)_3C_6H_2\}_2$ (**3**) cleanly in high yield from the reaction of **1** with neat $Me_3SiCl$ under reflux [eqn (3)]:

$$Ti(NMe_2)_2\{O\text{-}2,4,6\text{-}(t\text{-}Bu)_3C_6H_2\}_2 + \text{excess } Me_3SiCl \xrightarrow[\text{reflux}]{} TiCl_2(O\text{-}2,4,6\text{-}(t\text{-}Bu)_3C_6H_2)_2 + 2Me_2SiNMe_2, \quad (3)$$

**3**

**3** may be isolated as a deep red, hydrocarbon-soluble, air-stable crystalline material.

*X-ray structure of* **1**

A view of the molecule is shown in Fig. 1 and crystal data are given in Experimental. Relevant bond lengths and angles are presented in Table 1.

The coordination geometry about the Ti atom is a distorted tetrahedron. The distortions from idealized geometry are as expected considering the difference in size of the amide and phenoxide groups. Thus the N(1)—Ti(1)—N(2) angle [98.6(2)°] is considerably less than either the N(1)—Ti(1)—O(2) [107.2(2)°] or O(1)—Ti(1)—O(2) [115.2(2)°] angles. There are several features of the structure which suggest that both N → Ti $\pi$-bonding and O → Ti $\pi$-bonding are present to a significant degree.[3c] Both N(1) and N(2) are virtually planar (see Table 1) and the Ti—N distances of 1.897(5) and 1.864(4) Å are considerably shorter than a single bond length of *ca* 1.96 Å estimated from the sum of covalent radii.[4] The Ti—N distances can be compared to the Ti—N distance [1.852(4) Å] observed in $Et_2NTiCl_3$[5] which was also attributed to ($p \rightarrow d$) $\pi$-bonding involving an $sp^2$ hybridized nitrogen.

Table 1. Selected bond lengths (Å) and angles (°) for **1**

| Atom 1 | Atom 2 | Distance | Atom 1 | Atom 2 | Atom 3 | Angle |
|---|---|---|---|---|---|---|
| Ti1 | O1 | 1.813(4) | O1 | Ti1 | O2 | 115.2(2) |
| Ti1 | O2 | 1.860(3) | O1 | Ti1 | N1 | 116.7(2) |
| Ti1 | N1 | 1.897(5) | O1 | Ti1 | N2 | 102.4(2) |
| Ti1 | N2 | 1.864(4) | O2 | Ti1 | N1 | 107.2(2) |
| O1 | C11 | 1.375(6) | O2 | Ti1 | N2 | 115.9(2) |
| O2 | C21 | 1.366(5) | N1 | Ti1 | N2 | 98.6(2) |
| N1 | C101 | 1.491(7) | Ti1 | O1 | C11 | 171.0(3) |
| N1 | C102 | 1.471(8) | Ti1 | O2 | C21 | 152.0(3) |
| N2 | C201 | 1.482(7) | Ti1 | N1 | C101 | 127.9(4) |
| N2 | C202 | 1.505(7) | Ti1 | N1 | C102 | 124.5(4) |
| | | | C101 | N1 | C102 | 107.5(5) |
| | | | Ti1 | N2 | C201 | 121.0(4) |
| | | | Ti1 | N2 | C202 | 127.8(4) |

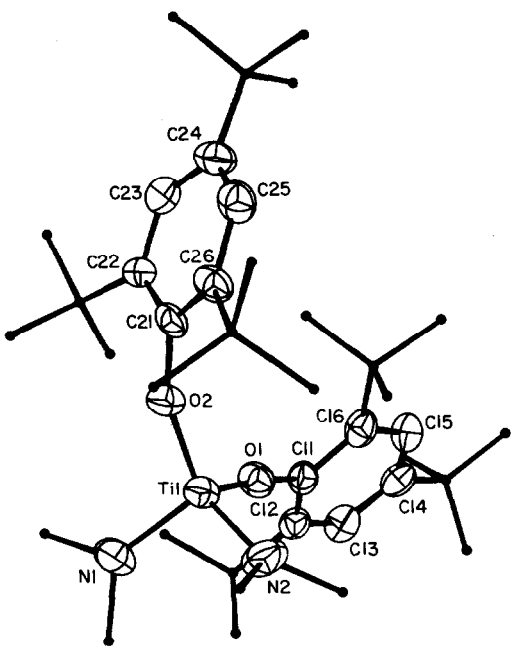



Fig. 1. A general view of **1**. Methyls on the t-Bu and $NMe_2$ groups are represented as sticks for clarity.

The bonding parameters of the phenoxides also indicate the presence of substantial O → Ti $\pi$-bonding. However, the degree of $\pi$-bonding appears to be different for the two phenoxides. Thus one phenoxide has a Ti—O(1) distance of 1.813(4) Å and a Ti—O(1)—C(11) angle of 171.0(3)° while the other has analogous values of 1.860(3) Å and 152.0(3)°. Both Ti—O distances are considerably shorter than the calculated single covalent bond length (*ca* 2.01 Å) and may be compared with an analogous Ti—O length of 1.744(10) Å found in $[TiCl_2(OPh)_2]_2$.[6] In this complex the Ti—O—C angle of 165.9(6)° was also taken as indicative of O → Ti $\pi$-bonding (*sp* hybridized O). In addition both O(1)—C(11) and O(2)—C(21) distances are quite short [1.375(6) and 1.366(5) Å, respectively], indicating an additional degree of $\pi$-bonding between these pairs of atoms. Although the precise reasons for the differences in bonding parameters for the two phenoxides are not

clear at present it appears that intramolecular crowding is not an important factor. The shortest contacts are between the t-Bu carbons of one phenoxide and the ring carbon atoms of the other and none of these is less than 3.48 Å.

## EXPERIMENTAL

All reactions were performed under oxygen-free nitrogen. Microanalyses were by the Schwartzkopf Microanalytical Laboratory (Woodside, NY). Hexane was dried over sodium and distilled from sodium/benzophenone under nitrogen before use. Toluene was distilled from sodium under nitrogen before use.

### *Instruments*

IR: Perkin–Elmer 1330. NMR: Varian EM 390 ($^1$H, 90 MHz), FT 80 ($^{13}$C, 20 MHz), Nicolet NT 200 ($^1$H and $^{13}$C). IR spectra were as nujol mulls (KBr plates) and NMR spectra were recorded in $C_6D_6$ at ambient temperature and are referenced to $Me_4Si$ ($\delta$0.0). M.ps were in sealed capillaries under nitrogen (1 atm) and are uncorrected.

$Ti(NMe_2)_4$[7] and $Zr(NMe_2)_4$[7] were prepared as previously described. 2,4,6-Tri-t-butylphenol was purchased from the Aldrich Chemical Company (Milwaukee, WI) and recrystallized from hexane before use.

### $Ti\{O\text{-}2,4,6\text{-}(t\text{-}Bu)_3C_6H_2\}_2(NMe_2)_2$ (1)

$Ti(NMe_2)_4$ (1.46 g, 6.512 mmol) was added to 2,4,6-tri-t-butylphenol (3.42 g, 13 mmol) at −78°C. The mixture was warmed slowly to room temperature (1 h). At −20°C gas evolution was noted. The mixture was then heated (120°C, oil bath) under nitrogen (2 h). The resulting red oil was cooled to 100°C and then placed under vacuum as it cooled to room temperature. The resulting waxy solid was extracted into toluene (50 cm$^3$), the solution was filtered and then evaporated to dryness under vacuum. Excess 2,4,6-tr-t-butylphenol was sublimed onto a cold probe (−78°C) at 110–120°C under vacuum. The remaining solid was extracted into hexane (100 cm$^3$) and the solution filtered and evaporated to *ca* 75 cm$^3$ under vacuum. Cooling (−20°C) yielded orange/yellow crystals of **1** which were collected and dried under vacuum. Yield 3.50 g, 82%. M.p. 189–193°C. The complex becomes dark red at its m.p. and returns to an orange/yellow color on solidification when cooled. NMR: $^1$H (90 MHz), $\delta$7.46 [*brs*, 4H, *O*-2,4,6-(t-Bu)$_3C_6H_2$]; $\delta$3.24 (*s*, 12H, N*Me*$_2$); $\delta$1.55 [*s*, 18H, *O*-2,4,6-(t-*Bu*)$_3C_6H_2$]; $\delta$1.29 [*s*, 9H, *O*-2,4,6-(t-*Bu*)$_3C_6H_2$]. $^{13}$C {$^1$H}: $\delta$ 161.81 (*s*), 122.94 (*s*), 139.13 (*s*), 142.00 (*s*) [phenyl C atoms of *O*-2,4,6-(t-Bu)$_3C_6H_2$]; $\delta$49.51 (*s*, N*Me*$_2$); $\delta$36.15 [*s*, *O*-2,4,6-(t-C*Me*$_3$)$C_6H_2$]; $\delta$31.95 [*s*, *O*-2,4,6-(t-C*Me*$_3$)$C_6H_2$]; quaternary carbon atoms of the t-Bu groups were not observed. IR (nujol mull) (cm$^{-1}$): 2850 s, 1416 m, 1360 m, 1293 w, 1263 w, 1220 s, 1048 w, 946 m, 915 m, 864 s, 844 s, 763 m, 749 w, 717 w, 572 m, 483 w. Found: C, 71.16; H, 10.48; N, 4.09%. Calc. for $C_{40}H_{70}N_2O_2Ti$: C, 72.91; H, 10.71; N, 4.25%.

### $Zr\{O\text{-}2,4,6\text{-}(t\text{-}Bu)_3C_6H_2\}_2(NMe_2)_2$ (2)

A solution of 2,4,6-tr-t-butylphenol (4.62 g, 18 mmol) in hexane (25 cm$^3$) was added to a solution of $Zr(NMe_2)_4$ (1.08 g, 4.1 mmol) in hexane (50 cm$^3$) at −78°C. The mixture was allowed to warm to room temperature and then heated under reflux (12 h). Volatile materials were removed under vacuum and the residue was heated at 120°C under vacuum (4 h). The solid was extracted into hexane (50 cm$^3$), the solution evaporated to *ca* 20 cm$^3$ under vacuum and filtered. Cooling (−20°C) gave white microcrystals of **2**. They were collected and dried under vacuum. Yield 2.53 g, 88%. M.p.: the complex becomes waxy at *ca* 107°C and melts over the range 168–175°C. NMR: $^1$H (in $CDCl_3$): $\delta$7.21 [*s*, 4H, *O*-2,4,6-(t-Bu)$_3C_6H_2$]; $\delta$3.09 (*s*, 12H, N*Me*$_2$); $\delta$1.44 [*s*, 36H, *O*-2,4,6-(t-*Bu*)$_3C_6H_2$]; $\delta$1.28 [*s*, 18H, *O*-2,4,6-(t-*Bu*)$_3C_6H_2$]. $^{13}$C {$^1$H} (in $CDCl_3$): $\delta$141.36 (*s*), 138.01 (*s*), 122.59 (*s*), [phenyl C atoms of *O*-2,4,6-(t-Bu)$_3C_6H_2$], and the quaternary *C*—O carbon of the phenyl rings were not observed; $\delta$44.44 (*s*, NMe$_2$); $\delta$36.03 [*s*, *O*-2,4,6-(t-C*Me*$_3$)$_3C_6H_2$]; $\delta$31.88 [*s*, *O*-2,4,6-(t-C*Me*$_3$)$C_6H_2$]; quaternary carbon atoms of the t-Bu groups were not observed. Found: C, 68.63; H, 10.17; N, 3.85%. Calc: C, 68.42; H, 10.05; N, 3.85%.

### $Ti\{O\text{-}2,4,6\text{-}(t\text{-}Bu)_3C_6H_2\}_2Cl_2$ (3)

$Me_3SiCl$ (20 cm$^3$) was added to **1** (2.5 g, 3.8 mmol) at room temperature. The mixture slowly turned red. The solution was refluxed (3 days), volatile materials were removed under vacuum and residual 2,4,6-tri-t-butylphenol was removed by sublimation onto a cold probe (−78°C) at 110–120°C under vacuum. The residue was extracted into toluene (50 cm$^3$) and the solution filtered. Cooling (−20°C) gave dark red crystals of **3**. The complex was recrystallized twice more from toluene (−20°C) and finally dried under vacuum. Yield 2.2 g, 90%. M.p. 288–293°C. NMR: $^1$H (90 MHz) in $C_6D_6$; $\delta$7.37 [*s*, 4H, *O*-2,4,6-(t-Bu)$_3$ $C_6H_2$]; $\delta$1.56 [*s*, 36H, *O*-2,4,6-(t-*Bu*)$_3C_6H_2$]; $\delta$1.18 [*s*, 18H, *O*-2,4,6-(t-*Bu*)$_3C_6H_2$]. $^{13}$C {$^1$H}: $\delta$169.81, 140.10, 129.22, 122.55 [*s*, phenyl C atoms of *O*-2,4,6-(t-Bu)$_3C_6H_2$]; $\delta$36.03 [*s*, *O*2,4,6-

$(t\text{-}Bu)_3C_6H_2]$; $\delta$32.13 [*s*, *O*-2,4,6-$(t\text{-}CMe_3)C_6H_2]$; quaternary carbon atoms of the t-Bu groups were not observed. Found: C, 67.54; H, 9.05; Cl, 10.91%. Calc: C, 67.39; H, 9.11; Cl, 11.05%.

*X-ray experimental*

Crystals of **1** were grown from hexane solutions at −20°C and were mounted in thin-walled glass capillaries under nitrogen. Final lattice parameters were determined from 25 high-angle reflections ($26.0° > 2\theta > 30.0°$) carefully centered on an Enraf–Nonius CAD-4 diffractometer. Data were collected by the $\omega/2\theta$ scan technique at 23 ± 2°C. Details of intensity data collection methods are as outlined in Ref. 8. The space group was uniquely determined by systematic absences. The data was corrected for Lorentz and polarization effects and an absorption correction was applied using an empirical psi-scan method. The structure was solved using a combination of direct and heavy-atoms methods and successive difference Fourier maps using the Enraf–Nonius software package "SDP-PLUS" (B. A. Frenz and Associates, College Station, TX 77840, 4th edition, 1981) on a PDP 11/44 computer. Scattering factors were taken from Ref. 9 and unit weights were used throughout. Hydrogen atoms were not located. The final full-matrix least-squares refinement used anisotropic thermal parameters for all atoms. No chemically significant peaks were present in the final difference Fourier map.

Crystal data (**1**): $C_{40}H_{70}N_2O_2Ti$, $M = 658.92$, monoclinic, $P2_1/n$, $a = 11.641(5)$Å, $b = 24.237(5)$ Å, $c = 14.375(2)$ Å, $\beta = 93.606(3)°$, $U = 4047.7(5)$ Å$^3$, $D_c = 1.081$ g cm$^{-3}$, $Z = 4$, $\lambda$(Mo-K$_\alpha$) = 0.71069 Å, $\mu$(Mo-K$_\alpha$) = 2.39 cm$^{-1}$, final $R = 0.0816$ ($R_w = 0.0945$) from 2747 observed reflections [$I > 3\sigma(I)$], 7689 measured, where $R = \sum(|F_o| - |F_c|)/\sum|F_o|$ and $R_w = [\sum\omega(|F_o| - |F_c|)^2/\sum\omega|F_o|^2]^{1/2}$. Tables of atomic coordinates, thermal parameters, bond lengths and angles and $F_o/F_c$ values have been deposited as supplementary material with the Editor from whom copies are available on request. Atomic coordinates have also been deposited with the Cambridge Crystallographic Data Centre.

*Acknowledgements*—We thank the Robert A. Welch Foundation (F-816), the University Research Institute of the University of Texas at Austin, the National Science Foundation (CHE82-11883), and the Research Corporation for support. The X-ray diffractometer was purchased with funds from the National Science Foundation (CHE82-05871) and the University of Texas at Austin.

## REFERENCES

1. L. Chamberlain, I. P. Rothwell and J. C. Huffman, *J. Am. Chem. Soc.* 1982, **104**, 7338; L. Chamberlain, J. Keddington and I. P. Rothwell, *Organometallics* 1982, **1**, 1098; L. Chamberlain, J. Keddington, I. P. Rothwell and J. C. Huffman, *Organometallics* 1982, **1**, 1538.
2. L. R. Chamberlain and I. P. Rothwell, *J. Am. Chem. Soc.* 1983, **105**, 1665.
3. M. F. Lappert, P. P. Power, A. R. Sanger and R. C. Srivastava, *Metal and Metalloid Amides* (a) p. 608, (b) Chap. 8, p. 503, (c) Chap. 8, p. 475. John Wiley, New York (1980).
4. L. E. Sutton (Ed.) *Tables of Interatomic Distances and Configurations in Molecules and Ions.* Special Publication No. 11, The Chemical Society, London.
5. J. Fayos and D. Mootz, *Z. Anorg. Allg. Chem.* 1971, **380**, 196.
6. K. Watenpaugh and C. N. Caughlan, *Inorg. Chem.* 1966, **5**, 1782.
7. D. C. Bradley and I. M. Thomas, *J. Chem. Soc.* (*A*) 1960, 3857.
8. R. A. Jones and T. C. Wright, *Organometallics* 1983, **2**, 1842.
9. *International Tables for X-ray Crystallography*, Vol. 4. Kynoch Press, Birmingham, U.K. (1974).

*Polyhedron* Vol. 3, No. 9/10, pp. 1125–1129, 1984
Printed in the U.S.A.

0277–5387/84 $3.00 + .00
© 1984 Pergamon Press Ltd.

# EXTRACTION OF TRIVALENT ACTINIDES WITH SOME SUBSTITUTED PYRAZOLONES AND THEIR SYNERGISTIC MIXTURES WITH TRI-*n*-OCTYLPHOSPHINE OXIDE IN CHLOROFORM

**J. N. MATHUR and P. K. KHOPKAR***
Radiochemistry Division, Bhabha Atomic Research Centre, Trombay, Bombay-400085, India

(*Received* 19 *March* 1984; *accepted* 23 *June* 1984)

**Abstract**—Trivalent actinides, Am, Cm, Bk and Cf, have been extracted with 1-phenyl-3-methyl-4-benzoyl pyrazolone-5 (HPMBP) or 1-phenyl-3-methyl-4-(3:5-dinitrobenzoyl) pyrazolone-5 (HDMPP) in chloroform. With HPMBP, Am, Bk and Cf are extracted as the self-adduct species $M(PMBP)_3 \cdot nHPMBP$ ($n = 1$ or 2) whereas in all the other systems formation of a non-adduct chelate species has been observed. With tri-*n*-octylphosphine oxide (TOPO), as the neutral donor, the synergistic adduct species are $M(A)_3 \cdot mTOPO$, where $m$ is 1 or 2 in the above systems. The equilibrium constants ($\beta_1$, $\beta_2$ and $K_2$) for the organic-phase synergistic reactions have been calculated. In Am(III)–different β-diketones–TOPO systems the equilibrium constants follow the order HPMBP < HDMPP < thenoyltrifluoroacetone < benzoyltrifluoroacetone.

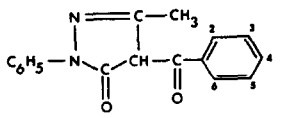
Synergistic extraction of metal ions has various advantages over ordinary solvent extraction systems, such as enhancement of extractability, widening the optimum extraction pH range, stabilization of an extracted species by forming an adduct and a favourable kinetic effect.[1] The continued interest in this field can be seen from various reviews[2–5] published by different authors. Extraction of the trivalent actinides and lanthanides has been extensively studied with mixtures of thenoyltrifluoroacetone (HTTA) and various neutral donors.[2–9] Among the various new chelating agents being tried for the extraction of metal ions 1-phenyl-3-methyl-4-benzoyl pyrazolone-5 (HPMBP) has proved to be a very promising reagent. HPMBP and its various 4-aroyl and acyl group derivatives have been extensively used for the preparation of solid compounds as well as for the extraction of several rare earth ions,[10–16] but the same have been used less frequently[17–19] for the extraction of trans-plutonium elements (TPE). Due to the lower $pK_a$ value (compared to HTTA) HPMBP has been found to extract TPE from more acidic solutions.[19,20] Another new derivative of HPMBP, namely, 1-phenyl-3-methyl-4-(3:5-dinitrobenzoyl) pyrazolone-5 (HDMPP), with the introduction of two electron-withdrawing nitro groups in the benzoyl ring would be expected to lower the $pK_a$ value (compared to HPMBP) and hence extract the TPE at a lower pH. The present study deals with the extraction of Am(III), Cm(III), Bk(III) and Cf(III) with HPMBP and HDMPP alone and with their synergistic mixtures with tri-*n*-octylphosphine (TOPO) in chloroform.

## EXPERIMENTAL

The tracer solutions of $^{241}Am$, $^{244}Cm$, $^{249}Bk$ and Cf (mainly $^{252}Cf$) were prepared and assayed as described earlier.[7,21,22] TOPO (Merck Pro Analysi), chloroform (BDH Analar) and other chemicals used were of A.R. grade. HPMBP (m.p. 92°C) and HDMPP (m.p. 225.5°C) were prepared in this laboratory. The structural formula of the β-diketones used in this work are given in Scheme 1.

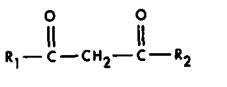
The experimental details of β-diketone variation, pH variation and extraction with the synergistic mixture of β-diketone + TOPO for the trivalent actinides were as given in Ref. 19.

* Author to whom correspondence should be addressed.



HPMBP

HDMPP – $NO_2$ GROUPS IN POSITION 3 AND 5 IN THE BENZOYL GROUP.



HTTA – $R_1$ – THENOYL GROUP
$R_2 - CF_3$

HBTFA – $R_1$ – BENZOYL GROUP
$R_2 - CF_3$

Scheme 1.

## RESULTS AND DISCUSSION

The extraction of Am(III), Cm(III), Bk(III) and Cf(III) with HDMPP and that of Cm(III) with HPMBP alone may be represented by:

$$M^{3+}_{aq} + 3HA_{org} \overset{K_{HA}}{\rightleftharpoons} M(A)_{3org} + 3H^{+}_{aq}, \quad (1)$$

whereas that of Am(III), Bk(III) and Cf(III) with HPMBP (where the formation of a self-adduct species has been observed) may be expressed as:

$$M^{3+}_{aq} + (3+n)HPMBP_{org} \overset{K_{HA}}{\rightleftharpoons} M(PMBP)_3 \cdot nHPMBP_{org} + 3H^{+}_{aq}, \quad (2)$$

where $n = 1$ for Am(III) and Bk(III), $n = 2$ for Cf(III), and HA is the $\beta$-diketone.

The formation of these species in the organic phase was arrived at by the slope analysis method where log $D$ (distribution coefficient) values were plotted against log [HA] (Figs 1 and 2) or pH. It

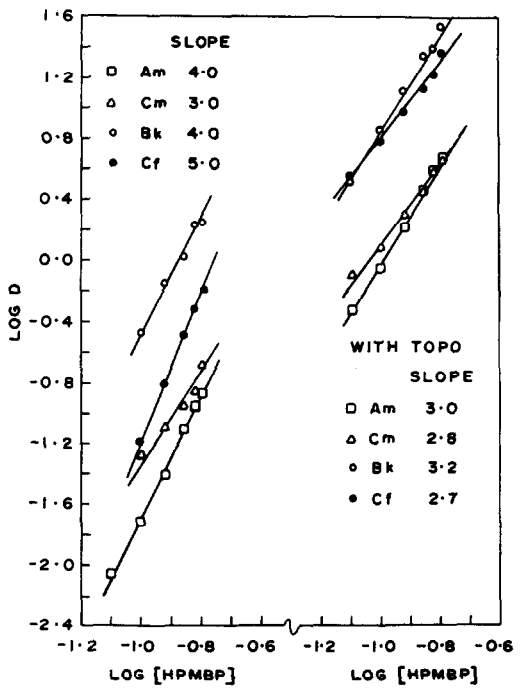



Fig. 1. Variation of log $D$ of trivalent actinides as a function of HPMBP (alone and in the presence of TOPO) concentration.

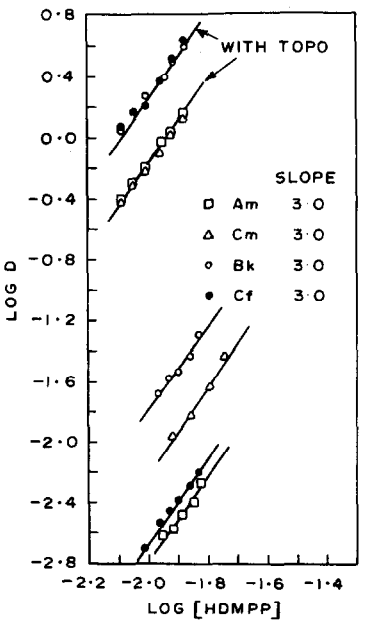



Fig. 2. Variation of log $D$ of trivalent actinides as a function of HDMPP (alone and in the presence of TOPO) concentration.

can be seen from Fig. 1 that the HPMBP variation gives a slope of 4 with Am(III) and Bk(III) and 5 with Cf(III). This, in conjunction with the slope of 3 observed with pH variation for all these systems, indicates the formation of the self-adduct species $M(PMBP)_3 \cdot HPMBP$ (M = Am, Bk) and $Cf(PMBP)_3 \cdot 2HPMBP$. The formation of these species was further ascertained from the plots of log $D$-3pH-3 log $[HA]_{org}$ vs log $[HA]_{org}$ as suggested by Hori *et al.*[23] Such plots gave a slope of 1 with Am and Bk and 2 with Cf. It is seen from the present study that Cm(III) does not form a self-adduct species with HPMBP in $CHCl_3$. Possibly the self-adduct formation with various trivalent actinides is connected with "tetrads" where Cm is on one of the minima. However, in xylene the formation of self-adduct species $M(PMBP)_3 \cdot HPMBP$ has been observed with all the four trivalent actinides,[19] which is commensurate with the generally increased extraction in this diluent as compared to $CHCl_3$. Formation of self-adduct species in different metal $\beta$-diketone systems has been established by many workers,[23–30] whereas extraction of simple chelates have been reported by others.[10,11,27,31] It looks likely that the formation of a self-adduct species depends on various factors such as concentration of the chelating agent, its ionization constant ($pK_a$), the comparative basicity of the undissociated ligand molecules, diluent and of course the complexing ability of the metal ion.

In the present study the formation of a self-adduct species with HPMBP and not with HDMPP could

possibly arise due to: (a) the lower $pK_a$ of HDMPP (nearly 2 log units) as compared to that of HPMBP leading to the availability of comparatively lesser amounts of the unionized HDMPP in the aqueous phase, and (b) the weaker basicity of the neutral HDMPP molecule (due to the presence of two $NO_2$ groups) leading to a reduced possibility of its successfully competing with the coordinated water molecules of the metal chelate in the organic phase.

The extraction of the trivalent actinides in the presence of HPMBP (or HDMPP) and TOPO may be represented by:

$$M^{3+}_{aq} + 3HA_{org} + YTOPO_{org} \overset{K_{syn_Y}}{\rightleftharpoons} MA_3 \cdot YTOPO_{org} + 3H^+_{aq}, \quad (3)$$

where $Y = 1$ or 2.

The organic-phase reactions may be represented either by the addition reactions:

$$M(A)_{3org} + TOPO_{org} \overset{\beta_1}{\rightleftharpoons} M(A)_3 \cdot TOPO_{org} \quad (4)$$

and

$$M(A)_{3org} + 2TOPO_{org} \overset{\beta_2}{\rightleftharpoons} M(A)_3 \cdot 2TOPO_{org} \quad (5)$$

or the substitution reactions:

$$M(A)_3 \cdot nHA_{org} + TOPO_{org} \overset{\beta_1}{\rightleftharpoons} M(A)_3 \cdot TOPO_{org} + nHA_{org} \quad (6)$$

and

$$M(A)_3 \cdot nHA_{org} + 2TOPO_{org} \overset{\beta_2}{\rightleftharpoons} M(A)_3 \cdot 2TOPO_{org} + nHA_{org}. \quad (7)$$

The formation of the second synergistic species in both the cases could, however, be represented by:

$$M(A)_3 \cdot TOPO_{org} + TOPO_{org} \overset{K_2}{\rightleftharpoons} M(A)_3 \cdot 2TOPO_{org}, \quad (8)$$

$K_2$ being the constant for this reaction.

It can be seen from Figs 1 and 2 (plots of log $D$ vs log [HA] at fixed TOPO concentrations) that only three $\beta$-diketone moieties are attached to the synergistic species in all the systems studied here. The plots of log $D$ vs log [TOPO] at fixed HPMBP concentration gave slopes of 0.8 (Bk) and 0.9 (Cf), indicating the attachment of only one TOPO molecule in these synergistic systems, whereas in all the other cases slopes of between 1 and 2 were obtained, showing the simultaneous extraction of the synergistic species $M(A)_3(TOPO)$ and $M(A)_3(TOPO)_2$ in the organic phase.

The organic-phase equilibrium constants ($\beta_1$, $\beta_2$ and $K_2$) and the two-phase equilibrium constants ($K_{syn_1}$ and $K_{syn_2}$) in these systems have been calculated from the plots of $D - D_{HA}/[TOPO]$ vs [TOPO] (Fig. 3) or log $D$ vs log [TOPO] (Fig. 4) as described earlier.[19,32] The equilibrium constant values mentioned here refer only to the concentration quotients which have been calculated on the assumption that the activity coefficients of the species involved do not change significantly under the experimental conditions employed.

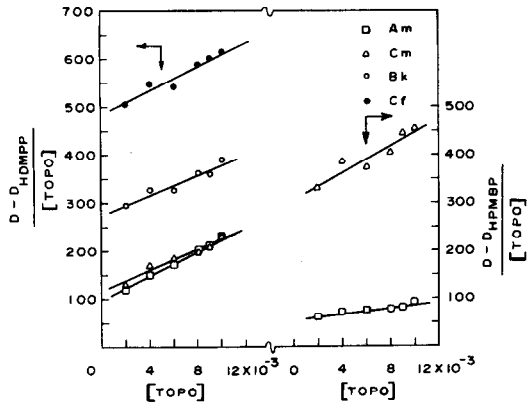



Fig. 3. Variation of $(D - D_{HA})/[TOPO]$ vs [TOPO] for the trivalent actinides (HA = HPMBP and HDMPP).

Table 1 gives the values of $K_{syn_1}$, $K_{syn_2}$ and $K_{HA}$ and Table 2 those of $\beta_1$, $\beta_2$ and $K_2$ for Am(III), Cm(III), Bk(III) and Cf(III) with HPMBP or HDMPP and TOPO in chloroform. In the HPMBP/TOPO system the values of $\beta_1$ and $\beta_2$ for Cm(III) are quite high compared to those with other trivalent actinides. This could possibly be due to the addition reaction in the case of Cm(III) and the substitution one with other actinides. Bacher and Keller[31] have reported values of log $\beta_1$ (0.9) and log $\beta_2$ (7.6) for the Am(III)/HPMBP/TOPO/$CHCl_3$ system. These values are quite different from those reported in the present work. These authors[31] have not reported the formation of any self-adduct species and their much

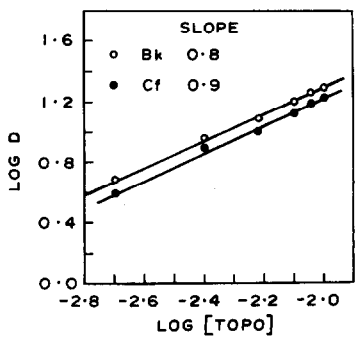



Fig. 4. Variation of log $D$ of Bk(III) and Cf(III) as a function of TOPO concentration at fixed HPMBP concentration.

Table 1. Two-phase equilibrium constants of the trivalent actinides in HPMBP and HDMPP+TOPO in $CHCl_3$ systems at 30°C

| M(III) | $\log K_{syn_1}$ | $\log K_{syn_2}$ | $\log K_{HA}$ |
|---|---|---|---|
| | HPMBP+TOPO | | |
| Am | −0.95±0.02 | 0.75±0.07 | −3.67 |
| Cm | −0.74±0.02 | 0.91±0.05 | −4.34 |
| Bk | −0.28±0.04 | — | −2.46 |
| Cf | −0.26±0.06 | — | −2.20 |
| | HDMPP+TOPO | | |
| Am | 1.74±0.01 | 3.88±0.01 | −2.81 |
| Cm | 1.83±0.02 | 3.79±0.03 | −2.20 |
| Bk | 2.20±0.01 | 3.78±0.01 | −1.82 |
| Cf | 2.44±0.01 | 3.86±0.04 | −2.70 |

Table 2. Equilibrium constants for the organic-phase synergistic reactions of trivalent actinides—HPMBP and HDMPP chelates with TOPO in $CHCl_3$

| M(III) | $\log \beta_1$ | $\log \beta_2$ | $\log K_2$ |
|---|---|---|---|
| | HPMBP+TOPO | | |
| Am | 2.72±0.02 | 4.42±0.07 | 1.70±0.07 |
| Cm | 3.59±0.02 | 5.25±0.05 | 1.66±0.06 |
| Bk | 2.18±0.04 | — | — |
| Cf | 1.94±0.06 | — | — |
| | HDMPP+TOPO | | |
| Am | 4.56±0.03 | 6.69±0.03 | 2.13±0.02 |
| Cm | 4.03±0.02 | 5.99±0.03 | 1.96±0.03 |
| Bk | 4.02±0.01 | 5.60±0.03 | 1.58±0.03 |
| Cf | 5.14±0.02 | 6.56±0.04 | 1.42±0.04 |

higher $\beta_2$-value leads to the conclusion that $K_2 \gg K_1$, which is quite unlikely under normal conditions.

There is no particular order in the $\beta_1$-values of the trivalent actinides/HPMBP/TOPO/$CHCl_3$ systems as also reported earlier for these trivalent actinides in HTTA[7] and HPMBP[19] systems in xylene. However, it was observed that in general these values are lower in $CHCl_3$ compared to those in xylene.[19] This follows the general observation[33] that extraction as well as synergistic extraction of these metal ions are higher in benzene or xylene as compared to that in $CHCl_3$. In a recent communication Sasayama *et al.*[11] have studied the synergistic extraction of Eu(III) with a mixture of HPMBP and TOPO in benzene. The equilibrium constants, $\log \beta_1$ (6.10) and $\log \beta_2$ (10.40), reported by these authors are much higher compared to those of the trivalent actinides of comparable ionic radii reported in xylene,[19] probably due to the unsupported assumption of the extraction of the non-adduct species by HPMBP alone.

As in the case of HPMBP systems the $\beta_1$-values in HDMPP systems also do not follow any particular order but the $K_2$-values do show an order, Am > Cm > Bk > Cf. Since the formation of a self-adduct species has not been observed with Cm(III) in both the HDMPP and HPMBP systems in $CHCl_3$, the synergistic equilibrium constants associated with these systems will be very much comparable. The $\beta_1$-values (Table 2) follow the order HDMPP > HPMBP. This may be explained on the basis of the lower $pK_a$ value for HDMPP (than HPMBP) leading to the lesser stability of the Cm–HDMPP chelates and in turn giving the higher $\beta_1$-value for its TOPO adduct species. A similar order is also observed in the $K_2$-values in these systems.

Table 3 gives the values of $\beta_1$, $\beta_2$ and $K_2$ for Am(III) with mixtures of different $\beta$-diketones and TOPO in $CHCl_3$. This follows the order HPMBP < HDMPP < HTTA < benzoyltrifluoroacetone (HBTFA), which is just the reverse of that obtained for $\log K_{HA}$ in these systems (Table 3) as discussed in the earlier work,[9] except in the case of HPMBP, where the formation of a self-adduct species has been observed.

Table 4 gives the separation factors [SFs $(D_{Bk}/D_{Cf})$] between Bk(III) and Cf(III) with different $\beta$-diketones using xylene or $CHCl_3$ as the diluent. It can be seen that the SF follows the order HPMBP > HDMPP > HBTFA > HTTA. It has been observed in general that the SF in xylene is about an

Table 3. Equilibrium constants for the organic-phase synergistic reaction of Am(III) with mixtures of $\beta$-diketones and TOPO in $CHCl_3$

| $\beta$-Diketone | $\log \beta_1$ | $\log \beta_2$ | $\log K_2$ | $\log K_{HA}$ |
|---|---|---|---|---|
| HPMBP | 2.72±0.02 | 4.42±0.07 | 1.73±0.07 | −3.67 |
| HDMPP | 4.56±0.03 | 6.69±0.03 | 2.13±0.02 | −2.81 |
| HTTA | 4.91±0.02 | 7.37±0.08 | 2.46±0.08 | −8.72 |
| HBTFA | 5.08±0.02 | — | — | −9.65 |

Table 4. SFs between Bk(III) and Cf(III) with different β-diketones

| β-Diketone | SF Xylene | SF $CHCl_3$ |
|---|---|---|
| HPMBP | 772 | 48 |
| HDMPP | — | 7.5 |
| HBTFA | 92.5 | 1.6 |
| HTTA | 14.7 | 0.55 |

order of magnitude higher than that in $CHCl_3$. The lower SFs in $CHCl_3$ could conceivably be due to an interaction between the diluent and the metal chelates themselves.

*Acknowledgement*—We thank Dr P. R. Natarajan, Head, Radiochemistry Division for his keen interest in this work.

## REFERENCES

1. H. Akaiwa and H. Kawamoto, *Rev. Anal. Chem.* 1982, **6**, 65.
2. H. Irving, *Solvent Extraction Chemistry*, p. 91. North-Holland, Amsterdam (1967).
3. T. V. Healy, *Solvent Extraction Research*, p. 257. Wiley, New York (1969).
4. G. Duyckaerts and J. F. Desreux, *International Solvent Extraction Conference, Toronto*, p. 73. CIM, Montreal (1977).
5. J. N. Mathur, *Solvent Extraction and Ion Exchange*, 1983, **1**, 349.
6. K. Akiba, M. Wada and T. Kanno, *J. Inorg. Nucl. Chem.* 1981, **43**, 1031.
7. P. K. Khopkar and J. N. Mathur, *Sep. Sci. Technol.* 1981, **16**, 957.
8. M. Wada, K. Akiba and T. Kanno, *Bull. Res. Inst. Min. Dress. Met. Tohoku Univ., Jpn* 1979, **35**, 11.
9. J. N. Mathur and P. K. Khopkar, *Radiochem. Radioanal. Lett.* 1983, **57**, 259.
10. S. Umetani, M. Matsui, J. Toei and T. Shigematsu, *Anal. Chim. Acta* 1980, **113**, 315.
11. K. Sasayama, S. Umetani and M. Matsui, *Anal. Chim. Acta* 1983, **149**, 253.
12. E. C. Okafor, *Talanta* 1982, **29**, 275.
13. E. C. Okafor, *J. Inorg. Nucl. Chem.* 1980, **42**, 1155.
14. E. C. Okafor, *Polyhedron* 1983, **2**, 309.
15. V. Giri and P. Indrasenan, *Polyhedron* 1983, **2**, 573.
16. Y. Sasaki and H. Freiser, *Inorg. Chem.* 1983, **22**, 2289.
17. M. K. Chmutova, B. F. Myasoedov, M. E. Kochetkova, B. Y. Spivakov and Y. A. Zolotov, *Radiokhimiya* 1974, **16**, 702.
18. G. A. Pribylova, M. K. Chmutova and B. F. Myasoedov, *Radiokhimiya* 1978, **20**, 719.
19. J. N. Mathur and P. K. Khopkar, *Sep. Sci. Technol.* 1982, **17**, 985.
20. J. N. Mathur and P. K. Khopkar, *Solvent Extraction and Ion Exchange* 1983, **1**, 597.
21. P. K. Khopkar and J. N. Mathur, *J. Inorg. Nucl. Chem.* 1974, **36**, 3819.
22. P. K. Khopkar and J. N. Mathur, *J. Inorg. Nucl. Chem.* 1977, **39**, 2063.
23. T. Hori, M. Kawashima and H. Freiser, *Sep. Sci. Technol.* 1980, **15**, 861.
24. D. Dyrssen, *Sven. Kem. Tidskr.* 1955, **67**, 311.
25. L. Newman and P. Klotz, *Inorg. Chem.* 1966, **5**, 461.
26. O. Navratil, *Proceedings of the International Solvent Extraction Conference, Liège*, 1980, Vol. 3, p. 2585. Association des Ingénieurs Sortis de l'Université de Liège (1980).
27. R. Lundqvist, *Proceedings of the International Solvent Extraction Conference, Liège*, 1980, 80-51. Association des Ingénieurs Sortis de l'Université de Liège (1980).
28. S. Peterson, *J. Inorg. Nucl. Chem.* 1960, **14**, 126.
29. E. L. King, USAEC Report TID-5290 paper 34 (1958), p. 269.
30. G. A. Pribylova, M. K. Chmutova and B. F. Myasoedov, *Radiokhimiya* 1981, **23**, 521.
31. W. Bacher and C. Keller, *J. Inorg. Nucl. Chem.* 1973, **35**, 2945.
32. J. N. Mathur, S. A. Pai, P. K. Khopkar and M. S. Subramanian, *J. Inorg. Nucl. Chem.* 1977, **39**, 653.
33. T. V. Healy, *J. Inorg. Nucl. Chem.* 1961, **19**, 328.

*Polyhedron* Vol. 3, No. 9/10, pp. 1131–1134, 1984
Printed in the U.S.A.

0277–5387/84 $3.00 + .00
© 1984 Pergamon Press Ltd.

# ELECTRONIC STATES OF HOT IONS IN IRRADIATED FROZEN ETHANOL SOLUTIONS OF DIAMAGNETIC Mo(0) AND Mo(IV) COMPLEXES

J. O. DZIEGIELEWSKI
Department of Inorganic and Radiation Chemistry, Institute of Chemistry, Silesian University, Katowice, Szkolna 9 Street, Poland

(*Received* 30 *April* 1984; *accepted* 23 *June* 1984)

**Abstract**—The irradiation of frozen ethanol solutions of $Mo(CO)_6$ and $[MoOCl(d)(dppe)_2]Cl$ results in bands at 21,500 $cm^{-1}$ due to $[Mo(CO)_6]^-$ and at 25,000 and 23,500 $cm^{-1}$ due to $[MoOCl(dppe)_2]$ in the excited state. On the basis of bands the electron configurations of Mo(−I) and Mo(III) in the excited state were determined. The behaviour of hot ions depends on the symmetry and charge of the central ion.

Although much has been published on hot ions so far, the influences of such basic factors as the symmetry of the central ion charge, the crystal field force, the degree of covalency of the coordinate bond or the acceptor ability of the ligands on the electronic states of the reduced or oxidized central ions have not yet been determined. It also remains to be explained to what degree these factors affect the lifetime of hot ions and the manner of their decay. In order to elucidate some of these problems, electronic states were studied as well as the manner of hot-ion decay. Hot ions were obtained by irradiation of the hexacarbonyl of molybdenum and the complex of Mo(IV) with 1,2-bis(diphenylphosphino)ethane (dppe). This paper reports an attempt to determine the influence of the electronic configuration and symmetry of the central atom charge on the electronic states and the reactivity of hot ions.

In another paper[1] it was shown that the decrease in symmetry from $O_h$ to $D_{4h}$ in complex compounds of Co(II), Ni(II) and Cu(II) with tetracycline resulted in an increased reactivity of those compounds in the presence of solvated electrons.

## EXPERIMENTAL

$Mo(CO)_6$ (Merck) (purest grade) was used. $[MoOCl(dppe)_2]Cl$ was prepared according to the literature.[2] Ethanol was of the purest grade and was not purified further. Ethanol solutions were prepared in dark flasks. Before the irradiation, they were flushed for 30 min with argon. The gas was introduced into the solutions through a bubbler filled with the solvent. Quartz cells were filled with solutions in an argon atmosphere and placed in a cryostat. The cryostat was filled with liquid nitrogen and irradiated by a cobalt source. In the second cryostat ethanol was irradiated in a cell as thick as those used for the solutions. After irradiation, the cryostats were placed in a Specord UV–VIS spectrophotometer, the temperature of the samples was gradually increased (by evaporating liquid nitrogen without heating) and the occurrence and decay of absorption bands was recorded. The dose rate was $1.8 \times 10^{16}$ eV $g^{-1}$ $s^{-1}$. It was determined with a Fricke dosimeter and converted into the electron density of ethanol.

Solid $[MoOCl(dppe)_2]Cl$ was irradiated at 77 K in spectrosil capillaries. In irradiated samples ESR signals were recorded using a JEOLCO JES-ME-3X spectrometer.

## RESULTS AND DISCUSSION

With the temperature increase from 77 to 100 K of the irradiated frozen solutions, the decay of the trapped electron band and the occurrence of bands at 21,500 $cm^{-1}$ for $Mo(CO)_6$ (Fig. 1) and at 25,500 and 23,500 $cm^{-1}$ for $[MoOCl(dppe)_2]Cl$ (Fig. 2) are observed. The latter bands overlap each other. A further increase in temperature results in a decrease in the intensity at 21,500 $cm^{-1}$ and in the occurrence of new bands at 24,170 $cm^{-1}$ for the $Mo(CO)_6$ solution. At 160 K both bands decay. In the glass containing $[MoOCl(dppe)_2]Cl$ the increase in temperature results in an intensity decrease and caused the decay of bands at 115–120 K. Considering the low intensity and width of the 21,500-$cm^{-1}$ band

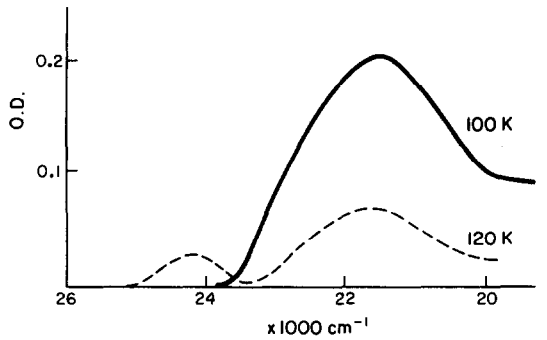



Fig. 1. Optical absorption spectra detected in irradiated frozen ethanol solution of $Mo(CO)_6$ saturated with argon: dose = 3.72 kGy, concentration = $6.8 \times 10^{-3}$ mol/l, cell thickness = 5 cm.

and taking into account the calculated MO levels for $Mo(CO)_6$,[3] it is possible to attribute this band to the $\sigma d^* \rightarrow t_{2g}^*$ transition. Thus, the $e_s^-$ freed from traps interact with $Mo(CO)_6$ producing the $[Mo(CO_6]^-$ ion. The production of this ion was confirmed by pulse radiolysis when $Mo(CO)_6$ was irradiated in cyclohexane and the band was recorded at 21,300 $cm^{-1}$.[4] The delocalized character of the $\sigma d$ orbital permits such a form of this ion.

Thus, the electronic state of the hot central Mo(−I) ion is the following: $(t_{2g})^6$, $(e_g^*)^1$. Due to the high value of 10 $Dq$ (= 33,000 $cm^{-1}$),[3] the $[Mo(CO)_6]^-$ ion is remarkably unstable. The decay of Mo(−I) may occur exclusively as a result of the intermolecular oxidation–reduction reaction since levels lower than $\sigma d^*$ are occupied. In an alcohol solution the most probable form of the oxidation–reduction reaction is as follows:

$$[Mo(CO)_6]^- + C_2H_5OH_2^+ \rightarrow [Mo(CO)_5] + C_2H_5OH + H + CO.$$

The band at 24,170 $cm^{-1}$ originates from $[Mo(CO)_5]$.[5,6]

$[MoOCl(dppe)_2]Cl$ is a diamagnetic compound as indicated by its band asssociated with the $d$–$d$ transition at 17,300 $cm^{-1}$ ($^1A_1 \rightarrow {}^3B_1$, $^3E$). Thus, Mo(IV) shows $C_{4v}$ symmetry. Unoccupied levels in $[MoOCl(dppe)_2]Cl$ are as follows (in order of increasing energies): $b_1$, $e$, $\pi^*$ and $a_1$ (originating only from $d$- and $p$-orbitals).[7] Taking into consideration the high intensity of these bands (Fig. 2), they may be attributed to the transitions $e \rightarrow \pi^*$ (at 25,500 $cm^{-1}$) and $\pi^* \rightarrow a_1$ (at 23,500 $cm^{-1}$). These bands are of the charge-transfer type. This attribution is accounted for by the occurrence of two bands and their high intensity. In the case of the octahedral complex $[Mo(CO)_6]^-$, where the transition $\sigma d^* \rightarrow \pi^*$ is forbidden, the intensity is significantly lower. It is possible to assume that the bands at 25,500 and 23,500 $cm^{-1}$ result from the reaction:

$$[MoOCl(dppe)_2]^+ + e_s^- \rightarrow [MoOCl(dppe)_2]^*.$$

Thus, the hot central ion in the neutral complex shows the following electronic configuration: $(b_2)^2$, $(e)^1$ or $(b_2)^2$, $(\pi^*)^1$. The decay of the hot ion in $[MoOCl(dppe)_2]^*$ is due to deactivation of the excitation state, $e \leftarrow \pi^*$, as well as to the lowering of the $e$-level below the $b_1$-level. These transitions account for the lower thermal stability of $[MoOCl(dppe)_2]^*$ compared to $[Mo(CO)_6]^-$. The

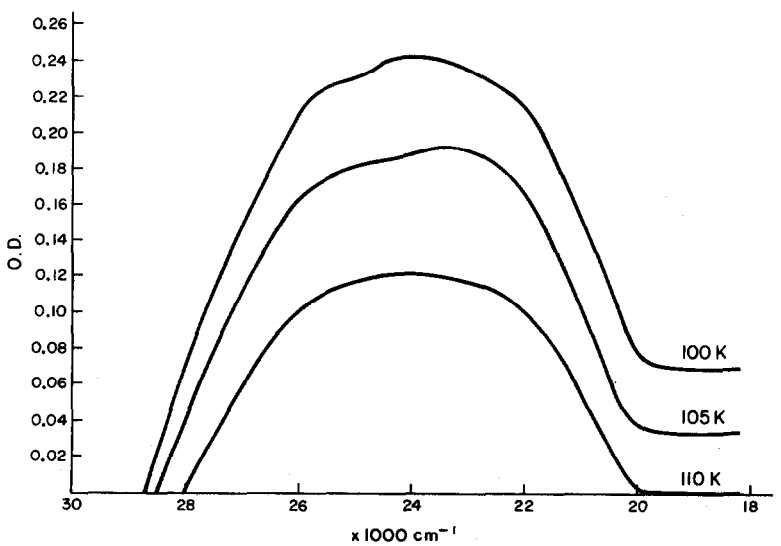



Fig. 2. Optical absorption spectra detected in irradiated frozen ethanol solution of $[MoOCl(dppe)_2]Cl$ saturated with argon: dose = 0.4 kGy, concentration = $3.7 \times 10^{-4}$ mol/l, cell thickness ≐ 1 cm.

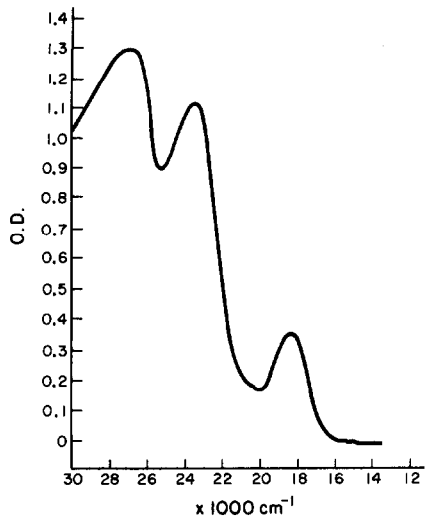



Fig. 3. Optical absorption spectra detected in aerated benzene solution of $[MoCl_2(dppe)_2]$: concentration = $4.26 \times 10^{-3}$ mol/l, cell thickness = 5 cm.

Mo(III) complex of electronic configuration $(b_2)^2, (e)^1$ is not stabilized by ligands because of the weakened $\pi$-bonding in the Mo—O group. In this situation the Mo(III) complex undergoes a disproportionation reaction in methanol solution:[8]

$$2[MoOCl(dppe)_2]^* \xrightarrow[2CH_3OH_2^+]{2Cl^-} [MoCl_2(dppe)_2] + [MoOCl(dppe)_2]Cl + H_2O + 2CH_3OH.$$

The $[MoOCl(dppe)_2]^*$ obtained from an aerated benzene solution of $[MoCl_2(dppe)_2]$ has the proposed electronic configuration as confirmed by the spectrum of Mo(III) in Fig. 3. The bands in Fig. 3 may be attributed to the following transitions: $^2B_2 \rightarrow {}^4E$ (at 18,500 $cm^{-1}$), $^2B_2 \rightarrow {}^2B_1$, $^4B_1$ (at 24,000 $cm^{-1}$) and $^2E \rightarrow {}^2A_1$ (at 27,000 $cm^{-1}$). Mo(III) does not disproportionate in benzene solution ($H^+$ ions not present).

It should be noted that the transition energy $2B_2 \rightarrow {}^4E$ is higher than that of $^1A_1 \rightarrow {}^3B_1$ which seems to confirm the decrease of the tetragonal ligand field factor of Mo(III) in comparison with that of Mo(IV), leading consequently to the lower $e$-level in comparison with $b_1$. The absence of interaction between $e_s^-$ and the ligand (dppe), in accordance with our interpretation of results, is confirmed by the fact that no changes in intensity at 39,690 $cm^{-1}$ (dppe band), after irradiation of the alcohol solution of $[MoOCl(dppe)_2]Cl$ at room temperature, are observed.

In the solid state no interaction between $e^-$ and the ligand is observed either. After irradiation of $[MoOCl(dppe)_2]Cl$ in the solid state ESR signals are observed (Fig. 4).

The ESR signals are unresolved as a result of interaction between the unpaired electron Mo(III) of the $e$-orbital and the P as well as the Cl nuclei. The value of $g$ (1.97), as well as the lack of changes in the signal within the range 120–300 K, indicate that the signal does not originate from organic radicals. $g_{av}$ equals 1.971 indicating that the ESR signal results from Mo(III). The higher $g$-value (1.971) follows from the delocalization of the unpaired electron on the ligand.[9,10] This delocalization is possible when oxygen is present in the coordination sphere. If the ESR signal resulted from Mo(II), the $g_{av}$-value would be lower[9,10] (about 1.94). According to the literature[11] the ligand field parameter of Mo(II) is distinctly lower than that of Mo(III). The lower ligand field parameter reduces the $g$-value.[10]

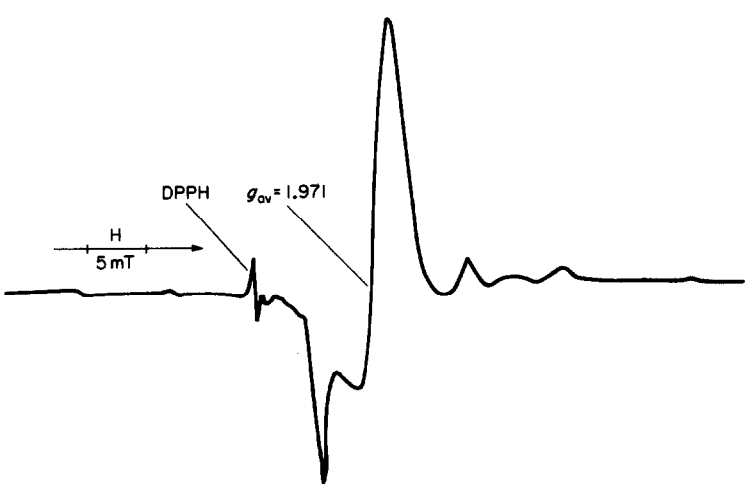



Fig. 4. ESR spectrum of irradiated $[MoOCl(dppe)_2]Cl$ at 77 K in solid state (powder): dose = 10.1 kGy.

Obscure satellite lines result from the interaction between electron e and the $^{95}$Mo and $^{97}$Mo nuclei [a sextet (8.33 mT)]. The anisotropy of the signal is due to the presence of axial symmetry, i.e. $g_{\parallel} = 1.997$ and $g_{\perp} = 1.956$. The relation $g_{\parallel} < g_e > g_{\perp}$ agrees with the assumed Mo(III) electronic configuration, $(b_2)^2, (e)^1$.

The results presented earlier suggested that different electronic configurations of central ions and the transition of symmetry from $O_h$ to $C_{4v}$ in Mo(0) and Mo(IV) compounds with acceptor ligands result in very different behaviours of the hot ions.

## REFERENCES


1. J. O. Dzięgielewski and P. Głowacki, submitted to *Pol. J. Chem.*
2. A. V. Butcher and J. Chatt, *J. Chem. Soc. A* 1971, 2356.
3. L. N. Beach and H. B. Gray, *J. Am. Chem. Soc.* 1968, **90**, 5713.
4. L. Flamigni, *Radiat. Phys. Chem.* 1979, **13**, 133.
5. R. N. Perutz and J. J. Turner, *J. Am. Chem. Soc.* 1975, **97**, 4791.
6. M. J. Boylan, P. S. Braterman and A. Fullarton, *J. Organomet. Chem.* 1971, **31**, C29.
7. B. Jezowska-Trzebiatowska and W. Wojciechowski, *Theoretical Problems of Coordination Chemistry*, p. 131. PWN, Warsaw (1970).
8. H. W. Czarnik-Matusewicz and J. O. Dzięgielewski, *Radioanal. Radiochem. Lett.* 1982, **51**, 355.
9. L. S. Meriwether, W. F. Marzluff and W. S. Hodgson, *Nature (London)* 1966, **212**, 465.
10. C. A. McAuliffe (General Editor), *Techniques and Topics in Bioinorganic Chemistry*, p. 272. Izdatielstwo MIR, Moscow (1978).
11. L. S. Meriwether, S. D. Robinson and G. Wilkinson, *J. Chem. Soc.* 1966, 1488.

*Polyhedron* Vol. 3, No. 9/10, pp. 1135–1140, 1984
Printed in the U.S.A.

0277-5387/84 $3.00 + .00
© 1984 Pergamon Press Ltd.

# SYNTHESIS, CHARACTERISATION AND COORDINATING PROPERTIES OF A NEW PYRAZOLE-DERIVED THIOSEMICARBAZONE, A POTENTIAL ANTIVIRAL AGENT: Co(III), Ni(II) AND Cu(II) COMPLEXES OF NEUTRAL AND DEPROTONATED 5(3)-METHYLPYRAZOLE-3(5)-ALDEHYDOTHIOSEMICARBAZONE

**NITYANANDA SAHA* and NIBEDITA MUKHERJEE**
Department of Chemistry, University College of Science, Calcutta 700009, India

(*Received* 5 *January* 1984; *accepted revised* 9 *July* 1984)

**Abstract**—The title compound (abbreviated as MPzATSH) has been synthesised and physico-chemically (IR, PMR and mass spectrum) characterised for the first time. The ligational behaviour of the thiosemicarbazone has been demonstrated by isolation and characterisation of its complex species with Co(III), Ni(II) and Cu(II) with different counterions. Magnetic and spectral features indicate $Co(MPzATS)_2X$ (X = Cl, Br, $ClO_4$, $BF_4$, $NO_3$ or $\frac{1}{2}SO_4$) as the diamagnetic octahedral species with the ligand in the deprotonated thiol form, while $Ni(MPzATSH)_2X_2$ and $Cu(MPzATSH)X_2$ are proposed as octahedral complexes with the ligand in the neutral "thione" form.

The coordination chemistry of pyrazole-derived ligands has received much attention[1] during recent years, including work from our laboratory,[2] primarily because of biological implications. In view of the well-documented antiviral activity of α-(*N*)-heterocyclic thiosemicarbazones[3] and the fact that such activity is often related to their chelating ability with a metal ion, we have embarked on an investigation relating to the synthesis, characterisation and coordination mode of pyrazole-based thiosemicarbazones. The present paper is intended to report the synthesis of a hitherto unknown pyrazole-based thiosemicarbazone, viz. 5(3)-methylpyrazole - 3(5) - aldehydothiosemicarbazone (Fig. 1a) (MPzATSH) and its characterisation by various physico-chemical data (IR, mass and PMR spectra) along with a comprehensive report on the coordinating properties of the title ligand by complexation with Co(III), Ni(II) and Cu(II) salts with various counterions: the solid metal complexes have also been physico-chemically characterised.

## EXPERIMENTAL

### *Synthesis of MPzATSH*

MPzATSH has been synthesised for the first time by a similar but modified method[4,5] involving: (1) the conversion of 5(3)-methylpyrazole-3(5)-carbohydrazide[6] into its benzene sulphonyl derivative (m.p. 179–180°C), followed (2) by treatment with thiosemicarbazide in alkaline ethylene glycol (160°C): the recrystallised product (ethanol) melts at 221–222°C. (Found: C, 39.01; H, 4.20; N, 37.51; S, 17.27%. Calc. for $C_6H_9N_5S$: C, 39.34; H, 4.92; N, 38.25; S, 17.48%.)

### *Synthesis of the metal complexes*

#### Co(III) *complexes*

$Co(MPzATS)_2X$ (*where* X = Cl, Br, $ClO_4$, $BF_4$, $NO_3$ *or* $\frac{1}{2}SO_4$)

Alcoholic solution of the hydrated Co(II) salt (0.005 mol) was mixed with a solution of the ligand (0.01 mol, 1.83 g) in the same solvent; the resulting mixture was diluted with water to double its volume and air was passed through this solution for 4–5 h for

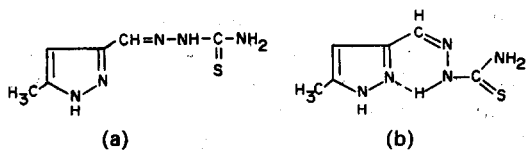



Fig. 1.

* Author to whom correspondence should be addressed.

oxidation. Large dark-brown crystals precipitated out in each case, which were filtered off, washed with water, alcohol and ether and dried in air.

### $Co(MPzATS)_2I$

The same procedure as outlined before was adopted using Co(II) acetate, the ligand and potassium iodide in the appropriate proportions and the desired complex was collected as above.

Ni(II) *complexes*: $Ni(MPzATSH)_2X_2$ (*where* X = Cl, Br, $NO_3$, $BF_4$, $ClO_4$ *or* $\frac{1}{2}SO_4$). A hot alcoholic solution of the hydrated Ni(II) salt (0.005 mol) [made slightly acidic (pH $\simeq$ 4)] is mixed with a solution of the ligand (0.01 mol, 1.8 g) in the same solvent. The resulting solution was filtered off and the clear greenish solution (pH $\simeq$ 3–4) was concentrated by heating at water bath temperature to half of its original volume and then cooled to room temperature ($\simeq$25°C): the desired complex in each case, separated out as micro-crystalline coloured species. The compounds were filtered off, washed with alcohol and dried over silica gel. The complexes were recrystallised from alcohol to obtain analytically pure samples.

Cu(II) *complexes*: $Cu(MPzATSH)X_2$ (*where* X = Cl, Br, $No_3$, $BF_4$ *or* $\frac{1}{2}SO_4$). The same preparative procedure as outlined earlier was adopted for the preparation of the monochelates of Cu(II) salts, using the respective Cu(II) salt (0.01 mol) and ligand (0.01 mol) and isolated in the usual way.

Elemental analyses of the ligand and complexes were carried out as described earlier.[2,7] The PMR spectrum of the ligand was recorded in a DMSO-$d_6$–TFA–$D_2O$ mixture in an EM-390 90 MHz NMR spectrometer. The mass spectrum of the ligand was recorded on an AEIMS 12 spectrometer at 70 eV.

Magnetic susceptibilities of the solid metal complexes were measured in a Gouy balance using GR $CuSO_4 \cdot 5H_2O$ as the calibrant. Electrolytic conductance measurements of the complexes were carried out in a Systronics (303 Model) direct reading conductivity meter: the concentration of the solution used for the purpose was $1.0 \times 10^{-3}$ *M*. The electronic diffuse reflectance spectra of the Co(III) and Ni(II) complexes were recorded in a Zeiss PMQ II spectrophotometer with a reflectance attachment RA3 while the reflectance spectra of the Cu(II) complexes and the solution spectra of all the complex species were taken in a Cary 17D spectrophotometer. The IR spectra of the ligand and metal complexes were recorded in a Beckman 20 IR spectrophotometer using KBr pellets in the range 4000–600 $cm^{-1}$ and in a Perkin–Elmer 221 IR spectrophotometer in the range 600–200 $cm^{-1}$.

## RESULTS AND DISCUSSION

### *Characterisation of the ligand*

The elemental analyses (C, H, N and S) and IR spectral data [characteristic bands ($cm^{-1}$) at 3300–3260 ($\nu_{NH}$), 1610 ($\nu_{C=N_{Pz}}$), 1535 ($\nu_{CH=N}$), 1010 ($\nu_{N-N_{Pz}}$), 800 ($\nu_{C=S}$)] are in quite good agreement with **1a**. The PMR spectrum in a DMSO-$d_6$–TFA–$D_2O$ mixture at 90 MHz gives singlets at $\delta$ 2.20 (3H) and $\delta$ 6.45 (1H) assigned to $-CH_3$ and $C_4-H$ protons. The one proton singlet at $\delta$ 7.93 ascribed to —CH=N indicates the existence of a hydrogen-bonded stabilised form of the compound (1*b*). The mass fragmentation patterns are compatible with the proposed structure. The strongest molecular ion peak appears at *m/z* 183. The subsequent strong peak at *m/z* 107 can be accounted for by a loss of $(H_2N)_2C{=}S$ followed by secondary fragmentation of the benzylic type to expel H from the $-CH_3$ group to give the next peak at *m/z* 106. The molecular ion peaks at 166, 149, 123 and 124 (in terms of decreasing intensities) can be reconciled by the loss of $H_3N$, $H_2S$, $C\begin{matrix}S\\ \diagdown\\ NH_2\end{matrix}$ and HNCS respectively.

### *Characterisation of the complex species*

The neutral form of the ligand, viz. MPzATSH, by interaction with Ni(II) salts in fairly acidic solution (pH = 3–4) produces greenish bis-species, $Ni(MPzATSH)_2X_2$ (X = Cl, Br, $NO_3$, $BF_4$, $ClO_4$ or $\frac{1}{2}SO_4$), whereas in slightly acidic solution (pH = 4–5) it forms monochelates, $Cu(MPzATSH)X_2$ (X = Cl, Br, $NO_3$, $\frac{1}{2}SO_4$, $BF_4$ or $ClO_4$). Starting with Co(II) salts, however, the ligand yielded Co(III) species, $Co(MPzATS)_2X$ (X = Cl, Br, I, $NO_3$, $ClO_4$, $BF_4$ or $\frac{1}{2}SO_4$), in the presence of air with the ligand presumably acting in its deprotonated form. This observation is quite consistent with earlier reports by several authors[8,9] using similar NNS ligands. All the compounds are insoluble in water but soluble in common organic solvents like methanol, acetone, DMF etc.

Co(III) *compounds*. All the reported Co(III) species, $Co(MPzATS)_2X$ (X = Cl, Br, I, $NO_3$, $ClO_4$, $BF_4$ or $\frac{1}{2}SO_4$), are diamagnetic as expected and have proved to be 1 : 1 electrolytes[10] ($\lambda_{max}$ = 80–104 $\Omega^{-1}$ $cm^2$ $mol^{-1}$) in methanol at 25°C (Table 1); the complexes could reasonably be formulated as $Co(MPzATS)_2X$. The diffuse reflectance spectra exhibit four bands in the regions 10,000–10,300, 14,500–15,150, 19,000–20,000 and 25,000–27,700 $cm^{-1}$ which may be assigned as $^1A_{1g} \rightarrow {}^3T_{1g}$, $^1A_{1g} \rightarrow {}^3T_{2g}$, $^1A_{1g} \rightarrow {}^1T_{1g}$ and $^1A_{1g} \rightarrow {}^1T_{2g}$ transitions[11] respectively in an idealised $O_h$-symmetry. As the

Table 1. Analytical, conductance and magnetic moment data for the complexes

| Compound* | M (%) | | N (%) | | Anion (X) (%) | | $\mu_{eff}$ at 298 K (B.M.) | Molar conductance at 30°C ($\Omega^{-1}$ cm$^2$ mol$^{-1}$) |
|---|---|---|---|---|---|---|---|---|
| | Calc. | Found | Calc. | Found | Calc. | Found | | |
| $Co(L)_2Cl$ | 12.87 | 12.79 | 30.53 | 30.48 | 7.74 | 7.70 | — | 104.6† |
| $Co(L)_2Br$ | 11.73 | 11.68 | 27.83 | 27.80 | 15.90 | 15.82 | — | 80.6† |
| $Co(L)_2I$ | 10.73 | 10.63 | 25.45 | 25.35 | — | — | — | 82.5† |
| $Co(L)_2(BF_4)$ | 11.59 | 11.49 | 27.50 | 27.45 | — | — | — | 80.1† |
| $Co(L)_2ClO_4$ | 11.28 | 11.20 | 26.77 | 26.68 | 6.79‡ | 6.71‡ | — | 81.7† |
| $Co(L)_2NO_3$ | 12.16 | 12.11 | 31.75§ | 31.65§ | — | — | — | 80.5† |
| $Co(L)_2(SO_4)_{1/2}$ | 12.53 | 12.47 | 29.72 | 29.65 | 10.19 | 10.10 | — | 81.4† |
| $Ni(LH)_2Cl_2$ | 11.86 | 11.78 | 28.24 | 28.15 | 14.32 | 14.22 | 3.0 | 218.2† |
| $Ni(LH)_2Br_2$ | 10.10 | 10.01 | 24.02 | 24.00 | 27.45 | 27.38 | 3.2 | 173.2† |
| $Ni(LH)_2(ClO_4)_2$ | 9.41 | 9.35 | 22.41 | 22.32 | 11.36‡ | 11.28‡ | 2.8 | 173.1† |
| $Ni(LH)_2SO_4$ | 11.29 | 11.21 | 26.88 | 26.79 | 18.43 | 18.39 | 3.0 | 160.5† |
| $Ni(LH)_2(NO_3)_2$ | 10.71 | 10.61 | 30.61§ | 30.58§ | — | — | 3.2 | 162.8† |
| $Ni(LH)_2(BF_4)_2$ | 9.85 | 9.76 | 23.46 | 23.41 | — | — | 2.8 | 164.7† |
| $Cu(LH)Cl_2 \cdot H_2O$ | 18.92 | 18.86 | 20.86 | 20.81 | 21.17 | 21.09 | 1.9 | 65.5‖ |
| $Cu(LH)Br_2 \cdot H_2O$ | 14.96 | 14.90 | 16.49 | 16.40 | 37.69 | 37.61 | 1.8 | 65.0‖ |
| $Cu(LH)(NO_3)_2 \cdot H_2O$ | 16.35 | 16.25 | 25.23§ | 25.15§ | — | — | 1.7 | 62.1‖ |
| $Cu(LH)(SO_4) \cdot H_2O$ | 17.61 | 17.56 | 19.42 | 19.35 | 26.63 | 26.61 | 1.8 | 66.2† |
| $Cu(LH)(BF_4)_2 \cdot H_2O$ | 14.55 | 14.50 | 16.04 | 16.00 | — | — | 1.8 | 111.3† |
| $Cu(LH)(ClO_4)_2 \cdot H_2O$ | 13.69 | 13.61 | 14.09 | 15.01 | 14.19‡ | 14.06‡ | 1.9 | 66.1‖ |

* L = MPzATS.
† Methanol.
‡ Percentage of chlorine.
§ Including nitrogen present in anion.
‖ DMF.

observed lower energy absorption bands are split to a very much greater extent, the examined complexes are indicated to be *trans*-isomers.[11] The observed spectral bands assist in finding the ligand field parameters, $10Dq$, $B$ and $C$, using the following known relationships:[11]

$$E(^1T_{1g} \leftarrow {}^1A_{1g}) = 10Dq - C,$$
$$E(^1T_{2g} \leftarrow {}^1A_{1g}) = 10Dq + 16B - C,$$
$$E(^3T_{1g} \leftarrow {}^1A_{1g}) = 10Dq - 3C,$$
$$E(^3T_{2g} \leftarrow {}^1A_{1g}) = 10Dq + 8B - 3C.$$

The calculated values of the ligand field parameters $C$ ($\simeq$5000 cm$^{-1}$), $B$ ($\simeq$ 500 cm$^{-1}$) and $10Dq$ ($\simeq$ 25,000 cm$^{-1}$) (Table 2) are quite consistent with the aforementioned proposition. Methanol solutions of the complexes show three bands in the regions 10,100–10,300, $\simeq$25,000 and 27,000–27,700 cm$^{-1}$ of which only the band around 10,000 cm$^{-1}$ could be due to a *d—d* transition, while the other two bands are reasonably taken as strong CT bands in view of high molar extinction coefficient values ($\varepsilon \simeq 10{,}500$ l cm$^{-1}$ mol$^{-1}$).

Ni(II) *complexes.* The molar conductance values in methanolic solution of these complexes ($\lambda_{max}$ = 160–220 $\Omega^{-1}$ cm$^2$ mol$^{-1}$) (Table 1) approach those expected for a 1:2 electrolyte.[10] The magnetic data of the present bis-Ni(II) species are in the range 2.8–3.3 B.M. (303 K) as expected for octahedral complexes. The diffuse reflectance spectra of the complexes are characterised by three main bands in the regions 11,100–11,905, 16,400–17,850 and 27,780–28,580 cm$^{-1}$ which may be assigned to $^3A_{2g}(F) \rightarrow {}^3T_{2g}(F)$ ($\nu_1$), $^3A_{2g}(F) \rightarrow {}^3T_{1g}(F)$ ($\nu_2$) and $^3A_{2g}(F) \rightarrow {}^3T_{1g}(P)$ ($\nu_3$) transitions respectively in an idealised $O_h$-symmetry. The calculated values of $\nu_2/\nu_1$ (1.45–1.50)[12] are consistent with an octahedral configuration suggesting strong $T_{1g}$-term interactions. The appearance of broad and diffused band envelopes without any recognisable splitting of the $\nu_1$- and $\nu_2$-bands in the examined spectral curves suggests a superimposition of more than one component into a single one.[13] The parameter $10Dq$ (Table 2) has been taken directly from the first energy transition ($\nu_1$), while the Racah parameter, $B$, has been calculated by the following diagonalised

Table 2. Ligand field parameters of the complexes

| Compound* | State | $\nu_2/\nu_1$ observed | $Dq$ ($cm^{-1}$) | $B$ ($cm^{-1}$) | $\beta$ | $C$ ($cm^{-1}$) |
|---|---|---|---|---|---|---|
| $Co(L)_2Cl$ | Solid | — | 2490 | 605.3 | — | 4895 |
| $Co(L)_2Br$ | Solid | — | 2500 | 673.1 | — | 5000 |
| $Co(L)_2I$ | Solid | — | 2490 | 577.0 | — | 4895 |
| $Co(L)_2ClO_4$ | Solid | — | 2540 | 563.6 | — | 4996 |
| $Co(L)_2BF_4$ | Solid | — | 2385 | 588.3 | — | 4615 |
| $Co(L)_2NO_3$ | Solid | — | 2200 | 522.5 | — | 3828 |
| $Co(L)_2(SO_4)_{1/2}$ | Solid | — | 2370 | 605.3 | — | 4465 |
| $Ni(LH)_2Cl_2$ | Solid | 1.48 | 1163 | 728.0 | 0.67 | — |
| | Solution | 1.46 | 1163 | | | |
| $Ni(LH)_2Br_2$ | Solid | 1.45 | 1176 | 650.0 | 0.61 | — |
| | Solution | 1.47 | 1163 | | | |
| $Ni(LH)_2SO_4$ | Solid | 1.45 | 1176 | 629.0 | 0.59 | — |
| | Solution | 1.45 | 1176 | | | |
| $Ni(LH)_2(NO_3)_2$ | Solid | 1.50 | 1111 | 741.0 | 0.69 | — |
| | Solution | 1.48 | 1163 | | | |
| $Ni(LH)_2(ClO_4)_2$ | Solid | 1.50 | 1190 | 714.0 | 0.66 | — |
| | Solution | 1.47 | 1190 | | | |
| $Ni(LH)_2(BF_4)_2$ | Solid | 1.49 | 1176 | 722.0 | 0.67 | |
| | Solution | 1.49 | 1176 | | | |
| $Cu(LH)Cl_2 \cdot H_2O$ | Solid | — | 781 | — | — | — |
| | Solution | | 794 | | | |
| $Cu(LH)Br_2 \cdot H_2O$ | Solid | — | 781 | — | — | — |
| | Solution | | 807 | | | |
| $Cu(LH)(NO_3)_2 \cdot H_2O$ | Solid | — | 807 | — | — | — |
| | Solution | | 794 | | | |
| $Cu(LH)(BF_4)_2 \cdot H_2O$ | Solid | — | 782 | — | — | — |
| | Solution | | 794 | | | |
| $Cu(LH)(ClO_4)_2 \cdot H_2O$ | Solid | — | 807 | — | — | — |
| | Solution | | 794 | | | |
| $Cu(LH)(SO_4) \cdot H_2O$ | Solid | — | 715 | — | — | — |
| | Solution | | 735 | | | |

*L = MPzATS.

secular equation:[14]

$$B = \frac{\nu_2 + \nu_3 - 3\nu_1}{15},$$

$\beta = B/B_o$, where $B_o = 1080\ cm^{-1}$ for the Ni(II) ion.

The calculated values of the ligand field parameters, $Dq$, $B$ and $\beta$ (Table 2) for the complexes give tacit support to the proposition made.

The methanolic solutions of the complexes record spectral data giving $\nu_1$ (11,500–11,900) and $\nu_2$ (16,300–17,800) bands which are not significantly different from those in the solid state, thereby suggesting no electronic or geometric change on dissolution in the said solvent; the molar extinction coefficient values ($\varepsilon \simeq 50$ l $cm^{-1}$ $mol^{-1}$) are in agreement with a pseudo-octahedral geometry.[12] The values of $\nu_2/\nu_1$ (Table 2) are also compatible with those in the solid. The band could not be located in the solution spectra of the species: the position of $\nu_3$ can, however, be computed[14] and is found, in all cases, to lie in the UV region where it might be obscured by intense internal $\pi$–$\pi^*$ transitions of the ligand or intense CT absorption.

Cu(II) *complexes.* The monoligated species, $Cu(MPzATSH)X_2$ show magnetic moment values (Table 1) of 1.8–1.9 B.M.: a distorted octahedral structure is suggested. Molar conductances recorded in DMF except for the fluoroborate complex (recorded in MeOH) afford values in the range 62–66 $\Omega^{-1}$ $cm^2$ $mol^{-1}$: the data can be reconciled in terms of 1:1 electrolyte behaviour[10] in accordance with the equilibrium:

$$[Cu(MPzATSH)X_2 \cdot H_2O] \overset{DMF}{\rightleftharpoons} [Cu(MPzATSH)X(DMF)_2]^+ + X^- + H_2O.$$

The electronic spectra of the complexes are characterised by a broad band around 16,000 $cm^{-1}$ both in the solid (d.r.s.) and in solution: the three transitions, $^2B_1 \rightarrow {}^2A_1$ ($\nu_1$), $^2B_1 \rightarrow {}^2B_2$ ($\nu_2$) and $^2B_1 \rightarrow {}^2E$ ($\nu_3$) expected are buried under one absorption envelope. The molar extinction coefficient values ($\varepsilon \simeq 10^2$ l $cm^{-1}$ $mol^{-1}$) and the *Dq* values (715–800 $cm^{-1}$) are also indicative of distorted octahedral structures[11] in these species. The reluctance to form an ionic bis-ligated complex with Cu(II) can be ascribed to the Jahn–Teller effect which causes elongation in the apical sites about Cu(II).[15]

A comparative study of the IR spectral data of the reported complexes with those of the uncomplexed ligand gives positive information regarding the bonding sites of the ligand molecule. The strong IR band appearing at 1610 $cm^{-1}$ in the free-ligand spectrum ($\nu_{CH=N}$) has been found to shift to a higher frequency region ($\simeq 1630$ $cm^{-1}$) in the spectra of the metal complexes due to positive involvement of the azomethine nitrogen[16] in bonding.

The positive shift of the $\nu_{N-N_z}$ frequencies from 1010 cm in the free-ligand spectrum to 1030 $cm^{-1}$ on complexation with a metal ion indicates involvement of the pyrazolyl hetero-nitrogen in bonding. However, in the spectrum of perchlorate, sulphate and fluoroborate complexes, this region is very much masked with characteristic anion bands and the expected bands could not be located.

An intense strong band at 845 $cm^{-1}$ in the free-ligand spectrum is due to $\nu_{C=S}$[17] which undergoes a downward shift by 10–25 $cm^{-1}$, pointing to the sulphur atom of the >C=S group as a possible coordination site in the case of Ni(II) and Cu(II) complexes. However, the band due to $\nu_{C=S}$ suffers an appreciable lowering by 50–100 $cm^{-1}$ in spectra of Co(III) complexes: this reasonably points to the presence of C—S—M bond formed through the deprotonation of the SH group (thio-enol of the ligand) during complexation.[18]

The diagnostic IR band frequencies of the counterions with appropriate assignments (Table 3) indicate the ionic nature of the nitrate,[19] perchlorate,[20] fluoroborate[21,22] and sulphate[23] in the case of Co(III) and Ni(II), whereas the anion nitrate,[19] sulphate,[23] fluoroborate[21,22] and perchlorate[20] are coordinated in the Cu(II) complexes.[23]

The free-ligand bands at 1535 and 650 $cm^{-1}$

Table 3. Some characteristic IR bands ($cm^{-1}$) of the complexes

| Compound* | IR band frequencies of the anion with probable assignments |
|---|---|
| $Ni(LH)_2(NO_3)_2$ | 1370–1320 br ($\nu_3$) $D_{3h}$-symmetry<br>850 vs ($\nu_2$) |
| $Ni(LH)_2(ClO_4)_2$ | 1140–1080 brs ($\nu_3$)<br>940 w ($\nu_1$) $T_d$-symmetry<br>620 ms ($\nu_4$) |
| $Ni(LH)_2(BF_4)_2$ | 1060–1020 br ($\nu_3$), $T_d$-symmetry |
| $Ni(LH)_2SO_4$ | 1150–1090 brs ($\nu_3$), $T_d$-symmetry |
| $Co(L)_2(NO_3)$ | 1380–1310 brs ($\nu_3$), $D_{3h}$-symmetry<br>830 vs ($\nu_2$) |
| $Co(L)_2(ClO_4)$ | 1090–1070 brs ($\nu_3$)<br>950 w ($\nu_1$), $T_d$-symmetry<br>620 ms ($\nu_4$) |
| $Co(L)_2(BF_4)$ | 1080–1030 brs ($\nu_3$), $T_d$-symmetry |
| $Co(L)_2(SO_4)_{1/2}$ | 1080–1060 brs ($\nu_3$), $T_d$-symmetry |
| $Cu(LH)(ClO_4)_2 \cdot H_2O$ | 1140 ms, $C_{3v}$-symmetry<br>1100 s, 1080 s components of $\nu_{Cl-O}$ |
| $Cu(LH)(NO_3)_2 \cdot H_2O$ | 1380 br ($\nu_3$), components of $\nu_3$<br>825 s ($\nu_2$), $C_{2v}$-symmetry |
| $Cu(LH)(BF_4)_2 \cdot H_2O$ | 1125 w, 1030 s split components of $\nu_3$, $C_{3v}$-symmetry |
| $Cu(LH)(SO_4) \cdot H_2O$ | 1110 mbr, 1165 wbr split components of $\nu_3$, $C_{2v}$-symmetry |

*L = MPzATS.

assignable to $\nu_{C=N}$ and in-plane deformation of the pyrazole ring respectively are shifted to a higher wave number ($\Delta\nu$ = 20–40 and 15–30 $cm^{-1}$ in $\nu_{C=N}$ and in-plane deformation) in all the spectra of the complexes indirectly suggesting the tertiary (iminic) nitrogen atom (of the pyrazole ring) as a possible bonding site. This conclusion is in agreement with the earlier observations[24,25] on metal complexes of other *N*-heterocycles and is also in conformity with crystallographic studies[26–28] of several pyrazole–metal complexes. This proposition is further supported by strong bands at 320 $cm^{-1}$ (absent in the free-ligand spectrum) assignable to the $\nu_{M-N(ring)}$.[2]

The other low-frequency bands in the regions 490–530 and 340–370 $cm^{-1}$ in all the complex species are tentatively attributed to $\nu_{M-N(azomethine)}$ and $\nu_{M-S}$ respectively.[29]

It appears, therefore, that the ligand MPzATSH behaves as a neutral (NNS) tridentate in its thio-keto form when complexed with Ni(II) and Cu(II), giving respectively bis- and mono-species, while, with Co(III), the deprotonated ligand in its thiol form exhibits a monoacidic (NNS) tridentate function, yielding bis-species.

*Acknowledgements*—We are grateful to Prof. Stanley Livingstone, University of New South Wales, Australia, and to Mr Micap, R.S.I.C., Calcutta-9, India, for providing us with the reflectance spectra of the complexes, and also to Dr S. Ganguli of Bose Institute, Calcutta-9, for the PMR spectrum of the ligand. One of us (N.M.) is thankful to the University Grants Commission, New Delhi, for the award of a fellowship (JRF) during the tenure of this work. We are thankful to Dr S. Roy of our Department for useful discussions on the PMR and mass spectrum of the ligand.

## REFERENCES

1. S. Trofimenko, *Chem. Rev.* 1972, 72, 500.
2. (a) N. Saha and K. M. Datta, *J. Inorg. Nucl. Chem.* 1981, **43**, 1405 and references therein. (b) N. Saha and D. Bhattacharya, *Indian J. Chem.* 1982, **21A**, 574 and references therein. (c) N. Saha and D. Mukherjee, *Polyhedron* 1983, **2**, 47. (d) N. Saha and K. M. Datta, *Synth. React. Inorg. Met.-Org. Chem.* 1983, **13**, 683.
3. D. D. Perrin and H. Stunzi, *Metal Ions in Biological Systems* (Edited by H. Sigel), Vol. 14, pp. 207–241. Marcel Dekker, New York (1982).
4. J. S. McFadyen and T. S. Stevens, *J. Chem. Soc.* 1936, 584.
5. C. Niemann, R. N. Lewis and J. T. Hays, *J. Am. Chem. Soc.* 1942, **64**, 1678.
6. M. J. S. Dewar and F. E. Kind, *J. Chem. Soc.* 1945, 114.
7. N. Saha and S. K. Kar, *J. Inorg. Nucl. Chem.* 1977, **39**, 195.
8. M. A. Ali and S. E. Livingstone, *Coord. Chem. Rev.* 1974, **13**, 101.
9. A. V. Ablov and N. I. Belichuk, *Russ. J. Inorg. Chem.* 1969, **14**, 93.
10. W. J. Geary, *Coord. Chem. Rev.* 1971, **7**, 81.
11. A. B. P. Lever, *Inorganic Electronic Spectroscopy*, pp. 307–322. Elsevier, Amsterdam (1968).
12. L. Sacconi, *Transition Metal Chemistry* (Edited by R. L. Carlin), Vol. 4, p. 199. Marcel Dekker, New York (1968).
13. G. Contrearas and E. Astigarrabia, *Inorg. Chim. Acta* 1971, **5**, 54.
14. C. J. Ballhausen, *Math. fys. Meddr.* 1954, **4**, 29.
15. M. A. Ali, S. E. Livingstone and D. J. Phillips, *Inorg. Chim. Acta* 1972, **6**, 11.
16. (a) D. M. Wiles and T. Suprunchuk, *Can. J. Chem.* 1969, **47**, 1087. (b) S. K. Sahni, R. P. Gupta, S. K. Sangal and V. B. Rana, *J. Indian Chem. Soc.* 1977, **54**, 200.
17. M. J. M. Campbell and R. Grzeskowiak, *J. Chem. Soc. A* 1967, 396.
18. M. S. Patil and J. R. Shah, *J. Indian Chem. Soc.* 1981, **58**, 944.
19. N. F. Curtis and Y. M. Curtis, *Inorg. Chem.* 1965, **4**, 804.
20. B. J. Hathway and A. E. Underhill, *J. Chem. Soc.* 1961, 3091.
21. S. Buffagni, L. M. Vallarino and J. V. Quagliano, *Inorg. Chem.* 1964, **3**, 480.
22. N. N. Greenwood, *J. Chem. Soc.* 1959, 3811.
23. K. Nakamoto, *Infrared Spectra of Inorganic Coordination Compounds*, p. 156. John Wiley, New York (1963).
24. (a) R. C. Agarwal, T. Prasad and N. N. Yadav, *J. Inorg. Nucl. Chem.* 1975, **37**, 899. (b) R. C. Agarwal and T. R. Rao, *ibid.* 1978, **40**, 171. (c) R. C. Agarwal and T. R. Rao, *ibid.* 1978, **40**, 1177.
25. J. R. Ferraro, *Appl. Spectrosc.* 1969, **23**, 160.
26. A. D. Mighell, C. W. Reimann and A. Santoro, *Acta Crystallogr.* 1969, **B25**, 595.
27. C. W. Reimann, A. Santoro and A. D. Mighell, *Acta Crystallogr.* 1970, **B26**, 521.
28. J. S. Reedijk, B. A. Blaisse and G. C. Vershoor, *Inorg. Chem.* 1971, **10**, 2594.
29. M. M. Mostafa, A. M. Shallaby and A. A. Elasmy, *J. Inorg. Nucl. Chem.* 1981, **43**, 2992.

*Polyhedron* Vol. 3, No. 9/10, pp. 1141–1145, 1984
Printed in the U.S.A.

0277–5387/84 $3.00 + .00
© 1984 Pergamon Press Ltd.

# INDUCED DISTANT COTTON EFFECTS IN COMPLEXES OF Cr(III) WITH L-MALIC ACID AND HETEROCYCLIC LIGANDS

S. BUNEL and E. MORAGA*
Departamento de Análisis Químico, Facultad de Ciencias Básicas y Farmacéuticas, Universidad de Chile, Santiago, Chile

(*Received* 26 *March* 1984; *accepted* 9 *July* 1984)

**Abstract**—Complexes of Cr(III) with L-malic acid and aromatic bases [2,2′-bipyridine (bipy) or 1,10-phenanthroline (phen)] and different counter ions were synthesized. Analyses and experiments carried out indicate that no more than one L-malate ligand enters the coordination sphere and that it behaves as a bidentate ligand. Optical rotatory dispersion and circular dichroism measurements always show a vicinal effect in the *d–d* transitions, and it is proposed that chromium adopts the lowest possible microsymmetry in all the complexes: induction of optical activity in the $\pi$–$\pi^*$ transitions in the UV region is not always present.

L-malic acid forms complexes with transition metal ions, acting either as a bi- or a tridentate ligand towards copper(II),[1] but these complexes have received little attention. The chiral malic acid can induce optical activity in the *d–d* transitions of the metallic ion. In mixed-ligand complexes there is also induction of optical activity in transitions originating in the other ligand.[2]

Optical induction as in malates and mixed malates of copper(II) may also be present in similar complexes of other transition metal ions. Therefore we synthesized 1 : 1 complexes of chromium(III) and L-malic acid and mixed-ligand complexes with L-malic acid and 2,2′-bipyridine (bipy) or 1,10-phenanthroline (phen) where the ratio chromium/malate/aromatic ligand is 1 : 1 : 1.

## EXPERIMENTAL

The syntheses gave two series of compounds: [Cr L-malate]$_2$(L-malate) and [Cr L-malate]$_2SO_4$, and their corresponding mixed-ligand complexes with phen and bipy.

The compound [Cr L-malate]$_2$(L-malate) was obtained by treating stoichiometric amounts of chromium(III) acetate and L-malic acid in aqueous solution at 100°C for an hour. The resulting solution was concentrated to dryness under vacuum. The crystalline solid was washed several times with acetone and then recrystallized from water. The same products were also obtained by heating L-malic acid and a suspension of chromium(III) hydroxide in water under reflux for an hour. The resulting solution was filtered and treated as previously described.

The compound [Cr L-malate]$_2SO_4$ was prepared by heating at 100°C for an hour a solution of stoichiometric amounts of chromium(III) sulphate and a suspension of freshly-prepared barium malate. The resulting solution was treated, after filtration, as previously described for the malates.

Both the malates and sulphates of chromium(III) are deep blue; they dissolve slowly in cold water but readily in hot water.

Aqueous solutions of the malates or sulphates and bipy or phen were heated for 30 min, giving the mixed-ligand complexes, which were isolated by the procedure previously described for the malate complexes. The mixed-ligand complexes are water-soluble and dark red in the solid.

Repeated efforts to prepare the complexes [Cr L-malate(bipy)$_2$]$^+$ or [Cr L-malate(phen)$_2$]$^+$ by the previously described method were unsuccessful.

The compositions of the new compounds (calculated values are given in parentheses) were: [Cr L-malate]$_2$(L-malate)·6H$_2$O: Cr, 14.59 (14.53); C, 20.99 (20.11)%. [Cr L-malate]$_2SO_4$·8H$_2$O: Cr, 16.97 (17.10); H, 3.90 (3.95); $SO_4^{2-}$, 15.73 (15.78)%; ratio $Cr^{3+}/SO_4^{2-}$, 1.08 (1.08). [Cr L-malate bipy]$_2$(L-malate)·1.5H$_2$O: Cr, 12.47(12.40); H, 3.64(3.69); N, 6.89 (6.67)%. [Cr L-malate bipy]$_2SO_4$·10H$_2$O: Cr, 10.86 (10.87); H, 4.05 (4.60); $SO_4^{2-}$, 11.15 (10.04)%; ratio $Cr^{3+}/SO_4^{2-}$, 0.97 (1.08). [Cr L-malate phen]$_2$(L-malate): Cr, 12.69 (12.09); C, 51.19 (50.23); H, 3.73

* Author to whom correspondence should be addressed.

(3.26); N, 6.38 (6.51)%. [Cr L-malate phen]$_2SO_4 \cdot 10H_2O$: Cr, 10.52 (10.36); H, 4.12 (4.38); $SO_4^{2-}$, 9.54 (9.56)%; ratio $Cr^{3+}/SO_4^{2-}$, 1.10 (1.08). Some values are missing because results of the corresponding analyses were out of agreement with calculations.

Optical rotatory dispersion (ORD) spectra were obtained using a modified Perkin–Elmer 141 polarimeter and circular dichroism (CD) spectra using a Cary 60 spectropolarimeter with a CD attachment at 27°C. Absorption spectra were obtained using a Zeiss IMR 21 spectrophotometer. The concentration of the solutions was generally $10^{-2}$ *M*.

The reagents came from Merck, Matheson-Coleman, Riedel de Haen and Aldrich; they were of analytical quality and were used without further purification.

## RESULTS AND DISCUSSION

In order to find out whether malic acid binds to Cr(III) as a bi- or tridentate ligand, reactions were performed using, for example, malic acid and chromium(III) acetate. The liberated acetic acid was separated by distillation and then titrated. Results indicate that malic acid is a bidentate ligand towards Cr(III) and also show that only one malate ion enters the coordination sphere of the metal. This bonding is different from that in copper(II)–malate complexes, where there is evidence for both bi- and tridenate coordination.[1]

The visible absorption spectra of [Cr L-malate]$^+$ ($\lambda_{max}$ = 17.54 and 23.81 kK); of $[Cr(H_2O)_6]^{3+}$ ($\lambda_{max}$ = 17.40 and 24.60 kK)[3] and of $[Cr(ox)_3]^{3-}$ ($\lambda_{max}$ = 17.50 and 23.85 kK)[4] are very similar, indicating that the separation of the energy levels is determined by the oxygen atoms around the Cr(III) ion rather than by the charge or nature of the ligand.

The visible absorption spectrum of [Cr L-malate]$^+$ consists of two well-defined bands (Fig. 1), whereas those of the mixed-ligand complexes [Cr L-malate bipy]$^+$ or [Cr L-malate phen]$^+$ exhibit one well-defined first band, plus several inflections replacing the second band of chromium malate, which probably correspond to overlapping of the second band with a $\pi$–$\pi^*$ transition of the aromatic ligand.

The visible CD spectra of all the complexes (Figs 1–3) show that there is induction of optical activity in the metal ion. The general features of these spectra are very similar, in spite of the changes of ligands around Cr(III). There are three CD signals under the first absorption band with a $-+-$ sequence of signs. The visible ORD spectra show a good

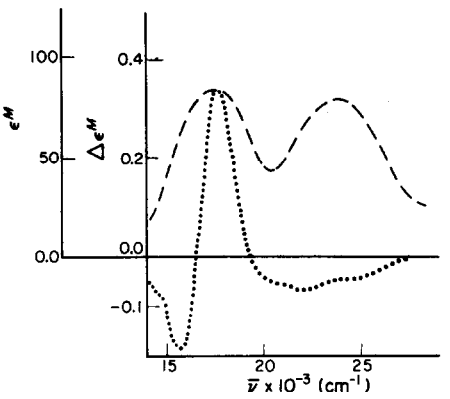



Fig. 1. Absorption (----) and CD (....) curves of [Cr L-malate]$_2SO_4$.

correlation with the positive CD band in each complex and confirm the results of the CD measurements (Table 1). Our results seem to show that the arrangement of the ligands around the metal ion is one resulting in the lowest possible microsymmetry. The magnetically allowed $^4T_{2g}$-state of Cr(III), which accounts for three CD bands, must split into three levels in this new low-symmetry state.

As the first negative CD signal under the first absorption band in the visible region is at approximately 15 kK (Table 1 and Figs 1–3), the question could arise as to whether the first negative CD signal corresponds to a component of the first absorption band or is due to a spin-forbidden transition. This second possibility is eliminated on

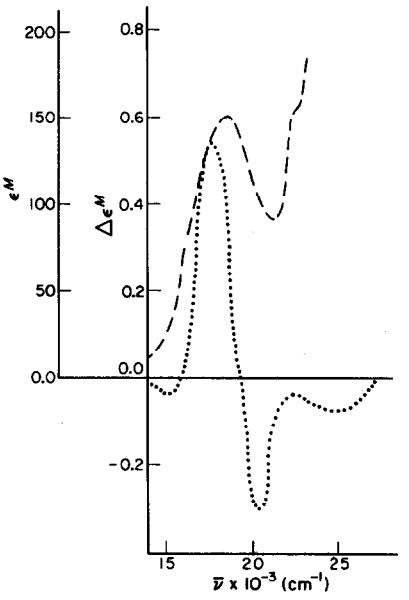



Fig. 2. Absorption (----) and CD (....) curves of [Cr L-malate bipy]$_2SO_4$.

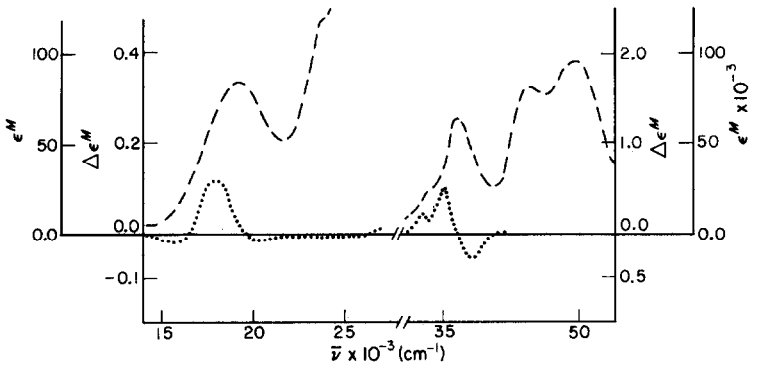



Fig. 3. Absorption (----) and CD (....) curves of [Cr L-malate phen]$_2$SO$_4$.

the grounds of the location and intensity of the CD signals.[5]

In the UV region, the absorption spectra of all these compounds show a large charge transfer band at approximately 51 kK. The mixed-ligand complexes also show several inflections corresponding to $\pi$–$\pi^*$ transitions of the aromatic ligand.

The CD spectra of [Cr L-malate phen]$^+$ malate and sulphate show distant Cotton effects under the typical first absorption bands of the aromatic ligand ($p$ and $\beta$ of phenanthroline)[6] with two CD signals of opposite sign, whereas in the [Cr L-malate bipy]$^+$ complexes the same effect is seen when the counter ion is malate.

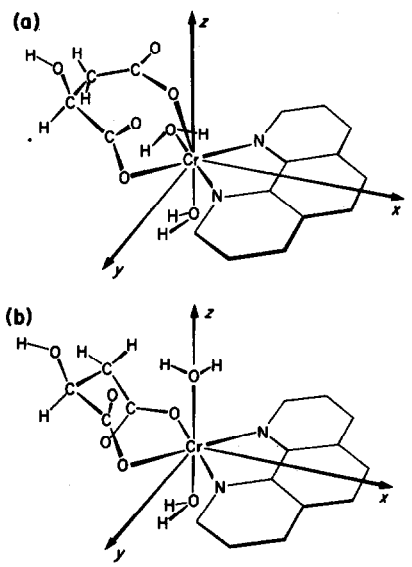



Fig. 4. Two possible structures of the complex formed by Cr(III), L-malic acid and phen. (a) The oxygen atoms belonging to the chiral ligand are placed out of the plane defined by the nitrogen atoms of the aromatic ligand and the metallic ion. (b) The oxygen and nitrogen atoms are in the same plane.

This induction of optical activity could be due to interaction of the $\pi$–$\pi^*$ and the ligand → metal charge transfer transition. Under Kirkwood's[7] coupled oscillator model for this type of complex, the requirement for a non-vanishing scalar product of electric and magnetic moments is that the aromatic and chiral ligand are in different planes.

It is interesting to note that, whereas in the visible region the absorption and CD spectra correspond to bonding of the metal to two nitrogen and four oxygen atoms, irrespective of their chemical nature, the CD UV spectra are sensitive to the presence and arrangement of the oxygen atoms belonging to the chiral ligand.

On the grounds of experimental results and considerations previously presented [Cr L-malate bipy]$_2$(L-malate) and [Cr L-malate phen]$_2$(L-malate) and sulphate should have similar structures with aromatic and chiral ligands in different planes.

ORD measurements of aqueous solutions of the compound [Cr L-malate bipy]$_2$SO$_4$ have shown that the amplitude of the Cotton effect (525 and 610 nm) increases with time. Besides, the CD spectra in the UV region measured 4 days after preparing the solution gave two signals of opposite signs under the first typical absorption band of the aromatic ligand ($\Delta\epsilon^M = -0.352$ at 30.8 kK and $+1.11$ at 33.3 kK). These results could be an indication that the malate ligand rearranges, changing from a structure where the oxygen atoms of the chiral ligand are located in the same plane as the nitrogen atoms of the aromatic ligand (Fig. 4b) to a disposition where the oxygen and nitrogen atoms stay in different planes (Fig. 4a). Terdentate coordination of the malate ligand would give the same effect in the UV region; but considering that the intensity of the CD signals under the first $d$–$d$ band does not change, we believe that the phenomenon observed is due to a rearrangement of the ligands around the central atom. We would expect terdentate coordination of the malate ligand

Table 1. Absorption and CD spectral data of chromium(III) complexes in the visible and UV regions

| COMPOUND | ABSORPTION | | CIRCULAR DICHROISM | |
|---|---|---|---|---|
| | $\bar{\nu}$ | $\varepsilon^M$ | $\bar{\nu}$ | $\Delta\varepsilon^M$ |
| [Cr L-malate]$_2$(L-malate) | 17.5 | 40.1 | 15.7 | -0.21 |
| | 23.9 | 37.4 | 17.9 | +0.33 |
| | 51.8 | $24.7\times10^3$ | 24.4 | -0.07 |
| | | | 35.7 | -0.25 |
| | | | 42.6 | +0.25 |
| | | | 47.6 | -4.64 |
| [Cr L-malate]$_2$SO$_4$ | 17.5 | 91.0 | 15.7 | -0.19 |
| | 23.9 | 70.0 | 17.5 | +0.34 |
| | 51.6 | $23.1\times10^3$ | 22.2 | -0.06 |
| [Cr L-malate phen]$_2$(L-malate) | 19.2 * | 42.5 | 15.6 | -0.08 |
| | (23.8) * | (73.4) | 17.9 | +0.18 |
| | (25.0) | (94.8) | 20.4 | -0.04 |
| | 33.8 | $11.8\times10^3$ | 35.1 | +0.89 |
| | 36.8 | $30.4\times10^3$ | 37.7 | -1.00 |
| | 44.4 | $40.5\times10^3$ | | |
| | 49.8 | $51.3\times10^3$ | | |
| [Cr L-malate phen]$_2$SO$_4$ | 19.2 | 93.2 | 15.8 | -0.02 |
| | (23.8) | (172.0) | 17.9 | +0.12 |
| | (25.0) | (218.9) | 20.4 | -0.02 |
| | (33.6) | $24.8\times10^3$ | 32.8 | +0.21 |
| | 36.4 | $63.8\times10^3$ | 34.5 | +0.49 |
| | 44.4 | $81.8\times10^3$ | 38.5 | -0.30 |
| | 49.5 | $95.9\times10^3$ | | |
| [Cr L-malate bipy]$_2$(L-malate) | 18.9 | 93.2 | 15.6 | -0.11 |
| | (22.5) | (62.3) | 17.9 | +0.47 |
| | (24.1) | (96.4) | 20.4 | -0.17 |
| | (25.5) | (124.5) | 25.0 | -0.12 |
| | 33.0 | $29.0\times10^3$ | 32.8 | +0.47 |
| | (40.0) | $(27.1\times10^4)$ | 34.5 | -0.27 |
| | 51.3 | $10.6\times10^4$ | | |
| [Cr L-malate bipy]$_2$SO$_4$ | 18.9 | 93.5 | 15.2 | -0.04 |
| | (22.5) | (95.2) | 17.7 | +0.54 |
| | (24.1) | (221.9) | 20.2 | -0.30 |
| | (25.6) | (319.1) | 24.9 | -0.08 |
| | 32.8 | $35.6\times10^3$ | | |
| | (40.8) | $31.0\times10^3$ | | |
| | 51.0 | $79.6\times10^3$ | | |

* Values in parentheses correspond to inflections.
$\varepsilon^M$ and $\Delta\varepsilon^M$ ($cm^{-1}\ M^{-1}$); $\bar{\nu}$ ($cm^{-1}$).

to give a marked increase of CD signals in the visible region arising from distortion of the chromium–oxygen bonds.

*Acknowledgements*—We thank Professor C. Ibarra, Universidad de Chile, Santiago, for discussion and Professor Dr. C. A. Bunton, University of California, Santa Barbara, for running the CD spectra and for helpful discussion and advice, which was made possible through the National Science Foundation. This work was supported by the Servicio de Desarrollo Científico, Artístico y de Cooperación Internacional de la Universidad de Chile.

## REFERENCES

1. S. Bunel, C. Ibarra, M. Rodríguez and A. Urbina, *J. Inorg. Nucl. Chem.* 1981, **43**, 967.
2. S. Bunel, C. Ibarra, M. Rodríguez and A. Urbina, *J. Inorg. Nucl. Chem.* 1981, **43**, 190.
3. C. K. Jorgensen, *Acta Chem. Scand.* 1954, **8**, 1495.
4. (a) C. K. Jorgensen, *Adv. Chem. Phys.* 1963, **5**, 33; (b) T. M. Dunn, *Seventh International Conference on Coordination Chemistry*. Butterworth, London (1963).
5. S. Kaisaki, J. Hidaka and Y. Shimura, *Bull. Chem. Soc. Jpn* 1970, **43**, 1100.
6. C. J. Hawkins, *Absolute Configuration of Metal Complexes*, Chap. 5. Wiley–Interscience, New York (1971).
7. I. Tinoco, *Adv. Chem. Phys.* 1962, **4**, 113.

*Polyhedron* Vol. 3, No. 9/10, pp. 1147–1150, 1984
Printed in the U.S.A.

0277-5387/84 $3.00+ .00
© 1984 Pergamon Press Ltd.

# NUCLEOPHILIC REACTION AND FORMATION OF COLIGAND ISOMERS IN THE Cu(II) - $NCO^-$ - BENZOPYRAZOLE SYSTEM

M. HVASTIJOVÁ, J. KOHOUT* and J. GAŽO+
Department of Inorganic Chemistry, Slovak Technical University, 812 37 Bratislava, Czechoslovakia

(Received 22 June 1984; accepted 24 July 1984)

Abstract - From the Cu(II) - $NCO^-$ - benzopyrazole (indazole; inz) system two coligand isomers were isolated, the cyanato complex $Cu(NCO)_2(inz)_2$ and the chelate 1-carbamoylindazolato complex $Cu(inz.NCO)_2$. Both compounds have been structurally characterized by IR, far IR and electronic spectroscopy.

In already published papers[1-4] it was shown, that in systems of Cu(II) - $NCO^-$ - pyrazole type base a nucleophilic addition of the cyanate carbon proceeds to the pyrazole imine nitrogen under the formation of new anionic chelate ligands. Since from the systems studied also the usual cyanato complexes were isolated, isomeric pairs were obtained which were called coligand isomers.[3,4]

The electron density in the pyrazole ring was found to be an important factor controlling the nucleophilic addition process. In order to obtain further information on this influence, we investigated the Cu(II) - $NCO^-$ system with benzopyrazole (indazole; inz) as the nucleophilic agent.

## EXPERIMENTAL

The compound $Cu(NCO)_2(inz)_2$ was prepared by treating a cool aqueous solution of $Cu(NO_3)_2$ and KNCO with a cool methanolic solution of inz. In a similar way using warm solution (40 °C) 1-carbamoylindazolato-copper(II), $Cu(inz.NCO)_2$, was obtained. A purer product was got, however, from $Cu(NCO)_2$(2,4-lutidine) in a methanolic suspension by treating it with inz.

$Cu(NCO)_2(inz)_2$, pale-green powder. Found: C, 49.62; H, 2.98; N, 21.38; Cu, 16.47. Calc.: C, 50.07; H, 3.15; N, 21.89; Cu, 16.55 %.

$Cu(inz.NCO)_2$, gray powder. Found: C, 50.01; H, 3.21; N, 21.46; Cu, 16.38. Calc.: C, 50.07; H, 3.15; N, 21.89; Cu, 16.55 %.

IR spectra (4000-400 $cm^{-1}$),[5] far IR spectra (400-50 $cm^{-1}$)[6] and electronic spectra (4.0-0.55 $\mu m^{-1}$)[7] were obtained as described in the cited papers.

*Author to whom correspondence should be addressed.
+Deceased.

## RESULTS AND DISCUSSION

Some selected IR spectral bands for the complexes under investigation are listed in Table 1. These bands were identified by comparing with the

Table 1. IR spectral data ($cm^{-1}$)[a]

| $Cu(NCO)_2(inz)_2$ | $Cu(inz.NCO)_2$ | Assignment |
|---|---|---|
| 3323ms | 3240ms,3180sh | $\nu$(NH) |
| 2227vs,2242vs | | $\nu_{as}$(NCO) |
| | 1705vs[b] | $\nu$(CO) |
| 1351ms | | $\nu_s$(NCO) |
| | 1333m | $\nu$(CN) |
| | 1213s | $\nu(CN_{ring})$ |
| 628m[c],619w[c],610m | | $\delta$(NCO) |
| | 508ms | $\gamma$(NCO) |
| 375s,360sh | 370s | $\nu$(Cu-NCO) |
| 275s | 309s | $\nu(Cu-N_{ring})$ |
| 102m,92sh | 73w[d] | $\nu$(Cu-OCN) |

[a]s=strong, m=medium, w=weak, v=very, sh=shoulder.
[b]An unresolved both-side splitting occurs.
[c]One of these bands belongs to indazole.
[d]The assignment is not certain (see text).

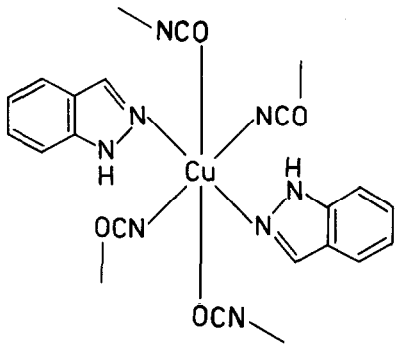
measured spectrum of the solid indazole[8] and assigned according to Ref. 3,4,9. From these data it is evident, that $Cu(NCO)_2(inz)_2$ contains nitrogen coordinated cyanate groups, but in $Cu(inz.NCO)_2$ the chelating ligands, 1-carbamoylindazolate anions, are present being formed by a nucleophilic addition between inz and NCO in the Cu(II) coordination sphere.[1-4] The electron density in the pyrazole ring of indazole, enhanced compared with pyrazole alone, should favour this reaction, and this was in fact proved as follows.

Examination of the IR spectra of $Cu(NCO)_2(inz)_2$ in course of time or by heating reveals, that the cyanato complex is changing into its coligand isomer. In accord with this, in heating $Cu(NCO)_2(inz)_2$ on its DTA curve an exothermic effect occurs which is attributed to the formation of $Cu(inz.NCO)_2$.[10]

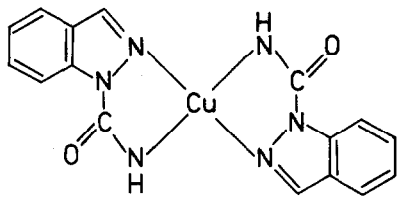
The ligand field spectrum of $Cu(NCO)_2(inz)_2$ shows a broad band with its maximum at 1.58 $\mu m^{-1}$ and a bulge on the low-wavenumber side. This band clearly indicates[9] the pseudooctahedral configuration of the cyanato species present, similar to that established for $Cu(NCO)_2(py)_2$.[11] Undoubtedly the

tertiary nitrogens of inz ligands are used for coordination[12] and the cyanate oxygens are in the copper axial sites[11] (see (I)).

The ligand field band of $Cu(inz.NCO)_2$, flattened and protracted to the IR region, has its maximum at 1.66 $\mu m^{-1}$ and a high-wavenumber shoulder at ca. 1.84 $\mu m^{-1}$. Starting from these spectral features, the strongly tetragonal arrangement may be attributed[13] to the 1-carbamoylindazolato complex which on the analogy of $Cu(3,5\text{-dimethylpyrazole.NCO})_2$ with solved crystal structure[1] may be represented as (II). The interaction of Cu(II) with axial donors (the carbamoyl oxygens are potentially available[2]) is only slight or does not occur at all. This fact agrees well with our previous assertion,[4] that chelate carbamoylpyrazolato complexes with multiple bonding in the




(I)




(II)

equatorial plane are generally more tetragonally distorted than isomeric cyanato complexes.

The tentative assignment of the Cu - donor stretching bands in the far IR region is made on the basis of Ref. 1,2,6,9 and given in Table 1. Remarkable is an increase of the $\nu(Cu\text{–}N_{ring})$ value when passing from $Cu(NCO)_2(inz)_2$ to $Cu(inz.NCO)_2$ which indicates a strengthening of the $Cu - N_{ring}$ bonds in the chelate system. In the case of $Cu(NCO)_2(inz)_2$ the band at 100 $cm^{-1}$ belongs to the axial Cu – OCN vibration, as it was for other similar species discussed elsewhere.[6] On the contrary, $Cu(inz.NCO)_2$ has the region of 100 $cm^{-1}$ blank and shows a band at 73 $cm^{-1}$ which could be originated by some lattice vibration, but could also be caused by a lowered copper axial vibration. However that may be, these facts confirm the strong tetragonality of $Cu(inz.NCO)_2$, issued from its d ← d spectrum.

## REFERENCES

[1] F. Valach, J. Kohout, M. Dunaj-Jurčo, M. Hvastijová and J. Gažo, J. Chem. Soc. Dalton 1979, 1867.
[2] M. Hvastijová, J. Kohout and J. Gažo, J. Inorg. Nucl. Chem. 1981, 43, 2337.
[3] M. Hvastijová, J. Kohout and J. Gažo, J. Coord. Chem. 1982, 12, 27.

[4]M. Hvastijová, J. Kohout and J. Gažo, Proc. 9th Conf. Coord. Chem., p. 121. Smolenice-Bratislava, ČSSR (1983).
[5]J. Kohout, M. Hvastijová, A. Mašlejová, J. Gažo and L. Omelka, Z. Anorg. Allg. Chem. 1977, 434, 29.
[6]J. Kohout, M. Hvastijová and J. Mroziński, J. Mol. Struct. 1984, 116, 211.
[7]M. Hvastijová, J. Kohout, H. Wusterhausen and H. Köhler, Z. Anorg. Allg. Chem. 1984, 510, 37.
[8]M. Hvastijová and J. Kohout. Unpublished results.
[9]J. Kohout, M. Hvastijová and J. Gažo, Coord. Chem. Rev. 1978, 27, 141.
[10]H. Langfelderová, M. Hvastijová, J. Kohout and P. Ambrovič. To be published.
[11]F. Valach, M. Dunaj-Jurčo and M. Handlovič, J. Cryst. Mol. Struct. 1980, 10, 61.
[12]J. Reedijk, Transition Met. Chem. 1979, 4, 335.
[13]B.J. Hathaway and D.E. Billing, Coord. Chem. Rev. 1970, 5, 143.

*Polyhedron* Vol. 3, No. 9/10, pp. 1151–1154, 1984
Printed in the U.S.A.

0277-5387/84 $3.00 + .00
© 1984 Pergamon Press Ltd.

# Synthesis, Reactions and Catalytic Activities of Cationic Rhodium(I) Complexes of Unsaturated Aldehydes

In Bum Kim and Chong Shik Chin*
Department of Chemistry, Sogang University, IPO Box 1142, Seoul 121, Korea

(Received 8 June 1984; accepted 21 August 1984)

Abstract : Reactions of $Rh(OClO_3)(CO)(Ph_3P)_2$(1)($Ph_3P$ = triphenylphosphine) with acrolein and trans-crotonaldehyde at 25°C produce the new cationic rhodium(I) complexes, $[Rh(CH_2{=}CHCHO)(CO)(Ph_3P)_2]ClO_4$(2) and $[Rh(CH_3CH{=}CHCHO)(CO)(Ph_3P)_2]ClO_4$(3) where $CH_2{=}CHCHO$ and $CH_3CH{=}CHCHO$ are coordinated to rhodium through the oxygen. $CH_2{=}CHCHO$ in 2 and $CH_3CH{=}CHCHO$ in 3 are readily replaced by $CH_2{=}CHCN$, $CH_3CH_2CN$, $CH_3COCH_3$ and $Ph_3P$. The complex 2 and 3 are catalytically active for the hydrogenation and oligomerization of acrolein and trans-crotonaldehyde, respectively, at 25°C under the atmospheric pressure of hydrogen.

We recently reported the synthesis of cationic rhodium(I)[1] and iridium(I)[2] complexes of an unsaturated nitrile($CH_2{=}CHCN$), $[M(CH_2{=}CHCN)(CO)(Ph_3P)_2]ClO_4$ (M = Rh, Ir) and their catalytic activities for hydrogenation of $CH_2{=}CHCN$ to $CH_3CH_2CN$[1] and polymerization of $CH_2{=}CHCN$.[1,2] We have subsequently become interested in the related complexes of unsaturated aldehydes.

In this paper, we wish to report the preparation, reactions and catalytic activities of new cationic rhodium(I) complexes, $[Rh(RCH{=}CHCHO)(CO)(Ph_3P)_2]ClO_4$(R = H, $CH_3$) which have been identified by elemental analyses, conductivity measurements, $^1$H-NMR, IR and electronic spectral data. There have been several other acrolein($CH_2{=}CHCHO$) and trans-crotonaldehyde($CH_3CH{=}CHCHO$) complexes reported such as Ni(t-BuNC)($CH_2{=}CHCHO$)(where acrolein is coordinated to Ni(0) through the π-system of the olefinic group)[3] and $ML_n(CH_3CH{=}CHCHO)$($ML_n$ = $TiCl_4$, $SnCl_4$, $AlCl_3$, etc.)(where trans-crotonaldehyde is coordinated to the metals through the oxygen).[4] To our knowledge, no cationic rhodium complexes of acrolein and crotonaldehyde coordinated through the oxygen have been reported thus far.

Addition of acrolein(or trans-crotonaldehyde) into the yellow solution of $Rh(OClO_3)(CO)(Ph_3P)_2$(1) in benzene at 25°C under nitrogen resulted within 5 minutes in solid of $[Rh(CH_2{=}CHCHO)(CO)(Ph_3P)_2]ClO_4$(2)[5](or $[Rh(CH_3CH{=}CHCHO)(CO)(Ph_3P)_2]ClO_4$(3)[6])(eq. 1). The complex 2 and 3 are stable in the solid state in air and in solution under nitrogen, and soluble in chloroform and dichloromethane, slightly soluble in benzene and insoluble in hexane.

$$Rh(OClO_3)(CO)(Ph_3P)_2 + RCH{=}CHCHO \longrightarrow [Rh(RCH{=}CHCHO)(CO)(Ph_3P)_2]ClO_4 \quad (1)$$

R = H, $CH_3$

The molar conductance(100 $ohm^{-1}cm^2mole^{-1}$ for 2 and 110 $ohm^{-1}cm^2mole^{-1}$ for 3 in dichloromethane) indicates that the complex 2 and 3 are 1:1 electrolytes.[7]

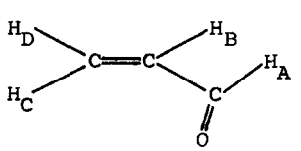
The IR spectra(in Nujol) of 2 and 3 suggest that both acrolein and

trans-crotonaldehyde are coordinated to rhodium through the oxygen. The $\nu_{CO}$ of aldehydes in 2(1639(s), 1623(s) $cm^{-1}$) and 3(1632(s), 1615(s) $cm^{-1}$) are much lower than those of free $CH_2$=CHCHO(1695(s), 1650(s) $cm^{-1}$) and $CH_3CH$=CHCHO(1689(s), 1642(s) $cm^{-1}$) while $\nu_{C=C}$ of $CH_2$=CHCHO in 2(1605 $cm^{-1}$(w)) is only slightly lower than that of free $CH_2$=CHCHO(1612 $cm^{-1}$(w)).[8] The $\nu_{CO}$ of acetone coordinated to iridium through the oxygen[9] has been observed at 1660 $cm^{-1}$ [10] while that of free acetone is seen at 1710 $cm^{-1}$. We also prepared the acetone complex, $[Rh(CH_3COCH_3)(CO)(Ph_3P)_2]ClO_4$(4)[11] for the comparison with 2 and 3, and found that the $\nu_{CO}$ of acetone in 4 is seen at 1654 $cm^{-1}$ (in Nujol). Coordination of an aldehyde to a metal through the π-system of the carbonyl group has not been observed yet. A broad and strong band at ca. 1100 $cm^{-1}$ observed for 2 and 3 attributable to the anionic tetrahedral $ClO_4$ group[12] supports that 2 and 3 are ionic compounds as confirmed by the conductivity data(see above). The $\nu_{CO}$ due to CO coordinated to rhodium are observed at 2016(vs) and 2017(vs) $cm^{-1}$ for 2 and 3, respectively.

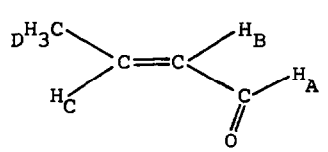
The rhodium-oxygen bond in 2 and 3 is also supported by the electronic spectral data. The electronic absorption spectra of 2 and 3 in benzene show bands at 353 nm(ε, 3780) and 359 nm(ε, 3420), respectively. It is well known that the four coordinated rhodium(I) complexes, $RhA(CO)(Ph_3P)_2$(A = halogen, ligand that coordinates through carbon, nitrogen, oxygen or sulfur) show a absorption band in the region of 350 - 400 nm(ε, 2600 - 4800) which sensitively shifts with respect to the ligating atom of A.[13] $RhA(CO)(Ph_3P)_2$ shows a absorption band at 350 - 363 nm(ε, 2600 - 3500) when A is the ligand that coordinates to rhodium through the oxygen such as $OClO_3$, $OReO_3$, $OCO_2H$, OH, $O_2P(OH)_2$ and $ONO_2$.[13] We also found that the complex 4 in benzene shows a absorption band at 350 nm(ε, 2790). It has been predicted that the absorption band of $RhA(CO)(Ph_3P)_2$ in the visible region would shifts to longer wave-length when the σ-donor strength of A increases,[13] which agrees with our electronic spectral data for 2 and 3.

The $^1$H-NMR spectra of 2 and 3 in the region where $CH_2$=CHCHO and $CH_3CH$=CHCHO show signals, are practically identical with those of free $CH_2$=CHCHO and $CH_3CH$=CHCHO except the small changes in chemical shifts(see table 1). The multiplet due to the phenyl hydrogens of triphenylphosphine is seen at ca. δ = 7.5 ppm(relative to TMS in $CDCl_3$) for 2 and 3, respectively. The coupling constants between the hydrogens of $CH_2$=CHCHO in 2 and of $CH_3CH$=CHCHO in 3 do not show any differences from those of free $CH_2$=CHCHO and $CH_3CH$=CHCHO. The spin coupling between $^{103}$Rh and the hydrogens of unsaturated aldehydes in 2 and 3 have not been observed.

Table 1. $^1$H-NMR spectral data for $[Rh(CH_2$=CHCHO$)(CO)(Ph_3P)_2]ClO_4$(2) and $[Rh(CH_3CH$=CHCHO$)(CO)(Ph_3P)_2]ClO_4$(3) in $CDCl_3$ at 25°C under nitrogen. The spectral data were obtained on a 60 MHz $^1$H-NMR spectrometer. Multiplicities and numbers of hydrogens are given in parentheses.




acrolein




trans-crotonaldehyde

| compound | chemical shift, ppm[b] | | | | |
|---|---|---|---|---|---|
| | $H_A$ | $H_B$ | $H_C$ | $H_D$ | $Ph_3P$ |
| $CH_2$=CHCHO | 8.75(d)(1) | 5.4 - 5.9(m)(3) | | | |
| $[L_3Rh(CH_2$=CHCHO)$]^+$[a] | 8.75(d)(1) | 6.2 - 6.6(m)(3) | | | 7.5(m)(30) |
| $CH_3CH$=CHCHO | 9.12(d)(1) | 5.54(ddq)(1) | 6.37(dq)(1) | 1.42(dd)(3) | |
| $[L_3Rh(CH_3CH$=CHCHO)$]^+$[a] | 8.52(d)(1) | 5.41(ddq)(1) | 6.63(dq)(1) | 1.67(dd)(3) | 7.5(m)(30) |

[a] $L_3$ = $(CO)(Ph_3P)_2$. [b] Relative to TMS.

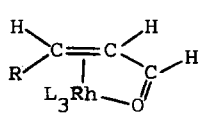
The unsaturated aldehydes in 2 and 3 are readily replaced by acrylonitrile, propionitrile, acetone and triphenylphosphine in chloroform under nitrogen at 25°C(eq. 2).

$$[Rh(RCH{=}CHCHO)(CO)(Ph_3P)_2]ClO_4 + L \longrightarrow [Rh(L)(CO)(Ph_3P)_2]ClO_4 + RCH{=}CHCHO \quad (2)$$

R = H, $CH_3$

L = $CH_2$=CHCN,[2] $CH_3CH_2CN$,[2] $CH_3COCH_3$,[11] $Ph_3P$[14]

It has been found that although no evidences have been obtained for the reactions of 2 and 3 with molecular hydrogen at 25°C under the atmospheric pressure of hydrogen(e.g. no $H_2$ uptake has been observed by 2 and 3 in chloroform), the complex 2 and 3 catalyze the hydrogenation and oligomerization of acrolein and crotonaldehyde. For example, a 10 ml of trans-crotonaldehyde solution of 3(0.16 g, 0.2 mmole) under hydrogen($P_{H_2}$ = 700 mmHg) produces 8.2 mmoles of butyraldehyde and ca. 0.11 g of crotonaldehyde oligomers(ca. 15 mmoles of crotonaldehyde monomer) for 100 hours at 25°C. The $^1$H-NMR spectrum of the oligomers shows the hydrogens of aldehyde groups(-CHO(1H)) at ca. 9.5 ppm, olefinic groups(18H) at 5.0 - 6.0 ppm and alkyl groups(-$CH_2$- and -$CH_3$(41H)) at 0.5 - 2.5 ppm. The solution of acrolein(5.0 ml, 75 mmole) and 2(0.16 g, 0.2 mmole) in benzene(5.0 ml)[15] under hydrogen(700 mmHg) in the dark catalytically produces propionaldehyde(10.6 mmole) and acrolein oligomers(0.12 g, ca. 22.0 mmoles of acrolein monomer) for 24 hours at 25°C. The $^1$H-NMR of the acrolein oligomers shows the hydrogens of olefinic groups(1.1H) at 5.0 - 6.0 ppm and alkyl groups(1H) at 0.5 - 2.5 ppm but does not show the hydrogens of aldehyde groups. These catalytic activities of 2 and 3 might be understood by the fact that an additional intramolecular rhodium-unsaturated aldehyde bond could be formed through the π-system of the olefinic group of RCH=CHCHO coordinated already through the oxygen(see below).



$L_3$ = $(CO)(Ph_3P)_2$

Acknowledgement. We wish to thank the Korean Science and Engineering Foundation and the Ministry of Education for the finantial support.

## References


1. T. Kwon, J. C. Woo and C. S. Chin, Polyhedron, 2, 1225-1228(1983).
2. J. C. Woo, S. H. Kim and C. S. Chin, J. Polymer Sci. Chem. Ed., 20, 1947-1948(1982).
3. S. D. Ittel, Inorg. Chem., 16, 2589-2597(1977).
4. D. F. Childs, D. L. Mulholland and A. Nixon, Can. J. Chem., 60, 801-803, 809-812(1982).
5. One drop of acrolein(ca. 0.74 mmole), 0.21 g(0.28 mmole) of 1 and 10 ml of benzene were used. The yellow solid(2) obtained by filtration was washed throughly with benzene(5 ml) and hexane(15 ml), and dried in vacuum. The yield was 0.14 g or 62 % based on $[Rh(CH_2=CHCHO)(CO)(Ph_3P)_2]ClO_4$. Anal. calcd for $RhC_{40}H_{34}ClO_6P_2$ : C, 59.23; H, 4.23; Cl, 4.38; P, 7.64. Found :C, 59.05; H, 4.38; Cl, 4.23; P, 7.79.
6. One drop of trans-crotonaldehyde( 0.61 mmole), 0.2 g(0.28 mmole) of 1 and 10 ml of benzene were used. The yield was 0.14 g or 61 % based on $[Rh(CH_3CH=CHCHO)(CO)(Ph_3P)_2]ClO_4$. Anal. Calcd for $RhC_{41}H_{36}ClO_6P_2$ : C, 59.68; H, 4.40; Cl, 4.30; P, 7.51. Found : C, 59.01; H, 4.21; Cl, 4.35; P, 7.71.
7. Molar conductance of a standard 1:1 electrolyte $[(C_3H_7)_4N]PF_6$ in dichloromethane at 25°C is 110 $ohm^{-1}cm^2mole^{-1}$.
8. $\nu_{C=C}$ of trans-$CH_3CH=CHCHO$ in 3 is not seen in the IR spectrum of 3 in Nujol, probably because of the strong $\nu_{CO}$ bands at 1632 and 1615 $cm^{-1}$.
9. R. H. Crabtree, G. G. Hlatky, C. P. Parnell, B. E. Segmüller and R. J. Uriate, Inorg. Chem., 23, 354-358(1984).
10. R. H. Crabtree, P. C. Demou, D. Eden, J. M. Mihelcic, C. A. Parnell, J. M. Quirk and G. E. Morris, J. Am. Chem. Soc., 104, 6994-7001(1982).
11. The complex 4 could be prepared in the same manner described for 2 and 3 (see text and reference 5). Detailed experimental data would be sumitted for publication.
12. J. Peone, Jr. and L. Vaska, Angew. Chem. Int. Ed., 10, 511-512(1971).
13. J. Brady, B. R. Flynn, G. L. Geoffroy, H. B. Gray, J. Peone, Jr. and L. Vaska, Inorg. Chem., 15, 1485-1488(1976).
14. L. Vaska and J. Peone, Jr., Suomen Kemistilehti, B44, 317-320(1971).
15. The yellow solution of 2(0.16 g, 0.2 mmole) in neat acrolein in the dark under the atmospheric pressure of hydrogen at 25°C become cloudy within 10 hours due to the large amount of acrolein polymers produced catalytically.

*Polyhedron* Vol. 3, No. 9/10, pp. 1155–1160, 1984
Printed in the U.S.A.

0277-5387/84 $3.00+ .00
© 1984 Pergamon Press Ltd.

# REACTION OF 2,2,3,4,4-PENTAMETHYLPHOSPHETANIC ACID, $C_8H_{16}PO_2H$, WITH FIRST ROW (3d) TRANSITION METAL IONS.

Colin E.J. Dowrick and David S. Moore*
Department of Chemistry, Dover College, Dover, Kent CT17 9RL.

(Received 18 June 1984; accepted after revision 28 September 1984)

Abstract:-

The interaction of the title acid as its conjugate base, $C_8H_{16}PO_2^-$, with first row (3d) transition metal ions has been investigated. Complex formation has been observed in all cases, and inverse solubilities noted for the water soluble complexes of scandium(III), manganese(III), cobalt(II), and nickel(II).

The synthesis of 1-chloro-2,2,3,4,4-pentamethylphosphetan-1-oxide from 2,3,3-trimethylpent-2-ene, phosphorus trichloride and aluminium trichloride has been well documented.[1,2] The subsequent conversion to 2,2,3,4,4-pentamethylphosphetanic acid, or its anhydride, upon hydrolysis with water has also been noted.[3,4]

Although few studies have been made on phosphetanic acid, its physical and spectral properties have been measured [5] and a preliminary study made into some of its reactions.[6]

The arrangement of atoms about the phosphorus atom in the phosphetanoate anion is similar to that observed for the carboxylate anion; for example both have a similar "bite" - for $RPO_2^-$ : O...O = ca.2.6Å ; for $RCO_2^-$ : O...O = ca.2.4Å. It was thought therefore that phosphetanic acid might show some reactions similar to those of a carboxylic acid. Ligating properties and hydrogen bonding to amines have been observed and initial findings reported.[6] A further study has now been made into the ability of the phosphetanoate anion to function as a ligand in its interactions with first row (3d) transition metal ions, (scandium to zinc inclusive). It is observed that rapid complex formation occurs, yielding under most conditions easily isolable products.

## Experimental

### Instruments:

Infrared spectra were run as hexachlorobutadiene mulls using a Perkin Elmer 457 Infrared spectrophotometer. $^{31}P$ - Nuclear magnetic spectra were taken on a Bruker HFX 90 spectrometer at 36.4MHz and referenced to external $H_3PO_4$. Analyses were (in part) carried out by the Imperial College, London, Microanalytical Department.

### Preparation of 2,2,3,4,4-pentamethylphosphetanic acid, $C_8H_{16}POOH$.

2,2,3,4,4-pentamethylphosphetanic acid was prepared from 1-chloro-2,2,3,4,4-pentamethyl-

phosphetan-1-oxide by literature methods.[1,2] The phosphetanic acid was recrystallised twice from boiling water, then dried in a desiccator, prior to use.

Reaction of 2,2,3,4,4-pentamethylphosphetanic acid with scandium(III)chloride hexahydrate.

Scandium chloride (1.0g, 0.004 mole) dissolved in hot water (20cm$^3$) was added to a hot solution of 2,2,3,4,4-pentamethylphosphetanic acid (2.1g, 0.012 mole) in water (30cm$^3$). A white precipitate formed instantly which was filtered from the hot solution and washed with hot water (20cm$^3$). This was tris(2,2,3,4,4-pentamethylphosphetanato)scandium(III), 1.40g, 68.8%.

In a similar manner, utilising appropriate mole ratios, the following complexes were prepared: tris(2,2,3,4,4-pentamethylphosphetanato)vanadium(III), (29.8%), as a pale green powder from vanadium(III) chloride under anaerobic conditions; tris(2,2,3,4,4-pentamethylphosphetanato)chromium(III), (63.8%), as dark green microcrystals from chromium(III) nitrate; bis(2,2,3,4,4-pentamethylphosphetanato)manganese(II) dihydrate, (42.5%), as a white powder from manganese(II) nitrate or sulphate, but not apparently from the chloride; tris(2,2,3,4,4-pentamethylphosphetanato)iron(III), (63.7%), as orange microcrystals from iron(III) nitrate; bis(2,2,3,4,4-pentamethylphosphetanato)nickel(II) nonahydrate, (25.0%), as green platelets from nickel(II) sulphate; bis(2,2,3,4,4-pentamethylphosphetanato)-copper(II), (48.0%), as a pale blue powder from copper(II) chloride; and bis(2,2,3,4,4-pentamethylphosphetanato)zinc(II), (45.0%), as a white powder from zinc(II) chloride.

Reaction of titanium(III) chloride with 2,2,3,4,4-pentamethylphosphetanic acid.

To titanium(III) chloride solution (12.5% w/v $TiCl_3$, 10cm$^3$) sodium hypochlorite solution was added dropwise until the purple colour just changed to yellow. A hot solution of 2,2,3,4,4-pentamethylphosphetanic acid (1g) in water (20cm$^3$) was then added and a very pale yellow precipitate instantly formed. This was filtered off, washed with water and dried in a desiccator. Yield of tetrakis(2,2,3,4,4-pentamethylphosphetanato)-titanium(III) 0.95g, 74%.

Bis(2,2,3,4,4-pentamethylphosphetanato)cobalt(II) has previously been reported and characterised.[6]

TABLE

| Complex | Mp | ANALYSIS | | | | | | | | | | $\mu_{eff}$ /BM | Conductance[b] |
|---|---|---|---|---|---|---|---|---|---|---|---|---|---|
| | | Metal | | C | | H | | P | | Water[a] | | | |
| | /°C | Found | Calc. | Found | Calc. | Found | Calc. | Found | Calc. | Found | Calc. | | /$\Omega^{-1}cm^2mol^{-1}$ |
| $Sc(O_2PC_8H_{16})_3$ | >360 | 7.78 | 7.89 | 50.38 | 50.53 | 8.49 | 8.42 | 16.10 | 16.30 | | | | |
| $Ti(O_2PC_8H_{16})_4$ | >360 | 6.40 | 6.42 | 51.30 | 51.34 | 8.50 | 8.56 | 16.70 | 16.58 | | | | |
| $V(O_2PC_8H_{16})_3$ | 98 | 8.60 | 8.85 | 50.12 | 50.00 | 8.37 | 8.33 | 16.13 | 16.15 | | | 2.80 | |
| $Cr(O_2PC_8H_{16})_3$ | 125 | 8.85 | 9.01 | 49.78 | 49.91 | 8.41 | 8.32 | 16.01 | 16.12 | | | 3.78 | |
| $Mn(O_2PC_8H_{16})_2.2H_2O$ | 230 | 12.54 | 12.47 | 43.29 | 43.54 | 8.14 | 8.16 | 14.27 | 14.06 | 8.20 | 8.16 | 5.87 | 4.20 |
| $Fe(O_2PC_8H_{16})_3$ | 290 | 9.21 | 9.64 | 49.65 | 49.57 | 8.22 | 8.26 | 16.11 | 16.00 | | | 5.68 | 2.8 |
| $Ni(O_2PC_8H_{16})_2.9H_2O$ | >360 | 10.18 | 10.33 | 33.49 | 33.63 | 8.78 | 8.76 | 10.79 | 10.86 | 28.20 | 28.40 | 3.30 | 252 |
| $Cu(O_2PC_8H_{16})_2$ | >360 | 15.27 | 15.39 | 46.47 | 46.43 | 7.77 | 7.74 | 15.08 | 14.99 | | | 1.84 | |
| $Zn(O_2PC_8H_{16})_2$ | >360 | 14.99 | 15.66 | 46.24 | 46.27 | 7.69 | 7.71 | 15.10 | 14.94 | | | | |

(a) by gravimetric analysis.

(b) conductivity measured at a concentration of 0.001 mol $dm^{-3}$ in water as solvent, except Fe when nitromethane was used.

## Discussion

Results are summarised in the Table.

All compounds are readily isolated using water as a solvent, however all products were filtered from hot solution as those complexes that were soluble in water (namely the complexes of scandium, manganese, cobalt and nickel) displayed inverse solubilities (i.e. soluble in cold water, largely insoluble in hot water). The nickel complex could also be obtained as diamond shaped platelets, upon slow evaporation of a saturated cold solution. All complexes isolated were air stable.

Characteristic phosphetan infra-red stretching frequencies were observed for all complexes at ca: 1238 (s), 931 (s), 670 (s) and 530 $cm^{-1}$ (s) - being recognised phosphetan ring absorptions [5]; and also at 1082 $cm^{-1}$ (s) due to $PO_2$ stretching.

As could be expected, chromium, manganese, iron and nickel phosphetan compounds, being paramagnetic, show very broad $^{31}P$ n.m.r. signals which cannot be resolved from the baseline. For the vanadium phosphetan complex however, although also paramagnetic, a very broad resonance signal centered on ca 63.4 ppm can just be resolved; this compares favourably with 59.04 ppm for the phosphetan acid. [6]

The interaction of scandium trichloride with phosphetanic acid produces $Sc(O_2PC_8H_{16})_3$, which is in accord with its most common coordination number of six, in which it resembles its

cogener aluminium. The complex is insoluble in common organic solvents, and is only slightly soluble in hot water, when it displays inverse solubility. In order to examine this inverse solubility, $Sc(O_2PC_8H_{16})_2$ was dissolved in cold water and recovered by filtering from hot solution. Over a number of determinations recovery was always better than 95%. Analytical and infrared spectral results indicated that the $Sc(O_2PC_8H_{16})_3$ was recovered unchanged after the dissolution.

Isolable products have only been obtained for titanium(IV) species in solution; there appears to be no apparent reaction of titanium(III) with phosphetanic acid, as in the latter case the bulk of the phosphetan can be recovered unchanged from the reaction mix. The infra-red spectrum did not reveal any bands that could have been due to $\nu$ (Ti-O), (between 350-400 and 520-620 $cm^{-1}$) [7], nor did the analysis results indicate any untoward stoicheiometric compositions, nor the presence of combined chlorine. The structure of the titanium(IV)-phosphetan complex is presumably octahedral. The very low solubility in water precluded any observations as to whether this too displayed inverse solubility in saturated solutions.

Although aqueous solutions of simple vanadium(III) salts are air sensitive and subject to aerial oxidation, [8] the vanadium(III) complex obtained was stable in air and was also stable in common organic solvents. The infrared spectrum showed no trace of absorptions due to $VO^{2+}$ or $VO_2^+$ species, and the presence of additional oxygen atoms did not show up in the analytical results. As with other vanadium(III) compounds, it would be expected that the complex adopted octahedral coordination. The occurrence of a small $^{31}P$ n.m.r. signal could possibly be due to a residual amount of a vanadium(V) complex which could not be removed by fractional crystallisation. The magnetic moment of 2.80 Bohr Magnetons was also consistent with a $d^2$ ion, ($V^{3+}$). [8]

The green chromium(III) phosphetanate compound is formed as a neutral complex of identical stoicheiometry as the analagous trifluoroacetate complex, $Cr(O_2CCF_3)_3$. [8] Analysis results did not support a bi- or tri-nuclear complex with, or without, oxocentering. The magnetic moment of 3.78 BM. is only slightly below the expected spin-only value of 3.88 BM. which is also in accord with the theory for octahedral chromium(III) complexes.

The interaction of manganese(II) sulphate or nitrate with phosphetanic acid in water produces $Mn(O_2PC_8H_{16})_2.2H_2O$ which then displays inverse solubility in water. The "insoluble" manganese complex, $Mn(O_2PC_8H_{16})_2$, previously isolated from manganese nitrate and phosphetanic acid in propanone solvent, has been reinvestigated and shown to dissolve in cold water, forming the hydrated complex when it then displays the same inverted solubility.

This observation tends to preclude the manganese complex from being of polymeric composition as has been suggested. [6]

In the interaction of iron salts with phosphetanic acid, isolable complexes have only been obtained from the more strongly oxidising iron(III); when iron(II) salts are used the starting materials can be recovered unchanged at the end of the reaction. The iron complexes obtained retain the iron in the +3 oxidation state, this has been confirmed by chemical methods. The iron(III) phosphetan complex is probably octahedrally coordinated, as is observed for the analagous phosphates, polyphosphates and polyols, all of which also coordinate through oxygen atoms. [9] Conductivity measurements in nitromethane show negligible conductance indicating that the compound formed is actually a complex and not an ordinary salt. The complex does not appear to be soluble to any appreciable extent in water.

The nickel(II) phosphetan complex crystallises from water as diamond shaped platelets. These green crystals analyse as the salt $Ni(O_2PC_8H_{16})_2.9H_2O$., and in water show a conductivity of 252 $\Omega^{-1}cm^2mol^{-1}$, as would be expected for a 2:1 electrolyte. [10] Heating these crystals results in the loss of water molecules and a colour change from green through to blue/purple. Gravimetric and analytical techniques have shown the water loss and colour change to be consistent with the following scheme. On increasing the temperature the green nickel(II) complex, $Ni(O_2PC_8H_{16})_2.9H_2O$ , loses seven water molecules to become the yellow, planar $Ni(O_2PC_8H_{16})_2.2H_2O$ complex (with unidentate phosphetanoate ligands), upon heating to a temperature higher than 110°C the remaining water molecules are lost and the blue/purple tetrahedral $Ni(O_2PC_8H_{16})_2$ complex formed. These changes, as would be expected, are reversible upon the addition of water at any stage; moreover the intermediates appear to be stable in a totally moisture free atmosphere. Similar colour changes for a wide range of nickel(II) complexes have been widely recognised for many years. [8] Concentrated aqueous solutions of the green nickel complex shows an inverse solubility in water on heating, as has been noted previously.

Treatment of copper(II) solutions with phosphetanic acid leads to the precipitation of the pale blue, water insoluble copper(II)-phosphetanate complex. This complex is probably of square-planar coordination, since in general most neutral four coordinate copper(II) complexes containing chelating ligands are planar. [11] However, since the product obtained is insoluble both in water and common organic solvents, it could

solution containing excess tetrabutylammonium bromide, which has been acidified by $HNO_3$. The precipitate was washed thoroughly with water and dried. Purification was possible by fractional crystallization from acetonitrile. Deposited metatungstates were repeatedly separated and the separation of product and metatungstate was monitored by the IR spectrum. The final acetonitrile solution was rather viscous and a deep red-brown. The product was reprecipitated by adding ethanol to the solution.

pH adjustment of the starting solution of $Na_2WO_4$ was allowed in the range 4.3–5.9, although Brown reported the addition of 1 *N* $HNO_3$ (194.4 $cm^3$) to a solution of $Na_2WO_4 \cdot 2H_2O$ (56.2 g, in 300 $cm^3$ of water).[4] The method of adjusting pH is experimentally more convenient than that of Brown's condition. This has already been confirmed for the preparations of dodecatungstopolyanions of M = Cu(II), Fe(III), Al(III) and Zn(II).[1,3]

The preparation and purufication of tungstochromate were performed by the same work-up, except that the pH of the starting solution of $Na_2WO_4$ was adjusted to about 4.1, and $Cr(NO_3)_3 \cdot 9H_2O$ (4.5 g, $1.1 \times 10^{-2}$ mol) was used in place of $MnSO_4 \cdot 4$–$6H_2O$, without addition of $K_2S_2O_8$. The lowest layer in the ether extraction was green and the product it contained was thermally unstable as reported by Brown.[5]

## RESULTS AND DISCUSSION

The IR spectra of the tungstopolyanion containing the Mn ion in the solid and in acetonitrile solution showed that the Keggin structure was retained and the metatungstate was completely removed. The absorption spectra were observed in the VIS–UV regions (Figs 1 and 2): 13,600 ($\varepsilon$ 4.7), 14,400 ($\varepsilon$ 9.2), *ca* 20,000 ($\varepsilon$ 222, broad), 26,400 ($\varepsilon$ 2910, shoulder) and 38,500 $cm^{-1}$ ($\varepsilon$ 38,000), but only absorptions due to water in the near-IR region. The 38,500-$cm^{-1}$ band can be assigned to the CT transition within the ligand as observed in many other tungstopolyanions.[1–3] However, MCD spectra in the UV region all consist of positive components, the pattern of which is quite different from that of the many dodecatungstopolyanions. In such polyanions, the MCD due to the W ← O CT transition within the $W_{12}O_{40}$ ligand shows apparently two positive and one negative component, where the negative one appears near the absorption maximum and exists between the two positive ones, although their positions and intensities can change with the central metal ion.[2,3] Thus, the results of IR and MCD indicate that the polyanion has the $MnW_{11}O_{39}$ skeleton rather than the $W_{12}O_{40}$ skeleton.

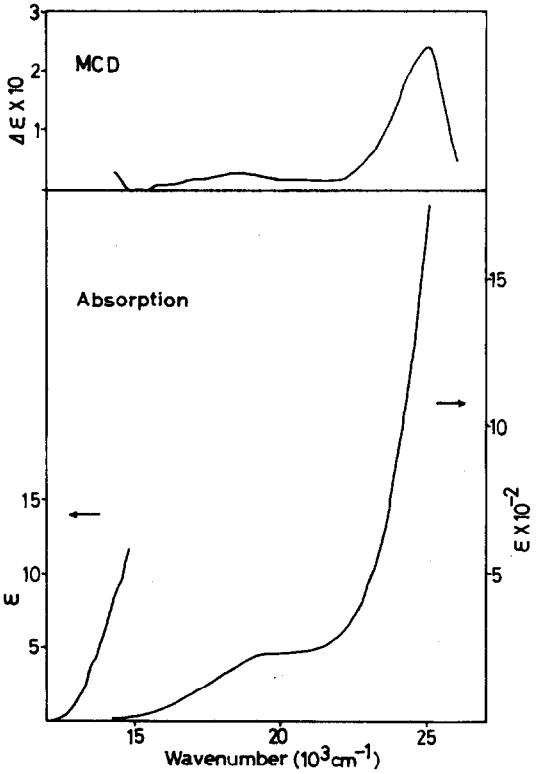



Fig. 1. VIS and MCD spectra of the tetrabutylammonium salt of tungstomanganate in acetonitrile solution.

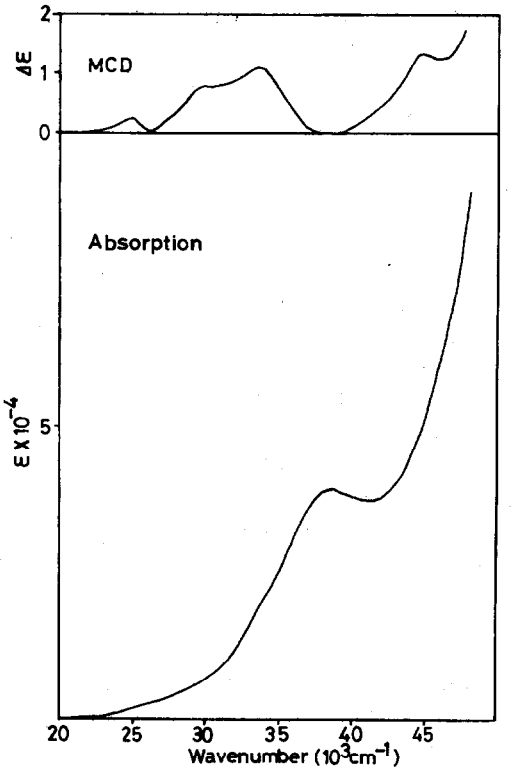



Fig. 2. UV and MCD spectra of the tetrabutylammonium salt of tungstomanganate in acetonitrile solution.

Four absorption bands in the VIS region resemble those observed in the usual octahedral Co(III) (low-spin $d^6$) and Cr(III) ($d^3$) complexes, where the shoulder band at 26,400 $cm^{-1}$ can be regarded as superimposed on the tail of the very intense CT band in the UV region. Moreover, the MCD spectrum in the VIS region suggests that two extremely weak bands at the lowest frequencies are due to the spin-forbidden transitions and the first and second absorptions come from the octahedral $d^3$-type configuration, and not from the octahedral low-spin $d^6$-type.[8] Taking account of no absorption in the near-IR region, these observations strongly suggest that the Mn ion with a valence of +4 is located in the octahedral site, and not in the tetrahedral one. Four absorptions in the VIS region and no absorption in the near-IR region were also observed in the spectra of the acetonitrile solutions on the way to purification.

If the Mn(IV) ion is located in the terahedral environment, some absorptions of the *d–d* transition due to the $d^3$-configuration should be observed with relatively strong intensities in the VIS and near-IR regions. These are caused by the facts that the ligand field separation, $\Delta_t$, becomes 4/9 of $\Delta_o$ and that the $t_2 \leftarrow e$ transition has little $p \leftarrow d$ transition character. Furthermore, some splittings are also expected from a spin–orbit coupling and a Jahn–Teller effect.[9] Brown reported a weak broad band ($\varepsilon$ 18) at 7000 $cm^{-1}$ and a strong peak ($\varepsilon$ 99,000) at 38,400 $cm^{-1}$:[4] the former should be due to the *d–d* transition and the latter to the CT transition within the ligand. However, it is unbelievable that only one absorption is observed in the near-IR region, the *d–d* transition due to the $d^3$-configuration, and, if so, its intensity is too low. We could not observe such a band, except for the absorptions due to the contaminated or coordinating water, in the neighbouring region of 7000 $cm^{-1}$.

The facts that the tungstomanganic acid is not so stable thermally and can be readily converted to metatungstic acid under treatment through the cation-exchange resin ($H^+$-form) are quite different from the chemical properties of all known dodecatungstometallic acids, suggesting that the Mn(IV) ion is located in the octahedral site in place of one W ion of metatungstate. For instance, the Keggin-type $[Co(II)W_{12}O_{40}]^{6-}$ polyanion has been prepared by acid hydrolysis of the dicobalt species, $[CoCoW_{11}O_{40}H_2]^{8-}$, in which two Co ions are located in the central tetrahedral and exterior octahedral sites, respectively.[2] Further, Ripan *et al.*[10] have reported that tri-heteropoly tungsto-polyanions, $[MM'W_{11}O_{40}H_2]$, were converted to polyanions of the type $[MW_{12}O_{40}]$ by passing through Amberlite IR-120 in the $H^+$-form, in which M and M′ ions are located in the tetrahedral and octahedral sites, respectively.

In the light of these considerations, we conclude that the Mn(IV) polyanion obtained by Brown's method has a mixed structure derived from the metatungstate, $[H_2Mn(H_2O)W_{11}O_{39}]^{6-}$. Analytical data of our sample support this conclusion. Found: C, 18.57; H, 3.78; N, 1.29%. Calc. for $[(C_4H_9)_4N]_{3.5}H_{2.5}[H_2MnW_{11}O_{40}H_2]$: C, 18.83; H, 3.74; N, 1.37%. In this structure, two protons occupy the central tetrahedral cavity as a hetero-atom and the Mn ion is located in the octahedral vacant site of $W_{11}O_{39}$, accompanied by one coordinating water molecule. This polyanion may be very close to the 1:11 compound with the analytical composition reported first by Mair and Waugh[6] and later by Singer and Waugh,[7] prior to Brown's paper,[4] although the valence of the Mn ion in the 1:11 compound has been estimated as +3.

For the acetonitrile solution of the green tungstopolyanion containing the Cr(III) ion, all absorption bands appeared only in the VIS and UV regions. Prominent bands in the VIS region, other than spin-forbidden bands, were observed at 16,400 (broad) and 22,500 $cm^{-1}$ (shoulder). Although Brown reported three absorption bands of 8300 ($\varepsilon$ 20), 16,000 ($\varepsilon$ 105) and 38,400 $cm^{-1}$ ($\varepsilon$ 99,000),[5] we could not observe the most important band in the near-IR region. Since the tungstochromic acid was also converted to the metatungstic acid by passing through the cation-exchange resin ($H^+$-form), this polyanion is also considered to have the 1:11 structure analogous to the Mn(IV) polyanion, rather than the 1:12 structure.

## REFERENCES


1. K. Nomiya, M. Miwa, R. Kobayashi and M. Aiso, *Bull. Chem. Soc. Jpn* 1981, **54**, 2983.
2. K. Nomiya, R. Kobayashi and M. Miwa, *Bull. Chem. Soc. Jpn* 1983, **56**, 2272.
3. K. Nomiya and M. Miwa, *Polyhedron* 1983, **2**, 955.
4. D. H. Brown, *J. Chem. Soc.* 1962, 4408.
5. D. H. Brown, *J. Chem. Soc.* 1962, 3322.
6. J. A. Mair and J. L. T. Waugh, *J. Chem. Soc.* 1950, 2372.
7. S. J. Singer and J. L. T. Waugh, *Proc. Nat. Acad. Sci. U.S.A.* 1952, **38**, 1027.
8. A. J. McCaffery, P. J. Stephens and P. N. Schatz, *Inorg. Chem.* 1967, **6**, 1614.
9. D. Sutton, *Electronic Spectra of Transition Metal Complexes*. McGraw-Hill, New York (1968).
10. R. Ripan, Al. Duca, D. Stanescu and M. Puscasu, *Z. Anorg. Allg. Chem.* 1966, **347**, 333. The tri-heteropoly compounds are described as $[MM'W_{12}O_{42}]$ in the paper.

*Polyhedron* Vol. 3, No. 9/10, pp. 1165–1167, 1984
Printed in the U.S.A.

0277-5387/84 $3.00 + .00
© 1984 Pergamon Press Ltd.

# COMMUNICATION

## HOMONUCLEAR SPIN–SPIN COUPLING THROUGH IRON IN SIMPLE INORGANIC IONS

**ANTHONY R. BUTLER, CHRISTOPHER GLIDEWELL,* ANDREW R. HYDE and JOSEPH McGINNIS**

Chemistry Department, University of St. Andrews, St. Andrews, Fife KY16 9ST, U.K.

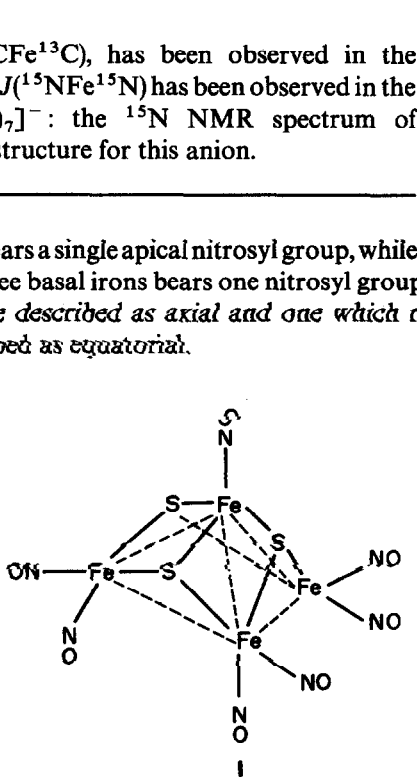
(*Received* 11 *April* 1984; *accepted* 14 *June* 1984)

**Abstract**—Homonuclear spin–spin coupling, $^2J(^{13}CFe^{13}C)$, has been observed in the nitroprusside ion, $[Fe(CN)_5NO]^{2-}$, and the coupling $^2J(^{15}NFe^{15}N)$ has been observed in the Roussin anions $[Fe_4S_3(NO)_7]^-$ and $[Fe_4Se_3(NO)_7]^-$: the $^{15}N$ NMR spectrum of $[Fe_4Se_3(^{15}NO)_7]^-$ provides a definitive proof of the structure for this anion.

We report that, by the use of isotopic enrichment and a high field spectrometer, homonuclear spin–spin coupling of type $^2J(XMX)$ is readily observable in simple inorganic ions. In particular we have observed $^2J(CFeC)$ in the nitroprusside anion, $[Fe(CN)_5NO]^{2-}$, and $^2J(^{15}NFe^{15}N)$ in the anion of Roussin's black salt, $[Fe_4S_3(NO)_7]^-$, and its selenium analogue $[Fe_4Se_3(NO)_7]^-$.

The nitroprusside anion has been shown[1] by X-ray analysis to possess $C_{4v}$ symmetry, in which there are four equivalent equatorial cyanide ligands and a unique axial cyanide. When nitroprusside is prepared from 90%-enriched $Na^{13}CN$, it follows, assuming that the $^{12}C$- and $^{13}C$-isotopes are statistically distributed between the two sites, that 59% of the spectral intensity is due to $[Fe(^{13}CN)_5NO]^{2-}$ and 26.2% to $[Fe(^{12}CN_{ax})(^{13}CN_{eq})_4NO]^{2-}$. No other isotopic species contributes more than 6.6% of the total intensity, and the $^{13}C$ NMR spectrum can be interpreted in terms of just two significant isotopic anions. At 20 MHz the spectrum is second-order, but it is first-order at 90 MHz: the spectrum (Fig. 1) then consists of a quintet and a doublet due to $[Fe(^{13}CN)_5NO]^{2-}$, having $\delta(^{13}C_{ax}) = +132.2$ ppm and $\delta(^{13}C_{eq}) = +134.4$ ppm respectively, and $^2J(^{13}C_{ax}Fe^{13}C_{eq}) = 18$ Hz; together with a singlet at $\delta(^{13}C_{eq}) = +134.4$ ppm due to $[Fe(^{12}C_{ax})(^{13}C_{eq})_4NO]^{2-}$.

In the anion $[Fe_4S_3(NO)_7]^-$ (**1**) of overall $C_{3v}$ symmetry, there are[2,3] three nitrosyl environments having relative abundances of 1:3:3. The unique iron bears a single apical nitrosyl group, while each of the three basal irons bears one nitrosyl group which may be described as axial and one which may be described as equatorial.




The $^{15}N$ NMR spectrum of a sample of $(Ph_3PNPPh_3)^+[Fe_4S_3(NO)_7]^-$ enriched to 99% $^{15}N$ in the anion only, and recorded at 36.5 MHz in $CD_2Cl_2$ solution is first-order (Fig. 2) and exhibits three resonances (Table 1): the unique apical nitrosyl group gives a singlet, while the resonances of the equatorial and axial ligands bonded to the basal irons exhibit doublet splittings due to a $^2J(^{15}N_{ax}Fe^{15}N_{eq})$ of 4.3 Hz. The $^{15}N$ NMR spectrum of $(Ph_3PNPPh_3)^+[Fe_4Se_3(NO)_7]^-$ recorded under similar conditions is very similar (Table 1).

The $^{15}N$ chemical shifts are all clearly compatible with the range of shifts, −37 to +49 ppm, reported[4] for a series of nitrosyl complexes containing MNO

* Author to whom correspondence should be addressed.

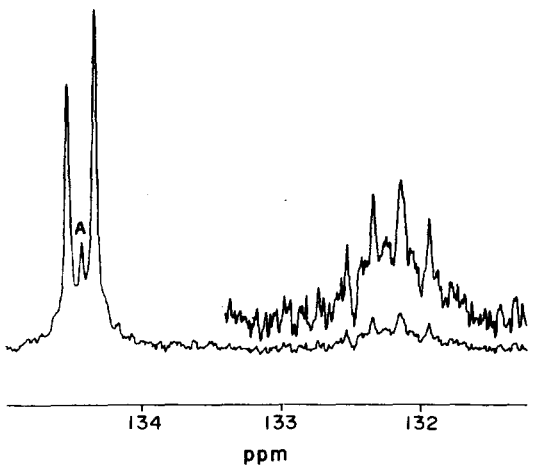



Fig. 1. $^{13}C$ NMR spectrum at 90 MHz of sodium nitroprusside, 90% enriched in $^{13}C$: the peak marked A is due to $[Fe(^{12}CN_{ax})(^{13}CN_{eq})_4NO]^{2-}$.

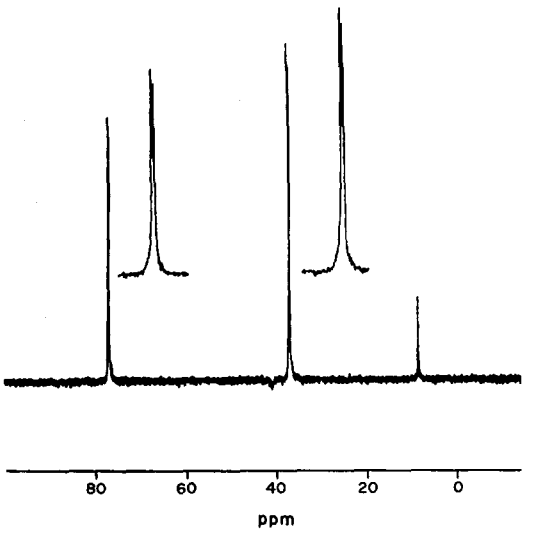



Fig. 2. $^{15}N$ NMR spectrum at 36.5 MHz of $(Ph_3PNPPh_3)^+[Fe_4S_3(NO)_7]^-$, 99% enriched in $^{15}N$ in the anion: natural abundance in the cation.

fragments which are linear, or nearly so. Bent nitrosyls, in contrast, have $^{15}N$-shifts in the range +360 to +720 ppm.[4] Although the selenium anion $[Fe_4Se_3(NO)_7]^-$ has been prepared[5] in analytically pure form as its $Ph_4As^+$ salt, its structure has never been definitively established, other than by inference from the known[2,3] structure of the sulphur analogue. The present $^{15}N$ NMR spectra provide proof of the structure.

We cannot at the present time establish which of the doublet resonances should be assigned to the axial ligands of the basal $Fe(NO)_2$ fragments, and which to the equatorial ligands. However we note that the chemical shifts of the apical nitrosyl groups are fairly close to those in the cubane-like complexes, $Fe_4X_4(NO)_4$ (X = S, Se), whose structures have both been established by X-ray analysis.[6,7] The shifts confirm the similarity of the nitrosyl groups in the $(ON)Fe^IX_3$ fragments of $[Fe_4X_3(NO)_7]^-$ and $Fe_4X_4(NO)_4$.

## EXPERIMENTAL

Samples of $Na_2[Fe(^{13}CN)_5NO]$ were prepared using 90% $^{13}C$-enriched $Na[^{13}CN]$ (MSD Isotopes, Inc.). Iron(II) sulphate was converted to sodium hexacyanoferrate(II), which was subsequently treated with concentrated nitric acid: the sodium nitroprusside was recrystallised from the minimum volume of water.[8]

Samples of $(PPN)^+[Fe_4S_3(^{15}NO)_7]^-$ and $(PPN)^+[Fe_4Se_3(^{15}NO)_7]^-$ ($PPN^+ \equiv Ph_3PNPPh_3^+$) were prepared as previously described[5] using 99% $^{15}N$-enriched $Na[^{15}NO_2]$ (MSD Isotopes, Inc.). $Fe_4S_4(NO)_4$ was prepared by reaction of $Na[Fe_4S_3(NO)_7]$ with elemental sulphur,[5] and $Fe_4Se_4(NO)_4$ was prepared similarly by reaction of $Na[Fe_4Se_3(NO)_7]$ with selenium.

NMR spectra were recorded using the Brüker WH-360 spectrometer at the University of Edinburgh.

Table 1. $^{15}N$ NMR data for iron–chalcogen–nitrosyl cluster compounds

| Compound | $\delta(^{15}N$ ppm)* | | |
|---|---|---|---|
| $(PPN)^+[Fe_4S_3(NO)_7]^-$ | 7.7 (s) | 36.0 (d, $J$ = 4.3 Hz) | 76.1 (d, $J$ = 4.3 Hz) |
| $(PPN)^+[Fe_4Se_3(NO)_7]^-$† | 7.8 (s) | 29.5 (d, $J$ = 4.1 Hz) | 74.9 (d, $J$ = 4.1 Hz) |
| $Fe_4S_4(NO)_4$ | 12.8 (s) | | |
| $Fe_4Se_4(NO)_4$† | 20.5 (s) | | |

*Chemical shifts (ppm) from $CH_3{}^{15}NO_2$ as external reference: spectra recorded in $CD_2Cl_2$ solution at 298 K.

† No satellite structure due to coupling of $^{15}N$ to $^{77}Se$ was detected.

*Acknowledgements*—We thank the Carnegie Trust for the Universities of Scotland, and the Cancer Research Campaign for financial support (to J.McG. and A.R.H. respectively), the Royal Society for a grant to purchase Na[$^{13}$CN], and Drs I. H. Sadler and D. Reed (University of Edinburgh) for recording the spectra.

## REFERENCES

1. P. T. Manoharan and W. C. Hamilton, *Inorg. Chem.* 1963, **2**, 1043.
2. G. Johansson and W. N. Lipscomb, *Acta Crystallogr.* 1958, **11**, 594.
3. C. T.-W. Chu and L. F. Dahl, *Inorg. Chem.* 1977, **16**, 3245.
4. L. K. Bell, D. M. P. Mingos, D. G. Tew, L. F. Larkworthy, B. Sandell, D. C. Povey and J. Mason, *J. Chem. Soc., Chem. Commun.* 1983, 125.
5. A. R. Butler, C. Glidewell, A. R. Hyde, J. McGinnis and J. E. Seymour, *Polyhedron* 1983, **2**, 1045.
6. C. T.-W. Chu, F. Y.-K. Lo and L. F. Dahl, *J. Am. Chem. Soc.* 1982, **104**, 3409.
7. L. L. Nelson, Ph.D. Thesis, University of Wisconsin-Madison (1981).
8. J. McGinnis, Ph.D. Thesis, University of St. Andrews (1983).

*Polyhedron* Vol. 3, No. 9/10, pp. 1169–1170, 1984
Pergamon Press Ltd. Printed in the U.S.A.

# BOOK REVIEWS

**Inorganic Coordination Compounds (Nobel Prize Topics in Chemistry).** George B. Kauffman. Heyden, 1981. ISBN 0-85501-683-3 and ISBN 0-85501-684-1 Pbk. Price not stated; xvi + 205 pp.

This book is a member of a series, each of which seeks to follow the development of an area of scientific study for which a Nobel prize was awarded. Through his writings, Professor Kauffman's name has come to be largely synonymous with Alfred Werner, and in this book he examines Werner's researches that led to the award of the 1913 Nobel Prize for Chemistry, putting them within the context of the development of Coordination Chemistry. As a combination of chemistry, history, and biography, it is not the easiest book to review.

The book is written for the non-specialist chemist, and Chapter 1 begins with definitions of various terms (coordination compound, ligand, complex, denticity, isomerism, etc.) and also includes what this reviewer found to be a most useful list of coordination compounds named after their discoverers (all apparently pre-World War I, but how many chemists since, bar Wilkinson and Vaska, can claim that distinction?) and another handy compilation of complex cobalt compounds with names based on colour (luteo, purpureo, roseo, etc.). Even though it would anticipated Werner's discoveries, it might have been helpful to have been given more diagrams to clarify structures.

Chapter 2 is an anecdotal biography of Werner. We learn that the young Werner often played truant from school and padded out his trousers with cardboard when in line for the cane. His interest in chemistry began at Technical school in Mulhouse, his birthplace, and initially he specialised in organic chemistry (which *Polyhedron* readers will recognise as a branch of inorganic chemistry). At the Hochschule in Zurich, Werner distinguished himself both in attaining the highest grades in chemistry and the lowest grades in mathematics and (believe it or not) descriptive geometry, which should give heart to us lesser mortals. Within a few months of becoming professor of organic chemistry (Sic; Werner spent much of his life teaching this area) at the University of Zurich, Werner had the 2 a.m. flash of inspiration that led to the development of his coordination theory. A vivid picture is drawn of the "Catacombs," the laboratories where his students worked, a space where gas lighting was needed at noon, which reeked of pyridine, and where pupils had steam pipes above their heads and concrete beneath their feet. Werner lived for science, slept little, spending his evenings either in the laboratory or drinking and playing cards. (How did he find time to marry and have two children?)

It is of course from his practical work that Werner obtained support for his theories; the compounds he prepared are still kept in Zurich. He only allowed a student to begin a research project that he had tested and knew to be feasible. (Contrary to the advice we always give, Werner never labelled any of the solutions on his bench—he could always remember the identity of each.) His tremendously sustained work, coupled with alcoholism, led to his premature death from arterioscloerosis in 1919 at the age of 53.

For Chapter 3, Kauffman has chosen to print a lecture (1912) on optical activity in coordination compounds. Werner was of course the first chemist to resolve a completely carbon-less coordination compound, $[Co\{Co(OH)_2(NH_3)_4\}_3]Br_6$ a distinction only shared with F. G. Mann {Na *cis*-$[Rh(H_2O)_2(SO_2(NH_2)_2)_2]$} and Gillard and Wimmer $[Pt(S_5)_3]^{2-}$ and Shimba, Fujinami and Shibata {*cis-cis-cis*-$[Co(NH_3)_2(H_2O)_2(CN)_2]^+$ and *cis-cis-cis*-$[Co(NH_3)_2(H_2O)_2(NO_2)_2]^+$}.

Chapter 4 considers historically significant coordination compounds of the pre-Werner period such as Prussian blue and early work on cobalt ammines, whilst Chapter 5 relates the theories advanced to explain the bonding in these compounds, such as the constant valency approach of Kekulé, and the Blomstrand-Jørgensen chain theory. It was Werner's achievement to distinguish between valency and coordination number, and to show from a consideration of the number of isomers that cobalt(III) complexes generally adopt an octahedral geometry. There is a detailed and interesting discussion of the principal types of cobalt ammine complexes and of the points where Werner's theories triumphed, together with an account of Werner's experiments in the field of optically active coordination compounds.

It was only after Werner's death that crystallographic pioneers such as Wyckoff and Dickenson carried out the determinations of crystal structure that confirmed his theories, and a final chapter traces developments such as this, whilst leaving the post-1945 developments to a final table, Appendix A, "Some historically significant events in coordination chemistry." This is inevitably subjective [e.g. the alkylamides $M\{N(SiMe_3)_2\}_3$ are earlier representatives of planar 3-coordination than the quoted examples], but is nevertheless a most valuable perspective. The book has a full bibliography.

The book is written in a style which makes it easy to read and has an excellent selection of portraits of the "great names" of the past. It could be read with profit by any university or college chemistry student.

*Stanground School*
*Peterborough*
*Cambridgeshire*
*England*

SIMON COTTON

**Gmelin: Handbook of Inorganic Chemistry. 8th Edn. Sc, Y, La-Lu—Rare Earth Elements. Part D6: Ion Exchange and Solvent Extraction Reactions. Organometallic Compounds.** 1983. 49 ills. xii + 304 pp. Springer-Verlag. ISBN 3-540-93491-X. DM 1012; approx $392.70.

This volume is the sixth in the series (though not in appearance) of that part of Gmelin's Handbook (Part D) dealing with Rare Earth coordination compounds. It consists of two authoritative compilations of information.

Approximately the first half of the book consists of a review by Yizhak Marcus of certain aspects of the ion exchange and solvent extraction of these metals that have not already been dealt with in the series. At a time when chemists are accustomed to purchase most lanthanides at quite reasonable prices in a high degree of purity, it is salutary to remember that until less than 40 yr ago they could only be separated from each other by repeated fractional crystallization, and that it was the advent of ion-exchange resins that opened the doorway to intensive study of lanthanide chemistry, a non-controversial spin-off from the Manhattan Project. In particular, there is a significant separation between "adjacent" rare earth cations when adsorbed on a cation-exchange resin in the presence of a suitable complexing medium. The early resins such as synthetic zeolites were subsequently supplanted with polystyrene sulphonic acid cation exchanged resins (crosslinked with divinylbenzene). There is a survey of the cation exchange data for all the rare earths on such resins, listing equilibrium constants, distribution ratios and thermodynamic data, followed by a tabulation of kinetic data listing self-diffusion coefficients, and a most thorough listing of separation factors. Data are also quoted for other resins that do not have sulphonate groups, including natural zeolites and zirconium phosphate exchangers. Later sections are devoted to results for anion-exchange resins.

The section on solvent extraction of rare earths covers a whole range of extractants, such as sulphonic acids, carboxylic acids, chelating agents such as $\beta$-diketones and hydroxyquinolines, and phosphoric acid derivatives, especially tributyl phosphate. Solvent extraction is a practical competitor to ion-exchange for large-scale separation of the rare earths and a knowledge of the behaviour of the rare earths is vital in view of the presence of them in the fission products encountered in spent fuel rods from nuclear power stations. In this section, too, the data are clearly tabulated.

The chemistry of organolanthanides and actinides has been one of the most exciting growth areas in inorganic chemistry over the last decade.

Simple compounds such as the cyclopentadienyl derivatives have been known for nearly thirty years, but the almost simultaneous discovery in the early 1970s by several workers of the isolability of sigma-bonded organometallics has led to mushrooming growth. Here, as in the previous section, the literature has been surveyed (by J. H. Forsberg and T. Moeller) through 1981, with many 1982 and 1983 publications included, so necessary in this fast-moving field (yet so difficult to achieve). The compounds with alkyl, alkenyl, alkynyl, and aryl groups are dealt with first, followed by the cyclopentadienyl derivatives, the substituted cyclopentadienyls, indenyls, fluorenyls, and cyclooctatetraenyls, in that order. For each compound, details are given of the preparative method, together with a description of its appearance and all available spectroscopic data. Where the crystal structure has been determined, a clear diagram of the structure is given. The authors give an extremely lucid account of the compounds under consideration; this reviewer found the text extremely readable. The formula index provided makes it easy to locate compounds, whether they appear in the test or in a table. This volume is obviously indispensible to libraries using the Gmelin system, but its price will put it out of the reach of all chemists except those with private means.

*Stanground School*
*Peterborough*
*Cambridgeshire*
*England*

SIMON COTTON

*Polyhedron* Vol. 3, No. 9/10, p. 1171, 1984
Pergamon Press Ltd. Printed in the U.S.A.

# ERRATUM

K. Nomiya and M. Miwa, Structural stability index of heteropoly- and isopoly-anions. *Polyhedron* 1984, **3**, 341–346.

The authors regret that of the structural parameters of the Waugh-type $XMo_9O_{32}^{6-}$ anion in Table 1 (p. 343), C should be 3, because there exist three closed loops over the three boat-like frameworks, each of which is formed by edge-sharing of six $MoO_6$ octahedra. Thus, the structural stability index $\eta$ should also be corrected from 1.33 to 2. Correspondingly, p. 343, column 1, lines 25 and 26 should read: ... edge-sharing; there are three closed loops over them and the index $\eta = 18/9 = 2$. Silverton-type ....

*Polyhedron* Vol. 3, No. 9/10, p. 1173, 1984
Pergamon Press Ltd. Printed in the U.S.A.

# ANNOUNCEMENT

The Fifth International Conference on the Chemistry and Uses of Molybdenum, sponsored by the Climax Molybdenum Co. Ltd and the Dalton Division, will be held at the University of Newcastle upon Tyne from 1 to 5 July 1985. Plenary lectures will be given by: R. Chevrel (Rennes), F. A. Cotton (Texas A & M), M. Green (Bristol), B. Kelley (Biotech, Sydney), R. E. McCarley (Ames, Iowa), A. Müller (Bielefeld), R. K. Murmann (Missouri), W. H. Orme-Johnson (MIT) and H. Wise (Stanford).

Further details can be obtained from: Professor A. G. Sykes, Department of Inorganic Chemistry, The University, Newcastle upon Tyne NE1 7RU, U.K.

The final selection of papers for 30-min lectures and posters will be based on abstracts submitted. Applications are invited for three RSC bursaries of £60 from graduate/post-doc students.

The proceedings will be published in *Polyhedron*.

*Polyhedron* Vol. 3, No. 11, pp. 1175–1225, 1984
Printed in the U.S.A.

0277–5387/84 $3.00 + .00
Pergamon Press Ltd.

# POLYHEDRON REPORT NUMBER 8

## REACTIONS OF TRIOSMIUM CLUSTERS WITH ORGANIC COMPOUNDS

KEVIN BURGESS
University Chemical Laboratory, Lensfield Road, Cambridge, CB2 1EW, England

### CONTENTS

INTRODUCTION ..... 1176
SYNTHESES OF TRIOSMIUM CLUSTERS IN GENERAL ..... 1176
(i) Nucleophilic attack on carbonyl ligands ..... 1176
(ii) "Unsaturated" triosmium clusters ..... 1177
(iii) Coordinatively flexible ligands ..... 1177
(iv) Oligomerization and fragmentation ..... 1178
ALCOHOLS AND PHENOLS ..... 1178
N-Benzyl(2-hydroxybenzene)methanimine (N-benzylsalicyladimine) ..... 1179
Alcohols also containing alkyne functionality ..... 1179
ALDEHYDES AND KETONES ..... 1181
ALKENES ..... 1183
(i) Simple alkenes ..... 1183
*Endocyclic alkenes* ..... 1185
(ii) Dienes ..... 1185
1,2–*Dienes (allene)* ..... 1185
1,3–*Dienes* ..... 1185
1,4–*Dienes* ..... 1187
(iii) Benzene ..... 1187
(iv) $\alpha,\beta$-Unsaturated esters ..... 1187
ALKYNES ..... 1188
(i) Diphenylethyne ..... 1188
(ii) Alkyl and monoaryl alkynes ..... 1189
(iii) Fluoroalkynes ..... 1191
AMIDES ..... 1192
AMIDINES ..... 1192
AMINES ..... 1193
(i) Primary and secondary ..... 1193
(ii) Tertiary ..... 1194
AZIDES ..... 1195
(i) With $[Os_3H_2(CO)_{10}]$ ..... 1195
(ii) With $[Os_3(CO)_{11}(NCMe)]$ and with $[Os_3(CO)_{11}(NC_5H_5)]$ ..... 1197
CARBANIONS AND CARBOCATIONS ..... 1199
CARBODIIMIDES ..... 1200
CARBON DISULPHIDE ..... 1200
CARBOXYLIC ACIDS ..... 1202
DIAZOCOMPOUNDS ..... 1202
(i) With $[Os_3H_2(CO)_{10}]$ and with $[Os_3H_2(CO)_9(PMePh_2)]$ ..... 1202
(ii) With $[Os_3H(CO)_{10}(NCMe)(SiPh_3)]$, $[Os_3(CO)_9(C_2Ph_2)]$ and $[Os_3(CO)_{11}(NCMe)]$ ..... 1204
A DIAZONIUM SALT ..... 1206
HETEROCYCLES ..... 1206
(i) Metallated heterocycles ..... 1206
(ii) 2-Substituted pyridines bound to triosmium via the pyridine nitrogen and the 2-substituent ..... 1209
(iii) Ligands coordinated solely by heterocyclic nitrogen ..... 1210

IMINES ..... 1210
ISOCYANATES AND ISOTHIOCYANATES ..... 1212
(i) Isocyanic acid ..... 1212
(ii) Methylisocyanate ..... 1213
(iii) Arylisocyanates ..... 1214
(iv) Arylisothiocyanates ..... 1214
ISOCYANIDES ..... 1215
KETENES ..... 1215
NITRILES ..... 1215
(i) Acetonitrile ..... 1215
(ii) Trifluoroacetonitrile ..... 1216
PHOSPHINES AND ARSINES ..... 1217
(i) Trialkylphosphines ..... 1217
(ii) Aryl phosphines and arsines ..... 1218
(iii) Phosphines and arsines with alkyne or alkene functionality ..... 1219
*Phosphine- and arsine-alkenes* ..... 1219
*Phosphine-alkynes* ..... 1219
SILANES AND STANNANES ..... 1220
THIOLS, SULPHIDES AND DISULPHIDES ..... 1220
REFERENCES ..... 1221

## INTRODUCTION

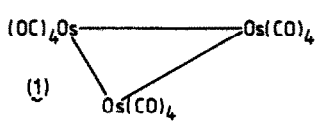
Some metal cluster compounds are models for adsorbates on a metallic surface in a heterogeneous catalytic system and some are potential homogeneous catalysts for reactions of industrial importance. Cluster chemistry has therefore drawn appreciable funding from industry over the last two decades and this has enabled organometallic chemists to record a great deal about the properties of metal clusters. A result of this research effort is that reactivity patterns are beginning to emerge in organic-substrate/cluster reactions and preferred modes of coordination of organic ligands to metal cluster skeletons are easier to predict. Also, in some cases, it is now possible to adopt a rational approach to cluster synthesis and avoid the haphazard preparative methods that were used in earlier days.

This review is an attempt to classify the reactions of triosmium clusters with organic compounds according to the functional groups in the organic substrate. The term "organic" is taken in a broad sense but not to include carbon monoxide.

## A. SYNTHESES OF TRIOSMIUM CLUSTERS IN GENERAL[1]

Triosmium dodecacarbonyl $[Os_3(CO)_{12}]$ (1)[2,3] is the fundamental starting material for syntheses of triosmium clusters.

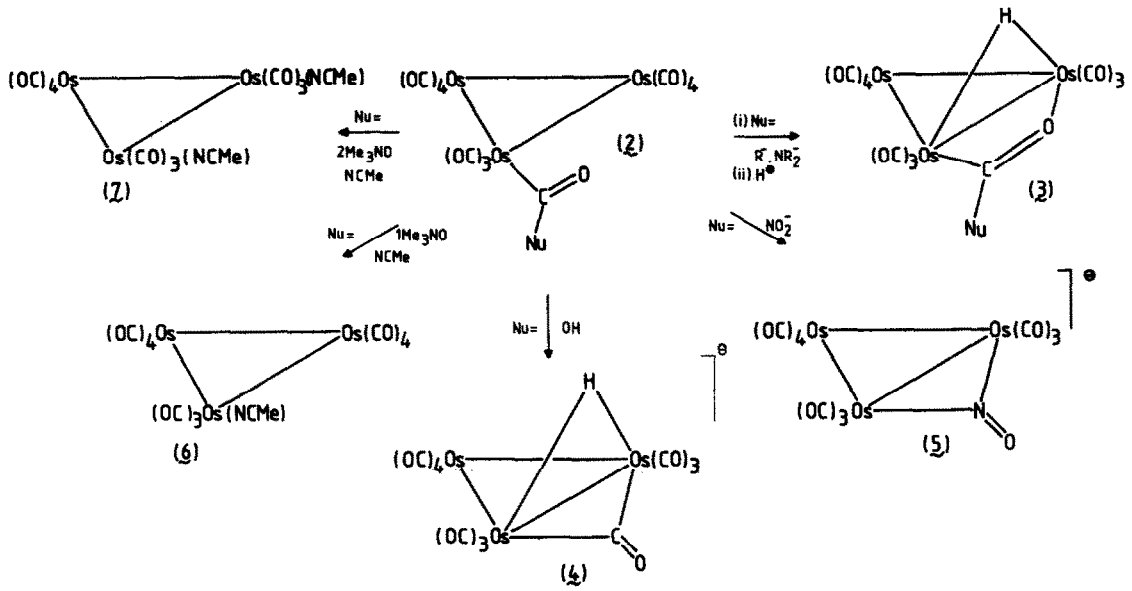
Each osmium atom of this complex is coordinated to four terminal carbonyl ligands and bonds to two other metal atoms and thus attains an eighteen valence electron shell [$d^8 + (4 \times 2) + (2 \times 1)$]. The metal frame of the complex is therefore *saturated* and fairly unreactive. Osmium–carbonyl bonds are relatively strong (*ca.* 201 kJ $mol^{-1}$)[4] so, in order to introduce a ligand onto the metal frame by cleavage of an osmium carbonyl bond, large activation energies must be surmounted. Thermal and photochemical reactions of $[Os_3(CO)_{12}]$ (1) can be useful but sometimes the conditions required to bring about a reaction facilitate decomposition of the product. Such syntheses are rarely product selective. Other methods of introducing functionality onto a triosmium frame are considered in the remainder of this section.



(1)

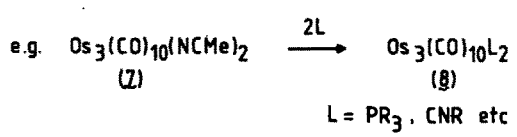
### (i) *Nucleophilic attack on carbonyl ligands*

Nucleophiles (Nu) can attack carbonyl ligands of $[Os_3(CO)_{12}]$ (1) to give a relatively unstable anion (2). Subsequent reactions of this intermediate are governed by the nature of the nucleophile.



Carbanions and dialkyl amido ($R_2N^-$) anions afford acyl complexes (3) (at 20°C after protonation) whereas hydroxide[6] and nitrite[7] give cluster anions, (4) and (5) respectively, useful starting materials for the synthesis of organotriosmium clusters. Trimethylamine-N-oxide oxidizes carbonyl ligands[8] on triosmium[9] to carbon dioxide leaving trimethylamine to fill the vacant coordination site. Trimethylamine is a poor ligand (if, indeed, it is ever coordinated at all) and is displaced by acetonitrile thus the clusters $[Os_3(CO)_{11}(NCMe)]$ (6) and $[Os_3(CO)_{10}(NCMe)_2]$ (7) can be prepared.[9]

Acetonitrile ligands of $[Os_3(CO)_{11}(NCMe)]$ (6) and $[Os_3(CO)_{10}(NCMe)_2]$ (7) are labile[11] and are readily substituted by other potential ligands.[9,10,12]



When the *functionalized* clusters (6) and (7) are reacted with organic compounds the reaction rarely affords simple substitution products, rearrangements are the norm.

Carbonyl ligands can also be removed under reducing conditions, i.e. by the action of benzophenone radical anions.[13]

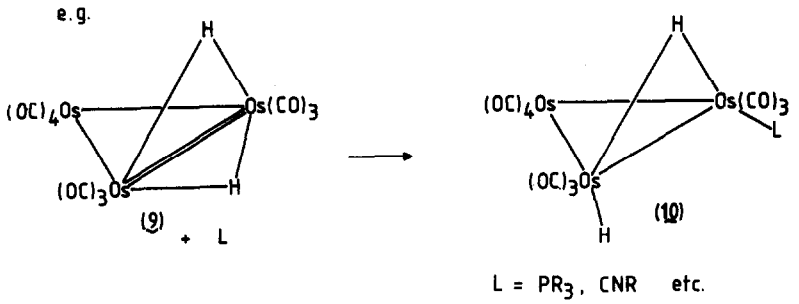
(ii) *"Unsaturated" triosmium clusters*

Several triosmium clusters are known in which the ligands and metal–metal single bonds cannot provide an eighteen valence electron shell about each metal; such complexes are *unsaturated.* Osmium–osmium double bonds are drawn to represent this unsaturation, the rationale being that metal atoms in such complexes will share electrons to complete their valence shells. The most studied of these electron-deficient triosmium compounds is $[Os_3H_2(CO)_{10}]$ (9)[14] (easily prepared[15] by the action of dihydrogen on $[Os_3(CO)_{12}]$ (1)). In the presence of electron donors these unsaturated clusters will accommodate another ligand, relinquishing their double bond thus achieving a saturated state.[16–20]

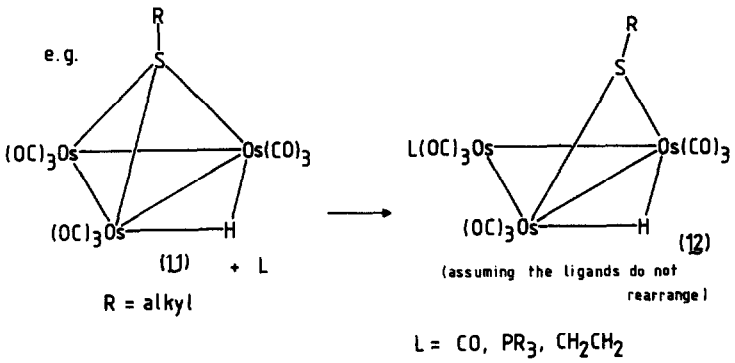
The metal core of an unsaturated triosmium cluster is therefore *activated.* Once again, if the electron donor is an organic compound, rearrangement usually ensues after the initial coordination.

(iii) *Coordinatively flexible ligands*

Nitrosyl,[21,22] thiol[23,24] and halogen[10] ligands are *flexible* in that they can donate or withdraw



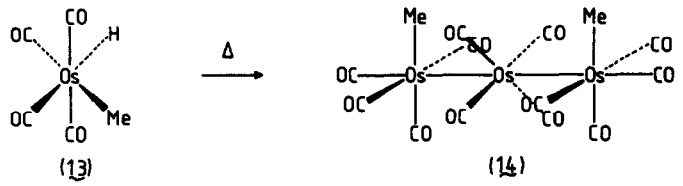

electrons by forming or breaking dative bonds to the metal core of a cluster. Coordinatively flexible ligands can be manipulated to introduce other functionality onto an osmium triangle.




This synthetic approach is not particularly general, it is limited to a few special clusters, and has rarely been used in syntheses of organotriosmium clusters.

(iv) *Oligomerization and fragmentation*

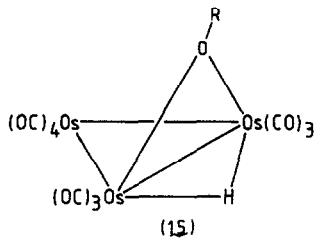
Organotriosmium chain clusters can be prepared by combination of monometallic complexes.[25,26]



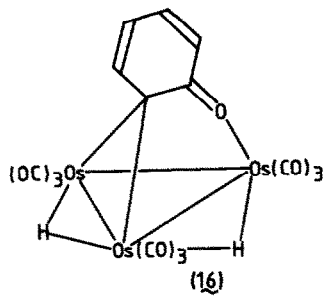

Conversely, it is possible that organotriosmium clusters could be prepared by degradation of polymetallic clusters bearing organic ligands. However, clusters with more than three osmium atoms are, usually, relatively difficult to prepare so this method has no practical advantage at present.

## B. ALCOHOLS AND PHENOLS

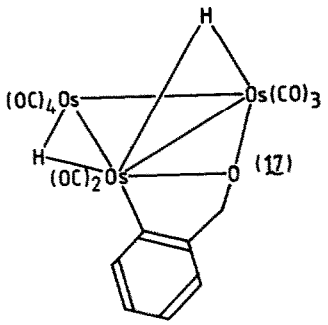
The predominant bonding mode of alcohols to triosmium is formation of an alkoxide bridge by hydrogen transfer from hydroxyl to metal triangle.



Such complexes are formed via thermal reactions of $[Os_3(CO)_{12}]$ (**1**)[27–29] or from clusters functionalized by labile ligands.[12,30] Where R is an aryl substituent further decarbonylation can occur via metallation of the aromatic rings giving, for example:



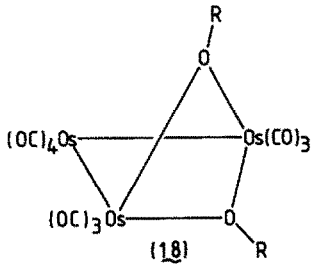

(16)




(17)

Complex (16) is illustrative of two general tendencies of *metallated, face capping, phenol ligands on triosmium*: (a) they *coordinate as the keto tautomer* and (b) *the coordinated carbon will bridge* metals in preference to the oxygen.

When two alkoxide ligands are present on triosmium they bridge the same edge of the osmium triangle thus opening it.[31]

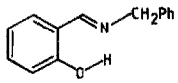



(18)

The diethoxide complex (R = Et) (**18**) is a minor product in the synthesis of $[Os_3(CO)_{12}]$ (**1**) in ethanol.[32]

*N-Benzyl(2-hydroxybenzene)methanimine (N-benzylsalicyladimine)*[33]

Reaction of $[Os_3(CO)_{11}(NCMe)]$ (**6**) with this imine initially gives a product (**19**) in which the



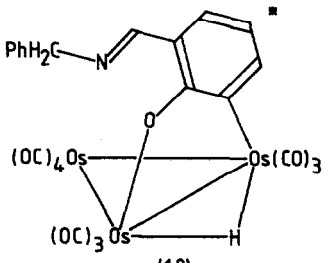

organic ligand is coordinated via the phenolic oxygen and metallation of the aromatic ring. Thermolysis of this product affords three isomers of $[Os_3(CO)_9$(salicyladimine)] (**20–22**).

The predominant product is the benzyne complex (**22**) in which neither the hydroxyl nor imine functionality is coordinated, this illustrates a "rule of thumb": *aromatic organic substrates tend to form aryne ligands on triosmium at elevated temperatures* unless an exceptionally favourable mode of coordination is available as an alternative.

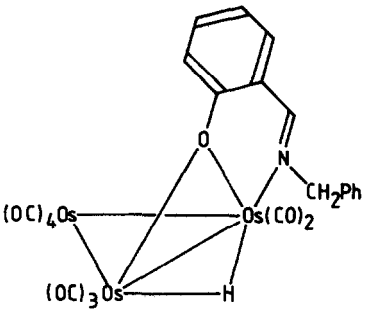
*Alcohols also containing alkyne functionality*

Reactions of $[Os_3(CO)_{12}]$[34,35,36] (**1**) or $[H_2Os_3(CO)_{10}]$[37] (**9**) with hydroxyalkynes give products (**23–25**) in which *the alkyne group is coordinated in preference to the oxygen of the alcohol.*

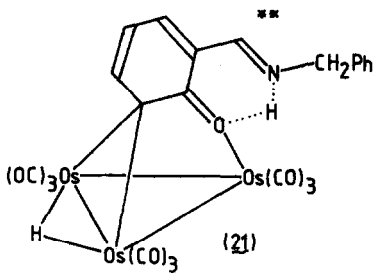
Hydroxyalkynes ($HOCR_2C{:}CYH$) ($R \neq H$) give clusters of type (**25**) via carbon–carbon bond cleavage; (HOCPhMeC:CPh), for instance, forms complex (**25**) (Y = Ph) and in doing so liberates



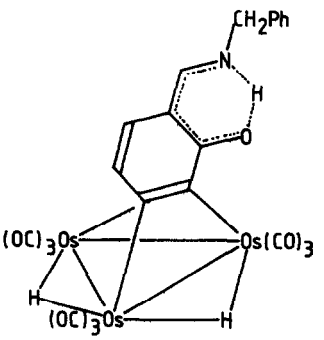

(19)




(20)

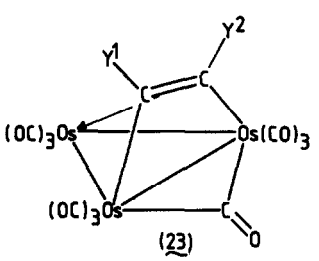



(21)



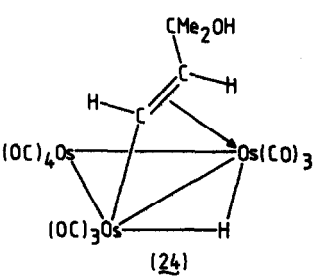

(22)

* Or the keto tautomer.
** Or an isomer with μ-oxygen.

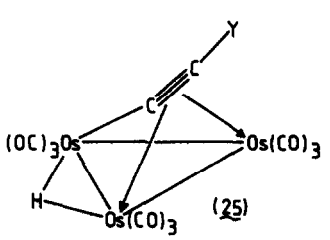



(23)

| $Y^1$ | $Y^2$ |
|---|---|
| $CH_2OH$ | $CH_2OH$ |
| H | $CMe_2OH$ |



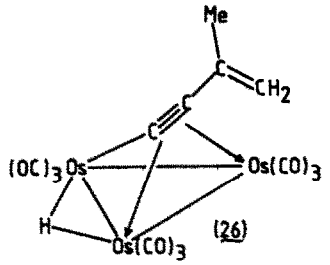

(24)



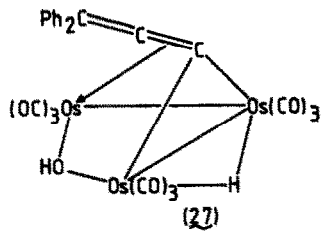

(25)

Y = Ph, $CMe_2OH$, $CPh_2OH$

an equivalent of phenylethanone (MeCOPh). Protonation of $[Os_3H(CO)_9(CCY)]$ (**25**) causes dehydration[34] ($Y = CMe_2OH$) giving cluster (**26**) or isomerization[36] with migration of the OH groups from the carbon to the metals ($Y = CPh_2OH$) affording complex (**27**).

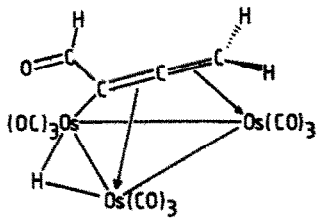



(26)

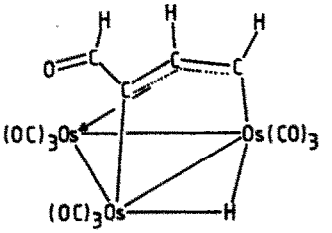



(27)

Thermolysis of $[Os_3(CO)_{10}(HOCH_2C{:}CCH_2OH)]$ (**23**) ($Y^1 = Y^2 = CH_2OH$) causes dehydration and decarbonylation giving complex (**28**); further heating causes rearrangement of the organic fragment to the allylic ligand of cluster (**29**).[37]



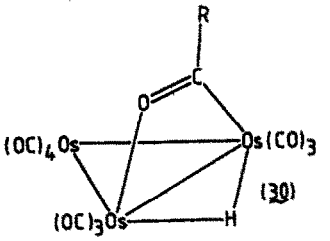

(28)




(29)

## C. ALDEHYDES AND KETONES

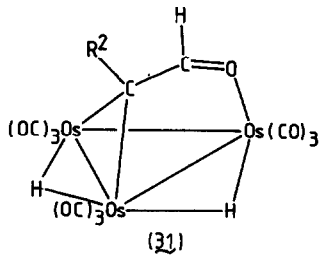
Thermolysis of aldehydes with $[Os_3(CO)_{12}]$ (**1**) at 130–150°C[38,39] or with $[Os_3(CO)_{10}(NCMe)_2]$ (**7**) at 40°C[40] affords acyl complexes.



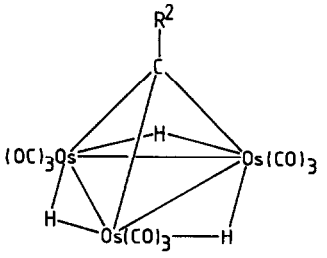

(30)

R = alkyl or aryl
≠ H

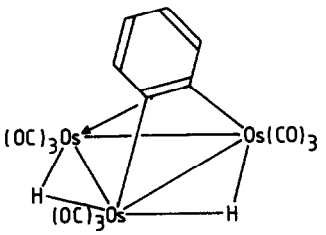
At elevated temperatures these clusters decarboxylate; four product types form depending on the group "R". Where there are $\alpha$-hydrogens R can be metallated to give (**31**) and alkylidyne clusters (**32**) presumably by loss of the organic carbonyl from (**30**). The benzyne cluster (**33**) and the metallated pyridine (**34**) are derived from benzaldehyde and pyridine-2-carboxyaldehyde via (**30**) (R = Ph and 2-$NC_5H_4$), in these cases the aromatic substituents preclude formation of a monometallated or alkylidyne cluster.



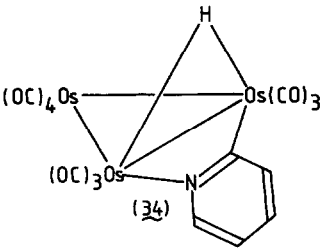

(31)




$R^2$ = Me, H (32)

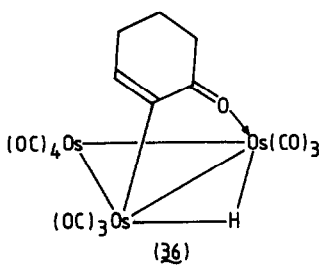



(33)



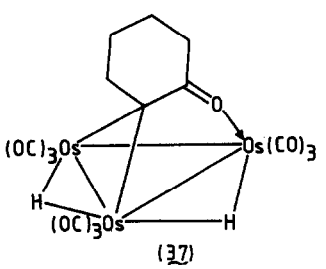

(34)

Cyclohexanone and $[Os_3(CO)_{12}]$ (**1**) combine in refluxing decane to give a complex (**37**) in which the metallated ketone spans a triosmium face. The same cluster is formed in a similar reaction of 2-cyclohexenone via hydrogen transfer. When $[Os_3H_2(CO)_{10}]$ (**9**) is heated with 2-cyclohexenone and the alkene functionality is metallated but not $\pi$-bonded in the product (**36**), the oxygen coordinates preferentially. Insertion of osmium at the 2-position is an anomaly of this organometallic chemistry, classically, 2-cyclohexenone is activated at the 3 and 6-positions. Decarbonylation of (**36**) at 128°C gives two isomers (**37**) and (**38**) which do not interconvert under the reaction conditions.



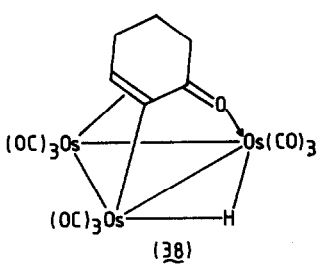

(36)




(37)

+




(38)

Propanone, cyclohexanone and cyclopentanone react with $[Os_3(CO)_{11}(NH_3)]$ perhaps via a dissociative mechanism (see Section *Q*).[165,166]

$$Os_3(CO)_{11}(NH_3)\ (39) \rightleftharpoons Os_3(CO)_{11} + NH_3$$
$$NH_3 + RCOR' \longrightarrow RCNHR' + H_2O$$
$$Os_3(CO)_{11} + RCNHR' \longrightarrow Os_3(CO)_{11}(NHCRR')\ (40)$$

Tetraphenylcyclopentadienone has been reacted with $[Os_3(CO)_{12}]$ (**1**) but the products were not characterized.[42]

## D. ALKENES

An extensive range of structural types of clusters are available from coordination of alkenes (and alkynes) to triosmium. These are valuable models for identification of species formed by chemisorption of hydrocarbons on metal surfaces;[43–45] this is done by comparison of vibrational spectra.[46] Hydrogen transfer, between carbon and osmium, and stereomutation of alkene groups are common in triosmium cluster chemistry. Therefore, it is not surprising that triosmium clusters can catalyse hydrogenation[47] and isomerization[17,47–49] of alkenes.

(i) *Simple alkenes.*

Formation of a dative bond from a $\pi$-cloud may often be the initial step in coordination of an alkene to a metal cluster. Several triosmium clusters bearing $\pi$-bound alkene ligands have been prepared by simple substitution[9,10]

$$Os_3(CO)_{11}(NCMe)\ (9) \xrightarrow{CH_2CH_2} Os_3(CO)_{11}(CH_2CH_2)\ (41)$$
$$Os_3H(CO)_{10}(SMe)\ (12) \xrightarrow{Me_3NO,\ CH_2CH_2} Os_3H(CO)_9(CH_2CH_2)(SMe)\ (12)$$

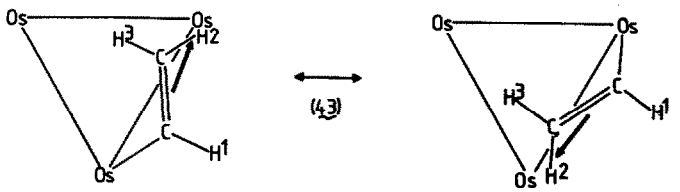
or by exploitation of coordinative flexibility.[23,24]

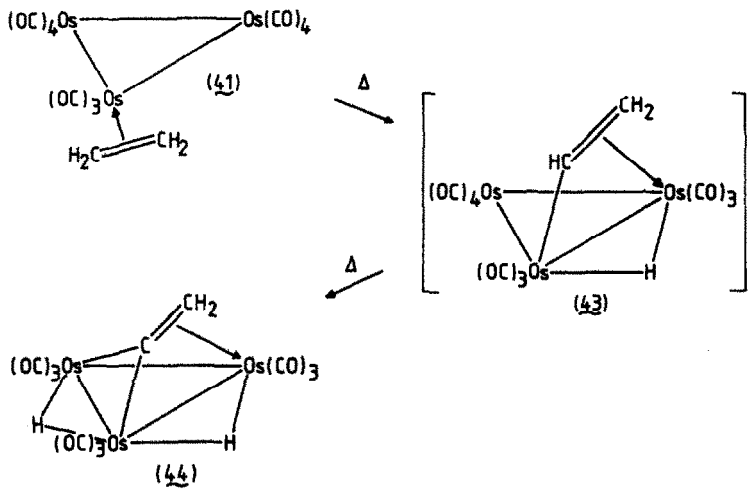
$$Os_3H(CO)_9(SMe)\ (11) \xrightarrow{CH_2CH_2} Os_3H(CO)_9(CH_2CH_2)(SMe)\ (12)$$

Thermolysis of triosmium clusters containing $\pi$-bonded alkenes causes oxidative addition.[10,23,24,50]

$$\text{e.g.}\quad Os_3H(CO)_9(CH_2CH_2)(SR)\ (12) \xrightarrow{\Delta} Os_3H(CO)_9(CHCH_2)(S) + RH\ (42)$$

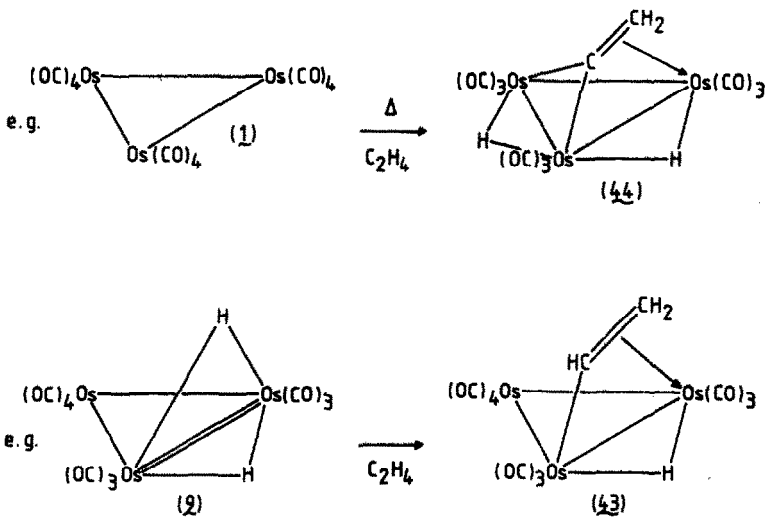
$^{13}C$ NMR spectra of the vinyl complexes reveal that the $\sigma$- and $\pi$-bonds to the organic ligand rapidly interchange between the bridged osmium atoms, for instance,[51] for $[Os_3H(CO)_{10}(CHCH_2)]$ (**43**).



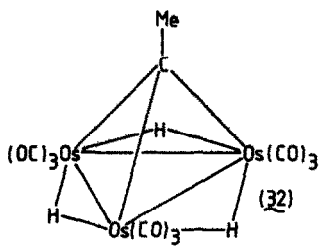


At higher temperatures a second oxidative addition occurs and vinylidene complexes, e.g. (**44**), result.[52,53]

In many cases, $\pi$-bound alkene[52] and, sometimes, vinyl intermediates are not observed presumably because of the conditions used to cause the reaction.[54–57]



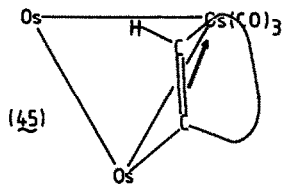
Hydride ligands migrate around the edge of the metal triangle of $[OsH_2(CO)_9(CCH_2)]$ (**44**) at 20°C but the organic fragment is relatively immobile at this temperature.[58–60,220,221] Dihydrogen may add to the methylene and the metal core of this cluster to give an ethylidyne complex (**32**).[61]



Reactions of $[Os_3H_2(CO)_{10}]$ (**9**) with cyclooctene in an ethene atmosphere afford $[Os_3(CO)_{10}(C_8H_{14})_2]$ which is a lightly stabilized (i.e. functionalized) cluster.[12]

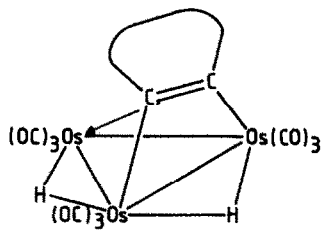
*Endocyclic alkenes*

An endocyclic alkene is 1,2-disubstituted and, unless the ring is large, must be a Z-geoisomer; this has important implications here. Clearly, the 1,1-vinylidene mode of coordination as in $[Os_3H_2(CO)_9(CCH_2)]$ (**44**) is precluded. The vinyl ligand of a complex of the same type as $[Os_3H(CO)_{10}(CHCH_2)]$ (**42**) but derived from an endocylic alkene, i.e.




(45)

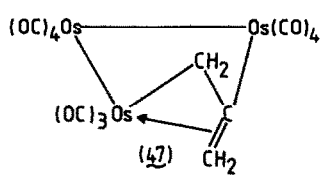
would encounter severe steric interactions with one of the $Os(CO)_3$ fragments and this might prevent $\sigma$-/$\pi$- bond fluxionality (*vide-supra*); such a complex would therefore be destabilized by both enthalpy and entropy factors. Triosmium clusters of this type have not been observed. Reaction of cyclopentene,[57] indene[60] and cyclooctene[62,63] with $[Os_3(CO)_{12}]$ (**1**) occurs with 1,2-elimination of dihydrogen from the alkene giving 1,2-metallated ligands.




(46)

(ii) *Dienes*

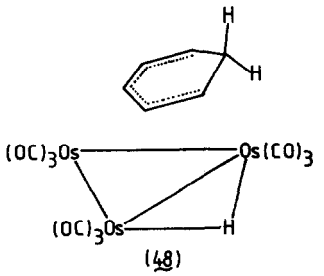
1,2-*Dienes* (*allene*). Allene displaces the nitrile ligand of $[Os_3(CO)_{11}(NCMe)]$ (**6**) and bridges an osmium–osmium edge perpendicularly; the ligand formed donates four electrons and thus opens the metal triangle.[64]



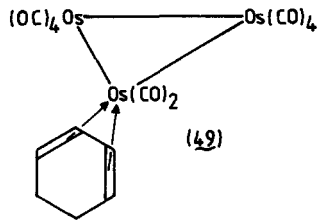

(47)

1,3-*Dienes*. Cyclopentadiene and $[Os_3(CO)_{12}]$ (**1**) react to form a cluster of type (**46**) (see endocyclic alkenes above).[155]

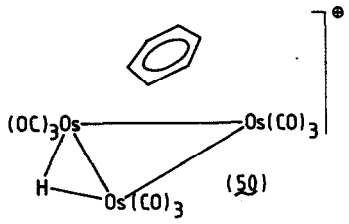
Reaction of $[Os_3H_2(CO)_{10}]$ (**9**) with cyclohexa-1,3-diene affords two isomers, (**48**) and (**49**), of the formula $[Os_3(CO)_{10}(diene)]$ and an equivalent of the monoene.[65] The diene ligand of complex (**49**) is both fluxional[66] and labile;[30] this cluster has been used as a starting material in syntheses of other compounds.[30] Triphenylmethyl carbocations ($Ph_3C^+$) abstract hydride, from either the organic ring, or the metal frame of the eta-five cluster (**48**) thus forming a cationic benzene complex (**50**), and a cationic eta-five complex (**51**), respectively.



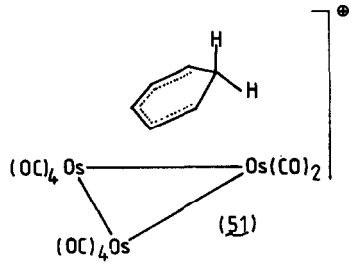

(48)




(49)



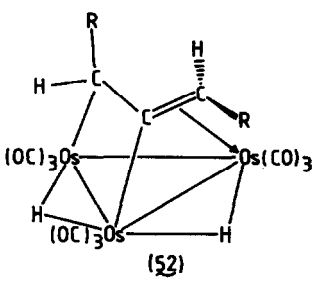

(50)



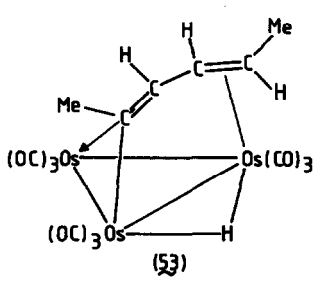

(51)

$[Os_3(CO)_{12}]$ (**1**) reacts with Z,E- and E,E-2,4-hexadiene to give $[Os_3H_2(CO)_9(C_6H_{10})]$ (**52**) (although the structure of this cluster was not established beyond question) and two isomers of the formula $[Os_3H(CO)_9(C_6H_9)]$ (**53**) and (**54**).[67] The NMR of complex (**54**) reveals that the alkene hydrogens readily interchange with the metal hydride.[68]

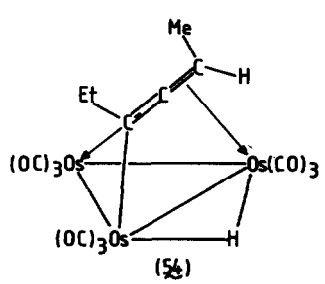
Hydrogen transfer from metal to carbon occurs when $[Os_3H_2(CO)_{10}]$ (**9**) is reacted with 1,3-cyclononadiene and an allyl complex (**55**) results.[69]



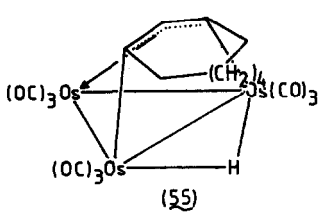

(52)




(53)

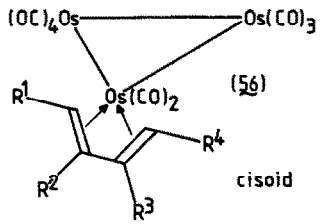



(54)




(55)

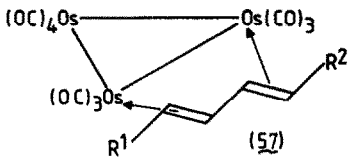
Butadiene and substituted butadienes form two products $[Os_3H_2(CO)_{10}]$ (**9**) corresponding to coordination of the diene as a *cisoid* or a *transoid* conformer.[70,71]




(56)

cisoid

| $R^1$ | $R^2$ | $R^3$ | $R^4$ |
|---|---|---|---|
| H | H | H | H |
| H | Me | H | H |
| H | Me | Me | H |



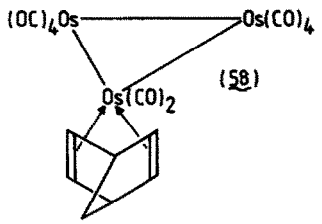

(57)

transoid

| $R^1$ | $R^2$ |
|---|---|
| H | H |
| Me | Me |

Butadiene can adopt either orientation of coordination whereas the coordination of more substituted dienes is apparently restricted by steric interactions between the diene substituents and adjacent carbonyl ligands.

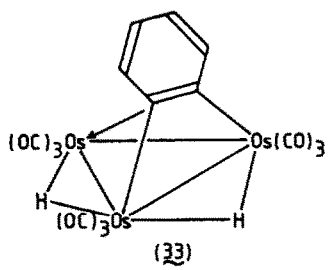
1,4-*Dienes*. Norbornadiene is restrained in a configuration similar to the *cisoid* conformer of 1,3-butadiene and coordinates to triosmium in an analogous way giving:[72]




(58)

(iii) *Benzene*

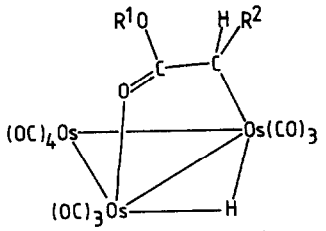
Thermal reaction of $[Os_3(CO)_{12}]$ (**1**) with benzene gives a coordinated benzyne (**33**). Yields in this reaction are variable and always poor;[57] better yields of (**33**) are obtained in the reaction of $[Os_3(CO)_{10}(NCMe)_2]$ (**7**) with benzene.[73]




(33)

(iv) *α,β-Unsaturated esters*

α,β-Unsaturated esters are hydrogenated at the 3-position by $[Os_3H_2(CO)_{10}]$ (**9**) the organic moiety then coordinates through the ester carbonyl and via metallation of the α-carbon.[74]



(59)

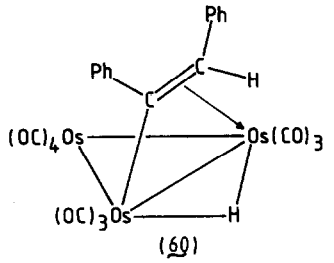
| $R^1$ | $R^2$ |
|---|---|
| Et | $CH_2COEt$ |
| OC | $CH_2$ |
| Et | H |

## E. ALKYNES

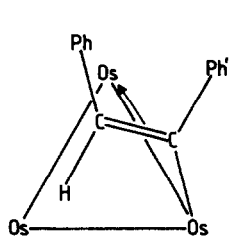
Some triosmium clusters are isolatable model compounds for cyclotrimerization, hydrogenation and hydroformylation in heterogenous or homogenous catalytic reactions of alkynes.

(i) *Diphenylethyne*

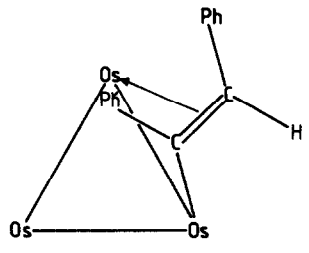
Treatment of $[Os_3H_2(CO)_{10}]$ (**9**) with 3–4 equivalents of diphenylethyne at 20°C affords a vinyl cluster $[Os_3H(CO)_{10}(PhCCHPh)]$ (**60**); metallation and hydrogenation of the alkyne occurs stereoselectively *cis*.[75]



(60)



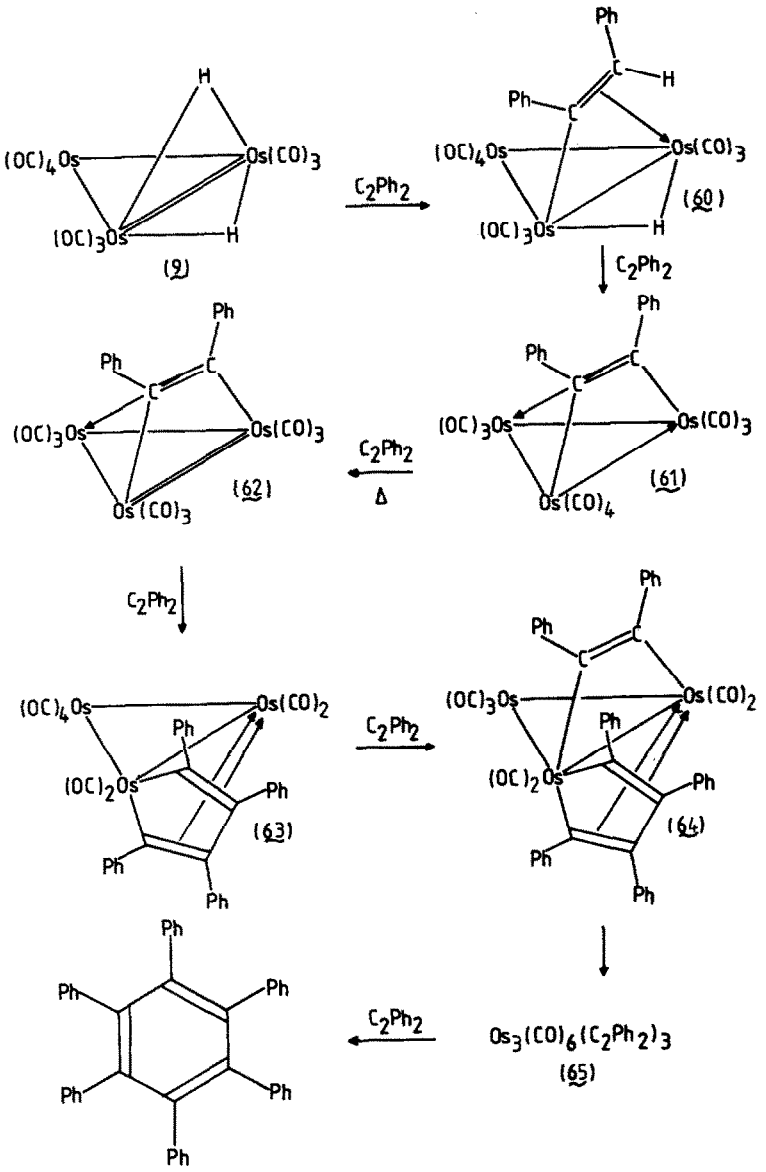
endo



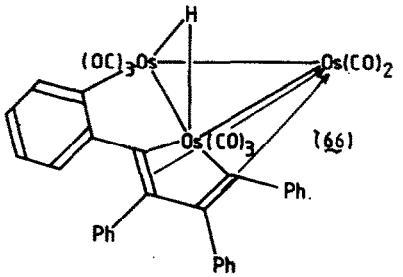
exo

There are two possible orientations of the vinyl ligand in this complex, *exo* or *endo* relative to the osmium triangle. The *endo* isomer has been observed in an X-ray analysis of the complex.[76] Steric interactions between the $\alpha$-phenyl substituent (Ph') and the $Os(CO)_4$ fragment of the molecule are minimized in this *endo* configuration.

Excess diphenylethyne adds to the vinyl complex (**60**) in steps which culminates in the formation of hexaphenylbenzene.[77–84]




An equivalent of 1,2-diphenylethene (mostly the Z isomer) is liberated in the formation of (**61**) from the vinyl complex (**60**). Evidence that $[Os_3(CO)_9(C_2Ph_2)]$ (**62**) is an intermediate is circumstantial.[75] The complex with two linked diphenylethynes (**63**) is also accessible by the action of carbon monoxide on a metallated complex[77]

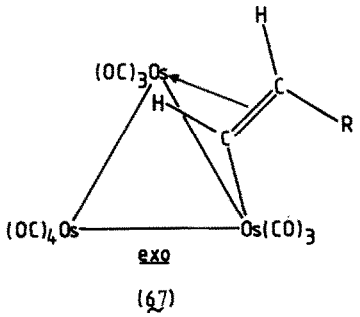



which is formed by thermal reaction of diphenylethyne with $[Os_3(CO)_{12}]$ (**1**).

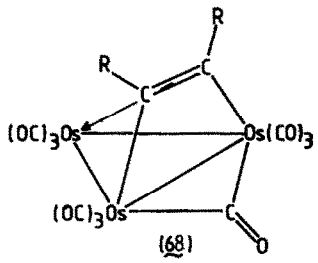
(ii) *Alkyl and monoaryl alkynes*

Reactions of alkyl and monoaryl alkynes are similar to those of diphenylethyne in that vinyl

complexes (**67**) and 1,2-dimetallated alkenes (**68**) are formed by reaction with $[Os_3H_2(CO)_{10}]$ (**9**)[52,85,86] $[Os_3(CO)_{12}]$ (**1**)[87] or $[Os_3H_2(CO)_9(\text{phosphine})]$.[88] Two such vinyl complexes (**67**) (R = Et, H) have been studied crystallographically[89,90] and both have the *exo* configuration (cf. *endo* stereoisomers are formed from diphenylethyne, *vide supra*).



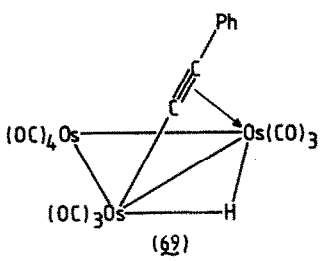

(67)



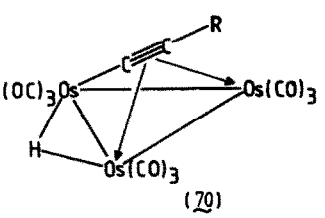

(68)

Vinylidene complexes $[Os_3H_2(CO)_9(CCR^1R^2)]$ (**67**) are fluxional as a result of migration of hydrogens about the metal triangle (*vide supra*) but fluxionality of the 1,2-dimetallated isomers $[Os_3H_2(CO)_9(CR^1CR^2)]$ (**68**) must occur via Os–C bond cleavage.[91]

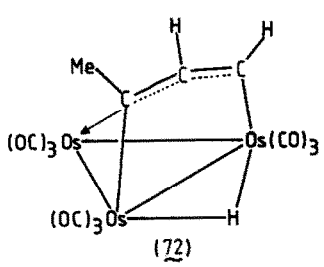
Alkynes and $\alpha$-hydrogen atoms and terminal alkynes are able to transfer hydrogen atoms to the triosmium frame consequently these give several other structural types of triosmium complex. Such clusters could not be formed from diphenylethyne unless rearrangement of the organic fragment occurred.



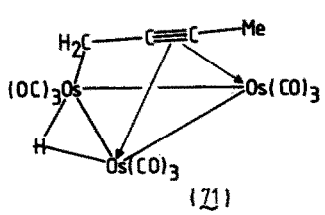

(69)




(70)



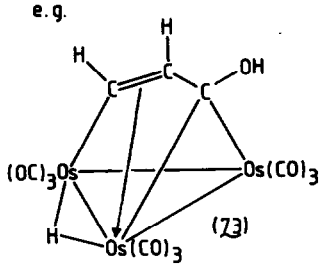

(72)




(71)

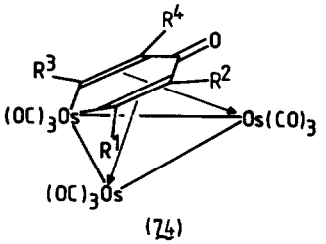
Whereas *diphenylethyne tends towards cyclotrimerization on a triosmium face, terminal alkynes form carbon–carbon bonds by coupling of one or more alkyne fragments to a carbonyl ligand.* Thus propyne and ethyne react with $[Os_3(CO)_{11}(NCMe)]$ (**6**) in the presence of water to give hydroxyallyl complexes.[92]

e.g.

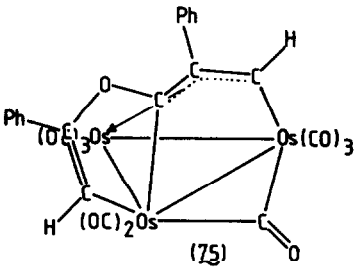


(73)

When two alkynes attach to a carbonyl ligand osmacyclic systems result; the following clusters are examples of this.[93–95]

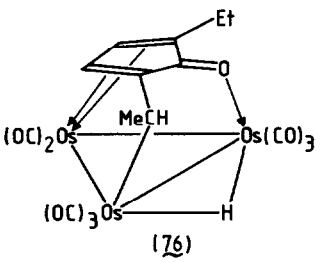


(74)

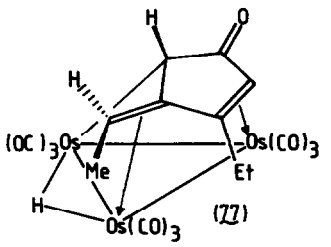


(75)

Clusters (**74**) when formed from an unsymmetrical alkyne may exist as three isomers.[95] Thermolysis of an isomer with ethyl substituents remote from the osmium in the organic ring (e.g. $R^1 = R^3 = H$, $R^2 = R^4 = Et$) gives decarbonylation at the cluster frame and ring contraction to give complex (**76**).[96,97] The isomer (**74**) with two ethyl substituents close to the osmium in the metallocyclic ring, $R^1 = R^3 = Et$, $R^2 = R^4 = H$, also decarbonylates via ring contraction on thermolysis but gives a different type of complex (**77**).[98] Thermolysis of the third isomer of (**74**) formed from 1-butyne affords a mixture of products that are analogous to (**76**) and (**77**).



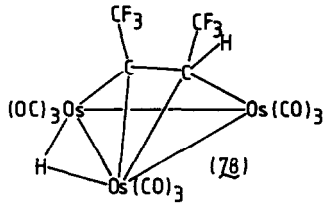
(76)



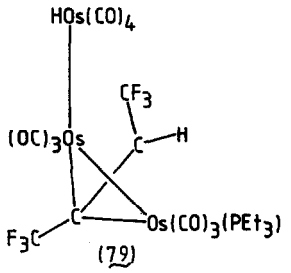
(77)

(iii) *Fluoroalkynes*

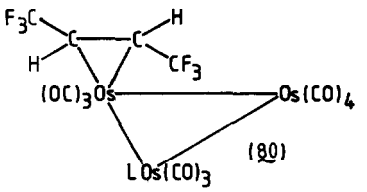
Electron withdrawing properties of a trifluoromethyl substituent are such that alkynes bearing this group have anomalous properties. Hexafluorobut-2-yne and $[Os_3H_2(CO)_{10}]$ (**9**) react to form a face capped cluster $[Os_3H(CO)_9(C_2F_3CCHCF_3)]$ (**78**).[99] This nonacarbonyl adds two electron donors to give a triosmium chain complex (**79**)[100] and/or $\pi$-bound alkene complexes (**80**).[101] It is interesting to compare this behaviour with that of $[Os_3H(CO)_{10}(CHCH_2)]$ (**43**) which, under similar conditions, forms a 1,3-dipolar ligand by addition of triphenylphosphine to the vinyl group (see Section V, "Phosphines").



(78)



(79)

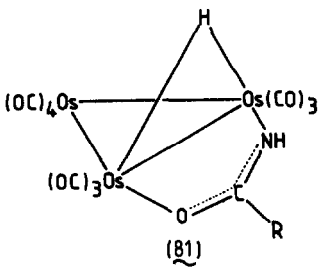


(80)

L = $Br^{\bullet}$, $PEt_3$

## F. AMIDES

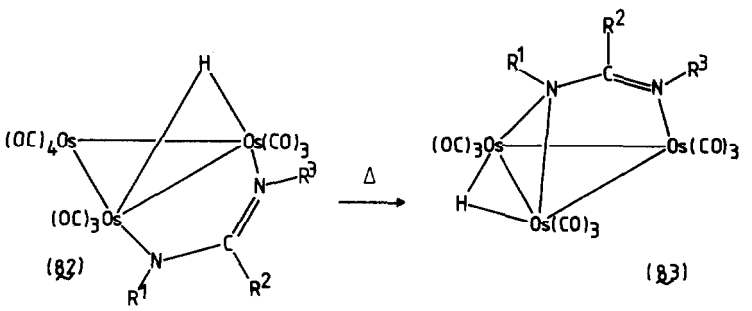
Primary amides ($RCONH_2$) react with $[Os_3(CO)_{10}(NCMe)_2]$ (7) to give complexes (**81**) in which the amide is metallated on the nitrogen and bound via the amide carbonyl.[40] N-Substituted analogues of these complexes $[Os_3H(CO)_{10}(OCHNHR)]$ have been prepared from isocyanates (see Section R).



(81)

## G. AMIDINES

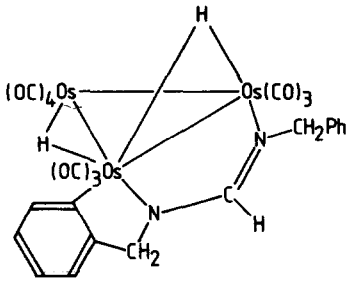
Functionalized clusters $[Os_3(CO)_{10}(L)_2]$ (L = NCMe(7)[102] or cyclo-$C_8H_{14}$[103]) react with amidines to form decacarbonyl complexes (**82**); these are isoelectronic with triosmium decacarbonyls bearing carboxylate ligands (see Section M) and with those supporting triazenato ligands (see Section I). Decarbonylation of these complexes (**82**) normally occurs via expansion of the coordination sphere of a nitrogen to give the organic moiety capping a triosmium nonacarbonyl frame.



(82) (83)

| $R^1$ | $R^2$ | $R^3$ |
|---|---|---|
| H | Me | H |
| Ph | Ph | Ph |
| $^i$Pr | H | $^i$Pr |
| $CH_2Ph$ | H | $CH_2Ph$ |

However, the complex derived from N,N'-diphenylmethamidine (PhNCHNHPh) ($R^1 = R^3 = CH^2Ph$, $R^2 = H$) metallates one aromatic ring on heating (**84**).

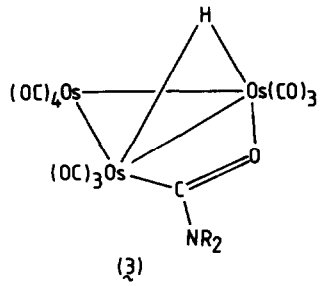


(84)

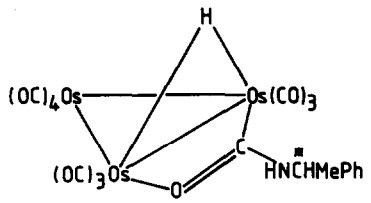
## H. AMINES

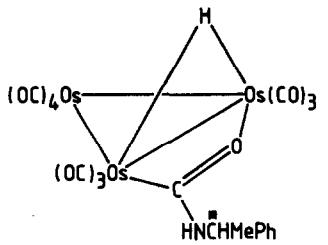
(i) *Primary and secondary*

Primary and secondary amines (and dialkyl amide ions, $\overset{\ominus}{N}R_2$) attack a carbonyl ligand of $[Os_3(CO)_{12}]$ (**1**) in polar solvents at 0 to −30°C to give clusters of type (**3**).[5,104] Chiral amines react to give separable diastereoisomers of this complex.[105]

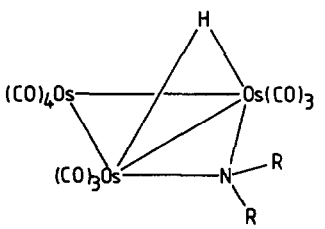


(3)

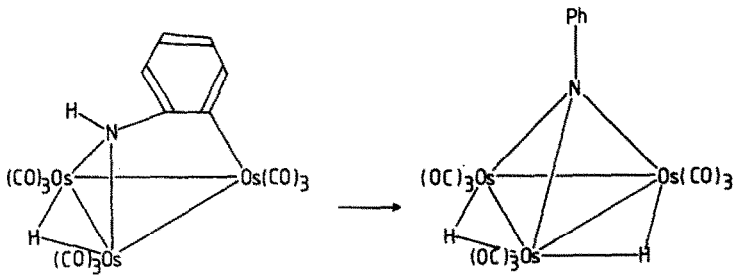




Amido-bridged clusters are formed by heating complexes of type (**3**). Amido ligands can also be formed by reaction of functionalized clusters $[Os_3(CO)_{11}L]$ (L = labile ligand(s)) with amines.[12,30]

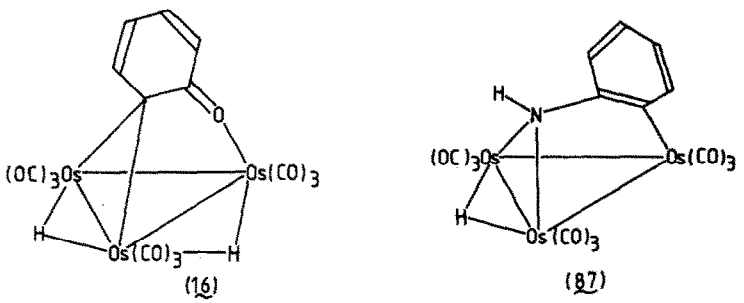


Thermolysis of $[Os_3(CO)_{12}]$ (**1**) in phenylamine affords $[Os_3H_2(CO)_8(NHC_6H_4)(NH_2Ph)]$ (**85**) (*structurally uncharacterized*); *this amine complex reacts with carbon monoxide to give a* nonacarbonyl (**87**) which may then isomerize to a nitrene cluster (**88**).[106]




(87) (88)

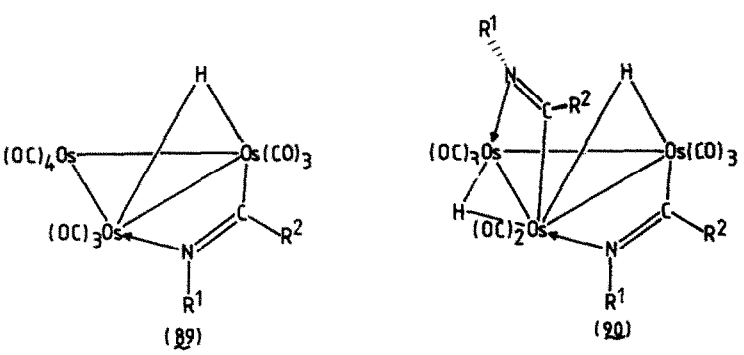
The fragments $NHC_5H_4$ (from phenylamine as in **(87)**) and $OC_6H_4$ (from phenol as in **(16)**) cap a triosmium cluster face in different ways.[107] *Nitrogen atoms of* $NHC_6H_4$ *ligands bridge and the carbon is bonded to just one osmium* whilst *oxygen atoms of* $OC_6H_4$ *ligands coordinate to only one osmium atom and the metallated carbon bridges.*




(16) (87)

(ii) *Tertiary*

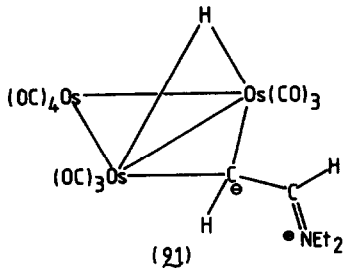
Thermal reactions of tertiary amines with $[Os_3(CO)_{12}]$ **(1)** usually involve metallation of an amine substituent; this is similar to the thermal reactions of $[Os_3(CO)_{12}]$ **(1)** with tertiary phosphines (see Section V). Thus, trimethylamine ($NMe_3$) with N,N-dimethylphenylmethanamine ($PhCH_2NMe_2$) eliminate an alkene and form complexes with one or two iminyl ligands.[108]




(89) (90)

Methylene carbons of benzyl groups are metallated in preference to methyl carbons in the reaction of $[Os_3(CO)_{12}]$ **(1)** with $(PhCH_2NMe_2)$.

Triethylamine is metallated at a $\beta$-carbon in its reaction with $[Os_3(CO)_{10}(NCMe)_2]$ **(7)** and a complexed zwitterionic, or 1,3-dipolar, ligand is formed.[109,110]



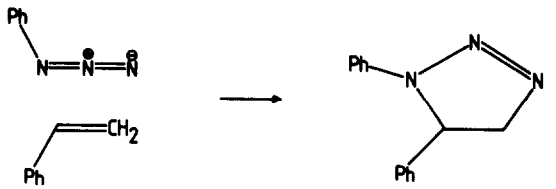

(91)

## I. AZIDES

Iodine azide degrades $[Os_3(CO)_{12}]$ (**1**) to monometallic products,[111] however the triosmium core is retained in the reactions of organic azides with activated and with functionalized clusters.

(i) *With* $[Os_3H_2(CO)_{10}]$

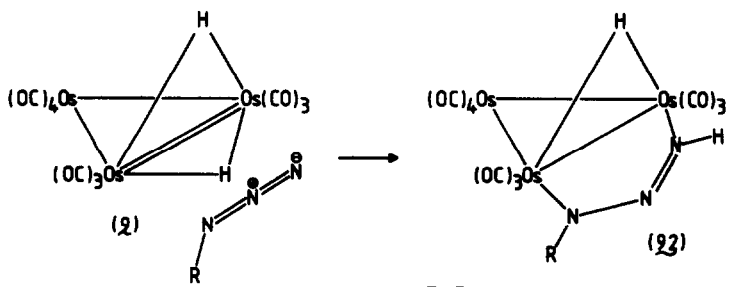
Reactions of organic azides with $[Os_3H_2(CO)_{10}]$ (**9**) are, to some extent, analogous to their reactions with alkenes. Alkyl and aryl azides form metallocycles (**92**) with $[Os_3H_2(CO)_{10}]$ (**9**) similar to a [2 + 3] adduct from a 1,3-dipolar cycloaddition of an alkene to an azide




1,3-Dipolar Cycloaddition

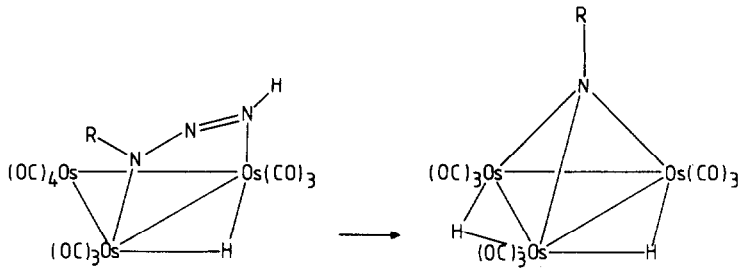
except that the azide is reduced to a triazenato ligand.[112,113]

The adducts (**92**) lose dinitrogen and carbon monoxide on heating and this provides a general synthesis for triosmium clusters with a capping nitrene (NR) ligand.

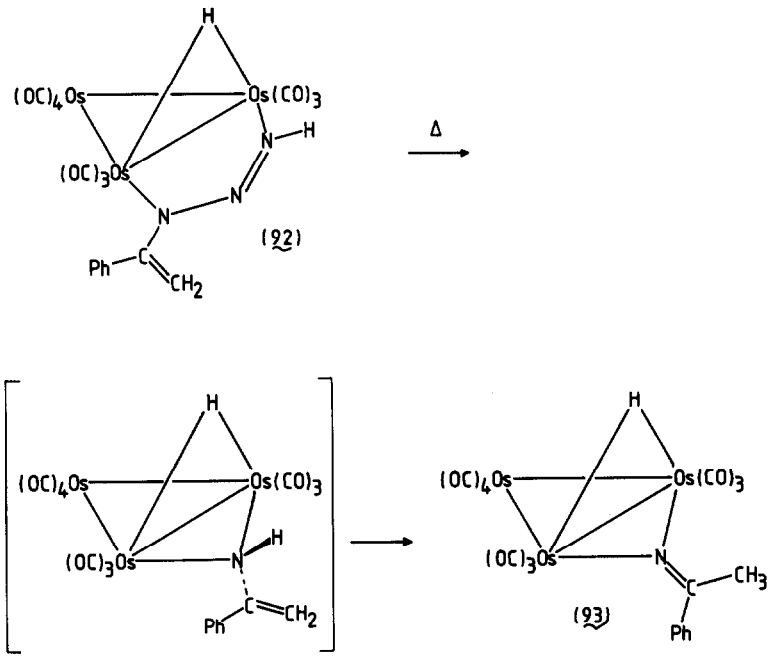



(2) (93)

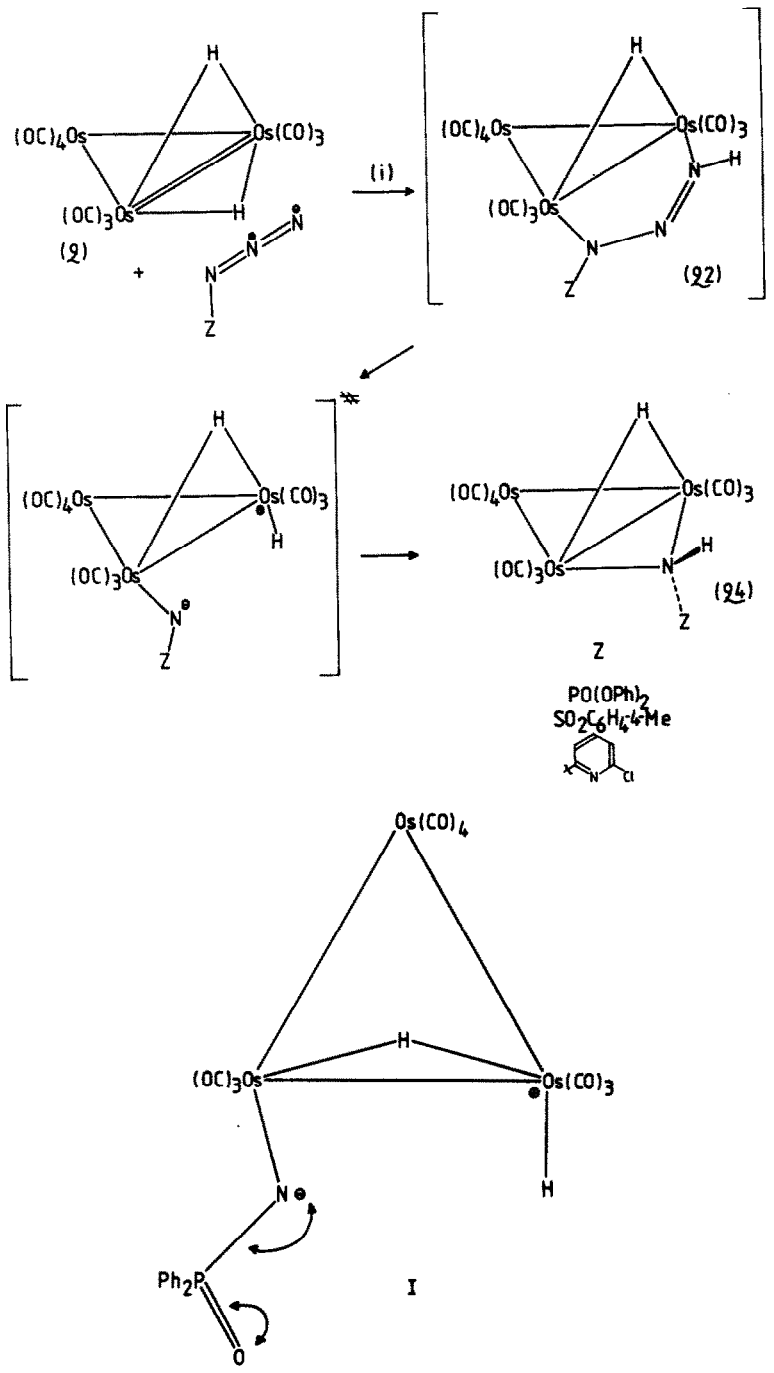
R = Ph, Me, n-Bu, $CH_2Ph$, cyclo-$C_6H_{11}$, $CPhCH_2$




Trimethylsilylazide ($N_3SiMe_3$) and $[Os_3H_2(CO)_{10}]$ (**9**) give, after a chromatographic separation, the symmetrical triazenato complex $[Os_3H(CO)_{10}(HNNNH)]$ (**92**) (R = H).[114] Presumably the silicon–nitrogen bond could not withstand chromatography. Thermolysis of this complex gives the amido-bridge cluster $[Os_3H(CO)_{10}(NH_2)]$ (**39**) rather than the expected complex $[Os_3H_2(CO)_9(NH)]$ or $[Os_3H_3(CO)_9N]$; these nitrene clusters are unknown at present. 1-Azidophenylethene $[PhC(CH_2)N_3]$ forms an adduct (**92**) (R = $C(CH_2)Ph$) with $[Os_3H_2(CO)_{10}]$ (**9**) but when this complex is heated tautomerization occurs and an imine coordinated to a triosmium decacarbonyl skeleton is isolated.[113]



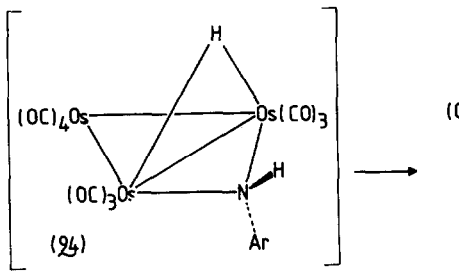

Electron withdrawing substituents facilitate ring contraction of $\Delta$-1,2,3-triazolines to aziridines under mild conditions. In just the same way azides with an electron withdrawing substituent $N_3Z$ (Z = $SO_2C_6H_4$–4–Me,[115] $PO(OPh)_2$,[113] $2(NC_5H_3$–6–Cl)[113]) and $[Os_3H_2(CO)_{10}]$ (**9**) react to give substituted-amido-bridged systems directly.[113] Presumably loss of dinitrogen from the expected triazenato cluster is relatively easy due to stabilization of the transition state I.

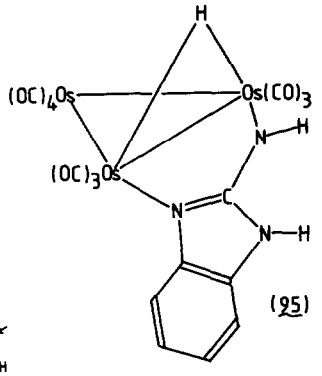



In two cases isomers of the amido-bridged system are isolated;[113] here the electron withdrawing substituent is able to coordinate to the cluster and rearrangement ensues. Thus, 2-azidobenzimidazole(2-$N_3$-$CN_2HC_6H_4$) and phenacylazide ($N_3COPh$) give complexes (**95**) and (**96**) in which the azide substituent has become coordinated.

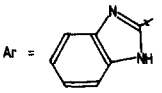
(ii) *With* $[Os_3(CO)_{11}(NCMe)]$ *and with* $[Os_3(CO)_{11}(NC_5H_5)]$

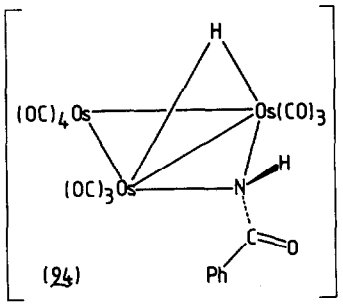
Azidobenzene ($PhN_3$) reacts with functionalized complexes $[Os_3(CO)_{11}L]$ (L = NCMe, $NC_5H_5$) to give products (**97**) in which a nitrogen atom of the azide has become bonded to the carbon atom of a carbonyl ligand.[11,12] The labile ligand L is essential for this reaction, $[Os_3(CO)_{12}]$ (**1**) does not react with azidobenzene under these conditions. Furthermore $[Os_3(CO)_{11}(NCMe)]$ (**6**) does not react with

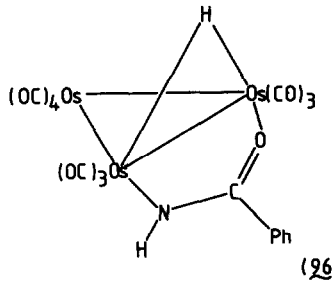



Ar =

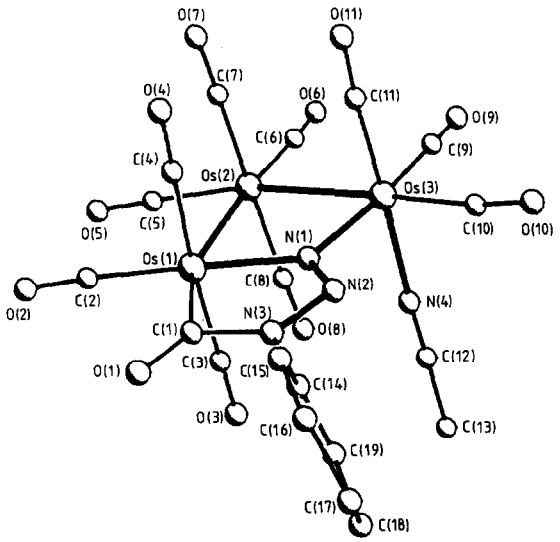


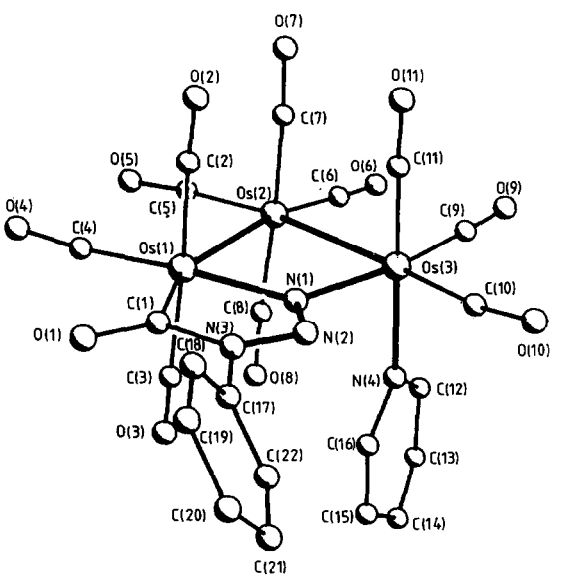



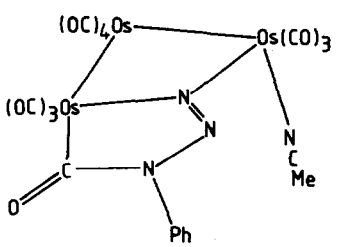




Molecular Structure of $[Os_3(CO)_{10}(\mu\text{-}n^2\text{-}CON_3Ph)(NC_5H_5)]$

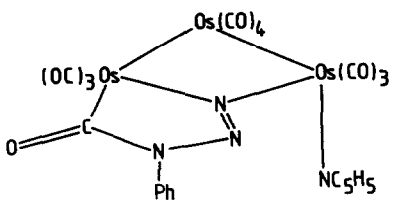
Molecular Structure of $[Os_3(CO)_{10}(\mu\text{-}n^2\text{-}CON_3Ph)(NCMe)]$




(97)

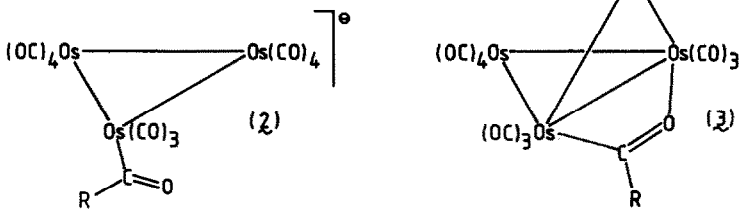



(97)

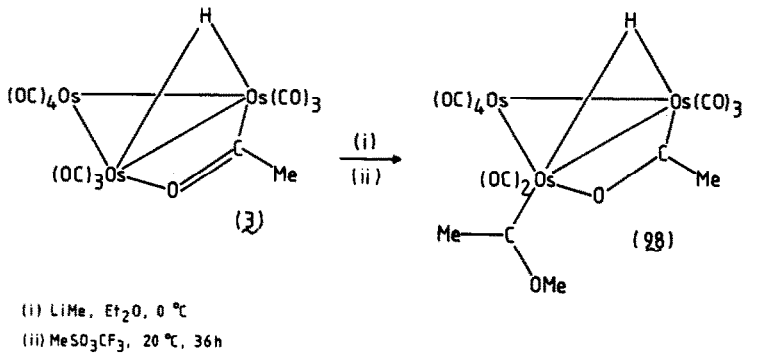
azidobenzene *in acetonitrile* under these conditions. Consequently, it seems that the reaction may involve dissociation to give an unsaturated intermediate $[Os_3(CO)_{11}]$ followed by similar interactions to those observed in the reaction of azidobenzene with $[Os_3H_2(CO)_{10}]$ (**9**).

## J. CARBANIONS AND CARBOCATIONS

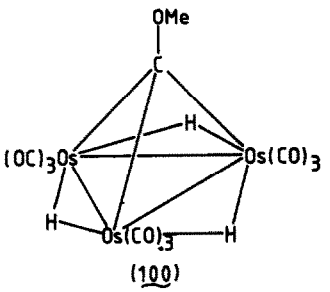
Nucleophilic attack by a carbanion[5,104] or hydride anion[116–120] on a carbonyl ligand of $[Os_3(CO)_{12}]$ (**1**) affords a $\sigma$-bound acyl complex (**2**) which will decarbonylate on standing at 20°C to give (**3**) after protonation.



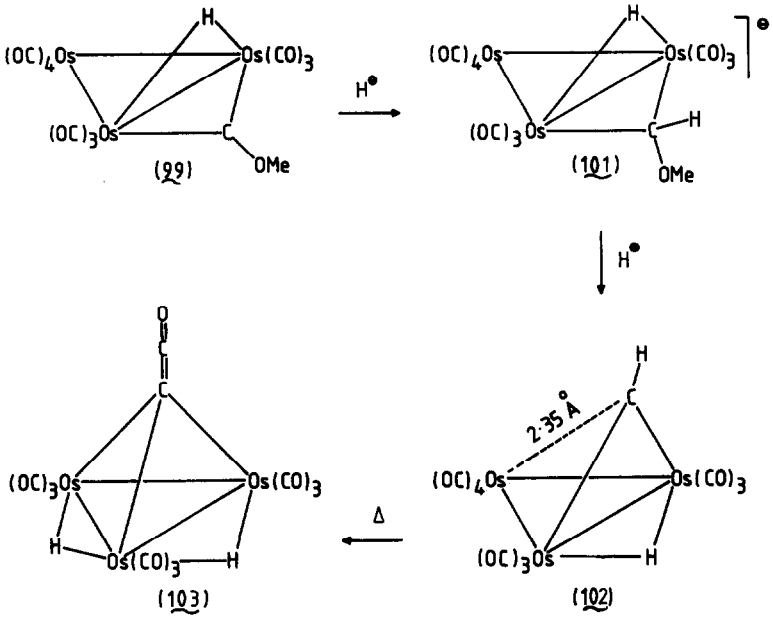

Addition of a second equivalent of methyl lithium to complex (**3**) (R = Me) and methylation with methyltrifluoromethylsulphonate gives a "Fischer-type" carbene complex.[121]




Alkylation of the triosmium anion $[Os_3H(CO)_{11}]^{\ominus}$ (**4**) affords carbyne clusters[122,123] (**99**) which in turn may be hydrogenated to a nonacarbonyl face capped complex (**100**)[124]

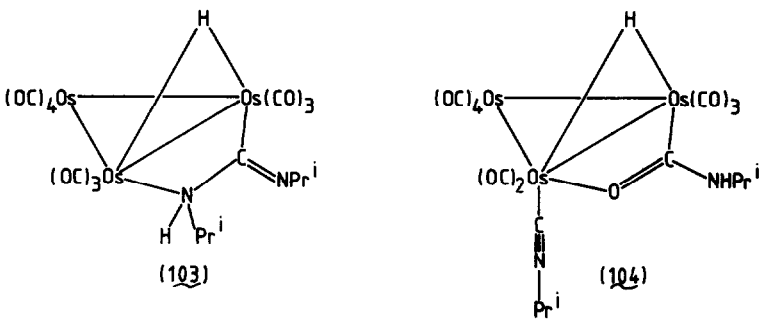



or converted to a semi-capping methylidyne[125] cluster by sequential reduction with hydride and protonation. At 69°C the methylidyne complex (**102**) rearranges to give a ketene ligand on triosmium (**102**). Ethene reacts with $[Os_3H(CO)_{11}]^{\ominus}$ (**4**) at 26°C to give $[Os_3H(CO)_{10}(OCEt)]$ (**30**) after protonation.[126]




## K. CARBODIIMIDES

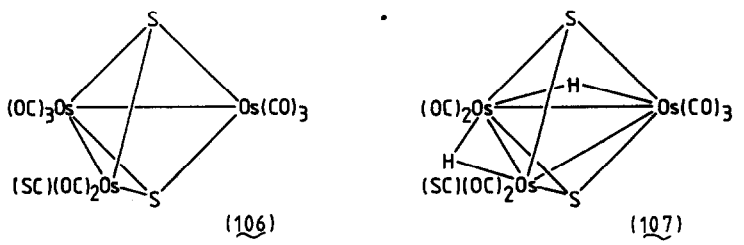
Diisopropylcarbodiimide ($^{i}$PrNCN$^{i}$Pr) and $[Os_3H_2(CO)_{10}]$ (**9**) react to give an amidinyl cluster (**103**) via transfer of hydrogen from the metal core to the organic substrate.[127] A second product (**104**) is formed via a hydrogen transfer. In this complex (**104**) the carbodiimide has been cleaved to give an isocyanide and a methanamido ligand. Thermolysis of the amidinyl complex (**103**) gives $[Os_3H(CO)_9(^{i}PrNHCN^{i}Pr)]$ (**105**) for which the structure is not known.



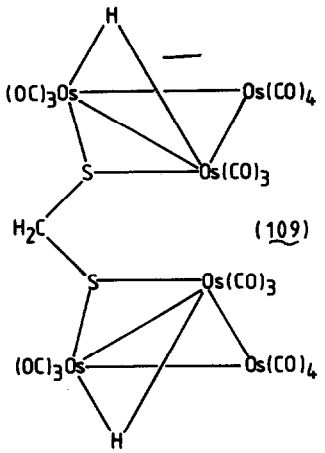

## L. CARBON DISULPHIDE

Triosmium clusters can cleave a carbon–sulphur bond of carbon disulphide and/or hydrogenate the carbon depending on the cluster substrate.

Thermolysis of $[Os_3(CO)_{12}]$ (**1**) with carbon disulphide gives a sulphur capped cluster $[Os_3(CO)_8(CS)(S)]$ (**106**)[128,129] containing a thiocarbonyl ligand. A homologue of this cluster, $[Os_3H_2(CO)_7(CS)(S)]$ (**107**), related by isoelectronic replacement of CO by $H_2$, is formed from $[Os_3H_2(CO)_8S(NCMe)]$ (**108**) and carbon disulphide.[130]

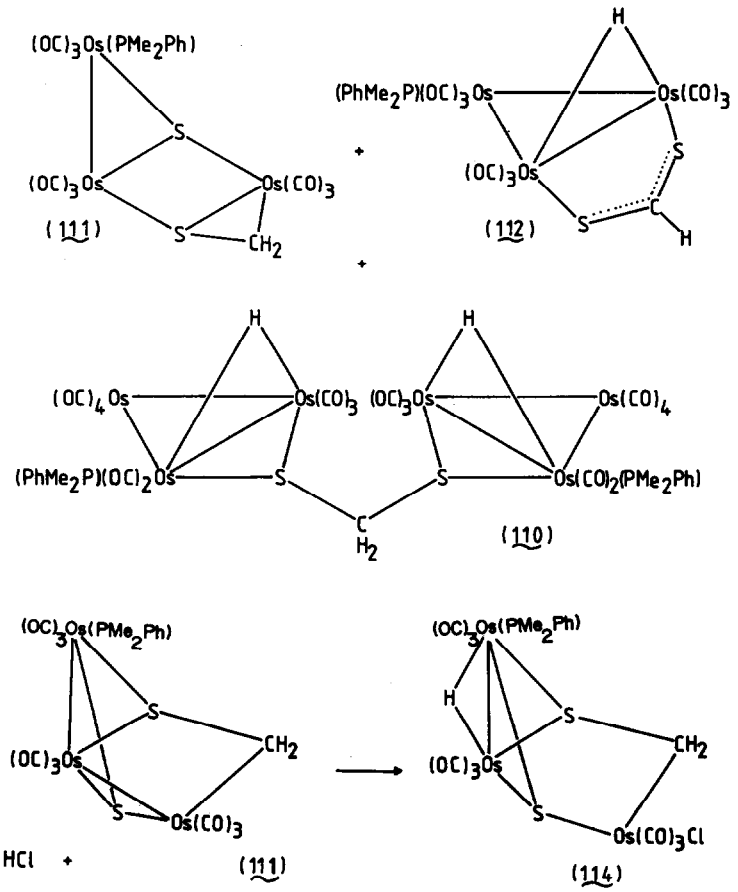


Reaction of $[Os_3H_2(CO)_{10}]$ (**9**) with carbon disulphide yields a bis(triosmium) complex (**109**).[131] In general, $[Os_3H_2(CO)_{10}]$ (**9**) and its phosphine substituted



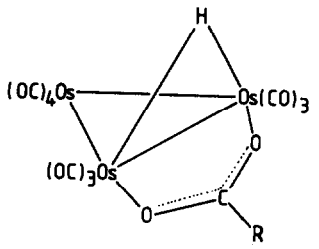

(109)

homologues $[Os_3H_2(CO)_9$ (phosphine)] give different product types or product distributions when reacted with the same organic substrate. Two triosmium complexes (**111**) and (**112**) as well as bis(triosmium) cluster (**110**) are formed in the reaction of $[Os_3H_2(CO)_9(PMe_2Ph)]$ (**113**) with carbon disulphide.[132–134] Cluster (**111**) relinquishes a metal–metal bond in its reaction with HCl.[135–136]



## M. CARBOXYLIC ACIDS

Only one mode of coordination of carboxylate ligands to triosmium has been observed to date.[30] These compounds can be prepared by reaction of carboxylic acids on a functionalized cluster; direct thermal reactions with $[Os_3(CO)_{12}]$ (**1**) give only monometallic complexes![37] Carboxylate complexes are formed in the reactions of aldehydes with some triosmium clusters (e.g. (**1**) and (**7**)). Indeed, methanal gives none of the expected acyl complex (**3**) only the methanoic acid derivative (**115**) (R = H).[138] This cluster (R = H) has been studied as a model for surface absorbates.[139]



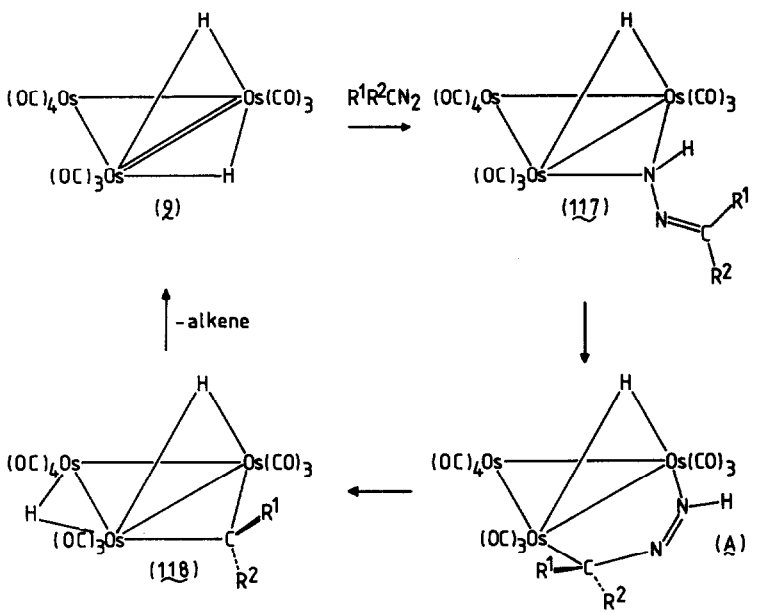

(115)

## N. DIAZOCOMPOUNDS

(i) *With* $[Os_3H_2(CO)_{10}]$ *and with* $[Os_3H_2(CO)_9(PMePh_2)]$

Both azides and diazocompounds are 1,3-dipolar. Consequently, there is an appreciable similarity between some of the reactions described here and in Section I on azides.

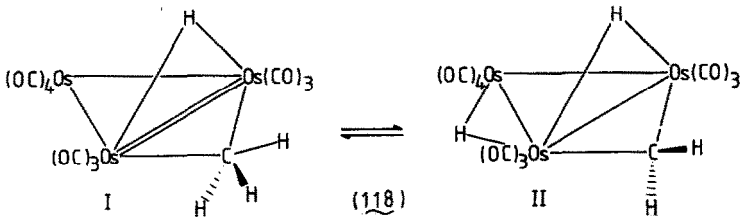
The following general reaction scheme has been invoked to rationalize the reactions of diazocompounds with $[Os_3H_2(CO)_{10}]$ (**9**).[140]

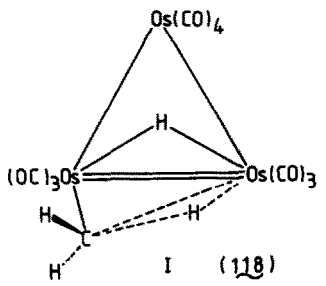


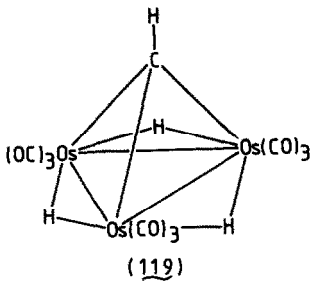

Hydrazone complexes (**117**)[140,141] are the isolated products of $R^1$ and $R^2$ are bulky; the diphenyl complex, for instance, is stable to *ca.* 180°C. If the substituents are smaller expulsion of dinitrogen and hydrogen transfer can occur. Intermediate (A) has not been observed but is directly analogous to the triazenato clusters (**92**) formed from alkyl azides; (A) may well be less stable than these complexes due to greater steric interactions. The carbene complex (**118**) is stable for $R^1 = R^2 = H$ but if $\beta$-hydrogens are present elimination occurs to give an alkene and $[Os_3H_2(CO)_{10}]$ (**9**)

($R^1 = R^2 = Me$,[140] $R^1 = Me, R^2 = H$[142]). The hydrazone complex (**117**) is isolatable for 2-diazopropane ($R^1 = R^2 = Me$) but it decomposes to propene and $[Os_3H_2(CO)_{10}]$ (**9**) on standing at 20°C.

Complex (**118**) in solution exists as a mixture of tautomers.[143–145] The methyl tautomer (I) is probably best represented as a complex with an appreciable C . . . H . . . Os interaction. Only the carbene form (II) has been observed in the solid state.[146] Heating a solution of (**118**) in methylbenzene at 110°C affords a methylidyne complex (**119**).[143]

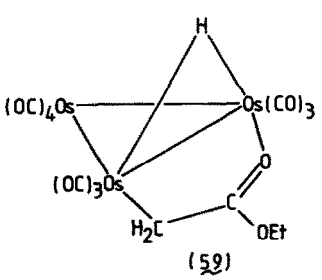


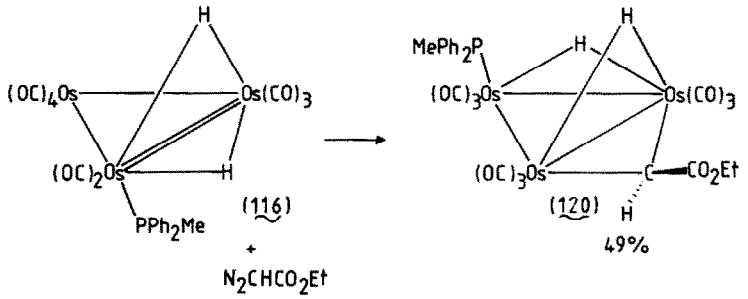




This is reminiscent of formation of nitrene ligands on triosmium from azides (see Section I). Calculations indicate that the methylidyne carbon of (**119**) should readily support a positive charge;[147] this could account for bromination of this ligand by boron tribromide presumably via an electrophilic attack.[148]

Ethyldiazoethanoate ($N_2CHCO_2Et$) and $[Os_3H_2(CO)_{10}]$ (**9**) may form a carbene complex ($R^1 = CO_2Et$, $R^2 = H$) initially but the isolated product involves coordination of the ester carbonyl.[74]

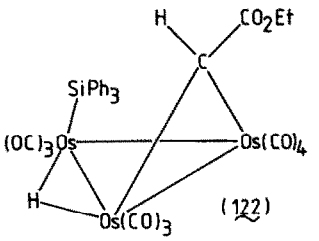


Ethyldiazoethanoate and $[Os_3H_2(CO)_9(PMePh_2)]$ (**116**) react to form a complex (**120**) bearing a carbene ligand.[149] This is another example of the marked effect of the substitution of a carbonyl by a phosphine on the reactivity of $[Os_3H_2(CO)_9(L)]$ complexes. No tautomeric equilibrium is observed in the variable temperature $^1H$ NMR spectrum of (**120**).



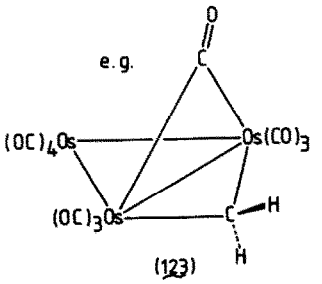

(ii) *With* $[Os_3H(CO)_{10}(NCMe)(SiPh_3)]$, $[Os_3(CO)_9(C_2Ph_2)]$, *and* $[Os_3(CO)_{11}(NCMe)]$

Ethyldiazoethanoate ($N_2CHCO_2Et$) and $[Os_3H(CO)_{10}(NCMe)(SiPh_3)]$ (**121**) (Section X) react to form a carbene complex (**122**).[223]

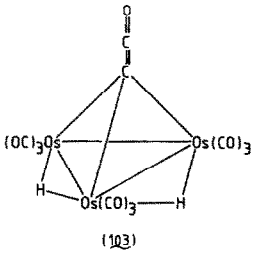



This product is similar to $[Os_3H_2(CO)_9(CHCO_2Et)(PMePh_2)]$ (**120**) described in Subsection (i). Thermolysis of (**122**) gives a nonacarbonyl and an undecacarbonyl cluster; these are currently under investigation.

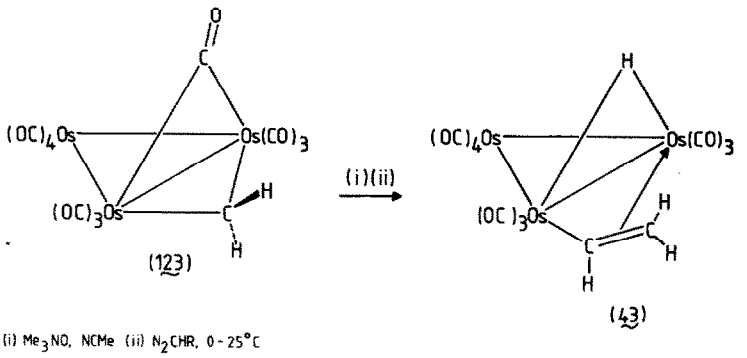
Diazocompounds add to $[Os_3(CO)_{11}(NCMe)]$ (**6**) to give carbene clusters such as (**123**) perhaps via 1,3-dipolar cycloaddition to an unsaturated intermediate "$[Os_3(CO)_{11}]$".[64,150]



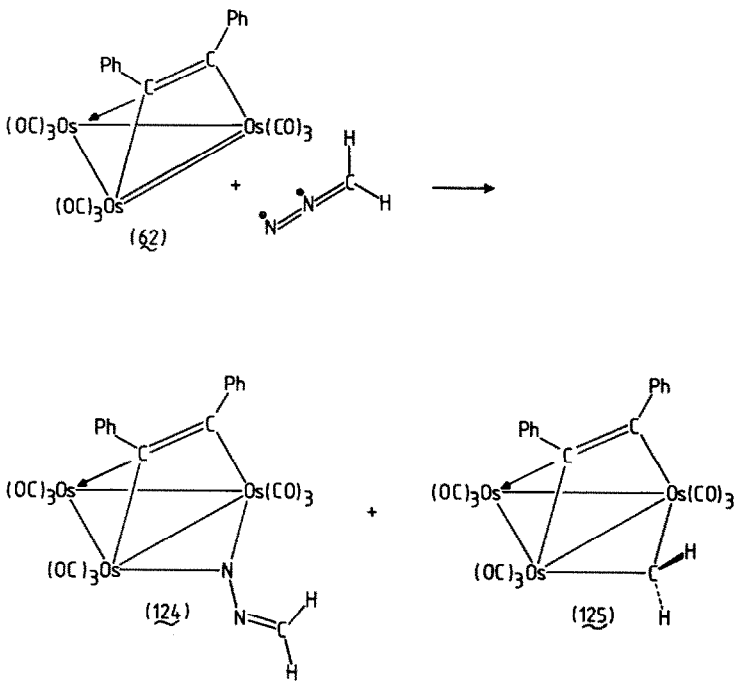

Triosmium clusters bearing carbene or carbyne ligands can often be precursors to carbon–carbon bond formation on the metal face. Thermolysis of (**123**)[151] or $[Os_3H(CO)_{10}(CH)]$ (**102**)[152] affords a coordinated ketene.



Thus the carbene has joined to a carbonyl ligand. Similarly, oxidative removal of a carbonyl ligand of $[Os_3(CO)_{11}(CH_2)]$ (**123**) and reaction of the product *in situ* with a diazocompound gives a vinyl cluster.[152] Addition of labelled diazomethane to the product of the amine oxide oxidation affords a scrambled label; $[Os_3H(CO)_{10}(\overset{*}{C}HCH_2)]$ (**43**) 50% $[Os_3H(CO)_{10}(CH\overset{*}{C}H_2)]$ (**43**) 50%. Carbon–carbon bond formation in this reaction therefore must precede carbon–hydrogen bond fission. A vinyl complex $[Os_3H(CO)_{10}(CHCH_2)]$ (**43**) is formed by a direct reaction of $[Os_3H(CO)_{10}(CH)]$ (**102**) with diazomethane.[152]

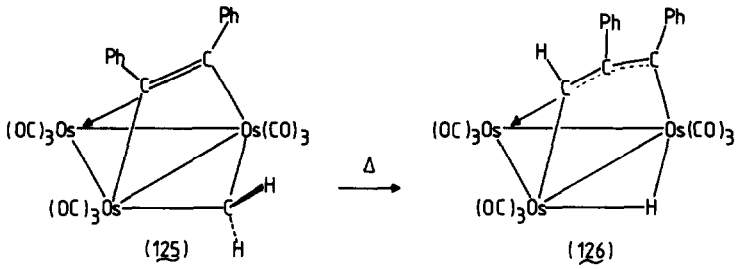



$[Os_3(CO)_9(C_2Ph_2)]$ (**62**) is unsaturated. It reacts with diazomethane to form two products.[153]




Photolysis (but not thermolysis) of the nitrene complex (**124**) converts it to the carbene (**125**). This is a similar reaction to the rearrangement proposed for decomposition of hydrazone complexes $[Os_3H(CO)_{10}(NHNCR^1R^2)]$ (**117**) (Subsection (i)).

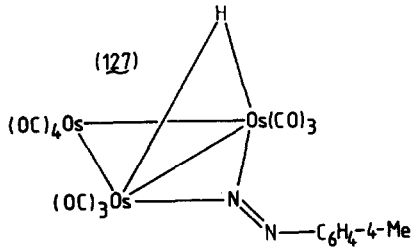
Another example of carbon–carbon bond formation via a carbene ligand on a triosmium face is the action of heat on $[Os_3(CO)_9(C_2Ph_2)(CH_2)]$ (**125**) which gives a coordinated allyl fragment.



(125) (126)

## O. A DIAZONIUM SALT[154]

4-Methylbenzenediazonium tetrafluoraborate adds to $[Os_3H_2(CO)_{10}]$ (**9**); the initial product (a cation) was not isolated but was deprotonated using ammonia to give an azo-cluster (**127**). A similar complex bearing a 2-azo-6-chloropyridine ligand has been prepared from 2-azido-6-chloropyridine ($2\text{-}N_3\text{-}6\text{-}ClNC_5H_3$) and $[Os_3(CO)_{10}(NCMe)_2]$ (**7**).[149]



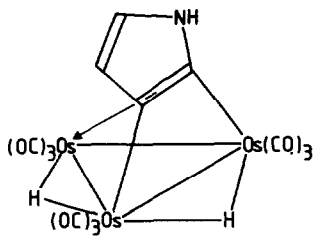
(127)

## P. HETEROCYCLES

There are several modes of coordination of heterocycles to triosmium. Complexes of pyridine on $Os_3$ are of particular value for comparison with metal absorbates.[156,157] Reactions of substituted heterocycles with triosmium can give coordination to the ring substituents and/or the heterocyclic functionality.

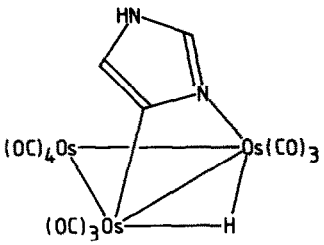
(i) *Metallated heterocycles*

Pyrrole and $[Os_3(CO)_{12}]$ (**1**) react at elevated temperatures to give a complex in which the nitrogen atom is not coordinated.[158]



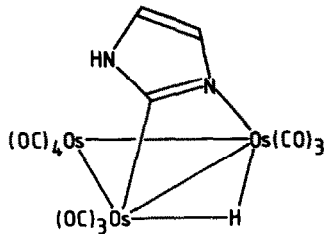
(128)

The lone pair on the nitrogen atom of pyrrole is part of the $6\pi e$ aromatic $(4n + 2)$ set and coordination is therefore unlikely. For imidazole and pyrazole this is not so. These heterocycles react with $[Os_3(CO)_{10}(NCMe)_2]$ (**7**) to form two isomeric clusters in each case, (**129**) & (**130**) and (**131**) & (**132**), respectively.[149,159] These isomers correspond to metallation on either side of the basic nitrogen in the heterocyclic rings.

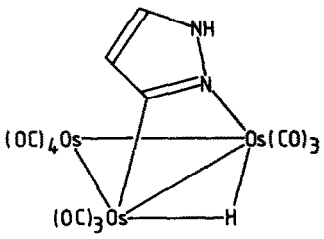



(129)

stable to 200 °C

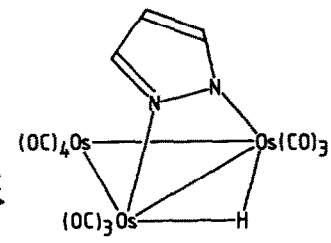



(130)

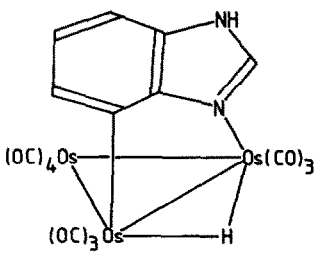



(131)

180 °C

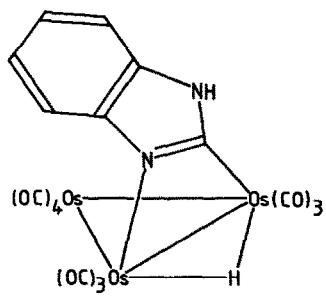



(132)

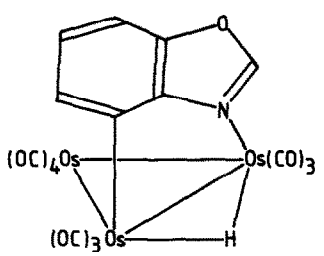



(133)

180 °C




(134)

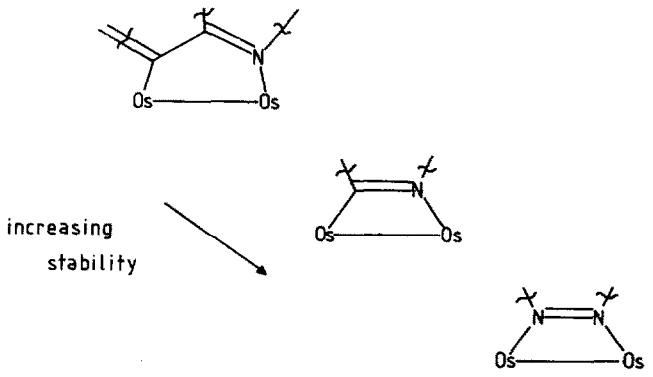



(135)

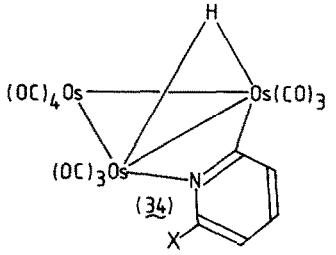
In a similar reaction with benzimidazole one of the expected isomers (**134**) forms readily but metallation on the other side of the basic nitrogen is precluded by the benzene ring so an osmium inserts into the next available carbon–hydrogen bond giving (**133**).

Benzoxazole and $[Os_3(CO)_{10}(NCMe)_2]$ (**7**) form a complex (**135**) in which metallation has occurred regioselectively at the $\beta$-position.[149]

As indicated above, two of these complexes (**129**) and (**131**) can be converted to the other isomers at elevated temperatures.[149] Hence the following order of thermodynamic stability is applicable to these systems.




Coordination of six membered ring heterocycles with triosmium gives analogous complexes to those discussed above. 2-Substituted pyridines when reacted with lightly stabilized clusters $[Os_3(CO)_{10}L_2]$ (e.g. L = NCMe (**7**)) can give metallated systems in which the pyridine substituent is not coordinated.[160,161,163]



(34)

X = H, Cl, CN, Me, $CH_2Ph$

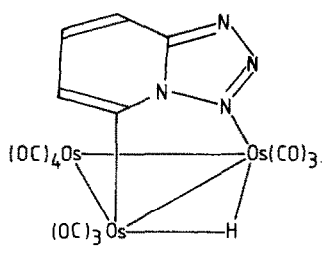
The complex of pyridine (X = H) can be formed from $[Os_3(CO)_{12}]$ (**1**).[162] Formation of such a complex from 2-chloropyridine[160] (X = Cl) demonstrates that a bridging hydrogen is preferred over a bridging chlorine despite the facile displacement of halide from 2-halopyridines.

2-Azidopyridine (I) exists mainly as its tetrazole tautomer (II) and it coordinates as the tetrazole when reacted with $[Os_3H_2(CO)_{10}]$ (**9**) to form the metallated product (**136**).[149] The elements of dihydrogen are lost in this reaction. One of these originates from the aromatic ring since $[Os_3D_2(CO)_{10}]$ (**1**) forms $[Os_3D(CO)_{10}(C_5H_4N_4)]$ in a similar reaction.

A triosmium cluster formed from 2,2-bipyridyl also contains a metallated ring; this is discussed in the next section.



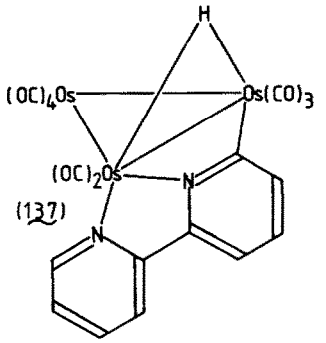
(I) (II)



(136)

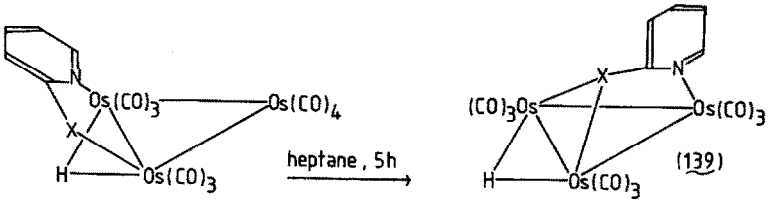
(ii) 2-*Substituted pyridines bound to triosmium via the pyridine nitrogen and the 2-substituent*

2,2'-Bipyridyl and $[Os_3(CO)_{12}]$ (**1**) react to give a complex (**137**) in which the heterocycle both chelates and is metallated.[163] Similar clusters from pyridine-2-hydroxymethylene and pyridine-2-carboxylic acid have been mentioned in a paper but not yet reported in full.[163]



(137)

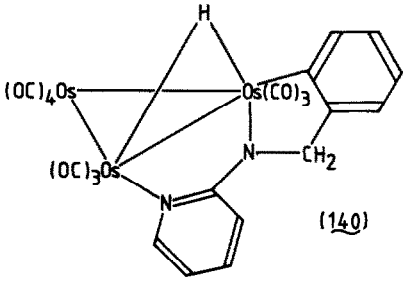
Triosmium decacarbonyls $[Os_3H(CO)_{10}(XC_5H_4N)]$ (X = NH, $NCH_2Ph$, S, O (**138**) are accessible by the reaction of the appropriate 2-substituted pyridine with $[Os_3(CO)_{10}(NCMe)]$ (**7**). These complexes decarbonylate on heating giving clusters of type (**139**).[160]



(138) (139)

| Z | °C | % |
|---|---|---|
| O | 200+ | - * |
| S | 160 | 67 |
| NH | 90 | 68 |

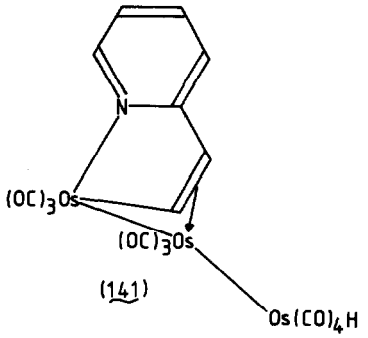
*But this reaction has been observed, see text.



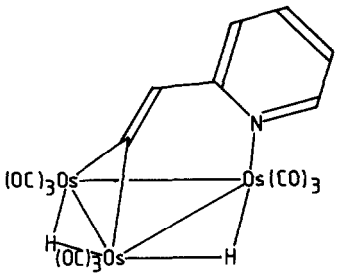
(140)

The temperatures at which this decarbonylation occurs increase in the order NR, S, O indicative of decreasing availability of a lone pair on the heteroatom for coordination. A metallated cluster (**140**) is also formed in the reaction of 2(phenylmethylamino)pyridine[$(PhCH_2NH)C_5H_4N$] (X = $NCH_2Ph$).[103]

Pyridines bearing *ortho* unsaturated hydrocarbon functionality tend to open the osmium triangle to form a triosmium chain complex (**141**).[149] In the vinylidene cluster (**142**) the pyridine nitrogen coordinates in preference to the alkene $\pi$-cloud.[149]




(141)

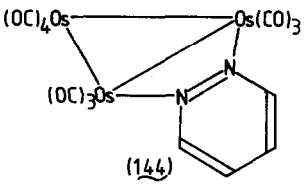



(142)

(iii) *Ligands coordinated solely by heterocyclic nitrogen*

The pyridine ligand of $[Os_3(CO)_{11}(NC_5H_5)]$ is labile hence the cluster is a possible starting material for the synthesis of other complexes. $[Os_3(CO)_{11}(NC_5H_5)]$ (**143**) can be prepared from $[Os_3(CO)_{11}(NCMe)]$ (**10**) or from $[Os_3(CO)_{12}]$ (**1**) in pyridine/dichloromethane with trimethylamine-N-oxide.

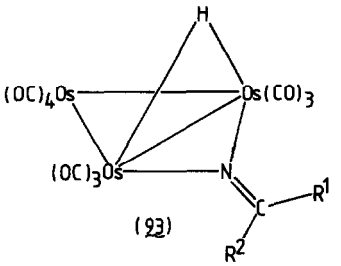
A metallocyclic cluster (**144**) is formed in the reaction of 1,2-pyridazine and $[Os_3(CO)_{12}]$ (**1**).[164] This complex is exceptional in that it has no osmium hydride.




(144)

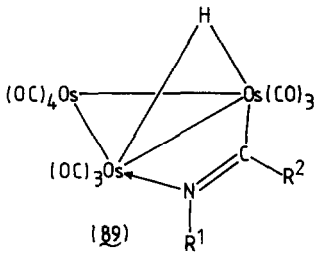
## Q. IMINES

Reaction of ketones with $[Os_3(CO)_{11}(NH_3)]$ (**145**) affords imine complexes $[Os_3(CO)_{11}(NHCR^1R^2)]$ (**146**) (Section C).[165] Thermolysis of these imine complexes causes decarbonylation and ligand to metal hydride transfer and an N-bound imine is formed.[166]



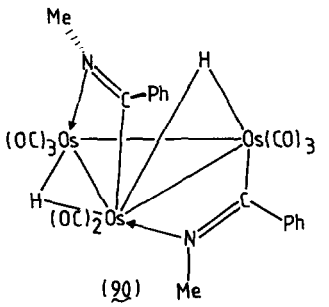

(93)

Such compounds have also been formed from trifluoroacetonitrile (Section V(ii)). Alternatively, imine functionality can be coordinated via both the carbon and the nitrogen.



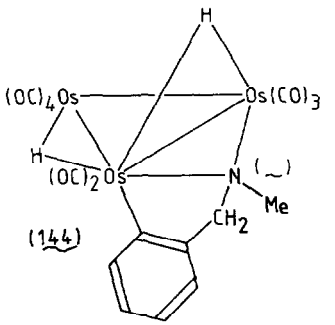

(89)

This type of complex can be formed from amines, trifluoroacetonitrile, isocyanides, isothiocyanates (Sections H, U, S and R) or by direct reaction of imines with $[Os_3H_2(CO)_{10}]$ (**9**)[167,168] or $[Os_3(CO)_{12}]$ (**1**).[108] The latter reaction with (N-methyl)phenylmethimine[108] (MeN : CPhH) gives a cluster with two such ligands as an additional product.



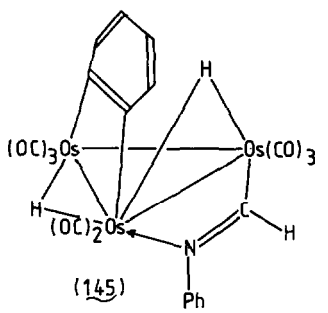

(90)

The thermal reaction of $[Os_3H_2(CO)_{10}]$ (**9**) with (MeN : CPhH) gives a cluster[167] in which metallation has occurred (**144**) as well as (**89**).[168]



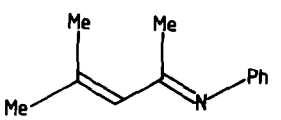

(144)

Thermolysis of a complex of type (**89**) ($R^1$ = H, $R^2$ = Ph) affords a cluster with a 1,2-dimetallated benzene ligand.[169]

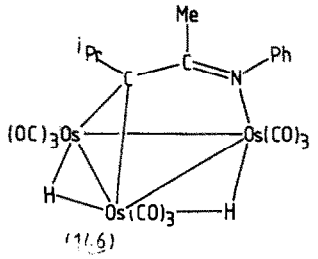



(145)

An $\alpha,\beta$-unsaturated imine

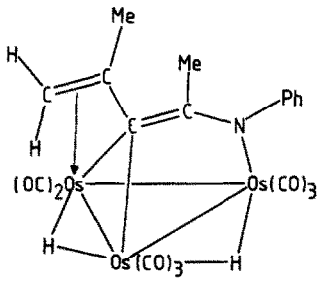



and $[Os_3H_2(CO)_{10}]$ (**9**) react to form a face capped cluster.[170]




(146)

Thus complexation of this imine causes hydrogen shifts within the ligand. This reaction is analogous to those of $[Os_3H_2(CO)_{10}]$ (**9**) with $\alpha,\beta$-unsaturated esters (Section D(v)) to give $[Os_3H(CO)_{10}(CHRCO_2R^1)]$ (**59**) complexes. Another product (**147**) is formed by the reaction of the imine with $[Os_3H_2(CO)_{10}]$ (**9**) or by maintaining complex (**146**) under the reaction conditions.

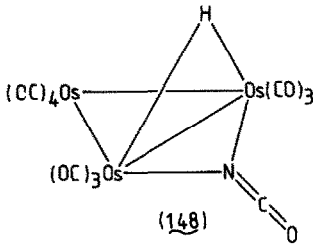



(147)

## R. ISOCYANATES AND ISOTHIOCYANATES

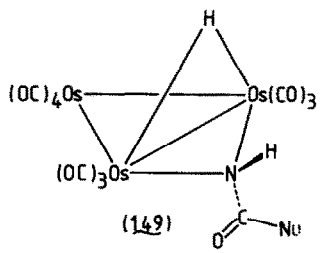
(i) *Isocyanic acid*

Isocyanic acid, generated *in situ*, reacts with $[Os_3(CO)_{10}(NCMe)_2]$ (**7**) to give an isocyanate complex.[171]




(148)

This cluster has been reported to add nucleophiles (NuH, Nu = $NR_2$, OR) onto the isocyanate functionality to give bridging-amido complexes.

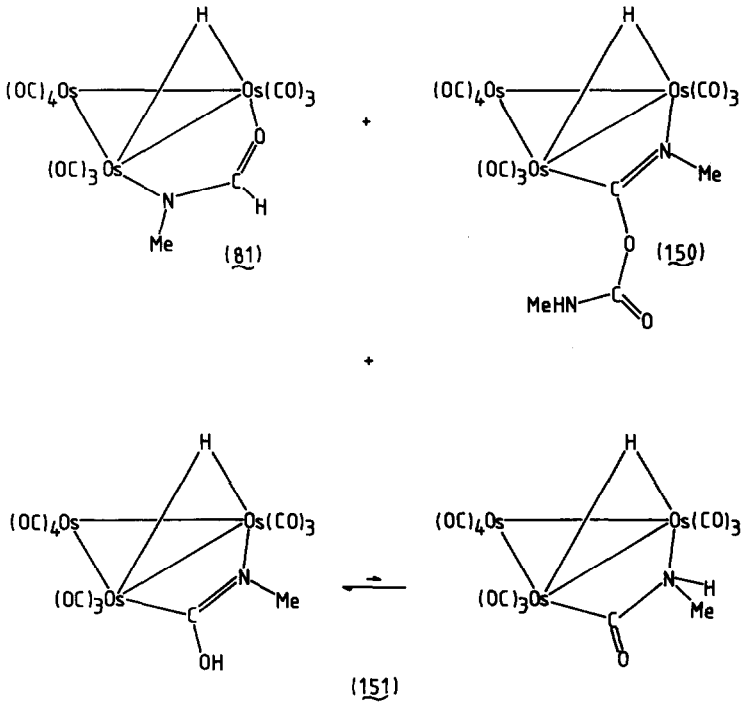



(149)

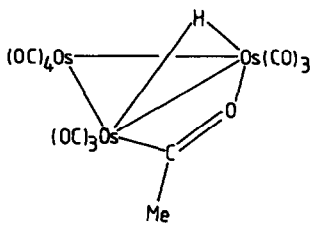
Details of such additions have not been published; however, similar reactivity of an analogous cluster $[Os_3(AuPEt_3)(CO)_{10}(NCO)]$ has been reported in full.[172]

(ii) *Methylisocyanate*

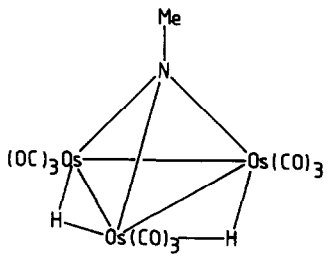
Methylisocyanate and $[Os_3H_2(CO)_{10}]$ (**9**) react to give three complexes.[173–175]




The major product (**81**) can alternatively be formed from an amide (Section F).[40] Complex (**150**) apparently results from addition of a second mole of methylisocyanate to cluster (**151**). The complex with an organic ligand coordinated by both the nitrogen and the carbon (**151**) exists in a tautomeric equilibrium; it isomerizes in solution to an acyl complex (**30**) (see Section H).

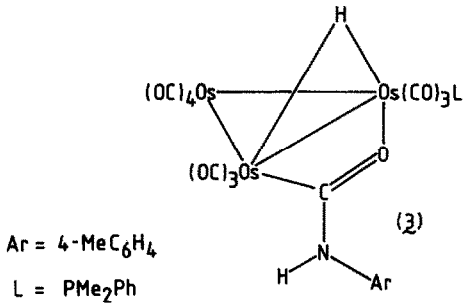



The methanamide and acyl complexes (**81**) & (**151**) respectively do not interconvert but it is possible to decarbonylate them both to the same nitrene cluster (**88**).



(iii) *Arylisocyanates*

Arylisocyanates react with $[Os_3H_2(CO)_{10}]$ (**9**) to form products analogous to (**81**) and traces of complexes of type (**3**).[174,175] However, reaction of $[Os_3H_2(CO)_9(PMePh_2)]$ (**113**) with phenylisocyanate affords an acyl complex (**3**) as the major product.[175]



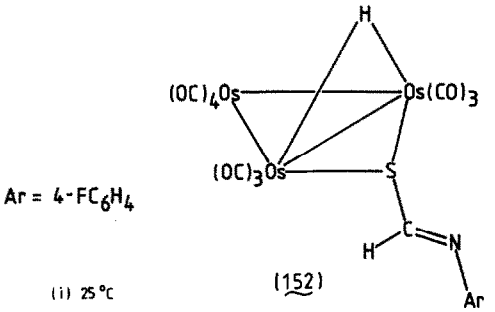

Ar = 4-$MeC_6H_4$

L = $PMe_2Ph$

(3)

(iv) *Arylisothiocyanates*[174,176]

Coordination of sulphur is the dominant feature of the reactions of isothiocyanates (RNCS) with triosmium clusters; cleavage of carbon–sulphur bonds is also observed at higher temperatures. Thus, the initial product from 4-fluorobenzisothiocyanate and $[Os_3H_2(CO)_{10}]$ (**9**) is a complex containing a bridging-sulphur atom.[176]

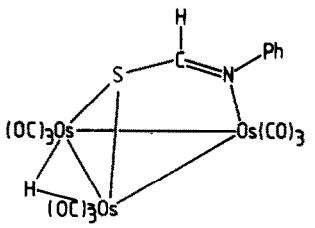



Ar = 4-$FC_6H_4$

(i) 25 °C

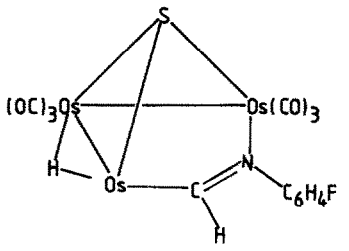
(152)

Photolysis of this complex transforms the organic ligand into a face capping mode via coordination of the nitrogen giving (**153**).




(153)

The carbon–sulphur bond in this complex is cleaved on heating and a side bound imine group is produced in the product (**154**).



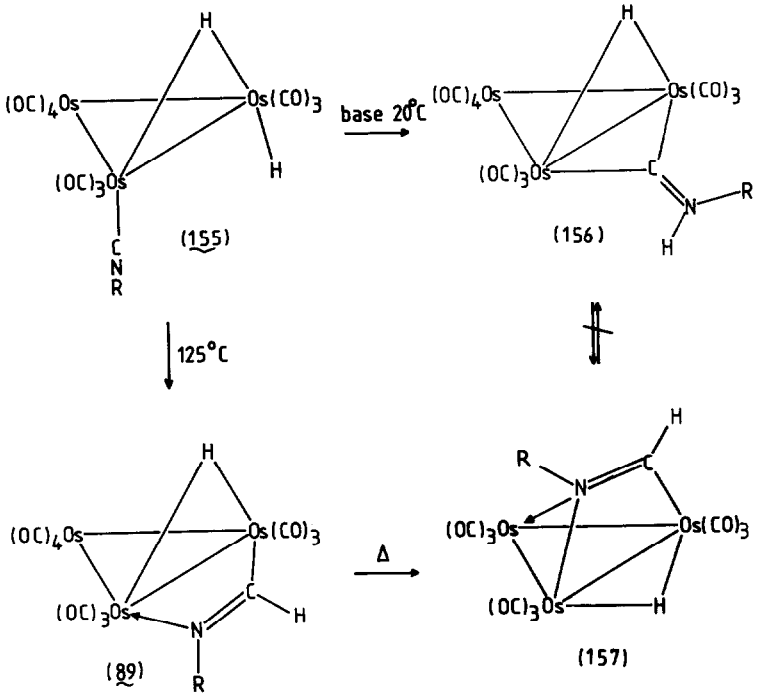

(154)

## S. ISOCYANIDES

Simple substitution reactions are not covered comprehensively here. Generally three isocyanides (at least) can be coordinated to a triosmium frame, they adopt axial positions unless exceptional steric crowding forces equatorial coordination.[177]

(i) *With* $[Os_3H_2(CO)_{10}]$ (**9**)

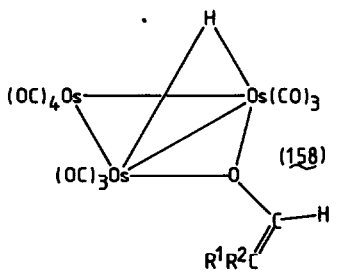
The expected adducts $[Os_3H_2(CO)_{10}(L)]$ (**155**) (L = CNR) are formed from $[Os_3H_2(CO)_{10}]$ (**9**) and isocyanides at ambient temperature.[178] In basic solvents or solvents containing a trace of base (e.g. triethylamine) the nitrogen atom of the adduct is hydrogenated presumably via a proton transfer. Heating the adducts (**155**) (L = CNR) in nonpolar solvents causes the nitrogen to coordinate.[179–181]




## T. KETENES

Ketenes (O : C : $R^1R^2$) and $[Os_3H_2(CO)_{10}]$ (**9**) react to form enolates stabilized by coordination to triosmium in complexes of general structure (**158**).[38,39]

When heated the methylketene complex ($R^1$ = H, $R^2$ = Me) is transformed into $[Os_3H(CO)_{10}(OCEt)]$ (**30**) and the ketene ($R^1$ = $R^2$ = H) complex affords $[Os_3H_2(CO)_9(CHCHO)]$ (**31**); both these product types are also accessible via reactions of aldehydes (Section C).




## U. NITRILES

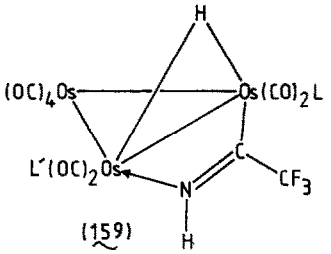
(i) *Acetonitrile*

Triosmium clusters bearing acetonitrile ligands are common starting materials for the synthesis

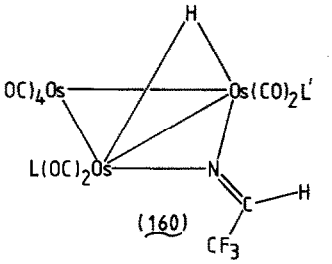
of other compounds. Only some general points about these complexes will be made here. Acetonitrile ligands can be introduced via the action of trimethylamine-N-oxide on metal carbonyls and they are easily displaced by two electron donors.[10] Like isonitriles, acetonitrile ligands occupy axial coordination sites; $[Os_3(CO)_{10}(NCMe)_2]$ (**7**) crystallizes in a *trans* diaxial configuration with the nitrile ligands on different osmium atoms.[182]

(ii) *Trifluoroacetonitrile*

Trifluoroacetonitrile and $[Os_3H_2(CO)_{10}]$ (**9**) react to form two isomers of $[Os_3H(CO)_{10}(NHCCF_3)]$ (**159**) and (**160**) L = L′ = CO).[183,184,185] The phosphine substituted dehydride $[Os_3H_2(CO)_9(PMePh_2)]$ (**113**) gives corresponding compounds but only the regioisomers of (**159**) and (**160**)(L = CO, L′ = $PMePh_2$) with the phosphine furthest away from the trifluoromethyl group.



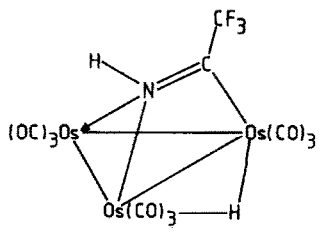

(159)



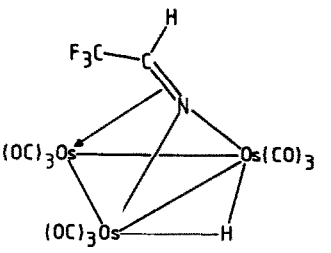

(160)

However, the reaction of dimethylphenyl phosphine with decacarbonyl (**160**) is non-regioselective, both isomers of (**160**) (with L = CO, L′ = $PMe_2Ph$ and L = $PMe_2Ph$, L′ = CO) form.[186]

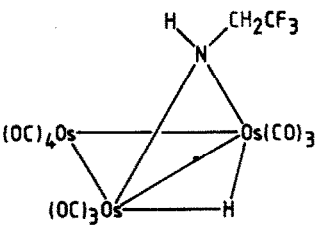
Thermal decarbonylation of $[Os_3H(CO)_{10}(NCHCF_3)]$ (**159**) and (**160**) affords corresponding isomers of the nonacarbonyls (**161**) and (**162**), respectively. Thus there is a stereochemical "memory" effect.



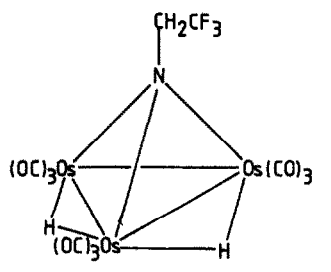

(161)



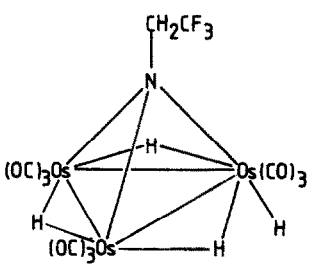

(162)




(163)




(88)



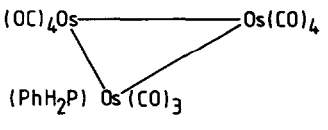

(164)

Hydrogenation of the terminally bound iminyl complex (**159**) (L = L' = CO) occurs in stages and several intermediates have been isolated. The first mole of dihydrogen adds to the carbon–nitrogen double bond to give an alkyl amido-bridged cluster (**163**), decarbonylation of this product affords a nitrene complex which in turn adds a second mole of dihydrogen to give $[Os_3H_4(CO)_8(NCH_2CF_3)]$ (**164**).[187] The tetrahydro cluster (**164**) is unique in that four hydrides are supported on the trimetal frame.

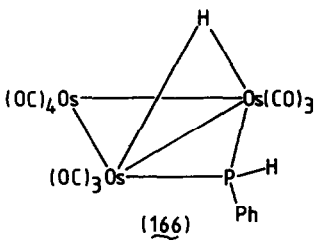
## V. PHOSPHINES AND ARSINES

Triosmium carbonyls bearing simple phosphine or arsine ligands as the only functionality are not covered comprehensively in this review. Generally phosphines can be introduced onto a triosmium frame via direct thermal reactions,[188–190] oxidative (or reductive) removal of carbonyl ligands[191] or reaction with an activated or functionalized cluster.[10] Capping, bridging and terminal coordination is possible by using phosphines with a suitable number of hydrogen substituents.[189,191]

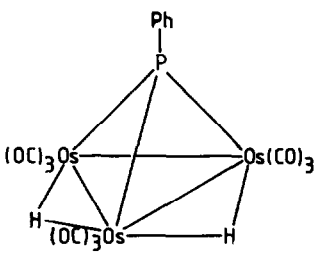
Terminal phosphines preferentially occupy equatorial coordination sites;[192,193] this contrasts the coordination of nitriles and isonitriles. It seems that *good π-acceptor ligands tend to adopt axial sites, π-donors occupy equatorial positions.* Bridging phosphido ligands tend to lie in the plane of the osmium triangle but asymmetry of other ligands or of the phosphide substituents perturb this favoured arrangement.




(165)



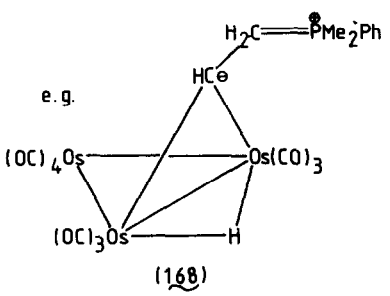

(166)




(167)

Complexes with four or more monodentate phosphine substituents on triosmium have not been isolated but higher substitution is possible with chelating phosphines.[194]

Phosphines add to vinyl ligands of complexes like $[Os_3H(CO)_{10}(CHCH_2)]$ (**43**) to form zwitterionic adducts (see also Section H (Amines) for other zwitterionic complexes).[195–197]

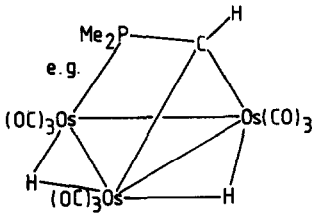



(168)

The remainder of this section is devoted to reactions in which phosphine or amine substituents become metallated.

(i) *Trialkylphosphines*

Thermolysis of $[Os_3(CO)_{11}P(CH_2R)_3]$ (**165**) (R = H, Me) gives nonacarbonyls by metallation of the α-methylene group.[198]

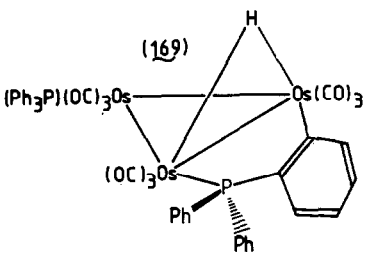



(166)

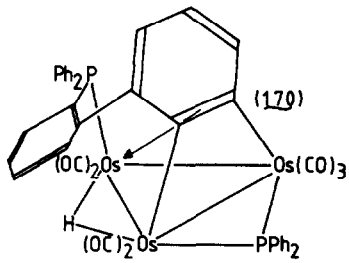
Similarly, $[Os_3(CO)_{10}(PCH_2RR)_2]$ (**167**) clusters give isomers of the formula $[Os_3H_2(CO)_9P(CH_2R)_3PCR(CH_2R)_2]$ (**167**). Metallation of an alkyl phosphine (or amine) is less favourable than of an aryl or vinyl phosphine; this is illustrated by some of the reactions (in the following section) in which some of the phosphines have both alkyl and aryl substituents.

(ii) *Aryl phosphines and arsines*

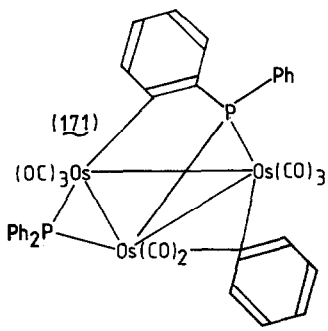
Thermal reactions of aryl phosphines (or arsines) give products: (a) in which phosphorus (or arsenic) carbon bonds are retained but the aryl group is metallated, e.g. (**169**)–(**171**);[199–201] (b) involving phosphorus (or arsenic)–carbon bond cleavage giving arene ligands.[199–206] Many products fall into both these categories.



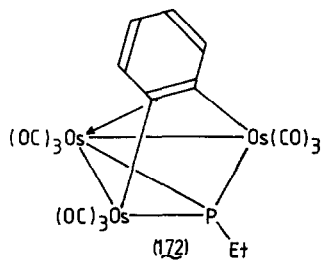

(169)



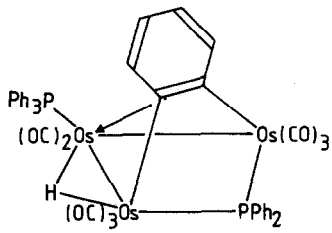

(170)



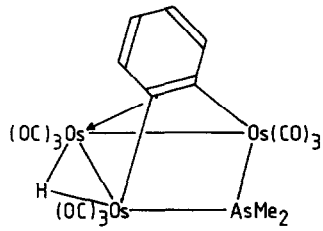

(171)



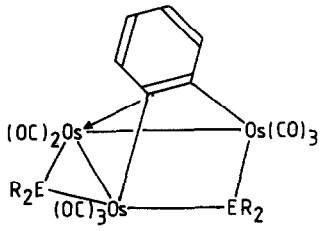

(172)



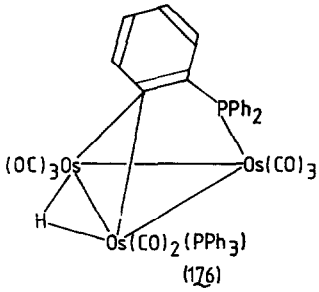

(173)




(174)

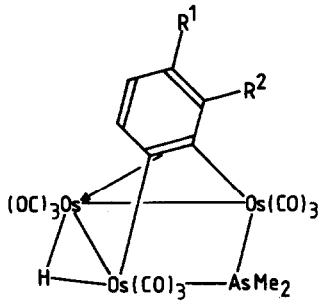



(175)
E = P or As




(176)

An extraordinary hydrogen transfer reaction must take place in the formation of arsine complexes (**177**) and (**178**) from $[Os_3(CO)_{11}\{AsMe_2(C_6H_4\text{-}4\text{-}OMe)\}]$ and $[Os_3(CO)_{11}\{AsMe_2(C_6H_4\text{-}2\text{-}Me)\}]$ (**179**) respectively since an arsenic–carbon bond is replaced by a hydrogen–carbon.[205]

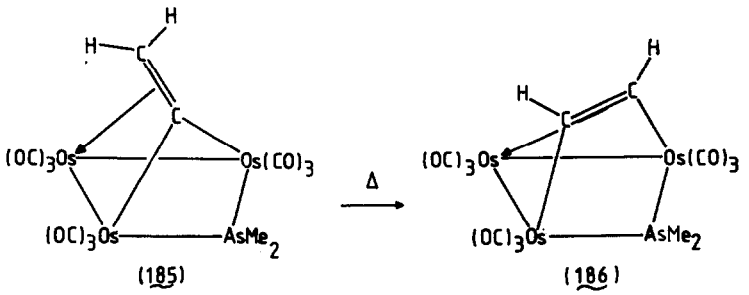



| $R^1$ | $R^2$ | |
|---|---|---|
| H | OMe | (177) |
| Me | H | (178) |

(iii) *Phosphines and arsines with alkyne or alkene functionality*

*Phosphine- and arsine-alkenes.* Ethenyldiphenylphosphine $[Ph_2P(CHCH_2)]$ reacts with $[Os_3(CO)_{10}(NCMe)_2]$ (**7**) to give a structurally uncharacterized cluster $[Os_3(CO)_8\{Ph_2P(CHCH_2)\}_2]$ (**180**) and $[Os_3(CO)_{11}(Ph_2PCHCH_2)]$ (**181**).[149] (2-Ethenylbenzene)diphenylphosphine $(CH_2CHC_6H_4\text{-}2\text{-}PPh_2)$ and $[Os_3H_2(CO)_{10}]$ (**9**) react to form $[Os_3H_2(CO)_8(Ph_2PC_6H_4C_2H)]$ (**182**) in which the phosphine is probably an equatorial substituent in such a configuration that the alkene can cap the triosmium face.[207]

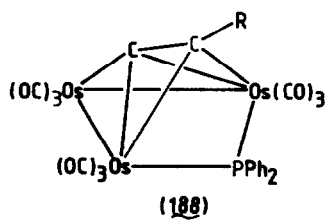
Thermolysis of $[Os_3(CO)_{11}(AsMe_2CHCH_2)]$ (**183**) affords $[Os_3(CO)_{10}(AsMe_2CHCH_2)]$ (**184**) but the structure of this is not established. At 125°C this decacarbonyl (**184**) forms $[Os_3H(CO)_9(C_2H_2)(AsMe_2)]$ (**185**) in which the organic fragment is coordinated as a vinylidene ligand.[208] This complex isomerizes at 150°C.




(185) (186)

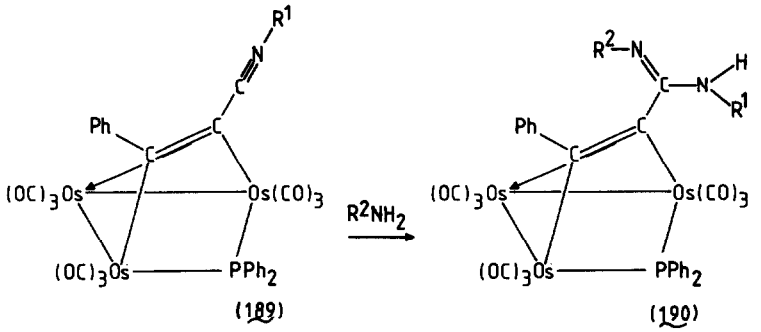
Presumably the alkene group is more stable spanning the open edge of the osmium triangle when it is 1,2-dimetallated. Such a rearrangement of an alkene ligand from 1,1- to 1,2-disubstitution is otherwise unknown in triosmium chemistry.

*Phosphine-alkynes.* Thermolysis of $[Os_3(CO)_{11}(PPh_2C_2R)]$ (**187**) causes carbon–phosphorus bond cleavage giving a complex with a face capping alkyne ligand.[209,210]




(188)

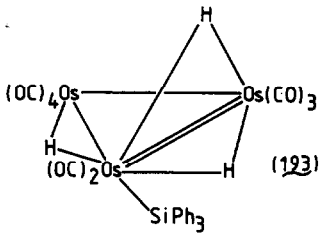
Isocyanides add to the alkyne functionality of (**188**) giving complex (**189**) which in turn may react with butylamine to give addition across the isocyanide group.[211]



(189) (190)

## W. SILANES AND STANNANES

Clusters consisting of silane ligands, on a triosmium chain $[Os_3(CO)_{12}(SiRCl_2)]$ (**191**), and on an osmium triangle $[Os_3H_3(CO)_9(SiRCl_1)_3]$ (**192**) (R = Cl,Me) have been prepared from silanes and $[Os_3(CO)_{12}]$ (**1**).[212–214] Triphenylsilane and $[Os_3H_2(CO)_{10}]$ (**9**) react to form a cluster with an osmium–osmium multiple bond.[149,†]



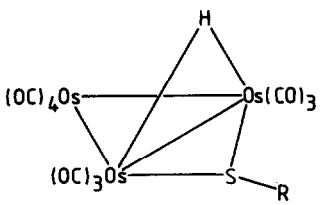
(193)

The reactivity of this cluster is of current interest. Triphenylsilane displaces only one acetonitrile from $[Os_3(CO)_{10}(NCMe)_2]$ (**7**) affording $[Os_3H(CO)_{10}(NCMe)(SiPh_3)]$ (**194**); the nitrile ligand of this complex can be displaced by other ligands (see Section M(ii)).[149]

Trimethylstannane displaces a carbonyl ligand from $[Os_3(CO)_8S(SCH_2)(PMePh)]$ (**111**) to form a substitution product $[Os_3H(CO)_7S(SCH_2)(PMe_2Ph)(SnMe_3)]$ (**195**).[215]

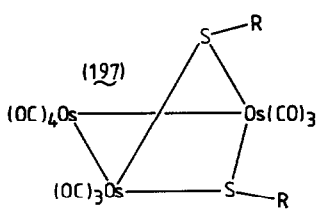
## X. THIOLS, SULPHIDES AND DISULPHIDES

The sulphur–aryl bond is cleaved in preference to the sulphur–alkyl bond just as in similar reactions of phosphines (Section V(ii)).



(196)

Disulphides react with $[Os_3(CO)_{10}(NCMe)_2]$ (**7**) to form open osmium triangles in which the long edge is bridged by two sulphur atoms.[218]

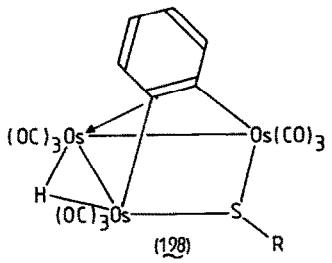


(197)

†See also Ref. 222.

*Exo* and *endo* isomerism of the R groups relative to the metal triangle has been observed by NMR.

Alkylphenylsulphides react with $[Os_3(CO)_{12}]$ (1) to give an aryne cluster.[219]




(198)

The sulphur-aryl bond is cleaved in preference to the sulphur-alkyl bond just as in similar reactions of phosphines (Section V(ii)).

*Acknowledgements*—I would like to acknowledge the help and advice given to me by Professor Sir Jack Lewis, F.R.S., Dr. Paul R. Raithby and Dr. B.F.G. Johnson throughout my stay at Cambridge. I would also like to thank ICI/SERC for financial support.

## Y. REFERENCES

1. B. F. G. Johnson, J. Lewis and D. A. Pippard, *J. Organomet. Chem.* 1978, **160**, 263.
2. B. F. G. Johnson, J. Lewis and P. A. Kilty, *J. Chem. Soc.* (*A*) 1968, 2859.
3. C. W. Bradford and R. S. Nyholm, *J. Chem. Soc. Chem. Commun.* 1967, 384.
4. C. E. Housecroft, M. E. O'Neill, K. Wade and B. C. Smith, *J. Organomet. Chem.* 1981, **213**, 35.
5. H. D. Kaesz, C. B. Knobler, M. A. Andrews, G. van Buskirk, R. Szostak, C. E. Strouse, Y. C. Lin and A. Mayr, *Pure Appl. Chem.* 1982, **54**, 131.
6. C. R. Eady, B. F. G. Johnson, J. Lewis and M. C. Maeatesta, *J. Chem. Soc. Dalton Trans.* 1978, 1358.
7. R. E. Stevens, T. J. Yanta and W. L. Gladfelter, *J. Am. Chem. Soc.* 1981, **103**, 4981.
8. Y. Shvo and E. Hazum, *J. Chem. Soc. Chem. Commun.* 1974, 336.
9. B. F. G. Johnson, J. Lewis and D. A. Pippard, *J. Organomet. Chem.* 1978, **145**, C4.
10. B. F. G. Johnson, J. Lewis and D. A. Pippard, *J. Chem. Soc. Dalton Trans.* 1981, 407.
11. K. Burgess, B. F. G. Johnson, J. Lewis and P. R. Raithby, *J. Chem. Soc. Dalton Trans.* 1982, 2085.
12. M. Tachikawa and J. R. Shapley, *J. Organomet. Chem.* 1977, **124**, C19.
13. M. I. Bruce, D. C. Kehoe, J. G. Matisons, B. K. Nicholson, P. H. Rieger and M. L. Williams, *J. Chem. Soc. Chem. Commun.* 1982, 442.
14. B. F. G. Johnson, J. Lewis and P. A. Kilty, *J. Chem. Soc.* (*A*) 1968, 2859.
15. S. A. R. Knox, J. W. Koepke, M. A. Andrews and H. D. Kaesz, *J. Am. Chem. Soc.* 1975, **97**, 3942.
16. A. J. Deeming and S. Hasso, *J. Organomet. Chem.* 1975, **88**, C21.
17. A. J. Deeming and S. Hasso, *J. Organomet. Chem.* 1976, **114**, 313.
18. J. R. Shapley, J. B. Keister, M. R. Churchill and B. G. DeBoer, *J. Am. Chem. Soc.* 1975, **97**, 4145.
19. M. R. Churchill and B. G. DeBoer, *Inorg. Chem.* 1977, **16**, 2397.
20. J. B. Keister and J. R. Shapley, *Inorg. Chem.* 1982, **21**, 3304.
21. S. Bhaderi, B. F. G. Johnson, J. Lewis, D. J. Watson and C. Zuccaro, *J. Chem. Soc. Chem. Commun.* 1977, 477.
22. S. Bhaderi, B. F. G. Johnson, J. Lewis, D. J. Watson and C. Zuccaro, *J. Chem. Soc. Dalton Trans.* 1979, 557.
23. B. F. G. Johnson, J. Lewis, D. A. Pippard and P. R. Raithby, *J. Chem. Soc. Chem. Commun.* 1978, 551.
24. B. F. G. Johnson, J. Lewis and D. A. Pippard, *J. Organomet. Chem.* 1981, **213**, 249.
25. J. Evans, S. J. Okrasinski, A. J. Pribula and J. R. Norton, *J. Am. Chem. Soc.* 1976, **98**, 4000.
26. W. J. Carter, J. W. Kelland, S. J. Okrasinski, K. E. Warner and J. R. Norton, *Inorg. Chem.* 1982, **21**, 3955.
27. K. A. Azam, A. J. Deeming, I. P. Rothwell, M. B. Hursthouse and L. New, *J. Chem. Soc. Chem. Commun.* 1978, 1086.
28. K. A. Azam, A. J. Deeming, R. E. Kimber and P. R. Shukla, *J. Chem. Soc. Dalton Trans.* 1976, 1853.
29. K. A. Azam, C. C. Yin and A. J. Deeming, *J. Chem. Soc. Dalton Trans.* 1978, 1201.
30. E. G. Bryan, B. F. G. Johnson and J. Lewis, *J. Chem. Soc. Dalton Trans.* 1977, 1328.
31. V. F. Allen, R. Mason and P. B. Hitchcock, *J. Organomet. Chem.* 1977, **140**, 297.

32. K. Burgess and M. A. Pearsall, Unpublished results.
33. A. J. Arce, A. J. Deeming and R. Shaunak, *J. Chem. Soc. Dalton Trans.* 1983, 1023.
34. S. Aime, L. Milone and A. J. Deeming, *J. Chem. Soc. Chem. Commun.* 1980, 1168.
35. S. Aime and A. J. Deeming, *J. Chem. Soc. Dalton Trans.* 1981, 828.
36. A. J. Deeming, M. B. Hursthouse and J. D. J. Backer-Dirks, *J. Chem. Soc. Dalton Trans.* 1982, 1625.
37. S. Aime, A. Tiripicchio, M. T. Camellini and A. J. Deeming, *Inorg. Chem.* 1981, **20**, 2027.
38. K. A. Azam, A. J. Deeming and I. P. Rothwell, *J. Organomet. Chem.* 1978, **178**, C20.
39. K. A. Azam, A. J. Deeming and I. P. Rothwell, *J. Chem. Soc. Dalton Trans.* 1981, 91.
40. B. F. G. Johnson, J. Lewis, T. I. Odiaka and P. R. Raithby, *J. Organomet. Chem.* 1981, **216**, C56.
41. K. A. Azam and A. J. Deeming, *J. Mol. Cat.* 1977, **3**, 207.
42. E. Sappa, G. Cetini, O. Gambino and M. Valle, *J. Organomet. Chem.* 1969, **20**, 201.
43. C. E. Anson, B. T. Keiller, I. A. Oxton, B. B. Powell and N. Sheppard, *J. Chem. Soc. Chem. Commun.* 1983, 470.
44. J. R. Andrews, S. F. A. Kettle, D. B. Powell and N. Sheppard, *Inorg. Chem.*, in press.
45. J. Evans and G. S. McNulty, *J. Chem. Soc. Dalton Trans.* 1983, 639.
46. I. A. Oxton, *Rev. Inorg. Chem.* 1982, **4**, 1.
47. J. B. Keister and J. R. Shapley, *J. Am. Chem. Soc.* 1976, **98**, 1056.
48. R. P. Ferrari and G. A. Vaglio, *Inorg. Chim. Acta* 1976, **20**, 141.
49. R. P. Ferrari, G. A. Vaglio and M. Valle, *Inorg. Chim. Acta* 1978, **31**, 177.
50. J. Lewis and B. F. G. Johnson, *Gazz. Chim. Ital.* 1979, **109**, 271.
51. J. R. Shapley, S. I. Richter, M. Tachikawa and J. B. Keister, *J. Organomet. Chem.* 1975, **94**, C43.
52. A. J. Deeming, S. Hasso and M. Underhill, *J. Chem. Soc. Dalton Trans.* 1975, 1614.
53. J. B. Keister and J. R. Shapley, *J. Organomet. Chem.* 1975, **85**, C29.
54. A. J. Deeming, S. Hasso, M. Underhill, A. J. Canty, B. F. G. Johnson, W. G. Jackson, J. Lewis and T. W. Matheson, *J. Chem. Soc. Chem. Commun.* 1974, 807.
55. W. G. Jackson, B. F. G. Johnson and J. Lewis, *J. Organomet. Chem.* 1977, **139**, 125.
56. R. Jackson, B. F. G. Johnson, J. Lewis, P. R. Raithby and S. W. Sankey, *J. Organomet. Chem.* 1980, **193**, C1.
57. A. J. Deeming and M. Underhill, *J. Chem. Soc. Dalton Trans.* 1974, 1415.
58. W. G. Jackson, B. F. G. Johnson and J. Lewis, *J. Organomet. Chem.* 1975, **90**, C13.
59. J. Evans, B. F. G. Johnson, J. Lewis and T. W. Matheson, *J. Organomet. Chem.* 1975, **97**, C16.
60. A. J. Deeming, *J. Organomet. Chem.* 1978, **150**, 123.
61. A. J. Deeming and M. Underhill, *J. Chem. Soc. Chem. Commun.* 1973, 277.
62. A. J. Canty, B. F. G. Johnson and J. Lewis, *J. Organomet. Chem.* 1972, **43**, C35.
63. A. J. Canty, A. J. P. Domingos, B. F. G. Johnson and J. Lewis, *J. Chem. Soc. Dalton Trans.* 1973, 2056.
64. B. F. G. Johnson, J. Lewis, P. R. Raithby and S. W. Sankey, *J. Organomet. Chem.* 1982, **231**, C65.
65. E. G. Bryan, B. F. G. Johnson, J. W. Kelland, J. Lewis and M. McPartlin, *J. Chem. Soc. Chem. Commun.* 1976, 254.
66. E. G. Bryan, B. F. G. Johnson and J. Lewis, *J. Chem. Soc. Dalton Trans.* 1977, 144.
67. R. P. Ferrari and G. A. Vaglio, *J. Organomet. Chem.* 1979, **182**, 245.
68. S. Aime, *Inorg. Chim. Acta* 1982, **62**, 51.
69. E. G. Bryan, B. F. G. Johnson and J. Lewis, *J. Organomet. Chem.* 1976, **122**, 249.
70. M. Tachikawa, J. R. Shapley, R. C. Haltiwanger and C. G. Pierpont, *J. Am. Chem. Soc.* 1976, **98**, 4651.
71. C. G. Pierpont, *Inorg. Chem.* 1978, **17**, 1976.
72. M. Tachikawa, S. I. Richter and J. R. Shapley, *J. Organomet. Chem.* 1977, **128**, C9.
73. R. Goudsmidt, B. F. G. Johnson, J. Lewis, P. R. Raithby and M. J. Rosales, *J. Chem. Soc. Dalton Trans.* 1983, 2257.
74. J. B. Keister and J. R. Shapley, *J. Am. Chem. Soc.* 1976, **98**, 1056.
75. M. Tachikawa, J. R. Shapley and C. G. Pierpont, *J. Am. Chem. Soc.* 1975, **97**, 7172.
76. A. D. Clauss, M. Tachikawa, J. R. Shapley and C. G. Pierpont, *Inorg. Chem.* 1981, **20**, 1528.
77. O. Gambino, G. A. Vaglio, R. P. Ferrari and G. Cetini, *J. Organomet. Chem.* 1971, **30**, 381.
78. R. P. Ferrari, G. A. Vaglio, O. Gambino, M. Valle and G. Cetini, *J. Chem. Soc. Dalton Trans.* 1972, 1998.
79. G. A. Vaglio, O. Gambino, R. P. Ferrari and G. Cetini, *Inorg. Chim. Acta* 1973, **7**, 193.
80. G. Ferraris and G. Gervasio, *J. Chem. Soc. Dalton Trans.* 1973, 1933.
81. G. Ferraris and G. Gervasio, *J. Chem. Soc. Dalton Trans.* 1974, 1813.
82. R. P. Ferrari and G. A. Vaglio, *Gazz. Chim. Ital.* 1975, **105**, 939.
83. C. G. Pierpont, *Inorg. Chem.* 1977, **16**, 636.
84. G. Ferraris and G. Gervasio, *J. Chem. Soc. Dalton Trans.* 1972, 1057.
85. A. J. Deeming, S. Hasso, and M. Underhill, *J. Organomet. Chem.* 1974, **80**, C53.
86. W. G. Jackson, B. F. G. Johnson, J. W. Kelland, J. Lewis and K. T. Schorpp, *J. Organomet. Chem.* 1975, **87**, C27.

87. R. P. Ferrari and G. A. Vaglio, *Gazz. Chim. Ital.* 1975, **105**, 939.
88. S. C. Brown and J. Evans, *J. Chem. Soc. Dalton Trans.* 1982, 1049.
89. A. G. Orpen, A. V. Rivera, E. G. Bryan, D. Pippard, G. M. Sheldrick and K. D. Rouse, *J. Chem. Soc. Chem. Commun.* 1978, 723.
90. J. J. Guy, B. E. Reichert and G. M. Sheldrick, *Acta Cryst.* 1976, **B32**, 3319.
91. J. Evans, B. F. G. Johnson, J. Lewis and T. W. Matheson, *J. Organomet. Chem.* 1975, **97**, C16.
92. B. E. Hanson, B. F. G. Johnson, J. Lewis and P. R. Raithby, *J. Chem. Soc. Dalton Trans.* 1980, 1852.
93. O. Gambino, R. P. Ferarri, M. Chinone and G. A. Vaglio, *Inorg. Chim. Acta* 1975, **12**, 155.
94. G. Gervasio, S. Aime, L. Milone, E. Sappa and M. Franchini-Angela, *Transition Met. Chem.* 1976, **1**, 96.
95. W. G. Jackson, B. F. G. Johnson, J. W. Kelland, J. Lewis and K. T. Schorpp, *J. Organomet. Chem.* 1975, **88**, C17.
96. M. R. Churchill, R. A. Lashewycz, M. Tachikawa and J. R. Shapley, *J. Chem. Soc. Chem. Commun.* 1977, 699.
97. M. R. Churchill and R. A. Lashewycz, *Inorg. Chem.* 1978, **17**, 1291.
98. M. R. Churchill and R. A. Lashewycz, *Inorg. Chem.* 1979, **18**, 156.
99. M. Laing, P. Sommerville, Z. Dawoodi, M. J. Mays and P. J. Wheatley, *J. Chem. Soc. Chem. Commun.* 1978, 1035.
100. Z. Dawoodi, M. J. Mays and P. R. Raithby, *J. Chem. Soc. Chem. Commun.* 1979, 721.
101. Z. Dawoodi, M. J. Mays and P. R. Raithby, *J. Chem. Soc. Chem. Commun.* 1980, 641.
102. K. Burgess, H. D. Holden, B. F. G. Johnson and J. Lewis, *J. Chem. Soc. Dalton Trans.* 1983, 1199.
103. A. J. Deeming and R. Peters, *J. Organomet. Chem.* 1980, **202**, C39.
104. A. Mayr, Y. C. Lin, N. M. Boag and H. D. Kaesz, *Inorg. Chem.* 1982, **21**, 1704.
105. A. J. Arce and A. J. Deeming, *J. Chem. Soc. Chem. Commun.* 1980, 1102.
106. C. C. Yin and A. J. Deeming, *J. Chem. Soc. Dalton Trans.* 1974, 1013.
107. K. A. Azam, A. J. Deeming, I. P. Rothwell, M. B. Hursthouse and J. D. J. Backer-Dirks, *J. Chem. Soc. Dalton Trans.* 1981, 2039.
108. C. C. Yin and A. J. Deeming, *J. Organomet. Chem.* 1977, **133**, 123.
109. J. R. Shapley, M. Tachikawa, M. R. Churchill and R. A. Lashewycz, *J. Organomet. Chem.* 1978, **162**, C39.
110. M. R. Churchill and R. A. Lashewycz, *Inorg. Chem.* 1979, **18**, 848.
111. Van K. Dehnicke and R. Dubgen, *Z. Anorg. Allg. Chem.* 1978, **44**, 61.
112. K. Burgess, B. F. G. Johnson, J. Lewis and P. R. Raithby, *J. Organomet. Chem.* 1982, **224**, C40.
113. K. Burgess, B. F. G. Johnson, J. Lewis and P. R. Raithby, *J. Chem. Soc. Dalton Trans.* 1982, 2119.
114. B. F. G. Johnson, J. Lewis, P. R. Raithby and S. W. Sankey, *J. Organomet. Chem.* 1982, **228**, 135.
115. M. R. Churchill, F. J. Hollander, J. R. Shapley and J. B. Keister, *Inorg. Chem.* 1980, **19**, 1272.
116. B. F. G. Johnson, J. Lewis, P. R. Raithby, G. M. Sheldrick and G. Suss, *J. Organomet. Chem.* 1978, **162**, 179.
117. R. L. Pruett, R. C. Schoening, J. L. Vidal and R. A. Fiato, *J. Organomet. Chem.* 1979, **182**, C57.
118. B. F. G. Johnson, R. L. Kelly, J. Lewis and J. R. Thornback, *J. Organomet. Chem.* 1980, **190**, C91.
119. R. C. Schoening, J. L. Vidal and R. A. Fiato, *J. Organomet. Chem.* 1981, **206**, C43.
120. G. R. Steinmetz and G. L. Geoffroy, *J. Am. Chem. Soc.* 1981, **103**, 1278.
121. C. M. Jensen, T. J. Lynch, C. B. Knobler and H. D. Kaesz, *J. Am. Chem. Soc.* 1982, **104**, 4679.
122. J. B. Keister, *J. Chem. Soc. Chem. Commun.* 1979, 214.
123. P. D. Gavens and M. J. Mays, *J. Organomet. Chem.* 1978, **162**, 389.
124. J. B. Keister, M. W. Payne and M. J. Muscatella, *Organometallics* 1983, **2**, 219.
125. J. R. Shapley, M. E. Cree-Uchiyama and G. M. St George, *J. Am. Chem. Soc.* 1983, **105**, 140.
126. C. E. Kampe, N. M. Boag and H. D. Kaesz, *J. Am. Chem. Soc.* 1983, **105**, 2896.
127. R. D. Adams, D. A. Katahira and J. P. Selegue, *J. Organomet. Chem.* 1981, **213**, 259.
128. P. V. Broadhurst, B. F. G. Johnson, J. Lewis and P. R. Raithby, *J. Organomet. Chem.* 1980, **194**, C35.
129. P. V. Broadhurst, B. F. G. Johnson, J. Lewis and P. R. Raithby, *J. Chem. Soc. Dalton Trans.* 1982, 1641.
130. P. V. Broadhurst, B. F. G. Johnson, J. Lewis, A. G. Orpen, P. R. Raithby and J. R. Thornback, *J. Organomet. Chem.* 1980, **187**, 141.
131. R. D. Adams and N. M. Golembeski, *J. Am. Chem. Soc.* 1979, **101**, 1306.
132. R. D. Adams, N. M. Golembeski and J. P. Selegue, *J. Am. Chem. Soc.* 1981, **103**, 546.
133. R. D. Adams and J. P. Selegue, *J. Organomet. Chem.* 1980, **195**, 223.
134. R. D. Adams, N. M. Golembeski and J. P. Selegue, *J. Am. Chem. Soc.* 1979, **101**, 5862.
135. R. D. Adams, N. M. Golembeski and J. P. Selegue, *J. Organomet. Chem.* 1980, **193**, C7.
136. R. D. Adams, N. M. Golembeski and J. P. Selegue, *Organometallics* 1982, **1**, 240.
137. G. C. R. Crooks, B. F. G. Johnson, J. Lewis, I. G. Williams and G. Gamlen, *J. Chem. Soc.* (*A*) 1969, 2761.
138. K. A. Azam and A. J. Deeming, *J. Chem. Soc. Chem. Commun.* 1977, 472.

139. J. R. Shapley, G. M. St George, M. R. Churchill and F. J. Hollander, *Inorg. Chem.* 1982, **21**, 3295.
140. K. Burgess, B. F. G. Johnson, J. Lewis and P. R. Raithby, *J. Chem. Soc. Dalton Trans.* 1982, 263.
141. M. R. Churchill and H. J. Wasserman, *Inorg. Chem.* 1981, **20**, 2905.
142. J. R. Shapley, Personal communication.
143. R. B. Calvert and J. R. Shapley, *J. Am. Chem. Soc.* 1977, **99**, 5225.
144. R. B. Calvert and J. R. Shapley, *J. Am. Chem. Soc.* 1978, **100**, 6544.
145. R. B. Calvert and J. R. Shapley, *J. Am. Chem. Soc.* 1978, **100**, 7726.
146. R. B. Calvert, J. R. Shapley, A. J. Schultz, J. M. Williams, S. L. Suib and G. D. Stucky, *J. Am. Chem. Soc.* 1978, **100**, 6240.
147. D. E. Sherwood and M. B. Hall, *Inorg. Chem.* 1982, **21**, 3458.
148. J. B. Keister and T. L. Horling, *Inorg. Chem.* 1980, **19**, 2304.
149. K. Burgess, Unpublished results.
150. J. R. Shapley, A. C. Sievert, M. R. Churchill and H. J. Wasserman, *J. Am. Chem. Soc.* 1981, **103**, 6975.
151. A. C. Sievert, D. S. Strickland, J. R. Shapley, G. R. Steinmetz and G. L. Geoffroy, *Organometallics* 1982, **1**, 214.
152. J. R. Shapley, D. S. Strickland and G. M. St George, *Organometallics* 1983, **2**, 185.
157. A. D. Clauss, J. R. Shapley and S. R. Wilson, *J. Am. Chem. Soc.* 1981, **103**, 7387.
154. M. R. Churchill and H. J. Wasserman, *Inorg. Chem.* 1981, **20**, 1580.
155. A. P. Humphries and S. A. R. Knox, *J. Chem. Soc. Dalton Trans.* 1975, 1710.
156. R. M. Wexler, M. C. Tsai, C. M. Friend and E. L. Muetterties, *J. Am. Chem. Soc.* 1982, **104**, 2034.
157. B. A. Monow, I. A. Cody, L. E. Moran and R. Palepu, *J. Catal.* 1976, **44**, 467.
158. C. C. Yin and A. J. Deeming, *J. Chem. Soc. Dalton Trans.* 1982, 2563.
159. J. R. Shapley, D. E. Samkoff, C. Bueno and M. R. Churchill, *Inorg. Chem.* 1982, **21**, 634.
160. K. Burgess, B. F. G. Johnson and J. Lewis, *J. Organomet. Chem.* 1982, **233**, C55.
161. A. J. Deeming, R. Peters, M. B. Hursthouse and J. D. J. Backer-Dirks, *J. Chem. Soc. Dalton Trans.* 1982, 1205.
162. C. C. Yin and A. J. Deeming, *J. Chem. Soc. Dalton Trans.* 1975, 2091.
163. A. J. Deeming, R. Peters, M. B. Hursthouse and J. D. J. Backer-Dirks, *J. Chem. Soc. Dalton Trans.* 1982, 787.
164. F. A. Cotton and B. E. Hanson, *Inorg. Chem.* 1977, **16**, 2820.
165. G. Suss-Fink, *Z. Naturforsch* 1980, **35b**, 454.
166. G. S. Fink, L. Kahn and P. R. Raithby, *J. Organomet. Chem.* 1982, **228**, 179.
167. R. D. Adams and J. P. Selegue, *Inorg. Chem.* 1980, **19**, 1791.
168. R. D. Adams and N. M. Golembeski, *Inorg. Chem.* 1978, **17**, 1969.
169. R. D. Adams and N. M. Golembeski, *J. Organomet. Chem.* 1979, **172**, 239.
170. R. D. Adams and J. P. Selegue. *Inorg. Chem.* 1980, **19**, 1795.
171. A. J. Deeming, I. Ghatak, D. W. Owen and R. Peters, *J. Chem. Soc. Chem. Commun.* 1982, 392.
172. K. Burgess, B. F. G. Johnson and J. Lewis, *J. Chem. Soc. Dalton Trans.* 1983, 1179.
173. Y. C. Lin, C. B. Knobler and H. D. Kaesz, *J. Am. Chem. Soc.* 1981, **103**, 1216.
174. R. D. Adams and N. M. Golembeski, *J. Organomet. Chem.* 1979, **171**, C21.
175. R. D. Adams, N. M. Golembeski and J. P. Selegue, *Inorg. Chem.* 1981, **20**, 1242.
176. R. D. Adams and Z. Dawoodi, *J. Am. Chem. Soc.* 1981, **103**, 6510.
177. M. J. Mays and P. D. Gavens, *J. Chem. Soc. Dalton Trans.* 1980, 911.
178. R. D. Adams and N. M. Golembeski, *Inorg. Chem.* 1979, **18**, 1909.
179. R. D. Adams and N. M. Golembeski, *J. Am. Chem. Soc.* 1979, **101**, 2579.
180. R. D. Adams and N. M. Golembeski, *J. Am. Chem. Soc.* 1978, **100**, 4622.
181. R. D. Adams and N. M. Golembeski, *Inorg. Chem.* 1979, **18**, 2255.
182. P. A. Dawson, B. F. G. Johnson, J. Lewis, J. Puga, P. R. Raithby and M. J. Rosales, *J. Chem. Soc. Dalton Trans.* 1982, 233.
183. Z. Dawoodi, M. J. Mays and P. R. Raithby, *J. Organomet. Chem.* 1981, **219**, 103.
184. R. D. Adams, D. A. Katahira and L. W. Yang, *J. Organomet. Chem.* 1981, **219**, 85.
185. Z. Dawoodi, M. J. Mays and A. G. Orpen, *J. Organomet. Chem.* 1981, **219**, 251.
186. R. D. Adams, D. A. Katahira and L. W. Yang, *J. Organomet. Chem.* 1981, **219**, 241.
187. J. Banford, Z. Dawoodi, K. Hendrick and M. J. Mays, *J. Chem. Soc. Chem. Commun.* 1982, 554.
188. A. J. Deeming, B. F. G. Johnson and J. Lewis, *J. Chem. Soc. (A)* 1970, 897.
189. F. Iwasaki, M. J. Mays, P. R. Raithby, P. L. Taylor and P. J. Wheatley, *J. Organomet. Chem.* 1981, **213**, 185.
190. S. C. Tripathi, S. C. Srivastava, R. P. Mani and A. K. Shrimal, *Inorg. Chim. Acta* 1975, **15**, 249.
191. K. Natarajan, L. Zsolnai and G. Huttner, *J. Organomet. Chem.* 1981, **220**, 365.
192. B. F. G. Johnson, J. Lewis, B. E. Reichert and K. J. Schropp, *J. Chem. Soc. Dalton Trans.* 1976, 1403.

193. E. Band and E. L. Muetterties, *Chem. Rev.* 1978, **78**, 639.
194. E. W. Ainscough, T. A. James, S. D. Robinson and J. N. Wingfield, *J. Chem. Soc. Dalton Trans.* 1974, 2384.
195. A. J. Deeming and S. Hasso, *J. Organomet. Chem.* 1976, **112**, C39.
196. M. R. Churchill, B. G. DeBoer, J. R. Shapley and J. B. Keister, *J. Am. Chem. Soc.* 1976, **98**, 2357.
197. M. R. Churchill and B. G. DeBoer, *Inorg. Chem.* 1977, **16**, 1141.
198. A. J. Deeming and M. Underhill, *J. Chem. Soc. Dalton Trans.* 1973, 2727.
199. C. W. Bradford, R. S. Nyholm, G. J. Gainsford, J. M. Guss, P. R. Ireland and R. Mason, *J. Chem. Soc. Chem. Commun.* 1972, 87.
200. G. J. Gainsford, J. M. Guss, P. R. Ireland and R. Mason, *J. Organomet. Chem.* 1972. **40**, C70.
201. C. W. Bradford and R. S. Nyholm, *J. Chem. Soc. Dalton Trans.* 1973, 529.
202. A. J. Deeming, R. S. Nyholm and M. Underhill, *J. Chem. Soc. Chem. Commun.* 1972, 224.
203. A. J. Deeming, R. E. Kimber and M. Underhill, *J. Chem. Soc. Dalton Trans.* 1973, 2589.
204. A. J. Deeming, I. P. Rothwell, M. B. Hursthouse and J. D. J. Backer-Dirks, *J. Chem. Soc. Dalton Trans.* 1981, 1879.
205. A. J. Arce and A. J. Deeming, *J. Chem. Soc. Dalton Trans.* 1982, 1155.
206. S. C. Brown and J. Evans, *J. Chem. Soc. Chem. Commun.* 1980, 1021.
207. A. J. Deeming and M. Underhill, *J. Organomet. Chem.* 1972, **42**, C60.
208. C. J. Cooksey, A. J. Deeming and I. P. Rothwell, *J. Chem. Soc. Dalton Trans.* 1981, 1718.
209. A. J. Carty, *Pure Appl. Chem.* 1982, **54**, 113.
210. A. J. Carty, S. A. Maclaughlin and N. J. Taylor, *J. Organomet. Chem.* 1981, **204**, C27.
211. S. A. Maclaughlin, J. P. Johnson, N. J. Taylor, A. J. Carty and E. Sappa, *Organometallics* 1983, **2**, 352.
212. G. N. van Buuren, A. C. Willis, F. W. B. Einstein, L. K. Peterson, R. K. Pomeroy and D. Sutton, *Inorg. Chem.* 1981, **20**, 4361.
213. A. C. Willis, G. N. van Buuren, R. K. Pomeroy and F. W. B. Einstein, *Inorg. Chem.* 1983, **22**, 1162.
214. R. K. Pomeroy, *J. Organomet. Chem.* 1981, **221**, 323.
215. R. D. Adams and D. A. Katahira, *Organometallics* 1982, **1**, 460.
216. G. R. Crooks, B. F. G. Johnson, J. Lewis and I. G. Williams, *J. Chem. Soc.* (*A*) 1969, 797.
217. A. J. Deeming, B. F. G. Johnson and J. Lewis, *J. Chem. Soc.* (*A*) 1970, 2517.
218. P. V. Broadhurst, Ph.D. Thesis. Cambridge (1982).
219. R. D. Adams, D. A. Katahira and L. W. Yang, *Organometallics* 1982, **1**, 235.
220. E. C. Bryan, W. G. Jackson, B. F. G. Johnson, J. W. Kelland, J. Lewis and K. T. Schorpp, *J. Organomet. Chem.* 1976, **108**, 385.
221. A. J. Deeming, S. Hasso, M. Underhill, A. J. Canty, B. F. G. Johnson, W. G. Jackson, J. Lewis and T. W. Matheson, *J. Chem. Soc. Chem. Commun.* 1974, 807.
222. A. C. Willis, F. W. B. Einstein, R. M. Ramadan and R. K. Pomeroy, *Organometallics* 1983, **2**, 935.
223. K. Burgess, *J. Chem. Soc. Dalton Trans.*, in press.

*Polyhedron* Vol. 3, No. 11, pp. 1227–1231, 1984
Printed in the U.S.A.

0277–5387/84 $3.00 + .00
© 1984 Pergamon Press Ltd.

# METAL COMPLEXES OF MERCAPTOAMINES—II

## NEW ASSIGNMENT OF THE STRUCTURE OF *BIS*(β-MERCAPTOETHYLAMINE)NICKEL(II) AND RELATED COMPOUNDS

**J. SUADES***
Departament de Química Inorgànica, Universitat Autònoma de Barcelona, Barcelona, Spain

**and**

**X. SOLANS and M. FONT-ALTABA**
Departament de Cristallografia i, Mineralogia, Universitat de Barcelona, Barcelona, Spain

(*Received* 1 *November* 1983; *accepted* 10 *January* 1984)

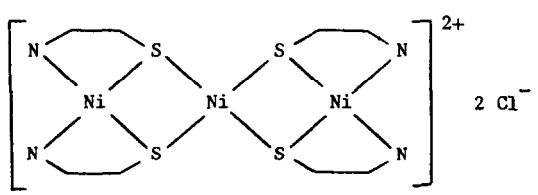
**Abstract**—A *cis*-geometry was proposed for the green complex *bis*(β-mercaptoethylamine)nickel(II) on the basis of its reactivity, IR spectroscopy and orbital geometry considerations. The crystal and molecular structure of this complex has been determined by X-ray diffraction and shows that the complex has a *trans* geometry. The crystal structure consists of *trans*-$NiL_2$ molecules strongly linked through NH–S hydrogen bonds. Electronic and IR spectroscopy, and powder X-ray analysis are in agreement with the same *trans* geometry for the complexes *bis*(β-mercaptoethylamine)palladium(II) and *bis*-(γ-mercaptopropylamine)nickel(II). As a result of the new assignment of the structure of these complexes some concepts, such as its reactivity with nickel(II), are reconsidered.

The green complex *bis*(β-mercaptoethylamine)-nickel(II) was first prepared by Jensen.[1] Some years later, Jicha and Busch[2,3] studied the behaviour of the β-mercaptoethylamine (MEA=$NH_2$–$CH_2$–$CH_2$–$S^-$) as a ligand. These investigators determined the magnetic moment of $Ni(MEA)_2$ and found it to be diamagnetic, so the configuration around the nickel atom has to be square-planar.

Two isomers, *cis* and *trans* might be expected for the complex $Ni(MEA)_2$ with square planar Ni(II). Although experimental conditions were changed no evidence of such isomerism was observed, and the methods usually employed in the separation of geometrical isomers were impracticable in view of the very slight solubility of $Ni(MEA)_2$.

Jicha and Busch suggested a *cis* isomer structure for the compounds $M(MEA)_2$ (M=Ni, Pd) and *facial* for $Co(MEA)_3$ on the basis of the pi-bonding tendencies of the donor atoms and the symmetry of the appropriate central atom *d* orbitals.[2] Moreover, these authors obtained another complex with MEA of stoichiometry $[Ni_3(MEA)_4]Cl_2$ and they suggested the structure (I) for this compound. This structure was corroborated by an X-ray diffraction study.[4]

(I)




The trinuclear nickel(II) complex was synthesized from the neutral $Ni(MEA)_2$ complex by reaction with a Ni(II) salt:[2]

$$2\,Ni(MEA)_2 + Ni(II) \rightarrow [Ni_3(MEA)_4]^{2+}.$$

This reaction was generalized by the use of different metal salts, and heterometallic trinuclear complexes were obtained:[2]

$$2\,Ni(MEA)_2 + M(II) \rightarrow [M(Ni(MEA)_2)_2]^{2+}.$$

*Author to whom correspondence should be addressed.

In view of all those results, it is reasonable to think that the *cis* orientation of the ligands is required in the $Ni(MEA)_2$ complex.

On the other hand, the structure of the brown complex $Ni(MEDMA)_2$[5] (MEDMA=$S^-$–$CH_2$–$CH_2$–$N(CH_3)_2$) was determined by X-ray diffraction,[6] and the $NiS_2N_2$ skeleton is *trans*-planar. This different behaviour between MEA and MEDMA was attributed to the steric requirements of methyl groups.[5]

Far-IR spectra of the complexes $M(MEA)_2$, $M(MEDMA)_2$ (M=Ni, Pd) and $Ni(MPA)_2$ was studied by Schläpfer and Nakamoto[7] using isotope substitution of the metal and the amino group. They also proposed a *cis* structure for the $M(MEA)_2$ and $Ni(MPA)_2$ complexes, and a *trans* structure for $M(MEDMA)_2$(MPA=$S^-$–$CH_2$–$CH_2$–$CH_2$–$NH_2$).

We are interested in the study of mercaptoamines[8] as ligands, and our work with the $NiL_2$ (L=MEA, MPA) complexes has shown that some physical and chemical properties of those complexes could be explained better with another structure. It seemed to us that the solution of the structure of one of these supposed *cis*-$NiL_2$ complexes could be interesting.

## EXPERIMENTAL

### *Preparations*

The synthesis of MPAh ligand (MPAh=$NH_2$–$(CH_2)_3$–SH) was reported earlier,[8,9] and MEAh · HCl (MEAh=$NH_2$–$(CH_2)_2$–SH) was supplied by Merck.

The $M(MEA)_2$ (M=Ni, Pd) complexes were prepared as previously described.[2] The $Ni(MPA)_2$ complex was prepared by adding an ethanolic solution of $Ni(ClO_4)_2$ to a thiolato solution of the ligand, in the molar ratio 1 : 3.

### *Preparation of single crystals of* $Ni(MEA)_2$

All those $ML_2$ compounds have very low solubilities. Single crystals were prepared by the slow diffusion method of aqueous solutions.

We used a H-shaped tube. In one arm was placed an aqueous solution of ammonia with solid $NiCl_2$ at the bottom. In the other one was placed water and solid MEAh–HCl. After a few days, single crystals were formed near the middle of the H-shaped tube.

### *X-ray data collection and reduction*

An equidimensional crystal (0.1 × 0.1 × 0.1 mm) was selected for crystal structure measurements and mounted on a Philips Pw-1100 four circle diffractometer. The unit cell was measured from 20 reflections within the range of $\theta$ angle 6–9°, $\omega$-scan technique and graphite monochromatized $MoK_\alpha$ radiation was used for intensity measurements. No absorption corrections were made.

### *Crystal data*

Formula $Ni(S–CH_2–CH_2–NH_2)_2$; Fw = 210.99; System = monoclinic; Space group = $P2_1/a$; $a = 7.298(1)$; $b = 10.290(2)$; $c = 4.864(1)$ Å; $\beta = 94.10(1)°$; $V = 364.3(2)$ Å$^3$; $Z = 2$; $F(000) = 220$: $\lambda(MoK_\alpha) = 0.71069$ Å; $\mu(MoK_\alpha) = 31.0$ cm$^{-3}$; measured intensities 905 (with $\theta \leqslant 32°$); observed intensities 887 (with $I \geqslant 2.5(I)$).

### *Structure solution and refinement*

The structure was determined by direct methods, using the MULTAN system of computer programs.[10] An E-map gave a set of peaks corresponding to all nonhydrogen atoms but with an incorrect origin, which was corrected with the TRADIR computer program.[11] Isotropic and anisotropic full-matrix refinements were carried out with the SHELX76 computer program.[12] A difference synthesis gave all hydrogen atoms which were refined with an overall isotropic temperature factor. The function minimized was $W\|F_0|-|F_c\|^2$, where $w = (\sigma^2(F_0) + 0.00946|F_0|^2)^{-1}$ and the final $R$ factor 0.050 ($Rw = 0.005$). Final atomic coordinates, thermal parameters and a list of $F_0/F_c$ values have been deposited with the Editor as supplementary data.†

### *Powder X-ray analysis*

Powder X-ray analysis of $Ni(MEA)_2$ and $Pd(MEA)_2$ compounds were carried out with a Philips PW-1310 diffractometer using $CuK_\alpha$ radiation ($\theta$ range 12–65°). Comparison between the two powder diffraction results show that the two compounds are isostructural. A refinement of cell-parameter from 30 diffraction peaks gave the following cell parameters: $Ni(MEA)_2$; $a = 7.307(6)$; $b = 10.295(12)$; $c = 4.871(4)$ Å; $\beta = 94.07(8)°$; $Pd(MEA)_2$, $a = 7.316(12)$, $b = 10.277(20)$, $c = 4.880(9)$ Å, $\beta = 93.87(26)°$.

## RESULTS AND DISCUSSION

### *Description of the structure*

Intramolecular bond lengths and bond angles are listed in Table 1. The numbering system employed is displayed in Fig. 1.

The crystal structure is made up of molecules of *trans* $Ni(MEA)_2$. The nickel atoms are placed on centres of symmetry at ($a/2$,0,0,0,$b/2$,0) and the molecules are linked by intermolecular N–H-----S

†Atomic coordinates have also been deposited with the Cambridge Crystallographic Data Centre.

Table 1. Intramolecular bond lengths (Å) and angles (Deg.)

| | | | |
|---|---|---|---|
| Ni - S | 2.159(1) | N - Ni - $S_{inner}$ | 90.8(1) |
| Ni - N | 1.868(3) | N - Ni - $S_{outer}$ | 89.2(1) |
| S - C(1) | 1.761(4) | C(1)-S-Ni | 96.9(1) |
| C(1)-C(2) | 1.523(6) | C(2)-C(1)-S | 108.2(3) |
| C(2)-N | 1.390(5) | N-C(2)-C(1) | 110.8(3) |
| C(1)-H(C1) | 0.97(6) | C(2)-N-Ni | 109.7(3) |
| C(1)-H(C1) | 0.87(6) | | |
| C(2)-H(C2) | 0.96(6) | | |
| C(2)-H(C2) | 0.91(6) | | |
| N - H(N) | 0.93(6) | | |
| N - H(N)' | 0.94(6) | | |

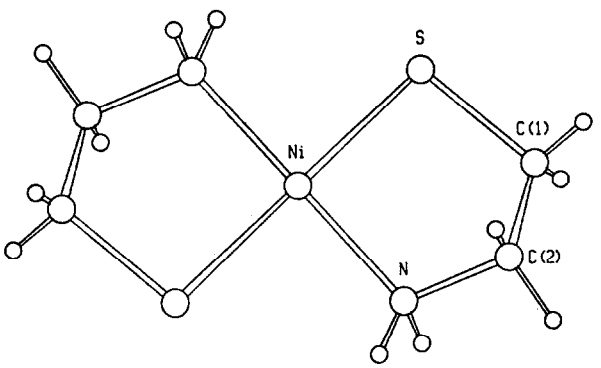



Fig. 1. A perspective view of $Ni(MEA)_2$ showing the numbering scheme.

hydrogen bonds, which essentially determine the packing of the structure. There are two NH-----S intermolecular hydrogen bonds (Table 2); one of them between the molecules of which the nickel atoms are situated on the same plane (001) (N–S = 3.367 Å), and another one between those planes (N–S = 3.427 Å) (Fig. 2). The hydrogen bond lengths are in good agreement with literature values (the average N–S distance in compounds with NH-----S hydrogen bonds is 3.4 Å).[13] The five-membered chelate ring shows an envelope form, where the C(2) atom deviates from the mean-plane defined by Ni, S, C, N.

Table 2. NH----S hydrogen bond distances and angles

| | N·····S(Å) | H·····S(Å) | NHS(deg.) |
|---|---|---|---|
| (inter) N-H(N)·····$S^{i}$ | 3.427(4) | 2.59(5) | 150.4(1) |
| (inter) N-H(N)'·····$S^{ii}$ | 3.367(4) | 2.57(5) | 145.8(1) |
| (intra) N-H(N)'·····$S^{iii}$ | 2.836(3) | 2.52(5) | 99.8(1) |

i= x + 1, -y, -z - 1
ii= -x + 3/2, y-½, -z
iii= -x + 1, -y, -z

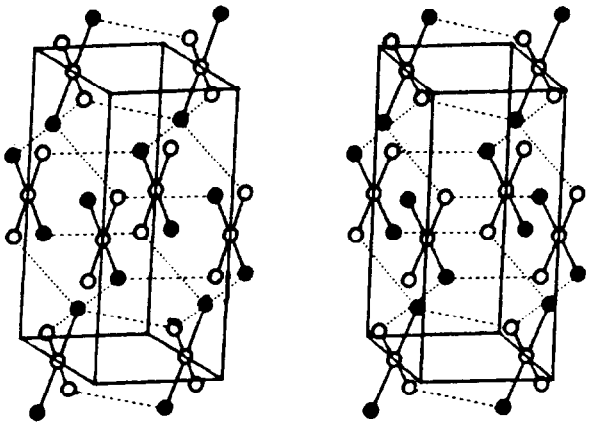


Fig. 2. Stereogram of the unit cell showing the intermolecular hydrogen bonds. In order to simplify the figure only $NiS_2N_2$ units are represented (sulphur atoms are represented by black circles). N–S = 3.367 Å (·····); N–S = 3.427 Å (----------).

The geometry around the metal atom is rigorously planar due to the presence of the crystallographic inversion centre at the nickel atom.

The Ni–S bond length is in good agreement with the values observed in thiolate nickel(II) complexes where sulphur atoms do not act as a bridge.[14] The Ni–N bond length is also in the range of 1.82–1.92 Å found for planar Ni(II) chelates.[6]

It is interesting to compare the *trans*-$NiS_2N_2$ unit of the complex $Ni(MEA)_2$ with that of the homologous $Ni(MEDMA)_2$ complex[6] (Ni–S = 2.198; Ni–N = 1.974 Å; SNiN inner = 87.9°; SNiN outer = 92.1°).

First of all, we can see that the largest SNiN angle is the outer in $Ni(MEA)_2$ and it is the inner in $Ni(MEDMA)_2$. This different geometry between both complexes may be probably attributed to the proximity of N and sulphur atoms in $Ni(MEA)_2$ as a result of the intramolecular NH-----S hydrogen bond (Table 2).

Another significant difference is the shortening of the Ni–S and Ni–N bond distances in the $Ni(MEA)_2$ in relation to the $Ni(MEDMA)_2$. The enlargement of Ni–N bond distance in the last complex is probably caused by nonbonded repulsions between the sulphur atom and the methyl groups.[6]

The difference between the Ni–S bond lengths could be probably also attributed to the proximity of N and S atoms by the NH-----S intramolecular hydrogen bonds.

Finally, powder X-ray analysis of $Ni(MEA)_2$ synthesized according to Jicha and Bush, shows that it has the same structure as that of the single crystals prepared by the slow diffusion method. The complex $Pd(MEA)_2$ is isostructural with the nickel complex.

*Electronic spectra*

On contrasting the electronic spectra of the complexes $Ni(MEA)_2$ and $Ni(MEDMA)_2$ (Table 3), we can see that all the four transitions of $Ni(MEA)_2$ are at higher energies than those of $Ni(MEA)_2$. It was attributed (on the hypothesis of a *cis* structure for $Ni(MEA)_2$ to the fact that, in agreement with the crystal field theory, a *cis*-square-planar complex absorbs at higher energies[15] than a *trans* complex. Now, we can see (on the basis of the X-ray diffraction analysis) that this probably has to be explained by the differences in metal–ligand bond lengths between both complexes. Those distances are significantly shortened in the $Ni(MEA)_2$ complex, so we should expect a shift to higher energies in its electronic spectrum.

The same *trans* structure should probably also be considered for $Ni(MPA)_2$ complex on the basis of its electronic spectrum (Table 3) which is very similar to that of $Ni(MEA)_2$. In addition the physical and chemical properties of both complexes are also similar.

*IR spectra*

The far-IR spectra of $NiL_2$ (L=MEA, MPA, MEDMA) and $PdL_2$ (L=MEA, MEDMA) have been studied.[7] They seemed consistent with *cis* isomers for the complexes where the ligand has an $-NH_2$ group, and *trans* when it has an $-N(CH_3)_2$ group.

Our X-ray study of $Ni(MEA)_2$ has shown that this complex has the *trans* configuration therefore it is difficult to use the far-IR spectra of mercaptoamine metal complexes to distinguish between the *cis* and *trans* isomers.

The far-IR spectra of $Ni(MEDMA)_2$ shows clearly two metal–ligand bands (sensitive to $^{62}Ni$–$^{58}Ni$ substitution).[7] It is in accordance with the $C_i$ symmetry of the *trans*-$NiS_2N_2$ skeleton, where only one Ni–N and Ni–S stretching mode should be infrared active.

The spectra of $M(MEA)_2$ (M=Ni, Pd) and $Ni(MPA)_2$ are much more complicated than that of $Ni(MEDMA)_2$. (There are more metal–ligand bands.) It was assigned on the basis that in the *cis*-$NiS_2N_2$ skeleton (local symmetry $C_{2v}$) two Ni–S and two Ni–N bands should be expected.[7]

The X-ray analysis of $Ni(MEA)_2$ has shown that this complex has the *trans* structure, and probably the same structure should be considered for $Ni(MPA)_2$ and $Pd(MEA)_2$. Consequently, the existence of more bands in the IR spectra of $Ni(MEA)_2$ in relation to $Ni(MEDMA)_2$ has to be attributed to other causes. Probably, the influence of the NH-----S hydrogen bonds in the IR spectrum should be considered. For instance, the NH-----S intramolecular hydrogen bond gives rise to a new Ni–S-----H–N ring. The vibrational modes associated with those rings have to be altered by $^{62}Ni$–$^{58}Ni$ and $NH_2$–$ND_2$ isotope substitution.[7] In addition, as a result of the NH-----S hydrogen bonds, coupling between modes with the same symmetry may be possible. All these facts make difficult a straightforward interpretation of bands in the far-IR spectra.

Table 3. Electronic spectra[7] ($\lambda$ nm)

| $Ni(MEA)_2$ | $Ni(MEDMA)_2$ | $Ni(MPA)_2$ |
|---|---|---|
| 617 | 714 | 617 |
| 467 | 493 | 476 |
| 377 (sh) | 392 (sh) | 370 |
| 325 | 340 | 325 |

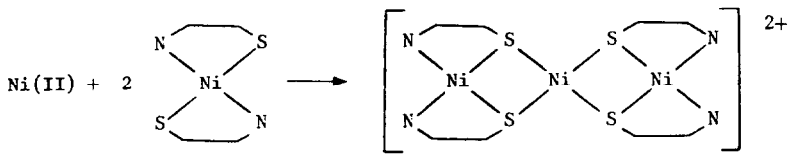
On the other hand, the influence of NH-----S hydrogen bonds can be observed in the region 3000–3500 $cm^{-1}$ of the IR spectrum. The $\nu$(N–H) stretching bands appear in the spectrum of $Ni(MEA)_2$ at the frequencies of 3190, 3140, 3070 $cm^{-1}$. Those bands are shifted to lower frequencies as a result of the coordination to metal atom. However, at the same time a significant shift due to hydrogen bond formation should be considered. The position of those bands is similar to that of metal mercaptoamine complexes where X-ray analysis has shown the existence of NH-----Cl hydrogen bonds[8] (position of $\nu$(N–H) bands in $[Ni_3(MPA)_4]Cl_2$: 3170, 3100, 3030 $cm^{-1}$). This result indicates that the strength of NH-----S bonds in $Ni(MEA)_2$ could be similar to the NH-----Cl bond.

The position of $\nu$(N–H) bands in the spectrum of $Ni(MPA)_2$ (3190, 3140, 3070 $cm^{-1}$) is the same as that in the $Ni(MEA)_2$ complex. It agrees well with the hypothesis of identical *trans*-$NiS_2N_2$ structures in both complexes with NH-----S hydrogen bonds.

## CONCLUSIONS

The solution of the structure of $Ni(MEA)_2$ has permitted us to understand the low solubilities of this complex. In polar solvents it is not soluble because the dipole moment is equal to zero. On the other hand, the complex has a rigid structure strongly hydrogen bonded. That bond cannot be broken by non-polar solvents, so this complex cannot be dissolved by those solvents either. In contrast, the $Ni(MEDMA)_2$ complex dissolves in non-polar solvents because the molecules are linked only by Van der Waals forces.

One of the most important reasons that adduced to assign the *cis*-configuration to this complex was its reactivity with Ni(II) salts to yield the trinuclear complex.[2]



Now, this process should be understood as a *trans–cis* isomerization reaction. It is easily comprehensible as a consequence of the great affinity of the sulphur atom to act as a bridge in thiolate metal complexes.

The different behaviour between $Ni(MPA)_2$ and $Ni(MEA)_2$ towards polar solvents [$Ni(MPA)_2$ is dissolved yielding $[Ni_3(MPA)_4]^{2+}$ while $Ni(MEA)_2$ remains practically insoluble] has been attributed to the greater stability of the five atom chelate rings in $Ni(MEA)_2$.[8] It could be also explained by the *trans–cis* isomerization. This process may be easier in the complex $Ni(MPA)_2$ than in $Ni(MEA)_2$, particularly if it would be an intermediate where one metal–ligand bond was broken.[16]

As a summary, this study has shown that probably, there is not a preference for the *cis* geometry in the $NiL_2$ (L = mercaptoamine) complexes. On the other hand, we can see that the NH-----S hydrogen bonds should be borne in mind as an important factor in the mercaptoamine complexes where the amine group is $-NH_2$.

## REFERENCES


1. K. A. Jensen, *Anorg. Allgem. Chem.* 1963, **229**, 265.
2. D. C. Jicha and D. H. Busch, *Inorg. Chem.* 1962, **1**, 872–887.
3. D. H. Busch, J. A. Burke, D. C. Jicha, M. C. Thompson and M. L. Morris, *Adv. Chem. Ser.* 1963, **37**, 125.
4. C. H. Wei and L. F. Dahl, *Inorg. Chem.* 1970, **9**, 1878.
5. C. A. Root and D. H. Busch, *Inorg. Chem.* 1968, **7**, 789.
6. R. L. Girling and E. L. Amma, *Inorg. Chem.* 1967, **6**, 2009.
7. C. W. Schläpfer and K. Nakamoto, *Inorg. Chim. Acta* 1972, **6**, 177.
8. H. Barrera, J. Suades, M. C. Perucaud and J. L. Briansó, submitted for publication.
9. T. C. Owen, *J. Chem. Soc.* (*C*) 1967, 1373.
10. P. Main, S. L. Fiske, S. E. Hull, L. Lessinger, G. Germain, J. P. Declercq and M. M. Woolfson, *MULLTAN. An Automatic System of Computer Programs for Crystal Structure Determination From X-Ray Diffraction Data.* University of York, England and University of Louvain, Belgium, 1980.
11. P. T. Beurskens, W. P. Bosman, H. M. Doesburg, R. O. Gould, Th. E. M. Van der Hark, P. A. J. Prick, J. H. Noordik, G. Beurskens and V. Parthasarathi, DIRDIF. Direct methods for difference structures. An automatic procedure for phase extension and refinement of difference structure factors. Tech. Rep. 1981–2. Crystallographic Lab. Toernoiveld, The Netherlands, 1981.
12. G. M. Sheldrick, *SHELX. A Computer Program for Crystal Structure Determination.* University of Cambridge, England, 1976.
13. R. Srinivasan and K. K. Chacko, Conform-Biopolym. *Pap. Int. Symp., Madras* 1967, **2**, 607–15.
14. Q. Fernando and P. I. Wheatley, *Inorg. Chem.* 1965, **4**, 1726.
15. G. Maki *J. Chem. Phys.* 1958, **29**, 1129.
16. M. L. Tobe, *Inorganic Reactions Mechanisms.* Thomas Nelson and Sons Ltd. 1972, p. 67.

*Polyhedron* Vol. 3, No. 11, pp. 1233–1236, 1984
Printed in the U.S.A.

0277-5387/84 $3.00 + .00
© 1984 Pergamon Press Ltd.

# ON BROMINATION OF 2,4-PENTANEDIONATO–COPPER(II)

**S. B. KULKARNI, G. N. NATU* and N. H. PAIKE†**
Department of Chemistry, University of Poona, Pune 411 007, India

(*Received* 1 *September* 1983; *accepted* 17 *February* 1984)

**Abstract**—Treatment of bis-2,4-pentanedionato–copper(II), with liquid bromine, at room temperature, gave a low melting dark green reaction product containing weakly coordinated tribromide ion. Characterization of this product using elemental analysis, conductivity, electronic, IR and ESR-spectra was carried out and suggested that the composition of the product was [Cu(HacacBr)Br($Br_3$)].

Extensive reports[1,2] on the studies of bis-2,4-pentanedionate–copper(II), $Cu(acac)_2$ are available. Halogenation reaction appears to be one of the earliest reported reactions,[3] where it was observed that chlorination of $Cu(acac)_2$ yields bis-3-chloro-2,4-pentanedionato–copper(II). The other recent investigations include an elaborate study of the bromination reaction in dichloromethane, carried out by Nakamura *et al.*[4] The salient features of their investigations were the formation of 3-bromo-2,4-pentanedione and reduction of Cu(II)→Cu(I) when bromine concentration was less than 1:2 mole ratio of $Cu(acac)_2$:$Br_2$. When $Ni_3(acac)_6$ was treated with excess bromine then nickel(III) bromide was formed, and the study of this reaction has been reported from this laboratory.[5] This initiated the study of oxidative decomposition reaction between $Cu(acac)_2$ and liquid bromine.

## EXPERIMENTAL

The title compound, $Cu(acac)_2$ was prepared using a standard procedure.[6] The bromination reaction was carried out using anhydrous Cu $(acac)_2$ and liquid bromine under the experimental conditions reported earlier[5] giving a dark green reaction product. Found: Cu, 11.5; C, 10.62; Br, 57.1; Calc. for $C_5H_7O_2Br_5Cu$:Cu, 11.3; C, 10.67; and Br, 56.9%.

Molecular weight of the reaction product was determined cryoscopically in dioxane. Solution conductivity in acetonitrile was measured on Philips GM 4144 conductivity bridge; electronic spectra were recorded in acetonitrile on Beckman DK2 ratio-recording spectrophotometer; and the EPR spectrum of the reaction product was recorded on a Varian E-4 spectrometer (at the Indian Institute of Technology, Madras, India).

The IR spectra were recorded on Perkin–Elmer-337 in the range 4000–400 $cm^{-1}$ and obtained from I.I.T. Madras (India) on Polytec FIR-30 instrument in the range 600–100 $cm^{-1}$.

## RESULTS AND DISCUSSION

(i) *Composition.* The earlier reports[4,5] were convincing enough that the experimental conditions play a deciding role in these reactions. Thus under the present conditions the nature of the reaction products was not the same as those reported[4] earlier. The reaction product obtained under the present conditions was a dark green viscous liquid. It could be crystallized at −70°C as dark needle-like crystals. Owing to experimental difficulties an exact m.p. of the compound could not be determined. The dark green mass decomposed at about 50°C evolving bromine and leaving behind a black sticky residue.

The viscous reaction product was subjected to polarographic analysis in acetonitrile using 0.1 M lithium perchlorate as supporting electrolyte. The $E_{1/2}$ (−0.34 V vs S.C.E.) was in excellent agreement with that reported[7] for the reduction process, Cu(II)→Cu(I). This observation suggested that the copper remained in the Cu(II) oxidation state.

Elemental analysis showed a high bromine content. Molecular weight of 500 in dioxane indicated a monomeric unit. Solution conductivity[8] at room temperature in acetonitrile corresponded to 1:1 electrolytic nature (Table 1). The electrolyte type was ascertained on the basis of the magnitude of solution conductivity and comparing it with simi-

*Author to whom correspondence should be addressed.

†Present address: Shri Sharanbasveshwar College of Science, Gulbarga, 585103, India.

Table 1. Solution conductivity of $Cu(HacacBr)Br(Br_3)$

| Solvent | $\Lambda_e$ ($ohm^{-1}.cm^2.mole^{-1}$) at concentration, at 27 °C ($mol.lit^{-1}$) | | | |
|---|---|---|---|---|
| | 0.01 | 0.005 | 0.0025 | $\Lambda_\infty$ |
| Acetone | 128.9 | 143.2 | 158.9 | 188.0 |
| Acetonitrile | 77.3 | 89.2 | 96.7 | 120.8 |

lar electrolytes reported in the literature.[8] Thus, the high bromine content, 1:1 electrolyte type and a molecular weight of 500 suggested the presence of the $Br_3^-$ ionic species.

It was attempted to prepare a solid crystalline adduct from the viscous mass. When pyridine was added to an acetonitrile solution of the reaction product a dark olive green crystalline compound separated out in quantitative yield while the filtrate contained bromine which on iodometric analysis showed the presence of two bromine atoms per molecule of the separated pyridine adduct, $Cupy_2Br_2$. The nature of this adduct was confirmed from its electronic spectral and magnetic studies.[9]

From all these results the formula of the dark green viscous product could be shown as:

$$Cu(HacacBr)Br(Br_3).$$

This formulation explains the solution conductivity due to the ionization equilibrium,

$$[Cu(HacacBr)Br(Br_3)] \rightleftharpoons [Cu(HacacBr)Br]^+ + Br_3^-,$$

and the formation of the pyridine adduct,

$$[Cu(HacacBr)Br(Br_3)] + 2py \rightarrow Cupy_2Br_2 + Br_2 + HacacBr.$$

HacacBr was confirmed as 3-bromo-2,4-pentanedione from its infrared and electronic spectra.

Attempts were made to isolate the tribromide adduct using tetra-*n*-butyl ammonium bromide, (tnba–bromide). The procedure used was similar to those reported[10] for mixed tetrahalocobaltates. However, the reaction resulted in the formation of a pale purple coloured crystalline compound, $(tnba)_2CuBr_4$, and bromine. The filtrate contained bromine and 3-bromo-2,4-pentanedione. The elemental analysis and spectral and magnetic properties of the purple crystalline tetrabromo cuprate were similar to those reported in the literature.[11] Thus the reaction of the dark green product may be formulated as:

$$[Cu(HacacBr)Br(Br_3)] + 2tnbaBr \rightarrow (tnba)_2CuBr_4 + Br_2 + HacacBr.$$

The dark green product was further characterized using spectral and magnetic studies.

(ii) *Spectral and magnetic studies.* Nakamura *et al.*[4] have reported the electronic spectrum of 3-bromo-2,4-pentanedionato–copper(II) and Popov and Swensen[12] has discussed the electronic spectra of polyhalogen compounds.[13] The characteristic feature of the spectrum of a polyhalide ion is its high absorptivity (about 55,000 l. $mol^{-1}$ for $Br_3^-$). The characteristic transitions associated with (a) ligand field transitions of copper(II) ion, (b) tribromide ion (c) 3-bromo-2, 4-pentanedione are exhibited in the electronic spectrum of the dark green reaction product in acetonitrile (Table 2). There are a number of medium intensity and one high intensity absorption bands in the spectrum. These were resolved on ICL-1904S computer system using a program developed in this laboratory based on a similar literature program.[14]

The electronic spectrum of 3-bromo-2,4-pentanedione was comparable with that reported in literature[4] for the compound 3-bromo-2,4-pentanedionato–copper(II). The red shift in the absorption maxima observed for the reaction product compared with former complex may be attributed to the weak interaction of the dione with copper in the reaction product. These two absorptions (31,746 and 45,045 $cm^{-1}$) assisted in the identification of the dione in the reaction product.

The characteristics of the charge-transfer absorptions of the tribromide ion are not greatly modified on complexation. This indicates a weak coordination of the tribromide ion with central

Table 2. Electronic spectral and magnetic susceptibility data of Cu(HacacBr)Br($Br_3$) and its reaction products

| Compound | Absorption maxima* (cm$^{-1}$) $\nu_1$ | $\nu_2$ | $\nu_3$ | $\mu_{eff}$ (e.p.r.†) | $g_{iso}$ (e.p.r) |
|---|---|---|---|---|---|
| Cu(HacacBr)·Br·$Br_3$ | 8037 | 15800 | 24800 | (1.8) | 2.06 |
| $(tnba)_2CuBr_4$ | 10900 | 16000 (16393) | 19600 (19048) | 1.88 (1.80) | 2.06 |
| $Cu(py)_2·Br_2$ | 11200 | 13800 (14598) | 22800 (23809) | 1.78 (1.78) | 2.05 |
| Hacac·Br | — | 31750 (31746) | 42000 (45045) | - | - |
| $Br_3^-$ | 27550 (27000) v.weak | 37280 (37175) | | - | - |

*Literature data is reported in parentheses
†Magnetic moments calculated from e.p.r. data at room temperature

metal. This, in turn, explains the ionization in solution of the green reaction product exhibiting 1:1 electrolyte behaviour.

The infrared spectrum of the dark green reaction product could not be recorded owing to experimental difficulties. The IR spectrum of the pale yellow liquid (separated after the reaction of tetra-*n*-butylammonium bromide with the dark green reaction product) was comparable with that reported by Nakamura.[4] This confirmed the formation of 3-bromo-2,4-pentanedione in the reaction product. The spectra of the products with pyridine and tetra-*n*-butylammonium bromide were recorded as nujol mulls and were identical to those reported in the literature.[15]

Measurements of paramagnetic susceptibility of the green mass was not attempted due to experimental difficulties. However an EPR spectrum of a dilute solution in acetonitrile at room temperature resulted in a single line with $g_{(ave)}$ value of 2.06 consistent with a magnetic moment of 1.8 B.M. This indicates a mononuclear species without spin–spin interaction.

In summary it could be stated that this product appears to be one of the few low melting transition metal complexes containing trihalide ions.[13] The characteristic features of the product are the presence of neutral 3-bromo-2,4-pentanedione and simultaneously coordinated $Br^-$ and $Br_3^-$ ions.

*Acknowledgement*—The authors gratefully acknowledge Prof. V. K. Phansalkar, Head of the Chemistry Department for his encouragements and facilities. One of the authors (NHP) is grateful to the University Grants Commission, New Delhi, for the financial aid under faculty improvement programme and the Principal Shri Sharanbasaveshwar College of Science, Gulbarga, for the grant of study leave.

## REFERENCES

1. J. P. Fackler, *Prog. Inorg. Chem.* 1966, **7**, 361.
2. D. W. Thompson, *Structure and Bonding* 1972, **9**, 27.
3. G. T. Morgan, H. D. K. Drew and T. V. Borker, *J. Chem. Soc.* 1922, **121**, 2457.
4. Y. Nakamura and S. Kawaguchi, *Bull. Chem. Soc. Jpn.* 1965, **38**, 954; and T. Ogura, Y. Kojima, Y. Nakamura and S. Kawaguchi, *Ibid.* 1965, **38**, 1468.
5. S. B. Kulkarni, G. N. Natu, S. S. Keni and S. P. Ghodke, *J. Inorg. Nucl. Chem.* 1977, **39**, 1238.
6. J. A. Bertrand and D. Caine, *J. Am. Chem. Soc.* 1964, **86**, 2298.
7. J. N. Burnett, L. K. Hiller, Jr. and R. W. Murray, *J. Electrochem. Soc.* 1970, **117**, 1028.
8. W. J. Geary, *Coord. Chem. Rev.* 1971, **7**, 81.
9. Van H. Crawford and W. E. Hatfield, *Inorg. Chem.* 1977, **16**, 1336.
10. N. K. Jha and A. Saxena, *Inorg. Chim. Acta* 1978, **26**, 201.
11. B. Morosin and K. Lawson, *J. Mol. Spec.* 1964, **12**, 98.

12. A. I. Popov and R. F. Swensen, *J. Am. Chem. Soc.* 1955, **77**, 3724.

13. V. Gutman (Editor) *Halogen Chemistry*, Vol. 1. Academic Press, New York (1967).

14. G. Beach, *Fortran IV in Chemistry*. Wiley, London (1975).

15. R. Colton and J. H. Canterford, *Halides of the First Row Transition Metals*. Wiley-Interscience, London (1969).

*Polyhedron* Vol. 3, No. 11, pp. 1237–1239, 1984
Printed in the U.S.A.

0277-5387/84 $3.00 + .00
© 1984 Pergamon Press Ltd.

# STRUCTURAL STUDIES OF BIOLOGICALLY ACTIVE COMPLEXES OF ZINC(II), CADMIUM(II), MERCURY(II) AND COPPER(II) WITH *P*-ANISALDEHYDE THIOSEMICARBAZONE

**K. N. THIMMAIAH,* G. T. CHANDRAPPA, RANGASWAMY and JAYARAMA**
Department of Postgraduate Studies & Research in Chemistry, University of Mysore, Manasagangotri, Mysore 570006, India

(*Received* 18 *October* 1982; *accepted after revision* 17 *February* 1984)

**Abstract**—*p*-Anisaldehyde thiosemicarbazone (PAT) has been used to isolate the complex compounds of the general formula $[M(PAT)X_2]\ H_2O$ where M(II) = Zn, Hg, Cd and Cu, and X = Cl or 1/2 $SO_4$. Probable structures for the complex compounds have been proposed on the basis of elemental analysis, conductometric, spectral and magnetic susceptibility data. The toxicity of the isolated complexes and ligand has been evaluated on pathogenic fungus.

Thiosemicarbazones have attracted special attention due to their activity against viruses, protozoa small-pox and certain kinds of tumour.[1-3] It is known that some drugs have increased activity when administered as metal complexes[4,5] and a number of metal chelates inhibit tumour growth.[6] Further, it is becoming increasingly clear that zinc plays a vital role in biological processes. Zinc deficiency can cause unusual disorder in the development of the body, disorder in the metabolic system and prostrate gland, and can result in mental retardation. Hence, it was thought worthwhile to study the complexation with divalent zinc. Thimmaiah *et al.* have proposed PAT as a selective and sensitive reagent for the spectrophotometric determination of nickel(II),[7] copper(II) and palladium(II).[8] In the present communication, the authors report the isolation and characterization of Zn, Hg, Cd and Cu complexes with PAT and the fungicidal activities of the complexes on pathogenic fungus (Alternaria Sp., Paecilomyces Sp., and Pestalotia Sp.). The strucure of PAT is shown opposite.

## EXPERIMENTAL

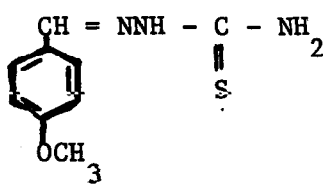
*Preparation of PAT.* PAT was prepared and purified by the method reported elsewhere.[9]

*Preparation of the complexes.* 50 $cm^3$ of a 0.05 M aqueous solution of the metal salts were mixed with 50 $cm^3$ of a 0.05 M solution of PAT in ethanol and the mixture was stirred for about 1 hr. This was kept overnight, filtered off, washed with water followed by ethanol until it was free from ligand, and dried *in vacuo*.

*Analysis.* Zn, Hg, Cd and Cu contents of the complexes were estimated by standard methods. Carbon, hydrogen, nitrogen and sulphur were determined in the Micro-Analytical Section of the Central Drug Research Institute, Lucknow. The analytical results were given in Table 1.

*Physical measurements.* Magnetic susceptibility measurements were carried out at room temperature (27°C) using a Gouy balance, and calculations were made using computed values of Pascal constants for diamagnetic corrections. Conductance measurements were made on $10^{-3}$ M solutions of the complexes in nitromethane using a Toshniwal conductivity bridge. IR spectra (200–4000 $cm^{-1}$) of the complexes and the ligand were recorded on a Perkin–Elmer 221 spectrophotometer in KBr discs.

In the evaluation of antifungal activity, the ligand and metal complexes were incorporated in




*Author to whom correspondence should be addressed. Present address: Bowman Gray School of Medicine, Winston-Salem, NC 27103, U.S.A.

Table 1. Analytical data, colour, melting point, magnetic moment and conductance* data of the complexes

| Complex | Colour | m.p. (°C) | C% Calc. (found) | H% Calc. (found) | N% Calc. (found) | S% Calc. (found) | Cl% Calc. (found) | M% Calc. (found) | $\Lambda_S$ | $\mu_{eff}$(BM) (27°C) |
|---|---|---|---|---|---|---|---|---|---|---|
| $[Zn(PAT)Cl_2]H_2O$ | White | 192–193 | 29.75 (28.72) | 3.58 (3.62) | 11.59 (11.14) | 8.18 (8.28) | 19.59 (19.03) | 17.91 (17.68) | 4.0 | Diamagnetic |
| $[Hg(PAT)Cl_2]H_2O$ | Yellow | 179–180 | 21.67 (20.68) | 2.59 (2.38) | 8.42 (8.12) | 6.41 (6.55) | 14.26 (13.92) | 40.23 (40.98) | 4.4 | Diamagnetic |
| $[Cd(PAT)Cl_2]H_2O$ | Yellow | above 360(d) | 26.34 (26.45) | 3.19 (3.12) | 10.24 (9.96) | 7.80 (7.98) | 17.31 (17.70) | 27.40 (26.32) | 4.6 | Diamagnetic |
| $[Cu(PAT)SO_4]H_2O$ | Yellowish green | above 360(d) | 27.90 (28.74) | 3.38 (3.62) | 18.88 (17.05) | 16.58 (15.98) | - - | 16.44 (17.08) | 4.8 | 1.87 |

d: decomposes

Table 2. Fungicidal screening data of complexes and ligand

| Compound | Average percentage inhibition after 8 days | | | | | |
|---|---|---|---|---|---|---|
| | Organism Alternaria Sp. Conen used | | Organism Paecilomyces Sp. Conen used | | Organism Pestalotia Sp. Conen used | |
| | 0.01% | 0.1% | 0.01% | 0.1% | 0.01% | 0.1% |
| $[Zn(PAT)Cl_2]H_2O$ | 49.39 | 73.79 | 46.9 | 74.46 | 84.79 | 92.79 |
| $[Hg(PAT)Cl_2]H_2O$ | 82.54 | 92.17 | 56.03 | 76.76 | 71.88 | 76.19 |
| $[Cd(PAT)Cl_2]H_2O$ | 58.74 | 75.90 | 51.15 | 75.57 | 67.56 | 84.77 |
| $[Cu(PAT)SO_4]H_2O$ | 55.80 | 58.74 | 33.70 | 63.10 | 80.81 | 88.57 |
| PAT | 43.06 | 68.67 | 65.01 | 81.43 | 79.74 | 89.33 |

Czapecks medium against Alternaria (Sp.), Paecilomyces (Sp.) and Pestalotia (Sp.). Dimethyl sulphoxide was used as a solvent for preparing different concentrations (0.01%, 0.1%) of the chelating agent and metal complexes. The growth inhibition percentage was calculated on the basis of the average diameter of the fungal colony.

$$\text{percentage inhibition} = \frac{(C - T) \times 100}{C}$$

where $C$ is the diameter of the fungus colony in the control plates after 8 days, $T$ is the diameter of the fungus colony in treated plates after 8 days. The values of percentage inhibition of various compounds are recorded in Table 2.

## RESULTS AND DISCUSSION

The elemental analyses of the complexes showed that Zn, Hg, Cd and Cu combine with PAT to form complexes of composition $[M(PAT)X_2]\,H_2O$. All the complexes are soluble in acetone, methanol, nitromethane, DMF, DMSO and acetonitrile.

*Magnetic moments.* The magnetic susceptibility values obtained for Zn(II), Hg(II) and Cd(II) complexes showed them to be diamagnetic. The value $\mu_{eff}$ = 1.87 BM for $[Cu(PAT)SO_4]H_2O$ showed that it was paramagnetic and confirmed the presence of Cu(II).

The low values of molar conductance in nitromethane indicate that the complexes are non-ionic.

*IR spectra.* An assignment of the important IR absorption bands is based on the study of IR spectra of the free ligand and its metal complexes. In the IR spectrum of the ligand, frequencies of various intensities are exhibited in the region 3400–3100, 1600–1520 and 1360–820 $cm^{-1}$ which may be assigned to $\nu(NH + NH_2)$, $\nu(C=N)$, $\nu(C=C)$, $\nu(C=S)$ and other phenyl ring vibrations respectively. On complexation with metals a negative shift in the $\nu(C=N)$ vibration indicates the coordination of azomethine nitrogen to the metal ion. The $\nu(C=S)$ vibration of the thiosemicarbonyl group located at 1360 $cm^{-1}$ in the IR spectrum of the free ligand is shifted downwards by about 40 $cm^{-1}$ in the spectra of the complexes suggesting the coordination of thiocarbonyl sulphur to the metal ion. In addition to the above changes, new bands which appeared in the spectra of the complexes in the regions 505–470, 380–330 and 270–250 $cm^{-1}$ have been assigned to $\nu(M–N)$, $\nu(M–S)$ and $\nu(M–Cl)$ bonds respectively. On the basis of the above evidence, it is concluded that the ligand "PAT" is bidentate in nature.

Alternaria (Sp.), Paecilomyces (Sp.) and Pestalotia (Sp.) were employed to check the antifungal activity of the ligand and its complexes. The toxicity of the complexes with Alternaria (Sp.) has been observed to be greater than that of PAT. In the case of Paecilomyces (Sp.), the ligand is more toxic than all the complexes, whereas in the case of Pestalotia (Sp.), Hg and Cd complexes are less toxic and the Zn complex more toxic than PAT. It is further observed that the toxicity of the complexes generally increases with increasing metal radius. The Hg complex displayed more toxicity than other metal complexes except against Pestalotia (Sp.).

The $>C=S$ and $>C=N$ groups in the ligand are free, and show higher toxicity as they can easily combine with the fungi-cells to check growth. On the other hand, in metal complexes, they are not free to inhibit fungal growth, as they are involved in bond formation with the metal ions. Hence the toxicity of the complexes decreases. The free ligand is highly soluble in the medium and may be easily absorbed by the fungal hyphae, but the complexes show less solubility and hence the toxicity differs between PAT and its metal complexes.

*Acknowledgements*—The authors wish to express their sincere thanks to Professor H. Sanke Gowda and Dr. S. Y. Ambekar, Department of Chemistry, University of Mysore, for their valuable suggestions. One of the authors (G. T. Chandrappa) gratefully acknowledges University Grants Commission, New Delhi, for awarding a Junior Research Fellowship.

## REFERENCES

1. N. Orlova, V. A. Aksensova, D. A. Selidovkin, N. S. Bogdanova and G. N. Perskin, *Russ. Pharm. Toxicol.* 1968, 348.
2. D. J. Bauer, L. S. Vincent, C. H. Kempe and A. W. Downie, *Lancet* 1963, **20**, 494.
3. H. G. Petering, H. H. Buskirk and G. E. Underwood, *Cancer Res.* 1964, **64**, 367.
4. D. R. Williams, *Chem. Rev.* 1972, **72**, 203.
5. A. Furst and R. T. Haro, *Progr. Exp. Tumor Res.* 1969, **12**, 102.
6. F. P. Dwyer, E. Mayhew, E. M. F. Roe and A. Shulman, *Brit. J. Cancer* 1965, **19**, 195.
7. H. Sanke Gowda, K. N. Thimmaiah and S. Maqbool Ahmed, *Ind. J. Chem.* 1982, **21A**, 327.
8. K. N. Thimmaiah, S. Maqbool Ahmed and H. Sanke Gowda, *Ind. J. Chem.* 1983, **22**, 690.
9. P. T. Peter Sah and T. C. Daniels, *Rev. Trav. Chim.* 1950, **69**, 1545.

*Polyhedron* Vol. 3, No. 11, pp. 1241–1245, 1984
Printed in the U.S.A.

0277–5387/84 $3.00 + .00
© 1984 Pergamon Press Ltd.

# ADDUCT FORMATION OF SOME TRIS(N,N DIALKYL-DITHIOCARBAMATO)Cr(III) COMPLEXES WITH IODINE

GUIDO CRISPONI,* PAOLA DEPLANO, VALERIA NURCHI and EMANUELE F. TROGU
Istituto di Chimica Generale, Inorganica ed Analitica dell'Università, 09100 Cagliari, Italy

(*Received* 4 *January* 1984; *accepted* 17 *February* 1984)

**Abstract**—Spectrophotometric studies of dichloromethane solutions containing iodine and some $Cr(S_2CNR_2)_3$ complexes (where $R_2NCS_2^-$ are: $OC_4H_8NCS_2^-$ = modtc; $(C_2H_5)_2NCS_2^-$ = $Et_2$dtc; $(C_6H_5CH_2)_2NCS_2^-$ = $Bz_2$dtc) have shown the formation of 1:1 adducts whose spectral features were studied and which suggested that charge-transfer interaction involving iodine and a sulphur atom of a coordinated dithiocarbamato ligand occurred.

A new BASIC non-linear least-squares program which performs an optimization of the absorbance data taken at several wavelengths was devised to evaluate reliable formation constants.

The thermodynamic parameters have been calculated and compared with those obtained in the same conditions as above by a reinvestigation of the known 1:1 complex formation of iodine with the corresponding tetraalkylthiuram-disulphides, where the donor site is also the sulphur atom of the thiocarbonyl group. The $-\Delta H^\circ$ values related to the $Cr(dtc)_3 \cdot I_2$ complexes are about 2 kcal lower than those of thiuram disulphides, showing a lowering of the donor strength of the thiocarbonyl sulphur as a consequence of the coordination to the metal.

The reaction of iodine with metal dithiocarbamates is widely used to prepare several types of products, including those in which the metal[1,2] or the ligand undergoes oxidation.[3,4]

However up to now a systematic study to clarify the mechanism of these reactions and possibly to find some generalization to predict their reactivities has not been undertaken.

We are at the moment investigating this subject and are working on the hypothesis that the formation of charge transfer (c.t.) adducts may be the first interaction between iodine and dithio- or diseleno-carbamato derivatives.

This working hypothesis is based on the following considerations: thio-[5] and especially seleno-[6] carbonyl derivatives form 1:1 c.t. adducts with iodine; also the coordinated, S and Se atoms of Co(III) dithio- and diseleno-carbamates retain basic properties and give 1:1 c.t. complexes with iodine;[7] and moreover a c.t. adduct may be precursory in oxidative reactions.[8]

Therefore the evaluation of reliable association constants of this kind of adduct is very important for our studies, and in an attempt to study a system which will not show any subsequent reaction, we have chosen the Cr(III) dithiocarbamates. In fact it was shown that $d^3$ and $d^6$ compounds (viz. $Cr(dtc)_3$ and $Co(dtc)_3$) possess remarkable stability both to oxidation and reduction[9,10] and that the well-known inertness of these complexes to ligand substitution suggests that $Cr(dtc)_3$ derivatives are suitable for the thermodynamic measurements of c.t. adducts with iodine.

We report here the results of 1:1 adduct formation of some $Cr(dtc)_3$ derivatives with iodine in $CH_2Cl_2$ and, in the same solvent for comparison, of those (tetraalkylthiuram)disulphides which have the same substituents on the N atom of the dtc ligand. Moreover a new least squares method for evaluating association constants ($\kappa$) and absorptivities ($\epsilon$) is proposed.

## EXPERIMENTAL

### *Reagents and products*

The $Cr(dtc)_3$ complexes were prepared according to the literature method.[11]

Doubly sublimed iodine was purchased from Carlo Erba.

*Author to whom correspondence should be addressed.

R.P.E. Carlo Erba Methylene Chloride was dried over 4Å molecular sieves.

The thiuramdisulphides $[OC_4H_8NC(S)S]_2$; $[(C_2H_5)_2NC(S)S]_2$ and $[(C_6H_5CH_2)_2NC(S)S]_2$ were prepared by oxidation of the inner salt of the corresponding dithiocarbamate in aqueous solution with 6% hydrogen peroxide. The cream solid formed was filtered off, dried and recrystallized twice from $CH_2Cl_2$/ethanol mixtures.

All the prepared compounds were checked by CHN analysis.

The slow evaporation of concentrated $CH_2Cl_2$/petroleum ether solutions of $Cr(dtc)_3$ with an excess of iodine (in an approximate 1:4 molecular ratio), and repeated washing of these solids with petroleum ether until iodine colourless, left pure $Cr(dtc)_3 \cdot I_2$ adducts. Found: C, 22.5; H, 2.9; N, 5.7; Calc. for $C_{15}H_{24}N_3O_3S_6CrI_2$: C, 22.73; H, 3.05; N, 5.30%.

Dark brown products, which contain an $I_2$:$Cr(dtc)_3$ ratio which is higher than 1:1, have been isolated using the above solutions without addition of petroleum ether.

They did not give satisfactory analytical results since they lost iodine slowly. The IR spectra of these iodine-rich adducts were very similar to those of $Cr(dtc)_3 \cdot I_2$ except for a low increase of the $\nu$(CN) absorption (see Results and Discussion).

The CHN analyses were performed by the Istituto di Chimica Farmaceutica, University of Cagliari.

*Apparatus*

The IR spectra were recorded in KBr pellets or in $CH_2Cl_2$ solutions on a Perkin–Elmer mod. 983 spectrophotometer.

The UV–vis. spectra in $CH_2Cl_2$ solution were run on a Cary mod. 219 spectrophotometer, equipped with a Lauda Thermostat ($\pm$ 0.1°C) using 0.10 or 1.00 cm matched quartz cells.

*Measurements*

The Job plots for the systems $Cr(dtc)_3$–$I_2$ were made at several appropriate wavelengths (see Fig. 1 as example) on $CH_2Cl_2$ solutions having a total concentration of $3 \times 10^{-3}$ mol. $l^{-1}$.

A first set of nine $CH_2Cl_2$ solutions containing constant $Cr(dtc)_3$ concentrations ($1 \times 10^{-4}$ mol. $l^{-1}$) and iodine ranging between $1 \times 10^{-4}$ and $2 \times 10^{-2}$ mol. $l^{-1}$ was made up and their spectra immediately recorded at 10, 20 and 30°C in the 350–410 nm wavelength range.

At the end of the whole time required for the recording of the spectra the decomposition of the solutions was spectrophotometrically found to be negligible.

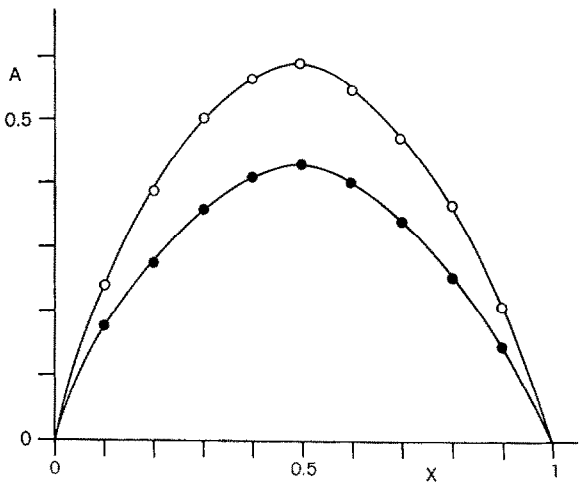



Fig. 1. The Job plot for the system $Cr(modtc)_3$ + $I_2$. $x$ = $Cr(modtc)_3$ molar fraction. $A$ = Absorbance arbitrary units. ○ = 410 nm; ● = 440 nm.

A second set of nine $CH_2Cl_2$ solutions containing constant iodine concentrations ($4 \times 10^{-4}$ mol.$l^{-1}$) and thiuram disulphides ranging between $4 \times 10^{-4}$ and $1.5 \times 10^{-2}$ mol.$l^{-1}$ was prepared and their measurements made as described above, in the 430–560 nm wavelength range.

At higher iodine concentrations the time evolution of the spectra was not negligible. Studies on the nature of the final products and kinetic measurements on the transformation reactions of these adducts are in progress and will be published in a forthcoming paper.

*Calculations*

To obtain the stability constants and the other parameters (see Results and Discussion), a new BASIC program "KEPS 1:1" was written by us (available on request), and used on a Hewlett Packard mod. 85 computer.

## RESULTS AND DISCUSSION

The addition of iodine to $Cr(dtc)_3$ derivatives in $CH_2Cl_2$ medium is accompanied by a change in the UV–vis. spectra of the solutions with respect to the added spectra of the components. By applying the continuous variation method, the Job plot shows the formation of a 1:1 complex between the reagents and no other stoichiometries in the explored concentration range.

Unfortunately the absorbances of the formed complex are masked by the absorption of the free $Cr(dtc)_3$ and its spectral features are obtained by subtracting the absorbances of the equilibrium concentrations of the components from the spectrum of their mixtures.

The spectrum so obtained is reported in Fig. 2 for the $Cr(modtc)_3 \cdot I_2$ case (the other complexes

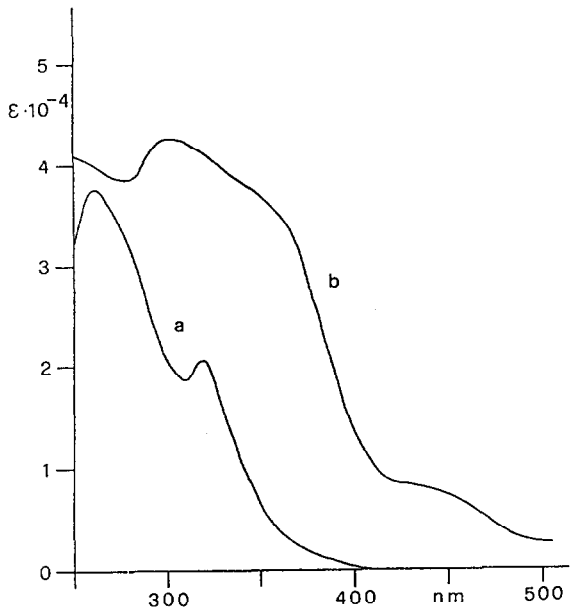



Fig. 2. The UV–vis. spectra of: (a) $Cr(modtc)_3$; (b) $Cr(modtc)_3 \cdot I_2$ (calculated, see text).

show similar features) and the band near 295 nm can be attributed to the charge-transfer band while the one near 450 nm to the blue-shifted iodine.

The most direct evidence that, of the several available electron-donor sites of $Cr(dtc)_3$ derivative, the site of interaction is one coordinated carbonyl sulphur, comes from infrared results.

*IR Results*

The IR spectra of metal dithiocarbamates have been largely studied[12] and the position of $\nu$(CN) ranging between 1450 and 1500 $cm^{-1}$ and of $\nu$(CS) (950–1050 $cm^{-1}$) can give valuable information on the electronic and structural characteristics of the dtc derivatives.

In our $CH_2Cl_2$ solutions we have observed a positive shift (5–10 $cm^{-1}$) of the $\nu$(CN) band and a splitting of the $\nu$(CS) band (1000, 990 $cm^{-1}$) on passing from $Cr(dtc)_3$ to the iodine complexes, and according to these studies our results suggest that the $\nu$(CS) vibrations are no longer equivalent, and according to the Bonati criterion[13,14] the dtc ligand becomes unsymmetrically bonded and its structure receives a greater contribution of the resonance form $R_2\overset{+}{N}{=}CS_2^{2-}$ as a consequence of the adduct formation with iodine.

Similar features were maintained in the products isolated in the solid state. Only the $\nu$(CN), $\nu$(CS) and $\nu$(CrS) (the last value shows a slight positive shift of a few wavenumbers) regions show a variation with respect to the additive spectra of the components.

*Calculations*

When A + B react to form a 1:1 complex, with association constant $\kappa$, the absorbance values are given at any fixed wavelength by the relation:

$$D_{ex} = \epsilon_A(a - x) + \epsilon_B(b - x) + \epsilon_x(x) \qquad (1)$$

where $\epsilon_A$, $\epsilon_B$ and $\epsilon_x$ are the absorptivities and $a$, $b$ and $x$ the concentrations of the starting reagents and the formed complex respectively.

By subtracting the known values of the starting reagents, it is possible to obtain a corrected value of the absorbance (1) as

$$D = (\epsilon_x - \epsilon_A - \epsilon_B)x. \qquad (2)$$

Having a set of absorbances at Q wavelengths for a number N of different concentrations of the starting reagents, we could express them in a matrix notation

$$D = E \cdot x. \qquad (3)$$

Where D is a matrix N · Q, E is the absorptivity vector and $x$ the concentration vector.

To obtain $\kappa$ and E together from eqn (3) we must minimize the function

$$\chi^2 = \sum_{1}^{N}{}_i \sum_{1}^{Q}{}_j (D_{ij} - \epsilon_j x_i(\kappa))^2 \qquad (4)$$

where

$$x_i(\kappa) = \{a_i + b_i + \kappa^{-1} - [(a_i + b_i + \kappa^{-1})^2 - 4a_ib_i]^{\frac{1}{2}}\}/2$$

The $\chi^2$ function is linearly dependent on $\epsilon$ while not on $\kappa$.

Therefore having an initial estimate of the association constant $\kappa_0$ it is possible to calculate $E_0$ by a linear least squares method[15,16] as:

$$E_0 = (X' \cdot X)^{-1}X'D \qquad (5)$$

(where the symbols are used according to matrix notation), and consequently also $\chi^2(\kappa_0, E_0)$ can be calculated.

The $\kappa$ value which minimizes the $\chi^2$ function is calculated by an iterative process, according to the Gauss–Newton non-linear least-squares method as previously described.[16]

The D function (eqn 2) may be developed in Taylor series

$$D_c = D(\kappa_0, E_0) + Z_{k_0}(\kappa - \kappa_0) \qquad (6)$$

where the series is truncated to the first term, Z is

the numerically calculated derivative of D with respect to $\kappa$ and the correction term $(\kappa - \kappa_0)$ is:

$$\kappa - \kappa_0 = (Z'Z)^{-1}Z'(D - D_c) \qquad (7)$$

(Z is the vector of derivatives).

Equations (5) and (7), the standard deviations of the parameters and some useful indexes of their reliability (as previously discussed[17]) were performed using a new program in BASIC language which allows a complete matricial formalism also on small personal computers.

This program was checked on some literature data in comparison with the Gauss–Newton method previously reported by Wentworth *et al.*[18] and by Rosseinsky[19] and with Conrow's[20] method, recently reproposed by Drago *et al.*[21]

All the programs converge to the same final results.

However (i) the first method needs good initial estimates of both $\kappa$ and $\epsilon$ since it gives some convergence problems with bad initial estimates or with highly correlated parameters; (ii) the second is very ineffective in the $\kappa'$ finding and can lead to a very long calculation time.

Our method has the advantage of obtaining very good convergence after a maximum of four iterations (it is advisable to use a damping factor of 0.3 for the correction term (7) in the first two iterations).

The program allows furthermore a preliminary check of the experimental data by a graphical and/or numerical analysis of the matrix D (eqn 3); the rows (and columns) must in fact be linearly dependent on each other, with straight lines passing through the origin[22] only when the stoichiometry of the complex formation is 1:1.

Therefore any deviation from linearity is indicative of the failure of the assumed model. Moreover such a graphical analysis reveals gross errors in the input data before the optimization procedure begins.

*Thermodynamic results*

The formation constants so calculated and the related thermodynamic parameters are reported in

Table 1. Stability constants and thermodynamic parameters of the formation of $Cr(S_2CNR_2)_3 \cdot I_2$ and $(R_2NC(S)S)_2 \cdot I_2$ adducts in methylene chloride

| Donor | T °C | K 1 mol$^{-1}$ | $-\Delta H^\circ$ Kcal mol$^{-1}$ | $-\Delta S^\circ$ e. u. |
|---|---|---|---|---|
| $Cr(S_2CNC_4H_8O)_3$ | 10 | 27 ± 1 | 2.1 ± 0.1 | 1.0 ± 0.4 |
| | 20 | 24 ± 2 | | |
| | 30 | 21 ± 2 | | |
| $Cr(S_2CN(C_2H_5)_2)_3$ | | 46 ± 3 | 2.2 ± 0.1 | 0.4 ± 0.8 |
| | | 39 ± 3 | | |
| | | 35 ± 3 | | |
| $Cr(S_2CN(CH_2C_6H_5)_2)_3$ | | 49 ± 2 | 1.9 ± 0.1 | -0.8 ± 0.4 |
| | | 43 ± 2 | | |
| | | 39 ± 3 | | |
| $(OC_4H_8NC(S)S)_2$ | | 136 ± 6 | 4.4 ± 0.1 | 5.8 ± 0.3 |
| | | 103 ± 7 | | |
| | | 81 ± 7 | | |
| $((C_2H_5)_2NC(S)S)_2$ | | 520 ± 30 | 4.6 ± 0.1 | 3.8 ± 0.7 |
| | | 400 ± 20 | | |
| | | 300 ± 20 | | |
| $((C_6H_5CH_2)_2NC(S)S)_2$ | | 87 ± 5 | 3.4 ± 0.2 | 3 ± 1 |
| | | 73 ± 6 | | |
| | | 53 ± 5 | | |

Table 1. As expected, the thermodynamic data on the variously N-substituted Cr dithiocarbamates are very similar to each other showing that the interactions between iodine and the various $Cr(dtc)_3$ are of the same kind and, according to IR results, involve predominantly one sulphur atom of a coordinated ligand, which acts as the donor.

We reinvestigated the known[5] reaction of iodine with tetraalkylthiuramdisulphides in order to compare the data obtained in the same medium and with the same calculation method. The decrease of the $-\Delta H^\circ$ values compared with those obtained with the iodine complexes with thiuramdisulphides (in which one carbonyl S atom acts as donor) takes into account a lowering of basicity as a consequence of the coordination of the C=S group to a metal atom.

Moreover, by comparing our results with those previously reported[5] for the tetraethylthiuramdisulphide derivatives, we observe that the earlier evaluation of the stability constants is given with a 50% error and therefore a comparison is meaningless, while the $-\Delta H^\circ$ values are quite similar within error limits and the differences in $\Delta S^\circ$ can be accounted for by a different solvent effect.

## REFERENCES


1. P. T. Beurskens, H. J. A. Blaauw, J. A. Cras and J. J. Steggerda, *Inorg. Chem.* 1968, **7**, 808.
2. H. C. Brinkhoff, *Rec. Trav. Chim. Pays-Bas* 1971, **90**, 377.
3. H. C. Brinkhoff, J. A. Cras, J. J. Steggerda and J. Willemse, *Rec. Trav. Chim. Pays-Bas* 1969, **88**, 633.
4. H. C. Brinkhoff, A. M. Grotens and J. J. Steggerda, *Rec. Trav. Chim. Pays-Bas* 1970, **89**, 11.
5. A. F. Grand and M. Tamres, *Inorg. Chem.* 1969, **8**, 2459.
6. F. A. Devillanova and G. Verani, *Tetrahedron* 1981, **37**, 1803.
7. G. Crisponi, P. Deplano and E. F. Trogu, *Inorg. Chim. Acta* 1983, **75**, 135.
8. F. Bigoli, G. Crisponi, P. Deplano, E. Leporati, M. A. Pellinghelli and E. F. Trogu, *J. Chem, Soc. Dalton Trans.* 1983, 1763.
9. A. R. Hendrickson, R. L. Martin and N. R. Rhode, *Inorg. Chem.* 1974, **13**, 1933.
10. R. L. Chant, A. R. Hendrickson, R. L. Martin and N. M. Rhode, *Inorg. Chem.* 1975, **14**, 1894.
11. A. F. Schreiner and P. J. Hauser, *Inorg. Chem.* 1972, **11**, 2706.
12. D. Coucouvanis, *Prog. Inorg. Chem.* 1979, **26**, 301.
13. F. Bonati and R. Ugo, *J. Organomet. Chem.* 1967, **10**, 257.
14. D. A. Brown, W. K. Glass and M. A. Burke, *Spectrochim. Acta* 1976, **32A**, 137.
15. F. R. Bevington, *Data Reduction and Error Analysis for the Physical Sciences*. McGraw-Hill, New York (1969).
16. N. Draper and H. Smith, *Applied Regression Analysis*. Wiley, New York (1966).
17. G. Carta and G. Crisponi, *J. Chem. Soc. Perkin II* 1982, 53.
18. W. E. Wentworth, W. Hirsch and E. Chen, *J. Phys. Chem.* 1967, **71**, 218.
19. D. R. Rosseinsky and H. Kellawi, *J. Chem. Soc. A* 1969, 1207.
20. K. Conrow, G. D. Johnson and R. E. Bowen, *J. Am. Chem. Soc.* 1964, **86**, 1025.
21. J. R. Long and R. S. Drago, *J. Chem. Ed.* 1982, **59**, 1037.
22. F. R. Hartley, C. Burgess and R. M. Alcock, *Solution Equilibria*. E. Horwood, Chichester, England (1980).

*Polyhedron* Vol. 3, No. 11, pp. 1247–1253, 1984
Printed in the U.S.A.

0277–5387/84 $3.00 + .00
© 1984 Pergamon Press Ltd.

# MONONUCLEAR, THREE-COORDINATE METAL THIOLATES: PREPARATION AND CRYSTAL STRUCTURES OF $[NBu^n_4][Hg(SPh)_3]$ AND $[NPr^n_4][Pb(SPh)_3]$

GEORGE CHRISTOU*†
Department of Chemistry, Imperial College of Science and Technology, London SW7 2AY, England

and

KIRSTEN FOLTING and JOHN C. HUFFMAN
Molecular Structure Center, Indiana University, Bloomington, IN 47405, U.S.A.

(*Received* 20 *November* 1983; *accepted* 17 *February* 1984)

**Abstract**—Dissolution of HgO or PbO in methanolic solutions of NaSPh yields homogeneous solutions from which highly crystalline $[NBu^n_4][Hg(SPh)_3]$ (**1**) or $[NPr^n_4][Pb(SPh)_3]$ (**2**) can be isolated on addition of appropriate quaternary ammonium salts. **1** crystallizes in monoclinic space group $P2_1/a$ with $a = 20.663(7)$, $b = 16.812(6)$, $c = 9.757(3)$ Å, $\beta = 95.52(2)°$ and $Z = 4$. The anion consists of a rare example of trigonal planar coordinated Hg; there are no weaker, intermolecular Hg...S axial interactions. **2** crystallizes in triclinic space group $P\bar{1}$ with $a = 12.689(7)$, $b = 11.255(6)$, $c = 12.046(7)$ Å, $\alpha = 107.93(3)$, $\beta = 109.64(3)$, $\gamma = 86.01(3)°$, and $Z = 2$. The anion consists of a trigonal pyramidal coordinated $PbS_3$ unit. The structures were solved using data collected at approx. −160°C and refined to conventional R values of 5.7 and 4.6%, respectively for **1** and **2**.

The biological chemistry of mercury has attracted considerable interest due to its high toxicity to living systems.[1] In particular, it is thought that this metal strongly interacts with the thiolate function of the cysteine amino acid residue, a belief supported by the high stability constant of the mercury–thiolate bond.[1,11] Some recent interest has focused on the metallothioneins[2] which are low molecular weight proteins believed to be involved in the control of zinc and copper metabolism and the detoxification of metals such as cadmium and mercury. In their native form they contain a total of seven Zn and/or Cd atoms bound in two polynuclear aggregates[3] by 20 cysteinyl thiolate groups;[4] the metal-free apoprotein can, however, bind other metals such as Cu, Ag, Co and Hg. Indeed, mercury-containing metallothionein has been isolated from mammals to which mercury has been administered.[5] Similar metal-thiolate interactions *in vivo* may also obtain for lead, another highly toxic metal to living systems.

Despite this, very few anionic complexes of Hg(II) and Pb(II) with small organic thiolates are known and in even fewer cases is structural information available. The isolation of the homoleptic species $[Hg(SR)_4]^{2-}$ (R = Ph,[6a] $C_6H_4$-*p*-Cl,[6b] $C_6F_5$[6c] and $C_6Cl_5$[6d]) have been reported and the R = $C_6H_4$-*p*-Cl species has been crystallographically shown to be a tetrahedrally-coordinated monomer.[6b] In contrast, $[Hg(SPh)_3]^-$, $[Hg(SBu^t)_3]^-$and $[Pb(SC_6F_5)_3]^-$ have not been structurally characterized and are reported to be trigonal pyramids based on vibrational evidence or comparison with the corresponding halides;[7,8a] the reaction of $Pb(SPh)_2$ and excess $PhS^-$ has been reported to yield $[Pb(SPh)_3]^-$ based on $^{207}Pb$ NMR studies and comparison with the corresponding Sn(II) reactions which are better characterized.[8b] Among Hg(II)- and Pb(II)-thiolate chemistry, the only complex with a ligand : metal ratio of 3 : 1 to be structurally characterized is $[Hg(SMe)_3]^-$ and this has been shown[6b] to be dimeric with four-

*Author to whom correspondence should be addressed.

†Present address: Department of Chemistry, Indiana University, Bloomington, IN 47405, U.S.A.

coordinate Hg(II) *viz.* $[(MeS)_2Hg(\mu\text{-}SMe)_2\text{-}Hg(SMe)_2]^{2-}$.

During our investigations into the reactions of HgO and PbO with four equivalents of NaSPh, we obtained in high yields crystalline materials of empirical formulation $[NR_4][M(SPh)_3]$ (M = Hg, Pb). To unambiguously determine their nuclearity and coordination geometry, we have obtained the crystal structures of $[NBu^n_4][Hg(SPh)_3]$ (**1**) and $[NPr^n_4][Pb(SPh)_3]$ (**2**) which both proved to be monomeric, and herein report the result of this work.

## EXPERIMENTAL

### *Synthesis*

All manipulations were performed under a nitrogen atmosphere employing standard inert-atmosphere techniques.

$[NBu^n_4][Hg(SPh)_3]$ (**1**). Sodium metal (1.84 g, 80 mmol) was dissolved in MeOH (100 $cm^3$) and benzenethiol (8.21 $cm^3$, 80 mmol) added, followed by solid HgO (4.33 g, 20 mmol). The solid slowly dissolved with stirring and slight warming to produce a pale yellow solution. After 0.5 hr, $NBu^n_4Br$ (12.9 g, 40 mmol) in EtOH (80 $cm^3$) was added to

Table 1. Summary of crystal data, intensity collection and structure refinement for $(NR_4)[M(SPh)_3]$ (M = Hg, R = Bu$^n$; M = Pb, R = Pr$^n$)

| Quantity | M = Hg(II) | M = Pb(II) |
|---|---|---|
| formula | $C_{34}H_{51}NS_3Hg$ | $C_{30}H_{43}NS_3Pb$ |
| molecular weight | 770.56 | 721.05 |
| cryst. system | monoclinic | triclinic |
| space group | $P2_1/a$ | $P\bar{1}$ |
| temperature, °C | approx. -160 | approx. -160 |
| a, Å | 20.663(7) | 12.689(7) |
| b, Å | 16.812(6) | 11.255(6) |
| c, Å | 9.757(3) | 12.046(7) |
| $\alpha$, deg | ------ | 107.93(3) |
| $\beta$, deg | 95.52(2) | 109.64(3) |
| $\gamma$, deg | ------ | 86.01(3) |
| V, $Å^3$ | 3373.50 | 1540.43 |
| Z | 4 | 2 |
| cryst. dimens., mm | 0.15x0.15x0.15 | 0.16x0.08x0.16 |
| radiation ($MoK_{\bar{\alpha}}$) | 0.71069 Å | 0.71069 Å |
| abs. coeff., $cm^{-1}$ | 47.613 | 57.327 |
| scan speed, deg. $mm^{-1}$ | 5($\theta/2\theta$) | 3($\theta/2\theta$) |
| scan range, deg | 1.8 + dispersion | 2.0 + dispersion |
| data collected | $6° \leq 2\theta \leq 45°$ | $6° \leq 2\theta \leq 45°$ |
| Unique data | 4406 | 4022 |
| data with $F > 2.33\sigma(F)$ | 3437 | 3487 |
| goodness of fit | 1.267 | 1.709 |
| R, % | 5.7 | 4.6 |
| $R_w$, % | 5.3 | 4.5 |

yield a copious precipitate of small plate-like crystals. The flask was left at 0°C overnight and the solid collected by filtration, washed copiously with EtOH and dried *in vacuo*. The crude material was dissolved in warm MeCN (45 $cm^3$, ~ 50°C), filtered and EtOH (45 $cm^3$) added at this temperature. Slow cooling to ambient temperature and then 0°C overnight produced large pale yellow prisms which were collected by filtration, washed copiously with EtOH and dried *in vacuo*. Yield: 11.8 g (77%). Found: C, 53.52; H, 6.80; N, 1.82; S, 11.40; Hg, 25.90. Calc. for $C_{34}H_{51}NS_3Hg$: C, 53.00; H, 6.67; N, 1.82; S, 12.48; Hg, 26.02%.

$[NPr^n_4][Pb(SPh)_3]$ (**2**). This material was prepared in an analogous manner employing PbO (4.46 g, 20 mmol) and recrystallized as yellow prisms from MeCN/EtOH. Yield: 9.1 g (64%). Found: C, 50.14; H, 5.97; N, 1.95; S, 12.30; Pb, 28.70. Calc. for $C_{30}H_{43}NS_3Pb$: C, 49.97; H, 6.01; N, 1.94; S, 13.34; Pb, 28.73%.

*X-Ray studies*

Suitable crystals were mounted on the goniostat of a Picker four-circle diffractometer and cooled to approx. − 160°C. The diffractometer system, low temperature apparatus and general techniques for collection and reduction of data have been described previously.[9] Unit cell dimensions were obtained from 30 and 41 centred reflections for **1** and **2**, respectively. The crystal and machine parameters employed in the subsequent data collection and structure solution are collected in Table 1.

$[NBu^n_4][Hg(SPh)_3]$ (**1**). The position of the Hg atom was located by a Patterson function and standard Fourier techniques located the remaining non-hydrogen atoms. After initial refinement cycles, a difference Fourier showed the positions of all the hydrogen atoms, which were included in the final refinement with isotropic thermal parameters; all other atoms were refined anisotropically. No absorption correction was performed. Final refinement parameters are included in Table 1.

$[NPr^n_4][Pb(SPh)_3]$ (**2**). The structure was solved and refined in a manner analogous to (**1**) except that hydrogen atoms were included in the final refinement cycles in calculated positions.

## RESULTS AND DISCUSSION

HgO and PbO readily dissolve in methanolic solutions of NaSPh to yield pale yellow solutions (eqn 1) from which the $[M(SPh)_3]^-$ (M = Hg, Pb) anions can be precipitated in high yield by the addition of bulky quaternary ammonium salts. We

$$MO + 4NaSPh \xrightarrow[N_2]{MeOH} Na[M(SPh)_3] + NaSPh + [Na_2O] \quad (1)$$

have employed the metal oxides rather than the halides as reagents to avoid the presence of potentially ligating halide ions. The use of MO (M = Zn or Pb) to prepare neutral $M(SC_6Cl_5)_2$ has been described elsewhere.[6d]

Previously it had been shown[6c] that $Hg(NO_3)_2$ will react with four equivalents of $NaSC_6H_4$-*p*-Cl to yield $[NMe_4]_2[Hg(SC_6H_4\text{-}p\text{-}Cl)_4]$ (**3**) in the presence of $NMe_4^+$ cations. Our isolation of a three-coordinate complex from a similar system suggests an equilibrium in solution between the mono- and di-anions (eqn 2). Such equilibria are

$$[Hg(SPh)_4]^{2-} \rightleftarrows [Hg(SPh)_3]^- + PhS^- \quad (2)$$

well established[10] for Hg(II) with monodentate ligands such as $CN^-$ and $Cl^-$ and, in addition, it has been shown[7] that $[Hg(SPh)_4]^{2-}$ can be obtained from solutions containing preformed $[Hg(SPh)_3]^-$ and added NaSPh. The stoichiometry of the precipitated anion (**1**) or (**3**) would thus seem to be a function of solubility dependent upon the cation employed. In contrast, only one species $[Pb(SPh)_3]^-$ is detected by $^{207}Pb$ NMR of $Pb(SPh)_2/PhS^-$ reaction mixtures, even in the presence of two equivalents of $PhS^-$.[8b]

*Description of structures*

(**1**) and (**2**) crystallize in monoclinic and triclinic space groups, respectively, and contain discrete cations and anions. The structure and metric parameters of the former and the phenyl groups of the latter are unexceptional and will not be discussed further.

The structure of the anion of (**1**) is depicted in Fig. 1. Relevant bond lengths and angles are listed in Table 2. Three $PhS^-$ groups are terminally ligated to a trigonal planar mercury atom which lies only 0.018 Å above the S(2, 3, 4) least squares plane. In $[Hg(TePh)_3]^-$, which also possesses trigonal planar coordination,[11] and Hg atom is 0.09 Å above the $Te_3$ plane. The central $HgS_3$ core is significantly distorted from local $D_{3h}$ symmetry, however, for two reasons no doubt due to lattice effects: (i) rotation about Hg in the $HgS_3$ plane of the Hg–S(4) vector by 17.1° towards Hg–S(2), yielding the S–Hg–S angles in Table 2; and (ii) significant variation in the Hg–S bond distances, 2.407(3)–2.507(3) Å (mean 2.448 Å). **3** possesses longer Hg–S distances,[6c] in accord with its greater

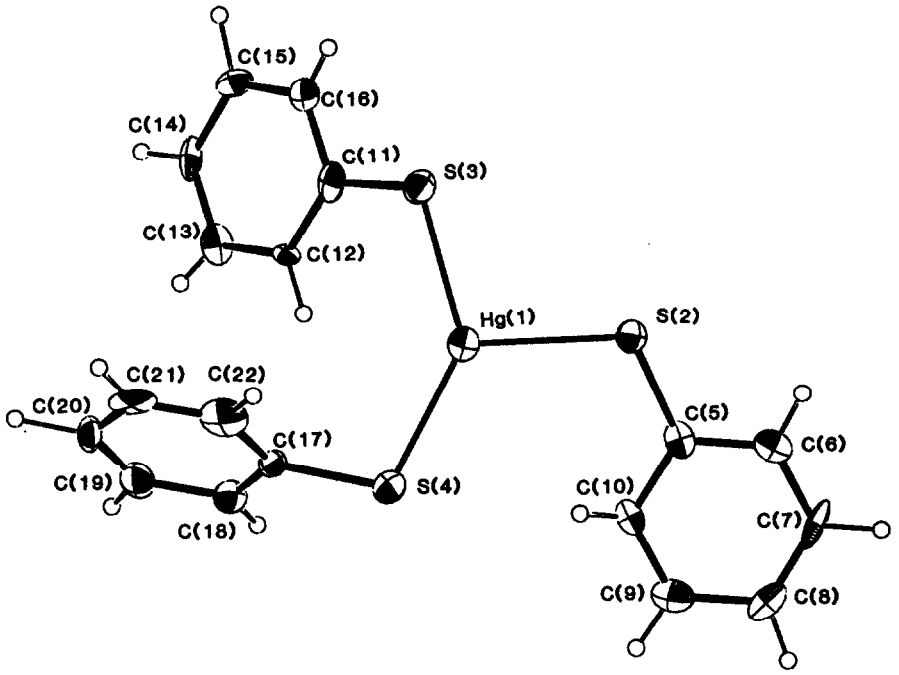



Fig. 1. The structure of the anion of 1 showing the atom labelling scheme. Non-hydrogen atoms are depicted as 50% probability ellipsoids.

coordination number, and in a much narrower range 2.537(1)–2.552(1) Å (mean 2.545 Å).

Mercury(II) usually forms complexes which are either linear two- or tetrahedral four-coordinate, but many species of empirical formulation Hg(ligand)$_3$ have been isolated. In many cases, however, crystallographic studies have shown these to be *bis*-($\mu$-bridged) dimers retaining four-coordination around each metal, e.g. $[Cl_2Hg(\mu\text{-}Cl)_2HgCl_2]^{2-}$,[12] $[(MeS)_2Hg(\mu\text{-}SMe)_2Hg(SMe)_2]^{2-}$,[6c] $[Cl_2Hg(\mu\text{-urea})_2HgCl_2]$[13] and $[X(PR_3)Hg(\mu\text{-}X)_2HgX(PR_3)]$ (X = Cl, Br, I).[14,15] Even for mononuclear species such as $[CH_3S][HgI_3]$,[16] $[NMe_4][HgX_3]$ (X = Cl, Br, I)[17] and $HgCl_2$(9-methyl-hypox anthine),[18] weaker intermolecular Hg···X interactions have been detected such that the coordination of the Hg

Table 2. Selected bond lengths (Å) and angles (°) in $[M(SPh)_3]^-$ (M = Hg(II), Pb(II)) anions

| Quantity | M = Hg(II) | M = Pb(II) |
|---|---|---|
| M-S(2) | 2.507(3) | 2.696(3) |
| M-S(3) | 2.407(3) | 2.665(3) |
| M-S(4) | 2.431(3) | 2.633(3) |
| Mean | 2.448(43) | 2.675(15) |
| S(2)-C(5) | 1.760(11) | 1.779(10) |
| S(3)-C(11) | 1.779(11) | 1.768(10) |
| S(4)-C(17) | 1.782(11) | 1.775(10) |
| S(2)-M-S(3) | 120.0(1) | 102.7(1) |
| S(2)-M-S(4) | 102.9(1) | 93.7(1) |
| S(3)-M-S(4) | 137.1(1) | 89.7(1) |
| Mean | 120.0 | 95.4 |
| M-S(2)-C(5) | 110.7(4) | 98.1(3) |
| M-S(3)-C(11) | 105.8(4) | 94.9(3) |
| M-S(4)-C(17) | 104.8(4) | 93.7(3) |

Table 3. Comparison of selected distances and angles in monomeric three-coordinate species

| Compound | M-L (Å) | L-M-L (°) | M-$L_3$ (Å)[a] | References |
|---|---|---|---|---|
| $[Hg(SPh)_3]^-$ (1) | 2.407-2.507<br>mean 2.448 | 102.9-137.1<br>mean 120.0 | 0.018 | b |
| $[Hg(TePh)_3]^-$ | 2.682-2.717<br>mean 2.697 | 110.7-125.2<br>mean 119.9 | 0.09 | 11 |
| $[HgI_3]^-$ | 2.683-2.688<br>mean 2.686 | 114.7-122.7<br>mean 120.0 | 0[c] | 12 |
| $[Cu(SPh)_3]^{2-}$ | 2.274-2.335<br>mean 2.295 | 111.7-135.4<br>mean 120.0 | 0.05 | 19 |

[a] M-$L_3$ denotes the displacement of the metal atom from the $L_3$ least squares plane.

[b] This work.

[c] The Hg atom lies on a $C_2$ axis through one Hg-I vector.

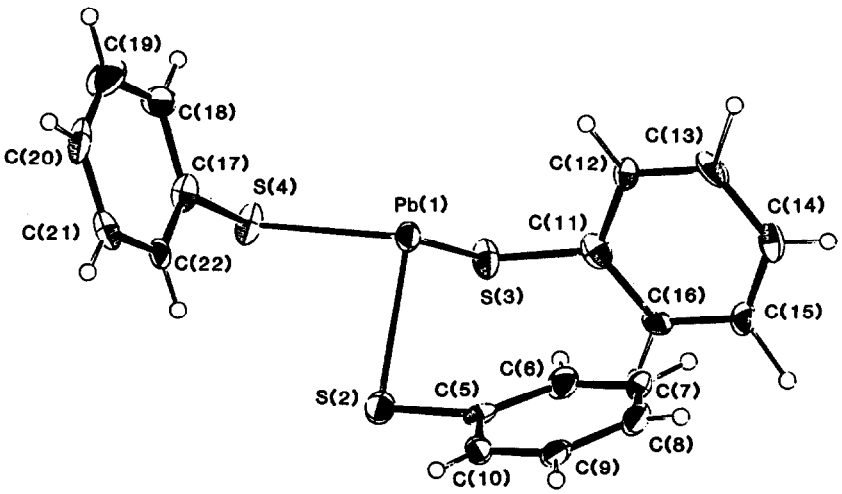



Fig. 2. The structure of the anion of **2** showing the atom labelling scheme. Non-hydrogen atoms are depicted as 50% probability ellipsoids.

atoms is best described as trigonal bipyramidal. **1** possesses no intermolecular Hg···S interactions within 5 Å and is thus a rare example of a true trigonal planar Hg(II) complex; $[Ph_4As][Hg(TePh)_3]$[12] and $[NBu^n_4][HgI_3]$[13] are two further examples, and pertinent structural data for these three compounds are compared in Table 3. Also included is the corresponding data for $[Cu(SPh)_3]^{2-}$,[19] the only established trigonal planar metal thiolate in the first transition series. In all cases, metal atom displacements ($M-L_3$) from the ligand least-squares plane are small ($\leq$ 0.09 Å) yielding mean L–M–L angles of ~120°, as expected for trigonal planar geometry. Metal–ligand distances are smaller in the Cu(I) complex reflecting the smaller radius of Cu(I)($3d^{10}$) vs Hg(II)($5d^{10}$), and, similarly, the size of the ligand atom is reflected in variation of Hg–L distances amongst the Hg(II) complexes. Otherwise the four complexes are very similar.

The structure of the anion of **2** is depicted in Fig. 2 and relevant bond lengths and angles are listed in Table 2. The coordination geometry of the lead(II) atom can be described as either trigonal pyramidal or pseudo-tetrahedral (with a stereochemically active lone pair occupying one site). The Pb atom lies 1.382 Å above the S(2, 3, 4) least squares plane of three terminally bound benzenethiolate groups. The $PbS_3$ core possesses essential $C_{3v}$ symmetry but, as in **1**, significant deviations from this symmetry are apparent. Thus, (i) the Pb–S distances range between 2.633(3)–2.696(3) Å (mean 2.675 Å) and (ii) S–Pb–S angles range between 89.7(1)–102.7(1)°. These angles are significantly less than the tetrahedral angle (109.5°) in accord with the steric requirements of a lone pair.

To our knowledge, **2** is the first structurally characterized example of an anionic lead(II) thiolate and supports the assignment of similar trigonal pyramidal coordination to $[Ph_4As][Pb(SC_6F_5)_3]$, which was based on the structures of $[MCl_3]^-$ (M = Pb, Sn) anions,[8] and $[Pb(SPh)_3]^-$ generated in solution.[8b]

Complexes **1** and **2** represent rare examples of mononuclear three-coordinate metal thiolates and may prove useful starting materials for the preparation of higher nuclearity metal-thiolate systems. Based on $^{113}Cd$ NMR studies of metallothionein,[3] the metals in this protein appear to be in two polynuclear aggregates of 3 and 4 metal atoms of postulated formulation $Cd_4(SPh)_{11}^{3-}$ and $Cd_3(SPh)_9^{3-}$. If mercury metallothionein binds the metal atoms similarly, the corresponding mercury species should be present; such units are unknown at the present time in mercury thiolate chemistry. It has been shown that trigonal planar $[Cu(SPh)_3]^{2-}$ can be converted to adamantane-like $[Cu_4(SPh)_6]^{2-}$ on treatment with equimolar Cu(I) salts.[19] We have, therefore, explored a similar reaction of **1** with $HgCl_2$ in an attempt to prepare $[Hg_4(SPh)_6]^{2+}$ or $[Hg_4(SPh)_6Cl_4]^{2-}$. Preliminary experimentation, however, has yielded only $Hg(SPh)_2$ as an isolable product but further investigation is obviously warranted.

*Supplementary material.* A listing of $F_o/F_c$, atomic coordinates, temperature factors, and bond lengths and angles have been deposited with the Editor from whom copies are available on request. Atomic coordinates have also been deposited with the Cambridge Crystallographic Data Base.

*Acknowledgements*—We thank the Science and Engineering Research Council for an Advanced Fellowship (G.C.) and the Bloomington Academic Computer Service for a gift of computer time.

## REFERENCES


1. T. W. Clarkson, *Ann. Rev. Pharm.* 1972, **12**, 375 and references therein.
2. J. H. R. Kagi and B. L. Vallee, *J. Biol. Chem.* 1961, **236**, 2435.
3. J. D. Otvos and I. M. Armitage, *Proc. Nat. Acad. Sci. U.S.A.* 1980, **77**, 7094.
4. Two crab metallothioneins contain only 18 cysteines; K. Lerch, D. Ammer and R. W. Olafson, *J. Biol. Chem.* 1982, **257**, 2420.
5. J. K. Piotrowski, B. Trojanowska, J. M. Wisniewski-Knypl and W. Bolanowska, *Toxicol. Appl. Pharmacol.* 1974, **27**, 11.
6. (a) G. K. Carson and P. A. W. Dean, *Inorg. Chim. Acta* 1982, **66**, 157; (b) S. Choudhury, I. G. Dance, P. J. Guerney and A. D. Rae, *Inorg. Chim. Acta* 1983, **70**, 227, and unpublished work referred to herein; (c) W. Beck, K. H. Stetter, S. Tadros and K. E. Schwarzhans, *Chem. Ber.* 1967, **100**, 3944; (d) C. R. Lucas and M. E. Peach, *Inorg. Nucl. Chem. Lett.* 1969, **5**, 73.
7. J. Liesk, P. Schulz and G. Klar, *Z. Anorg. Allg. Chem.* 1977, **435**, 103.
8. (a) M. Muller, R. J. H. Clark and R. S. Nyholm, *Trans. Met. Chem.* 1978, **3**, 369; (b) J. J. I. Arsenault and P. A. W. Dean, *Can. J. Chem.* 1983, **61**, 1516.
9. J. C. Huffman, L. N. Lewis and K. G. Caulton, *Inorg. Chem.* 1980, **19**, 2755.
10. F. A. Cotton and G. Wilkinson, *Advanced Inorganic Chemistry*, Chap. 19. Interscience, New York (1980), and references therein.
11. U. Behrens, K. Hoffman and G. Klar, *Chem. Ber.* 1977, **110**, 3672.
12. P. L. Goggin, P. King, D. E. McDawn, G. E. Taylor, P. Woodward and M. Sandstrom, *J. Chem. Soc. Dalton Trans.* 1982, 875.
13. K. Lewinski, J. Sliwinski and L. Lebioda, *Inorg. Chem.* 1983, **22**, 2339.
14. N. A. Bell, M. Goldstein, T. Jones, L. A. March and I. W. Nowell, *Inorg. Chim. Acta* 1982, **61**, 83.
15. N. A. Bell, M. Goldstein, T. Jones and I. W. Nowell, *Inorg. Chim. Acta* 1983, **69**, 155.
16. R. H. Fenn, *Acta Cryst.* 1978, **B34**, 273.
17. E. Fatuizzo, R. Nitsche, H. Roetschi and S. Zingg, *Phys. Rev.* 1962, **125**, 514.
18. N. B. Behrens, B. A. Cartwright, D. M. L. Goodgame and A. C. Skapski, *Inorg. Chim. Acta* 1978, **31**, L471.
19. D. Coucouvanis, C. N. Murphy and S. K. Kanodia, *Inorg. Chem.* 1980, **19**, 2993.

*Polyhedron* Vol. 3, No. 11, pp. 1255–1265, 1984
Printed in the U.S.A.

0277–5387/84 $3.00 + .00
Pergamon Press Ltd.

# ALKYL, HYDRIDO AND RELATED COMPOUNDS OF RUTHENIUM WITH TRIMETHYLPHOSPHINE AND BIS(1,2-DIMETHYLPHOSPHINO)ETHANE. X-RAY CRYSTAL STRUCTURES OF *CIS*-HYDRIDO-ETHYLTETRAKIS(TRIMETHYLPHOSPHINE)-RUTHENIUM(II) AND ETHYLENE TETRAKIS-(TRIMETHYLPHOSPHINE)RUTHENIUM(0)

**WAI-KWOK WONG, KWOK W. CHIU, JOHN A. STATLER and GEOFFREY WILKINSON***

Chemistry Department, Imperial College of Science and Technology, London SW7 2AY, England

and

**MAJID MOTEVALLI and MICHAEL B. HURSTHOUSE***

Chemistry Department, Queen Mary College, London E1 4NS, England

(*Received* 28 *February* 1984, *accepted* 30 *March* 1984)

**Abstract**—The interaction of *trans*-$RuCl_2(PMe_3)_4$ with $R_2Mg$, depending on the reaction conditions and the alkyl groups gives either $(C_2H_4)Ru(PMe_3)_4$ or *cis*-$Ru(H)(C_2H_5)(PMe_3)_4$ for R = ethyl, and *cis*-$Ru(H)(^nC_3H_7)(PMe_3)_4$ for R = *n*-propyl. The interaction of $Et_2Mg$ with *trans*-$RuX_2(dmpe)_2$ (X = Cl, $CO_2Me$) gives either *cis*-$Ru(Et_2)(dmpe)_2$ for X = Cl or *trans*-$Ru(Et)_2(dmpe)_2$ for X = $CO_2Me$. NMR data for $(C_2H_4)Ru(PMe_3)_4$ suggest that ethylene is bound in the $\eta^2$ or metallocyclopropane form, which is confirmed by a single-crystal X-ray diffraction study. This shows a relatively long carbon–carbon bond distance of 1.44(1)Å between the "ethylene" carbons. The structure of *cis*-$Ru(H)(C_2H_5)(PMe_3)_4$ has also been confirmed by a single-crystal X-ray diffraction study. Possible mechanisms for the observed reactivities are considered.

Metal hydridoalkyl complexes have long been postulated as key intermediates in metal catalysed hydroformylation and hydrogenation of olefins but relatively few mono-nuclear hydridoalkyl complexes are known. We have recently described the synthesis of *cis*-$Ru(H)(Me)(PMe_3)_4$[1] and we report here the synthesis of *cis*-$Ru(H)(R)(PMe_3)_4$, R = Et, $^n$Pr, via the interaction of *trans*-$RuCl_2(PMe_3)_4$ with the dialkyl magnesium. The synthesis of the ethylene complex, $(C_2H_4)Ru(PMe_3)_4$, and the results of the interaction of *trans*-$RuX_2(dmpe)_2$ (X = Cl, $CO_2Me$) with $Et_2Mg$ are also reported. NMR data for new compounds are collected in Tables 1–3.

*Authors to whom all correspondence should be addressed.

## RESULTS AND DISCUSSION

1. *Reactions of trans*-$RuCl_2(PMe_3)_4$ *with* $Et_2Mg$

(a) *In diethylether at* −78°C. When *trans*-$RuCl_2(PMe_3)_4$ was treated with slight excess of $Et_2Mg$ in diethylether at −78°C a pale yellow compound (major product) and a white compound (minor product) were isolated. Both compounds are extremely air sensitive; they are soluble in most organic solvents, although they react with alcohols and chlorinated solvents.

The pale yellow compound *A* has the stoichiometry $Ru(C_2H_4)(PMe_3)_4$. Cryoscopic molecular weight measurement indicates that *A* is a monomer in benzene solution. The $^{31}P\{^1H\}$ spectrum shows two triplets at $\delta$ 0.9 ($J_{PP}$ = 35.4 Hz) and $\delta$ −14.6 ppm ($J_{PP}$ = 35.4 Hz) with relative intensity

Table 1. $^1$H NMR data[a]

| Compound | δ,ppm | J(Hz) | Assignment |
|---|---|---|---|
| cis-Ru($C_2H_4$)($PMe_3$)$_4$ | 1.32,d[b](9) | 2.3 | cis-$PMe_3$ |
| | 1.30,d(9) | 1.5 | cis-$PMe_3$ |
| | 1.02,t(18) | 2.1 | trans-$PMe_3$ |
| | 0.92,t(4) | 7.7 | $CH_2$ |
| cis-Ru(H)(Et)($PMe_3$)$_4$ | 1.33,t(18) | 2.5 | trans-$PMe_3$ |
| | 1.18,d(9) | 4.7 | cis-$PMe_3$ |
| | 1.02,d(9) | 4.9 | cis-$PMe_3$ |
| | 1.76,m(2) | | Ru-$CH_2$-$CH_3$ |
| | 0.68,t(3) | 2.2 | Ru-$CH_2$-$CH_3$ |
| | -9.87,m(1) | | Ru-H |
| cis-Ru(H)($^n$$C_3H_7$)($PMe_3$)$_4$ | 1.32,t(18) | 2.2 | trans-$PMe_3$ |
| | 1.19,d(9) | 4.9 | cis-$PMe_3$ |
| | 1.04,d(9) | 4.9 | cis-$PMe_3$ |
| | 1.87,m(2) | | Ru-$CH_2$-$CH_2CH_3$ |
| | 1.43,m(3) | | Ru-$CH_2CH_2CH_3$ |
| | 0.58,m(2) | | Ru-$CH_2CH_2CH_3$ |
| | -9.85,m | | Ru-H |
| cis-Ru(Et)$_2$(dmpe)$_2$ | 1.80,m(6) | | Ru$CH_2CH_3$ |
| | 1.37,m(8) | | P$CH_2CH_2$P |
| | 1.14,m(24) | | $Me_2PCH_2CH_2PMe_2$ |
| | 0.45,m(4) | | Ru$CH_2CH_3$ |
| trans-Ru(Et)$_2$(dmpe)$_2$ | 1.33,m(8) | | P$CH_2CH_2$P |
| | 1.20,m(24) | | $Me_2$P |
| | 1.42,t(6) 7.8Hz | | Ru$CH_2CH_3$ |
| | -0.22,m(4) | | Ru$CH_2CH_3$ |

[a] In $C_6D_6$ with reference to $Me_4Si$(60.0), relative areas are in parenthesis; d, doublet; t, triplet; m, multiplet.

Table 2. $^{31}P$-{$^1H$} NMR data[a]

| Compound | δ, ppm | $J_{PP}$ Hz | Assignment |
|---|---|---|---|
| cis-$Ru(C_2H_4)(PMe_3)_4$ | 0.9, t(2) | 35.4 | trans-$PMe_3$ |
| | −14.6, t(2) | 35.4 | cis-$PMe_3$ |
| cis-$RuH(C_2H_5)(PMe_3)_4$ | −1.3, t(2) | 25.5 | trans-$PMe_3$ |
| | −12.9, t(1) | 25.5 | cis-$PMe_3$ |
| | −13.1, t(1) | 25.5 | cis-$PMe_3$ |
| cis-$RuH(^nC_3H_7)(PMe_3)_4$ | −1.4, t(2) | 24.4 | trans-$PMe_3$ |
| | −12.9, t(1) | 24.4 | cis-$PMe_3$ |
| | −13.1, t(1) | 24.4 | cis-$PMe_3$ |
| cis-$Ru(Et)_2(dmpe)_2$ | 36.7, t | 17.8 | trans-$PMe_2$ |
| | 29.8, t | 17.8 | cis-$PMe_2$ |
| trans-$Ru(Et)_2(dmpe)_2$ | 44.7, s | | $Me_2P$ |

[a] In $C_6D_6$ referenced to external 85% $H_3PO_4$ (δ0.0), relative areas are in parenthesis. Chemical shifts in ppm; negative upfield from 85% $H_3PO_4$. s, singlet; t, triplet.

1:1 for the four $PMe_3$ groups. The triplet at δ 0.9 ppm can be assigned to the two *trans*- and the triplet at −14.6 ppm to the two *cis*-$PMe_3$ groups respectively. These assignments are consistent with those for $^{31}P$ NMR data on the similar complex $Ru(C_2H_4)(dmpe)_2$ [dmpe = bis(1,2-dimethylphosphino)ethane][2]; X-ray data on the latter complex is not available. There are two extreme resonance forms for the binding of $C_2H_4$ to a metal, namely $\eta^2$-ethylene and metallacyclopropane.[3] The $^{13}C$-{$^1H$} spectrum of $Ru(C_2H_4)(PMe_3)_4$ shows a quintet ($J = 5.8$ Hz) for the $CH_2$ carbons at δ 14.3 ppm; this relatively high field shift when compared with data[4] for ($\eta^2$-$CH_2CHCO_2Me$)$Ru(CO)_4$(δ 35.5, 23.9 ppm) suggests that the contribution of the metallocyclopropane resonance form may be significant. This is also supported by the $^1H$ NMR data of *A*, which shows a triplet ($J_{PH} = 7.7$ Hz) in the aliphatic region (δ 0.92 ppm) for the $CH_2$ protons. This shift may be compared to δ 0.77 (at 80°C) for $(C_2H_4)Ru(dmpe)_2$ and δ 0.59 (at 80°C) for $(C_2H_4)Fe(dmpe)_2$, which was said to be the highest field shift reported to date for a metal ethylene complex and consistent with a high electron density on the metal.[3] Similarly for $(C_2H_4)Pt(PEt_3)_2$ the ethylene protons appear at δ 2.15 ppm[5] and for ($\eta^2$-$CH_2CHCO_2Me$)$Ru(CO)_4$[4] at δ 1.74 and 2.47 ppm.

The metallacycle formulation is confirmed by the X-ray structural data: the molecular structure is shown in Fig. 1 and bond lengths and angles in Table 4. The most notable feature of the structure is that the $C_2H_4$ group is co-ordinated in an almost symmetrical fashion [Ru–C = 2.16, 2.18(1)Å], with the C–C bond lying close to the "equatorial" plane of the metal co-ordination polyhedron. The latter can be described either as a distorted octahedron with the $C_2H_4$ group occupying two co-ordination sites (and therefore forming a metallacyclopropane ring in a formally ruthenium(II) complex), or as a distorted trigonal bipyramid with the $C_2H_4$ group

Table 3. $^{13}C$-{$^1H$} NMR data[a]

| Compound | δppm | $J_{PC}$Hz | Assignment |
|---|---|---|---|
| $Ru(C_2H_4)(PMe_3)_4$[b] | 29.1,t | 8.3 | trans-$P\underline{Me}_3$ |
| | 20.9,g | 5 | cis-$P\underline{Me}_3$ |
| | 20.4,g | 5 | cis-$P\underline{Me}_3$ |
| | 14.3,p | 5.8 | $\underline{CH}_2$ |
| $RuH(C_2H_5)(PMe_3)_4$ | 28.6,d,f,m | 13.1 | cis-$P\underline{Me}_3$ |
| | 24.9, t of t | 11.5;4.1 | trans-$P\underline{Me}_3$ |
| | 23.0, d Of m | 12.3 | cis-$P\underline{Me}_3$ |
| | 27.6,d | 12.3 | $CH_2\underline{CH}_3$ |
| | 0.25,m | | Ru-$\underline{CH}_2CH_3$ |
| $RuH(n\text{-}C_3H_7)(PMe_3)_4$ | 28.6, d of m | 13.3 | cis-$P\underline{Me}_3$ |
| | 24.8, t of t | 12.5, 3.3 | trans-$P\underline{Me}_3$ |
| | 23.1, d of m | 14 | cis-$P\underline{Me}_3$ |
| | 37.0, d | 10.8 | Ru-$CH_2\underline{CH}_2CH_3$ |
| | 22.7,s | | Ru-$CH_2CH_2\underline{CH}_3$ |
| | 12.5, m | | Ru-$\underline{CH}_2CH_2CH_3$ |

[a] In $C_6D_6$ referenced to $Me_4Si$(δ0.0). [b] In $d_8$-toluene; s, singlet; d, doublet; t, triplet; q, quartet; p, pentuplet; m, multiplet.

occupying one co-ordination site (and therefore π-bonding as an ethylene molecule in a formally ruthenium(0) complex). The former model is obviously to be considered a significant contributor to the bonding description in view of the C(4)–C(2) bond length of 1.44(1)Å and the particular orientation of the $RuC_2$ plane. Indeed, the five atoms Ru, P(1), P(4), C(1) and C(2) define a very good plane, with a maximum atomic deviation of 0.002Å. Apart from the obvious deviation from ideal octahedral geometry caused by the restricted bite of the $C_2H_4$ ligand, the only other distortions are an asymmetry in the equatorial P–Ru–C angles, 96.2 and 118.8°, and a bending over of the two axial phosphines towards the $C_2H_4$ group giving a P(2)–Ru–P(3) angle of 166.1°. Both deformations arise from a need to accommodate acceptable phosphine Me ... Me interactions. The Ru–P distances show differences which clearly reflect the structural inequivalence of the axial and equatorial sites. The Ru–P(2) and Ru–P(3) bonds, which are *trans* to each other, are some 0.02–0.03Å longer than the equatorial Ru–P(1), Ru–P(4) bonds, which in turn are *trans* to the Ru–C bonds.

(b) *In tetrahydrofuran at* ca. 20°C. As noted above a white minor product was also isolated from the reaction in diethylether. In tetrahydrofuran at ambient temperature with a slight excess of $Et_2Mg$ this is the sole product. The compound is extremely air and moisture sensitive. It is soluble in most organic solvents but reacts with alcohols and chlorinated solvents.

The white compound *B* has the stoichiometry $Ru(C_2H_6)(PMe_3)_4$. Cryoscopic molecular weight measurement indicates that it is a monomer in benzene solution. The IR spectrum shows a metal–

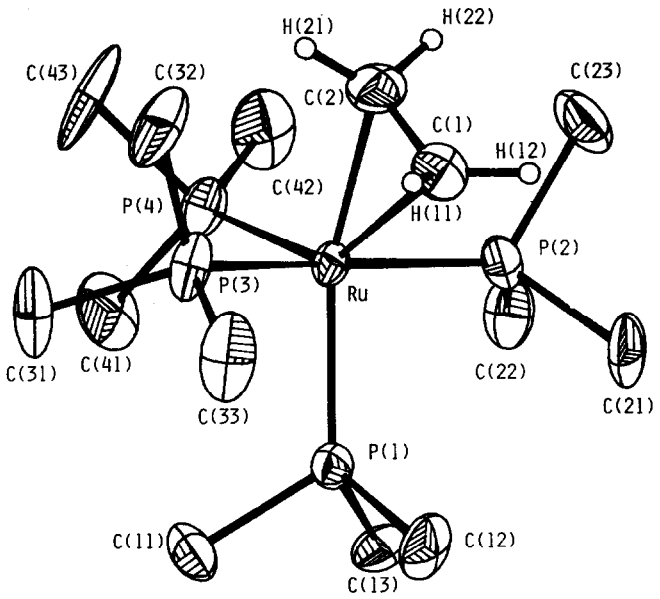



Fig. 1. The structure of $Ru(C_2H_4)(PMe_3)_4$.

Table 4. Bond lengths and angles for $Ru(C_2H_4)(PMe_3)_4$

a) Bond lengths (Å)

| | | | |
|---|---|---|---|
| P(1)-Ru | 2.309(3) | P(2)-Ru | 2.324(3) |
| P(3)-Ru | 2.327(3) | P(4)-Ru | 2.297(3) |
| C(1)-Ru | 2.178(6) | C(2)-Ru | 2.155(7) |
| C(11)-P(1) | 1.847(7) | C(12)-P(1) | 1.851(7) |
| C(13)-P(1) | 1.838(6) | C(21)-P(2) | 1.835(7) |
| C(22)-P(2) | 1.849(6) | C(23)-P(2) | 1.850(6) |
| C(31)-P(3) | 1.857(7) | C(32)-P(3) | 1.839(7) |
| C(33)-P(3) | 1.837(7) | C(41)-P(4) | 1.842(7) |
| C(42)-P(4) | 1.825(7) | C(43)-P(4) | 1.837(7) |
| H(11)-C(1) | 1.014(44) | H(12)-C(1) | 1.040(60) |
| C(2)-C(1) | 1.439(9) | H(21)-C(2) | 1.024(43) |
| H(22)-C(2) | 1.085(58) | | |

b) Bond angles (deg.)

| | | | |
|---|---|---|---|
| P(2)-Ru-P(1) | 89.5 | P(3)-Ru-P(1) | 90.1 |
| P(3)-Ru-P(2) | 166.1 | P(4)-Ru-P(1) | 106.2 |
| P(4)-Ru-P(2) | 96.9 | P(4)-Ru-P(3) | 96.5 |
| C(1)-Ru-P(1) | 118.8(3) | C(1)-Ru-P(2) | 83.9(3) |
| C(1)-Ru-P(3) | 84.2(3) | C(1)-Ru-P(4) | 135.0(2) |
| C(2)-Ru-P(1) | 157.6(2) | C(2)-Ru-P(2) | 87.0(3) |
| C(2)-Ru-P(3) | 88.1(3) | C(2)-Ru-P(4) | 96.2(3) |
| C(2)-Ru-C(1) | 38.8(2) | C(11)-P(1)-Ru | 121.0(3) |
| C(12)-P(1)-Ru | 118.8(3) | C(12)-P(1)-C(11) | 97.7(4) |
| C(13)-P(1)-Ru | 121.2(3) | C(13)-P(1)-C(11) | 94.8(4) |
| C(13)-P(1)-C(12) | 97.8(4) | C(21)-P(2)-Ru | 115.6(3) |
| C(22)-P(2)-Ru | 123.4(3) | C(22)-P(2)-C(21) | 99.2(4) |
| C(23)-P(2)-Ru | 118.8(3) | C(23)-P(2)-C(21) | 97.5(4) |
| C(23)-P(2)-C(22) | 97.5(4) | C(31)-P(3)-Ru | 122.5(3) |
| C(32)-P(3)-Ru | 118.7(3) | C(32)-P(3)-C(31) | 97.5(4) |
| C(33)-P(3)-Ru | 116.0(3) | C(33)-P(3)-C(31) | 100.1(4) |
| C(33)-P(3)-C(32) | 97.3(4) | C(41)-P(4)-Ru | 122.9(3) |
| C(42)-P(4)-Ru | 119.9(3) | C(42)-P(4)-C(41) | 96.6(4) |
| C(43)-P(4)-Ru | 116.3(3) | C(43)-P(4)-C(41) | 99.3(5) |
| C(43)-P(4)-C(42) | 96.7(5) | H(11)-C(1)-Ru | 114.4(26) |
| H(12)-C(1)-Ru | 113.7(32) | H(12)-C(1)-H(11) | 119.5(42) |
| C(2)-C(1)-Ru | 69.7(4) | C(2)-C(1)-H(11) | 119.0(26) |
| C(2)-C(1)-H(12) | 110.6(34) | C(1)-C(2)-Ru | 71.5(4) |
| H(21)-C(2)-Ru | 109.7(25) | H(21)-C(2)-C(1) | 117.8(26) |
| H(22)-C(2)-Ru | 115.3(31) | H(22)-C(2)-C(1) | 116.6(34) |
| H(22)-C(2)-H(21) | 117.2(42) | | |

hydride stretch at 1832 $cm^{-1}$ and the $^1H$ NMR spectrum shows the hydride resonance as a multiplet at $\delta -9.87$ ppm. The resonance for the ethyl moiety consists of a triplet at $\delta$ 0.68 ($J_{HH} = 2.2$ Hz) for the methyl protons and a multiplet centred around $\delta$ 1.76 ppm for the methylene protons. The spectrum also shows a triplet ($J_{PH} = 2.5$ Hz), a doublet ($J_{PH} = 4.7$ Hz), and a doublet ($J_{PH} = 4.9$ Hz) of relative intensities 2:1:1 at $\delta$ 1.33, 1.18 and 1.02 ppm respectively for the trimethylphosphine protons. This resonance pattern indicates that *B* has a *cis*-hydridoalkyl configuration with the proton resonance of the two equivalent *trans*-$PMe_3$ groups centred at $\delta$ 1.33 ppm and that of the two non-equivalent *cis*-$PMe_3$ groups centred at $\delta$ 1.18 and $\delta$ 1.02 ppm. The $^{31}P$-$\{^1H\}$ spectrum also exhibits a resonance pattern expected for the *cis* isomer. This shows three triplets of relative intensity of 2:1:1 centred at $\delta$ 1.3 ($J_{PP} = 25.5$ Hz), $-12.9$ ($J_{PP} = 25.5$ Hz) and $-13.1$ ($J_{PP} = 25.5$ Hz) ppm for the two equivalent *trans* and the two non-equivalent *cis*-$PMe_3$ groups respectively. Based on the spectroscopic data, *B* is formulated as *cis*-$Ru(H)(C_2H_5)(PMe_3)_4$ and this molecular geometry is confirmed by an X-ray crystallographic study. The structure of the molecule is shown in Fig. 2 whilst bond lengths and angles are given in Table 5. Points to note in the structure of this ruthenium(II) complex are the close similarity between the Ru–P bonds here and in the ethylene complex, *A*, and between all Ru–P bonds in the present complex, indicating only small differences in *trans* influencing properties between phosphines themselves and the hydride and ethyl ligands, and no differences between the hydride and ethyl.

Angular deformations in the octahedral geometry again reflect balancing of the steric interactions between the $PMe_3$ and other ligands.

2. *Reactions of trans*-$RuCl_2(PMe_3)_4$ *with* (*n-propyl*)$_2$Mg

When *trans*-$RuCl(PMe_3)_4$ was treated with slight excess of $^nPr_2Mg$ in tetrahydrofuran at room temperature a white compound, *C*, was isolated in high yield (70%). It is also the only product isolated from the reaction in $Et_2O$ at $-78°C$. The compound has stoichiometry $Ru(C_3H_8)(PMe_3)_4$ and is monomeric in benzene.

The IR spectrum shows a metal–hydride stretch at 1806 $cm^{-1}$. The $^1H$ NMR spectrum shows a multiplet centred at $\delta -9.85$ ppm for the hydride and three multiplets of relative intensity 2:3:2 centred at $\delta$ 1.87, 1.43 and 0.58 ppm, respectively, for the *n*-propyl moiety. The proton resonance pattern for the trimethylphosphine groups is similar to that of *B* and suggests a *cis*-configuration for *C*. It shows a triplet ($J_{PH} = 2.2$ Hz), a doublet ($J_{PH} = 4.9$ Hz), and a doublet ($J_{PH} = 4.9$ Hz), of intensity of 2:1:1 centred at $\delta -1.32$, 1.19 and 1.04 ppm for the two equivalent *trans*- and the two non-equivalent *cis*-$PMe_3$ groups, respectively. The $^{31}P$-$\{^1H\}$ NMR spectrum is also remarkably similar to that of *B* and further supports the *cis*-configuration. This shows three triplets of relative intensity of 2:1:1 centred at $\delta$ 1.4 ($J_{PP} = 24.4$ Hz), $-12.9$ ($J_{PP} = 24.4$ Hz) and $-13.1$ ppm ($J_{PP} = 24.4$ Hz) for the two equivalent *trans*, and the two

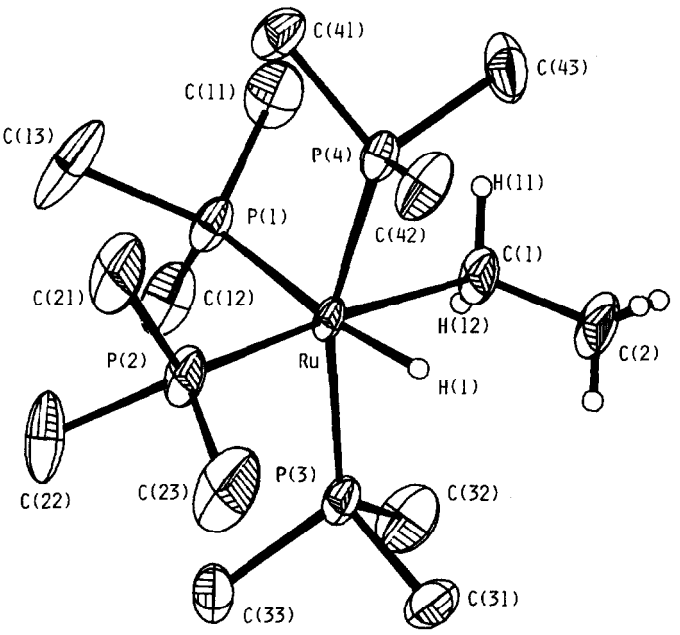



Fig. 2. The structure of $Ru(H)(Et)(PMe_3)_4$.

Table 5. Bond lengths and angles for $Ru(H)(Et)(PMe_3)_4$

a) Bond lengths (A)

| | | | |
|---|---|---|---|
| P(1)-Ru | 2.326(3) | P(2)-Ru | 2.320(3) |
| P(3)-Ru | 2.314(3) | P(4)-Ru | 2.312(3) |
| C(1)-Ru | 2.214(6) | H(1)-Ru | 1.553(41) |
| C(11)-P(1) | 1.828(6) | C(12)-P(1) | 1.834(6) |
| C(13)-P(1) | 1.831(6) | C(21)-P(2) | 1.838(7) |
| C(22)-P(2) | 1.853(7) | C(23)-P(2) | 1.829(7) |
| C(31)-P(3) | 1.833(6) | C(32)-P(3) | 1.837(6) |
| C(33)-P(3) | 1.842(6) | C(41)-P(4) | 1.843(6) |
| C(42)-P(4) | 1.829(6) | C(43)-P(4) | 1.836(6) |
| C(2)-C(1) | 1.523(8) | H(11)-C(1) | 0.978(37) |
| H(12)-C(1) | 1.023(42) | H(21)-C(2) | 1.023(53) |
| H(22)-C(2) | 0.963(55) | H(23)-C(2) | 0.981(53) |

b) Bond angles (deg.)

| | | | |
|---|---|---|---|
| P(2)-Ru-P(1) | 98.6 | P(3)-Ru-P(1) | 100.2 |
| P(3)-Ru-P(2) | 92.9 | P(4)-Ru-P(1) | 97.5 |
| P(4)-Ru-P(2) | 93.6 | P(4)-Ru-P(3) | 160.0 |
| C(1)-Ru-P(1) | 87.1(2) | C(1)-Ru-P(2) | 174.1(1) |
| C(1)-Ru-P(3) | 84.5(2) | C(1)-Ru-P(4) | 87.1(2) |
| H(1)-Ru-P(1) | 172.1(14) | H(1)-Ru-P(2) | 86.4(16) |
| H(1)-Ru-P(3) | 85.6(16) | H(1)-Ru-P(4) | 76.0(16) |
| H(1)-Ru-C(1) | 88.2(16) | C(11)-P(1)-Ru | 116.0(3) |
| C(12)-P(1)-Ru | 120.1(3) | C(12)-P(1)-C(11) | 97.5(3) |
| C(13)-P(1)-Ru | 121.4(3) | C(13)-P(1)-C(11) | 98.7(4) |
| C(13)-P(1)-C(12) | 98.4(4) | C(21)-P(2)-Ru | 121.8(3) |
| C(22)-P(2)-Ru | 121.1(3) | C(22)-P(2)-C(21) | 94.9(4) |
| C(23)-P(2)-Ru | 115.8(3) | C(23)-P(2)-C(21) | 98.7(4) |
| C(23)-P(2)-C(22) | 99.8(4) | C(31)-P(3)-Ru | 114.9(3) |
| C(32)-P(3)-Ru | 120.6(3) | C(32)-P(3)-C(31) | 98.2(3) |
| C(33)-P(3)-Ru | 123.6(3) | C(33)-P(3)-C(31) | 98.4(3) |
| C(33)-P(3)-C(32) | 96.2(4) | C(41)-P(4)-Ru | 122.8(3) |
| C(42)-P(4)-Ru | 115.4(3) | C(42)-P(4)-C(41) | 99.3(3) |
| C(43)-P(4)-Ru | 119.8(3) | C(43)-P(4)-C(41) | 96.5(3) |
| C(43)-P(4)-C(42) | 98.3(4) | C(2)-C(1)-Ru | 117.4(4) |
| H(11)-C(1)-Ru | 108.9(21) | H(11)-C(1)-C(2) | 110.5(22) |
| H(12)-C(1)-Ru | 108.7(23) | H(12)-C(1)-C(2) | 109.6(24) |
| H(12)-C(1)-H(11) | 100.4(30) | H(21)-C(2)-C(1) | 117.6(31) |
| H(22)-C(2)-C(1) | 114.2(32) | H(22)-C(2)-H(21) | 100.6(40) |
| H(23)-C(2)-C(1) | 112.4(31) | H(23)-C(2)-H(21) | 106.6(44) |
| H(23)-C(2)-H(22) | 104.1(42) | | |

non-equivalent *cis*-phosphines, respectively. Thus, based on the spectroscopic data, *C* is formulated as *cis*-$Ru(H)(^nC_3H_7)(PMe_3)_4$.

3. *Reaction of trans*-$RuCl_2(dmpe)_2$ *with* $Et_2Mg$

No reaction was observed between *trans*-$RuCl_2(dmpe)_2$ and diethylmagnesium in thf even after prolonged refluxing (2 weeks). However, if the reaction was performed in toluene at 90°C for 2 days, a complex mixture was obtained. The $^{31}P\text{-}\{^1H\}$ NMR spectrum of the filtered solution showed the presence of the following compounds: *cis*-$RuH_2(dmpe)_2$,[2] $(C_2H_4)Ru(dmpe)_2$,[2] *cis*- and *trans*-$Ru(Et)_2(dmpe)_2$ (see below). After several crystallizations a pure, white crystalline compound of stoichiometry $Ru(C_2H_5)_2(dmpe)_2$ was isolated. The $^1H$ NMR spectrum shows two complex multiplets of relative intensity 3:2 at $\delta$ 1.80 and 0.45 ppm for the methyl and the methylene protons of the ethyl moiety respectively. The $^{31}P\text{-}\{^1H\}$ NMR spectrum shows two triplets of relative intensity 1:1 at $\delta$ 35.7 ($J = 17.8$ Hz) and 29.8 ($J = 17.8$ Hz) ppm. This suggests that the compound has a *cis*-configuration with the resonances at $\delta$ 36.7 and 29.8 ppm assigned to the two axial and two equatorial phosphorus atoms, respectively. The compound thus appears to be *cis*-$RuEt_2(dmpe)_2$.

4. *Reaction of trans*-$Ru(CO_2Me)_2(dmpe)_2$ *with* $Et_2Mg$

When *trans*-$Ru(CO_2Me)_2(dmpe)_2$ was treated with $Et_2Mg$ in thf at ambient temperature, an air sensitive white compound of stoichiometry $Ru(C_2H_5)_2(dmpe)_2$ was isolated. The $^1H$ NMR spectrum shows a triplet and a multiplet of relative

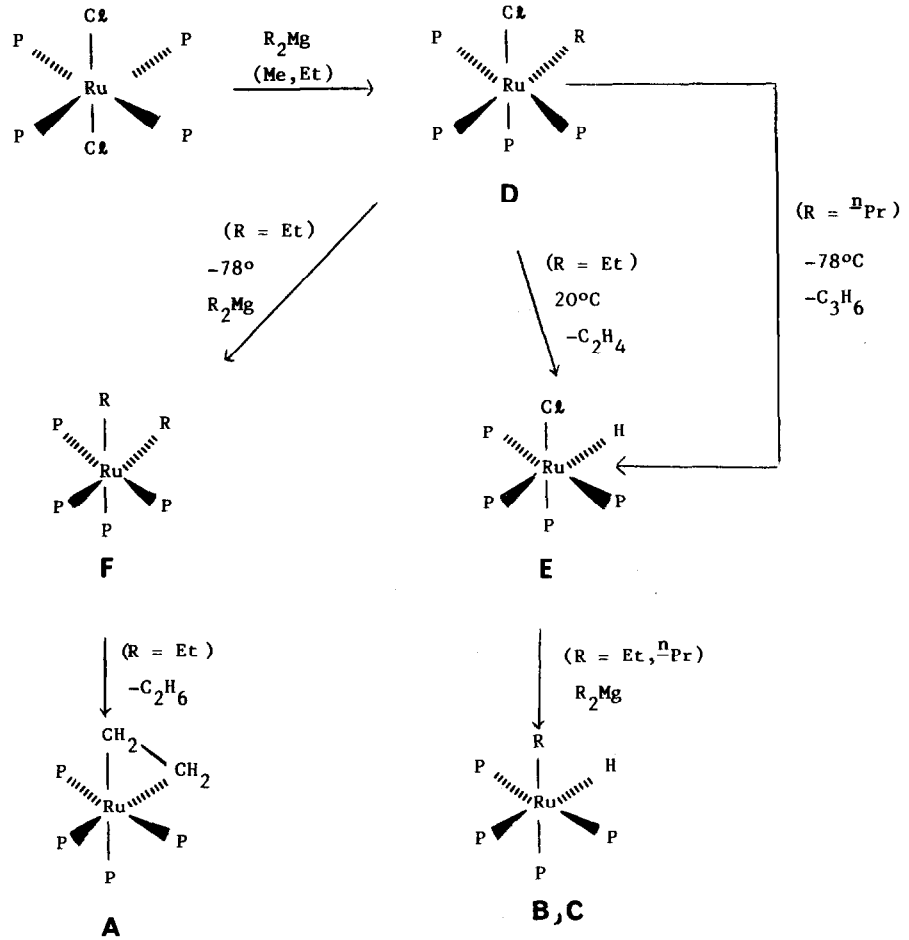
intensity 3:2 at $\delta$ 1.42 ($J = 7.8$ Hz) and $-0.22$ ppm for the methyl and the methylene protons of the ethyl moiety, respectively. The $^{31}P\text{-}\{^1H\}$ NMR spectrum shows a singlet at $\delta$ 44.7 ppm and is consistent with a *trans*-configuration. Thus the compound is formulated as *trans*-$Ru(Et)_2(dmpe)_2$.

## DISCUSSION

The reaction scheme, shown in Scheme I could account for the observed reactivities of *trans*-$RuCl_2(PMe_3)_4$ towards dialkyl magnesium. Initially, *trans*-$RuCl_2(PMe_3)_4$ reacts with dialkyl magnesium to form the alkylchloro-complex intermediate, *D*, which, depending on the alkyl group and the reaction conditions, undergoes either $\beta$-hydride transfer to give the hydridochloro complex *E* or further substitution to give the corresponding dialkyl complex, *F*. With an ethyl group, at room temperature *D* undergoes $\beta$-hydride transfer with the elimination of ethylene to give *E*, which in turn undergoes further substitution with diethyl magnesium to give *B*. At $-78$°C, *D* undergoes further substitution to give the diethyl complex, *F*, which then loses ethane through $\beta$-hydride transfer to give *A*. However, with a *n*-propyl group, *D* undergoes $\beta$-hydride transfer with elimination of ethylene even at $-78$°C to give *E* which then undergoes further substitution to give *C*.

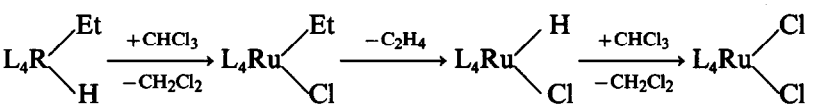
Ruthenium complexes of the types *E* and *F* are well known.[6,7] The intermediacy of *D* is supported by the isolation of the methyl analogue, *cis*-$RuMeCl(PMe_3)_4$.[1] The transformation of *D* into *E* is indirectly supported by the attempted synthesis of $Ru(Et)_2(PMe_3)_4$ through the reaction of diethyl magnesium with $Ru_2(CO_2Me)_4Cl$ in the presence of excess trimethylphosphine, in which *E* was isolated in low yield. The reaction probably proceeds via *cis*-$RuEtCl(PMe_3)_4$ which then eliminates ethylene to give *cis*-$RuHCl(PMe_3)_4$. It is of interest that there is an equilibrium[8] in solution between $[C_6H_6Ru(PMe_3)H(C_2H_4)]^+$ and $[C_6H_6Ru(PMe_3)(C_2H_5)]^+$; again this provides support for the $D \rightarrow E$ conversion.

To illustrate that the Ru–Et moiety does un-




Scheme I. Possible reaction sequences in alkylation of *trans*-$RuCl_2(PMe_3)_4$ by $R_2Mg$ ($P = PMe_3$).

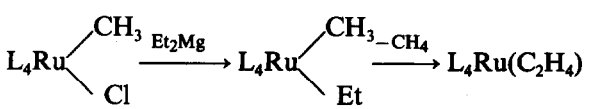
dergo facile ethylene elimination, the thermolysis of *cis*-RuH(Et)$(PMe_3)_4$ (*B*), and its reaction with chloroform were studied. The progress of the reactions was monitored by $^1H$ and $^{31}P\text{-}\{^1H\}$ NMR spectroscopy. *B* was thermally stable in $C_6D_6$ solution and did not decompose at 75°C even after 48 hr. However, at room temperature, it reacted instantaneously with chloroform to give an orange species in quantitative (NMR) yield with liberation of ethylene. The $^{31}P\text{-}\{^1H\}$ NMR spectrum of the orange species shows two triplets of equal intensity centred at $\delta$ 9.8 ($J_{PP} = 31$ Hz) and $\delta$ −11.5 ppm ($J_{PP} = 31$ Hz), which suggests a *cis*-configuration for the complex. The $^1H$ NMR spectrum shows a triplet ($J_{PH} = 3.8$ Hz), a doublet ($J_{PH} = 3.8$ Hz) and a doublet ($J_{PH} = 4.5$ Hz) of relative intensity of 2:1:1 centred at $\delta$ 1.44, 1.31 and 1.26 ppm for the two *trans*- and the two *cis*-$PMe_3$ groups, respectively. No other proton resonance corresponding to the complex was observed. The spectroscopic data suggest the product to be *cis*-$RuCl_2(PMe_3)_4$. The $^1H$ NMR spectrum of the resultant solution also showed two singlets at $\delta$ 5.37 and $\delta$ 4.98 ppm which correspond to the proton resonances of $CH_2Cl_2$ and ethylene, respectively. The observation can be explained by the following equation where L = $PMe_3$:



The formation of the hydridoalkyl complex from the hydridochloro complex *E* has been demonstrated[1] for methyl and thus supports the view that *B* is produced via the hydridochloro complex *E*.

Elimination of ethane from the *cis*-diethyl complex, *F*, to give the ethylene complex, *A*, is further supported by the thermolysis[5] of *cis*-$(Et)_2Pt(PEt_3)_2$ which eliminates ethane to give $(C_2H_4)Pt(PEt_3)_2$ in quantitative yield. This suggests that *F* is a plausible intermediate for the formation of *A*.

The reaction of *cis*-RuMeCl$(PMe_3)_4$ with diethyl magnesium in diethyl ether at −78°C also gives $(C_2H_4)Ru(PMe_3)_4$ in high yields. This can also be explained by the sequences in Scheme I and in the following equation (L = $PMe_3$):



which is further support for the intermediacy of *F* in the alkylation of *trans*-$RuCl_2(PMe_3)_4$ at low temperature.

In the case of *n*-propyl, the alkylchloro intermediate, *D*, is more prone to $\beta$-hydride transfer than the ethyl analogue and undergoes $\beta$-hydride transfer at low temperature with the elimination of propene to give intermediate, *E*, which then undergoes further substitution to give *C*.

This is consistent with the fact that propylene complexes are much more labile than the corresponding ethylene complexes.[7]

## EXPERIMENTAL

Microanalyses were by Pascher (Bonn). IR spectra (in $cm^{-1}$) were obtained on a Perkin–Elmer 683 spectrometer using Nujol mulls unless otherwise specified. Nuclear magnetic resonance spectra were recorded using either Bruker WM 250 or Jeol FX90Q spectrometers. Molecular weights were determined cryoscopically in benzene.

All operations were carried out under argon or *in vacuo*. All chemicals used were of reagent grade. Solvents were dried by standard procedures, distilled, and deaerated prior to use. Melting points were taken in sealed capillaries and are uncorrected.

*Syntheses.* *trans*-$RuCl_2(PMe_3)_4$;[6,9] *cis*-RuClMe$(PMe_3)_4$;[1] *trans*-$RuCl_2(dmpe)_2$ was prepared by refluxing *trans*-$RuCl_2(PMe_3)_4$ with two equivalents of dmpe in toluene and crystallising; *trans*-$Ru(CO_2Me)_2(dmpe)_2$ was prepared from $Ru(CO_2Me)_2(PPh_3)_2$[10] by refluxing a hexane solution containing a slight excess of dmpe, then filtering and washing the solid with petroleum and ether.

1. *($\eta^2$-ethene)tetrakis(trimethylphosphine)ruthenium(II)(A)*

*Method* 1. To an $Et_2O$ (50 $cm^3$) suspension of *trans*-$RuCl_2(PMe_3)_4$ (1.51 g, 3.2 mmol) at −78°C was added dropwise 4.5 $cm^3$ of 0.8M $Et_2Mg$ solution in ether. The reaction mixture was stirred at −78°C for 2 hr and then warmed slowly to room temperature. After stirring *ca.* 12 hr the solvent was removed under vacuum and the residue extracted with hexane (2 × 30 $cm^3$), and filtered. The filtrate was concentrated to *ca.* 10 $cm^3$ and cooled to −20°C to give light yellow needles. Yield: 0.72 g (51%); m.p., 140°C decomp. with gas evolution. [Found (required): C 38.4(38.4); H, 9.3(9.3); P, 28.5(28.6)%. *M*, 460 (436).] IR: 1425 m, 1296 m, 1279 m, 1271 m, 1095 m, 935 s, 893 w, 855 m, 707 m, 698 m.sh, 662 m, 605 m.

The mother liquor contains both *A* and *B* according to $^{31}P-\{^1H\}$ NMR spectra.

*Method* 2. To a suspension of *cis*-$RuMeCl(PMe_3)_4$ (0.9 g, 2 mmol) in $Et_2O$ (50 $cm^3$) at −78°C was added dropwise 1.4 $cm^3$ of a 0.8 M $Et_2Mg$ solution in $Et_2O$. The reaction mixture was stirred at −78°C for 2 hr and the product isolated as above. Yield (2 crops from hexane): 80%.

2. *cis-Hydridoethyltetrakis(trimethylphosphine)ruthenium(II)(B)*

To a solution of *trans*-$RuCl_2(PMe_3)_4$ (2.19 g, 4.6 mmol) in thf (50 $cm^3$) was added 6 $cm^3$ of solution of $Et_2Mg$(0.8 M in $Et_2O$, 4.8 mmol) at room temperature. The solution was stirred *ca.* 12 hr at room temperature, when the colour was light yellow. The solvent was removed under vacuum and the residue extracted with hexane (2 × 30 $cm^3$). The filtrated solution was concentrated to *ca.* 10 $cm^3$ and cooled to −20°C to yield white crystals. Yield: 1.4 g (70%); m.p., 154°C decomp. [Found (required): C, 38.5(38.6); H, 9.7(9.7); P, 28.5(28.5)%. *M*, 470(435).]

IR: 1832 m, 1420 m, 1292 s, 1273 s, 1156 m, 932 s, 846 m, 698 m, 668 w, 652 s.

3. *cis-Hydrido-n-propyltetrakis(trimethylphosphine)ruthenium(II)*

To a solution of *trans*-$RuCl_2(PMe_3)_4$ (1.43 g; 3 mmoles) in 50 $cm^3$ of thf was added dropwise at room temperature 6 $cm^3$ of a 0.53 M $(^nPr)_2Mg$ solution in $Et_2O$. The solution was stirred *ca.* 12 hr and the product isolated as in **2** as white needles. Yield: 0.95 g(70%); m.p., 110°C decomp. [Found (required): C, 40.0(40.1); H, 9.9(9.8); P, 27.3 (27.6)%. *M*, 460(449).]

IR: 1806 s, 1420 m, 1366 w, 1296 s, 1277 s, 1148 m, 938 s, 882 w, 858 m, 713 m, 708 m.sh, 682 w, 667 s.

The same product was isolated when the reaction was performed at −78°C in either $Et_2O$ or thf.

4. *Reactions of cis-hydridoethyltetrakis(trimethylphosphine)ruthenium(II)*

(a) Thermolysis. 20 mg of *cis*-$Ru(H)(Et)(PMe_3)_4$ in 0.5 $cm^3$ of $C_6D_6$ was heated at 75°C for 48 hr. No apparent reaction took place. The $^1H$ and $^{31}P-\{^1H\}$ NMR spectra of the solution showed no other species other than the starting material.

(b) With $CHCl_3$: To a solution of 30 mg of *cis*-$Ru(H)(Et)(PMe_3)_4$ in 0.5 $cm^3$ of $C_6D_6$ was added 0.05 $cm^3$ of $CHCl_3$ at room temperature. The colourless solution turned light orange within a few seconds. The $^1H$ and $^{31}P-\{^1H\}$ NMR spectra of the solution showed the quantitative formation of *cis*-$RuCl_2(PMe_3)_2$ plus $CH_2Cl_2$ and $C_2H_4$.

5. *trans-Diethylbis[bis-1,2-(dimethylphosphino)ethane]ruthenium(II)*

To a suspension of $Ru(CO_2Me)_2(dmpe)_2$ (0.74 g: 1.43 mmol) in thf (50 $cm^3$) at −78°C was added $Et_2Mg$(2 $cm^3$ of a 0.8 M solution in $Et_2O$). After stirring at −78°C for *ca.* 1 hr the solution was allowed to warm and stirred for *ca.* 12 hr when the solvent removed under vacuum. The residue was extracted into hexane (2 × 30 $cm^3$) and filtered. The pale yellow filtrate was concentrated to *ca.* 5 $cm^3$ and cooled to −20°C to give white crystals. Yield: 0.37 g, 60%; m.p., 220°C decomp. [Found (required): C, 41.3(41.8); H, 9.2(9.2); P, 27.0(27.0)%.]

IR: 1448 m, 1345 w, 1288 s, 1269 s, 1224 w, 1156 m, 1112 w, 1068, 955 w, 928 vs, 898 s, 878 s, 848 w, 825 s, 785 s, 784 m, 709 s, 687 s, 632 s.

6. *cis-Diethylbis[bis-1,2-(dimethylphosphino)ethane]ruthenium(II)*

$Et_2Mg$(2.2 $cm^3$ of 0.8 M in $Et_2O$; 1.8 mmol) was added to a solution of *trans*-$RuCl_2(dmpe)_2$ (0.76 g; 1.61 mmol) in toluene (50 $cm^3$) at −78°C. Since no reaction occurred at room temperature the solution was heated at 90°C for *ca.* 24 hr when a white precipitate was formed. The solvent was removed, the residue extracted into hexane (2 × 30 $cm^3$) and the filtered solution concentrated to *ca.* 5 $cm^3$ and cooled to −20°C to give a mixture of compounds. A pure, white crystalline compound was finally obtained after several crystallizations from hexane. Yield: 0.07 g, 10%; m.p., 150° decomp. with evolution of gas. [Found (required): C, 41.1(41.8); H, 9.0(9.2); P, 26.3(27.0)%.]

IR: 1420 m, 1290 m, 1273 m, 1260 w, 1230 w, 1164 m, 1068 m, 1028 m, 926 s, 902 m, 883 s, 828 m, 786 w, 710 m, 682 m, 639 s, 462 m.

*Crystallographic studies*

Crystals of both compounds were sealed under argon in Lindemann capillaries. All crystallographic measurements were made at T = 294K using a CAD4 diffractometer, operating in the $\theta/2\theta$ mode with graphite monochromated Mo–$K\alpha$ radiation ($\lambda = 0.71069$Å), in a manner previously described in detail.[11] The structures were solved and refined using routine procedures and standard computer programs.[11] In the refinements all non-hydrogen atoms were assigned anisotropic thermal parameters. In both compounds most of the hydrogen atoms present were located experimentally although many of those on the phosphine methyl groups did not refine well. Accordingly those on the ethylene group in *A* and the metal and ethyl group in *B* were freely refined with isotropic thermal parameters whilst those on phosphine methyl groups were inserted in idealised

positions and the $CH_3$ groups refined as rigid bodies. The weighting scheme $\omega = [1/\sigma^2(Fo) + gFo^2]$ was used in each case, with the parameter g determined in the refinement process so as to give acceptable agreement analyses. Experimental details are as follows:

*Compound A*

*Crystal data.* $Ru(C_2H_4)(PMe_3)_4$, $M = 433.44$, monoclinic, $a = 13.744(2)$, $b = 18.174(3)$, $c = 9.379(1)$Å, $\beta = 108.03(1)°$, $V = 2227.7$Å$^3$, space group $P2_1/n$, $Z = 4$, $D_c = 1.29$ g cm$^{-3}$, $F(000) = 912$, $\mu$(Mo–$K\alpha$) = 8.84 cm$^{-1}$.

*Data collection.* Crystal size 0.52 × 0.22 × 0.17 mm, scan width $\omega = 0.8 + 0.35 \tan\theta$, scan times 1.35–6.77 deg. min$^{-1}$, $1.5 \leq \theta \leq 25°$, 3919 unique data, 3035 observed [$I > 1.5\sigma(I)$].

*Structure refinement.* Number of parameters = 228, weighting factor g = 0.0003, R = 0.0336, $R_\omega = 0.0331$.

*Compound B*

*Crystal data.* $RuH(Et)(PMe_3)_4$, $M = 435.45$, triclinic, $a = 9.237(4)$, $b = 9.562(2)$, $c = 15.133(3)$Å, $\alpha = 103.50(2)$, $\beta = 90.68(3)$, $\gamma = 118.21(2)°$, $V = 1133.59$Å$^3$, space group $P1$, $Z = 2$, $D_c = 1.27$ g cm$^{-3}$, $F(000) = 456$, $\mu$(Mo–$K\alpha$) = 8.69$^{-1}$.

*Data Collection.* Crystal size 0.55 × 0.35 × 0.05 mm, scan parameters as above, 3971 unique data, 3300 observed.

*Structural refinement.* Number of parameters 236, weighting factor g = 0.0001, R = 0.0287, $R_\omega = 0.0269$.

Final atomic positional and thermal parameters full lists of bond lengths and angles and Fo/Fc values have been deposited as supplementary material with the Editor, from whom copies are available on request. Atomic co-ordinates have also been submitted to the Cambridge Crystallographic Data Centre.

*Acknowledgements*—We thank S.E.R.C. for provision of the X-ray and computing facilities, and for support, the National Science Foundation for a N.A.T.O. Postdoctoral Fellowship (J.A.S.) and Johnson Matthey PLC for a loan of ruthenium chloride.

## REFERENCES

1. J. A. Statler, G. Wilkinson, M. Thornton-Pett and M. B. Hursthouse, *J. Chem. Soc., Dalton Trans.* 1984, 1731.
2. C. A. Tolman, S. D. Ittel, A. D. English and J. P. Jesson, *J. Am. Chem. Soc.* 1978, **100**, 4080.
3. For discussion see (a) M. J. S. Dewar and G. P. Ford, *J. Am. Chem. Soc.* 1979, **101**, 783. (b) D. M. P. Mingos, In *Comprehensive Organometallic Chemistry* (Edited by G. Wilkinson, F. G. A. Stone and E. W. Abel), Vol. 3, Chap. 19. Pergamon Press, Oxford (1982). (c) A. J. Schultz, R. K. Brown, J. M. Williams and R. R. Schrock, *J. Am. Chem. Soc.* 1981, **103**, 169.
4. F. Grevels, J. G. A. Reuvers and J. Takats, *J. Am. Chem. Soc.* 1981, **103**, 4069.
5. R. G. Nuzzo, J. J. McCarthy and G. M. Whitesides, *Inorg. Chem.* 1981, **20**, 1312.
6. R. A. Jones, F. Mayor Real, G. Wilkinson, A. M. R. Galas, M. B. Hursthouse and K. M. A. Malik, *J. Chem. Soc. Dalton Trans.* 1980, 551.
7. R. A. Andersen, R. A. Jones and G. Wilkinson, *J. Chem. Soc. Dalton Trans.* 1978, 446.
8. R. Werner and H. Werner, *Chem. Bev.* 1983, **116**, 2074.
9. D. Sellman and E. Bohlen, *Z. Naturf. B.* 1982, **37B**, 1026.
10. J. D. Gilbert and G. Wilkinson, *J. Chem. Soc.* (*A*) 1969, 1749.
11. M. B. Hursthouse, R. A. Jones, K. M. A. Malik and G. Wilkinson, *J. Am. Chem. Soc.* 1979, **101**, 4128.

Polyhedron Vol. 3, No. 11, pp. 1267–1269, 1984
Printed in the U.S.A.

0277-5387/84 $3.00 + .00
Pergamon Press Ltd.

# NOTE

## STRUCTURAL STUDIES OF SIALON CERAMICS BY HIGH-RESOLUTION SOLID-STATE NMR

**J. KLINOWSKI* and J. M. THOMAS**

Department of Physical Chemistry, University of Cambridge, Lensfield Road, Cambridge CB2 1EP, England

**D. P. THOMPSON, P. KORGUL and K. H. JACK**

Wolfson Research Group for High-Strength Materials, Crystallography Laboratory, The University, Newcastle-upon-Tyne NE1 7RU, England

**and**

**C. A. FYFE and G. C. GOBBI**

Guelph-Waterloo Centre for Graduate Work in Chemistry, University of Guelph, Guelph, Ontario N1G 2W1, Canada

(*Received* 20 *January* 1984; *accepted* 17 *February* 1984)

**Abstract**—High-resolution solid-state $^{27}Al$ NMR with magic-angle spinning (MASNMR) readily monitors the quantity and coordination (four- and six-fold) of aluminium in two ceramic materials of the Si–Al–O–N system. Sialon X-phase, of approximate composition $Si_3Al_6O_{12}N_2$, contains aluminium-centred octahedra and tetrahedra in the ratio *ca.* 1.9 : 1.0, while another sample containing a mixture of sialon polytypoids shows $AlO_6$ octahedra and a large quantity of what is most probably nitrogen-coordinated tetrahedral aluminium. In addition, $^{29}Si$ MASNMR detects two different kinds of silicon in the latter sample in a 2 : 1 ratio. These observations are interpreted satisfactorily in terms of the crystal structures of the compounds and provide further examples of the potential of MASNMR in the investigation of complex ceramic systems.

Sialons[1,2] are phases in the Si–Al–O–N and M–Si–Al–O–N systems, many of which are structurally related to the mineral silicates and aluminosilicates. They are built of three-dimensional arrangements of $(Si, Al)(O, N)_4$ tetrahedra and sometimes also contain aluminium in six-fold (octahedral) coordination. Some of the sialons are of considerable technological interest as engineering ceramics because of their exceptional thermal and mechanical properties,[3] but among them are several phases which have not been completely or unequivocally characterized.

For example, sialon X-phase with an approximate composition $Si_3Al_6O_{12}N_2$ has a complex and faulted triclinic structure[4] related to that of mullite and contains aluminium in both four- and six-fold coordination. Then, in the aluminium nitride-rich corner of the Si–Al–O–N system there are six polytypoid phases[3] designated by the Ramsdell symbols 8H, 15R, 12H, 21R, 27R and $2H^{\delta}$; they have compositions $M_mX_{m+1}$ where M = Si, Al; X = O, N; and $m = 4$, 5, 6, 7, 9 and $\sim 11$ respectively. Their structures are determined by their compositions and consist of a sequence of tetrahedra similar to that in wurtzite but with every $m$th layer of tetrahedra replaced by a layer of $AlO_6$ octahedra.[5,6]

*Author to whom correspondence should be addressed.

$^{29}Si$ and $^{27}Al$ MASNMR has already provided considerable insight into the structures of silicates and aluminosilicates such as zeolite catalysts[7] and cements.[8] In these materials aluminium and silicon are present as $AlO_4$ and $SiO_4$ tetrahedra and $AlO_6$ octahedra. $^{29}Si$ MASNMR is sensitive to the type of linking of the tetrahedra and can distinguish between the five possible types of $Si(OAl)_n(OSi)_{4-n}$ structural units where $n = 0$, 1, 2, 3 or 4. $^{27}Al$ MASNMR readily distinguishes between tetrahedrally and octahedrally bonded Al. In the sialons a much greater structural variety is in principle possible in view of the presence of nitrogen. Thus, in addition to $SiO_4$ tetrahedra there may be $SiO_3N$, $SiO_2N_2$, $SiON_3$ and $SiN_4$ tetrahedra and, moreover, each type can be linked to neighbouring tetrahedra in five possible ways as described above. A similar situation can in principle be obtained with Al-centred structural units. MASNMR is uniquely equipped to monitor these various possibilities.

## EXPERIMENTAL

$^{29}Si$ and $^{27}Al$ MASNMR spectra were obtained at 79.80 and 104.22 MHz respectively using a Bruker WH-400 spectrometer with a narrow-bore superconducting magnet. Spinners of the Andrew-Beams type were made of Delrin and spun at *ca.* 3.5 kHz using nitrogen as the driving gas. Proton decoupling and cross-polarization were not used. Further details of the technique are given elsewhere.[7] The two sialon samples were finely powdered before measurement.

## RESULTS AND DISCUSSION

Figure 1(a) shows the $^{27}Al$ MASNMR spectrum of sialon X-phase. By reference to the data bank of $^{27}Al$ NMR shifts in various materials,[7] the signal at 0.82 ppm from $Al(H_2O)_6^{3+}$ is attributed to octahedral aluminium as $AlO_6$ and the signal at 66.9 ppm to $AlO_4$ tetrahedra. The observed 1.9 : 1.0 intensity ratio of tetrahedral : octahedral aluminium is in complete agreement with the structure[4] which provides for 20–22 tetrahedral and 12 octahedral aluminium atoms per unit cell. Because of the very long $^{29}Si$ $T_1$ relaxation times, it proved impossible to obtain $^{29}Si$ MASNMR spectra of sialon X-phase.

Figure 1(b) gives the $^{27}Al$ MASNMR spectrum of the sialon polytypoid. X-Ray and electron microscopic examination showed the sample to be a mixture of mainly 15R with appreciable amounts of 12H and 21R phases plus some unreacted AlN. The spectrum indicates the presence of only *two* types of aluminium. The small signal at 2.3$\bar{4}$ ppm is unambiguously attributed to $AlO_6$ octahedra and the intense signal at 108.2 ppm is tentatively assigned to Al coordinated by four nitrogen atoms, i.e. to $AlN_4$. The intensity ratio of the two signals is 9 : 1.

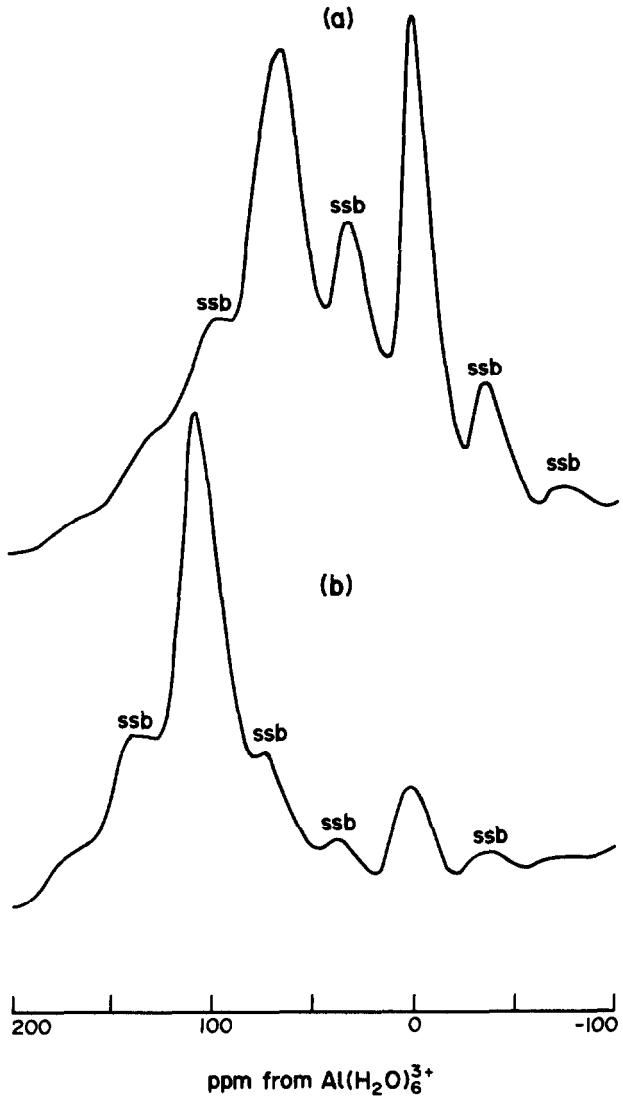



Fig. 1. $^{27}Al$ MASNMR spectra of sialons at 104.22 MHz. Chemical shifts are given in ppm from $Al(H_2O)_6^{3+}$. ssb denotes spinning sidebands. (a) Sialon X-phase. (b) Sialon polytypoid.

The $^{29}Si$ MASNMR spectrum of the same sample is given in Fig. 2. There are two distinct signals at −36.0 and −48.1 ppm from TMS in the intensity ratio 1 : 2 respectively. These chemical shifts are very different from those previously found, for example in zeolites[7] or synthetic cordierite.[9] In their extensive study of various silicates, Mägi *et al.*[10] found the range of $^{29}Si$ chemical shifts to extend from −60 ppm for some $Q^0$ silicates (i.e. those containing isolated $SiO_4$ tetrahedra) to −114 ppm for certain $Q^4$ (i.e. three-dimensional) silicates.

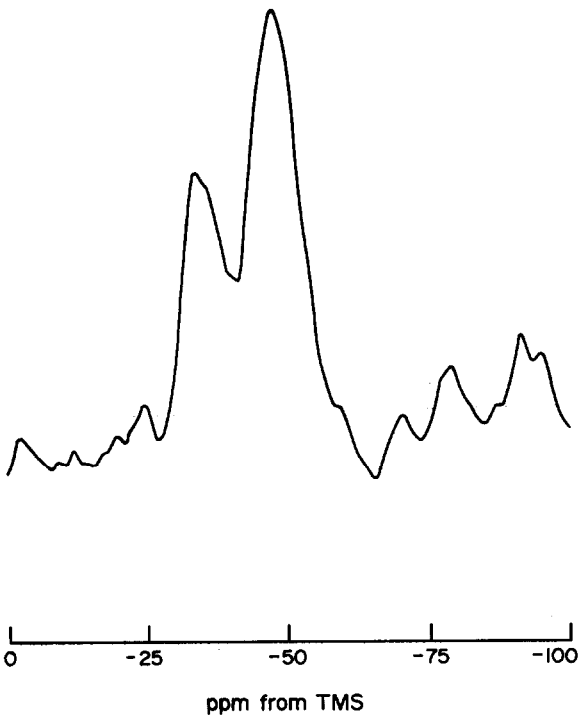



Fig. 2. $^{29}$Si MASNMR spectrum of the sialon polytypoid at 79.80 MHz. Chemical shifts are given in ppm from tetramethylsilane (TMS).

The observed signals are outside this range and are tentatively ascribed to silicon in a predominantly nitrogen environment. The $M_mX_{m+1}$ compositions of the sialon polytypoid phases deviate only slightly from $SiO_2.(m-1)AlN$. Thus, the simplest unit of structure containing only one $MX_2$ layer and one layer of octahedra also contains only two oxygen atoms that coordinate the octahedral aluminium. For example, for the 15R polytypoid, the $M_5X_6$ unit has the composition *ca.* $SiO_2.4AlN = AlO_2.SiAl_3N_4$. The metal atoms adjacent to the octahedral layer are therefore tetrahedrally coordinated by one oxygen and three nitrogen atoms, while the remaining 4-coordinated metal atoms (Si or Al) are surrounded by four nitrogen atoms. This is true for any sialon polytypoid in the series, but as the composition approaches AlN (i.e. as $m$ increases) the proportion of $MN_4$ tetrahedra increases relative to $MN_3O$ tetrahedra. The observed $^{29}$Si MASNMR peak intensities clearly depend on the relative numbers of $MN_4$ and $MN_3O$ tetrahedra and also on the distribution of silicon between these two kinds of tetrahedral sites. Even though further work is needed for a complete interpretation, the two-peak $^{29}$Si spectrum is in good agreement with expectations.

The results of this preliminary examination show that MASNMR can readily and quantitatively distinguish the various types of Si and Al in complex oxynitride ceramics.

*Acknowledgement*—We are grateful to B. P. Research Centre, Sunbury, for support.

## REFERENCES

1. Y. Oyama and O. Kamigaito, *Jap. J. Appl. Phys.* 1971, **10**, 1637.
2. K. H. Jack and W. I. Wilson, *Nature Phys. Sci.* 1972, **238**, 28.
3. K. H. Jack, *J. Mat. Sci.* 1976, **11**, 1135.
4. D. P. Thompson and P. Korgul, *Progress in Nitrogen Ceramics, NATO ASI Series* (Edited by F. L. Riley), p. 375. Martinus Nijhoff, The Hague (1973).
5. D. P. Thomson, *Nitrogen Ceramics, NATO ASI Series* (Edited by F. L. Riley), p. 129. Noordhoff, Leyden (1977).
6. D. P. Thompson, P. Korgul and A. Hendry, *Progress in Nitrogen Ceramics, NATO ASI Series* (Edited by F. L. Riley), p. 61. Martinus Nijhoff, The Hague (1983).
7. C. A. Fyfe, J. M. Thomas, J. Klinowski and G. C. Gobbi, *Angew Chem. Intl. Edn. Engl.* 1983, **22**, 259, and references therein.
8. E. Lippmaa, M. Mägi, M. Tarmak, W. Wieker and A. R. Grimmer, *Cement Concr. Res.* 1982, **12**, 537.
9. C. A. Fyfe, G. C. Gobbi, J. Klinowski, A. Putnis and J. M. Thomas, *J. Chem. Soc. Chem. Commun.* 1983, 556.
10. M. Mägi, E. Lippmaa, A. Samoson, G. Engelhardt and A. R. Grimmer, *J. Phys. Chem.* 1984, **88**, 1518.

*Polyhedron* Vol. 3, No. 11, pp. 1271–1276, 1984
Printed in the U.S.A.

0277–5387/84 $3.00 + .00
© 1984 Pergamon Press Ltd.

# NOTE

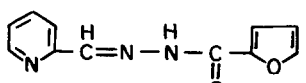
## STUDIES ON THE REACTION PRODUCTS OF *BIS*(2-FURANTHIOCARBOXYHYDRAZIDATO)M(II) WITH PYRIDINE-2- AND -4-CARBOXALDEHYDES

**N. K. SINGH*, SEEMA AGRAWAL and R. C. AGGARWAL**
Department of Chemistry, Banaras Hindu University, Varanasi 221005, India

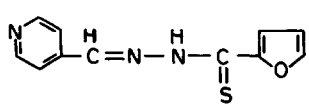
(*Received* 26 *September* 1983; *accepted after revision* 17 *February* 1984)

**Abstract**—Condensation of *bis*(2-furanthiocarboxyhydrazidatometal(II), $M(fth)_2$; [M (II) = Mn, Fe, Co, Ni, Cu and Zn] with pyridine-2- and -4-carboxaldehydes gave complexes of the formula $M(pfth)_2$ [$pfth^-$ = pyridine-2-carboxaldehyde-2-furanthiocarboxyhydrazonato], $Ni(Ifth)_2$, $Zn(Ifth)_2$, Cu(Ifth) and $Co(Ifth)_3$ ($Ifth^-$ = pyridine-4-carboxaldehyde-2-furanthiocarboxyhydrazonato). The magnetic and electronic spectral studies coupled with photoacoustic or Mössbauer spectra suggested octahedral geometry for the M(II) complexes with low-spin states for $Co(Ifth)_3$ and $Fe(pfth)_2$. IR and $^1H$ NMR spectral studies of diamagnetic complexes suggested bonding through "azomethine" nitrogen and "thiolo" sulphur. IR spectra also showed the involvement of pyridine ring nitrogen in coordination in all the complexes except Cu(Ifth), $Co(Ifth)_3$ and $Zn(Ifth)_2$. Some of the compounds possessed antimicrobial activity.

Although a few papers are available on the transition metal complexes of thiohydrazides[1–3] there is no previous work on the complexes of thiohydrazones except for the reported synthesis and characterization of *bis*(acet-thiohydrazonato) Ni(II).[4] In view of this and the potential biologically active nature of transition metal complexes of thiosemicarbazones,[5,6] which are structurally very similar to thiohydrazones the 3*d*-metal complexes of pyridine-2-carboxaldehyde-2-furanthiocarboxy hydrazone (Hpfth, *a*) and pyridine-4-carboxaldehyde-2-furanthiocarboxy hydrazone (HIfth, *b*) were synthesized and characterized by various physicochemical methods. The antibacterial activity of 2-furanthiocarboxyhydrazide (Hfth), $Cu(fth)_2$, $Zn(fth)_2$, $Cu(pfth)_2$ and $Zn(pfth)_2$ has also been studied.



a – Hpfth



b – HIfth

## EXPERIMENTAL

All the chemicals used were of BDH or equivalent quality. Pyridine-2- and -4-carboxaldehydes were prepared by reported literature method.[7] *Bis*(2-furanthiocarboxyhydrazidato)M(II) were prepared as described in our earlier paper.[3] Attempts to prepare the hydrazones by the condensation of 2-furanthiocarboxyhydrazide and pyridine-2- and -4-carboxaldehydes were not successful. Therefore, $M(pfth)_2$ [M(II) = Mn, Fe, Co, Ni, Cu and Zn] were prepared by refluxing the ethanolic suspension of the respective $M(fth)_2$ and an excess of pyridine-2-carboxaldehyde for about ~3 hr. Cu(Ifth), $Co(Ifth)_3$, $Ni(Ifth)_2$ and $Zn(Ifth)_2$ were, however, prepared in a homogeneous reaction by refluxing for ~4 hr the DMSO solution of the respective $M(fth)_2$ and pyridine-4-carboxaldehyde. After cooling to room temperature the compounds which separated were

*Author to whom correspondence should be addressed.

Table 1. Characterization data of pyridine-2- and pyridine-4-carboxaldehyde-2-furanthiocarboxyhydrazonato complexes

| Compound | Colour | Metal(%) | Nitrogen(%) | Sulphur(%) | $\mu_{eff}$ (B.M.) | M.P. (°C) |
|---|---|---|---|---|---|---|
| $Mn(pfth)_2$ | Violet | 10.94 (10.69) | 16.17 (16.31) | 12.52 (12.43) | 6.02 | >300 |
| $Fe(pfth)_2$ | Bottle green | 10.30 (10.81) | 16.04 (16.29) | 12.56 (12.41) | diamagnetic | >300 |
| $Co(pfth)_2$ | Dark brown | 10.55 (11.36) | 16.10 (16.19) | 12.49 (12.33) | 2.58 | 250(d) |
| $Ni(pfth)_2$ | Dark brown | 10.85 (11.32) | 16.04 (16.19) | 12.39 (12.34) | 3.16 | >300 |
| $Cu(pfth)_2$ | Dark brown | 12.92 (12.14) | 15.99 (16.04) | 12.38 (12.23) | 1.77 | 200 |
| $Zn(pfth)_2$ | Yellow | 12.17 (12.45) | 14.84 (15.99) | 12.28 (12.18) | diamagnetic | >300 |
| Cu(Ifth) | Dark brown | 21.32 (21.65) | 14.02 (14.31) | 11.02 (10.90) | diamagnetic | 290 |
| $Ni(Ifth)_2$ | Dark brown | 11.53 (11.29) | 15.96 (16.10) | 12.44 (12.31) | 2.60 | >300 |
| $Co(Ifth)_3$ | Yellowish brown | 7.93 (7.86) | 16.60 (16.83) | 13.02 (12.82) | diamagnetic | 230 |
| $Zn(Ifth)_2$ | Yellow | 12.72 (12.45) | 15.86 (15.99) | 12.64 (12.18) | diamagnetic | 240 |

Calculated values are given in parentheses.

Table 2. Electronic and photoacoustic spectral bands, their assignments and stereochemistry of the complexes

| Complex | Band maxima ($cm^{-1}$) | Assignments | B ($cm^{-1}$) | β | LFSE (kJ/mole) | Stereochemistry (References) |
|---|---|---|---|---|---|---|
| $Fe(pfth)_2$ | 9805,10200 | $^1A_{1g} \rightarrow {}^3T_{1g}; \rightarrow {}^3T_{2g}$ | - | - | - | l.s.oct (19) |
| $Co(pfth)_2$ | 16000 | $^4T_{1g}(F) \rightarrow {}^4A_{2g}(\nu_2)$ | - | - | - | oct (11) |
| | 20000 | $^4T_{1g}(F) \rightarrow {}^4T_{1g}(P)(\nu_3)$ | | | | |
| $Co(Ifth)_3$ | (760) | $^1A_{1g} \rightarrow {}^3T_{2g}$ | - | - | - | l.s.oct (20) |
| | 21050(480) | $^1A_{1g} \rightarrow {}^1T_{1g}$ | | | | |
| $Ni(pfth)_2$ | 12120(800) | $^3A_{2g}(F) \rightarrow {}^3T_{2g}(F)(\nu_1)$ | 571.5 | 0.53 | 174.11 | h.s.oct (16) |
| | 17390(550) | $^3A_{2g}(F) \rightarrow {}^3T_{1g}(F)(\nu_2)$ | | | | |
| | 26670(375) | $^3A_{2g}(F) \rightarrow {}^3T_{1g}(P)(\nu_3)$ | | | | |
| $Ni(Ifth)_2$ | 9525(1140) | $^3A_{2g}(F) \rightarrow {}^3T_{2g}(F)(\nu_1)$ | 791.8 | 0.73 | 136.79 | h.s.oct (16) |
| | 15380(700) | $^3A_{2g}(F) \rightarrow {}^3T_{1g}(F)(\nu_2)$ | | | | |
| | (440) | $^3A_{2g}(F) \rightarrow {}^3T_{1g}(P)(\nu_3)$ | | | | |
| $Cu(pfth)_2$ | 20000(460) | Envelope of $^2B_{1g} \rightarrow {}^2A_{1g}; \rightarrow {}^2B_{2g}; \rightarrow {}^2E_g$ | - | - | - | oct (21) |

Photoacoustic spectral bands (nm) are given in parentheses.

suction filtered, washed with ethanol and dried *in vacuo*.

The experimental details pertaining to the elemental analysis of the complexes and recording of molar conductance, magnetic susceptibility, IR and electronic spectra were the same as described in our previous paper.[3] The room temperature Mössbauer spectrum of $Fe(pfth)_2$ shown in Fig. 1 was obtained on a constant acceleration Mössbauer spectrometer using sodium nitroprusside as a calibrant and the spectrum was fitted by least squares to the Lorenzian line shape by means of the programme—Mösfit. The photoacoustic spectra were recorded in the solid state on a Princeton Applied Research Instrument, Model 6001 in the range 200–1500 nm using carbon black as a reference. The $^1H$ NMR spectra of the complexes were recorded on a Perkin–Elmer R-32 spectrophotometer in DMSO($d_6$). The antibacterial activity of the compounds was tested *in vitro* using agar plate diffusion technique[8] and the results are given in Table 3.

## RESULTS AND DISCUSSION

All the complexes are insoluble in water but are slightly soluble in DMF and DMSO; complexes $M(pfth)_2$ are slightly soluble in ethanol and methanol also. The molar conductance values of the soluble complexes in DMF show them to be non-ionic in nature. The formation of $Co(Ifth)_3$ and Cu(Ifth) is most probably connected with the redox behaviour of metal ions and the ligand and also the geometry of the ligand.[9,10] The magnetic moment and electronic spectral data are consistent with the stereochemistry of the complexes indicated against each complex in Table 2. The anomalous magnetic moment of $Co(pfth)_2$ may be due to the existence of low-spin and high-spin equilibrium arising from nearly equi-energetic $^4T_1$ and $^2E$ terms in the metal ions.[11] The values of the isomer shift ($0.50 \pm 0.01$ mm sec$^{-1}$) and quadrupole splitting ($0.40 \pm 0.005$ mm sec$^{-1}$) for $Fe(pfth)_2$ support its low-spin octahedral geometry. The non-zero quadrupole splitting may be due to the distorted octahedral geometry of the complex owing to non-identical donor atoms.[12]

Photoacoustic spectroscopy is an important tool for studying complexes in the sense that the scattered light which creates a severe problem in other conventional technique, has no effect on PAS since only the absorbed light is converted to sound.[13] The PAS bands at 760 and 480 nm in $Co(Ifth)_3$, at 800, 550 and 375 nm in $Ni(Ifth)_2$ are due to *d–d* transitions which are in accord with the octahedral geometry of these complexes[14] as shown by their electronic spectra. It may be mentioned that the first band of $Co(Ifth)_3$ and the third band of $Ni(Ifth)_2$ are not observed in their electronic spectra. The PAS of $Cu(pfth)_2$ is also in good agreement with its proposed structure.[14]

The presence of $\nu$(NH) band in $M(fth)_2$ and its disappearance in the complexes under present

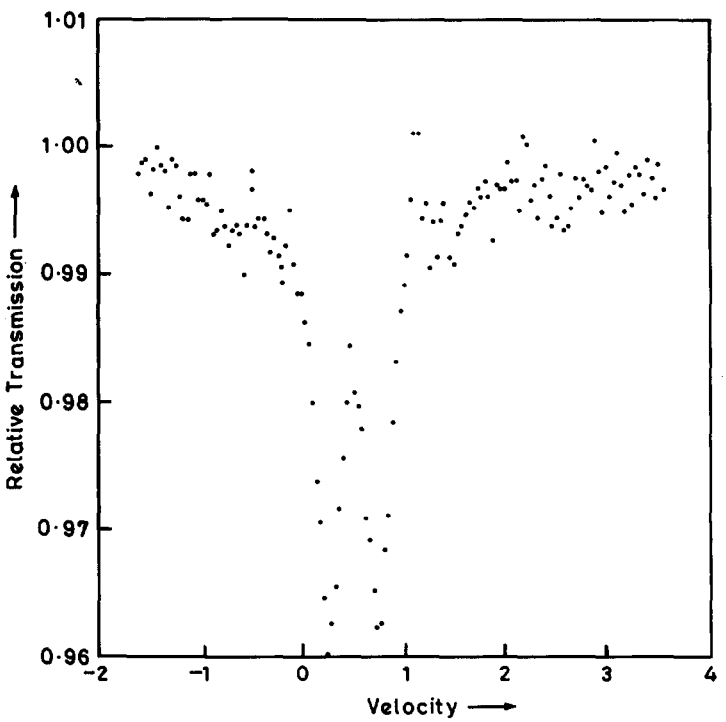



Fig. 1. Mössbauer spectrum of $Fe(pfth)_2$ at 300 K.

Table 3. Antimicrobial activity of Cu(II) and Zn(II) complexes

| Compound | Conc. used (mg/ml) | Microbial species | | |
|---|---|---|---|---|
| | | a | b | c |
| Hfth | 1 | + | - | + |
| | 10 | + | + | + |
| $Cu(fth)_2$ | 1 | + | - | - |
| | 10 | + | + | - |
| $Zn(fth)_2$ | 1 | + | - | - |
| | 10 | + | - | + |
| $Cu(pfth)_2$ | 1 | + | - | - |
| | 10 | + | - | + |
| $Zn(pfth)_2$ | 1 | + | - | - |
| | 10 | + | - | + |
| DMSO (Control) | | - | - | - |

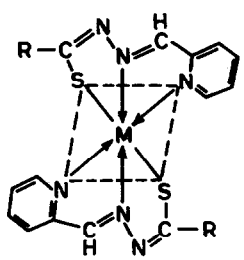
+inhibition; – no inhibition; a — *Staphylococcus aureus;* b — *Proteus mirabilis* and c — *Klebsillea pneumoniae*

study is due to the removal of $-NH_2$ protons of the former complexes during their condensation with pyridine carboxaldehydes. The presence of $\nu$ (C–S) band at 720 $cm^{-1}$ in $M(fth)_2$ as well as the present complexes indicates bonding through "thiolo" sulphur.[15] Pyridine nitrogen coordination in $M(pfth)_2$ and $Ni(Ifth)_2$ is shown by the presence of bands[16,17] at ~1595, ~620 and ~440 $cm^{-1}$. However, the occurrence of the corresponding pyridine ring vibrations in $Co(Ifth)_3$, Cu(Ifth) and $Zn(Ifth)_2$ at comparatively lower frequencies (~1580, ~605 and ~410 $cm^{-1}$) shows the non-involvement of the pyridine ring nitrogen in these complexes. The non-ligand bands due to $\nu$(M–S) and $\nu$(M–N) observed for all the complexes in 350–370 and 290–320 $cm^{-1}$ regions further support coordination through "thiolo" sulphur and azomethine nitrogen.[15]

$^1H$ NMR spectra of Zn(II) and Co(III) complexes lack resonances due to $-NH_2$ protons and show a downfield shift of ~1 ppm in –CH=N as compared to its position in 2-formylpyridinethiosemicarbazone.[18] These results suggest condensation of $-NH_2$ protons with pyridine aldehydes and participation of the resulting azomethine nitrogen in bonding.

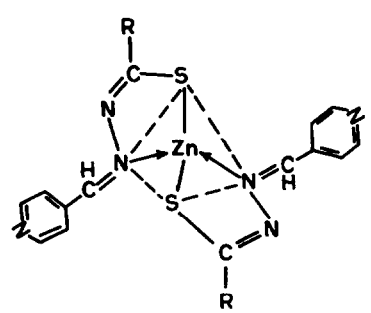
All the complexes inhibit the growth of *Staphylococcus aureus* but towards other bacteria the inhibition is not very pronounced. Cu(II) and Zn(II) complexes have weak antimicrobial action as compared to 2-furanthiocarboxyhydrazide for which significant inhibitory effect against all the bacteria tested have been observed.

Based on analytical data and physicochemical studies discussed above, structures I–IV are proposed for the complexes.

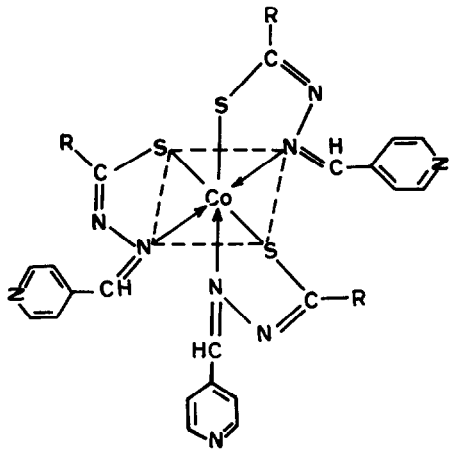


M (II) = Mn (II), Fe (II), Co (II), Ni (II), Zn (II)

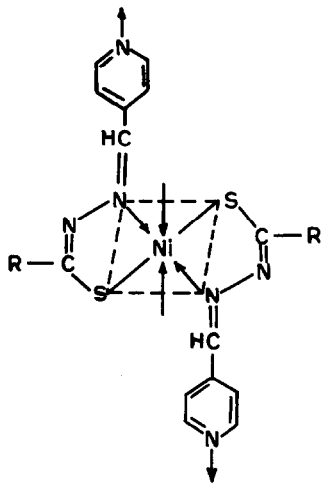
I



II



III



IV R = 2-furyl

*Acknowledgement*—Sincere thanks are due to Prof. S. S. Sandhu, G.N.D. University, Amritsar for Mössbauer spectrum, to Prof. P. C. Sen, I.M.S., B.H.U., for providing facilities for antimicrobial testing and also to the Head, Department of Chemistry, School of Physical Science, University of Hyderabad for photoacoustic spectra. One of us (Miss Seema Agrawal) is also thankful to C.S.I.R. for the award of S.R.F.

## REFERENCES

1. E. Larsen and P. Trinderup, *Acta Chem. Scand.* 1970, **24**, 261.
2. J. Gabel and E. Larsen, *Acta Chem. Scand.* 1978, **A32**, 929.
3. N. K. Singh, (Miss) Seema Agrawal and R. C. Aggarwal, *Ind. J. Chem.* 1982, **21A**, 973.
4. J. Gabel, E. Larsen and P. Trinderup, *Acta Chem. Scand.* 1977, **A31**, 657.
5. W. E. Antholine, J. M. Knight and David H. Petering, *J. Med. Chem.* 1976, **19**, 339.
6. C. H. Chan-Stier, D. Minkel and D. H. Petering, *Bioinorg. Chem.* 1976, **6**, 203.
7. A. Markovac, C. L. Stevens, A. B. Ash and B. C. Hackley, *J. Org. Chem.* 1970, **35**, 841.
8. R. S. Varma and W. L. Nobles, *J. Pharm. Sci.* 1968, **57**, 1801.
9. M. Akbar Ali and R. Bose, *J. Inorg. Nucl. Chem.* 1977, **39**, 265.
10. Hans Stunzi, *Aust. J. Chem.* 1981, **34**, 2549.
11. H. A. Goodwin, D. W. Mather and F. E. Smith, *Aust. J. Chem.* 1973, **26**, 2623.
12. A. Bond, R. L. Martin and I. A. G. Roos, *Aust. J. Chem.* 1974, **27**, 2307.
13. A. Rosenwaig, *Anal. Chem.* 1975, **47**, 592.
14. R. Singh and R. S. S. Rao, *J. Mol. Struct.* 1981, **71**, 23.
15. K. Geetharani and D. N. Sathyanarayana, *Aust. J. Chem.* 1977, **30**, 1617.
16. M. Akbar Ali and M. T. H. Tarafdar, *J. Inorg. Nucl. Chem.* 1977, **39**, 1785.
17. I. S. Ahuja and R. Singh, *J. Inorg. Nucl. Chem.* 1974, **36**, 1505.
18. I. Antonini, F. Claudi, P. Franchetti, M. Grifantini and S. Martelli, *J. Med. Chem.* 1977, **20**, 447.
19. A. B. P. Lever, *Inorganic Electronic Spectroscopy*, p. 302. Elsevier, Amsterdam (1968).
20. *Ibid.* pp. 307, 277.
21. K. C. Patel and D. E. Goldberg, *J. Inorg. Nucl. Chem.* 1972, **34**, 637.

*Polyhedron* Vol. 3, No. 12, p. 1277, 1984
Pergamon Press Ltd. Printed in Great Britain.

# INTRODUCTION

**B. F. G. JOHNSON**
University Chemical Laboratory, Lensfield Road, Cambridge CB2 1EW, U.K.

Cluster compounds now occupy a central role in inorganic chemistry. This situation is apparent not only by the large number of publications ranging from the purely synthetic to the more sophisticated theoretical studies but also by the sustained interest shown by workers outside inorganic chemistry. An enormous variety of stable chemical species have been prepared containing both transition and non-transition metals and involving a range of ligand systems.

Of all cluster compounds, those of boron have been by far the most systematically studied, and, as a consequence, have provided the closest insight into the structure and bonding of this class of compound. Within the past few years, however, a variety of investigations into transition-metal clusters has served to indicate that there consists a huge new class of compounds which possess structures hitherto not found and which are clearly not bound by the bonding rules applicable to the main group elements, notably boron and carbon.

This symposium is devoted to current views of bonding within transition-metal clusters and it is our intention to acquaint the reader with the more up-to-date approaches commonly applied to the understanding of the multifarious structures adopted, especially those of the noble metals and gold, which show rather special structural features. Also included is a discussion of carbido-clusters which are unique to the transition metals but which are attracting considerable attention at present.

During the course of the preparation of this symposium-in-print, which is largely based on a one-day meeting held in Cambridge in November 1983, several new approaches came up as a result of post-paper discussions. One of these ideas reached fruition in time for publication and is a joint effort between Drs Mingos and McPartlin.

Such is the rate of progress in this subject that we expect some of the ideas reported will have been superseded. Nevertheless, we hope that this symposium will serve its intention of bringing the subject more or less up to date.

*Polyhedron* Vol. 3, No. 12, pp. 1279–1288, 1984
Printed in Great Britain

0277–5387/84 $3.00 + .00
Pergamon Press Ltd

# ELECTRON-COUNTING PROCEDURES IN CLUSTERS OF THE IRON TRIAD

MARY McPARTLIN

School of Chemistry, The Polytechnic of North London, Holloway, London N7 8DB, U.K.

(*Received* 28 *April* 1984)

**Abstract**—Until recently all known high-nuclearity carbonyl clusters of the iron triad had metal core structures based on an octahedron with formulations corresponding to seven skeletal electron pairs ($S = 7$), in agreement with the predictions of polyhedral skeletal electron counting procedures. The isolation of the monoanion $[HOs_8(CO)_{22}]^-$, which also has $S = 7$, first broke this pattern, as it has a fused tetrahedral core geometry. The extension of skeletal electron counting procedures to include multiple "capping" of incomplete polyhedra permits a simple rationalisation of this structure as a tetra-capped *arachno*-octahedral. This approach has allowed the development of a matrix correlation for the main structural types observed in this triad. Structural relationships between the first members of a new class of high-nuclearity clusters based on the fusion of *two* are also discussed.

Electron-counting procedures have proved very useful in rationalising and classifying the cluster species of the iron triad. As the range and variety of cluster compounds increases the existence of a simple set of electron-counting rules is a helpful aid for remembering both structures and formulae. This is particularly true for osmium species where the range of structural types and nuclearities is greatest. The most widely applied approaches are all related to the qualitative proposals put forward by Wade in 1971.[1] In its original form the Wade theory stated that the *closo*-, *nido*- or *arachno*-forms of an *n*-vertex polyhedron all require $n+1$ pairs of skeletal-bonding electrons ($S = n+1$).[1] In addition to the electrons required for skeletal bonding, Wade assumed that every metal would require 12 non-skeletal electrons, that is 12e per metal occupy six low-lying metal–ligand orbitals. Therefore, to give the required *S*-value of $n+1$, a *closo*-(*n*-vertex) polyhedron will require a total polyhedral electron count of $12n+2(n+1)$e.* As a *nido*-polyhedron requires the same value of *S* but has one metal atom less than the *closo*-polyhedron it follows that its total electron requirement will be 12e less: similarly an *arachno*-polyhedron, which has two metal atoms less, will require 24 fewer electrons. The predicted total electron counts are therefore:

| | |
|---|---|
| *closo*-(*n*-vertex), | $12n+2(n+1)$; |
| *nido*-(*n*-vertex), | $12(n-1)+2(n+1)$; |
| *arachno*-(*n*-vertex), | $12(n-2)+(2n+1)$. |

Even simple formulae like this can prove difficult to remember and it is often more convenient to apply directly the principle that *the skeletal electron pairs* (S) *are those left over after* 12e *have been assigned to every metal, and the number of vertices in the fundamental polyhedron* (n) *will be one less than this, i.e.* $S-1$. If the total number of metal atoms in the cluster is less than *n* (the number of vertices in the parent polyhedron) then the corresponding *nido*- or *arachno*-polyhedron will result. For example the $M_4$-cluster monoanion $[H_3Ru_4(CO)_{12}]^-$ has a total electron count of $3+(4\times 8)+(12\times 2)+1 = 60$e. Assigning 12e to each of the metals leaves an excess of 12e or six skeletal electron pairs (S = 6): the basic polyhedron therefore has five vertices (a trigonal bipyramid) and as there are only four metal atoms present the observed geometry is *nido*-(5-vertex) or tetrahedral (Fig. 1a).[3]

The most common cluster types for the iron triad are based on an octahedral metal arrangement (6-vertex) and therefore have seven skeletal electron pairs ($S = 7$). For the octahedron a total polyhedral count of $(12\times 6)+2(6+1) = 86$e is required and there are many alternative ways in which the 86e can arise. For example the dianion $[Os_6(CO)_{18}]^{2-}$, the hydrido-species $H_2Ru_6(CO)_{18}$ and the interstitial-carbido cluster $Ru_6C(CO)_{17}$ all have 86e and have been shown to be octahedral.[4–6] The dihydride

* Later calculations[2] have provided a firm theoretical basis for the $(n+1)$ rule and for this electron count: the original Wade approach, with its easy relationship to cluster geometry, is therefore still valid. Throughout this paper the value of *n* refers to the number of vertices in the parent polyhedron, not to the number of metal atoms.

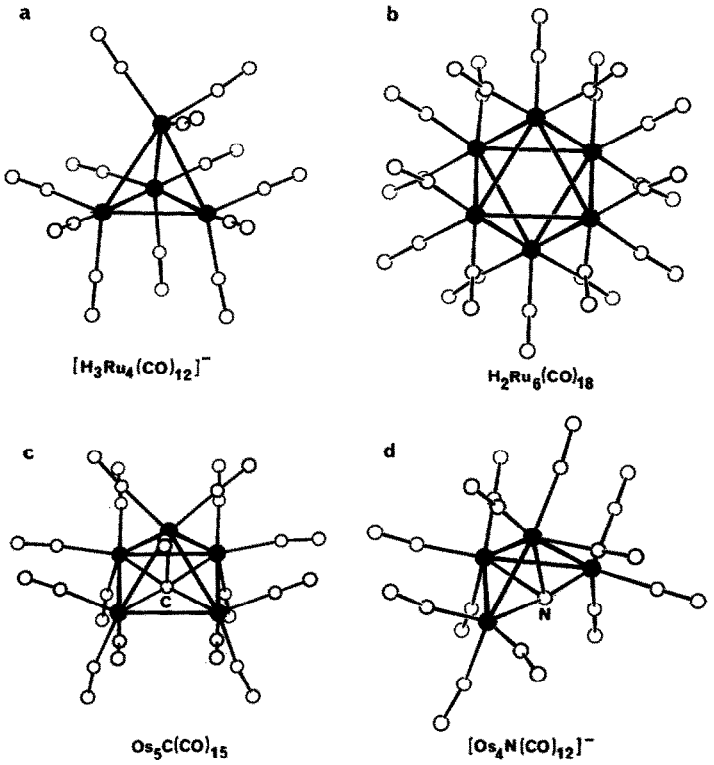



Fig. 1. The overall structures of some clusters related to the number of skeletal electrons ($S$): (a) $[H_3Ru_4(CO)_{12}]^-$, 60e, $S = 6$, *nido*-(5-vertex) or tetrahedral; (b) $H_2Ru_6(CO)_{18}$, 86e, $S = 7$, *closo*-(6-vertex) or octahedral; (c) $Os_5C(CO)_{15}$, 74e, $S = 7$, *nido*-(6-vertex) or square-pyramidal; (d) $[Os_4N(CO)_{12}]^-$, 62e, $S = 7$, *arachno*-(6-vertex) or "butterfly".

$H_2Ru_6(CO)_{18}$ was the first octahedral cluster of the iron triad to be structurally characterised and is shown in Fig. 1b.[5]

There are also well-established examples of *nido*-(6-vertex) polyhedral (square-pyramidal) clusters, which require 12e less, that is a total polyhedral count of $(12\times5)+2(6+1) = 74$e to give the predicted skeletal electron count of $S = 7$. The neutral carbido-cluster species $M_5C(CO)_{15}$ occurs for all the metals of this triad,[7] and has 74e with the square-pyramidal geometry illustrated in Fig. 1c for $Os_5C(CO)_{15}$. Formation of an *arachno*-(6-vertex) polyhedron, or "butterfly" metal arrangement, requires the loss of a further 12e, giving a total polyhedral count of $12(6-2)+2(6+1) = 62$e, and many examples are known: Fig. 1d shows the structure of the recently discovered[8] interstitial nitrido-osmium species $[Os_4N(CO)_{12}]^-$. Therefore summarising these changes it can be seen that successive removal of vertices from a polyhedron produces successive reductions of 12e in the total polyhedral count, i.e.:

The Wade theory also successfully predicted that the addition of 2e to an $n$-vertex polyhedron, which increases the $S$-value by 1, would produce a metal core rearrangement giving the corresponding *nido*-[$(n+1)$-vertex] polyhedron and the addition of a further 2e would give the *arachno*-[$(n+2)$-vertex] polyhedron. This principle is illustrated in Fig. 2 using the structural relationships of the metal core geometries of some pentaosmium species.[7,9] In practice this type of cluster rearrangement is relatively rare except for the trivial opening of a tetrahedron (*nido*-trigonal bypyramid) on addition of 2e to give the "butterfly" (*arachno*-octahedral) arrangement: this occurs frequently, not only for isolated $M_4$-species but also for the surface tetrahedra of large clusters.[10]

The number of structures that could be rationalised in this way was greatly increased when the capping principle was introduced to electron-counting procedures for metal cluster compounds.[11,12] Basically this states that if an extra

| | −12e | | −12e | |
|---|---|---|---|---|
| octahedral | ⟶ | *nido*-octahedral | ⟶ | *arachno*-octahedral |
| (6-vertex) | | (square-pyramid) | | ("butterfly") |
| 86e | | 74e | | 62e |

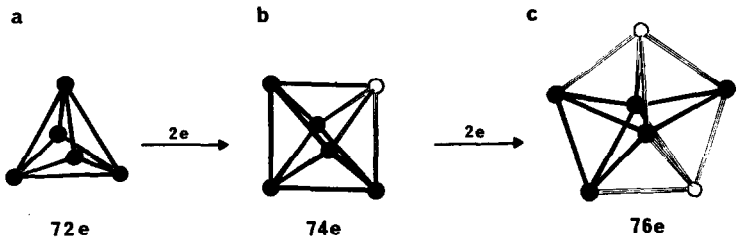



Fig. 2. The relationship between the metal cores in some pentaosmium species: (a) $Os_5(CO)_{16}$, 72e, $S = 6$, trigonal bipyramidal;[9] (b) $Os_5C(CO)_{15}$, 74e, $S = 7$, *nido*-octahedral;[7] (c) $[Os_5C(CO)_{15}I]^-$, 76e, $S = 8$, *arachno*-pentagonal bipyramidal.[7]

atom is added to bridge a triangular face of a polyhedron the skeletal electron requirement of the cluster is unchanged. Therefore, because each added atom requires 12e for non-cluster bonding, it follows that when a polyhedron is capped by an extra atom the total electron count must increase by 12e. If $m$ extra atoms are added in this way to an $n$-vertex polyhedron the electron count will increase by $12m$ electrons so that the $S$-value of $n+1$ is maintained and the total polyhedral count becomes $12(n+m) + 2(n+1)$e. Applying this principle to an octahedron would give a mono-capped octahedral structure with a total electron requirement of $12(6+1)+2(6+1) = 98$e, i.e. 12e more than the 86e for an uncapped octahedron. The first cluster with this core geometry[13] was $Os_7(CO)_{21}$ which has the predicted electron count of 98e. More recently it has been shown that a bi-capped octahedral structure (Fig. 3a) occurs for $[Os_8(CO)_{22}]^{2-}$.[14] This cluster dianion has a total of 110e valence electrons overall, i.e. 12e more than $Os_7(CO)_{21}$ and 24e more than $[Os_6(CO)_{18}]^{2-}$, these extra electrons being required for non-skeletal bonding by the extra Os atoms. A tri-capped octahedral cluster species of this type has not been found so far but such an $M_9$-cluster would have $86+(3\times12)$e, i.e. 122e. The tetra-capped octahedral geometry, first observed for the dianion $[Os_{10}C(CO)_{24}]^{2-}$,[15] is now widely known and is illustrated in Fig. 3b. As predicted the addition of four caps to the basic octahedron results in these clusters having $86+(4\times12) = 134$e. Even with the addition of the capping principle to electron-counting procedures, the deduction of the probable polyhedral type remains as simple as it was with the basic Wade approach. It is still possible to think of *the total number of skeletal electron pairs* (S) *as equal to the pairs left over after* 12e *have been assigned to every metal, and the parent polyhedron has one vertex less than this number* (n = S − 1). *Any metal atoms in excess of the number of vertices* (n) *occupy capping positions.* For example the cluster $Os_8(CO)_{23}$ has 110 valence electrons $[(8\times8+(23\times2)$e$]$ and assigning $12\times8$ to the metal atoms leaves 14e over. The value of $S$ is therefore 7 so that the parent polyhedron will be octahedral (six vertices). As there are eight metal atoms in the cluster the two extra occupy capping positions, giving the observed bi-capped octahedral geometry.[16] Three different arrangements for the two caps on the octahedron surface can be envisaged. The structure of $[Os_8(CO)_{22}]^{2-}$ shows one, a second with *trans*-capping metal atoms occurs in $[Re_8C(CO)_{24}]^{2-}$,[17] and a third, in which the

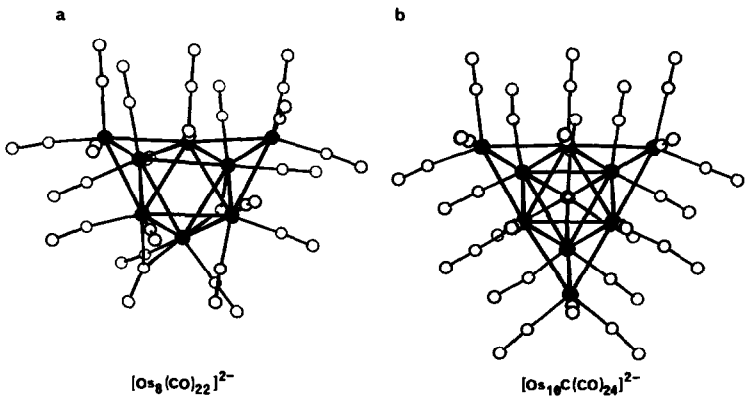



Fig. 3. The structures of two cluster dianions with capped-octahedral metal cores: (a) $[Os_8(CO)_{22}]^{2-}$, 110e, $2S = 110-(8\times12)$, $S = 7$, bi-capped-(6-vertex); (b) $[Os_{10}C(CO)_{24}]^{2-}$, 134e, $2S = 134-(10\times12)$, $S = 7$, tetra-capped-(6-vertex).

Table 1. A chart showing the relationship between structure and total polyhedral electron count for osmium cluster species with $S = 7$

| *closo*-(6-vertex) | −12e → | *nido*-(6-vertex) | −12e → | *arachno*-(6-vertex) |
|---|---|---|---|---|
| $[Os_6(CO)_{18}]^{2-}$ octahedron 86e | | $Os_5C(CO)_{15}$ square-pyramid 74e | | $[Os_4N(CO)_{12}]^-$ "butterfly" 62e |
| +12e | | | | |
| $Os_7(CO)_{21}$ mono-capped 98e | | $H_2Os_6(CO)_{18}$ mono-capped 86e | | $H_2Os_5(CO)_{16}$ edge-bridged tetrahedron 74e |
| +12e | | | | |
| $[Os_8(CO)_{22}]^{2-}$ bi-capped 110e | | "$Os_7$" bi-capped 98e | | "$Os_6$" bi-tetrahedron 86e |
| +12e | | | | |
| "$Os_9$" tri-capped 122e | | "$Os_8$" tri-capped 110e | | — |
| +12e | | | | |
| $[Os_{10}C(CO)_{24}]^{2-}$ tetra-capped 134e | | "$Os_9$" tetra-capped 122e | | — |

capping tetrahedra share a common edge, has not been observed.

The geometric cluster types discussed so far are related by increments of 12e to the parent 6-vertex (octahedral) polyhedron and to emphasise this they are shown in a flow-chart form in Table 1. The horizontal rows represent successive removal of a vertex from the polyhedron with the corresponding successive losses of 12e. The vertical columns represent successive additions of capping groups and therefore give corresponding increases of 12e to the total count. Some clusters do not fall readily into this classification. For example, $H_2Os_6(CO)_{18}$ has 86e and from electron-counting procedures and by analogy with known clusters it was expected to be octahedral. X-ray analysis established that in fact the core geometry is a capped square pyramid[4] (Fig. 4a). This was an unexpected observation because it had not been anticipated that the capping of a polyhedron would occur before all the vertices had been occupied by metal atoms. As any polyhedron can be capped without effecting its skeletal electron requirements it follows that the addition of a cap to a *nido*-octahedron will maintain the skeletal electron value of $S = 7$ and so give the observed total electron count for this geometry as $74 + 12 = 86$e. The capped square-pyramidal geometry is therefore a valid alternative to the more common octahedral one for hexanuclear clusters with 86e. Conversely this unexpected geometry can be rationalised by regarding it as a *nido*-(capped octahedron) and as such it would require 98 − 12e, i.e. 12e less than $Os_7(CO)_{21}$, giving the observed total of 86e. The position of $H_2Os_6(CO)_{18}$ in Table 1 may therefore be described as vertically below the square-pyramidal $Os_5C(CO)_{15}$ cluster [cap (+ 12e)] or alternatively as one position to the right of $Os_7(CO)_{21}$ [remove vertex (−12e)]. Another example of the capping of incomplete polyhedra is given by the structure of $H_2Os_5(CO)_{16}$.[18] This cluster has a total count of 74e and would have been expected to have a square-pyramidal [*nido*-octahedral ($S = 7$)] metal arrangement. Instead the metal core has an edge-bridged tetrahedral geometry which may be rationalised if it is derived from the mono-capped octahedral metal core of $Os_7(CO)_{21}$ by removal of two vertices [a horizontal displacement of two positions in the chart (Table 1)]. Thus $H_2Os_5(CO)_{16}$ may be classified as

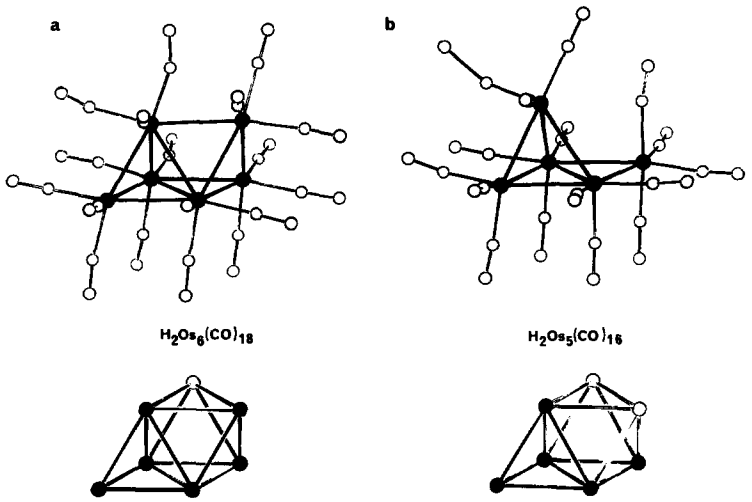



Fig. 4. The structures of two hydrido-cluster molecules which illustrate the capping of incomplete polyhedra: (a) $H_2Os_6(CO)_{18}$, 86e, $2S = 86-(6\times12)$, $S = 7$, capped-[*nido*-(6-vertex)]; (b) $H_2Os_5(CO)_{16}$, 74e, $2S = 74-(5\times12)$, $S = 7$, capped-[*arachno*-(6-vertex)].

an *arachno*-(capped octahedron) ($S = 7$) and as such would require $98-(2\times12) = 74$e. This alternative geometry for 74e may also be derived by capping a "butterfly" [i.e. capping an *arachno*-octahedron ($S = 7$)] and therefore its position in Table 1 is vertically below the "butterfly" structure of $[Os_4N(CO)_{12}]^-$. In this way the same total electron count is required, viz. $62+12 = 74$e.

Until 1981 all the osmium clusters known with $S = 7$ had octahedrally related structures and the metal cores could be regarded as small fragments of the close-packed array found in bulk metals (Fig. 5). The largest of this group of cluster species is illustrated by the dianion $[Os_{10}C(CO)_{24}]^{2-}$ where the metal atoms define all but four of the lattice points of a face-centred cubic (fcc) unit cell (Fig. 6a).[15]

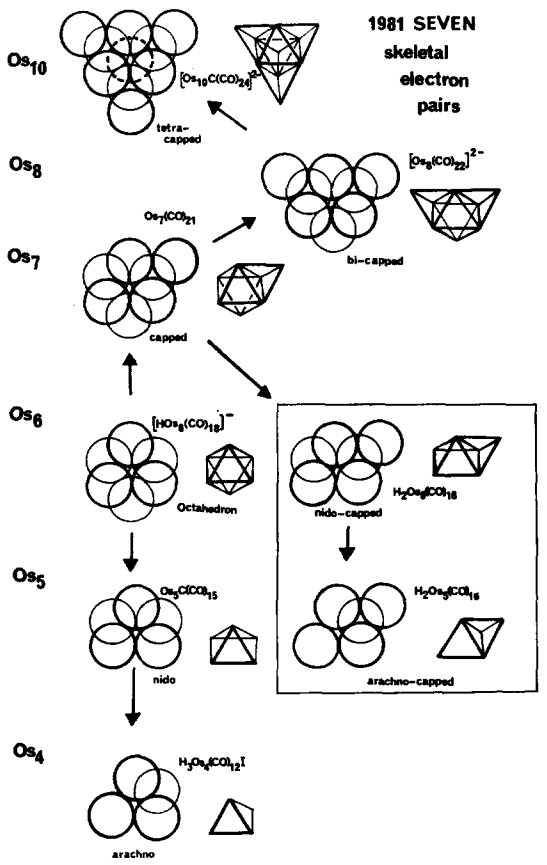



Fig. 5. A slide shown in 1981 to summarise all the polynuclear osmium geometries for $S = 7$ known at that time, and to illustrate their relationship to the close-packed array found in bulk metals.

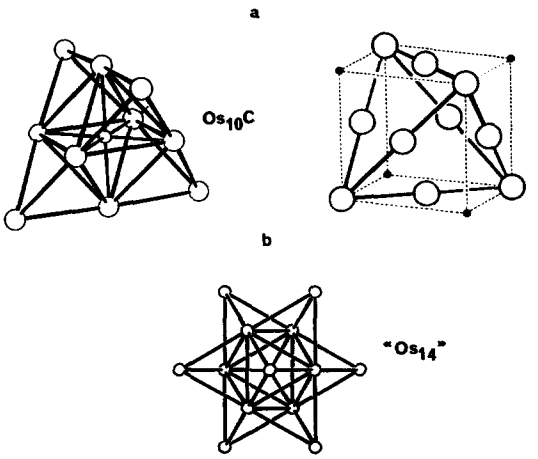
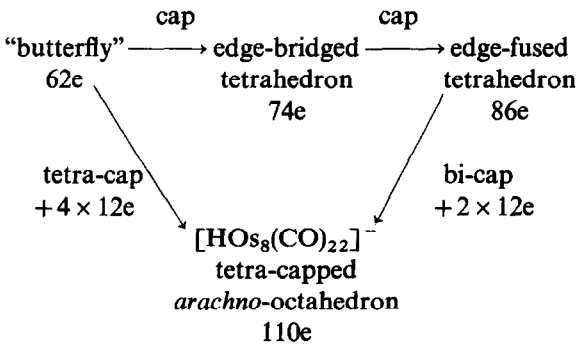



Fig. 6. (a) The relationship between the $Os_{10}$ core of $[Os_{10}C(CO)_{24}]^{2-}$ and the lattice points of an fcc unit cell. (b) The octa-capped metal core that may be envisaged for the hypothetical dianion $[H_4Os_{14}C(CO)_{30}]^{2-}$ ($S = 7$): the metal atoms occupy all the lattice points of the fcc unit cell.

The type of metal core has proved so stable that continuing the capping process to all faces of the octahedron one might expect to obtain an $Os_{14}$ cluster with a valence electron count of $86+(8\times12)$ = 182e and with a metal arrangement corresponding to all the lattice points of the complete fcc unit cell. Such a structure (Fig. 6b) has not been observed so far, and may be precluded by surface ligand overcrowding. However with a maximum number of interstitial atoms (i.e. four H atoms in the tetrahedral cavities and one C atom in the octahedral cavity) one could envisage a reasonable surface ligand distribution for a hypothetical dianion such as $[H_4Os_{14}C(CO)_{30}]^{2-}$ with one CO ligand in the centre of the fcc face and three CO groups on the eight corners.

The sequence of high-nuclearity osmium cluster compounds based on capped octahedra was interrupted by the isolation[19] of the hydrido-monoanion $[HOs_8(CO)_{22}]^-$, which has the same electron count (110e) as the dianion $[Os_8(CO)_{22}]^{2-}$ and by analogy would be expected to have a similar bi-capped octahedral structure. The observed geometry, which did not seem to have any relationship to an octahedron, closely resembled that of $Os_6(CO)_{18}$,[11] from which it had been prepared. This neutral cluster, $Os_6(CO)_{18}$, was one of the first non-octahedral hexanuclear species discovered, and its total electron count of 84e ($S=6$) allowed the observed geometry to be rationalised as a capped trigonal bipyramid ($S=6$).[11] The structure of $[HOs_8(CO)_{22}]^-$ (Fig. 7a) may be regarded as derived from this by the addition of two Os atoms to give an extra edge-fused tetrahedron. Shortly after the characterisation of $[HOs_8(CO)_{22}]^-$ the heptaosmium dihydrido-molecule $H_2Os_7(CO)_{20}$ was shown to have a related structure (Fig. 7b), which can also be derived from $Os_6(CO)_{18}$ but by addition of one edged-bridging osmium atom.[20] Again the metal geometry was unexpected as this cluster has the same electron count (98e) as the $Os_7(CO)_{21}$ molecule ($S=7$) and it would also have been expected to have a mono-capped octahedral metal core.

As all the previous osmium clusters with $S=7$ have fitted readily onto the $S=7$ chart (Table 1), derived from the application of the Wade theory and the capping principle, it seemed worth reconsidering the approach to the structure of the two "fused-tetrahedral" hydrido-species. A significant feature, if one is attempting to relate them to the other octahedrally derived $S=7$ structures, is that both $[HOs_8(CO)_{22}]^-$ and $H_2Os_7(CO)_{20}$ have "butterfly" components in their overall structure. Now the edge-bridged tetrahedral structure of $H_2Os_5(CO)_{16}$ was fitted into the $S=7$ matrix (Table 1) by recognising that it could be described as a capped *arachno*-octahedron. If an $Os_8$ species were to be derived by a similar rationale one would require a tetra-capped *arachno*-octahedron. The *arachno*-octahedron or "butterfly" only has two triangular faces available to be capped and, although the bi-capped octahedral structure derived in this way can be envisaged as an alternative structure for 86e (Table 1), it has not been observed so far in this triad: further capping for this geometry was ruled out in Table 1. However the whole approach may be extended if extra capping atoms are accommodated on triangular faces generated by conventional capping groups already present:




The validity of such a double capping is intrinsic in the fundamental hypothesis that addition of a capping group does not change the original skeletal electron requirement of a cluster. It is more explicitly stated in the new Mingos approach to electron counting in fused polyhedra,[21] i.e. the addition of an extra metal atom to any polyhedron, by fusion of a tetrahedron through a triangular face, requires an increase in the overall polyhedral electron count of $60-48=12$e. Placing this in the context of the Wade approach to skeletal electron counting it follows that addition of such a cap anywhere in the cluster, providing as it does one metal atom and 12e, will not effect the value of $S$ nor require any alteration in the order of the parent polyhedron. This therefore allows a description of both the "problem" species, $H_2Os_7(CO)_{20}$ and $[HOs_8(CO)_{22}]^{2-}$, as *arachno*-octahedra which have been tri-capped and tetra-capped respectively. They therefore can be accommodated satisfactorily on the expanded version of the chart for $S=7$ illustrated in Fig. 8. The possibility of the capping groups being distributed in different ways not only on the faces of the basic polyhedron but also on a variety of triangular faces generated by earlier capping groups increases the number of possible structures greatly. In Fig. 8 only one example of each type structure is given: the alternative structures derived by redistribution of the capping groups are not illustrated.

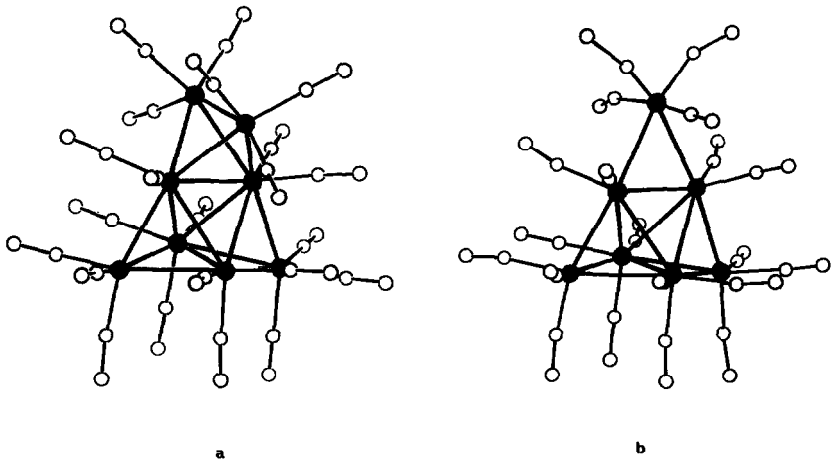



Fig. 7. The structures of two hydrido-cluster species with $S = 7$ and "fused-tetrahedral" structures related to that of $Os_6(CO)_{18}$ ($S = 6$): (a) $[HOs_8(CO)_{22}]^-$ and (b) $H_2Os_7(CO)_{20}$.

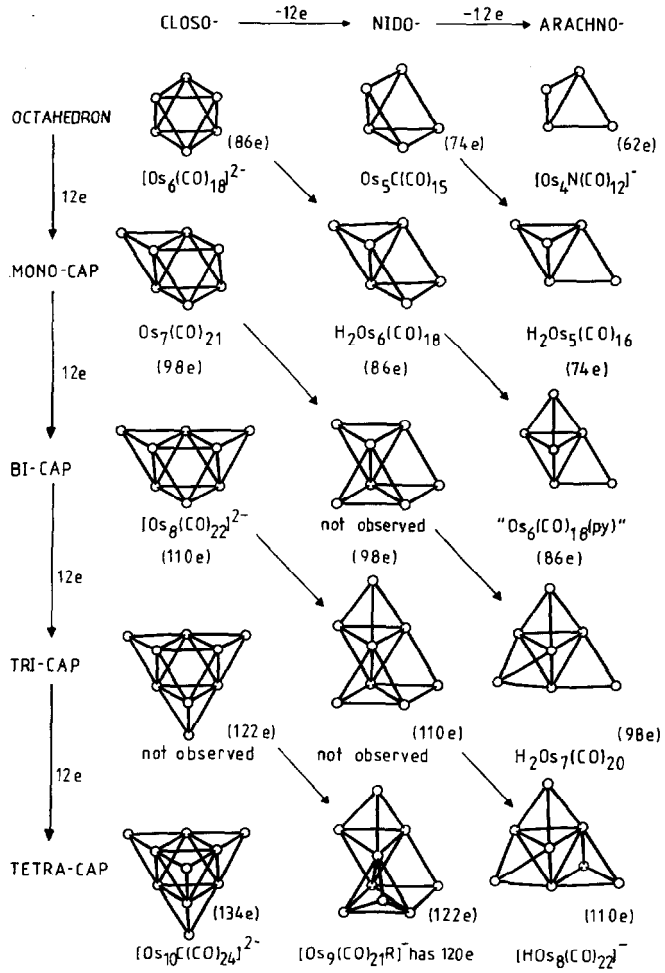



Fig. 8. A chart relating the structures and total polyhedral electron count for clusters species with $S = 7$. For the multi-capped geometries "isomers" differing in the distribution of the "caps" are possible but only one is illustrated in each case. The structures lying along the diagonals represent alternative geometries for the same total electron count and result from the removal of vertices ($-12$e) and their replacement with capping groups ($+12$e).

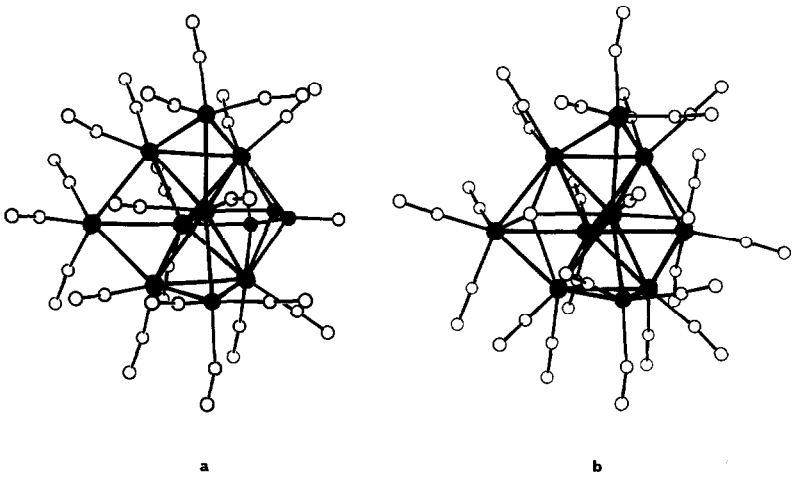



Fig. 9. The structures of two recently discovered high-nuclearity osmium cluster species: (a) $[Os_9(CO)_{21}(CHCMeCH)]^-$ and (b) $Os_{10}(S)_2(CO)_{23}$.

Examination of the chart shows that all the "abnormal" structures, i.e. those derived from the unexpected capping of incomplete octahedra, lie along the diagonals and provide alternative structures for a given number of metal atoms and electrons. Some positions in the "matrix" correspond to possible structures for cluster species which are as yet unknown. For example an $Os_9$ species with $S = 7$ would have 122e and would be expected to have one of the following structures: tri-capped octahedral, tetra-capped *nido*-octahedral or penta-capped *arachno*-octahedral.

Nonaosmium species have proved very elusive but the first was obtained recently[22] by the reaction of $Os(CO)_{12}$ in isobutanol solution and is a rare high-nuclearity cluster hydrocarbon derivative $[Os_9(CO)_{21}(CHCMeCH)]^-$ (Fig. 9a). The $Os_9$ core appears to fit well into the matrix for the other osmium clusters as a tetra-capped square-pyramidal structure which should be related to the tetra-capped octahedral structure of $[Os_{10}C(CO)_{24}]^{2-}$ by removal of one vertex and 12e (the four caps being redistributed):

tetra-capped octahedron 134e $\xrightarrow{-12e}$ tetra-capped *nido*-octahedron 122e

Unexpectedly the cluster has only 120 polyhedral valence electrons, two less than expected from skeletal electron counting, and it is unique among high-nuclearity clusters of this triad in having 2e less than expected from the E.A.N. rule.

It seemed significant that all the species in the matrix which occur on the diagonals, that is which have the apparently "unnecessary" capped *nido*- and capped *arachno*-octahedral cores, have so far been hydrides. This observation may be related to theoretical calculations on boranes which indicate that high-energy occupied orbitals localised round the "open" faces of *nido*- and *arachno*-clusters may be stabilised by hydrogen ligands.[23]

Recently[24] it has been shown that, when the pyrolysis of $Os_3(CO)_{12}$ is carried out in the presence of elemental sulphur, a neutral molecule, $Os_{10}(S)_2(CO)_{23}$, is among the products and that it has a new type of $Os_{10}$ core (Fig. 9b) quite unlike the tetra-capped octahedral arrangement found in all previous $Os_{10}$ clusters with 134e. There are interesting structural relationships between the new $Os_{10}$ core geometry and that of the $Os_9$ cluster and of the recently reported[25] $Ru_{10}$ species $[Ru_{10}(C)_2(CO)_{24}]^{2-}$ (Fig. 10). As the

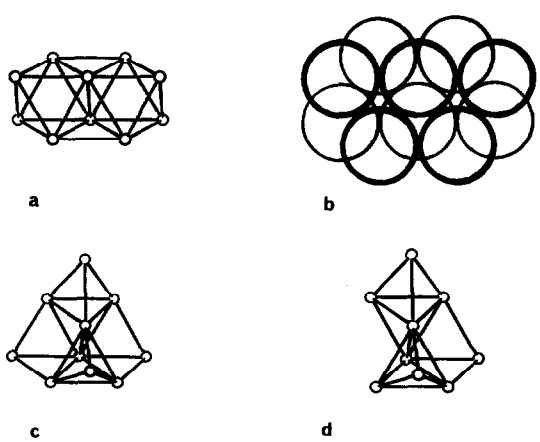



Fig. 10. The structural relationship between high-nuclearity cluster species of the iron triad: (a) the $Ru_{10}$ core in $[Ru_{10}(C)_2(CO)_{24}]^{2-}$; (b) the $Ru_{10}$ core shown as a fragment of a close-packed array; (c) the $Os_{10}$ core in $Os_{10}(S)_2(CO)_{23}$; (d) the $Os_9$ in $[Os_9(CO)_{21}(CHCMeCH)]^-$.

$Os_{10}(S)_2(CO)_{23}$ core can be derived from the bi-octahedral structure of the $Ru_{10}$ cluster by removing two vertices ($-2\times12$e) and replacing the atoms as caps ($+2\times12$e) the two cluster would be expected to have the same electron count. In fact there is a discrepancy of 4e between them, the $Ru_{10}$ cluster having 138e and the $Os_{10}$ only 134e. The theoretical count for these clusters can most readily be calculated using the recent Mingos approach to electron counting in condensed polyhedra.[21] This is summarised by saying that the total electron count for the condensed polyhedron is equal to the sum of the counts for the component individual polyhedra from which it is constructed minus the characteristic electron count for any surfaces or edges that are shared. Thus $Os_{10}(S)_2(CO)_{23}$ may be built up from a square pyramid (74e) fused through two triangles ($-2\times48$e) to two tbp ($+2\times72$e) and this composite polyhedron then fused through a "butterfly" surface ($-62$e) to a second square pyramid ($+74$e), giving the observed total polyhedral count of 134e. Therefore the $Ru_{10}$ dianion would also be expected to have 134e and the $Os_9$ to have 12e less, i.e. 122e. The observation that the $[Ru_{10}(C)_2(CO)_{24}]^{2-}$ dianion has 138e, 4e more than expected, is no doubt related to the marked distortions in the structure which has six unusually long Ru—Ru distances. Similar polyhedral "elongation" distortions have also been observed in several trigonal bipyramidal $M_5$-clusters, e.g. $[Ni_5(CO)_{12}]^{2-}$ and $[Rh_5(CO)_{15}]^{-}$,[26] and significantly allow accommodation of 4e more than predicted,[27] whereas in clusters with more regular tbp geometries, e.g. $Os_5(CO)_{16}$,[9] the predicted electron count of 72e occurs. The $[Os_9(CO)_{21}(CHCMeCH)]^{-}$ monoanion is at first sight more difficult to explain as it is 2e short of the required count. However the unusual electron count in this case arises from the observation for the first time of a hydrocarbon ligand isolated on a high-nuclearity osmium cluster. It is necessary to apply the Mingos condensed-polyhedral approach to the overall $Os_9C_3$ polyhedron and this then gives a predicted electron count that agrees with the observed overall count. Thus the cluster may be regarded as a square pyramid (74e) fused through two triangles ($-2\times48$e) to two trigonal bipyramids ($+2\times27$e) and this composite polyhedron then fused through a "butterfly" ($-62$e) to an $Os_4C_3$ pentagonal bipyramid [$+70$e (main-group atoms only require 2e for non-skeletal bonding)], giving a total electron count of 130e which is the observed total when the valency electrons of the three cluster carbon atoms are included.

The highest nuclearity cluster observed so far in the iron triad is the dianion $[Os_{11}C(CO)_{27}]^{2-}$,[28] which is unusual in having a central trigonal prismatic cavity (Fig. 11), a geometry common in the cobalt triad but previously not observed for these atoms. The electron count of this cluster may be explained[28] using the condensed-polyhedral approach. It is obtained in trace amounts in the pyrolysis of $Os_3(CO)_{12}$ together with a wide range of the more typical octahedrally derived clusters, including $[Os_{10}C(CO)_{24}]^{2-}$. On reaction with iodine it ultimately loses one "$Os(CO)_3$" unit to give the $[Os_{10}C(CO)]^{2-}_{24}$ dianion (Fig. 11). It seems likely that the $[Os_{11}C(CO)_{27}]^{2-}$ dianion represents a step in the sequence of cluster growth immediately before the formation of the extremely stable $[Os_{10}C(CO)_{24}]^{2-}$ dianion. Although the $Os_{11}$ species is the highest nuclearity cluster so far obtained in the iron triad it seems unlikely that it is the prototype for larger clusters of these metals. It is more probable that many high-nuclearity clusters related in geometry to the $Ru_{10}$, the $Os_{10}(S)_2$ and the $Os_9$ species will be obtained. These three clusters may be regarded as the first members of a family of high-nuclearity clusters of the iron triad based on the fusion of two or more octahedra through tetrahedral linking units: alternation of octahedra and tetrahedra in the ratio of 1 : 2 is fundamental to the structures of all close-packed arrays, and the structure of the $Ru_{10}$ cluster forms part of two layers in such an array (Fig. 10b). These clusters therefore provide a link between the mono-octahedral clusters, to which the species of the iron triad have previously been limited, and the more extended close-packed arrays observed for clusters of rhodium and platinum.[29]

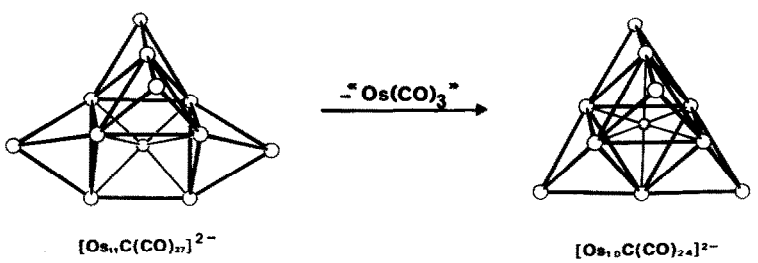



Fig. 11. The relationship between the metal core geometry of $[Os_{11}C(CO)_{27}]^{2-}$ and that of $[Os_{10}C(CO)_{24}]^{2-}$.

## REFERENCES


1. K. Wade, *J. Chem. Soc., Chem. Commun.* 1971, 792; *Inorg. Nucl. Lett.* 1972, **8**, 559.
2. E.g. D. M. P. Mingos, *J. Chem. Soc., Dalton Trans.* 1974, 133; A. J. Stone, *Inorg. Chem.* 1981, **20**, 563.
3. P. F. Jackson, B. F. G. Johnson, J. Lewis, M. McPartlin and W. J. H. Nelson, *J. Chem. Soc., Chem. Commun.* 1978, 920.
4. M. McPartlin, C. R. Eady, B. F. G. Johnson and J. Lewis, *J. Chem. Soc., Chem. Commun.* 1976, 833.
5. M. R. Churchill, J. Wormwald, J. Knight and M. J. Mays, *J. Chem. Soc., Chem. Commun.* 1970, 458.
6. A. Sirugu, M. Bianchi and E. Benedetti, *J. Chem. Soc., Chem. Commun.* 1969, 596.
7. E. H. Braye, L. F. Dahl, W. Hubel and D. L. Wampter, *J. Am. Chem. Soc.* 1962, **84**, 4633; D. H. Farrar, P. F. Jackson, B. F. G. Johnson, J. Lewis, J. N. Nicholls and M. McPartlin, *J. Chem. Soc., Chem. Commun.* 1981, 415; P. F. Jackson, B. F. G. Johnson, J. Lewis, J. N. Nicholls, M. McPartlin and W. J. H. Nelson, *J. Chem. Soc., Chem. Commun.* 1980, 564.
8. M. A. Collins, B. F. G. Johnson, J. Lewis, J. M. Mace, J. Morris, M. McPartlin, W. J. H. Nelson, J. Puga and P. R. Raithby, *J. Chem. Soc., Chem. Commun.* 1983, 689.
9. B. E. Reichert and G. M. Sheldrick, *Acta Crystallogr.* 1977, **B33**, 173.
10. D. H. Farrar, P. F. Jackson, B. F. G. Johnson, J. Lewis, W. J. H. Nelson, M. D. Vargas and M. McPartlin, *J. Chem. Soc., Chem. Commun.* 1981, 1009.
11. R. Mason, K. M. Thomas and D. M. P. Mingos, *J. Am. Chem. Soc.* 1973, **95**, 3803.
12. C. R. Eady, B. F. G. Johnson and J. Lewis, *J. Chem. Soc., Dalton Trans.* 1975, 2606.
13. C. R. Eady, B. F. G. Johnson, J. Lewis, R. Mason, P. B. Hitchcock and K. M. Thomas, *J. Chem. Soc., Chem. Commun.* 1977, 385.
14. P. F. Jackson, B. F. G. Johnson, J. Lewis and P. R. Raithby, *J. Chem. Soc., Chem. Commun.* 1980, 60.
15. P. F. Jackson, B. F. G. Johnson, J. Lewis, M. McPartlin and W. J. H. Nelson, *J. Chem. Soc., Chem. Commun.* 1980, 224; P. F. Jackson, B. F. G. Johnson, J. Lewis, W. J. H. Nelson and M. McPartlin, *J. Chem. Soc., Dalton Trans.* 1982, 2099.
16. P. R. Raithby, personal communication, 1983.
17. G. Ciani, G. D'Alfonso, M. Freni, P. Romiti and A. Sironi, *J. Chem. Soc., Chem. Commun.* 1982, 705.
18. J. J. Guy and G. M. Sheldrick, *Acta Crystallogr.* 1978, **B34**, 1725.
19. D. Braga, K. Henrick, B. F. G. Johnson, J. Lewis, M. McPartlin, W. J. H. Nelson and M. D. Vargas, *J. Chem. Soc., Chem. Commun.* 1982, 419.
20. E. J. Ditzel, H. D. Holden, B. F. G. Johnson, J. Lewis, A. Saunders and M. J. Taylor, *J. Chem. Soc., Chem. Commun.* 1982, 1373.
21. D. M. P. Mingos, *J. Chem. Soc., Chem. Commun.* 1983, 706.
22. B. F. G. Johnson, J. Lewis, M. McPartlin, W. J. H. Nelson, P. R. Raithby, A. Sironi and M. D. Vargas, *J. Chem. Soc., Chem. Commun.* 1983, 1476.
23. J. Evans, *J. Chem. Soc., Dalton Trans.* 1978, 25; A. J. Stone and M. J. Alderton, *Inorg. Chem.* 1982, **21**, 2297.
24. J. P. Attard, B. F. G. Johnson, J. Lewis, J. M. Mace, M. McPartlin and A. Sironi, *J. Chem. Soc., Chem. Commun.* 1984, 595.
25. C.-M. T. Hayward, J. R. Shapley, M. R. Churchill, C. Bueno and A. L. Rheingold, *J. Am. Chem. Soc.* 1982, **104**, 7347.
26. G. Longoni, P. Chini, L. D. Lower and L. Dahl, *J. Am. Chem. Soc.* 1975, **97**, 5034; A. Fumagalli, T. F. Koetzle, F. Takusagawa, P. Chini, S. Martinengo and B. T. Heaton, *J. Am. Chem. Soc.* 1980, **102**, 1740.
27. J. W. Lauher, *J. Am. Chem. Soc.* 1978, **100**, 5305.
28. D. Braga, K. Henrick, B. F. G. Johnson, J. Lewis, M. McPartlin, W. J. H. Nelson, A. Sironi and M. D. Vargas, *J. Chem. Soc., Chem. Commun.* 1983, 1131.
29. C. Ciano, A. Sironi and S. Martinengo, *J. Chem. Soc., Dalton Trans.* 1981, 519; S. Martinengo, G. Ciani and A. Sironi, *J. Am. Chem. Soc.* 1980, **102**, 7564.

*Polyhedron* Vol. 3, No. 12, pp. 1289–1297, 1984
Printed in Great Britain

0277-5387/84 $3.00 + .00
Pergamon Press Ltd

# STRUCTURE AND BONDING IN CLUSTER COMPOUNDS OF GOLD

D. MICHAEL P. MINGOS
Inorganic Chemistry Laboratory, University of Oxford, South Parks Road, Oxford OX1 3QR, U.K.

(*Received* 1 *April* 1984)

**Abstract**—Recently a number of high nuclearity gold cluster compounds of the type $[Au(AuPR_3)_n]^{x+}$ have been synthesised and structurally characterised using single crystal X-ray crystallographic measurements. The structures and properties of these compounds are contrasted with those of comparable high nuclearity metal carbonyl cluster compounds. In order to account for the structures of $[Au(AuPR_3)_n]^{x+}$ in the solid state and in solution it has proved necessary to develop a flexible bonding model which emphasises the topologies of the clusters rather than their detailed geometries. In this fashion the observed stereochemical non-rigidity of these compounds in solution is readily accounted for. In the solid state the structures of the higher nuclearity cluster cations can be derived either from the centred chair $[Au(AuPR_3)_6]$, or the centred crown $[Au(AuPR_3)_8]$ by adding edge or face capping $AuPR_3$ fragments. The bonding in heterometallic clusters containing the $AuPR_3$ fragment is also considered.

The last 20 years has seen an enormous growth of interest in those compounds having a sufficient number of metal atoms to define a three-dimensional polyhedral core. Metal carbonyl cluster compounds have been particularly well investigated because of their relevance to the chemisorbed state of heterogeneous metal catalysts and their potential as catalysts in $CO/H_2$ chemistry.[1] The higher nuclearity cluster compounds of gold $[Au(AuPR_3)_n]^{x+}$ are unlikely to lead to a better understanding of these particular processes, but nevertheless are of some interest both from an academic and industrial point of view. The possible importance of gold clusters in the extractive metallurgy of gold using reduced carbon and the utilisation of molecular gold cluster compounds in electron microscopy studies can be cited as examples of the applications of these compounds.[2,3] From a structural and theoretical point of view the cluster compounds of gold are particularly interesting because they do not conform to the structural patterns which have emerged for metal carbonyl cluster compounds in recent years.[4,5] In this review I shall try and emphasise the ways in which the cluster compounds of gold differ from those of the related metal carbonyl cluster compounds of osmium and rhodium. In particular the following differences in their chemistries can be identified:

(a) The cluster compounds of gold undergo cluster aggregation and degradation reactions much more readily than the corresponding metal carbonyl cluster compounds.

(b) The potential energy surfaces connecting alternative polyhedral geometries of gold cluster compounds appear to be much softer than those of metal carbonyl cluster compounds. This is manifested in the higher degree of fluxionality associated with gold cluster compounds and the observation of more than one skeletal geometry in the solid state for a particular cluster nuclearity.

(c) The structures of gold cluster compounds cannot be easily described in terms of deltahedra, condensed deltahedra and deltahedral fragments. The gold cluster compounds frequently adopt more open structures than those reported for comparable metal carbonyl clusters and which can only be related to deltahedra by the loss of three or four vertices.

(d) The addition of electron pairs to gold cluster cations does not lead to geometric changes which follow the *closo*-, *nido*- and *arachno*-pattern common to boranes and other metal clusters.

Having highlighted these differences the following section of the review will give a more detailed account of the chemical and structural aspects of gold cluster compounds. In addition semi-empirical molecular orbital calculations will be presented which have been used to rationalise the electronic

factors responsible for these differences. More detailed accounts of gold cluster chemistry are to be found in recent reviews.[6]

## CLUSTER AGGREGATION AND DEGRADATION REACTIONS

Tertiary phosphine gold cluster compounds are generally synthesised by the reduction of the linear gold(I) compounds $AuXPR_3$.[6] For triaryl–phosphine complexes $NaBH_4$ has proved to be an effective reducing agent,[7] but for phosphines with alkyl groups a mixture of cluster compounds is obtained. In our laboratories we have established that the sandwich compound $[Ti(\eta\text{-}C_6H_5CH_3)_2]$ is a more effective reducing agent.[8] Examples of its use are given below:

$$AuCl(PMe_2Ph) + Ti(\eta\text{-}C_6H_5CH_3)_2 \rightarrow [Au_{11}(PMe_2Ph)_{10}]^{3+},$$

$$AuCl(PPh_3) + Ti(\eta\text{-}C_6H_5CH_3)_2 \rightarrow [Au_9(PPh_3)_8]^{3+}.$$

These high nuclearity gold cluster cations undergo cluster aggregation and degradation reactions with a remarkable facility. For example, the addition of chloride ions to $[Au_{11}(PMe_2Ph)_{10}]^{3+}$ leads to the formation of the icosahedral cluster $[Au_{13}Cl_2(PMe_2Ph)_{10}]^{3+}$ in high yield and within a few minutes at room temperature. This may be contrasted with many aggregation reactions of metal carbonyl cluster compounds which occur only if the temperature is raised to 100–200°C. Degradation reactions of gold cluster compounds also occur with the same facility and result from the addition of mono- or polydentate phosphine ligands, e.g.[9]

$$[Au_{13}Cl_2(PMe_2Ph)_{10}]^{3+} + PMe_2Ph \rightarrow [Au_{11}(PMe_2Ph)_{10}]^{3+}.$$

It seems, therefore, that cluster aggregation is kinetically a very fast process for gold cluster compounds and that the extent of growth is limited primarily by the steric requirements of the peripheral ligands. Therefore, reagents which result in the replacement of a bulky phosphine ligand by a smaller halide ligand permit cluster aggregation. Similarly the replacement of halide ligands by phosphines leads to cluster degradation. These processes do not occur by simple replacement steps, but frequently involve the simultaneous formation of either neutral or cationic mononuclear gold complexes. For example, degradation reactions involving phosphine ligands generally proceed with the simultaneous formation of $[Au(PR_3)_2]^+$.[10]

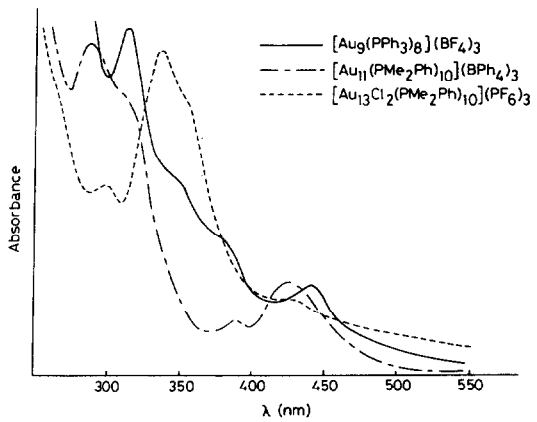



Fig. 1. Electronic spectral data for $Au_9$, $Au_{11}$ and $Au_{13}$ cluster compounds illustrating the way in which the differences in band maxima can be used to distinguish the compounds in solution.

Attempts have been made to put these steric effects on a more quantitative basis by the development of a *cluster cone angle* concept analogous to that developed by Tolman for mononuclear complexes.[11,12] The cluster cone angle is based on a model derived from the van der Waal's radii of the ligand atoms and is defined in terms of the angle at the origin of the polyhedron which is subtended by the peripheral ligand atoms. The recognition that steric effects of this type were significant was an important component in the successful synthesis of the first example of an icosahedral metal cluster compound, viz. $[Au_{13}Cl_2(PMe_2Ph)_{10}]^{3+}$.[8] Simple calculations had demonstrated that the cluster cone angles of $PMe_2Ph$ and $PMePh_2$ were more compatible with the steric requirements of a metal icosahedron than those of the bulkier $PPh_3$ ligand.

The liabilities of gold phosphine cluster compounds influences the way in which the compounds are purified and crystallised. Mixtures of the cluster compounds are frequently formed in the initial reduction of $AuClPR_3$ and their precipitation with large counter anions does not result in pure crystalline materials. Fortunately, the electronic spectral characteristics of these highly coloured compounds are distinctive and can be used to monitor their reactions. Figure 1 illustrates the spectra of some of the cluster compounds and demonstrates the way in which the nuclearity of the cluster influences the spectral characteristics. Using this technique it becomes much simpler to judge when a cluster aggregation or degradation reaction has gone to completion and when the cluster is in a sufficiently pure state for effective crystallisation.

## STRUCTURES OF GOLD CLUSTER COMPOUNDS IN THE SOLID STATE

The formation of crystalline samples of gold cluster compounds which diffract well in a single crystal X-ray experiment is sometimes problematical because of the large scope for disorder associated with these molecules and the high absorption coefficient of gold. These problems have been discussed in detail by Steggarda *et al.*[13] Fortunately, a number of compounds have now been structurally characterised by this technique. The results are summarised in Table 1 and some of the structures are illustrated in Fig. 2. The bonding in "naked" gold cluster species originates primarily from the overlap of gold 6*s* orbitals and is multicentred in nature. Therefore, the bonding interactions between the nearest neighbour gold atoms are maximised for deltahedral molecules. However, the attainment of this type of polyhedral geometry is not always compatible with the steric requirements of the ligands in tertiary phosphine gold cluster cations. For low nuclearity clusters deltahedral geometries are electronically and sterically favourable and therefore are observed in: $[Au_4I_2(PPh_3)_4]$—tetrahedral;[14] $[Au_6(Ptol_3)_6]^{2+}$—octahedral[15] and $[Au_7(PPh_3)_7]^+$—pentagonal bipyramidal.[16] Alternatively, non-spherical polyhedra formed from the condensation of smaller deltahedral fragments are sometimes seen, e.g. $[Au_6(PPh_3)_6]^{2+}$—edge sharing pair of tetrahedra[17]—and $[Au_6(dppp)_4]^{2+}$—tetrahedral with edge bridging gold atoms.[18]

The higher nuclearity clusters are characterised by the presence of an additional gold atom at the centre of polyhedron. The presence of this gold atom is most important to the stabilisation of the high nuclearity gold cluster compounds because it reinforces the radial bonding. X-ray crystallographic studies have established that these radial interactions are more significant than the tangential interactions. For example, the radial gold–gold bond lengths are generally 0.1–0.2 Å shorter than the peripheral gold–gold bond lengths.[6,19]

The higher nuclearity gold cluster compounds can initially be distinguished on the basis of a simple topological feature—those compounds with a total of $12n+18$ valence electrons have the peripheral gold atoms lying approximately on the surface of a sphere, whereas those with a total of $12n+16$ valence electrons have the peripheral gold atoms lying approximately on a ring or torus. Since attention has been focussed on the topologies of the clusters, rather than a precise description of the polyhedron formed by the metal atoms, then the most flexible bonding model is one that is independent of the spherical co-ordinates of the gold atoms. Such a model has been developed for borane and metal carbonyl clusters by Stone.[20] Using his notation, the out-pointing $s$—$d_{z^2}$—$p_z$ hybrids of $AuPR_3$ fragments on the peripherary of the cluster can combine to form cluster molecular orbitals, which can be expressed as

Table 1. Summary of known gold cluster cations

| Stoichiometry | Polyhedral geometry | Number of valence electrons |
|---|---|---|
| Non-centred polyhedra | | |
| $Au_4(\mu\text{-}I)_2(PPh_3)_4$ | Tetrahedral | 54 |
| $[Au_6(P(p\text{-}C_6H_4CH_3)_3)_6]^{2+}$ | Octahedral | 76 |
| $[Au_7(PPh_3)_7]^+$ | Pentagonal bipyramid | 88 |
| Condensed non-centred polyhedra | | |
| $[Au_6(PPh_3)_6]^{2+}$ | Edge-sharing bitetrahedral | 76 |
| $[Au_6(dppp)_4]^{2+}$ | Di-$\mu$-bridged tetrahedral | 80 |
| Toroidal centred clusters ($12n+16$ electrons) | | |
| $[Au_8(PPh_3)_7]^{2+}$ | Icosahedron—five vertices | 100 |
| $[Au_9(P(p\text{-}C_6H_4CH_3)_3)_8]^{3+}$ | Icosahedron—four vertices | 112 |
| $[Au_9(P(p\text{-}C_6H_4OMe)_3)_8]^{3+}$ | Centred crown | 112 |
| $[Au_{10}Cl_3(PCy_2Ph)_6]^+$ | Ring of six tetrahedra | 124 |
| Spherical centred clusters ($12n+18$ electrons) | | |
| $[Au_8(PPh_3)_8]^{2+}$ | Capped centred chair | 102 |
| $[Au_9(PPh_3)_8]^+$ | Bicapped centred chair | 114 |
| $[Au_{11}I_3(P(p\text{-}C_6H_4F)_3)_7]$ | Tridecahedron | 128 |
| $[Au_{13}Cl_2(PMe_2Ph)_{10}]^{3+}$ | Icosahedral | 152 |

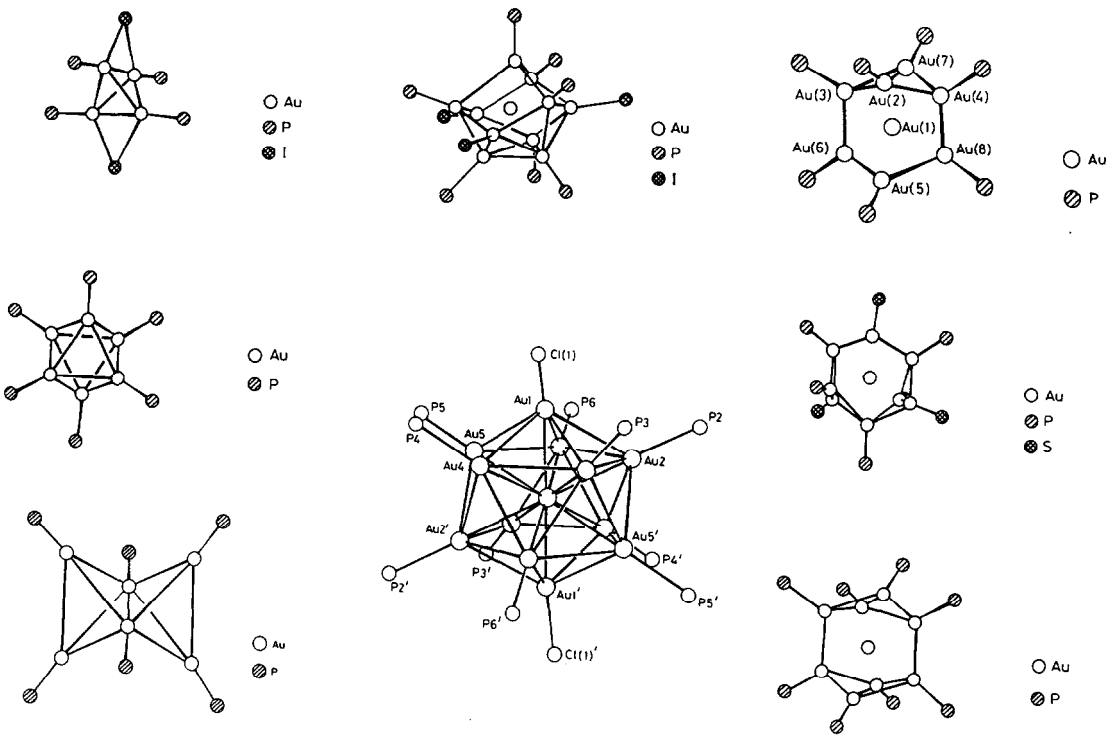
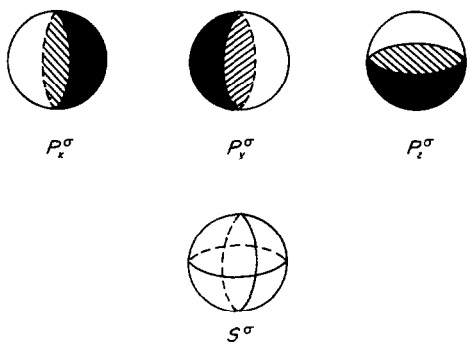



Fig. 2. Some examples of structurally characterised gold cluster compounds. The non-centred clusters are represented by $[Au_4I_2(PPh_3)_4]$, $[Au_6(Ptol_3)_6](BPh_4)_2$ and $[Au_6(PPh_3)_6](NO_3)_2$. The centred spherical clusters include $[Au_{11}I_3(PAr_3)_7]$ and $[Au_{13}Cl_2(PMe_2Ph)_{10}](PF_6)_2$. The toroidal centred clusters are represented by $[Au_8(PPh_3)_7]^{2+}$, $[Au_9(SCN)_3(PCy_3)_5]$ and $[Au_9(Ptol_3)_8](BF_4)_3$.

spherical harmonics, and classified according to their azimuthal and magnetic quantum numbers $l$ and $m$, i.e. as $S^\sigma$ ($l = 0, m = 0$); $P^\sigma$ ($l = 1, m = 0, \pm 1$); $D^\sigma$ ($l = 0, \pm 1, \pm 2$) etc. In common with atomic orbitals, which are also expressed in terms of spherical harmonics, these cluster molecular orbitals are characterised by the number of nodal planes which they possess. Furthermore, because of the significant 6*s*–6*s* overlap integrals between adjacent gold atoms the number of nodal planes accurately reflects the relative energies of the molecular orbitals. Indeed, when $12 > n > 6$ then only the $S^\sigma$ and $P^\sigma$, which are illustrated below, are bonding.




It follows that all spherical clusters of the type $Au_n$ ($12 > n > 6$) are characterised by a total of four bonding skeletal molecular orbitals. The central gold atoms reinforces this pattern because it has 6*s* and 6*p* atomic orbitals which overlap effectively with the $S^\sigma$ and $P^\sigma$ molecular orbitals localised on the peripheral atoms.

The $12n + 18$ electron rule for the spherical gold clusters $[Au(AuPR_3)_n]^{x+}$ is a direct consequence of the formation of the four skeletal molecular orbitals, designated above as $S^\sigma$ and $P^\sigma$, i.e. eight electrons occupy these orbitals, $10(n + 1)$ electrons occupy the 5*d* shells of the gold atoms and $2n$ electrons the Au—P $\sigma$-bonding orbitals. Table 1 gives specific examples of these clusters and in some instances they are illustrated in Fig. 2.[21–24]

In contrast, the toroidal clusters are characterised by a total of $12n + 16$ electrons (see Table 1 and Fig. 2 for some examples). This difference can be traced to a removal of the degeneracy of the $P_x^\sigma$, $P_y^\sigma$ and $P_z^\sigma$ set of skeletal bonding molecular orbitals when the symmetry is reduced from spherical to eliptical. In an eliptical or toroidal cluster the $P_x^\sigma$- and $P_y^\sigma$-functions retain their bonding character, but the $P_z^\sigma$-function becomes either nonbonding or antibonding. The

reason for this can be appreciated by reference to the illustration below.



$P_z^\sigma$

In the toroidal cluster the adjacent gold atoms lie above and below the nodal plane and consequently the interactions between them is overall anti-bonding.

A more detailed analysis of the structures of high nuclearity gold clusters, which is summarised in Fig. 3, suggests that the structures of these compounds are derived from two basic components—the centred crown, $[Au_9(PR_3)_8]$, and the centred chair, $[Au_7(PR_3)_6]$.[24,25] The latter is the more important and the majority of toroidal and spherical clusters can be derived from it in the manner illustrated in the figure. The toroidal clusters are generated by the addition of edge bridging $AuPR_3^+$ fragments to three atom sequences of the peripheral gold atoms. This process retains the $S^\sigma$, $P_x^\sigma$ and $P_y^\sigma$ bonding skeletal molecular orbitals. The spherical clusters are generated by the addition of either $AuPR_3$ or $Au_3(PR_3)_3$ fragments along the three-fold symmetry axis of the centred chair. The addition of these fragments stabilises the $P_z^\sigma$ skeletal molecular orbital and therefore leads to an electron count of $12n + 18$. The centred crown geometry shown at the top of Fig. 3 has been found in $[Au_9\{P(C_6H_4OMe)_3\}_8]^{3+}$.[21]

## SKELETAL REARRANGEMENTS ASSOCIATED WITH REDOX PROCESSES

For boranes and metal carbonyl clusters increases in the total number of valence electrons originating either from redox processes or the coordination of additional ligands generally results in the opening up of the structure. If the original cluster has a *closo*-geometry the successive addition of electron pairs

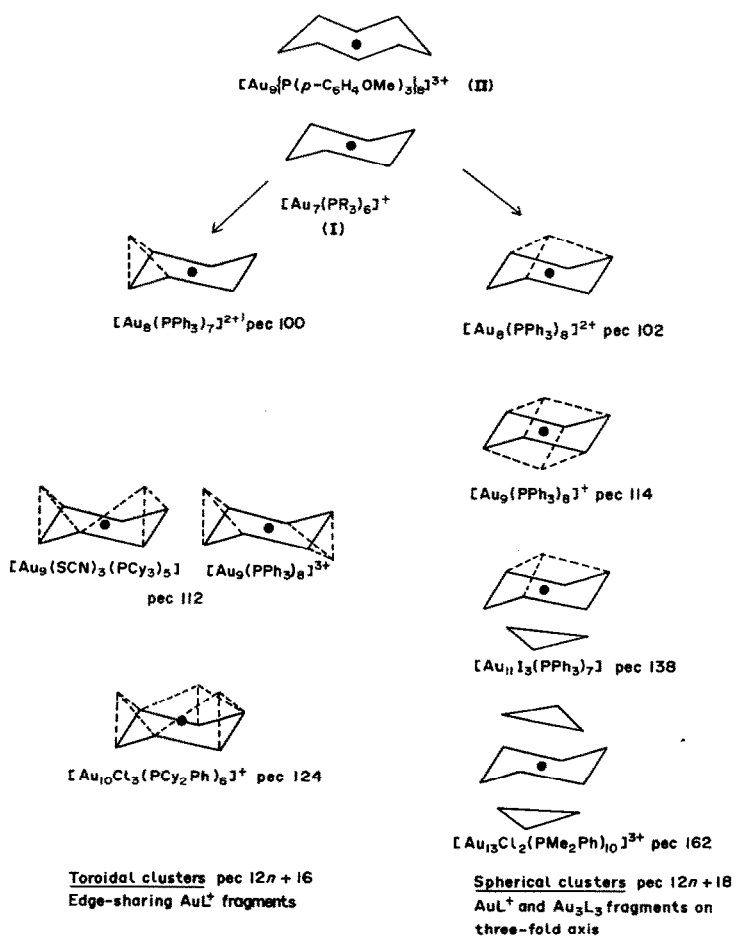
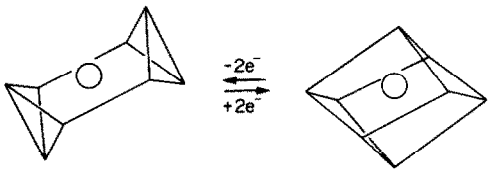



Fig. 3. Description of high-nuclearity clusters based on the addition of edge- and face-capping groups to the centred chair, $[Au_7(PR_3)_6]$. pec, polyhedral electron count.

results in *nido*- and *arachno*-deltahedral fragments.[4] The more restricted use of valence orbitals by the gold fragments in $[Au(AuPR_3)_n]^{x+}$ leads to a different pattern of behaviour. The addition of an electron pair to a toroidal cluster with $12n+16$ electrons results in a more compact spherical cluster with $12n+18$ valence electrons. Such a transformation has recently been studied using electrochemical techniques and the conclusions are summarised in a schematic fashion below.[26]

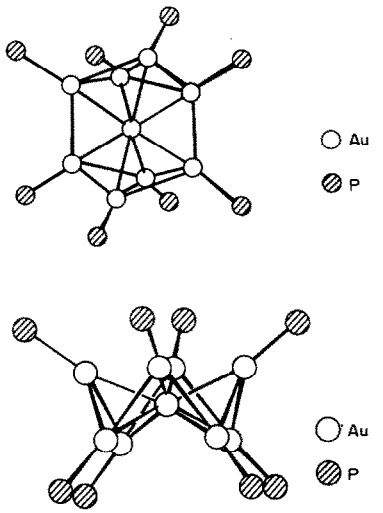



$[Au_9(PAr_3)_8]^{3+}$ $[Au_9(PAr_3)_8]^{+}$

Interestingly both structures are based on a centred chair but in the oxidised form the additional $AuPPh_3$ fragments occupy edge bridging positions, whereas in the reduced form they occupy positions along the three fold axis. The latter can also be described in terms of a distorted cube. The distortions can in part be ascribed to steric effects since cluster cone angle considerations suggest that this ion must be very sterically crowded.

## STEREOCHEMICAL NON-RIGIDITY IN GOLD CLUSTER COMPOUNDS

During the last few years it has become apparent that transition metal cluster compounds may have alternative structures which are separated by only small energy differences. In particular solution NMR studies have suggested that $[Rh_9P(CO)_{21}]^{2-}$ is undergoing rapid skeletal rearrangements in solution and that in the stacked platinum cluster anions $[Pt_3(CO)_6]_n^{2-}$ the triangles of platinum atoms rotate in an independent fashion.[27,28] In addition Lewis, Johnson and their coworkers have noted that osmium carbonyl cluster anions undergo dramatic rearrangements on protonation.[29] Our studies on gold cluster complexes has demonstrated that the potential energy surfaces connecting alternative polyhedral geometries must be very soft. For example, $\{Au_9[P(C_6H_4OMe)_3]_8\}(NO_3)_3$ crystallizes in two modifications. The green modification is tetragonal and the golden brown modification is orthorhombic. Single crystal X-ray crystallographic determinations on these modifications have demonstrated that they have the very different skeletal geometries illustrated below.[30]




The former is based on a centred chair and the latter a centred crown and their interconversion requires substantial atom movements. Yet in solution NMR and electronic spectral data indicate that they share a common structure. Detailed NMR experiments by Vollenbroek *et al.*[31] have confirmed that $[Au_9(PPh_3)_8]^{3+}$ is stereochemically non-rigid in solution.[31] CP/MAS[32] NMR studies on the two crystalline modifications in the solid state have confirmed that they do not undergo similar rearrangements at room temperature under these conditions.

Similar behaviour has been noted for some of the lower nuclearity gold cluster cations. Thus although $[Au_6(Ptol_3)_6](BPh_4)_2$ has an octahedral structure in the solid state is the closely related complex $[Au_6(PPh_3)_6](NO_3)_2$ has a structure based on two tetrahedra sharing a common edge.[17] Furthermore, although the $^{31}P\{^1H\}$ NMR spectrum of the latter in $CH_2Cl_2$ at 203 K shows two resonances at 49.6 and 60.7 ppm with relative integration ratios of 4/2, i.e. consistent with the solid state structure, only a weighted average signal is observed at room temperature.[17]

We conclude from these observations that the steric and electronic effects in these gold cluster compounds are finely balanced and that the observed structure in the solid state often represents only a shallow minimum in the potential energy surface for the molecule. It was these considerations which initially led us to propose a topologically based bonding model to account for the bonding in gold cluster compounds rather than one based on clearly identifiable polyhedral geometries, which carry with them the implication of stereochemical rigidity.

## HETEROMETALLIC CLUSTERS CONTAINING $AuPR_3$ FRAGMENT

Recently a large number of mixed metal cluster compounds containing the $AuPPh_3$ fragment have been characterised. The relatively easy synthesis of such compounds either from metal carbonyl cluster anions and $AuPPh_3^+$ or from hydrido-cluster cations and $AuMePPh_3$ has been a major factor in the rapid growth of this area.[33–36] Bruce and Nicholson have used a variant of the former method, viz. utilising $(Ph_3PAu)_3O^+$ rather than $AuPPh_3^+$, to synthesise a related series of complexes with one, two and three gold atoms.[37] Similar compounds have been reported by Stone *et al.*[38] from mononuclear gold precursors. In these compounds compact structures based on face sharing tetrahedra are formed with the $AuPR_3$ fragments adding to the least hindered triangular faces. In related compounds, however, the $AuPPh_3$ fragment occupies a $\mu_2$ bridging mode between two transition metal atoms. In a previous paper we have developed a fragment molecular orbital analysis which accounts for the bonding in low nuclearity gold cluster compounds and heterometallic compounds containing the $AuPPh_3$ fragment.[23] However, two aspects of these compounds appear to be causing some confusion in the current literature. The first concerns the validity of the *polyhedral skeletal electron pair approach* to such heterometallic clusters and the second concerns the stereochemical non-rigidity of those compounds containing several gold atoms.[37,38] These two aspects are interrelated and may be interpreted in terms of the fragment molecular orbital analysis developed previously for $AuPR_3$.[23]

The frontier molecular orbitals of the $AuPR_3$ fragment are represented in a schematic fashion in Fig. 4. The orbitals with a predominance of *d* orbital character are filled and the bonding characteristics of the $AuPR_3$ fragment are determined primarily by the $hy(s-z)$ and higher lying pair of metal $p_x$- and $p_y$-orbitals. For gold the energy separation between these two classes of orbital is large and the bonding is dominated by the $hy(s-z)$ frontier orbital. For comparative purposes the frontier molecular orbitals of the $Mn(CO)_3$ and the $Mn(CO)_4$ fragments are also illustrated in the figure.

Some years ago we developed a capping principle from a consideration of the interactions between the fragment molecular orbitals of a $M(CO)_3$ capping group and the bonding molecular orbitals of the polyhedron which was being capped on a triangular or square face.[40] It was argued that on the basis of pseudo-symmetry considerations the polyhedron would have a set of three bonding molecular orbitals with nodal characteristics matching those of the higher lying $2e$ and $2a_1$ frontier orbitals of the $M(CO)_3$ fragment. Conventional perturbation theory arguments suggested that the introduction of the capping $M(CO)_3$ fragment would stabilise the three bonding polyhedral molecular orbitals and destabilise the $M(CO)_3$ frontier orbitals to such an

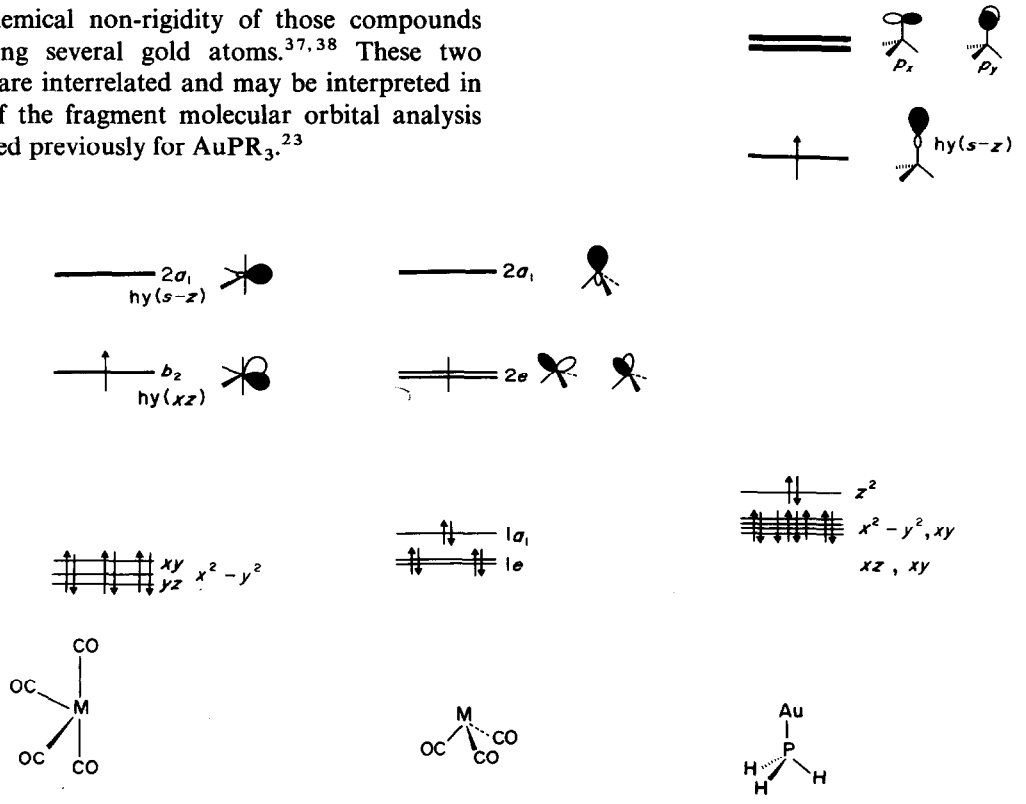



Fig. 4. Comparison of the frontier orbitals of $Au(PH_3)$, $Mn(CO)_3$ and $Mn(CO)_4$.

extent that they would not be available for skeletal bonding. It follows from this analysis that each capping $M(CO)_3$ fragment results in an increment in the total electron count of 12. The following compounds illustrate this general principle:[29]

| | | |
|---|---|---|
| Octahedron, | e.g. $Rh_6(CO)_{16}$, | polyhedral electron count 86 |
| Capped octahedron, | e.g. $Rh_7(CO)_{16}^{3-}$, | polyhedral electron count 98 |
| Bicapped octahedron, | e.g. $Re_8C(CO)_{24}^{2-}$, | polyhedral electron count 110 |
| Tetracapped octahedron, | e.g. $Os_{10}C(CO)_{24}^{2-}$, | polyhedral electron count 134 |

The same arguments apply for the capping of a polyhedron by an $AuPR_3$ fragment, because this fragment (see Fig. 4) also has a set of high lying $a_1$ and $e$ frontier orbitals which are destabilised by the capping interactions. Therefore, the $AuPR_3$ fragment effectively functions as $AuPR_3^+$ and results also in an increment in the polyhedral electron count 12. The following examples illustrate this point:

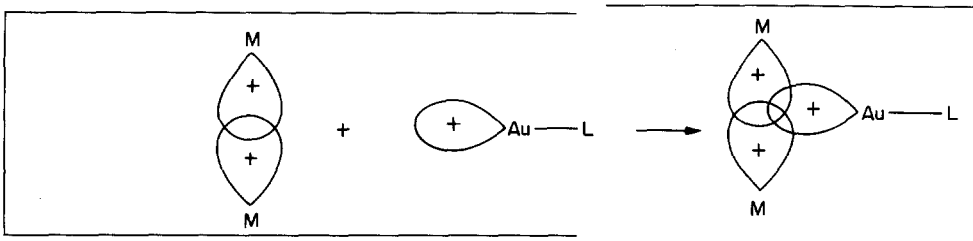
| | | |
|---|---|---|
| Tetrahedron, | e.g. $Os_4H_4(CO)_{12}$, | polyhedral electron count 60 |
| Capped tetrahedron, | e.g. $FeCo_3Au(CO)_{12}(PPh_3)$, | polyhedral electron count 72 |
| Bicapped tetrahedron, | e.g. $Ru_4H_2(AuPPh_3)_2(CO)_{12}$, | polyhedral electron count 84 |
| Tricapped tetrahedron, | e.g. $Ru_4H(AuPPh_3)_3(CO)_{12}$, | polyhedral electron count 96 |

| | | |
|---|---|---|
| Butterfly, | e.g. $Os_3Au(PPh_3)H(CO)_{10}$, | polyhedral electron count 60 |
| Capped butterfly, | e.g. $Os_4Au(PEt_3)H(CO)_{13}$, | polyhedral electron count 72 |

However, an important difference arises when a polyhedron is expanded by edge bridging rather than by capping. The frontier orbitals of the $M(CO)_4$ fragment, illustrated in Fig. 4, are ideally suited to interact with a pair of metal atoms connected by a metal–metal bond.[39] Using arguments related to those developed above for capping, the $M(CO)_4$ frontier orbitals are destabilised by their interaction with the orbitals of the parent polyhedron. Consequently, edge bridging by $M(CO)_4$ fragments leads to an increment in the electron count of 14. The $M(CO)_3$ fragment does not function effectively as an edge bridging group because one component of the $e$-set is not utilised in bonding. The redundant component can accommodate an additional electron pair making it isoelectronic with $M(CO)_4$. Either way, edge bridging in a metal carbonyl cluster results in an increment of 14 electrons. The following compounds illustrate this generalisation:[29]

| | | |
|---|---|---|
| Triangle, | e.g. $Os_3(CO)_{12}$, | polyhedral electron count 48 |
| Butterfly, | e.g. $Re_4(CO)_{16}^{2-}$, | polyhedral electron count 62 |
| Planar raft, | e.g. $Os_6(CO)_{21}$, | polyhedral electron count 90 |

The $AuPR_3^+$ moiety can bridge a metal–metal bond by utilising its $a_1 - hy(s-z)$ orbital in a three-centre two-electron interaction of the type illustrated below. The $e$-set of $p_x$- and $p_y$-orbitals are too high lying to make an effective contribution.




Consequently, edge bridging by an $AuPR_3$ fragment leads to an increment in the polyhedral electron count of 12. Therefore the polyhedral electron count in heterometallic clusters containing gold will be two electrons fewer than that predicted from the polyhedral skeletal electron pair approach for each $AuPR_3$ fragment which edge bridges. The following compounds illustrate this point:

The fact that that $AuPR_3$ fragment can function as either a face or edge bridging group and in each instance cause an increment in the polyhedral electron count of 12 also provides an explanation for the stereochemical non-rigidity of this type of heterometallic cluster. In some respects it resembles the carbonyl ligand which acts as a two-electron donor irrespective of whether it is in a terminal, edge bridging or face bridging location. In contrast the transformation of face to edge bridging of a metal carbonyl fragment requires the donation of an electron pair. Consequently, these cluster compounds are generally stereochemically rigid.

In conclusion, our studies of homo- and heterometallic cluster compounds of gold have demonstrated that the initial impression of cluster compounds based on rigid platonic solids is invalid. Some cluster compounds, and particularly those

containing gold are exceptionally flexible and undergo skeletal rearrangements which are rapid on the NMR time scale. The implications of this mobility to the properties of clusters and crystallites on inert supports are difficult to ignore.

*Acknowledgements*—The SERC is thanked for financial support, Johnson-Matthey Ltd for the loan of gold metal and my students for generously dedicating a great deal of effort and expertise converting my ill-formed ideas into scientific facts. In particular I should like to thank Brian Theobald and Kevin Hall for synthesising the gold cluster compounds, David Evans for assistance with the theoretical investigations and Clive Briant for his crystallographic skills.

## REFERENCES

1. E. L. Muetterties, *Chem. Eng. News.* 30 August, 1982, 28.
2. G. T. McDougal and R. D. Hancock, *Gold Bull.* 1981, **14**, 138.
3. D. Safer, J. Hainfield, J. S. Wall and J. E. Reardon, *Science* 1982, **218**, 290.
4. K. Wade, *Adv. Inorg. Chem. Nucl. Chem.* 1976, **18**, 1.
5. D. M. P. Mingos, *J. Chem. Soc., Chem. Commun.* 1983, 706; *Accounts Chem. Res.* 1984, **17**, 311; *J. Chem. Soc., Dalton Trans.* 1976, 1163.
6. K. P. Hall and D. M. P. Mingos, *Prog. Inorg. Chem.* 1984, **32**, 37; D. M. P. Mingos, *Gold Bull.* 1984, **17**, 5.
7. L. Malatesta, *Gold Bull.* 1975, **8**, 48.
8. C. E. Briant, B. R. C. Theobald, J. W. White, L. K. Bell, D. M. P. Mingos and A. J. Welch, *J. Chem. Soc., Chem. Commun.* 1981, 201.
9. C. E. Briant, K. P. Hall and D. M. P. Mingos, *J. Organomet. Chem.* 1982, **229**, C5; *J. Organomet. Chem.* 1983, **254**, C18.
10. J. J. Steggarda, J. J. Bour and J. W. A. van der Welden, *Recl Trav. Chim. Pays-Bas* 1982, **101**, 164.
11. C. A. Tolman, *Chem. Rev.* 1977, **77**, 313.
12. D. M. P. Mingos, *Inorg. Chem.* 1982, **21**, 466.
13. J. M. M. Smits, P. T. Beurskens and J. J. Steggarda, *J. Crystallogr. Spec. Res.* 1983, **13**, 381.
14. F. DeMartin, M. Manasserro, L. Naldini, R. Ruggeri and M. Sansoni, *J. Chem. Soc., Chem. Commun.* 1981, 222.
15. P. L. Bellon, M. Manasserro and M. Sansoni, *J. Chem. Soc., Dalton Trans.* 1973, 2423.
16. J. W. A. van der Velden, P. T. Beurskens, J. J. Bour, W. P. Bosman, J. H. Noordik, M. Kolenbrander and J. A. K. M. Buskes, *Inorg. Chem.* 1984, **23**, 497.
17. C. E. Briant, K. P. Hall and D. M. P. Mingos, *J. Organomet. Chem.* 1982, **229**, C5.
18. J. W. A. van der Velden, J. J. Bour, J. J. Steggarda, P. T. Beurskens, M. Roseboom and J. H. Noordik, *Inorg. Chem.* 1982, **21**, 4321.
19. P. G. Jones, *Gold Bull.* 1981, **14**, 102, 159; **16**, 114.
20. A. J. Stone, *Inorg. Chem.* 1981, **20**, 563.
21. K. P. Hall, B. R. C. Theobald, D. I. Gilmour, D. M. P. Mingos and A. J. Welch, *J. Chem. Soc., Chem. Commun.* 1982, 528.
22. D. M. P. Mingos, *Proc. R. Soc.* 1982, **A308**, 75.
23. D. G. Evans and D. M. P. Mingos, *J. Organomet. Chem.* 1982, **232**, 171.
24. K. P. Hall, D. I. Gilmour and D. M. P. Mingos, *J. Organomet. Chem.* **268**, 275.
25. C. E. Briant, K. P. Hall and D. M. P. Mingos, *J. Chem. Soc., Chem. Commun.* 1984, 248.
26. J. G. M. van der Linden, M. L. H. Paulissen and J. E. J. Schmitz, *J. Am. Chem. Soc.* 1983, **105**, 1903.
27. J. L. Vidal, W. E. Walker, R. L. Pruett and R. C. Schoning, *Inorg. Chem.* 1979, **18**, 129.
28. C. Brown, B. T. Heaton, A. D. C. Towl, G. Longoni, A. Fumagalli and P. Chini, *J. Organomet. Chem.* 1979, **181**, 233.
29. J. Lewis and B. F. G. Johnson, *Pure Appl. Chem.* 1982, **54**, 97.
30. C. E. Briant, K. P. Hall and D. M. P. Mingos, *J. Chem. Soc., Chem. Commun.* 1984, 290.
31. F. A. Vollenbroek, J. P. van der Berg, J. W. A. van der Velden and J. J. Bour, *Inorg. Chem.* 1980, **19**, 2685.
32. J. W. Diesveld, E. M. Menger, H. T. Edzes and W. S. Veeman, *J. Am. Chem. Soc.* 1980, **102**, 7935.
33. M. J. Freeman, M. Green, A. G. Orpen, I. D. Salter and F. G. A. Stone, *J. Chem. Soc., Chem. Commun.* 1983, 1332.
34. B. F. G. Johnson, J. Lewis, J. W. H. Nelson, M. D. Vargas, D. Braga and M. McPartlin, *J. Organomet. Chem.* 1983, **246**, C69.
35. M. Green, K. A. Mead, R. M. Mills, I. D. Salter, F. G. A. Stone and P. Woodward, *J. Chem. Soc., Chem. Commun.* 1982, 51.
36. C. E. Briant, K. P. Hall and D. M. P. Mingos, *J. Chem. Soc., Chem. Commun.* 1983, 843.
37. M. I. Bruce and B. K. Nicholson, *J. Organomet. Chem.* 1983, **252**, 243.
38. L. W. Bateman, M. Green, K. A. Mead, R. M. Mills, I. D. Salter, F. G. A. Stone and P. Woodward, *J. Chem. Soc., Dalton Trans.* 1983, 2599.
39. D. G. Evans and D. M. P. Mingos, *Organometallics* 1983, **2**, 435.
40. M. I. Forsyth and D. M. P. Mingos, *J. Chem. Soc., Dalton Trans.* 1977, 610.

*Polyhedron* Vol. 3, No. 12, pp. 1299–1306, 1984
Printed in Great Britain

0277–5387/84 $3.00 + .00
Pergamon Press Ltd

# THE BONDING IN BORON AND TRANSITION-METAL CLUSTER COMPOUNDS

A. J. STONE
University Chemical Laboratory, Lensfield Road, Cambridge CB2 1EW, U.K.

(*Received* 28 *April* 1984)

**Abstract**—A method is described for constructing qualitatively the molecular orbitals of an approximately spherical cluster of boron or transition-metal atoms. The method gives a way of understanding the electron-counting rules for such clusters, the preference for deltahedral structures, the relationship between *closo* boranes on the one hand and *nido* and *arachno* boranes on the other, and Mingos' capping and condensation principles for transition-metal clusters.

## 1. INTRODUCTION

It is not necessary in the present company to enlarge on the importance of Wade's electron-counting rules[1] to our understanding of the structures of cluster molecules such as the boranes and the transition-metal cluster carbonyls. Nor is it necessary to expound the relationships between the structures of different types of borane, as set out by Williams,[2] or describe the way in which Mingos' capping principle,[3] and more recently his condensation principle,[4] have clarified our understanding of transition-metal structures. The purpose of the present article is to explain how these rules may be understood in simple terms with the help of some elementary pictorial molecular orbital theory.

It is helpful to begin with a familiar example. The molecular orbitals of a cyclic hydrocarbon like benzene can be written in terms of atomic orbitals $\eta_r$ as

$$\psi_{Mc} = \sum_r \eta_r \cos(2\pi Mr/n),$$
$$\psi_{Ms} = \sum_r \eta_r \sin(2\pi Mr/n), \tag{1.1}$$

where $n$ is the number of atoms. (These expressions are not normalized, but we need not concern ourselves with that here.) For $M = 0$, we get only the orbital $\psi_0 \equiv \psi_{0c} = \sum_r \eta_r$, since $\psi_{0s}$ vanishes, and then the orbitals occur in pairs for $M = 1, 2, \ldots$ until $n$ orbitals have been found. If we were to construct more than $n$ orbitals by taking more values of $M$, we would find they were not new ones but repetitions of the first $n$.

Now observe that these orbitals can be constructed from the orbitals for a particle on a ring, which are

$$\psi_{Mc} = \cos M\theta,$$
$$\psi_{Ms} = \sin M\theta, \tag{1.2}$$

if we interpret the value of one of these functions, evaluated at the position of an atom, as the coefficient of the atomic orbital on that atom in the LCAO wavefunction. If the position of one atom defines $\theta = 0$, then the other atoms are at $\theta = 2\pi r/n$, so $\cos M\theta$ becomes $\cos(2\pi Mr/n)$ and we arrive at eqn (1.1). This is not an accident: it reflects the cyclic symmetry of both systems. Moreover the energies of these orbitals increase with $M$; $\psi_0$ has no nodes and is bonding in the cyclic $n$-atom system, $\psi_{1c}$ and $\psi_{1s}$ each have one node bisecting the ring and are less strongly bonding, and the energy increases steadily with the number $M$ of nodes.

What now if we consider a less symmetrical system—a distorted benzene, say, in which the bond lengths are all different? Symmetry appears to offer no help in such a case. But we can be confident, if the distortion is not too extreme, that the lowest-energy orbital will have no nodes, that the next two orbitals will have one node each and be close to each other in energy, and so on. So a very good first guess at the molecular orbitals will be given by the recipe above: take the LCAO coefficient of atomic orbital $\eta_r$ to be $\cos M\theta_r$ (or $\sin M\theta_r$). The position $\theta_r$ will not now be exactly $2\pi r/n$ because of the distortion. This simple model will not give the exact orbitals, but for qualitative and approximate quantitative purposes it is sure to contain all the important features.

There is another way to arrive at the same result. If we start from the electron on a ring, which we can imagine to be uniformly charged to keep the electron from leaving it, we can concentrate the charge at a number of points (the nuclei) distributed around the ring. As a result, the electronic wavefunction will tend to be concentrated near the nuclear charges, and to resemble an atomic wavefunction there, so that an LCAO description becomes more appropriate; but the relative importance of each atomic function in the LCAO description will be related to the amplitude of the original ring wavefunction at the position of the atom.

## 2. *CLOSO* CLUSTERS

Such ideas were extensively used at one time as a way of understanding the electronic spectra of condensed aromatic hydrocarbons—naphthalene, for example, being treated as a perturbed 10-member ring.[5] The extension to globular clusters as distinct from planar ring-like systems was used by Longuet-Higgins in the 1950s (though not, I think, published) and by Hoffman, Ruedenberg and Verkade.[6] Here the model system is a particle confined to the surface of a sphere, and the model wavefunctions are the spherical harmonics $Y_{LM}(\theta, \phi)$. $Y_{LM}$ has $L$ nodal surfaces, and the energies increase steadily with $L$, being proportional to $L(L+1)$ for the simple model. There are $2L+1$ functions with a given $L$; these all have the same energy, and are distinguished by the label $M$ which usually runs from $-L$ to $L$. However the $Y_{LM}$ are complex when $M \neq 0$, and it is often convenient to use real functions $Y_{LMc}$ and $Y_{LMs}$, with $M > 0$, defined so that

$$\left.\begin{aligned} Y_{LM} &= \sqrt{\tfrac{1}{2}}(-1)^M(Y_{LMc}+iY_{LMs}),\\ Y_{L-M} &= \sqrt{\tfrac{1}{2}}(Y_{LMc}-iY_{LMs}) \end{aligned}\right\} \quad M > 0. \quad (2.1)$$

For example, the functions $Y_{10}$, $Y_{11c}$ and $Y_{11s}$ with $L = 1$ are proportional respectively to $\cos\theta$, $\sin\theta\cos\phi$ and $\sin\theta\sin\phi$, and describe the angular behaviour of $p_z$, $p_x$ and $p_y$ atomic orbitals.

If now we have a cluster of atoms distributed over the surface of a sphere, at positions $(\theta_r, \phi_r)$, we may generate a cluster wavefunction by taking the values of the spherical harmonic $Y_{LM}(\theta, \phi)$ at the positions of the atoms as the LCAO coefficients:

$$\psi^\sigma_{LM} = \sum \eta_r Y_{LM}(\theta_r, \phi_r). \quad (2.2)$$

This procedure will generate cluster orbitals with the same nodal structure as the spherical harmonics $Y_{LM}$, and for the reasons adduced in the case of the ring these orbitals are likely to be good approximations to the true molecular orbitals of the cluster. Moreover we can expect that their energies will increase steadily with the number of nodes, and that orbitals $\psi^\sigma_{LM}$ with the same $L$ but different $M$ will have similar energies.

This procedure leads to cluster orbitals like those illustrated in Fig. 1 for an octahedral cluster. It is convenient to use the labels $S$, $P$, $D$, ... for orbitals generated from the spherical harmonics with $L = 0$, $1, 2, \ldots$, and these are labelled $S^\sigma$, $P^\sigma$ and $D^\sigma$ because they are constructed from $\sigma$-orbitals of the constituent atoms. The label $\sigma$ here denotes cylindrical symmetry about the radius vector, as it would if the atoms were ligand atoms surrounding a central transition-metal ion. There is a single $S^\sigma$ orbital corresponding to $Y_{00}$, a set of three $P^\sigma$-orbitals corresponding to $Y_{10}$, $Y_{11c}$ and $Y_{11s}$ and each having one nodal plane, and a set of $D^\sigma$-orbitals corresponding to $Y_{20}$ and $Y_{22c}$. The spherical harmonics $Y_{21c}$, $Y_{21s}$ and $Y_{22s}$ are all zero at all the atom positions, so they do not generate cluster orbitals, but in any case we expect only six independent cluster orbitals from the six atomic orbitals. The high symmetry makes this a rather special case, but it has the advantage of familiarity for the inorganic chemist.

It is possible to estimate the energies of these orbitals using the rather crude approximations of extended Hückel theory;[7] the details will not be given here but the result is instructive. The orbitals with a given value of $L$ are expected to have similar energies, and the average of those energies is

$$W^\sigma_L = \alpha^\sigma + \frac{2b}{n}\beta^\sigma P_L(\cos\omega). \quad (2.3)$$

In this expression, $\alpha^\sigma$ and $\beta^\sigma$ are Coulomb and resonance integrals, and $n$ and $b$ are the number of

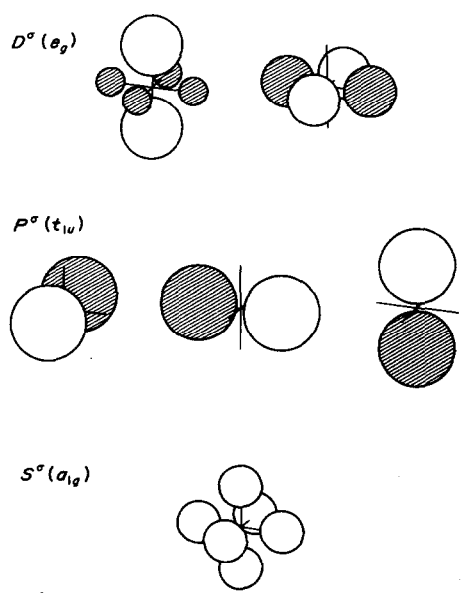



Fig. 1. $\sigma$-Orbitals for an octahedral cluster.

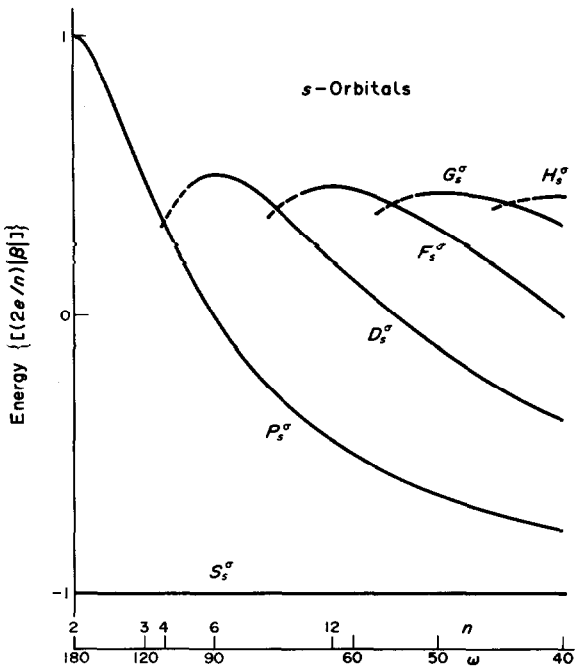



Fig. 2. Energy of $L^\sigma$-orbitals as a function of cluster size.

atoms and the number of bonds in the cluster. $P_L(\cos\omega)$ is a Legendre polynomial, and $\omega$ is the angle subtended at the centre of the cluster by one of the bonds, and decreases as the cluster size increases. Figure 2 shows how the $P_L(\cos\omega)$ factor varies with the size of the cluster, and it is apparent that the energy always increases steadily with $L$. Note that clusters with 4 or fewer atoms have only $S^\sigma$ and $P^\sigma$ cluster orbitals ($L = 0$ and 1) so the $D^\sigma$-energy is not shown for these small clusters. Similarly $F^\sigma$-energies are not shown for $n < 9$. The horizontal scale shows the value of $\omega$ as well as $n$, since they are quite closely related.

An important feature of the energy formula is the factor $2b/n$, which is the average coordination number of the atoms in the cluster. The formula shows quite plainly that the bonding energy of the orbitals is proportional to the coordination number, and if only bonding orbitals are occupied the most stable structure is the one with the maximum number of bonds. Such a structure is a polyhedron composed entirely of triangular faces—a deltahedron.

Equation (2) can be applied to any kind of $\sigma$ atomic orbital, but not to atomic $\pi$-orbitals. The $\pi$-orbitals have intrinsic nodes, so the nodal pattern in the cluster orbital is no longer a useful guide to its energy. To handle atomic $\pi$-orbitals, such as are present in the BH units comprising a *closo* borane, a further development is needed.

A set of atomic $p$-functions behaves in many ways like a set of unit vectors; by combining them, with suitable coefficients, it is possible to construct $p$-functions pointing in any direction. The two $\pi$-orbitals of a BH unit have a similar property, except that because there are only two of them it is only possible to construct orbitals with them which are directed along the surface of the sphere on which the BH units sit. If we can find a function of the polar angles $(\theta, \phi)$ analogous to the spherical harmonic $Y_{LM}$, but whose value at the point $(\theta, \phi)$ is a vector parallel to the surface of the sphere, then the direction and magnitude of that vector can be taken to specify the direction and magnitude of a $\pi$-orbital contribution to a cluster wavefunction.

There are in fact two such functions for each $LM$ except for $L = M = 0$. One is defined by

$$\mathbf{V}_{LM} = \nabla Y_{LM}(\theta, \phi), \tag{2.4}$$

where $\nabla$ is the gradient operator:

$$\nabla = \left(\frac{\partial}{\partial x}, \frac{\partial}{\partial y}, \frac{\partial}{\partial z}\right)$$

$$= \left(\frac{\partial}{\partial r}, \frac{1}{r}\frac{\partial}{\partial \theta}, \frac{1}{r \sin\theta}\frac{\partial}{\partial \phi}\right)$$

in Cartesian coordinates or spherical polar coordinates respectively. Since $Y_{LM}(\theta, \phi)$ does not depend on $r$, the radial component of $\mathbf{V}_{LM}$ is zero, so that $\mathbf{V}_{LM}$ is a tangential vector function as required.

The other type of function is defined by

$$\bar{\mathbf{V}}_{LM}(\theta, \phi) = \hat{\mathbf{r}}(\theta, \phi) \times \mathbf{V}_{LM}(\theta, \phi), \tag{2.5}$$

where $\hat{\mathbf{r}}(\theta, \phi)$ is a unit vector in the direction of the radius vector at the position $(\theta, \phi)$ on the sphere. The direction of $\bar{\mathbf{V}}_{LM}$ at any point on the sphere is perpendicular to both the radius vector at the point and the direction of $\mathbf{V}_{LM}$, so it is also tangential, but orthogonal to $\mathbf{V}_{LM}$. This is a very important feature; it means that the orbital constructed from the $\bar{\mathbf{V}}_{LM}$ can be obtained from the orbital constructed from the corresponding $\mathbf{V}_{LM}$ by rotating every atomic $\pi$-function through 90° about the radius vector. A further rotation recovers the original function, except for a change of sign.

$Y_{00}$ is a constant, so its gradient is zero and there is no $\mathbf{V}_{00}$ or $\bar{\mathbf{V}}_{00}$. The $\mathbf{V}_{1M}$ and $\bar{\mathbf{V}}_{1M}$ are illustrated in Fig. 3: at each of the selection of points on the sphere, the direction and magnitude of each function are represented by an arrow of suitable direction and length.

From these vector functions, then, we can construct cluster orbitals. The relationship between vector function and cluster orbital is illustrated in a general way for a part of the spherical surface of a hypothetical (and very large!) cluster in Fig. 4. The direction of the gradient is at right angles to the contours, as shown, and its magnitude, which

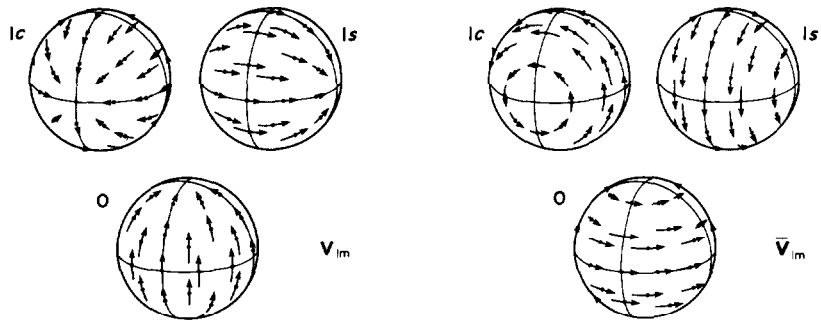



Fig. 3. The surface vector harmonics $\mathbf{V}_{1M}$ and $\bar{\mathbf{V}}_{1M}$.

describes the steepness of the function, is large when the contour lines are close together and zero at a maximum or minimum. Far from a maximum or minimum the contours are as shown in Fig. 4(a), and the gradient does not vary greatly in direction or magnitude. The corresponding LCAO wavefunction has its $p$–$\pi$ orbitals arranged parallel to one another, and is $\sigma$-antibonding but $\pi$-bonding. Consequently such a region is more or less non-bonding in character.

Near a maximum, on the other hand [Fig. 4(b)] the arrows representing the gradient all point towards the maximum, and the corresponding region of the LCAO wavefunction is strongly bonding. The same is true near a minimum. Another similar feature, which occurs for example when $\theta = 90°$ in the $d_{z^2}$ function, is a line along which the function has a maximum or minimum, as illustrated in Fig. 4(c). The wavefunction in this type of region is also strongly bonding.

The characteristics of the $\bar{\mathbf{V}}_{LM}$ are complementary to these, and are obtained by rotating all the gradient vectors through 90°. The non-bonding region remains non-bonding [Fig. 4(d)]—it is still $\sigma$-antibonding and $\pi$-bonding—but the bonding regions of the $\mathbf{V}_{LM}$ become antibonding regions in the $\bar{\mathbf{V}}_{LM}$, as shown in Figs 4(e) and 4(f).

Thus we expect the $\psi_{LM}$, constructed from the

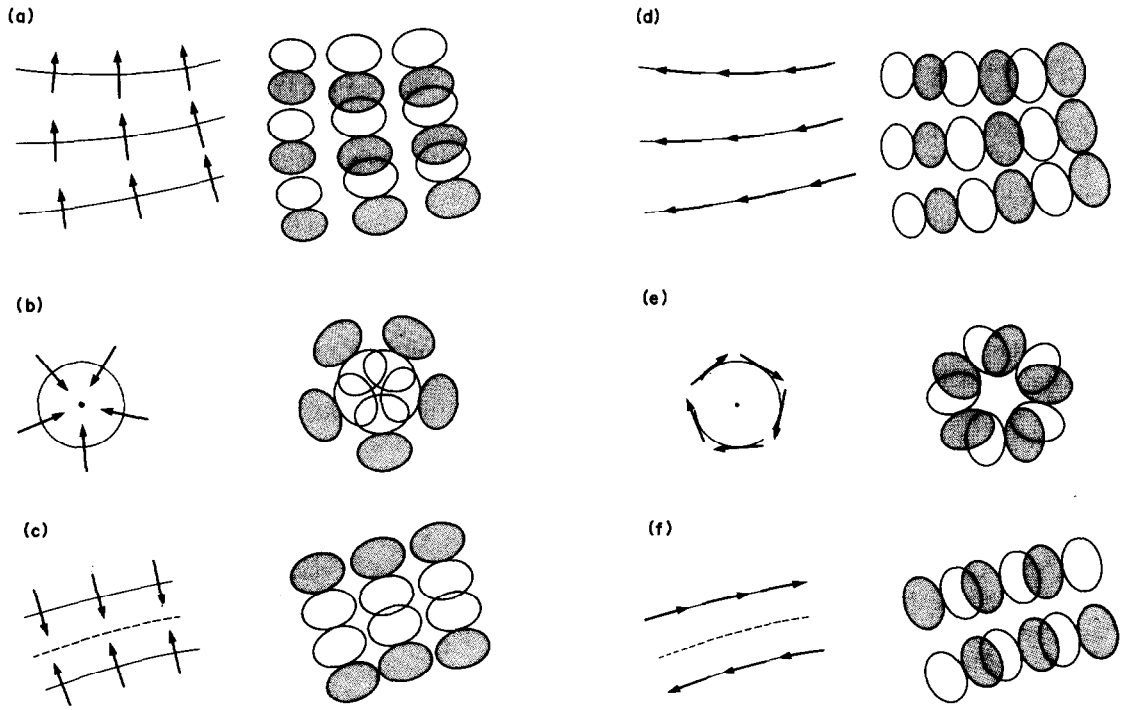



Fig. 4. Relationship between vector surface harmonics and cluster orbitals. The lines in each part of the diagram represent schematically the contours of a region of a spherical harmonic, plotted on the surface of the sphere. The arrows in (a), (b) and (c) show the magnitude and direction of the gradient vector function $\mathbf{V}_{LM}$, and the corresponding region of the LCAO wavefunction $\psi^{\pi}_{LM}$ is also shown. (d), (e) and (f) illustrate the corresponding regions of $\bar{\mathbf{V}}_{LM}$ and $\bar{\psi}^{\pi}_{LM}$.

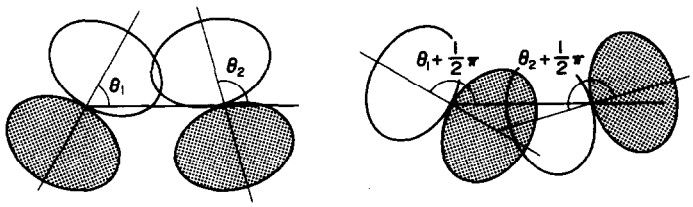



Fig. 5. Bonding between two adjacent $\pi$-orbitals of a cluster.

$\mathbf{V}_{LM}$, to be bonding orbitals and the $\bar{\psi}^{\pi}_{LM}$, constructed from the $\bar{\mathbf{V}}_{LM}$, to be antibonding. This expectation is confirmed by explicit calculation.[7]

Indeed we can go further. If we consider the atomic orbitals on two neighbouring atoms in a cluster $\pi$-orbital [Fig. 5(a)], it is easy enough to establish, by resolving each $\pi$-orbital into components parallel and perpendicular to the bond, that the contribution of this pair to the cluster orbital energy is

$$E_{12} = 2c_1c_2(\beta_\pi \sin\theta_1 \sin\theta_2 - \beta_\sigma \cos\theta_1 \cos\theta_2), \tag{2.6}$$

where $c_1$ and $c_2$ are the orbital coefficients and $\beta_\sigma$ and $\beta_\pi$ are suitable resonance integrals for the $\sigma$–$\sigma$ and $\pi$–$\pi$ interactions. If now we rotate each orbital through 90°, [Fig. 5(b)] then the energy is obtained by replacing each $\theta$ in eqn (2.6) by $\theta+\frac{1}{2}\pi$, and is

$$\bar{E}_{12} = 2c_1c_2(\beta_\pi \cos\theta_1 \cos\theta_2 - \beta_\sigma \sin\theta_1 \sin\theta_2), \tag{2.7}$$

so that if $\beta_\sigma = \beta_\pi$ (which is approximately true for boranes) then $\bar{E}_{12} = -E_{12}$. In other words, the operation of rotating each $\pi$ orbital through 90° about the radius vector, which takes $\psi^{\pi}_{LM}$ into $\bar{\psi}^{\pi}_{LM}$ and vice versa, changes bonding interactions into antibonding ones and vice versa.

We see, then, that the $\pi$ cluster orbitals come in pairs, $\psi^{\pi}_{LM}$ and $\bar{\psi}^{\pi}_{LM}$, one of each pair being bonding and the other antibonding. Since there are $2n$ $\pi$-orbitals, two for each of the $n$ atoms in the cluster, we have $n$ bonding $\pi$-orbitals and $n$ antibonding ones.

Just as in the case of the cyclic hydrocarbons, we expect these $\sigma$- and $\pi$-orbitals to be good first approximations to the molecular orbitals. However the cluster case is more complicated, because we have a $\psi^{\sigma}_{LM}$, a $\psi^{\pi}_{LM}$ and a $\bar{\psi}^{\pi}_{LM}$ for each set of values of $L$ and $M$, except $L = M = 0$. Orbitals with different $L$ and $M$ do not normally mix much with each other, but those with the same $L$ and $M$ can do so. However a further approximate symmetry determines that, although $\psi^{\sigma}_{LM}$ and $\psi^{\pi}_{LM}$ mix with each other, neither mixes with $\bar{\psi}^{\pi}_{LM}$. This further symmetry is inversion.

Inversion of a spherical harmonic $Y_{LM}$ leaves it unchanged or changes its sign according as $L$ is even or odd. The same is true of the $\mathbf{V}_{LM}$, but the $\bar{\mathbf{V}}_{LM}$ behave in the opposite way: that is, they are unchanged or changed in sign according as $L$ is odd or even. The $\mathbf{V}_{1M}$ and $\bar{\mathbf{V}}_{1M}$ shown in Fig. 3 display these contrasting properties. This means that the antibonding $\bar{\psi}^{\pi}_{LM}$ do not mix much with the other orbitals, but the bonding $\psi^{\pi}_{LM}$ mix with the $\psi^{\sigma}_{LM}$ to give in each case a more strongly bonding orbital and a non-bonding or antibonding one. The details of this mixing are unimportant, though we can see from Fig. 2 that the $\psi^{\sigma}_{LM}$ with small $L$ will contribute more to the bonding functions than those with large $L$. The effect is that all the $\psi^{\pi}_{LM}$ are more or less stabilized, giving $n$ bonding orbitals, while the $\psi^{\sigma}_{LM}$ are destabilized and will be unoccupied.

But all this applies only for $L = 1, 2, \ldots$ and not for $L = 0$, because there is no $\mathbf{V}_{00}$ or $\bar{\mathbf{V}}_{00}$, so the $S^{\sigma}$ function, the most strongly bonding of all the $\psi^{\sigma}_{LM}$, is unaffected by this mixing. Consequently there are $n+1$ bonding cluster orbitals in all.

More detailed analysis[7] confirms this qualitative picture, and also shows that the binding energy is proportional to the coordination number, as it was when there were only $\sigma$ orbitals to consider. Consequently the theory predicts that clusters such as the boranes should have deltahedral structures and $n+1$ bonding cluster orbitals—results which are well-established empirical observations. Explicit MNDO calculations on a series of boranes[8] show that the cluster orbitals do indeed behave as this qualitative theory leads us to expect. A study of electronic structures of small molecules like $N_2$, $C_2H_2$ and $C_3H_3^+$ shows that they too can be viewed in this way.[7]

Tetrahedral molecules however provide a particularly interesting exception to the general rule. The tetrahedron has three bonding cluster $\pi$ orbitals (the $T_2$-set) which are classified as $\psi^{\pi}_{1M}$, and three antibonding ones (the $T_1$ set) which are $\bar{\psi}^{\pi}_{1M}$, and the pairing principle pairs each of the $T_2$ orbitals with a corresponding member of the $T_1$ set. This means that the remaining two orbitals, one of which is $D^{\pi}$ and the other $\bar{D}^{\pi}$, can only be paired with each other. (Notice that it is not possible for an orbital to be paired with itself, as can happen in alternant hydrocarbons where a pairing principle also applies, because the pairing operation in the present case is guaranteed to produce a different orbital.) But they belong to the $E$-

representation, so they must be degenerate and by the pairing principle must be approximately non-bonding. In fact the analytic formula for the energies $W_2^\pi$ and $\bar{W}_2^\pi$ of the $D^\pi$-orbitals, obtained using Hückel approximations,[7] shows that this is indeed true for the tetrahedron. Since this degenerate pair of orbitals must be either full or empty for a stable structure, we see that the tetrahedron can have either four cluster orbitals occupied ($S^\sigma$ and $P^\pi$, as in $B_4Cl_4$) or six ($S^\sigma$, $P^\pi$ and the $E$-set, as in $P_4$ or tetrahedrane), but there is no possibility of a tetrahedral cluster with five skeletal electron pairs, electron-counting rules notwithstanding.

## 3. *NIDO* CLUSTERS

So far we have considered only *closo* clusters. However, the principles can be extended to *nido* clusters,[9] which can be regarded as derived from *closo* clusters by the removal of a vertex. To see what happens to the orbital pattern in this case, we imagine the original *closo* cluster to be oriented so that the departing vertex is on the $+z$-axis. Then we can classify the orbitals of both the *closo* and the *nido* cluster under $C_{\infty v}$-symmetry. The cluster orbitals could then be labelled as $\Sigma^+$ or $\Sigma^-$ when $M = 0$, $\Pi$ when $M = 1$, and so on, but it is more convenient to use the notation $E_1, E_2, \ldots$ for orbitals with $M = 1, 2, \ldots$. This is more directly related to the $LM$ classification for the spherical cluster, and also corresponds to the notation used in any finite group to which the molecule may in fact belong.

The $2L+1$ orbitals $\psi_{LM}^\pi$ are now classified under this scheme as $\Sigma^+, E_1, E_2, \ldots, E_L$. Similarly the $\bar{\psi}_{LM}^\pi$ are $\Sigma^-, E_1, E_2, \ldots, E_L$. Each bonding $E_M^\pi$-set of orbitals is paired with an antibonding $E_M^\pi$-set, so that there is an even number of $E_M^\pi$-sets in total. In particular there is an even number of $E_1^\pi$-sets, half of them bonding and half antibonding.

Now in constructing a *nido* cluster we remove a vertex, which we have arranged to lie on the $+z$-axis. It takes with it one $\sigma$-orbital, which transforms as $\Sigma^+$, and a set of $\pi$-orbitals which transform as $E_1^\pi$. Consequently there is now an *odd* number of $E_1^\pi$-orbital sets. Each bonding $E_1^\pi$-set is paired with an antibonding set, so at least one $E_1^\pi$-set must now be non-bonding and paired with itself. Normally we would expect just one such non-bonding set, so if there were $2k$ $E_1^\pi$-sets in the *closo* cluster, we now have $k-1$ bonding sets, $k-1$ antibonding ones and one non-bonding. If therefore we fill the bonding and non-bonding orbitals we have $k$ filled $E_1^\pi$-sets—the same number as in the *closo* cluster—and the electron count is unchanged.

This will happen only if something is done to stabilise the structure. Removing a BH unit from $B_nH_n^{2-}$, but leaving two of its electrons behind to maintain the electron count, leaves $B_{n-1}H_{n-1}^{4-}$, an improbable species. The simplest way to stabilise it is to add four protons to give $B_{n-1}H_{n+3}$, and indeed *nido* boranes typically have this formula. The non-bonding $E_1^\pi$-set must have substantial amplitude at the open face of the *nido* polyhedron, because it must be able to interact strongly enough with the orbitals of a BH unit to recover the bonding and antibonding orbitals of the original *closo* structure. Consequently the additional protons should be found around the open face. Brint[10] has remarked that the orbitals of a square array of four protons can be regarded as $\sigma$, two $\pi$s and a $\delta$, and that the $\sigma$- and $\pi$-orbitals allow the $H_4$-unit to mimic a BH unit. Other species, notably transition metal ions, have suitable $\pi$ acceptor orbitals to allow them to coordinate with a $B_{n-1}H_{n-1}^{4-}$ unit.

Notice too that the energy of the frontier $E_1^\pi$-orbital is minimized if the open face extends over as many atoms as possible, because then the single node bisecting the open face has less extreme antibonding effects. [Compare the $M = 1$ orbitals of cyclopropenyl (antibonding) and benzene (bonding).] Consequently it is to be expected that the *nido* cluster is derived by removing the atom of highest coordination number from the *closo* cluster.[9]

A similar argument can be applied to *arachno* clusters,[9] where a pair of $E_2$-orbitals, as well as a pair of $E_1$, become frontier orbitals. It has to be admitted, however, that the electron count becomes less well defined, because the structure of an *arachno* cluster is not very close to the notional $C_{\infty v}$-symmetry.

## 4. TRANSITION-METAL CLUSTERS

Transition-metal clusters are more complicated, because of the presence of $d$-orbitals on each cluster atom. If we take a local $z$-axis along the radius vector, then the $d_{z^2}$-orbital is cylindrically symmetrical about the radius vector and is therefore a $d^\sigma$-orbital. The $d_{xz}$- and $d_{yz}$-orbitals have a single nodal plane containing the radius vector and are classified as $d^\pi$, and finally the $d_{xy}$- and $d_{x^2-y^2}$-orbitals have two nodes containing the radius vector and must be classified as $d^\delta$. These $\delta$-type atomic orbitals are a new feature of transition-metal clusters. They can be handled by an extension of the methods described above,[7] or by a more elegant method described by Qian-er.[11] It emerges that there are no $\delta$-type cluster orbitals with $L = 0$ or 1, so the $\delta$-series starts with $D^\delta$. Also, just as with the $\pi$-orbitals, there is a pairing principle, and we can identify $D^\delta$, $F^\delta$, ... bonding orbitals and corresponding $\bar{D}^\delta$, $\bar{F}^\delta$, ... antibonding orbitals, though the energy separation is not very great.

We now have an embarassingly large collection of orbitals. Each atom contributes one *s*-function (the 4*s* for first-row transition metals), a set of *p*-functions, one of which is a $p^\sigma$ and the other two $p^\pi$, and the *d*-functions $d^\sigma$, $d^\pi$ and $d^\delta$. But the surface harmonic approach allows us to classify the orbitals according to the approximate spherical symmetry, and so to reduce very greatly the number of orbitals which needs to be considered at one time. For each value of $L$ up to a limit determined by the size of the cluster, we can construct $L_s^\sigma$-, $L_p^\sigma$-, $L_p^\pi$-, $L_d^\sigma$-, $L_d^\pi$- and $L_d^\delta$-functions, all behaving like the $Y_{LM}$ under inversion, and $\bar{L}_p^\pi$-, $\bar{L}_d^\pi$- and $\bar{L}_d^\delta$-functions having the opposite parity to the $Y_{LM}$. The notation now includes a subscript *s*, *p* or *d* to indicate the type of atomic orbital; the symbol $L$ stands for $S$, $P$, $D$, ... as the case may be.

Consider first the $\bar{L}_p^\pi$ and $\bar{L}_d^\pi$. Both sets are initially antibonding, but by mixing $p_x$ with $d_{xz}$ we can construct an inward-pointing $\pi$-orbital which will contribute to a more strongly antibonding function, and an outward-pointing one which will contribute to a cluster orbital which will be much less strongly antibonding and can act as an acceptor for ligand electrons. The $\bar{L}_d^\delta$ will mix with these, when $L > 1$, to push the bonding and antibonding orbitals even further apart. Of these orbitals, therefore, we identify n strongly antibonding ones, inaccessible to electrons by virtue of their high energy. Moreover they are directed towards the centre of the cluster and so cannot help to stabilize electrons in ligand orbitals, having negligible amplitude in the ligand region. The remaining $2n$ orbitals are relatively low-lying, and can contain electrons on their own account, or act as acceptor orbitals for ligand electrons.

The $L_s^\sigma$, $L_p^\sigma$, $L_p^\pi$, $L_d^\sigma$, $L_d^\pi$ and $L_d^\delta$ will all mix with each other in a similar fashion. Here, however, the $S_s^\sigma$-, $S_p^\sigma$- and $S_d^\sigma$-orbitals cannot combine to produce an antibonding orbital. An inward-pointing combination is bonding between the cluster atoms, while an outward-pointing combination can accept ligand electrons. Only the $P$, $D$, ... cluster orbitals can generate inaccessible orbitals in the manner of the $\bar{P}$, $\bar{D}$, .... Consequently there are only $n-1$ inaccessible orbitals derived from this series.[7]

So there are in total $2n-1$ unoccupied orbitals in such a cluster. Moreover they correspond precisely, as Mingos[12] pointed out in the special case of the octahedron, to the vacant orbitals of a boron hydride. It is really in this sense that the electron-counting rules carry over from boron hydrides to transition-metal clusters. The picture is however much less clear-cut than the boron hydrides, and as Woolley has explained[13] the analogy should not be pressed too far.

The electron-counting rules do work satisfactorily for cluster carbonyls, however, and if we interpret them in terms of the *antibonding* orbitals, too high in energy to be occupied in their own right, and too inaccessible to take part in the stabilisation of ligand donor orbitals (because strongly antibonding in the metal cluster and therefore necessarily directed inwards, rather than outwards towards the ligands) we can obtain a simple interpretation not only of *closo* clusters but also of vertex, edge and face-linked clusters.

Imagine a polyhedral transition-metal cluster, with $n$ atoms and $N$ inaccessible orbitals, from which we extract a vertex, edge or face ($j = 1, 2$ or 3 atoms) to leave an open cluster of $n-j$ atoms. The extracted unit has a number $J$ of inaccessible orbitals arising from its own internal bonding—$J = 0$, 1 or 3 for an atom, diatom or triatom—so the original number of inaccessible orbitals is reduced at least to $N-J$. Some of these $N-J$ orbitals will drop in energy through the removal of antibonding interactions with the departing unit, but they are necessarily localized in the region of the open face. These frontier orbitals would interact strongly with ligands replacing the departing vertex, edge or face, just as in the boranes (Fig. 6).

However we now form a linked structure, consisting of an $(n-j)$-atom open cluster on one side of a linking $j$-atom unit, and an $(m-j)$-atom open cluster, derived from an $m$-atom closed cluster with $M$ inaccessible orbitals, on the other. If now there are orbitals of the linking unit which can mix with the frontier orbitals of both open clusters, which will usually be the case when it comprises transition-metal atoms, then the frontier orbitals will be pushed up again in energy and will become inaccessible again. The total number of inaccessible orbitals is now $N-J$ from one open cluster (including its frontier orbitals), $M-J$ from the other, and $J$ from the linking unit, making $N+M-J$ in all.

Thus the total number of inaccessible orbitals in a linked structure is the sum of the numbers associated

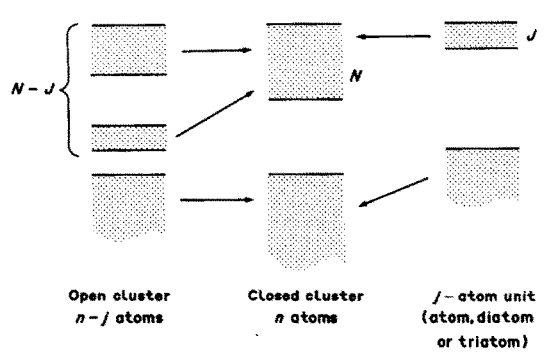



Fig. 6. Schematic orbital energy diagram for removal of an atom, edge or face from a closed cluster with $M$ inaccessible orbitals.

with the two separate structures, less the number associated with the atom, edge or face that they have in common. Since the total number of valence orbitals is fixed at 9 for each atom, this leads directly to Mingos' electron-counting rule[4] for such structures, if in every case all orbitals but the inaccessible ones are to be occupied either by metal electrons or by electrons donated from the ligands.

This does not in itself explain why such structures are adoped—it merely rationalizes the electron counts that are observed when they *are* adopted. But we are used to the idea that stable structures are those in which the occupied orbitals have energies as low as possible, and that if electrons are removed it will often be advantageous for the structure to rearrange so as to lower the energy of the orbitals still occupied at the expense of those newly vacated. In other words, the stable structure is generally that in which the occupied orbitals, and no others, have low energies.

In these electron-rich compounds we see the converse effect. An increase in the energy of the vacant orbitals is associated with a reduction in the energy of the remaining, occupied, orbitals, and the optimum structure will usually be one in which the vacant orbitals, and no others, have high energies. Adding a pair of electrons will obviously favour a structure in which there is one strongly-antibonding orbital fewer. Removing a pair of electrons will, less obviously, favour a structure in which there is one more strongly antibonding orbital, and the reason for this is, as stated above, that an increase in the energy of the newly-vacated orbital is associated with a decrease in the energy of the orbitals still occupied.

Two examples will suffice.

(i) The octahedron has 11 inaccessible orbitals, leaving 43 occupied (86 electrons), as in $Os_6(CO)_{18}^{2-}$. Removing a pair of electrons favours a structure with 12 inaccessible orbitals. The bicapped tetrahedron (capped trigonal-bipyramid) of $Os_6(CO)_{18}$ has $9+6-3=12$ inaccessible orbitals as required.

(ii) A *closo* deltahedral structure with 10 atoms should have $2\times10-1=19$ inaccessible orbitals and $2\times(9\times10-19)=142$ valence electrons, as in the bicapped square antiprism adopted by $Rh_{10}X(CO)_{22}^{2-}$ (X = S, P, As).[14–16] Removing 4 electrons as in $Ru_{10}C_2(CO)_{24}^{2-}$ (138 valence electrons) favours a structure with 21 inaccessible orbitals; the observed structure has two octahedra of Ru atoms sharing an edge[17] and has just this number of inaccessible orbitals—11 for each octahedron, less 1 for the shared edge. (The interstitial carbon atoms do not affect the electron count,[7,18] though they undoubtedly help to stabilize the two $Ru_6$ octahedra.)

The theory outlined here is not to be regarded as a complete predictive picture of the bonding in such clusters. Rather it is a guide to understanding. The detailed pattern of energy levels in these molecules is very complex, and our understanding of them is far from complete.[13] Even the numerical values quoted above for the numbers of inaccessible orbitals are appropriate only for one class of cluster compounds, the transition-metal cluster carbonyls, and must be modified for other types of cluster.[3] Moreover ideas based on molecular-orbital theory must be used cautiously, since it is becoming clear that electron correlation effects are very important in transition-metal compounds; while the simple molecular-orbital methods such as extended Hückel theory, which must by necessity be used at present for these large systems, are unreliable even within the molecular-orbital model.[13] Nevertheless the ideas set out here may serve as a guide through the forest of energy-level diagrams in the literature, and help us towards a clearer understanding of these fascinating substances.

## REFERENCES


1. K. Wade, *Adv. Inorg. Radiochem.* 1976, **18**, 1.
2. R. E. Williams, *Adv. Inorg. Radiochem.* 1976, **18**, 67.
3. D. M. P. Mingos, *Nature Phys. Sci.* 1972, **236**, 99; D. M. P. Mingos and M. I. Forsyth, *J. Chem. Soc., Dalton Trans.* 1977, **1977**, 610.
4. D. M. P. Mingos, *J. Chem. Soc., Chem. Commun.* 1983, **1983**, 706; D. M. P. Mingos and D. G. Evans, *J. Organomet. Chem.* 1983, **251**, C13.
5. J. R. Platt, *J. Chem. Phys.* 1949, **17**, 484.
6. D. K. Hoffman, K. Ruedenberg and J. G. Verkade, *Struct. Bonding (Berlin)* 1977, **33**, 57.
7. A. J. Stone, *Inorg. Chem.* 1981, **20**, 563; *Mol. Phys.* 1980, **41**, 1339.
8. P. Brint, J. P. Cronin, E. Seward and T. Whelan, *J. Chem. Soc., Dalton Trans.* 1983, **1983**, 975.
9. A. J. Stone and M. Alderton, *Inorg. Chem.* 1982, **21**, 2297.
10. P. Brint (in press).
11. Zhang Qian-er, *J. Mol. Struct. (Theochem.)* 1984, **18**, 215.
12. D. M. P. Mingos, *J. Chem. Soc., Dalton Trans.* 1974, **1974**, 133.
13. R. G. Woolley, submitted for publication.
14. G. Ciani, L. Garleschelli, A. Sironi and S. Martinengo, *J. Chem. Soc., Chem. Commun.* 1981, **1981**, 563.
15. J. L. Vidal, W. E. Walker and R. C. Schoening, *Inorg. Chem.* 1981, **20**, 238.
16. J. L. Vidal, *Inorg. Chem.* 1981, **20**, 243.
17. C.-M. T. Hayward, J. R. Shapley, M. R. Churchill, C. Bueno and A. L. Rheingold, *J. Am. Chem. Soc.* 1982, **104**, 7347.
18. J. W. Lauher, *J. Am. Chem. Soc.* 1978, **100**, 5305; *ibid.*, 1979, **101**, 2604.

*Polyhedron* Vol. 3, No. 12, pp. 1307–1319, 1984
Printed in Great Britain

0277-5387/84 $3.00 + .00
Pergamon Press Ltd

# MAIN GROUP HETEROATOMS IN TRANSITION METAL CLUSTERS*

J. NICOLA NICHOLLS
University Chemical Laboratory, Lensfield Road, Cambridge, U.K.

(*Received* 25 *March* 1983)

**Abstract**—The class of transition metal cluster compounds which contain individual main group heteroatoms is surveyed. Hydrido-clusters and clusters containing group IV, V, VI and VII atoms are dealt with in turn with reference to their synthesis, structure and reactivity.

As a result of the anticipation of similarities between transition metal clusters and fragments of bulk metals, particular attention has been paid during the development of metal cluster chemistry to complexes containing isolated main group atoms. Such clusters have been compared with simple metallic interstitial compounds and atoms bound to metal surfaces and have been postulated as models for intermediates in catalytic processes.[1,2] This may or may not prove to be a useful analogy, but interest in these molecules has resulted in the synthesis and characterisation of a fascinating and extensive class of transition metal clusters containing main group atoms. These range from truly interstitial compounds with high metal : main group atom ratios, as illustrated by $[PtRh_{10}N(CO)_{21}]^{3-}$ [3] and $[Os_{10}C(CO)_{24}]^{2-}$,[4] through "semi-interstitials" like $[Ru_5C(CO)_{15}]$ [5] and $[Fe_4N(CO)_{12}]^-$,[6] to highly exposed surface species such as $[Os_6(\mu_3O)(CO)_{19}]$[7] and $[Ni_3(C_5H_5)_3(\mu_3S)_2]$[8] (see Fig. 1).

The heteroatoms display a wide range of bonding modes and coordination numbers, from eight, in $[Rh_9As(CO)_{21}]^{2-}$,[9] to three, in $[Fe_3(CO)_9As_2]$,[10] for arsenic and six in $[HRu_6(CO)_{18}]^-$ [11] to one in $[H_2Os_3(CO)_{11}]$ [12] for hydrogen. They have been found to stabilise unusual metal cluster geometries like square prismatic or butterfly arrangements and to increase resistance to cluster degradation. Interstitial heteroatoms also allow the synthesis of high nuclearity clusters of metals like rhenium, which require more electrons than could conveniently be provided by external ligands, by furnishing electrons from *within* the cluster. This principle is illustrated by the recent report of the synthesis of the high nuclearity rhenium cluster $[Re_7C(CO)_{21}]^{3-}$ [13] which contains an interstitial carbon atom. In addition when the heteroatom is exposed it provides a possible alternative site of attack for incoming ligands.

It is often difficult to draw the line between which heteroatoms in transition metal clusters should be described as "interstitial" and which "surface" species. The extremes are well defined : for example, in $[Ru_6C(CO)_{17}]$ [14] the carbido-atom is completely enclosed by an octahedron of ruthenium atoms, while the oxygen atom in $[Os_6O(CO)_{19}]$ [7] sits above a triangle of osmium atoms. The carbide in the former is therefore described as interstitial while the oxygen in the latter is clearly a surface species. There is, however, a "grey" area in between consisting of clusters containing heteroatoms displaying a wide range of bonding modes which cannot easily be classified. For example, in $[Ru_5C(CO)_{15}]$ [5] the carbon atom lies slightly below the plane of metal atoms making up the case of the square pyramid and could therefore be described as a surface species. However, since it is also bound to the fifth ruthenium atom and is partially enclosed by the metal cage it could be described as occupying an interstitial site, the carbon being in the centre of a *nido*-octahedral structure and a "semi-interstitial" carbide. For the purposes of this article, since the whole spectrum of bonding modes and coordination numbers of heteroatoms will be covered, I do not intend to dwell on classification, but rather to illustrate the wide variety of structures adopted by transition metal–heteroatom clusters.

At present the range of main group atoms found in transition metal clusters consists of H, C, Si, Ge, Sn, P, N, As, Sb, O, S, Se and the halogens. In the following pages is summarised what is known to date

* In this article the term "cluster" is used to describe any discrete molecule containing three or more metal atoms held together, although not necessarily in a *closo*-polygonal or polyhedral array, by metal–metal bonds.

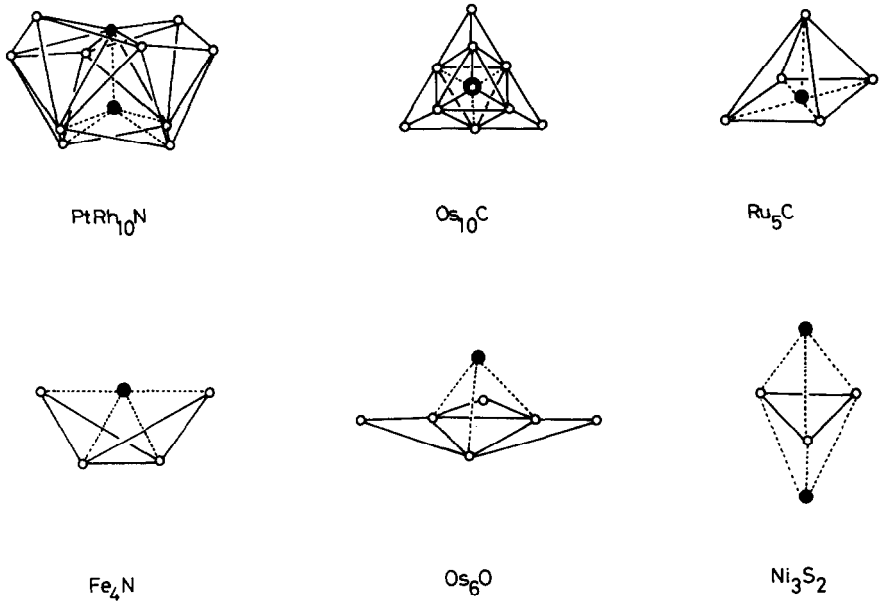



Fig. 1. The transition metal–heteroatom cores of $[PtRh_{10}N(CO)_{21}]^{3-}$, $[Os_{10}C(CO)_{24}]^{2-}$, $[Ru_5C(CO)_{15}]$, $[Fe_4N(CO)_{12}]^-$, $[Os_6O(CO)_{19}]$ and $[Ni_3(C_5H_5)_3S_2]$.

in the field of coordinated heteroatoms in transition metal cluster chemistry. The systems that will be dealt with are those in which the heteroatom is bound exclusively to metal atoms, excluding, for example, "carbido"-species in which the "carbido"-atoms are actually present as $C_2$-units and can therefore be alternatively described as organic fragments. Firstly the hydrido-clusters, which include interstitial, terminal and bridging hydrides will be discussed. Clusters involving group IV heteroatoms will be taken next followed by groups V, VI and VII. It will become apparent that in moving from group IV to VII there is an increased tendency for the heteroatom to be found coordinated to the surface of the cluster rather than in an interstitial site.

## THE HYDRIDO-CLUSTERS

The interstitial nature of hydrogen in binary metallic hydrides is well established but it was not until 1967 that the first genuine example of a transition metal cluster containing an interstitial hydride ligand was reported. That compound was the halide cluster $[HNb_6I_{11}]$ [15] and the hydride was located directly using neutron diffraction methods. In the following year the report of another interstitial hydride, this time in a metal carbonyl as opposed to a metal halide cluster, was the subject of some controversy. It was suggested[16] that despite the highly symmetrical packing of carbonyl ligands and the lack of $^{13}C$—$^1H$ coupling in $[HRu_6(CO)_{18}]^-$, which the authors had used as evidence for the interstitial nature of the hydride,[11] the fact that the $^1H$ NMR showed a large downfield shift indicated a hydride associated with a carbonyl, i.e. a formyl group. The authors' original formulation was later vindicated after a neutron study resulted in the direct location of the hydride at the centre of the octahedron of ruthenium atoms[17] (see Fig. 2). Since then, several examples of hydrogen occupying regular or distorted octahedral cavities in clusters have been seen. It has also been shown that a wide range of $^1H$ NMR shifts exists for interstitial hydrides, from $-23.2$[17] to $29.3\delta$.[19]

Another series of hydrido-clusters is now known in which hydrogen occupies a semi- or *nido*-octahedral cavity. That is to say the hydride is located in the square plane of a square pyramid of metal atoms and may therefore be considered to be five-coordinate (see Fig. 2). The series is made up of the cluster $[HRh_{14}(CO)_{25}]^{3-}$ [18] and the family $[Rh_{13}H_{5-n}(CO)_{24}]^{n-}$ $(n = 2,3,4)$.[19] In each case the hydrides have not been directly located but their positions within the clusters may be inferred from solid state bond length considerations. In solution, however, $^1H$ and $^{13}C$ NMR studies have shown that the hydrides migrate freely within their cluster frameworks.[20]

Mobility of a slightly different nature has been demonstrated for the octahedrally coordinated hydride in the cluster $[HRu_6(CO)_{18}]^-$, described previously. The preparation of this cluster, as for many hydrido-clusters, involves protonation of an anion, in this case the octahedral dianion $[Ru_6(CO)_{18}]^{2-}$. The hydride immediately occupies a position at the centre of the octahedron: however,

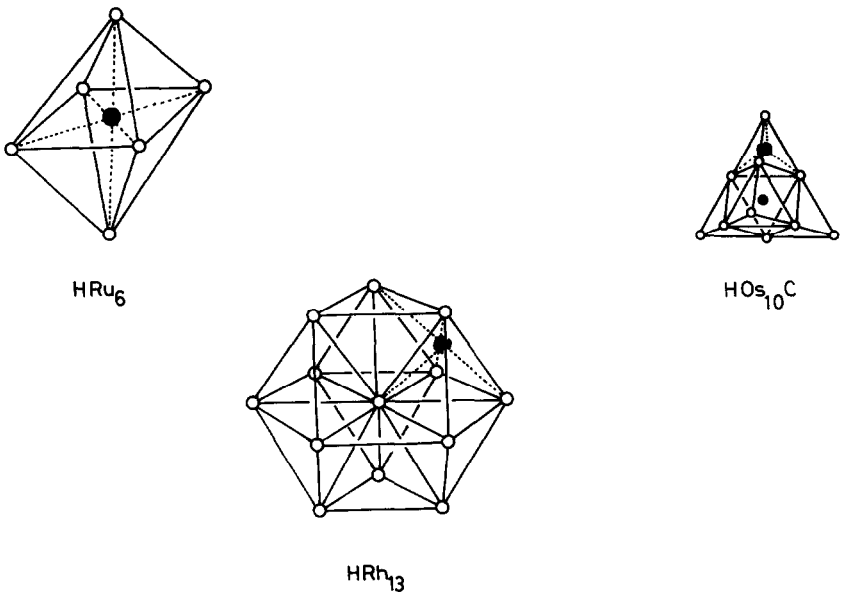



Fig. 2. The ruthenium–hydrogen core of $[HRu_6(CO)_{18}]^-$ and the proposed locations of the hydride ligands in $[HRh_{13}(CO)_{24}]^{4-}$ and $[HOs_{10}C(CO)_{24}]^-$.

on further protonation the interstitial hydride leaves the central cluster cavity and adopts a bridging site on the surface of the octahedron in $[H_2Ru_6(CO)_{18}]$.[21]

In 1982 an interstitial hydride having an even lower coordination number was reported.[22] Since the ligand distribution in the cluster $[HOs_{10}C(CO)_{24}]^-$ was found to be remarkably similar to that of $[Os_{10}C(CO)_{24}]^{2-}$, from which it was prepared, and since the $^1H$ NMR signal at 15.45$\delta$ indicated that the hydride ligand was directly bonded to the metal core, it was supposed that the hydride was in an interstitial site. The octahedral cavity was already occupied by a carbido-atom, so it seemed reasonable to suggest that the hydride was sited within a tetrahedral cap (see Fig. 2), and from bond length considerations it appeared to be disordered over two sites. Observation of $^{187}Os$—$^1H$ coupling in a high resolution $^1H$ NMR study of $[HOs_{10}C(CO)_{24}]^-$ has recently allowed confirmation of this proposal in that the $^{187}Os$—$^1H$ couplings and satellite intensities have proved to be entirely as expected for a tetrahedrally coordinated hydride.[23] A similar situation is observed in the case of the non-carbido cluster $[H_4Os_{10}(CO)_{24}]^{2-}$ for which it is proposed that three hydrides are to be found in tetrahedral capping sites while the fourth occupies the octahedral cavity filled by carbon in the isoelectronic $[Os_{10}C(CO)_{24}]^{2-}$.[24]

The majority of cluster bound hydrogen atoms are found on the surfaces of clusters in $\mu_3$- or $\mu_2$-bonding situations, as illustrated by $[H_4Re_4(CO)_{12}]$[25] and $[H_4Ru_4(CO)_{12}]$[26] respectively (see Fig. 3) and in many such clusters the hydride ligands are found to fluxional. For example the hydrides in $[H_4Ru_4(CO)_{12}]$ were found to be mobile, even in the solid state, and although for the analogous osmium cluster they were static in the solid state at temperatures of up to 300 K, the hydrides in $[H_4Os_4(CO)_{12}]$ are dynamic in solution.[23]

Although well known in mononuclear chemistry, terminal hydride ligands are rarely observed on clusters: in one example, $[H_2Os_3(CO)_{11}]$,[12] both terminal and $\mu_2$-bridging hydrides are seen. However, this molecule is only moderately stable and reverts back to $[Os_3(\mu_2H)_2(CO)_{10}]$ in the absence of CO (see Fig. 4).

Hydrido-clusters may be prepared by the protonation of anions, reactions involving mol-

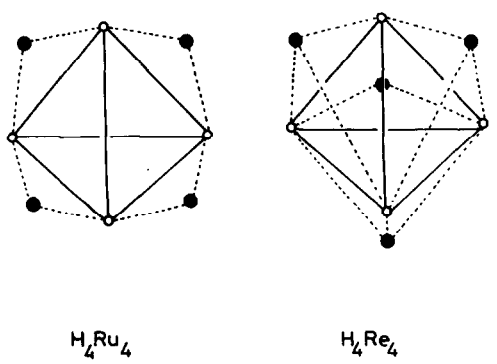
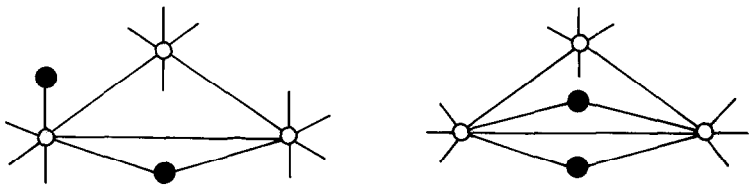



Fig. 3. The structures of $[H_4Ru_4(CO)_{12}]$ and $[H_4Re_4(CO)_{12}]$ (carbonyl ligands omitted).



$[H_2Os_3(CO)_{11}]$ $[H_2Os_3(CO)_{10}]$

Fig. 4. The structures of $[H_2Os_3(CO)_{10}]$ and $[H_2Os_3(CO)_{11}]$.

ecular hydrogen, or by the addition of molecules containing hydrogen atoms, examples of which are given below:

$$[Co_6(CO)_{15}]^{2-} + H^+ \rightarrow [HCo_6(CO)_{15}]^-,^{28}$$

$$[Os_3(CO)_{12}] + H_2 \rightarrow [H_4Os_4(CO)_{12}],^{29}$$

$$[Ru_5C(CO)_{15}] + HBr \rightarrow [HRu_5C(CO)_{15}Br].^{30}$$

The main reaction of the coordinated hydrogen atoms in these clusters is their removal in deprotonation experiments. Interstitial hydrides such as $[HOs_{10}C(CO)_{24}]^-$ and $[HCo_6(CO)_{15}]^-$ are moderately stable in non-coordinating solvents but in the presence of solvents like THF, $CH_3OH$ and $(CH_3)_2CO$ are readily deprotonated.[22] Other interstitial hydrides, like $[HRu_6(CO)_{18}]^-$ and $[H_4Os_{10}(CO)_{24}]^{2-}$, however, resist deprotonation, even under severe conditions. Deprotonation has also been observed for surface bound $\mu_2$- and $\mu_3$-hydrides, for example $[H_2Os_6(CO)_{18}]$ loses a proton to give $[HOs_6(CO)_{18}]^-$,[31] in basic solvents and a proton is readily removed from $[HRu_5C(CO)_{15}Br]$ by treatment with proton sponge [1,8-bis-(dimethylamino)-naphthalene].[32]

## GROUP IV HETEROATOMS

Simple interstitial binary carbides have been known for some time, but it was not until 1962 that the first carbido-cluster was reported in the literature.[33] An X-ray structure revealed that the carbonyl cluster $[Fe_5C(CO)_{15}]$ contained a carbon atom bound to five iron atoms. The carbido-atom was found to be only partially shielded by the $Fe_5$ square pyramidal cage and therefore open to attack by incoming ligands, although no such attack was actually observed.

Since then the number of carbido-carbonyl clusters has increased enormously and carbides have become the largest and most widely studied group of interstitial clusters. The maximum number of metal atoms to which carbon has been found to be coordinated is eight: $[Co_8C(CO)_{18}]^{2-}$ provides a rare example of carbon occupying a tetragonal antiprismatic cluster cavity.[34] More commonly,

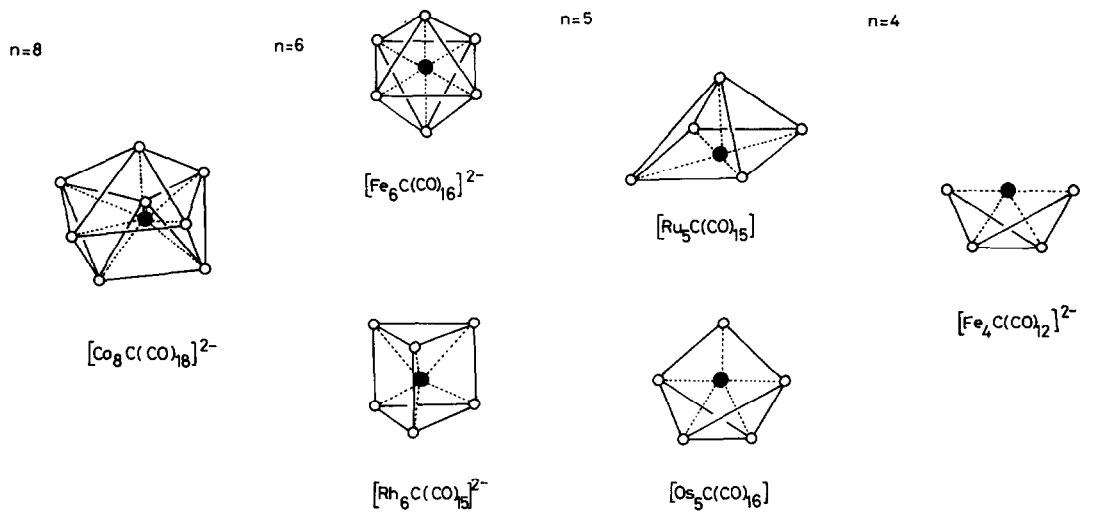



Fig. 5. The $M_nC$ core geometries displayed by transition metal carbide clusters.

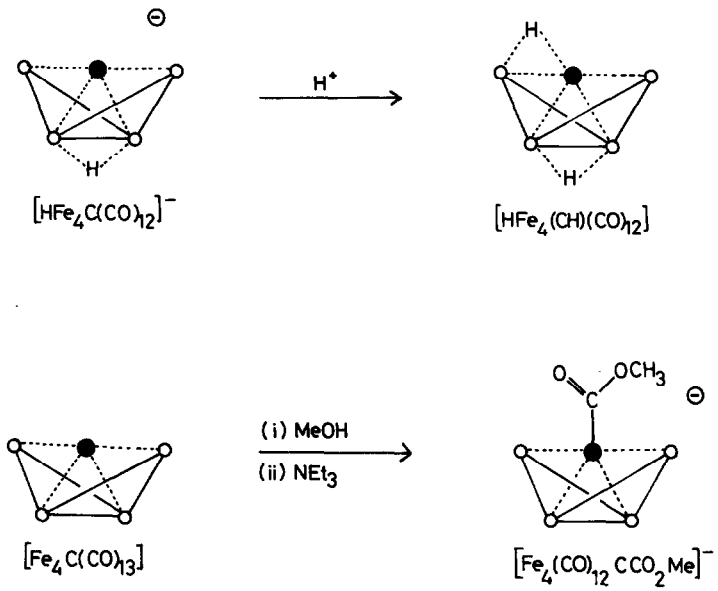



Fig. 6. Reactions occurring at the carbido-carbon atoms of $Fe_4C$ clusters.

carbon is bound to six metal atoms, in octahedral or trigonal prismatic cages, or five metals, in square pyramidal (*nido*-octahedral) or bridged butterfly (*arachno*-pentagonal bipyramidal) sites. Recent developments have also included the discovery of carbon bound to four metals in an open butterfly arrangement. The various $M_nC$ skeletons described above are illustrated in Fig. 5.

As yet no carbido-clusters have been observed in which carbon is less than four coordinate, although there is evidence for low coordinate carbido-cations in the mass spectra of carbonyl clusters.[35]

It has now been established by $^{13}C$-labelling that the carbido-atom in carbide clusters can be derived either from a carbonyl group, via disproportionation of CO to give $CO_2$ and C or loss of the elements of water from a hydrido-cluster, or from an external source:

$$[Os_3(CO)_{11}py] \rightarrow [Os_{10}C(CO)_{24}]^{2-} + CO_2,^{4}$$

$$[Ru_3(CO)_{12}] \rightarrow [Ru_6C(CO)_{17}] + CO_2,^{14}$$

$$[H_2Ru_6(CO)_{18}] \rightarrow [Ru_6C(CO)_{17}] + \text{“}H_2O\text{”},^{36}$$

$$[Rh(CO)_4]^- + CCl_4 \rightarrow [Rh_6C(CO)_{15}]^- + Cl^-,^{37}$$

$$[Co_2(CO)_8] + CS_2 \rightarrow [Co_6C(CO)_{12}S_2].^{38}$$

New carbido-clusters may also be prepared via the controlled degradation of performed carbido-species:

$$[Ru_6C(CO)_{17} \xrightarrow{CO} [Ru_5C(CO)_{15}] + [Ru(CO)_5],^{5}$$

$$[Fe_6C(CO)_{16}]^{2-} \xrightarrow[MeOH]{C_7H_7^+Br^-} \xrightarrow{H^+} [Fe_4C(CO)_{13}].^{39}$$

Alternatively, preformed carbides may be used as building blocks in the synthesis of larger clusters:

$$[Fe_4C(CO)_{12}]^{2-} + [W(CO)_3(NCCH_3)] \rightarrow [Fe_4WC(CO)_{15}]^{2-},^{40}$$

$$[Fe_5C(CO)_{14}]^{2-} + [W(CO)_3(NCCH_3)] \rightarrow Fe_5WC(CO)_{15}]^{2-}.^{40}$$

Most of the studies on the classes of heteroatom-containing complexes which follow have concentrated on the synthesis and structural analysis of the molecules in question. The study of carbido-clusters, however, has also involved an investigation of their reactivity towards a variety of reagents.

Direct attack at the carbido-carbon atom has been observed for the tetranuclear iron carbido-clusters: reaction of $[HFe_4C(CO)_{12}]^-$ with $H^+$ leads to the formation of a methylidyne (CH) group bound to the tetranuclear cluster[41] and treatment of $[Fe_4C(CO)_{13}]$ with methanol and then base yields a butterfly (carbomethoxy) methylidyne complex[42] (see Fig. 6). No such direct attack at the carbon atom has been seen for the higher nuclearity iron clusters or any of the Re, Ru, Os, Rh or Co carbides.* However, the carbon atom does confer on the cluster considerable stability towards degradation and in addition allows the metal framework to be relatively

* This observation is in accordance with recent MO calculations on iron carbide clusters which predict that the metal-carbide orbitals are not sufficiently high lying for the carbon atom to be involved in reactions until the number of metal atoms is reduced to four.[90]

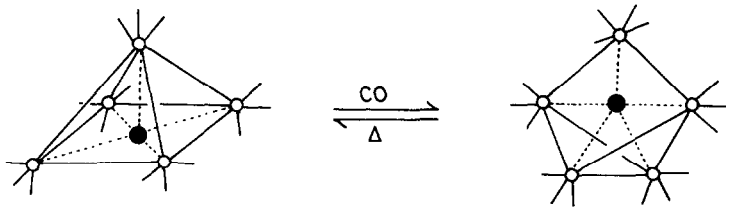



Fig. 7. The reversible carbonylation of $[Os_5C(CO)_{15}]$.

flexible. Facile structural transformations therefore result from addition or removal of electrons, giving rise to a wide range of $M_nC$ framework geometries. For example, addition of CO to $[Os_5C(CO)_{15}]$ results in the opening up of the square based pyramid to give a bridged butterfly arrangement of metals, while further heating of the product $[Os_5C(CO)_{16}]$, even under CO, results in the ejection of CO and regeneration of $[Os_5C(CO)_{15}]$ (see Fig. 7).[43]

Similarly, reaction of $[Ru_6C(CO)_{17}]$ with HSEt results in the opening up of an octahedron of ruthenium atoms to give another wing tip bridged butterfly structure, but in this case a sixth metal atom is found bridging an edge of the basic five atom unit[44] (see Fig. 8).

It is hoped that we shall soon see the synthesis of other low nuclearity carbido-clusters and it will be interesting to compare their reactivity, in particular that of the carbido-carbon atom with that of the tetranuclear iron carbides.

As far as other group IV heteroatom clusters are concerned, a much less extensive series of compounds is known. Complexes of the type $[Co_3(CO)_9-ECo(CO)_4]$ (E = Si, Ge) have been reported in which the silicon or germanium atom is bound to four cobalt atoms, of which three form a cluster and the fourth is held in place by the tetrahedrally coordinated heteroatom (see Fig. 9):[45,46] a similar situation is observed in the tetrahedrally coordinated tin complex $\{[(C_5H_5)Fe(CO)_2]_2Sn_2Fe_3(CO)_9\}$.[47] In this molecule both faces of the triangular $Fe_3(CO)_9$ cluster unit are capped by tin atoms. From the limited number of examples known it would appear that although these atoms are from the same periodic group as carbon they show a much reduced tendency for the formation of complexes with transition metal clusters.

## GROUP V HETEROATOMS

Many features of carbido-clusters are paralleled by nitrido-clusters. Nitrogen, like carbon, appears to stabilise the less frequently observed cluster geometries. Indeed, $[Rh_6N(CO)_{15}]^-$ [50] and $[Rh_6C(CO)_{15}]^{2-}$ [51] have the same trigonal prismatic structures, $[Fe_5C(CO)_{15}]$ [33] and $[HFe_5N(CO)_{14}]$ [52] are both square prismatic and $[Os_4N(CO)_{12}]^-$ [53] and $[Fe_4C(CO)_{12}]^{2-}$ [6] contain the same open butterfly of metal atoms (see Fig. 10). In clusters having high transition metal : heteroatom ratios, however, it has been said that nitrides tend towards lower coordination than carbides and lie in less regular cavities.[3] Thus while the carbon atoms in $[Os_{10}C(CO)_{24}]^{2-}$ and $[Os_{11}C(CO)_{27}]^{2-}$ occupy octahedral and trigonal prismatic sites respectively,[54] the nitrogen atom in $[PtRh_{10}N(CO)_{21}]^{3-}$ [3] is found in a distorted trigonal prismatic cavity.

Outside cluster chemistry, nitrogen atoms have

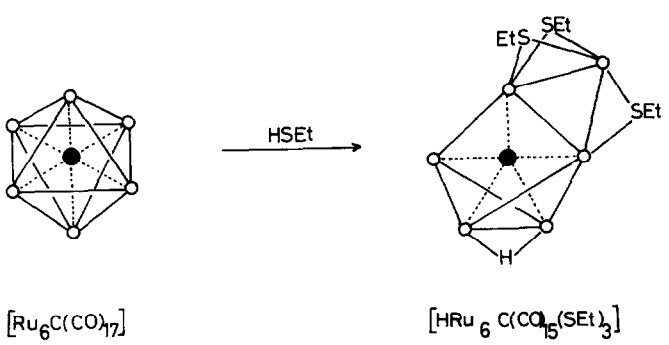



Fig. 8. The reaction of $[Ru_6C(CO)_{17}]$ with ethane-thiol.

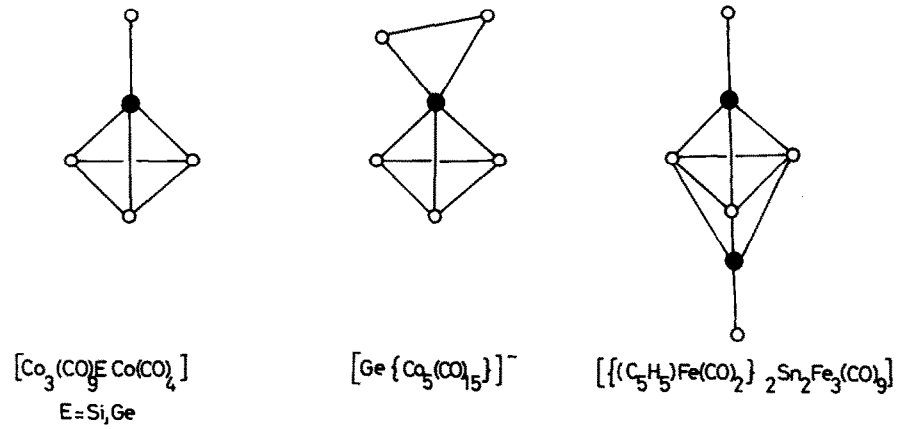



Fig. 9. The core geometries adopted by $M_nE$ clusters (E = Si, Ge, Sn).

been found bound to a single metal centre, as in $[Re(N)Cl_2(PPh_3)_2]$,[55] linking two metal atoms, as in $[Ru_2NCl_8(H_2O)_2]^{3-}$ [56] or three metals as in $[Ir_3(N)(SO_4)_6(H_2O)_3]$ [57] in which nitrogen sits in the centre of a plane of three iridium atoms which are not bound to each other. Within cluster chemistry, however, such low metal : heteroatom ratios are rare. The lowest coordination observed for atomic nitrogen in a cluster is three: in $[Mo_3(N)(O)(CO)_4Cp_3]$ [58] the nitrogen atom occupies an unusual site in the plane of the three molybdenum atoms. In this case two metal–metal bonds hold the $Mo_3$ unit in an open triangular arrangement, as shown in Fig. 10 and result in a very exposed nitrogen atom.

Just as with the carbido-clusters the source of nitrogen in nitrido-clusters may be either external or internal. For example, addition of $NO^+$ to $[HRu_4(CO)_{13}]^-$ and $[Co_6(CO)_{15}]^{2-}$ gives $[HRu_4N(CO)_{12}]$ [59] and $[Co_6N(CO)_{15}]^-$ [60] respectively while treatment of $[Rh_7(CO)_{16}]^{3-}$ with CO/NO mixtures yields $[Rh_6N(CO)_{15}]^-$,[60] all three reactions involving an external source of nitrogen. An example of an internal source of nitrogen would be a coordinated nitrosyl group: pyrolysis of $[FeRu_3(NO)(CO)_{12}]$ yields the nitride $[FeRu_3N(CO)_{12}]^-$ [61] and the reaction of $[Mo(CO)_2(NO)(C_5H_5)]$ with $[Mo_2(CO)_6(C_5H_5)_2]$ is used to prepare the trinuclear cluster $[Mo_3(N)(O)(CO)_4(C_5H_5)_3]$.[62] In the latter case it has been proved

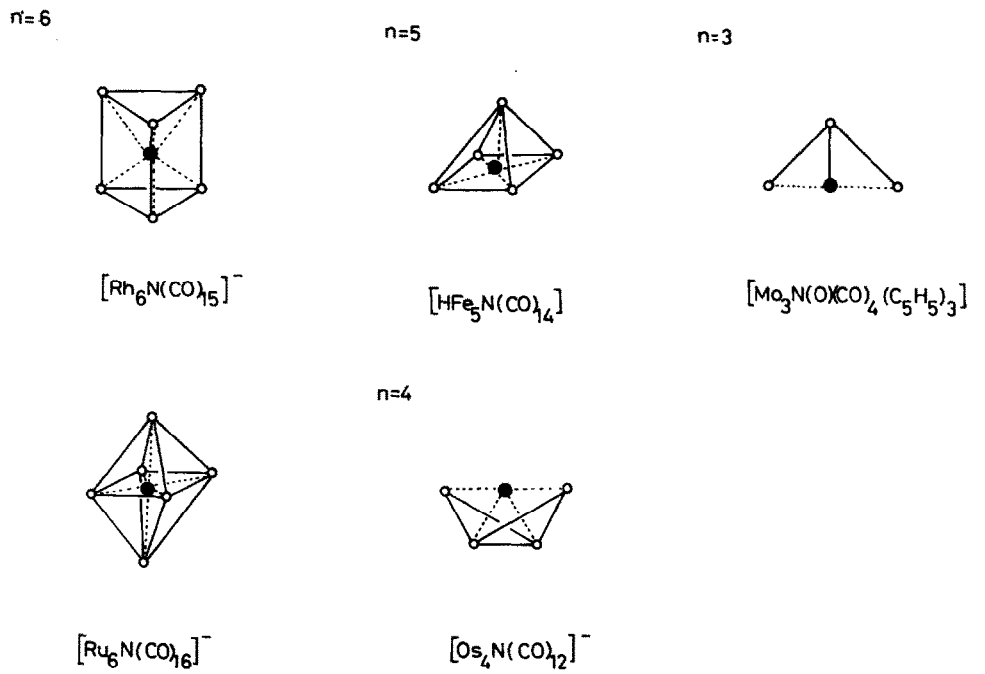



Fig. 10. The various $M_nN$ core geometries found in nitrido-clusters. $[Ru_6N(CO)_{16}]^-$ has been characterised spectroscopically but not crystallographically.[62]

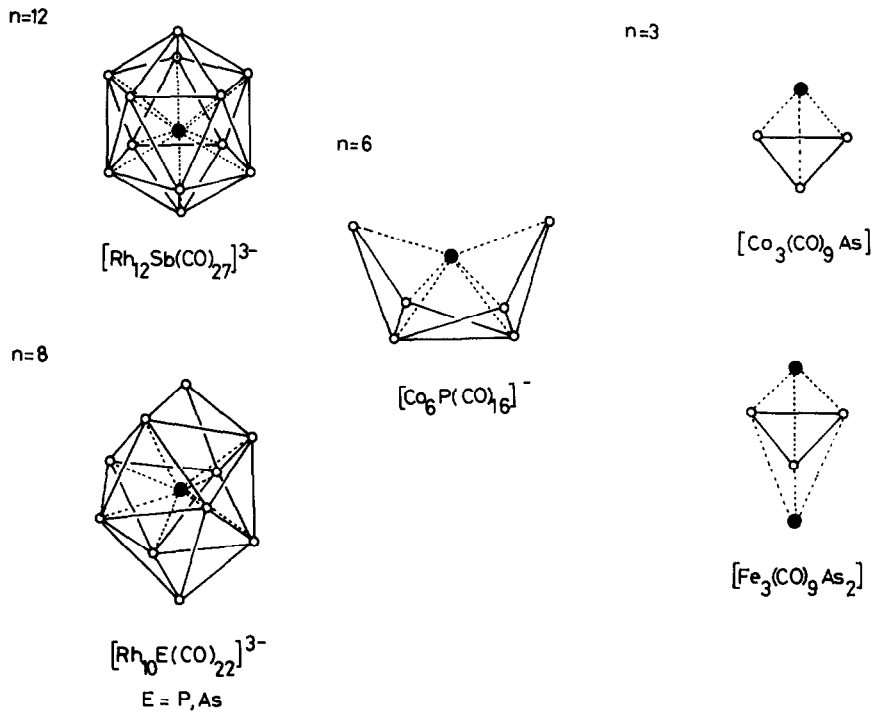



Fig. 11. The transition metal–heteroatom core geometries displayed by clusters involving atomic phosphorus, arsenic or antimony as ligands.

conclusively by $^{18}O$ labelling that on conversion of the nitrosyl ligand to a nitride the nitrosyl oxygen is lost as $CO_2$. The final method available for the synthesis of new nitrido-clusters is the breakdown or build up of preformed nitrido-clusters. For example, reaction of $[Rh_6N(CO)_{15}]^-$ with $[PtRh_4(CO)_{14}]^{2-}$ results in the formation of $[PtRh_{10}N(CO)_{21}]^{3-}$.[3]

In contrast with clusters involving group IV heteroatoms which are as yet mainly limited to carbides, there are several examples of the coordination of the other group V elements, P, As and Sb to transition metal clusters. The first organometallic complex containing naked phosphorus as a ligand was reported in 1973:[63] in $[Co_4Cp_4P_4]$ each phosphorus atom bridges three transition metals, however this molecule only contains two metal–metal bonds and so does not qualify for inclusion as a cluster compond. Arsenic and antimony have been found in $\mu_3$-sites in metal cluster compounds and in $[Fe_3(CO)_9As_2]$ an arsenic atom caps either side of the $Fe_3$ triangle,[10] but the main interest in the group V heteroatom–transition metal clusters is in those containing interstitial P, As or Sb atoms (see Fig. 11). It is interesting to compare such species with the nitride clusters to see just what effect these larger heteroatoms will have on the metal geometries: they will certainly be unable to adopt the same structures as the nitrides since even the smallest, phosphorus, is too big to fit into an octahedral or trigonal prismatic cavity.

Clusters involving interstitial phosphorus and arsenic atoms show a preference for the square antiprism[65,66] as the primary building block (see Fig. 11) although when fewer metals are available, as in $[Co_6P(CO)_{16}]^-$, a more open structure must be adopted in order to accommodate the large phosphorus atom.[67] When antimony, which is even larger takes up a five electron donor interstitial coordination mode it requires an even larger cavity and in $[Rh_{12}Sb(CO)_{27}]^{3-}$ [68] we see the first example of an icosahedral cluster geometry, made possible by the stabilising effect of the central antimony atom.

In terms of synthesis the phosphorus, arsenic and antimony clusters all result from pyrolysis reactions in the presence of an external source of the heteroatom: $PCl_3$, white phosphorus or $PPh_3$, $AsPh_3$ and $SbCl_3$ or $SbPh_3$ respectively. It is worth noting that while pyrolysis of phosphite derivatives of osmium clusters results in the formation of carbido-clusters,[69] pyrolysis of $[Rh(CO)_2(acac)]$ with triphenyl phosphine gives a phosphido-cluster.[66] This difference may simply be due to the P—O bonds in the phosphite being stronger than the P—C bonds in the phosphine or it may reflect differences between the metals, in which case it could have wider implications for the possible synthesis of

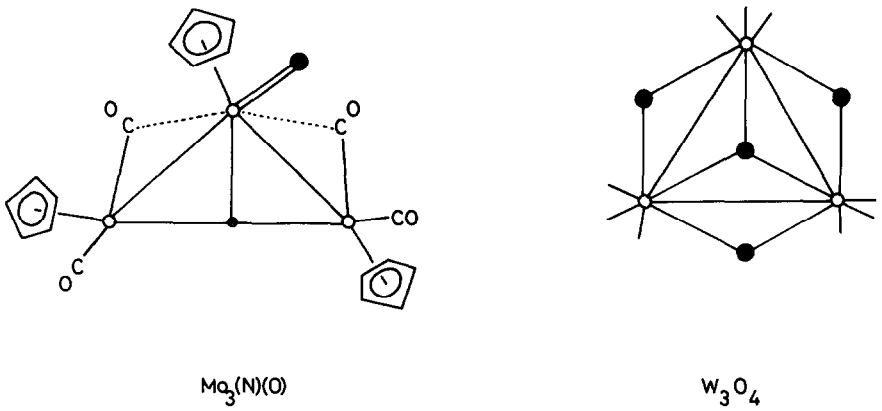



Fig. 12. Essential features of the structures of $[Mo_3(N)(O)(CO)_4Cp_3]$ and $[W_3O_4F_9]\cdot 3H_2O$.

phosphido-clusters from other than the cobalt subgroup metals.

Once again the presence of the heteroatoms in the group V atom–metal clusters gives added stability towards cluster breakdown: rhodium clusters are usually transformed to $[Rh_5(CO)_{15}]^-$ and $[Rh(CO)_4]^-$ under $CO/H_2$ but $[Rh_9P(CO)_{21}]^{2-}$ is stable to 600–800 atm $CO/H_2$ at 230°C[66] and $[Rh_{12}Sb(CO)_{27}]^{3-}$ is stable under 500 atm $CO/H_2$ at 150°C.[68] There has been only one report of the reactivity of an exposed group V heteroatom in a metal cluster. Carbonylation of $[Ru_6N(CO)_{16}]^-$ results in the formation of $[Ru_5N(CO)_{14}]^-$ which reacts further with CO to give $[Ru_4(NCO)(CO)_{13}]^-$ in which process the nitrido-nitrogen atom is converted to an isocyanato-ligand.[62] No reactivity has been reported for the cluster-bound nitrogen atom in $[Fe_4N(CO)_{12}]^-$ or the phosphorus atom in $[Co_6P(CO)_{16}]^-$, although they, too, might be expected to undergo reaction.

## GROUP VI HETEROATOMS

Examples of naked oxygen atoms as ligands are well known in mononuclear transition metal complexes like $OsO_4$, where the metal is in a high formal oxidation state and, unlike the nitrides, terminal oxides are also occasionally found in transition metal clusters. Thus $[Mo_3(N)(O)(CO)_4Cp_3]$ contains an (Mo=O) unit, the oxygen atom of which derives from an external and as yet unknown source of oxygen[61] (see Fig. 12).

Atomic oxygen is also found in W,[70] Mn,[71] Ti,[72] Ru[73] and Os[7] clusters, as a $\mu_2$- or $\mu_3$-bridging ligand, as illustrated by the complexes $[W_3O_4F_9]\cdot 3H_2O$ [70] and $[Os_6O(CO)_{19}]$ [7] whose structures are shown in Figs. 1 and 12. In the syntheses of $[Os_6O(CO)_{19}]$ and $[Ru_3(\mu_3O)(O)(CO)_6(Ø_2AsCH_2AsØ_2)]$ molecular oxygen has been found to be the source of the oxygen atom[73] but in most other cases the oxygen source has not been identified.

In no case has an interstitial oxygen atom in a metal cluster been reported, a feature of oxide chemistry which is in contrast with that of sulphides since two examples of interstitial sulphur containing clusters are known.

Atomic sulphur displays a wide variety of bonding modes in its coordination to transition metal clusters. In $[Mo_3(C_5H_5)_3S_4]^+$ the $\mu_2$- and $\mu_3$-modes are demonstrated[74] and in $[Os_6(CO)_{17}S_2]$ two $\mu_4$S ligands have been identified as a result of a crystallographic investigation[75] (see Fig. 13).

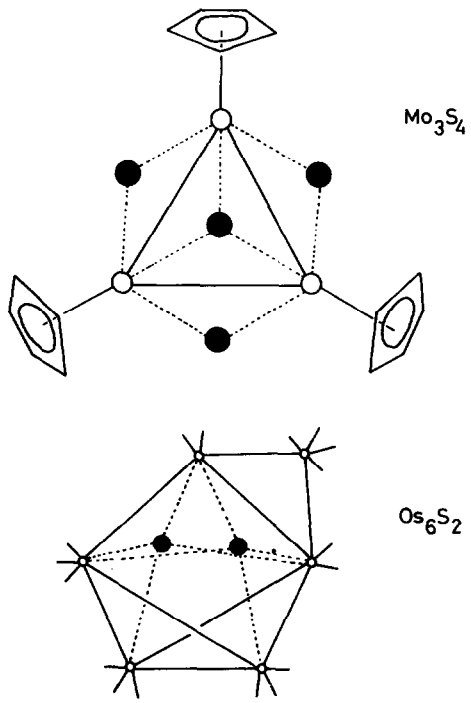
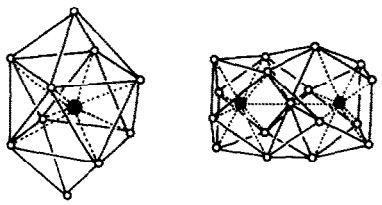



Fig. 13. The molecular structures of the complexes $[Mo_3(C_5H_5)_3S_4]$ and $[Os_6(CO)_{17}S_2]$.



$Rh_{10}S$ $Rh_{17}S_2$

Fig. 14. The Rh–S core geometries of the clusters $[Rh_{10}S(CO)_{22}]^{2-}$ and $[Rh_{17}S_2(CO)_{32}]^{3-}$.

Selenium, too, has been found to act as a $\mu_3$-ligand capping a triangle of metal atoms in, for example $[Co_3(CO)_9Se]$.[76] The exposed sulphur and selenium atoms in these molecules appear to be characterised by their reluctance to undergo reactions. There is, however, at least one example of reaction at a $\mu_3S$ centre. In 1978 reaction of $[(CH_3)_3O]^+$ with $[HOs_3(CO)_9S]^-$ was found to give $[HOs_3(CO)_9(\mu_3SMe)]$, although the product was never fully characterised.[77]

Clusters containing interstitial sulphur atoms involve much higher coordination numbers: in $[Rh_{10}S(CO)_{22}]^{2-}$ sulphur is found to stabilise an unusual square prismatic cavity,[78] while in $[Rh_{17}S_2(CO)_{32}]^{3-}$ each sulphur atom is bound to nine rhodium atoms,[79] as shown in Fig. 14.

As far as the source of the sulphur atom is concerned, $H_2S$, $SO_2$, S and $CS_2$ have all been used to introduce atomic sulphur into metal clusters. Alternatively, a cluster which already contains sulphur in the form of, say, an SCN ligand may be used as the starting material. An example of the use of such a route is the preparation of $[Rh_{10}S(CO)_{22}]^{2-}$ from $[Rh_6(CO)_{14}(SCN)_2]^{2-}$.[78]

## GROUP VII HETEROATOMS

A series of transition metal clusters exists in which halide atoms are the only ligands present. They display a range of halide bonding modes from $\mu_3$- to $\mu_2$- to terminal and are characterised by two main structural types, illustrated in Fig. 15, containing either octahedral $M_6(\mu_3X)_8$ or $M_6(\mu_2X)_{12}$ units, which are very stable and only broken up under vigorous conditions. Thus, the salt $[Mo_6Cl_8Cl_6]^{2-}$ contains eight face capping and six terminal chlorines[80] while $[Nb_6Br_{12}Cl_6]^{4-}$ has 12 edge bridging bromine and six terminal chlorine ligands.[81] Such clusters are not limited to the early transition metals and, in an example from the other end of the transition series, $[Pt_6Cl_{12}]$ displays an octahedral structure with 12 $\mu_2$Cl ligands[82] very similar to that of the core of $[Nb_6X_{18}]^{4-}$.

Generally speaking, however, clusters of the later transition metals containing halide atoms are mainly mixed halide-carbonyl species having terminal or $\mu_2$-bridging halogens. For example in $[Os_5C(CO)_{15}I]^-$ the iodide atom is found in a terminal position[83] on the cluster while in $[Ru_4(CO)_{13}Cl]^-$ chlorine bridges the wing tips of an open butterfly of ruthenium atoms[84] (see Fig. 16). Synthesis of the early transition metal halide clusters normally involves the reduction of the higher mononuclear or

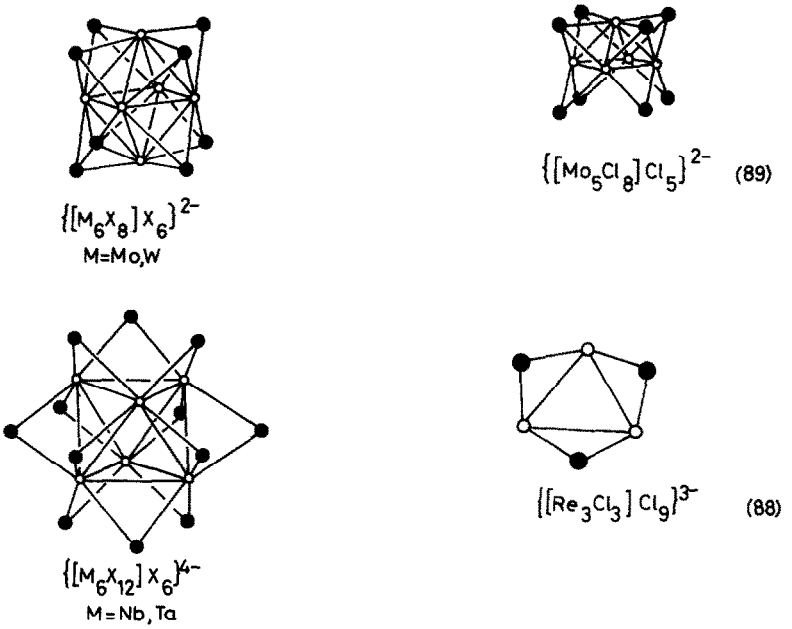



Fig. 15. The structures of the metal–halide clusters. The terminally bound halide ligands are omitted for clarity.

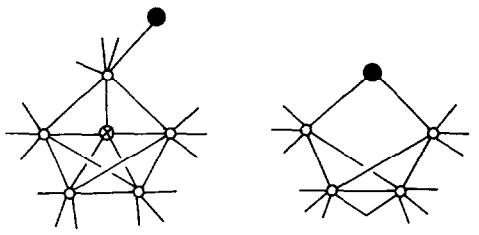



Fig. 16. The structures of $[Os_5C(CO)_{15}I]^-$ and $[Ru_4(CO)_{13}Cl]^-$.

dinuclear halides in the presence of an excess of the metal in question at elevated temperatures, while in the case of the carbonyl halides addition of $X_2$, HX or $[Au(PPh_3)X]$ to a neutral carbonyl cluster or reaction of an anion with $I_2$ is the usual route.

As has been mentioned above the $M_6X_8$ and $M_6X_{12}$ cores of the early transition metal halides are very stable to degradation as these central units contain the bridging halides in each case. The terminally bound halogen atoms may however be removed, as the halide ions $X^-$, and the cations $[M_6X_8]^{4+}$ and $[M_6X_{12}]^{2+}$ have been studied as solutions in neutral monodentate ligand solvents like amines, alcohols or water.[85] It has also proved possible to remove the halogen atoms from some of the carbonyl halide clusters, or to persuade them to change from being terminal one electron donors to bridging three electron donor ligands and vice versa. Thus the two bridging iodine ligands in $[Os_{10}C(CO)_{24}I_2]$ are removed stepwise on treatment with $I^-$, pyridine or phosphite[86] giving first $[Os_{10}C(CO)_{24}I]^-$ and then the dianion $[Os_{10}C(CO)_{24}]^{2-}$ (see Fig. 17); the iodine atoms are removed as $I^+$ to give $I_2$ or $IL_2$ (L = py, $P(OR)_3$) respectively. The halide ligand in $[HRu_5C(CO)_{15}Cl]$ is removed in a different way: simple thermolysis of the pentanuclear chloro-cluster in hydrocarbon solvents results in the ejection of molecular HCl, leaving the carbonyl cluster $[Ru_5C(CO)_{15}]$ in solution.[32] On heating $[HRu_5C(CO)_{15}Cl]$ in the presence of an excess of HCl, however, this reaction is suppressed in favour of loss of CO and formation of the $\mu_2$Cl species $[HRu_5C(CO)_{14}Cl]$, a step which may be reversed by addition of CO to this or any of the formally analogous series $[ARu_5C(CO)_{14}X]$ (A = $Au(PR_3)$, H; X = Cl, Br), to give the $[ARu_5C(CO)_{15}X]$ molecules[87] (see Fig. 18). This example clearly demonstrates the ease with which halide heteroatoms may be converted from two to four electron donors and back in transition metal carbonyl clusters.

## CONCLUSION

A large number of clusters are known which contain main group heteroatoms bound exclusively to transition metals. The heteroatoms display a wide range of bonding modes and their coordination

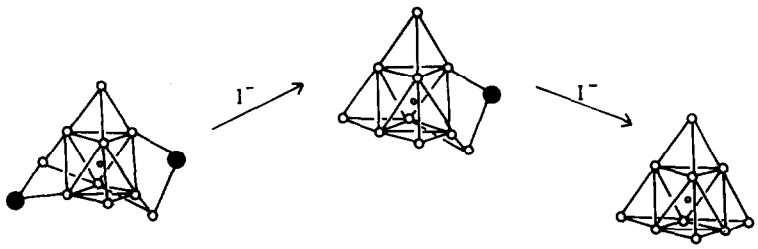



Fig. 17. The stepwise removal of iodine ligands from $[Os_{10}C(CO)_{24}I_2]$.

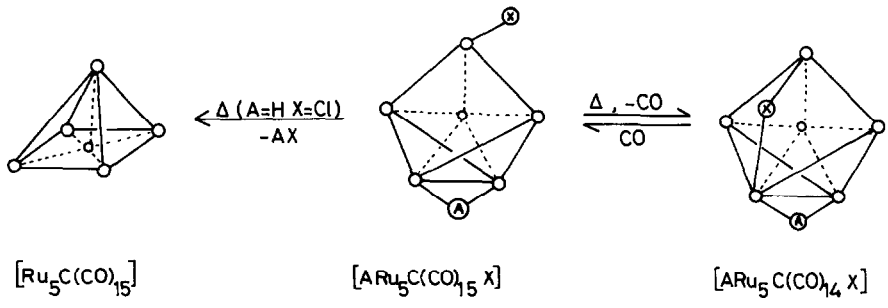



Fig. 18. The conversion of halide ligands between terminal and bridging bonding modes in $Ru_5C$ clusters.

numbers range from 12, for antimony, to one, for hydrogen, oxygen and the halogens. When found in interstitial sites they often impart considerable stability towards degradation to the metal cluster, as seen by comparison with the stability of simple metal carbonyl clusters. They are often associated with the less commonly observed metal geometries such as icosahedral $M_{12}$, square antiprismatic $M_8$, square pyramidal $M_5$ and open butterfly $M_4$ structures and, when exposed, provide possible alternative sites for attack by incoming reagents.

Hydride and halide ligands can often be removed from their parent clusters. The group IV, V and VI heteroatoms, however, seem to be more firmly bound and direct attack at these cluster-bound heteroatoms has as yet been limited to the carbon atom in $Fe_4$ clusters, the sulphur atom in $[HOs_3(CO)_9S]^-$ and the nitrogen atom in $[Ru_5N(CO)_{14}]^-$ which are converted to (CH) or ($CCO_2Me$), $SCH_3$) and (NCO) groups respectively.

While many carbido-, hydrido- and nitrido-clusters are known few clusters have been prepared which contain heteroatoms like phosphorus, arsenic and sulphur. The study of these species has also largely been directed towards synthesis and there is therefore insufficient information to allow a real comparison of the reactivity of the cluster-bound heteroatoms. Clearly this is an area which will receive more attention as the study of transition metal clusters containing main group heteroatoms progresses.

*Acknowledgement*—I wish to thank Gonville and Caius College, Cambridge, for the award of a Research Fellowship.

## REFERENCES

1. M. Tachikawa and E. L. Muetterties, *Prog. Inorg. Chem.* 1981, **28**, 203.
2. E. L. Muetterties, T. N. Rhodin, E. Bard, C. F. Brucker and W. R. Pretzer, *Chem. Rev.* 1979, **79**, 91.
3. S. Martinengo, G. Ciani and A. Sironi, *J. Am. Chem. Soc.* 1982, **104**, 328.
4. P. F. Jackson, B. F. G. Johnson, J. Lewis, W. J. H. Nelson and M. McPartlin, *J. Chem. Soc., Dalton Trans.* 1982, 2099.
5. D. H. Farrar, P. F. Jackson, B. F. G. Johnson, J. Lewis, J. N. Nicholls and M. McPartlin, *J. Chem. Soc., Chem. Commun.* 1981, 415.
6. D. E. Fjare and W. L. Gladfelter, *J. Am. Chem. Soc.* 1981, **103**, 1572.
7. R. J. Goudsmit, B. F. G. Johnson, J. Lewis, P. R. Raithby and K. H. Whitmire, *J. Chem. Soc., Chem. Commun.* 1983, 246.
8. H. Varenkamp, V. A. Uchtman and L. F. Dahl, *J. Am. Chem. Soc.* 1968, **90**, 3272.
9. J. L. Vidal, *Inorg. Chem.* 1981, **20**, 243.
10. L. F. J. Delbaere, L. J. Kruczynski and D. W. McBride, *J. Chem. Soc., Dalton Trans.* 1973, 307.
11. C. R. Eady, B. F. G. Johnson, J. Lewis, M. C. Malatesta, P. Machin and M. McPartlin, *J. Chem. Soc., Chem. Commun.* 1976, 945.
12. J. R. Shapley, J. B. Keister, M. R. Churchill and B. G. de Boer, *J. Am. Chem. Soc.* 1975, 4145.
13. G. Ciani, G. D'Alfonso, M. Freni, P. Romiti and A. Sironi, *J. Chem. Soc., Chem. Commun.* 1982, 339.
14. A. Sirugi, M. Bianchi and E. Benedetti, *J. Chem. Soc., Chem. Commun.* 1969, 596.
15. A. Simon, *Z. Anorg. Chem.* 1967, **355**, 311.
16. P. Chini, G. Longoni, S. Martinengo and A. Ceriotti, *Adv. Chem.* 1978, **167**, 1.
17. P. F. Jackson, B. F. G. Johnson, J. Lewis, P. R. Raithby, M. McPartlin, K. D. Rouse, J. Allibon and S. A. Mason, *J. Chem. Soc., Chem. Commun.* 1980, 295.
18. G. Ciani, A. Sironi and S. Martinengo, *J. Organomet. Chem.* 1980, **192**, C42.
19. G. Ciani, A. Sironi and S. Martinengo, *J. Chem. Soc., Dalton Trans.* 1981. 519.
20. B. T. Heaton, S. Martinengo, R. J. Goodfellow and P. Chini, *J. Chem. Soc., Chem. Commun.* 1977, 39.
21. M. R. Churchill and J. Wormald, *J. Am. Chem. Soc.* 1971, **93**, 5670.
22. P. F. Jackson, B. F. G. Johnson, J. Lewis, M. McPartlin and W. J. H. Nelson, *J. Chem. Soc., Chem. Commun.* 1982, 48.
23. E. C. Constable, B. F. G. Johnson, J. Lewis, G. N. Pain and M. J. Taylor, *J. Chem. Soc., Chem. Commun.* 1982, 754.
24. D. Braga, J. Lewis, B. F. G. Johnson, M. McPartlin, W. J. H. Nelson and M. D. Vargas, *J. Chem. Soc., Chem. Commun.* 1983, 241.
25. R. Bau, S. W. Kirtley, T. N. Sorrell and S. Winarko, *J. Am. Chem. Soc.* 1974, **96**, 998.
26. R. D. Wilson, S. M. Wu, R. A. Love and R. Bau, *Inorg. Chem.* 1978, **17**, 1271.
27. A. T. Nicol and R. W. Vaughan, *Adv. Chem. Ser.* 1978, **167**, 245.
28. D. W. Hart, R. G. Teller, C. Y. Wei, R. Bau, G. Longoni, S. Campanella, P. Chini and T. F. Koetzle, *Angew. Chem. Int. Ed. Engl.* 1979, **18**, 80.
29. K. Wong, Ph.D. thesis, Cambridge University, 1978.
30. I. A. Oxton, D. B. Powell, D. H. Farrar, B. F. G. Johnson, J. Lewis and J. N. Nicholls, *Inorg. Chem.* 1981, **20**, 4302.
31. C. R. Eady, B. F. G. Johnson and J. Lewis, *J. Chem. Soc., Chem. Commun.* 1976, 302.
32. B. F. G. Johnson, J. Lewis, J. N. Nicholls, J. Puga, P. R. Raithby, M. J. Rosales, M. McPartlin and W. Clegg, *J. Chem. Soc., Dalton Trans.* 1983, 277.
33. E. H. Braye, L. F. Dahl, W. Hübel and D. L. Wampler, *J. Am. Chem. Soc.* 1962, **84**, 4633.
34. V. G. Albano, P. Chini, G. Ciani, S. Martinengo, D. Strumolo and M. Sansoni, *J. Chem. Soc., Dalton Trans.* 1978, 463.
35. B. F. G. Johnson and J. Lewis, *Acc. Chem. Res.* 1968, 245.
36. J. N. Nicholls, D. H. Farrar, B. F. G. Johnson, J. Lewis

and P. F. Jackson, *J. Chem. Soc., Dalton Trans.* 1982, 1395.
37. V. G. Albano, P. Chini, S. Martinengo, D. J. A. McCaffrey and D. Strumolo, *J. Am. Chem. Soc.* 1974, **96**, 8106.
38. G. Bor, G. Gervasio, R. Rossetti and P. L. Stanghellini, *J. Chem. Soc., Chem. Commun.* 1978, 841.
39. J. S. Bradley, E. W. Hill, G. B. Ansell and M. A. Modrick, *Organometallics* 1982, **1**, 1634.
40. M. Tachikawa, R. L. Geerts and E. L. Meutterties, *J. Organomet. Chem.* 1981, **213**, 11.
41. M. Tachikawa and E. L. Meutterties, *J. Am. Chem. Soc.* 1980, **102**, 4541.
42. J. S. Bradley, G. B. Ansell, M. E. Leonowicz and E. W. Hill, *J. Am. Chem. Soc.* 1981, **103**, 4968.
43. B. F. G. Johnson, J. Lewis, J. N. Nicholls, W. J. H. Nelson, J. Puga, P. R. Raithby and M. D. Vargas, *J. Chem. Soc., Dalton Trans.* 1983, 2447.
44. B. F. G. Johnson, J. Lewis, K. Wong and M. McPartlin, *J. Organomet. Chem.* 1980, **185**, C17.
45. G. Schmid, V. Bärzel and G. Etzrodt, *J. Organomet. Chem.* 1976, **112**, 345.
46. D. N. Duffy, K. M. Mackay, B. K. Nicholson and W. T. Robinson, *J. Chem. Soc., Dalton Trans.* 1981, 381.
47. T. J. McNeese, S. S. Wreford, D. L. Tipton and R. Bau, *J. Chem. Soc., Chem. Commun.* 1977, 390.
48. R. A. Croft, D. N. Duffy and B. K. Nicholson, *J. Chem. Soc., Dalton Trans.* 1982, 1023.
49. M. R. Churchill and J. Wormald, *J. Chem. Soc., Dalton Trans.* 1974, 2410.
50. R. Bonfichi, G. Ciani, A. Sironi and S. Martinengo, *J. Chem. Soc., Dalton Trans.* 1983, 253.
51. V. G. Albano, M. Sansoni, P. Chini and S. Martinengo, *J. Chem. Soc., Dalton Trans.* 1973, 651.
52. M. Tachikawa, J. Stein, E. L. Muetterties, R. G. Teller, M. A. Beno, E. Gebert and J. M. Williams, *J. Am. Chem. Soc.* 1980, **102**, 6648.
53. M. A. Collins, B. F. G. Johnson, J. Lewis, J. M. Mace, J. Morris, M. McPartlin, W. J. H. Nelson, J. Puga and P. R. Raithby, *J. Chem. Soc., Chem. Commun.* 1983, 689.
54. B. F. G. Johnson, J. Lewis, W. J. H. Nelson, J. N. Nicholls and M. D. Vargas, *J. Organomet. Chem.* 1983, **249**, 255.
55. R. J. Doedens and J. A. Ibers, *Inorg. Chem.* 1967, **6**, 204.
56. M. Ciechanowicz and A. C. Skapski, *J. Chem. Soc. (A)* 1971, 1792.
57. M. Ciechanowicz, W. P. Griffith, D. Pawson, A. C. Skapski and M. J. Cleare, *J. Chem. Soc., Chem. Commun.* 1971, 876.
58. N. D. Feasey, S. A. R. Knox and A. G. Orpen, *J. Chem. Soc., Chem. Commun.* 1982, 75.
59. D. Braga, B. F. G. Johnson, J. Lewis, J. M. Mace, M. McPartlin, J. Puga, W. J. H. Nelson, P. R. Raithby and K. H. Whitmire, *J. Chem. Soc., Chem. Commun.* 1982, 1081.
60. S. Martinengo, G. Ciani, A. Sironi, B. T. Heaton and J. Mason, *J. Am. Chem. Soc.* 1979, **101**, 7095.
61. N. D. Feasey and S. A. R. Knox, *J. Chem. Soc., Chem. Commun.* 1982, 1062.
62. M. L. Blohm, D. E. Fjare and W. L. Gladfelter, *Inorg. Chem.* 1983, **22**, 1004.
63. G. L. Simon and L. F. Dahl, *J. Am. Chem. Soc.* 1973, **95**, 2175.
64. A. Vizi-Orosz, V. Galamb, G. Palyi, L. Marko, G. Bor and G. Natile, *J. Organomet. Chem.* 1976, **107**, 235.
65. J. L. Vidal, W. E. Walker and R. C. Schoening, *Inorg. Chem.* 1981, **20**, 238; J. L. Vidal, *Inorg. Chem.* 1981, **20**, 243.
66. J. L. Vidal, W. E. Walker, R. L. Pruett and R. C. Schoening, *Inorg. Chem.* 1979, **18**, 129.
67. G. Ciani and A. Sironi, *J. Organomet. Chem.* 1983, **241**, 385.
68. J. L. Vidal and J. M. Troup, *J. Organomet. Chem.* 1981, **213**, 351.
69. J. M. Fernandez, B. F. G. Johnson, J. Lewis and P. R. Raithby, *J. Chem. Soc., Dalton Trans.* 1981, 2250.
70. K. Mennemann and R. Mattes, *Angew. Chem. Int. Ed. Engl.* 1976, **15**, 118.
71. A. Bino, F. A. Cotton, Z. Dori and B. W. S. Kolthammer, *J. Am. Chem. Soc.* 1981, **103**, 5779.
72. J. C. Huffman, J. G. Stone, W. C. Krusell and K. G. Caulton, *J. Am. Chem. Soc.* 1977, **99**, 5830.
73. G. Lavigne, N. Lugan and J. J. Bonnet, *Nouv. J. Chim.* 1981, **5**, 423.
74. P. J. Vergamini, H. Varenkamp and L. F. Dahl, *J. Am. Chem. Soc.* 1971, **93**, 6327.
75. R. D. Adams, I. T. Horvath and L. W. Yang, *J. Am. Chem. Soc.* 1983, **105**, 1533.
76. C. E. Strouse and L. F. Dahl, *J. Am. Chem. Soc.* 1971, **93**, 6032.
77. B. F. G. Johnson, J. Lewis, D. Pippard and P. R. Raithby, *J. Chem. Soc., Chem. Commun.* 1978, 551.
78 G. Ciani, L. Garlaschelli, A. Sironi and S. Martinengo, *J. Chem. Soc., Chem. Commun.* 1981, 563.
79. J. L. Vidal, R. A. Fiato, L. A. Cosby and R. L. Pruett, *Inorg. Chem.* 1978, **17**, 2574.
80. F. A. Cotton, R. M. Wing and R. A. Zimmerman, *Inorg. Chem.* 1967, **6**, 12.
81. B. Spreckelmeyer and H. G. v. Schnering, *Z. Anorg. Allg. Chem.* 1971, **386**, 27.
82. K. Brodersen, G. Thiele and H. G. v. Schnering, *Z. Anorg. Allg. Chem.* 1965, **337**, 120.
83. P. F. Jackson, B. F. G. Johnson, J. Lewis, J. N. Nicholls, M. McPartlin and W. J. H. Nelson, *J. Chem. Soc., Chem. Commun.* 1980, 564.
84. G. R. Steinmetz, A. D. Harley and G. L. Geoffroy, *Inorg. Chem.* 1980, 2985.
85. J. C. Sheldon, P. A. Vaughan, J. H. Sturtevant and L. Pauling, *J. Am. Chem. Soc.* 1950, **72**, 5477.
86. D. H. Farrar, P. F. Jackson, B. F. G. Johnson, J. Lewis, W. J. H. Nelson, M. D. Vargas and M. McPartlin, *J. Chem. Soc., Chem. Commun.* 1981, 1009.
87. B. F. G. Johnson, J. Lewis, J. N. Nicholls, J. Puga and K. H. Whitmire, *J. Chem. Soc., Dalton Trans.* 1983, 787.
88. J. A. Bertrand, F. A. Cotton and W. A. Dollase, *Inorg. Chem.* 1963, **2**, 1166.
89. K. Jodden, H. G. V. Schnering and H. Schafer, *Angew. Chem. Int. Ed. Engl.* 1975, **14**, 570.
90. J. Kolis, F. Basolo and D. F. Schriver, *J. Am. Chem. Soc.* 1982, **104**, 5626.

*Polyhedron* Vol. 3, No. 12, pp. 1321–1328, 1984
Printed in Great Britain

0277-5387/84 $3.00 + .00
Pergamon Press Ltd

# SOME STRUCTURAL SYSTEMATICS IN METAL CARBONYL CLUSTER CHEMISTRY

**MARY McPARTLIN**
School of Chemistry, The Polytechnic of North London, Holloway, London N7 8DB, U.K.

**and**

**D. MICHAEL P. MINGOS***
Inorganic Chemistry Laboratory, University of Oxford, South Parks Road, Oxford OX1 3QR, U.K.

(*Received* 28 *April* 1984)

**Abstract**—The recently developed electron-counting rules for condensed polyhedral metal carbonyl clusters have been utilised to develop a systematic approach for enumerating the structural alternatives for metal cluster compounds which are isoelectronic. The more usual cluster degradation and aggregation processes are represented in a matrix form which relates the change in electron count to the number of new bonds formed (or broken). The matrices for cluster degradation and aggregation are represented in a complementary fashion so that the search for isoelectronic clusters is greatly simplified. The utility of the approach is illustrated by reference to some recent examples from metal carbonyl cluster chemistry.

The rapid development of cluster chemistry which has occurred in recent years has revealed a degree of structural complexity and variety quite unparalleled in main-group chemistry.[1] Thus, although borane anions adopt either spherical deltahedra, or fragments derived from them,[2] metal carbonyl clusters adopt only a limited number of polyhedra of this type and their observed structures are often better described in terms of condensed polyhedra derived from triangular, tetrahedral, trigonal prismatic and octahedral components.[3] The permutational possibilities resulting from the combination of these fragments are large, particularly for clusters containing more than five metal atoms, and even for a given electron count several polyhedral possibilities exist. Recently a generalised principle has been derived,[4] which can be used to evaluate the electron count in condensed polyhedra from those of its component polyhedra. In particular, it has been proposed that the total electron count in a condensed polyhedron is equal to the sum of the electron counts for the parent polyhedra minus the electron count characteristic of the atom, pair of atoms, or face of atoms common to both polyhedra.[4]

This economical generalisation has provided a convenient *aufbau* procedure for deriving the electron counts in condensed polyhedra which contain metal atoms which conform either to the 18- or 16-electron rules.[4,5] This procedure is useful for exploring the electronic requirements for some alternative polyhedral geometries, but in its present form is less useful for defining in a systematic fashion the number and types of polyhedra for a series of cluster compounds with the same number of transition metals and valence electrons.

The need for such a systematic procedure is going to increase with the more widespread use of EXAFS[6] and FABS[7] in the study of high-nuclearity clusters, both of which require the examination of alternative structures which are possible for a given set of data. Furthermore, recent structural and NMR studies have led to the recognition that the potential energy surfaces connecting alternative polyhedral geometries are relatively soft for metal carbonyl and related clusters and therefore the observation of a particular structure in the solid state may be the result of rather subtle electronic and steric effects.[8–10] This paper attempts to define in a more precise geometrical fashion the type of structures which are consistent with a particular electron count, and proposes a systematic method for evaluating the more important structural alternatives. This method is based on the electron-counting rules derived previously for condensed polyhedra.[4]

The starting point of the analysis is the knowledge that spherical metal carbonyl deltahedral molecules, containing $n$ atoms, are characterised by a total of $14n+2$ valence electrons. The corresponding *nido*- and *arachno*-polyhedral molecules are characterised

* Author to whom correspondence should be addressed.

by a total of $14n+4$ and $14n+6$ valence electrons respectively.[11] The degradation of an $n$-atom *closo*-metal carbonyl cluster which results in the removal of $m$ metal atoms can result in the formation of *closo*-, *nido*- or *arachno*-polyhedral molecules with $n-m$ atoms. However, each of these processes is characterised by a different change in the total electron count, i.e. $14m$ for *closo*-($n$) to *closo*-($n-m$), $14m-2$ for *closo*-($n$) to *nido*-($n-m$), and $14m-4$ for *closo*-($n$) to *arachno*-($n-m$). These degradation processes can be conveniently represented in a matrix form such as that shown in Fig. 1. The vertical columns represent transformations involving a retention of polyhedral type, i.e. *closo*- to *closo*- and *nido*- to *nido*-, and involve increments of 14 electrons, and the horizontal columns represent changes in polyhedral type with retention of nuclearity, e.g. *closo*-($n$) to *nido*-($n$), to *arachno*-($n$) etc. Degradation processes involving changes in both the nuclearity and polyhedral type are represented by diagonal relationships between the matrix elements and involve increments of 12 electrons. For reasons which will become clear later the changes in electron count are referenced to the *closo*-($n$) atomed polyhedral molecule which forms the first element of the matrix.

For those deltahedra containing vertices with differing connectivities the degradation processes indicated in Fig. 1 can lead to alternative isomeric possibilities. For boranes it has been observed that it is the vertex of highest connectivity which is invariably lost in the *closo*- → *nido*- degradation process.[12] The trigonal-bipyramid is the major exception to this generalisation and consequently the tetrahedron rather than the butterfly represents a *nido*-trigonal-bipyramid. The generalisation is not valid for transition metal carbonyl and post-transition metal clusters and the loss of either the higher- or the lower-connectivity vertex may be observed. For example, $[Rh_9P(CO)_{21}]^{2-}$ and $Sn_9^{4-}$ have *nido*-structures based on the loss of a low-connectivity capping atom from a bicapped square-antiprism.[13,14] The corresponding nine-vertex carborane, $C_2B_7H_9^{2-}$, has a structure based on the loss of a high-connectivity vertex from the bicapped square-antiprism.[15]

The *nido*- → *arachno*- transformation can similarly lead to greater structural diversity for transition metal carbonyl clusters, because the vertex lost is not necessarily one that is adjacent to that lost in the *closo*- → *nido*- transformation. For example the skeletal geometry in *arachno*-$B_5H_{11}$ is derived from a pentagonal-bipyramid by the loss initially of the higher-connectivity axial vertex followed by an adjacent equatorial vertex. The skeletal geometry observed for $[Os_5C(CO)_{16}]$, which has a total of 76 valence electrons, can be described also in terms of an *arachno*-pentagonal-bipyramid, but with two non-adjacent vertices missing. This structural difference is illustrated later.[16]

A higher-nuclearity example is provided by the 118-electron *arachno*-$[Ni_8C(CO)_{16}]^{2-}$ cluster[17]

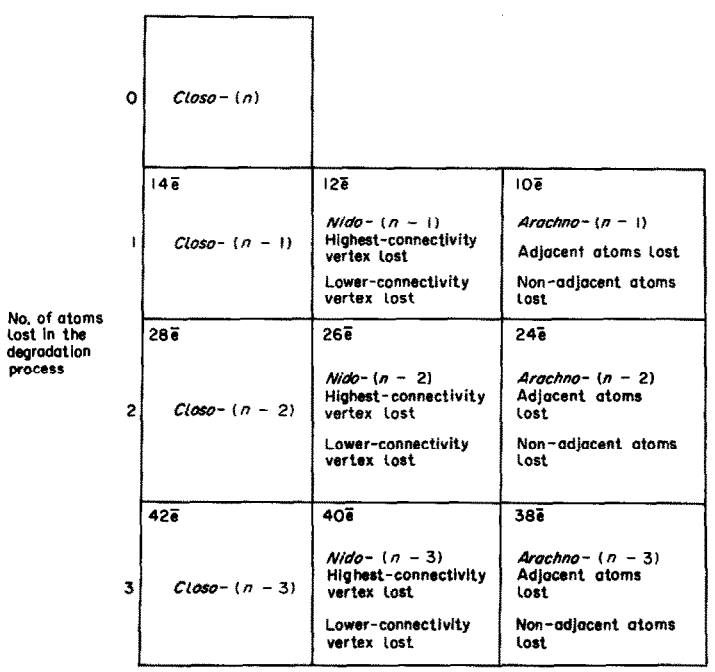



Fig. 1. Summary of changes in the polyhedral electron count associated with cluster degradation processes in transition metal carbonyl clusters with deltahedral geometries.

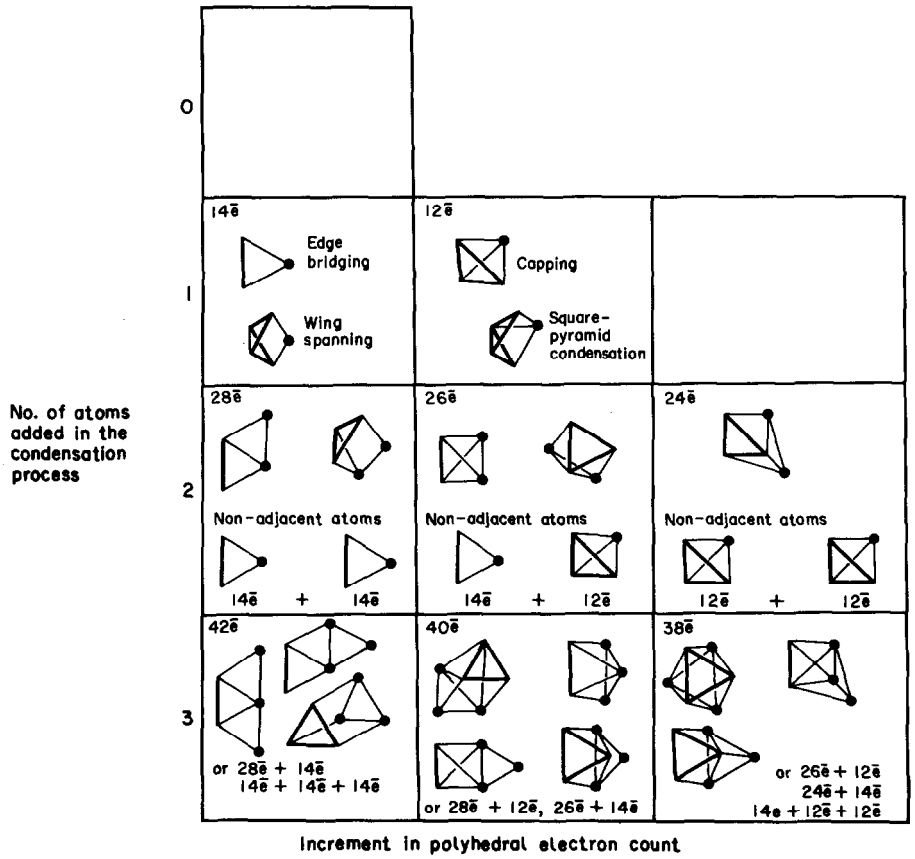



Fig. 2. Summary of changes in total electron count associated with cluster condensation processes. The number of atoms added are indicated by the black circles and the edges common to both polyhedra by the bolder lines.

which has a structure derived from the bicapped square-antiprism by the loss of the non-adjacent capping atoms, i.e. it is a square-antiprism.

In Fig. 1 some attempt has been made to illustrate the way in which alternative structures can arise by the loss of vertices with different connectivities and geometrical relationships. The adoption of a particular *nido*- or *arachno*-structure in preference to others will of course depend not only on the electronic requirements of the metal carbonyl fragments, but also on the nature of any bridging groups and the method of isolation.

Figure 2 summarises the consequences to the total electron count of some condensation processes which lead to cluster aggregation. For the addition of a single metal atom this can be achieved either by the fusion of a triangular moiety to an edge of the parent polyhedron or the fusion of a tetrahedron through a triangular face. The former leads to an increment in the total electron count of 14 and the latter to an increase of 12. These processes can also be described as edge bridging and face capping.

For the addition of two or more atoms alternative condensation modes can arise. The atoms can either be added separately or together. For example, a 26-electron increment in the total electron count can be achieved with the addition of two metal atoms either by the sequential fusion of a triangle to an edge ($+14\bar{e}$) and a tetrahedron to a face ($+12\bar{e}$), the fusion of a tetrahedron through an edge ($+26\bar{e}$) or a square-pyramid through a triangular face ($+26\bar{e}$). Of course, for the addition of three metal atoms the permutations become greater and only the more significant ones are indicated in Fig. 2.

For higher-nuclearity clusters ($n \geqslant 8$) capping and related processes can lead to non-spherical polyhedra, i.e. polyhedra with adjacent triangular faces which define re-entrant angles. In these situations an increment of 12 electrons for the addition of a single vertex can be achieved by fusing a square-pyramid to the butterfly defined by the two adjacent triangular faces. This process is illustrated in Fig. 2.

The degradation and aggregation matrices in Figs 1 and 2 have been constructed in a complementary fashion in order to emphasise the relationships between the number of atoms lost (or gained) and the changes in the polyhedral electron counts. In order

to establish which polyhedral structures have the same polyhedral electron count and the same number of metal atoms it is necessary to place restrictions on the possible degradation and aggregation processes illustrated in Figs 1 and 2. In particular, *sets of polyhedral molecules with the same polyhedral electron counts will only be obtained if a degradation process represented by a matrix element in Fig.* 1 *is matched by the corresponding matrix element for the aggregation process in Fig.* 2.

For example, the degradation process *closo-* ($n$ atoms) → *nido-* ($n-2$ atoms) results in a decrease in the polyhedral electron count of 26 electrons (see Fig. 1) and therefore must be matched by condensation processes which add two atoms and result in an increase in the polyhedral electron count of 26. Such processes are illustrated in the identical matrix element of Fig. 2, and involve edge fusion of a tetrahedron, face fusion of a square-pyramid or the sequential addition of an edge-bridging triangle and a face-bridging tetrahedron. In the case of a specific polyhedron, e.g. a *closo*-octahedral metal carbonyl cluster such as $[Os_6(CO)_{18}]^{2-}$ (**I**), the degradation process *closo* ($n$) → *nido-* ($n-2$) leads to a tetrahedron with a total of 60 valence electrons, e.g. $[Os_4H_4(CO)_{12}]$. The three condensation processes described earlier lead to the formation of three alternative polyhedral structures with 86 valence electrons. These are a capped square-pyramid (**II**), a pair of tetrahedra fused through a common edge (**III**) and an edge-bridged trigonal-bipyramid, which can exist in two isomeric forms (**IVa** and **IVb**) depending on whether the edge bridging occurs across an axial or an equatorial edge. The ways in which these polyhedra are generated from the parent octahedron are illustrated in Fig. 3.

The fact that four alternative structures have been obtained from the consideration of a pair of matching matrix elements from Figs 1 and 2 gives the impression that a large number of alternative structures must exist. In fact it is an easy matter to demonstrate that consideration of the alternative matrix elements for the octahedron generates no additional structures. Indeed the elimination of three vertices from a low-nuclearity cluster such as the octahedron has little meaning, although for higher-nuclearity clusters it could prove to be important. By utilising this systematic approach it can be stated that the four polyhedra (**I–IV**) represent the most likely geometric forms for 86-electron metal carbonyl clusters. Furthermore, because of the *isolobal* relationships connecting transition metal and main-group fragments the analysis can be extended to metalloboranes, organometallic, and sulphur- and phosphorus-containing polyhedral molecules.

The octahedral (**I**) and capped square-pyramid (**II**) structures have been established for the 86-electron $[Os_6(CO)_{18}]^{2-}$ and $[Os_6H_2(CO)_{18}]$ clusters respectively.[18,19] The structure based on the pair of tetrahedra sharing a common edge has not been observed in metal carbonyl clusters but an *isolobal* analogue, i.e. $[Mo_2Fe_2S_2(\eta C_5H_5)_2(CO)_8]$ has structure **III**.[20] The edge-bridged trigonal bipyramidal structure (**IV**) has not been characterised to date, but there is evidence that it is the initial

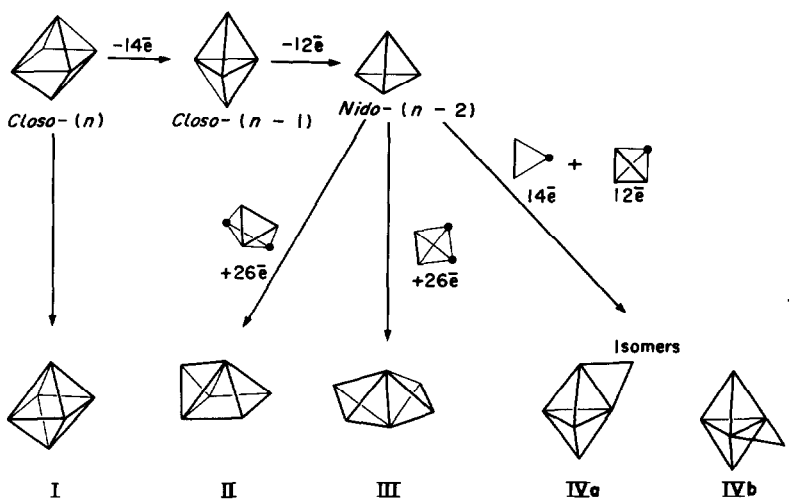



Fig. 3. Illustration of the way the matrices of Figs 1 and 2 can be utilised to generate alternative 86-electron cluster structures. The loss of 26 electrons associated with the process *closo*-octahedron to *nido*-($n-2$) tetrahedron is matched by the three alternative 26-electron condensation processes illustrated.

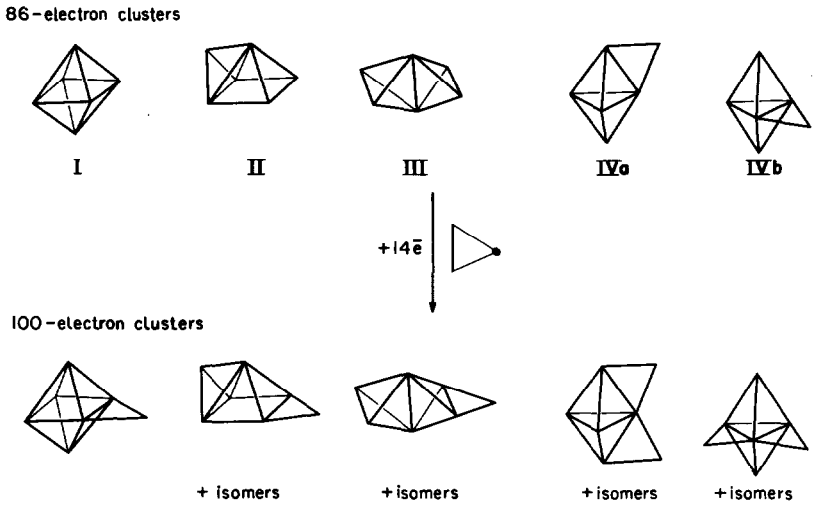



Fig. 4. Some examples of 100-electron cluster structures derived by edge bridging polyhedra I–IV.

intermediate formed when nucleophiles are added to $[Os_6(CO)_{18}]$. For example, structure **IVa** has been proposed for the adduct $[Os_6(CO)_{18}(py)]$.[21]

It is clear that this methodology can be applied to higher-nuclearity *closo*-metal carbonyl clusters, although, of course, a rapidly increasing number of structures would be generated using it. However, since many of the known metal carbonyl cluster compounds have structures based on polyhedra I–IV, particularly in the iron triad, it is also instructive to use these polyhedra as fundamental building blocks for generating either higher- or lower-nuclearity cluster compounds. Such an analysis is greatly facilitated by the degradation and aggregation matrices which have been illustrated in Figs 1 and 2, because they define the electronic requirements for aggregation and degradation processes. To take a trivial example, if a series of heptanuclear clusters with 100 valence electrons is required then an aggregation process involving the addition of a single atom and an increment of 14 electrons is required from Fig. 2. This can be achieved by the fusion of a triangle to the 86-electron polyhedra (I–IV), i.e. by adding an edge-bridging group. The polyhedra which result from these aggregation processes are illustrated in Fig. 4. Similarly, if a series of pentanuclear clusters with 74 electrons is required then the matrix in Fig. 1 is examined for processes which lead to an electron loss of 12 electrons. These are the diagonal elements representing the degradation processes: *closo*- $(n) \rightarrow$ *nido*- $(n-1)$, *nido*- $(n) \rightarrow$ *arachno*- $(n-1)$ etc. Figure 5 illustrates the consequences of these 12-electron degradation processes for I–IV and gives some examples of clusters which have 74 electrons.

Figures 6 and 7 illustrate the consequences of capping polyhedra I–IV by fusing either one or two tetrahedra to triangular faces. A large number of

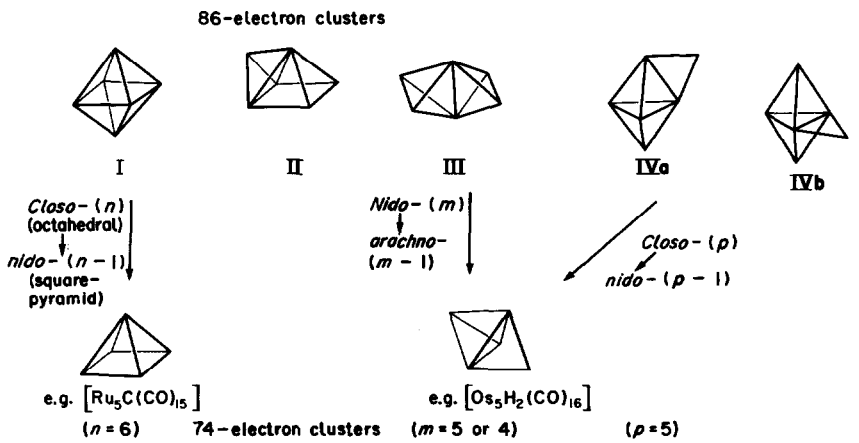



Fig. 5. Some examples of the alternative geometries for 74-electron clusters derived from the alternative 12-electron degradation processes illustrated in Fig. 1.

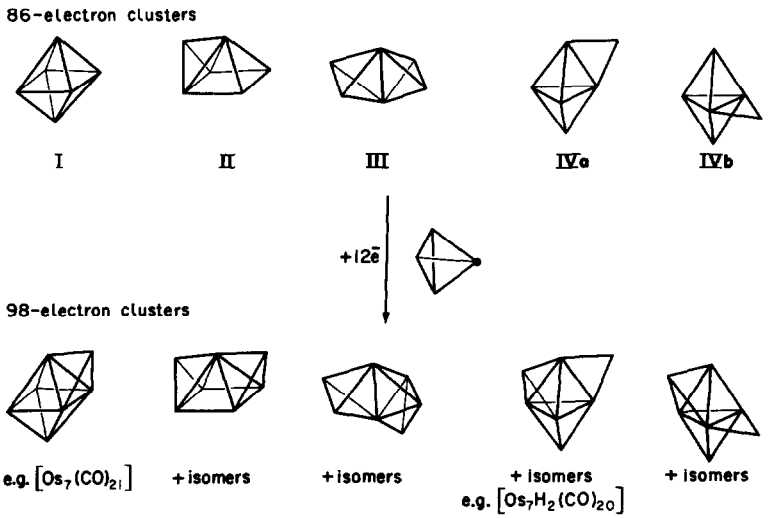



Fig. 6. Structures of 98-electron clusters derived by face-capping aggregation processes.

isomeric possibilities begin to be generated and therefore only some illustrative examples are given in Figs 6 and 7. Using these procedures the observed structures for hepta- and octanuclear metal carbonyl anions of osmium and related clusters are generated.

By increasing the number of aggregation processes selected from Fig. 2 a wide range of higher-nuclearity clusters may be generated. For example, starting with the 86ē polyhedron I the application of four 12ē capping steps leads to the tetra-capped

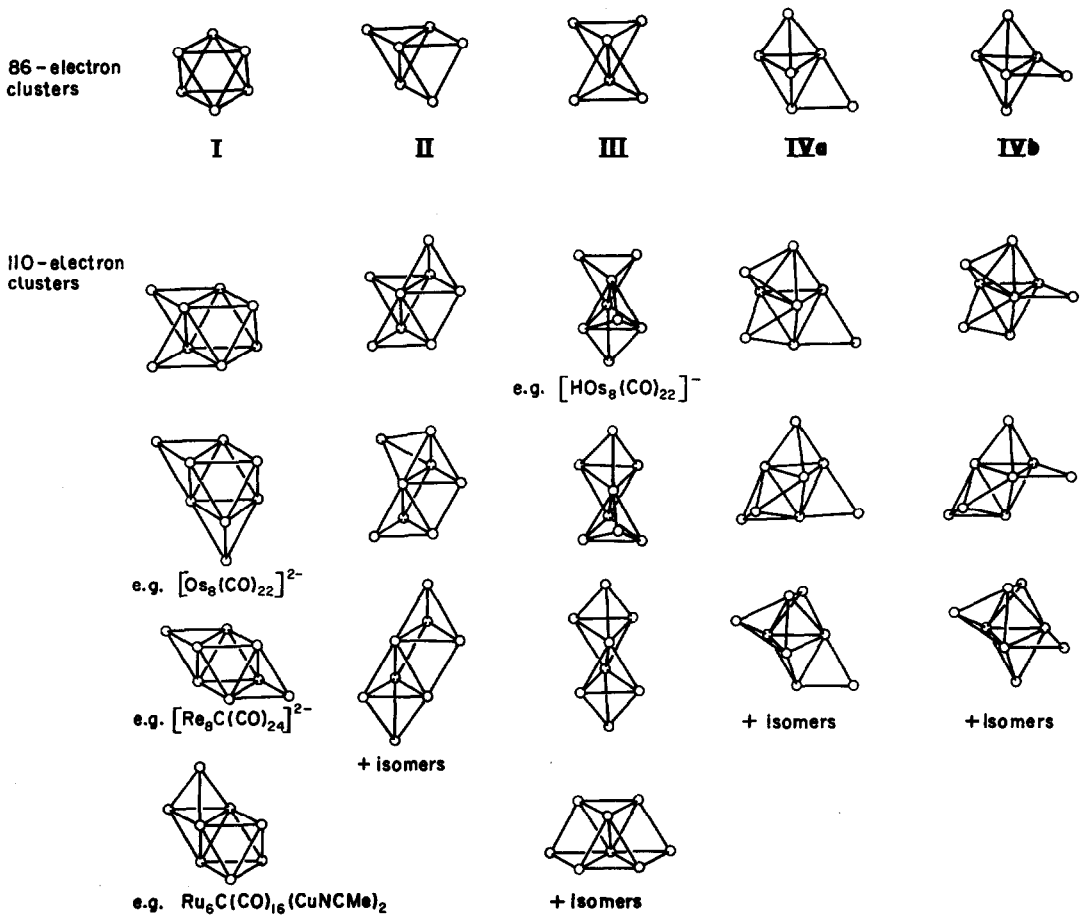



Fig. 7. Some examples of the possible structures for clusters with 110 electrons.

octahedral metal core found in a number of osmium clusters with 134ē, e.g. $[Os_{10}C(CO)_{24}]^{2-}$ and $[H_4Os_{10}(CO)_{24}]^{2-}$.[22] When a combination of both 12ē (capping) and 14ē (edge-bridging) processes are selected the "open-cap" structures, found for $Os_{10}$ derivatives with bridging ligands, are obtained, e.g.

$[Os_{10}C(CO)_{24}]^-$ and

$[Os_{10}C(CO)_{24}NO]^-$ (136ē),[23,24] and

$Os_{10}C(CO)_{24}I_2$ and

$Os_{10}C(CO)_{23}(NO)I$ (138ē).[23,25]

The number of isomeric polyhedral structures that can be derived in this way is very high and only those so far observed are illustrated in Fig. 8.

The types of aggregation process that can be applied to the 86ē polyhedron **III** are more varied because this geometry has four triangular faces defining re-entrant angles. For example application of two 12ē square-pyramidal condensation processes (Fig. 2) to **III** gives a metal core with *two nido*-octahedral (square-pyramidal) units. This makes possible two extra "octahedron-closing" 12ē aggregation processes (not illustrated in Fig. 2) and so leads to a new range of polyhedral geometries based not on one octahedral unit but on *two* linked through the tetrahedra of **III** (134e). High-nuclearity cluster species are still relatively rare, but recently a new type of metal core geometry was characterised in $[Os_{10}(S)_2(CO)_{23}]$ (134e) and it consists of the two square-pyramidal units, derived from the bi-tetrahedron (**III**) as described earlier, together with two capping groups obtained from the more common 12ē capping aggregation processes (Fig. 8).[26] The double octahedral geometry has only been observed in the slightly distorted form found in $[Ru_{10}(C)_2(CO)_{24}]^{2-}$. This cluster has 138e and the distortions from regular geometry have been attributed to the presence of four electrons in anti-bonding skeletal molecular orbitals.[27] The $Ru_{10}$ geometry has also been described in terms of a pair of octahedra sharing a common edge and it is noteworthy that the predicted electron count for this geometry is 138.[4]

Although the procedures developed in this paper provide a rational basis for enumerating the polyhedral structures associated with a particular electron count it does not provide a basis for discriminating between the alternative structures. The soft potential energy surfaces connecting these alternative geometric possibilities suggests that the development of rules which unambiguously predict the structures for metal clusters, isolobal heterometallic clusters and main-group clusters will be problematical. Nevertheless, some patterns are beginning to emerge. For example, hydrido-metal carbonyl clusters tend to form clusters of lower symmetry and with fewer edges than the parent cluster carbonyl anions. This can be attributed to the larger stabilisation energies associated with protonation for this class of polyhedron.

## REFERENCES

1. B. F. G. Johnson (Ed.), *Transition Metal Cluster Compounds*, Wiley–Interscience, Chichester (1980)

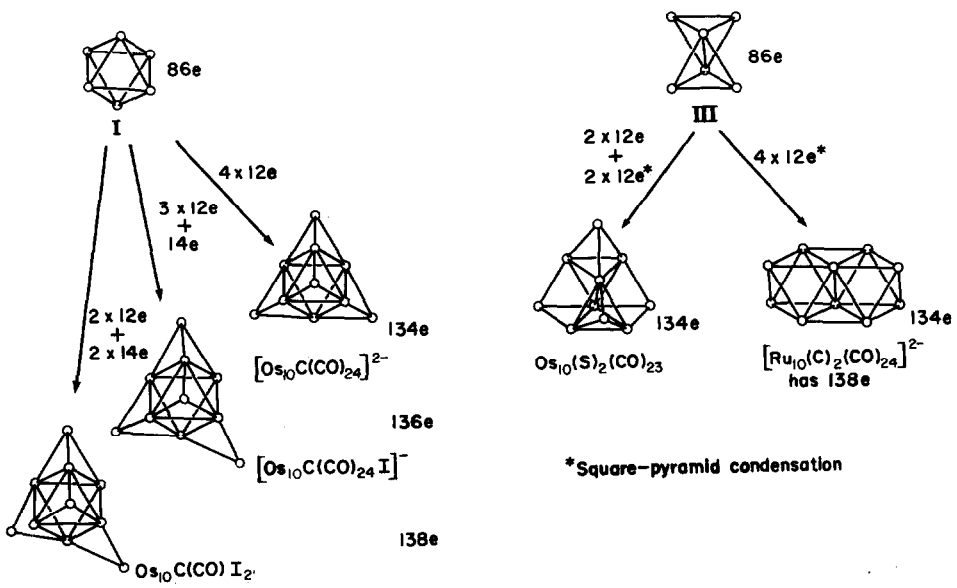



Fig. 8. Examples of the way the degradation and aggregation matrices can be used to derive the structures of the decanuclear cluster compounds of osmium and ruthenium.

gives an introduction to transition metal carbonyl cluster chemistry.
2. K. Wade, *Adv. Inorg. Radiochem.* 1976, **18**, 1; M. E. O'Neill and K. Wade, in *Metal Interactions with Boron Clusters* (Edited by R. N. Grimes), p. 1. Plenum Press, New York (1982).
3. D. M. P. Mingos, *Acc. Chem. Res.*, submitted for publication.
4. D. M. P. Mingos, *J. Chem. Soc., Chem. Commun.* 1983, 706.
5. D. G. Evans and D. M. P. Mingos, *J. Organomet. Chem.* 1983, **251**, C13.
6. S. L. Cook, J. Evans, G. V. Greaves, B. F. G. Johnson, J. Lewis, P. R. Raithby, P. B. Wells and P. Worthington, *J. Chem. Soc., Chem. Commun.* 1983, 777.
7. D. Braga, K. Henrick, B. F. G. Johnson, J. Lewis, M. McPartlin, W. J. H. Nelson, A. Sironi and M. D. Vargas, *J. Chem. Soc., Chem. Commun.* 1983, 1131.
8. C. E. Briant, K. P. Hall and D. M. P. Mingos, *J. Chem. Soc., Chem. Commun.* 1984, 290.
9. J. L. Vidal, W. E. Walker, R. L. Pruett and R. C. Schoning, *Inorg. Chem.* 1979, **18**, 129.
10. J. Lewis and B. F. G. Johnson, *Pure Appl. Chem.* 1982, **54**, 97.
11. A. J. Stone, *Inorg. Chem.* 1981, **20**, 563 and references therein.
12. R. E. Williams, *Inorg. Chem.* 1971, **10**, 210.
13. J. L. Vidal, W. E. Walker, R. L. Pruett and R. C. Schoening, *Inorg. Chem.* 1979, **18**, 129.
14. J. D. Corbett and P. A. Edwards, *J. Am. Chem. Soc.* 1977, **99**, 3313.
15. R. E. Williams, *Adv. Inorg. Radiochem.* 1976, **18**, 66.
16. B. F. G. Johnson, *Philos. Trans. R. Soc. London* 1982, **A308**, 5.
17. G. Longoni, A. Ceriotti, R. Della, Pergola, M. Manasserro, M. Perogo, G. Piro and M. Sansoni, *Philos. Trans. R. Soc. London* 1982, **A308**, 47.
18. M. McPartlin, C. R. Eady, B. F. G. Johnson and J. Lewis, *J. Chem. Soc., Chem. Commun.* 1976, 883.
19. C. R. Eady, B. F. G. Johnson and J. Lewis, *J. Chem. Soc., Chem. Commun.* 1976, 302.
20. T. P. Fehlner, C. E. Housecroft and K. Wade, *Organometallics* 1983, **2**, 1426.
21. B. F. G. Johnson, J. Lewis, M. McPartlin, M.-A. Pearsall and A. Sironi, *J. Chem. Soc., Chem. Commun.* 1984, 1089.
22. P. F. Jackson, B. F. G. Johnson, J. Lewis, W. J. H. Nelson and M. McPartlin, *J. Chem. Soc., Dalton Trans.* 1982, 2099; D. Braga, B. F. G. Johnson, J. Lewis, M. McPartlin, W. J. H. Nelson and M. D. Vargas, *J. Chem. Soc., Chem. Commun.* 1983, 241.
23. D. H. Farrar, P. F. Jackson, B. F. G. Johnson, J. Lewis, W. J. H. Nelson, M. D. Vargas and M. McPartlin, *J. Chem. Soc., Chem. Commun.* 1981, 1009.
24. D. Braga, K. Henrick, B. F. G. Johnson, J. Lewis, M. McPartlin, W. J. H. Nelson and J. Puga, *J. Chem. Soc., Chem. Commun.* 1982, 1083.
25. M. McPartlin, unpublished results.
26. J. P. Attard, B. F. G. Johnson, J. Lewis, J. M. Mace, M. McPartlin and A. Sironi, *J. Chem. Soc., Chem. Commun.*, 1984, 595.
27. C.-M. T. Hayward, J. R. Shapley, M. R. Churchill, C. Bueno and A. L. Rheingold, *J. Am. Chem. Soc.* 1982, **104**, 7347.

*Polyhedron* Vol. 3, No. 12, pp. 1329–1331, 1984
Printed in Great Britain

0277–5387/84 $3.00 + .00
Pergamon Press Ltd

# POTENTIOMETRIC STUDIES ON MIXED COMPLEXES OF Ni(II) WITH TAURINE, DL-METHIONINE AND DL-ETHIONINE IN AQUEOUS SOLUTION*

J. MASŁOWSKA† and L. CHRUŚCIŃSKI
Institute of General Food Chemistry, Technical University, 90-924 Łódź, Stefanowskiego 4/10, Poland

(*Received* 17 *January* 1984; *accepted* 14 *June* 1984)

**Abstract**—The formation and stability of the simple and mixed complexes of Ni(II) with taurine, DL-methionine and DL-ethionine have been investigated by means of potentiometric measurement of hydrogen ion concentration at 25°C and in a 0.1 *M* $NaClO_4$ medium. Mixed complexes, [$Ni(Met_2)Tau$] and [$Ni(Eth_2)Tau$], have been considered, where Met = DL-methionine, Eth = DL-ethionine and Tau = taurine.

Ternary coordination complexes are known to play important roles in many biological processes. Such mixed complexes of amino acids are likely to be important as a model for metalloenzyme–substrate complexes and also as a component of the multi-metal–multi-ligand systems in biological fluids.

Continuing our studies on complexes of transition metal ions with amino acids containing sulphur,[1,2] we proceed now to investigations of mixed-complex formation in the Ni(II)–DL-methionine– and Ni(II)–DL-ethionine–taurine systems. Taurine (2-amino-ethanosulphonic acid) is a main component of free amino acids in many organs of animal organisms, particularly in the heart.[3]

## EXPERIMENTAL

### *Reagents*

Taurine (BDH Biochemicals), DL-methionine (Reanal), DL-ethionine (Fluka) of Analar grade were crystallised from ethanol–water solutions. Nickel perchlorate was prepared and its concentration was determined as described previously.[2] The pH-metric titrations were carried out with the use of carbonate-free NaOH.

To maintain a constant ionic strength, $\mu = 0.1$, a solution of $NaClO_4$ was used.

### *Apparatus*

The pH-metric titrations were performed under oxygen-free nitrogen with an OP-208 pH-meter (Radelkis), using a special vessel described elsewhere.[4] The glass electrode was calibrated with a potassium hydrogen phthalate buffer, pH = 4.008, and a phosphate buffer, pH = 6.865, at 25°C.

### *Methods*

The pH-metric titrations were carried out by the Calvin–Bjerrum technique. Dissociation constants of ligands and stability constants of simple and mixed complexes were calculated by the method of Irving and Rossotti[5] using an ODRA 1305 computer.

The following systems were examined:

(i) $HClO_4$ ($5.00 \times 10^{-3}$ *M*),
(ii) $HClO_4$ ($5.00 \times 10^{-3}$ *M*) + ligand X ($5.00 \times 10^{-3}$ *M*),
(iii) $HClO_4$ ($5.00 \times 10^{-3}$ *M*) + ligand Y ($5.00 \times 10^{-3}$ *M*),
(iv) $HClO_4$ ($5.00 \times 10^{-3}$ *M*) + ligand X ($5.00 \times 10^{-3}$ *M*) + Ni(II) ($5.00 \times 10^{-3}$ *M*),
(v) $HClO_4$ ($5.00 \times 10^{-3}$ *M*) + ligand Y ($5.00 \times 10^{-3}$ *M*) + Ni(II) ($5.00 \times 10^{-3}$ *M*),
(vi) $HClO_4$ ($5.00 \times 10^{-3}$ *M*) + ligand X ($5.00 \times 10^{-3}$ *M*) + ligand Y ($5.00 \times 10^{-3}$ *M*) + Ni(II) ($5.00 \times 10^{-3}$ *M*),

where X = DL-methionine or DL-ethionine and Y = taurine.

* The work has been carried out within the research problem MR-I-11.

† Author to whom correspondence should be addressed.

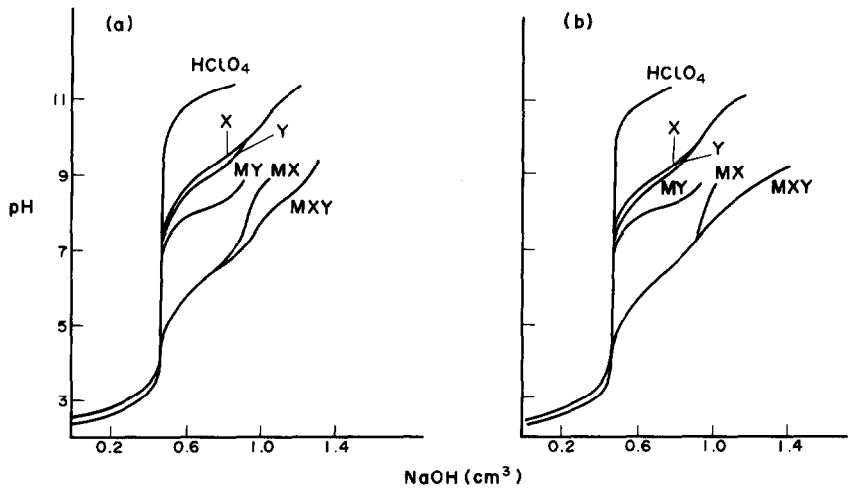



Fig. 1. Titration curves for the systems. (a) Ni(II)–DL-methionine–taurine. (b) Ni(II)–DL-ethionine–taurine.

The concentration of NaOH used for titrations was 1.041 *M*. The titration curves are shown in Fig. 1.

## RESULTS AND DISCUSSION

### *Simple complexes*

The values of stability constants for complexes of Ni(II) with DL-methionine and DL-ethionine have been discussed elsewhere.[2] The present constants were found at an ionic strength of 0.1 M $NaClO_4$. The values of those constants are given in Table 1. The values for the complexes of Ni(II) with DL-methionine are in agreement with the data given by Lenz and Martell,[6] but our log $K_1 = (5.08)$ is somewhat different from that given by Swash and Pettit[7] (5.34) and by Fridman *et al.*[8] (5.50). The value of log $K_2$ (4.57) is consistent with that given in the literature.

The values of stability constants for Ni(II) complexes with DL-ethionine are absent from the literature, but Pettit *et al.*[9] have determined the stability constants for complexes of Ag(I) with methionine and ethionine and found that the ethionine complexes are more stable than the methionine ones. According to our results, the methionine complexes of Ni(II) are slightly more stable than the ethionine ones. Ni(II) only forms a 1 : 1 complex with taurine. Its log $K_1 = 3.62$. There are only a few data in the literature concerning stability constants of metal complexes with taurine. Farooq *et al.*[10–12] have found that taurine forms 1:1 and 1:2 complexes with such metals as Cr(II), Pd(II) and Rh(III), whose stability constants are higher than those found by us. Mittal *et al.*[13] have determined the stability constant for a Cu(II) complex with taurine (log $K_1 = 4.67$). The value of the log $K_1$ for the Ca(II) complex with taurine (composition 1:1) found by Irving *et al.*[14] is 0.217.

The comparison of the stability constant for the Ni(II) complex with β-alanine[15] (log $K_1 = 4.63$) (β-alanine contains a carboxylic group instead of a sulphonic one as in taurine) with the stability constant found by us shows that β-alanine forms more stable complexes. The complex-forming ability of the carboxylic group is greater than that of the sulphonic group.

Table 1. Stability constants for simple complexes of Ni(II) with DL-methionine, DL-ethionine and taurine: temperature 25°C, $\mu = 0.1$ *M* ($NaClO_4$), SDs in parentheses

| Ligand | Dissociation constant | | Stability constant | |
|---|---|---|---|---|
| | $pK_1$ | $pK_2$ | log $\beta_1$ | log $\beta_2$ |
| DL-methionine | 2.30 (0.02) | 9.12 (0.03) | 5.08 (0.04) | 9.65 (0.05) |
| DL-ethionine | 2.18 (0.03) | 8.93 (0.03) | 4.97 (0.04) | 9.24 (0.06) |
| Taurine | 1.54 (0.04) | 8.91 (0.05) | 3.62 (0.04) | — |

*Mixed complexes*

The titration curves (Fig. 1) show that the formation of a mixed complex in the Ni(II)–DL-methionine– and Ni(II)–DL-ethionine–taurine systems probably occurs within the pH range where Ni(II) chelates are formed with methionine and ethionine (composition 1 : 2). Therefore, the possible complexing reaction of taurine should be considered in terms of the addition of a taurine molecule to the 1 : 2 complex according to the following reaction:

$$MX_2 + Y \rightleftharpoons MX_2Y. \quad (1)$$

The reaction constant for the formation of such a complex can be designated as $K_{2XY}$ in accordance with the designations used elsewhere.[16,17] A similar case of the addition of a second ligand to a simple double complex has been considered by Shelke and Jahagirdar.[16] Using the calculation procedure of Ramamoorthy and Manning,[17] we have calculated the equilibrium constant for reaction (1). The calculated values are given in Table 2. The values of $\Delta \log K$ for mixed complexes were also calculated. They allow one to estimate the possibility of mixed-complex formation.[18,19] The positive value of $\Delta \log K$ shows that reaction (1) is shifted to the right.

Table 2. Formation constants for mixed complexes of Ni(II) with DL-methionine, DL-ethionine and taurine: temperature 25°C, $\mu = 0.1$ $M$ ($NaClO_4$), SDs in parentheses

| System | Formation constant ($K_{2XY}$) | $\Delta \log K$* |
|---|---|---|
| DL-methionine–taurine | 3.75 (0.05) | 0.13 |
| DL-ethionine–taurine | 3.68 (0.05) | 0.06 |

* $\Delta \log K = \log K_{2XY} - \log K_{MY_1}$.

## REFERENCES


1. J. Masłowska and L. Chruściński, *J. Inorg. Nucl. Chem.* 1981, **43**, 3398.
2. J. Masłowska and L. Chruściński, *Polyhedron* 1984, **3**, 523.
3. J. G. Jackobsen and L. H. Smith, Jr, *Physiology* 1968, **48**, 424.
4. D. D. Perrin and I. G. Sayce, *Chem. Ind.* 1966, 661.
5. H. Irving and H. S. Rossotti, *J. Chem. Soc.* 1953, 3397; 1954, 2904.
6. G. R. Lenz and A. E. Martell, *Biochemistry* 1964, **3**, 745.
7. J. L. M. Swash and L. D. Pettit, *Inorg. Chim. Acta* 1976, **19**, 19.
8. Y. D. Fridman, S. D. Gorkhov and L. G. Ilyasova, *Koord. Khim.* 1982, **8**, 362.
9. L. D. Pettit, K. F. Siodigui, H. Kozłowski and T. Kowalik, *Inorg. Chim. Acta* 1981, **55**, 87.
10. O. Farooq, A. U. Malik and N. Ahmad, *J. Electroanal. Chem.* 1970, **26**, 411.
11. O. Farooq, N. Ahmad and A. U. Malik, *J. Electroanal. Chem.* 1973, **48**, 475.
12. O. Faroog and N. Ahmad, *J. Electroanal. Chem.* 1974, **57**, 121.
13. R. K. Mittal, M. Chandra and A. K. Dey, *Montsh. Chem.* 1976, **109**, 953.
14. C. S. Irving, B. E. Hammer, S. S. Danyluk and P. D. Klein, *J. Inorg. Biochem.* 1980, **13**, 137.
15. H. Irving, R. P. J. Williams, D. J. Ferrett and A. E. Williams, *J. Chem. Soc.* 1954, 3494.
16. D. N. Shelke and D. V. Jahagirdar, *J. Inorg. Nucl. Chem.* 1979, **41**, 1635.
17. S. Ramamoorthy and P. G. Manning, *J. Inorg. Nucl. Chem.* 1972, **34**, 1977.
18. Y. Marcus and I. Eliezer, *Coord. Chem. Rev.* 1969, **4**, 273.
19. R. B. Martin and R. Prados, *J. Inorg. Nucl. Chem.* 1974, **36**, 1665.

*Polyhedron* Vol. 3, No. 12, pp. 1333–1335, 1984
Printed in Great Britain

0277–5387/84 $3.00 + .00
Pergamon Press Ltd

# SYNTHESIS AND VIBRATIONAL SPECTRA OF BIMETALLIC COMPOUNDS OF THE TYPE $[(NH_3)(L)ZnFe(CO)_4]$ (L = BIDENTATE AMINE)

**A. E. MAURO* and M. N. G. MANCINI**
Instituto de Química de Araraquara, UNESP, C.P. 174, 14.800 Araraquara, S.P. Brasil

(*Received* 2 *February* 1984; *accepted* 14 *June* 1984)

**Abstract**—New compounds with the general formulae $[(NH_3)(L)ZnFE(CO_4]$ (L = ethylenediamine, *N*-methylethylenediamine, *N,N'*-dimethylethylenediamine and 1,3-propanediamine) were prepared and studied by vibrational spectroscopy. The data suggest that they may be formulated as monomers with a trigonal bipyramidal configuration around the iron atom.

Many metal carbonyls containing iron bonded to a metal of group IIB are known.[1–4] While the oligomer $[HgFe(CO)_4]_4$ does not react with amines its halogen derivatives,[1] $(HgX)_2Fe(CO)_4$ (X = Cl, Br, I), form stable adducts with nitrogen ligands, such as $py_2(HgCl)_2Fe(CO)_4$. However, several adducts of $[MFe(CO)_4]_4$ (M = Zn, Cd) have been reported,[4] and, while $[CdFe(CO)_4]_4$ has been known since 1938,[5] only recently has the synthesis of $[ZnFe(CO)_4]_4$ from $(NH_3)_3ZnFe(CO)_4$ been reported.[6] This latter complex, the first one having an iron–zinc bond, was synthesized by Hieber and Fack[7] by adding $ZnCl_2$ to an ammoniacal solution of $[HFe(CO)_4]^-$. In this paper compounds of the type $[(NH_3)(L)ZnFe(CO)_4]$ [L = ethylenediamine (en), *N*-methylethylenediamine (Meen), *N,N'*-dimethylethylenediamine (s-diMeen) and 1,3-propanediamine (tn)] were obtained when $ZnCl_2$ and the bidentate amine were added to the ammoniacal solution of $[HFe(CO)_4]^-$. Their structures are discussed on the basis of IR and Raman data.

## EXPERIMENTAL

### *Synthesis of the compounds*

All operations involved in this work, except the weighings, were carried out under an atmosphere of prepurified nitrogen in a Schlenk apparatus. The $Fe(CO)_5$ (Fluka) and the other reagents (p.a. grade) were used without further purification.

To a solution of 35 $cm^3$ of $NH_4OH$ and 15 $cm^3$ of $H_2O$ was added 1 $cm^3$ (7.45 mmol) of $Fe(CO)_5$. The mixture was stirred for 5 h at room temperature producing $[HFe(CO)_4]^-$. Then 11.1 mmol of the amine (en, Meen, s-diMeen and tn) and 1.02 g (7.45 mmol) of $ZnCl_2$ were added causing a microcrystalline solid to appear. The insoluble product was filtered off, washed with four 20-$cm^3$ portions of water, followed by three 20-$cm^3$ portions of diethylether and dried under vacuum.

The analytical data for the complexes prepared are shown in Table 1.

### *Vibrational spectra*

The IR spectra, at room temperature, were recorded as nujol mulls between CsI plates on a Perkin–Elmer 567 spectrophotometer. The Raman spectra were recorded from solid samples on a Jarrel–Ash 25-300 spectrometer using an $Ar^+$ laser with an excitation line at 514.5 nm from coherent radiation. Since the samples were decomposed by the laser beam, the rotating-cell technique[8] was employed.

Table 1. Analytical data of the complexes

| Complex | Calculated(%) | | | | Found(%) | | | |
|---|---|---|---|---|---|---|---|---|
| | C | H | N | Fe | C | H | N | Fe |
| $(NH_3)(en)ZnFe(CO)_4$ | 23.2 | 3.6 | 13.5 | 18.0 | 22.7 | 3.4 | 13.6 | 17.8 |
| $(NH_3)(Meen)ZnFe(CO)_4$ | 25.9 | 4.0 | 12.9 | 17.2 | 25.2 | 3.9 | 12.6 | 16.9 |
| $(NH_3)(s\text{-}diMeen)ZnFe(CO)_4$ | 28.4 | 4.4 | 12.4 | 16.5 | 28.1 | 4.6 | 12.4 | 16.5 |
| $(NH_3)(tn)ZnFe(CO)_4$ | 25.9 | 4.0 | 12.9 | 17.2 | 25.3 | 4.3 | 12.6 | 16.9 |

* Author to whom correspondence should be addressed.

## RESULTS AND DISCUSSION

The metal–metal-bonded species of general formula $MFe(CO)_4$ (M = Zn, Cd, Hg) show the interesting structure of a nearly square planar centrosymmetric eight membered ring.[4] While the attempts to prepare adducts of $HgFe(CO)_4$ with amines were unsuccessful many derivatives of $ZnFe(CO)_4$ and $CdFe(CO)_4$ were synthesized and they have quite different structures, e.g. $[(bpy)CdFe(CO)_4]$ is a trimer,[9] $[(bpy)ZnFe(CO)_4]$ is a dimer,[6] and $[(NH_3)_3ZnFe(CO)_4]$ is a monomer.[3] For the complexes reported in this paper, $[(NH_3)(L)ZnFe(CO)_4]$, where mono- and bidentate nitrogen ligands are coordinated to the zinc atom, the following solid-state structures may be possible:

(a) An ionic structure of $[Zn(L)(NH_3)]^{2+}$ and $[Fe(CO)_4]^{2-}$ ions (L = bidentate amine).

(b) Monomers with a bipyramidal configuration around the iron atom having the $Zn(L)(NH_3)$ group at the axial position, in agreement with the rules of symmetry pointed out by Haas and Sheline.[10] For these compounds axial substitution is predicted, since the $Zn(L)(NH_3)$ fragment muxt be a good $\sigma$-donor and an extremely weak $\pi$-acceptor.

(c) Cyclic polymers with an octahedral configuration for the iron atom and the zinc atoms bridging $Fe(CO)_4$ units.

$[(NH_3)(L)Zn]^{2+}[Fe(CO)_4]^{2-}$
Ionic (a)

$(NH_3)(L)ZnFe(CO)_4$
Monomer (b)

$[(NH_3)(L)ZnFe(CO)_4]_2$
Cyclic polymer (c)

The complexes of this study are air-sensitive and show a low solubility in suitable solvents for molecular weight measurements. The vibrational spectra in the CO stretching region (Table 2) allow the exclusion of both the ionic and the cyclic structure. The ionic structure is excluded since only one $\nu$(CO) would be expected. The cyclic structure with $D_{2h}$ local symmetry is excluded since the four $\nu$(CO) in the IR ($2B_{3u}+B_{1u}+B_{2u}$) and the four Raman frequencies ($2A_g+B_{1g}+B_{2g}$) would not be coincident. The monomeric structure with a $C_{3v}$-symmetry around the iron atom agrees best with the experimental data since, as expected, the $\nu$(CO) in the IR ($2A_1+E$) and Raman ($2A_1+E$) spectra coincide.

For the $ZnFe(CO)_4$ skeleton there are 24 fundamental vibrations distributed in the following symmetry species: $7A_1+1A_2+8E$. The most important bands in the study of metal carbonyl compounds are CO stretching and three are expected for the $ZnFe(CO)_4$ skeleton: $2A_1+E$. The assignment for these three carbonyl stretching modes, and their force constants calculated using the Cotton–Kraihanzel model[11] are given in Table 2. In these compounds, where a splitting of the degenerated vibrational mode occurred, an average value of the two frequencies was employed in calculating the force constants. It is seen that $K_1$, the axial CO stretching force constant, is significantly larger than $K_2$, the equatorial CO stretching force constant. At the same time these constants are significantly lower than those reported for $Fe(CO)_5$ ($K_1 = 16.92$, $K_2 = 16.59$).[12]

Table 2. CO stretching frequencies, tentative assignments and approximate force constants

| Compound | | Frequencies ($cm^{-1}$) $A_1^{ax}$ | $A_1^{eq}$ | E | Force constants ($mdyn\,A^{o-1}$) $K_1$ | $K_2$ | $K_i$ |
|---|---|---|---|---|---|---|---|
| $(NH_3)(en)ZnFe(CO)_4$ | IR | 1947m | 1840sh | 1826s<br>1808sh | 15.27 | 13.49 | 0.13 |
| | R | 1948vw | 1843s | 1829sh<br>1809vs | | | |
| $(NH_3)(Meen)ZnFe(CO)_4$ | IR | 1944s | 1850sh | 1820vs<br>1807vs | 15.13 | 13.51 | 0.25 |
| | R | 1946w | 1854vs | 1818vs<br>1803sh | | | |
| $NH_3(s\text{-}diMeen)ZnFe(CO)_4$ | IR | 1945s | 1843sh | 1820vs<br>1796sh | 15.26 | 13.40 | 0.20 |
| | R | 1947w | 1841w | 1820s<br>1798vs | | | |
| $(NH_3)(tn)ZnFe(CO)_4$ | IR | 1940s | 1856s | 1820vs<br>1797w | 15.00 | 13.48 | 0.30 |
| | P | 1946vw | 1849vs | 1824s<br>1790s | | | |

vs, very strong; s, strong; m, medium; w, weak; vw, very weak. ax, axial; eq, equatorial.

The assignment proposed, $\nu(CO^{ax}) > \nu(CO^{eq})$, is based on the fact that the intensity of the $A_1^{ax}$-mode is greater than that of the $A_1^{eq}$-mode. An anomalous situation is observed for $(NH_3)(tn)ZnFe(CO)_4$, where the $A_1^{eq}$-mode has a great intensity. This may be caused by a mixing with the $A_1^{ax}$-mode and also by a distortion of the carbonyl groups from planarity. This would lead to a decrease in the $C^{ax}$–Fe–$C^{eq}$ angle ($\theta$) and, consequently, to an increase in the intensity of the $CO^{eq}$ mode, since the intensity of this mode is a function[13] of cos $\theta$.

The band due to metal–metal stretching was expected to appear in the region of the far-IR spectra, but could not be observed in the IR due to the limitations of the spectrophotometer. However, a strong band observed at 190 $cm^{-1}$ in the Raman spectra of these compounds can be assigned to the zinc–iron stretching mode.

The compounds $[(NH_3)(L)ZnFe(CO)_4]$ are clearly monomeric in the solid state; however, when there is only a bidentate amine bonded to the Zn

atom the adducts, $LZnFe(CO)_4$, have a cyclic dimeric structure.[3] By comparison[6] with the CO bands of $ZnFr(CO)_4$ (the mean value in the IR is 1961 $cm^{-1}$), it is seen that in the adducts the nitrogen ligands coordinated to the Zn atom displace the CO bands to lower energies (the mean value in the IR is 1854 $cm^{-1}$) since there is, in these complexes, an increase in the population of the CO $\pi^*$-orbitals and a decrease in the CO bond order.

The others bands observed in the spectra are probably due to the vibrational modes of the amines, the FeC stretchings, FeCO deformations, ZnN stretchings and combination modes. The complete IR data are:

$[(NH_3)(en)ZnFe(CO)_4]$: 3367w, 3325w, 3249w, 3045w, 1947m, 1840sh, 1826s, 1808sh, 1598sh, 1585m, 1327vw, 1273w, 1235m, 1136w, 1105w, 1030m, 1020sh, 973w, 633s, 550w, 505w, 445vw, 367vw, 320vw, 248w.

$[(NH_3)(Meen)ZnFe(CO)_4]$: 3360w, 3352vw, 3290w, 3204w, 1944s, 1850sh, 1820vs, 1807vs, 1623m, 1600s, 1310m, 1262s, 1130w, 1095w, 1052m, 1000m, 950s, 932sh, 868vw, 633vs, 622vs, 555w, 532m, 517m, 499vw, 425w, 380vw, 310vw, 235w.

$[(NH_3)(s\text{-}diMeen)ZnFe(CO)_4]$: 3360m, 3290w, 3220w, 1945s, 1843sh, 1820vs, 1796sh, 1620sh, 1604s, 1270s, 1250sh, 1130w, 1078w, 1065w, 1002w, 965vw, 950m, 845w, 634vs, 608s, 558w, 529w, 415w, 360w, 330w, 240w.

$[(NH_3)(tn)ZnFe(CO)_4]$: 3358w, 3306w, 3198w, 1940s, 1856vs, 1820vs, 1797w, 1608vw, 1583m, 1313w, 1282vw, 1248m, 1168m, 1143w, 1019m, 905m, 763vw, 640vs, 546vw, 536w, 483vw, 370w, 230w.

*Acknowledgement*—We thank the Fundação de Amparo Pesquisa do Estado de São Paulo for financial support.

## REFERENCES

1. A. A. Chalmers, J. Lewis and S. B. Wild, *J. Chem. Soc (A)* 1968, 1013.
2. D. M. Adams, D. J. Cook and R. D. Kemmitt, *J. Chem. Soc. (A)* 1968, 1067.
3. A. E. Mauro, Y. Hase and O. Sala, *J. Mol. Struct.* 1979, **51**, 9.
4. R. D. Ernst, T. J. Marks and J. A. Ibers, *J. Am. Chem. Soc.* 1977, **99**, 2090.
5. F. Feigl and P. Krumholz, *Z. Anorg. Chem.* 1938, **215**, 242.
6. R. J. Neustadt, J. H. Cymbaluk, R. D. Ernst and F. W. Cagle, *Inorg. Chem.* 1980, **19**, 2375.
7. H. Hieber and E. Fack, *Z. Anorg. Allg. Chem.* 1938, **236**, 83.
8. W. Kiefer and J. Bernstein, *J. Appl. Spectrosc.* 1971, **25**, 609.
9. R. D. Ernst, T. J. Marks and J. A. Ibers, *J. Am. Chem. Soc.* 1977, **99**, 2098.
10. H. Haas and R. K. Sheline, *J. Chem. Phys.* 1967, **47**, 2996.
11. F. A. Cotton and C. S. Kraihanzel, *J. Am. Chem. Soc.* 1962, **84**, 4432.
12. G. Bor, *Inorg. Chim. Acta* 1968, **3**, 191.
13. D. J. Darensbourg, H. H. Nelson and C. L. Hyde, *Inorg. Chem.* 1974, **13**, 2135.

*Polyhedron* Vol. 3, No. 12, pp. 1337–1345, 1984
Printed in Great Britain

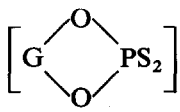
0277–5387/84 $3.00 + .00
Pergamon Press Ltd

# ALKYLENEDITHIOPHOSPHATE DERIVATIVES OF ARSENIC(III), ANTIMONY(III) AND BISMUTH(III)

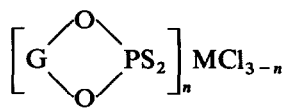
**H. P. S. CHAUHAN, G. SRIVASTAVA and R. C. MEHROTRA***
The Chemical Laboratories, University of Rajasthan, Jaipur-302004, India

(*Received* 6 *March* 1984; *accepted* 23 *June* 1984)

**Abstract**—Tris(alkylenedithiophosphates) of arsenic(III), antimony(III) and bismuth(III),



M (M = As, Sb or Bi; G = —$CH_3CHCHCH_3$—, —$(CH_3)_2CC(CH_3)_2$—, —$(CH_3)_2CCH_2CH(CH_3)$—, —$CH_2C(CH_3)_2CH_2$— or —$CH_2C(C_2H_5)_2CH_2$—) have been synthesized by the reactions of alkylenedithiophosphoric acids with metal oxides and chlorides and of their ammonium salts with metal chlorides in suitable solvents. Mixed chloride alkylenedithiophosphates of arsenic(III) and antimony(III),



(M = As or Sb; G = —$CH_3CHCHCH_3$— or —$CH_2C(C_2H_5)_2CH_2$—) have been obtained by the reactions of metal chlorides with ammonium alkylenedithiophosphates at 1 : 1 and 1 : 2 molar ratios or alternatively by the co-disproportionation reactions of metal chlorides with metal tris(alkylenedithiophosphates) at different (2 : 1 and 1 : 2) molar ratios. These new compounds have been characterized by elemental analyses, molecular weight measurements and spectroscopic (IR, and $^1H$ and $^{31}P$ NMR) data. Chelated structures with bidentate alkylenedithiophosphate groups have been proposed for all these derivatives.

Dialkyldithiophosphate derivatives of arsenic(III), antimony(III) and bismuth(III) are well known for their utility as analytical reagents,[1–3] as lubricant additives [4–6] and for regeneration of cracking catalysts.[7–9] We have recently reported the synthesis, reactions and spectroscopic characterization of mixed halide dialkyldithiophosphate derivatives of arsenic(III),[10] antimony(III)[10] and bismuth(III).[11] X-ray crystal structures of a few tris(dialkyldithiophosphates) of antimony(III)[9,12] and bismuth(III)[13] have already been reported. A number of alkylenedithiophosphoric acids which are cyclic analogues of dialkyldithiophosphoric acids have been synthesized[14] recently and their organotin[15] and nickel[16] derivatives have also been reported. However, alkylenedithiophosphate derivatives of arsenic, antimony and bismuth have not previously been reported.

In view of the exciting chemistry and various applications of corresponding dialkyldithiophosphate derivatives of arsenic(III), antimony (III) and bismuth(III), it was thought worthwhile to synthesize tris as well as mixed chloride alkylenedithiophosphate derivatives of these elements and to investigate their various physicochemical properties.

## EXPERIMENTAL

### *Materials*

Solvents (benzene, $CHCl_3$, $CCl_4$ and light petroleum etc.) were dried by standard methods. Arsenic trichloride (b.p. 130°C), anitmony trichloride (b.p. 223°C) and glycols (butane-2,3-diol, 2,3-dimethylbutane-2,3-diol, 2-methylpentane-2,4-

* Author to whom correspondence should be addressed.

diol, 2,2-dimethylpropane-1,3-diol and 2,2-diethylpropane-1,3-diol) were distilled before use. Bismuth trichloride was obtained by passing chlorine gas through a boiling solution of BiOCl in concentrated HCl and simultaneously distilling the volatile solvents. The solid mass thus obtained was sublimed under reduced pressure to yield bismuth trichloride as a white crystalline solid. Alkylenedithiophosphoric acids as well as their ammonium salts were prepared by the previously reported methods.[14] Phosphorus pentasulphide (Reidel), arsenic trioxide (Sisco), antimony trioxide (Loba), bismuth trioxide (E. Merck) and bismuth oxychloride (Mayfair and Croydon) were used as received.

*Product analyses*

Sulphur was estimated gravimetrically as barium sulphate. Arsenic[10,18] and antimony[10] were estimated by decomposing the compound by sulphuric acid followed by the oxidation of As(III) and Sb(III) to As(V) and Sb(V) respectively by heating with $KMnO_4$; excess $KMnO_4$ was decolourized by $H_2O_2$ and excess $H_2O_2$ was removed by evaporation. The remaining solid mass was dissolved in HCl, KI was added to it and liberated iodine was titrated against standard sodium thiosulphate solution using starch as an internal indicator. Bismuth was estimated by titrating against standard EDTA solution using xylenol-orange as indicator.[19]

*Measurements*

Molecular weights were measured cryoscopically as well as ebullioscopically in benzene. IR spectra were recorded in nujol mulls in the range 4000–200 $cm^{-1}$ using CsI optics on a Perkin–Elmer Model 577 spectrophotometer. $^1H$ NMR spectra were recorded on a Perkin–Elmer R12B spectrometer in $CDCl_3$ or $CCCl_4$ solutions using tetramethylsilane as a reference. $^{31}P$ NMR spectra in $CDCl_3$ solutions were recorded on a Varian XL-100A spectrophotometer using $H_3PO_4$ as an internal standard.

*General methods of syntheses of various alkylenedithiophosphate derivatives of arsenic*(III), *antimony*(III) *and bismuth*(III)

*Reaction of metal (As, Sb or Bi) chloride with alkylenedithiophosphoric acid at* 1 : 3 *molar ratio.* The mixture of alkylenedithiophosphoric acid and metal (arsenic, antimony or bismuth) trichloride in benzene was refluxed for 3–4 h until liberation of hydrogen chloride gas ceased. In the cases of the corresponding 2,2-dimethylpropane-1,3-diol derivatives, the insoluble metal tris(alkylenedithiophosphate) so formed was separated as the reaction proceeded, while in the cases of the corresponding butane-2,3-diol derivatives the metal tris(alkylenedithiophosphate) was soluble in hot benzene and crystallized on standing.

*Reaction of metal chloride with ammonium alkylenedithiophosphate at* 1 : 3 *molar ratio.* A benzene solution of metal (arsenic or antimony) chloride was mixed with the ammonium salt of alkylenedithiophosphoric acid and stirred with slight heating (50–60°C) for about 3 h. In the cases of the corresponding hexyleneglycol and 2,2-diethylpropane-1,3-diol derivatives, where metal tris(alkylenedithiophosphates) are soluble in benzene, the reaction mixture was filtered to remove the precipitated ammonium chloride followed by removal of the solvent from the filtrate under reduced pressure giving a yellow solid product. In the cases of the corresponding pinacol derivatives where the metal tris(alkylenedithiophosphates) are insoluble in benzene the contents were filtered followed by washing the precipitate with water to remove the soluble ammonium chloride. On drying the residue a yellow solid powder was obtained.

*Reaction of bismuth trichloride with ammonium hexylenedithiophosphate at* 1 : 3 *molar ratio in dilute HCl.* On addition of bismuth trichloride (prepared *in situ* by dissolving $Bi_2O_3$ in HCl) to an alcoholic solution of $\underline{OC(CH_3)_2CH_2CHCH_3OP(S)SNH_4}$ slowly with constant stirring, an exothermic reaction with the precipitation of yellow bismuth tris(hexylenedithiophosphate) occurred. The precipitate was washed several times with water and dried, when a yellow solid compound was obtained.

*Reaction between metal (As or Sb) trioxide and* 2,3-*butylenedithiophosphoric acid at* 1 : 6 *molar ratio.* A benzene solution of 2,3-butylenedithiophosphoric acid was added to the metal oxide ($As_2O_3$ or $Sb_2O_3$) and the contents were heated for 3–4 h, when a clear solution was obtained. The metal tris(butylenedithiophosphate) crystallized out from this solution on standing overnight.

*Reaction between antimony trichloride and* $\underline{OCH_2C(C_2H_5)_2CH_2OP(S)SNH_4}$ *at* 1 : 1 *or* 1 : 2 *molar ratio.* A benzene solution of antimony trichloride and solid $\underline{OCH_2C(C_2H_5)_2CH_2OP(S)}$ $SNH_4$ (at 1 : 1 or 1 : 2 molar ratio respectively) were mixed and stirred for about 2 h. Precipitated ammonium chloride was removed by filtration. On removing the solvent from the filtrate, the desired mixed chloride alkylenedithiophosphate was obtained.

*Reaction between metal (As or Sb) trichloride and metal (As or Sb) tris*(2,3-*butylenedithiophosphate) at* 2 : 1 *or* 1 : 2 *molar ratio.* The benzene solutions of metal (arsenic or antimony) trichlorides and

Table 1. Synthesis and properties of alkylenedithiophosphate derivatives of arsenic(III), antimony(III) and bismuth(III)

| Sl. No. | Compound | Route of synthesis | Yield (%) | Physical state | M.p. (°C) | Solubility* | Analysis: Metal found (calc.) | Analysis: Sulphur found (calc.) | Molecular weight found (calc.) |
|---|---|---|---|---|---|---|---|---|---|
| 1 | $[OCH(Me)CH(Me)OPS_2]_3As$ | a, d | 90 | White crystalline solid | 180 | Soluble in benzene and $CHCl_3$ | 11.79 (11.98) | 31.22 (30.75) | 650 (624) |
| 2 | $[OC(Me)_2C(Me)_2OPS_2]_3As$ | b | 68 | Yellow solid powder | Does not melt up to 300°C | Insoluble in common organic solvents | 10.94 (10.57) | 27.31 (27.14) | — |
| 3 | $[OC(Me)_2CH_2CH(Me)OPS_2]_3As$ | b | 96 | Pale yellow low m.p. solid | 55 | Soluble in benzene $CCl_4$ and $CHCl_3$, on standing becomes insoluble | 10.82 (10.57) | 27.67 (27.14) | 674 (709) |
| 4 | $[OCH_2C(Me)_2CH_2OPS_2]_3As$ | a | 73 | Yellow solid | 210 | Insoluble in benzene | 11.39 (11.24) | 28.54 (28.86) | — |
| 5 | $[OCH_2C(Et)_2CH_2OPS_2]_3As$ | b | 90 | Light yellow solid | 125 | Soluble in benzene, $CCl_4$, $CHCl_3$ etc. | 9.94 (9.98) | 25.08 (25.62) | 784 (751) |
| 6 | $[OCH(Me)CH(Me)OPS_2]_2AsCl$ | f | 98 | Yellow sticky solid | — | Soluble in benzene, $CHCl_3$ etc. | 15.94 (15.71) | 27.76 (26.90) | 447 (476) |
| 7 | $[OCH(Me)CH(Me)OPS_2]AsCl_2$ | f | 98 | Yellow viscous liquid | — | Soluble in benzene and $CHCl_3$ | 23.14 (22.77) | 18.68 (19.49) | 307 (329) |
| 8 | $[OCH(Me)CH(Me)OPS_2]_3Sb$ | a, d | 92 | Yellow crystalline solid | — | Soluble in benzene and $CHCl_3$ | 18.87 (18.14) | 28.85 (28.65) | 679 (675) |
| 9 | $[OC(Me)_2C(Me)_2OPS_2]_3Sb$ | b | 73 | Yellow solid powder | Does not melt up to 300°C | Insoluble in common organic solvents | 18.08 (16.12) | 24.80 (25.46) | — |

Table 1. Synthesis and properties of alkylenedilhiophosphate derivatives of arsenic (III), antimony (III) and bismuth (III)—*cont.*

| Sl. No. | Compound | Route of synthesis | Yield (%) | Physical state | M.p. (°C) | Solubility* | Analysis: Metal found (calc.) | Analysis: Sulphur found (calc.) | Molecular weight found (calc.) |
|---|---|---|---|---|---|---|---|---|---|
| 10 | $[OC(Me)_2CH_2CH(Me)OPS_2]_3Sb$ | b | 92 | Pale yellow low m.p. solid | 55 | Freshly prepared soluble in benzene, $CCl_4$ etc., on standing a few weeks becomes insoluble in them | 14.99 (16.12) | 24.94 (25.46) | 732 (755) |
| 11 | $[OCH_2C(Me)_2CH_2OPS_2]_3Sb$ | a | 75 | Yellow solid | 200 | Insoluble in benzene, $CHCl_3$ and $CCl_4$ | 17.73 (17.07) | 26.56 (26.96) | — |
| 12 | $[OCH_2C(Et)_2CH_2OPS_2]_3Sb$ | b | 94 | Light yellow solid | 112 | Soluble in benzene, $CHCl_3$ and $CCl_4$ | 15.01 (15.27) | 24.42 (24.12) | 765 (797) |
| 13 | $[OCH(Me)CH(Me)OPS_2]_2SbCl$ | f | 94 | Yellow low m.p. (sticky) solid | 65 | Soluble in benzene | 23.41 (23.25) | 25.51 (24.49) | 496 (524) |
| 14 | $[OCH(Me)CH(Me)OPS_2]SbCl_2$ | f | 97 | Yellow sticky solid | — | Soluble in benzene | 32.54 (32.39) | 16.63 (17.06) | 484 (376) |

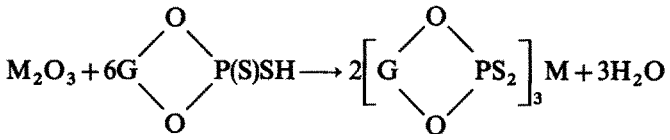
| | | | | | | | | | |
|---|---|---|---|---|---|---|---|---|---|
| 15 | $[OCH_2C(Et)_2CH_2OPS_2]_2SbCl$ | e | 68 | Light yellow sticky solid | — | Soluble in benzene | 19.99 (20.03) | 20.92 (21.18) | — |
| 16 | $[OCH_2C(Et)_2CH_2OPS_2]SbCl_2$ | e | 69 | Yellow sticky solid | — | Soluble in benzene | 29.48 (29.13) | 14.94 (15.35) | — |
| 17 | $[OCH(Me)CH(Me)OPS_2]_3Bi$ | a | 81 | Yellow solid | 260 | Soluble in benzene and $CCl_4$ (crystallized from benzene) | 27.97 (27.55) | 25.04 (25.36) | 744 (759) |
| 18 | $[OC(Me)_2CH_2CH(Me)OPS_2]_3Bi$ | c | 93 | Yellow solid | 80 (decomposed) | Soluble in benzene and $CHCl_3$ | 24.63 (24.80) | 22.67 (22.83) | 822 (842) |
| 19 | $[OCH_2C(Me)_2CH_2OPS_2]_3Bi$ | a | 45 | Yellow solid | 290 (decomposed without melting) | Insoluble in benzene | 25.92 (26.10) | 24.49 (24.03) | — |
| 20 | $[OCH_2C(Et)_2CH_2OPS_2]_3Bi$ | a | 59 | Yellow solid | 255 | Insoluble in acetone, less soluble in benzene | 24.14 (23.62) | 22.58 (21.74) | 857 (885) |

* All the compounds are insoluble in water. Compounds 6, 7, 13, 14, 15 and 16 are hydrolyzed by water.

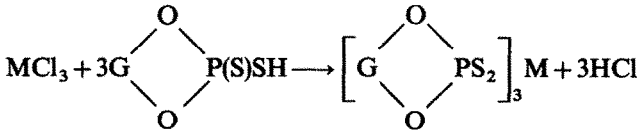
$[OCHCH_3CHCH_3OPS_2]_3M$ (M = As or Sb) were mixed and heated for about 1 h followed by removal of the solvent, giving the desired mixed chloride 2,3-butylenedithiophosphate derivative of the metal.

## RESULTS AND DISCUSSION

Tris(alkylenedithiophosphates) of arsenic(III), antimony(III) and bismuth(III) have been synthesized by the reactions of alkylenedithiophosphoric acids with the corresponding metal oxides and chlorides:



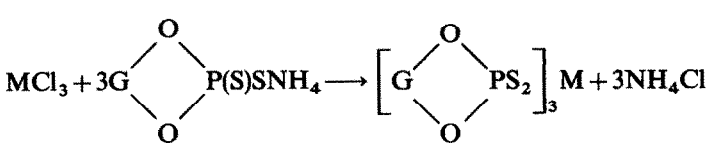
[M = As or Sb; G = —(Me)CHCH(Me)—] and



[M = As, Sb or Bi; G = $—CH_3CHCHCH_3—$, $—CH_2C(CH_3)_2CH_2$ or $—CH_2C(C_2H_5)_2CH_2—$].

All these reactions are quite facile and are completed by refluxing the reactants in benzene for 3–4 h.

Although the alkylenedithiophosphoric acids can be obtained in a purer form compared to dialkyldithiophosphoric acids (only the hexyleneglycol derivative is not of high purity) and they seem to be more stable to atmospheric oxidation and hydrolysis, even then it was conjectured that their alkali (ammonium) salts might be more pure and stable and the reactions of these salts with metal chlorides may be more facile. In view of these advantages, the majority of these derivatives (Table 1) have been synthesized by the reactions of ammonium alkylenedithiophosphates with metal chlorides:



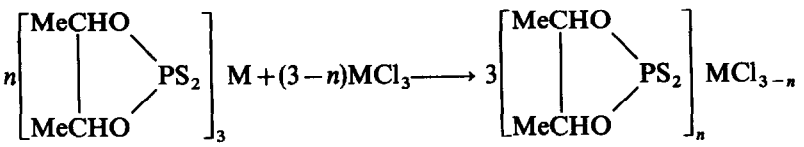
[M = As, Sb or Bi; G = $—(CH_3)_2CC(CH_3)_2—$, $—(CH_3)_2CCH_2CH(CH_3)—$ or $—CH_2C(C_2H_5)_2CH_2—$].

These reactions are even more facile than those of the corresponding free acids and are completed by stirring the reactants in benzene for 3–4 h at 50–60°C, with the precipitation of ammonium chloride. Some of the metal tris(alkylenedithiophosphates) are soluble in benzene and they can, therefore be easily separated from ammonium chloride by filtration. In the cases of derivatives which are insoluble in benzene, the products along with ammonium chloride are filtered out and washed with water to remove the soluble ammonium chloride.

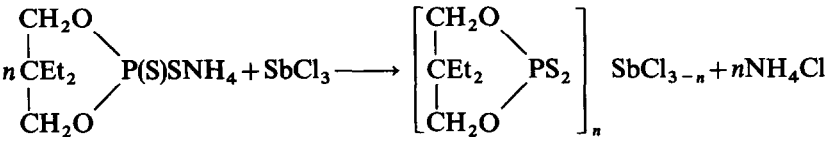
The reaction of bismuth trichloride (BiOCl in HCl) with an aqueous solution of ammonium hexylenedithiophosphate has been carried out with the immediate precipitation of bismuth tris(hexylenedithiophosphate).

Mixed chloride alkylenedithiophosphates of arsenic(III) and antimony(III) have been prepared either by the co-disproportionation reactions between metal trichlorides and metal tris(alkylenedithiophosphates) at different (2:1 and 1:2) stoichiometric ratios or by the reaction of antimony trichloride with ammonium alkylenedithio-

phosphate at 1:1 and 1:2 molar ratios:



(M = As or Sb; $n$ = 1 or 2).



($n$ = 1 or 2).

Table 2. $^1$H NMR spectral data for some alkylenedithiophosphates of arsenic(III), antimony(III) and bismuth(III)

| Sl. No. | Compound | Chemical shifts ($\delta$) (ppm)* |
|---|---|---|
| 1 | $[OCH(Me)CH(Me)OPS_2]_3As$ | 1.40–1.54 [$q$ (four peaks), 18H, $CH_3$]<br>4.30 [$s$ (broad), 6H, CHO] |
| 2 | $[OCH(Me)CH(Me)OPS_2]_3Bi$ | 1.46–1.57 ($d$, 18H, $CH_3$)<br>4.20–4.90 ($m$, 6H, CHO) |
| 3 | $[OC(Me)_2CH_2CH(Me)OPS_2]_3As$ | 1.42–2.24 ($m$, 33H, $CH_3$, $CH_2$)<br>4.88 [$s$ (broad, 3H, CHO] |
| 4 | $[OC(Me)_2CH_2CH(Me)OPS_2]_3Sb$ | 1.42–2.24 ($m$, 33H, $CH_3$, $CH_2$)<br>4.90 $s$ (broad, 3H, CHO] |
| 5 | $[OC(Me)_2CH_2CH(Me)OPS_2]_3Bi$ | 1.35–2.20 ($m$, 33H, $CH_3$, $CH_2$)<br>4.75 [$s$ (broad), 3H, CHO] |
| 6 | $[OCH_2C(Me)_2CH_2OPS_2]_3Sb$ | 1.13 ($s$, 18H, $CH_3$)<br>4.00–4.28 ($d$, 12H, $CH_2O$) |
| 7 | $[OCH_2C(Et)_2CH_2OPS_2]_3As$ | 0.78–0.97 ($t$, 18H, $CH_3$)<br>1.37–1.56 ($q$, 12H, $CH_2$)<br>4.12–4.27 ($d$, 12H, $CH_2O$) |
| 8 | $[OCH_2C(Et)_2CH_2OPS_2]_3Sb$ | 0.81–0.98 ($t$, 18H, $CH_3$)<br>1.38–1.57 ($q$, 12H, $CH_2$)<br>4.11–4.30 ($d$, 12H, $CH_2O$) |
| 9 | $[OCH_2C(Et)_2CH_2OPS_2]_3Bi$ | 0.78–1.04 ($t$, 18H, $CH_3$)<br>1.37–1.61 ($q$, 12H, $CH_2$)<br>4.12–4.40 ($d$, 12H, $CH_2O$) |

* $d$, doublet; $m$, multiplet; $q$, quartet; $s$, singlet; $t$, triplet.

All these reactions are quite facile and are carried out by heating the reactants in benzene for about 1 h.

Metal tris(alkylenedithiophosphates) are yellow crystalline solids or yellow powders. A few of these are soluble in common organic solvents while others are insoluble (Table 1). All of these, however, are insoluble in water and do not show any tendency to hydrolyse even after long contact. These compounds are non-volatile even under reduced pressure and generally melt with decomposition except for the pinacol derivatives which do not melt even up to 300°C. The soluble compounds amongst these are found to be monomeric in freezing as well as in refluxing benzene.

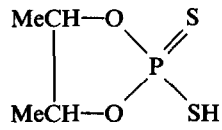
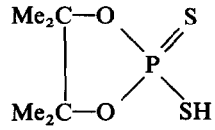
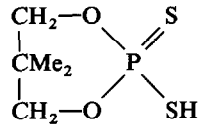
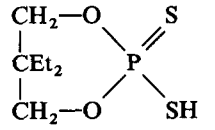
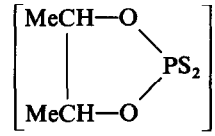
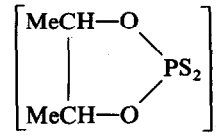
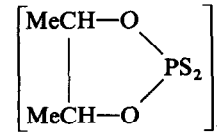
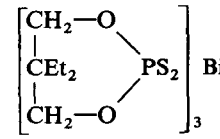
Mixed chloride alkylenedithiophosphate derivatives of arsenic and antimony are yellow sticky solids or yellow viscous liquids. When prepared freshly these are soluble in benzene, $CHCl_3$ and $CCl_4$ and are monomeric in nature. However, on standing for a few days they tend to become partially insoluble in these solvents.

IR spectra of these new derivatives have been recorded in the region 4000–200 $cm^{-1}$ and tentative assignments have been made on the basis of earlier reports.[14,15,17,20,21] The bands present in the region 1090–980 and 880–770 $cm^{-1}$ have been assigned to (P)–O–C and P–O–(C) stretching vibrations respectively. A strong band (also of medium intensity in some of the cases) in the region 940–910 $cm^{-1}$ is most probably due to the dioxaphospholane and dioxaphosphorinane rings.[22] A strong band present in the region 685–620 $cm^{-1}$ in alkylenedithiophosphoric acids and assigned to $\nu$(P=S) does not appear to be shifted in arsenic and antimony complexes but a shifting of 50–25 $cm^{-1}$ towards lower wave numbers is observed in the corresponding bismuth complexes, this shifting is probably due to comparatively strong bidentate chelation in bismuth complexes. The bands of medium intensities in the region 600–485 $cm^{-1}$ may be attributed to $\nu$(P—S) asymmetric and symmetric vibrations. The bands of medium intensities in the region 400–200 $cm^{-1}$ are most probably due to $\nu$(M—S)[23,24] and $\nu$(M—Cl).[25]

The $^1$H NMR spectra of the soluble compounds have been recorded in $CCl_4$ or $CDCl_3$ and the data are summarised in Table 2. The spectra show the characteristic proton resonances for the corresponding alkylene moieties. The coupling of α-protons of alkylene groups with phosphorus is also observed.

$^{31}$P NMR spectral data for some alkylenedithiophosphoric acids and a few representative metal derivatives have been recorded in $CDCl_3$ solutions. In the proton-decoupled $^{31}$P NMR spectra only one $^{31}$P chemical shift for each compound is observed (Table 3).

Table 3. $^{31}$P NMR spectral data for alkylenedithiophosphoric acids and their arsenic(III), antimony(III) and bismuth(III) derivatives

| Sl. No. | Compound | $^{31}$P chemical shift (δ) (ppm) |
|---|---|---|
| 1 |  | 95.49 |
| 2 |  | 93.07 |
| 3 |  | 78.58 |
| 4 |  | 77.80 |
| 5 |  | 103.23 |
| 6 |  | 107.93 |
| 7 |  | 115.29 |
| 8 |  | 97.90 |

The $^{31}$P chemical shift values appear to be dependent on the size of the heterocyclic ring. In the spectra of dioxaphospholanes (where the ring is five-membered) the chemical shift values are between 93 and 96 ppm (in parent acids) and between 103 and 116 ppm (in corresponding arsenic, antimony and bismuth complexes), while in the corresponding dioxaphosphorinane derivatives (where the ring is six-membered) the chemical shift values are between 77 and 79 ppm (in the parent acids) and 97.9 ppm (for a bismuth complex). Like open-chain dialkyldithiophosphates,[10,11,26] the $^{31}$P chemical shift

values observed in parent alkylenedithiophosphoric acids are shifted towards down field in the corresponding arsenic, antimony and bismuth complexes (by 8–20 ppm) and this shifting is in the order As < Sb < Bi.

Preliminary X-ray investigations, details of which would be published elsewhere, show that $[OCHCH_3CHCH_3OPS_2]_3Bi$ has a distorted octahedral structure.

*Acknowledgements*—One of the authors (H. P. S. Chauhan) wishes to thank the University Grants Commission for the financial support in the form of a Senior Research Fellowship under the Special Assistance Programme and to Prof. B. N. Bhattacharya, Head, Regional Sophisticated Instrumentation Centre, Indian Institute of Technology, Bombay for recording $^{31}P$ NMR spectra.

## REFERENCES

1. A. I. Busev and M. I. Ivanyutin, *Tr. Kom. Anal. Khim., Akad. Nauk SSSR* 1960, **11**, 172; *Chem. Abstr.* 1961, **55**, 24381.
2. I. S. Levin, Yu. M. Yukhin, I. A. Bykhovskaya, I. A. Vorsina and V. V. Sergeeva, *Ser. Khim. Nauk* 1973, **5**, 83; *Chem. Abstr.* 1974, **80**, 7593.
3. I. S. Levin, V. V. Sergeeva and I. A. Vorsina, *Ser. Khim. Nauk* 1975, **2**, 107; *Chem. Abstr.* 1975, **83**, 66255.
4. H. H. Farmer, B. W. Malone and H. F. Tompkins, *Lubr. Eng.* 1967, **23**, 57.
5. U.S. Patent 3,428,563; *Chem. Abstr.* 1969, **70**, 69976.
6. L. S. Kharchenko, G. G. Kupko, G. M. Rykhlevskii and Yu. T. Tordash, *Khim. Tekhnol. Topl. Masel* 1974, **1**, 46; *Chem. Abstr.* 1974, **81**, 123954.
7. Belgian Patent, 845,345; *Chem. Abstr.* 1978, **88**, 25448.
8. D. L. McKay, Fr. Demande 2,362,207; *Chem. Abstr.* 1979, **90**, 41172.
9. R. O. Day, M. M. Chauvin and W. E. McEwen, *Phosphorus Sulfur* 1980, **8**, 121.
10. H. P. S. Chauhan, G. Srivastava and R. C. Mehrotra, *Polyhedron* 1983, **2**, 359.
11. H. P. S. Chauhan, G. Srivastava and R. C. Mehrotra, *Phosphorus Sulfur* 1983, **17**, 161.
12. D. B. Sowerby, I. Haiduc, A. B. Rusu and M. Salajan, *Inorg. Chim. Acta* 1983, **68**, 87.
13. S. L. Lawton, C. J. Fuhrmeister, R. G. Hass, C. S. Jarman and F. G. Lothmeyer, *Inorg. Chem.* 1974, **13**, 135.
14. H. P. S. Chauhan, C. P. Bhasin, G. Srivastava and R. C. Mehrotra, *Phosphorus Sulfur* 1983, **15**, 99.
15. R. J. Rao, G. Srivastava and R. C. Mehrotra, *J. Organomet. Chem.* 1983, **258**, 155.
16. C. P. Bhasin, G. Srivastava and R. C. Mehrotra, *Inorg. Chim. Acta* 1983, **77**, L131.
17. B. P. Singh, G. Srivastava and R. C. Mehrotra, *J. Organomet. Chem.* 1979, **171**, 35.
18. H. P. S. Chauhan, G. Srivastava and R. C. Mehrotra, *Synth. React. Inorg. Met.-Org. Chem.* 1981, **11**, 565.
19. A. I. Vogel, *Quantitative Inorganic Analysis*, 3rd edition. Longman, London (1961).
20. D. E. C. Corbridge, *Top. Phosphorus Chem.* 1969, **6**, 235.
21. J. R. Wasson, G. M. Woltermann and H. J. Stoklosa, *Top. Curr. Chem.* 1973, **35**, 65.
22. R. A. Y. Jones and A. R. Katritzky, *J. Chem. Soc.* 1960. 4376.
23. T. B. Brill and N. C. Campbell, *Inorg. Chem.* 1973, **12**, 1884.
24. D. M. Adams and J. B. Cornell, *J. Chem. Soc. A* 1968, 1299.
25. E. Maslowsky, Jr, *J. Organomet. Chem.* 1974, **70**, 153.
26. C. Glidewell, *Inorg. Chim. Acta* 1977, **25**, 159.

*Polyhedron* Vol. 3, No. 12, pp. 1347–1350, 1984
Printed in Great Britain

0277-5387/84 $3.00 + .00
© 1984 Pergamon Press Ltd

# INFRARED SPECTRA OF $\eta^5$-CYCLOPENTADIENYLBERYLLIUM CHLORIDE AND BROMIDE AND OF DICYCLOPENTADIENYLBERYLLIUM: A COMPARATIVE STUDY

**S. J. PRATTEN, M. K. COOPER and M. J. ARONEY***
Department of Inorganic Chemistry, University of Sydney, Sydney, N.S.W., 2006, Australia

(*Received* 16 *April* 1984; *accepted* 9 *July* 1984)

**Abstract**—The IR spectra of $\eta^5$-cyclopentadienylberyllium chloride and bromide and of dicyclopentadienylberyllium in solution are compared. Evidence is given for *pentahapto*- and *monohapto*-attachment of the cyclopentadienyl rings for the structure of dicyclopentadienylberyllium in solution.

Since the discovery of dicyclopentadienylberyllium,[1] $Cp_2Be$, its structure and bonding have been in doubt. Spectroscopic and diffraction studies have led to structural interpretations which are often in conflict.[2–12] $Cp_2Be$ is dipolar in solution[13,14] indicating that, in this state at least, it does not have a metallocene $D_{5d}$ or $D_{5h}$ structure. The observation of a sharp proton singlet in the NMR spectrum down to $-135°C$ is clear evidence for fluxional behaviour.[15] An X-ray study of the crystal at $-120°C$ indicated a slip sandwich structure with the two cyclopentadiene rings parallel and the Be $\pi$-bonded ($\eta^5$) to one ring and $\sigma$-bonded ($\eta^1$) to the other.[16] Theoretical MO studies[12,17–21] suggest $\pi$-Cp, $\sigma$-Cp bonding and generally favour a non-parallel arrangement of the rings, as required by a localised Cp group with a tendency towards tetrahedral geometry about the carbon atom $\sigma$-bonded to Be (Fig. 1).

In this work a comparative study was made of the solution IR spectra of $Cp_2Be$ and of $\eta^5$-cyclopentadienylberyllium chloride and bromide, CpBeX (X = Cl or Br). From this we propose the solution-state structure of $Cp_2Be$.

## EXPERIMENTAL

All operations, except where otherwise stated, were carried out under oxygen-free dry nitrogen using Schlenk techniques. Analytical-grade diethylether was distilled immediately prior to use from sodium wire and benzophenone under an atmosphere of nitrogen. All other solvents were dried over phosphorus pentoxide or molecular sieves and were outgassed with nitrogen.

IR spectra were recorded from 4000 to 250 $cm^{-1}$ on a Perkin–Elmer 457 double-beam grating spectrophotometer using a 0.2-mm pathlength KBr solution cell or a 1.0 mm pathlength polyethylene cell in the sample beam. Different solvents were used to overcome the problem of solvent absorption. Polystyrene was used as the calibrant.

NMR spectra were recorded on a Jeol FX60Q spectrometer. The solutions containing TMS as internal reference were sealed under nitrogen in 5-mm tubes.

### *Syntheses*

$Cp_2Be$ was prepared by the method of Fischer and Hofmann.[1] Yields of up to 90% were obtained when

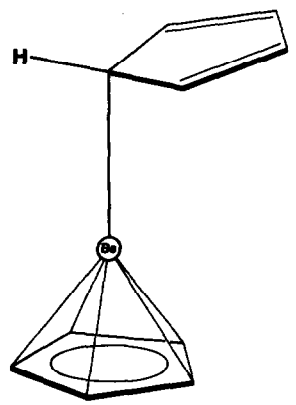



Fig. 1.

* Author to whom correspondence should be addressed.

a two-fold excess of sodium cyclopentadienide was used. The product was purified by vacuum sublimation to yield colourless air- and moisture-sensitive crystals [m.p. 59°C, lit. 59–60°C (Ref. 1)]. CpBeCl was prepared by reacting molten $Cp_2Be$ with an excess of finely divided beryllium chloride for 2 h.[22] The product was removed and vacuum sublimed to yield colourless crystals [m.p. 43–44°C, lit. 43–44°C (Ref. 22)]. CpBeBr was prepared using the following synthesis.* A two-fold stoichiometric excess of $Cp_2Be$ dissolved in diethylether was added to anhydrous iron(II) bromide in diethylether with stirring at −78°C. The mixture was allowed to warm to room temperature and stirred for a further 2 h. After the solvent was removed under reduced pressure a cold trap (0°C) was connected to the reaction flask and colourless crystals slowly sublimed (0.1 mm Hg) at room temperature into the trap in low yield. The ferrocene ($Cp_2Fe$) by-product and the unreacted $Cp_2Be$ remained in the reaction flask. The product, apparently more volatile than $Cp_2Be$, was found to have a singlet at $\delta$ 6.29 ppm ($C_6D_{12}$) in the proton NMR. The mass spectrum recorded at a source temperature of 65°C, inlet temperature of 40°C and an ionising voltage of 70 eV, showed parent peaks of nearly equal abundance at 153 and 155 mass units ($^{79}Br$ 50.54% and $^{81}Br$ 49.46% natural abundance).

## RESULTS AND DISCUSSION

The solution spectra of $Cp_2Be$, CpBeCl and CpBeBr are recorded in Table 1 together with the spectra of $Cp_2Fe$, $\eta^1$-cyclopentadienylmercury chloride (CpHgCl) and $\eta^1,\eta^1$-dicyclopentadienylmercury ($Cp_2Hg$), which are included for comparison.

The IR spectrum of $Cp_2Be$ now reported agrees essentially with the solution-state spectrum of Fritz and Sellman.[8] Our solution spectrum of CpBeCl resembles, though it is not identical with, the spectra reported for the low-temperature solid state.[24,25] The literature contains a vapour-phase spectrum of CpBeBr which, however, lists only a few absorptions.[22] No significant change was found in the IR spectra of the compounds examined with variation of solvent ($CS_2$, $C_6D_{12}$ and $CDCl_3$).

The dominant feature of the spectra of CpBeCl and CpBeBr is the occurrence of very intense bands at 994 and 898 $cm^{-1}$ (CpBeCl) and at 973 and 899 $cm^{-1}$ (CpBeBr). In a spectral comparison of the two halides the most significant difference is the change of the 994-$cm^{-1}$ peak in the chloride to 973 $cm^{-1}$ in the bromide. These absorptions are thus attributed to the respective Be–halogen stretches. Gaseous, monomeric beryllium chloride has an antisymmetric stretching frequency of 1113 $cm^{-1}$, reflecting the shorter Be–Cl bond length.[26,27] The other absorptions at 898 and 899 $cm^{-1}$, which are virtually invariant for the two halides (and for which no comparable absorptions exist in the spectrum of $Cp_2Fe$), are assigned to the Be–$\eta^5$–Cp stretch. Be is known to have a *pentahapto*-attachment to Cp for all states of CpBeX.[28,29] The similarity of the Cp groups in the two CpBeX complexes is underscored by the near-identical proton NMR shifts of $\delta$ 6.27 ppm for CpBeCl and 6.29 ppm for CpBeBr (in $C_6D_{12}$). Assignment of very intense absorptions to vibrations involving Be would reasonably be expected as the small size and high charge density and hence high polarising power of this atom will result in a substantive change of the bond dipole with vibrational movement.[30] For example the most intense band in the IR spectrum of di-t-butylberyllium, assigned by comparison with the spectrum of the deuterated analogue, is that of the anti-symmetric Be–C stretch.[31] The remaining bands in the spectra of CpBeCl and CpBeBr between 4000 and *ca* 700 $cm^{-1}$ (other than combinations and overtones that occur between *ca* 1600 and 3000 and near 4000 $cm^{-1}$) compare closely with absorptions in $Cp_2Fe$ and are due to vibrational modes associated with the centrally bonded *pentahapto*-Cp rings.[30] The Be–Cp stretching frequencies for CpBeCl and CpBeBr are predictably higher than the Fe–Cp stretch of $Cp_2Fe$ (484 $cm^{-1}$ by analogy with data in Ref. 30). Be–halogen and Be–ring deformation modes would be expected to be below *ca* 700 $cm^{-1}$. These bands are very difficult to observe due to the high absorption of the polyethylene cells used—no attempt has been made to assign them.

The spectrum of $Cp_2Be$ is more complicated than those of the other solutes with which it is compared (Table 1). McVicker and Morgan[9] have reported that the gas-phase spectrum of $Cp_2Be$ is significantly simpler than that of the solid state and they attribute this to a "change from considerable central $\sigma$-bonding of the metal to the rings in the solid state to predominantly ionic character in the gas phase". This interpretation is suspect since the reported gas-phase spectrum closely resembles our solution-state spectra for low solute concentrations where only the strongest absorptions are apparent. The ease of sublimation of $Cp_2Be$ and its ready solubility in organic solvents also attest to its predominantly covalent character.

The spectrum of $Cp_2Be$ shows all the bands in the spectra of CpBeCl and CpBeBr which are due to the

* Beryllium bromide was not available to us.

Table 1.

| $Cp_2Fe$[a] | $CpBeBr$[b] | $CpBeCl$[c] | $Cp_2Be$[d] | $CpHgCl$[e] | $Cp_2Hg$[f] |
|---|---|---|---|---|---|
| | 3980 vw | 3980 vw | 3970 w | | |
| | | | 3910 w | | |
| | | | 3170 vw | | |
| | | | | 3105 m | 3090 s |
| | | | 3110 sh | 3098 m | 3088 s |
| 3090 s | 3120 m | 3120 ms | 3080 s | 3072 s | 3076 sh |
| | | | 3050 sh | 3040 w | 3040 sh |
| | | | | 2950 w | 2970 w |
| | 2700 vw | 2700 m | 2710 w | | |
| | | 2495 w | 2500 vw | | |
| | 2420 vw | 2420 m | 2420 w | | |
| | 2275 vw | 2275 mw | | | |
| | 2065 vw | 2085 m | 2085 w | | |
| | 1835 w | 1840 m | 1818 w | 1830 w | 1808 w |
| | | | | 1810 w | |
| 1755 mw | 1742 m | 1745 ms | 1737 m | | |
| 1715 vw | | | | | |
| 1680 w | 1590 mw | 1615 m | 1605 m | | 1630 w |
| | | | | 1543 w | 1530 w |
| 1410 ms | 1430 m | 1427 ms | 1428 m | 1461 m | 1427 m |
| | | | 1410 sh | | |
| | | | 1365 m | 1379 m | 1383 m |
| | | | 1305 vw | 1290 m | 1296 m |
| | | 1260 w | | | |
| | | | 1235 vw | 1228 m | 1234 m |
| 1106 s | 1125 s | 1125 s | 1124 s | | |
| | | | 1106 w | 1108 w | 1109 m |
| | | 1090 mw | 1090 sh | | |
| | | | 1074 mw | 1089 m | 1084 m |
| 1050 w | 1060 vw | 1062 mw | 1060 sh | | |
| | | | | 1026 m | 1026 m |
| 1003 s | 1017 s | 1017 s | 1015 s | | |
| | | | | 990 m | 988 m |
| | | 994 vvs+ | | | |
| | 973 vvs+ | | | | |
| | | | 965 vs,b+ | | |
| | | | | 962 m | 957 m |
| | | | 915 sh | 941 s | 907 vs |
| | 899 vvs+ | 898 vs+ | | | |
| | | | 890 sh | 902 s | 885 vs |
| | 880 sh | | | 885 w | |
| 855 vw | 860 sh | 860 ms | 862 ms | | |
| 835 w | | 835 mw | 829 m | 819 m | 822 m |
| 814 s | | | | | |
| 780 w | 775 mw | 780 s | 785 sh | | |
| | | | 770 ms | 756 vs | 748 vs |
| | | | 740 vs+ | | |
| | 730 vw | 730 vw | | 720 w | 720 w |
| | | 685 vw | | | |
| | | | 663 s | 653 s | 646 s |
| | 610 vw | 610 vw | 590 vw | | |
| | | | | 565 w | 575 w |
| 499 s+ | 500 vw | 495 w | | | |
| 484 ms+ | 480 vw | 475 w | | | |
| | 410 vw | | 425 w | | |
| | | | | 359 s+ | 348 s+ |
| | | 312 ms | 313 w | | |

v, very; s, strong; m, medium; w, weak; sh, shoulder; b, broad.

+ Metal–ligand vibration.

[a] Present work—recorded in $CS_2$.

[b] Present work—recorded in $CS_2$ and $C_6D_{12}$.

[c] Present work—recorded in $CS_2$.

[d] Present work—recorded in $CS_2$ and $CDCl_3$.

[e] Quoted from Ref. 23 (in $CS_2$).

[f] Quoted from Ref. 23 (in $CS_2$ and $CHCl_3$).

*pentahapto*-ring. The remaining absorptions compare well with the bands previously assigned[23] to Cp ring vibrational modes in the spectra of CpHgCl and $Cp_2Hg$ (for which the rings are known to be *monohapto* and fluxional). Both $\pi$-bonded and $\sigma$-bonded Cp groups have been found to exhibit consistent and characteristic absorption patterns in the various metal–Cp complexes (Ref. 30, p. 391, and Ref. 32). It is concluded that in the solution state $Cp_2Be$ is *pentahapto*-bonded to one Cp ring and *monohapto* to the other. This instantaneous structure for $Cp_2Be$ in the solution state satisfies the well-established preference shown by Be for covalent bonding and a maximum coordination number of four.[28] The bands at 965 and 740 $cm^{-1}$ deserve comment. Their high intensity relative to all other absorptions in the spectrum suggests that they are due to stretching vibrations involving Be atom displacements. The broad band at 965 $cm^{-1}$ (which possibly obscures a weaker $\eta^1$-Cp ring deformation absorption in that region[8]) could reasonably be assigned to the Be–*pentahapto*-ring stretch on the basis of its greater bond strength. The peak at 740 $cm^{-1}$, though assigned to a CH vibration mode by Fritz and Sellman,[8] could on such grounds be due to the Be–*monohapto*-ring vibration.

*Acknowledgement*—The award of a Commonwealth Research Studentship to S. J. Pratten is gratefully acknowledged.

## REFERENCES

1. E. O. Fischer and H. P. Hofmann, *Chem. Ber.* 1959, **92**, 482.
2. A. Almenningen, O. Bastiansen and A. Haaland, *J. Chem. Phys.* 1964, **40**, 3434.
3. A. Haaland, *Acta Chem. Scand.* 1968, **22**, 3030.
4. A. Almenningen, A. Haaland and J. Lusztyk, *J. Organometal. Chem.* 1979, **170**, 271.
5. H. P. Fritz, *Chem. Ber.* 1959, **92**, 780.
6. H. P. Fritz and R. Schneider, *Chem. Ber.* 1960, **93**, 1171.
7. H. P. Fritz, *Adv. Organometal. Chem.* 1964, **1**, 262.
8. H. P. Fritz and D. Sellman, *J. Organometal. Chem.* 1966, **5**, 501.
9. G. B. McVicker and G. L. Morgan, *Spectrochim. Acta* 1970, **26A**, 23.
10. G. L. Morgan and G. B. McVicker, *J. Am. Chem. Soc.* 1968, **90**, 2789.
11. J. Lusztyk and K. B. Starowieyski, *J. Organometal. Chem.* 1979, **170**, 293.
12. R. Gleiter, M. C. Böhm, A. Haaland, R. Johansen and J. Lusztyk, *J. Organometal. Chem.* 1979, **170**, 285.
13. E. O. Fischer and S. Schreiner, *Chem. Ber.* 1959, **92**, 938.
14. W. Strohmeier and D. von Hobe, *Z. Elektrochem.* 1960, **64**, 945.
15. C. H. Wong and S. M. Wang, *Inorg. Nucl. Chem. Lett.* 1975, **11**, 677.
16. C. H. Wong, T. Y. Lee, K. J. Chao and S. Lee, *Acta Crystallogr.* 1972, **B28**, 1662.
17. D. S. Marynick, *J. Am. Chem. Soc.* 1977, **99**, 1436.
18. M. J. S. Dewar and H. S. Rzepa, *J. Am. Chem. Soc.* 1978, **100**, 777.
19. N. S. Chiu and L. Schäfer, *J. Am. Chem. Soc.* 1978, **100**, 2604.
20. E. D. Jemmis, S. Alexandratos, P. R. Schleyer, A. Streitwieser and H. F. Schaefer, *J. Am. Chem. Soc.* 1978, **100**, 5695.
21. J. Demuynck and M. M. Rohmer, *Chem. Phys. Lett.* 1978, **54**, 567.
22. D. A. Drew and G. L. Morgan, *Inorg. Chem.* 1977, **16**, 1704.
23. E. Maslowsky and K. Nakamoto, *Inorg. Chem.* 1969, **8**, 1108.
24. D. A. Coe, J. W. Nibler, T. H. Cook, D. Drew and G. L. Morgan, *J. Chem. Phys.* 1975, **63**, 4842.
25. K. B. Starowieyski and J. Lusztyk, *J. Organometal. Chem.* 1977, **133**, 281.
26. A. Büchler and W. Klemperer, *J. Chem. Phys.* 1958, **29**, 121.
27. D. A. Drew and A. Haaland, *Acta Chem. Scand.* 1972, **26**, 3351.
28. N. A. Bell, *Comprehensive Organometallic Chemistry* (Edited by G. Wilkinson, F. G. A. Stone and E. W. Abel), Chap. 3. Pergamon Press, Oxford (1982).
29. A. Bjørseth, D. A. Drew, K. M. Marstokk and H. Møllendal, *J. Mol. Struct.* 1972, **13**, 233.
30. K. Nakamoto, *Infrared and Raman Spectra of Inorganic and Coordination Compounds.* Wiley–Interscience, New York (1978).
31. G. E. Coates, P. D. Roberts and A. J. Downs, *J. Chem. Soc. (A)* 1967, 1085.
32. D. M. Adams, *Metal–Ligand and Related Vibrations*, p. 189. Edward Arnold, London (1967).

*Polyhedron* Vol. 3, No. 12, pp. 1351–1355, 1984
Printed in Great Britain

0277–5387/84 $3.00 + .00
© 1984 Pergamon Press Ltd

# UNUSUAL DEMETHYLATION OF 1-DIMETHYLAMINE-1-CARBA-*CLOSO*-DODECABORANE(11)

**JAROMÍR PLEŠEK, TOMÁŠ JELÍNEK and BOHUMIL ŠTÍBR***
Institute of Inorganic Chemistry Prague, Czechoslovak Academy of Sciences, 250 68 Řež near Prague, Czechoslovakia

(*Received* 16 *May* 1984; *accepted* 9 *July* 1984)

**Abstract**—1-Dimethylamine-1-carba-*closo*-dodecaborane(11), 1-$(CH_3)_2NH$-1-$CB_{11}H_{11}$, can be smoothly demethylated with iodine in weakly alkaline solution to produce 1-methylamine-1-carba-*closo*-dodecaborane(11), 1-$CH_3NH_2$-1-$CB_{11}H_{11}$. The latter compound undergoes formylation with formaldehyde and iodine to give 1-hydroxymethylene-methylamine-1-carba-*closo*-dodecaborane(11). Further chemical transformations of both compounds are reported.

We have recently[1] described the reaction of *nido*-7-$(CH_3)_3N$-7-$CB_{10}H_{12}$ with triethylamineborane, resulting in a high-yield isolation of 1-dimethylamine-1-carba-*closo*-dodecaborane(11), 1-$(CH_3)_2NH$-1-$CB_{11}H_{11}$ (**I**). Its methylation in alkaline solution produced the *N*-trimethyl derivative, 1-$(CH_3)_3N$-1-$CB_{11}H_{11}$ (**IIb**), which can be easily deaminated to the parent anion, $[1\text{-}CB_{11}H_{12}]^-$, with sodium in liquid ammonia. We wish to report herein further reactions of the *N*-dimethyl derivative leading to some other interesting *C*-substituted compounds of the $[CB_{11}H_{12}]^-$ family.

## EXPERIMENTAL

### *Physical measurements*

$^1H$ (60 MHz) and $^{11}B$ (64.18 MHz) NMR spectra in hexadeuterioacetone were recorded on a Tesla BS 467 and a Varian XL-200 spectrometer, respectively: chemical shifts are given in $\delta$-values [ppm, referenced to tetramethylsilane and $BF_3$-$O(C_2H_5)_2$, positive values downfield]. IR spectra were obtained in nujol mulls using a Perkin–Elmer 684 spectrometer. Mass spectra were collected at 70 eV on a GC/MS HP-5989 device. TLC was performed on Silufol sheets [silica gel on aluminium foil (Kavalier n.p., Votice, Czechoslovakia): detection by $I_2$ vapours followed by $AgNO_3$ spray] in acetonitrile–chloroform (1 : 3). The $pK_a$ values were determined by potentiometric titration in 50% ethanol.

### *Chemicals*

The starting compound *closo*-1-$(CH_3)_2NH$-1-$CB_{11}H_{11}$ was prepared according to the recently described procedure.[1] Tetrahydrofuran and ether were distilled with $NaAlH_2(OC_2H_4OCH_3)_2$ prior to use. Other chemicals were reagent grade and used as received.

### *Syntheses*

Except for operations involving manipulation with sodium hydride, performed under dry nitrogen, no inert atmosphere is required in other syntheses due to the relatively high stability of the compounds involved. Properties of all the isolated derivatives are summarized in Tables 1 and 2.

### *Demethylation of* I

A solution of **I** (5.6 g, 0.03 mol) and sodium carbonate (11.0 g, 0.1 mol) in water (250 $cm^3$) was stirred with iodine (7 g, 0.03 mol) until the solution had decolourized (*ca* 6 h). The mixture was then filtered, acidified with conc. hydrochloric acid (30 $cm^3$) and the last traces of iodine were removed with sodium sulphite (2.0 g). The voluminous white precipitate was filtered, washed with three 30-$cm^3$ portions of water and dried in air to recover 1.4 g (25%) of the starting compound **I** (identified by its $^1H$ and $^{11}B$ NMR spectra). Trimethylamonium hydrochloride (2.5 g, 0.025 mol) in water (10 $cm^3$) was added to separate a white precipitate of $[(CH_3)_4N]^+[1\text{-}O\text{-}CH{=}(CH_3)N\text{-}1\text{-}CB_{11}H_{11}]^-$ (**IIIa**) which was filtered, washed twice with water (50

* Author to whom correspondence should be addressed.

Table 1. Properties of 1-L-1-$CB_{11}H_{11}$ compounds.

| Compound | $R_F$ | *m/z* | δ ($^1$H NMR) | | | δ ($^{11}$B NMR) | | |
|---|---|---|---|---|---|---|---|---|
| | | | $CH_3N$ | $[(CH_3)_4N]^+$ | Other | B(12) | B(5–11) | B(2–6) |
| **I** | 0.57 | 189 | 3.14 | — | — | −8.37 | −16.65 | −15.69 |
| **II** | 0.35 | 175 | 2.88* | — | 8.98† | −9.93 | −13.70 | −15.77 |
| **IIa** | 0.35 | — | 2.50 | 3.45 | — | −12.95 | −14.40 | −14.40 |
| **IIb** | 0.59 | 203 | 3.47 | — | — | −7.40 | −13.63 | −15.07 |
| **IIc** | 0.62 | 203 | 3.08 | — | 3.55‡<br>1.40§ | — | — | — |
| **III** | 0.10 | 203 | 3.26 | — | — | −9.92 | −14.45 | −14.45 |
| **IIIa** | 0.10 | — | 2.82 | 3.45 | 8.45‖ | −9.92 | −14.45 | −14.45 |
| **IIIb** | 0.18 | — | 3.31 | — | 7.66¶ | −7.10 | −13.89 | −13.89 |
| **IIIc** | 0.18 | — | 2.91 | 3.45 | 7.37¶ | −8.88 | −13.50 | −14.57 |

* Triplet.
† Broad $NH_2$ singlet.
‡ $(CH_3)CH_2$ quartet.
§ $CH_3(CH_2)$ triplet.
‖ CH=N signal.
¶ $C_6H_5$ signal.

$cm^3$) and dissolved in 5% aqueous potassium hydroxide (30 $cm^3$). The trimethylamine evolved was removed *in vacuo*, the solution was filtered, the clear filtrate was acidified with conc. hydrochloric acid (20 $cm^3$) and extracted with two 30-$cm^3$ portions of ether. The semi-solid residue, remaining after evaporating the ether *in vacuo*, was dried at 120°C/1.3 Pa to obtain 0.6 g (10%) of the formyl derivative 1-HO-CH=$(CH_3)$N-1-$CB_{11}H_{11}$ (**III**). The filtrate obtained after removing the **IIIa** anion was extracted twice with ether (50 $cm^3$), the ether layer was separated and stripped off *in vacuo* to give a

Table 2. IR spectra of compounds **III**–**IIIc** and their assignment.

| **III** | **IIIa** | **IIIb** | **IIIc** | Assignment |
|---|---|---|---|---|
| 3618 (m) | — | 3590 (w) | — | ν(O—H) |
| 3545 (m) | — | 3220 (m) | — | ν(N—H) |
| 3400 (m) | — | — | — | $\nu_{assoc}$(O—H) |
| 2550 (vs) | 2520 (vs) | 2550 (vs) | 2515 (vs) | ν(B—H) |
| 1680 (vs) | 1655 (vs) | 1590–1570* | 1660–1640* | ν(C=O) |
| 1630 (sh) | — | 1625 (m) | — | ν(C=N) |
| — | — | 1605 (m) | 1610 (m) | ν(C—C) ring |
| — | 1485 (s) | — | 1485 (s) | $\delta_{asym}(CH_3—N)$ |
| — | — | 1445 (s) | 1440 (s) | ν(C—C) ring |
| 1420 (m) | 1415 (m) | 1420 (m) | 1415 (m) | $\delta_{sym}(CH_3{}^tN)$ |
| — | 1350 (s) | — | 1360 (s) | |
| 1337 (s) | 1265 (m) | 1270 (m) | 1270 (m) | ν(C—N) amidic |
| — | — | 1210 (m) | 1210 (m) | |
| 1125 (s) | 1125 (s) | — | — | |
| — | — | 1075 (m) | 1070 (m) | |
| 1060 (m) | — | 1060 (m) | — | ν(C—O) |
| 1050 (m) | 1050 (m) | 1050(m) | 1050 (m) | $CB_{11}H_{11}$ skeletal |
| 985 (m) | 990 (m) | — | — | |
| 955 (m) | 950 (m) | 945 (m) | 950 (m) | $\nu_{asym}$(C—N) |
| 765 (m) | 765 (m) | 775 (m) | 775 (m) | $\nu_{sym}$(C—N) |
| — | — | 710 (m) | 710 (m) | δ(C—H) ring |

* Doublet of the *cis*- and *trans*-forms.

white solid which was washed with benzene (50 $cm^3$) and air dried to isolate 3.3 g (63%) of 1-$CH_3NH_2$-1-$CB_{11}H_{11}$ (**II**).

$[(CH_3)_4N]^+[1\text{-}CH_3NH\text{-}1\text{-}CB_{11}H_{11}]^-$ (**IIa**)

To a solution of compound **II** (1.7 g, 0.01 mol) in 2% aqueous potassium hydroxide, 30 $cm^3$ of an aqueous solution containing tetramethylammonium iodide (2.5 g, 0.013 mol) were added. The separated precipitate was recrystallized from hot ethanol to obtain 1.9 g (85%) of the tetramethylammonium salt (**IIa**) as white leaflets.

**IIIa**

Compound **III** (1.0 g, 5 mmol) was dissolved in water (50 $cm^3$) and the solution was treated with 30 $cm^3$ of an aqueous solution containing tetramethylammonium iodide (1.5 g, 7 mmol). The separated coarse white precipitate was washed twice with hot water (50 $cm^3$) and air dried to give 1.2 g (65%) of the salt **IIIa**.

*Formylation of* **II**

Sodium carbonate (5.0 g, 0.03 mol) and compound **II** (1.7 g, 0.01 mol) were dissolved in water (150 $cm^3$). After adding paraformaldehyde (0.9 g, 0.03 mol) and iodine (7.1 g, 0.02 mol), the mixture was stirred at ambient temperature for 6 hr, filtered, acidified with diluted hydrochloric acid to slightly acidic reaction and decolourized with sodium sulphite (2.0 g). Addition of trimethylammonium hydrochloride (1.0 g, 0.01 mol) caused precipitation of the trimethylammonium salt of the *N*-formyl derivative (**III**) which was filtered and dissolved in aqueous potassium hydroxide. The evolved trimethylamine was removed *in vacuo*, the remaining solution was filtered and precipitated with tetramethylammonium iodide (2.0 g, 0.01 mol). The precipitate was filtered, washed with water and air dried to give 1.6 g (70.5%) of the salt **IIIa**. The recovered starting compound **II** (0.5 g, 29.4%) was obtained after working up the filtrate as in the first experiment (extraction with ether).

*Hydrolysis of* **III**

A solution of compound **III** (1.0 g, 5 mmol) in conc. hydrochloric acid (10 $cm^3$) was heated on a water bath for 3 hr. After cooling down to ambient temperature, it was extracted twice with ether (30 $cm^3$). Pure compound **II** [identified by TLC and $^1H$ NMR spectrum (0.8 g, 95%)] was obtained on removing the ether *in vacuo* and drying the residue in air.

*Improved preparation of* **II**

To a solution containing compound **I** (11.2 g, 0.06 mol) and sodium carbonate (21.1 g, 0.2 mol) in water (350 $cm^3$), iodine (24.0 g, 0.095 mol) was successively added in four 6-g doses. After stirring for 8 hr, the mixture was filtered, acidified with conc. hydrochloric acid (60 $cm^3$) and the last traces of iodine were removed with sodium sulphite (5.0 g). The separated starting compound **I** (1.4 g, 12.5%) was recovered after filtering and drying it in air. The clear filtrate was extracted with two 100-$cm^3$ portions of ether, the combined organic extracts were stripped off *in vacuo*, the solid residue was dissolved in dilute (1 : 5) hydrochloric acid and heated in a water bath for 5 hr. The solution was then cooled, extracted twice with ether (50 $cm^3$) and the solid obtained after removing the ether *in vacuo* was dried at 80°C/1.3 Pa to give 8.9 g [84.7% (96.7% based on compound **I** consumed)] of compound **II**.

*Methylation of* **II**

To a solution of compound **II** (1.7 g, 0.01 mol) in tetrahydrofuran (50 $cm^3$), sodium hydride (1.0 g, 0.04 mol) and dimethyl sulphate (4 $cm^3$, 0.04 mol) were added and the mixture was stirred for 8 hr. The mixture was then filtered, the tetrahydrofuran was distilled off *in vacuo* and the solid residue was treated with hot methanol, filtered and dried. After recrystallization from an acetone–water mixture, 1.7 g (85%) of **IIb** was obtained.

*Ethylation of* **II**

To a solution of compound **II** (1.7 g, 0.01 mol) in tetrahydrofuran (50 $cm^3$), sodium hydride (1.0 g, 0.04 mol) and ethyl bromide (2 $cm^3$, 0.03 mol) were added and the mixture was left to stand for 48 hr. Ethanol (50 $cm^3$) and water (50 $cm^3$) were added to the mixture which was then filtered. The filtrate was then basified and refiltered. The filtrate was acidified with dilute hydrochloric acid, extracted with two 30-$cm^3$ portions of ether and the combined organic extracts were evaporated *in vacuo*. The solid residue was washed with dilute hydrochloric acid and dissolved in chloroform. After removing the chloroform *in vacuo*, the crude product was recrystallized from benzene to give 1.5 g (75%) of 1-$C_2H_5(CH_3)NH$-1-$CB_{11}H_{11}$ (**IIc**).

*Benzoylation of* **II**

To a solution of compound **II** (3.4 g, 0.02 mol) in tetrahydrofuran (50 $cm^3$), sodium hydride (2.0 g, 0.08 mol) and benzoyl chloride (5 $cm^3$, 0.04 mol) were

carefully added. After stirring for 6 hr, the mixture was filtered and water (50 $cm^3$) was added to the filtrate. The tetrahydrofuran was then removed *in vacuo*, the residual solution was acidified with conc. hydrochloric acid (20 $cm^3$), filtered and extracted with two 30-$cm^3$ portions of ether. The product obtained after evaporating the combined organic extracts *in vacuo* was dried at 120°C/1.3 Pa to isolate 2.5 g (45%) of 1-$C_6H_5(OH)C{=}(CH_3)N$-1-$CB_{11}H_{11}$ (**IIIb**).

$[(CH_3)_4N]^+[1\text{-}C_6H_5(O)C{=}(CH_3)N\text{-}1\text{-}CB_{11}H_{11}]^-$ (**IIIc**)

To a solution of compound **IIIb** (1.0 g, 3.6 mmol) in 2% aqueous potassium hydroxide (30 $cm^3$), aqueous 1 *M* tetramethylammonium chloride (10 $cm^3$) was added. The suspension so formed was then heated to 70°C and ethanol was successively added to obtain a clear solution. After allowing the filtered solution to stand overnight, 1.2 g (82%) of crystalline **IIIc** was separated from the solution.

## RESULTS AND DISCUSSION

Formation of two new species with a 1-carba-*closo*-dodecaborane(12) framework was revealed by TLC on treatment of **I**[1] with 1 molar equivalent of iodine in aqueous sodium carbonate solution. Besides iodoform of an obscure origin and recovered starting compound **I** (25%), a pure main product **II** (64%) along with a side product (**III**) (10%) can be simply separated from the reaction mixture.

The main product was identified as a hitherto unknown zwitterionic 1-methylamine-1-carba-*closo*-dodecaborane(11) (**II**), the side product being the corresponding formyl derivative in its tautomeric form, i.e. 1-hydroxymethylenemethylamine-1-carba-*closo*-dodecaborane(11) (**III**). Evidence for the suggested constitutions is based on the results of relevant mass, IR, $^1H$ and $^{11}B$ NMR spectra (see Tables 1 and 2). The results are also in agreement with various chemical transformations of compounds **II** and **III**.

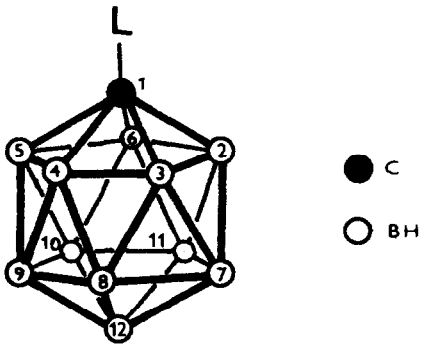



Fig. 1. Simplified structure of *closo*-1-L-1-$CB_{11}H_{11}$ compounds [L=$NH(CH_3)_2$ (**I**), $NH_2CH_3$ (**II**), $\bar{N}HCH_3$ (**IIa** anion), $N(CH_3)_3$ (**IIb**), $NH(CH_3)C_2H_5$ (**IIc**), $N(CH_3){=}CH{-}OH$ (**III**), $N(CH_3){=}CH{-}O$ (**IIIa** anion), $N(CH_3){=}C(OH)C_6H_5$ (**IIIb**) and $N(CH_3){=}C(O)C_6H_5$ (**IIIc** anion)].

Compound **II** resulted apparently as a consequence of a curious demethylation of **I** and the formyl derivative (**III**) is produced by a no less extraordinary formylation of its precursor (**II**). The following array of reactions (Scheme 1) may explain the observed facts:

$$[(CH_3)_2\bar{N}CB_{11}H_{11}]^- \xrightarrow{I_2} (CH_3)_2N(I)CB_{11}H_{11}$$

$$\xrightarrow{-HI} CH_2{=}N(CH_3)CB_{11}H_{11}$$

$$\xrightarrow{OH^-} [HOCH_2\bar{N}(CH_3)CB_{11}H_{11}]^-$$

$$\xrightarrow{I_2} HOCH_2NI(CH_3)CB_{11}H_{11}$$

$$\xrightarrow{-HI} HOCH{=}N(CH_3)CB_{11}H_{11}$$

**III**

$$[HOCH_2\bar{N}(CH_3)CB_{11}H_{11}]^- \xrightleftharpoons{-CH_2O,\,H^+} CH_3NH_2CB_{11}H_{11}$$

**II**

Scheme 1.

Compound **II** is essentially inert towards iodine in aqueous sodium carbonate; however, in the presence of formaldehyde, compound **III** is obtained in good yield. This observation strongly supports the proposed reaction pathway.

On heating briefly with hydrochloric acid, the formyl derivative (**III**) quantitatively hydrolyses to species **II**, which was used for modifying the original procedure, and pure compound **II** can be obtained in almost quantitative yield in this way.

Derivative **II** is a solid, not melting up to 250°C, very soluble in polar solvents such as water, ethanol, acetone, ether etc., but sparingly soluble in chloroform and virtually insoluble in benzene. It is a weak acid ($pK_a$ = 6.51 in 50% ethanol) and the [1-$CH_3NH$-1-$CB_{11}H_{11}]^-[N(CH_3)_4]^+$ salt can be isolated from alkaline solutions on addition of tetramethylammonium chloride.

Methylation of **II** with dimethyl sulphate in the presence of sodium hydride affords quantitatively the recently described[1] 1-trimethylamine-1-carba-*closo*-dodecaborane(11) (**IIb**). However, with ethyl bromide, only 1-methylethylamine-1-carba-*closo*-dodecaborane(11) (**IIc**) can be obtained.

The formyl derivative (**III**) is a much stronger acid than **II** ($pK_a = 2.68$ in 50% ethanol), and its $[(CH_3)_3NH]^+$, $[(CH_3)_4N]^+$ and $[(CH_2)_6N_4H]^+$ salts can be obtained without complication even from acidic solutions. The tetramethylammonium salt, $[(CH_3)_4N]^+[O\text{-}CH{=}N(CH_3)\text{-}1\text{-}CB_{11}H_{11}]^-$, was chosen for identification by spectral methods. The **IIIa** anion is very stable in neutral or alkaline solutions: however, it slowly hydrolyses in acidic medium to give the parent compound (**II**). Nevertheless, practically pure free acid can be obtained if the salt **IIIa**, suspended in 10% hydrochloric acid, is extracted with ether.

Treatment of **II** with benzoyl chloride and sodium hydride in tetrahydrofuran results in the formation of 1-hydroxybenzylidenemethylamine-1-carba-*closo*-dodecaborane(11) (**IIIb**), which was isolated as the salt **IIIc**. The free acid (**IIIb**) is then readily obtained from its salt (**IIIc**) as in the case of acid **III**.

Both acids **III** and **IIIb** cannot be crystallized in the usual way because of either their extreme solubility (chloroform, ether, ethanol and water) or extreme insolubility (benzene and parafinic hydrocarbons) and they were obtained as amorphous hydroscopic powders, despite their TLC purity. Such unpleasant properties can be explained in terms of possible *cis–trans* isomerism, due to the presence of the C=N bond, complicated by tautomeric equilibria between corresponding amide and hydroxymethylenic forms. Some evidence for the mentioned *cis*- and *trans*-forms of **III** and **IIIb** can be shown by the IR absorptions assigned to both OH and NH groups (see Table 2).

The ready availability of compounds of the general formula $1\text{-L-}1\text{-}CB_{11}H_{11}$ as described now opens wide possibilities of synthesizing further diverse *C*-substituted representatives of the $[1\text{-}CB_{11}H_{12}]^-$ family of carbaboranes. The relevant research is now in progress.

*Acknowledgements*—The $^1H$ and $^{11}B$ NMR spectra were measured by Drs F. Mareš and S. Heřmánek, mass spectra were collected by Dr Z. Weidenhoffer and the potentiometric $pK_a$ measurements were performed by Mr M. Skalický, all of the Institute of Inorganic Chemistry, Czechoslovak Academy of Sciences, Prague. We wish to thank these colleagues for their kind assistance.

## REFERENCE

1. J. Plešek, T. Jelínek, E. Drdáková and B. Štíbr, *Collect. Czech. Chem. Commun.* 1984, **49**, 1559.

*Polyhedron* Vol. 3, No. 12, pp. 1357–1363, 1984
Printed in Great Britain

0277–5387/84 $3.00 + .00
© 1984 Pergamon Press Ltd

# PREPARATION AND CHARACTERIZATION OF A NOVEL MACROCYCLIC LIGAND—DINITRO-TETRAAZACYCLOTETRADECA-TETRAENE—AND APPLICATION AS A HIGHLY SELECTIVE EXTRACTANT FOR COPPER(II)

MANABU FUJIWARA, TAKAYUKI MATSUSHITA* and TOSHIYUKI SHONO

Department of Applied Chemistry, Faculty of Engineering, Osaka University, Yamadaoka, Suita, Osaka 565, Japan

(*Received* 30 *May* 1984; *accepted* 9 *July* 1984)

**Abstract**—A novel tetraaza macrocyclic Schiff base ligand, 6,13-dinitro-5,7,12,14-tetramethyl-1,4,8,11-tetraazacyclotetradeca-1,5,7,12-tetraene, was prepared and its copper(II) and nickel(II) complexes were characterized. This ligand was found to be an excellent extractant for copper(II).

Many tetraaza macrocyclic compounds and their metal complexes have been prepared and characterized.[1,2] Of them, unsaturated Schiff base ligands have been intensively investigated in connection with their resemblance to naturally occurring porphyrins.[3] In addition, substituent effects on the properties of the metal complexes with these ligands have been reported.[4,5] These tetraaza ligands can be expected to form selectively complexes with transition metal ions. However, the extraction properties of these ligands for transition metal ions have been little studied.[6] Recently, Zolotov *et al.*[7,8] reported the extraction of transition and post-transition metal ions by several tetraaza macrocyclic compounds and found that copper(II) is selectively extracted.

In this paper, we describe the preparation of 6,13-dinitro - 5,7,12,14 - tetramethyl - 1,4,8,11 - tetraaza-cyclotetradeca-1,5,7,12-tetraene ($H_2L^2$) and the characterization of its copper(II) and nickel(II) complexes. Moreover, the extraction properties of $H_2L^2$ and its parent macrocycle ($H_2L^1$) (see Fig. 1) for transition metal ions such as copper(II), nickel(II) and zinc(II) will be described.

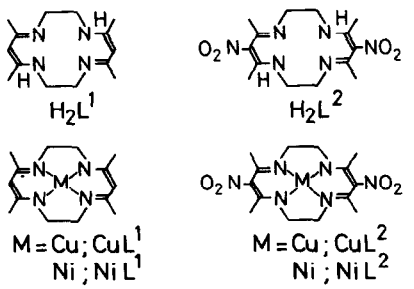



Fig. 1. Macrocycles and their complexes studied.

## EXPERIMENTAL

### *Preparation of bis(3-nitro-2,4-pentanedionato) copper(II)*[9]

To an acetic anhydride solution (50 $cm^3$) of acetylacetone (10 $cm^3$) was added very slowly copper(II) nitrate trihydrate (7.5 g) while cooling with an ice-water bath. The mixture was stirred vigorously at 0°C for 5 hr, and then at room temperature for 24 hr. The blue solution turned green gradually. The mixture was poured into an aqueous solution (1 $dm^3$) of sodium acetate (10%). It was stirred for 3 hr while cooling at 0°C to give a dark green precipitate. It was collected on a glass filter,

* Author to whom correspondence should be addressed.

washed with water, and then recrystallized from a mixture of ethanol and chloroform. The yield was 40%. Found: C, 33.97; H, 3.79; N, 7.96%. Calc. for $CuC_{10}H_{12}N_2O_8$: C, 34.14; H, 3.45; N, 7.97%. IR (in KBr disk): 3420, 1585, 1520, 1395, 1340, 1105, 1000, 935 and 825 $cm^{-1}$.

*Preparation of* (6,13-*dinitro*-5,7,12,14-*tetramethyl*-1,4,8,11-*tetraazacyclotetradeca*-1,5,7,12-*tetraenato*)*copper*(II) ($CuL^2$)

To a xylene solution (100 $cm^3$) of the aforementioned copper complex (3.0 g) was added dropwise ethylenediamine (1.1 g) with stirring at 80°C. The green solution turned gray with a precipitate. The mixture was stirred vigorously for 8 hr at 120°C. The precipitate was redissolved and developed a deep brown color. The solution was evaporated to dryness under reduced pressure. The resulting brown residue was recrystallized from a mixture of ethanol and chloroform. The yield was 70%. Found: C, 41.92; H, 5.24; N, 20.87%. Calc. for $CuC_{14}H_{20}N_6O_4$: C, 42.04; H, 5.05; N, 21.02%. IR (in KBr disk): 3420, 1560, 1475, 1425, 1340, 1310, 1135, 1010 and 800 $cm^{-1}$.

*Preparation of* $H_2L^2$

Hydrogen sulphide gas was passed very slowly through a chloroform solution (100 $cm^3$) of $CuL^2$ (1.5 g) with stirring for 3 hr. A few drops of a 2-propanol solution saturated with hydrogen chloride gas were added to the chloroform solution for aggregation of a precipitate of copper sulphide. It was filtered off and the yellow filtrate was stirred vigorously with a large excess of sodium hydrogen carbonate for 2 hr while nitrogen gas was passed through the solution. The mixture was filtered and the filtrate was evaporated to dryness under reduced pressure. The resulting solid was recrystallized from ethanol to give orange crystals. The yield was 65%. M.p.: 203.5–204.0°C (decomp.). Found: C, 49.55; H, 6.62; N, 24.63%. Calc. for $C_{14}H_{22}N_6O_4$: C, 49.68; H, 6.57; N, 24.84%. MS found: *m/z* 338. Calc. for $C_{14}H_{22}N_6O_4$: *M* 338. IR (in KBr disk): 3400, 1600, 1495, 1425, 1350, 1290, 1270, 1155 and 990 $cm^{-1}$. $^1$H-NMR (in $CDCl_3$): $\delta$ 2.21 (12H, *s*, $C\underline{H}_3$), 3.56 (8H, *s*, $C\underline{H}_2$) and 13.78 (2H, *s*(*br*), N<u>H</u>) ppm.

*Preparation of copper*(II) *and nickel*(II) *complexes with* $H_2L^2$, $CuL^2$ *and* $NiL^2$

To an ethanol solution (50 $cm^3$) of copper(II) acetate monohydrate (0.20 g, 1.0 mmol) was added an equimolar amount of $H_2L^2$ (0.34 g). The solution was refluxed for 1 hr, and then cooled to room temperature. The resulting precipitate was collected on a glass filter, and recrystallized from a mixture of ethanol and chloroform to give the copper complex ($CuL^2$) as brown crystals. The yield was 0.29 g. This complex was identical to that obtained by the reaction of Cu($\gamma$-$NO_2$ acac)$_2$ with ethylenediamine, on the basis of IR and electronic spectra.

A nickel complex of $H_2L^2$ was obtained in a similar manner to that described for the copper complex, using nickel(II) acetate tetrahydrate in place of a copper salt. It was recrystallized from a mixture of ethanol and chloroform. The yield was 0.24 g. Found: C, 42.67; H, 5.33; N, 21.16%. Calc. for $NiC_{14}H_{20}N_6O_4$: C, 42.56; H, 5.11; N, 21.28%. IR (in KBr disk): 3420, 1575, 1480, 1425, 1355, 1285, 1165, 1010 and 805 $cm^{-1}$.

A zinc complex of $H_2L^2$ could not be obtained in a similar manner to that described for the copper complex.

*Preparation of* $H_2L^1$ *and its copper*(II) *and nickel*(II) *complexes*

These compounds were prepared according to the literature.[10]

*Materials*

All reagents were reagent grade. Chloroform was refluxed over $P_2O_5$ and distilled. *N*,*N*-dimethylformamide (DMF) was distilled over $CaH_2$ under reduced pressure prior to use. Other solvents were purified by a usual manner. Water was deionised. Acetate buffer solutions (0.2 mol $dm^{-3}$) were used for adjusting pH from 3.5 to 5.5. pH below 3.5 or above 5.5 were adjusted by addition of an adequate amount of 1.0 mol $dm^{-3}$ hydrochloric acid or sodium hydroxide.

*Measurements*

UV and visible absorption spectra were recorded on a Hitachi 340 recording spectrophotometer. IR spectra were recorded on a Hitachi 215 grating spectrophotometer. Atomic absorption spectra were obtained using a Nippon Jarrel Ash AA-1. $^1$H-NMR spectra were taken with a JEOL JNM-PS 100 spectrometer, using $CDCl_3$ as the solvent and TMS as the internal standard. Polarograms were measured in DMF at 25°C by use of a Yanaco P-8 Polarograph. A dropping mercury electrode and a mercury pool were used as the working and counter electrodes, respectively. Tetrabutylammonium perchlorate (0.1 mol $dm^{-3}$) was used as the supporting electrolyte. The pH of a sample solution was measured with a Shibata 671 pH meter.

*Procedure for solvent extraction*

Solvent extractions were carried out by using a 10-$cm^3$ test tube with a stopper in which an aqueous solution (5 $cm^3$) of metal acetate ($Cu^{2+}$, $Ni^{2+}$ or $Zn^{2+}$) and a chloroform solution (5 $cm^3$) of the ligand were contained as aqueous and organic phases, respectively. The concentrations of the materials varied from $2.0 \times 10^{-2}$ to $2.0 \times 10^{-4}$ mol $dm^{-3}$. The test tube was shaken for an adequate time, from 2 min to 72 hr, at room temperature by use of a shaker. After shaking, the concentrations of metal ions remained in the aqueous phase were determined by atomic absorption spectrometry. Moreover, the concentrations of metal complexes transferred into the organic phase were determined by measuring visible absorption spectra of the chloroform solution.

## RESULTS AND DISCUSSION

In the present work, the novel tetraaza macrocyclic Schiff base ligand $H_2L^2$ was obtained by demetallation of its copper complex in a good yield. The copper(II) and nickel(II) complexes were prepared by using the free ligand and characterized by their electronic absorption spectra and polarograms. These were compared with those for the metal complexes of $H_2L^1$ in order to investigate substituent effects of nitro groups. Moreover, $H_2L^2$ has been applied to solvent extraction of transition metal ions and found to be a highly selective extractant for copper(II).

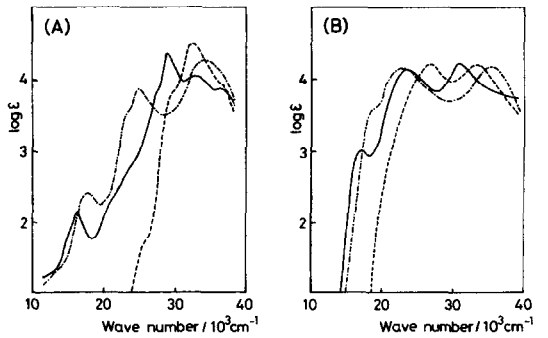



Fig. 2. Electronic spectra in chloroform. (A) (– – –) $H_2L^1$, (——) $CuL^1$ and (–·–·–) $NiL^1$. (B) (– – –) $H_2L^2$, (——) $CuL^2$ and (–·–·–) $NiL^2$.

*Electronic spectra*

Figure 2 shows the electronic spectra of the ligands $H_2L^1$ and $H_2L^2$ and their complexes with copper(II) and nickel(II) in chloroform. The band positions of the absorption maxima are listed in Table 1, together with the extinction coefficients. The spectrum of $H_2L^1$ exhibits three absorption bands centered at 308 nm [Fig. 2(A)], which can be assigned to $\pi$–$\pi^*$ transitions. The spectrum of either $CuL^1$ or $NiL^1$ shows an absorption band with moderate intensity in the visible region. The absorption bands at 615 nm for $CuL^1$ and at 562 nm for $NiL^1$ can be assigned to the ligand field transitions. The absorption bands observed in the UV region for these complexes may be due to the charge-transfer transitions.[5] On the other hand, the spectrum of $H_2L^2$ exhibits two broad

Table 1. Absorption maxima and half-wave potentials of the macrocycles and their copper(II) and nickel(II) complexes

| Compound | $\lambda_{max}$ / nm (log ε)[a] | $-E_{1/2}$ (vs Hg pool)[b] / V |
|---|---|---|
| $H_2L^1$ | 308(4.48) | |
| $CuL^1$ | 302(4.03), 343(4.34), 615(2.15) | 2.23 |
| $NiL^1$ | 292(4.26), 399(3.87), 562(2.40) | 2.50 |
| $H_2L^2$ | 297(4.23), 371(4.21) | |
| $CuL^2$ | 323(4.24), 427(4.14), 586(3.01) | 1.27, 2.28 |
| $NiL^2$ | 283(4.18), 442(4.15), 540$^{sh}$(3.54) | 1.51, 1.88 |

[a] Measured in chloroform. sh, shoulder.
[b] Measured in DMF at 25°C.

absorption bands at 297 and 371 nm [Fig. 2(B)], which also can be assigned to $\pi$–$\pi^*$ transitions. The spectrum of $CuL^2$ shows an absorption band at 586 nm, in the visible region assignable to the ligand field transitions. This band is more intense than that of $CuL^1$ and its position is shifted to shorter wavelengths by 29 nm compared to that of $CuL^1$. A similar spectral feature is observed for $NiL^2$: the absorption band at 540 nm in the visible region is more intense and its position is shifted to shorter wavelengths by 22 nm compared to that of $NiL^1$. These higher energy shifts and increases in intensity may be caused by substitution of $NO_2$ for H. Such substituent effects have been reported for the nickel(II) complexes of 15-membered tetraaza macrocyclic ligands.[5]

*Electrochemical properties*

The half-wave potentials of the complexes measured in DMF are summarized in Table 1. The polarograms of $CuL^1$ and $NiL^1$ show one cathodic wave at half-wave potentials of $-2.23$ and $-2.50$ V (vs Hg pool), respectively. On the other hand, those of $CuL^2$ and $NiL^2$ show two-step cathodic waves at half-wave potentials of $-1.27$ and $-2.28$ and $-1.51$ and $-1.88$ V, respectively. These first waves can be assigned to one-electron reduction of the central metal ion from bivalent to univalent. Introduction of the nitro groups on the $\gamma$-carbon atoms of $H_2L^1$ results in a large positive shift (*ca* 1 V) for the reduction potentials of the copper(II) and nickel(II) complexes. This can be interpreted in terms of a decrease in electron density on the central metal ion of the complex caused by the electron-withdrawing nitro groups. Such substituent effects have been reported for the nickel(II) complexes with 15-membered tetraaza macrocyclic ligands.[5]

*Complexation of copper*(II) *and nickel*(II) *with* $H_2L^1$ *and* $H_2L^2$

The rates of complexation of copper(II) and nickel(II) with $H_2L^1$ and $H_2L^2$ were spectrophotometrically determined in a homogeneous DMF solution at 25°C. A DMF solution of each ligand ($8.0 \times 10^{-5}$ mol dm$^{-3}$) and a DMF solution of the equimolar amount of each metal ion were mixed, and then its absorption spectrum was measured over the range 270–500 nm at regular time intervals. In the case of copper(II) with $H_2L^2$, the absorption spectrum remarkably changes during the initial 2 min and then gradually until 150 min: the absorption maximum of the ligand at 370 nm decreases in intensity and the new absorption bands which appeared at 323 and 430 nm increase in intensity, having isosbestic points at 333 and 386 nm [Fig. 3(A)]. These spectral changes indicate the formation of a $CuL^2$ complex. Similar spectral changes were observed for other cases: with $H_2L^1$ and copper(II) the absorption maximum of the ligand was shifted from 305 to 341 nm, having an isosbestic point at 322 nm, with $H_2L^1$ and nickel(II) it was shifted from 305 to 398 nm, having an isosbestic point at 348 nm, and with $H_2L^2$ and nickel(II) it was shifted from 370 to 448 nm, having an isosbestic point at 389 nm [Fig. 3(B)]. The extent of complexation for these systems was calculated from these spectral changes. The results are shown in Fig. 4. Clearly, the rates of complexation of copper(II) with both ligands were found to be much faster than

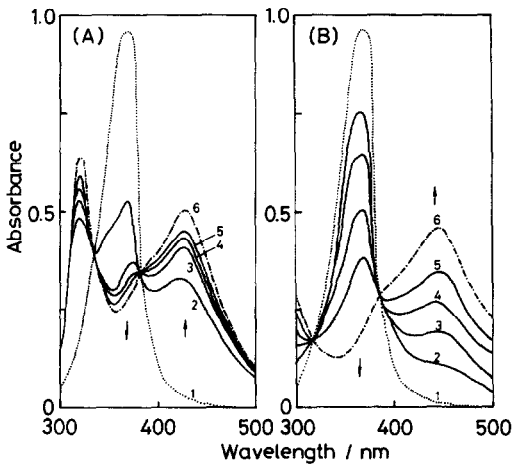



Fig. 3. Absorption spectral changes caused by complexation of copper(II) (A) and nickel(II) (B) with $H_2L^2$ in DMF at 25°C. $[H_2L^2]$ = [metal] = $4.0 \times 10^{-5}$ mol dm$^{-3}$; cell length = 1 cm. (A) 1, $H_2L^2$; 2, 3, 4 and 5, after 2, 20, 45 and 75 min, respectively; 6, $CuL^2$. (B) 1, $H_2L^2$; 2, 3, 4 and 5, after 45, 100, 200 and 400 min, respectively; 6, $NiL^2$.

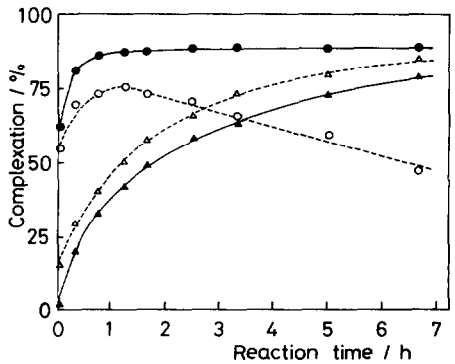



Fig. 4. The time-courses of complexation of copper(II) and nickel(II) with either $H_2L^1$ or $H_2L^2$ in DMF at 25°C. [ligand] = [metal] = $4.0 \times 10^{-5}$ mol dm$^{-3}$. (--○--) $CuL^1$, (--△--) $NiL^1$, (——●——) $CuL^2$ and (——▲——) $NiL^2$.

those for nickel(II). The extent of complexation of copper(II) with $H_2L^2$ reaches *ca* 90% after 2 hr. However, in the course of complexation of copper(II) with $H_2L^1$, it reaches a maximal value (75%) after 75 min and then decreases gradually. This may be caused by the instability of $CuL^1$ formed in the DMF solution. In the fact, on standing a DMF solution of the isolated $CuL^1$, its absorption spectrum was decreased in intensity over the range 330–500 nm, suggesting that decomposition of the complex occurs.[11] Such behaviour was not observed for the complexes $CuL^2$, $NiL^1$ and $NiL^2$. On the other hand, the rates of complexation of nickel(II) with $H_2L^1$ and $H_2L^2$ are slow and not so different between the two ligands. Complex formation was still incomplete after 7 hr. These results clearly reflect on solvent extractions of these metal ions by the ligands, which will be described later.

### *Solvent extraction of transition metal ions by* $H_2L^1$ *and* $H_2L^2$

Solvent extractions of copper(II), nickel(II) and zinc(II) by $H_2L^2$ were carried out under the conditions mentioned in Experimental compared with those by $H_2L^1$. Figure 5 shows the plots of the percentages of these metal ions extracted by $H_2L^1$ and $H_2L^2$ against shaking time. The concentrations of the extractants in chloroform and of the metal ions in water were $2.0 \times 10^{-2}$ and $2.0 \times 10^{-3}$ mol $dm^{-3}$, respectively, and the pH of the aqueous phase was adjusted to nearly 5.7 without using a buffer solution. The rates of extraction of copper(II) by both extractants were found to be much faster than those of nickel(II) and zinc(II). With $H_2L^2$ nearly 100% copper(II) in the aqueous phase could be extracted within 30 min, whereas, with $H_2L^1$, nearly 90% copper(II) was transferred into the organic phase after 2 hr. Moreover, in the former case, the percentage of extracted copper(II) was constant until 24 hr, whereas, in the latter case, it decreased gradually after 6 hr. This may be caused by instability of the complex $CuL^1$ transferred into the chloroform solution as mentioned earlier.

As for nickel(II), the rate of extraction by $H_2L^1$ was slightly faster than that by $H_2L^2$, in contrast to the copper case. However, the extent of extraction of nickel(II) by both extractants was much lower than those of copper(II). On the other hand, as for zinc(II), its extraction by $H_2L^1$ was observed at a slightly faster rate than that for nickel(II), whereas no extraction of zinc(II) by $H_2L^2$ was observed after shaking for 72 hr under the same conditions. These results indicate that $H_2L^2$ is considered to be a better extractant than $H_2L^1$ in extraction rate, selectivity for copper(II) and stability. Such properties of the former may result from introduction of nitro groups which provide adequate hydrophobicity and ligand field strength. In fact, the distribution ratios of the extractants ($[H_2L]_{org}/[H_2L]_{aq}$), which were determined at pH 5.7 after shaking for 3 hr, were 0.67 and 1.56 for $H_2L^1$ and $H_2L^2$, respectively. In addition, the distribution ratios of the copper(II) complexes were determined to be 0.83 and 500 for $CuL^1$ and $CuL^2$, respectively.

### *Effect of pH on extraction*

Figure 6 shows the effects of the pH of the aqueous phase on extractions of copper(II) and nickel(II) by $H_2L^1$ and $H_2L^2$. The extractions were made under the following conditions: the concentrations of the extractants and metal ions were $2.0 \times 10^{-3}$ mol $dm^{-3}$, and shaking times were 4, 3 and 24 hr for the

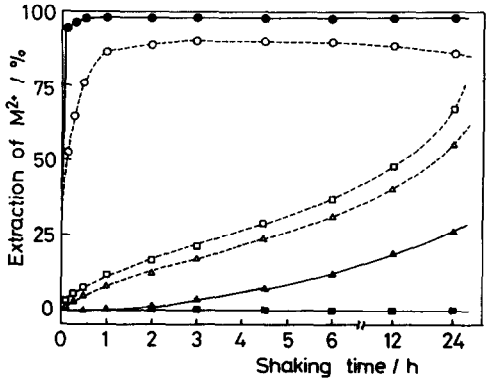



Fig. 5. Extractabilities of $H_2L^1$ and $H_2L^2$ ($2.0 \times 10^{-2}$ mol $dm^{-3}$) for copper(II), nickel(II) and zinc(II) ($2.0 \times 10^{-3}$ mol $dm^{-3}$). (--○--) Cu(II)-$H_2L^1$, (--△--) Ni(II)-$H_2L^1$, (--□--) Zn(II)-$H_2L^1$, (——●——) Cu(II)-$H_2L^2$, (——▲——) Ni(II)-$H_2L^2$ and (——■——) Zn(II)-$H_2L^2$.

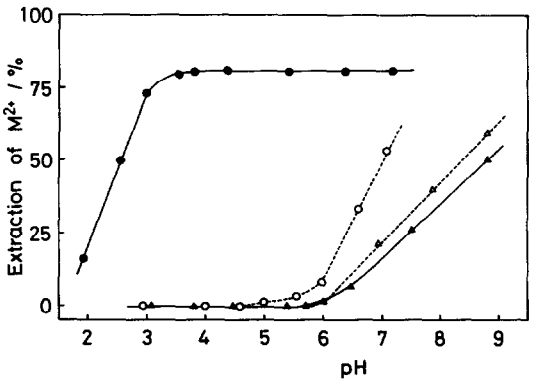



Fig. 6. Effect of pH on extraction of copper(II) and nickel(II) ($2.0 \times 10^{-3}$ mol $dm^{-3}$) by $H_2L^1$ and $H_2L^2$ ($2.0 \times 10^{-3}$ mol $dm^{-3}$). (--○--) Cu(II)-$H_2L^1$, (--△--) Ni(II)-$H_2L^1$, (——●——) Cu(II)-$H_2L^2$ and (——▲——) Ni(II)-$H_2L^2$.

systems of copper(II) and $H_2L^1$, copper(II) and $H_2L^2$, and nickel(II) and both extractants, respectively. With $H_2L^1$ both metal ions could not be extracted in acidic regions (pH less than 4.5). The extraction of copper(II) by $H_2L^1$ began to occur at pH 5.0 and its percentage increased with increasing pH of the aqueous phase. At pH 5.7, the percentage of copper(II) extracted by $H_2L^1$ is much lower than that obtained in the experiment shown in Fig. 5. This was ascribed to the extraction conditions being different in the two experiments: in the former case, $H_2L^1$ was used at 10-molar fold excess over copper(II) and a buffer solution was not used for adjusting the pH of the aqueous phase. On the other hand, with $H_2L^2$ the extraction of copper(II) began to occur in more acidic conditions than that by $H_2L^1$ and its constant extraction (*ca* 80%) was achieved in the pH range from 3.5 to 7.5. The extractions of nickel(II) by $H_2L^1$ and $H_2L^2$ were observed at pHs above 6.0.

The $pH_{50\%}$ values indicate that $H_2L^2$ possesses a high selectivity and extractability to copper(II).

*Effect of molar ratios of* $H_2L^2$ *to copper*(II) *on extraction*

Figure 7 shows the plots of the percentage of copper(II) extracted by $H_2L^2$ against shaking time at various molar ratios. When the concentration of the extractant ($2.0 \times 10^{-2}$ mol dm$^{-3}$) was equal to that of copper(II), the extraction attained equilibrium at 88% after 90 min. As the molar ratios of $H_2L^2$ to copper(II) were increased to 10 and 100, the shaking times needed for attaining equilibrium were remarkably shortened to 30 and 10 min, respectively, and nearly 100% copper(II) in the aqueous phase was transferred into the organic phase.

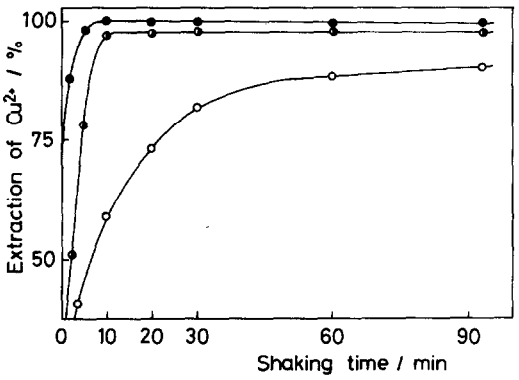



Fig. 7. Effect of molar ratios of $H_2L^2$ to copper(II) on extraction. $[H_2L^2] = 2.0 \times 10^{-2}$ mol dm$^{-3}$; [Cu(II)] = (—○—) $2.0 \times 10^{-2}$, (—◑—) $2.0 \times 10^{-3}$ and (—●—) $2.0 \times 10^{-4}$ mol dm$^{-3}$.

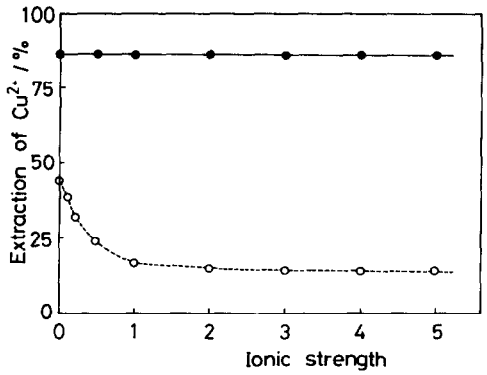



Fig. 8. Effect of ionic strength on extraction of copper(II) ($2.0 \times 10^{-3}$ mol dm$^{-3}$) by $H_2L^1$ and $H_2L^2$ ($2.0 \times 10^{-3}$ mol dm$^{-3}$). Ionic strength was adjusted by addition of sodium nitrate. (-- ○ --) Cu(II)-$H_2L^1$ and (—●—) Cu(II)-$H_2L^2$.

*Effect of ionic strength*

Figure 8 shows the effect of the ionic strength of the aqueous phase on extraction of copper(II) by $H_2L^1$ and $H_2L^2$. The extractions were carried out under the following conditions: the concentrations of the extractants and copper(II) were $2.0 \times 10^{-3}$ mol dm$^{-3}$, the pH of the aqueous phase was 5.7, and the shaking times were 4 and 3 hr for $H_2L^1$ and $H_2L^2$, respectively. The ionic strength of the aqueous phase was varied from 0.0 to 5.0 by addition of sodium nitrate. The extraction of copper(II) by $H_2L^1$ was strongly influenced by the ionic strength of the aqueous phase. The percentage of copper(II) extracted decreased from 43 to 17% as the ionic strength increased from 0.0 to 1.0 and came to a constant value of 14% when the ionic strength was above 2.0. On the contrary, the extraction of copper(II) by $H_2L^2$ was not affected by the ionic strength, and a constant extraction (88%) was achieved in the range of ionic strength from 0.0 to 5.0. These results suggest that $H_2L^2$ can be applied as a useful extractant of copper(II) from aqueous solutions containing a large amount of alkali metal salts.

## REFERENCES

1. (a) D. H. Busch, *Helv. Chim. Acta* Special Issue, 1967, 174; (b) D. H. Busch, *Acc. Chem. Res.* 1978, **11**, 392.
2. G. A. Melson, *Coordination Chemistry of Macrocyclic Compounds*. Plenum Press, New York (1979).
3. L. F. Lindoy, *Chem. Soc. Rev.* 1972, 421.
4. D. G. Pillsbury and D. H. Busch, *J. Am. Chem. Soc.* 1976, **98**, 7836.
5. J. A. Streeky, D. G. Pillsbury and D. H. Busch, *Inorg. Chem.* 1980, **19**, 3148.
6. E. A. Krasnushkina and Yu. A. Zolotov, *Trends Anal. Chem.* 1983, **2**, 158.

7. Yu. A. Zolotov, V. P. Bodnja, G. A. Larikova, N. V. Niz'eva, G. E. Vlasova and E. V. Rybakova, *Zh. Anal. Khim.* 1982, **37**, 1543.
8. Yu. A. Zolotov, N. V. Niz'eva, V. P. Ionov, D. M. Kumina and O. V. Ivanov, *Mikrochim. Acta* 1983, **1**, 381.
9. J. P. Collman, R. L. Marshall, W. L. Young and S. D. Goldby, *Inorg. Chem.* 1962, **1**, 704.
10. T. Hayashi, *Bull. Chem. Soc. Jpn* 1981, **54**, 2348.
11. T. J. Trux and R. H. Holm, *J. Am. Chem. Soc.* 1972, **94**, 4529.

*Polyhedron* Vol. 3, No. 12, pp. 1365–1367, 1984
Printed in Great Britain

0277–5387/84 $3.00 + .00
© 1984 Pergamon Press Ltd

# COMMUNICATION

## THE PREPARATION AND CHARACTERISATION OF DICHLORO(1,2,4-TRITHIA-3-AZABUT-2-ENE)GOLD(III), $AuCl_2(S_3N)$

J. D. WOOLLINS
Department of Chemistry, Imperial College of Science and Technology, South Kensington, London SW7 2AY, U.K.

(*Received* 22 *May* 1984; *accepted* 9 *July* 1984)

**Abstract**—Deprotonation of heptasulphurmonoimide at −78°C using BuLi followed by reaction with $HAuCl_4$ yields $AuCl_2(S_3N)$, in moderate yield (21%), characterised by IR/Raman and UV/Vis spectroscopies.

In recent years there has been a lively interest in sulphur–nitrogen chemistry[1] largely as a result of the discovery of the unusual electrical properties of polymeric sulphur–nitride, $(SN)_x$. Despite the advances that have been made in the synthesis of S–N clusters there still remain few examples of metal complexes containing cyclic sulphur–nitrogen ligands with many of the complexes known being prepared in poor yield from reactions involving explosive tetrasulphurtetranitride.[2] It is the purpose of this paper to report a simple synthesis of $AuCl_2(S_3N)$, **1**, in reasonable yield from heptasulphurmonoimide and chloroauric acid. Characterisation of **1** was accomplished by microanalysis, IR/Raman and UV/Vis spectroscopies.

## EXPERIMENTAL

All solvents were of reagent grade, dried using standard procedures: reactions were carried out under argon. Heptasulphurmonoimide was prepared by the literature method,[3] and $HAuCl_4$ was from Johnson Matthey Chemicals. IR spectra were recorded as pressed discs using a Perkin–Elmer 683. Raman spectra were obtained from rotating KBr discs using a Spex Ramalog system (647.1-nm excitation). UV/Vis spectra were measured with a Pye–Unicam SP8100.

### *Preparation of* $AuCl_2(S_3N)$

Heptasulphurmonoimide (0.48 g, 2 mmol) was dissolved in diethyl ether (10 $cm^3$) and the solution cooled to −78°C, whereupon BuLi [0.75 $cm^3$, 2 mmol (Aldrich Chemical Co.)] was added. To the resulting pale yellow solution was slowly added $HAuCl_4$ (0.36 g, 1.05 mmol) in diethyl ether (4 $cm^3$). The reaction mixture was allowed to warm to room temperature, filtered, reduced in volume to *ca* 6 $cm^3$ and cooled to −15°C to give the product as black crystals (85 mg, 21%). Found: N, 3.59; Cl, 17.34; S, 25.91%. Calc. N, 3.70; Cl, 18.78; S, 25.40%. Mass spectrum: parent ion not detected, peaks at *m/z* 111 ($S_3NH$), 78 ($NS_2$) and 46 (NS) being the only NS fragments.

## RESULTS AND DISCUSSION

Previously[2] we have reported conditions for the preparation and separation of $M(S_3N)_2$ complexes (M = Co, Ni, Pd or Pt) in low yield from the reaction of the appropriate metal halide with $S_4N_4$. More recently Bojes *et al.*[3,4] have successfully used $PPN[S_3N]$ ($PPN^+ = [(Ph_3P)_2N]^+$) to prepare $Ni(S_3N)_2$, **2**, $PPN[Cu(S_3N)_2]$, **3**, $PPN[Ag(S_3N)_2]$, **4**, and $PPN[CuCl(S_3N)]$, **5**, in 30, 46, 17 and 23% yields respectively. This latter route has the advantage of being a rational synthesis but does require the conversion of heptasulphurmonoimide into $PPN[S_4N]$ which is then desulphurated to $PPN[S_3N]$. The reaction described here takes advantage of the solution equilibrium of $S_7N^-$ [eqn (1)]:

$$S_7N^- = NS_4^- + 3/8S_8 = \tfrac{1}{2}S_6N_2^{2-} + \tfrac{1}{2}S_8 \quad (1)$$

to give the first example of a gold complex containing the $S_3N^-$ ligand, obtained in 21% yield. It is noteworthy that this yield is comparable to that

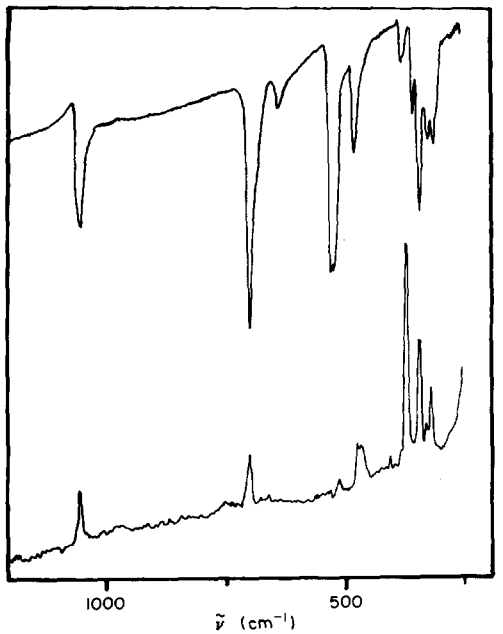



Fig. 1. IR (upper trace) and Raman (lower trace) spectra of $AuCl_2(S_3N)$.

reported for the preparation of **2–5** from $PPN[S_3N]$ mentioned earlier. Indeed, bearing in mind its simplicity, the "one-pot" method described here seems preferable. Attempts to improve the yield by addition of triphenylphosphine or carrying out the reaction at room temperature were not successful.

The characterisation of **1** was accomplished by microanalysis and UV/Vis and vibrational spectroscopies. The IR and Raman spectra (Fig. 1 and Table 1) are comparable with those previously reported for complexes of the type $M(S_3N)_2$ with bands due to $\nu$(SN) at 1052 and 696 $cm^{-1}$ in **1** compared to 994 and 700 $cm^{-1}$ in $Pt(S_3N)_2$. As was the case for the $M(S_3N)_2$ complexes difficulties are encountered in making an unequivocal assignment of the $\nu$(S—S) vibration because of the presence of a $\delta$(SN) vibration in the same region of the spectrum. Our assignment assumes that the (SN) vibrations are generally stronger in the IR than in the Raman spectra whilst the $\nu$(S—S) vibrations are of reasonable strength in both [cf. $S_3N^-$ (Ref. 4)]. It is of interest to note the effect of co-ordination upon the

Table 1. Vibrational frequencies ($cm^{-1}$) and assignments for $AuCl_2(S_3N)$, $Pt(S_3N)_3$ and $PPN[S_3N]$*

| $AuCl_2(S_3N)$ | | $Pt(S_3N)_2$[a] | $PPN[S_3N]$[b] | | Assignment |
|---|---|---|---|---|---|
| IR | Raman | | IR | Raman | |
| 1058sh<br>1052m | 1052w | 1001sh<br>994m | 893vs | 894m | $\nu(S^2-N^3)$ |
| 696s<br>643w | 697w | 710sh<br>700s | 666s | 686s | $\nu(S^4-N^3)$ |
| 524s | 509w | 524mw<br>514m | – | – | $\delta$(SN) |
| 477mw | 475w | 492w<br>480w | 564s | 574vs | $\nu$(S–S) |
| 372vw | 368s | – | – | – | $\nu$(M–S) |
| 357m | – | – | – | – | $\nu$(M–Cl) |
| 342s | 339m | – | – | – | $\nu$(M–Cl) |
| 328m | 324vw | 329mw | – | – | $\nu$(M–S) |
| 315m | 314 | 311w | – | – | ring def. |

* The numbering of the ring atoms is $M—S^1—S^2—N^3—S^4$.

[a] From Ref. 2.

[b] From Ref. 4.

vibrational spectrum of $S_3N^-$ the $\nu$(SN) vibrations increasing in frequency with the $\nu$(S—S) vibration decreasing. This observation is at variance with the predicted effect since *ab initio* calculations by Bojes *et al.*[4] indicate that the lowest unoccupied $\pi^*$-orbital in $S_3N^-$ is antibonding to all linkages and thus one might expect $\pi$-back-bonding from the gold to the $S_3N^-$ to weaken all of the bonds in the ligand.

The UV/Vis spectrum of **1** has absorption maxima (in MeCN) at 350 ($\varepsilon = 2.8 \times 10^3$ dm$^3$ mol$^{-1}$ cm$^{-1}$) and 458 nm ($\varepsilon = 1.9 \times 10^3$ dm$^3$ mol$^{-1}$ cm$^{-1}$) which are consistent with previously reported[2,4,5] data on $S_3N^-$ and suggest only minor perturbation of the energy levels upon co-ordination.

*Acknowledgement*—I am grateful to Johnson Matthey Chemicals for loans of precious metals.

## REFERENCES

1. H. G. Heal, *The Inorganic Heterocyclic Chemistry of Sulfur, Nitrogen and Phosphorus.* Academic Press, New York (1980).
2. J. D. Woollins, R. Grinter, M. K. Johnson and A. J. Thomson, *J. Chem. Soc., Dalton Trans.* 1980, 1910.
3. J. Bojes, T. Chivers and I. Drummond, *Inorg. Synth.* 1978, **XVIII**, 203.
4. J. Bojes, T. Chivers, W. G. Laidlaw and M. Trsic, *J. Am. Chem. Soc.* 1982, **104**, 4837.
5. J. Bojes, T. Chivers and P. W. Codding, *J. Chem. Soc., Chem. Commun.* 1981, 1171.